

DESIGN OF REINFORCED CONCRETE STRUCTURES

N SUBRAMANIAN

*Consulting Engineer
Maryland, USA*

OXFORD
UNIVERSITY PRESS

OXFORD
UNIVERSITY PRESS

Oxford University Press is a department of the University of Oxford. It furthers the University's objective of excellence in research, scholarship, and education by publishing worldwide. Oxford is a registered trade mark of Oxford University Press in the UK and in certain other countries.

Published in India by
Oxford University Press
YMCA Library Building, 1 Jai Singh Road, New Delhi 110001, India

© Oxford University Press 2013

The moral rights of the author/s have been asserted.

First published in 2013

All rights reserved. No part of this publication may be reproduced, stored in a retrieval system, or transmitted, in any form or by any means, without the prior permission in writing of Oxford University Press, or as expressly permitted by law, by licence, or under terms agreed with the appropriate reprographics rights organization. Enquiries concerning reproduction outside the scope of the above should be sent to the Rights Department, Oxford University Press, at the address above.

You must not circulate this work in any other form
and you must impose this same condition on any acquirer.

ISBN-13: 978-0-19-808694-9

ISBN-10: 0-19-808694-6

Typeset in Times
by Cameo Corporate Services Limited, Chennai
Printed in India by Yash Printographics, Noida 201301

Third-party website addresses mentioned in this book are provided
by Oxford University Press in good faith and for information only.
Oxford University Press disclaims any responsibility for the material contained therein.

*Respectfully dedicated to the memory of my beloved teacher
Prof. P. Purushothaman*

PREFACE

According to the World Business Council for Sustainable Development (www.wbcd.org), *concrete* is the most widely used material on earth (apart from water), with nearly three tons being used annually for each human being. Concrete is a construction material composed primarily of coarse and fine aggregates, cement, and water. Nowadays, various chemical and mineral admixtures are also added to concrete to achieve the required properties. It is also one of the oldest materials known to humans—the 43.3 m diameter Pantheon dome in Rome, which remains the largest coffered dome in the world, is nearly 1900 years old. Since concrete is weak in tension and strong in compression, reinforcements are added to make it a composite material called *reinforced concrete* (RC), which can resist both tensile and compressive stresses. The wide popularity of RC is due to its many advantages over other materials such as structural steel or wood.

The behaviour of RC structural elements is difficult to predict; one of my professors (late) Dr S.R. Srinivasan used to quip, the behaviour of RC is comparable to that of a drunken monkey bitten by a scorpion! The design rules for RC structures developed in the past were mostly empirical in nature and were based on extensive tests conducted on scaled specimens (which also introduced *size effects*). Design of an RC structure involves the proportioning of different elements of the structure and detailing them in such a way that the structure will be able to resist all the loads that are likely to act on it during its service life, without excessive deformation or collapse. Such designs should also be aesthetic, economical, durable, stable, and sustainable. RC design is often considered as much an art as a science. It must balance theoretical analysis with practical considerations such as the probability of loads acting on it, the actual behaviour of the structure as distinguished from the idealized analytical and design model, the actual properties of materials used compared to the assumed ones, and the actual behaviour of the material compared to the assumed elastic behaviour.

Structural knowledge is increasing continuously and rapidly as techniques for analysis, design, fabrication, and erection of structures are being improved constantly and new types of structures are being introduced. Hence, designers need to have a sound knowledge of the behaviour—both material behaviour of the reinforced concrete and structural behaviour of the individual elements as well as the complete structure. Unless the structural engineers are abreast of the recent developments and understand the relationship between the structural behaviour and design criteria implied by the rules of the design codes, they will be following the codal rules rigidly and blindly and may even apply them incorrectly in situations beyond their scope.

This text attempts to guide students and practising structural engineers in understanding and using the design codes correctly and wisely. It also strives to make them aware of the recent developments and the latest technologies and methods in use in the area of reinforced concrete.

ABOUT THE BOOK

Design of Reinforced Concrete Structures is designed to meet the requirements of undergraduate students of civil and structural engineering. This book will also be an invaluable reference to postgraduate students, practising engineers, and researchers.

This text is based on the latest Indian Standard code of practice for plain and reinforced concrete (IS 456:2000) released in July 2000 (reaffirmed 2005) and the three amendments released in June 2001, September 2005, and August 2007. Even though this fourth revision of the code gives greater emphasis to the limit states method of design, it also provides working stress method in Annex B as an alternative method. SI units have been used throughout the book.

Focusing on the modern limit states design, the book covers topics such as the properties of concrete, structural forms, loadings, behaviour of various structural elements (compression and tension members, beams, slabs, foundations, walls, and joints) and design and detailing for flexure, shear, torsion, bond, tension, compression, and compression with uniaxial and biaxial bending. It also discusses the design of flat plates, footing and pile caps, shear walls, staircases, RC joints, and multi-storey buildings.

The following features in the book make it stand out among the other books in this area:

- Even though IS 456 was revised in 2000, most of the design provisions remain unchanged from the previous 1978 edition of the code. Hence, IS 456 code provisions are compared with the provisions of other recent codes, especially with the provisions of ACI 318:2011 (in the global economy, many engineers are required to design structures using codes of other countries also).
- As per the seismic zone map of India (as given in IS 1893), more than 60 per cent of the land area in India is susceptible to seismic damage. Hence, seismic design and ductile detailing are given equal importance in this book. The behaviour of various elements of structures and the basis for the codal rules are also explained.
- Several topics that are usually not found in other books such as high-strength concrete, high-strength reinforcement, structural forms, sustainable design, integrity reinforcement, various shear design procedures, various shear and punching shear reinforcement, bond of coated and headed bars, space truss model of torsion design, size effect in beams and slabs, yield line analysis of slabs, design of flat slabs, pile caps, staircases, joints, shear walls, and strut-and-tie model design are discussed in this book.
- Detailed case studies of structural failures and innovations are provided in most of the chapters to help students relate to the concepts learnt through the book.

- A rich pedagogy provides the required rigour for students to excel in this subject in the examinations: over 160 examples with step-by-step solutions, over 850 review questions, 160 numerical problems, and over 750 illustrative figures and 200 tables. An exhaustive reference list at the end of each chapter helps interested readers to pursue topics further.
- Last but not the least, this book provides the most updated information in this subject covering the state-of-the-art trends and developments.

USING THE BOOK

The text is divided into 20 chapters and completely covers the undergraduate curriculum of most universities and the postgraduate (PG) course of several universities. The teacher adopting this book is requested to exercise discretion in selecting portions of the text to be presented for a particular course. It is suggested that portions of Chapters 6–8, 11, 13, 16, and 18–20 may be taught at PG level and Chapters 1–4 may be left for self-study.

Although relevant information from the Indian Standard code of practice has been included in the text, readers are advised to refer to the latest codes published by the Bureau of Indian Standards, New Delhi—IS 456:2000, codes on design loads (IS 875 and IS 1893), design aids to IS 456 (SP 16:1980), handbook on concrete reinforcement and detailing (SP 34:1987), explanatory handbook on IS 456:1978 (SP 24:1980), and code on ductile detailing of RC structures (IS 13920:1993).

CONTENTS AND COVERAGE

The book comprises 20 chapters and five appendices.

Chapter 1 provides information about the historical developments, advantages, ingredients, and proportioning of concrete mixes. It also covers types of concrete and reinforcing bars and properties of fresh and hardened concrete, since a designer should have a sound knowledge of the material that is used for designing.

Chapter 2 discusses the various RC elements and possible structural forms to resist gravity as well as lateral loads and a brief discussion on formwork. This information will be useful in practice to select the structural form.

Many failures are attributed to the lack of determination of the actual loads acting on structures. Hence the various loads and their combinations to be considered in the analysis are provided in *Chapter 3*.

Chapter 4 introduces the design considerations and the role of the structural designer in the complete design process. Various design philosophies are explained with their advantages and drawbacks. Sampling and acceptance criteria are also discussed. An introduction to the evolving performance-based design is also provided.

The flexural analysis and design of beams is discussed in *Chapter 5*. This chapter deals with the analysis and design of singly and doubly reinforced rectangular beams, flanged beams, deep, wide and hidden beams, and lintel and plinth beams. Limits on minimum and maximum reinforcement, slenderness limits, and design using

charts available in SP 16 are also explained. Emphasis is given to ductility and earthquake resistance.

Chapter 6 deals with the design to resist shear forces. In addition to explaining the behaviour of beams under shear, factors affecting the behaviour, design and maximum shear strength, minimum and maximum shear reinforcement, critical section for shear as well as design and detailing of various types of shear reinforcement based on different theories are discussed. Details on shear in beams with high-strength concrete and steel and shear strength of members with axial force are also included.

Chapter 7 discusses the bond between steel reinforcement and concrete as it is necessary for the composite action of RC members. Local and anchorage bonds are distinguished and development length provisions for various types of bars are discussed. Anchoring rebars with hooks/bends and headed bars are explained and discussions on splicing and curtailment of reinforcement are included.

IS 456 considers the design of torsion approximately as additional bending moment and shear force. The plastic space truss model considered in ACI and other codes is fully explained. The design method based on this model and graphical methods for torsion are discussed in *Chapter 8*. Detailing for torsion is also explained.

Chapters 9–11 deal with the design of one-way, two-way, and flat slabs/flat plates respectively. In each of these chapters, the behaviour of these slabs is explained and considerations for the design are discussed. The design for concentrated load is considered and design procedures as well as design using charts are explained. Topics such as non-rectangular slabs, opening in slabs, ribbed or voided slabs, slabs on grade, waffle slabs, hollow-core slabs, and yield-line analysis are also covered. Flat plates are susceptible to failure in punching shear. Hence, greater emphasis has been given to the design and detailing to prevent punching shear.

Serviceability checks for deflection and cracking at working loads are important for the proper functioning of structural elements during their design life. This aspect is covered in *Chapter 12*, with a comparison of the provisions found in other codes. Vibration and fatigue control are also briefly discussed.

The design of short and slender columns subjected to axial load as well as combined axial load and bending moment is covered in *Chapters 13* and *14*. Different classifications of columns are provided and the determination of effective length of columns is explained. The design methods as well as the use of design aids are illustrated with examples. Biaxially loaded columns as well as L-, T-, and +-shaped columns are also discussed.

Chapter 15 deals with the design of different types of footings, piles, and pile caps. Soil as well as structural design and detailing are explained.

Chapter 16 discusses the design of load-bearing walls, retaining walls, and shear walls. Behaviour of these walls is discussed and theories of earth pressures provided. Practical topics such as opening in walls, construction joints, drainage and compaction of backfill are also included.

The design of different types of staircases is provided in *Chapter 17* and design of tension members are covered in *Chapter 18*. The design of beam-column joints, and beam-to-beam joints are provided in *Chapter 19*. This chapter also discusses the design of corbels and anchors and detailing of obtuse- and acute-angled corners.

As RC designs are carried out in design offices using standard computer programs, a typical analysis and design of a multi-storey building is carried out using the STAAD.Pro software in *Chapter 20*. This chapter gives the students an exposure to how designs are handled in practice and also guide them to use such software packages.

Appendices A–E provide some useful information such as properties of soils, strut-and-tie method of design, design aids, conversion factors, and some rules of thumb and practical tips.

Though care has been taken to present error-free material, some errors might have crept in inadvertently. I would highly appreciate if these errors are brought to the attention of publishers. Any suggestions for improvement are also welcome.

ACKNOWLEDGEMENTS

Sir Isaac Newton once said, *‘If I have seen farther than others, it is because I have stood on the shoulders of giants.’* In the same way, I have been greatly influenced in the preparation of this book by the books, papers, and lectures of great professors and designers. I would like to apologize for any phrase or illustrations used in this book inadvertently without acknowledgement.

I am grateful to my teachers (late) Prof. P. Purushothaman of College of Engineering, Guindy (now belonging to Anna University), and Prof. P. Sabapathy of Thiagarajar College of Engineering, Madurai, who cultivated great interest in me about designing RC structures. My understanding of this subject was greatly influenced by the books and publications of several authors listed in the Bibliography section at the end of the book. I have also learnt a lot from the discussions I had on several occasions with Prof. A.R. Santhakumar (former Dean of Anna University and Professor at IIT Madras).

I thank the following organizations/publishers for permitting me to reproduce material from their publications: American Concrete Institute (ACI), Farmington Hills, Michigan; American Society of Civil Engineers (ASCE), Reston, Virginia; Mr Toru Kawai, Executive Director of Japan Concrete Institute (JCI); Structural Engineers Association of California (SEAOC), The Indian Concrete Journal, Mumbai; Indian Concrete Institute, Chennai; NBM & CW, New Delhi; Elsevier Ltd; Oxford, UK; Wiley-VCH Verlag GmbH & Co. KGaA, Weinheim, Germany; NISEE-PEER Library, University of California, Berkeley; Prof. Durgesh Rai, Coordinator, NICEE, IIT Kanpur; and Ar. Daniel Safarik, Editor, Council on Tall Buildings and Urban Habitat (CTBUH), Chicago. I also thank Concrete Reinforcing Steel Institute (CRSI), Schaumburg, Illinois; Portland Cement Association (PCA), Skokie, Illinois; Mr Chris

Shaw of UK; Architects Jesse Reiser and Chad Oppenheim; Prof. Mir M. Ali of University of Illinois at Urbana-Champaign; Prof. K.S. Moon of Yale University; Prof. C.V.R. Murty of IIT, Madras; Prof. Mete Sozen of Purdue University; M/s Tata Steel Ltd; Taylor & Francis; William Palmer Jr (Editor-in-Chief, Concrete Construction); Er Hanns U. Baumann of BauTech, California; Mr Stefan Sommerand of Cobiax, Switzerland; Mr Kate Stevenson of Max Frank Ltd, UK; C.M. Dordi of M/s Ambuja Cements Ltd; Ar. Jan Lorant of Gabor Lorant Architetts, Inc., Phoenix, Arizona; Mr Casper Ålander of Celsa Steel Service, Finland; Ms Sabrina Bénétteau of Compagnie Eiffage du Viaduc de Millau, France; Er S.A. Reddi, former Deputy Managing Director of Gammon India Ltd; Dr V.S. Parameswaran, Former Director of SERC; Kenaidan Contracting Ltd, Ontario, Canada; Mr Cary Kopczynski of Cary Kopczynski & Company, Bellevue, Washington; Insul-Deck, LLC, Villa Rica, Georgia; Er Cliff Schwinger, Vice-President of The Harman Group, Inc.; and Er N. Prabhakar, Mumbai and several others for giving me permission to use photos and figures originated by them (they are acknowledged below the figures). My special thanks go to Mrs Anuthama Srisailam for her help in getting photos of high-rise buildings in Chicago.

I am privileged and grateful to Prof. B. Vijaya Rangan, Emeritus Professor of Civil Engineering, Curtin University of Technology, Perth, Australia, for his encouraging words and for writing the foreword to this book.

I also thank all those who assisted me in the preparation of this book. First and foremost, I thank Er Yogesh Pisal, Senior Engineer (Civil), Aker Powergas Private Ltd, Mumbai for writing Chapter 20 on Design of Multi-storey Buildings. My sincere thanks are due to Prof. P. Suryanarayana, retired Professor and former Dean (planning and development) of Maulana Azad National Institute of Technology, Bhopal (MP), for going through all the chapters patiently and offering useful comments; Er R.K. Desai, Former Chief Engineer (Civil), ITI Ltd, Bangalore for providing many tables of Appendix C; Er V.M. Rajan, Superintending Engineer (Civil) TANGEDCO, Chennai for providing many tables of Appendix D; Er Rahul Leslie for his help in providing computer solutions to some problems; Er Naseef Ummer of IIT Delhi and Er Hemal Mistry for their help in locating the literature; and Er Pankaj Gupta of Roark Consulting, Noida, UP, for sharing Australian and New Zealand codes. I also thank my several friends at www.sefindia.org (in particular, Er T. Rangarajan, Er Vikramjeet, Er P.K.Mallick, Er Vivek Abhyankar, and Er E.S. Jayakumar) for sharing their knowledge, and Er Siddique and Er Ganesh of Nagpur for their encouragement.

I will be failing in my duty if I do not acknowledge the help and wonderful assistance I received from Ms S. Chithra at all the stages of this book. Lastly, I acknowledge the excellent support and coordination provided by the editorial team of Oxford University Press, India.

Dr N. Subramanian
Gaithersburg, Maryland, USA

FOREWORD

The global use of concrete is second only to water. We have been designing, constructing, using, and maintaining numerous concrete structures in the past century to fulfil our infrastructure demands. All this professional experience, along with extensive research, has guided us to understand the construction and behaviour of concrete structures. This vast knowledge is transferred through books and research publications.

This book on concrete structures is outstanding in every way; congratulations to Dr Subramanian for writing such a marvellous and useful book! Dr Subramanian has an extensive professional and research experience. He has been involved in the design and construction of over 650 projects, and published several books and over 200 research papers. He has received many awards and prizes for his contributions, including the Scientist of the Year Award from the Tamil Nadu Government in India. He has used his vast professional experience, in-depth knowledge, and research outputs to produce this outstanding book.

This book is unique in many aspects. It contains extensive information on design and construction of concrete structures. The following are some of the highlights of this book:

- Numerous photographs and well-labelled illustrations
- Clear numerical examples that are helpful to both young readers and professional engineers
- Case studies that clearly illustrate the topic discussed
- Subject matter in each chapter is extensively covered with useful information
- Review questions and exercises at the end of each chapter, which are again useful to students and refreshing for professional engineers
- Extensive list of references at the end of each chapter for further reading

This book will be highly cherished by the budding and professional engineers alike. Dr Subramanian has performed a great service to concrete construction by writing this book. I am privileged and honoured to write this Foreword. Congratulations once again to Dr Subramanian, and wish this book a great success!

Dr B. Vijaya Rangan

Emeritus Professor of Civil Engineering

Curtin University

Perth, Australia

BRIEF CONTENTS

Features of the Book iv

Foreword vi

Preface vii

Detailed Contents xi

List of Symbols xvii

1. Introduction to Reinforced Concrete	1
2. Structural Forms	45
3. Loads and Load Combinations	70
4. Basis of Structural Design	102
5. Flexural Analysis and Design of Beams	142
6. Design for Shear	214
7. Design for Effective Bond between Concrete and Steel	262
8. Design for Torsion	306
9. Design of One-way Slabs	334
10. Design of Two-way Slabs	362
11. Design of Flat Plates and Flat Slabs	415
12. Serviceability Limit States: Deflection and Crack Control	467
13. Design of Axially Loaded Short Columns	506
14. Design of Columns with Moments	546
15. Design of Footings and Pile Caps	585
16. Design of RC Walls and Structural Walls	644
17. Design of Staircases	702
18. Design of Tension Members	726
19. Design of Joints	743
20. Design of Multi-storey Buildings	790

Appendix A: Properties of Soils 809

Appendix B: Design Using Strut-and-tie Model 813

Appendix C: Analysis and Design Aids 822

Appendix D: Practical Tips and Some Rules of Thumb 839

Appendix E: Conversion Factors 850

Bibliography 853

Index 854

DETAILED CONTENTS

Features of the Book iv

Foreword vi

Preface vii

Brief Contents x

List of Symbols xvii

1. Introduction to Reinforced Concrete	1		
1.1 Introduction	1		
1.1.1 Brief History	2		
1.1.2 Advantages and Disadvantages of Concrete	3		
1.2 Concrete-making Materials	4		
1.2.1 Cement (Portland Cement and Other Cements)	4		
1.2.2 Aggregates	8		
1.2.3 Water	10		
1.2.4 Admixtures	11		
1.3 Proportioning of Concrete Mixes	13		
1.4 Hydration of Cement	16		
1.5 Types of Concrete	17		
1.5.1 Ready-mixed Concrete	17		
1.5.2 High-performance Concrete	18		
1.5.3 Structural Lightweight Concrete	20		
1.5.4 Fibre-reinforced Concrete	21		
1.5.5 Ductile Fibre-reinforced Cementitious Composites	21		
1.5.6 Ferrocement	23		
1.6 Reinforcing Steel	24		
1.6.1 Corrosion of Rebars	26		
1.7 Concrete Mixing, Placing, Compacting, and Curing	27		
1.8 Properties of Fresh and Hardened Concrete	29		
1.8.1 Workability of Concrete	29		
1.8.2 Compressive Strength	29		
1.8.3 Stress–Strain Characteristics	32		
1.8.4 Tensile Strength	33		
1.8.5 Bearing Strength	33		
1.8.6 Modulus of Elasticity and Poisson’s Ratio	33		
1.8.7 Strength under Combined Stresses	35		
1.8.8 Shrinkage and Temperature Effects	35		
1.8.9 Creep of Concrete	36		
1.8.10 Non-destructive Testing	36		
1.9 Durability of Concrete	36		
2. Structural Forms	45		
2.1 Introduction	45		
2.2 Basic Structural Elements	46		
2.2.1 Footings	47		
2.2.2 Columns	47		
2.2.3 Beams	48		
2.2.4 Slabs	48		
2.2.5 Walls	48		
2.2.6 Trusses	49		
2.3 Floor and Roof Systems	51		
2.3.1 Bearing Wall Systems	51		
2.3.2 One-way and Two-way Slab Systems	52		
2.3.3 Two-way Flat Plates and Flat Slabs	54		
2.3.4 Grid Floors	56		
2.3.5 Composite Floors	56		
2.4 Precast and Prestressed Concrete Buildings	56		
2.5 Lateral Load Resisting Systems	57		
2.5.1 Rigid or Moment-resisting Frames	58		
2.5.2 Shear-walled Frame Systems	58		
2.5.3 Outrigger and Belt Truss Systems	59		
2.5.4 Framed-tube Systems	60		
2.5.5 Braced-tube Systems	60		
2.5.6 Tube-in-tube and Bundled-tube Systems	61		
2.5.7 Diagrid Systems	62		
2.5.8 Other Systems	62		
2.5.9 Transfer Girders	62		
2.6 Structural Integrity	64		
2.7 Slip-form and Jump-form Constructions	66		
2.7.1 Slip-form Construction	66		
2.7.2 Jump-form Construction	66		
3. Loads and Load Combinations	70		
3.1 Introduction	70		
3.2 Characteristic Actions (Loads)	70		
3.3 Dead Loads	72		
3.4 Imposed Loads	72		
3.4.1 Consideration of Slab Loads on Beams	73		
3.4.2 Consideration of Wall Loads on Beams	74		
3.5 Impact Loads	75		
3.6 Snow and Ice Loads	75		
3.7 Wind Loads	75		
3.7.1 Vortex Shedding	77		
3.7.2 Dynamic Effects	78		
3.7.3 Wind Effects on Tall Buildings	79		
3.8 Earthquake Loads	80		
3.8.1 Natural Frequencies	82		
3.8.2 Equivalent Static Method	83		
3.8.3 Rules to be Followed for Buildings in Seismic Areas	84		
3.8.4 Devices to Reduce Earthquake Effects	85		
3.9 Other Loads and Effects	86		
3.9.1 Foundation Movements	87		
3.9.2 Thermal and Shrinkage Effects	87		
3.9.3 Soil and Hydrostatic Pressure	88		
3.9.4 Erection and Construction Loads	89		
3.9.5 Flood Loads	89		
3.9.6 Axial Shortening of Columns	89		

3.10	Pattern Loading	90		
3.11	Load Combinations	90		
4.	Basis of Structural Design	102		
4.1	Introduction	102		
4.2	Steps Involved in Construction	102		
4.3	Roles and Responsibilities of Designers	103		
4.4	Design Considerations	105		
4.4.1	Safety	105		
4.4.2	Stability	108		
4.4.3	Serviceability	109		
4.4.4	Economy	109		
4.4.5	Durability	109		
4.4.6	Aesthetics	116		
4.4.7	Environment Friendliness	116		
4.4.8	Functional Requirements	118		
4.4.9	Ductility	120		
4.5	Analysis and Design	121		
4.5.1	Relative Stiffness	122		
4.5.2	Redistribution of Moments	124		
4.6	Codes and Specifications	125		
4.7	Design Philosophies	126		
4.7.1	Working Stress Method	127		
4.7.2	Ultimate Load Design	129		
4.7.3	Principles of Limit States Design	129		
4.7.4	Sampling and Acceptance Criteria	131		
4.8	Limit States Method	132		
4.8.1	Limit States of Strength	133		
4.8.2	Serviceability Limit States	135		
4.9	Design by Using Model and Load Tests	136		
4.10	Strut-and-tie Model	136		
4.11	Performance-based Design	136		
5.	Flexural Analysis and Design of Beams	142		
5.1	Introduction	142		
5.2	Behaviour of Reinforced Concrete Beams in Bending	143		
5.2.1	Uncracked Section	143		
5.2.2	Cracking Moment	145		
5.2.3	Cracked Section	145		
5.2.4	Yielding of Tension Reinforcement and Collapse	146		
5.3	Analysis of and Design for Flexure	146		
5.3.1	Effective Span	146		
5.4	Analysis of Singly Reinforced Rectangular Sections	146		
5.4.1	Assumptions Made to Calculate Ultimate Moment of Resistance	146		
5.4.2	Design Bending Moment Capacity of Rectangular Section	149		
5.4.3	Balanced, Under-reinforced, and Over-reinforced Sections	150		
5.4.4	Depth of Neutral Axis	151		
5.4.5	Resisting Moment Strength for Balanced Sections	152		
5.5	Design of Singly Reinforced Rectangular Sections	153		
5.5.1	Minimum Depth for Given M_u	153		
5.5.2	Limiting Percentage of Steel	153		
5.5.3	Factors Affecting Ultimate Moment Capacity	154		
5.5.4	Minimum Tension Reinforcement	154		
5.5.5	Maximum Flexural Steel	156		
5.5.6	Slenderness Limits for Rectangular Beams	157		
5.5.7	Guidelines for Choosing Dimensions and Reinforcement of Beams	158		
5.5.8	Procedure for Proportioning Sections for Given Loads	160		
5.5.9	Design of Over-reinforced Sections	162		
5.5.10	Design Using Charts and Design Aids	162		
5.6	Doubly Reinforced Rectangular Beams	162		
5.6.1	Behaviour of Doubly Reinforced Beams	164		
5.6.2	Analysis of Doubly Reinforced Rectangular Beams	165		
5.6.3	Limiting Moment of Resistance and Compression Steel	166		
5.6.4	Design of Doubly Reinforced Rectangular Beams	166		
5.6.5	Design Using Charts and Design Aids	168		
5.7	Flanged Beams	168		
5.7.1	Effective Width of Flange	169		
5.7.2	Behaviour of Flanged Beams	170		
5.7.3	Analysis of Flanged Beams	171		
5.7.4	Minimum and Maximum Steel	174		
5.7.5	Doubly Reinforced Flanged Beams	176		
5.7.6	Design of Flanged Beams	178		
5.7.7	Design of Flanged Beams Using Charts and Design Aids	179		
5.7.8	Design of L-beams	180		
5.8	Minimum Flexural Ductility	180		
5.9	Deep Beams	181		
5.10	Wide Shallow Beams	185		
5.11	Hidden Beams	185		
5.12	Lintel and Plinth Beams	186		
5.13	High-strength Steel and High-strength Concrete	187		
5.14	Fatigue Behaviour of Beams	188		
6.	Design for Shear	214		
6.1	Introduction	214		
6.2	Behaviour of Reinforced Concrete Beams under Shear	215		
6.2.1	Behaviour of Uncracked Beams	215		
6.2.2	Behaviour of Beams without Shear Reinforcement	218		
6.2.3	Types of Shear or Web Reinforcements	220		
6.2.4	Behaviour of Beams with Shear/Web Reinforcements	227		
6.3	Factors Affecting Shear Strength of Concrete	229		
6.4	Design Shear Strength of Concrete in Beams	231		
6.4.1	Maximum Shear Stress	233		
6.4.2	Effects Due to Loading Condition	234		
6.5	Critical Section for Shear	234		
6.6	Minimum and Maximum Shear Reinforcement	236		
6.6.1	Maximum Spacing	236		
6.6.2	Upper Limit on Area of Shear Reinforcement	237		
6.7	Design of Shear Reinforcement	237		
6.7.1	The Ritter-Mörsch Truss Model	238		
6.7.2	Modified Compression Field Theory	240		
6.7.3	Design Procedure for Shear Reinforcement	241		
6.7.4	Transverse Spacing of Stirrups in Wide Beams	242		
6.7.5	Design Aids	242		
6.7.6	Anchoring of Shear Stirrups	242		
6.8	Shear Design of Flanged Beams	243		
6.9	Shear Design of Beams with Varying Depth	243		
6.10	Shear Design of Beams Located in Earthquake Zones	244		

6.11	Shear in Beams with High-strength Concrete and High-strength Steel	245	8.5.3	Consideration of Flanged Beams	315
6.12	Shear Design Beams with Web Opening	246	8.5.4	Area of Stirrups for Torsion	315
6.13	Shear Strength of Members with Axial Force	247	8.5.5	Area of Longitudinal Reinforcement for Torsion	316
6.14	Design of Stirrups at Steel Cut-off Points	248	8.5.6	Limiting Crack Width for Combined Shear and Torsion	317
6.15	Shear Friction	248	8.6	Skew Bending Theory	318
7. Design for Effective Bond between Concrete and Steel		262	8.6.1	Interaction Curves for Combined Flexure and Torsion	319
7.1	Introduction	262	8.6.2	Interaction Curves for Combined Shear and Torsion	320
7.2	Local or Flexural Bond Stress	263	8.7	Indian Code Provisions for Design of Longitudinal and Transverse Reinforcements	320
7.3	Anchorage Bond	264	8.7.1	Equivalent Shear and Moment	321
7.4	Bond Behaviour	266	8.7.2	Minimum Longitudinal Reinforcement for Torsion	321
7.4.1	Test Specimens	266	8.7.3	Design of Transverse Reinforcement	321
7.4.2	Factors Affecting Bond Strength	267	8.7.4	Distribution of Torsional Reinforcement	322
7.5	Development Length	269	8.8	Design and Detailing for Torsion as per IS 456 Code	323
7.5.1	Critical Sections for Development of Reinforcement	270	8.9	Graphical Methods	323
7.5.2	Derivation of Analytical Development Length	270	8.10	Other Considerations	324
7.5.3	Codal Provisions for Development Length	271	9. Design of One-way Slabs		
7.5.4	Design Aids	273	9.1	Introduction	334
7.5.5	Recent Research	273	9.2	Types of Slabs	334
7.5.6	Reduction in Development Length due to Excess Reinforcement	274	9.3	Behaviour of One-way Slabs	335
7.5.7	Development Length of Bars in Compression	274	9.4	General Considerations for Design of Slabs	335
7.5.8	Development Length of Bundled Bars	274	9.4.1	Effective Span	335
7.5.9	Development of Welded Deformed Wire Reinforcement in Tension	275	9.4.2	Minimum Thickness	336
7.6	Anchoring Reinforcing Bars	276	9.4.3	Concrete Cover	338
7.6.1	Behaviour of Hooks or Bends in Tension	276	9.4.4	Analysis of Continuous One-way Slabs	338
7.6.2	Headed and Mechanically Anchored Bars in Tension	279	9.4.5	Calculation of Reinforcements	340
7.6.3	Anchoring Bent-up Bars and Shear Reinforcement	281	9.4.6	Detailing of Reinforcement in One-way Slabs	341
7.7	Splicing of Reinforcement	282	9.4.7	Use of High-strength Steel and High-strength Concrete in Slabs	342
7.7.1	Indirect Splices	282	9.5	Design of Slabs for Shear and Size Effect	343
7.7.2	Direct Splices	288	9.6	Design Procedure for One-way Slabs	344
7.8	Curtailement of Reinforcement	293	9.7	Concentrated Load on One-way Slabs and Design of Culverts	345
7.8.1	Curtailement of Tension Reinforcement in Flexural Members	293	9.7.1	Effective Width of Cantilever Slabs	346
7.8.2	Curtailement of Positive Moment Reinforcement	293	9.7.2	Design of Culvert	346
7.8.3	Curtailement of Negative Moment Reinforcement	294	9.8	Ribbed, Hollow Block, or Voided Slabs	347
7.8.4	Curtailement of Bundled Bars	294	9.9	Earthquake Considerations	349
7.8.5	Special Members	295	9.10	Slabs-on-grade	350
7.9	Seismic Considerations	295	10. Design of Two-way Slabs		
8. Design for Torsion		306	10.1	Introduction	362
8.1	Introduction	306	10.2	Behaviour of Two-way Slabs	362
8.2	Equilibrium and Compatibility Torsion	306	10.3	Minimum Thickness of Slabs	364
8.2.1	Torsion in Curved Beams	308	10.4	Wall- and Beam-supported Two-way Slabs	367
8.2.2	Semicircular Beams Supported on Three Columns	309	10.4.1	Analysis of Wall-supported Slabs	367
8.3	Behaviour of Beams in Torsion	309	10.4.2	Beam-supported Two-way Slabs	378
8.3.1	Torsional Analysis	309	10.4.3	Design Procedure for Two-way Slabs	378
8.3.2	Behaviour of Plain Concrete Members	311	10.4.4	Use of Design Aids	379
8.3.3	Behaviour of Beams with Torsional Reinforcement	311	10.4.5	Detailing of Reinforcements	379
8.4	Theoretical Models for Torsion	312	10.5	Design of Non-rectangular Slabs	381
8.5	Plastic Space Truss Model	313	10.5.1	Circular Slabs	382
8.5.1	Design Strength in Torsion	313	10.5.2	Triangular Slabs	384
8.5.2	Cracking Torque	313	10.5.3	Trapezoidal and Polygonal Slabs	385

10.6	Concentrated Loads on Two-way Slabs	386	12.5	Deflection of Two-way Slabs	483
10.7	Openings in Two-way Slabs	387	12.6	Cracking in Reinforced Concrete Members	484
10.8	Yield-line Analysis for Slabs	388	12.6.1	Types of Cracks	485
10.8.1	Upper and Lower Bound Theorems	389	12.6.2	Mechanism of Cracking	486
10.8.2	Characteristics of Yield Lines	389	12.6.3	Limiting the Crack Width	486
10.8.3	Orthotropic Reinforcement and Skewed Yield Lines	390	12.6.4	Crack Control Provisions in Codes	487
10.8.4	Ultimate Load on Slabs	391	12.6.5	Distribution of Tension Reinforcement in Flanges of I-beams	489
10.8.5	Yield-line Analysis by Virtual Work Method	391	12.7	Side Face Reinforcement in Beams	490
10.8.6	Yield-line Analysis by Equilibrium Method	394	12.8	Frame Deflections	490
10.8.7	Limitations of Yield-line Theory	394	12.9	Vibration Control	491
10.9	Sloped and Pyramidal Roofs	395	12.10	Fatigue Control	492
10.10	Earthquake Considerations	396	12.11	Slenderness Limits for Beams for Stability	493
10.11	Simplified Design	397	12.12	Deflection of Cantilevers	493
11. Design of Flat Plates and Flat Slabs		415	13. Design of Axially Loaded Short Columns		506
11.1	Introduction	415	13.1	Introduction	506
11.2	Proportioning of Flat Slabs	416	13.2	Classification of Columns	506
11.2.1	Thickness of Slab	416	13.2.1	Based on Cross Section	506
11.2.2	Drop Panel	416	13.2.2	Based on Type of Reinforcement	507
11.2.3	Column Heads	416	13.2.3	Based on Type of Loading	507
11.2.4	Shear Caps	417	13.2.4	Based on Slenderness Ratio	507
11.3	Behaviour of Flat Slabs	417	13.3	Unsupported and Effective Lengths of Columns	508
11.4	Methods of Analysis	419	13.3.1	Unsupported Length	508
11.4.1	Direct Design Method	420	13.3.2	Buckling of Columns and Effective Length	509
11.4.2	Equivalent Frame Method	424	13.4	Determination of Effective Length of Columns in Frames	511
11.4.3	Transfer of Moments to Columns	425	13.4.1	Sway and Non-sway Frames	513
11.5	Shear in Flat Plates and Flat Slabs	427	13.4.2	Fixity at Footing	514
11.5.1	One-way or Beam Shear	427	13.5	Behaviour of Short Columns	515
11.5.2	Two-way or Punching Shear	428	13.5.1	Confining Reinforcement for Circular Columns	516
11.5.3	Reinforcement for Punching Shear	435	13.5.2	Confining Reinforcement for Rectangular and Square Columns	517
11.6	Design Procedure for Flat Slabs and Plates	441	13.6	Practical Provisions on Reinforcement Detailing	517
11.7	Detailing of Reinforcements	441	13.6.1	Dimensions	518
11.7.1	Detailing at Edge Columns	443	13.6.2	Concrete Cover	518
11.7.2	Structural Integrity Reinforcement	444	13.6.3	Longitudinal Reinforcement	518
11.8	Openings in Flat Slabs	445	13.6.4	Transverse Reinforcement	519
11.9	Earthquake Effects	446	13.6.5	Columns in Multi-storey Frames	521
11.9.1	Diaphragm Action	447	13.7	Other Codal Provisions	522
11.9.2	Effective Slab Width for Earthquake Loads	447	13.7.1	Slenderness Limit	522
11.9.3	Deformation Capacity of Slab–Column Connections	448	13.7.2	Minimum Eccentricity	522
11.10	Waffle Slabs	449	13.8	Design of Short Columns Under Axial Compression	523
11.11	Grid Slabs	450	13.8.1	Design of Rectangular Columns with Axial Loading	523
11.12	Hollow-core Slabs	450	13.8.2	Design of Circular or Square Columns with Spiral Reinforcement	524
12. Serviceability Limit States: Deflection and Crack Control		467	13.8.3	Steps in the Design of Short Columns	525
12.1	Introduction	467	13.8.4	Design Aids	525
12.2	Design for Limit State of Deflection	468	13.9	Design of Pedestals	525
12.2.1	Limiting Deflection	469	13.10	Earthquake and other Considerations	526
12.3	Short-term Deflections	469	13.10.1	Strong Column–Weak Beam Concept	526
12.3.1	Moment of Inertia of Member	470	13.10.2	Detailing of Longitudinal Reinforcement	527
12.3.2	Load–Deflection Behaviour of RC Beam	472	13.10.3	Detailing of Transverse Reinforcement	528
12.3.3	Other Factors that Influence Deflection	476	13.10.4	Special Confining Reinforcement	530
12.3.4	Deflection of Continuous Beams	476			
12.3.5	Design Aids	477			
12.4	Long-term Deflections	477			
12.4.1	Deflection due to Creep	477			
12.4.2	Deflection due to Differential Shrinkage	481			
12.4.3	Deflection due to Temperature	482			

14. Design of Columns with Moments	546		
14.1	Introduction	546	
14.2	Design of Column with Axial Load and Uniaxial Bending	547	
14.2.1	Assumptions Made in Limit States Design for Columns	547	
14.2.2	Derivation of Basic Equations	547	
14.2.3	Sections with Asymmetric Reinforcement and Plastic Centroid	551	
14.2.4	Analysis of Circular Columns	551	
14.2.5	Interaction Curves	552	
14.2.6	Design Aids	553	
14.2.7	Design Procedure	554	
14.2.8	Splicing of Reinforcement	555	
14.2.9	Transverse Reinforcement	556	
14.3	Design of Columns with Axial Load and Biaxial Bending	557	
14.3.1	Methods of Superposition	559	
14.3.2	Methods of Equivalent Uniaxial Eccentricity	559	
14.3.3	Methods Based on Approximations for Shape of Interaction Surface	560	
14.3.4	Design Procedure for Columns with Biaxial Moments	561	
14.3.5	Design Aids	561	
14.3.6	Design of L, T, and + Columns	562	
14.4	Slender Columns	562	
14.4.1	Definition	562	
14.4.2	Behaviour	563	
14.4.3	Design Approaches	565	
14.4.4	Slender Columns Bent about Both Axes	569	
14.4.5	Design Procedure	570	
14.5	Earthquake Considerations	570	
15. Design of Footings and Pile Caps	585		
15.1	Introduction	585	
15.2	Types of Footings	585	
15.3	Soil Pressure under Footings	587	
15.3.1	Soil Pressure under Footings Subjected to Lateral Moments	587	
15.3.2	Safe Bearing Capacity	589	
15.3.3	Settlement of Foundation	589	
15.3.4	Depth of Foundation	590	
15.3.5	Gross and Net Soil Pressures	591	
15.4	Design Considerations	592	
15.5	Structural Design of Individual Footings	594	
15.5.1	Shear Design Considerations	595	
15.5.2	Bending Moment Considerations	596	
15.5.3	Providing Development Length	597	
15.5.4	Transfer of Load at Base of Column	597	
15.5.5	Design of Wall Footings	599	
15.5.6	Design of Square Column Footings	599	
15.5.7	Design of Rectangular Footings	600	
15.5.8	Design of Sloped Footings	601	
15.6	Design of Combined Footings	602	
15.6.1	Two-column Footings	604	
15.6.2	Design of Combined Slab and Beam Footing	606	
15.6.3	Design of Combined Footing with Strap Beam	608	
15.7	Design of Plain Concrete Footings	609	
15.8	Design of Piles	610	
15.8.1	Behaviour of Piles	610	
15.8.2	Static Formula for Pile Capacity	611	
15.8.3	Dynamic Pile Formula	612	
15.8.4	Pile Groups	612	
15.8.5	Structural Design of Piles	613	
15.8.6	Design of Under-reamed Piles	615	
15.9	Design of Pile Caps	617	
15.9.1	Sectional Method of Design of Pile Cap	618	
15.9.2	Strut-and-tie Model for Pile Caps	619	
15.9.3	Detailing of Pile Caps	622	
15.10	Earthquake Considerations	622	
15.10.1	Use of Grade Beams	623	
15.10.2	Failures due to Liquefaction	623	
16. Design of RC Walls and Structural Walls	644		
16.1	Introduction	644	
16.2	Types of Reinforced Concrete Walls	645	
16.3	Load-bearing Walls	645	
16.3.1	Braced and Unbraced Walls	645	
16.3.2	Eccentricities of Vertical Load	646	
16.3.3	Slenderness Ratio and Effective Height of Walls	646	
16.3.4	Empirical Design Method	647	
16.3.5	Design of Walls Subjected to Combined Horizontal and Vertical Loads	647	
16.3.6	Detailing of Concrete Walls	649	
16.4	Design of Retaining Walls	650	
16.4.1	Types of Retaining Walls	650	
16.4.2	Theories of Earth Pressure	652	
16.4.3	Earth Pressure during Earthquakes	656	
16.4.4	Preliminary Proportioning of Retaining Walls	657	
16.4.5	Drainage and Compaction of Backfill	658	
16.4.6	Stability Requirements	659	
16.4.7	Soil Bearing Pressure Requirements	660	
16.4.8	Procedure for Design	660	
16.4.9	Behaviour and Design of Cantilever-retaining Walls	661	
16.4.10	Behaviour and Design of Counterfort-retaining Walls	662	
16.4.11	Bridge Abutments or Basement Walls	664	
16.5	Structural Walls	665	
16.5.1	Types of Structural Walls	665	
16.5.2	Behaviour of Structural Walls	666	
16.5.3	Design of Structural Walls	668	
16.5.4	Detailing of Structural Walls	673	
16.5.5	Procedure for Design of Reinforced Concrete Structural Walls	675	
16.5.6	Coupling Beams	676	
16.5.7	Openings in Structural Walls	680	
16.5.8	Construction Joints	680	
17. Design of Staircases	702		
17.1	Introduction	702	
17.2	Types of Staircases	703	
17.2.1	Structural Classifications	704	
17.2.2	Effective Span	706	
17.3	Loads on Stair Slabs	707	
17.4	Design of Stair Slabs Spanning Transversely	707	
17.5	Design of Stair Slabs Spanning Longitudinally	709	
17.6	Helicoidal Staircases	711	
17.7	Earthquake Considerations	712	

18. Design of Tension Members	726		
18.1 Introduction	726		
18.2 Behaviour of Tension Members	726		
18.3 Design Methods for Members in Direct Tension	727		
18.3.1 Minimum Concrete Grade and Cover of Reinforcement for Liquid Retaining Structures	728		
18.3.2 Minimum Reinforcement	728		
18.3.3 Spacing of Reinforcement	729		
18.4 Design Procedure for Direct Tension	729		
18.5 Design of Members Subjected to Tension and Bending	729		
18.5.1 Tension with Small Eccentricity	729		
18.5.2 Tension with Large Eccentricity	730		
18.5.3 Checking for Crack Width	731		
18.6 Interaction Curves for Bending and Tension	732		
18.7 Design for Bending, Shear, and Tension	733		
18.8 Detailing for Tension Members	733		
18.9 Earthquake and Other Considerations	733		
18.10 Design of Water Tanks	734		
19. Design of Joints	743		
19.1 Introduction	743		
19.2 Beam-column Joints	744		
19.2.1 Requirements of Beam-column Joints	745		
19.2.2 Design and Detailing of Joints	745		
19.2.3 Corner Joints	746		
19.2.4 T-joints	747		
19.2.5 Beam-column Joints in Frames	748		
19.2.6 Design of Beam-column Joints	748		
19.2.7 Anchorage of Bars at Joints	753		
19.2.8 Constructability Issues	755		
19.3 Beam-to-beam Joints	756		
19.4 Design of Corbels	758		
19.5 Design of Anchors	761		
19.5.1 Types of Anchors	761		
19.5.2 Code Provisions for Design	763		
19.5.3 Steel Strength of Anchor in Tension	764		
19.5.4 Concrete Breakout Strength of Anchor in Tension	764		
19.5.5 Pull-out Strength in Tension	766		
19.5.6 Concrete Side-face Blowout Strength in Tension	767		
19.5.7 Failure Modes in Shear Loading	767		
19.5.8 Steel Strength of Anchor in Shear	767		
19.5.9 Concrete Breakout Strength of Anchor in Shear	768		
19.5.10 Concrete Pryout Strength of Anchor in Shear	770		
19.5.11 Bond Strength of Adhesive Anchor in Tension	770		
19.5.12 Required Strength of Anchors	772		
19.5.13 Interaction of Tensile and Shear Forces	773		
19.5.14 Seismic Design Requirements	773		
19.5.15 Influence of Reinforcements to Resist Shear	774		
19.5.16 Required Edge Distances and Spacing to Prevent Splitting of Concrete	775		
19.6 Obtuse-angled and Acute-angled Corners	775		
20. Design of Multi-storey Buildings	790		
20.1 Introduction	790		
20.2 Example Frame	791		
20.3 Detailed Structural Layouts	792		
20.4 Estimation of Loads	794		
20.4.1 Calculation of Dead Load—STAAD.Pro Load Case 11	794		
20.4.2 Calculation of Live Load—STAAD.Pro Load Case 12	794		
20.4.3 Calculation of Earthquake Load	794		
20.5 Analysis of Structure	795		
20.5.1 Gravity Load Analysis	796		
20.5.2 Lateral Load Analysis	796		
20.6 Load Combinations	796		
20.7 Reinforced Concrete Design Using STAAD.Pro for Indian Codes	796		
20.7.1 Design Parameters as per IS 456	796		
20.7.2 Design Parameters as per IS 13920	797		
20.7.3 Design Parameters for Building under Consideration	798		
20.8 Serviceability Checks	798		
20.9 Strength Design of Columns	798		
20.10 Strength Design of Beams	799		
20.11 Design of Foundations	801		
20.11.1 Design Parameters	801		
20.11.2 Design Forces	801		
20.11.3 Summary of Foundation Design	801		
20.12 Design of Slabs	802		
20.12.1 Summary of Loading on Slab	802		
20.12.2 Design Data	802		
20.12.3 Summary of Slab Reinforcement	802		
20.13 STAAD.Pro Input File	802		

Appendix A: Properties of Soils 809

Appendix B: Design Using Strut-and-tie Model 813

Appendix C: Analysis and Design Aids 822

Appendix D: Practical Tips and Some Rules of Thumb 839

Appendix E: Conversion Factors 850

Bibliography 853

Index 854

INTRODUCTION TO REINFORCED CONCRETE

1.1 INTRODUCTION

The word ‘concrete’ comes from the Latin word *concretus* (meaning compact or condensed), the perfect passive participle of *concrecere*, from *con* (together) and *crescere* (to grow). This name was chosen perhaps due to the fact that this material *grows together*, due to the process of *hydration*, from a visco-elastic, moldable liquid into a hard, rigid, solid rock-like substance. The Romans first invented what is today known as *hydraulic cement-based concrete* or simply *concrete*. They built numerous concrete structures, including the 43.3 m diameter concrete dome, the *Pantheon*, in Rome, which is now over 2000 years old but is still in use and remains the world’s largest non-reinforced concrete dome (see case study in Chapter 2 for more details about the Pantheon).

Concrete is used in nearly every type of construction. Traditionally, concrete has been primarily composed of cement, water, and aggregates (aggregates include both coarse and fine aggregates). Although aggregates make up the bulk of the mix, it is the hardened cement paste that binds the aggregates together and contributes to the strength of concrete, with the aggregates serving largely as low-cost fillers (though their strength also is important).

Concrete is not a homogeneous material, and its strength and structural properties may vary greatly depending upon its ingredients and method of manufacture. However, concrete is normally treated in design as a homogeneous material. Steel reinforcements are often included to increase the tensile strength of concrete; such concrete is called *reinforced cement concrete* (RCC) or simply *reinforced concrete* (RC).

As of 2006, about 7.5 billion cubic metres of concrete were produced each year—this equals about one cubic metre per year for every person on the earth (see Table 1.1). The National Ready Mixed Concrete Association (NRMCA) estimates that ready-mixed concrete production in 2005 was

about 349 million cubic metres in the USA alone, which is estimated to have about 6000 ready-mixed concrete plants.

TABLE 1.1 Annual consumption of major structural materials in the world

Material	Unit Weight (kg/m ³)	Million Tonnes	Tonnes/Person
Structural steel	7850	1244	0.18
Cement	1440	3400	0.48
Concrete	2400	~18,000	2.4 (990 litres)
Timber	700	277	0.04
Drinking water ⁺	1000	5132	0.73 (730 litres)

Notes: The estimated world population as of August 2012 is 7.031 billion.

⁺Assumed as two litres/day/person

Concrete technology has advanced considerably since its discovery by the Romans. Now, concrete is truly an engineered material, with a number of ingredients, which include a host of mineral and chemical admixtures. These ingredients should be precisely determined, properly mixed, carefully placed, vibrated (not required in self-compacting concretes), and properly cured so that the desired properties are obtained; they should also be inspected at regular intervals and maintained adequately until their intended life. Even the cement currently being used has undergone a number of changes. A variety of concretes is also being used, some tailored for their intended use and many with improved properties. Few specialized concretes have compressive strength and ductility matching that of steel. Even though this is a book on RC design, it is important for the designers to know about the nature and properties of the materials they are going to specify for the structures designed by them. As concrete technology has grown in parallel with concrete design, it is impossible to describe all the ingredients, their chemistry, the different kinds of concretes, and their properties in this chapter. Hence, only a brief introduction is given about them, and interested readers should consult a book on concrete technology (many references are given at the end) for further details.

1.1.1 Brief History

Many researchers believe that the first use of a truly cementitious binding agent (as opposed to the ordinary lime commonly used in ancient mortars) occurred in southern Italy around second century BC. Volcanic ash (called *pozzuolana*, found near Pozzuoli, by the Bay of Naples) was a key ingredient in the Roman cement used during the days of the Roman empire. Roman concrete bears little resemblance to modern Portland cement concrete. It was never put into a mould or formwork in a plastic state and made to harden, as is being done today. Instead, Roman concrete was constructed in layers by packing mortar by hand in and around stones of various sizes. The Pantheon, constructed in AD 126, is one of the structural marvels of all times (Shaeffer 1992).

During the Middle Ages, the use of concrete declined, although isolated instances of its use have been documented and some examples have survived. Concrete was more extensively used again during the Renaissance (14th–17th centuries) in structures like bridge piers. Pozzolanic materials were added to the lime, as done by the Romans, to increase its hydraulic properties (Reed, et al. 2008).

In the eighteenth century, with the advent of new technical innovations, a greater interest was shown in concrete. In 1756, John Smeaton, a British Engineer, rediscovered hydraulic cement through repeated testing of mortar in both fresh and salt water. Smeaton's work was followed by Joseph Aspdin, a bricklayer and mason in Leeds, England, who, in 1824, patented

the first 'Portland' cement, so named since it resembled the stone quarried on the Isle of Portland off the British coast (Reed, et al. 2008). Aspdin was the first to use high temperatures to heat alumina and silica materials, so that cement was formed. It is interesting to note that cement is still made in this way. I.K. Brunel was the first to use Portland cement in an engineering application in 1828; it was used to fill a breach in the Thames Tunnel. During 1959–67, Portland cement was used in the construction of the London sewer system.

The small rowboats built by Jean-Louis Lambot in the early 1850s are cited as the first successful use of reinforcements in concrete. During 1850–1880, a French builder, Francois Coignet, built several large houses of concrete in England and France (Reed, et al. 2008). Joseph Monier of France, who is considered to be the first builder of RC, built RC reservoirs in 1872. In 1861, Monier published a small book, *Das System Monier*, in which he presented the applications of RC. During 1871–75, William E. Ward built the first landmark building in RC in Port Chester, NY, USA. In 1892, François Hennebique of France patented a system of steel-reinforced beams, slabs, and columns, which was used in the construction of various structures built in England between 1897 and 1919. In Hennebique's system, steel reinforcement was placed correctly in the tension zone of the concrete; this was backed by a theoretical understanding of the tensile and compressive forces, which was developed by Cottançin in France in 1892 (Reed, et al. 2008).

CASE STUDY

The Ingalls Building

The Ingalls Building, built in 1903 in Cincinnati, Ohio, is the world's first RC skyscraper. This 15-storey building was designed by the Cincinnati architectural firm Elzner & Anderson and engineer Henry N. Hooper. Prior to 1902, the tallest RC structure in the world was only six storeys high. Since concrete possesses very low tensile strength, many at that time believed that a concrete tower as tall as the Ingalls Building would collapse under wind loads or even its own weight. When the building was completed and the supports removed, one reporter allegedly stayed awake through the night in order to be the first to report on the building's failure.

Hooper designed a monolithic concrete box of 200 mm walls, with the floors, roof, beams, columns, and stairs all made of concrete. Columns measured 760 mm by 860 mm for the first 10 floors and 300 mm² for the rest. It was completed in eight months, and the finished building measured 15 m by 30 m at its base and was 64 m tall.

Still in use, the building was designated a National Historic Civil Engineering Landmark in 1974 by the American Society of Civil Engineers; in 1975, it was added to the American National Register of Historic Places.



15-storey Ingalls Building in Cincinnati, Ohio
(Source: http://en.wikipedia.org/wiki/Ingalls_Building)

Earnest L. Ransome patented a reinforcing system using twisted rods in 1884; he also built the first RC framed building in Pennsylvania, USA, in 1903. In 1889, the first concrete reinforced bridge was built. The Ingalls building, which is the first concrete skyscraper, was built in 1904 using the Ransome system and is still in use.

By the 1900s, concrete was generally used in conjunction with some form of reinforcement, and steel began to replace wrought iron as the predominant tensile material. A significant advance in the development of RC was the pre-stressing of steel reinforcing, which was developed by Eugène Freyssinet, in the 1920s, but the technique was not widely used until the 1940s. Victoria skyscraper in Montreal, constructed in 1964, with a height of 190 m and utilizing 41 MPa concrete in the columns, paved way for high-strength concretes (HSCs) (Shaeffer 1992).

In 1908, Prof. Mörsch and Bach of the University of Stuttgart conducted a large number of tests to study the behaviour of RC elements. Prof. Mörsch's work can be considered to be the starting point of modern theory of RC design. Thaddeus Hyatt, an American, was probably the first to correctly analyse the stresses in an RC beam and in 1877 published a small book. In 1895, A. Considère of France tested RC beams and columns and in 1897 published the book *Experimental Researches on Reinforced Concrete*. Several early studies of RC members were based on ultimate strength theories, for example, flexure theory of Thullie in 1897 and the parabolic stress distribution theory of Ritter in 1899. However, the straight line (elastic) theory of Coignet and Tedesco, developed in 1900, was accepted universally because of its simplicity. The ultimate strength design was adopted as an alternative to the working stress method only in 1956–57. Ecole des Ponts et Chaussées in France offered the first teaching course in RC design in 1897. The first British code was published in 1906 and the first US code in 1916. The first Indian code was published in 1953 and revised in 1957, 1964, 1978, and 2000.

1.1.2 Advantages and Disadvantages of Concrete

Reinforced concrete has been used in a variety of applications, such as buildings, bridges, roads and pavements, dams, retaining walls, tunnels, arches, domes, shells, tanks, pipes, chimneys, cooling towers, and poles, because of the following advantages:

Moulded to any shape It can be poured and moulded into any shape varying from simple slabs, beams, and columns to complicated shells and domes, by using *formwork*. Thus, it allows the designer to combine the architectural and structural functions. This also gives freedom to the designer to select any size or shape, unlike steel sections where the designer is constrained by the standard manufactured member sizes.

Availability of materials The materials required for concrete (sand, gravel, and water) are often locally available and are relatively inexpensive. Only small amounts of cement (about 14% by weight) and reinforcing steel (about 2–4% by volume) are required for the production of RC, which may have to be shipped from other parts of the country. Moreover, reinforcing steel can be transported to most construction sites more easily than structural steel sections. Hence, RC is the material of choice in remote areas.

Low maintenance Concrete members require less maintenance compared to structural steel or timber members.

Water and fire resistance RC offers great resistance to the actions of fire and water. A concrete member having sufficient cover can have one to three hours of fire resistance rating without any special fire proofing material. It has to be noted that steel and wood need to be fireproofed to obtain similar rating—steel members are often enclosed by concrete for fire resistance. If constructed and cured properly, concrete surfaces could provide better resistance to water than steel sections, which require expensive corrosion-resistant coatings.

Good rigidity RC members are very rigid. Due to the greater stiffness and mass, vibrations are seldom a problem in concrete structures.

Compressive strength Concrete has considerable compressive strength compared to most other materials.

Economical It is economical, especially for footings, basement walls, and slabs.

Low-skilled labour Comparatively lower grade of skilled labour is required for the fabrication, erection, and construction of concrete structures than for steel or wooden structures.

In order to use concrete efficiently, the designer should also know the weakness of the material. The disadvantages of concrete include the following:

Low tensile strength Concrete has a very low tensile strength, which is about one-tenth of its compressive strength and, hence, cracks when subjected to tensile stresses. Reinforcements are, therefore, often provided in the tension zones to carry tensile forces and to limit crack widths. If proper care is not taken in the design and detailing and also during construction, wide cracks may occur, which will subsequently lead to the corrosion of reinforcement bars (which are also termed as *rebars* in the USA) and even failure of structures.

Requires forms and shoring Cast in situ concrete construction involves the following three stages of construction, which are not required in steel or wooden structures: (a) Construction of formwork over which concrete will be

poured—the formwork holds the concrete in place until it hardens sufficiently, (b) removal of these forms, and (c) propping or shoring of new concrete members until they gain sufficient strength to support themselves. Each of these stages involves labour and material and will add to the total cost of the structure. The formwork may be expensive and may be in the range of one-third the total cost of an RC structure. Hence, it is important for the designer to make efforts to reduce the formwork cost, by reusing or reducing formwork.

Relatively low strength Concrete has relatively low strength per unit weight or volume. (The compressive strength of normal concrete is about 5–10% steel, and its unit density is about 31% steel; see Table 1.2.) Hence, larger members may be required compared to structural steel. This aspect may be important for tall buildings or long-span structures.

TABLE 1.2 Physical properties of major structural materials

Item	Mild Steel	Concrete ¹ M20 Grade	Wood
Unit mass, kg/m ³	7850 (100) ³	2400 (31) ³	290–900 (4–11) ³
Maximum stress in MPa			
Compression	250 (100)	20 (8)	5.2–23 ² (2–9)
Tension	250 (100)	3.13 (1.3)	2.5–13.8 (1–5)
Shear	144 (100)	2.8 (1.9)	0.6–2.6 (0.4–1.8)
Young's modulus, MPa	2×10^5 (100)	22,360 (11)	4600–18,000 (2–9)
Coefficient of linear thermal expansion, °C × 10 ⁻⁶	12	10–14	4.5
Poisson's ratio	0.3	0.2	0.2

Notes:

¹ Characteristic compressive strength of 150 mm cubes at 28 days

² Parallel to grain

³ The values in brackets are relative percentage values as compared to steel.

Time-dependent volume changes Concrete undergoes drying shrinkage and, if restrained, will result in cracking or deflection. Moreover, deflections will tend to increase with time due to creep of the concrete under sustained loads (the deflection may possibly double, especially in cantilevers). It has to be noted that both concrete and steel undergo approximately the same amount of thermal expansion or contraction; see Table 1.2.

Variable properties The properties of concrete may widely vary due to variation in its proportioning, mixing, curing, and curing. Since cast in situ concrete is site-controlled, its quality may not be uniform when compared to materials such as structural steel and laminated wood, which are produced in the factory.

CO₂ emission Cement, commonly composed of calcium silicates, is produced by heating limestone and other

ingredients to about 1480 °C by burning fossil fuels, and it accounts for about 5–7 per cent of CO₂ emissions globally. Production of one ton of cement results in the emission of approximately one ton of CO₂. Hence, the designer should specify cements containing cementitious and waste materials such as fly ash and slags, wherever possible. Use of fly ash and other such materials not only reduces CO₂ emissions but also results in economy as well as improvement of properties such as reduction in heat of hydration, enhancement of strength and/or workability, and durability of concrete (Neville 2012; Subramanian 2007; Subramanian 2012).

1.2 CONCRETE-MAKING MATERIALS

As already mentioned, the present-day concrete is made up of cement, coarse and fine aggregates, water, and a host of mineral and chemical admixtures. When mixed with water, the cement becomes adhesive and capable of bonding the aggregates into a hard mass, called *concrete*. These ingredients are briefly discussed in the following sections.

1.2.1 Cement—Portland Cement and Other Cements

The use of naturally occurring limestone will result in natural cement (*hydraulic lime*), whereas carefully controlled computerized mixing of components can be used to make manufactured cements (*Portland cement*). Portland cements are also referred to as *hydraulic cements*, as they not only harden by reacting with water but also form a water-resistant product. The raw materials used for the manufacture of cement consist of limestone, chalk, seashells, shale, clay, slate, silica sand, alumina and iron ore; lime (calcium) and silica constitute about 85 per cent of the mass.

The process of manufacture of cement consists of grinding the raw materials finely, mixing them thoroughly in certain proportions, and then heating them to about 1480 °C in huge cylindrical steel rotary kilns 3.7–10 m in diameter and 50–150 m long and lined with special firebrick. (The rotary kilns are inclined from the horizontal by about 3° and rotate on its longitudinal axis at a slow and constant speed of about 1–4 revolutions/minute.) The heated materials sinter and partially fuse to form nodular shaped and marble- to fist-sized material called *clinker*. (It has to be noted that at a temperature range of 600–900 °C, *calcination* takes place, which results in the release of environmentally harmful CO₂.) The clinker is cooled (the strength properties of cement are considerably influenced by the cooling rate of clinker) and ground into fine powder after mixing with 3–5 per cent gypsum (*gypsum* is added to regulate the setting time of the concrete) to form Portland cement. (In modern plants, the heated air from the coolers is returned to the kilns, to save fuel and to increase the burning efficiency.) It is then loaded into bulk carriers or packaged into bags; in India, typically 50 kg bags are used.

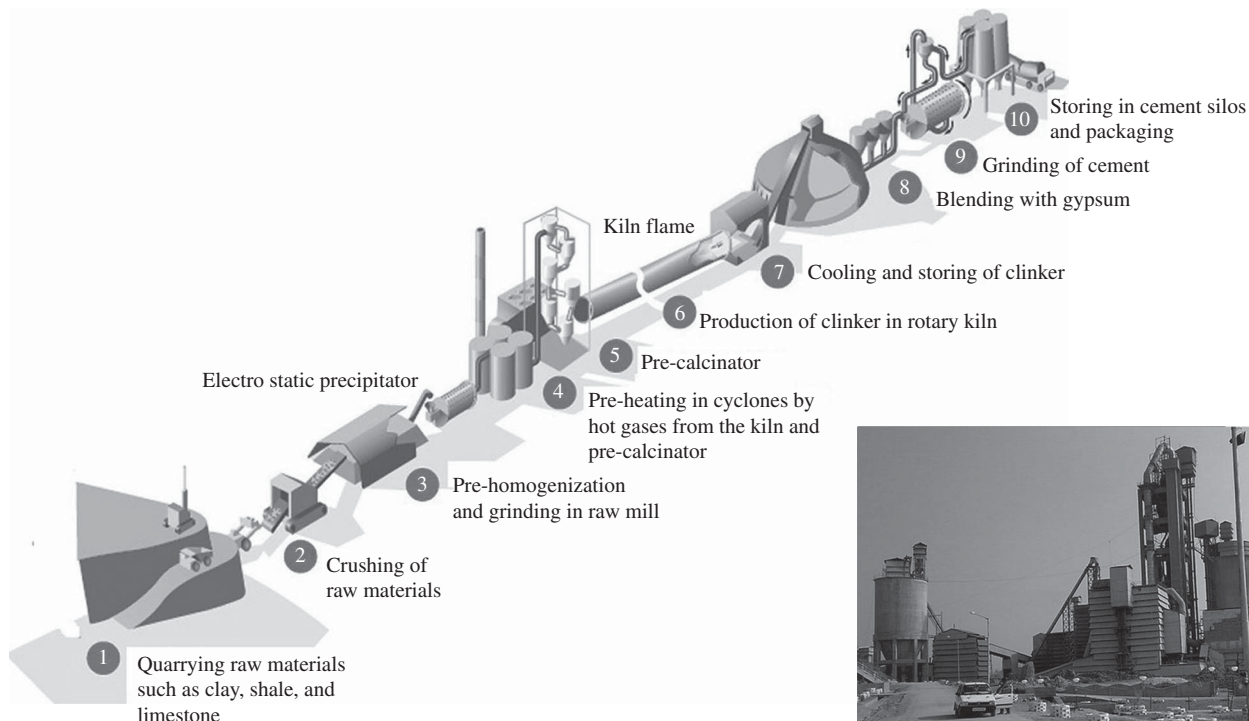


FIG. 1.1 Dry process of cement manufacture (a) Schematic representation (b) View of MCL Cement plant, Thangskai, Meghalaya

Sources: www.cement.org/basics/images/flashtour.html and http://en.wikipedia.org/wiki/File:Cement_Plant_MCL.jpg (adapted)

Two different processes, known as *dry* and *wet*, are used in the manufacture of Portland cement, depending on whether the mixing and grinding of raw materials is done in dry or wet conditions. In addition, a semi-dry process is also sometimes employed in which the raw materials are ground dry, mixed with water, and then burnt in the kilns. Most modern cement factories use either a dry or a semi-dry process. The schematic representation of the dry process of cement manufacture is shown in Fig. 1.1.

Portland Cement

Portland cement (often referred to as *ordinary Portland cement* or *OPC*) is the most common type of cement in general use around the world. The different types of cements covered by the Indian and US standards and their chemical compounds are shown in Table 1.3. Cement production in India consists mainly of the following three types (see Fig. 1.2): OPC ~39 per cent, Portland pozzolana cement (PPC) ~52 per cent, and Portland slag cement (PSC) ~8 per cent. All other varieties put together comprise only 1 per cent of the total production (Mullick 2007).

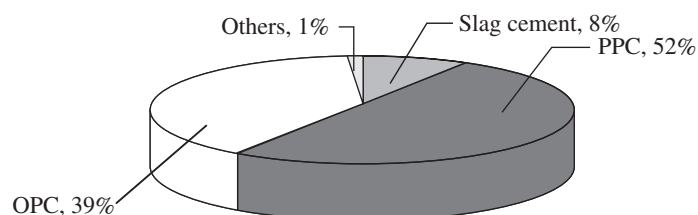


FIG. 1.2 Production trend of different varieties of cement in India

Source: Mullick 2007

TABLE 1.3 Types of Portland cements

India/UK	USA (ASTM)	Typical Compounds ³
OPC (IS 269, IS 8112 and IS 12269)	Type I ¹	C ₃ S 55%, C ₂ S 19%, C ₃ A 10%, C ₄ AF 7%, MgO 2.8%, SO ₃ 2.9%, Ignition loss 1.0%, and free CaO 1.0% (C ₃ A < 15%)
	Type II ¹	C ₃ S 51%, C ₂ S 24%, C ₃ A 6%, C ₄ AF 11%, MgO 2.9%, SO ₃ 2.5%, Ignition loss 1.0%, and free CaO 1.0% (C ₃ A < 8%)
Rapid hardening Portland cement (IS 8041:1990)	Type III ¹	C ₃ S 57%, C ₂ S 19%, C ₃ A 10%, C ₄ AF 7%, MgO 3.0%, SO ₃ 3.1%, Ignition loss 0.9%, and free CaO 1.3% Its seven day compressive strength is almost equal to Types I and II 28 day compressive strengths.
Low heat Portland cement (IS 12600:1989)	Type IV	C ₃ S 28%, C ₂ S 49%, C ₃ A 4%, C ₄ AF 12%, MgO 1.8%, SO ₃ 1.9%, Ignition loss 0.9%, and free CaO 0.8% (C ₃ A < 7% and C ₃ S < 35%)
Sulphate resisting Portland cement (IS 12330:1988)	Type V	C ₃ S 38%, C ₂ S 43%, C ₃ A 4%, C ₄ AF 9%, MgO 1.9%, SO ₃ 1.8%, Ignition loss 0.9%, and free CaO 0.8% [C ₃ A < 5% and (C ₄ AF) + 2(C ₃ A) < 25%]
PSC (IS 455:1989, IS 12089:1987)	Type IS	Made by grinding granulated high-quality slag with Portland cement clinker

(Continued)

TABLE 1.3 (Continued)

India/UK	USA (ASTM)	Typical Compounds ³
PPC [IS 1489-Part 1:1991 (fly ash based), IS 1489-Part 2:1991 (calcined clay based)]	Type IP	A blended cement made by inter-grinding Portland cement and pozzolanic materials without burning
Ternary blended cement	Type IT(SX)(PY) ²	A blended cement made by inter-grinding Portland cement, slag, and pozzolana without burning

Notes:

¹ Types Ia, IIa, and IIIa have the same composition as Types I, II, and III, but have an air-entraining agent ground into the mix.

² The letters X and Y stand for the percentage of supplementary cementitious material (SCM) included in the blended cement, and S and P are the types of SCMs, where S is for slag and P for pozzolan. For example, Type IT(S25)(P15) contains 25 per cent slag and 15 per cent pozzolans.

³ See Table 1.5 for explanation of these compounds.

There are other types, such as high alumina cement (IS 6452:1989), super sulphated cement (IS 6909:1990), hydrophobic Portland cement (IS 8043: 1991), white cement (IS 8042:1989), concrete sleeper grade cement (IRS-T 40:1985), expanding cements, and masonry cement (IS 3466:1988), which are used only in some special situations. (Refer to Mehta and Monteiro (2006) and Shetty (2005) for details regarding these cements.) Geopolymer cements are inorganic hydraulic cements that are based on the polymerization of minerals (see Section 4.4.7 of Chapter 4).

Ordinary Portland cement is the most important cement and is often used, though the current trend is to use PPC (see Fig. 1.2). Most of the discussions to follow in this chapter pertain to this type of cement. The Bureau of Indian Standards (BIS) has classified OPC into the following three grades:

1. 33 grade OPC, IS 269:1989
2. 43 grade OPC, IS 8112:1989
3. 53 grade OPC, IS 12269:1987

TABLE 1.4 Physical properties of various types of cements

S. No.	Type of Cement	IS Code	Fineness m ² /kg (min.)	Setting Time in Minutes		Soundness		Compressive Strength in MPa		
				Initial (min.)	Final (max.)	Le Chatelier (max.) (mm)	Auto Clave, for MgO, (max.) (%)	3 days	7 days	28 days
1.	OPC 33	269:1989	225	30	600	10	0.8	16	22	33
2.	OPC 43	8112:1989	225	30	600	10	0.8	23	33	43
3.	OPC 53	12269:1987	225	30	600	10	0.8	27	37	53
4.	PPC (fly ash-based)	1489:1991 (Part 1)	300	30	600	10	0.8	16	22	33
5.	PSC (slag)	455:2002	225	30	600	10	0.8	16	22	33
6.	SRC	12330:1988	225	30	600	10	0.8	10	16	33

TABLE 1.5 Chemical composition of OPC (Bogue's Compounds)

S. No.	Compound	Cement Chemist Notation (CCN)*	Typical Composition as %	Mineral Phase
1.	Tricalcium silicate 3(CaO)·SiO ₂	C ₃ S	45–65	Alite
2.	Dicalcium silicate 2(CaO)·SiO ₂	C ₂ S	15–30	Belite
3.	Tricalcium aluminate 3(CaO)·Al ₂ O ₃	C ₃ A	5–10	Aluminate
4.	Tetracalcium alumino ferrite 4(CaO)·Al ₂ O ₃ ·Fe ₂ O ₃	C ₄ AF	5–15	Ferrite
5.	Gypsum CaSO ₄ ·2 H ₂ O		2–10	

*Cement chemists use the following shorthand notation:
C = CaO, S = SiO₂, A = Al₂O₃, F = Fe₂O₃, M = MgO,
H = H₂O, N = Na₂O, K = K₂O, \bar{S} = SO₃.

The number in the grade indicates the compressive strength of the cement in N/mm² at 28 days. The 33 grade cement is suitable for producing concrete up to M25. Both 43 grade and 53 grade cement are suitable for producing higher grades of concrete. The important physical properties of the three grades of OPC and other types of cements are compared in Table 1.4. The chemical composition of OPC is given in Table 1.5 and Fig. 1.3.

Approximately 95 per cent of cement particles are smaller than 45 micrometres, with the average particle being around 15 micrometres. The overall particle size distribution of cement is called *fineness*. Fineness affects the heat released and the rate of hydration; greater fineness causes greater early strength (especially during the first seven days) and more rapid generation of heat. *Soundness* refers to the ability of the cement paste to retain its volume after setting and is related to the presence of excessive amounts of free lime or

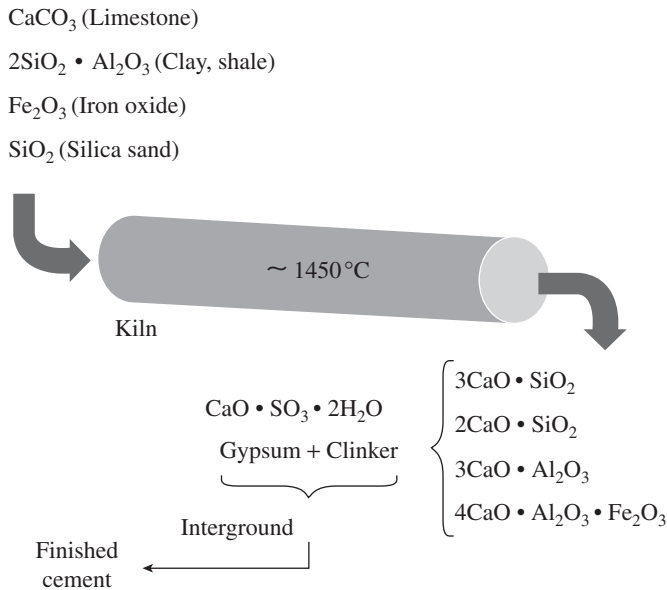


FIG. 1.3 Chemical compounds of cement

magnesia in the cement. *Consistency* indicates the degree of density or stiffness of cement. *Initial setting* of cement is that stage when the paste starts to lose its plasticity. *Final setting* is the stage when the paste completely loses its plasticity and attains sufficient strength and hardness. The specific gravity of Portland cement is approximately 3.15.

As seen in Table 1.5 and Fig. 1.3, there are four major compounds in cement and these are known as tricalcium silicate (C₃S), dicalcium silicate (C₂S), tricalcium aluminate (C₃A), and tetracalcium aluminoferrite (C₄AF). Their composition varies from cement to cement and plant to plant. (The levels of the four clinker minerals can be estimated using a method of calculation first proposed by Bogue in 1929 or by the X-ray diffraction analysis, which gives the exact measurement.) In addition, to these compounds, there are other minor compounds such as MgO, Na₂O, K₂O, SO₃, fluorine, chloride, and trace metals, which are present in small quantities (Moir 2003). Of these K₂O and Na₂O are called *alkalis* and are found to react with some aggregates, resulting in *alkali-silica reaction* (ASR), which causes disintegration of concrete at a later date.

The silicates C₃S and C₂S are the most important compounds and are mainly responsible for the strength of the cement paste. They constitute the bulk of the composition. C₃A and C₄AF do not contribute much to the strength, but in the manufacturing process they facilitate the combination of lime and silica and act as a flux. The role of the different compounds on different properties of cement is shown in Table 1.6.

Portland Pozzolana Cement

As mentioned already, the Romans and Greeks were aware that the addition of volcanic ash results in better performance of concrete. The name pozzolan is now frequently used to describe a range of materials both natural and artificial. [A *pozzolan*

TABLE 1.6 Role of different compounds on properties of cement

Characteristic	Different Compounds in Cement			
	C ₃ S	C ₂ S	C ₃ A	C ₄ AF
Setting	Quick	Slow	Rapid	–
Hydration	Rapid	Slow	Rapid	–
Heat liberation (Cal/g) 7 days	Higher	Lower	Higher	Higher
Early strength	High up to 14 days	Low up to 14 days	Not much beyond 1 day	Insignificant
Later strength	Moderate at later stage	High at later stage after 14 days	–	–

may be defined as a siliceous or siliceous and aluminous material, which in itself possesses little or no cementitious value. However, in finely divided form and in the presence of water, it reacts chemically with calcium hydroxide released by the hydration of Portland cement, at ordinary temperature, to form calcium silicate hydrate and other cementitious compounds possessing cementitious properties (Mehta 1987)]. Fly ash, ground granulated blast furnace slag (GGBS), silica fume, and natural pozzolans, such as calcined shale, calcined clay or metakaolin, are used in conjunction with Portland cement to improve the properties of the hardened concrete. The latest amendment (No. 3) to IS 1489 requires that PPC be manufactured by the inter-grinding of OPC clinker with 15–35 per cent of pozzolanic material. The generally used pozzolanic materials in India are fly ash (IS 1489-Part 1) or calcined clay (IS 1489-Part 1). Mixtures using three cementitious materials, called *ternary mixtures*, are becoming common, but no Indian specification regarding this has been developed yet. UltraTech PPC, Suraksha, Jaypee Cement (PPC) are some of the brand names of PPC in India. As of now, in India, PPC is considered equivalent to 33 grade OPC.

PPC offers the following advantages:

1. Economical than OPC as the costly clinker is replaced by cheaper pozzolanic material
2. Converts soluble calcium hydroxide into insoluble cementitious products, thus improving permeability and durability
3. Consumes calcium hydroxide and does not produce as much calcium hydroxide as OPC
4. Improves pore size distribution and reduces micro-cracks at the transition zone due to the presence of finer particles than OPC
5. Reduces heat of hydration and thermal cracking
6. Has high degree of cohesion and workability in concrete and mortar

The main disadvantage is that the rate of development of strength is initially slightly slower than OPC. In addition, its

effect of reducing the alkalinity may reduce the resistance to corrosion of steel reinforcement. However, as PPC significantly lowers the permeability, the risk of corrosion is reduced. The setting time is slightly longer.

Portland Slag Cement

Blast furnace slag is a non-metallic product consisting essentially of silicates and aluminosilicates of calcium developed in a molten condition simultaneously with iron in a blast furnace. *GGBS* is obtained by rapidly cooling the molten slag, which is at a temperature of about 1500°C, by quenching in water or air to form a glassy sand-like granulated material. Every year about nine million tons of blast furnace slag is produced in India. The *GGBS* should conform to IS I2089:1987. *PSC* is obtained either by intimate inter-grinding of a mixture of Portland cement clinker and granulated slag with the addition of gypsum or calcium sulphate or by an intimate and uniform blending of Portland cement and finely ground granulated slag. Amendment No. 4 of IS 455 requires that the slag constituent not be less than 25 per cent or more than 70 per cent of the *PSC*. It has to be noted that *PSC* has physical properties similar to those of *OPC*.

The following are some advantages of *PSC*:

1. Utilization of slag cement in concrete not only lessens the burden on landfills; it also conserves a virgin manufactured product (*OPC*) and decreases the embodied energy required to produce the cementitious materials in concrete. Embodied energy can be reduced by 390–886 million Joules with 50 per cent slag cement substitution. This is a 30–48 per cent reduction in the embodied energy per cubic metre of concrete (<http://www.slagcement.org>).
2. By using a 50 per cent slag cement substitution less CO₂ is emitted (amounting to about 98 to 222 kg per cubic metre of concrete, a 42–46% reduction in greenhouse gas emissions) (<http://www.slagcement.org>).
3. Using slag cement to replace a portion of Portland cement in a concrete mixture is a useful method to make concrete better and more consistent. *PSC* has a lighter colour, better concrete workability, easier finishability, higher compressive and flexural strength, lower permeability, improved resistance to aggressive chemicals, and more plastic and hardened consistency.
4. The lighter colour of slag cement concrete also helps reduce the heat island effect in large metropolitan areas.
5. It has low heat of hydration and is relatively better resistant to soils and water containing excessive amounts of sulphates and is hence used for marine works, retaining walls, and foundations.

Both *PPC* and *PSC* will give more strength than *OPC* at the end of 12 months. UltraTech Premium, Super Steel (Madras Cement), and S 53 (L&T) are some of the brand names of *PSC* available in India.

Storage of Cement

Cement is very finely ground and readily absorbs moisture; hence, care should be taken to ensure that the cement bags are not in contact with moisture. They should be stored in airtight and watertight sheds and used in such a way that the bags that come in first are the first to go out. Cement stored for a long time tends to lose its strength (loss of strength ranges from 5–10% in three months to 30–40% in one year). It is better to use the cement within 90 days of its production. In case it is used at a later date, it should be tested before use.

Tests on Cement

The usual tests carried out for cement are for chemical and physical requirements. They are given in IS 4031 (different parts) and IS 4032. Most of these tests are conducted at a laboratory (Neville 2012).

Fineness is measured by the *Blaine air permeability test*, which indirectly measures the surface area of the cement particles per unit mass (m²/kg), or by actual sieving (IS 4031-Part 1:1996 and Part 2:1999). Most cement standards have a minimum limit on fineness (in the range 225–500 m²/kg). Soundness of cement is determined by Le-Chatelier and autoclave tests, as per IS 4031-Part 3:1988. *Consistency* is measured by *Vicat apparatus*, as per IS 4031-Part 4:1988. The paste is said to be of standard consistency when the penetration of plunger, attached to the *Vicat apparatus*, is 33–35 mm. The initial and final setting times of cement are measured using the *Vicat apparatus* with different penetrating attachments, as per IS 4031-Part 5:1988. It has to be noted that the setting time decreases with increase in temperature; the setting time of cement can be increased by adding some admixtures. The compressive strength of cement is the most important of all the properties. It is found using a cement–sand mortar (ratio of cement to sand is 1:3) cube of size 70.6 mm, as per IS 4031-Part 6:1988. The compressive strength is taken as the average of strengths of three cubes. The heat of hydration is tested in accordance with IS 4031-Part 9:1988 using vacuum flask methods or by conduction calorimetry.

A web-based computer software called *Virtual Cement and Concrete Testing Laboratory* (eVCCTL) has been developed by scientists at the National Institute of Standards and Technology (NIST), USA, which can be used to explore the properties of cement paste and concrete materials. This software may be found at http://www.nist.gov/el/building_materials/evcctl.cfm.

1.2.2 Aggregates

The fine and coarse aggregates occupy about 60–75 per cent of the concrete volume (70–85% by mass) and hence strongly influence the properties of fresh as well as hardened concrete, its mixture proportions, and the economy. Aggregates used in concrete should comply with the requirement of

IS 383:1970. Aggregates are commonly classified into fine and coarse aggregates. *Fine aggregates* generally consist of natural sand or crushed stone with particle size smaller than about 5 mm (materials passing through 4.75 mm IS sieve). Coarse aggregates consist of one or a combination of gravels or crushed stone with particle size larger than 5 mm (usually between 10 mm and 40 mm). Aggregates can also be classified in two more ways. Depending on the source, they could be either naturally occurring (gravel, pebbles, sand, etc.) or synthetically manufactured (bloomed clay aggregates, sintered fly ash aggregate, etc.). Moreover, depending on the bulk density, aggregates can either be normal weight (1520–1680 kg/m³), lightweight (less than 1220 kg/m³), or heavyweight (more than 2000 kg/m³). The normal weight aggregates—sand, gravel, crushed rock (e.g., granite, basalt, and sand stone), and blast furnace slag—are used to produce normal weight concrete with a density of 2200–2400 kg/m³. Aggregates such as expanded shale, clay, slate, slag, pumice, perlite, vermiculite, and diatomite are used to produce structural lightweight concrete (SLWC) with density ranging from about 1350 kg/m³ to 1850 kg/m³. Heavyweight aggregates consist of hematite, steel, or iron and are used in special applications such as providing radiation shielding and abrasion resistance (ACI 301M:10 2010, ACI Committee E-701 2007).

The factors of aggregates that may directly or indirectly influence the properties of concrete are given in Table 1.7 (Ambuja technical booklets 5:1996, 125:2007). Only normal weight aggregates are discussed here and should confirm to IS 383:1970. The coarse aggregates form the main matrix of the concrete and hence provide strength to the concrete, whereas the fine aggregates form the filler matrix and hence reduce the porosity of concrete. Some properties of aggregates are shown in Table 1.8.

TABLE 1.7 Factors of aggregates that may affect properties of concrete

S. No.	Factors	Influence on Concrete Property
1.	Specific gravity/Porosity	Strength/Absorption of water
2.	Crushing strength	Strength
3.	Chemical stability	Durability
4.	Surface texture	Bond grip
5.	Shape (see Fig. 1.4)	Water demand (strength)

S. No.	Factors	Influence on Concrete Property
6.	Gradation or particle size distribution	Water demand (strength), cohesion, bleeding, and segregation
7.	Maximum size of aggregate	Strength and water demand
8.	Presence of deleterious materials such as dust, clay, silt, or mud	Water demand (strength), cohesion, bond, and durability

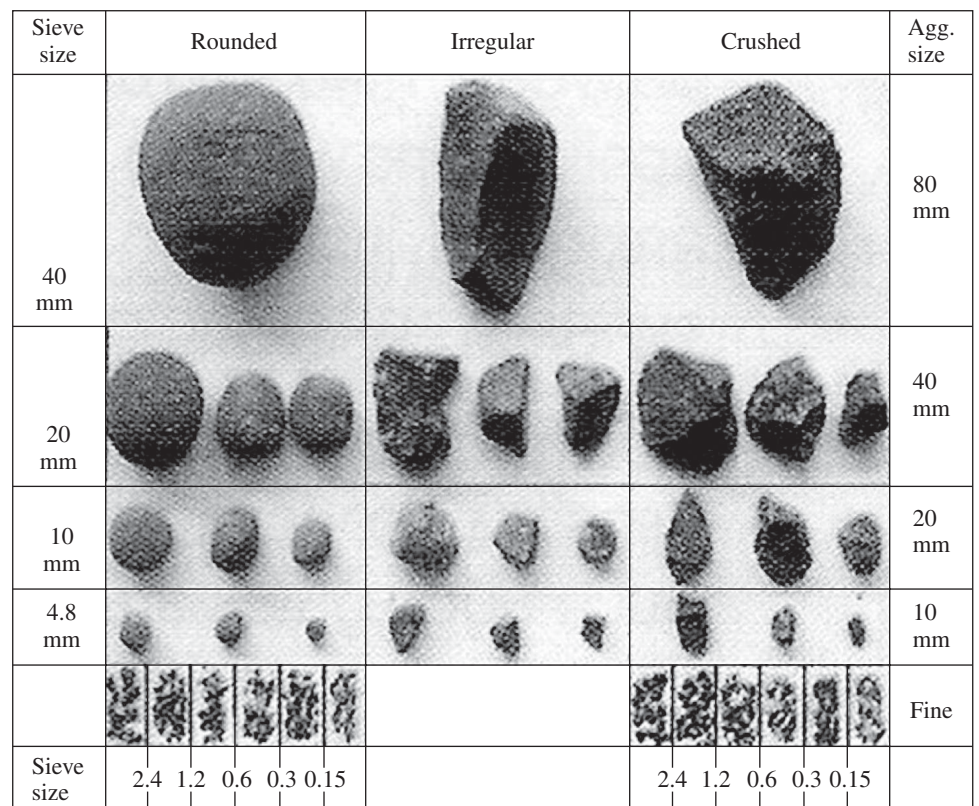


FIG. 1.4 Different shapes and sizes of aggregates

Source: Ambuja technical booklet 125:2007

TABLE 1.8 Properties of aggregates

Aggregate	Property	Aggregate	Property
	Specific Gravity		Minimum Voids (%)
Gravel	2.67	River sand	
Granite	2.80	Fine	43
Sand	2.65	Coarse	35
Basalt	2.85	Mixed and moist	38
Bottom ash	1.57	Mixed and dry	30
	<i>Bulk density (kg/l)</i>		
Broken granite	1.68	Broken stone, graded	
Broken stone	1.60	Maximum size: 25 mm	46
Stone screening	1.45	Maximum size: 50 mm	45

(Continued)

TABLE 1.8 (Continued)

Aggregate	Property	Aggregate	Property
	Specific Gravity		Minimum Voids (%)
Beach or river Shingle	1.60	Maximum size: 63 mm	41
River sand		Stone screening	48
Fine	1.44		Fineness Modulus
Medium	1.52	Sand	2.70
Coarse	1.60	Bottom ash	2.08

In several countries including India, natural coarse aggregates and river sand are scarce; at the same time, the waste from the demolition of buildings is escalating. The amount of construction waste in India alone is estimated to be around 12–14.7 million tons per annum (Rao, et al. 2011). In such places, *recycled coarse aggregates* (RCA) could be used profitably. More details about RCA and their use in concrete may be found in the works of Dhir and Paine (2010), Rao, et al. (2011), and Subramanian (2012). In general, mechanical properties such as compressive strength, split and tensile strengths, and modulus of elasticity are reduced with increasing percentage of RCA. It is suggested that 25 per cent of RCA may be used in concrete, as it will not affect the properties significantly (Rao, et al. 2011). Other substitutes for coarse aggregate include incinerator bottom ash aggregate and sintered fly ash pellets. Recycled glass aggregates, bottom ash from thermal power plants, and quarry dust have significant potential for use as fine aggregates in concrete (Dhir and Paine 2010; Mullick 2012). Clause 5.3.1 of IS 456 stipulates that such aggregates should not contain more than 0.5 per cent of sulphates as SO_3 and should not absorb more than 10 per cent of their own mass of water. Before using these materials, it is better to study their effect on the properties of concrete. For example, manufactured sand, often referred to as *M-sand*, from crushed gravel or rock is cubical in shape and results in increased water demand of the concrete mix.

Aggregates must be clean, hard, strong, and durable; they should be free from coatings of clay, absorbed chemicals, and other fine materials that could affect the hydration and bond of the cement paste. Aggregates are usually washed to remove impurities and graded at the site or plant. Grading or particle size distribution of aggregates is a major factor determining the workability, segregation, bleeding, placing, and finishing characteristics of concrete. The grading of fine aggregates has been found to influence the properties of green (fresh) concrete more than those of coarse aggregates. The grading requirements recommended by the Indian and US standards for fine aggregates is given in Table 1.9. Combined gradation

of fine and coarse aggregate may result in better control of workability, pumpability, shrinkage, and other properties of concrete (Kosmatka, et al. 2011). In general, aggregates that do not have a large deficiency or excess of any size and give a smooth grading curve will produce the most satisfactory results (Kosmatka, et al. 2011). Coarse and fine aggregates should be batched separately.

TABLE 1.9 Grading requirements for fine aggregates

IS Sieve Designation	Percentage Passing by Weight for Grading Zone				ASTM Standard C 33
	I	II	III	IV	
10 mm	100	100	100	100	100
4.75 mm	90–100	90–100	90–100	95–100	95–100
2.36 mm	60–95	75–100	85–100	95–100	80–100
1.18 mm	30–70	55–90	75–100	90–100	50–85
600 μ m	15–34	35–59	60–79	80–100	25–60
300 μ m	5–20	8–30	12–40	15–50	5–30
150 μ m	0–10	0–10	0–10	0–15	0–10

The *fineness modulus* (FM) of either fine or coarse aggregate is calculated by adding the cumulative percentages by mass retained on each of the series of sieves and dividing the sum by 100. The higher the FM, the coarser will be the aggregate. The maximum size of coarse aggregate should not be greater than the following: one-fourth of the maximum size of member, 5 mm less than the maximum clear distance between the main bars, or 5 mm less than the minimum cover of the reinforcement. For RCC works, 20 mm aggregates are preferred. In thin concrete members with closely spaced reinforcement or small cover and in HSC, Clause 5.3.3 of IS 456 allows the use of 10 mm nominal maximum size. Rounded aggregates are preferable to angular or flaky aggregates, as they require minimum cement paste for bond and demand less water. Flaky and elongated aggregates are also susceptible to segregation and low strength.

It should be noted that the amount of water added to make concrete must be adjusted for the moisture conditions of the aggregates to accurately meet the water requirement of the mix design. Various testing methods for aggregates to concrete are described in IS 2386-Parts 1 to 8:1963.

1.2.3 Water

Water plays an important role in the workability, strength, and durability of concrete. Too much water reduces the concrete strength, whereas too little will make the concrete unworkable. The water used for mixing and curing should be clean and free from injurious amounts of oils, acids, alkalis, salts, sugars, or organic materials, which may affect the concrete or steel. As per Clause 5.4 of IS 456, potable water is considered satisfactory for mixing as well as curing concrete; otherwise, the water to be used should be tested as per IS 3025-Parts 1 to 32 (1984

to 1988). In general, sea water should not be used for mixing or curing concrete. The permissible limits for impurities as per Clause 5.4 of IS 456 are given in Table 1.10. The pH value of water used for mixing should be greater than six.

TABLE 1.10 Permissible limits for impurities in mixing water

Impurity	Maximum Permissible Limit	
	IS 456 (mg/l)	ASTM C 94 (ppm)
Organic	200	–
Inorganic	3000	–
Sulphates (such as SO ₃)	400	3000
Chlorides (such as Cl)	2000 (for plain concrete work) 500 (for RCC)	1000 ¹
Suspended matter	2000	50,000
Alkalis (such as Na ₂ O + 0.658K ₂ O)	–	600

Note:

¹ Prestressed concrete or concrete in bridge decks 500 ppm (ppm and mg/l are approximately equal)

In general, the amount of water required to be added for cement hydration is less compared to that required for workability. For complete hydration of Portland cement, only about 36–42 per cent water (this is represented by the water/cement or water/cementitious ratio, usually denoted by *w/c ratio* or *w/cm ratio*), that is, *w/c* of 0.36–0.42, is needed. If a *w/c* ratio greater than about 0.36 is used, the excess water, which is not required for cement hydration, will remain in the capillary pores or may evaporate in due course. This process leads to *drying shrinkage* (drying shrinkage is destructive as it leads to micro-cracking and may eventually weaken concrete). Similarly, when a *w/c* ratio of less than about 0.36 is used, some cement will remain unhydrated. The space initially taken up by water in a cementitious mixture will be partially or completely replaced over time by the hydration products. If a *w/c* ratio of more than 0.36 is used, then porosity in the hardened material will remain, even after complete hydration. This is called *capillary porosity* and will lead to corrosion of reinforcement.

1.2.4 Admixtures

It is interesting to note that the Romans were the first to use admixtures in concrete in the form of blood, milk, and lard (pig fat). Present-day admixtures may be classified as chemical and mineral admixtures.

Chemical Admixtures

Chemical admixtures are materials in the form of powder or fluids that are added to the concrete immediately before or

during mixing in order to improve the properties of concrete. They should comply with the requirements of IS 9103:1999. Admixtures are used for several purposes, such as to increase flowability or pumpability of fresh concrete, obtain high strength through lowering of *w/c* ratio, retard or accelerate time of initial setting, increase freeze–thaw resistance, and inhibit corrosion (Krishnamurthy 1997). Normal admixture dosage is about 2–5 per cent by mass of cement. The effectiveness of an admixture depends upon factors such as type, brand, and amount of cementing materials; water content; aggregate shape, gradation, and proportions; mixing time; slump; and temperature of the concrete (Kosmatka, et al. 2011).

The common types of admixtures are as follows (Rixom and Mailvaganan 1999; Aitcin, et al. 1994; Kosmatka, et al. 2011):

1. *Accelerators* enhance the rate of hydration of the concrete and, hence, result in higher early strength of concrete and early removal of formwork. Typical materials used are calcium chloride, triethanolamine, sodium thiocyanate, calcium formate, calcium nitrite, and calcium thiosulphate. Typical commercial products are Mc-Schnell OC and Mc-Schnell SDS. Typical dosage is 2–3 per cent by weight of cement. As the use of chlorides causes corrosion in steel reinforcing, they are not used now.
2. *Retarders* slow down the initial rate of hydration of cement and are used more frequently than accelerators. They are often combined with other types of admixtures like water reducers. Typical retarders are sugars, hydroxides of zinc and lead, calcium, and tartaric acid. Typical dosage is 0.05 per cent to 0.10 per cent by weight of cement. Commonly used retarders are lignosulphonic acids and hydroxylated carboxylic acids, which act as water-reducing and water-retarding admixtures; they delay the initial setting time by three to four hours when used at normal ambient temperatures.
3. *Water-reducing admixtures* are used to reduce the quantity of mixing water required to produce concrete. Water-reducing admixtures are available as *ordinary water-reducing admixtures* (WRA) and *high-range water-reducing admixtures* (HRWRA). WRA enable up to 15 per cent water reduction, whereas HRWRA enable up to 30 per cent. Popularly, the former are called *plasticizers* and the latter *superplasticizers*. In modern day concreting, the distinction seems to be disappearing. Compounds used in India as superplasticizers include sulphonated naphthalene formaldehyde condensates (SNF), sulphonated melamine formaldehyde condensates (SMF), and modified lignosulphonates (MLS). Some new generation superplasticizers include acrylic polymer based (AP) superplasticizers, copolymers of carboxylic acid with acrylic ether (CAE), polycarboxylate ethers (PCs), and multi-polycarboxylate ethers (MCEs). The naphthalene

and melamine types of superplasticizers or HRWRA are typically used in the range 0.7–2.5 per cent by weight of cement and give water reductions of 16–30 per cent. The PCs are more powerful and are used at 0.3–1.0 per cent by weight of cement to typically give 20 per cent to over 40 per cent water reduction. Use of superplasticizers with reduced water content and w/c ratio can produce concretes with (a) high workability (in fresh concretes), with increased slump, allowing them to be placed more easily, with less consolidating effort, (b) high compressive strengths, (c) increased early strength gain, (d) reduced chloride ion penetration, and (e) high durability. It has to be noted that it is important to consider the compatibility of superplasticizers with certain cements (Jayasree, et al. 2011; Mullick 2008).

4. *Air entraining admixtures* are used to entrain tiny air bubbles in the concrete, which will reduce damage during freeze–thaw cycles, thereby increasing the concrete’s durability. Furthermore, the workability of fresh concrete is improved significantly, and segregation and bleeding are reduced or eliminated. However, entrained air entails a trade off with strength, as each 1 per cent of air may result in 5 per cent decrease in compressive strength. The materials used in such admixtures include salts of wood resins, some synthetic detergents, salts of petroleum acids, fatty and resinous acids and their salts, and salts of sulphonated hydrocarbons.
5. *Corrosion inhibitors* are used to minimize the corrosion of steel and steel bars in concrete.

The other chemical admixtures include foaming agents (to produce lightweight foamed concrete with low density), alkali–aggregate reactivity inhibitors, bonding admixtures (to increase bond strength), colouring admixtures, shrinkage reducers, and pumping aids. It is important to test all chemical admixtures adequately for their desired performance. It is also desirable to prepare trial mixes of concrete with chemical admixtures and test their performance before using them in any large construction activity (see also Clause 5.5 of IS 456). They should not be used in excess of the prescribed dosages, as they may be detrimental to the concrete.

Mineral Admixtures

Mineral admixtures are inorganic materials that also have pozzolanic properties. These very fine-grained materials are added to the concrete mix to improve the properties of concrete (mineral admixtures) or as a replacement for Portland cement (blended cements). Pozzolanic materials react with the calcium hydroxide (lime) released during the hydration process of cement to form an additional C-S-H gel. This can reduce the size of the pores of crystalline hydration products, make the microstructure of concrete more uniform, and improve the impermeability and durability of concrete. These improvements can lead to an increase in strength and service life of concrete. Some of the mineral admixtures are briefly described here:

1. *Fly ash* is a by-product of coal-fired thermal power plants. In India, more than 120 million tons of fly ash is produced every year, the disposal of which poses a serious environmental problem. Any coal-based thermal power station may produce four kinds of ash: fly ash, bottom ash, pond ash, and mound ash. The quality of fly ash to be used in concrete is governed by IS 3812 (Parts 1 and 2):2003, which groups all these types of ash as *pulverized fuel ash* (PFA). PFA is available in two grades: Grade I and grade II (Class F—siliceous fly ash and Class C—calcareous fly ash, as per ASTM). Both these grades can be used as admixtures. Up to 35 per cent replacement of cement by fly ash is permitted by the Indian codes. Fly ash is extracted from flue gases through electrostatic precipitator in dry form. It is a fine material and possesses good pozzolanic properties. The properties of fly ash depend on the type of coal burnt. The lower the loss on ignition (LOI), the better will be the fly ash. The fineness of individual fly ash particles range from 1 micron to 1 mm in size. The specific gravity of fly ash varies over a wide range of 1.9 to 2.55. For a majority of site-mixed concrete, fly ash-based blended cement is the best option. Fly ash particles are generally spherical in shape and reduce the water requirement for a given slump. The use of fly ash will also result in reduced heat of hydration, bleeding, and drying shrinkage.
2. *Ground granulated blast furnace slag* is a by-product of steel production and has been used as a cementitious material since the eighteenth century. It is currently inter-ground with Portland cement to form blended cement, thus partially replacing Portland cement. It reduces the temperature in mass concrete, permeability, and expansion due to alkali–aggregate reaction and improves sulphate resistance. See Section 1.2.1 for more details on PSC.
3. *Silica fume* is also referred to as *micosilica* or *condensed silica fume*. It is a by-product of the production of silicon and ferrosilicon alloys. Silica fume used in concrete should conform to IS 15388:2003; as per Clause 5.2.1.2 of IS 456, its proportion is 5–10 per cent of cement content of a mix. Silica fume is similar to fly ash, with spherical shape, but has an average particle size of about 0.1 micron, that is, it is 100 times smaller than an average cement particle. This results in a higher surface to volume ratio and a much faster pozzolanic reaction. Silica fume addition benefits concrete in two ways: (a) The minute particles physically decrease the void space in the cement matrix—this phenomenon is known as packing. (b) Silica fume is an extremely reactive pozzolan; it increases the compressive strength and improves the durability of concrete. Silica fume for use in concrete is available in wet or dry form. It is usually added during concrete production at a concrete plant. However, it generally requires the use of superplasticizers for workability.
4. *Rice husk ash* (RHA) is produced by burning rice husk in controlled temperature, without causing environmental

pollution. (India produces about 125 million tons of paddy and 30 million tons of rice husk.) It exhibits high pozzolanic characteristics and its use in concrete results in high strength and impermeability. Water demand and drying shrinkage should be studied before using rice husk.

5. *High-reactivity Metakaolin* (HRM) is obtained by calcination of pure or refined *kaolinitic* clay at a temperature between 650 °C and 850 °C followed by grinding to achieve a fineness of 700–900 m²/kg. The strength and durability of concrete produced with the use of HRM is similar to that produced with silica fume. Whereas silica fume is usually dark grey or black in colour, HRM is usually bright white in colour, making it the preferred choice for architectural concrete, where appearance is important.

More details about mineral admixtures may be found in the works of Bapat (2012) and Ramachandran (1995).

1.3 PROPORTIONING OF CONCRETE MIXES

Concrete mix design is the process of proportioning various ingredients such as cement, cementitious materials, aggregates, water, and admixtures optimally in order to produce a concrete at minimal cost and will have specified properties of workability and homogeneity in the green state and strength and durability in the hardened state (SP 23:1982).

Earlier mix design procedures such as minimum voids method, Fuller's maximum density method, Talbot–Richart method, and fineness modulus method are based on the principles of minimum voids and maximum density (Krishna Raju 2002). The modern mix design methods include the Road Note No. 4 method, the ACI (American Concrete Institute) method, the USBR (United States Bureau of Reclamation) method, the Bolomeya model, the British mix design method, and the BIS method (Krishna Raju 2002; Nataraja and Reddy 2007). All these methods are mostly based on empirical relations, charts, graphs, and tables developed through extensive experiments using locally available materials. Although the older BIS code (IS 10262:1982) differed from the ACI method (ACI 211.1, 1991) in some aspects, the present BIS code (IS 10262:2009) is in line with the ACI code method (Nataraja and Das 2010). In all these mix proportioning methods, the ingredients are proportioned by weight per unit volume of concrete.

The main objective of any concrete mix proportioning method is to make a concrete that has the following features:

1. Satisfies workability requirements in terms of slump for easy placing and consolidating
2. Meets the strength requirements as measured by the compressive strength
3. Can be mixed, transported, placed, and compacted as efficiently as possible
4. Will be economical to produce

5. Fulfills durability requirements to resist the environment in which the structure is expected to serve

Changes in Procedure for Mix Proportioning in IS 10262:2009

As per Clause 9.1.1 of IS 456, the minimum grade of concrete to be used in an RCC should not be less than M20. Moreover, all concretes above M20 grade for RCC work must be *design mixes*. Concrete grades above M60 fall under the category of HSC and hence should be proportioned using the guidelines given in specialist literature, such as ACI 211.4-93 and the work of Krishna Raju (2002) and de Larrard (1999).

The 2009 version of the code does not contain the graph of w/c ratio versus 28-day compressive strength. Now, the relationship between w/c ratio and the compressive strength of concrete needs to be established for the materials actually used or by using any other available relationship based on experiments. The maximum w/c ratio given in IS 456:2000 for various environmental conditions may be used as a starting point. The water content per cubic metre of concrete in the earlier version of the standard was a constant value for various nominal maximum sizes of aggregates. However, in the revised version, the maximum water content per cubic metre of concrete is suggested. Another major inclusion in the revised standard is the estimation of volume of coarse aggregate per unit volume of total aggregate for different zones of fine aggregate. As air content in normal (non-air entrained) concrete will not affect the mix proportioning significantly, it is not considered in the revised version; it is also not considered in IS 456:2000.

Data for Mix Proportioning

The following basic data is required for concrete mix proportioning of a particular grade of concrete:

1. Exposure condition of the structure under consideration (see Table 3 of IS 456:2000 and Table 4.4 in Chapter 4 of this book for guidance)
2. Grade designation—The minimum grade of concrete to be designed for the type of exposure condition under consideration (see Tables 3 and 5 of IS 456:2000 and Table 4.4 in Chapter 4 and Table 1.11 of this book for guidance)
3. Type of cement (OPC, PPC, PSC, etc.)

TABLE 1.11 Grades of concrete

Group	Grade Designation	Specified Characteristic 28-day Compressive Strength of 150 mm cube, N/mm ²
Ordinary concrete	M10–M20	10–20
Standard concrete	M25–M60	25–60
High-strength concrete	M65–M100	65–100

4. Minimum and maximum cement content (see Tables 3, 4, 5, and 6 of IS 456:2000 and Tables 4.4 and 4.5 in Chapter 4 of this book for guidance)
5. Type of aggregate (basalt, granite, natural river sand, crushed stone sand, etc.)
6. Maximum nominal size of aggregate to be used (40 mm, 20 mm, or 12.5 mm)
7. Maximum w/c ratio (see Tables 3 and 5 of IS 456:2000 and Tables 4.4 and 4.5 in Chapter 4 of this book for guidance)
8. Desired degree of workability (see Table 1.12, which is based on Clause 7 of IS 456)
9. Use of admixture, its type, and conditions of use
10. Maximum temperature of concrete at the time of placing
11. Method of transporting and placing
12. Early age strength requirements, if required

TABLE 1.12 Workability of concrete

Placing Conditions	Degree of Workability	Slump, mm
Mud mat, shallow section, pavement using pavers	Very low	0.70–0.80 (compacting factor)
Mass concrete; lightly reinforced slabs, beams, walls, columns; strip footings	Low	25–75
Heavily reinforced slabs, beams, walls, columns	Medium	50–100
Slip formwork, pumped concrete	Medium	75–100
In situ piling, trench fill	High	100–150
Tremie concrete	Very high	150–200 (flow test as per IS 9103:1999)

Note: Internal (needle) vibrators are suitable for most of the placing conditions. The diameter of the needle should be determined based on the density and spacing of reinforcements and the thickness of sections. Vibrators are not required for tremie concrete.

The step-by-step mix proportioning procedure as per IS 10262 is as follows (IS 10262:2009; Nagendra 2010):

Step 1 Calculate the target mean compressive strength for mix proportioning. The 28-day target mean compressive strength as per Clause 3.2 of IS 10262 is

$$f'_{ck} = f_{ck} + 1.65 \times s \quad (1.1)$$

where f'_{ck} is the target mean compressive strength at 28 days (N/mm^2), f_{ck} is the characteristic compressive strength at 28 days (N/mm^2), and s is the standard deviation (N/mm^2).

Standard deviation should be calculated for each grade of concrete using at least 30 test strength of samples (taken from

site), when a mix is used for the first time. In case sufficient test results are not available, the values of standard deviation as given in Table 1.13 may be assumed for proportioning the mix in the first instance. As soon as sufficient test results are available, actual standard deviation shall be calculated and used to proportion the mix properly.

TABLE 1.13 Assumed standard deviation

S. No.	Grade of Concrete	Assumed Standard Deviation, N/mm^2
1.	M10	3.5
2.	M15	
3.	M20	4.0
4.	M25	
5.	M30	5.0
6.	M35	
7.	M40	
8.	M45	
9.	M50	
10.	M55	

Note: These values correspond to strict site control of storage of cement, weigh batching of materials, controlled addition of water, and so on. The values given in this table should be increased by 1 N/mm^2 when the aforementioned are not practised.

Step 2 Select the w/c ratio. The concrete made today has more than four basic ingredients. We now use both chemical and mineral admixtures to obtain concretes with improved properties both in fresh and hardened states. Even the qualities of both coarse and fine aggregates in terms of grading, shape, size, and texture have improved due to the improvement in crushing technologies. As all these variables will play a role, concretes produced with the same w/c ratio may have different compressive strengths. Therefore, for a given set of materials, it is preferable to establish the relationship between the compressive strength and free w/c ratio. If such a relationship is not available, maximum w/c ratio for various environmental exposure conditions as given in Table 5 of IS 456 (Table 4.5 in Chapter 4 of this book) may be taken as a starting point. Any w/c ratio assumed based on the previous experience for a particular grade of concrete should be checked against the maximum values permitted from the point of view of durability, and the lesser of the two values should be adopted.

Step 3 Select the water content. The quality of water considered per cubic metre of concrete decides the workability of the mix. The use of water-reducing chemical admixtures in the mix helps to achieve increased workability at lower water contents. The water content given in Table 1.14 (Table 2 of IS 10262) is the maximum value for a particular nominal maximum size of (angular) aggregate, which will achieve a slump in the range of 25 mm to 50 mm. The water content per

TABLE 1.14 Maximum water content per cubic metre of concrete for nominal maximum size of (angular) aggregate

S. No.	Nominal Maximum Size of Aggregate, mm	Maximum Water Content*, kg
1.	10	208
2.	20	186
3.	40	165

Note: These quantities of mixing water are for use in computing cementitious material contents for trial batches.

*Water content corresponding to saturated surface dry aggregate

unit volume of concrete can be reduced when increased size of aggregate or rounded aggregates are used. On the other hand, the water content per unit volume of concrete has to be increased when there is increased temperature, cement content, and fine aggregate content.

In the following cases, a reduction in water content is suggested by IS 10262:

1. For sub-angular aggregates, a reduction of 10 kg
2. For gravel with crushed particles, a reduction of 20 kg
3. For rounded gravel, a reduction of 25 kg

For higher workability (greater than 50 mm slump), the required water content may be established by trial, an increase by about 3 per cent for every additional 25 mm slump, or alternatively by the use of chemical admixtures conforming to IS 9103:1999.

Use of water reducing admixture Depending on the performance of the admixture (conforming to IS 9103:1999) that is proposed to be used in the mix, a reduction in the assumed water content can be made. Water-reducing admixtures will usually decrease water content by 5–10 per cent and superplasticizers decrease water content by 20 per cent and above at appropriate dosages. As mentioned earlier, the use of PC-based superplasticizers results in water reduction up to 30–40 per cent.

Step 4 Calculate the content of cementitious material. The cement and supplementary cementitious material content per unit volume can be calculated from the free w/c ratio of Step 2. The total cementitious content so calculated should be checked against the minimum content for the requirements of durability and the greater of the two values adopted. The maximum cement content alone (excluding mineral admixtures such as fly ash and GGBS) should not exceed 450 kg/m³ as per Clause 8.2.4.2 of IS 456.

Step 5 Estimate the proportion of coarse aggregate. Table 1.15 (Table 3 of IS 12062) gives the volume of coarse aggregate for unit volume of total aggregate for different zones of fine aggregate (as per IS 383:1970) for a w/c ratio of 0.5, which requires to be suitably adjusted for other w/c ratios. This table is based on ACI 211.1:1991. Aggregates of

TABLE 1.15 Volume of coarse aggregate per unit volume of total aggregate for different zones of fine aggregate

Nominal Maximum Size of Aggregate, mm	Volume of Coarse Aggregate* Per Unit Volume of Total Aggregate for Different Zones of Fine Aggregate (for w/c Ratio = 0.5)			
	Zone IV	Zone III	Zone II	Zone I
10	0.50	0.48	0.46	0.44
20	0.66	0.64	0.62	0.60
40	0.75	0.73	0.71	0.69

Note: The volume of coarse aggregate per unit volume of total aggregate needs to be changed at the rate of ± 0.01 for every ± 0.05 change in w/c ratio.

*Volumes are based on aggregate in saturated surface dry condition.

essentially the same nominal maximum size, type, and grading will produce concrete of satisfactory workability when a given volume of coarse aggregate per unit volume of total aggregate is used. It can be seen that for equal workability, the volume of coarse aggregate in a unit volume of concrete is dependent only on its nominal maximum size and the grading zone of fine aggregate.

Step 6 Identify the combination of different sizes of coarse aggregate fractions. Coarse aggregates from stone crushes are normally available in two sizes, namely 20 mm and 12.5 mm. Coarse aggregates of different sizes can be suitably combined to satisfy the gradation requirements (cumulative per cent passing) of Table 2 in IS 383:1970 for the given nominal maximum size of aggregate.

Step 7 Estimate the proportion of fine aggregate. The absolute volume of cementitious material, water, and the chemical admixture is found by dividing their mass by their respective specific gravity, and multiplying by 1/1000. The volume of all aggregates is obtained by subtracting the summation of the volumes of these materials from the unit volume. From this, the total volume of aggregates, the weight of coarse and fine aggregate, is obtained by multiplying their fraction of volumes (already obtained in Step 5) with the respective specific gravities and then multiplying by 1000.

Step 8 Perform trial mixes. The calculated mix proportions should always be checked by means of trial batches. The concrete for trial mixes shall be produced by means of actual materials and production methods. The trial mixes may be made by varying the free w/c ratio by ± 10 per cent of the pre-selected value and a suitable mix selected based on the workability and target compressive strength obtained. Ribbon-type mixers or pan mixers are to be used to simulate the site conditions where automatic batching and pan mixers are used for the production of concrete. After successful laboratory trials, confirmatory field trials are also necessary.

The guidelines for mix proportioning for HSC are provided by ACI 211.4R:93, for concrete with quarry dust by Nataraja,

et al. (2001), and for concrete with internal curing by Bentz, et al. (2005). Rajamane (2004) explains a procedure of mix proportioning using the provisions of IS 456:2000. Optimal mixture proportioning for concrete may also be performed using online tools such as COST (Concrete Optimization Software Tool) developed by NIST, USA (<http://ciks.cbt.nist.gov/cost/>).

1.4 HYDRATION OF CEMENT

When Portland cement is mixed with water, a series of chemical reactions takes place, which results in the formation of new compounds and progressive setting, hardening of the cement paste, and finally in the development of strength. The overall process is referred to as *cement hydration*. Hydration involves many different reactions, often occurring at the same time. When the paste (cement and water) is added to aggregates (coarse and fine), it acts as an adhesive and binds the aggregates together to form concrete. Most of the hydration and about 90 per cent strength development take place within 28 days; however, the hydration and strength development continues, though more slowly, for a long time with adequate moisture and temperature (50% of the heat is liberated between one and three days, 75% in seven days, and about 90% in six months). Hydration products formed in hardened cement pastes are more complicated, and the chemical equations are shown in Table 1.16. More details

of the chemical reactions may be found in the works of Johansen, et al. (2002), Lea (1971), Powers (1961), and Taylor (1997).

As shown in Fig. 1.5, tricalcium silicate (C₃S) hydrates and hardens rapidly and is mainly responsible for the initial set and early strength of concrete. Thus, OPC containing increased percentage of C₃S will have high early strength. On the other hand, dicalcium silicate (C₂S) hydrates and hardens slowly and contributes to strength increase only after about seven days. Tricalcium aluminate (C₃A) is responsible for the large amount of heat of hydration during the first few days of hydration and hardening. It also contributes slightly to the strength development in the first few days. Cements with low percentages of C₃A are more resistant to soils and waters containing sulphates. Tetracalcium aluminoferrite (C₄AF) contributes little to strength. The grey colour of cement is due to C₄AF and its hydrates. As mentioned earlier, gypsum (calcium sulphate dihydrate) is added to cement during final grinding to regulate the setting time of concrete and reacts with C₃A to form *ettringite* (calcium trisulphoaluminate or AFt). In addition to controlling setting and early strength gain, gypsum also helps control drying shrinkage (Kosmatka, et al. 2003). Figure 1.5 shows the relative reactivity of cement compounds. The ‘overall curve’ has a composition of 55 per cent C₃S, 18 per cent C₂S, 10 per cent C₃A, and 8 per cent C₄AF.

TABLE 1.16 Portland cement compound hydration reactions

Basic Cement Compounds		Hydrated Compounds	
2(C ₃ S) Tricalcium silicate	+11H Water	= C ₃ S ₂ H ₈ Calcium silicate hydrate (C-S-H)	+3 (CH) Calcium hydroxide
2(C ₂ S) Dicalcium silicate	+9H Water	= C ₃ S ₂ H ₈ Calcium silicate hydrate (C-S-H)	+CH Calcium hydroxide
C ₃ A Tricalcium aluminate	+3(C \bar{S} H ₂) Gypsum	+26H Water	= C ₆ A \bar{S} ₃ H ₃₂ Ettringite (AFt)
2(C ₃ A) Tricalcium aluminate	+C ₆ A \bar{S} ₃ H ₃₂ Ettringite (AFt)	+4H Water	= 3(C ₄ A \bar{S} H ₁₂) Calcium mono-sulphoaluminate (AFm)
C ₃ A Tricalcium aluminate	+CH Calcium hydroxide	+12H Water	= C ₄ A13H Tetracalcium aluminate hydrate
C ₄ AF Tetracalcium aluminoferrite	+10H Water	+2(CH) Calcium hydroxide	= 6CAF12H Calcium aluminoferrite hydrate

\bar{S} = SO₃ (Sulfur trioxide)

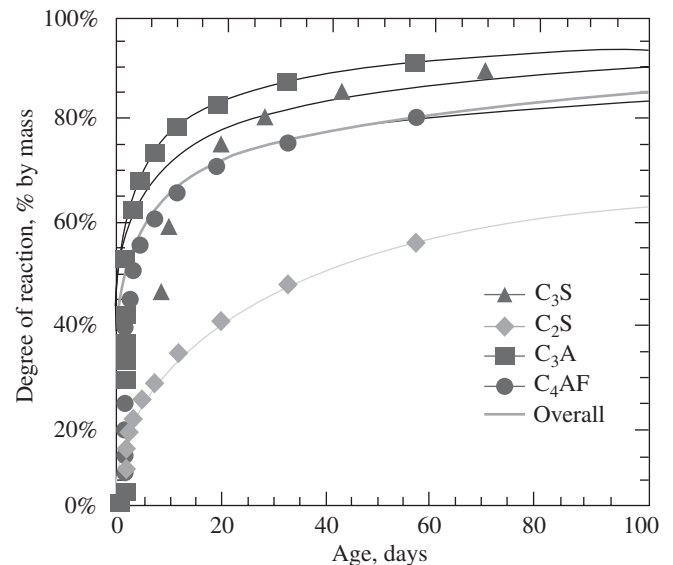


FIG. 1.5 Relative reactivity of cement compounds

Source: Reprinted from Tennis, P.D. and H.M. Jennings 2000, ‘A Model for Two Types of Calcium Silicate Hydrate in the Microstructure of Portland Cement Pastes’, *Cement and Concrete Research*, Vol. 30, No. 6, pp. 855–63, with permission from Elsevier.

Heat of hydration When Portland cement is mixed with water, heat is liberated as a result of the exothermic chemical reaction. This heat is called the *heat of hydration*. The heat generated by the cement’s hydration raises the temperature

of concrete; temperature rises of 55°C have been observed with mixes having high cement content. Such a temperature rise will result in the cracking of the concrete. As a rule of thumb, the maximum temperature differential between the interior and exterior concretes should not exceed 20°C to avoid crack development. ACI 211.1:91 states that as a rough guide, hydration of cement will generate a concrete temperature rise of about 4.7–7.0°C per 50 kg of cement per cubic metre of concrete. Usually, the greatest rate of heat of hydration occurs within the first 24 hours and a large amount of heat evolves within the first three days. Factors influencing heat development in concrete include the cement content (cements with higher contents of tricalcium silicate (C₃S) and tricalcium aluminate (C₃A) and higher fineness have higher rates of heat generation), w/c ratio, placing and curing temperature, the presence of mineral and chemical admixtures, and the dimensions of the structural element. Higher temperatures greatly accelerate the rate of hydration and the rate of heat liberation at early stages (less than seven days). Kulkarni (2012) observed that over the years there is a large increase in the C₃S content and fineness of cement, both of which speed up the hydration reaction and provide high early strength and accompanying side effect of higher heat of hydration (for example, in 1920s, the cement in the USA contained 21% of C₃S and 48% of C₂S; now their proportion is completely reversed and it is 56% of C₃S and 17% of C₂S). In view of these changes in the cement characteristics, design strengths could be achieved with low cement content and higher w/c ratio.

Mineral admixtures (e.g., fly ash), can significantly reduce the rate and amount of heat development. The methods to minimize the rise in concrete temperature include cooling the mixing water, using ice as part of the mixing water, using a moderate-heat Portland cement or moderate- or low-heat blended cement, using chemical admixtures (water-reducer or water-retarder), keeping cement contents to a minimum level, or cooling the aggregate. Moreover, curing with water helps to control temperature increases and is better than other curing methods.

1.5 TYPES OF CONCRETE

Depending on where it is mixed, concrete may be classified as *site-mixed concrete* or *ready-mixed* (factory-mixed) *concrete* (RMC). Site mixing is not always recommended as the mixing may not be thorough and the control on the w/c or w/cm ratio cannot be strictly maintained. Hence, it is used only in locations where RMC is not readily available. Concrete without reinforcement is called plain concrete and with reinforcement is called RCC or RC. Even though concrete is strong in compression, it is weak in tension and tends to crack when subjected to tensile forces; reinforcements are

designed to resist these tensile forces and are often provided in the tension zones. Hence, only RCC is used in structures. Depending on the strength it may attain in 28 days, concrete may be designated as ordinary concrete, standard or *normal strength concrete* (NSC), HSC, and *ultra-high-strength concrete* (UHSC). In IS 456, the grades of concrete are designed as per Table 1.11. Clause 6.1.1 of IS 456 defines the *characteristic strength* as the strength of the concrete below which not more than five per cent of the test results will fall (refer to Section 4.7.3 and Fig. 4.25 of Chapter 4). The minimum grade for RC as per IS 456 is M20; it should be noted that other international codes specify M25 as the minimum grade. In general, the usual concretes fall in the M20 to M50 range. In normal buildings M20 to M30 concretes are used, whereas in bridges and prestressed concrete construction, strengths in the range of M35 to M50 are common. Very high-strength concretes in the range of M60 to M70 have been used in columns of tall buildings and are normally supplied by ready-mix concrete companies (Kumar and Kaushik 2003).

Concrete with enhanced performance characteristics is called *high-performance concrete* (HPC). *Self-compacting concrete* (SCC) is a type of HPC, in which maximum compaction is achieved using special admixtures and without using vibrators. Structural engineers should aim to achieve HPC through suitable mix proportioning and the use of chemical and mineral admixtures.

When fibres are used in concrete, it is called *fibre-reinforced concrete* (FRC). (Fibres are usually used in concrete to control cracking due to plastic shrinkage and drying shrinkage.) High-performance FRCs are called *ductile fibre-reinforced cementitious composites* (DFRCCs); they are also called *ultra-high-performance concretes* (UHPCs) or *engineered cementitious composites* (ECCs). Due to the non-availability of standard aggregates or to reduce the self-weight, lightweight aggregates may be used; such concretes are called SLWCs or *autoclaved aerated concretes* (AACs). A brief description of these concretes is given in the following sections.

1.5.1 Ready-mixed Concrete

Ready-mixed concrete is a type of concrete that is manufactured in a factory or batching plant, based on standardized mix designs, and then delivered to the work site by truck-mounted transit mixers. This type of concrete results in more precise mixtures, with strict quality control, which is difficult to follow on construction sites. Although the concept of RMC was known in the 1930s, this industry expanded only during the 1960s. The first RMC plant started operating in Pune, India, in 1987, but the growth of RMC picked up only after 1997. Most of the RMC plants are located in seven large cities of India,

and they contribute to about 30–60 per cent of total concrete used in these cities. (Even today, a substantial proportion of concrete produced in India is volumetrically batched and site-mixed, involving a large number of unskilled labourers in various operations.) The fraction of RMC to total concrete being used is 28.5 per cent. RMC is being used for bridges, flyovers, and large commercial and residential buildings (Alimchandani 2007).

The RMC plants should be equipped with up-to-date equipment, such as transit mixer, concrete pump, and concrete batching plant. RMC is manufactured under computer-controlled operations and transported and placed at site using sophisticated equipment and methods. The major disadvantage of RMC is that since the materials are batched and mixed at a central plant, travelling time from the plant to the site is critical over longer distances. It is better to have the ready mix placed within 90 minutes of batching at the plant. (The average transit time in Mumbai is four hours during daytime.). Though modern admixtures can modify that time span, the amount and type of admixture added to the mix may affect the properties of concrete.

1.5.2 High-performance Concrete

High-performance concrete may be defined as any concrete that provides enhanced performance characteristics for a given application. It is difficult to provide a unique definition of HPC without considering the performance requirements of the intended use. ACI has adopted the following broad definition of HPC: ‘A concrete meeting special combinations of performance and uniformity requirements that cannot always be achieved routinely by using only conventional materials and normal mixing, placing, and curing practices. The requirements may involve enhancements of characteristics such as easy placement, compaction without segregation, long-term mechanical properties, early-age strength, permeability, density, heat of hydration, toughness, volume stability, and long service life in severe environments’ (ACI 363 R-10). Table 1.17 lists a few of these characteristics. Concretes possessing many of these characteristics often achieve higher strength (HPCs usually have strengths greater than 50–60 MPa). Therefore, HPCs will often have high strength, but a HSC need not necessarily be called HPC (Mullick 2005; Muthukumar and Subramanian 1999).

The HPCs are made with carefully selected high-quality ingredients and optimized mixture designs (see Table 1.18). These ingredients are to be batched, mixed, placed, compacted, and cured with superior quality control to get the desired characteristics. Typically, such concretes will have a low water–cementitious materials ratio of 0.22 to 0.40.

TABLE 1.17 Desired characteristics of HPCs

Property	Criteria that may be specified
High strength	70–140 MPa at 28–91 days
High early compressive strength	20–28 MPa at 3–12 hours or 1–3 days
High early flexural strength	2–4 MPa at 3–12 hours or 1–3 days
High modulus of elasticity	More than 40 GPa
Abrasion resistance	0–1 mm depth of wear
Low permeability	500–2000 Coulombs
Chloride penetration	Less than 0.07% Cl at 6 months
Sulphate attack	0.10% or 0.5% maximum expansion at 6 months for moderate or severe sulphate exposures
Low absorption	2–5%
Low diffusion coefficient	1000×10^{-14} m/s
Resistance to chemical attack	No deterioration after 1 year
Low shrinkage	Shrinkage strain less than 0.04% in 90 days
Low creep	Less than normal concrete

TABLE 1.18 Typical HPC mixtures used in some structures

Ingredients	Structure				
	Two Union Square, Seattle, 1988	Great Belt Link, East Bridge, Denmark, 1996	Kaiga Atomic Project Unit 2, India, 1998	Petronas Tower, Malaysia, 1999	Urban Viaduct, Mumbai, India, 2002
Water kg/m ³	130	130	136	152	148
Portland cement, kg/m ³	513	315	400	186	500
Fly ash, kg/m ³	–	40	–	345*	–
Silica fume, kg/m ³	43	23	25	35	50
Coarse aggregates, kg/m ³	1080	1140	1069	1000	762 (20 mm) + 384 (10 mm)
Fine aggregates, kg/m ³	685	710	827	725	682
Water reducer, L/m ³	–	1.5	–	–	–
Air content %	–	5.5	2	–	1.5
Superplasticizer, L/m ³	15.7	5.0	5.82	9.29	8.25

(Continued)

TABLE 1.18 (Continued)

Ingredients	Structure				
	Two Union Square, Seattle, 1988	Great Belt Link, East Bridge, Denmark, 1996	Kaiga Atomic Project Unit 2, India, 1998	Petronas Tower, Malaysia, 1999	Urban Viaduct, Mumbai, India, 2002
W/cm ratio	0.25	0.34	0.32	0.25–0.27	0.269
Slump, mm	–	–	175 + 25	180–220	130–180 (at plant) 80–120 (at site)
Strength at 28 days, MPa	119	–	75.9	80	79.6–81.3
Strength at 91 days, MPa	145	–	81.4 (180 days)	100 (56 days)	87.2–87.4

*Mascrete, which is a cement–fly ash compound in the ratio 20:80

Superplasticizers are usually used to make these concretes fluid and workable. It should be noted that without superplasticizers, the w/cm ratio cannot be reduced below a value of about 0.40. Typically, 5–15 L/m³ of superplasticizer can effectively replace 45–75 L/m³ of water (Aïtcin and Neville 1993). This drastic reduction in mixing water reduces the distance between cement particles, resulting in a much denser cement matrix than NSC. The optimal particle-packing mixture design approach may be used to develop a workable and highly durable design mixture (with cement content less than 300 kg/m³), having compressive strength of 70–80 MPa (Kumar and Santhanam 2004).

As the crushing process takes place along any potential zones of weakness within the parent rock, and thus removes them, smaller particles of coarse aggregates are likely to be stronger than the large ones. Hence, for strengths in excess of 100 MPa, the maximum size of aggregates should be limited to 10–12 mm; for lesser strengths, 20 mm aggregates can be used (Aïtcin and Neville 1993; Aïtcin, 1998). Strong and clean crushed aggregates from fine-grained rocks, mostly cubic in shape, with minimal flaky and elongated shapes are suitable for HPC. In order to have good packing of the fine particles in the mixture, as the cement content increases, the fine aggregates should be coarsely graded and have fineness modulus of 2.7–3.0.

As the HPC has very low water content, it is important to effectively cure HPC as early as possible. Membrane curing is not suitable for HPC, and hence fogging or wet curing should be adopted to control plastic and autogenous shrinkage cracking (see Section 1.7).

HPC has been primarily used in tunnels, bridges, pipes carrying sewage, offshore structures, tall buildings, chimneys, and foundations and piles in aggressive environments for its strength, durability, and high modulus of elasticity. It has also been used in shotcrete repair, poles, parking garages, and agricultural

applications. It should be noted that in severe fires, HPC results in bursting of the cement paste and spalling of concrete. More information on HPC may be obtained from ACI 363R-10 and IS 9103:1999 codes and the works of Zia, et al. (1991), Zia, et al. (1993), Aïtcin and Neville (1993), and Aïtcin (1998).

Self-compacting Concrete

Self-compacting concrete, also known as *high-workability concrete*, *self-consolidating concrete*, or *self-levelling concrete*, is a HPC, developed by Prof. Okamura and associates at the University of Tokyo (now Kochi Institute of Technology), Japan, in 1988 (Okamura and Ouchi 2003). SCC is a highly workable concrete that can flow through densely reinforced and complex structural elements under its own weight and adequately fill all voids without segregation, excessive bleeding, excessive air migration, and the need for vibration or other mechanical consolidation. The highly flowable nature of SCC is due to very careful mix proportioning, usually replacing much of the coarse aggregate with fines and cement, and adding chemical admixtures (EFNARC 2005). SCC may be manufactured at a site batching plant or in an RMC plant and delivered to site by a truck mixer. It may then be placed by either pumping or pouring into horizontal or vertical forms. To achieve fluidity, new generation superplasticizers based on polycarboxylic esters (PCE) are used nowadays, as it provides better water reduction and slower slump loss than traditional superplasticizers. The stability of a fluid mix may be achieved either by using high fines content or by using viscosity-modifying agents (VMA).

Several new tests have evolved for testing the suitability of SCC (see Fig. 1.6). They essentially involve testing the (a) flowability (slump flow test), (b) filling ability (slump flow test, V-funnel, and Orimet) (It may be noted that in the slump flow test, the average spread of flattened concrete is measured horizontally, unlike the conventional slump test, where vertical slump is measured.), (c) passing ability (L-box, J-ring, which is a simpler substitute for U-box), (d) robustness, and (e) segregation resistance or stability (simple column box test, sieve stability test). The details of these test methods may be found in the works of Okamura and Ouchi (2003) and Hwang, et al. (2006).

The SCC has been used in a number of bridges and precast projects in Japan, Europe, and USA (Ouchi 2003). Recently, SCC has been used in a flyover construction in Mumbai, India (ICJ, August 2009). The various developments in SCC undertaken in India may be found in ICJ (2004, 2009). An amendment (No. 3, August 2007) in the form of Annex J was added to IS 456, which prescribes the following for SCC:

1. Minimum slump flow: 600 mm
2. Amount of fines (< 0.125 mm) in the range of 400–600 kg/m³, which may be achieved by having sand content more than 38 per cent and using mineral admixture to the order of 25–50 per cent by mass of cementitious materials
3. Use of HRWRA and VMA

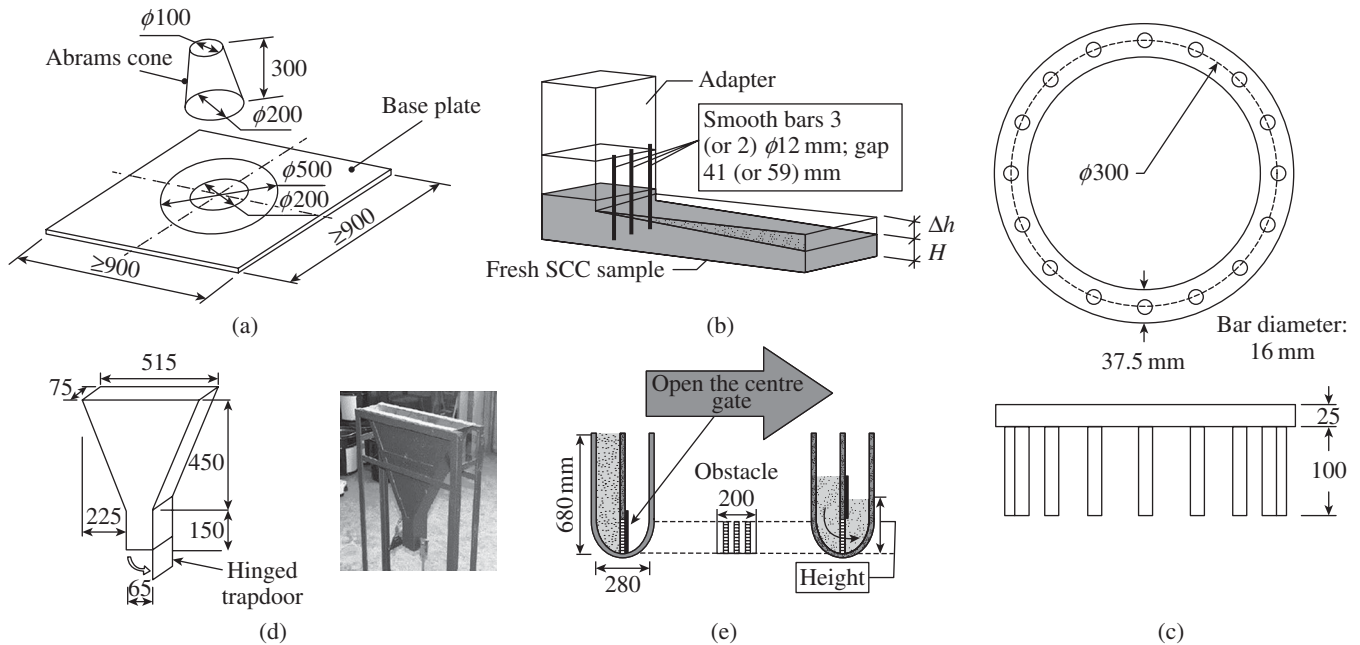


FIG. 1.6 Tests on self-consolidating concrete (a) Slump flow test (b) L-box (c) J-ring (d) V-funnel (e) U-flow test

Source: Okamura and Ouchi 2003, reprinted with permission from JCI.

1.5.3 Structural Lightweight Concrete

Some of the early structures from the Roman Empire that still survive today, including the Pantheon, have elements that were constructed with lightweight concrete. The use of lightweight concrete in modern times started when Steven J. Hayde, a brick-maker from Kansas City, Missouri, developed a rotary kiln method for expanding clays, shales, and slates in the early 1900s. SLWC is made with lightweight coarse aggregates such as natural *pumice* or *scoria* aggregates and expanded slags; sintering-grate expanded shale, clay, or fly ash; and rotary-kiln expanded shale, clay, or slate (ACI E1-07). The in-place density (unit weight) of such SLWC will be of the order of 1360–1850 kg/m³, compared to the density of normal weight concrete of 2240–2400 kg/m³. For structural applications, the strength of such SLWC should be greater than 20 MPa. The use of SLWC allows us to reduce the deadweight of concrete elements, thus resulting in overall economy. In most cases, the slightly higher cost of SLWC is offset by reductions in the weight of concrete used. Seismic performance is also improved because the lateral and horizontal forces acting on a structure during an earthquake are directly proportional to the inertia or mass of a structure. Companies like Lafarge produce varieties of industrial lightweight aggregates; examples include Aglite™, Haydite™, Leca™, Litex™, Lytag™, True Lite™, and Vitrex™ (www.escsi.org). As a result of these advantages, SLWC has been used in a variety of applications in the past 80 years. The reduced strength of SLWC is considered in the design of the ACI code by the factor λ .

An effective technique developed to help mitigate and overcome the issues of autogenous shrinkage and self-desiccation is *internal curing*; *autogenous shrinkage* is defined as a concrete volume change occurring without moisture transfer to the environment, as a result of the internal chemical and structural reactions (Holt 2001). Autogenous shrinkage is accompanied by self-desiccation during hardening of the concrete, which is characterized by internal drying. *Self-desiccation*, or internal drying, is a phenomenon caused by the chemical reaction of cement with water (Persson and Fagerlund 2002). The reaction leads to a net reduction in the total volume of water and solid (Persson, et al. 2005). The porosity of lightweight aggregates provides a source of water for internal curing, resulting in continued enhancement of the strength and durability of concrete. However, this does not prevent the need for external curing. More details about the mix design, production techniques, properties, and so on may be found in the ACI 213R-03 manual and the works of Neville (1996), Clarke (1993), Bentz, et al. 2005, and Chandra and Berntsson (2002).

Autoclaved Aerated Concrete

Autoclaved aerated concrete, also known as *autoclaved cellular concrete* (ACC) or *autoclaved lightweight concrete* (ALC) with commercial names Siporex, e-crete, and Ytong, was invented in the mid-1920s by the Swedish architect Johan Axel Eriksson. It is a lightweight, strong, inorganic, and non-toxic precast building material that simultaneously provides strength, insulation, and fire, mould, and termite resistance. Though relatively unknown in countries such as the USA,

India, Australia, and China, AAC now accounts for over 40 per cent of all construction in the UK and more than 60 per cent of construction in Germany.

Autoclaved aerated concrete is a precast product manufactured by combining silica (either in the form of quartz/silica sand or recycled fly ash), cement, lime, water, and an expansion agent—aluminium powder—at the rate of 0.05–0.08 per cent (it has to be noted that no coarse aggregates are used). Aluminium powder reacts with calcium hydroxide and water to form numerous hydrogen bubbles, resulting in the expansion of concrete to roughly two to five times its original volume. The hydrogen subsequently evaporates, leaving a highly closed-cell aerated concrete.

When the forms are removed from the material, it is solid but still soft. It is then cut into either blocks or panels and placed in an autoclave chamber for 12 hours. AAC blocks (typically 600 mm long, 200 mm high, and 150–300 mm thick) are stacked one over the other using thin-set mortar, as opposed to the traditional concrete masonry units (CMU) construction.

1.5.4 Fibre-reinforced Concrete

Fibres are added to concrete to control cracking caused by plastic shrinkage and drying shrinkage. The addition of small closely spaced and uniformly dispersed fibres will act as crack arresters and enhance the tensile, fatigue, impact, and abrasion resistance of concrete. They also reduce the permeability of concrete. Though the flexural strength may increase marginally, fibres cannot totally replace flexural steel reinforcement (the concept of using fibres as reinforcement is not new; fibres have been used as reinforcement since ancient times, for example, horsehair in mortar and asbestos fibres in concrete).

Clause 5.7 (Amendment No. 3) of IS 456:2000 permits the use of fibres in concrete for special applications to enhance its properties. Steel, glass, polypropylene, carbon, and basalt fibres have been used successfully; steel fibres are the most common (see Fig. 1.7). Steel fibres may be crimped, hooked, or flat. This type of concrete is known as FRC.

The amount of fibres added to a concrete mix is expressed as a percentage of the total volume of the composite (concrete and fibres) and termed *volume fraction*, which is denoted by V_f and typically ranges from 0.25 per cent to 2.5 per cent (of

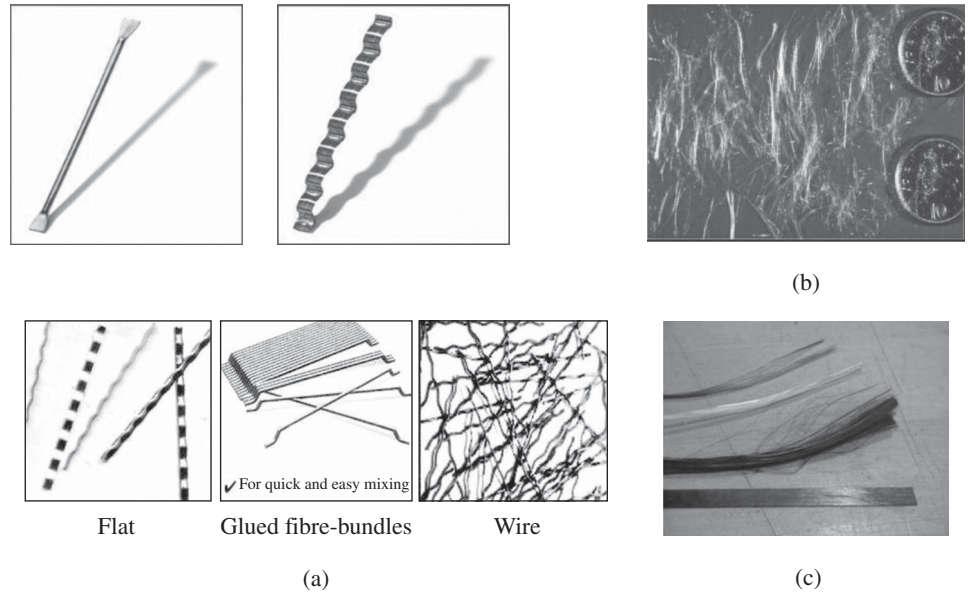


FIG. 1.7 Fibres used in concrete (a) Different types and shapes of steel fibres (b) Fine fibrillated polypropylene fibres (c) Glass fibres

Courtesy: Dr V.S. Parameswaran

which 0.75–1.0 is the most common fraction). The aspect ratio of a fibre is the ratio of its length to its diameter. Typical aspect ratio ranges from 30 to 150. The diameter of steel fibres may vary from 0.25 mm to 0.75 mm. Increasing the aspect ratio of the fibre usually increases the flexural strength and toughness of the matrix. However, fibres that are too long tend to ‘ball’ in the mix and create workability problems (Subramanian 1976b). To obtain adequate workability, it is necessary to use superplasticizers. The ultimate tensile strength of steel fibres should exceed 350 MPa. More information on FRC may be had from the works of Parameswaran and Balasubramanian (1993) and Bentur and Mindess (2007) and ACI 544.1R-96 report.

1.5.5 Ductile Fibre-reinforced Cementitious Composites

Ductile fibre-reinforced cementitious composite is a broader class of materials that has properties and superior performance characteristics compared to conventional cementitious materials such as concrete and FRC. DFRCCs have unique properties including damage reduction, damage tolerance, energy absorption, crack distribution, deformation compatibility, and delamination resistance (*delamination* is a mode of failure in composite materials—splitting or separating a laminate into layers) (Matsumoto and Mihashi 2003). The various subgroups of DFRCC are shown in Fig. 1.8 and Table 1.19 (Matsumoto and Mihashi 2003). It should be noted that DFRCC encompasses a group of high-performance fibre-reinforced cementitious composites (HPRCC). UHPC, also known as *ultra-high performance fibre-reinforced concrete* (UHPRFC) or *reactive powder concrete* (RPC), developed in France in the late 1990s, is a new class

of DFRCCs that have ultra-strength and ultra-performance characteristics.

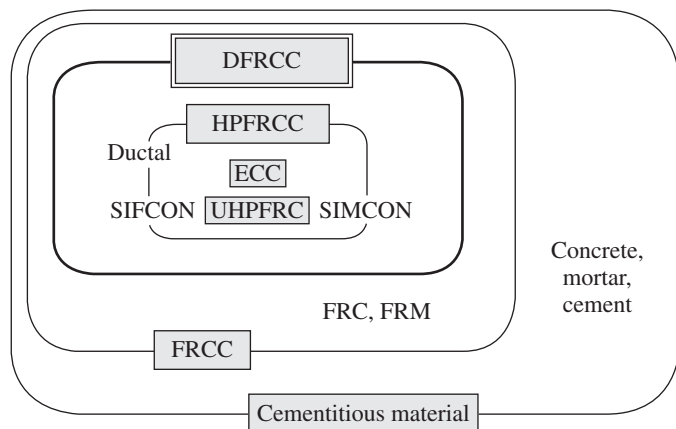


FIG. 1.8 Classification of cementitious materials

Source: Matsumoto and Mihashi 2003, reprinted with permission from JCI

TABLE 1.19 Characteristics of different cementitious materials

Characteristics	Cement, Mortar	Concrete, FRC	DFRCC	HPFRCC
Material response	Brittle	Quasi brittle	Quasi-brittle (tension) or ductile (flexure)	Ductile
Strain softening or hardening (see Fig. 1.9)	–	Strain softening	Strain softening (tension) or hardening (flexure)	Strain hardening
Cracking behaviour (flexure)*	Localized cracking	Localized cracking	Multiple cracking	Multiple cracking
Cracking behaviour (tension)	Localized cracking	Localized cracking	Localized cracking	Multiple cracking

*Cracking behaviour in flexure is dependent on specimen size. This comparison is based on specimen size of 100 × 100 × 400 mm

Source: Matsumoto and Mihashi 2003, reprinted with permission from JCI

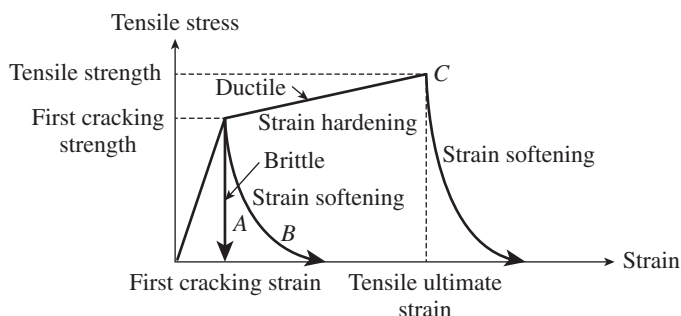


FIG. 1.9 Definitions of brittle, ductile, strain softening, and strain hardening under uniaxial tensile loading

Source: Matsumoto and Mihashi 2003, reprinted with permission from JCI

Engineered Cementitious Composites

Engineered cementitious composites are a special type of HPFRCC that has been micro-structurally tailored based on micro-mechanics. ECC is systematically engineered to achieve high ductility under tensile and shear loading. By employing material design based on micro-mechanics, it can achieve maximum ductility in excess of three per cent under uniaxial tensile loading with only two per cent fibre content by volume. Experiments have shown that even at the ultimate load (5% strain), the crack width remains at about 60µm and is even lower at strain below one per cent.

As shown in Fig. 1.10, extensive experimental studies have demonstrated superior seismic response as well as minimum post-earthquake repair (Fischer and Li 2002). It should be noted that even at high drift level of 10 per cent, no spalling of the reinforced ECC was observed; in contrast, the RCC column lost the concrete cover after bond splitting and being subjected to heavy spalling. The test results also illustrated the potential reduction or elimination of steel stirrups by taking advantage of the shear ductility of ECC. The tensile ductility in ECC also translates into shear ductility since the material undergoes diagonal tensile multiple cracking when subjected to shear (Li, et al. 1994).

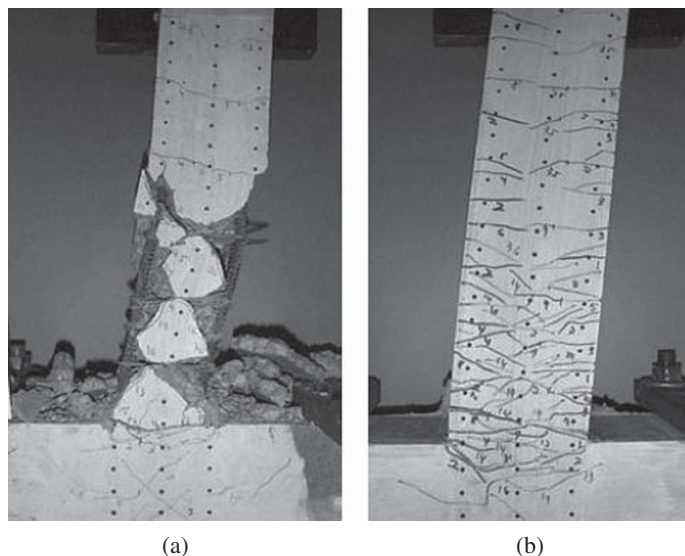


FIG. 1.10 Damage of column at 10% drift after reverse cyclic loading (a) RCC (b) ECC without stirrups

Source: Fischer and Li 2002, reprinted with permission from ACI

Life cycle cost comparison showed that ECC slab systems provide 37 per cent cost efficiency, consume 40 per cent less total primary energy, and produce 39 per cent less carbon dioxide compared to conventional RCC systems (Li 2003). More details about the behaviour and application of ECC may be found in the study of Li (2003).

Ultra-high-performance Concrete

Ultra-high-performance concrete is a high-strength, high-stiffness, self-consolidating, and ductile material, formulated by combining Portland cement, silica fume, quartz flour, fine silica sand, high-range water reducer, water, and steel or organic fibres. Originally it was developed by the Laboratoire Central des Ponts et Chaussées (LCPC), France, containing a mixture of short and long metal fibres and known as *multi-scale fibre-reinforced concrete* (Rossi 2001). It has to be noted that there are no coarse aggregates, and a low w/cm ratio of about 0.2 is used in UHPC compared to about 0.4–0.5 in NSC. The material provides compressive strengths of 120–240 MPa, flexural strengths of 15–50 MPa, and post-cracking tensile strength of 7.0–10.3 MPa and has modulus of elasticity from 45 GPa to 59 GPa [Ductal® (Lafarge, France), CoreTUFF® (US Army Corps of Engineers), BSI®, Densit® (Denmark), and Ceracem® (France and Switzerland) are some examples of commercial products]. The enhanced strength and durability properties of UHPC are mainly due to optimized particle gradation that produces a very tightly packed mix, use of steel fibres, and extremely low water to powder ratio (Nematollahi, et al. 2012).

Some of the potential applications of UHPC are in prestressed girders and precast deck panels in bridges, columns, piles, claddings, overlays, and noise barriers in highways. The 60 m span Sherbrooke pedestrian bridge, constructed in 1997 at Quebec, Canada, is the world's first UHPC bridge without any bar reinforcement. More details of this bridge may be had from the works of Blais and Couture (1999) and Subramanian (1999). The 15 m span Shepherds Creek Road Bridge, New South Wales, Australia, built in 2005 is the world's first UHPC bridge for normal highway traffic. Since then, a number of bridges and other structures have been built utilizing UHPC all over the world (see www.fhwa.dot.gov).

The materials for UHPC are usually supplied by the manufacturers in a three-component premix: powders (Portland cement, silica fume, quartz flour, and fine silica sand) pre-blended in bulk bags; superplasticizers; and organic fibres. Care should be exercised during mixing, placing, and curing. The ductile nature of this material makes concrete to deform and support flexural and tensile loads, even after initial cracking. The use of this material for construction is simplified by the elimination of reinforcing steel and its ability to be virtually self-placing. More details about UHPC may be found in the works of Schmidt, et al. (2004), Fehling, et al. (2008), and Schmidt, et al. (2012). A comparison of stress–strain curves in concretes is provided in Fig. 1.11. The influence of fibres and confinement on the ductility of RPC should be noted.

Slurry Infiltrated Fibrous Concrete and Slurry Infiltrated Mat Concrete

Slurry infiltrated fibrous concrete (SIFCON), invented by Lankard in 1979, is produced by infiltrating cement slurry

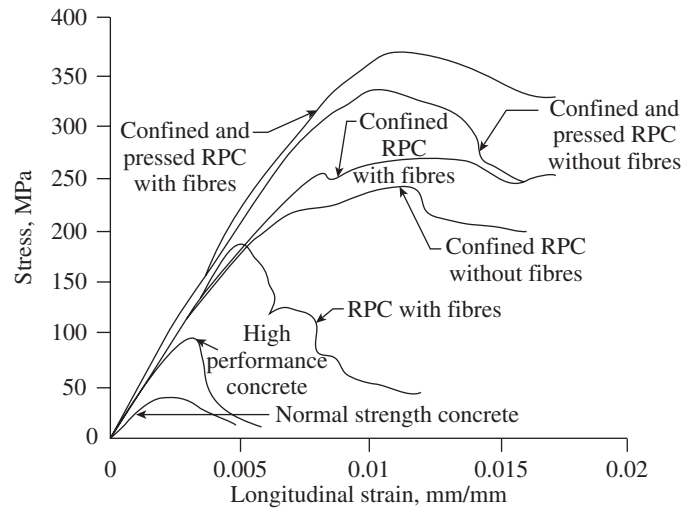


FIG. 1.11 Comparison of stress–strain curves of NSC, HPC, and RPC

Source: Blais and Couture 1999

(made of cement and sand in the proportion 1:1, 1:1.5, or 1:2, with fly ash and silica fume equal to 10–15% by weight of cement, w/cm ratio of 0.3–0.4, and superplasticizer equal to 2–5% by weight of cement) into pre-placed steel fibres (single plain or deformed fibres) in a formwork. It has to be noted that it does not contain any coarse aggregates but has a high cementitious content. Due to the pre-placement of fibres, its fibre volume fraction may be as high as 6–20 per cent. The confining effect of numerous fibres yields high compressive strengths from 90 MPa to 210 MPa, and the strong fibre bridging leads to tensile strain hardening behaviour in some SIFCONs. Slurry infiltrated mat concrete (SIMCON) is similar to SIFCON, but uses pre-placed fibre mat instead of steel fibres. SIFCON and SIMCON are extremely ductile and hence ideally suitable for seismic retrofit of structures (Dogan and Krstulovic-Opara 2003). They also have improved uniaxial tensile strength, flexural, shear, impact strengths, and abrasion resistance (Parameswaran 1996). They are best suited for the following applications: pavement rehabilitation, safety vaults, strong rooms, refractory applications, precast concrete products, bridge decks and overlays, repair and rehabilitation of structures, especially in seismic zones, military applications, and concrete mega-structures, such as offshore platforms and solar towers. More details about SIFCON and SIMCON may be found in the works of Parameswaran, et al. (1990), Parameswaran (1996), Lankard (1984), Naaman, et al. (1992), Sashidhar, et al. (2010, 2011) and Hackman, et al. (1992).

1.5.6 Ferrocement

Ferrocement also known as *ferrocrete*, invented by Jean Louis Lambot of France, in 1848, is a composite material like RCC. In RCC, the reinforcement consists of steel bars placed in the tension zone, whereas ferrocement is a thin RC made

of rich cement mortar (cement to sand ratio of 1:3) based matrix reinforced with closely spaced layers of relatively small diameter wire mesh, welded mesh, or chicken mesh. (The diameter of wires range from 4.20mm to 9.5mm and are spaced up to 300mm apart.) The mesh may be metallic or synthetic (Naaman 2000). The mortar matrix should have excellent flow characteristics and high durability. The use of pozzolanic mineral admixtures such as fly ash (50% cement replacement with fly ash is recommended) and use of superplasticizers will not only permit the use of water–binder ratio of 0.40–0.45 by mass but will also enhance the durability of the matrix. A mortar compressive strength of 40–50 MPa is recommended.

During the 1940s, Pier Luigi Nervi, an Italian engineer, architect, and contractor, had used ferrocement for the construction of aircraft hangars, boats and buildings. It has to be noted that though Nervi used a large number of meshes in his structures, in many present-day applications, only two layers of mesh reinforcement are used. Applications of ferrocement include boats, barges, water tanks, pipes, biogas digesters, septic tanks, toilet blocks, and monolithic or prefabricated housing (Subramanian 1976a). Recently, Spanos, et al. (2012) studied the use of ferrocement panels as permanent load bearing formwork for one-way and two-way slabs. Such panels provide economic advantages and the slabs incorporating them will provide superior serviceability performance. At the new Sydney Opera House, the sail-shaped roofs (built of conventional RC) have been covered with tile-surfaced panels of ferrocement, which serve as waterproofs for the concrete underneath. More information about the design and construction of ferrocement may be had from the study of Naaman (2000) and ACI 549.1R-93 manual.

Polymer concrete Polymer concrete is obtained by impregnating ordinary concrete with a monomer material and then polymerizing it by radiation, by heat and catalytic ingredients, or by a combination of these two techniques. Depending on the process by which the polymeric materials are incorporated, they are classified as (a) polymer concrete (PC), (b) polymer impregnated concrete (PIC), and (c) polymer modified concrete (PMC). Due to polymerization, the properties are much enhanced and polymer concrete is also used to repair damaged concrete structural members (Subramanian and Gnana Sambanthan 1979).

In addition to these types of concrete, *prestressed concrete* is often used in bridges and long-span structures; however, it is outside the scope of this book. A prestressed concrete member is one in which internal stresses (compressive in nature) are introduced, which counteract the tensile stresses resulting from the given external service level loads. The prestress is commonly introduced by tensioning the high-strength steel reinforcement (either by using the pre-tensioning or the

post-tensioning method), which applies pre-compression to the member. The design of prestressed concrete members should conform to IS 1343:1980.

1.6 REINFORCING STEEL

As stated earlier, steel reinforcements are provided in RCC to resist tensile stresses. The quality of steel used in RCC work is as important as that of concrete. Steel bars used in concrete should be clean and free from loose mill scales, dust, loose rust and any oily materials, which will reduce bond. Sand blasting or similar treatment may be done to get clean reinforcement.

As per Clause 5.6 of IS 456, steel reinforcement used in concrete may be of the following types (see Table 1.1 of SP 34 (S&T):1987 for the physical and mechanical properties of these different types of bars):

1. Mild steel and medium tensile steel bars (MS bars) conforming to IS 432 (Part 1):1982
2. High-yield strength-deformed steel bars (HYSD bars) conforming to IS 1786:2008
3. Hard drawn steel wire fabric conforming to IS 1566:1982
4. Structural steel conforming to Grade A of IS 2062:2006

It should be noted that different types of rebars, such as plain and deformed bars of various grades, say grade Fe 415 and Fe 500, should not be used side by side, as this may lead to confusion and error at site. Mild steel bars, which are produced by hot rolling, are not generally used in RCC as they have smooth surface and hence their bond strength is less compared to deformed bars (when they are used they should be hooked at their ends). They are used only as ties in columns or stirrups in beams. Mild steel bars have characteristic yield strength ranging from 240 N/mm² (grade I) to 350 N/mm² (medium tensile steel) and percentage elongation of 20–23 per cent over a gauge length of $5.65 \sqrt{\text{area}}$.

Hot rolled *high-yield strength-deformed bars* (HYSD bars) were introduced in India in 1967; they completely replaced mild steel bars except in a few situations where acute bending was required in bars greater than 30mm in diameter. They were produced initially by cold twisting (CTD bars) and later by heat treatment (TMT bars) and micro-alloying. They were introduced in India by Tata Steel as Tistrong bars and later as Tiscon/Torsteel bars. *Cold twisted deformed bars* (CTD bars or *Torsteel bars*) are first made by hot rolling the bars from high-strength mild steel, with two or three parallel straight ribs and other indentations on it. After cooling, these bars are cold twisted by a separate operation, so that the steel is strained beyond the elastic limit and then released. As the increase in strength is due to cold-working, this steel should not be normally welded. In CTD bars, the projections will form a helix around the bars; if they are over-twisted, the pitch of the helixes will be too close. Cold twisting introduces residual stresses in steel,

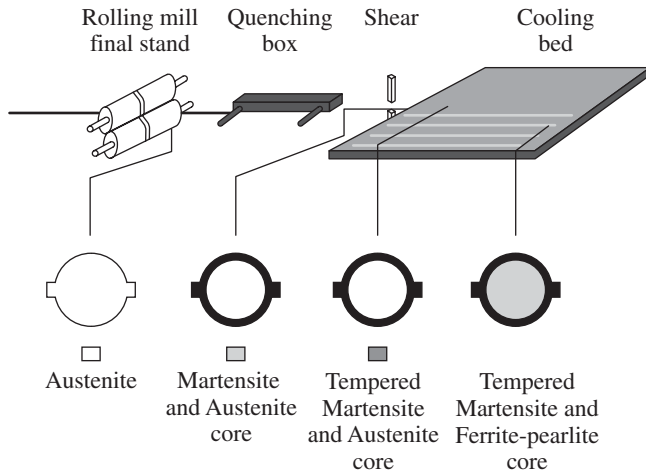


FIG. 1.12 Manufacturing process of TMT bars

Source: Tata steel-TISCON CRS-Corrosion Resistant Steel Bars, *Tata Steel Catalog*, Tata Steel, Kolkata, August 2004.

and as a result, these bars corrode much faster than other bars; hence, these are not recommended in many advanced countries.

Thermo-mechanically treated reinforcement bars (TMT Bars) are a class of hot rolled HYSD bars, which are rapidly cooled to about 450°C by a controlled quenching process using water when they are leaving the last stand of the rolling mill at a temperature of about 950°C . This sudden partial quenching, along with the final cooling, transforms the surface layer of the bars from austenite to tempered martensite, with a semi-tempered middle ring of martensite and bainite and a fine-grained ferrite-pearlite core (see Fig. 1.12). TMT bars can be welded as per IS 9417 using ordinary electrodes and no extra precautions are required. Strength, weldability, and ductility are the main advantages of TMT bars; in addition, they are also economical. TMT bars produced by SAIL or Tata are known as SAIL-TMT or TISCON-TMT. Bars produced by RINL are called REBARS. As it is visually difficult to distinguish TMT bars from mild steel deformed bars, the following procedure is suggested in IS 1786: A small piece

(about 12 mm long) can be cut and the transverse face lightly ground flat on progressively finer emery papers up to '0' size. The sample can be macro-etched with nital (five % nitric acid in alcohol) at ambient temperature for a few seconds to reveal a darker annular region corresponding to martensite or bainite microstructure and a lighter core region.

By micro-alloying with elements such as copper, phosphorus, and chromium, *thermo-mechanically treated corrosion resistant steel bars* (TMT CRS bars) are produced, which have better corrosion resistance than ordinary TMT bars.

It is better to adopt precautions against corrosion even while using such bars, as they are not 100% corrosion-resistant. Though IS 1786 specifies four grades for these HYSD bars, namely Fe 415, Fe 500, Fe 550, and Fe 600, and additional three grades with a suffix D, denoting that they are ductile, the availability of Fe 550, Fe 600, Fe 415D, Fe 500D, and Fe 550D grades are limited (the numbers after Fe denoting the 0.2% proof or yield stress, in N/mm^2).

The most important characteristic of the reinforcing bar is its stress-strain curve; the important property is its characteristic yield strength or 0.2 per cent proof stress as the case may be (see Fig. 1.13 and Table 1.20), and as per Clause 5.6.3 of IS 456, the modulus of elasticity E_s for these steels may be taken as 200 kN/mm^2 . (For HYSD bars the yield point is not easily defined based on the shape of the stress-strain curve; hence an offset yield point is arbitrarily defined at 0.2% of the strain. Thus by drawing a line parallel to the elastic portion of the stress-strain curve from the 0.2% strain, the yield point stress is located on the stress-strain curve as shown in Fig. 1.13b.) The design stress-strain curves for steel reinforcements (both mild steel and HYSD bars) are given in Fig. 5.5 of Chapter 5. The inelastic strains in HYSD bars for some design stress values, as per IS 456, are given in Table 5.1 (see Section 5.4). The chemical composition of various grades of steel is given in IS 1786:2008 specifications.

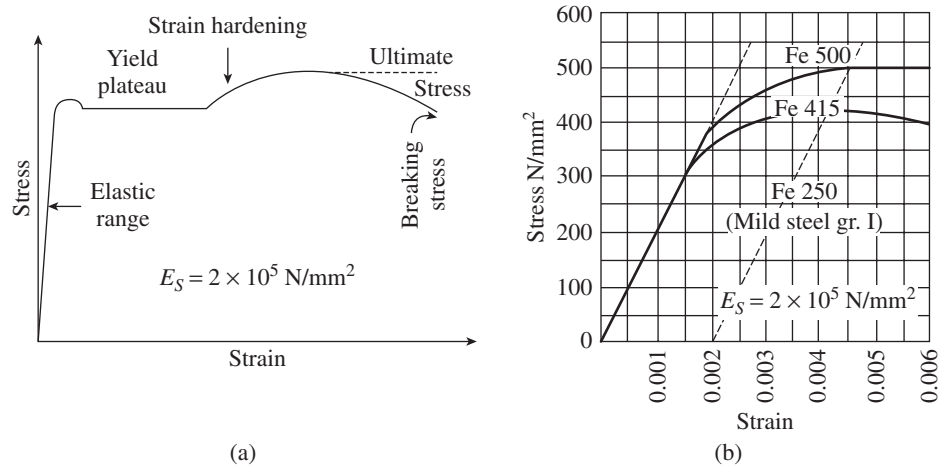


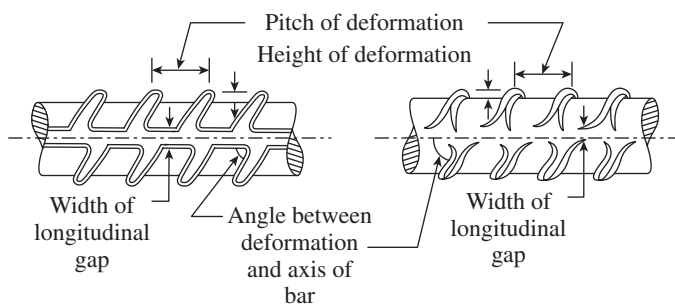
FIG. 1.13 Stress-Strain curve (a) Mild steel (b) HYSD bars (only initial portions of the curves are shown)

Clause 5.3 of IS 13920 stipulates that steel reinforcements of grade Fe 415 or less should be used in structures situated in earthquake zones. However, TMT bars of grades Fe 500 and Fe 550, having elongation more than 14.5 per cent, are also allowed. For providing sufficient bond between the bars and the concrete, the area, height, and pitch of ribs should satisfy Clause 5 of IS 1786 (see Fig. 1.14). The nominal size (in millimetres) of the available bars as per IS 1786 are 4, 5, 6, 8, 10, 12, 16, 20, 25, 28, 32, 36, and 40. A density of $7,850/\text{kgm}^3$ may be taken for calculating the nominal mass.

TABLE 1.20 Mechanical properties of high-strength deformed bars as per IS 1786:2008

S. No.	Property	Fe 415	Fe 415D	Fe 500	Fe 500D	Fe 550	Fe 550D	Fe 600
1.	0.2% proof stress/yield stress, min. N/mm ²	415.0	415.0	500.0	500.0	550.0	550.0	600.0
2.	Elongation, percentage, min. on gauge length $\frac{5.65\sqrt{A}^*}{}$	14.5	18.0	12.0	16.0	10.0	14.5	10.0
3.	Tensile strength, min.	10% more than the actual 0.2% proof stress/yield stress but not less than 485.0 N/mm ²	12% more than the actual 0.2% proof stress/yield stress but not less than 500.0 N/mm ²	8% more than the actual 0.2% proof stress/yield stress but not less than 545.0 N/mm ²	10% more than the actual 0.2% proof stress/yield stress but not less than 565.0 N/mm ²	6% more than the actual 0.2% proof stress/yield stress but not less than 585.0 N/mm ²	8% more than the actual 0.2% proof stress/yield stress but not less than 600.0 N/mm ²	6% more than the actual 0.2% proof stress/yield stress but not less than 660.0 N/mm ²
4.	Total elongation at maximum force, percentage, min. on gauge length $\frac{5.65\sqrt{A}^*}{}$	—	5%	—	5%	—	5%	—

*A is the cross-sectional area of the test piece.

**FIG. 1.14** Deformation on bars

Welded wire fabrics (WWF) consist of hard drawn steel wire mesh made from medium tensile steel, drawn out from higher diameter steel bars. As they undergo cold-working, their strength is higher than that of mild steel. WWF consists of longitudinal and transverse wires (at right angles to one another) joined by resistant spot welding using machines. They are available in different widths and rolls and as square or oblong meshes; see Table C-1 of SP 34 (S&T):1987 and SP 1566:1982. Their use in India is limited to small size slabs.

1.6.1 Corrosion of Rebars

Corrosion of steel rebars is considered the main cause of deterioration of numerous RCC structures throughout the world. In fact, the alkaline environment of concrete (pH of 12–13) provides a thin oxide passive film over the surface of steel rebars and reduces the corrosion rate considerably.

For steel bars surrounded by sound concrete, the passive corrosion rate is typically 0.1 μm per year. Without the passive film, the steel would corrode at rates at least 1000 times higher (ACI 222R-01). The destruction of the passive layer occurs when the alkalinity of the concrete is reduced or when the chloride concentration in concrete is increased to a certain level. In many cases, exposure of RC to chloride ions is the primary cause of premature corrosion of steel reinforcement. Although chlorides are directly responsible for the initiation of corrosion, they appear to play only an indirect role in the rate of corrosion after initiation. The primary factors controlling the corrosion rate are the availability of oxygen, electrical resistivity and relative humidity of the concrete, pH, and prevailing temperature. *Carbonation* is another cause for corrosion. Carbonation-induced corrosion often occurs in building facades that are exposed to rainfall, are shaded from sunlight, and have low concrete cover over the reinforcing steel. Carbonation occurs when carbon dioxide from the air penetrates the concrete and reacts with hydroxides (e.g., calcium hydroxide), to form carbonates. In the reaction with calcium hydroxide, calcium carbonate is formed. This reaction reduces the pH of the pore solution to as low as 8.5, destroying the passive film on steel rebars. It has to be noted that carbonation is generally a slow process. In high-quality concrete, carbonation is estimated to proceed at a rate up to 1.0 mm per year. The highest rates of carbonation occur

when the relative humidity is maintained between 50 per cent and 75 per cent. The amount of carbonation is significantly increased in concrete with a high water-to-cement ratio, low cement content, short curing period, low strength, and highly permeable paste. Corrosion can also occur when two different metals are in contact within concrete. For example, *dissimilar metal corrosion* can occur in balconies where embedded aluminium railings are in contact with the reinforcing steel.

Conventional concrete contains pores or micro-cracks. Detrimental substances or water can penetrate through these cracks or pores, leading to corrosion of steel bars. When corrosion takes place, the resulting rust occupies more than three times the original volume of steel from which it is formed. This drastic expansion creates tensile stresses in the concrete, which can eventually cause cracking, delamination, and spalling of cover concrete (see Fig. 4.5 of Chapter 4). The presence of corrosion also reduces the effective cross-sectional area of the steel reinforcement and leads to the failure of a concrete element and subsequently the whole structure. Mitigation measures to reduce the occurrence of corrosion include (a) decreasing the w/c or w/cm ratio of concrete and using pozzolans and slag to make the concrete less permeable (pozzolans and slag also increase the resistivity of concrete, thus reducing the corrosion rate, even after it is initiated), (b) providing dense concrete cover, as per Table 16 of IS 456, using controlled permeability formwork (CPF), thus protecting the embedded steel rebars from corrosive materials (see Section 4.4.5 for the details of CPF), (c) including the use of corrosion-inhibiting admixtures, (d) providing protective coating to reinforcement, and (e) using of sealers and membranes on the concrete surface. It should be noted that the sealers and membranes, if used, have to be reapplied periodically (Kerkhoff 2007).

As mentioned, one of the corrosion mitigation methods is by using the following reinforcements:

Fusion-bonded epoxy-coated reinforcing bars Typical coating thickness of these bars is about 130–300 μm . Damaged coating on the bars, resulting from handling and fabrication and the cut ends, must be properly repaired with patching material prior to placing them in the structure. These bars have been used in RC bridges from the 1970s and their performance is found to be satisfactory (Smith and Virmani 1996). They may have reduced bond strength.

Galvanized reinforcing bars The precautions mentioned for epoxy-coated bars are applicable to these bars as well. The protective zinc layer in galvanized rebars does not break easily and results in better bond.

Stainless steel bars Stainless steel is an alloy of nickel and chromium. Two types of stainless steel rods, namely SS304 and SS316, are used as per BS 6744:2001. Though the initial cost of

these bars is high, life cycle cost is lower and they may provide 80–125 years of maintenance-free service. The Progresso Bridge in New Mexico, USA, was built during 1937–41 using stainless rebar and has not required maintenance until now.

Fibre-reinforced polymer bars (FRP bars) These are aramid fibre (AFRP), carbon fibre (CFRP) or glass fibre (GFRP) reinforced polymer rods. They are non-metallic and hence non-corrosive. Although their ultimate tensile strength is about 1500 MPa, their stress–strain curve is linear up to failure. In addition, they have one-fourth the weight of steel reinforcement and are expensive. The modulus of elasticity of CFRP is about 65 per cent of steel bars and the bond strength is almost the same. As the Canadian Highway Bridge Design Code, CSA-S6-06, has provisions for the use of GFRP rebars, a number of bridges in Canada are built using them. More details about them may be obtained from the work of GangaRao, et al. (2007) and the ACI 440R-07 report.

Basalt bars These are manufactured from continuous basalt filaments and epoxy and polyester resins using a pultrusion process. It is a low-cost, high-strength, high-modulus, and corrosion-resistant alternative to steel reinforcement. More information about these bars may be found in the study of Subramanian (2010).

In addition, *Zbar*, a pretreated high-strength bar with both galvanizing and epoxy coating, has been recently introduced in the USA. High-strength *MMFX steel bars*, conforming to ASTM A1035, with yield strength of 827 MPa and having low carbon and 8–10 per cent chromium have been introduced in the USA recently, which are also corrosion-resistant, similar to TMT CRS bars (www.mmfx.com).

Clause 5.6.2 of IS 456 suggests the use of coating to reinforcement, and Amendment No. 3 of this clause states that the reduction of design bond strength of coated bars should be considered in design, but it does not elaborate. See Sections 7.4.2 and 7.5.3 of Chapter 7 for the reduction of design bond strength based on the ACI code provisions.

Viswanatha, et al. (2004), based on their extensive experience of testing rebars, caution about the availability of substandard rebars in India, including rerolled bars and inadequately quenched or low carbon content TMT bars. Hence, it is important for the engineer to accept the rebars only after testing them in accordance with IS 1608:2005 and IS 1786:2008. Basu, et al. (2004) also provide an overview of the important characteristics of rebars and a comparison of specifications of different countries.

1.7 CONCRETE MIXING, PLACING, COMPACTING, AND CURING

The measurement of materials for making concrete is called *batching* (see also Clause 10.2 of IS 456). Though volume

batching is used in small works, it is not a good method and weigh batching should always be attempted (fully automatic weigh batching equipment are used in RMC plants). The mixing of materials should ensure that the mass becomes homogeneous, uniform in colour and consistency. Again, hand mixing is not desirable for obvious reasons and machine mixing is to be adopted for better quality. Several types of mixtures are available; pan mixtures with revolving star blades are more efficient (Shetty 2005; IS 1791:1985; IS 12119:1987). Clause 10.3 of IS 456 stipulates that if there is segregation after unloading from the mixer, the concrete should be remixed. It also suggests that when using conventional tilting type drum mixtures, the mixing time should be at least two minutes and the mixture should be operated at a speed recommended by the manufacturer (normal speeds are 15–20 revolutions/minute). Clause 10.3.3 of IS 456 restricts the dosage of retarders, plasticizers, superplasticizers, and polycarboxylate-based admixtures to 0.5 per cent, 1.0 per cent, 2.0 per cent, and 1.0 per cent, respectively, by weight of cementitious materials.

Concrete can be transported from the mixer to the formwork by a variety of methods and equipment such as mortar pans, wheel barrows, belt conveyors, truck-mixer-mounted conveyor belts, buckets used with cranes and cable ways, truck mixer and dumpers, chutes or drop chutes, skip and hoist, transit mixer (in case of RMC), tremies (for placing concrete under water) or pumping through steel pipes. As there is a possibility of segregation during transportation, care should be taken to avoid it. More details about the methods of transportation may be found in the works of Panarese (1987), Kosmatka (2011), and Shetty (2005).

It is also important that the concrete is placed in the formwork properly to yield optimum results. Prior to *placing*, reinforcements must be checked for their correctness (location and size), cover, splice, and anchorage requirements, and any loose rust must be removed. The formwork must be cleaned, its supports adequately braced, joints between planks or sheets effectively plugged, and the inside of formwork applied with mould-releasing agents for easy stripping. Details of different kinds of formwork and their design may be found in the work of Hurd (2005) and IS 14687:1999 guidelines. It is necessary to thoroughly clean the surface of previous lifts with a water jet and treat them properly. Concrete should be continuously deposited as near as possible to its final position without any segregation. In general, concrete should be placed in thicker members in horizontal layers of uniform thickness (about 150 mm thick for reinforced members); each layer should be thoroughly consolidated before the next is placed. Chutes and drop chutes may be used when the concrete is poured from a height, to avoid segregation. Though Clause 13.2 of IS 456 suggests a permissible free fall of 1.5 m, it has been found that a free fall of even high-slump concrete of

up to 46 m directly over reinforcing steel does not result in segregation or reduction of compressive strength (Suprenant 2001).

Concreting during hot or cold weather should conform to the requirements of IS 7861(Part 1):1975 and IS 7861(Part 2):1981. More guidance on *hot weather concreting* is given in the work of Venugopal and Subramanian (1977) and ACI 305R-10 manual. Guidance for underwater concreting is provided in Clause 14 of IS 456.

Right after placement, concrete contains up to 20 per cent entrapped air. Vibration consolidates concrete in two stages: first by moving the concrete particles and then by removing entrapped air. The concrete should be deposited and compacted before the commencement of initial setting of concrete and should not be disturbed subsequently. Low-slump concrete can be consolidated easily, without adding additional water, by the use of superplasticizers. High frequency power driven internal or external vibrators (as per IS 2505, IS 2506, IS 2514, and IS 4656) also permit easy consolidation of stiff mixes having low w/cm ratio (manual consolidation with tamping rod is suitable only for workable and flowing mixtures). The internal vibrator or needle vibrator is immersed in concrete and the external vibrator is attached to the forms. (The radius of action of a needle vibrator with a diameter of 20–40 mm ranges between 75 mm and 150 mm; ACI 309R:05 provides more data on consolidation.) Good compaction with vibrators prevents honeycombing and results in impermeable and dense concrete, better bond between concrete and reinforcement, and better finish. Guidance on construction joints and cold joints is provided in Clause 13.4 of IS 456.

All newly placed and finished concrete slabs should be cured and protected from drying and from extreme changes in temperature. *Wet curing* should start as soon as the final set occurs and should be continued for a minimum period of 7–15 days (longer curing is required in case of concretes with fly ash). It has to be noted that in concretes without the use of retarders or accelerators, final set of cement takes place at about six hours. Concreting in hot weather conditions requires special precautions against rapid evaporation and drying due to high temperatures. More information on curing is provided in Clause 13.5 of IS 456 and also in Section 4.4.5 of Chapter 4.

Removal of forms It is advantageous to leave forms in place as long as possible to continue the curing period. As per Clause 11.3 of IS 456, the vertical supporting members of formwork (shoring) should not be removed until the concrete is strong enough to carry at least twice the stresses to which the concrete may be subjected to at the time of removal of formwork. When the ambient temperature is above 15°C and where Portland cement is used and adequate curing is done, the vertical formwork to columns, walls, and beams can be

removed in 16–24 hours after concreting. Beam and floor slab forms and supports (props) may be removed between 3 and 21 days, depending on the size of the member and the strength gain of the concrete (see Clause 11.3.1 of IS 456). If high early strength concrete is used, these periods can be reduced. Since the minimum stripping time is a function of concrete strength, the preferred method of determining stripping time in other cases is to be determined based on the tests of site-cured cubes or concrete in place. More details including shoring and reshoring of multi-storey structures may be found in ACI 347-04 guide.

1.8 PROPERTIES OF FRESH AND HARDENED CONCRETE

A designer needs to have a thorough knowledge of the properties of concrete for the design of RC structures. As seen in the previous sections, present-day concrete is much complicated and uses several different types of materials, which considerably affect the strength and other properties. Complete knowledge of these materials and their use and effects on concrete can be had from the works of Gambhir (2004), Mehta and Monteiro (2006), Mindess, et al. (2003), Neville (2012), Neville and Brooks (2010), Santhakumar (2006), and Shetty (2005). An introduction to some of the properties, which are important for the designer and construction professionals, is presented in this section.

1.8.1 Workability of Concrete

As discussed in Section 1.2.3, water added to the concrete mix is required not only for hydration purposes but also for workability. *Workability* may be defined as the property of the freshly mixed concrete that determines the ease and homogeneity with which it can be mixed, placed, compacted, and finished. The desired degree of workability of concrete is provided in Table 1.12. The main factor that affects workability is the water content (in the absence of admixtures). The other interacting factors that affect workability are aggregate type and grading, aggregate/cement ratio, presence of admixtures, fineness of cement, and temperature. It has to be noted that finer particles require more water to wet their large specific surface, and the irregular shape and rough texture of angular aggregate demand more water. Workability should be checked frequently by one of the standard tests (*slump, compacting factor, Vee Bee consistency,*

or flow table) as described in IS 1199:1955. Although it does not measure all factors contributing to workability, *slump test* is the most commonly used method to measure the consistency of the concrete, because of its simplicity. This test is carried out using an open-ended cone, called the *Abrams cone*. This cone is placed on a hard non-absorbent surface and filled with fresh concrete in three stages, and each time the concrete is tamped using a rod of standard dimensions. At the end of the third stage, the concrete is struck off level with a trowel at the top of the mould. Now, the mould is carefully lifted vertically upwards without disturbing the concrete in the cone, thereby allowing the concrete to subside. This subsidence is termed as *slump* and is measured to the nearest 5 mm. Figure 1.15 shows the slump testing mould, measurement, and types of slumps. If a shear slump (indicates concrete is non-cohesive) or collapse slump (indicates a high workability mix) is achieved, a fresh sample should be taken and the test repeated. A slump of about 50–100 mm is used for normal RC (see Table 1.12)

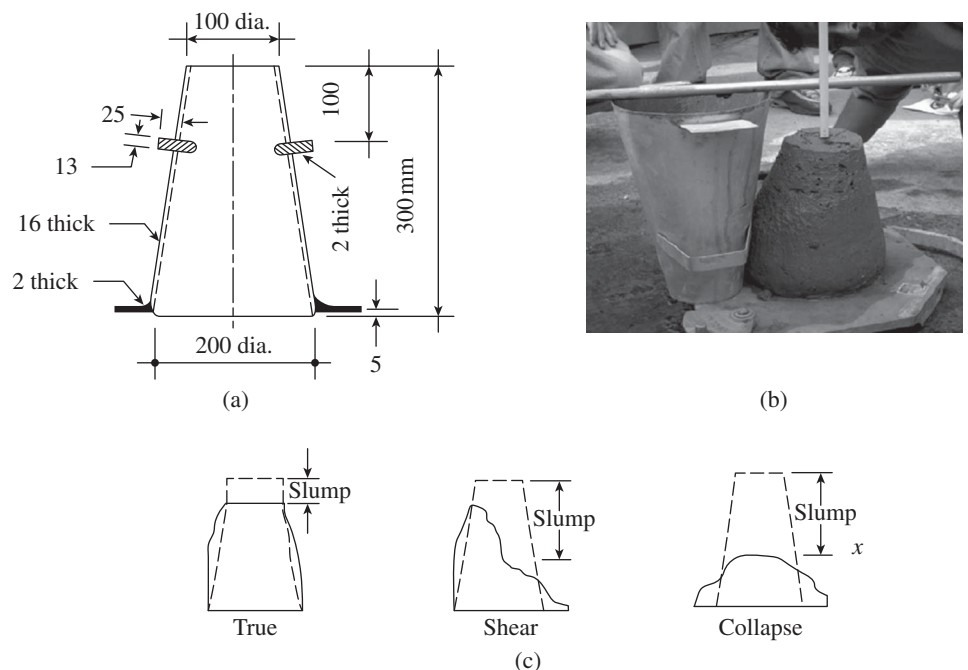


FIG. 1.15 Slump testing (a) Typical mould for slump test (b) Measuring slump (c) Types of slump

1.8.2 Compressive Strength

Compressive strength at a specified age, usually 28 days, measured on standard cube or cylinder specimens, has traditionally been used as the criterion for the acceptance of concrete. It is very important for the designer because concrete properties such as stress–strain relationship, modulus of elasticity, tensile strength, shear strength, and bond strength are expressed in terms of the uniaxial compressive strength. The compressive strengths used in structural applications vary from 20 N/mm² to as high as 100 N/mm². (In One, World Trade Center, New York, USA, a concrete with a compressive strength of 96.5 MPa was used with a modulus of elasticity of 48,265 MPa).

Cube and Cylinder Tests

In India, the UK, and several European countries, the characteristic compressive strength of concrete (denoted by f_{ck}) is determined by testing to failure 28-day-old concrete cube specimens of size 150 mm × 150 mm × 150 mm, as per IS 516:1959. When the largest nominal size of aggregate does not exceed 20 mm, 100 mm cubes may also be used. However, in the USA, Canada, Australia, and New Zealand, the compressive strength of concrete (denoted by f'_c) is determined by testing to failure 28-day-old concrete cylinder specimens of size 150 mm diameter and 300 mm long. Recently, 70 mm cube or 75 mm cylinder HSC or UHSC specimen is being recommended for situations in which machine capacity may be exceeded (Graybeal and Davis 2008).

The concrete is poured in the cube or cylinder mould in layers of 50 mm and compacted properly by either hand or a vibrator so that there are no voids. The top surface of these specimens should be made even and smooth by applying cement paste and spreading smoothly on the whole area of the specimen. The test specimens are then stored in moist air of at least 90 per cent relative humidity and at a temperature of $27^\circ\text{C} \pm 2^\circ\text{C}$ for 24 hours. After this period, the specimens are marked and removed from the moulds and kept submerged in clear fresh water, maintained at a temperature of $27^\circ\text{C} \pm 2^\circ\text{C}$ until they are tested (the water should be renewed every seven days). The making and curing of test specimen at site is similar (see also Clause 3.0 of IS 516).

These specimens are tested by a compression testing machine after 7 days of curing or 28 days of curing. Load should be applied gradually at the rate of 140 kg/cm² per minute until the specimen fails. Load at the failure divided by the area of specimen gives the compressive strength of concrete. A minimum of three specimens should be tested at each selected age. If the strength of any specimen varies by more than ± 15 per cent of average strength, results of such a specimen should be rejected (Clause 15.4 of IS 456). The average of *three* specimens gives the compressive strength of concrete. Sampling and acceptance criteria for concrete strength, as per IS 456, are provided in Section 4.7.4 of Chapter 4. (In the USA, the evaluation of concrete strength tests is done as per ACI 214R-02.) Figure 1.16 shows the cube testing and various failure modes of concrete cubes. The ideal failure mode, with almost vertical cracks (see Fig. 1.16b) is rarely achieved due to the rough contact surface between the concrete cube and the plate of testing machine. When the stress level reaches about 75–90 per cent of the

maximum, internal cracks are initiated in the mortar throughout the concrete mass, parallel to the direction of the applied load. The concrete tends to expand laterally due to Poisson's effect, and the cube finally fails leaving two truncated pyramids one over the other (see Fig. 1.16b). Sometimes the failure may be explosive, especially in cubes of HSC; to avoid injuries, proper precautions should be taken to contain the debris using high resistance and transparent polycarbonate or steel mesh shields around the testing machine.

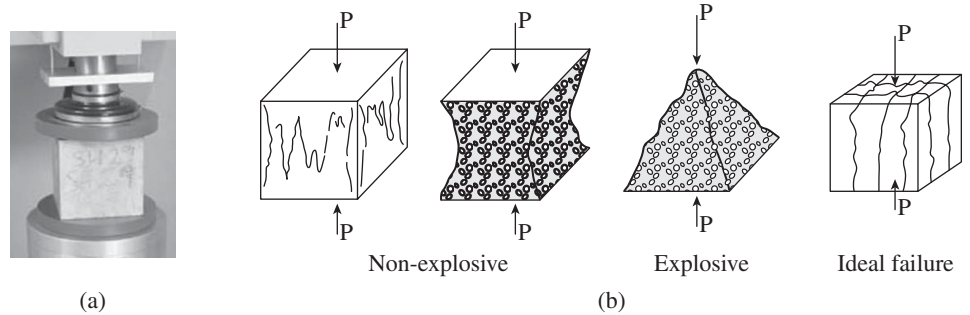


FIG. 1.16 Cube testing and failure of concrete cubes (a) Cubes in testing machine (b) Failure of concrete cubes

Factors Affecting Compressive Strength

The compressive strength of concrete is affected by the following important factors: w/c or w/cm ratio, type of cement, use of supplementary cementitious materials, type of aggregates, quantity and quality of mixing water, moisture and temperature conditions during curing, age of concrete, rate of loading during the cube or cylinder test (the measured compressive strength of concrete increases with increasing rate of loading), and the size of specimen.

The w/c ratio is inversely related to concrete strength: the lower the ratio, the greater the strength. It is also directly linked to the spacing between cement particles in the cement paste. When the spacing is smaller, cement hydrates fill the gaps between the cement particles faster and the links created by the hydrates will be stronger, resulting in stronger concrete (Bentz and Aitcin, 2008). Various mathematical models have been developed to link strength to the porosity of the hydrates. In 1918, Abrams presented his classic law of the following form (Shetty 2005):

$$f_{c,28} = \frac{k_1}{k_2^{wc}} \quad (1.2a)$$

where $f_{c,28}$ is the 28-day compressive strength, k_1 and k_2 are the empirical constants, and wc is the w/c ratio by volume. For 28-day strength of concrete recommended by ACI 211.1-91, the constants k_1 and k_2 are 124.45 MPa and 14.36, respectively. Popovics (1998) observed that these values are conservative and suggested the values 187 MPa and 23.07, respectively, for k_1 and k_2 . Abrams' w/c ratio law states that

the strength of concrete is dependent only upon the w/c ratio, provided the mix is workable. Abram's law is a special case of the following Feret formula developed in 1897 (Shetty 2005):

$$f_{c,28} = k \left(\frac{V_c}{V_c + V_w + V_a} \right) \quad (1.2b)$$

where V_c , V_w , and V_a are the absolute volumes of cement, water, and entrained air, respectively, and k is a constant. In essence, strength is related to the total volume of voids and the most significant factor in this is the w/c ratio. The graph showing the relationship between the strength and w/c ratio is approximately hyperbolic in shape (see Fig. 1.17).

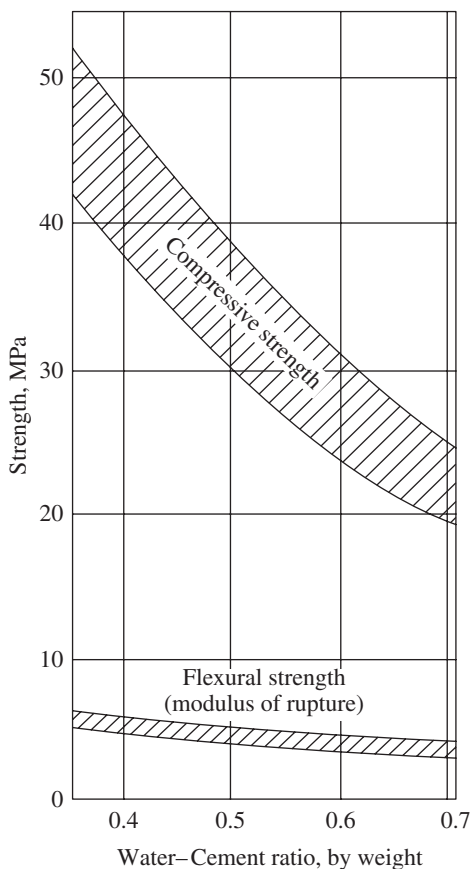


FIG. 1.17 Relation between strength and w/c ratio of normal concrete

At a more fundamental level, this relation can be expressed as a function of the gel/space ratio (x), which is the ratio of the volume of the hydrated cement paste to the sum of the volumes of the hydrated cement and the capillary voids. The data from Powers (1961) gives the following relationship:

$$f_{c,28} = 234x^3 \text{ MN/m}^2 \quad (1.2c)$$

where x is the gel/space ratio and 234 is the intrinsic strength of the gel in MPa for the type of cement and specimen used by

Powers. It has to be noted that this relation is independent of the age of the concrete and the mix proportions. This equation is valid for many types of cement, but the values of the numerical coefficients vary a little depending on the intrinsic strength of the gel. Such models that focus only on the cement paste ignore the effects of the aggregate characteristics on strength, which can be significant. A comparison of these mathematical models is provided by Popovics (1998). Based on the strength vs w/c ratio curves provided in the earlier version of IS 10262, Rajamane (2005) derived the following equation.

$$f_{c,28} = 0.39 f_{cem} [(1/wc) - 0.50] \quad (1.2d)$$

where f_{cem} is the 28-day compressive strength of cement tested as per IS 4031 (MPa) and wc is the w/c ratio by weight.

Many researchers have also attempted to estimate the strength of concrete at 1, 3, or 7 days and correlate it to the 28-day strength. This relationship is useful for formwork removal and to monitor early strength gain; however, it depends on many factors such as the chemical composition of cement, fineness of grinding, and temperature of curing. The 7-day strength is often estimated to be about 75 per cent of the 28-day strength (Neville 2012). Neville, however, suggests that if the 28-day strength is to be estimated using the strength at 7 days, a relationship between the 28-day and 7-day strengths has to be established experimentally for the given concrete. For concrete specimens cured at 20°C, Clause 3.1.2(6) of Eurocode 2 (EN 1992-1-1:2004) provides the following relationship.

$$f_{cm}(t) = \exp \left[s \left(1 - \left(\frac{28}{t} \right)^{0.5} \right) \right] f_{cm} \quad (1.3a)$$

where $f_{cm}(t)$ is the mean compressive strength at age t days, f_{cm} is the mean 28-day compressive strength, and s is a coefficient depending on the type of cement; $s = 0.2, 0.25,$ and 0.38 for high early strength, normal early strength, and slow early strength cement, respectively. ACI Committee 209.2R-08 recommends the relationship for moist-cured concrete made with normal Portland concrete as given here:

$$f_{cm}(t) = \left(\frac{t}{a + bt} \right) f_{c28} \quad (1.3b)$$

The values of constants a and b are 4.0 and 0.85, respectively, for normal Portland cement and 2.3 and 0.92, respectively, for high early strength cement. The 1978 version of IS 456 specified an 'age factor', based on Eq. (1.3b), using $a = 4.7$ and $b = 0.833$, but that provision has been deleted in the 2000 version of the code.

Influence of Size of Specimen

The pronounced effect of the height/width ratio and the cross-sectional dimension of the test specimen on the compressive

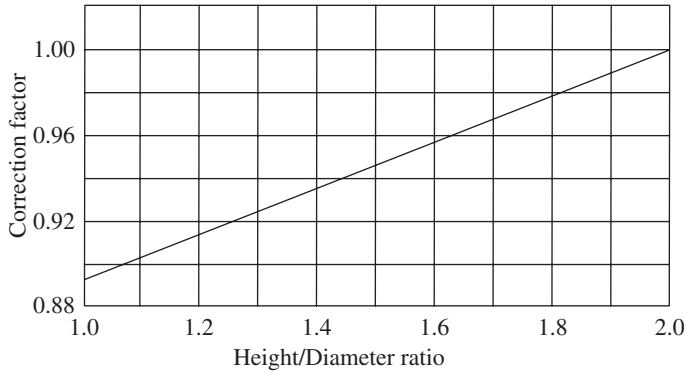


FIG. 1.18 Correction factor for height/diameter ratio of cylinder

strength has been observed by several researchers. The difference in compressive strength of different sizes of specimens may be due to several factors such as St Venant’s effect, size effect, or lateral restraint effect due to the testing machine’s platen (Pillai and Menon 2003). In addition, the preparation of the end conditions (cappings) of the concrete cylinder can significantly affect the measured compressive strength. When the height/diameter ratio of cylinders is less than 2.0, IS 516:1959, suggests a correction factor as shown in Fig. 1.18. Standard cubes with height/width ratio of 1.0 have been found to have higher compressive strength than standard cylinders with height/diameter ratio of 2.0. The ratio of standard cylinder strength and standard cube strength is about 0.8–0.95; higher ratio is applicable for HSC. Similarly 100 mm × 200 mm cylinders exhibit 2–10 per cent higher strengths than 150 mm × 300 mm cylinders; the difference is less for higher strength concrete (Graybeal and Davis 2008). It has to be noted that the ACI code formulae, which are based on standard cylinder strength, f'_c have been converted to standard cube strength, f_{ck} , for easy comparison, by using the relation $f'_c = 0.8f_{ck}$ throughout this book. A more precise coefficient R to convert cylinder strength to cube strength is $R = 0.76 + 0.2 \log(f'_c/20)$.

In the case of cubes, the specimens are placed in the testing machine in such a way that the load is applied on opposite sides of the cube as cast, that is, not to the top and bottom. On the other hand, cylinders are loaded in the direction in which they are cast. Due to this reason and also because the standard cylinders have height/width ratio of two, the compressive strengths predicted by cylinders are more reliable than cubes.

1.8.3 Stress–Strain Characteristics

Typical stress–strain curves of normal weight concrete of various grades, obtained from uniaxial compression tests, are shown in Fig. 1.19(a) and a comparison of normal weight and lightweight concrete is shown in Fig. 1.19(b). (The idealized stress–strain curve for concrete, and the assumed stress block adopted in IS 456 are given in Fig. 5.4 in Section 5.4 of Chapter 5). It has to be noted that, for design, the value of maximum compressive strength of concrete in structural elements is taken as 0.85 times the cylinder strength, f'_c , which is approximately equal to $0.67f_{ck}$.

It is seen from Fig. 1.19 that the curves are initially linear and become non-linear when the stress level exceeds about 40 per cent of the maximum stress. The maximum stress is reached when the strain is approximately 0.002; beyond this point, the stress–strain curve descends. IS 456 limits the maximum failure strain in concrete under direct compression to 0.002 (Clause 39.1a) and under flexure to 0.0035 (Clause 38.1b). The shape of the curve is due to the formation of micro-cracks within the structure of concrete. The descending branch of the curve can be fully traced only with rigid testing machines. In axially flexible testing machines, the test cube or cylinder will fail explosively when the maximum stress is reached.

Numerical approximations of stress–strain curves of concretes have been provided by various researchers, and a comparison of these formulae is provided by Popovics (1998).

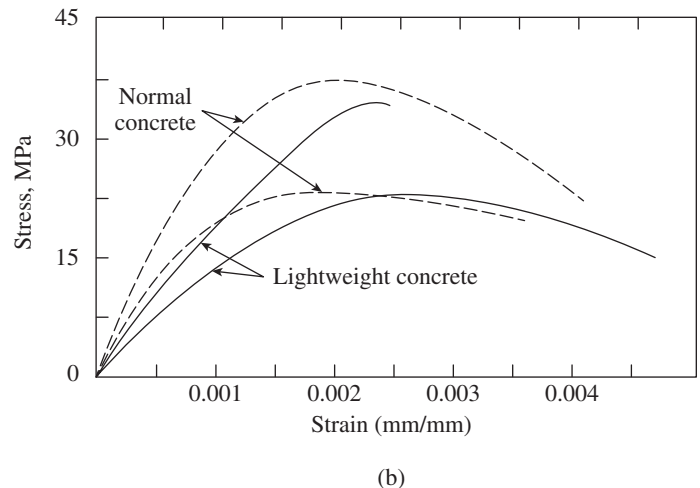
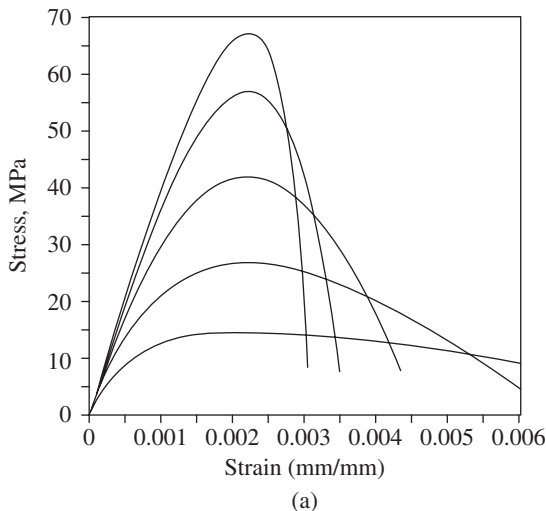


FIG. 1.19 Typical stress–strain curves of concrete in compression (a) Concrete with normal weight aggregates (b) Normal weight vs lightweight aggregate concrete

Such a mathematical definition of stress–strain curve is required for non-linear analysis of concrete structures. HSCs exhibit more brittle behaviour, which is reflected by the shorter horizontal branch of stress–strain curves.

1.8.4 Tensile Strength

As mentioned earlier, concrete is very weak in tension, and direct tensile strength is only about 8–11 per cent of compressive strength for concretes of grade M25 and above (Shetty 2005). The use of pozzolanic admixtures increases the tensile strength of concrete. Although the tensile strength of concrete increases with an increase in compressive strength, the rate of increase in tensile strength is of the decreasing order (Shetty 2005). The tensile strength of concrete is generally not taken into account in the design of concrete elements. Knowledge of its value is required for the design of concrete structural elements subject to transverse shear, torsion, and shrinkage and temperature effects. Its value is also used in the design of prestressed concrete structures, liquid retaining structures, roadways, and runway slabs. Direct tensile strength of concrete is difficult to determine. The *splitting (cylinder) tensile test* on 150 mm × 300 mm cylinders, as per IS 5816:1999, or the *third-point flexural loading test* on 150 mm × 150 mm × 700 mm concrete beams, as per IS 516:1959, is often used to find the tensile strength. The splitting tensile test is easier to perform and gives more reliable results than other tension tests; though splitting strength may give 5–12 per cent higher value than direct tensile strength (Shetty 2005). According to Mehta and Monteiro (2010), the third-point flexural loading test tends to overestimate the tensile strength of concrete by 50–100 per cent.

The theoretical maximum flexural tensile stress occurring in the extreme fibres of RC beams, which causes cracking, is referred to as the *modulus of rupture*, f_{cr} . Clause 6.2.2 of IS 456 gives the modulus of rupture or flexural tensile strength as

$$f_{cr} = 0.7\sqrt{f_{ck}} \quad (1.4)$$

It should be noted that Clause 9.5.2.3 of ACI 318 code suggests a lower, conservative value for the modulus of rupture, which equals $\lambda 0.55\sqrt{f_{ck}}$, where λ is the modification factor for lightweight concrete and equals 1.0 for normal weight concrete, 0.85 for sand-lightweight concrete, and 0.75 for all lightweight concrete. IS 456 does not provide an empirical formula for estimating the direct tensile strength, f_{ct} . Clause R8.6.1 of ACI 318 suggests an average splitting tensile strength of

$$f_{ct} = 0.5\sqrt{f_{ck}} \quad (1.5)$$

Shear strength Pure shear is a rare occurrence; usually a combination of flexural and shear stresses exists, resulting in a

diagonal tension failure. The design shear strength of concrete is given in Table 19 of IS 456 as a function of percentage flexural reinforcement. The maximum shear stress in concrete with shear reinforcement is restricted in Clause 40.2.3 to the following value:

$$\tau_{c,max} = 0.63\sqrt{f_{ck}} \quad (1.6)$$

More discussions on shear strength of concrete are provided in Chapter 6.

Bond strength The common assumption in RC that plane sections remain plane after bending will be valid only if there is perfect bond between concrete and steel reinforcement. Bond strength depends on the shear stress at the interface between the reinforcing bar and the concrete and on the geometry of the reinforcing bar. Clause 26.2.1.1 of IS 456 provides a table for design bond stress and is approximately represented by

$$\tau_{bd} = 0.16(f_{ck})^{2/3} \quad (1.7)$$

More discussions on bond strength of concrete are provided in Chapter 7.

1.8.5 Bearing Strength

The compressive stresses at supports, for example, at the base of column, must be transferred by bearing (Niyogi 1974). Clause 34.4 of IS 456 stipulates that the permissible bearing stress on full area of concrete in the working stress method can be taken as $0.25f_{ck}$ and for limit state method it may be taken as $0.45f_{ck}$. According to Clause 10.4.1 of ACI 318, the design bearing strength of concrete should not exceed $\phi 0.85 f'_c$, where ϕ is the strength reduction factor, which is taken as 0.65. Thus, it is approximately equal to $0.442f_{ck}$.

1.8.6 Modulus of Elasticity and Poisson's Ratio

Concrete is not an elastic material, that is, it will not recover its original shape on unloading. In addition, it is non-linear and exhibits a non-linear stress–strain curve. Hence, the elastic constants such as *modulus of elasticity* and *Poisson's ratio* are not strictly applicable. However, they are used in the analysis and design of concrete structures, assuming elastic behaviour. The modulus of elasticity of concrete is a key factor for estimating the deformation of buildings and members as well as a fundamental factor for determining the *modular ratio*, m . The use of HSC will result in higher modulus of elasticity and in reduced deflection and increased tensile strengths. The modulus of elasticity is primarily influenced by the elastic properties of the aggregates and to a lesser extent by the curing conditions, age of the concrete, mix proportions, porosity of concrete, and the type of cement. It is normally related to the compressive strength of concrete and may be determined by means of an extensometer attached to the compression test specimen as described in IS 516:1959.

The Young’s modulus of elasticity may be defined as the ratio of axial stress to axial strain, within the elastic range. When the loading is of low intensity and of short duration, the initial portion of the stress–strain curve of concrete in compression is linear, justifying the use of modulus of elasticity. However, when there is sustained load, inelastic creep occurs even at relatively low stresses, making the stress–strain curve non-linear. Moreover, the effects of creep and shrinkage will make the concrete behave in a non-linear manner. Hence, the initial tangent modulus is considered to be a measure of *dynamic modulus of elasticity* (Neville and Brooks 2010).

When linear elastic analysis is used, one should use the *static modulus of elasticity*. Various definitions of modulus of elasticity are available: initial tangent modulus, tangent modulus (at a specified stress level), and secant modulus (at a specified stress level), as shown in Fig. 1.20. Among these, the *secant modulus*, which is the slope of a line drawn from the origin to the point on the stress–strain curve corresponding to 40 per cent of the failure stress, is found to represent the average value of E_c under service load conditions (Neville and Brooks 2010). Clause 6.2.3.1 of IS 456 suggests that the short-term static modulus of elasticity of concrete, E_c , may be taken as

$$E_c = 5000 \sqrt{f_{ck}} \text{ N/mm}^2 \quad (1.8a)$$

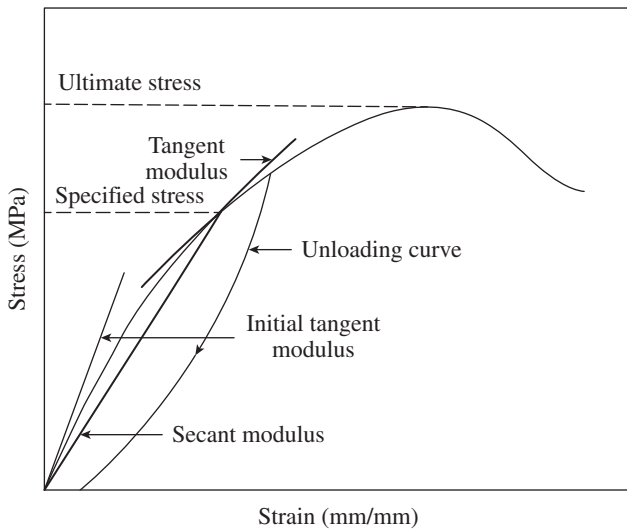


FIG. 1.20 Various definitions of modulus of elasticity of concrete

As per Clause 8.5.1 of ACI 318, the modulus of elasticity for concrete may be taken as

$$E_c = \rho_c^{1.5} 0.038 \sqrt{f_{ck}} \text{ N/mm}^2 \quad (1.8b)$$

where ρ_c is the unit weight of concrete (varies between 1440 kg/m³ and 2560 kg/m³). For normal weight concrete, ACI code allows it to be taken as (assuming $\rho_c = 2300 \text{ N/mm}^2$)

$$E_c = 4200 \sqrt{f_{ck}} \text{ N/mm}^2 \quad (1.8c)$$

Both IS 456 and ACI 318 caution that the actual measured values may differ by ± 20 per cent from the values obtained from Eq. (1.8). Moreover, the US code value is 16 per cent less than the value specified by the Indian code. It has to be noted that the use of lower value of E_c will result in a conservative (higher) estimate of the short-term elastic deflection.

The ACI committee report on HSC (ACI 363R-92) suggests the following equation, which has been adopted by NZS 3101-Part 1:2006 and CSA A23.3-04:

$$E_c = (2970 \sqrt{f_{ck}} + 6900) (\rho_c / 2300)^{1.5} \text{ N/mm}^2 \quad (1.8d)$$

for 26 MPa < f_{ck} < 104 MPa

Noguchi, et al. (2009) proposed the following equation, which is applicable to a wide range of aggregates and mineral admixtures used in concrete.

$$E_c = k_1 k_2 \times 3.36 \times 10^4 (\rho_c / 2400)^2 (f_{ck} / 75)^{1/3} \text{ N/mm}^2 \quad (1.8e)$$

where the correction factors k_1 and k_2 are given in Tables 1.21 and 1.22.

TABLE 1.21 Values of correction factor k_1

Type of Coarse Aggregate	Value of k_1
Crushed limestone, calcined bauxite	1.20
Crushed quartzite aggregate, crushed andesite, crushed basalt, crushed clay slate, crushed cobblestone	0.95
Coarse aggregate other than above	1.0

TABLE 1.22 Values of correction factor k_2

Type of Mineral Admixture	Value of k_2
Silica fume, GGBS, fly ash fume	0.95
Fly ash	1.10
Mineral admixture other than the above	1.0

The *dynamic modulus of elasticity* of concrete, E_{cd} , corresponds to a small instantaneous strain. It can be determined by the non-destructive electro-dynamic method, by measuring the natural frequency of the fundamental mode of longitudinal vibration of concrete prisms, as described in IS 516:1959. The dynamic modulus of elasticity has to be used when concrete is used in structures subjected to dynamic loading (i.e., impact or earthquake). The value of E_{cd} is generally 20 per cent, 30 per cent, and 40 per cent higher than the secant modulus for high-, medium-, and low-strength concretes, respectively (Mehta and Monteiro 2006).

Poisson’s ratio is defined as the ratio of lateral strain to the longitudinal strain, under uniform axial stress. Experimental studies have predicted widely varying values of Poisson’s ratio, in the range of 0.15–0.25. A value of 0.2 is usually suggested for design for both NSCs and HSCs. For lightweight concretes, the Poisson’s ratio has to be determined from tests.

1.8.7 Strength under Combined Stresses

Structural members are usually subjected to a combination of forces, which may include axial force, bending moments, transverse shear, and twisting moments. Any state of combined stress acting at any point in a member may be reduced to three principal stresses acting at right angles to each other on an appropriately oriented elementary cube in the material. Any or all of the principal stresses can be either compression or tension. When one of these three principal stresses is zero, a state of *biaxial* stress exists; if two of them are zero, the state of stress is *uniaxial*. In most of the situations, only the uniaxial strength properties are known from simple tests described in this chapter. The failure strength under combined stresses is usually defined by an appropriate failure criterion. Until now, neither a general theory of strength of concrete under combined stresses nor a universally accepted failure criterion has been proposed.

However, the strength of concrete for biaxial state of stress has been established experimentally by Kupfer, et al. (1969) (see Fig. 1.21). This figure shows that under biaxial tension, the strength is close to that of uniaxial tension. When one principal stress is tension and other is compressive, the concrete cracks at a lower stress than it would have in uniaxial tension or compression. Under biaxial compression, the strength is greater than the uniaxial compression by about 27 per cent.

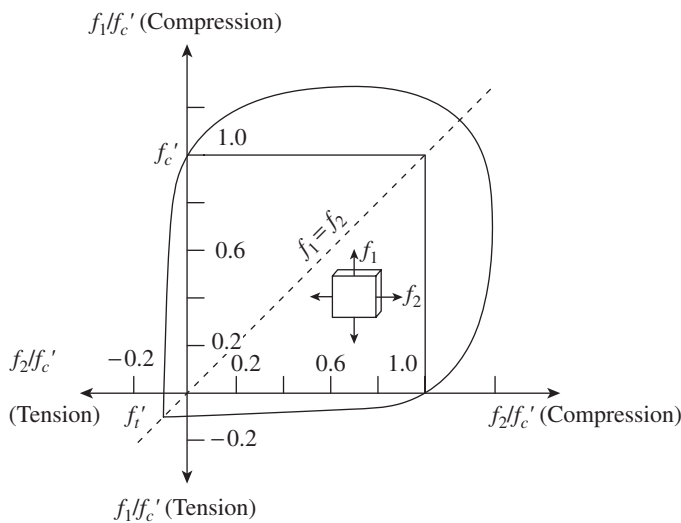


FIG. 1.21 Strength of concrete in biaxial stress

Source: Kupfer, et al. 1969, reprinted with permission from ACI

1.8.8 Shrinkage and Temperature Effects

As shrinkage and temperature effects are similar, they are both considered in this section.

Shrinkage Effects

Shrinkage and creep are not independent phenomena. For convenience, their effects are treated as separate, independent,

and additive. The total shrinkage strain in concrete is composed of the following:

1. *Autogenous shrinkage*, which occurs during the hardening of concrete (Holt 2001)
2. *Drying shrinkage*, which is a function of the migration of water through hardened concrete

Drying shrinkage, often referred to simply as *shrinkage*, is caused by the evaporation of water from the concrete. Both shrinkage and creep introduce time-dependent strains in concrete. However, shrinkage strains are independent of the stress conditions of concrete. Shrinkage can occur before and after the hydration of the cement is complete. It is most important, however, to minimize it during the early stages of hydration in order to prevent cracking and to improve the durability of the concrete. Shrinkage cracks in RC are due to the differential shrinkage between the cement paste, the aggregate, and the reinforcement. Its effect can be reduced by the prolonged curing, which allows the tensile strength of the concrete to develop before evaporation occurs. The most important factors that influence shrinkage in concrete are (a) type and content of aggregates, (b) w/c ratio, (c) effective age at transfer of stress, (d) degree of compaction, (e) effective section thickness, (f) ambient relative humidity, and (f) presence of reinforcement (ACI 209R-92).

Shrinkage strain is expressed as a linear strain (mm/mm). In the absence of reliable data, Clause 6.2.4.1 of IS 456 recommends the approximate value for the total shrinkage strain for design as 0.0003. (ACI 209R-92 suggests an average value of 780×10^{-6} mm/mm for the ultimate shrinkage strain, ϵ_{sh}). Different models for the prediction of creep under compression and shrinkage induced strains in hardened concrete are presented and compared in ACI 209.2R-08. Long-term deflection calculations considering the effects of shrinkage and creep are covered in Chapter 12.

Temperature Effects

Concrete expands with rise in temperature and contracts with fall in temperature. The effects of thermal contraction are similar to the effects of shrinkage. To limit the development of temperature stresses, expansion joints are to be provided, especially when there are marked changes in plan dimensions. In addition, when the length of the building exceeds 45 m, expansion joints are to be provided, as per Clause 27 of IS 456. Temperature stresses may be critical in the design of concrete chimneys and cooling towers. Roof slabs may also be subjected to thermal gradient due to solar radiation. In large and exposed surfaces of concrete such as slabs, nominal reinforcements are usually placed near the exposed surface to take care of temperature and shrinkage stresses. The coefficient of thermal expansion depends on the type of cement and aggregate, cement content, relative humidity, and

the size of section. Clause 6.2.6 of IS 456 provides a table to choose the value of coefficient of thermal expansion based on the aggregate used. However, SP 24:1983 recommends a value of 11×10^{-6} mm/mm per degree Celsius for the design of liquid storage structures, bins and chimneys, which is close to the thermal coefficient of steel (about 11×10^{-6} mm/mm per degree Celsius). The calculation of deflection due to temperature effects is discussed in Section 12.4.3 of Chapter 12. More discussions on thermal and shrinkage effects are provided in Section 3.9.2 of Chapter 3.

Fire design of concrete structures is outside the scope of this book. When exposed to fire, both concrete and steel reinforcement of RC members lose 60 per cent of their characteristic strength at a temperature of 500°C. Where HSCs are used, consideration should be given to mitigate the effects of spalling (e.g., use of fibre reinforcement, sacrificial concrete layers, thermal barriers, and fire-resisting concrete.). More information on fire design may be found in fib reports (2007, 2008).

1.8.9 Creep of Concrete

Creep in concrete is the gradual increase in deformation (strain) with time in a member subjected to sustained loads. The creep strain is much larger than the elastic strain on loading (creep strain is typically two to four times the elastic strain). If the specimen is unloaded, there is an immediate elastic recovery and a slower recovery in the strain due to creep (see Fig. 1.22). Both amounts of recovery are much less than the original strains under load. If the concrete is reloaded at a later date, instantaneous and creep strains develop again. Creep occurs under both compressive and tensile stresses and always increases with temperature. HSCs creep less than NSCs. When the stress in concrete does not exceed one-third of its characteristic compressive strength, creep may be assumed proportional to the stress (Clause 6.2.5 of IS 456). It has to be noted that, unlike concrete, steel will creep only above 700°F.

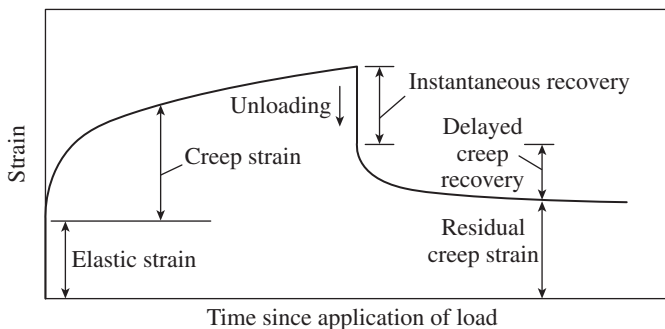


FIG. 1.22 Typical creep curve

The main factors affecting creep strain are the concrete mix and strength, the type of aggregate used, curing, ambient relative humidity, and the magnitude and duration of sustained

loading. As per IS 456, the ultimate creep strain ϵ_{cp} is to be calculated from the creep coefficient C_t (θ in IS nomenclature) given in Clause 6.2.5.1. Calculation of long-term deflection due to creep is provided in Section 12.4.1 of Chapter 12.

More information on creep, shrinkage, and temperature effects may be obtained from the work of Bamforth, et al. (2008).

1.8.10 Non-destructive Testing

Non-destructive tests are used to find the strength of existing concrete elements. They are classified as follows:

1. *Half-cell electrical potential method* to detect the corrosion potential of reinforcing bars in concrete
2. *Schmidt/Rebound hammer test* (IS 13311-Part 2:1992) to evaluate the surface hardness of concrete
3. *Carbonation depth measurement test* to determine whether moisture has reached the depth of the reinforcing bars, thereby leading to corrosion
4. *Permeability test* to measure the flow of water through the concrete
5. *Penetration resistance* or *Windsor probe test* to measure the surface hardness and hence the strength of the surface and near-surface layers of the concrete
6. *Covermeter test* to measure the distance of steel reinforcing bars beneath the surface of the concrete and the diameter of the reinforcing bars
7. *Radiographic test* to detect voids in the concrete and the position of prestressing ducts
8. *Ultrasonic pulse velocity test* (IS 13311-Part 1:1992) mainly to measure the time of travel of ultrasonic pulse passing through the concrete and hence concrete quality
9. *Sonic methods*, which use an instrumented hammer providing both sonic echo and transmission methods, to predict the integrity of piles and bridge decks
10. *Tomographic modelling*, which uses the data from ultrasonic transmission tests in two or more directions, to detect voids in concrete
11. *Impact echo testing* to detect voids, delamination, and other anomalies in concrete
12. *Ground penetrating radar* or *impulse radar testing* to detect the position of reinforcing bars or stressing ducts
13. *Infrared thermography* to detect voids, delamination, and other anomalies in concrete and also to detect water entry points in buildings

The details of these tests may be found in ACI 228.1R-03 manual and the work of Malhotra and Carino (2003).

1.9 DURABILITY OF CONCRETE

Although several unreinforced concrete structures, built 2000 years ago, such as the Pantheon in Rome and several

aqueducts in Europe, are still in excellent condition, many RC structures built in the twentieth century have deteriorated within 10–20 years. In several countries like the USA, about 40–50 per cent of the expenditure in the construction industry is spent on repair, maintenance, and rehabilitation of existing structures. These deteriorating concrete structures not only affect the productivity of the society but also have a great impact on our resources, environment, and human safety. It has been realized that the deterioration of concrete structures is due to the main emphasis given to mechanical properties and the structural capacity and the neglect of construction quality and life cycle management (ACI 201.2R-08). Strength and durability are two separate aspects of concrete; neither will guarantee the other. Hence, clauses on durability were included for the first time in the fourth revision of IS 456, published in 2000 (see Clause 8 of the code).

As per Clause 8.1 of IS 456, a *durable concrete* is one that performs satisfactorily in the working environment of anticipated exposure conditions during its service life. The following factors affect the durability of concrete: (a) Environment, (b) concrete cover to the embedded steel, (c) quality and type of constituent materials, (d) cement content and w/c ratio of concrete, (e) degree of compaction and curing of concrete, and (f) shape and size of member. The prescriptive requirements given in IS 456 are discussed in Section 4.4.5 of Chapter 4. The requirement of concrete exposed to sulphate attack is provided in Clause 8.2.2.4 and Table 4 of IS 456. Guidance to prevent alkali–aggregate reaction is given in Clause 8.2.5.4 of IS 456.

EXAMPLES

EXAMPLE 1.1 (Mix proportioning for M25 concrete): Calculate the mix proportioning for M25 concrete if the following are the stipulations for proportioning:

1. Grade designation: M25
2. Type of cement: OPC 43 grade conforming to IS 8112
3. Maximum nominal size of aggregate: 20 mm
4. Exposure condition: Moderate
5. Minimum cement content (Table 5 of IS 456): 300 kg/m³
6. Workability: Slump 75 mm
7. Method of concrete placing: Pumping
8. Degree of supervision: Good
9. Type of aggregate: Crushed angular aggregate
10. Maximum cement content: 450 kg/m³
11. Chemical admixture type: Superplasticizer

The test data for materials is as follows:

1. Cement used: OPC 43 grade conforming to IS 8112
2. Specific gravity of cement: 3.15
3. Chemical admixture: Superplasticizer conforming to IS 9103

4. Specific gravity of materials is as follows:
 - (a) Coarse aggregate: 2.68
 - (b) Fine aggregate: 2.65
 - (c) Chemical admixture: 1.145
5. Water absorption is as follows:
 - (a) Coarse aggregate: 0.6 per cent
 - (b) Fine aggregate: 1.0 per cent
6. Free (surface) moisture data is as follows:
 - (a) Coarse aggregate: Nil (absorbed moisture also nil)
 - (b) Fine aggregate: Nil
7. Sieve analysis data is as follows:
 - (a) Coarse aggregate: Conforming to Table 2 of IS 383:1970
 - (b) Fine aggregate: Conforming to grading zone 1 of Table 4 of IS 383:1970

SOLUTION:

Step 1 Calculate the target strength for mix proportioning. From Eq. (1.1)

$$f'_{ck} = f_{ck} + 1.65 \times s$$

From Table 8 of IS 456 (see Table 1.13), standard deviation for M25, $s = 4 \text{ N/mm}^2$

$$\text{Therefore, target strength} = 25 + 1.65 \times 4 = 31.6 \text{ N/mm}^2$$

Step 2 Select the w/c ratio. From Table 5 of IS 456 (Table 4.5), maximum water cement ratio for moderate exposure is 0.50. Adopt w/c ratio as $0.45 < 0.50$.

Step 3 Select water content. From Table 2 of IS 10262, Maximum water content = 186 kg (for 25–50 mm slump and for 20 mm aggregate)

$$\text{Estimated water content for 75 mm slump} = 186 + 3/100 \times 186 = 191.58 \text{ kg}$$

As superplasticizer is used, the water content can be reduced to more than 20 per cent. Based on trials with superplasticizer, water content reduction of 20 per cent has been achieved. Hence, the assumed water content = $191.58 \times 0.80 = 153.2 \text{ kg}$.

Step 4 Calculate the cement content.

$$\text{w/c ratio} = 0.45$$

$$\text{Cement content} = 153.2/0.45 = 340.4 \text{ kg/m}^3$$

From Table 5 of IS 456 (Table 4.5), minimum cement content for moderate exposure condition = 300 kg/m³. Since $340.4 \text{ kg/m}^3 > 300 \text{ kg/m}^3$, it is acceptable.

Step 5 Determine the proportion of volume of coarse aggregate and fine aggregate content. From Table 3 of IS 10262 (Table 1.15), volume of coarse aggregate corresponding to 20 mm size aggregate and fine aggregate (Zone 1) for w/c ratio of 0.50 is 0.60. We now have w/c ratio as 0.45. Therefore, the volume of coarse aggregate has to be increased to decrease the fine aggregate content. As the w/c ratio is lower by 0.05,

the proportion of volume of coarse aggregate is increased by 0.01 (at the rate of $-/+0.01$ for every $+0.05$ change in the w/c ratio). Therefore, corrected proportion of volume of coarse aggregate for the w/c ratio of 0.45 is 0.61.

Note: Even if the selected coarse aggregate is not angular, the volume of coarse aggregate has to be increased suitably, based on experience.

For pumpable concrete, these values should be reduced by 10 per cent.

Therefore, volume of coarse aggregate = $0.61 \times 0.09 = 0.55$

Volume of fine aggregate content = $1 - 0.55 = 0.45$

Step 6 Perform the mix calculations. The mix calculations per unit volume of concrete are as follows:

1. Volume of concrete = 1 m^3
2. Volume of cement = Mass of cement/Specific gravity of cement $\times 1/1000$

$$a = 340.4/3.15 \times 1/1000 = 0.108 \text{ m}^3$$

3. Volume of water = Mass of water/Specific gravity of water $\times 1/1000$

$$b = 153.2/1 \times 1/1000 = 0.153 \text{ m}^3$$

4. Volume of chemical admixture (superplasticizer) (at 1.0 per cent by mass of cementitious material)

$$\begin{aligned} c &= \text{Mass of chemical admixtures/Specific gravity of admixture} \times 1/1000 \\ &= 3.4/1.145 \times 1/1000 = 0.00297 \text{ m}^3 \end{aligned}$$

5. Total volume of aggregate (coarse + fine)

$$\begin{aligned} d &= [1 - (a + b + c)] = 1 - (0.108 + 0.153 + 0.00297) \\ &= 0.736 \text{ m}^3 \end{aligned}$$

6. Mass of coarse aggregate = $d \times \text{volume of coarse aggregate} \times \text{specific gravity of coarse aggregate} \times 1000 = 0.736 \times 0.55 \times 2.68 \times 1000 = 1084.86 \text{ kg}$
7. Mass of fine aggregate = $d \times \text{volume of fine aggregate} \times \text{specific gravity of fine aggregate} \times 1000 = 0.736 \times 0.45 \times 2.65 \times 1000 = 877.68 \text{ kg}$

Step 7 Determine the mix proportions for trial number 1.

Cement = 340.40 kg/m^3

Water = 153.2 kg/m^3

Fine aggregate = 878 kg/m^3

Coarse aggregate = 1085 kg/m^3

Chemical admixture = 3.4 kg/m^3

w/c ratio = 0.45

The following are the adjustments for moisture in aggregates and water absorption of aggregates and the correction for aggregates:

Free (surface) moisture is nil in both fine and coarse aggregates.

Corrected water content = $153.2 + 878 (0.01) + 1085 (0.006) = 168.49 \text{ kg}$

The estimated batch masses (after corrections) are as follows:

Cement = 340.4 kg/m^3

Water = 168.5 kg/m^3

Fine aggregate = 878.0 kg/m^3

Coarse aggregate = 1085 kg/m^3

Superplasticizer = 3.4 kg/m^3

Two more trial mixes with variation of ± 10 per cent of w/c ratio should be carried out to achieve the required slump and dosage of admixtures. A graph between the three w/c ratios and their corresponding strengths should be plotted to correctly determine the mix proportions for the given target strength.

EXAMPLE 1.2 (Mix proportioning for M25 concrete, using fly ash as part replacement of OPC):

Calculate the mix proportioning for M25 concrete with the same stipulations for proportioning and the same test data for materials as given in Example 1.1, except that fly ash is used as part replacement of OPC.

SOLUTION:

Considering the same data as in Example 1.1 for M25 concrete, the mix proportioning steps from 1 to 3 will remain the same.

The procedure of using fly ash as a partial replacement to OPC has been explained in step 4.

Step 4 Calculate the cement content.

From Example 1.1, cement content = 340.4 kg/m^3

Now, to proportion a mix containing fly ash, the following steps are suggested:

1. Decide percentage of fly ash to be used based on project requirement and quality of materials.
2. In certain situations, increase in cementitious material content may be warranted.

The decision to increase cementitious material content and its percentage may be based on experience and trial. Let us consider an increase of 10 per cent in the cementitious material content.

Cementitious material content = $340.4 \times 1.1 = 374.4 \text{ kg/m}^3$

Water content = 153.2 kg/m^3 (from Example 1.1)

Hence, w/c ratio = $153.2/374.4 = 0.41$

Fly ash at 35 per cent of total cementitious material content = $374.4 \times 35\% = 131 \text{ kg/m}^3$

Cement (OPC) content = $374.4 - 131 = 243.4 \text{ kg/m}^3$

Saving of cement while using fly ash = $374.4 - 243.4 = 97 \text{ kg/m}^3$

Fly ash being utilized = 131 kg/m^3

Step 5 Determine the proportion of volume of coarse aggregate and fine aggregate content. From Table 3 of IS 10262 (Table 1.15), the volume of coarse aggregate corresponding to 20 mm size aggregate and fine aggregate (Zone I) for w/c ratio

of 0.50 is 0.60. In this example, w/c ratio is 0.41. Therefore, the volume of coarse aggregate is required to be increased to decrease the fine aggregate content. As the w/c ratio is lower by approximately 0.10, the proportion of volume of coarse aggregate is increased by 0.02 (at the rate of $-/+0.01$ for every $+0.05$ change in the w/c ratio). Therefore, the corrected proportion of volume of coarse aggregate for the w/c ratio of 0.41 is 0.62.

Note: Even if the selected coarse aggregate is not angular, the volume of coarse aggregate has to be increased suitably, based on experience.

For pumpable concrete, these values should be reduced by 10 per cent.

Therefore, volume of coarse aggregate = $0.62 \times 0.09 = 0.56$
Volume of fine aggregate content = $1 - 0.56 = 0.44$

Step 6 Perform the mix calculations. The mix calculations per unit volume of concrete shall be as follows:

1. Volume of concrete = 1 m^3
2. Volume of cement = Mass of cement/Specific gravity of cement $\times 1/1000$

$$a = 243.4/3.15 \times 1/1000 = 0.0773 \text{ m}^3$$

3. Volume of fly ash = Mass of fly ash/Specific gravity of fly ash $\times 1/1000$

$$b = 131/2.0 \times 1/1000 = 0.0655 \text{ m}^3$$

4. Volume of water = Mass of water/Specific gravity of water $\times 1/1000$

$$c = 153.2/1 \times 1/1000 = 0.153 \text{ m}^3$$

5. Volume of chemical admixture (superplasticizer) (at 0.8 per cent by mass of cementitious material)

$$d = \text{Mass of chemical admixture/Specific gravity of admixture} \times 1/1000 \\ = 3/1.145 \times 1/1000 = 0.0026 \text{ m}^3$$

6. Total volume of aggregate (coarse + fine)

$$e = [1 - (a + b + c + d)] \\ = 1 - (0.0773 + 0.0655 + 0.153 + 0.0026) = 0.7016 \text{ m}^3$$

7. Mass of coarse aggregate

$$= e \times \text{volume of coarse aggregate} \times \text{Specific gravity of coarse aggregate} \times 1000 \\ = 0.7016 \times 0.56 \times 2.68 \times 1000 = 1053 \text{ kg}$$

8. Mass of fine aggregate

$$= e \times \text{volume of fine aggregate} \times \text{specific gravity of fine aggregate} \times 1000 \\ = 0.7016 \times 0.44 \times 2.65 \times 1000 \\ = 818 \text{ kg}$$

Step 7 Determine the mix proportions for trial number 1.

$$\text{Cement} = 243.4 \text{ kg/m}^3$$

$$\text{Fly ash} = 131 \text{ kg/m}^3$$

$$\text{Water} = 153 \text{ kg/m}^3$$

$$\text{Fine aggregate} = 818 \text{ kg/m}^3$$

$$\text{Coarse aggregate} = 1053 \text{ kg/m}^3$$

$$\text{Chemical admixture} = 3 \text{ kg/m}^3$$

$$\text{w/c ratio} = 0.41$$

Note: The aggregate should be used in saturated surface dry condition. As mentioned in Example 1.1, three trial mixes with slightly varying w/cm ratio has to be made to determine experimentally the exact mix proportions that will result in the required workability, strength, and durability.

SUMMARY

Concrete technology has advanced considerably since the discovery of the material by the Romans more than 2000 years ago. A brief history of developments that resulted in the current day RC is provided. The advantages and drawbacks of concrete as a construction material are listed. Cement is the most important ingredient of concrete as it binds all the other ingredients such as fine and coarse aggregates. The cements that are in use today include OPC, rapid hardening Portland cement, low heat Portland cement, sulphate-resisting Portland cement, PSC, PPC, and ternary blended cement. The making and properties of these various types of cements are briefly discussed. The three grades of cement and their properties are also provided. The fine and coarse aggregates occupy about 60–75 per cent of the concrete volume (70–85% by mass) and hence strongly influence the properties of fresh as well as hardened concrete, its mixture proportions, and the economy. Mixing water plays an important role in the workability, strength, and durability of concrete. Hence, their properties and use in concrete are briefly discussed.

As we now use a variety of chemical and mineral admixtures to improve properties of concrete, a brief introduction to them is also provided. It is important to realize the chemical interaction of these

admixtures with the ingredients of cement, as they may ultimately affect the performance of concrete. Proportioning of concrete mixes, as per the latest IS 10262:2009, is described. Hydration of cement and heat of hydration are also described. In addition to the ordinary concrete, we now have a host of different types of concretes, such as RMC, HPC, SCC, SLWC, AAC, FRC, DFRC (which include ECC, UHPC, SIFCON and SIMCON), polymer concrete, and ferrocement. They are used in some situations to achieve strength and durability.

When reinforcing steel (often called *rebar*) is placed inside a concrete mass (they are often placed in the tension zone, as concrete is weak in tension), the solidified mass is called RC. Though traditionally mild steel was used as rebar, a number of different types of rebars are now available and include hot rolled HYSD, hard drawn wire fabric, TMT bars, and TMT CRS bars. The mechanical properties of these steel bars are also provided. A brief description of the corrosion of steel bars, which is mainly responsible for the deterioration of RCC structures all over the world, is also included. Corrosion may be mitigated by the use of fusion-bonded epoxy-coated rebars, galvanized rebars, FRP bars, basalt bars, or TMT CRS bars.

In order to get quality concrete, careful mixing, placing, compacting, and curing of concrete is necessary at site. Forms should be removed only after concrete has gained sufficient strength to carry at least twice the stresses it may be subjected to at the time of removal of forms. Important properties of concrete such as workability of concrete (usually measured by slump test), compressive strength (measured by conducting tests on carefully made and cured cubes or cylinders on the 28th day), stress–strain characteristics, tensile and bearing strength, modulus of elasticity, and Poisson’s ratio are

discussed. Expressions for finding compression strength at any day, modulus of elasticity, and tensile, shear, bond, and bearing strengths, are provided as per Indian codes and compared with the provisions of the US code. Discussions on strength under combined stresses and shrinkage, temperature, and creep effects are also included. Various non-destructive tests performed on concrete to assess the strength of existing structures are also listed. Two examples are provided to explain the mix proportioning of concrete.

REVIEW QUESTIONS

- Write a short history of concrete, beginning with the Roman concrete.
- What are the advantages and drawbacks of concrete?
- Compare the major properties of steel, concrete, and wood.
- What are the processes by which modern cement is made? Explain the dry process of cement manufacture.
- List five different cements that are in use today.
- What are the three different grades of cements used in India? How is the grade of cement fixed?
- How does the fineness of cement affect the concrete?
- What are the four major compounds used in cement? How do they affect the different properties of concrete?
- How is PPC manufactured? What are its advantages?
- How is PSC manufactured? What are its advantages?
- Name any three tests that are conducted on cement.
- What are the different classifications of aggregates? List five factors of aggregates that may affect the properties of concrete.
- The specific gravity of gravel is _____.
(a) 2.80 (c) 2.67
(b) 2.85 (d) 3.10
- The maximum size of coarse aggregate used in concrete is the lesser of _____.
(a) one-fourth the size of member, 5 mm less than max. clear distance between bars, and min. cover
(b) one-fourth the size of member and 20 mm
(c) one-fourth the size of member, 5 mm less than max. clear distance between bars, and 10 mm less than min. cover
- Can sea water be used for mixing or curing of concrete? State the reason.
- Name any three chemical admixtures used in concrete.
- Name any two compounds used as superplasticizers in India.
- Name any three mineral admixtures used in concrete.
- Write short notes on the following:
(a) Fly ash
(b) Silica fume
(c) GGBS
- What are the main objectives of concrete mix proportioning?
- How is target mean compressive strength fixed for mix proportioning?
- How is initial w/c ratio assumed in mix proportioning?
- What is meant by hydration of cement? What is heat of hydration?
- Name any three types of concretes.
- Why is it better to use RMC than site-mixed concrete?
- As per IS 456, which of the following is considered standard concrete (NSC)?
(a) M25–M60, (c) M50–M75,
(b) M30–M50, (d) M20–M40
- As per IS 456, which of the following is considered HSC?
(a) M50–M80, (c) M60–M90,
(b) M65–M100, (d) M50–M90
- How does HPC differ from HSC?
- Write short notes on the following:
(a) HPC (e) DFRCC
(b) SCC (f) SIFCON and SIMCON
(c) FRC (g) Ferrocement
(d) SLWC
- How are TMT bars manufactured? How do they differ from cold twisted deformed bars?
- Draw the stress–strain curve for mild steel bars and HYSD bars.
- As per IS 13920, which of the following should not be used in earthquake zones?
(a) Bars of grade Fe 500 and above
(b) Bars of grade Fe 550 and above
(c) Bars of grade Fe 600 and above
(d) All of these
- When does corrosion of rebars take place? What are the different methods adopted to mitigate corrosion?
- Name three types of rebars that are used in corrosive environments.
- State the three methods by which concrete is compacted.
- What is workability of concrete? Name and describe the test to measure workability.
- How is compressive strength of concrete determined?
- Name any three factors that may affect the compressive strength of concrete.
- How does the stress–strain curve of HSC differ from NSC?
- Write the expressions of modulus of elasticity, tensile, shear, and bearing strength of concrete as per IS 456.
- Write short notes on shrinkage, temperature, and creep effects of concrete.
- Name any three non-destructive tests performed on concrete.

EXERCISES

- Determine the mix proportioning for M30 concrete for the data given in Example 1.1.
- Determine the mix proportioning for M30 concrete for the data given in Example 1.1, with fly ash as part replacement of OPC.

REFERENCES

- ACI 201.2R-08 2008, *Guide to Durable Concrete*, American Concrete Institute, Farmington Hills, p. 49.
- ACI 209R-92 1992, *Prediction of Creep, Shrinkage, and Temperature Effects in Concrete Structures*, American Concrete Institute, Farmington Hills, p. 47.
- ACI 211.1-91 1991, *Standard Practice for Selecting Proportions for Normal, Heavyweight, and Mass Concrete*, American Concrete Institute, Farmington Hills, p. 38.
- ACI 211.4R-93 1993, *Guide for Selecting Proportions for High-strength Concrete with Portland Cement and Fly Ash*, American Concrete Institute, Farmington Hills, p. 13.
- ACI 213R-03 2003, 'Guide for Structural Lightweight Aggregate Concrete', in *ACI Manual of Concrete Practice, Part 1: Materials and General Properties of Concrete*, American Concrete Institute, Farmington Hills, p. 38.
- ACI 214R-02 2002, *Evaluation of Strength Test Results of Concrete*, American Concrete Institute, Farmington Hills, p. 20.
- ACI 222R-01 2001, *Protection of Metals in Concrete against Corrosion*, American Concrete Institute, Farmington Hills, p. 41.
- ACI 228.1R-03 2003, *In-Place Methods to Estimate Concrete Strength*, American Concrete Institute, Farmington Hills, p. 44.
- ACI 301M:10 2010, *Specifications for Structural Concrete*, American Concrete Institute, Farmington Hills, p. 75.
- ACI 305R:10 2010, *Guide to Hot Weather Concreting*, American Concrete Institute, Farmington Hills, p. 23.
- ACI 309R:05 2005, *Guide for Consolidation of Concrete*, American Concrete Institute, Farmington Hills, p. 39.
- ACI 347-04, *Guide to Formwork for Concrete*, American Concrete Institute, Farmington Hills, p. 32.
- ACI 363R-10 2010, *State-of-the-art Report on High-strength Concrete*, American Concrete Institute, Farmington Hills, p. 65.
- ACI 440R-07 2007, *Report on Fiber-reinforced Polymer (FRP) Reinforcement in Concrete Structures*, American Concrete Institute, Farmington Hills, p. 100.
- ACI 544.1R-96 1996, *Report on Fiber-reinforced Concrete*, American Concrete Institute, Farmington Hills, p. 64.
- ACI 549.1R-93 1993 (reapproved 1999), *Guide for the Design, Construction, and Repair of Ferrocement*, American Concrete Institute, Farmington Hills, p. 30.
- ACI Committee E-701 2007, *Aggregates for Concrete*, American Concrete Institute, Farmington Hills, p. 29.
- Aïtcin, P.-C. 1998, *High Performance Concrete*, CRC Press, Boca Raton, FL, p. 624.
- Aïtcin, P.-C., C. Jolicouer, and J.G. MacGregor 1994, 'Superplasticizers: How They Work and Why They Occasionally Don't', *Concrete International, ACI*, Vol. 16, No. 5, pp. 45–52.
- Aïtcin, P.-C. and A. Neville 1993, 'High-performance Concrete Demystified', *Concrete International, ACI*, Vol. 15, No. 1, pp. 21–6.
- Alimchandani, C.R. 2007, 'The Indian Experience of Ready Mixed Concrete', *32nd Conference on Our World in Concrete & Structures*, 28–29 August 2007, Singapore, (also see http://www.cipremier.com/e107_files/downloads/Papers/100/32/100032002.pdf, last accessed on 12 October 2012).
- Ambuja Technical Booklets: No. 5, *Aggregates for Mortar and Concrete*, May 1996, p. 11, No. 125, *FAQs on Aggregates*, May 2007, p. 20, Ambuja Cements Ltd, Mumbai.
- Bamforth, P., D. Chisholm, J. Gibbs, and T. Harrison 2008, *Properties of Concrete for Use in Eurocode 2*, The Concrete Centre, Surrey, p. 53.
- Bapat, J.D. 2012, *Mineral Admixtures in Cement and Concrete*, CRC Press, Boca Raton, p. 310.
- Basu, P.C., P. Shylamoni, and A.D. Roshan 2004, 'Characterisation of Steel Reinforcement for RC Structures: An Overview and Related Issues', *The Indian Concrete Journal*, Vol. 78, No. 1, pp. 19–30.
- Bentur, A. and Mindess, S. 2007, *Fibre Reinforced Cementitious Composites*, 2nd edition, Taylor and Francis, Oxon, p. 624.
- Bentz, D.P. and P.-C. Aïtcin 2008, 'Meaning of Water–Cement ratio: Distance between Cement Particles is Fundamental', *Concrete International, ACI*, Vol. 30, No. 5, pp. 51–4.
- Bentz, D.P., P. Lura, and J.W. Roberts 2005, 'Mixture Proportioning for Internal Curing', *Concrete International, ACI*, Vol. 27, No. 2, pp. 35–40.
- Blais, P.Y. and M. Couture 1999, 'Precast, Prestressed Pedestrian Bridge: World's First Reactive Powder Concrete Structure', *PCI Journal*, pp. 60–71.
- Chandra, S. and L. Berntsson 2002, *Lightweight Aggregate Concrete: Science, Technology, and Applications*, William Andrew Publishing, Norwich, p. 430.
- Clarke, J.L. (ed.) 1993, *Structural Lightweight Aggregate Concrete*, Blackie Academic and Professional, London, p. 148.
- de Larrard, F. 1999, *Concrete Mixture Proportioning: A Scientific Approach*, CRC Press, Boca Raton, p. 448.
- Dhir, R.K. and K.A. Paine 2010, 'Value Added Sustainable Use of Recycled and Secondary Aggregates in Concrete', *The Indian Concrete Journal*, Vol. 84, No. 3, pp. 7–26.
- Dogan, E. and N. Krstulovic-Opara 2003, 'Seismic Retrofit with Continuous Slurry-infiltrated Mat Concrete Jackets', *ACI Structural Journal*, Vol. 100, No.6, pp.713–22.
- EFNARC-2005, *The European Guidelines for Self-Compacting Concrete: Specification, Production and Use*, (also see <http://www.efnarc.org/pdf/SCCGuidelinesMay2005.pdf>, last accessed on 11 October 2012).
- Fehling, E., M. Schmidt, and S. Stürwald, (eds) 2008, *Proceedings of the Second International Symposium on Ultra High Performance Concrete*, University of Kassel, Germany, 5–7 March 2008, Kassel University Press, p. 920, (also see <http://www.uni-kassel.de/upress/online/frei/978-3-89958-376-2.volltext.frei.pdf>, last accessed on 12 January 2013).
- fib 2007, *Fire Design of Concrete Structures: Materials, Structures and Modeling*, State-of-the-art Report, Bulletin 38, fédération internationale du béton (fib), Lausanne, p. 98.
- fib 2008, *Fire Design of Concrete Structure: Structural Behaviour and Assessment*, State-of-the-art Report, Bulletin 46, fédération internationale du béton (fib), Lausanne, p. 209.
- Fischer, G. and V.C. Li 2002, 'Influence of Matrix Ductility on the Tension-stiffening Behavior of Steel Reinforced ECC', *ACI Structural Journal*, Vol. 99, No. 1, pp. 104–11.

- Gambhir, M.L. 2004, *Concrete Technology*, Tata McGraw-Hill Education, New Delhi, p. 658.
- GangaRao, H.V.S., N. Taly, and P.N. Vijay 2007, *Reinforced Concrete Design with FRP Composites*, CRC Press, Boca Raton, p. 382.
- Graybeal, B. and M. Davis 2008, 'Cylinder or Cube: Strength Testing of 80 to 200MPa (11.6 to 29 ksi) Ultra-high-performance Fiber-reinforced Concrete', *ACI Materials Journal*, Vol. 105, No. 6, pp. 603–9.
- Hackman, L.E., M.B. Farrell, and O.O. Dunham 1992, 'Slurry Infiltrated Mat Concrete (SIMCON)', *Concrete International, ACI*, Vol. 14, No. 12, pp. 53–6.
- Holt E.E. 2001, *Early Age Autogenous Shrinkage of Concrete*, Technical Research Center of Finland, ESPOO, VTT Publication No. 446, p. 197, (also see <http://vtt.fi/inf/pdf/publications/2001/P446.pdf>, last accessed on 12 September 2012).
- Hurd, M.K. 2005, *Formwork for Concrete*, SP-4, 7th edition, American Concrete Institute, Farmington Hills, p. 500.
- IS 269:1989 (reaffirmed 1998), *Specifications for 33 Grade Portland cement*, Bureau of Indian Standards, New Delhi.
- IS 383:1970 (reaffirmed 1997), *Specifications for Coarse and Fine Aggregates from Natural Sources for Concrete*, Bureau of Indian Standards, New Delhi.
- IS 432 (Part 1):1982 (reaffirmed 1995), *Specification for Mild Steel and Medium Tensile Steel Bars and Hard-drawn Steel Wire for Concrete Reinforcement, Part 1 Mild Steel and Medium Tensile Steel Bars*, 3rd revision, Bureau of Indian Standards, New Delhi.
- IS 455:1989 (reaffirmed 2000), *Specification for Portland Slag Cement*, Bureau of Indian Standards, New Delhi.
- IS 516:1959 (reaffirmed 1999), *Methods of Tests for Strength of Concrete*, Bureau of Indian Standards, New Delhi.
- IS: 1489 (Part-1):1991(reaffirmed 2000), *Specification for Portland Pozzolana Cement, Part 1: Fly Ash Based*, Bureau of Indian Standards, New Delhi.
- IS: 1489 (Part-2):1991(reaffirmed 2000), *Specification for Portland Pozzolana Cement, Part 2: Calcined Clay Based*, Bureau of Indian Standards, New Delhi.
- IS 1786:2008, *Specification for High Strength Deformed Steel Bars and Wires for Concrete Reinforcement*, 4th revision, Bureau of Indian Standards, New Delhi.
- IS: 3812:2003, *Specification for Pulverized Fuel Ash, Part 1: For Use as Pozzolana in Cement, Cement Mortar and Concrete, Part 2: For Use as Admixture in Cement Mortar and Concrete*, Bureau of Indian Standards, New Delhi.
- IS 4031 (Parts 1–15):1988 (reconfirmed 2000) *Methods of Physical Tests for Hydraulic Cement, Part 6: Determination of Compressive Strength of Hydraulic Cement other than Masonry Cement*, Bureau of Indian standards, New Delhi, p. 3.
- IS 5816-1999, *Methods of Tests for Splitting Tensile Strength of Concrete Cylinders*, 1st revision, Bureau of Indian Standards, New Delhi.
- IS: 8112-1989 (reaffirmed 2000), *Specifications for 43 Grade Portland Cement*, 1st revision, Bureau of Indian Standards, New Delhi.
- IS 9103:1999, *Specifications for Admixtures for Concrete*, 1st revision, Bureau of Indian Standards, New Delhi.
- IS 10262:2009, *Concrete Mix Proportioning: Guidelines*, Bureau of Indian Standards, New Delhi.
- IS 12269:1987 (reaffirmed 1999), *Specification for 53 Grade Ordinary Portland Cement*, Bureau of Indian Standards, New Delhi.
- IS 12089:1987 (reconfirmed 1999), *Specification for Granulated Slag for Manufacture of Portland Slag Cement*, Bureau of Indian Standards, New Delhi.
- IS 15388:2003, *Silica Fume-Specification*, Bureau of Indian Standards, New Delhi.
- Indian Concrete Journal (ICJ)*, *Special Issues on Self-compacting Concrete*, July 2004, June 2009, and August 2009.
- Jayasree, C., M. Santhanam, and R. Gettu 2011, 'Cement–Superplasticiser Compatibility Issues and Challenges', *The Indian Concrete Journal*, Vol. 85, No.7, pp. 48–60.
- Johansen, V.C., W.A. Klemm, and P.C. Taylor 2002, 'Why Chemistry Matters in Concrete?', *Concrete International, ACI*, Vol. 24, No. 3, pp. 84–9.
- Kerkhoff, B. 2007, *Effects of Substances on Concrete and Guide to Protective Treatments*, Portland Cement Association, p. 36.
- Kosmatka, S.H., B. Kerkhoff, and W.C. Panarese 2011, *Design and Control of Concrete Mixtures*, 15th edition, Portland Concrete Association, Skokie, p. 444.
- Krishnamurthy, S. (ed.) 1997, *ICI Monograph on Concrete Admixtures*, Indian Concrete Institute, Chennai, p. 35.
- Krishna Raju, N. 2002, *Design of Concrete Mixes*, 4th edition, CBS Publishers and Distributors Pvt. Ltd, New Delhi, p. 316.
- Kupfer, H., H.K. Hilsdorf, and H. Rüschi 1969, 'Behavior of Concrete under Biaxial Stresses', *Journal of ACI*, Vol. 66, No. 8, pp. 656–66.
- Kulkarni, V.R. 2012, *E-conference on Durability of Concrete*, 27 February to 11 March, 2012, (also see <http://www.sefindia.org/forum/viewtopic.php?t=11706&view=next>, last accessed on 12 January 2013).
- Kumar P., and S.K. Kaushik 2003, 'Some Trends in the Use of Concrete: Indian Scenario', *The Indian Concrete Journal*, Vol. 77, No. 12, pp. 1503–8.
- Kumar, S. and M. Santhanam 2004, 'Use of Particle Packing Model to Produce HPC at Optimum Cement Content', *The Indian Concrete Journal*, Vol. 78, No. 12, pp. 22–8.
- Lea, F.M., 1971 *The Chemistry of Cement and Concrete*, 3rd edition, Chemical Publishing Co., Inc., New York, p. 740.
- Hwang, S-D, K.H. Khayat, and O. Bonneau 2006, 'Performance-based Specifications of Self-consolidating Concrete used in Structural Applications', *ACI Materials Journal*, Vol. 103, No. 2, pp. 121–9.
- Lafarge-Ductal®, *Executive Summary: Completed North American Ductal® Bridges*, http://www.fhwa.dot.gov/hfl/innovations/uhpc_bridges_in_north_america.cfm, last accessed on 12 January 2013.
- Lankard, D.R. 1984, 'Properties and Applications of Slurry Infiltrated FiberConcrete (SIFCON)', *Concrete International, ACI*, Vol. 6, No. 12, pp. 44–7.
- Li, V.C. 2003, 'On Engineered Cementitious Composites (ECC): A Review of the Material and its Applications', *Journal of Advanced Concrete Technology*, Vol. 1, No. 3, pp. 215–30.
- Li, V.C., D.K. Mishra, A.E. Naaman, J.K. Wight, J.M. LaFave, H.C. Wu, and Y. Inada 1994, 'On the Shear Behavior of ECC', *Journal of Advanced Cement Based Materials*, Vol. 1, No. 3, pp. 142–9.
- Malhotra, V.M. and N.J. Carino 2003, *Handbook on Nondestructive Testing of Concrete*, 2nd edition, CRC Press, Boca Raton, p. 384.
- Matsumoto, T. and H. Mihashi 2003, 'JCI-DFRCC Committee Report: DFRCC Terminology and Application Concepts', *Journal of Advanced Concrete Technology*, Vol. 1, No. 3, pp. 335–40.

- Mehta, P.K. 1987, 'Natural Pozzolans: Supplementary Cementing Materials in Concrete', *CANMET Special Publication*, Vol. 86, pp. 1–33.
- Mehta, P.K. and P.J.M. Monteiro 2006, *Concrete: Microstructure, Properties and Materials*, 3rd edition, McGraw-Hill, New York, p. 659 (also contains a CD-ROM with numerous PowerPoint slides, videos, and additional material).
- Mindess, S., J.F. Young, and D. Darwin 2003, *Concrete*, 2nd edition, Prentice Hall and Pearson Education, Harlow, p. 644.
- Moir, G. 2003, *Cements in Advanced Concrete Technology*, edited by J. Newman and B.S. Choo, Elsevier Butterworth-Heinemann, Amsterdam, p. 1–45.
- Mullick, A.K. 2005, 'High Performance Concrete in India: Development, Practices and Standardisation', *ICI Journal*, Vol. 5, No. 2, pp. 7–14.
- Mullick, A.K. 2007, 'Performance of Concrete with Binary and Ternary Cement Blends', *Indian Concrete Journal*, Vol. 81, No. 1, pp. 15–22.
- Mullick, A.K. 2008, 'Cement–Superplasticiser Compatibility and Method of Evaluation', *The Indian Concrete Journal*, Vol. 82, No. 6, pp. 8–15.
- Mullick, A.K. 2012, 'Green Options for Binder System and Aggregate in Sustainable Concrete', *Indian Concrete Journal*, Vol. 86, No. 6, pp. 9–17.
- Muthukumar, D. and N. Subramanian 1999, 'Characteristics of High Strength Concrete with Respect to Ageing', *Civil Engineering & Construction Review (CE & CR)*, Vol. 12, No. 2, pp.14–7.
- Naaman, A.E. 2000, *Ferrocement and Laminated Cementitious Composites*, Techno Press 3000, Ann Arbor, p. 372.
- Naaman, A.E., D. Otter, and H. Najm 1992, 'Elastic Modulus of SIFCON in Tension and Compression', *ACI Materials Journal*, Vol. 88, No. 6, pp. 603–13.
- Nagendra, R. 2010, 'Concrete Mix Proportioning as per New Revised IS 10262:2009', *The Indian Concrete Journal*, Vol. 84, No. 9, pp. 9–21.
- Nataraja, M.C. and L. Das 2010, 'Concrete Mix Proportioning as per Draft IS 10262:2009: Comparison with IS 10262:2009 and ACI 211.1-91', *The Indian Concrete Journal*, Vol. 84, No. 9, pp. 64–70.
- Nataraja, M.C., Nagaraj, T.S. and Ashok Reddy 2001, 'Proportioning Concrete Mixes with Quarry Waste', *International Journal of Cement, Concrete and Aggregates*, ASTM, Vol. 23, No. 2, pp. 1–7.
- Nataraja, M.C. and B.M.R. Reddy 2007, Mix proportioning of plain and rice husk ash concrete as per draft IS 10262, *The Indian Concrete Journal*, Vol. 81, No. 3, pp. 36–42, and Discussions by M.P. Rajamane, Vol. 81, No. 5, pp. 44–6, 55–56.
- Nematollahi, B., M.R.R. Saifulnaz, M.S. Jaafar, and Y.L. Voo 2012, 'A Review on Ultra High Performance “ductile” Concrete (UHPdC) Technology', *International Journal of Civil and Structural Engineering*, Vol. 2, No. 3, pp. 1003–18.
- Neville, A.M. 2012, *Properties of Concrete*, 5th edition, Prentice Hall Harlow, p. 872.
- Neville, A.M. and J.J. Brooks 2010, *Concrete Technology*, 2nd edition, Prentice Hall & Pearson Education, Harlow, p. 442.
- Niyogi, S.M. 1974, 'Concrete Bearing Strength: Support, Mix, Size Effect', *Journal of the Structural Division*, ASCE, Vol. 100, No. 8, pp. 1685–1702.
- Noguchi, T., F. Tomosawa, K.M. Nemati, B.M. Chiaia, and A.P. Fantilli 2009, 'A Practical Equation for Elastic Modulus of Concrete', *ACI Structural Journal*, Vol. 106, No. 5, pp. 690–6.
- Okamura, H. and M. Ouchi 2003, 'Self-compacting Concrete', *Journal of Advanced Concrete Technology*, Vol. 1, No. 1, pp. 5–15.
- Ouchi, M., S.A. Nakamura, T. Osterberg, S-E. Hallberg, M. Lwin 2003, *Applications of Self-compacting Concrete in Japan, Europe, and the United States*, ISHPC, p. 20, (also see <http://www.fhwa.dot.gov/bridge/scc.pdf>, last accessed on 5 October 2012).
- Panarese, W.C. 1987, *Transporting and Handling Concrete*, IS178, Portland Cement Association.
- Parameswaran, V.S. 1996, *Behaviour and Applications of Slurry Infiltrated Fibrous Concrete (SIFCON)*, Technical Manual: ICFRC-TM 2, International Centre for Fibre Reinforced Concrete Composites, Madras, p. 13.
- Parameswaran, V.S. and K. Balasubramanian 1993, *Fibre Reinforced Concrete (Theory, Properties and Applications)*, Technical Manual: ICFRC-TM1, International Centre for Fibre Reinforced Concrete Composites, Madras, p. 45.
- Parameswaran, V.S., T.S. Krishnamoorthy, and K. Balasubramanian 1990, 'Behaviour of High Volume Fibre Cement Mortar in Flexure', *Cement and Concrete Composites*, Vol. 12, No. 4, pp. 293–301.
- Persson, B. and G. Fagerlund, (eds) 2002, 'Self-desiccation and its Importance in Concrete Technology', *Proceedings of the Third International Research Seminar in Lund*, 14–15 June 2002, (also see <http://lup.lub.lu.se/luur/download?func=downloadFile&recordId=633777&fileId=634557>, last accessed on 12 September 2012).
- Persson, B., D. Bentz, and L.-O. Nilsson 2005, 'Self-desiccation and its Importance in Concrete Technology', *Proceedings of the Fourth International Research Seminar*, Gaithersburg, (also see <http://ciks.cbt.nist.gov/~bentz/Lund2005/TVBM-3126hp1.pdf>, last accessed on 12 September 2012).
- Pillai, S.U. and Menon, D. 2003, *Reinforced Concrete Design*, 2nd edition, Tata McGraw Hill Publishing Company Ltd, New Delhi, p. 875.
- Popovics, S. 1998, *Strength and Related Properties of Concrete*, John Wiley, New York, p. 552.
- Powers, T.C. 1961, *Some Physical Aspects of the Hydration of Portland Cement*, Research Department Bulletin RX125, Portland Cement Association.
- Rajamane, N.P. 2004, 'A Procedure for Concrete Mix Design Using Provisions of IS 456:2000', *New Building Materials and Construction World*, Vol. 10, No. 12, pp. 74–89.
- Rajamane, N.P. 2005, 'A General Formula to Replace Concrete BIS Mix Design Curves of SP:23 (S&T):1981', *New Building Materials and Construction World*, Vol. 10, No. 11, pp 124–9.
- Ramachandran, V.S. (ed.) 1995, *Concrete Admixtures Handbook: Properties, Science and Technology*, 2nd edition,, Noyes Publications, Park Ridge, Indian edition by Standard Publishers, New Delhi, 2002, p. 1183.
- Rao, M.C., S.K. Bhattacharyya, and S.V. Barai 2011, 'Recycled Course Aggregate and Its Use in Concrete', *ICI Journal*, Vol. 11, No. 4, pp. 27–40.
- Reed, P., K. Schoonees, and J. Salmond 2008, *Historic Concrete Structures in New Zealand: Overview, Maintenance and Management*, Science & Technical Publishing, Wellington, p. 90, (also see <http://www.doc.govt.nz/upload/documents/science-and-technical/sap248.pdf>, last accessed on 12 October 2012).
- Rixom, R. and N.P. Mailvaganam 1999, 'Chemical Admixtures for Concrete', 3rd edition, CRC Press, Boca Raton, p. 456.

- Rossi, P. 2001, 'Ultra-high-performance Fiber-reinforced Concretes', *Concrete International, ACI*, Vol. 23, No. 12, pp. 46–52.
- SP 23:1982, *Handbook on Concrete Mixes*, Bureau of Indian Standards, New Delhi, p. 122.
- Santhakumar, A.R. 2006, *Concrete Technology*, Oxford University Press, New Delhi, p. 784.
- Sashidhar, C., H. Sudarsana Rao, N.V. Ramana and K. Gnanaswar 2010, 'Compression and Tension Behaviour of SIFCON Produced with Low Tensile Strength Steel Fibre', *Indian Concrete Journal*, Vol. 84, No. 10, pp. 31–36, and 'Flexural Behaviour of SIFCON Produced with Low Tensile Strength Steel Fibre', Vol. 85, No. 10, October 2011.
- Schmidt, M., E. Fehling, C. Geisenhanslüke (eds) 2004, 'Ultra High Performance Concrete (UHPC)', *Proceedings of the International Symposium on UHPC*, University of Kassel, Germany, 13–15 September 2004, Kassel University Press, p. 868, (also see <http://www.uni-kassel.de/upress/online/frei/978-3-89958-086-0.volltext.frei.pdf>, last accessed on 12 January 2013).
- Schmidt, M., E. Fehling, C. Glotzbach, S. Fröhlich, and S. Piotrowski (eds) 2012, *Proceedings of the 3rd International Symposium on UHPC and Nanotechnology for High Performance Construction Materials*, University of Kassel, Germany, 7–9 March 2012, Kassel University Press, p. 1058, (also see <http://www.uni-kassel.de/upress/online/frei/978-3-86219-264-9.volltext.frei.pdf>, last accessed on 12 January 2013).
- Shaeffer, R.E. 1992, *Reinforced Concrete: Preliminary Design for Architects and Builders*, McGraw-Hill, p. 196.
- Shetty, M.S. 2005, *Concrete Technology: Theory and Practice*, 6th revised edition, S. Chand and Company Ltd, New Delhi, p. 624.
- Smith, J.L. and Y.P. Virmani 1996, *Performance of Epoxy-coated Rebars in Bridge Decks*, Report No. FHWA-RD-96-092, Federal Highway Administration.
- SP 34 (S & T):1987, *Handbook on Concrete Reinforcement and Detailing*, Bureau of Indian Standards, New Delhi 1987.
- Spanos, A., R.S. Ravindrarajah, and R.N. Swamy 2012, 'Material and Structural Implications of Using Ferrocement as Permanent Formwork', *The Indian Concrete Journal*, Vol. 86, No. 8, pp. 9–23.
- Subramanian, N. 1976a, 'Ferrocement: A Review', *Science & Engineering*, Vol. XXIX, No. 9, pp. 121–5.
- Subramanian, N. 1976b, 'Fibre Reinforced Concrete', *Science & Engineering*, Vol. XIX, No. 6, pp. 82–7.
- Subramanian, N. 1999, 'Reactive Powder Concrete: A Material of the Future?', *Civil Engineering & Construction Review*, Vol. 12, No. 2, pp. 33–6.
- Subramanian, N. 2007, *Space Structures: Principles and Practice*, 2 volumes, Multi-Science Publishing Co., Essex, p. 820.
- Subramanian, N. 2010, 'Sustainability of RCC Structures using Basalt Composite Rebars', *The Master Builder*, Vol. 12, No. 9, pp. 156–64.
- Subramanian, N. 2012, 'The Principles of Sustainable Building Design', in G.M. Sabnis (ed.), *Green Building with Concrete: Sustainable Design and Construction*, CRC Press, Boca Raton, p. 333.
- Subramanian, N. and T. Gnana Sambanthan 1979, 'Polymers to Improve the Properties of Concrete', *Proceedings, All India Seminar on Prestressed Concrete Structures*, Thiagarajar College of Engineering, Madurai, 2–3 May, pp. 7–11.
- Suprenant, B.A. 2001, 'Free Fall of Concrete', *Concrete International, ACI*, Vol. 23, No. 6, pp. 44–5.
- Taylor, H.F.W. 1997, *Cement Chemistry*, Thomas Telford Publishing, London, p. 477.
- Tennis, P.D. and H.M. Jennings 2000, 'A Model for Two Types of Calcium Silicate Hydrate in the Microstructure of Portland Cement Pastes', *Cement and Concrete Research*, Vol. 30, No.6, pp. 855–63.
- Venugopal, M.S. and Subramanian, N. 1977, 'Hot Weather Concreting', *Indian Concrete Journal*, Vol. 51, No. 11, pp. 348–9.
- Viswanatha, C.S., L.N. Prasad, Radhakrishna, and H.S. Nagaraj 2004, 'Sub-standard Rebars in the Indian Market: An Insight', *The Indian Concrete Journal*, Vol. 78, No. 1, pp. 52–5, (also see http://www.mmfx.com/wp-content/uploads/2012/06/MMFX_Product_Information2011.pdf, last accessed on 12 January 2013).
- Zia, P., M.L. Leming, and S.H. Ahmad 1991, *High-performance Concretes: A State-of-the-art Report*, SHRP-C/FR-91-103 and FHWA-RD-97-030, Strategic Highway Research Program, National Research Council, Washington, DC, p. 236, (also see <http://www.fhwa.dot.gov/publications/research/infrastructure/structures/hpc/97030/index.cfm#toc>, last accessed on 5 October 2012).
- Zia, P., M.L. Leming, S.H. Ahmad, J.J. Schemmel, R.P. Elliott, and A.E. Naaman 1993, *Mechanical Behavior of High-Performance Concretes, Volume 1: Summary Report*. SHRP-C-361, Strategic Highway Research Program, National Research Council, Washington, DC, p. 98, (also see <http://onlinepubs.trb.org/onlinepubs/shrp/SHRP-C-361.pdf>, last accessed 5 October 2012).

STRUCTURAL FORMS

2.1 INTRODUCTION

The art of structural design is manifested in the selection of the most suitable structural system for a given structure. The arrangement of beams and columns to support the vertical (gravity) loads and the selection of a suitable structural system to resist the horizontal (lateral) loads pose a great challenge to the structural engineer, as these factors will determine the economy and functional suitability of the building. In bridge design, the choice of continuous or simple span structures, box girders, cable suspension or cable-stayed girders, and steel orthotropic (bridge floor) or concrete decks will determine not only the economy but also the resulting aesthetics of the bridge (Subramanian 1987). The selection of a suitable system is made mainly based on previous data or experience.

Depending upon the way a structure resists loads and on the different forms, reinforced concrete (RC) structures may be classified as follows:

1. *Gravity masonry structures*: This consists of load-bearing walls, which resist loads transmitted to them by floor slabs. The stability of the structure depends on gravity loads. These are suitable only for buildings with up to two or three floors.
2. *Framed structures*: This consists of a concrete skeleton that collects loads from plate elements (concrete floors and masonry/RC walls) and transmits them to the foundations.
3. *Shell or folded plate structures*: These are curved or folded surfaces enclosing the area and carrying loads.
4. *Other structures*: These include structures and structural elements such as silos or bunkers, retaining walls, liquid retaining structures, chimneys, poles, and foundations for which RC is the ideal material of construction.

Examples of these structures are shown in Fig. 2.1. The structures are also sometimes classified as *non-habitat structures* (e.g., bridges, transmission line towers, silos,

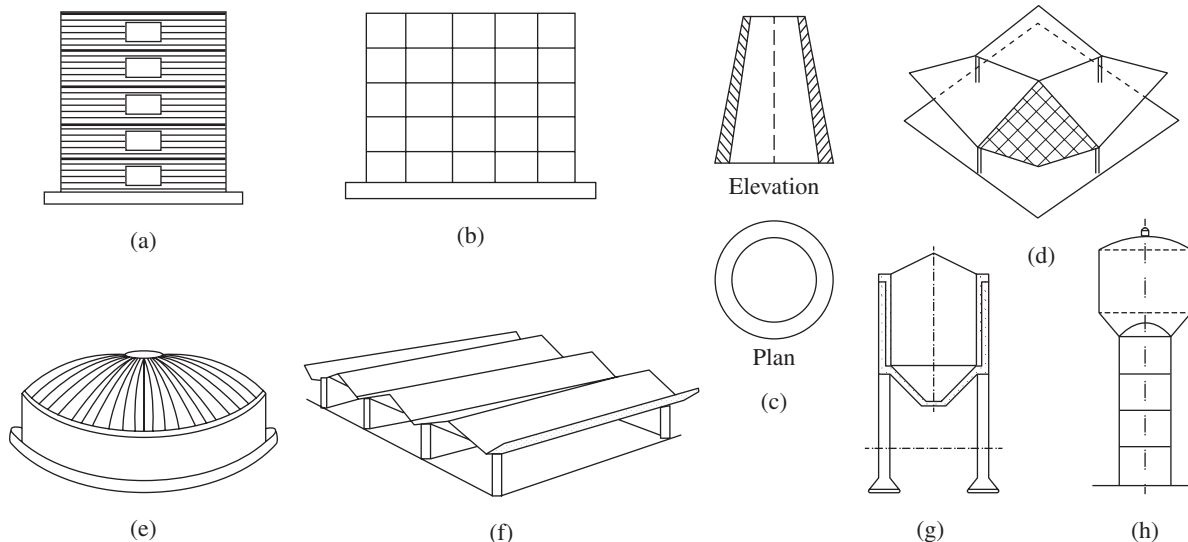
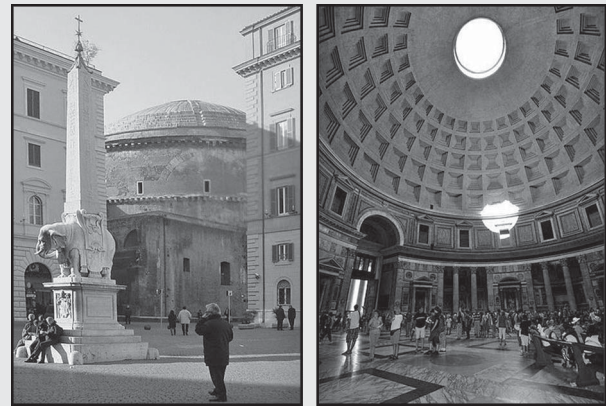


FIG. 2.1 Examples of RC structures (a) Load-bearing brick wall with concrete slabs (b) Rigid frame building (c) Chimney (d) Hyperbolic paraboloid roof (e) Concrete dome (f) Folded plate roof (g) Bunker (h) Water tank

CASE STUDY

Pantheon in Rome

The oldest-known concrete shell, the Pantheon in Rome, Italy, completed in about AD 125, is still standing and is the world's largest unreinforced concrete dome. It has a massive concrete dome 43.3 m in diameter, with an oculus at its centre. The downward thrust of the dome is carried by eight barrel vaults in the 6.4 m thick drum wall into eight piers. The thickness of the dome varies from 6.4 m at the base of the dome to 1.2 m around the oculus. The stresses in the dome were found to be substantially reduced by the use of successively less-dense aggregate stones in the higher layers of the dome. The interior coffering was not only decorative but also reduced the weight of the roof, as did the elimination of the apex by means of the oculus.



Pantheon with concrete dome

television towers, liquid retaining structures, and chimneys) and *habitat structures* (e.g., buildings and stadiums). We are concerned only with RC buildings in this book. Hence an introduction to the different types of structural systems and elements that are used in RC buildings is given in this chapter.

2.2 BASIC STRUCTURAL ELEMENTS

An RC structure consists of different structural elements. It may also contain non-structural elements, such as partitions and false ceilings. The function of any structure is to resist the applied loads (gravitational, for example, dead and imposed loads, and lateral, for example, wind and earthquake) effectively and to transmit the resulting forces to the supporting

ground without differential settlement. At the same time, the structure should satisfy serviceability requirements, be durable, and should not pose problems of maintenance.

The most common RC construction is the building. Hence, consider a typical two-storey building as shown in Fig. 2.2. It has a slab-and-beam system, in which the slabs span between the beams. The loads (dead, imposed, or snow) applied on the slabs are transferred to the beams, which are, in turn, transferred to the columns and through the columns to the footing. The footings distribute the load over sufficient area of soil underneath. Sometimes, the floor or roof slab loads may be transferred to secondary beams. The reactions of the secondary beams, in turn, are transferred to the main girders, which are supported by columns. In Fig. 2.2, the roof is shown as a *concrete joist-slab construction*, which is popular in the

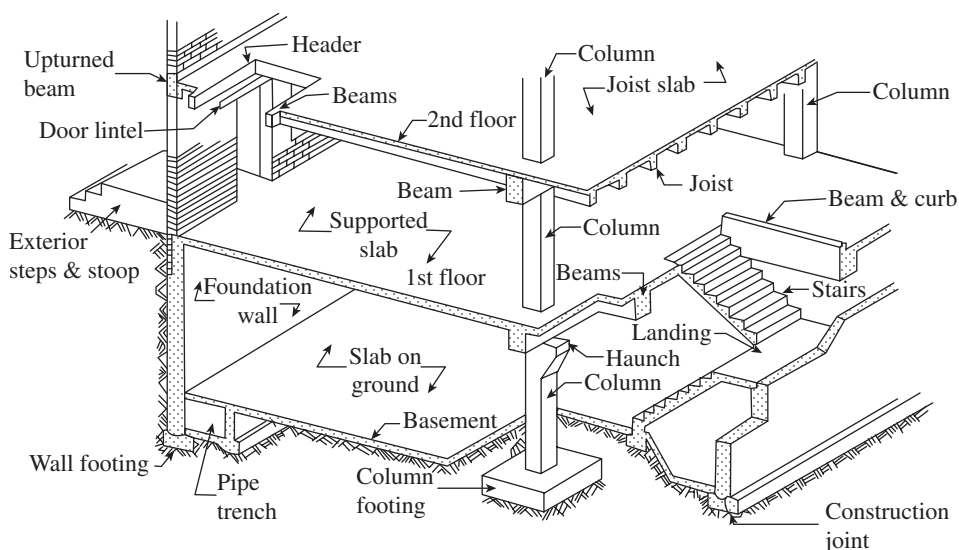


FIG. 2.2 Different elements of a typical RC structure

Courtesy: Concrete Reinforcing Steel Institute, USA

USA. Here, a series of parallel ribs or joists support the load from the roof slab. The slabs carry the loads in the north-south direction and are considered as one-way slabs (see also Section 2.3).

In load-bearing wall systems, instead of the beam and column, the concrete slabs rest directly on the masonry wall. As mentioned earlier, such systems are suitable only up to two or three floors. As the height of the building increases, the behaviour of the system is affected by lateral loads such as wind and earthquake. Several structural systems have been developed in the past for resisting the lateral loads and are discussed in Section 2.5.

2.2.1 Footings

As mentioned in Section 2.2, *footings* distribute the load they receive from columns or walls to the soil underneath in such a way that settlement, particularly uneven or relative settlement, of the structure is limited and failure of the underlying soil is avoided. Hence, the size of footings is so chosen that the pressure under them is less than the *allowable bearing pressure* of the soil. When there are lateral or uplift loads, footings are required to provide sufficient resistance to sliding and overturning. The depth of footing may vary between 1 m and 2 m, depending on the availability of proper bearing material at the site. If good bearing strata are not available at a reasonable depth, the use of deep foundations, for example, *piles*, may be warranted. The design of footing requires proper understanding of soil mechanics.

Among the several types of RC footings in common use are the wall, isolated spread, combined, raft foundations, pile, and pile cap types, which are shown in Fig. 2.3. The design of footings is discussed in detail in Chapter 15.

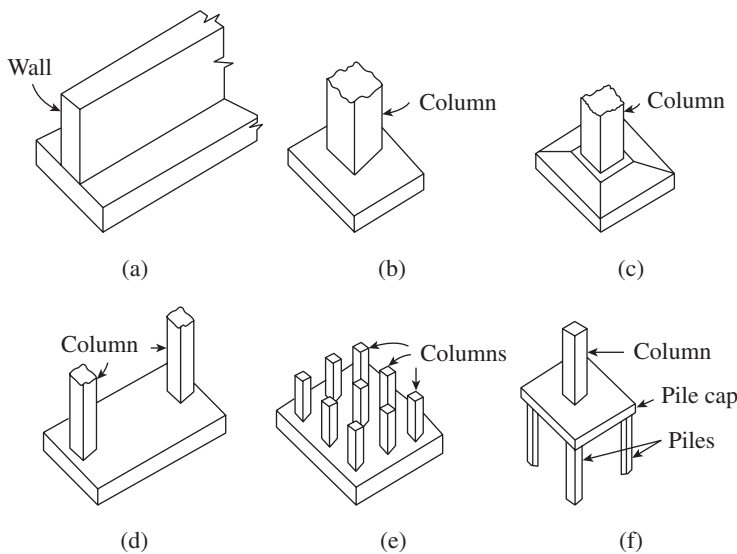


FIG. 2.3 Types of footings (a) Wall footing (b) Isolated spread footing (c) Sloped footing (d) Combined footing (e) Raft foundation (f) Pile foundation

to increase the load-carrying capacity of plain concrete columns. Closely spaced ties and helical spirals wrapped around the longitudinal reinforcement are provided to resist shear forces, avoid buckling of longitudinal bars, provide confinement of concrete in potential *plastic hinge regions*, and increase *ductility*. It is also possible to have *composite compression members* or *composite columns*, which are reinforced longitudinally with structural steel shapes, such as hollow tubes, I-sections, with or without additional longitudinal bars and other transverse reinforcements. These are shown in Fig. 2.5.

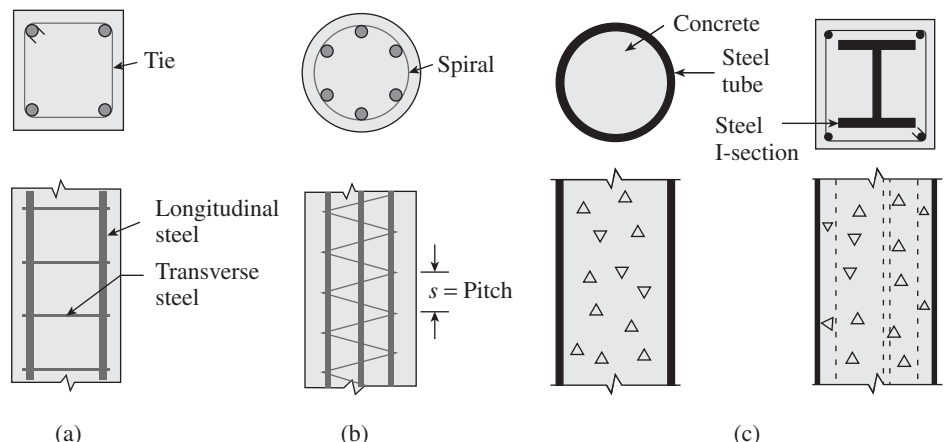


FIG. 2.5 Different types of columns (a) Square-tied column (b) Circular spirally reinforced column (c) Composite columns

2.2.2 Columns

Columns are vertical structural elements that transfer the load from the beams to the foundations. When they carry only axial load they are called *axially loaded columns*. However, in actual practice, there are no perfect axially loaded columns. Due to the eccentricity of loads, imperfections in their construction, and so forth, there may be secondary moments in the columns. There may be bending moments due to the rigid frame actions or lateral loads. Such columns with large bending moments are called *beam columns*. Beam columns may carry uniaxial or even biaxial bending moments.

Reinforced concrete columns with rectangular or square shapes are often used because of the simplicity of constructing the *formwork*. However, when they are used in open spaces, circular shapes are attractive. Square and circular shapes are also preferable in high earthquake zones. L-, +-, and T-shaped columns are also used on rare occasions (see Fig. 2.4). Reinforcement in the form of longitudinal bars is often provided

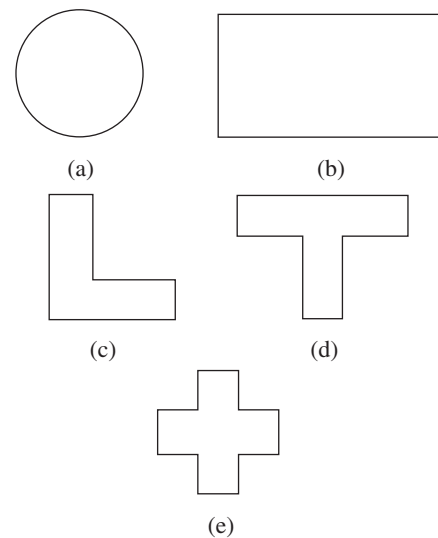


FIG. 2.4 Different shapes of columns (a) Circular (b) Rectangular (c) L-section (d) T-section (e) Cross section

Columns are often classified either as *short* or *stocky* columns, when they fail essentially by squashing and their strength is governed by the material properties, or as *long* or *slender* columns, when they fail by buckling. The design of columns is discussed in detail in Chapters 13 and 14.

2.2.3 Beams

A *beam* is a structural element that is primarily subjected to bending. Beams support the slabs and transfer the load applied on slabs to columns. Secondary beams may transfer the load to main beams, which, in turn, transfer the load to columns. RC beams are normally cast monolithically with slabs. As a result, the two parts act together to resist the loads. Hence, though beams are normally rectangular in shape, some extra slab width at the top, called *flange*, is assumed to act together in the design. The resulting beams are called *L-beams* or *T-beams*, depending on whether flanges are on only one side or on both the sides, as shown in Figs 2.6(b) and (c), respectively.

The most efficient cross section for a simply supported beam is an I- or H-section beam (see Fig. 2.6d). I-section and box section beams are normally adopted in bridges.

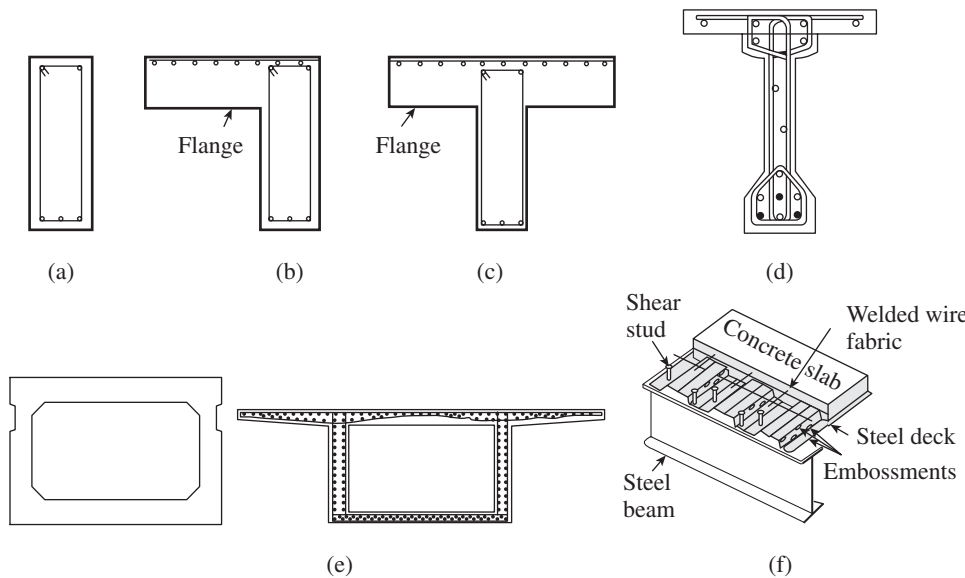


FIG. 2.6 Different types of beams (a) Rectangular (b) L-section (c) T-section (d) I-section (e) Box section (f) Steel–Concrete composite beam

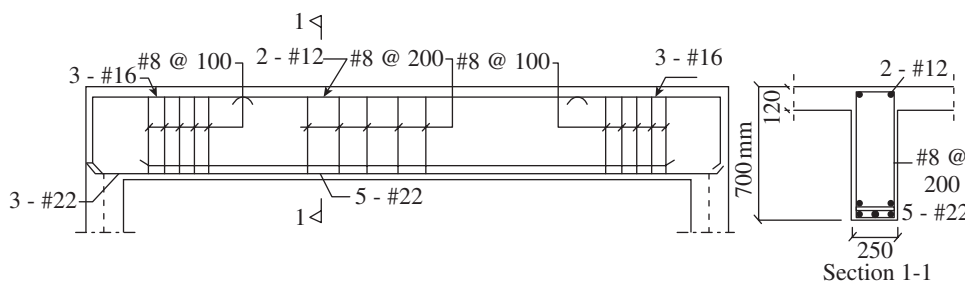


FIG. 2.7 Typical reinforcement details in a beam

A steel–concrete composite beam, as shown in Fig. 2.6(f), which consists of a steel wide-flange shape attached to a concrete floor slab, may also be employed in bridge structures.

Normally, RC beams are designed for bending moment and shear force. Longitudinal reinforcements are provided to resist the tension produced by bending moments and stirrups are provided to resist the shear forces, as shown in Fig. 2.7. In some situations, wherein the beams may also be subjected to torsion, the longitudinal and transverse stirrups jointly resist the torsional moments (see Chapter 8). Beams in frames subjected to lateral loads may have to be designed to resist reversal of moments and additional axial forces. Beams can be *singly* or *doubly reinforced*, depending on whether they are reinforced only in the tension zone or reinforced with steel in both the compression and tension zones, respectively. They can also be simply supported, continuous, or cantilevered. The design of beams is discussed in detail in Chapters 5, 6, and 8.

2.2.4 Slabs

Buildings and bridges require a floor slab to provide protection for occupants and for the vehicles to pass through, respectively. Concrete is the ideal material of choice for the slab because its mass and stiffness can be used to reduce deflections and vibrations of the floor system and to provide the required fire protection. Slabs can be simply supported, continuous, or cantilevered. Slabs are supported on beams, which are, in turn, supported by columns. They are classified in many ways such as *one-way*, *two-way*, *flat plates*, *flat slabs*, *waffle slabs*, and *ribbed (joist) slabs*. Details of floor and roof systems are provided in Section 2.3. The design of slabs is discussed in detail in Chapters 9–11.

2.2.5 Walls

Walls are vertical elements and are of masonry or RC construction. Walls may be of different types such as load-bearing walls, shear walls, retaining walls, and partition walls. When they support gravity loads in buildings, they are called *load-bearing walls* and when they resist lateral

loads due to wind or earthquake, they are called *shear walls*.

When walls are provided as non-structural dividing elements, their thickness is decided based on sound insulation and fire resistance requirements, and only nominal reinforcements are provided. In general, several walls or wall systems (walls connected monolithically, around the lift cores of buildings) placed symmetrically in the plan in two perpendicular directions resist the lateral loads (see Fig. 2.8a). A *coupled wall* is a form of shear wall, often found in practice, which consists of two or more shear walls in the same plane, connected at the floor levels by beams, as shown in Fig. 2.8(b). Load-bearing walls may have thickness in the range of 150 mm to 200 mm, whereas shear walls may be considerably thicker. They may be considered as a series of vertical strips and designed as a column, when designing vertical reinforcement. Slenderness effects must also be considered, as for columns. If the walls are subjected mainly to lateral bending, they may be designed as slabs.

Retaining walls are used to retain earth in a vertical position, at locations where abrupt changes occur in the ground levels. Designing any retaining wall requires knowledge of *lateral earth pressure*. The wall and the supporting foundation have to be designed for the lateral pressure exerted by soil, and checked for strength, overturning, and sliding. Retaining walls are of the following types (see Fig. 2.9):

1. *Gravity wall* (Fig. 2.9a): In this type of wall, stability is provided by its own weight. It is usually of masonry or plain concrete construction. Plain concrete wall is preferred only if the height is less than about 3 m.
2. *Cantilever retaining wall* (Fig. 2.9b): This is the most common type of wall and consists of a vertical stem and base slabs. The stem acts as a vertical cantilever, and the heel and toe slabs act as horizontal cantilevers. Reinforcements should be provided as shown in Fig. 2.9(b).
3. *Counterfort retaining wall* (Fig. 2.9c): When the height of the material to be retained is more than about 7–8 m, cantilever walls become uneconomical; hence, counterfort retaining walls are adopted. The counterforts behave like vertical cantilever beams with a T-section and varying depth. The vertical slab (stem) is designed with

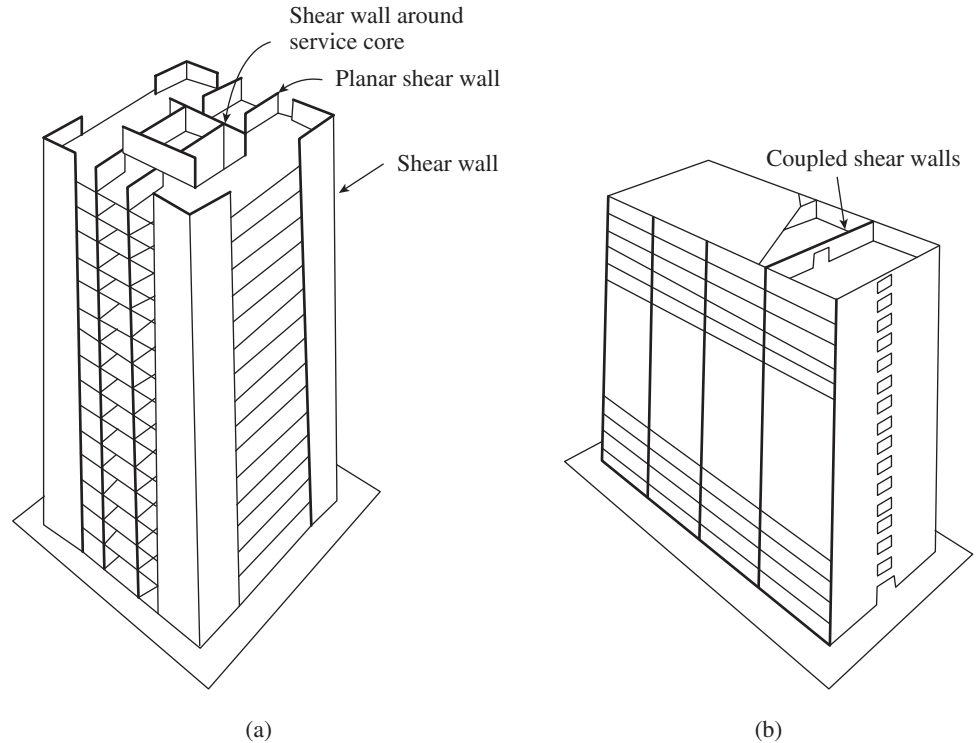


FIG. 2.8 Types of shear walls (a) Solid shear walls (b) Coupled shear walls

a fixed boundary condition on three sides and is free at the top.

4. *Buttress retaining wall* (Fig. 2.9d): A buttress wall is similar to a counterfort retaining wall, except that the transverse support walls are located on the side of the stem opposite the retaining material and act as compression struts. Hence, they are more efficient than the tension counterforts and are economical for heights over 7–8 m. However, counterforts are widely used as they are hidden behind the retained material, unlike the buttress walls that also occupy usable space in front of the wall.
5. *Basement wall* (Fig. 2.9e): The exterior walls at the basement of a building also act as retaining walls, with the top of the wall being restrained, due to the RC slab at the ground floor level. The wall may be designed as a propped cantilever.

The design of shear walls and retaining walls are discussed in detail in Chapter 16.

2.2.6 Trusses

For covering long-span industrial buildings, precast RC *trusses* with prestressed tie member, as shown in Fig. 2.10, are often employed. These types of trusses are often advantageous and economical compared to steel trusses for use in coastal areas, where corrosion is the main concern. The configuration of the truss depends on the general layout and span of the roof to be covered. Usually, high-strength concrete of grade M35–M60 is used for these trusses. The members of these trusses are subjected

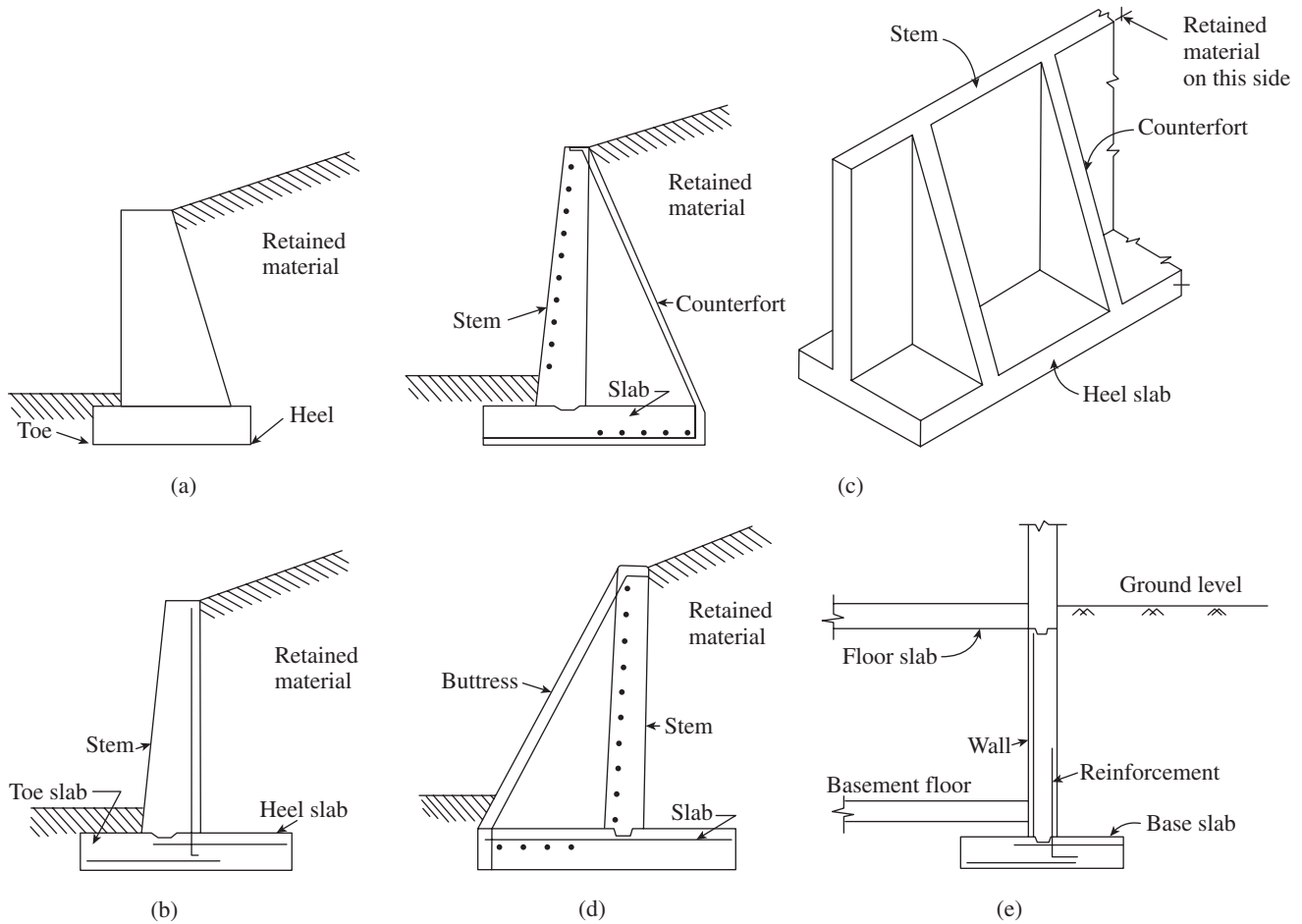


FIG. 2.9 Types of retaining walls (a) Gravity wall (b) Cantilever retaining wall (c) Counterfort wall (d) Buttress wall (e) Basement wall

to axial tension or compression, though the top chord may be subjected to additional bending if there are intermediate purlins.

The *bowstring configuration* is preferable and economical when compared to polygonal truss configuration. This is because the web members in bowstring configuration are subjected to forces of low magnitude, and the bottom tie is subjected to very high tension and is hence ideal for prestressing.

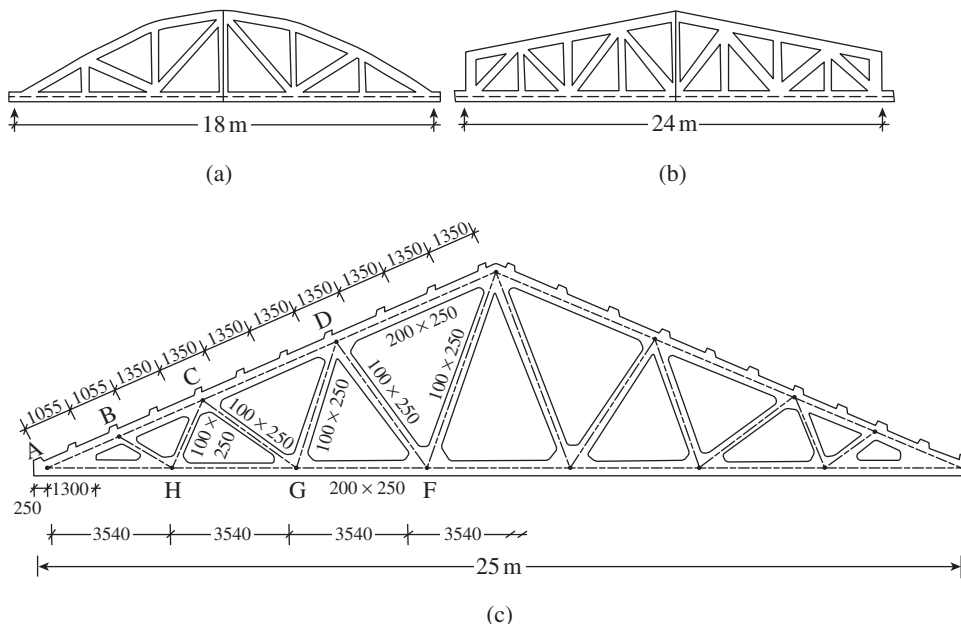


FIG. 2.10 Typical configuration of precast RC trusses with prestressed tie member (a) Bowstring configuration (b) Trapezoidal truss (c) Polygonal truss configuration with typical member sizes

The height of these trusses may be in the range of 1/7 to 1/9 of their span and the span is normally in the range of 15 m to 30 m. The width of members other than diagonals are kept in the range of 200 mm to 300 mm. The diagonal members can have a depth of 100 mm to 150 mm, as they will carry forces of less magnitude. Precast roof slabs of width 3 m are used as roof covering. Such trusses have been used extensively to cover industrial buildings in countries such as Russia, Poland, Slovakia, Serbia (erstwhile Yugoslavia), and Germany. The analysis of these trusses is

similar to any steel truss and is done assuming that the joints are hinged. It is important to consider the fabrication and erection loads as well as the initial stresses due to prestressing in the bottom chord member in the analysis. More details about the design and construction of these trusses may be found in Indian Standard (IS) 3201 (1988); Murashev, et al. (1976); and Krishna Raju (2007).

2.3 FLOOR AND ROOF SYSTEMS

The structural system of any building may be conveniently considered to be composed of two load-transmission mechanisms, namely *gravity load resisting* and *lateral load resisting* mechanisms, even though the two mechanisms, in reality, are inseparable. Moreover, although real buildings are three-dimensional structures, it is convenient to consider them to be composed of two-dimensional or planar subsystems in the vertical and horizontal planes. Now, let us consider a few *gravity load resisting floor systems*. Floors and roofs are elements in the horizontal plane, supported by beams and vertical elements such as walls or columns. They support dead loads such as their own weight, partition walls, and finishes, together with imposed loads. Floors are stiff in the horizontal plane and act as *diaphragms*. The factors that influence the choice of a floor system include architectural concerns, its role in resisting lateral loads, and speed of erection.

Reinforced concrete floor systems may be categorized as one-way or two-way depending on whether the slab spans in one direction between the supporting beams or walls, or spans in orthogonal directions. In both systems, continuity over interior supports may be advantageously considered by providing negative moment reinforcement in the slab at the interior supports.

2.3.1 Bearing Wall Systems

Bearing walls can be of different types such as (a) masonry walls, (b) confined masonry walls, (c) insulated RC walls, and (d) tilt-up concrete walls, which are briefly discussed in the following sub-sections.

Masonry Walls

The bearing wall systems, as shown in Fig. 2.1(a), consist of 100–200 mm thick floor slabs, which are supported on load-bearing masonry walls. The slabs may be square or rectangular, with spans ranging between 3 m and 7 m. This

system is adopted for buildings up to four floors. Though they may be economical, they do not provide freedom in plan layout; slabs should be placed on walls below and openings in walls are restricted. Further, it may be necessary to provide horizontal RC bands and vertical reinforcement in walls as per IS 4326 (see Fig. 2.11) to resist earthquake loads.

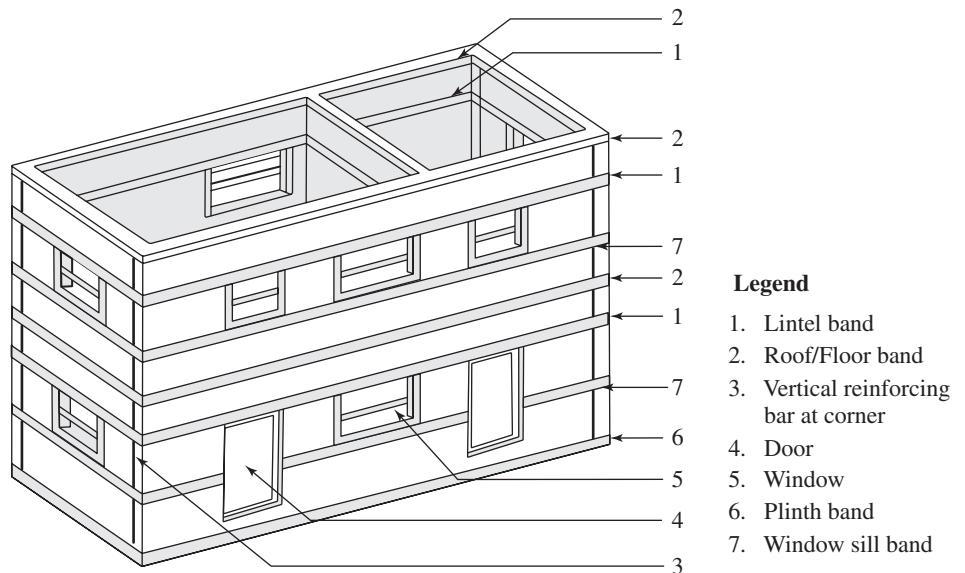


FIG. 2.11 Vertical and horizontal bands in masonry walls to resist earthquakes

Confined Masonry Construction

An innovative system, as shown in Fig. 2.12, called *confined masonry construction* offers an alternative to both unreinforced masonry and RC frame constructions. In fact, confined masonry construction has features of both these technologies. It consists of

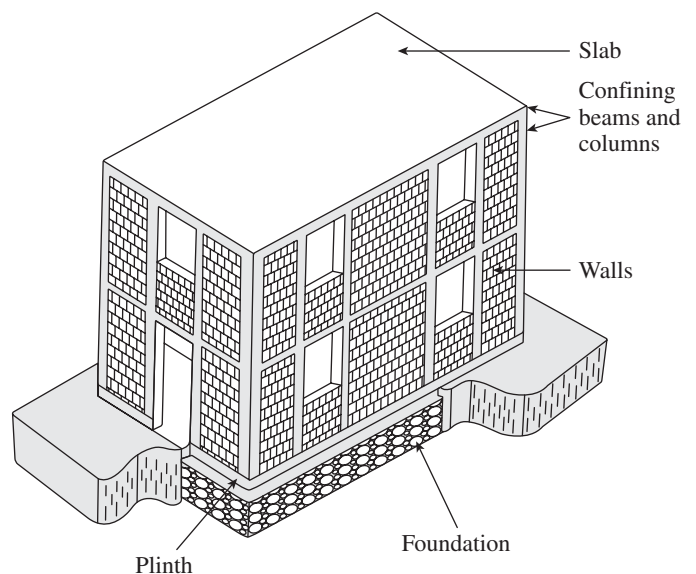


FIG. 2.12 Typical confined masonry construction

Source: Brzev 2007

Courtesy: NICEE, IIT Kanpur

masonry walls (made of either clay brick or concrete block units) and horizontal and vertical RC confining members built on all four sides of a masonry wall panel. Vertical members, called *tie-columns*, resemble columns in RC frame construction, except that they tend to be of a far smaller cross section. Horizontal elements, called *tie-beams*, resemble beams in RC frame construction. A very important feature of confined masonry is that tie-columns are cast-in-place after the masonry wall construction has been completed (Brzev 2007 and Schacher 2009).

In this system, the vertical load is resisted by the beam-column system and the lateral loads by the brick walls acting as boxed units. The size of columns is restricted to 230 mm × 230 mm and the columns are designed to carry only vertical loads. The beams are designed as continuous beams. This system is suitable for buildings with four to five floors.

Confined masonry construction is similar to *reinforced masonry*. In reinforced masonry, vertical reinforcement bars are placed in the hollow cores of hollow concrete or masonry blocks, which are subsequently grouted with a cement-based grout to protect the reinforcement from corrosion.

Insulated Reinforced Concrete Walls

When RC walls are used, *insulated concrete forms* (ICFs), made of polystyrene, can be used to achieve greater energy efficiency. Once the concrete is poured inside these forms, the forms stay in place as a permanent part of the wall assembly (see Fig. 2.13). There are many benefits in using insulated concrete forms. Once left in place, the forms provide not only a continuous insulation and sound barrier, but also a backing for drywall on the inside or brick on the outside. ICF walls are also more resistant to fire and provide up to four hours of fire-resistance rating. They also offer resistance to many pests such as rodents, termites, and insects. The form material on either side of the walls can easily accommodate electrical and plumbing installations.

These walls may have a uniform R-value of up to R-35 as well as 30–50 per cent less air infiltration than a conventional frame building. Studies show that buildings with ICF exterior walls require an estimated 44 per cent less energy to heat and 32 per cent less energy to cool than comparable wood-frame buildings.

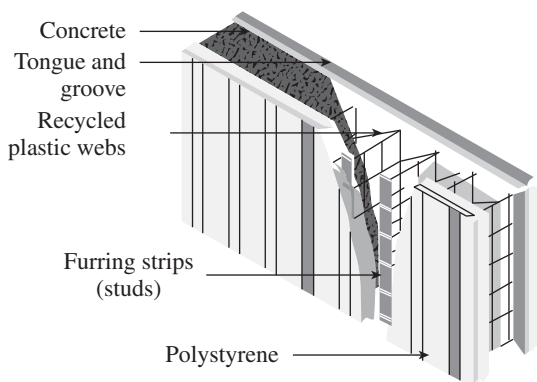


FIG. 2.13 Insulated RC walls

Moreover, ICFs do not produce any harmful gases that might affect indoor air quality. The material is very resource efficient and ICF construction generates very little waste, most of which can be recycled on the job site. The use of ICF can help projects earn several *Leadership in Energy and Environmental Design* (LEED) points. More details about ICF are available in Vanderwerf, et al. (1997).

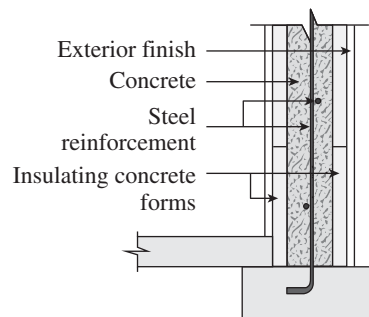
Tilt-up Concrete Wall Panels

Tilt-up (also called *tilt-slab* or *tilt-wall*) is a cost-effective and efficient type of construction method. In this method, concrete walls are horizontally cast on the building floor. After the concrete is cured and has attained sufficient strength, the forms are removed. A crane is used to lift or ‘tilt up’ the panel into a vertical position above the footings. The crew members help to guide the concrete panel into position and the crane sets it into place. The wall elements are braced into position until the remaining building structural components (roofs, intermediate floors, and walls) are secured (see Fig. 2.14). An experienced tilt-up crew can erect as many as 30 panels in a single day. Once all the panels are erected, the crew members apply finishes and patch any imperfections in the walls. Now, the roof system is installed and the work inside the building begins.

Tilt-up construction is a dominant method of construction throughout North America, several Caribbean nations, Australia, and New Zealand. However, this method is not yet popular in Europe and Asia. Tilt-up differs from prefabrication or plant cast construction in that all elements are constructed on the job site. This eliminates the size limitation imposed by transporting elements from a factory to the project site. More information on this type of construction may be found in TCA Manual 2006 or American Concrete Institute (ACI) Guide 2005.

2.3.2 One-way and Two-way Slab Systems

Irrespective of the supporting system (wall or beam), slabs are classified as one-way or two-way slabs depending on the way in which they bend. Thus, *one-way slabs*, supported by parallel walls or beams, bend in only one direction and



transfer their loads to the two opposite support walls or beams. Even when a rectangular slab is supported on all the four edges, the slab may be considered as a one-way slab if the length-to-breadth (L/B) ratio of the slab is equal to or greater than two. In this case, the slab spans predominantly in the direction parallel to the shorter edge, as shown in Fig. 2.15. The spanning direction in each case is shown by the double-headed arrow.



FIG. 2.14 Tilt-up wall construction
 Courtesy: Insul-Deck LLC, www.insuldeck.com

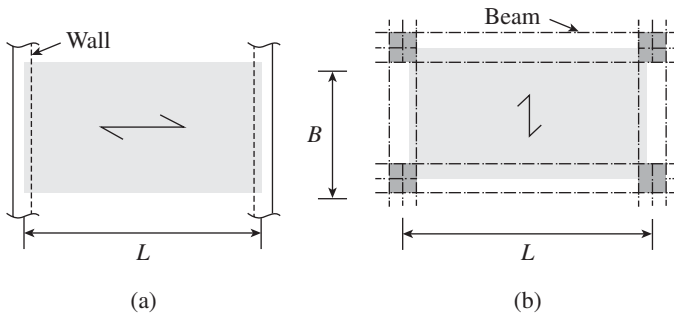


FIG. 2.15 Plan view of one-way slab (a) Supported on two opposite edges (b) Supported on all edges ($L/B > 2$)

A one-way slab is designed for the spanning direction alone; the main tension reinforcing bars of such slabs run parallel to the span. For the transverse direction, a minimum amount of shrinkage reinforcement is provided. The slab thickness is governed by deflection considerations and varies between 100mm and 150mm. One-way slabs may be economically provided up to a span of 3.60m. One-way slab action is assumed in a ribbed floor (slab with joist beams) made of precast double tee sections, in ribbed floor with integral beams, and also in hollow-block or -cored slabs (see Figs 2.16a and 2.17). The design of one-way slabs is elaborated in Chapter 9. Ambalavanan, et al. (1999) have analysed the cost effectiveness of alternate one-way floor or roof systems.

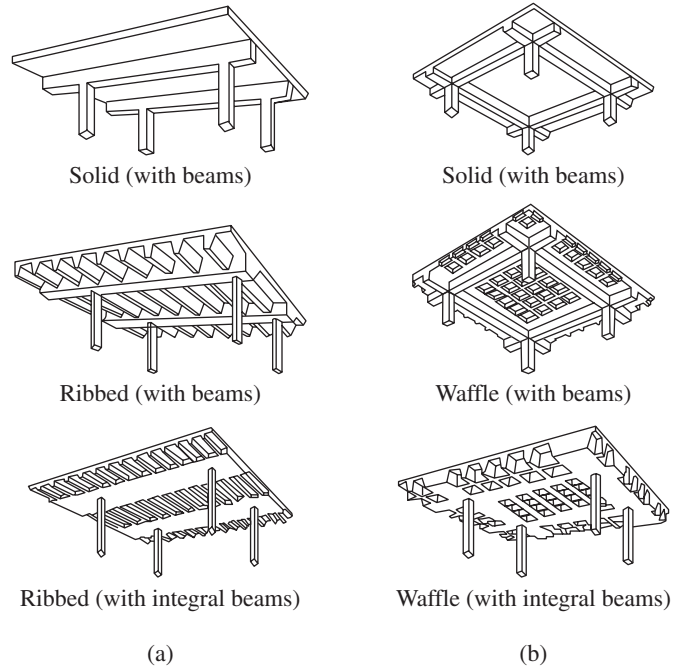


FIG. 2.16 Types of slab designs (a) One-way slabs (b) Two-way slabs

When the ratio of long side to short side of a slab is less than two, it is called *two-way slab* (see Fig. 2.16b). The panel will deflect in a dish- or saucer-like form under the action of external load, as shown in Fig. 2.18 and its corners will lift if the slab is not monolithically cast with the supports. Two-way slabs are designed to transfer their loads to all the four support walls. It should be noted that a slab supported on three edges

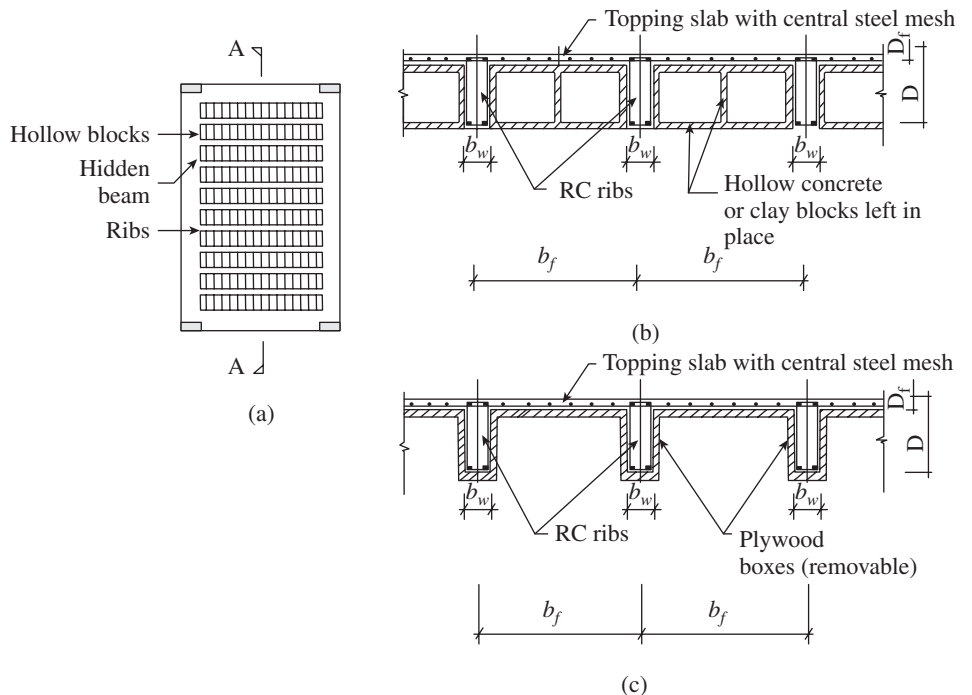


FIG. 2.17 One-way slab with hollow blocks (a) Plan of slab (b) Section A-A (c) Section A-A for slabs with only ribs

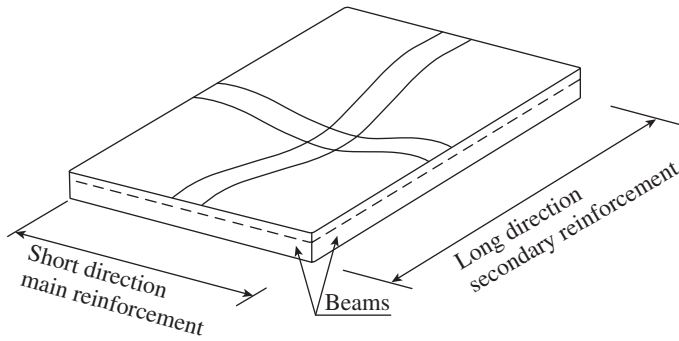


FIG. 2.18 Two-way slabs bend and deflect in double curvature

or two adjacent edges may also be considered as a two-way slab. The load gets divided in the two directions, depending on the ratio of the sides.

Two-way slabs are suitable for panel sizes up to $6\text{ m} \times 6\text{ m}$. The usual thickness of these slabs is in the range of 100 mm to 200 mm. In two-way slabs, the main bars are provided in both directions, mutually at right angles. Two-way slab behaviour is assumed in a waffle floor and in a waffle floor with integral beams (see Fig. 2.16b). In *waffle slabs*, also called *two-way ribbed slabs*, ribs are provided in both directions of span. The ribs are formed by using temporary or permanent shuttering, and the slab and joists are poured integrally over square, domed forms that are omitted around the columns to create solid panels. The *hollow-block floor* is constructed with blocks made of clay tile or lightweight concrete blocks (see Fig. 2.17). The principal advantage of these floors is the reduction of self-weight, which is achieved by removing a part of concrete below the neutral axis or, in the case of hollow-block

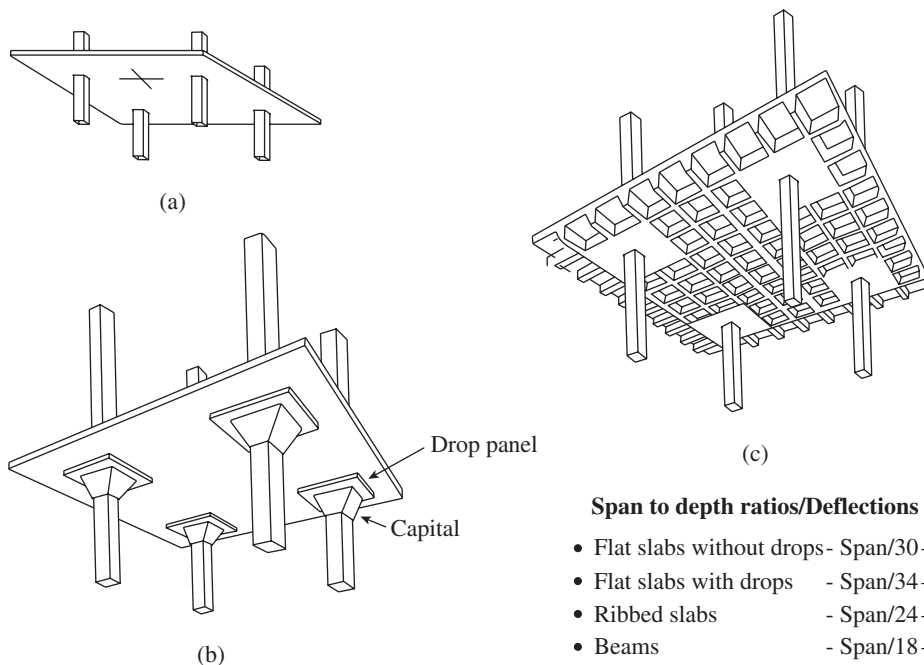


FIG. 2.19 Flat plates and flat slabs (a) Two-way flat plate (b) Two-way flat slab with column capitals/drop panels (c) Waffle flat slab

floor, replacing it with a lightweight material. Clause 30 of IS 456 deals with the ribbed, hollow block, or voided slabs. The design of two-way slabs is discussed in Chapter 10.

2.3.3 Two-way Flat Plates and Flat Slabs

Two-way flat plates, directly supported on columns, two-way flat slabs, supported by column capitals or drop panels, waffle flat slabs, and voided two-way flat plates are considered in this section (Fig. 2.19). In addition, the lift slab method of construction used to construct these types of slabs is also described.

Flat Plates

Flat plate floors are uniformly thick two-way reinforced slabs, supported by columns or masonry walls (Fig. 2.19a). They can be used for spans up to 8 m using RC and up to 11 m when post-tensioned. Due to its simplicity, it is the most economical floor system in terms of formwork and reinforcement. Its uniform thickness gives the architects freedom in locating the supporting columns and walls and provides exposed flat ceilings and minimum storey height. It also results in fast construction. However, these floors have low punching shear capacity (special shear reinforcements are needed around columns) and low stiffness for deflection. Often, beams are provided at the periphery of the floor to stiffen the free edges and to support brick walls. They are not recommended in earthquake zones. Shear walls may be provided to resist entire lateral loads due to earthquakes, so that the flat slab with column may resist only the vertical loads.

Flat Slabs

Two-way flat slabs are similar to flat plates, but have column capitals or drop panels, or both, at the top of the columns (Fig. 2.19b). The capitals increase the shear capacity of slabs, and the drop panels increase both the shear and negative moment capacities at the supports, where the effect is maximal. Thus, flat slabs are used for heavier loading and longer spans and require less concrete and reinforcement than flat plates. However, they need more formwork for capital and panels and take more time to construct than flat plates. They are used in spans that are square or nearly square. Flat slabs may be used for spans up to 10 m and imposed loads up to 7 kN/m^2 .

Waffle Flat Slabs

Waffle flat slabs have a square grid of closely spaced joists with filler panels over the columns, as shown in Fig. 2.19(c). Similar to ordinary waffle

CASE STUDY

The L'Ambiance Plaza Collapse

L'Ambiance Plaza was planned as a 16-storey building, with 13 storeys of apartments and 3 levels of parking, at Bridgeport, Connecticut. It consisted of two offset rectangular towers, 19.2 m by 34 m each, connected by an elevator. These towers were being constructed by the lift slab method. Floor and roof slabs were two-way, unbonded, post-tensioned flat plates. On 23 April 1987, during construction, the entire structure suddenly collapsed, killing 28 workers and injuring many more. At the time of collapse, slabs 3, 4, and 5 of the east tower had been placed into final position, and slabs 9, 10, and 11 for the west tower had just been lifted. The entire collapse took only five seconds. The collapse was one of the worst disasters in the USA. This was the first serious failure of a lift slab structure, a system that had been in use for over 40 years.

An unusually prompt legal settlement prematurely ended all investigations of the collapse. Consequently, the exact cause of the collapse has never been established. The building had a number of deficiencies, any one of which could have triggered the collapse. The report by the National Bureau of Standards (NBS) concluded that an overloaded steel angle welded to a shear head arm channel deformed, causing the jack rod and lifting nut to slip out, thereby starting the collapse. Failure was possibly due to high concrete stresses on the floor slabs by the placement process, resulting in cracking of the slab concrete and ending in a punching shear failure. Moreover, the ACI code states that 'a minimum of two tendons shall be provided in each direction through the critical shear section over the columns'. This was not followed in the L'Ambiance Plaza structure.

While buildings constructed by the lift slab method are stable once they are completed, they may be unstable during construction, if the following measures are not taken during construction (Martin www.eng.uab.edu; Cuoco, et al. 1992):

- Provision of temporary lateral bracing during all stages of construction
- Provision of redundancies in concrete punching shear and connections in the structure
- Provision of temporary posts to support the concrete slab until it is completely attached to the column
- Provision of sway bracing (cables that keep the stack of floors from shifting sideways). Though this is required, it was not used in L'Ambiance Plaza.



Collapse of L'Ambiance Plaza
(Courtesy: The National Institute of Standards and Technology,
US Department of Commerce)

slabs, lightweight concrete blocks, on temporary or permanent shuttering, may be used in their construction and domed forms are omitted around the columns to create solid panels. The concrete in the ribs and slabs are poured integrally, creating aesthetic soffits, with up to 750 mm² and up to 500 mm deep pockets.

Lift Slab Construction

Lift slab construction is a method of erecting post-tensioned RC floor and roof slabs. This technique was invented in the USA by Raymond A. Burkland in the late 1940s. In this system, flat roof and flat slabs are cast one on the other at ground level around the column. Special lifting collars or shear heads are provided in the slabs at the columns. Bond-breaking compounds are applied between slabs to separate them. The slabs are cured to reach the prescribed strength; they are then pulled up into their respective positions by using powerful hydraulic jacks mounted on top of the columns to lift the slabs. More details about the lift slab method can be found in Subramanian (1999).

Voided Two-way Flat Plates

A relatively new technology of voided two-way flat plates has been developed by the Swiss firm Cobiax (www.cobiax.ch)

and already used in the construction of office buildings in Switzerland, Germany, Austria, and the UK, with floor spans up to 17 m and overall slab thicknesses up to 600 mm. In these slabs, the overall weight of slabs are reduced by 35 per cent by incorporating industrially produced spherical hollow shells made from recycled polyethylene between the top and bottom steel reinforcement, as shown in Fig. 2.20. The reduced slab weight also results in reduction in the weight of columns and foundations. The concept is similar to the waffle slab, that is, removing concrete near the neutral axis which is stressed less.

The plastic modules are placed on the lower reinforcing mat, on top of which the upper reinforcing mat is then placed. In the vicinity of the column, the slab is designed to resist punching shear stresses using a solid cross section, with additional shear reinforcement as required to maintain a flat soffit throughout the slab. Voided slabs can also be coupled with post-tensioning to minimize dead load deflections. Post-tensioning results in an almost 'crack-free' cross section, making the slab stiffer and reducing the deflection (since the full cross-sectional rigidity is available to resist the applied loads).

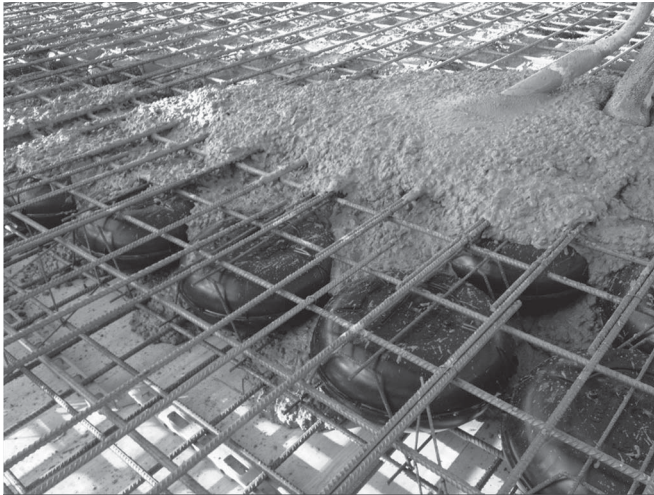


FIG. 2.20 Voided two-way flat slabs

Courtesy: Cobiax Technologies AG, Zug, Switzerland

2.3.4 Grid Floors

Grid floor consists of beams spaced at regular intervals in perpendicular directions, cast monolithic with the concrete slab. They are suitable for large panels with spans greater than 10 m and are more often used as floor or roof systems for large assembly halls and auditoriums. Grid floors offer large column-free areas and are ideally suited for concealed architectural lighting; the coffered soffits are aesthetically superior to other floor systems. The layout of grid floors is shown in Fig. 2.21. Grids with diagonal members are called diagrids. It is more economical to space the grid beams at larger intervals, in the range of 2 m to 2.5 m. It should be noted that the behaviour of grid slabs is different from that of ribbed slabs, as the torsional rigidity is negligible in grids.

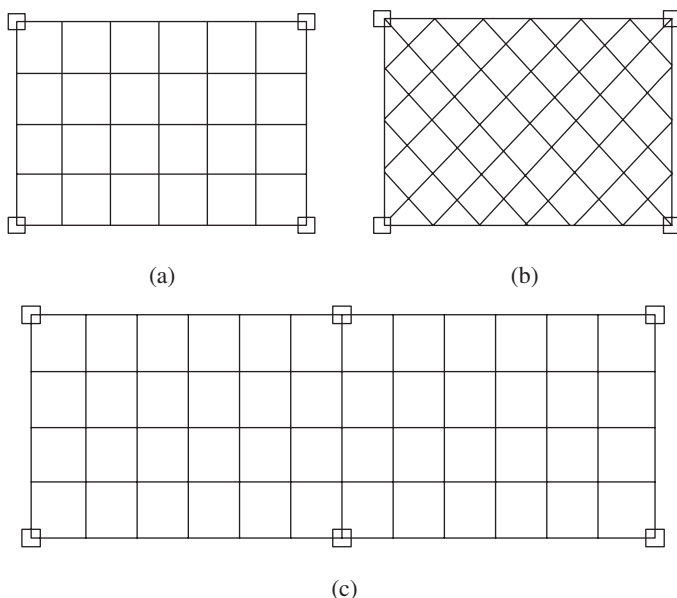


FIG. 2.21 Layout of grid floors (a) Rectangular grid (b) Diagrid (c) Continuous grid

Large grid floors may be analysed by the following methods:

1. Method based on Timoshenko's anisotropic plate theory
2. Computer programs based on stiffness matrix method

More detail on grids may be found in the National Buildings Organization (1968) book on grids and Varghese (2006).

2.3.5 Composite Floors

Composite floors consisting of profiled steel decking and in situ RC slabs are often used in bridge construction and commercial and industrial buildings. This type of construction is structurally efficient as it exploits the tensile resistance of steel and the compressive resistance of concrete. The steel decking acts as permanent formwork to the concrete and, after the concrete gains sufficient strength, acts together compositely to resist the applied loads. The composite interaction is achieved by the attachment of shear connectors to the top flange of the beam. The embossments in the decking provide additional composite action. The beam is often made of hot rolled or fabricated steel sections. The studs are normally welded to the beam through the decking, using *through-deck* welding, prior to placing the concrete. Only minimal wire mesh reinforcement is required to resist shrinkage or temperature movements and to improve fire resistance (see Fig. 2.6f).

Composite slabs are usually shallower than conventional RC slabs, which leads to a reduction in the overall construction depth. Moreover, the use of steel decking as a working platform speeds up the construction process. The decking also acts as an effective lateral restraint for the beams, increasing their load-carrying capacity. More than 40 per cent of all new multi-storey buildings in the UK and the USA use composite floor construction. The behaviour and design of such composite slabs are outside the scope of this book and interested readers may consult Oehlers and Bradford (1999) and Nethercot (2003).

2.4 PRECAST AND PRESTRESSED CONCRETE BUILDINGS

Common precast and prestressed concrete products are shown in Fig. 2.22. Double tee and hollow-core slabs are the most widely used building products (PCI Design Handbook 2004).

A *hollow-core slab*, also known as a voided slab or hollow-core plank, is a precast slab of prestressed concrete typically used in the construction of floors in multi-storey apartment buildings. The precast concrete slab has tubular voids extending over the full length of the slab, typically with a diameter slightly smaller than the thickness of the slab. This makes the slab much lighter than a massive floor of equal thickness or strength.

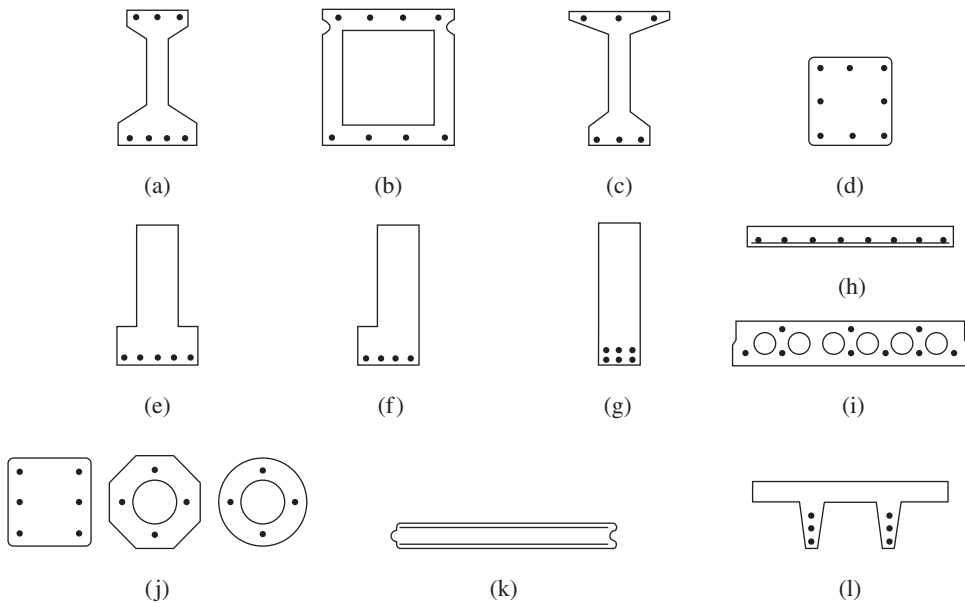


FIG. 2.22 Common precast and prestressed concrete products (a) I-beam (b) Box beam (c) Bulb tee (d) Column (e) Inverted tee beam (f) Ledger beam (g) Rectangular beam (h) Slab (i) Hollow-core slab (j) Pile sections (k) Sheet pile (l) Double tee

The most common floor and roof elements employed are 1220 mm wide, 200 mm deep untopped hollow-core units. These slabs can span up to 9 m without intermediate supports. Longer spans can be achieved by using 250 mm or 300 mm deep hollow-core units (PCI Manual 1998).

Precast or prestressed double tees are ideal for floor and roof systems requiring medium to long, uninterrupted spans and heavy load-carrying capabilities. Double tees come in a variety of widths and depths to suit different spans and loading conditions. These are considered for spans and loads that exceed the capacity of hollow-core slabs. More details about these precast or prestressed products may be obtained from PCI Design Handbook (2004). The Central Building Research Institute, Roorkee, and the Structural Engineering Research Centre, Chennai, have also developed several precast concrete products. Interested readers may contact them for further details. B.G. Shirke Construction Technology Private Limited has also pioneered and patented a system using partial precast structural components such as dense concrete hollow-core columns, dense concrete partially precast beams, lintels, and staircases, and Siporex blocks and slabs. Provisions for the design and construction of floor and roof with precast RC planks and joists are given in IS 13994 and with channel unit are given in IS 14215.

2.5 LATERAL LOAD RESISTING SYSTEMS

In the structures constructed at the beginning of the 20th century, structural members were primarily assumed to carry the gravity loads. However, the advances in structural engineering analysis and design procedures as well as the invention of high-strength materials have resulted in tall

structures with reduced building weight and increased slenderness. It has also become more important to develop systems for these buildings that will effectively resist lateral loads such as wind and earthquake. As a general rule, all other things being equal, the taller the building, the more necessary it is to identify the proper structural system for resisting the lateral loads (Subramanian 2004). Currently, there are many structural systems that can be used for the lateral resistance of tall buildings (El Nimeiri and Khan 1983).

In 1969, Fazlur Rahman Khan classified structural systems for buildings in relation to their heights and later upgraded them as shown in Fig. 2.23 (Ali 2001). According to him, feasible structural systems are rigid frames, shear walls, interactive frame–shear wall combinations, and the various other tubular systems.

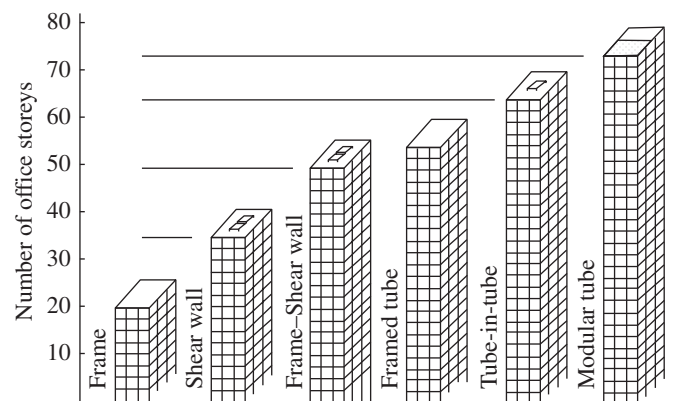


FIG. 2.23 Classification of structural systems by Fazlur Kahn

Source: Subramanian 1995

Taking into consideration the systems reported in the literature, the following classification has been identified for the structural systems of tall concrete buildings (Taranath 1998 and Varyani 1999):

1. Rigid frame systems
2. Shear-walled frame systems
3. Outrigger and belt truss systems
4. Framed-tube systems
5. Braced-tube systems
6. Bundled-tube systems

These systems are briefly discussed in the following subsections.

2.5.1 Rigid or Moment-resisting Frames

Rigid or moment-resisting frame systems for resisting lateral and vertical loads have been in practice for a number of years. Rigid or moment-resisting frames are structures having the traditional beam-column framing. The joints in these frames are considered rigid, because it is assumed that beam-to-column connections have enough rigidity to hold the nearly unchanged original angles between intersecting components. Owing to the monolithic behaviour and hence the inherent stiffness of the joint, rigid framing is ideally suitable for RC buildings.

Rigid frames carry the gravity loads that are imposed on the floor system. The floors also function as horizontal diaphragms that transfer lateral forces to the girders and columns. In addition, the girders or beams resist high moments and shears at the ends of their lengths, which are, in turn, transferred to the column system. For a rigid frame, the strength and stiffness are directly proportional to the size of the beam and the column and inversely proportional to the column spacing. As a result, columns and beams can become quite large as the height of the building increases. In order to obtain an efficient frame action, closely spaced columns and deep beams at the building exterior must be used. Especially for the buildings in seismic zones, special attention should be given to the design and detailing of joints, since rigid frames are more ductile and vulnerable to severe earthquakes when compared to braced steel or shear-walled structures. Rigid frame systems are not efficient for buildings with more than 20 storeys, because lateral deflection due to the bending of columns causes excessive drift. Many of the buildings built in India are of this type (see Fig. 2.24).



FIG. 2.24 Typical rigid, jointed RC framed buildings under construction in Chennai, India

Courtesy: Akshaya Homes

2.5.2 Shear-walled Frame Systems

Systems composed of shear walls alone or interacting with the rigid frames may be considered as an improvement of the

rigid frame system. *Shear walls*, first used in 1940, are vertical, cantilevered walls, which resist lateral wind and seismic loads acting on a building transmitted to them by the floor diaphragms. RC shear walls have the ability to dampen vibration and provide mass to a building. Shear walls may be constructed in a variety of shapes such as rectangular, C- or L-shaped, circular, curvilinear, or box type. Shear walls often exist as core walls surrounding internal services such as elevators and stairwells. When carefully planned, these walls may be used as partitions in a structure serving as both gravity and lateral load resisting systems. Wall thickness varies from 140 mm to 500 mm, depending on the number of storeys and thermal insulation requirements. In general, shear walls are continuous throughout the building height. They are usually provided along *both* length and width of buildings. They could be placed symmetrically along one or both directions in plan. Shear walls are more effective when located along exterior perimeter of the building; such a layout increases the resistance of the building to twisting.

The *tunnel form construction* method may be used to cast the walls and the slabs in a single operation using specially designed half-tunnel-steel forms (upside down ‘U’ shape), thereby reducing the construction time significantly. Since shear walls carry *large* horizontal earthquake forces, the overturning effects on them are large. Thus, design of their foundations requires special attention. Shear walls may be effective for buildings with up to 35 storeys.

A combined system called *shear wall-frame system* was first considered by Fazlur Khan. In this system, a central core or dispersed shear walls interact with the remaining beam-column or slab-column framing in the building through rigid floor diaphragms (see Fig. 2.25). The columns are designed to primarily carry the *gravity* loads and the shear walls are designed to carry the lateral loads. These systems are stiffer when compared to the rigid frame system and can be used for buildings with up to 50 storeys. The 88-storeyed Petronas Towers, Malaysia, completed in 1998 (tallest buildings in the world from 1998 to 2004 until surpassed by Taipei 101, but remain the tallest twin buildings in the world), also utilized this system in composite construction. The City Hall of Toronto, Ontario, Canada, designed by the Finnish architect Viljo Revell and engineered by Hannskarl Bandel in 1965, has curved shear walls (Fig. 2.25b).

As mentioned in Section 2.2.5, shear walls that are perforated with openings are called *coupled walls*. These walls act as isolated cantilevered walls connected by coupling beams (also called spandrel beams) designed for bending and shear effects. When designed in a ductile manner,



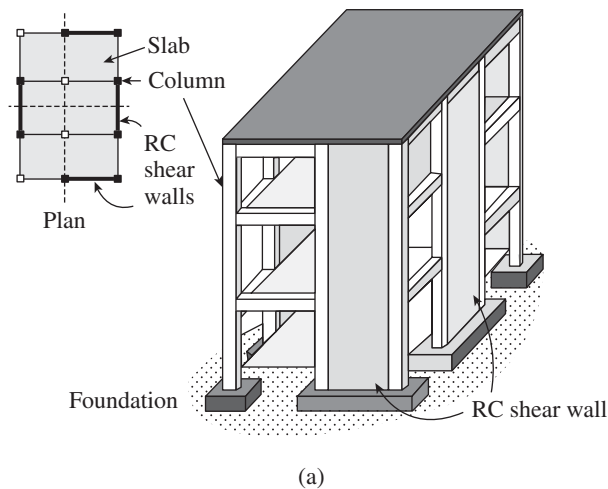


FIG. 2.25 Typical shear wall-frame system (a) Plan (b) The City Hall of Toronto, Ontario, Canada

these beams may act as fuses and are used to dissipate seismic energy. Coupling beams are often provided with diagonal reinforcement to ensure ductile seismic response. More details about the design of shear walls are provided in Chapter 16.

2.5.3 Outrigger and Belt Truss Systems

Outrigger systems have been historically used by sailing ships to help resist the wind forces in their sails, making the tall and slender masts stable and strong. The core in a tall building is analogous to the mast of the ship, with outriggers acting as the spreaders and the exterior columns like the stays (Ali and Moon 2007). As an innovative and efficient structural system, the outrigger system comprises a central core, including either braced frames

or shear walls, with horizontal ‘outrigger’ trusses or girders connecting the core to the external columns. Furthermore, in most cases, the external columns are interconnected by exterior belt girder, as shown in Fig. 2.26(a). If the building is subjected to horizontal loading, the rotation of the core is prevented by the column-restrained outriggers. The outriggers and belt girder are often one or two storeys deep to provide adequate stiffness. Hence, they are generally positioned at plant levels to reduce the obstruction created by them. Multi-storey outriggers have better lateral resistance than single-storey outrigger structures and thus better efficiency in the structural behaviour. However, the lateral stiffness is enhanced only marginally by each extra outrigger storey (Günel and Ilgin 2007).

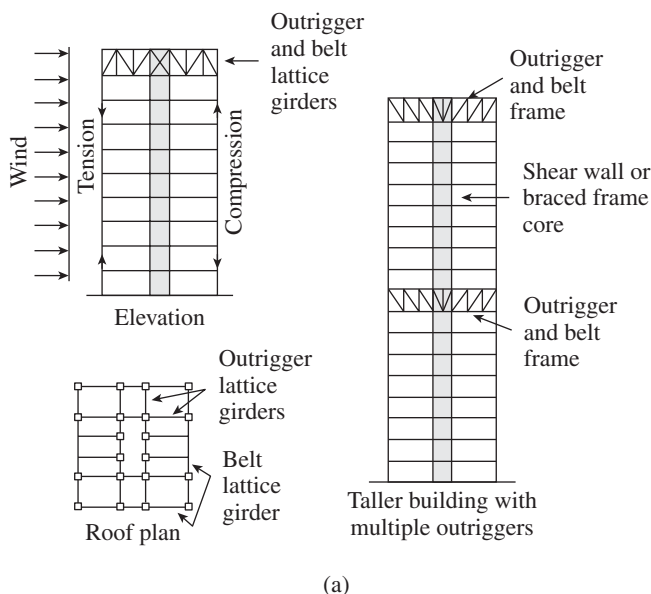


FIG. 2.26 Outrigger and belt truss system (a) Typical plan and section (b) Jin Mao Building, Shanghai, China (Photo: Mates II) (c) Taipei 101, Taipei (Photo: Connor Powell)

Outrigger structures can be used for buildings with over 100 storeys. The 421 m tall, 88-storey Jin Mao Building, Shanghai, China, designed by the Chicago office of Skidmore, Owings, and Merrill, completed in 1999 (Fig. 2.26b), and the 509.2 m tall, 101-storey Taipei 101, Taipei, completed in 2004 (Fig. 2.26c), are excellent examples of this system. The 88 floors of the Jin Mao Building are divided into 16 segments. The tower is built around an octagon-shaped concrete shear wall core surrounded by eight exterior composite super columns and eight exterior steel columns. Three sets of 8 two-storey high outrigger trusses connect the columns to the core at six of the floors to provide additional support.

2.5.4 Framed-tube Systems

The framed-tube structural system was invented by Fazlur Rahman Khan in the 1960s. A framed tube consists of closely spaced perimeter columns interconnected by deep spandrels, so that the whole building works as a huge vertical cantilever tube to resist overturning moments. Window openings usually cover about 50 per cent of the exterior wall surface. Larger openings such as retail store and garage entries are accommodated by large transfer girders, albeit disrupting the tubular behaviour of the structure locally at that location. It is an efficient system to provide lateral resistance with or without interior columns. The exterior tube carries all the lateral loading. Gravity loading is shared by the tube and the interior columns or shear walls, if any. Besides its structural efficiency, framed-tube buildings leave the interior floor plan relatively free of core bracing and heavy columns, enhancing the net usable floor area, as a result of the perimeter framing system resisting the entire lateral load

(Günel and Işın 2007). However, the closely spaced perimeter columns may hinder views from the interior of the building. The 43-storey DeWitt-Chestnut apartment building in Chicago completed in 1965, designed by Fazlur Rahman Khan, and shown in Fig. 2.27, is the first RC building in the world to implement the framed-tube system, which was later used in the steel-framed World Trade Center, New York.

Several configurations of tubes exist, namely framed, braced, tube-in-tube, and bundled tubes, and are discussed in the following sub-sections.

2.5.5 Braced-tube Systems

By adding multi-storey diagonal bracings to the face of the tube, the rigidity and efficiency of the framed-tube can be improved (Fig. 2.28a). The resulting system called *braced-tube system*, or *trussed-tube system*, could be utilized for greater heights and allows larger spacing between the columns. The bracing helps the perimeter columns to act together in carrying both gravity and horizontal wind loads. Its unique feature is that the members have axial but little or no flexural deformation; it also eliminates the risk of the corner columns being stressed excessively. Although braced-tube system is more effective than framed tube, it is not widely used because of its problems in curtain wall detailing.

New York's 50-storey-high 780 Third Avenue building was the first RC building to use this concept in 1985. The 174 m tall, 60-storey Onterie Center, Chicago, designed by Fazlur Rahman Khan of Skidmore, Owings, and Merrill, and completed in 1986, is the first concrete high-rise building in the world to use diagonal shear walls at the building perimeter. The diagonal bracing is achieved by blocking out

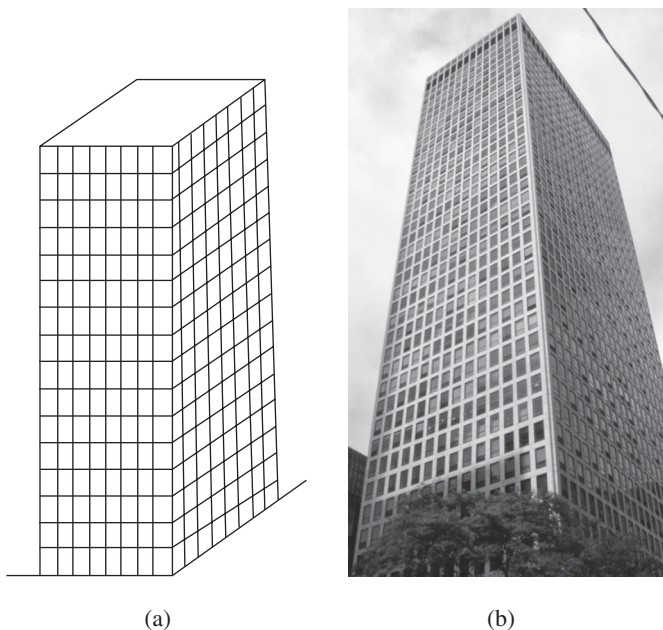


FIG. 2.27 Framed-tube system (a) Typical framing (b) DeWitt-Chestnut apartment building in Chicago

Courtesy: Anuthama Srisailam

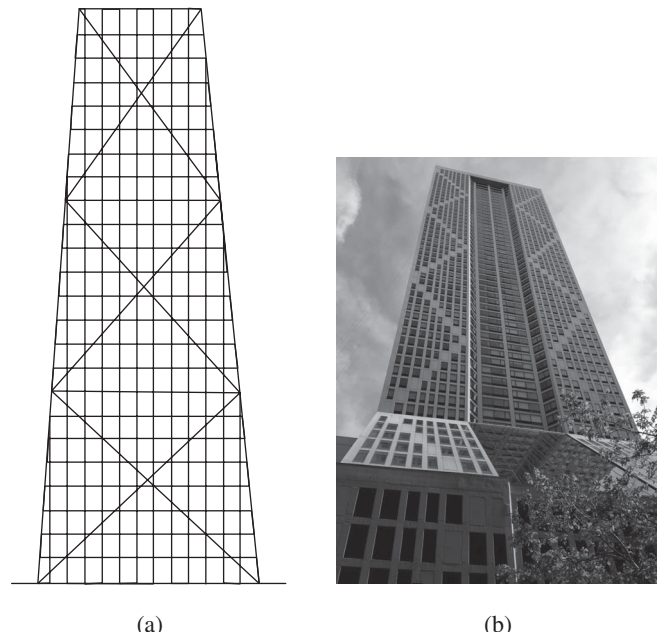


FIG. 2.28 Braced-tube systems (a) Typical bracing (b) Onterie Center, Chicago

Courtesy: Anuthama Srisailam

the windows along the facades by filling them with concrete (Fig. 2.28b).

2.5.6 Tube-in-tube and Bundled-tube Systems

When the building dimension increases in both horizontal and vertical directions, a single framed tube may not have adequate structural efficiency; the wider the structure is in plan, the less effective is the tube. In such cases, *bundled tube*, also known as *modular tube*, with larger spaced columns is preferred. It is nothing but a cluster of tubes interconnected with common interior panels to generate a perforated multi-cell tube, as shown in Fig. 2.29(b).

The stiffness of a framed tube can also be enhanced by using the core to resist part of the lateral load resulting in a *tube-in-tube* system, as shown in Fig. 2.29(a). The floor diaphragm connecting the core and the outer tube transfer the lateral loads to both the tubes. The core itself could be made up of a solid tube, a braced tube, or a framed tube. It is also possible to introduce more than one tube inside the perimeter tube. The 50-storey, 218 m tall One Shell Plaza in Houston, Texas, was built in 1971 using the tube-in-tube concept.

A bundled-tube system, shown in Fig. 2.29(b), reduces the *shear lag* problem, which is more serious if a single tube is used. Shear lag is a phenomenon in which the stiffer or more rigid regions of the structure or structural component attract more stresses than the more flexible regions. Shear lag causes stresses to be unevenly distributed over the cross section of the structure or structural component.

The analysis of a tube structure may be carried out using a space frame program (Subramanian 1995; 2007). The main feature exhibited in the analysis for horizontal load is the drop-off in load taken by the columns in the flange faces. This is caused by shear lag in the beam-column frame, as shown in Fig. 2.29(c). The use of simple beam theory will result in uniform stress distribution as shown in Fig. 2.29(c).

Since the bundled-tube design is derived from the layout of individual tubes, the cells can be of different shapes such as triangular, hexagonal, or semicircular units. Moreover, by terminating a tube at any desired height, it is possible to have setbacks in the elevation, without sacrificing structural stiffness. The disadvantage, however, is that the floors are divided into tight cells by a series of columns that run across the building width (Günel and İlgin 2007).

The 57-storey, 205 m tall One Magnificent Mile building in Chicago completed in 1983 is an example of RC bundled tube, designed by Skidmore, Owings, and Merrill and is one of the last buildings engineered by Khan. The structural system of this building consists of three hexagonal tubes bundled together (Fig. 2.29d). The tied tubes give the building added stiffness. As in the Sears Tower (which is also a bundled tube made of structural steel members), the tubes terminate at different heights, as the gravity loads decrease.

The 62-storey, 257 m tall One Peachtree Center, built in 1991 in Atlanta, Georgia, is also a bundled tube, with three different strengths of concrete (58.6 MPa, 68.9 MPa, and 82.7 MPa) being used in its columns and shear walls.

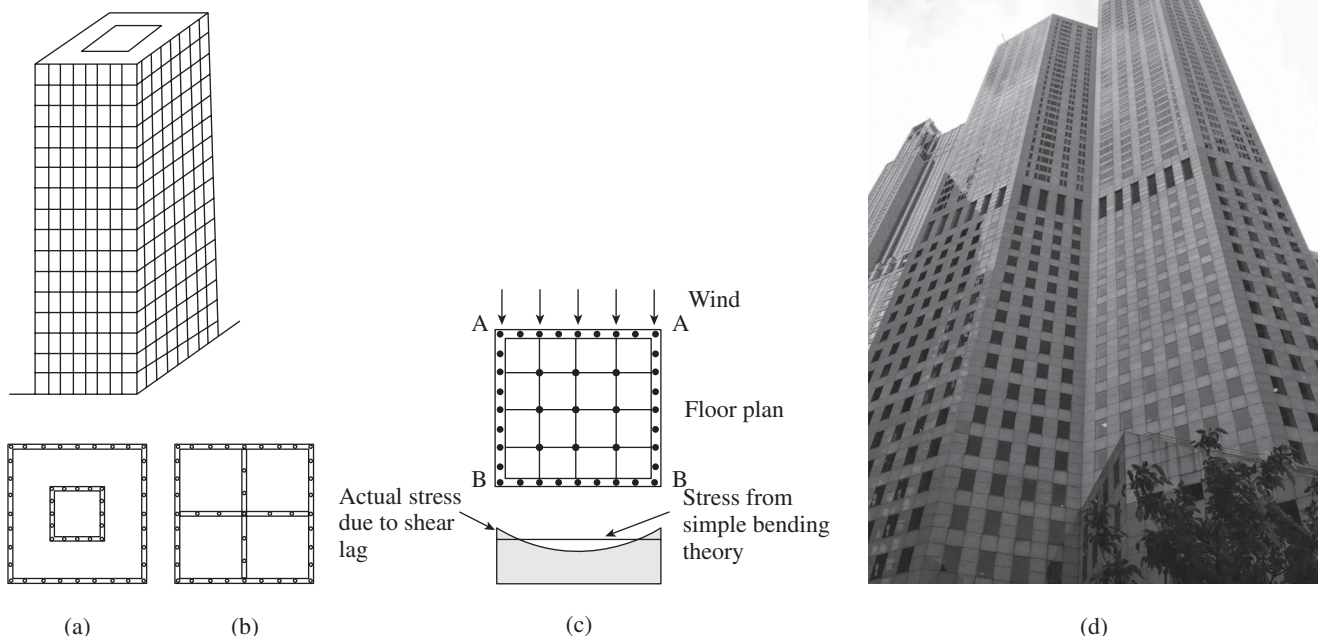


FIG. 2.29 Tube systems (a) Tube-in-tube system (b) Bundled-tube systems (c) Stress distribution (d) One Magnificent Mile, Chicago

Courtesy: Anuthama Srisailam

2.5.7 Diagrid Systems

Recently, there has been a renewed interest among architectural and structural designers of tall buildings in *diagrid systems*, which use perimeter diagonals for structural effectiveness and lattice-like aesthetics. The difference between braced-tube structures and diagrid structures is that almost all the conventional vertical columns are eliminated in the latter (see Figs 2.30a and b). This is possible because the diagonal members in diagrid structural systems can carry gravity loads as well as lateral forces due to their triangulated configuration in a distributive and uniform manner (Ali and Moon 2007). Compared with conventional framed tubular structures without diagonals, diagrid structures are much more effective in minimizing shear deformation. This is because they carry shear by the axial action of diagonal members, whereas conventional tubular structures carry shear by the bending of the vertical columns and horizontal spandrels (Moon, et al. 2007).

Diagrid structures provide both bending and shear rigidity. Thus, unlike outrigger structures, diagrid structures do not need high shear rigidity cores because shear can be carried by the diagrids located on the perimeter, even though super-tall buildings with a diagrid system can be further strengthened and stiffened by engaging the core, generating a system similar to a tube-in-tube (Moon, et al. 2007). The optimum angle for the diagonals was found to be 63° for up to 40–60 storeys and 69° for 60–100 storeys (Moon, et al. 2007).

The COR Building in Miami (see Fig. 2.30c) designed by Chad Oppenheim Architecture and Ysrael Seinuk of YAS Consulting Engineers and the O-14 Building in Dubai (see Fig. 2.30d) designed by RUR Architecture employ RC diagrids as their primary lateral load resisting systems. Due to the properties of concrete, the structural diagrid patterns, which are directly expressed as building façade aesthetics, are more fluid and irregular in these buildings and are different from the explicit and pristine features of steel diagrids (Ali and Moon 2007).

2.5.8 Other Systems

For the 828 m tall, 162-storey Burj Khalifa (the world's tallest structure, which was completed in October 2009) in Dubai, United Arab Emirates, designers Skidmore, Owings, and Merrill utilized a bundled shear wall system, which is also called *buttressed core system*. In this system, as shown in Fig. 2.31, each wing, with its own high-performance concrete corridor walls and perimeter columns, buttresses the other via a six-sided central core or hexagonal hub. This resulted in a tower that is extremely stiff both laterally and torsionally (Subramanian 2010).

Other types of lateral load resisting systems include *space trusses*, *super frames*, and *exoskeleton*. These have been occasionally used for tall buildings. Space truss structures are modified braced tubes with diagonals connecting the exterior to the interior. In space trusses, some diagonals penetrate the interior of the building. Examples include the Bank of China Tower of 1990 by I.M. Pei in Hong Kong. More details of such systems may be found in Ali and Moon (2007) and Moon, et al. (2007).

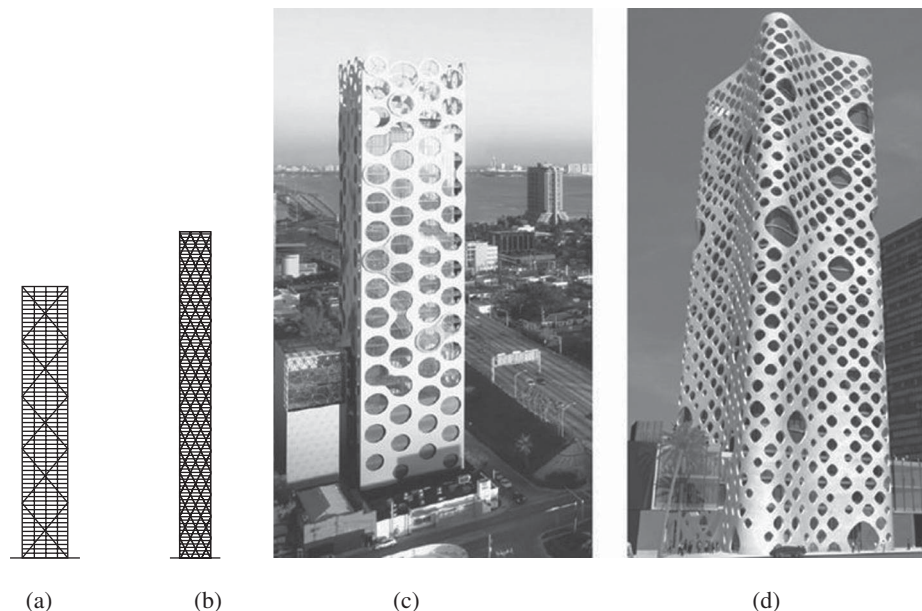


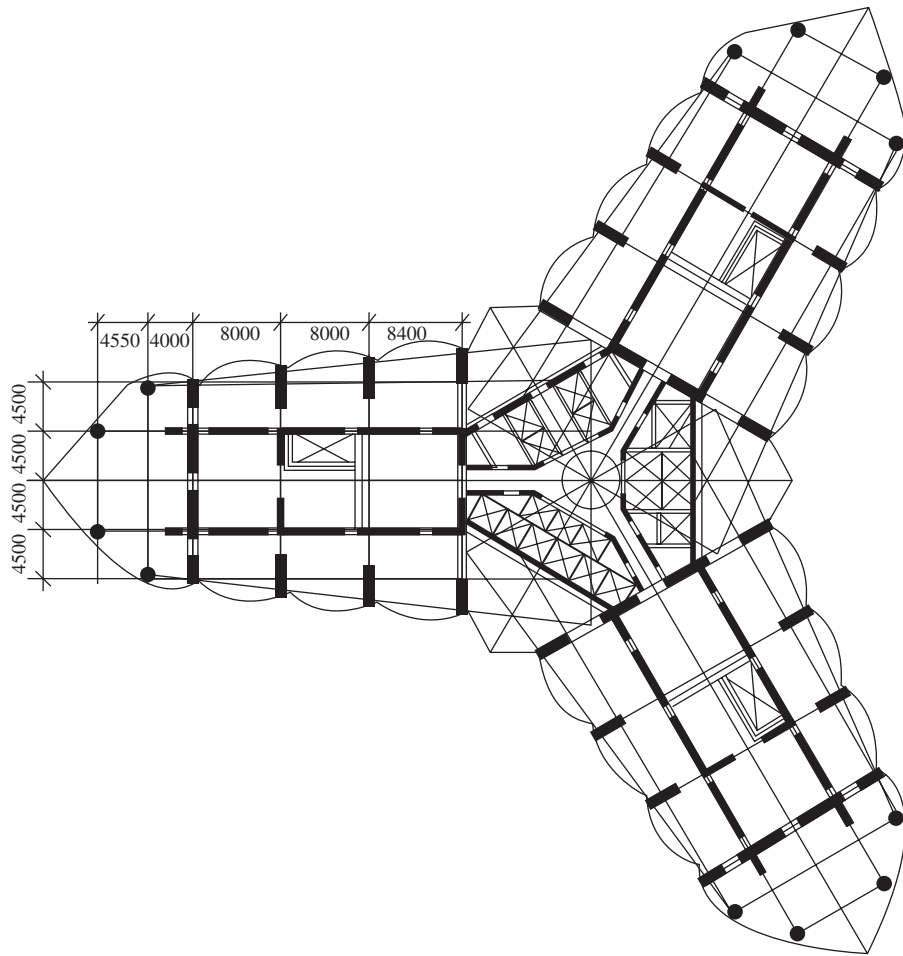
FIG. 2.30 Braced-tube and diagrid structures (a) 60-storey braced tube with 12-storey module (b) 100-storey diagrid with 69° angle (c) COR Building, Miami (d) O-14 Building, Dubai (Ali and Moon 2007)

Courtesy: (c) Ar. Chad Oppenheim (d) Ar. Jesse Reiser

2.5.9 Transfer Girders

In several buildings, large column-free spaces are required at the lower floors for parking areas, banquet or convention halls, lobbies, and so forth. For providing such large openings, the tube frame or shear walls must be interrupted with transfer girders or trusses (see Fig. 2.32). These transfer girders or trusses are often deep, and their depth may extend over one full storey.

The upper storey columns or shear walls terminate above the transfer girders or trusses, and the loads from these columns are transmitted to the transfer girder or trusses, which are, in turn, transferred to the columns below by truss or beam action. The columns that terminate at the transfer girder are



(a)

(b)

FIG. 2.31 Buttressed core system of Burj Khalifa (a) Plan (b) Elevation

called *floating columns*. When the buildings with such transfer girders are situated in earthquake zones, sufficient care should be taken in their design and detailing as they result in soft storeys and are vulnerable for collapse. Moreover, the failure of transfer girder will affect the stability of the whole building, and catastrophic failure of the structure can occur. Hence, their use must be strictly regulated, if not prohibited. If necessary, redundant transfer girders may be provided close to the ones that are near public streets to maintain structural integrity. It should

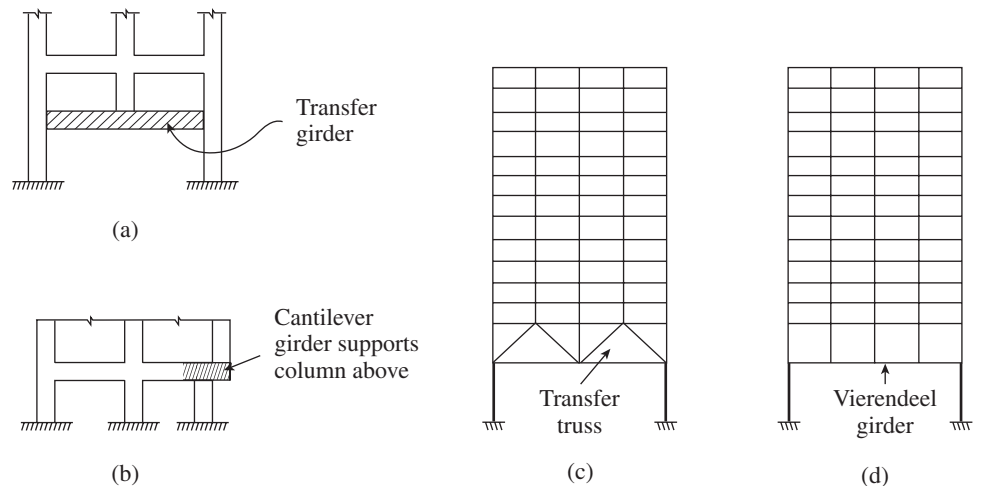


FIG. 2.32 Use of transfer girder or truss (a) Typical transfer girder (b) Cantilevered transfer girder (c) Transfer truss (d) Vierendeel girder

be noted that the columns near public streets are vulnerable to accidental loads, such as collision of automobiles and terrorist blast attack.

2.6 STRUCTURAL INTEGRITY

Localized damage (due to accidental loads, blast loads, etc.) of a major structural support may spread from element to element, resulting in the collapse of the entire structure. Hence, the extent of total damage may be disproportionate to the original cause. This sequence of failure is usually termed *progressive collapse*. The tragic events of 11 September 2001, in which several buildings in the World Trade Center complex collapsed, killing 2752 people (Subramanian 2002), and the bombing of the nine-storey Alfred P. Murrah Federal Building in Oklahoma City on 19 April 1995 (in which 168 people were killed and more than 680 people were injured and 324 buildings damaged causing a financial loss of \$652 million) underline the importance of designing certain buildings to address the threat of explosions.

Except for some special and important structures, it is impractical or expensive to design structures to resist this kind of collapse. Protection against progressive collapse requires analysis and design assuming loss of one member at a time. The potential for progressive collapse is evaluated based on a *demand-to-capacity ratio* (DCR). DCR is defined as the ratio of the force (bending moment, axial force, or shear force) in the structural member after the instantaneous removal of a column to the member capacity. A structural member is considered to have failed if its DCR exceeds 2.0 for typical structural configurations with simple layout and 1.5 for atypical structural configurations.

Structural integrity can be accomplished by providing sufficient continuity, redundancy, or energy-dissipating capacity (ductility), or a combination thereof, in the members of the structure. Minor changes in reinforcement detailing or provision of ties can be made to provide continuity and redundancy, which will also increase the ductility of the structure, and thus limit the effects of local damage or minimize progressive collapse.

To reduce the risk of localized damage, buildings should be effectively tied together at each principal floor level. It is important to effectively hold each column in position by means of horizontal ties (beams) in two directions (preferably at right angles), at each principal floor level supported by the column. Horizontal ties are also required at the roof level. At re-entrant corners, the tie member nearest to the edge should be anchored into the framework, as shown in Fig. 2.33.

Each portion of a building between expansion joints should be treated as a separate building. By tying the structure together as shown in Fig. 2.33, alternative load paths, which enhance the safety, should be made available. To ensure sway

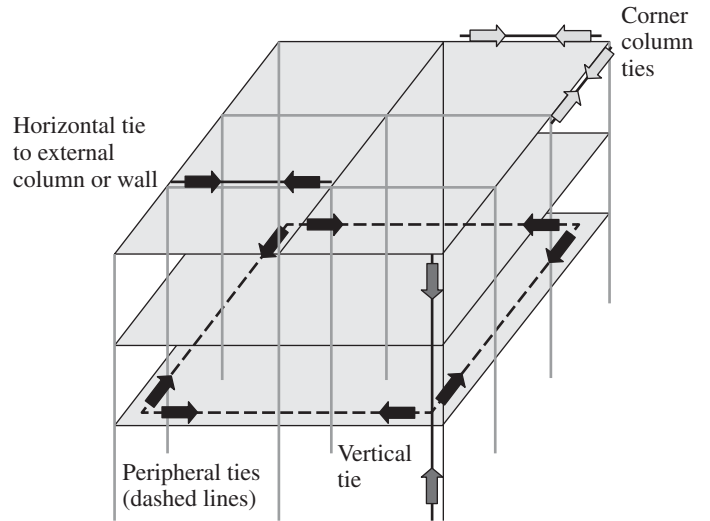


FIG. 2.33 Tying columns to building to achieve structural integrity

resistance, no portion of the structure should be dependent on only one lateral resisting system. All columns should be continuous vertically through the floors.

All the perimeter or spandrel beams should be provided with continuous top and bottom reinforcement. This reinforcement provides a continuous tie around the structure and would act as a catenary in case of loss of a support. Lack of continuous reinforcement across the beam-to-column connection can lead to progressive collapse.

The Indian code IS 456 does not contain provisions for structural integrity requirements. The ACI 318:08 code (Clause 7.13) requirements for structural integrity are as follows (PCA-IS 184 2006):

1. At least one-sixth of the tension reinforcement required for negative moment at support, but not less than two bars, must be continuous or spliced at or near mid-span (Fig. 2.34a).
2. At least one-fourth of the positive moment reinforcement in continuous members must extend into the support to a length of 150mm (Fig. 2.34b). The same amount of reinforcement should be continuous or spliced at or near the support. If the depth of a continuous beam changes at a support, the bottom reinforcement in the deeper member should be terminated with a standard hook and that in the shallower member should be extended into and fully developed in the deeper member.
3. The continuous top and bottom reinforcement required for structural integrity of perimeter beams are to be enclosed by the corners of U-stirrups with not less than 135-degree hooks around the continuous top bars or by one-piece closed stirrups with not less than 135-degree hooks around one of the continuous top bars (Fig. 2.34c).
4. At least one-fourth of the positive moment reinforcement, but not less than two bars, must be continuous (Fig. 2.34d).

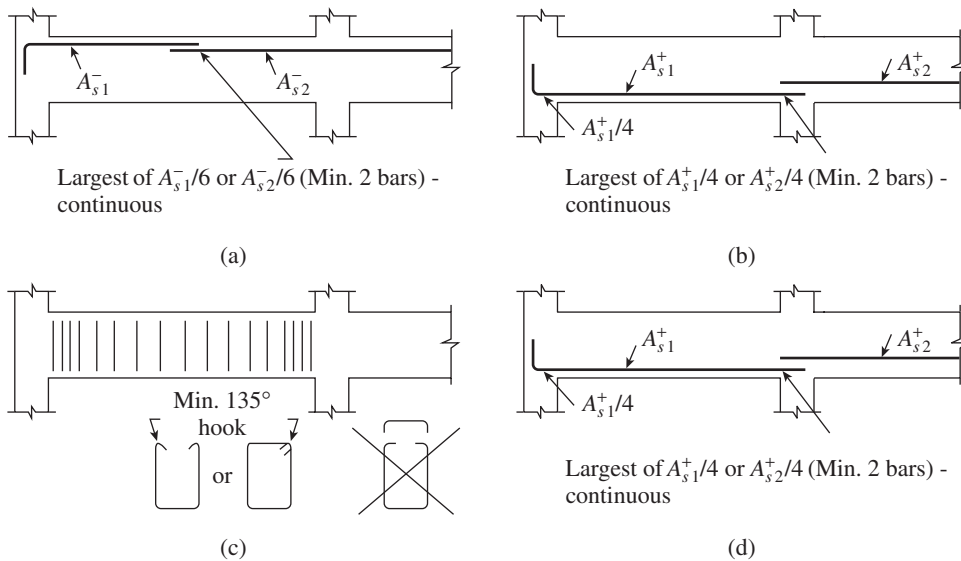


FIG. 2.34 Structural integrity requirements in beams (a) Top bars of perimeter beams (b) Bottom bars of perimeter beams (c) Stirrups in perimeter beams (d) Bottom reinforcement interior beams

Source: PCA-IS 184 2006

5. In joist construction, at least one bottom bar must be continuous and lap splices provided should provide full development length. At the discontinuous end of the joist, the bars must be terminated with a standard hook.

In cast-in-place two-way flat slabs, all bottom bars within the column strip, in each direction, should be continuous. Continuous column strip bottom bars through the column core give the slab some residual capacity in case of a punching shear failure at a single support. In addition, as shown in Fig. 2.35, at least two of the column strip bottom bars in each direction must pass within the column core without any laps in the column region and must be anchored at exterior supports (PCA-IS 184 2006).

Precast concrete or other heavy floor or roof units must be properly anchored at both ends. Precast members shall be adequately braced and supported during erection to ensure proper alignment and structural integrity until permanent

connections are completed. In precast concrete structures, tension ties should be provided in the transverse, longitudinal, and vertical directions and around the perimeter of the structure to tie all the elements together effectively. The ACI code Clause 16.5.1.2 requires these ties (see Fig. 2.33) should be designed to carry a minimum of 4.4 kN/m. Key elements that would risk the collapse of the greater area (greater than 15 per cent of floor area or 70 m², whichever is less) should be identified and designed for accidental loading. More details about blast effects and design of structural integrity may be found in Mays and Smith (1995) and Ellingwood, et al. (2007).

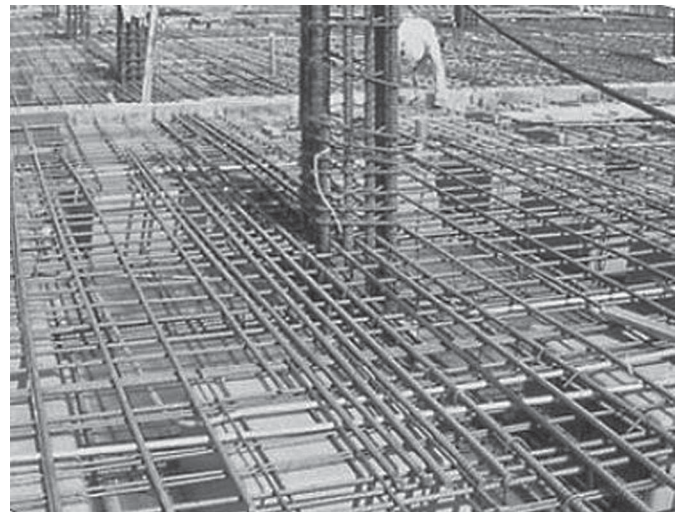


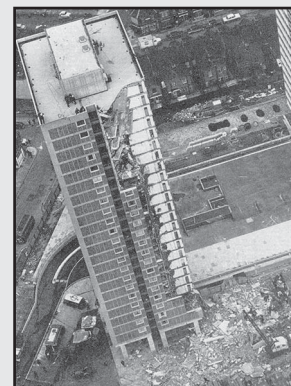
FIG. 2.35 Continuous column strip bottom bars through the column core
Source: PCA-IS 184 2006

CASE STUDIES

Ronan Point Collapse

Progressive collapse provisions were introduced in the British code as early as 1970. This was a direct result of the Ronan Point collapse in 1968. This involved a 23-storey tower block in Newham, East London, which suffered a partial collapse when a gas explosion demolished a load-bearing wall, causing the collapse of one entire corner of the building. Four people were killed in the incident, and seventeen were injured. (Ronan Point was repaired after the explosion, but it was demolished in 1986 to make way for a new low-rise housing development project.)

Due to the failure of Ronan Point apartment building, many other similar large panel system buildings were demolished.



Ronan point apartment

(Continued)

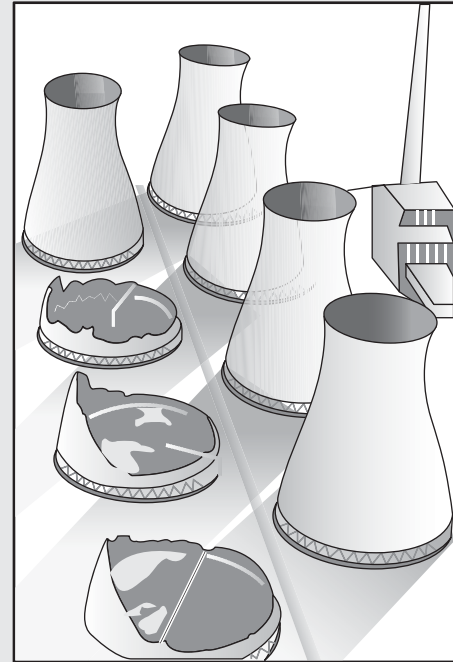
(Continued)

The Building Research Establishment, UK, published a series of reports in the 1980s to advise councils and building owners on what they should do to check the structural stability of their blocks. As a result of terrorist attacks on embassies abroad, along with the Murrah Federal Building in Oklahoma City, abnormal load requirements were introduced in the US codes. Structural integrity requirements are yet to be introduced in IS 456.

Failure of Ferrybridge Cooling Towers

Large cooling towers are susceptible to wind damage, and several failures have occurred in the past. Three 115 m tall, hyperbolic cooling towers failed by snap-through buckling at Ferrybridge power station, UK, on 1 November 1965 due to vibrations caused by winds blowing at 137 km/h. The structures were designed to withstand higher wind speeds. However, the following two factors caused the collapse: The average wind speed over a one-minute period was used in design, whereas the structures were susceptible to much shorter gusts, which were not considered in the design. The designers used wind loading based on experiments using a single isolated tower. However, in reality, the shape and arrangement of these cooling towers created turbulence and vortex on the leeward towers that collapsed. An eyewitness said that the towers were moving like belly dancers. Three out of the original eight cooling towers were destroyed and the remaining five were severely damaged. The failed towers were rebuilt and the others strengthened. Occurrences of failure of cooling towers have also been reported in Ardeer, UK, in 1973, Bouchain, France, in 1979, Fiddler's Ferry, UK, in 1984, and Willow Island, West Virginia,

USA, and Port Gibson, Mississippi, USA, in the 1980s. These failures resulted in the revision of building codes all over the world to include provisions regarding improved structural support and necessity of performing wind tunnel tests for complicated configurations and arrangements.



Three collapsed cooling towers at Ferrybridge, UK

2.7 SLIP-FORM AND JUMP-FORM CONSTRUCTIONS

The two forms of construction often employed in tall structures are the slip- and jump-form constructions. A brief discussion about these two forms of construction follows.

2.7.1 Slip-form Construction

Slip-form construction is used for various applications such as bridge piers, building cores, shear walls, chimneys, communication towers, cooling towers, and silos. In many cases, the procedure can be used to erect a structure in half the time required for conventional form work. In addition, the working platforms rise with the form and reduce the labour costs of dismantling and re-erecting scaffolds at each floor.

Vertical slip-form construction is a process of placing concrete continuously with a single form that is constructed on the ground and raised as the concrete is cast (it is also possible to move the form in the horizontal direction). Forms are not removed; they slip over the concrete, which can support itself by the time it is out of the form. Casting is done at a rate

that prevents the formation of a cold joint in previously placed concrete. The result is a continuous placing sequence resulting in a monolithically erected structure or wall with no visible joints (see Fig. 2.36). This construction process utilizes lifting jacks located on the ground or on the working platform that elevates the form and the workers' scaffolding attached with smooth rods or pipes. These rods or pipes are embedded in the hardened concrete. The construction technique is similar to an extrusion process. The slip form moves upwards as it extrudes the concrete wall. The rate of the extrusion process is controlled by the setting time of the concrete and the crew's ability to prepare the wall for the pour. The average time of lift for any project is 150–200 mm/h, placing approximately 100 mm to 250 mm layers of concrete per lift. More details about slip-form construction may be obtained from McConnell (2008).

2.7.2 Jump-form Construction

As the name implies, in jump-form construction, the wall form is jumped from one lift to the other. The system is supported by the lower lift of concrete. Forms are released and

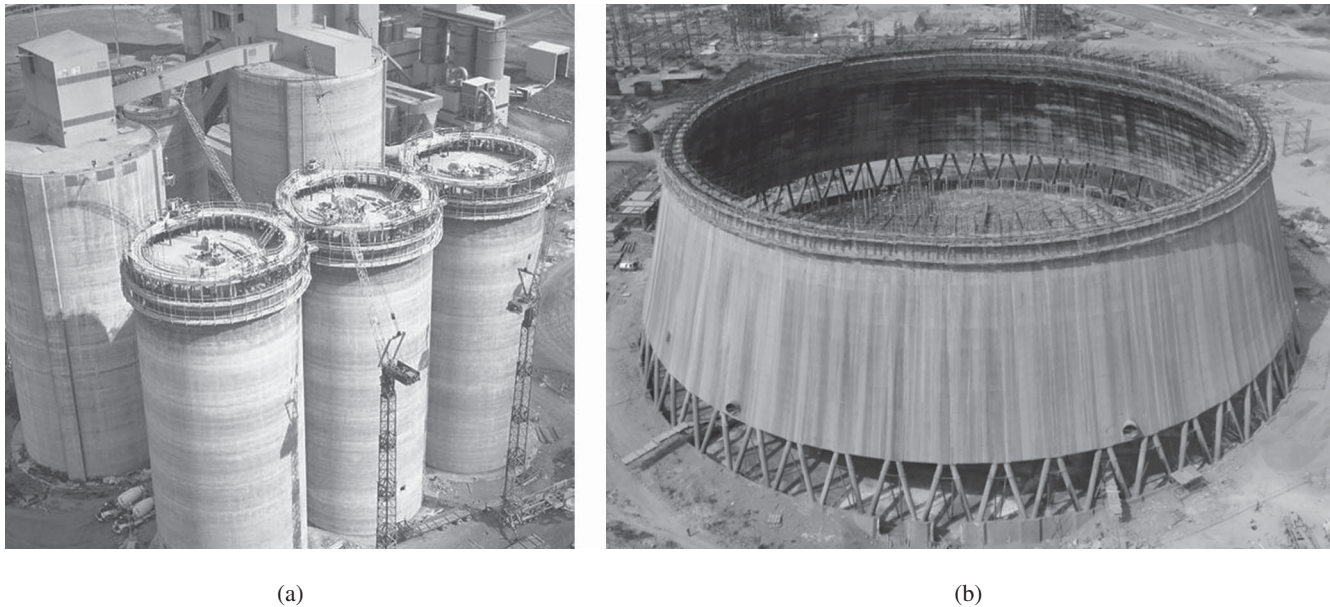


FIG. 2.36 Slip-form and jump-form construction (a) Slip forming 65 m tall, 23 m diameter clinker silos, which stand 1 m apart (b) Jump forming a hyperbolic paraboloidal cooling tower

Courtesy: (a) Kenaidan Contracting Ltd (b) Gammon India Ltd

stripped after the concrete has adequately cured. Embeds are provided in the concrete to receive the form system when it is jumped up to the next level. Instead of using expensive long reach cranes to bring up materials, lifting is done by a self-climbing form system (see Fig. 2.36b). Jump-form system may involve less crew than the conventional slip form operation, and the work is done only during day shift. It may be 15 per cent less expensive and in some cases faster than slip

forming. The system comes with adjustable steel forms, work platforms, hoist, jib cranes, concrete bucket, and powered concrete distributor buggy.

It should be noted that jump form and slip form are proprietary systems. More information about these systems may be obtained from companies such as PERI, Doka, and ULMA.

SUMMARY

After the architect finalizes the plan of a building, the structural engineer has to develop a suitable structural system that will resist the applied external loads. The engineer has to select a system that is safe, efficient, durable, economical, and environment friendly. A number of systems have been evolved in the past for different types of structures such as buildings and bridges. Normal buildings have elements such as footings, columns, beams, beam-columns, slabs, walls (shear walls and cantilever, counterfort, and buttress retaining walls), and trusses. These elements can be cast in situ or precast. Even prestressed elements can be used in long-span constructions. A short introduction of these elements has been provided. The load resisting system may be classified into gravity load resisting and lateral load resisting systems. Gravity load resisting systems include bearing wall systems (masonry walls, confined masonry walls, insulated RC walls, tilt-up concrete walls), one-way and two-way slab systems, two-way flat plates and flat slabs including waffle slabs and voided slabs, grid floors, and composite floors. Several techniques have been evolved for the erection of slab systems like lift slab system, which can be used to construct buildings economically and quickly. Several precast and prestressed concrete elements are available for gravity load resisting systems.

As the height of building increases beyond 20 or more floors, gravity load resisting systems with rigid frames will not be economical and efficient (Fintel and Ghosh, 1983). Moreover, for such high-rise buildings, lateral loads such as wind and earthquake will govern the design (Subramanian, 2001). Several innovative systems have been developed in the past for such lateral load resistance. They include shear walls, frame shear walls, outrigger and belt truss systems, framed tube, tube-in-tube, braced tube, bundled or modular tube, diagrid systems, and buttressed core systems. The details of all these systems have been explained and examples provided.

In any system, collapse due to progressive collapse or due to the failure of one or few elements should not occur. Such structural integrity may be achieved by tying all the elements effectively and by using reinforcement details, which will redistribute the forces to other unaffected parts.

Slip- and jump-form constructions, which are often employed in high-rise structures, are also explained. Using the information provided in this chapter, the structural engineer can select a suitable load resisting system for the building at hand.

REVIEW QUESTIONS

1. State the classification of RC structures.
2. What are the basic structural elements of a normal RC structure?
3. What is the basic function of footing?
4. List the different types of footings.
5. What is the function of columns? How do beam-columns differ from columns?
6. Describe the different types of columns.
7. What are beams? Sketch the different types of beams.
8. List the different classifications of slabs.
9. What are the different types of walls?
10. State the different checks to be performed on retaining walls.
11. What are the different types of retaining walls?
12. What is the difference between counterfort and buttress type retaining walls?
13. What is the shape that is economical for RC trusses?
14. Explain the role of slab in integrating the gravity and lateral load-resisting systems of tall buildings.
15. Why are brick walls considered unsafe in earthquake zones? What are the methods to make them earthquake resistant?
16. What is confined masonry construction?
17. How are insulated reinforced masonry walls constructed? What are the advantages offered by these walls over other types of walls?
18. Write a short note on tilt-up wall construction.
19. How can we classify one-way and two-way slabs?
20. What are the types of one-way and two-way slabs?
21. What are two-way ribbed slabs? How are they constructed?
22. How do flat plates and flat slabs differ?
23. Are flat plates suitable in earthquake zones? How are they strengthened to resist lateral loads?
24. What are waffle slabs? How are they constructed?
25. Explain the lift slab method of construction.
26. Write short notes on the following:
 - (a) Voided two-way flat slabs
 - (b) Grid floors
 - (c) Composite floors
 - (d) Precast and prestressed concrete construction
 - (e) Hollow-cored slabs
27. List the structural systems adopted for tall buildings.
28. How do rigid frames resist lateral loads? What is the drawback of this system if the number of floors is more than 20?
29. What are the advantages of shear walls over moment-resistant frames?
30. What are the different types of shear wall systems?
31. Explain how lateral loads are resisted by outrigger and belt truss systems?
32. What are framed-tube systems? How do they differ from moment-resisting frames?
33. In what way is a braced tube different from a framed tube and how is it advantageous?
34. How is it possible to build super-tall structures using tube-in-tube or bundled-tube systems?
35. What is the main difference between the diagrid system and the other tube systems?
36. What is the system that has been adopted in Burj Khalifa, the world's tallest building?
37. What is the function of transfer girders? Can they be adopted in severe earthquake-prone areas?
38. A ten-storey RC building is to be built in Chennai. It should have a large column-free area at the ground floor and the structural engineer has the freedom to choose column layout in the upper floor. Suggest a suitable lateral and gravity loading system.
39. An 80-storey RC commercial building has to be built in New Delhi, with service core in the middle of the building. The architect wants a column-free interior. Suggest a suitable lateral and gravity loading system.
40. Why are structural integrity provisions important in building design. Give a few examples of detailing procedures that will safeguard buildings in case of accidental loads.
41. How does slip form differ from jump-form construction?

REFERENCES

- Ali, M.M. 2001, *Art of the Skyscraper: The Genius of Fazlur Khan*, Rizzoli, New York, (also see: <http://www.fazlurrkhan.com/milestones.htm>, last accessed on 05 October 2012).
- Ali, M.M. and K.S. Moon 2007, 'Structural Developments in Tall Buildings: Current Trends and Future Prospects', *Architectural Science Review*, Vol. 50, No. 3, pp. 205–23, (also see <http://sydney.edu.au/architecture/documents/publications/ASR/Structural%20Developments%20in%20Tall%20Buildings.pdf>, last accessed on 5 October 2011).
- Ambalavanan, R., N. Narayanan, and K. Ramamurthy 1999, 'Cost Effectiveness Analysis of Alternate One-way Floor/Roof Systems', *The Indian Concrete Journal*, Vol. 73, No. 3, pp. 171–7.
- Brzev, B. 2007, *Earthquake-resistant Confined Masonry Construction*, National Information Centre of Earthquake Engineering, Kanpur, p. 99, (also see http://www.preventionweb.net/files/2732_ConfinedMasonry14Dec07.pdf, last accessed on 05 October 2012).
- Cuoco, D., D. Peraza, and T. Scarangelo 1992, 'Investigation of L'Ambiance Plaza Building Collapse', *Journal of Performance of Constructed Facilities*, ASCE, Vol. 4, No. 4, pp. 211–31.
- Ellingwood, B.R., R. Smilowitz, D.O. Dusenbeery, D. Duthinh, H.S. Lew, and N.J. Carino 2007, *Best Practices for Reducing the Potential for Progressive Collapse in Buildings*, National Institute of Standards and Technology Interagency Report (NISTIR) 7396, Gaithersburg, p. 216, (also see <http://www.fire.nist.gov/bfrlpubs/build07/art008.html>, last accessed on 5 October 2012).
- El Nimeiri, M.M. and F.R. Khan 1983, 'Structural Systems for Multi-use High-rise Buildings', in *Developments in Tall Buildings*, Van Nostrand Reinhold Company, New York, p. 221.
- Fintel, M. and S.K. Ghosh 1983, 'Economics of Long-span Concrete Slab Systems for Office Buildings—A Survey', *Concrete International*, ACI, Vol. 5, No. 2, pp. 21–34.

- Gunel, M.H. and H.E. Ilgin 2007, 'A Proposal for the Classification of Structural Systems of Tall Buildings', *Building and Environment*, Vol. 42, pp. 2667–75.
- IS 1893, *Criteria for Earthquake Resistant Design of Structures, Part 1: General Provisions and Buildings* (2002), *Part 4: Industrial Structures including Stack-like Structures* (2005), Bureau of Indian Standards, New Delhi.
- IS 3201:1988, *Criteria for Design and Construction of Precast-trusses and Purlins*, 1st revision, Bureau of Indian Standards, New Delhi.
- IS 4326:1993, *Indian Standard Code of Practice for Earthquake Resistant Design and Construction of Buildings*, 2nd revision, Bureau of Indian Standards, New Delhi.
- Krishna Raju, N. 2005, *Advanced Reinforced Concrete Design (IS 456:2000)*, 2nd edition, CBS Publishers and Distributors, New Delhi.
- Krishna Raju, N. 2007, *Prestressed Concrete*, 4th edition, Tata McGraw Hill Publishing Company Ltd, New Delhi, pp. 657–63.
- Martin, R. 2010, *L'Ambiance Plaza Collapse*, Bridgeport, Connecticut, April 23, 1987, (also see http://www.eng.uab.edu/cee/faculty/ndelatte/case_studies_project/L%27Ambiance%20Plaza/ambiance.htm#design, last accessed on 20 December 2010).
- Mays, G.C. and P.D. Smith 1995, *Blast Effects on Buildings: Design of Buildings to Optimize Resistance to Blast Loading*, Thomas Telford, New York.
- McConnell, S.W. 2008, 'Structural Concrete Systems', in E.G. Nawy (ed.), *Concrete Construction Engineering Handbook*, 2nd edition, CRC Press, Boca Raton, Florida, Chap. 10.
- Moon, K.S., J.J. Connor, and J. E. Fernandez 2007, 'Diagrid Structural Systems for Tall Buildings: Characteristics and Methodology for Preliminary Design', *The Structural Design of Tall and Special Buildings*, Vol. 16, No. 2, pp. 205–30.
- Murashev, V., E. Sigalov, and V.N. Baikov 1976, *Design of Reinforced Concrete Structures*, Mir Publishers, Moscow.
- National Buildings Organization 1968, *Analysis of Grids*, New Delhi.
- Nethercot, D.A. (ed.) 2003, *Composite Construction*, Spon Press, London and New York.
- Oehlers, D.J. and M.A. Bradford 1999, *Elementary Behaviour of Composite Steel and Concrete Structural Members*, Butterworth Heinemann, Oxford, p. 259.
- PCA-IS 184 2006, *Structural Integrity Requirements for Concrete Buildings*, Portland Cement Association, Skokie, Illinois, p. 6, www.cement.org.
- PCI 1998, *PCI Manual for the Design of Hollow Core Slabs*, 2nd edition, Precast/Prestressed Concrete Institute Chicago, Illinois.
- PCI 2004, *PCI Design Handbook—Precast and Prestressed Concrete* (MNL-120-04), 6th edition, Precast/ Prestressed Concrete Institute, Chicago, Illinois.
- Rai, D.C., K. Kumar, and H.B. Kaushik 2006, 'Ultimate Flexural Strength of Reinforced Concrete Circular Hollow Sections', *The Indian Concrete Journal*, Vol. 80, No. 12, pp. 39–45.
- Reynolds, C.E., J.C. Steedman, and A.J. Threlfall 2008, *Reynolds's Reinforced Concrete Designer's Handbook*, 11th edition, Taylor and Francis, London and New York, p. 401.
- Subramanian, N. 1980, 'Optimum Design of Concrete Circular Tanks', *Science and Engineering*, Vol. 33, No. 7, pp. 139–43.
- Subramanian, N. 1982, 'Failure of Congress Hall, Berlin', *The Indian Concrete Journal*, Vol. 56, No. 11, pp. 290–1.
- Subramanian, N. 1987, 'Aesthetics of Non-habitat Structures', *The Bridge and Structural Engineer*, Journal of ING/IABSE, Vol. 17, No. 4, pp. 75–100.
- Subramanian, N. 1995, 'Computer Analysis and Design of Tall Structures', *Civil Engineering and Construction Review*, Vol. 8, No. 4, pp. 42–6.
- Subramanian, N. 1999, 'Top-to-bottom Construction for High-rise Buildings', *Bulletin of the Indian Concrete Institute*, No. 68, pp. 43–5.
- Subramanian, N. 2002, 'Collapse of WTC – Its Impact on Skyscraper Construction', *The Indian Concrete Journal*, Vol. 76, No. 3, pp. 165–79.
- Subramanian, N. 2004, 'Tall Buildings', in *International Conference on World Innovations in Structural Engineering*, 1–3 December 2004, Hyderabad, India.
- Subramanian, N. 2007, *Space Structures: Principles and Practice*, 2 volumes, Multi-Science Publishing Co., Essex, p. 820.
- Subramanian, N. 2010, 'Burj Khalifa: World's Tallest Structure', *New Building Materials and Construction World*, Vol. 16, No. 7, pp. 198–206.
- TCI 2006, *The Tilt-Up Construction and Engineering Manual*, 6th edition, The Tilt-up Concrete Association (www.tilt-up.org).
- Vanderwerf P.A, S.J. Feige, P. Chammas, and L.A. Lemay 1997, *Insulating Concrete Forms for Residential Design and Construction*, McGraw-Hill Professional, New York, p. 326.
- Varghese, P.C. 2006, *Advanced Reinforced Concrete Design*, 2nd edition, Prentice Hall of India, New Delhi, p. 534.

LOADS AND LOAD COMBINATIONS

3.1 INTRODUCTION

Before designing any structure or the different elements such as beams and columns, one has to first determine the various natural and man-made loads acting on them (see Fig. 3.1). These loads on a structure may be due to the following:

1. Mass and gravitational effect ($m \times g$): Examples of these types of loads are dead loads, imposed loads, snow, ice, and earth loads, and hydraulic pressure.
2. Mass and its acceleration effect ($m \times a$): Examples of such loads are earthquake, wind, impact, and blast loads.
3. Environmental effects: Examples are the loads due to temperature difference, settlement, and shrinkage. These are also termed as *indirect loads*.

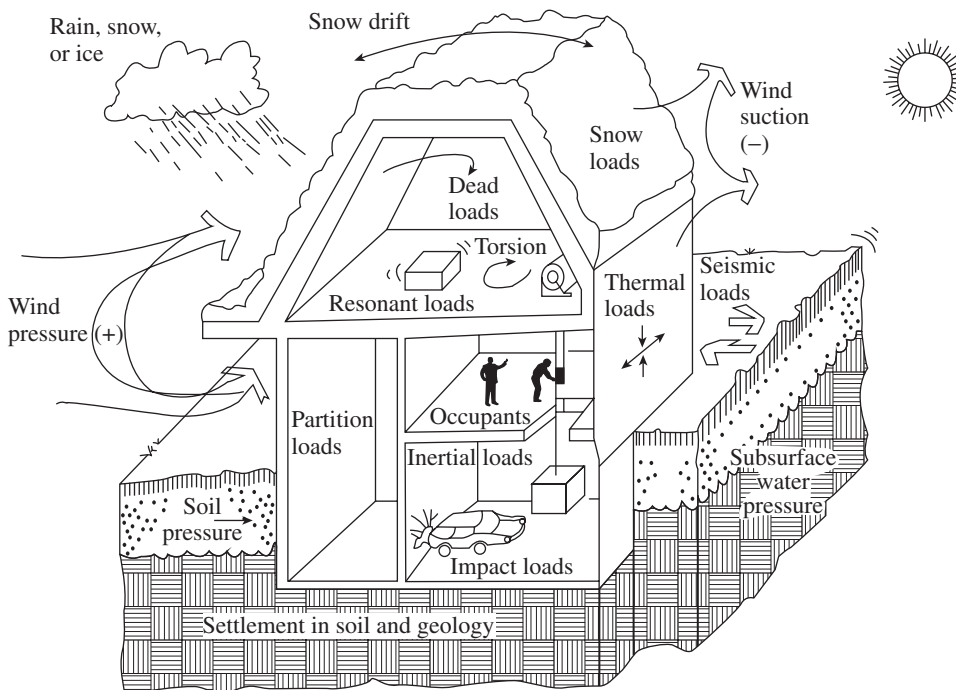


FIG. 3.1 Types of loads

In India, the basic data on dead, imposed, and wind loads for buildings and their combinations to be considered in design are given in Indian Standard (IS) 875, Parts 1–5. Data regarding earthquake loads is specified in IS 1893. For chimneys and other forms of structures, the necessary loading data is provided in the code of practice appropriate to that type of structure (e.g., IS 4995, IS 4998, IS 11504). We shall briefly discuss a few important loads in this chapter.

3.2 CHARACTERISTIC ACTIONS (LOADS)

The determination of the loads for which a given structure has to be proportioned is one of the most difficult problems in design and is often not taught in course work. Decisions are to be made on the type of loads the structure may experience during its lifetime, combinations of loads, and so forth. The probability that a specific load will be exceeded during the life of a structure usually depends on the period of exposure (or life) of the structure and the magnitude of design load. For example, wind loads acting on a structure at a given location varies every day based on the wind speed; for design, we need to consider the maximum wind speed (load) that may occur in that location only once in several years. The average time period between the occurrences of such maximum wind speeds is called (mean) *return period*. Thus, a return period is defined as the number of years, the reciprocal of which provides the probability of an extreme wind exceeding a given wind speed in any

one year. (In general, the return period may be defined as the average time between consecutive occurrences of the same event. It is only an average duration and not the actual time between occurrences, which would be highly variable). Such return periods can be determined from statistical analysis of wind speed records. Of course, extremes of other natural phenomena such as snow, earthquake, or flood also occur infrequently and the return periods for specific extremes can be similarly determined.

Thus, if the return period R of a wind speed of 200 km/h at a certain locality is 50 years, then the probability that it will be exceeded in any one year is $1/R = 1/50 = 0.02$. However, for design purposes we are interested not in the probability that it will be exceeded in any one year but rather in the probability that it will be exceeded during the life of the structure. It should be noted that if $1/R$ is the probability that the wind speed will be exceeded in any year, $(1 - 1/R)$ is the probability that it will not be exceeded in that year. If we consider N as the life of the structure in years, then the probability that it will not be exceeded during the life of the structure will be $(1 - 1/R)^N$. Therefore, the probability P_N that it will be exceeded at least once in N years is

$$P_N = 1 - (1 - 1/R)^N \quad (3.1)$$

Thus, the probability that a wind speed of 200 km/h with a return period of 50 years will be exceeded at least once in 50 years (life of the structure) is

$$P_{50} = 1 - (1 - 0.02)^{50} = 0.635$$

That is, there is a 63.5 chance that the structure will be exposed to a wind exceeding 200 km/h. The code (IS 875, part 3) states that a value of $P_N = 0.63$ is normally considered sufficient for the design of buildings and structures against wind effects. Thus, if the acceptable risk is 0.63, it is sufficient to design the structure to resist the wind load from a 200 km/h wind. It has to be remembered that there will be a margin of safety (due to the partial safety factors for loads and materials) and hence the structure may not collapse under a wind of this speed.

Ideally, loads applied to a structure during its life should be considered statistically and a characteristic load determined. Thus, the *characteristic load* may be defined as the load that shall not be exceeded by a certain accepted or pre-assigned probability (usually 5%) during the life of the structure as shown in Fig. 3.2. For all practical purposes, the specified load in the codes is taken as the characteristic load in the absence of statistical data.

When the statistical data is available, the probability that a load may exceed the characteristic load is expressed as

$$p_f = \phi_c (Q_m - Q_c) / \sigma \quad (3.2)$$

where p_f is the probability that the load exceeds the characteristic load Q_c , Q_m the statistical mean of the observed

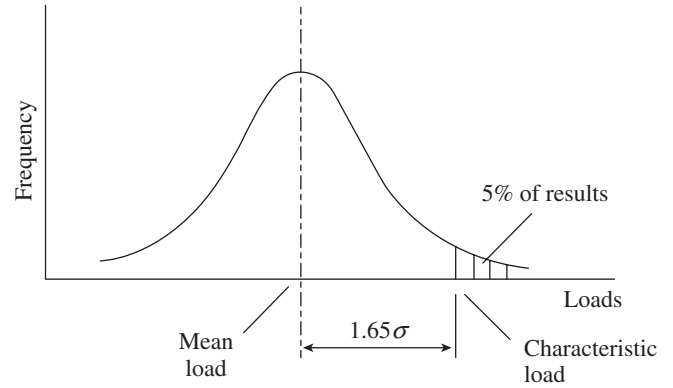


FIG. 3.2 Definition of characteristic load

maximum loads, σ the standard deviation of the loads, and ϕ_c the cumulative distribution function.

The value of the *cumulative distribution function* depends on the statistical distribution of loads. Statistical distribution of dead loads and live loads are often assumed to be a *normal distribution* (as shown in Fig. 3.2), though some codes assume it to be of *Weibull-type distribution*. Equation (3.2) can be rewritten as

$$(Q_m - Q_c) / \sigma = \phi_c^{-1}(p_f) = -k \quad (3.3)$$

$$\text{or} \quad Q_c = Q_m + k\sigma \quad (3.4)$$

$$\text{where} \quad -k = \phi_c^{-1}(p_f) \quad (3.5)$$

k is a coefficient associated with the pre-assigned probability of failure

For a characteristic load that shall not be exceeded by a probability of five per cent, we have

$$p_f = (5/100) \text{ or}$$

$$k = \phi_c^{-1}(0.05)$$

From standard tables for normal distribution, the value of k for $p_f = 0.05$ is obtained as $k = 1.65$. Thus, Eq. (3.4) can now be written as follows:

$$Q_c = Q_m + 1.65\sigma \quad (3.6)$$

Example 3.1 illustrates the concept of characteristic load.

Design Actions—Loads

The design action Q_d is arrived at by multiplying the characteristic actions (loads), Q_c , by partial safety factors, γ_f , as follows (these factors are often referred to as *load factors*):

$$Q_d = \Sigma \gamma_f Q_c \quad (3.7)$$

Here, γ_f is the partial safety factor for the load, given in Table 3.1.

TABLE 3.1 Ultimate loads using partial safety factor, γ_f , as per IS 456

Load Combination	Limit State of Collapse	Limit State of Serviceability
Dead load (DL) and imposed load (IL)	1.5DL + 1.5IL	DL + IL
Dead load and wind load (WL) Case 1: Stability against overturning is not critical Case 2: Stability against overturning is critical	1.5DL + 1.5WL	DL + WL
	0.9DL + 1.5WL	DL + WL
Dead, imposed, and wind/ earthquake loads (EL)	1.2(DL + IL + WL)	1.0DL + 0.8IL + 0.8WL

Note: While considering earthquake loads, substitute EL for WL. When differential settlement, creep, shrinkage, or temperature effects are significant, use the following partial safety factors for limit state of collapse: $UL = 0.75(1.4DL + 1.4TL + 1.7IL)$ must be greater than $(1.4DL + TL)$. For serviceability limit states, γ_f can be taken as unity for this case.

These partial safety factors are provided to take into account the following factors:

1. Possibility of unfavourable deviation of the load from the characteristic value
2. Possibility of inaccurate assessment of load
3. Variation in dimensional accuracy
4. Uncertainty in the assessment of effects of the load
5. Uncertainty in the assessment of the limit state being considered

When more than one imposed load can act simultaneously, the leading load is considered as that load causing the larger action effect. The load factor for water may be taken as 1.4 (as per BS 8007). This value may appear to be very conservative. However, if used for the design of a tank, for example, it allows for the tank overflowing, dimensional changes, and the possibility of the tank being filled with a denser liquid.

3.3 DEAD LOADS

The load that is fixed in magnitude and position is called the *dead load*. Determination of the dead load of a structure requires the estimation of the weight of the structure together with its associated 'non-structural' components. Thus, one needs to calculate and include the weight of slabs, beams, walls, columns, partition walls, false ceilings, façades, claddings, water tanks, stairs, brick fillings, plaster finishes, and other services (cable ducts, water pipes, etc.). After the design process, the initially assumed dead load of the structure (based on experience) has to be compared with

the actual dead load. If the difference between the two loads is significant, the assumed dead load should be revised and the structure redesigned. Dead weights of different materials are provided in code IS 875 (Part 1: Dead loads). The weights of some important building materials are given in Table 3.2. The self-weight computed on the basis of nominal dimensions and unit weights as given in IS 875 (Part I) may be taken to represent the characteristic dead load.

TABLE 3.2 Weights of some building materials as per IS 875 (Part 1)

S. No.	Material	Unit Weight
1.	Brick masonry in CM 1:4	20 kN/m ³
2.	Plain concrete	24 kN/m ³
3.	Reinforced cement concrete	25 kN/m ³
4.	Stone masonry	20.4–26.5 kN/m ³
5.	Cement mortar	20.4 kN/m ³
6.	Steel	78.5 kN/m ³
7.	20 mm cement plaster	450 N/m ²
8.	5 mm glass	125 N/m ²
9.	Floor finishes	600–1200 N/m ²
10.	Water	10 kN/m ³

3.4 IMPOSED LOADS

Imposed loads (previously referred to as *live loads*) are gravity loads other than dead loads and include items such as occupancy by people, movable equipment and furniture within the buildings, stored materials such as books, machinery, and snow. Hence, they are different for different types of buildings such as domestic, office, and warehouse. They often vary in space and in time. Imposed loads are generally expressed as static loads for convenience, although there may be minor dynamic forces involved. The code provides uniformly distributed loads (UDLs) as well as concentrated loads for various occupational categories. The reason for considering concentrated loads is that there are some localized loads (e.g., heavy items of furniture, equipment, or vehicles) that may not be adequately represented by a UDL. The distributed and concentrated imposed loads shall be considered separately and the design carried out for the most adverse conditions. The magnitudes of a few imposed loads are given in Table 3.3.

TABLE 3.3 Live loads on floors as per IS 875 (Part 2)

S. No.	Type of Floor Usage	Imposed Load (kN/m ²)
1.	Residential	2.0
2.	Office	2.5 4.0
	(a) with separate storage (b) without separate storage	
3.	Shops, classrooms, restaurants, theatres, etc.	4.0 5.0
	(a) with fixed seating (b) without fixed seating	
4.	Factories and warehouses	5.0–10.0

(Continued)

TABLE 3.3 (Continued)

S. No.	Type of Floor Usage	Imposed Load (kN/m ²)
5.	Book stores and stack rooms in libraries	10.0
6.	Garages with light vehicles	4.0
7.	Stairs, landings, and balconies (a) not liable to overcrowding (b) liable to overcrowding	4.0 5.0

Note: In cantilever steps, a minimum of 1.3 kN concentrated load at the free edge should be considered at each cantilever step.

It should be noted that the imposed load may change from room to room. Where there is such variation, to account for the most adverse load cases, analysis should be carried out for the following:

1. Factored live load on all spans
2. Factored live load on two adjacent spans
3. Factored live load on alternate spans

The second case results in high bending moment (BMs) over the support between the two loaded spans and the third case results in high BMs at mid-span in the loaded beams.

When the load due to partition is considered, the floor load should be increased by 33.3 per cent per metre run of partition wall subject to a minimum of 1 kN/m²; total weight per metre run must be less than 4 kN/m. For complete guidance, the engineer should refer to IS 875 (Part 2).

When large areas are considered, the code allows for a reduction in the imposed load; for single beam or girders, a reduction of five per cent for each 50m² floor area, subjected to a maximum of 25 per cent, is allowed. In multi-storey buildings, the probability that all the floors will be simultaneously loaded with the maximum imposed load is remote, and hence, reduction to column loads is allowed. Thus, imposed loads may be reduced in the design of columns, walls, and foundations of multi-storey buildings as given in Table 3.4. It should be noted that such reduction is not permissible if earthquake loads are considered.

TABLE 3.4 Reduction in imposed load applicable to columns

Floor Measured from Top	Percentage
1 (top or roof)	0
2	10
3	20
4	30
5 to 10	40
11 to ground floor	50

Code IS 875 (Part 2) also provides the values of *horizontal loads* acting on parapets and balustrades. These loads should be assumed to act at handrail or coping level.

Roofs are considered non-accessible except for normal maintenance and minor repairs. If roofs are frequently accessible and used for floor-type activities, they should be treated as floors and the corresponding loads should be considered.

Srinivasa Rao and Krishnamurthy (1993) conducted load survey on imposed loads acting on office buildings and found that the maximum imposed load is only of the order of 2.35 kN/m² in office buildings without separate provision for store rooms (this value is much smaller than the 4 kN/m² specified in IS 875—Part 2). A similar survey was conducted by Sunil Kumar (2002) and Sunil Kumar and Kameswara Rao (1994) on residential buildings, and it was found that the design imposed loads specified in the code are much higher than those estimated by the load survey.

3.4.1 Consideration of Slab Loads on Beams

When a slab is supported on four sides and the length to width ratio is greater than two, the slab acts as a one-way slab and the beams along the long spans are assumed to carry the load from the slab, as shown in Fig. 3.3(a). However, in two-way slabs (i.e., when a slab is supported on four sides and the length to width ratio is lesser than or equal to two), the load distribution

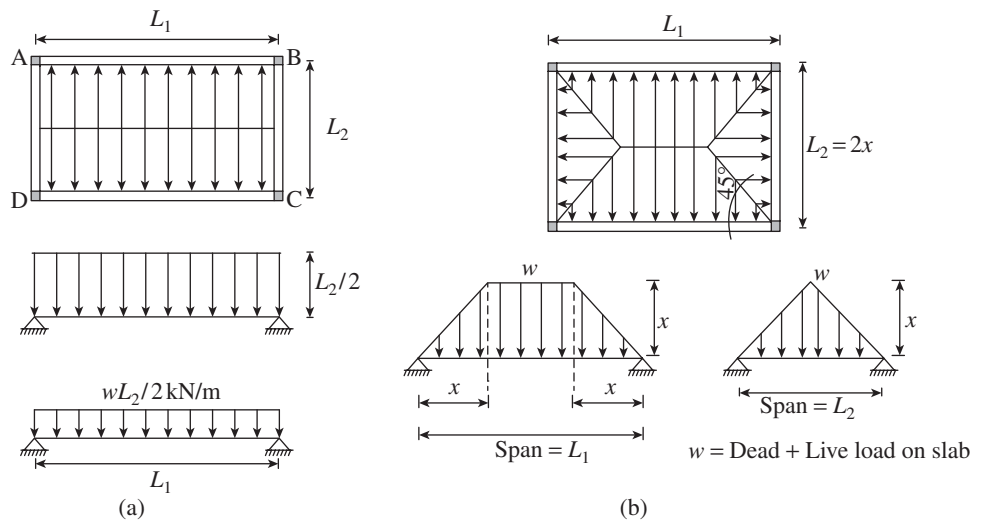


FIG. 3.3 Load distribution (a) One-way slabs (b) Two-way slabs

is based on yield-line analysis. In a square slab, the yield lines running at 45° from each corner will meet at a single point in the centre. On the other hand, in a rectangular slab, the same four yield lines will not meet at one point, and hence, there will be a fifth yield line running between the intersections of these yield lines, as shown in Fig. 3.3(b). Thus, the long beams will be subjected to a trapezoidal load and the short beams to a triangular load, as shown in Fig. 3.3(b).

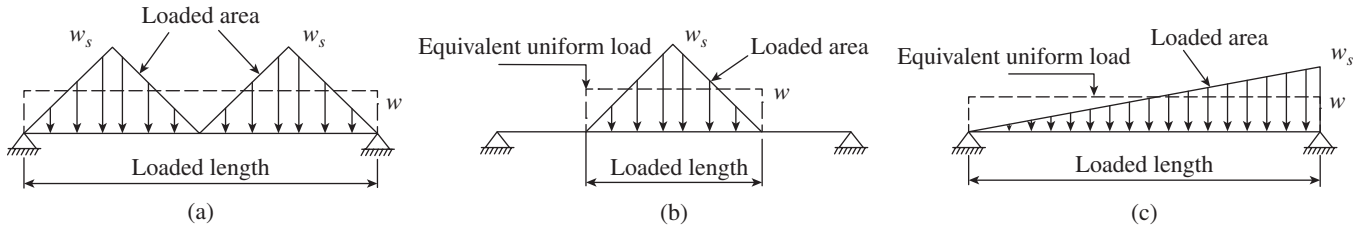


FIG. 3.4 Other possible loadings on beams and equivalent uniform loads (a) Two triangular loads in span (b) Triangular load in the middle of span (c) Triangularly varying load

The triangular and trapezoidal loads can be replaced by the equivalent UDLs for the analysis of the beams. Let α and β be the coefficients for the equivalent UDLs, which convert these triangular or trapezoidal loads to obtain the same amount of maximum bending moment and shear force. Equating the maximum bending moment of the UDL and triangular load, we get

$$\frac{wL_2^2}{8} = \frac{\alpha L_2^2}{12} \text{ or } \alpha = 0.667w \quad (3.8)$$

where w is the total dead and imposed loads on slab in kN/m^2 .

In the same way, equating the maximum shear force of the UDL and the triangular load, we get

$$\frac{wL_2}{4} = \frac{\beta L_2}{2} \text{ or } \beta = 0.5w \quad (3.9)$$

Similarly, in the case of trapezoidal loading, it can be shown that

$$\alpha = \left(1 - \frac{1}{3r^2}\right) \quad (3.10)$$

$$\beta = \left(1 - \frac{1}{2r}\right)$$

where $r = \frac{\text{Length}}{\text{Width}} = \frac{L_1}{L_2} = \frac{L_1}{2X} \geq 1$

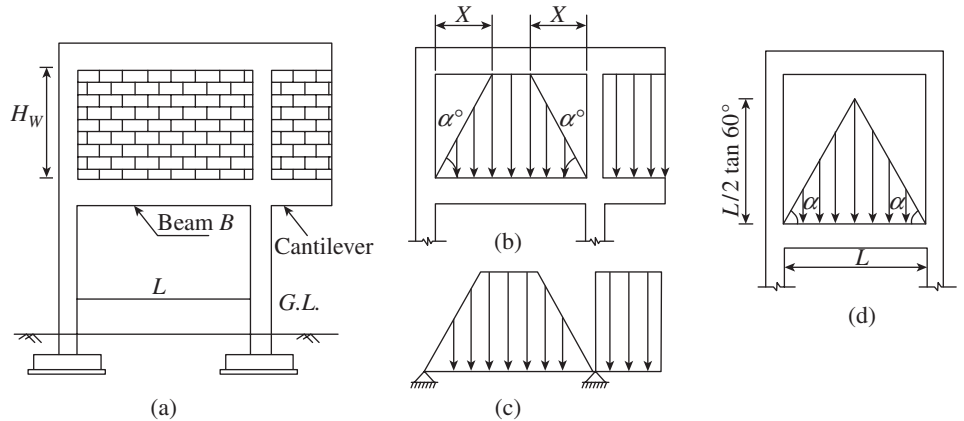


FIG. 3.5 Consideration of wall loads (a) Typical frame with walls (b) Loads transferred to columns and beams (c) Load on beam due to walls (d) Short span walls

The coefficients α and β have been calculated for various values of r and are given in Table 3.5.

TABLE 3.5 Coefficients to convert trapezoidal loads to equivalent UDLs

$L_1/2X$	1.0	1.1	1.2	1.4	1.6	1.8	2.0	> 2.0
α (B.M.)	0.667	0.725	0.769	0.830	0.870	0.897	0.917	~1.0
β shear force (S.F.)	0.500	0.545	0.583	0.643	0.688	0.722	0.750	~1.0

It should be noted that when the loading is as shown in Fig. 3.4, the non-uniform loads must be approximated to an equivalent UDL, as given by the following equation:

$$w = w_s(\text{loaded area/loaded length}) \quad (3.11)$$

3.4.2 Consideration of Wall Loads on Beams

When the height of the masonry over a beam is greater than about 0.6 times the span of the beam, it can be assumed that there will be an arch action in the masonry and hence some part of the load will be transferred to the columns on either side. In such situations, only wall loads bounded by α° lines from the columns cause bending moment and shear force in the beam, as shown in Fig. 3.5(b). The value of α ranges between 45° and 60° ; let us assume it to be 60° . This trapezoidal wall load can be replaced by equivalent uniform loads, using the coefficients given in Table 3.5, for bending moment and shear force. Thus,

$$\text{Wall load for bending} = \alpha H_w g_w \quad (3.12a)$$

$$\text{Wall load for shear} = \beta H_w g_w \quad (3.12b)$$

where H_w is the height of the wall and $g_w = \gamma_w t_w$ where γ_w is the weight of wall material (for brickwork with plastering, it may be taken as 20 kN/m^3) and t_w the thickness of the wall.

It should be noted that arch action will not develop for walls supported on cantilever beams or for walls containing openings, and hence the total value of the wall load should be transferred to the beam. Arch action may also not develop in partition walls of thickness 115 mm. When the height of the wall, H_w , is greater than $0.5L \tan \alpha^\circ$, the beam will experience only a triangular load, as shown in Fig. 3.5(d).

In such a case, the equivalent wall load is calculated as follows:

$$\text{Wall load for bending} = 2/3(0.5L \tan 60^\circ)g_w \quad (3.12c)$$

$$\text{Wall load for shear} = 0.5(0.5L \tan 60^\circ)g_w \quad (3.12d)$$

When there is no opening in the wall, the beam can be designed by considering the *composite action* of the brick wall above it, with a bending moment of $wL^2/30$, where w is the uniform load on the beam (Govindan and Santhakumar 1985; IS 2911). The brick strength should not be less than 3.5 N/mm^2 . For composite action to take place, the first course of brickwork may be laid on the reinforced concrete (RC) beam, as soon as the concrete is poured and levelled.

3.5 IMPACT LOADS

Impact due to vertical crane, moving machinery, and so on is converted empirically into equivalent static loads through an impact factor, which is normally a percentage (20% to 100%) of the machinery load (see Clause 6.0 of IS 875—Part 2). Thus, if the impact is 25 per cent, the machinery load is multiplied by 1.25. The loads due to cranes and other machineries are often obtained from the manufacturers or suppliers. For a lift machine room above the roof of a multi-storey building, we may consider an imposed load of 10 kN/m^2 . Assuming an impact allowance of 100 per cent, this will result in 20 kN/m^2 . It should be noted that the impact load is an important criterion in industrial buildings where machinery will be mounted on floors and also in bridges. Indian Road Congress (IRC) codes should be consulted for considering such loads on bridges.

3.6 SNOW AND ICE LOADS

Snow and ice loads are to be considered in the mountainous (Himalayan) regions in the northern parts of India. Thus, the roofs in these regions should be designed for the actual load due to snow or for the imposed loads specified in IS 875 (Part 2), whichever is more severe. Freshly fallen snow weighs up to 96 kg/m^3 and packed snow 160 kg/m^3 . The procedure for obtaining snow load on roof consists of multiplying the ground snow (corresponding to a 50-year mean return period) with a coefficient to take care of the effect of roof slope, wind exposure, non-uniform accumulation of snow on pitched or curved roofs, multiple series roofs or multi-level roofs, and roof areas adjacent to projections on a roof level. Although maximum snow and maximum wind loads are not considered to act simultaneously, it is important to consider drift formation due to wind, since the majority of snow-related roof damage is due to drifted snow. The reader is advised to consult IS 875 (Part 4), ASCE/SEI 07–10, and O'Rourke (2010) for more information on snow loading.

3.7 WIND LOADS

Winds are produced by the differences in atmospheric pressures, which are primarily due to the differences in temperature. Wind flow manifests itself into gales, cyclones, hurricanes, typhoons, tornadoes, thunderstorms, and localized storms. Tropical *cyclone* is the generic term used to denote *hurricanes* and *typhoons*. The wind speeds of cyclones can reach up to $30\text{--}36 \text{ m/s}$ and in the case of severe cyclones up to 90 m/s . Cyclones in India far exceed the design wind speed given in IS 875 (Part 3). Horizontal wind flow exerts lateral pressure on the building envelope and hence has to be considered in the design.

Tornadoes consist of a rotating column of air, accompanied by a funnel-shaped downward extension of a dense cloud having a vortex of about $60\text{--}240 \text{ m}$ diameter, whirling destructively at speeds of $75\text{--}135 \text{ m/s}$. Tornadoes are the most destructive of all wind forces, and in the USA alone the damage is in excess of \$100 million per year. More details of tornado-resistant design may be found in Whalen, et al. (2004), Minor (1982), and Coulbourne, et al. (2002). An animated guide to the causes and effects of tornadoes is provided by <http://news.bbc.co.uk/2/hi/science/nature/7533941.stm>.

Code IS 875:1987 (Part 3) provides the basic wind speeds, averaged over a short interval of 3 seconds and having a 50-year return period at 10 m height above ground level in different parts of the country. The entire country is divided into six wind zones (see Fig. 1 of this code). The wind pressure or load acting on the structural system and the structural or non-structural component being considered depends on the following:

1. Velocity and density of air
2. Height above ground level
3. Shape and aspect ratio of the building
4. Topography of the surrounding ground surface
5. Angle of wind attack
6. Solidity ratio or openings in the structure
7. Susceptibility of the structural system under consideration to steady and time-dependent (dynamic) effects induced by the wind load

Depending on these factors, the wind can create positive pressure or negative pressure (suction) on the sides of the building.

The design wind speed is obtained from the basic wind speed, as per IS 875 (Part 3), after modifying it to include the risk level, terrain roughness, height and size of structure, and local topography as

$$V_z = V_b k_1 k_2 k_3 \quad (3.13)$$

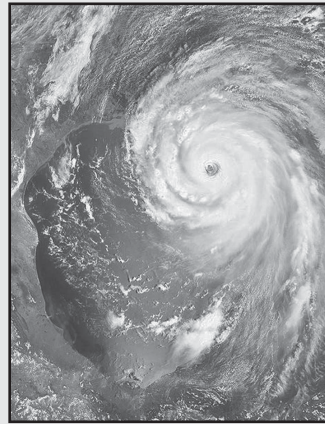
where V_z is the design wind speed at any height z in m/s , V_b the basic wind speed (given in Fig. 1 of the code), k_1

CASE STUDY

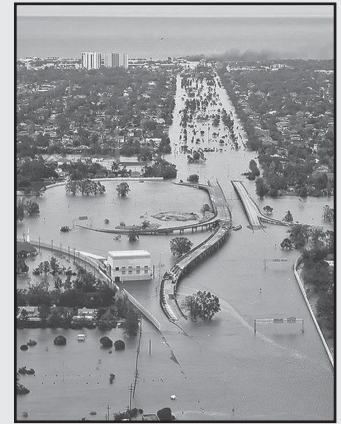
Hurricane Katrina

Hurricane Katrina struck the New Orleans area of USA on the early morning of 29 August 2005. It developed into a powerful category-five hurricane, on the *Saffir–Simpson scale* of hurricane intensity, with the highest wind speed of 280 km/h (77.78 m/s). It caused severe destruction along the Gulf coast from central Florida to Texas. Much of the destruction was due to the storm surge, which breached the levees of Louisiana at 53 different points, with 80 per cent of the city being submerged, leaving several victims clinging to rooftops and sending several others to shelters around the country. At least 1836 people lost their lives in the actual hurricane and in the subsequent floods, making it the deadliest US hurricane since the 1928 Okeechobee hurricane. NASA satellite images showed that the floods that had buried up to 80 per cent of New Orleans subsided only by 15 September 2005. Katrina redistributed over one million people from the central Gulf coast elsewhere across the USA, which became the largest diaspora in the history of that country.

The total damage from Katrina is estimated at \$81.2 billion (2005 US dollars), nearly double the cost of the previously most expensive storm, Hurricane Andrew, when adjusted for inflation. Federal disaster declarations covered 233,000 km² of USA, an area almost as large as the UK. The hurricane left an estimated three million people without electricity. The Superdome, which was



(a)



(b)

(a) Satellite image of the 25 mile wide eye of Hurricane Katrina (Photo: NASA)
 (b) Flooded I-10/I-610/West End Blvd interchange and surrounding area of northwest New Orleans and Metairie, Louisiana (Photo: US Coast Guard, Kyle Niemi)

sheltering many people who were evacuated from their homes, sustained significant damage.

the probability factor or risk coefficient (given in Table 1 of the code), k_2 the terrain, height, and structure size factor (given in Table 2 of the code), and k_3 the topography (ground contours) factor (given in Section 5.3.3 of the code). It should be noted that the design wind speed up to 10 m height from mean ground level is considered to be a constant.

The design wind pressure p_d is obtained from the design wind velocity as

$$p_d = 0.6V_z^2 \quad (3.14)$$

The wind load on a building can be calculated for the following:

1. The building as a whole
2. Individual structural elements such as roofs and walls
3. Individual cladding units including glazing and their fixings

The code provides the pressure coefficients (derived on the basis of models tested in wind tunnels) for a variety of buildings. Force coefficients are also given for clad buildings, unclad structures, and structural elements.

Wind causes pressure or suction normal to the surface of a structure. Pressures are caused both on the exterior as well as the interior surfaces, the latter being dependent on the

openings (or permeability) in the structure, mostly in the walls. Wind pressure acting normal to the individual element or cladding unit is given by

$$F = (C_{pe} - C_{pi})Ap_d \quad (3.15)$$

where F is the net wind force on the element, A the surface area of element or cladding, C_{pe} the external pressure coefficient, C_{pi} the internal pressure coefficient, and p_d the design wind pressure.

The wind pressure coefficients depend on the following factors:

1. Shape of the building or roof
2. Slope of the roof
3. Direction of wind with respect to building
4. Zone of the building

A typical industrial building elevation is shown in Fig. 3.6 along with the wind pressure coefficients, C_{pe} and C_{pi} . The building is divided into four zones and four local zones. External pressure coefficients (C_{pe}) for walls and pitched roofs of rectangular clad buildings are given in Tables 4 and 5, respectively, of this code. The internal pressure is considered positive if acting from inside to outside, whereas external pressure coefficient is considered positive when acting from outside to inside, as shown in Fig. 3.6. All buildings are

classified into four types depending on the permeability, and the corresponding internal pressure coefficients are listed in Table 3.6. Figure 3 of this code provides the internal wind pressure coefficients in buildings with large openings, exceeding 20 per cent permeability.

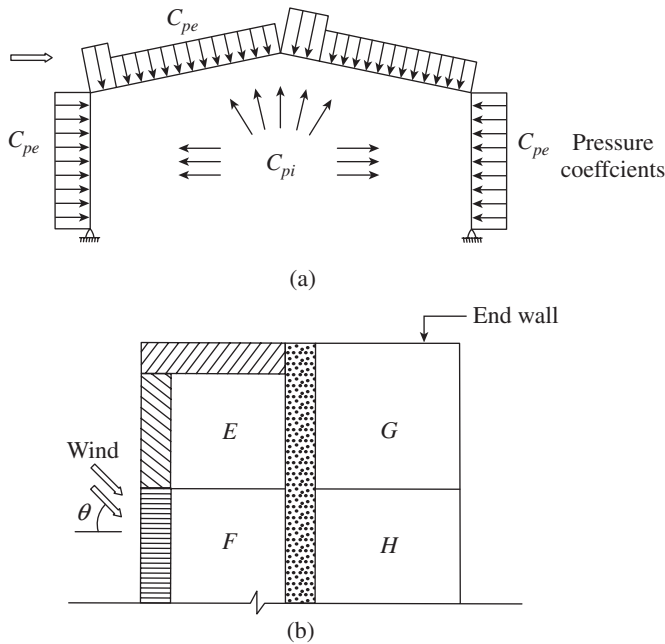


FIG. 3.6 Typical industrial building elevation along with the wind pressure coefficients (a) Typical elevation with wind pressure coefficients C_{pe} and C_{pi} (b) Half plan

TABLE 3.6 Internal pressure coefficient C_{pi}

S. No.	Type of Building	C_{pi}
1.	Buildings with low permeability (less than 5% openings in wall area)	± 0.2
2.	Buildings with medium permeability (5–20% openings in wall area)	± 0.5
3.	Buildings with large permeability (openings in wall area > 20%)	± 0.7
4.	Buildings with one side large openings	See Fig. 3 of code

It should be noted that in addition to C_{pe} local pressure coefficients are also given in Tables 4 and 5 of the code. These local pressure coefficients should not be used for calculating the force on structural elements such as roof and walls or the structure as a whole. They should be used only for the calculation of forces on the local areas affecting roof sheeting, glass panels, and individual cladding units including their fixtures.

Code IS 875 (Part 3) provides the external coefficient for mono-slope and hipped roofs, canopy roofs (e.g., open-air parking garages, railway platforms, stadiums, and theatres), curved roofs, pitched and saw-tooth roofs of multi-span

buildings, overhangs from roofs, cylindrical structures, roof and bottom of cylindrical structures, combined roofs, and roofs with skylight, grand stands, and spheres.

The total wind load for a building as a whole is given by the code as follows:

$$F = C_f A_e p_d \quad (3.16)$$

Here, F is the force acting in the specified direction, C_f the force coefficient of the structure, A_e the effective frontal area, and p_d the design wind pressure.

The code provides the force coefficients for rectangular clad buildings in uniform flow and for other clad buildings of uniform sections. The force coefficients for free-standing walls and hoardings, solid circular shapes mounted on a surface, unclad buildings, and frameworks are also given.

In certain buildings, a force due to frictional drag shall be taken into account in addition to those loads specified for rectangular clad buildings. This addition is necessary only where the ratio d/h or d/b is greater than four (where b , d , and h stand for breadth, depth, and height of the structure). The frictional drag force F' in the direction of the wind is given by the following formulae:

$$\text{If } h \leq b, \quad F' = C'_f (d - 4h) b p_d + C'_f (d - 4h) 2h p_d \quad (3.17a)$$

$$\text{If } h > b, \quad F' = C'_f (d - 4b) b p_d + C'_f (d - 4b) 2h p_d \quad (3.17b)$$

In each case, the first and second terms give the drag on the roof and on the walls, respectively. The term C'_f has the following values:

1. $C'_f = 0.01$ for smooth surfaces without corrugations or ribs across the wind direction
2. $C'_f = 0.02$ for surfaces with corrugations across the wind direction
3. $C'_f = 0.04$ for surfaces with ribs across the wind direction

3.7.1 Vortex Shedding

In general, the wind blowing past a body can be considered to be diverted in three mutually perpendicular directions, giving rise to forces and moments about the three axes. However, in structural engineering applications, the force and moment with respect to the vertical axes are not considered important (they are significant in aeronautical engineering applications). Thus, the effects of wind are considered in two dimensions, as shown in Fig. 3.7. *Along-wind* or simply wind is the term used to refer to *drag forces* and *transverse wind* is used to refer to cross-wind. The *cross-wind response*, that is, motion in a plane perpendicular to the direction of wind, dominates the along-wind response for many tall buildings (Taranath 1998). While the maximum lateral wind loading and deflection are generally in the direction parallel to the wind (along-wind direction), the maximum acceleration of the building (which

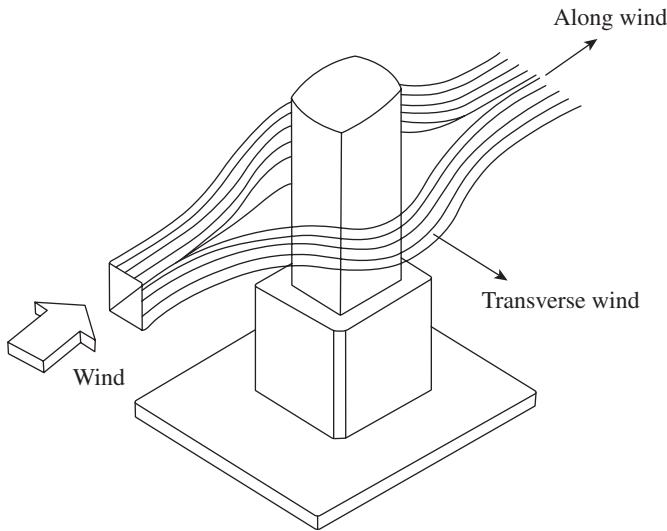


FIG. 3.7 Simplified two-dimensional flow of wind

will lead to possible human perception of motion or even discomfort) may occur in the cross-wind direction (direction perpendicular to the wind). This complex nature of wake-excited response is due to the interaction of turbulences, building motion, and dynamics of negative pressure wake formation.

Consider a circular chimney subject to wind flow, as shown in Fig. 3.8(a). The originally parallel stream lines of the wind are now displaced at the boundary of the building. These result in spiral vortices being shed (break away from the surface of the building) periodically from the sides of the building into the downstream flow of wind called the *wake*. As a result of these vortices, an impulse is applied to the building in the transverse direction. At high wind speeds, the vortices are shed alternatively first from one and then from the other side. This kind of shedding, which gives rise to vibration in the flow as well as the transverse directions of the wind, is called

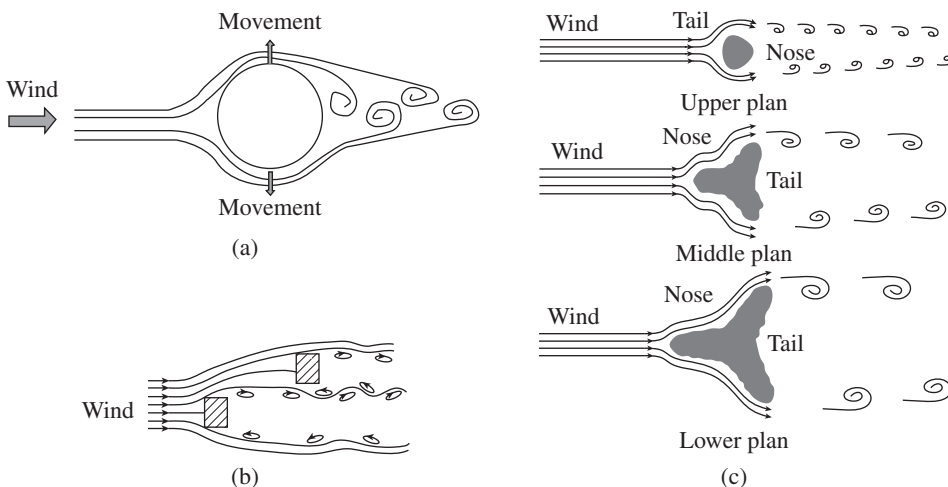


FIG. 3.8 Vortex shedding and interference effect (a) Flow around isolated building (b) Flow around two close buildings (c) Disorganized vortex shedding behaviour in Burj Khalifa due to the shape

Source: Baker, et al. 2008, CTBUH

vortex shedding. When the wind velocity is such that the frequency of vortex shedding becomes approximately equal to the natural frequency of the building, a resonance condition is created, and hence the vortex shedding will be critical. As per IS 875 (Part 3), if the length to maximum transverse width ratio is less than 2.0, vortex shedding need not be considered.

It may be of interest to note that while designing Burj Khalifa (the world’s tallest building), extensive *wind tunnel testing* was conducted. Based on this data, the number and spacing of the setbacks as well as the shape of the wings were determined. This resulted in substantial reduction in wind loads by the disorganized vortex shedding over the height of the tower, as shown in Fig. 3.8(c) (Baker, et al. 2008).

When one or more similar or dissimilar tall structures are placed downstream or upstream of the structure, the ‘stand-alone’ values of pressures and forces get altered. This is termed as the *interference effect*. Interferences will occur irrespective of whether the structures involved are rigid or flexible. In the former, it is the ‘wake’ of one structure that affects the other, whereas in the latter, the deflections of the structure affect the wake itself (see Fig. 3.8b). It is very difficult to quantify the interference effect. Systematic wind tunnel studies have to be conducted to study these effects.

3.7.2 Dynamic Effects

Dynamic response is attributed to the following actions of wind:

1. Non-correlation of the fluctuating along-wind pressures over the height and width of the structure
2. Resonant vibrations of a structure
3. Vortex shedding forces acting in a direction normal to the wind causing a cross-wind as well as torsional response

As per IS 875 (Part 3), the *dynamic effects* of winds (excitations along and across the direction of wind) should be studied for the following cases of buildings (flexible slender buildings):

1. Buildings and closed structures with a height to minimum lateral dimension ratio of more than 5.0 ($h/b > 5.0$), or heights greater than 120 m
2. Buildings and close structures whose fundamental natural frequency (first mode) is less than 1.0 Hz

For these buildings, the calculated wind pressure at height z should be multiplied by the gust factor G_f .

It should be noted that IS 875 (Part 3) is under revision, and the draft code contains several major changes, based on recent research, especially for calculating the dynamic effects of wind. The draft code stipulates that the wind pressure for flexible buildings should be multiplied by the dynamic response factor C_{dyn} , instead of the gust factor G_f (see <http://www.iitk.ac.in/nicee/IITK-GSDMA/W03.pdf>).

3.7.3 Wind Effects on Tall Buildings

High-rise buildings (more than 10 storeys) are affected by wind. For buildings with less than 10 storeys and with regular configurations, wind load will not govern the design. However, if not properly addressed, wind stress from the vortex shedding could theoretically cause major structural damage or even collapse of tall and slender buildings or structures. Skyscrapers are normally engineered according to a 50- or 100-year return period, meaning that, on an average, engineers expect winds to reach structurally dangerous speeds only once in a half century or more. Often, very tall structures are designed to resist an additional wind load of up to 60 per cent, or novel methods are incorporated to account for the uncertainty in their measurements. For example, in the Burj Khalifa towers, the setbacks in different levels were cleverly oriented, in an upward spiralling pattern, decreasing the cross section of the tower as it reached towards the sky. These

setbacks also have the advantage of providing a different width to the tower for each differing floor plate. This stepping and shaping of the tower has the effect of ‘confusing the wind’: wind vortices never get organized over the height of the building, because at each new tier the wind encounters a different building shape (see Section 2.5.8 and Figs 2.31 and 3.8c).

Buildings with shorter fundamental periods attract higher seismic forces as the code-based design spectrum exhibits higher accelerations at shorter periods. For wind design, the opposite behaviour is observed. Longer fundamental periods are indicative of buildings that are more susceptible to dynamic amplification effects from sustained wind gusts and result in higher design forces (Jacobs 2008).

It should be noted that the prescribed forces in codes are only for ‘regular-shaped’ buildings. Wind tunnel analysis should be performed for all unusually shaped structures. In the case of Burj Khalifa, wind tunnel testing led to a dramatic design change: the entire building was rotated 120° to reduce wind loading. It has also been found that wind tunnel analysis is beneficial for buildings exceeding 30 storeys in height in terms of accelerations, cladding pressures, and base overturning moments.

Wind stress can cause all kinds of problems in tall buildings. It can break windowpanes, damage the outer façade, stress

CASE STUDY

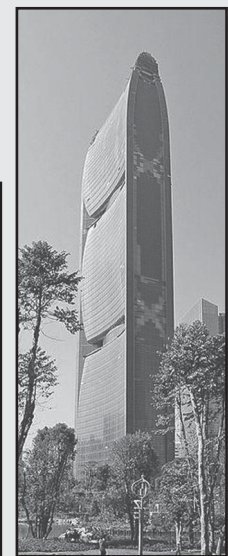
Wind as a Source of Energy in Tall Buildings

In future, wind will be treated not just as an obstacle to be overcome, but as a source of energy to be harnessed. Several skyscrapers that are under construction integrate large wind turbines into their design. The 50-storey Bahrain World Trade Center in the centre of Manama was the first to include such a wind turbine. Three 225 kilowatts, 29m diameter wind turbines hang from separate walkways connecting the identical, sail-shaped towers. Together, these turbines supply about 15 per cent of the towers’ electricity, the equivalent of the energy needed to power over 300 homes. The unique shape of the buildings directs the wind gusts towards the turbines, thereby increasing wind speeds and creating an artificial wind tunnel between the two towers (as shown in the figure).

Wind can also provide skyscrapers with natural ventilation, which along with lighting, heating, and cooling systems represents the major energy expenditure in most buildings. Some advanced building façades, like that in Pearl River Tower, Guangzhou, China, have a system for regulating natural airflow into the building. In such façades, vents in the building’s ‘skin’ are used to provide energy-efficient ventilation, powered by the prevailing winds outside (Frechette and Gilchrist 2008).



(a)



(b)

(a) Bahrain World Trade Centre, Bahrain (b) Pearl River Tower, Guangzhou, China

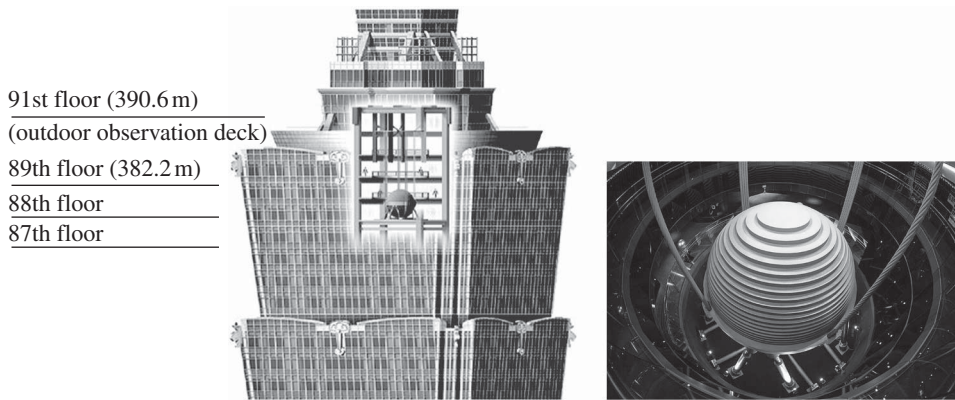


FIG. 3.9 Tuned mass damper installed at the top of Taipei 101 tower, Taiwan

building joints, cause leaking, crack walls, and create various other issues. In addition, it can result in unnerving and even nauseating or swaying the occupants. Indeed, measures to counteract the wind are undertaken as much for comfort as for safety. The happiness of the occupants is an especially important issue for structural engineers. For example, in the 508 m tall Taipei 101 tower, Taiwan (the world's tallest building from 2004 to 2010), a gold-coloured, 730-ton giant pendulum, known as a tuned mass damper, is placed between the 88th and 92nd storeys, which swings gently back and forth, balancing the tower against the forces of the wind and ensuring the comfort of its occupants (see Fig. 3.9). Tuned mass dampers are also employed in Boston's John Hancock building and New York City's Citigroup Center, for reducing the action of the wind. The size and shape of the damper is 'tuned' based on the height and mass of each particular tower. As the wind pushes the building in one direction, the damper swings or slides the other way, reducing sway, similar to the way shock absorbers on a car soften bumps in the road.

3.8 EARTHQUAKE LOADS

The crust of the earth is composed of about 13 large plates and several small ones ranging in thickness from 32 km to 240 km. The plates are in constant motion. When they collide at their boundaries, *earthquakes* occur. Some think that earthquakes may also be caused by actions such as underground explosions due to the testing of nuclear bombs, construction of dams, and so forth. Though most of the earthquakes have occurred in well-defined 'earthquake belts', a few earthquakes have hit seismically inactive parts of the world, for example, the Kutch earthquake of 26 January 2001. Hence, it is important to incorporate some measure of earthquake resistance into the design of all structures, since failures of structures due to earthquakes are catastrophic. Moreover, tall buildings may be at greater risk than single-storey buildings.

Earthquakes cause the ground to shake violently in all directions, lasting for a few seconds in a moderate earthquake or for a few minutes in very large earthquakes. Earthquakes are recorded using *accelerometers* or *seismometers*. The intensity of an earthquake reduces with the distance from the epicentre of the earthquake (*epicentre* is the location on the surface of the earth that is above the *focal point of an earthquake*). The magnitude and intensity of an earthquake are of interest to the

structural engineer. The *magnitude* is a measure of the amount of energy released by the earthquake, whereas *intensity* is the apparent effect of the earthquake. Unlike the intensity, which can vary with the location, the magnitude is constant for a particular earthquake. The magnitude is measured by the *Richter scale*, which is a logarithmic scale; for example, an earthquake that measures 5.0 on the Richter scale has a shaking amplitude 10 times larger than the one that measures 4.0 and has a 31.6 times greater energy release.

The intensity at a place is evaluated considering the three features of shaking, namely perception by people, performance of buildings, and changes to natural surroundings. Two commonly used intensity scales are the *modified Mercalli intensity (MMI) scale* and the *Medvedev-Sponheuer-Karnik (MSK) scale*. Both the MMI and MSK scales are quite similar and range from I (least perceptible) to XII (most severe). An animated guide to earthquakes is available at <http://news.bbc.co.uk/2/hi/science/nature/7533950.stm>.

In addition to the peak ground acceleration of an earthquake, the following factors also influence the seismic damage: (a) amplitude, (b) duration and frequency of ground vibration, (c) magnitude, (d) distance from epicentre, (e) geographical conditions between the epicentre and the site, (f) soil properties at the site and foundation type, and (g) the building type and characteristics.

Soil liquefaction is another effect caused by earthquakes, which produces a quicksand-type condition, resulting in the loss of the bearing capacity of the soil. Soil liquefaction may result in settlement and total collapse of structures.

Earthquake loads are dynamic and produce different degrees of response in different structures. When the ground under a structure having a mass suddenly moves, the inertia of the mass tends to resist the movement as shown in Fig. 3.10 and creates forces, called *inertia forces*, which are equal to the product of the mass of the structure and the acceleration ($F = ma$). The mass is equal to the weight (W) divided by the acceleration due to gravity, that is, $m = W/g$.

CASE STUDY

The Sichuan Earthquake, 2008

The *Sichuan earthquake* that hit Sichuan Province in western China on 12 May 2008 was of magnitude 7.9 and had a duration of about two minutes. The epicentre was in Wenchuan County, 80km west/northwest of the provincial capital city of Chengdu. More than 87,400 people lost their lives, 374,176 were injured, and 4.8 million were left homeless (estimates range from 4.8 million to 11 million). Approximately 15 million people lived in the affected area.

It was the deadliest earthquake to hit China since the 1976 Tangshan earthquake (which killed at least 240,000 people) and the strongest since the Chayu earthquake (8.5 Richter scale) of 1950. Strong aftershocks, some exceeding a magnitude of 6, continued to hit the area months after the main quake, causing more casualties and damage. This very disastrous earthquake was classified as XI, under the Modified Mercalli intensity scale. Over 7000 schoolrooms and numerous buildings collapsed in the earthquake.



Complete collapse of RC buildings during the 2008 Sichuan earthquake

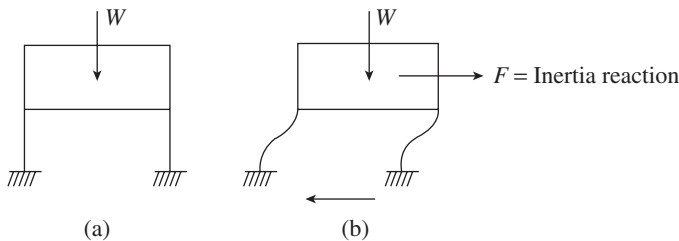


FIG. 3.10 Force developed due to an earthquake (a) At rest (b) Under horizontal motion from the earthquake

In IS 1893 (Part 1) code, the following seismic design philosophy has been adopted:

1. Minor and frequent earthquakes should not cause any damage to the structure.

2. Moderate earthquakes should not cause significant structural damage but could have some non-structural damage (structure will become operational once the repair and strengthening of the damaged main members are completed).
3. Major and infrequent earthquakes should not cause collapse (the structure will become dysfunctional for further use, but will stand so that people can be evacuated and property recovered).

Hence, the structures are designed for much smaller forces than actual seismic loads during strong ground shaking. It should be noted that this approach is different from that adopted in the case of wind, dead, imposed, and other loads, where the structure is designed for the anticipated loads.

CASE STUDY

The Indian Ocean Tsunami, 2004

The Indian Ocean tsunami was due to an undersea earthquake (Sumatra–Andaman earthquake) that occurred on 26 December 2004, with an epicentre off the west coast of Sumatra, Indonesia. The quake, with a Richter magnitude of 9.1 to 9.3, is the second largest earthquake ever recorded on a seismograph. It had the longest duration ever observed, between 8.3 and 10 minutes.

This earthquake caused an estimated 1600km fault surface to slip under the ocean to about 15m, resulting in the earthquake (followed by the tsunami) to be felt simultaneously as far away as Bangladesh, India, Malaysia, Myanmar, Thailand, Singapore, and the Maldives. The slip did not happen instantaneously but

took place in two phases over a period of several minutes. Due to the slip, the sea floor is estimated to have risen by several metres, displacing an estimated 30km³ of water and triggering devastating tsunami waves. Because of the distances involved, the tsunami took from fifteen minutes to seven hours to reach the various coastlines. In many places, the waves reached as far as 2km inland. The wave reached a height of 24m when coming ashore along large stretches of the coastline, rising to 30m in some areas when travelling inland.

An analysis by the United Nations found that a total of 229,866 people were lost, including 186,983 dead and 42,883 missing,

(Continued)

(Continued)

due to the tsunami in towns and villages along the coast of the Indian Ocean. The livelihoods of over three million survivors were destroyed. Beyond the heavy toll on human lives, it had caused an enormous environmental impact that will affect the region for many years to come.

Guidelines for the design of structures against tsunami are scarce (it is generally not feasible or practical to design normal structures to withstand tsunami loads), but warning and evacuation systems have been developed (see FEMA 55 and FEMA P646 at www.fema.gov).

For the purpose of determining seismic forces, India is classified into four *seismic zones* (zones II to V) by IS 1893 (Part 1) code (see Fig. 1 of the code). Recently, the National Disaster Management Authority, Government of India, has developed the *Probabilistic Seismic Hazard Map* (PSHM) of India, which provides better estimates of seismic intensity (<http://ndma.gov.in/ndma/disaster/earthquake/Indiapshafinalreport.pdf>). The code requires that the designer either use a dynamic analysis of the structure or, for the usual generally rectangular medium height buildings (regular buildings), use an empirical lateral base shear force (see Table 3.7). The dynamics of earthquake action on structures is outside the scope of this book, and the reader may refer to Chopra (2000), Clough and Penzien (1993), and Kappos and Penelis (1996) for the details of these dynamic analysis methods.

TABLE 3.7 Requirement of dynamic analysis as per IS 1893 (Part 1)

Seismic Zone	Regular Buildings	Irregular Buildings
II and III	Height > 90 m	Height > 40 m
IV and V	Height > 40 m	Height > 12 m

Notes:

1. Large-span industrial buildings may also require dynamic analysis.
2. Buildings with a high level of torsion irregularity are prohibited in zones IV and V.

For regular buildings, IS 1893 (Part 1) code suggests that the *design horizontal seismic coefficient* A_h for a structure may be determined by the following simplified expression:

$$A_h = ZI(S_d/g)/(2R) \quad (3.18)$$

Here, Z is the *zone factor*, given in Table 2 of IS 1893 (Part 1), for the *maximum considered earthquake* (MCE) (the factor of two in the denominator of Eq. (3.18) is used to reduce the MCE to *design basis earthquake*). I is the *importance factor*, depending on the functional use of the structure; it is given in Table 2 of IS 1893 (Part 1). R is the *response reduction factor*, depending on the perceived seismic damage performance of the structure, characterized by ductile or brittle deformations. The values of R for different types of RC buildings are given in Table 7 of IS 1893 (Part 1); a value of $R = 3$ is assumed for ordinary RC moment-resistant frames or for ordinary RC shear walls, $R = 4$ for ductile shear walls, and $R = 5$ for special RC moment-resistant frames. (S_d/g) is the *response acceleration coefficient* as given by Fig. 2 of IS 1893 (Part 1),

or Eqs 3.19 to 3.21, based on the appropriate natural periods and damping of the structure.

A plot of the maximum response (for example, acceleration, velocity, or displacement) against the period of vibration or the natural frequency of vibration is called a *response spectrum*. Using several earthquake spectra, a smooth spectrum representing an upper bound response to ground motion is normally used in the codes. Figure 2 of the code shows such a spectrum adopted by the code. The values given in Fig. 2 of the code can be represented mathematically by the following equations:

1. For rocky or hard soil sites:

$$S_d/g \begin{cases} = 2.50 & 0.0 \leq T \leq 0.10 \text{ (for fundamental mode)} \\ = 1 + 15T & 0.0 \leq T \leq 0.10 \text{ (for higher modes)} \\ = 2.50 & 0.10 \leq T \leq 0.40 \\ = 1.0/T & 0.40 \leq T \leq 4.00 \\ = 0.25 & T > 4.00 \end{cases} \quad (3.19)$$

2. For stiff soil sites:

$$S_d/g \begin{cases} = 2.50 & 0.0 \leq T \leq 0.10 \text{ (for fundamental mode)} \\ = 1 + 15T & 0.0 \leq T \leq 0.10 \text{ (for higher modes)} \\ = 2.50 & 0.0 \leq T \leq 0.55 \\ = 1.36/T & 0.55 \leq T \leq 4.0 \\ = 0.34 & T > 4.0 \end{cases} \quad (3.20)$$

3. For soft soil sites:

$$S_d/g \begin{cases} = 2.50 & 0.0 \leq T \leq 0.10 \text{ (for fundamental modes)} \\ = 1 + 15T & 0.0 \leq T \leq 0.10 \text{ (for higher modes)} \\ = 2.50 & 0.0 \leq T \leq 0.67 \\ = 1.67/T & 0.67 \leq T \leq 4.00 \\ = 0.42 & T > 4.00 \end{cases} \quad (3.21)$$

The multiplying factors for obtaining S_d/g values for other *damping* (these should not be applied to the point at zero period) are given in Table 3 of IS 1893 (Part 1).

3.8.1 Natural Frequencies

A structure with n degrees of freedom has N *natural frequencies* and N *mode shapes*. The lowest of the natural frequencies of the structure is called its *fundamental natural frequency* or just *natural frequency* expressed in Hz. The associated natural period is called the *fundamental natural period*, which is the reciprocal of the natural frequency and is expressed in seconds. Where a number of modes are to be considered for dynamic analysis, the value of A_h (see

Eq. 3.18) should be determined using the natural period of vibration of that mode. For underground structures and foundations at depths of 30m or more, the design horizontal acceleration spectrum value is taken as half the value obtained from Eq. (3.18). For structures and foundations placed between the ground level and 30m depth, the value can be linearly interpolated between A_h and $0.5A_h$. For vertical motions, the value shall be taken as two-thirds the design horizontal acceleration spectrum; see Clause 6.4 of IS 1893 (Part 1):2002.

The approximate fundamental natural period of vibration, T_a , in seconds, for a *moment-resisting concrete frame* without *brick infill* panels is given by the code as follows (FEMA 450 2003; Goel and Chopra 1997):

$$T_a = 0.075h^{0.75} \quad (3.22a)$$

where h is the height of the building in metres.

ASCE/SEI 07–10 provides the following equation:

$$T_a = 0.0466h^{0.9} \quad (3.22b)$$

For buildings with up to 12 storeys and having a storey height of at least 3 m,

$$T_a = 0.1n \quad (3.22c)$$

where n is the number of storeys.

For all other buildings, including moment-resisting frame buildings with brick infill, T_a is given by IS 1893 (Part 1) as

$$T_a = 0.09h/\sqrt{d} \quad (3.22d)$$

where d is the base dimension of the building at the plinth level, along the considered direction of the lateral force, in metres.

More accurate estimates of natural period may be obtained by using Rayleigh's method, as follows:

$$T_1 = 2\pi \frac{\sum_{i=1}^n W_i \Delta_i}{\sum_{i=1}^n F_i \Delta_i} \quad (3.23)$$

where F_i are the lateral loads applied at levels $i = 1$ to n , Δ_i refers to the corresponding lateral displacements, and W_i are the floor weights. It should be noted that for the evaluation of Eq. (3.23), the displacements Δ_i are required, and these may be obtained by any computer program based on stiffness analysis.

ASCE/SEI 07–10 provides the following approximate equation for *shear walled buildings* (Goel and Chopra 1998):

$$T_a = \frac{0.0062}{\sqrt{C_w}} h \quad (3.24a)$$

where $C_w = \frac{100}{A_B} \sum_{i=1}^x \left(\frac{h}{h_i} \right)^2 \left[\frac{A_i}{1 + 0.83 \left(\frac{h_i}{D_i} \right)^2} \right]$, A_B is the area of

the base of the structure in m^2 , A_i is the web area of the shear wall i in m^2 , D_i is the length of the shear wall i in m, h_i is the height of the shear wall i in m, and x is the number of shear walls in the building effective in resisting the lateral forces in the direction under consideration. For buildings with up to 12 storeys and having a storey height of at least 3 m,

$$T_a = 0.05n \quad (3.24b)$$

where n is the number of storeys.

It is suggested by the code to adopt only the approximate natural period given by Eq. (3.22) or (3.23) in the calculations, even though one may obtain an exact value, especially for irregular structures (which may be more than this value) by using a dynamic analysis computer program. It is to safeguard the structure against the application of lower design seismic forces calculated using the large natural period obtained by the programs. Several approximate methods for structural seismic design may be found in Scarlat (1995).

3.8.2 Equivalent Static Method

In the *equivalent static method* (also referred to as the *seismic coefficient method*), which accounts for the dynamics of the building in an approximate manner, the total design seismic base shear is determined by the following relation:

$$V_B = A_h W \quad (3.25)$$

Here, A_h is the design horizontal acceleration spectrum value as per Eq. (3.18) using the approximate fundamental natural period T_a as given in Eq. (3.22) in the considered direction of vibration and W is the seismic weight of the building.

Buildings provide a certain amount of damping due to internal friction, slipping, and so forth. It is usually expressed as a percentage of critical damping. A damping of five per cent of the critical is considered for the RC structures as per Clause 7.8.2.1 of IS 1893 (Part 1).

The seismic weight of each floor is calculated as its full dead load plus the appropriate amount of imposed load (Table 3.8). While computing the seismic weight of each floor, the weight of the columns and walls in any storey should be appropriately apportioned to the floors above and below the storey. It has to be noted that buildings designed for storage purposes are likely to have large percentages of service load present at the time of earthquake shaking. Other appropriate loads such as snow and permanent equipment should also be considered.

TABLE 3.8 Percentage of imposed load to be considered in seismic weight calculation

Imposed Uniformly Distributed Floor Load (kN/m ²)	Percentage of Imposed Load
Up to and including 3.0	25
Above 3.0	50

Note: The imposed load on roof need not be considered. No further reduction for large areas or for the number of storeys above the one under consideration (as envisaged in IS 875—Part 2) for static load cases is allowed.

After the base shear force V_B is determined, it should be distributed along the height of the building (to the various floor levels) using the following expression:

$$Q_i = V_B \left(\frac{W_i h_i^k}{\sum_{j=1}^n W_j h_j^k} \right) \quad (3.26)$$

where Q_i is the design lateral force at floor i , W_i is the seismic weight of floor i , h_i is the height of floor i measured from base, and n is the number of storeys in the building. The value of k equal to two is adopted in the Indian code. The use of the equivalent static method is explained in Example 3.5.

After obtaining the seismic forces acting at different levels, the forces and moments in the different members can be obtained by using any standard computer program for the various load combinations specified in the code. The structure must also be designed to resist the overturning effects caused by the seismic forces. Moreover, storey drifts and member forces and moments due to P-delta effects must be determined. It should be noted that all cantilever vertical projections are to be designed for five times the design horizontal seismic coefficient A_h and the horizontal projections should be checked for stability for five times the design vertical component (i.e., $10/3A_h$).

In tall buildings the contribution of higher modes may be important, in irregular buildings the mode shape may not be regular, and in industrial buildings (with large spans and heights) the assumptions of the static procedure (the fundamental mode of vibration is the most dominant, and mass and stiffness are evenly distributed) may not be valid. Hence, for these buildings, the code suggests dynamic analysis methods, which are grouped into *response spectrum method* (multi-storey buildings, irregular buildings, overhead water tanks, and bridge piers are often designed using this method) and *time-history response analysis* (very important structures such as nuclear reactors, large-span structures, or very tall buildings are designed using this method). These methods require some knowledge of structural dynamics and are not covered in this book. For more details, the reader may refer to Bozorgnia and Bertero (2004).

3.8.3 Rules to be Followed for Buildings in Seismic Areas

For better seismic response, proper precautions need to be taken at the planning stage itself (Murty 2005). It is preferable

to select a site where the bedrock is available close to the surface, so that foundations can be laid directly on the rock. The differential movement of foundation due to seismic motions is an important cause of structural damage, especially in heavy, rigid structures that cannot accommodate these movements. Hence, if the foundation is on soft soil with spread footings, adequate plinth or tie beams should be provided to counter differential settlement. If the loads are heavy, pile foundations with strong pile caps may be provided. Raft foundation is also good to resist differential settlements, but may prove to be expensive. In sandy or silty soils, if the water table is near the foundation level, appropriate methods must be adopted to prevent liquefaction.

To perform well in an earthquake, a building should possess the following four main attributes: (a) simple and regular configuration, (b) adequate lateral strength, (c) adequate stiffness, and (d) adequate ductility. Figure 3.11 shows the irregular configurations that are to be avoided and the regular configurations that result in better earthquake performance. The openings in a wall should be centrally located and should be of a small size so that the wall is not unduly weakened. (Ventilators provided near the edges of walls, adjacent to columns, will create a *short column effect* and result in the failure of the column. Similar effect will be created if openings are provided from column to column.) Long cantilevers and floating columns should be avoided. Appendages such as sunshades (*chajjas*) and water tanks should be designed for higher safety levels, or best avoided.

Concrete stairways often suffer seismic damage due to their inhibition of drift between connected floors. This can be avoided by providing a slip joint at the lower end of each stairway to eliminate the bracing effect of stairway or by tying the stairways to stairway shear walls.

Masonry and infill (non-structural) walls should be reinforced by vertical and horizontal reinforcing bands to avoid their failure during a severe earthquake. Other non-structural elements should be carefully detailed or tied so that they may not fall under severe shaking.

It should be noted that the failure of a beam causes localized effect whereas the failure of a column may affect the stability of the whole building. Hence, it is better to make columns stronger than beams. This can be achieved by appropriate sizing of the member and detailing. This concept is called *strong column-weak beam* design (see also Section 13.9.1).

When buildings are too close to each other, they may pound on each other. Connections and bridges between buildings should be avoided and buildings with different sizes and shapes should have an adequate gap between them to avoid *pounding*. When building heights do not match, the roof of the shorter building may pound at the mid-height of the columns of the taller one, which will result in dangerous consequences (Bachmann 2003). The buildings or two adjacent units of the


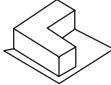
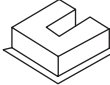




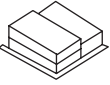


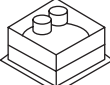

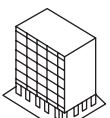
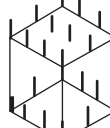

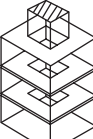
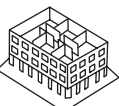
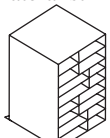
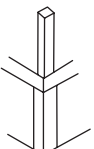
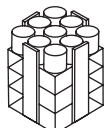
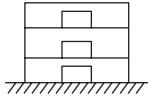
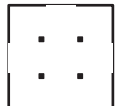
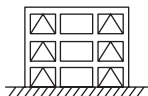
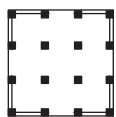
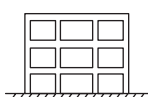
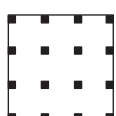
Irregular configurations						Regular configurations	
(a) Buildings with irregular configuration							
							
T-shaped plan	L-shaped plan	U-shaped plan	Cruciform plan	Other complex shapes			
							
Setbacks	Multiple towers	Split levels	Unusually high storey	Unusually low storey	Outwardly uniform appearance but non-uniform mass distribution or converse		
(b) Buildings with abrupt changes in lateral resistance							
							
'Soft' lower levels	Large openings in shear walls	Interruption of columns	Interruption of beams	Openings in diaphragms			
(c) Buildings with abrupt changes in lateral stiffness							
							
Shear walls in some storeys, moment-resisting frames in others	Interruption of vertical-resisting elements	Abrupt changes in size of members	Drastic change in mass/stiffness ratio				
							
							Shear walls
							
							Braced frames
							
							Moment-resistant frames

FIG. 3.11 Irregular and regular configurations with reference to earthquake performance

Source: Ar. Gabor Lorant of Gabor Lorant Architects Inc.

same building should be separated by a distance equal to R times the sum of the calculated storey displacements to avoid pounding; the value of R is given in Table 7 of IS 1893 (Part 1). This value may be multiplied by a factor of 0.5 if the two units have the same floor elevation.

Buildings having simple regular geometry and uniformly distributed mass and stiffness in plan and elevation (regular structures) have been found to suffer less damage in earthquakes than buildings with irregular structures. Hence, columns and walls should be arranged in grid fashion and should not be staggered in plan. The effect of asymmetry will induce torsional oscillations of structures and stress concentrations at re-entrant corners (Murthy 2005). These irregularities may be grouped as *plan irregularities* and *vertical irregularities* (see also Fig. 3.11).

3.8.4 Devices to Reduce Earthquake Effects

In addition to the aforementioned guidelines for analysis and design, the structural engineer now has the option of using a variety of devices to ensure the safety or serviceability

of the structure under severe earthquakes. These devices either isolate the structure from ground vibration or absorb the energy provided by the earthquake to the building (similar to the shock absorbers provided in motor vehicles, which absorb the vibrations caused by the undulated road surfaces).

Base Isolation

The concept of *base isolation* is to introduce springs or special rubber pads between the ground and the foundation of the structure, such that the building is isolated from the ground. (This concept is similar to the provision of neoprene bearings at the supports below the bridge decks.) These flexible pads, called *base isolators*, introduce flexibility in the structure, thereby increasing the time period. Thus, the forces induced by ground shaking will be much smaller than that experienced by 'fixed-base buildings' directly resting on the ground. The buildings resting on such base isolators are called *base-isolated buildings*. Moreover, the isolators are designed to absorb the energy and thus increase the

damping of the building. These base isolators may be either coiled springs or laminated rubber bearing pads, made of alternate layers of steel and rubber (Fig. 3.12a) and have a low lateral stiffness. Figure 3.12(b) shows an actual base isolator.

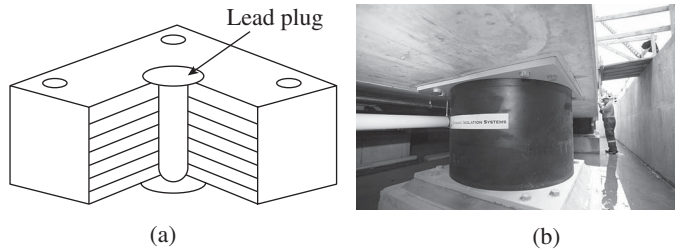


FIG. 3.12 Seismic base isolators (a) Laminated rubber bearing pad (b) External view

Base isolators are found to be useful for short-period structures, those with fundamental periods including soil–structure interaction that is less than 0.7 seconds. IS 1893 code permits the use of only standard devices having detailed experimental data on the performance. In India, rubber base isolators have been used in two single-storey brick masonry buildings (a school and a shopping centre) in Killari, Maharashtra, and in a four-storey Bhuj hospital after the 2001 Bhuj (Gujarat) earthquake. Base isolation has been successfully implemented in several hundreds of buildings in countries such as USA, Japan, New Zealand, and Italy.

Energy-absorbing Devices

Another approach for controlling seismic damage in buildings and improving seismic performance is by installing *dampers* (seismic energy dissipating devices) mounted on structures (especially on diagonal braces). They act like the hydraulic shock absorbers provided in automobiles, which absorb the vibration of sudden jerks and transmit only a part of the vibration above the chassis of the vehicles. Dampers were first used in the 1960s to absorb the vibration caused by winds in tall buildings and are being used to protect buildings against the effects of earthquakes only since the 1990s. When the device merely absorbs the energy during vibration without any energy input from outside, it is termed as a *passive device*. On the other hand, if it opposes the vibration by means of an

external energy source, it is called an *active device*. Commonly used dampers include the following (see Fig. 3.13):

1. *Viscous dampers*: They consist of a piston–cylinder arrangement filled with a viscous silicon-based fluid, which absorbs the energy.
2. *Friction dampers*: The energy is absorbed by the friction between two layers, which are made to rub against each other.
3. *Hysteretic dampers*: The energy is absorbed by yielding metallic parts.
4. *Visco-elastic dampers*: They contain a visco-elastic material sandwiched between two steel plates, which undergoes shear deformation, thus dissipating energy.

The following are the other types of dampers:

1. *Tuned mass dampers (TMD)*: They are extra masses attached to the structure by a spring–dashpot system and designed to vibrate out of phase with the structure. Energy is dissipated by the dashpot due to the relative motion between the mass and the structure (see Section 3.7.3 and Fig. 3.9).
2. *Tuned liquid dampers (TLD)*: They are essentially water tanks mounted on the structures, which dissipate energy by the splashing of the water. The motion of the liquid may be hindered by orifices to obtain additional energy dissipation.
3. *Hydraulic activators*: They are active vibration control devices and have a sensor to sense the vibration and activate the activator to counter it. These devices require an external energy source and are expensive.

More information on base isolators and energy-absorbing devices may be found in Naeim and Kelly (1999).

3.9 OTHER LOADS AND EFFECTS

The guidelines for special loads due to foundation movements, temperature effects, soil and hydrostatic pressure, erection loads, accidental loads, and so forth are provided by IS 875 (Part 5) and Taly (2003). Details of blast loading are provided in IS 6922. It is important for the engineer to accurately calculate, as per the codal provisions, the different loads acting on a structure, as overestimation of loads will result in uneconomical structures and underestimation will result in sudden failures.

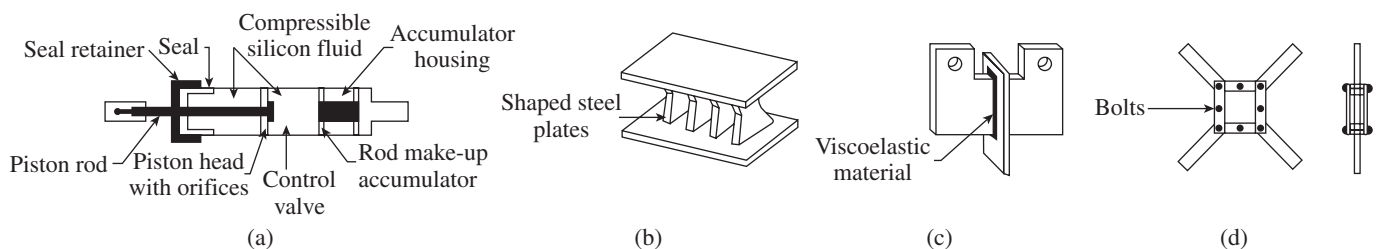


FIG. 3.13 Types of dampers (a) Typical viscous damper (b) Typical hysteretic damper (c) Typical visco-elastic damper (d) Typical friction damper

3.9.1 Foundation Movements

Foundation movements result in three types of distortions: (a) maximum (absolute settlement), (b) average (vertical) tilt, and (c) angular distortion. It has been found that angular distortion due to differential settlement is responsible for the major cracking of buildings (Venugopal and Subramanian 1977). Permissible values of total settlement, differential settlement, and angular distortion are given in IS 1904. It is prudent to design the foundations in such a way as to limit the angular distortion within the permissible limits. Plinth beams, connecting the foundations, may be provided to take care of differential settlements. While designing the plinth beams, a possible differential settlement of 12 mm may be considered.

3.9.2 Thermal and Shrinkage Effects

As per Clause 19.5.1 of IS 456, temperature fluctuations and shrinkage and creep effects may be ignored in buildings whose lateral dimension does not exceed 45 m. As per Clause 27.2 of the code, if the lateral dimension of the building exceeds 45 m, temperature effects must be considered in the design, or suitable expansion or contraction joints in accordance with IS 3414 should be provided. Similarly, structures that have abrupt changes in plan should be provided with expansion joints at places where such changes occur. These expansion joints facilitate the necessary movements to occur with minimum resistance at the joint. Usually, the two separated structures are supported on separate columns or walls, but need not necessarily be on separate foundations. Reinforcements should not extend across the expansion joint, and there should be a complete break between the sections.

Guidance for the design and construction of joints in RC buildings is provided by CIRIA Report 146 (1995), Varyani and Radhaji (2005), and Pfeiffer and Darwin (1987). Length between the expansion joints versus design temperature change ΔT , as given in ACI 224.3R (1995), by two different methods is provided in Fig. 3.14. Because of the additive volume change due to drying shrinkage (which is taken care of by the term $T_s = 17^\circ\text{C}$), the joint spacing given by Fig. 3.14(a) is governed by contraction instead of expansion.

The maximum variation in temperature in a particular location can be determined from Figs 1 and 2 of IS 875 (Part 5). A few software packages, such as ANSYS and ABAQUS, are capable of doing temperature analysis (Saetta, et al. 1995). As per Clause 6.2.6 of IS 456, the *coefficient of thermal*

expansion for concrete, α_c , varies from 6×10^{-6} mm/mm per degree Celsius (for concrete with limestone aggregates) to 12×10^{-6} mm/mm per degree Celsius (for concrete with siliceous aggregates—sandstone and quartzite). An average value of 10×10^{-6} mm/mm per degree Celsius may be taken for concrete members. The displacement Δ , due to temperature differential Δt , for a length of L , may be computed as (Fintel 1974)

$$\Delta = \alpha_c \Delta t L \tag{3.27}$$

The spacing of expansion joints is affected by many factors such as building shape, material type and associated properties (such as shrinkage of concrete or long-term axial shortening due to pre-stress), fixed or pinned bases, restraints to movement such as walls and bracing and their relative location in the structure, heated or air conditioned interiors and the reliability of those systems, expected diurnal and seasonal temperature differential, storey height, column stiffness, and effective reserve capacity of the column section available for resisting temperature loading, which, in turn, depends mainly on the percentage of reinforcement and the width of the building. Square buildings may require smaller spacing than rectangular ones (Varyani and Radhaji 2005). As mentioned previously, temperature stresses are important in the design of chimneys, cooling towers, and structures designed to resist loads due to fires.

Shrinkage and Temperature Reinforcement

Slabs and other elements exposed to the sun’s radiation also develop temperature stresses. In such occasions, nominal reinforcements are often provided, close to the surface that is being affected, to take care of temperature and shrinkage.

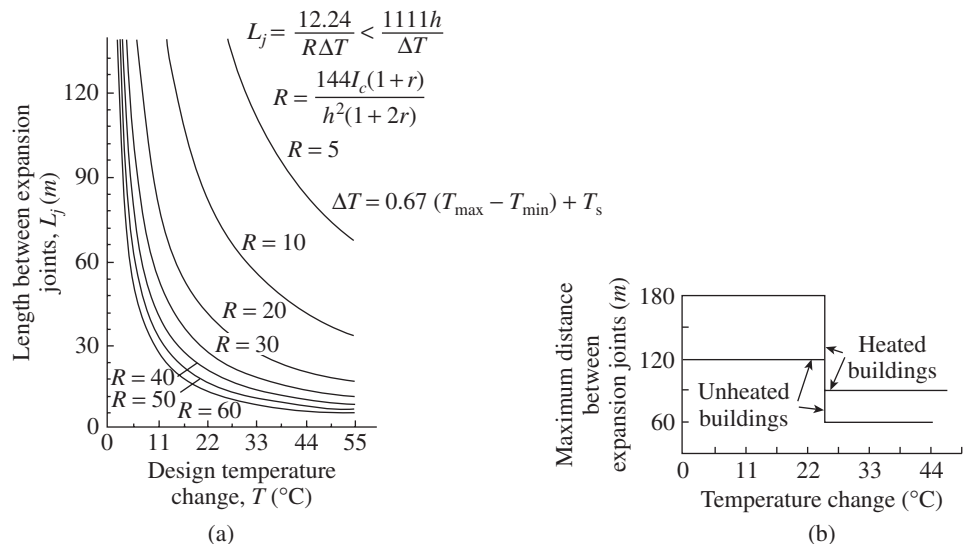


FIG. 3.14 Length between expansion joints versus design temperature change ΔT , as given in ACI 224.3R (1995) (a) Graph as per Martin and Acosta method (1970) (b) Graph as per National Academy of Sciences (1974) (Reprinted with permission from ACI)

Where shrinkage and temperature movements are permitted to occur freely, the codes specify the amount of shrinkage and temperature reinforcement, as shown in Table 3.9. These values specified in the codes have not changed for a long time and are empirical, but they have been used satisfactorily for many years. ACI 318 also suggests that such reinforcements should have a maximum spacing of five times the slab thickness or 450 mm, whichever is smaller. Splices and end anchorages of shrinkage and temperature reinforcements should be designed for the full specified yield strength, according to the ACI code. In one-way slabs, shrinkage and temperature reinforcement are provided normal to the flexural reinforcement (over the flexural reinforcement, or bottom bars, in the positive moment region and below the flexural reinforcement, or top bars, in the negative moment region).

TABLE 3.9 Minimum ratios of temperature and shrinkage reinforcement in slabs based on gross concrete area

Code	IS 456:2000 (Clause 26.5.2.1)	ACI 318:2008 (Clause 7.12.2.1)	NZS 3101:2006 (Clause 8.8.1)
Slabs with mild steel bars	0.0015	0.0020 ($f_y = 280$ MPa and 350 MPa)	0.7/ $f_y \geq 0.0014$
Slabs with high-strength deformed bars or welded wire fabric	0.0012	0.0018 ($f_y = 420$ MPa)	
Slabs with reinforcements having yield strength greater than 420 MPa	NA	0.0018 \times 420/ f_y ≥ 0.0014	

Concrete shrinks as it dries out, as pointed out in Section 1.8.8. Usually, slabs and other members are joined rigidly to other parts of the structure and cannot contract freely. This will result in tensile stresses, known as *shrinkage stresses*. In such situations, it may be necessary to provide more reinforcement than that suggested for minimum steel; otherwise, the slabs will crack due to shrinkage stresses. However, analysing the effects of shrinkage or temperature change is complicated and neither the Indian nor the ACI code provides guidance for determining these effects. However, Clause 9.4.3 of the Australian code, AS 3600:2001, and ACI 209 R-92 provide some guidance. The shrinkage and temperature reinforcement required for a fully restrained slab could be double that required by ACI 318 (Gilbert 1992). Cracks due to restrained drying shrinkage can be serious because, unlike flexural cracks, they can extend over the full depth of the member. The minimum steel requirements will not eliminate shrinkage cracking but will control crack widths. More details on shrinkage

and temperature reinforcement can be found in Suprenant (2002).

Shrinkage Strip and Shrinkage Compensating Concrete

A *shrinkage strip* or *pour strip* is a temporary joint in the structure that is left open for a certain time during construction to allow a significant part of shrinkage to take place. However, they are expensive and delay the construction because of the following reasons:

1. Reshores must be left in place for an extended time (in 12 weeks, pour strips may address only about half the potential shrinkage).
2. The presence of reshores in pour strip bays delays the completion of the mechanical, electrical, and plumbing systems, as well as the installation of final finishes.
3. The process of forming, placing, and finishing pour strips is labour intensive; additional reinforcing bars and labour are often required in pour strip bays (Suprenant 2002).

Hence, the better alternative would be to use *shrinkage compensating concrete*, also known as *K-concrete* (containing calcium aluminates) in USA. Shrinkage compensating concrete is a concrete made with expansive cement, which will expand by an amount equal to or slightly greater than the anticipated drying shrinkage. Ideally, a residual compression will remain in the concrete, reducing the risk of shrinkage cracking (Eskildsen, et al. 2009). In USA and Russia, expansive cements are available, whereas in Japan they are produced by adding expansive admixtures to ordinary Portland cement. These cements contain or are blended with combinations of calcium sulphate, calcium aluminates, and calcium aluminate sulphates. Although their characteristics are in most respects similar to those of Portland cement concrete, the materials, selection of proportions, placement, and curing must be such that sufficient expansion is obtained to compensate for subsequent drying shrinkage. The cost of shrinkage compensating concrete may be 20 per cent more than comparable Portland cement concrete. More details about shrinkage compensating concrete may be found in ACI 223 R-10.

3.9.3 Soil and Hydrostatic Pressure

In the design of structures below ground level, for example, basement walls and retaining walls, the pressure exerted by the soil or water, or both, must be considered (see Fig. 3.15). Permissible bearing pressures on subsoil are given in Appendix A. The water pressure, p_w , is given by

$$p_w = \gamma_w H \quad (3.28)$$

where γ_w is the unit weight of water (10 kN/m³) and H is the height of the (subsoil) water retained.

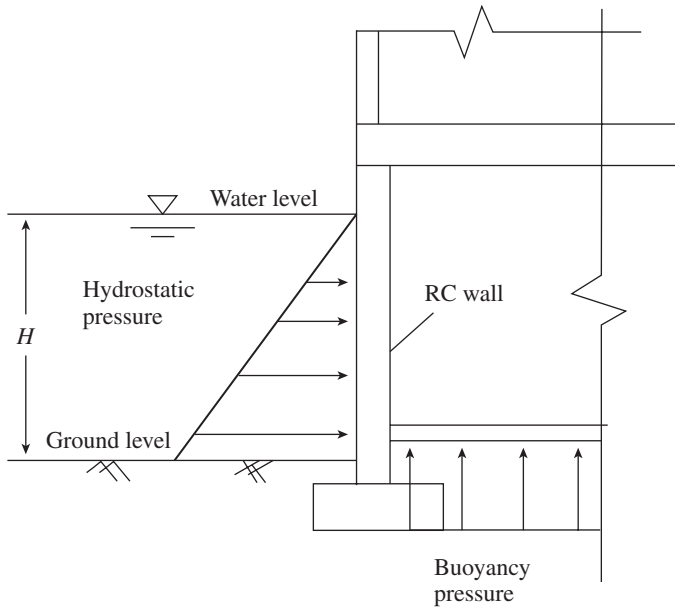


FIG. 3.15 Soil or hydrostatic pressure on retaining wall

Many established theories are available (Bowles 1990) to calculate the active earth pressures. The active earth pressure as per Rankine's theory for cohesionless soil is given by

$$p_e = \frac{1 - \sin \phi}{1 + \sin \phi} \gamma_e H \quad (3.29)$$

where γ_e is the unit weight of earth and ϕ is the angle of repose of the soil.

When a portion or whole of the soil is below the free water table, lateral earth pressure shall be evaluated by considering the reduced weights of soil (due to buoyancy) and the full hydrostatic pressure. All foundation slabs and other footings below the water table should be designed to resist a uniformly distributed uplift equal to the full hydrostatic pressure.

The structures should be checked against overturning and horizontal sliding. Imposed loads having favourable effect should be disregarded for this purpose. Due consideration should be given to the possibility of the soil being permanently or temporarily removed and for the foundation under submerged condition (only buoyant weight of the foundation or soil should be taken in the calculation for overturning). More details on earth pressures and retaining wall design are provided in Chapter 16.

3.9.4 Erection and Construction Loads

Erection loads are very important for precast concrete members. It is also important to temporarily brace the structures during erection for safety and stability. In addition, the construction of slabs in multi-storey RC construction often employs shoring and formwork such that the weight of the newly cast slab plus the working load are transferred to one or more previously placed slabs. The construction loads on the supporting floors may often exceed the slab design loads during maturity, especially when the design live load is small

compared with the dead load. (This situation is encountered in residential multi-storey buildings.) Insufficient support will result in serviceability problems such as deflected slabs and beams with radial cracks around columns. At an early age, concrete is susceptible to tensile cracking. Concrete failure due to deficiency in tensile strength, and consequently low shear resistance, is the most serious type of slab failure.

Hence, formwork should not be removed until the concrete attains the strength sufficient to carry the construction loads. It is also important to have one level of shores and two levels of reshores to distribute the load to several levels. Such a system will also permit the placement of one storey per week in the most economical manner. Adequate temporary lateral bracing of shores reduces the possibility of formwork collapse due to overloading forms and lateral pressure caused by wind, movement of heavy equipment, and impact of placement of concrete.

Simulation of construction sequence in the analysis of the frames of multi-storey buildings leads to a considerable variation in the design moments obtained by conventional one-step analysis. Hence, for an accurate evaluation of the forces in the members, frames must be analysed considering the construction sequence. More details about this type of analysis and shoring/reshoring may be found in Chen and Mosallam (1991) and ACI 347.2R-05.

3.9.5 Flood Loads

The warming up of the atmosphere has resulted in heavy, unprecedented floods in several parts of the world. Hence, it has now become necessary to protect structures against such floods. Storm-induced erosion and localized scour can lower the ground surface around the foundations of buildings and cause loss of load-bearing capacity and loss of resistance to lateral and uplift loads. Flood loads include the following: (a) hydrostatic, including buoyancy or floatation effects, (b) breaking wave, (c) hydrodynamic, and (d) debris impact (from waterborne objects). Provisions regarding this are lacking in the Indian code and interested readers may refer to ASCE/SEI 07-10 and ASCE 24-05 for more details.

3.9.6 Axial Shortening of Columns

Axial shortening of columns due to long-term creep and shrinkage is inevitable in tall RC buildings having 30 storeys or more. However, calculation of the exact values of axial shortening is not a straight forward task since it depends on a number of parameters such as the type of concrete, reinforcement ratio, and the rate and sequence of construction. All these parameters may or may not be available to the design engineer at the preliminary design stage of construction. Furthermore, long-term shortening of columns could affect the horizontal structural members such as beams and floors and hence could affect the finishes and partitions. The axial

shortening at any floor level n , Δ_n , could be calculated by using the following formula:

$$\Delta_n = \frac{1}{E} \sum_{k=1}^{NS} \frac{L_k}{A_k} P_k \quad (3.30)$$

where E is the Young's modulus, which can be taken as $5000\sqrt{f_{ck}}$ as per IS 456, P_k is the load in the column at the k th storey, NS is the number of storeys, and L_k and A_k are the length and area, respectively, of the column at the k th storey.

Assuming that the column area is varying linearly, instead of the actual discrete variation, Taranath (1998) developed the following formula to calculate the axial shortening of a column at a height z in a single step.

$$\Delta_z = \frac{P_b}{E} \left[-\frac{1}{\alpha} \ln \left(1 - \frac{\alpha z}{A_b} \right) \right] - \frac{\beta}{E} \left[-\frac{1}{\alpha^2} \left\{ \alpha z + A_b \ln \left(1 - \frac{\alpha z}{A_b} \right) \right\} \right] \quad (3.31)$$

where α is the rate of change of area of the column given by $(A_b - A_t)/L$, β is the rate of change of axial load given by $(P_b - P_t)/L$, A_t is the area of the column at the top, A_b is the area of the column at the bottom, P_t is the axial load at the top, P_b is the axial load at the bottom, E is the Young's modulus, and L is the height of the building.

Jayasinghe and Jayasena (2004) provide a set of guidelines so that the effect of axial shortening of column could be taken into account approximately, especially at the preliminary design stage and also during the construction phase. Samara (1995) has presented a new rational approach for the evaluation of the effects of creep on RC axially loaded column at sustained service stresses. This approach has been found to correlate well with experimental results and also the measured values at Water Tower place and Lake Point Tower in Chicago.

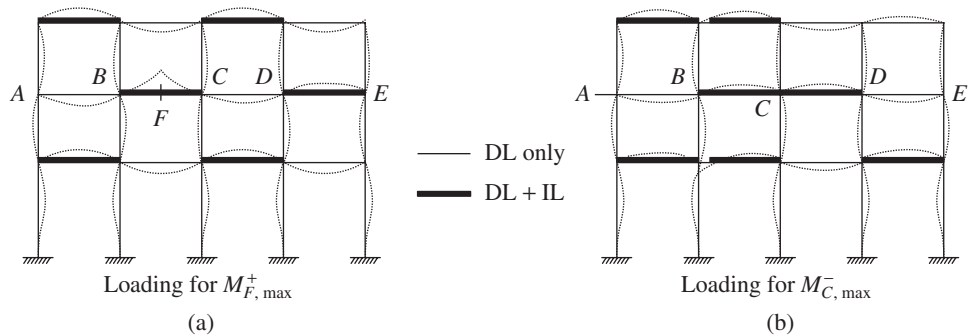


FIG. 3.16 Gravity load patterns and the influence lines for bending moment (a) Loading for maximum positive mid-span moment (b) Loading for maximum negative support moment

3.10 PATTERN LOADING

For continuous structures, connected by rigid joints or continuous over supports, vertical loads should be arranged in the most unfavourable but realistic pattern for each element. The arrangement of live loads considered in the analysis may be limited to the following combinations (see IS 456, Clause 22.4.1):

1. Where the nominal design imposed load does not exceed three quarters of the nominal dead load, design imposed load and design dead load on all spans (design imposed

load is the characteristic imposed load multiplied by the appropriate partial safety factor)

2. Where the nominal live load exceeds three quarters of the nominal dead load
 - (a) design dead load on all spans with full design imposed load on alternate spans (see Fig. 3.16b)
 - (b) design dead load on all spans with full design imposed load on two adjacent spans (see Fig. 3.16a)
 - (c) design dead load plus design imposed load on all spans

For continuous beams and slabs continuous over supports, the arrangement as given in point 2 may be used. Moreover, it should be noted that the redistribution of moments cannot be applied in this case.

Loading arrangements given in point 2(c) is required to find the maximum load on the columns and points 2(a) and (b) are required to determine the maximum moments occurring in the beams of rigid frames (as shown in Fig. 3.16).

When lateral loads are also considered (dead load + imposed load + wind or earthquake load combination), it is not necessary to apply pattern loading.

From this discussion, it is obvious that the critical loading condition for the strength of a simply supported beam is when it supports the maximum design dead load and imposed load at the ultimate limit state. The size of the beam can be determined from the bending moment and the shear derived from this loading condition, and should be checked for deflection at the serviceability limit state.

3.11 LOAD COMBINATIONS

If we do not consider accidental loads, as per Table 18 of IS 456, we should consider the following 13 loading cases for a building in which lateral load is resisted by the frames or walls oriented in two orthogonal directions, say x and y (see Fig. 3.17):

1. 1.5(DL + IL)
2. 1.2(DL + IL + EL_x)
3. 1.2(DL + IL - EL_x)
4. 1.2(DL + IL + EL_y)
5. 1.2(DL + IL - EL_y)

6. $1.5(DL + EL_x)$
7. $1.5(DL - EL_x)$
8. $1.5(DL + EL_y)$
9. $1.5(DL - EL_y)$
10. $0.9DL + 1.5EL_x$
11. $0.9DL - 1.5EL_x$
12. $0.9DL + 1.5EL_y$
13. $0.9DL - 1.5EL_y$

Here, DL is the dead load, IL is the imposed load (live load), WL is the wind load, and EL_x and EL_y are the design earthquake loads in x and y directions, respectively. The factors 1.5, 1.2, and 0.9 are the *partial safety factors* for the loads.

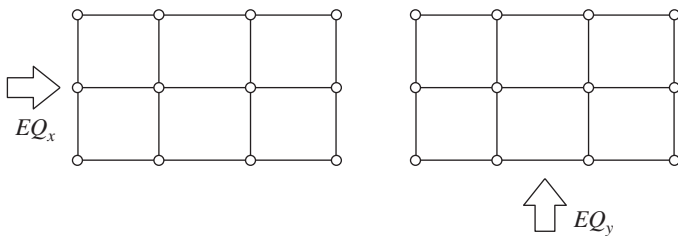


FIG. 3.17 Earthquake loading in two orthogonal directions

Since the horizontal loads are reversible in direction, in some cases the design is governed by the effect of lateral load minus the effect of gravity loads. In such situations, a load factor greater than 1.0 for gravity loads will make the calculations un-conservative. Hence, a load factor of 0.9 is specified on gravity loads in load combinations 10–13. Many designs of footings, corner columns, and beams at the ends in framed structures are found to be governed by this load combination. Central columns may be governed by combinations 6–9.

Since dead loads can be precisely estimated than live loads, several codes assume a smaller value of load factor for dead loads (e.g., 1.25 in the Canadian code, 1.4 in the US and UK code) and a higher value of load factor for imposed loads (e.g., 1.5 in the Canadian code and 1.6 in the US and UK codes). However, in the Indian code the same load factor of 1.5 is used for both dead and imposed loads.

Since the code assumes that maximum earthquake and wind loads will not occur simultaneously, in the given combinations, EL_x or EL_y may be replaced by WL_x or WL_y in places where wind load is predominant. It may be noted that in many occasions, loading combinations 6–9 may govern the design.

When snow load is present on the roofs, the imposed load on the roof should be replaced by the snow load on the roof for the purpose of load combinations. When imposed load is combined with earthquake load, the effect of the earthquake should be calculated for the full dead load plus the percentage of the imposed load as given in Table 3.8.

Load Combinations for Non-orthogonal Buildings

In structures with non-orthogonal lateral load resisting system, the lateral load resisting elements may be oriented in

a number of directions. In such buildings, considering x and y direction loads acting separately, as discussed in the previous section, may be un-conservative for elements not oriented in the x and y directions.

A lateral load resisting system in the form of frames or walls offers maximum resistance when the load is in the direction of the element. However, in non-orthogonal structures, it may be tedious to apply lateral loads in each of the directions in which the lateral load resisting elements are oriented. Hence, in such buildings, as shown in Fig. 3.18, IS 1893 suggests that the buildings be designed for the following:

1. 100 per cent design earthquake load in x direction and 30 per cent design earthquake load in y direction, acting simultaneously
2. 100 per cent design earthquake load in y direction and 30 per cent design earthquake load in x direction, acting simultaneously

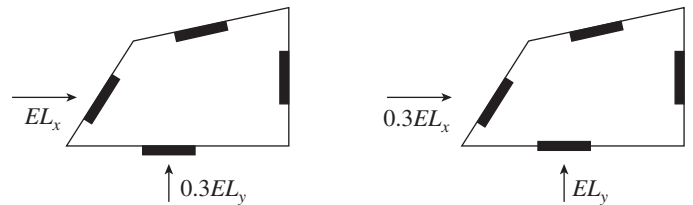


FIG. 3.18 100% + 30% rule for non-orthogonal lateral load resisting systems

Code IS 1893 suggests that this rule should also be applied to buildings that are torsionally unbalanced about both the orthogonal axes. Since the directions of the earthquake forces are reversible, it results in the following eight additional possibilities:

1. $EL_x + 0.3EL_y$
2. $0.3EL_x + EL_y$
3. $EL_x - 0.3EL_y$
4. $0.3EL_x - EL_y$
5. $-(EL_x + 0.3EL_y)$
6. $-(0.3EL_x + EL_y)$
7. $-(EL_x - 0.3EL_y)$
8. $-(0.3EL_x - EL_y)$

It is important to note that the corner columns of buildings with orthogonal lateral load resisting systems will be governed by this 100% + 30% rule. However, the code dispenses with this rule for orthogonal buildings to save the design effort.

EXAMPLES

EXAMPLE 3.1:

An industrial building has been designed to resist a floor live load of 5 kN/m^2 , as per IS 875 (Part 2), but later on statistical readings were taken on similar slabs and the observed live loads in kN/m^2 on the various slabs are as follows:

- $13 \times 3.2, 15 \times 3.8, 35 \times 4, 10 \times 4.2, 10 \times 4.4$

(13×3.2 means 13 number of slabs, each having a load of 3.2 kN/m^2)

Determine the characteristic load if the accepted probability of the load is not to exceed five per cent, assuming normal distribution.

SOLUTION:

The measured live loads are denoted by Q_{vi} .

$$Q_{vi} = 13 \times 3.2, 15 \times 3.8, 35 \times 4, 10 \times 4.2, 10 \times 4.4$$

Total number of samples, $n = 13 + 15 + 35 + 10 + 10 = 83$

The mean value, $Q_{vm} = 3.91$

Standard deviation, $\sigma = 0.3512$

Coefficient of variation, $C_v = \sigma/Q_{vm} = 0.09$

(These values can be obtained by using a scientific calculator.)

The characteristic live load, $Q_{vk} = Q_{vm} + 1.65s$

$$= 3.91 + 1.65 \times 0.3512 = 4.489 \text{ kN/m}^2$$

Thus, the characteristic value that should have been used in the design is 4.489 or 4.5 kN/m^2 , which is less than that assumed in the design. Hence, it is safe.

EXAMPLE 3.2:

Calculate the loads acting on beam B2 of a two-storey residential RC building, as shown in Fig. 3.19. Assume the floor finish to be of 1.6 kN/m^2 .

SOLUTION:

Calculation of Loads

Span of beam B2 = 7 m

Assume the thickness of wall to be 230 mm and width of beam to be 230 mm. The depth of beam may be assumed to be 85 mm per 1 m span.

Hence, depth = $7 \times 85 = 595$ or say 600 mm

Weight of beam = $0.23(0.6 - 0.15) \times 25 = 2.59 \text{ kN/m}$

For residential buildings, imposed load as per IS 875 (Part 2) = 2 kN/m^2

Assuming a slab thickness of 150 mm, weight of slab = $0.15 \times 25 = 3.75 \text{ kN/m}^2$

Total dead load including floor finish = $3.75 + 1.6 = 5.35 \text{ kN/m}^2$

Total load on slab = $5.35 + 2.0 = 7.35 \text{ kN/m}^2$

The distribution of slab load on beams is shown in Fig. 3.19(d). The slab load transmitted to beam B2 consists of three parts: (a) direct load from slab S_1 (trapezoidal) and slab S_2 (triangular), as shown in Fig. 3.19(e), (b) reaction from beam B5, with half the load from one-way slab S_3 (UDL), and (c) trapezoidal wall load on beam B2, as shown in Fig. 3.19(f).

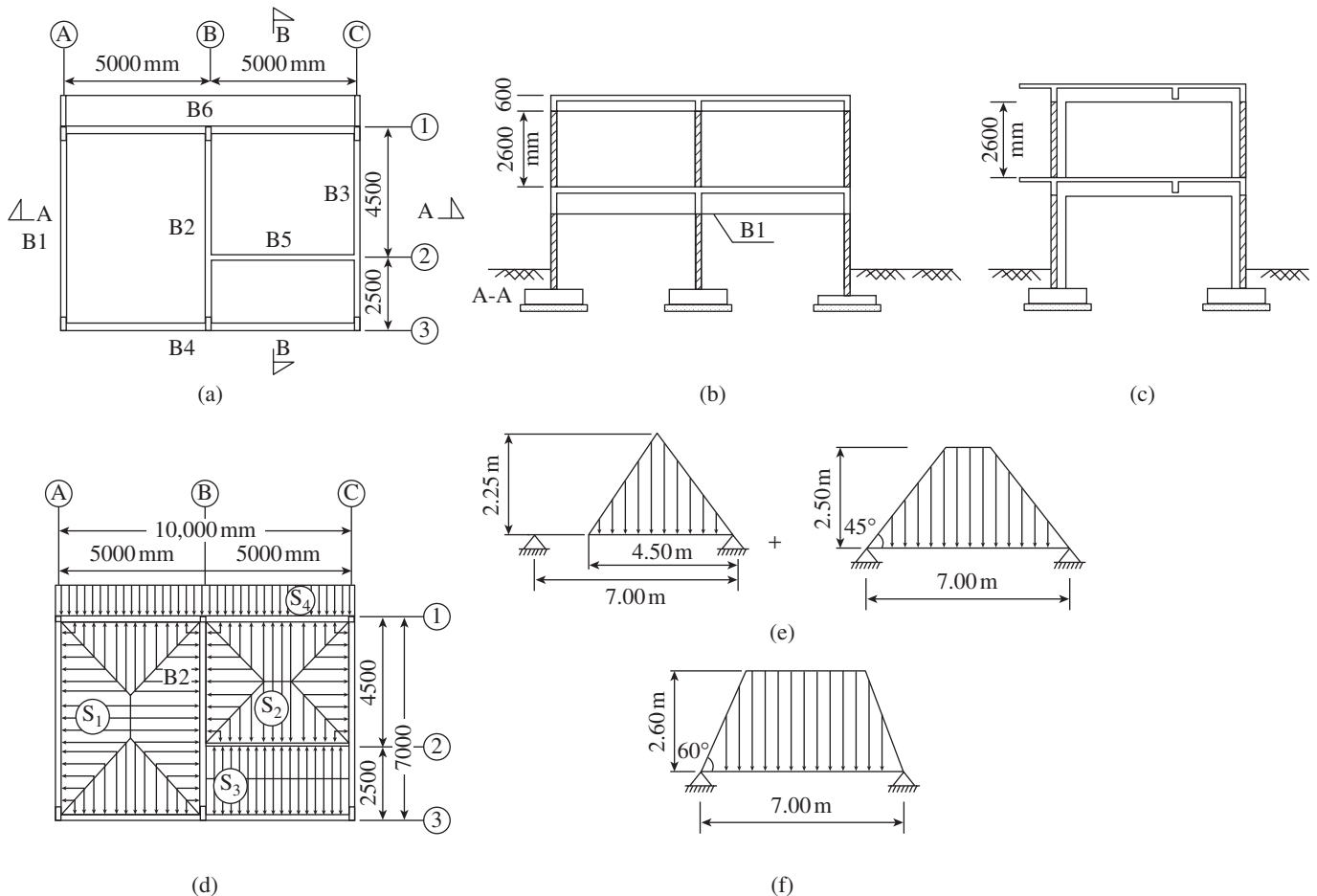


FIG. 3.19 Slab of Example 3.2 (a) Plan (b) Section A-A (c) Section B-B (d) Load distribution of slabs (e) Direct slab load on beam B2 (f) Direct wall load on beam B2

Load Due to Slabs S₁ and S₂

The trapezoidal load can be converted into UDL using Table 3.5.

$L_1/L_2 = 7.0/5.0 = 1.4$. Hence, from Table 3.5, $\alpha = 0.83$ and $\beta = 0.643$.

Equivalent load for bending = $7.35 \times 0.83 \times 2.5 = 15.25 \text{ kN/m}$

Equivalent load for shear = $7.35 \times 0.643 \times 2.5 = 11.80 \text{ kN/m}$

Equivalent UDL Due to Triangular Loading

Equivalent UDL for the loaded part of the beam = $w \frac{\text{Loaded area}}{\text{Loaded length}} = \frac{7.35 \times (0.5 \times 4.5 \times 2.25)}{4.5} = 8.27 \text{ kN/m}$

Load Due to Wall

Refer to Fig. 3.19(f).

Height of the wall = 2.6 m

Let us calculate the equivalent UDL.

$$X = h_w / \sqrt{3} = 2.6 / \sqrt{3} = 1.5 \text{ m}$$

$$L_1/2X = \frac{7.0}{2 \times 1.5} = 2.33$$

Since $L_1/(2X) > 2$, the coefficient for calculating the equivalent UDL for B.M. or S.F. of the beam may be taken as 1.0 (see Table 3.5).

Hence, $g_w \times h_w = 1.0 \times 20 \times 2.3 \times 2.6 = 11.96 \text{ kN/m}$

Calculation of Reaction Due to Beam B5

Refer to Fig. 3.20(a).



FIG. 3.20 Equivalent beam loading (a) Slab load on secondary beam B5 (b) Equivalent load for bending for beam B2 (c) Equivalent load for shear for beam B2

Assume the size of beam B5 to be 230 × 500 mm.

Self-weight of beam = $0.23 \times (0.5 - 0.15) \times 25 = 2.01 \text{ kN/m}$

$L_1/L_2 = 5.0/4.5 = 1.11$; from Table 3.5, $\beta = 0.55$

Slab load due to dead and imposed loads = $7.35 \times 1.25 + 7.35 \times 2.25 \times 0.55 = 18.28 \text{ kN/m}$

Total equivalent UDL = $2.01 + 18.28 = 20.3 \text{ kN/m}$

Reaction due to dead and imposed loads = $20.3 \times 5/2 = 50.75 \text{ kN}$

Equivalent Load for B.M. for Beam B2

Part ab: $2.59 + 15.25 + 11.96 = 29.8 \text{ kN/m}$

Part bc: $2.59 + (15.25 + 8.27) + 11.96 = 38.07 \text{ kN/m}$

Equivalent Load for S.F. for Beam B2

Part ab: $2.59 + 11.8 + 11.96 = 26.35 \text{ kN/m}$

Part bc: $2.59 + (11.8 + 8.27) + 11.96 = 34.62 \text{ kN/m}$

These loadings are shown in Fig. 3.20(b) and (c).

EXAMPLE 3.3:

A commercial building shown in Fig. 3.21 has seven storeys. The roof is accessible and all the floors are used as offices. Calculate the load on interior column AB on the first floor, assuming the spacing of columns in the perpendicular direction to be 4 m.

Live load on each floor = 4000 N/m^2

Live load on roof with access = 1500 N/m^2

Assuming 150 mm thick slab, dead load = 3750 N/m^2

Add dead load of floor finish, etc. (say) = 1000 N/m^2

Total dead load = 4750 N/m^2

Height of each storey = 3 m

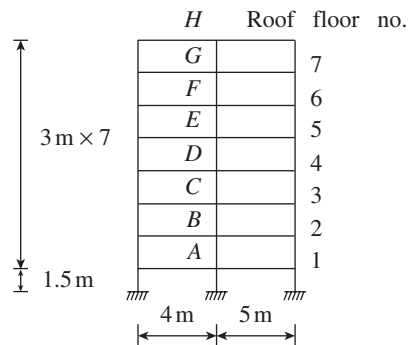


FIG. 3.21 Seven-storey building of Example 3.3

SOLUTION:

The loads from the various floor levels are computed as shown in Table 3.10. The live load has been reduced as per IS 875 (Part 2).

TABLE 3.10 Imposed load reduction for a seven-storey building

Column	Floor	Live Load (N/m ²)	Dead Load (N/m ²)	Total Load from Floor (N/m ²)
GH	Roof	1500	4750	6250
FG	7	$0.9 \times 4000 = 3600$	4750	8350
EF	6	$0.8 \times 4000 = 3200$	4750	7950
DE	5	$0.7 \times 4000 = 2800$	4750	7550
CD	4	$0.6 \times 4000 = 2400$	4750	7150
BC	3	$0.6 \times 4000 = 2400$	4750	7150
AB	2	$0.6 \times 4000 = 2400$	4750	7150

$$\begin{aligned} \text{Design load on column AB} &= 1.5(6250 + 8350 + 7950 + 7550 \\ &\quad + 3 \times 7150) \times 4 \times (4 + 5)/2 \\ &= 1,391,850/1000 = 1391.9 \text{ kN} \end{aligned}$$

It should be noted that if the live load reduction is not considered, the load on column AB will be $1.5(6250 + 8750 \times 6) \times 4 \times (4 + 5)/2 = 1,586,250/1000 = 1586.3 \text{ kN}$. Thus, there is an increase of 14 per cent load. It should also be noted that the dead load on the roof in a real structure may be more due to the type of weathering course adopted.

EXAMPLE 3.4:

A rectangular building situated in an industrial area is to be designed in Chennai city. The height of the building is 4.5 m and the size of the building is 10 m × 40 m. The walls of the building have 20 openings of size 1.2 m × 1.5 m. The building has a flat roof supported on load-bearing walls (see Fig. 3.22). Compute the design wind pressure and design forces on walls and roofs of the building.

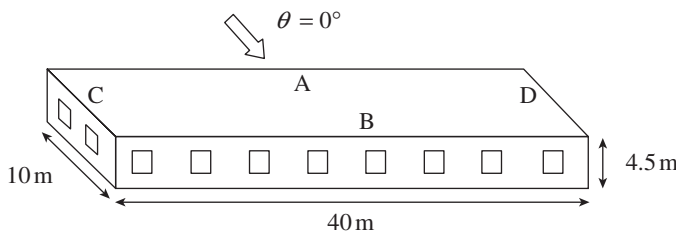


FIG. 3.22 Single-storey building of Example 3.4

SOLUTION:

Basic wind speed in Chennai, as per wind zone map or Appendix A of IS 875 (Part 3)

$$V_b = 50 \text{ m/s}$$

Assume that the building is to be designed for a 50-year life. Then, the risk coefficient from Table 1 of IS 875 (Part 3) is

$$k_1 = 1$$

The building is proposed to be erected in a city's industrial area, and hence, it is considered as belonging to category 3. The terrain factor from Table 2 of IS 875 (Part 3) for a height of 4.5 m is

$$k_2 = 0.91$$

The ground is assumed to be plain; hence, the topography factor is

$$k_3 = 1$$

$$\begin{aligned} \text{Design wind speed } V_z &= V_b k_1 k_2 k_3 \\ &= 50 \times 1 \times 0.91 \times 1 = 45.5 \text{ m/s} \end{aligned}$$

$$\begin{aligned} \text{Wind pressure } p_z &= 0.6 V_z^2 = 0.6 \times (45.5)^2 \\ &= 1242 \text{ N/m}^2 = 1.242 \text{ kN/m}^2 \end{aligned}$$

Permeability of Building

$$\begin{aligned} \text{Area of the walls} &= 4.5(2 \times 10 + 2 \times 40) = 450 \text{ m}^2 \\ \text{Area of all the openings} &= 20 \times 1.5 \times 1.2 = 36 \text{ m}^2 \end{aligned}$$

Percentage opening area is 8 per cent, which is between 5 per cent and 20 per cent. Hence, the building is of medium permeability.

Wind Load Calculation

$$F = (C_{pe} - C_{pi}) A p_d$$

Internal Pressure Coefficient

This is obtained from Table 3.6.

$$C_{pi} = \pm 0.5$$

External Pressure Coefficient

On roof: Using Table 5 of IS 875 (Part 3), with roof angle 0° without local coefficients, for $h/w = 0.45$, the coefficients are obtained as shown in Table 3.11.

TABLE 3.11 External pressure coefficients for roof

Portion of Roof	Wind Incidence Angle	
	0°	90°
E	-0.8	-0.8
F	-0.8	-0.4
G	-0.4	-0.8
H	-0.4	-0.4

Design Pressure Coefficients for Walls

For $h/w = 0.45$, $l/w = 4$, and C_{pe} for walls using Table 4 of IS 875 (Part 3), we obtain the coefficients as shown in Table 3.12:

TABLE 3.12 Design pressure coefficients for walls

Wall	Wind Incidence Angle	
	0°	90°
A	+0.7	-0.5
B	-0.25	-0.5
C	-0.6	+0.7
D	-0.6	-0.1

It should be noted that the pressure coefficients are given only for buildings with l/w ratio up to four. For longer buildings, that is, $l/w > 4.0$, the values given in the table up to $l/w = 4.0$ should be used.

These values have to be combined with the internal pressure coefficients $C_{pi} = \pm 0.5$.

Thus, net pressure for roof as per Fig. 3.6 is shown in Fig. 3.23.

$$\begin{aligned} C_{pnet} \text{ for walls A or B} &= 0.7 - (-0.5) = +1.2 \text{ pressure} \\ &= -0.5 - (+0.5) = -1.0 \text{ suction} \end{aligned}$$

$$\begin{aligned} C_{pnet} \text{ for walls C or D} &= 0.7 - (-0.5) = +1.2 \text{ pressure} \\ &= -0.6 - (+0.5) = -1.1 \text{ suction} \end{aligned}$$

Design Pressure for Walls

$$F = C_{pnet} \times p_d$$

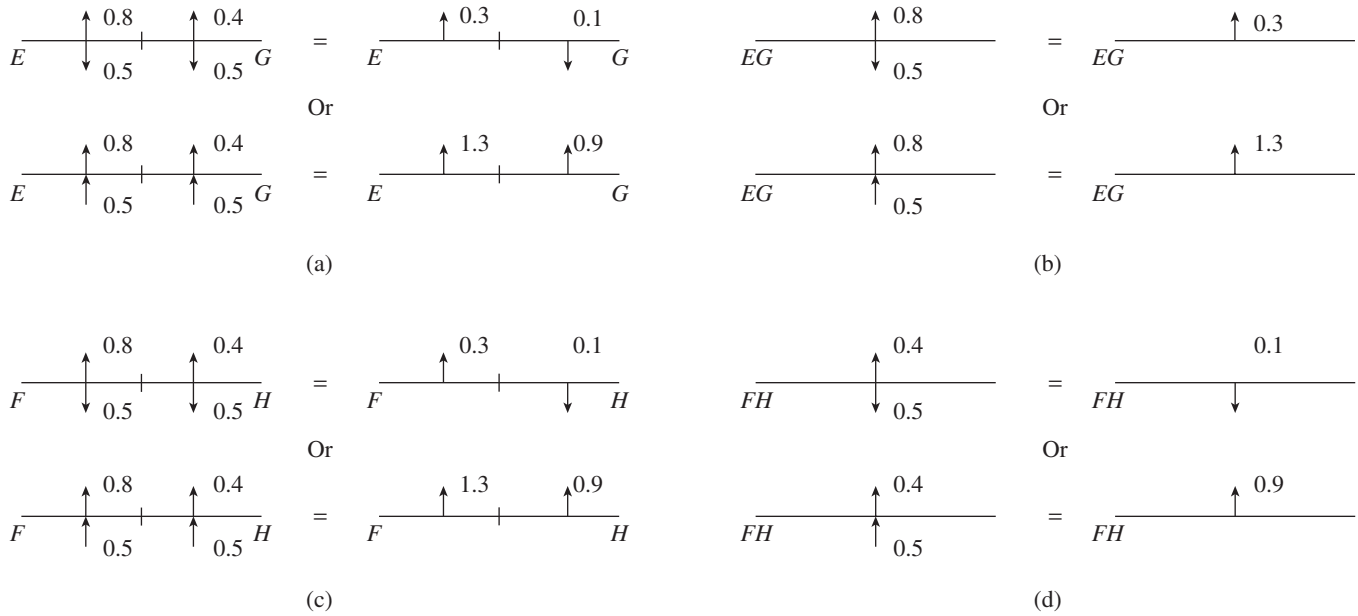


FIG. 3.23 Net roof pressure coefficients for different zones and combinations (a) For 0° wind incidence, for E/G (end zone) (b) For 90° wind incidence, for E/G (end zone) (c) For 0° wind incidence, for F/H (mid-zone) (d) For 90° wind incidence, for F/H (mid-zone)

For long walls,

$$F = 1.2 \times 1.242 = 1.4904 \text{ kN/m}^2 \text{ pressure}$$

$$= -1 \times 1.242 = -1.242 \text{ kN/m}^2 \text{ suction}$$

For short walls

$$F = 1.2 \times 1.242 = 1.4904 \text{ kN/m}^2 \text{ pressure}$$

$$= -1.1 \times 1.242 = -1.3662 \text{ kN/m}^2 \text{ suction}$$

For roof

$$F = 1.3 \times 1.242 = 1.6146 \text{ kN/m}^2 \text{ pressure}$$

$$= -0.1 \times 1.242 = -0.1242 \text{ kN/m}^2 \text{ suction}$$

For 0° wind,

$$\text{Force} = 1.2 \times (40 \times 4.5) \times 1.314 = 283.824 \text{ kN}$$

For 90° wind,

$$\text{Force} = 1 \times (10 \times 4.5) \times 1.314 = 59.13 \text{ kN}$$

EXAMPLE 3.5:

Consider a three-storey concrete building shown in Fig. 3.24. The building is located in Roorkee (seismic zone IV). The soil conditions are medium stiff and the entire building is supported on raft foundation. The concrete frames are infilled with unreinforced brick masonry. Determine the seismic load on the structure as per IS 1893 (Part 1). The seismic weights as shown in the figure have been calculated with 50 per cent of the live load lumped at the floors and no live load on roof.

Calculation of Force Due to Frictional Drag

Since $40/4.5 = 8.8 > 4.0$ (even though $40/10 = 4.0$), the frictional drag due to wind has to be considered. This will act in the longitudinal direction of the building along the wind. Here $h < b$, and hence Eq. (3.17a) is used.

$$F' = 0.01 (40 - 4 \times 4.5) 10 \times 1.242 + 0.01 (40 - 4 \times 4.5) 2 \times 4.5 \times 1.242$$

$$= 3.7324 + 3.4592 = 5.192 \text{ kN/m}^2$$

This frictional drag will act on the roof of the building.

Alternate Calculation using Force Coefficients Given in Code

Size of the building = 40 m × 10 m × 4.5 m

Therefore, $h/b = 4.5/10 = 0.45$

$a/b = 10/40 = 0.25$ and $b/a = 40/10 = 4$

As per Fig. 4 of code IS 875 (Part 3)

$$C_{f1} = 1.2 \quad C_{f2} = 1.0$$

The force acting on the building = $C_f A_e p_a$

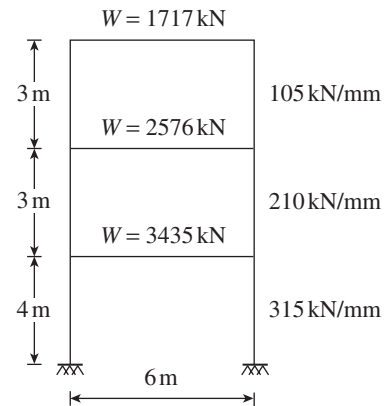


FIG. 3.24 Frame of Example 3.5

SOLUTION:

For seismic zone IV, the zone factor is 0.24, according to Table 2 of IS 1893 (Part 1). Being an office building, the importance

factor is 1.0 (Table 6 of IS 1893). The building has a special moment-resisting frame and hence $R = 5$.

Total seismic weight of the structure $= \Sigma W_i = 1717 + 2576 + 3435 = 7728 \text{ kN}$

$$h = 4 + 3 + 3 = 10 \text{ m}$$

Assume the depth of the building to be 15 m.

Fundamental Period

The lateral load resistance is provided by moment-resisting frames infilled with brick masonry panels. Hence, for EL in x direction,

$$\begin{aligned} T &= 0.09h/\sqrt{d} \quad (\text{Clause 7.6.2 of IS 1893}) \\ &= 0.09 \times 10/\sqrt{5} = 0.23 \text{ s} \end{aligned}$$

From Fig. 2 of IS 1893 for $T = 0.23 \text{ s}$, $S_d/g = 3.5$

$$\begin{aligned} A_h &= ZI(S_d/g)/(2R) \quad (\text{Clause 6.4.2 of IS 1893}) \\ &= 0.24 \times 1 \times 3.5/(2 \times 5) = 0.06 \end{aligned}$$

$$\begin{aligned} \text{Design base shear } V_B &= A_h W \\ &= 0.06 \times 7728 = 463.68 \text{ kN} \end{aligned}$$

Force Distribution with Building Height

The design base shear is distributed with height as per Clause 7.7.1 and the relevant calculations are shown in Table 3.13.

TABLE 3.13 Lateral load distribution as per static method

Storey level	W_i (kN)	h_i (m)	$W_i h_i^2$	$(W_i h_i^2)/(\Sigma W_i h_i^2)$	Lateral force at i th level for EL in direction (kN)	
					X	Y
3	1717	10	171,700	0.486	225.35	225.35
2	2576	7	126,224	0.358	166.00	166.00
1	3435	4	54,960	0.156	73.33	73.33
Σ	7728	—	352,884	1.000	463.68	463.68

EL in y Direction

$$T = 0.09 \times 10/\sqrt{6} = 0.367 \text{ s}$$

Therefore, $S_d/g = 3.5$ and $A_h = 0.06$

Hence, for this building, the design seismic force in y direction is the same as that in the x direction.

EXAMPLE 3.6:

Calculate the maximum axial shortening of column at the top of a 50-storey building, assuming that the variation in the cross-sectional area of the column is a linear function, with the following data: grade of concrete is M40, $P_t = 230 \text{ kN}$, $P_b = 12,000 \text{ kN}$, column of size is $230 \text{ mm} \times 300 \text{ mm}$ at the top and $680 \text{ mm} \times 1000 \text{ mm}$ at the bottom, and height of the building is 200 m.

SOLUTION:

For 40 MPa concrete, $E = 5000 \sqrt{f_{ck}} = 5000 \sqrt{40} = 31,622 \text{ MPa}$

$$A_t = 230 \times 300 = 69,000 \text{ mm}^2, A_b = 680 \times 1000 = 680,000 \text{ mm}^2$$

$$P_t = 230 \text{ kN}, P_b = 12,000 \text{ kN}$$

$$\Delta_z = \frac{P_b}{E} \left[-\frac{1}{\alpha} \ln \left(1 - \frac{\alpha z}{A_b} \right) \right] - \frac{\beta}{E} \left[-\frac{1}{\alpha^2} \left\{ \alpha z + A_b \ln \left(1 - \frac{\alpha z}{A_b} \right) \right\} \right]$$

$$\alpha = \frac{(A_b - A_t)}{L} = \frac{680,000 - 69,000}{200,000} = 2.715 \text{ mm}^2/\text{mm}$$

$$\beta = \frac{(P_b - P_t)}{L} = \frac{12,000 - 230}{200,000} = 0.05885 \text{ kN/mm} = 58.85 \text{ N/mm}$$

$$\begin{aligned} \ln \left(1 - \frac{\alpha L}{A_b} \right) &= \ln \left(1 - \frac{2.715 \times 200,000}{680,000} \right) \\ &= \ln(0.7985) = -0.225 \end{aligned}$$

$$\begin{aligned} \Delta_{top} &= \frac{12,000 \times 10^3}{31,622} \left[-\frac{(-0.225)}{2.715} \right] - \frac{58.85}{31,622} \\ &\quad \left[-\frac{1}{2.715^2} \{ 2.715 \times 200,000 + 680,000 \times (-0.225) \} \right] \\ &= 31.45 + 98.47 = 129.92 \text{ mm} \end{aligned}$$

It should be noted that the reinforcements in the columns are not considered in this example. They may also be included by converting their area to the equivalent area of concrete, using the modular ratio. In addition, creep and shrinkage effect have to be considered (see the example in Samara 1995).

EXAMPLE 3.7:

Roof design loads include a dead load of 1.60 kN/m^2 , a live load of 1.15 kN/m^2 , and a wind pressure of 0.70 kN/m^2 (upward or downward). Determine the governing loading.

SOLUTION:

The load combinations are as follows:

- $1.5(\text{DL} + \text{LL}) = 1.5(1.6 + 1.15) = 4.125 \text{ kN/m}^2$
- $1.2(\text{DL} + \text{LL} + \text{WL}) = 1.2(1.6 + 1.15 + 0.70) = 4.14 \text{ kN/m}^2$
- $1.2(\text{DL} + \text{LL} - \text{WL}) = 1.2(1.6 + 1.15 - 0.70) = 3.46 \text{ kN/m}^2$
- $0.9\text{DL} + 1.5\text{WL} = 0.9 \times 1.6 + 1.5 \times 0.70 = 3.49 \text{ kN/m}^2$
- $0.9\text{DL} - 1.5\text{WL} = 0.9 \times 1.6 - 1.5 \times 0.70 = 0.39 \text{ kN/m}^2$
- $1.5(\text{DL} + \text{WL}) = 1.5(1.6 + 0.70) = 3.45 \text{ kN/m}^2$
- $1.5(\text{DL} - \text{WL}) = 1.5(1.6 - 0.70) = 1.35 \text{ kN/m}^2$

The second load combination is the governing loading. Hence, the roof has to be designed for a total factored load of 4.14 kN/m^2 . It may be noted that the fifth loading combination produces the minimum load. When the dead load is comparatively small, it will result in a negative value for the combination, which will be critical for the overturning or stability checks. Moreover, since it is a simple calculation, we are in a position to find the governing load combination. In a complex structural system, it may not be easy to evaluate the governing loading condition. Moreover, one loading

combination may be critical for one set of members (say columns) and another combination may be critical for another set of members (say bracings). Hence, in these cases, a computer program will be quite useful to calculate the critical forces in any member due to any combination of loads.

EXAMPLE 3.8:

Calculate the gap required between two parts of a building for thermal expansion. Check it with the gap required to avoid pounding as per Clause 7.11.3 of IS 1893 (Part 1):2002. Assume that the coefficient of thermal expansion, α , is 12×10^{-6} mm/mm per degree Celsius and that the building is in Hyderabad. It has five floors and each part has a length of 45 m and a storey of height 3.3 m.

SOLUTION:

Gap for Expansion Joint

Required gap for expansion joint = 2Δ

where $\Delta = \alpha_c tL$

From Figs 1 and 2 of IS 875 (Part 5):1987, for Hyderabad, the maximum and minimum temperatures are 45°C and 7.5°C.

Temperature differential ($T_{\max} - T_{\min}$) = 37.5°C
 Required gap = $2 \times 12 \times 10^{-6} \times 37.5 \times 45 = 0.045 \text{ m} = 45 \text{ mm}$

Gap for Seismic Requirements

The permissible storey drift as per IS 1893 (Clause 7.11.1) is $0.004 \times H$.

Permissible drift per storey = $0.004 \times 3.3 \times 1000 = 13 \text{ mm}$ per storey

As per Table 7 of IS 1893 (Part 1), for special moment-resisting frame,

Response reduction factor, $R = 5.0$

Since the two units will be at the same elevation levels,

Seismic separation gap = $(13 + 13) \times 5/2 = 65 \text{ mm}$ per storey

For the five-storey building,

Separation required at top = $65 \times 5 = 325 \text{ mm}$

Hence, the gap required to prevent pounding (325 mm) governs, as it is much higher than the gap required for contraction or expansion (45 mm).

SUMMARY

The four main phases in a structural design process are as follows: (a) determination of the structural system, (b) calculation of the various loads acting on the system, (c) analysis of the structural system for these loads, and (d) design of the various members as per the codal provisions. Out of these phases, determination of the various loads is the most difficult and important phase, since the final design is based on these loads. Several failures have been reported in the past, which clearly show that one of the main reasons for these failures is the lack of consideration of the loads acting on the structures. Hence, in this chapter, a brief review of all the loads that may act on any structure is given. Of the several natural and man-made loads, the following loads are considered important: (a) dead loads, (b) imposed loads (live and snow loads) (c) wind loads, and (d) earthquake loads. Though dead loads can be evaluated accurately based on the dimensions, the determination of imposed, wind, and earthquake loads are difficult due to the probability of occurrence of the loads. Through continued research, we are now able to define these loads fairly accurately. However, when calibrating the codal loads, some simplifying assumptions are often made. In order to ascertain the value of these loads, it is important to know their characteristics. Hence, some details about wind and earthquake loads are given, in addition to the provisions given in

the Indian wind (IS 875—Part 3) and earthquake (IS 1893—Part 1) codes.

Some of the loads such as impact loads due to traffic on a bridge, crane loads, wind loads, and earthquake loads are dynamic in nature. However, most often they are converted to equivalent static loads. Dynamic analysis is resorted to only in the case of flexible structures, whose natural frequency in the first mode is less than 1.0Hz or whose height to least lateral dimension ratio is more than about five. Complicated structures should be avoided especially in earthquake zones, since their analysis and modelling is difficult. For structures with complicated geometrics, wind loading parameters should be derived from the model analysis in wind tunnels. It is very important to realize that the earthquake codes require the designer to design the structure only for a fraction of the load that may act on the building. Hence, the designer has to detail the structure in such a way that during a major earthquake, the structure may be damaged but will allow the occupants to escape by using the ductility of the material and over-strength factors. The examples provided at the end of this chapter may clarify the concepts discussed, and the references given at the end may be consulted for more details. More examples may be found in the IS explanatory hand books on IS 1893 (Part 1) and IS 875 (Part 3).

REVIEW QUESTIONS

1. Write the IS code numbers that need to be used to evaluate wind, dead, live, earthquake, and crane loads.
2. Define return period and characteristic load.
3. In the absence of statistical data, which of the following options must be chosen?
 - (a) Take the load specified in the codes as characteristic load.
 - (b) Consider the characteristic load based on previous data or experience.
 - (c) Obtain the data from the weather bureau.
 - (d) Consult specialist literature.
4. Which of the following options gives the partial safety factors for DL and WL for limit state of collapse when stability against overloading is critical?

(a) 1.5DL + 1.5WL	(c) 0.9DL + 1.5WL
(b) 1.2DL + 1.2WL	(d) 1.4DL + 1.6WL

5. Can you guess why a uniform partial safety factor has been adopted for limit state of collapse, when DL and IL are acting together?
6. Is it safe to overestimate the dead load? If your answer is no, provide the reason.
7. The unit weight of RC members can be assumed as _____.
(a) 23 kN/m³ (c) 24.5 kN/m³
(b) 24 kN/m³ (d) 25 kN/m³
8. Provide the imposed floor loads for the following occupancies:
(a) Residential
(b) Assembly building with fixed seats
(c) Balconies in residential buildings
(d) Staircases in residential buildings
(e) Libraries
9. Loads due to partition walls may be considered by increasing the floor load by a minimum of _____.
(a) 1.5 kN/m² (c) 2 kN/m²
(b) 1 kN/m²
10. Why and how do we reduce the live loads in the columns of multi-storey buildings?
11. State the coefficients that are used to convert the triangular and trapezoidal loads into equivalent UDL for obtaining the maximum B.M.
12. How are wall loads on beams considered in the analysis?
13. Total load (including impact) due to lift machine room is taken as _____.
(a) 10 kN/m² (c) 10 × 1.25 kN/m²
(b) 20 kN/m² (d) 15 kN/m²
14. What are tornadoes? How are they different from cyclones?
15. What are the factors that affect the wind pressure or load acting on the structures?
16. What is the significance of local pressure coefficients?
17. Frictional drag coefficients are to be taken into account when _____.
(a) $d/h > 4$ (c) d/h or $d/b > 4$
(b) $d/b > 4$ (d) d/h or $d/b > 2$
18. Explain along-wind and cross-wind response.
19. What is vortex shedding? When can we neglect the effects of vortex shedding?
20. How were wind load effects minimized in the design of Burj Khalifa, the tallest building in the world?
21. What is interference effect? Why is it considered important in the design of tall structures?
22. Under what conditions are the dynamic effects of wind to be considered?
23. Why is wind tunnel testing important in the design of tall buildings?
24. State a few methods by which wind-induced oscillations may be reduced.
25. Is it possible to consider wind as a source of energy in tall buildings?
26. Define epicentre of an earthquake.
27. The earthquake on a Richter scale 7 is _____.
(a) 10 times larger than magnitude 6
(b) 100 times larger than magnitude 5
(c) 1000 times larger than magnitude 4
(d) All of these
28. List the factors that influence the seismic damage.
29. What is soil liquefaction? What are its effects on structures?
30. State the seismic design philosophy adopted in IS 1893 (Part 1). How is it different from the other load effects?
31. For the purpose of determining seismic forces, India is classified into _____.
(a) three zones (c) five zones
(b) four zones (d) six zones
32. State the equation given in IS 1893 for design horizontal seismic coefficient A_h of a structure. How is the design base shear obtained from A_h ?
33. The response reduction factor R for special RC moment-resistant frames is _____.
(a) 3 (c) 8
(b) 4 (d) 5
34. Define response spectrum, natural frequency, and natural period.
35. What are the important factors that influence earthquake-resistant design?
36. What is the significance of response reduction factor?
37. How is the base shear of a building calculated using the equivalent static method?
38. State the formulae given in the IS 1893 code for finding the fundamental natural period of vibration of RC buildings for the following:
(a) Moment-resisting frames with brick infill panels
(b) Moment-resisting frames without brick infills
(c) Moment-resisting frames with concrete and masonry shear walls
39. How is the base shear force distributed along the height of the building as per IS 1893?
40. State the various rules to be followed while planning and designing a building in an earthquake-prone zone.
41. What are the plan irregularities that should be considered?
42. State the various vertical irregularities.
43. Write short notes on the following:
(a) Base isolation (b) Energy-absorbing devices
44. How can we take care of differential settlement in foundations?
45. How can we calculate the axial shortening of columns in multi-storey buildings?
46. What are the factors that affect the choice of spacing of expansion joints?
47. The percentage of high-strength deformed bars in one-way slabs to cater for shrinkage or temperature, as per IS 456, is _____.
(a) 0.12% (c) 0.20%
(b) 0.15% (d) 1.2%
48. What is a shrinkage strip? What are the difficulties of using a shrinkage strip? What is the better alternative to shrinkage strip?
49. State the formula to calculate the active earth pressure as per Rankine's theory.
50. Are loads occurring during erection critical? What are the erection loads that should be considered in design?
51. What are the arrangements of live loads, as per the code, that produce maximum load effects?
52. List the 8 loading combinations to be considered and the 13 combinations when considering only DL, LL, and EL.
53. What are the additional eight loading cases to be considered for non-orthogonal buildings?

EXERCISES

- Measurement of loads on floor slabs of residential buildings are as follows in kN/m^2 :
 $8 \times 0.90, 12 \times 1.1, 15 \times 1.2, 30 \times 1.4, 40 \times 1.5, 15 \times 1.6, 5 \times 1.7$
 (8×0.90 means eight samples of 0.9 kN/m^2 each)
 Determine the characteristic load on the floors if the acceptable probability of load is not to exceed five per cent of the specified load.
- An office building was designed to resist a floor load of 4 kN/m^2 . After the building was constructed, measurements were taken on the various floors and were found to be as follows:
 $12 \times 3.2, 10 \times 3.8, 20 \times 4, 15 \times 4.2, 8 \times 4.4$
 Determine the probability of the loads exceeding the specified load of 4 kN/m^2 .
 Hint: After calculating $(Q_m - Q/\sigma)$, the probability of exceeding the specified load (Q) can be found by referring to the statistical table for normal distribution, given in any standard book on statistics.
- A six-storey building is to be used for residential purposes. Calculate the load on an interior column in the ground floor, assuming that the columns are placed in a grid of $6 \text{ m} \times 4 \text{ m}$. Consider the live load reduction as per IS 875, Part 3.
- A tall building is proposed in Mumbai where there are some existing tall buildings. Use the following data:
 - Level ground
 - Design for a return period of 50 years
 - Basic wind speed = 44 m/s
 - Size of the building = $30 \text{ m} \times 40 \text{ m}$ and height = 60 m
 Estimate the risk, topography, and terrain coefficients and compute the design wind speed and pressure.
- Compute the design wind pressure and design forces on the walls and roofs of a two-storey building having a height of 6.5 m and size $10 \text{ m} \times 30 \text{ m}$. Assume there are six openings on each floor of size $1.2 \text{ m} \times 1.2 \text{ m}$ in the wall of length 30 m and two similar openings in each floor in the 10 m long wall. The building has a flat roof and is supported on load-bearing walls.
- Consider a four-storey office building, as shown in Fig. 3.25, located in Shillong (seismic zone V). The soil condition is

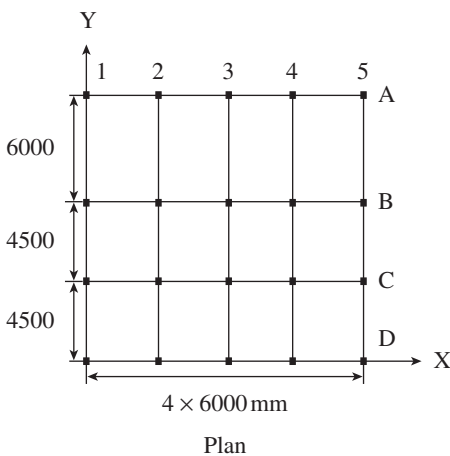
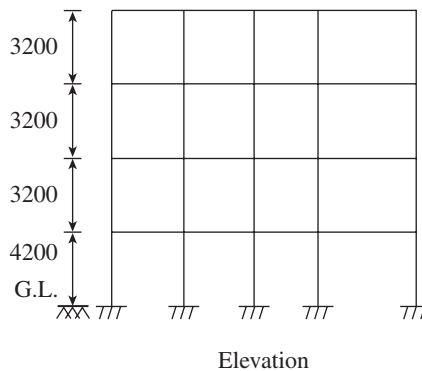


FIG. 3.25



medium stiff and the entire building is supported on raft foundation. The RC frames are infilled with brick masonry. The lumped weight due to dead loads is 12 kN/m^2 on the floors and 10 kN/m^2 on the roof. The floors carry a live load of 4 kN/m^2 and roof of 1.5 kN/m^2 . Determine the design seismic load on the structure by the equivalent static method. Assume that the frames are moment-resisting frames with $R = 5$.

[Ans.: Design base shear = 1560 kN]

- A three-storey building and the seismic weights acting on it are shown in Fig. 3.26. Assuming that the building is in seismic zone IV and supported by soft soil, determine the design seismic load on the structure by the following methods:
 - Equivalent static method
 - Response spectrum method
 The free vibration properties of this building are provided in Table 3.14.

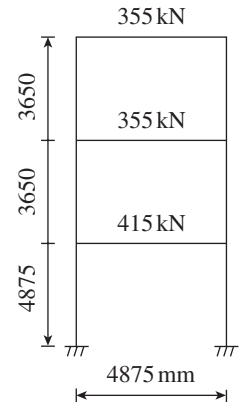


FIG. 3.26

TABLE 3.14

Natural period (Seconds)	Mode 1	Mode 2	Mode 3
	0.114	0.040	0.021
Mode shapes			
Roof	1.000	1.000	1.000
2nd floor	0.726	-0.583	-3.377
1st floor	0.340	-1.146	1.378

- Calculate the gap required between two parts of a building for thermal expansion. Check it with the gap required to avoid pounding as per Clause 7.11.3 of IS 1893 (Part 1):2002. Assume that the coefficient of thermal expansion, α , is $12 \times 10^{-6} \text{ mm/mm}$ per degree Celsius and that the building is in New Delhi. The building has six floors and each part has a length of 40 m and a storey of height 3.5 m .
- Calculate the maximum axial shortening of column at the top of a 60-storey building, assuming that the variation in the cross-sectional area of the column is a linear function, with the following data: grade of concrete is M50, $P_t = 250 \text{ kN}$, $P_b = 15,000 \text{ kN}$, column of size is $230 \text{ mm} \times 300 \text{ mm}$ at the top and $800 \text{ mm} \times 1000 \text{ mm}$ at the bottom, and height of the building is 210 m .
- Roof design loads include a dead load of 1.75 kN/m^2 , a live (or snow) load of 1.25 kN/m^2 , and a wind pressure of 0.75 kN/m^2 (upward or downward). Determine the governing loading.

REFERENCES

- ACI 209 R-92 1992 (reapproved 2008), *Prediction of Creep, Shrinkage, and Temperature Effects in Concrete Structures*, American Concrete Institute, Farmington Hills, p. 47.
- ACI 223 R-10 2010, *Guide for the Shrinkage Compensating Concrete*, American Concrete Institute, Farmington Hills, p. 16.
- ACI 224.3R-95 1995 (reapproved 2008), *Joints in Concrete Construction*, American Concrete Institute, Farmington Hills, p. 41.
- ACI 347.2R-05 2005, *Guide for Shoring/Reshoring of Concrete Multistory Buildings*, American Concrete Institute, Farmington Hills, p. 18.
- ASCE 24-05 2006, *Flood Resistant Design and Construction*, American Society of Civil Engineers, Reston, p. 74.
- ASCE/SEI 07-10 2010, *Minimum Design Loads for Buildings and Other Structures*, American Society of Civil Engineers, Reston, p. 608.
- Bachman, H. 2003, *Seismic Conceptual Design of Buildings: Basic Principles for Engineers, Architects, Building Owners and Authorities*, National Information Centre for Earthquake Engineering, Kanpur, p. 84.
- Baker, W.F., D.S. Korista, and L.C. Novak 2008, 'Burj Dubai: Engineering the World's Tallest Building', *Proceedings, Council on Tall Buildings and Urban Habitat's 8th World Congress*, Dubai, United Arab Emirates, pp. 1-10.
- BS 8007:1987, *Code of Practice for Design of Concrete Structures for Retaining Aqueous Liquids*, British Standard Institution, London.
- Bowles, J.E. 1990, *Foundation Analysis and Design*, 4th edition, McGraw Hill Book Co., New York.
- Bozorgnia, Y. and V.V. Bertero (ed.) 2004, *Earthquake Engineering: From Engineering Seismology to Performance-based Engineering*, CRC Press, Boca Raton, p. 1152.
- Chen W.F. and K.H. Mosallam (ed.) 1991, *Concrete Buildings: Analysis for Safe Construction*, CRC Press, Boca Raton, p. 232.
- Chopra, A.K. 2000, *Dynamics of Structures: Theory and Applications to Earthquake Engineering*, 2nd edition, Prentice Hall Inc., Englewood Cliffs, p. 844.
- CIRIA Report 146 1995, *Design and Construction of Joints in Concrete structures*, Construction Industry Research and Information Association, London.
- Clough, R.W. and J. Penzien 1993, *Dynamics of Structures*, McGraw Hill, New York.
- Coulbourne, W.L., E.S. Tezak, and T.P. McAllister 2002, 'Design Guidelines for Community Shelters for Extreme Wind Events', *Journal of Architectural Engineering*, ASCE, Vol. 8, No. 2, pp. 69-77.
- Eskildsen, S., M. Jones, and J. Richardson 2009, 'No More Pour Strips: Shrinkage Compensating Concrete Eliminates Need', *Concrete International*, ACI, Vol. 31, No. 10, pp. 42-7.
- FEMA 450 2003, *NEHRP Recommended Provisions for Seismic Regulations for New Buildings and Other Structures, Part 1: Provisions, Part 2: Commentary*, Building Seismic Safety Council, National Institute of Building Sciences, Washington, DC., (also see <http://www.fema.gov/library/viewRecord.do?id=2020/>, last accessed on 5 October 2012).
- FEMA P55 2011, *Coastal Construction Manual. Principles and practices of Planning, Siting, Designing, Constructing, and Maintaining Residential Buildings in Coastal Areas*, 4th edition, 2 Volumes, Federal Emergency Management Agency, Washington D.C., 2011.
- FEMA P646 June 2008, *Guidelines for Design of Structures for Vertical Evacuation from Tsunamis*, Applied Technology Council, California and Federal Emergency Management Agency, Washington, DC, p. 158.
- Fintel, M. 1974, 'Joints in Buildings', *Handbook of Concrete Engineering*, Van Nostrand Reinhold Company, New York, pp. 94-110.
- Frechette, R.E. and R. Gilchrist 2008, 'Towards Zero Energy: A Case Study of the Pearl River Tower, Guangzhou, China', *Proceedings, Council on Tall Buildings and Urban Habitat's 8th World Congress*, Dubai, United Arab Emirates.
- Gilbert, R.I. 1992, 'Shrinkage Cracking in Fully Restrained Concrete Members', *ACI Structural Journal*, Vol. 89, No. 2, pp. 141-9.
- Goel, R.K. and A.K. Chopra 1997, 'Period Formulas for Moment-resisting Frame Buildings', *Journal of Structural Engineering*, ASCE, Vol. 123, No. 11, pp. 1454-61.
- Goel, R.K. and A.K. Chopra 1998, 'Period Formulas for Concrete Shear Wall Buildings', *Journal of Structural Engineering*, ASCE, Vol. 124, No. 4, pp. 426-33.
- Govindan, P. and A.R. Santhakumar 1985, 'Composite Action of Reinforced Concrete Beams with Plain Masonry Infills', *The Indian Concrete Journal*, Vol. 59, No. 8, pp. 204-8.
- IS 875 (Part 1-Part 5):1987, *Code of Practice for Design Loads (Other than Earthquake) for Buildings and Structures, Part 1: Dead loads—Unit Weights of Building Material and Stored Materials, Part 2: Imposed Loads, Part 3: Wind Loads, Part 4: Snow Loads, Part 5: Special Loads and Load Combinations*, Bureau of Indian Standards, New Delhi.
- IS 1893, *Criteria for Earthquake Resistant Design of Structures, Part 1: General Provisions and Buildings (2002), Part 4: Industrial Structures including Stack-like Structures (2005)*, Bureau of Indian Standards, New Delhi.
- IS 1904:1986, *Code of Practice for Design and Construction of Foundations in Soils: General Requirements*, Bureau of Indian Standards, New Delhi.
- IS 2911 (Part 3):1980, *Code of Practice for Design and Construction of Pile Foundations (Under-reamed Piles)*, Bureau of Indian Standards, New Delhi.
- IS 3414:1968, *Code of Practice for Design and Installation of Joints in Buildings*, Bureau of Indian Standards, New Delhi.
- IS 4995 (Parts 1 and 2):1974, *Criteria for Design of Reinforced Concrete Bins for Storage of Granular and Powdery Materials, Part 1: General Requirements and Assessment of Bin Loads, Part 2: Design Criteria*, Bureau of Indian Standards, New Delhi.
- IS 4998 (Parts 1 and 2):1992, *Criteria for Design of Reinforced Concrete Chimneys, Part 1: Assessment of Loads, Part 2: Design Criteria*, Bureau of Indian Standards, New Delhi.
- IS 6922:1973, *Criteria for Safety and Design of Structures Subject to Underground Blasts*, Bureau of Indian Standards, New Delhi.
- IS 11504:1985, *Criteria for Structural Design of Reinforced Concrete Natural Draught Cooling Towers*, Bureau of Indian Standards, New Delhi.

- Jacobs, W.P. 2008, 'Building Periods: Moving Forward (and Backward)', *Structure Magazine*, ASCE, June, pp. 24–7.
- Jayasinghe, M.T.R. and W.M.V.P.K. Jayasena 2004, 'Effects of Axial Shortening of Columns on Design and Construction of Tall Reinforced Concrete Buildings', *Practice Periodical on Structural Design and Construction*, ASCE, Vol. 9, No. 2, pp. 70–8.
- Kappos, A. and G.G. Penelis 1996, *Earthquake Resistant Concrete Structures*, Spon Press, London, p. 572.
- Minor, J.E. 1982, 'Tornado Technology and Professional Practice', *Journal of Structural Division*, ASCE, Vol. 108, No. 11, pp. 2411–22.
- Murty, C.V.R. 2005, *Earthquake Tips. Learning Earthquake Design and Construction*, Indian Institute of Technology, Kanpur, and Building Material and Technology Promotion Council, New Delhi, p. 48.
- Naeim, F. and J.M. Kelly 1999, *Design of Seismic Isolated Structures: From Theory to Practice*, John Wiley, New York, p. 304.
- O'Rourke, M.O. 2010, *Snow Loads: Guide to Snow Load Provisions of ASCE 7–10*, ASCE Press, American Society of Civil Engineers, Reston, p. 176.
- Pfeiffer, M.J. and D. Darwin 1987, *Joint Design for Reinforced Concrete Buildings*, Report of University of Kansas, p. 80, (also see <http://www2.ku.edu/~iri/publications/sm20.pdf>, last accessed on 5 October 2012).
- Saetta, A., R. Scotta, and R. Vitaliani 1995, 'Stress Analysis of Concrete Structures Subjected to Variable Thermal Loads', *Journal of Structural Engineering*, ASCE, Vol. 121, No. 3, pp. 446–57.
- Samara, R.M. 1995, 'New Analysis for Creep Behaviour in Concrete Columns', *Journal of Structural Engineering*, ASCE, Vol. 121, No. 3, Mar., pp. 399–07.
- Scarlat, A.S. 1995, *Approximate Methods in Seismic Structural Design*, E & FN Spon, London, p. 277.
- Srinivasa Rao, P. and G.S. Krishnamurthy 1993, 'Imposed Loads on Floors of Office Buildings—Results of Load Survey', *The Indian Concrete Journal*, Vol. 67, No. 11.
- Sunil Kumar 2002a, 'Live Loads in Residential Buildings. Part I: The Results of the Survey', *The Indian Concrete Journal*, Vol. 76, No. 3.
- Sunil Kumar 2002b, 'Live Loads in Residential Buildings. Part II: Life Time Maximum Loads', *The Indian Concrete Journal*, Vol. 76, No. 4.
- Sunil Kumar and C.V.S. Kameswara Rao 1994, 'Live Loads in Residential Buildings in Urban and Rural Areas', *The Indian Concrete Journal*, Vol. 68, No. 10.
- Suprenant, B.A. 2002, 'Shrinkage and Temperature Reinforcement: Simple Topic, Not-so-simple Design Issues', *Concrete International*, ACI, Vol. 24, No. 9, pp. 72–6.
- Taly, N. 2003, *Loads and Load Paths in Buildings: Principles of Structural Design*, ICC International Code Council, Washington, DC, p. 866.
- Taranath, B.S. 1998, *Steel, Concrete and Composite Design of Tall Buildings*, 2nd edition, McGraw Hill, New York, p. 998.
- Varyani, U.H. and A. Radhaji 2005, *Design Aids for Limit State Design of Reinforced Concrete Members*, 2nd edition, Khanna Publishers, New Delhi, Chap. 15, pp. 243–60.
- Venugopal, M.S. and N. Subramanian 1977, 'Differential Movements in Soils', *Seminar on Problems of Building Foundations*, 20 February 1977, Madras.
- Whalen, T.M., S. Gopal, and D.M. Abraham 2004, 'Cost–Benefit Model for the Construction of Tornado Shelters', *Journal of Construction Engineering and Management*, ASCE, Vol. 130, No. 6, pp. 772–9.
- <http://www.iitk.ac.in/nicee/IITK-GSDMA/W03.pdf>, last accessed on 8 October 2011.
- <http://news.bbc.co.uk/2/hi/science/nature/7533950.stm>, last accessed on 8 October 2011.
- <http://ndma.gov.in/ndma/disaster/earthquake/Indiapshafinalreport.pdf>, last accessed on 8 October 2011.
- <http://news.bbc.co.uk/2/hi/science/nature/7533941.stm>, last accessed on 8 October 2011.
- http://www.wbdg.org/resources/seismic_design.php, last accessed on 20 December, 2012.

BASIS OF STRUCTURAL DESIGN

4.1 INTRODUCTION

The construction of a reinforced concrete (RC) structure requires several sequential steps. Several professionals, such as architects, electrical and mechanical engineers, geotechnical engineers, and builders, are involved in the execution of these steps. Hence, during the process, the structural engineer may have to interact with them in order to provide an efficient design. Many of the design steps are iterative in nature.

While designing any structure, the designer should consider several criteria, which include safety, stability, serviceability, economy, durability, sustainability, constructionability, ductility, and aesthetics (see Section 4.4). The engineer is usually guided in his/her efforts by the codes of practices, which provide a set of rules or standards based on which the designs are to be made. In India, the code IS 456, published by the Bureau of Indian Standards (BIS), is to be used for the design of RC structures. Other related codes on materials, mix design, detailing, and so forth are also referred to. Several design philosophies have been developed in the past including the working stress method (WSM), ultimate load method, limit states method, and performance-based design method. In general, the codes also allow designs based on experimental methods. A brief introduction to these aspects is given in this chapter, which will be useful while designing structures and their component elements.

4.2 STEPS INVOLVED IN CONSTRUCTION

The construction of any structure involves many steps. Although the structural designer is not responsible for each of these steps, he/she should be involved in most of them. This is to ensure that the resulting structure satisfies the considerations discussed in Section 4.4 and the structure does not have any adverse impact on the environment.

The following list provides the necessary steps involved in the construction of a structure:

1. A prospective owner identifies a location and arranges for necessary finance for construction. He/She also chooses the architect or project manager, who in turn chooses the various consultants (structural, geotechnical, survey, etc.).
2. A land surveyor surveys the land and draws the contours.
3. An architect or engineer (project manager) studies the applicable by-laws and draws a plan of the structure in such a way that it meets the town planning, fire protection, health, and safety requirements.
4. The competent authority approves the plan.
5. The geotechnical engineer investigates the site conditions, level of water table, nature of soil (whether expansive or not), and so forth, and gives a soil report.
6. The form, shape, and size of the structure is determined by the architect with the help of the structural engineer (based on preliminary design), such that the resulting structure is stable, economical, and efficiently resists the external loads.
7. Suitable materials of construction (steel, concrete, wood, brick, plastics, etc.) are selected after considering the required performance, cost, supply, availability of labour, and transportation to site. While choosing the materials, consideration should be given to the design and detailing procedures and control procedures for shop fabrication and field construction.
8. The structural engineer estimates the probable loads (dead, imposed, wind, snow, earthquake, etc.) that will be acting on the structure, in consultation with the current codes of practices.
9. The structural engineer arrives at the structural system after comparing various possible systems. In a building, heating and air conditioning requirements or other functional

requirements may dictate the use of a structural system that is not the most efficient from a purely structural viewpoint, but which is the best in the overall consideration of the total building. While choosing the structural forms, layouts, and details, the following points should be considered:

- (a) The structure has low sensitivity to hazardous conditions.
 - (b) The structure, as a whole, survives with only local damage, even after any one individual element suffers serious damage by the hazard.
 - (c) The structure gives ample warning before any collapse (should have various load paths and redistribution of loads).
10. A suitable structural analysis, mostly with the aid of computers, is done to determine the internal forces acting on various elements of the structural system based on the various loads and their combinations.
 11. Considering the critical loading conditions, the sizes of various elements are determined following the provisions contained in the codes. The design should be made in such a way that the following points are considered:
 - (a) The structure shall remain fit with adequate reliability and be able to sustain all actions (loads) and other influences experienced during the construction and use.
 - (b) The structure should have adequate durability and serviceability under normal maintenance.
 - (c) The structure should not be seriously damaged or collapse under accidental events such as explosions, impact, or due to consequences of human error.
 12. The detailed structural drawings are then prepared once again following provisions contained in the codes and approved by the structural engineer.
 13. The architect or project manager develops detailed architectural drawings and specifications.
 14. The estimator arrives at the quantities involved and the initial cost of construction.
 15. Based on these quantities, a tender for the building is floated.
 16. Comparing the cost quoted by different contractors, the general contractor for the structure is chosen.
 17. The contractor, based on the structural drawings, prepares the fabrication and erection drawings and bill of quantity of materials (BOQ). The structural engineer again approves these drawings.
 18. The contractor constructs the building based on the specifications given by the architect or project manager. While constructing, the contractor consults the architect, project manager, or structural engineer for any changes due to the site conditions. The structural engineer must also convey to the fabricator and erector his/her concept of the structure and specific methods of execution (if any).

19. The structural engineer with the help of quality control inspectors inspects the work of the fabricator and erector to ensure that the structure has been fabricated or erected in accordance with his/her designs and specifications. Similarly, the architect and project manager also inspect the construction periodically to check whether it is built as per specifications.
20. In some important buildings, 'as-built' drawings are prepared as a permanent record of the building.
21. After the structure is constructed, it is handed over to the owner, who, by appointing suitable consultants and contractors, maintains the building until its intended life.

From these steps, it may be clear that accurate calculations alone *may not* produce safe, serviceable, and durable structures. Suitable materials, quality control, adequate detailing, good supervision, and maintenance are also equally important.

These 21 steps briefly summarize the various activities involved in the construction of a structure. While executing the various steps, the structural engineer has to interact with the architect or project manager and also with others (electrical engineers, mechanical engineers, civil engineers, geotechnical engineers, surveyors, urban planners, estimators etc.) and incorporate their requirements, if any, into the design (e.g., load due to mechanical and electrical systems). It has to be noted that steps 8 to 14, which are done mainly in the design office, are not straightforward operations but are iterative as shown in Figs 4.1 and 4.2. This book mainly covers only step 11—the design of structural elements to safely carry the expected loads and to ensure that the elements and the structure perform satisfactorily. Some guidelines and discussions are included about steps 8–10 and 12.

Compared to analysis (where all the parameters are known), design is a creative process. It involves the selection of span, assessment of loads, choice of material, choice of cross section, choice of jointing method and system, and so forth. Hence, there is no unique solution to a design problem. The designer has to make several decisions, which will affect the final construction and its cost. Hence, the designer has to use his/her engineering judgment and experience in order to reduce the cost and arrive at an efficient solution to the problem.

4.3 ROLES AND RESPONSIBILITIES OF DESIGNERS

The objective of design should be the achievement of an acceptable probability that the structure will perform satisfactorily for the intended purpose during the design life. With the appropriate degree of safety, the structure should sustain all the loads and deformations during construction and its designed life and also have adequate resistance to accidental loads and fire.

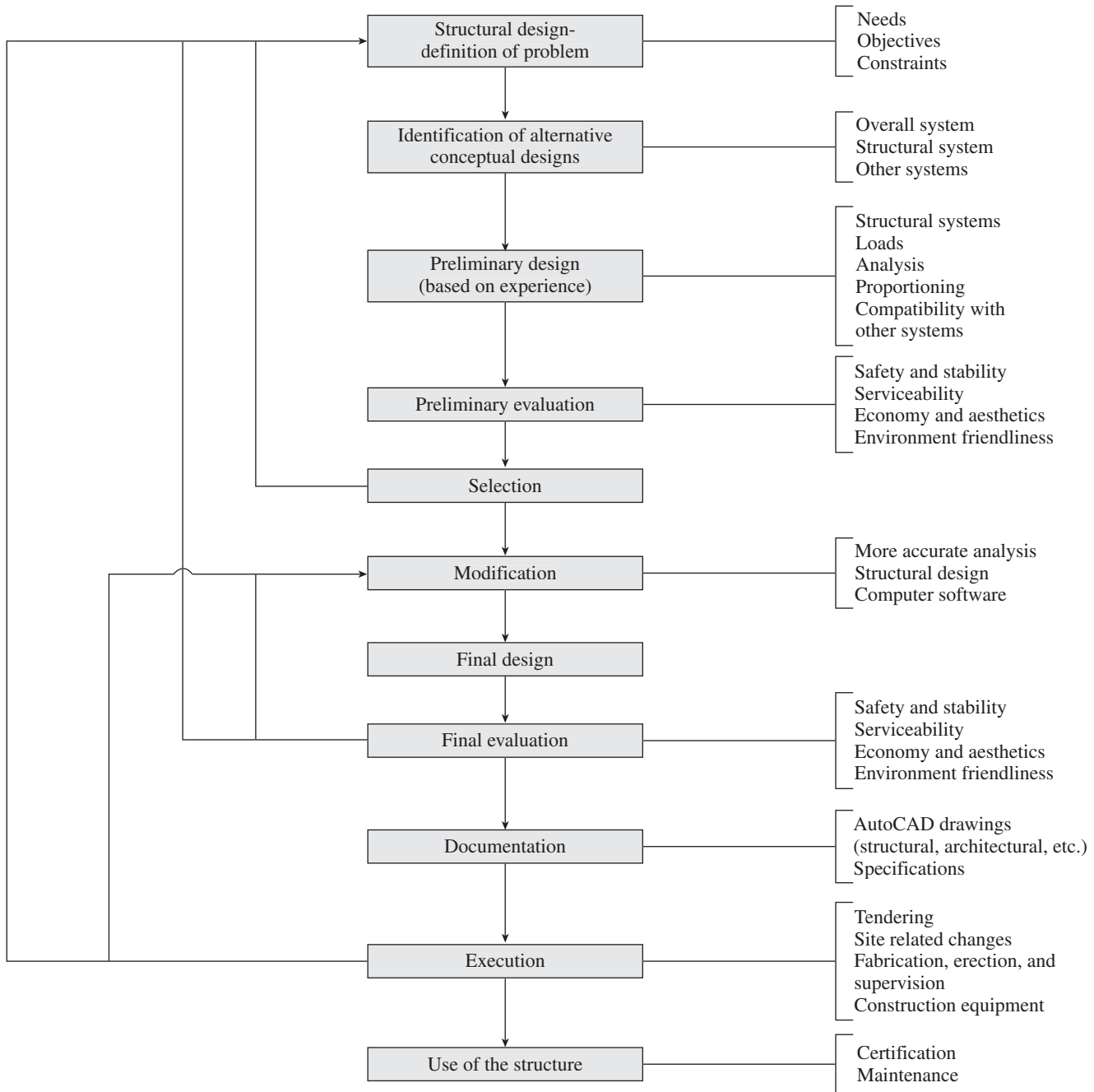


FIG. 4.1 Overall iterative design process

As already discussed, the designer has to take several factors into consideration, while designing the structure. These factors include the following:

1. Material to be used
2. Arrangement of structural system (e.g., gravitational and lateral load resisting system)
3. Method of fabrication (cast in situ or prefabricated) and erection
4. Installation of services (lift, water supply, power, ventilation, heating and cooling, etc.).

5. Safety, economy, and aesthetics
6. Required fire protection
7. Operating/Maintenance and life cycle costs

It is the structural designer's role to ensure that the best structural system is selected, within the scope of the imposed constraints. Today's structural engineer has several aids such as computer programs, handbooks, and charts and hence should spend more time on thinking about the design concepts and select the best structural system for the project at hand (see Chapter 2 for a discussion of various structural systems).

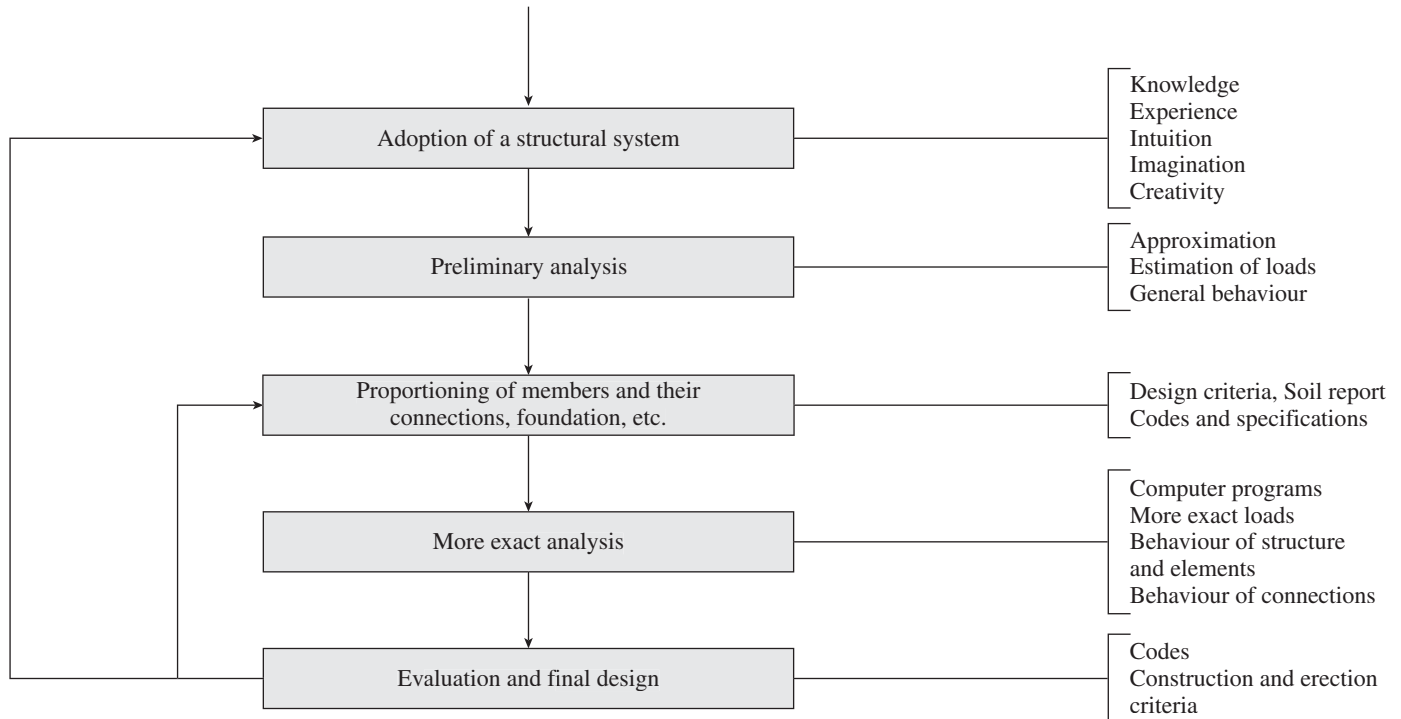


FIG. 4.2 Iterative structural design process

For most structures, the designer should specify a grade and type of concrete that is suitable for the environment, keep the structural layout and structural details (e.g., connections) as simple as possible, and use the maximum possible repetition of member sections and connection details.

The designer should also have some knowledge about the material (concrete) and acceptance criteria. He/She should also be aware of the non-destructive testing techniques that are available and their limitations (brief details are presented in Chapter 1).

It is advantageous for the structural designer to read the description of actual projects (reported in several magazines and journals), discuss with practising engineers, attend technical meetings organized by professional bodies such as the *Indian Concrete Institute*, and visit construction sites and visualize and appreciate the structural behaviour of various structural systems. In comparison with these aspects of actual design practice, the actual proportioning of members, detailing of connections, and so forth is normally much more straightforward.

4.4 DESIGN CONSIDERATIONS

Structural design, though reasonably scientific, is also a creative process. The aim of a structural designer is to design a structure in such a way that it fulfils its intended purpose during the intended lifetime and has the following: (a) adequate safety (in terms of strength, stability, and structural integrity), (b) adequate serviceability (in terms of

stiffness, durability, etc.), (c) economy (in terms of cost of construction and maintenance), (d) durability, (e) aesthetics, (f) environment friendliness, (g) functional requirements, and (h) adequate ductility.

4.4.1 Safety

Safety requirement is paramount to any structure and requires that the collapse of the structure (partial or total) is acceptably low, not only under the normal expected loads (service loads), but also under less-frequent loads (such as due to earthquake or extreme wind) and accidental loads (blast, impact, etc.). Collapse due to various possibilities such as exceeding the load-bearing capacity, overturning, sliding, buckling, and fatigue fracture should be prevented.

Table 4.1 shows the minimum size requirements for earthquake safety as per different codes. It should be noted that American Concrete Institute (ACI) and draft IS 13920 suggest a minimum column size of 300 mm. In India, a beam width of 230 mm is often selected in order to match with the 230 mm thick brick wall. A minimum cover of 40 mm is often specified for columns (the cover should be based on durability and fire resistance, as per Tables 16 and 16a of IS 456). Hence, if the column size is also selected as 230 mm, the beam rods will have to be cranked in order to pass within column reinforcement, which is not a good practice (see Fig. 4.12 also). In addition, for better performance in earthquakes, one must adopt the *strong column–weak beam concept*. These two factors necessitate the column size to be bigger than the beam size.

TABLE 4.1 Minimum size requirement for seismic beam and columns as per various codes

S. No.	Code	Beam		Column	
		B (min.), mm	B/D (min.)	B (min.), mm	B/D (min.)
1.	ACI 318:11	250	0.30	300	0.4
2.	EC 8:1998	200	0.25	250	0.4
3.	IS 13920:1993	200*	0.3	200	0.4
4.	Draft IS 13920	200*	0.3	300 or 15d _b	0.4

* 300 mm for beam when span > 5 m and column clear height > 4 m,
 d_b = Largest longitudinal reinforcement bar diameter of beam
 B, D = Breadth and depth of the member respectively

Similarly, the minimum and maximum limits on longitudinal and transverse reinforcement ratios are often prescribed in the codes of practices for RC flexural members and columns. The minimum limit is prescribed to avoid sudden and brittle failure in case of accidental overload or to take care of additional tensile forces due to shrinkage, temperature, creep, or differential settlement. The maximum limit is prescribed to avoid compression failure of concrete before the tension failure of steel, thus ensuring sufficient rotation capacity at the ultimate limit state. Similar limits are prescribed on transverse reinforcement, as shear failures are more catastrophic than flexural failures. When shear reinforcements are provided, they restrain the growth of inclined cracking and increase the safety margin against failure. Ductility is also increased and a warning of failure is provided. Table 4.2

TABLE 4.2 Minimum steel requirement for beams as per various codes (Subramanian 2010a)

Requirement	Code Provision as per				
	IS 456 Clause 26.5	ACI 318**	CSA A23.3**	Eurocode 2	NZS 3101**
Minimum tensile steel for flexure ⁺ , $\frac{A_s}{b_s d} \geq$	$\frac{0.85}{f_y}$ For T-sections, use b _w alone	$\frac{0.224\sqrt{f_{ck}}}{f_y} \geq \frac{1.4}{f_y}$ For T-sections, use 2b _w or b _f whichever is smaller	$\frac{0.18\sqrt{f_{ck}}}{f_y}$ for T-beams b _w is replaced by a value in the range 1.5b _w to 2.5b _w	$\frac{0.26f_{cm}}{f_y}$ ≥ 0.0013 For T-beams, b _w is taken as the mean breadth	$\frac{0.224\sqrt{f_{ck}}}{f_y}$ For T-beams, b _w is taken as the smaller of 2b _w or width of flange
Maximum tensile steel for flexure ≤	0.04bD	Net tensile strain in extreme tensile steel ≥ 0.005. This will result in approximately $p_t = 15.5 \frac{f_{ck}}{f_y} \leq 2.5$	Tension reinforcement limited to satisfy $\frac{x_u}{d} \leq \frac{700}{700 + f_y}$	0.04bD	$\frac{0.9f_{ck} + 10}{6f_y} \leq 0.025$
Minimum shear reinforcement, $\frac{A_{sv}}{b_w s_v} \geq$	$\frac{0.4}{0.87f_y}$ when τ _v > 0.5 τ _c	$\frac{0.056\sqrt{f_{ck}}}{f_y} \geq \frac{0.35}{f_y}$ when applied shear is greater than 0.5 × concrete strength	$\frac{0.054\sqrt{f_{ck}}}{f_y}$ when applied shear is greater than concrete strength	$\frac{0.08\sqrt{f_{ck}}}{f_y}$ when applied shear is less than shear strength of concrete	$\frac{0.9\sqrt{f_{ck}}}{16f_y}$ when applied shear is greater than 0.5 × concrete strength
Spacing of minimum stirrups ≤	0.75d ≤ 300 mm	0.5d ≤ 600 mm and 0.25d ≤ 300 mm, when V _s > 0.3√f _{ck} b _w d	0.63d ≤ 600 mm 0.32d ≤ 300 mm when V _u > φ (0.1f _{ck} b _w d)	0.75d ≤ 600 mm	0.5d ≤ 600 mm 0.25d ≤ 300 mm, when V _s > 0.3√f _{ck} b _w d

** The cylinder strength is assumed to be 0.8 times the cube strength.

+ Alternatively, it may be at least one-third greater than that required by the analysis, as per ACI code clause 10.5.3.

f_{cm} = Mean axial tensile strength = 0.30 (f_{ck})^{0.666}, f_{ck} = Characteristic cube strength of concrete,

b_f = Breadth of flange, b_w = Breadth of web, b = Breadth of beam

φ = Resistance factor for concrete in shear = 0.65.

A_s = Minimum tensile steel for flexure

A_{sv} = Minimum shear reinforcement

D = Depth of beam, d = Effective depth of the beam

f_y = Characteristic yield strength of reinforcement

p_t = Percentage of tension steel

s_v = Spacing of vertical stirrups

V_s = Nominal shear carried by vertical shear reinforcement

V_u = Factored shear force

x_u = Depth of neutral axis

τ_c = Design shear strength of concrete, τ_v = Nominal shear stress.

provides the minimum steel requirement for beams as per various codes.

The provisions for minimum tensile reinforcement ratio in flexural members of Indian, American, Eurocode 2, New Zealand, and Canadian codes are compared in the first row of Table 4.2. All the codes, except the Indian code, have a similar format and the minimum tensile steel in beams is dependent on the compressive strength of concrete. However, in the IS code, it is independent of f_{ck} ; it might have been assumed to be a constant value of 25 MPa. In some situations, large beams designed with the minimum steel requirement of the IS code have experienced extensive cracking, although there are no reported failures (Varghese 2006).

An area of compression reinforcement at least equal to one-half of tension reinforcement should be provided, in order to ensure adequate ductility at potential *plastic hinge zones* and to ensure that the minimum tension reinforcement is present for moment reversal (Wight and MacGregor 2009). As per Clause 26.5.1.2 of IS 456, the maximum area of compression reinforcement should not exceed $0.04bD$, where b and D are the breadth and depth of the beam.

An upper limit to the tension reinforcement ratio in flexural RC members is also provided to avoid the compression failure of concrete before the tension failure of steel, thus ensuring sufficient rotation capacity at the ultimate limit state. Upper limit is also required to avoid congestion of reinforcement, which may cause insufficient compaction or poor bond between reinforcement and concrete. The provisions for maximum tensile reinforcement in flexural members of Indian, Eurocode 2, American, New Zealand, and Canadian codes are compared in the second row of Table 4.2. Except the Indian code and Eurocode 2, all the other codes have a similar format and involve both f_{ck} and f_y .

When the principal tensile stress within the *shear span* exceeds the tensile strength of concrete, diagonal tension cracks are initiated in the web of concrete beams. The shear span is the distance between the support and the point where the load is applied; for more complex loading cases, the shear span is more difficult to define. Leonhardt and Walther (1962) define the shear span of a beam with uniform load over its entire length as one-fourth of the span. These cracks later propagate through the beam web, resulting in brittle and sudden collapse, when web reinforcement is not provided. (The diagonal cracking strength of the RC beams depends on the tensile strength of concrete, which in turn is related to its compressive strength.) Hence, minimum shear reinforcements are often stipulated in different codes. Such reinforcement is of great value if a member is subjected to an unexpected tensile force due to creep, shrinkage, temperature, differential settlement, or overload.

The provisions for maximum shear reinforcement in flexural members of Indian, Eurocode 2, American, New Zealand, and Canadian codes are compared in the third row of

Table 4.2. Tests conducted on high-strength concrete (HSC) beams indicated that the minimum area of shear reinforcement is also a function of concrete strength (Roller and Russell 1990). Hence, the equation given by ACI provides better correlation with test results.

Stirrups will not be able to resist shear unless an inclined crack crosses them. Hence, ACI code Section 11.4.5.1 sets the maximum spacing of vertical stirrups as the smaller of $d/2$ or 600 mm, so that each 45° crack will be intercepted by at least one stirrup. If $V_u/\phi - V_c$ exceeds $0.3\sqrt{f_{ck}}b_wd$, the maximum allowable stirrup spacing is reduced to half of the earlier-mentioned spacing. Thus, for vertical stirrups, the maximum spacing is the smaller of $d/4$ or 300 mm. This stipulation is provided because closer stirrup spacing leads to narrower inclined cracks and also provides better anchorage for the lower ends of the compression diagonals (see Fig. 6.14 of Chapter 6). The last row of Table 4.2 compares the minimum stirrup spacing of the different codes.

If the area of shear reinforcement is large, failure may occur due to the compression failure of concrete struts prior to the yielding of steel shear reinforcement. Hence, an upper limit to the area of shear reinforcement is necessary. Based on this, the maximum shear force carried by the beam is limited. IS 456 recommends that this value should not exceed $\tau_{c,max}$ given by (see Table 20 of IS 456)

$$\tau_{c,max} = 0.85 \times 0.83\sqrt{f_c} = 0.631\sqrt{f_{ck}} \quad (4.1)$$

Lee and Hwang (2010) compared the test results of 178 RC beams reported in the literature with that of the 18 beams tested by them and found that the shear failure mode changes from under-reinforced to over-reinforced shear failure when $p_v f_y / f_c$ is approximately equal to 0.2. Hence, they suggested the maximum amount of shear reinforcement for ductile failure as

$$p_{v,max} = \frac{A_{sv}d}{sb_w} = 0.2 \frac{f_c}{f_y} \quad (4.2a)$$

where A_{sv} is the area of cross section of transverse stirrups, d is the effective depth of beam, s is the spacing of stirrups and b_w is the breadth of web. In terms of f_{ck} , Eq. (4.2a) may be rewritten as

$$p_{v,max} = 0.16 \frac{f_{ck}}{f_y} \quad (4.2b)$$

Lee and Hwang (2010) also found that the amount of maximum shear reinforcement, as suggested by Clause 11.4.7.9 of ACI 318:11, and given in Eq. (4.3), needs to be increased for high-strength concrete beams, as test beams with greater than 2.5 times $p_{v,max}$, as given by Eq. (4.3), failed in shear after yielding of the stirrups:

$$p_{v,max} = 0.6 \frac{\sqrt{f_{ck}}}{f_y} \quad (4.3)$$

TABLE 4.3 Minimum steel requirement for columns as per various codes

S. No.	Code	Longitudinal Steel		Minimum Transverse Steel (Spiral), A_{sh}	Minimum Transverse Ties, A_{sh}
		Minimum(%)	Maximum(%)		
1.	ACI 318:11**	$> 1A_g$	$< 8A_g$	$> 0.09sD_k \left(\frac{A_g}{A_k} - 1 \right) \frac{f_{ck}}{f_{yt}}$ $> 0.096sD_k \frac{f_{ck}}{f_{yt}}$	$> 0.24sh \left(\frac{A_g}{A_k} - 1 \right) \frac{f_{ck}}{f_{yt}}$ $> 0.072sh \frac{f_{ck}}{f_{yt}}$
2.	IS 456:2000	$> 0.8A_g$	$< 6A_g^*$	$0.09sD_k \left(\frac{A_g}{A_k} - 1 \right) \frac{f_{ck}}{f_{yt}}$	NA
3.	IS 13920:1993	$> 0.8A_g$	$< 6A_g^*$	$> 0.09sD_k \left(\frac{A_g}{A_k} - 1 \right) \frac{f_{ck}}{f_{yt}}$	$0.18sh \left(\frac{A_g}{A_k} - 1 \right) \frac{f_{ck}}{f_{yt}}$
4.	Draft IS 13920	$> 0.8A_g$	$< 6A_g^*$	$> 0.09sD_k \left(\frac{A_g}{A_k} - 1 \right) \frac{f_{ck}}{f_{yt}}$ $> 0.024sD_k \frac{f_{ck}}{f_{yt}}$	$> 0.18sh \left(\frac{A_g}{A_k} - 1 \right) \frac{f_{ck}}{f_{yt}}$ $> 0.05sh \frac{f_{ck}}{f_{yt}}$

* It is suggested to adopt $0.04A_g$ to avoid practical difficulties in placing and compacting concrete.

** The cylinder strength is assumed as 0.8 times the cube strength.

A_{sh} = Area of transverse reinforcement, s = Pitch of spiral/hoop, D_k = Diameter of the core measured to the outside of spiral or hoop, A_g = Gross area of the column cross section, A_k = Area of the confined concrete core measured to the outside of spiral or hoop, h = Longer dimension of the rectangular confining hoop, measured to its outer face, and f_{yt} = Yield stress of spiral or hoop reinforcement.

More details on minimum steel requirements for flexural members may be found in Chapter 5 and in Subramanian (2010a).

The minimum amount of shrinkage and temperature reinforcement specified in the codes for slabs is already shown in Table 3.9. The minimum amount of longitudinal and transverse reinforcement specified in the codes for columns is shown in Table 4.3. These are further discussed in Section 13.5 of Chapter 13.

4.4.2 Stability

Another related aspect of safety is structural integrity and stability. Unlike steel structures where the members are made

of plated elements, concrete structures have massive members and are hence not susceptible for local buckling. Due to the massiveness of the members, buckling of members is also not very critical, except in slender columns. In such cases, the concepts such as *critical load* and *effective length* developed for steel structures are also made use of in concrete structures (see Fig. 4.3). Normally, concrete structures can be considered as *braced frames* (frames that do not sway), with bracing in the form of shear walls, stairwells, or elevator shafts that are considerably stiffer than columns. Unlike steel columns, concentric axial loading is not considered and all codes stipulate that concrete columns must be designed for a certain minimum eccentricity. A concrete column subjected to an ultimate compressive force P

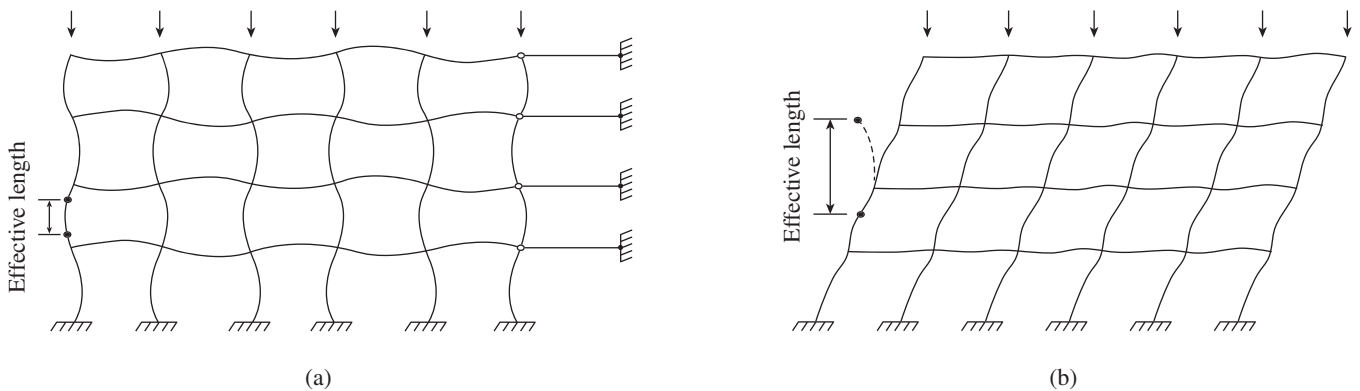


FIG. 4.3 Buckling modes of braced and unbraced frames and the effective length concept (a) Braced frame (b) Unbraced frame

and an ultimate bending moment M is related by an *interaction diagram* (also called the *failure envelope* or *failure surface*). These interaction diagrams are discussed in detail in Chapter 14.

The structure as a whole should be stable under all conditions. Even if a portion of the structure is affected or collapses, the remaining parts of the structure should be able to redistribute the loads. In other words, *progressive failure* should be minimized (see Section 2.6 of Chapter 2). As per Clause 20.1 of IS 456, the stability of the structure as a whole against overturning may be achieved by considering a restoring moment that is not less than 1.2 times the maximum overturning moment caused by the characteristic dead load and 1.4 times the maximum overturning moment caused by the characteristic imposed loads. In cases where the dead load assists the restoring moment, the moment due to the imposed loads should be ignored and only 0.9 times the characteristic dead load shall be considered to provide stability. The anchorages or counterweights provided for the stability of cantilevers during construction and service should be designed for a factor of safety of 2.0. For safety against sliding, a factor of safety of 1.4 should be considered for the adverse combination of applied characteristic loads, with only 0.9 times characteristic dead loads acting on the structure. As per Clause 20.5 of IS 456, lateral sway of the building should not exceed $H/500$, where H is the total height of the building. More discussions on stability against overturning or sliding may be found in Chapters 15 and 16.

4.4.3 Serviceability

Serviceability requirement is related to the utility of the structure. It means that the structure should satisfactorily perform under service loads, without discomfort to the user due to excessive deflection, cracking, vibration, and so forth. Some other considerations of serviceability are durability, impermeability, and acoustic and thermal insulation. It may be noted that a design that adequately satisfies the safety requirement *need not* necessarily satisfy the serviceability requirement. For example, a beam at the roof level may have sufficient stiffness for the applied loads but may result in excessive deflections, leading to cracking of the slab it is supporting, which will result in loss of permeability (leaking). Similarly, members not placed and compacted properly and exposed to weather become vulnerable to corrosion, thereby affecting their *durability*. Slabs may have sufficient strength to withstand the designed load effects but may vibrate causing discomfort. These serviceability aspects are considered in Chapter 12.

4.4.4 Economy

Increasing the design margins of safety may enhance safety and serviceability, but will increase the cost of the structure. For overall *economy* one should consider not only the initial cost but also the *life cycle cost* and the long-term environmental effects on the community. For RC structures, economy may

not be achieved by minimizing the amount of concrete or reinforcement alone. It is because a large part of the construction cost involves cost of labour, formwork, and falsework. The following points will help in achieving economy:

1. Using repetitive member sizes and simple reinforcement detailing that result in easy and faster construction may be more economical than a design with optimum material quantities.
2. Regular-shaped buildings with rectangular or square columns may be economical than irregular shaped buildings with L- or T-shaped columns.
3. Uniform floor-to-floor height will also result in the reuse of formwork.
4. Limiting column sizes to only a few, and consistency with column forms allow for greater formwork reuse and efficiency.
5. Using consistent beam sizes, spacing, and depth allows for greater formwork reuse and installation and standardized forms as well as reduces cut and fits.
6. Use of waste materials, for example, fly ash in the construction products such as cement and bricks will also result in savings.
7. The cost of the floors in a low- to mid-rise building may be 80–90% of the total cost of the concrete frame. Hence, the choice of the right floor framing system for a given bay dimensions may be critical in economizing the cost.
8. For high-rise buildings, choosing a proper lateral load resisting system plays a critical role in the final cost.
9. Precasting and prefabricating techniques will ensure quality and economy.
10. Avoiding transfer beams wherever possible will reduce the cost as columns are cheaper than beams.
11. High-strength concrete and steel reinforcement in columns have shown to reduce weight as well as cost.

More discussions on economy may be found in Webb (1993), Subramanian (1995a), and Delahay and Christopher (2007).

4.4.5 Durability

Several unreinforced concrete structures, which are more than 2000 years old, such as the Pantheon in Rome and several aqueducts in Europe, made of slow-hardening, *lime-pozzolan cements*, are still in excellent condition, whereas many RC structures built in the 20th century, constructed with Portland cement, have deteriorated within 10–20 years (Subramanian 1979; Mehta and Burrows 2001). In most countries in the European Union and other countries such as the USA, approximately 40–50 per cent of the expenditure in the construction industry is spent on repair, maintenance, and remediation of existing structures. The growing number of deteriorating concrete structures not only affects the productivity of the society, but also has a great impact on

our resources, environment, and human safety. It has now been realized that the reason for the deterioration of concrete structures is that emphasis is mainly given to mechanical properties and structural capacity, while neglecting construction quality and life cycle management (ACI 202.2R-2008). Strength and durability are two separate aspects of concrete; neither guarantees the other. Hence, clauses on durability were included for the first time in the fourth revision of IS 456, published in 2000 (see Clause 8 of the code).

A *durable concrete* is one that will continue to perform its intended functions, that is, maintain its required strength and serviceability in the working environment during the specified or traditionally expected service life. The durability of a concrete may be affected by a number of parameters, which include the environment, temperature or humidity gradients, abrasion and chemical attack, permeability of concrete to the ingress of water, oxygen, carbon dioxide, chloride, sulphate and other deleterious substances, alkali–aggregate reaction (chemical attack within the concrete), chemical decomposition of hydrated cement, corrosion of reinforcement, concrete cover to the embedded steel, quality and type of constituent materials, cement content and water–cement ratio, degree of compaction and curing of concrete, shape and size of members, and presence of cracks (see Table 4.4).

TABLE 4.4 Different exposure conditions for concrete

S. No.	Environment	Exposure Conditions Table 3 of Code IS 456	Allowable Maximum Crack Width as per Clause 35.3.2 (mm)
1.	Mild	Protected concrete surfaces, except those situated in coastal area	0.3
2.	Moderate	Concrete surfaces sheltered from rain, continuously under water, or in contact with non-aggressive soil or groundwater	0.25*
3.	Severe	Concrete surfaces exposed to severe rain, coastal environment, alternate wetting and drying, or completely immersed in sea water	0.20
4.	Very severe	Concrete surfaces exposed to sea water spray, corrosive fumes, severe freezing conditions while wet, or in contact with aggressive sub-soil or ground water	0.10
5.	Extreme	Concrete surface of members in tidal zone or in direct contact with aggressive chemicals	< 0.10

* Assumed to be in between severe and mild

The prescriptive requirements given in the code relate to the use of the specified maximum water–cement ratios, minimum cement content, minimum grade of concrete for various exposure conditions, and minimum cover (see Table 4.5). The durability requirements of the different codes were compared by Kulkarni (2009) and Ramalingam and Santhanam (2012), who have also provided suggestions to improve the exposure condition clause of IS 456.

TABLE 4.5 Prescriptive durability requirements of cement content, water–cement ratio, and grade of concrete for different exposures

S. No.	Exposure	Reinforced Concrete		
		Minimum Cement Content (kg/m ³)	Maximum Free Water– Cement Ratio	Minimum Grade of Concrete
1.	Mild	300	0.55	M20
2.	Moderate	300	0.50	M25
3.	Severe	320	0.45	M30
4.	Very severe	340	0.45	M35
5.	Extreme	360	0.40	M40

Notes:

1. The cement content prescribed in this table is irrespective of the grade and type of cement and the grade of concrete, and it is inclusive of additions such as fly ash, silica fume, rice husk ash, metakaoline, and ground granulated blast furnace slag. The additions such as fly ash or ground granulated blast furnace slag may be taken into account in the concrete composition with respect to the cement content and water–cement ratio, if the suitability is established and as long as the maximum amounts taken into account do not exceed the limit of pozzolan and slag specified in IS 1489 (Part 1) and IS 455, respectively.
2. The minimum cement content, maximum free water–cement ratio, and minimum grade of concrete are individually related to the exposure conditions given in Table 4.4.

Low water–cementitious materials (w/cm) ratio produces dense and impermeable concrete, which is less sensitive to *carbonation*. Well-graded aggregates also reduce the w/cm ratio. The coefficient of permeability increases more than 100 times from w/cm ratio of 0.4 to 0.7. It is now possible to make concretes with w/cm ratio as low as 0.25 using *super-plasticizers*, also called *high-range water-reducing admixtures* (HRWRA). It should be noted that the super-plasticizer used must be compatible with the other ingredients such as Portland cement (Jayasree, et al. 2011). Micro-cracks that are produced in the interface between the cement paste and aggregates (called the *transition zone*) are also responsible for the increased permeability. Use of pozzolanic material, especially silica fume, reduces the permeability of the transition zone as well as the bulk cement paste. When silica fume is included, use of super-plasticizers is mandatory. *Self-compacting concrete* (SCC), in which the ingredients are proportioned in such a way that the concrete is compacted by its own weight without the use of vibrators and assures complete filling of the formwork, even when access is hindered by congested reinforcement detailing, may be adopted in severe and extreme environmental conditions.

Currently available cements are more finely ground and are hardened rapidly at an earlier age. Moreover, they may contain more tricalcium silicate (C_3S) and less dicalcium silicate (C_2S), resulting in rapid development of strength. Compared to old concrete mixtures, modern concrete tends to crack more easily due to lower creep and higher thermal shrinkage, drying shrinkage, and elastic modulus (Mehta and Burrows 2001). There is a close relationship between cracking and deterioration of concrete structures exposed to severe exposure conditions.

Curing of Concrete

For concrete to achieve its potential strength and durability, it has to be properly cured. *Curing* is the process of preventing loss of moisture from the surface of concrete and maintaining satisfactory moisture content and favourable temperature in the concrete during the *hydration* of cementitious materials so that the desired properties are developed. Prevention of moisture loss is particularly important when the adopted w/cm ratio is low, the cement used has a high rate of strength development (grade 43 and higher cements), or *supersulphated cement* is used in the concrete (it requires moist curing for at least seven days). Curing primarily affects the concrete in the cover of the reinforcement, and the cover protects the reinforcement from corrosion by the ingress of aggressive agents. Curing is often neglected in practice and is the main cause of deterioration of concrete structures in India and abroad.

Many methods of curing exist—ponding of water on the surface of concrete slabs, moist curing using wet hessian (called burlap in the USA), sacking, canvas, or straw on concrete columns, curing by spraying membrane-forming *curing compounds* on all exposed surfaces (approximate coverage rate of $4\text{ m}^2/\text{l}$ for untextured surface and $6\text{ m}^2/\text{l}$ for textured surface), covering concrete by polyethylene sheets or water-proof paper (with adequate lapping at the junctions), as soon as concreting is completed to prevent evaporation of moisture from the surface, and *steam curing* (the high temperature in the presence of moisture accelerates the hydration process, resulting in faster development of strength). Keeping the formwork intact and sealing the joints with any sealing compound is also good for the curing of beams.

In India, several builders adopt the wrong practice of commencing curing only on the next day of concreting. Even on the next day, curing is started after making arrangements to build bunds with mud or lean mortar to retain water. This further delays the curing. The time of commencement of curing depends on several parameters such as prevailing temperature, humidity, wind velocity, type of cement, fineness of cement, w/cm ratio used, and the size of member. However, the main objective is to keep the surfaces of concrete wet. Enough moisture must be present to promote hydration. Curing compound should be applied or wet curing should start immediately after the bleeding

water, if any, dries up. In general, concrete must be cured until it attains about 70 per cent of the specified strength. Clause 13.5.1 of IS 456 suggests curing for a period of seven days (with the temperature being maintained above 10°C) in case of ordinary Portland cement concrete and ten days (with a recommendation to extend it for 14 days) when mineral admixtures or blended cements are used or when the concrete is exposed to dry and hot weather conditions. At lower temperatures, the curing period must be increased. Mass concrete, heavy footings, large piers, and abutments should be cured for at least two weeks. Further precautions to be undertaken during hot or cold weather concreting are discussed in IS 7861 (Parts 1 and 2) and Venugopal and Subramanian (1977). More details on curing may be found in Subramanian (2002).

Cover

Cover is the shortest distance between the surface of a concrete member and the nearest surface of the reinforcing steel. The concrete cover protects the steel reinforcement against corrosion in two ways—providing a barrier against the ingress of moisture and other harmful substances and forming a passive protective (calcium hydroxide) film on the steel surface. The cover provides corrosion resistance, fire resistance, and a wearing surface and is required to develop the bond between reinforcement and concrete. It should exclude plaster and any other decorative finish. Too large a cover reduces the effective depth and is prone to cracking, whereas too less may lead to corrosion due to carbonation of concrete. The nominal cover required to meet the durability requirements is given in Table 4.6. These values should be increased when lightweight or porous aggregates are used.

TABLE 4.6 Required cover (mm) for durability

Exposure Condition	Concrete Grade with Aggregate Size 20 mm				
	M20	M25	M30	M35	M40
Mild	20	20	20	20	20
Moderate	–	30	30	30	30
Severe	–	–	45	40*	40*
Very Severe	–	–	–	50	45*
Extreme	–	–	–	–	75

Notes:

1. For main reinforcement up to 12 mm diameter bar in mild exposure, the nominal cover may be reduced by 5 mm.
2. A tolerance in nominal cover of +10 mm and –0 mm is permissible as per IS 456.
3. To develop proper bond, a cover of at least one bar diameter is required.
4. Cover should allow sufficient space so that the concrete can be placed or consolidated around the bars. For this reason, the cover should be 5 mm more than the size of aggregate.
5. Cover at the end of bars should be $\geq 25\text{ mm}$ and $\geq 2.0d_b$, where d_b is the diameter of the bar.

* For *severe* and *very severe* conditions, 5 mm reduction in cover is permissible, if M35 and above concrete is used.

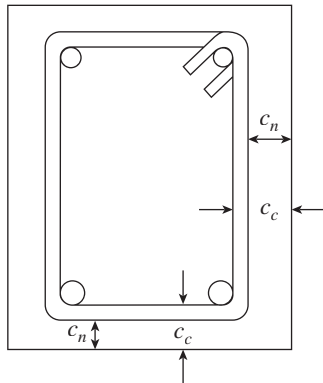


FIG. 4.4 Clear (c_c) and nominal (c_n) covers to reinforcements

The *nominal cover* is the design depth of cover to all steel reinforcements including links (see Fig. 4.4). Moreover,

according to Clause 26.4 of IS 456, the nominal cover for longitudinal reinforcement in columns should not be less than 40 mm, and it should not be less than 50 mm for footings. In addition to providing the nominal cover, it should be ensured that the cover concrete is well compacted, dense, and impermeable. Otherwise, heavy corrosion of reinforcement will take place as shown in Fig. 4.5.

Adequate cover, in thickness and in quality, is necessary for other purposes too—to transfer the forces in the reinforcement by bond action, to provide fire resistance to steel, and to provide an alkaline environment on the surface of steel. The nominal cover requirement for different hours of fire resistance is given in Table 4.7.

It has been found that a thick cover leads to increased crack widths in flexural RC members, defeating the very



FIG. 4.5 Heavy corrosion of rebars in a 4-star hotel in Chennai due to permeable or less than nominal cover

purpose for which it is provided. Hence, the engineer should adopt a judicious balance between the cover depth and crack width requirements. The German code, DIN 1045, stipulates that concrete cover greater than 35 mm should be provided with a wire mesh within 10 mm of surface to prevent spalling due to shrinkage or creep. A novel method called *supercover concrete* has been developed by researchers at South Bank University, UK, for preventing reinforcement corrosion in concrete structures with thick covers using glass fibre reinforced plastic (GFRP) rebars (see Fig. 4.6). This method involves using conventional steel reinforcement together with concrete covers in excess of 100 mm, with a limited amount of GFRP rebars in cover zones. This method is found to be cheaper than cathodic protection (Arya and Pirathapan 1996; Subramanian and Geetha 1997).

TABLE 4.7 Nominal cover (mm) for fire resistance

Fire resistance (hours)	Beams		Slabs		Ribs		Columns
	Simply supported	Continuous	Simply supported	Continuous	Simply supported	Continuous	
0.5	20	20	20	20	20	20	40
1.0	20	20	20	20	20	20	40
1.5	20	20	25	20	35	20	40
2.0	40*	30	35	25	45*	35	40
3.0	60*	40*	45*	35*	55*	45*	40
4.0	70*	50*	55*	45*	65*	55*	40

Notes:

These nominal covers relate to the minimum member dimensions given in Fig. 1 of IS 456.

* When the cover exceeds 40 mm in flexural members, additional measures, such as sacrificial steel in tensile zone, are required to reduce the risk of spalling (see Clause 21.3.1 of the code).

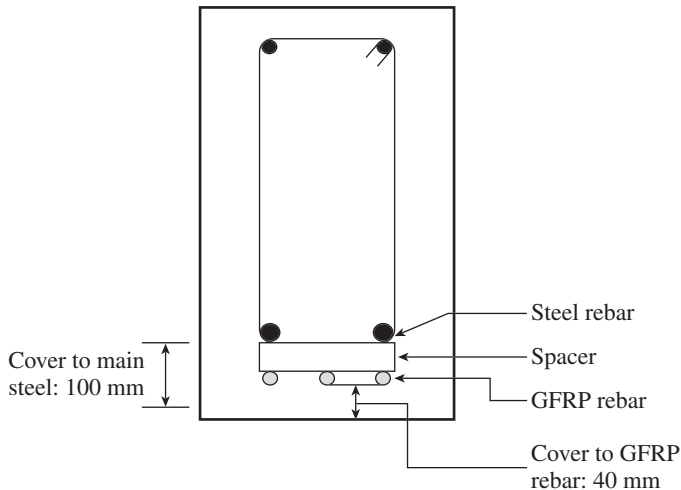


FIG. 4.6 Schematic diagram of supercover concrete system

Source: Arya and Pirathapan 1996

A holistic approach to durability of concrete structures must consider the following: component materials, mixture proportions, placement, consolidation and curing, and structural design and detailing. Air-entraining admixture has to be used under conditions of freezing and thawing.

The philosophies to tackle corrosion in concrete and their representative costs (given as a percentage of the first cost of the concrete structure) include the following (Mehta 1997):

1. Use of fly ash or slag as a partial replacement of the concrete mixture (0%)

2. Pre-cooling of the concrete mixture (3%)—pre-cooling will mitigate the effects of heat of hydration and may reduce the extent of cracking.
3. Use of silica fume and a super-plasticizer (5%)
4. Increasing cover by 15 mm (4%)
5. Addition of corrosion-inhibiting admixture (8%)
6. Using epoxy-coated or galvanized reinforcing bars (8%)
7. External coatings (20%)
8. Cathodic protection (30%).

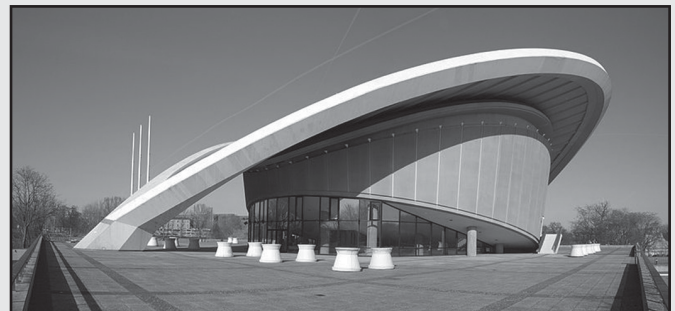
Where thermal cracking is of concern, the most cost-effective solution would be to use as less Portland cement content as possible with large amounts of cementitious or pozzolanic admixture (Mehta 1997).

Plastic and cementitious spacers and steel wire chairs should be used to maintain the specified nominal cover to reinforcement (see Figs 4.7 and 4.8). Spacers go between the formwork and the reinforcement, and chairs go between the layers of reinforcement (e.g., top reinforcements supported off bottom reinforcement). *Spacers* and *chairs* should be fixed at centres not exceeding $50d$ in two directions at right angles for reinforcing bars and 500 mm in two directions at right angles for welded steel fabric, where d is the size of the reinforcement to which the spacers are fixed. The material used for spacers should be durable, and it should not lead to corrosion of the reinforcement nor cause spalling of the concrete cover. Cementitious spacers must be factory-made and should be comparable in strength, durability, porosity, and appearance of the surrounding concrete. It is important to check the cover

CASE STUDY

Failure of Congress Hall, Berlin, Germany

The Benjamin Franklin Hall, as the building was officially known, also called the conference hall (Der Kongresshalle) and nicknamed 'pregnant oyster' (Schwangere Auster), is a gift from the USA to the Berlin International Building Exhibition in 1957. The American architect Hugh A. Stubbins Jr designed the building in collaboration with two Berlin architects, Werner Duettmann and Franz Mocken. This one-third curved and cantilevered roof (see figure) collapsed on 21 May 1980, killing one and injuring numerous people. It started rumbling and vibrating in the morning and hence most people inside had time to leave the building before it collapsed. The 76 mm thick RC shell roof resembles an open human eye with a tension ring as the pupil and the two arches at the edges representing the upper and lower lids. The two arch support points represent the corners of the 'eye'. The report of the failure cited that the collapse was mainly due to the planning and execution of the roof, which led to cracks and corrosion



Congress Hall, Germany

and finally to the failure of the tensioning elements. The hall was rebuilt in its original style and reopened again in 1987 at the 750th anniversary of Berlin. More details of the failure may be found in Subramanian (1982).

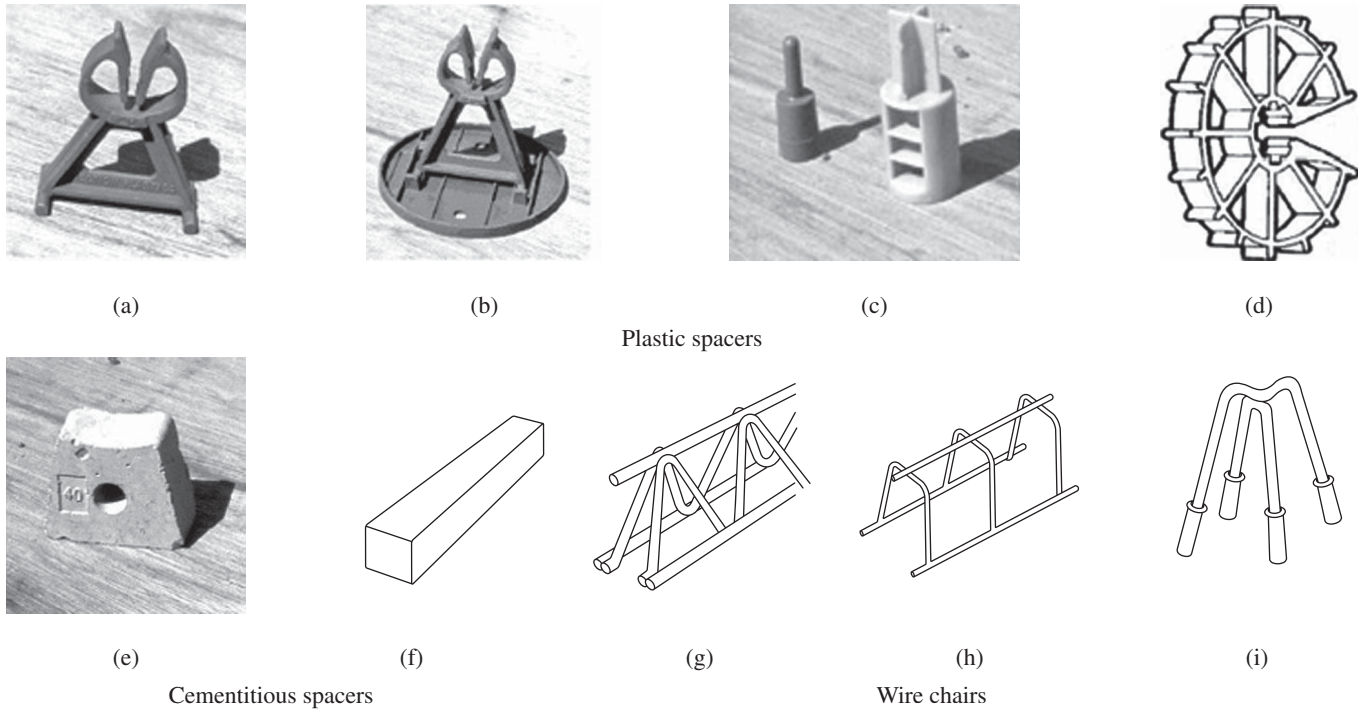


FIG. 4.7 Spacers and chairs to ensure good and uniform concrete cover (a) Single cover 'A' spacer (b) Soft substrate 'A' spacer (c) End spacer (d) Circular spacers (e) Single cover spacer (f) Line spacer (g) Lattice type continuous chair (h) Goalpost type continuous chair (i) Individual chair
 Source: Shaw, C., Durability of Reinforced Concrete, <http://www.localsurveyorsdirect.co.uk/sites/default/files/attachments/reinforcedconcrete.pdf>

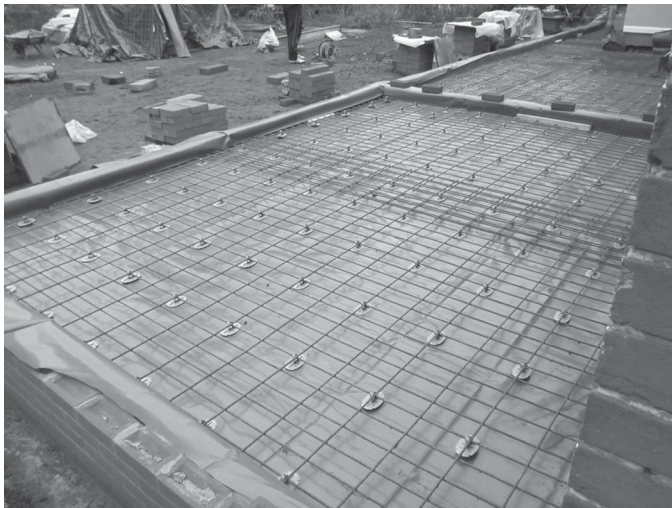


FIG. 4.8 Spacers for welded steel fabric with new soft substrate spacers
 Photo copyright: C.B. Shaw, UK

before and during concreting. The position of reinforcement in the hardened concrete may be checked using a *cover meter*. The reinforcements need to be tied together to prevent displacement of the bars before or during concreting. The six types of ties used in practice are shown in Fig. 4.9. Slash ties are used in slabs, ring slash and crown ties in walls, and crown or hairpin ties in beams and columns. British Standard (BS) 7973-1 contains complete details of the product requirements for the spacers and chairs, and BS 7973-2 specifies how they

are to be used, including the tying of the reinforcement. More discussions on cover, spacers, and chairs may be found in Prakash Rao (1995) and Subramanian and Geetha (1997).

To assist designers in choosing the concrete mix, minimum cover, and minimum thickness of slab based on Tables 3, 5, 16, and 16A of IS 456:2000, Varyani (2001) developed the table shown in Table 4.8.

Controlled Permeability Formwork Systems

It is well known that the use of conventional impermeable formworks (wood or steel) results in cover zones having reduced cement content and increased w/cm ratio. As a result, the presence of blowholes and other water-related blemishes are often observed upon removal of the formwork. The concept of using permeable formwork (PF) to produce better quality cover concrete was first originated by John J. Earley in the 1930s. The US Bureau of Reclamation developed the first type of PF, known as *absorptive form liner*, in 1938. This technology was revived in Japan in 1985, and a number of Japanese companies have developed *controlled permeable formwork* (CPF) systems, using textile and silk form. A company (DuPont) has also developed a less-expensive CPF liner system known as *Zemdrain*. CPF systems have been used in a number of projects in Europe and Australia (Basheer, et al. 1993). It has been proved both in the laboratory and on the field that these systems increase the cement content of the cover region,

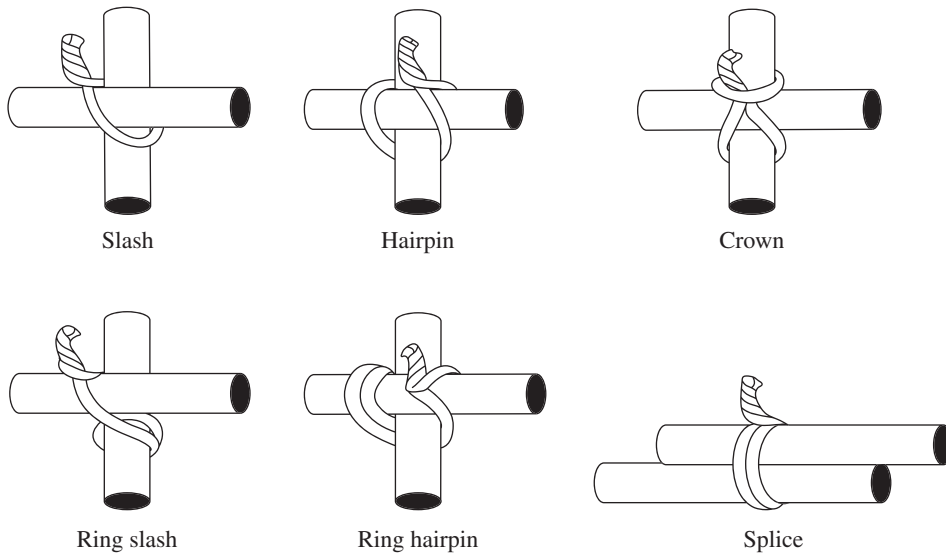


FIG. 4.9 Six types of ties used in binding wires

Note: The ends of the tying wire should not encroach into the concrete cover.

Source: Shaw, C., Durability of Reinforced Concrete, <http://www.localsurveyorsdirect.co.uk/sites/default/files/attachments/reinforcedconcrete.pdf>

while at the same time reducing the w/cm ratio, porosity, and permeability (Basheer, et al. 1993).

Typically, CPFs are thermally bonded permeable liners that consist of a polyester filter and polyethylene drain elements, attached in tension to the internal face of a structural support, as shown in Fig. 4.10 (Reddi 1992; Annie Peter and Chitharanjan 1995). During concreting, due to the action of vibrators, the

entrapped air and excess mix water, which would otherwise become trapped at the surface causing blemishes, pass through the liner, as shown in Fig. 4.10. The pore structure of the liners is so chosen that they will retain majority of the cement and other smaller fines. A proportion of water is held within the liner, which, under capillary action, imbibes back into the concrete to assist curing. The forms can be removed with the normal level of care and cleaned with high-pressure water and reused. Release agents are not required as CPF liners easily debond from the concrete during formwork striking. The main advantage of CPF are surface finish with very few blowholes, aesthetically pleasing textured surfaces giving good bond for plaster or tiles, and improved initial surface strength,

allowing earlier formwork striking. Recently, the influence of SCC, which does not require any vibration effort for its compaction, on CPF was studied by Barbhuiya, et al. (2011). They found that the degree of improvement in the cover region is significantly lower in the case of SCC when compared to conventional concrete.

TABLE 4.8 IS 456:2000 requirements for durability and fire resistance (Varyani 2001)

Exposure Zone	Where Applicable	Minimum Concrete Mix	Nominal Cover for Members, mm		Minimum Thickness of Slabs, mm	Remarks
Mild	Concrete surface protected against weather or aggressive conditions in non-coastal regions	M20	Slab	20	110	For buildings in mid-land areas like Delhi
			Beam	25		
			Column	40		
			Footing	50		
Moderate	Concrete surface sheltered from saturated salt air in coastal areas	M25	Slab	30	110	For buildings in coastal areas such as Mumbai, Chennai, and Kolkata
			Beam	30		
			Column	40		
			Footing	50		
Severe	Concrete exposed to coastal environment or completely immersed in sea water	M30	Slab	45	140	For structures immersed in sea water
			Beam	45		
			Column	45		
			Footing	50		

Notes:

1. The other two exposure zones, very severe and extreme, being applicable to special situations, have not been given here.
2. Slab covers have been reduced in moderate and severe exposure zones in order to restrict crack width and to also reduce dead load of buildings.

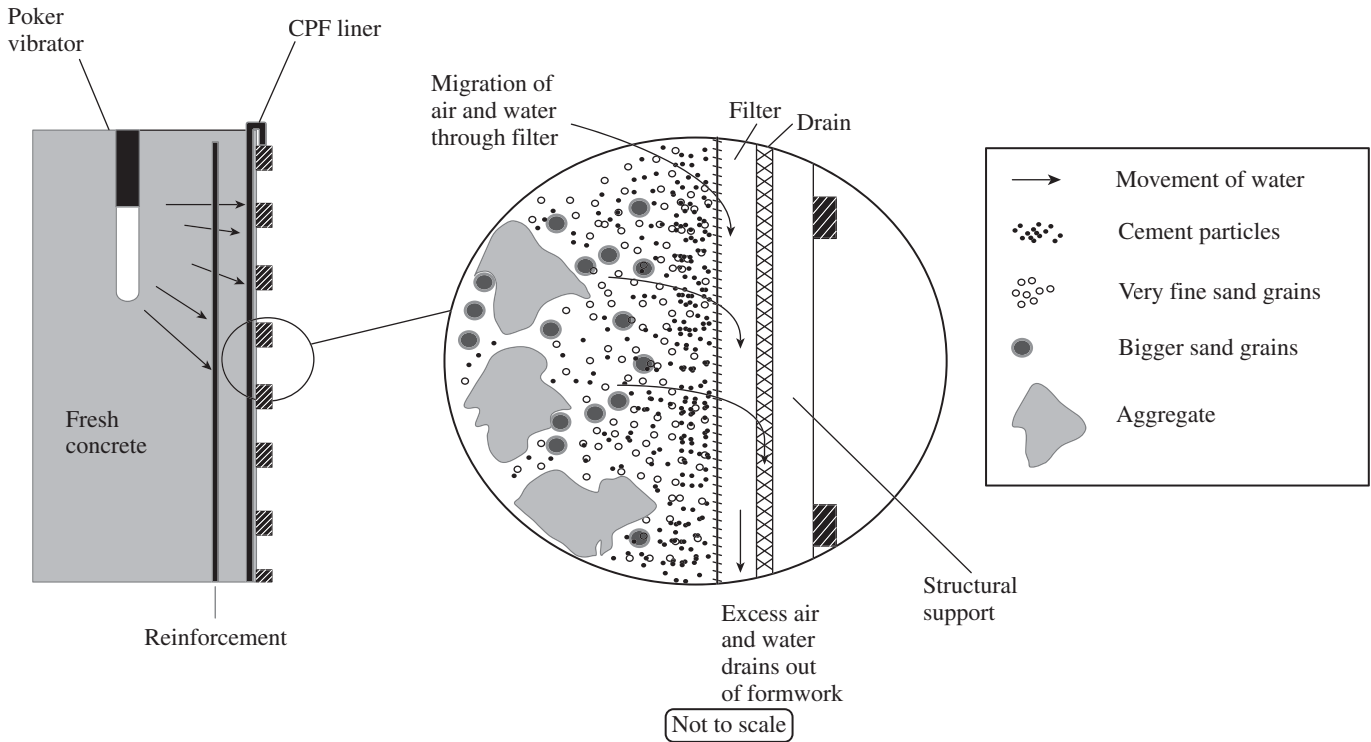


FIG. 4.10 Controlled permeability formwork

4.4.6 Aesthetics

Aesthetics is important not only for structures of high visibility but also for all other structures, as it gives a sense of pride to the owner. Aesthetic consideration may include selection of shape, geometrical proportions, symmetry, surface texture, colour, and harmony. Aesthetics is an art and cannot be objectively quantified or subjected to fixed rules. The structural engineer must work in close coordination with the architects, planners, and other design professionals to design aesthetic structures that are elegant and at the same time economical and functional. The impact of the structure on its surrounding has to be considered by the architect, by choosing local materials and architectural styles. A few examples of aesthetic concrete structures include the replica of the classical ancient Greek Parthenon, constructed with combined cast-in-place and precast concrete facades during 1925–31 and located in Nashville, Tennessee, USA; the Marina City complex, designed in 1959 by architect Bertrand Goldberg and completed in 1964; and the Lotus Temple Bahá'í House of Worship, New Delhi, which is composed of 27 free-standing marble clad 'petals' arranged in clusters of three to form nine sides and designed by the Iranian architect, Fariborz Sahba. The consultants were Flint & Neill Partnership of London while the contractors were the ECC Construction Group of Larsen & Toubro Limited. These are shown in Fig. 4.11. More information on aesthetics and examples of aesthetic concrete buildings may be found in

Subramanian (1987), Schlaich (1995), Collins (2001), Steiger (1996; 1997), and Kaushik (2003).

4.4.7 Environment Friendliness

Climate change resulting from the high concentration of greenhouse gases, such as carbon dioxide (CO₂), methane (CH₄), nitrous oxide (N₂O), and fluorinated gases, in the atmosphere is threatening the world's environment. The concentration of CO₂, one of the primary greenhouse gases, has risen from 316 ppm in 1959 to 390 ppm in 2010. To avoid a *global warming* of 2.1°C, it is estimated that a CO₂ concentration of less than 450 ppm needs to be maintained.

The construction industry consumes 40 per cent of the total energy and about one-half of the world's major resources. Hence, it is imperative to regulate the use of materials and energy in this industry. CO₂ is a major by-product in the manufacturing of the two most important materials of construction—Portland cement and steel. Thus, while selecting the material and system for the structure, the designer has to consider the long-term *environmental effects*, which include maintenance, repair and retrofit, recyclability, environmental effects of demolished structure, adoptability of fast track construction, and demountability and dismantling of the structure at a future date. In concrete structures, in addition to performance, the concrete mixture has to be considered in terms of the waste or by-product material content, embodied energy, and carbon footprint.



(a)



(b)



(c)

FIG. 4.11 Examples of aesthetic concrete structures (a) Replica of the Parthenon (b) The Marina City complex (c) Bahá'í Lotus Temple

Source: http://www.wpclipart.com/buildings/famous/US_famous/Parthenon_replica_Nashville_Tenenssee.jpg.html

Mehta (2009) has shown that by simultaneously using the following three tools, major reductions in concrete consumption and carbon emissions can be achieved (see Table 4.9).

1. *Consuming less concrete by rehabilitating old buildings:* One of the best solutions to improve sustainability is to increase the service life of concrete structures from the present 50 years to 100–150 years, and enhancing the long-term durability (by careful selection of constituents of concrete). Use of *demountable precast products*, which can be reused, is also an efficient solution.
2. *Consuming less cement in concrete mixtures:* Using high-range water-reducing admixtures to reduce 20–25 per cent of water, thereby reducing cement content; optimizing aggregate size and grading; and using 56–90-day compressive strength instead of the traditional 28-day strength (especially in Portland Pozzolana Cement, PPC) in the design may result in 15–20% cement savings. It should be noted that concretes with mineral admixtures tend to develop strength slowly and hence their 56th to 90th day strength will be much higher than the 28th day strength. Moreover, the 28th day strength was adopted as the standard when the concretes were made only with Portland cement.
3. *Minimizing the quantity of cement in a concrete mix:* The use of industrial by-products such as fly ash, blast furnace slag, silica fume, and reactive rice-husk ash can lead to significant reductions in the amount of cement needed to make concrete, and hence reduces the emissions of CO₂ and consumption of energy and raw materials, in addition to reducing the landfill or disposal burdens. (India produces over 270 million tonnes of fly ash per year, which is harmful and difficult to dispose.) Fly ash can be readily substituted for over 30 per cent of cement volume and blast furnace slag for more than

35 per cent. *High volume fly ash (HVFA) concretes* with 50–70 per cent of cementitious content have been studied extensively and are found to be feasible in certain situations. They are found to have better properties than concretes produced with Portland cement (Malhotra 2002).

Table 4.9 is based on the following assumptions: Combined use of tools 1 and 2 will reduce cement consumption by 30 per cent (2.80 billion tonnes in 2010 to 1.96 billion tonnes in 2030). The clinker factor is reduced by 20–30 per cent by the use of alternate cementitious materials. Carbon emission factor is decreased by 10–20 per cent by the use of waste material as fuel.

TABLE 4.9 Projected cement and CO₂ reduction

Description	Year 2010	Year 2030	Percentage Reduction
Cement requirement, billion tonnes	2.8	1.96	30
Clinker factor*	0.83	0.60	27
Clinker requirement, billion tonnes	2.3	1.18	49
CO ₂ emission factor ⁺	0.9	0.8	10
Total CO ₂ emission, billion tonnes	2.07	0.94	55

* Tonne of clinker per tonne of cement

⁺ Tonne of CO₂ per tonne of clinker

Source: Mehta 2009, reprinted with permission from Concrete International

It is interesting to note that the use of Portland cement containing *limestone filler* (which does not have pozzolanic properties) is a common practice in European countries, especially in France. Bentz, et al. (2009) carried out a study using the *Power's model* and suggested that for low w/cm ratios in the range of 0.30 to 0.35, it is possible to replace cement with limestone powder to the extent of 15 per cent. Such incorporation of coarse limestone powder, with a median particle diameter of about 100 micron, could also significantly increase durability by reducing autogenous deformation and inclination for related early age cracking.

The use of ready-mixed concrete can also help in obtaining quality concrete that will increase the durability and life of concrete structures. Modern concretes such as fibrous concrete, geopolymer concrete, high-performance concrete, reactive powder concrete, SCC, and self-curing concrete not only enhance the properties of concrete but also increase the life of structures built with them.

Geopolymer Concrete

The *geopolymer concrete* can be used as a greener alternative to Portland cement concrete. It can be produced by blending

three elements, namely calcined alumino-silicates (from clay), alkali-disilicates, and granulated blast furnace slag or fly ash. The cement hardens at room temperatures and provides compressive strengths of 20 MPa after 4 hours and up to 70–100 MPa after 28 days. Geopolymer binder can be used in applications to replace or partially replace ordinary Portland cement with environmental and technical benefits, including an 80–90% reduction in CO₂ emissions. This is mainly due to the absence of the high-temperature calcination step in geopolymer synthesis. The silicon and aluminium oxides in the low-calcium fly ash chemically react with the alkaline liquid to form the geopolymer paste that binds the loose coarse aggregates, fine aggregates, and other unreacted materials together to form the geopolymer concrete (Rangan 2008).

More information on the sustainability of concrete structures may be had from Vangeem and Marceau (2002); Swamy (2003); Subramanian (2007); Subramanian (2008); Mehta (2009); Subramanian (2010c); and Subramanian (2012).

4.4.8 Functional Requirements

A structure must always be designed to serve its intended function as specified by the owner and architect. Constructability is a major part of the functional requirement and is also related to safety and durability. During the planning and design stages, it is important and crucial to consider constructability, that is, consideration should be given to the way in which all the elements on the drawing board can be constructed practically. The collapse of the Hyatt Regency Hotel walkways in the 1980s provides a classical example of the error in constructability. In this building, a flawed alteration was made in the rod hangers by the contractor, which was approved by the designer without verifying its effects, leading to the collapse. The contractor made this flawed alteration because of the difficulty of constructing the original detail in the field (see Subramanian 2010b for the details of this failure).

In addition to such careless review of detailed drawings, especially when changes to the original details are made, another undesirable practice is to ignore the warning signals occurring during construction. These signals might be in the form of excessive deflections, vibrations, wrong construction practices adopted by the contractor, or the change in loading conditions during construction.

Troubles in buildings may also result due to design engineers not visiting the job site. Job site visits are crucial as they will confirm if the contractors are following the original details on the drawings. Site visit gives the engineer an opportunity to correct anything that contractors might have missed or misunderstood. Many times, loads and conditions unanticipated during design might be discovered during the site visit, when the structure is actually built.

Building information modelling (BIM) is used nowadays to facilitate collaboration among the various disciplines and systems and to identify any misconceptions before the beginning of the construction. Integrating BIM and constructability solves potential design issues and minimizes problems at the construction site as construction knowledge is also utilized during the design process.

The term *constructability* with respect to *cast in situ* concrete construction refers primarily to the ease with which reinforcements can be placed and concrete is poured. In order to achieve constructability, engineers should imagine the possible situations that may be encountered in the field when they are preparing the detailed drawings. Visualizing the construction process will aid in catching constructability flaws. For example, many times junior engineers make the mistake of supporting bigger size beams on small size beams. Moreover, having the same size of beams and columns will result in cranking the beam bars to be placed inside the column, which is not a good practice (see Figs 4.12a and b). Figures 4.13(a) and (b) show another example where the engineer is attempting to fit too much reinforcing steel into too little space (Schwinger 2011). Of course, such problems caused by the 135° hooks of transverse reinforcement may be solved by using *welded reinforcement grids* (WRG) (see Figs 4.14a and b). The one-piece WRG improves not only the constructability but also the ductile performance and speed of construction.

Similarly, using 180° bar hooks in slabs may complicate the placement of reinforcing steel, as shown in Fig. 4.15. While bars with 90° hooks can be dropped straight down into place, bars with 180° hooks cannot be dropped into place unless the perpendicular edge bar is temporarily moved out of the way and then re-positioned after the hooked bars are installed (Schwinger 2011).

Although IS 456 permits up to six per cent longitudinal reinforcement in columns, it is better to limit the percentage of longitudinal steel to two per cent for economy and four per cent for constructability. It should be noted that columns reinforced with six per cent steel using lap splices will have twelve per cent steel at splice locations, unless mechanical splice couplers are used. Figure 4.16 shows the reinforcing steel at the splice location of two columns of size 600 mm × 600 mm—one reinforced with eight 36 mm rods ($\rho = 2.26\%$) and another reinforced with sixteen 36 mm rods ($\rho = 4.52\%$). It should also be noted that the column with

16 vertical bars results in congestion of reinforcement. Large numbers of vertical bars also require more ties. Moreover, installing beam and slab reinforcing through heavily reinforced columns can be difficult. Heavily reinforced columns are not only difficult to build, but also not economical.

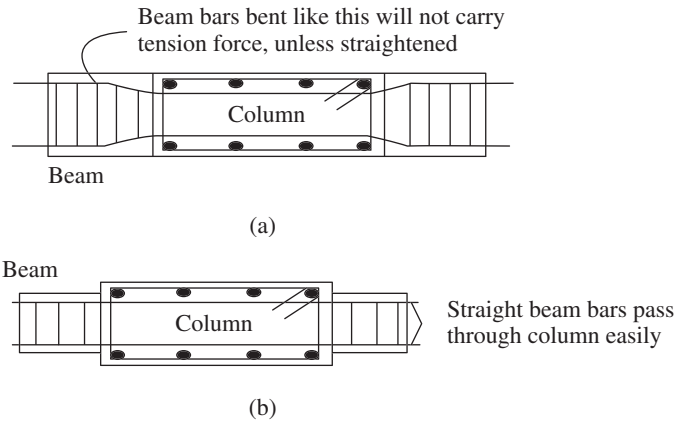


FIG. 4.12 Bigger column sizes result in better reinforcement detailing (a) Beam and column of same size (b) Column width bigger than beam width
Source: Murty 2005, NICEE, IIT Kanpur

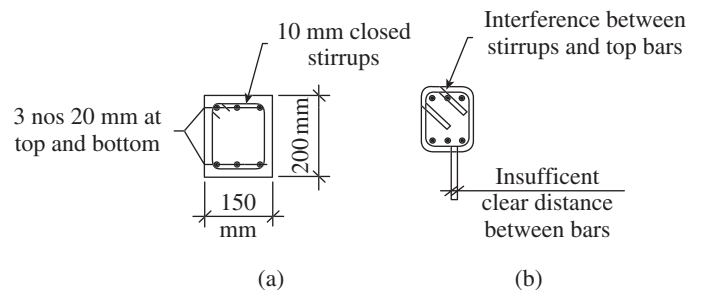


FIG. 4.13 Assumed conditions in drawings resulting in difficulties at site (a) Details as given by engineer (b) Actual condition at site
Source: Schwinger 2011

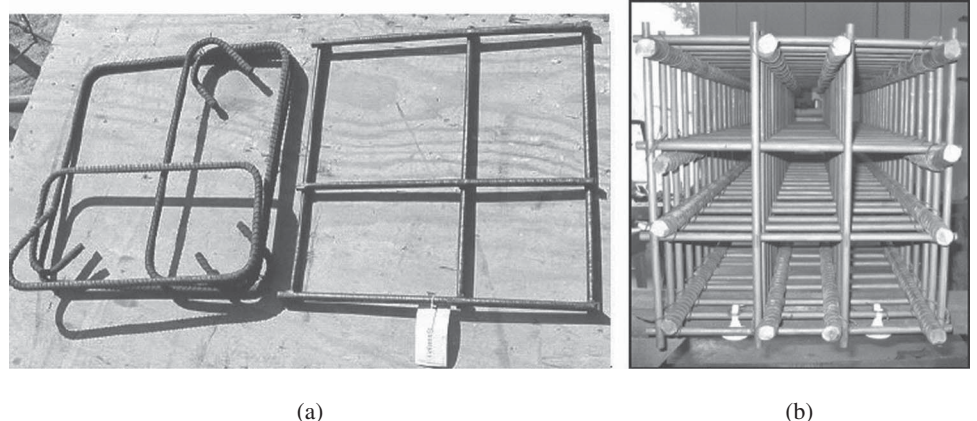


FIG. 4.14 Transverse reinforcement in beams/columns (a) Conventional and welded reinforcement grids (b) Better constructability of column with BauGrid® WRG™
Source: Baumann 2008

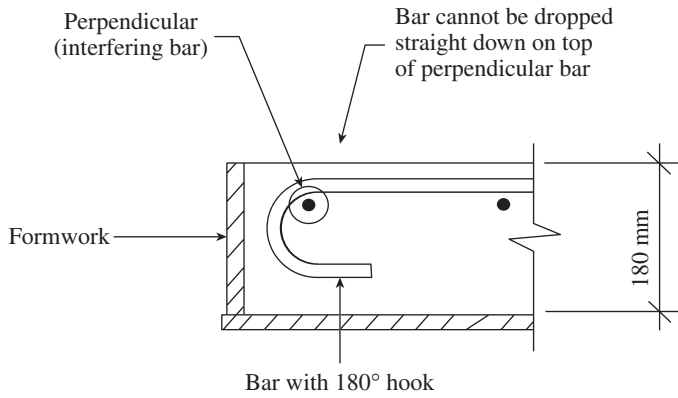


FIG. 4.15 Problem in using 180° hooks in slabs

Source: Schwinger 2011

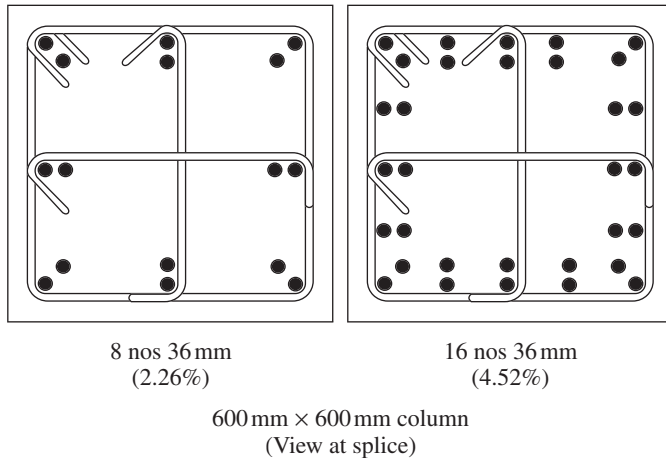


FIG. 4.16 More than 4% reinforcing steel in columns results in practical problems

Hence, bundled bars should be avoided in columns. Splices in bundled bars must be staggered, which adds another level of complexity. Likewise, mechanical splice couplers, when required, cannot be easily installed on bundled bars.

Designers must specify the criteria for installing a slab-embedded cable and conduit in the floor slabs. Specifying such criteria on the general notes will, at a minimum, facilitate awareness that caution must be taken in coordinating where and how cables and conduits may be installed without compromising the structural integrity of the floor framing (Schwinger 2011).

4.4.9 Ductility

Ductility is more commonly defined as the ability of the materials or structures to absorb energy by deforming into an inelastic range upon the application

of a tensile force, or as the ability of a material to withstand plastic deformation without rupture. Ductile materials show large deformation before fracture. Thus, ductility (μ) may also be defined as the ratio of the ultimate deformation Δ_{max} at an assumed collapse point to the yield deformation Δ_y . See Figs 4.17 and 4.18. The lack of ductility is often termed brittleness. This capacity of the structure to absorb energy, with acceptable deformations and without failure, is a very desirable characteristic in any earthquake-resistant design. Thus,

$$\mu = \Delta_{max} / \Delta_y > 1 \tag{4.4}$$

It should be noted that the displacement Δ_{max} and Δ_y in this equation may represent strain, curvature, rotation, or deflection.

Paulay and Priestley (1992) provide the following relationship between the response reduction factor, R , and the displacement ductility, μ .

$$\text{For long period structure: } R = \mu \tag{4.5a}$$

$$\text{For short period structure: } R = \sqrt{(2\mu - 1)} \tag{4.5b}$$

$$\text{For long period structure: } R = 1 \text{ (regardless of } \mu) \tag{4.5c}$$

Ductility is often measured by the *hysteretic behaviour* of critical components such as column-beam assembly of a moment-resisting frame. The hysteretic behaviour is usually predicted by the cyclic moment-rotation or force-deflection behaviour of the assembly as shown in Fig. 4.19. The slope of the curve represents the stiffness of the structure and the enclosed area represents the dissipated energy. Perfect ductility is defined by the ideal elastic or perfectly plastic (also called elasto-plastic) curves, which are difficult to achieve in materials like concrete. *Hysteretic energy* is the energy dissipated by inelastic cyclic deformations and is given by the area within the load deformation curve shown in Fig. 4.19, also called the *hysteretic curve*. Under

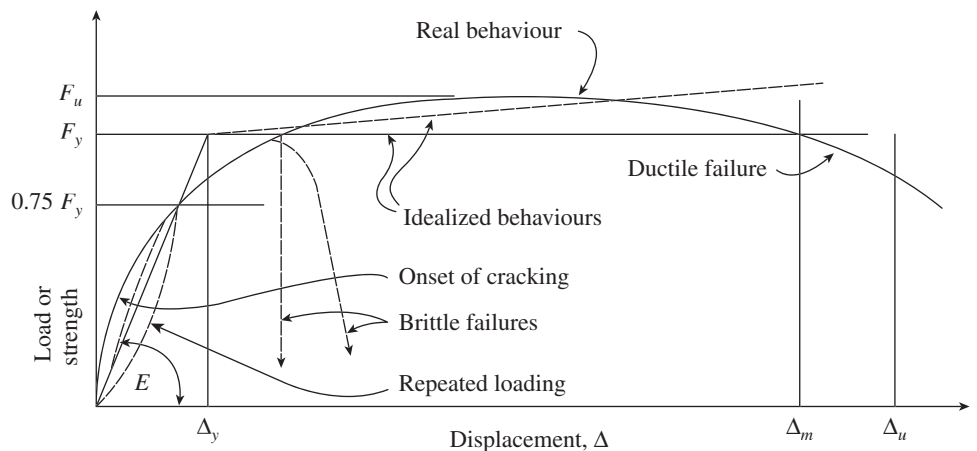


FIG. 4.17 Typical load-displacement curve for an RC element

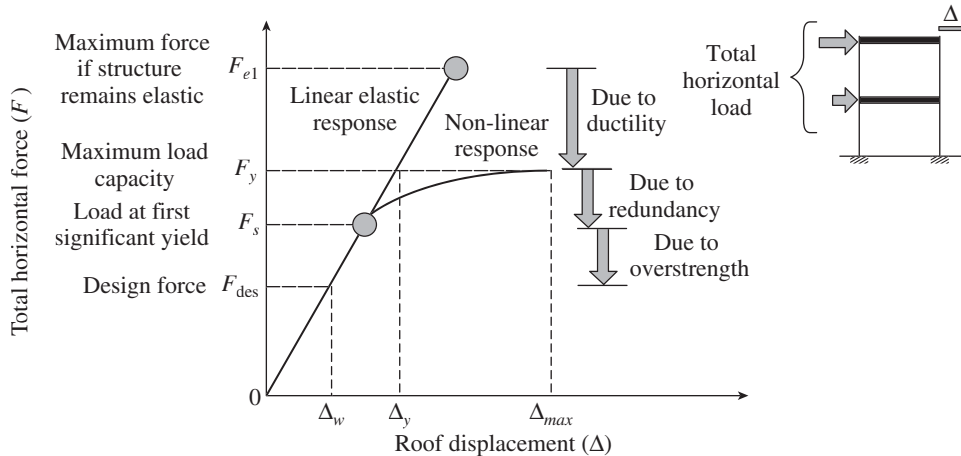


FIG. 4.18 Concept of response reduction factor

Source: Jain and Murty 2005, NICEE, IIT Kanpur

ideal conditions, *hysteresis loops* of the form shown in Fig. 4.19(a) result, where the energy absorbed will be about 70–80 per cent of that of an equivalent elasto-plastic loop. Limited energy dissipation curves are shown in Fig. 4.19(b). The degradation of strength and stiffness under repeated inelastic cycling is called *low-cycle fatigue*.

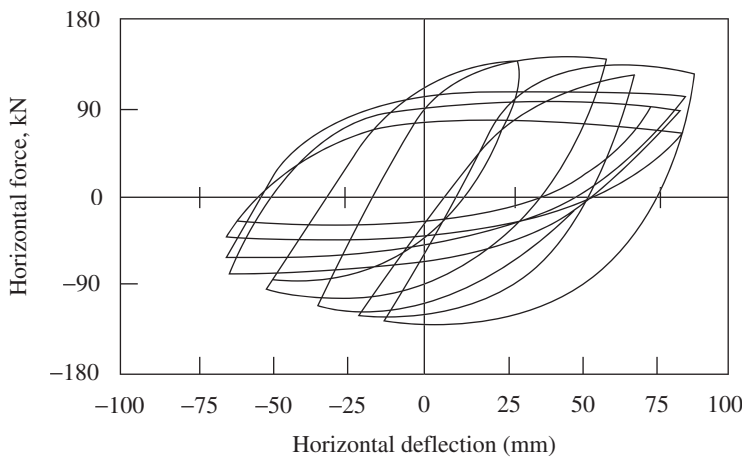
When a structure yields, it will result in the following:

1. There is more energy dissipation in the structure due to hysteresis.

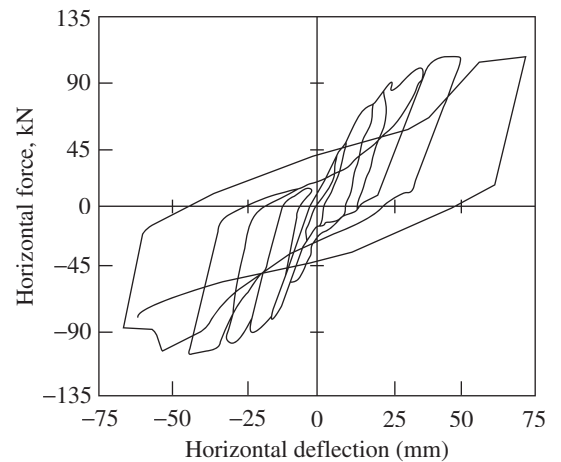
2. The structure becomes softer and its natural period increases; hence, the structure has to resist a lower seismic force (see Fig. 2 of IS 1893, Part 1).

Thus, higher ductility indicates that the structure can withstand stronger earthquakes without complete collapse. The values prescribed in IS 1893 (Part 1) for R are based on the observed performance of buildings in the past earthquakes, expected ductility (toughness), over strength, and values in practice in other countries and include all the factors discussed here (Jain 1995).

As indicated earlier, large areas enclosed by the force–deformation loops indicate more dissipation of hysteretic energy. One way of ensuring good ductility and energy dissipation capacity is to provide sufficient transverse reinforcement in plastic hinge zones to confine concrete. Slenderness ratio and axial load ratio of the members may also control ductility. Both ductility and energy dissipation capacity are required to resist severe earthquakes (it should be noted that these two quantities are inter-related and a large demand on one tends to decrease the other).



(a)



(b)

FIG. 4.19 Hysteretic behaviour (a) Curve representing large energy dissipation (b) Curve representing limited energy dissipation

4.5 ANALYSIS AND DESIGN

In the structural design process, the term *analysis* means the determination of the axial forces, bending moments, shears, and torsional moments acting on the different members of a structure, due to the applied loads and their combinations

(static or dynamic). In general, the term *design* may mean the development of the structural layout and system for the structure or arrangement of different members. However, for the design engineer, the term design means the selection of sizes of members to safely and economically resist the forces and moments found in the analysis phase. In the design

phase, one will normally design not only the members but also its connections and the foundations, so that the loads are transmitted to the soil.

The analysis is relatively simple for statically determinate structures (simply supported beams, cantilever, trusses, etc.), and the laws of statics can be used to determine the forces and moments on each member. The relative stiffness of intersecting members does not affect the analysis. After the analysis is completed and the critical moments and forces in the different members are tabulated, the design of the member is a straightforward process using an appropriate design method (e.g., working stress method, limit states method, etc.). For statically determinate structures, there will not be any need for re-analysis or re-design of the members.

However, for statically indeterminate structures, the analysis procedure is rather complex. A number of analytical methods have been developed, which include slope deflection method, moment distribution method, Kani's method, portal method, cantilever method, and matrix methods. In these methods, assumptions are usually made regarding the distribution of applied load among the members according to the relative stiffness of connecting members, the response and behaviour of members and structures to the applied loads, the rigidity of joints, and so forth. Moreover, to perform the analysis, the proportions of various structural elements should be known in advance, which generally requires a preliminary design. Thus, in these types of structures, analysis and design are interactive processes.

After the first cycle of analysis is completed, and the different members are designed as per the codal rules, it is usually necessary to re-analyse the structure to check the validity of the original member sizes. For complex structures, several cycles of analysis and design may be required (many times, three cycles are found to be sufficient).

As already mentioned, a statically indeterminate analysis requires preliminary member sizes, which are often assumed based on experience or using approximate methods. Hand books often provide formulae and coefficients to simplify the preliminary design of continuous beams or simple rigid jointed frames like portal frames (Reynolds and Steedman 1988; Young and Budynas 2001).

Various computer programs are available for the analysis and design of different types of structures. They include ADINA, ANSYS, SAP2000, STAAD III and STAAD PRO (www.reiworld.com), ETABS (www.csiberkeley.com), and STRUDS. These programs are quite general in terms of loading, geometric configurations, and support conditions. With these programs, it is now possible to analyse any structure with any complicated geometry subjected to any pattern of loading (static or dynamic) and having any boundary condition or discontinuity (Subramanian, 1995b).

Analytical methods and modelling techniques used by these computer programs offer various levels of sophistication and refinement. While using these programs, the designer should be aware of any assumptions used and the limitations of these programs. This is because no amount of mathematical precision can make up for the use of an analytical method that is not applicable for the structure being designed.

Clause 22.1 of code IS 456 suggests the use of linear elastic (first-order) analysis to calculate the internal actions produced by design loads. Such elastic analysis allows superposition of desired combination of load effects. The code allows for moment redistribution, if desired, as per Clause 37.1.1. It also allows for the effects of deflections on moments and forces in frames with slender columns (see Clause 39.7). The code also states that plastic methods such as yield-line analysis may be used for the analysis of two-way slabs (see Clause 37.1.2).

Though the code allows substitute frame analysis for reasonably regular frames subjected to gravity loads in Clause 22.4.2, designers analyse the whole frame, due to the availability of software packages. In case of a regular structural system, the space frame can be divided into planar frames for analysis. However, consideration of the whole space frame is advisable in the case of irregular configuration, as the torsional effects are considered automatically by the computer program. The code also gives the moment and shear coefficients for continuous beams of uniform cross section and supporting uniformly distributed loads (see Tables 12 and 13 of the code). When such coefficients are used, redistribution of moments is not permitted by the code.

4.5.1 Relative Stiffness

Under service gravity loading, the cracking of RC frames will be relatively minor. Clause 22.3.1 of IS 456 suggests that the relative stiffness to be used in linear elastic analysis can be based on the following:

1. *Gross concrete section ignoring reinforcement*: The most frequently used method in practice because the reinforcement data is not known before the design
2. *Transformed section*: The gross concrete section including area of reinforcement on the basis of modular ratio (as per Annex B-1.3 of the code, the modular ratio m is given by $280/(3\sigma_{cbc})$, where σ_{cbc} is the permissible compressive stress due to bending as given in Table 21 of the code)
3. *Cracked section*: The area of concrete in compression and the transformed area of reinforcement based on modular ratio

While analysing the frames for seismic loading, most members will either yield or reach yielding and hence the cracking will be significant. Therefore, it is essential to use the realistic stiffness of members. The use of realistic stiffness is also important because it directly affects the building periods

and dynamic response, deflection and drift, and internal force distribution. The calculation of relative stiffness as given in Clause 22.3.1(c) of the code is difficult to estimate. The parameters that affect the effective stiffness include the following:

1. The amount and distribution of reinforcement, especially those in the tension zone
2. Yield strength of longitudinal reinforcement
3. The extent of cracking, which affects the magnitude of tension stiffening
4. Tensile strength of concrete
5. The initial conditions in the member (such as shrinkage and creep, which induce compression in the reinforcement) before the structural actions are imposed

The effective stiffness to be considered in the frame analysis has been studied by a number of investigators and the values suggested by them and other codes are given in Tables 4.10 and 4.11. Elwood and Eberhard (2009) proposed equations for the effective stiffness of columns, which are more accurate than the existing models. The equations proposed by Khuntia

TABLE 4.10 Effective stiffness for beams and columns as per different sources

Type of Member	IS 456 2000	ACI 318 2011	Khuntia and Ghosh (2004)	Kumar and Singh (2010)
Beam $P/(f_{ck}A_g) < 0.08$	I_g, I_{tr} , or I_{cr}	$0.35I_g$ For T-beam take as two times the I_g of the web, i.e., $2(b_w h_c^3/12)$	$I_g(0.1 + 25A_{st}/A_g)$ [1.2 – $0.2(b_w/d)$] ≤ $0.6I_g$ and [1.2 – $0.2(b_w/d)$] ≤ 1.0	$0.35I_g$ for $P_u/(f_{ck}A_g) ≤ 0.16$
Column $P/(f_{ck}A_g) ≥ 0.08$	I_g, I_{tr} , or I_{cr}	$0.70I_g$	$I_g(0.8 + 25A_{st}/A_g)$ [1 – $(M_u/P_u h_c)$ – $(0.5P_u/P_o)$] ≤ $0.875I_g$	(a) [0.175 + $0.875P_u/(f_{ck}A_g)]I_g$ for $0.2 ≤ P_u/(f_{ck}A_g) ≤ 0.48^*$ (b) $0.7I_g$ for $P_u/(f_{ck}A_g) ≥ 0.48$
Walls Uncracked	–	$0.70I_g$	–	–
Cracked	–	$0.35I_g$	–	–

* For high-strength concrete the following equations are to be used:

(a) $[0.24 + 1.1P_u/(f_{ck}A_g)]I_g$ for $0.1 ≤ P_u/(f_{ck}A_g) ≤ 0.48^*$

(b) $0.9I_g$ for $P_u/(f_{ck}A_g) ≥ 0.48$

where A_g is the gross cross section area in mm², A_{st} is the gross steel area in mm², I_g is the gross moment of inertia of cross section in mm⁴, P_u is the factored axial load on column in kN, P_o is the nominal axial load strength in kN, M_u is the factored moment on column in kNm, b is the width of member in mm, b_w is the web width of T- or L-beam in mm, d is the effective depth in mm, and h_c is the overall depth of column in mm.

TABLE 4.11 Effective stiffness as per New Zealand Standard NZS 3101

Type of Member		Ultimate Limit State ($f_y = 500$ MPa)	Serviceability Limit State		
			$\mu = 1.25$	$\mu = 3$	$\mu = 6$
Beams	Rectangular beam	$0.32I_g^+$	I_g	$0.7I_g$	$0.40I_g^+$
	T- or L-beam	$0.27I_g^+$	I_g	$0.6I_g$	$0.35I_g^+$
Columns	$P_u/(f_{ck}A_g) > 0.5$	$0.80I_g$	I_g	$1.0I_g$	$1.0I_g$
	$P_u/(f_{ck}A_g) = 0.2$	$0.50I_g$	I_g	$0.8I_g$	$0.66I_g$
	$P_u/(f_{ck}A_g) = 0.0$	$0.30I_g$	I_g	$0.7I_g$	$0.45I_g$
Walls	$P_u/(f_{ck}A_g) = 0.2$	$0.42I_g$	I_g	$0.7I_g$	$0.42I_g$
	$P_u/(f_{ck}A_g) = 0.1$	$0.33I_g$	I_g	$0.6I_g$	$0.33I_g$
	$P_u/(f_{ck}A_g) = 0.0$	$0.25I_g$	I_g	$0.5I_g$	$0.25I_g$
Diagonally reinforced coupling beams	–	$0.60I_g$ for flexure Shear area A_{shear}	I_g 1.5 A_{shear} for ULS	$0.75I_g$ 1.25 A_{shear} for ULS	$0.60I_g$ for flexure Shear area A_{shear}

μ = Maximum ductility demand

+ Use with a E value of M40 concrete regardless of the actual concrete strength

ULS = Ultimate limit state

A_{shear} = Effective shear area

$A_{shear} = \frac{V_y}{GL\delta_y}$, where the shear deformation,

$\delta_y = \left[\frac{L}{\sin \alpha} + \frac{f_y d_b}{15} \right] \frac{f_y}{E_s}$

G = Shear modulus = $0.4E_c$

d_b = Diameter of rebar in the coupling beam

E_c and E_s = Young's modulus of concrete and steel respectively

f_y = Yield strength of steel diagonal rebars

L = Clear length of coupling beam

V_y = Shear force

α = Inclination of the bars to the axis of the beam

and Ghosh (2004) are suggested as alternate values in ACI 318:2011 (by using the effective moment of inertias, the non-linear effects are considered approximately in the ACI code). These effective flexural stiffness values are intended to provide an estimate of the secant stiffness to the yield point (see Figs 4.17 and 4.18). Under sustained lateral loads, for example the earth pressure, the effective moment of inertia needs to be further reduced by dividing it by $(1 + \beta_{ds})$. As per ACI code, the term β_{ds} denotes the ratio of the maximum factored sustained shear within a story to the maximum factored shear in that story associated with the same load combination, but shall not be taken greater than 1.0.

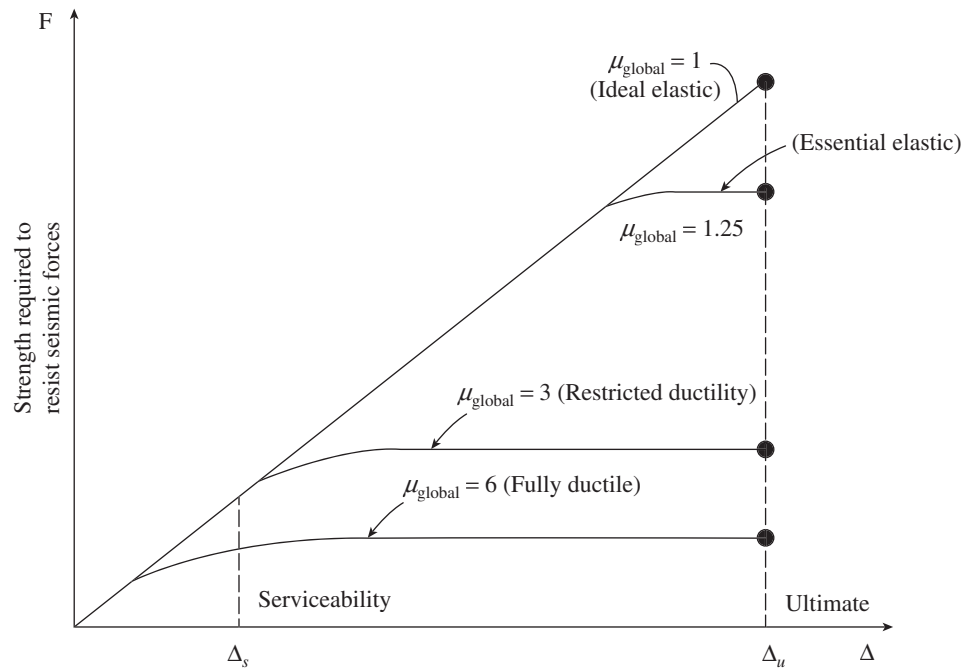
The idealized static pushover plots in Fig. 4.20 may help to interpret the NZS 3101 provisions for the stiffness coefficients for the three different ductility demands given in Table 4.11. It is seen that the New Zealand code provisions are extensive and may be adopted in the analysis. According to ACI code Clause 10.10.4.1, the stiffness modification factor for flat plates and flat slab may be assumed as 0.25 and area can be taken as $1.0A_g$ for all types of members. For more information on modelling and acceptance criteria for seismic design and analysis of tall buildings, refer to the report PEER/ATC 72-1 (2010).

4.5.2 Redistribution of Moments

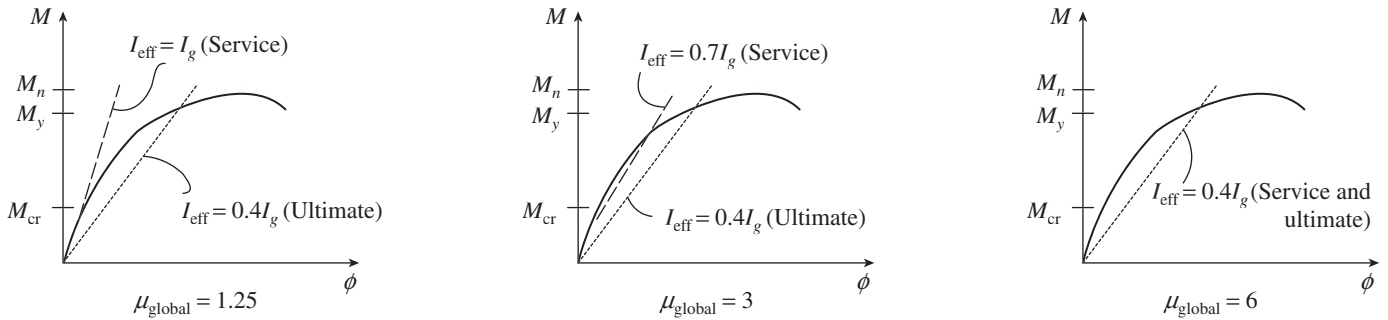
In engineering practice, bending moment and shear force distributions in an RC indeterminate structure are normally arrived at by using any standard *linear elastic analysis* computer

package. Such a linear analysis has the virtue of simplicity and permits results from a series of analyses to be combined using the *principle of superposition*. The assumption of linear elastic behaviour is reasonable at working loads but may become invalid at higher loads due to cracking and the development of plastic deformations. Once an element cracks, the behaviour becomes non-linear, but it is still reasonable to assume that the tension reinforcement and the concrete in compression both behave elastically up to the yield of the reinforcement.

Design codes permit elastic analysis to be used at the ultimate limit state but acknowledge this non-linear behaviour by allowing a limited amount of *moment redistribution* from one part of the structure to another. Such moment redistribution in concrete structures is similar to plastic moment distribution in steel structures. In steel structures, as the external load is



(a)



(b)

FIG. 4.20 Interpretation of NZS effective stiffness recommendations (a) Force deformation of system (global response) (b) Moment curvature of beam (local response)

Source: Mehanny, et al. 2001, reprinted with permission from ACI

increased, the section experiencing the maximum bending moment reaches its plastic moment capacity (thus forming a *plastic hinge*); then, the moment gets distributed to other sections. This process continues until sufficient number of plastic hinges is formed and the structure fails by forming a *mechanism* (Subramanian 2010b). In concrete structures too, as the loads are increased, tension reinforcement yields at the location of maximum bending moment and the section undergoes inelastic rotation. Thus, after yielding first, the moments are redistributed to the other sections of the member, which are still elastic. When the load is increased further, plastic hinges will eventually form in other locations, until the structure fails due to a mechanism. However, this redistribution can take place safely only when ductile detailing is adopted as per IS 13920 at critical plastic hinge locations, and when the crack widths are controlled (Beeby 1997; Scott and Whittle 2005). The plastic hinges permit the utilization of the full capacity of more cross sections of a flexural member at the ultimate loads.

Moment redistribution is useful in practical design as it allows some flexibility in the arrangement of reinforcement. It can be used to transfer moment away from the congested areas (e.g., beam-column connections) to less-congested areas (e.g., mid-spans of beams) or help to allow standard reinforcement layouts where small differences occur in the bending moment distributions for a series of beams, thus avoiding the need to detail each beam separately. In addition, useful economies can be achieved when moment redistribution is applied to different load combinations, resulting in a smaller bending moment envelope, which still satisfies the equilibrium (Scott and Whittle 2005).

Implicit in the current use of moment redistribution is the assumption that sections possess sufficient ductility for the requisite plastic deformations to occur. Design codes achieve this by specifying rules that ensure that the tension steel must have yielded, explicitly in the case of ACI 318 (which allows 20% moment redistribution when ϵ_t is equal to or greater than 0.0075 at the section at which moment is reduced) and implicitly in the case of IS 456, BS 8110, and Eurocode 2 (which link percentage redistribution to neutral axis depth). Clause 37.1.1 of code IS 456 allows redistribution of moments provided the following conditions are satisfied:

1. Equilibrium is maintained at all times between the internal forces and external loads. Thus, for example, when the end support of a continuous beam has a cantilever moment, the moment cannot be reduced by redistribution.
2. The ultimate moment of resistance provided at any section is not less than 70 per cent of the maximum elastic moment obtained using elastic analysis for all appropriate load combinations.

3. The redistribution at any section should not be more than 30 per cent of the numerically largest elastic moment obtained using elastic analysis for all appropriate load combinations. It should be noted that the code allows only 15 per cent redistribution in the case of the WSM (see Clause B-1.2 of code IS 456).

At locations where moment capacity provided is less than the moment obtained from elastic analysis (i.e., at locations from where moments are reduced due to redistribution), the following relation should be satisfied:

$$\frac{x_u}{d} + \frac{\delta M}{100} \leq 0.6 \quad (4.6)$$

Here, x_u is the depth of neutral axis, d is the effective depth, and δM is the percentage reduction in moment. Substituting the 30 per cent maximum allowable redistribution in this condition, we get $x_u/d \leq 0.3$. For structures having four or more storeys, the maximum redistribution is limited to 10 per cent, if the frames are designed to provide lateral stability also.

It should be noted that as per Clause 22.7 of IS 456 and Clause 6.2.4 of IS 13920:1993, moment redistribution is not allowed under the following conditions:

1. Simplified analysis using moment coefficients is adopted as per Table 12 of the code.
2. The frames are designed for earthquake forces and for lateral loads (the draft IS 13920 allows 10% redistribution).
3. Based on experimental results of 33 two-span continuous beams, Scott and Whittle (2005) confirmed that the 30 per cent redistribution of moment as recommended in the codes is conservative and that there is redistribution even during the elastic stage. Reynolds and Steedman (2008) (see Tables 2.34 and 2.35 of their book) provide moment coefficients for 10 per cent and 30 per cent redistribution.

4.6 CODES AND SPECIFICATIONS

A structural engineer is often guided in his/her efforts by the *code of practice*. A code represents the consensus of opinion of experienced engineers and professionals. It may not cover in detail every situation a designer may encounter. Often the designer must exercise judgment in interpreting and applying the requirements of a code. It has to be noted that strict adherence to codes will hamper the adoption of innovative designs. Codes are basically written for the purpose of protecting the public. These codes provide the guidelines for the design and construction of structures. They are revised at regular intervals to reflect new developments (in research, materials, construction techniques, etc.), based on the experience gained from past design practice, behaviour

of existing structures, and failure of structures. Codes contain the recommended loads for a given locality and the recommended fire and corrosion protection. They also contain rules governing the ways in which loads are to be applied and design rules for steel, concrete, and other materials. These rules may be in the form of detailed recommendations or by reference to other standards that provide specific design rules. The codes should be regarded as aids to design, which contain stress levels, design formulae, and recommendations for good practice, rather than as a manual or textbook on design.

The codes serve at least the following four distinct functions:

1. They ensure adequate structural safety, by specifying certain essential minimum requirements for the design.
2. They aid the designer in the design process. Often, the results of sophisticated analysis are made available in the form of simple formulae or charts.
3. They ensure consistency among different engineers.
4. They protect the structural engineer from disputes, though codes in many cases do not provide legal protection.

On the other hand, *project specifications* along with the design drawings are given to the builder by the architect or project manager. These specifications and the way in which the drawings are prepared and presented vary from organization to organization. However, they include the following items:

1. Materials that must be used in the structure
2. Sizes of structural members
3. Joint details
4. Expected quality and tolerance
5. Instructions on how the construction work is to be done

Whoever writes the specification, the structural engineer should be involved in preparing or approving the technical contents of a specification.

In India, the BIS issues the codes and standard handbooks. Committees representing producers, designers, educators, fabricators, government bodies, and other interested bodies formulate them. The draft is circulated to a larger section of engineers, designers, and professionals. The committee considers their comments and finally the BIS prints the code. It is strongly advised that the reader possess a copy of the following codes, which will be referred to frequently in this book:

1. IS 456:2000, *Code of Practice for Plain and Reinforced Concrete* (Fourth revision)
2. IS 875:1987, *Code of Practice for Design Loads for Buildings and Structures* (Part 1: *Dead Loads*, Part 2: *Imposed Loads*, Part 3: *Wind Loads*, Part 4: *Snow Loads*, and Part 5: *Special Loads and Load Combinations*)

3. IS 1893 (Part 1):2002, *Criteria for Earthquake-resistant Design of Structures*
4. IS 13920:1993, *Code of Practice for Ductile Detailing of Reinforced Concrete Structures Subjected to Seismic Forces*
5. IS 4326:1993, *Code of Practice for Earthquake-resistant Design and Construction of Buildings*
6. IS 10262:2009, *Guidelines for Concrete Mix Design Proportioning*

In addition, the designer may need to refer to a number of other codes covering topics such as specification for Portland cement, pozzolan cement, fly ash, slag cement, coarse and fine aggregates, ready-mixed concrete, admixtures, and high-strength deformed bars, and also codes for the design of foundations, liquid retaining structures, bridges, and silos.

In certain cases, it may be useful for the designer to consult codes of other countries. The following are some of these codes that will be helpful:

1. ACI 318-11 2011, *Building Code Requirements for Structural Concrete and Commentary*, American Concrete Institute, Farmington Hills.
2. NZS 3101-06 July 2006, *Concrete Structures Standard, Part 1: The Design of Concrete Structures, Part 2: Commentary on the Design of Concrete Structures*, Standards Council of New Zealand, Wellington.
3. BS 81101: 97 September 1998, *Structural Use of Concrete, Part I: Code of Practice for Design and Construction*, British Standards Institution, London.
4. CSA-A23.3-04 2004, *Design of Concrete Structures*, Canadian Standards Association, Toronto.
5. ENV 1992-1-1:1992, Eurocode 2, *Design of Concrete Structures, Part 1: General Rules and Rules for buildings*, European Committee for Standardization (CEN), Brussels.
6. AS 3600:09 Australian Standard 2009, *Concrete Structures*, Standards Australia, Sydney.
7. DIN 1045-1:01 July 2001, *Tragwerke aus Beton, Stahlbeton und Spannbeton, Teil 1: Bemessung und Konstruktion*, Deutsches Institut für Normung, Berlin.

4.7 DESIGN PHILOSOPHIES

Over the years, various design philosophies have evolved in different parts of the world, with regard to structural concrete design. The earliest codified design philosophy is the *working stress method* of design, which evolved around 1900 when the theory proposed by Coignet and Tedesco was accepted. The elastic theory has been the basis of RC design for many years. In the recent (2000) revision of code IS 456, the provisions relating to this method of design procedure have been relegated from the main text of the Code to Annex B at the end of the code (with only a few pages devoted to it)

'so as to give greater emphasis to limit states design'. Prior to 2002, Appendix A of ACI 318 code allowed the design of concrete structures either by strength design or by working stress design. In 2002, the appendix was deleted. However, it should be noted that serviceability checks are performed only on unfactored or service loads in all the codes.

The WSM was followed by the *ultimate strength design*, which was developed in the 1950s. This design became accepted as an alternative to WSM in the ACI code in 1956 and in the British code in 1957. It was based on the ultimate load carrying capacity of the RC at collapse. This method was introduced as an alternative to WSM in Appendix B of IS 456 code in 1964.

In the mid-1960s, the probabilistic concepts of design received a major impetus (Madsen, et al. 1986; Subramanian 1974). The philosophy was based on the theory that the various uncertainties in design could be handled more rationally in the mathematical framework of probability theory. The risk involved in the design was quantified in terms of the probability of failure. Such probabilistic methods are known as *reliability-based methods*. However, this theory was not accepted in professional practice, mainly because the theory appeared to be complicated (mathematically and numerically).

For codification, the probabilistic *reliability method* approach was simplified and reduced to a deterministic format involving multiple (partial) *safety factors* (rather than the probability of failure). Based on the CEB-FIP recommendations, the philosophy of limit states method was introduced in the British code CP 110 in 1972 (now BS 8110), and the Indian Concrete Code IS 456 in 1978. In the USA, the ACI introduced the limit states method in the form of *Load and Resistant Factor Design* (LRFD) in 1963. In the 1971 version of the code (ACI 318-71), the LFRD method was fully adopted and the WSM was moved to an Appendix and later deleted in 2002.

4.7.1 Working Stress Method

This was the traditional method of design not only for RC but also for structural steel and timber design. The conceptual basis of the WSM is simple. It basically assumes that the structural material behaves in a linear elastic manner and that adequate safety can be ensured by suitably restricting the stresses in the material due to the expected *working loads* (service loads) on the structure.

It assumes that both the steel reinforcement and concrete act together and are perfectly elastic at all stages, and hence the *modular ratio* (ratio between the moduli of elasticity of steel and concrete) can be used to determine the stresses in steel and concrete (it is interesting to note that a few codes such as CP 114, used in the UK until 1973, used a constant modular ratio of 15, independent of the strength of concrete and steel).

The stresses under the working loads are obtained by applying the methods of 'strength of materials' like the simple bending theory. The limitations due to non-linearity (geometric as well as material) and buckling are neglected.

The stresses caused by the 'characteristic' or service loads are checked against the *permissible (allowable) stress*, which is a fraction of the ultimate or yield stress; for example, for compression in bending, one-third of the cube strength of the concrete is assumed as the permissible stress. The permissible stress may be defined in terms of a *factor of safety*, which takes care of the overload or other unknown factors. Thus, the permissible stress is defined by

$$\text{Permissible (allowable) stress} = \frac{\text{Ultimate or yield stress}}{\text{Factor of safety}} \quad (4.7a)$$

Thus, in WSM,

$$\text{Working stress} \leq \text{Permissible stress} \quad (4.7b)$$

Therefore, the basic assumptions in the elastic theory in bending are as follows:

1. At any cross section, plane sections will remain as plane even after bending.
2. The stress-strain relationship of steel and concrete under working loads is a straight line, and hence stresses σ can be calculated from the strains ε using the relationship $\sigma = E \times \varepsilon$.
3. The tensile stresses are taken up only by the reinforcement and not by the concrete.
4. In order to consider creep effects, the modular ratio m is taken as $(280/3\sigma_{cbc})$, where σ_{cbc} is the permissible compressive stress due to the bending in the concrete expressed in N/mm² (see Table 4.12 for the various values of σ_{cbc} for various grades of concrete).

TABLE 4.12 Permissible stresses in concrete (MPa)

Grade of Concrete	Permissible Stress in Compression		Modular Ratio $m = 280/$ $(3\sigma_{cbc})$	Permissible Average Stress in Bond for Plain Bars in Tension* τ_{bd}
	Bending Compression σ_{cbc}	Direct Compression σ_{cc}		
M20	7.0	5.0	13.33	0.8
M25	8.5	6.0	10.98	0.9
M30	10.0	8.0	9.33	1.0
M35	11.5	9.0	8.11	1.1
M40	13.0	10.0	7.18	1.2
M45	14.5	11.0	6.44	1.3
M50	16.0	12.0	5.83	1.4
M55	18.0	13.5	5.19	1.5
M60	20.0	15.0	4.67	1.6

* Bond stress may be increased by 25 per cent for bars in compression.

Based on these assumptions, the total compressive force C (see Fig. 4.21) is given as follows:

$$C = 0.5 \sigma_{cbc} b(kd)$$

b, d = Breadth and effective depth of beam respectively

k = Neutral axis factor

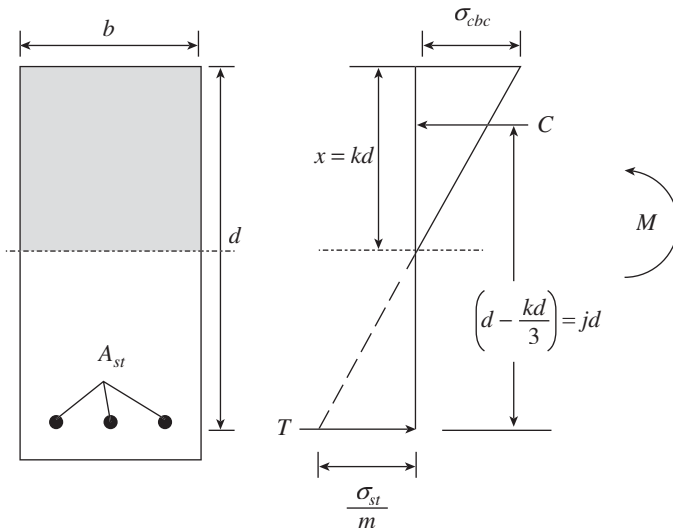


FIG. 4.21 Stress distribution in rectangular section

This force acts at the centroid of the triangular stress block, at a distance $x/3$ from the top. Hence, the lever arm distance is

$$jd = d - \frac{kd}{3} = d \left(1 - \frac{k}{3} \right); \text{ Hence, } j = \left(1 - \frac{k}{3} \right) \quad (4.8)$$

If the moment at service load is M_s , then

$$M_s = Cjd = 0.5 \sigma_{cbc} b(kd)jd \quad (4.9a)$$

and $d = \sqrt{\frac{M_s}{Qb}}$ where Q is a constant and is taken as

$$Q = 0.5 \sigma_{cbc} jk \quad (4.9b)$$

Similarly, taking moments about C yields

$$M_s = Tjd = \sigma_{st} A_{st} jd \quad (4.10a)$$

Using this equation, we get

$$A_{st} = \frac{M_s}{\sigma_{st} jd} \quad (4.10b)$$

where A_{st} is the area of tension steel and σ_{st} is the permissible stress in the steel in tension.

These equations are used in the design of rectangular beams using WSM. However, this analysis ignores the effect of creep, which tends to slightly increase the stress in the tension steel.

Each member of the structure is checked for a number of different combinations of loadings. Usually, a factor of safety of about 3 is adopted for cube strength of concrete

and a factor of safety of about 1.8 is used for steel, with respect to its yield stress (see Tables 4.12 and 4.13). Since dead, live, and wind or earthquake loads are all unlikely to simultaneously act on the structure, the stresses are checked as follows:

Stress due to dead load + live load < permissible stress

Stress due to dead load + live load + wind or earthquake load < 1.33 (permissible stress)

TABLE 4.13 Permissible stresses in steel reinforcement

Type of Stress in Steel Reinforcement	Permissible Stress in MPa	
	Mild Steel Bars as per IS 432(Part 1) (Grade Fe 250)	High-yield Strength-deformed Bars as per IS 1786 (Grade Fe 415)
Tension (σ_{st} or σ_{sv}) Up to and including 20 mm	140	230
Over 20 mm	130	230
Compression in column bars (σ_{sc})	130	190
Compression in beam or slab bars Up to and including 20 mm	140	190
Over 20 mm	130	190

Note: For high-yield strength-deformed bars of grade Fe 500, permissible stress in direct tension and flexural tension shall be $0.55f_y$. The permissible stresses for shear and compression steel shall be as for grade Fe 415.

There are many limitations in and shortcomings of WSM. Some of them are listed as follows:

1. The main assumption of a linear elastic behaviour and the implied assumption that the stresses under working loads can be kept within the 'permissible stresses' are found to be unrealistic. Many factors are responsible for this, such as the long-term effects of creep and shrinkage and other secondary effects. All such effects result in significant local increases in and redistribution of the calculated stresses. For example, the compression steel in columns may reach the yield strength during the sustained application of service loads, which is not indicated by WSM. Thus, the method does not provide a realistic measure of the actual strength or factor of safety underlying a design.
2. The use of the imaginary concept of modular ratio results in larger percentage of compression steel and generally larger member sizes than the members designed using ultimate load or limit states design. However, as a result of the larger member sizes, they result in better performance during service (less deflection, crack width, etc.).
3. The stress-strain curve for concrete is non-linear and is time dependent. This is particularly so at higher ranges of stress. Thus, the elastic modulus is a function of the stress

level (it may also change with age) and hence the modular ratio is not really constant. This method does not consider the consequences of this material non-linearity.

4. WSM does not discriminate between the different types of loads that act simultaneously, but have different degrees of uncertainty. This may result in unconservative designs, particularly when two different loads (say, dead loads and wind loads) have counteracting effects.

In spite of these shortcomings, most structures designed in accordance with this method have performed satisfactorily for many years. Its popularity is due to its simplicity—in concept as well as application (see Examples 4.1 and 4.2 for the application of WSM).

It has to be noted that serviceability requirements such as deflection and crack width limits are always investigated at service load conditions, even when the limit states design is used to satisfy strength requirements (see Chapter 12). Members subjected to tension are often governed by WSM requirements (see Chapter 18).

4.7.2 Ultimate Load Design

The shortcomings of WSM led to the development of the ultimate load design. This method is also referred to as the *load factor method* or the *ultimate strength method*. This method was introduced in the USA in 1956, the UK in 1957, and as an alternative in the second revision of IS 456 in 1964. In this method, the non-linear stress–strain curves of concrete and steel and the stress condition just before collapse are considered. Thus, the problems associated with the concept of modular ratio are avoided in this method. Sufficient safety is achieved by the use of a *load factor*, which is defined as the ratio of the ultimate load (design load) to the working load (IS 456:1964 specified a load factor of 1.5 for service dead load and 2.2 for service live load). In this method of design, different types of loads are assigned with different load factors under combined loading conditions, thereby overcoming the related shortcomings of WSM. For example, a low load factor is used for a load that is known more exactly (e.g., the dead load) and a higher load factor for less-certain loads, (e.g., the live loads). Thus, in the ultimate load design, the strength of the member must be more than the ultimate load acting on the member.

$$\text{Design resistance } (R_n) \geq \text{Design load effect } (\sum \gamma_i Q_i) \quad (4.11)$$

where R_n is the nominal strength of the member, Q_i are the various load effects (such as dead, live, and wind loads), and γ_i are the respective load factors. It should be noted that even though non-linear stress–strain behaviour is considered in the design, the analysis is still based on linear elastic theory. It is because non-linear analysis of RC structures may be complicated and time consuming for regular design

office practice. Before collapse, redistribution of internal moments and forces takes place. Hence, the error is on the safer side by not considering the redistribution of forces in the elastic analysis. Since elastic moments and forces are statically admissible distribution of forces, the strength of the resulting structure is lower bound according to the *lower bound theorem of plasticity*. More details of this method of design may be found in Ramakrishnan and Arthur (1969).

One of the disadvantages of this method is that the performance at the normal service loads is not considered. Hence, it was realized that the design approach that combines the best features of the ultimate strength design and working stress design will result in better structural performance in strength and serviceability. This realization led to the development of limit states design.

4.7.3 Principles of Limit States Design

Before discussing the limit states design, let us look at some of the principles behind this method.

Uncertainties in Design

To safeguard against the risk of failure (collapse or unserviceability), safety margins are normally provided in the design. In the aforementioned designs, these safety margins were assigned (in terms of ‘permissible stresses’ in WSM and ‘load factors’ in the ultimate load design) primarily on the basis of past experience and engineering judgment. Structures designed according to these methods were found, in general, to be safe and reliable. However, the safety margins provided in these methods lacked scientific basis. Hence, reliability-based design methods were developed with the objective of obtaining rational solutions, which provide adequate safety.

The variables such as loads, material strength, and member dimensions (see, for example, Fig. 4.22) are subject to varying degrees of uncertainty and randomness. The deviations in the dimensions of members or strength of material, even though within acceptable tolerance, can result in a member having less than computed strength. Hence, the design should take into account the possibility of overload or under strength. Further, some idealization and simplifying assumptions are often used in the theories of structural analysis and design. There are also several unforeseen factors that influence the prediction of strength and serviceability. They include construction methods, workmanship and quality control, intended service life of the structure, human errors, possible future change of use, and frequency of loading. These uncertainties make it difficult for the designer to guarantee the absolute safety of the structure. Hence, in order to provide reliable safety margins, the design must be based on the probabilistic methods of design.

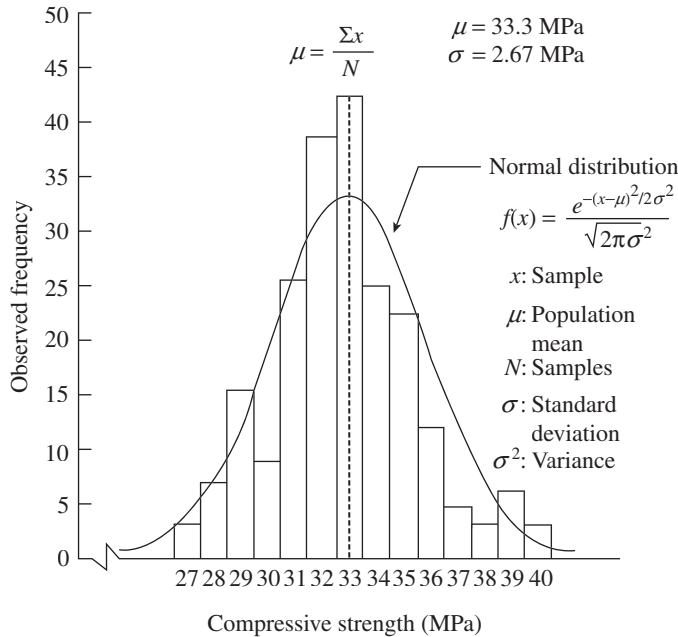


FIG. 4.22 Typical variation in compressive strength of concrete cubes

Limit States

In the limit states design, the term ‘limit states’ is preferably used instead of the term ‘failure’. Thus, a *limit state* is a state of impending failure, beyond which a structure ceases to perform its intended function satisfactorily.

The limit states usually considered relevant for RC are normally grouped into the following three types (Wight and MacGregor 2009; SP 24:1983):

1. *Ultimate (safety) limit states*, which correspond to the maximum load carrying capacity and are concerned with the following: (a) loss of equilibrium (collapse) of a part or the whole structure when considered as a rigid body, (b) progressive collapse, (c) transformation of the structure into a plastic mechanism collapse, (d) rupture of critical sections due to the stress exceeding material strength (in some cases reduced by repeated loading) or by deformations, (e) loss of stability (buckling, overturning, or sliding), and (f) fracture due to fatigue.
2. *Serviceability limit states*, which deal with the discomfort to occupancy and/or malfunction, caused by excessive deflection, excessive crack width, undesirable vibration (e.g., wind induced oscillations, floor vibration), and so forth.
3. *Special limit states*, which deal with the abnormal conditions or abnormal loading such as damage or collapse in extreme earthquakes, damage due to fire, explosions, or vehicle collisions, damage due to corrosion or deterioration (and subsequent loss of durability), elastic, plastic, or creep deformation, or cracking leading to a change of geometry, which necessitates the replacement of the structure.

The attainment of one or more ultimate limit states may be regarded as the inability to sustain any increase in load, whereas the serviceability limits states denote the need for remedial action or some loss of utility. Hence, ultimate limit states are conditions to be avoided and serviceability limit states are conditions that are undesirable. Thus, it is clear that any realistic, rational, and quantitative representation of safety must be based on statistical and probabilistic analysis, which caters for both *overload* and *under strength*.

The design for the ultimate limit state may be conveniently explained with reference to the type of diagram shown in Fig. 4.23. This figure shows the hypothetical frequency distribution curves for the effect of loads on the structural element and the resistance (strength) of the structural element. When the two curves overlap, shown by the shaded area, the effect of the loads is greater than the resistance of the element, and the element will fail. Thus, the structure and its elements should be proportioned in such a way that the overlap of the two curves are small, which means that the probability of failure is within the acceptable range.

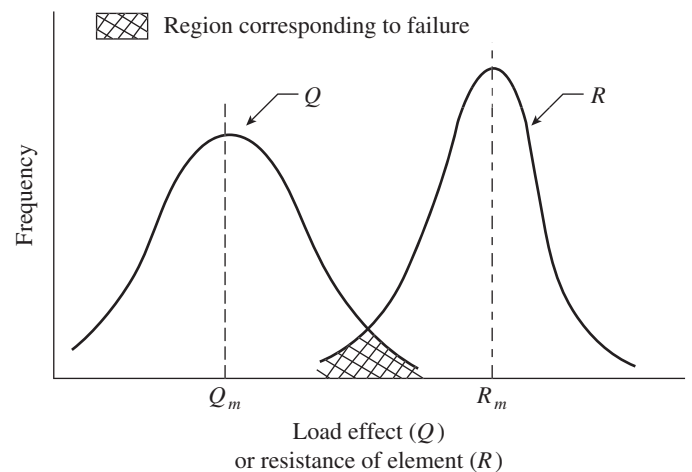


FIG. 4.23 Frequency distribution curves

Levels of Reliability Methods

There exists a number of levels of reliability analysis. These are differentiated by the extent of probabilistic information that is used (Pillai and Menon 2003).

A full-scale probabilistic analysis is generally described as a *level III reliability method*, which uses the probability of failure P_f to evaluate the risk involved. It is highly advanced, mathematically involved, and generally used as a research tool. It is not suitable for general use in design offices.

The problem may be simplified by limiting the probability information of the basic variables to their ‘second moment statistics’ (i.e., *mean* and *variance*). Such a method is called a *level II reliability method*. In this method, the structural failure (the achievement of a limit state) is examined by comparing the resistance R with the load effect Q in a logarithmic

form observing $\ln(R/Q)$ as shown in Fig. 4.24. In this figure, the hatched region shows the failure. The distance between the failure line and the mean value of the function, $\ln(R/Q)_m$, is defined by β called the *reliability index*, the concept of which was first proposed by Freudenthal (1956). The larger the value of β , the greater is the margin of safety of the system. The expression for β may be written as (see also Fig. 4.24)

$$\beta = \frac{\ln(R_m/Q_m)}{\sqrt{(V_r^2 + V_q^2)}} \quad (4.12)$$

where $V_R = (\sigma_R/R_m)$, $V_Q = (\sigma_Q/R_m)$, R_m and Q_m are the mean values of resistance and load, respectively, and σ_R and σ_Q are the standard deviations of resistance and load, respectively.

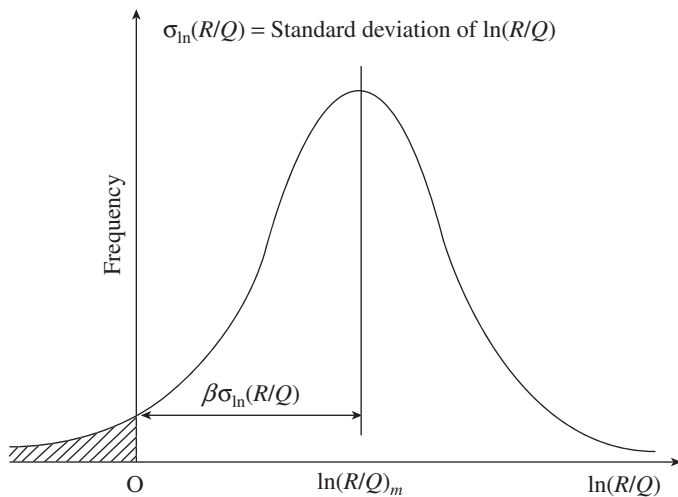


FIG. 4.24 Level II reliability method

However, even such a ‘simplified method’ is unsuitable for use in a design office, as the determination of β requires an iterative procedure; it may require special software and is therefore time consuming (Galambos 1981; Ranganathan 1990).

The values of the reliability index β corresponding to various failure probabilities P_f can be obtained from the standardized normal distribution function of the cumulative densities and are given in Table 4.14.

TABLE 4.14 Reliability index for various failure probabilities

β	2.32	3.09	3.72	4.27	4.75	5.2	5.61
$P_f = \varphi(\beta)$	10^{-2}	10^{-3}	10^{-4}	10^{-5}	10^{-6}	10^{-7}	10^{-8}

It has to be noted that the values given in Table 4.14 are valid only if the safety margin is normally distributed.

For code use, the method must be as simple as possible using deterministic rather than probabilistic data. Such a method, called *level I reliability method* or first-order second moment reliability method, is used in the code to obtain a probability-based assessment of structural safety.

Characteristic Load and Characteristic Strength

In normal design calculations, a single value is usually used for each load and for each material property, with a margin to take care of all uncertainties. Such a value is termed the *characteristic strength* (or resistance) or *characteristic load*.

The *characteristic strength* of a material (such as steel, concrete, or wood) is defined as the value of strength below which more than a prescribed percentage of test results will fall. This prescribed percentage is normally taken as 95. Thus, the characteristic strength, f_{ck} , of concrete is the value of cube/cylinder strength, below which not more than five per cent of the test values may fall (see Fig. 4.25).

Similarly, the *characteristic load*, Q_c , is defined as the load that is not expected to be exceeded with more than five per cent probability during the lifespan of a structure. Thus, the characteristic load will not be exceeded 95 per cent of the time (see Section 3.2 and Fig. 3.2 of Chapter 3).

The design values are derived from the characteristic values through the use of partial safety factors, both for materials and for loads. The acceptable failure probability, P_f , for particular classes of structures is generally derived from experiences with past practice, consequences of failure, and cost considerations. Having chosen P_f and β , the determination of partial safety factors is an iterative process (Galambos 1981).

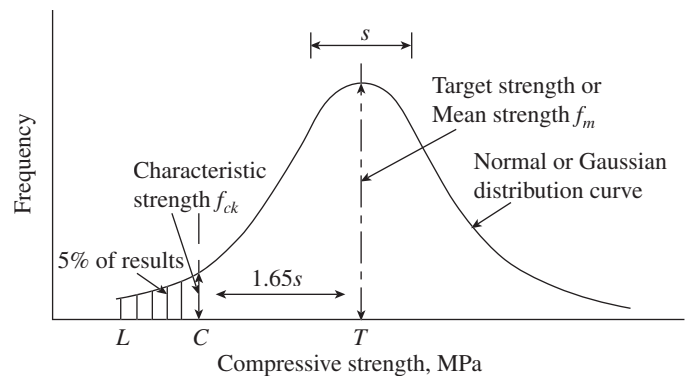


FIG. 4.25 Normal frequency distribution of concrete strengths

4.7.4 Sampling and Acceptance Criteria

The relationship between mean and characteristic strength is given by

$$\varphi_c^{-1}(P_f) = (f_{ck} - f_m)/s = -k \quad (4.13)$$

where φ_c is the cumulative normal distribution function, f_m and s are the mean value and standard deviation of the normal distribution, respectively, f_{ck} is the characteristic strength, and k is an index that signifies the acceptable probability of failure. As the five per cent is on the negative end of the curve, the minus sign is assigned to k . The value of k is 1.65 for

five per cent acceptability of failure. Thus, Eq. (4.13) may be written as

$$f_m = f_{ck} + 1.65s \tag{4.14}$$

The minimum size of the sample needs to be about 50 for normal distribution, but Clause 9.2.4.1 of IS 456 accepts a size of 30. When insufficient test results (less than 30 samples) are available, an assumed value of standard deviation, s , has to be used; the code suggests a value of 4.0 N/mm² for concrete of grades M20 and M25 and 5.0 N/mm² for concrete of grades M30 and above (see Table 8 of IS 456). The standard deviation of the results from the mean value is regarded as an index of the scatter and hence may reveal the site control. A small value of standard deviation will result in a curve with a dominant peak, while a larger value will result in a flatter curve as shown in Fig. 4.26. Three test specimens form a sample. The minimum frequency of sampling depends on the quantity of concrete, as shown in Table 4.15. It has to be noted that IS 456 specifies both compressive and flexural strength tests (Clauses 16.1 and 16.2); flexural strength test is considered only in some special situations, where the tensile strength of concrete plays an important role.

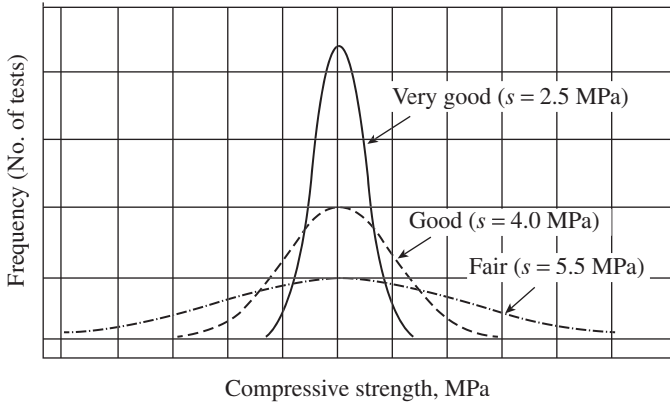


FIG. 4.26 Typical normal frequency curves for different levels of control

TABLE 4.15 Sampling frequency

Quantity of Concrete Involved, m ³	Required Number of Samples
1–5	1
6–15	2
16–30	3
31–50	4
> 51	4 + 1 additional for each additional 50 m ³

Note: A minimum of one sample in each shift is required.

In most constructions, it may be difficult to obtain 30 samples, and hence four consecutive non-overlapping samples (it means that the test results of one group should not be taken in another group too) are considered to be a practicable size to test the acceptability of concrete. As this size is smaller than the minimum

population size, the following expression, which satisfies the five per cent acceptability criterion, may be used (SP 24:1983):

$$f_{m1} = f_{ck} + 1.65s (1 - 1/\sqrt{n}) \tag{4.15a}$$

where n is the size of the sample and f_{m1} is the mean value of the smaller size sample. Equation (4.15a) for four non-overlapping samples reduces to

$$f_{m1} = f_{ck} + 0.825s \tag{4.15b}$$

The concrete strength (for grades M20 and above) is acceptable if the following relations are satisfied according to Table 11 of IS 456:

$$f_{m1} \geq f_{ck} + 0.825s \tag{4.16a}$$

$$f_{m1} \geq f_{ck} + 3 \text{ MPa} \tag{4.16b}$$

$$f_i \geq f_{ck} - 3 \text{ MPa} \tag{4.16c}$$

where f_{ck} is the characteristic strength, f_{m1} is the mean strength of any four consecutive non-overlapping samples, and f_i is the strength of a sample.

These *acceptability criteria* are supposed to be valid for concretes up to grade M60. It means that even if the concrete is of M60 grade, a mean value of the order of 63 MPa of four consecutive samples is acceptable. Hence, this criterion is liberal for HSC. However, Eq. 4.16(a) is more stringent for HSC, as the margin for individual sample strength is small.

As per ACI 318:18, the concrete may be accepted if the strength is larger than (a) $0.8f_{ck} + 1.34s$ and (b) $0.8f_{ck} + 2.33s - 3.45$ for concrete of grades less than M44 (with cylinder strength converted to cube strength). If the concrete strength is greater than M44, the strength should be larger than (a) $0.8f_{ck} + 1.34s$ and (b) $0.72f_{ck} + 2.33s$, where s is the standard deviation (it should be noted that the ACI values have been converted from cylinder to cube strength to compare with IS code values). As per Clause 5.6.3.3 of ACI, the concrete strength is considered to be satisfactory as long as the averages of any three consecutive strength tests remain above the specified strength and no individual strength test falls below the specified strength by more than 3.5 MPa if f_{ck} is 44 MPa or less or falls below f_{ck} by more than 10 per cent if f_{ck} is over 44 MPa.

It has to be noted that these strengths denote the 28th day strength. Concrete made with Portland cement attains about 85–90 per cent of strength on the 28th day; however, in PPC using pozzolanic materials such as fly ash, such a percentage of strength will be attained only after the 56th day. More details on acceptance criteria may be found in Rajamane, et al. 2012.

4.8 LIMIT STATES METHOD

The philosophy of the *limit states method of design* represents advancement over the traditional design philosophies. Unlike

WSM, which based calculations on service load conditions alone, or ultimate load method, which based calculations on ultimate load conditions alone, limit states method aims for a comprehensive and rational solution to the design problem, by considering *safety* at ultimate loads and *serviceability* at working loads.

The limit states method philosophy uses a multiple safety factor format that attempts to provide adequate safety at the ultimate loads as well as adequate serviceability at the service loads, by considering all possible *limit states*. The selection of the various multiple safety factors is supposed to have a sound probabilistic basis, involving the separate consideration of the different kinds of failure, types of materials, and types of loads.

4.8.1 Limit States of Strength

The three different design formats used in the limit states method are the multiple safety factor format, LRFD format, and the partial safety factor format. These are briefly described in the following sub-sections.

Multiple Safety Factor Format

The limit states design has to ensure that the probability of any limit state being reached is acceptably low. This is accomplished by specifying appropriate *multiple safety factors* for each limit state (level I reliability). The values of multiple safety factors are chosen by a careful reliability study in order to achieve the *target reliability*.

Several national codes introduced multiple safety factors in the limit states design during the 1970s. The values of these factors were chosen based on tradition, experience, and engineering judgement. Subsequently, several studies were made to determine the range of the reliability index (or its equivalent probability of failure P_f), in order to calibrate the codal values of specified safety factors. With every code revision, conscious attempts are made to specify more rational reliability-based safety factors, in order to achieve practical designs that are safe, reliable, and economical.

Load and Resistance Factor Design Format

Of the many available multiple safety factor formats, perhaps the simplest is the LRFD format that has been adopted by the ACI's code (ACI 318, 2011). As per LRFD, the expression for structural safety is given as follows:

$$\text{Design resistance } (\phi R_n) \geq \text{Design load effect } (\Sigma \gamma_i Q_i) \quad (4.17)$$

where the left-hand side of the equation represents the strength (or resistance) of the system or component and the right-hand side represents the load expected to be carried by the system or component. The nominal strength R_n is multiplied by a strength reduction (or resistance reduction factor) ϕ to

obtain the *design strength*. Similarly, the various load effects Q_i (such as dead, live, and wind loads) are multiplied by their respective overload factors γ_i to obtain the sum $\Sigma \gamma_i Q_i$.

Resistance factor accounts for the 'under strength' and is less than unity, and the values adopted in the current version of ACI 318:11 are given in Table 4.16. It will take care of the following aspects:

1. The possibility of unfavourable deviation of material strength from the characteristic value
2. The possibility of unfavourable reduction in member strength due to fabrication and tolerances.
3. The possibility of unfavourable variation of member sizes
4. The uncertainty in the theoretical assumptions
5. The uncertainty in the calculation of strength of members.

TABLE 4.16 Resistance or strength reduction factor ϕ as per ACI 318:11 (Clause 9.3.2)

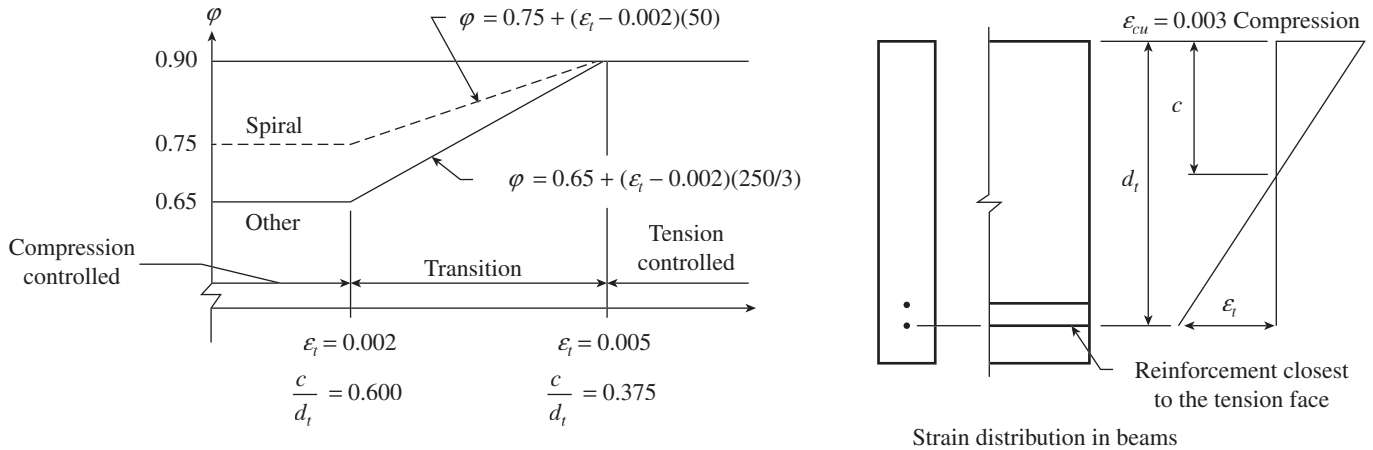
Structural Element	Factor ϕ
Tension-controlled sections:*	
Beam or slab: bending or flexure	0.9
Axial tension	
Compression-controlled sections:*	
Members with ties	0.65
Members with spirals	0.75
Beam: shear and torsion	0.75
Bearing except for strut-and-tie	0.65
Bearing areas in strut-and-tie	0.75
Flexural shear and bearing in plain structural concrete	0.60

* When the beam reaches its nominal flexural capacity, a *tension-controlled section* will have a net tensile strain in the extreme tension steel equal to or greater than 0.005, whereas in a *compression-controlled section*, the strain in the steel is less than or equal to the yield strain, which may be taken as 0.002. A *transition zone section* has a strain in between 0.002 and 0.005 (see Fig. 4.27). This classification was introduced in the 2002 edition of the code in order to control ductility.

It was observed during the 1994 Northridge earthquake that short structural walls in many of the parking structures sustained significant damage. Hence, the ACI code Section 9.3.4(b) suggests the shear strength reduction factor for diaphragms as 0.60 if the shear strength reduction factor for the walls is 0.60.

On the contrary, the load factors γ_i , which accounts for 'overloading' and the uncertainties associated with Q_i , are generally greater than unity. These loads factors will account for the following:

1. The possibility of unfavourable deviation of the load from the characteristic value
2. The possibility of inaccurate assessment of the load
3. The uncertainty in the assessment of the effects of the load
4. The uncertainty in the assessment of the limit state being considered



Interpolation on c/d_t :
 Spiral $\phi = 0.75 + 0.15 [(1/c/d_t) - (5/3)]$
 Other $\phi = 0.65 + 0.25 [(1/c/d_t) - (5/3)]$

FIG. 4.27 Variation of ϕ with net tensile strain in extreme tension steel, ϵ_t , and c/d_t for grade 420 reinforcement, as per ACI 318, reprinted with permission from ACI

The method used to develop LRFD uses the mean values R_m and Q_m (see Fig. 4.23) and the standard deviations σ_R and σ_Q of the resistance and the load, respectively.

The strength reduction factors (ϕ) were derived with the objective of obtaining the values of β as shown in Table 4.17 (Nowak and Szerszen 2003).

TABLE 4.17 Reliability indices based on recent recalibration

S. No.	Types of Member	Reliability Index, β
1.	RC beam, cast-in-place, flexure	3.54
2.	RC beam, cast-in-place, shear	3.95
3.	RC tied column, cast-in-place	3.98

Equation (4.17) may be rewritten as

$$\sum Q_i < R_n (\gamma/\phi) \tag{4.18}$$

This equation is representative of the safety concept underlying WSM. The term (γ/ϕ) here denotes the ‘factor of safety’ applied to material strength, in order to arrive at the permissible stress for design.

Alternatively, Eq. (4.17) can be rewritten as

$$R_n \geq (\gamma/\phi) \sum Q_i \tag{4.19}$$

This equation is representative of the safety concept underlying the ultimate load design method. The term (γ/ϕ) here denotes the so-called ‘load factor’ used in that method, applied to the load in order to arrive at the ultimate load for design.

Partial Safety Factor Format

The multiple safety factor format adopted by the Indian code was initially recommended by CEB-FIP 1970. (The

provisions found in both the Indian and British codes for limit states design are similar, as both are based on the model code released by CEB-FIP.) It is called the *partial safety factor format* and is expressed as follows:

$$R_d \geq \sum \gamma_{if} Q_{id} \tag{4.20}$$

Here, R_d is the design strength (or resistance) computed using the reduced material strengths R_u/γ_m where R_u is the characteristic material strength and γ_m is the *partial safety factors* for the material that allows for uncertainties of element behaviour and possible strength reduction due to manufacturing tolerances and imperfections in the material. Q_{id} is the design action (load effect) computed for the enhanced loads ($\gamma_{Df} \cdot DL, \gamma_{Lf} \cdot IL, \gamma_{Qf} \cdot EL$), involving separate partial load factors γ_{Df} (for dead load), γ_{Lf} (for imposed load), and γ_{Qf} (for wind or earthquake load).

Partial Safety Factors for Loads The *partial safety factors for loads* γ_f , make allowances for possible deviation of loads and the reduced possibility of all loads acting together. The values suggested by the code have already been discussed in Section 3.11 of Chapter 3. It is to be noted that when more than one imposed load acts simultaneously, the leading load is that causing the larger action effect.

It may be noted that whereas the multiplication factor ϕ is generally less than unity, the dividing factor γ_m is greater than unity—giving the same effect. All the load factors are generally greater than unity, because overestimation usually results in improved safety. However, one notable exception to this rule is the dead load factor γ_{Df} , which is taken as 0.9 whenever dead load contributes to stability against overturning or sliding, or while considering reversal stresses when dead loads are combined with wind or earthquake loads.

In such cases, underestimating the counteracting effects of dead load results in greater safety.

It should be noted that the load factors are reduced when different types of loads (DL, LL, and WL or EL) are acting simultaneously at their peak values. (This is sometimes referred to as the *load combination effect*.) It is because of the reduced probability of all the loads acting concurrently. The reader may refer Section 3.11 of Chapter 3 and Clause 35.4.1 of SP 24:1983 for more discussions.

Partial Load Factors for Materials The material partial safety factors γ_m for concrete and reinforcing steel is taken as 1.5 and 1.15, respectively. The partial safety factor of 1.15 as applied to steel reinforcement accounts for (a) the reduction in strength of any member as a result of inaccurate positioning of steel and (b) the reduction in strength of steel reinforcement due to any manufacturing defect—for example, deviation in the nominal diameter. Thus, the design strength of steel reinforcement equals $f_y/1.15 = 0.87f_y$.

A higher value of γ_m is prescribed by the code for concrete, as unlike steel, the strength of concrete may deviate much from the assumed strength due to several parameters such as deviation in properties of aggregates and defects or variations that may occur during mixing, transporting, placing, compacting, and curing of concrete.

It has been observed in experiments conducted on beams or columns that the strength of concrete in the compression zone at failure is approximately 0.85 times the strength of cylinders cast and tested in laboratories (Hognestad, et al. 1955; Rüsck 1960). This is approximately equal to $0.85 \times 0.8f_{ck} = 0.68$ times the characteristic cube strength (taking the cylinder strength as approximately equal to 0.8 times the cube strength). Thus, the characteristic strength of concrete in the actual structure is taken as $0.68f_{ck}$ and applying the partial safety factor of 1.5 for concrete, the design strength of concrete equals $0.68f_{ck}/1.5 = 0.45f_{ck}$.

4.8.2 Serviceability Limit States

In this limit state, the variable to be considered is a serviceability parameter Δ (representing deflection, vibration, etc.). Limit state or failure is considered to occur when a specified maximum limit of serviceability, Δ_{all} is exceeded. The limiting failure is deterministic and not probabilistic. Serviceability limit states relate to satisfactory performance and correspond to excessive deflection, vibration, local deformation, durability, and fire resistance.

The load factor γ_f should be taken as unity for all serviceability limit state calculations, since they relate to the criteria governing normal use.

Deflections and Crack Widths

The maximum deflection affecting the strength and stability of the structure is controlled by the strength limit state.

However, excessive deflection should not produce sagging appearance, plaster cracking, or failure to align plant and machinery (e.g., lifts). Excessive deflection of beams causes damage to supported non-structural elements such as partitions, excessive vibrations of floors, or impair the usefulness of the structure (e.g., distorting door frames so that doors will not open or close). On roofs, a major deflection-related concern is ponding of water. Excessive deflections are often indicative of excessive vibration and noise transmission, both of which are serviceability problems. Deflections are to be calculated for all combinations of loads specified in the code, by using an elastic analysis and checked for the maximum values specified in the code. Some of the deflection limits specified by Clause 23.2 of IS 456 are shown in Table 4.18.

Serviceability, instead of strength, may often control the design of beams. The code suggests an empirical method (by limiting the span to effective depth ratios) and a theoretical method to calculate the deflection (by considering the effective moment of inertia) and compare it with the limiting deflection.

Similarly, for controlling crack widths too, the code recommends an empirical method (detailing by spacing of bars, minimum steel ratios, etc.) and a theoretical method to calculate the actual width of cracks and compare it with the limiting crack width (see Table 4.4). More discussions on deflection and crack width considerations are provided in Chapter 12.

TABLE 4.18 Limiting deflection for flexural members as per IS 456

Type of Member	Deflection to be Considered	Deflection Limitation
Floor or roofs	Final due to all loads, including long-term effects of temperature, creep, and shrinkage	Span/250
Floor or roofs	Deflection including long-term effects of temperature, creep, and shrinkage that occur after the construction of partitions and finishes	Lesser of span/350 or 20 mm
Lateral drift of tall buildings	Due to wind or earthquake	Height/250 ⁺
Member supporting masonry partitions	Deflection that occurs after the addition of partitions	Span/500 [*]

⁺ As per Clause 7.11.1 of IS 1893 (Part 1):2002. As per Clause 20.5 of IS 456, lateral sway should not exceed $H/500$, where H is the total height of the building.

^{*} As per Table 2.4.2 of AS 3600-2001

Vibration

With the development of lighter construction using high-strength concrete and use of longer spans, there is a higher risk of vibrations becoming critical in a number of situations. *Vibration* will have to be checked when vibrating loads such as due to machinery, washing machines, and cranes applied to slabs. Activities such as dancing, aerobics, marching of soldiers, drilling, and impact loads also produce vibration. In these cases, care must be taken to ensure that the structural response will not amplify the disturbing motion. IS 456 does not give any recommendation for vibration control. However, IS 800:2007, Clause 5.6.2 recommends that flexible structures (with height to effective width ratio exceeding 5:1) should be investigated for lateral vibration under dynamic loads. Annex C of IS 800:2007 gives the guidelines to estimate floor frequency, damping, and acceleration due to vibration. When vibration becomes a problem, one may have to change the natural frequency of the structure by some means. Changing the load factor will not help in reducing this problem. Design charts for floor vibration, design criteria for vibration due to walking, and other information regarding building vibration may be found in Allen (1990); Ellingwood and Tullin (1984); Lancaster (2007); and Murray (1991).

Software packages (e.g., Floorvibe—www.floorvibe.com) are also available using which the frequency and amplitude resulting from transient vibration caused by human activity can be quickly estimated.

4.9 DESIGN BY USING MODEL AND LOAD TESTS

Clause 18.2.3 of IS 456 allows design based on experimental investigations conducted on models or full-size structure or element. The conditions given in Clause 18.2.3.1 must be fulfilled while conducting the experiments. These tests reveal not only the ultimate strength but also the behaviour of the structure, such as deflection and cracking performance of the structure under the considered loading. Even though a few products such as the *prestressed concrete sleepers* have been developed based on prototype testing, they are expensive and time consuming. Hence, prototype testing is resorted to only when a new theory is being applied or when a novel or new type of detail or structure is adopted.

4.10 STRUT-AND-TIE MODEL

The *strut-and-tie method* presents an alternative method for designing RC members with force and geometric discontinuities. This method is also useful for designing deep beams for which the usual assumptions of linear strain distribution is not

valid. Similarly, pile caps supported on piles can be designed using three-dimensional strut-and-tie models. These models are also useful for designing diaphragms with openings. The strut-and-tie model gives the lower bound estimates of the capacity of concrete structures, provided the following conditions are satisfied:

1. The strut-and-tie model of the structure represents a statically admissible distribution of forces.
2. The strengths of struts, ties, and nodal zones are chosen to be safe, relative to the computed forces in the strut-and-tie model.
3. The members and joint regions have enough ductility.

Strut-and-tie method of design was developed by Schlaich and associates during the late 1980s and was incorporated in the ACI code in 2002 (Schlaich, et al. 1987; Marti 1985). More details of this method are given in Appendix B.

4.11 PERFORMANCE-BASED DESIGN

Historically, the design basis of current prescriptive building codes is intended to provide a minimum level of safety and a relatively economical means to design and build buildings. For example, the buildings designed as per IS 1893 resist minor level earthquakes without damage, moderate level earthquakes with some non-structural damage, and major earthquakes without total collapse. *The performance-based design* codes are intended to design and build for a higher level of performance.

The development and use of the performance-based design has been in progress for several years, primarily for the seismic and blast design. It was introduced in FEMA 283/349 and refined and extended in FEMA 445. They allow the building owners to choose the performance of their buildings. For example, they may consider spending more money to achieve higher performance than provided in normal codes, thereby reducing risk and potential losses. This design is not limited to the design of new buildings. With it, existing buildings or bridges can be evaluated and/or retrofitted to reliable performance objectives (ASCE/SEI 41-2007).

Performance-based seismic design explicitly evaluates how a building is likely to perform, given the potential hazard it is likely to experience, considering uncertainties inherent in the quantification of potential hazard and uncertainties in the assessment of the actual building response. It permits the design of new buildings or upgrade of existing buildings with a realistic understanding of the risk of casualties, occupancy interruption, and economic loss that may occur as a result of future earthquakes. The methodology of this design is explained in Fig. 4.28 (FEMA 445).

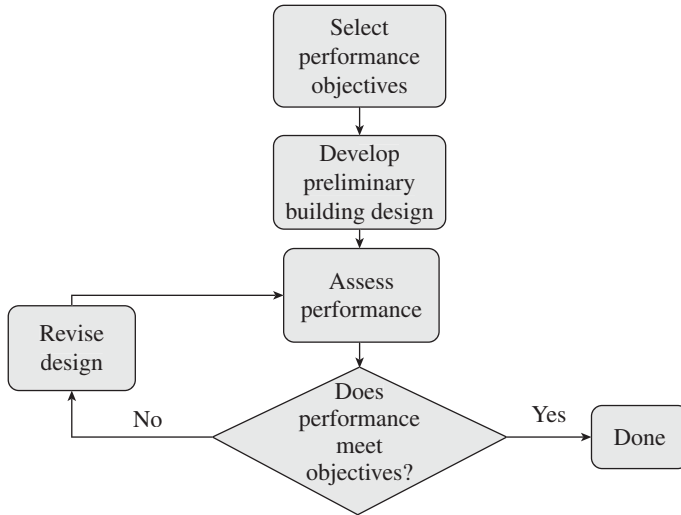


FIG. 4.28 Flow diagram of performance-based design

Source: FEMA 445

It also establishes a vocabulary that facilitates meaningful discussion between stakeholders and design professionals on the development and selection of design options. It provides a framework for determining the level of safety and the level of property protection, along with the cost, which are acceptable to building owners, tenants, lenders, insurers, regulators, and other decision-makers based upon the specific needs of a project (FEMA 445).

In contrast to the prescriptive design approaches, performance-based design provides a systematic methodology for assessing the performance capability of a building, system, or component (Klemencic, 2008). It can be used to verify the equivalent performance of alternatives, deliver standard performance at a reduced cost, or confirm higher performance needed for critical facilities. More information about this design may be found in ASCE 41 and FEMA 445. Though this has not yet been codified in India, with the current awareness about sustainability, it may be incorporated in the future editions of the Indian codes.

EXAMPLES

EXAMPLE 4.1:

Design an RC rectangular beam to carry a B.M. of 100kNm. Assume the width of the beam as 300 mm and use M20 concrete and high-strength deformed bars with $f_y = 415 \text{ N/mm}^2$.

SOLUTION:

From Tables 4.10 and 4.11,

Permissible compressive stress due to bending, σ_{cbc} , of M20 concrete = 7.0 N/mm^2

Permissible tensile stress of Fe 415 steel $\sigma_{st} = 230.0 \text{ N/mm}^2$

Modular ratio = 13.33

Neutral axis constant, k

$$= \frac{1}{1 + \frac{\sigma_{st}}{m\sigma_{cbc}}} = \frac{1}{1 + \frac{230}{13.33 \times 7}} = 0.2886$$

Lever arm constant, $j = 1 - k/3 = 1 - 0.2886/3 = 0.904$

Moment of resistance constant, $Q = 0.5kj\sigma_{cbc} = 0.5 \times 0.2886 \times 0.904 \times 7 = 0.913$

$$\text{Effective depth, } d = \sqrt{\frac{M}{Qb}} = \sqrt{\frac{100 \times 10^6}{0.913 \times 300}} = 604 \text{ mm}$$

Using 20 mm bars and a clear cover of 25 mm, provide total depth = 650 mm

$$\text{Hence, } d \text{ provided} = D - \text{cover} - \text{diameter of bar}/2 = 650 - 25 - 10 = 615 \text{ mm} > 604 \text{ mm.}$$

Required area of steel, A_{st}

$$= \frac{M}{\sigma_{st}jd} = \frac{100 \times 10^6}{230 \times 0.904 \times 615} = 782 \text{ mm}^2$$

Provide two #20 mm and one #16 mm bars, provided area = $829 \text{ mm}^2 > 782 \text{ mm}^2$

EXAMPLE 4.2:

Design a short square RC column to carry a load of 675 kN. Use M20 concrete and high-strength deformed bars with $f_y = 415 \text{ N/mm}^2$.

SOLUTION:

The permissible axial load of a short column

$$P = \sigma_{cc}A_c + \sigma_{sc}A_{sc}$$

From Tables 4.10 and 4.11, for M 20 concrete and grade Fe 415 steel:

Permissible stress in concrete in direct compression, $\sigma_{cc} = 5.0 \text{ N/mm}^2$

Permissible compressive stress in steel, $\sigma_{sc} = 190.0 \text{ N/mm}^2$

Assuming the size of column as 300 mm × 300 mm,

$$P = \sigma_{cc}A_c + \sigma_{sc}A_{sc}$$

Hence, $675 \times 10^3 = 5(300 \times 300 - A_{sc}) + 190A_{sc}$

Hence $A_{sc} = 1216 \text{ mm}^2$

Provide four 20 mm diameter bars, provided $A_{sc} = 1256 \text{ mm}^2 > 1216 \text{ mm}^2$. Hence, safe.

EXAMPLE 4.3:

In a concrete work, concrete of grade M25 is to be used. The standard deviation has been established as 4.0 N/mm^2 . In the course of testing concrete cubes, the following results were obtained (average strength of three specimens tested at 28 days, in each case expressed in N/mm^2): 29.8, 32.0, 33.6, 28.6, 23.0, 27.7, and 22 N/mm^2 . Determine whether the concrete is acceptable.

SOLUTION:

(a) The first four tests are straightaway accepted, the sample strength being greater than the characteristic strength of 25 MPa in each case.

- (b) The fifth test result of 23.0 N/mm^2 is less than the characteristic strength of 25 MPa, but greater than $f_{ck} - 3 \text{ N/mm}^2$, or 22 N/mm^2 . Average strength of the samples = $(29.8 + 32.0 + 33.6 + 28.6 + 23.0)/5 = 29.4$, which is greater than $f_{ck} + 1.65s(1 - 1/\sqrt{n}) = 25 + 1.65 \times 4(1 - 1/\sqrt{5}) = 25 + 0.912 \times 4 = 28.65 \text{ N/mm}^2$ and greater than $f_{ck} + 3 = 28 \text{ N/mm}^2$. Hence, acceptable.
- (c) The sixth result is also acceptable, being greater than the characteristic strength of 25 MPa.
- (d) The seventh one is equal to 22 N/mm^2 . The average strength of all seven samples is: $(29.8 + 32.0 + 33.6 + 28.6 + 23.0 + 27.7 + 22)/7 = 28.1$, which is less than $f_{ck} + 1.65s(1 - 1/\sqrt{n}) = 25 + 1.65 \times 4(1 - 1/\sqrt{7}) = 25 + 1.026 \times 4.1 = 29.1 \text{ N/mm}^2$ but greater than $f_{ck} + 3 = 28 \text{ N/mm}^2$. The seventh sample thus does not comply with all the requirements given in Table 11 of IS 456. However, the acceptance will depend upon the discretion of the site engineer. In this case, as only one specimen fails to meet a single criterion, the concrete may be accepted.

SUMMARY

The various steps involved in the construction activities are listed and the role and responsibilities of the designer while carrying out these activities are emphasized in this chapter. Structural design is considered a science as well as an art. The aim of any structural designer should be to design a structure in such a way that it will fulfil its intended purpose during its intended lifetime and have (a) adequate safety (in terms of strength, stability, and structural integrity), (b) adequate serviceability (in terms of stiffness, durability, etc.), (c) economy (in terms of cost of construction and maintenance), (d) durability, (e) aesthetics, (f) environment friendliness, (g) functional requirements, and (h) adequate ductility.

The term analysis means the determination of the internal forces acting on different members of a structure, due to the application of external actions (forces). The analysis is followed by design, which is the selection of the sizes of different members based on the criteria stipulated in the national code of practices. A brief description of the methods of analysis and the available computer program are given.

A discussion on code and specifications that will guide the designer in the design process has been provided. The codes published by the Bureau of Indian Standards for the design of RC structures are listed and the reader is advised to obtain a copy of

these codes, since they may be required to understand the material that is provided in the chapters to follow.

The various design philosophies that have been evolved in the past, namely working stress method, ultimate strength (load) design, and limit states design, are briefly discussed. The various limit states to be considered in the design are explained. A brief description of the reliability of these methods of design is also provided.

The terms characteristic load and characteristic strength are explained. The basis of the limit states method is explained along with the various partial safety factors adopted by the code for materials and loads. The various serviceability limit states, related to the satisfactory performance of the structure (as opposed to the ultimate or safety limit states, which are concerned with strength, stability, fatigue, etc.), are also briefly explained along with the deflection limits specified by the code. Brief discussions on the design based on experimental results and performance-based design are also provided.

As explained in this chapter, though analysis and design are interactive processes, for convenience they are presently performed as separate activities, with the design phase following the analysis phase. The design of RC flexural members is discussed in Chapter 5.

REVIEW QUESTIONS

- What are the various steps involved in the construction of RC structures?
- What are the roles and responsibilities of the designer?
- What are the main design considerations during the design of RC structures?
- The minimum size of a column as per IS 13920 is _____.
(a) 200 mm (c) 300 mm
(b) 250 mm (d) 350 mm
- Why is an area of compression reinforcement at least equal to 50 per cent of the tension reinforcement necessary in beams?
- Why is an upper limit to tension reinforcement in beams necessary?
- What is the purpose of shear reinforcement and why should we provide at least minimum shear reinforcement in beams?
- What are the elements that will provide bracing effect in RC frames?
- What is the purpose of serviceability requirement?
- Will optimum quantities of materials provide an economic structure? State the reason for your answer.
- What are the five exposure conditions considered for durability?
- The allowable maximum crack width under mild exposure is _____.
(a) 0.3 mm (c) 0.1 mm
(b) 0.2 mm (d) 0.4 mm
- List a few parameters that will affect the durability of concrete.
- The minimum grade of concrete for moderate environment is _____.
(a) M30 (c) M25
(b) M15 (d) M20
- Why is curing important for the development of strength? List the methods of curing.
- The minimum number of days concrete elements have to be cured when blended cements or mineral admixtures are used is _____.
(a) 3 days (c) 7 days
(b) 10 days (d) 15 days
- Minimum cover to be provided for columns as per IS 456 is _____.
(a) 50 mm (c) 40 mm
(b) 25 mm (d) 30 mm

18. Will providing thick covers always provide the required durability? State the reason for your answer.
19. List a few methods that are used to tackle corrosion in RC structures.
20. Spacers and chairs should be provided at a maximum spacing of _____.
(a) 500 mm (c) 2 m
(b) 1000 mm (d) 300 mm
21. What is controlled permeability formwork? Write a short note on it.
22. Write a short note on aesthetics of RC structures.
23. List the three tools suggested by Mehta to reduce CO₂ emissions in concrete structures.
24. What is geopolymer concrete? How is it better than ordinary concrete?
25. Why are site visits considered necessary and important for the structural designer?
26. List a few constructability issues connected with detailing of reinforcement bars.
27. What is ductility? Why should it be considered in design?
28. Distinguish the differences between analysis and design.
29. List the names of a few computer programs suitable for linear elastic analysis of structures.
30. What is meant by relative stiffness? State the three relative stiffness values suggested in Clause 22.3.1 of IS 456:2000.
31. List the parameters that affect the relative stiffness of members.
32. Why are codes of practices necessary and what is the function of these codal provisions?
33. List a few Indian standard codes that are followed while designing structures made of RC.
34. Distinguish the differences between the working stress method, ultimate load design, and limit states design.
35. What are the limitations and shortcomings of the working stress method?
36. What is modular ratio?
37. The permissible stress used for HYS bars of grade Fe 415 in columns is _____.
(a) 415 N/mm² (c) 190 N/mm²
(b) 230 N/mm² (d) 250 N/mm²
38. What are the three types of limit states that are considered in the limit states method?
39. What are characteristic load and characteristic strength?
40. The standard deviation suggested by IS 456:2000 for grade M20 concrete is _____.
(a) 4 N/mm² (c) 5 N/mm²
(b) 3.5 N/mm² (d) 4.5 N/mm²
41. How many cube specimens form a sample?
(a) 4
(b) 3
(c) 5 consecutive non-overlapping
(d) 2
42. State the three acceptability criteria as per Table 11 of IS 456:2000.
43. What are the features of load and resistant factor design?
44. What are the partial safety factors (of resistance) for materials adopted by the IS 456 code?
45. What are the partial load factors adopted for the following loading combinations:
(a) DL (c) WL
(b) LL (d) DL + LL
46. Write a brief note on the various serviceability limit states considered by the IS 456 code.
47. The final deflection limitation for floors and roofs as per IS 456 is _____.
(a) Span/250 (c) 20 mm
(b) Span/350 (d) Both (b) and (c)
48. When is model testing adopted as an alternative method of design.
49. Under what circumstances is the strut-and-tie method of design useful?
50. What is performance-based design?

EXERCISES

1. Design a RC rectangular beam to carry a B.M. of 75 kNm. Assume the width of the beam as 230 mm and use M20 concrete and high-strength deformed bars with $f_y = 415 \text{ N/mm}^2$.
2. Design a short square RC column to carry a load of 500 kN. Use M30 concrete and high-strength deformed bars with $f_y = 415 \text{ N/mm}^2$.
3. In a concrete work, concrete of grade M30 is to be used. The standard deviation has been established as 4.0 N/mm^2 . In the course of testing the concrete cubes, the following results were obtained (average strength of three specimens tested at 28 days, in each case expressed in N/mm^2): 35.1, 36.9, 38.7, 34.6, 27.9, 33.0, and 28 N/mm^2 . Determine whether the concrete is acceptable.

REFERENCES

- ACI 318-08 2008, *Building Code Requirements for Structural Concrete and Commentary*, American Concrete Institute, Farmington Hills, p. 473.
- Allen, D.E. 1990, 'Building Vibration from Human Activities', *Concrete International*, Vol. 12, No. 6, pp. 66–73.
- ACI 202.2R-2008, *Guide to Durable Concrete*, American Concrete Institute, Farmington Hills, p. 49.
- ACI-ASCE Committee 426 1973, 'Shear Strength of Reinforced Concrete Members', *Proceedings, ASCE, Journal of the Structural Div.*, Vol. 99, No. ST6, pp. 1091–187.
- Annie Peter, J. and N. Chitharanjan 1995, 'Evaluation of Indigenous Filter Fabrics for Use in Controlled Permeable Formwork', *Indian Concrete Journal*, Vol. 69, No. 4, pp. 215–9.
- Arya, C. and G. Pirathapan 1996, 'Supercover Concrete: A New Method for Preventing Reinforcement Corrosion in Concrete Structures using GFRP Rebars', in R. K. Dhir and M. J. McCarthy (eds), *Appropriate Concrete Technology*, E & FN Spon, London, pp. 408–19.
- ASCE/SEI 41/06 2007, *Seismic Rehabilitation of Existing Buildings*, American Society of Civil Engineers, Reston, p. 428.

- Barbhuiya, S.A., A. Jaya, and P.A.M. Basheer 2011, 'Influence SCC on the Effectiveness of Controlled Permeability Formwork in Improving Properties of Cover Concrete', *The Indian Concrete Journal*, Vol. 85, No. 2, pp. 43–50.
- Basheer, P.A.M., A.A. Sha'at, A.E. Long, and F.R. Montgomery 1993, 'Influence of Controlled Permeability Formwork on the Durability of Concrete', *Proceedings, International Conference on Concrete 2000, Economic and Durable Construction Through Excellence*, Vol. 1, E & FN Spon, London, pp. 737–48.
- Baumann, H.U. 2008, 'Evolving Technology for Design and Construction of Tall Concrete Structures', *CTBUH 8th World Congress*, Dubai, p. 5.
- Beeby A.W. 1997, 'Ductility in Reinforced Concrete: Why Is It Needed and How Is It Achieved?', *The Structural Engineer*, Vol. 75, No. 18, pp. 311–18.
- Bentz, D.P., E.F. Irassar, B.E. Bucher, and W.J. Weiss 2009, 'Limestone Fillers Conserve Cement, Part 1: An Analysis Based on Powers' Model, Part 2: Durability Issues and the Effects of Limestone Fineness on Mixtures', *Concrete International*, ACI, Vol. 31, No. 11, pp. 41–6, No.12, pp. 35–9.
- BS 7973 (Parts 1 and 2) 2001, *Spacers and Chairs for Steel Reinforcement and their Specification*, British Standards Institution, London.
- CEB-FIP 1970, *International Recommendations for the Design and Construction of Concrete Structures*, Comité Européen du Béton-Fédération Internationale de la Précontrainte, Paris.
- Collins, M.P. 2001, 'In Search of Elegance: The Evolution of the Art of Structural Engineering in the Western World', *Concrete International*, ACI, Vol. 23, No. 7, pp. 57–72.
- Delahay, J. and B. Christopher, 'Current Trends in Economical Reinforced Concrete Construction, Part 3: Reinforcement, Materials and Other Factors', *Structure Magazine*, ASCE, July 2007, pp. 19–21, October 2007, pp. 20–21, January 2008, pp. 43–46.
- Ellingwood, B. and A. Tullin, 'Structural Serviceability: Floor Vibration', *Journal of Structural Engineering*, ASCE, Vol. 110, No. ST2, February 1984, pp. 401–418, Disc, Vol. 111, No. ST5, May 1985, pp. 1158–1161.
- Elwood, K.J. and M.O. Eberhard 2009, 'Effective Stiffness of Reinforced Concrete Columns', *ACI Structural Journal*, Vol. 106, No. 4, pp. 476–84.
- FEMA 445 2006, *Next-Generation Performance-based Seismic Design Guidelines Program Plan for New and Existing Buildings*, Applied Technology Council, California, and Federal Emergency Management Agency, Washington, DC, p. 154.
- Feld, J. and K. Carper 1997, *Construction Failures*, 2nd edition, Wiley-Interscience, New York, p. 528.
- Freudenthal, A.M. 1956, 'Safety and the Probability of Structural Failure', *ASCE Transactions*, Vol. 121, pp. 1337–97.
- Galambos, T.V. 1981, 'Load and Resistance Factor Design', *Engineering Journal*, AISC, Vol. 18, No. 3, pp. 74–82.
- Hognestad, E., N.W. Hanson, and D. McHenry 1955, 'Concrete Stress Distribution in Ultimate Strength Design', *ACI Journal*, Vol. 52, pp. 455–79.
- IS 7861, *Code of Practice for Extreme Weather Concreting, Part 1: Recommended Practice for Hot Weather Concreting (1975), Part 2: Recommended Practice for Cold Weather Concreting (1981)*, Bureau of Indian Standards, New Delhi.
- Jain, S.K. 1995, 'A Proposed Draft for IS:1893 Provisions on Seismic Design of Buildings, Part II: Commentary and Examples', *Journal of Structural Engineering*, SERC, Vol. 22, No. 2, pp. 73–90.
- Jain, S.K. and C.V.R. Murty 2005, *Proposed Draft Provisions and Commentary on Indian Seismic Code, IS 1893 (Part 1)*, p. 158, (also see <http://www.iitk.ac.in/nicee/IITK-GSDMA/EQ05.pdf>, last accessed on 6 October 2012).
- Jayasree, C., M. Santhanam, and R. Gettu 2011, 'Cement–Superplasticiser Compatibility – Issues and Challenges', *The Indian Concrete Journal*, Vol. 85, No. 7, pp. 48–58.
- Kaushik, S.K. 2003, 'Aesthetics and Structural Design', *Proceedings, International Symposium on Innovative World of Concrete*, Indian Concrete Institute, Pune, 19– 21 September 2003, pp. 75–84.
- Khuntia, M. and S.K. Ghosh 2004, 'Flexural Stiffness of Reinforced Concrete Columns and Beams: Analytical Approach', *ACI Structural Journal*, Vol. 101, No. 3, pp. 351–63.
- Klemencic, R. 2008, 'Performance-based Seismic Design–Rising', *STRUCTURE Magazine*, ASCE, pp. 10–13.
- Kulkarni, V.R. 2009, 'Exposure Classes for Designing Durable Concrete', *The Indian Concrete Journal*, Vol. 83, No. 3, pp. 23–43.
- Kumar R. and Y. Singh 2010, 'Stiffness of Reinforced Concrete Frame Members for Seismic Analysis', *ACI Structural Journal*, Vol. 107, No. 5, pp. 607–15.
- Lancaster, F.D. 2007, 'Subduing Vibration in Laboratory Buildings', *STRUCTURE Magazine*, ASCE, Nov. 2007, pp. 66–9.
- Lee, J.-Y. and H.-B. Hwang 2010, 'Maximum Shear Reinforcement of Reinforced Concrete Beams', *ACI Structural Journal*, Vol. 107, No. 5, pp. 580–8.
- Madsen, H.O., S. Krenk, and N.C. Lind 1986, *Methods of Structural Safety*, Prentice Hall, Inc., Englewood Cliffs, p. 416.
- Malhotra, V.M. 2002, 'High-performance High-volume Fly Ash Concrete: An Environmentally Friendly Solution to the Infrastructure Needs of Developing Countries', *Concrete International*, ACI, Vol. 24, No. 7, pp. 30–4.
- Marti, P. 1985, 'Truss Models in Detailing', *Concrete International*, ACI, Vol. 7, No. 12, pp. 66–73.
- Mehanny, S.S.F., H. Kuramoto, and G.G. Deierlein 2001, 'Stiffness Modeling of Reinforced Concrete Beam-columns for Frame Analysis', *ACI Structural Journal*, Vol. 107, No. 2, pp. 215–25.
- Mehta, P.K. 1997, 'Durability: Critical Issues for the Future', *Concrete International*, ACI, Vol. 19, No. 7, pp. 27–33.
- Mehta, P.K. 2009, 'Global Concrete Industry Sustainability: Tools for Moving Forward to Cut Carbon Emissions', *Concrete International*, ACI, Vol. 31, No. 2, pp. 45–8.
- Mehta, P.K. and R.W. Burrows 2001, 'Building Durable Structures in the 21st Century', *Concrete International*, ACI, Vol. 23, No. 3, pp. 57–63.
- Murray, T.M., 1991, 'Building Floor Vibrations', *Engineering Journal*, 3rd Qtr., AISC, pp. 102–109.
- Murty, C.V.R. 2005, *Earthquake Tips. Learning Earthquake Design and Construction*, Indian Institute of Technology, Kanpur, and Building Material and Technology Promotion Council, New Delhi, p. 48.
- Nowak, A.S. and M.M. Szerszen 2003, 'Calibration of Design Code for Building (ACI 318), Part 1: Statistical Models for Resistance, Part 2: Reliability Analysis and Resistance Factor', *ACI Structural Journal*, Vol. 100, No. 3, pp. 377–91.

- Paulay T. and M.J.N. Priestley 1992, *Seismic Design of Reinforced concrete and Masonry Buildings*, John Wiley and Sons, Inc., New York, p. 744.
- PEER/ATC 72-1 2010: *Modeling and Acceptance Criteria for Seismic Design and Analysis of Tall Buildings*, Applied Technology Council, Pacific Earthquake Engineering Research Center, p. 242, (also see http://peer.berkeley.edu/tbi/wp-content/uploads/2010/09/PEER-ATC-72-1_report.pdf, last accessed on 10 October 2002).
- Pillai, S.U. and D. Menon 2003, *Reinforced Concrete Design*, 2nd edition, Tata McGraw-Hill Publishing Company Ltd, New Delhi, p. 875.
- Prakash Rao, D.S. 1995, *Design Principles and Detailing of Concrete Structures*, Tata McGraw-Hill Publishing Company Ltd, New Delhi, pp. 207–8, 299–309.
- Rajamane, N.P., M.C. Nataraja, and T.P. Ganesan 2012, 'A Technical Look at "Individual Test Result" Criterion for Concrete Acceptance as per IS 456:2000', *The Indian Concrete Journal*, Vol. 86, No. 4, pp. 26–37.
- Ramakrishnan, V. and P.D. Arthur 1969, *Ultimate Strength Design for Structural Concrete*, Sir Isaac Pitman and Sons Ltd, London, p. 264.
- Ramalingam, S. and M. Santhanam 2012, 'Environmental Exposure Classifications for Concrete Construction – A Relook', *The Indian Concrete Journal*, Vol. 86, No. 5, pp. 18–28.
- Rangan, B.V. 2008, 'Low-calcium Fly Ash-based Geopolymer Concrete', in E. G. Nawy (ed.), *Concrete Construction Engineering Handbook*, 2nd edition, CRC Press, Boca Raton, Chap. 26.
- Ranganathan, R. 1990, *Reliability Analysis and Design of Structures*, Tata McGraw-Hill Publishing Company Ltd, New Delhi, p. 354.
- Reddi, S.A. 1992, 'Permeable Formwork for Impermeable Concrete', *Indian Concrete Journal*, Vol. 66, No. 1, pp. 31–5.
- Reynolds, C.E. and J.C. Steedman 1988, *Reinforced Concrete Designer's Handbook*, 10th edition, E & FN Spon, London, p. 436.
- Roller, J.J. and H.G. Russell 1990, 'Shear Strength of High-strength Concrete Beams with Web Reinforcement', *ACI Structural Journal*, Vol. 87, No. 2, pp. 191–8.
- Rüsch, H. 1960, 'Researches Towards a General Flexural Theory for Structural Concrete', *ACI Journal*, Vol. 57, pp. 1–28.
- Schlaich, J. 1995, 'The Gap between Quality and Technology', *Concrete International*, ACI, Vol. 17, No. 8, pp. 58–64.
- Schlaich, J., K. Schafer, and M. Jennewein 1987, 'Towards a Consistent Design of Structural Concrete', *PCI Journal*, Vol. 32, No. 3, pp. 74–150.
- Schwinger, C.W. 2011, 'Tips for Designing Constructible Concrete Structures, Part 1', *STRUCTURE Magazine*, ASCE, pp. 42–3.
- Scott, R.H. and R.T. Whittle 2005, 'Moment Redistribution Effects in Beams', *Magazine of Concrete Research*, Vol. 57, No. 1, pp. 9–20.
- SP 24:1983, *Explanatory Handbook on Indian Standard Code of Practice for Plain and Reinforced Concrete (IS 456:1978)*, Indian Standards Institution, New Delhi, p. 164.
- Steiger, R.W., 'Aesthetics, Part 1: Beauty Is in the Mind of the Beholder, Part 2: Design Excellence – How Can We Achieve It?', *Concrete International*, ACI, Vol. 18, No. 12, December 1996, pp. 65–70, Vol. 19, No. 1, January 1997, pp. 65–70.
- Subramanian, N. 1974, 'Safety in Engineering Structures', *Fourth National Conference on Industrial Safety*, College of Engineering, Guindy, Chennai, November 1974.
- Subramanian, N. 1979, 'Deterioration of Concrete Structures: Causes and Remedial Measures', *The Indian Highways*, Vol. 7 No. 3, pp. 5–10.
- Subramanian, N. 1982, 'Failure of the Congress Hall, Berlin', *The Indian Concrete Journal*, Vol. 56, No. 11, pp. 290–1.
- Subramanian, N. 1987, 'Aesthetics of Non-Habitat Structures', *The Bridge and Structural Engineer, Journal of ING/IABSE*, Vol. 17, No. 4, pp. 75–100.
- Subramanian, N. 1995a, 'Economy in Building Construction', *Bulletin of the Indian Concrete Institute*, No. 50, pp. 15–21.
- Subramanian, N. 1995b, 'Computer Analysis and Design of Tall Structures', *Civil Engineering and Construction Review*, Vol. 8, No. 4, pp. 42–6.
- Subramanian N. 2002, 'Curing – The Last and the Least Considered Aspect in Concrete Making', *Journal of the Indian Concrete Institute*, Vol. 3, No. 1, pp. 13–20.
- Subramanian, N. 2007, 'Sustainability – Challenges and Solutions', *The Indian Concrete Journal*, Vol. 81, No. 12, pp. 39–50.
- Subramanian, N. 2008, 'Pervious Concrete – A Green Material that Helps Reduce Water Run-off and Pollution', *The Indian Concrete Journal*, Vol. 82, No. 12, pp. 16–34.
- Subramanian, N. 2010a, 'Limiting Reinforcement Ratios For RC Flexural Members', *The Indian Concrete Journal*, Vol. 84, No. 9, pp. 71–80.
- Subramanian, N. 2010b, *Steel Structures: Design and Practice*, Oxford University Press, New Delhi, pp.133–4.
- Subramanian, N. 2010c, 'Sustainability of RCC Structures Using Basalt Composite Rebars', *The Master Builder*, Vol. 12, No. 9, pp. 156–64.
- Subramanian, N. 2012, 'The Principles of Sustainable Building Design', in G.M. Sabnis (ed.), *Green Building with Concrete: Sustainable Design and Construction*, CRC Press, Boca Raton, pp. 37–87.
- Subramanian, N. and K. Geetha 1997, 'Concrete Cover for Durable RC Structures', *The Indian Concrete Journal*, Vol. 71, No. 4, pp. 197–201.
- Swamy, R.N. 2003, 'Holistic Design: Key to Sustainability in Concrete Construction', *The Indian Concrete Journal*, Vol. 77, No. 9, pp. 1291–9.
- Vangeem, M.G. and M.L. Marceau 2002, 'Using Concrete to Maximize LEED™ Points', *Concrete International*, ACI, Vol. 24, No. 11, pp. 69–73.
- Varghese, P.C. 2006, *Limit States Design of Reinforced Concrete*, 2nd edition, Prentice Hall of India Ltd, New Delhi, p. 545.
- Varyani, U.H. 2001, 'Discussion on Cement Content, Exposure Conditions, and Grades of Concrete', by Reddi, S.A., *The Indian Concrete Journal*, Vol. 75, No. 7, pp. 433–4.
- Venugopal, M.S. and N. Subramanian 1977, 'Hot Weather Concreting', *Indian Concrete Journal*, Vol. 51, No. 11, pp. 348–9.
- Webb, J. 1993, 'High-strength Concrete: Economics, Design and Ductility', *Concrete International*, ACI, Vol. 15, No. 1, pp. 27–32.
- Wight, J.K. and J.G. MacGregor 2009, *Reinforced Concrete: Mechanics and Design*, 5th edition, Pearson Prentice Hall, New Jersey, p. 1112.
- Young, W.C. and R.G. Budynas 2001, *Roark's Formulas for Stress and Strain*, 7th edition, McGraw-Hill Professional, New York, p. 832.

FLEXURAL ANALYSIS AND DESIGN OF BEAMS

5.1 INTRODUCTION

A reinforced concrete (RC) structure has several members in the form of beams, columns, slabs, and walls that are rigidly connected to form a monolithic frame. Each individual member must be capable of resisting the forces acting on it. *Beams* are members that are primarily subjected to *flexure* or bending and often support slabs. The term *girder* is also used to represent beams, but is usually a large beam that may support several beams. It may be noted that slabs are also predominantly subjected to flexure. Columns and walls may also be subjected to flexure when they experience eccentric loading or lateral pressures. Beams support the loads applied on them by slabs and their own weight by internal moments and shears. The behaviour of RC beams under flexure alone is covered in this chapter. The effects of shear, torsion, and axial force are covered in subsequent chapters.

In an RC beam of rectangular cross section, if the reinforcement is provided only in the tension zone, it is called a *singly reinforced rectangular beam*, whereas if the reinforcements are provided in both the compression and tension zones, it is called a *doubly reinforced rectangular beam*. In many practical situations, the beams will be supporting slabs and a portion of the slab will be acting along with the beam in resisting the applied bending moments. These beams can be designed by taking into account the contribution of the slab in resisting the compression at mid-span. These beams are called *T-beams* or *L-beams* (also called *spandrel beams*) depending on whether the beam is at the centre of the building or at the edge, respectively. At the supports, due to negative moment, the flanges of T- or L-beams will be in tension, and hence they have to be designed only as rectangular beams. T- or L-beams can also be singly or doubly reinforced.

In all these types of beams, two types of problems are encountered—analysis and design. Analysis is a situation existing in an already-constructed building, where the geometry of the beam and the reinforcement details are known, and the engineers are required to calculate the capacity to check

whether the existing beam is capable of resisting the external loads. Design situations occur in new buildings where one has to arrive at the depth, breadth, and reinforcement details for the beam to safely and economically resist the externally applied loads. It is important to know the behaviour of each type of beam before designing them in order to correctly place the reinforcement. When subjected to increasing external moment, the beam cracks after a certain load and then the reinforcement comes into play. The cracks keep increasing in size, eventually leading to the failure of the beam, and the corresponding moment is termed the *ultimate moment*. This moment is resisted by the internal resisting moment created by the couple of compressive force in concrete and the tensile force in steel.

Beams are classified as under-reinforced, over-reinforced, and balanced, depending on their behaviour. *Over-reinforced beams* are to be avoided as they result in brittle failure of concrete under compression, which are sudden and do not give any warning before failure. *Balanced sections* are those in which both the concrete and steel fail at the same time. In *under-reinforced beams*, failure is initiated by the yielding of steel, even though the final failure may be due to concrete compression. This type of failure is ductile (due to inelastic deformation in steel reinforcement) and hence gives enough warning before failure. In the codes of practices, under-reinforced beam or ductile behaviour is ascertained by controlling the value of tension strain at the level of steel reinforcement, when the extreme concrete fibre in compression reaches the maximum compression strain. Several assumptions are made in the general theory for the design of beams, of which the most important one is that there is a linear strain variation across the depth of the member. In IS 456, the maximum strain in concrete is taken as 0.0035 and that in steel as $f_y/1.15E_s + 0.002$ (the extra strain of 0.002 is to ensure ductile behaviour). The IS code also considers a *parabolic-rectangular stress block* for concrete. Based on the equilibrium and compatibility of strains, the neutral axis depth and the moment of resistance of any beam's cross section can be obtained.

In beams with span less than 2.5 times the depth, the linear stress–strain behaviour is not valid. Such beams are called *deep beams*. Based on the experimental data, some guidelines have been suggested in IS 456; more accurate assessment of the behaviour of the beams can be made by using the strut-and-tie models. In order to reduce the floor heights, wide shallow beams (WSBs) are sometimes employed, and for shorter spans, beams may also be concealed inside the slab thickness. High-strength concrete (HSC) and high-strength steel (HSS) are also employed in tall buildings or bridges to reduce the size or to reduce reinforcement congestion.

5.2 BEHAVIOUR OF REINFORCED CONCRETE BEAMS IN BENDING

Let us first consider the behaviour of a singly reinforced rectangular beam under increasing moment. As mentioned, the beam behaves as a plain concrete beam until it cracks. Once the cracks are developed, the reinforcements resist the tensile forces. Near the ultimate load, in under-reinforced sections, the steel reinforcements start to yield in a ductile manner, and when the steel yields, or the concrete crushes in compression, the beam fails. This behaviour is explained in detail in the following sub-sections.

5.2.1 Uncracked Section

Bending causes tensile and compressive stresses in the cross section of the beam, and the nature of these stresses depends

upon the position of the fibre in the beam and also the type of support conditions. For example, assuming gravity loading, the top fibres near the mid-span of a simply supported beam will be under compression and the bottom fibres will be in tension. In contrast, in a cantilever beam, the top fibres will be in tension and the bottom fibres will be under compression. Figures 5.1(a) and (c) show a rectangular, simply supported, and singly reinforced RC beam subjected to uniformly distributed gravity loads. Figure 5.1(d) shows the variation of elastic stresses across the depth of the beam. It should be noted that the tensile stresses are indicated by the positive sign and the compressive stresses by the negative sign.

As long as the moment is small and does not induce cracking, the strains across the cross section are small and the neutral axis is at the centroid of the cross section (see Fig. 5.2a). The *neutral axis* is an imaginary line that separates the tension zone from the compression zone. By this definition, the stress at the neutral axis is equal to zero as shown in Fig. 5.2.

The stresses are related to the strains and the deflection is proportional to the load, as in the case of isotropic, homogeneous, linearly elastic beams. The following applied mechanics formulae for pure flexure (called the *Euler–Bernoulli* equations) hold good:

$$\frac{M}{I} = \frac{f}{y} = \frac{E_c}{R} \tag{5.1a}$$

i.e.,
$$M = \frac{fI}{y} = fZ \quad \text{and} \quad f = \frac{M}{Z} \tag{5.1b}$$

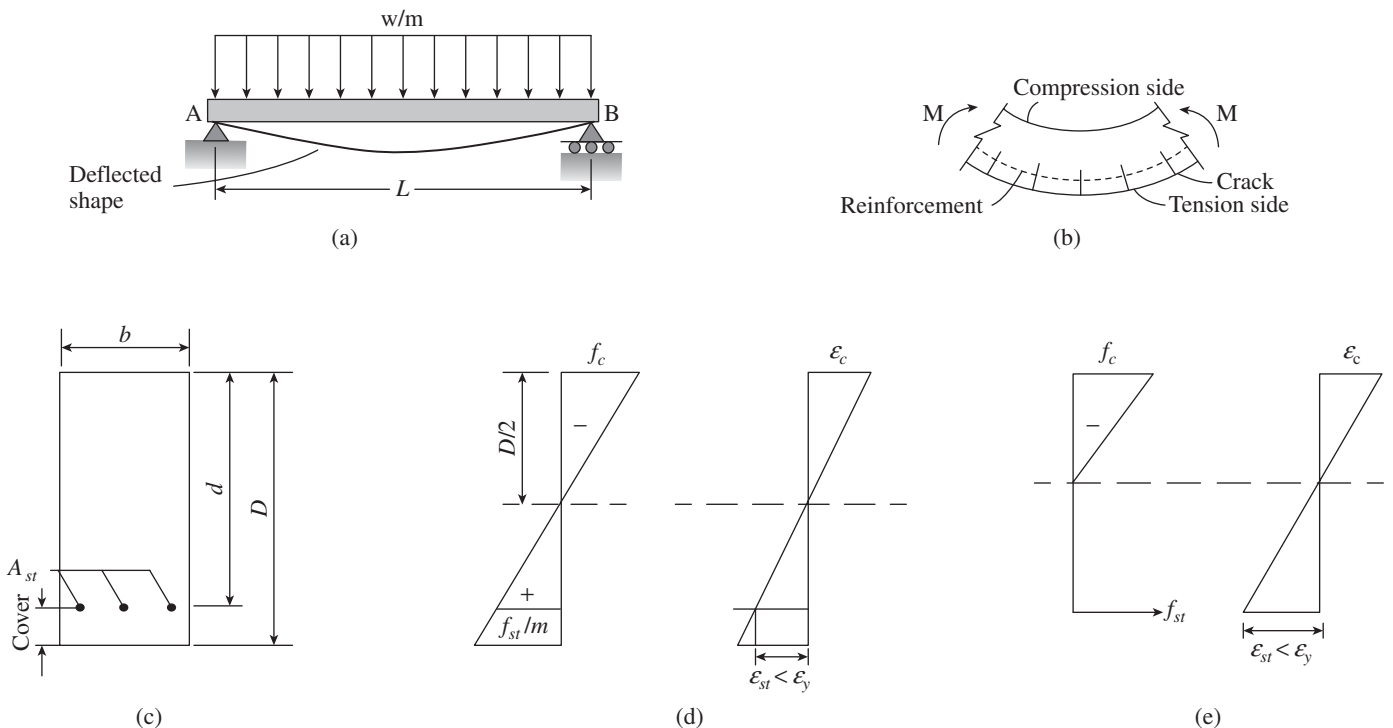


FIG. 5.1 Mechanics of RC beam under flexure (a) Simply supported beam (b) Segment of beam at mid-span (c) Cross section of beam (d) Elastic stress–strain distribution (e) Stress–Strain distribution after cracking (*Continued*)

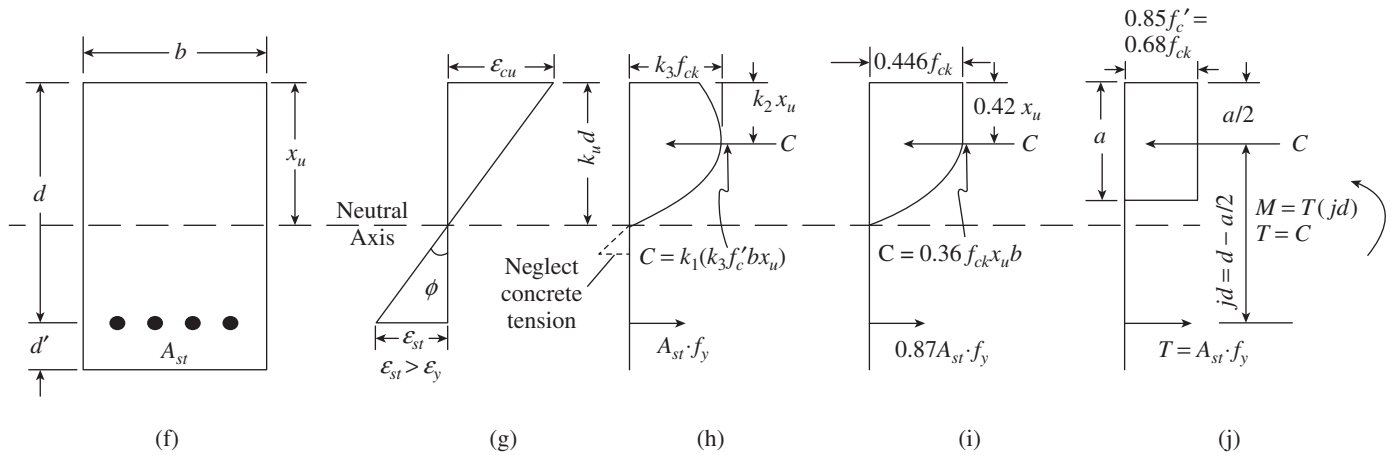


FIG. 5.1 (Continued) (f) Cross section of beam (g) Strain distribution at failure (h) Actual stress distribution at failure (i) Assumed stresses as per IS 456 (j) Equivalent rectangular stress distribution as per ACI 318 $\epsilon_{cu} = 0.0035$ (IS 456), $\epsilon_{cu} = 0.003$ (ACI 318)

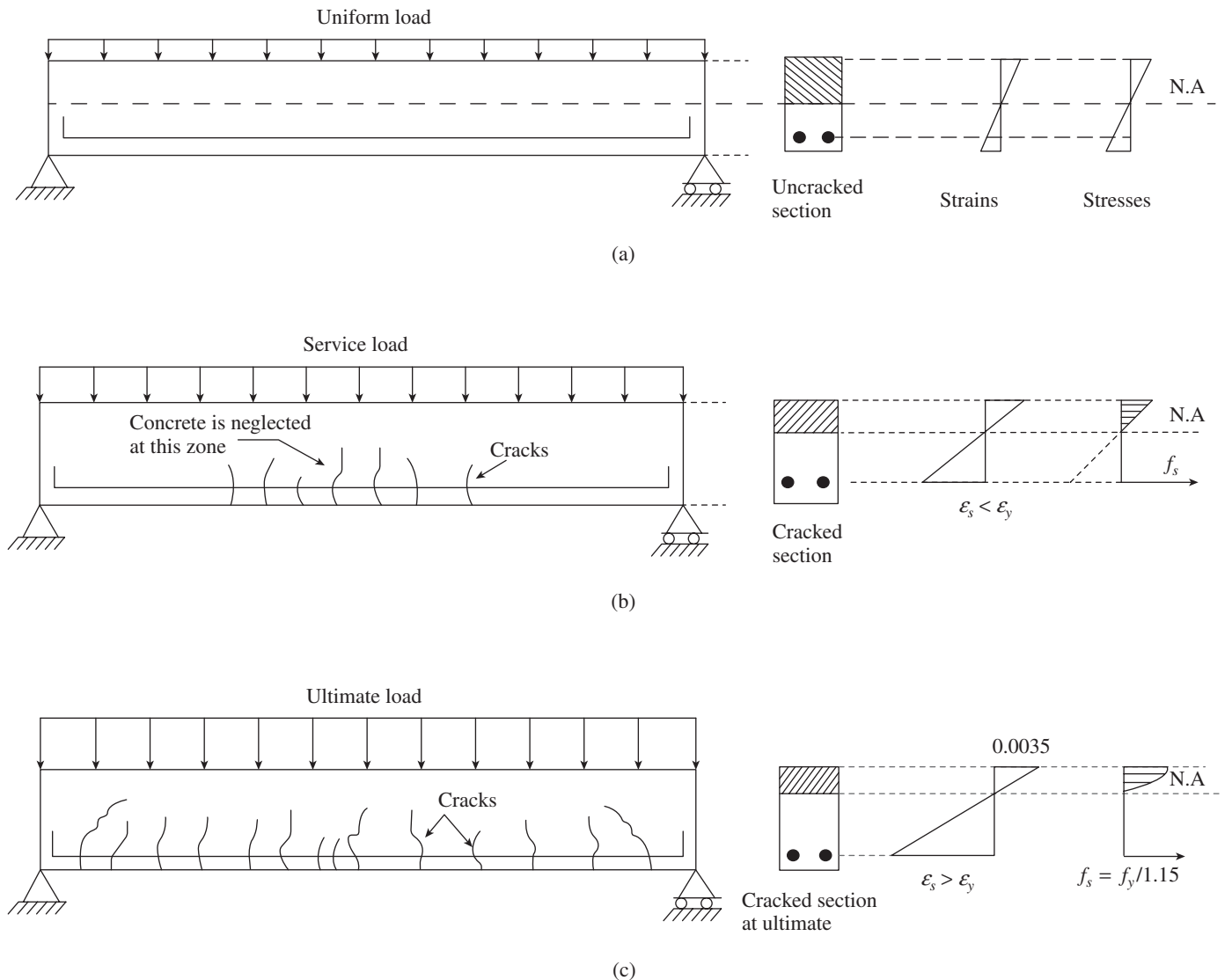


FIG. 5.2 Behaviour of an RC beam under different stages of loading (a) Before cracking (b) After cracking but before yielding of steel (working load) (c) Ultimate and final stage

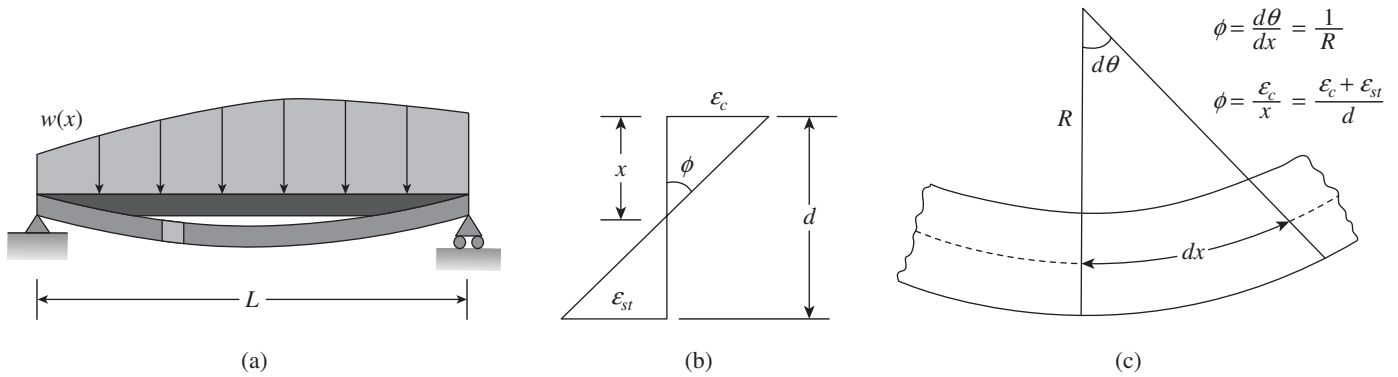


FIG. 5.3 Rotation of a section in bending (a) Simply supported beam (b) Strain distribution across the section (c) Element of a bent beam

or

$$\frac{M}{E_c I} = \frac{1}{R} \approx \frac{d^2 y}{dx^2} \quad (5.1c)$$

$$\phi = \frac{d\theta}{dx} = \frac{1}{R} = \frac{\epsilon_{cu}}{x_u} = \frac{\epsilon_{st}}{d - x_u} \quad (\text{see Figs 5.1g and 5.3}) \quad (5.2)$$

$$V = \frac{dM}{dx} \quad (5.3)$$

where d is the effective depth of the beam (as per Clause 23.0 of IS 456 the *effective depth* of a beam is defined as the distance between the centroid of the area of tension reinforcement and the maximum compression fibre), E_c is the Young's modulus of elasticity of concrete, f is the bending stress at a layer, I is the second moment of area (moment of inertia) of the beam, M is the applied bending moment, R is the radius of curvature, V is the shear force, x_u is the depth of neutral axis, y is the distance of the layer from the neutral axis, Z is the section modulus, ϵ_{cu} is the ultimate compressive strain in concrete, ϵ_{st} is the strain at the centroid of tension steel, ϵ_y is the yield strain in steel, and ϕ is the curvature of the beam (equals the slope of the strain diagram). These formulae cannot be used in cracked beams, as the stress–strain relationship for concrete becomes non-linear at higher strain levels.

5.2.2 Cracking Moment

As the load is increased, the extreme tension fibre of the beam cracks as the stress reaches the value of modulus of rupture, f_{cr} (see Fig. 5.2b). Most of these cracks are so small that they are not visible to the naked eye. At this stage, the maximum strains in concrete in tension and compression are still low; hence, assuming a linear stress–strain relation, the moment that produces the first crack or the *cracking moment*, M_{cr} , is given by

$$M_{cr} = \frac{f_{cr} I_g}{y_t} = f_{cr} Z \quad (5.4)$$

where y_t is the distance of extreme tension fibre from the neutral axis, I_g is the second moment of gross area ignoring reinforcement, and f_{cr} is the modulus of rupture, which is taken as

$0.7 \sqrt{f_{ck}}$, as per Clause 6.2.2 of the code. (It should be noted that the ACI 318 code suggests a lower, conservative value for modulus of rupture, which equals $\lambda 0.55 \sqrt{f_{ck}}$, where λ is the modification factor for lightweight concrete. For normal weight concrete λ equals 1.0; for lightweight concrete λ equals $f_{ct}/(0.5 \sqrt{f_{ck}}) \leq 1.0$, where f_{ct} is the splitting tensile strength of lightweight concrete.) Even though the reinforcements can be included in the calculation of I_g using the transformed section method, this will not make any appreciable change in the value of M_{cr} .

The section curvature at cracking, ϕ_{cr} , can also be calculated using the elastic bending theory as

$$\phi_{cr} = \frac{M_{cr}}{E_c I_g} \quad (5.5a)$$

where the Young's modulus of elasticity of concrete, E_c , may be taken as $5000 \sqrt{f_{ck}}$ N/mm².

5.2.3 Cracked Section

As the load is increased further, extensive cracking occurs as shown in Figs 5.1(b) and 5.2(b). The cracks also widen and propagate gradually towards the neutral axis. The cracked portion of the concrete beam is ineffective in resisting the tensile stresses. The steel reinforcements come into play now, and there is a sudden transfer of tension force from the concrete to the reinforcements in the tension zone. This results in increased strains in the reinforcements. If the minimum amount of tensile reinforcement is not provided, the beam will suddenly fail.

The relatively large increase in the tensile strains of reinforcements results in an upward shifting of the neutral axis (see Figs 5.1e and 5.2b). The deflections and rotations also increase at a faster rate, resulting in increased curvature at the cracked section. If the concrete stresses do not exceed approximately $0.33 f_{ck}$, the stresses and strains continue to be approximately proportional and close to linear. The relationship between the moment and curvature is again approximately linear, but the slope is different from that of the uncracked section. This is called the *working load stage*, which was the basis of the *working stress method*.

5.2.4 Yielding of Tension Reinforcement and Collapse

If the loads are increased further, the tensile stress in the reinforcement and the compression stress in the concrete increase further. The stresses over the compression zone will become non-linear. However, the strain distribution over the cross section is linear. This is called the *ultimate stage* (see Fig. 5.2c). The distribution of stress in the compression zone will have the same shape of the concrete stress–strain curve.

At one point, either the steel or concrete will reach its respective capacity; steel will start to yield or the concrete will crush. Let us assume that the section under consideration is *under-reinforced*. In this case, the steel will yield first before the concrete fails, giving sufficient warning before failure. For normally reinforced beams, the yield load is approximately 90–95 per cent of the ultimate load. There will be a considerable shift in the neutral axis position; non-linear deflections will increase leading to extensive cracking, and finally the beam will collapse due to the crushing of concrete in the compression zone. It has to be noted that in the over-reinforced beams the steel will not yield, and hence, the concrete in the compression zone will crush and the beam will collapse (rather explosively) suddenly without giving any warning. Such failures are sudden and catastrophic; this is not the preferred mode of failure.

Hence, most codes do not permit the use of over-reinforced beams. Let us now develop a mathematical model for these phases of behaviour.

The yield curvature is calculated as the slope of the strain diagram by setting the strain in the steel equal to the yield strain.

$$\phi_y = \frac{\epsilon_y}{d - x_u} \quad (5.5b)$$

5.3 ANALYSIS OF AND DESIGN FOR FLEXURE

The analysis of flexure should not be confused with the *structural analysis*, which is concerned with the determination of forces and moments acting in the different elements (such as beams and columns) of a structure due to the application of external loads. The analysis of flexure deals with the calculation of the nominal or theoretical moment strength of the beam (or stresses, deflections, crack width, etc.) for a given cross section and reinforcement details. It is determined from the equilibrium of internal compressive and tensile forces, based on the assumed compressive stress block of concrete. The moment strength of the beam is determined from the couple of internal compressive and tensile forces.

On the other hand, the design for flexure deals with the determination of the cross-sectional dimensions and the reinforcement for a given ultimate moment acting on the beam. Many times, the breadth of the beam may be fixed based on architectural considerations. Sometimes, both the breadth and depth may be fixed for standardization of sizes and only the reinforcement needs to be determined. It should be noted that

there may be several possible solutions to a design problem, whereas the solution to an analysis problem is unique.

5.3.1 Effective Span

As the bending moment varies with the square of effective span, it is important to correctly fix the effective span. Clause 22.2 of IS 456 suggests the following:

1. For beams that are not built integrally with their supports, for example, beams supported on brick walls:
Effective span, $L = (L_n + d)$ or c/c of supports, whichever is less (where L_n is the clear span, d is the effective depth of slab, and c/c denotes the centre-to-centre distance)
2. For continuous beams:
 - (a) If width of support, $b_w \leq L_n/12$,
Effective span, $L = (L_n + d)$ or c/c of supports, whichever is less
 - (b) If width of support, $b_w > L_n/12$ or 600 mm, whichever is less, the following cases can arise:
 - (i) For end span with one end fixed and the other continuous or for intermediate spans,
Effective span, $L = L_n$
 - (ii) For end span with one end free and the other continuous,
Effective span, $L = L_n + d/2$ or $L_n + \text{Half width of discontinuous support}$, whichever is less
 - (iii) Spans with roller or rocker bearings,
Effective span, $L = \text{Distance between the centres of bearings}$
3. For cantilevers:
 - (a) Normally,
Effective span, $L = L_n + d/2$
 - (b) If it forms the end of a continuous beam,
Effective span, $L = L_n + b_w/2$

5.4 ANALYSIS OF SINGLY REINFORCED RECTANGULAR SECTIONS

Some assumptions need to be made in order to analyse the beams subjected to flexure. These assumptions and the derivation of the theoretical moment capacity of beams are discussed in this section.

5.4.1 Assumptions Made to Calculate Ultimate Moment of Resistance

The mathematical models for shallow beams (span to depth ratio greater than 2.5) are based on the following assumptions (see Clause 38 of IS 456):

1. Plane sections normal to the axis remain plane after bending, that is, strains are proportional to the distance from the neutral axis. This assumption holds good until collapse for all slender members.

- The maximum strain in concrete, ϵ_{cu} , at the outermost compression fibre is assumed to be 0.0035 in bending. (It should be noted that the value of ϵ_{cu} will reduce as the concrete strength increases, especially for HSC. CEB-FIP model code 1990 suggests $\epsilon_{cu} = 0.0035$ for $f_{ck} \leq 50$ MPa and $\epsilon_{cu} = 0.0035 \left(\frac{50}{f_{ck}} \right)$ for $50 \text{ MPa} < f_{ck} \leq 80 \text{ MPa}$.)
- Compressive stress distribution is assumed to correspond with the assumed stress-strain diagram of concrete, as shown in Fig. 5.4(a). The stress block in IS 456 is assumed as parabolic-rectangular, as shown in Fig. 5.4(b). It has to be noted that the geometrical shape of the stress distribution depends on a number of factors, such as cube/cylinder strength and the rate and duration of loading. Several studies have indicated that the ratio of maximum compressive strength in beams or columns to the cylinder compressive strength, f'_c can be taken as being equal to 0.85 for most practical purposes (Hognestad 1952a). This accounts for the *size effect* and the fact that the actual beam

is subjected to sustained loading, whereas the test cylinder is subjected to short-term loading alone. Furthermore, the cylinder strength, f'_c is about 0.80 of the cube strength, f_{ck} . Hence, the maximum compressive strength of concrete in any structure is assumed to be $0.85 \times 0.8 = 0.67$ times the characteristic cube compressive strength. With an additional partial material safety factor γ_m of 1.5, the maximum compressive strength will be equal to $0.67/1.5 = 0.447f_{ck}$, which is normally rounded off to $0.45f_{ck}$. It should be noted that the partial safety factor is applied over the whole stress-strain curve to obtain the design stress-strain curve, as shown in Fig. 5.4(a). The stress-strain curve shown in Fig 5.4(a) is parabolic from the starting point of zero strain up to a strain of 0.002, and then a straight line from this point up to the crushing strain of 0.0035. The same shape is adopted for the stress block too in the Indian code. If the distance up to 0.0035 strain is denoted as x , then the distance of 0.002 strain is obtained as $(0.002/0.0035) x = (4/7)x = 0.57x$.

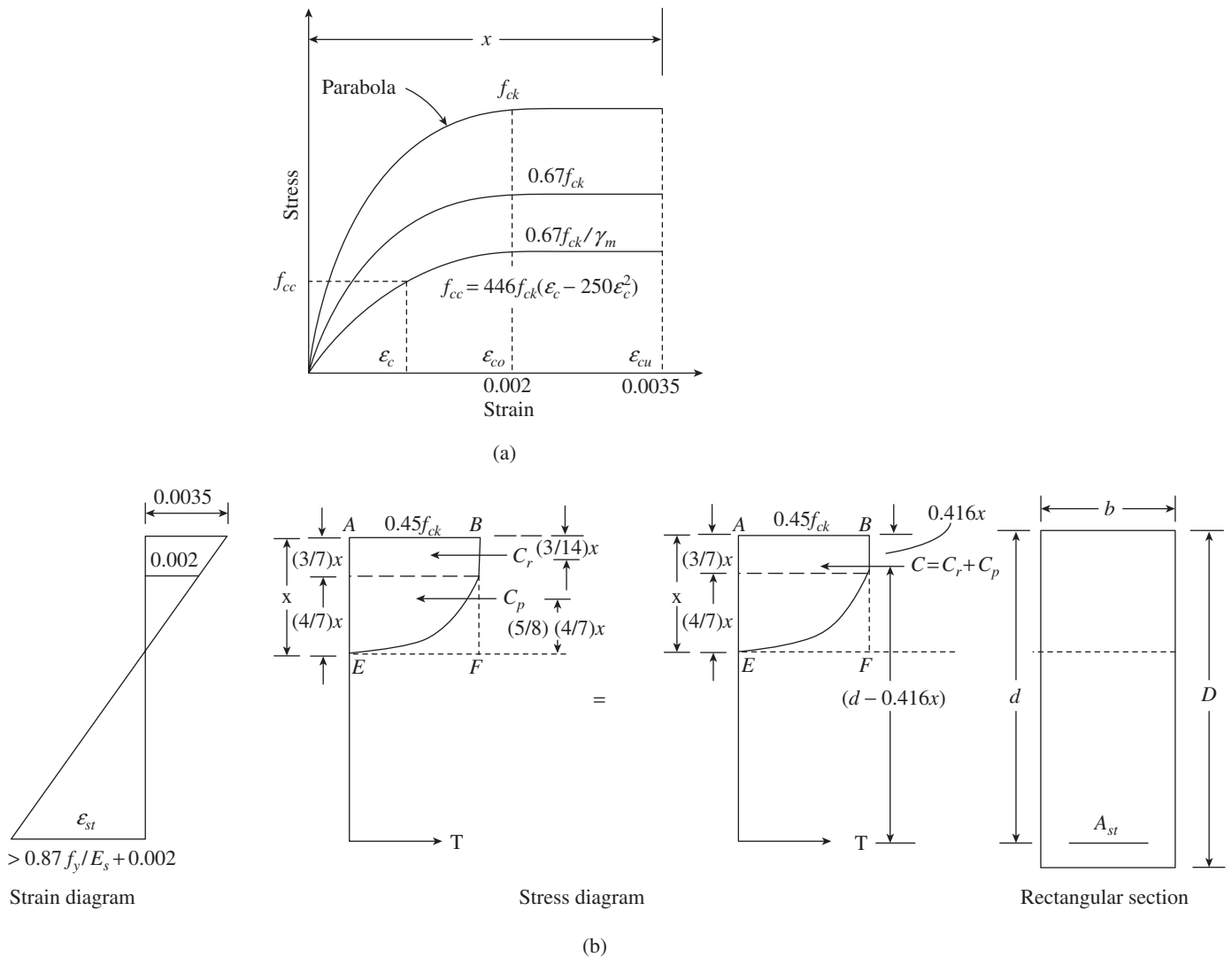


FIG. 5.4 Stress-Strain curve for concrete (a) Idealized (b) Stress block adopted in IS 456:2000

The design compressive stress f_c corresponding to any strain $\epsilon_c \leq 0.0035$, as shown in Fig. 5.4(a), may be approximated by a parabola. The equation for this parabola was first introduced by Hognestad (1952b) as

$$f_c = 0.447 f_{ck} \left[2 \left(\frac{\epsilon_c}{\epsilon_{co}} \right) - \left(\frac{\epsilon_c}{\epsilon_{co}} \right)^2 \right]$$

for $\epsilon_c < 0.002$, with $\epsilon_{co} = 0.002$ (5.6a)

$$f_c = 0.447 f_{ck} \text{ for } 0.002 \leq \epsilon_c \leq 0.0035 \text{ (5.6b)}$$

4. The tensile strength of concrete may be neglected. It should be noted that the ultimate tensile strain of concrete is of the order of 0.00015, which is less than one-twentieth of the compressive strain. However, the tensile strength of concrete is taken into account to check the deflection and crack widths in the limit state of serviceability. All the tensile forces are assumed to be carried by the reinforcement.
5. The stresses in the reinforcement are derived from the representative stress–strain curve for the type of steel used. Typical curves for mild steel bars (grade Fe 250) and high-yield strength-deformed (HYSD) bars (generally cold-twisted) of grade Fe 415 are shown in Figs 5.5(a) and (b), respectively. For design purposes, a partial material safety factor γ_m of 1.15 is suggested by the code. Thus, the maximum stress in steel is limited to $f_y/1.15 = 0.87f_y$, where f_y is the characteristic strength of steel, which equals yield

stress in mild steel and is taken as proof stress for HYSD bars at a 0.2 per cent residual strain. For mild steel bars and for HYSD bars up to $\epsilon_s < 0.8f_y/(1.15E_s)$, the stress–strain relationship is linear. Hence,

$$\text{Stress in steel, } f_s = \epsilon_s E_s \text{ for } \epsilon_s < 0.8f_y/(1.15E_s) \text{ (5.7)}$$

The dotted inclined line in Fig. 5.5(b) is parallel to the elastic curve with a residual strain of 0.2 per cent. It should be noted that in the case of steel the partial material safety factor of $\gamma_m = 1.15$ is used only in the region starting from $0.8f_y$ of the actual stress–strain curve (see Figs 5.5a and b). The design stress–strain curve given in Fig. 5.5(b) is linear up to a strain of $0.8f_y/(1.15E_s)$ (i.e., $\epsilon_s = 0.0014435$ for grade Fe 415 and $\epsilon_s = 0.0017391$ for grade Fe 500) and thereafter non-linear up to the design stress of $f_y/1.15$, corresponding to a strain equal to or greater than $f_y/(1.15E_s) + 0.002$. Table 5.1 gives the inelastic strains for HYSD bars for a few design stress values and Table 5.2 gives the values of design stress at some selected strain values for Fe 415 and Fe 500 grade steels.

TABLE 5.1 Inelastic strain in HYSD bars for some design stress values

Design Stress	$0.8f_{yd}$	$0.85f_{yd}$	$0.9f_{yd}$	$0.95f_{yd}$	$0.975f_{yd}$	$1.0f_{yd}$
Inelastic Strain	0.000	0.0001	0.0003	0.0007	0.0010	0.0020

Table 5.2 is difficult to implement in computer codes or spreadsheets, and hence, the following equations have been derived to calculate f_{yd} from the given value of strain.

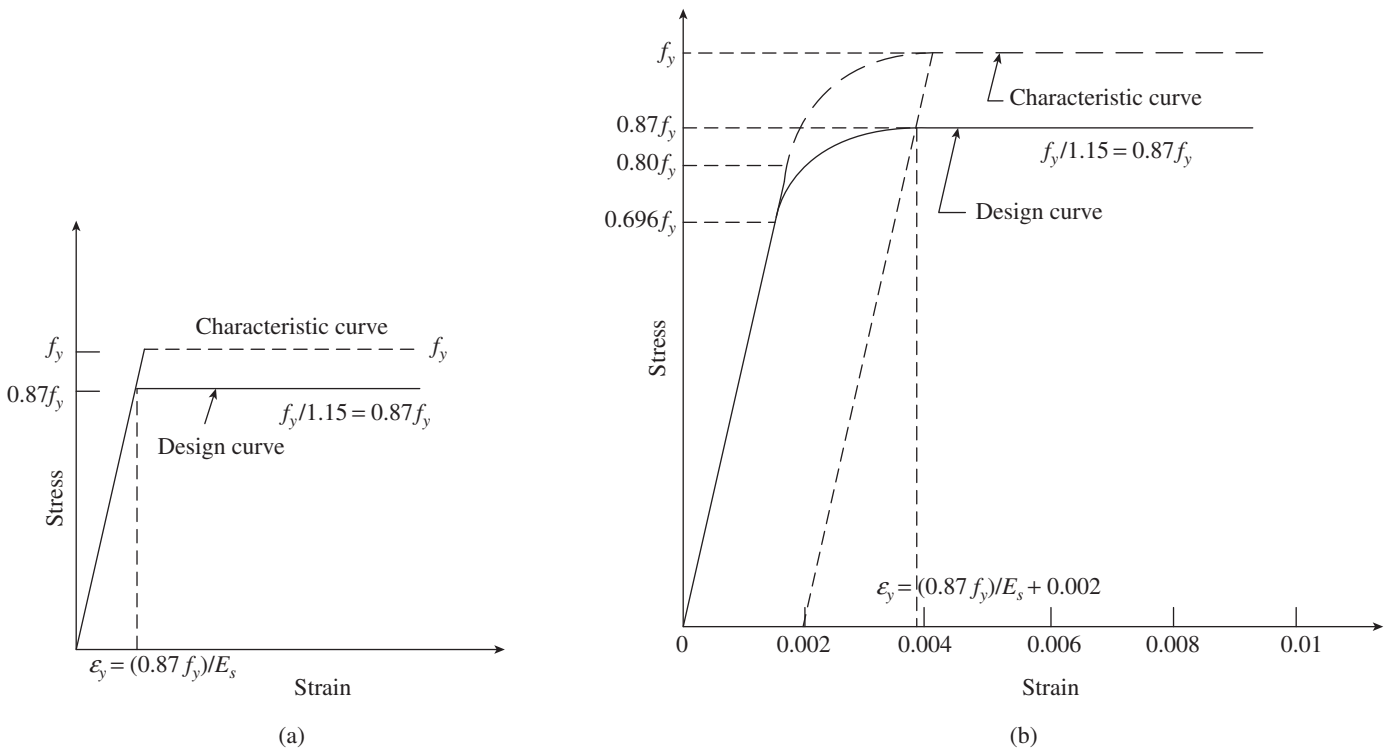


FIG. 5.5 Stress–Strain curves for steel reinforcements (a) Mild steel bars (b) HYSD bars as per IS 456 ($E_s = 2 \times 10^5 \text{ N/mm}^2$)

TABLE 5.2 Design stress at salient strain as per Fig. 5.5(b) for HYSD bars

Stress Level	$f_y = 415 \text{ N/mm}^2$		$f_y = 500 \text{ N/mm}^2$	
	Strain $\times 10^{-3}$	Stress (N/mm ²)	Strain $\times 10^{-3}$	Stress (N/mm ²)
0.0	0.00	0.0	0.0	0.0
$0.80f_{yd}$	1.444	288.7	1.74	347.8
$0.85f_{yd}$	1.63	306.7	1.95	369.6
$0.90f_{yd}$	1.92	324.8	2.26	391.3
$0.95f_{yd}$	2.41	342.8	2.77	413.0
$0.975f_{yd}$	2.76	351.8	3.12	423.9
$1.0f_{yd}$	≥ 3.81	360.9	≥ 4.17	434.8

Note: Linear interpolation may be done for intermediate values.

$f_{yd} = 0.87f_y$

For Fe 415 steel:

$$f_{yd} = -109.1569 + 537,276.6\varepsilon - 250,905 \times 10^3 \varepsilon^2 + 5,528,249 \times 10^4 \varepsilon^3 - 4,709,357 \times 10^6 \varepsilon^4$$

For Fe 500 steel:

$$f_{yd} = 1707.624 - 2,356,626\varepsilon - 1,444,077 \times 10^3 \varepsilon^2 + 3,666,904 \times 10^5 \varepsilon^3 - 3,318,089 \times 10^7 \varepsilon^4$$

In order to avoid sudden and brittle compression failure of concrete in singly reinforced beams, IS 456 stipulates that the maximum strain in the tension reinforcement in the section at failure should obey the following condition:

$$\varepsilon_{su} \geq 0.002 + \frac{f_y}{1.15E} = 0.002 + \frac{0.87f_y}{E_s} \quad (5.8)$$

where ε_{su} is the strain in steel at ultimate failure, f_y is the characteristic strength of steel, and E_s is the modulus of elasticity of steel, which is taken as $2 \times 10^5 \text{ N/mm}^2$. Thus, for grade Fe 415 steel, ε_{su} should not be less than 0.0038. This assumption assures ductile failure, that is, the tensile reinforcement will undergo a certain degree of inelastic deformation before the brittle concrete failure in compression.

It has been found from experiments that the strain in concrete at collapse is in the range of 0.003–0.008. (It should be noted that in contrast to concrete, steel reinforcements can sustain very high tensile strains, due to the ductile behaviour of steel after yielding. The ultimate tensile strain in steel is in the range 0.12–0.20, i.e., 25–35 times more strain than concrete.). However, the codes of India, Belgium, Sweden, UK, Germany, and Canada restrict this value to 0.0035 in design, whereas the US codes restrict it to 0.003. The strain and stress distributions at failure are shown in Figs 5.1(g) and (h). The curved stress block may be replaced by an equivalent rectangular stress distribution, with the intensity equal to $0.85f'_c = 0.68f_{ck}$ and depth $a = \beta_1 x_u$, as suggested by Whitney (1937) and shown in Fig. 5.1(j). The area of this stress block should be equivalent to the curved stress block and the centroids of the two blocks should coincide. The ACI code suggests the value of β_1 as 0.68

for concrete cube strengths up to and including 35 MPa. For cube strengths above 35 MPa, β_1 is to be reduced at a rate of 0.05 for each 8.75 MPa of strength in excess of 35 MPa but shall not be taken less than 0.52. This is expressed as

$$\beta_1 = 0.68 - 0.05 \left(\frac{f_{ck} - 35}{8.75} \right) \geq 0.52 \quad (5.9)$$

The values of β_1 are reduced for HSC primarily because of the different shapes of the stress–strain curves. It should be noted that most of the codes (such as the US, UK, Australian, and New Zealand codes) adopt a similar equivalent rectangular stress block, whereas the Indian code has adopted a parabolic–rectangular stress block, which, though more accurate, results in lengthy calculations.

- The embedded reinforcement is bonded with concrete, even when the section is cracked. Adequate bond length is available at all critical sections (see Chapter 7 for more details on bond). The strain in the reinforcement is equal to the strain in the concrete at the same level. The most economical solution is to place the steel bars far away from the neutral axis; however, some cover has to be provided to protect them from the environment.

5.4.2 Design Bending Moment Capacity of Rectangular Section

The analysis of the cross section is carried out by satisfying the following two requirements:

- Equilibrium:** This demands that the sum of the internal forces be equal to the sum of the external forces. For sections subjected to pure bending, there are no external forces. This leads to the following:

$$\sum \text{Internal forces} = 0; \text{ Thus, } T - C = 0 \text{ or } T = C$$

$$\sum \text{Internal } M = \sum \text{External } M \text{ (taken about any point in the section), where } T \text{ is the tension force, } C \text{ is the compressive force, and } M \text{ is the moment.}$$
- Compatibility of strains:** The strain at any point is proportional to its distance from the neutral axis.

Hence, if the problem has more than two unknowns, they should be reduced to two by using some suitable assumptions. Normally, the stress in the tension steel is assumed to be equal to the yield strength, f_y . It has to be noted that this assumption should be verified after determining the position of the neutral axis. Based on this, the nominal or theoretical moment strength of the beam may be obtained using the following simple steps:

- Compute total tensile strength, $T = A_{st} f_{st} = 0.87 A_{st} f_y$.
- As the compressive force C and the tensile force T must be equal to maintain the equilibrium of the section, equate T with the total compressive force C and solve for x .
- Calculate the distance between the centres of gravity of T and C , called the lever arm, z (for rectangular stress block, $z = d - x/2$).

4. Determine M_n , which is equal to T or C multiplied by the lever arm, z .

Considering the area of parabolic and rectangular portions of the stress block, the compressive force of concrete is determined as follows (see Fig. 5.4b):

$$C_p = 0.45f_{ck}b(4x/7) (2/3) = 0.171f_{ck}bx,$$

$$C_r = 0.45f_{ck}b(3x/7) = 0.193f_{ck}bx$$

Thus, $C = C_p + C_r = 0.36f_{ck}bx$ (5.10)

where C_p is the compressive force of concrete due to the parabolic portion of stress block and C_r is the compressive force of concrete due to the rectangular portion of stress block,

The distance from the top fibre at which the compressive force acts may be obtained by taking the moment of the forces about the top fibre. Denoting this distance as x_c ,

$$C(x_c) = C_p[x - (5/8)(4x/7)] + C_r(3x/14)$$

Substituting the values of C_p , C_r , and C and simplifying, we get

$$x_c = 0.416x \quad (5.11a)$$

The lever arm, z , that is, the distance between the centre of gravities of T and C is given by

$$z = d - 0.416x \quad (5.11b)$$

Having determined the stress block distance x , the assumption of the tension steel yielding can be verified by using compatibility of strains as follows:

$$f_s = E_s \varepsilon_{st} \quad (\text{as per Hook's law})$$

$$\varepsilon_{st} = 0.0035 \frac{d-x}{x} \quad (\text{Compatibility of strains})$$

Substituting the value of $E_s = 2 \times 10^5$, we get

$$f_s = 700 \frac{d-x}{x} \leq \frac{f_y}{1.15} \quad (5.12)$$

If the stress in steel, f_s , calculated by using Eq. (5.12) exceeds $f_y/1.15$, then the assumption of yielding of tension steel is valid ($f_s = f_y/1.15$), as used to calculate tension force.

The second equilibrium equation can be used to determine the moment capacity of the section by equating the internal moment, M_n , to the external applied moment, M_u . The internal moment capacity may be computed by taking the moment of the internal forces T and C about any point. Thus, the nominal or theoretical moment of resistance of the beam, M_n , is obtained in terms of concrete compressive strength as

$$M_n = Cz = 0.36f_{ck}bx (d - 0.416x) \quad (5.13)$$

Alternatively, in terms of the steel tensile strength,

$$M_n = Tz = 0.87f_y A_{st} (d - 0.416x) \quad (5.14a)$$

If the tension steel does not yield, Eq. (5.14a) becomes

$$M_n = f_{st} A_{st} (d - 0.416x) \quad (5.14b)$$

If an equivalent rectangular stress block as shown in Fig. 5.1(j) is adopted, the calculations are simple and will result in Eqs (5.15a and b) and (5.16) (with partial safety factor of 1.5 for concrete and 1.15 for steel):

$$T = 0.87f_y A_{st} \quad (5.15a)$$

$$C = 0.68/1.5 f_{ck}ba = 0.45f_{ck}ba \quad (5.15b)$$

$$M_n = Tz = 0.87f_y A_{st} (d - 0.5a) = 0.45f_{ck}ba(d - 0.5a) \quad (5.16)$$

5.4.3 Balanced, Under-reinforced, and Over-reinforced Sections

The RC sections under flexure are generally assumed to fail when the compressive strain in concrete reaches the failure strain in bending compression, which is assumed by IS 456 as 0.0035. The RC sections in which the tension steel reaches yield strain at the same load as the concrete reaches failure strain in bending compression are called *balanced sections*. The RC sections in which the tension steel reaches yield strain before the load that causes the concrete to reach failure strain in bending compression are called *under-reinforced sections*. The RC sections in which the failure strain of concrete in bending compression is reached earlier than the load that causes yield strain in tension steel are called *over-reinforced sections*. Figure 5.6 shows the location of the neutral axis for the balanced and under- and over-reinforced sections (it also shows the $x_{u,lim}$ case, which is considered the balanced section in the IS code, in order to ensure ductility and to avoid over-reinforced sections).

It should be noted that in the case of under-reinforced beams, yielding of the tensile steel will not result in the sudden collapse of the beam. As discussed in Section 5.2.4, yielding of the tensile steel results in non-linear deflections, leading to extensive cracking. Finally the beam will collapse due to the crushing of concrete in the compression zone. This is because the rupture of steel takes place at a much higher strain, of the order of 0.20–0.25 (i.e., 0.20–0.25% elongation based on the original length), compared to the yield strain of 0.0038 for grade Fe 415 steel, and the concrete ultimate strain is 0.0035. Since the failure initiated by the yielding of steel gives ample warning before the final failure, this failure is called *ductile failure*. Thus, the member will experience large deflections, large strains, and wide cracks before the final failure, and hence, repairs can be performed in case of overload.

Moreover, the cost of reinforcement is about 70 times that of concrete by volume. Hence, the designer should try to use as minimum a quantity of steel as possible. In addition, in under-reinforced concrete sections the strength of steel is fully utilized, and hence, it will be economical in addition to being ductile.

The moment capacity of an under-reinforced beam is controlled by the steel, whereas for an over-reinforced beam it is controlled by the concrete. The value of (x/d) of a singly

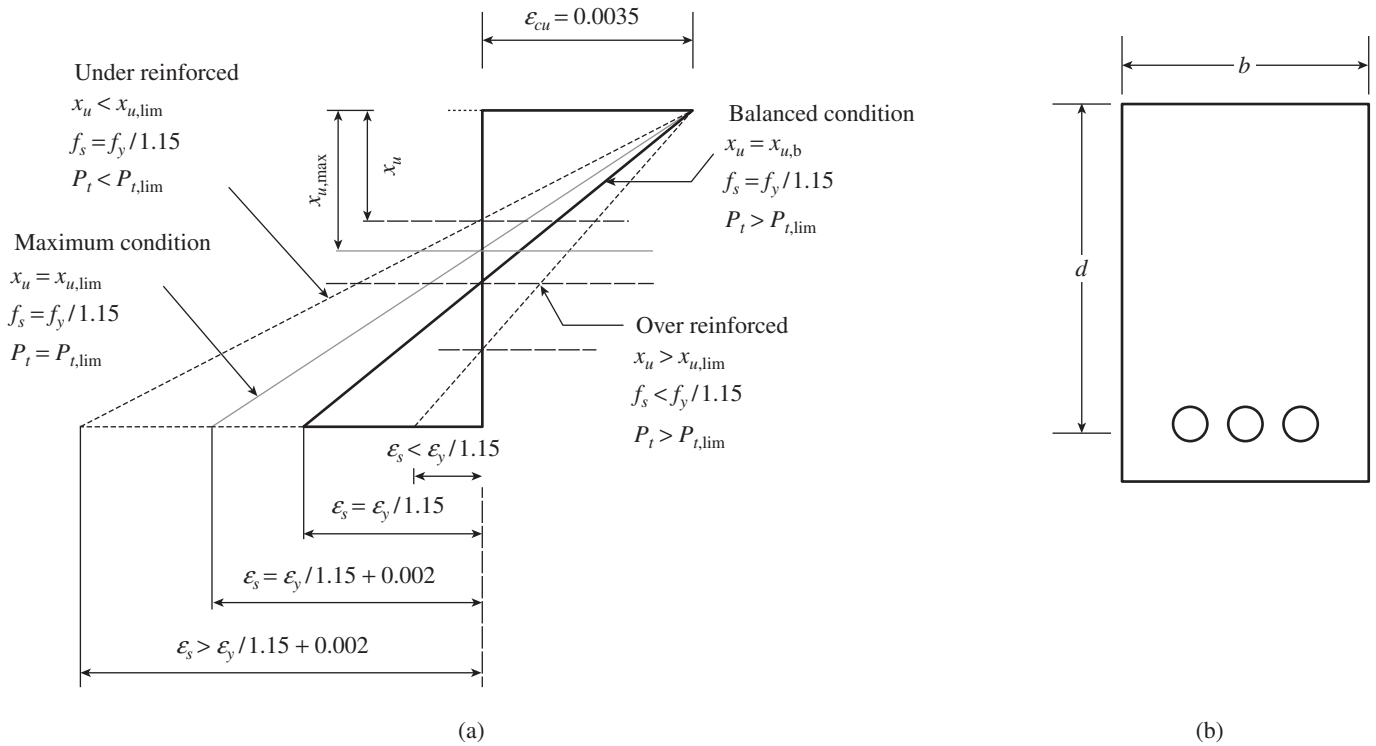


FIG. 5.6 Neutral axis for balanced and under- and over-reinforced sections (a) Strain distribution (b) Beam cross section

reinforced concrete beam is not allowed to exceed the limiting values of (x_u/d) specified in Table 5.3. However, when compression steel is provided, the ductility of the section is improved and the limiting value of (x_u/d) may be relaxed.

TABLE 5.3 Limiting values of x_u/d , j , k_1 , and k_2

Type of Steel	f_y (N/mm ²)	Yield Strain (ϵ_{su}) $\times 10^{-3}$	$(x_u/d)_{\text{limit}}$	j	k_1	k_2
Mild steel	250	3.088	0.531	0.78	0.191	0.149
HYSD	415	3.805	0.479	0.80	0.172	0.138
HYSD	500	4.175	0.456	0.81	0.164	0.133

5.4.4 Depth of Neutral Axis

As already discussed, beams are assumed to fail when the failure compression strain is reached in concrete. The steel need not reach yield stress at the same time, unless it has been specifically designed to fulfil this condition. For example, steel also yields when concrete fails in balanced or under-reinforced beams. However, in over-reinforced beams, the stress in steel at failure will be below its yield stress. As an equilibrium of forces is required at all times, the tensile forces will be equal to compressive forces. Thus, we have

$$\begin{aligned} \text{Total tension, } T &= f_{st} A_{st} \\ \text{Total compression, } C &= 0.36 f_{ck} b x \end{aligned}$$

where f_{st} is the actual tension in steel corresponding to the strain in steel.

Equating the two expressions, we get

$$f_{st} A_{st} = 0.36 f_{ck} b x$$

or

$$x = \frac{f_{st} A_{st}}{0.36 f_{ck} b} \quad (5.17)$$

In under-reinforced beams, the yield stress of $0.87f_y$ is reached first in steel reinforcement. Substituting this value in Eq. (5.17) and dividing both sides by the effective depth, we get the equation presented in Annex G of IS 456.

$$\frac{x_u}{d} = \frac{0.87 f_y A_{st}}{0.36 f_{ck} b d} \quad (5.18a)$$

where x_u is the depth of the neutral axis at ultimate failure of under-reinforced beam in flexure.

If an equivalent rectangular stress block as shown in Fig. 5.1(j) is adopted, equating tension and compression (Eqs 5.15a and b), we get

$$0.87 f_y A_{st} = 0.45 f_{ck} b a$$

or

$$a = \frac{1.93 f_y A_{st}}{f_{ck} b} \quad (5.18b)$$

where a is the depth of the neutral axis at ultimate failure of the under-reinforced beam in flexure.

Limiting Values of x_u/d

From assumption 5 given in Section 5.4.1, in order to avoid brittle failure, the steel strain ϵ_{su} at failure should not be less than the following:

$$\epsilon_{su} = 0.002 + \frac{f_y}{1.15 E} \quad (5.19)$$

Assuming $E_s = 2 \times 10^5 \text{ N/mm}^2$, the yield strain for different grades of steel may be worked out and is given in Table 5.3. It should be noted that there is no balanced strain condition specified in the Indian code provisions; the tensile strain in reinforcement is permitted to reach any value more than the specified minimum.

From the similar triangles of Fig 5.4(b), we get

$$\frac{\varepsilon_{cu}}{\varepsilon_{su}} = \frac{x_u}{d - x_u}$$

From this, we get

$$x_u = \frac{\varepsilon_{cu} d}{\varepsilon_{cu} + \varepsilon_{su}} = \frac{0.0035d}{0.0035 + 0.002 + [f_y / (1.15E_s)]} \quad (5.20a)$$

Substituting for $E_s = 2 \times 10^5 \text{ N/mm}^2$ and simplifying, we get

$$\left(\frac{x_u}{d}\right)_{\text{lim}} = \frac{805}{1265 + f_y} = k_u \quad (5.20b)$$

Substituting the values of f_y for various grades of steel, the limiting values of x_u/d are obtained as shown in Table 5.3 for various grades of steel.

The lever arm distance as given by Eq. (5.21) is

$$z = jd = d - x_c = d - 0.416x_u = d[1 - 0.416(x_u/d)] \quad (5.21)$$

where j is the ratio of the lever arm distance coefficient. The values of j for different grades of steel may be calculated and are shown in Table 5.3.

The maximum or limiting value of concrete compression, C_L , is obtained by substituting the limiting values of (x_u/d) in Eq. (5.10). Thus

$$C_L = 0.36f_{ck}bd(x_u/d) = k_1f_{ck}bd$$

The values of $k_1 = 0.36(x_u/d)$ for different values of (x_u/d) are also given in Table 5.3.

The nominal or theoretical moment strength of the beam, M_n , can be obtained in terms of concrete compressive strength as

$$\begin{aligned} M_n &= Cz = 0.36f_{ck}bx_u(d - 0.416x_u) \\ &= 0.36f_{ck}b(x_u/d)djd = k_2f_{ck}bd^2 \end{aligned} \quad (5.22a)$$

where $k_2 = 0.36(x_u/d)j$. The values of k_2 for different steel grades are given in Table 5.3.

Alternatively, in terms of the steel tensile stress,

$$\begin{aligned} M_n &= Tz = f_{st}A_{st}(d - 0.416x_u) \text{ for all } x_u \\ &= 0.87f_yA_{st}(d - 0.416x_u) \text{ for all } x_u < x_{u,\text{lim}} \end{aligned} \quad (5.22b)$$

5.4.5 Resisting Moment Strength for Balanced Sections

In Section 5.4.2, the nominal or theoretical moment strength of the beam was derived in terms of the steel tensile strength as

$$M_n = Tz = 0.87f_yA_{st}(d - 0.416x_u)$$

Substituting the value of x_u/d from Eq. (5.18) as

$$x_u = \frac{0.87f_yA_{st}}{0.36f_{ck}b}$$

we get

$$M_n = 0.87f_yA_{st} \left[d - \frac{0.416(0.87f_yA_{st})}{0.36f_{ck}b} \right]$$

Simplifying and rounding off the coefficient, we obtain the equation given in Annex G of IS 456, which should be used when x_u/d is less than the limiting value.

$$M_n = 0.87f_yA_{st}d \left[1 - \frac{f_yA_{st}}{f_{ck}bd} \right] \quad (5.23)$$

Let the area of tensile steel be denoted as a percentage of the effective beam area as follows:

$$p_t = \frac{A_{st}}{bd} \times 100$$

where p_t is the percentage of steel. Substituting p_t for (A_{st}/bd) in Eq. (5.23), we get

$$M_n = 0.87f_y \frac{p_t}{100} bd^2 \left[1 - \frac{f_y p_t}{100f_{ck}} \right]$$

Dividing both sides by bd^2 , we get

$$\frac{M_n}{bd^2} = 0.87f_y \left(\frac{p_t}{100} \right) \left[1 - \frac{f_y p_t}{f_{ck} 100} \right] \quad \text{for } p_t < p_{t,\text{lim}} \quad (5.24)$$

Based on Eq. (5.24), SP 16:1980 has provided tables (Tables 1–4), using which for any value of M_u/bd^2 the percentage of steel may be obtained for different values of f_y and f_{ck} . It must be noted that the value of p_t found from Eq. (5.24) is not directly proportional to M_u/bd^2 . Moreover, this equation should be used only for under-reinforced beams, where the tensile stress in steel will reach yield stress before failure.

Solving the quadratic equation given in Eq. (5.24) in p_t , we get

$$p_{t,\text{lim}} = 50 \frac{f_{ck}}{f_y} \left[1 - \sqrt{1 - \frac{4.6M_u}{f_{ck}bd^2}} \right] \quad (5.25)$$

where $p_{t,\text{lim}}$ is the limiting percentage tensile steel corresponding to the limiting moment of resistance, $M_{u,\text{lim}}$.

When the value of x/d is equal to the limiting value, Eq. (5.22) must be used. Dividing both sides of Eq. (5.22a) by bd^2 we obtain the other equation given in Annex G of IS 456:

$$\frac{M_{n,\text{lim}}}{bd^2} = 0.36f_{ck} \left(\frac{x_{u,\text{lim}}}{d} \right) \left(1 - 0.416 \frac{x_{u,\text{lim}}}{d} \right) \quad (5.26)$$

Substituting the values of x_u/d from Table 5.3, we get the limiting moment of resistance for various grades of steel as

shown in Table 5.4. Substituting these values in Eq. (5.25), we get the reinforcement index, $\left(\frac{p_t, \text{lim} f_y}{f_{ck}}\right)$, as given in Table 5.4.

TABLE 5.4 Limiting moment of resistance and reinforcement index for singly reinforced rectangular sections

$f_y, \text{N/mm}^2$	250	415	500
$M_{u, \text{lim}}/f_{ck} b d^2$	0.149	0.138	0.133
$p_t, \text{lim} f_y/f_{ck}$	21.97	19.82	18.87

Thus, the moment capacity of a singly reinforced section is restricted to $M_{n, \text{lim}}$. Even if the beam has more reinforcement than that required for a balanced section, the increase in strength will be very minimal. Such an over-reinforced beam is not adopted in practice, as the failure of the beam will be brittle, without any warning, and hence catastrophic. If the applied moment, M_u , exceeds $M_{n, \text{lim}}$, the section has to be redesigned by (a) changing the cross-sectional dimensions of the member, (b) increasing the concrete strength, or (c) designing the member as a doubly reinforced section.

5.5 DESIGN OF SINGLY REINFORCED RECTANGULAR SECTIONS

As mentioned in Section 5.3, the design for flexure deals with the determination of the cross-sectional dimensions and the reinforcement for a given ultimate moment acting on the beam. The basic requirement of safety at the ultimate limit state of flexure is that the factored applied moment due to external loads and self-weight, M_u , should not exceed the ultimate moment of resistance, M_n , and that the failure at the limit state should be ductile. Hence, the basic design equation is given by

$$M_u \leq M_n \quad \text{with} \quad x_u \leq x_{u, \text{limit}} \quad (5.27)$$

Many times, the breadth of the beam may be fixed based on architectural considerations. Hence, let us discuss how the depth and area of reinforcement are determined.

5.5.1 Minimum Depth for Given M_u

As per Eq. (5.22a), the nominal moment capacity of the beam is

$$M_n = k_2 f_{ck} b d^2$$

where $k_2 = 0.36(x_u/d)j$ and its value is given in Table 5.3 for various grades of steel.

From this equation, we get

$$d = \sqrt{\frac{M_u}{k f_{ck} b}} \quad (5.28a)$$

For Fe 415 grade steel, the value of $k_2 = 0.138$. Hence,

$$d = \sqrt{\frac{M_u}{0.138 f_{ck} b}} = \sqrt{\frac{7.2 M_u}{f_{ck} b}} \quad (5.28b)$$

For Fe 250 and Fe 500 grades steel, the coefficient 7.2 in Eq. (5.28b) is to be replaced by 6.71 and 7.52, respectively.

Similarly the value of (x/d) can be derived as follows:

From Eq. (5.26)

$$M_u = 0.36 f_{ck} \left(\frac{x_u}{d}\right) \left(1 - 0.416 \frac{x_u}{d}\right) b d^2$$

Dividing both sides of this equation by $(0.36)(0.416) f_{ck} b d^2$, we get

$$\frac{6.68 M_u}{f_{ck} b d^2} = 2.4 \left(\frac{x_u}{d}\right) - \left(\frac{x_u}{d}\right)^2$$

Rearranging the terms, we get the following quadratic equation in (x_u/d)

$$\left(\frac{x_u}{d}\right)^2 - 2.4 \left(\frac{x_u}{d}\right) + \frac{6.68 M_u}{f_{ck} b d^2} = 0$$

Solving for (x_u/d) , we get the following:

$$\left(\frac{x_u}{d}\right) = 1.2 - \sqrt{1.44 - \frac{6.68 M_u}{f_{ck} b d^2}} \quad (5.29a)$$

This equation may also be written in the following format:

$$\left(\frac{x_u}{d}\right) = \frac{1 - \sqrt{1 - 4\beta m}}{2\beta}, \quad \text{with} \quad m = \frac{M_u}{0.36 f_{ck} b d^2}$$

and

$$\beta = 0.416 \quad (5.29b)$$

From Eq. (5.29b), we may determine the value of (x_u/d) for the given values of M_u, f_{ck}, b , and d .

5.5.2 Limiting Percentage of Steel

From Eq. (5.18a), with x_u as the depth of the neutral axis at ultimate load, we get

$$\frac{x_u}{d} = \frac{0.87 f_y A_{st}}{0.36 f_{ck} b d}$$

Rearranging the terms and simplifying, we get

$$\frac{A_{st}}{b d} = \frac{0.414 f_{ck} x_u}{f_y d} \quad (5.30)$$

Denoting the area of tensile steel as a percentage of effective beam area,

$$p_t = \frac{A_{st}}{b d} \times 100$$

Rewriting Eq. (5.30) in terms of p_t , we get

$$p_t = \frac{41.38 f_{ck}}{f_y} \left(\frac{x_u}{d}\right) \quad (5.31a)$$

Thus

$$\frac{p_t, \text{lim} f_y}{f_{ck}} = 41.38 \left(\frac{x_{u, \text{lim}}}{d}\right) \quad (5.31b)$$

Using Eq. (5.20b), we get

$$\frac{p_{t,lim} f_y}{f_{ck}} = \left(\frac{33310}{1265 + f_y} \right) \quad (5.31c)$$

The value of $p_{t,lim}(f_y/f_{ck})$ for various steel grades are shown in Table 5.5 along with the limiting percentage of steel for concrete grades M20 to M50.

TABLE 5.5 Percentage of limiting steel areas for balanced section

Grade of Steel	(x_u/d) Limit	$p_{t,lim}(f_y/f_{ck})^*$	Limiting Percentage of Steel for Grades M20 to M50
Fe 250	0.531	21.97	1.758–4.396
Fe 415	0.479	19.82	0.955–2.389
Fe 500	0.456	18.87	0.755–1.887

*Until 2002, the ACI code permitted p_t values up to 75 per cent of the steel required for balanced sections; see also Sections 5.5.4 and 5.5.5.

5.5.3 Factors Affecting Ultimate Moment Capacity

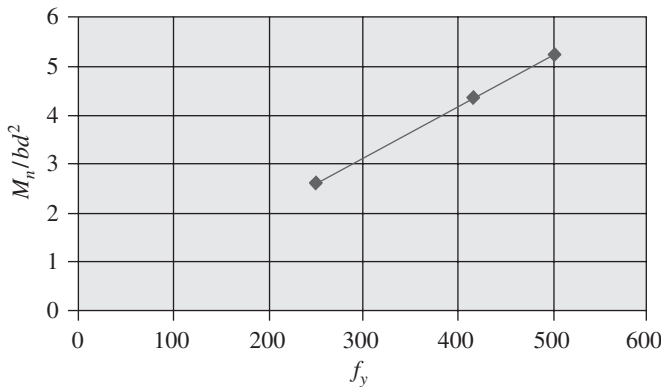
The following factors affect the nominal ultimate strength of a beam subjected to bending (Subramanian 1975):

1. Yield strength of steel reinforcement, f_y
2. Compressive strength of concrete, f_{ck}
3. Depth of beam, d
4. Breadth of beam, b
5. Percentage of reinforcement, p_t

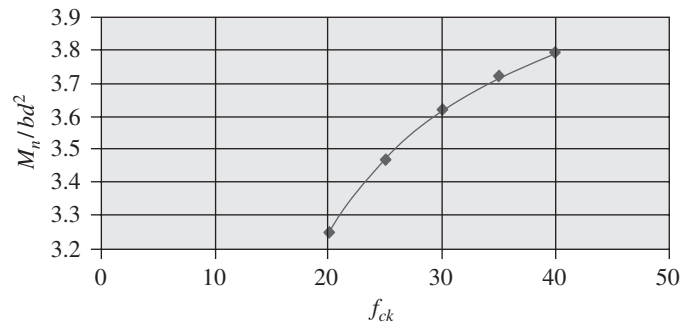
The effects of these parameters are shown in Fig. 5.7. As shown in Fig. 5.7(a), the yield strength of steel reinforcement has a considerable impact on its ultimate moment capacity. Increasing the yield strength of steel from 250 N/mm² to 415 N/mm² increases the ultimate capacity by 51 per cent. However, the compressive strength of concrete has only a slight effect on the ultimate capacity, as shown in Fig. 5.7(b). Changing the compressive strength of concrete from 20 N/mm² to 40 N/mm² increases the ultimate moment capacity by only 16.5 per cent. With the other factors remaining the same, the moment capacity of the beam is directly proportional to the breadth and square of the depth. Thus, the depth of the beam has more influence on the ultimate moment capacity than its width. Increasing the depth from 500 mm to 1000 mm increases the capacity of the beam four times. Increasing the percentage of tensile reinforcement also has a significant effect on the ultimate moment capacity, as shown by Fig. 5.7(c).

5.5.4 Minimum Tension Reinforcement

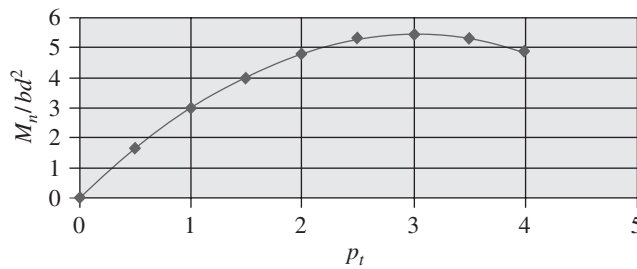
For architectural or other reasons, beams may be provided in a larger size than required for flexural strength. With a small amount of tensile reinforcement, the computed strength of the member using cracked section analysis (using Eq. 5.23) may become less than that of the corresponding strength of an unreinforced concrete section, computed using the modulus



(a)



(b)



(c)

FIG. 5.7 Effect of different parameters on ultimate moment capacity (a) Effect of yield strength of steel (b) Effect of compressive strength of concrete (c) Effect of percentage of steel reinforcement

of rupture. This will result in sudden and brittle failure of such beams. To prevent such possibilities, codes of practices often prescribe a minimum amount of tension reinforcement. Minimum steel is also provided from the shrinkage and creep considerations, which often control the minimum steel requirement of slabs. Minimum steel will also guarantee accidental overloads due to vibration and settlements, control cracks, and ensure ductility.

Hence, the required condition for the minimum percentage of steel may be stated as follows:

$$\frac{\text{Strength as RC beam}}{\text{Strength as plain concrete beam}} > \quad (5.32)$$

The moment of resistance for an unreinforced concrete beam, M_{cr} , may be calculated using elastic theory from Eq. (5.4). Substituting the values of I_g/y_t (equal to $b_w D^2/6$, for a rectangular section) and f_{cr} in Eq. (5.4), we get

$$M_{cr} = 0.117 b_w D^2 \sqrt{f_{ck}} \quad (5.33)$$

where D is the total depth of the beam and b_w is the width of the rectangular beam (for T -beams, b_w denotes the width of the web).

The nominal moment of resistance as given by the cracked section theory in Eq. (5.22), without the partial safety factors may be approximately written as

$$M_n = A_s f_y (d - 0.416 x_u) \quad (5.34a)$$

The term $(d - 0.416 x_u)$, representing the lever arm, may range from $1.00d$ (when steel area is zero) to $0.71d$ (at balanced failure). Safely assuming it to be $0.71d$, we get

$$M_n = 0.71 A_s f_y d \quad (5.34b)$$

In rectangular beams, the ratio D/d will be in the range 0.8–0.95. Safely assuming it to be 1.0 in Eq. (5.33) and equating Eqs (5.33) and (5.34b), we get

$$0.71 A_s f_y d = 0.117 b_w d^2 \sqrt{f_{ck}} \quad (5.35a)$$

Rearranging the terms, we get

$$\frac{A_s}{b_w d} = \frac{0.17 \sqrt{f_{ck}}}{f_y} \quad (5.35b)$$

It should be noted that the minimum steel as per Eq. (5.35b) is dependent on the compressive strength of concrete and hence will increase with increasing f_{ck} . However, in IS 456, f_{ck} might have been assumed to be 25 MPa, and the equation is given in Clause 26.5.1.1 as

$$\frac{A_s}{b_w d} = \frac{0.85}{f_y} \quad (5.35c)$$

The explanatory handbook SP 24:1983 states that this requirement will result in 0.34 per cent for mild steel, thus matching the 0.3 per cent minimum as required in the 1964

version of the code. For cold-worked deformed bars ($f_y = 415 \text{ N/mm}^2$), the value of minimum steel will be given as 0.20 per cent.

Varghese (2006) reports that in some situations, large beams designed with the minimum steel requirement of the IS code have experienced extensive cracking, although there are no reported failures. Hence, there is a need to revise the minimum tensile steel provisions of IS 456:2000. It should be noted that cantilever T -beams, with their flange in tension, will require significantly higher reinforcement than specified in this clause to prevent brittle failure caused by concrete crushing; however, IS 456 suggests calculating the minimum reinforcement for such T -beams by taking b_w as the width of the web alone.

It is interesting to note that the US code, until the 1995 edition, used Eq. (5.36a) (which is similar in format to the Indian code equation and uses a factor of safety of 2.5):

$$\frac{A_s}{b_w d} = \frac{1.4}{f_y} \quad (5.36a)$$

This equation provides a minimum tension steel of about 0.5 per cent (as against the 0.3% minimum in the Indian code) for mild steel grade, as required by the earlier editions of the ACI code. The 1995 version of the code recognized that the minimum steel as given by Eq. (5.36a) may not be sufficient for HSC with strength greater than 35 MPa. Hence, the code introduced Eq. (5.36b), which has a format similar to Eq. (5.35b):

$$\frac{A_s}{bd} = \frac{0.25 \sqrt{f_c}}{f_y} \geq \frac{1.4}{f_y} \quad (5.36b)$$

where f_c is the cylinder compressive strength of concrete. Equation 5.36(b) may be rewritten in terms of cube compressive strength as follows:

$$\frac{A_s}{b_w d} = \frac{0.224 \sqrt{f_{ck}}}{f_y} \geq \frac{1.4}{f_y} \quad (5.36c)$$

It should be noted that $0.224 \sqrt{f_{ck}}$ and 1.4 are equal when f_{ck} equals 39 MPa. Hence, $(1.4/f_y)$ will control only when f_{ck} is less than 39 MPa. Thus, for HSC, the concrete strength should also be considered while providing minimum tensile reinforcement. It makes sense as HSC is normally brittle when compared to normal strength concrete. It has to be remembered that for T -beams with the flange in tension, ACI 318-08 specifies the use of Eq. (5.36b), with b_w replaced by $2b_w$ or the width of the flange b_f , whichever is smaller.

In this connection, it should be noted that Clause 6.2.1 of IS 13920 uses Eq. (5.36d), which is similar to Eq. (5.36c):

$$\frac{A_s}{b_w d} = \frac{0.24 \sqrt{f_{ck}}}{f_y} \quad (5.36d)$$

A comparison of the minimum flexural reinforcement provisions of different codes is provided in Fig. 5.8. It can be seen that unlike Eurocode 2, the minimum flexure reinforcement requirements for the slabs of the Indian, Canadian, and US codes are not a function of concrete strength (Subramanian 2010).

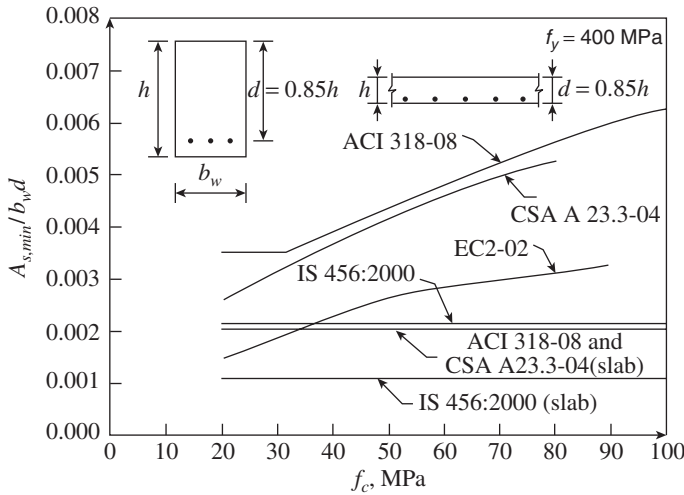


FIG. 5.8 Comparison of minimum flexural reinforcement provisions of different codes

Source: Li and Zhang 2005 (adapted)

An area of compression reinforcement equal to at least one-half of the tension reinforcement should be provided, in order to ensure adequate ductility at the potential plastic hinge zones and to ensure that minimum tension reinforcement is present for moment reversal (NZS 3101:2006; Wight and MacGregor 2009).

5.5.5 Maximum Flexural Steel

An upper limit to the tension reinforcement ratio in flexural RC members is also provided to avoid the compression failure of concrete before the tension failure of steel, thus

ensuring sufficient rotation capacity at the ultimate limit state. The upper limit is also required to avoid congestion of reinforcement, which may cause insufficient compaction or poor bond between the reinforcement and concrete.

Until 2002, the ACI code permitted p_t values up to 75 per cent of the steel required for balanced sections as the maximum flexural reinforcement (see Table 5.5 for the percentage of limiting steel areas for balanced section). Using this rule and selecting M25 concrete and grade 415 steel, the maximum percentage of steel = $0.75 \times 19.82 \times 25/415 = 0.90$. However, IS 456 stipulates that the maximum percentage of tension reinforcement in flexural members be four per cent, which is very high (if both tension and compression steel are provided, it amounts to 8%). It should be noted that Clause 6.2.2 of IS 13920 suggests a percentage of steel of 2.5 per cent, which is also high.

Tension- and Compression-controlled Sections

Although the US code specified the maximum percentage of steel as 75 per cent of the balanced reinforcement ratio in the earlier versions, in the 2002 version of the code, the provision was changed, as it may become complicated for flanged sections and sections that use compression reinforcement. In the present edition of ACI 318-11, the ductility of the section is controlled by controlling the tensile strain, ϵ_t , in the extreme layer of tensile steel, as suggested by Mast (1992) (see Fig. 5.9). Thus, when the net tensile strain in the extreme tension steel, ϵ_t , is equal to or greater than 0.005 and the concrete compressive strain reaches ϵ_{cu} , the section is defined as a *tension-controlled* section. Sections with ϵ_t less than 0.002 are considered *compression controlled* and are not used in singly reinforced sections. Sections with ϵ_t in the range 0.002–0.005 are considered as transition between tension and compression controlled. Such a tension-controlled section

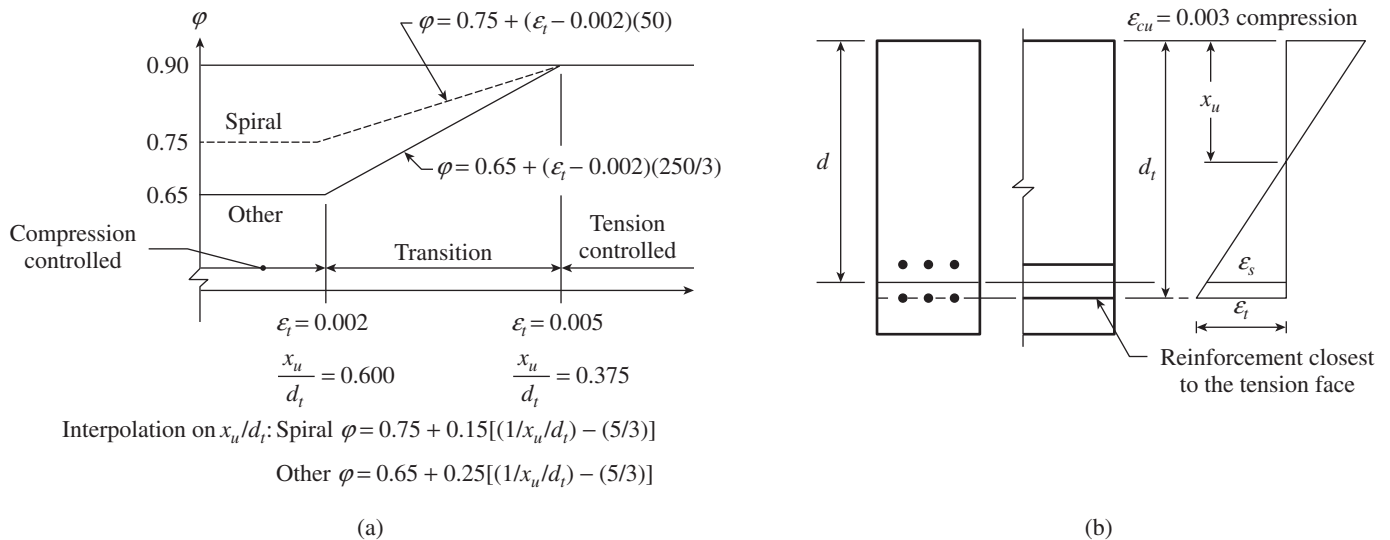


FIG. 5.9 Definition of tension- and compression-controlled sections (for grade 420 reinforcement) in ACI 318 code (a) Tension- and compression-controlled sections (b) Strain distribution (Reprinted with permission from ACI)

will give ample warning of failure with excessive deflection and cracking. For grade 415 steel, the tensile yield strain is $\epsilon_y = 415/(200 \times 10^3) = 0.00208$. Thus, the tension-controlled limit strain of 0.005 was chosen to be 2.5 times the yield strain. Such tension-controlled sections will result in a moment–curvature diagram similar to that shown in Fig. 5.10 (the one with area of reinforcement equal to 2900 mm^2).

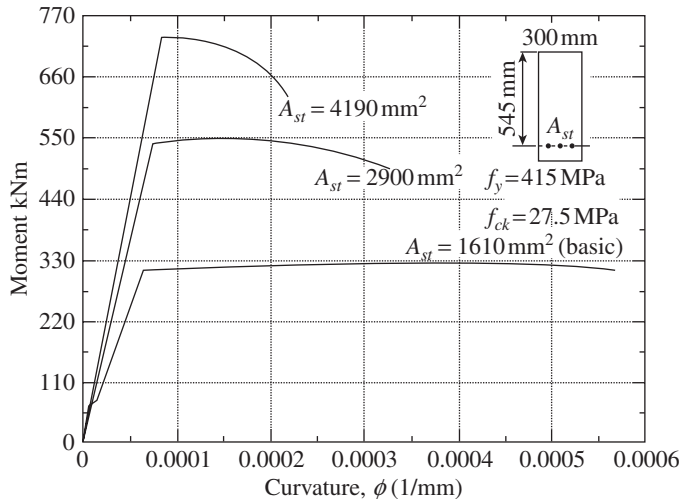


FIG. 5.10 Moment–Curvature diagram of a beam with varying steel areas

It should be noted that in the ACI code different strength reduction factors (called ϕ factors) are used—ranging from 0.9 (tension-controlled) to 0.65 (compression-controlled)—to calculate the design strength of members from the calculated nominal strength. Moreover, flexural members are usually chosen as tension controlled, whereas compression members are usually chosen as compression controlled. The net tensile strain limit of 0.005 for tension-controlled sections was chosen to be a single value that applies to all types of steel—prestressed and non-prestressed (Mast 1992).

From the similar triangles of Fig. 5.9(b), and assuming ϵ_{cu} as 0.0035 according to IS 456, for tension-controlled flexural members we may deduct $x_u/d_t = 0.0035/(0.003 + 0.005) = 3.5/8$. Substituting this value in Eq. (5.31a), we get,

$$p_t = 18.1 \frac{f_{ck}}{f_y} \leq 2.5 \quad (5.37)$$

For M25 concrete and grade 415 steel, we get $p_t = 1.09$ per cent, compared to $0.75 \times 19.82 \times 25/415 = 0.90$ per cent obtained using the earlier rule specified in the older version

of the ACI code (i.e., 75% of steel required for the balanced section, as per Table 5.4).

Comparison of the provisions for maximum tensile reinforcement in flexural members of the Indian, Eurocode 2, US, New Zealand, and Canadian codes shows that except the Indian and Eurocode 2 codes, all the other codes have a similar format and involve both f_{ck} and f_y (Subramanian 2010).

5.5.6 Slenderness Limits for Rectangular Beams

When slender beams are used, the beam may fail by lateral buckling accompanied by a twist, as shown in Fig. 5.11, before the development of flexural strength. The lateral buckling of concrete beams is less critical than that of steel beams. It is because RC beams are often less slender and accompanied by floor slabs attached to the compression zone of beams (see Fig. 5.12a).

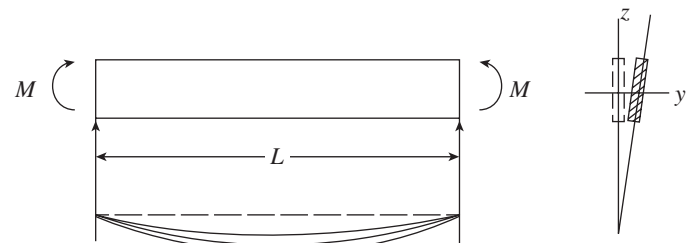


FIG. 5.11 Lateral buckling of slender beams

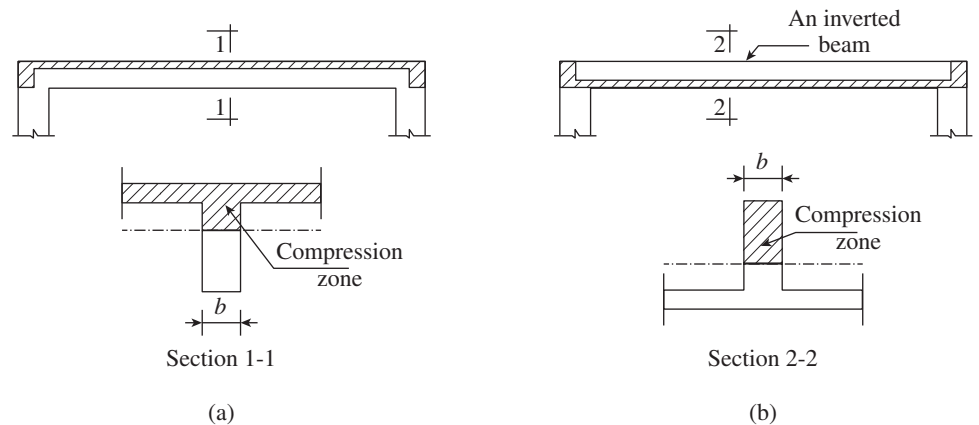


FIG. 5.12 Lateral supports to beams (a) Laterally supported beams (b) Laterally unsupported beams

However, lateral torsional instability may be important in the case of beams lacking lateral support, if the flexural stiffness in the plane of bending is very large compared to its lateral stiffness. Critical situations may arise during the erection of precast concrete structures before adequate lateral restraint to components is provided (Park and Paulay 1975).

Figure 5.12(b) shows a case where the compression zone of the beam is not laterally supported against lateral buckling by the floor slabs. In such cases, and in other cases where the floor slabs do not exist, Clause 23.3 of the code sets the

following limits on the clear distance, l , between the lateral restraints:

1. For simply supported or continuous beams, the lesser of $60b$ and $250b^2/d$
2. For cantilever beams with lateral restraint only at support, lesser of $25b$ and $100b^2/d$

where d is the effective depth of the beam and b is the breadth of the compression face midway between the lateral restraints. These slenderness limits are based on UK code CP 110:1972 and BS 8110:1997. According to ACI 318, Clause 10.4.1, the distance between lateral restraints shall not exceed $50b$, where b is the least width of compression flange or face. If these limits are exceeded, the critical moment M_{cr} will govern the strength of the beam. The approximate value for this critical moment is (Park and Paulay 1975)

$$M_{cr} = \frac{64f_{ck}b^3d}{l} \quad (5.38)$$

Based on experimental investigations, Revathi and Menon (2007) proposed the following moment reduction factor, η (ranging in value from 1.0 to 0.6), to be applied on the ultimate moment capacity of beams, M_n (see Eq. 5.23), in the transition zone of slenderness $0.3\lambda < ld/b^2 < 1.6\lambda$:

$$\eta = 1.1 - \frac{1}{3} \left(\frac{ld/b^2}{\lambda} \right) \quad (5.39a)$$

where l is the clear distance between lateral restraints, d is the effective depth of beam, b is the breadth of beam, and λ is the limiting slenderness ratio, defined as follows:

$$\lambda = \frac{C_1}{10C_2} \frac{E_c}{R} \sqrt{\alpha\beta} \quad (5.39b)$$

Here, E_c is the short-term elastic modulus of concrete, R is the flexural resistance factor (without partial safety factors), α is the flexural rigidity coefficient, β is the torsional rigidity coefficient, constant C_1 depends on the nature of loading (equals π for pure bending and 3.54 for uniformly loaded case), and constant C_2 is the effective length ratio (equals 1.0 for simply supported case and 0.5 for fixed-fixed boundary condition). Simplified equations for α and β are provided by Revathi and Menon (2007). Equation 5.39 incorporates the effects of design variables such as grade of concrete, grade of steel, amount of tension and compression reinforcement, and transverse reinforcement ratio. Typical limiting slenderness ratios, λ_{max} , for beams with various boundary conditions for $p_t = 1.1$ per cent, $p_c = 0.46$ per cent, and $C_1 = 3.54$ (Revathi and Menon 2009) are provided in Table 5.6.

TABLE 5.6 Typical limiting slenderness ratios for beams with various boundary conditions

Boundary Condition	$f_y = 415 \text{ MPa}$		$f_y = 250 \text{ MPa}$	
	$f_{ck} = 20 \text{ MPa}$	$f_{ck} = 45 \text{ MPa}$	$f_{ck} = 20 \text{ MPa}$	$f_{ck} = 45 \text{ MPa}$
Simply supported	215	178	285	243
Cantilever	107	89	142	121
Fixed-Fixed	430	356	570	486

5.5.7 Guidelines for Choosing Dimensions and Reinforcement of Beams

It should be noted that the selection of the sizes of flexural members is also dictated by the serviceability criteria (need to control deflections and crack widths; see Clause 23.2 of IS 456:2000), and requirement related to placement of reinforcement (providing proper cover for durability, spacing of reinforcement bars for proper compaction of concrete, etc.; see Clauses 26.3 and 26.4 of IS 456:2000), in addition to strength considerations. Moreover, architectural considerations may also dictate the size of beams in some situations.

Unlike analysis, design will not yield a unique solution. Many choices of beam sizes (breadth and depth) and reinforcements are feasible. The following may be useful while selecting the sizes of beams:

1. It is economical to select singly reinforced sections with moderate percentage of tension reinforcement ($p_t \approx 0.5-0.8$ times $p_{t,lim}$), which will result in ductile sections.
2. The minimum percentage of steel is around 0.3 per cent. Choose the depth of the beam such that the percentage of steel required is less than 75 per cent of the balanced steel.
3. At least two rods must be provided as tension steel, and not more than six bars are to be used in one layer. It is preferable to adopt a single size of bars or two sizes at the most. When two sizes of bars are adopted, it is better to choose such that the sizes do not vary much (say, 16 mm and 12 mm, 20 mm and 16 mm, and so on).
4. Often two bars are used as hanger bars, which are placed in the compression side of the beam. Their purpose is to provide support for the stirrups and to hold them in position (stirrups are provided to resist shear, as explained in Chapter 6). The minimum diameter of the main tension bar should be 12 mm and that of the hanger bar 10 mm (unless the hanger bars are significant, say, greater than 0.2%, they are not considered as compression steel).
5. The usual diameters of bars adopted in practice are 10, 12, 16, 20, 22, 25, and 32 mm. If two different sizes are used as reinforcement in one layer, the larger diameter bars are

placed near the faces of the beam. It is preferable to keep the rods symmetrical about the centre line of the beam.

6. The width of the beam necessary to accommodate the required number of rods is dependent on the side cover and minimum spacing. Table 4.6 of Chapter 4 gives the required cover to main steel reinforcement for beams. Assuming a nominal cover of 20mm for mild exposure and a stirrup size of 8mm, the clear cover to steel works out to 28mm. The cover and arrangement of bars within a beam should be such that there is provision for the following:
- Sufficient concrete on all sides of each bar to transfer forces into or out of the bar, that is, to develop sufficient bond
 - Sufficient space for the fresh concrete to flow around the bar and get compacted
 - Sufficient space to allow vibrators to reach up to the bottom of the beam

As per Clause 26.3.2 of IS 456:2000, the minimum horizontal distance between bars (the dimension ' s_h ' shown in Fig. 5.13) should be greater than the diameter of the larger bar (if the diameters are unequal) or nominal/maximum size of aggregate plus 5 mm. In India, 20mm aggregate is usually used in RC members and hence the clear minimum distance between bars should be 25 mm or the diameter of the larger bar used. Assuming 8 mm bar for stirrups, the required minimum width for different bar diameters can be worked out and one such calculation is shown in Table 5.7.

From this table, it is clear that for two bars a minimum width of only 200mm is to be adopted. The minimum vertical spacing between bars (dimension ' s_v ' in Fig. 5.13) should be greater than (a) 15 mm, (b) the diameter of the larger bar (if the diameters are unequal), and (c) two-thirds the nominal or maximum size of aggregate. The dimensions

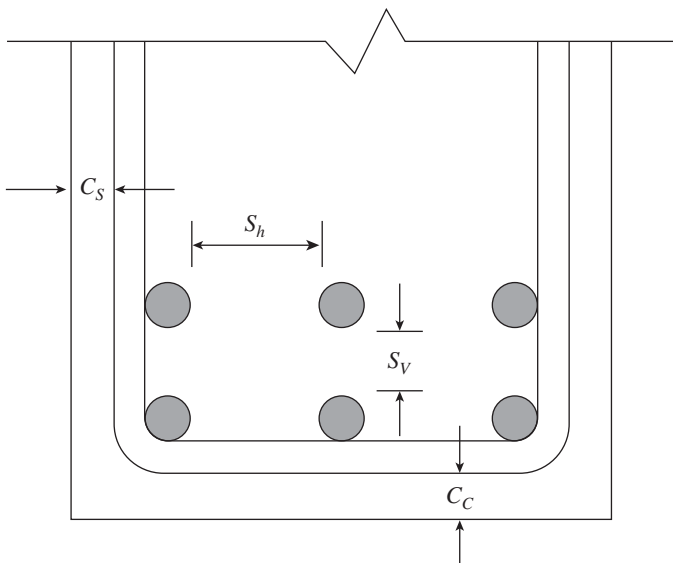


FIG. 5.13 Clear cover, clear side cover, and spacing between bars

' c_c ' and ' c_s ' in Fig. 5.13 are the clear cover and clear side cover, respectively, for the main reinforcement. The value of c_s should be greater than 25 mm or the diameter of the larger bar (if the diameters are unequal).

TABLE 5.7 Minimum width of beam based on minimum spacing of bars

Main Bar Diameter (mm)	Nominal Cover (See Table 4.6 and Fig. 5.13) (mm)	Minimum Distance between Bars (See Fig. 5.13) (mm)	Beam Width for Two Main Bars (mm)	Additional Width for Every Extra Bar (mm)
12	15*	25	95	37
16	20	25	113	41
20	20	25	121	45
22	25 ⁺	25	135	47
25	25	25	141	50
28	30	28	160	56

Notes:

- This table is for mild environment, 20mm aggregates, and 8mm stirrup.
- Increase cover for other environmental conditions, check cover for fire resistance.
- Increase width for stirrup diameter of 10mm and above.

* As per Table 16 of IS 456:2000, nominal cover is reduced by 5 mm for bars less than 12 mm diameter.

⁺ As per Clause 26.4.1, nominal cover should not be less than the diameter of the bar.

If the rods are placed in many layers, the effective depth should be calculated with reference to the centroid of reinforcement. The following formula can be used to calculate the centroidal distance of bars from the bottom fibre:

$$g_1 = (\sum \text{Area of rods in each layer} \times \text{Distance of C.G. from bottom}) / \text{Total area}$$

Then, effective depth, $d = D - g_1$

- In building frames, the width of the beams is often selected based on the lateral dimension of columns into which they frame. In India, in most of the buildings (with up to four to five floors), the column and beam widths are often selected as 230mm, just to match the size of the walls, so that column sides are flush with the finished surface of the wall. However, proper detailing requires the minimum size of the columns to be 300mm, so that the reinforcement bars of beams are properly accommodated inside the column. Sometimes, the beam width is also selected as 115 mm to support a half brick wall, which is often used as a partition wall. However, it should be noted that as per draft IS 13920 a minimum width of 200mm must be provided for the beam and a minimum b/D ratio of 0.3 must be adopted (see Table 4.1). The usual widths of beams adopted in practice are 150, 200, 230, 250, and 300mm. Again, it must be noted that these widths should be equal to or less than the dimension of the column into which they frame.

8. When architectural considerations restrict the size of the beam, the required moment of resistance may be achieved by increasing the strength of concrete or steel or by providing compression steel to make the beam doubly reinforced (see Section 5.6). It has to be noted that one may also take advantage of the slabs cast integrally with the beams by considering them as flanged beams: T- or L-beams (see Section 5.7).
9. As discussed in Section 5.5.3, increasing the depth is more advantageous than increasing the width (which is often fixed on architectural considerations) and results in an enhanced moment of resistance and a flexural stiffness with reduced deflections, curvatures, and crack widths. However, very deep beams are not desirable, as such deep beams reduce the height of headroom and may increase the height of the building too. Moreover, if the depth of the beam increases beyond 750 mm, side face reinforcement (not less than 0.1% of the web area and distributed equally on two faces at a spacing lesser of 300 mm and web thickness) has to be provided to reduce cracking, as per Clause 26.5.1.3 of IS 456:2000 (see Fig. 5.14). Increasing the compressive strength of concrete will not produce a large change in the nominal moment strength, but it will increase the ductility of the section (Wight and MacGregor 2009).

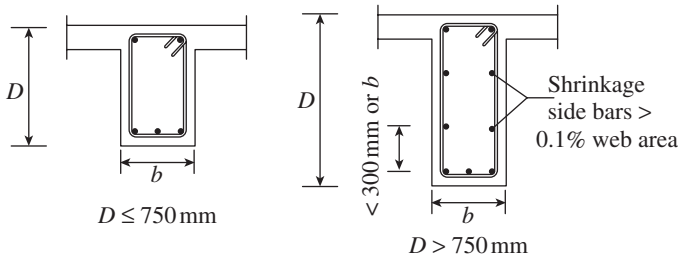


FIG. 5.14 Side face reinforcement

It should be noted that in the Indian building construction industry, the structural designs are found to be greatly influenced by the available construction infrastructure, namely timber suppliers. They mainly work in the foot-pound-second (FPS) system rather than the International System of Units (the SI system). The timber planks available are usually of size 4" (≈ 100 mm), 6" (≈ 150 mm), 9" (≈ 230 mm), 12" (≈ 300 mm), and 14" (≈ 350 mm). Thus, the usual depths of beams adopted in India are 350 mm (in order to avoid cutting or wastage of timber), 450 mm, 500 mm, and 600 mm. This fact equally holds good for the width of the beam, which are selected as 150 mm, 230 mm, or 300 mm. In beams of other sizes, plywood with timber framing is used (Vivek 2011).

10. It is often recommended to have the overall depth to width ratio (D/b) of rectangular beams in the range 1.5–2.0, though it may be higher (up to 3.0) for beams carrying heavy loads or having larger spans. It has to be noted that

the width and depth may also be governed by the shear force acting on the section (see Chapter 6).

11. The deflection requirements often control the depth of the beam. Clause 23.2.1 of IS 456:2000 suggests the following minimum span to effective depth (L/d) ratios for spans up to 10 m:

$$L/d = (L/D)_{\text{basic}} \times k_t \times k_c \quad (5.40a)$$

Here $(L/D)_{\text{basic}}$ is as follows:

Cantilever beams: 7

Simply supported beams: 20

Continuous beams: 26

For spans above 10 m, these values may be multiplied by 10/span in metres, except for cantilevers, for which the deflection calculations are necessary to fix the depth. The modification factors k_t (dependent on p_t and f_{st}) and k_c (dependent on p_c) are shown in Figs 4 and 5 of the code (Beeby 1971) and are given by the following:

$$k_t = \frac{1}{[0.225 + 0.00322f_s - 0.625 \log_{10}(1/p_t)]} \quad (5.40b)$$

$$k_c = 1 + \frac{p_c}{p_c + 3.0} \leq 1.5 \quad (5.40c)$$

Where

$$p_c = \frac{100A_{sc}}{bd}, p_t = \frac{100A_{st}}{bd},$$

and $f_s = 0.58 f_y = \frac{\text{Area of steel required}}{\text{Area of steel provided}}$

The L/d ratios of 10–15 have been found to result in economic depths for simply supported and continuous beams. An L/d ratio of 5–7 may be adopted for cantilevers. However, for cantilevers, though it is possible to taper the depth along the length, such tapering may not be economical due to the increased cost of the formwork.

12. It is desirable to limit the number of different sizes of beams in a structure to a few standard modular sizes, as they will reduce the cost of the formwork and permit reusability of forms.

5.5.8 Procedure for Proportioning Sections for Given Loads

A typical design problem involves the determination of the size and reinforcement of the beam subjected to a bending moment. It must be noted that the bending moment due to the self-weight of the beam should also be included in the calculation of the bending moment. As discussed, it is advisable to adopt under-reinforced beams with $p_t < p_{t,\text{lim}}$. The various steps involved are as follows:

1. Assume suitable concrete and steel grade.
2. Fix the beam width, b , based on the architectural and other considerations.

3. Calculate the effective depth of beam as per Eq. (5.28):

$$d = \sqrt{\frac{M_u}{kf_{ck}b}} = \sqrt{\frac{k_3 M_u}{f_{ck}b}}$$

where $k_3 = 6.71, 7.2,$ and 7.52 for Fe 250, Fe 415, and Fe 500 grade steels, respectively.

4. Round off to the next 50 mm and adopt an effective depth. Adopting a depth greater than the required depth results in an under-reinforced section. One may now assume the diameter of the bar and calculate the effective cover. Based on this, determine the total depth (expressed in multiples of 25 mm or 50 mm). Check whether the D/b ratio is within the range 1.5–2.0.
5. Now calculate the adopted effective depth (assuming the bars are accommodated in single layer) as follows:

$$D = d + \text{clear cover} + \text{diameter of stirrup} + \text{diameter of main bar}/2$$

If the bars cannot be accommodated in one layer, the value of d should be calculated accordingly. As shown in Fig. 5.15, the effective depth is the distance between the extreme compression fibre to the centroid of the longitudinal tensile steel reinforcement.

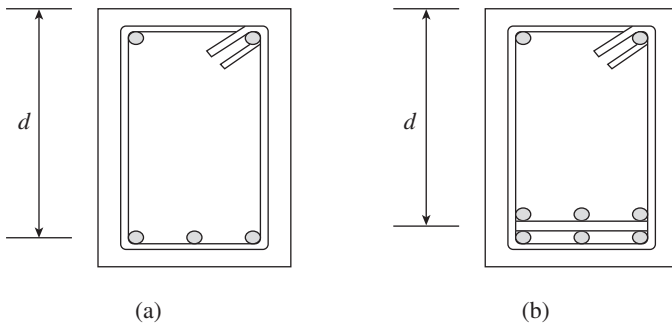


FIG. 5.15 Effective depth of an RC beam (a) Beam with single layer of reinforcement (b) Beam with two layers of reinforcement

6. The effective span of a beam of simply supported beams may be calculated as the clear span plus the effective depth of beam or c/c of supports, whichever is less (see Clause 22.2 of IS 456 and Section 5.3.1 for guidance to calculate the effective span of continuous beams, cantilevers, and members in frames).
7. Using the effective span and the considered loading, calculate the factored bending moment, M_u , acting on the beam. When the beam is a part of a frame and the bending moments are determined using a computer program (which will give the values at the centre lines), it is required to calculate the moment values at the face of the column for the design; this will result in considerable economy.

8. Calculate (x_u/d) using Eq. (5.29).

$$\left(\frac{x_u}{d}\right) = 1.2 - \sqrt{1.44 - \frac{6.68 M_u}{f_{ck} b d^2}}$$

This value should be less than $(x_u/d)_{lim}$.

9. Find the required area of steel.

$$\text{Required } A_{st} = \frac{M_u}{0.87 f_y z} \text{ with } z = d \left(1 - 0.416 \frac{x_u}{d}\right)$$

Provide the area of steel equal to or slightly greater than the required area and calculate the required number of bars for the chosen diameter of bar.

10. Check for minimum and maximum area of reinforcement. The minimum area of reinforcement is given by Eq. (5.35c) or (5.36c).

$$\frac{A_s}{b_w d} = \frac{0.85}{f_y} \text{ as per IS 456}$$

$$\frac{A_s}{b_w d} = \frac{0.224 \sqrt{f_{ck}}}{f_y} \geq \frac{1.4}{f_y} \text{ as per ACI 318}$$

The maximum area of steel according to Table 5.5 is given as follows:

$$p_{t,lim} = k \left(\frac{f_{ck}}{f_y}\right)$$

Here $k = 21.97, 19.82,$ or 18.87 for Fe 250, Fe 415, and Fe 500 grade steels, respectively. The provided p_t should be less than or equal to $p_{t,lim}$.

11. Check for ductility. Assuming the tension steel is yielding, calculate x_u as follows:

$$x_u = \frac{0.87 f_y A_{st}}{0.36 f_{ck} b}$$

Using strain compatibility, calculate ϵ_{st} as follows:

$$\epsilon_{st} = \left(\frac{d - x_u}{x_u}\right) \epsilon_{cu}$$

This calculated value of strain in steel should be greater than 0.005, so that we achieve enough ductility and the section can be classified as ‘tension controlled’ as per ACI 318. If the value of ϵ_{st} is less than 0.005, the depth should be increased and steps 5–8 repeated until ϵ_{st} is greater than 0.005. Increasing the concrete compressive strength will also change the transition zone section (with ϵ_{st} values 0.002–0.005) to tension-controlled section.

12. If the beam is an inverted beam, then the lateral slenderness has to be checked, as discussed in Section 5.5.6.
13. If the web of the beam is more than 750 mm, side face reinforcement has to be provided (not less than 0.1% of

- the web area and distributed equally on the two faces at a spacing equal to the lesser of 300 mm and web thickness).
14. The beam reinforcements should be detailed properly. At least one-third of the positive moment reinforcement in simple supports and one-fourth of the positive moment reinforcement in continuous beams should be extended along the same face of the member into the support to a length equal to $L_d/3$, where L_d is the development length (see Chapter 7 of this book and Clause 4.6.3 of SP 34:1987).
 15. The shear capacity should also be checked, as per Chapter 6, and if it is not sufficient, shear reinforcements should be designed. In any case, a minimum amount of shear reinforcement should be provided. In some cases, the beam has to be designed for torsion (see Chapter 8). When the beam is a part of a frame and the shear forces are determined using a computer program (which will give the values at the centre lines), it is required to calculate the shear values at a distance d from the face of the column.
 16. It should be noted that in addition to these steps, the beam should be checked for deflection and crack control.

5.5.9 Design of Over-reinforced Sections

It has to be noted that over-reinforced sections are not permitted by the code, that is, when $p_t < p_{t,lim}$ and $x_u > x_{u,lim}$ the steel will not yield and the stress in steel will be $f_{st} < 0.87f_y$. Now the failure will be by compression failure of concrete and the expression for M_n is of the following form:

$$\frac{M_n}{bd^2} = f_{st} \frac{p_t}{100} \left[1 - \frac{0.416f_{st}}{0.36f_{ck}} \frac{p_t}{100} \right] \quad \text{for } f_{st} < 0.87f_y \quad (5.41)$$

The strain ϵ_{st} corresponding to the stress f_{st} must satisfy the strain compatibility condition. The following are the steps involved in the strain compatibility method for determining M_n for a given p_t :

1. Apply equilibrium equation $T = C$, assuming the steel has yielded. Calculate the first trial value of x_u .
2. Now, $f_s = 700 \frac{d - x_u}{x_u}$.
3. Recalculate x_u . With the stress in the steel as $A_s f_s$, we get

$$0.36f_{ck}bx_u = A_s f_s$$

Substitute the value of f_s from step 2 in this equation and solve the quadratic equation for x_u .

4. Determine f_s by using the equation given in step 2.
5. Determine the moment capacity of the section, M_n , using the following equation:

$$M_n = A_s f_s (d - 0.416x_u)$$

This procedure is illustrated in Example 5.5. Thus, it is clear that the determination of M_u of over-reinforced section requires considerable computational effort. A conservative estimate of

the ultimate moment capacity of such over-reinforced section is given by $M_{n,lim}$ (see Eq. 5.26).

5.5.10 Design Using Charts and Design Aids

In practice, spreadsheets or computer programs are used to design beams. The Bureau of Indian Standards (BIS) has also published a special publication SP 16, which contains charts and tables that may be used for the quick design of beams. These tables are based on Eq. (5.24). Charts 1 to 18 of SP 16 have been developed by assigning different values of M_u per unit width and plotting in terms of depth, d , and percentage of tensile reinforcement, p_t . One such chart for $f_y = 415 \text{ N/mm}^2$ and $f_{ck} = 20 \text{ N/mm}^2$ is shown in Fig. 5.16. Tables 1 to 4 of SP 16 show various values of M_u/bd^2 for a number of p_t values. Using Excel, similar tables have been generated and are included in Appendix C.

The following procedure has to be adopted to determine the value of A_{st} from Tables 1 to 4 of SP 16 (or Tables C.1 to C.6 of Appendix C), for the given values of M_u, f_{ck}, f_y, b , and d .

1. Calculate M_u/bd^2 .
2. Choose the table corresponding to the given values of f_{ck} and f_y .
3. Read the percentage of steel corresponding to the value of M_u/bd^2 . Interpolate for in between values.

5.6 DOUBLY REINFORCED RECTANGULAR BEAMS

It is always economical to design beams as singly reinforced. However, occasionally beam sections are designed to have both tension and compression steel reinforcement. These are called *doubly reinforced beams*. If the required area of tension steel is more than the limiting area of steel recommended by the code (when $\epsilon_{st} = 0.0038$), compression steel may be provided to increase the moment-resisting capacity. Adding compression steel may change the mode of failure from compression failure of concrete to tension failure of steel. It may even change the section from over-reinforced to under-reinforced. Compression steel, in addition to increasing the resisting moment, also increases the amount of curvature that a member can take before failure in flexure. Thus, the ductility of the section is increased substantially (see Fig. 5.17, where p_t denotes tension steel and p_c denotes compression steel). Due to this fact, several earthquake codes specify a certain minimum amount of compression reinforcement to be included. For example, Clause 6.2.3 of IS 13920:1993 requires a minimum of 50 per cent tension steel to be provided as compression steel. As per AS 1480, compression steel must be used even in normal beams if the percentage of tension steel exceeds three-fourths of the balanced percentage.

Compression steel is also effective in reducing the long-term deflections due to shrinkage and creep, as shown in Fig. 5.18. The reader can also check the equation given

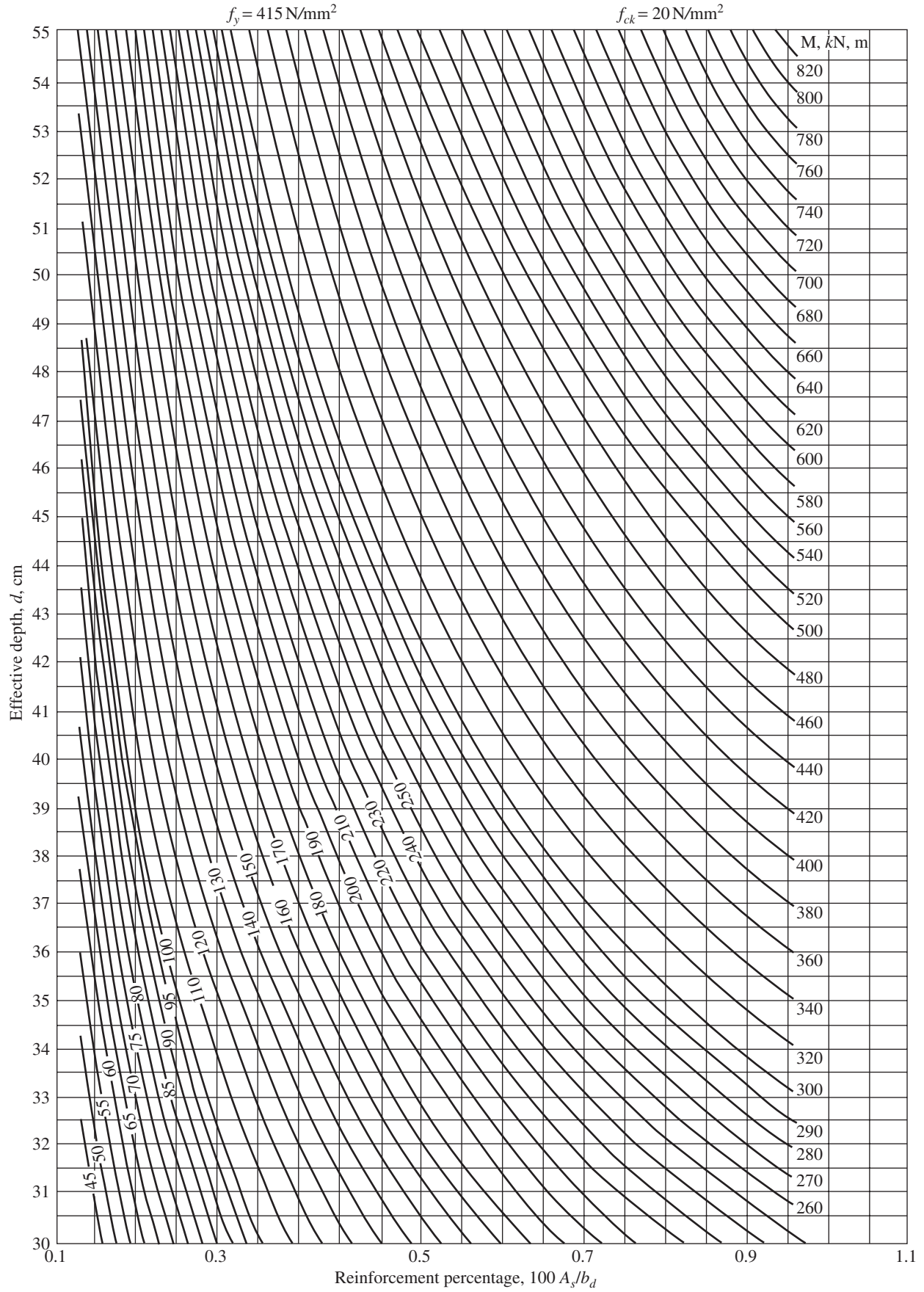


FIG. 5.16 Design chart for singly reinforced rectangular section for M_u (kNm) per metre width, as per SP 16

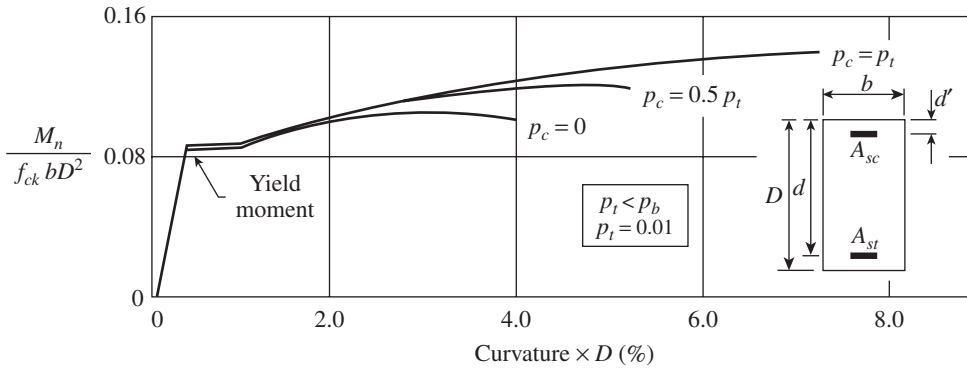


FIG. 5.17 Effect of compression reinforcement on strength and ductility of under-reinforced beams

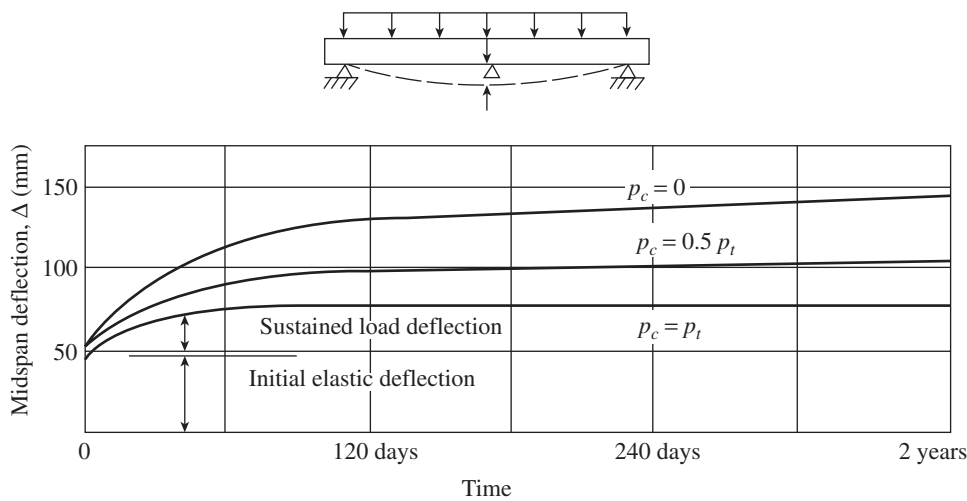


FIG. 5.18 Effect of compression reinforcement on sustained deflection

Source: Washa and Fluck 1952, reprinted with permission from ACI

in Annex C of IS 456 (Clause C-3.1) for calculating the deflection due to shrinkage, which clearly shows the effect of compression reinforcement on long-term deflection.

Compression reinforcement is used in the following situations:

1. In many cases, doubly reinforced sections may be necessary when architectural (space or aesthetic) requirements restrict the depth of beams. In such cases, the beam has to carry moments greater than the limiting capacity of the beam given by Table 5.4.
2. When the bending moment at a section changes sign (as may occur in the span of a continuous beam with moving loads in a bridge girder or in beams subjected to lateral loads such as earthquake or wind), compression reinforcement is used.
3. While assembling the reinforcement cage for a beam, it is advantageous to provide continuous compression reinforcement, which will hold the shear stirrups in place and also help to anchor the stirrups. If it is not provided,

the stirrups will not be held in proper position during concrete placement and vibration.

5.6.1 Behaviour of Doubly Reinforced Beams

The experiments conducted on doubly reinforced beams have shown that the beam will not collapse even if the compression concrete crushes, when the compression steel is enclosed by stirrups. Once the compression concrete reaches its crushing strain of about 0.0035, the cover concrete spalls (similar to the process in columns), and the beam deflects in a ductile manner. If the compression bars are confined by closely spaced stirrups, the bars will not buckle and will continue to take additional moment. This additional moment is not considered in practice, since the beam is considered to have practically reached its limiting strength once the cover spalls. However, the additional moment will provide extra safety and ductility.

In spite of the advantages mentioned, adding compression steel in beams will not appreciably increase the moment capacity of the section.

The depth of compression steel from the top fibre will be in the range of 10–30 per cent of the neutral axis distance. In such a case, the strain in compression steel is in the range of 0.0024–0.003. The corresponding stress in Fe 415 grade steel will be in the range of 342–354 MPa, which is near the design yield stress ($415/1.15 = 360.8$ MPa). Hence, usually an initial assumption is made that in addition to tension steel the compression steel also yields. In fact, this assumption may be perfect because the creep and shrinkage occurring in the compression concrete will help the compression steel to yield. It should be noted that if the calculated neutral axis is close to compression steel (this will happen in beams with a low percentage of tensile steel), the addition of compression steel is not advisable, as it will not contribute to the moment capacity of the section. To increase the moment capacity, it is required to add reinforcing steel in both tension and compression sides of the beam. This is because even if compression steel is added, the value $M = Tz$ will remain the same, as the lever arm z of the internal couple is not affected by the presence of compression steel alone (see also Section 5.6.4 and Fig. 5.19).

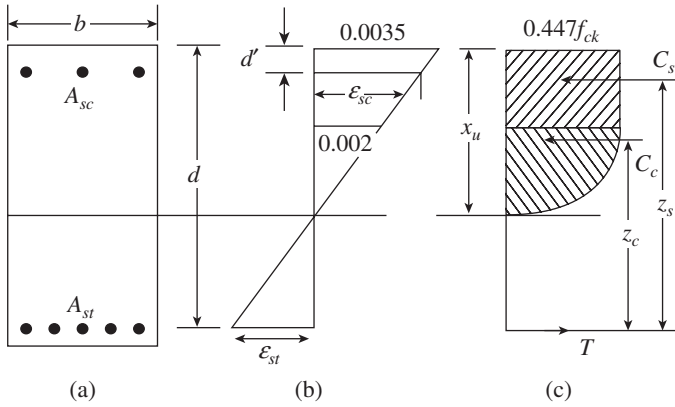


FIG. 5.19 Doubly reinforced rectangular section (a) Beam section (b) Strain (c) Stresses

Clause 26.5.1.2 of IS 456 states that the compression reinforcement must be enclosed by stirrups for effective lateral restraint. Section 26.5.3.2(c) stipulates that the spacing of the stirrups should not exceed 300 mm, least lateral dimension of the beam cross section, or sixteen times the smallest diameter of the longitudinal bar. It also states that the diameter of the stirrups should be greater than one-fourth of the diameter of the largest longitudinal bar or 6 mm.

5.6.2 Analysis of Doubly Reinforced Rectangular Beams

The distribution of stresses and strains in a doubly reinforced rectangular section are similar to that of a singly reinforced section, shown in Fig. 5.1, except that there is now an additional stress f_{sc} in the compression steel. This stress may or may not reach the design yield stress $0.87f_y$, depending on the magnitude of strain in the compression steel.

Considering the strain compatibility, the strain in compression steel is easily obtained as

$$\epsilon_{sc} = 0.0035 \left(1 - \frac{d'}{x_u} \right) \quad (5.42)$$

where d' is the distance between the centroid of the compression steel and the extreme compression fibre (effective cover for compression steel), as shown in Fig. 5.19.

The stress in compression steel corresponding to this strain is given as follows:

For mild steel:

$$f_{sc} = \epsilon_{sc} E_s \leq 0.87 f_y \quad (5.43a)$$

For HYSD bars:

$$f_{sc} = \epsilon_{sc} E_s \text{ for } \epsilon_{sc} \leq 0.696 f_y / E_s \quad (5.43b)$$

This is calculated from Table 5.2 or design stress–strain curve (Fig. 5.5) for $\epsilon_{sc} > 0.696 f_y / E_s$.

The limiting moment of resistance of the section will depend on whether it is a balanced or under- or over-reinforced

section, which may be ascertained by comparing the depth of the neutral axis (x_u) obtained by assuming either balanced or under-reinforced section with the neutral axis depth of the balanced section.

Considering a balanced section, the neutral axis can be obtained from the equilibrium of the internal compressive and tensile forces as follows:

$$C_s + C_c = T \quad (5.44a)$$

where C_s and C_c denote the compressive force in concrete and compression steel, respectively. Thus,

$$0.36 f_{ck} b x_u + (f_{sc} - f_{cc}) A_{sc} = 0.87 f_y A_{st} \quad (5.44b)$$

Rearranging, we get

$$x_u = \frac{0.87 f_y A_{st} - (f_{sc} - f_{cc}) A_{sc}}{0.36 f_{ck} b} \quad (5.44c)$$

where f_{sc} is the stress in compression steel, determined using Eq. (5.43), and f_{cc} is the stress in concrete at the level of centroid of the compression steel corresponding to the strain given by Eq. (5.45).

$$\begin{aligned} f_{cc} &= 0.447 f_{ck} \left[2 \left(\frac{\epsilon_c}{0.002} \right) - \left(\frac{\epsilon_c}{0.002} \right)^2 \right] \text{ for } \epsilon_c < 0.002, \\ &= 0.447 f_{ck} \text{ for } 0.002 \leq \epsilon_c \leq 0.0035 \end{aligned} \quad (5.45)$$

The ultimate moment of resistance can be calculated by considering the moments of C_c and C_s about the centroid of the tension steel (Fig. 5.19) as follows:

$$M_n = C_c z_c + C_s z_s$$

$$M_n = 0.36 f_{ck} b x_u (d - 0.416 x_u) + (f_{sc} - f_{cc}) A_{sc} (d - d') \quad (5.46)$$

The value of x_u given by Eq. (5.44c) can be determined only by iteration using the following procedure:

Step 1 Assume $x_u = x_{u,lim} = \frac{0.0035}{0.0055 + 0.87 f_y / E_s} d$.

Step 2 Calculate $\epsilon_{sc} = \frac{0.0035(x_u - d')}{x_u}$ and the corresponding values of f_{sc} and f_{cc} using Eqs (5.43) and (5.45).

Step 3 Compute $x_u = \frac{0.87 f_y A_{st} - (f_{sc} - f_{cc}) A_{sc}}{0.36 f_{ck} b}$

Repeat Steps 2 and 3 until the value of x_u converges.

Comparison of x_u with $x_{u,lim}$ will give rise to the following two cases:

Case 1 If $x_u \leq x_{u,lim}$ then it is a balanced or an under-reinforced section and the value of x_u as determined by the given procedure is correct. The ultimate moment of resistance can be calculated using Eq. (5.46).

Case 2 If $x_u > x_{u,\text{lim}}$ then it is an over-reinforced section and the value of x_u as determined by this procedure is not correct. It may be determined from the equilibrium of internal forces as follows:

$$C_s + C_c = T$$

Thus,

$$0.36f_{ck}bx_u + (f_{sc} - f_{cc})A_{sc} = f_{st}A_{st}$$

or

$$x_u = \frac{f_{st}A_{st} - (f_{sc} - f_{cc})A_{sc}}{0.36f_{ck}b}$$

where f_{st} is the stress in tension steel, corresponding to the strain $\epsilon_{st} = 0.0035(d - x_u)/x_u$ and f_{sc} and f_{cc} are the stresses in compression steel and concrete, respectively, at the level of centroid of the compression steel corresponding to the strain $\epsilon_{sc} = 0.0035(x_u - d')/x_u$.

The value of x_u can be determined by iteration using the following procedure:

Step 1 Assume $x_u = x_{u,\text{lim}} = \frac{0.0035}{0.0055 + 0.87f_y/E_s} d$.

Step 2 Calculate $\epsilon_{st} = \frac{0.0035(d - x_u)}{x_u}$ and the corresponding values of f_{st} .

Step 3 Calculate $\epsilon_{sc} = \frac{0.0035(x_u - d')}{x_u}$ and the corresponding values of f_{sc} and f_{cc} using Eqs (5.43) and (5.45).

Step 4 Compute $x_u = \frac{f_{st}A_{st} - (f_{sc} - f_{cc})A_{sc}}{0.36f_{ck}b}$.

Repeat Steps 2 and 4 until the value of x_u converges.

The ultimate moment of resistance can now be calculated using Eq. 5.46.

5.6.3 Limiting Moment of Resistance and Compression Steel

The limiting moment of resistance $M_{n,\text{lim}}$ is obtained for the condition $x_u = x_{u,\text{lim}}$ and is given by the following expression:

$$M_{n,\text{lim}} = 0.36f_{ck}bx_{u,\text{lim}}(d - 0.416x_{u,\text{lim}}) + (f_{sc} - 0.447f_{ck})A_{sc}(d - d') \quad (5.47a)$$

where the value of f_{sc} depends on ϵ_{sc} , obtained from Eq. (5.43) and Table 5.2. For convenience, the values of the stress f_{sc} (corresponding to $x_u = x_{u,\text{lim}}$) for various grades of steel and the ratios of (d'/d) as derived using Eqs (5.43) and (5.20) and Table 5.2 are given in Table 5.8.

Similarly, the compression reinforcement for the balanced section is given by

$$p_{c,\text{lim}} = \frac{0.87f_y}{f_{sc} - 0.447f_{ck}}(p_t - p_{t,\text{lim}}) \quad (5.47b)$$

where f_{sc} may be obtained from Table 5.8. If the p_c provided in a beam section exceeds $p_{c,\text{lim}}$, then $x_u < x_{u,\text{lim}}$ and the beam is under-reinforced. Similarly, if $p_c < p_{c,\text{lim}}$ the beam is over-reinforced.

TABLE 5.8 Design stress f_{sc} for different values of d'/d

d'/d	Stress f_{sc} (MPa)			d'/d	Stress f_{sc} (MPa)		
	Fe 250	Fe 415	Fe 500		Fe 250	Fe 415	Fe 500
0.04	217.5	355.72	424.66	0.13	217.5	346.40	401.60
0.05	217.5	355.08	423.78	0.14	217.5	344.52	398.36
0.06	217.5	354.44	421.41	0.15	217.5	342.58	395.06
0.07	217.5	353.80	419.01	0.16	217.5	339.90	391.82
0.08	217.5	353.17	416.61	0.17	217.5	337.22	386.75
0.09	217.5	352.53	414.21	0.18	217.5	334.53	381.43
0.10	217.5	351.89	411.43	0.19	217.5	331.85	376.04
0.11	217.5	350.18	408.15	0.20	217.5	329.17	370.65
0.12	217.5	348.28	404.87	—	—	—	—

To find the limiting compression steel, let us consider p_t as consisting of two components—one component is $p_{t,\text{lim}}$ and the other is $(p_t - p_{t,\text{lim}})$. Let us also assume that the tensile force due to $p_{t,\text{lim}}$ is balanced by the compressive force in concrete $C_c = 0.36f_{ck}bx_{u,\text{max}}$, and the tensile force due to $(p_t - p_{t,\text{lim}})$ is balanced by the compressive force in the compression steel, C_s , alone. Now, considering the force equilibrium of the second part, the balanced compression steel, $p_{c,\text{lim}}$, may be obtained as follows:

$$0.87f_y \frac{(p_t - p_{t,\text{lim}})bd}{100} = (f_{sc} - 0.447f_{ck}) \frac{p_{c,\text{lim}}}{100} bd$$

From this equation, we get

$$p_{c,\text{lim}} = \frac{0.87f_y}{(f_{sc} - 0.447f_{ck})} (p_t - p_{t,\text{lim}}) \quad \text{for } x_u = x_{u,\text{lim}} \quad (5.48)$$

In this equation, f_{sc} should be calculated based on Table 5.2. As in the case of singly reinforced beams, the following can be deduced:

If the provided p_c in the beam is greater than $p_{c,\text{lim}}$ given by Eq. (5.48), then $x_u < x_{u,\text{lim}}$, and the beam may be considered under-reinforced, whereas if $p_c < p_{c,\text{lim}}$, then $x_u > x_{u,\text{lim}}$, and the beam is over-reinforced. The limiting moment of resistance $M_{n,\text{lim}}$ for the balanced condition can be derived in terms of percentage tensile steel as follows:

$$M_{n,\text{lim}} = 0.87f_y \left[\frac{p_{t,\text{lim}}}{100} bd(d - 0.416x_{u,\text{lim}}) + \frac{(p_t - p_{t,\text{lim}})}{100} bd(d - d') \right] \quad (5.49)$$

5.6.4 Design of Doubly Reinforced Rectangular Beams

The procedure similar to the one used for designing singly reinforced sections can be used for the design of doubly

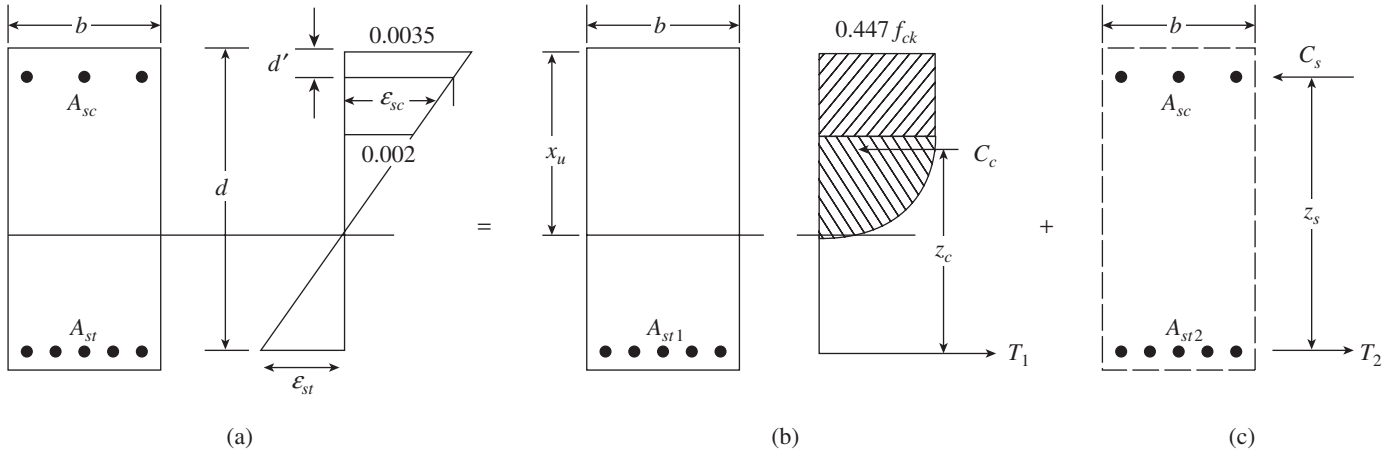


FIG. 5.20 Design of doubly reinforced rectangular section (a) Beam section (b) Strain (c) Stresses

reinforced sections, assuming that the beam is equivalent to two beams as shown in Fig. 5.20. Thus, the real beam may be considered as consisting of one singly reinforced beam, which reaches its ultimate strength, and another imaginary steel beam (without any concrete) but has only compression and tension steel. The moment of resistance of the doubly reinforced beam is thus the sum of the moment of resistance of the two beams shown in Fig. 5.20. This concept is referred to as *steel beam theory*.

Thus,
$$M_n = M_{n1} + M_{n2}$$

where M_{n1} is the limiting moment of resistance of the singly reinforced beam and M_{n2} is the moment capacity of the steel beam.

The limiting moment of resistance of singly reinforced beam is given by

$$\begin{aligned} M_{n,\text{lim}} &= 0.149f_{ck}bd^2 \text{ for grade Fe 250 steel with } p_{t,\text{lim}} = 21.97 \frac{f_{ck}}{f_y} \\ &= 0.138f_{ck}bd^2 \text{ for grade Fe 415 steel with } p_{t,\text{lim}} = 19.82 \frac{f_{ck}}{f_y} \\ &= 0.133f_{ck}bd^2 \text{ for grade Fe 500 steel with } p_{t,\text{lim}} = 18.87 \frac{f_{ck}}{f_y} \end{aligned} \quad (5.50a)$$

$$(5.50b)$$

$$(5.50c)$$

The moment capacity of the steel beam is given by (considering the effect of replacement of concrete in the compression zone by the compression steel too)

$$M_{n2} = (f_{sc} - f_{cc})A_{sc}(d - d')$$

where f_{sc} is the stress in compression steel, corresponding to the strain given by $\epsilon_{sc} = 0.0035 \left(\frac{x_{u,\text{lim}} - d'}{x_{u,\text{lim}}} \right)$ determined

using Eq. (5.43), and f_{cc} is the stress in concrete at the level of the centroid of the compression steel. The value of f_{cc} will be much smaller than that of f_{sc} and hence can be neglected for all practical purposes; hence, we get the value of M_{n2} as given in Annexure G-1.2 of IS 456 as

$$M_{n2} = M_u - M_{n,\text{lim}} = (f_{sc} - f_{cc})A_{sc}(d - d') \quad (5.51)$$

The total area of tension reinforcement is obtained as

$$A_{st} = A_{st1} + A_{st2}$$

where A_{st} is the area of total tension reinforcement, A_{st1} is the area of tensile reinforcement for a singly reinforced section with a moment resistance capacity of $M_{n,\text{lim}}$, and $A_{st2} = A_{sc}f_{sc}/0.87f_y$.

The compression steel area (A_{sc}) may be expressed as a ratio of tension steel, A_{st} , as follows:

$$A_{sc} = \alpha A_{st} \quad (5.52)$$

The value of α is usually in the range 0.1–0.6. For economy, it is always better to restrict the amount of compression reinforcement to only 40 per cent of the tension steel.

The following steps are adopted in the design of doubly reinforced sections, subjected to an external moment M_u , where the depth is restricted for architectural or other considerations and it is required to find A_{st} and A_{sc} :

1. Assume a reasonable breadth for the beam and the limiting moment of resistance of the section $M_{n,\text{lim}}$, considering the beam as singly reinforced and using Eq. (5.50).
2. Compare $M_{n,\text{lim}}$ with the factored applied moment M_u . If $M_{n,\text{lim}} > M_u$, a singly reinforced section itself is adequate to resist the external moment. Otherwise, the beam has to be designed as doubly reinforced.
3. Determine the area of tensile reinforcement A_{st1} required to resist $M_{n,\text{lim}}$ given by

$$A_{st1} = \frac{M_{n,\text{lim}}}{0.87f_y(d - 0.416x_{u,\text{lim}})} \quad (5.53)$$

This can also be determined from the $p_{t,lim}$ given in Eq. (5.50).

4. Calculate the additional moment to be resisted by the beam, $M_{u2} = M_u - M_{n,lim}$.

This moment has to be resisted by the internal couple produced by the additional tensile steel A_{st2} and the compressive steel A_{sc} .

5. Compute A_{st2} and A_{sc} using the following relations:

$$A_{st2} = \frac{M_{u2}}{0.87f_y(d-d')} \quad (5.54a)$$

$$A_{sc} = \frac{M_{u2}}{(f_{sc} - f_{cc})(d-d')} \quad (5.54b)$$

Here, f_{sc} and f_{cc} are the design stresses in compression steel and concrete at the level of centroid of the compression steel.

6. Compute total tensile steel, $A_{st} = A_{st1} + A_{st2}$.

Check if the provided p_c is greater than the $p_{c,lim}$ given by Eq. (5.47b). Only when p_c provided in a beam section exceeds $p_{c,lim}$, the beam is under-reinforced. Hence, if it is less, revise the reinforcement.

7. Other checks regarding shear, deflection, and maximum crack width should also be made on the designed beam.

5.6.5 Design Using Charts and Design Aids

As mentioned in Section 5.5.10, in practice, spreadsheets or computer programs are used to design doubly reinforced beams. The special publication SP 16, published by BIS, contains charts and tables that may be used for the quick design of doubly reinforced beams. Charts 19 and 20 of SP 16 can be used to determine A_{st2} , the additional steel, for the beam for different $(d-d')$ values for Fe 250 grade steel alone. For other grades of steel, multiplication factors are provided in Table G of SP 16 for four different values of (d'/d) . Tables 45 to 56 of SP 16 show the reinforcement percentages (p_t and p_c) for various M_u/bd^2 values, and for four different values of (d'/d) ratios (0.05, 0.10, 0.15, and 0.20), three steel grades (Fe 250, Fe 415, and Fe500), and three concrete grades (M15, M20, and M30). These tables are based on Eqs (5.55)–(5.57):

$$\frac{M_u}{bd^2} = \frac{M_{u,lim}}{bd^2} + \frac{p_{t2}}{100}(0.87f_y)\left(1 - \frac{d'}{d}\right) \quad (5.55)$$

Here, p_{t2} is the additional percentage of tensile reinforcement and $(M_{u,lim}/bd^2)$ values are given by Eq. (5.50).

$$p_t = p_{t,lim} + p_{t2} \quad (5.56)$$

$$p_c = p_{t2} \left(\frac{0.87f_y}{f_{sc} - f_{cc}} \right) \quad (5.57)$$

The values of $p_{t,lim}$ are also given in Eq. (5.50).

The following procedure has to be adopted to determine the value of A_{st} from Tables 45 to 56 of SP 16, for the given values of M_u, f_{ck}, f_y, b , and d .

1. Calculate M_u/bd^2 .
2. Choose the table corresponding to the given values of f_{ck}, f_y , and (d'/d) .
3. Read the percentage of tension and compression steel (p_t and p_c) corresponding to the value of M_u/bd^2 . Interpolate for in between values.

Using Excel, similar tables have been generated and are included as Tables C.7 and C.8 in Appendix C. It has to be noted that IS 13920 requires 50 per cent of tension steel as compression steel for the beams to perform as ductile beams. Desai (2003) also developed tables that give the $M_u/f_{ck}bd^2$ values for the given values of $p_t, p_c, d'/d, f_{ck}$, and f_y . These tables (given as Tables C.9–C.16 in Appendix C) will be very useful to analyse a given section for its moment capacity. During design, extra reinforcement is normally provided, according to the available bar sizes. Thus, these tables can be used to find the additional moment capacity that is available in the designed beams.

Moreover, when the beams are subjected to reversal of stresses, designers generally design them separately for sagging (positive) and hogging (negative) moments and provide reinforcements at the appropriate face of the beam. Since reinforcements are available on both the faces of the beam, such beams can be designed using these tables, resulting in considerable saving of reinforcements. Sinha (1996) and Varyani and Radhaji (2005) also developed design charts for singly and doubly reinforced rectangular beams.

5.7 FLANGED BEAMS

With the exception of precast systems, beams in RC buildings are often cast monolithically with concrete slabs. Naturally, in this case, both the beam and the slab act together to resist the external loads. (If the beam and the slab are not cast monolithically, some kind of shear connector has to be provided in order to assume composite action.) Due to this, some portion of the slab is often considered to act together with the beam. This extra width of the slab at the top (if the beam is an inverted beam, the slab will be at the bottom) is often called a *flange*. If the slab is present on both the sides, the beam is called a *T-beam*, and if the slab is present only on one side (at the end of the slabs), it is called an *L-beam* (see Fig. 5.21). The part of the T- or L-beam below the slab is called the *web* or *stem* of the beam (it should be noted that the entire rectangular portion of the beam other than the overhanging parts of the flange is considered as the web in shear calculations, described in Chapter 6). The integral action of the slab with the beam is ensured by the stirrups (described

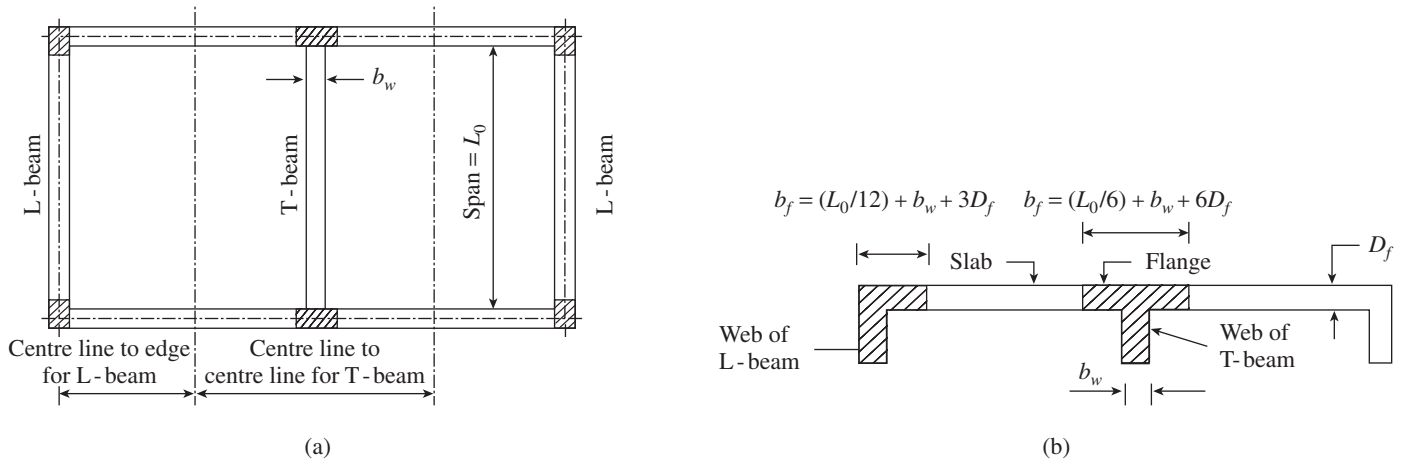


FIG. 5.21 T- and L-beams (a) Plan (b) Section

in Chapter 6), which extend from the web into the slab, and also by the bent-up bars in slabs.

5.7.1 Effective Width of Flange

The effective flange width concept allows us to use the rectangular beam design methodology in the design of T- or L-beams. There is always a question of the width of the slab that acts with the beam integrally to resist the applied loads. When the flange is relatively wide, the flexural compressive stress is not uniform over its width. It has been found from experiments that this stress has the maximum value near the web of the beam and reduces to a minimum value midway between the webs, as shown in Fig. 5.22(a). This is because the shearing deformation of the flange relieves some compression at the points away from the web. This effect is referred to as the *shear lag* effect.

Although the actual longitudinal compression varies as shown in Fig. 5.22(a), it is simple and convenient to consider an effective flange width, b_f , smaller than the actual flange width, which is uniformly stressed at the maximum value (Lee 1962). This effective width was found to depend primarily on the type of loading (concentrated, uniformly distributed, etc.) and four important dimensional parameters, namely b_0/L , L_0/D , b_w/D , and b_f/d , where b_0 , L_0 , D , b_w , and b_f are the beam spacing, span, overall depth, web thickness, and flange width, respectively (Loo and Sutandi 1986). The equivalent flange width may be less for the concentrated load than for uniformly

distributed loads. Different codes adopt different formulae for calculating the effective width, and there is considerable lack of agreement among the code methods in predicting the b_f values. However, all codes were found to predict conservative estimates of b_f for uniformly distributed loads, but give unsafe values for concentrated loading cases, when the beam spacing is small (Loo and Sutandi 1986). The Indian (Clause 23.1.2), US (Clause 8.12), and New Zealand code provisions are compared in Table 5.9.

The Indian code also specifies that for isolated beams the effective flange width should not be greater than the actual width or the following:

$$\text{T-beams: } b_f = \frac{L_0}{\left(\frac{L_0}{b}\right) + 4} + b_w \quad (5.58a)$$

$$\text{L-beams: } b_f = \frac{0.5L_0}{\left(\frac{L_0}{b}\right) + 4} + b_w \quad (5.58b)$$

According to ACI, for isolated beams, the T-flange thickness should not be less than one-half the width of the web and the effective flange width should not be more than four times the width of the web (b_w). The New Zealand code clearly states that only one-half of the effective overhanging parts of flanges used for the evaluation of flexural strength

Distribution of longitudinal compressive stress in top fibre

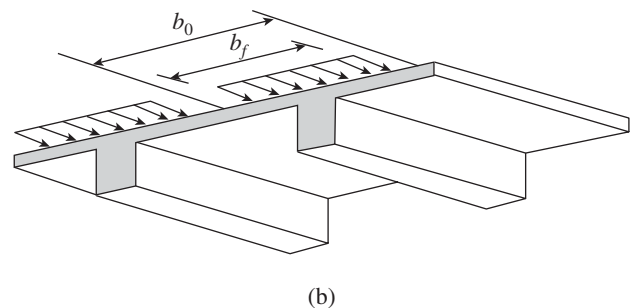
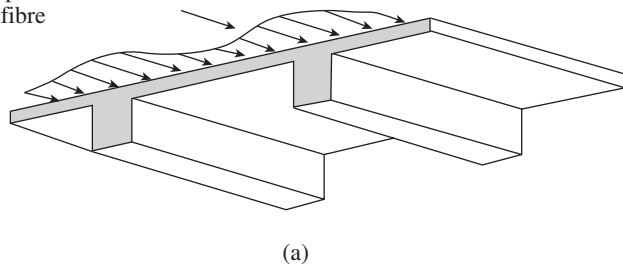


FIG. 5.22 Distribution of flexural compressive stresses across the flange (a) Actual distribution (b) Assumed in design

TABLE 5.9 Effective flange width, b_f , as per different codes

Type of Beam	IS 456:2000	ACI 318:08	NZS 3101:2006
T-beam	Least of (a) $b_w + 6D_f + L_0/6$ (b) $b_w + b_0$	Least of (a) $b_w + 16D_f$ (b) $L_0/4$ (c) $b_w + b_0$	Least of (a) $b_w + 16D_f$ (b) $b_w + L_0/4$ (c) $b_w + 2D_1$ (d) $b_w + b_0$ $\left(\frac{D_1}{D_1 + D_2} \right)$
L-beam	Least of (a) $b_w + 3D_f + L_0/12$ (b) $b_w + b_0$	Least of (a) $b_w + 6D_f$ (b) $b_w + L_0/12$ (c) $b_w + b_0/2$	Least of (a) $b_w + 8D_f$ (b) $b_w + L_0/8$ (c) $b_w + D_1$ (d) $b_w + b_0$ $\left(\frac{D_1}{D_1 + D_2} \right)$

L_0 = Distance between the points of contra flexure (zero moments) or effective span for simply supported beams and 0.7 times the effective span for continuous beams, b_w = Breadth of web, D_f = Thickness of flange, b_0 = Half the sum of the clear distances to the adjacent beams on either side, D_1 = Total depth of beam being considered, and D_2 = Total depth of the adjacent beam.

(see Table 5.9) should be used for the evaluation of stiffness (moment of inertia). Thus, it is clear that the code formulae for calculating the effective flange width differ considerably and the provisions of NZ 3101 are more stringent.

It should be noted that the direction of bending moment plays a role in the decision regarding the design of the beam as a rectangular or T-beam. Consider the example of a continuous beam shown in Fig. 5.23. If the flange resists the compressive stresses due to the bending moment, then it can be designed as a T-beam. On the other hand, if the web resists the compressive

stresses, it has to be designed as a rectangular beam. Thus, in a normal beam (where the slab is at the top) subjected to gravity loading, near the mid-span there is a positive bending moment (section A–A); the flange resists the compressive stresses due to the bending moment, and hence the beam is designed as a T-beam. On the other hand, near the support (section B–B), there is a negative bending moment; the compressive stresses due to the bending moment are resisted by the web of the same beam, and hence it has to be designed only as a rectangular beam. However, as shown in Case 2 of Fig. 5.23, for an inverted beam, the position of the slab is reversed, and hence near support (section D–D), it is designed as a T-beam and near mid-span (section C–C), the same beam has to be designed only as a rectangular beam.

5.7.2 Behaviour of Flanged Beams

The behaviour of the flanged beams is similar to that of the rectangular beams. For the case of ‘sagging’ moment (referred to as positive moment in this book), which occurs at mid-span, the top fibres (above neutral axis) are subjected to compression and the bottom fibres (below the neutral axis) are subjected to tension, and hence the effect of the flange (which is effective in resisting compression in concrete) can be considered in the design; due to this, the area of reinforcement is reduced. However, near the supports in continuous beams or at the support of cantilevers, there will be a ‘hogging’ moment (referred to as negative moment in this book), and hence the top fibres will be in tension and bottom fibres will be in compression. Now, the flanges are subjected to tension; since concrete is weak in tension, it will crack, and hence only the reinforcement should be considered to be effective in the calculations. Thus, the flange concrete is ignored for the hogging moment. Thus, in effect, the T-beam action is taken only at the mid-span, whereas near supports only the rectangular beam action is considered. In the same manner, the behaviour of doubly reinforced T-beams will be similar to that of doubly reinforced rectangular sections; again, only at the portion near the mid-span, the flanges are effective and considered in resisting the external moment. It has to be noted that under reversal of stresses (as happens due to the action of lateral loads), there will be a negative moment near the mid-span and a positive moment near the support. Hence, the T-beam action may be utilized near the supports and should not be considered near the mid-span.

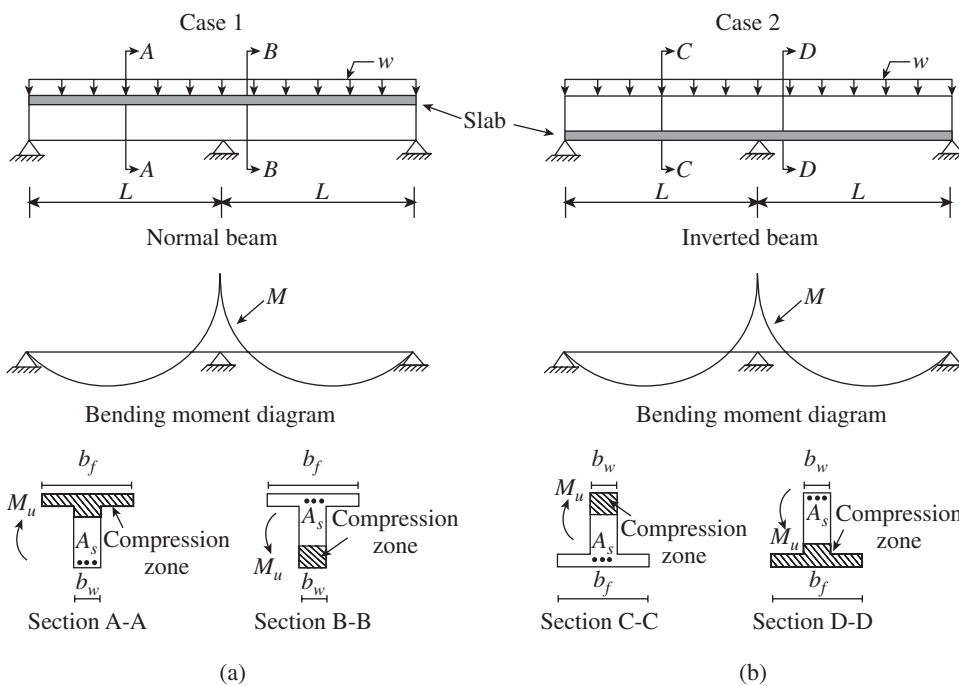


FIG. 5.23 Compression zones (a) Normal beams (b) Inverted beams

5.7.3 Analysis of Flanged Beams

The basic assumptions stated in Section 5.4 for the rectangular sections, including that of the plane sections remaining plane after bending, are also applicable for T-beams. It is assumed that the concrete begins to crush in compression at a strain equal to 0.0035. Depending on the magnitude of the applied bending moment, the neutral axis may lie within or outside the flange, resulting in the following three cases:

Case 1 Neutral axis within the flange ($x_u \leq D_f$), as shown in Fig. 5.24(a). As shown in this figure, the compression zone

in this case occupies only a part of the flange. Hence, the concrete section in the flange on the tension side of the neutral axis can be assumed to be ineffective, and the beam can be treated as a normal rectangular beam of width b_f and depth d . Thus, Eqs (5.18a), (5.22a), and (5.29) are applicable with b being replaced by b_f , as follows:

$$\frac{x_u}{d} = \frac{0.87 f_y A_{st}}{0.36 f_{ck} b_f d} \tag{5.59}$$

$$\left(\frac{x_u}{d}\right) = \frac{1 - \sqrt{[1 - 4\beta m]}}{2\beta};$$

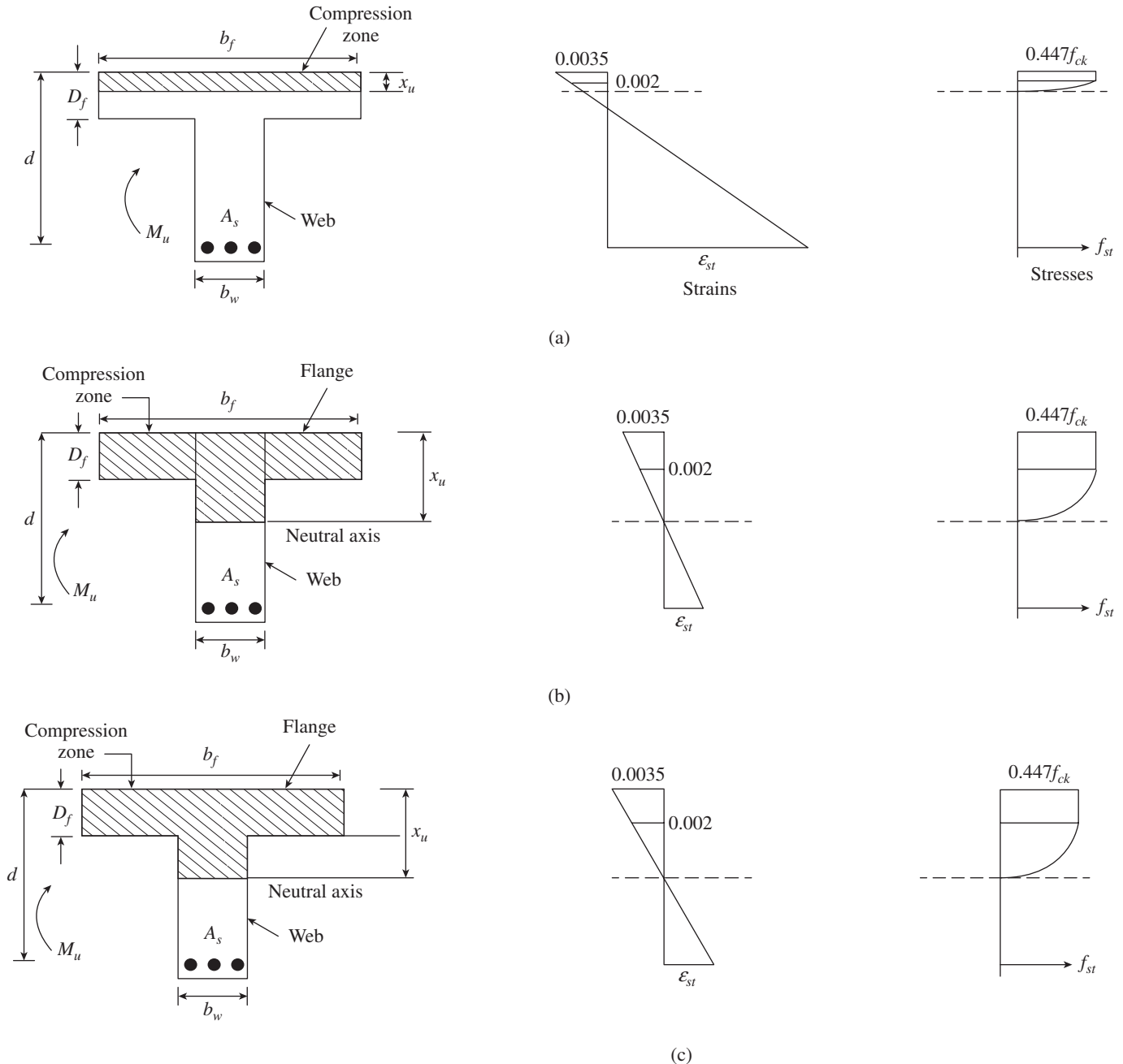


FIG. 5.24 Behaviour of flanged T-beams at ultimate load (a) Neutral axis within flange $x_u \leq D_f$ (b) Neutral axis outside flange $x_u > D_f$ (c) Neutral axis outside flange $x_u > D_f$ and $D_f > 0.2d$

$$\text{with } m = \frac{M_u}{0.36f_{ck}b_f d^2} \quad \text{and} \quad \beta = 0.416 \quad (5.60)$$

$$M_n = 0.36f_{ck} \left(\frac{x_u}{d} \right) \left(1 - 0.416 \frac{x_u}{d} \right) b_f d^2 \quad \text{for all } x_u \quad (5.61)$$

As in the case of rectangular beams

$$\left(\frac{x_u}{d} \right)_{\text{lim}} = \frac{805}{1265 + f_y}$$

The T-beam is considered under-reinforced when $x_u < x_{u,\text{lim}}$.

Case 2 Neutral axis outside the flange, which happens when $(3x_u/7) \geq D_f$, as shown in Fig. 5.24(b). As shown in this figure, the compression zone in this case occupies the full flange and a portion of the web. When the thickness of the flange is small compared to the depth of the beam, that is, when D_f is less than $0.2d$, the compressive stress in the flange will be uniform (and equals $0.447f_{ck}$) or nearly uniform, as shown in Fig. 5.24(b). The moment of resistance of the T-beam can now be taken as the sum of the moment of resistance of the concrete in the web of width b_w and the contribution due to the flanges of width b_f . The centroid of the compressive force in the flange can also be taken at $D_f/2$ from the extreme compression fibre.

From Fig. 5.24(b), with b_f as the breadth of the flange, the total compression in concrete

$$C_{uw} + C_{uf} = 0.36f_{ck}x_u b_w + 0.447f_{ck}D_f(b_f - b_w)$$

Total tension in steel: $T_u = 0.87f_y A_{st}$

Equating total compression and total tension and rearranging, we get

$$x_u = \frac{0.87f_y A_{st} - 0.447f_{ck}D_f(b_f - b_w)}{0.36f_{ck}b_w} \quad (5.62)$$

The moment of resistance of the section can be considered as having two parts:

$$M_n = M_{n1}[\text{rectangular web of size } b_w \times d] \\ + M_{n2}[\text{flange of size } (b_f - b_w) \times D_f]$$

Taking the moment of forces about the tension steel, we get for the web portion alone

$$M_{n1} = 0.36f_{ck} \left(\frac{x_u}{d} \right) \left(1 - 0.416 \frac{x_u}{d} \right) b_w d^2 \quad (5.63a)$$

For the remaining flange of size $(b_f - b_w) \times D_f$, we get

$$M_{n2} = 0.447f_{ck}(b_f - b_w)D_f \left(d - \frac{D_f}{2} \right) \quad (5.63b)$$

Thus, we get the moment of resistance of the T-beam as given in Annex G (Eq. G-2.2) of IS 456:2000 as

$$M_n = 0.36f_{ck} \left(\frac{x_u}{d} \right) \left(1 - 0.416 \frac{x_u}{d} \right) b_w d^2$$

$$+ 0.447f_{ck}(b_f - b_w)D_f \left(d - \frac{D_f}{2} \right) \quad (5.63c)$$

where M_n , x_u , d , and f_{ck} are as defined earlier, b_f is the breadth of flange, b_w is the breadth of web, and D_f is the thickness of flange.

From this equation, the value of (x_u/d) may also be derived as follows:

Dividing both sides of the equation by $(0.1497f_{ck}b_f d^2)$, we get

$$\frac{6.68M_n}{f_{ck}b_f d^2} = \left[2.4 \left(\frac{x_u}{d} \right) - \left(\frac{x_u}{d} \right)^2 \right] \frac{b_w}{b_f} \\ + 3 \frac{b_w}{b_f} \left(\frac{b_f}{b_w} - 1 \right) \left(\frac{D_f}{d} \right) \left(1 - \frac{D_f}{2d} \right)$$

Rearranging the terms in this equation, a quadratic equation in (x_u/d) is obtained as

$$\left(\frac{x_u}{d} \right)^2 - 2.4 \left(\frac{x_u}{d} \right) + \frac{6.68M_n}{f_{ck}b_f d^2} \left(\frac{b_f}{b_w} \right) - 3 \left(\frac{b_f}{b_w} - 1 \right) \left(\frac{D_f}{d} \right) \left(1 - \frac{D_f}{2d} \right)$$

$$\text{Denoting } k_4 = \frac{6.68M_n}{f_{ck}b_f d^2} \left(\frac{b_f}{b_w} \right) - 3 \left(\frac{b_f}{b_w} - 1 \right) \left(\frac{D_f}{d} \right) \left(1 - \frac{D_f}{2d} \right)$$

and solving, we get

$$\left(\frac{x_u}{d} \right) = 1.2 - \sqrt{1.44 - k_4} \quad (5.64)$$

Case 3 Neutral axis outside the flange; this occurs when $(3x_u/7) < D_f$ or when the flange thickness is greater than about $0.2d$, as shown in Fig. 5.24(c). As seen from the stress and strain distribution, shown in Fig. 5.24(c), the parabolic portion of the stress block extends to a height of $4/7x_u$ from the neutral axis, beyond which it is rectangular for the remaining $3/7x_u$. The limiting x_u/d for Fe 250, Fe 415, and Fe 500 grade steel are approximately 0.531, 0.479, and 0.456, respectively (see Table 5.3). Hence, considering the worst case, the rectangular stress distribution may extend to a depth of $3/7 \times 0.456d = 0.195d \approx 0.2d$ (for grade 500 steel). Hence, a depth of $0.2d$ has been chosen as the limiting depth for the shallow flanges in Clause G-2.2 of IS 456:2000.

In this case, the estimation of compressive force in the flange is difficult as the stress distribution is non-linear and the stress block in the flange consists of a rectangular area plus a truncated parabolic area (see Fig. 5.24c). It has to be noted that the calculations will become simpler if an equivalent rectangular stress block is adopted, as suggested by Whitney (1937) and adopted in the ACI code (see Section 5.4.1 and Fig. 5.1j). Let us assume a rectangular stress block as a substitute for the complex stress block in the flange as shown in Fig. 5.25.

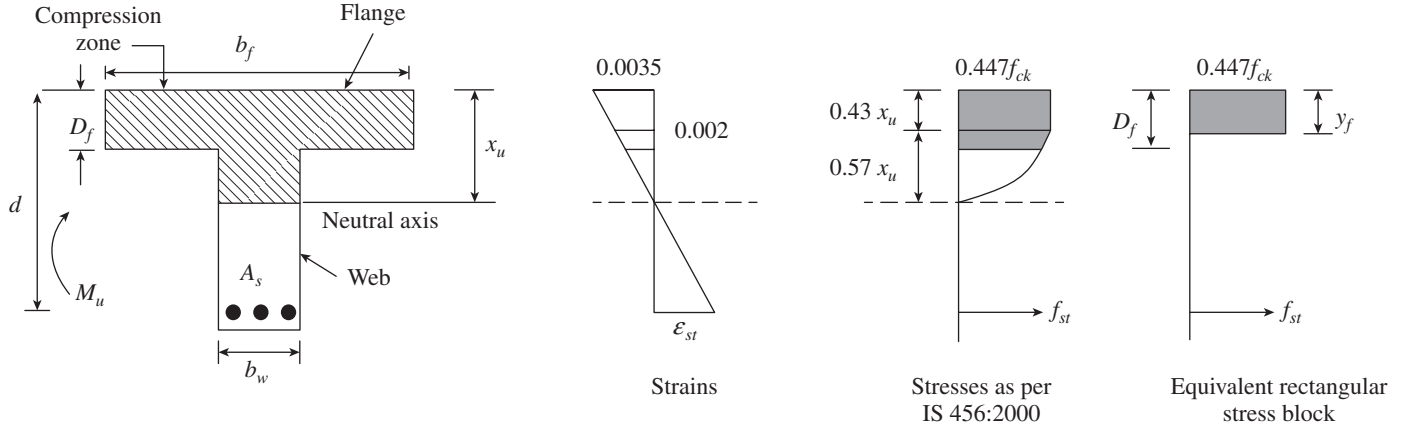


FIG. 5.25 Neutral axis outside flange $x_u > D_f$ and $D_f > 0.2d$ and an equivalent rectangular stress block for the flange portion

Let y_f be the depth of the equivalent rectangular stress block.

Let $y_f = Ax_u + BD_f$.

The values of constants A and B can be found by substituting the following conditions:

1. When $D_f = 3/7x_u$, $y_f = 0.43$.
2. When $D_f = x_u$, $y_f = 0.8x_u$ (assumed).

Solving for the two constants, we get $A = 0.15$ and $B = 0.65$. Hence,

$$y_f = 0.15x_u + 0.65D_f \quad \text{for } 1 < x_u/D_f < 7/3 \quad (5.65)$$

$$= D_f \quad \text{for } x_u/D_f \geq 7/3$$

It should be noted that this approximation of equivalent depth will not satisfy the two conditions of equivalence, in terms of the area of stress block as well as the centroidal location, at the same time (Pillai and Menon 2003).

From Fig. 5.24(c), with b_f as the breadth of the flange, the total compression in concrete is

$$C_{uw} + C_{uf} = 0.36f_{ck}x_ub_w + 0.447f_{ck}y_f(b_f - b_w)$$

$$= 0.36f_{ck}x_ub_w + 0.447f_{ck}(0.15x_u + 0.65D_f)(b_f - b_w)$$

$$= x_u[0.36f_{ck}b_w + 0.447f_{ck} \times 0.15(b_f - b_w)]$$

$$+ 0.447f_{ck} \times 0.65D_f(b_f - b_w)$$

Total tension in steel: $T_u = 0.87f_yA_{st}$

Equating total compression and total tension and rearranging, we get

$$x_u = \frac{0.87f_yA_{st} - 0.447f_{ck} \times 0.65D_f(b_f - b_w)}{0.36f_{ck}b_w + 0.447f_{ck} \times 0.15(b_f - b_w)}$$

$$= \frac{0.87f_yA_{st} - 0.29f_{ck}D_f(b_f - b_w)}{0.36f_{ck}b_w + 0.067f_{ck}(b_f - b_w)} \quad (5.66)$$

The moment of resistance in this case can be written as

$M_n = M_{n1}$ [rectangular web of size $b_w \times d$] + M_{n2} [flange of size $(b_f - b_w) \times D_f$]

Taking the moment of forces about the tension steel, for the web portion alone

$$M_{n1} = 0.36f_{ck} \left(\frac{x_u}{d} \right) \left(1 - 0.416 \frac{x_u}{d} \right) b_w d^2 \quad (5.67a)$$

For the remaining flange of size $(b_f - b_w) \times D_f$, we get

$$M_{n2} = 0.447f_{ck}(b_f - b_w)y_f \left(d - \frac{y_f}{2} \right) \quad (5.67b)$$

Hence, we get the moment of resistance of the T-beam as given in Annex G (Eq. G-2.2.1) of IS 456:2000 as

$$M_n = 0.36f_{ck} \left(\frac{x_u}{d} \right) \left(1 - 0.416 \frac{x_u}{d} \right) b_w d^2$$

$$+ 0.447f_{ck}(b_f - b_w)y_f \left(d - \frac{y_f}{2} \right) \quad (5.67c)$$

For this case, the value of (x_u/d) may be derived as discussed earlier from this value of M_n as

$$\left(\frac{x_u}{d} \right) = 1.2 - \sqrt{1.44 - k_5} \quad (5.68a)$$

$$\text{with } k_5 = \frac{6.68M_n}{f_{ck}b_f d^2} \left(\frac{b_f}{b_w} \right) - 3 \left(\frac{b_f}{b_w} - 1 \right) \left(\frac{y_f}{d} \right) \left(1 - \frac{y_f}{2d} \right) \quad (5.68b)$$

The limiting value for the moment of resistance is obtained for the condition $x_u = x_{u,\text{lim}}$, where $x_{u,\text{lim}}$ takes the values of 0.531, 0.479, and 0.456 for Fe 250, Fe 415, and Fe 500 grades of steel, respectively (see Table 5.3). Thus, the limiting moment of resistance is given by

$$M_{n,\text{lim}} = 0.36f_{ck} \left(\frac{x_{u,\text{lim}}}{d} \right) \left(1 - 0.416 \frac{x_{u,\text{lim}}}{d} \right) b_w d^2$$

$$+ 0.447f_{ck}(b_f - b_w)y_f \left(d - \frac{y_f}{2} \right) \quad (5.69)$$

where

$$y_f = \begin{cases} 0.15x_{u,lim} + 0.65D_f & \text{for } D_f/d > 0.2 \\ D_f & \text{for } D_f/d \leq 0.2 \end{cases} \quad (5.70)$$

As discussed in the case of rectangular sections, if it is found from the analysis of a given T-section that $x_u > x_{u,lim}$ the section is over-reinforced; hence, the strain compatibility method needs to be applied to calculate the exact value of x_u , and based on this value, the moment of resistance M_n can be calculated. $M_{n,lim}$, as given in Eq. (5.69), may be taken as a conservative estimate of the moment of resistance.

5.7.4 Minimum and Maximum Steel

Similar to rectangular beams, T-beams should also be provided with a minimum amount of reinforcement. According to Clause 26.5.1.1 of IS 456, the minimum amount of reinforcement to be provided in the T-beams is the same as that for rectangular beams, as given by Eq. (5.35c).

$$\frac{A_s}{b_w d} = \frac{0.85}{f_y}$$

In this equation, b_w is the breadth of the web of the T-beam. For grade Fe 415 bars, this equation will give about 0.20 per cent minimum steel. As discussed in Section 5.5.4, the minimum area equation should also include concrete strength and hence the ACI code expression is more appropriate. According to the ACI code, which was based on the derivation made by Wang and Salmon (2002), for T-beams, with the flange in tension, the minimum reinforcement should be

$$\frac{A_s}{b_w d} = \frac{0.448\sqrt{f_{ck}}}{f_y} \geq \frac{1.4}{f_y} \quad (5.71)$$

where b_w is the breadth of the web or the effective width of the flange b_f , whichever is smaller. This requirement can be waived if the following over-strength equation is satisfied:

$$M_n \geq \frac{1.33M_u}{\phi} \quad (5.72)$$

Here, M_n is the ultimate nominal flexural capacity of the section, M_u is the applied external factored moment, and ϕ is the resistance factor, which can be taken equal to 0.9 for flexure. It should also be remembered that lesser minimum reinforcement will be necessary for indeterminate structures than for determinate members, due to

their ability to redistribute moments. Recently, Seguirant, et al. (2010) developed an equation for minimum steel requirement that provides the most reasonable and consistent margins of safety for all grades of reinforcement than the available and present codal methods. They also found that the minimum reinforcement not only prevents the fracture of the reinforcement at first cracking but in many cases also prevents the concrete from crushing at first cracking.

In the same Clause 26.5.1.1 of IS 456, the maximum steel is specified as four per cent, based on web width. The discussions on minimum and maximum reinforcement as given in Sections 5.5.4 and 5.5.5 for rectangular beams are also applicable for T-beams. More discussions on the minimum reinforcement for beams may be found in Medhekar and Jain (1993).

Transverse Reinforcement in Flange

If the main reinforcement in the slab (flange portion) of a T- or an L-beam is parallel to the beam, it is necessary to provide transverse reinforcement at the top of the slab, over full effective width (see Fig. 5.26). This situation normally occurs when a number of smaller beams supporting a one-way slab are supported by a girder, which is therefore parallel to the one-way slab (see Fig. 5.26). This steel not only makes the girder and slab act together but is also useful to resist the horizontal shear stresses produced by the variation of compressive stress across the width of the slab (see Fig. 5.22a).

Clause 23.1.1(b) of IS 456 specifies that such reinforcement should not be less than 60 per cent of the main reinforcement at the mid-span of the beam. This reinforcement should be placed at the top and bottom of the slab as shown in Fig. 5.26

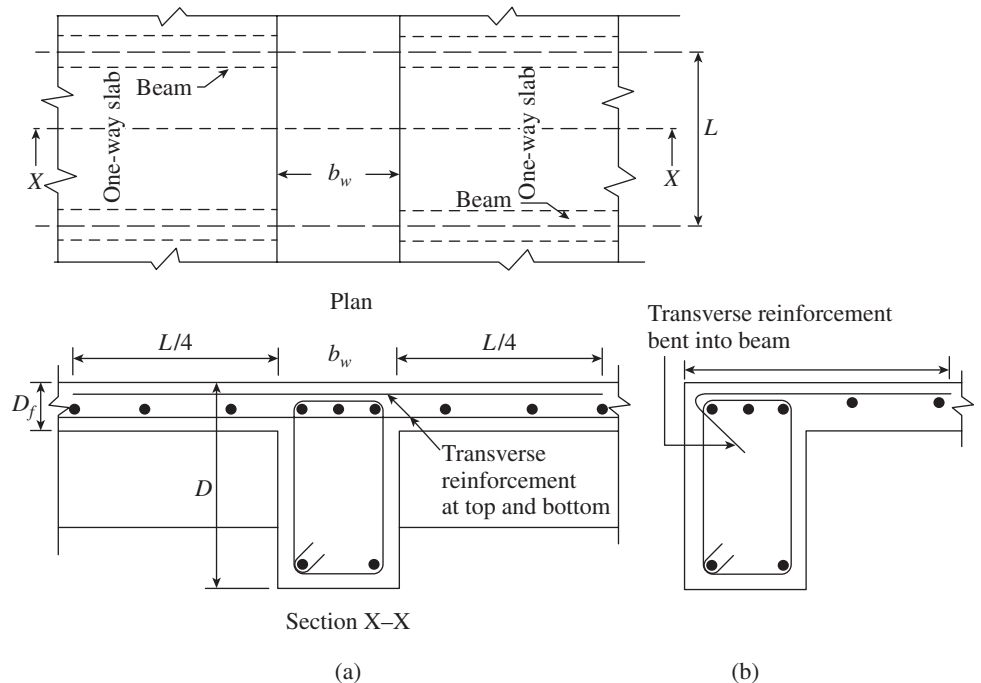


FIG. 5.26 Transverse reinforcement in flanges of T-beams (a) Internal beam (b) External beam

and should either pass below the longitudinal bars anchoring the stirrups in the beam or be bent into the beam (see the L-beam section in Fig. 5.26). The purpose of the clause is to control the cracks that will tend to occur in the flange above the edge of the web and to avoid the necessity of complex computations to determine the amount of reinforcement. Tests on simply supported T-beams have shown that the cracks are parallel to the web, as shown in Fig. 5.27, rather than at a 45° angle as frequently assumed (Placas and Regan 1971). This mode of cracking indicates direct shear and normal stress failure along the shear plane rather than diagonal tension failure. If adequate reinforcement is not provided, the cracks will lead to the separation of flanges from the web, resulting in premature failure of the beam. It should be noted that BS 8110, as per Table 3.25 of the code, specifies that this steel should not be less than 0.15 per cent of the longitudinal cross-sectional area of the flange. Thus, for a T-beam, with a flange thickness of 100 mm and with the area of main reinforcement at mid-span as 400 mm²/m, the transverse steel according to IS 456 is $0.6 \times 400 = 240 \text{ mm}^2/\text{m}$, whereas as per BS 8110 it is only $(0.15/100) \times 100 \times 1000 = 150 \text{ mm}^2/\text{m}$.

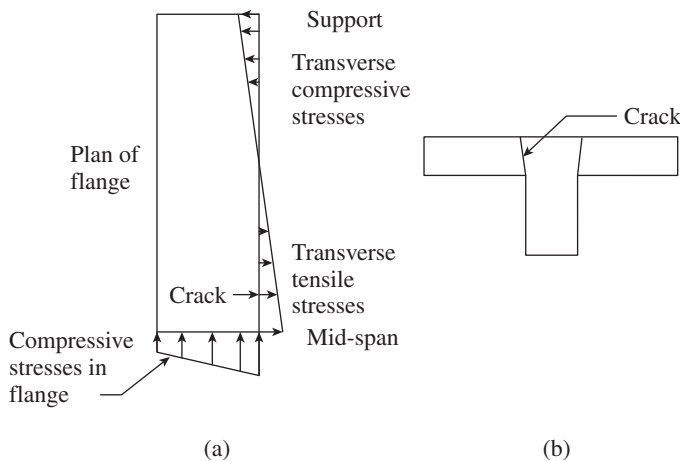


FIG. 5.27 Flange cracking in T-beams (a) Plan (b) Section

The US code ACI 318-08 does not consider this type of transverse reinforcement, whereas the Canadian code suggests a minimum reinforcement similar to that given in Eq. (5.36c). In this connection, it is to be noted that NZS 3101:2006 code stipulates that the tensile strength of the reinforcement in the effective overhanging flange should not exceed 15 per cent of the total flexural tensile strength of the beam. More discussion on transverse reinforcement in the flanges of T-beams and a refined method of calculation may be found in Razaqpur and Ghali (1986).

According to the US code, transverse reinforcement should be designed to carry the factored load on the overhanging slab width assuming it to act as a cantilever. For isolated beams, it is necessary to consider the full width of the overhanging flange; for other T-beams, it is enough to consider only the effective overhanging slab width. Moreover, the spacing of

such transverse reinforcement should be the lesser of five times the slab thickness and 450 mm.

Flexural Tension Reinforcement

When the beam is subjected to negative bending moment, some of the longitudinal reinforcement in the flange (slab reinforcement) will also act as tension steel, in addition to the main steel provided in the beam. The tensile force is transferred across the flange into the web by the shear in the flange, similar to the case of compressive force transfer when positive bending moment acts on the beam. IS 456 does not specify the effective width over which the slab steel can be considered to be acting as tension reinforcement. Park and Paulay (1975) suggest that the slab steel within a width of four times the slab thickness on each side of the web could also be considered as tension steel for the T-beam (see Fig. 5.28).

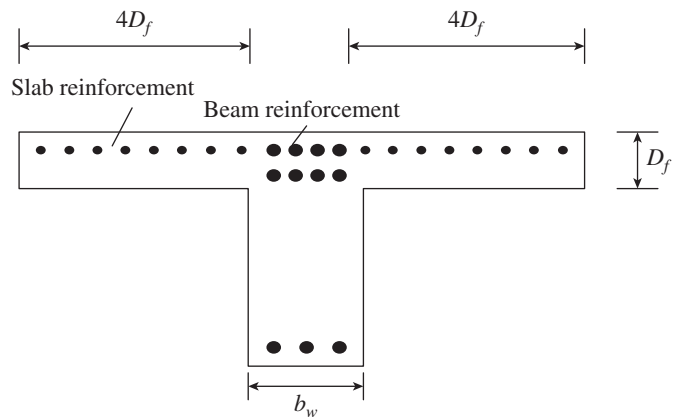


FIG. 5.28 Tension steel in slab width that resists negative bending moment

Clause 26.5.1.8 of IS 456 code (similar to Clause 10.6.6 of ACI 318) suggests that for control of flexural cracking in the flanges of T-beams, flexural reinforcement must be distributed over the flange width not exceeding the effective flange width or a width equal to one-tenth of the span, whichever is smaller. If the effective flange width is greater than one-tenth of the span, additional nominal longitudinal reinforcement as shown in Fig. 5.29 should be provided in the outer portions of the flange (Fanella and Rabbat 2002). As per Clause 26.5.2.2, the diameter of the bar shall not exceed one-eighth of the flange thickness.

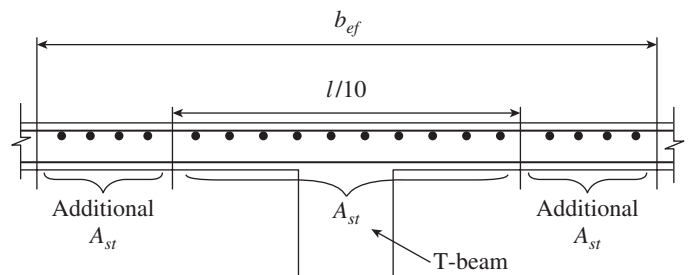


FIG. 5.29 Placement of beam reinforcement to resist negative moment for T-beams

Clause 26.3.3(a) stipulates that near the tension face of a beam, the spacing should not be greater than that given in Table 15 of the code, depending on the redistribution of moment carried out in the analysis. For no redistribution, the maximum spacing as per the code is 300mm, 180mm, and 150mm for Fe 250, Fe 415, and Fe 500 grades of steel, respectively.

5.7.5 Doubly Reinforced Flanged Beams

The analysis and design of doubly reinforced T-sections are similar to that of doubly reinforced rectangular sections. In these sections, the tensile force developed in the tension steel has to balance the compression developed in concrete in the compression zone as well as the compressive force due to compression steel. As discussed in the previous sections on singly reinforced flanged beams, the ultimate moment of resistance of the section will depend on whether it is balanced, under-reinforced, or over-reinforced; this may be found by comparing the value of neutral axis depth x_u with the limiting value $x_{u,lim}$. Again there will be two cases—the neutral axis lying either in the flange or in the web. This may be found by comparing the value of x_u with D_f . Moreover, when the neutral axis is outside the flange, depending on whether $3x_u/7$ is greater or less than D_f , the flange will be subjected to uniform rectangular compressive stress distribution or non-linear stress distribution.

Case 1: Neutral axis in the flange Consider a balanced or under-reinforced section with the neutral axis lying in the flange, as shown in Fig. 5.30(a).

Stress in compression steel = $(f_{sc} - f_{cc})A_{sc}$

Equating the compressive and tensile forces, we get

$$0.36f_{ck}b_f x_u + (f_{sc} - f_{cc})A_{sc} = 0.87f_y A_{st}$$

$$\text{Thus, } x_u = \frac{0.87f_y A_{st} - (f_{sc} - f_{cc})A_{sc}}{0.36f_{ck}b_f} \quad (5.73)$$

where f_{sc} and f_{cc} are the stresses in compression steel and concrete, respectively, corresponding to strain $\epsilon_{sc} = 0.0035(x_u - d')/x_u$, where d' is the distance between the centroid of the compression steel and the extreme compression fibre (effective cover for compression steel) as shown in Fig. 5.30. The stress in compression steel corresponding to this strain is given as follows (Eq. 5.43a):

$$\text{For mild steel: } f_{sc} = \epsilon_{sc} E_s \leq 0.87f_y$$

For HYSD bars: $f_{sc} = \epsilon_{sc} E_s$ for $\epsilon_{sc} \leq 0.696f_y/E_s$ and is calculated from Table 5.2 or design stress-strain curve (Fig. 5.5) for $\epsilon_{sc} > 0.696f_y/E_s$.

The value of x_u can be determined from the solution of this equation by iterative procedure as discussed in Section 5.6.2 for doubly reinforced rectangular sections. The moment of

resistance may be found similar to that of rectangular sections, with the breadth as b_f .

$$M_n = C_c z_c + C_s z_s$$

$$M_n = 0.36f_{ck}b_f x_u (d - 0.416x_u) + (f_{sc} - f_{cc})A_{sc} (d - d')$$

Case 2: Neutral axis lies in the web If $x_u > D_f$, then the neutral axis lies in the web and the section is to be analysed as a flanged section. The triangular distribution of strains and non-linear distribution of stresses in the section are shown in Fig. 5.30(b). The position of the neutral axis may be determined from the equilibrium of the compressive and tensile forces as

$$T = C_c + C_s$$

$$C_c = C_{uw} + C_{uf} = 0.36f_{ck}b_w x_u + 0.447f_{ck}(b_f - b_w)y_f$$

or

$$0.87f_y A_{st} = 0.36f_{ck}b_w x_u + 0.447f_{ck}(b_f - b_w)y_f + (f_{sc} - f_{cc})A_{sc} \quad (5.74)$$

where f_{sc} and f_{cc} are the stresses in compression steel and concrete, respectively, corresponding to strain $\epsilon_{cc} = 0.0035(x_u - d')/x_u$ and can be determined, as discussed for the previous case, with $y_f = 0.15x_u + 0.65D_f$ or D_f , whichever is smaller.

The value of x_u shall depend on whether $y_f = 0.15x_u + 0.65D_f$ or $y_f = D_f$.

For $y_f = 0.15x_u + 0.65D_f$, substituting the value of y_f in Eq. (5.74) and simplifying,

$$x_u = \frac{0.87f_y A_{st} - 0.29(b_f - b_w)D_f f_{ck} - (f_{sc} - f_{cc})A_{sc}}{0.36f_{ck}b_w + 0.067f_{ck}(b_f - b_w)} \quad (5.75)$$

For $y_f = D_f$

$$x_u = \frac{0.87f_y A_{st} - 0.447f_{ck}(b_f - b_w)D_f - (f_{sc} - f_{cc})A_{sc}}{0.36f_{ck}b_w} \quad (5.76)$$

The value of x_u can be determined from the solution of these equations by an iterative procedure as follows:

Step 1 Assume $x_u = x_{u,lim} = \frac{0.0035}{0.0055 + 0.87f_y/E_s} d$.

Step 2 Compute $\epsilon_{sc} = 0.0035(x_u - d')/x_u$ and the corresponding values of f_{sc} and f_{cc} as discussed in Section 5.6.2.

Step 3 Compute the appropriate value of x_u given by Eq. (5.75) or (5.76) depending on whether $y_f = 0.15x_u + 0.65D_f$ or $y_f = D_f$.

Repeat Steps 2 and 3 until the value of x_u converges. Comparison of x_u with $x_{u,lim}$ gives rise to either of the following cases.

Case 2a: Neutral axis lies in the web—balanced or under-reinforced If $x_u \leq x_{u,lim}$, then it is a balanced or an under-reinforced section and the value of x_u as determined

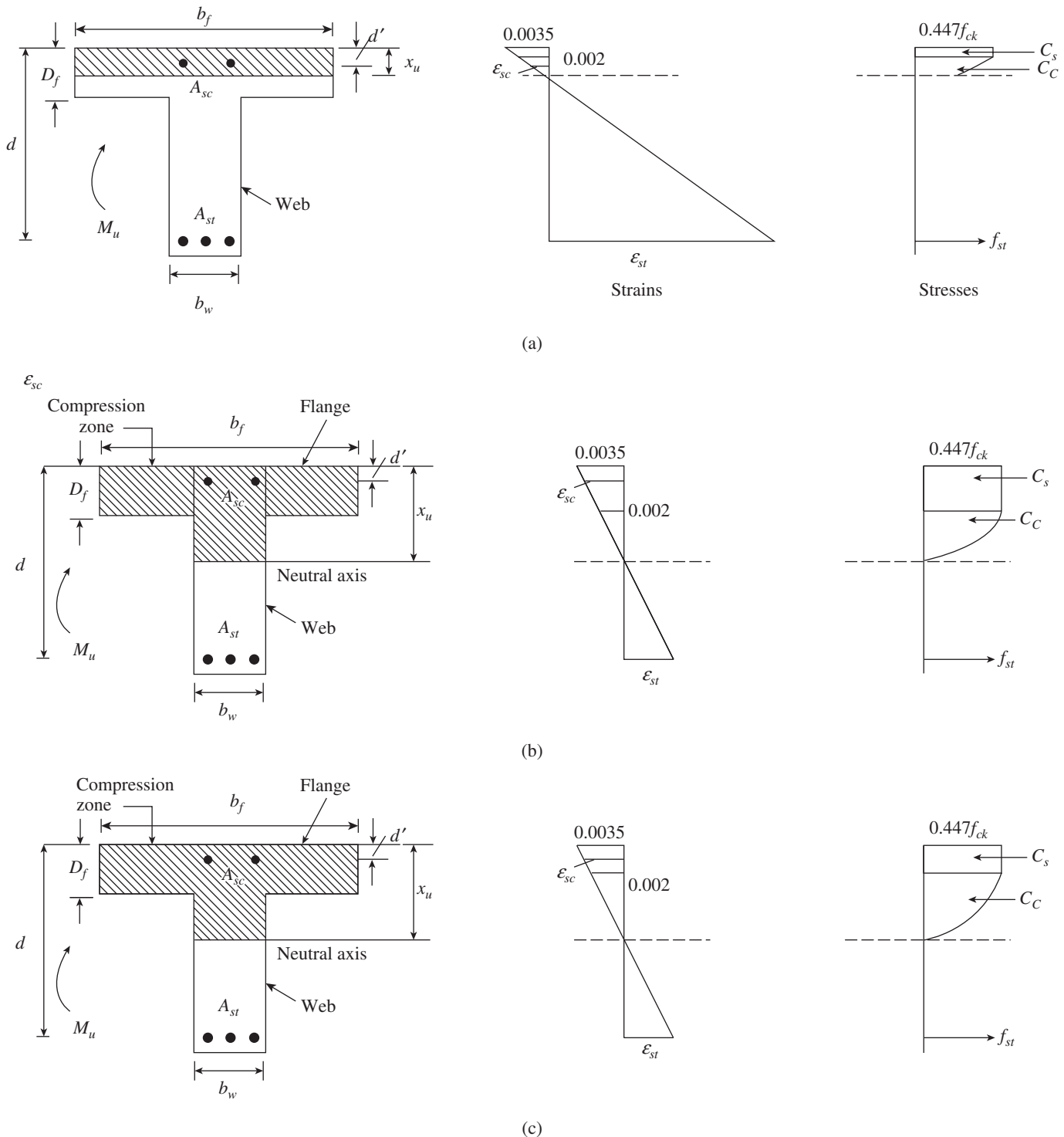


FIG. 5.30 Behaviour of doubly reinforced T-beam (a) Neutral axis within flange $x_u \leq D_f$ (b) Neutral axis outside flange $x_u > D_f$ (c) Neutral axis outside flange $x_u > D_f$ and $D_f > 0.2d$

is correct. If $x_u \leq D_f$ then the neutral axis lies in the flange, and the analysis of the section can be made as that of a rectangular section of width b_f , as discussed in Section 5.6.2. If $x_u > D_f$ then the neutral axis lies in the web.

The ultimate moment of resistance can be determined by taking the moment of compressive forces in concrete and steel about tensile force as

$$\begin{aligned}
 M_u = & 0.36 f_{ck} b_w x_u (d - 0.416 x_u) \\
 & + d 0.447 f_{ck} (b_f - b_w) y_f (d - 0.5 y_f) \\
 & + (f_{sc} - f_{cc}) A_{sc} (d - d') \quad (5.77)
 \end{aligned}$$

Case 2b: Neutral axis lies in the web—over-reinforced If $x_u > x_{u,lim}$, then it is an over-reinforced section and the value of x_u as determined is not correct. It will depend on whether

the neutral axis lies in the flange or in the web. For the neutral axis lying in the flange (i.e., $x_u < D_f$), the value of x_u can be determined using

$$0.36f_{ck}b_f x_u + (f_{sc} - f_{cc})A_{sc} = f_{st}A_{st}$$

Thus,
$$x_u = \frac{f_{st}A_{st} - (f_{sc} - f_{cc})A_{sc}}{0.36f_{ck}b_f} \quad (5.78)$$

where f_{st} is the stress in the tension steel corresponding to strain $\epsilon_{st} = 0.0035(d - x_u)/x_u$ and f_{sc} and f_{cc} are the stresses in compression steel and concrete, respectively, corresponding to strain $\epsilon_{sc} = 0.0035(x_u - d')/x_u$. The value of x_u can be determined by solving Eq. (5.78) by using the iterative procedure already described in Section 5.6.2.

If $x_u \leq D_f$, then the analysis of the section can be done as that of a rectangular section of width b_f as discussed in Section 5.6.2. If $x_u > D_f$, then the value of x_u can be determined from the equilibrium of internal forces as follows:

$$0.36f_{ck}b_w x_u + 0.447f_{ck}(b_f - b_w)y_f + (f_{sc} - f_{cc})A_{sc} = f_{st}A_{st}$$

where $y_f = 0.15x_u + 0.65D_f$ or D_f , whichever is smaller, f_{st} is the stress in tension steel corresponding to strain $\epsilon_{st} = 0.0035(d - x_u)/x_u$ and f_{sc} and f_{cc} are the stresses in the compression steel and concrete, respectively, corresponding to strain $\epsilon_{sc} = 0.0035(x_u - d')/x_u$. The value of x_u shall depend on whether $y_f = 0.15x_u + 0.65D_f$ or $y_f = D_f$.

For $y_f = 0.15x_u + 0.65D_f$,

$$x_u = \frac{f_{st}A_{st} - 0.29(b_f - b_w)D_f - (f_{sc} - f_{cc})A_{sc}}{0.36f_{ck}b_w + 0.067f_{ck}(b_f - b_w)} \quad (5.79)$$

For $y_f = D_f$,

$$x_u = \frac{f_{st}A_{st} - 0.447f_{ck}(b_f - b_w)D_f - (f_{sc} - f_{cc})A_{sc}}{0.36f_{ck}b_w} \quad (5.80)$$

The value of x_u can be determined by solving these two equations, using an iterative procedure as follows:

Step 1 Assume $x_u = x_{u,lim} = \frac{0.0035}{0.0055 + 0.87f_y/E_s} d$.

Step 2 Compute $\epsilon_{st} = 0.0035(d - x_u)/x_u$ and the corresponding value of f_{st} as described in Section 5.6.2.

Step 3 Compute $\epsilon_{sc} = 0.0035(x_u - d')/x_u$ and the corresponding values of f_{sc} and f_{cc} as described in Section 5.6.2.

Step 4 Compute x_u from either Eq. (5.79) or (5.80) as appropriate depending on whether $y_f = 0.15x_u + 0.65D_f$ or $y_f = D_f$.

Repeat Steps 2 to 4 until the value of x_u converges. Then, the ultimate moment of resistance of the section with respect to compressive force can be determined from Eq. (5.77).

5.7.6 Design of Flanged Beams

The design of a flanged section for a given applied external moment requires the determination of its cross-sectional dimensions and the area of the steel. As discussed, a part of the slab that deflects monolithically with the web of the beam forms the flange of the beam and can be determined as per the codal rules (see Table 5.9). The thickness of the slab is fixed by the design of the slab. The width of the web is mainly fixed by architectural considerations (such as to be flush with the wall), requirement for resisting shear at supports, and minimum width requirement for placing reinforcing steel. Thus, the design of a T-beam or an L-beam requires the determination of the depth and area of the steel.

The depth is initially fixed based on deflection considerations. As per Clause 23.2.1 of IS 456, the deflection of the beam will be within limits if the span to depth ratio is not greater than the following:

- For spans up to 10 m, the following L/d ratios are suggested:

(a) Cantilever	7
(b) Simply supported beam	20
(c) Continuous beam	26
- If the span of the beam is above 10 m, the values given in point 1 are multiplied by 10/span in metres, except for cantilevers, which require deflection calculations.

The following steps are necessary for the design of a flanged beam:

Step 1 Determine the factored ultimate moment to be carried by the beam for the given span and loading conditions.

Step 2 Initially assume the beam depth to be in the range of one-twelfth to one-fifteenth of the span depending on whether it carries heavy or light loads.

However, in many cases, the depth of the beam is decided by the architect or fixed such that the beam section throughout a structure is standardized; in such cases, only the area of steel needs to be determined. Once the overall depth is fixed, the effective depth of the beam can be determined by subtracting the effective cover based on environmental conditions.

Flanged Beam under Negative Moment

In designing for a factored negative moment, M_u (i.e., designing top reinforcement), the reinforcement area is calculated in exactly the same way as described previously for singly or doubly reinforced rectangular beams.

Flanged Beam under Positive Moment

With the flange in compression, initially the neutral axis is assumed to be located within the flange. On the basis of this assumption, the depth of the neutral axis is calculated. If the stress block does not extend beyond the flange thickness, the

section is designed as a rectangular beam of width b_f . If the stress block extends beyond the flange depth, the contribution of the web to the flexural strength of the beam is taken into account. See Fig. 5.30.

Assuming the neutral axis lies in the flange, the depth of the neutral axis is calculated as

$$\frac{x_u}{d} = \frac{1 - \sqrt{1 - 4 \times 0.416m}}{2 \times 0.416}$$

where the normalized design moment, m , is given by

$$m = \frac{M_u}{0.36f_{ck}b_f d^2}$$

1. If $\frac{x_u}{d} \leq \frac{D_f}{d}$, the neutral axis lies within the flange and the subsequent calculations for A_{st} are exactly the same as previously defined for the rectangular beam design. However, in this case, the width of the beam is taken as b_f . Compression reinforcement is required when $M_u > M_{n,lim}$ (see Eq. 5.50).

2. If $\frac{x_u}{d} > \frac{D_f}{d}$, the neutral axis lies below the flange and the calculation for A_{st} has two parts. The first part is for balancing the compressive force from the flange, C_f , and the second one is for balancing the compressive force from the web, C_w , as shown in Fig. 5.30.

Calculate the ultimate resistance moment of the flange as

$$M_f = 0.447f_{ck}(b_f - b_w)y_f(d - \frac{y_f}{2}) \quad (5.81a)$$

where y_f is taken as

$$y_f = \begin{cases} D_f & \text{if } D_f \leq 0.2d \\ 0.15x_u + 0.65D_f & \text{if } D_f > 0.2d \end{cases} \quad (5.81b)$$

Calculate the moment taken by the web as

$$M_w = M_u - M_f$$

Calculate the limiting ultimate moment of resistance of the web for the tension reinforcement as

$$M_{w,lim} = 0.36f_{ck}b_w d^2 \frac{x_{u,lim}}{d} \left[1 - 0.416 \frac{x_{u,lim}}{d} \right] \quad (5.82a)$$

where

$$\begin{aligned} \frac{x_{u,lim}}{d} &= 0.531 & \text{for } f_y \leq 250 \text{ MPa} \\ &= 0.531 - 0.052 \frac{f_y - 250}{165} & \text{for } 250 < f_y \leq 415 \text{ MPa} \\ &= 0.479 - 0.023 \frac{f_y - 415}{85} & \text{for } 415 < f_y \leq 500 \text{ MPa} \\ &= 0.456 & \text{for } f_y > 500 \text{ MPa} \end{aligned} \quad (5.82b)$$

3. If $M_w \leq M_{w,lim}$, the beam is designed as a singly reinforced concrete beam. The area of reinforcement is calculated as the sum of two parts, one to balance the compression in the flange and the other to balance the compression in the web.

$$A_{st} = \frac{M_f}{0.87f_y(d - 0.5y_f)} + \frac{M_w}{0.87f_y z} \quad (5.83a)$$

where

$$z = d \left(1 - 0.416 \frac{x_u}{d} \right) \quad (5.83b)$$

$$\frac{x_u}{d} = \frac{1 - \sqrt{1 - 4 \times 0.416 \times m}}{2 \times 0.416} \quad (5.83c)$$

$$m = \frac{M_w}{b_w d^2 0.36f_{ck}} \quad (5.83c)$$

4. If $M_w > M_{w,lim}$, the area of compression reinforcement, A_{sc} , is given by

$$A_{sc} = \frac{M_w - M_{w,lim}}{(f_{sc} - 0.447f_{ck})(d - d')} \quad (5.84)$$

where d' is the depth of the centroid of compression reinforcement from the concrete compression face. The stress in compression steel corresponding to the strain

$\epsilon_{sc} = 0.0035 \left[1 - \frac{d'}{x_{u,lim}} \right]$ is found from Table 5.2. The

required tension reinforcement is calculated as follows:

$$A_{st} = \frac{M_f}{0.87f_y(d - 0.5y_f)} + \frac{M_{w,lim}}{0.87f_y z} + \frac{M_w - M_{w,lim}}{0.87f_y(d - d')} \quad (5.85a)$$

where

$$z = d \left(1 - 0.416 \frac{x_{u,lim}}{d} \right) \quad (5.85b)$$

5.7.7 Design of Flanged Beams Using Charts and Design Aids

As mentioned, in practice, spreadsheets or computer programs are used to design flanged T- or L-beams. Most of the T-beams encountered in practice have their neutral axis within the flange and hence the area of steel can be calculated by using Tables 1–4 of SP 16:1980, considering them as rectangular beams having width b_f and effective depth d . However, when the neutral axis falls below the bottom of the flange, these tables cannot be used. Tables 57–59 of SP 16 also give the limiting moment of resistance factor $M_{u,lim}/(f_{ck}b_w d^2)$ for three grades of steel for different values of D_f/d and b_f/b_w . The amount of steel necessary for the moment is not indicated in these tables. As such, these tables are of limited practical use, as the steel area required for the actual beams will be much less than that required for full capacity. Hence, they may be used perhaps to check the capacity of the designed concrete

section. The special publication SP 24:1983, published by the BIS, contains three tables (E-9–E-11) providing the reinforcement percentage factor for $M_{u,lim}/(f_{ck}b_wd^2)$ for three grades of steel for different values of d/D and b_f/b_w , which are also of limited use because they are again based on the limiting moment of resistance. Desai (2006) developed equations and design aids for doubly reinforced T-beams (see Tables C.17–C.20 of Appendix C). The design charts for singly reinforced T-beams are also available in Iyengar and Viswanatha (1990), Sinha (1996), and Varyani and Radhaji (2005).

5.7.8 Design of L-beams

An L-beam is similar to a T-beam, except that the slab is connected to one side of the web. The same formulae derived for T-beams can also be used for the analysis and design of L-beams. However, it has to be noted that since the area and the loading on an L-beam are not symmetrical about the centre of the beam, L-beams are subjected to torsion. This torsion is assumed to be resisted by the rectangular portion of the L-beam. To resist torsion, extra longitudinal top reinforcement and special stirrups are to be provided. The design for torsion is covered in Chapter 8. In practice, such L-beams (also called *spandrel beams*), occurring at the edge of buildings, are not designed for torsion; when the distance between the L-beam and the next T-beam is excessive, shear stirrups are provided liberally to take into account the torsion.

Isolated L-beams are allowed to deflect both horizontally and vertically. Hence, their neutral axis will be inclined as shown in Fig. 5.31, which also shows the forces and strains occurring in such a beam. It is easier to arrive at the moment of resistance, if a rectangular stress block, as in ACI code, is

adopted. The force in the compression zone equals the area of the compressive zone multiplied by the concrete stress. Thus,

$$C_{uc} = 0.447f_{ck}(X_1Y_1/2) \tag{5.86a}$$

$$T_u = 0.87A_{st}f_y \tag{5.86b}$$

The distance X_1 may be assumed as $1.5b_w$. Equating C_{cu} and T_u , the value of Y_1 can be obtained.

Because the moment due to gravity load is about a horizontal axis, the lever arm must be vertical and equals $(d - Y_1/3)$. Thus, the moment of resistance is given by

$$M_n = 0.87A_{st}f_y \left(d - \frac{Y_1}{3} \right) \tag{5.87}$$

It should be noted that these equations apply only to the triangular compression zone, as shown in Fig. 5.31. Trial-and-error solutions are generally used for other shapes. Rüschi (1960) has shown that the triangular stress block is applicable to a wide variety of shapes of compression zones.

5.8 MINIMUM FLEXURAL DUCTILITY

In the flexural design of RC beams, in addition to providing adequate strength, it is often necessary to provide a certain minimum level of ductility. For structures subjected to seismic loads, the design philosophy called *strong column–weak beam* is adopted, which is supposed to guarantee the following behaviour: The beams yield before the columns and have sufficient flexural ductility such that the potential plastic hinges in the beam maintain their moment resistant capacities until the columns fail. To ensure the ductile mode of failure, all beams should be designed as under-reinforced. More stringent reinforcing detailing like provision of confining reinforcement in the plastic hinge zones is also generally imposed. In addition, traditionally limits were also imposed on either the tension steel ratio (should not be more than 0.75 of the balanced steel ratio or the strain in steel should be greater than 0.005) or the neutral axis depth. This kind of limitation may result in a variable level of curvature ductility depending on the concrete grade and yield strength of steel.

Studies conducted by Ho, et al. (2004) revealed that the flexural ductility of an RC beam is dependent not only on the tension and compression steel ratios but also on the concrete

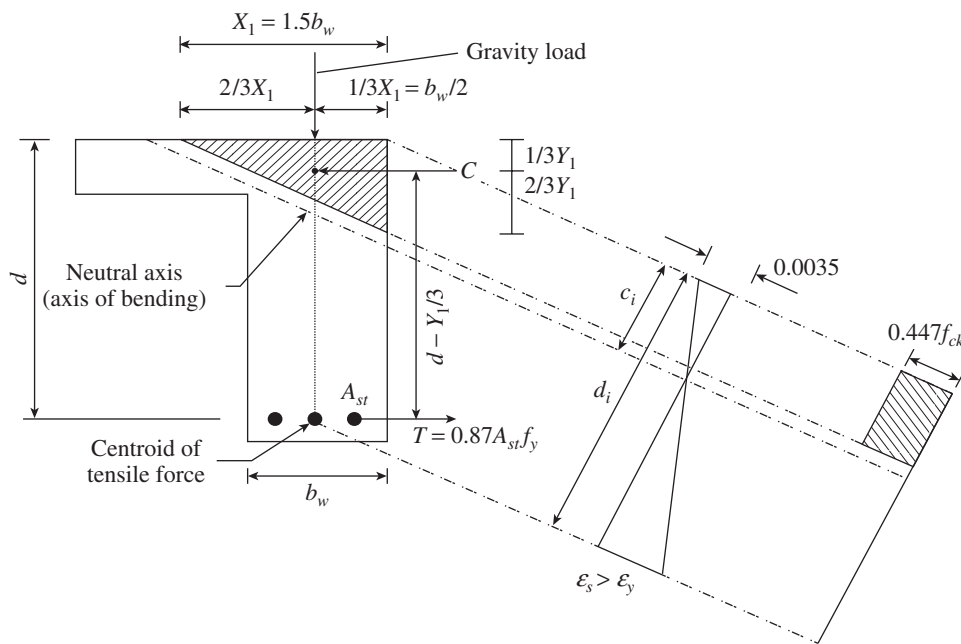


FIG. 5.31 Stresses and strains in an isolated L-beam

grade and the steel yield strength. They also observed that the current practices of providing minimum flexural ductility in the existing design codes would not really provide a consistent level of minimum flexural ductility. Moreover, they observed that when HSC and/or HSS are used, the flexural ductility so provided would be lower than that provided in the past to beams made of conventional materials.

In order to provide a consistent level of minimum curvature ductility, Ho, et al. (2004) proposed to set a fixed minimum value for the curvature ductility factor. By studying the curvature ductility factors provided in the various existing design codes, they recommended a minimum curvature ductility factor of 3.32 and suggested the following guidelines to attain this minimum curvature ductility factor:

1. When the yield strength of the compression and tension steel is less than or equal to 460 MPa, the value of x_u should not exceed $0.50d$ when $f_{ck} \leq 30$ MPa, should not exceed $0.40d$ when $30 \text{ MPa} < f_{ck} \leq 50$ MPa, and should not exceed $0.33d$ when $50 \text{ MPa} < f_{ck} \leq 80$ MPa.
2. When the yield strength of the compression and tension steel is between 460 MPa and 600 MPa, the value of x_u should not exceed $0.45d$ when $f_{ck} \leq 30$ MPa, should not exceed $0.35d$ when $30 \text{ MPa} < f_{ck} \leq 50$ MPa, and should not exceed $0.28d$ when $50 \text{ MPa} < f_{ck} \leq 80$ MPa.
3. Similarly, when the yield strength of the compression and tension steel is less than or equal to 600 MPa, the value of $(p_t - p_c)$ should not exceed $0.70p_b$ when $f_{ck} \leq 30$ MPa, should not exceed $0.60p_b$ when $30 \text{ MPa} < f_{ck} \leq 50$ MPa, and should not exceed $0.50p_b$ when $50 \text{ MPa} < f_{ck} \leq 80$ MPa, where p_b is the balanced steel ratio, $p_c = A_{sc}/bd$, and $p_t = A_{st}/bd$. These guidelines are applicable to both singly and doubly reinforced sections.

5.9 DEEP BEAMS

A deep beam is a structural member whose span to depth ratio is relatively small so that shear deformation dominates the behaviour. According to Clause 29.1 of IS 456, a beam is considered a deep beam when the effective span to overall depth ratio (L/D ratio) is less than (a) 2.0 for simply supported beams and (b) 2.5 for continuous beams. According to ACI 318 Clause 10.7.1, the beam is considered deep in either of the following cases:

1. The clear span to overall depth ratio (L/D) is less than or equal to 4.0.
2. There are concentrated loads in a beam within twice the member depth from the face of the support.

The assumptions of linear-elastic flexural theory and plane sections remaining plane even after bending are not valid for deep beams. Hence, these beams have to be designed taking into account non-linear stress distribution along the depth

and lateral buckling. Arch action is more predominant than bending in deep beams. Hence, these beams require special considerations for their design and detailing. RC deep beams are often found as single-span or continuous transfer girders, pile-supported foundations, foundation walls supporting strip footings or raft slabs, walls of silos and bunkers, bridge bents, or shear wall structures, and in offshore structures. One such example of a deep beam is shown in Fig. 5.32.

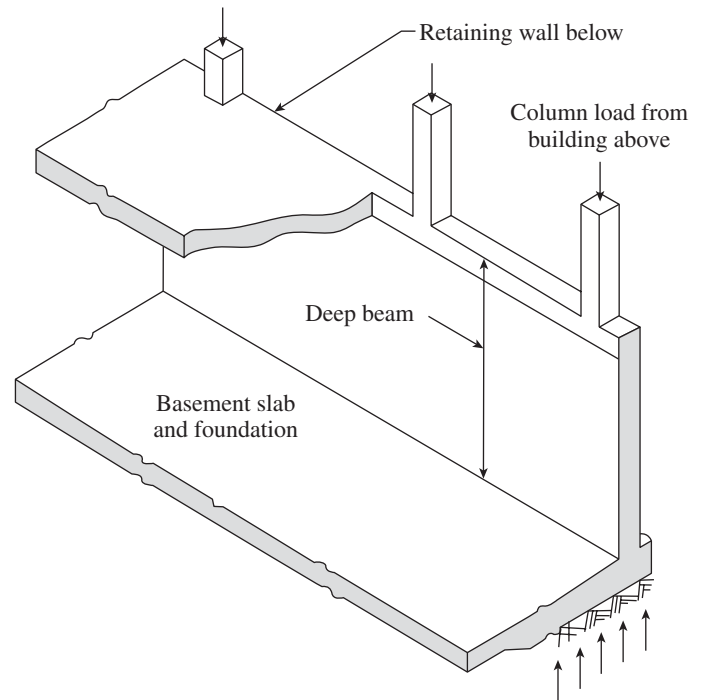


FIG. 5.32 Example of deep beam

During the 1970s, Kong and his associates at the University of Newcastle upon Tyne tested over 200 beams with many different configurations and studied the effect of variables such as shear span to depth ratio, reinforcement configurations, weight of concrete, and position of any web openings (Kong 1990). This work, together with the earlier research by Leonhardt and Walther (1966), formed the basis of the CIRIA Guide 2 published by Ove Arup and Partners (1977). The Indian code provisions are based on this guide. More reliable assessment of the behaviour of deep beams may be obtained by using the strut-and-tie model (Wight and Parra-Montesinos 2003). The strut-and-tie model provisions may be found in Appendix A of ACI 318 (see Appendix B of this book).

A brief introduction to the IS code provisions are provided here and strut-and-tie modelling is discussed in Appendix B. It should be noted that deep beams are sensitive to loading at the boundaries, and the length of bearing may affect the stress distribution in the vicinity of the supports. Similarly, stiffening ribs, cross walls, or extended columns at supports will also influence the stress distribution (Park and Paulay 1975). The concrete compression stresses are seldom critical. However,

the considerable increase of diagonal compression stresses near the support after the onset of cracking and anchorage of tensile steel are important considerations in the design and detailing (Park and Paulay 1975).

The ‘Simple Rules’ provided in IS 456, based on the CIRIA Guide 2, are intended primarily for uniformly loaded (from the top) deep beams and are intended to control the crack width rather than the ultimate strength. In addition, the active height of a deep beam is limited to a depth equal to the span; the part of the beam above this height is merely taken as a load-bearing wall between the supports. These rules are provided for single-span and continuous beams. The steps required for the flexural design of deep beams as per IS 456 are as follows (Kong 1990):

Step 1 Calculate the bending moment as in ordinary beams:

1. Simply supported beam with uniformly distributed load, w_u

$$M_{Max}^+ = \frac{w_u L^2}{8} \tag{5.88a}$$

2. Continuous beams with uniformly distributed load, w_u , as per ACI 318-89

- (a) Mid-span: $M_{Max}^+ = \frac{w_u L^2}{24} (1 - e^2)$ (5.88b)

- (b) Face of support: $M_{Max}^- = \frac{w_u L^2}{24} (2 - 3e + e^2)$ (5.88c)

where e is the ratio of the width of the support to the effective span of the beam.

Step 2 Calculate the capacity of the concrete section.

$$M_n = 0.12 f_{ck} b D^2 \tag{5.89}$$

where f_{ck} is the characteristic compressive strength of concrete and b and D are the thickness and overall depth of the beam, respectively. It has to be noted that D of a deep beam is limited to a depth equal to the span.

Step 3 If $L/D \leq 1.5$, go to step 4. If $L/D > 1.5$, check whether the applied moment M_u does not exceed M_n of Eq. (5.89),

where L is the effective span taken as the c/c between the supports or 1.15 times the clear span, whichever is lesser (see Clause 29.2 of IS 456), and D is the overall depth.

Step 4 Calculate the area A_{st} of the main longitudinal reinforcement:

$$A_{st} \geq \frac{M_u}{0.87 f_y z} \tag{5.90}$$

where M_u is the factored applied moment, f_y the characteristic yield strength of steel, and z the lever arm, which is to be taken as follows (Clause 29.2 of IS 456):

$$z = 0.2L + 0.4D \text{ if } (1 \leq L/D \leq 2) \text{ and } 0.6L \text{ if } (L/D < 1) \text{ for single-span beams} \tag{5.91a}$$

$$z = 0.2L + 0.3D \text{ if } (1 \leq L/D \leq 2.5) \text{ and } 0.5L \text{ if } (L/D < 1) \text{ for continuous beams} \tag{5.91b}$$

It should be noted that in deep beams the requirement of flexural reinforcement is not large, and hence the approximate lever arms, as determined from experiments and given here, are sufficient to arrive at them. It is also important to detail the reinforcement properly as the deep beam behaviour is different from that of normally sized beams. The recommendations given in IS 456 are as follows:

Reinforcement for positive moment In a simply supported beam, due to the arching action, the tension steel serves as a tie connecting the concrete compression struts (see Figs 5.33a and b). The cracking will occur at one-third to one-half of the ultimate load (Wight and MacGregor 2009). The flexural stress at the bottom is constant over much of the span. The non-uniform stress distribution due to uniformly distributed load is also shown in Fig. 5.33(c). The tests on deep beams have shown that the tension zone in the bottom is relatively small (Leonhardt and Walther 1966). Accordingly, Clause 29.3.1 of IS 456 suggests that the tensile reinforcement for a positive moment should be placed within a tension zone of depth equal to $0.25D - 0.05L$ from the extreme tension fibre at the mid-span as shown in Fig. 5.34(a). The suggested distribution, as

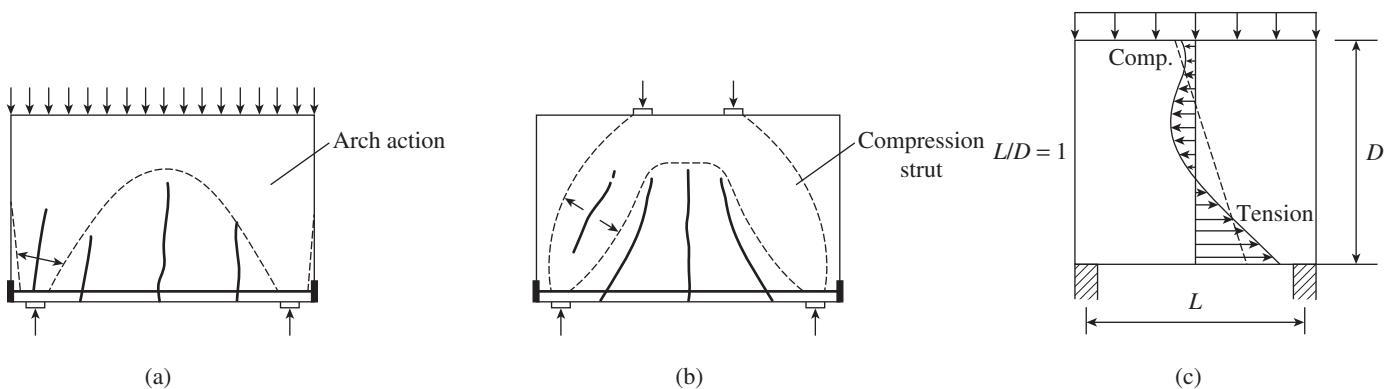


FIG. 5.33 Typical inclined compression failure of deep beams under various stress distributions (a) Uniform (b) Two-point loading (c) Non-linear

per Leonhardt and Mönning (1977), for downward loading from the soffit is shown in Fig. 5.34(b).

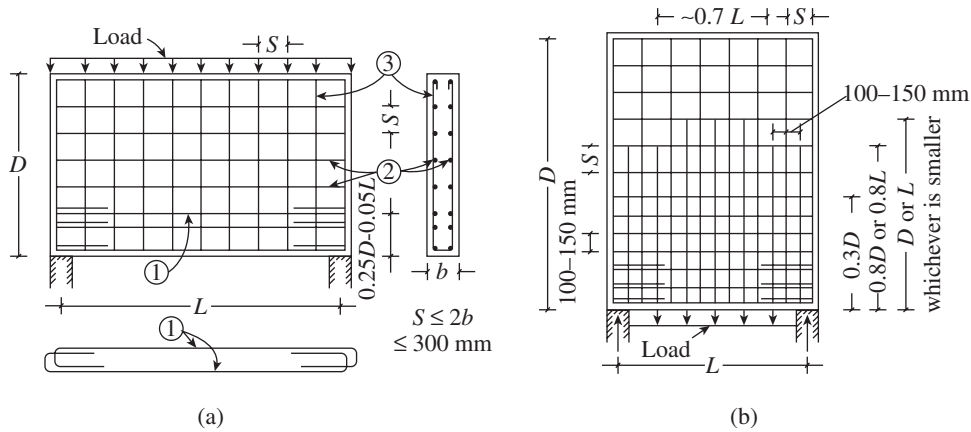


FIG. 5.34 Detailing of reinforcement in simply supported deep beams (a) Loaded from top (b) Loaded from soffit

The force in the longitudinal tension ties will be constant along the length of the deep beam. This implies that the force must be well anchored at the supports; else, it will result in major cause of distress. Hence, Clause 29.3.1(b) of IS 456 suggests that the bottom reinforcement should be extended into the supports without curtailment and embedded beyond the face of each support to a length of $0.8L_d$, where L_d is the development length for the design stress in the reinforcement (see Chapter 7 for the calculation of L_d). If sufficient embedment length is not available, the longitudinal reinforcement may be adequately anchored by hooks or welding to special mechanical anchorage devices (Seo, et al. 2004). Bent-up bars are not recommended. The beam should be proportioned in such a way that the strength of the steel tension ties governs the design.

Reinforcement for negative moment In the case of continuous deep beams, the tensile reinforcement for negative moment should satisfy the following requirements (Clause 29.3.2 of IS 456):

1. **Termination of reinforcement:** Negative reinforcement can be curtailed only in deep beams with $l/D > 1.0$. Not more than 50 per cent of the reinforcement may be terminated at a distance of $0.5D$ from the face of the support and the remaining should be extended over the full span (it has to be noted that l denotes the clear span and not the effective span of deep beam).

2. **Distribution of reinforcement:** When the l/D ratio is less than 1.0, the negative reinforcement should be evenly distributed

over a depth of $0.8D$ measured from the top tension fibre at the support, as shown in Fig. 5.35 (Leonhardt and Mönning 1977). However, when the l/D ratio is in the range 1.0–2.5, the negative reinforcement should be provided in two zones as shown in Fig. 5.36 and described as follows (Leonhardt and Mönning 1977):

- (a) A zone of depth $0.2D$ from the tension fibre should be provided with $\left(\frac{0.5l}{D} - 0.25\right)$ times the reinforcement calculated for negative moment, where l is clear span of beam.

- (b) A zone of $0.6D$ from this zone should contain the remaining reinforcement for negative moment and shall be evenly distributed.

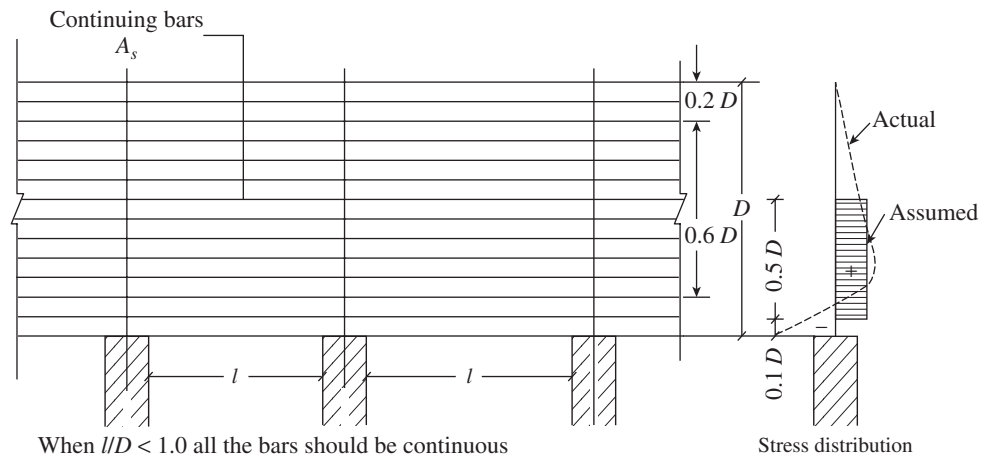


FIG. 5.35 Detailing of negative reinforcement in continuous deep beams ($l/D \leq 1.0$)

When the depth of the beam is much larger than the span, the portion above a depth equal to 0.8 times the span can be merely considered a load-bearing wall. Beam action should be considered only in the lower portion. Continuous deep beams are very sensitive to differential settlement of their supports.

Vertical reinforcement The loads applied at the bottom of the beam, as shown in Fig. 5.34(b), induce hanging action (for example, as in the face of bunker walls). Hence, Clause 29.3.3 of IS 456 suggests that suspension stirrups should be provided to carry the concerned loads (see also SP 24:1983 for detailing of suspended stirrups). Tests have shown that vertical shear reinforcement (perpendicular to the longitudinal axis of the member) is more effective for member strength than

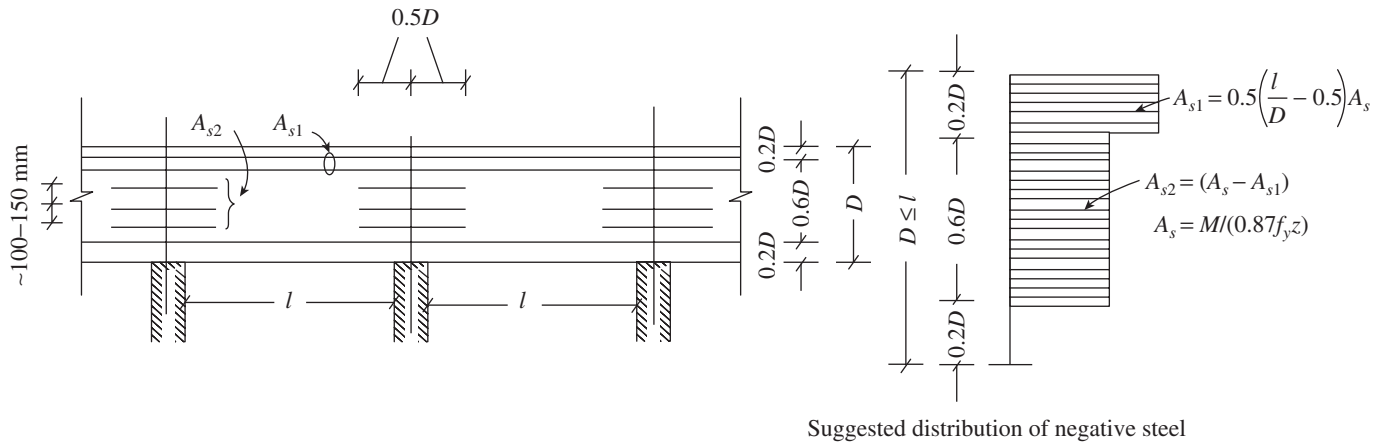


FIG. 5.36 Detailing of negative reinforcement in continuous deep beams ($1.0 \leq l/D \leq 2.5$)

horizontal shear reinforcement (parallel to the longitudinal axis of the member) in deep beams (Rogowsky and MacGregor 1986). However, equal minimum reinforcement in both directions is specified in the ACI code to control the growth and width of diagonal cracks, as shown in Table 5.10. The maximum spacing of bars has also been reduced in the ACI code from 450 mm to 300 mm. Hence, there is an urgent need to revise the IS code clauses. IS 456 stipulates that the spacing of vertical reinforcement should not exceed three times the thickness of the beam or 450 mm (see Table 5.10). Suspender stirrups should completely surround the bottom reinforcement and extend into the compression zone of the beam (see SP 24).

Side face or web reinforcement IS 456 suggests that the side face reinforcements should be provided as per the minimum requirements of walls. The requirement of minimum vertical and horizontal side face reinforcements, as per the code, is given in Table 5.10. For deep beams of thickness more than 200 mm, the vertical and horizontal reinforcements should be provided in two grids, one near each face of the beam (Clause 32.5.1). The horizontal and vertical steel placed on both the faces of the deep beam serve not only as shrinkage and temperature reinforcement but also as shear reinforcement.

TABLE 5.10 Side face reinforcement (Clause 32.5 of IS 456:2000)

Type of Reinforcement	Side Face Reinforcement of Gross Area of Concrete (Percentage)	
	Vertical	Horizontal
Bars of diameter ≤ 16 mm and $f_y \geq 415$ MPa	0.12*	0.20
Bars of Fe 250 grade steel	0.15	0.25
Welded wire fabric made with bars of diameter ≤ 16 mm	0.12	0.20

* It should be noted that as per the 2011 version of the ACI code, both vertical and horizontal reinforcement should not be less than $0.0025b_w s$ and the spacing s should not exceed the smaller of $d/5$ and 300 mm. As per Clause 32.5(b) and (d) of IS 456, both vertical and horizontal spacing of reinforcement should not exceed three times the thickness of the beam or 450 mm.

Shear reinforcement A deep beam provided with the reinforcements is deemed to satisfy the provision for shear, that is, the main tension and the web steels together with concrete will carry the applied shear, and hence, a separate check for shear is not required. However, Clause 11.7.3 of ACI 318:2011 code stipulates that the shear in deep beams should not exceed $0.74\phi\sqrt{f_{ck}}b_wd$ (where ϕ is the strength reduction factor = 0.75). More discussions on shear strength of deep beams may be found in Aguilar, et al. (2002) and Russo, et al. (2005).

Bearing strength In addition, the local failure of deep beams due to bearing stresses at the supports as well as loading points should be checked. To estimate the bearing stress at the support, the reaction may be considered uniformly distributed over the area equal to the beam width $b_w \times$ effective support length. The permissible ultimate stress is limited to $0.45f_{ck}$, as per Clause 34.4 of IS 456. The support areas may be strengthened by vertical steel and spiral reinforcement to prevent brittle failure at support.

Lateral buckling check To prevent the lateral buckling of simply supported deep beams, the breadth, b , should be such that the following conditions are satisfied (Clause 23.3 of IS 456):

$$\frac{l}{b} \leq 60 \quad \text{and} \quad \frac{ld}{b^2} \leq 250 \quad (5.92)$$

where L is the clear distance between the lateral restraints and d is the effective depth of the beam. A more accurate slenderness limit formula for rectangular beams is provided by Revathi and Menon (2007).

Brown and Bayrak (2008) critically evaluated the US provisions related to strut-and-tie models for deep beams and concluded that these provisions may lead to an unconservative calculation of nominal capacities in some cases. They also developed new lower bound provisions based on 596 published test results that incorporate parameters such as effect of strut inclination, concrete strength, geometry of bottle shaped strut, and shear reinforcement.

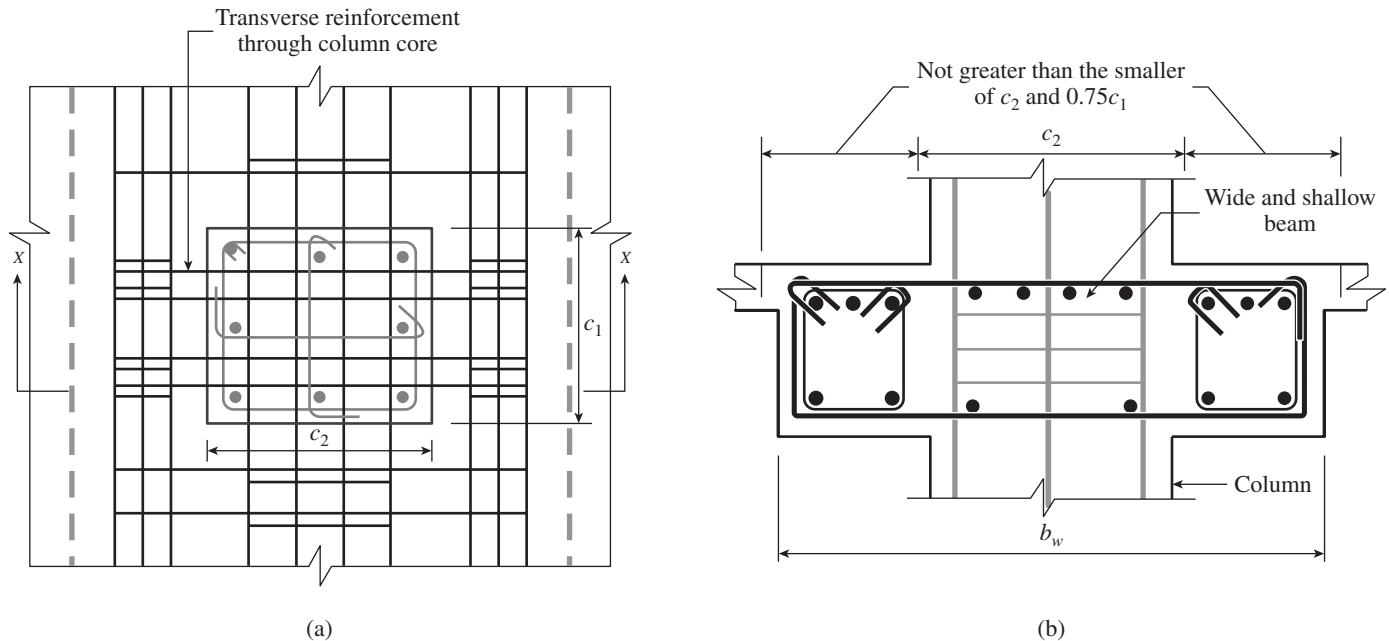


FIG. 5.37 WSB and column joint (ACI 318) (a) Plan (b) Section X-X (Reprinted with permission from ACI)

5.10 WIDE SHALLOW BEAMS

Wide shallow beams (WSB) are often found in one-way concrete joist systems and in other concrete buildings where floor-to-ceiling heights are restricted and congestion of column core is expected. WSB systems differ from normal beam systems discussed until now (normal beams are also designated as *floor drop beams* (FDBs) to distinguish them from WSBs) in the sense that they have beams of substantial width and usually have the same depth as that of the interconnected joists. Moreover, column widths are usually much narrower than the WSBs (see Fig. 5.37).

Studies on these types of floors are limited. Recently, Shuraim and Al-Negheimish (2011) studied the behaviour of joist floors with WSBs using finite element method (FEM) and found that the distribution of moments in WSB floor is complex and differs from what is normally assumed in practice. They developed an analytical procedure using equivalent frames with modified stiffness properties. They also proposed a scheme to laterally distribute the moments, obtained from a two-dimensional frame, such that the final distributions match with experimental as well as FEM results. In general, the design of wide beams may be carried out similar to the normally sized beams. Since they have limited depth, they require more longitudinal steel than normally sized beams. Shear and deflection may also be critical in such shallow beams; usually multi-legged shear stirrups are provided (see also Chapter 6).

According to the ACI 318 code, the width of the beam, b_w , should not exceed $3c_2$ or $c_2 + 1.5c_1$ as shown in Fig. 5.37, where c_1 and c_2 are the sizes of column as shown in this figure. At least a few transverse reinforcements should pass through the column core to tie the beam effectively with the column, as shown in Fig. 5.37. Additional transverse reinforcements

outside the column core may be required to resist torsional moments. Chow and Selna (1994) found that this type of WSB and floor system is likely to have good ductile behaviour as the beams deform inelastically. Wide beam–Narrow column systems are currently prohibited in high seismic zones by ACI-ASCE Committee 352.

5.11 HIDDEN BEAMS

In many situations, the architect may want to have a flat soffit of slab, without beams projecting out of the slab. In such situations, the structural engineer has to resort to *hidden beams* (also known as *concealed or flush beams*), which are beams having depth exactly equal to the thickness of the slab, as shown in Fig. 5.38. The span of such hidden beams should not exceed about 1.8–2 m. They are used to support 115 mm thick brick (partition) walls and may have a width equal to the wall thickness plus two times the slab thickness. The normal method of design, as explained in Section 5.4, can be used for the design of such beams. Since the depth is limited, the required area of reinforcement will be higher than for normal beams.

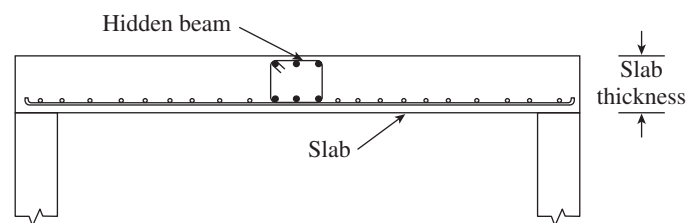


FIG. 5.38 Hidden beam

Deodhar and Dubey (2004) conducted experimental investigations on hidden beams in slabs of size 1.2×1.5 m and thickness 50 mm. Based on their behaviour, they found

that the provision of hidden beams improves the stiffness and stability of the slabs. They also found that the provision of hidden beams is more effective along the longer span than along the shorter span and that the negative reinforcement, provided in the location of the hidden beam, improves the load-carrying capacity of the slabs. It has to be noted that they studied only the stiffening effect of such beams and did not apply any partition load on the hidden beam.

5.12 LINTEL AND PLINTH BEAMS

Lintels are beams that support masonry above openings in walls. Typically, lintels for concrete or masonry walls are constructed as in situ or precast concrete beams. Vertical loads carried by lintels typically include the following: (a) distributed loads from the dead weight of the lintel and the masonry wall above the lintel and any floor and/or roof, (b) dead and live loads supported by the masonry, and (c) concentrated loads from floor beams, roof joists, and other members that frame directly into the wall. When there is sufficient height of brick wall over the lintel and sufficient bearing is provided, *arching action* in masonry is possible, and hence the entire wall load above the lintel is not transferred to it. The length of bearing of the lintel at each end shall not be less than 100 mm or one-tenth of the span, whichever is higher, and the area of the bearing shall be sufficient to ensure that stresses in the masonry do not exceed the permissible stresses. For well-bonded brickwork, a 45° triangular load dispersion is often assumed, as shown in Fig. 5.39(a). In practice, when the length of the walls on both sides of an opening is at least half the effective span of the opening, arch action is assumed. Concentrated loads transferred from beams on the wall above

the lintel may be considered to have a dispersion angle of 30° to the vertical on either side (see Fig. 5.39b).

When the loads are applied below the apex of the triangle, arch action is not possible, and in such a case, all the loads from the wall above the lintel must be carried by the lintel. Assuming a triangular load on the lintel, the bending moment at mid-span due to the weight of the brick wall above the lintel is

$$M = \frac{WL}{6} \tag{5.93}$$

where W is the total weight of the triangular brickwork and L is the effective span of the lintel. After calculating the bending moment, the lintel beam may be designed as a normal rectangular beam. More details on the design of lintel beams may be found in Rai (2008) and Dayaratnam (1987).

Plinth beams are provided at plinth level in load-bearing masonry walls to resist uneven settlements. In buildings situated in seismic zones, they are provided as a continuous band at plinth level, in addition to similar beams at lintel and roof levels. The depth of these beams ranges between 100 mm and 150 mm and the beams are normally provided with a minimum of two 8 mm bars at the top and bottom and 6 mm stirrups at 230 mm spacing.

Grade beams are provided to connect the column foundations together, whether the columns are supported on individual spread footings, individual piles, or pile groups. These beams are not required to support significant structural loads directly. They also support walls and are often stronger than plinth beams. Normally, they are 150 mm deep with three 8 mm diameter bars at the top and bottom and 6 mm stirrups at 150–200 mm spacing.

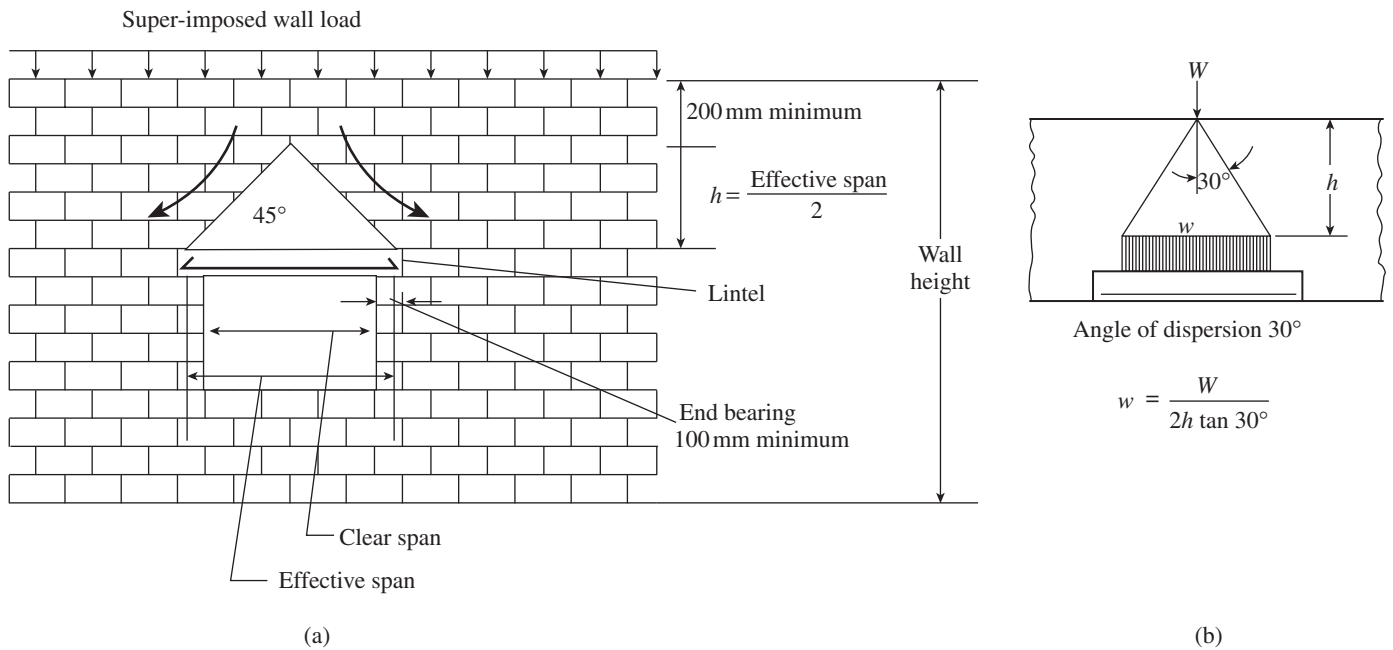


FIG. 5.39 Lintel beam (a) Dispersion of uniformly distributed load (b) Dispersion of concentrated load

Research conducted at the Indian Institute of Technology, Chennai, as well as other research organizations has established that there is an arching effect of masonry similar to that observed in lintel beams (Jagadish 1988; Govindan and Santhakumar 1985). In addition, the beam acts as a deep composite beam along with the brickwork. Recognizing these effects, Clause 5.3.1 of IS 2911 states that the grade beams supporting brick walls should be designed considering the arching effect of masonry above the beam. It suggests that the maximum bending moment may be taken as $wL^2/50$ (instead of the usual $wL^2/8$), where w is the uniformly distributed load per metre run worked out by assuming a maximum height of two storeys in a structure with load-bearing walls and one storey in framed structures and L is the effective span in metres. The value of the bending moment should be increased to $(wL^2/30)$ if the beams are not supported during construction until the masonry above it gains strength. Moreover, for considering composite action, the minimum height of the wall should be 0.6 times the beam span. For concentrated loads and other loads that come directly over the beam, full bending moment should be considered. The design of plinth and grade beams may be made considering them as rectangular beams.

5.13 HIGH-STRENGTH STEEL AND HIGH-STRENGTH CONCRETE

Strictly speaking, the provisions of IS 456 are applicable only up to a concrete strength of 40MPa; this is because these provisions are based on the results of experiments conducted on specimens having strength up to only 40MPa. However, due to the continued use of HSC, especially in tall buildings and bridges, in August 2007 the BIS amended that these design provisions are applicable up to a concrete strength of M60. It should also be noted that the latest version of the ACI code (ACI 318-11) does not impose any restriction on the maximum strength of concrete for seismic design, though Canadian and New Zealand codes limit concrete strength to 80MPa and 70 MPa, respectively, for ductile elements. As stated in Section 5.4.1, the stress distribution in HSC will be triangular instead of rectangular–parabolic, as assumed by IS 456. The American code provisions, as discussed in Section 5.4.1, which consider this stress distribution, should be followed for HSC.

The advantages and disadvantages of using higher strength materials are now clear. The use of a higher strength concrete would allow a higher flexural strength to be achieved while maintaining the same minimum level of flexural ductility, even though a higher strength concrete by itself is generally less ductile. On the other hand, the use of a higher strength steel would not allow a higher flexural strength to be achieved while maintaining the same minimum level of flexural ductility; it only allows the use of a smaller steel area for a given flexural strength requirement to save the amount of steel

needed. The other advantages of HSS are reduction of steel congestion in highly reinforced members, improved concrete placement, saving in cost of labour, reduction in construction time, and in some cases resistance to corrosion. However, the IS code provisions are applicable up to Fe 500 grade of steel.

Based on a series of investigations, the researchers at North Carolina State University suggested a design methodology in a format similar to that of ACI 318 provisions for the flexural design of concrete beams reinforced with ASTM A1035-07 grade 100 (690MPa) steel bars, commercially known as MMFX; it should be noted that this methodology is not suitable for structures in high seismic zones (Mast, et al. 2008). The stress–strain behaviour of this MMFX steel bar may be represented as follows:

$$f_s = 1172 - \frac{2.379}{\varepsilon_s + 0.00104} \text{MPa for } 0.00241 < \varepsilon_s < 0.060 \quad (5.94)$$

$$= 200,000\varepsilon_s \text{MPa for } \varepsilon_s \leq 0.00241$$

where f_s is the stress in steel and ε_s is the corresponding strain. They also suggested a tension-controlled strain limit of 0.009 (instead of the strain limit of 0.005, used up to 520 MPa steel in ACI 318-11) and a compression-controlled strain limit of 0.004 (The New Zealand code has specified 0.004 as the limiting compression strain in concrete and 0.018 as the limiting tensile strain in reinforcement for nominally ductile plastic regions in beams and walls, which have been found to be overly conservative (Walker and Dhakal 2009)). Based on this, they also developed the following simple equation for strength reduction factor ϕ in the transition zone between the tension- and compression-controlled sections (see also Section 5.5.5 and Fig. 5.9):

$$\phi = 0.45 + 50\varepsilon_t \text{ for } 0.004 < \varepsilon_t < 0.009 \quad (5.95)$$

$$= 0.9 \text{ for } \varepsilon_t \geq 0.009$$

$$= 0.65 \text{ for } \varepsilon_t \geq 0.004$$

They cautioned that for compression steel the present ACI yield strength limit of 550MPa should be maintained. An example based on this philosophy of design is presented in Example 5.30.

The seismic behaviour of ultra-high-strength concrete (UHSC) beams, that is, beams with strength greater than 100MPa, has been studied by Elmenhawi and Brown (2010). They found that UHSC can improve the energy dissipation capacity provided that the beams have symmetric reinforcement and less shear demand and the plastic hinge zone (may be taken as about 0.8–1.0 depth of the beam) is well confined. More details on UHSC elements may be found in Fehling, et al. (2008) and Schmidt and Fehling (2007).

The flexural performance of recycled concrete beams was studied by Fathifazl, et al. 2009, who observed a performance of these beams comparable with those of conventional natural aggregates and suggested the same general flexural theory for these beams too.

5.14 FATIGUE BEHAVIOUR OF BEAMS

The RC beams subjected to moving loads are prone to fatigue. Concrete bridge decks, elements of offshore structures, and concrete pavements are subjected to a large number of loading cycles. Fatigue strength is influenced by the range of loading, rate of loading, eccentricity of loading, load history, material properties, and environmental conditions. The effect of the range of stress will usually be represented in the form of stress–fatigue life curves, commonly referred to as *S–N curves*. The reinforcement of these concrete elements may fail by fatigue if there are more than one million load cycles and the tensile stress range (the maximum tensile stress in a cycle minus the algebraic minimum stress) is above a threshold or *endurance limit* of about 165 MPa. It has to be noted that fatigue strength is independent of the yield strength.

Fatigue strength is greatly reduced in the vicinity of tack welds or bends in the region of maximum stress; fatigue failure is possible in such locations if the stress range exceeds about 70 MPa. Fatigue will not be a problem if the number of cycles is less than 20,000. Due to the significant dead load of RC structures, compared to steel structures, a stress range exceeding 165 MPa is rare in most concrete structures. An overview of the fatigue strength of RC structures is provided by ACI 215 and the fatigue strength of bridges by ACI 343.

Fatigue failure of the concrete occurs through progressive growth of micro-cracking. Since the tests conducted by Feret in 1906, many researchers have carried out laboratory experiments to investigate the fatigue behaviour of plain as well as steel fibre RC. Lee and Barr (2004) provide a general overview of recent developments in the study of the fatigue behaviour of plain and fibre RC. The fatigue strength of plain concrete in compression or tension in 10 million cycles is about 55 per cent of the static strength and is not sensitive to stress concentration (Wight and MacGregor 2009). It has to be noted that the cumulative damage theory based on Palmgren-Miner’s hypothesis is not applicable for the fatigue behaviour of concrete beams (Sain and Kishen 2007). Sain and Kishen (2007) also found that the rate of fatigue crack propagation decreases along with an increase in percentage reinforcement. Structural size effect on fatigue in bending of concrete was studied by Zhang, et al. (2001). ACI 215 recommends that the compressive stress range f_{sr} should not exceed

$$f_{sr} = 0.32f_{ck} + 0.47f_{\min} \tag{5.96}$$

where f_{\min} is the minimum compressive stress in the cycle (compression is taken as positive). It is better to limit the compressive stress at service load to $0.4 f_{ck}$. The fatigue strength of stirrups may be less than that of longitudinal bars due to the kinking, and hence, it may be reasonable to limit the stirrup stress range to 0.75 times f_{sr} .

EXAMPLES

The following are a few examples of analysis of singly reinforced rectangular beams.

EXAMPLE 5.1 (Calculation of cracking moment of section): Assuming that the concrete is uncracked, compute the bending stresses in the extreme fibres of the beam having a size of 600 mm × 300 mm, as shown in Fig. 5.40, for a bending moment of 60 kNm. Assume the concrete is of grade 25 MPa. In addition, determine the cracking moment of the section.

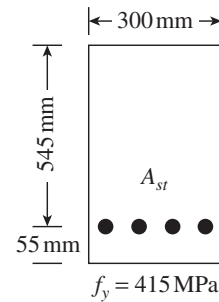


FIG. 5.40 Beam of Example 5.1

SOLUTION:

Bending stress:

$$I_g = bd^3/12 = 300 \times 600^3/12 = 5.4 \times 10^9 \text{ mm}^4$$

Bending stress in extreme fibre,

$$f = \frac{My}{I_g} = \frac{60 \times 10^6 \times 300}{5.4 \times 10^9} = 3.33 \text{ MPa}$$

$$M_{cr} = \frac{f_{cr} I_g}{y_t} = f_{cr} Z \text{ with } f_{cr} = 0.7 \sqrt{f_{ck}} = 0.7 \sqrt{25} = 3.5 \text{ MPa}$$

$$\text{Hence, } M_{cr} = \frac{3.5 \times 5.4 \times 10^9}{300} = 63 \times 10^6 \text{ MPa} > 60 \times 10^6 \text{ MPa}$$

EXAMPLE 5.2 (Determination of under- or over-reinforced section):

Determine whether the section shown in Fig. 5.40 is under or over-reinforced with $f_{ck} = 27.5 \text{ N/mm}^2$, $f_y = 415 \text{ N/mm}^2$, and the following values of A_{st} : (a) 1610 mm² (b) 2100 mm² (c) 2960 mm² (d) 4190 mm².

SOLUTION:

To determine whether the section is over or under-reinforced, the maximum permitted area of steel has to be calculated.

From Table 5.5, we get

$$p_{t,\text{lim}} = \frac{19.82 f_{ck}}{f_y} = \frac{19.82 \times 27.5}{415} = 1.313$$

$$A_{st,\text{lim}} = 1.313 \times 545 \times 300/100 = 2147 \text{ mm}^2$$

(a) $A_{st} = 1610 \text{ mm}^2 < A_{st,\text{lim}}$; hence it is an under-reinforced section.

- (b) $A_{st} = 2100 \text{ mm}^2 < A_{st,lim}$; hence it is an under-reinforced section.
- (c) $A_{st} = 2960 \text{ mm}^2 > A_{st,lim}$; hence it is an over-reinforced section.
- (d) $A_{st} = 4190 \text{ mm}^2 > A_{st,lim}$; hence it is an over-reinforced section.

Let us investigate case (c) further, by assuming that the steel has yielded.

As per Eq. (5.18a)

$$\frac{x_u}{d} = \frac{0.87 f_y A_{st}}{0.36 f_{ck} b d} = \frac{0.87 \times 415 \times 2960}{0.36 \times 27.5 \times 545 \times 300} = 0.6602$$

Hence $x_u = 0.6602 \times 545 = 359.8 \text{ mm}$

Hence, stress in steel,

$$f_s = 700 \frac{d - x}{x} = 700 \frac{545 - 359.8}{359.8} = 360.3 \approx \left(\frac{f_y}{1.15} = 360.8 \right)$$

Hence, it shows that the reinforcement represents the balanced condition, that is, the concrete and steel will fail at the same load. As discussed earlier, there is no balanced strain condition specified in IS 456. Due to the extra strain of 0.002 considered in the IS code equation for $A_{st,lim}$, this section is considered as over-reinforced. This shows the extra cushion (27.5% less reinforcement in this case) provided in the code to make the section ductile.

EXAMPLE 5.3 (Analysis of singly reinforced rectangular section—IS and ACI methods):

Determine the nominal ultimate moment strength of the beam section shown in Fig. 5.40, with $A_{st} = 3$ bars of 25 mm diameter = 1473 mm^2 , $f_y = 415 \text{ MPa}$, and $f_{ck} = 20 \text{ MPa}$ using the following methods:

- (a) Parabolic–rectangular stress block as per IS 456
 (b) Equivalent rectangular stress block as in ACI 318.

SOLUTION:

(a) Using the parabolic–rectangular stress block as per IS 456:

$$p_{t,lim} = \frac{19.82 f_{ck}}{f_y} = \frac{19.82 \times 20}{415} = 0.955,$$

$$A_{st,lim} = 0.955 \times 545 \times 300 / 100 = 1561 \text{ mm}^2 > A_{st}$$

Hence, the beam is *under-reinforced*.

Assuming the tension steel yields, the tensile and compressive forces are computed as follows:

$$T = A_{st} f_{st} = 0.87 A_{st} f_y = (0.87)(1473) 415 = 531,827 \text{ N}$$

$$C = 0.36 f_{ck} b x_u = (0.36)(20)(300)x_u = 2160 x_u \text{ N}$$

Equating T and C and solving for x_u ,

$$x_u = 531,827 / 2160 = 246.2 \text{ mm}$$

Lever arm $z = d - 0.416 x_u = 545 - 0.416(246.2) = 442.6 \text{ mm}$

Hence, $M_n = (531,827)(442.6) 10^{-6} = 235.4 \text{ kNm}$

- (b) Using the equivalent rectangular stress block as in ACI 318, the tensile and compressive forces are calculated as follows:

$$T = A_{st} f_{st} = 0.87 A_{st} f_y = 0.87(1473) 415 = 531,827 \text{ N}$$

$$C = 0.45 f_{ck} b a = (0.45)(20)(300)a = 2700a \text{ N}$$

Equating T and C and solving for a ,

$$a = 531,827 / 2700 = 197 \text{ mm}$$

Lever arm $z = d - a/2 = 545 - 197/2 = 446.5 \text{ mm}$

$M_n = Tz = 0.87 f_y A_{st} (d - 0.5a) = (531,827)(446.5) 10^{-6} = 237.46 \text{ kNm}$

It should be noted that this value of $M_n = 237.46 \text{ kNm}$ compares well with the value of 235.4 kNm calculated using the parabolic–rectangular stress block of IS 456.

EXAMPLE 5.4 (Capacity of singly reinforced rectangular section):

Determine whether the section shown in Fig. 5.41 can withstand a factored applied bending moment of 100 kNm , with $A_{st} = 2$ numbers 20 diameter = 628 mm^2 , $f_y = 415 \text{ MPa}$, and $f_{ck} = 30 \text{ MPa}$.

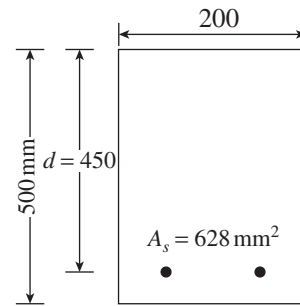


FIG. 5.41 Beam of Example 5.4

SOLUTION:

Assume a concrete cover of 50 mm. Then $d = 500 - 50 = 450 \text{ mm}$

$$p_{t,lim} = \frac{19.82 f_{ck}}{f_y} = \frac{19.82 \times 30}{415} = 1.432,$$

$$A_{st,lim} = 1.432 \times 450 \times 200 / 100 = 1289 \text{ mm}^2 > A_{st}$$

Hence, the beam is *under-reinforced*.

$$\begin{aligned} M_n &= 0.87 f_y A_{st} d \left(1 - \frac{f_y A_{st}}{f_{ck} b d} \right) \\ &= 0.87 \times 415 \times 628 \times 450 \left(1 - \frac{415 \times 628}{30 \times 450 \times 200} \right) 10^{-6} \\ &= 92.18 \text{ kNm} \end{aligned}$$

Let us check the capacity of the beam for concrete failure:

$$\begin{aligned} M_{n,lim} &= 0.138 f_{ck} b d^2 \\ &= 0.138 \times 30 \times 200 \times 450^2 \times 10^{-6} \\ &= 167.67 \text{ kNm} \end{aligned}$$

This confirms that the failure by steel yielding governs.

Since M_n (92.18 kNm) is less than the applied moment M_u (100 kNm), the cross section is not adequate and is unsafe.

EXAMPLE 5.5 (Analysis of over-reinforced rectangular beam): Calculate the maximum moment that the beam shown in Fig. 5.42 can sustain. Assume $f_{ck} = 25$ MPa and $f_y = 415$ MPa.

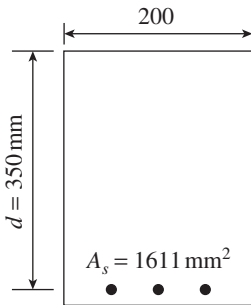


FIG. 5.42 Beam of Example 5.5

SOLUTION:

$$p_{t,lim} = \frac{19.82 f_{ck}}{f_y} = \frac{19.82 \times 25}{415} = 1.194,$$

$$\begin{aligned} A_{st,lim} &= 1.194 \times 350 \times 200 / 100 \\ &= 835.8 \text{ mm}^2 < A_s \end{aligned}$$

Hence, the section is *over-reinforced*.

Step 1 Assume tension reinforcement has yielded and calculate x_u .

As per Eq. (5.18a)

$$\begin{aligned} \frac{x_u}{d} &= \frac{0.87 f_y A_{st}}{0.36 f_{ck} b d} = \frac{0.87 \times 415 \times 1611}{0.36 \times 25 \times 350 \times 200} \\ &= 0.923 > \left(\frac{x_u}{d} \right)_{lim} = 0.479 \end{aligned}$$

which shows that the tension reinforcement has not yielded.

Trial value of $x_u = 0.923 \times 350 = 323.1$ mm

Step 2 Determine the stress in steel.

$$\text{Stress in steel, } f_s = 700 \frac{350 - x_u}{x_u} = \frac{2,45,000 - 700x_u}{x_u}$$

Step 3 Recalculate x_u .

$$0.36 f_{ck} b x_u = A_s f_s$$

$$\text{i.e., } 0.36 \times 25 \times 200 \times x_u = 1611 \times \frac{2,45,000 - 700x_u}{x_u}$$

$$x_u^2 + 626.5x_u - 2,19,275 = 0$$

This is a quadratic equation in x_u . Solving, we get

$$x_u = 250.13 \text{ mm, } \left(\frac{x_u}{d} \right) = 0.7146 > \left(\frac{x_u}{d} \right)_{lim} = 0.479$$

$$\begin{aligned} f_s &= 700 \frac{350 - x_u}{x_u} = 700 \frac{350 - 250.13}{250.13} \\ &= 279.5 \text{ N/mm}^2 < 415 / 1.15 = 360.9 \text{ N/mm}^2 \end{aligned}$$

Step 4 Calculate the moment capacity.

$$\begin{aligned} M_n &= f_s A_{st} (d - 0.416 x_u) \\ &= 279.5 \times 1611 (350 - 0.416 \times 250.13) \times 10^{-6} \\ &= 110.74 \text{ kNm} \end{aligned}$$

EXAMPLE 5.6 (Analysis of rectangular beam with a steel plate): Find the ultimate moment capacity of a rectangular beam shown in Fig. 5.43, which has been found to be inadequate to carry the external loading and hence repaired by gluing a steel plate of thickness 3 mm (yield strength 250 N/mm²) at the bottom of the beam. Assume $f_{ck} = 20$ MPa and $f_y = 250$ MPa.

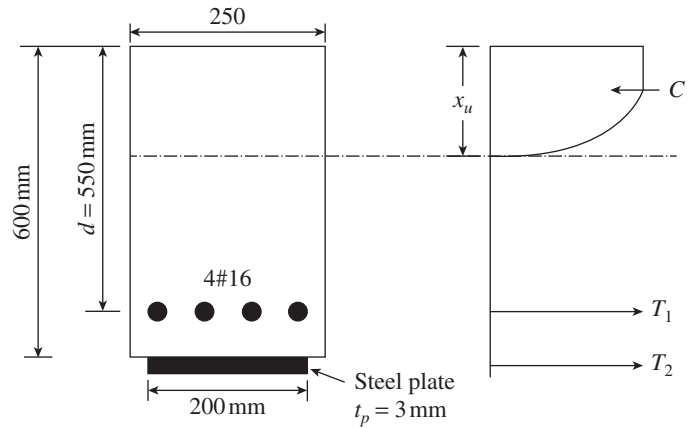


FIG. 5.43 Beam of Example 5.6

SOLUTION:

Area of the plate $A_p = 3 \times 200 = 600 \text{ mm}^2$

Area of steel bars $= 4 \times 201 = 808 \text{ mm}^2$

Now, $C = T_1 + T_2$

Assume that both the steel bars and the plate yield.

$$0.36 f_{ck} b x_u = A_{st} f_y / 1.15 + A_p f_{yp} / 1.15$$

$$\begin{aligned} 0.36 \times 20 \times 250 x_u &= 808 \times 250 / 1.15 + 600 \times 250 / 1.15 \\ x_u &= 170.05 \text{ mm} \end{aligned}$$

Check for steel yielding

As per Table 5.5, $\left(\frac{x_u}{d} \right)_{lim}$ for $f_y = 250 \text{ N/mm}^2 = 0.531$

Hence $x_{u,lim} = 0.531 \times 550 = 292.05 \text{ mm} < 170.05 \text{ mm}$

Hence, steel yielding governs.

The stress in the plate

$$\begin{aligned} f_{sp} &= 700 \frac{d_p - x_u}{x_u} \\ &= 700 \frac{(601.5 - 170.05)}{170.05} \\ &= 1776 \text{ N/mm}^2 > 250/1.15 \end{aligned}$$

Hence, the steel plate also yields.

Calculation of ultimate moment capacity

Taking moment about the concrete force C , we get

$$\begin{aligned} M_n &= T_1(d - 0.416x_u) + T_2(d_p - 0.416x_u) \\ M_n &= 0.87 \times 250 \times 808(550 - 0.416 \times 170.05) \\ &\quad + 0.87 \times 250 \times 600 \times (601.5 - 0.416 \times 170.05) \\ M_n &= (84.22 + 69.26) \times 10^6 \text{ Nmm} = 153.48 \text{ kNm} \end{aligned}$$

EXAMPLE 5.7 (Analysis of trapezoidal section):

Find the ultimate moment capacity of an RC trapezoidal section as shown in Fig. 5.44. The beam has a top width of 400 mm, depth of 550 mm, and width at the level of centroid of reinforcement as 250 mm. Assume $A_{st} = 1473 \text{ mm}^2$, $f_{ck} = 25 \text{ MPa}$, and $f_y = 415 \text{ Pa}$.

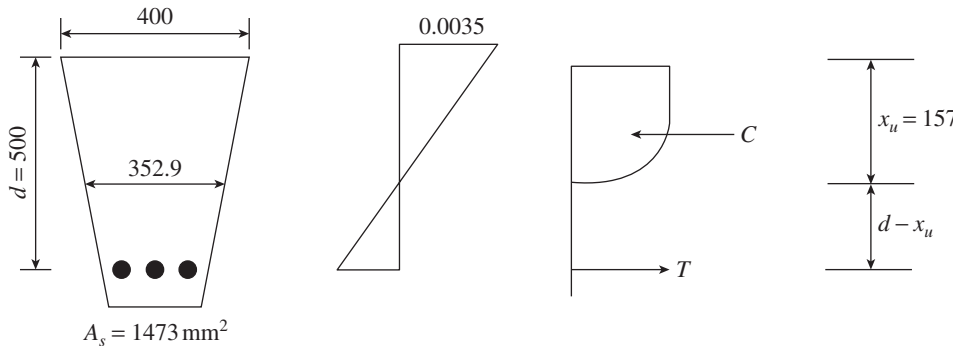


FIG. 5.44 Trapezoidal beam of Example 5.7

SOLUTION:

Step 1 Compute x_u .

Assume tension steel has yielded. Then

$$\begin{aligned} 0.36f_{ck}A_c &= 0.87f_yA_s \\ (0.36 \times 25)A_c &= 0.87 \times 415 \times 1473 \\ A_c &= \frac{0.87 \times 415 \times 1473}{0.36 \times 25} = 59,091.85 \text{ mm}^2 \\ A_c &= \text{Average width} \times x_u \text{ mm}^2 \\ \text{Average width} &= \frac{1}{2} \left[400 + \left(250 + \frac{150 \times (500 - x_u)}{500} \right) \right] \\ &= \frac{1}{2} [650 + 0.3(500 - x_u)] \\ &= (-0.15x_u + 400) \end{aligned}$$

Hence, $A_c = (-0.15x_u + 400)x_u = 59,091.85$

Expanding we get

$$\begin{aligned} 0.15x_u^2 - 400x_u + 59,091.85 &= 0 \\ x_u^2 - 2666.7x_u + 3,93,945 &= 0 \end{aligned}$$

$$x_u = \frac{2,666.7 - \sqrt{2,666.7^2 - 4 \times 3,93,945}}{2} = 157 \text{ mm}$$

Step 2 Check for ϵ_s .

$$d - x_u = 500 - 157 = 343 \text{ mm}$$

$$\epsilon_s = \frac{0.0035(d - x_u)}{x_u} = \frac{0.0035 \times 343}{157} = 0.0076 > 0.0038$$

Hence, the tension steel yields.

$$\frac{x_u}{d} = \frac{157}{500} = 0.314 < \frac{x_{u,\text{lim}}}{d} = 0.479$$

Hence, it is acceptable.

Step 3 Check $T = C$.

$$T = 0.87f_yA_{st} = 0.87 \times 415 \times 1473 \times 10^{-3} = 531.8 \text{ kN}$$

$$C = 0.36f_{ck}A_c = 0.36 \times 25 \times 59,091.85 \times 10^{-3} = 531.8 \text{ kN}$$

Hence, it is acceptable.

Step 4 Find the centre of compression and lever arm.

Width b of beam at neutral axis = $b = 250 + (150/500)(500 - 157) = 352.9 \text{ mm}$

Let CG be y from the top fibre. Then

$$\begin{aligned} y &= \frac{h}{3} \left(\frac{a + 2b}{a + b} \right) \\ &= \frac{157}{3} \left[\frac{400 + 2 \times 352.9}{400 + 352.9} \right] \\ &= 76.86 \text{ mm} \end{aligned}$$

Step 5 Calculate M_u .

$$z = 500 - 76.86 = 423.14 \text{ mm}$$

$$M_u = Tz = 531.8 \times 0.423 = 225 \text{ kNm}$$

Check using SP 16

$$\text{Average breadth} = \frac{400 + 250}{2} = 325 \text{ mm}$$

$$\text{With } d = 500, \frac{A_s \times 100}{bd} = \frac{1473 \times 100}{500 \times 325} = 0.906\%$$

From Table 3 of SP 16, $M_u/bd^2 = 2.755$

$$\text{Hence, } M_u = 2.755 \times 325 \times 500^2 \times 10^{-6} = 223.8 \text{ kNm}$$

EXAMPLE 5.8 (Analysis of cross-shaped section):
 Find the ultimate moment capacity of the cross section shown in Fig. 5.45. Assume $f_{ck} = 25 \text{ N/mm}^2$ and $f_y = 415 \text{ N/mm}^2$.

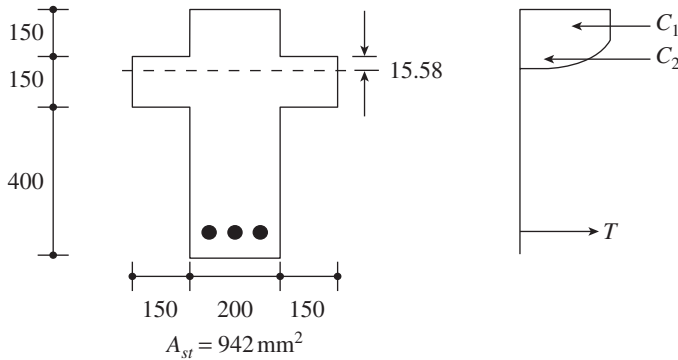


FIG. 5.45 +shaped beam of Example 5.8

SOLUTION:

Step 1 Compute x_u .

Assuming tension steel has yielded,

$$0.36f_{ck}A_c = 0.87f_yA_{st}$$

$$0.36 \times 25 \times A_c = 0.87 \times 415 \times 942$$

Hence, $A_c = 37,789.9 \text{ mm}^2$

Since A_c is greater than $200 \text{ mm} \times 150 \text{ mm} = 30,000 \text{ mm}^2$ (top portion of the beam shown in Fig. 5.45), let us assume that the neutral axis distance is below the top portion, at a distance equal to x_2 .

$$x_2 \times 500 + 150 \times 200 = 37,789.9$$

$$x_2 = 15.58 \text{ mm}$$

Therefore, $x_u = 150 + 15.58 = 165.58 \text{ mm}$

Step 2 Check the yielding of steel. Assuming a cover of 50 mm,

$$d = 150 + 150 + 400 - 50 = 650 \text{ mm}$$

$$\frac{x_u}{d} = \frac{165.58}{650} = 0.255 < (x_u/d)_{lim} = 0.479$$

Hence, tension steel will yield.

Step 3 Compute M_n .

Taking moment about tension force, T

$$M_n = C_1y_1 + C_2y_2$$

$$C_1 = 0.36 \times 25 \times 200 \times 150/1000 = 270 \text{ kN}$$

$$y_1 = 650 - 150/2 = 575 \text{ mm}$$

$$C_2 = 0.36 \times 25 \times 500 \times 15.58/1000 = 70.11 \text{ kN}$$

$$y_2 = 650 - 150 - 15.58/2 = 492.21 \text{ mm}$$

$$M_n = 270 \times 575/1000 + 70.11 \times 492.21/1000$$

$$= 189.75 \text{ kNm}$$

The following are a few examples for the design of singly reinforced rectangular beams.

EXAMPLE 5.9 (Design of singly reinforced rectangular concrete):

Design a singly reinforced concrete beam of width 250 mm, subjected to an ultimate moment of 130 kNm. Assume $f_{ck} = 20 \text{ MPa}$ and $f_y = 415 \text{ MPa}$.

SOLUTION:

Step 1 Determine the depth of the beam.

From Eq. (5.28)

$$d = \sqrt{\frac{7.2M_u}{f_{ck}b}} = \sqrt{\frac{7.2 \times 130 \times 10^6}{20 \times 250}} = 433 \text{ mm}$$

Provide $d = 460 \text{ mm}$ with cover as 40 mm. Thus $D = 460 + 40 = 500 \text{ mm}$.

Step 2 Check for x_u/d (Eq. 5.29a).

$$\left(\frac{x_u}{d}\right) = 1.2 - \sqrt{1.44 - \frac{6.68M_u}{f_{ck}bd^2}}$$

$$= 1.2 - \sqrt{1.44 - \frac{6.68 \times 130 \times 10^6}{20 \times 250 \times 460^2}} = 0.407$$

The value of (x_u/d) is less than that of $(x_u/d)_{lim} = 0.479$ for Fe 415 steel. Thus, the section is *under-reinforced* and also the depth provided is more than the balanced section.

Step 3 Determine the area of reinforcement.

$$z = d \left(1 - 0.416 \frac{x_u}{d}\right) = 460(1 - 0.416 \times 0.407) = 382.12 \text{ mm}$$

$$A_{st} = \frac{M_u}{0.87f_y z} = \frac{130 \times 10^6}{0.87 \times 415 \times 382.12} = 942.2 \text{ mm}^2$$

Provide three 20 mm diameter bars with $A_{st} = 942 \text{ mm}^2$. In addition, provide two 8 mm diameter hanger rods. The designed beam is shown in Fig. 5.46.

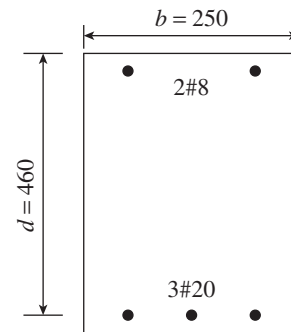


FIG. 5.46 Designed beam of Example 5.9

Check for minimum area of steel

$$\text{Minimum area } \frac{A_{st}}{b_w d} = \frac{0.85}{f_y}$$

$A_{st, \min} = 0.85 \times 250 \times 460/415 = 236 \text{ mm}^2 < 942 \text{ mm}^2$;
hence, the beam is safe.

According to the equation given in ACI 318,

$$\frac{A_s}{b_w d} = \frac{0.224 \sqrt{f_{ck}}}{f_y} \geq \frac{1.4}{f_y}$$

$$A_{st, \min} = 0.224 \times 250 \times 460 \times \sqrt{20}/415 = 278 \text{ mm}^2$$

or $1.4 \times 250 \times 460/415 = 388 \text{ mm}^2 < 942 \text{ mm}^2$

Hence, the beam is safe.

Check for maximum area of steel

$$p_{t, \lim} = 19.82 \left(\frac{f_{ck}}{f_y} \right) = 19.82 \times \frac{20}{415} = 0.955 > p_t = 0.8208$$

Hence, it is acceptable.

Check for ductility

Assuming tension steel is yielding,

$$x_u = \frac{0.87 f_y A_{st}}{0.36 f_{ck} b} = \frac{0.87 \times 415 \times 942}{0.36 \times 20 \times 250} = 188.9 \text{ mm}$$

Using strain compatibility,

$$\epsilon_{st} = \left(\frac{d - x_u}{x_u} \right) \epsilon_{cu} = \left(\frac{460 - 188.9}{188.9} \right) \times 0.0035 = 0.00502 > 0.005$$

Hence, the section is tension controlled and will have enough ductility.

EXAMPLE 5.10 (Design of singly reinforced rectangular beam):

Design a singly reinforced concrete beam subjected to an ultimate moment of 315 kNm. Assume $f_{ck} = 25 \text{ N/mm}^2$ and $f_y = 415 \text{ N/mm}^2$. In this beam, due to architectural considerations, the width has to be restricted to 230 mm.

SOLUTION:

Step 1 Calculate the depth of the beam.

$$d = \sqrt{\frac{7.2 M_u}{f_{ck} b}} = \sqrt{\frac{7.2 \times 315 \times 10^6}{25 \times 230}} = 628 \text{ mm}$$

Provide $d = 650 \text{ mm}$ and cover = 50 mm; hence $D = 700 \text{ mm}$.

Step 2 Check whether (x_u/d) exceeds $(x_u/d)_{\lim}$.

$$\begin{aligned} (x_u/d) &= 1.2 - \left(1.44 - \sqrt{1 - \frac{6.68 M_u}{f_{ck} b d^2}} \right) \\ &= 1.2 \left(1.44 - \sqrt{1 - \frac{6.68 \times 315 \times 10^6}{25 \times 230 \times 650^2}} \right) \\ &= 0.436 < 0.479. \text{ Hence, it is under-reinforced.} \end{aligned}$$

Step 3 Calculate A_{st} .

$$z = d \left(1 - 0.416 \frac{x_u}{d} \right) = 650 (1 - 0.416 \times 0.436) = 532.1 \text{ mm}$$

$$A_{st} = \frac{M_u}{0.87 f_y z} = \frac{315 \times 10^6}{0.87 \times 415 \times 532.1} = 1640 \text{ mm}^2$$

Provide six 20 mm bars (area provided = 1885 mm²). It should be noted that the six bars cannot be provided in one level and hence has to be provided in two levels as shown in Fig. 5.47. When providing rods in two layers, we have to check whether the assumed effective depth is still maintained. Assuming a spacer bar of 20 mm and clear cover of 30 mm, the effective depth provided for this bar arrangement is 700 – 30 – 20 – 10 = 640 mm. Let us check whether this effective depth is adequate to resist the external moment.

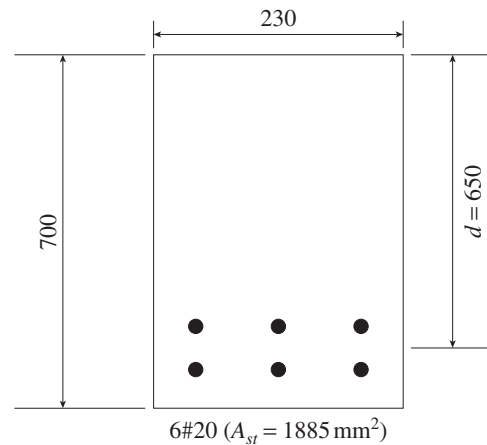


FIG. 5.47 Designed beam of Example 5.10

$$\begin{aligned} M_n &= 0.87 f_y A_{st} d \left(1 - \frac{f_y A_{st}}{f_{ck} b d} \right) \\ &= 0.87 \times 415 \times 1885 \times 640 \left(1 - \frac{415 \times 1885}{25 \times 230 \times 640} \right) \times 10^{-6} \\ &= 342.97 \text{ kNm} > M_u = 315 \text{ kNm} \end{aligned}$$

Hence, the provided effective depth is adequate.

EXAMPLE 5.11 (Design of singly reinforced rectangular section using design aids):

Design a singly reinforced concrete beam of width 250 mm, subjected to an ultimate moment of 130 kNm, using the design tables of SP 16. Assume $f_{ck} = 20 \text{ MPa}$ and $f_y = 415 \text{ MPa}$.

SOLUTION:

This example is the same as Example 5.9, except that we are going to use design tables. Hence, Steps 1 and 2 are the same as in Example 5.9. Let us proceed from Step 3.

Step 3 Determine the area of reinforcement.

The area of steel may be determined from the design charts as follows:

$$\text{Calculate } M_u/bd^2 = 130 \times 10^6 / (250 \times 460^2) = 2.457$$

Choose Table 2 of SP 16 (or Table C.1 of Appendix C). For $M_u/bd^2 = 2.457$, we obtain $p_t = 0.822$ for $f_y = 415 \text{ N/mm}^2$ and $f_{ck} = 20 \text{ N/mm}^2$. Hence, $A_{st} = 0.822 \times 460 \times 250 / 100 = 945 \text{ mm}^2$.

Provide three 20 mm diameter bars with $A_{st} = 942 \text{ mm}^2 \approx 945 \text{ mm}^2$.

The other steps are similar to Example 5.9.

EXAMPLE 5.12 (Design of over-reinforced rectangular beam):

Design a singly reinforced concrete beam, subjected to an ultimate moment of 150 kNm. Assume M25 concrete and Fe 415 grade steel. Due to architectural considerations, the breadth and depth of beam are restricted to 230 mm and 400 mm, respectively.

SOLUTION:

Step 1 Confirm whether it is an over- or under-reinforced beam. Calculate M_n limit for concrete failure:

$$M_n = 0.138 \times 25 \times 230 \times 400^2 = 126.96 \text{ kNm}$$

Since $M_u > M_n$, the beam is over-reinforced and is not recommended to be used by IS 456. However, we shall design it as over-reinforced to explain the steps involved.

Step 2 Determine the depth of the neutral axis.

$$\left(\frac{x_u}{d}\right) = 1.2 - \sqrt{\left[1.44 - \frac{6.68M_u}{f_{ck}bd^2}\right]}$$

$$= 1.2 - \sqrt{\left[1.44 - \frac{6.68 \times 150 \times 10^6}{25 \times 230 \times 400^2}\right]} = 0.597$$

It has to be noted that (x_u/d) is greater than 0.479 (the limiting value).

$$x_u = 0.597 \times 400 = 238.8 \text{ mm}$$

Step 3 Calculate ϵ_s and f_s .

$$\epsilon_s = 0.0035 \left(\frac{d}{x_u} - 1\right) = 0.0035 \left(\frac{400}{238.8} - 1\right) = 2.36 \times 10^{-3}$$

$$\text{From Table 5.2, } f_s = 324.8 + (342.8 - 324.8) \left(\frac{236 - 192}{241 - 192}\right) = 340.96 \text{ N/mm}^2$$

Step 4 Calculate the required area of steel.

$$A_{st}f_s = 0.36f_{ck}bx_u$$

$$A_{st} \times 340.96 = 0.36 \times 25 \times 230 \times 238.8$$

Hence, $A_{st} = 1450 \text{ mm}^2$

The designed beam section is shown in Fig. 5.48.

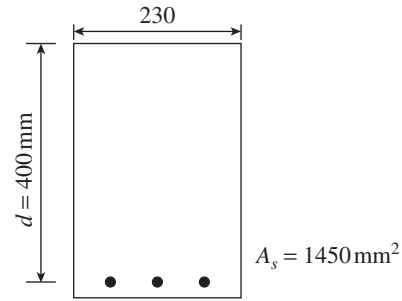


FIG. 5.48 Designed beam of Example 5.12

Once again, it is stressed that this design is not acceptable, and it is preferable to design it as doubly reinforced beam (see Example 5.17).

EXAMPLE 5.13 (Analysis of singly reinforced beam using design aids):

Determine the value of the ultimate uniformly distributed load w_u that can be carried by the beam shown in Fig. 5.49, using design aids. Use M25 concrete and Fe 415 grade steel.

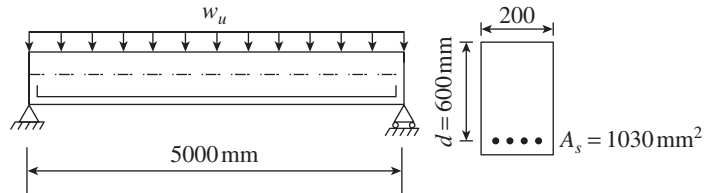


FIG. 5.49 Beam of Example 5.13

SOLUTION:

$$p_t = 1030 \times 100 / (600 \times 200) = 0.858$$

From Table C.2 of Appendix C, $M_u/bd^2 = 2.656$

$$\text{Hence, } M_u = 2.656 \times 200 \times 600^2 = 191.23 \times 10^6 \text{ Nmm}$$

$$\text{The maximum moment at mid-span} = w_u L^2 / 8$$

Equating these two, we get

$$w_u = 191.23 \times 10^6 \times 8 / 5000^2 = 61.19 \text{ N/m}$$

The following examples illustrate the analysis and design of doubly reinforced beams.

EXAMPLE 5.14 (Analysis of doubly reinforced rectangular beam):

Calculate the ultimate moment of resistance of a doubly reinforced beam having $b = 250 \text{ mm}$, $d = 500 \text{ mm}$, $d' = 40 \text{ mm}$, $A_{st} =$ four 25 mm diameter bars (1963 mm^2), $A_{sc} =$ three 16 mm bars (603.2 mm^2), $f_y = 250 \text{ MPa}$, and $f_{ck} = 20 \text{ MPa}$.

SOLUTION:

For Fe 250, $x_{u, \max} / d = 0.531$; hence $x_u = 0.531 \times 500 = 265.5 \text{ mm}$

Assuming $f_{sc} = f_{st} = 0.87f_y$ and considering force equilibrium,

$$C_c + C_s = T_u$$

$$C_c = 0.36f_{ck}bx_u = (0.36 \times 20 \times 250)x_u = 1800x_u$$

$$C_s = (0.87f_y - 0.447f_{ck})A_{sc} = (0.87 \times 250 - 0.447 \times 20) \times 603.2 = 125,803 \text{ N}$$

$$T_u = 0.87f_yA_{st} = 0.87 \times 250 \times 1963 = 426,952 \text{ N}$$

Hence $1800x_u + 1,25,803 = 4,26,952$, or $x_u = 167.3 \text{ mm} < x_{u,\max}$

Thus, the assumption $f_{st} = 0.87f_y$ is justified.

$$\begin{aligned} \epsilon_{sc} &= 0.0035 \frac{(x_u - d')}{x_u} = 0.0035 \frac{(167.3 - 40)}{167.3} \\ &= 0.00287 > \epsilon_y = \frac{0.87 \times 250}{2 \times 10^5} = 0.00109 \end{aligned}$$

Thus, the assumption $f_{sc} = 0.87f_y$ is justified. The ultimate moment of resistance

$$\begin{aligned} M_n &= C_c(d - 0.416x_u) + C_s(d - d') \\ &= (1800 \times 167.3) \times (500 - 0.416 \times 167.3) \\ &\quad + 1,25,803 \times (500 - 40) \times 10^{-6} \\ &= 187.48 \text{ kNm} \end{aligned}$$

EXAMPLE 5.15 (Analysis of doubly reinforced rectangular beam):

An RC beam has a width of 200 mm and an effective depth of 450 mm. The effective covers for tension and compression reinforcement are 50 mm and 30 mm, respectively. The beam is reinforced with three bars of 20 mm diameter in tension and three bars of 16 mm diameter of Fe 415 grade in compression (see Fig. 5.50). Assuming M20 concrete, calculate the ultimate moment carrying capacity of the beam.

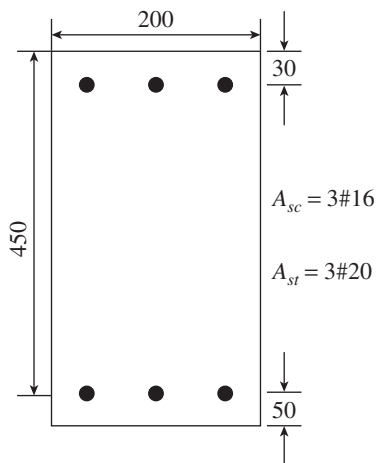


FIG. 5.50 Doubly reinforced beam of Example 5.15

SOLUTION:

The given values are as follows:

$$b = 200 \text{ mm}, d = 450 \text{ mm}, d' = 30 \text{ mm}, d'/d = 0.067, f_{ck} = 20 \text{ MPa}, f_y = 415 \text{ MPa},$$

$$A_{st} (3 \times 20 \text{ mm bars}) = 942.5 \text{ mm}^2, \text{ and } A_{sc} (3 \times 16 \text{ mm bars}) = 603.2 \text{ mm}^2$$

Step 1 Calculate x_u .

Let us assume as first trial, $x_u = x_{u,\text{lim}}$

$$\begin{aligned} x_u &= \frac{0.0035}{0.0055 + 0.87f_y/E_s} d \\ &= \frac{0.0035}{0.0055 + 0.87 \times 415/2 \times 10^5} 450 = 215.6 \text{ mm} \end{aligned}$$

Step 2 Calculate ϵ_{sc}

$$\epsilon_{sc} = \frac{0.0035(x_u - d')}{x_u} = \frac{0.0035(215.6 - 30)}{215.6} = 0.00301$$

Corresponding value of f_{sc} (from Table 5.2) = 355.9 MPa

$$f_{cc} = 0.447f_{ck} = 0.447 \times 20 = 8.94 \text{ MPa}$$

$$f_{st} = 0.87f_y = 0.87 \times 415 = 361.05 \text{ MPa}$$

Step 3 Compute x_u

$$\begin{aligned} x_u &= \frac{0.87f_yA_{st} - (f_{sc} - f_{cc})A_{sc}}{0.36f_{ck}b} \\ &= \frac{361.05 \times 942.5 - (355.9 - 8.94) \times 603.2}{0.36 \times 20 \times 200} \\ &= 90.97 \text{ mm} \end{aligned}$$

Since $x_u < x_{u,\text{lim}}$, the section is under-reinforced. Let us now assume $x_u = 90.97$ and repeat Steps 2 and 3 until the value of x_u converges.

$$\epsilon_{sc} = \frac{0.0035(x_u - d')}{x_u} = \frac{0.0035(90.97 - 30)}{90.97} = 0.00234$$

The stress f_{sc} corresponding to the strain of 0.00234 is 341.5 MPa:

$$f_{cc} = 0.447f_{ck} = 0.447 \times 20 = 8.94 \text{ MPa}$$

$$f_{st} = 0.87f_y = 0.87 \times 415 = 361.05 \text{ MPa}$$

The modified value of x_u is calculated as

$$\begin{aligned} x_u &= \frac{0.87f_yA_{st} - (f_{sc} - f_{cc})A_{sc}}{0.36f_{ck}b} \\ &= \frac{361.05 \times 942.5 - (341.5 - 8.94) \times 603.2}{0.36 \times 20 \times 200} \\ &= 97.0 \text{ mm} \end{aligned}$$

The modified x_u may also be assumed as the average of the previous two x_u values, that is, in this case $x_u = (90.97 + 97)/2 = 93.98 \text{ mm}$.

This procedure is repeated until the solution converges. The converged values are as follows:

$$x_u = 96.24 \text{ mm}, f_{cc} = 8.94 \text{ MPa}, f_{sc} = 343.3 \text{ MPa}, \text{ and } f_{st} = 361.05 \text{ MPa}$$

The moment of resistance of the section may be computed as

$$M_n = 0.36f_{ck}bx_u(d - 0.416x_u) + (f_{sc} - f_{cc})A_{sc}(d - d')$$

$$= [0.36 \times 20 \times 200 \times 96.24 \times (450 - 0.416 \times 96.24) + (343.3 - 8.94) \times 603.2 \times (450 - 30)]/10^6$$

$$= 56.8 + 84.7 = 141.5 \text{ kNm}$$

EXAMPLE 5.16 (Analysis of doubly reinforced rectangular beam using design aids):

Determine the ultimate moment capacity of a doubly reinforced concrete beam 300 mm wide and 600 mm deep. This beam is provided with two 16 mm bars on the compression side and five 16 mm bars on the tension side. Adopt M20 concrete and Fe 415 grade steel. Assume effective concrete cover, $d' = 40$ mm. Use design aids.

SOLUTION:

The given values are as follows:

$$d = 600 - 40 = 560 \text{ mm}, b = 300 \text{ mm}, A_{st} = 5\#16 = 5 \times 201.1 = 1005.5 \text{ mm}^2,$$

$$A_{sc} = 2\#16 = 2 \times 201.1 = 402.2 \text{ mm}^2$$

$$d'/d = 40/560 = 0.07; \text{ choose the next higher value of } 0.10.$$

Calculate p_t/f_{ck} and p_c/f_{ck} .

$$p_t/f_{ck} = 1005.5 \times 100 / (300 \times 560 \times 20) = 0.0299, \text{ say } 0.03$$

$$p_c/f_{ck} = 402.2 \times 100 / (300 \times 560 \times 20) = 0.01197$$

From Table C.10, referring to the column corresponding to $p_t/f_{ck} = 0.03$, we get by linear interpolation

$$M_n/(f_{ck}bd^2) = 0.0982 + (0.0993 - 0.0982)/(0.02 - 0.01) \times (0.01195 - 0.01) = 0.0984$$

Hence, the moment capacity of the section

$$M_n = 0.0984 \times 20 \times 300 \times 560^2/10^6 = 185.15 \text{ kNm}$$

EXAMPLE 5.17 (Design of doubly reinforced rectangular beam):

Design a simply supported rectangular RC beam, having a span of 5.5 m, subjected to a uniformly distributed load of 33.8 kN/m. Compute the required reinforcement, assuming the breadth of beam as 230 mm and the effective cover for compression and tension reinforcement as 50 mm. Assume that the beam is supported by load-bearing masonry of thickness 230 mm. Use M20 concrete and Fe 415 grade steel.

SOLUTION:

The given values are as follows:

$$b = 230 \text{ mm}, d' = 50 \text{ mm}, f_{ck} = 20 \text{ MPa}, f_y = 415 \text{ MPa}$$

Step 1 Calculate factored maximum bending moment.

Assume depth as $L/10 = 550/10 = 550$ mm. Hence, effective depth,

$$d = 550 - 50 = 500 \text{ mm}$$

Effective span = Lesser of distance between supports and clear span plus d
 $= 5.5 \text{ m or } (5.5 - 0.23 + 0.5) = 5.77 \text{ m}$
 $= 5.5 \text{ m (as per Clause 22.2 of IS 456)}$

Distributed load due to self-weight = $25 \times 0.23 \times 0.55 = 3.2 \text{ kN/m}$

Total load = $33.8 + 3.2 = 37 \text{ kN/m}$

Bending moment = $wL^2/8 = 37 \times 5.5^2/8 = 140 \text{ kNm}$

Factored moment at mid-span, $M_u = 1.5 \times 140 = 210 \text{ kNm}$

Step 2 Calculate the limiting neutral axis depth:

$$x_{u,lim} = 0.479 \times 500 = 239.5 \text{ mm}$$

Step 3 Calculate $M_{n,lim}$ and $p_{t,lim}$ for singly reinforced section.

$$M_{n,lim} = 0.138f_{ck}bd^2 = 0.138 \times 20 \times 230 \times 500^2/10^6 = 158.7 \text{ kNm}$$

$$p_{t,lim} = 19.82 \times f_{ck}/f_y = 19.82 \times 20/415 = 0.96$$

Hence, $A_{st1} = 0.96 \times 230 \times 500/100 = 1098 \text{ mm}^2$

Step 4 Check $M_{n,lim} > M_u$.

Since $M_{n,lim} = 158.7 \text{ kNm} < M_u = 210 \text{ kNm}$, a doubly reinforced beam is required.

The additional moment of resistance required to be resisted by the beam is

$$M_{u2} = 210 - 158.7 = 51.3 \text{ MPa}$$

Step 5 Compute A_{st2} and A_{sc} .

$$A_{st2} = \frac{M_{u2}}{0.87f_y(d - d')} = \frac{51.3 \times 10^6}{0.87 \times 415 \times (500 - 50)} = 316 \text{ mm}^2$$

Compute total tensile steel, $A_{st} = A_{st1} + A_{st2} = 1098 + 316 = 1414 \text{ mm}^2$

Provide four 22 diameter bars (area provided = 1520 mm^2).

The compression steel can be calculated as

$$A_{sc} = \frac{M_{u2}}{(f_{sc} - f_{cc})(d - d')}$$

Strain at the level of centroid of compression steel

$$\epsilon_{sc} = 0.0035 \frac{(x_u - d')}{x_u} = \frac{0.0035(239.5 - 50)}{239.5} = 0.002769$$

From Table 5.2, for a strain of 0.002769, $f_{sc} = 351.63 \text{ MPa}$.

Stress in concrete at the level of centroid of compression steel is

$$f_{cc} = 0.447f_{ck} = 0.447 \times 20 = 8.94 \text{ MPa}$$

$$\text{Thus, } A_{sc} = \frac{51.3 \times 10^6}{(351.63 - 8.94)(500 - 50)} = 333 \text{ mm}^2$$

Provide three 12 mm diameter rods as compression steel (A_{sc} provided = 339.3 mm^2).

Step 6 Check for ductility.

$$p_t \text{ provided} = \frac{1520}{230 \times 500} \times 100 = 1.32; \quad p_c \text{ provided} = \frac{339.3}{230 \times 500} \times 100 = 0.295$$

$$\begin{aligned} p_{c,\text{lim}} &= \frac{0.87f_y}{f_{sc} - 0.447f_{ck}} (p_t - p_{t,\text{lim}}) \\ &= \frac{0.87 \times 415}{351.63 - 0.447 \times 20} (1.32 - 0.96) \\ &= 0.379 > p_c = 0.295 \end{aligned}$$

Hence, the section is *over-reinforced* and the design should be revised to ensure ductile behaviour.

$$A_{sc} > \frac{p_{c,\text{lim}}}{100} bd = \frac{0.379}{100} \times 230 \times 500 = 435.85 \text{ mm}^2$$

Hence, provide two 16 mm diameter and one 12 mm diameter bars as compression steel (area provided = 515 mm², p_c provided = 0.448). The designed beam is shown in Fig. 5.51.

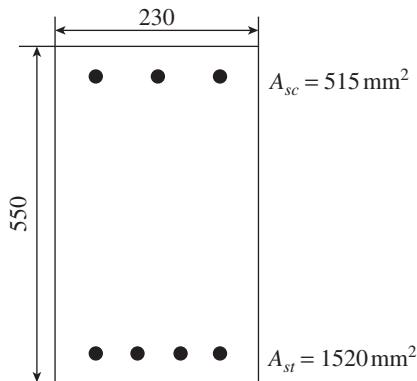


FIG. 5.51 Designed beam of Example 5.17

Step 7 Check for deflection (see Chapter 12 for more details).

$$\begin{aligned} f_s &= 0.58f_y \frac{\text{Area of steel required}}{\text{Area of steel provided}} \\ &= 0.58 \times 415 \times \frac{1414}{1520} = 223.9 \text{ MPa} \\ k_t &= \frac{1}{[0.225 + 0.00322f_s - 0.625 \log_{10}(1/p_t)]} \\ &= \frac{1}{[0.225 + 0.0032 \times 223.9 - 0.625 \log_{10}(1/1.32)]} \\ &= 1/1.021 = 0.979 \\ k_c &= 1 + \frac{p_c}{p_c + 3.0} = 1 + \frac{0.448}{0.448 + 3.0} = 1.13 \leq 1.5 \end{aligned}$$

$$(L/d)_{\text{max}} = 20 \times 0.979 \times 1.13 = 22.13$$

$$\text{Actual } (L/d) = 5500/500 = 11 < 22.13$$

Hence, the beam is safe with regard to deflection considerations.

EXAMPLE 5.18 (Design of doubly reinforced rectangular beam using design aids):

Design the doubly reinforced concrete beam given in Example 5.17 using design aids.

SOLUTION:

The given values are as follows:

$$b = 230 \text{ mm}, \quad d = 550 - 50 = 500 \text{ mm}, \quad d' = 50 \text{ mm},$$

$$f_{ck} = 20 \text{ MPa}, \quad f_y = 415 \text{ MPa} \text{ and } M_u = 210 \text{ kNm}$$

Step 1 Calculate the parameters given in the tables.

$$(d'/d) = 50/500 = 0.1; \quad (M_u/bd^2) = 210 \times 10^6/(230 \times 500^2) = 3.652$$

Step 2 Find p_t and p_c from design aids.

Using Table 50 of SP 16, under the column $(d'/d) = 0.1$, by interpolating we get $p_t = 1.23$ and $p_c = 0.288$. It should be noted that as per Table C.7 of Appendix C of the book, we get $p_t = 1.144$ and $p_c = 0.572$, as the table is based on IS 13920 and provides ductile beams.

$$A_{st} = (1.23/100) \times 230 \times 500 = 1414.5 \text{ mm}^2$$

Provide four 22 mm diameter bars (area provided = 1520 mm²).

$$A_{sc} = (0.288/100) \times 230 \times 500 = 331.2 \text{ mm}^2$$

Provide three 12 mm diameter rods as compression steel (A_{sc} provided = 339.3 mm²).

Step 3 Check for minimum area of steel.

$$\text{Minimum area } \frac{A_{st}}{b_w d} = \frac{0.85}{f_y}$$

$A_{st,\text{min}} = 0.85 \times 230 \times 500/415 = 236 \text{ mm}^2 < 1520 \text{ mm}^2$; hence, the beam is safe.

According to the equation given in ACI 318,

$$\frac{A_s}{b_w d} = \frac{0.224\sqrt{f_{ck}}}{f_y} \geq \frac{1.4}{f_y}$$

$$A_{st,\text{min}} = 0.224 \times 230 \times 500 \times \sqrt{20}/415 = 278 \text{ mm}^2$$

$$\text{or } 1.4 \times 230 \times 500/415 = 388 \text{ mm}^2 < 1520 \text{ mm}^2$$

Hence, the beam is safe.

EXAMPLE 5.19 (Analysis of cantilever beam):

Find the maximum cantilever span L_c for the beam shown in Fig. 5.52 and subjected to a factored uniformly distributed load of 20 kN/m² and a factored point load 75 kN acting at the tip of the cantilever. Assume $f_{ck} = 30 \text{ MPa}$ and $f_y = 415 \text{ MPa}$.

SOLUTION:

It has to be noted that the tension steel is at the top of beam. This is because the cantilever action will result in tension at the top (negative moment) and compression at the bottom of

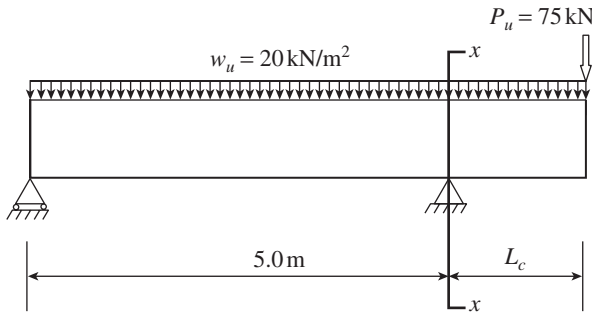


FIG. 5.52 Cantilever beam of Example 5.19

the beam at the support. Similar negative moment will occur at the support of continuous beams.

Assume an effective cover of 50 mm for the tension and compression steel. Hence,

$$d' = 50 \text{ mm} \quad \text{and} \quad d = 550 - 50 = 500 \text{ mm}$$

$$A_{st} = 4\#25 = 1963 \text{ mm}^2, A_{sc} = 2\#22 = 760 \text{ mm}^2, \alpha = 760/1963 = 0.387 < 0.4$$

Step 1 Check for under- or over-reinforced condition. For Fe 415 steel, $x_{u,max}/d = 0.479$. Hence, $x_{u,max} = 0.479 \times 500 = 239.5 \text{ mm}$

Assuming both tension and compression steel yield,

$$x_u = \frac{f_{st}A_{st} - (f_{sc} - f_{cc})A_{sc}}{0.36f_{ck}b}$$

$$= \frac{0.87 \times 415 \times 1963 - (0.87 \times 415 - 0.447 \times 30) \times 760}{0.36 \times 30 \times 230}$$

$$= 178.95 \text{ mm} < 239.5 \text{ mm}$$

Hence, the assumption of tension steel yielding is correct.

Step 2 Check for yielding of compression steel.

$$\epsilon_{sc} = 0.0035(1 - d'/x_u) = 0.0035(1 - 50/178.95) = 0.00252$$

For Fe 415 steel,

$$\epsilon_y = \frac{0.87f_y}{E_s} + 0.002 = \frac{0.87 \times 415}{2 \times 10^5} + 0.002 = 0.0038$$

Since $\epsilon_{sc} < \epsilon_y$, compression steel does not yield. Hence, we should compute the correct value of x_u iteratively by using strain compatibility.

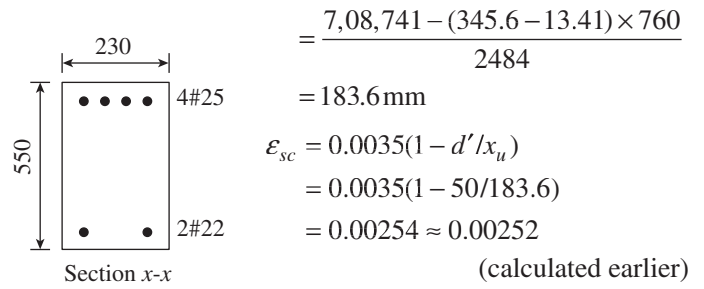
Step 3 Determination of x_u .

For $\epsilon_{sc} = 0.00252$, from Table 5.2, we get

$$f_{sc} = 342.8 + (351.8 - 342.8) \frac{252 - 241}{276 - 241} = 345.6 \text{ MPa}$$

$$x_u = \frac{f_{st}A_{st} - (f_{sc} - f_{cc})A_{sc}}{0.36f_{ck}b}$$

$$= \frac{0.87 \times 415 \times 1963 - (345.6 - 0.447 \times 30) \times 760}{0.36 \times 30 \times 230}$$



$$= \frac{7,08,741 - (345.6 - 13.41) \times 760}{2484}$$

$$= 183.6 \text{ mm}$$

$$\epsilon_{sc} = 0.0035(1 - d'/x_u)$$

$$= 0.0035(1 - 50/183.6)$$

$$= 0.00254 \approx 0.00252$$

(calculated earlier)

Let us do one more cycle of calculation for x_u .

$$f_{sc} = 342.8 + (351.8 - 342.8) \frac{254 - 241}{276 - 241} = 346.1 \text{ MPa}$$

$$x_u = [708,741 - (346.1 - 13.41) \times 760]/2484 = 183.5 \text{ mm}$$

$$\approx 183.6 \text{ mm}$$

Hence, take the value of x_u as 183.5 mm.

Step 4 Determine M_n .

$$M_n = 0.36f_{ck}bx_u(d - 0.416x_u) + (f_{sc} - f_{cc})A_{sc}(d - d')$$

$$= [0.36 \times 30 \times 230 \times 183.5 \times (500 - 0.416 \times 183.5)$$

$$+ (346.1 - 13.41) \times 760 \times 450]/10^6$$

$$= 306.89 \text{ kNm}$$

Step 5 Equate the internal and external moments to find L_c . The external moment due to the uniformly distributed load and point load is

$$M_u = \frac{w_u L_c^2}{2} + P_u L_c = \frac{20L_c^2}{2} + 75L_c = 306.89$$

Solving this quadratic equation in L_c , we get

$$L_c = 2.94 \text{ m}$$

EXAMPLE 5.20 (Analysis of singly reinforced isolated T-beam):

Determine the ultimate moment of resistance of an isolated T-beam, having a span of 6 m and cross-sectional dimensions as shown in Fig. 5.53, assuming $f_{ck} = 20 \text{ MPa}$ and grade 415 steel.

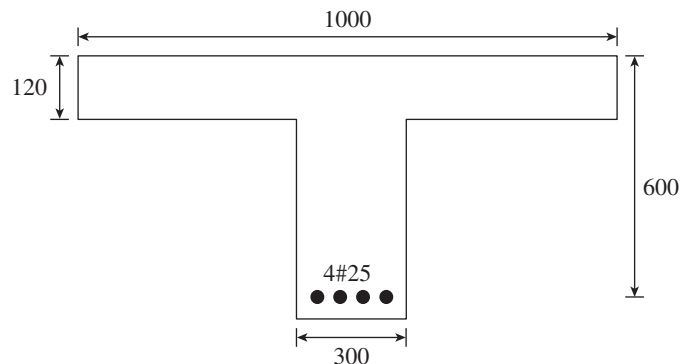


FIG. 5.53 T-beam of Example 5.20

SOLUTION:

The given values are as follows:

$$D_f = 120 \text{ mm}, b_w = 300 \text{ mm}, d = 600 \text{ mm}, A_{st} = 4\#25 = 1963 \text{ mm}^2, f_y = 415 \text{ MPa}, f_{ck} = 20 \text{ MPa}$$

Step 1 Calculate the effective width of the slab.

$$b_f = \frac{L_0}{(L_0/b) + 4} + b_w = \frac{6000}{(6000/1000) + 4} + 300 = 900 \text{ mm}$$

Step 2 Check the position of the neutral axis.

$$x_{u,\text{lim}} = 0.479d = 0.479 \times 600 = 287.4 \text{ mm}$$

Assume that the neutral axis coincides with the bottom fibre of the flange, that is, $x_u = D_f$.

$$\begin{aligned} \text{Total compression in flange} &= 0.36f_{ck}b_fD_f \\ &= 0.36 \times 20 \times 900 \times 120/10^3 \\ &= 777.6 \text{ kN} \end{aligned}$$

$$\text{Total tension in steel} = 0.87f_yA_{st} = 0.87 \times 415 \times 1963/10^3 = 708.7 \text{ kN}$$

Since the total compression in flange is greater than the total tension in steel, the neutral axis is within the flange.

Step 3 Calculate x_u .

Equating compression and tension, we get

$$0.36f_{ck}b_fx_u = 0.87f_yA_{st}$$

$$\begin{aligned} \text{Thus, } x_u &= \frac{0.87f_yA_{st}}{0.36f_{ck}b_f} = \frac{0.87 \times 415 \times 1963}{0.36 \times 20 \times 900} \\ &= 109.37 \text{ mm} < D_f = 120 \text{ mm} \end{aligned}$$

Hence, the assumption that the neutral axis is within the flange is confirmed.

Moreover, $x_u < x_{u,\text{lim}}$. Hence, the section is under-reinforced.

Step 4 Calculate the ultimate moment of resistance.

$$\begin{aligned} M_u &= 0.87f_yA_{st}(d - 0.416x_u) \\ &= 0.87 \times 415 \times 1963 \times (600 - 0.416 \times 109.37) \times 10^{-6} \\ &= 393 \text{ kNm} \end{aligned}$$

Alternate approximate values:

1. Approximate formula

$$\begin{aligned} M_u &= 0.87f_yA_{st}(d - 0.5D_f) \\ &= 0.87 \times 415 \times 1963 \times (600 - 120/2) \\ &= 382.72 \text{ kNm} \end{aligned}$$

This formula may be used to get a preliminary estimate of the capacity.

2. Using design aids—SP 16 tables

Using this table, only the limiting moment capacity can be found.

$$\frac{D_f}{d} = \frac{120}{600} = 0.2, \frac{b_f}{b_w} = \frac{900}{300} = 3$$

From Table 58, $\frac{M_{u,\text{lim}}}{b_w d^2 f_{ck}} = 0.299$. Hence,

$$M_{u,\text{lim}} = 0.299 \times 300 \times 600^2 \times 20/10^6 = 645.84 \text{ kNm}$$

EXAMPLE 5.21 (Analysis of isolated singly reinforced T-beam):

Determine the ultimate moment of resistance of an isolated T-beam, having a span of 6 m and cross-sectional dimensions as shown in Fig. 5.54, assuming $f_{ck} = 20 \text{ MPa}$ and grade 415 steel.

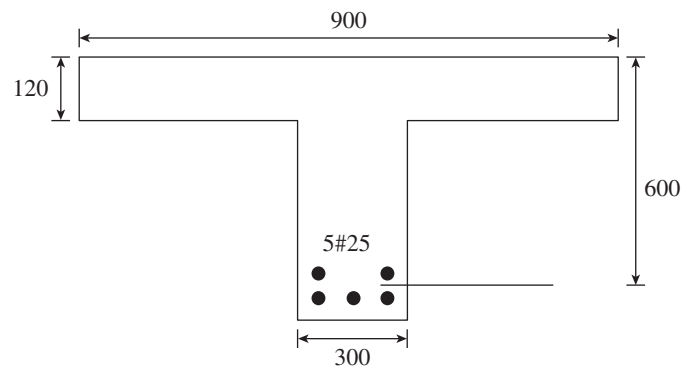


FIG. 5.54 T-beam of Example 5.21

SOLUTION:

The given values are as follows:

$$D_f = 120 \text{ mm}, b_w = 300 \text{ mm}, b_f = 900 \text{ mm}, d = 600 \text{ mm}, A_{st} = 5\#25 = 2454 \text{ mm}^2, f_y = 415 \text{ MPa}, f_{ck} = 20 \text{ MPa}$$

Step 1 Check the position of the neutral axis.

$$x_{u,\text{lim}} = 0.479d = 0.479 \times 600 = 287.4 \text{ mm}$$

Assume that the neutral axis coincides with the bottom fibre of the flange, that is, $x_u = D_f$.

$$\begin{aligned} \text{Total compression in flange} &= 0.36f_{ck}b_fD_f \\ &= 0.36 \times 20 \times 900 \times 120/10^3 \\ &= 777.6 \text{ kN} \end{aligned}$$

$$\text{Total tension in steel} = 0.87f_yA_{st} = 0.87 \times 415 \times 2454/10^3 = 886 \text{ kN}$$

Since the total compression in flange is less than the total tension in steel, the neutral axis is in the web.

Step 2 Calculate x_u .

Assuming the stress is uniform in the flange,

$$\begin{aligned} x_u &= \frac{0.87f_yA_{st} - 0.447f_{ck}D_f(b_f - b_w)}{0.36f_{ck}b_w} \\ &= \frac{0.87 \times 415 \times 2454 - 0.447 \times 20 \times 120 \times (900 - 300)}{0.36 \times 20 \times 300} \\ &= 112.19 < D_f = 120 \text{ mm} \end{aligned}$$

Hence, our assumption that the neutral axis coincides with the bottom fibre of flange is not valid. Let us now calculate x_u assuming that the compressive stress in the flange is non-uniform.

Replacing D_f with y_f , $y_f = 0.15x_u + 0.65D_f$

Now, the neutral axis depth is calculated as

$$x_u = \frac{0.87f_y A_{st} - 0.447f_{ck} \times 0.65D_f(b_f - b_w)}{0.36f_{ck}b_w + 0.447f_{ck} \times 0.15(b_f - b_w)}$$

$$= \frac{0.87 \times 415 \times 2454 - 0.447 \times 20 \times 0.65 \times 120 \times (900 - 300)}{0.36 \times 20 \times 300 + 0.447 \times 20 \times 0.15 \times (900 - 300)}$$

$$= 157.74 \text{ mm}$$

$$x_u > D_f = 120 \text{ mm}; \text{ also, } (3/7) x_u = 67.6 \text{ mm} < D_f.$$

Hence, the neutral axis is in the web and the stress block in the flange is non-linear.

$$y_f = 0.15x_u + 0.65D_f = 0.15 \times 157.74 + 0.65 \times 120 = 101.66 \text{ mm}$$

Step 3 Check whether the beam is under-reinforced.

$$x_{u,\text{lim}} = 0.479d = 0.479 \times 600 = 287.4 \text{ mm}$$

Since $x_u < x_{u,\text{lim}}$, the section is under-reinforced.

Step 4 Calculate M_n .

$$M_n = 0.36f_{ck} \left(\frac{x_u}{d} \right) \left(1 - 0.416 \frac{x_u}{d} \right)$$

$$b_w d^2 + 0.447f_{ck}(b_f - b_w)y_f \left(d - \frac{y_f}{2} \right)$$

$$= 0.36 \times 20 \times \frac{157.74}{600} \left(1 - 0.416 \frac{157.74}{600} \right) \times 300 \times$$

$$600^2 + 0.447 \times 20 \times (900 - 300) \times 101.66 \times$$

$$\left(600 - \frac{101.66}{2} \right)$$

$$= 182.07 \times 10^6 + 299.47 \times 10^6 \text{ Nmm} = 481.54 \text{ kNm}$$

EXAMPLE 5.22 (Analysis of isolated singly reinforced T-beam):

Determine the ultimate moment of resistance of the isolated T-beam of Example 5.21 with $D_f = 100$ mm and $A_{st} =$ five 28 mm diameter bars and assuming $f_{ck} = 20$ MPa and grade 415 steel.

SOLUTION:

The given values are as follows:

$$D_f = 100 \text{ mm}, b_w = 300 \text{ mm}, b_f = 900 \text{ mm}, d = 600 \text{ mm}, A_{st} = 5 \text{ #28} = 3078 \text{ mm}^2, f_y = 415 \text{ MPa}, f_{ck} = 20 \text{ MPa}$$

Step 1 Check the position of the neutral axis.

Assume that the neutral axis coincides with the bottom fibre of the flange, that is, $x_u = D_f$.

$$\text{Total compression in flange} = 0.36f_{ck}b_f D_f$$

$$= 0.36 \times 20 \times 900 \times 100/10^3$$

$$= 648 \text{ kN}$$

$$\text{Total tension in steel} = 0.87f_y A_{st}$$

$$= 0.87 \times 415 \times 3078/10^3$$

$$= 1111.3 \text{ kN}$$

Since the total compression in flange is less than the total tension in steel, the neutral axis is in the web.

Step 2 Calculate x_u .

Assuming stress is uniform in the flange,

$$x_u = \frac{0.87f_y A_{st} - 0.447f_{ck} D_f (b_f - b_w)}{0.36f_{ck}b_w}$$

$$= \frac{0.87 \times 415 \times 3078 - 0.447 \times 20 \times 100 \times (900 - 300)}{0.36 \times 20 \times 20}$$

$$= 266.16 > D_f = 100 \text{ mm}$$

$$\text{Check } (3/7)x_u = (3/7) \times 266.16 = 114 > D_f = 100 \text{ mm}$$

Hence, our assumption that the flange is uniformly stressed is correct.

Step 3 Check whether the beam is under-reinforced.

$$x_{u,\text{lim}} = 0.479d = 0.479 \times 600 = 287.4 \text{ mm}$$

Since $x_u < x_{u,\text{lim}}$, the section is under-reinforced.

Step 4 Calculate M_n .

$$M_n = 0.36f_{ck}x_u(d - 0.416x_u)b_w + 0.447f_{ck}(b_f - b_w)$$

$$D_f \left(d - \frac{D_f}{2} \right)$$

$$= 0.36 \times 20 \times 266.16(600 - 0.416 \times 266.16) \times$$

$$300 + 0.447 \times 20 \times (900 - 300) \times 100 \times \left(600 - \frac{100}{2} \right)$$

$$= 281.28 \times 10^6 + 295.02 \times 10^6 \text{ Nmm} = 576.3 \text{ kNm}$$

EXAMPLE 5.23 (Analysis of singly reinforced T-beam):

Determine the limiting moment of resistance by concrete failure of a T-beam with the following dimensions: $D_f = 140$ mm, $b_w = 300$ mm, $b_f = 1200$ mm, $d = 600$ mm, $A_{st} = 6\text{#}28 = 3695 \text{ mm}^2$, Assume Fe 415 steel and M 30 concrete.

SOLUTION

$$\text{For Fe 415, } (x_{u,\text{lim}}/d) = 0.479; x_{u,\text{lim}} = 0.479 \times 600 = 287.4 \text{ mm}$$

$$D_f/d = 140/600 = 0.23 > 0.2$$

$$\text{Hence, } y_f = 0.15x_{u,\text{lim}} + 0.65D_f = 0.15 \times 287.4 + 0.65 \times 140 = 134.11 \text{ mm}$$

$$M_{n,\text{lim}} = 0.36f_{ck} \left(\frac{x_{u,\text{lim}}}{d} \right) \left(1 - 0.416 \frac{x_{u,\text{lim}}}{d} \right) b_w d^2$$

$$+ 0.447f_{ck}(b_f - b_w)y_f \left(d - \frac{y_f}{2} \right)$$

$$\begin{aligned}
&= 0.36 \times 0.479 \times (1 - 0.416 \times 0.479) \times 300 \times 600^2 \\
&\quad + 0.447 \times 30 \times (1200 - 300) \times 134.11 \times \left(600 - \frac{134.11}{2} \right) \\
&= (447.38 + 862.61) \times 10^6 \text{ Nmm} = 1310 \text{ kNm}
\end{aligned}$$

EXAMPLE 5.24 (Design of singly reinforced T-beam):

Determine the area of required steel for the T-beam with the following dimensions: $D_f = 200$ mm, $b_w = 300$ mm, $b_f = 1500$ mm, and $d = 650$ mm. It is required to carry a factored moment of 1200 kNm. Assume Fe 415 steel and M30 concrete.

SOLUTION:

Step 1 Determine the neutral axis depth and lever arm depth.

$$\begin{aligned}
\frac{x_u}{d} &= 1.2 - \sqrt{\left(1.44 - \frac{6.68 M_u}{f_{ck} b_f d^2} \right)} \\
&= 1.2 - \sqrt{\left(1.44 - \frac{6.68 \times 1200 \times 10^6}{30 \times 1500 \times 650^2} \right)} = 0.191 \\
x_u &= 0.191 \times 650 = 124.05 \text{ mm} < 200 \text{ mm}
\end{aligned}$$

Hence, the neutral axis is within the flange.

Lever arm depth

$$z = d \left(1 - 0.416 \frac{x_u}{d} \right) = 650(1 - 0.416 \times 0.191) = 598.39 \text{ mm}$$

Step 2 Determine the area of steel.

$$A_{st} = \frac{M_u}{0.87 f_y z} = \frac{1200 \times 10^6}{0.87 \times 415 \times 598.39} = 5554.3 \text{ mm}^2$$

Approximate value of A_{st}

$$\begin{aligned}
A_{st} &= \frac{M_u}{0.87 f_y (d - D_f/2)} \\
&= \frac{1200 \times 10^6}{0.87 \times 415 \times (650 - 100)} = 6043 \text{ mm}^2
\end{aligned}$$

This formula may be used to get a preliminary estimate of the area of steel.

Using design aids

As the neutral axis lies within the flange, this beam may be designed using the tables of SP 16.

Using Table 4:

$$\frac{M_u}{b_w d^2} = \frac{1200 \times 10^6}{1500 \times 650^2} = 1.893, \text{ Hence for } f_y = 415, p_t = 0.5698\%$$

$$\text{Thus, } A_{st} = \frac{0.5698 \times 1500 \times 650}{100} = 5555.2 \text{ mm}^2$$

EXAMPLE 5.25 (Design of singly reinforced T-beam):

Design a T-beam with the following dimensions: $D_f = 100$ mm, $b_w = 230$ mm, and $b_f = 900$ mm. It is required to carry a

factored moment of 250 kNm. Assume Fe 415 steel and M25 concrete.

SOLUTION:

Step 1 Assume the depth. Let us assume the depth of the beam as 350 mm and a clear cover of 25 mm. Assuming 20 mm rods, effective depth = $350 - 25 - 10 = 315$ mm.

Step 2 Calculate approximate A_{st} . Assume a lever arm z equal to the larger of $0.9d = 283.5$ mm or $d - 0.5D_f = 265$ mm. Hence, adopt $z = 283.5$ mm.

$$A_{st,app} = \frac{M_u}{0.87 f_y z} = \frac{250 \times 10^6}{0.87 \times 415 \times 283.5} = 2442 \text{ mm}^2$$

Step 3 Check for the location of the neutral axis.

$$x_{u,max} = 0.479 \times 315 = 150.88 \text{ mm} > D_f$$

Assuming the neutral axis at the bottom layer of flange, that is, at 100 mm from the top fibre of the beam

$$\begin{aligned}
M_{u,lim} &= 0.36 f_{ck} b_f D_f (d - 0.416 D_f) \\
&= 0.36 \times 25 \times 900 \times 100 \times (315 - 41.6)/10^6 \\
&= 221.45 \text{ kNm} < M_u = 250 \text{ kNm}
\end{aligned}$$

Hence, $x_u > D_f$ and the neutral axis is below the flange and in the web.

Step 4 Determine the neutral axis depth and lever arm depth.

$$M_n = C_{uw}(d - 0.416 x_u) + C_{uf}(d - y_f/2)$$

where C_{uw} and C_{uf} are the compressive force contributions of the web and flange, respectively.

$$C_{uw} = 0.362 f_{ck} b_w x_u = 0.362 \times 25 \times 230 \times x_u = 2081.5 x_u$$

$$\begin{aligned}
C_{uf} &= 0.447 f_{ck} (b_f - b_w) y_f = 0.447 \times 25 \times (900 - 230) \\
&\quad \times y_f = 7487.25 y_f
\end{aligned}$$

$$\text{Also, } y_f = 0.15 x_u + 0.65 D_f = 0.15 x_u + 65$$

Substituting these values and equating with the external moment, we get

$$\begin{aligned}
250 \times 10^6 &= 2081.5 x_u (315 - 0.416 x_u) + 7487.25 (0.15 x_u + 65) \\
&\quad [315 - (0.15 x_u + 65)/2]
\end{aligned}$$

Simplifying, we get

$$250 \times 10^6 = -950.13 x_u^2 + 9,36,420 x_u + 137.48 \times 10^6$$

$$\text{or } x_u^2 + 985.6 x_u + 1,18,426 = 0$$

Solving this quadratic equation, we get $x_u = 140.05$ mm

$$y_f = 0.15 x_u + 0.65 D_f = 0.15 \times 140.05 + 0.65 \times 100 = 86 \text{ mm}$$

Step 5 Calculate A_{st} . Equating the tensile and compressive forces, we get

$$0.87 f_y A_{st} = 0.36 f_{ck} b_w x_u + 0.447 f_{ck} y_f (b_f - b_w)$$

Hence,

$$A_{st} = \frac{0.36 \times 25 \times 230 \times 140.05 + 0.447 \times 25 \times 86 \times (900 - 230)}{0.87 \times 415}$$

$$= 2587 \text{ mm}^2 \text{ (as against } A_{st,app} = 2442 \text{ mm}^2)$$

There is a difference of only six per cent between the approximate and exact values, and hence, this value can be used for the preliminary design.

Provide three 25 mm diameter and three 22 mm diameter bars (area provided = 2613 mm²). It should be noted that the bars have to be provided in two layers, and hence the effective depth will be reduced. Assuming a spacer of 20 mm diameter, Effective depth provided = 350 – 25 – 20 – 10 = 295 mm

Hence, the area of steel should be increased by using

$$A_{st,app} = \frac{M_u}{0.87 f_y z} = \frac{250 \times 10^6}{0.87 \times 415 \times (0.9 \times 295)}$$

$$= 2608 \text{ mm}^2 < 2613 \text{ mm}^2$$

Provide three 25 mm diameter and three 22 mm diameter rods, with area = 2987 mm² > 2655 mm². The designed section is shown in Fig. 5.55.

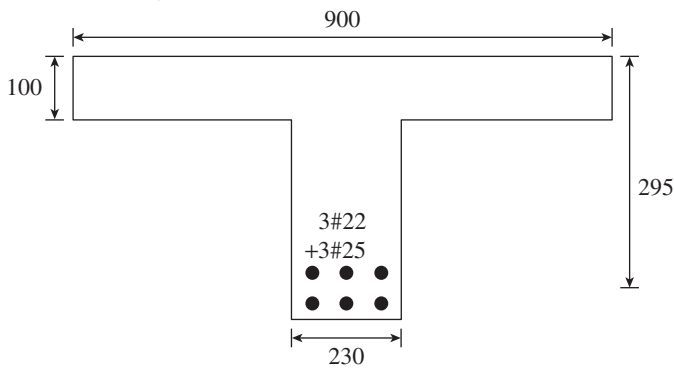


FIG. 5.55 Designed T-beam of Example 5.25

The analysis of this section for the designed dimensions and reinforcement yields a capacity of 256.33 kNm > applied moment. Hence, the beam is safe.

EXAMPLE 5.26 (Analysis of T-beam with compression steel): Calculate the ultimate moment of resistance of a T-beam with the following dimensions: $D_f = 140$ mm, $b_w = 200$ mm, $b_f = 675$ mm, $d = 390$ mm, $d' = 25$ mm, and $A_{st} = 6\#25$ diameter bars and $A_{sc} = 2\#20$ (see Fig. 5.56). Assume Fe 415 steel and M30 concrete.

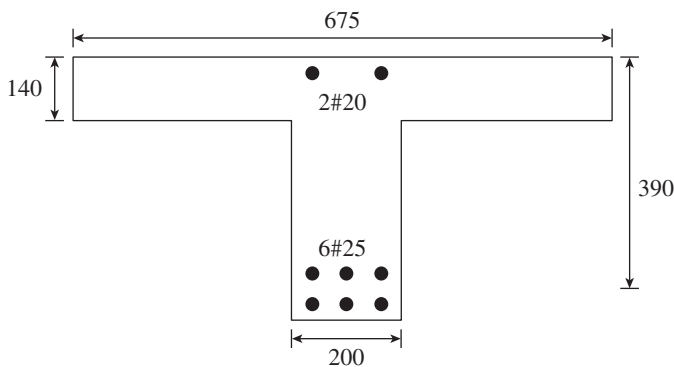


FIG. 5.56 Doubly reinforced T-beam of Example 5.26

SOLUTION:

Step 1 Calculate x_u .

$$A_{st} = 6\#25 = 2945 \text{ mm}^2; A_{sc} = 2\#20 = 628 \text{ mm}^2$$

Assuming that both tension and compression steel yield,

$$0.36 f_{ck} b_f x_u = 0.87 f_y (A_{st} - A_{sc})$$

$$\text{Thus, } x_u = \frac{0.87 \times 415 \times (2945 - 628)}{0.36 \times 30 \times 675} = 114.75 \text{ mm}$$

Hence, the neutral axis is in the flange.

Step 2 Check the strain in the steel. From the strain diagram, we calculate the strains in the tension and compression steel as

$$\epsilon_{st} = \frac{0.0035 \times (390 - 114.75)}{114.75} = 0.0084 > 0.0038$$

It is also greater than 0.005, showing that the tension steel yields and has good ductility.

$$\epsilon_{sc} = \frac{0.0035 \times (114.75 - 25)}{114.75} = 0.0027 > \frac{0.87 f_y}{E_s} = 0.0018$$

Hence, the compression steel also yields.

Step 3 Calculate M_u . As failure is due to the yielding of steel,

$$M_u = M_{u1} + M_{u2}$$

$$M_{u1} = 0.87 f_y (A_{st} - A_{sc}) (d - 0.416 x_u)$$

$$= 0.87 \times 415 \times (2945 - 628) (390 - 0.416 \times 114.75) / 10^6$$

$$= 286.32 \text{ kNm}$$

$$M_{u2} = 0.87 f_y A_{sc} (d - d')$$

$$= 0.87 \times 415 \times 628 (390 - 25) / 10^6$$

$$= 82.76 \text{ kNm}$$

Hence $M_u = 286.32 + 82.76 = 369.08 \text{ kNm}$

EXAMPLE 5.27 (Design of T-beam):

Design a T-beam to span 8 m supporting a one-way slab of thickness 150 mm and subjected to a live load of 4 kN/m² and a dead load (due to floor finish, partition, etc.) of 1.5 kN/m², in addition to its self-weight. Assume Fe 415 steel and M20 concrete and the c/c of beams as 4 m.

SOLUTION:

The given details are as follows:

$$L_0 = 8 \text{ m}, D_f = 150 \text{ mm}, f_y = 415 \text{ MPa}, f_{ck} = 20 \text{ MPa}$$

Step 1 Fix the dimensions of the beam. Assume $b_w = 300$ mm. Effective flange width (as per Clause 23.1.2 of IS 456)

$$b_f = \frac{L_0}{6} + b_w + 6D_f = \frac{8000}{6} + 300 + 6 \times 150 = 2533 \text{ mm}$$

Check: $b_w + c/c$ of beams = $300 + 4000 = 4300 \text{ mm} > 2533 \text{ mm}$;
hence, $b_f = 2533 \text{ mm}$

Let us assume the overall depth as $L/15$. Thus,

$$D = 8000/15 = 533 \text{ mm}; \text{ let us adopt } D = 550 \text{ mm}$$

Again assuming an effective cover of 50 mm, $d = 500 \text{ mm}$.

Step 2 Determine the bending moment.

Distributed load from slab, $w_{LL} = 4 \times 4 = 16 \text{ kN/m}$

Dead load due to slab = $25 \text{ kN/m}^3 \times 0.15 = 3.75 \text{ kN/m}^2$

Total dead load = $3.75 + 1.5 = 5.25 \text{ kN/m}^2$

$$w_{DL} = 5.25 \times 4 = 21 \text{ kN/m}$$

Dead load due to the self-weight of the web of beam = $25 \text{ kN/m}^3 \times 0.3 \times (0.55 - 0.15) = 3 \text{ kN/m}$

Factored load = $w_u = 1.5(16 + 21 + 3) = 60 \text{ kN/m}$

Factored moment $M_u = w_u L^2/8 = 60 \times 8^2/8 = 480 \text{ kNm}$

Step 3 Determine the approximate A_{st} . The approximate lever arm z is the larger of

$$(a) \quad 0.9d = 0.9 \times 500 = 450 \text{ mm}$$

$$(b) \quad d - D_f/2 = 500 - 150/2 = 425 \text{ mm}$$

Hence, approximate value of $z = 450 \text{ mm}$

$$\text{Approximate } A_{st} = \frac{M_u}{0.87 f_y z} = \frac{480 \times 10^6}{0.87 \times 415 \times 450} = 2954 \text{ mm}^2$$

Let us assume that we are going to provide four 32 mm bars. Assuming 8 mm diameter stirrups and 32 mm clear cover (it has to be noted that the clear cover should not be less than the diameter of bar),

$$\text{Actual } d = 550 - 32 - 8 - 32/2 = 494 \text{ mm}$$

Step 4 Calculate the neutral axis depth. Let us assume that the neutral axis lies within the flange. Using Eq. (5.60)

$$m = \frac{M_u}{0.36 f_{ck} b_f d^2} = \frac{480 \times 10^6}{0.36 \times 20 \times 2533 \times 494^2} = 0.1078;$$

$$\beta = 0.416$$

Hence,

$$\frac{x_u}{d} = \frac{1 - \sqrt{1 - 4\beta m}}{2\beta} = \frac{1 - \sqrt{1 - 1.664 \times 0.1078}}{0.832} = 0.1131$$

Thus, $x_u = 0.1131 \times 494 = 55.87 \text{ mm}$ and $D_f = 150 \text{ mm}$

Hence, the neutral axis is within the flange.

Step 5 Determine A_{st} .

Lever arm distance,

$$z = d \left(1 - 0.416 \frac{x_u}{d} \right) = 494 \times (1 - 0.416 \times 0.1131) \\ = 470.75 \text{ mm}$$

$$A_{st} = \frac{M_u}{0.87 f_y z} = \frac{480 \times 10^6}{0.87 \times 415 \times 470.75} = 2824 \text{ mm}^2 < \text{approximate } A_{st} = 2954 \text{ mm}^2$$

Provide two 32 mm diameter and two 28 mm diameter bars in a single row (A_{st} provided = 2839 mm^2).

EXAMPLE 5.28 (Design of T-beam with compression steel):

Design a T-beam with 1600 mm width of flange, 110 mm depth of flange, 250 mm width of web, and 500 mm effective depth to carry a factored bending moment of (a) 620 kNm and (b) 730 kNm. Assume M20 concrete and Fe 415 steel.

SOLUTION:

(a) $M_u = 620 \text{ kNm}$

The following values are given:

$b_f = 1600 \text{ mm}$, $D_f = 110 \text{ mm}$, $b_w = 250 \text{ mm}$, $d = 500 \text{ mm}$,
 $f_y = 415 \text{ MPa}$, $f_{ck} = 20 \text{ MPa}$

Step 1 Check for the location of the neutral axis. Assuming the neutral axis is within the flange, its depth

$$\frac{x_u}{d} = \frac{1 - \sqrt{1 - 1.664m}}{0.832} \quad \text{and}$$

$$m = \frac{M_u}{0.36 f_{ck} b_f d^2} = \frac{620 \times 10^6}{0.36 \times 20 \times 1600 \times 500^2} = 0.2152$$

$$\text{Hence, } \frac{x_u}{d} = \frac{1 - \sqrt{1 - 1.664 \times 0.2152}}{0.832} = 0.2389$$

Thus, $x_u = 0.2389 \times 500 = 119.45 \text{ mm}$

$\frac{D_f}{d} = \frac{110}{500} = 0.22 < \frac{x_u}{d}$. Hence, the neutral axis is in the web.

Step 2 Calculate the moment of resistance of the flange.

$$M_f = 0.447 f_{ck} (b_f - b_w) y_f \left(d - \frac{y_f}{2} \right)$$

Since $D_f/d > 0.2$, $y_f = 0.15x_u + 0.65D_f = 0.15 \times 119.45 + 0.65 \times 110 = 89.42 \text{ mm}$

$$M_f = 0.447 \times 20 \times (1600 - 250) \times 89.42 \times (500 - 89.42/2) / 10^6 \\ = 491.35 \text{ kNm}$$

Step 3 Calculate the moment taken by the web and the limiting moment of the web.

$$M_w = M_u - M_f = 620 - 491.35 = 128.65 \text{ kNm}$$

For Fe 415 grade steel $M_{w,\text{lim}} = 0.138 f_{ck} b_w d^2 = 0.138 \times 20 \times 250 \times 500^2 / 10^6 = 172.5 \text{ kNm}$

$M_{w,\text{lim}} > M_w$. Hence, the beam may be designed as singly reinforced.

Step 4 Calculate the area of steel.

$$A_{st} = \frac{M_f}{0.87f_y(d - 0.5y_f)} + \frac{M_w}{0.87f_y z}, \text{ with } y_f = 89.42 \text{ mm}$$

$$z = d \left(1 - 0.416 \frac{x_u}{d} \right) = 500(1 - 0.416 \times 0.2389) = 450.3 \text{ mm}$$

$$A_{st} = \frac{491.35 \times 10^6}{0.87 \times 415 \times (500 - 0.5 \times 89.42)} + \frac{128.65 \times 10^6}{0.87 \times 415 \times 450.3}$$

$$= 2989.07 + 791.3 = 3780.36 \text{ mm}^2$$

Provide five 32 mm diameter bars (A_{st} provided = 4021 mm²) in two rows.

Note: The effective depth is reduced since the bars are provided in two rows. Hence, provided area should be checked for this effective depth.

(b) $M_u = 730 \text{ kNm}$

Step 1 Check for the location of the neutral axis. Assuming the neutral axis is within the flange,

$$\frac{x_u}{d} = \frac{1 - \sqrt{1 - 1.664m}}{0.832} \text{ and}$$

$$m = \frac{M_u}{0.36f_{ck}b_f d^2} = \frac{730 \times 10^6}{0.36 \times 20 \times 1600 \times 500^2} = 0.2535$$

$$\text{Hence, } \frac{x_u}{d} = \frac{1 - \sqrt{1 - 1.664 \times 0.2535}}{0.832} = 0.288$$

$$\text{Thus, } x_u = 0.288 \times 500 = 144 \text{ mm}$$

$$\frac{D_f}{d} = \frac{110}{500} = 0.22 < \frac{x_u}{d}. \text{ Hence, the neutral axis is in the web.}$$

Step 2 Calculate the moment of resistance of the flange.

$$M_f = 0.447f_{ck}(b_f - b_w)y_f \left(d - \frac{y_f}{2} \right)$$

Since $D_f > 0.2$, $y_f = 0.15x_u + 0.65D_f = 0.15 \times 144 + 0.65 \times 110 = 93.1 \text{ mm}$

$$M_f = 0.447 \times 20 \times (1600 - 250) \times 93.1 \times (500 - 93.1/2) / 10^6$$

$$= 509.5 \text{ kNm}$$

Step 3 Calculate the moment taken by the web and the limiting moment of the web.

$$M_w = M_u - M_f = 730 - 509.5 = 220.5 \text{ kNm}$$

For Fe 415 grade steel $M_{w,lim} = 0.138f_{ck}b_w d^2 = 0.138 \times 20 \times 250 \times 500^2 / 10^6 = 172.5 \text{ kNm}$

$M_w > M_{w,lim}$. Hence, the beam has to be designed as doubly reinforced.

Step 4 Calculate the area of steel.

$$A_{sc} = \frac{M_w - M_{w,lim}}{(f_{sc} - 0.447f_{ck})(d - d')}$$

Assuming 20 mm diameter bars for compression reinforcement and 8 mm diameter bars for stirrups,

$$d' = \text{Clear cover} + \text{Diameter of stirrup} + \text{Bar diameter}/2$$

$$= 25 + 8 + 20/2 = 43 \text{ mm}$$

For Fe 415 steel, $\frac{x_{u,lim}}{d} = 0.479$. Hence, $x_{u,lim} = 0.479 \times 500 = 239.5 \text{ mm}$

$$\varepsilon_{sc} = 0.0035 \left(1 - \frac{d'}{x_{u,lim}} \right) = 0.0035 \left(1 - \frac{43}{239.5} \right) = 0.00287$$

From Table 5.2,

$$f_{sc} = 351.8 + \frac{360.9 - 351.8}{381 - 276} (287 - 276) = 352.76 \text{ N/mm}^2$$

Hence,

$$A_{sc} = \frac{(220.5 - 172.5) \times 10^6}{(352.76 - 0.447 \times 20)(500 - 43)} = 305.5 \text{ mm}^2$$

Provide two 16 mm diameter bars (A_{sc} provided = 402 mm²).

Calculation of tensile steel

Lever arm distance,

$$z = d \left(1 - 0.416 \frac{x_{u,lim}}{d} \right) = 500 \times (1 - 0.416 \times 0.479)$$

$$= 400.37 \text{ mm}$$

$$A_{st} = \frac{M_f}{0.87f_y(d - 0.5y_f)} + \frac{M_{w,lim}}{0.87f_y z} + \frac{M_w - M_{w,lim}}{0.87f_y(d - d')}, \text{ with}$$

$$y_f = 93.1 \text{ mm}$$

Thus,

$$A_{st} = \frac{509.5 \times 10^6}{0.87 \times 415 \times (500 - 0.5 \times 93.1)} +$$

$$\frac{172.5 \times 10^6}{0.87 \times 415 \times 400.37} +$$

$$\frac{(220.5 - 172.5) \times 10^6}{0.87 \times 415 \times (500 - 43)}$$

$$= 3112.06 + 1193.33 + 290.91 = 4596.30 \text{ mm}^2$$

Provide five 32 mm diameter and one 28 mm diameter bars in two rows (A_{st} provided = 4637 mm²).

EXAMPLE 5.29 (Design of deep beam):

Design a simply supported, 300 mm thick RC vertical deep beam of height 4.0 m, which is supported over 500 mm wide piers having a clear spacing of 5 m. The beam carries a service superimposed load of 200 kN/m. Assume M20 grade concrete and steel of grade Fe 415.

SOLUTION:

For Fe 415 steel, $f_{st} = 0.87 \times 415 = 361.05$ MPa

Effective span $L =$ Smaller of c/c between supports $= 5 + 0.5 = 5.5$ m

and $1.15 \times 5 = 5.75$ m

Hence $L = 5.5$ m

Deep beam parameters

Thickness of beam $t = 300$ mm. Depth of beam $= 4$ m.

Assume effective depth as 3625 mm.

Aspect ratio $L/D = 5.5/4.0 = 1.375 < 2.0$

$L/b = 5.5/0.3 = 18.3 < 60$

$Ld/b^2 = 5.5 \times 3.625/0.3^2 = 221.5 < 250$

Hence, lateral buckling is prevented. Moreover, L/D is within the range 1.0–2.0.

Hence, lever arm $z = 0.20 \times 5 + 0.4 \times 4 = 2.6$ m

Factored dead load $w_{u,d} = 1.5 \times (25 \times 4 \times 0.3) = 45$ kN/m

Factored superimposed load $w_{u,t} = 1.5 \times 200 = 300$ kN/m

Total factored load $w_u = w_{u,d} + w_{u,t} = 345$ kN/m

For simply supported deep beam

Maximum bending moment $M_u = (345 \times 5.5^2)/8 = 1304.5$ kN/m

Hence, $A_{st} = \frac{M_u}{0.87 f_y z} =$

$$\frac{1304.5 \times 10^6}{0.87 \times 415 \times 2600} = 1389.6 \text{ mm}^2$$

Consider seven 16 mm bars ($A_{st} = 1408 \text{ mm}^2$).

Percentage of steel

$$p_t = \frac{1408 \times 100}{300 \times 4000}$$

$$= 0.117\% < \frac{0.24 \sqrt{f_{ck}}}{f_y} \times 100$$

$$= \frac{0.24 \times \sqrt{20}}{415} \times 100 = 0.26\%$$

The steel considered is less than the minimum specified. Hence, we should provide at least $0.26 \times 300 \times 4000/100 = 3120 \text{ mm}^2$. Hence, provide five 20 mm diameter and eight 16 mm diameter bars (A_{st} provided $= 1571 + 1608 = 3179 \text{ mm}^2$).

Zone or depth of placement $= 0.25D - 0.05L = 0.25 \times 4000 - 0.05 \times 5500 = 725$ mm

Distribute eight 16 mm diameter bars within a depth of 725 mm from the bottom fibre of the beam with a nominal cover of 50 mm. The bars should be anchored into the support and the minimum embedment length as per Clause 29.3.1 and 26.2.1 of IS 456

$$0.80L_d = \frac{0.8 f_{st} d_b}{4 \tau_{bd}}$$

$$= \frac{0.8 \times 361.05 \times 16}{4 \times 1.92} = 601.75 \text{ mm}$$

Embed the bars beyond the face of each support by 450 mm (assuming a cover of 50 mm) and provide 90° hook to obtain anchorage length of 605 mm. Mechanically anchored headed bars provide better anchorage (see Section 7.6.2 of Chapter 7).

Nominal horizontal and vertical reinforcements—provided as per ACI 318

Vertical/Horizontal steel per metre length/height of beam,

$$A_{st,v} = \frac{0.25 \times 300 \times 1000}{100} = 750 \text{ mm}^2$$

Provide 10 mm vertical and horizontal bars at 210 mm c/c on both the faces (A_{st} provided $= 748 \text{ mm}^2/\text{m}$). The maximum spacing is the lesser of $d/5 = 3625/5 = 725$ mm and 300 mm. Hence, the provided spacing is satisfactory.

Check for shear is not necessary as per Clause 29.1(b) of IS 456:2000. The designed beam is shown in Fig. 5.57.

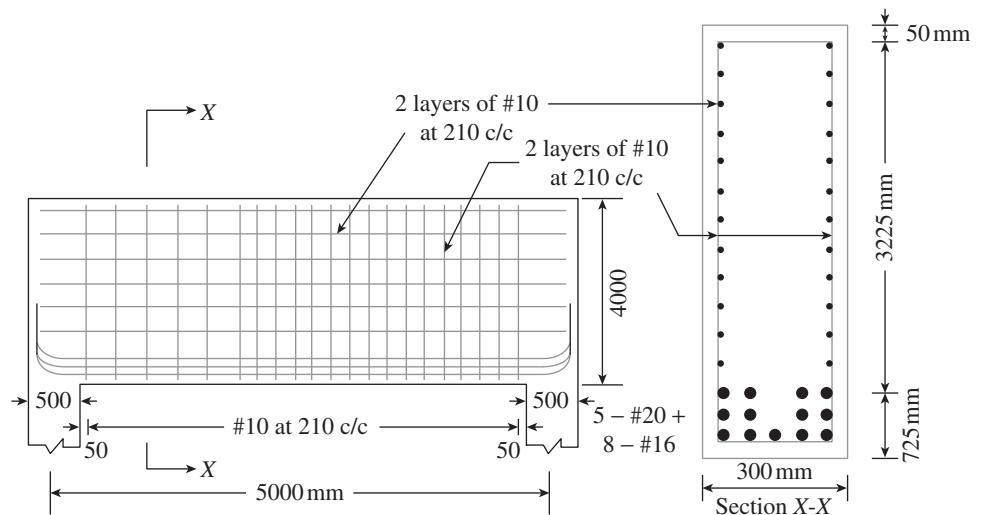


FIG. 5.57 Deep beam of Example 5.29

It should be noted that a more accurate design of deep beams is made using the strut-and-tie method (see Appendix B).

EXAMPLE 5.30 (Beam with high-strength steel):

A simply supported beam of span 4.57 m and loaded with four point loads is shown in Fig. 5.58. The beam has a width of 305 mm and depth of 460 mm. It is reinforced with three HSS bars (MMFX Steel) of 19 mm diameter at the bottom and two Fe 400 grade bars at the top. The effective cover for the top and bottom steel are 60 mm and 40 mm, respectively. Assuming M50 concrete calculate the moment capacity and the value of concentrated loads it can sustain using the ACI code (note that this beam was tested by Mast, et al. 2008).

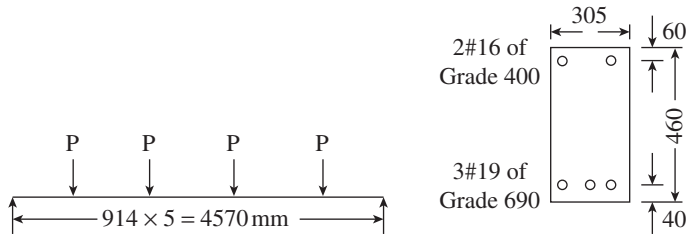


FIG. 5.58 Beam with HSS of Example 5.30

SOLUTION:

Let us assume ϵ_{cu} as 0.003 as per ACI code for this example.

The following values are given:

$$A_{st} = 3\#19 = 850 \text{ mm}^2, A_{sc} = 2 \times 16 = 402 \text{ mm}^2,$$

$$f_{yt} = 690 \text{ MPa}, f_{yc} = 400 \text{ MPa}, f'_c = 50 \text{ MPa}$$

$$a = \frac{A_{st} f_{yt}}{0.85 f'_c b} = \frac{850 \times 690}{0.85 \times 50 \times 305} = 45.2 \text{ mm}$$

Assuming that the steel has yielded at nominal strength,

$$T = 850 \times 690/1000 = 586.5 \text{ kN}$$

As per Clause 10.2.7.3 of ACI 318, for f'_c between 17 MPa and 28 MPa, β_1 is 0.85. For f'_c above 28 MPa, β_1 shall be reduced linearly at a rate of 0.05 for each 7 MPa of strength in excess of 28 MPa, but β_1 should not be taken less than 0.65.

$$\beta_1 = 0.85 - 0.05 \frac{50 - 28}{7} = 0.69$$

$$x_u = a/\beta_1 = 45.2/0.69 = 65.5 \text{ mm}$$

From the strain diagram,

$$\begin{aligned} \epsilon_{st} &= \epsilon_{cu} \left(\frac{d - x_u}{x_u} \right) = 0.003 \left(\frac{420 - 65.5}{65.5} \right) \\ &= 0.016 > 0.009 \end{aligned}$$

Hence, the section is tension controlled.

It should be noted that the tension-controlled strain limit of 0.009 was proposed by Mast, et al. (2008) for HSS with $f_y \geq 690$ MPa.

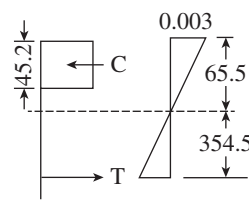
$$\begin{aligned} M_u &= A_{st} f_y (d - a/2) = 850 \times 690 (420 - 45.2/2)/10^6 \\ &= 233.07 \text{ kNm} \end{aligned}$$

With a ϕ factor of 0.9 for flexure, the capacity it can withstand $= 0.9 \times 233.07 = 209.76$ kNm.

$$\text{Bending moment} = 2P \times 2285 - P \times 1371 - P \times 457 = 2742P$$

$$\text{Hence, } P = 233.07 \times 10^3 / 2742 = 85 \text{ kN}$$

It should be noted that if we include the self-weight of the beam also in the calculation, the value of P will be slightly reduced.



EXAMPLE 5.31:

Design a lintel for a window opening of span 2 m. The thickness of the wall is 230 mm and the height of the brickwork above the lintel is 1.2 m. The length of the wall on either side of the lintel is more than half the span of the lintel. Use Fe 415 steel and M20 concrete.

SOLUTION:

Step 1 Calculate the effective span. Assume the depth of lintel as 115 mm. With an effective cover of 25 mm, effective depth, $d = 90$ mm and breadth of lintel = thickness of wall = 230 mm. Effective span = Clear span + Half width of bearing on either side or
 $= \text{Clear span} + \text{Effective depth} = 2.0 + 0.09 = 2.09 \text{ m}$

Step 2 Calculate the bending moment. The load on lintel is as follows:

$$\text{Weight of brickwork} = 20 \text{ kN/m}^3$$

$$\text{Height of apex of triangle} = \text{Effective span}/2 = 2.09/2 = 1.045 \text{ m}$$

Since the height of the brickwork above the lintel is 1.2 m and there is sufficient length of wall on either side of the lintel, arch action is possible.

$$\text{Self-weight of lintel, } w = 0.23 \times 0.115 \times 25 = 0.66 \text{ kN/m}$$

$$\text{Weight of triangular brickwork, } W = (2.09 \times 1.045)/2 \times 0.23 \times 20 = 5.02 \text{ kN}$$

$$\text{Bending moment } M = wl^2/8 + WL/6$$

$$= 0.66 \times 2.09^2/8 + 5.02 \times 2.09/6$$

$$= 2.11 \text{ kNm}$$

$$\text{Factored design moment, } M_u = 1.5 \times 2.11 = 3.165 \text{ kNm}$$

$$\frac{M_u}{bd^2} = \frac{3.165 \times 10^6}{230 \times 90^2} = 1.698 \text{ N/mm}^2$$

From Table 2 of SP 16, we get for this value of M_u/bd^2 , $p_t = 0.53\%$.

$$\text{Hence } A_{st} = \frac{0.53 \times 90 \times 230}{100} = 110 \text{ mm}^2$$

Balanced area of steel,

$$p_{t,\text{lim}} = 19.82 f_{ck} / f_y = 19.82 \times 20 / 415 = 0.965\%$$

$$\text{Hence, } A_{st,\text{lim}} = 0.965 \times 90 \times 230 / 100 = 197.6 \text{ mm}^2$$

Provide two 8 mm diameter and one 6 mm diameter bars.

$$\text{Area provided} = 128 \text{ mm}^2 < A_{st,\text{lim}}$$

Provide two 6 mm diameter hanger bars and also minimum shear reinforcement (see Chapter 6 for details).

SUMMARY

Beams are primarily subjected to flexure or bending and often support slabs. They support the loads applied on them by the slabs and their own weight by internal moments and shears. The behaviour of a rectangular RC beam is explained. It is seen that the reinforcement comes into play only after the concrete cracks in the tension zone. As the moment is increased, the beam fails by the yielding of reinforcement and subsequently secondary compression failure in the concrete.

Two types of problems are often encountered—analysis of the beam section and design for the given moment. In the analysis problem, the geometry of the beam and the reinforcement details are known, and one needs to calculate the capacity to check whether the existing beam is capable of resisting the external loads. Design situations occur in new buildings where the depth, breadth, and reinforcement details required for the beam to safely and economically resist the externally applied loads need to be calculated.

In an RC beam of rectangular cross section, if the reinforcement is provided only in the tension zone, it is called a singly reinforced rectangular beam; if the reinforcements are provided in both the compression and tension zones, it is called a doubly reinforced rectangular beam. T- or L-beams are often encountered in practice, which have a flange consisting of the slab. T- or L-beams may also be singly or doubly reinforced.

All these beams are also classified as under-reinforced, over-reinforced, and balanced beams, depending on their behaviour. Over-reinforced beams are to be avoided as they result in brittle failure of concrete under compression, which is sudden and without any warning. Balanced sections are those in which both the concrete and steel fail at the same time. In under-reinforced beams, the failure is initiated by the yielding of steel; hence, this type of failure is ductile (due to inelastic deformation in steel reinforcement) and gives enough warning before failure.

In the codes of practices, the ductile behaviour is ascertained by controlling the value of tension strain at the level of steel reinforcement when the extreme concrete fibre in compression reaches the maximum compression strain. In IS 456, the maximum strain in concrete is taken as 0.0035 and that in steel as $f_y/1.15E_s + 0.002$ (the extra strain of 0.002 is specified to assure the ductile behaviour). Several assumptions are made in the general theory for the design of beams; there is a linear strain variation across the depth of the member, plane sections remain plane after bending, and so on. All these assumptions are explained. The parabolic–rectangular stress block for concrete assumed by the IS code and the equivalent rectangular stress block of the ACI code are explained.

The equations for the neutral axis depth, moment of resistance of rectangular under- and over-reinforced beams (both singly reinforced and doubly reinforced), and their limiting reinforcements and limiting moments of resistance are derived. The factors affecting the moment of resistance are discussed. To avoid sudden failure, some minimum reinforcement is necessary in the beams. Similarly, for proper behaviour, a limit on the maximum reinforcement is also specified. The Indian code provisions and the latest provisions in the ACI code are discussed for both minimum and maximum steel. The tension- and compression-controlled sections are explained with respect to the ACI code provisions. The slenderness limits proposed in the code to avoid lateral buckling along with the latest research on this topic are presented. Some guidelines for the design of singly and doubly reinforced rectangular beams are provided.

In T- or L-beams, the contribution of slab acting along with the web can be considered. The expressions to determine the effective width of the flange as per different codes are given. The transverse reinforcement necessary for the slab to act in unison with the beam is also discussed. At the supports, under gravity loading, the flanges of T- or L-beams will be subjected to negative moment and hence will be in tension; hence, they have to be designed only as rectangular beams. However, at mid-spans, the flange will be under compression and considered in design. It should be noted that under reversal of loading, the direction of bending moments will be reversed. T- or L-beams can also be singly or doubly reinforced. The expressions necessary for their analysis and design are also derived. The procedure for design is outlined. Design charts have been developed in the past for all these types of beams. The use of these design aids are also explained and illustrated by examples. Based on the latest research, the minimum flexural ductility requirements of the beams are provided.

In beams with span less than 2.5 times the depth, the linear stress–strain behaviour is not valid. Such beams are called deep beams. The simplified guidelines suggested in IS 456 for these beams are explained along with the reinforcement detailing (more accurate assessment of their behaviour can be made by using the strut-and-tie models). In order to reduce the floor heights, WSBs are sometimes employed and for shorter spans, beams may also be concealed inside the slab thickness. These beams are discussed along with lintel, plinth, and grade beams. HSC and HSS are also employed in tall buildings or bridges to reduce the size or to reduce reinforcement congestion. Some discussions are included about HSC and HSS. Fatigue behaviour, which may be critical in beams subjected to moving or impact loads, is also discussed. Ample examples are provided to clarify the derived expressions and design procedures.

REVIEW QUESTIONS

- Which of the following are correct statements under gravity loading?
 - In simply supported beams, the top fibres will be under compression near the mid-span.
 - In continuous beams, near the support, the top fibres will be under tension.
 - In cantilevers, the top fibres will be under tension.
 - All of these
- Define the following:
 - Neutral axis
 - Cracking moment of beam
 - Section curvature at cracking
- Will the reinforcement be acting before cracking? Why?
- When the beam starts to crack, the neutral axis _____.
 - shifts downwards
 - remains in the same position
 - shifts upwards

5. How will you distinguish the working stage from the limit stage of behaviour?
6. Differentiate between analysis and design of sections.
7. State the basic assumptions used in the theory of bending as applied to limit states design of beams.
8. The ultimate strain in concrete in bending is assumed in the IS code as _____.
 (a) 0.002 (c) 0.0035
 (b) 0.003 (d) 0.004
9. What is meant by strain compatibility? State the fundamental assumption that ensures strain compatibility.
10. State the shape of the stress block used in the following codes:
 (a) IS 456 (b) ACI 318
11. What are the partial safety factors used for concrete compressive strength and steel tensile strength? Can you guess why a higher factor of safety is used for concrete than steel?
12. Sketch the stress–strain curve of concrete as adopted in IS 456.
13. The maximum strain in the tension reinforcement in the section at failure should be _____.
 (a) more than $\frac{f_y}{1.15E_s} + 0.002$
 (b) equal to 0.0035
 (c) more than $\frac{f_y}{E_s} + 0.002$
 (d) less than $\frac{f_y}{1.15E_s} + 0.002$
14. The ultimate tensile strain in steel is in the range of _____.
 (a) 0.012–0.020 (c) 0.12–0.20
 (b) 0.0012–0.0020 (d) None of these
15. What are the two requirements that are to be satisfied in the flexural analysis of beams?
16. What do you understand by (a) balanced section, (b) under-reinforced section, and (c) over-reinforced section? Why is it preferable to design a beam as under-reinforced?
17. A rectangular RC beam has a width of b mm and effective depth of d mm. Derive expressions for the following:
 (a) Neutral axis depth
 (b) Lever arm
 (c) Moment of resistance
 (d) Limiting percentage of steel
18. Can you guess why $x_{u,max}$ is dependent only on the grade of steel and not on the grade of concrete?
19. What are the limiting values of x_u/d for grade 250, 415, and 500 steels?
20. What are the limiting values of M_u/bd^2 for grade 250, 415, and 500 steels?
21. What are the limiting values of $p_f f_y / f_{ck}$ for grade 250, 415, and 500 steels?
22. Why is it necessary to restrict the moment capacity of beam to the limiting value of M_n ?
23. If the applied moment, M_u , exceeds $M_{n,lim}$, the section may be redesigned by _____.
 (a) changing the cross-sectional dimensions of the member
 (b) increasing the concrete strength
 (c) designing the member as a doubly reinforced section
 (d) all of these
24. What is the basic design equation of a singly reinforced beam?
25. List the factors that may affect the nominal ultimate strength of a beam subjected to bending.
26. Why is it necessary to impose minimum and maximum limits on flexural tension reinforcement? What are the values given in IS 456? Why are the values given in IS 456 not relevant?
27. How are tension- and compression-controlled sections defined in the ACI code?
28. Why is it necessary to impose slenderness limits on the section of beams? How are the Indian code provisions different from the ACI provisions in this aspect?
29. State a few guidelines for choosing the dimensions and reinforcement for beams.
30. How is the effective cover for beams calculated?
31. The cover and spacing between bars provide _____.
 (a) concrete on all sides of each bar to develop sufficient bond
 (b) space for the fresh concrete to flow around the bar and get compacted
 (c) space to allow vibrators to reach up to the bottom of the beam
 (d) all of these
32. The minimum horizontal distance between the bars in a beam should be _____.
 (a) greater than the diameter of the larger bar
 (b) greater than the cover
 (c) greater than the maximum size of aggregate + 5 mm
 (d) both (a) and (c)
33. Side face reinforcement should be provided, when the depth exceeds _____.
 (a) 550 mm (c) 750 mm
 (b) 650 mm (d) 1000 mm
34. Basic L/D ratio for cantilever beams is given in IS 456 as _____.
 (a) 10 (b) 20 (c) 8 (d) 7
35. Basic L/D ratio for simply supported beams is given in IS 456 as _____.
 (a) 10 (b) 20 (c) 8 (d) 7
36. Why is it better to limit the different sizes of beams in a project to a few standard sizes?
37. What is the equation to determine the depth of a beam for a given external moment?
38. Why is ductility considered important in beam design? How can we achieve the required ductility by the design methods?
39. List the steps involved in the strain compatibility method of design of over-reinforced beams.
40. What are the advantages of using design charts presented in SP 16? Can they be used for the design of non-rectangular sections?
41. List the steps involved to determine A_{st} using design aids presented in SP 16.
42. Why is it necessary to limit x_u/d in the design of singly reinforced beams? Can the condition be relaxed in doubly reinforced beams? State the reasons.
43. A depth greater than the calculated depth is normally chosen. Will it produce an under-reinforced or over-reinforced section? Why?

44. Under what circumstances are doubly reinforced beams used? What are the advantages of doubly reinforced beams over singly reinforced beams?
45. What is the effect of creep and shrinkage on doubly reinforced beams?
46. By the use of compression steel in doubly reinforced beams _____ .
 - (a) ductility is increased
 - (b) compression failure of concrete may be changed to tension failure of steel
 - (c) long-term deflections are reduced
 - (d) all of these
47. Why is it necessary to tie the compression steel with stirrups at closer intervals?
48. Will adding compression steel increase the moment capacity appreciably? State the reason for your answer.
49. How will you decide whether a doubly reinforced section is under- or over-reinforced?
50. What is the minimum percentage of steel to be provided as compression steel to consider the beam as doubly reinforced?
51. What are the minimum and maximum percentages of tension and compression reinforcement in doubly reinforced beams?
52. How is it determined whether a beam of given dimensions is to be designed as doubly reinforced?
53. Derive the expression for determining the area of steel for a doubly reinforced beam of given dimension and external moment.
54. What is the difference between an L- and a T-beam?
55. How is the effective flange width calculated for a T-beam using the IS code?
56. What is meant by shear lag in T-beams?
57. When is a T-beam designed as a rectangular beam?
58. What are the possible positions of neutral axis in the design of T-beams?
59. Describe the method of locating the position of neutral axis in T-beams.
60. At what location of neutral axis will the flange of a T-beam be subjected to non-linear stress distribution?
61. What is the role of transverse reinforcement in the slab portion of T-beams?
62. Is the minimum percentage of tension steel in a T-beam different from a rectangular beam? Is it determined based on web width or flange width?
63. What is the maximum percentage of steel that is allowed in T-beams?
64. Give the approximate formula that is used to determine the area of steel for T-beams subjected to factored moment.
65. What is the flange width on either side of a web, the reinforcement of which can be considered to act as tension reinforcement, when a negative bending moment is acting on the beam?
66. What is the distance over which the reinforcement should be distributed to control flexural cracking in T-beam flanges?
67. What are deep beams? When is a beam considered a deep beam according to IS 456?
68. List the design procedure of deep beams according to the IS code.
69. Describe the detailing to be adopted in simply supported deep beams according to IS 456:2000.
70. What is the percentage and spacing of steel to be provided as vertical and horizontal reinforcement in deep beams as per the IS and ACI codes?
71. How are bearing stresses checked in deep beams?
72. What are wide shallow beams? Sketch the beam-column joint detail of a WSB.
73. What are hidden beams? How are they designed?
74. What is the difference in structural action between a normal beam and a lintel?
75. Distinguish between grade and plinth beams.
76. Will the stress distribution of high-strength concrete also be parabolic-rectangular?
77. Under what conditions should the fatigue behaviour be considered?
78. Fatigue will not be a problem if the number of cycles is less than _____.
 - (a) 20,000
 - (b) 2,00,000
 - (c) 1,00,000

EXERCISES

1. Assuming that the concrete is uncracked, compute the bending stresses in the extreme fibres of the beam having a size 500×250 mm as shown in Fig. 5.59 for a bending moment of 120 kNm. Assume concrete of grade 30 MPa. In addition, determine the cracking moment of the section.
2. Determine whether the section shown in Fig. 5.59 is under or over-reinforced with $f_{ck} = 30$ N/mm², $f_y = 500$ N/mm², and with the following values of A_{st} : (a) 1140 mm² (b) 1415 mm² (c) 2413 mm² (d) 3217 mm².

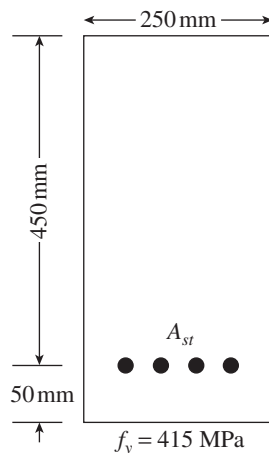


FIG. 5.59

3. Determine the nominal ultimate moment strength of the beam section shown in Fig. 5.59, with $A_{st} = 4\#20$ diameter = 1257 mm², $f_y = 415$ MPa, and $f_{ck} = 30$ MPa using the following methods:
 - (a) Parabolic-Rectangular stress block as per IS 456
 - (b) Equivalent rectangular stress block as in ACI 318.
4. Determine whether the section having the dimensions given below can withstand a factored applied bending moment of 310 kNm: $b = 230$ mm, $D = 600$ mm, effective cover = 40 mm, $A_{st} = 3\#25$ diameter = 1473 mm², $f_y = 500$ MPa, and $f_{ck} = 35$ MPa.

[Ans.: $M_n = 300.2$ kNm and hence is not safe]
5. Calculate the maximum moment that can be sustained by a beam with $b = 250$ mm, $d = 400$ mm, and $A_{st} = 3600$ mm². Assume $f_{ck} = 20$ MPa and $f_y = 415$ MPa.

[Ans.: $M_n = 110$ kNm]
6. Find the ultimate moment capacity of a rectangular beam with $b = 250$ mm, $d = 400$ mm, $A_{st} = 942$ mm², which has been found

to be inadequate to carry a factored moment of 145 kNm and hence repaired by gluing a steel plate of thickness 3 mm and size 175 mm (yield strength 250 N/mm²) at the bottom of the beam, as shown in Fig. 5.60. Assume $f_{ck} = 20$ MPa and $f_y = 415$ MPa.

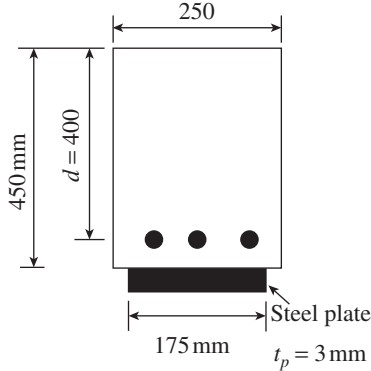


FIG. 5.60

7. Find the ultimate moment capacity of an RC trapezoidal section as shown in Fig. 5.61 with $A_{st} = 1963$ mm². The beam has a top width of 500 mm, depth of 550 mm, and width at the level of centroid of reinforcement as 300 mm. Assume $f_{ck} = 20$ MPa and $f_y = 415$ MPa. [Ans.: $M_n = 317$ kNm]

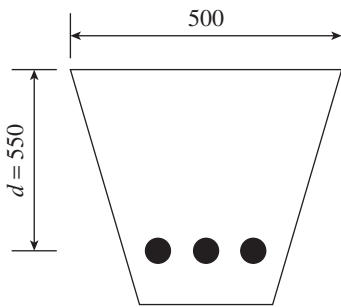


FIG. 5.61

8. Find the ultimate moment capacity of the cross section shown in Fig. 5.62, with $A_{st} = 1847$ mm². Assume $f_{ck} = 35$ N/mm² and $f_y = 415$ N/mm².

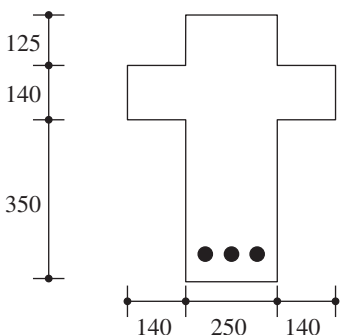


FIG. 5.62

9. Design a singly reinforced concrete beam of width 300 mm, subjected to an ultimate moment of 250 kNm. Assume $f_{ck} = 30$ MPa and $f_y = 415$ MPa. [Ans.: $d = 460$ mm and A_{st} required = 1849 mm²]
10. Design a singly reinforced concrete beam subjected to an ultimate moment of 350 kNm. Assume $f_{ck} = 35$ N/mm² and $f_y = 415$ N/mm². In this beam, due to architectural considerations,

the width has to be restricted to 250 mm.

[Ans.: $d = 550$ mm and A_{st} required = 2169.2 mm²]

11. Design a singly reinforced concrete beam of width 230 mm, subjected to an ultimate moment of 200 kNm. Assume $f_{ck} = 30$ MPa and $f_y = 250$ MPa, using design tables of SP 16. [Ans.: $d = 475$ mm, A_{st} required = 2364.2 mm²]
12. Design a singly reinforced concrete beam, subjected to an ultimate moment of 130 kNm. Assume M20 concrete and Fe 415 grade steel. Due to architectural considerations, the breadth and overall depth of the beam are restricted to 230 mm and 450 mm, respectively. Assume effective cover as 50 mm.
13. Determine the value of ultimate uniformly distributed load, w_u , that can be carried by the beam shown in Fig. 5.63, using design aids. Use M25 concrete and Fe 415 grade steel and assume $A_{st} = 1383.8$ mm².

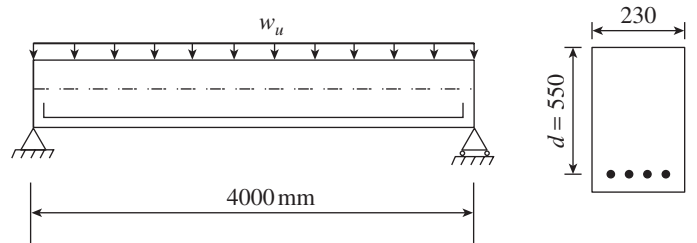


FIG. 5.63

14. Determine the ultimate moment of resistance of a doubly reinforced beam section with the following data: $b = 300$ mm, $d = 550$ mm, $d' = 50$ mm, $A_{st} = 4\#32$ mm diameter bars (3217 mm²), $A_{sc} = 2\#25$ mm bars (982 mm²), $f_y = 250$ MPa, and $f_{ck} = 20$ MPa. [Ans.: $x_u = 229.12$ mm and $M_n = 327.37$ kNm]
15. Determine the ultimate moment of resistance of a doubly reinforced beam section with the following data: $b = 350$ mm, $d = 550$ mm, $d' = 60$ mm, $A_{st} = 5\#32$ mm diameter bars (4021 mm²), $A_{sc} = 3\#25$ mm bars (1473 mm²), $f_y = 415$ MPa, and $f_{ck} = 30$ MPa. [Ans.: $x_u = 253.66$ mm and $M_n = 668.8$ kNm]
16. Determine the ultimate moment capacity of a doubly reinforced concrete beam 250 mm wide and 520 mm deep. This beam is provided with two 20 mm bars on the compression side and two 28 mm bars and one 25 mm bar on the tension side. Adopt M30 concrete and Fe 415 grade steel. Assume effective concrete cover, $d' = 40$ mm. Use design aids.
17. A rectangular RC beam of overall size 200 × 450 mm is subjected to a factored moment of 160 kNm. Compute the required reinforcement, assuming effective cover for compression and tension reinforcement as 50 mm. Use M20 concrete and Fe 415 grade steel.
18. Design the doubly reinforced concrete beam of Exercise 17 using design aids.
19. Find the maximum cantilever span L_c for the beam shown in Fig. 5.64 and subjected to a factored uniformly distributed load of 15 kN/m² and a factored point load 50 kN acting at the tip of the cantilever. Assume $f_{ck} = 25$ MPa and $f_y = 415$ MPa.

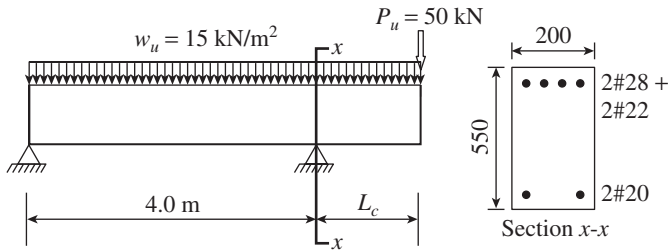


FIG. 5.64

20. Determine the ultimate moment of resistance of an isolated T-beam, shown in Fig. 5.65, assuming $f_{ck} = 20$ MPa and grade 415 steel. [Ans.: $x_u = 71.15$ mm and $M_n = 217.89$ kNm]

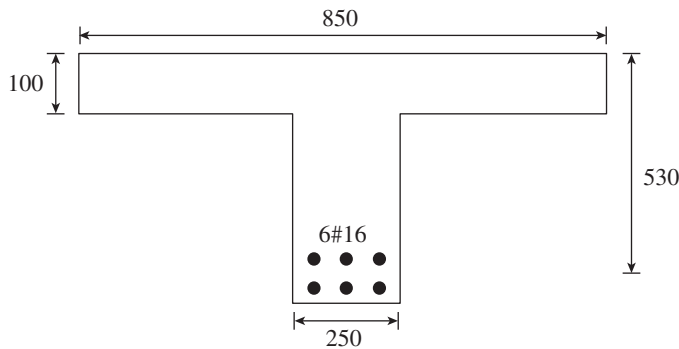


FIG. 5.65

21. Determine the ultimate moment of resistance of the isolated T-beam of the previous exercise, assuming $A_{st} = 1884$ mm², $f_{ck} = 20$ MPa, and grade 415 steel. [Ans.: $x_u = 127.44$ mm, $y_f = 84.12$ mm, and $M_n = 329.57$ kNm]
22. Determine the limiting moment of resistance by concrete failure of a T-beam with the following dimensions: $D_f = 125$ mm, $b_w = 250$ mm, $b_f = 1000$ mm, $A_{st} = 2454$ mm² and $d = 550$ mm. Assume Fe 415 steel and M 25 concrete. [Ans.: $M_{n,lim} = 756.64$ kNm]

23. Determine the area of steel required for a T-beam with the following dimensions: $D_f = 150$ mm, $b_w = 250$ mm, $b_f = 1200$ mm, $d = 550$ mm. It is required to carry a factored moment of 750 kNm. Assume Fe 415 steel and M 25 concrete.

[Ans.: $x_u = 141.73$ mm and $A_{st} = 4230$ mm²]

24. Design a T-beam with the following dimensions: $D_f = 120$ mm, $b_w = 230$ mm, $b_f = 1000$ mm. It is required to carry a factored moment of 400 kNm. Assume Fe 415 steel and M25 concrete ($d = 400$ mm, $x_u = 141.87$ mm, and $A_{st} = 3184$ mm²).
25. Calculate the ultimate moment of resistance of a T-beam with the following dimensions: $D_f = 150$ mm, $b_w = 250$ mm, $b_f = 800$ mm, $d = 415$ mm, $d' = 35$ mm, $A_{st} = 6\#28$ diameter bars, and $A_{sc} = 2\#22$. Assume Fe 415 steel and M20 concrete. [Ans.: $x_u = 122.65$ mm and $M_n = 490$ kNm]
26. Design a T-beam spanning 6m supporting a one-way slab of thickness 140mm and subjected to a live load of 3.5 kN/m² and a dead load (due to floor finish, partition, etc.) of 1.2 kN/m², in addition to its self-weight. Assume Fe 415 steel and M25 concrete and the centre-to-centre distance of beams as 4 m.
27. Design a T-beam with 1300 mm width of flange, 120 mm depth of flange, 300 mm width of web, and 550 mm effective depth to carry a factored bending moment of (a) 650 kNm and (b) 800 kNm. Assume M25 concrete and Fe 415 steel.
28. Design a simply supported, 270 mm thick RC vertical deep beam of height 3.5 m, which is supported over 500 mm wide piers having a clear spacing of 4.5 m. The beam carries service superimposed load of 200 kN/m. Assume M20 grade concrete and steel of grade Fe 415.
29. Design a lintel for a window opening of span 1.5 m. The thickness of the wall is 230 mm and the height of the brickwork above the lintel is 1.1 m. The length of the wall on either side of the lintel is more than half the span of the lintel. Use Fe 415 steel and M20 concrete.

REFERENCES

- ACI 215R-74 (Revised 1992/Reapproved 1997), *Considerations for the Design of Concrete Structures Subjected to Fatigue Loading*, American Concrete Institute, Farmington Hills, p. 24.
- ACI 318M-2008, *Building Code Requirements for Structural Concrete and Commentary*, American Concrete Institute, Farmington Hills, p. 473.
- ACI-ASCE Committee 343R-1995, *Analysis and Design of Reinforced Concrete Bridge Structures*, American Concrete Institute, Farmington Hills, p. 158.
- ACI-ASCE Committee 352R-02 2002, *Recommendations for Design of Beam-column Connections in Monolithic Reinforced Concrete Structures*, American Concrete Institute, Farmington Hills, p. 38.
- Aguilar, G., A.B. Matamoros, G.J. Parra-Montesinos, J.A. Ramirez, and J.K. Wight 2002, 'Experimental Evaluation of Design Procedures for Shear Strength of Deep Reinforced Concrete Beams', *ACI Structural Journal*, Vol. 99, No. 4, pp. 539-48.
- Beeby, A.W. 1971, *Modified Proposals for Controlling the Deflection by Means of Ratios of Span to Effective Depth*, Cement and Concrete Association, Publication No. 42.456, London.
- Brown M.D. and O. Bayrak 2008, 'Design of Deep Beams Using Strut-and-tie Models, Part I: Evaluating U.S. Provisions, Part II: Design Recommendations', *ACI Structural Journal*, Vol. 105, No. 4, pp. 395-413.
- CEB-FIP 1993, *CEB-FIP Model Code 1990: Design Code*, Comité-Euro-International du Béton/Fédération Internationale de la Précontrainte, Thomas Telford, London, p. 462.
- CIRIA Guide 2 1977, *The Design of Deep Beams in Reinforced Concrete*, Construction Industry Research and Information Association and Ove Arup and Partners, London, p. 131.
- Chow, H.-L. and L.G. Selna 1994, 'Seismic Response of Shallow-floor Buildings', *The Structural Design of Tall Buildings*, Vol. 3, No. 2, pp. 107-17.
- Cohn, M.Z. and S.K. Ghosh 1972, 'Flexural Ductility of Reinforced Concrete Sections', *Publications, International Association of Bridge and Structural Engineers*, Vol. 32-II, pp. 53-83.
- CP 110-Part 1 1972, *Code of Practice for Structural Use of Concrete*, British Standards Institution, London, p. 154.
- Dayaratnam, P. 1987, *Brick and Reinforced Brick Structures*, Oxford and IBH Publishing Co. Pvt. Ltd, New Delhi, p. 181.
- Deodhar, S.V. and S.K. Dubey 2004, 'Hidden Beam: A New Concept of Slab Design', *CE & CR*, pp. 54-8.

- Desai, R.K. 2003, 'Limiting Moment Capacities of a Doubly Reinforced Concrete Section', *ICI Journal*, Vol. 4, No. 1, pp. 29–32.
- Desai, R.K. 2006, 'Moment of Resistance of Doubly Reinforced T-beam Section', *ICI Journal*, Vol. 7, No. 2, pp. 17–21.
- Elmenschawi, A. and T. Brown 2010, 'Seismic Behavior of 150MPa (22 ksi) Concrete Flexural Members', *ACI Structural Journal*, Vol. 107, No. 3, pp. 311–320.
- Fanella, D.A. and B.G. Rabbat (ed.) 2002, *PCA Notes on ACI 318-02 Building Code Requirements for Structural Concrete with Design Applications*, 8th edition, Portland Cement Association, Illinois.
- Fathifazl, G., A.G. Razaqpur, O.B. Isgor, A. Abbas, B. Fournier, and S. Foo 2009, 'Flexural Performance of Steel Reinforced Recycled Concrete Beams', *ACI Structural Journal*, Vol. 106, No. 6, pp. 858–67.
- Fehling, E., M. Schmidt, and S. Stürwald 2008, 'Ultra High Performance Concrete (UHPC)', *Proceedings of the Second International Symposium on Ultra High Performance Concrete Kassel*, Germany, 5–7 March 2008, Schriftenreihe Baustoffe und Massivbau, Heft 10, Kassel University Press, p. 902, (also see <http://www.uni-kassel.de/upress/online/frei/978-3-89958-376-2.volltext.frei.pdf>, last accessed on 21 May 2011).
- Feret, R. 1906, *Etude Experimentale du Ciment Arme*, Grauthier-Villiers, Paris, Chap. 3.
- Ghoneim, M.A., and M.T. El-Mihilmy 2008, *Design of Reinforced Concrete Structures*, Vol.1, 2nd edition, Al-Balagh Lel Tebaah Wal-Nashr Wattawoza, Cairo, p. 411.
- Govindan P. and A.R. Santhakumar 1985, 'Composite Action of Reinforced Concrete Beams with Plain Masonry Infills', *The Indian Concrete Journal*, Vol. 59, No. 8, pp. 204–8.
- Ho, J.C.M., A.K.H. Kwan, and H.J. Pam 2004, 'Minimum Flexural Ductility Design of High-strength Concrete Beams', *Magazine of Concrete Research*, Vol. 56, No. 1, pp. 13–22.
- Hognestad, E. 1952a, 'Fundamental Concepts in Ultimate Load Design of Reinforced Concrete Members', *Proceedings, ACI Journal*, Vol. 23, No. 10, pp. 809–30.
- Hognestad, E. 1952b, 'Inelastic Behavior in Tests of Eccentrically Loaded Short Reinforced Concrete Columns', *Proceedings, ACI Journal*, Vol. 24, No. 2, pp. 117–139.
- IS 2911 (Part III):1979, *Code of Practice for Design and Construction of Pile Foundations (Under-reamed Piles)*, Bureau of Indian Standards, New Delhi.
- IS 13920:1993, *Indian Standard Code of Practice for Ductile Detailing of Reinforced Concrete Structures Subjected to Seismic Forces*, Bureau of Indian Standards, New Delhi, p. 14, (also see <http://www.iitk.ac.in/nicee/IITK-GSDMA/EQ11.pdf>, last accessed on 17 October 2012, for the draft revised edition of the code).
- Iyengar, K.T.S. and C.S. Viswanatha 1990, *Torsteel Design Handbook for Reinforced Concrete Members with Limit State Design*, Torsteel Research Foundation in India, Mumbai, p. 190.
- Jagadish, R. 1988, *Influence of Openings on the Behaviour of Infilled Frames*, Ph.D. Thesis, IIT, Chennai.
- Kong, F.K. (ed.) 1990, *Reinforced Concrete Deep Beams*, Blackie and Son Ltd, Glasgow and London, and Van Nostrand Reinhold, New York, p. 288.
- Lee, J.A.N. 1962, 'Effective Widths of Tee-Beams', *The Structural Engineer*, Vol. 40, No. 1, pp. 21–7.
- Lee, M.K. and B.I.G. Barr 2004, 'An Overview of the Fatigue Behaviour of Plain and Fibre Reinforced Concrete', *Cement & Concrete Composites*, Elsevier Science, Vol. 26, No. 4, pp. 299–305.
- Leonhardt, F. and E. Mönning 1977, *Vorlesungen über Massivebau, Dritter Teil, Grundlagen zum Bewehren im Stahlbetonbau*, Dritte Auflage, Springer-Verlag, Berlin, p. 246.
- Leonhardt, F. and R. Walther 1966, *Wandartige Träger*, Bulletin No. 178, Wilhelm Ernst und Sohn, Berlin, p. 159.
- Li, Z. and Y. Zhang 2005, 'High-performance Concrete', in W. F. Chen and E.M. Lui (eds), *Handbook of Structural Engineering*, 2nd edition, CRC Press, Boca Raton, p. 1768.
- Loo, Y.-C. and T.D. Sutandi 1986, 'Effective Flange Width Formulas for T-beams', *Concrete International*, ACI, Vol. 8, No. 2, pp. 40–5.
- Mast, R.F. 1992, 'Unified Design Provisions for Reinforced and Prestressed Concrete Flexural and Compression Members', *ACI Structural Journal*, Vol. 89, No. 2, pp. 185–99.
- Mast, R.F., M. Dawood, S.H. Rizkalla, and P. Zia 2008, 'Flexural Strength of Concrete Beams Reinforced with High-strength Steel Bars', *ACI Structural Journal*, Vol. 105, No. 5, pp. 570–7.
- Medhekar, M.S. and S.K. Jain 1993, 'Proposed Minimum Reinforcement Requirements for Flexural Members', *The Bridge and Structural Engineer*, ING-IABSE, Vol. 23, No. 2, pp. 77–88.
- NZS 3101:2006, *Part 1: The Design of Concrete Structures, Part 2: Commentary*, Standards New Zealand, Wellington.
- Park, R. and T. Paulay 1975, *Reinforced Concrete Structures*, John Wiley and Sons, New York, p. 769.
- Pillai, S.U. and Menon, D. 2003, *Reinforced Concrete Design*, 2nd edition, Tata McGraw Hill Publishing Company Ltd, New Delhi, p. 875.
- Placas, A. and P.E. Regan 1971, 'Shear Failures of Reinforced Concrete Beams', *Proceedings, American Concrete Institute*, Vol. 68, No. 10, pp. 763–73.
- Rai, D.C. 2008, *Structural Use of Unreinforced Masonry*, <http://www.iitk.ac.in/nicee/IITK-GSDMA/EQ12b.pdf>, last accessed on 17 October 2012.
- Rao, Prakash D.S., *Design Principles and Detailing of Concrete Structures*, Tata McGraw-Hill Publishing Company Ltd, 1995, p. 360.
- Razaqpur, A.G. and A. Ghali 1986, 'Design of Transverse Reinforcement in Flanges of T-beams', *ACI Structural Journal*, Vol. 83, No. 6, pp. 680–9.
- Revathi P. and D. Menon 2007, 'Slenderness Effects in Reinforced Concrete Beams', *ACI Structural Journal*, Vol. 104, No. 4, pp. 412–9.
- Revathi P. and D. Menon 2009, 'Assessment of Flexural Strength of Slender RC Rectangular Beams', *The Indian Concrete Journal*, Vol. 83, No. 5, pp. 15–24.
- Rogowsky, D.M. and J.G. MacGregor 1986, 'Design of Reinforced Concrete Deep Beams', *Concrete International*, ACI, Vol. 8, No. 8, pp. 46–58.
- Rüsch, H. 1960, 'Research Toward a General Flexural Theory for Structural Concrete', *ACI Journal*, Vol. 57, No. 1, pp. 1–28.
- Russo, G., R. Venir, and M. Pauletta 2005, 'Reinforced Concrete Deep Beams—Shear Strength Model and Design Formula', *ACI Structural Journal*, Vol. 102, No. 3, pp. 429–37.

- Sain, T. and J.M. Kishen 2007, 'Prediction of Fatigue Strength in Plain and Reinforced Concrete Beams', *ACI Structural Journal*, Vol. 104, No. 5, pp. 621–8.
- Schmidt, M. and E. Fehling 2007, *Ultra High Performance Concrete (UHPC), 10 Years of Research and Development at the University of Kassel*, Schriftenreihe Baustoffe und Massivbau, Heft 7, Kassel University Press, p. 475, (also see <http://www.uni-kassel.de/upress/online/frei/978-3-89958-347-2.volltext.frei.pdf>, last accessed on 21 May 2011).
- Seguirant, S.J., R. Brice, and B. Khaleghi 2010, 'Making Sense of Minimum Flexural Reinforcement Requirements for Reinforced Concrete Members', *PCI Journal*, Vol. 55, pp. 64–85.
- Seo, S.-Y., S.-Y. Yoon, and W.-J. Lee 2004, 'Structural Behavior of R.C. Deep Beam with Headed Longitudinal Reinforcement', *13th World Conference on Earthquake Engineering*, Vancouver, 1–6 August 2004, Paper No. 58, (also see http://www.iitk.ac.in/nicee/wcee/article/13_58.pdf, last accessed on 20 June 2012).
- Shuraim A.B. and A.I. Al-Negheimish 2011, 'Design Considerations for Joist Floors with Wide-shallow Beams', *ACI structural Journal*, Vol. 108, No. 2, pp. 188–96.
- Sinha, S.N. 1996, *Handbook of Reinforced Concrete Design*, Tata McGraw-Hill Publishing Company Ltd, New Delhi, p. 530.
- SP 24(S&T):1983, *Explanatory Handbook on Indian Standard Code of Practice for Plain and Reinforced Concrete*, Bureau of Indian Standards, New Delhi, p.164.
- Subramanian, N. 1975, 'Optimum Design of Rectangular Beams in Accordance with IS:456-1964', *Design Incorporating Indian Builder*, Vol. 19, No. 8, pp. 38–9.
- Subramanian, N. 2010, 'Limiting Reinforcement Ratios for RC Flexural Members', *The Indian Concrete Journal*, Vol. 84, No. 9, pp. 71–80.
- Varghese, P.C. 2006, *Limit States Design of Reinforced Concrete*, 2nd edition, Prentice Hall of India Ltd, New Delhi, p. 545.
- Varyani, U.H., and A. Radhaji 2005, *Design Aids for Limit State Design of Reinforced Concrete Members*, Khanna Publishers, Nai Sarak, Delhi, p. 420
- Vivek Abhyankar, Personal communication, 19 April 2011.
- Walker, A. and A.P. Dhakal 2009, 'Assessment of Material Strain Limits for Defining Plastic Regions in Concrete Structures', *Bulletin of the NZSEE*, Vol. 42, No. 2, pp. 86–95.
- Wang, C.K. and C.G. Salmon 2002, *Reinforced Concrete Design*, 6th edition, John Wiley and Sons Inc., Hoboken, pp. 558–60.
- Washa, G.W. and P.G. Fluck 1952, 'Effect of Compressive Reinforcement on the Plastic Flow of Reinforced Concrete Beams', *Proceedings, ACI Journal*, Vol. 49, No. 4, pp. 89–108.
- Whitney, C.S., 'Design of reinforced concrete members under flexure or combined flexure and direct compression', *ACI Journal Proceedings*, Vol. 8, No.4, Mar-April 1937, pp. 483–498.
- Wight, J.K. and J.G. MacGregor 2009, *Reinforced Concrete: Mechanics and Design*, 5th edition, Pearson Prentice Hall, New Jersey, p. 1112.
- Wight, J.K. and G.J. Parra-Montesinos 2003, 'Strut-and-tie Model for Deep Beam Design', *Concrete International, ACI*, Vol. 25, No. 5, pp. 63–70.
- Zhang, J., V.C. Li, and H. Stang 2011, 'Size Effect on Fatigue in Bending of Concrete', *Journal of Materials in Civil Engineering, ASCE*, Vol. 13, No. 6, pp. 446–53.

DESIGN FOR SHEAR

6.1 INTRODUCTION

A beam may be subjected to shear, axial thrust or tension, or torsion, in addition to the predominant flexure. Chapter 5 dealt with flexure alone, whereas this chapter deals with flexural shear, which is simply referred to as *shear*, associated with varying bending moments. According to traditional design philosophy, bending moment and shear force are treated separately, even though they coexist. It is important to realize that shear analysis and design are not really concerned with shear as such. The shear stresses in most beams may be below the direct shear strength of concrete. We are in fact concerned with *diagonal tension stress*, which is a result of the combination of flexural and shear stress. Hence, shear failure is often termed as *diagonal tension failure*.

The method followed in major parts of this chapter, which is often called the *sectional design model*, is intended to be used in the 'flexural regions' of members. The sectional design model is one in which the assumption that plane sections remain plane after bending is reasonably valid. In this model, the flexural longitudinal reinforcement is designed for the effects of flexure and any additional axial force, and the transverse reinforcement is designed for shear and torsion. In the case of slabs, this type of shear is called *one-way shear*, which is different from the *two-way* or *punching shear*, which normally occurs in flat slabs near the slab-column junctions.

The shear behaviour of reinforced beams has been researched for more than a century and the foundations of knowledge on shear were provided by Mörch in 1909. Earlier, research on shear behaviour has established that the behaviour before cracking is not affected significantly by shear reinforcements and they come into play only after cracking (Fergusson 1973; Park and Paulay 1975). Furthermore, after cracking, the efforts to represent the behaviour on the basis of stresses were not satisfactory. Hence, the behaviour after cracking is often explained in terms of strength, rather than stresses (Regan and Yu 1973; Warner, et al. 1976). It must also

be remembered that reinforced concrete (RC) is a composite material and shows non-isotropic mechanical properties, which complicates the formulation of relationships between stresses and strains in the material. The design recommendations of several codes of practice are based on the empirical relations derived from laboratory tests. An excellent review of research is provided by the report of the ACI-ASCE Committee 326 (now 426) (1962 and 1973), Regan (1993), Duthinh and Carino (1996), and the ACI-ASCE Committee 445 report (1998).

The Canadian code and AASHTO LRFD sectional design model for shear is a hand-based shear design procedure derived from the *modified compression field theory* (MCFT), developed at the University of Toronto by Prof. Collins, Prof. Vecchio, and associates, which is also discussed briefly in this chapter. This method considers the combined efforts of flexure, shear, axial load (compression or tension), and torsion.

The other model called *strut-and-tie model* is described in Appendix B. This method is suitable at regions where plane sections do not remain plane after bending, that is, in deep beams, members with shear span to effective depth ratio (a_v/d) less than 1.5 (for a beam subjected to a concentrated load, the distance from the load to the support, usually denoted by a_v , is called the *shear span*), pile caps, brackets, and regions near discontinuities or changes in cross section. The strut-and-tie method may require several trials to produce an efficient model and does not provide a unique solution.

There may be certain circumstances where consideration of direct shear is important. One such example is the design of composite members combining precast beams and cast-in-place to slabs, where horizontal shear stresses at the interface between the beam and slab have to be considered. As it is inappropriate to use the methods developed for diagonal tension in such cases, one has to resort to the *shear friction* concept. This concept, used for the design of brackets and corbels, is also explained.

It is well known that inadequate shear design is inherently more dangerous than inadequate flexural design, since shear failures normally exhibit fewer significant signs of distress and warnings than flexural failures. However, unlike flexural design for which the classical beam theory (plane sections remain plane) allows for an accurate, rational, and simple design for both uncracked and cracked members, the determination of shear strength of RC members is based on several assumptions, all of which are not yet proved to be correct. It is important to realize that there is a considerable disagreement in the research community about the factors that most influence shear capacity.

As learnt from Chapter 5, the main objective of an RC designer is to produce ductile behaviour in the members such that ample warning is provided before failure. To achieve this goal, RC beams are often provided with *shear reinforcement*. Moreover, the codes are usually more conservative with regard to shear (by providing larger safety factors) compared to bending (for example, in the ACI code, a strength reduction factor of 0.75 is used for shear compared to 0.9 used for tension-controlled flexure). Thus, the design methods and detailing rules prescribed in the code will result in a strength that is governed by bending failure rather than shear failure, if the member is overloaded.

6.2 BEHAVIOUR OF REINFORCED CONCRETE BEAMS UNDER SHEAR

The behaviour of RC beams under shear may be categorized into the following three types:

1. Behaviour when the beam is not cracked
2. Cracked beam behaviour when no shear reinforcements are provided
3. Cracked beam behaviour when shear reinforcements are provided

These three types of behaviour are briefly discussed in the following subsections.

6.2.1 Behaviour of Uncracked Beams

The loads acting on a structural element is in equilibrium with the reactions, and the bending moment and shear force diagrams can be drawn for the entire span as shown in Fig. 6.1. Before cracking, the RC beam may be assumed to behave like a homogenous beam. Thus, using basic mechanics of materials, the flexural stress f_x and the shear stress τ at any point in the section located at a distance y from the neutral axis is given by

$$\begin{aligned} f_x &= \frac{My}{I} \\ \tau &= \frac{VQ_v}{Ib} \end{aligned} \quad (6.1)$$

where M is the bending moment at any cross section, I is the moment of inertia about the neutral axis ($bD^3/12$), y is the distance of fibre from the neutral axis, V is the shear force from the shear diagram at the point where shear stress is calculated, Q_v is the first moment of the area about the neutral axis of the portion of the section above the layer at distance y from the neutral axis $Q_v = \int y dA = \sum \bar{y}_j A_j$, b is the width of the beam at the point where shear stress is calculated, and A_j is the sectional area from the top fibre to the level y from the neutral axis. The bending and shear stress distributions across the cross section of rectangular beam are shown in Fig. 6.2. It should be noted that the shear stress variation is parabolic, with the maximum value at the neutral axis (with $Q_{v,\max} = (bD/2)(D/4) = bD^2/8$, $\tau_{\max} = 1.5V/bD$) and zero values at the top and bottom of the section. Thus, the maximum shear stress is 50 per cent more than the average shear stress.

Neglecting any vertical normal stress f_y caused by the surface loads, the combined flexural and shear stresses can be resolved into equivalent *principal stresses* f_1 and f_2 , acting on orthogonal planes and inclined at an angle α to the beam axis, as shown in Figs 6.3(a)–(f). The direction of the principal compressive stresses is in the shape of an arch, whereas that of the principal tensile stresses is in the shape of a catenary or suspended chain. As we know, the maximum bending stresses occur at mid-span and the direction of stresses tends to be parallel to the axis of the beam. Near the supports, the shear forces have the greatest value and hence the principal stresses become inclined; greater the shear force, greater the angle of inclination.

These principal stresses are given by the classical formula

$$f_1 = \frac{f_x}{2} + \sqrt{\frac{f_x^2}{4} + \tau^2} \quad (6.2a)$$

$$f_2 = \frac{f_x}{2} - \sqrt{\frac{f_x^2}{4} + \tau^2} \quad (6.2b)$$

where f_1 is the major principal stress and f_2 is the minor principal stress, tension being taken as positive. The direction of the major principal stress from the beam axis is given by

$$\tan 2\alpha = \frac{2\tau}{f_x} \quad (6.2c)$$

The principal stresses and their angle of inclination at any point can be found using Mohr's circle for stress, as explained in any mechanics of material textbook like Subramanian (2010). The elements located at the neutral axis are subjected to pure shear (see Figs 6.3b and c) where τ is the maximum and $f_x = 0$. Hence, $f_1 = f_2 = \tau_{\max}$ and $\alpha = 45^\circ$. Since concrete is weak in tension, tension cracks as shown in Fig. 6.3(c) will develop

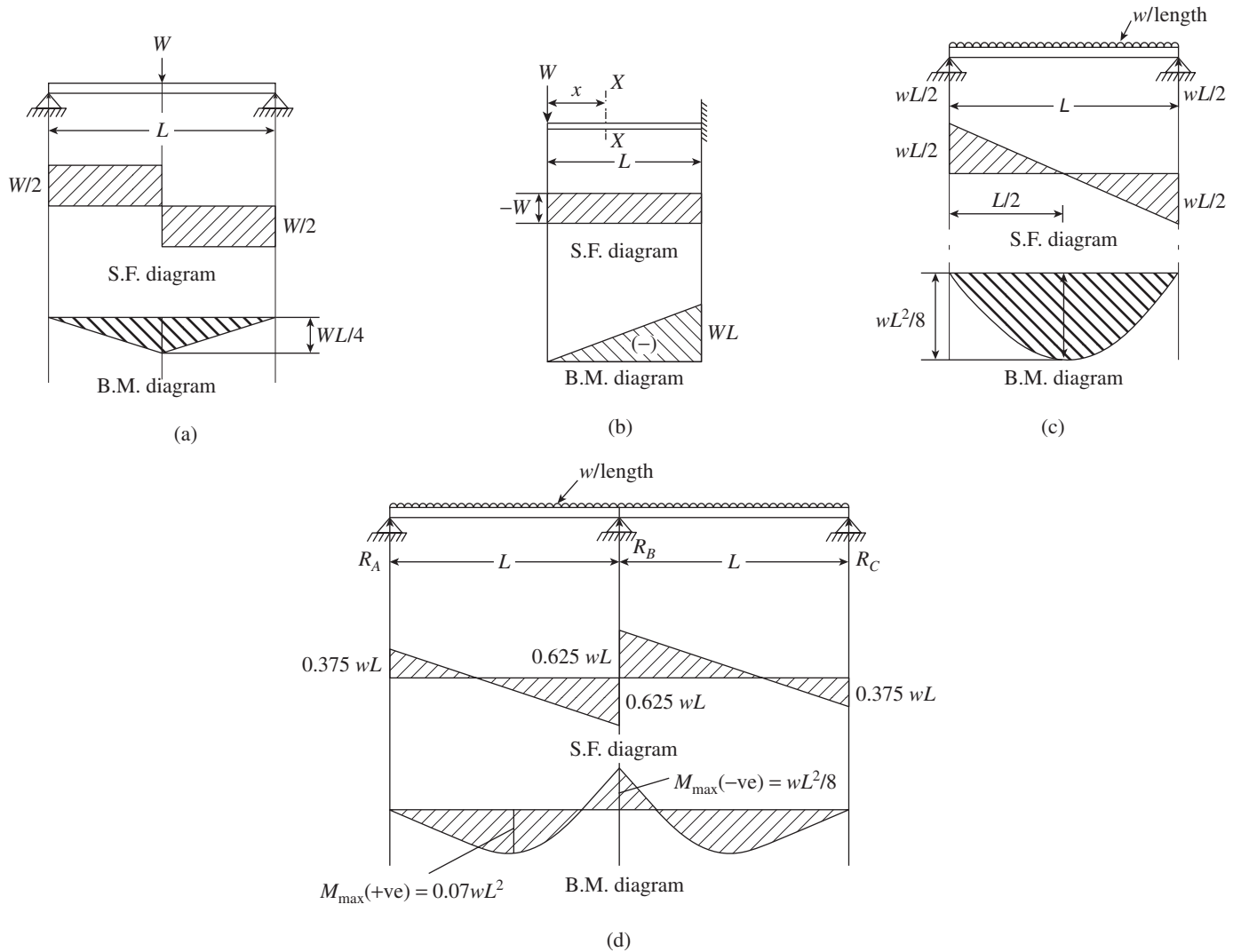


FIG. 6.1 Shear force (S.F.) and bending moment (B.M.) diagrams for typical beam elements (a) Simply supported beam with concentrated load (b) Cantilever beam (c) Simply supported beam with uniformly distributed load (d) Continuous beam

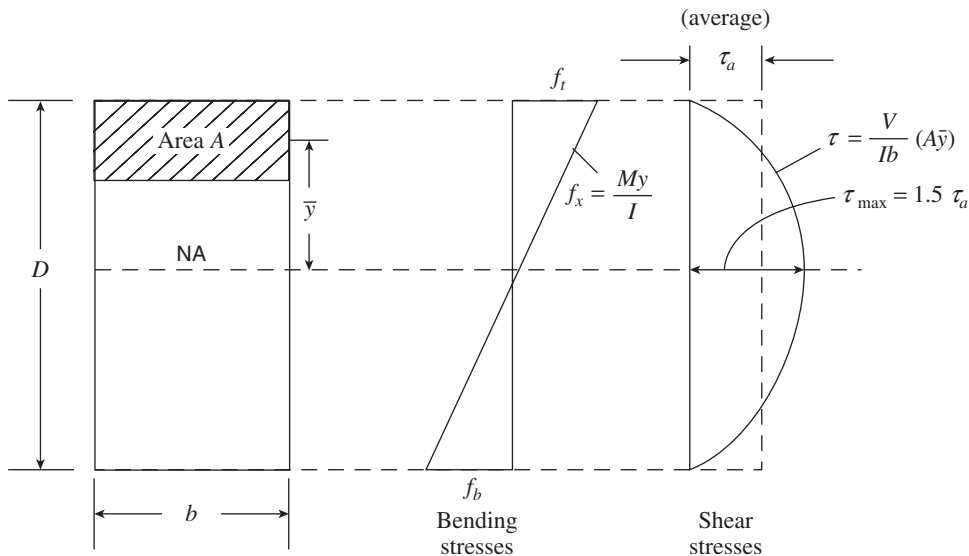


FIG. 6.2 Flexural and shear stress variation across the cross section of a rectangular beam

in a direction perpendicular to the principal tensile stresses. Thus, the compressive stress trajectories (see Fig. 6.4a) indicate the potential crack pattern (depending on the magnitude of tensile stresses developed). It should be noted that once a crack develops, the stress distribution shown in Fig. 6.3 is no longer valid in that region, as the effective section properties get altered and Eq. (6.2) is no longer valid. The theoretical reinforcement required to resist such cracking is shown in Fig. 6.4(b), which is difficult to provide. Hence, transverse reinforcement, as discussed in Section 6.2.3 is often provided.

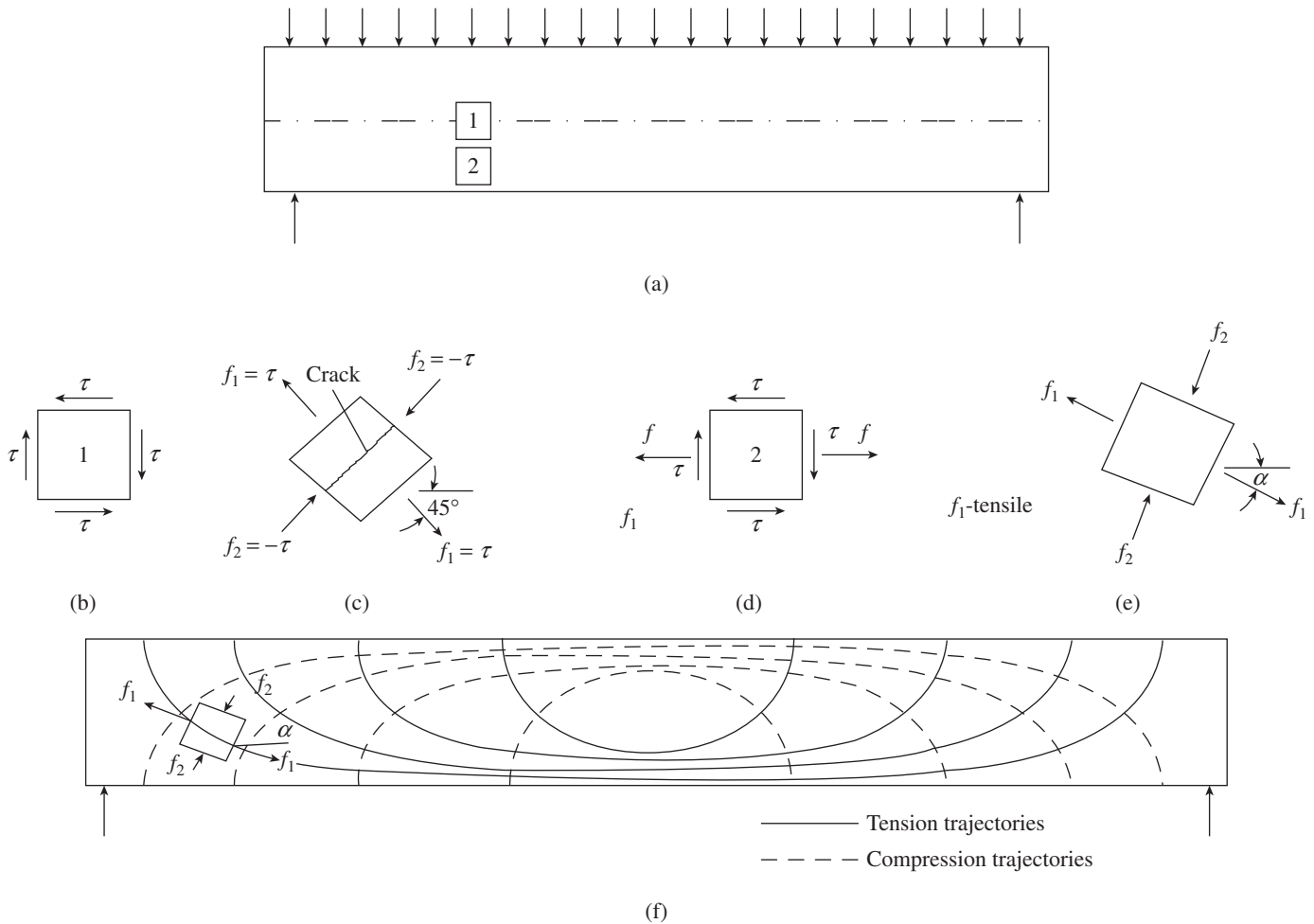


FIG. 6.3 Stress distribution in RC beams (a) Beam with loading (b)–(e) Stresses in elements 1 and 2 (f) Principal stress distribution

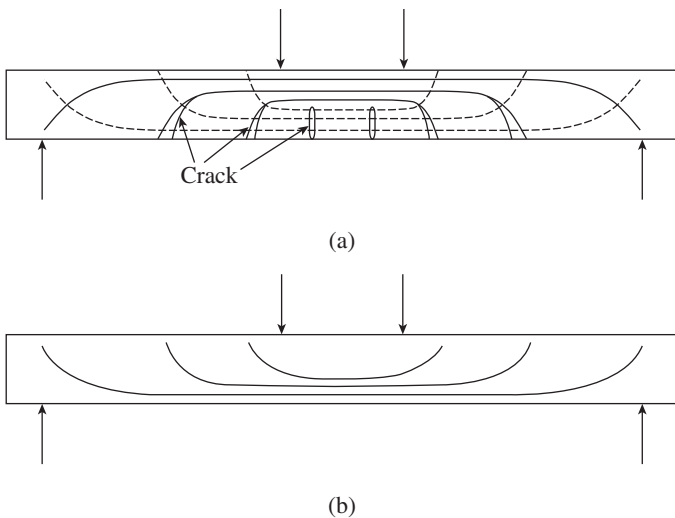


FIG. 6.4 Cracking of beams due to tensile stresses (a) Typical cracking (b) Theoretical reinforcement required to resist such cracking

Types of Cracks

The typical crack pattern of a beam subjected to loads is shown in Fig. 6.5. Near the mid-span, where the bending moment predominates, the tensile stress trajectories are

crowded and are horizontal in direction as shown in Fig. 6.3(f). Hence, *flexural cracks* perpendicular to the horizontal stress trajectories (i.e., cracks will be vertical) will appear even at small loads. These flexural cracks are controlled by the longitudinal tension bars.

In the zones where shear and bending effects combine together, that is, in zones midway between the support and mid-span, the cracks may start vertically at the bottom, but will become inclined as they approach the neutral axis due to shear stress (see Fig. 6.5). These cracks are called *flexure shear cracks*.

Near the supports that contain concentrated compressive forces, the stress trajectories have a complicated pattern. As shear forces are predominant in this section, the stress trajectories are inclined (see Fig. 6.3f) and cracks inclined at about 45° appear in the mid-depth of the beam (these cracks are rare and occur mainly near the supports of deep and thin-webbed beams, as in I-section beams, or at inflection points of continuous beams). These cracks are termed as *web-shear cracks* or *diagonal tension cracks*. Appropriate *shear reinforcement* has to be provided to prevent the propagation of these cracks.

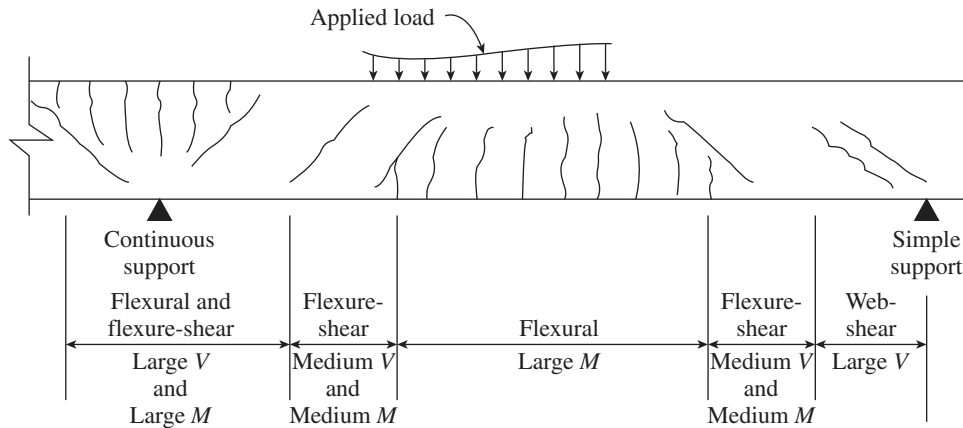


FIG. 6.5 Typical crack pattern in an RC beam

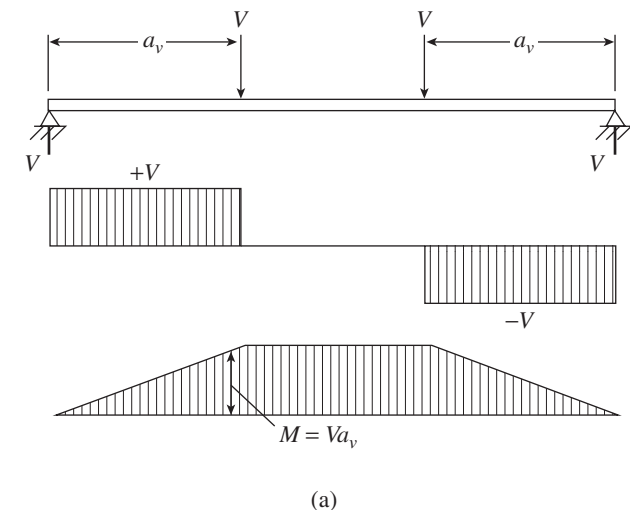
The direct tensile strength ranges between $0.22 \sqrt{f_{ck}}$ and $0.37 \sqrt{f_{ck}}$ for normal density concrete. Thus, in regions of the beam where there is a large shear and small moment, diagonal tension cracks appear at an average or nominal shear stress of about $0.27 \sqrt{f_{ck}}$. Hence,

$$\tau_{cr} = \frac{V_{cr}}{b_w d} = 0.27 \sqrt{f_{ck}} \quad (6.3a)$$

where V_{cr} is the shear force at which the diagonal tension crack may occur, τ_{cr} is the average critical shear stress at which the crack appears, b_w is the breadth of web, and d is the effective depth of beam.

However, in the presence of large moments (for which adequate longitudinal bars are provided), the nominal shear stress at which diagonal tension cracks form has been found from experiments as

$$\tau_{cr} = \frac{V_{cr}}{b_w d} = 0.15 \sqrt{f_{ck}} \quad (6.3b)$$

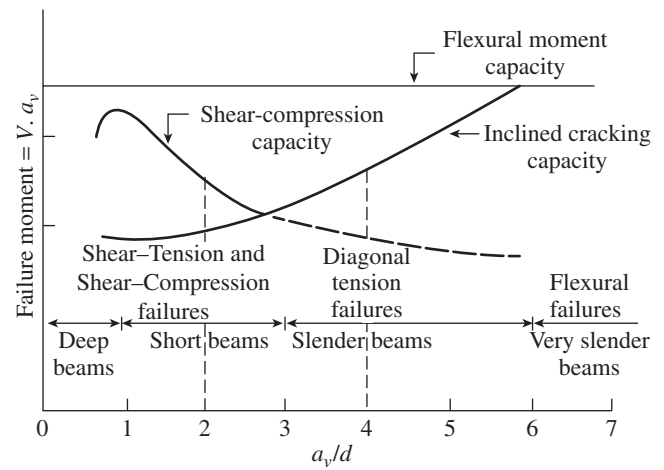


(a)

6.2.2. Behaviour of Beams without Shear Reinforcement

The mechanism of the brittle-type diagonal tensile failure of RC beams with no shear reinforcement (stirrups) is complex and not yet fully understood. The behaviour of beams failing in shear may vary widely, depending on the a_v/d ratio (shear span to effective depth ratio) and the amount of web reinforcement (see Fig. 6.6).

Very short shear spans, with a_v/d ranging from zero to one, develop inclined cracks joining the load and the support. These cracks, in effect, change the behaviour from beam action to *arch action*. Such beams with the a/d ratio of zero to one are termed as *deep beams*. In these beams, the longitudinal tension reinforcement acts as the tension tie of a tied arch and has uniform tensile force from support to support (see Fig. 6.7). These beams normally fail due to the anchorage failure at the ends of the tension tie (see Fig. 6.7).



(b)

FIG. 6.6 Effect of a/d ratio on shear strength of beams without stirrups (a) Beam, shear force, and moment diagrams (b) Variation in shear capacity with a/d for rectangular beams

Source: ACI-ASCE Committee 426 1973, reprinted with permission from ASCE

Comparison of Eqs (6.3b) and (6.3a) shows that the large values of bending moments reduce the shear force at which diagonal shear cracks form to about 50 per cent of the value at which they would form if the bending moment is nearly zero.

Sometimes, inclined cracks propagate along the longitudinal tension reinforcement towards the support. Such cracks are termed as *tensile splitting cracks* or *secondary cracks*.

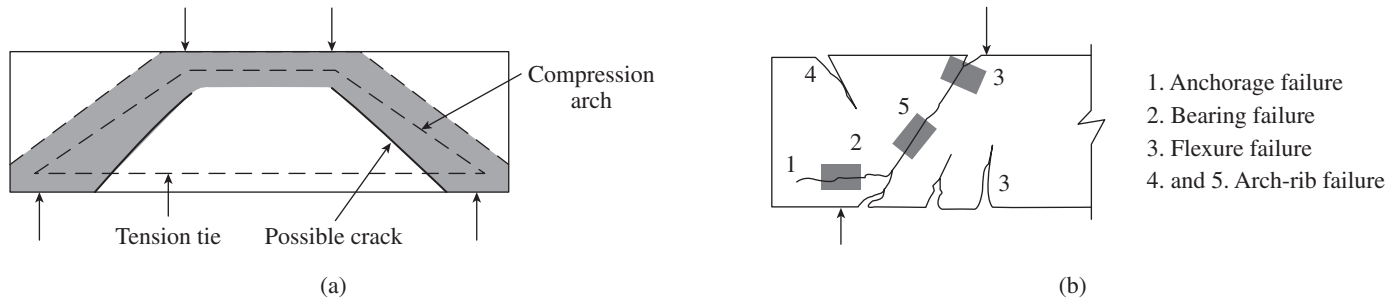


FIG. 6.7 Modes of failure of deep beams (a) Arch action (b) Types of failures

Source: ACI-ASCE Committee 426 1973, reprinted with permission from ASCE

Beams with a/d ranging from 1 to 2.5 develop inclined cracks and, after some internal redistribution of forces, carry some additional loads due to arch action. These beams may fail by splitting failure, bond failure, shear tension, or shear compression failure (see Fig. 6.8).

For slender shear spans, having a_v/d ratio in the range of 2.5 to 6, the crack pattern will be as shown in Figs 6.8(a) and (b). When the load is applied and gradually increased, flexural cracks appear in the mid-span of the beams, which are more or less vertical in nature. With further increase of load, inclined shear cracks develop in the beams, at about $1.5d-2d$ distance from the support, which are sometimes called *primary shear cracks*. The typical cracking in the slender beams without transverse reinforcement, leading to the failure, involves two branches. The first branch is the slightly inclined shear crack, with the typical height of the flexural crack. The second branch of the crack, also called secondary shear crack or *critical crack*, initiates from the tip of the first

crack at a relatively flatter angle, splitting the concrete in the compression zone. It is followed by a tensile splitting crack (destruction of the bond between steel reinforcement and concrete near the zone of support), as shown in Fig. 6.8(a). Depending on some geometric parameters of the beam, the critical crack further extends in the compression zone and finally meets the loading point, leading to the collapse of the beam. The failure is by shear compression (see Fig. 6.8c) due to the crushing of concrete, without ample warning and at comparatively small deflection. The nominal shear stress at the diagonal tension cracking at the development of the second branch of inclined crack is taken as the shear capacity of the beam.

Very slender beams, with a/d ratio greater than 6.0, will fail in flexure prior to the formation of inclined cracks. It should be noted that the inclined cracking loads of short shear spans and slender shear spans are approximately equal. Hence, the a_v/d ratio is not considered in the equations for shear at

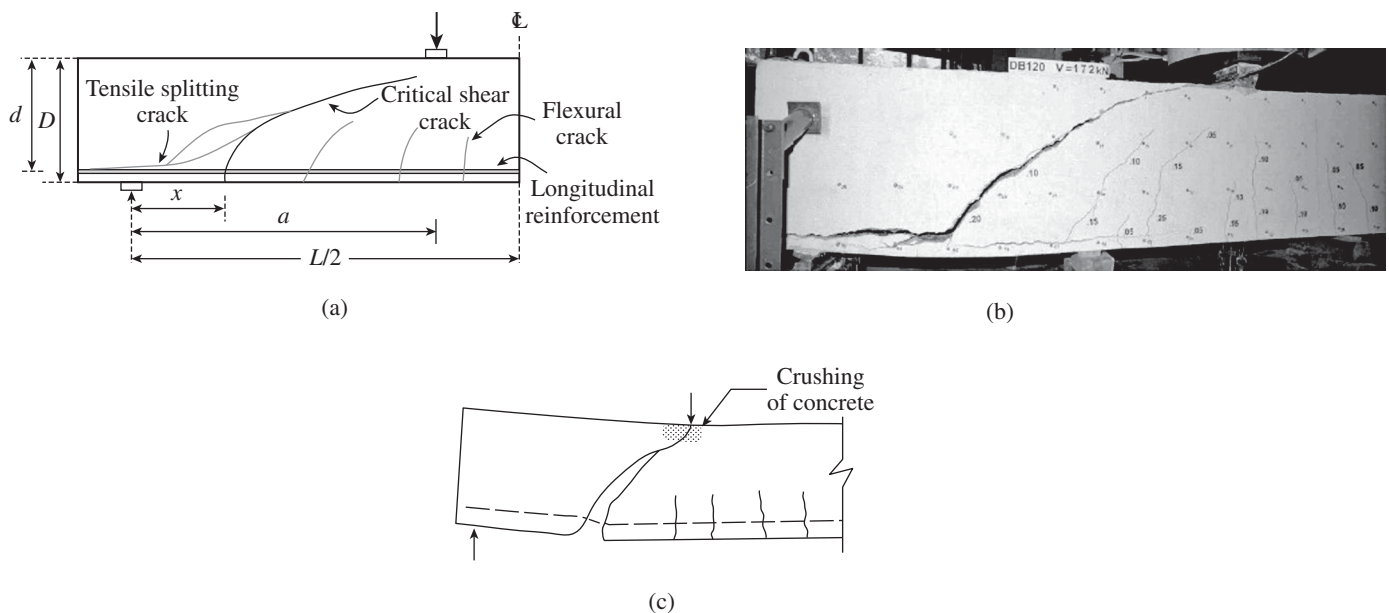


FIG. 6.8 Behaviour of beam without shear reinforcement (a) Typical crack pattern (b) Typical failure of beam without shear reinforcement (c) Shear-compression failure

Sources: (a) and (c)—ACI-ASCE Committee 426 1973, reprinted with permission from ASCE

(b)—Angelakos, et al. 2001, reprinted with permission from ACI

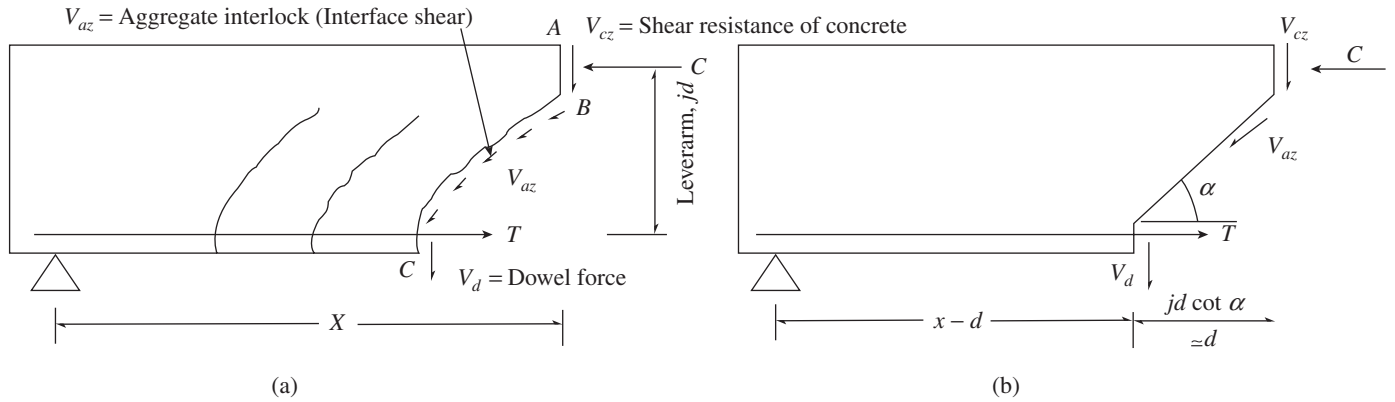


FIG. 6.9 Equilibrium of internal forces in a cracked beam without stirrups (a) Actual (b) Idealized

inclined cracking. In the case of slender beams, inclined cracking causes sudden failure if the beam does not have shear reinforcement.

Flexural shear cracking load cannot be calculated by computing the principal stresses in an uncracked beam. Hence, empirical equations have been derived to calculate these loads. The internal forces across an inclined crack in a cracked beam without shear reinforcement are shown in Fig. 6.9. Thus, shear is transferred across the line ABC by the (a) shear in the compression zone of concrete, V_{cz} , (b) vertical component of the shear transferred across the crack by the interlock of aggregate particles on the two faces of the concrete, V_{az} , and (c) dowel action of the longitudinal reinforcement, V_d .

The equilibrium of vertical forces gives the following equation:

$$V = V_{cz} + V_{az} + V_d \quad (6.4)$$

For rectangular sections, V_{cz} , V_{az} , and V_d may be in the range 20–40 per cent, 33–50 per cent, and 15–25 per cent, respectively (ACI-ASCE Committee 426 1973).

Taylor (1969) observed that 40–60 per cent of the shear forced is carried by V_d and V_{az} , after the inclined cracking. As the load is increased, the crack widens, the contribution of V_{az} decreases, and the contribution of V_{cz} and V_d increases. Due to the doweling action, a splitting crack appears along the longitudinal reinforcement (see Fig. 6.8a), resulting in the reduction of V_d to a minimum value and the beam fails subsequently by the crushing of concrete. In general, the shear failure of a slender beam without stirrups is sudden and dramatic. In high-strength concrete (HSC) beams, the failure is sudden and explosive.

6.2.3 Types of Shear or Web Reinforcements

Shear or web reinforcements, called *stirrups*, *links*, or *studs*, may be provided to resist shear in several different ways such as the following (NZS 3101-06, Subramanian 2012):

1. Stirrups perpendicular to the longitudinal flexural (tension) reinforcement of the member, normally vertical (Fig. 6.10a)

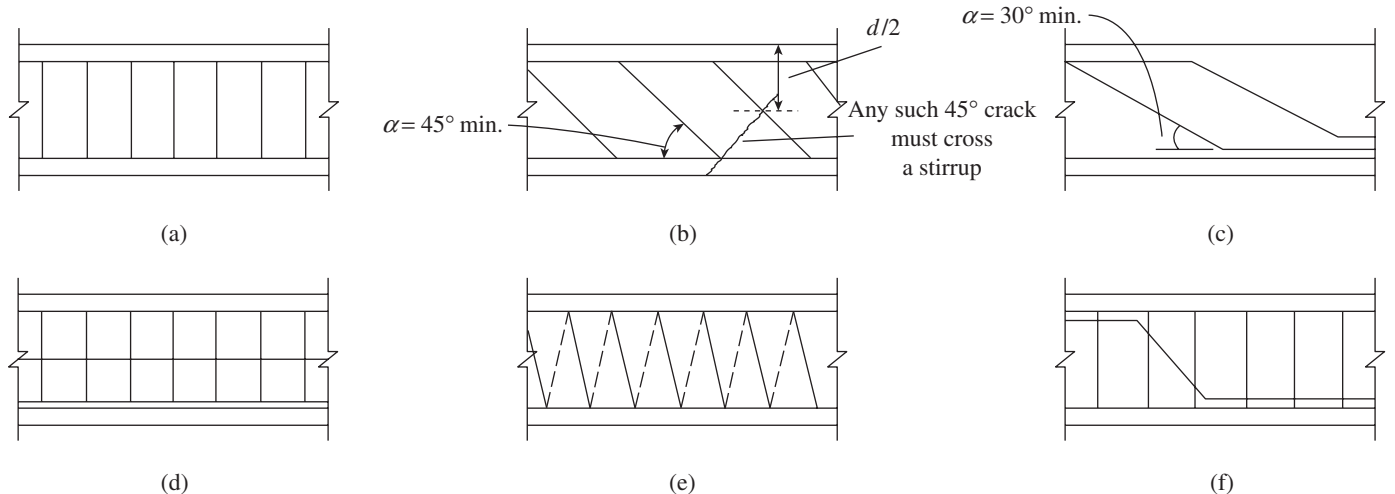


FIG. 6.10 Types and arrangement of stirrups (a) Vertical stirrups (b) Inclined stirrups (c) Longitudinal bent bars (d) Welded wire fabric (e) Spirals (f) Combined bent bars and vertical stirrups

- Inclined stirrups making an angle of 45° or more with the longitudinal flexural reinforcement of the member (Fig. 6.10b)
- Bent-up longitudinal reinforcement, making an angle of 30° or more with the longitudinal flexural reinforcement (Fig. 6.10c)
- Welded wire mesh, which should not be used in potential plastic hinge locations (Fig. 6.10d). They are used in small, lightly loaded members with thin webs and in some precast beams (Lin and Perng 1998).
- Spirals (Fig. 6.10e)
- Combination of stirrups and bent-up longitudinal reinforcement (Fig. 6.10f)
- Mechanically anchored bars (head studs) with end bearing plates or a head having an area of at least 10 times the cross-sectional area of bars (see Fig. 6.11)
- Diagonally reinforced members (as in diagonally reinforced coupling beams; see Chapter 16 for details)
- Steel fibres in potential plastic hinge locations of members

IS 456 allows the use of only vertical stirrups, bent-up bars along with stirrups, and inclined stirrups.

The inclusion of web reinforcement such as stirrups does not fundamentally change the previously described mechanism of shear resistance. The presence of stirrups contributes to the strength of shear mechanisms in the following ways (Park and Paulay 1975):

- They carry part of the shear.
- They improve the contribution of the dowel action. The stirrup can effectively support a longitudinal bar that is being crossed by a flexural shear crack close to a stirrup.

- They limit the opening of diagonal cracks within the elastic range, thus enhancing and aiding the shear transfer by aggregate interlock.
- When stirrups are closely spaced, they provide confinement to the core concrete, thus increasing the compression strength of concrete, which will be helpful in the locations affected by the arch action.
- They prevent the breakdown of bond when splitting cracks develop in the anchorage zones because of the dowel and anchorage forces.
- The strength of the 'concrete tooth' between two adjacent shear cracks of the beam and located below the neutral axis is important for developing shear strength (see Fig. 6.9). Each of these small blocks acts as a cantilever with its base at the compression zone. The resistance of the tooth is a function of flexural resistance, dowel effects, and interface forces. The stirrups suppress the flexural tensile stresses in the cantilever blocks by means of the diagonal compressive force C_d resulting from the truss action (see also Section 6.2.4).

Leonhardt and Walther (1964) found that compared to the other types of shear or web reinforcement, inclined stirrups yield the best performance in terms of cracking or crack width and ultimate capacity for the same area of steel followed by vertical stirrups and bent-up bars (see Fig. 6.12).

Vertical Stirrups

The transverse reinforcement in the form of shear stirrups will usually be vertical and taken around the outermost tension and compression longitudinal reinforcements along the faces

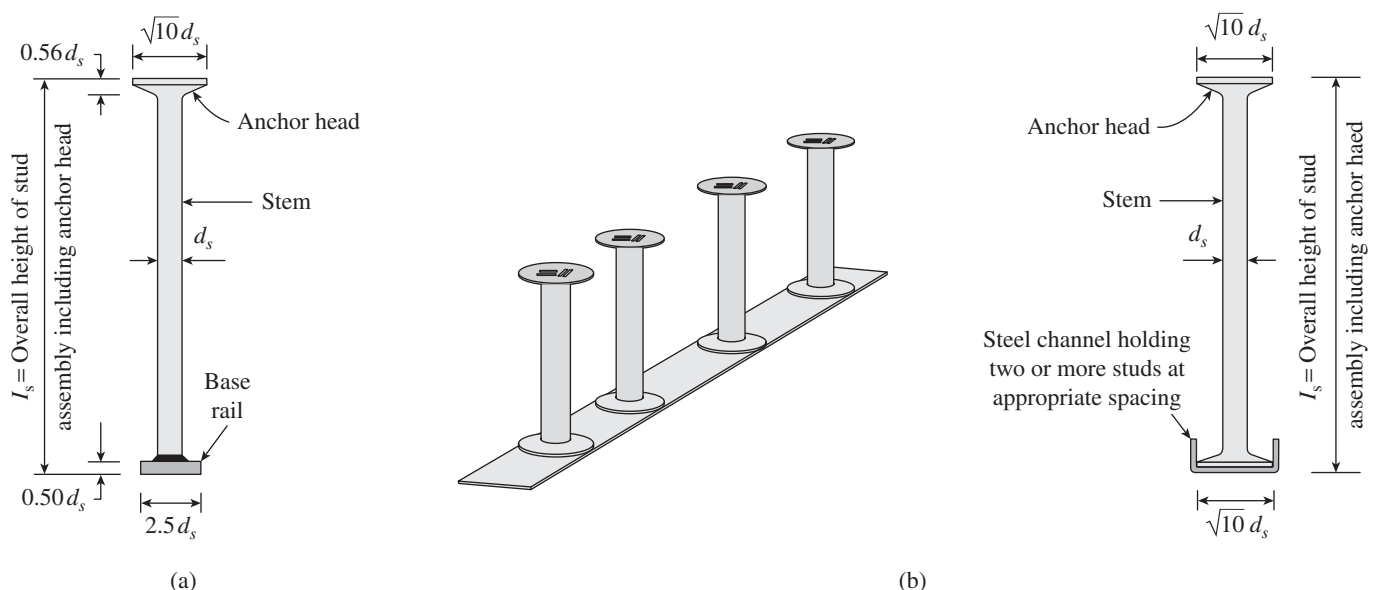


FIG. 6.11 Headed shear stud reinforcement conforming to ASTM A1044/A1044M (a) Single-headed studs welded to base rail (b) Double-headed studs crimped into a steel channel

Source: ACI 421.1 R-08, reprinted with permission from ACI

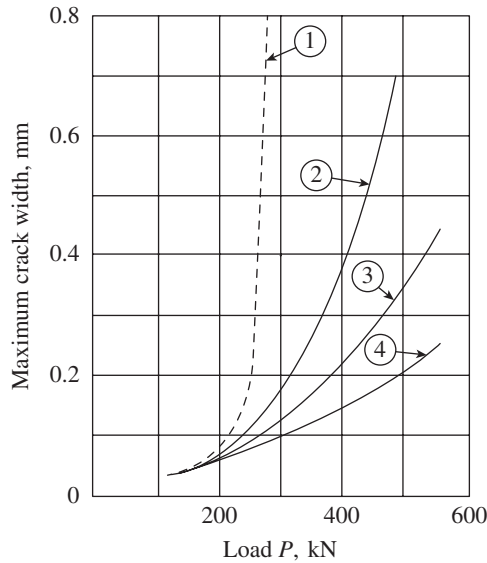
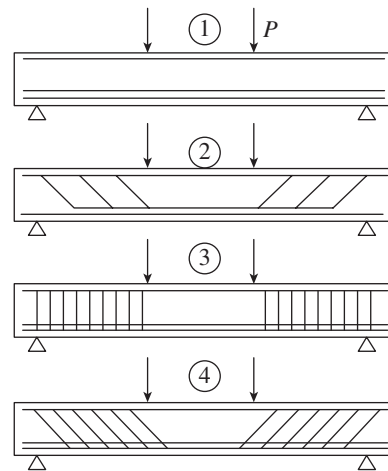


FIG. 6.12 Performance of different types of web reinforcement

of the beam, as shown in Fig. 6.13. In T- and I-beams, they should pass around the longitudinal bars located close to the outer face of the web. The most common types are \sqsubset shaped, but it can be in the form of single vertical prong or in the shape of $\sqsubset \sqsubset$ as shown in Figs 6.13(a)–(e). Multiple stirrups in the shape as shown in Fig. 6.13(e) may prevent splitting in the plane of the longitudinal bars. Hence, they are more desirable for wide beams than the arrangement shown in Fig. 6.13(d). The stirrup arrangements shown in Figs 6.13(a)–(e) are not closed at the top and hence their placement at site is relatively easy compared to the closed stirrups. However, they should be used in beams with negligible torsional moment.



Closed stirrups, which are suitable for beams with significant torsion and in earthquake zones, are shown in Figs 6.13(f)–(k). The type shown in Fig. 6.13(f) is frequently adopted in India—the vertical hoop is a closed stirrup having a 135° hook with a 6–10 diameter extension (but not greater than 65–75 mm) at each end that is embedded in the confined core (see Figs 6.13f and j). It can also be made of two pieces of reinforcement as shown in Fig. 6.13(g) with a U-stirrup having a 135° hook and a 10 diameter extension (but not lesser than 75 mm) at each end, embedded in concrete core and a cross-tie. A cross-tie is a bar having a 135° hook with a

10 diameter extension (but not lesser than 75 mm) at each end. It should be noted that the draft IS 13920 code suggests a six diameter extension, which is not greater than 65 mm. It is also possible to have the cross-tie with a 135° hook at one end and 90° hook at the other end for easy fabrication, as shown in Figs 6.13(h) and (k). The hooks engage peripheral longitudinal bars. Consecutive cross-ties engaging the same longitudinal bars should have their 90° hooks at the opposite sides of the flexural member (i.e., the cross-ties should be alternated). If the longitudinal reinforcement bars secured by the cross-ties are confined by a slab on only one side of the beam, the 90° hooks of the cross-ties can be placed on that side (see Fig. 6.13(h)). In deep members (especially those with gradually

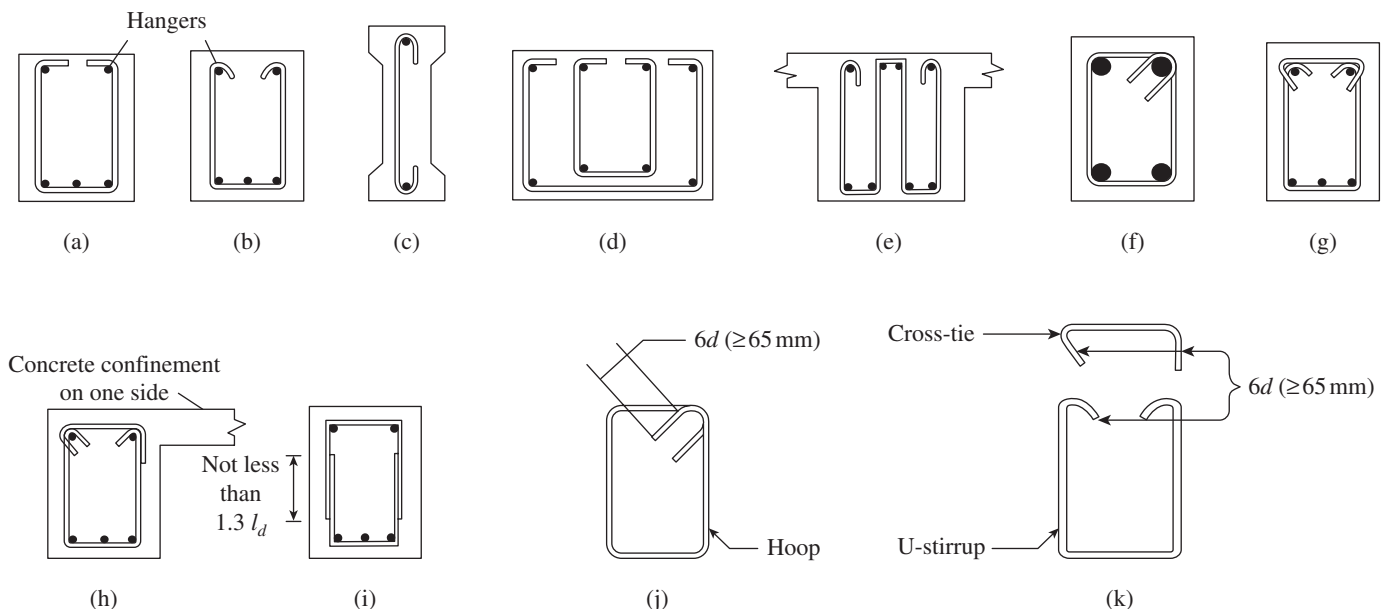


FIG. 6.13 Types of vertical stirrups (a)–(e) Open stirrups for beams with negligible torsion (f)–(i) Closed stirrups with significant torsion (j)–(k) Detail of 135° hook

varying depths), it may be convenient to use lap-spliced stirrups (with a lap length equal to 1.3 times the development length; see Chapter 7 for details), as shown in Fig. 6.13(i). However, this arrangement should not be adopted in seismic zones.

The legs of stirrups should not be too wide apart in order to avoid vertical cracks through the web (see Fig. 6.14). The corner longitudinal bars being rigid attract compression forces to flow towards them, whereas the other inner bars are relatively flexible. If the beam width is greater than 400 mm (> 500 mm if the beam is deeper than 1.0 m), it is desirable to provide four-legged stirrups instead of the usual two-legged ones. This ensures uniform distribution of compression stresses and reduces the possibility of web splitting. When multi-legged stirrups are used, especially in shallow beams, two different arrangements of providing vertical stirrups are feasible, as shown in Fig. 6.15. IS 13920 suggests that the minimum diameter of bars forming hoops should be 6 mm for beams having a clear span less than 5 m and 8 mm if the clear span exceeds 5 m. SP 34:1987 suggests that an arrangement in which overlap of stirrups should be avoided (Fig. 8.8 of SP 34), since such a pattern will make it difficult to fix the reinforcement.

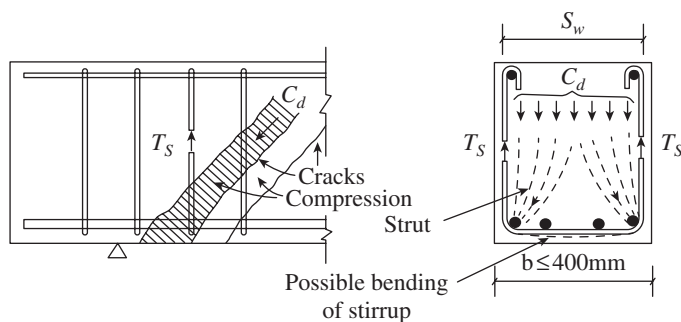


FIG. 6.14 Flow of forces in beams with stirrups

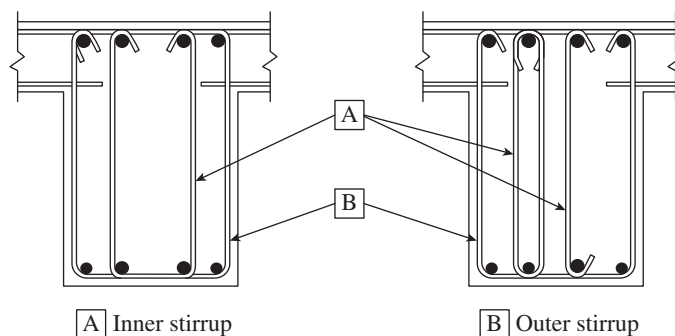


FIG. 6.15 Alternate arrangement of vertical stirrups

Bars called hangers (usually having the same or slightly greater diameter than the stirrups) are placed in the compression side of the beams to support the stirrups, as shown in Figs 6.13–6.15. The stirrups are placed around the tensile longitudinal bars and, to meet anchorage requirements,

hooked around the hangers with 90° or 135° hooks, and placed with 6–10 diameter extensions, as shown in Figs 6.13(j) and (k) (it should be noted that a 90° bend may not ensure satisfactory performance at the ultimate loads, since the concrete cover may spall off in the compression region due to the high tensile forces in the stirrups, which tries to straighten the bend). Bending of the stirrups around the hangers reduces the bearing stresses under the hooks. If the bearing stresses are too high, the concrete may crush and the stirrups will tear out.

Bent-up Bars

The performance of bent-up bars in shear is illustrated in Fig. 6.16. As seen in this figure, large stresses concentrate in the region of such bars, leading to the splitting of concrete when spaced far apart or when placed asymmetrically with reference to the vertical axis of cross section.

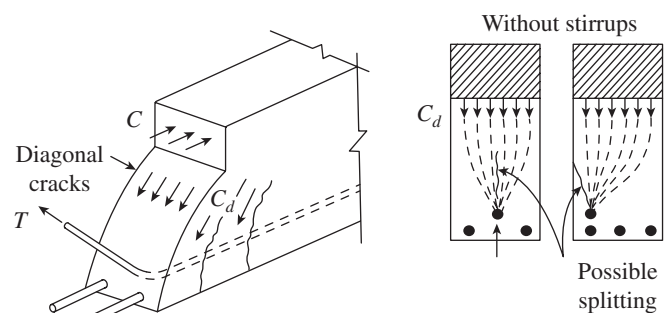


FIG. 6.16 Performance of bent-up bars in shear

The following are some of the disadvantages of bent-up bars (Prakash Rao 1995):

1. They are widely spaced and are few in number. Hence, a crack may not be intercepted by more than one bar, thus resulting in wider cracks than those in beams with stirrups.
2. When some of the bars at a section are bent up, the remaining flexural bars are subjected to higher stresses, resulting in wider flexural cracks.
3. Concrete at the bends may be subjected to splitting forces, resulting in possible web cracking.
4. They do not confine the concrete in the shear region.
5. Reduction of flexural steel due to bent-up bars may result in the shifting of the neutral axis upwards, causing wider cracks in the tension zone.
6. They are less efficient in tying the compression flange and web together.

Due to these reasons and also the fact that bent-up bars do not contribute to the reversal of shear force (as may occur during earthquakes), Clause 6.3.4 of IS 13920 discourages the use of bent-up bars in earthquake zones (SP:24-1983).

However, Clause 40.4 of IS 456 recommends bent-up bars and stirrups together, by specifying that the design capacity of the bent-up bars should not exceed half that of total shear reinforcement. Most designers prefer to design vertical stirrups to take up all the shear requirements and bent-up bars, if any, to provide additional safety against diagonal tension failure.

Inclined Stirrups

Inclined stirrups are similar to vertical stirrups, except that they are placed at an angle of about 45° to the longitudinal axis of the beam. Their behaviour is similar to the bent-up bars. However, they have the following advantages over the bent-up bars:

1. They can be closely spaced, and hence the cracks may be intercepted by more than one bar, resulting in less wider cracks than those in beams with bent-up bars.
2. They confine the concrete in the shear region.
3. They are efficient as vertical stirrups in tying the compression flange and web together.

Moreover, as they are nearly perpendicular to the cracks, they are more efficient than all other shear reinforcements (see Fig. 6.12). However, they are difficult to fabricate and construct. Furthermore, when there is a reversal of shear force (due to earthquakes), they may be inefficient. It has to be noted that experimental investigations on inclined stirrups are very limited compared to the extensive investigations on vertical stirrups (Leonhardt and Walther 1964; Bach, et al. 1980).

Spirals

The increase in strength of core concrete and ductility due to confinement reinforcement in the form of helical reinforcement in RC columns is well known (see Chapter 13). However, its effect in RC beams has not been studied extensively. Helical reinforcement is bound to increase the ductility in high-strength RC beams. If the correct pitch is

utilized for effective confinement, helical reinforcement will provide an economical solution for enhancing the strength of flexural members (Hadi and Schmidt 2003). Several ways of providing spirals such as spirals in tensile zone, spirals in compression zone, double spirals, and interlocking spirals have been studied by Jaafar (2007), as shown in Fig. 6.17. It was found that interlocking spirals and double spirals provide better performance under cyclic loading due to the confinement action and shear contribution. Cracks were found to be terminated by hoops and stopped from spreading. As the shear strength of concrete is mainly provided by the uncracked compression zone, it may be sufficient to confine the compression zone alone. Design codes have not yet provided equations for the design of spirals.

Headed Studs

The use of standard hooks in conventional stirrups may result in steel congestion, making fabrication and construction difficult. In addition, geometric limitations often prevent the use of large diameter reinforcement bars due to the construction limitations arising from lengthy hook extensions and large bend diameters. Moreover, the concrete inside the bend of conventional stirrups may be crushed before the yield stress in the stirrup is reached. In order to maintain equilibrium, the tensile force T in a bent bar must receive a radial reaction per unit length of magnitude $T/(Rd_b)$ from the concrete, where R is the radius of curvature and d_b is the diameter of bar (see Fig. 6.18). In other words, the bearing stress at bends f_{br} is given by (see Clauses 26.2.2.5 and 4.5.2.1 of SP 34:1987)

$$f_{br} = \frac{T}{Rd_b} \leq \frac{1.5f_{ck}}{1 + (2d_b/a_1)} \tag{6.5}$$

where a_1 is the centre-to-centre distance (c/c) between bars for internal bars and cover plus size of bar for bars adjacent to the face of the member.

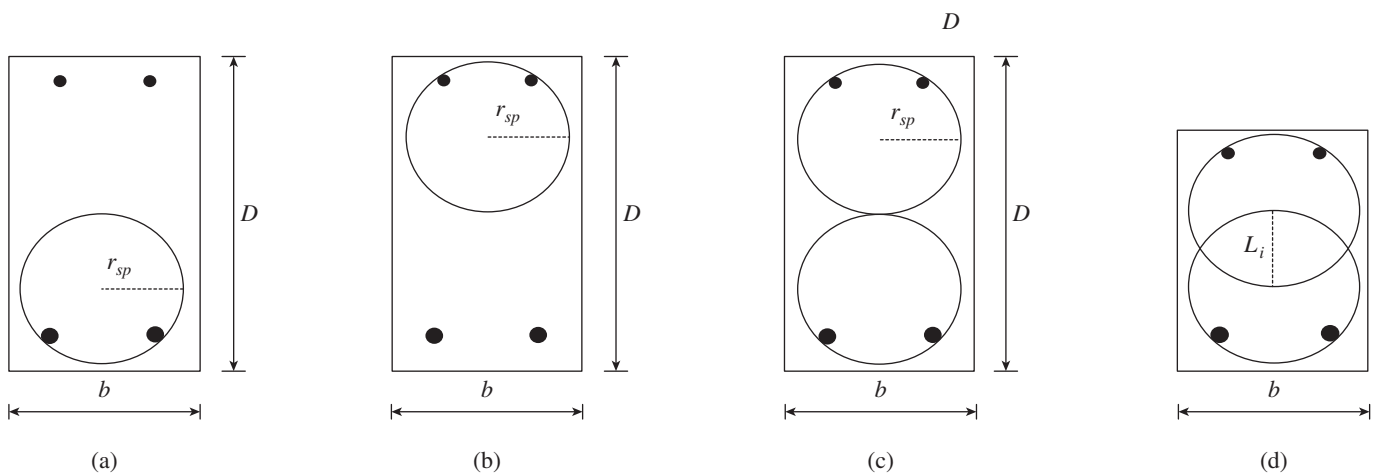


FIG. 6.17 Ways of providing spirals (a) Spirals (tensile zone) (b) Spirals (compression zone) (c) Double spirals (d) Interlocking spirals

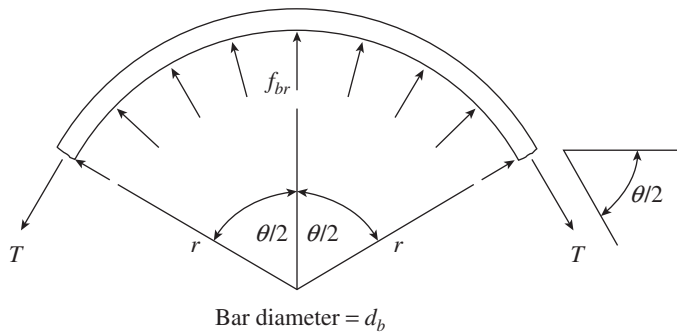


FIG. 6.18 Stress conditions at bend of shear reinforcing bar

For standard hooks and bends, Table 4.1 of SP 34:1987 requires that $R \geq 4d_b$ (as per ACI 318, $R \geq 2d_b$ for $d_b \leq 16$ mm). With this radius, the average bearing stress on concrete when the stress in the reinforcement reaches f_y is

$$f_{br} = \frac{f_y \pi (d_b^2 / 4)}{(4d_b) d_b} = 0.2 f_y \quad (6.6)$$

Thus, when the stress in the bar reaches f_y , the bearing stress can damage (split or crush) the concrete inside the bend and result in bend slip; hence, the hook cannot develop the stress f_y in the bar. (However, it should be noted that Clause 26.2.2.5 of IS 456 provides exemption from checking for bearing stress in concrete for standard hooks and bends given in Table 4.1 of SP 34 or IS 2502:1963, as the concrete within the bend may be subjected to triaxial stress field and can withstand high stresses locally.) Hence, the building codes require the minimum values of inner radius R and also that the bend engages a heavier bar, running perpendicular to the plane of the bend.

It was also observed that the slip occurs before the development of the full f_y in the legs of the stirrups at its connection with the bend (Leonhardt and Walther 1964; ACI-ASCE Committee 1973). It was found to occur in spite of the mechanical anchorage provided by the relatively heavy bar placed inside the bend. The flexural reinforcing bar, however, cannot be placed any closer to the vertical leg of the stirrup, without reducing the effective depth, d . Flexural reinforcing bars can provide such improvement to shear reinforcement anchorage only if the attachment and direct contact exist at the intersection of the bars, which is difficult to attain due to the workmanship involved or improper stirrup details. Under normal construction, however, it is very difficult to ensure such conditions for all stirrups. Thus, such support is normally not fully effective and the end of the vertical leg of the stirrup can move. In shallow beams or slabs, conventional stirrups typically cannot develop yield stress prior to shear failure due to the anchorage slip. This is indirectly accounted for in codes by limiting the shear stress resisted by concrete (for example, in ACI it is limited to $0.15 \sqrt{f_{ck}}$). These problems are largely avoided if the shear reinforcement is

provided with mechanical anchorage, as provided in headed studs (see Fig. 6.11).

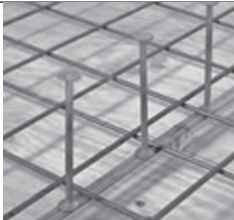
Conventional stirrups are being increasingly replaced by *headed studs*, which are smooth or deformed bars provided with forged or welded heads for anchorage at one or both the ends, as shown in Figs 6.11 and 6.19.

Several types and configurations of shear studs have been reported in the literature. The two common types are the single-headed studs welded to a continuous base rail and the double-headed studs welded to spacer rails (see Fig. 6.11). The base rail is used to position the studs at the required spacing, which is determined by readymade software or calculation. This *shear stud rail system* is sometimes referred to as SSR on drawings. Several manufacturers produce readymade systems and the details of Shearail® system by Max Frank Ltd, UK, are given in Table 6.1. To be fully effective, the size of the heads should be capable of developing the specified yield strength of the studs. Experiments have shown that an anchor



FIG. 6.19 Headed stud with deformed stem and heads at both ends
Courtesy: HALFEN GmbH, Germany and Max Frank Ltd, UK

TABLE 6.1 Details of Shearail® system

Stud diameter, mm		10	12	14	16	20
Head diameter, mm		30	36	42	48	60
Twin rail width, mm		2 × 16	2 × 16	2 × 16	2 × 16	3 × 16

Note: Stud lengths available in increments of 10 mm; rail thickness 3 mm; overhangs of twin rails are kept the same at both ends to eliminate site fixing errors.

Courtesy: Max Frank Ltd, UK

head three times the diameter of the shaft can provide a secure mechanical anchorage with negligible slip and develop full yield force for studs of yield stress f_y up to 500 MPa (Ghali and Dilger 1998; Ghali and Youakim 2005). The studs are usually placed in the forms above the reinforcement supports to ensure the specified concrete cover.

A tapered head is found to be sufficient for anchorage and strength (see Fig. 6.20). When the studs are used, it is not essential to place longitudinal bars behind the heads. Without the longitudinal bars, the heads can produce sufficient anchorage to develop yield force in the studs. Headed studs reduce congestion in beam-column joints and in zones of lap splices. Headed studs have been used in a number of projects that include offshore structures, bridges, flat plates, and other structures located in Europe, Australia, Asia, and North America (Ghali and Youakim 2005). The lower bearing stress and smaller slip make the studs more effective than conventional stirrups in controlling concrete cracks that intersect the stems at any location between the heads. A stud is longer than the effective part of a stirrup and this can intersect more shear cracks. When stirrups are used in lieu of studs, the distance d between the centroid of tensile reinforcement and the extreme compression fibre has to be smaller by the amount equal to the diameter of the stirrups (see Fig. 6.20). The reduction in flexural and shear strength of the member due to the smaller d has to be compensated by providing greater amount of flexural and shear reinforcements; this additional reinforcement may be significant in thin slabs (Ghali and Youakim 2005).

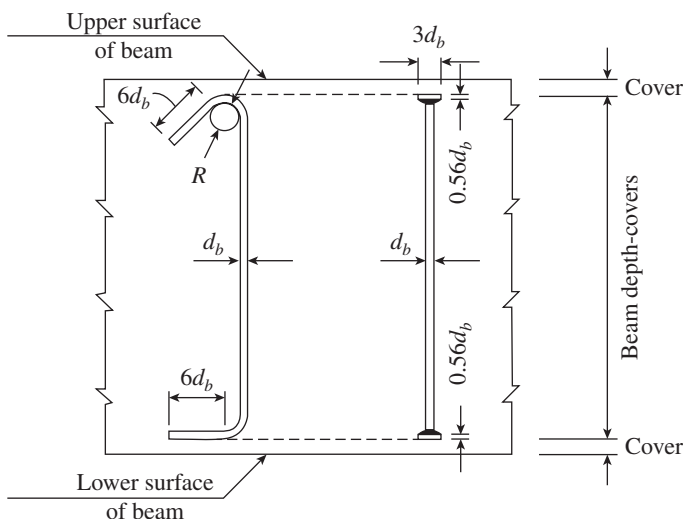


FIG. 6.20 Conventional single-leg stirrup and headed stud

Experiments have shown that higher shear stress in concrete can be allowed in slabs and beams when using stud reinforcement with anchor heads exhibiting no measurable slip. This superior effectiveness of studs is recognized in Canadian code CSA A-23:2004 by allowing a 50 per cent higher shear stress in concrete with the use of headed studs

than with conventional stirrups. Clause 11.11.5 of ACI 318 permits the use of headed studs. As per this clause, in beams where the flexural tension reinforcement is at the bottom of the section, the overall height of the shear stud assembly should not be less than the thickness of the member less the sum of: (a) the concrete cover on the bottom flexural reinforcement, (b) the concrete cover on the head of the stud, and (c) one-half the bar diameter of the bottom flexural reinforcement. When studs are used as shear reinforcement, Clause 11.11.5.1 of ACI 318 allows a higher nominal shear strength, τ_n (MPa), resisted by the concrete and steel, which is given as

$$\tau_n = 0.6\sqrt{f_{ck}} \quad (6.7a)$$

It also recommends the shear strength of concrete within the shear reinforced zone to be

$$\tau_c = 0.224\lambda\phi\sqrt{f_{ck}} \quad (6.7b)$$

where λ is the modification factor for lightweight concrete and ϕ is the strength reduction factor for shear = 0.75.

When stirrups are used, only lower stresses are permitted by ACI 318-05 as follows:

$$\tau_n = 0.45\sqrt{f_{ck}} \quad (6.8a)$$

$$\tau_c = 0.15\lambda\phi\sqrt{f_{ck}} \quad (6.8b)$$

In addition, the ACI code allows the spacing between the studs to be $\leq 0.75d$ compared to $0.5d$ for stirrups (when maximum shear stresses due to the factored loads are less than or equal to $0.445\phi\sqrt{f_{ck}}$). These differences in design rules permit lesser amount of shear reinforcement or a thinner slab or beam when studs are used. The use of studs also has the advantage of saving labour costs due to simplified installation of reinforcement. IS 456 does not contain provisions for design using headed studs as shear reinforcement.

Steel Fibres

Fibre-reinforced concrete (FRC) with a minimum volume fraction of 0.5 per cent fibres can be used to replace minimum shrinkage and temperature reinforcement. The replacement of stirrups by fibres in FRC has the following advantages: (a) The random distribution of fibres throughout the volume of concrete at much closer spacing than is practical for the stirrups can lead to distributed cracking with reduced crack width. (b) The first-crack tensile strength and the ultimate tensile strength of the concrete are increased by the fibres. (c) The shear friction strength is increased by resistance to pull-out and by fibres bridging cracks. Thus, steel fibres (crimped or hooked) increase the post-cracking resistance across an inclined crack, which in turn increases the aggregate interlock and shear resistance of concrete (Narayanan and Darwish 1987). The use of fibres also results in multiple inclined

cracks and gradual shear failure, unlike the sudden failure of concrete beams without shear reinforcement. Clause 11.4.6(f) of the ACI code allows the use of fibre reinforcement instead of shear reinforcement, when the factored design shear V_u is in the following range $0.5\phi V_c < V_u \leq \phi V_c$ ($\phi = 0.75$). Clause 5.6.6.2 of the ACI code specifies that a minimum of 60kg of deformed fibres per cubic metre should be used, which is approximately equal to a volume fraction of 0.75 per cent. The use of fibres to enhance shear strength is restricted to normal strength concrete (NSC) with f_{ck} less than 32MPa, beams with depth less than 600mm, and V_u less than $\phi 0.15\sqrt{f_{ck}} b_w d$. Such a minimum quantity of fibres has shown to exhibit shear strengths larger than $0.26\sqrt{f_{ck}} b_w d$ in laboratory tests (Parra-Montesinos 2006; ACI 544.1R:1996). IS 456 does not contain any provision to use fibres as shear reinforcement.

It is also possible to use the stirrup and fibre reinforcement effectively in combination. However, although the increase in shear capacity has been quantified in several investigations, it has not yet been used in practical applications.

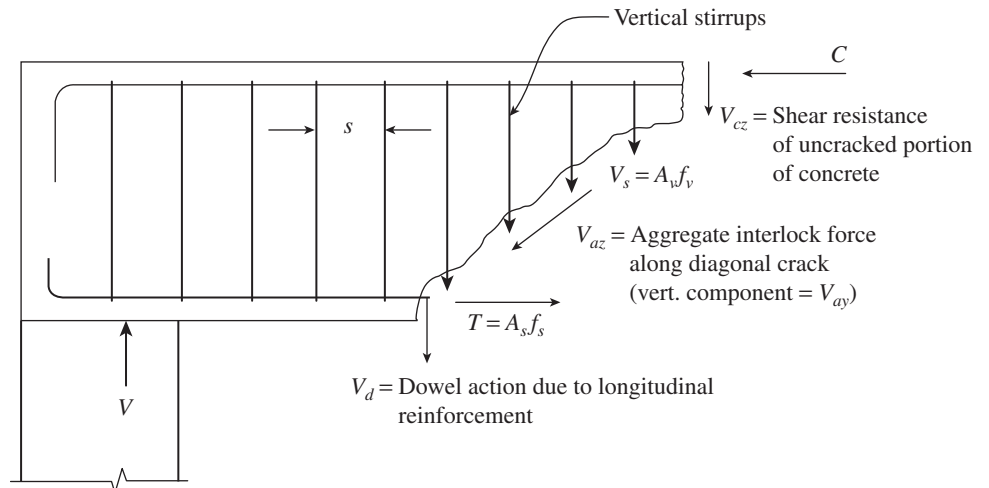


FIG. 6.21 Equilibrium of internal forces in a cracked beam with stirrups

The presence of shear reinforcements restricts the growth of diagonal cracks and reduces their penetration into the compression zone. This leaves more uncracked concrete in the compression zone for resisting the combined action of shear and flexure. The stirrups also counteract the widening of cracks, making available significant interface shear between the cracks. They also provide some measure of restraint against the splitting of concrete along the longitudinal reinforcement as shown in Fig. 6.8(a), thus also increasing the dowel action.

With further loading and opening of cracks, the interface shear V_{az} decreases, forcing V_d and V_{cz} to increase at an accelerated

6.2.4 Behaviour of Beams with Shear/Web Reinforcements

When a beam with transverse shear reinforcement is loaded, most of the shear force is initially carried by the concrete. Between flexural and inclined cracking, the external shear is resisted by the concrete V_{cz} , the interface shear transfer V_{az} , and the dowel action V_d (see Fig. 6.21). The first branch of shear cracking of the beams with transverse reinforcement is typically the same in nature as that of beams without transverse reinforcement. The shear crack in this case also involves two branches. The formation of the second crack and the corresponding load may be assumed to be the same. After the first inclined crack, redistribution of shear stresses occurs, with some parts of the shear being carried by the concrete and the rest by the stirrups, V_s . Further loading will result in the shear stirrups carrying increasing shear, with the concrete contribution remaining constant, as shown in Fig. 6.22.

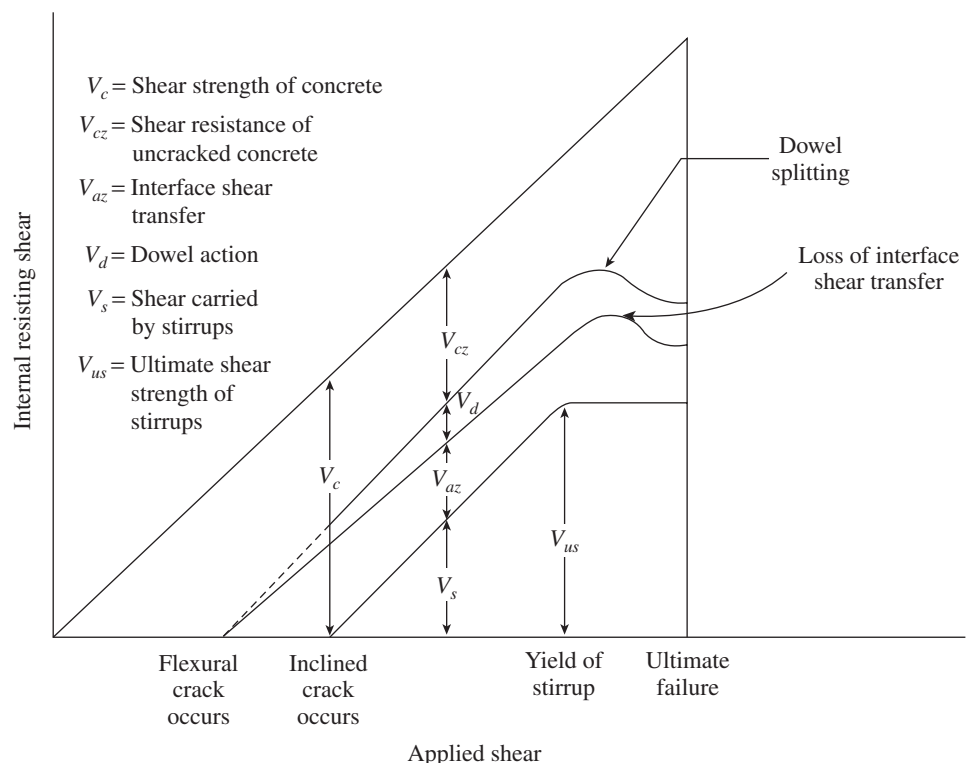


FIG. 6.22 Distribution of internal shears in beam with web reinforcement

Source: ACI-ASCE Committee 426 1973, reprinted with permission from ASCE

rate; the stirrups also start to yield. Soon, the failure of the beam follows either by splitting (dowel) failure or by compression zone failure due to the combined shear and compression.

It is clear from the given description that once a crack is formed, the behaviour is complex and dependent on the crack location, inclination, length, and so on. Hence, it is difficult to develop a rational procedure for the design, and past codal methods are based partly on rational analysis and partly on experimental data. Since it is difficult to quantify the contributions from V_{cz} , V_d , and V_{az} , they are often lumped together as V_c and referred somewhat incorrectly as ‘the shear carried by the concrete’ (Wight and MacGregor 2009). Thus, the nominal shear strength V_n is assumed to be

$$V_n = V_c + V_s \tag{6.9}$$

The term V_c is often taken as the failure capacity of the beam without stirrups and V_s the shear carried by the stirrups. The design strength is given in the ACI code as ϕV_n , where ϕ is the strength reduction factor in shear = 0.75.

If a stirrup happens to be near the bottom of a major diagonal crack, it is very effective in maintaining the dowel force and restraining the splitting failure, provided that the stirrups are of sufficient size, well anchored, and closely spaced (Kani 1969; ACI-ASCE Committee 426, 1973).

Due to the complexity of the shear behaviour, a committee of senior US engineers in 1973 (ACI-ASCE Committee 426 1973) concluded that ‘a full rational shear design approach does not seem possible at this time’. A semi-empirical shear design procedure was developed as an interim measure. The design procedure was based on the assumption that the shear strength of reinforced or prestressed concrete members is equal to the inclined cracking strength of the concrete, V_c (which included the contributions of V_{cz} , V_d , and V_{az}), plus the strength of the shear reinforcement, V_s (Wight and MacGregor 2009). The inclined cracking strength of the concrete, V_c , was obtained from curve fitting to the available experimental results (see Fig. 6.23), and the strength of the shear reinforcement, V_s , was calculated using the 45° truss model developed by Ritter in 1899. More discussion on the truss model as well as the other improved models developed after the publication of ACI-ASCE Committee 426 report (1973) is given in Section 6.7.

Thus, the semi-empirical ACI code equation for concrete strength is given by (see Fig. 6.23)

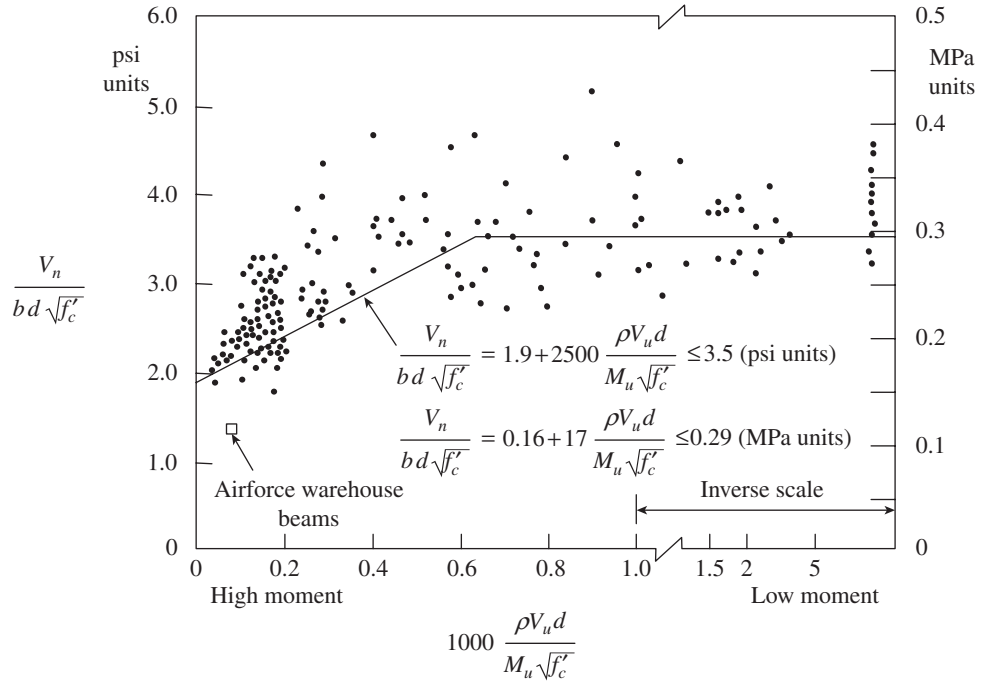


FIG. 6.23 Shear strength of concrete as a function of shear to moment ratio
Source: ACI-ASCE 326 1962, reprinted with permission from ACI

$$\frac{V_c}{b_w d} = 0.143 \lambda \sqrt{f_{ck}} + \frac{17 \rho V_u d}{M_u} \leq 0.26 \lambda \sqrt{f_{ck}} \tag{6.10}$$

where λ is the modification factor for lightweight concrete, $\rho = A_{st}/b_w d$, A_s is the area of longitudinal steel, and d is the effective depth of the beam. It should be noted that $M_u/(V_u d) = a_v/d$. Consequently, Eq. (6.10) accounts indirectly for the shear span to depth ratio and the slenderness of the member. When computing V_c by Eq. (6.10), $V_u d/M_u$ shall not be taken greater than 1.0, where M_u occurs simultaneously with V_u at the section considered. Transforming Eq. (6.10) into force format for the evaluation of the nominal shear resistance of the web of the beam of normal concrete and including the shear strength of vertical stirrups, we get

$$V_n = \left(0.143 \lambda \sqrt{f_{ck}} + \frac{17 \rho V_u d}{M_u} \right) b_w d + A_v f_{ys} d/s \tag{6.11}$$

where $A_v f_{ys}$ is the vertical force in the stirrup of area, A_v , and yield strength, f_{ys} , and s is the stirrup spacing.

For a number of reasons, Eq. (6.11) is now considered inappropriate, and in 1977, ASCE-ACI Committee 426 suggested that this equation should no longer be used!

ACI 318 also suggests the following simplified equation by assuming that the second term of Eq. (6.11) equals $0.007 \sqrt{f_{ck}}$:

$$V_c = 0.15 \lambda \sqrt{f_{ck}} b_w d \tag{6.12}$$

This design procedure was considered reasonably safe and accurate. It is worth mentioning that the aforementioned design procedure is the basis of the ACI design code and has remained unchanged since 1971. Similar design procedures had been

used in the CSA code, until 1994, and the IS code and continue to be used in the current European Code (Eurocode 2).

As already seen, cracked RC transmits shear in a relatively complex manner involving the opening and closing of cracks, formation of new cracks, interface shear transfer at rough crack surfaces, significant tensile stress in the cracked concrete, and a great variation of local stresses in both the concrete and reinforcement from point to point in the cracked concrete. The highest reinforcement stresses and the lowest concrete tensile stresses occur at the cracks.

6.3 FACTORS AFFECTING SHEAR STRENGTH OF CONCRETE

The following factors were found to affect the shear strength of beams without web reinforcement (Wight and MacGregor 2009; ACI-ASCE Committee 426 1973).

Tensile strength of concrete The inclined cracking load in shear is a function of the tensile strength of concrete, f_{ct} . The flexural cracking that precedes the inclined cracking disturbs the elastic stress field in such a way that the inclined cracking occurs at a principal tensile stress approximately equal to 50 per cent of f_{ct} for the uncracked section. The empirical equations suggested by the codes consider this parameter by including f_{ck} in the equations.

Longitudinal reinforcement ratio p_t The shear strength of the RC beams is found to drop significantly if the longitudinal reinforcement ratio ($p_t = A_s/b_w d$) is decreased below 1.2–1.5 per cent (Rajagopalan and Ferguson 1968). When p_t is reduced, the dowel action, V_d , is reduced. Moreover, the flexural cracks extend higher into the beam and are wider, reducing both the shear capacity of the compression zone and the interface shear transfer. The practical range of p_t for beams developing shear failure is 0.0075–0.025. In this range, the shear strength of concrete may be approximately estimated using Eq. (6.11). This equation may overestimate the shear strength for beams with small steel percentages. The longitudinal reinforcement ratio, p_t , is often included in the empirical equations suggested by the codes (see Section 6.4).

Shear span to effective depth ratio The effect of this ratio on the behaviour has already been discussed in Section 6.2.2. Its effect is pronounced when a_v/d is less than two and has no effect when it is greater than six. The CEB-FIP model code includes the shear span in the empirical equation.

Lightweight aggregate concrete Lightweight aggregate concrete often has lower tensile strength than concrete with normal aggregates (Yang 2010). ACI accounts for this effect by using a factor λ —the value of λ is taken as 0.85 for sand-lightweight concrete (where the entire fine aggregate is replaced by sand) and as 0.75 for all other lightweight concretes.

Size of beam As the depth of the beam increases, the shear stress at failure decreases. Many codes consider this by including a factor in the form of $(k_1/d)^a$. See also Section 6.3.1 for more discussions on this effect.

Axial forces It has to be noted that axial tension decreases the inclined cracking load and the shear strength of concrete, whereas axial compression increases the inclined cracking load and the shear strength of concrete. Axial compression also delays flexural cracking and increases the shear failure load. See Section 6.13 for more discussions.

Size of coarse aggregate Increasing the size of coarse aggregates increases the roughness of the crack surfaces, thus allowing higher shear stresses to be transferred across the cracks (Collins and Kuchma 1999). However, in HSC beams and in beams with lightweight aggregates, the cracks cross through the aggregates, instead of going through them. This may reduce the shear transferred by the aggregate interlock along the cracks and thereby the shear strength of concrete. The Canadian code expression considers the aggregate size while calculating the shear strength of concrete.

Size Effect

The failure of large RC elements during earthquakes resulted in several experimental investigations (Leonhardt and Walther 1964; Kani 1967; Bažant and Kim 1984; Taylor 1972; Shioya, et al. 1989; Collins and Kuchma 1999; Lubell, et al. 2004; Collins, et al. 2008; Mihaylov, et al. 2010). In 1967, Kani showed the importance of the *size effect* and demonstrated that as the depth of the beam increases, the shear stress at failure decreases for a given f_{ck} , p_t , and a/d . With increasing beam depth, the crack spacing and crack width tend to increase. This result was reconfirmed by the extensive experimental investigations conducted by Shioya, et al. (1989) in Japan. The main results of this work are summarized in Fig. 6.24, which shows that the shear stress at failure decreases when the member depth increases or the maximum aggregate size decreases. The largest beam of this series of tests spanned 36 m and had an effective depth of 3 m and a maximum aggregate size of 25 mm. However, it has been found that the failure shear stress does not significantly change when the width of beams is increased (Collins, et al. 2008). Hence, members with high values of steel stress parameter $M/(V\rho_w d)$ or members with large depths could fail at shear stresses much less than $0.15\sqrt{f_{ck}}$ MPa, as given in ACI 318-08 (which does not consider the size effect), and could lead to overestimating their strength by 50 per cent or more.

It is of interest to note that the beams tested by Shioya, et al. had the same concrete strength and percentage of longitudinal reinforcement as that of the failed Air Force warehouse beams (see the case study). From Fig. 6.24, it is clear that the difference in failure loads between the one-third model conducted by the Portland Cement Association and the

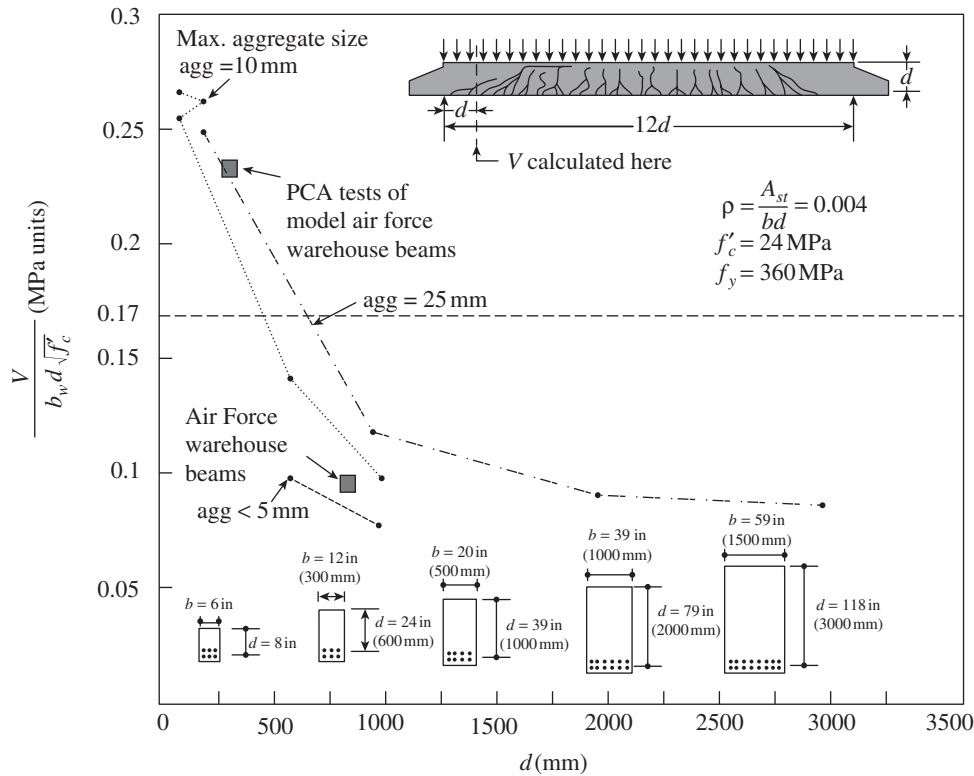


FIG. 6.24 Influence of member depth and maximum aggregate size on shear stress at failure; tests by Shioya, et al. (1989)

Source: Lubell, et al. 2004, reprinted with permission from Concrete International, ACI

actual beam of warehouse was primarily due to the size effect in shear, rather than the influence of axial tensile stresses, as concluded by PCA (Elstner and Hognestad 1957).

Since then, several experimental and analytical investigations have been conducted to study the size effect, which resulted in the simplest explanation of size effect in shear: larger crack widths that occur in larger members reduce the aggregate interlock (Walraven 1981). Crack widths increase nearly linearly with the tensile strain in reinforcement and the spacing between cracks. Hence, for the same reinforcement strains, doubling the depth of the beam will

double the crack width at mid-depth (Shioya, et al. 1989). Until 1980, the size effect in shear was not considered in the design codes. After that, based on the experimental and analytical results, some codes (Australian, UK, New Zealand, and Eurocode 2) incorporated this important effect by using some empirical relations (Subramanian 2003).

Recent fracture mechanics-based finite element analysis coupled with the statistical analysis of 234 test results by Yu and Bažant (2011) showed that the size effects are mitigated considerably if the depth of the beam is less than 1 m. However, in beams having depths greater than 1 m, the size effect cannot be neglected.

In beams with at least a minimum amount of web reinforcement, the web reinforcement reduces the crack spacing and holds the crack faces together, and hence, the shear transfer across the cracks due to aggregate interlock is not reduced. Hence, the size effect is not felt in beams with web reinforcement (Collins and Kuchma 1999).

The comparison of test results from beams with and without intermediate layers of crack control reinforcement showed that the intermediate longitudinal reinforcement (specified as side face reinforcement, which should not be less than 0.1 per cent of the web area as per Clause 26.5.1.3 of IS 456) greatly reduced the crack spacing near mid-depth and increased the shear capacity by more than 50 per cent, thus mitigating the size effect (Lubell, et al. 2004). The influence of the distribution of longitudinal reinforcement on the cracking pattern is shown in Fig. 6.25.

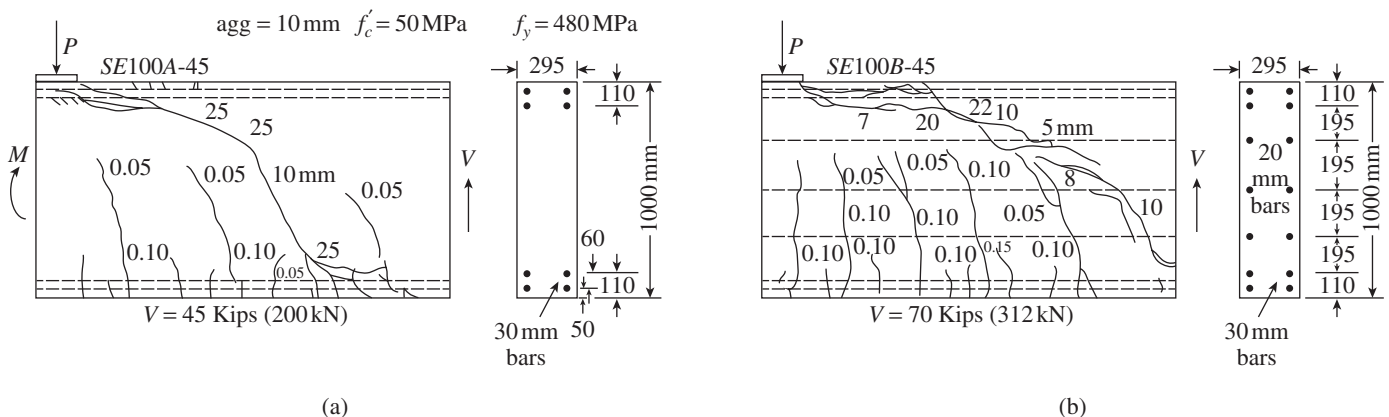


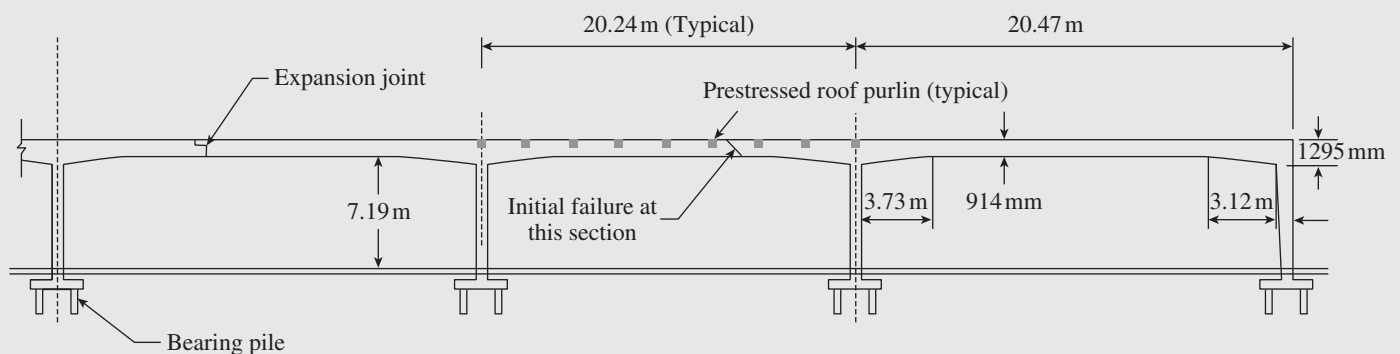
FIG. 6.25 Influence of distribution of longitudinal reinforcement on shear cracking pattern in a beam (a) Without side face reinforcement (b) With side face reinforcement

Source: Lubell, et al. 2004, reprinted with permission from Concrete International, ACI

CASE STUDY

Partial Collapse of Wilkins Air Force Depot in Shelby, Ohio

It is interesting to note that the shear provisions of the ACI code were revised after the partial collapse of the Wilkins Air Force Depot in Shelby, Ohio, in 1955 (Feld and Carper 1997). It was a six-span rigid frame building, 122m wide and 610m long. The haunched rigid frames had six 20.24m spans each and were spaced at approximately 10.06m. The concrete for each frame was placed continuously in a single working day. Severe cracking was observed two weeks before the collapse, so the girder was supported by temporary shoring. About 370m² of the roof suddenly collapsed on 17 August 1955. At the time of collapse, there were no loads other than the self-weight of the roof. The 914mm deep beams of this warehouse did not contain stirrups and had 0.45 per cent of longitudinal reinforcement (Feld and Carper 1997). The concrete alone was expected to carry the shear forces and had no shear capacity once cracked. The beams failed at a shear stress of only about 0.5MPa, whereas the ACI Code (1951 version) at the time permitted an allowable working stress of 0.62MPa for the M20 concrete used in the structure.



Shear failure of 900 mm deep beams in Air Force warehouse, Shelby, Ohio (Photo: C.P. Seiss)

Source: Lubell, et al. 2004, reprinted with permission from Concrete International, ACI

Experiments conducted at the Portland Cement Association (PCA) on 305 mm deep model beams indicated that the beams could resist a shear stress of about 1.0MPa prior to failure (Feld and Carper 1997). However, application of an axial tensile stress of about 1.4MPa reduced the shear capacity of the beam by 50 per cent. Thus, it was concluded that tensile stresses caused by the restraint of shrinkage and thermal movements caused the beams of the

Wilkins Air Force Depot to fail at such low thermal shear stresses (Feld and Carper 1997). The expansion joints locked and did not function to relieve stresses. This failure outlines the importance of providing minimum shear reinforcement in beams. It has to be noted that repeated loading will result in failure loads that may be 50–70 per cent of the static failure loads (ACI-ASCE Committee 426 1973).

Sleipner A is a combined accommodations, production, and processing concrete gravity base offshore platform at the Sleipner East gas field in the Norwegian sector of the North Sea. Even though it was analysed and designed using sophisticated finite element software, it resulted in a catastrophic failure on 23 August 1991 (resulting in an economic loss of about \$700 million), due to the underestimation of applied shear in the analysis and overestimation of shear strength in the design of the tricell walls. It may probably be considered the

most expensive shear failure, and about a 15 m height of the tricell walls did not contain any stirrup. (See case study in Chapter 7.)

6.4 DESIGN SHEAR STRENGTH OF CONCRETE IN BEAMS

As already discussed, the design shear strength of concrete, τ_c , depends on factors such as the grade of concrete,

longitudinal reinforcement ratio, shear span to depth ratio, type of aggregate used, size of beam, axial force, and size of coarse aggregate used (Subramanian 2007). The Indian code suggests an empirical formula based on the work of Rangan (1972), which considers the grade of concrete and longitudinal reinforcement ratio, as follows:

$$\tau_c = 0.85\sqrt{0.8f_{ck}}(\sqrt{(1+5\beta_{ss})}-1)/(6\beta_{ss}) \quad (6.13)$$

where $\beta_{ss} = \begin{cases} (0.8f_{ck})/(6.89p_t) \\ 1.0 \end{cases}$, whichever is greater

The factor 0.8 in the formula is for converting the cylinder strength to cube strength and the factor 0.85 is a reduction factor similar to partial safety factor ($1/\gamma_m$), according to SP 24:1983. The values of τ_c , based on Eq. (6.13), have been worked out for different values of f_{ck} and p_t and are presented in Table 6.2 (see Table 19 of the code).

TABLE 6.2 Design shear strength of concrete, τ_c , N/mm²

$p_t = \frac{100A_{st}}{b_w d}$	Grade of Concrete				
	M20	M25	M30	M35	M40
≤ 0.15	0.288	0.291	0.294	0.296	0.297
0.2	0.326	0.331	0.334	0.337	0.339
0.3	0.388	0.395	0.400	0.403	0.407
0.4	0.437	0.446	0.452	0.457	0.461
0.5	0.478	0.489	0.497	0.503	0.508
0.6	0.514	0.526	0.536	0.543	0.549
0.7	0.546	0.559	0.570	0.578	0.585
0.8	0.574	0.589	0.601	0.611	0.618
0.9	0.599	0.616	0.630	0.640	0.649
1.0	0.623	0.641	0.656	0.667	0.677
1.1	0.644	0.664	0.680	0.692	0.703
1.2	0.664	0.686	0.703	0.716	0.727
1.3	0.682	0.706	0.724	0.738	0.750
1.4	0.700	0.725	0.744	0.759	0.771
1.5	0.716	0.742	0.762	0.779	0.792
1.6	0.731	0.759	0.780	0.797	0.811
1.7	0.746	0.775	0.797	0.815	0.830
1.8	0.760	0.790	0.813	0.832	0.847
1.9	0.773	0.804	0.828	0.848	0.864

2.0	0.785	0.818	0.843	0.864	0.880
2.1	0.797	0.831	0.857	0.878	0.896
2.2	0.808	0.843	0.871	0.893	0.911
2.3	0.819	0.855	0.883	0.906	0.925
2.4	0.821	0.867	0.896	0.919	0.939
2.5	0.821	0.878	0.908	0.932	0.952
2.6	0.821	0.888	0.919	0.944	0.965
2.7	0.821	0.899	0.930	0.956	0.978
2.8	0.821	0.909	0.941	0.968	0.990
2.9	0.821	0.918	0.952	0.979	1.001
3.0	0.821	0.918	0.962	0.989	1.013
3.1	0.821	0.918	0.971	1.000	1.024
3.2	0.821	0.918	0.981	1.010	1.034
3.3	0.821	0.918	0.990	1.020	1.045
3.4	0.821	0.918	0.999	1.029	1.055
3.5	0.821	0.918	1.006	1.039	1.065
3.6	0.821	0.918	1.006	1.048	1.074
3.7	0.821	0.918	1.006	1.056	1.084
3.8	0.821	0.918	1.006	1.065	1.093
3.9	0.821	0.918	1.006	1.073	1.102
≥ 4.0	0.821	0.918	1.006	1.081	1.110

Note: The term A_{st} denotes the area of longitudinal tensile reinforcement and should continue for at least one effective depth beyond the section being considered.

As already discussed, the American code (ACI 318-08) formula is semi-empirical and based on experiments conducted in 1962 on concretes having strength less than 40 MPa.

Previous research has shown that the expression, which is a function of one-third power of concrete compressive strength, truly represents the shear strength (Subramanian 2003). Hence, the latest Eurocode 2 (EN 1992-1-1:2004) expression for nominal shear strength as given in Eq. (6.14), which also considers the size effect, may be considered as more rational for NSCs and HSCs.

$$V_n = (0.18/\gamma_c)k(p_t f_{ck})^{1/3}b_w d \geq 0.035k^{1.5}\sqrt{f_{ck}}b_w d \quad (6.14)$$

where k is a factor to consider size effect = $1 + (200/d)^{0.5} \leq 2.0$ (d in mm), γ_c is the partial factor of safety for concrete = 1.5, $p_t = 100A_{st}/b_w d \leq 2$, A_{st} is the area of tensile reinforcement,

f_{ck} is the cube compressive strength of concrete, and b_w and d are the breadth and effective depth of beam, respectively.

The UK code (BS 8110-1:1997) formula is also based on one-third power of concrete compressive strength and considers the size effect and is given as follows:

$$V_n = (0.79/\gamma_m)(p_t)^{1/3}(f_{ck}/25)^{0.333}(400/d)^{0.25}b_w d \quad (6.15)$$

with $p_t = 100A_{st}/b_w d \leq 3$, $400/d \geq 1.0$, $25 \text{ MPa} \leq f_{ck} \leq 40 \text{ MPa}$, and $\gamma_m = 1.25$.

The New Zealand code (NZS 3101, Part 1:2006) considers the size of aggregates and size effect and is given as follows:

$$V_n = k_a k_d v_b \quad (6.16)$$

where $v_b = 0.89(0.07 + 10\rho)\sqrt{f_{ck}}$ or $0.18\sqrt{f_{ck}}$, whichever is smaller, but is greater than or equal to $0.07\sqrt{f_{ck}}$; $\rho = A_{st}/b_w d$; k_a is the aggregate factor; $k_a = 1.0$ for aggregate size $\geq 20 \text{ mm}$ and $k_a = 0.85$ for aggregate size $\leq 10 \text{ mm}$; k_d is the size effect factor; $k_d = (400/d)^{0.25}$ for $d \geq 400 \text{ mm}$ and $k_d = 1.0$ if $d < 400 \text{ mm}$.

Equations (6.17a and b), derived based on the statistical studies of the beam data, by Zsutty is often referred to in the literature and models the actual effects of f'_c , $\rho_w (= A_{st}/b_w d)$, and a_v/d more closely than Eq. (6.10) given in the ACI code (Zsutty 1968).

$$V_n = 2b_w d (f_{ck} \rho_w)^{1/3} (d/a_v)^{1/3} \text{ for } a_v/d > 2.5 \quad (6.17a)$$

$$V_n = 5b_w d (f_{ck} \rho_w)^{1/3} (d/a_v)^{4/3} \text{ for } a_v/d \leq 2.5 \quad (6.17b)$$

A comparison of the formulae given in the different codes and the experimental results of 149 specimens is given in Fig. 6.26, which shows that the formula given in IS 456 is very conservative (Pendyla and Mendis 2000; Subramanian 2003; Gayed and Ghali 2004).

6.4.1 Maximum Shear Stress

The recommendation given in the codes for the design of shear reinforcements (see Section 6.7) will result in the yielding of shear reinforcement at the ultimate load conditions; hence, the failure will be ductile. However, the shear strength of beams cannot be increased beyond a certain limit, even with the addition of closely spaced shear reinforcement. It is because large shear forces in the beam will result in compressive

stresses that may cause crushing of web concrete, as shown in Fig. 6.8(c), which is brittle (SP 24:1983). To avoid such failures, an upper limit on τ_c is often imposed by the codes. IS 456 imposes a maximum shear stress, $\tau_{c,max}$, which should not be exceeded even when the beam is provided with shear reinforcement, as follows:

$$\tau_{c,max} = \gamma [0.83\sqrt{f'_c}] \quad (6.18a)$$

where γ is a safety factor = 0.85. Converting it to cube strength, we get

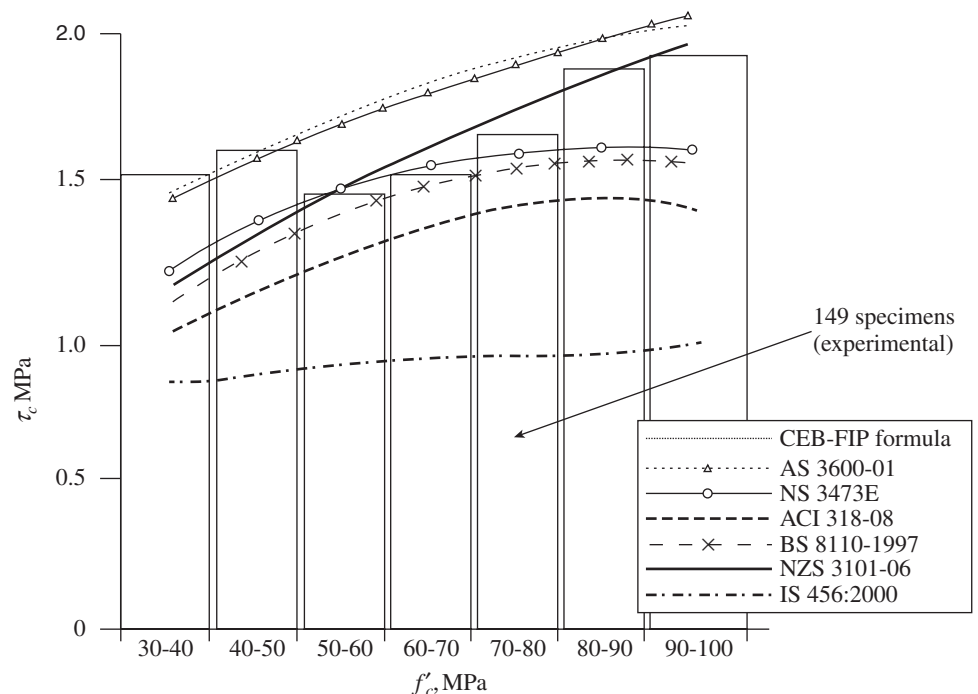


FIG. 6.26 Comparison of the formulae given in different codes with experimental results

Source: Subramanian 2003; Pendyla and Mendis 2000, reprinted with permission from ACI

$$\tau_{c,max} = 0.85[0.83\sqrt{(0.8f_{ck})}] = 0.631\sqrt{f_{ck}} \quad (6.18b)$$

Using Eq. (6.18b), the $\tau_{c,max}$ values for different grades of concretes can be arrived at and are presented in Table 6.3 (Table 20 of the code).

TABLE 6.3 Maximum shear stress $\tau_{c,max}$, N/mm² (Clause 40.2.3)

Grade of Concrete	M15	M20	M25	M30	M35	M40	M45	M50	M55 and Above
$\tau_{c,max}$, N/mm ²	2.5	2.8	3.1	3.5	3.7	4.0	4.3	4.6	4.8

Note: $\tau_{c,max} = 0.631\sqrt{f_{ck}}$

Clauses 11.2.2.1 and 11.4.7.9 of ACI 318 also have a similar limit (with $\tau_{s,max}$ as $0.66\sqrt{f_{ck}}$ and $\tau_{c,max}$ as $0.29\lambda\sqrt{f'_c}$) of $0.95\sqrt{f'_c} = 0.85\sqrt{f_{ck}}$. The UK code, BS 8110, limits the maximum

shear stress to $0.8\sqrt{f_{ck}}$ or 5 MPa, whereas the New Zealand code NZS 3101 limits it to $0.16f_{ck}$ or 8 MPa, whichever is smaller.

6.4.2 Effects Due to Loading Condition

Experiments have shown that the shear strength of beams, either slender or deep, under the uniform load (which is often encountered in practice, as loads are transferred to beams through slabs) is much higher than that of beams under a loading arrangement of two concentrated loads at quarter points or one concentrated load at mid-span (Zararis and Zararis 2008; Brown, et al. 2006). Hence, the shear strength equations presented in the codes, which are mostly derived from tests on beams with concentrated loads, can also be safely applied to uniformly distributed loading cases. In this case, the splitting failure along the line of the second branch of the critical diagonal crack occurs near the support reaction and not near a concentrated load. If any concentrated load is applied between $2d$ and $6d$ from

the face of the support, it is advisable to reduce the shear strength of concrete, V_c , given in the codes by half (Brown, et al. 2006).

6.5 CRITICAL SECTION FOR SHEAR

Before designing the beam for shear, we should first locate the critical section for shear. The maximum shear force in a beam usually occurs at the face of the support and reduces progressively away from the support. When there are concentrated loads, then the shear force remains high in the span between the support and the first concentrated load (Figs 6.27a–f).

Clause 22.6.2 of IS 456 allows a section located at a distance d (effective depth) from the face of the support to be treated as a *critical section* in the following cases (see Figs 6.27a–c):

1. Support reaction, in the direction of applied shear force, introduces compression into the end regions of the member.

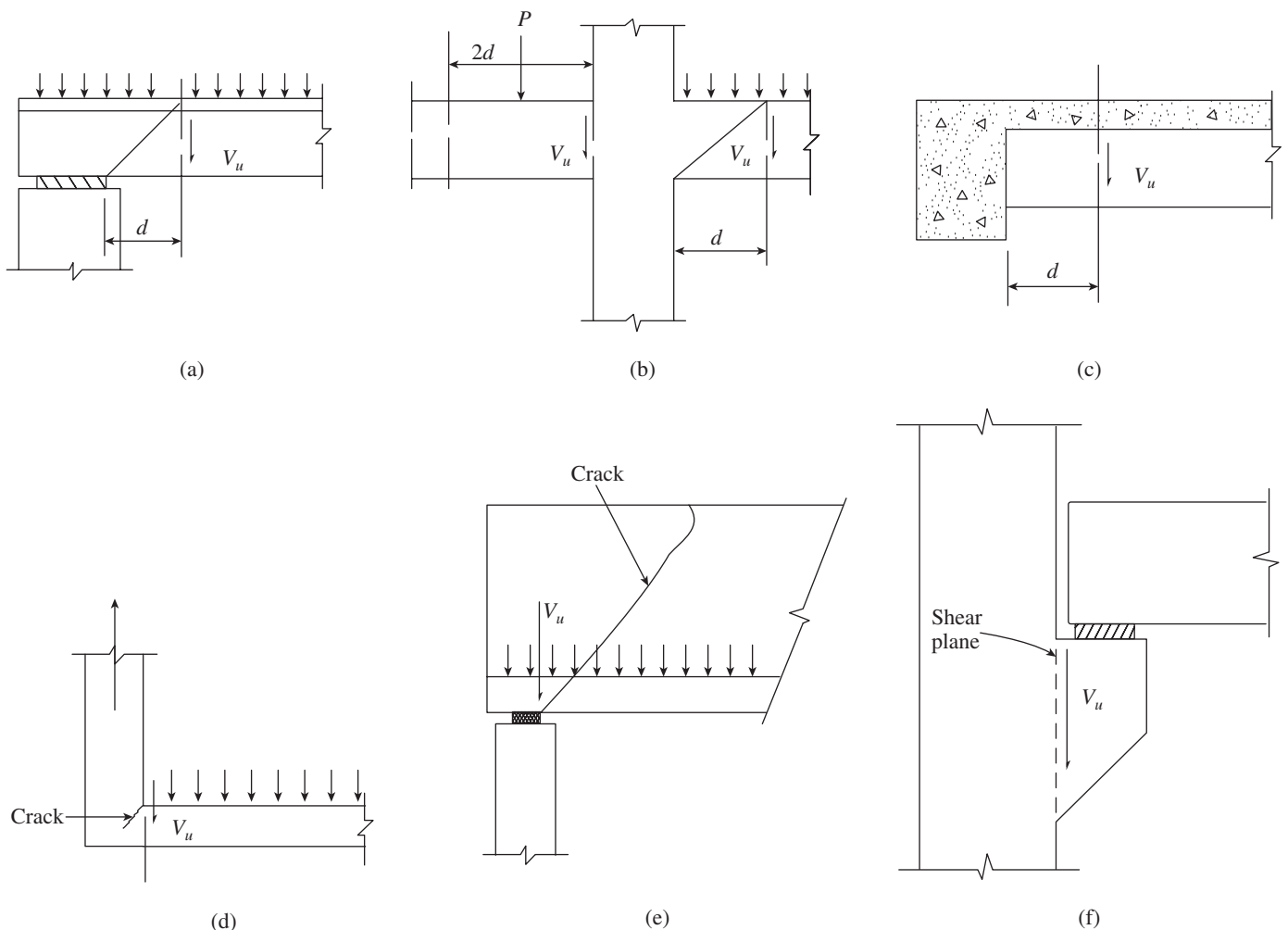


FIG. 6.27 Critical sections for shear near support (a)–(c) Critical section at a distance ‘d’ from the face of the support (d)–(f) Critical section at the face of the support

2. Loads are applied at or near the top of the member.
3. No concentrated load occurs between the face of the support and the location of the critical section, which is at a distance d from the face of the support

In these cases, it is enough to design the beam segment between the critical section and the face of the support for the shear force calculated at the critical section. This clause is useful in designing the base slabs of footings, where flexural (one-way) shear is a major structural consideration (see Chapter 15).

This clause cannot be applied in the following situations:

1. Beams framing into a supporting member in tension (see Fig. 6.27d)
2. Beams loaded near the bottom, as in the case of inverted beam (see Fig. 6.27e)
3. Concentrated load introduced within a distance $2d$ from the face of the support, as in the beam on the left side of Fig. 6.27(b). In this case, closely spaced stirrups should be designed and provided in the region between the support and the concentrated load (see also Section 6.6).

In all these cases, the critical section for shear must be taken at the face of the support. For brackets and corbels too, the shear at the face of the support must be considered, as shown in Fig. 6.27(f). It should be noted that brackets and corbels are more appropriately designed for shear using the shear friction provisions.

Enhanced Shear Strength near Supports

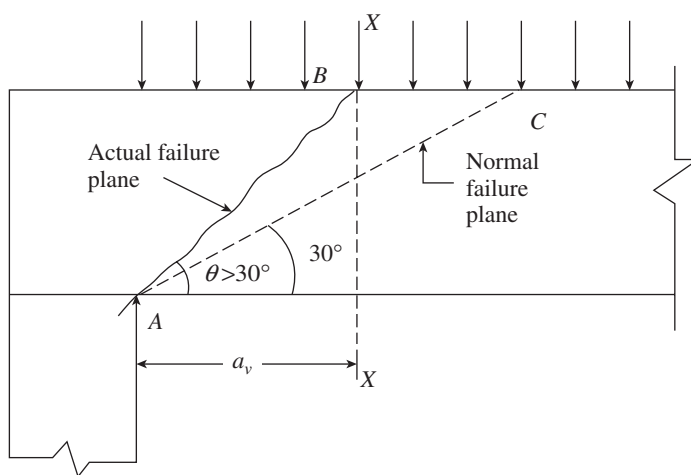
It has been observed from tests that shear failure at sections of beams and cantilevers without shear reinforcement occurs at a plane inclined at an angle 30° as shown in Fig. 6.28(a).

When the failure plane is inclined more steeply than this, for example, when the shear span to effective depth ratio is less than two, the shear force required to produce the failure is increased. As this ratio increases from 0.5 to 2.0, the enhanced shear strength to normal shear strength ratio of concrete (τ_{ce}/τ_c) decreases rapidly from 4.0 to 1.0 (see Fig. 6.28b). Clause 40.5 of IS 456 allows the designer to consider this enhancement of shear strength near a support, provided the tensile longitudinal reinforcement is well anchored into the support (by a distance at least equal to the effective depth), by using the following relation:

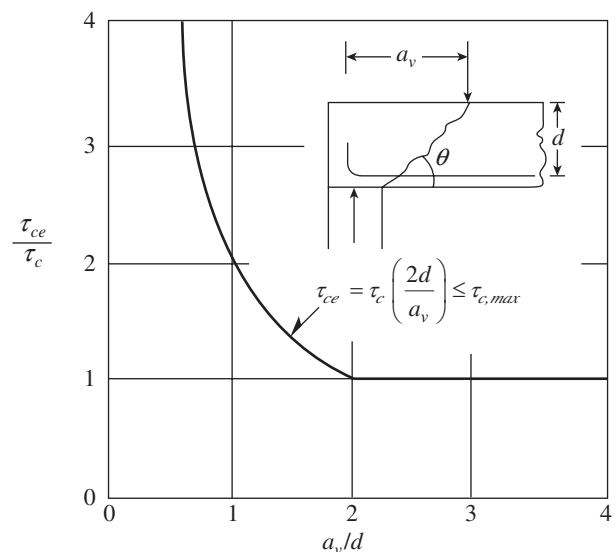
$$\text{Enhanced design shear strength, } \tau_{ce} = \frac{2d\tau_c}{a_v} \leq \tau_{c,max} \quad (6.19)$$

where a_v is the shear span as shown in Fig. 6.28(a). However, the maximum shear strength $\tau_{c,max}$ should be limited to the values specified in Table 20 of the code. Clause 40.5.2 of IS 456 also recommends reducing the shear reinforcement near the support, due to this enhanced shear strength.

A good design is one in which shear failure is eliminated such that the flexure design governs the behaviour. Hence, Clause 40.5.2 of the code, which tends to reduce the shear reinforcement near the supports and increases the vulnerability to shear failure, is not advisable, especially in seismic zones. Moreover, in comparison to the total reinforcement in the beam, the reduction in the quantity of shear reinforcement achieved through this clause is marginal and hence may also not result in much economy. This clause is particularly non-conservative for structures to be built in earthquake-prone areas, wherein we design in such a way that ductile flexure failure occurs before the brittle shear failure. Hence, this clause may be applicable only in structures subjected to static loads.



(a)



(b)

FIG. 6.28 Enhanced shear strength (a) Steep failure plane (b) Influence of shear span to depth ratio

Furthermore, Clause 40.5 of IS 456 also seeks to increase the shear strength of concrete near the supports up to the maximum shear stress, $\tau_{c,max}$. This implies that there could be situations where the shear force at the critical section is large but only minimum shear reinforcement is provided, owing to this peculiar provision in the code (Murty 2001). Moreover, it is difficult to apply the clause in the case of commonly applied uniformly distributed loads, since a designer does not know the failure plane angle, and hence the value of a_v to be used in Eq. (6.19) is unknown.

6.6 MINIMUM AND MAXIMUM SHEAR REINFORCEMENT

As discussed earlier, when the principal tensile stress within the shear span exceeds the tensile strength of concrete, diagonal tension cracks are initiated in the web of concrete beams. These cracks later propagate through the beam web, resulting in brittle and sudden collapse, when web reinforcement is not provided. (The diagonal cracking strength of the RC beams depends on the tensile strength of concrete, which in turn is related to its compressive strength.) Hence, minimum shear reinforcements are often stipulated in different codes. When shear reinforcements are provided, they restrain the growth of inclined cracking. Ductility is also increased and a warning of failure is provided. Such reinforcement is of great value if a member is subjected to an unexpected tensile force due to creep, shrinkage, temperature, differential settlement, or an overload.

As per Clause 26.5.1.6 of IS 456:2000, minimum shear reinforcement should be provided in all the beams when the calculated nominal shear stress, τ_v , is less than half of design shear strength of concrete, τ_c , as given in Table 19 of the code. The minimum stirrup to be provided is given as follows:

$$\frac{A_{sv}}{b_w s_v} \geq \frac{0.4}{0.87 f_y} = \frac{0.46}{f_y} \quad (6.20)$$

Here, A_{sv} is the area of cross section of transverse reinforcement and s_v is the stirrup spacing along the length of the member. It has to be noted that the code restricts the characteristic yield strength of stirrup reinforcement to 415 N/mm².

Until the 2002 version, the ACI code used a formula similar to that given in the Indian code, with a coefficient equal to one-third instead of 0.46; thus, the requirement for the minimum area of transverse reinforcement was independent of the concrete strength. Tests conducted by Roller and Russell on HSC beams indicated that the minimum area of shear reinforcement as per Eq. (6.20) was inadequate to prevent brittle shear failures. This is because cracking occurred through the aggregates and hence the contribution from the aggregate interlock was minimal. They also suggested that the minimum shear reinforcement should also be a function of concrete strength (Roller and Russell 1990).

Hence, the current version of the ACI code provides the following equation for minimum shear reinforcement:

$$\frac{A_{sv}}{b_w s_v} = \frac{0.9 \sqrt{f_{ck}}}{16 f_y} \geq \frac{1}{3 f_y} \quad (6.21)$$

It should be noted that Eq. (6.21) provides for a gradual increase in the minimum area of transverse reinforcement while maintaining the previous minimum value. In seismic regions, web reinforcement is required in most beams because the shear strength of the concrete is taken as equal to zero if the earthquake-induced shear exceeds half the total shear (Wight and MacGregor 2009).

6.6.1 Maximum Spacing

As per Clause 26.5.1.5 of IS 456, for vertical stirrups, the maximum spacing of shear reinforcement shall not exceed 0.75d or 300 mm, whichever is less. It should be noted that the IS code limits the maximum yield strength of web reinforcement to 415 N/mm² to avoid the difficulties encountered in bending high-strength stirrups (they may be brittle near sharp bends) and also to prevent excessively wide inclined cracks. For inclined stirrups at 45°, the same clause of the code stipulates the maximum spacing as 1.0d or 300 mm, whichever is less.

The stirrups will not be able to resist the shear unless an inclined crack crosses them. Hence, ACI code Section 11.4.5.1 sets the maximum spacing of vertical stirrups as the smaller of $d/2$ or 600 mm, so that each 45° crack will be intercepted by at least one stirrup. If $V_u/d\phi - V_c$ exceeds $\sqrt{f_c} b_w d/3$, the maximum allowable stirrup spacing is reduced to half of the aforementioned spacing. Thus, for vertical stirrups, the maximum spacing is the smaller of $d/4$ or 300 mm. This stipulation is provided because closer stirrup spacing leads to narrower inclined cracks and will also provide better anchorage for the lower ends of the compression diagonals (Wight and MacGregor 2009). Clause 6.3.5 of IS 13920 also stipulates a spacing of stirrups as $d/4$ or eight times the diameter of the smallest longitudinal bar, but not less than 100 mm at either end of the beams over a length of $2d$ (in plastic hinge regions) and a spacing of $d/2$ elsewhere. The first hoop should be placed at a distance not exceeding 50 mm from the joint face. The ACI code also restricts the maximum yield strength of web reinforcement to 415 N/mm², although the New Zealand code allows a design yield strength up to 500 MPa. Based on these discussions, it is clear that the IS 456 should also adopt Eq. (6.21) with the spacing as stipulated in IS 13920 (Subramanian 2010). A comparison of the shear design provisions of various codes is provided in Table 6.4. The provisions for minimum shear reinforcement in flexural members of the Indian, Eurocode 2, US, New Zealand, and Canadian codes are compared in Table 6.4 and Fig. 6.29. Except the Indian code, all the other codes have a similar format and consider both f_{ck} and f_y .

TABLE 6.4 Comparison of shear design provisions of different codes

Requirement	Code Provision as per				
	IS 456	ACI 318*	CSA A23.3*	Eurocode 2	NZS 3101*
Minimum shear reinforcement, $\frac{A_s}{b_w s_v} \geq$	$\frac{0.4}{0.87 f_y}$ when $\tau_v > 0.5 \tau_c$	$\frac{0.9 \sqrt{f_{ck}}}{16 f_y} \geq \frac{0.33}{f_y}$ when applied shear is greater than $0.5 \times$ concrete strength	$\frac{0.054 \sqrt{f_{ck}}}{f_y}$ when applied shear is greater than concrete strength	$\frac{0.08 \sqrt{f_{ck}}}{f_y}$ when applied shear is greater than shear strength of concrete	$\frac{0.9 \sqrt{f_{ck}}}{16 f_y}$ when applied shear is greater than $0.5 \times$ concrete strength
Spacing of minimum stirrups \leq	$0.75d \leq 300$ mm	$0.5d \leq 600$ mm and $0.25d \leq 300$ mm, when $V_s > \sqrt{f'_c} b_w d/3$	$0.63d \leq 600$ mm and $0.32d \leq 300$ mm when $V_u > \phi_c f'_c b_w d/11.4$	$0.75d \leq 600$ mm	$0.5d \leq 600$ mm and $0.25d \leq 300$ mm, when $V_s > \sqrt{f'_c} b_w d/3$

*The cylinder strength is assumed to be equal to 0.8 times the cube strength.
Source: Subramanian 2010

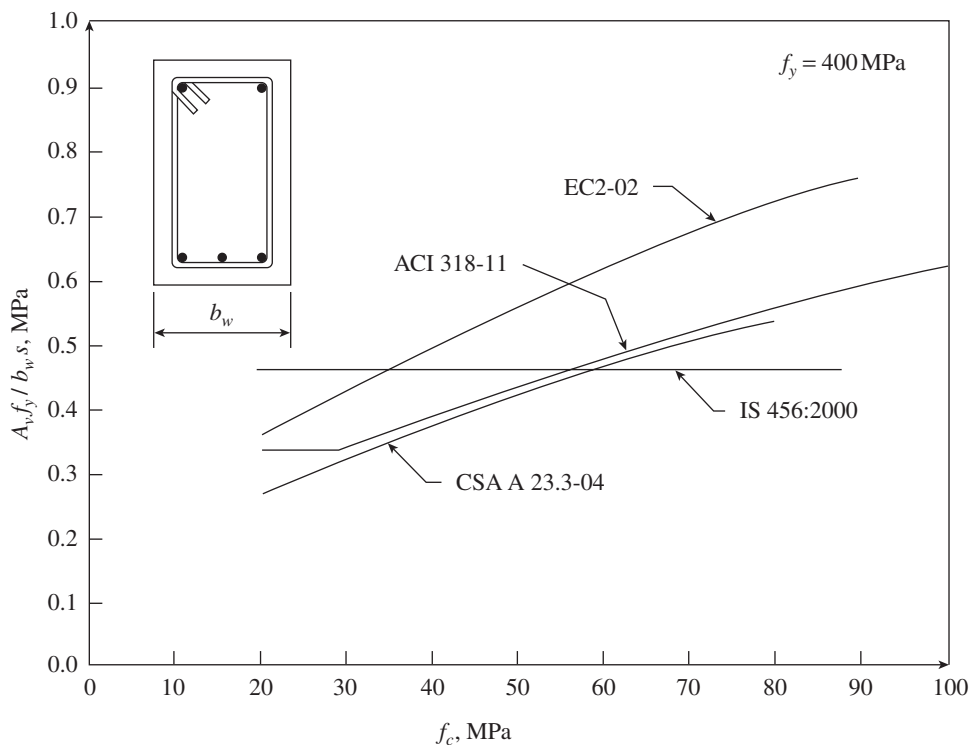


FIG. 6.29 Minimum shear reinforcement as a function of f_c as per different codes
Source: Li and Zhang 2005 (adapted), Copyright Taylor and Francis Group LLC Books, 2005

6.6.2 Upper Limit on Area of Shear Reinforcement

As discussed in Section 6.4.2, IS 456 recommends that maximum shear stress should not exceed $\tau_{c,max} = 0.631 \sqrt{f_{ck}}$ (see Eq. 6.18b).

Lee and Hwang compared the test results of 178 RC beams reported in the literature and the 18 beams tested by them and found that the shear failure mode changes from under-reinforced to over-reinforced shear failure when $p_v f_y / f_c$

is approximately equal to 0.2. Hence, they suggested the following maximum amount of shear reinforcement for ductile failure (Lee and Hwang 2010):

$$p_{v,max} = 0.2(f_c/f_y) \quad (6.22a)$$

where $p_{v,max} = A_{sv}/(s_v b_w)$

In terms of f_{ck} , Eq. (6.22a) may be written as

$$p_{v,max} = 0.16(f_{ck}/f_y) \quad (6.22b)$$

Lee and Hwang also found that the amount of maximum shear reinforcement, as suggested by Clause 11.4.7.9 of ACI 318-08, and given in Eq. (6.23) need to be increased for HSC beams, as test beams with greater than 2.5 times the $p_{v,max}$ given by Eq. (6.22), failed in shear after the yielding of the stirrups (Lee and Hwang 2010).

$$p_{v,max} = 2 \sqrt{f_c} / (3f_y) \quad (6.23)$$

The expressions suggested by the Canadian code and Eurocode are more complicated but are found to agree with the test results reasonably (Lee and Hwang 2010). However, these equations for maximum shear reinforcement are proportional to the concrete compressive strength, whereas the Indian and American code equations are proportional to the square root of the concrete compressive strength. It is also interesting to note that the Canadian code and Eurocode equations are based on analytical methods such as the variable angle truss method, whereas the Indian and American code equations are based on the experimental results. Based on this discussion, it may be seen that the Indian code should also adopt

Eq. (6.22b) for maximum shear reinforcement (Subramanian 2003).

6.7 DESIGN OF SHEAR REINFORCEMENT

The behaviour of beams failing in shear has to be represented in terms of a mechanical mathematical model in order to use it in the design. A number of models have been developed for shear design and analysis. The Truss model adopted by the American

and Indian codes and the MCFT adopted by the Canadian code are two major models for shear design. Other models are also available, such as the rotating-angle softened-truss model and the fixed-angle softened-truss model (Hsu 1993; Belarbi and Hsu 1995; Pang and Hsu 1996), the truss model with crack friction (Dei Poli, et al. 1987; 1990; Kirmair 1987; Kupfer and Bulicek 1991; Reineck 1991), compression force path method (Kotsovos and Pavlovic 1999), and the critical crack theory, which has been adopted in the Swiss code SIA 262 (Muttoni and Ruiz 2008). Eurocode 2 uses the ‘variable angle truss model’. However, these models will not be discussed here since they are not as widely used in practice as the ACI and the CSA models. An excellent review of most of these models is available in ACI-ASCE Committee 445 report (1998).

6.7.1 The Ritter–Mörsch Truss Model

The truss model was originally introduced by Ritter, who proposed a 45° truss model for computing the shear strength of the RC members; this model was refined by Mörsch (Ritter 1899; Mörsch 1909). The Ritter–Mörsch truss model became the basis of many design codes around the world. Ritter assumed that after the cracking of concrete, the behaviour of an RC member is similar to that of a truss with a top longitudinal concrete chord, a bottom longitudinal steel chord (consisting of longitudinal reinforcement), vertical steel ties (stirrups), and diagonal concrete struts inclined at 45° , as shown in Fig. 6.30(a). It was further assumed that the diagonally cracked concrete cannot resist tension and the shear force is resisted by transverse steel, commonly referred to as the steel contribution (V_s) and the uncracked concrete contribution (V_c). When a shear force is applied to this truss, the concrete struts are subjected to compression whereas tension is produced in the transverse ties and in longitudinal chords. The force component in each can be determined by statics. The design of stirrups is usually based on the vertical component of diagonal tension, whereas the horizontal component is resisted by the longitudinal tensile steel of the beam.

As already discussed, the concrete contribution, V_c , is generally considered to be a combination of force transfer by the dowel action of the main flexural steel, aggregate interlock

along a diagonal crack, and uncracked concrete beyond the end of the crack. It is also difficult to calculate the exact proportion of each of these forces. Hence, it was vaguely rationalized to adopt the diagonal cracking load of the beam *without* web reinforcement as the concrete contribution to the shear strength of an identical beam *with* web reinforcement.

The truss analogy formed the basis of several code procedures (including the ACI and IS codes) as it was simple to understand and apply. Experience with the 45° truss analogy revealed that the results of this model were quite conservative, particularly for beams with small amounts of web reinforcement. However, the results overestimated the concrete shear strength for beams with low reinforcement ratios ($\rho < 1.0\%$), overestimated the gain in shear strength resulting from the use of HSC, and underestimated the influence of $V_u d/M_u$ (ACI-ASCE Committee 426 1973; Roller and Russel 1990; Collins and Kuchma 1999). Moreover, as already mentioned, the truss model does not consider the size effects.

The truss model has been modified by several others in the past 30 years, which include the works of Schlaich, Thürlimann, Marti, and MacGregor (Thürlimann, et al. 1983; Schlaich, et al. 1987; Marti 1985; Collins and Mitchell 1991; Wight and Macgregor 2009). Based on their work, it was realized that the angle of inclination of the concrete struts, θ , may be in the range $25\text{--}65^\circ$, instead of the constant 45° assumed in the Ritter–Mörsch model. These developments lead to the *variable angle truss model* (see Fig. 6.30b). The choice of small value of θ reduces the number of required stirrups, but increases the compression stresses in the web and the horizontal component to be resisted by the longitudinal tensile steel of the beam.

Ad hoc procedures, also developed empirically, were added into the codes to adjust for some of these deficiencies of the Ritter–Mörsch model and for some specific classes of members (e.g., deep beams vs normal-sized beams, beams with axial forces, prestressed vs non-prestressed beams, HSC beams, etc.), with additional restrictions on their range of applicability. As a result, the number of equations for shear provisions in the ACI code alone has grown from 4 prior to 1963 to about 43 in 2008 (ACI-ASCE Committee 445, 1998).

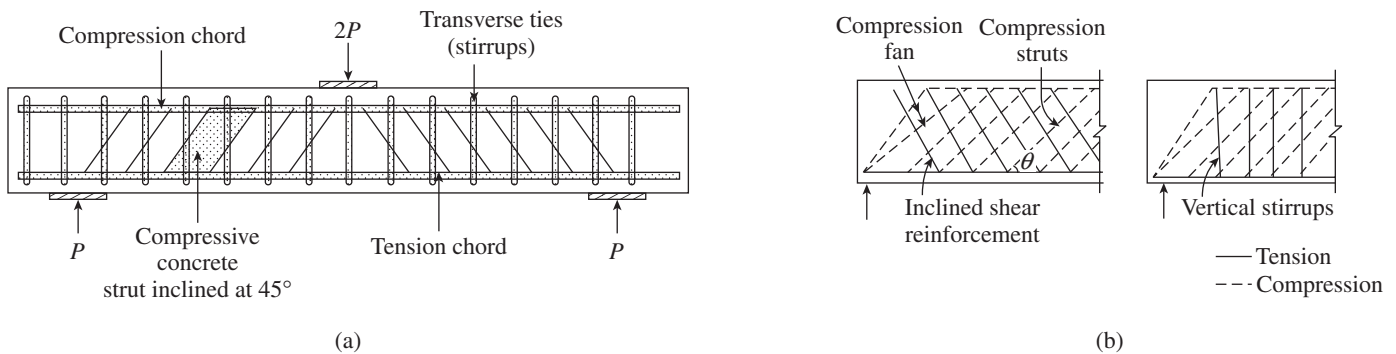


FIG. 6.30 Truss models for beams with web reinforcement (a) Ritter–Mörsch truss model (b) Variable angle truss model

Let us now consider how the truss model is applied to the design. As per limit states design philosophy,

Capacity \geq demand, or

$$V_n \geq V_u \quad (6.24a)$$

where V_u is the design factored shear force acting at the section under consideration and V_n is the nominal shear capacity of beam with uniform depth, which is obtained by using the following equation (Clause 40.1 of the code):

$$V_n = \tau_v b_w d \quad (6.24b)$$

As discussed, using the truss model, the nominal shear capacity V_n of the beam with transverse reinforcement is considered as the sum of the contributions of concrete, V_c , and that of the stirrups, V_s , as follows:

$$V_n = V_c + V_s \quad (6.24c)$$

where V_c is the nominal shear resistance provided by the concrete (V_c is calculated as given in Section 6.4; $V_c = \tau_c b_w d$) and V_s is the nominal shear provided by the shear reinforcement.

It is important to realize that the assumption shear stresses are uniform over the shear area arises from the simplification originally made in the ACI 318 code in 1967. In fact, in reality, shear stresses may be far from uniform.

Beams with Vertical Stirrups

In the truss model, the crack is assumed to form at an angle 45° to the neutral axis. Hence, the horizontal distance of the crack is approximately d . If we consider a stirrup with the total area of legs as A_{sv} , and the stirrups spaced at a distance s_v apart (see Fig. 6.31a),

$$\text{Number of stirrups crossed by the crack, } n = d/s_v \quad (6.25a)$$

Assuming that the stress in the stirrups is equal to the design yield stress ($= 0.87f_{yv}$), we get the equation given in Clause 40.4 (a) of IS 456 for the shear resistance of the vertical stirrups as follows:

$$V_s = 0.87f_{yv}A_{sv}(d/s_v) \quad (6.25b)$$

Substituting this value in Eq. (6.24c) and using Eq. (6.24b), we get

$$V_n = \tau_v b_w d = \tau_c b_w d + 0.87 f_{yv} A_{sv} (d/s_v)$$

Simplifying, we get

$$\frac{A_{sv}}{s_v} = \frac{(\tau_v - \tau_c) b_w}{0.87 f_{yv}} \quad (6.25c)$$

where A_{sv} is the total cross-sectional area of a 'single' stirrup leg effective in shear, s_v is the stirrup spacing along the length of the member, τ_v is the calculated nominal shear stress ($V_u/b_w d$) in MPa, τ_c is the design shear strength of concrete in MPa, and f_{yv} is the yield stress of the stirrup steel.

Comparing Eq. (6.20) and Eq. (6.25c), we get $(\tau_v - \tau_c) = 0.40$ MPa. This shows that the amount of required minimum stirrups corresponds to a nominal shear stress resisted by stirrups of 0.40 MPa (the Joint ASCE-ACI Committee (1973) on shear recommended 0.34 MPa).

Thus, when τ_v exceeds τ_c (calculated using Table 19 of the code), shear reinforcement has to be provided.

Although while deriving the formula it was assumed that all the links crossing the crack inclined at an angle of 45° are effective, tests have shown that the links that intercept the crack near the top are relatively ineffective (Tompos and Frosch 2002). To rectify this, the code (Clause 26.5.1.5) limits the spacing to $0.75d$ (see also Section 6.7.3).

From Eq. (6.24c), it is possible to write as

$$V_s = V_u - V_c = (\tau_v - \tau_c) b_w d \quad (6.25d)$$

where V_u is the applied factored shear force due to the external loads and V_c is the shear strength provided by concrete. The other terms are defined already.

It should be noted that in Eq. (6.25a), d/s_v is used to compute the number of stirrups crossing a shear crack forming at an angle of about 45° . This ratio seldom results in whole numbers, allowing for fractional shear contribution to shear strength. In reality, a crack cannot cross a fractional portion of a stirrup. This can be easily incorporated by truncating the decimal portion of d/s_v , thus producing an integer quantity (Tompos and Frosch 2002).

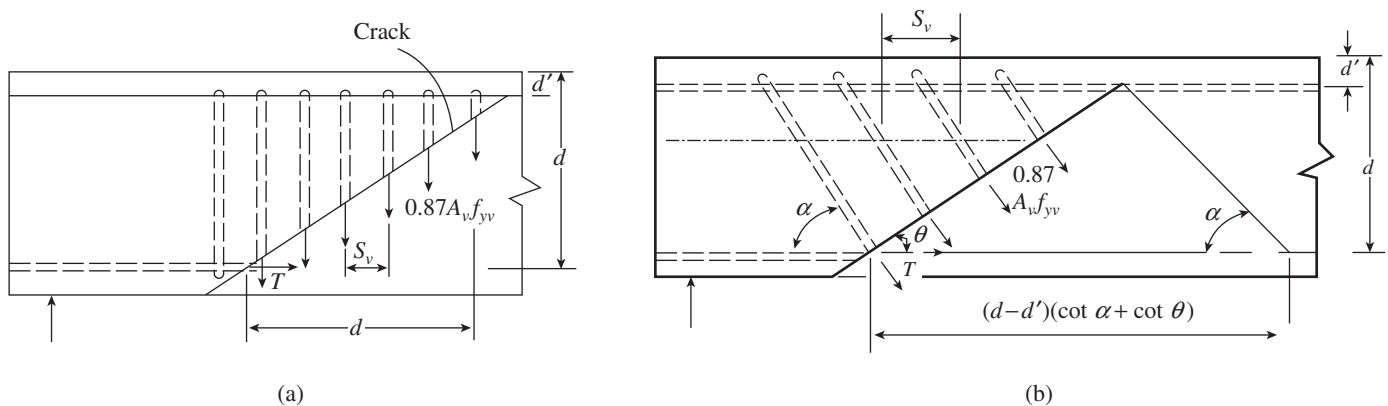


FIG. 6.31 Design of stirrups (a) Vertical stirrups (b) Inclined stirrups

Beams with Inclined Stirrups

The inclined stirrups are assumed to be placed at angle α (usually, not less than 45°) with the axis of the beam and spaced s_v apart, as shown in Fig. 6.31(b). Let us consider a stirrup with a total area of legs as A_{sv} and with design yield stress equal to $0.87f_{yv}$. The horizontal length over which the bar is effective is given by

$$L_h = (d - d')(\cot \theta + \cot \alpha)$$

The number of effective stirrups is given by

$$n = \frac{(d - d')(\cot \theta + \cot \alpha)}{s_v}$$

Using truss analogy,

Vertical component of shear carried by one stirrup = $0.87f_{yv}A_{sv}\sin \alpha$

Hence, the shear resistance of all the stirrups intercepting the crack is given by

$$V_{us} = 0.87f_{yv}A_{sv}\sin \alpha \times \frac{(d - d')(\cot \theta + \cot \alpha)}{s_v} \quad (6.26a)$$

As per truss analogy, the crack angle θ is taken as 45° and $(d - d')$ may be taken approximately as d ; using the aforementioned equation and simplifying, we get the formula given in Clause 40.4(b) of IS 456 as

$$V_{us} = \frac{0.87f_{yv}A_{sv}d}{s_v} (\sin \alpha + \cos \alpha) \quad (6.26b)$$

The case of vertical stirrups may be considered as a special case of inclined stirrups, with $\alpha = 90^\circ$. Thus, if we substitute 90° for angle α in Eq. (6.26b), we get Eq. (6.25b).

Bent-up Bars

The shear force V_{us} resisted by the bent-up bars inclined at an angle α is equal to the vertical component of the forces in the bars. Hence, we get the formula given in Clause 40.4(c) of IS 456 as

$$V_{us} = T \sin \alpha = 0.87f_{yv}A_{sv}\sin \alpha \quad (6.26c)$$

As stated earlier, bent-up bars alone cannot suffice as shear reinforcement.

6.7.2 Modified Compression Field Theory

Compression field theory is the reverse of the *tension field theory*, originally developed by Wagner in 1929 to simplify the post-buckling analysis of flexible shear panels used in aircraft construction. He assumed that the applied shear was carried by a diagonal tension field after the buckling of the thin metal web. Then, he considered the deformations of the system by assuming that the angles of inclination of the diagonal tensile stresses would coincide with the angles of inclination of the principal tensile strains.

The compression field theory developed by Collins and Mitchell is similar to Wagner's tension field theory and assumes that a diagonal compression field carries shear after cracking (Collins 1978; and Collins and Mitchell 1991). It was modified and simplified later by Collins, Vecchio, and Bentz (Vecchio and Collins 1986; Bentz, et al. 2006). Unlike the traditional truss models, the *modified compression field theory* (MCFT) uses the strain conditions in the web to determine the inclination θ of the diagonal compressive stresses (see Fig. 6.32). The equilibrium conditions, compatibility conditions, and stress-strain relationships (constitutive relationships) are formulated in terms of average stresses and average strains. The compatibility conditions used in the compression field theory are derived from Mohr's circle for strains. The constitutive relationships in this theory resulted from the tests of over 200 RC panels, using the panel element tester and shell element tester of the University of Toronto, under pure shear or combinations of shear and normal stresses. Figure 6.32 gives the 15 equations used in MCFT. The MCFT assumed that the directions of the inclined compression field (i.e., the strut angle and the crack angle) and the principal compressive stress coincide. Solving the equations of the MCFT is tedious, if attempted by hand, and hence software programs called *Membrane-2000* and *Response-2000* were developed (Bentz 2000). Over the last 20 years, the MCFT has been applied to the analysis of numerous RC structures and found to provide accurate simulations of behaviour.

The simplified MCFT has been found to give similar results to the full MCFT, but is simple to apply. The following equations are incorporated in the Canadian code, CSA S23-2004, based on the simplified MCFT. For vertical stirrups,

$$V = V_c + V_s = \phi_c \beta_m \sqrt{f'_c} b_w d_v + \frac{\phi_s A_v f_{yv}}{s_v} d_v \cot \theta \leq 0.25 \phi_c f'_c b_w d_v \quad (6.27a)$$

In Eq. (6.27a), the effective shear depth d_v can be taken as the greater of $0.9d$ or $0.72D$; the resistance factor ϕ_c for concrete is 0.65 and ϕ_s for steel is 0.85. The term β_m models the ability of the cracked concrete to transfer shear. It is a function of (a) the longitudinal strain at the mid-depth of the member ϵ_x , (b) the crack spacing at mid-depth, and (c) the maximum course aggregate size, a_g . It is calculated using the following expression, which also takes into account the size effect:

$$\beta_m = \frac{0.40}{(1 + 1500\epsilon_x)} \cdot \frac{1300}{(1000 + s_{ze})} \quad (\text{mm}) \quad (6.27b)$$

This equation may be simplified to the following if $a_g \geq 20$ mm:

$$\beta_m = \frac{230}{(1000 + d_v)} \quad (\text{mm}) \quad (6.27c)$$

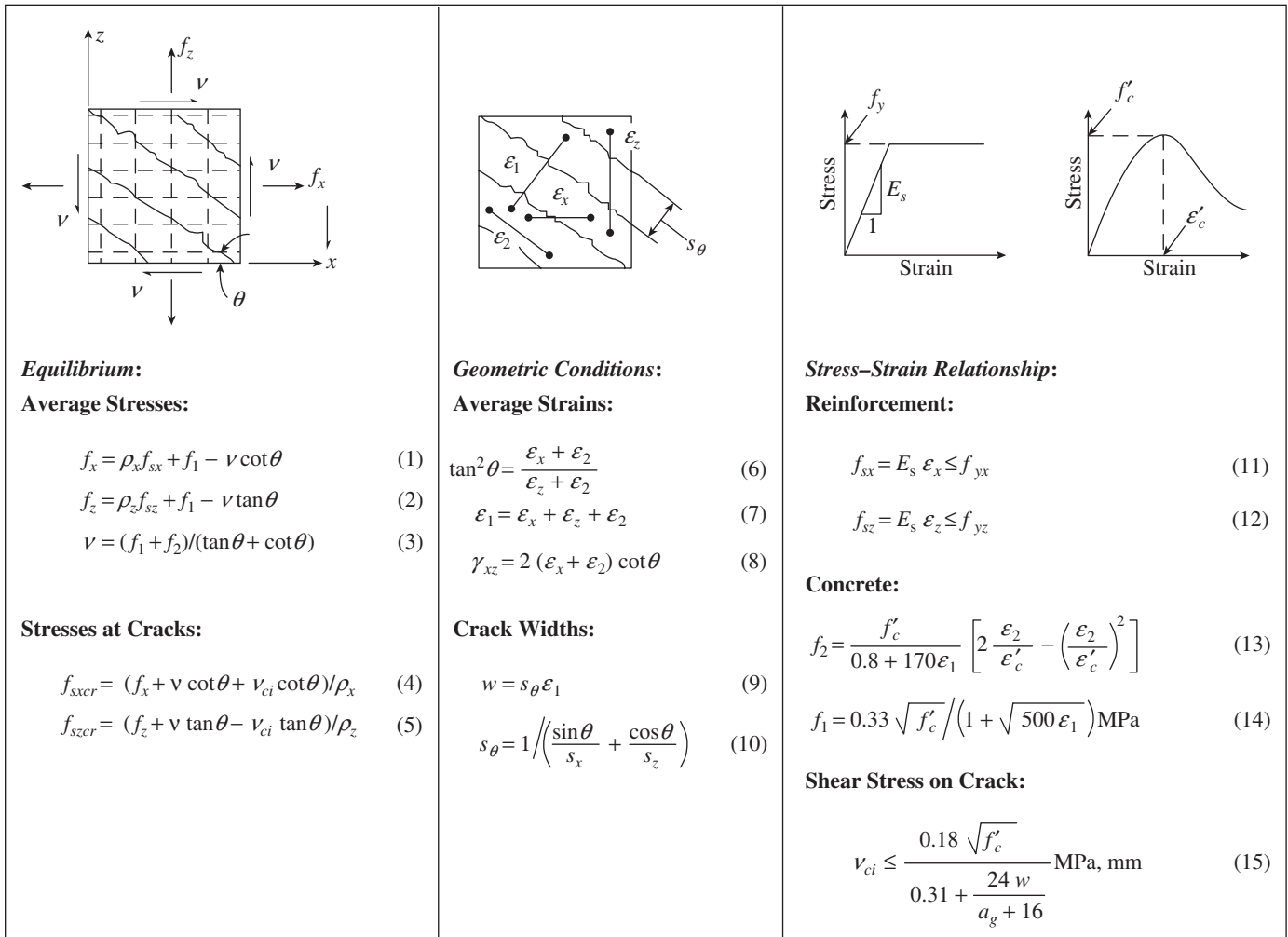


FIG. 6.32 Equations of modified compression field theory

Source: Bentz, et al. 2006, reprinted with permission from ACI

The longitudinal strain at mid depth ϵ_x is conservatively assumed to be equal to half the strain in the longitudinal tensile steel and is given by

$$\epsilon_x = \frac{M/d_v + V}{2E_s A_s} \leq 3.0 \times 10^{-3} \quad (6.27d)$$

The equivalent crack spacing factor s_{ze} is given by

$$s_{ze} = 35s_z / (15 + a_g) \geq 0.85 s_z \text{ (mm)} \quad (6.27e)$$

In this equation, s_z can be taken as d_v .

The aggregate size does not influence the aggregate interlock capacity in HSC because the cracks pass through the aggregate. To account for this, a_g is reduced linearly to zero as $\sqrt{f'_c}$ increases from 60 to 70 MPa; for concrete grades higher than M70, it is taken as zero. The value of $\sqrt{f'_c}$ is limited to 8.3 MPa. When the following relation holds good, the members do not exhibit size effects:

$$\frac{A_v f_{yv}}{b_w s_v} \geq 0.062 \sqrt{f'_c} \quad (6.27f)$$

If this equation is satisfied, s_{ze} is taken as 300 mm.

The angle of inclination of the cracks at mid-depth, θ in degrees, is calculated using

$$\theta = (29 + 7000 \epsilon_x) \leq 75^\circ \quad (6.27g)$$

Finally, the longitudinal reinforcement at the critical section for shear must be capable of resisting a tensile force F_{lt} given by

$$F_{lt} = M/d_v + 0.5(V + V_c) \cot \theta \quad (6.27h)$$

It is seen that these equations are much complicated than the equations based on the truss model.

6.7.3 Design Procedure for Shear Reinforcement

The design of an RC beam for shear using vertical stirrups involves the following steps:

1. Determine the maximum factored shear force V_u at the critical sections of the member (see Fig. 6.27).
2. Check the adequacy of the section for shear. Compute the nominal shear stress $\tau_v = V_u / (b_w d)$. Check whether τ_v is less than the maximum permissible shear stress, $\tau_{c,max}$, as given in Table 20 of the code. If τ_v is greater than $\tau_{c,max}$,

increase the size of the section or the grade of concrete and recalculate steps 1 and 2.

3. Determine the shear strength provided by the concrete (for the percentage of tensile reinforcement available at the critical section) V_c , using design shear strength τ_c given by Eq. (6.13) or Table 19 of the code; $V_c = \tau_c bd$.
4. If $V_u > V_c$, shear reinforcements have to be provided for $V_{us} = V_u - V_c$.
5. Compute the distance from the support beyond which only minimum shear reinforcement is required (i.e., where $V_u < 0.5V_c$).
6. Design of stirrups (Clause 40.4):

Where stirrups are required, it is usually advantageous to select a bar size and type (e.g., 8 mm diameter double-legged stirrups) and determine the required spacing. The total cross-sectional area of stirrup, $A_{sv} = \text{Number of legs} \times \text{Area of stirrup}$. Though the minimum diameter of 6 mm is specified in Clause 26.5.3.2(c), usually bars of 8 mm or greater is adopted in practice.

- (a) If vertical stirrups are chosen, calculate the spacing using

$$s_v = \frac{0.87 f_y A_{sv} d}{V_{us}} \quad (6.28a)$$

- (b) If inclined stirrups at 45° are chosen, calculate the spacing using

$$s_v = \frac{0.87 f_y A_{sv} d}{V_{us}} (\sin \alpha + \cos \alpha) \quad (6.28b)$$

- (c) In regions where only minimum stirrups are required (Clause 26.5.1.6)

$$s_v = \frac{0.87 f_y A_{sv}}{0.4 b_w} \quad (6.28c)$$

The calculated spacing s_v should be smaller than the following maximum spacing (Clause 26.5.1.5):

- (a) For vertical stirrups, the lesser of $0.75d$ or 300 mm
- (b) For inclined stirrups, the lesser of d or 300 mm

Adopt the spacing accordingly.

7. Check anchorage requirements and details.

Although Clause 26.5.1.6 of the code states that shear reinforcement need not be provided in the regions of the beam where $\tau_v < 0.5\tau_c$, it is a better practice to provide nominal (minimum) shear reinforcement in such regions of the beam to improve ductility and to prevent failure due to accidental loading.

It should be noted that while larger diameter stirrups at wider spacing are more cost effective than smaller stirrup sizes at closer spacing (due to fabrication and placement costs), closely spaced stirrups of smaller diameter gives better crack control. Usually, the stirrup diameter is kept the same throughout the span of the beam. Changing the stirrup spacing as few times as possible over the required length also results in cost savings. If possible, no more than three different stirrup spacings should be specified along the length of a beam, with the first stirrup located 50 mm from the face of the support.

6.7.4 Transverse Spacing of Stirrups in Wide Beams

In wide beams with large number of longitudinal rods and carrying heavy shear forces (such as those encountered in raft foundations), it is advisable to provide multi-legged stirrups as shown in Figs 6.13(d) and (e) and 6.15, so that the longitudinal forces are evenly distributed among the longitudinal rods of the beam. From the tests conducted on wide members, it was found that the effectiveness of the shear reinforcement decreases as the spacing of the web reinforcement legs across the width of the member increases (see Fig. 6.14). The IS and ACI codes do not provide stirrup leg spacing limits across the width of sections. Leonhardt and Walther (1964) recommend a maximum transverse spacing, s_w , of 200 mm; Eurocode 2 suggests spacing limits of $0.75d$ or 600 mm in both width and longitudinal directions; and Lubell, et al. (2009) suggest a limiting spacing lesser of d or 600 mm, with a suggestion to reduce it to half when the nominal shear stress exceeds $0.37 \sqrt{f_{ck}}$.

6.7.5 Design Aids

For a given arrangement of vertical stirrup (with a given number of legs, diameter of bar, and spacing), the shear resistance V_{us}/d (N/mm) is constant. It can be obtained by rearranging Eq. (6.25b) as

$$\frac{V_{us}}{d} = \frac{0.87 f_y A_{sv}}{s_v} \quad (6.29)$$

Design aids can be generated using this equation (see Table C.21 of Appendix C for the design aid of a two-legged vertical stirrup and Table C.22). Such design aids for vertical stirrups and bent-up bars may be found in SP 16:1980, Tables 62 and 63, respectively.

6.7.6 Anchoring of Shear Stirrups

The stirrups should be well anchored to develop the yield stress in the vertical legs, as follows:

1. The stirrups should be bent close to the compression and tension surfaces, satisfying the minimum cover.
2. The ends of the stirrups should be anchored by standard hooks (see Fig. 6.13).
3. Each bend of the stirrups should be around a longitudinal bar. The diameter of the longitudinal bar should not be less than the diameter of the stirrups.

In addition to providing anchorage, these specifications are provided for other reasons too, including the following:

1. Constructability purposes
2. Prevention of presumed concrete crushing at the corner of the stirrup, resulting from the high stress concentrations that develop in this region when the member is loaded

The bent-up bars should be anchored adequately as shown in Fig. 6.33. As per SP 34 (Clause 4.3.5), the development length should be provided in the compression zone, measuring from the mid-depth of the beam (see Chapter 7 for discussion on development

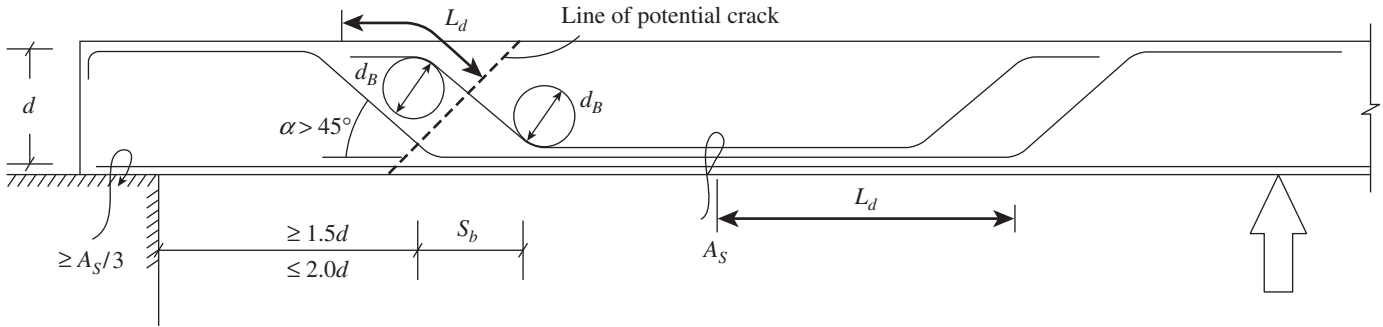


FIG. 6.33 Anchoring of bent-up bars

length). If the bent-up bars are anchored in the tension zone, the development length can be measured from the end of the sloping or inclined portion of the bar, as shown in Fig. 6.33. The maximum longitudinal spacing of the bent-up bars should not exceed $s_{b,max}$. Eurocode 2:2004 suggests the following equation for $s_{b,max}$:

$$s_{b,max} = 0.6d(1 + \cot \alpha) \quad (6.30)$$

Here, the angle α should be between 45° and 90° to the longitudinal axis of the beam.

The minimum diameter of bend, d_b , may be taken as 20 times the diameter of the bar.

6.8 SHEAR DESIGN OF FLANGED BEAMS

The behaviour and cracking pattern of T-beams under two-point loading or one-point loading in the middle of the beam are similar to that of rectangular beams (Leonhardt and Walther 1964; Zararis, et al. 2006; Tureyen, et al. 2006). IS 456 and several other codes ignore the flanges of T- or L-beams that are integrally cast with slabs and consider only the web in concrete shear strength computations. Although this approach provides conservative results, it may become uneconomically conservative. An increase in the shear capacity results from an increase of the cross-sectional area of the compressive zone of a beam. It has been found that the shear capacity of T-beams is 30–40 per cent higher than the shear strength of their web (Zararis, et al. 2006). This increased strength is due to the size of the flanges, an increase in the tensile strength of concrete, and the neutral axis depth, though there is a wide scatter of test results.

To account for the effect of flange thickness on the shear area of the T-beams, the concept of *shear funnel*, as shown in Figs 6.34(a) and (b), was developed by Zararis, et al. (2006) and Tureyen, et al. (2006). According to this concept, the area of concrete bounded by the neutral axis and the two angled lines is defined as the effective shear area. The angle θ may be conveniently and conservatively taken as 45° . Using the *form factor approach*, Tureyen, et al. provided the following formula for calculating the shear strength of concrete in T-beams:

$$V_c = 0.37\sqrt{f_{ck}}(b_f x_u \sqrt{(b_w/b_f)}) \quad \text{when } x_u \leq D_f \quad (6.31a)$$

$$V_c = 0.37\sqrt{f_{ck}}[b_f D_f \sqrt{(b_w/b_f)} + b_w(x_u - D_f)] \quad \text{when } x_u > D_f \quad (6.31b)$$

where b_f and D_f are the breadth and depth of flange, respectively, and x_u is the neutral axis depth, which can be calculated as shown in Chapter 5. As the term $\sqrt{(b_w/b_f)}$ yields a value of one when there are no flanges, the form factor approach unifies the calculation of shear strength of both the rectangular and T-beams.

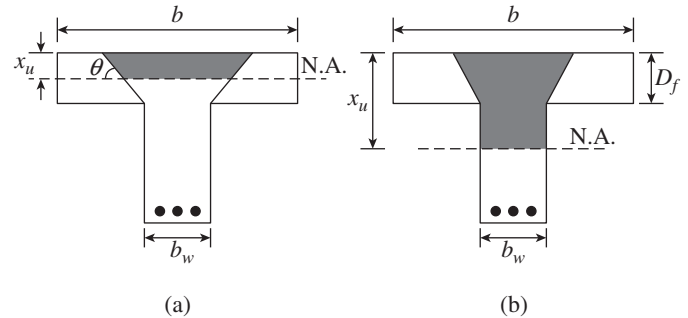


FIG. 6.34 Concept of shear funnel (a) Neutral axis within flange (b) Neutral axis outside flange

6.9 SHEAR DESIGN OF BEAMS WITH VARYING DEPTH

Beams of varying depth are encountered in haunched beams. In such members, it is necessary to account for the contribution of the vertical component of the flexural tensile force T_u , which is inclined at an angle β to the longitudinal direction, in the nominal shear stress, τ_v . The following two cases may arise in practice:

1. The bending moment M_u increases numerically in the same direction in which the effective depth d increases. In this case, as seen in Fig. 6.35(a), the net shear force is

$$V_{u,net} = V_u - (M_u/d)\tan \beta \quad (6.32)$$

The nominal shear stress (Clause 40.1.1 of IS 456) is obtained as

$$\tau_v = \frac{V_u - (M_u/d)\tan \beta}{b_w d} \quad (6.33a)$$

2. The bending moment M_u decreases numerically in the direction in which the effective depth d increases: In this case, as seen in Fig. 6.35(b), the net shear force is

$$V_{u,net} = V_u + (M_u/d)\tan \beta$$

The nominal shear stress (Clause 40.1.1 of IS 456) is obtained as

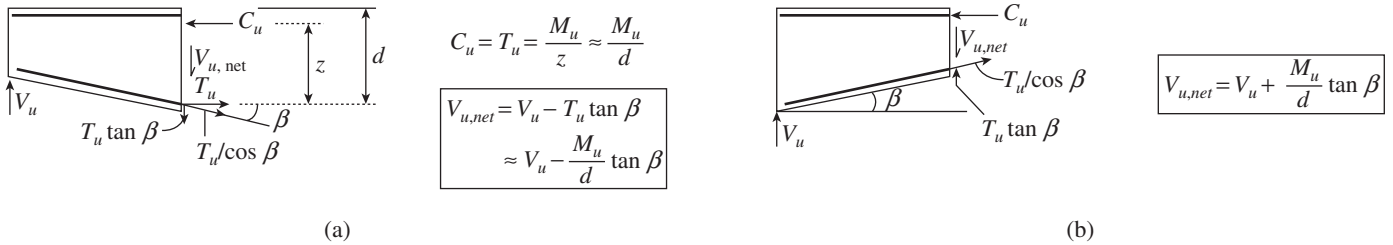


FIG. 6.35 Beams of variable depth (a) Bending moment increases with increasing depth (b) Bending moment decreases with increasing depth

$$\tau_v = \frac{V_u + (M_u/d) \tan \beta}{b_w d} \quad (6.33b)$$

A similar situation arises in tapered base slabs or footings, where flexural compression is inclined to the longitudinal axis of the beam, since the compression face may be sloping. Equation (6.30) may be used in such situations too.

It should be noted that in the case of cantilever beams, the depth increases in the same direction as the bending moment, and hence Eq. (6.30a) can be used to check for reduced shear stress.

6.10 SHEAR DESIGN OF BEAMS LOCATED IN EARTHQUAKE ZONES

When there is a reversal of stresses, due to earthquakes or reversed wind directions, the shear strength of concrete cannot be relied

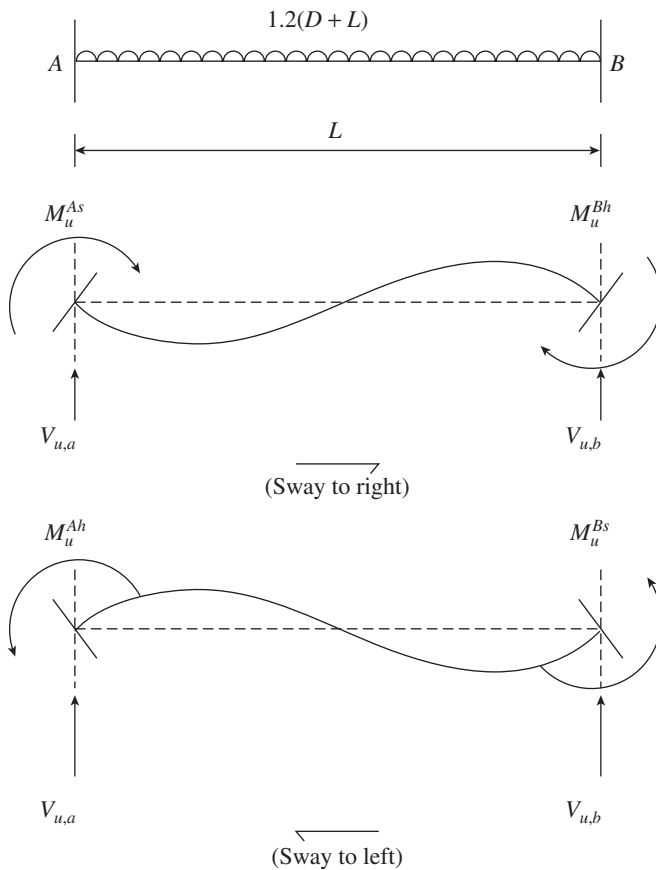
upon, as the cracks will criss-cross the cross section and hence cracked concrete will be present in the tension and compression zones. Hence, the stirrups should be designed to take the entire shear with zero contribution from concrete. Moreover, only vertical closed stirrups or those placed perpendicular to the member axis are to be used, with 135° hooks.

According to Clause 6.3.3 of IS 13920:1993, the shear capacity of the beam shall be more than the following:

1. Calculated factored shear force as per analysis
2. Shear force due to the formation of plastic hinges at both ends of the beam plus the factored gravity load on the span. This is given by the following (see Fig. 6.36):

(a) For sway to right:

$$V_{u,a} = V_a^{D+L} - 1.4 \frac{[M_u^{As} + M_u^{Bh}]}{L_{AB}} \quad \text{and} \quad (6.34a)$$



$$V_{u,a} = V_a^{D+L} - 1.4 \left[\frac{M_u^{As} + M_u^{Bh}}{L_{AB}} \right]$$

$$V_{u,b} = V_b^{D+L} + 1.4 \left[\frac{M_u^{As} + M_u^{Bh}}{L_{AB}} \right]$$

$$V_{u,a} = V_a^{D+L} + 1.4 \left[\frac{M_u^{Ah} + M_u^{Bs}}{L_{AB}} \right]$$

$$V_{u,b} = V_b^{D+L} - 1.4 \left[\frac{M_u^{Ah} + M_u^{Bs}}{L_{AB}} \right]$$

FIG. 6.36 Calculation of design shear force in case of earthquake loading

$$V_{u,b} = V_b^{D+L} + 1.4 \frac{[M_u^{As} + M_u^{Bh}]}{L_{AB}} \quad (6.34b)$$

(b) For sway to left:

$$V_{u,a} = V_a^{D+L} + 1.4 \frac{[M_u^{Ah} + M_u^{Bs}]}{L_{AB}} \quad \text{and} \quad (6.34c)$$

$$V_{u,b} = V_b^{D+L} - 1.4 \frac{[M_u^{Ah} + M_u^{Bs}]}{L_{AB}} \quad (6.34d)$$

Here, M_u^{As} , M_u^{Ah} , M_u^{Bs} , and M_u^{Bh} are the sagging and hogging moment of resistance of the beam section at ends A and B, respectively, L_{AB} is the clear span of the beam, V_a^{D+L} and V_b^{D+L} are the shears at ends A and B, respectively, due to the vertical loads with a partial safety factor of 1.2 for loads. The design shear at end A should be larger of the two values of $V_{u,a}$ computed earlier. Similarly, the design shear at end B should be larger of the two values of $V_{u,b}$ computed earlier. As mentioned in Chapter 5, the calculation of the moment of resistance of a section for the given area of reinforcement is too laborious. Hence, design aids have been developed by Desai (2003), which can be used for the shear design of beams.

Clause 6.3.3 of IS 13920:1993 ensures that a brittle shear failure does not precede the actual yielding of the beam in flexure. This clause also simplifies the process of calculating the plastic moment capacity of a section by taking it to be 1.4 times the calculated moment capacity with usual partial safety factors. This factor of 1.4 is based on the consideration that the plastic moment capacity of a section is usually calculated by assuming the stress in flexural reinforcement as $1.25f_y$ as against $0.87f_y$ in the moment capacity calculation (see Eq.6.34).

If the building is located in an earthquake zone, as per IS 13920, the spacing of stirrups over a length of $2d$, at either end of the beam (where flexural yielding due to plastic hinges may occur), shall not exceed (a) $d/4$ and (b) eight times the diameter

of the smallest bar, but need not be less than 100 mm. The first hoop should be at a distance of about 50 mm from the face of the joint. In the remaining portions of the beam, the spacing should be less than $d/2$ or 300 mm (see Fig. 6.37).

6.11 SHEAR IN BEAMS WITH HIGH-STRENGTH CONCRETE AND HIGH-STRENGTH STEEL

As already mentioned, in HSC the cracks pass through the aggregates instead of going around them due to the smaller difference between the strengths of aggregate and concrete matrix. This creates smoother crack surfaces, reducing the contribution of aggregate interlock and, hence, reducing the shear force carried by the concrete. As a result, higher dowel forces occur in the longitudinal reinforcing bars. These higher dowel forces, together with the high bond stresses in HSC beams, result in higher bond-splitting stresses where the shear cracks cross the longitudinal tension bars. These combined effects can ultimately lead to brittle shear failures. Hence, the formula similar to that in the IS code, which was derived based on the tests on NSC beams, should not be used. The reserve strength beyond diagonal cracking strength may decrease as the concrete strength increases (Lee and Kim 2008). However, due to the several assumptions involved in deriving the shear strength equation, the codal formulae are found to be conservative for HSC too (Subramanian 2003).

Xiao and Ma (1998) conducted experimental and analytical studies on the seismic performance of HSC beams with strength 70MPa (with a length to depth ratio of 6.0 and shear span ratio of 3.0) in moment-resisting frame structures (see Figs 6.38 a and b). Based on these tests, it was found that HSC beams exhibited increased capacity and improved hysteretic performance compared to NSC beams. Flexure deformation-dominated ductile responses were achieved by designing the

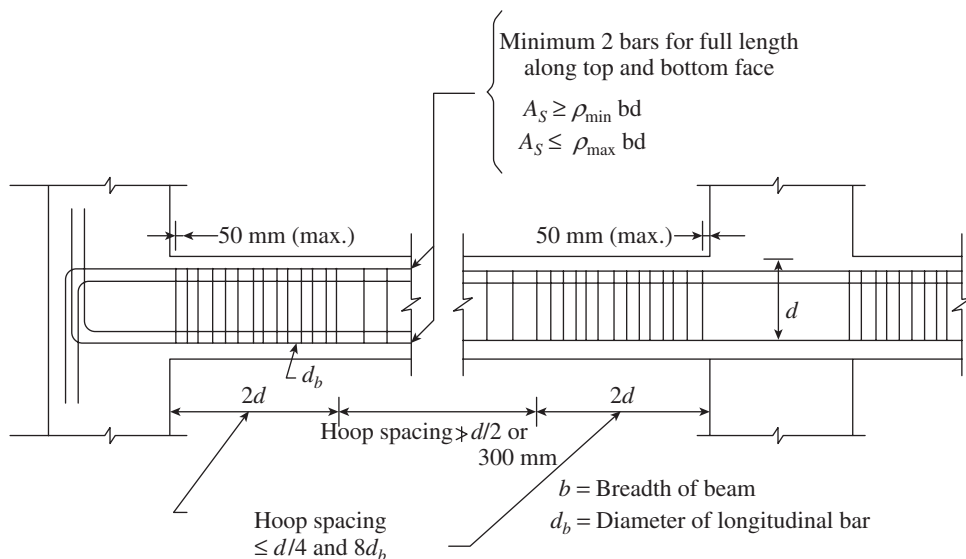


FIG. 6.37 Stirrup arrangement for beams located in earthquake zones

beam shear strength based on the seismic provision of the current ACI 318 code (by ignoring the shear strength contribution of concrete).

Beams made of HSC were found to exhibit more significant size effect than NSC beams (Collins and Kuchma 1999).

The width of the diagonal cracks is directly related to the strain in the stirrups. Hence, the Indian and US codes do not permit the design yield stress of stirrups to exceed 415MPa. This requirement limits the width of cracks that can develop. Such a requirement is important for both the appearance and development of aggregate interlock. When the

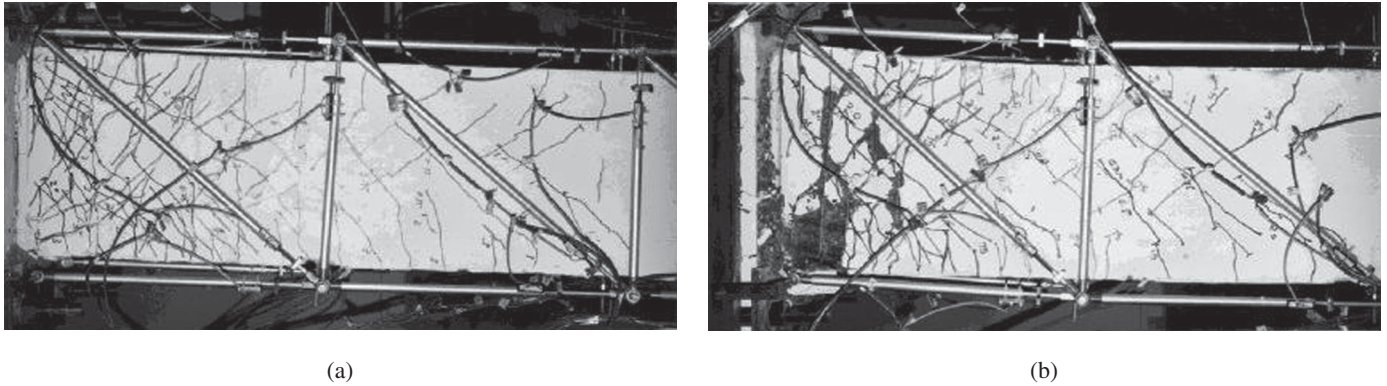


FIG. 6.38 Comparison for HSC beams with different transverse reinforcement details (a) HSC beam with 10 mm diameter stirrups (b) HSC beam with 6 mm diameter stirrups

Source: Xiao and Ma 1998, Copyright John Wiley & Sons Ltd 1998

width of the crack is limited, the aggregate interlock is enhanced. A further advantage of a limited yield stress is that the required anchorage length at the top of the stirrups is not as stringent as it would be for stirrups with higher yield strength. Hassan, et al. (2008) and Sumpter, et al. (2009) used MMFX steel with yield strength of 827 MPa as shear reinforcement in concrete beams with M27 to M51 concrete and found that the shear strength was significantly higher than that of beams with grade 420 steel. However, the failure was controlled by the crushing of concrete strut and not by the yielding of stirrup; hence, the stirrup strength beyond 552 MPa could not be used. They suggest that pairing high-strength steel (HSS) with HSC will be more beneficial.

It should be noted that the limitation of 420 MPa for design yield stress of stirrups is relaxed for deformed welded wire fabric because previous research has shown the use of higher strength wires to be quite satisfactory. Tests have shown that the width of inclined shear cracks at service loads is less for beams with higher strength wire fabric than for beams with stirrups having yield strength of 415 MPa. The ACI code permits a maximum stress of 550 MPa for high-strength wire fabric.

6.12 SHEAR DESIGN BEAMS WITH WEB OPENING

Transverse openings are provided in concrete beams for accommodating utility services, which will result in compact design and overall saving in terms of total building height. The provision of openings changes the behaviour of the beam from a simple one to a more complex one. Even though several codes contain detailed provisions for openings in floor slabs, they do not contain guidelines for openings in the web of beams. Although numerous shapes of openings are possible, circular (to accommodate service pipes) and rectangular (to accommodate air-conditioning ducts) openings are most common. Sometimes, the corners of rectangular openings are rounded off to reduce stress concentrations.

The openings must be located in such a way that no potential failure planes passing through several openings

could develop. In considering this, the possible reversal of the shear forces, in the case of earthquakes, should be taken into account. NZS 3101, Part1:06, suggests that small openings may be placed in the mid-depth of the web of beams, provided (a) the size of these openings does not exceed 1000 mm^2 for beams with an effective depth lesser than or equal to 500 mm or $0.004d^2$ when $d > 500$ mm, (b) the clear distance between these openings is greater than or equal to 150 mm, and (c) they do not encroach the compression zone of the member; the edge of the small opening should be no closer than $0.33d$ to the compression face of the member.

When a beam contains a small opening, the nominal shear strength of the beam without shear reinforcement may be taken as (Mansur and Tan 1999)

$$V_c = \tau_c b_w (d - d_o) \quad (6.35)$$

where d_o is the depth or diameter of the opening.

When the largest dimension of the opening exceeds 25 per cent of the effective depth, it is considered large, and the beam should be subjected to rational analysis to ensure that the failure at the opening does not occur under adverse loading conditions. This will require orthogonal or diagonal reinforcement of the member as shown in Fig. 6.39.

Such large openings should not be placed when the design shear force exceeds $0.36\sqrt{f_{ck}} b_w d$ or closer than $1.5D$ to the plastic region; the height of the opening should never exceed $0.4d$ and width $2d$ or its edge be closer than $0.33d$ to the compression face of the beam (see Fig. 6.39). The horizontal clear distance between adjacent large openings should be greater than $2d$ or $2L_o$, whichever is higher.

Entire shear resistance may be assigned to the compression chord. Longitudinal and transverse reinforcements should be placed in both sides of the opening to resist 1.5 times the shear force and bending moment generated by the shear across the opening. Shear reinforcement in the chords adjacent to the opening must resist 1.5 times the design shear force. This is to ensure that no failure occurs due

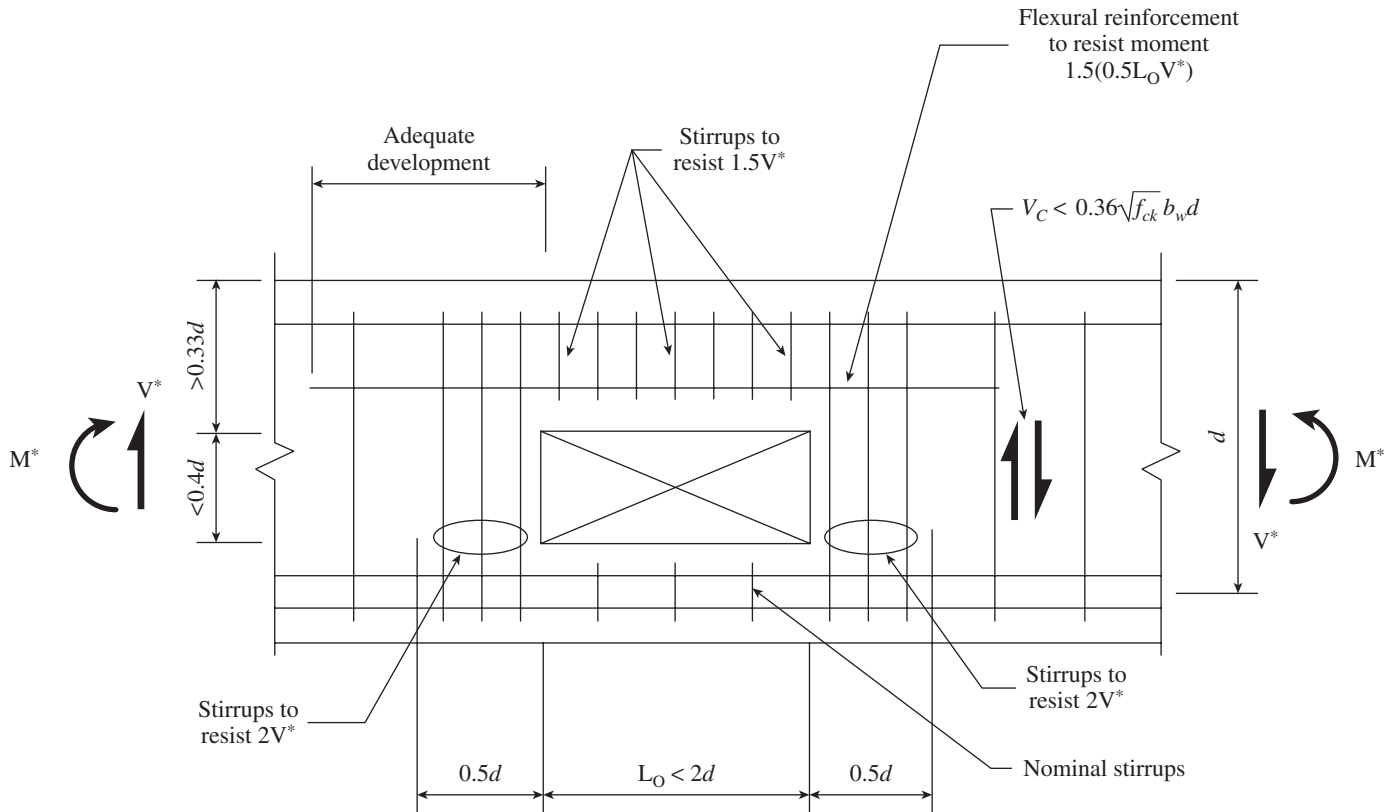


FIG. 6.39 Beams with large web openings

to the weakening of the beam by the opening. To control the horizontal splitting and diagonal tension cracks at the corners of the opening, transverse reinforcements should be designed for two times the design shear force and provided over a distance not less than $0.5d$ on both sides of the opening. All these design rules are shown in Fig. 6.39. More information on beams with openings may be found in Mansur and Tan (1999).

6.13 SHEAR STRENGTH OF MEMBERS WITH AXIAL FORCE

The beams in moment-resistant frames are often subjected to axial forces in addition to the bending moments and shears. Columns are also subjected to axial loads, bending moments, and shear forces. It has been found that axial tensile forces tend to decrease the shear strength of concrete, whereas axial compression tends to increase it (Bhide and Collins 1989; Gupta and Collins 2001). The compressive force acts like prestressing and delays the onset of flexural cracking; also, flexural cracks do not penetrate to a greater extent into the beam. However, tensile forces directly increase the stress and hence the strain in the longitudinal reinforcement. Axial tension increases the inclined crack width and reduces the aggregate interlock, and hence, the shear strength provided by the concrete is reduced.

Clause 40.2.2 of IS 456 allows an increase in the design shear strength of concrete due to compressive forces, using

the following factor, which should be multiplied with the values given in Table 19 of the code (Table 6.2 of this book):

$$\delta = 1 + \frac{3P_u}{A_g f_{ck}} \leq 1.5 \quad (6.36a)$$

where P_u is the axial compressive force acting on the member in N, A_g is the gross area of concrete section in mm^2 , and f_{ck} is the characteristic compressive strength of concrete in MPa. IS 456 does not give the guidelines for the detrimental effects of the tensile force, but may be considered with P_u taken negative for tension and using the following expression (NZS 3101, Part 1:2006):

$$\delta = 1 + \frac{12P_u}{A_g f_{ck}} \geq 0 \quad (6.36b)$$

Interestingly, Clause 11.2.1.2 of ACI 318-08 gives the following expression for the design shear strength of members with shear and axial compression:

$$V_c = 0.15 \left(1 + \frac{P_u}{14A_g} \right) \lambda \sqrt{f_{ck}} b_w d \quad (6.37)$$

In this equation, P_u/A_g is expressed in MPa.

For members subjected to significant axial tension, the following expression is suggested by ACI 318-08 (Clause 11.2.2.3):

$$V_c = 0.15 \left(1 + \frac{0.29P_u}{A_g} \right) \lambda \sqrt{f_{ck}} b_w d \geq 0 \quad (6.38)$$

where P_u is taken as negative for tension and P_u/A_g is expressed in MPa.

6.14 DESIGN OF STIRRUPS AT STEEL CUT-OFF POINTS

Longitudinal tension reinforcement is often curtailed in order to provide the required reduced area of steel in locations where the bending moment is less than the maximum value (see Chapter 7). The termination of flexural tensile reinforcement gives rise to sharp discontinuity in the steel, causing early appearance of flexural cracks, which in turn may turn into diagonal shear cracks. Clause 26.2.3.1 of IS 456 insists that the bars should extend beyond the theoretical cut-off point to reduce stress concentration (except at simple supports and end of cantilevers) by a distance greater than the effective depth d or 12 times the bar diameter. Experiments have shown that bar curtailment, especially when deformed bars are used, may adversely affect the shear strength of beams.

Hence, Clause 26.2.3.2 of IS 456 stipulates that flexural reinforcement in beams may be terminated in the tension zone, only if *any one* of the following conditions is satisfied:

1. The shear at the cut-off point does not exceed $2/3$ of V_u (i.e., cut-off is allowed in low shear zones). Writing it in terms of the stress, we get

$$\tau_v \leq \frac{2(\tau_c + \tau_s)}{3} \quad (6.39)$$

where $\tau_v = V_u/b_wd$

This may be rewritten as

$$\tau_s \leq (1.5\tau_v - \tau_c) \quad (6.40)$$

where τ_s is the shear for which the stirrups at the cut-off point should be designed.

2. Extra shear reinforcements are provided over a distance equal to $0.75d$ from the cut-off point. The excess stirrup area (in excess of that required for shear and torsion), A_{sv1} , given by

$$A_{sv1} = \frac{0.4b_s s_v}{f_{yv}} \quad (6.41)$$

where the spacing s_v should not exceed $d/(8\beta_b)$, where β_b is the ratio of area of bars cut off to the total area of bars at the section.

3. When 36mm diameter or smaller bars are used, excess flexural steel is available (continuing bars provide double the area required for flexure) along with excess shear capacity (shear capacity is greater than $1.33V_u$). It has to be noted that curtailment is not permitted for rods greater than 36mm.

Similar provisions are available in Clause 12.10.5 of ACI 318:05. As only one of these conditions needs to be satisfied, it is easier to consider only the first requirement. To avoid this check, designers may opt to extend all bars into the supports in simply supported beams or past the points of inflection in continuous beams.

6.15 SHEAR FRICTION

Shear friction is used where direct shear is transferred across a given plane. The situations where this concept will be useful include the interface between concretes cast at different times, interface between concrete and steel, connections of precast constructions, and corbels (see Fig. 6.40). The correct application of this concept depends on the proper selection of the assumed location of crack or slip. In the typical edge or end bearing applications, a crack of about 20° to the vertical is often assumed. The reinforcement must be provided crossing the potential or actual crack or shear plane to prevent direct shear failure.

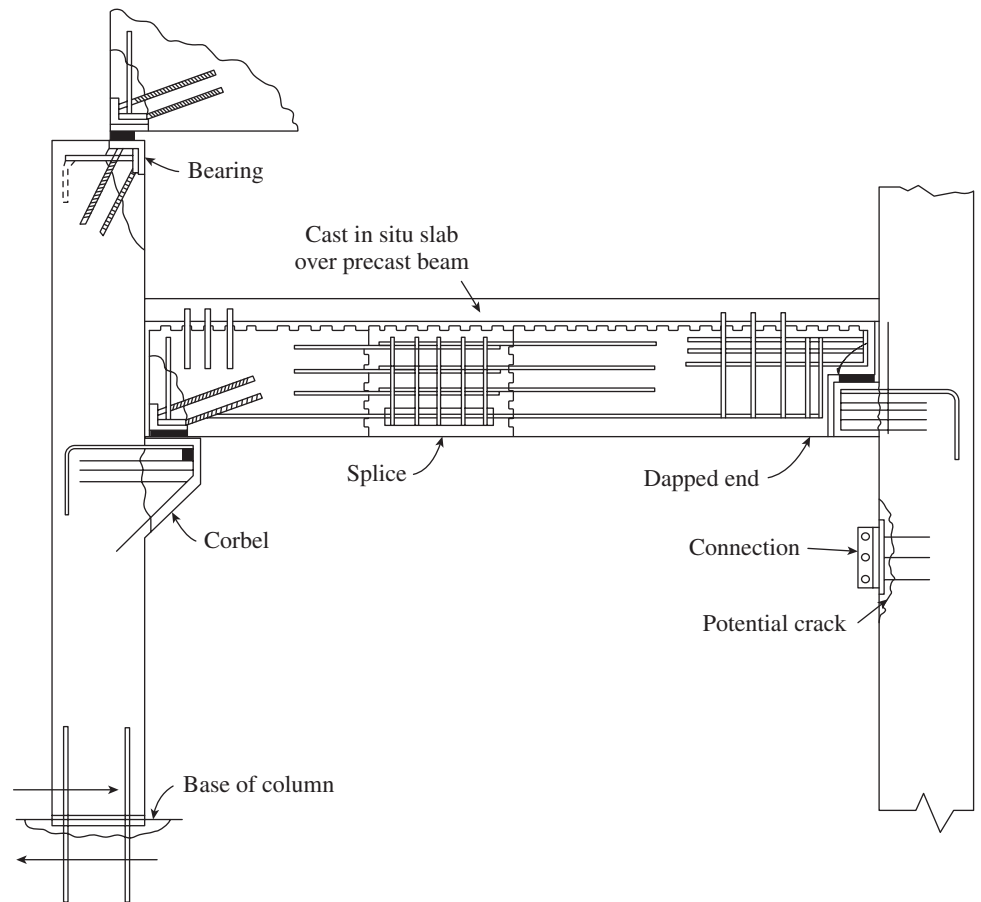


FIG. 6.40 Locations of potential cracks where shear friction concept is applied

The shear friction design method is quite simple and the behaviour can be easily visualized. As shown in Figs 6.41(a)–(c), a cracked block of concrete with the intercepted reinforcement is assumed. The shear force V_u acts parallel to the crack, and the tendency for the upper block to slip relative

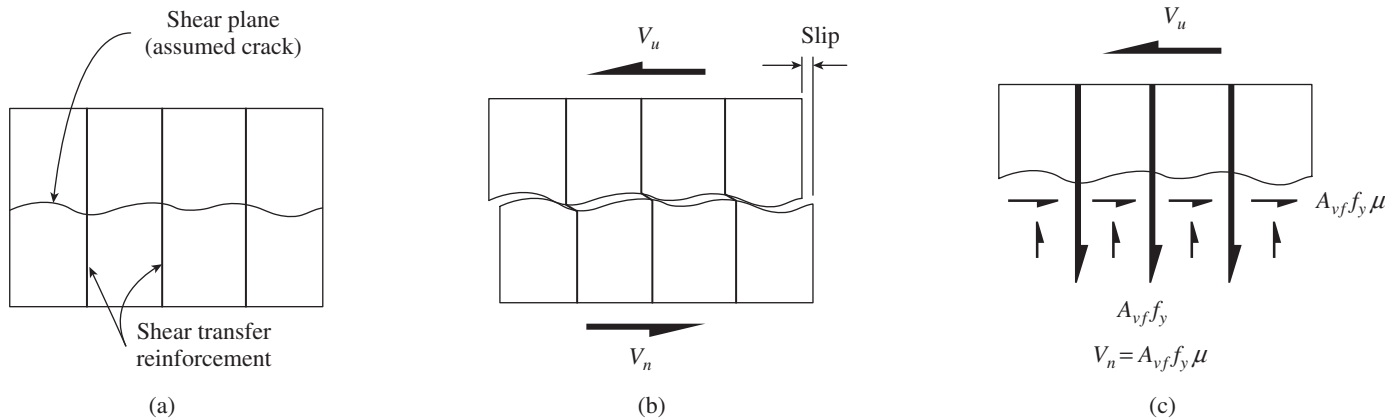


FIG. 6.41 Basis of shear friction design (a) Applied shear (b) Enlarged crack surface (c) Free body of concrete above crack

to the lower block has to be resisted by the friction along the interface of the crack, by the resistance to the shearing off of protrusions on the crack faces, and by the dowel action of the reinforcement crossing the crack. The dowel effect is usually neglected for simplicity, and to compensate for this factor a high value of friction coefficient is assumed. The irregular surface may separate the two blocks slightly, as shown in Fig. 6.41(b). If the crack surface is rough, the coefficient of friction may be high. The reinforcement provides a clamping force $A_{vf}f_y$ across the crack faces.

The tests have confirmed that well-anchored reinforcements will be stressed up to yield strength when the shear failure occurs. From the free body of the concrete above the crack, the nominal shear resistance V_{sn} due to friction between the crack surfaces is given as follows (Mattock and Hawkins 1972):

$$V_{sn} = A_{vf}f_y\mu \quad (6.42a)$$

where A_{vf} is the area of shear friction reinforcement placed normal to the possible crack, f_y is the yield strength of the reinforcement, and μ is the coefficient of friction (see Table 6.5). As per Clause 11.6 of the ACI code, the design strength is ϕV_{sn} , where $\phi = 0.75$ for shear friction design (we may adopt a partial safety factor of material as $1/1.5 = 0.67$), and to avoid the failure of concrete by crushing, V_{sn} should not exceed the lesser of $0.16f_{ck}A$ and $5.5A_c$ MPa, where A_c is area of concrete section resisting shear transfer. The yield stress of reinforcement is limited to 415 MPa.

TABLE 6.5 Values of coefficient of friction, μ

Case	Concrete Cast Against	Coefficient μ
1.	Monolithic construction	$1.4\lambda^*$
2.	Hardened concrete with surface intentionally roughened	1.0λ
3.	Hardened concrete with surface not intentionally roughened	0.6λ
4.	As-rolled structural steel and anchored by headed studs or reinforcing bars	0.7λ

*The value of λ is taken as 1.0 for normal weight concrete and 0.75 for lightweight concrete.

If V_u is the external factored shear force, the required steel area is given by

$$A_{vf} = \frac{V_u}{\phi\mu f_y} = \frac{V_u}{0.75\mu f_y} \quad (6.42b)$$

In some cases, the shear friction reinforcement may not cross the shear plane at 90° as discussed until now. If the shear friction reinforcement is inclined to the shear plane such that the shear force produces tension in the shear friction reinforcement, V_{sn} is computed by (see Fig. 6.42)

$$V_{sn} = A_{vf}f_y(\mu \sin \alpha + \cos \alpha) \quad (6.43)$$

where α is the angle between the shear friction reinforcement and the crack or shear plane. It should be noted that Eq. (6.43) should be used only when the shear force component parallel to the reinforcement produces tension in the reinforcement, as shown in Fig. 6.42; when α is greater than 90° , the relative moments of the surfaces try to compress the bars and Eq. (6.39) is not valid. See commentary to Clause 11.6.3 of ACI 318:08 for the *modified shear friction method*.

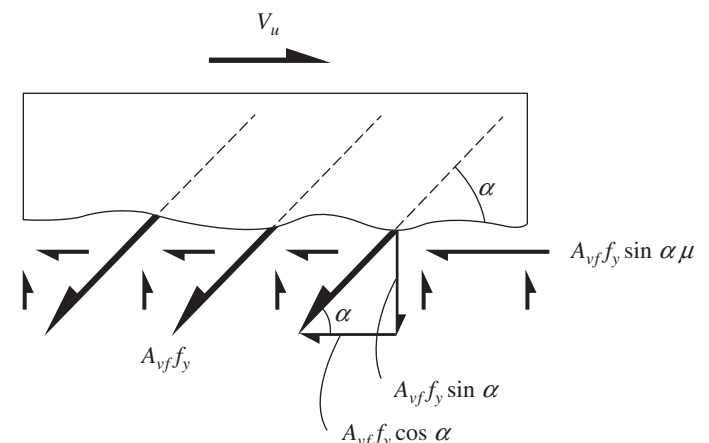


FIG. 6.42 Shear friction reinforcement at an angle to assumed crack

While using the shear friction method of design, reinforcement should be well anchored to develop the yield strength of steel, by full development length, hooks, or bends in the case of

reinforcement bars and by proper heads or welding in the case of studs joining the concrete to structural steel. Furthermore, the shear friction reinforcement anchorage should engage the primary reinforcement; otherwise, a potential crack may pass between the shear friction reinforcement and the body of the concrete (NZS 3101, Part 2:2006). Care must be exercised to consider all possible failure planes and to provide sufficient well-anchored reinforcement across the planes. It should be noted that IS 456 does not give any guidance for the shear friction method of design.

EXAMPLES

EXAMPLE 6.1 (Design of vertical stirrups):

A rectangular beam of size 230 mm width and 450 mm effective depth is reinforced with four bars of 20 mm diameter. Determine the required vertical shear reinforcement to resist the factored shear force of (a) 70 kN, (b) 250 kN, and (c) 400 kN. Consider concrete of grade M25 and steel of grade Fe 415.

SOLUTION:

(a) $V_u = 70$ kN

$$\text{Nominal shear stress, } \tau_v = V_u / (b_w d) \\ = 70 \times 10^3 / (230 \times 450) = 0.68 \text{ N/mm}^2$$

For M25 concrete, $\tau_{c, \max}$ from Table 20 of the code = 3.1 N/mm².

$$\text{Area of tension steel} = 4\#20 = 4 \times 314 = 1256 \text{ mm}^2$$

$$100A_s / bd = 100 \times 1256 / (230 \times 450) = 1.21\%$$

From Table 19 of the code, design shear strength

$$\tau_c = 0.69 \text{ N/mm}^2$$

$$\tau_v < \tau_c < \tau_{c, \max} \text{ but } \tau_v > 0.5\tau_c$$

$$V_{uc} = \tau_c b_w d = 0.69 \times 230 \times 450 / 10^3 = 71.42 \text{ kN} > V_u$$

(Let us just compare the value with that given in ACI 318:11

$$V_c = 0.15 \lambda \sqrt{f_{ck}} b_w d = 0.15 \times 1 \times \sqrt{25} \times 230 \times 450 / 10^3 = 77.6 \text{ kN}$$

It shows that the Indian code underestimates the concrete shear strength. In some cases, the difference may even be 50%.)

Hence, only minimum reinforcement has to be provided.

Consider 8 mm diameter two-legged vertical stirrups ($A_{sv} = 100 \text{ mm}^2$) at spacing s_v (Clauses 26.5.1.5 and 26.5.1.6).

$$s_v = \frac{0.87 A_{sv} f_y}{0.4b} = \frac{0.87 \times 100 \times 415}{(0.4 \times 230)} = 392 \text{ mm}$$

$$s_{v, \max} = 0.75d = 0.7 \times 450 = 315 \text{ or } 300 \text{ mm. Hence, } \\ s_{v, \max} = 300 \text{ mm}$$

Hence, provide 8 mm diameter two-legged stirrups at a spacing of 300 mm.

Using design aids

Design of nominal shear is equivalent to designing the section for a shear stress of 0.4 Pa.

$$\frac{V_{us}}{d} = \frac{0.4 \times 230 \times 450}{45 \times 1000} = 0.92 \text{ kN/cm}$$

From Table 62 of SP 16, provide two-legged 8 mm diameter stirrups at 350 mm c/c (spacing $> s_{v, \max}$). Hence, provide two-legged 8 mm diameter stirrups at 300 mm c/c.

(b) $V_u = 250$ kN

$$\text{Nominal shear stress } \tau_v = V_u / (b_w d) = 250 \times 10^3 / (230 \times 450) = 2.42 \text{ N/mm}^2$$

$\tau_{c, \max}$ from (a) = 3.1 N/mm² $> \tau_v$. Hence, it is acceptable.

$$\tau_c \text{ from (a)} = 0.69 \text{ N/mm}^2$$

$$V_{uc} = \tau_c b_w d = 71.42 \text{ kN from (a)} < V_u$$

Hence, shear reinforcement has to be provided.

Consider 8 mm diameter two-legged vertical stirrups ($A_{sv} = 100 \text{ mm}^2$)

From Clause 40.4(a)

$$s_v = \frac{0.87 f_y A_{sv} d}{(V_u - V_{uc})} = \frac{0.87 \times 415 \times 100 \times 450}{(250 - 71.42)} \times 10^{-3}$$

$$= 91 \text{ mm} < s_{v, \max} = 300 \text{ mm}$$

Hence, 8 mm diameter two-legged stirrups at a c/c of 90 mm may be provided.

However, it may be desirable to provide a larger spacing of stirrups for convenience in construction. Hence, let us choose 10 mm diameter stirrups ($A_{sv} = 157 \text{ mm}^2$).

$$s_v = \frac{0.87 \times 415 \times 157 \times 450}{(250 - 71.42)} \times 10^{-3} = 142.8 \text{ mm} < 300 \text{ mm}$$

Hence, provide two-legged 10 mm diameter stirrups at a spacing of 140 mm c/c.

Using design aids

$$\frac{V_{us}}{d} = \frac{(250 - 71.42)}{45} = 3.97 \text{ kN/cm}$$

From Table 62 of SP 16, use 10 mm diameter stirrups at 140 mm c/c.

(c) $V_u = 400$ kN

$$\text{Nominal shear strength } \tau_v = V_u / (b_w d) = 400 \times 10^3 / (230 \times 450) = 3.86 \text{ N/mm}^2$$

$$\tau_{c, \max} \text{ from (a)} = 3.1 \text{ N/mm}^2 < 3.86 \text{ N/mm}^2$$

Hence, the section is not sufficient to carry the applied shear.

The section has to be modified (say to 230 mm \times 600 mm) and the design for shear may be carried out as shown earlier.

EXAMPLE 6.2 (Design of bent-up bars as shear reinforcement):

A rectangular beam of section 300 mm width by 500 mm effective depth is reinforced with four 20 mm bars, out of which two bars are bent at the ends of the beam at 45°. Determine the additional shear reinforcement required, if the factored shear force at the critical section is 320 kN. Consider concrete of grade M25 and steel of grade Fe 415.

SOLUTION:

Step 1 Determine nominal shear stress.

$$V_u = 320 \text{ kN; } \tau_v = \frac{V_u}{b_w d} = \frac{320 \times 10^3}{300 \times 500} = 2.13 \text{ N/mm}^2$$

Step 2 Check for shear stress.

$$p = \frac{A_s \times 100}{b_w d} = \frac{628 \times 100}{300 \times 500} = 0.42 \%$$

From Table 19 of IS 456, $\tau_c = 0.45 \text{ N/mm}^2$

From Table 20 of IS 456, $\tau_{c,\max} = 3.1 \text{ N/mm}^2$

$$\tau_v > \tau_c \text{ but } \tau_v < \tau_{c,\max}$$

Hence, shear reinforcement has to be provided.

Step 3 Calculate the shear to be carried by steel, V_s .

$$V_s = (2.13 - 0.45) \times 300 \times 500 \times 10^{-3} = 252 \text{ kN}$$

Step 4 Determine the shear resistance of the bent-up bars.

As per Clause 40.4(c) of IS 456

$$\begin{aligned} V_{us} &= 0.87 f_y A_{sv} \sin \alpha \\ &= 0.87 \times 415 \times 628 \times \sin 45^\circ \times 10^{-3} \\ &= 160.3 \text{ kN} > 252/2 = 126 \text{ kN} \end{aligned}$$

These results can also be obtained from Table 63 of SP 16 as follows:

V_{us} of single 20 diameter bar (Fe 415) = 80.21; hence for two bars = 160.42 kN.

These bars are effective over a distance of

$$d(1 + \cot \alpha) = 500(1 + \cot 45^\circ) = 1000 \text{ mm}$$

Step 5 Determine the shear provided by the additional vertical stirrups. As per Clause 40.4 of IS 456 at least $V_s/2$ should be provided by the vertical stirrups. Hence, the shear to be provided by vertical stirrups

$$V'_{us} = \frac{1}{2} \times 252 = 126 \text{ kN}$$

$$\frac{V'_{us}}{d} = \frac{126}{500} = 2.52 \text{ kN/cm}$$

From Table 62 of SP 16, use additional two-legged vertical stirrups of 8 mm diameter bars at 140 mm c/c.

Check: Max allowed spacing = 75×500 or $300 = 300 \text{ mm}$.

EXAMPLE 6.3 (Design of a T-beam for shear):

A T-beam and slab system is having beams spaced at 3 m centre to centre with clear span of 6 m and supported by 300 mm brick walls. The T-beam has the following dimensions: $D_f = 100 \text{ mm}$, $b_w = 250 \text{ mm}$, $D = 550 \text{ mm}$, and clear cover = 30 mm. The beam has to carry a live load of 4 kN/m and is reinforced with four 20 mm diameter bars as longitudinal tension steel. Design the shear reinforcement using M20 concrete and grade Fe 415 steel. In addition, design the beam for a shear of 150 kN.

SOLUTION:

Step 1 Calculate the maximum shear force at critical section:

Spacing of beam = 3 m

As per Clause 22.2 of IS 456

Effective span = Lesser of clear span + Effective depth or c/c of supports

$$= (6 + 0.5) \text{ or } (6 + 0.3) = 6.3 \text{ m}$$

$$\begin{aligned} \text{Dead load of beam} &= (3 \times 0.10 \times 25) + (0.25 \times 0.45 \times 25) \\ &= 10.32 \text{ kN/m} \end{aligned}$$

$$\text{Live load of beam} = 3 \times 1 \times 4 = 12 \text{ kN/m}$$

$$\text{Factored load} = 1.5(10.32 + 12) = 33.48 \text{ kN/m}$$

$$\text{Factored shear force} = 33.48 \times 6.3/2 = 105.46 \text{ kN}$$

Assuming 10 mm stirrups, effective depth, $d = 550 - 30 - 10 - 20/2 = 500 \text{ mm}$

Shear force at critical section, that is, at d from the face of the support

$$V_u = 33.48 (6.3 - 2 \times 0.5)/2 = 88.72 \text{ kN}$$

Step 2 Calculate the nominal shear stress.

$$\text{Nominal shear stress, } \tau_v = V_u/(b_w d) = 88.72 \times 10^3/(250 \times 500) = 0.71 \text{ N/mm}^2$$

Step 3 Check for shear stresses.

For M20 concrete, $\tau_{c,\max}$ from Table 20 of code = $2.8 \text{ N/mm}^2 > \tau_v$,

Area of tension steel near support = $4\#20 = 4 \times 314 = 1256 \text{ mm}^2$

$$p_t = 100A_s/bd = 100 \times 1256/(250 \times 500) = 1.00\%$$

Hence, from Table 19 of the code,

$$\text{Design shear strength of concrete, } \tau_c = 0.62 \text{ N/mm}^2$$

$$\tau_v > \tau_c < \tau_{c,\max}$$

Hence, shear reinforcement has to be provided to carry a shear equal to $V_u - \tau_c b d$.

Step 4 Design the shear reinforcement.

Shear carried by concrete = $0.62 \times 250 \times 500 \times 10^{-3} = 77.5 \text{ kN}$

$$\text{Shear to be carried by stirrups} = 88.72 - 77.5 = 11.22 \text{ kN}$$

Assuming two-legged 8 mm diameter stirrups, $A_{sv} = 2 \times 50.3 = 100.6 \text{ mm}^2$

Shear to be carried by nominal steel at $0.4 \text{ N/mm}^2 = 0.4 \times 250 \times 500 \times 10^{-3} = 50 \text{ kN} > 11.22 \text{ kN}$

Hence, only nominal steel has to be provided.

Minimum steel as per Clause 26.5.1.6

$$\frac{A_{sv}}{bs_v} = \frac{0.4}{0.87 f_y} \text{ or } s_v = \frac{0.87 f_y A_{sv}}{0.4 b} = \frac{0.87 \times 415 \times 100.6}{0.4 \times 250}$$

$$= 363.2 \text{ mm}$$

Maximum spacing = $0.75d$ ($0.75 \times 500 = 375 \text{ mm}$) or 300 mm

Hence, provide two-legged 8 mm stirrups at a spacing of 300 mm throughout the beam length. The details of shear reinforcement are provided in Fig. 6.43.

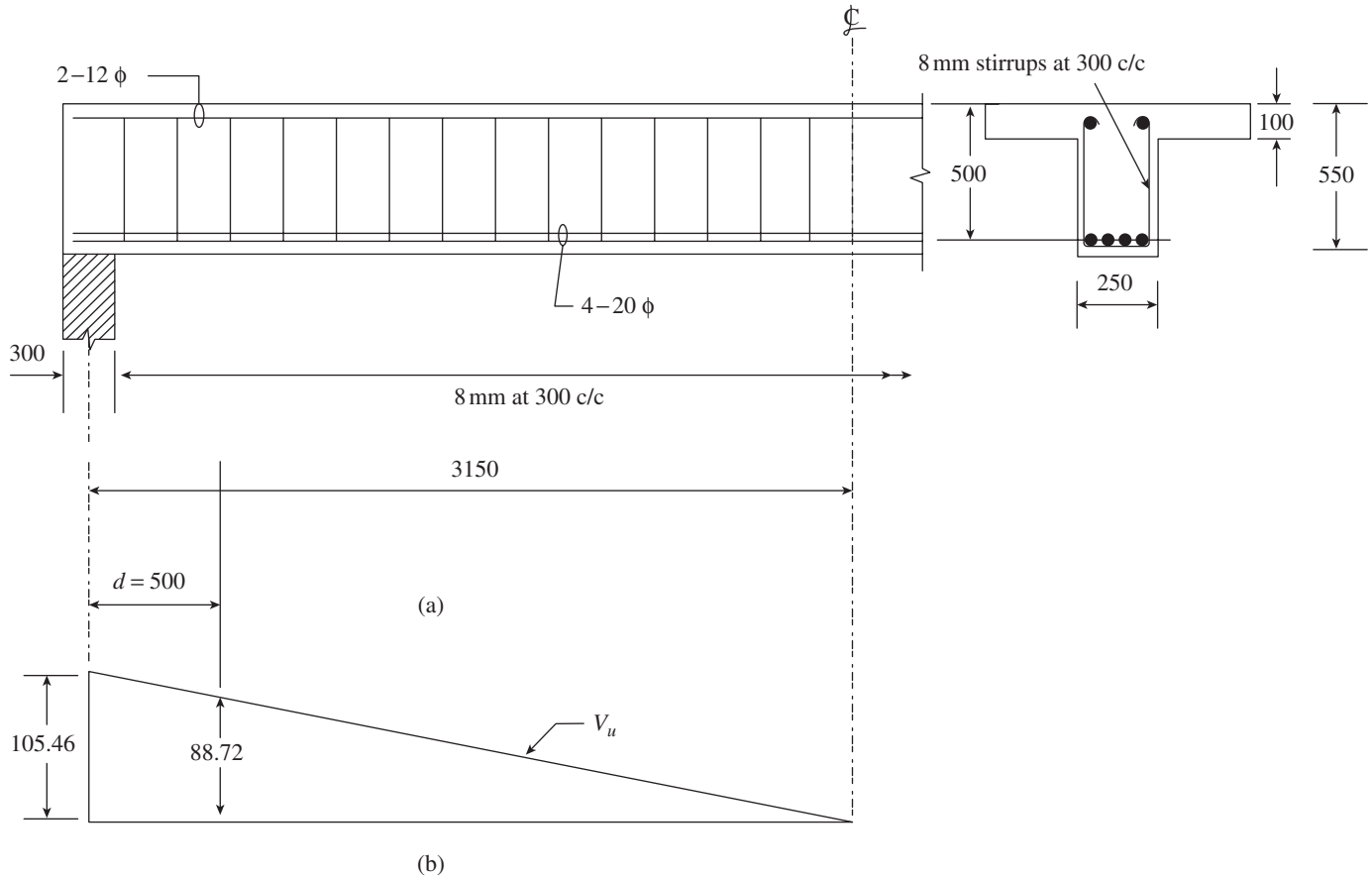


FIG. 6.43 Beam of Example 6.3 (a) Shear reinforcement (b) Shear force diagram

(Let us just check the minimum steel as per ACI code,

$$\frac{A_{sv}}{bs_v} = \frac{0.9\sqrt{f_{ck}}}{16f_y} \geq \frac{1}{3f_y}$$

Hence, $s_v = \frac{16f_y A_{sv}}{0.9\sqrt{f_{ck}} b} = \frac{16 \times 415 \times 100.6}{0.9 \times \sqrt{20} \times 250} = 663 \text{ mm}$ or

$$s_v = \frac{3f_y A_{sv}}{b} = \frac{3 \times 415 \times 100.6}{250} = 500 \text{ mm}$$

Both are greater than 363.2 mm.)

Design for $V_u = 150 \text{ kN}$

Step 1 Calculate shear stresses.

Nominal shear stress, $\tau_v = V_u / (b_w d) = 150 \times 10^3 / (250 \times 500) = 1.2 \text{ N/mm}^2$

$$\tau_c = 0.62 \text{ N/mm}^2; \tau_{c,max} = 2.8 \text{ N/mm}^2$$

$$\tau_v > \tau_c < \tau_{c,max}$$

Hence, shear reinforcement has to be provided to carry a shear equal to $V_u - \tau_c b d$.

Step 2 Design the shear reinforcement.

Stirrups have to be provided for $V_s = 150 - 77.5 = 72.5 \text{ kN} > 50 \text{ kN}$

$$V_s / d = 72.5 / 50 = 1.45 \text{ kN/cm}$$

Hence, from Table 62 of SP 16, adopt two-legged 8 mm diameter stirrups at 250 mm c/c.

Step 3 Calculate the region of nominal shear.

Shear that can be carried by concrete = 77.5 kN

Distance from the centre line of beam where this can be achieved

$$= \frac{(6.3/2 - 0.5)}{150} \times 77.5 = 1.37 \text{ m}$$

Hence provide two-legged 8 mm diameter stirrups at 250 mm c/c from support to $6.3/2 - 1.37 = 1.78 \text{ m}$ on both ends of the beam and two-legged 8 mm diameter stirrups at 300 mm c/c in the central 2.74 m portion of the beam.

Note: In practice, it is better to provide two-legged 8 mm diameter stirrups at 250 mm c/c throughout the beam.

EXAMPLE 6.4 (Shear resistance of a given beam):

Calculate the shear resistance of a beam of width 300 mm and effective depth 500 mm reinforced with five 20 mm bars at the mid-span of which two bars are bent at the ends at 45°. The beam is provided with shear reinforcement of 8 mm diameter two-legged vertical stirrups throughout the beam at a spacing of 160 mm. M20 concrete and Fe 415 steel have been adopted.

Step 1 Calculate τ_c .

Tension steel at support, $A_s = 3\#20 \text{ mm} = 942 \text{ mm}^2$

$$p_t = \frac{100A_s}{b_w d} = \frac{100 \times 942}{300 \times 500} = 0.628\%$$

Step 2 Calculate the shear strength. As per Table 19 of IS 456,

$$\tau_c = 0.52 \text{ N/mm}^2$$

Shear taken by concrete $V_c = 0.52 \times 300 \times 500 \times 10^{-3} = 78 \text{ kN}$

Step 3 Calculate the shear strength of vertical stirrups.

Shear taken by stirrups (8 mm at 160 mm c/c)

$$V_s = \frac{A_{sv}}{s_v} 0.87 f_y d = \frac{(2 \times 50.3)}{160} \times 0.87 \times 415 \times 500 \times 10^{-3} = 113.5 \text{ kN}$$

Step 4 Determine the shear strength of bent-up bars.

$$V_s = A_{sv} (0.87 f_y) \sin \alpha = 2 \times 314 (0.87 \times 415) \sin 45^\circ \times 10^{-3} = 160.3 \text{ kN}$$

Step 5 Calculate the total shear resistance of the beam.

$$V = 78 + 113.5 + 160.3 = 351.8 \text{ kN}$$

It should be noted that considerable shear is taken by bent-up bars. However, it is not advisable to provide bent-up bars alone due to the reasons discussed in the text.

EXAMPLE 6.5 (Shear in tapered beam):

Design shear reinforcement for a tapered cantilever beam of span 3 m, having a section of 250 mm effective depth and 300 mm width at the free end, and 550 mm effective depth and 300 mm width at the support (see Fig. 6.44). The beam has to support a factored uniform load of 80 kN/m, including its self-weight. Assume an effective cover of 50 mm, Fe 415 steel, and M25 concrete.

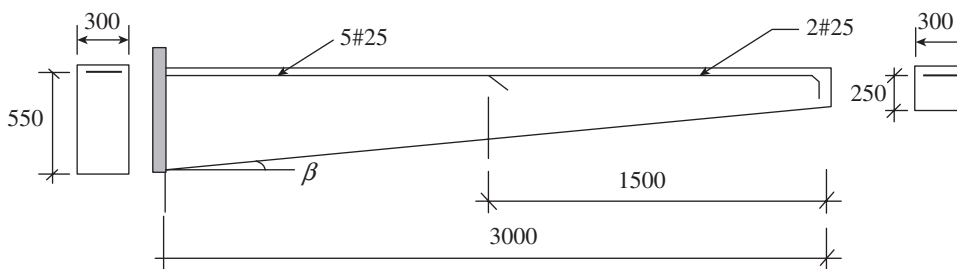


FIG. 6.44 Tapered cantilever beam of Example 6.5

SOLUTION:

In cantilever, the critical section for shear should be taken at the support.

Step 1 Calculate shear force and bending moment at the critical section.

Shear force at support, $V = 80 \times 3 = 240 \text{ kN}$

Bending moment at support, $M = 80 \times 3^2/2 = 360 \text{ kNm}$

$$\tan \beta = \frac{550 - 250}{3000} = 0.1$$

Step 2 Find the type of variation of the bending moment. The bending moment increases numerically in the same direction in which the depth of the section increases. Hence, as per Clause 40.1.1 of IS 456

$$V_u = V - (M/d) \tan \beta = 240 - (360/0.55) \times 0.1 = 174.55 \text{ kN}$$

The shear design is similar to the other examples.

Step 3 Calculate the shear stresses.

Nominal shear stress, $\tau_v = V_u/(b_w d) = 174.55 \times 10^3/(300 \times 550) = 1.06 \text{ N/mm}^2$

$$p_t = \frac{100A_s}{b_w d} = \frac{100 \times 5 \times 490}{300 \times 550} = 1.48\%$$

$\tau_c = 0.737 \text{ N/mm}^2$ (Table 19 of IS 456); $\tau_{c,\max} = 3.1 \text{ N/mm}^2$ (Table 20 of IS 456)

$$\tau_v > \tau_c < \tau_{c,\max}$$

Hence, shear reinforcement has to be provided to carry a shear equal to $V_u - V_c$.

Step 4 Design the shear reinforcement.

$$V_c = 0.737 \times 300 \times 550 \times 10^{-3} = 121.6 \text{ kN}$$

Stirrups has to be provided for $V_s = 174.55 - 121.6 = 52.95 \text{ kN}$

$$V_s/d = 52.95/55 = 0.963 \text{ kN/cm}$$

Hence, from Table 62 of SP 16, adopt two-legged 8 mm diameter stirrups at 300 mm c/c.

EXAMPLE 6.6 (Shear in curtailed steel locations):

Consider the cantilever beam of Example 6.5 and design a shear reinforcement at 1.5 m from the free end, if the longitudinal reinforcement of five 25 bars is curtailed to two 25 bars.

SOLUTION:

Step 1 Calculate the shear force and bending moment at the section.

Shear force, $V = 80 \times 1.5 = 120 \text{ kN}$

Bending moment, $M = 80 \times 1.5^2/2 = 90 \text{ kNm}$

$\tan \beta = 0.1$ (from Example 6.5)

Effective depth at this section = $(250 + 550)/2 = 400 \text{ mm}$

Step 2 Identify the type of variation of bending moment. The bending moment increases numerically in the same direction in which the depth of the section increases. Hence, as per Clause 40.1.1 of IS 456

$$V_u = V - (M/d) \tan \beta = 120 - (90/0.40) \times 0.1 = 97.5 \text{ kN}$$

Step 3 Calculate the shear stresses.

Nominal shear stress, $\tau_v = V_u/(b_w d) = 97.5 \times 10^3/(300 \times 400) = 0.81 \text{ N/mm}^2$

$$p_t = \frac{100A_s}{b_w d} = \frac{100 \times 2 \times 490}{300 \times 400} = 0.82\%$$

$\tau_c = 0.59 \text{ N/mm}^2$ (Table 19 of IS 456); $\tau_{c,\max} = 3.1 \text{ N/mm}^2$ (Table 20 of IS 456)

$$\tau_v > \tau_c < \tau_{c,\max}$$

Hence, shear reinforcement has to be provided to carry a shear equal to $V_u - V_c$.

Step 4 Design the shear reinforcement.

$$V_c = 0.59 \times 300 \times 400 \times 10^{-3} = 70.8 \text{ kN}$$

Stirrups have to be provided for $V_s = 97.5 - 70.8 = 26.7 \text{ kN}$

$$V_s/d = 26.7/40 = 0.668 \text{ kN/cm}$$

Hence, from Table 62 of SP 16, adopt two-legged 8 mm diameter stirrups at 300 mm c/c.

Step 5 Provide extra stirrup at cut-off. As per Clause 26.2.3.2 (a) of IS 456, the shear at cut-off point should not exceed $2/3(V_c + V_s)$.

V_s of two-legged 8 mm diameter stirrups at 300 mm c/c

$$V_s = \frac{A_{sv}}{s_v} 0.87 f_y d = \frac{(2 \times 50.3)}{300} \times 0.87 \times 415 \times 400 \times 10^{-3} = 48.4 \text{ kN}$$

Hence $2/3(V_c + V_s) = 2/3(70.8 + 48.4) = 79.5 \text{ kN}$

$$V_u = 97.5 > 79.5$$

Hence, provide two-legged 8 mm diameter stirrups at 190 mm c/c, with $V_s = 76.46 \text{ kN}$.

The other condition is also shown just for calculation, as only one condition needs to be satisfied.

Since the longitudinal steel is curtailed, we have to provide extra steel for a distance of $0.75d$ ($0.75 \times 400 = 300 \text{ mm}$) in the direction of curtailment from the point of curtailment as per Clause 26.2.3.2(b) of IS 456.

$\beta_b = \text{Area of cut-off bars/Total area of bars} = 3 \times 490/(5 \times 490) = 0.6$

$$\text{Maximum } s_v = \frac{d}{8\beta_b} = \frac{400}{8 \times 0.6} = 83.33 \text{ mm, say } 80 \text{ mm}$$

$$A'_{sv} = \frac{0.4bs_v}{f_y} = \frac{0.4 \times 300 \times 80}{415} = 23.1 \text{ mm}^2$$

Area of two-legged 6 mm diameter stirrups = $56.5 \text{ mm}^2 > 23.1 \text{ mm}^2$.

Hence, provide two-legged 6 mm diameter extra stirrups beyond the point of cut-off for a distance of 300 mm at 80 mm spacing, in addition to the two-legged 8 mm diameter stirrups at 300 mm c/c (see Fig. 6.45).

EXAMPLE 6.7 (Shear strength when shear and axial forces are present):

A rectangular beam of section 230 mm width by 450 mm effective depth is reinforced with four 20 mm bars and is made of concrete of grade M25 and steel of grade Fe 415.

Determine the shear strength of concrete, if (a) a compressive force of 100 kN is acting on the beam (b) a tensile force of 50 kN is acting on the beam.

SOLUTION:

(a) Compressive force of 100 kN

The shear strength of the section has already been calculated in Example 6.1 as 71.42 kN.

The augmentation factor due to compressive force as per Clause 40.2.2 is

$$\delta = 1 + \frac{3P_u}{A_g f_{ck}} = 1 + \frac{3 \times 100 \times 10^3}{230 \times 450 \times 25} = 1.116 \leq 1.5;$$

hence

$$V_c = 1.116 \times 71.42 = 82.8 \text{ kN}$$

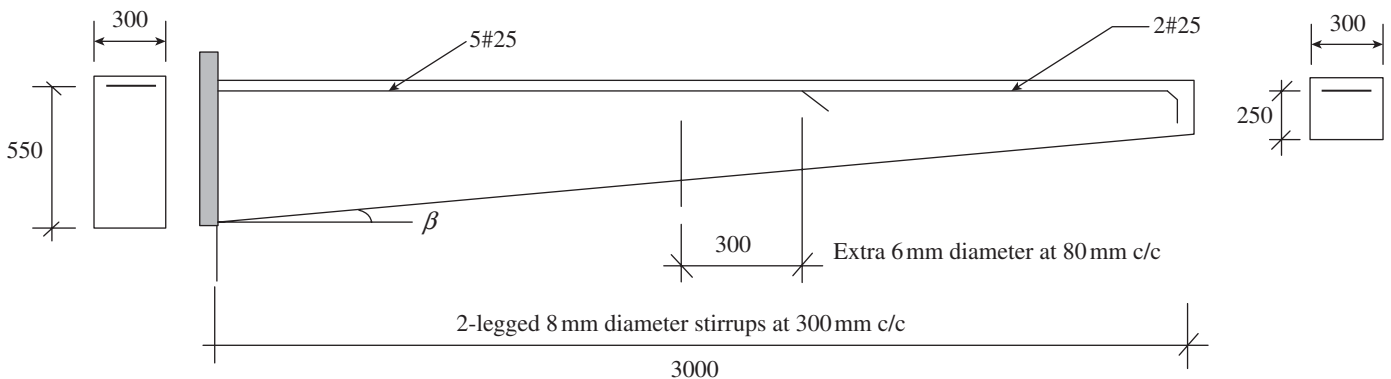


FIG. 6.45 Details of shear reinforcement for cantilever beam of Example 6.6

The shear strength as per ACI 318 is

$$\begin{aligned} V_c &= 0.15 \left(1 + \frac{P_u}{14A_g} \right) \lambda \sqrt{f_{ck}} b_w d \\ &= 0.15 \left(1 + \frac{100 \times 10^3}{14 \times 230 \times 450} \right) \\ &\quad 1.0 \times \sqrt{25} \times 230 \times 450 \times 10^{-3} \\ &= 82.98 \text{ kN} \end{aligned}$$

(b) Tensile force of 50 kN

The reduced shear strength as per ACI 318 is

$$\begin{aligned} V_c &= 0.15 \left(1 + \frac{0.29P_u}{A_g} \right) \lambda \sqrt{f_{ck}} b_w d \\ &= 0.15 \left(1 - \frac{0.29 \times 50 \times 10^3}{230 \times 450} \right) 1.0 \times \sqrt{25} \times 230 \times 450 \times 10^{-3} \\ &= 66.75 \text{ kN} \end{aligned}$$

Note: Minus sign denotes tension

EXAMPLE 6.8 (Shear friction):

Design the bearing of a precast beam of size 400 mm width and 600 mm depth to resist a support reaction of $V_u = 400$ kN applied to a $75 \times 75 \times 6$ mm steel angle as shown in Fig. 6.46. Assume a horizontal reaction, N_u , of 20 per cent of the vertical reaction, owing to restrained volume change, or 80 kN. Assume the use of M30 concrete and Fe 415 steel.

SOLUTION:

Let us first assume a crack at 20° initiated at 100 mm at the end of the beam as shown in Fig. 6.46. Required A_{vf} as per shear friction theory

$$\begin{aligned} A_{vf} &= \frac{V_u \cos 20^\circ + N_u \sin 20^\circ}{\phi \mu f_y} = \frac{(400 \times 0.9396 + 80 \times 0.342) 10^3}{0.75 \times 1.4 \times 415} \\ &= 925.3 \text{ mm}^2 \end{aligned}$$

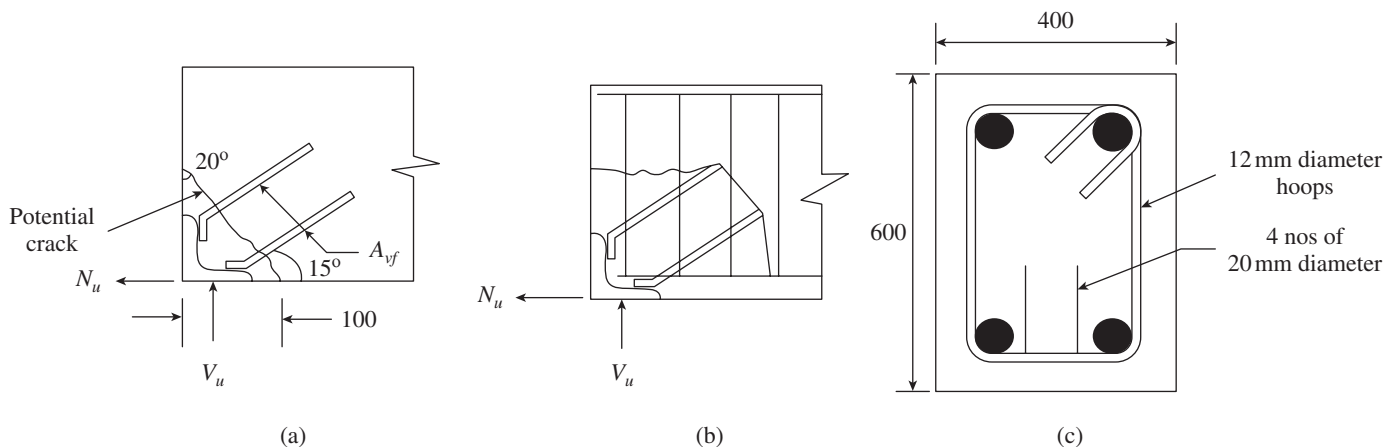


FIG. 6.46 Precast beam of Example 6.8 (a) Detail at bearing with assumed crack (b) Second possible crack (c) Shear reinforcement

Use four 20 mm diameter bars (area = 1256 mm^2), which are to be welded to the base at an angle of 15° with the bottom face of the beam and extended into the beam to a length of 760 mm (development length as per Clause 26.2.1 of IS 456 for M30).

As per Clause 11.6 of the ACI code, the design strength is ϕV_{sn} ($\phi = 0.75$). To avoid the failure of concrete by crushing, external shear should not exceed the smaller of $0.16f_{ck}A$ and $5.5A_c \text{ MPa}$, where A_c is the area of concrete section resisting the shear transfer.

$$\text{Area of concrete } A_c = 400 \frac{100}{\sin 20^\circ} = 116,952 \text{ mm}^2$$

$$V_n = 0.16f_{ck}A = 0.16 \times 30 \times 116,952/1000 = 561 \text{ kN or } 5.5 \times 116,952/1000 = 643 \text{ kN}$$

The design strength = $0.75 \times 561 = 420$ kN

Applied shear, $V_u = 400 \cos 20 + 80 \sin 20 = 403.2 \text{ kN} < 420$ kN; hence, it is safe.

Let us consider another crack as shown in Fig. 6.46(b), which may result if the entire anchorage pulls out of the beam horizontally.

$$\text{For this case, } A_{sh} = \frac{A_{vf} f_y \cos 15^\circ}{\phi \mu f_y} = \frac{1256 \times 0.966}{0.75 \times 1.4} = 1155 \text{ mm}^2$$

Provide four two-legged 16 mm diameter hoops with area = 1608 mm^2 .

EXAMPLE 6.9 (Shear design of Beam in seismic zone):

A 450 mm wide and 600 mm deep RC beam spans between two interior columns in a building frame located in a high seismic zone. The clear span of the beam is 7 m and the reinforcement at the face of the support consists of four 32 mm diameter bars at the top and four 25 mm bars at the bottom. The effective depth is 535 mm for both top and bottom steel. The maximum factored shear for $1.2(\text{DL} + \text{LL})$ is 140 kN at each end of the beam. Using M30 concrete and Fe 415 steel, determine the shear reinforcement for the region adjacent to column faces.

SOLUTION:

For negative bending, the area of steel is $A_{sc} = 4 \times 804 \text{ mm}^2$ at both ends.

$$p_{top} = \frac{4 \times 804 \times 100}{450 \times 535} = 1.34\%$$

Hence, from Table 4 of SP 16, $M_u^{Bh} = 3.93 \times 450 \times 535^2 \times 10^{-6} = 506 \text{ kNm}$

For positive bending, the area of steel is $A_{st} = 4 \times 490 \text{ mm}^2$ at both ends.

$$p_{bottom} = \frac{4 \times 490 \times 100}{450 \times 535} = 0.82\%$$

Hence, from Table 4 of SP 16, $M_u^{As} = 2.62 \times 450 \times 535^2 \times 10^{-6} = 337.4 \text{ kNm}$

Note: For simplicity, the top and bottom reinforcements have been taken separately; for more accuracy, we should calculate the moment of resistance of the beam at both ends considering it as a doubly reinforced section.

Hence, as per Clause 6.3.3 of IS 13920, $V_{u,a} = V_a^{D+L} + 1.4 \frac{[M_u^{Ah} + M_u^{Bs}]}{L_{AB}}$

Design shear force at each end of beam, $V_u = 140 + 1.4 \left(\frac{506 + 337.4}{7.0} \right) = 308.68 \text{ kN}$

Since the beam is located in a seismic zone, the shear strength of concrete has to be omitted and the transverse reinforcement has to be designed for the full value of V_u .

$$\frac{V_u}{d} = \frac{308.68}{53.5} = 5.769 \text{ kN/cm}$$

Hence, as per Table 62 of SP 16, provide four-legged 10 mm diameter vertical stirrups at 190 mm c/c having $V_u/d = 5.97 \text{ kN/cm}$ for a distance $= 2d = 2 \times 535 = 1070 \text{ mm}$ at both ends. Spacing should be lesser of $d/4 = 535/4 = 134 \text{ mm}$ and $8d_b = 8 \times 25 = 200 \text{ mm}$. Hence, reduce spacing to 130 mm. The remaining portion of the beam can be designed for a shear force of 140 kN as in the previous examples.

SUMMARY

In general, a beam may be subjected to shear, axial thrust or tension, or torsion in addition to the predominant flexure. According to traditional design philosophy, bending moment and shear force are treated separately, even though they coexist. Shear analysis and design are in many cases concerned with the *diagonal tension stress*, which is a result of the combination of flexural and shear stresses. Hence, shear failure is often termed as *diagonal tension failure*. Unlike flexural failures, shear failures are sudden and catastrophic.

The design recommendations of several codes of practice are based on the empirical relations derived from laboratory tests. Most of the codes (for example, ACI 318 and IS 456) follow the Truss model developed by Ritter in 1899 and modified by Mörsch in 1909, which assumes that vertical stirrups and the longitudinal steel resist tension while the diagonal strut and the uncracked concrete above the neutral axis (constituting the compression chord) resist compression. Stirrups act only after the concrete is cracked and if the crack angle is 45° . In this method, it has been vaguely rationalized to adopt the diagonal cracking load of the beam *without* web reinforcement as the concrete contribution to the shear strength of an identical beam *with* web reinforcement. This is why the values of concrete strength calculated using ACI and IS code formulae are quite conservative. This model has been refined by several others and it was later realized that the angle of inclination of the concrete struts, θ , may be in the range 25–65. These developments led to the variable angle truss model (adopted by the Eurocode). The choice of small value of θ reduces the number of required stirrups, but increases the compression stresses in the web and the horizontal component to be resisted by the longitudinal tensile steel of the beam.

The Canadian code and AASHTO LRFD sectional design model for shear are derived from the MCFT, which considers the combined efforts of flexure, shear force, axial load (compression or tension), and torsion.

The other model called *strut-and-tie model* is described in Appendix B. This method is suitable at regions where plane sections

do not remain plane after bending, that is, in deep beams, members with shear span to effective depth ratio (a_v/d) less than 1.5, pile caps, brackets, and regions near discontinuities or change in cross section. The strut-and-tie method may require several trials to produce an efficient model and does not provide a unique solution.

There may be certain circumstances where consideration of direct shear is important. One such example is in the design of composite members combining precast beams and cast-in-place slabs, where horizontal shear stresses at the interface between the beam and slab have to be considered. In these situations, the *shear friction* concept is utilized.

The main objective of an RC designer is to produce ductile behaviour in members such that ample warning is provided before failure. To achieve this goal, RC beams are often provided with *shear reinforcement*. Shear reinforcement may be provided in different ways—vertical stirrups, inclined stirrups, bent-up bars, welded wire mesh, spirals, headed studs, steel fibres, etc. Several design methods and detailing rules that are prescribed in the code will result in a strength that is governed by bending failure rather than shear failure, if the member is overloaded.

Design aids in the form of tables are available in SP 16 for vertical stirrups and bent-up bars. Flanged beams are designed conservatively by taking only the contribution of web. Shear funnel concept may be used to economically design T-beams. Formulae are also given for designing beams of variable depth.

In beams of frames located in earthquake zones, the shear strength of concrete has to be ignored and only vertical stirrups should be used. Discussions on HSC, HSS, and beams with web openings, which are increasingly used are also included. Axial tensile stresses are detrimental to the shear strength. Though the IS code gives the formula to consider axial compression, which will increase the shear strength, other national code formulae should be used for axial tension. The codes also suggest rules to increase shear reinforcement at longitudinal tensile steel cut-off points.

REVIEW QUESTIONS

1. What are the three types of shear behaviour of RC beams?
2. Why is shear failure termed as diagonal tension failure?
3. Describe the behaviour of uncracked beams subjected to shear loads.
4. State the situations under which the following modes of cracking occur in RC beams:
 - (a) Flexural cracks
 - (b) Diagonal tension cracks
 - (c) Flexural shear cracks
 - (d) Splitting cracks
5. How does the shear span influence the mode of shear failure?
6. What are the components that participate in the shear transfer mechanism at a flexural shear crack location in an RC beam?
7. What are the different types of web reinforcements?
8. Lists the ways in which stirrups contribute to the strength of shear mechanism?
9. Rank the performance of the following in resisting shear:
 - (a) Vertical stirrups
 - (b) Bent-up bars
 - (c) Inclined stirrups
10. Write short notes on the following:
 - (a) Vertical stirrups
 - (b) Bent-up bars
 - (c) Inclined stirrups
 - (d) Spirals
 - (e) Headed studs
 - (f) Steel fibres to increase shear strength
11. Closed stirrups are better for beams _____.
 - (a) with BM and shear
 - (b) in frames located in earthquake zones
 - (c) in resisting torsion
 - (d) in all of these
12. Why are lap-spliced stirrups and 90° hooks not preferable?
13. Why does the IS code discourage the use of bent-up bars alone?
14. What are the advantages of inclined stirrups over bent-up bars?
15. Why are inclined stirrups not preferred in seismic zones?
16. Why are the hooks placed in such a way that they engage a longitudinal bar of slightly higher diameter?
17. Describe the behaviour of beams with shear or web reinforcements.
18. Explain the action of an RC beam (with shear reinforcement) with the aid of the truss analogy model.
19. List the factors that affect the shear strength of concrete.
20. What is meant by size effect? How does it affect the shear strength of concrete?
21. Write the expression that is used in IS 456 to calculate the shear strength of concrete? Is it applicable to HSC? Does it consider size effect?
22. Why is the design shear strength of concrete (τ_c) related to the percentage tension steel p_t ?
23. Why is an upper limit $\tau_{c,max}$ imposed on the shear strength of an RC beam with shear reinforcement?
24. Is uniformly distributed load more critical than concentrated loads?
25. In general, the critical section for shear in an RC beam is located at a distance d (effective depth) away from the face of the support. Why? Under what circumstances is this not permitted?
26. Why is the provision of minimum stirrup reinforcement mandatory in all RC beams?
27. The maximum spacing of a vertical stirrup is _____.
 - (a) $1.0d$
 - (b) $0.75d$ or 300 mm, whichever is less
 - (c) 300 mm
 - (d) $1.0d$ or 300 mm, whichever is less
28. The maximum spacing of an inclined stirrup is _____.
 - (a) $1.0d$
 - (b) $0.75d$ or 300 mm, whichever is less
 - (c) 300 mm
 - (d) $1.0d$ or 300 mm, whichever is less
29. The maximum spacing of vertical stirrups at beam ends (plastic hinge locations) as per IS 13920 is _____.
 - (a) $0.75d$ or 300 mm, whichever is less
 - (b) $0.5d$ or 200 mm, whichever is less
 - (c) smaller of $0.25d$ or 8 times the diameter of the smallest longitudinal bar
 - (d) $0.25d$ or 300 mm, whichever is less
30. In the traditional method of design for shear, how is the influence of shear on longitudinal reinforcement requirement taken care of?
31. The model adopted for shear reinforcement design by IS 456 code is _____.
 - (a) modified compression field theory
 - (b) 45° truss model
 - (c) variable angle truss model
 - (d) compression force-path method
32. Why is it that the variable angle truss model may give more accurate results than the 45° truss model?
33. Explain the Ritter–Mörsch Truss model.
34. Derive the formula for the spacing of vertical stirrups.
35. State the steps involved in the design of shear stirrups.
36. Why is it better to provide multi-legged stirrups in wide beams?
37. Why is it necessary to anchor stirrups in the compression zone of beams?
38. Is the shear design of flanged beams different from that of rectangular beams? What is the simplifying assumption made in codes? What is shear funnel concept?
39. How is the computation of nominal shear stress for beams with variable depth different from that for prismatic beams?
40. How does the shear design of beams located in seismic zones differ from that of normal beams?
41. Why is the shear strength of HSC different from that of NSC?
42. Why does IS 456 restrict the strength of stirrups?
43. Sketch the shear reinforcement details to be adopted in the case of large openings in the web.
44. How does the presence of an axial force (tension or compression) influence the shear strength of concrete?
45. The location of curtailment of tension reinforcement in an RC beam is considered a critical section for shear. Why?
46. Explain the concept of interface shear and shear friction theory. Where is this concept relevant?

EXERCISES

1. A rectangular beam of size 250 mm width and 500 mm effective depth is reinforced with four bars of 25 mm diameter. Determine the required vertical shear reinforcement to resist factored shear force of (a) 80 kN, (b) 300 kN, and (c) 600 kN. Consider concrete of grade M20 and steel of grade Fe 415.
[Ans.: (a) Two-legged 8 mm at 300 mm c/c (b) Two-legged 10 mm at 135 mm c/c (c) Size of beam to be changed]
2. A rectangular beam of section 250 mm width by 500 mm effective depth is reinforced with four 25 mm bars, out of which two bars are bent at the ends of the beam at 60°. Determine the additional shear requirement required if the factored shear force

at the critical section is 350 kN. Consider concrete grade M25 and steel of grade Fe 415.

[Ans.: V_{us} bent up = 250.64 kN, provide additional two-legged 10 mm at 200 mm c/c]

3. A simply supported T-beam of 7.5 m span (c/c) is subjected to a factored dead load (including self-weight) of 40 kN/m and a factored live load of 50 kN/m. The details of the section and bar cut-offs are shown in Fig. 6.47. Design and detail the shear reinforcement using 'vertical' stirrups. Assume M20 concrete and Fe 415 steel.

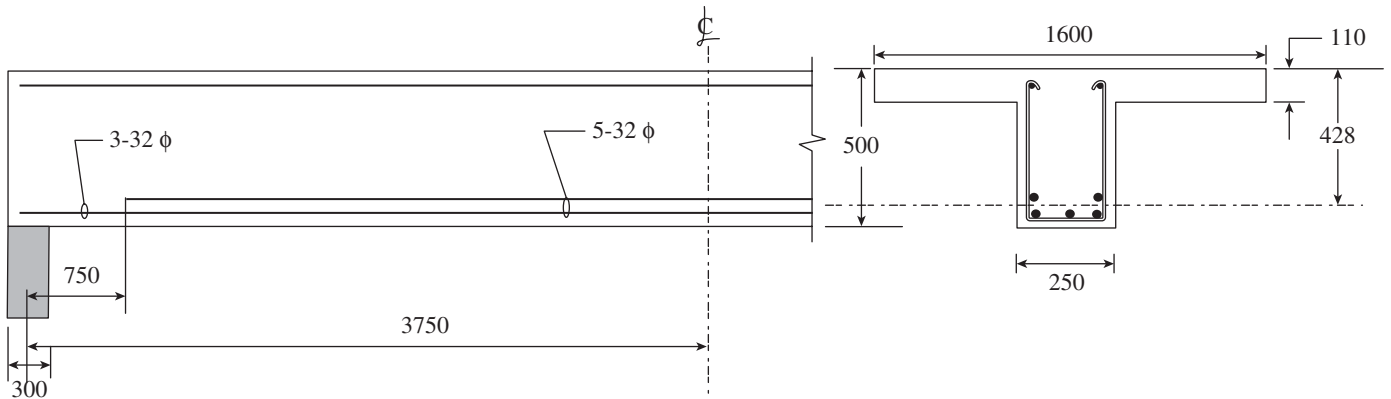


FIG. 6.47

4. Calculate the shear resistance of a beam of width 250 mm and effective depth 450 mm reinforced with four 22 mm bars at mid-span of which two bars are bent at the ends at 45°. The beam is provided with shear reinforcement of two-legged 10 mm diameter vertical stirrups throughout the beam at a spacing of 220 mm c/c. M25 concrete and Fe 415 steel have been adopted.
5. Design the shear reinforcement for a tapered cantilever beam of span 3 m, having a section of 300 mm depth and 350 mm width at the free end, and 700 mm depth and 350 mm width at the support (see Fig. 6.48). The beam has to support a factored uniform load of 105 kN/m, including self-weight. Assume an effective cover of 45 mm, Fe 415 steel, and M20 concrete.
6. Consider the cantilever beam of Exercise 5 and design the shear reinforcement at 2 m from the free end, if the longitudinal reinforcement of five 25 bars is curtailed to two 25 bars.
7. A rectangular beam of section 300 mm width by 450 mm effective depth is reinforced with five 22 mm bars and is made of concrete grade M30 and steel of grade Fe 415. Determine the shear strength of concrete, if (a) a compressive force of 125 kN is acting on the beam and (b) a tensile force of 80 kN is acting on the beam.
8. Design the bearing of a precast beam of size 300 mm width and 550 mm depth to resist a support reaction of $V_u = 340$ kN applied to a $75 \times 75 \times 6$ mm steel angle as shown in Fig. 6.46. Assume a horizontal reaction, N_u , of 20 per cent of the vertical reaction, owing to restrained volume change, or 68 kN. Assume M 25 concrete and Fe 415 steel

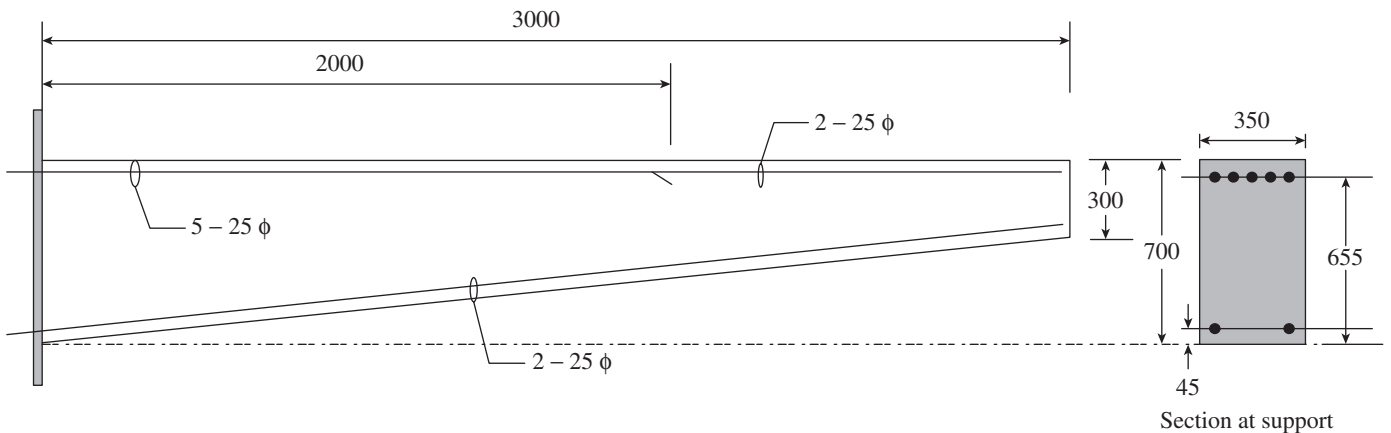


FIG. 6.48

REFERENCES

- ACI-ASCE Committee 326 (now 426) 1962, 'Shear and Diagonal Tension', *Journal of ACI*, Vol. 59, No.1-3, pp. 1-30, 277-334, 352-396; also discussion and closure Vol. 59, No.10, pp.1323-49.
- ACI 421.1 R-08 2008, *Guide to Shear Reinforcement for Slabs*, reported by Joint ACI-ASCE Committee 421, American Concrete Institute, Farmington Hills, p. 23.
- ACI-ASCE Committee 426 1973, 'Shear Strength of Reinforced Concrete Members', *Proceedings, ASCE, Journal of the Structural Division*, Vol. 99, No. ST6, pp. 1091-187 (contains extensive bibliography).
- ACI-ASCE Committee 426 1978, *Suggested Revisions to Shear Provisions for Building Codes*, American Concrete Institute, Detroit, p. 88.
- ACI-ASCE Committee 445 on Shear and Torsion 1998, 'Recent Approaches to Shear Design of Structural Concrete', *Journal of Structural Engineering*, ASCE, Vol. 124, No. 1, pp. 1375-417.
- ACI 544.1R-96 1996 (reapproved 2009), *State-of-the-Art Report on Fiber Reinforced Concrete*, American Concrete Institute, Farmington Hills, p. 64.
- Anderson, N. and J.A. Ramirez 1989, 'Detailing of Stirrup Reinforcement', *ACI Structural Journal*, Vol. 86, No. 5, pp. 507-15.
- Angelakos, D., E.C. Bentz, and M.P. Collins 2001, 'Effect of Concrete Strength and Minimum Stirrups on Shear Strength of Large Members', *ACI Structural Journal*, Vol. 98, No. 3, pp. 290-300.
- Bach, F., M.P. Nielsen, and M.W. Braestrup 1980, *Shear Tests on Reinforced Concrete T-beams*, Structural Research Lab, Technical University of Denmark, Copenhagen, p. 89, (also see <http://cbs.biocentrum.sitecore.dtu.dk/upload/institutter/byg/publications/rapporter/abk-r120.pdf>, last accessed on 24 October 2012).
- Bažant, Z.P. and J.K. Kim 1984, 'The Size Effect in Shear Failure of Longitudinally Reinforced Beams', *ACI Structural Journal*, Vol. 81, No. 5, pp. 456-68.
- Belarbi, A. and Hsu, T.T.C. 1995, 'Constitutive Laws of Softened Concrete in Biaxial Tension-Compression', *ACI Structural Journal*, Vol. 92, No. 5, pp. 562-573.
- Bentz E.C. 2000, *Sectional Analysis of Reinforced Concrete Members*, PhD thesis, Department of Civil Engineering, University of Toronto, Ontario, p. 198, (also see http://www.ecf.utoronto.ca/~bentz/appen_a.pdf and user manuals for Membrane-2000: <http://www.ecf.utoronto.ca/~bentz/m2k.htm> and Response-2000: <http://www.ecf.utoronto.ca/~bentz/r2k.htm>, last accessed on 24 October 2012).
- Bentz, E.C., F.J. Vecchio, and M.P. Collins 2006, 'The Simplified MCFT for Calculating the Shear Strength of Reinforced Concrete Elements', *ACI Structural Journal*, Vol. 103, No. 4, pp. 614-24.
- Bhide, S.B. and M.P. Collins 1989, 'Influence of Axial Tension on the Shear Capacity of Reinforced Concrete Members', *ACI Structural Journal*, Vol. 86, No. 5, pp. 570-81.
- Brown, M.D., O. Bayrak, and J.O. Jirsa 2006, 'Design for Shear Based on Loading Condition', *ACI Structural Journal*, Vol. 103, No. 4, pp. 541-50.
- Collins, M.P. 1978, 'Towards a Rational Theory for RC Members in Shear', *Proceedings*, *Journal of the Structural Division*, ASCE, Vol. 104, No. ST4, pp. 649-66.
- Collins, M.P. and D. Kuchma 1999, 'How Safe Are Our Large, Lightly Reinforced Concrete Beams, Slabs and Footings?', *ACI Structural Journal*, Vol. 96, No. 4, pp. 482-90.
- Collins, M.P. and D. Mitchell 1991, *Prestressed Concrete Structures*, Prentice Hall, Englewood Cliffs, p. 720.
- Collins, M.P., E. Bentz, and E.G. Sherwood 2008, 'Where is Shear Reinforcement Required? Review of Research Results and Design Procedures', *ACI Structural Journal*, Vol. 105, No. 5, pp. 590-600.
- Collins, M.P., F.J. Vecchio, R.G. Selby, and P.R. Gupta 1997, 'The Failure of an Offshore Platform', *Concrete International*, ACI, Vol. 19, No. 8, pp. 29-35.
- CSA A23.3-2004, *Design of Concrete Structures*, Canadian Standards Association, Ontario, p. 232, (also see www.csa.ca, last accessed on 24 October 2012).
- Dei Poli, S., P.G. Gambarova, and C. Karakoc 1987, 'Aggregate Interlock Role in RC Thin-webbed Beams in Shear', *Journal of Structural Engineering*, ASCE, Vol. 113, No. 1, Jan. 1987, pp. 1-19.
- Dei Poli, S., M.D. Prisco, and P. G. Gambarova 1990, 'Stress Field in Web of RC Thin-webbed Beams Failing in Shear', *Journal of Structural Engineering*, ASCE, Vol. 116, No. 9, pp. 2496-515.
- Desai, R.K. 2003, 'Design of Shear Reinforcement for Reinforced Cement Concrete Beams as per IS 13920 Design Aids', *Journal of the Institution of Engineers (India)*, Civil Engineering Division, Vol. 84, pp. 43-6.
- Duthinh D. and N.J. Carino 1996, *Shear Design of High-strength Concrete Beams: A Review of the State-of-the-Art*, Report No. NISTIR 5870, Building and Fire Research Laboratory, National Institute of Standards and Technology, Gaithersburg, p. 206.
- Elstner, R.C. and E. Hognestad 1957, 'Laboratory Investigations of Rigid Frame Failure', *Proceedings of the ACI Journal*, Vol. 53, No. 1, pp. 637-68.
- EN 1992-1-1:2004, *Eurocode 2: Design of Concrete Structures, Part 1-1: General Rules and Rules for Buildings*, European Committee for Standardization (CEN), Brussels.
- Feld, J. and K. Carper 1997, *Construction Failures*, 2nd edition, Wiley-Interscience, New York, p. 528.
- Fergusson, P.M. 1973, *Reinforced Concrete Fundamentals*, John Wiley and Sons, New York.
- Gayed, R.B. and A. Ghali 2004, 'Double Head Studs as Shear Reinforcement in Concrete I-beams', *ACI Structural Journal*, Vol. 101, No. 4, pp. 549-57.
- Ghali, A. and W.H. Dilger 1998, 'Anchoring with Double Headed Studs', *Concrete International*, ACI, Vol. 20, No. 11, pp. 21-4.
- Ghali A. and S.A. Youakim 2005, 'Headed Studs in Concrete: State of the Art', *ACI Structural Journal*, Vol. 102, No. 5, pp. 657-67.
- Gupta, P.R. and M.P. Collins 2001, 'Evaluation of Shear Design Procedures for Reinforced Concrete Members under Axial Compression', *ACI Structural Journal*, Vol. 98, No. 4, pp. 537-47.
- Hadi, M.N.S. and L.C. Schmidt 2003, 'Use of Helices for Enhancing the Properties of Reinforced Concrete Beams', *International Journal of Materials and Product Technology*, Vol. 19, No. 3/4, pp. 247-58.
- Hassan, T.K., H.M. Seliem, H. Dwairi, S.H. Rizkalla, and P. Zia 2008, 'Shear Behavior of Large Concrete Beams Reinforced with High-strength Steel', *ACI Structural Journal*, Vol. 105, No. 2, pp. 173-9.
- Hsu, T.T.C. 1993, *Unified Theory of Reinforced Concrete*, CRC Press, Boca Raton.

- IS 456: 2000, *Indian Standard Code of Practice for Plain and Reinforced Concrete*, Bureau of Indian Standards, New Delhi, p. 100.
- Jaafar, K. 2007, 'Shear Behavior of Reinforced Concrete Beams with Confinement near Plastic Hinges', *Morley Symposium on Concrete Plasticity and its Application*, University of Cambridge, 23 July 2007, pp. 163–72.
- Kani, G.N.J. 1967, 'How Safe Are Our Large Reinforced Concrete Beams?', *ACI Journal, Proceedings*, Vol. 64, No. 3, pp. 128–41.
- Kani, G.N.J. 1969, 'A Rational Theory for the Function of Web Reinforcement', *ACI Journal, Proceedings*, Vol. 66, No. 3, pp. 185–97.
- Kirmair, M. 1987, *Das Schubtragverhalten Schlanker Stahlbetonbalken—Theoretische und Experimentelle Untersuchungen für Leicht- und Normalbeton*, Dissertation, University of Munich, Germany.
- Kotsovos M.D. and M.N. Pavlovic' 1999, *Ultimate Limit-state Design of Concrete Structures: A New Approach*, Thomas Telford, London, p. 164.
- Kupfer, H. and H. Bulicek 1991, 'Comparison of Fixed and Rotating Crack Models in Shear Design of Slender Concrete Beams', in D.E. Grierson, et al. (eds), *Progress in Structural Engineering*, Kluwer, Dordrecht, pp. 129–38.
- Lee, J.Y. and H.B. Hwang 2010, 'Maximum Shear Reinforcement of Reinforced Concrete Beams', *ACI Structural Journal*, Vol. 107, No. 5, pp. 580–8.
- Lee, J.-Y. and U.-Y. Kim 2008, 'Effect of Longitudinal Tensile Reinforcement Ratio and Shear Span-depth Ratio on Minimum Shear Reinforcement in Beams', *ACI Structural Journal*, Vol. 105, No. 2, pp. 134–144.
- Leonhardt, F. 1965, 'Reducing the Shear Reinforcement in Reinforced Concrete Beams and Slabs', *Magazine of Concrete Research*, Vol. 17, No. 53, pp. 187–94.
- Leonhardt, F. and E. Mönig 1977, *Vorlesungen über Massivebau, Dritter Teil: Grundlagen zum Bewehren im Stahlbetonbau*, 3rd edition, Springer-Verlag, Berlin, p. 246.
- Leonhardt, F. and R. Walther 1964, 'The Stuttgart Shear Tests, 1961', *Cement and Concrete Association*, London, Library Translation No 111, Translation by C. V. Amerongen, p. 136.
- Li, Z. and Y. Zhang 2005, 'High-performance Concrete', in W.F. Chen and E.M. Lui (eds.), *Handbook of Structural Engineering*, 2nd edition, CRC Press, Boca Raton, p. 1768.
- Lin, C.H. and S.M. Perng 1998, 'Flexural Behaviour of Concrete Beams with Welded Wire Fabric as Shear Reinforcement', *ACI Structural Journal*, Vol. 95, No. 5, pp. 540–6.
- Lubell, A., E.C. Bentz, and M.P. Collins 2009, 'Shear Reinforcement Spacing in Wide Members', *ACI Structural Journal*, Vol. 106, No. 2, pp. 205–15.
- Lubell, A., T. Sherwood, E.C. Bentz, and M.P. Collins 2004, 'Safe Shear Design of Large, Wide Beams', *Concrete International*, ACI, Vol. 26, No. 1, pp. 66–78.
- Mansur, M.A. and K.H. Tan 1999, *Beams with Openings: Analysis and Design*, CRC Press, Boca Raton, p. 224.
- Marti, P. 1985, 'Basic Tools of Reinforced Concrete Beam Design', *ACI Structural Journal*, Vol. 82, No. 1, pp. 46–56, (see also Marti, P. 1985, 'Truss Models in Detailing', *Concrete International*, ACI, Vol. 7, No. 12, pp. 66–73).
- Mattock, A.H. and N.M. Hawkins 1972, 'Shear Transfer in Reinforced Concrete: Recent Research', *Journal of Prestressed Concrete Institute*, Vol. 17, No. 2, pp. 55–75.
- Mihaylov, B.I., E.C. Benz, and M.P. Collins 2010, 'Behavior of Large Deep Beams Subjected to Monotonic and Reversed Cyclic Shear', *ACI Structural Journal*, Vol. 107, No. 6, pp. 726–34.
- Mörsch, E. 1909, *Der Eisenbetonbau, seine Theorie und Anwendung (Reinforced Concrete Theory and Application)*, 3rd edition, Verlag Konrad Wittner, Stuttgart, p. 118.
- Murty, C.V.R. 2001, 'Shortcomings in Structural Design Provisions of IS 456: 2000', *The Indian Concrete Journal*, Vol. 75, No. 2, pp. 150–7.
- Muttoni, A. and M.F. Ruiz 2008, 'Shear Strength of Members without Transverse Reinforcement as Function of Critical Shear Crack Width', *ACI Structural Journal*, Vol. 105, No. 2, pp. 163–72.
- Narayanan, R. and I.Y.S. Darwish 1987, 'Use of Steel Fibers as Shear Reinforcement', *ACI Structural Journal*, Vol. 84, No. 3, pp. 216–27.
- NZS 3101:2006, *Part 1: The Design of Concrete Structures and Part 2: Commentary*, Standards New Zealand, Wellington, (also see www.standards.co.nz, last accessed on 24 October 2012).
- Pang, X.B.D. and T.T.C. Hsu 1996, 'Fixed-angle Softened-truss Model for Reinforced Concrete', *ACI Structural Journal*, Vol. 93, No. 2, pp. 197–207.
- Park, R. and T. Paulay 1975, *Reinforced Concrete Structures*, John Wiley and Sons, New York, p. 769.
- Parra-Montesinos, G.J. 2006, 'Shear Strength of Beams with Deformed Steel Fibers', *Concrete International*, ACI, Vol. 28, No. 11, pp. 57–66.
- Pendyala, R.S. and P. Mendis, 'Experimental Study on Shear Strength of High-strength Concrete Beams', 2000, *ACI Structural Journal*, Vol. 97, No. 4, pp. 564–571.
- Rajagopalan, K.S. and P.N. Ferguson 1968, 'Exploratory Shear Tests Emphasizing Percentage of Longitudinal Steel', *ACI Journal, Proceedings*, Vol. 65, pp. 634–8.
- Rangan, B.V. 1972, 'Diagonal Cracking Strength in Shear of Reinforced Concrete Beams', *Civil Engineering Transactions, Institution Engineers Australia*, Vol. CE14, No. 1.
- Rao, Prakash D.S. 1995, *Design Principles and Detailing of Concrete Structures*, Tata McGraw Hill Publishing Co., New Delhi, p. 360.
- Regan, P.E. 1993, 'Research on Shear: A Benefit to Humanity or a Waste of Time?', *Structural Engineer*, Vol. 71, No. 19/5, pp. 337–47.
- Regan, P.E. and C.W. Yu 1973, *Limit State Design of Structural Concrete*, Chatto and Windus, London.
- Reineck, K.H. 1991, 'Modelling of Members with Transverse Reinforcement' and 'Model for Structural Concrete Members without Transverse Reinforcement', *IABSE Colloquium on Structural Concrete*, IABSE Report-62, IABSE, Zurich, pp. 481–8, 643–8.
- Ritter, W. 1899, 'Die bauweise hennebique', *Schweizerische Bauzeitung*, Vol. 33, No. 7, pp. 59–61.
- Roller, J.J. and H.G. Russell 1990, 'Shear Strength of High-strength Concrete Beams with Web Reinforcement', *ACI Structural Journal*, Vol. 87, No. 2, pp. 191–8.
- Schlaich, J., K. Shafer, and J. Jannewein 1987, 'Toward a Consistent Design of Structural Concrete', *Journal of Prestressed Concrete Institute*, Vol. 32, No. 3, pp. 74–150.
- Shioya, T., M. Iguro, Y. Nojiri, H. Akiyama, and T. Okada 1989, 'Shear Strength of Large Reinforced Concrete Beams', in V.C. Li and Z. P. Bazant (eds), *Fracture Mechanics: Applications to Concrete*, SP-118, American Concrete Institute, Detroit, pp. 259–79.

- SP:24(S&T) 1984, *Explanatory Handbook on Indian Standard Code of Practice for Plain and Reinforced Concrete*, Bureau of Indian Standards, New Delhi, p. 164.
- Subramanian N. 2003, 'Shear Strength of High Strength Concrete Beams: Review of Codal Provisions', *The Indian Concrete Journal*, Vol. 77, No. 5, pp. 1090–4.
- Subramanian, N. 2007, Discussion on 'Shear Behaviour of Steel Fibre Reinforced Concrete Beams with Low Shear Span to Depth Ratio', *The Indian Concrete Journal*, Vol. 81, No. 6, pp. 47–50.
- Subramanian, N. 2010, 'Limiting Reinforcement Ratios for RC Flexural Members', *The Indian Concrete Journal*, Vol. 84, No. 9, pp. 71–80.
- Subramanian, N. 2012, 'Alternate Transverse Reinforcement in Beams', ICI Journal, *The Indian Concrete Institute*, Vol. 13, No. 3, pp. 7–12.
- Subramanian, R. 2010, *Strength of Materials*, 2nd edition, Oxford University Press, New Delhi, p. 1052.
- Sumpter, M.S., S.H. Rizkalla, and P. Zia 2009, 'Behavior of High-performance Steel as Shear Reinforcement for Concrete Beams', *ACI Structural Journal*, Vol. 106, No. 2, pp. 171–7.
- Taylor, H.P.J. 1969, 'Investigation of the Dowel Shear Forces Carried by the Tensile Steel in Reinforced Concrete Beams', *Cement and Concrete Association*, London, TRA 431, p. 24.
- Taylor, H.P.J. 1972, 'Shear Strength of Large Beams', *Journal of the Structural Division, Proceedings*, ASCE, Vol. 98, No. ST11, pp. 2473–90.
- Thürliamann, B., P. Marti, J. Pralong, P. Ritz, and B. Zimmerli 1983, *Vorlesung zum Fortbildungskurs für Bauingenieure*, Institut für Baustatik und Konstruktion, ETH Zürich.
- Tompos, E.J. and R.J. Frosch 2002, 'Influence of Beam Size, Longitudinal Reinforcement and Stirrup Effectiveness on Concrete Shear Strength', *ACI Structural Journal*, Vol. 99, No. 5, pp. 559–67.
- Tureyen, A.K., T.S. Wolf, and R.J. Frosch 2006, 'Shear Strength of Reinforced Concrete T-beams without Transverse Reinforcement', *ACI Structural Journal*, Vol. 103, No. 5, pp. 656–63.
- Vecchio, F.J. and M.P. Collins 1986, 'The Modified Compression Field Theory for Reinforced Concrete Elements Subjected to Shear', *ACI Structural Journal*, Vol. 83, No. 2, pp. 219–31.
- Walraven, J.C. 1981, 'Fundamental Analysis of Aggregate Interlock', *Proceedings, Journal of the Structural Division*, ASCE, Vol. 107, No. ST11, pp. 2245–70.
- Warner, R.F., B.V. Rangan, and A.S. Hall 1976, *Reinforced Concrete*, Pitman, Australia.
- Wight, J.K. and J.G. MacGregor 2009, *Reinforced Concrete: Mechanics and Design*, 5th edition, Pearson Prentice Hall, New Jersey, p. 1112.
- Xiao, Y. and R. Ma 1998, 'Seismic Behavior of High Strength Concrete Beams', *The Structural Design of Tall Buildings*, Vol. 7, pp. 73–90.
- Yang, K.H. 2010, 'Tests of Lightweight Concrete Deep Beams', *ACI Structural Journal*, Vol. 107, No. 6, pp. 663–70.
- Yu, Q. and Z.P. Bažant 2011, 'Can Stirrups Suppress Size Effect on Shear Strength of RC Beams?', *Journal of Structural Engineering*, ASCE, Vol. 137, No. 5, pp. 607–17.
- Zararis, P.D. and I.P. Zararis 2008, 'Shear Strength of Reinforced Concrete Beams under Uniformly Distributed Loads', *ACI Structural Journal*, Vol. 105, No. 6, pp. 711–9.
- Zararis, I.P., M.K. Karaveziroglou, and P.D. Zararis 2006, 'Shear Strength of Reinforced Concrete T-beams', *ACI Structural Journal*, Vol. 103, No. 5, pp. 693–700.
- Zsutty, T.C. 1971, 'Shear Strength Prediction for Separate Categories of Simple Beam Tests', *ACI Journal, Proceedings*, Vol. 68, No. 2, pp. 138–43.
- Zsutty, T.C. 1968, 'Beam shear strength prediction by analysis of existing data', *Proceedings, American Concrete Institute*, Vol. 65, No. 11, pp. 943–951 and Discussions May 1969, Vol. 66, No. 5, pp. 435–437.

DESIGN FOR EFFECTIVE BOND BETWEEN CONCRETE AND STEEL

7.1 INTRODUCTION

The term 'bond' in reinforced concrete (RC) refers to the interaction between the reinforcing steel and the surrounding concrete that allows for transfer of stress from the steel into the concrete. The bond between the steel and concrete ensures strain compatibility (the strain at any point in the steel is equal to that in the adjoining concrete) and thus the composite action of concrete and steel. Proper bond also ensures that there is no slip between the steel bars relative to the surrounding concrete under service load. Bond is the mechanism that allows for anchorage of straight reinforcing bars and influences many other important features of structural concrete such as crack control and section stiffness. The common assumption in RC that plane sections remain plane after bending will be valid only if there is a perfect bond between the concrete and steel reinforcement.

As shown in Fig. 7.1, bond in RC is achieved through the following mechanisms (ACI 408R-03):

1. Chemical adhesion due to the products of hydration
2. Frictional resistance due to the surface roughness of the reinforcement and the grip exerted by the concrete shrinkage
3. Mechanical interlock due to the ribs provided in the deformed bars

Each component contributes to the overall bond performance in varying degrees depending on the type of reinforcing bar. The chemical bond can be lost at a very small slip between the reinforcing bar and concrete. Since the plain bars do not provide a mechanical interlock, many foreign codes prohibit their use in RC and allow their use only for transverse spirals, stirrups, and ties smaller than 10mm in diameter. However, there is no such restriction in the Indian code. Many experimental studies show that the bond behaviour of steel reinforcing bars is highly dependent on the 'relative rib area'.

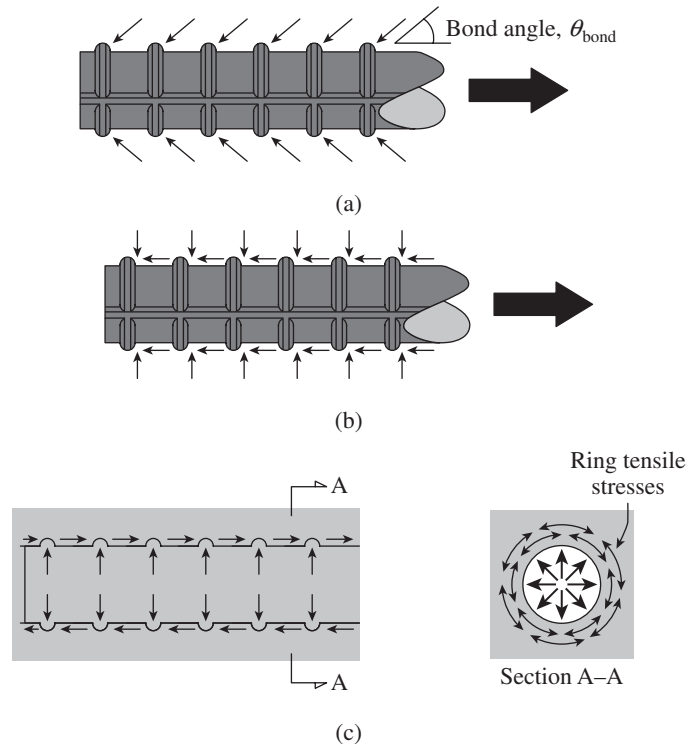


FIG. 7.1 Bond force transfer mechanism for deformed reinforcing bars (a) Bearing forces on deformations (b) Parallel and perpendicular components of bearing (c) Corresponding radial splitting and longitudinal bearing forces on concrete

Source: Thompson, et al. 2002

Traditionally, the design for bond required the consideration of both flexural (local) bond stress u_f and development (anchorage) bond stress u_{av} . It was later realized that the exact value of flexural bond stress could not be accurately computed owing to the unpredictable and non-uniform distribution of the actual bond stress. It was also found that localized bond failures can and do occur and they do not impair the ultimate load carrying capacity of the beams, provided the bars are adequately anchored at their ends. Thus, in the limit state

design, the focus shifted from checking the flexural bond to the development of the required bar stresses through provision of adequate anchorage at simple supports and at bar cut-off points. Special checking of anchorage length is required in the following cases:

1. In flexural members that have relatively short length
2. At simple supports and points of inflection
3. At points of bar cut-off
4. At cantilever supports
5. At beam-column joints in lateral load (wind and earthquake) resisting frames
6. For stirrups and transverse ties
7. At lap splices

Several failures have occurred due to the non-provision of adequate anchorage lengths, especially at cantilever supports, lap splices, and beam-column joints. Hence, the provision for anchorage length assumes greater importance.

The bond behaviour is affected by several factors that include concrete cover and bar spacing, bar size, transverse reinforcement, bar geometry, concrete properties, steel stress and yield strength, bar surface condition, bar casting position, development and splice length, distance between spliced bars, and concrete consolidation.

An excellent summary of the bond and anchorage length is provided by the ACI Committee 408 reports (ACI 408R-03 2003; ACI 408.2R-92 1992; ACI 408.3R-09 2009), Lutz and Gergely (1967), Orangun, et al. (1977), Jirsa, et al. (1979), and Darwin, et al. (1996).

The bond between the reinforcing bars and concrete was recognized as the key factor for the proper performance of RC structures more than 125 years ago (Hyatt 1877). Based on extensive research conducted until then, the ACI Committee 408 issued its first report on the subject in 1966. The committee issued suggested provisions for development, splice, and hook design (ACI 408.1R-79) in 1979, a state-of-the-art report on bond under cyclic loads in 1992 (ACI 408.2R-92), and design provisions for splice and development design for high relative rib area bars (bars with improved bond characteristics) in 2001 (ACI 408.3-01). These extensive ACI provisions have been adopted in several other national codes (e.g., New Zealand and Canada).

For many years, bond strength was considered in terms of the shear stress at the interface between the reinforcing bar and the concrete, thus treating it as a material property. (The term *bond force* is used to represent the force that tries to move a reinforcing bar parallel to its length with respect to the surrounding concrete; *bond strength* represents the maximum bond force that may be sustained by a bar.) Nevertheless, research has shown that bond, anchorage, development, and splice strength are structural properties that are dependent not only on the concrete strength but also on

the geometry of the reinforcing bar and the structural member itself. However, in the design codes, bond and its design provisions are still treated empirically. One should realize that an understanding of the empirical behaviour is critical to the development of rational analysis and design techniques (ACI 408R-03).

7.2 LOCAL OR FLEXURAL BOND STRESS

Suppose an RC beam is constructed using plain round bars that are greased or lubricated smoothly, before the concrete is poured (Fig. 7.2a). If this beam is loaded as shown in Fig. 7.2(b), the reinforcement bars will tend to maintain their original length by slipping longitudinally, as shown in Fig. 7.2(b), without sharing the bending stresses.

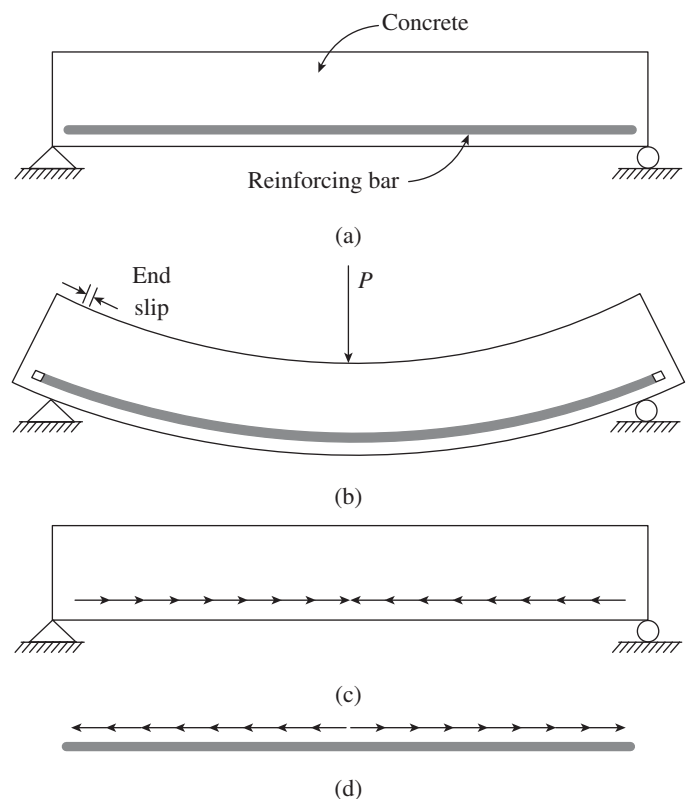


FIG. 7.2 Bond stresses due to flexure (a) Beam before loading (b) Unrestrained slip between steel and concrete (c) Bond forces acting on concrete (d) Bond forces acting on steel

However, when the bars are not greased, bond forces will develop at the interface of concrete, as a result of bending, as shown in Fig. 7.2(c). This will result in equal and opposite bond forces acting on the reinforcement as shown in Fig. 7.2(d). These interface bond forces prevent the slip as indicated in Fig. 7.2(b).

If plain bars are used, the bond due to the relatively weak chemical adhesion and mechanical friction between the concrete and steel is easily broken at large loads, and

hence the beam will collapse as the bars are pulled through the concrete. To prevent this, end anchorage in the form of hooks are often provided, as shown in Fig. 7.3. Such a beam will not collapse even if the bond is destroyed over the entire length, provided the anchorage is adequate. This is because the beam will now behave as a tied arch, with the uncracked concrete (shown shaded in Fig. 7.3) acting as an arch and the reinforcing bars acting as the tie. In this case, the bond stress will be zero over the entire unbonded length and the force in the steel is constant and equals M_{\max}/jd . It has to be noted that the total steel elongation in such a beam will be greater than the elongation in a beam with bonded reinforcement, thus resulting in greater deflections and crack widths. To prevent such a situation, deformed bars are now recommended by the codes of practices. The projecting ribs of deformed bars bear on the surrounding concrete and increase the bond strength considerably, while reducing the crack widths and deflections. The use of deformed bars also enables the designer to dispense with anchorage devices like hooks.

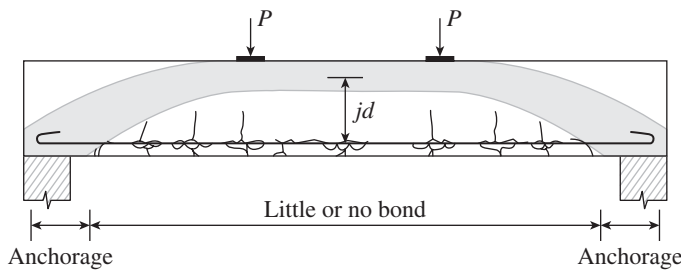


FIG. 7.3 Tied arch action in beams with little or no bond

Let us consider a short piece of beam of length Δx , as shown in Fig. 7.4. The moment at one end will differ from that at the other end by a small amount $\Delta M = M_2 - M_1$. Assuming that concrete does not resist any tensile stresses after cracking, the change in the steel bar force due to the change in bending moment is

$$\Delta T = \frac{\Delta M}{jd} \quad (7.1)$$

where jd is the internal lever arm between the tensile and compressive force resultants. If the bond force in the bar per unit length U is defined as the change in tensile force per unit length, then

$$U = \frac{\Delta T}{\Delta x} = \frac{1}{jd} \frac{\Delta M}{\Delta x} = \frac{V}{jd} \quad (7.2)$$

where V is the shear force at the section. If τ_{bf} is designated as the flexural bond stress, we get

$$\tau_{bf} = \frac{V}{jd} \left(\frac{1}{\pi d_b} \right)_n = \frac{V}{jd \sum_n o} \quad (7.3)$$

where n is the number of bars at the cross section, $(\pi d_b)_n$ is the sum of perimeters of n bars, and $\sum_n o$ is also the sum of the perimeters of n bars. This derivation is based on highly idealized situations, where bond stresses are assumed to be uniformly distributed, the effect of cover is ignored, the effect of cracking is neglected, and the type of steel (plain or deformed) is not considered.

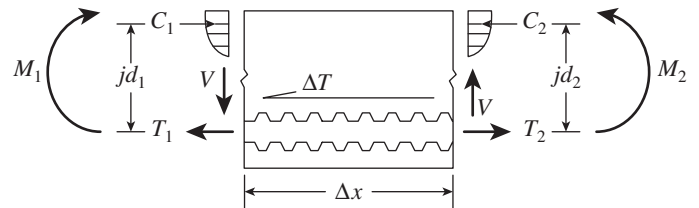


FIG. 7.4 Forces and stresses acting on an element of beam

Source: ACI 408 R-03, reprinted with permission from ACI

For many years, Eq. (7.3) was used to calculate the bond stress. Over time, however, it was realized that the change in force in the reinforcing bars ΔT does not vary strictly with the change in moment per unit length as suggested by Eq. (7.3); rather, it varies simply with the force in the bar T , which varies from a relatively high value at the cracks to a low value between the cracks, where the concrete shares the tensile force with the reinforcing steel (see Fig. 7.5). It may also be noted that the actual bond stress will be influenced by flexural cracking, local slip, splitting, and other secondary effects—which are not accounted for in Eq. (7.3). In particular, flexural cracking has a major influence in governing the magnitude and distribution of local bond stresses.

Tests on beams have shown that longitudinal splitting cracks tend to get initiated near the flexural crack locations where the local peak bond stresses can be high. Beams with large diameter bars are particularly vulnerable to splitting and/or local slip. In addition, flexural cracks are generally not present in the compression zone. Hence, flexural bond is less critical in compression bars compared to tension bars with a similar axial force.

7.3 ANCHORAGE BOND

As mentioned earlier, anchorage or development bond is the bond developed near the extreme ends (or cut-off point) of a bar subjected to tension (or compression).

To explain this, let us consider the cantilever beam shown in Fig. 7.6(a). Here, the bar must extend a distance L_d beyond the support to develop its full yield strength so that sufficient bond resistance is mobilized. Though the bond stress τ_{ba} may possibly vary as shown in Fig. 7.6(b), it is customary to assume an average uniform bond stress along the length as shown in Fig. 7.6(c).

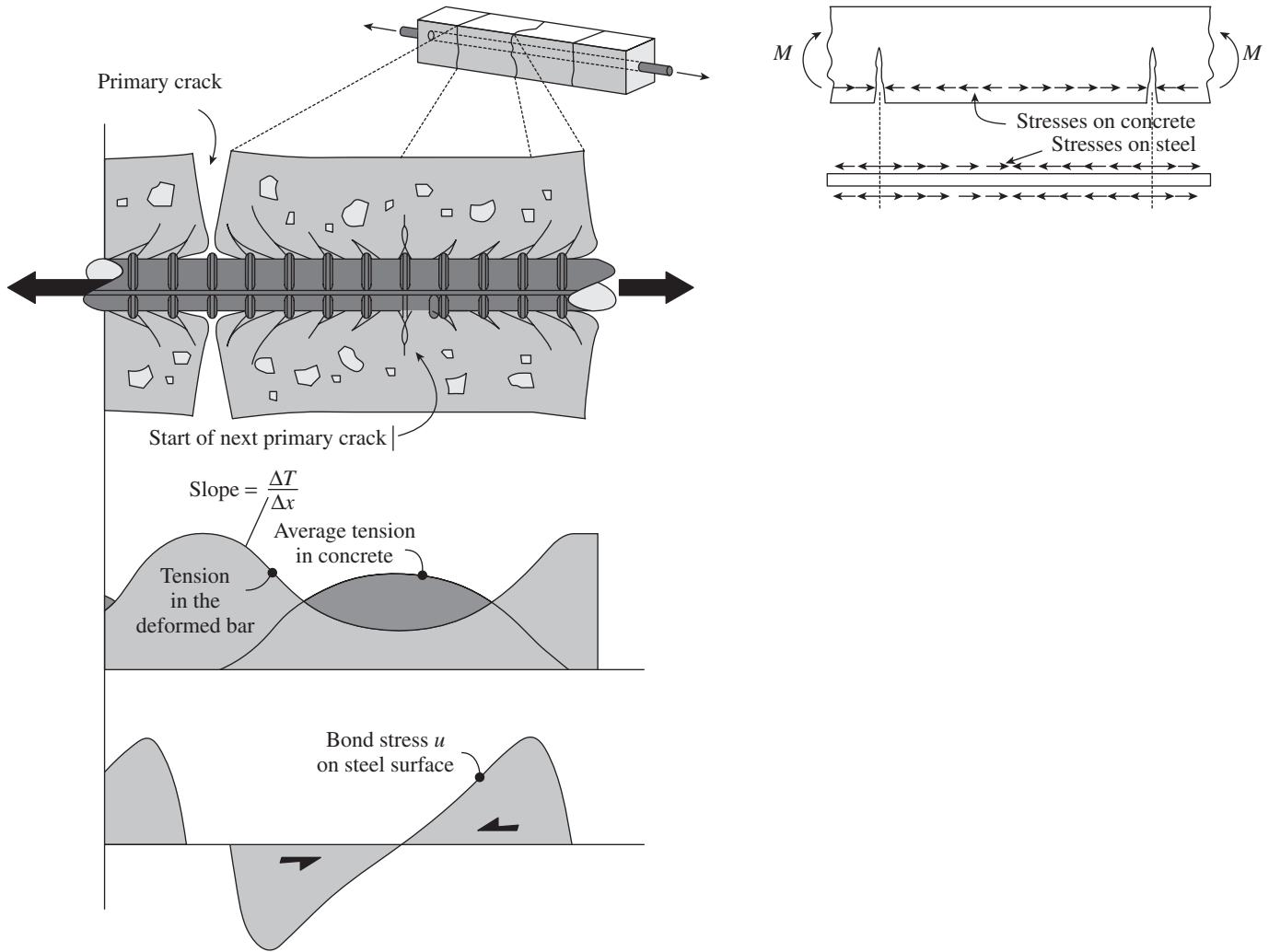
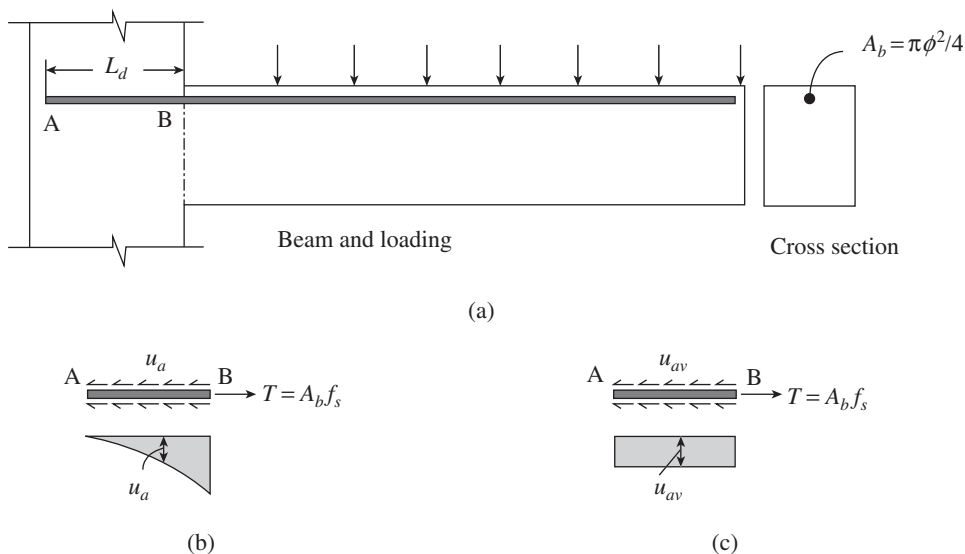


FIG. 7.5 Effect of flexural cracks on flexural bond stress in constant moment region

Source: Goto 1971; Thompson, et al. 2002



Consideration of equilibrium yields the following relationship:

$$T = A_b f_s = \tau_{ba} (\pi d_b) L_d$$

With area of bar, $A_b = \frac{\pi d_b^2}{4}$, we get

the anchorage bond stress

$$\tau_{ba} = \frac{f_s}{4L_d} d_b \quad (7.4)$$

where τ_{ba} is the anchorage bond stress (N/mm²), d_b is the diameter of bar (mm), f_s is the stress in the bar (N/mm²), and L_d is the development length (mm).

FIG. 7.6 Generation of anchorage bond stress (a) Cantilever beam (b) Possible variation of anchorage bond stress (c) Assumed uniform average bond stress

7.4 BOND BEHAVIOUR

Deformed bars have significant bond capacity due to the interlocking of the ribs with the surrounding concrete. When a deformed bar is subjected to tension in a confined mass of surrounding concrete, surface adhesion is overcome and the bearing forces on the ribs and the friction forces on the ribs and barrel of the bar are mobilized. As the slip increases, the friction on the barrel of the reinforcing bar is also overcome, leaving the forces at the contact faces between the ribs and the surrounding concrete as the principal mechanism of force transfer (see Fig. 7.7a). The forces on the bar surface are balanced by the compressive and shear stresses on the contact surfaces of concrete. The forces on the concrete have both longitudinal and radial components as shown in Figs 7.1 and 7.7(a). The latter causes hoop tensile stresses in the concrete around the bar as shown in Fig. 7.7(b).

Bond failures are generally characterized by two modes—*pull-out* and *splitting*. For most structural applications, bond failures are governed by the splitting of the concrete rather than by pull-out.

When the ribs are high and spaced too closely, the shear stresses will govern the behaviour and the bar will pull out, as shown in Fig. 7.7(d). When the rib spacing is larger than approximately 10 times the rib height, crushing takes place ahead of the ribs immediately adjacent to the bar interface and forms a wedge in front of the rib. This wedging action results in transverse cracks as shown in Fig. 7.7(b) and will form if the concrete cover or the spacing between the bars is sufficiently small, leading to splitting cracks, as shown in Fig. 7.7(c). The splitting cracks follow the reinforcement bars along the bottom or side surfaces of the beam. If the concrete cover, bar spacing, and transverse reinforcement are sufficient to prevent splitting failure, a ‘pull-out’ failure will occur due to shearing, along a surface at the top of the ribs around the bars, as shown in Fig. 7.7(d). If the anchorage to the concrete is adequate, the stress in the reinforcement may become high enough to yield and even strain harden the bar.

Tests have demonstrated that bond failures can occur at bar stresses up to the tensile strength of the steel (ACI 408R-03).

Rehm (1968), based on experiments, concluded that an optimal ratio of a/c of ribs in the region of 0.065 ensured satisfactory bond performance of ribbed bars. (The deformation requirement of ASTM A 305 is such that $0.057 < a/c < 0.072$. See Fig. 7.7(a) for the definition of a and c .) ACI 408.3R-09 defines the relative rib area as

$$R_r = \frac{A_r}{\pi d_b c_r} \approx \frac{a}{c} \tag{7.5}$$

where A_r is the projected rib area normal to the reinforcing bar axis, mm^2 , and c_r is the average centre-to-centre rib spacing, mm. Conventional deformed reinforcement has relative rib areas of 0.06 to 0.085. A high relative rib area bar is defined as a reinforcing bar with R_r greater than or equal to 0.10. Based on experimental results, ACI 408.3R-09 provides guidelines for bars with a relative rib area up to 0.14. As per IS 1786:2008, the mean area of ribs (in mm^2) per unit length (in mm) above the core of the bar, projected on a plane normal to the axis of the bar, should not be less than the following values:

- 0.12 d_b for $d_b \leq 10$ mm
- 0.15 d_b for $10 \text{ mm} < d_b \leq 16$ mm
- 0.17 d_b for $d_b > 16$ mm

where d_b is the nominal diameter of the bar in mm. The mean projected area of transverse ribs alone should not be less than one-third of the values given.

7.4.1 Test Specimens

Different types of tests have been used to study the bond between the reinforcing bars and concrete. The four most common configurations are shown in Fig. 7.8. It is important to note that the details of the specimen not only affect the measured bond strength but also the nature of the bond response. The pull-out specimen is widely used because of its ease of fabrication and the simplicity of the test. Here, a concrete cylinder containing a bar is mounted on a stiff plate and a jack is used to pull the bar out of the cylinder, as shown in Fig. 7.8(a). The variation

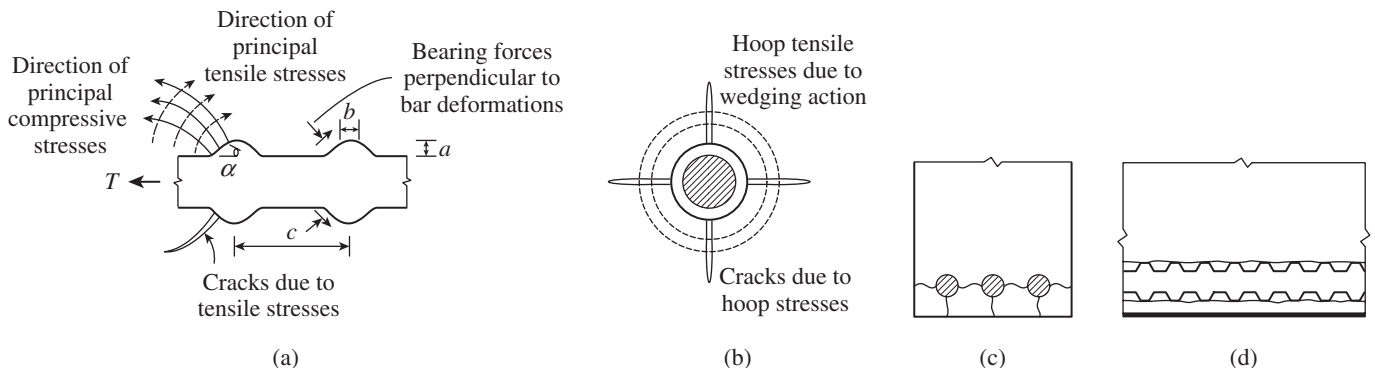


FIG. 7.7 Cracking mechanisms in bond (a) Deformed bar with deformation face angle α and possible cracks (b) Formation of splitting cracks parallel to the bar (c) Splitting cracks between bars and along the reinforcement (d) Shear crack and/or local concrete crushing due to bar pull-out

Source: ACI 408R-03, reprinted with permission from ACI

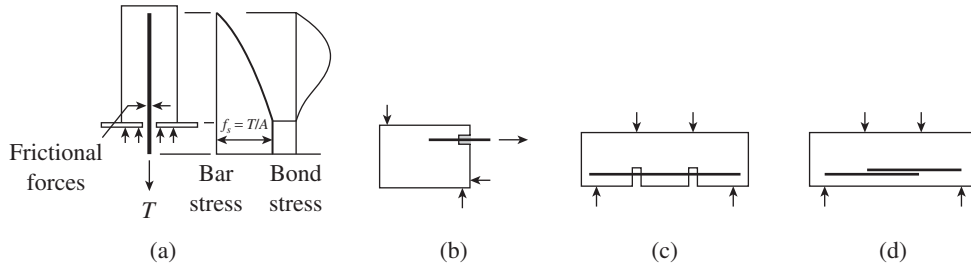


FIG. 7.8 Test methods (a) Pull-out specimen (b) Beam-end specimen (c) Beam-anchorage specimen (d) Splice specimen

of stress in the bar and the bond stress are also shown in Fig. 7.8(a). In this test, the concrete is compressed and hence does not crack. This specimen is the least realistic of the four shown in Fig. 7.8, because the concrete is not cracked and hence does not match the condition in actual construction. Moreover, the friction that is produced during the test on the stiff plates resist the transverse expansion due to Poisson's effect.

The specimens shown in Figs 7.8(b)–(d) provide more realistic bond strength values. The details of these tests may be found in ACI 408R-03. Because of both its relative simplicity of fabrication and realistic stress state in the vicinity of the bars, the splice specimen shown in Fig. 7.8(d) was used for the development of design provisions in ACI 318-11. A typical bond stress versus slip curve for a bar loaded monotonically and failing by pull-out is shown in Fig. 7.9 (Eligehausen, et al. 1983).

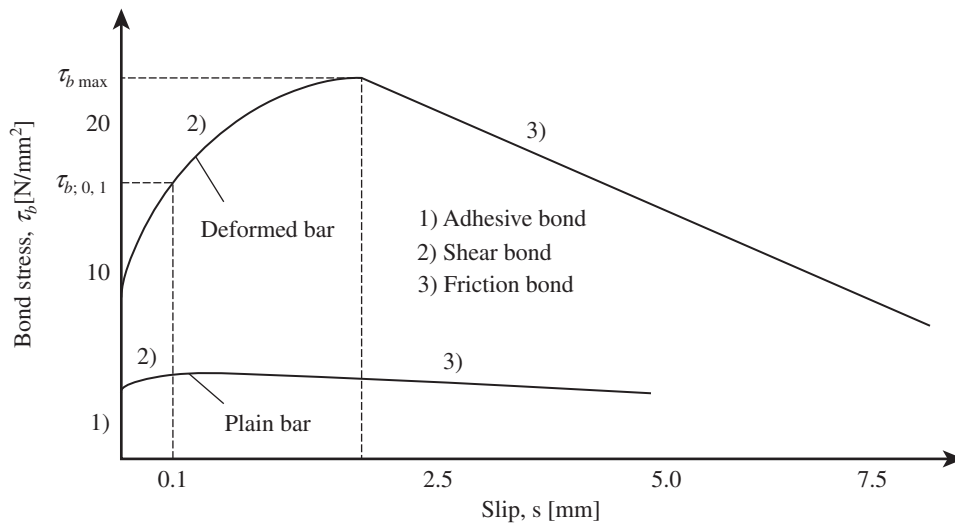


FIG. 7.9 Typical bond stress vs slip curve for bar loaded monotonically and failing by pull-out

From the results of the bond tests, the design bond stress (permissible average anchorage bond stress) τ_{bd} is determined for various grades of concrete.

7.4.2 Factors Affecting Bond Strength

Under static monotonically increasing loads, the following are the most important factors that affect the bond behaviour (ACI 408R-03):

Mechanical properties of concrete—tensile and bearing strength Up to M55 concrete, the effect of concrete

properties on the bond strength may be represented using the square root of the compressive strength $\sqrt{f_{ck}}$ (Tepfers 1973; Orangun, et al. 1977). For higher strength concrete, however, the average bond strength at failure, normalized with respect to $\sqrt{f_{ck}}$, decreases with an increase in compressive strength (Azizinamini, et al. 1993; Azizinamini, et al. 1995). Zsutty (1985) found that $f_{ck}^{(1/3)}$ provided an improved match with data compared to $\sqrt{f_{ck}}$. Darwin, et al. (1996) and Zuo and Darwin (2000) based on their own test results and a large international database observed that a best fit is provided by using $f_{ck}^{(1/4)}$.

Surface condition of bars The surface of a reinforcing bar plays an important role in the development of the bond as it may affect the friction between the reinforcing steel and concrete and the ability of the ribs to transfer force between the two materials. Bar surface condition involves the cleanliness of reinforcement, the presence of rust on the bar surface (rust, mill scale, or a combination of the two is considered satisfactory provided the weight and dimensions of the bar are within tolerable limits as per Johnston and Cox 1940), and the application of epoxy coatings to protect the reinforcement from corrosion.

Grade of concrete A higher grade of concrete has improved tensile strength and hence enhanced bond strength.

Bar diameter A beam reinforced with a larger number of small bars requires a smaller development length than one reinforced with a smaller number of large bars of the same total area. For a given length of a bar, the bond force mobilized by both the concrete and transverse reinforcement increases as the bar diameter increases.

Geometry of bars—deformation height, spacing, width, and face angle Based on the work of Clark (1946; 1950), the following requirements for deformed bars are specified in the ASTM specifications: The maximum average spacing of deformations should be equal to 70 per cent of the nominal diameter of the bar and a minimum height of deformations should be equal to four per cent of the nominal diameter for bars with a nominal diameter of 13 mm or smaller, 4.5 per cent of the nominal diameter for bars with a nominal diameter of

16 mm, and five per cent for larger bars. Lutz, et al. (1966), Lutz and Gergely (1967), and Darwin and Graham (1993) studied the effect of deformation pattern and found that for a deformed bar with a rib face angle greater than 40°, slip occurs by progressively crushing the concrete in front of the ribs; a region of crushed concrete occurs with a rib face angle of 30–40° (which acts as a wedge); and no crushing of concrete occurs if the rib face angle is less than 30°.

Cover concrete over bars and spacing of bars Bond force–slip curves become steeper and the bond strength increases as the cover and bar spacing increase. As already mentioned, the mode of failure also depends on the cover and bar spacing (Orangun, et al. 1977; Darwin, et al. 1996). For larger cover and bar spacing, it is possible to obtain a pull-out failure, and the use of smaller cover and bar spacing may result in a splitting tensile failure and lower bond strength. Recent studies have hypothesized that the action of splitting arises from a stress condition analogous to a concrete cylinder surrounding a reinforcing bar and acted upon by the outward radial components of the bearing forces from the bar. The cylinder would have an inner diameter equal to the bar diameter and a thickness c equal to the smaller of c_b , the clear bottom or top cover, and c_{si} , half of the clear spacing to the next adjacent bar (see Fig. 7.10). When splitting failures occur, the nature of the failure depends, in general, on whether the concrete cover c_b is smaller than either the concrete side cover c_{so} or half of the bar clear spacing c_{si} . When c_{so} and c_{si} are smaller than c_b , splitting cracks form through the side cover and between the reinforcing bars (see Fig. 7.10a). When c_{so} equals c_b and both c_{so} and c_b are less than c_{si} , cracks form in

the side and bottom cover (see Fig. 7.10b). When c_b is smaller than c_{so} and c_{si} , the splitting crack occurs through the bottom cover (see Fig. 7.10c).

Darwin, et al. (1996) found that compared to cases in which the minimum value of c_{so} or c_{si} equals c_b , the bond strength of bars for which the minimum value c_{so} or c_{si} does not equal c_b increases by the ratio

$$\left(0.1 \frac{c_{\max}}{c_{\min}} + 0.9 \right) \leq 1.25 \quad (7.6)$$

where $c_{\max} = \text{maximum}(c_b, c_s)$, $c_{\min} = \text{minimum}(c_b, c_s)$, $c_s = \text{minimum}(c_{so}, c_{si} + 6.4 \text{ mm})$.

Presence of confinement in the form of transverse reinforcement, like stirrups The bond strength of bars confined by transverse reinforcement, like stirrups, increases with an increase in the relative rib area. Stirrups, in general, confine developed and spliced bars by limiting the progression of splitting cracks and, thus, increase the bond strength. The additional bond strength provided by the transverse reinforcement increases approximately with the three-fourth power of the compressive strength.

Confinement of concrete around bars An increase in slump and the use of workability enhancing admixtures tend to have a negative effect on the bond strength. The longer the concrete has time to settle and bleed, the lower is the bond strength. This effect is especially important for top bars (ACI 408-03). The bond strength of non-vibrated concrete specimens is found to be lower than that of vibrated specimens.

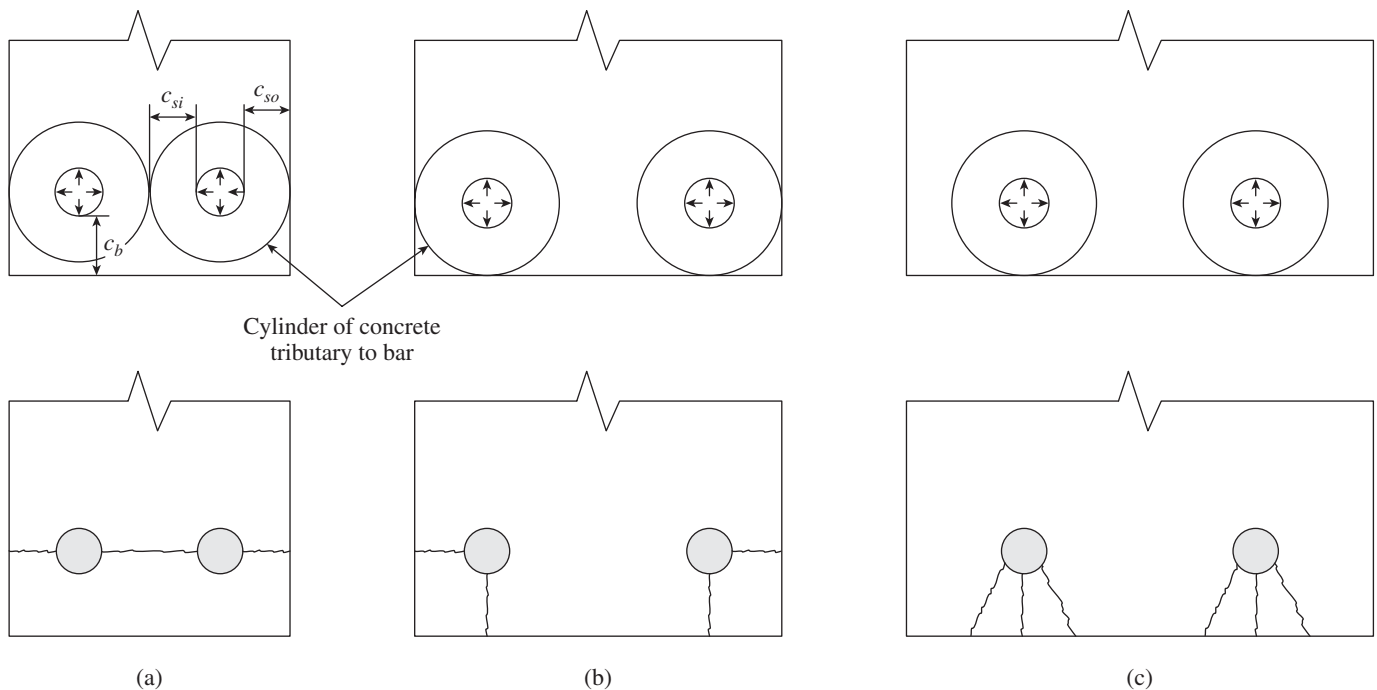


FIG. 7.10 Effect of cover and spacing of bars (a) c_{so} and $c_{si} < c_b$ (b) c_{so} and $c_b < c_{si}$, $c_{so} = c_b$ (c) $c_b < c_{so}$ and c_{si}

Aggregates used in concrete The bond strength of bars cast in lightweight concrete, with or without transverse reinforcement, is lower than that of bars cast in normal weight concrete. ACI 318 includes a factor for development length of 1.3 to reflect the lower tensile strength of lightweight aggregate concrete when compared with normal weight concrete with the same compressive strength, and allows that factor to be taken as $6\sqrt{f_{ck}/f_{ct}} \geq 1.0$, if the average splitting strength f_{ct} of the lightweight aggregate concrete is specified. Zuo and Darwin (2000) observed that a higher-strength coarse aggregate (basalt) increased the concrete contribution to bond strength, T_c , by up to 13 per cent compared with a weaker coarse aggregate like limestone.

Coating applied on reinforcement to reduce corrosion

Epoxy coating and galvanization (with typical thickness of 175–300 μm) is used to improve the corrosion resistance of reinforcing bars. It is well established that the presence of epoxy coatings reduces the bond strength of reinforcement (Choi, et al. 1991; Cleary and Ramirez 1993; Miller, et al. 2003). Choi, et al. (1991) and Idun and Darwin (1999) found that the thickness of coating has little effect on the bond strength and the average bond strength ratio for epoxy-coated bars to uncoated bars, C/U , was observed to be 0.82 for 15 splice specimens. In ACI 318, the development length is multiplied by a factor of 1.5 for epoxy-coated bars with a cover of less than $3d_b$ or clear spacing between bars less than $6d_b$ and a factor of 1.2 for other cases, with a maximum of 1.7 for the product of top-bar factor and epoxy-coating factors.

Type of reinforcement Deformed (ribbed) bars have enhanced bond strength when compared to plain bars. Fibre reinforcements, especially steel fibre, tend to act as transverse reinforcement and increase the bond strength of reinforcement bars.

Bar casting position Another factor that influences the bond strength is the depth of fresh concrete below the bar during casting. Excess water (often used in the mix for workability) and entrapped air invariably rise towards the top of the concrete mass during vibration and tend to get trapped beneath the horizontal reinforcement, thereby weakening the bond at the underside of these bars, as shown in Fig. 7.11 (Jirsa and Breen 1981; Jeanty, et al. 1988; Thompson, et al. 2002). This effect is called the *top-cast bar effect*. (As early as 1913, Abrams observed that the bar position during concrete placement plays an important role in the bond strength between the concrete and reinforcing steel). Thus, top-cast bars have lower bond strengths than bars cast lower in a member. ACI 318 defines top bars as horizontal bars placed so that more than 300 mm of concrete is cast below the bar and accounts for this effect by multiplying the development length of a top bar by an arbitrary factor of 1.3 for concretes with slump less than 100 mm (reduced from 1.4 since 1989).

It has to be noted that this effect becomes more pronounced with increasing concrete fluidity (Brettmann, et al. 1986). Jirsa and Breen (1981) observed that the slump of concrete is a very important variable in determining the effects of casting position. For slumps of 100–150 mm, they recommended a multiplier ranging from 1.0 to 1.6, and for slumps greater than 150 mm, it ranged from 1.0 to 2.2.

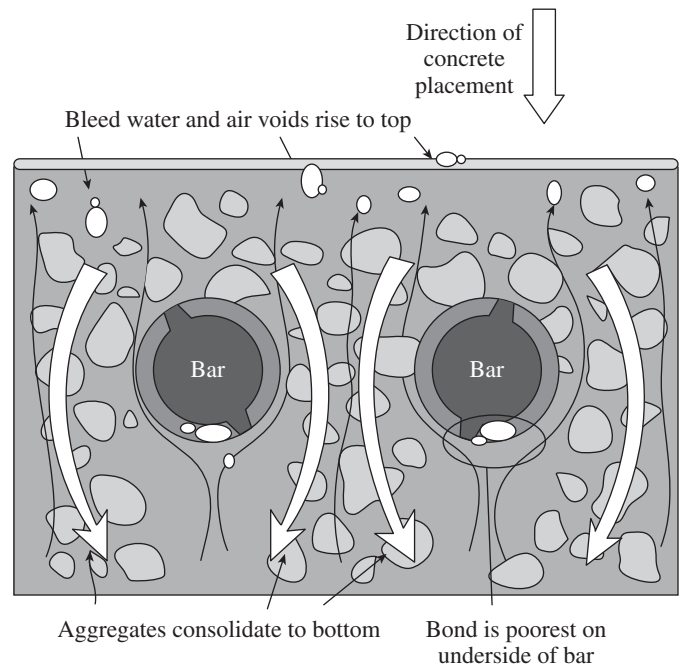


FIG. 7.11 Top-cast bar effect

Source: Thompson, et al. 2002

In addition to these parameters, the following factors should also be given importance under cyclic loading (Rehm and Eligehausen 1979; ACI 408.2R-92):

1. Bond stress range—stress ranges in excess of 40 per cent of the yield strength of the reinforcement in anchorages are found to reduce bond strength; studies show that these losses can be as high as 50 per cent of the static ultimate pull-out bond strength
2. Type of loading—reversed cyclic stresses tend to deteriorate bond at a higher rate; an important factor in high-cycle fatigue is the fatigue strength of the concrete itself
3. Maximum imposed bond stress

The code provisions should include all these factors in order that the development length is correctly computed.

7.5 DEVELOPMENT LENGTH

As discussed in relation to Fig. 7.3, when the end anchorage is reliable, sufficient bond will be available for the beam to carry the applied load even if the *local* bond is not available in other parts of the beam. Thus, the *development length* may be defined as the length of embedment necessary to develop

the full tensile strength of the bar, controlled by either pull-out or splitting. In other words, a certain minimum length of the bar, called the development length, has to be provided on either side of a point of maximum steel stress to prevent the bar from pulling out under tension (or pushing in under compression). If the actual length L is equal to or greater than L_d , no premature bond failure will occur; thus the beam is supposed to fail in bending or shear rather than undergo bond failure. It has to be noted that in the case of bond, we are considering the overall mechanism of failure rather than the limiting stresses to govern the design.

When the required development length could not be provided in certain practical situations, *bends*, *hooks*, and *mechanical anchorages* can be used to supplement with an equivalent development length (refer to Section 7.6). In situations where the embedment portion of the bar is not subjected to any flexural bond, the term *anchorage length* is used instead of the term development length.

7.5.1 Critical Sections for Development of Reinforcement

The *critical sections for development* of reinforcement in flexural members are at points of maximum stress and at points within the span where the adjacent reinforcement terminates or is bent. In general, the development lengths need to be checked in the following situations or locations:

1. Maximum moment sections
2. At all sections where bars are cut-off (refer to Section 7.8)
3. At lap splices (refer to Section 7.7)
4. At supports of simply supported beams and *points of contraflexure* (the point of contraflexure may be defined as the point where the sign of bending moment changes)
5. At cantilever supports
6. In flexural members that have relatively short spans
7. At beam-column joints in lateral load resisting frames
8. For stirrups and transverse ties

It has to be noted that the required development length will be usually available near the mid-span of normal beams (where generally sagging moments are maximum) and the support locations of continuous beams (where generally hogging moments are maximum).

7.5.2 Derivation of Analytical Development Length

Most of the codal equations on bond strength are empirical and based on statistical analysis of test results. Thus, these equations are highly dependent on the test data used, which

may limit their validity in different situations. Wight and MacGregor (2009) developed the following analytical development length. Consider the circular prism of length L shown in Fig. 7.12(a), which may be assumed to represent the zones of highest radial tensile stresses in concrete, as shown in Fig. 7.10 by larger circles. Let us assume that this

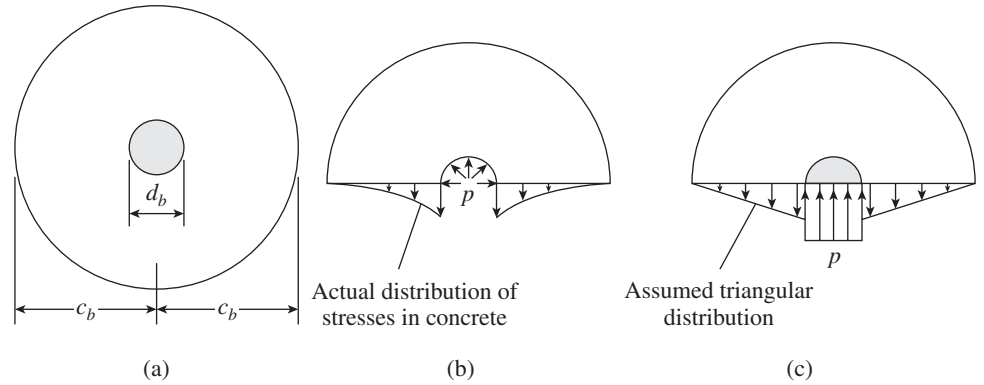


FIG. 7.12 Stress distribution in concrete of a circular concrete prism (a) Circular concrete prism around rebar (b) Actual stress distribution (c) Assumed stress distribution

cylindrical concrete prism has a diameter $2c_b$, and contains a bar of diameter d_b . The radial component of the forces on the concrete causes a pressure p , as shown in Figs 7.12(b) and (c). The tensile stresses in concrete, which equilibrate the pressure p on either side of the concrete, may be assumed to have a triangular distribution as shown in Fig. 7.12(c) for simplicity.

The splitting of concrete will occur when the maximum stress in concrete reaches the flexural tensile strength of concrete f_{cr} . In order to maintain equilibrium in the vertical direction, we should have

$$\frac{pd_b L}{2} = k_t (c_b - \frac{d_b}{2}) f_{cr} L \quad (7.7a)$$

where k_t is the ratio of average tensile stress to the maximum tensile stress in concrete. For triangular stress distribution, k_t may be taken as 0.5. Assuming that the forces shown in Fig. 7.7(a) are acting at an angle of 45° , the average bond stress $\tau_{b,ave}$ at the onset of splitting will be equal to p . Substituting the value of k_t , and considering $f_{cr} = 0.7\sqrt{f_{ck}}$ as per Clause 6.2.2 of IS 456:2000 and rearranging, we get

$$\tau_{b,ave} = \left(\frac{0.7c_b}{d_b} - 0.35 \right) \sqrt{f_{ck}} \quad (7.7b)$$

The development length L_d , which is required to raise the bar from zero to f_y , is obtained from Eq. (7.4) as

$$L_d = \frac{f_y}{4\tau_{b,ave}} d_b \quad (7.8a)$$

Substituting the value of $\tau_{b,ave}$ from Eq. (7.7b) and assuming $c_b = 1.5d_b$, we get

$$L_d = \frac{f_y}{2.8\sqrt{f_{ck}}} d_b \quad (7.9)$$

The reader may observe the similarity of this equation with the statistically derived expressions of the ACI code (Eqs 7.14 and 7.18–7.20).

Wang (2009) also proposed an analytical model based on the splitting bond mechanisms (which is the most common bond failure mode in real structures) and found that the equation proposed by him provides more reliable results than the ACI code formula.

7.5.3 Codal Provisions for Development Length

In this section, the Indian code provisions are given and compared with the codal provisions of other countries.

Indian Code Provisions

According to Clause 26.2.1 of the Indian code (IS 456), the calculated tension or compression in any bar at any section shall be developed at each side of the section by an appropriate development length L_d given by

$$L_d = \frac{d_b f_s}{4\tau_{bd}} \quad (7.10)$$

where d_b is the nominal diameter of the bar, f_s is the stress in the bar at the section considered at design load (for fully stressed bars, $f_s = 0.87f_y$), and τ_{bd} is the design bond stress as per Table 7.1. The development length includes the anchorage values of hooks in tension reinforcement. The note under the clause states that for non-circular bars, the development length should be sufficient to develop stress in the bar by bond. Howell and Higgins (2007) compared the available pull-out test results and found that the computation of development length according to the ACI code formula, considering square bars as equivalent round bars (with diameter, $d = a/0.886$, where a is the side of the square), is reasonable and conservative.

TABLE 7.1 Design bond stress in limit state method for plain bars in tension

Grade of Concrete	M20	M25	M30	M35	M40 and Above
Design bond stress τ_{bd} , MPa	1.2	1.4	1.5	1.7	1.9
As per Eq. (7.12), MPa	1.18	1.37	1.54	1.71	1.87

Notes:

1. For deformed bars in tension, τ_{bd} values can be increased by 60 per cent.
2. For bars in compression, the values of bond stress in tension can be increased by 25 per cent.
3. In case nominal reinforcement is provided, τ_{bd} is taken as 1.0N/mm^2 .

For fully stressed deformed bars in tension, Eq. (7.10) in conjunction with Table 7.1 will result in

$$L_d = \frac{0.136d_b f_y}{\tau_{bd}} \quad (7.11)$$

Though it is not clear how the values given in Table 7.1 have been derived, they may be approximated by the following equation

$$\tau_{bd} = 0.16(f_{ck})^{2/3} \quad (7.12)$$

Substituting this value in Eq. (7.11) and considering deformed bars, we get

$$L_d = \frac{d_b f_s}{1.177(f_{ck})^{2/3}} \quad (7.13)$$

The present Indian code formula considers only the diameter, yield stress, and grade of concrete as variables. In addition, the Indian code provisions are not generally applicable to high-strength concretes or HSCs (though the same bond stress of 1.9 MPa is suggested to be taken for concretes of strength M40 and above) and do not consider other later developments like epoxy-coated bars as reinforcement (Subramanian 2005). Table 7.2 provides the development length in terms of L_d/d_b for high-yield strength-deformed (HYSD) bars, that is, $f_y = 415\text{MPa}$.

TABLE 7.2 Development length in terms of L_d/d_b for HYSD bars ($f_y = 415\text{MPa}$)

Name of Code/Formula	Grade of Concrete				
	M20	M25	M30	M35	M40
IS 456:2000 limit state $L_d = \frac{d_b f_s}{1.177(f_{ck})^{2/3}}$	47	41	38	33	29.7
IS 456:2000 working stress	45	40	36	33	30
BS 8110-1:97* Type 1 deformed ($\beta_1 = 0.4$)** $L_d = \frac{f_s d_b}{4\beta_1 \sqrt{f_{ck}}}$ Type 2 deformed ($\beta_1 = 0.5$)	50	45	41	38	35.7
	40	36	33	30.5	28.5
DIN 1045-1:2001, Bond class I Bond class II	39.2	33.4	30	26.5	24.4
	56	47.7	43	38	35
AS 3600:2001+ $L_d = \frac{k_1 k_2 f_s A_b}{0.89(2a + d_b)\sqrt{f_{ck}}}$ $\geq 25k_1 d_b$	52	47	43	39	37

*Lap length to be increased by 40–100 per cent depending on the position of the bar.

** β_1 is a coefficient defined in BS 8110 and depends on the type of bar.

+ Assuming that clear cover, $a = \text{bar size}$, d_b ; $k_1 = 1.0$, and $k_2 = 2.2$

US Code Provisions

The 1999 version of the US code provision was based on the work of Orangun, et al. (1977), who developed a best-fit equation to estimate the average bond stress (bond strength u). The equation was modified in the subsequent editions of the ACI code and according to the 2011 version, the development length of straight deformed bars and wires in tension, expressed in terms of bar or wire diameter, is given by

$$L_d = \frac{f_y}{\lambda \sqrt{f_{ck}}} \frac{\alpha \beta \gamma}{\left(\frac{c + k_{tr}}{d_b} \right)} d_b \geq 300 \text{ mm} \quad (7.14)$$

where

L_d = development length in mm

d_b = nominal diameter of bar or wire in mm

f_y = specified yield strength of bar or wire in MPa

f_{ck} = specified cube compressive strength of concrete in MPa

α = reinforcement location factor

= 1.3 for horizontal reinforcement in beams and walls cast in lifts greater than 300 mm of fresh concrete

= 1.0 for other reinforcement

β = coating factor (based on the work of Treece and Jirsa 1989)

= 1.5 for epoxy-coated bars or wires with cover less than $3d_b$ or clear spacing less than $6d_b$, as splitting may occur at lower longitudinal force

= 1.2 for all other epoxy-coated bars or wires

= 1.0 for uncoated and galvanized reinforcement

(The product of α and β should not be greater than 1.7.)

γ = reinforcement size factor

= 0.8 for 20 mm and smaller bars and deformed wires

= 1.0 for 22 mm and larger bars

λ = lightweight aggregate concrete factor

= 0.75 when lightweight aggregate concrete is used

= $f_{ct}/(0.5\sqrt{f_{ck}})$ but less than 1.0 when f_{ct} (split cylinder tensile strength) is specified

= 1.0 for normal weight concrete

c = spacing or cover dimension (mm)

= smallest of the side cover (c_s), the cover for the bar or wire, c_b (in both cases measured from the centre of the bar or wire to the top or bottom surface), or one-half the centre-to-centre spacing of the bars or wires.

$$k_{tr} = \text{transverse reinforcement index} = \frac{40A_{tr}}{sn}$$

where

A_{tr} = total cross-sectional area of all transverse reinforcement within the spacing s , which crosses the potential plane of splitting through the reinforcement being developed within the development length, mm²

f_{yt} = specified yield strength of transverse reinforcement, N/mm²

s = maximum centre-to-centre spacing of transverse reinforcement within L_d , mm

n = number of bars being developed or spliced along the plane of splitting

It has to be noted that the term $(c + k_{tr})/d_b$ cannot be greater than 2.5 to safeguard against pull-out type failures. It has to be emphasized that Eq. (7.14) does not contain the strength reduction factor ϕ ; instead it was developed to implicitly account for the reinforcement overstress factor of approximately 1.25; hence, the development length is intended to provide strength for bar stress = $1.25f_y$.

As a design simplification, it is conservative to assume $k_{tr} = 0$, even if transverse reinforcement is present. The term $(c + k_{tr})/d_b$ in the denominator of Eq. (7.14) accounts for the effects of small cover, close bar spacing, and confinement provided by transverse reinforcement. The ACI code also gives some simplified versions of Eq. (7.14) for pre-selected values of $(c + k_{tr})/d_b$. However, the development lengths L_d computed by Eq. (7.14) could be substantially shorter than that computed from the simplified equations. It should be noted that the development length of straight deformed bars or wires including all modification factors must not be less than 300 mm.

It is difficult to compare the IS code provisions with those of the ACI code, since they do not have the same format. Prakash Rao (1991) has shown that the anchorage and lap lengths prescribed in various codes of practice differ significantly. Table 7.3 shows the comparison for grade 415 reinforcement ($f_y = 415$ MPa) and different concrete compressive strengths, for normal weight concrete ($\lambda = 1.0$) and uncoated ($\beta = 1.0$) bottom bars ($\alpha = 1.0$), with $k_{tr} = 0$.

TABLE 7.3 Comparison of L_d/d_b for bars in tension (for Fe 415 grade steel)

Name of Code	Bar Diameter mm	Grade of Concrete				
		M20	M25	M30	M35	M40
IS 456:2000	All bars	47	40	38	33	29.7
ACI 318:08 $c_c = 1.5d_b$	< 19	49.5	44.2	40.4	37.4	35
	> 22	61.9	55.3	50.5	46.8	43.7
ACI 318:08 $c_c = 1.0d_b$	< 19	74.4	66.4	60.6	56	52.5
	> 22	93	83	75.8	70	65.6
Eq. (7. 15) $c_c = 1.5d_b$; $\omega = 1$	All bars	71.2	66.4	62.5	59.2	56.5

It is seen from Table 7.3 that the IS code requires less development length than the ACI code. The ACI code accounts for the increase in bond length for smaller diameter bars. As the cover increases, the ACI code gives less development length, which is not considered in the Indian code. The Indian code provisions were based on experiments with concrete strength up to only 40 MPa, whereas Clause 12.1.2 of the ACI code limits the value of $\sqrt{f'_c}$ to 8.3 (i.e., for concrete cube strength up to 86 MPa).

It has to be noted that the Indian code formula does not consider most of the parameters that affect the bond strength as discussed in Section 7.4.2. In contrast, the US, Canadian, and New Zealand codes, which have the same format, consider several important parameters that affect the bond strength such as location of rebars, yield strength of steel, grade of concrete, surface condition of rebars, reinforcement size, lightweight aggregates, spacing between rebars, size of cover, and the effect of transverse reinforcement. Hence, these codes truly represent the bond behaviour of reinforcement.

7.5.4 Design Aids

Tables 64–66 of SP 16:1980 directly provide the value of development length for fully stressed bars for M15 to M30 for three different values of $f_y = 250, 415, \text{ and } 500 \text{ MPa}$, respectively. Similar tables for $f_y = 415 \text{ MPa}$ and $f_y = 500 \text{ MPa}$ are presented in Tables 7.4 and 7.5, respectively.

TABLE 7.4 Development length for fully stressed deformed bars as per IS 456, mm (for $f_y = 415 \text{ MPa}$)

Bar Diameter, mm	Tension Bars—Grade of Concrete					Compression Bars—Grade of Concrete				
	M20	M25	M30	M35	M40	M20	M25	M30	M35	M40
6	282	242	226	199	178	226	193	181	159	143
8	376	322	301	265	238	301	258	241	212	190
10	470	403	376	332	297	376	322	301	265	238
12	564	484	451	398	356	451	387	361	319	285
16	752	645	602	531	475	602	516	481	425	380
18	846	725	677	597	534	677	580	542	478	428
20	940	806	752	664	594	752	645	602	531	475
22	1034	887	827	730	653	827	709	662	584	523
25	1175	1007	940	830	742	940	806	752	664	594
28	1316	1128	1053	929	831	1053	903	842	743	665
32	1504	1289	1204	1062	950	1204	1032	963	850	760
36	1692	1451	1354	1195	1069	1354	1161	1083	956	855

Note: The development lengths given here are for a stress of $0.87f_y$ in the bars.

TABLE 7.5 Development length for fully stressed deformed bars as per IS 456, mm (for $f_y = 500 \text{ MPa}$)

Bar Diameter, mm	Tension Bars—Grade of Concrete					Compression Bars—Grade of Concrete				
	M20	M25	M30	M35	M40	M20	M25	M30	M35	M40
6	340	291	272	240	215	272	233	218	192	172
8	453	388	363	320	286	363	311	290	256	229
10	566	485	453	400	358	453	388	363	320	286
12	680	583	544	480	429	544	466	435	384	343
16	906	777	725	640	572	725	621	580	512	458
18	1020	874	816	720	644	816	699	653	576	515
20	1133	971	906	800	715	906	777	725	640	572
22	1246	1068	997	880	787	997	854	798	704	630
25	1416	1214	1133	1000	894	1133	971	906	800	715
28	1586	1359	1269	1119	1002	1269	1088	1015	896	801
32	1813	1554	1450	1279	1145	1450	1243	1160	1024	916
36	2039	1748	1631	1439	1288	1631	1398	1305	1151	1030

Note: The development lengths given here are for a stress of $0.87f_y$ in the bars.

7.5.5 Recent Research

Globally, there is an increased usage of high-strength and high-performance concrete (HPC) with compressive strength

70–120 MPa. Yet, the bulk of knowledge on bond and anchorage behaviour between steel and concrete that is used in practice is from the experience on RC elements having much lower concrete strength (Yerlici and Özturan 2000). For higher strength concrete, a higher degree of elastic and stiffer bond behaviour is expected due to the improved strength and the higher modulus of elasticity (Rashid 2004). The average bond strength is increased in HSC as the porosity is reduced due to the addition of much finer materials such as fly ash and silica fume. However, more brittle bond behaviour has been reported for HSC (Ezeldin and Balaguru 1989). Though the bond characteristics of normal concrete are reasonably well established, the bond characteristics of HPC using supplementary cementitious materials such as ground-granulated blast-furnace slag (GGBS), fly ash, and silica fume are not yet fully established (Azizinamini, et al. 1993; Gjrov 1990; Hamad 1998). Balasubramanian, et al. (2004) have shown that the addition of slag (up to 50% as cement replacement material) did not result in any reduction in the bond strength characteristic.

Azizinamini, et al. (1995) studied the effect of high concrete strength on bond and found that the average bond stress at failure normalized with respect to the square root of concrete compressive strength $\sqrt{f_{ck}}$ decreases with an increase in the compressive strength. The rate of decrease becomes more pronounced as the splice length increases. Darwin and co-workers compared a large data of experimental investigations and found that the best fit for experimental results is provided by $f_c'^{1/4}$ and not $f_c'^{1/2}$ as given in the ACI and other codes (Darwin, et al. 1996; Zuo and Darwin 2000). They also suggested that the effect of transverse reinforcement on the splice strength is better characterized using $f_c'^{3/4}$. They proposed the following equation for the development length (Zuo and Darwin 2000; Darwin, et al. 2005), which has been adopted in ACI 408R-03:

$$\frac{L_d}{d_b} = \frac{\left(\frac{f_y}{f_c'^{1/4}} - 48\omega \right) \alpha \beta}{1.5 \lambda \left(\frac{c_b \omega + K'_{tr}}{d_b} \right)} \quad (7.15a)$$

in which $\left(\frac{c_b \omega + K'_{tr}}{d_b} \right)$ should be less than 4.0; the factor ω can be taken as 1.0 or calculated as

$$\omega = 0.1 \frac{c_{\max}}{c_{\min}} + 0.9 \leq 1.25$$

The transverse reinforcement index K'_{tr} is calculated as

$$K'_{tr} = \frac{6t_d A_{tr} \sqrt{f'_c}}{sn} \quad (7.15b)$$

The bar diameter factor t_d is calculated as

$$t_d = 0.03d_b + 0.22 \quad (7.15c)$$

The other symbols α, β, k_{tr} , and so on are as defined in Section 7.5.3. Though the format of Eq. (7.15) is similar to that of

Eq. (7.14) of the ACI 318:11 code, the application of Eq. (7.15) differs from that of Eq. (7.14) due to the following reasons:

1. Eq. (7.14) distinguishes 19mm diameter and smaller bars from larger bars using the γ term, leading to a 20 per cent drop in the development or splice length for the smaller bars.
2. The development length L_d calculated using Eq. (7.14) must be increased by 30 per cent for class B splices (splices in which the area of steel provided is less than two times the area of steel required or where more than 50 per cent of the steel is spliced). A comparison of this equation is made in Table 7.3 for $c_c = 1.5d_b$.

Seliem, et al. (2009) found that Eq. (7.15) with a strength reduction factor (ϕ factor) of 0.82 provides a reasonable estimate of bond strength for both unconfined and confined splices of high-strength ASTM A1035 (MMFX) bars. The following equation was proposed by El-Hacha, et al. (2006) for *MMFX high-strength steel reinforcement*, with $f_y = 827$ MPa.

$$\frac{L_d}{d_b} = \frac{9 \left(\frac{f_y}{\sqrt{f'_c}} - 51 \right) \alpha \beta}{4 \lambda \left(\frac{c_{\min} + 0.5d_b + k_{tr}}{d_b} \right)}; k_{tr} = \frac{A_{tr} f_{yt}}{556sn} \quad (7.16)$$

where the symbols α , β , k_{tr} , and so on are as defined in Section 7.5.3. Several other alternative equations have been proposed by other researchers (Yerlici and Özturan 2000; Canbay and Frosch, 2006).

The development of bond strength of reinforcement in *self-consolidating concrete* (SCC) (which is cast without applying any consolidation) was studied by Chan, et al. (2003) and Cattaneo and Rosati (2009). They observed that as compared to NSC, SCC exhibits significantly higher bond strength and less significant top-bar effect. SCC also exhibited significant size effect; smaller bar diameter exhibited higher bond strength than the larger one. Recently, Darwin and Browning (2011), based on their splice tests of beams with high-strength reinforcement (ASTM A 1035-MMFX bars with $f_y = 690$ – 827 MPa) and concrete of strength ranging from 43 MPa to 68 MPa, concluded that the ACI 408R equation, Eq. (7.15), provides a reasonable estimate of the strength for both unconfined and confined splices along with a reasonable margin of safety compared to the ACI equation, Eq. (7.14).

7.5.6 Reduction in Development Length due to Excess Reinforcement

The Indian and US codes allow for the *reduction in development length* by the ratio $(A_{st} \text{ required}) / (A_{st} \text{ provided})$ when excess reinforcement is provided to resist the factored applied moment in a flexural member (SP 24:1983). Thus, we have

$$L'_d = L_d \frac{(A_{st})_{\text{required}}}{(A_{st})_{\text{provided}}} \quad (7.17)$$

where L'_d is the actual required development length and L_d is the development length of the fully stressed bars (where $f_s = 0.87f_y$).

However, such a reduction is not allowed for tension lap splices, development of positive moment reinforcement at support, and development of shrinkage and temperature reinforcement (where we have to provide development length as for fully stressed bars). This reduction is also not permitted for reinforcement in structures located in regions of high seismic risk.

7.5.7 Development Length of Bars in Compression

The real performance of *bond in compression* is not precisely known. The present practice is to consider it similar to that of tension. However, the development length required is shorter for bars in compression than in tension because of the absence of tension cracking in the concrete and the beneficial effect of end bearing of the bars in compression. In the Indian code, the values of bond stress in tension (see Table 7.2) are increased by 25 per cent. The development lengths for compression bars for $f_y = 415$ MPa and $f_y = 500$ MPa may be directly read from Tables 7.4 and 7.5, respectively. The US, Canadian, and New Zealand codes specify the following equation:

$$L_{dc} = \frac{0.268 f_y}{\lambda \sqrt{f_{ck}}} d_b \geq 0.043 f_y d_b \quad \text{or} \quad 200 \text{ mm} \quad (7.18)$$

This development length may be reduced when excess reinforcement is provided and/or where confining ties or spirals are provided around the reinforcement (25% reduction). Comparison of Eq. (7.18) with the Indian code provisions shows that the development length as per the IS 456 code is about 1.5–1.8 times longer than that required by the ACI 318 code (Kalyanaraman 1984). For example, the development length in compression for Fe 415 steel in M25 concrete as per IS 456 is $32.2d_b$ and according to Eq. (7.18) is only $22.2d_b$.

As per Clause 26.2.2.2 of IS 456, the projected lengths (and not equivalent lengths as in tension) of hooks, bends, and straight lengths beyond the bends alone are considered effective for the development length for bars in compression (see also Section 7.6.1).

7.5.8 Development Length of Bundled Bars

For situations requiring heavy concentration of reinforcement, bundles of bars can save space and reduce congestion for placement and consolidation of concrete. *Bundling of bars* in columns will result in better locating and orienting of the reinforcement for increased column capacity; also, fewer ties are required if column bars are bundled. While using bundled bars, the following points should be remembered:

1. Bars may be arranged singly, in pairs in contact, or in groups of three or four bars bundled in contact (see

Fig. 7.13). It is better to restrict the number of bars in a bundle to three in beams and to four in columns.

2. Clause 26.1.1 of IS 456 prohibits the bundling of bars larger than 32 mm, except in columns, whereas as per the ACI code bars greater than 36 mm should not be bundled. This is primarily because of crack control problems.
3. Bundled bars should be enclosed within stirrups or ties.
4. Bundled bars should be tied together to ensure that the bars remain together.

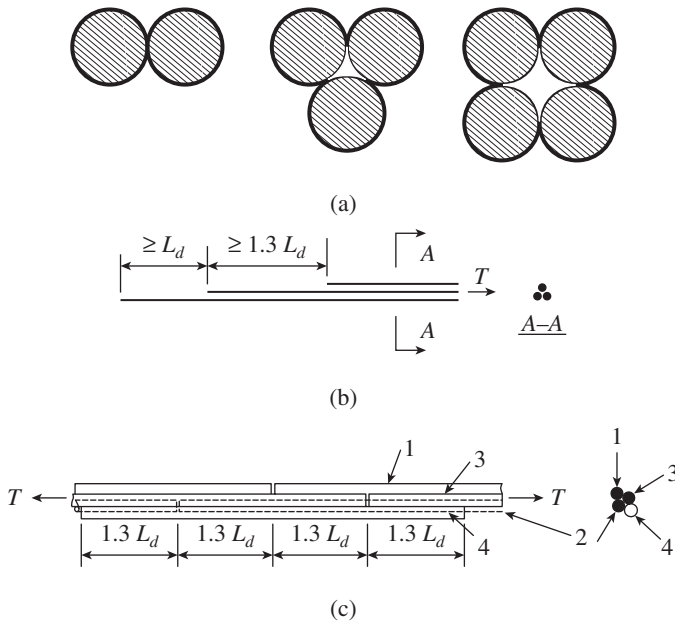


FIG. 7.13 Bundling of bars (a) Possible bundling schemes of reinforcing bars and effective perimeter (b) Anchorage of staggered bars in a bundle (c) Lap joint in tension including a fourth bar

For spacing and concrete cover, a unit of bundled bars must be treated as a single bar with an area equivalent to the total area of all the bars in the bundle. Equivalent diameters of bundled bars are given in Table 7.6.

TABLE 7.6 Equivalent diameters and perimeter of bundled bars

Bar Diameter (d_b), mm	Equivalent Diameter, mm ($d_{eq} = d_b \sqrt{n_b}$)		
	Two-bar Bundle	Three-bar Bundle	Four-bar Bundle
12	16.97	20.78	24
16	22.63	27.71	32
20	28.28	34.64	40
22	31.11	38.11	44
25	35.36	43.30	50
28	39.60	48.50	56
32	45.25	55.43	64

Increased development length for individual bars within a bundle, whether in tension or compression, is required when bars are bundled together. The additional length is required because there is no 'core' of concrete between the bars to provide

resistance to slipping. The ACI code gives a modification factor of 1.2 for a three-bar bundle and 1.33 for a four-bar bundle. For the factors of Eq. (7.14), which are based on bar diameter d_b , a unit of bundled bar must be treated as a single bar of a diameter derived from the total equivalent area. In Clause 26.2.1.2 of the Indian code, the development length is increased by 10 per cent for two bars in contact, 20 per cent for three bars in contact, and 33 per cent for four bars in contact, which are similar to the ACI code. The codes do not explicitly state how these factors were derived, but they may be based on the change in effective perimeter when the bars are grouped together (see Fig. 7.13).

If end hooks are required, it is preferable to stagger the hooks of the individual bars within the bundle. When individual bars in a bundle are cut-off within the span of beams, they should terminate at different points. The ACI code suggests that the stagger should be at least 40 bar diameters. More information on bundled bars can be had from Jirsa, et al. (1995) and Bashandy (2009).

7.5.9 Development of Welded Deformed Wire Reinforcement in Tension

The development requirements for *wire fabric* primarily depend on the location of the cross wire rather than the bond characteristics of the plain or deformed wire. It has to be noted that some of the development is assigned to the welds and some assigned to the length of deformed wire. An embedment of at least two cross wires, with the first cross wire at 50 mm or more beyond the point of critical section, as shown in Fig. 7.14, is adequate to develop the yield strength of anchored wires, according to the ACI code. However, development length L_{dw} measured from the critical section to the outermost cross wire, calculated using Eq. (7.19) should be greater than 200 mm, as shown in Fig. 7.14.

$$L_{dw} = L_d (\text{Eq. 7.14}) \times \psi_w \quad (7.19)$$

where ψ_w is the greater of $(f_y - 240)/f_y$ and $(5d_b)/s$, but less than 1.0, and s is the spacing between the wires to be developed. Epoxy-coated welded wire reinforcements have been found to have the same development and splice strengths as uncoated welded wire reinforcement because the primary anchorage for the wire reinforcement is provided by the cross wires. Hence, an epoxy-coating factor of 1.0 is suggested by the ACI code for development and splice lengths of epoxy-coated welded wire reinforcement with cross wires within the splice or development length. Readers may refer to Clause 12.8 of the ACI code for calculating the development length of welded *plain* wire reinforcement in tension.

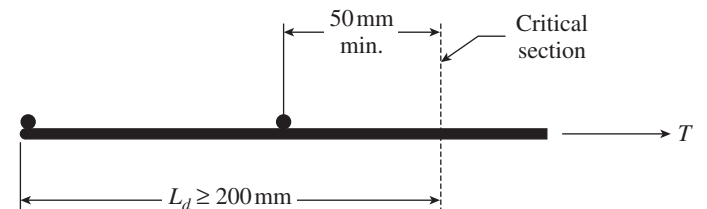


FIG. 7.14 Development of welded wire fabric

7.6 ANCHORING REINFORCING BARS

Often, the space available at the ends of a beam is limited to accommodate the development length L_d . This is particularly true in the case of *beam-column junctions* (refer to Chapter 19). In such situations, any deficiency in the required development length may be made up by suitably *anchoring the reinforcements* using bends, hooks, or any mechanical devices. As mentioned previously, hooks *should be* provided for plain bars in tension. However, as deformed bars have superior bond characteristics due to mechanical bearing, provision of bends, hooks, or mechanical devices is not absolutely essential.

7.6.1 Behaviour of Hooks or Bends in Tension

When a 90° bar is loaded in tension, the stresses in the bar are resisted by the bond on the surface and also by the bearing on the concrete inside the hook (Marques and Jirsa 1975). The bend tries to straighten out, since the compressive force inside the bend is not collinear with the applied tensile force. This action produces compressive forces on the outside of the tail (Fig. 7.15).

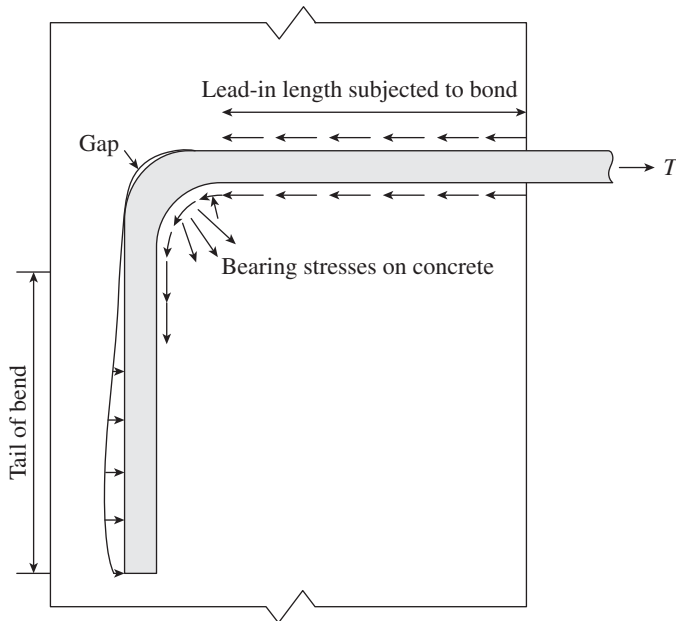
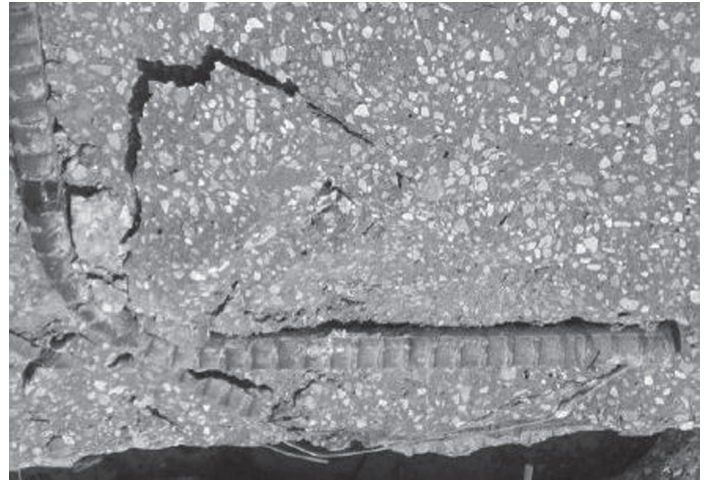


FIG. 7.15 Forces acting on the bend

Due to the high local stress concentrations of bearing stresses, the concrete inside the bend crushes as shown in Fig. 7.16. If the cover is less, the crushing will extend to the surface of the concrete, resulting in splitting of the concrete cover (see Fig. 7.17). Typical stress distribution and slip of 90° and 180° bends are shown in Fig. 7.18. It has to be noted that the slip is considerable for a 180° hook (1.75 times higher) compared to a 90° hook. Top-bar effect was also found in 180° hooks (Rehm 1969). Thus, hook development is a direct function of bar diameter d_b , which governs the magnitude of compressive stresses on the inside of the hook. Only standard hooks, as shown in Fig. 7.19(a), were considered in the experiments and the influence of larger radius of bend has not been studied yet.



(a)



(b)

FIG. 7.16 Crushed concrete inside of bend radius (a) 90° hook (b) 180° hook

Source: Hamilton III, et al. 2008



FIG. 7.17 Splitting bond failure in Surajbari bridge during Bhuj earthquake

Courtesy: Er S.A. Reddi, former deputy managing director, Gammon India Ltd

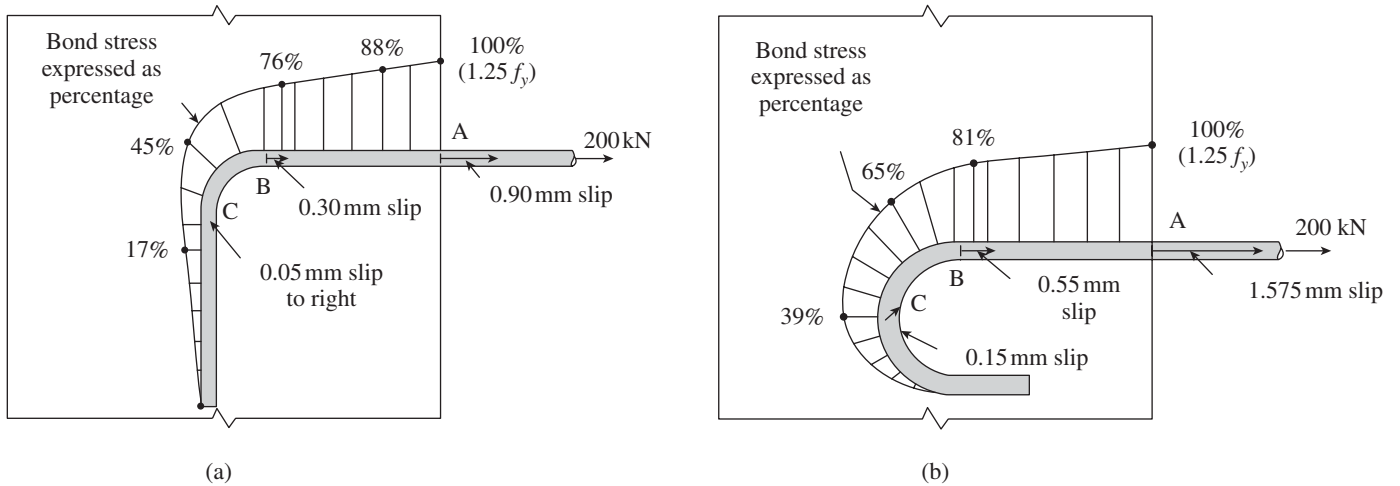


FIG. 7.18 Typical stress distribution and slip in bends and hooks (a) 90° standard hook (b) 180° standard hook

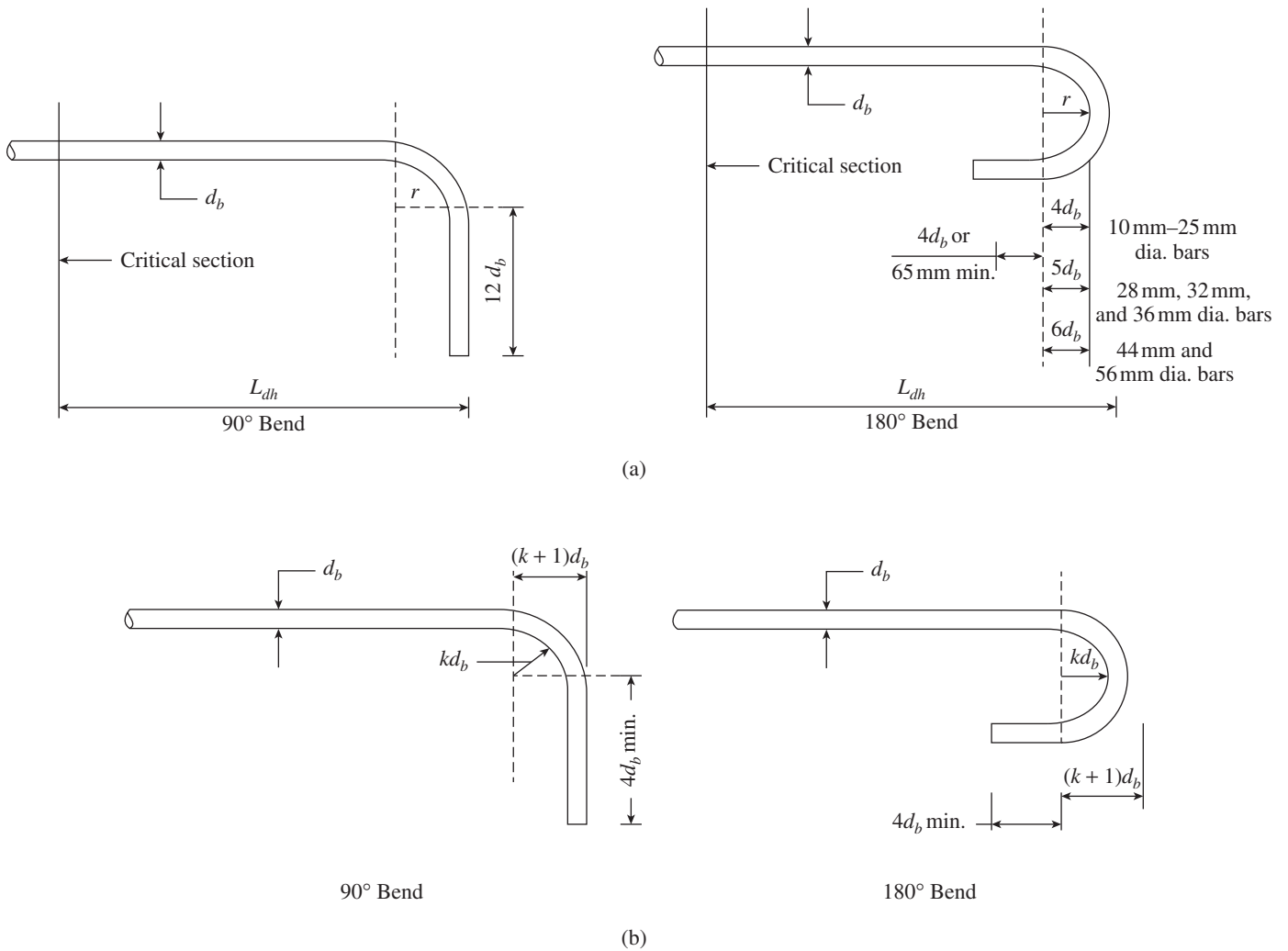


FIG. 7.19 Development length of standard bends and hooks (a) As per ACI code (b) As per IS 456

The treatment of hooked anchorages in the Indian and US codes is entirely different. As per Clause 26.2.2.1 of IS 456:2000, the anchorage value or *equivalent length* of bend is taken as four times the diameter of the bar for each 45° bend

subject to a maximum of 16 times the diameter of the bar. The anchorage value of a standard U-type hook is taken as 16 times the diameter of the bar (see Table 7.7). Standard bend and hooks as per IS 456 are given in Fig. 7.19(b) (minimum

value of k in Fig. 7.19b is two for mild steel and four for cold-worked deformed bars). Amendment 4 of IS 456 (March 2009) states that the design bond stress for fusion-bonded epoxy-coated deformed bars should be taken as 80 per cent of the values given in Table 7.1.

TABLE 7.7 Equivalent length of bends and hooks

Type of Bar	Bend		Hook		Equivalent Length	
	Angle	Extension	Angle	Extension	90°	180°
Straight or inclined bar	90°	$4d_b$	180°	$4d_b$	$2(4d_b) = 8d_b$	$4(4d_b) = 16d_b$
Stirrups	90°	$8d_b$	135° 180°	$6d_b$ $4d_b$	Full anchorage is assumed	

In compression, hooks and bends are ineffective and should not be used as anchorage. As per Clause 26.2.2.2 of IS 456, only the projection length (and not the equivalent length as in tension) beyond the bends (if provided) is taken as effective for bars in compression (see Fig. 7.20). Hence, in the design for compression steel, the sizes of bars are selected so as to satisfy the available development length. As known from Table 7.1, the development length required for compression is 25 per cent less than that required for tension. Thus, in IS 456, the development length is calculated as per Eq. (7.10) and reduced as per Eq. (7.17), and provided with or without bends or hooks, by using the equivalent length of bends and hooks (see Table 7.7). Table 7.8 gives the anchorage value of hooks and bends for bars subjected to tension.

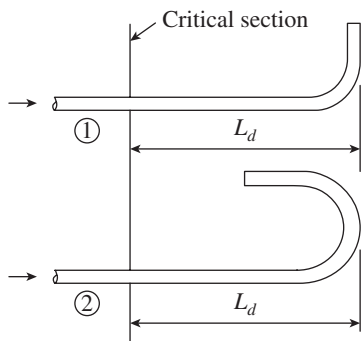


FIG. 7.20 Development length in compression

Note: In compression, hooks and bends are ineffective and hence should not be used as anchorage.

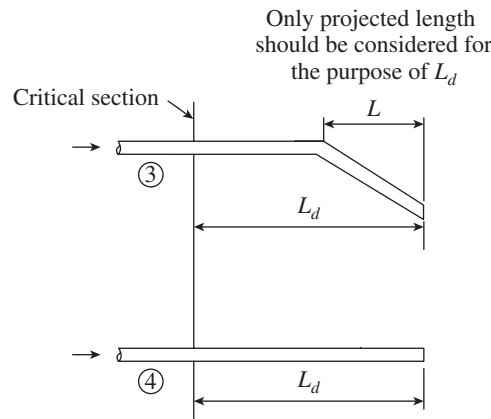
TABLE 7.8 Anchorage value (equivalent length) of hooks and bends

Bar Diameter, d_b , mm	6	8	10	12	16	20	22	25	28	32	36
Anchorage value of hook, mm	96	128	160	192	256	320	352	400	448	512	576
Anchorage value of 90° bend, mm	48	62	80	96	128	160	176	200	224	256	288

In the US, Canadian, and New Zealand codes, the development length L_{dh} , measured from the critical section to the outside end of the standard hook (i.e., the straight embedment length between the critical section and the start of the hook, plus the radius of bend of the hook, plus one bar diameter), is given by (see Fig. 7.19)

$$L_{dh} = \frac{0.268\beta f_y}{\lambda\sqrt{f_{ck}}} d_b \geq 8d_b \quad \text{or} \quad 150 \text{ mm} \quad (7.20)$$

As in Eq. (7.14), modifiers are included to represent the influence of bar size, cover, epoxy coating, lightweight concrete, confinement by transverse ties or stirrups, and more reinforcement provided than required by analysis (Hamad, et al. 1993). Some of these modifiers are $\beta = 1.2$ for epoxy-coated and $\lambda = 0.75$ for lightweight concrete. For other cases, β and λ are taken as 1.0. The length L_{dh} may be multiplied by 0.7 for a 90° hook with cover or bar extension beyond the hook not less than 50 mm and for 36 mm bar with smaller hooks and side cover > 65 mm (see Section 12.5.3 of the ACI code for other multipliers). Fig. 7.19 shows L_{dh} and the standard hook details for all standard ACI bar sizes. Comparing Eq. (7.20) with Eq. (7.14) (without the modifiers), we may find that the development length is decreased 3.75 times by using the hooks. It has to be noted that the design process in the ACI code does not distinguish between the 90° bend and 180° hook or between the top and bottom bar hooks.



Thus, the ACI code directly gives the anchorage length of different bends and hooks as a function of the bar size and strength of bars and concrete, whereas the IS code specifies the anchorage value of bends and hooks as a multiple of the bar diameter. It should be noted that the straight extension of bars beyond a standard bend is allowed by IS 456 to be included as additional anchorage length provided, whereas the ACI code does not do so. Tests have shown that this straight extension beyond a standard bend is not effective and should not be included (Orangun, et al. 1977; Jirsa, et al. 1979).

As discussed in Section 6.2.3 of Chapter 6 and as per Clause 26.2.2.5 of the code, the bearing stress in concrete for standard bends (as given in IS 2502 and shown in Fig. 7.20) need not be checked as the bearing stress will be of the order of only $0.2f_y$. IS 456 also allows the use of non-standard hooks, in which case the bearing stress inside the bend or hook should be checked using Eq. (6.5) given in Chapter 6 (Clause 26.2.2.5). For fully stressed bars, this equation results in

$$\frac{0.87 f_y (\pi d_b^2 / 4)}{r d_b} \leq \frac{1.5 f_{ck}}{1 + (2d_b / a)}$$

Simplifying, we get

$$r \geq 0.456 d_b \left(\frac{f_y}{f_{ck}} \right) \left(1 + \frac{2d_b}{a} \right) \quad (7.21)$$

where r is the internal radius of the bend, d_b is the size of the bar, or, in bundle, the equivalent size of bar, and a is the centre-to-centre distance between the bars or group of bars perpendicular to the plane of the bend; it can be taken as cover plus size of bar.

It has to be noted that bar hooks are especially susceptible to concrete splitting failure if both the side cover (normal to plane of hook) and top or bottom cover (in plane of hook) are small. Hence, confinement reinforcement in the form of ties or stirrups perpendicular to the bar being developed is suggested by the ACI code, when both the side and top (or bottom) covers over hook are less than 65 mm . These ties or stirrups should be spaced not greater than $3d_b$ along L_{dt} . The first tie or stirrup shall enclose the bent portion of the hook, within $2d_b$ of the outside of the bend (ACI code Clause 12.5.4). Such ties or stirrups should be provided for confinement at ends of simply supported beams, at free end of cantilevers, and at ends of members framing into a joint where members do not extend beyond the joint. In compression, hooks are ineffective and may not be used as anchorage (ACI code Clause 12.5.5).

7.6.2 Headed and Mechanically Anchored Bars in Tension

Use of hooks often results in steel congestion, difficult fabrication and construction, and greater potential for poor concrete placement. In addition, cyclic loading tends to degrade the anchorage capacity due to the slip. The use of anchor plates or heads either welded or threaded to the longitudinal bar (often called *headed bars*) have been identified as a viable alternative to hooked bars for exterior joints and also provide ease of fabrication, construction, and concrete placement. Headed bars with rectangular, round, or elliptical heads are available. The heads may be welded, forged, or threaded (Fig. 7.21). Thompson, et al. (2006a) suggested that the headed bar anchorage is provided by a combination of head bearing and bond. The initial anchorage is provided by bond. As additional load is applied to the bar, the bond achieves peak capacity and begins to decline. As the process of bond deterioration occurs, bond anchorage is transferred to the head, causing rise in head bearing. The anchorage capacity

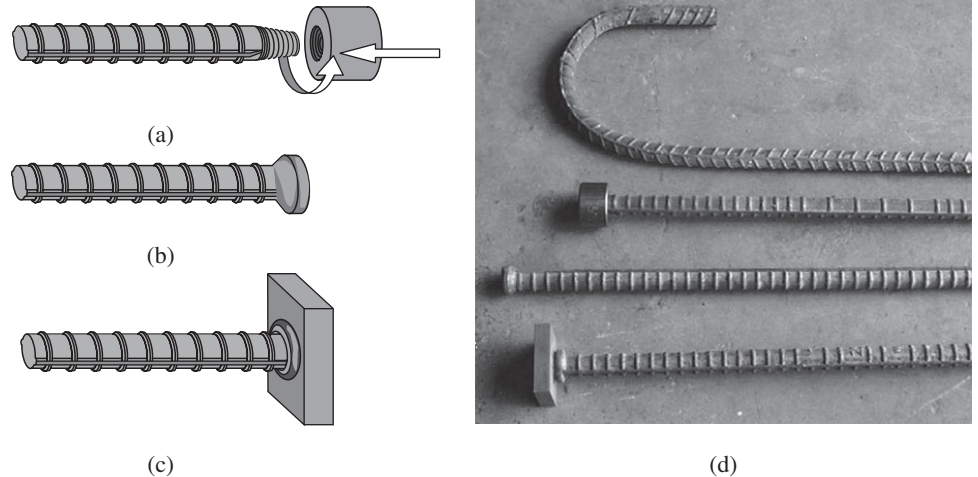


FIG. 7.21 Types of heads and various headed bars compared to a standard hook (25 mm size) (a) Threaded head (b) Forged head (c) Friction welded head (d) Photo showing bars with standard hook and various heads

Source: Thompson, et al. 2002

at failure is provided by a combination of peak head bearing and reduced bond. According to Thompson, et al. (2006c), the strut-and-tie models are the best for determining the anchorage length and the node and strut dimensions play a critical role in defining the anchorage length. They also recommended a minimum anchorage length of $6d_b$.

Tests conducted by Chun, et al. (2007) and Kang, et al. (2010) reveal that the hysteretic behaviour of exterior joints constructed with headed bars was similar or even superior to that of joints with hooked bars. The head size with a net area of three to four times the bar area was sufficient to anchor the beam reinforcement effectively (with a development length shorter than that needed for hooked bars) within the exterior beam-column joint. For roof level connections, anchoring the column heads above the beam bars and adding an additional layer of transverse reinforcement led to improved behaviour.

Though IS 456:2000 states that mechanical devices can be used to anchorage bars with the approval of the engineer in charge, it does not contain any clause to calculate the anchorage length. Clause 12.6.1 of the ACI code suggests Eq. (7.22) to determine the development length of headed deformed bars in tension, L_{dt} , provided the following conditions are satisfied (see Fig. 7.22):

1. Yield strength of bar f_y does not exceed 420 MPa
2. Diameter of bar does not exceed 36 mm
3. Normal weight concrete is used
4. Net bearing area of head A_{brg} is not less than $4A_b$, where A_b is the area of bar
5. Clear cover for bar is not less than $2d_b$
6. Clear spacing between bars is not less than $4d_b$

$$L_{dt} = \frac{0.215 \beta f_y}{\sqrt{f_{ck}}} d_b \geq 8d_b \text{ or } 150 \text{ mm} \quad (7.22)$$

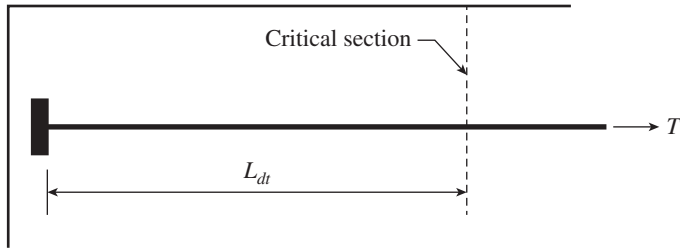


FIG. 7.22 Development of headed deformed bars

These restrictions are based on available experimental results (Thompson, et al. 2006a and 2006b). Modifier β is taken as 1.2 for epoxy-coated reinforcement and 1.0 for all other cases. It should be noted that Eq. (7.22) results in a development length approximately 80 per cent of that required for hooked bars, as per Eq. (7.20). Moreover, Eq. (7.22) is not a function of the head size, though it is indirectly accounted for through the minimum requirements.

To avoid congestion, it may be desirable to stagger the heads. When longitudinal headed bars from a beam or a slab terminate at a supporting member, the bars should be extended up to the far face of the confined core of the supporting member, for example, in a column as shown in Fig. 7.23 (allowing for cover and avoiding interference with column reinforcement). Thus, in this case, the resulting anchorage length will exceed L_{dt} . It has to be noted that the additional reduction in development length, such as those allowed for standard hooks with additional confinement provided by transverse reinforcement, is not allowed for headed deformed reinforcing bars, as the test data does not show significant improvement in the behaviour due to confinement. However, transverse reinforcement, which may help to limit splitting cracks in the vicinity of the head, is

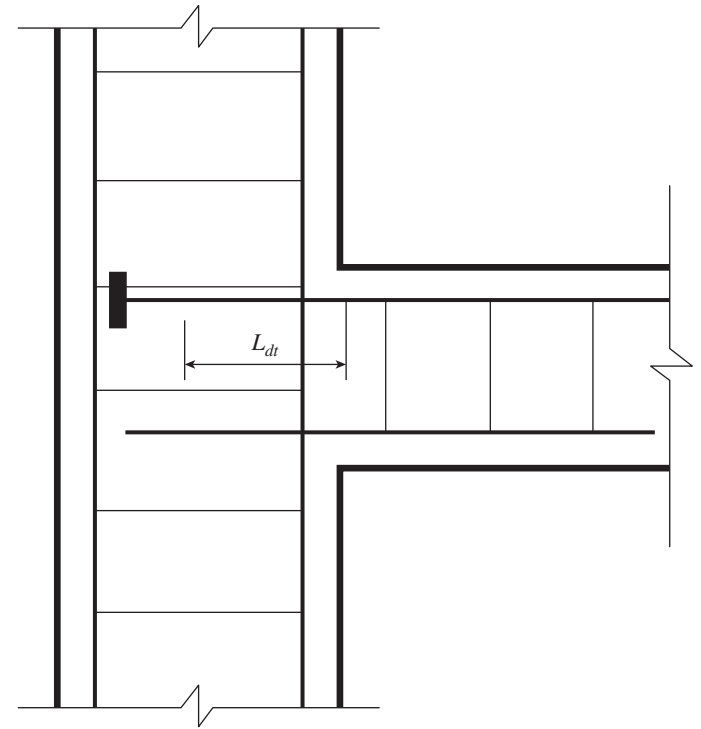


FIG. 7.23 Headed deformed bar extended to far side of column core

recommended. In addition, as per ACI 318, headed bars should not be considered effective in compression, as no test data is available yet to show that the use of heads are beneficial in compression. Thompson, et al. (2006c) also cautioned that the location of the critical section based on the strut-and-tie model will be different from the one assumed based on the beam theory.

CASE STUDY

Sinking of the Sleipner 'A' Offshore Platform

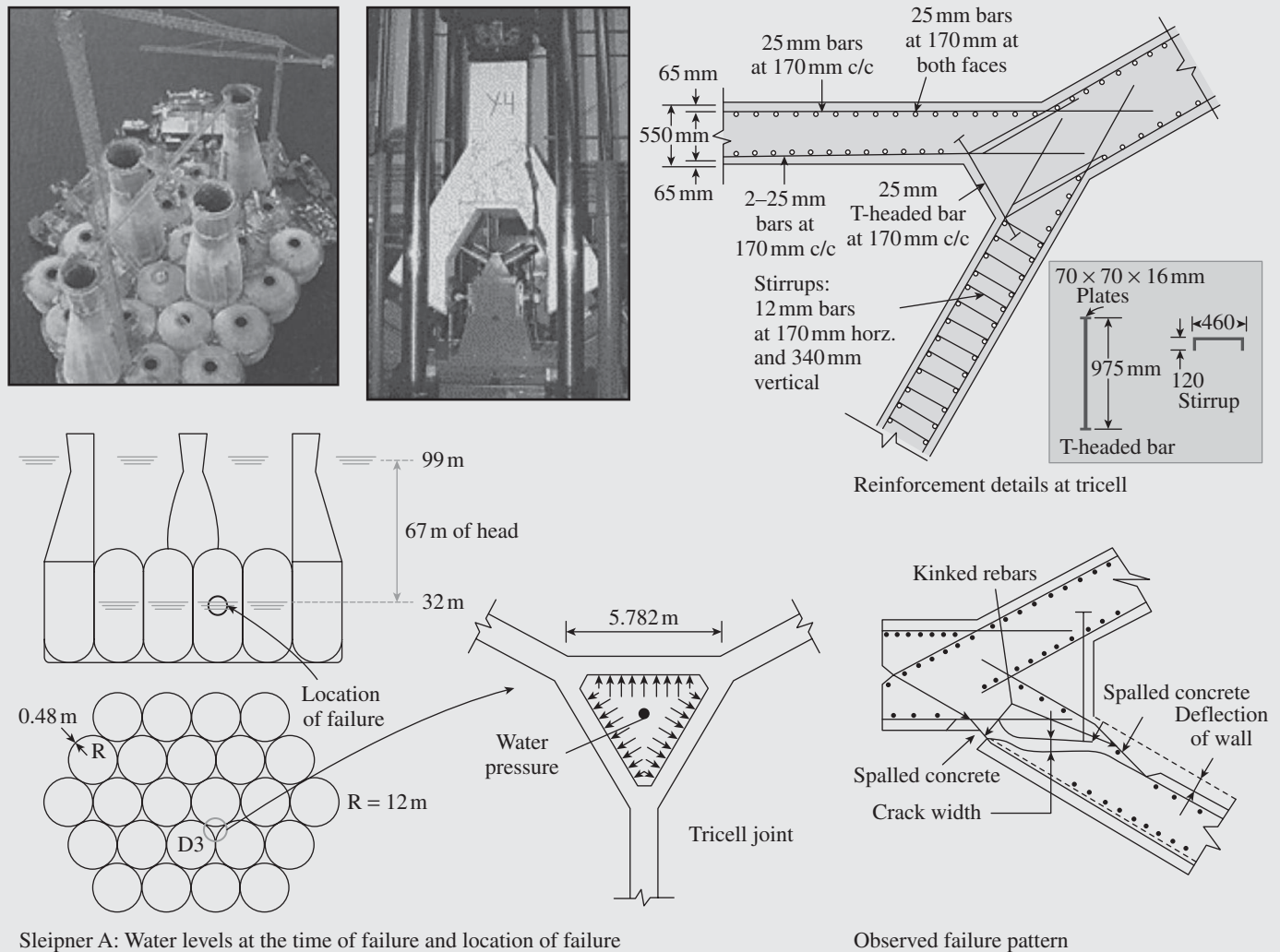
Sleipner 'A' is an offshore oil and gas drilling platform in the North Sea, operated by Statoil, and supported on the seabed at a water depth of 82m. The *condeep*-type platform consists of two units, the hull and the deck. The hull is a gravity base (with a total base area of 16,000m²) made up of support pilings and concrete ballast chambers from which three or four shafts rise and upon which the deck sits. Once fully ballasted, the hull sits on the sea floor. Moreover, the platform consisted of 24 chambers, of which 4 formed the 'legs' supporting the facility on top (see figure). The top deck weighs 57,000 tons and provides accommodation for about 200 people and support for drilling equipment weighing about 40,000 tons.

In August 1991, prior to the mating of the hull and the deck unit, the hull was towed into Gandsfjord, outside Stavanger, Norway,

where it was to be lowered in the water in a controlled ballasting operation at a rate of 1 m per 20 minutes. As the hull was lowered to the 99 m mark, on 23 August 1991, rumbling noises were heard followed by the sound of water pouring into the unit. A cell wall had failed and a serious crack had developed, and the sea water poured in at a rate that was too great for the de-ballasting pumps to deal with. Within a few minutes, the hull began sinking at a rate of 1m per minute. As the structure sank deeper, the buoyancy chambers imploded and the rubble struck the floor of the 220m deep seabed creating a 3.0 magnitude earthquake, which was recorded in a local seismograph station. The failure involved a total economic loss of about \$700 million. The cell wall failure was traced to a *tricell*, a triangular concrete frame placed where the cells meet (see figure).

(Continued)

(Continued)



Sleipner A: Water levels at the time of failure and location of failure

Sleipner 'A' Offshore Platform

(Source: Selby, et al. 1997, reprinted with permission from Concrete International, ACI)

Immediately after the accident, the owner of the platform conducted investigations. The conclusion of the investigation was that the loss was caused by a failure in a cell wall, resulting in a serious crack and a leakage that the pumps were not able to cope with (Selby, et al. 1997; Holand 1997).

The post-accident investigation traced the error to inaccurate finite element approximation of the linear elastic model of the tricerell. Test specimens also revealed a mode of failure in which the shear cracks in the walls of the tricerell joint bypassed the ends of the double-headed tie bars, thus resulting in *insufficient anchorage of the reinforcement* in a critical zone (see figure). The shear stresses

were also underestimated by 47 per cent, leading to insufficient design. In particular, certain concrete walls did not have sufficient thickness (Jakobsen and Rosendahl 1994; Selby, et al. 1997).

During redesign, the length of the double-headed ties was increased by 500mm, shifting the termination point of the ties into the compression zone of the joint walls. Much more stirrup reinforcement was additionally provided in the region of the joint to carry the recalculated shear forces. The improvement to the joint specimens provided about 70 per cent increase in capacity. The base structure was redesigned and the Sleipner 'A' Platform was successfully completed in June 1993.

7.6.3 Anchoring Bent-up Bars and Shear Reinforcement

In this section, we look at inclined bars and stirrups.

Inclined bars According to Clause 26.2.2.4(a) of IS 456,

the development length should be calculated as per Eq. (7.10) and the length should be measured from the end of the inclined portion of the bar in the tension zone (see Fig. 7.24a) and from the mid-depth of the beam in the compression zone (see Fig. 7.24b). See also Section 6.7.6 and Fig. 6.33 of Chapter 6.

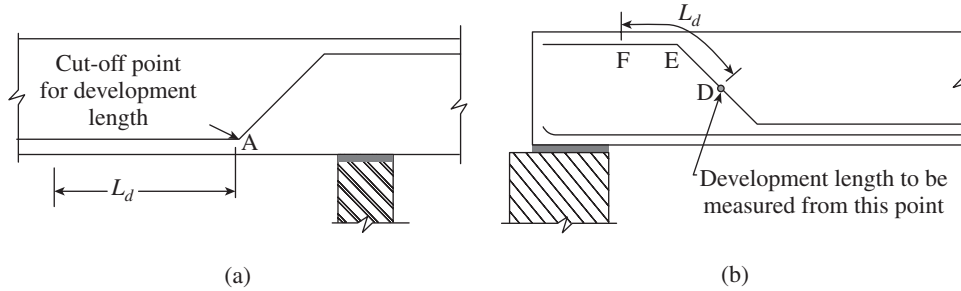


FIG. 7.24 Anchoring bent-up bars (a) Tension zone (b) Compression zone

Stirrups According to Clause 26.2.2.4(b) of IS 456, complete development length and anchorage is achieved in the following situations:

1. When the bar is bent through an angle of at least 90° around a bar of at least the same diameter and is continued beyond the end of the curve for a length of at least $8d_b$ (see Fig. 7.25a)
2. When the bar is bent through an angle of 135° and is continued beyond the end of the curve for a length of at least $6d_b$ (see Fig. 7.25b)
3. When the bar is bent through an angle of 180° and is continued beyond the end of the curve for a length of at least $4d_b$ (see Fig. 7.25c)

However, the cover over a 90° hook in a stirrup may result in the spalling of cover concrete if it is thin, as shown in Fig. 7.25(a). It is because the 90° hook has the tendency to straighten out under overloads. Hence, it is preferable to have a cover greater than or equal to twice the diameter of stirrup bar in such situations. It has to be noted that Clause 6.3.1 of IS 13920 allows only 135° hooks with an extension of $6d_b > 65$ mm in stirrups or ties in earthquake zones. Further, the recommended length beyond the bend decreases with increases in the angle of bend; the larger the angle, the greater is the anchorage value of the bar (see Section 7.6.1 and Table 7.7).

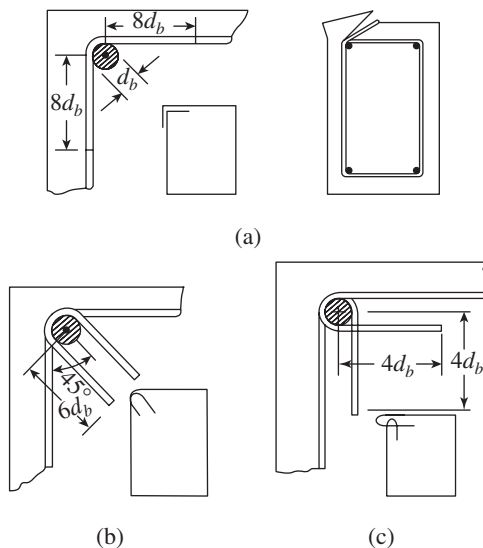


FIG. 7.25 Anchoring stirrups (a) With 90° hook (b) With 135° hook (c) With 180° hook

7.7 SPLICING OF REINFORCEMENT

Commercially available reinforcement bars are usually limited to about 12 m in length and mats to widths of 3.5 m. It is thus not always possible to obtain reinforcement of the required length. Moreover, it is convenient to work at site with bars of shorter

length. Hence, the bars and mats often have to be overlapped or *spliced*. It will be a better practice to avoid splices by proper planning and ordering bars to the required length. Splices increase the quantity of the required steel and may cause congestion if not detailed properly.

Splices are required when the bars are shorter than the required length or when the diameter has to be changed along the length (often occurs in columns). The purpose of splicing is to transfer effectively the forces from the terminating bar to the continuing (connected) bar without eccentricity at the junction.

Splices can be classified into tension and compression splices (also called *end-bearing splices*) depending on the nature of force transferred by them. They may also be classified as direct and indirect splices depending on the mechanical coupling between the bars. *Direct splices* transfer forces from one bar to the other without straining the surrounding concrete; welded splices and mechanical couplers are examples of such direct splicing. In *indirect splices*, the forces are transferred through the bond between the steel reinforcement and the concrete. Such a transfer will result in stress concentrations and cracking of the surrounding concrete. These effects should be minimized by the following methods:

1. Using proper splicing techniques
2. Keeping the splice locations away from sections with high flexural or shear stresses
3. Staggering the locations of splicing in the individual bars of a group

7.7.1 Indirect Splices

The most common method of splicing is to lap the two bars one over the other for an adequate length. Such *lap splices* where no other device is involved are called *indirect splices*. Lapped bars may be either separated from each other, as shown in Fig. 7.26, or placed in contact as shown in Fig. 7.27. As per Clause 12.14.2.3 of the ACI code, the separation of bars in non-contact lap splices of flexural members can be 150 mm or one-fifth the lap splice length (L_{sp}), whichever is less. Contact splices are much preferred as they may be tied together using wires and hence will remain in position while concreting. The IS code does not mention non-contact splices.

As already mentioned, in the lapped splice, the force in one bar is first transferred to the concrete and then to the adjacent

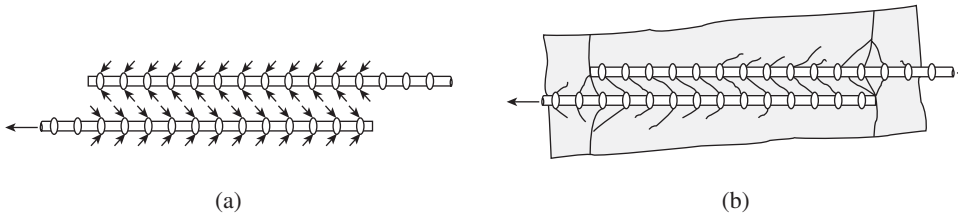


FIG. 7.26 Non-contact tension splices (a) Forces on bars at splice (b) Internal cracks at splice
Source: ACI 408R-03, reprinted with permission from ACI

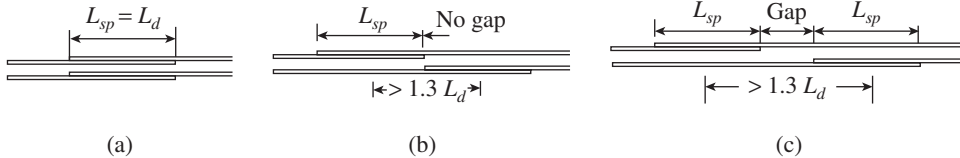


FIG. 7.27 Various options of contact lap splices (a) Aligned (b) Staggered, with no gap (c) Staggered, with a gap

bar. The force transfer mechanism in a lapped splice is shown in Fig. 7.26(a) and the resulting crack pattern is shown in Fig. 7.26(b). The mechanism of force transfer can be modelled by a truss analogy. The transfer of forces causes outward pressure similar to that shown in Fig. 7.1(c), which results in transverse cracks along the bars. The free ends of the splice bars act as crack initiators, due to the discontinuity. Such transverse cracks trigger splitting cracks. When several highly stressed bars are terminated at the same section, the splitting cracks will have a cumulative effect and will result in the spalling of concrete and eventual failure of the splice, unless the spacing of bars is greater than about $12d_b$ (Ferguson and Breen 1965). The presence of suitable transverse reinforcement will prevent the widening of cracks and spalling of concrete (see Section 7.7.1). Lap splices must also have adequate concrete cover for corrosion protection similar to continuous bars. It is important to ensure that the spacing between the lap splices allows for the adequate flow of concrete around the splice.

Although it is allowed, the reinforcing bar layout configuration shown in Fig. 7.27(b) is not the most ideal. In this case, as the bar ends of successive terminated bars are aligned, there is a strong tendency for a splitting crack to develop in the concrete, coincident with the bar ends. This is illustrated in Fig. 7.28(a). The superimposed effects can be adverse, resulting in large crack width even when the lap length L_{sp} exceeds the tension development length L_d . Transverse reinforcement in this region may provide confinement and help the situation, but providing a gap

between the ends of the staggered lap splices will result in a more desirable behaviour (Stöckl 1972). The layout condition shown in Fig. 7.27(c) is better, as the crack width developed at the bar ends will be narrower, as shown in Fig. 7.28(b). Clause 26.2.5 of IS 456 recommends that the splices in flexural members should be located where the bending moment is less than 50 per cent of the moment of resistance and not more than 50 per cent of the bars should be spliced at any section. On the other hand, Clause 12.5.1 of the ACI code classifies lap splices into two categories depending on the magnitude of tensile stress in the reinforcement and the percentage of bars spliced at the section and gives the lap length for each category as a multiple of the development length ($1.0L_d$ or $1.3L_d$). Both the codes require the splice length to be equal to the development length when less than 50 per cent of the bars are spliced at a section and stressed to less than 50 per cent of the capacity due to flexure at a section. Clause 26.2.5.1 of IS 456 lists several rules for the length of lap splice, L_{sp} . They are summarized as follows and are also given in Fig. 7.29:

1. For bars in flexural tension:

$L_{sp} = L_d \geq 30d_b$ (including anchorage value of hooks and cogs, if provided)

- (a) Flexural tension bars at the top-of the beam (top-bar effect):
When minimum cover is less than $2d_b$, $L_{sp} = 1.4L_d$

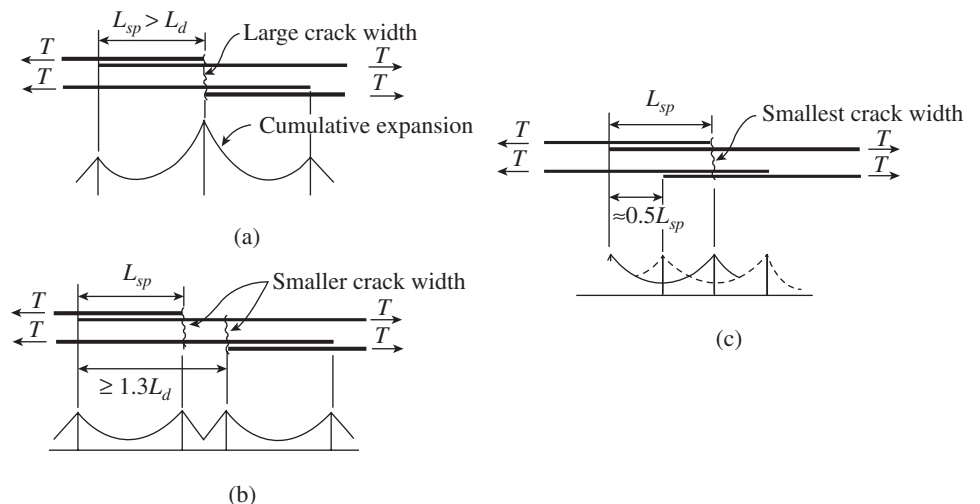


FIG. 7.28 Crack widths as functions of splice locations (a) Large crack width due to superimposed effects (b) Reduced crack width due to avoidance of superimposition (c) Smallest crack width due to low superimposition effects

Source: Stöckl, S. 1972, Copyright Wilhelm Ernst & Sohn Verlag für Architektur und Technische Wissenschaften GmbH & Co. KG, reproduced with permission.

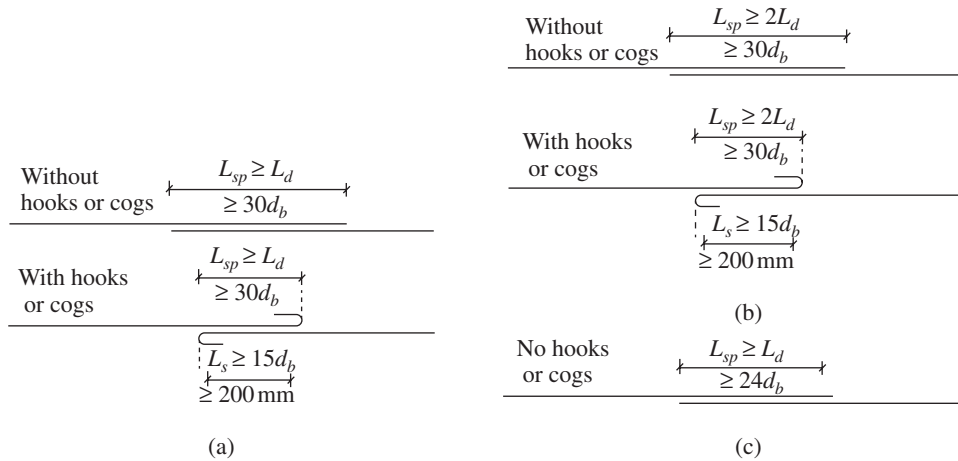


FIG. 7.29 Lap length as per Clause 26.2.5.1 of IS 456 (a) Bars in flexural tension (b) Bars in direct tension (c) Bars in compression

Notes:

L_{SP} includes anchorage value of hooks or cogs

L_S = straight length of bar excluding hooks or cogs

L_d = basic anchorage length

For plain bars in tension, hooks at the end of splices is mandatory.

- (b) Flexural tension bars at the corner of the section:
 - When minimum cover to either face is less than $2d_b$, $L_{sp} = 1.4L_d$
 - When clear distance between adjacent laps < 75 mm or $6d_b$, $L_{sp} = 1.4L_d$
 - When both 1(a) and 1(b) are applied, $L_{sp} = 2L_d$

2. For bars in direct tension:

$L_{sp} = 2L_d \geq 30d_b$ (including anchorage value of hooks and cogs, if provided)

(Splices in tension members should be enclosed by spirals of 6 mm diameter bars or more and with a pitch of 100 mm or less. It has to be noted that as per the ACI code, splices in tension tie members are required to be made with full mechanical or welded splice with 750 mm stagger between the adjacent splices. SP 24:83 also suggests the use of such welded or mechanical connections.)

3. For bars in compression:

$L_{sp} = L_d \geq 24d_b$ (with enhanced design bond stress, as per Table 7.1)

4. For bundled bars:

Entire bundles shall not be lap spliced. They should be spliced one bar at a time. Such individual splices within a bundle should be staggered.

5. Welded wire fabric:

Overlap measured between the extreme cross wires should be greater than the spacing of cross wire plus 100 mm (also see Fig. 4.6 of SP 34:1987).

The codes also stipulate that in the calculation of development length for splices, the factor for excess area of steel must not be used and the full strength of the member ($0.87f_y$) should be used (SP 24:83). Alternative equations have also been proposed

by other researchers for splice length (Canbay and Frosch 2006).

As per Clause 26.2.5.1 of IS 456, when bars of two different sizes are lap spliced in tension, the splice length shall be calculated on the basis of the diameter of the smaller bar. Moreover, lap splices are not permitted in bars having diameter greater than 32 mm (due to insufficient data on their behaviour at the spliced location); for such bars one should use either mechanical splices or welded splices.

As per Clause 26.2.5.1(b) of IS 456, lap splices are considered staggered if the centre-to-centre distance of the splices is greater than 1.3 times the lap length as calculated in Fig. 7.29 (see also Fig. 7.27). According to Clause 12.15.5.1 of ACI 318, splices should be staggered by at

least 600 mm. Individual splices of bars within a bundle should be staggered by 1.3 times the increased lap length (SP 24:83).

When more than 50 per cent of the bars are spliced at a section or where splices are made at points of maximum stress, the lap length should be increased as per Fig. 7.30 and/or spirals or closely spaced stirrups should be used around the length of the entire splice.

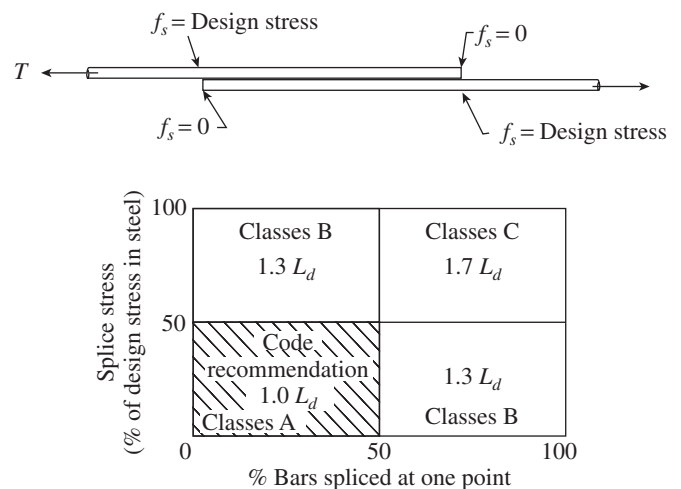


FIG. 7.30 Lap splices for flexural tension members

Note: ACI code has classified splices as Class A, B, and C. The current version of ACI code has eliminated Class C.

Transverse Reinforcement at Lap Splices

Transverse tensile stresses will develop as a result of splicing (see Fig. 7.26), which will lead to cracking unless transverse reinforcements are provided to take care of them. Usual transverse reinforcements provided to resist shear forces may

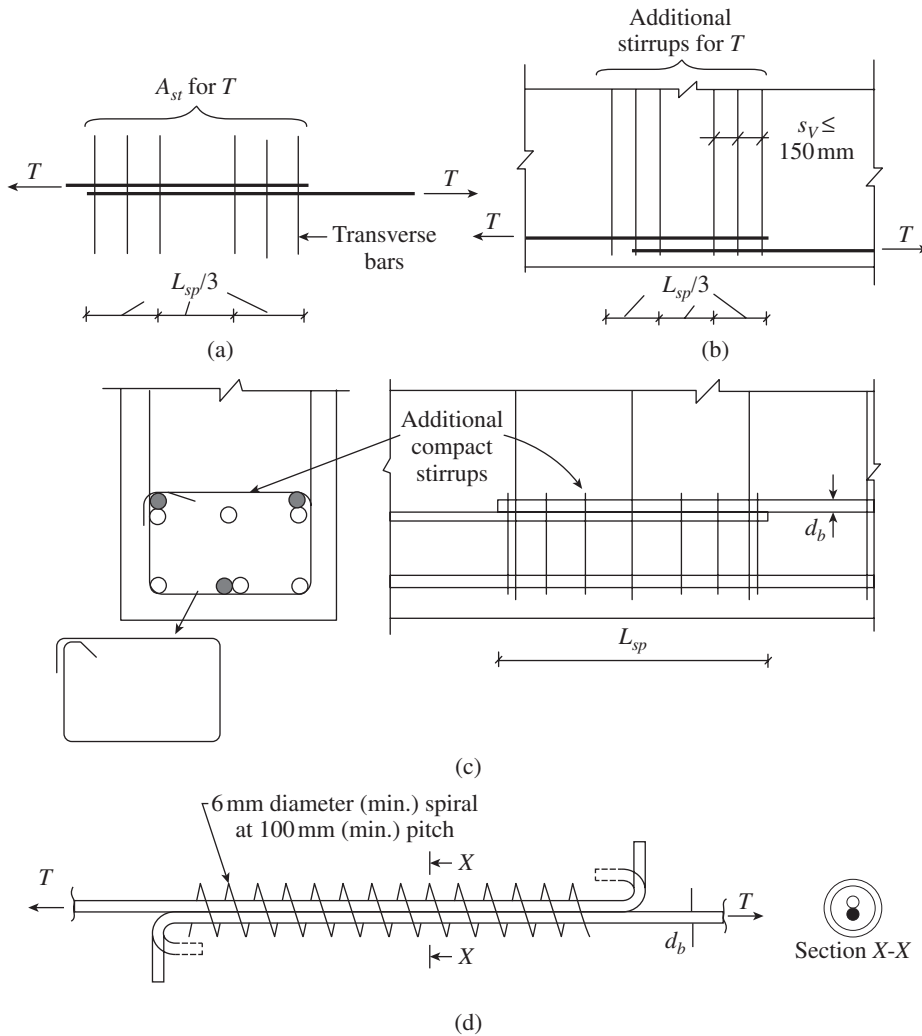


FIG. 7.31 Transverse reinforcement at tension splice (a) Tension splice (b) Transverse reinforcement at the end 1/3rd lengths of splice with minimum three stirrups at each end (c) Additional compact stirrups when large bars are spliced in two rows (d) Splices in direct tension members to be enclosed in spirals

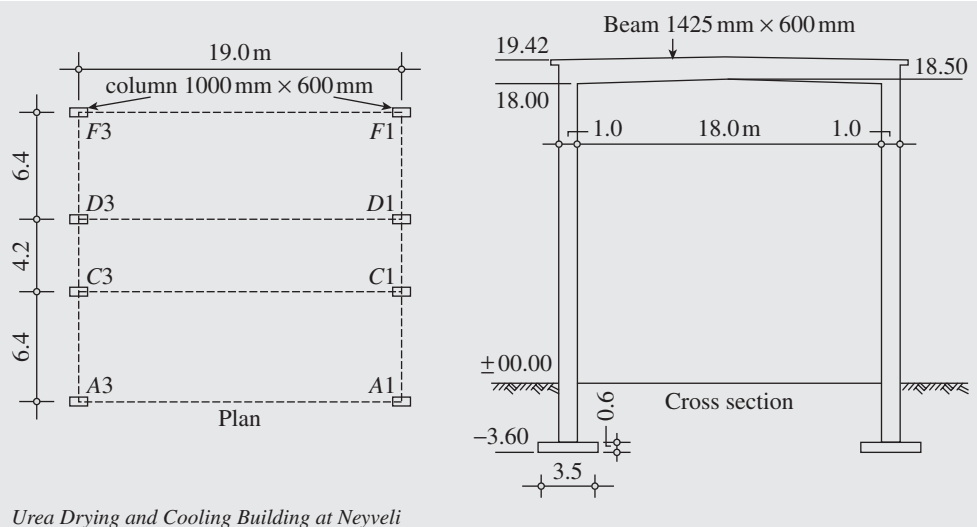
not always be adequate. It is good practice to check the adequacy of transverse reinforcement whenever bars of size large than 10 mm are spliced; however, IS 456 recognizes the necessity of transverse reinforcement only in situations where more than 50 per cent of the bars are spliced at a section or where splices are made at points of maximum stress (Clause 26.2.5).

It is a better practice to provide additional transverse reinforcement at a splice. According to Clause 4.4.1 of SP 34:1987, the transverse reinforcement should be designed to resist a tension equal to the full tensile force in the lapped bars, and they are most effective when provided in one-third length of the splice at both ends. The transverse bars for splices should be a minimum of three at each end with a spacing not exceeding 150 mm, as shown in Figs 7.31(a) and (b). It also recommended that for bars greater than 28 mm diameter, lap splices should be completely enclosed by transverse reinforcement, in the form of compact stirrups (with a minimum of 6 mm diameter and spacing not exceeding 150 mm) or spirals (with a minimum of 6 mm diameter and pitch not exceeding 100 mm), as shown in Figs 7.31(c) and (d).

CASE STUDY

Failure of Industrial Building at Neyveli

A single span RC structure with a span of 19 m, as shown in the figure, was constructed for a urea drying and cooling building at Neyveli, Tamil Nadu, in January 1962. The roof beams in the end bays were reinforced with seven 38 mm diameter bars at the bottom and seven 22 mm diameter bars plus one 16 mm diameter bar at the top. The beams in the central bay were reinforced with seven 38 mm diameter bars plus one 20 mm bar at the bottom and one 38 mm diameter



Urea Drying and Cooling Building at Neyveli

(Continued)

(Continued)

bar plus six 32 mm diameter bar at the top. The beam had a cross section of 1425 mm × 600 mm and was made of M15 concrete.

During the removal of the shuttering of the last bay on 26 January 1962, a sudden heavy cracking sound was heard and within a few seconds the roof caved in along the ridge. The beams had cracked in the middle and the main reinforcements were pulled out. The collapsed roof came to rest on the centring props underneath.

The testing of the concrete cubes revealed that the compressive strength of the concrete was more than that required according to the design. The materials used, including the steel reinforcement, were of high quality, and yet the structure failed. A close examination of the failed area disclosed that most of the reinforcement bars

were lapped at the centre of the beam, where failure had occurred. Naturally, a beam with a clear span of 18 m could not be reinforced without resorting to lapping, as the bars were supplied at a standard length of 12 m. To use the bars more economically, and to avoid more than one lap, all the lapping had been done in only one place, that too at the centre. This resulted in heavy congestion of bars and the bond between steel and concrete was poor. The version of IS 456 in vogue at that time did not prohibit the lapping of tensile reinforcement. Even the revised 1964 code only suggested that laps should be avoided in maximum stressed zones as far as possible and lapped splices in tension should not be used in the case of bars greater than 36 mm diameter; such splices should be welded (Srinivasan 1975).

Recently, Darwin and Browning (2011), based on their splice tests of beams with high-strength reinforcement (ASTM A 1035-MMFX bars with $f_y = 690\text{--}827\text{ MPa}$) and concrete of strength ranging from 43 MPa to 68 MPa, concluded that transverse confining reinforcement increases the load and deformation capacity of all beam splice specimens and that increasing splice lengths may not be sufficient to develop high bar stresses unless transverse reinforcement is used.

Compression Splices

A compression lap splice transfers a force by the combination of the bond and the end bearing as shown in Fig. 7.32(a). Thus, combined compressive and tensile stresses are developed

in compression splices, whereas biaxial tensile stresses are developed in tension splices (Chun, et al. 2010). Furthermore, the end of compression bar bearing on the concrete leads to bursting force, resulting in side face blow-out failure of concrete cover as shown in Fig. 7.32(b), especially when the concrete cover is less than about $1.2d_b$ (Leonhardt and Teichen 1972). The end bearing was found to be responsible for the majority of splice failures, irrespective of the splice length tested; the splice lengths varied between nine and 38 times the d_b (Leonhardt and Teichen 1972). The bearing capacity of concrete at the spliced ends could be improved by confining the transverse reinforcement placed close to the end of the bar, with a spacing not exceeding $4d_b$, as indicated in Fig. 7.32(b).

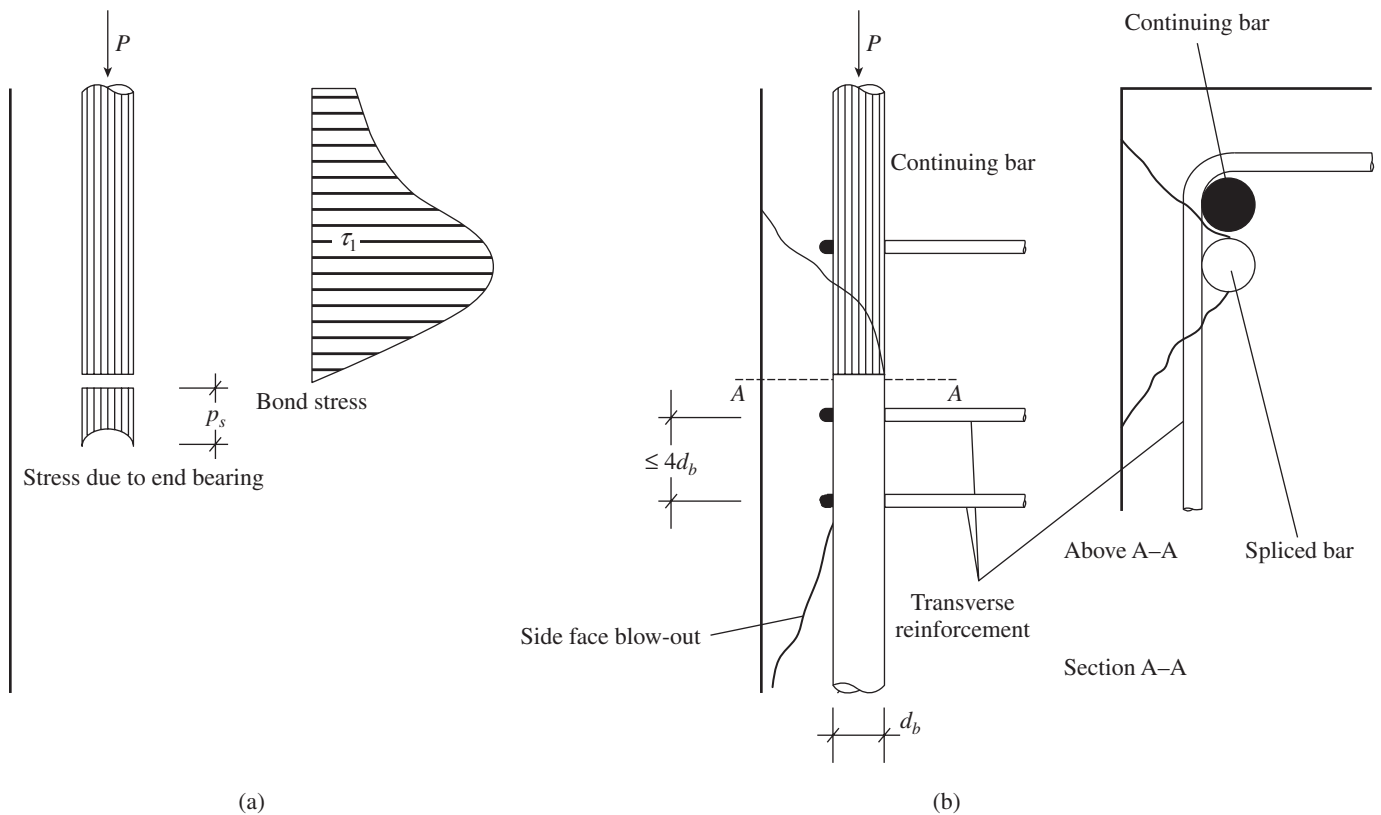


FIG. 7.32 Resistance of compression splices (a) Components of resistance (b) Side face blow-out failure due to end bearing

The spacing between the bars and increase in cover thickness had little effect on the splice strength in compression (Leonhardt and Teichen 1972).

The compressive forces in steel bars can be directly transferred from bar to bar by end bearing, provided the bars will never experience tension and the ends of the bars are square-cut (maximum deviation of 1.5° from a right angle at the end surfaces of the bar is permitted in the codes).

As a result of the force transfer in end bearing in addition to the bond in concrete, the required length of compression lap splice will be smaller than that of a tension splice. The Indian code suggests that the compression splice length may be taken as the development length in compression as follows:

$L_{sp} = L_d \geq 24d_b$ (with enhanced design bond stress, as per Table 7.1)

The US, Canadian, and New Zealand codes provide the following equation for compression splice length (see Clause 12.16.1 of ACI 318)

$$L_{sp} = 0.071f_y d_b \geq 300 \text{ mm for } f_y \leq 420 \text{ MPa} \quad (7.23a)$$

$$L_{sp} = (0.13f_y - 24)d_b \geq 300 \text{ mm for } f_y > 420 \text{ MPa} \quad (7.23b)$$

For f_{ck} less than 26 MPa, the length of the lap should be increased by one-third. These equations are based on the research conducted on 11 column tests with lapped splices over 45 years ago, on concretes having strength less than 30 MPa (Pfister and Mattock 1963). It should be noted that Eqs (7.23a and b) do not contain concrete compressive strength. Moreover, the compression lap splice length calculated using these equations may be longer than a tension lap splice in HSC. To remove this anomaly, Chun, et al. (2010b) derived the following equation for compression splices in confined concrete based on their experimental results:

$$L_{sp} = \psi_{comp} \frac{(f_y)^2}{100f_{ck}} d_b \quad (7.24a)$$

where $\psi_{comp} = \frac{1}{\left(1 + 0.134 \frac{K_{tr}}{d_b}\right)^2}$ with $\frac{K_{tr}}{d_b} \leq 1.76$ and

$$K_{tr} = \frac{40A_{tr}}{ns_{tr}} \leq \left(2 - \frac{c}{d_b}\right)$$

It should be noted that this equation takes into account the concrete strength as well as the effect of transverse reinforcement using the transverse reinforcement index, K_{tr} .

Chun, et al. (2010a) also derived the following equation for compression splices in unconfined concrete based on their experimental results:

$$L_{sp} = \frac{\left(\frac{f_y}{0.72\sqrt{f_{ck}}} - 16.4\right)^2}{123} d_b \quad (7.24b)$$

They also suggested the upper limits for Eqs (7.24a and b) as those predicted by the ACI code equation (Eqs 7.23a and b). These equations were found to yield reliable results compared to the ACI code formula.

Conical failures are possible when compression bars do not have adequate cover at their ends (see Fig. 7.33a). To prevent such failures, the concrete cover at the ends of the bar near free surface should be greater than $3d_b$, as shown in Fig. 7.33(b) or the bars should be bent as shown in Fig. 7.33(c).

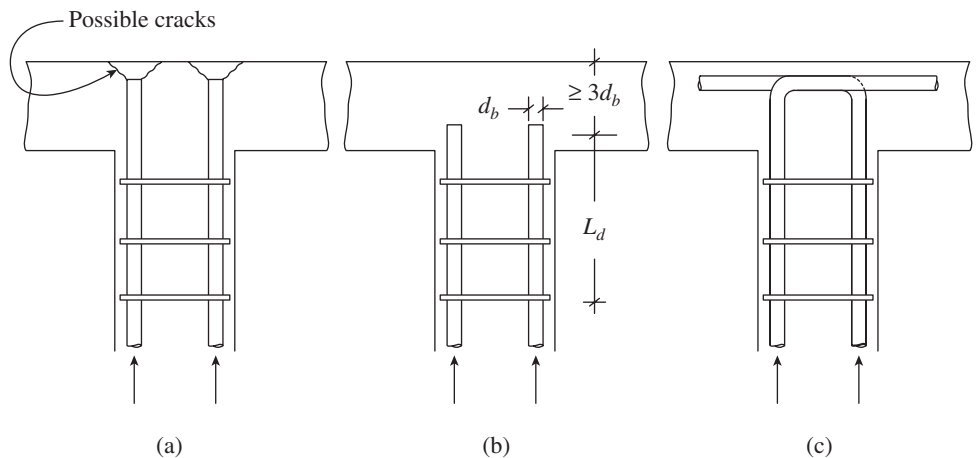


FIG. 7.33 Anchoring compression bars near free surface of concrete (a) Bar ends too close to surface (b) Adequate cover at the free ends (c) Bars bent in

Hooks and cogs are not desirable at the ends of spliced bars in compression, as they may induce buckling when the stresses are high.

Transverse Reinforcement in Compression Splices

Compression bars require a slightly different layout of transverse reinforcement due to the splitting forces caused by the direct bearing of bar ends on concrete (see Fig. 7.34). It is recommended to provide at least two bars within a distance of four times the diameter of the spliced bar from the ends; the remaining bars are to be provided within the end one-third lap length, as shown in Fig. 7.34(a).

Where longitudinal bars are offset at a splice, the slope of the inclined portion of the bar with the axis of the column should not exceed one in six, and the portions of the bar above and below

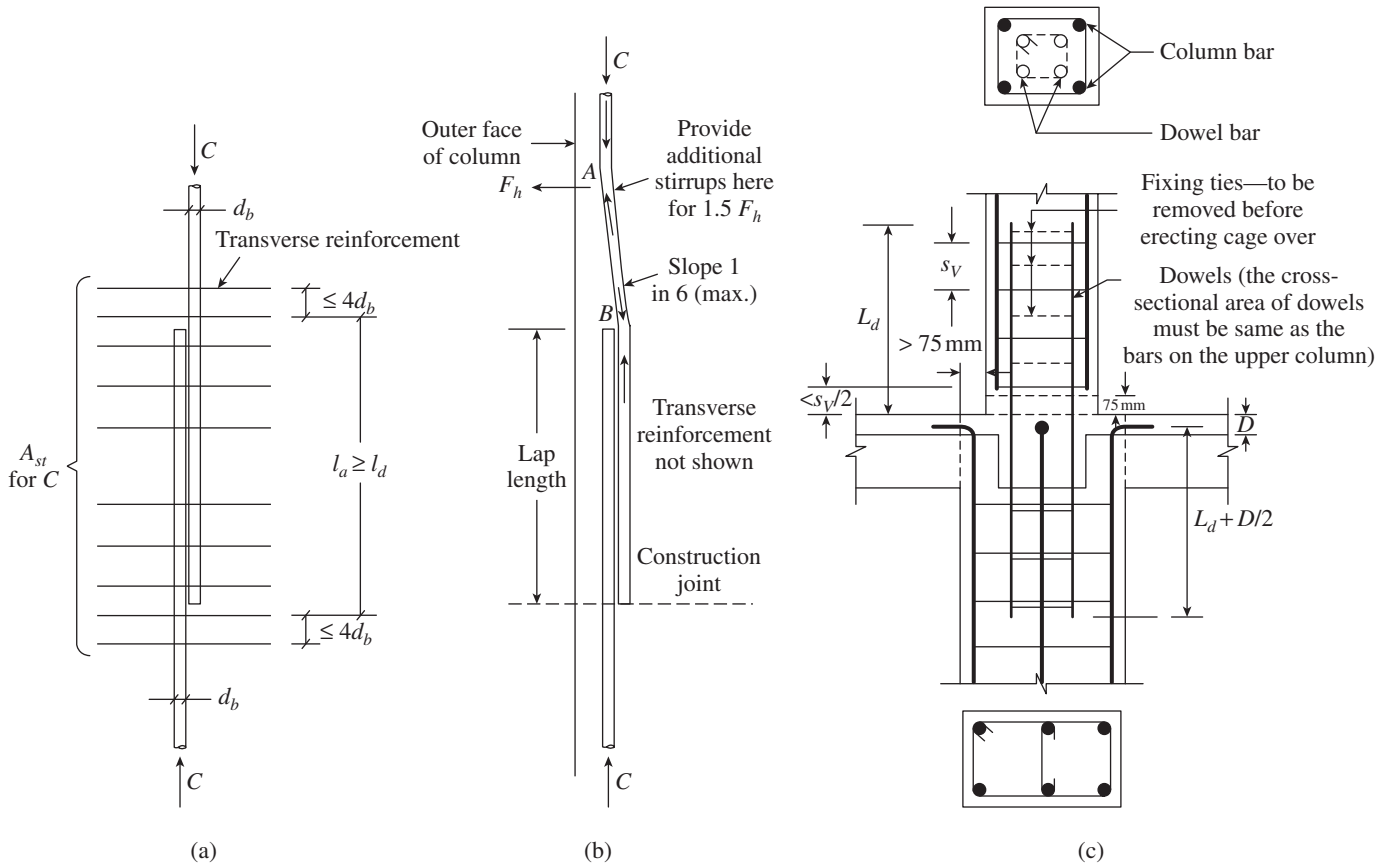


FIG. 7.34 Transverse reinforcement for compression splices (a) Straight bars (b) Cranked bars (c) Splicing when column faces are offset by more than 75 mm

the offset should be parallel to the axis of the column, as shown in Fig. 7.34(b). It should be noted that the offset bars should be bent before they are placed in the form to avoid damaging the hardened concrete. Additional transverse reinforcement should be provided at the bend to resist the horizontal thrust of the bar force. Clause 26.5.3.3 of IS 456 recommends that this horizontal thrust should be taken as 1.5 times the horizontal component of the nominal stress in the inclined portion of the bar. It has to be noted that additional links are required only at end A and not at end B in Fig. 7.34(b), and they should be placed near the point of bend (within $8d_b$), as per Clause 4.4.2 of SP 34:1987. When the column faces are offset by 75 mm or more, splices of vertical bars adjacent to the offset face should be made by separate dowels overlapped as shown in Fig. 7.34(c).

7.7.2 Direct Splices

As mentioned earlier, welded splices and mechanical splices are considered as direct splices as they do not strain the surrounding concrete and result in the direct transfer of forces from one set of reinforcement bars to the other.

Welded Splices

Lapped splices may extend over one-third the height of a column in a multi-storey RC frame, and hence their weight

may be significant. Moreover, lapped splices may produce congestion of reinforcement, and may interfere with the proper compaction of concrete. To overcome these difficulties, methods that result in direct transfer of forces from bar to bar without assistance from the concrete have been employed in the past. *Flash butt welding* of bars, end to end, using electric arc welding has been used in the past. In gas pressure welding, the ends of the bars are pressed against each other, after heating to the correct temperature, resulting in a bulb forming at the contact section and subsequent fusion. Complete specifications for welding hot-rolled deformed bars and cold-worked steel bars are available in Appendix A of SP 34:1987. The bars spliced should be of the same diameter. The types of butt welds that can be adopted are shown in Fig. 7.35. Direct butt welding has to be adopted for bars greater than 20 mm.

For bars of diameter less than 20 mm, indirect splicing may be used, although lap welding is the preferred option for such bars. Butt splices are often used for compression bars and require edge preparation before butt welding—V-grooves or bevels—depending upon whether the bars will be placed in a horizontal or vertical position (see Table A-1 of SP 34:1987 for the preparation of edges of different types of butt welds). Fig. 7.36 shows a few *indirect butt splices*.

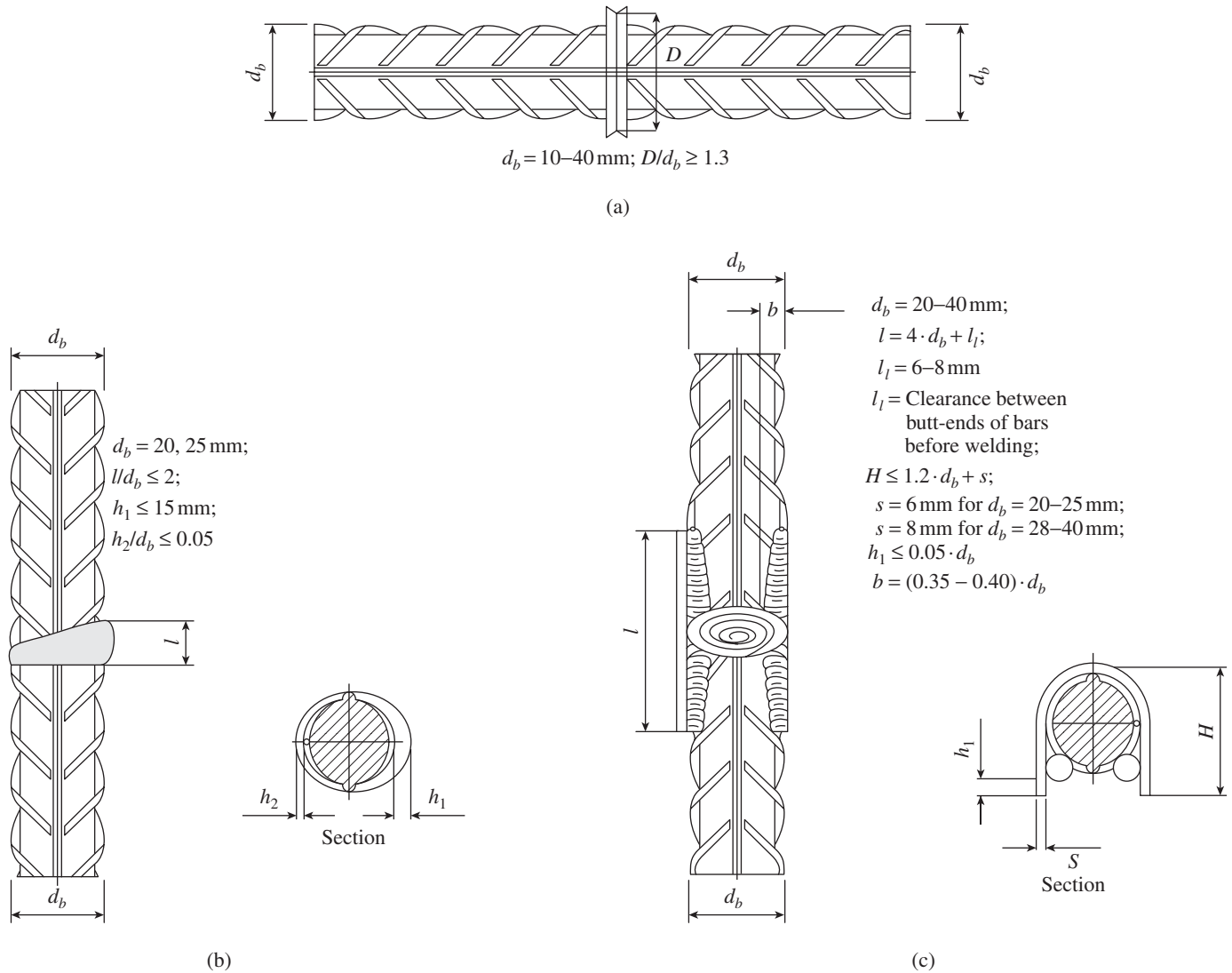


FIG. 7.35 Details of welded butt joints (a) Flash welding (b) Enclosed welding (c) Enclosed welding with lap strap
 Source: Degtyarev 2007, reprinted with permission from ACI

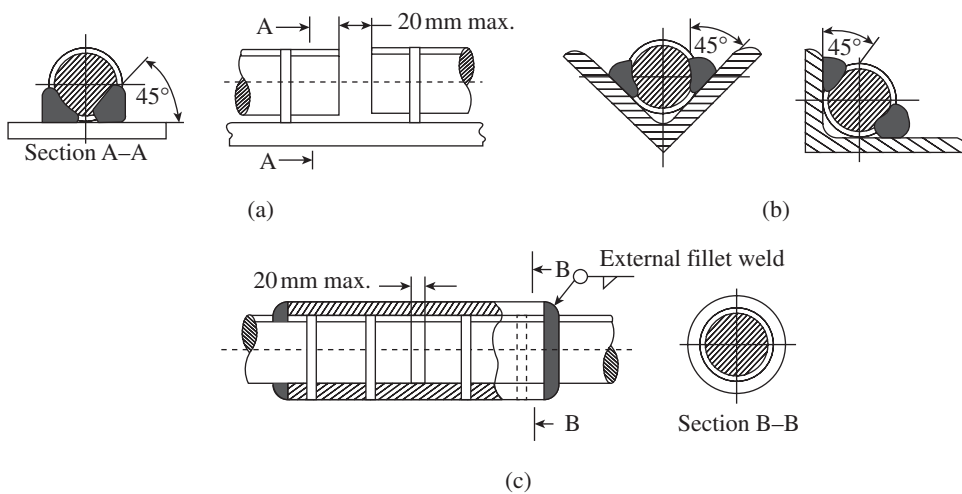


FIG. 7.36 Indirect butt splices (a) Using a plate (b) Using an angle (c) Using a sleeve

In indirect butt splices, as shown in Fig. 7.36, both bars are welded to a common splice member such as a plate, angle, or some other shape. The bars are nearly aligned; bar ends are separated no more than 20 mm; and the cross section of the bars is not welded.

Lap-welded splices can also be used and may be of single or double lap, as shown in Fig. 7.37. Single lap splices shown in Fig. 7.37(a) result in eccentric load application and require transverse reinforcement to avoid splitting of concrete in the region of splicing. Double lap-welded splices, as shown in Fig. 7.37(b), eliminate

eccentric loading, but require more space and material than single lap splices. The area of the additional bars provided at the double lap splice should be at least equal to that of the spliced bars; this may be ensured by using bars having a diameter greater than 0.71 times the diameter of the spliced bars. All these splices are suitable for cold-rolled deformed bars of diameter 12 mm or more, but should not be used in situations involving cyclic or varying loads of high amplitude.

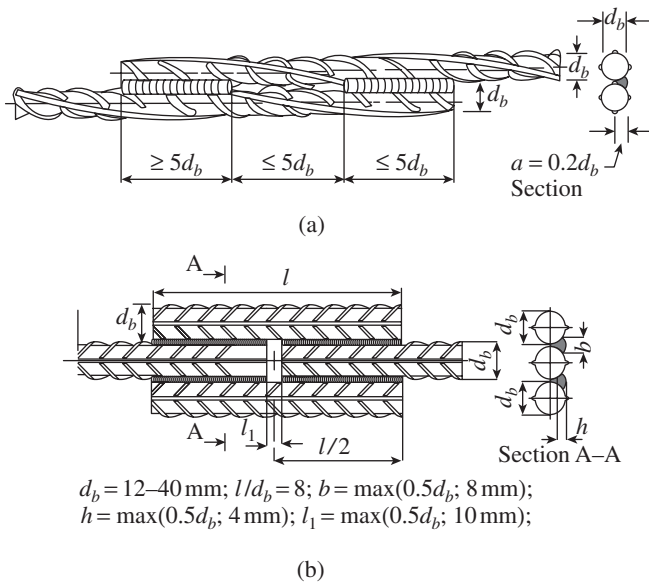


FIG. 7.37 Details of welded lap joints (a) Single lap (b) Double lap
 Source: SP 34:1987; Degtyarev 2007, reprinted with permission from ACI

It has to be noted that American Welding Society (AWS) Structural welding code—Reinforcing steel, D1.4-92, states that welded lap joints shall be limited to bar size 19 mm and smaller. Moreover, lap joints made with double flare V-groove welds are preferable, and single flare V-groove welds may be used only when the joint is accessible from only one side and should be approved by the engineer. The bars may be lap welded using the details given in Table 7.9.

TABLE 7.9 Details of lap-welded joints as per SP 34:1987

Bar Diameter	Throat Thickness, mm	Gap between Rebars, mm
$d_b < 12 \text{ mm}$	3	1.5
$12 \text{ mm} \leq d_b \leq 16 \text{ mm}$	3	3
$d_b > 16 \text{ mm}$	5	3

Note:

- Minimum size of electrode (E70XX and E80XX) up to 6mm: 1.6mm, 6–10mm: 2.0mm, 10–14mm: 2.5mm, 14–20mm: 3.15mm, and over 20mm: 4mm.
- Strength of weld per mm length, is $N = \frac{f_u}{(\sqrt{3} \times \gamma_{mw})} \times 0.7 \times \text{size}$

where $\gamma_{mw} = 1.5$ for site welding and f_u may be taken as 410MPa.

As per SP 34:1987, welded joints should also be staggered in the length of the RC components and should not be located

in highly stressed areas or in bends. The weldability of bars should be ascertained before welding any steel reinforcement. As per IS 1786, for guaranteed weldability, the Carbon Equivalent (CE), calculated using the formula

$$CE = C + \frac{Mn}{6} + \frac{Cr + Mo + V}{5} + \frac{Cu + Ni}{15} \quad (7.25a)$$

should be less than 0.53 per cent, when micro alloys or low alloys are used. When micro alloys or low alloys are not used, the CE, calculated using the formula

$$CE = C + \frac{Mn}{6} \quad (7.25b)$$

should be less than 0.42 per cent. The symbols in these equations represent the chemical elements in per cent by mass (C: carbon, Mn: manganese, Cr: chromium, Mo: molybdenum, V: vanadium, Cu: copper, and Ni: nickel). Welding is usually performed with shielded metal arc welding (SMAW), gas metal arc welding (GMAW), flux cored arc welding (FCAW), or thermite welding (not used currently in bar splices) processes, and as per IS 2751 and IS 9417.

Clause 12.4 of the code (IS 456) recommends that in important connections, tests should be done to prove the adequacy of strength. In addition, Clause 26.2.5.2 limits the strength of welded splice to 80 per cent of the design strength of the bar for tension splices (100% can be assumed for compression splices), whereas Clause 12.14.3.4 of ACI 318 stipulates that a fully welded splice should develop at least $1.25f_y$ of the bar.

End-bearing splices are permitted by Clause 26.2.5.3 of IS 456 for bars subjected to compression. To adopt it, the ends of bars have to be square-cut and welded to suitable bearing plates, which should be embedded within the concrete cover. Recently, Degtyarev (2007) developed equations for calculating the tensile strength of welded quench and self-tempered (QST) bars.

It should be noted that tack welding can cause a metallurgical notch effect in large longitudinal bars, reducing their original tensile strength, bendability, and impact resistance. Hence, tack welding of bars is prohibited.

Mechanical Splices

Many types of *mechanical splicing* products (often called *couplers*) are available, some of which are listed as follows (ACI 439.3R-2007):

- Cold-swaged steel coupling sleeve
- Cold-swaged steel coupling sleeve with threaded ends
- Extruded steel coupling sleeve
- Hot-forged steel coupling sleeve
- Grout-filled coupling sleeve
- Coupler for thread-deformed reinforcing bars
- Steel-filled coupling sleeve
- Taper-threaded steel coupler
- Couplers with standard national coarse (NC) threads

Couplers are categorized as tension couplers and compression couplers. Unless specified otherwise, tension couplers should always be used. Couplers may also be categorized as *in-line couplers*, in which the centre line of each spliced bar coincides, and *offset couplers*, where the centre lines have an eccentricity. The latter splice type is alternatively referred to as an *offset mechanical splice* or a *mechanical lap splice*.

As shown in Fig. 7.38, mechanical splices generally use threaded annular sleeve, slightly larger than the diameter of the bars, which is placed around the bars at the joint. The sleeves are normally cold pressed against the bars, forcing the ribs of the deformed bars to become embedded in the wall thickness of the sleeve. With suitable bar deformations, a sleeve embedment length of only $2d_b$ for each of the two bars may be sufficient to transfer the load of the bar in tension. They can also be formed by filling the annular space between the bars

and the sleeve with molten metal. Direct threading of bars is avoided to prevent reduction in bar size and consequently its strength. A solution to this is to increase the size of the ends over a small length through tapering, as shown in Fig. 7.38(a).

A new type of coupler called *set screw couplers* is not threaded, swaged, or metal-filled; instead it consists of a steel tube with a series of lock-shear bolts—generally six to eight—and two serrated strips that run the inside length of the coupler, as shown in Fig. 7.38(g). The installation of this coupler is carried out as follows: After sliding one length of rebar halfway into the coupler, the bolts are tightened to fit snugly. The second bar is then inserted into the coupler until it butts against the other bar end, and the remaining bolts are tightened to a snug fit. A ratchet or an impact wrench is used to tighten the bolts until their heads shear off, implanting the bolt ends into the rebar and embedding the serrated strips into both

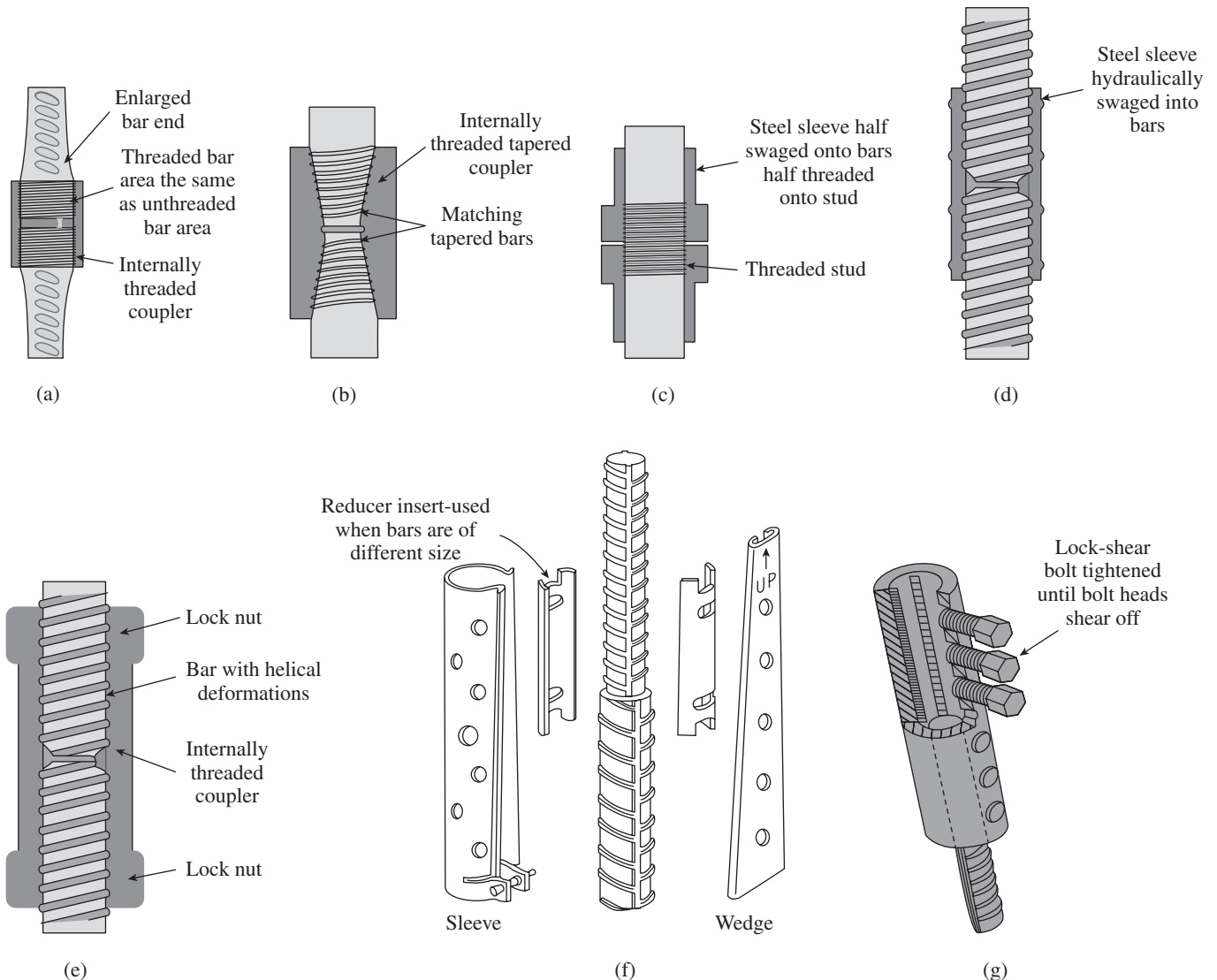


FIG. 7.38 Types of mechanical couplers (a) Couplers with parallel threads (b) Couplers with taper-cut threads (c) Cold-swaged steel coupling sleeve with threaded ends (d) Cold-swaged steel coupler (e) Coupler with counter nuts (f) Wedge-locking coupling sleeve (g) Set screw couplers

Source: Cresswell Riol 2006 (adapted), reprinted with permission from Institution of Structured Engineers, UK

the rebar and the interior coupler wall. This type of splicing system does not require any special bar-end preparation and can be used in projects where bars are in place or access is limited. More details about mechanical couplers may be

found in ACI 439.3R-2007, SP 34:1987, and Prakash Rao (1995). A comparison of these couplers is made in Table 7.10 and the use of couplers in column reinforcement is shown in Fig. 7.39.

TABLE 7.10 Available mechanical connection types (adapted from ACI 439.3R 2007, reprinted with permission from ACI)

	Cold-swaged Steel Coupling Sleeve	Cold-swaged Steel Coupling Sleeve with Threaded Ends	Extruded Steel Coupling Sleeve	Hot-forged Steel Coupling Sleeve	Grout-filled Coupling Sleeve	Coupler for Thread-deformed Reinforcing Bars	Steel-filled Coupling Sleeve	Taper-threaded Steel Coupler	Couplers with Standard NC Threads
Bar size range (mm)	10–56	10–56	16–56	16–56	16–56	20–56	12–56	12–56	12–56
Special bar-end preparation	None	None	None	Remove loose particles and rust	None	Cut square within 1.5°	Remove loose particles and rust	End must be threaded	None
Installation tools	Special tools required	Hand-held	Special tools required	Special tools required	Grout pump	Yes: < 36 mm No: >36 mm	Hand-held	Hand-held	Hand-held
Weather restrictions	None	None	None	Bars must be dry	None	None	Bars must be dry	None	None
Special precautions	None	None	None	Fire hazard during installation	None	None	Fire hazard during installation and proper ventilation required	None	None

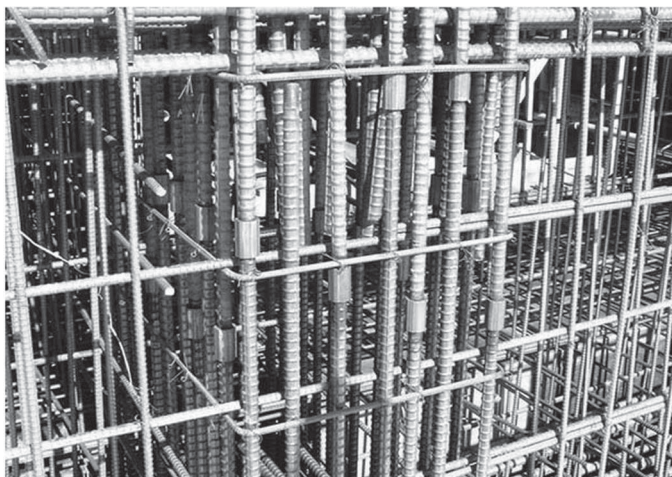


FIG. 7.39 Use of mechanical coupler in column reinforcement (note staggering of couplers)

Based on the experimental results on offset mechanical splices, as shown in Fig. 7.40, Coogler, et al. (2008) found the following:

1. Offset splices are not recommended for use with bar sizes greater than 16 mm, unless tests indicate to satisfy the performance criteria.
2. Offset splices should not be used in applications subject to seismic load reversals.

3. Offset splices should be included in the second category of mechanical splices (having a fatigue limit of 80 MPa).

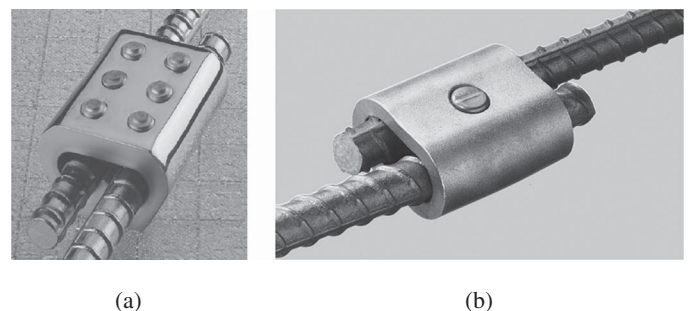


FIG. 7.40 Offset mechanical splice (a) BarSplice Double Barrel Zap Screwlok© (b) Lenton Quick Wedge©

Source: Coogler, et al. (2008), reprinted with permission from ACI

Clause 12.14.3.2 of the ACI code requires that the mechanical splices should have at least 25 per cent higher design strength than lap splices, though Clause 26.2.5.2 of IS 456 suggests 100 per cent design strength to be assumed for mechanical connections. It should be noted that couplers should be provided with a concrete cover similar to that specified for the reinforcement.

Mechanical butt splices provide superior strength during load transfer. Superior cyclic performance and greater

structural integrity during seismic events are other advantages of mechanical butt splices. From the structural standpoint, the most important benefit of mechanical splices is that they ensure load path continuity of the structural reinforcement. Use of mechanical butt splices results in using larger diameter rebar in a smaller column, while minimizing congestion. In addition, use of mechanical splicing eliminates the tedious calculations needed to determine proper lap lengths and the possible errors associated with the calculations. Mechanical splices are also fast to install and involve no specialized labour.

7.8 CURTAILMENT OF REINFORCEMENT

It is not necessary to provide the same amount of reinforcement throughout the beam or slab. The amount of reinforcement may be reduced in places where there is less bending moment. This section deals with the rules provided in the codes for such *curtailment of reinforcement*.

7.8.1 Curtailment of Tension Reinforcement in Flexural Members

In simply supported beams, the bending moment will be the maximum at mid-span and hence requires maximum area of steel reinforcement. Towards the support points, the bending moment will be less and hence some reinforcements may be curtailed to achieve economy. In practice, *theoretical cut-off point* (TCP), that is, points at which the bars are desired to be cut-off, and the actual or *physical cut-off point* (PCP) differ. Clause 26.2.3 of IS 456 requires that the distance at which PCP occurs for all steels (whether in tension or compression) should be more than $12 d_b$ or the effective depth. In addition, the bar as a whole should satisfy the requirement of development length (see Fig. 7.41).

Tests have shown that when bars are cut-off in tension zones, shear strength and ductility are reduced. Hence, the code does not permit termination of flexural reinforcement in a tension zone unless the following additional conditions are satisfied (Clause 26.2.3.2 and 26.2.3.3 of IS 456); see Fig. 7.41.

1. When shear stresses are low, diagonal cracks are less likely to form. Hence, the code stipulates that the actual shear capacity at the PCP should be greater than 1.5 times the factored shear force at the section (Clause 3.12.9.1 of BS 8110 requires it to be twice), that is, $V_u \leq (2/3)V_n$.
2. To reduce the probability of diagonal cracking, we should allow lower stress in steel reinforcement. Hence, the code states that for 36 mm and smaller bars, the continuing bars should provide double the area required for flexure at the PCP, and the factored shear should not exceed three-fourth the actual shear capacity (i.e., $V_u \leq 0.75V_n$).
3. As discussed in Section 6.14 of Chapter 6, experiments have shown that bar curtailment may adversely affect the shear strength of beams; the diagonal cracks due to shear can be restrained by closely spaced stirrups. Hence, the code

stipulates that extra stirrup area should be provided along each terminated bar (see also Section 6.14 of Chapter 6 for the explanation of the code clause).

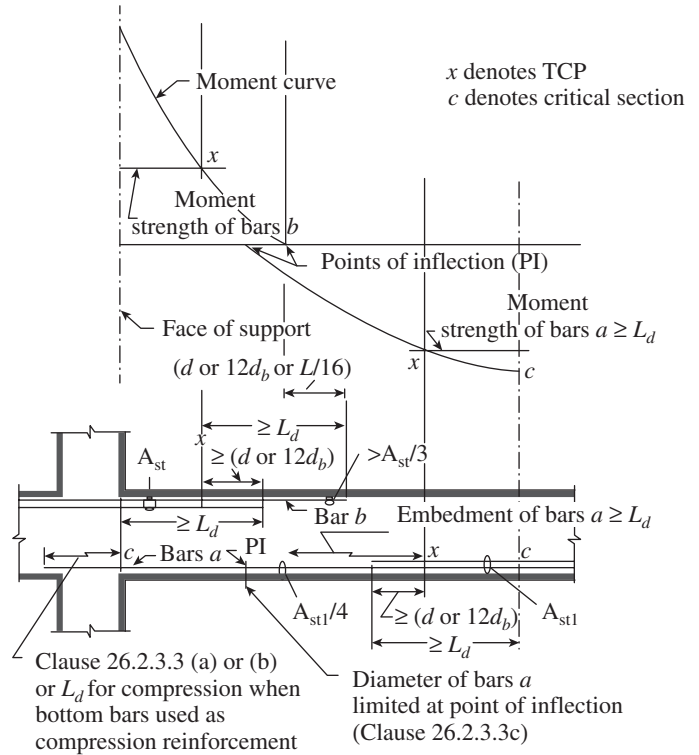


FIG. 7.41 Development of flexural reinforcement in a typical continuous beam

7.8.2 Curtailment of Positive Moment Reinforcement

Positive moment reinforcement should be carried into the support to provide for some shifting of the moments due to changes in loading, settlement of supports, and lateral loads. Hence, the following rules are specified in the code:

1. At least one-third of the positive reinforcement in simply supported beam and one-fourth of the positive reinforcement of continuous beam must be continued over the support (see Fig. 7.42(a)). Such bars should extend over the support by a length not less than one-third of the development length ($L_d/3$). The ACI code stipulates that they should extend into the support by at least 150 mm.
2. When a flexural member is part of a primary seismic load resisting system, loads greater than those anticipated in design may cause reversal of moment at supports; to ensure ductile behaviour, some positive reinforcement should be well anchored into the support. Hence, the code stipulates that in such cases, the positive moment reinforcement should be extended into the support as described and should be anchored to develop f_y in tension at the face of the support (Fig. 7.42b).

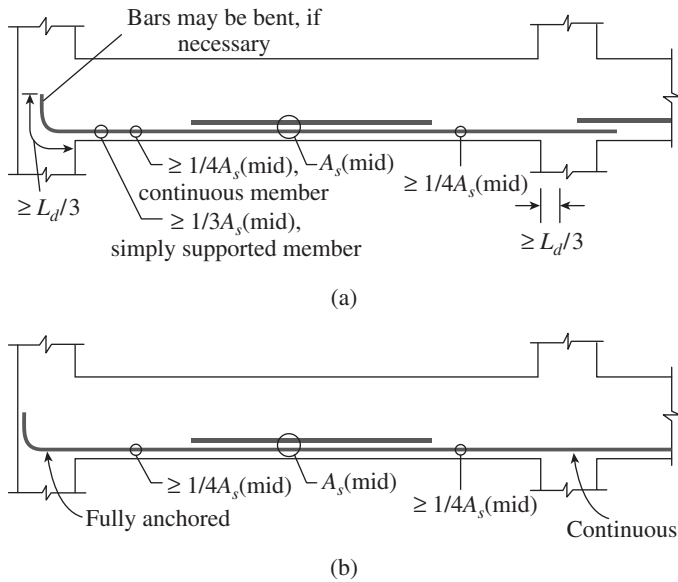


FIG. 7.42 Positive moment reinforcement requirements (a) Beams that are not part of primary lateral load resisting system (b) Beams that are part of primary load resisting system

3. At simple supports and at points of inflection, positive moment tension reinforcement shall be limited to a diameter such that L_d computed for f_d satisfies the following relation:

$$L_d \leq \frac{M_{n1}}{V_u} + L_o \quad (7.26)$$

where M_{n1} is the moment of resistance of the section, calculated assuming all reinforcement at the section to be stressed to f_d , $f_d = 0.87f_y$, V_u is the factored shear force at the section due to design loads, and L_o at a support is the embedment length beyond the centre of support or L_o at a point of inflection shall be limited to d or $12d_b$, whichever is greater (see Section 25.2.3.3 of SP 24:1983 for more discussions).

An increase of 30 per cent in the value of M_n/V_u is permitted in Eq. (7.26) when the ends of reinforcement are confined by a compressive reaction. This concept is explained in Fig. 7.43.

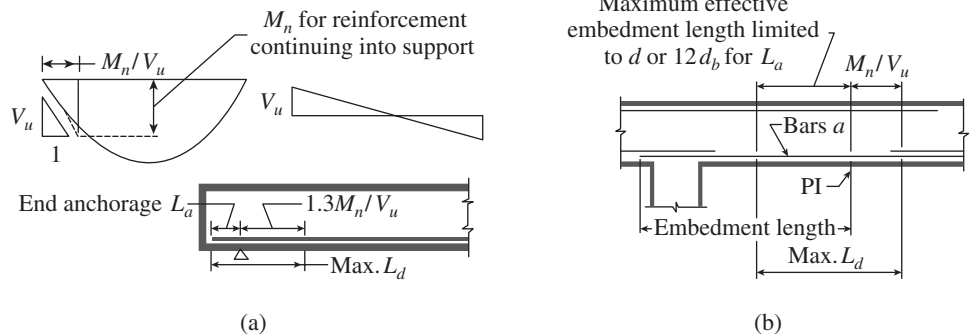


FIG. 7.43 Concept for determining maximum bar size (a) Maximum size of bar at simple support (b) Maximum size of bar 'a' at point of inflection

Note: The 1.3 factor is usable only if the reaction confines the ends of the reinforcement.

7.8.3 Curtailment of Negative Moment Reinforcement

Negative moment reinforcement in a continuous beam or cantilever beam,

or in any beam of a rigid frame, should be anchored in or through the supporting member by embedment length, hooks, or mechanical anchorage (see Fig. 7.44). Clause 26.2.3.4 of IS 456 stipulates that at least one-third of the total tension reinforcement provided for the negative moment at the support should have an embedment length beyond the point of inflection not less than the effective depth d , $12d_b$, or $L/16$, whichever is greater, where L is the clear span. At interior supports of deep flexural members, the negative moment tension reinforcement shall be continuous with that of the adjacent spans, as shown in Fig. 7.44(b).

When adjacent spans are unequal, the extension of negative reinforcement beyond each face of column support shall be based on the longer span. Thus, if the adjacent span is relatively much shorter, the top reinforcement might have to be provided throughout the span in the shorter span.

7.8.4 Curtailment of Bundled Bars

All the bars in a bundle should not terminate in a single point. As per Clause 26.2.3.5 of IS 456, the bundled bars must

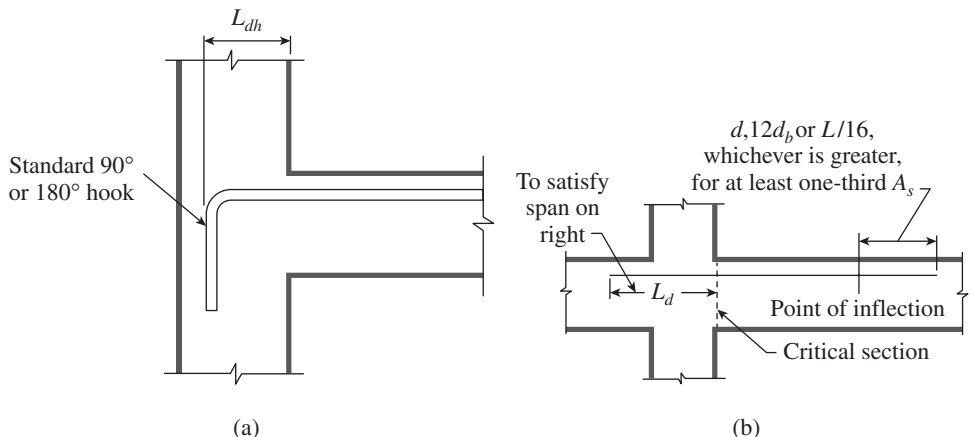


FIG. 7.44 Development of negative moment reinforcement (a) Anchorage into exterior column (b) Anchorage into adjacent beam

Note: Usually such anchorage becomes part of the adjacent beam reinforcement.

terminate at different points separated by a distance greater than 40 times the diameter of a bar. However, all the bundled bars can be terminated at the support.

7.8.5 Special Members

Adequate anchorage should be provided for tension reinforcement in flexural members where reinforcement stress is not directly proportional to moment, such as sloped, stepped, or tapered footings; brackets; deep flexural members; or members in which tension reinforcement is not parallel to the compression face.

All these provisions in the Indian code are similar to those provided in the US code (see Clause 12.10 of ACI 318-2011), New Zealand, Canadian, and Australian codes. It should be noted that at least two bars are required at the supports; the economic number of compression and tension steel in beams should perhaps be chosen as six bars of suitable diameter. If four bars are used, then 50 per cent of the bars will go into the supports, as against the 25 per cent or 33.33 per cent required by the codes. Moreover, it has to be noted that all curtailment should be such that the arrangement of steel is kept symmetrical and extra shear reinforcement has to be provided in the cut-off points. Thus, if there is no significant economy in the curtailment of reinforcements, it is perhaps simpler to carry the top and bottom bars throughout the span.

The calculation of bar cut-off points from equations of moment diagrams is tedious and may be difficult to apply; more detailed discussions on curtailment of reinforcement may be found in Wight and MacGregor (2009), who suggest a graphical method for simplicity. Hence, simplified empirical rules have been developed for detailing reinforcements for slabs and beams having nearly equal spans with uniformly distributed load to comply with anchorage and other requirements. They are discussed in Chapters 10, 11, and 17.

7.9 SEISMIC CONSIDERATIONS

As already mentioned in Section 7.4.2, seismic modification factors are needed to account for the reduction in bond strength due to cyclic loading (ACI 408.2R-92). ACI 318 formula (Eq. 7.14) requires an increase in development length of 30 per cent. For practice, a seismic modification factor of 1.5 would be conservative and will result in a seismic development length of 10 bar diameters (Steuck, et al. 2009).

During an earthquake, the zone of inelastic deformation that exists at the end of a beam may extend for some distance into the column. This makes the bond between the concrete and steel ineffective in this region. Hence, Clause 6.2.5 of IS 13920 recommends that in an external joint, both the top and

the bottom bars of the beam shall be provided with anchorage length beyond the inner face of the column. This anchorage length should not be less than the development length in tension plus 10 times the bar diameter minus the allowance for 90° bend(s), as shown in Fig. 7.45. In an internal joint, both face bars of the beam should be taken continuously through the column.

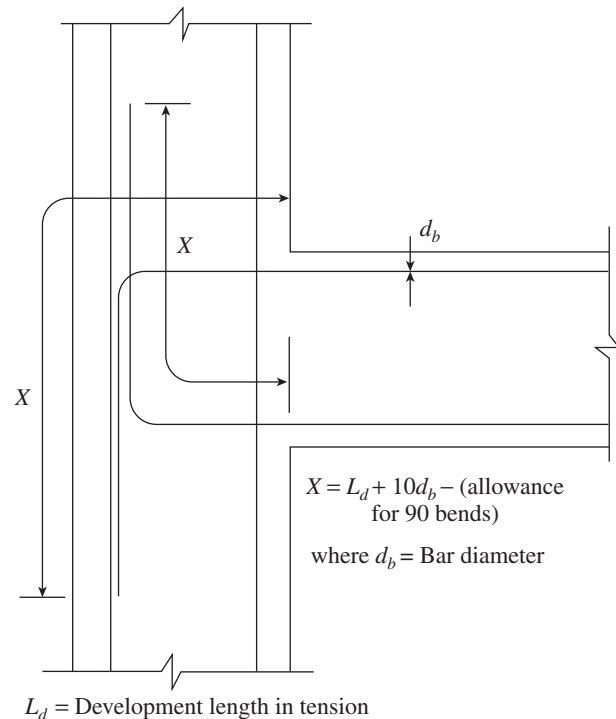
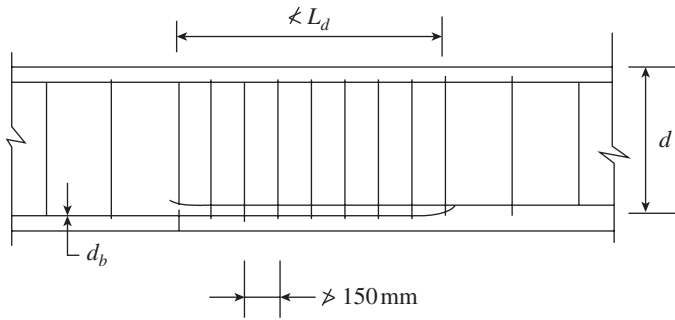


FIG. 7.45 Anchorage of beam bars in an external joint

According to Clause 6.2.6 of IS 13920, longitudinal bars in beams are allowed to be spliced only if hoop or spiral reinforcement is provided over the entire splice length, at a spacing not exceeding 150 mm, as shown in Fig. 7.46. (As per ACI 318 spacing of such transverse reinforcement should not exceed the smaller of $d/4$ and 100 mm.) Transverse reinforcement for lap splices at any location is mandatory because of the likelihood of loss of shell concrete. In addition, lap splices of reinforcement are prohibited at regions where flexural yielding is anticipated because such splices are not reliable under conditions of cyclic loading into the inelastic range. Thus, lap splices should not be provided at the following locations:

1. Within the joints
2. Within a distance of $2d$ from the face of the joint
3. Within a quarter length of the member, where flexural yielding may generally occur due to earthquake loading

Not more than 50 per cent of the bars should be spliced at one section.



L_d = Development length in tension d_b = Bar diameter

FIG. 7.46 Lap splices in beams located in earthquake zones

Lap splices in columns near the ends of the column in frames are vulnerable due to the spalling of the shell concrete in these locations. Hence, IS 13920, Clause 7.2.3, stipulates that lap splices should be located only near the centre half of the member length, where stress reversal is likely to be limited to a smaller stress range than at locations near the joints (see Fig. 7.47). It also suggests that it should be proportioned as a *tension splice* (it is because columns can develop substantial reversible moments during earthquakes and all the bars are liable to go under tension).

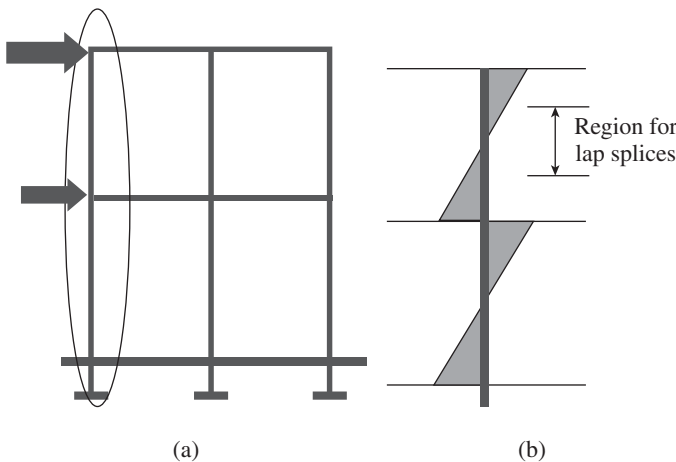


FIG. 7.47 Location for lap splices for frames subjected to lateral loads
(a) Typical frame (b) Typical bending moment diagram under lateral loads

Transverse reinforcement is required along the lap splice length due to the uncertainty in moment distributions along the height and the need for confinement of lap splices subjected to stress reversals. Hence, IS 13920, Clause 7.2.3, stipulates that hoops should be provided over the entire splice length with a spacing of 150mm from centre to centre or less. It is preferable to splice only up to 50 per cent of the bars at a section. When more than 50 per cent of the bars are spliced at one section, a lap length of $1.3L_d$, where L_d is the development length of bar in tension, should be provided. It has to be noted that this provision means that in normal multi-storey

buildings, only half the bars can be spliced in one storey and the other half in the next storey; however, when one wants to splice all the bars in the same storey, an increased lap length of $1.3L_d$ has to be provided.

In general, welding of stirrups, ties, or other similar elements to longitudinal reinforcement can lead to local embrittlement of the steel. According to Clause 6.2.7 of IS 13920, use of welded splices and mechanical connections can be used only when alternate bars in each layer of longitudinal reinforcement are spliced at a section and the centre-to-centre distance between the splices of adjacent bars, measured along the longitudinal axis of the member, is greater than 600 mm. However, welding of stirrups, ties, or inserts to longitudinal reinforcement is prohibited.

As discussed in Chapter 6, stirrups and ties should have a 135° hook with a six diameter extension (but not less than 65 mm) at each end that is embedded in the concrete core.

EXAMPLES

EXAMPLE 7.1 (Development length):

An RC wall footing has a width of 1.8m and supports a 300mm thick wall, as shown in Fig. 7.48. Check whether there is sufficient space for 20mm diameter bars to develop the required bond, if they are stressed fully. Use M30 concrete and Fe 415 grade steel.

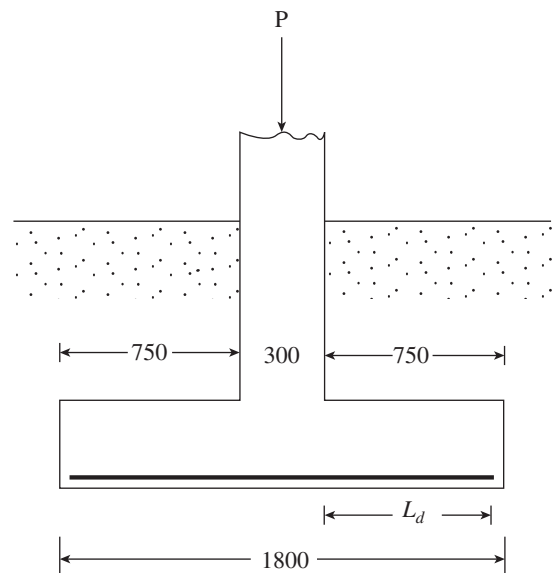


FIG. 7.48 Figure for Example 7.1

SOLUTION:

Available development length = 750 – cover

Cover at the end of bar should be ≥ 25 mm and $\geq 2d_b$

Hence, available development length = $750 - 2 \times 20 = 710$ mm

Design bond stress for deformed bars, τ_{bd} , for M30 concrete as per Table in Clause 26.2.1.1 of IS 456 = $1.5 \times 1.6 = 2.4$ N/mm²

Required development length as per Clause 26.2.1

$$= L_d = \frac{f_s d_b}{4\tau_{bd}} = \frac{0.87 \times 415 \times 20}{4 \times 2.4} = 752 \text{ mm} > 710 \text{ mm}$$

(Note that this value can be directly obtained from Table 7.4.)

Hence, we have to provide bends or hooks at the ends of the bar to anchor them.

Anchorage value of 90° bend with $4d_b$ extension (Clause 26.2.2.1a) $= (4 + 4)d_b = 160 \text{ mm}$.

Hence, total anchorage length $= 710 + 160 = 870 \text{ mm} > 752 \text{ mm}$.

Hence, provide standard 90° bend at the end to satisfy development length requirement.

EXAMPLE 7.2 (Development of epoxy-coated bar):

Calculate the required development length for the 20 mm diameter epoxy-coated bottom bar as shown in Fig. 7.49. Assume M20 concrete and Fe 415 steel. Compare the values of L_d obtained by using IS 456 and ACI 318 code.

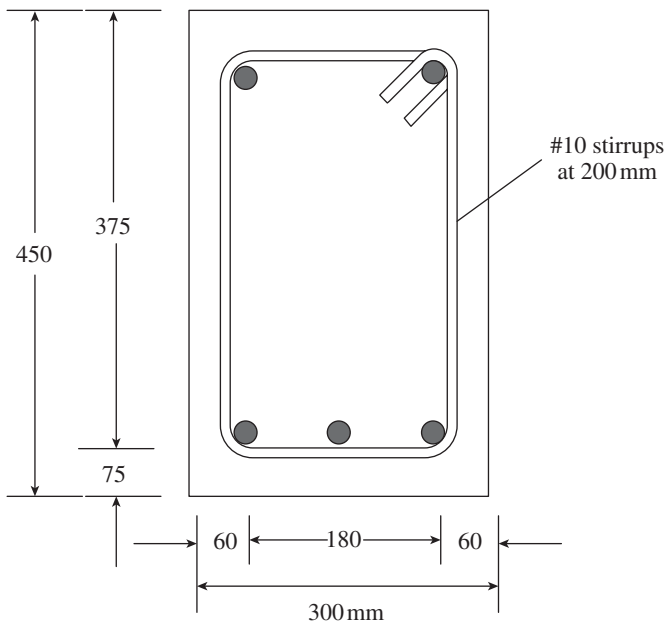


FIG. 7.49 Figure for Example 7.2

SOLUTION:

(a) Development length as per IS 456:

From Table 7.4, L_d for 20 mm Fe 415 grade tension bar in M20 concrete $= 940 \text{ mm}$.

Amendment to IS 456 suggests that for epoxy-coated steel, the design bond stress should be taken as 80 per cent of the values given in the table of Clause 26.2.1.1.

Hence, development length $= 940/0.8 = 1175 \text{ mm}$

As the IS 456 formula does not consider the effect of transverse reinforcement, let us calculate the development length as per ACI 318.

(b) Development length as per ACI 318:

Spacing of main reinforcement $= 180/2 = 90 \text{ mm}$

Total area of transverse reinforcement (2-legged 10 mm), $A_{tr} = 2 \times 78.54 \text{ mm}^2$

Spacing of transverse reinforcement, $s = 200 \text{ mm}$

Characteristic strength of transverse reinforcement,

$f_{yt} = 415 \text{ MPa}$

Number of bars being anchored, $n = 3$

$c =$ smallest of the side cover, c_s , the cover for the bar, c_b , or one-half the centre-to-centre spacing of the bars $=$ Smallest of $(60, 75, 1.5 \times 90) = 60 \text{ mm}$

Transverse reinforcement factor,

$$k_{tr} = \frac{40A_{tr}}{sn} = \frac{40 \times 2 \times 78.54}{200 \times 3} = 10.47 \text{ mm}$$

$(c + k_{tr})/d_b = (60 + 10.47)/20 = 3.52 > 2.5$. Hence, adopt 2.5.

$\alpha =$ reinforcement location factor $= 1.0$ (bottom bar)

$\beta =$ coating factor $= 1.5$ [epoxy-coated bar with cover $= 75 \text{ mm} (> 3d_b = 60 \text{ mm})$ but spacing between bars $= 90 \text{ mm} (< 6d_b = 120 \text{ mm})$]

$\gamma =$ reinforcement size factor $= 0.8$ (bar size 20 mm)

$\lambda =$ lightweight aggregate factor $= 1$ (normal concrete)

$$L_d = \frac{f_y}{\lambda \sqrt{f_{ck}}} \frac{\alpha \beta \gamma}{\left(\frac{c + k_{tr}}{d_b}\right)} d_b = \frac{415}{1 \times \sqrt{20}} \frac{1.0 \times 1.5 \times 0.8}{2.5} 20 = 891 \text{ mm} > 300 \text{ mm}$$

Thus, we get $L_d = 891 \text{ mm}$ using ACI code, compared to 1175 mm as obtained in IS 456 (about 30% less length using ACI 318).

EXAMPLE 7.3 (Anchorage of bars):

Consider the cantilever beam of Example 6.5. Check whether the anchorage provided for the longitudinal bars in the beam, as shown in Fig. 7.50, is adequate and suggest appropriate modifications, if required. The beam is subjected to a uniformly distributed factored load of 80 kN/m, including self-weight. Assume M25 concrete and Fe 415 steel.

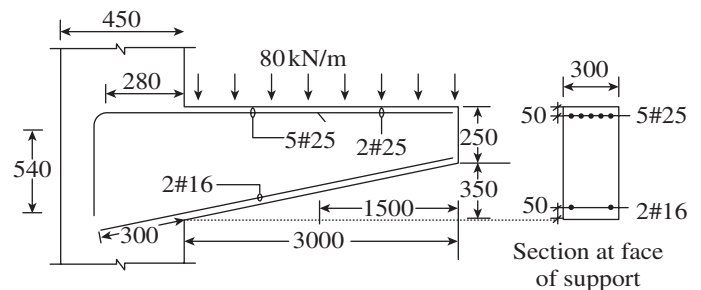


FIG. 7.50 Figure for Example 7.3

SOLUTION:

Assuming the bars are fully stressed at the location of maximum moment (i.e., face of column support), full development length L_d is required for anchorage of the bars inside the column, beyond this section.

For the tension bars (5#25 at top):

$$L_d = \frac{f_s d_b}{4 \tau_{bd}} = \frac{0.87 \times 415 \times 25}{4 \times (1.4 \times 1.6)} = 1007 \text{ mm}$$

Actual anchorage length provided (including effect of the 90° bend ($4d_b$) and extension of bar beyond bend) = $280 + (4 \times 25) + 540 = 920 \text{ mm} < L_d = 1007 \text{ mm}$. Hence, it is not acceptable.

For the compression bars (2#16 at bottom):

For compression, τ_{bd} can be increased by 25 per cent

$$L_d = \frac{0.87 \times 415 \times 16}{4 \times (1.4 \times 1.6 \times 1.25)} = 516 \text{ mm}$$

Actual anchorage length provided = $300 \text{ mm} < L_d = 516 \text{ mm}$; hence, it is not acceptable.

Actual Anchorage Length Required

Before providing the increased anchorage length, let us verify whether the bars are fully stressed under the given loading and calculate the precise development length.

Maximum factored moment at the critical section (at support):

From Example 6.5, factored bending moment = 360 kNm
 $b = 300 \text{ mm}$, $d = 600 - 50 = 550 \text{ mm}$

$$\frac{M_u}{bd^2} = \frac{360 \times 10^6}{300 \times 550^2} = 3.967 \text{ MPa} > M_{u, \text{lim}} / bd^2 = 0.138 \times 25 = 3.45 \text{ MPa (Table 5.4)}$$

Hence, the beam has to be doubly reinforced.

Using design aids (Table 51 or SP 16) with $d'/d = 50/550 = 0.09$

$$(p_t)_{\text{req}} = 1.352; (A_{st})_{\text{required}} = (1.352/100) \times (300 \times 550) = 2230.8 \text{ mm}^2$$

$$(p_c)_{\text{req}} = 0.165; (A_{sc})_{\text{required}} = (0.165/100) \times (300 \times 550) = 272 \text{ mm}^2$$

$$(A_{st})_{\text{provided}} = 5 \times 491 = 2455 \text{ mm}^2 > 2230.8 \text{ mm}^2$$

$$(A_{sc})_{\text{provided}} = 2 \times 201 = 402 \text{ mm}^2 > 272 \text{ mm}^2$$

Actual anchorage length required = $L_d \times (A_s)_{\text{required}} / (A_s)_{\text{provided}}$

For the *tension* bars = $\frac{2230.8}{2455} \times 1007 = 915 \text{ mm} < 920 \text{ mm}$ provided. Hence, it is acceptable.

For the *compression* bars = $\frac{272}{402} \times 516 = 349 \text{ mm} > 300 \text{ mm}$ provided. Hence, it is not acceptable.

Proposed Modification for Compression Bars

We may reduce the anchorage length requirements by providing smaller diameter bars. Hence, for compression bars (at bottom), provide 3#12 mm (instead of 2#16).

Now, $A_{sc} = 3 \times 113 = 339 \text{ mm}^2 > 272 \text{ mm}^2$ required L_d in compression for M25 from Table 7.4, and using $(A_{sc})_{\text{required}} / (A_{sc})_{\text{provided}}$ ratio
 = $387 \times (272/339) = 310 \text{ mm} > 300 \text{ mm}$ provided

Hence, extend the compression bars by providing a standard 90° bend (additional anchorage obtained = $8d_b = 8 \times 12 = 96 \text{ mm}$). Hence, it is acceptable.

EXAMPLE 7.4 (Hooked bar anchorage):

The exterior end of a 400 mm wide and 600 mm deep beam frames into a 600 mm square column as shown in Fig. 7.51. The column is reinforced with four 32 mm bars. The negative moment reinforcement at the exterior end of the beam consists of four 25 mm bars. Assuming Fe 415 steel and M30 concrete, design the anchorage for the four 25 mm bars into the column as per IS 456 and ACI 318.

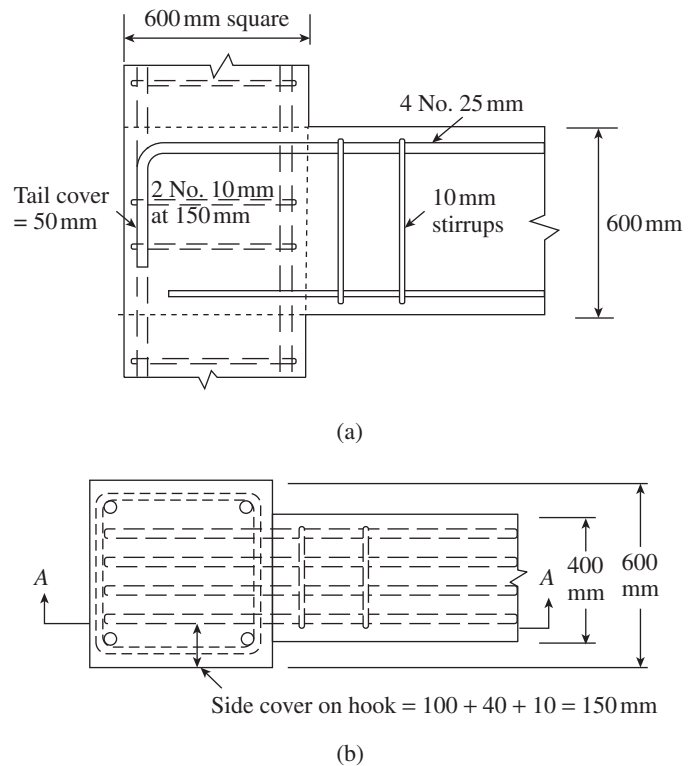


FIG. 7.51 Figure for Example 7.4

SOLUTION:

(a) As per IS 456:

Required development length for 25 mm grade Fe 415 bar in M30 concrete (from Table 7.4) = 940 mm .

Assuming a 90° bend with $12d_b$ extension,

$$\begin{aligned} \text{Length provided} &= (600 - \text{cover}) + 4d_b + 12d_b \\ &= (600 - 50) + 16 \times 25 \\ &= 950 \text{ mm} > 940 \text{ mm}. \end{aligned}$$

Check for vertical height of bend within the joint:

The vertical height = $4d_b + 12d_b = 16 \times 25 = 400 \text{ mm}$. This is less than the depth of beam minus covers. Hence, it will fit within the joint and is acceptable.

(b) As per ACI 318:

$$\begin{aligned} L_{dh} &= \frac{0.268 f_y}{\sqrt{f_{ck}}} d_b = \frac{0.268 \times 415}{\sqrt{30}} 25 = 20.3 \times 25 = 508 \text{ mm} \\ &\geq 8d_b \text{ or } 150 \text{ mm} \end{aligned}$$

The requirement is less than 550mm, but this equation assumes a standard hook at the end, with a bend and $12d_b$ extension. Hence, provide the same arrangement as discussed in the IS code.

Minimum ties have to be provided in the joint. Assuming 10mm ties, the required spacing may be found using Eq. (6.20) or (6.21) given in Chapter 6.

$$\frac{A_{sv}}{b_w s_v} = \frac{0.9\sqrt{f_{ck}}}{16f_y} \geq \frac{1}{3f_y}$$

The second expression governs. Hence,

$$s_v = \frac{(2 \times 78.5) \times 3 \times 415}{600} = 326 \text{ mm}$$

Provide 10mm ties in the joint at 150mm centre-to-centre spacing.

EXAMPLE 7.5 (Compression lap and welded laps):

A tied column of a multi-storeyed building has sixteen 28 mm longitudinal bars (see Fig. 7.52). Assuming $f_y = 500 \text{ MPa}$ and $f_{ck} = 60 \text{ MPa}$, calculate the compression lap length required as per (a) IS 456, (b) ACI 318, and (c) equations proposed by Chun, et al. (d) How can the length be reduced by using welded lap joint?

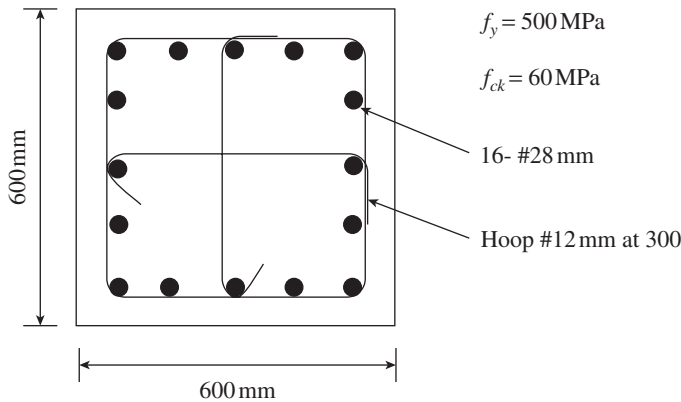


FIG. 7.52 Figure for Example 7.5

SOLUTION:

(a) Lap length as per Clause 26.2.5.1 of IS 456:

$$\text{Development length in compression} = L_d = \frac{f_s d_b}{4\tau_{bd}} \geq 24 d_b$$

with τ_{bd} for tension bars from Clause 26.2.1.1 (table) increased for deformed bars (60%) and for compression (25%).

$$\text{Hence, } L_d = \frac{0.87 \times 500}{4 \times (1.9 \times 1.6) \times 1.25} d_b = 28.62 \times 28 = 801 \text{ mm}$$

Note that the IS 456 values of τ_{bd} are valid only up to M40. Using Eq. (7.13), we get

$$L_d = \frac{d_b f_s}{1.177(f_{ck})^{2/3}} = \frac{0.87 \times 500}{1.177 \times (60)^{2/3}} d_b = 24.12 \times 28 = 675 \text{ mm}$$

(b) As per the ACI 318 code, for $f_y = 500 \text{ MPa}$, Eq. (7.23b)

$$L_{sp} = (0.13f_y - 24)d_b = (0.13 \times 500 - 24)d_b = 41 \times 28 = 1148 \text{ mm}$$

(c) As per Eq. (7.24a) proposed by Chun, et al.

$$\frac{K_{tr}}{d_b} = \frac{40A_{tr}}{ns_{tr}d_b} = \frac{40 \times (3 \times 113)}{5 \times 300 \times 28} = 0.322 < 1.76$$

$$\psi_{comp} = \frac{1}{\left(1 + 0.134 \frac{K_{tr}}{d_b}\right)^2} = \frac{1}{(1 + 0.134 \times 0.322)^2} = 0.92$$

$$\text{Thus, } L_{sp} = \psi_{comp} \frac{(f_y)^2}{100f_{ck}} d_b = 0.92 \frac{500^2}{100 \times 60} d_b = 38.33d_b$$

$$\text{Hence, } L_{sp} = 38.33 \times 28 = 1073 \text{ mm}$$

Thus, it is seen that in the present case, the IS code values are much lower than the accurate values (37% less) and the ACI code values are seven per cent higher than the accurate values.

(d) Reduction of lap length by using welded lap joint:

As 28 mm bars weigh 4.833 kg/m, the weight of lapping sixteen 28 mm bars with a lap length of 801 mm will result in 62 kg.

Hence, let us adopt a single lap welding as shown in Fig. 7.37(a) of total length of $15d_b$ with $10d_b$ lap welding and $5d_b$ gaps ($L_w = 10 \times 28 = 280 \text{ mm}$). The welds are designed to carry the equivalent force (F) for a lap of $(28.62 - 15)d_b = 13.62d_b$.

$$F = (0.87 \times 500) \times \frac{\pi \times 28^2}{4} \times \frac{13.62}{28.62} = 127.5 \text{ kN}$$

Thus, the size of the weld is calculated as

$$\text{Size} = \frac{F}{L_w} \left(\frac{\sqrt{3} \times \gamma_{mw}}{0.7f_u} \right) = \frac{127.5 \times 1000}{280} \left(\frac{\sqrt{3} \times 1.5}{0.7 \times 410} \right) = 4.2 \text{ mm}$$

Provide the size of weld as $0.2 \times d_b = 0.2 \times 28 = 5.6$, say, 5 mm weld of length 280 mm. Note that AWS Structural welding code—Reinforcing steel, D1.4-92, does not allow welded lap joints (with double flare V-groove welds) for bars greater than 19 mm.

EXAMPLE 7.6 (Curtailment of reinforcement):

An RC beam of span 6 m, subjected to uniformly distributed loads, requires six 20 mm Fe 415 bars as tension reinforcement. Determine the TCP and PCP where two and four of these bars can be curtailed. Assume M25 concrete, $b = 400 \text{ mm}$, and $d = 450 \text{ mm}$.

SOLUTION:

Two of the bars (denoted as bars A in Fig. 7.53) should continue into the supports. Considering that symmetry should be maintained, two bars (bars B in Fig. 7.53) can be cut-off at x_1 ($2/3M_o$ location, where M_o is the maximum bending moment at the centre), and two more bars (bars C in Fig. 7.53) can be curtailed at x_2 ($1/3M_o$ location).

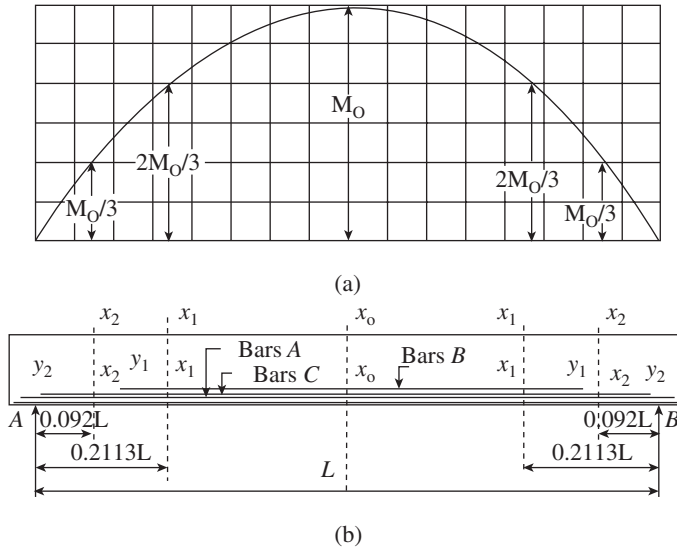


FIG. 7.53 (a) Moment diagram for uniform loading (b) Theoretical and modified cut-off points for $(2/3) M_0$ and $(1/3) M_0$

Step 1 Calculate TCP.

TCP for bars B from bending moment considerations:

$$\frac{(wL^2/8) - (wx^2/2)}{(wL^2/8)} = (4/6) \text{ bars}$$

where x is measured from mid-span. Simplifying, we get $6(L^2 - 4x^2) = 4L^2$ with $L = 6$ m, $x_2 = 1.732$ m from mid-span or $3 - 1.732 = 1.268$ m ($0.2113L$) from support.

In the same way, the TCP for bars C from bending moment considerations can be found as $x_2 = 2.449$ m from mid-span or $0.092L = 0.552$ m from support.

Step 2 Calculate development length. The development length for 20 mm bars of grade Fe 415 for M 25 concrete from Table 7.4, $L_d = 806$ mm.

Step 3 Determine the PCPs. Clause 26.2.3.4 of the code requires that the distances x_1y_1 and x_2y_2 should be at least equal to d (400 mm) or $12d_b$ ($12 \times 20 = 240$ mm), whichever is larger. Thus, the PCPs should be located at 400 mm from the TCPs (i.e., $x_1y_1 = x_2y_2 = 400$ mm).

Step 4 Check for development length at the cut-off points

PCP y_1 for B bars from support = $1268 - 400 = 868$ mm

PCP y_2 for C bars from support = $552 - 400 = 152$ mm

It is evident that bars A, B and C have adequate development length of more than 806 mm on either side of mid-span. At section x_1 , B bars are cut-off and bars A and C have a development length of $0.2113L = 1268$ mm and 1112 mm ($1268 - 152$), respectively, and both lengths are greater than 806 mm. Hence, the development lengths at x_1 are adequate. At section x_2 only bars A are available, and the development

length available up to the centre of support is $0.092L = 552$ mm < 806 mm. However, these bars will continue into the support and this additional length should be $(806 - 552) = 254$ mm or $L_d/3 = 806/3 = 269$ mm (Clause 26.2.3.3). Extend the bars A into the support by 150 mm and bend the bars using 90° bend with $4d_b$ extension, which will give an extra length of $8 \times 20 = 160$ mm (total 310 mm > 269 mm).

Note that additional checks are required for shear and additional stirrups are to be provided at all cut-off points as per Clause 26.2.3.2 of the code.

EXAMPLE 7.7 (Development length at support of simply supported beam):

Consider the beam of Example 5.10, which is a simply supported beam of span 6 m that carries a factored load of 78 kN/m, including the self-weight. Suppose the beam is of size 700 mm by 300 mm, with effective depth 660 mm and reinforced with six 20 mm bars at the centre. If only four bars are continued into the support, check the development at the supports assuming M20 concrete and Fe 415 steel.

SOLUTION:

Step 1 Calculate the maximum bending moment and shear force.

Maximum bending moment at mid-span,

$$M_u = \frac{wL^2}{8} = \frac{78 \times 6^2}{8} = 351 \text{ kNm}$$

Maximum shear force at support,

$$V_u = wL/2 = 78 \times 6 / 2 = 234 \text{ kN}$$

Step 2 Calculate the moment of resistance at the support. At support, with four 20 bars

$$p_t = \frac{100A_{st}}{bd} = \frac{100 \times 1257}{300 \times 660} = 0.635$$

From Table 2 of SP 16:1980, $\frac{M_u}{bd^2} = 1.987$.

Hence, $M_u = 1.987 \times 300 \times 660^2 \times 10^{-6} = 259.66 \text{ kNm}$.

Step 3 Check the development length at the support.

L_d for 20 mm bars from Table 7.4 for M20 concrete and grade Fe 415 steel = 940 mm.

Using 30 per cent increase as per Clause 26.2.3.3(c) of IS 456, the condition to be satisfied is:

$$L_d \leq 1.3 \frac{M_1}{V_u} + L_o$$

$$L_o = \text{Greater of } d \text{ and } 12 d_b = 660 \text{ mm}$$

$$1.3 \frac{M_1}{V_u} + L_o = \frac{1.3 \times 259.66 \times 10^6}{234 \times 10^3} + 660$$

$$= 1442 + 660 = 2102 \text{ mm} > 940 \text{ mm}$$

Hence, it is adequate.

SUMMARY

The composite action of concrete and steel in RC structures is provided by the bond between the steel reinforcement and the surrounding concrete. The required bond strength is achieved by

providing sufficient development length. Non-provision of adequate development lengths often results in failures, especially in cantilever supports, lap splices, and beam-column joints. The bond strength is

influenced by several factors, which include the bar diameter, cover concrete, spacing of reinforcement, transverse reinforcement (e.g., stirrups), grade of concrete, confinement of concrete around the bars, aggregates used in concrete, coating applied on bars to reduce corrosion, and type of reinforcement bars used.

Though the Indian concrete code was revised in 2000, the development length (L_d) provisions remain unchanged and do not cover the effect of several parameters. However, the US code considers all these parameters. Hence, the provisions of the Indian code are discussed and then compared with the provisions of the US code.

Recent research has shown that the best fit for experimental results is provided by $f_{ck}^{1/4}$ and not $f_{ck}^{1/2}$ as given in the ACI code. Hence, formulae based on recent research have also been included. Design aids in the form of tables, which will be useful for providing development lengths of bars of different diameters, have also been provided. If excess reinforcement than that is required is provided, the L_d values can be reduced proportionately. In the same way, transfer of forces in compression is less critical and hence L_d required for compression is less than that required for tension. Tables are also provided to directly get the L_d values in compression. Discussions on development length of bundled bars and welded meshes are also included.

When space available at the ends of beam or slabs is limited, the deficiency in the required development length may be made up by suitably anchoring the reinforcements using bends, hooks, or any mechanical devices. Indian code provisions for such devices are provided and compared with other codal provisions, wherever necessary.

In practice, it is often required to splice the bar, as we cannot get bars of the exact required length. Indirect splices in the form of lap splices are often used, though they are not efficient and economical. Welded and mechanical couplers can be used as an economic alternative to lap splices. Mechanical couplers and butt welding of bars also eliminate the eccentricity involved in lap splices. The Indian code provisions for splicing bars are discussed both for tension and compression splices and the recent developments are also included.

Depending upon the forces acting in the RC members, the reinforcement can be curtailed to achieve economy. However, the bars have to be extended beyond the TCPs to reduce the stresses and cracks. The Indian code provides certain rules for such curtailment of reinforcement, based on experimental research and experience. These rules are explained. Finally, the development length requirements in seismic situations are also discussed. Ample examples are provided to explain the concepts discussed in this chapter.

REVIEW QUESTIONS

- List the three mechanisms through which bond is achieved in RC.
- Distinguish between local bond and anchorage bond.
- Why are plain bars considered to develop weak bond? When plain bars are used, what should we do to mobilize bond strength?
- Derive expressions for flexural bond stress.
- Why is flexural bond stress not reliable?
- What is anchorage bond? Derive the expression for anchorage bond.
- Explain bond behaviour.
- The height/spacing ratio of ribs, (a/c) ratio that is optimal is _____.
(a) 0.057 (c) 0.065
(b) 0.072 (d) 0.10
- What is the normal specimen used for finding the bond stress of bars?
- Sketch the typical bond stress vs slip curves.
- List the factors that affect the bond strength.
- Current research shows that the bond strength is closely represented by _____.
(a) $\sqrt{f_{ck}}$ (c) $f_{ck}^{1/3}$
(b) f_{ck} (d) $f_{ck}^{1/4}$
- Why do the cover and spacing of bars affect the bond strength?
- How does confinement in the form of transverse reinforcement affect the bond strength?
- Will surface conditions of the bar like coating affect the bond resistance?
- What is meant by top-bar effect? Why is the required development length of top bars greater than that of bottom bars?
- Define development length.
- Name the devices that can be used to obtain the required development length if it is not achievable with straight bars.
- List a few locations that can be considered as critical sections for the development of reinforcement.
- Write the equation that is used in IS 456 for development length. What are the drawbacks of using this equation?
- Write the US code equation for development length. Why is it considered superior to the Indian code equation?
- How are the tabled design bond stress for plain bars in the Indian code modified to take into account the deformed bars and bars under compression?
- If the theoretical steel needed is A_s and if more than the required steel is provided, can the development length for bars be reduced? Write the expression for the reduced development length.
- Why is the bond stress in compression assumed to be more than that in tension bars?
- Can we consider equivalent length for hooks and bends in compression bars for development?
- What is meant by bundling of bars? How many bars can be bundled together? State the points to be considered while calculating development length in the bundled bars.
- Write short notes on development length in welded fabrics.
- What is meant by anchorage of bars?
- What is meant by equivalent length or anchorage value of bends and hooks? Can they be used to increase the theoretical development length of tension as well as compression bars?
- Anchorage value of standard 90° bend as per IS 456 is _____.
(a) eight times the diameter of the bar with a maximum of 16 times the diameter of the bar

- (b) 16 times the diameter of the bar
 - (c) four times the diameter of the bar for each 45° bend, which should not exceed 16 times the diameter of bar
 - (d) four times the diameter of the bar
31. The anchorage vale of a standard U hook is _____.
 - (a) eight times the diameter of the bar
 - (b) 16 times the diameter of the bar
 - (c) four times the diameter of the bar for each bend, which should not exceed 16 times the diameter of the bar
 - (d) four times the diameter of the bar
 32. Write the equation for checking the bearing stress of concrete inside the hook.
 33. Do we have to check the bearing stress inside the standard hooks? Why is it not considered necessary?
 34. What are headed bars? How are they superior to hooks and bends? Describe the behaviour of headed bars in tension.
 35. To anchor reinforcement properly, the head size of headed bar should have an area that is _____.
 - (a) 2–3 times the bar area
 - (c) 4–5 times the bar area
 - (b) 3–4 times the bar area
 - (d) 1.5–2.5 times the bar area
 36. When can we assume that stirrups are fully anchored as per Clause 26.2.2.4 of IS 456?
 37. In earthquake situations, we should use only stirrups with _____.
 - (a) 90° hooks with $8d_b$ mm extension
 - (b) 180° hooks with $4d_b$ mm extension
 - (c) 135° hooks with $6d_b$ mm extension
 - (d) 135° hooks with $8d_b$ mm extension
 38. What is the length of bars that are usually available in the market? When does a steel bar require splicing? What is the purpose of splicing?
 39. List the various classifications of splicing.
 40. Why are lap splices called as indirect splicing?
 41. According to IS 456, it is recommended that the splices are located where the bending moment is less than _____.
 - (a) 75 per cent of moment of resistance and less than 50 per cent bars are spliced
 - (b) 65 per cent of moment of resistance and less than 25 per cent bars are spliced
 - (c) 50 per cent of moment of resistance and less than 50 per cent bars are spliced
 - (d) 60 per cent of moment of resistance and less than 50 per cent bars are spliced.
 42. For flexural tension bars, the splice should be the larger of L_d and _____.
 - (a) $40d_b$
 - (c) $25d_b$
 - (b) $50d_b$
 - (d) $30d_b$
 43. Why do the cover and spacing of bars affect the development length? How is the top-bar effect considered in the splicing of top bars in beams?
 44. For bars in direct tension, the splice should be the larger of $30d_b$ and _____.
 - (a) L_d
 - (c) $1.3L_d$
 - (b) $1.4L_d$
 - (d) $2L_d$
 45. How should the bundled bars be spliced?
 46. Up to what diameter bars are allowed to be extended by splicing? If the bar diameter exceeds this limit, what will you do?
 47. Is it advisable to splice more than 50 per cent at a section? If it is required, what are the additional precautions to be taken as per the Indian code to reduce the possibility of cracking?
 48. Why does the code prescribe transverse reinforcements at spliced locations? Discuss these specifications regarding transverse reinforcements.
 49. In what way does the compression splice behave differently from the tension splices? Enumerate the rules for compression splices.
 50. How should we provide transverse reinforcements for compression splices?
 51. Write short notes on the following:
 - (a) Butt and lap-welded splices
 - (b) Mechanical splices
 - (c) Curtailment of reinforcement in beams
 52. List a few points to be considered in the seismic locations while providing development length and splices.

EXERCISES

1. An RC footing has a width of 1.5 m and supports a 250 mm thick column. Check whether there is sufficient space for 16 mm diameter bars to develop the required bond if they are stressed fully. Assume M20 concrete and Fe 415 grade steel.
2. Determine the development length required for the tension bars of beams shown in Fig. 7.54. Assume M20 concrete, Fe 415 grade steel and
 - (a) uncoated bar in normal weight concrete;
 - (b) epoxy-coated bar in normal weight concrete;
 - (c) epoxy-coated bar in lightweight concrete.
 Compare the values by using the IS and ACI code formulae.

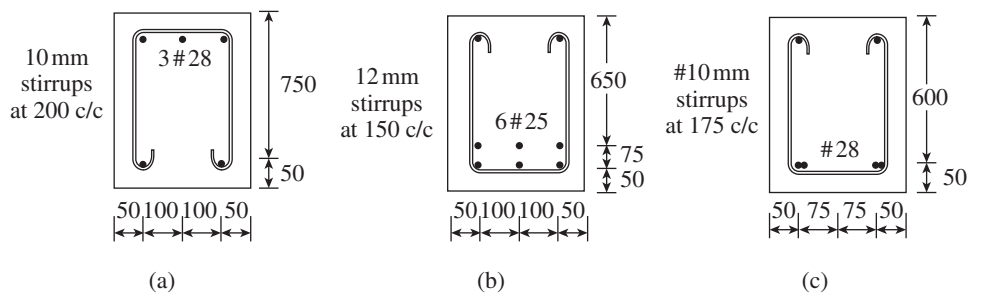


FIG. 7.54

3. Calculate the required development length for the 25 mm diameter epoxy-coated bottom bar shown in Fig. 7.55. Assume M20 concrete and Fe 415 steel. Compare the values of L_d obtained by using IS 456 and ACI 318 codes.

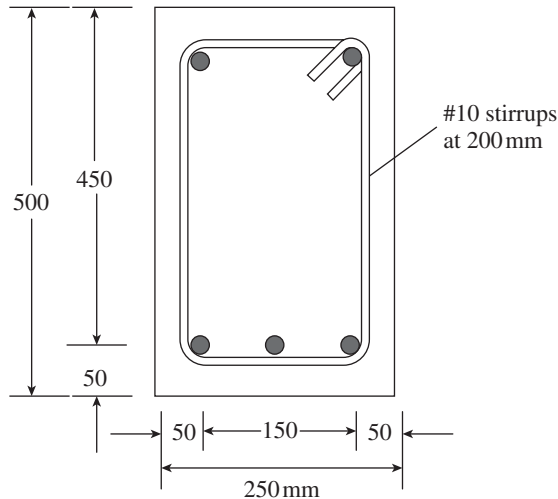


FIG. 7.55

4. The cantilever beam shown in Fig. 7.56 frames into a column of size 450×450 mm. Calculate and sketch the anchorage to be provided for the four 28 longitudinal bars in the beam. The beam is subjected to a uniformly distributed factored load of 70 kN/m , including the self-weight. Assume M20 concrete and deformed bars of grade Fe 415 steel.

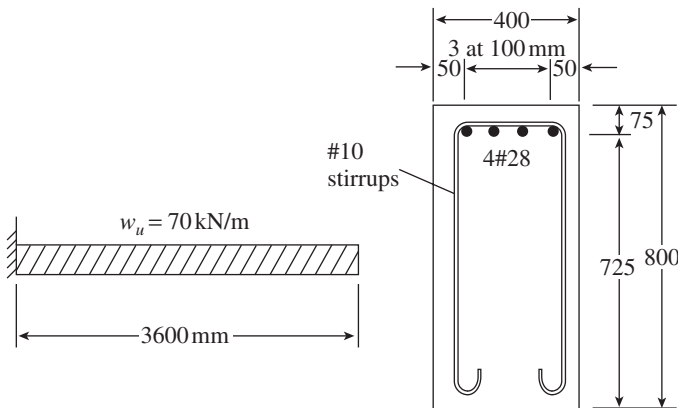


FIG. 7.56

5. In the cantilever beam of Exercise 4, determine the point where the two bars can be cut-off. Show a sketch indicating the TCP and PCP.
6. A tied column of a multi-storeyed building has sixteen 20 mm longitudinal bars (see Fig. 7.57). Assuming $f_y = 415 \text{ MPa}$ and $f_{ck} = 30 \text{ MPa}$, calculate the compression lap length required (a) as per IS 456 and (b) ACI 318. (c) In addition, how can the length be reduced by using welded lap joints?

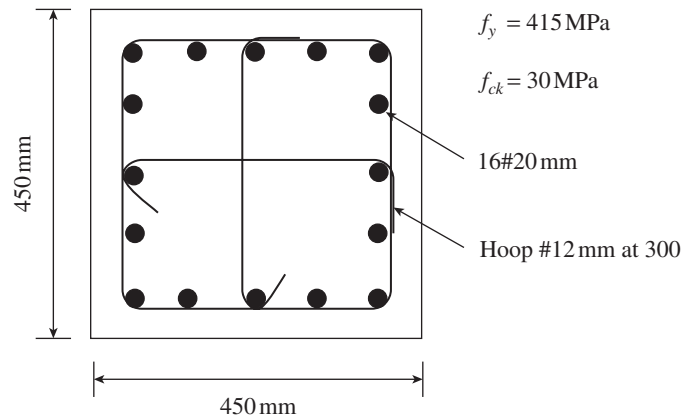


FIG. 7.57

7. An RC beam of span 5 m, subjected to uniformly distributed loads, requires six 16 mm Fe 415 bars as tension reinforcement. Determine the TCP and PCP where two and four of these bars can be curtailed. Assume M20 concrete, $b = 400$ mm, and $d = 550$ mm.
8. Explain why IS 456 does not insist on the condition $L_d < M_1/V + L_o$ for negative steel at the interior supports of a continuous beam. How does one check the anchorage length of bar at the interior support? Consider a continuous beam ABC, simply supported at A and C and continuous over B. The design requires four bars of 28 mm at the top and three bars of 28 mm at the bottom for a moment of 575 kNm at the support. Check the anchorage length that should be provided for the tension steel. What are the requirements to be fulfilled for the negative moment reinforcement?

REFERENCES

- ACI 408R-03 2003, *Bond and Development of Straight Reinforcing Bars in Tension*, American Concrete Institute, Farmington Hills, p. 49.
- ACI 408.2R-92 1992, *Bond Under Cyclic Loads*, American Concrete Institute, Farmington Hills, p. 32.
- ACI 408.3R-09 2009, *Guide for Lap Splice and Development Length of High Relative Rib Area Reinforcing Bars in Tension and Commentary*, American Concrete Institute, Farmington Hills, p. 8.
- ACI 439.3R-07 2007, *Mechanical Connections of Reinforcing Bars*, American Concrete Institute, Farmington Hills, p. 20.
- Aziznamini, A., M. Chisala, and S.K. Ghosh 1995, 'Tension Development Length of Reinforcing Bars Embedded in High-strength Concrete', *Engineering Structures*, Vol. 17, No. 7, pp. 512–22.
- Aziznamini, A., M. Stark, J.J. Roller, and S.K. Ghosh 1993, 'Bond Performance of Reinforced Bars Embedded in High-strength Concrete', *ACI Structural Journal*, Vol. 90, No. 5, pp. 554–61.
- Balasubramanian, K., T.S. Krishnamurthy, S. Gopalakrishnan, B.M. Bharathkumar, and Girish Kumar 2004, 'Bond Characteristics of Slag-based HPC', *The Indian Concrete Journal*, Vol. 78, No. 8, pp. 39–44.
- Bashandy, T.R. 2009, 'Evaluation of Bundled Bar Lap Splices', *ACI Structural Journal*, Vol. 106, No. 2, pp. 215–21.
- Brettmann, B.B., D. Darwin, and R.C. Donahey 1986, 'Bond of Reinforcement to Superplasticized Concrete', *ACI Journal*, Vol. 83, No. 1, pp. 98–107.
- Cambay, E. and R.J. Frosch 2006, 'Design of Lap-spliced Bars: Is Simplification Possible?', *ACI Structural Journal*, Vol. 103, No. 3, pp. 443–51.
- Cattaneo S. and G. Rosati 2009, 'Bond between Steel and Self-consolidating Concrete: Experiments and Modeling', *ACI Structural Journal*, Vol. 106, No. 4, pp. 540–50.

- Chan, Y.W., Y.S. Chen, and Y.S. Liu 2003, 'Development of Bond Strength of Reinforcement Steel in Self-consolidating Concrete', *ACI Structural Journal*, Vol. 100, No. 4, pp. 490–8.
- Choi, O.C., H. Hadje-Ghaffari, D. Darwin, and S.L. McCabe 1991, 'Bond of Epoxy-coated Reinforcement: Bar Parameters', *ACI Materials Journal*, Vol. 88, No. 2, pp. 207–17.
- Chun S-C., S-H. Lee, T.H.-K. Kang, B. Oh, and J.W. Wallace 2007, 'Mechanical Anchorage in Exterior Beam-column Joints Subjected to Cyclic Loading', *ACI Structural Journal*, Vol. 104, No. 1, pp. 102–12.
- Chun S-C., S-H. Lee, and B. Oh 2010a, 'Compression Lap Splice in Unconfined Concrete of 40MPa and 60MPa (5800 psi and 8700 psi) Compressive Strengths', *ACI Structural Journal*, Vol. 107, No. 2, pp. 170–8.
- Chun S-C., S-H. Lee, and B. Oh 2010b, 'Compression Lap Splice in Confined Concrete of 40MPa and 60MPa (5800 psi and 8700 psi) Compressive Strengths', *ACI Structural Journal*, Vol. 107, No. 4, pp. 476–85.
- Clark, A.P. 1946, 'Comparative Bond Efficiency of Deformed Concrete Reinforcing Bars', *ACI Journal, Proceedings*, Vol. 43, No. 4, pp. 381–400.
- Clark, A.P. 1950, 'Bond of Concrete Reinforcing Bars', *ACI Journal, Proceedings*, Vol. 46, No. 3, pp. 161–84.
- Cleary, D.B. and J.A. Ramirez 1993, 'Epoxy-coated Reinforcement under Repeated Loading', *ACI Structural Journal*, Vol. 90, No. 4, pp. 451–8.
- Coogler, K.L., K.A. Harries, and M. Gallick 2008, 'Experimental Study of Offset Mechanical Lap Splice Behavior', *ACI Structural Journal*, Vol. 105, No. 4, pp. 478–87.
- Cresswell Riol, B.H.G. (ed) 2006, *Standard Method of Detailing Structural Concrete: A Manual for Best Practice*, 3rd edition, The Institution of Structural Engineers and Concrete Society, London, p. 188.
- Degtyarev, V.V. 2007, 'Tensile Strength of Welded Splices of QST Reinforcing Bars', *ACI Structural Journal*, Vol. 104, No. 1, pp. 95–102.
- Darwin, D. and J.A. Browning 2011, 'Splice Tests of Beams with High-strength Reinforcement', *ACI Fall Convention, Bridging Theory and Practice*, Cincinnati, 16–20 October 2011.
- Darwin, D. and E.K. Graham 1993, 'Effect of Deformation Height and Spacing on Bond Strength of Reinforcing Bars', *ACI Structural Journal*, Vol. 90, No. 6, pp. 646–57.
- Darwin, D., L.A. Lutz, and J. Zuo 2005, 'Recommended Provisions and Commentary on Development Length and Lap Splice Lengths for Deformed Reinforcing Bars in Tension', *ACI Structural Journal*, Vol. 102, No. 6, pp. 892–900.
- Darwin, D., J. Zuo, M.L. Tholen, and E.K. Idun 1996, 'Development Length Criteria for Conventional and High Relative Rib Area Reinforcing Bars', *ACI Structural Journal*, Vol. 95, No. 4, pp. 347–59.
- El-Hacha, R., H. El-Agroudy, and S.H. Rizkalla 2006, 'Bond Characteristics of High-strength Steel Reinforcement', *ACI Structural Journal*, Vol. 103, No. 6, pp. 771–782.
- Eligehausen, R., E.P. Popov, and V.V. Bertero 1983, *Local Bond Stress-Slip Relationships of Deformed Bars under Generalized Excitations*, Report No. UCB/EERC-82/23, Earthquake Engineering Research Center, University of California at Berkeley, California, p. 169.
- Ezeldin, A.S. and P.N. Balaguru 1989, 'Bond Behavior of Normal and High-strength Fibre Reinforced Concrete', *ACI Materials Journal*, Vol. 86, No. 5, pp. 515–24.
- Ferguson, P.M. and J.E. Breen 1965, 'Lapped Splices for High-Strength Reinforcing Bars', *ACI Journal, Proceedings*, Vol. 62, No. 9, pp. 1063–78.
- Gjrov 1990, 'Effect of Condensed Silica Fume on the Steel Concrete Bond', *ACI Materials Journal*, Vol. 87, No. 6, pp. 573–80.
- Goto, Y. 1971, 'Cracks Formed in Concrete around Deformed Tension Bars', *ACI Journal, Proceedings*, Vol. 68, No. 4, pp. 244–51.
- Hamad, B.S. 1998, 'Bond Strength of Reinforcement in High Performance Concrete: Role of Silica Fume, Casting Position and Super Plasticizer Dosage', *ACI Materials Journal*, Vol. 95, No. 5, pp. 499–511.
- Hamad B.S., J.O. Jirsa, and N.I. D'abreu de Paulo 1993, 'Anchorage Strength of Epoxy-coated Hooked Bars', *ACI Structural Journal*, Vol. 90, No. 2, pp. 210–7.
- Hamilton III, H.R., G.G. Ciancone, and A.P. Michael 2008, *Behavior of Standard Hook Anchorages Made with Corrosion Resistant Reinforcement*, Final Report, Department of Civil and Coastal Engineering, University of Florida, Gainesville, p. 110, (also see http://www.dot.state.fl.us/research-center/Completed_Proj/Summary_STR/FDOT_BD545_40_rpt.pdf, last accessed on 27 October 2012).
- Holand I. 1997, *Sleipner A GBS Loss, Report 17: Main Report*, SINTEF, Report No. STF22 A97861, Trondheim, p. 25.
- Howell, D.A. and C. Higgins 2007, 'Bond and Development of Deformed Square Reinforcing Bars', *ACI Structural Journal*, Vol. 104, No. 3, pp. 333–43.
- Hyatt, T. 1877, *An Account of Some Experiments with Portland-Cement-Concrete Combined with Iron, as a Building Material*, Chiswick Press, London, p. 47.
- Idun, E.K. and D. Darwin 1999, 'Bond of Epoxy-coated Reinforcement: Coefficient of Friction and Rib Face Angle', *ACI Structural Journal*, Vol. 96, No. 4, pp. 609–615.
- IS 2751:1979 (reaffirmed 1998), *Code of Practice for Welding of Mild Steel Plain and Deformed Bars for Reinforced Concrete Construction*, 1st revision, Bureau of Indian Standards, New Delhi.
- IS 9417:2008, *Recommendations for Welding Cold Worked Bars for Reinforced Concrete Construction*, 1st revision, Bureau of Indian Standards, New Delhi.
- Jakobsen B. and F. Rosendahl 1994, 'The Sleipner Platform Accident', *Structural Engineering International*, Vol. 4, No. 3, pp. 190–3.
- Jeanty, P.R., D. Mitchell, and M.S. Mirza 1988, 'Investigation of "Top Bar" Effects in Beams', *ACI Structural Journal*, Vol. 85, No. 3, pp. 251–7.
- Jirsa, J.O. and J.E. Breen 1981, *Influence of Casting Position and Shear on Development and Splice Length—Design Recommendation*, Research Report No. 242-3F, Center for Transportation Research, University of Texas at Austin, Austin, p. 46.
- Jirsa, J.O., W. Chen, D.B. Grant, and R. Elizondo 1995, *Development of Bundled Reinforcing Bars*, Report No. 1362-2Ff, Center for Transportation Research, University of Texas at Austin, p. 123, (also see <http://fsel.engr.utexas.edu/publications/docs/1363-2.pdf>, last accessed on 27 October 2012).
- Jirsa, J.O., L.A. Lutz, and P. Gergely 1979, 'Rationale for Suggested Development, Splice and Standard Hook Provisions for Deformed Bars in Tension', *Concrete International*, Vol. 1, No. 7, pp. 47–61.

- Johnston, B. and K.C. Cox 1940, 'The Bond Strength of Rusted Deformed Bars', *Journal of the American Concrete Institute, Proceedings*, Vol. 37, No. 9, pp. 57–72.
- Kalyanaraman, V. 1984, 'Special Design Requirements: A Comparison of IS: 456-1978 with ACI 318-77', *Journal of the Institution of Engineers, Civil Engineering Division*, Vol. 65, pp. 76–81.
- Kang, T. H.-K., S.-S. Ha, and D.-U. Choi 2010, 'Bar Pullout Tests and Seismic Tests of Small-headed Bars in Beam-column Joints', *ACI Structural Journal*, Vol. 107, No. 1, pp. 32–42.
- Leonhardt, F. and K.-T. Teichen 1972, *Druck-Stösse von Bewehrungsstößen*, Deutscher Ausschuss für Stahlbeton Bulletin No. 222, Wilhelm Ernst und Sohn, Berlin, pp. 1–53.
- Leonhardt, F. and E. Mönning 1977, *Vorlesungen über Massivbau, Dritter Teil-Grundlagen zum Bewehren im Stahlbetonbau*, 3rd edition, Springer-Verlag, Berlin, p. 246.
- Lutz, L.A. and P. Gergely 1967, 'Mechanics of Bond and Slip of Deformed Bars in Concrete', *ACI Journal, Proceedings*, Vol. 64, No. 11, pp. 711–21, and Discussions, Vol. 65, pp. 412–4.
- Lutz, L.A., P. Gergely, and G. Winter 1966, *The Mechanics of Bond and Slip of Deformed Reinforcing Bars in Concrete*, Report No. 324, Department of Structural Engineering, Cornell University, Ithaca, pp. 711–21.
- Marques, J.L.G. and J.O. Jirsa 1975, 'A Study of Hooked Bar Anchorages in Beam-column Joints', *ACI Structural Journal*, Vol. 72, No. 5, pp. 198–209.
- Miller, G. G., J.L. Kepler, and D. Darwin 2003, 'Effect of Epoxy Coating Thickness on Bond Strength of Reinforcing Bars', *ACI Structural Journal*, Vol. 100, No. 3, pp. 314–20.
- Orangun, C.O., J.O. Jirsa, and J.E. Breen 1977, 'A Reevaluation of Test Data on Development Length and Splices', *ACI Journal, Proceedings*, Vol. 74, No. 3, pp. 114–22.
- Pfister, J.F. and A.H. Mattock 1963, 'High-strength Bars as Concrete Reinforcement, Part 5: Lapped Splices in Concentrically Loaded Columns', *Journal, PCA Research and Development Laboratories*, Vol. 5, No. 2, pp. 27–40.
- Prakash Rao, D.S. 1991, 'Detailing of Reinforced Concrete Structures', *Proceedings of the IABSE Conference on Structural Concrete*, Stuttgart, pp. 819–24.
- Rashid, M.A. 2004, 'Consideration in Using HSC in RC Flexural Members: A Review', *The Indian Concrete Journal*, Vol. 78, No. 5, pp. 20–8.
- Rehm, G. 1968, *The Basic Principles of the Bond between Steel and Concrete*, Translation No. 134, Cement and Concrete Association, London, p. 66.
- Rehm, G. 1969, *Kriterien zur Beurteilung von Bewehrungsstößen mit hochwertigem Verbund (Criteria for the Evaluation of High Bond Reinforcing Bars)*, Stahlbetonbau-Berichte aus Forschung und Praxis-Hubert Rüsche gewidmet, Berlin, pp.79–85.
- Rehm, G. and R. Eligehausen 1979, 'Bond of Ribbed Bars under High-cycle Repeated Loads', *ACI Journal, Proceedings*, Vol. 76, No. 2, pp. 297–310.
- Selby, R.G., F.J. Vecchio, and M.P. Collins 1997, 'The Failure of An Offshore Platform', *Concrete International, ACI*, Vol. 19, No. 8, pp. 28–35.
- Seliem, H.M., A. Hosny, S. Rizkalla, P. Zia, M. Briggs, S. Miller, D. Darwin, J. Browning, G.M. Glass, K. Hoyt, K. Donnelly, and J.O. Jirsa 2009, 'Bond Characteristics of ASTM A 1035 Steel Reinforcing Bars', *ACI Structural Journal*, Vol. 106, No. 4, pp. 530–7.
- SP:34-1984 1987, *Handbook on Concrete Reinforcement and Detailing*, Special Publication, Bureau of Indian Standards, New Delhi.
- Srinivasan, D. 1975, 'Case Study of a Building Failure', *The Indian Concrete Journal*, Vol. 49, No. 6, pp.164–5, 178.
- Steuck, K.P., M.O. Eberhard, and J.F. Stanton 2009, 'Anchorage of Large Diameter Reinforcing Bars in Ducts', *ACI Structural Journal*, Vol. 106, No. 4, pp. 507–13.
- Subramanian, N. 2005, 'Development Length of Reinforcing Bars: Need to Revise Indian Codal Provisions', *The Indian Concrete Journal*, Vol. 79, No. 8, pp. 39–46.
- Stöckl, S. 1972, 'Übergreifungsstöße von zugbeanspruchten bewehrungsstäben (Lap Splicing of Reinforcing Bars Subject to Tension)', *Beton-und Stahlbetonbau*, Vol. 10, pp. 229–34.
- Tepfers, R. 1973, *A Theory of Bond Applied to Overlapped Tensile Reinforcement Splices for Deformed Bars*, Chalmers University of Technology, Publication No. 73:2, Göteborg.
- Thompson, M.K., J.O. Jirsa, J.E. Breen, and R.E. Klingner 2002, *Anchorage Behavior of Headed Reinforcement: Literature Review*, Research Report FHWA/TX-0-1855-1, Center for Transportation Research, The University of Texas at Austin, p. 102.
- Thompson, M.K., J.O. Jirsa, and J.E. Breen 2006a, 'CCT Nodes Anchored by Headed Bars, Part 2: Capacity of Nodes', *ACI Structural Journal*, Vol. 103, No. 1, pp. 65–73.
- Thompson, M.K., A. Ledesma, J.O. Jirsa, and J.E. Breen 2006b, 'Lap Splices Anchored by Headed Bars', *ACI Structural Journal*, Vol. 103, No. 2, pp. 271–9.
- Thompson, M.K., J.O. Jirsa, and J.E. Breen 2006c, 'Behavior and Capacity of Headed Reinforcement', *ACI Structural Journal*, Vol. 103, No. 4, pp. 522–530.
- Treece, R.A. and J.O. Jirsa 1989, 'Bond Strength of Epoxy-coated Reinforcing Bars', *ACI Materials Journal*, Vol. 86, No. 2, pp. 167–74.
- Wang, H. 2009, 'An Analytical Study of Bond Strength Associated with Splitting of Concrete Cover', *Engineering Structures*, Vol. 31, No. 4, pp. 968–75.
- Wight, J.K. and J.G. MacGregor 2009, *Reinforced Concrete: Mechanics and Design*, Pearson-Prentice Hall, Upper Saddle River, NJ, p. 1112.
- Yerlici, V.A. and T. Özturan 2000, 'Factors Affecting Anchorage Bond Strength in High-performance Concrete', *ACI Structural Journal*, Vol. 97, No. 3, pp. 499–507.
- Zuo, J. and D. Darwin 2000, 'Splice Strength of Conventional and High Relative Rib Area Bars in Normal and High-strength Concrete', *ACI Structural Journal*, Vol. 97, No. 4, pp. 630–41.
- Zsutty, T. 1985, 'Empirical Study of Bar Development Behavior', *Journal of Structural Engineering*, ASCE, Vol. 111, No. 1, pp. 205–219.

DESIGN FOR TORSION

8.1 INTRODUCTION

Structural concrete members are often subjected to torsional moments in addition to bending moments and axial or shear forces. Torsion develops in structural members as a result of asymmetrical loading, member geometry, or structural framing. In complex structures such as helical stairways, curved beams, and eccentrically loaded box girders, torsional effects dominate the structural behaviour. Earthquakes can cause dangerous torsional forces, especially in asymmetrical structures where the centres of mass and rigidity do not coincide. Torsional moment tends to twist the structural member around its longitudinal axis, inducing shear stresses. However, structural members are rarely subjected to torsional moment alone. Usually, torsional moments act concurrently with bending moment (B.M.) and shear or axial forces.

Earlier structural codes were silent regarding torsion design. Torsion was considered to be a secondary effect and covered by the factor of safety. Improved methods of analysis and new design approaches resulted in the better understanding of the behaviour of reinforced concrete (RC) members subjected to torsion. Research conducted by several researchers, notably by Hsu and his associates at the University of Houston, USA, Collins and his associates in Canada, and Pandit and his associates in India, resulted in better understanding of the behaviour of and design and detailing for torsion. An excellent overview of torsion as applicable to RC design is provided by Zia (1968), Tamberg and Mikluchin (1973), Collins and Mitchell (1980), Warwaruk (1981), Hsu (1984), Pandit and Gupta (1991), and Hsu and Mo (2010).

The behaviour under torsion is discussed in this chapter along with the design and detailing for torsion. It has to be noted that unlike shear, which is a two-dimensional (2D) problem, torsion is a three-dimensional (3D) problem, involving both the shear problem of membrane elements and the warping of the cross section. Although the diagonal tension stresses produced

by torsion are very similar to those caused by shear, they occur on all the faces of the member; hence, they have to be added to the stresses caused by the shear on one face whereas subtracted from the stresses on the other face. As the torsional cracks spiral around the beams, it is necessary to provide closed stirrups as well as additional longitudinal reinforcement, especially at the corners of the faces of the beams.

As the Indian code provisions on torsion are not precise, the ACI code provisions are also provided. Interaction between torsion, bending moment, and shear force (S.F.) is also discussed. The effects of torsion and design for various cross sections, such as rectangular, T-, and box sections, are also considered. Thin, open C-, and U-shaped sections subject to torsion suffer distortions (referred to as *Vlasov torsion*) and are not covered in this chapter.

8.2 EQUILIBRIUM AND COMPATIBILITY TORSION

While considering torsion in RC structures, it is useful to distinguish between primary and secondary torsions (see Fig. 8.1). *Primary torsion*, also called *equilibrium torsion* or *statically determinate torsion*, exists when the external load has no alternative load path but must be supported by torsion (see Figs 8.1a and b). For such cases, the torsion required to maintain static equilibrium can be uniquely determined from statics alone. For example, in the cantilevered slab shown in Fig. 8.1(a), the loads applied to the slab surface cause twisting moments T to act along the length of the supporting beam. These are equilibrated by the resisting torque T provided at the columns. The structure will collapse if the beam is not designed for the applied torsional moments. Other examples of primary torsion may be found in eccentrically loaded box girders (Fig. 8.1c), edge beams of concrete shell roofs, ring beams at the bottom of circular water tanks, as shown in Fig. 8.1(e) (particularly the Intz type), continuous curved bridge girders (Fig. 8.2a), and helicoidal stairway slabs (Fig. 8.2b).

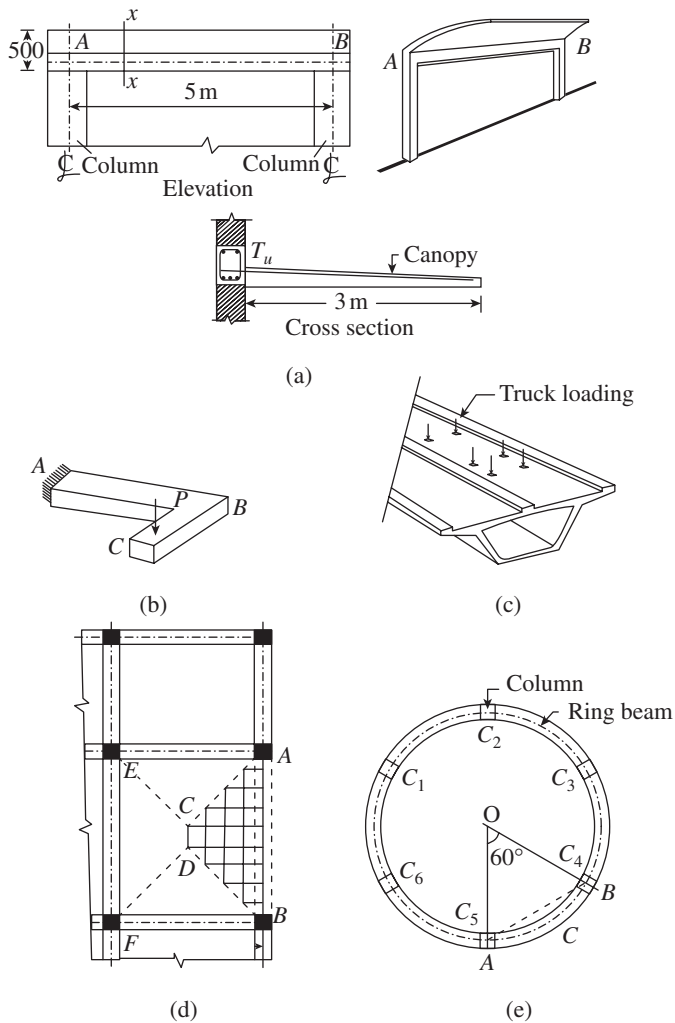
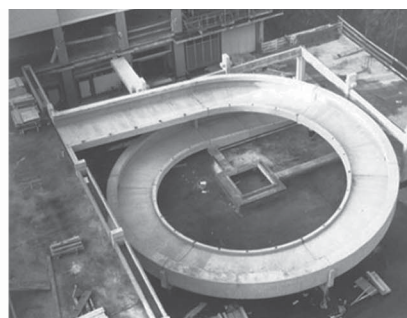


FIG. 8.1 Structural elements subjected to torsion (a) Beams supporting cantilevered canopy slabs (b) Cantilever beam supporting eccentric load (c) Box-girder bridges (d) Edge beams in framed structures (e) Circular ring beams



(a)



(b)

FIG. 8.2 Structures subjected to torsion (a) Curved continuous beams or box girders in Bandra–Worli sea link bridge (b) Helicoidal girders

Sources: (a) https://en.wikipedia.org/wiki/File:Worli_skyline_with_BSWL.jpg

(b) Beguin 2007, reprinted with permission from Concrete International, ACI

requirements of continuity, that is, due to compatibility of deformation between the adjacent elements of a structure (see Fig. 8.1d). In this case, the torsional moments cannot be found based on static equilibrium alone. The beams in a grid structure also have compatibility torsion. The torsion acting on the members can be found using a 3D analysis program and by specifying the torsional stiffness to the members. The explanatory handbook SP 24:1983, based on experimental results, suggests that torsional rigidity (GC) may be calculated by assuming the modulus of rigidity G as $0.4E_c$ and the torsional stiffness C equal to half of the St Venant value calculated for the plain concrete section (see also Section 8.3). In general, G is defined as follows:

$$G = \frac{E}{2(1 + \nu)} \quad (8.1)$$

where E is the Young's modulus and ν is the Poisson's ratio. Poisson's ratio for concrete is frequently taken as 0.15–0.25. The suggested value of $G = 0.4E_c$ is obtained by taking ν as 0.25.

Disregard to compatibility torsion in the design will often lead to extensive cracking, but generally will not cause collapse. An internal readjustment of forces will take place and an alternative equilibrium of forces will be found. For example, edge or spandrel beams built monolithically with the floor slab are subjected to torsional moment resulting from the restraining negative bending moment at the exterior end of the slab. The restraining moment is proportional to the torsional stiffness of the spandrel beam (Fig. 8.1d).

The amount of torsion in a member depends on its torsional stiffness in relation to the torsional stiffness of the interconnecting members. If the spandrel beam is torsionally stiff and suitably reinforced, and if the columns can provide the necessary resisting torque, then the slab moments will

approximate those of a rigid exterior support. However, if the beam has little torsional stiffness and inadequate torsional reinforcement, the beam will twist and crack to further reduce its torsional stiffness, and the slab moments will approximate those for a hinged edge. If the slab is designed to resist the altered moment diagram, collapse will not occur. However, when the cracks are excessive, the structure may become unserviceable.

The torsional stiffness, K_t , of a member is defined as the ratio of torsional moment to the angle of

twist (or rotation), ϕ . Thus, if ϕ is the total angle of twist in a length L , we get

twist (or rotation), ϕ . Thus, if ϕ is the total angle of twist in a length L , we get

$$K_t = \frac{T}{\phi} = \frac{GC}{L} \tag{8.2a}$$

From this, the angle of twist can be written as

$$\phi = \frac{TL}{GC} \tag{8.2b}$$

The ratio of bending stiffness to torsional stiffness may now be expressed as

$$\frac{EI}{L} : \frac{GC}{L}$$

Considering a rectangular section with $D = 2b$, the value of I is about three times that of C (see Section 8.3). Using $G = 0.4E_c$, we find that the bending stiffness of a beam is approximately 7.5 times the torsional stiffness. This shows that the members will attract more bending moment than torsion.

8.2.1 Torsion in Curved Beams

As discussed earlier, curved beams (e.g., ring beams under circular water tanks supported by columns) are subjected to bending and torsion. The magnitude and distribution of the bending and torsional moments along the circumference are influenced by the number of supports and the radius of the curved beam. A typical curved beam circular in plan and supported by eight columns is shown in Fig. 8.3(a). By considering Fig. 8.3(b), the maximum positive and negative bending moments and the torsional moments can be expressed in the following form (Varyani and Radhaji 2005):

$$\text{Negative maximum bending moment} = K_1WR^2$$

$$\text{Positive maximum bending moment} = K_2WR^2$$

$$\text{Maximum torsional moment} = K_3WR^2$$

where W is the total load on the curved beam $= 2\pi R w$, w is the uniformly distributed load per unit length of beam in kN/m, R is the radius of the circular beam, K_1 , K_2 , and K_3 are the moment coefficients, as given in Table 8.1, and θ is the angle subtended at the centre by the ends of the beam.

TABLE 8.1 Moment coefficients in circular beams supported on columns

Number of Columns	θ (Degrees)	Maximum Shear at Support	Negative Bending Moment at Support, K_1	Positive Bending Moment at Centre of Spans, K_2	Maximum Torsion, K_3	Angular Distance for Maximum Torsion, β
4	90	$W/8$	-0.2023	0.1106	0.0333	$19^\circ 21'$
6	60	$W/12$	-0.0930	0.0471	0.0094	$12^\circ 44'$
8	45	$W/16$	-0.0522	0.0264	0.0038	$9^\circ 33'$
10	36	$W/20$	-0.0327	0.0201	0.0025	$7^\circ 30'$
12	30	$W/24$	-0.0232	0.0119	0.0013	$6^\circ 21'$
16	22.5	$W/32$	-0.0129	0.0065	0.0005	$4^\circ 45'$
20	18	$W/40$	-0.0082	0.0041	0.0002	$3^\circ 48'$
24	15	$W/48$	-0.0057	0.0028	0.0001	$3^\circ 10'$

The critical sections for design are the support sections subjected to maximum negative and positive bending moments and the

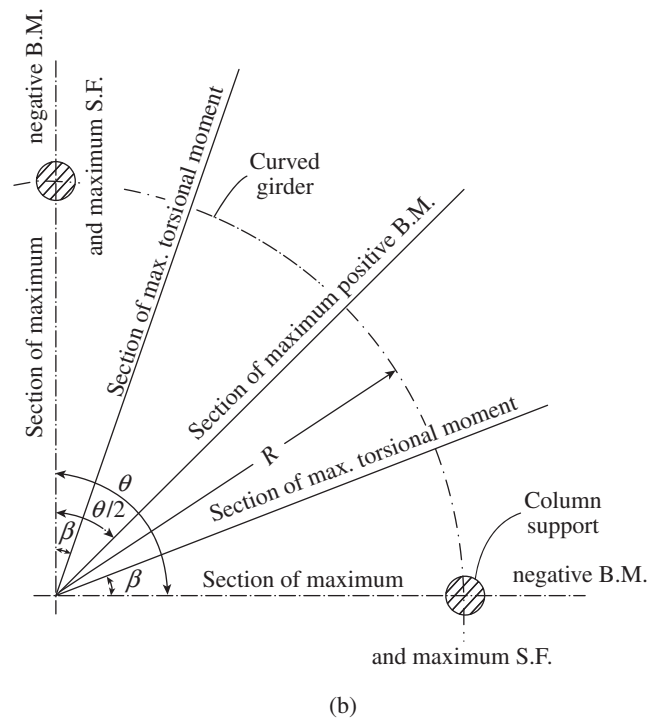
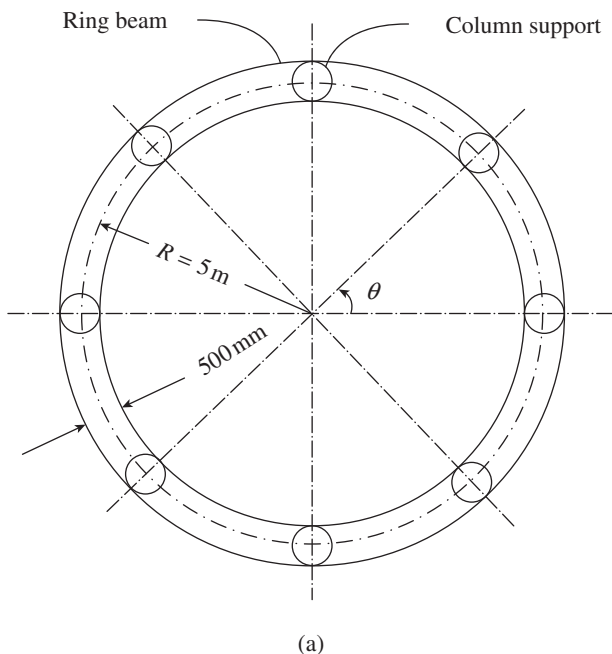


FIG. 8.3 Beams curved in plan (a) Ring beam supported on eight columns (b) Position of maximum moments

sections subjected to maximum torsion associated with some shear force; at this section, the bending moment will be zero. Hence, it has to be designed for combined torsion and shear.

It has to be noted that the values given in Table 8.1 should not be used for beams with single circular span with fixed ends (Varyani and Radhaji 2005). Tables and equations for a variety of end conditions and load cases may be found in Young and Budynas (2002).

8.2.2 Semicircular Beams Supported on Three Columns

The magnitude and position of maximum positive and negative bending moments and torsional moments in a semicircular beam supported on three equally spaced supports are as follows:

Maximum positive bending moment
 = $0.152wR^2$ acting at a section $29^\circ 44'$ from the end columns

Maximum negative bending moment
 = $-0.429wR^2$ acting at the central support

Maximum positive bending moment
 = $0.103wR^2$ acting at a section $59^\circ 29'$ from the end columns

8.3 BEHAVIOUR OF BEAMS IN TORSION

In this section, a brief introduction is given about torsional analysis, which is followed by the behaviour of plain concrete members and RC members.

8.3.1 Torsional Analysis

The analysis for torsion may be either in the elastic range of behaviour or in the plastic range. We shall consider both types of analysis in this section.

Elastic Analysis

Navier was the first to develop, in 1826, a theory for torsion of homogeneous elastic members with circular cross sections. This theory was based on the three principles of mechanics of materials, namely equilibrium, compatibility conditions, and Hooke's law. St Venant, in 1856, recognized that Navier's method using polar moment of inertia could not be applied to the rectangular cross sections. Hence, he extended the theory to take into account the warping displacements of the rectangular cross sections. This theory applicable to homogeneous material such as steel of prismatic circular, non-circular, and thin-walled cross sections is described in any mechanics of a materials book (e.g., Timoshenko and Goodier 1970). From this theory, it may be observed that torsion causes shear stresses. In non-circular sections, there is considerable warping of the cross section and the plane sections do not remain plane, as shown in Fig. 8.4.

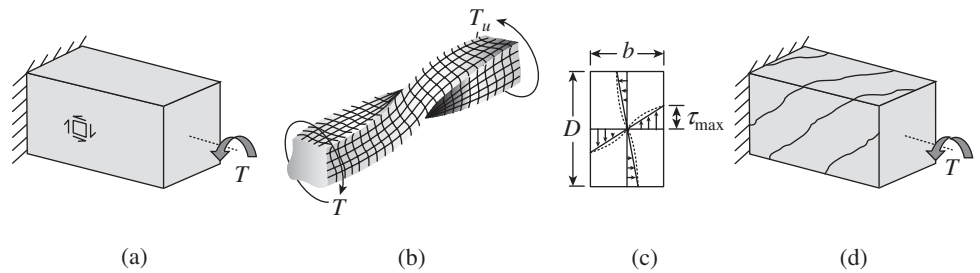


FIG. 8.4 Elastic torsional behaviour of rectangular beams (a) Beam subjected to torsion (b) Warping of the cross section (c) Torsional stress (d) Crack pattern

The elastic torsional stress distribution for rectangular beams is as shown in Fig. 8.4(c), with the maximum shear stress, $\tau_{t,max}$, occurring on the outside face of the rectangular section at the mid-point of each of the wider side, with a value

$$\tau_{t,max} = \frac{T}{\alpha_2 b^2 D} \quad (8.3a)$$

and the torsional constant, C , has a value

$$C = \beta_2 b^3 D \quad (8.4a)$$

where T is the torque or twisting moment, b and D are the dimensions of the shorter and wider faces of the rectangle, respectively, and α_2 and β_2 are constants that vary depending on the value of D/b , as shown in Table 8.2.

TABLE 8.2 Values of constants C and K

D/b	Value of		D/b	Value of	
	α_2	β_2		α_2	β_2
1.0	0.208	0.141	3.0	0.267	0.263
1.2	0.219	0.166	4.0	0.282	0.281
1.5	0.231	0.196	5.0	0.291	0.291
2.0	0.246	0.229	10.0	0.313	0.313
2.5	0.258	0.249	∞	0.333	0.333

The torsional constant C of T-, L-, or I-sections may be approximated by (Bach's formula proposed in 1911)

$$C = \sum \frac{x^3 y}{3} \quad (8.4b)$$

where x and y are the side and thickness, respectively, of each of the component rectangles into which the section may be divided.

The following more exact expression for torsional constant, C , was derived by Timoshenko and Goodier (1970) for sections composed of rectangular elements having $D/b < 10$:

$$C = \sum \left(\frac{x^3 y}{3} \right) \left(1 - 0.63 \frac{x}{y} \right) \quad (8.4c)$$

Because of the advantageous distribution of shear stresses, thin-walled tubular sections are more efficient in resisting torsion. When the wall thickness, t , is small relative to the

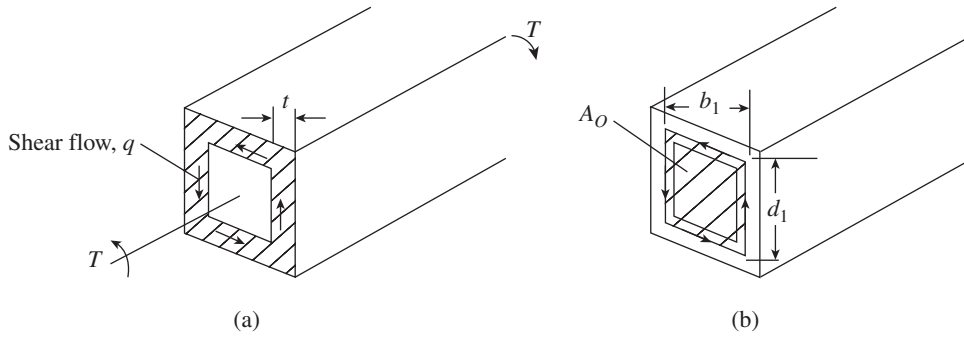


FIG. 8.5 Torsion in a thin-walled rectangular tube (a) Thin-walled tube (b) Area enclosed by shear flow path

overall dimensions of the section, a uniform *shear flow* q across the thickness can be assumed, and from Timoshenko and Goodier (1970), we get (see also Fig. 8.5).

$$q = \frac{T}{2A_o} \tag{8.5}$$

where A_o is the area enclosed by the centre line of the thickness (see Fig. 8.5b) and later on referred to as the *lever arm area* by Hsu (1988). Equation (8.5) was first derived by Bredt in 1896. The concept of shear flow around the thin-walled tube is useful when the role of reinforcement in torsion is considered in Section 8.5.

In the case of compatibility torsion, if the spandrel beam as shown in Fig. 8.1(d) is *uncracked*, its torsional stiffness $GCIL$ computed as given, and a 3D analysis performed, the torsional moment carried by it may be very large. As the beam cracks, the torsional stiffness reduces considerably and the beam will rotate, reducing the torsional moment carried by it. It has to be noted that the stiffness needs to be specified in the 3D analysis to determine the torsional moment. Cracked section stiffness requires the knowledge of the steel reinforcement. To solve this problem, Lampert (1973) and Collins and Lampert (1973) proposed expressions for torsional rigidity of cracked sections based on their studies. As mentioned in Section 8.2, the explanatory handbook SP 24:1983 suggests adopting a C value equal to half of the St Venant value calculated for the plain concrete section.

Alternatively, Collins and Lampert (1973) also suggest carrying out the analysis based on zero torsional stiffness; such an analysis and the subsequent design based on flexure and shear, neglecting torsion, were found to produce satisfactory design, similar to the analysis using uncracked stiffness and the subsequent design based on flexure, shear, and torsion. It was found that the added reinforcement increases the torsional moment in the member, but had little effect on the twist. The purpose of the torsional reinforcement in this case would be to provide more ductility and distribute the cracks caused by the torsional moments. Clause 41.1 of IS 456 reflects this philosophy.

Plastic Analysis

It has to be noted that the value of stress to be used in the limit states design should be based on plastic analysis, even though the assumption of fully plasticized section is not justifiable for materials like concrete. In plastic analysis, a uniform shear stress over the cross section is assumed, whereas the elastic analysis shows a non-linear stress distribution, as shown in Fig. 8.4(c). The ultimate torque can now be easily obtained by using the *sand heap*

analogy, which is based on the following principles [Prandtl's *soap-film or membrane analogy* applicable to elastic behaviour was extended by Nadai in 1931 to develop the sand heap analogy for plastic or ultimate torsion (Nadai 1950)]:

1. Ultimate torque = Twice the volume of sand heap
2. Slope of sand heap = $2 \times$ constant plastic shear stress

Let H be the height of the sand heap (see Fig. 8.6a).

$$\text{Volume of the sand heap} = \frac{1}{3}b^2H + \frac{1}{2}b(D-b)H = bH \left(\frac{b}{3} + \frac{D-b}{2} \right) = \frac{bH}{2} \left(D - \frac{b}{3} \right)$$

$$\text{Slope, } \theta = \frac{H}{(b/2)} = \tau_{t,\max}; \quad H = \frac{\tau_{t,\max}b}{2}$$

$$\text{Hence, volume} = \frac{\tau_{t,\max}b^2}{4} \left(D - \frac{b}{3} \right)$$

$$\text{or } T_{u,cr} = \frac{\tau_{t,\max}b^2}{2} \left(D - \frac{b}{3} \right) \tag{8.6}$$

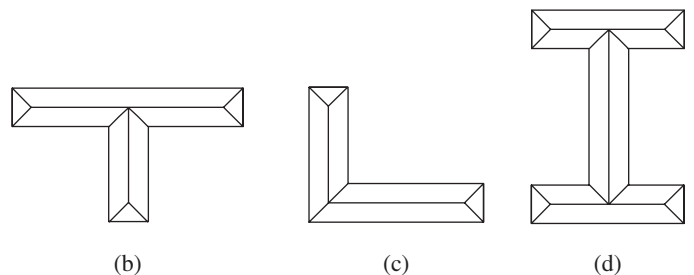
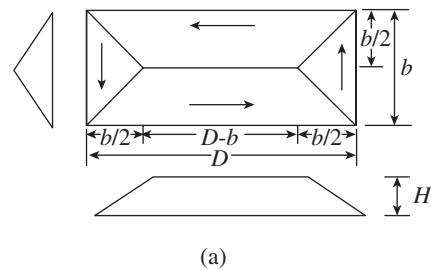


FIG. 8.6 Sand heap analogy for different sections (a) Rectangle (b) T-section (c) L-section (d) I-section

The ultimate torque of T-, L-, or I-sections can be obtained in a similar manner by dividing them into component rectangles (see Fig. 8.6). The test results indicate an ultimate torsional stress, $\tau_{t,max}$, value of about $0.2\sqrt{f_{ck}}$ to be used with Eq. (8.6).

As the torque–twist relationship is approximately linear up to torsional cracking (as shown in Section 8.3.3), the torsional shear stress τ_t corresponding to any factored torque $T_u \leq T_{u,cr}$ for rectangular sections may be obtained from Eq. (8.6) as

$$\tau_t = \frac{2T_u}{b^2(D - b/3)} \quad (8.7a)$$

In IS 456, this expression is extended to RC sections with effective depth d by rewriting Eq. (8.7a) to the form

$$\tau_t = \frac{2T_u}{b^2 dk}, \text{ with } k = [(D/d) - b/(3d)] \quad (8.7b)$$

For practical beams, the D/d ratios may range from 1.05 to 1.20 and b/d values range from 2 to 3, with k ranging from 0.75 to 1.1. Considering an average value and also providing a correction factor for the non-realistic full plastification of materials like concrete, Eq. (8.7a) may be reduced to the following form:

$$\tau_t = \frac{1.6(T_u/b)}{bd} \quad (8.7c)$$

Thus, the shear stress due to torsion is also brought to a similar form to that of shear stress ($\tau_v = V_u/bd$), so that the equivalent shear may be calculated as per Clause 41.3.1 of the code as

$$V_e = V_u + 1.6 \frac{T_u}{b} \quad (8.8)$$

where V_e is the equivalent shear force including torsion in N, V_u is the factored shear force due to external loads excluding torsion in N, T_u is the factored torsional moment due to external loads in Nmm, and b and d are the breadth and effective depth, respectively, of the beam in mm.

8.3.2 Behaviour of Plain Concrete Members

The theories of Navier, St Venant, Bredt, and Bach are applicable to the RC beams before cracking. They also laid

the foundation for the development of theories to predict the behaviour of RC members subjected to torsion after cracking.

When a rectangular concrete beam is subjected to pure torsion, a state of pure shear develops at the top and side faces of the beam, with direct tensile and compressive stresses along the diagonal directions, similar to the beam subjected to shear. The principal tensile and compressive stress trajectories form in orthogonal directions at 45° to the axis of the beam. When the principal tensile stress reaches the value of tensile strength of concrete f_t , cracks form at the maximum stressed location centre of the beam (at the middle of wider face). These inclined cracks tend to extend around the member in a spiral fashion, as shown in Figs 8.7(b) and 8.4(d). Once the crack is formed, the crack will penetrate inwards from the outer surface of the beam, due to the brittle nature of the concrete and will lead to a sudden failure of the beam unless torsional reinforcements are provided.

The *cracking torque*, T_{cr} , provides an idea about the ultimate torsional resistance of plain concrete beams. In general, it can be computed by equating the theoretical nominal maximum torsional shear stress to the tensile strength of concrete (Clause 11.5.1 in the ACI code assumes that cracking due to torsion occurs when the principal tensile stress reaches $0.3\lambda\sqrt{f_{ck}}$). Different expressions for T_{cr} can be derived based on different methods (see Section 8.4). IS 456 has adopted the design shear strength of concrete τ_c (Table 19 of code) for the simplicity of combining the effects of torsional shear and flexural shear.

8.3.3 Behaviour of Beams with Torsional Reinforcement

Prior to cracking, the behaviour is similar to plain concrete beams; the torsional moment is resisted by internal shear stresses. When the diagonal tension exceeds the tensile strength of the concrete, diagonal cracking occurs, and as described earlier, the cracks spiral around the perimeter of the member. Simultaneously, torsional stiffness of the beam drops significantly. Upon further torsional loading, excessive twisting deformations lead to the spalling of the concrete cover over the transverse reinforcement and the beam eventually fails. Hence, transverse reinforcement must be properly anchored with 135° hooks.

The torsional reinforcements come into play only after the cracks form due to diagonal tensile stresses. As the cracks spiral around the beam, the best way to provide reinforcement is to have them in the form of spirals to resist the tensile stresses. However, it is impractical to provide such reinforcement. Hence, usually torsional reinforcement is provided in the form of a combination of

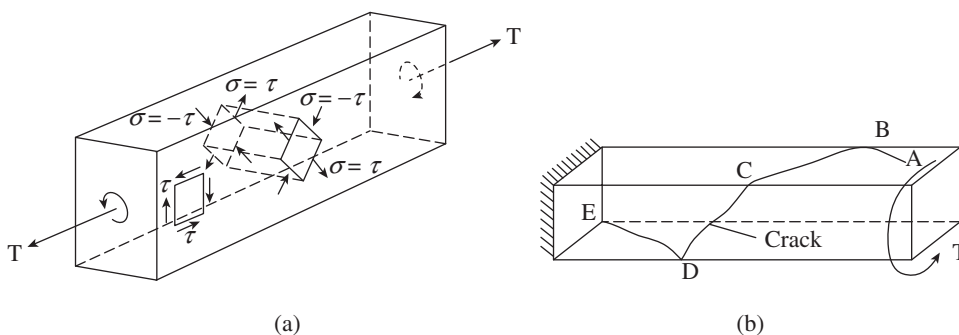


FIG. 8.7 Stresses caused by torsion (a) Shear and principal stresses (b) Crack pattern

longitudinal bars at the corners of the beam and stirrups placed perpendicular to the beam axis. Since the cracks spiral around the beam, four-sided closed stirrups are required. It has to be noted that the longitudinal bars are also required to resist the bending moments and the stirrups to resist the shear forces.

The torque–twist behaviour of a typical torsionally reinforced rectangular concrete beam is shown in Fig. 8.8. It is seen that the behaviour is similar to that of a plain concrete beam until the formation of the first crack (corresponding to the cracking torque $M_{t,cr}$). After cracking, the strength and behaviour depend on the amount of torsional reinforcement provided. It should be noted that the addition of longitudinal reinforcement without stirrups has little effect on the strength of the beam subjected to torsion, as it resists only the longitudinal component of the diagonal tension forces.

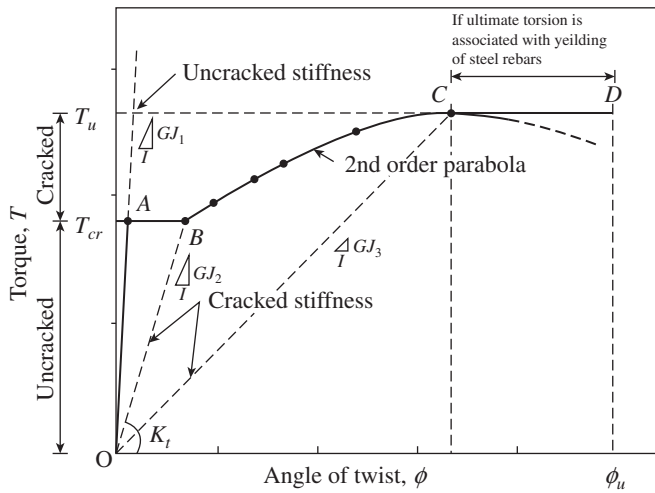


FIG. 8.8 Typical torque–twist curve for an RC rectangular beam

Once the crack is formed, the angle of twist increases without any increase in the external torque, as the forces are redistributed to the torsional reinforcement. Then, the cracking extends to the central core of the member, rendering the central core ineffective. After this, the failure may take several forms, such as (a) the yielding of longitudinal reinforcement or the stirrups or yielding of both at the same time and (b) the crushing of concrete between the inclined cracks due to principal compression before the yielding of steel (this happens in beams that are over-reinforced in torsion). Ductile behaviour is achieved only when both the longitudinal and transverse reinforcements yield prior to the crushing of concrete.

8.4 THEORETICAL MODELS FOR TORSION

As mentioned in Chapter 6, the first theory for the shear design of structural concrete using a 45° plane truss model based on the *struts-and-ties concept* was developed by Ritter in 1899 and later improved by Mörsch in 1902. Rausch (1929) extended the 2D plane truss model to a 3D truss model and developed a

theory for the torsion of RC members. In Rausch's model, the member was idealized as a *space truss* formed by connecting a series of component plane trusses capable of resisting the shear action. The circulatory shear stresses, developed in the cross section of the space truss, form an internal torsional moment capable of resisting the applied torsional moment. However, the prediction based on this truss model consistently overestimated the shear and torsional strengths of the tested specimens and was found to be unconservative by more than 30 per cent for under-reinforced beams (Hsu 1968a; 1968b). This model treated the concrete struts and steel ties as line elements without assigning any cross-sectional dimensions. Hence, this model did not consider the beams as continuous material and the calculation of stresses and strains in the beam was not possible.

Since the late 1960s, the truss model theory for torsion has undergone the following four major developments: (a) Lampert and Thürlimann (1968; 1969) introduced the *variable angle truss model* and discovered that the diagonal concrete struts are subjected to bending in addition to compression. (b) Collins (1973) derived compatibility equations using which the angle of the diagonal concrete struts could be determined. Mitchell and Collins (1974) developed a *space truss model* with concrete cover spalling to determine the thickness of the shear flow zone. (c) Robinson and Demorieux (1972) discovered the softening phenomenon in the concrete struts. This fact was quantified by Vecchio and Collins (1981) using a softened coefficient. (d) Combining the equilibrium, compatibility, and softened stress–strain relationships, Hsu and Mo (1985) developed a *softened truss model* to determine the shear and torsional behaviour of the RC members throughout the postcrack loading history up to the peak point.

In addition, the following models have also been developed: (a) the *softened membrane model* (the softened truss and softened membrane models consider the non-linear theory of shear and torsion and are used in finite element computer software); (b) the *modified compression field theory* (MCFT); and (c) the *cyclic softened membrane model*, for predicting the behaviour of membrane elements under dynamic loads like earthquakes. More details about these developments may be found in Hsu and Mo (2010) and Jeng and Hsu (2009). Non-linear finite element programs called *Simulation of Concrete Structures* on the platform of open domain *OpenSees* and *Membrane-2012* have also been developed at the University of Houston and the University of Toronto, respectively, and are available for download on the Internet (Bentz 2010). The development of non-linear theory for shear and torsion was made possible by the installation of the multi-channel servo-controlled Universal Panel Tester and the Membrane Element Tester at the University of Houston and the University of Toronto, respectively, which enabled the researchers to perform strain-controlled tests (Hsu and Mo 2010).

8.5 PLASTIC SPACE TRUSS MODEL

The design theory called the thin-walled tube or plastic space truss model was developed by Lampert and Thürlimann (1971) and Lampert and Collins (1972) and was adopted by the ACI code in 1995 and by several European design recommendations. This theory combines the thin-walled tube analogy with the plastic truss analogy for shear and leads to simpler calculations than the skew bending theory (Hsu 1997 and MacGregor and Ghoneim 1995).

8.5.1 Design Strength in Torsion

The test data (Hsu 1968b; Lampert and Thürlimann 1968) for solid and hollow beams suggests that once cracking has occurred, the concrete in the centre of the member has little effect on the torsional strength of the cross section and can be ignored. The beams can be considered to be equivalent tubular members. Hence, solid members can be considered as equivalent tubes.

The solid rectangular or square beams may be idealized as a thin-walled tube as shown in Fig. 8.9(a) and the applied torsion, T , is assumed to be resisted by a shear flow $q = T/(2A_o)$ acting around the centre line of the tube, where A_o is the area enclosed by the centre line of the thickness. This shear flow, q , occupies a zone called the *shear flow zone*, which has an equivalent thickness denoted by $t_o = A_{cp}/p_{cp}$, where A_{cp} and p_{cp}

are the area and perimeter of the full concrete cross section. This thickness is a variable determined from the equilibrium and compatibility conditions. It is not the same as the given wall thickness, t , of a hollow member.

This hollow trussed tube consists of closed stirrups forming transverse *tension tie members*, longitudinal bars in the corners of the stirrups that act as *tension chords*, and *concrete compression diagonals*, which spiral around the member between the torsional cracks at an angle θ (which can take load parallel to but *not* perpendicular to the torsional cracks), as shown in Fig. 8.9(b). This theory assumes that the concrete carries no tension and the reinforcement yields. After torsional cracking develops, the torsional resistance is provided mainly by a space truss consisting of closed stirrups, longitudinal bars, and compression diagonals, as shown in Fig. 8.9(c). Experiments have shown that the thickness of the walls of the imaginary tube, t_e , representing a solid member is large and is in the range of one-sixth to one-fourth of the minimum width of the rectangular beam.

8.5.2 Cracking Torque

For a tube wall of thickness t , the unit shear stress acting within the walls of the tube can be written using Eq. (8.5) as

$$\tau = \frac{T}{2A_o t} \quad (8.9)$$

where A_o is the area enclosed by the centre line of the thickness or the *lever arm area*. As shown in Fig. 8.7(a), the principal tensile stress $\sigma = \tau$. Thus, the concrete will crack when the tensile stress exceeds the tensile strength of concrete f_{cr} . It has to be noted that in this situation, concrete is under biaxial tension and compression. Hence, instead of taking the usual value of modulus of rupture of concrete (i.e., $f_{ct} = 0.7\sqrt{f_{ck}}$) for normal weight concrete, we may consider a conservative value of $f_{ct} = 0.3\sqrt{f_{ck}}$. Substituting this value for $f_{ct} = 0.3\sqrt{f_{ck}}$ in Eq. (8.9) and rearranging, we get

$$T_{cr} = 0.3\sqrt{f_{ck}}(2A_o t) \quad (8.10a)$$

As A_o represents the area enclosed by the shear flow path, it should be a fraction of the area enclosed by the outside perimeter of the full concrete cross section A_{cp} . As mentioned earlier, the thickness of the walls of

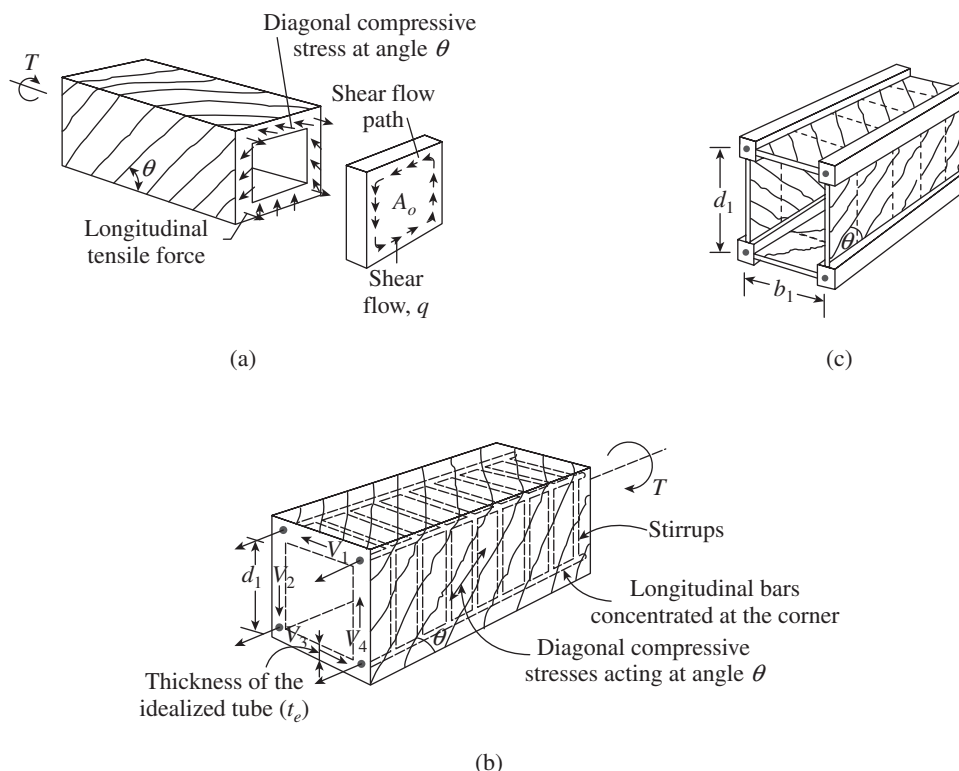


FIG. 8.9 Thin-walled tube or plastic space truss analogy (a) Thin-walled tube analogy (b) Space truss analogy (c) Idealized section of the truss

Source: MacGregor and Ghoneim 1995, reprinted with permission from ACI

the imaginary tube is in the range of one-sixth to one-fourth of the minimum width. Using the value of $t = b/4$, with a width to depth ratio of 0.5, results approximately in $A_o = (2/3)A_{cp}$. In the same way, the thickness t may be written in terms of A_{cp} and p_{cp} as $t = (3/4)A_{cp}/p_{cp}$, where p_{cp} is the perimeter of the full concrete cross section. Substituting these values in Eq. (8.10a), we get the equation given in Clause 11.5.1 of ACI 318-11 and suggested by Hsu and Burton (1974) as

$$T_{cr} = \phi 0.3 \lambda \sqrt{f_{ck}} \frac{A_{cp}^2}{P_{cp}} d \quad (8.10b)$$

where ϕ is the capacity reduction factor for torsion = 0.75 and λ is the factor for lightweight concrete (see Section 8.10).

If the member is subjected to compression or tension, Eq. (8.10b) is modified as

$$T_{cr} = \phi 0.3 \lambda \sqrt{f_{ck}} \frac{A_{cp}^2}{P_{cp}} \sqrt{1 + \frac{P_u}{0.3 \lambda A_g \sqrt{f_{ck}}}} \quad (8.10c)$$

For members with hollow sections, the T_{cr} values calculated using these expressions have to be multiplied by (A_g/A_{cp}) because tests of solid and hollow beams indicate that the cracking torque of a hollow section is approximately (A_g/A_{cp}) times the cracking torque of a solid section with the same outside dimensions (Hsu 1968a). In Eq. (8.10), T_{cr} is the cracking torque, A_{cp} is the area enclosed by the outside perimeter of the concrete cross section, p_{cp} is the outside perimeter of the concrete cross section, λ is the lightweight concrete factor, and P_u is the tension or compression force acting on the member; negative sign should be used for P_u in the case of tension. Experiments have shown that Eq. (8.10) gives a reasonable estimate of the cracking torque of solid RC members, regardless of the cross-sectional shape. For hollow sections, the value of T_{cr} given by Eq. (8.10a) should be reduced by the ratio A_g/A_{cp} , where A_g is the gross cross-sectional area of the concrete.

When there is combined shear and torsion, the interaction between cracking torsion and shear may be expressed as follows (see Section 8.6):

$$\left(\frac{T}{T_{cr}}\right)^2 + \left(\frac{V}{V_{cr}}\right)^2 = 1 \quad (8.11)$$

where V_{cr} is the inclined cracking shear in the absence of the torque and T_{cr} the cracking torsion in the absence of shear. If we substitute $T = 0.25T_{cr}$ in Eq. (8.11) and simplify, we get

$$V = 0.97V_{cr}$$

This calculation shows that the value of T up to $0.25T_{cr}$ will reduce the inclined cracking shear by only three per cent, which is negligible. Hence, Clause 11.5.1 of the ACI code

allows the designer to neglect torsion effects if the factored torsional moment T_u is less than 25 per cent of the cracking torque. Hence, the *threshold torsion*, T_{th} , below which torsion can be ignored in solid cross section is written as

$$T_{th} = \phi 0.075 \lambda \sqrt{f_{ck}} \frac{A_{cp}^2}{P_{cp}} \quad (8.12a)$$

where ϕ is the strength reduction factor = 0.75 for torsion and λ is the lightweight concrete factor.

When the member is subjected to an axial compression or tension P_u in addition to torsion,

$$T_{th} = \phi 0.075 \lambda \sqrt{f_{ck}} \frac{A_{cp}^2}{P_{cp}} \sqrt{1 + \frac{P_u}{0.3 \lambda A_g \sqrt{f_{ck}}}} \quad (8.12b)$$

It has to be noted that the interaction between torsional cracking and shear cracking for thin-walled hollow sections with large voids is represented by a straight-line relationship. For such a straight-line interaction, a torque of $0.25T_{cr}$ would cause a reduction of about 25 per cent in the inclined cracking shear. Hence, the cracking torque is multiplied by (A_g/A_{cp}) a second time to reflect the transition from the circular interaction between the inclined cracking loads in shear and torsion for solid members to the approximately linear interaction for thin-walled hollow sections. Thus, for thin-walled hollow sections, Eq. (8.12a) has to be modified as

$$T_{th} = \phi 0.075 \lambda \sqrt{f_{ck}} \frac{A_g^2}{P_{cp}} \quad (8.12c)$$

In the case of compatibility torsion, as present in statically indeterminate structures such as the one shown in Fig. 8.10, the design torsional moment can be reduced, because there will be redistribution of internal forces to other adjoining members after cracking (see also Section 8.2). In such a case, Clause 11.5.2.2 of the ACI code allows the designer to reduce the design T_u by an amount equal to the cracking torsion, as given by Eq. (8.10). (The replacement of A_{cp} with A_g , as in the calculation of the threshold torque for the hollow sections, is not applied here. Thus, the torque after redistribution is larger and hence more conservative.) If the calculated torsional moment is reduced as per Eq. (8.10), it is necessary to redistribute these bending moments to the adjoining members. This reduction is applicable in typical and regular framing conditions, as that shown in Fig. 8.10. When a structural layout imposes significant torsional rotations within a short length of the member, for example, when there is heavy torque loading located close to a stiff column, or when a column rotates in the reverse direction due to other loading, a more exact analysis should be used to determine the exact amount of torsion. It has to be noted that the IS code does not have such a provision of reducing the torsional moment in the case of indeterminate structures.

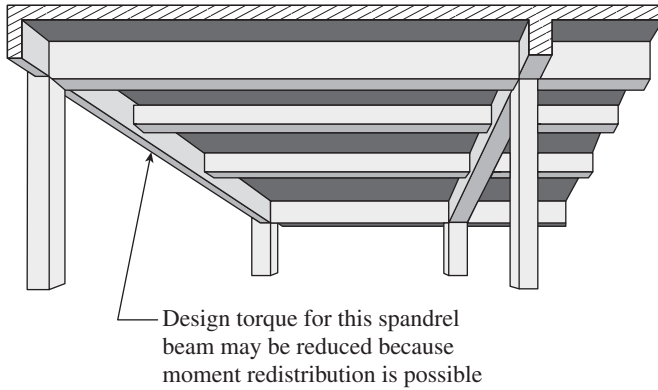


FIG. 8.10 Example of an indeterminate structure where design torque can be reduced

8.5.3 Consideration of Flanged Beams

For beams cast monolithically with a floor slab, Clause 11.5.1.1 of the ACI code states that the values A_{cp} and p_{cp} should be calculated by including the parts of adjacent slabs of the resulting T- or L-shaped beams. The width of the slab that should be included is shown shaded in Fig. 8.11 and should not exceed the projection of beam above or below the slab or four times the thickness of slab (NZS 3101 allows only $3d_f$), whichever is smaller. It has to be noted that Clause 41.1.1 of IS 456 suggests omitting the contribution of flanges, as it will be conservative to omit them (Kirk and Loveland 1972).

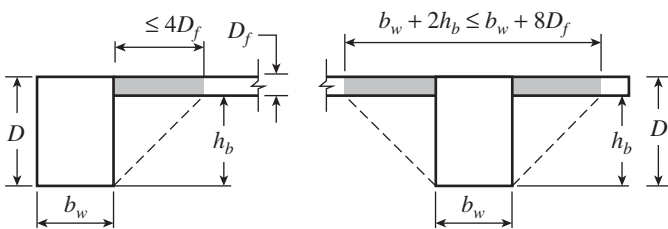


FIG. 8.11 Consideration in the case of flanged beams

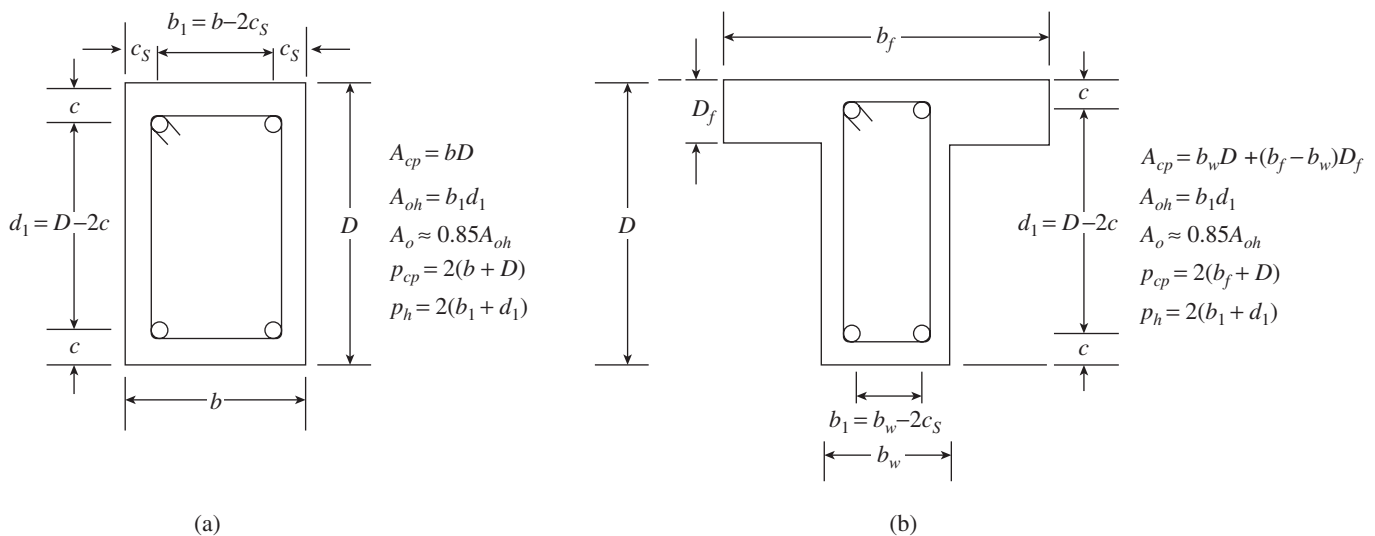


FIG. 8.12 Stirrups for torsion (a) Closed stirrup in rectangular beam (b) Closed stirrup in T-beam section

8.5.4 Area of Stirrups for Torsion

To find out the area of stirrups that is necessary to resist torsion, let us consider Figs 8.9(b) and 8.12(a). The height and width of the space truss are d_1 and b_1 , respectively, which are the distances between the centres of the longitudinal corner bars. The angle of the cracks is θ , which is initially about 45° but may become flatter at higher torques. (The angle θ may vary between 30° and 60° .) The ACI code Clause 11.5.3.6 suggests taking the angle as 45° , as this corresponds to the assumed angle in the derivation of the equation for designing stirrups for shear.

With reference to Fig. 8.9(b), the torsional resistance provided by the member with a rectangular cross section can be found to be the sum of the contributions of the shears in each of the four walls of the equivalent hollow tube. The shear flow or shear force per unit length of the perimeter of the tube obtained from Eq. (8.5) is

$$q = \frac{T}{2A_o}$$

The shear forces acting in the right- and left-hand vertical walls of the tube are

$$V_2 = V_4 = \frac{T}{2A_o}d_1 \quad (8.13a)$$

Similarly, the shear forces acting in the top and bottom walls of the tube are

$$V_1 = V_3 = \frac{T}{2A_o}b_1 \quad (8.13b)$$

Assuming that the stirrups crossing the crack are yielding, the shear in vertical walls may be written as

$$V_2 = V_4 = A_t(f_{yt}/\gamma_s)n \quad (8.13c)$$

where A_t is the area of one leg of a closed stirrup, f_{yt} is the yield strength of transverse reinforcement, γ_s is the partial safety factor for steel = 1.15, and n is the number of stirrups intercepted by the torsional crack.

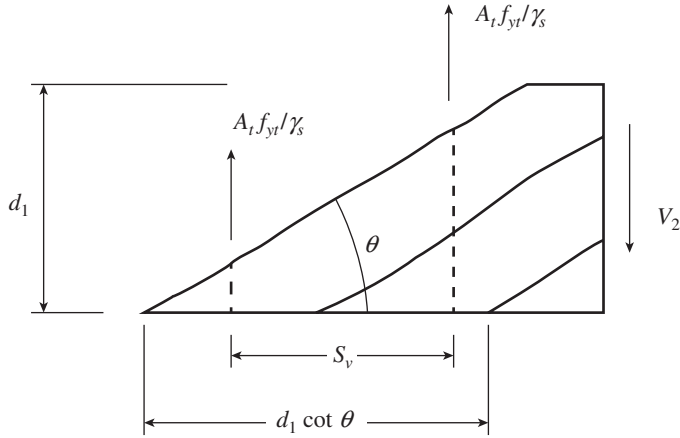


FIG. 8.13 Free body of vertical equilibrium

From Fig. 8.13, the horizontal projection of the crack is $d_1 \cot \theta$. Hence, the number of stirrups intercepted by the crack is

$$n = \frac{d_1 \cot \theta}{s_v} \tag{8.13d}$$

where θ is the slope angle of strut and s is the spacing of stirrups.

From Eqs (8.13c) and (8.13d), we get

$$V_2 = V_4 = \frac{A_t (f_{yt} / \gamma_s) d_1 \cot \theta}{s} \tag{8.13e}$$

Replacing V_2 with Eq. (8.13a) and taking T equal to nominal torsion capacity, T_n , we get

$$T_n = \frac{2A_o A_t (f_{yt} / \gamma_s)}{s_v} \cot \theta \tag{8.14a}$$

Tests have shown that the concrete outside the stirrups is relatively ineffective. Hence, the gross area enclosed by the shear flow path around the perimeter of the tube, A_o , after cracking may be defined in terms of the area enclosed by the centre line of the outermost closed transverse torsional reinforcement, A_{oh} (see Fig. 8.14). Section 11.5.3.6 of the ACI code allows the area A_o to be taken as $0.85A_{oh}$. If greater accuracy is required, the expression for A_o given by Hsu (1968a) may be used. It should also be noted that as the angle

θ gets smaller, the amount of stirrups required by Eq. (8.14a) decreases; however, the amount of longitudinal steel required (see Eq. 8.17) increases.

For the rectangular section shown in Fig. 8.12(a), with $\theta = 45^\circ$, $A_o = 0.85A_{oh}$, and $A_{oh} = b_1 d_1$, Eq. (8.14a) yields

$$T_n = \frac{1.7 b_1 d_1 A_t (f_{yt} / \gamma_s)}{s_v} \tag{8.14b}$$

where b_1 and d_1 are the dimensions of the stirrup.

From Eq. (8.14a), we get the required area of stirrup to resist the applied torque, T_u , as

$$A_t = \frac{T_u s_v}{2A_o (f_{yt} / \gamma_s)} \tan \theta \tag{8.15}$$

It has to be noted that when significant torsion is present, it is economical to select a larger beam than a smaller one with closely spaced stirrups and longitudinal steel required for the torsion design.

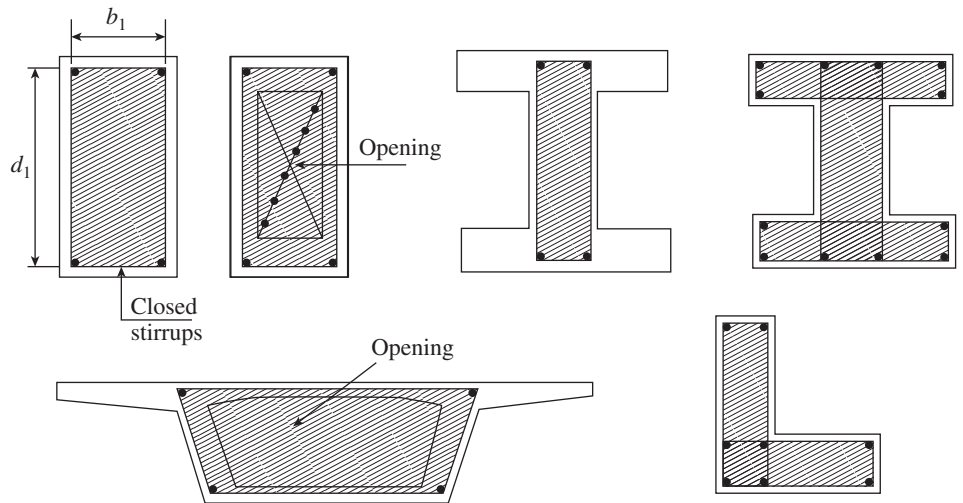


FIG. 8.14 Area enclosed by centre line of the outermost closed transverse torsional reinforcement for rectangular, I, L, and box section beams (A_{oh})

8.5.5 Area of Longitudinal Reinforcement for Torsion

The longitudinal reinforcement must be proportioned to resist the longitudinal tensile forces that occur due to torsion. As

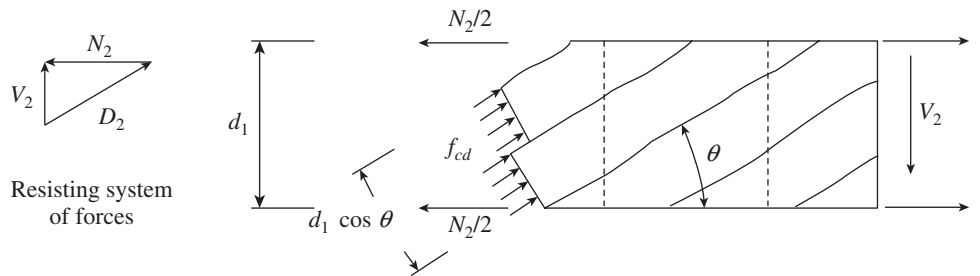


FIG. 8.15 Free body of horizontal equilibrium

shown in Fig. 8.15, the shear force V_2 can be resolved into a diagonal compressive force D_2 parallel to the inclined concrete compression struts and an axial tension force N_2 . From Fig. 8.15, we get

$$D_2 = V_2/\sin \theta \quad (8.16a)$$

$$N_2 = V_2 \cot \theta \quad (8.16b)$$

Since the shear flow q is constant along the side of the member, the forces D_2 and N_2 act at mid-height of the side. For a beam with longitudinal bars in the top and bottom corners as shown in Fig. 8.9(b), half of the tension force N_2 in side 2 will be resisted by each corner bar. Similar force components exist in the other three sides of the space truss. For a rectangular member, the total longitudinal force can be written as

$$N = 2(N_1 + N_2) \quad (8.16c)$$

Substituting the values of V_1 and V_2 from Eqs (8.13b) and (8.13a), using Eq. (8.16b), and taking T equal to nominal torsional capacity, T_n , we get

$$N = \frac{T_n}{2A_o} 2(d_1 + b_1) \cot \theta \quad (8.16d)$$

where $2(d_1 + b_1)$ is the perimeter of the closed stirrup, p_h . Longitudinal reinforcement should be provided to resist this longitudinal force N . Assuming that this reinforcement yields at the ultimate load, we get

$$A_l (f_y/\gamma_s) = N$$

Hence, using Eq. (8.16d), we get the required longitudinal reinforcement as

$$A_l = \frac{T_n p_h}{2A_o (f_y/\gamma_s)} \cot \theta \quad (8.17a)$$

If we substitute $A_o = 0.85A_{oh}$, we get

$$A_l = \frac{T_n p_h}{1.7A_{oh} (f_y/\gamma_s)} \cot \theta \quad (8.17b)$$

Alternatively, the required longitudinal steel, A_l , can also be expressed in terms of the area of torsional stirrups. Substituting Eq. (8.14a) into Eq. (8.17a), we get

$$A_l = \left(\frac{A_t}{s_v} \right) \left(\frac{f_{yt}}{f_y} \right) p_h \cot^2 \theta \quad (8.17c)$$

Equation (8.17a) is easier to use than Eq. (8.17c), as the term (A_t/s_v) is avoided in this equation. It should also be noted that as the forces N_1 through N_4 each act at the middle of one of the walls, the resultant force N acts along the centroidal axis of the cross section of the space truss. Thus, the line of action of the force in the longitudinal bars should coincide with that of N . Hence, it is required to distribute the longitudinal torsional steel around the perimeter of the cross section. We should use the same value of θ in Eqs (8.14) and (8.17) when designing a member for torsion. Equation (8.17a) can also be written as

$$T_n = \frac{2A_t A_o (f_y/\gamma_s)}{p_h \cot \theta} \quad (8.17d)$$

Combining Eq. (8.17d) with Eq. (8.14a), we may get the capacity of the section taking into account the areas of both transverse and longitudinal reinforcements. For a rectangular section, using $\theta = 45^\circ$, $A_o = b_1 d_1$, and $p_h = 2(b_1 + d_1)$ and simplifying, we get

$$T_n = 2b_1 d_1 \times 0.87 f_y \sqrt{\left(\frac{A_t}{s_v} \right) \left(\frac{A_l}{2(b_1 + d_1)} \right)} \quad (8.18a)$$

8.5.6 Limiting Crack Width for Combined Shear and Torsion

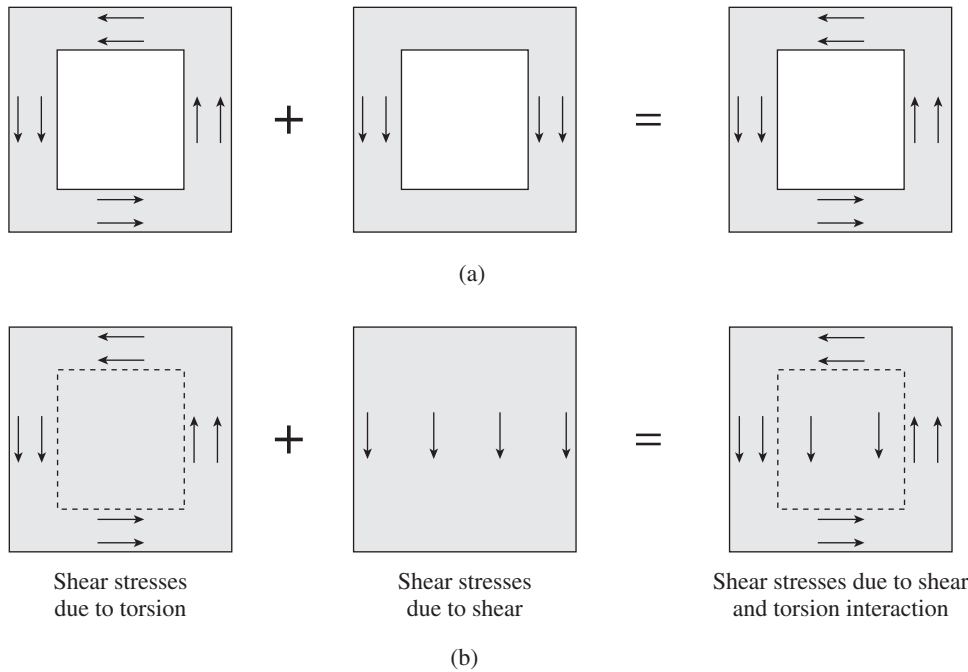
In the ACI codes prior to 1995, a portion of both the shear and torsion is resisted by the concrete terms V_c and T_c . This complexity arises due to the circular interaction assumed in the code between V_c and T_c (see Section 8.6). As seen in the previous derivations, the space truss analogy assumes that all the torsion is carried by the reinforcements, without any torsion being carried by the concrete, that is, T_c is always taken equal to zero. This has greatly simplified the calculations. For a low value of V_u and high T_u , with τ_v less than about $0.8(\phi 0.15\sqrt{f_{ck}})$ the older code required more stirrups, whereas for τ_v greater than this value, the new method required fewer or similar stirrups than the old method (Wight and MacGregor 2009).

We have seen in Section 6.4.1 of Chapter 6 that the codes often limit the maximum shear stresses (approximately $\tau_{c,\max} = 0.631\sqrt{f_{ck}}$) carried by stirrups in order to control the crack width (see Table 20 of IS 456). This concept is extended in the case of torsion too and an upper limit of $0.6\sqrt{f_{ck}}$ plus the stress causing shear cracking is specified; this limit is intended to control the crack width due to shear and torsion (Clause 11.5.3.1 of the ACI code). As we have seen in Chapter 6, the shear stress due to shear in the member is $\tau_v = V_u/b_w d$, and the shear stress caused by torsion as given by Eq. (8.9) is $\tau_t = T/(2A_o t)$. In hollow sections, these stresses have to be added directly on one side of the member (see Fig. 8.16a)]. Thus, for a cracked concrete cross section with $A_o = 0.85A_{oh}$ and $t = A_{oh}/p_h$, the maximum shear stress can be written as

$$\tau = \tau_v + \tau_t = \frac{V_u}{b_w d} + \frac{T_u p_h}{1.7A_{oh}^2} \leq \phi (\tau_c + 0.6\sqrt{f_{ck}}) \quad (8.18b)$$

For members with solid sections, τ_t is predominantly distributed around the perimeter, but the full cross section contributes to carrying τ_v (see Fig. 8.16b). Experimental results show that Eq. (8.18) is overconservative and a better correlation is achieved when the square root of the sum of the squares of nominal shear stresses is used. Thus, Eq. (8.19) is suggested for solid sections with the specified limit for crack control.

$$\tau = \sqrt{\left(\frac{V_u}{b_w d} \right)^2 + \left(\frac{T_u p_h}{1.7A_{oh}^2} \right)^2} \leq \phi (\tau_c + 0.6\sqrt{f_{ck}}) \quad (8.19)$$



$$f_{cd} = \sqrt{\left(\frac{T_u p_h}{1.7 A_{oh}^2 \cos \theta \sin \theta}\right)^2 + \left(\frac{V_u}{b_w d \cos \theta \sin \theta}\right)^2} \quad (8.22)$$

The value of f_{cd} in this equation should not exceed the crushing strength of the cracked concrete in the tube, f_{ce} . Collins and Mitchell (1980) predicted that f_{ce} will be equal to $0.44f_{ck}$. Setting f_{cd} in Eq. (8.22) equal to $0.44f_{ck}$ and assuming $\theta = 45^\circ$, the upper limit on shears and torques as determined by the crushing of concrete in the web becomes

$$\sqrt{\left(\frac{T_u p_h}{1.7 A_{oh}^2}\right)^2 + \left(\frac{V_u}{b_w d}\right)^2} \leq \phi (0.22 f_{ck}) \quad (8.23)$$

FIG. 8.16 Addition of torsional and shear stresses (a) Hollow sections (b) Solid sections

Either member dimensions or concrete strength must be increased if the criteria specified in Eq. (8.18) or (8.19) are not satisfied. In Eqs (8.18) and (8.19), τ_c is assumed to be $0.15\sqrt{f_{ck}}$ in the US code and hence the right-hand side of these equations gives the limit as $\phi 0.75\sqrt{f_{ck}}$; with the capacity reduction factor for torsion of 0.75, the limit is set as $0.56\sqrt{f_{ck}}$. However, it has to be noted that Clause 41.3.1 of the Indian code states that the value of equivalent nominal shear stress should not exceed $\tau_{c,max}$ given in Table 20 of the code, which is approximately equal to $0.63\sqrt{f_{ck}}$.

Failure can also occur due to the crushing of the concrete in the web. The diagonal compressive force in the vertical side of the member shown in Fig. 8.9(b) is given in Eq. 8.16(a). This force acts on a width $d_1 \cos \theta$ as shown in Fig. 8.15. The resulting compressive stress is

$$f_{cd} = \frac{V_2}{t d_1 \cos \theta \sin \theta} \quad (8.20a)$$

Substituting V_2 from Eq. (8.13a), and using $A_o = 0.85A_{oh}$ and $t = A_{oh}/p_h$, we get

$$f_{cd} = \frac{T_u p_h}{1.7 A_{oh}^2 \cos \theta \sin \theta} \quad (8.20b)$$

The compressive stress due to shear may be derived in a similar fashion as

$$f_{cd} = \frac{V_u}{b_w d \cos \theta \sin \theta} \quad (8.21)$$

For a solid section, they will be added via square root as explained in the derivation of Eq. (8.19). Hence, we get the combined compressive stress in the diagonals as

The limit $\phi(0.22f_{ck})$ in Eq. (8.23) will always exceed the limit $\phi(0.75\sqrt{f_{ck}})$ set in Eq. (8.19), for $f_{ck} \geq 11.62$ MPa. Because the RC members always have $f_{ck} > 20$ MPa, it is enough if we check Eq. (8.19). MacGregor and Ghoneim (1995) compared the test results of beams failed in pure torsion due to crushing of concrete in the tube and found that the limit in Eq. (8.19) gives an acceptable lower bound to the test results.

8.6 SKEW BENDING THEORY

The *skew bending theory* developed by Lessig (1959) and extended by Hsu (1968b) was the basis for the torsion design provisions of the codes issued during 1971–1990. The provisions in the Indian code are also based on the skew bending theory. This theory assumes that some shear and torsion is resisted by the concrete and the rest by the shear or torsion reinforcement. Hsu (1968a) used high-speed photography to record the failure process and visually observed that plain concrete members failed abruptly in a skew bending mode (i.e., the plane of failure is not perpendicular to the beam axis, but inclined at an angle). This may be easily demonstrated by applying a torque to a piece of chalk and observing the failure mode.

In this theory, the behaviour is studied on the basis of the mechanism of failure, rather than on the basis of stresses. Under the action of bending, the failure is vertical, with the primary yielding of tension steel in under-reinforced beams and secondary compression crushing of concrete. The effect of adding even a little torque skews the failure surface. The skewing is in the direction of the resultant moment–torque

vector. The compression face is at an angle θ to the vertical face of the beam cross section. This compression failure can occur at the top, sides, or bottom of the beam as shown in Fig. 8.17. Such a failure surface intersects some of the stirrups, which essentially provide torsional resistance.

The tension steel may yield first followed by the stirrups. If both yield before the crushing of concrete, the beam is under-reinforced. If the concrete crushes before both types of steel yield, it is over-reinforced.

Beams with large bending moment and small torsion fail with the compression fibres crushing at the top; this type of failure is termed as Mode 1 or *modified bending failure* (Fig. 8.17a). Mode 1 is the most common type of failure and likely to occur in wide beams, even if the torsion is relatively high. However, if the beam is narrow ($D \gg b$) and deep with equal amounts of top and bottom steel, the failure may be by crushing at the sides. This failure is termed as Mode 2 or *lateral bending failure* (Fig. 8.17b). If the top longitudinal steel is much less than the bottom steel, the failure may occur by crushing at the bottom fibre. This type of failure is termed as Mode 3 or *negative bending failure* (Fig. 8.17c). Large torsion and low flexure may result in Mode 2 and Mode 3 failures. Large moment may force the Mode 1 failure. High shear and low torsion sometimes result in Mode 4 failure. It is necessary to investigate these several modes systematically and choose the lowest capacity for a given beam.

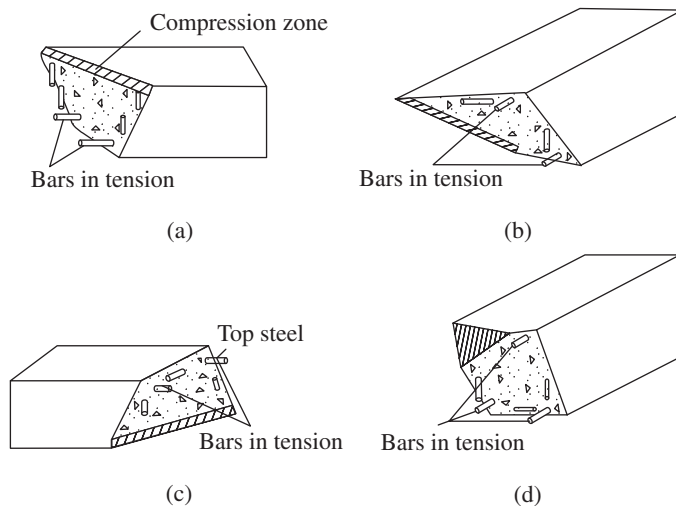


FIG. 8.17 Failure modes as per skew bending theory (a) Mode 1 (bending and torsion) (b) Mode 2 (low shear–high torsion) (c) Mode 3 (low bending–high torsion; weaker top steel) (d) Mode 4 (high shear–low torsion)

Source: Collins, et al. 1968, reprinted with permission from ACI

The torsional strength under Mode 1 failure of a beam subjected to a bending moment of M_u and torsion of T_u is given as follows (Warner, et al. 1976; Purushothaman 1984):

$$T_{n1} = M_n \left(\frac{2\gamma}{1+2\alpha} \right) \tan \theta \quad (8.24a)$$

$$\text{where } \tan \theta = \sqrt{\frac{1}{\beta^2} + \frac{(1+2\alpha)}{\gamma}} - \frac{1}{\beta}, \quad (8.24b)$$

M_n = pure flexural capacity = $A_{st} f_y (0.9d)$ (approximately),

$$\alpha = D/b, \quad \beta = T_u/M_u, \quad \gamma = \left(\frac{0.9A_v f_{yt}}{s_v} \right) \left(\frac{b_1}{A_{st} f_y} \right), \quad A_v = \text{area of}$$

one leg of stirrup, D , d , and b = overall depth, effective depth, and breadth of beam, respectively, s_v = spacing of stirrups, and d_1 = length of stirrup in the horizontal direction.

The torsional strength under Mode 3 failure is given by

$$T_{n3} = M_n \left(\frac{2\gamma}{1+2\alpha} \right) \tan \theta_1 \quad (8.25a)$$

$$\text{where } \tan \theta_1 = \sqrt{\frac{1}{\beta^2} + R_3 \frac{(1+2\alpha)}{\gamma}} + \frac{1}{\beta} \quad (8.25b)$$

where R_3 is the ratio of pure negative flexural strength and pure positive flexural strength = A_{sc}/A_{st} .

The torsional strength under Mode 2 failure is given by

$$T_{n2} = M_n \sqrt{R_2 \frac{4\gamma}{1+2\alpha}} \quad (8.26)$$

where $R_2 = M_{uy}/M_n$.

In a square beam with symmetrical longitudinal reinforcement subjected to pure torsion, the three modes will become identical. Warner, et al. (1976) have shown that similar expressions for T_{n1} to T_{n3} can be derived using the space truss analogy. It has to be noted that the presence of shear in addition to the bending and torsion will cause the beam to fail at a lower strength. The Indian code attempts to prevent such a possibility by suggesting the designing of the beam using the concept of equivalent shear.

8.6.1 Interaction Curves for Combined Flexure and Torsion

Torsion is normally accompanied by bending and shear. In general, flexural and torsional shears are of significance in those regions where the bending moment is low. Thus, for design purposes it is necessary to know the strength interaction relationship between shear and torsion. The experimental studies conducted at the University of Texas on rectangular, L-shaped, and T-shaped beams have indicated that a quarter circle interaction relationship is acceptable for members without web reinforcement. For members with web reinforcement, the interaction curve is found to be flatter than the quarter circle. The behaviour of asymmetrically reinforced beams may differ significantly from that of symmetrically reinforced beams.

In pure torsion, the additional bottom longitudinal steel available in asymmetrically reinforced sections does not increase the ultimate capacity because the weaker top steel is critical. The presence of bending moment introduces compression in the weaker steel and increases its resistance to

the torsional shear stresses. An increase of up to 30 per cent in torsional capacity was observed with the addition of bending moment equal to 40 per cent of the pure bending moment capacity in the under-reinforced tests. However, the presence of bending moment reduces the torsional ductility of beams with symmetrical or asymmetric longitudinal steel. It has to be noted that the presence of torsion invariably reduces the flexural strength of RC members.

Two simple interaction equations have been suggested by Lampert and Collins (1972). The first is for the case where the bottom longitudinal reinforcement yields along with the stirrups:

$$r \left(\frac{T_n}{T_{no}} \right)^2 + \frac{M_n}{M_{no}} = 1 \tag{8.27a}$$

The second equation is for the case where the weaker top longitudinal reinforcement yields along with the stirrups:

$$\left(\frac{T_n}{T_{no}} \right)^2 - \frac{1}{r} \frac{M_n}{M_{no}} = 1 \tag{8.27b}$$

where T_n and M_n are the nominal strengths in torsion and bending moment, respectively, acting simultaneously, T_{no} is the nominal strength under torsion alone, M_{no} is the nominal strength under bending alone, and r is the ratio of yield force in longitudinal compression steel to tension steel yield force = $A_{sc} f_y / A_s f_y$. Equation (8.27) is shown graphically in Fig. 8.18.

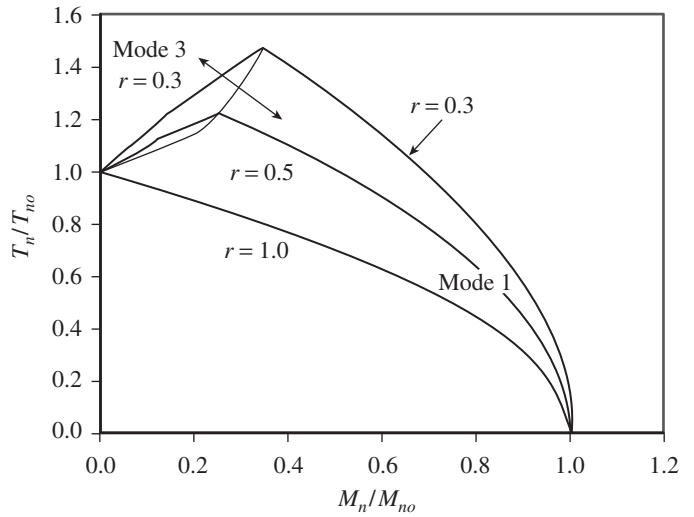


FIG. 8.18 Torsion–Flexure interaction curves for asymmetrically reinforced members with transverse reinforcement

Source: Adapted from ACI 445.1R-12, reprinted with permission from ACI

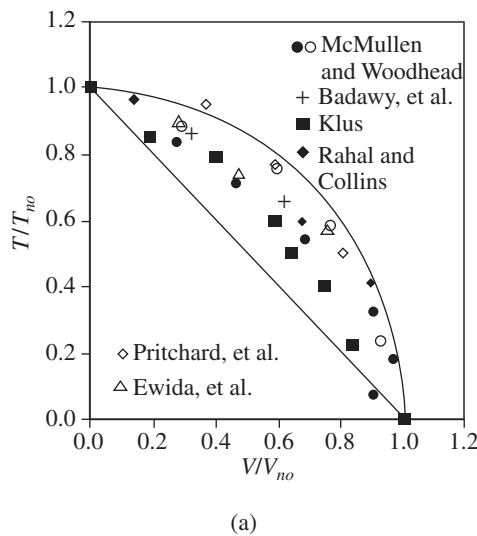


FIG. 8.19 Torsion–Shear interaction (a) Experimental results (b) Curves in the literature

Source: ACI 445.1R-12, reprinted with permission from ACI

8.6.2 Interaction Curves for Combined Shear and Torsion

Various torsion–shear interaction curves have been proposed, similar to the torsion–flexure interaction curves (Mattock 1968; ACI Committee 445: 2012). Various other linear interaction curves have also been suggested and are shown in Fig. 8.19. In general, the interaction curves may be represented by the following interaction equation:

$$\left(\frac{T}{T_{no}} \right)^n + \left(\frac{V}{V_{no}} \right)^n = 1 \tag{8.28}$$

where T and V are the applied torsion and shear, respectively, acting simultaneously, T_{no} is the nominal strength under torsion alone, V_{no} is the nominal strength under shear alone, and n is a constant (see Fig. 8.19). A value of $n = 1$ results in a linear interaction curve and provides conservative results (see Fig. 8.19a).

Victor and his associates (Victor 1966; Victor, et al. 1976; Victor and Aravindan 1978) and Elfgrén (1972) also studied the interaction of combined torsion, bending, and shear. Recently, Lu and Huang (2011) derived a unified formula for calculating the ultimate state of RC members under combined bending, shear, torsion, and axial compression. They also compared the interaction suggested by them with the available test results and found reasonable correlation.

8.7 INDIAN CODE PROVISIONS FOR DESIGN OF LONGITUDINAL AND TRANSVERSE REINFORCEMENTS

The Indian code provisions are based on the simplified skew bending theory (Iyengar and Ram Prakash 1974). In

this approach, the longitudinal and torsional reinforcements are not calculated separately. Instead, the total longitudinal reinforcement is calculated based on a *fictitious, equivalent bending moment*, which is a function of the actual bending moment and torsion. Similarly, the transverse reinforcement is determined from a *fictitious, equivalent shear*, which is a function of the actual shear and torsion. Furthermore, in T-beams, the flanges are neglected and the beam is designed by considering the rectangular web alone (Clause 41.1.1), which is justifiable (see Example 8.4).

Clause 41.2 of the code also states that the sections located at a distance less than the effective depth, d , from the face of the support may be designed for the same torsion as computed at a distance d from the support.

8.7.1 Equivalent Shear and Moment

The equivalent bending moment, M_{e1} , is calculated as follows (Clause 41.4.2):

$$M_{e1} = M_t + M_u \quad (8.29a)$$

where

$$M_t = T_u \left(\frac{1 + D/b}{1.7} \right), \quad (8.29b)$$

M_u is the factored bending moment at the cross section due to external loads in Nmm, T_u is the factored torsional moment in Nmm, M_t is the additional bending moment due to torsion as per the code in Nmm, and D and b are the overall depth and width of the beam in mm, respectively. The code assumes that the beam will fail by Mode 1 if the beam is designed for flexural strength M_{e1} (SP 24:1983). The derivation of Eq. (8.29) is explained in SP 24:1983.

As per Clause 41.4.2.1, if the numerical value of M_t exceeds the numerical value of M_u , we should provide additional longitudinal reinforcement for a moment M_{e2} applied in the opposite sense of M_u . Effectively, this will result in additional longitudinal reinforcement on the compression face of the beam due to the reversal of the moment sign. The additional moment M_{e2} is computed as

$$M_{e2} = M_t - M_u \quad (8.29c)$$

It follows from these provisions that for the case of pure torsion, that is, $M_u = 0$, equal longitudinal reinforcement is required at the top and bottom of the rectangular beam, each capable of resisting the equivalent bending moment equal to M_t . The code assumes that if the beam is designed for flexural strength M_{e2} Mode 3 failure can be avoided (SP 24:1983). The equivalent shear, V_e , is to be calculated as per Clause 41.3.1 of the code (see Eq. 8.8).

$$\text{Equivalent nominal stress, } \tau_{ve} = V_e/bd \quad (8.30a)$$

If τ_{ve} exceeds $\tau_{c,max}$ given in Table 20 of the code, the section has to be revised or a higher grade of concrete should be chosen. If τ_{ve} lies between τ_c (given in Table 19 of the code)

and $\tau_{c,max}$, transverse reinforcement for torsion, as discussed in Section 8.7.2, has to be provided (Clause 41.3.3).

It has to be noted that τ_c as given in Table 19 can also be estimated approximately by the following formula:

$$\tau_c = 0.64 \left(\frac{100A_s}{bd} \right)^{1/3} \left(\frac{f_{ck}}{25} \right)^{1/4} \quad (8.30b)$$

Clause 41.3.2 stipulates that if τ_{ve} is less than τ_c , minimum shear reinforcement should be provided.

8.7.2 Minimum Longitudinal Reinforcement for Torsion

When torsion is significant, that is, when $T_u/M_u > 0.5$, brittle failures have been observed. In order to avoid a brittle torsional failure, a minimum amount of torsional reinforcement (including both transverse and longitudinal steel) is required in a member subjected to torsion. The basic criterion for determining this minimum torsional reinforcement is to equate the postcracking strength T_n to the cracking strength T_{cr} . Based on this criteria, the formula for minimum longitudinal reinforcement was derived by Hsu (1997) and provided in the ACI code as

$$A_{l,min} = \frac{0.37 \sqrt{f_{ck}} A_{cp}}{f_y} - \left(\frac{A_t}{s_v} \right) p_h \left(\frac{f_{yt}}{f_y} \right) \text{ with } \left(\frac{A_t}{s_v} \right) \geq \frac{b_w}{6f_{yt}} \quad (8.31)$$

where $A_{l,min}$ is the total area of minimum longitudinal steel in mm^2 , A_{cp} is the area enclosed by the outside perimeter of the concrete cross section in mm^2 , A_t is the area of one leg of closed stirrup in mm^2 , and p_h is the perimeter of the centre line of the outermost closed torsional stirrup, mm. At least one longitudinal bar having a diameter of not less than $s_v/16$ or 10 mm should be placed inside each corner of the closed stirrups.

8.7.3 Design of Transverse Reinforcement

The code assumes that both the longitudinal and transverse steel reach design strength before failure occurs. Clause 41.4.3 of the code, based on the skew bending theory, stipulates that two-legged closed stirrups enclosing the corner longitudinal bars are to be provided to resist the torsion, with an area, A_{sv} , given by

$$\frac{A_{sv}}{s_v} = \frac{T_u}{b_1 d_1 (0.87 f_{yt})} + \frac{V_u}{2.5 d_1 (0.87 f_{yt})} \quad (8.32a)$$

Clause 41.4.3 also specifies the following minimum limit to the *total* area of transverse reinforcement.

$$\frac{A_{sv}}{s_v} \geq \frac{(\tau_{ve} - \tau_c) b}{(0.87 f_{yt})} \quad (8.32b)$$

where A_{sv} is the area of cross section of transverse stirrups in mm^2 , s_v is the spacing of transverse stirrup reinforcement in mm, b_1 is the centre-to-centre distance between the corner bars in the direction of the width in mm, d_1 is the centre-to-centre distance between the corner bars in the direction of the depth, mm, and f_{yt} is the characteristic strength of stirrup

reinforcement in N/mm^2 . Also see Fig. 8.12 for the definitions of b_1 and d_1 .

It has to be noted that Eq. (8.32a) is derived to resist Mode 2 failure (high torsion and low shear) of the skew bending theory. Moreover, in the case of pure torsion (i.e., when $V_u = 0$), this equation becomes exactly equal to Eq. (8.15), which was derived based on the space truss analogy. Equation (8.32b) safeguards against flexural shear failure in situations of high shear and low torsion. Only the outer two legs of the closed stirrups should be considered for computing the torsional resistance contribution of the web steel. If the stirrup consists of more than two legs, the interior legs should be ignored for torsion and considered only to take shear.

If τ_{ve} is less than τ_c , minimum shear reinforcement as per Clause 26.5.1.6 of the code should be provided as follows (also see Section 6.6 of Chapter 6):

$$\frac{A_{sv}}{s_v} \geq \frac{0.4b}{(0.87f_y)} \tag{8.33}$$

It should be noted that the minimum transverse reinforcement requirement is given in the ACI code as

$$(A_v + 2A_t) = 0.055\sqrt{f_{ck}} \frac{b_w s_v}{f_{yt}} \geq \frac{0.35b_w s_v}{f_{yt}} \tag{8.34}$$

where A_v is the area of shear reinforcement and A_t is the area of one leg of the closed stirrup resisting torsion.

To ensure ductile behaviour, the torsion member should be under-reinforced. To achieve this, the following maximum percentage of steel for pure torsion in the presence of equal volume of longitudinal reinforcement was derived by Park and Paulay (1975):

$$p_{t,max} = \frac{A_t}{s_v b} \leq \frac{0.24bD\sqrt{f_{ck}}}{\alpha_t b_1 d_1 f_y} \tag{8.35a}$$

where the value of A_t as derived experimentally by Hsu (1968b) is given by

$$a_t = 0.66 + 0.33\left(\frac{d_1}{b_1}\right) \leq 1.5 \tag{8.35b}$$

8.7.4 Distribution of Torsional Reinforcement

To ensure crack width control, Clause 26.5.1.7(a) stipulates that the spacing of transverse stirrups should not exceed x_1 , $(x_1 + y_1)/4$, and 300mm, where x_1 and y_1 are the short and long

dimensions of the stirrups, respectively. Similar provisions are found in the US code. In addition, the torsional stirrups should be extended to a distance of at least $(x_1 + y_1)$ beyond the point of zero torsion.

Clause 26.5.1.7(b) stipulates that the longitudinal reinforcement for torsion should be placed as close as possible to the corners of the cross section and that at least one longitudinal bar should be placed at the corners of the stirrups. The hooks of the closed stirrup should be developed into the core with 135° bends, as tests conducted by Mitchell and Collins (1976) showed that the corners of the beam may spall off if 135° hooks are not used (see Fig. 8.20). The inclined compressive stress in the concrete, f_{cd} , has components parallel to the top and side surfaces; the components acting towards the corner are balanced by the tensions in the stirrups, as shown in Fig. 8.20(b). If the concrete outside the reinforcing cage is not well anchored, the shaded region may fall off when the compression in the concrete is large (see Fig. 8.20).

The 135° bends ensure that the hooks are well developed into the member core and prevent hook pull-out under high torsional loads. In India, closed stirrups are often used. If the concrete around the stirrup anchorage is restrained against spalling by a slab, the anchorage details shown in Fig. 8.21 may be used (Mitchell and Collins 1976). Examples of ineffective stirrups for members under high torsion are shown in Fig. 8.22. It is also important to anchor the longitudinal rods adequately into the supports.

Clause 26.5.1.7(b) also states that when the size of the member exceeds 450 mm, additional longitudinal reinforcement with an area not less than 0.1 per cent of the web area should be provided in the side faces of the member.

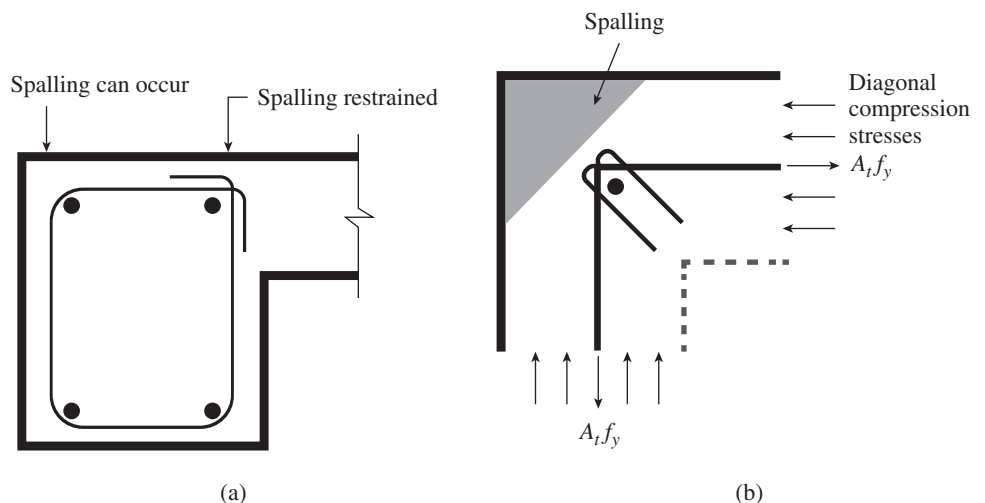


FIG. 8.20 Possible spalling of concrete at the corners due to torsion (a) Spandrel beam with 90° hooks—spalling prevented by an adjacent slab (b) Concrete spalling can be prevented by 135° hooks (Reprinted with permission from ACI)

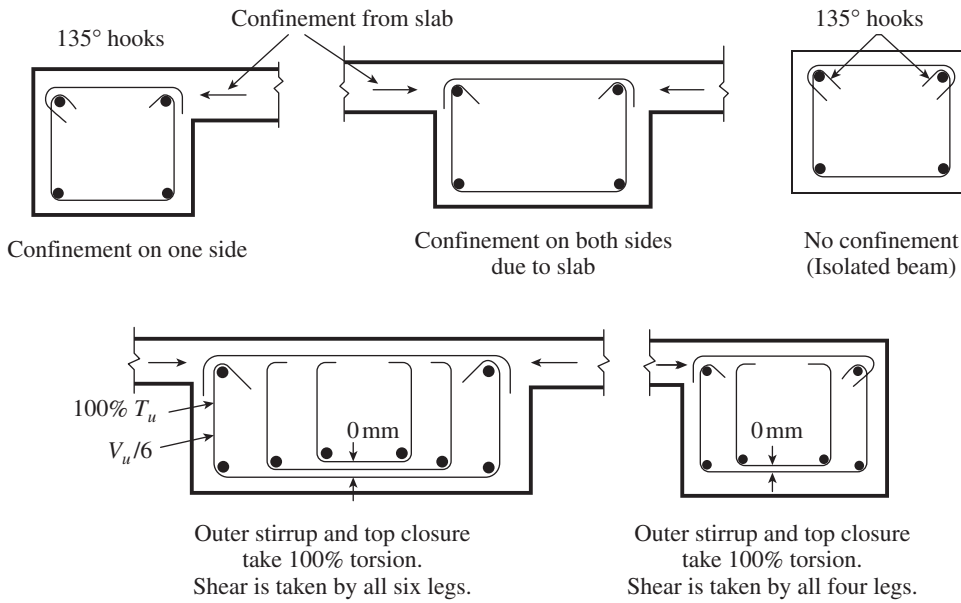


FIG. 8.21 Recommended closed stirrups for torsion

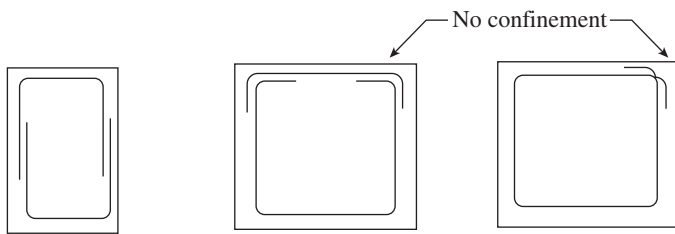


FIG. 8.22 Ineffective closed stirrups for members under high torsion

8.8 DESIGN AND DETAILING FOR TORSION AS PER IS 456 CODE

The following design steps are required for the design of flexural and shear reinforcement as per IS 456.

1. Determine the equivalent bending moment, $M_{e1} = M_u + M_t$, as per Eqs (8.29a) and (8.29b) and equivalent shear, V_e , as per Eq. (8.8).
2. Calculate the required longitudinal steel for M_{e1} as per the methods given in Chapter 5 (see Section 5.5.8 and 5.5.9) or by using design charts 1–18 of SP 16. If M_t exceeds M_u , provide additional reinforcement for the moment M_{e2} applied in the opposite sense of M_u (in the compression face).
3. Check for shear. Calculate the equivalent shear stress, τ_{ve} as per Eq. (8.30a). The value of τ_{ve} should not exceed the value of $\tau_{c,max}$ as given in Table 20 of the code; if it exceeds, revise the section or increase the grade of concrete.
4. Calculate the transverse reinforcement as follows:
 - (a) If the value of τ_{ve} does not exceed the value of τ_c given in Table 19 or calculated using Eq. (8.30b), provide minimum reinforcement as per Eq. (8.33).
 - (b) If the value of τ_{ve} exceeds the value of τ_c given in Table 19, provide *two-legged closed stirrups*, enclosing the corner longitudinal bars with an area of cross section A_{sv}

taken as the minimum of Eqs (8.32a and b).

5. Check the spacing as per Clause 26.5.1.7(a). It should not exceed x_1 , $(x_1 + y_1)/4$, and 300 mm, where x_1 and y_1 are the short and long dimensions of the stirrups, respectively.
6. Check if side face reinforcement is required. If the size is greater than 450 mm, provide 0.05 per cent side face reinforcement at each face.

8.9 GRAPHICAL METHODS

Two graphical methods have also been developed. Rahal developed a simplified method for combined stress resultants based on the MCFT (Rahal 2007). Leu and Lee (2000) proposed a

graphical solution to the softened truss model developed by Hsu (1988). A short description of the use of Rahal's method alone is given here. Interested readers may consult the publications mentioned for further details.

Rahal's graphical method is applied to beams subjected to torsion by idealizing the section as a hollow tube and by adopting simplified assumptions regarding the thickness of the hollow tube and the size of the shear flow zone. Based on the assumptions of the method, the reinforcing indices ω_t and ω_l in the transverse and longitudinal directions, respectively, are given as follows:

$$\omega_t = \frac{A_t f_{yt} p_{co}}{0.42 s_v A_{cp} f_{ck}} \quad (8.36a)$$

$$\omega_l = \frac{A_l f_y}{0.375 A_{cp} f_{ck}} \quad (8.36b)$$

The ultimate torsional moment of the section is also related to the ultimate shear strength in the walls as follows:

$$T_n = 0.67 \frac{A_{cp}^2}{p_{cp}} v_u \geq T_{cr} \quad (8.37)$$

Figure 8.23 gives the relationship between the indices and the normalized shear strength obtained using the results of the MCFT (Collins and Mitchell 1991). It should be noted that at relatively low ω_t values, the strains in the transverse steel exceed the yield strains before the ultimate capacity is reached. Beyond a specific level, the concrete crushes before the steel yields. Figure 8.23 shows a curve passing through those points beyond which concrete crushes before the transverse steel yields (over-reinforced case). The figure also shows a similar curve for the over-reinforced case in the longitudinal direction. The two balanced yield curves divide the graph into

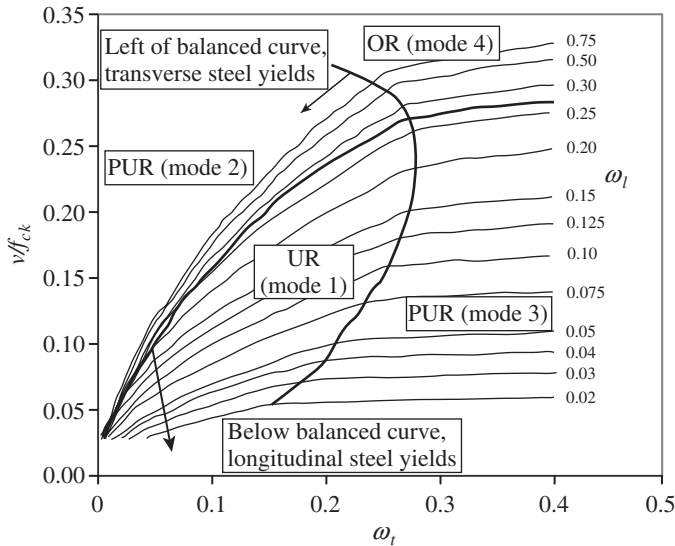


FIG. 8.23 Normalized shear strength curve for RC members
 Source: Rahal 2007, reprinted with permission from ACI

four regions (see Fig. 8.23). The relative position of a point of coordinates (ω_t, ω_l) with respect to these curves or regions indicates the expected mode of failure of an element with these reinforcement ratios. Four modes of failure are possible: partially over-reinforced (only longitudinal steel yields, Mode 3), or only transverse reinforcement yields, Mode 2), completely over-reinforced (concrete crushing before steel yielding, Mode 4), and completely under-reinforced (longitudinal and transverse steel yield, Mode 1).

8.10 OTHER CONSIDERATIONS

The following are the other considerations that should be taken into account:

Maximum yield strength of torsional reinforcement It is interesting to note that when transverse reinforcement is calculated for a member subjected to torsion, there is no restriction on the characteristic strength of stirrup reinforcement f_{yt} as per Clause 41.4.3 of IS 456, though f_{yv} is restricted to 415 MPa for shear design in Clause 40.4. Clause 11.5.3.4 of the ACI code limits this to 420 MPa in order to limit crack widths at service loads.

High-strength concrete Due to the absence of tests of high-strength concrete beams in torsion, Clause 11.1.2 of the ACI code limits the value of f_{ck} to 86 MPa.

Lightweight concrete As we have seen, the ACI code provisions are also applicable to lightweight concrete, using the factor λ . The value of λ is taken as 1.0 for normal weight concrete, 0.75 for all lightweight concrete, and 0.85 for sand-lightweight concrete.

Size effect Usually small scale models are tested in laboratories and the results are extrapolated and applied on

actual bigger size members. However, larger specimens have been found to fracture under relatively smaller applied load; this phenomenon is called the *size effect*. Bazant and Sener (1987) evaluated the existing test data on torsional failures and found that the size effect is present for rectangular plain concrete beams and beams with longitudinal steel bars without stirrups, that is, the nominal stress at failure decreases as the cross section increases. However, no such size effects were found on beams with both transverse and longitudinal reinforcements.

Precast L-shaped spandrel beams Precast L-shaped spandrel beams are most common in precast construction. They are characterized by a plate-like (wall-like) web with a continuous ledge running along the bottom of one side of the web, which provides support for the deck beams. These spandrel beams are subjected to significant torsion caused by a series of large, concentrated, eccentric loads along their span. Design methods for such beams are provided by Zia and Hsu (2004) and Lucier, et al. (2011).

EXAMPLES

EXAMPLE 8.1 (Computation of torsional moments):
 Compute the torsional moments in the canopy slab that is cantilevered 3 m from a beam of span 5 m, as shown in Fig. 8.1(a). The beam has a size 300 mm \times 500 mm and is well anchored into the two RC columns. Assuming a live load of 1.5 kN/m² on the canopy slab, compute the design torsional moment to be resisted by the beam.

SOLUTION:
 Assuming a thickness of 150 mm for the slab,
 Self-weight of slab = 0.15 \times 25 = 3.75 kN/m²
 Factored load on slab = 1.5 \times (DL + LL) = 1.5(1.5 + 3.75) = 7.875 kN/m²
 Torsion per unit length of the beam = 7.875 \times 3/2 = 11.82 kN/m
 Maximum torsion at the ends of the beam = 11.82 \times 5/2 = 29.55 kNm

Note that the torsion will be zero at mid-span.
 Torsion at critical section (at a distance d from support)
 = 11.82(2.5 - 0.46) = 24.12 kNm

EXAMPLE 8.2 (Calculation of cracking torque):
 Determine the cracking torque of a rectangular concrete beam of size 250 mm by 500 mm, assuming M25 concrete using (a) plastic theory, (b) IS code, and (c) ACI code formulae.

SOLUTION:

(a) Using plastic theory:

$$T_{cr} = \frac{1}{2} \tau_{t,max} b^2 (D - b/3)$$

Assuming $\tau_{t,\max} = 0.2\sqrt{f_{ck}} = 0.2\sqrt{25} = 1\text{MPa}$

$$T_{cr} = \frac{1}{2} \times 1 \times 250^2 (500 - 250/3) = 13.02 \times 10^6 \text{ Nmm} \\ = 13.02 \text{ kNm}$$

(b) Using IS code formula:

The Indian code does not give a direct formula for calculating τ_{cr} . However, it states that if $\tau_{ve} > \tau_c$ reinforcement has to be provided.

$$\tau_{ve} = [V_u + 1.6T_u/b]/(bd)$$

Assuming $V_u = 0$ and $d \approx 0.9D = 0.9 \times 500 = 450 \text{ mm}$

From Table 19 of IS 456, τ_c for M25 (with $p_t \leq 0.15$) = 0.29 MPa

Hence $0.29 = (0 + 1.6 \times T_{cr}/250)/(250 \times 500)$

$$T_{cr} = 5.66 \times 10^6 \text{ Nmm} = 5.66 \text{ kNm}$$

(c) Using ACI code formula:

$$T_{cr} = \phi 0.3 \sqrt{f_{ck}} \left(\frac{A_{cp}^2}{p_{cp}} \right)$$

$$A_{cp} = bD; p_{cp} = 2(b + D)$$

$$T_{cr} = 0.75 \times 0.3 \sqrt{25} \left[\frac{250^2 \times 500^2}{2(250 + 500)} \right] = 11.72 \text{ kNm}$$

Note: The value of the cracking torque predicted by the IS code is very conservative.

EXAMPLE 8.3 (Determination of torsional capacity):

The beam of Example 8.2 is reinforced with grade Fe 415 steel rebars as shown in Fig. 8.24. Determine the torsional capacity of the beam under pure torsion. Assume moderate exposure.

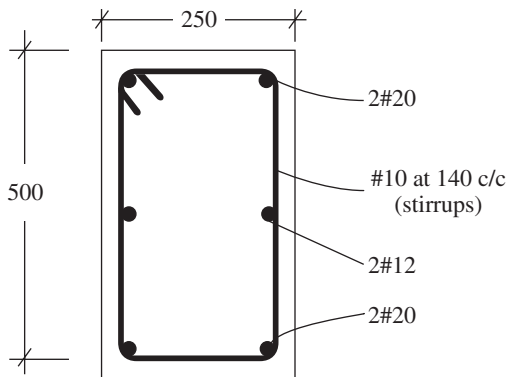


FIG. 8.24 Reinforcement of beam with steel rebars

SOLUTION:

The following values are given: $b = 250 \text{ mm}$, $D = 500 \text{ mm}$, $f_{ck} = 25 \text{ MPa}$, $f_y = f_{yt} = 415 \text{ MPa}$.

For moderate exposure, take clear cover = 30 mm (Table 16 of IS 456).

$$A_t (4\#20 + 2\#12) = 4 \times 314 + 2 \times 113 = 1482 \text{ mm}^2$$

$$A_t (\#10 \text{ stirrup}) = 78.5 \text{ mm}^2 \quad A_{sv} = 2A_t = 157 \text{ mm}^2$$

$$s_v = 140 \text{ mm}$$

$$b_1 = 250 - 30 \times 2 - 10 \times 2 - 20 = 150 \text{ mm}$$

$$d_1 = 500 - 30 \times 2 - 10 \times 2 - 20 = 400 \text{ mm}$$

From space truss theory, considering the contribution of both transverse and longitudinal reinforcements:

$$T_n = 2b_1d_1 \times 0.87f_y \sqrt{\left(\frac{A_t}{s_v}\right) \left(\frac{A_l}{2(b_1 + d_1)}\right)} \\ = 2 \times 150 \times 400 \times 0.87 \times 415 \sqrt{\left(\frac{78.5}{140}\right) \left[\frac{1482}{2(150 + 400)}\right]} \\ = 37.66 \times 10^6 \text{ Nmm} = 37.66 \text{ kNm} > T_{cr} = 11.72 \text{ kNm}$$

Alternatively, the torsional capacity can be calculated using the IS code formula considering shear-torsion interaction, with $V_u = 0$.

$$T_n = A_{sv} b_1 d_1 (0.87 f_y) / s_v \\ = 157 \times 150 \times 400 \times (0.87 \times 415) / 140 \\ = 24.29 \times 10^6 \text{ Nmm} = 24.29 \text{ kNm}$$

Note: The torsional capacity as per the IS code formula is conservative.

EXAMPLE 8.4 (Torsion in T-beams):

A T-beam as shown in Fig. 8.25 is subjected to a factored torsion of 160 kNm. Calculate the amount of torsion resisted by the two main rectangular portions of the T-beam using (a) elastic theory and (b) plastic theory.

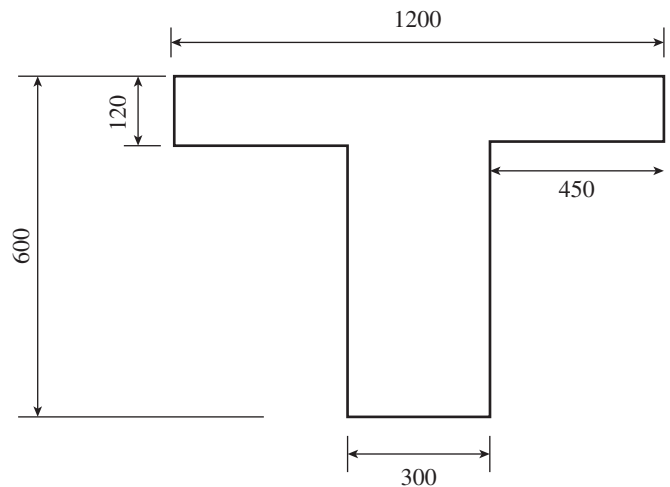


FIG. 8.25 T-beam

SOLUTION:

Check whether the effective overhang $\leq 4D_f$ and $D - D_f$.

Effective overhang = $(1200 - 300)/2 = 450\text{ mm} < 4 \times 120\text{ mm}$

Also, $D - D_f = 600 - 120 = 480 = 480\text{ mm} = 4 \times 120\text{ mm}$

Hence, it is adequate.

(a) Proportioning of torsion using elastic theory:

$$T_1 = T \frac{K_1 D_1 b_1^3}{\sum K D b^3}$$

For flange $\frac{D}{b} = \frac{900}{120} = 7.5 \quad K_1 = \left(1 - 0.63 \frac{b}{D}\right)/3 = 0.305$

For web $\frac{D}{b} = \frac{600}{300} = 2 \quad K_2 = \left(1 - 0.63 \times \frac{300}{600}\right)/3 = 0.228$

$$K_1 D_1 b_1^3 + K_2 D_2 b_2^3 = 0.305 \times 900 \times 120^3 + 0.228 \times 600 \times 300^3$$

$$= (4.74 + 36.94) \times 10^8 = 41.68 \times 10^8 \text{ mm}^4$$

$$T_1 = \frac{160 \times 4.74}{41.68} = 18.2 \text{ kNm}$$

$$T_2 = \frac{160 \times 36.94}{41.68} = 141.8 \text{ kNm}$$

This calculation shows that the web carries 88.6 per cent of the applied torsion. Hence, the provision in Clause 40.1.1 of IS 456 that the flanged beam can be designed by ignoring the contribution of flanges is reasonable.

(b) Calculation as per plastic theory:

$$T_1 = T \frac{D_1 b_1^3}{D_1 b_1^3 + d_2 b_2^3}$$

$$\sum_{i=1}^2 D_i b_i^3 = 900 \times 120^3 + 600 \times 300^3 = (15.55 + 162) \times 10^8$$

$$= 177.55 \times 10^8 \text{ mm}^4$$

$$T_1 = 160 \left(\frac{15.55}{177.55} \right) = 14.01 \text{ kNm}$$

$$T_2 = 160 \left(\frac{162}{177.55} \right) = 145.99 \text{ kNm}$$

EXAMPLE 8.5 (Determination of mode of failure):

Determine the torsional capacity and the mode of failure for the beam given in Example 8.3 using skew bending theory.

SOLUTION:

The following values are given: $b = 250\text{ mm}$, $D = 500\text{ mm}$, $f_{ck} = 25\text{ MPa}$, $f_y = f_{yt} = 415\text{ MPa}$.

Clear cover = 30 mm , $s_v = 140\text{ mm}$

$$A_{st} = 2 \times 314 = 628 \text{ mm}^2, A_{sc} = 2 \times 314 = 628 \text{ mm}^2, A_v = 78.5 \text{ mm}^2$$

$$b_1 = 250 - 2 \times 30 - 10 = 180 \text{ mm}, d = 500 - 30 - 10 - 10 = 450 \text{ mm}$$

$$M_n = A_{st} f_y (0.9d) = 628 \times 415 \times 0.9 \times 450 \times 10^6 = 105.55 \text{ kNm}$$

For Mode 1 failure,

$$\gamma = \left(\frac{0.9 A_v f_{yt}}{s_v} \right) \left(\frac{b_1}{A_{st} f_y} \right) = \left(\frac{0.9 \times 78.5 \times 415}{140} \right) \left(\frac{180}{628 \times 415} \right) = 0.144$$

$$\alpha = D/b = 500/250 = 2$$

$$\beta = M_u/T_u = \infty \text{ as } M_u = 0.0$$

$$\tan \theta = \sqrt{\frac{1}{\beta^2} + \frac{(1+2\alpha)}{\gamma}} - \frac{1}{\beta} = \sqrt{\frac{1+2 \times 2}{0.144}} = 5.36$$

$$T_{n1} = M_n \left(\frac{2\gamma}{1+2\alpha} \right) \tan \theta = 105.55 \left(\frac{2 \times 0.144}{1+2 \times 2} \right) 5.36 = 32.58 \text{ kNm}$$

For Mode 2 failure,

$$T_{n2} = M_n \sqrt{R_2 \frac{4\gamma}{1+2\alpha}}$$

$$R_2 = M_{ny}/M_n = \frac{0.9 \times (250 - 30 - 10 - 10) \times (3 \times 214) \times 415}{105.55 \times 10^6} = 47.95/105.55 = 0.45$$

$$T_{n2} = 105.55 \sqrt{\frac{0.45 \times 4 \times 0.144}{1+2 \times 2}} = 24.03 \text{ kNm}$$

For Mode 3 failure, $R_3 = 1$. Hence, $\tan \theta = 5.36$.

$$T_{n3} = T_{n1} = 32.58 \text{ kNm}$$

The failure will be by Mode 2 and the torsional capacity = 24.03 kNm .

Note: In this case, the failure load predicted by the skew bending theory (24.03 kNm) is less than that predicted by the plastic space truss theory (37.66 kNm).

EXAMPLE 8.6 (Design of T-beam):

The T-beam given in Example 8.4 is subjected to the following factored loads: bending moment of 150 kNm , shear of 120 kN , and torsion of 60 kNm . Assuming M30 concrete and Fe 415 steel, design the reinforcements as per IS 456. Assume severe environment.

SOLUTION:

As per Clause 40.1.1 of IS 456, we will design the flanged beam by ignoring the contribution of flanges.

The following values are given: $M_u = 150\text{ kNm}$, $V_u = 120\text{ kN}$, $T_u = 60\text{ kNm}$, $f_{ck} = 20\text{ MPa}$, $f_y = 415\text{ MPa}$.

From Table 16 of IS 456, for severe environment, clear cover = 45 mm

Assuming 25 mm diameter main rods and 10 mm diameter stirrups,

$$d = 600 - 45 - 10 - 12.5 = 522.5 \text{ mm}$$

Step 1 Calculate the equivalent bending moment and shear force.

$$M_{el} = M_u + M_t = M_u + T_u \left(\frac{1+D/b}{1.7} \right)$$

$$= 150 + 60 \left(\frac{1 + 600/300}{1.7} \right) = 150 + 105.9 = 255.9 \text{ kNm}$$

$$V_e = V_u + 1.6 \frac{T_u}{b} = 120 + 1.6 \frac{60}{0.3} = 120 + 320 = 440 \text{ kN}$$

Step 2 Calculate longitudinal steel.

$$M_t = 105.9 \text{ kNm} < M_u = 150 \text{ kNm}$$

(If $M_t > M_u$, extra compression steel for $M_t - M_u$ has to be provided)

$$\begin{aligned} M_{u,\text{lim}} \text{ for M30 concrete} &= 0.138 f_{ck} b d^2 \\ &= 0.138 \times 30 \times 300 \times 532.5^2 \\ &= 352.2 \text{ kNm} > 255.9 \text{ kNm} \end{aligned}$$

Hence, the section can be designed as singly reinforced.

$$\frac{M_{el}}{b d^2} = \frac{255.9 \times 10^6}{300 \times 532.5^2} = 3.00$$

From Table 4 of SP 16, $p_t = 0.959$

$$A_{st} = \frac{0.959}{100} \times (300 \times 532.5) = 1532 \text{ mm}^2$$

Provide 2#25 + 2#20 ($A_{st} = 1608 \text{ mm}^2$)

Note: We may also provide 5#20 ($A_{st} = 1570 \text{ mm}^2$), but the space between the bars will be $(300 - 2 \times 45 - 2 \times 10 - 5 \times 20)/4 = 22.5 \text{ mm} < 25 \text{ mm}$ required as per Clause 26.3.2 of the code. Hence, 2#25 + 2#20 is chosen, which has slightly more area but provides better flow of concrete.

Step 3 Check for shear.

$$\tau_{ve} = \frac{V_e}{b d} = \frac{440 \times 10^3}{300 \times 532.5} = 2.754 \text{ MPa}$$

$$p_{t,\text{provided}} = \frac{1608 \times 100}{300 \times 532.5} = 1.0\%$$

From Table 19 of IS 456, $\tau_c = 0.66 \text{ N/mm}^2 < 2.754 \text{ N/mm}^2$

From Table 20 of IS 456 $\tau_{c,\text{max}} = 3.5 \text{ N/mm}^2 > 2.754 \text{ N/mm}^2$

Hence, stirrups should be provided.

Step 4 Design the stirrups.

As per Clause 41.4.3, two conditions should be satisfied.

Condition 1:

$$b_1 = 300 - 45 \times 2 - 2 \times 10 - 25 = 165 \text{ mm}$$

$$d_1 = 600 - 45 \times 2 - 2 \times 10 - 25 = 465 \text{ mm}$$

$$\begin{aligned} \frac{A_{sv}(0.87f_y)}{s_v} &= \frac{T_u}{b_1 d_1} + \frac{V_u}{2.5 d_1} = \frac{60 \times 10^6}{165 \times 465} + \frac{120 \times 10^3}{2.5 \times 465} \\ &= 885.2 \text{ N/mm} \end{aligned}$$

Condition 2:

$$\frac{A_{sv}(0.87f_y)}{s_v} = (\tau_{ve} - \tau_c) b = (2.754 - 0.66) \times 300 = 628.2 \text{ N/mm}$$

Hence, let us design for 885.2 N/mm.

Using Table 62 of SP16

$$\frac{A_{sv}(0.87f_y)}{s_v} = \frac{V_{us}}{d} = \frac{885.2}{1000} \times 10 = 8.852 \text{ kN/cm}$$

Provide 12 mm diameter stirrups at 90 mm centre-to-centre spacing with $V_{us}/d = 9.074 \text{ kN/cm}$. Adopt two-legged 12 mm diameter stirrups at 90 mm centre-to-centre spacing.

Step 5 Check for spacing as per Clause 26.5.1.7.

$$x_1 = 300 - 45 \times 2 - 10 = 200 \text{ mm}$$

$$d_1 = 600 - 45 \times 2 - 10 = 500 \text{ mm}$$

Spacing should not exceed $x_1 = 165 \text{ mm}$ or 300 mm or

$$\frac{x_1 + y_1}{4} = \frac{(200 + 500)}{4} = 175 \text{ mm} > 90 \text{ mm}$$

Hence, it is adequate.

Step 6 Check for side face reinforcement.

As per Clause 26.5.1.7(b), side face reinforcement should be provided as per Clause 26.5.1.3 if the depth exceeds 450 mm.

At each face, $A_s = 0.05/100 \times 600 \times 300 = 90 \text{ mm}^2$ at spacing less than 300 mm or web thickness.

Provide one bar of 12 mm (area = 113 mm^2) on each face at mid-depth and two 12 mm diameter nominal hangers at top, as shown in Fig. 8.26.

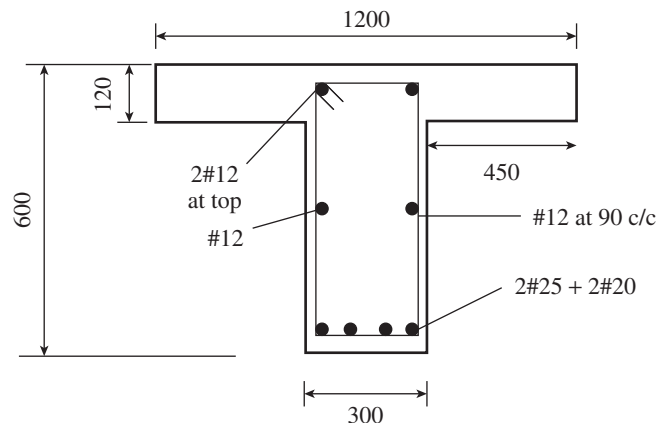


FIG. 8.26 Figure for Example 8.6

EXAMPLE 8.7 (Design of circular girder):

An Intz type water tank is supported on a ring beam of diameter 10 m, which in turn is supported by eight equally spaced columns along its perimeter, as shown in Fig. 8.3(a). A vertical load of 120 kN/m acts on the ring beam (excluding its self-weight). Design the ring beam, using M20 concrete and Fe 415 grade high-yield strength-deformed steel bars.

SOLUTION:

$w = 120 \text{ kN/m}$, $R = 5 \text{ m}$, 8 columns; hence $\theta = 45^\circ$

Self-weight of beam (assuming $300 \times 600 \text{ mm}$)

$$= 0.3 \times 0.6 \times 25 = 4.5 \text{ kN/m}$$

Total service load = 120 + 4.5 = 124.5 kN/m
 Total design ultimate load = 1.5 × 124.5 = 186.75 kN/m
 Total design ultimate load on circular beam, W
 $= 2\pi wR = 2 \times 3.14 \times 186.75 \times 5 = 5867 \text{ kN}$

Step 1 Design bending moments and shear forces.

Using Table 8.1, we get
 Negative maximum bending moment over support, $M_{nu} = K_1 wR^2$
 $= -0.0522 \times 186.75 \times 5^2 = 243.7 \text{ kNm}$
 Positive maximum bending moment, $M_{pu} = K_2 wR^2$
 $= 0.0264 \times 186.75 \times 5^2 = 123.3 \text{ kNm}$ acting at sections
 22° 30' from the columns
 Maximum torsional moment, $T_u = K_3 wR^2$
 $= 0.0038 \times 186.75 \times 5^2 = 17.74 \text{ kNm}$ acting at sections
 9° 33' from the columns
 Maximum shear force = $W/16 = 5867/16 = 366.7 \text{ kN}$
 Shear force at the section of maximum torsion

$$V_u = 366.7 - \frac{186.75 \times 5 \times \pi \times 9.5}{180} = 211.9 \text{ kN}$$

Step 2 Design beam at support.

$$M_{us} = 243.7 \text{ kNm}, V_u = 366.7 \text{ kN}$$

Assuming the width of beam as 300 mm,

$$\text{Effective depth} = d = \sqrt{\frac{M_{us}}{0.138 f_{ck} b}} = \sqrt{\frac{243.7 \times 10^6}{0.138 \times 20 \times 300}}$$

$$= 543 \text{ mm}$$

Adopt $D = 600 \text{ mm}$ and $d = 560 \text{ mm}$.

The required amount of reinforcement may be obtained from the formula

$$M_u = 0.87 f_y A_{st} d \left(1 - \frac{A_{st} f_y}{b d f_{ck}} \right)$$

Substituting, we get

$$243.7 \times 10^6 = 0.87 \times 415 \times A_{st} \times 560 \left(1 - \frac{415 \times A_{st}}{300 \times 560 \times 20} \right)$$

Solving this, we get $A_{st} = 1338 \text{ mm}^2$

Hence, provide 3#20 + 1#25 bars with $A_{st} = 1432 \text{ mm}^2$.

Transverse reinforcement:

$$\tau_v = \frac{V_u}{bd} = \frac{366.7 \times 1000}{300 \times 560} = 2.18 \text{ N/mm}^2 < \tau_{c,max} = 2.8 \text{ N/mm}^2$$

(Table 20 of IS 456)

$$p_t = \frac{100 A_s}{bd} = \frac{100 \times 1432}{300 \times 560} = 0.85$$

τ_c from Table 19 of IS 456 (for $p_t = 0.85$) = 0.584 N/mm²

$$\text{Shear taken by concrete} = \tau_c b d = 0.584 \times 300 \times 560 \times 10^{-3} = 98.12 \text{ kN}$$

Using 10 mm diameter, four-legged stirrups, spacing is given by

$$s_v = \frac{0.87 f_y A_{sv} d}{V_u - V_c} = \frac{0.87 \times 415 \times (4 \times 78.5) \times 560}{(366.7 - 98.12) \times 1000} = 236 \text{ mm}$$

Hence, provide 10 mm diameter stirrups at 225 mm centre-to-centre spacing.

Step 3 Design beam at mid-span.

$$M_{um} = 123.3 \text{ kNm}, V_u = 0 \text{ kN}$$

As before, the required amount of reinforcement may be obtained from

$$123.3 \times 10^6 = 0.87 \times 415 \times A_{st} \times 560 \left(1 - \frac{415 \times A_{st}}{300 \times 560 \times 20} \right)$$

Solving this equation, we get $A_{st} = 665 \text{ mm}^2$

Check for minimum A_{st} as per Clause 26.5.1.1

$$A_{st,min} = \frac{0.85 b d}{f_y} = \frac{0.85 \times 300 \times 560}{415} = 344 \text{ mm}^2 < 665 \text{ mm}^2$$

Hence, provide 4#16 mm diameter bars with $A_{st} = 804 \text{ mm}^2$.

Design for Shear

Since shear force is zero, we should provide minimum transverse reinforcement as per Clauses 26.5.1.5 and 26.5.1.6. Assuming 10 mm diameter stirrups,

$$s_v = \frac{0.87 f_y A_{sv}}{0.4 b} = \frac{0.87 \times 415 \times (2 \times 78.5)}{0.4 \times 300} = 472 \text{ mm} > s_{v,max}$$

$$= 0.75 d = 0.75 \times 560 = 420 \text{ mm}$$

Provide 10 mm diameter stirrups at 225 mm centre-to-centre spacing.

Step 4 Design the section subjected to torsion and shear.

$$T_u = 17.74 \text{ kNm}, V_u = 211.9 \text{ kN}, M_u = 0.0$$

As per Clause 41.4.2

$$M_t = T_u \left(\frac{1+D/b}{1.7} \right) = 17.74 \left(\frac{1+600/300}{1.7} \right) = 31.3 \text{ kNm}$$

$$M_{el} = M_u + M_t = 0.0 + 31.3 = 31.3 \text{ kNm}$$

Since the equivalent bending moment is small, we should provide at least minimum area of steel = 344 mm². Let us provide 4#16 bars with $A_{st} = 804 \text{ mm}^2$.

Note: We should provide equal amount of reinforcement in the compression side too. To provide easy detailing, let us provide 3#20 mm (area = 942 mm²).

Design of Transverse Reinforcement

As per Clause 41.3.1,

$$\text{Equivalent shear force, } V_e = V_u + \frac{1.6 T_u}{b} = 211.9 + \frac{1.6 \times 17.74}{0.3} = 306.5 \text{ kN}$$

$$\tau_{ve} = \frac{V_e}{bd} = \frac{306.5 \times 1000}{300 \times 560} = 1.82 \text{ N/mm}^2 < \tau_{c,\max} = 2.8 \text{ N/mm}^2$$

(Table 20 of IS 456)

$$p_t = \frac{100A_s}{bd} = \frac{100 \times 804}{300 \times 560} = 0.478$$

τ_c from Table 19 of IS 456 (for $p_t = 0.478$) = $0.47 \text{ N/mm}^2 < 1.82 \text{ N/mm}^2$

Hence, shear reinforcement has to be provided.

Using 10 mm diameter, two-legged stirrups, with side effective covers of 25 mm and bottom and top effective covers of 40 mm,

$$b_1 = 300 - 2 \times 25 = 250 \text{ mm}$$

$$d_1 = 600 - 2 \times 40 = 520 \text{ mm}$$

$$A_{sv} = 2 \times 78.5 = 157 \text{ mm}^2$$

Spacing should be less than the following (Clause 41.4.3):

$$s_{v1} = 0.87 f_y A_{sv} \left[\frac{b_1 d_1}{T_u} + \frac{2.5 d_1}{V_u} \right]$$

$$= 0.87 \times 415 \times 157 \left[\frac{250 \times 520}{17.74 \times 10^6} + \frac{2.5 \times 520}{211.9 \times 10^3} \right] = 763 \text{ mm}$$

$$s_{v2} = \frac{0.87 f_y A_{sv}}{(\tau_{ve} - \tau_c) b} = \frac{0.87 \times 415 \times 157}{(1.82 - 0.47) 300} = 140 \text{ mm}$$

Provide two-legged 10 mm stirrups at 140 mm centre-to-centre spacing.

Check for spacing as per Clause 26.5.1.7:

Height of stirrup leg, $y_1 = 250 + 20 + 10 = 280 \text{ mm}$

Width of stirrup leg, $x_1 = 520 + 20 + 10 = 550 \text{ mm}$

Spacing should not exceed $x_1 = 280 \text{ mm}$ or 300 mm or

$$\frac{x_1 + y_1}{4} = \frac{(280 + 550)}{4} = 207.5 \text{ mm} > 140 \text{ mm}$$

Hence, it is adequate.

Step 5 Check for side face reinforcement.

According to Clause 26.5.1.7(b), side face reinforcement should be provided as per Clause 26.5.1.3 if the depth exceeds 450 mm.

At each face, $A_s = 0.05/100 \times 600 \times 300 = 90 \text{ mm}^2$ at spacing less than 300 mm or web thickness.

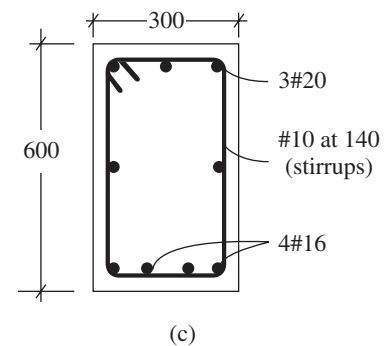
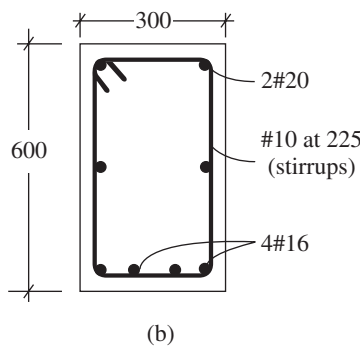
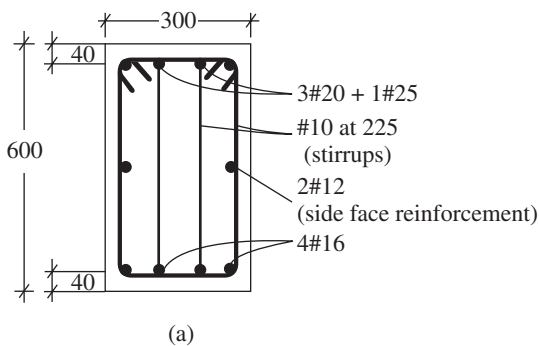


FIG. 8.27 Reinforcement of beam at different sections (a) At support (b) At mid-span (c) At section subjected to maximum torsion and shear

Provide one bar of 12 mm (area = 113 mm^2) on each face at mid-depth.

The reinforcement details of the beam at different sections are shown in Fig. 8.27.

EXAMPLE 8.8:

Design the reinforcement for a rectangular beam of size 300 mm by 500 mm, subjected to a torsional moment of $T_u = 30 \text{ kNm}$, using Rahal's graphical method. Assume $f_{ck} = 20 \text{ MPa}$ and $f_y = 415 \text{ MPa}$.

SOLUTION:

The outer perimeter of the gross section and the area enclosed within this perimeter are

$$A_{cp} = b \times d = 300 \times 500 = 150,000 \text{ mm}^2 \text{ and } p_{cp} = 2(b + d) = 2(300 + 500) = 1600 \text{ mm.}$$

Step 1 Check if the torsion effects can be neglected. As per the ACI code, the torsion effects can be neglected if $T_u \leq 0.25T_{cr}$.

$$T_{cr} = \phi 0.3 \sqrt{f_{ck}} \left(\frac{A_{cp}^2}{p_{cp}} \right) = 0.75 \times 0.3 \times \sqrt{20} \left(\frac{150,000^2}{1600} \right) \times 10^{-6}$$

$$= 14.15 \text{ kNm}$$

The torque is neglected if $T_u = 30 \text{ kNm}$ is less than $0.25T_{cr} = 0.25 \times 14.15 = 3.54 \text{ kNm}$. Since this requirement is not satisfied, the beam has to be designed for the applied torsion.

Step 2 Calculate the normalized shear stress and check adequacy of size of cross section. The shear stress in the walls of the cross section is calculated using Eq. (8.37) as

$$\frac{v_u}{f_{ck}} = \frac{(T_u / \phi) p_{cp}}{0.67 A_{cp}^2 f_{ck}} = \frac{(30 \times 10^6 / 0.75) \times 1600}{0.67 \times 150,000^2 \times 20} = 0.212$$

The normalized shear stress fits well within region I (Mode 1) in Fig. 8.23. Hence, the section can be designed to be under-reinforced and the section dimensions are adequate.

Step 3 Calculate the amounts of reinforcement. The most straightforward design of an under-reinforced section is to select equal amounts of longitudinal and transverse reinforcement indices ($\omega_t = \omega_l = v_u / f_{ck}$). Hence, $\omega_t = 0.212$ and

$\omega_t = 0.212$. From Eqs (8.36a and b), the amounts of transverse and longitudinal reinforcements are as follows:

$$\frac{A_t}{s_v} = \frac{0.42 A_{cp} f_{ck}}{f_{yt} \rho_{co}} \omega_t = \frac{0.42 \times 150,000 \times 20}{415 \times 1600} \times 0.212$$

$$= 0.402 \text{ mm}^2/\text{mm}$$

$$A_l = \frac{0.375 A_{cp} f_{ck}}{f_y} \omega_t = \frac{0.375 \times 150,000 \times 20}{415} \times 0.212$$

$$= 575 \text{ mm}^2$$

Choosing 8 mm diameter stirrups, $A_t = 50.3 \text{ mm}^2$, and spacing = $50.3/0.402 = 125 \text{ mm}$.

Provide 8 mm stirrups at 120 mm centre-to-centre spacing.

Provide six longitudinal bars of 12 mm diameter with $A_l = 6 \times 113 = 678 \text{ mm}^2$, as shown in Fig. 8.28. The spacing of the bars is less than 300 mm. Hence, it is adequate. Side face reinforcement = $0.05 \times 500 \times 300/100 = 75 \text{ mm}^2$; provided = 113 mm^2 . Hence, it is adequate.

Check for spacing:

The spacing should be the smallest of x_1 , $(x_1 + y_1)/4$, and 300 mm.

Assuming a clear cover of 30 mm and side cover of 25 mm,

$$x_1 = 300 - 2 \times 25 - 8 = 242 \text{ mm}$$

$$y_1 = 500 - 2 \times 30 - 8 = 432 \text{ mm}$$

Hence, spacing should be less than 242 mm, $(242 + 432)/4 = 168.5 \text{ mm}$, and 300 mm. Provided spacing = 120 mm. Hence, it is adequate.

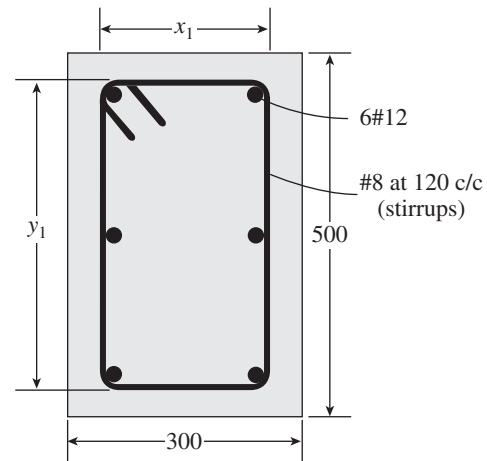


FIG. 8.28 Reinforcement of a rectangular beam

SUMMARY

Torsion develops in structural members as a result of asymmetrical loading, member geometry, or structural framing. Primary torsion, also called equilibrium torsion, exists when the external load has no alternative load path. Examples of such a situation include beams supporting canopy slabs, helicoidal stairway slabs, curved bridge girders, and ring beams at the bottom of circular water tanks. On the other hand, secondary torsion, or compatibility torsion, is due to the compatibility of deformation between the adjacent elements of a structure; edge beams or grid beams are examples of such secondary torsion. The expressions for calculating torsion in curved beams are provided. Torsional moments in edge beams may be determined by using a 3D analysis. Elastic and plastic torsional analyses are explained and the corresponding expressions are derived.

Torsional moment tends to twist the structural member around its longitudinal axis, inducing shear stresses. Unlike shear, which is a 2D problem, torsion is a 3D problem, involving both the shear problem of membrane elements and warping of the cross section. The behaviour of plain concrete beams as well as beams with torsional reinforcement is described.

A number of theoretical models have been developed in the past. The plastic space truss model, which has been adopted in several international codes, and the earlier skew bending theory, which forms the basis of the IS code, are fully explained. The equations for cracking torque, threshold torsion, nominal torsion capacity, and area of longitudinal as well as transverse reinforcements to resist torsion have been derived based on the space truss analogy. Although the diagonal tension stresses produced by torsion are very similar to those

caused by shear, they occur on all the faces of the member; hence, they have to be added to the stresses caused by shear on one face whereas subtracted from the stresses on the other face. The equations for controlling cracks based on the ACI code are also given.

The various failure modes as per the skew bending theory are explained and the equations for torsional strength for the three modes of failure are also given. The lowest of these strengths will be the strength of the beam. Interaction curves for combined torsion and moment and combined torsion and shear are provided. The simplified Indian code provisions based on the skew bending theory are explained.

The expression for minimum torsional reinforcement, which is required for ductility, is provided. The expression for maximum percentage of steel for pure torsion such that the beam is under-reinforced in torsion is also given. As the torsional cracks spiral around the beams, it is necessary to provide closed stirrups as well as additional longitudinal reinforcement, especially at the corners of the faces of the beams. Spacing requirements as per the IS code are also described. The importance of anchoring the stirrups to resist torsion is explained. The considerations for the design of T- and L-beams are also included.

The design steps necessary for designing a member subjected to combined torsion, bending moment, and shear as per the IS code are given. A graphical method for combined stresses, based on the MCFT, is explained. Other important considerations of size effect and high-strength concrete and steel are briefly discussed. Ample examples are provided to explain the formulae and concepts discussed in this chapter.

REVIEW QUESTIONS

1. Explain and differentiate between equilibrium and compatibility types of torsion.
2. Cite two examples of situations where there will be equilibrium torsion.
3. Cite two examples of situations where we have to consider compatibility torsion.
4. Many designers ignore compatibility torsion. Give your views about this. Is it acceptable? What are the consequences?
5. Will concrete columns be subjected to torsion? Can you site an example of this situation, that is, torsion existing with axial compression, flexure, and shear?
6. Write the expressions for torsional stiffness and angle of twist.
7. What are the critical sections for design in a curved beam?
8. Write the expression for τ_{\max} in a rectangular section as per the elastic theory.
9. What is the exact expression for torsional constant, C , derived by Timoshenko and Goodier?
10. Write down Bredt's equation for shear flow.
11. The explanatory handbook SP 24 suggests adopting a torsional stiffness C value equal to _____.
 - (a) half of the St Venant value
 - (b) one-third of the St Venant value
 - (c) one-fourth of the St Venant value
 - (d) none of these
12. In sand heap analogy, the ultimate torque is assumed to be _____.
 - (a) the volume of sand heap
 - (b) twice the volume of sand heap
 - (c) 1.5 times the volume of sand heap
 - (d) none of these
13. Write the expression of cracking torque of rectangular section based on the plastic (sand heap) theory.
14. Describe the behaviour of a plain rectangular beam subjected to torsion.
15. Describe the behaviour of a rectangular beam with torsional reinforcement subjected to torsion.
16. The best way to resist torsion is to provide _____.
 - (a) vertical open stirrups
 - (b) vertical closed stirrups and longitudinal bars
 - (c) spiral reinforcement
 - (d) none of these
17. Bent-up longitudinal bars can be used as shear reinforcement, but cannot be utilized as torsional reinforcement. Why?
18. Draw the typical torque–twist curve for an RC rectangular beam.
19. List any three models developed for the torsion of RC beams.
20. Explain the space truss analogy and derive the equation for the torsional capacity of a rectangular beam.
21. Write the expression given in the ACI code for cracking torque.
22. When the applied torque is equal to _____ per cent of the cracking torque, it can be ignored in the design.
 - (a) 10
 - (b) 20
 - (c) 25
 - (d) none of these
23. In the case of L-beams, the width of a slab that can be considered as per the ACI code is less than the projection of the beam below the slab or _____.
 - (a) two times the thickness of the slab
 - (b) three times the thickness of the slab
 - (c) four times the thickness of the slab
 - (d) five times the thickness of the slab
24. Derive the expression for the required longitudinal reinforcement for a rectangular RC beam based on plastic space truss theory.
25. Write the expression given in the ACI code for limiting the crack width.
26. Briefly discuss the different modes of failure under combined flexure and torsion as per skew bending theory.
27. Discuss the torsion–bending moment interaction of RC beams.
28. Discuss the torsion–shear interaction of RC beams.
29. Write down the equivalent shear and moment provisions of the IS code for designing beams subjected to torsion.
30. Why should minimum longitudinal reinforcement be provided when torsion is negligible?
31. State the equations provided in IS 456 for the design of stirrups for torsion.
32. Is the minimum stirrup reinforcement provision for torsion of the IS code different from that of shear? Write down the expression for minimum stirrup area as per IS 456.
33. What are the requirements for the spacing of torsional stirrups?
34. Why is it necessary to adequately anchor torsion reinforcement? Sketch a few recommended stirrup arrangements for rectangular, T-, and L- beams.
35. List the steps for designing rectangular beams for torsion as per the IS code provisions.
36. Why is the yield strength of stirrup reinforcement restricted in the codes?
37. What is size effect? Is it to be considered in the design of RC beams with stirrups subjected to torsion?
38. Which of the following statements is/are true?
 - (a) The presence of torsion invariably reduces the flexural strength of beams.
 - (b) The additional bottom longitudinal steel in asymmetrically reinforced sections increases the ultimate capacity in pure torsion.
 - (c) Side face reinforcement has to be provided only when the depth exceeds 750 mm.
 - (d) In order to limit crack width, f_y of stirrups should be restricted to 415 MPa.

EXERCISES

1. Compute the torsional moments in the canopy slab that is cantilevered 3 m from a beam of span 6 m, as shown in Fig. 8.1(a). The size of the beam is 300 mm \times 700 mm and is well anchored into the two RC columns. Assuming a live load of 2 kN/m² on the canopy slab, compute the design torsional moment to be resisted by the beam at critical section.

[Ans.: $T = 31.72$ kNm]

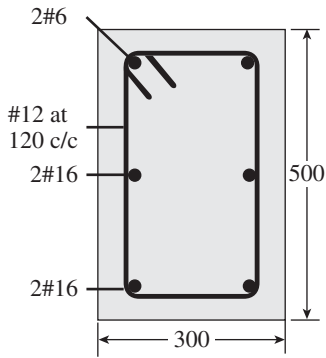


FIG. 8.29

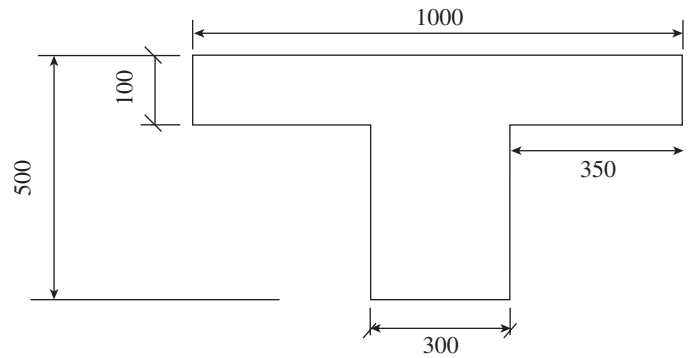


FIG. 8.30

- Determine the cracking torque of a rectangular concrete beam of size 300 mm by 500 mm, assuming M20 concrete using (a) plastic theory, (b) IS code, and (c) ACI code formulae. Assume $\tau_c = 0.3$ MPa.

[Ans.: (a) 16.09 kNm (b) 7.59 kNm (c) 13.99 kNm]

- The beam of Exercise 2 is reinforced with grade Fe 415 steel rebars as shown in Fig. 8.29. Determine the torsional capacity of the beam under pure torsion. Assume moderate exposure.
- A T-beam as shown in Fig. 8.30 is subjected to a factored torsion of 130 kNm. Calculate the amount of torsion resisted by the two main rectangular portions of the T-beam using (a) elastic theory and (b) plastic theory.
- Determine the torsional capacity and mode of failure for the beam given in Exercise 3 using skew bending theory.
- Design a rectangular beam for a section 300 mm wide with 535 mm effective depth subjected to the following factored loads: bending moment of 50 kNm, shear of 50 kN, and torsion of (a) 20 kNm

and (b) 40 kNm. Assuming M20 concrete and Fe 415 steel, design the reinforcements as per IS 456. Assume an effective cover of 35 mm. [Ans.: (a) Provide 2#16 + 1#12 at the bottom and top, two-legged 8 mm stirrups at 150 mm centre-to-centre spacing, and 2#10 as side face reinforcement. (b) Provide 2#20 + 1#12 at the bottom and top, two-legged 10 mm stirrups at 130 mm centre-to-centre spacing, and 2#10 as side face reinforcement.]

- A circular girder of an Intz type water tank of mean diameter 10 m is supported on six symmetrically placed columns. Assume that the circular girder supports a uniformly distributed load of 300 kN/m exclusive of its own self-weight. Design the girder using M25 concrete and Fe 415 grade HYSD bars.
- Design a semicircular beam supported on three equally spaced columns. The centre line of the columns is on a circle of diameter 8 m. Assuming that the superimposed load on the beam (excluding its self-weight) is 20 kN/m, design the beam using Fe 415 grade steel and M20 concrete.

REFERENCES

- ACI 445.1R-12, 'Report on Torsion in Structural Concrete', American Concrete Institute, Farmington Hills, MI.
- Bazant, Z.P. and S. Sener 1987, 'Size Effect in Torsional Failure of Concrete Beams', *Journal of Structural Engineering*, ASCE, Vol. 113, No. 10, pp. 2125–36.
- Beguín, G.H. 2007, 'A Helicoidal Concrete Ramp—A Graceful Prestressed Structure with Asymmetrical Section Built in Four Stages', *Concrete International*, ACI, Vol. 29, No. 7, pp. 37–42.
- Bentz, E.C. 2010, *Membrane-2012*, <http://www.ecf.utoronto.ca/~bentz/m2k.htm>, last accessed on 30 October 2012.
- Collins, M.P. 1973, 'Torque–Twist Characteristics of Reinforced Concrete Beams', *Inelasticity and Non-linearity in Structural Concrete*, SM Study No.8, University of Waterloo Press, Waterloo, pp. 211–31.
- Collins, M.P. and D. Mitchell 1991, *Prestressed Concrete Structures*, Prentice Hall, Englewood Cliffs, NJ, p. 720.
- Collins, M.P., P.F. Walsh, F.E. Archer, and A.S. Hall 1968, Ultimate strength of reinforced concrete beams subjected to combined torsion and bending, ACI Publication SP-18, Torsion of Structural Concrete, American Concrete Institute, Detroit.
- Collins, M.P. and P. Lampert 1973, 'Redistribution of Moments at Cracking—The Key to Simpler Torsion Design?', *Analysis of Structural Systems for Torsion*, SP-35, American Concrete Institute, Farmington Hills, pp. 343–83.
- Collins, M.P. and D. Mitchell 1981, 'Shear and Torsion Design of Prestressed and Non-prestressed Concrete Beams', *PCI Journal*, Vol. 25, No. 4, pp. 32–100, 'Discussion', Vol. 26, pp. 96–118.
- Elfgren, L. 1972, *Reinforced Concrete Beams Loaded in Combined Torsion, Bending and Shear—A Study of the Ultimate Load-carrying Capacity*, Ph. D. thesis, Publ. 71:1, Division of Concrete Structures, Chalmers University of Technology, 2nd edition, Göteborg, p. 230.
- Hsu, T.T.C. 1968a, 'Torsion of Structural Concrete—Plain Concrete Rectangular Sections', *Torsion of Structural Concrete (SP-18)*, American Concrete Institute, Detroit, pp. 203–38.
- Hsu, T.T.C. 1968b, 'Torsion of Structural Concrete—Behavior of Reinforced Concrete Rectangular Members', *Torsion of Structural Concrete (SP-18)*, American Concrete Institute, Detroit, pp. 261–306.
- Hsu, T.T.C. 1984, *Torsion of Structural Concrete*, Van Nostrand Reinhold, New York, p. 516.
- Hsu, T.T.C. 1988, 'Softening Truss Model Theory for Shear and Torsion', *ACI Structural Journal, Proceedings*, Vol. 85, No.6, pp. 624–35.
- Hsu, T.T.C. 1997, 'ACI Shear and Torsion Provisions for Prestressed Hollow Girders', *ACI Structural Journal*, Vol. 94, No. 6, pp. 787–99.

- Hsu, T.T.C. and K. Burton 1974, 'Design of Reinforced Concrete Spandrel Beams', *Journal of the Structural Division*, ASCE, Vol. 100, No. ST1, pp. 209–29.
- Hsu, T.T.C. and Y.L. Mo 1985, 'Softening of Concrete in Torsional Members—Theory and Tests', *ACI Journal, Proceedings*, Vol. 82, No. 3, pp. 290–303.
- Hsu T.T.C. and Y.L. Mo 2010, *Unified Theory of Concrete Structures*, John Wiley and Sons, Inc., New York.
- Iyengar, K.T.S. and N. Ram Prakash 1974, 'Recommendations for the Design of Reinforced Concrete Beams for Torsion, Bending and Shear', *The Bridge and Structural Engineer, Journal of ING/IABSE*, Vol. 4, No. 1, pp. 25–37.
- Jeng, C.H. and T.T.C. Hsu 2009, 'A Softened Membrane Model for Torsion in Reinforced Concrete Members', *Engineering Structures*, Vol. 31, No. 9, pp. 1944–54.
- Kirk, D.W. and N.C. Loveland 1972, 'Unsymmetrically Reinforced T-beams Subject to Combined Bending and Torsion', *Journal of the ACI*, Vol. 69, No. 8, pp. 492–499.
- Lampert, P. 1973, 'Postcracking Stiffness of Reinforced Concrete Beams in Torsion and Bending', *Analysis of Structural Systems for Torsion*, SP-35, American Concrete Institute, Farmington Hills, pp. 385–433.
- Lampert, P. and M.P. Collins 1972, 'Torsion, Bending and Confusion—An Attempt to Establish the Facts', *ACI Journal, Proceedings*, Vol. 69, No. 8, pp. 500–4.
- Lampert, P. and B. Thürlimann 1968 and 1969, *Torsionsversuch an Stahlbetonbalken* (Torsion Tests on Reinforced Concrete Beams) and *Torsion-Biege-Versuche an Stahlbetonbalken* (Torsion Bending Tests on Reinforced Concrete Beams), Bericht Nr. 6506-2 and 6506-3, Institut der Baustatik, ETH, Zurich (in German).
- Lampert, P. and B. Thürlimann 1971, 'Ultimate Strength and Design of Reinforced Concrete Beams in Torsion and Bending', *Publications, International Association for Bridge and Structural Engineering*, Vol. 31-1, pp. 107–31.
- Lessig, N.N. 1959, *Determination of Load-Carrying Capacity of Rectangular Reinforced Concrete Elements Subjected to Flexure and Torsion*, Work No. 5, Institute Betona I Zhelezobetona (Concrete and Reinforced Concrete Institute), Moscow, pp. 4–28 (in Russian), translated by Portland Cement Association, Foreign Literature Study No. 371.
- Leu, L.J. and Y.S. Lee 2000, 'Torsion Design Charts for Reinforced Concrete Rectangular Members', *Journal of Structural Engineering*, ASCE, Vol. 126, No. 2, pp. 210–8.
- Lu, Y. and L. Huang 2011, 'Research of Strength Interaction of Reinforced Concrete Members under Combined Loading', *Structural Engineers World Congress (SEWC) 2011*, 4–6 April 2011, Como–Villa Erba.
- Lucier, G., C. Walter, S. Rizkalla, P. Zia, and G. Klein 2011, 'Development of a Rational Design Methodology for Precast Concrete Slender Spandrel Beams, Part 2: Analysis and Design Guidelines', *PCI Journal*, pp. 106–32.
- MacGregor, J.G. and M.G. Ghoneim 1995, 'Design for Torsion', *ACI Structural Journal*, Vol. 92, No. 2, pp. 211–8.
- Mattock, A.H. 1968, 'How to Design for Torsion', *Torsion of Structural Concrete (SP-18)*, American Concrete Institute, Detroit, pp. 469–95.
- Mitchell, D. and M.P. Collins 1974, 'Diagonal Compression Field Theory—A Rational Model for Structural Concrete in Pure Torsion', *ACI Journal, Proceedings*, Vol. 71, No. 8, pp. 396–408.
- Mitchell, D. and M.P. Collins 1976, 'Detailing for Torsion', *ACI Journal, Proceedings*, Vol. 73, No. 9, pp. 506–11.
- Nadai, A. 1950, *Theory of Flow and Fracture of Solids*, 2nd edition, McGraw-Hill Book Company, New York, p. 572.
- Pandit, G.S. and S.P. Gupta 1991, *Torsion in Concrete Structures*, CBS Publishers and Distributors, Delhi, p. 512.
- Park, R. and T. Paulay, *Reinforced Concrete Structures*, John Wiley & sons, New York, 1975, p. 769.
- Purushothaman, P. 1984, *Reinforced Concrete Structural Elements, Behaviour, Analysis and Design*, Tata McGraw-Hill Publishing Co. Ltd, New Delhi, and Torsteel Research Foundation in India, Bangalore, p. 709.
- Rahal, K.N. 2007, 'Combined Torsion and Bending in Reinforced and Prestressed Concrete Beams using Simplified Method for Combined Stress Resultants', *ACI Structural Journal*, Vol. 104, No. 4, pp. 402–11.
- Rausch, E. 1929, *Berechnung des Eisenbetons gegen Verdrehung und Abscheren* (Design of Reinforced Concrete for Torsion and Shear), Springer Verlag, Berlin.
- Robinson, J.R. and J.M. Demorieux, *Essais de Traction-Compression sur Modèles d'Ame de Poutre en Béton Arme*, IRABA Report, Institut de Recherches Appliquées du Béton de L'Ame, Part 1, June 1968, p. 44, Part 2, May 1972, p. 53 (in French).
- Tamberg, K.G. and P.T. Mikluchin 1973, 'Torsional Phenomena Analysis and Concrete Structure Design', *Analysis of Structural systems for Torsion (SP-35)*, American Concrete Institute, Detroit, pp. 1–102.
- Timoshenko, S. and J.N. Goodier 1970, *Theory of Elasticity*, 3rd edition, McGraw Hill, New York, p. 608.
- Varyani U.H. and A. Radhaji 2005, *Design Aids for Limit States Design of Reinforced Concrete Members*, Khanna Publishers, Delhi, pp. 360–1.
- Vecchio, F.J. and M.P. Collins 1981, 'Stress–Strain Characteristic of Reinforced Concrete in Pure Shear', *IABSE Colloquium, Advanced Mechanics of Reinforced Concrete*, Delft, Final Report, IABSE, Zurich, pp. 221–25.
- Victor, D.J. 1966, *Semi-continuous Concrete T-beams without Stirrups under Combined Moment, Shear and Torsion*, Ph. D. thesis, The University of Texas at Austin.
- Victor D.J. and P.K. Aravindan 1978, 'Prestressed and Reinforced Concrete T-Beams under Combined Bending and Torsion', *ACI Journal, Proceedings*, Vol. 75, No 10, pp. 526–532.
- Victor, D.J., N. Lakshmanan, and N. Rajagopalan 1976, 'Ultimate Torque of Reinforced Concrete Sections', *Journal of the Structural Division*, ASCE, Vol. 102, No. ST7, pp. 1337–52.
- Warner, R.F., B.V. Rangan, and A.S. Hall 1976, *Reinforced Concrete*, Pitman, Australia.
- Warwaruk, J. 1981, 'Torsion in Reinforced Concrete', *Significant Developments in Engineering Practice and Research (SP-72)*, American Concrete Institute, Detroit, pp. 247–77.
- Wight, J.K. and J.G. MacGregor 2009, *Reinforced Concrete—Mechanics & Design*, 5th edition, Pearson-Prentice Hall, Upper Saddle River, NJ, p. 1112.
- Young, W.C. and R.G. Budynas 2002, *Roark's Formulas for Stress and Strain*, 7th edition, McGraw-Hill, New York, p. 851.
- Zia, P. 1968, 'Torsion Theories for Concrete Members', in *Torsion of Structural Concrete (SP-18)*, American Concrete Institute, Detroit, pp. 103–32.
- Zia, P. and T. Hsu 2004, 'Design for Torsion and Shear in Prestressed Concrete Flexural Members', *PCI Journal*, Vol. 49, No. 3, pp. 34–42.

DESIGN OF ONE-WAY SLABS

9.1 INTRODUCTION

Slabs are the most widely used structural elements whose thickness is considerably smaller than their other dimensions. They are frequently used as floors and roofs in buildings, decks in bridges, top and bottom of tanks, slabs-on-grade (directly supported on soil), staircases, and so on. They support and transmit loads to the walls or beams supporting them and sometimes transmit the loads directly to the columns by flexure, shear, and torsion. In addition to supporting vertical loads, slabs also act as deep horizontal girders to resist lateral wind and earthquake loads. Their action as *rigid diaphragms* of great stiffness is important in restricting the lateral deformation of multi-storeyed frames. It must be remembered that the very large volume and hence the mass of the slabs attract large lateral forces due to earthquake-induced accelerations. The maximum volume of concrete that goes into a structure is in the form of floor and roof slabs and footings. Due to this, the slightest reduction in the design depth will lead to considerable economy.

Slabs may have different shapes and support conditions. They can be of solid, ribbed, and waffle types. Depending on their load-carrying behaviour, they are classified as one-way or two-way slabs. In practice, the choice of slabs for a particular structure will largely depend upon the economy, buildability, loading conditions, and length of the span.

Slabs may be visualized as consisting of intersecting and closely spaced grid beams and hence are highly indeterminate. This high indeterminacy is very helpful to design engineers, as multiple load paths are available, and approximations in the analysis and design of slabs are compensated by heavy cracking and large deflections, without significantly affecting the load-carrying capacity (Purushothaman 1984).

A slab is generally designed as a flexural element considering a strip of 1 m width, even though it is cast in one

piece and not in strips of unit width. Hence, for the purpose of design, a slab is equivalent to a rectangular beam, with $b = 1000$ mm. The moment of resistance and the required area of reinforcement are expressed per unit width. The formulae derived for beams in Chapter 5 also apply to slabs, with $b = 1000$ mm. As slabs are thin compared to beams, the serviceability limit state of deflection is normally critical in slabs, rather than the ultimate limit states of bending and shear. Since slabs have relatively larger surface area compared to their volume, they are more affected by temperature and shrinkage stresses. Often, secondary reinforcement is provided to resist these stresses. Shear stresses are not critical in slabs, and hence, reinforcements to resist shear forces are generally not necessary in one-way slabs, unless the span is small and the load is large.

9.2 TYPES OF SLABS

Depending on the support conditions, slabs may be simply supported, continuous, or cantilevered. Slabs may also take various shapes such as rectangular, square, trapezoidal, circular, and triangular. While the rectangular slabs are frequently used, the circular slabs are often found in tanks. As mentioned earlier, a variety of slabs are possible, which include solid, ribbed, waffle, flat, and flat plate types. They can also be classified based on their method of construction as precast, prestressed, or cast in situ. In India, cast in situ slabs are common, whereas precast slabs are common in some countries like the USA.

In addition to these classifications, slabs may be categorized into one-way and two-way slabs depending on the way they support the loads. *One-way slabs* are those in which most of the load is carried on the shorter span. Some examples of one-way slabs are shown in Fig. 9.1. As seen in this figure, one-way slabs may be continuous or even cantilevered.

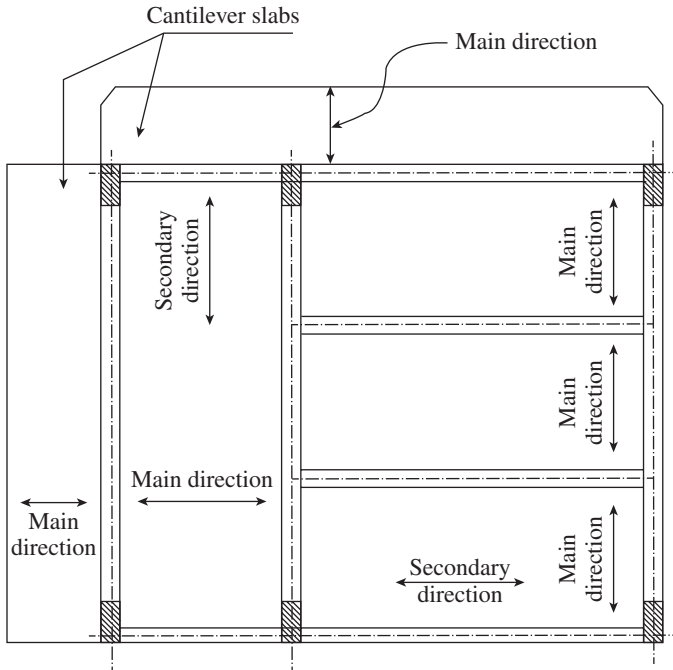


FIG. 9.1 Examples of one-way slab

One-way slab behaviour is evident when the ratio of the longer span to shorter span is greater than two or when a slab is supported only along two opposite sides. When the ratio of the longer span to the shorter span is less than two, the load sharing is done in both the directions, provided the slab is supported on all the four sides. These slabs are called two-way slabs and are discussed in Chapter 10.

9.3 BEHAVIOUR OF ONE-WAY SLABS

One-way slabs are usually made to span in the shorter direction alone, as the corresponding bending moments (B.M.) and shear forces are the maximum. The direction in which the load is carried—the short side—is called the *span*. The direction in which the slab bends is called the *main direction*, as shown in Fig. 9.1. The main reinforcement is placed at the tension face of the slab (usually at the bottom) in this direction alone (see Fig. 9.2a). Steel is provided in the transverse direction too to take care of the temperature and shrinkage effects in that direction. This steel is called the *distribution steel* or *secondary reinforcement*. It also helps in distributing the load. For example, point loads have a tendency to punch through the slab, and the distribution steel aids in distributing the load transversely over a larger width, thus offsetting the local effect. Even when a slab with $L_y/L_x \geq 2$ (where L_y is the long span and L_x is the shorter span) is supported on all four sides, one-way slab behaviour alone is to be expected, as evident from the deflection contour shown in Fig. 9.2(b). However, at the slab near the edges, some of the load is also transferred in the longitudinal direction, thereby producing two-way action. To account for this action, top reinforcement should be provided. If this reinforcement is not provided, wide cracks may appear on the top of the support along the shorter edges.

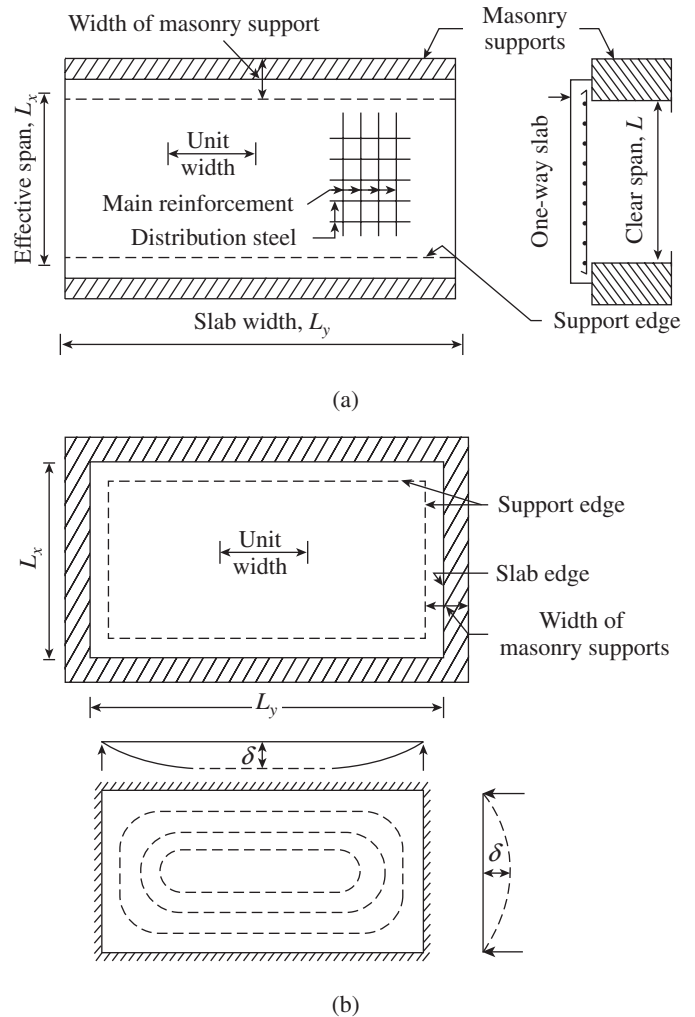


FIG. 9.2 One-way action in slabs (a) Typical one-way slab resting on masonry walls (b) Deflection contours of long slabs ($L_y/L_x \geq 2.0$)

It is important to note that if a slab panel is supported on only two parallel sides, it will act only as a one-way slab, regardless of the ratio of the long to short sides.

9.4 GENERAL CONSIDERATIONS FOR DESIGN OF SLABS

Before we attempt to design a one-way slab, we shall discuss the factors that affect the design of these slabs: effective span, control of deflection, behaviour of slabs cast monolithically with the supporting beams, effect of concentrated loads, minimum and maximum reinforcement, cover to reinforcement, and permissible shear stress in the following sections.

9.4.1 Effective Span

As the bending moment varies with the square of the effective span, it is important to fix the effective span correctly. Clause 22.2 of IS 456 suggests the following:

1. For slabs that are not built integrally with their supports, for example, slabs supported by brick walls or rolled-steel joists,

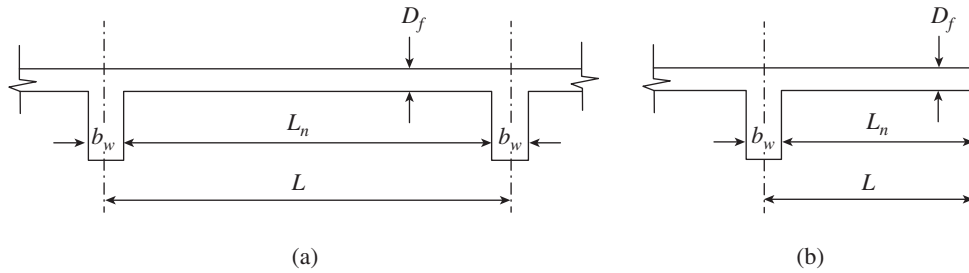


FIG. 9.3 Effective span of slabs (a) Continuous span (b) Cantilever span

Effective span, $L = (\text{Clear span, } L_n + \text{Effective depth of slab, } d)$ or c/c of supports, whichever is less (where L_n is the clear span, as shown in Fig. 9.3a, and c/c is the centre-to-centre distance)

2. For continuous slabs cast monolithically with supporting beams (see Fig. 9.3a),
 - (a) If width of support $b_w \leq L_n/12$
Effective span, $L = (\text{Clear span, } L_n + \text{Effective depth of slab, } d)$ or c/c of supports, whichever is less
 - (b) If width of support $b_w > L_n/12$ or 600 mm, whichever is less
 - (i) For end span with one end fixed and the other continuous or for intermediate spans,
Effective span, $L = L_n$
 - (ii) For end span with one end free and the other continuous,
Effective span, $L = L_n + d/2$ or $L_n + \text{Half width of discontinuous support, whichever is less}$
 - (iii) For spans with roller or rocker bearings,
Effective span, $L = \text{Distance between the centres of bearings}$
3. For cantilevers,
 - (a) Normally
Effective span, $L = L_n + d/2$
 - (b) If it forms the end of a continuous beam
Effective span, $L = L_n + b_w/2$

9.4.2 Minimum Thickness

The deflection requirements for slabs, which are the same as those for beams, will often control the required depth of the slabs. Most codes offer two methods for control of deflections: (a) checking the actual deflections against the allowable limits and (b) adopting specified maximum span to depth ratios for which serviceability can be assumed to be satisfied (limiting deflection of span/250 will not be exceeded) and hence detailed calculations for deflections are not required.

Explicit or direct computation of deflection using the equations given in Annexure C of IS 456 is lengthy and time consuming for normal building design (see Chapter 12 for these calculations). In addition, calculating the immediate deflection of the reinforced concrete (RC) members is difficult and inaccurate due to concrete cracking in the tension zone, caused

by early-age construction loads. Calculating the additional deflections due to shrinkage, creep, and the consequent redistribution of stresses is extremely difficult (Gardner 2011). Hence, the second method is generally adopted by the designers.

The following principle is involved in arriving at the basic values of the span to effective depth ratios:

Consider a fully elastic, simply supported rectangular member supporting a uniformly distributed load of w per unit length. If the permissible bending stress is f_b , then the section can support a moment M given by

$$M = f_b Z = \frac{f_b D^2}{6} = \frac{wL^2}{8} \quad (9.1)$$

The deflection of this beam will be

$$\delta = \frac{5}{384} \frac{wL^4}{EI} \quad (9.2)$$

From Eq. (9.1), we get

$$w = \frac{4}{3} f_b \left(\frac{D}{L} \right)^2 \quad (9.3)$$

Substituting the value of w in Eq. (9.2) and considering $I = bD^3/12$, with $b = 1$ m, we get

$$\frac{\delta}{L} = \frac{5}{24} \left(\frac{f_b}{E} \right) \left(\frac{L}{D} \right) \quad (9.4)$$

This equation can be generalized for other types of support conditions and loading and written as

$$\frac{\delta}{L} = K \left(\frac{L}{D} \right) \quad (9.5)$$

Thus, for a given elastic material, if the ratio of (L/D) is kept constant, the ratio of deflection to span will remain constant. By setting a limit to the ratio of span to depth, the deflections will be limited to a given fraction of the span (SP 24:1983; Beeby 1971). The basic ratios for different support conditions of the slab, as given in Clause 23.2.1 of IS 456, are shown in Table 9.1. For comparison, the values given by the ACI code are given in Table 9.2. More discussions on the (L/d) ratios may be found in Scanlon and Choi (1999) and Bischoff and Scanlon (2009).

TABLE 9.1 Basic span to effective depth ratios for flexural members as per IS 456:2000 and BS 8110:97

Support Condition	Rectangular Sections
Simply supported	20
Continuous	26
Cantilever	7

Note: For spans above 10m, these values may be multiplied by 10/span in metres, except for cantilevers, in which case deflection calculations should be made.

TABLE 9.2 Minimum thickness of flexural members as per Clause 9.5.2 of ACI 318-11

Member	Simply Supported	One End Continuous	Both Ends Continuous	Cantilever
	Members <i>Not</i> Supporting or Attached to Partitions or Other Construction Likely to be Damaged by Large Deflection			
Solid one-way slab	L/20	L/24	L/28	L/10
Beams or ribbed one-way slabs	L/16	L/18.5	L/21	L/8

Notes:

1. For f_y other than 415MPa, the values should be multiplied by $(0.4 + f_y / 700)$.
2. For lightweight concrete having density w_c in the range 1440–1840kg/m³, the values should be multiplied by $(1.65 - 0.0003w_c)$ but not less than 1.09.

Deflection is influenced by several parameters, which include the percentage of tension reinforcement and the stress at the service loads. In general, the percentage of reinforcement in slabs is low. Hence, we can use the span to effective depth ratios that are larger than those used for beams. In addition, the provision of compression reinforcement reduces the shrinkage and creep effects, and in turn reduces the long-term deflections. These facts are recognized by the code and it has given two modification factors, k_t and k_c , as shown in Figs 9.4 and 9.5 (Beeby 1971). It should be noted that while estimating k_t , the value of p_t and f_{st} should be considered at the *mid-span region*; however, in the case of cantilevers, p_t and f_{st} should be considered at the support.

The curves for the different grades of steel specified in Fig. 9.4 are based on the assumption

$$f_s = 0.58 f_y \frac{A_{st,required}}{A_{st,provided}} \quad (9.6)$$

where f_s is the stress in steel at service loads and f_y is the characteristic yield strength of the steel. It has to be noted that in this equation, 0.58 f_y is obtained from $(0.87/1.5)f_y$.

The multiplication factor k_t given in Fig. 9.4 can also be expressed by the following empirical formula suggested by Beeby (1971):

$$k_t = \frac{1}{0.225 + 0.00322 f_s - 0.625 \log_{10} \left(\frac{bd}{100 A_{st}} \right)} \quad (9.7)$$

The multiplication factor k_c given in Fig. 9.5 can also be expressed by the following empirical formula suggested by Beeby (1971):

$$k_c = 1 + \frac{p_c}{p_c + 3} \leq 1.5 \quad (9.8)$$

where p_c is the percentage of compression reinforcement = $\frac{100 A_{sc}}{bd}$.

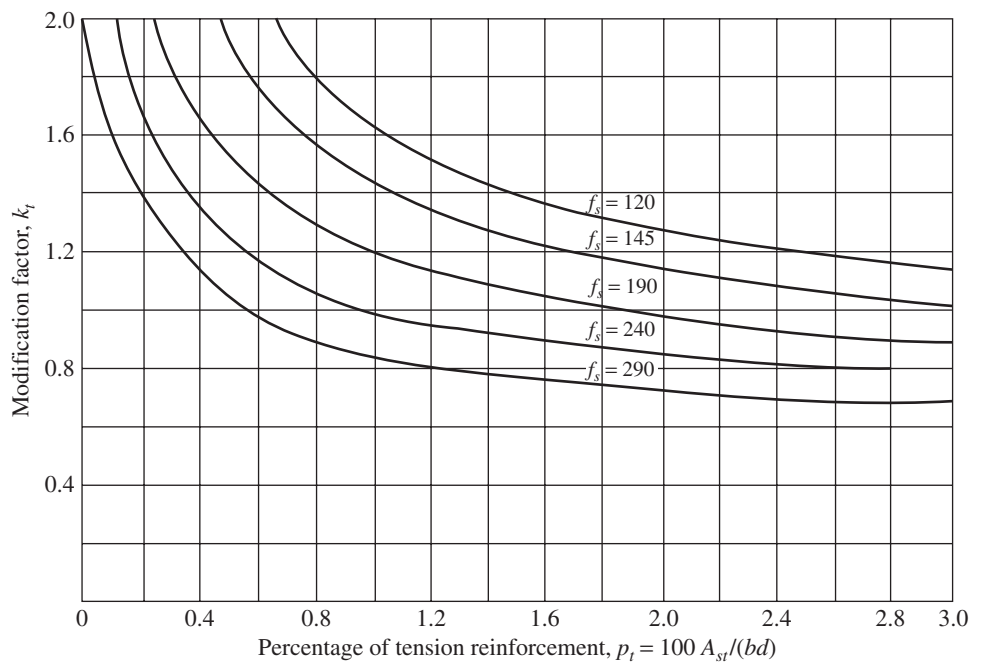


FIG. 9.4 Modification factor for tension reinforcement

Note: f_s is the steel stress at service loads in N/mm²

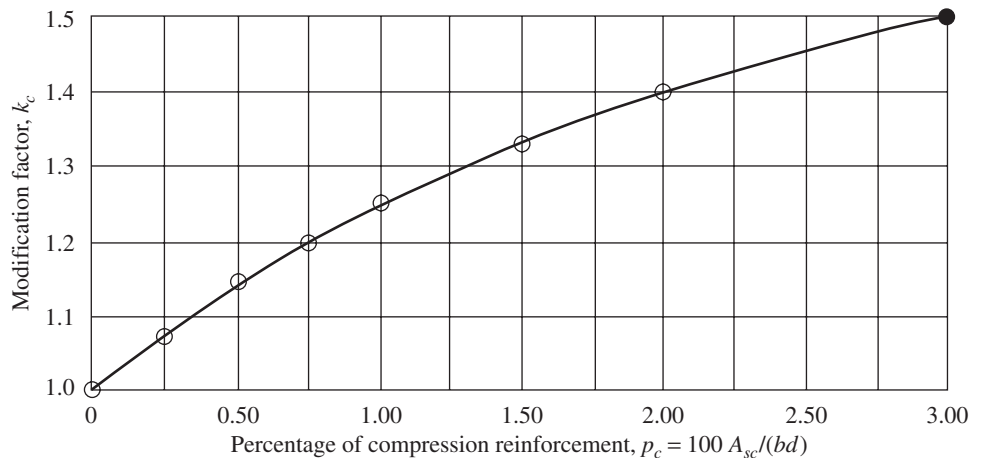


FIG. 9.5 Modification factor for compression reinforcement

Thus, the minimum effective depth of slab, d_{min} , can be calculated using

$$d_{min} = \frac{\text{Span}}{\text{Basic}(L/d)\text{ratio} \times k_t \times k_c} \quad (9.9)$$

With an initial estimate of $k_t = 1.4$, corresponding to a tension steel of 0.3 per cent, the L/d ratio for a simply supported slab with Fe 415 steel works out to 28. Hence, an effective depth of $L/25$ may be assumed for simply supported one-way slabs and about $L/32$ for continuous one-way slabs. (It is interesting to note that IS 456 also gives a reduction factor as applicable to the flanged beam in Fig. 6 of the code. However, SP 24:1983 states this may give abnormal results in some cases; hence, it may be advisable to ignore the flanges and consider only the rectangular web for calculating the L/d ratios.)

Thus, it is clear that when one desires to have a shallower member, the deflection can be kept within the required limits by providing more tension reinforcements than that required from strength considerations. Increasing the percentage of compression steel is the best method to control deflections without decreasing the strain in the tension steel beyond the limit specified in Clause 37.1(f) of the code.

The minimum thickness should also be checked against the required fire resistance (ranges between 75 mm for 0.5 hours and 170 mm for 4.0 hours; see Fig. 1 of IS 456).

9.4.3 Concrete Cover

The nominal cover specified for durability under different exposure conditions is given in Section 4.2.4 (see Table 4.6) of Chapter 4. If the local authorities specify fire protection, the cover should be selected based on the required hours of fire resistance (see Table 4.7). More information on the calculation methods for structural fire protection may be found in ASCE/SEI/SFPE 29-05. The minimum cover for slabs should not be less than 15 mm and the maximum cover not more than 75 mm as per Tables 4.6 and 4.7. As increased covers increase the dead load and the cost of any slab, the designer should exercise his/her judgment in the choice of the cover. In addition, the cover at each end of the reinforcing bar should not be less than 25 mm or less than twice the diameter of such a bar.

9.4.4 Analysis of Continuous One-way Slabs

For a simply supported, fixed, or cantilever one-way slab, the maximum bending moment and shear force can be calculated using Fig. 9.6, where w_u is the uniformly distributed load/m, $W = w_u L$, and L is the effective span.

In a continuous one-way slab, the precise determination of the theoretical bending moments may involve mathematical labour. Moreover, the probability of theoretical bending moments being greater than those actually realized due to

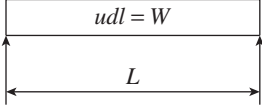
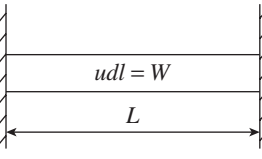
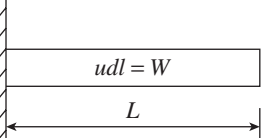
Loading	Maximum bending moment	Maximum shear force	Maximum deflection
	$\frac{WL}{8}$	$\frac{W}{2}$	$\frac{5WL^3}{384EI}$
	$\frac{WL}{12}$ at supports	$\frac{W}{2}$	$\frac{WL^3}{384EI}$
	$\frac{WL}{2}$	W	$\frac{WL^3}{8EI}$

FIG. 9.6 Bending moment, shear force, and deflection for single-span one-way slabs; udl —uniformly distributed load

the simplifying assumptions of knife-edge supports and uniform moment of inertia should also be considered. Hence, approximate bending moment coefficients for continuous beams are often suggested by the codes. The coefficients suggested by Clause 22.5.1 of IS 456 are given in Fig. 9.7. The dead loads (w_d) and live (imposed) loads (w_l) acting on the slab may be assumed as per IS 875: Parts 1 and 2 (see Sections 3.3 and 3.4 of Chapter 3). The live load moment coefficients are different from the dead load coefficients because of the combinations of adjacent spans loaded or alternate spans loaded cases (see Section 3.10).

The coefficients given in Fig. 9.7 are valid when the following conditions are satisfied:

1. Beams and slabs have uniform sections and are substantially subjected to a uniformly distributed load.
2. They are continuous over at least three spans.
3. Spans are more or less equal and the differences in spans are not more than 15 per cent of the longest span.
4. Unfactored live load does not exceed three times the unfactored dead load.
5. For moments at supports where two unequal spans meet or in case the spans are not equally loaded, the average of the two values for the negative moment at support may be considered for design.

It has to be noted that for members built into partially restraining supports, a negative bending moment coefficient of $w_u L^2/24$ at the face of the end support has to be considered. For this case, the shear force coefficient at the end support may be increased by 0.05, as per Clause 22.5.2 of IS 456.

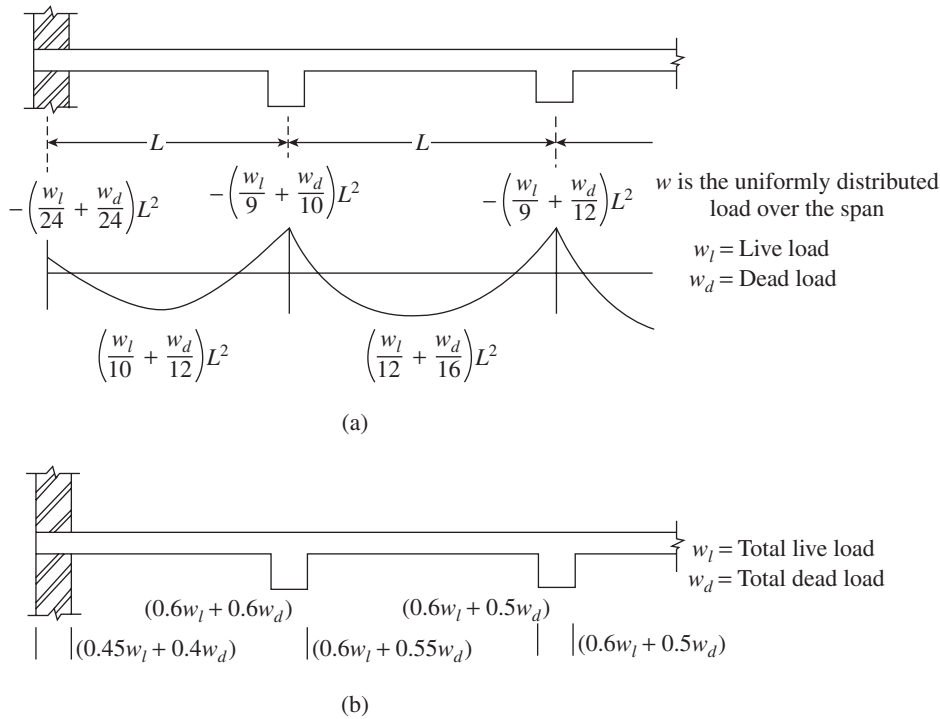


FIG. 9.7 Coefficients for continuous one-way slabs as per IS 456 (a) Bending moment (b) Shear force

When the coefficients given in Fig. 9.7 are considered, redistribution of moments is *not* allowed by the code. This is because the moment coefficients given in the code are derived only after performing the redistribution. *Moment redistribution* refers to the behaviour of statically indeterminate concrete members or structures that are not completely elastic, but have some reserve plastic capacity. When one location first yields, further load applied to the member or structure causes inelastic rotation at the yielded section and the bending moment is redistributed to other cross sections of the member that are still elastic. Further increases in load will make other sections to yield and develop hinges. This process continues until enough hinges are formed to produce a mechanism and the member or structure fails (Bondy 2003).

It is permissible to obtain the values of bending moments and shear forces using computer analysis by considering pattern loading (see Section 3.10), in which case redistribution is allowed. It should be noted that there is a slight difference in the values of coefficients suggested by the Indian and US codes (see Clause 8.3.3 of ACI 318).

From Fig. 9.7, it may be noted that the end span is more critical

than the interior spans. As the mid-span moment in the end span is larger than that in the interior spans, the end span will require more reinforcement and may govern the thickness. In practice, the same thickness is provided for interior spans too, unless there is a significant difference in the thicknesses.

Critical Sections for Moment and Shear

The moment diagram for continuous beams or slabs is usually quite steep in the region of support and there may be substantial difference between the support centre line (C.L.) moment and the moment at the face of the support (see Fig. 9.8). If the former is used in proportioning the member, a large section will result unnecessarily. Hence, for monolithic constructions, Clause 22.6.1 of the code allows the

slab or beam to be designed for the reduced moments computed at the face of the support. For non-monolithic constructions, such reductions are not possible at the support. Clause 24.3.1 of the code suggests that the beams supporting monolithic slabs may be assumed to be rigid and do not deform in relation to the slab.

For simple supports, Clause 22.6.2 of the code stipulates that the shear computed at the face of the support is to be considered in the design of the member.

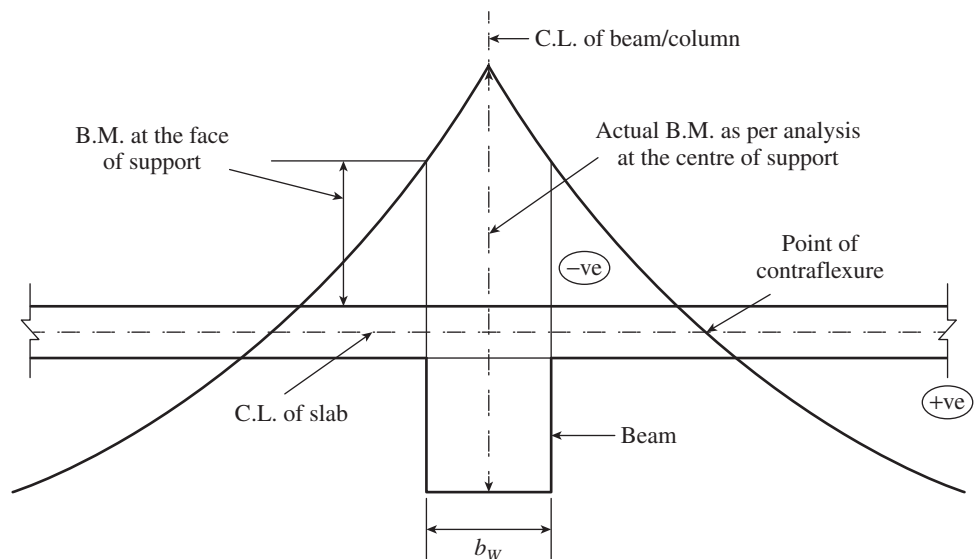


FIG. 9.8 Reduced bending moment at face of support

9.4.5 Calculation of Reinforcements

As the depth chosen based on the deflection criteria will normally be greater than that required for bending, the tension steel required will be less than the balanced steel, and the section will be under-reinforced. A check may be made for the effective depth, d , required for bending using Eq. (5.28a):

$$d = \sqrt{\frac{M_u}{k f_{ck} b}}$$

For Fe 415 grade steel, the value of $k_2 = 0.138$; hence, using Eq. (5.28b), we have

$$d = \sqrt{\frac{M_u}{0.138 f_{ck} b}} = \sqrt{\frac{7.2 M_u}{f_{ck} b}}$$

For Fe 250 and Fe 500 grade steel, the coefficient 7.2 in Eq. (5.28b) is to be replaced by 6.71 and 7.52, respectively. It has to be noted that in these equations, b is taken as 1000 mm.

From Section 5.5.1 of Chapter 5, the depth of neutral axis at the ultimate load x_u may be determined using Eq. (5.29a)

$$\left(\frac{x_u}{d}\right) = 1.2 - \sqrt{1.44 - \frac{6.68 M_u}{f_{ck} b d^2}}$$

The required amount of steel, A_{st} , may be calculated using the formula derived for beams in Section 5.4.4 of Chapter 5 (given here again for completeness) or by using the charts and tables given in SP 16 (p_t should be less than $p_{t,lim}$ given in Table 5.5 of Chapter 5 for ductile behaviour):

$$A_{st} = \frac{M_u}{0.87 f_y z} \tag{9.10a}$$

where the lever arm, $z = d \left(1 - 0.416 \frac{x_u}{d}\right)$. (9.10b)

The area of reinforcement may also be found using the following approximate formula:

$$A_{st} = \frac{M_u}{0.8 d f_y} \tag{9.10c}$$

This formula has been found to give a fairly good estimation of the area of bars.

The area of secondary or distribution steel is 0.12 per cent of the cross-sectional area for high-yield strength bars and 0.15 per cent for mild steel bars. The spacing of bars may be calculated as

$$s = \frac{1000(\pi d_b^2 / 4)}{A_{st}} \tag{9.11}$$

where d_b is the diameter of the chosen bar.

The use of compression reinforcement in slabs is unusual. However, when required it can be calculated in the same way as for a rectangular beam (see Section 5.6 of Chapter 5). Links or other means of preventing compression bars from buckling should be provided at centres not exceeding 12 times the diameter of the compression bars; otherwise, the bars in compression

should be neglected when computing the resistance (Reynolds and Steedman 2008).

Minimum and Maximum Flexural Reinforcement in Slabs

Clause 26.5.2 of IS 456 stipulates the following minimum reinforcement ($A_{st,min}$) in either direction of the slab:

$$\left. \begin{aligned} A_{st,min} &= 0.0015bD \text{ for Fe 250 grade steel} \\ &0.0012bD \text{ for Fe 415 grade steel} \\ &\text{or welded wire fabric} \end{aligned} \right\} \tag{9.12}$$

It has to be noted that these minimum requirements are based on the considerations of shrinkage and temperature effects alone, and not on strength. However, SP 24:1983 states that the minimum reinforcement required for slabs is less than that required for beams, since the overload will be distributed laterally and sudden failure will be less likely, and is therefore based on the shrinkage and temperature effects.

Moreover, as shown in Fig. 9.9, the spacing of such bars should not exceed $3d$ or 300mm in the case of main reinforcement and $5d$ or 300mm, whichever is less, in the case of secondary reinforcement (it has to be noted that this change from 450mm to 300mm in the case of secondary reinforcement was made in the third amendment to IS 456 in August 2007. However, Clause 7.12.2.2 of ACI 318 specifies $5D$ or 450mm). In addition, Clause 26.5.2.2 stipulates that the diameter of the reinforcing bars should not exceed one-eighth of the total depth of the slab, that is, $d_b \leq D/8$.

It should be noted that the minimum flexural tension reinforcement for each direction of a slab given by the ACI code (Clause 7.12.2.1) is higher than that given by IS 456 and takes into account higher steel grades (see Table 3.9). In addition, the ACI code imposes an upper limit of 0.04 times the gross cross-sectional area on both the tension and compression reinforcements.

It has to be noted that these requirements are satisfactory when shrinkage and temperature movements are permitted to occur. When structural walls or columns provide significant restraint to shrinkage and temperature movements, it causes tension in the slabs in addition to displacements, shear forces, and flexural moments in columns or walls. In such cases, it may be necessary to increase the amount of shrinkage and thermal reinforcements in the slabs in both the principal directions

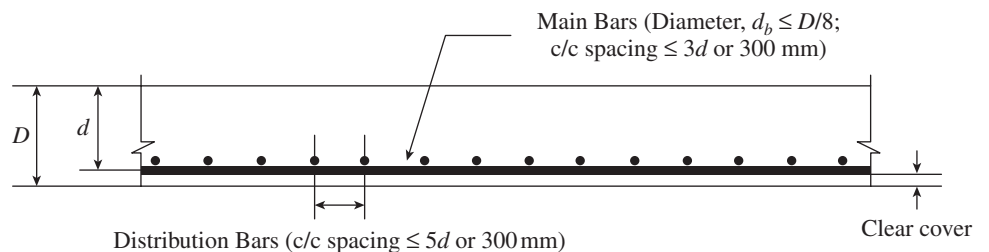


FIG. 9.9 Spacing of reinforcement in one-way slabs for crack control

(Gilbert 1992; Suprenant 2002a). In such cases, approximately *two to three times* the minimum shrinkage and temperature reinforcements specified in codes may be required to limit the shrinkage cracks to reasonable widths. Alternatively, unconcreted shrinkage control strips may be left during construction, which are filled in with concrete after the initial shrinkage has occurred (Suprenant 2002b). See Section 3.9.2 of Chapter 3 for more information on shrinkage control strips.

Recently, Rizk and Marzouk (2009) pointed out that the following formula, Eq. (5.36c), given in the ACI 318-08 code for minimum flexural reinforcement does not account for the member size effect:

$$\frac{A_s}{bd} = \frac{0.224\sqrt{f_{ck}}}{f_y} \geq \frac{1.4}{f_y}$$

Hence, using fracture mechanics, they proposed the following equations for minimum flexural reinforcement in slabs. For slabs with thickness ranging from 100 mm to 200 mm and covers up to 50 mm

$$\left(\frac{A_s}{bd}\right)_{\min} = \frac{0.415f_r}{f_y} \left(\frac{l_{ch}}{2h_{ef}}\right)^{0.33} \quad (9.13a)$$

For slabs with thickness ranging from 200 mm to 400 mm and covers up to 75 mm

$$\left(\frac{A_s}{bd}\right)_{\min} = \frac{0.358f_r}{f_y} \left(\frac{l_{ch}}{2h_{ef}}\right)^{0.33} \quad (9.13b)$$

where f_r is the modulus of rupture of concrete and may be taken as $0.67\sqrt{f_{ck}}$, l_{ch} is the characteristic length $= \left(\frac{E_c G_f}{f_t^2}\right)$, E_c is the modulus of elasticity of concrete, G_f is the fracture energy, f_t is the tensile strength of concrete, determined from split cylinder tests, h_{ef} is the effective embedment thickness $\approx D/2$, and D is the depth of slab. The characteristic length, l_{ch} , was estimated to have an average value of 500 mm (with $G_f = 110\text{N/m}$) and 250 mm (with $G_f = 160\text{N/m}$) for normal strength concrete (NSC) and high-strength concrete (HSC), respectively.

9.4.6 Detailing of Reinforcement in One-way Slabs

Unless the actual crack widths have been checked by direct calculation,

the following rules given in the code (see Clause 26.3.3b) will ensure that crack widths will not generally exceed 0.3 mm (refer to Fig. 9.9). This limit on crack widths is based on considerations of appearance and durability.

1. The horizontal spacing between parallel main reinforcement bars is less than $3d$ or 300 mm.
2. The horizontal spacing between parallel reinforcement bars of shrinkage and temperature steel is less than $5d$ or 300 mm.

Figure 9.10 shows the detailing of reinforcement in simply supported single-span one-way slabs. It should be noted that alternate main reinforcement bars are bent up near the supports at a distance of $0.1L$ from the support, as per Clause D-1.6 of the code, to resist any tension that may arise on account of partial fixity of support.

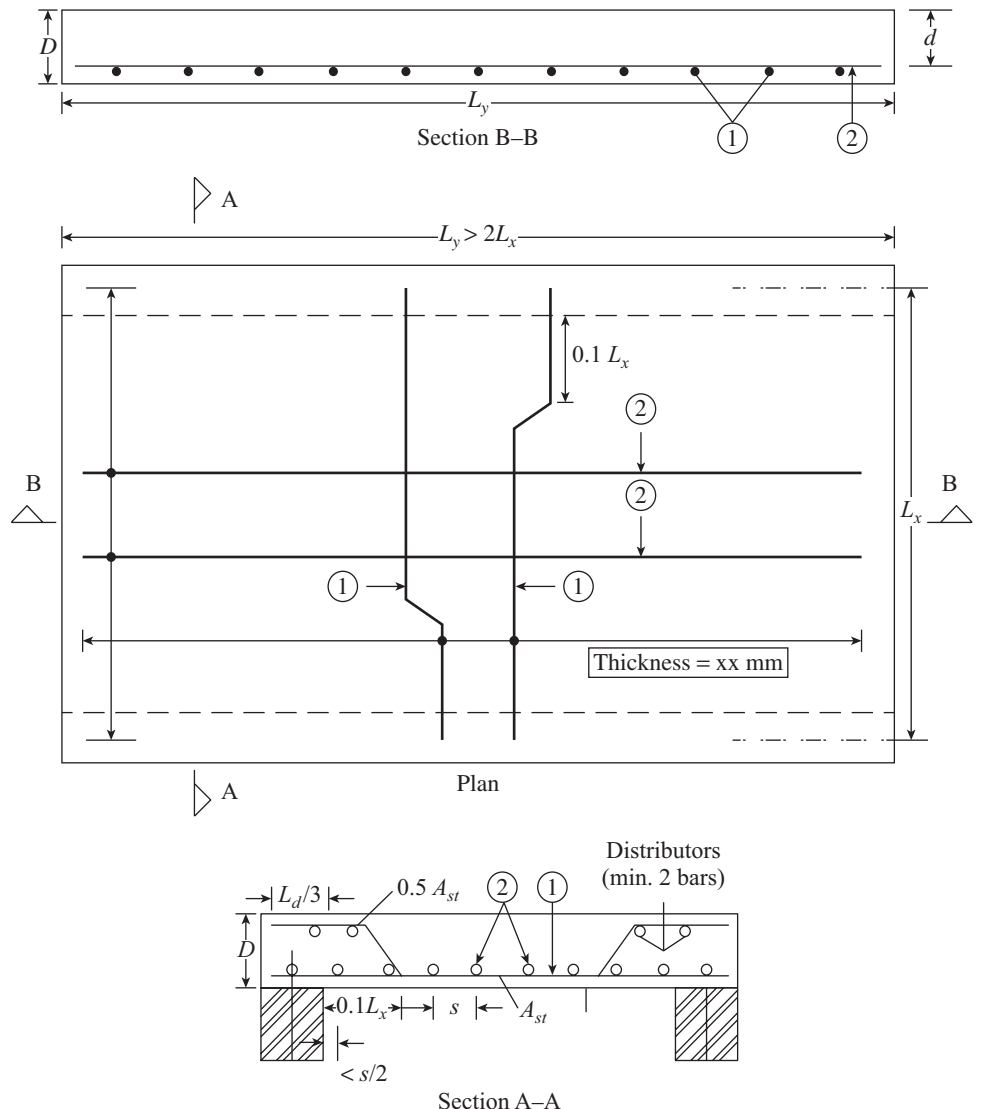


FIG. 9.10 Detailing of reinforcement in simply supported one-way slab with uniformly distributed load

Notes: Bark mark (1): Main bars; > 8 mm for Fe 415 grade and 10 mm for Fe 250 grade - $s < 3d$ or 300 mm.

Bark mark (2): Secondary bars; > 6 mm - $s < 5d$ or 300 mm

Two alternative arrangements of reinforcements are shown for continuous one-way slabs in Figs 9.11(a) and (b). In the first method, separate straight bar reinforcements are used for the positive moments and the negative moments (Fig. 9.11a), whereas in the second method, the top reinforcement for the negative moment over a support region is provided by bending up alternate bars of the bottom positive moment reinforcement from either side of the support, with some additional top bars (Fig. 9.11b).

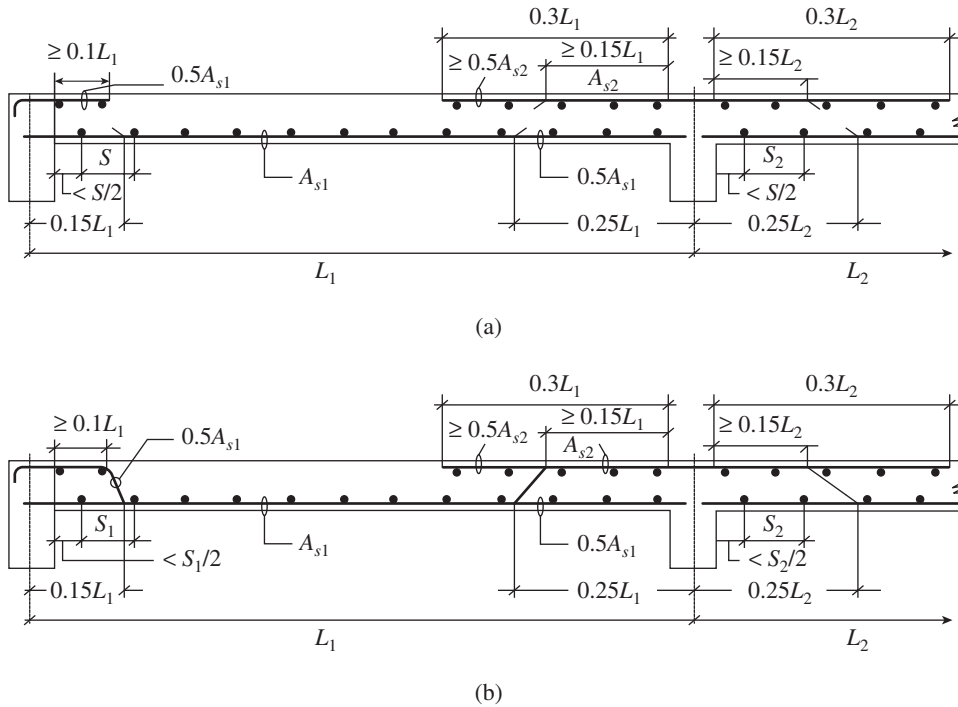


FIG. 9.11 Detailing of continuous one-way slab as per SP 34-1987 (a) Using straight bars (b) Using bent-up bars

9.4.7 Use of High-strength Steel and High-strength Concrete in Slabs

It is better to use bars of a smaller diameter at closer spacing in slabs rather than larger bars at large spacing. Thus, TOR-KARI bars (grade 550 steel), which are available at smaller diameters, may be used advantageously in slabs as well as in columns and beams as ties (though IS code restricts the use of yield stress as 415N/mm² only for stirrups and ties). Conventional high-strength deformed bars of Fe 415 grade of 8 mm and 10 mm diameter can be conveniently replaced by TOR-KARI reinforcement bars of 7 mm and 9 mm diameter, respectively (see Table 9.3). TOR-KARI of diameter 5 mm can also economically replace mild steel bars of diameter 6/8 mm often used as secondary reinforcement. The savings in cost is in the order of 8–10 per cent when TOR-KARI is used in place of Fe 415 grade steel and as much as 35 per cent when used in place of mild steel bars (Subramanian 1992; Suryanarayana 2000; <http://www.prosteel.in>).

TABLE 9.3 Substitution chart based on strength considerations

Fe 415 Steel	TOR-KARI (Fe 550) Steel
8 mm @ S mm spacing	7 mm @ S mm spacing
10 mm @ S mm spacing	9 mm @ 1.07S mm spacing or 8.5 mm @ S mm spacing
12 mm @ S mm spacing	9 mm @ 0.75 S mm spacing
16 mm @ S mm spacing	9 mm @ 0.42 S mm spacing

The use of HSC in slabs may not be beneficial, as there is no reason for the slab concrete to be particularly strong to meet the flexural requirements. Moreover, it is extremely uneconomical to design slabs with HSC. Hence, it is sufficient if the concrete is specified to meet the durability considerations, as given in Tables 4.6 and 4.8 of Chapter 4.

Transmission of High-strength Concrete Column Loads through Normal Strength Concrete Slabs

The HSC is often used in columns of high-rise buildings to achieve economy, reduce column cross section, and increase the carpet area of buildings. As mentioned, only NSC is used in slabs. The use of two different concrete mixtures at the joint region of beam/slab and

column poses a design and construction problem. Although the Indian code is silent on this aspect, the ACI code suggests the following three approaches:

1. The first method called *mushrooming* involves placing the column concrete within the joint region and extending it to about 500–600 mm into the slab from the face of the column. This method requires the placing of two different concrete mixtures in the floor system near the beam/slab-column junction and they need to be well integrated. Thus, the NSC should be placed while the HSC is still plastic and should be adequately vibrated to ensure that the concretes are well integrated. This also implies that the HSC in the floor in the region of column be placed before the NSC in the remainder of the floor to prevent the accidental placing of NSC in the column area. Thus, this method demands careful coordination of the designer and contractor, possible use of retarders, and high level of supervision. Due to these factors, this method is seldom practised.

2. The second method involves the addition of vertical dowels and spirals in the joint region in order to increase the axial load capacity of the slab concrete. The ACI code suggests this method when the column concrete strength is greater than 1.4 times the slab concrete strength. Experiments conducted at the University of Illinois and the University of Melbourne showed that the addition of dowels did not lead to increase in joint strength though they resulted in increased ductility (Subramanian 2006). Moreover, the use of this method will result in the congestion of the beam/slab-column region, which is already likely to be heavily reinforced. The addition of extra dowels and spirals will also increase the cost of construction. Hence, this method is also not adopted in practice.
3. The third strategy is to design the column-slab or column-beam joint using an *effective* concrete strength. Because the joint is confined to some degree by the surrounding slab or beam (the degree of confinement will differ for each of the three types of columns—interior, edge, and corner), the effective strength of the joint is higher than its cube strength. For columns laterally supported on four sides by beams of approximately equal depth or by slabs, the ACI code gives the following formulae for *effective* concrete strength based on the work of Bianchini, et al. (1960).
- (a) For interior columns:

$$\text{if } f_{cc}/f_{cs} \leq 1.4, f_{ce} = f_{cc} \quad (9.14a)$$

$$\text{if } f_{cc}/f_{cs} > 1.4, f_{ce} = 0.75f_{cc} + 0.35f_{cs} \quad (9.14b)$$

and (b) for corner or edge columns:

$$\text{if } f_{cc}/f_{cs} > 1.4, f_{ce} = 1.4f_{cs} \quad (9.14c)$$

where f_{ce} is the cube or cylinder strength of some hypothetical concrete that combines the properties of the column and slab concrete, f_{cc} is the cube or cylinder strength of column concrete, and f_{cs} is the cube or cylinder strength of slab concrete. As heavily loaded slabs do not provide as much confinement as lightly loaded slabs, the ACI code restricts that f_{cc}/f_{cs} should be less than 2.5 for design (Ospina and Alexander 1998). Subramanian (1998; 2006) also compared the provisions of the US, Canadian, and Australian codes as well other equations proposed by researchers and has suggested equations that correlate well with the experimental results.

Shah, et al. (2005), based on the observed problem in the flat plate structure of the Main Tower, Japan Center, at Frankfurt am Main, Germany, tested eight large-scale specimens of column-slab joints. Based on their research, they concluded that the strength of an interior column-slab joint is highly dependent upon the following parameters: the restraint to the joint by the surrounding slab, referred to as the *confinement factor* (represented by λ), the intensity of the slab load, the joint aspect ratio (represented by D_s/h , where D_s is the overall depth of slab and h is the side dimension of the square column), the slab reinforcement

ratio (ρ), and the column and slab concrete strength. They proposed the following formula:

$$f_{ce} = 0.35f_{cc} + 0.384 \left(\frac{\rho + 4.12}{D_s/h + 1.47} \right) \lambda f_{cs} \quad (9.14d)$$

They suggested a constant average value of 1.385 for λ . This equation was found to have better correlation with all available test results.

9.5 DESIGN OF SLABS FOR SHEAR AND SIZE EFFECT

The thickness selected based on the deflection criterion will be safe for shear for the normal case of uniformly distributed loads. Shear reinforcements may be required only in cases where there are heavy concentrated loads, as in deck slabs, culverts, and bridges and flyovers (see Section 9.7). In general, it is better to avoid shear reinforcement in slabs (by providing extra thickness) as they are thin and placing the shear reinforcements may be cumbersome.

Experimental tests indicate that there is size effect in slabs in shear as in beams. Thus, for slabs without stirrups, the shear stress at failure decreases as the slab becomes thicker and as the percentage of longitudinal reinforcement becomes lower (Angelakos, et al. 2001; Lubell, et al. 2004; Lubell, et al. 2009). Thick slabs are those with thickness greater than approximately one-tenth of the span and thin slabs are those with thickness less than approximately one-fortieth of the span. It should be noted that thick slabs transmit a portion of the loads by flat arch action and have significant in-plane compressive forces. Thin slabs act as thin membranes and medium-thick slabs do not exhibit either arch action or membrane action.

IS 456, based on the work of Taylor (1972), suggests that the shear strength of solid slabs up to a depth of 300 mm is comparatively more than that of depth greater than 300 mm. Hence, Clause 40.2.1.1 of IS 456 has specified an enhancement factor k for shear for solid slabs (i.e., not including *ribbed slabs*), which may be multiplied with the design shear strength, τ_c , given in Table 19 of IS 456 (see Table 6.2 of Chapter 6) for different overall depths of slab, as shown in Table 9.4. It has to be noted that according to Clause 40.2.3.1 of the code, the calculated nominal shear stress (V_u/bd) should not exceed *half* the maximum shear stress, $\tau_{c,max}$, given in Table 20 of the code (see Table 6.3 of Chapter 6). Shear reinforcements have to be provided only when the calculated nominal shear stress is in between $k\tau_c$ and $\tau_{c,max}$.

TABLE 9.4 Values of the multiplying factor k for shear in slabs

Overall Depth of Slab (mm)	300 or more	275	250	225	200	175	150 or less
k	1.00	1.05	1.10	1.15	1.20	1.25	1.30

9.6 DESIGN PROCEDURE FOR ONE-WAY SLABS

The different steps involved in the design of one-way slabs, considering them as *beams of one metre width*, are as follows:

Step 1 Calculate the effective span of the slab (Clause 22.2 of code).

Step 2 Estimate the required thickness of the slab based on the serviceability limit state criteria of deflection, using the limiting value of effective span to depth ratio given in Clause 23.2 of the code (as we do not know the amount of steel at this stage, an initial value of 25–30 may be assumed). It should be noted that a minimum depth of 100mm is required for ease of construction of slabs (also see Table 4.8 of Chapter 4 for minimum thickness based on exposure, durability, and fire resistance). Adopt suitable cover depending on the exposure condition and fire resistance (Table 16 of IS 456). Assuming rebar size, determine the overall depth. The calculated value of the thickness should be rounded off to the nearest multiple of 5 mm or 10 mm.

Step 3 Considering 1.0m wide strip of slab, calculate the maximum ultimate bending moment, M_u , and shear, V_u , due to factored (DL + LL) acting at the mid-span and support, respectively (see Fig. 9.6). For continuous slabs, the coefficients given in Tables 12 and 13 of IS 456 (see Fig. 9.7) may be used.

Step 4 Check the depth for bending. Assuming balanced section, calculate the depth required for bending using Eq. (5.28) given in Chapter 5. Check this effective depth with that assumed in Step 2. If the assumed depth in Step 2 is less, revise the depth and repeat Steps 3 and 4 again. However, in general, the depth assumed based on the deflection criteria will be higher than that required for the bending strength.

Step 5 Calculate the required main and distribution steel. The required amount of steel, A_{st} , may be calculated by using Eq. (9.10) or by using the charts and tables given in SP 16 (p_t should be less than $p_{t,lim}$ given in Table 5.5 of Chapter 5 for ductile behaviour). Adopt the main and distribution steel. The spacing of bars may be calculated using Eq. (9.11).

Step 6 Check for control of cracking using detailing rules (Clause 26.5.2.1). Check whether the adopted main steel and distribution steel are not less than the minimum percentage specified for slabs in the code (Eq. 5.35c of Chapter 5 or Eq. 9.12 or 9.13). Provide at least the minimum steel. The guidance for spacing, based on the selected bar diameter, for the distribution steel is provided in Table 9.5. Check whether the spacing adopted is less than the maximum spacing permitted by the code, as per Clause 26.3.3 ($3d$ or 300mm for main steel and $5d$ or 300mm for distribution steel). If not, adopt a spacing less than the maximum permitted spacing.

TABLE 9.5 Spacing of distribution steel for one-way slabs

Thickness of Slab (mm)	Fe 415 Grade Steel (0.12%)			Fe 250 Grade Steel (0.15%)			
	6	8	10	6	8	10	12
100	235	300	–	185	–	–	–
110	210	300	–	170	300	–	–
120	195	300	–	155	275	–	–
130	180	300	–	140	255	–	–
140	165	295	–	130	235	–	–
150	155	275	–	125	220	300	–
175	130	235	–	105	190	295	–
200	115	205	300	90	165	260	–
225	100	185	290	80	145	230	–
250	90	165	260	75	130	205	300

Step 7 Check the section for shear stresses at the critical section, that is, at a distance d from the support: Calculate the nominal shear stress, $\tau_v = V_u/bd$ (use $b = 1000$ mm). Assuming half the designed area of reinforcement at mid-span is available at support, determine τ_c from Table 19 of IS 456 (see Table 6.2 of Chapter 6). This value can be increased by multiplying the factor k given in Table 9.4. Check whether the calculated nominal shear stress τ_v exceeds *half* the maximum shear stress, $\tau_{c,max}$, given in Table 20 (see Table 6.3 of Chapter 6) of the code; otherwise, increase the section. Shear reinforcements have to be provided only when the calculated nominal shear stress is in between τ_c and $\tau_{c,max}$. It should be noted that usually one-way slabs will not be critical in shear.

Step 8 Check the adequacy of the adopted depth for deflection using the empirical method given in the code. Calculate the modification factor, k_f , given in Fig. 4 of IS 456 (see Fig. 9.4) for the adopted p_t . Multiply the value of k_f with the basic span to depth ratio and calculate the required depth again. If it is greater, adopt this depth and redo Steps 2–8.

Step 9 Check for development length as per Clauses 26.2.3.3(c) and 26.2.1 of the code. The embedment length at the support should be greater than $L_d/3$ and at simple support $L_d \leq 1.3 \frac{M_{n1}}{V_u} + L_o$ where M_{n1} is the moment of resistance of the section, V_u is the shear at support, and L_o is the end anchorage $\leq d$ or $12d_b$, whichever is greater.

Step 10 Sketch the reinforcement details.

Use of Design Aids

Design charts (Charts 1–18) and tables are available in SP 16:1980 for the rapid design of slabs. The tables are generally more convenient to deal with than charts and are often used in practice. Tables 1–4 of SP 16, presented for the design of singly reinforced beams, may be used for the design of slabs

assuming $b = 1000\text{mm}$. For a given value of M_u/bd^2 , the reinforcement percentage, p_t , can be read from these tables. Tables 5–44 give the moment of resistance of slabs, per metre width, of specific thicknesses ranging from 100 mm to 250 mm for different values of f_{ck} and f_y . These tables assume a standard clear cover of 15 mm for slab reinforcement. Charts 21–23 can also be used for finding the maximum ratio of span to effective depth for a given tension reinforcement and Table 96 for finding the spacing of bars for the designed area of steel.

9.7 CONCENTRATED LOAD ON ONE-WAY SLABS AND DESIGN OF CULVERTS

When concentrated loads act on a one-way slab, the simplified effective width method given in Clause 24.3.2 of the code may be adopted. (It should be noted that in two-way slabs, a similar effect is analysed by Pigeaud’s method. Even though this method can also be used to analyse one-way slabs, the effective width method is often used.)

Concentrated loads in slabs induce sharply varying moments in the direction of the main span as well as in the

transverse direction, as shown in Fig. 9.12(a). The bending moment M_x in a one-way slab due to the concentrated load can be determined using Slater’s formula, as recommended by IS 456 and IRC 21 (Westergaard and Slater 1921). The bending moment is assumed to be resisted by an effective width, b_e , of the slab. For a single concentrated load, the effective width is given as follows (see also Fig. 9.12b):

$$b_e = kx \left(1 - \frac{x}{L}\right) + t_y \tag{9.15}$$

where b_e is the effective width of the slab, k is a constant having values given in Table 9.6, depending upon the ratio of B/L , x is the distance of the centroid of the concentrated load from the nearest support, B is the width of the slab, L is the effective length, and t_y is the width of the contact area of the concentrated load from the nearer support measured parallel to the supported edge (dispersion is taken at 45° through the wearing coat).

The design moment M_{dx} per unit width of slab is given by

$$M_{dx} = \frac{M_x}{b_e} \tag{9.16}$$

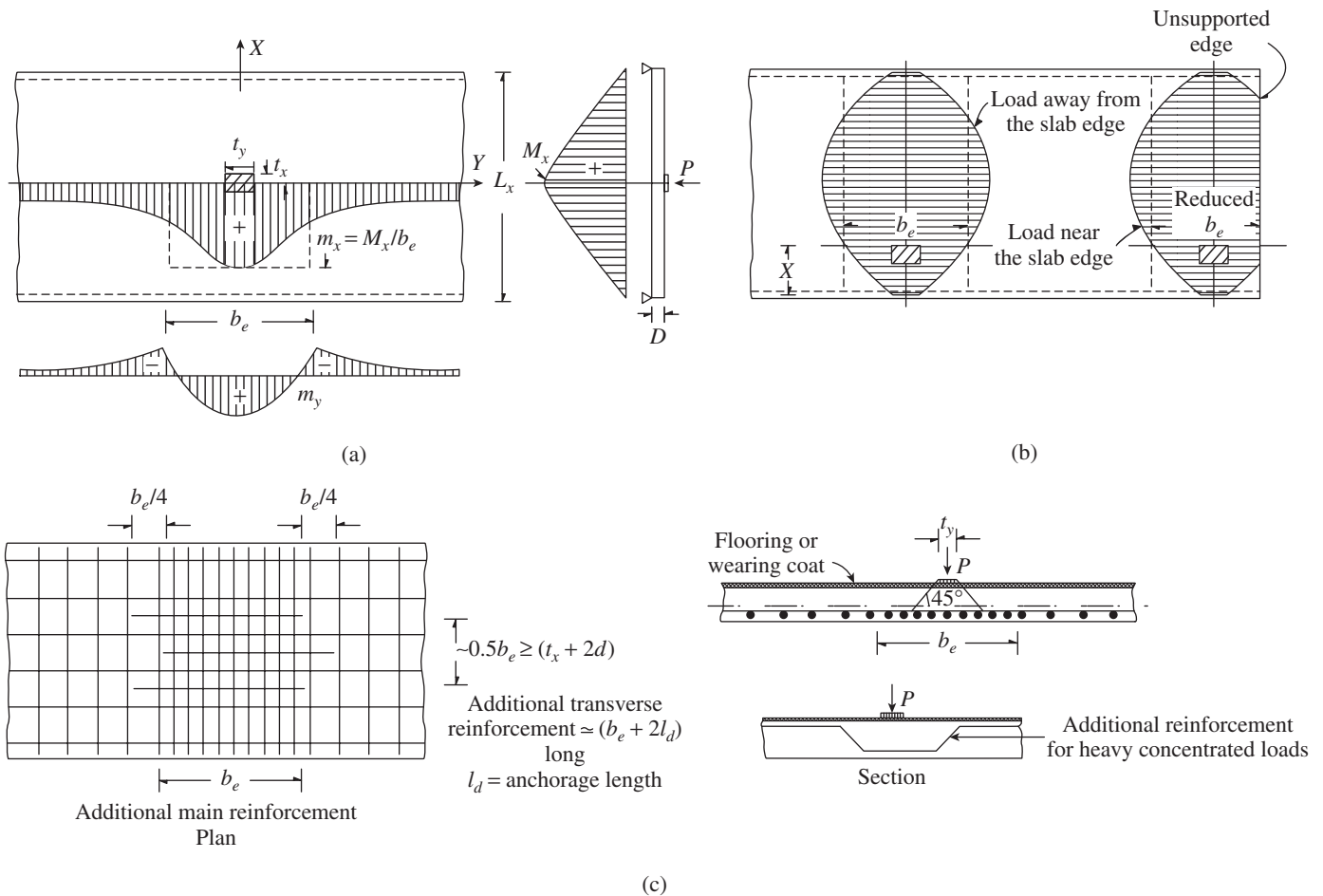


FIG. 9.12 Effect of concentrated load (a) Variation of moments (b) Variation of b_e with load position (c) Reinforcement

TABLE 9.6 Values of k

B/L	Value of k		B/L	Value of k	
	Simply Supported Slab	Continuous Slab		Simply Supported Slab	Continuous Slab
0.1	0.40	0.40	1.1	2.60	2.28
0.2	0.80	0.80	1.2	2.64	2.36
0.3	1.16	1.16	1.3	2.72	2.40
0.4	1.48	1.44	1.4	2.80	2.48
0.5	1.72	1.68	1.5	2.84	2.48
0.6	1.96	1.84	1.6	2.88	2.52
0.7	2.12	1.96	1.7	2.92	2.56
0.8	2.24	2.08	1.8	2.96	2.60
0.9	2.36	2.16	1.9	3.00	2.60
1.0	2.48	2.24	2.0 and above	3.00	2.60

The shear force in slab per unit width can be computed by

$$V_d = \frac{V_u}{b_e} \tag{9.17}$$

The variation of the effective width b_e for various positions of the load along the span is shown in Fig. 9.12(b). As shown in this figure, the effective width should be reduced as indicated when the load is close to the free edge. This effective width should never exceed the actual width of the slab. Furthermore, when the concentrated load is close to an unsupported edge of the slab, effective width should not exceed B or $B/2$ plus the distance of the load from the unsupported edge, whichever is less. For determining the effective length of the load in the direction of the span, the dispersion of the load through the full effective depth of the slab is taken, assuming a 45° angle of dispersion through both the wearing coat and the effective depth. Figure 9.12(c) shows the reinforcement details when there is a fixed concentrated load on the slab.

9.7.1 Effective Width of Cantilever Slabs

For cantilever slabs, Clause 24.3.2.1(d) of the code stipulates the effective width, assuming that full dispersion can occur on both sides of the load, as

$$b_e = 1.2a_1 + t_y \tag{9.18}$$

where a_1 is the distance of the concentrated load from the face of the cantilever support and t_y is the width of the contact area of the concentrated load parallel to the support. The effective width should not exceed $B/3$ or $B/6$ plus the distance of the load from the free edge, both measured parallel to the fixed edge.

9.7.2 DESIGN OF CULVERT

Bridges and culverts are constructed to cross rivers or to provide traffic at different levels. When the span is small, the word *culvert* is used instead of bridge. The span of these culverts may be up to 8 m. Figure 9.13 shows a typical deck slab culvert.

The width of the deck slab will be more than 3.8 m for culverts on single-lane highways, increasing by 3 m for every additional lane. In the case of combined road and rail bridges, this is increased by 4 m for single-track train way and 7.6 m for double-track train way.

In addition to the dead load of the slab and wearing coat (may be taken as 2.2 kN/m^3), an imposed load of $4\text{--}5 \text{ kN/m}^2$ is taken on the kerbs or footway. The deck slabs are subjected

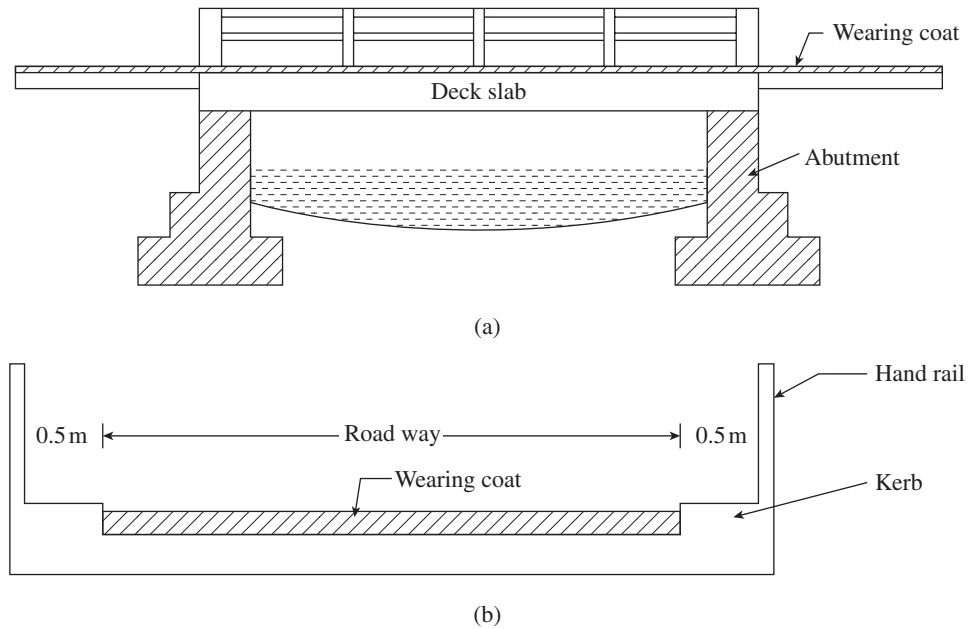


FIG. 9.13 Typical culvert (a) Longitudinal section (b) Cross section

to loads from various moving vehicles. The Indian Roads Congress (IRC) has classified these loads into Class AA loading, Class A loading, and Class B loading. The bridges designed for Class AA loading should also be checked for Class A loading. Class AA loading is shown in Fig. 9.14. For other loading and more information, the IRC code should be consulted. The minimum clearance between the road face of the kerb and the outer edge of the wheel or truck, C , is shown in Table 9.7.

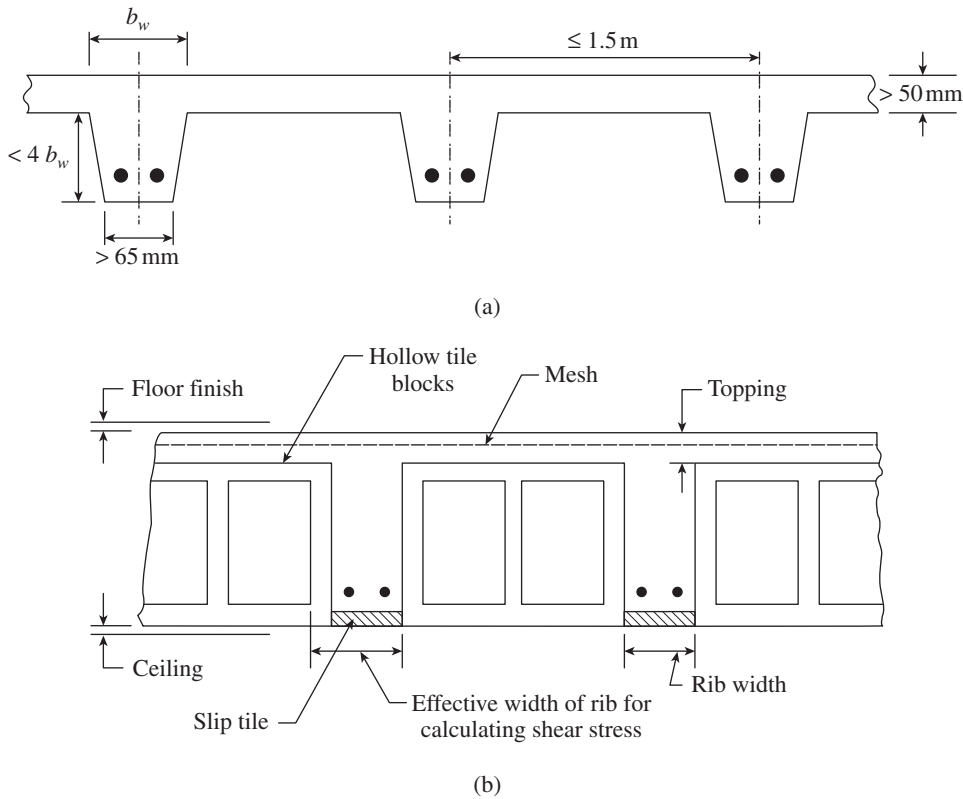


FIG. 9.15 Ribbed slabs (a) Without hollow blocks (b) With hollow blocks

have reduced self-weight and are economical compared to solid slabs (Ambalavanan, et al. 1999). However, they may have higher formwork costs than the solid slabs.

Clause 30.2 of the code suggests that the ribbed slabs may be designed similar to the continuous solid slabs or alternatively as a series of simply supported spans (since it may not be feasible to arrange the reinforcement over the supports within the restricted space available in the ribs), provided they are not exposed to severe conditions. In such cases, however, crack control reinforcement, as given in Clause 30.7 of the code, should be provided in the support region.

When hollow blocks (they should conform to IS 3951—Part 1 or IS 6061) are included in shear stress calculations, an increased rib width (by considering the wall thickness of the block on one side of the rib) may be used (see Fig. 9.15b); with narrow precast units, the width of the joining mortar or concrete may also be included.

For deflection requirements, the span to effective depth ratios as per the flanged beam (see Clause 23.2.1(d) of the code and Table 9.1) are also applicable for these slabs. The following reduction factor can be applied on the L/d ratio (see also Fig. 6 of IS 456):

$$RF = 0.8 \quad \text{for } 0 < (b_w/b_f) \leq 0.3 \quad (9.19a)$$

$$RF = \frac{2}{7} \left(\frac{b_w}{b_f} \right) + \frac{5}{7} \quad \text{for } 0.3 \leq (b_w/b_f) \leq 1.0 \quad (9.19b)$$

where b_w is the rib width and b_f is the flange width. (As already mentioned in Section 9.4.2, as per SP 24:1983 this reduction factor may result in abnormal results and hence may be ignored.) The rib width for a system with hollow-block slabs may be assumed to include the walls of the blocks on both sides of the rib. According to Clause 30.4, for voided slabs, an effective rib width can be calculated assuming all material below the upper flange of the unit to be concentrated in a rectangular rib having the same cross-sectional area and depth. Moreover, as per Clause 30.2, if the slab is designed as simply supported, even though it is continuous it should be treated as simply supported for checking the (L/d) ratio.

As per Clause 30.5 of the code, the width of in situ ribs should be greater than 65 mm, the rib spacing should be less than 1.5 m c/c, and the depth of rib, excluding any topping, should be less than four times their average

width (see Fig. 9.15a). The minimum rib width is normally determined from the considerations of cover, bar spacing, and fire resistance. There should be a minimum of five ribs in one-way slabs. The ribs may be slightly tapered as shown in Fig. 9.15(a) for easy removal of forms.

As the topping transfers the load by arching action, its depth should be at least one-tenth of the clear distance between the ribs or 50 mm (as per IS 6061—Part 2). It should be noted that the code is silent on whether the topping can be used for computing the structural strength. The design of ribbed slabs is covered in Clause 8.13 of the ACI code, under the heading of joist construction, and allows for a 10 per cent increase in the allowable shear stress of concrete.

Arrangement of Reinforcement in Ribbed Slabs

The following rules are suggested in Clause 30.7 of the code:

1. As a general rule, 50 per cent of the mid-span reinforcement in slabs should extend into the support. The bars should be anchored properly as per Clause 26.2.3.3 of the code.
2. Where the slab, which is continuous over supports, has been designed as simply supported (due to the difficulty of providing enough top steel in the ribs over support), reinforcements should be provided over supports to control cracking. This reinforcement should have an area not less than one-fourth of that required in the middle of the adjoining spans and should extend at least one-tenth of the clear span into the

adjoining spans. Designers should be aware of the risks of serious cracking (which will be hidden under floor finishes) associated with this method of design (see SP 24-1983).

3. A single layer of steel reinforcement mesh with a minimum of 0.12 per cent area of topping should be provided in each direction in the topping as per SP 24:1983. The spacing of wires should not exceed one half of the *c/c* of the ribs. The mesh is placed in the centre of the topping. If the ribs are widely spaced, it may be necessary to design the topping for moments and shears as a continuous one-way slab between ribs.

In slabs with permanent blocks, the side cover to the reinforcement should be a minimum of 10 mm. In other cases, cover should be provided as per Clause 26.4. Example 9.5 provides the necessary calculations involved in the design of ribbed slabs.

9.9 EARTHQUAKE CONSIDERATIONS

The horizontal forces generated by earthquake excitations are transferred to the ground by the vertical systems of the buildings that are designed for lateral load resistance (e.g., frames, bracing, and walls). These vertical systems are generally tied together as a unit by means of the building floors and roof, acting as *diaphragms*. Diaphragms transmit inertial forces from the floor system to the vertical elements of the seismic force resisting system. Thus, the floors or roofs, used primarily to create enclosures and resist gravity (or out of plane) loads, have to be designed as horizontal diaphragms to resist and transfer horizontal (or in-plane) loads to the appropriate vertical elements (see Fig. 9.16).

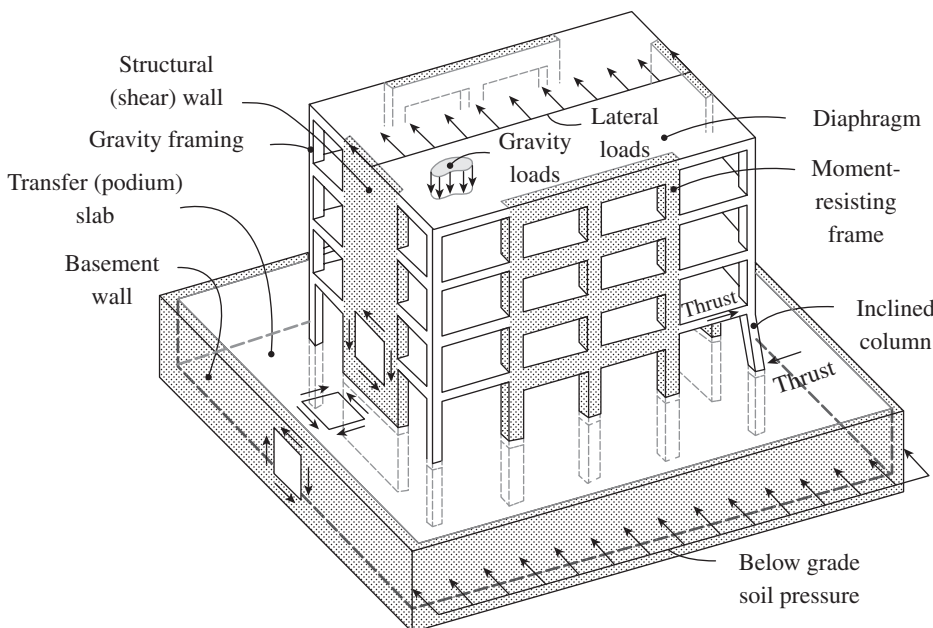


FIG. 9.16 Roles of diaphragms
Source: Moehle, et al. 2010

The simplified analysis procedure consists of considering the behaviour of diaphragm under the influence of horizontal loads as a horizontal continuous beam supported by the vertical lateral load resisting elements (often referred to as VLLR elements). The floor deck is assumed to act as the web of the continuous beam and the beams at the floor periphery are assumed to act as the compression and tension chords (flanges) of the (continuous) beam (see Fig. 9.17).

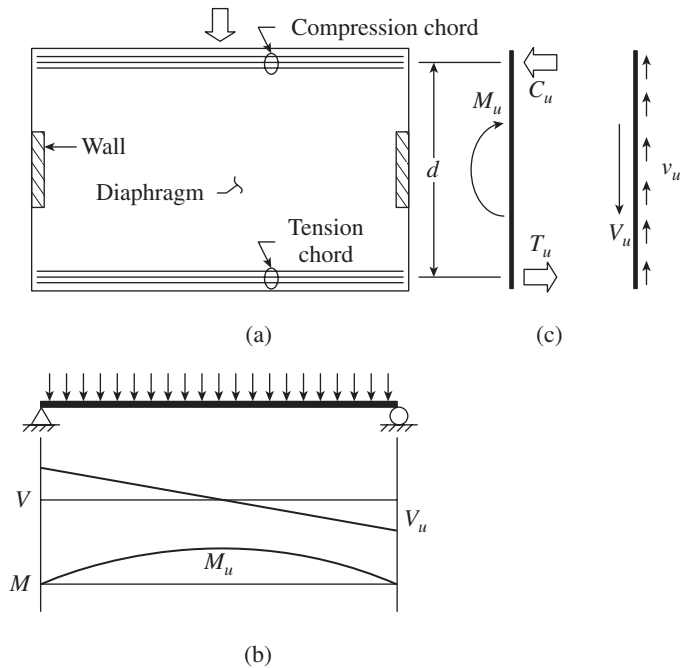


FIG. 9.17 Simple idealization of diaphragms and tension and compression chords (a) Plan (b) Simple beam idealization (c) Internal moment and shear resistance

Source: Moehle, et al. 2010

Diaphragms are classified as rigid, flexible, and semi-rigid based on this relative rigidity. No diaphragm is perfectly rigid or perfectly flexible, and the exact analysis of structural systems containing *semi-rigid diaphragms* is complex. A note below Clause 7.7.2.2 of IS 1893:2002 (Part 1) suggests that the floor diaphragm should be considered to be flexible if the maximum lateral displacement measured from the chord of the deformed shape at any point of the diaphragm is more than 1.5 times the average displacement of the entire diaphragm.

In general, low-rise buildings and buildings with very stiff vertical elements, like shear walls, are more susceptible to floor diaphragm flexibility problems than taller structures.

If sufficient bond is not provided between the walls and the diaphragm, the two will be separated from each other starting at the wall corners. This separation results in a dramatic increase in the wall torsion and might lead to collapse, as in the case of the Arvin High School Administrative Building in California during the Kern County earthquake of 21 July 1952 (Naeim and Boppana 2001).

Another potential problem in diaphragms can be due to any abrupt and significant changes in wall stiffness below and above a diaphragm level. In buildings with significant plan irregularities, such as multi-wing plans and L-, H-, or V-shaped plans, particular attention should be paid to accurately assess the in-plane diaphragm stress at the joints of the wings and to design for them. Other classes of buildings deserving special attention to diaphragm design include those with relatively large openings in one or more of the floor slabs and tall buildings resting on a significantly larger low-rise part, as shown in Fig. 9.16.

Neither IS 456 nor IS 13920 contains provisions for the design of diaphragms. Interested readers should consult the ACI code (Section 21.11), Bull (2004), Naeim and Boppana (2001), and Moehle, et al. (2010) for details of analysis, design, and constructional aspects of diaphragms.

9.10 SLABS-ON-GRADE

A *slab-on-ground* or *slab-on-grade* is defined as a slab supported by ground whose main purpose is to support the applied loads by bearing on the ground. Soils in the subgrade are generally the ultimate supporting materials. A typical slab-on-grade consists of (a) compacted *subgrade*, with gravel or crushed stone sub-base usually 150–300 mm thick, (b) *vapour barrier* (if needed) covered with sand layer, and (c) the slab itself with joints, reinforcement, and finishes (see Fig. 9.18). Proper preparation of the subgrade is critical for the performance of the slab, since even a most carefully constructed slab may fail when placed on poorly compacted or unsuitable soil.

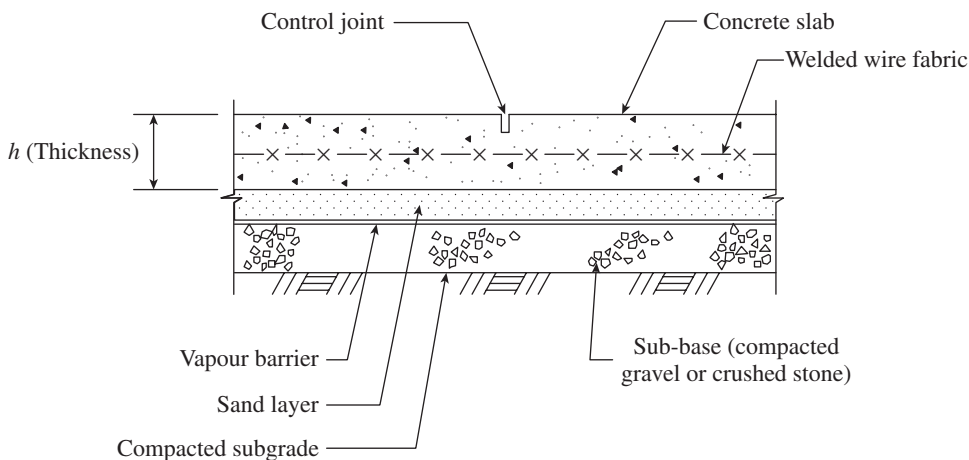


FIG. 9.18 Components of slab-on-grade

The sub-base, generally 150–300 mm thick, helps the slab to span over any poorly compacted spots by spreading concentrated loads over a larger area. It also provides effective drainage under the slab; the effectiveness of the sub-base increases with its depth. Though the use of vapour barriers (polyethylene sheets) is debatable, it prevents the dissipation of water during curing and may result in slab curling. A sand layer on the top of the vapour layer will mitigate the curling problem. The structural analysis (Westergaard 1926) and design of the slab is straightforward and is covered in ACI 360-06.

The reinforcement is mainly provided to limit the crack widths resulting from shrinkage and temperature restraint and the applied loads. Grade slabs generally have 150–200 mm thickness with two layers of grade 415 steel of 8 mm diameter both ways at 200 c/c or equivalent welded wire fabric reinforcement. The reinforcement for crack width control is provided at or above mid-depth of the slab-on-ground, but never below mid-depth. A common practice is to specify that the steel has a 38–51 mm cover below the top surface of the concrete. The reinforcement for moment capacity should be at the centroid of the tensile area of the uncracked concrete section. It can be calculated using the following formula:

$$A_s = \frac{370f_{cr}h}{f_s} \quad (9.20)$$

where A_s is the cross-sectional area of steel (mm^2/m of slab), f_{cr} is the modulus of rupture of concrete and may be taken as $0.7\sqrt{f_{ck}}$, h is the thickness of slab (mm), and f_s is the stress in steel (N/mm^2), which may be assumed to be equal to or less than $0.75f_y$ (the designer may consider using less than 75 per cent of f_y to limit the width of the cracks).

Slabs-on-ground have unique serviceability requirements and are used to minimize cracking and curling, increase surface durability, optimize joint locations and type of joints for joint stability (the differential deflection of the adjacent slab panel edges as wheel loads cross the joint), and maximize long-term flatness and levelness (ACI 360-06). Joints are used in

slab-on-ground construction to limit the frequency and width of random cracks caused by volume changes. Three types of joints are commonly used—*isolation joints*, *saw-cut contraction joints*, and *construction joints*. The use of *shrinkage-compensating concrete* allows the construction of joint spacing of 12–46 m and elimination of saw-cut contraction joints. More details about the design, construction, and other aspects may be found in ACI 360-06, Kiamco (1997), and Suprenant (2002b).

EXAMPLES

EXAMPLE 9.1 (Design of simply supported one-way slab):
Design a floor slab for an interior room, with clear dimensions of 3.5 m × 9 m, for a building located in Chennai. The slab is resting on 230 mm thick masonry walls. Assume live load as 4.0 kN/m² and dead load due to finish, partition, etc., as 1.5 kN/m². Use M25 concrete and Fe 415 steel.

SOLUTION:

Even though Chennai is a coastal city, the slab under consideration is for an interior room and thus protected against weather. Hence, we can consider the exposure condition as moderate. The required nominal cover as per Table 16 of IS 456 is 30 mm.

The following values are given: $f_{ck} = 25$ MPa, $f_y = 415$ MPa.

Since L/B ratio of slab = $9/3.5 = 2.57 > 2$, the slab will be designed as a one-way slab.

Step 1 Calculate the loads and effective span.

Assume $d = \text{span}/25 = 3500/25 = 140$ mm (Clause 24.1. of IS 456)

Assuming 10 mm main bars,

Total depth $D = 140 + 30 + 5 = 175$ mm

Dead load = $0.175 \times 25 = 4.375$ kN/m²

Dead load due to finish = 1.50 kN/m²

Total dead load = 5.875 kN/m²

Live load = 4 kN/m²

Factored load, $w_u = 1.5(4 + 5.875) = 14.82$ kN/m²

Effective span is the lesser of the following (Clause 22.2 of code):

1. Clear span + Effective depth = $3.5 + 0.14 = 3.64$ m
2. c/c of supports = $3.5 + 0.23 = 3.73$ m

Hence, effective depth = 3.64 m

Step 2 Calculate M_u and V_u .

$$M_u = \frac{w_u L_x^2}{8} = \frac{14.82 \times 3.64^2}{8} = 24.54 \text{ kNm}$$

$$V_u = \frac{w_u L_x}{2} = \frac{14.82 \times 3.64}{2} = 26.97 \text{ kN}$$

Step 3 Check the depth for bending moment. Assuming balanced section

$$M_{n,\text{lim}} = 0.138 f_{ck} b d^2 \text{ (with } b = 1000 \text{ mm for slab)}$$

$$d = \left(\frac{M_u}{0.138 f_{ck} b} \right)^{0.5} = \left(\frac{24.54 \times 10^6}{0.138 \times 25 \times 1000} \right)^{0.5} \\ = 84.3 \text{ mm} < 140 \text{ mm}$$

Hence, assumed depth is adequate.

Note: In slabs, the depth will mostly be governed by serviceability limit state criterion of deflection.

Step 4 Calculate the reinforcement. The depth is greater than that required for bending. Hence, the section is under-reinforced. We may use Eq. (5.29a) of Chapter 5 to calculate x_u/d and A_{st} .

$$\frac{x}{d} = 1.2 - \sqrt{1.44 - \frac{6.68 M_u}{f_{ck} b d^2}} \\ = 1.2 - \sqrt{1.44 - \frac{6.68 \times 24.54 \times 10^6}{25 \times 1000 \times 140^2}} = 0.149 < 0.479$$

Hence, it is under-reinforced.

$$z = d \left(1 - 0.416 \frac{x}{d} \right) = 140(1 - 0.416 \times 0.149) = 131.3 \text{ mm}$$

$$A_{st} = \frac{M}{0.87 f_y z} = \frac{24.54 \times 10^6}{0.87 \times 415 \times 131.3} = 518 \text{ mm}^2$$

Alternatively, the reinforcement can also be calculated in the following way using SP 16:

$$\frac{M}{b d^2} = \frac{24.54 \times 10^6}{1000 \times 140^2} = 1.252$$

From Table 3, $p_t = 0.3696$

$$A_{st} = \frac{0.3696 \times 1000 \times 140}{100} = 517 \text{ mm}^2$$

Provide 10 at 150 mm c/c (A_{st} provided = 524 mm²).
Distribution steel (Clause 26.5.2.1)

$$A_{sty} = \frac{0.12 b D}{100} = \frac{0.12 \times 1000 \times 175}{100} = 210 \text{ mm}^2$$

Provide 8 mm diameter bars at 220 mm c/c (A_{sty} provided = 228 mm²).

Spacing less than $5d = 5 \times 140 = 700$ mm or 300 mm > 220 mm. Hence, it is adequate.

Step 5 Check for control of cracks (Clause 26.5.2.1).

Minimum $p_t = 0.12\% < p_t$ provided = 0.374%

Hence, it is adequate. As per Clause 26.5.2.2 of IS 456,

Diameter of bar $< D/8$; we have $10 < 175/8 = 21.8$ mm

Also as per Clause 26.3.3, maximum spacing should be less than $3d$ or 300.

$$3d = 3 \times 140 = 420 \text{ or } 300 > 150 \text{ mm}$$

Hence, spacing is adequate.

Step 6 Check for shear.

$$\text{Nominal shear stress} = \frac{V_u}{b d} = \frac{26.97 \times 10^3}{1000 \times 140} = 0.193 \text{ N/mm}^2$$

$$p_t = \frac{524 \times 100}{1000 \times 140} = 0.374$$

Assume tension steel at support = $0.374/2 = 0.19\%$

From Table 19 of IS 456, $\tau_c = 0.318 \text{ N/mm}^2 > 0.193 \text{ N/mm}^2$

Hence, the slab is safe in shear, even without shear enhancement using factor k .

Step 7 Check for deflection (Clause 23.2.1).

Basic span to depth ratio = 20,

$$f_s = 0.58 f_y \frac{\text{Area}_{\text{required}}}{\text{Area}_{\text{provided}}} = 0.58 \times 415 \times \frac{517}{524} = 237.5 \text{ N/mm}^2$$

From Fig. 4 of IS 456, factor k_t for $p_t = 0.374$ and $f_s = 237.5$ is 1.384.

Hence, allowable $L/d = 1.384 \times 20 = 27.68 > 25$ (assumed)

Hence, the slab is safe against deflection.

Step 8 Check for development length (Clause 26.2.1).

$$L_d = \frac{0.87 f_y d_b}{4 \tau_{bd}} = \frac{0.87 \times 415 d_b}{4 \times (1.6 \times 1.4)} = 40.4 d_b$$

1. Embedment length into the support $> L_d/3$ (Clause 26.2.3.3a)

For 10 diameter bars, $L_d/3 = 40.4 \times 10/3 = 134.3 \text{ mm}$

Length of bar embedment at support = Width of support – Clear cover = $230 - 30 = 200 \text{ mm} > L_d/3$

2. At simple support (Clause 26.2.3.3d)

$$L_d \leq 1.3 \left(\frac{M_{nl}}{V_u} \right) + L_o$$

As alternate bars are bent up at support, the moment of resistance may be taken as half of span moment. Since $A_{st, \text{provided}}$ is approximately equal to $A_{st, \text{required}}$, let us assume that the moment of resistance is equal to M_u .

$$M_u = M_{nl} = 0.5 \times 24.54 = 12.27 \text{ kNm}$$

$V_u = 26.97 \text{ kN}$, $L_o = 8 d_b$ (for 90° bend from the centre of support)

$$\text{Thus, } 1.3 \times \left(\frac{12.27 \times 10^6}{26.97 \times 10^3} \right) + 8 \times 10 = 671 \text{ mm} > 403 \text{ mm}$$

Hence, $d_b = 10 \text{ mm}$ is satisfactory.

Figure 9.19 shows the reinforcement details of the slab at the mid-span of a long edge. It should be noted that alternate bars are bent up at a distance of 0.1 times the span from the edge of support to resist any secondary bending moment arising at the support. Extra nominal bars are shown in the section at edges and kinks for construction purposes.

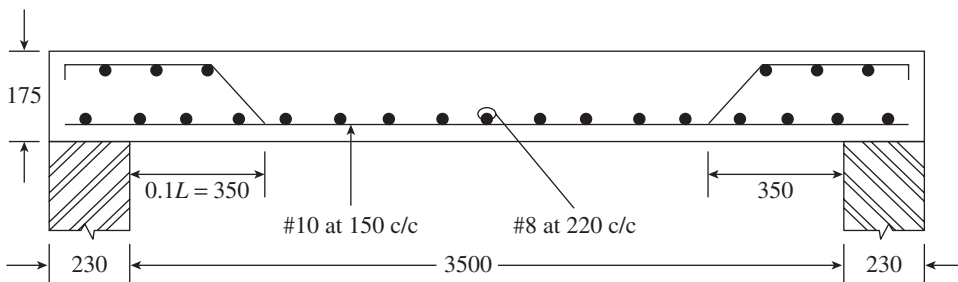


FIG. 9.19 Reinforcement details of slab of Example 9.1

EXAMPLE 9.2 (Design of one-way continuous slab):

A hall in a building has a floor consisting of a one-way continuous slab cast monolithically with simply supported 250 mm wide beams spaced at 4 m c/c, as shown in Fig. 9.20. The clear span of the beam is 9 m. Assuming a live load on the slab as 3.0 kN/m^2 , partition load as 1 kN/m^2 , and load due to finishes as 0.6 kN/m^2 , design the slab with M20 grade concrete and Fe 415 steel.

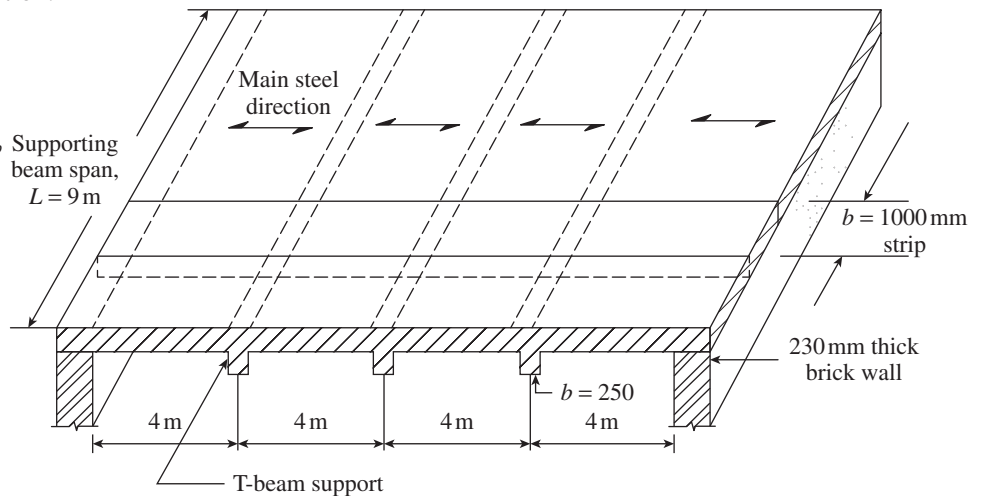


FIG. 9.20 One-way continuous slab of Example 9.2

SOLUTION:

The following values are given: $f_{ck} = 20 \text{ MPa}$, $f_y = 415 \text{ MPa}$.

Step 1 Calculate the loads.

Assume $d = \text{span}/30 = 4000/30 = 133.33$

With 10 mm diameter rebars, overall depth

$D = 133.33 + 15$ (assumed cover) $+ 5 = 153.33 \text{ mm}$

Adopt $D = 160 \text{ mm}$ and $d = 140 \text{ mm}$.

Dead load of slab = $0.16 \times 25 = 4.0 \text{ kN/m}^2$

Floor finish = 0.6 kN/m^2

Partition = 1.0 kN/m^2

Total dead load = 5.6 kN/m^2

Imposed load = 3.0 kN/m^2

Factored dead load, $w_{u,d} = 8.4 \text{ kN/m}^2$

Factored live load, $w_{u,l} = 4.5 \text{ kN/m}^2$

Ratio of LL/DL = $4.5/8.4 = 0.54 < 0.75$

As per Clause 22.4.1(a), the loading arrangement is design dead load plus design imposed load on all the spans.

Step 2 Calculate M_u and V_u . The maximum factored moment occurs in the end span (using Table 12 of IS 456).

$$\begin{aligned} M_{u, \text{mid}} &= \frac{w_{u,d} L^2}{12} + \frac{w_{u,l} L^2}{10} \\ &= \frac{8.4 \times 4^2}{12} + \frac{4.5 \times 4^2}{10} \\ &= 18.4 \text{ kNm} \end{aligned}$$

and

$$M_{u,\text{support}} = \frac{w_{u,d}L^2}{10} + \frac{w_{u,l}L^2}{9} = \frac{8.4 \times 4^2}{10} + \frac{4.5 \times 4^2}{9} = 21.44 \text{ kNm}$$

Maximum shear force at support (using Table 13 of IS 456)

$$V_u = 0.6(w_{u,d} + w_{u,l}) \times L = 0.6(8.4 + 4.5) \times 4 = 30.9 \text{ kN}$$

Step 3 Check the depth for bending moment. Assuming balanced section

$$d = \left(\frac{M}{0.138 f_{ck} b} \right)^{0.5} = \left(\frac{21.44 \times 10^6}{0.138 \times 20 \times 1000} \right)^{0.5} \\ = 88.1 \text{ mm} < 140 \text{ mm}$$

Hence, the assumed depth is adequate.

Step 4 Calculate the reinforcement. The section is under-reinforced and hence the formula derived in Chapter 5 may be used.

1. Steel required at support, for $M_u = 21.44 \text{ kNm}$:

$$\frac{x_u}{d} = 1.2 - \sqrt{1.44 - \frac{6.68 M_u}{f_{ck} b d^2}} \\ = 1.2 - \sqrt{1.44 - \frac{6.68 \times 21.44 \times 10^6}{20 \times 1000 \times 140^2}} = 0.163 < 0.479$$

Hence, it is under-reinforced.

$$z = d \left(1 - 0.416 \frac{x}{d} \right) = 140(1 - 0.416 \times 0.163) = 130.5 \text{ mm}$$

$$A_{st} = \frac{M}{0.87 f_y z} = \frac{21.44 \times 10^6}{0.87 \times 415 \times 130.5} = 455 \text{ mm}^2$$

Provide 10 mm bars at 170 mm c/c ($A_{st} = 462 \text{ mm}^2$) at support.

$$p_t = \frac{100 \times 462}{1000 \times 140} = 0.33\% > \text{Minimum steel } 0.12\%$$

2. Steel required at mid-span for $M_u = 18.4 \text{ kNm}$:

Using Table 2 of SP16

$$\frac{M_u}{b d^2} = \frac{18.4 \times 10^6}{1000 \times 140^2} = 0.938, \text{ hence, } p_t = 0.276\%$$

$$A_{st} = \frac{0.276 \times 1000 \times 140}{100} = 386 \text{ mm}^2$$

Provide 10 mm diameter bars at 200 mm c/c ($A_{st} = 393 \text{ mm}^2$) at mid-span.

Spacing limit: $3d = 3 \times 140 = 420 \text{ mm}$ or 300 mm ; hence,

$$s_{\text{max}} = 300 \text{ mm} > 200 \text{ mm}$$

3. Distribution steel

$$A_{st} = \frac{0.12 b D}{100} = \frac{0.12 \times 1000 \times 160}{100} = 192 \text{ mm}^2$$

Provide 8 mm diameter bars at 260 mm c/c ($< 5d$ or 300 mm); $A_{st} = 193 \text{ mm}^2$.

Step 5 Calculate curtailment of positive steel. Alternate main bars may be curtailed at distances not more than $0.15L = 600 \text{ mm}$ and $0.25L = 1000 \text{ mm}$ from discontinuous and continuous edges, respectively.

1. At simply supported end (see Fig. 9.11)

(a) Length beyond cut-off point =

$$0.15 \times 4000 - 0.5 \times 230 + 140 = 625 \text{ mm} > L_d = 470 \text{ mm}$$

(b) Length of curtailed bar from mid-span

$$= 0.5L - 0.15L = 0.35L = 0.35 \times 4000 = 1400 \text{ mm} > L_d$$

Hence, it is adequate.

2. At interior support

$$(a) 0.25 \times 4000 - 0.50 \times 250 + 140 = 1015 \text{ mm} > L_d = 470 \text{ mm}$$

$$(b) 0.50 \times 4000 - 0.25 \times 4000 = 1000 \text{ mm} > L_d = 470 \text{ mm}$$

Calculate the curtailment of negative steel. The length of bars extending from the discontinuous and continuous edges should not be less than L_d .

Length of bar from centre of edge support = $0.1L$ or L_d , that is, 470 mm

Length of bar from centre of interior support = $0.15L$ or L_d , that is, 600 mm

Step 6 Check for shear.

$$\text{Nominal shear stress, } \tau_v = \frac{V_u}{b d} = \frac{30.90 \times 10^3}{1000 \times 140} = 0.221 \text{ MPa}$$

From Table 19 of IS Code for $p_t = 0.33$ and M20, $\tau_c = 0.398 \text{ MPa} > 0.221 \text{ MPa}$

Hence, shear reinforcement is required. It should be noted that for solid slabs, τ_c may be multiplied by k as per Clause 40.2.1.1.

$$\text{Hence, } \tau_c = 1.3 \times 0.398 = 0.518 \text{ N/mm}^2 > \tau_v$$

Step 7 Check for development length as in Example 9.1.

1. At simple supports, L_d should be less than $1.3 \frac{M_{n,1}}{V_u} + L_o$

2. At points of inflection, $L_d < \frac{M_{n,1}}{V_u} + L_o$

At simple supports, assuming 50 per cent of the bars are bent up, the moment of resistance (assuming $M_n = M_u$)

$$M_{n,1} = 0.50 \times 1.84 = 9.2 \text{ kNm}$$

$$V_u \text{ (Table 13 of IS 456)} = (0.4 + 0.05) \times 8.4 \times 4 + (0.45 + 0.05) \\ \times 4.5 \times 4 = 24.12 \text{ kN}$$

Note: 0.05 is added due to partial restraint offered by the masonry wall as per Clause 22.5.2.

Considering $L_o = 8d_b$ for a 90° bend

$$1.3 \times \frac{9.2 \times 10^6}{24.12 \times 10^3} + 8 \times 10 = 575.8 < L_d = 470 \text{ mm}$$

Hence, the diameter of the chosen bar is satisfactory.

The development length at the inflection points will be adequate as $M_{n,1}$ remains the same and the value of V_u will be small.

Minimum length of bar embedded at support = $L_d/3 = 470/3 = 157$ mm or $(47 \times 8)/3 = 125$ mm for 8 mm bar < width of support – side cover = $230 - 25 = 205$ mm

Step 8 Check for deflection.

Basic L/d ratio = 20; $p_t = \frac{393 \times 100}{1000 \times 140} = 0.28\%$

Modification factor

$$k_t = \frac{1}{0.225 + 0.00322f_s - 0.625 \log(1/p_t)} \leq 2.0$$

$$f_s = 0.58f_y \frac{A_{s,required}}{A_{s,provided}} = 0.58 \times 415 \times \frac{386}{393} = 236.4 \text{ N/mm}^2$$

Hence, $k_t = 1.56$ (the same value may be obtained from Fig. 4 of IS 456).

Span/depth ratio = $20 \times 1.56 = 31.2$

L/d adopted = $30 < 31.2$. Hence, it is adequate.

Check top steel for T-beam action (Clause 23.1.1b):

The detailing arrangements (see Fig. 9.21) provide more than 60 per cent of the main steel in mid-span of the slab as transverse steel. Hence, the T-beam action is acceptable.

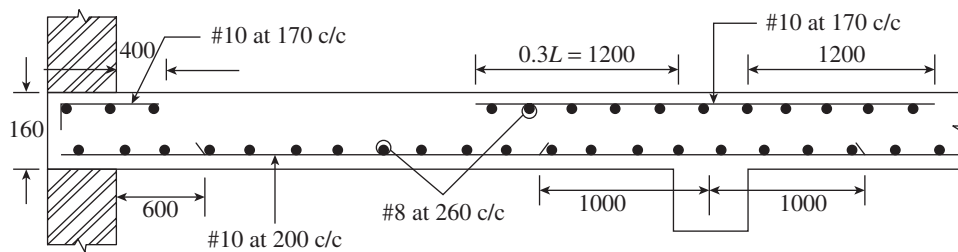


FIG. 9.21 Detailing of slab of Example 9.2

EXAMPLE 9.3 (Design of cantilever one-way slab):

Design a cantilevered portico slab of 5 m width and 2 m clear span. Assume moderate environment, with M25 concrete and Fe 415 grade steel.

SOLUTION:

The following values are given: $B = 6$ m, $L = 2$ m, $f_y = 415$ MPa, and $f_{ck} = 25$ MPa. The live load as per IS 875—Part 2 is 1.5 kN/m². However, it is better to assume 3 kN/m², as the slab may be crowded in the event of a procession.

Step 1 Calculate the loads. Assume the thickness at free end as 100 mm. As per Clause 23.2.1, for deflection consideration,

$$L/d \text{ for cantilever} = 7;$$

$$d = L/7 = 2000/7 = 285 \text{ mm}$$

Adopt $D = 300$ mm.

Assuming 10 mm diameter bars and clear cover of 15 mm, $d = 300 - 15 - 5 = 280$ mm. Adopt a total depth of 100 mm at the free end.

Effective span (Clause 22.2 c):

$$L = \text{Clear span} + 1/2 d = 2 + 0.140 = 2.14 \text{ m}$$

Self-weight of slab = $0.5(0.3 + 0.1)25 = 5.0$ kN/m²

Assumed weight of finishes = 0.85 kN/m²

Live load = 3.0 kN/m²

Total working load = 8.85 kN/m²

Design ultimate load $w_u = 8.85 \times 1.5 = 13.28$ kN/m²

Step 2 Calculate ultimate bending moment and shear.

$$M_u = 0.5w_u L^2 = 0.5 \times 13.28 \times 2.14^2 = 30.4 \text{ kNm}$$

$$V_u = w_u L = 13.28 \times 2.14 = 28.42 \text{ kN}$$

Step 3 Check for depth.

$$M_{u,lim} = 0.138f_{ck}bd^2$$

$$d = \left(\frac{M}{0.138f_{ck}b} \right)^{0.5} = \left(\frac{30.4 \times 10^6}{0.138 \times 25 \times 1000} \right)^{0.5} = 93.9 \text{ mm}$$

Hence, the assumed depth is adequate and the section is under-reinforced.

Step 4 Calculate the reinforcements. Let us use SP16, Table 3.

$$\frac{M_u}{bd^2} = \frac{30.4 \times 10^6}{1000 \times 280^2} = 0.388$$

From Table 3, $p_t = 0.11\% < A_{st,min} = 0.12\%$

Hence,

$$A_t = \frac{0.12 \times 1000 \times 280}{100} = 336 \text{ mm}^2$$

However, since cantilevers are prone to creep deflection, let us provide minimum reinforcement as per Clause 26.5.1.1.

$$A_{st} = \frac{0.85bd}{f_y} = \frac{0.85 \times 1000 \times 280}{415} = 574 \text{ mm}^2$$

From Table 96 of SP 16, provide 12 mm bars at 190 mm c/c, $A_{st} = 595$ mm².

Step 5 Check for control of cracks (Clause 26.5.2.1).

Diameter of bar $< D/8$; we have $12 < 300/8 = 37.5$ mm

Moreover, as per Clause 26.3.3, maximum spacing should be less than $3d$ (3×280) or 300 mm > 190 mm. Hence, the spacing is adequate.

Distribution steel = 0.12%

Hence, provide 10 at 230 mm c/c (spacing $< 5d$ or 300 mm).

Step 6 Check for shear.

Nominal shear stress $\tau_v = \frac{V_u}{bd} = \frac{28.4 \times 10^3}{1000 \times 280} = 0.102$ N/mm²

From Table 19 of IS 416, for M25 and $p_t = 0.212$, $\tau_c = 0.333$ N/mm² > 0.102 N/mm².

Hence, the slab is safe in shear.

Step 7 Check the development length. For M25 concrete and 12 mm diameter bars, with $f_y = 415$ MPa, from Table 65 of SP 16,

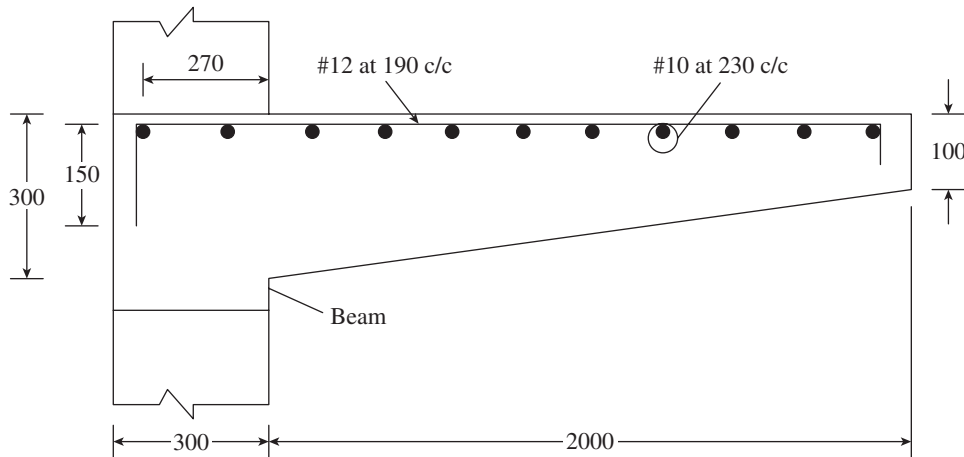


FIG. 9.22 Detailing of cantilever slab of Example 9.3

Anchorage length, $L_d = 484$ mm

Provide a 90° bend as in Fig. 9.22, which depicts cantilever one-way slab.

Anchorage provided = $270 + 150 + 8 \times 10 = 500$ mm > 484 mm

Hence, it is adequate.

Step 8 Check for deflection.

Basic L/d ratio = 7, $p_t = 0.212$

$$f_y = 0.58 f_y \frac{A_{s, \text{required}}}{A_{s, \text{provided}}} = 0.58 \times 415 = 240.7 \text{ N/mm}^2$$

Hence, k_t from Fig. 4 of IS 456 = 1.73

Hence, $(L/d)_{\text{max}} = 7 \times 1.73 = 12.1$

$$(L/d)_{\text{actual}} = 2140/280 = 7.6 < 12.1$$

Hence, the slab satisfies the deflection criteria.

Note: Since the creep deflection may be high in cantilever slabs, it is better to keep L/d ratio closer to 7.0–8.0.

Step 9 Calculate the curtailment of reinforcement. The bending moment is proportional to the square of the cantilever span. Half the bars can be curtailed at L_1 . This length is obtained as

$$\frac{1}{2} = \frac{L_1^2}{L^2} = \frac{L_1^2}{2.14^2}$$

or $L_1 = \sqrt{\frac{2.14^2}{2}} = 1.513$ m or $2.14 - 1.513 = 0.627$ m from support

The actual curtailment is done at a distance beyond the development length. Thus, curtailment length = $627 + 403 = 1030$ mm. However, since only minimum reinforcement is provided, the bars should not be curtailed for this beam.

Note: Cantilever slabs tend to be uneconomical due to substantial depths at the support. Hence, it will be economical to provide cantilever beams and simply-supported slabs cast over them.

EXAMPLE 9.4 (Design of culvert):
Design an RC slab culvert for a state highway for the following data (see Fig. 9.23):

Carriageway: Two lane 7.5 m wide
Kerbs: 600 mm wide on the sides
Clear span: 6 m, wearing coat: 80 mm thick

Loading: IRC Class AA loading: 2 wheels each 850×3600 mm area at 2.05 m centres with a load of 350 kN
Minimum clearance of wheel from kerb as per IRC = 1.2 m

Assume Fe 415 steel and M25 concrete.

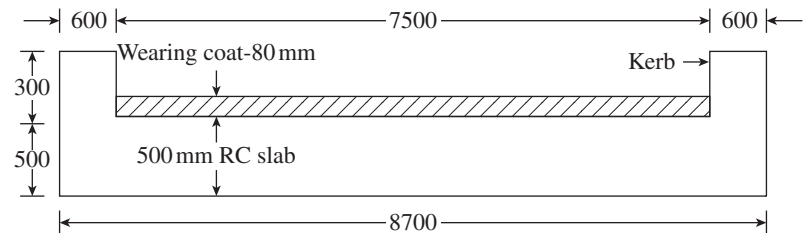


FIG. 9.23 Culvert of Example 9.4

SOLUTION:

Step 1 Calculate the depth of the slab and effective span. The thickness of the slab may be assumed as 80 mm per metre of span for highway bridge decks.

Overall slab thickness = $80 \times 6 = 480$ mm, say 500 mm

Using 25 mm diameter bars with clear cover of 35 mm

Effective depth = $500 - (35 + 12.5) = 452.5$ mm

Assume width of bridge bearing = 400 mm

Effective span is the lesser of the following:

1. Clear span + Effective depth = $6 + 0.4525 = 6.4525$ m
2. c/c of bearing = $6 + 0.4 = 6.4$ m

Hence, effective span $L = 6.4$ m.

Step 2 Calculate the dead load bending moment.

Dead weight of slab = $0.5 \times 25 = 12.50$ kN/m²

Weight of wearing coat = $0.08 \times 22 = 1.76$

Total load = 14.26 kN/m²

Dead load bending moment = $\frac{14.26 \times 6.4^2}{8} = 73$ kNm

Step 3 Calculate the live load bending moment.

Impact factor for the Class AA tracked vehicle is 25 per cent for 5 m span and decreasing linearly to 10 per cent for 9 m span, as per the IRC code.

Hence, for 6.4 m span, impact factor = $25 - \frac{15}{4}(6.4 - 5) = 19.75\%$

The tracked vehicle is placed symmetrically on the span.

Assuming 45° dispersion, effective width of load is given by

$$b_e = kx \left(1 - \frac{x}{L} \right) + t_y$$

For this case (see Fig. 9.24), $x = 3.2\text{ m}$, $L = 6.4\text{ m}$, $B = 8.7\text{ m}$

$$\frac{B}{L} = \frac{8.7}{6.4} = 1.36; t_y = 0.85 + 2 \times 0.08 = 1.01\text{ m}$$

From Table 9.6, for $B/L = 1.36$, $k = 2.768$

$$b_e = 2.768 \times 3.2 \times \left(1 - \frac{3.2}{6.4}\right) + 1.01 = 5.439\text{ m}$$

When the tracked vehicle is placed close to the kerb (Fig. 9.24), we see that the effective width of two loads overlap and the net effective width of dispersion

$$= 2225 + 2050 + \frac{5439}{2} = 6994.5\text{ mm}$$

Total load of two tracks with impact = $700 \times 1.1975 = 838.125\text{ kN}$

$$\text{Average intensity of load} = \frac{838.125}{4.76 \times 6.9945} = 25.11\text{ kN/m}^2$$

Maximum bending moment due to live load is (see Fig. 9.25)

$$M_{\max} = \frac{25.18 \times 4.76}{2} \times 3.2 - \frac{25.18 \times 4.76}{2} \times \frac{4.76}{4} = 191.77 - 71.31 = 120.46\text{ kNm}$$

Design bending moment = $1.5(120.46 + 73) = 290.19\text{ kNm}$

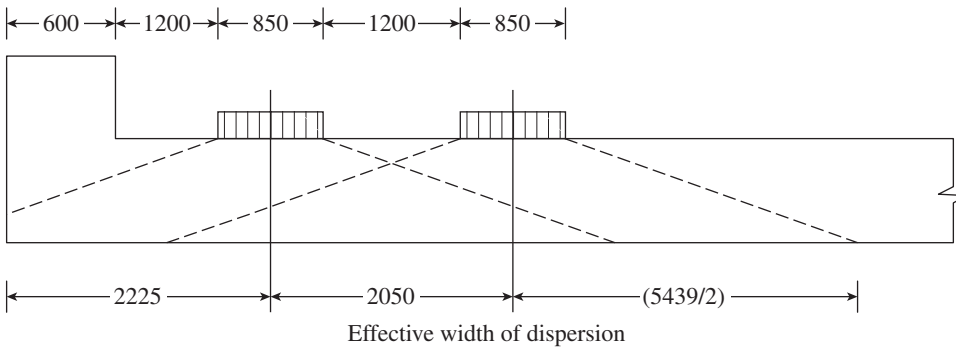


FIG. 9.24 Effective width of dispersion

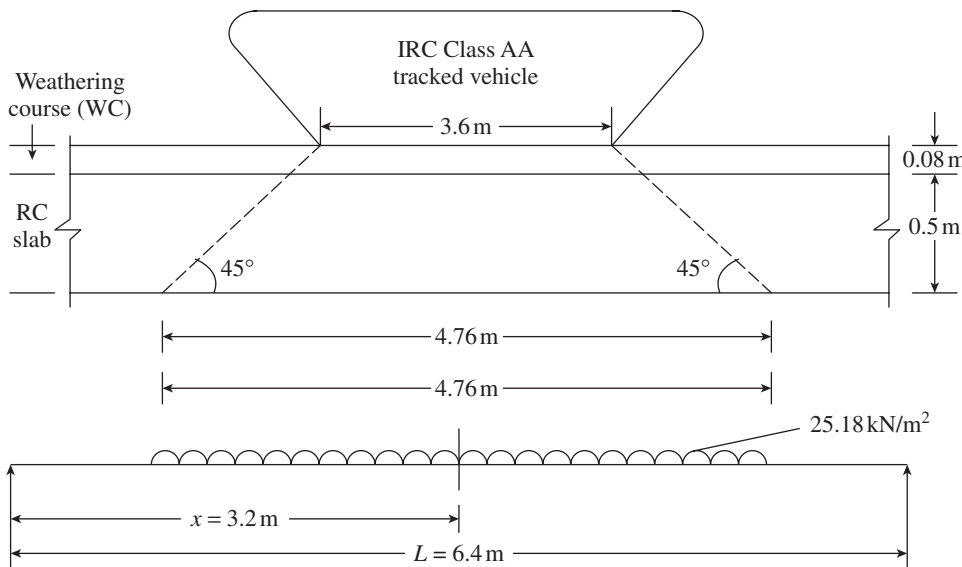


FIG. 9.25 Loading for maximum bending moment

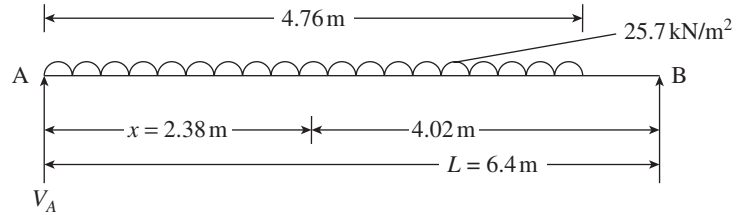


FIG. 9.26 Loading for maximum shear

Step 4 Calculate the shear due to Class AA tracked vehicle. For maximum shear at support, the loading is arranged as shown in Fig. 9.26:

Effective width of dispersion

$$b_e = kx \left(1 - \frac{x}{L}\right) + t_y$$

For this case, $t_y = 1.01\text{ m}$, $B = 8.7\text{ m}$, $x = 2.38\text{ m}$, $L = 6.4\text{ m}$, and $k = 2.768$ (Table 9.6).

$$b_e = 2.768 \times 2.38 \left(1 - \frac{2.38}{6.4}\right) + 1.01 = 5.15\text{ m}$$

Width of dispersion = $2225 + 2050 + 5150/2 = 6850\text{ mm}$

Hence, average intensity of load = $\frac{838.125}{4.76 \times 6.85} = 25.7\text{ kN/m}^2$

$$\text{Shear force } V_A = \frac{25.7 \times 4.76 \times 4.02}{6.4} = 76.84\text{ kN}$$

$$\text{Dead load shear} = \frac{14.26 \times 6.4}{2} = 45.63\text{ kN}$$

$$\text{Design shear, } V_u = 1.5(76.84 + 45.63) = 183.7\text{ kN}$$

Step 5 Design the deck slab.

$$d = \sqrt{\frac{M_u}{0.138 f_{ck} b}} = \sqrt{\frac{290.19 \times 10^6}{0.138 \times 25 \times 1000}} = 290\text{ mm}$$

Effective depth provided = $452.5\text{ mm} > 290\text{ mm}$. Hence, the depth provided is sufficient and the section is under-reinforced.

$$\frac{M_u}{bd^2} = \frac{290.19 \times 10^6}{1000 \times 452.5^2} = 1.417$$

From Table 3 of SP 16, $p_t = 0.422\%$

$$A_{st} = \frac{0.422 \times 1000 \times 452.8}{100} = 1909.6\text{ mm}^2$$

$$\text{Spacing of } 25\text{ mm bars} = \frac{1000 \times 490}{1909.6} = 257\text{ mm}$$

Provide 25 mm diameter bars at 250 mm c/c (spacing $< 3d$ or 300 mm).

$$A_{st, \text{ provided}} = 1963 \text{ mm}^2; p_t = 0.433\%$$

Bending moment for distribution reinforcement is

$$(0.3M_L + 0.2M_d) = 0.3 \times 120.46 + 0.2 \times 73 = 50.74 \text{ kNm}$$

Ultimate design moment = $1.5 \times 50.74 = 76.1 \text{ kNm}$

Using 12 mm bars, effective depth = $452.5 - (12.5 + 6) = 434 \text{ mm}$

$$\frac{M_u}{bd^2} = \frac{76.1 \times 10^6}{1000 \times 434^2} = 0.404$$

From Table 3 of SP 16, $p_t = 0.114\% < 0.12\%$ (minimum)

$$\text{Hence, } A_{st} = \frac{0.12 \times 1000 \times 434}{100} = 520.8 \text{ mm}^2$$

$$\text{Spacing of 12 mm bars} = \frac{1000 \times 113}{520.8} = 217 \text{ mm}$$

Provide 12 mm bars at 200 mm c/c (spacing $< 5d$ or 300 mm).

Step 6 Check for shear.

$$\text{Nominal shear stress, } \frac{V_d}{bd} = \frac{183.7 \times 10^3}{1000 \times 452.5} = 0.406 \text{ N/mm}^2$$

Providing reinforcement for a length of $0.1L$ at support with 20 mm bars at 200 c/c at top, we get

$$A_{st} = 1571 \text{ mm}^2; p_t = \frac{100 \times 1571}{1000 \times 452.5} = 0.347\%$$

From Table 19 of IS 456, with $p_t = 0.347$ and M25 concrete

$$\tau_c = 0.410 \text{ N/mm}^2 > 0.406 \text{ N/mm}^2$$

Hence, the section is safe against shear.

Design of kerbs:

Let the height of kerb above road surface = 220 mm

Total depth of kerb = $220 + 80 + 500 = 800 \text{ mm}$

Taking effective cover as 47.5 mm, effective depth = 752.5 mm

Loads on kerb:

$$\text{DL} = 0.6 \times 0.8 \times 25 = 12.0 \text{ kNm}$$

$$\text{LL} = 0.6 \times 4 \times 1 = 2.4 \text{ kNm}$$

$$\text{Weight of railing, etc.} = 0.6 \text{ kN/m}$$

$$\text{Total load} = 15 \text{ kN/m}$$

$$\text{Bending moment} = \frac{wl^2}{8} = \frac{15 \times 6.4^2}{8} = 76.8 \text{ kNm}$$

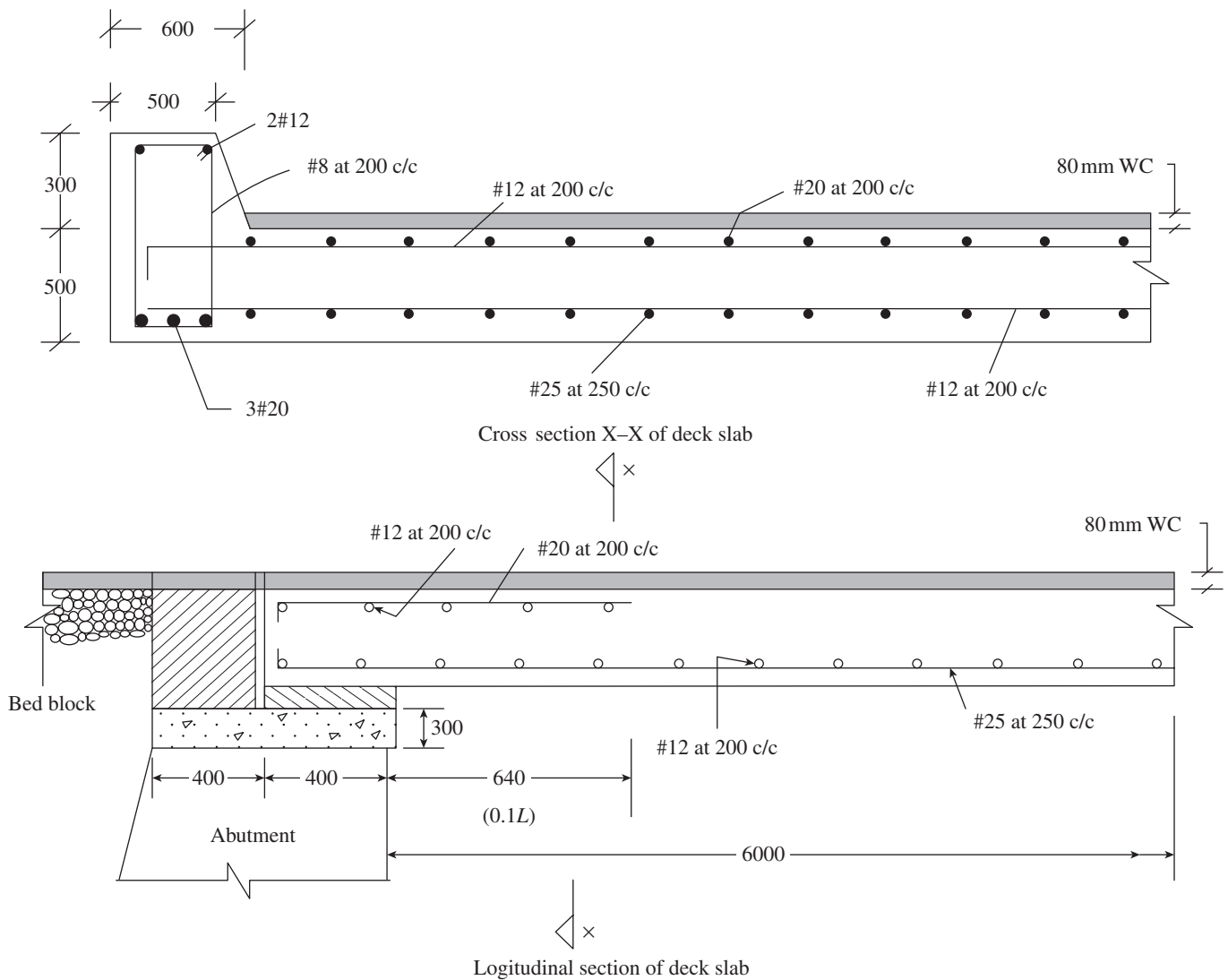


FIG. 9.27 Detailing of reinforcement of culvert slab

$$\frac{M_u}{bd^2} = \frac{76.8 \times 10^6}{600 \times 752.5^2} = 0.226$$

From Table 3 of SP 16, for M25 concrete, $p_t = 0.084\%$, $A_{st} = 379 \text{ mm}^2$

As per Clause 26.5.1.1, minimum $A_{st} = \frac{0.85bd}{f_y} = \frac{0.85 \times 600 \times 752.5}{415} = 925 \text{ mm}^2$

Hence, provide three 20 bars, with $A_{st} = 942 \text{ mm}^2$.

Check for shear:

$$V_u = 15 \times 6.4/2 = 48 \text{ kN}$$

Nominal shear = $48 \times 10^3 / (600 \times 752.5) = 0.106 \text{ N/mm}^2$

Hence, provide nominal 8 mm vertical stirrups at 200 mm spacing with two 12 mm diameter bars at the corners to support the stirrups. The details of reinforcement in culvert slab are given in Fig. 9.27.

Note: Although the principles of design are the same, the design using the IRC code may differ slightly.

EXAMPLE 9.5 (Design of ribbed slab):

A ribbed slab of 3.5 m span is to be designed to carry an imposed load of 3 kN/m^2 , using M25 concrete and Fe 415 grade steel. Assume dimensions as per IS 456 and design the reinforcement.

SOLUTION:

Assume that the ribs are spaced at 900 mm as shown in Fig. 9.28.

Imposed load = 3 kN/m^2

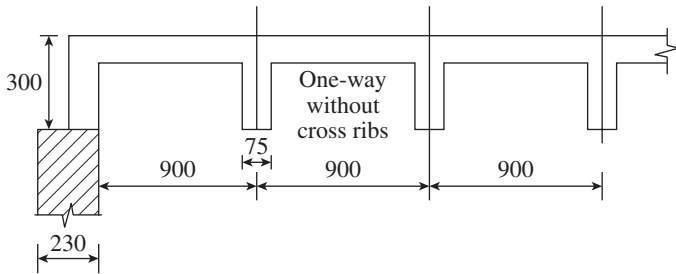


FIG. 9.28 Dimensions of ribbed slab

Step 1 Fix the dimensions of the rib.

Basic L/d ratio = 20 (Clause 23.2.1)

Assuming 0.8 per cent reinforcement, k_t as per Fig. 4 of IS 456 is (with $f_s = 0.58 \times f_y = 0.58 \times 415 = 240.7$) = 1.06.

Adopt $D_f = 75 \text{ mm}$ and $b_w = 75 \text{ mm}$.

The flange width $b_f = L_o/6 + b_w + 6D_f$ (Clause 23.1.2)
 $= 3500/6 + 75 + 6 \times 75$
 $= 1108 \text{ mm} > 900 \text{ mm}$ (spacing)

Ratio of web width/flange width = $75/900 = 0.083$

Hence from Fig. 6 of IS 456, reduction factor = 0.8.

Required rib depth = $L / (20 \times 1.06 \times 0.8) = 3500 / 16.96 = 206 \text{ mm}$

Adopt depth of rib as 300 mm. As per Clause 30.5, the width of the rib should be greater than 65 mm. Hence, adopt 75 mm. This clause also stipulates that spacing of rib $< 1.5 \text{ m}$; we have

adopted 900 mm spacing. Hence, it is adequate. Moreover, the depth of the rib should be less than four times the width of the rib.

Now, $300 - 75 = 225 \text{ mm} < 4 \times 75 = 300 \text{ mm}$

Hence, all the dimensions satisfy the code stipulations.

Step 2 Calculate the loads. The self-weight of the slab for 900 mm spacing is computed in the following way:

Assume slab thickness ($< 1/12^{\text{th}}$ spacing of ribs) = $900/12 = 75 \text{ mm}$

Self-weight of slab = $0.9 \times 1.0 \times 0.075 \times 25 = 1.69 \text{ kN}$

Self-weight of rib = $(0.3 - 0.075) \times 0.075 \times 1.0 \times 25 = 0.42 \text{ kN}$

Now $1.69 + 0.42 = 2.11 \text{ kN}$ is the self-weight of the system covering an area of $1 \text{ m} \times 0.9 \text{ m}$. Hence,

Load per square metre = $2.11/0.9 = 2.34 \text{ kN/m}^2$

Assume weight of finishes, etc. = 0.66 kN/m^2

Hence, total design load = $(3 + 2.34 + 0.66) \times 1.5 = 9 \text{ kN/m}^2$

Step 3 Calculate reinforcement in rib.

Maximum bending moment, $M_u = wL^2/8 = 9 \times 3.5^2/8 = 13.78 \text{ kNm}$

Assuming a clear cover of 25 mm and 10 mm diameter bars,

$$d = 300 - 25 - 5 = 270 \text{ mm}$$

For simplicity, let us ignore T-beam action and consider only the rectangular rib for design.

$$M_u/bd^2 = 13.78 \times 10^6 / (75 \times 270^2) = 2.52$$

From Table 3 of SP 16, $p_t = 0.807\%$.

$$A_{st} = \frac{0.807 \times 75 \times 270}{100} = 164 \text{ mm}^2$$

Provide one 16 bar with $A_{st} = 201 \text{ mm}^2$.

Step 4 Check for shear.

$$V_u = wL/2 = 9 \times 3.5/2 = 15.75 \text{ kN}$$

Nominal shear stress, $\tau_v = \frac{15.75 \times 10^3}{75 \times 270} = 0.78 \text{ N/mm}^2$

$$100A_s/bd = 100 \times 201 / (75 \times 270) = 0.993 \text{ N/mm}^2$$

From Table 19 of IS 456, for M25, $\tau_c = 0.559 \text{ N/mm}^2$ (0.81 N/mm^2)

Hence, shear reinforcement has to be provided.

Spacing of 6 mm links (Clause 40.4)

$$s_v = \frac{0.87f_y A_{sv} d}{(V_u - \tau_c bd)} = \frac{0.87 \times 415 \times 28 \times 270}{(15.75 \times 10^3 - 0.559 \times 75 \times 270)} = 718 \text{ mm}$$

Maximum spacing = $0.75d = 0.75 \times 270 = 202.5 \text{ mm}$ or 300 mm (Clause 26.5.1.5)

Provide 6 mm diameter stirrups at 200 mm c/c.

Check for minimum shear reinforcement (Clause 26.5.1.6):

$$\frac{A_{sv}}{s_v} \geq \frac{0.4b}{0.87f_y} \quad \text{or} \quad \frac{28}{200} \geq \frac{0.4 \times 75}{0.87 \times 415}$$

$0.14 \geq 0.083$; hence, it is suitable,

Step 5 Check for deflection. Since assumed reinforcement (0.8%) is approximately equal to the reinforcement provided (0.807%), the slab is satisfactory for deflection.

Step 6 Calculate reinforcement in slab portion.

$$\text{Area required per metre width} = \frac{0.12}{100} \times 75 \times 1000 = 90 \text{ mm}^2/\text{m}$$

As per Table 96 of SP 16, 6 mm at 300 mm c/c gives $94 \text{ mm}^2/\text{m}$.

Spacing shall not be greater than $3 \times d_s$, or 300 mm; $3 \times d_s = 3 \times (75 - 15 - 3) = 171 \text{ mm}$

Hence, provide 5 mm at 170 mm c/c both ways. (TOR-KARI 4.5 mm diameter bars at 170 mm c/c can also be used, giving an area of $93.5 \text{ mm}^2/\text{m}$.) The reinforcement details of the ribbed slab are given in Fig. 9.29.

Note: Normally, this topping slab will be reinforced with wire mesh reinforcement.

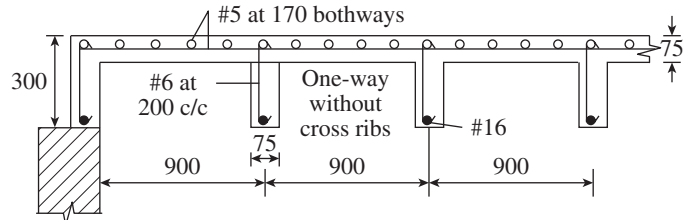


FIG. 9.29 Detailing of ribbed slab of Example 9.5

SUMMARY

Slabs are the most widely used structural elements whose thickness is considerably smaller than their other dimensions. They are frequently used as floors and roofs in buildings, decks in bridges, staircases, and so on. Depending on the support conditions, slabs may be simply supported, continuous, or cantilevered. Slabs may also take various shapes, but rectangular slabs are frequently used. Slabs may be categorized into one-way and two-way slabs depending on the way they support the loads. One-way slabs are those in which most of the load is carried on the shorter span. One-way slab behaviour is evident when the ratio of the longer span to the shorter span is greater than two or when a slab is supported only along two opposite sides.

The direction in which the slab bends is called the main direction. The main reinforcement is placed at the tension face of the slab. Steel is also provided in the transverse direction to take care of the temperature and shrinkage effects; this steel is called the secondary or distribution steel. However, near the supports two-way action may occur, and hence top reinforcement should be provided at least for a distance of $0.1L$ from the support, where L is the effective span. Clause 22.2 of IS 456 gives some rules for calculating the effective span, depending on the support condition.

Usually, the deflection criterion of slabs is considered to be met if the specified ratios of maximum span to depth given in Clause 23.2.1 of the code are satisfied. Modification factors are also given to the basic L/d ratios, depending on the percentage of tension and compression steel. Minimum thickness and cover should also be checked against the required fire rating of slabs.

One-way slabs may be analysed either by exact analysis using computer software or by using the moment and shear coefficients given in the codes, in which case the moment redistribution is not permitted. The critical section for bending in the case of monolithic beam and slab construction is at mid-span (simply supported slabs) or at the face of the beams (continuous slabs). For shear, the critical section is at the face of the support, and when applied shear

introduces compression, it may be taken at a distance d from the support, where d is the effective depth.

A slab is generally designed as a flexural element considering a strip of 1 m width, even though it is cast in one piece and not in strips of unit width. The computation for the depth required for resisting the moment and for required reinforcement is identical to the design of the rectangular beam (or the flanged beam if the slab is ribbed), described in Chapter 5. Minimum and maximum reinforcements are also specified to prevent sudden failure and to ensure ductile behaviour, respectively. The detailing should also consider the maximum permitted diameter and spacing of bars to control the crack width within acceptable limits. Though HSC is not advantageous, high-strength steel may result in economical constructions. The ACI code provides guidelines for cases where the HSC column loads are transferred through NSC slabs.

The size effect should be considered while designing for moment and shear. One-way slabs are often designed by using the design tables provided in SP 16. The code uses the effective width concept for tackling concentrated loads applied on slabs. Concentrated loads are often encountered in bridge slabs; one-way slabs in bridges are called culverts and their design is explained.

As in the case of beams, the concrete below the neutral axis is cracked and does not contribute to the strength of the slabs. Ribbed slabs with or without hollow blocks or voided slabs achieve economy by eliminating the cracked concrete. Minimal recommendations are given in the code for the design of such ribbed slabs. They are discussed and explained with an example.

Under earthquakes, the slabs act as diaphragms; the Indian code is silent on this aspect and hence a brief discussion is added to consider the design in such situations. Finally, slabs may also be used in pavements and industrial floors, in which case they are supported directly by the soil below. Brief discussions are included about the design of such slabs-on-grade. Ample examples are included to explain the concepts presented in this chapter.

REVIEW QUESTIONS

- How are slabs classified? List the various classifications.
- Distinguish between one-way and two-way slabs. Cite the situations in which one-way behaviour can be assumed.
- Slabs can be assumed as one-way slabs, when the L/B ratio of the slabs is greater than _____.
(a) 2.0 (b) 1.5 (c) 3.0 (d) none of these
- Should we have to provide reinforcement at the top of simply supported one-way slabs? Why?
- State the rules given in Clause 22.2 of IS 456 for calculating the effective span of slabs.
- What are the two methods suggested in the codes to limit deflections?

7. The basic L/d ratio for one-way simply supported slab specified in IS 456 is _____.
(a) 25 (c) 20.8
(b) 20 (d) none of these
8. The basic L/d ratio for one-way cantilevered slab specified in IS 456 is _____.
(a) 8 (b) 10 (c) 5.6 (d) none of these
9. Why is the span to effective depth ratio of slabs larger than that of beams?
10. What are the two modification factors applied on the basic L/d ratios?
11. What value will you assume for the initial design depth of simply supported and continuous one-way slabs?
12. What are the conditions to be satisfied when using the bending moment and shear force coefficients given in the code for continuous one-way slabs?
13. The positive bending moment coefficient at the middle of the end span of a continuous one-way slab is _____.
(a) $w_l L^2/10 + w_d L^2/12$ (c) $w_l L^2/12 + w_d L^2/16$
(b) $w_l L^2/9 + w_d L^2/10$ (d) none of these
14. At what points on the span should the bending moment be considered for the design of continuous one-way slabs?
15. How are slab reinforcements calculated?
16. Can we use the equations derived for under-reinforced beams in slabs? State the reason.
17. What are the minimum steel requirements for slabs as per Clauses 26.5.2 and 26.5.1.1 of IS 456?
18. What are the spacing requirements of slab reinforcement?
19. What is the importance of the spacing limitations of reinforcement imposed by the code?
20. Show with the help of a sketch how the distribution steel is placed with respect to main reinforcement at the following positions:
(a) At the mid-span of the slab
(b) Near supports of the slab
Explain the reasons for placing them according to your choice.
21. Sketch the reinforcement detailing of simply supported and continuous one-way slabs.
22. What are TOR-KARI bars? What is the advantage of using them in slabs?
23. State the three methods by which we can consider transferring HSC column loads through the normal strength concrete (NSC) slabs.
24. How are slabs designed for shear forces?
25. Briefly state the different steps involved in the design of one-way slabs.
26. Minimum distribution steel to be provided in slab for Fe 415 grade steel is _____.
(a) 0.12% (b) 0.10% (c) 0.15% (d) 1.2%
27. What value of clear cover to main steel is assumed in the tables provided by SP 16? How does one find the distribution steel from these tables?
28. How are concentrated loads considered in the design of slabs as per IS 456?
29. Write brief notes on the following:
(a) Design of culverts
(b) Slabs-on-grade
(c) Diaphragm action of slabs
30. List the three different ways in which ribbed slabs can be constructed as per Clause 30.1 of IS 456.

EXERCISES

1. Design a floor slab for an interior room, with clear dimensions of 3.0m × 8 m, for a building located in Mumbai. The slab is resting on 230mm thick masonry walls. Assume live load as 3.0kN/m² and dead load due to finish, partition, and so on as 1.2kN/m². Use M20 concrete and Fe 415 steel.
2. A hall in a building has a floor consisting of continuous slab cast monolithically with simply supported 230mm wide beams spaced at 3.5 m c/c. The clear span of the beam is 6m. Assuming the live load on slab as 3.0kNm² and partition plus load due to finishes as 1.5kN/m², design the slab with M25 grade concrete and Fe 415 steel.
3. Design a cantilevered portico slab of 6 m width and 1.75 m clear span, assuming moderate environment, with M20 concrete and Fe 415 grade steel.
4. Design an RC slab culvert for a state highway for the following data: Carriageway: Two lane 7.0m wide, Kerbs: 600mm wide on the sides, Clean span: 5 m, Wearing coat: 80 mm thick, Loading: IRC Class AA loading: Two wheels each 850 × 3600mm area at 2.05 m centres with a load of 350kN. Minimum clearance of wheel from kerb as per IRC = 1.2m. Assume Fe 415 steel and M20 concrete.
5. A ribbed slab of 4.0 m span is to be designed to carry an imposed load of 1.5kN/m², using M20 concrete and Fe 415 grade steel. Assume dimensions as per IS 456 and design the reinforcement.

REFERENCES

- ACI 360R-06 2006, *Design of Slabs on Grade*, American Concrete Institute, Farmington Hills, p. 74.
- Ambalavanan, R., N. Narayanan, and K. Ramamurthy 1999, 'Cost Effectiveness Analysis of Alternate One-way Floor/Roof Systems', *The Indian Concrete Journal*, ACC Ltd, Vol. 73, No. 3, pp.171-74.
- Angelakos, D., E.C. Bentz, and M.D. Collins 2001, 'Effect of Concrete Strength and Minimum Stirrups on Shear Strength of Large

- Members', *ACI Structural Journal*, American Concrete Institute, Farmington Hills, Vol. 98, No. 3, pp. 290–300.
- ASCE/SEI/SFPE 29-05 2006, *Standard Calculation Methods for Structural Fire Protection*, American Society of Civil Engineers, Reston, p. 80.
- Beeby, A.W. 1971, 'Modified Proposals for Controlling Deflections by Means of Ratios of Span to Effective Depth', *Technical Report 456 (Publication 42.456)*, Cement and Concrete Association, London, p. 19.
- Bianchini, A.C., R.E. Woods, and C.E. Kesler 1960, 'Effect of Floor Concrete Strength on Column Strength', *Proceedings, ACI Journal*, American Concrete Institute, Farmington Hills, Vol. 56, No. 11, pp. 1149–69.
- Bischoff, P.H. and A. Scanlon 2009, 'Span-depth Ratios for One-way Members based on ACI 318 Deflection Limits', *ACI Structural Journal*, American Concrete Institute, Farmington Hills, Vol. 106, No. 5, pp. 617–26.
- Bondy, K. 2003, 'Moment Redistribution: Principles and Practice Using ACI 318-02', *PTI Journal*, Post-Tensioning Institute, Phoenix, Vol. 1, pp. 3–21, (also see <http://www.kenbondy.com/images/ProfessionalArticles/MomentRedistributionPTIJJournal.pdf>, last accessed on 2 November 2012).
- Bull, D.K. 2004, 'Understanding the Complexities of Designing Diaphragms in Buildings for Earthquakes', *Bulletin of the New Zealand Society of Earthquake Engineering*, Wellington, Vol. 37, No. 2, pp. 70–88.
- Gardner, N.J. 2011, 'Span/Thickness Limits for Deflection Control', *ACI Structural Journal*, American Concrete Institute, Farmington Hills, Vol. 108, No. 4, pp. 453–60.
- Gilbert, R.I. 1992, 'Shrinkage Cracking in Fully Restrained Concrete Members', *ACI Structural Journal*, American Concrete Institute, Farmington Hills, Vol. 89, No. 2, 1992, pp. 141–9, and Beeby, A. W. 1993, 'Discussion', Vol. 90, No. 1, pp. 123–6.
- IS 6061:1981, *Code of Practice for Construction of Floor and Roof with Joists and Filler Blocks, Part 1: With Hollow Concrete Filler Blocks, Part 2: With Hollow Clay Filler Blocks, Part 3: With Precast Hollow Clay Block Joists and Hollow Clay Filler Blocks, and Part 4: With Precast Hollow Clay Block Slab Panels*, Bureau of Indian Standards, New Delhi.
- Kiamco, C. 1997, 'The Structural Look at Slabs on Grade', *Concrete International*, ACI, American Concrete Institute, Farmington Hills, Vol. 19, No. 7, pp. 45–9.
- Lubell, A.S., E.C. Bentz, and M.P. Collins 2009, 'Influence of Longitudinal Reinforcement on One-way Shear in Slabs and Wide Beams', *Journal of Structural Engineering*, ASCE, Vol. 135, No. 1, pp. 78–87.
- Lubell, A.S., E.G. Sherwood, E.C. Bentz, and M.P. Collins 2004, 'Safe Shear Design of Large Wide Beams', *Concrete International*, ACI, American Concrete Institute, Farmington Hills, Vol. 26, No. 1, pp. 66–78.
- Moehle, J.P., J.D. Hooper, D.J. Kelly, and T.R. Meyer 2010, 'Seismic Design of Cast-in-place Concrete Diaphragms, Chords, and Collectors: A Guide for practicing engineers', *NEHRP Seismic Design Technical Brief No. 3*, National Institute of Standards and Technology, Gaithersburg, p. 29, (also see <http://www.nehrp.gov/pdf/nistgcr10-917-4.pdf>, last accessed on 2 November 2012).
- Naeim, F. and R.R. Boppana 2001, 'Seismic Design of Floor Diaphragms', in F. Naeim (ed.), *The Seismic Design Handbook*, 2nd edition, Kluwer Academic Publishers, New York.
- Ospina, C.E. and S.D.B. Alexander 1998, 'Transmission of Interior Concrete Column Loads through Floors', *Journal of Structural Engineering*, ASCE, Vol. 124, No. 6, pp. 602–10.
- Purushothaman, P. 1984, *Reinforced Concrete Structural Elements: Behaviour, Analysis and Design*, Tata McGraw-Hill Publishing Company Ltd and Torsteel Research Foundation in India, New Delhi, pp. 377–638.
- Reynolds, C.E., and J.C. Steedman 1988, *Reinforced Concrete Designer's Handbook*, E & FN Spon, London, p. 436.
- Rizk, E. and H. Marzouk 2009, 'New Formula to Calculate Minimum Flexural Reinforcement for Thick High-strength Concrete Plates', *ACI Structural Journal*, American Concrete Institute, Farmington Hills, Vol. 106, No. 5, pp. 656–66.
- Scanlon, A. and B.-S. Choi 1999, 'Evaluation of ACI 318 Minimum Thickness Requirements for One-way Slabs', *ACI Structural Journal*, American Concrete Institute, Farmington Hills, Vol. 96, No. 4, pp. 616–21.
- Shah, A.A., J. Dietz, N.V. Tue, and G. König 2005, 'Experimental Investigation of Column-slab Joints', *ACI Structural Journal*, American Concrete Institute, Farmington Hills, Vol. 102, No. 1, pp. 103–13.
- Subramanian, N. 1992, 'Torkari Saves 30% Steel in Slabs', *Civil Engineering and Construction Review*, Trend-Set Engineers Pvt. Ltd, Vol. 5, No. 7, pp. 47–53.
- Subramanian, N. 1998, 'Effective Concrete Strength of Column-Slab/Beam Joints', *ICI Bulletin*, Indian Concrete Institute, Chennai, No. 65, pp. 29–31.
- Subramanian, N. 2006, 'Transmission of HSC Column Loads through NSC Slabs', *The Indian Concrete Journal*, ACC Ltd, Vol. 80, No. 1, pp. 44–9.
- Suprenant, B.A. 2002a, 'Shrinkage and Temperature Reinforcement: Simple Topic; Not-so-simple Design Issues', *Concrete International*, American Concrete Institute, Farmington Hills, Vol. 24, No. 9, pp. 72–6.
- Suprenant, B.A. 2002b, 'Why Slabs Curl, Part 1: A Look at the Curling Mechanisms and the Effect of Moisture and Shrinkage Gradients on the Amount of Curling', *Concrete International*, American Concrete Institute, Farmington Hills, Vol. 24, No. 3, pp.56–61, 'Part 2: Factors Affecting the Amount of Curling', Vol. 24, No. 4, pp. 59–64, and 'Discussions', October 2002, pp. 10–3.
- Suryanarayana, P. 2000, 'Use of Torkari Steel for Economic Designs', *Civil Engineering and Construction Review*, Vol. 15, No. 9, pp. 11–4.
- Taylor, H.P.J. 1972, 'Shear Strength of Large Beams', *Journal of Structural Engineering*, ASCE, Vol. 98, No. ST11, pp. 2473–90.
- Westergaard, H.M. 1926, 'Stresses in Concrete Pavements Computed by Theoretical Analysis', *Public Roads*, Vol. 14, No. 2, pp. 25–35.
- Westergaard, H.M. and W.A. Slater 1921, 'Moments and Stresses in Slabs', *Proceedings, American Concrete Institute*, Vol. 17, pp. 415–538. <http://www.prosteel.in>, last accessed on 2 November 2012.

DESIGN OF TWO-WAY SLABS

10.1 INTRODUCTION

In Chapter 9, we studied the behaviour and design of one-way slabs, in which the aspect ratio (ratio of the longer to the shorter span, L_y/L_x) is greater than 2.0. In such one-way slabs, the slab deflects in the shorter direction alone in a cylindrical fashion and hence the main reinforcement is placed in the same direction. However, when the aspect ratio of a floor panel is less than two, the contribution of the longer span in carrying the floor load becomes substantial. Since the floor load is transmitted in two directions, this type of slab is called a *two-way slab*, and the flexural reinforcement has to be designed in both the directions (see Section 2.3.2). Two-way slabs, when loaded, will deflect into a dish-shaped surface, similar to a saucer, rather than a cylindrical one as in one-way slabs (see Fig. 10.1).

Two-way slab systems include two-way solid slabs supported by beams, *flat plates*, *flat slabs*, and *waffle slabs* (see Section 2.3.3 and Figs 2.16 and 2.19 of Chapter 2 and Fig. 10.2). Usually, a choice between these different two-way slab systems is made based on the architectural, structural (magnitude of the design loads, span lengths, and provided

lateral load-resisting systems), and construction considerations (C & CAA T36 2003). As already discussed in Section 2.3.3 of Chapter 2, flat plate is simply a slab of uniform thickness directly supported on columns, generally suitable for relatively light loads. For larger loads and spans, a flat slab becomes more suitable since the *drop panels* and/or *column capitals* provide higher shear and flexural strength. A slab supported on beams on all sides of each floor panel is generally referred to as a two-way slab system. A waffle slab is equivalent to a two-way joist system or may be visualized as a solid slab with recesses, which are provided to decrease the weight of the slab (see Section 2.3.3). The analysis, design, and detailing of flat slabs and flat plates are provided in Chapter 11.

In this chapter, we will first consider the behaviour, analysis, design, and detailing of wall- and beam-supported two-way slabs. Slabs with non-rectangular shapes are also encountered in buildings and tanks. The design of such slabs is also covered briefly. Concentrated loads are encountered in industrial buildings and also in bridges. Slabs may be provided with openings for various reasons. Such slabs with openings are briefly discussed and possible solutions provided. Finally,

an introduction to yield-line analysis, which may be useful for designing slabs of unusual shapes or boundary conditions, is also provided.

10.2 BEHAVIOUR OF TWO-WAY SLABS

Let us first consider the behaviour of two-way slabs simply supported at all four edges by unyielding supports (stiff beams or walls), as shown in Fig. 10.3(a). It may be convenient to consider the slab as consisting of

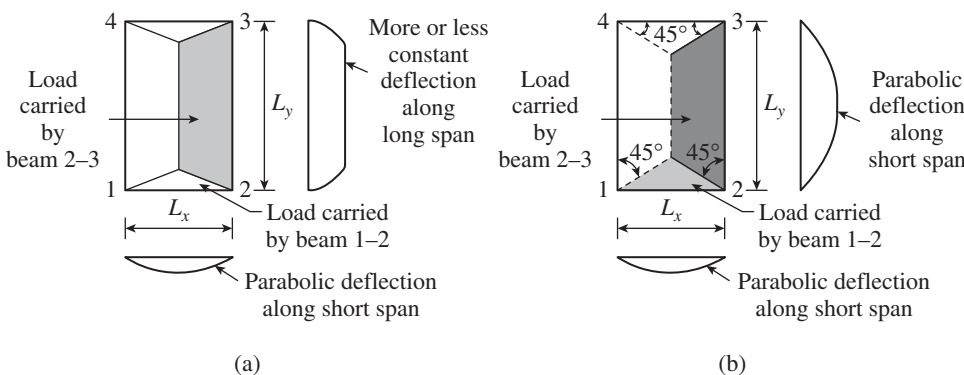


FIG. 10.1 Difference in behaviour of one-way and two-way slabs (a) One-way slab ($L_y/L_x > 2.0$) (b) Two-way slab ($L_y/L_x \leq 2$)

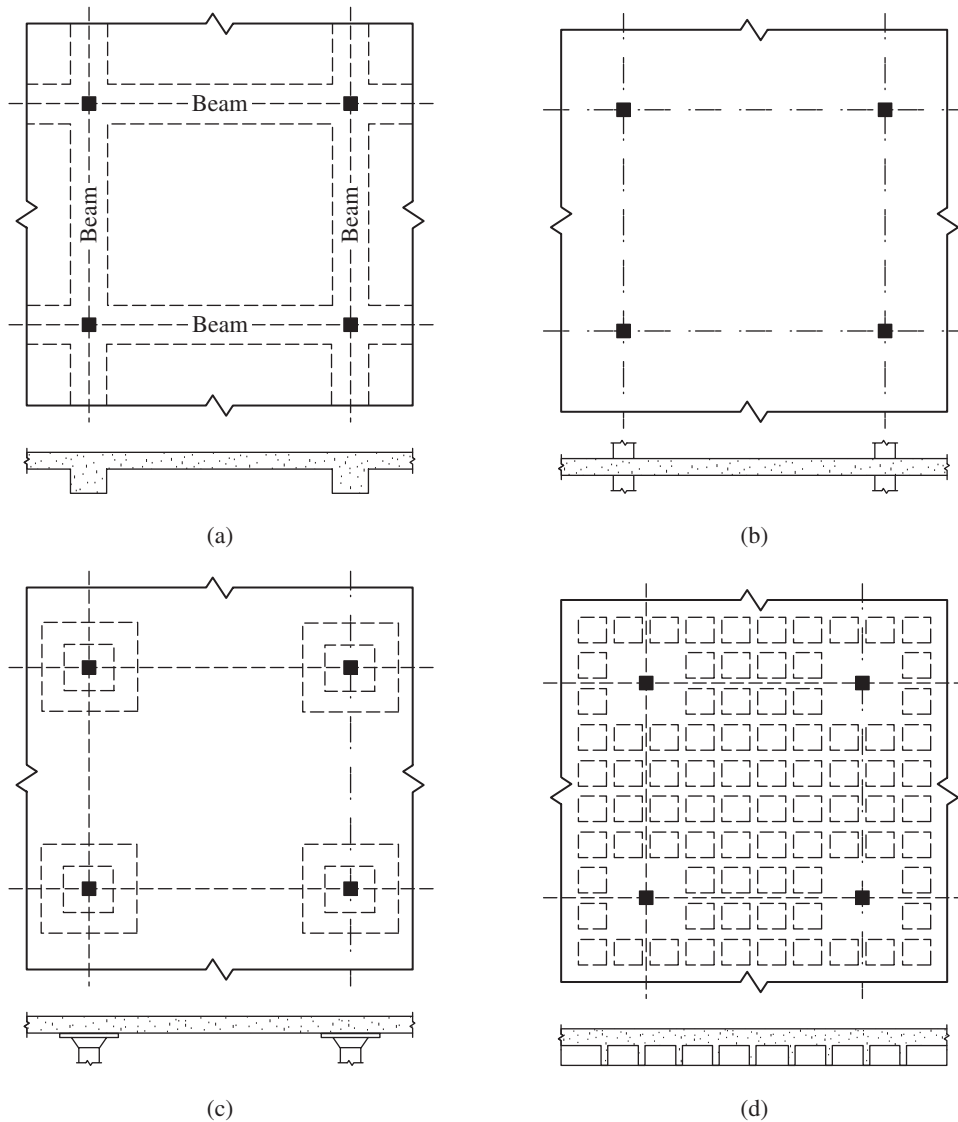


FIG. 10.2 Types of two-way slabs (a) Two-way slab (b) Flat plate (c) Flat slab (d) Grid or waffle slab

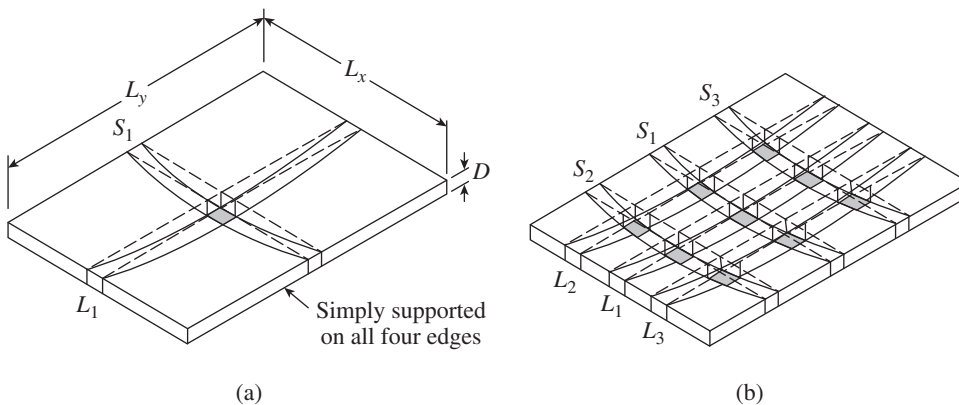


FIG. 10.3 Behaviour of two-way slabs (a) Single beam strip in each direction (b) Multiple beam strips in each direction

beam strips in each of the two directions, intersecting each other. Two such strips, L_1 in the longer direction and S_1 in the shorter direction, are shown in Fig. 10.3(a). When acted upon

When the load is increased, hairline cracks start to appear from the point of maximum deflection as shown in

by the applied load (say, uniformly distributed load of w), each of the two strips acts similar to a beam, sharing the applied load w and transferring it to their respective edge supports. Thus, bending exists in both directions. To resist these moments, the slab must be reinforced in both directions by two layers of reinforcements that are perpendicular to each other. These reinforcements have to be designed to take a proportionate share of the applied load. However, it has to be noted that the actual behaviour of the slab is more complex than that of the visualization of the slab being made of a series of orthogonal (intersecting at right angles) beams in two directions.

Now consider the same slab with two sets of three strips in two perpendicular directions as shown in Fig. 10.3(b). As shown in the figure, the behaviour of the outer strips S_2 , L_2 , S_3 , and L_3 are different from that of the centre strips S_1 and L_1 . These outer strips are bent as well as twisted. This twisting results in torsional stresses and torsional moments, especially near the corners, which in turn will result in lifting up of the corners, unless restrained. Thus, the total load is carried not only by the bending moments in the two directions but also by the torsional moments.

Consider a square slab, assuming that only a bending moment is present. The maximum bending moment will be

$$\frac{(w/2)L^2}{8} = 0.0625wL^2$$

However, actual analysis of square plates using the plate theory shows that the maximum bending moment is only $0.048wL^2$, thus indicating that the twisting moments reduce the bending moment by about 25 per cent.

Fig. 10.4(a). The slab no longer has constant stiffness, as the cracked regions have lower stiffness than the other regions. In rectangular slabs, the crack pattern may differ in the two directions and the slab may not remain isotropic (*isotropic* means that the mechanical properties are the same in every direction, whereas *orthotropic* means that the properties are different along each axis). Even though such a condition may violate the assumptions of elastic analysis, the elastic theory is found to predict the moments reasonably. It has to be noted that most of the slabs will have hairline cracks under service loading.

When the load is further increased, yielding of reinforcements takes place at the mid-span. Now the bending moments get redistributed to the non-yielding portions that still remain elastic. As the load is increased further, this inelastic redistribution will continue until a large area of steel in the central portion of the slab yields and a mechanism is formed when the slab fails (see Fig. 10.4b). The yield lines divide the slab into a series of trapezoidal or triangular elastic plates in the case of rectangular slabs and triangular plates in the case of square slabs (see Fig. 10.4b). The load corresponding to this stage of behaviour may be estimated using the yield-line analysis, which is discussed in Section 10.8.

Experiments on slabs have shown that even after forming a mechanism, they deform further, forming a flat compression arch as shown in Fig. 10.5, with the surrounding structure providing the necessary stiffness to resist the reaction of the arch and the reinforcement acting as a tie to the arch (Westergaard and Slater 1921; Ockelton 1955; Vecchio and Tang 1990). This stage of behaviour is usually disregarded in design.

This discussion shows that the elastic analysis does not accurately predict the behaviour beyond service loads and significant redistribution of moments takes place after the first yielding.

Similar behaviour has been observed in the case of flat slabs, except that first cracking usually appears on the top of the slab around the column as shown in Fig. 10.6, which is followed by the cracking of the slab at the bottom, midway between the columns. Even though the slabs supported by the unyielding supports exhibit ductile behaviour, flat slabs may fail suddenly in the punching shear.

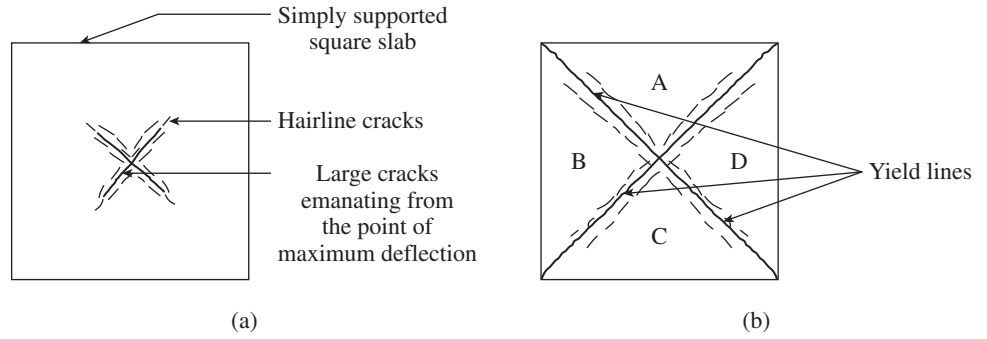


FIG. 10.4 Mode of failure of simply supported two-way slabs (a) Onset of yielding of bottom reinforcement at point of maximum deflection (b) Bottom steel yielding along yield lines forming a mechanism

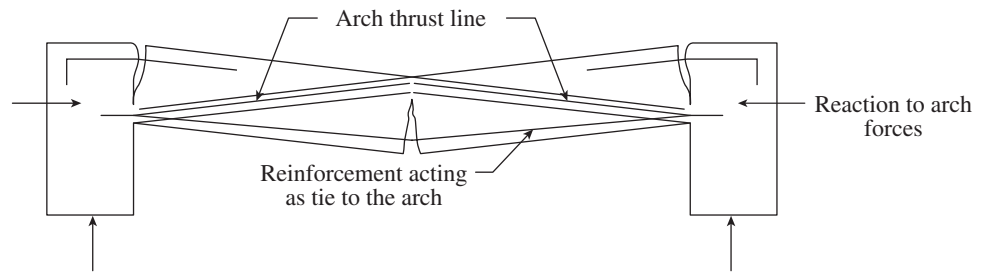


FIG. 10.5 Arch action in slabs

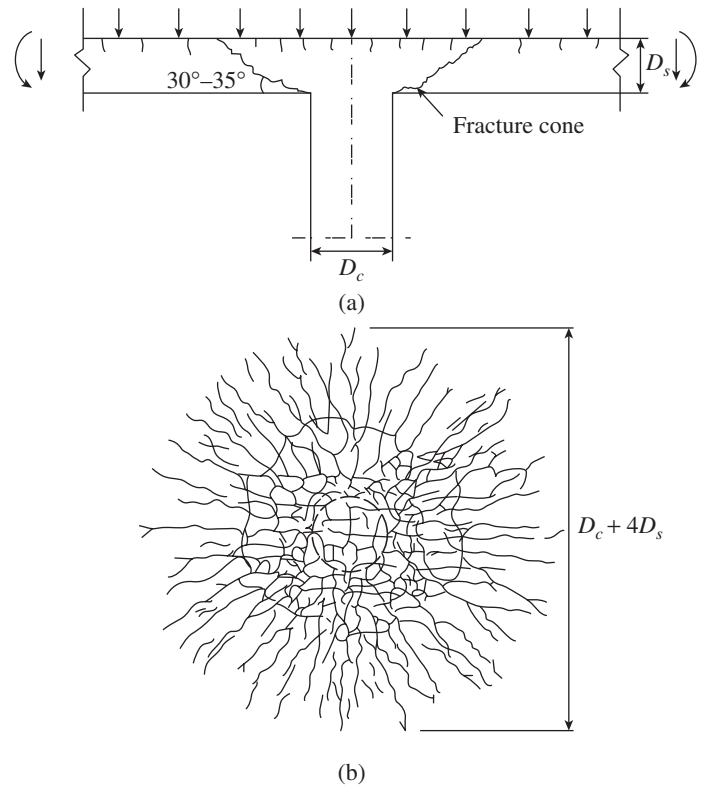


FIG. 10.6 Mode of failure of flat slab in shear (a) Crack pattern section at column (b) Crack pattern at the top of slab

10.3 MINIMUM THICKNESS OF SLABS

Slab thickness is the primary factor affecting the serviceability and shear strength. Fire resistance requirements may also

govern both the cover and slab thickness (guidance for fire resistance is provided in Fig. 1 and Table 16A of IS 456).

Clauses 23.2 and 24.1 of IS 456 suggest that the vertical deflection limits may be assumed to be satisfied in two-way slabs with short spans up to 3.5 m with mild steel reinforcement and for loading class up to 3 kN/m², when the *span to overall depth* ratios are not greater than the following values:

- 1. Simply supported slabs 35
- 2. Continuous slabs 40

This value should be multiplied by the factor 0.8 for Fe 415 grade steel. Moreover, for two-way slabs, the shorter of the two spans should be used for calculating the span to effective depth ratios. The basic ratios are modified according to the ratios of tension and compression reinforcements provided and the service load steel stress at mid-span (or at the support in the case of cantilevers), as per Figs 9.4 and 9.5 of Chapter 9, that is, Figs 4 and 5 of IS 456.

It has to be noted that IS 456 and the American Concrete Institute (ACI) codes allow *thinner slabs* to be used, provided the calculated deflections satisfy the limits given in the respective codes; for example, Clause 23.2 of IS 456 states that the final deflection due to all loads should not exceed span/250 (this restriction is to prevent the sagging appearance and can easily be countered by giving a suitable camber to the formwork; hence, the ACI code does not specify this limit), and the deflection after erection of partition and application of finishes should not exceed either span/350 or 20 mm (this restriction is to prevent the cracking of brittle partitions and finishing resting directly on the slab; the ACI code limits range from span/240 to span/480 depending on the material of the partition and an additional limit of span/360 for immediate deflection due to imposed load, when there are no partitions). Similarly, deflection calculations are to be made for cantilevers exceeding 10 m length. It must be remembered that the thickness of the slab may also be governed by shear, especially for flat plates. The shortcomings of the *L/d* provisions of IS 456 are discussed by Varyani (1998), who has suggested that the 20 mm limit is unreasonable and be eliminated in future editions of the code, in line with the ACI code.

Minimum Thickness of Flat Slabs and Flat Plates

For flat slabs with drops, the aforementioned span to effective depth ratios can be applied directly. As per Clause 31.2.1, for flat slabs without drops, these ratios should be multiplied by 0.9 and the minimum thickness of flat slab without drops should be 125 mm. The clause also stipulates that for flat slabs with or without drops, the *long span* has to be considered in the calculation of minimum depth. However, it does not specify the span to depth ratios for spans greater than 3.5 m and/or loading class greater than 3 kN/m².

The ACI code recommendations for calculating the minimum thickness of slabs without interior beams are as per Table 10.1 (ACI provides a unified approach to the design of two-way slabs, that is, unlike IS 456, slabs with and without beams are not considered in different provisions).

TABLE 10.1 Minimum thickness of slabs, *d_s*, without interior beams as per ACI 318-2011

Yield Strength, <i>f_y</i> (N/mm ²)	Without Drop Panels			With Drop Panels (Drop Panel Length ≥ <i>L_n</i> /3, depth ≥ 1.25 <i>D_s</i>)		
	Exterior Panels		Interior Panels	Exterior Panels		Interior Panels
	Without Edge Beams	With Edge Beams ³		Without Edge Beams	With Edge Beams	
280	<i>L_n</i> /33	<i>L_n</i> /36	<i>L_n</i> /36	<i>L_n</i> /36	<i>L_n</i> /40	<i>L_n</i> /40
420	<i>L_n</i> /30	<i>L_n</i> /33	<i>L_n</i> /33	<i>L_n</i> /33	<i>L_n</i> /36	<i>L_n</i> /36
520	<i>L_n</i> /28	<i>L_n</i> /31	<i>L_n</i> /31	<i>L_n</i> /31	<i>L_n</i> /34	<i>L_n</i> /34

Notes:

- 1. *L_n* is the length of clear span (in mm) in the longer direction measured face to face of supports in slabs without beams and face to face of beams or other supports in other cases.
- 2. The minimum thickness of the slab should not be less than 125 mm for slabs without drop panels and 100 mm for slabs with drop panels.
- 3. For slabs with beams between columns along exterior edges, the stiffness ratio of the edge beam to slab, *α_b*, should not be less than 0.8.

It has to be noted that in Table 10.1 (Note 3), it is stipulated that the stiffness ratio of the edge beam to slab, *α_b*, should not be less than 0.8. An edge beam that has an overall height of at least twice the slab thickness, *D_s*, and a gross area of at least 4*D_s*² will always have an *α_b* value greater than 0.8. It must also be noted that the ACI code suggests the use of the *long span* for calculating the minimum thickness and the values given in Table 10.1 are based on the yield strength of steel and not on the loading class. Fanella (2001) presented a chart based on the ACI code recommendations, which simplifies the calculation of the minimum slab thickness for the various types of two-way slabs. A modified chart in SI units is shown in Fig. 10.7, which will be useful to fix the minimum thickness.

The deflection and hence the minimum thickness of slab panels with beams on all sides depend not only on the panel aspect ratio but also on the relative stiffness of the supporting beams in the two directions. Realizing this, the following equation is provided in Clause 13.2.5 of the Canadian code to calculate the minimum thickness of a slab with beams between supports:

$$D \geq \frac{L_n(0.6 + f_y/1000)}{30 + 4\beta_s\alpha_{bm}} \geq \frac{\text{Perimeter}}{140} \text{ with } \alpha_{bm} \leq 2.0 \quad (10.1a)$$

where *D* is the overall thickness of slab in mm, *f_y* is the characteristic yield strength of steel in N/mm², *L_n* is the longer clear span, *β_s* is the ratio of clear spans *L_y*/*L_x*, *α_{bm}* is the average value of *α_b* for all beams on the edges of the slab

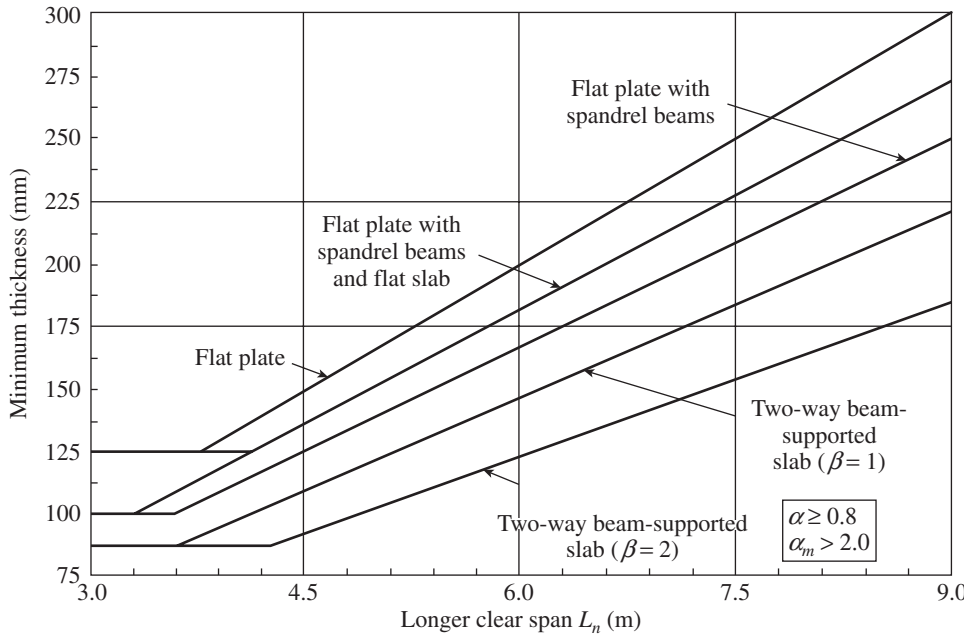


FIG. 10.7 Minimum slab thickness for two-way slabs
 Source: Fanella 2002 (Adapted), Structural Engineers Association of California (SEAOC)

panel, and α_b is the ratio of flexural stiffness of the beam ($4E_b I_b / L$) to the flexural stiffness of a width of the slab bounded laterally by the centre lines of adjacent panels (if any) on each side of the beam. (The sections to be considered for computing the moment of inertia of uncracked beam and slab, I_b and I_s , respectively, are shown shaded in Fig. 10.8.) From Fig. 10.8,

$$\alpha_b = \frac{4E_{cb} I_b / L}{4E_{cb} I_s / L} \tag{10.1b}$$

The lengths L of the beam and slab are equal and the values of modulus of elasticity, E , for the beam and

slab will not usually differ. Hence, Eq. (10.1b) may be simplified as

$$\alpha_b = \frac{I_b}{I_s} \tag{10.1c}$$

The Canadian code suggests that the value of I_b may be computed approximately as

$$I_b = \frac{b_w h^3}{12} \left(2.5 \left(1 - \frac{D_s}{h} \right) \right) \tag{10.1d}$$

where h is the height of the beam, b_w is the breadth of the beam, and D_s is the overall thickness of the slab. The limit of $\alpha_{b,m}$ at less than or equal to 2.0 in Eq. (10.1a) is to ensure that the slab will not become too thin when heavy beams are provided around the slab edges. It should be noted that the use of Eq. (10.1d)

requires that an initial assumption be made on the slab thickness.

The advantage of Eq. (10.1a) is that it also considers the yield strength of steel, f_y , while selecting the minimum thickness (it may be noted that the use of Fe 250 grade steel will result in a reduction in the slab thickness, although with increased steel quantity).

The Canadian code also recommends the following equation for the minimum thickness of two-way slabs without drop panels:

$$D_s \geq \frac{L_n (0.6 + f_y / 1000)}{30} \tag{10.2}$$

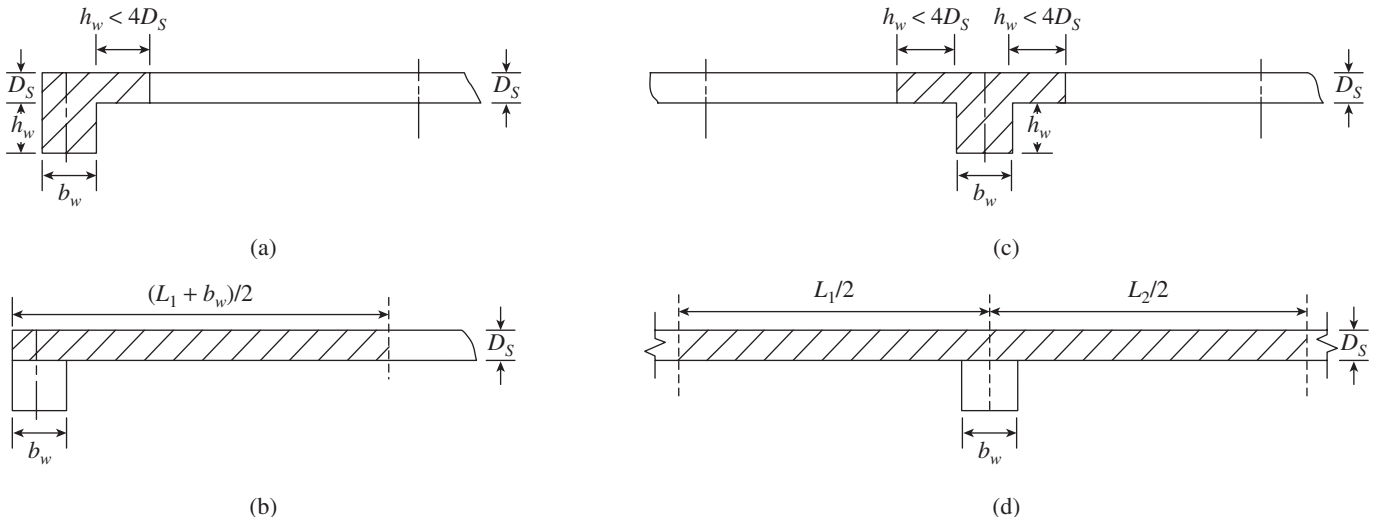


FIG. 10.8 Definition of beam and slab sections for the calculation of α_b (a) Section for I_b —edge beam (b) Section for I_s —edge beam (c) Section for I_b —interior beam (d) Section for I_s —interior beam

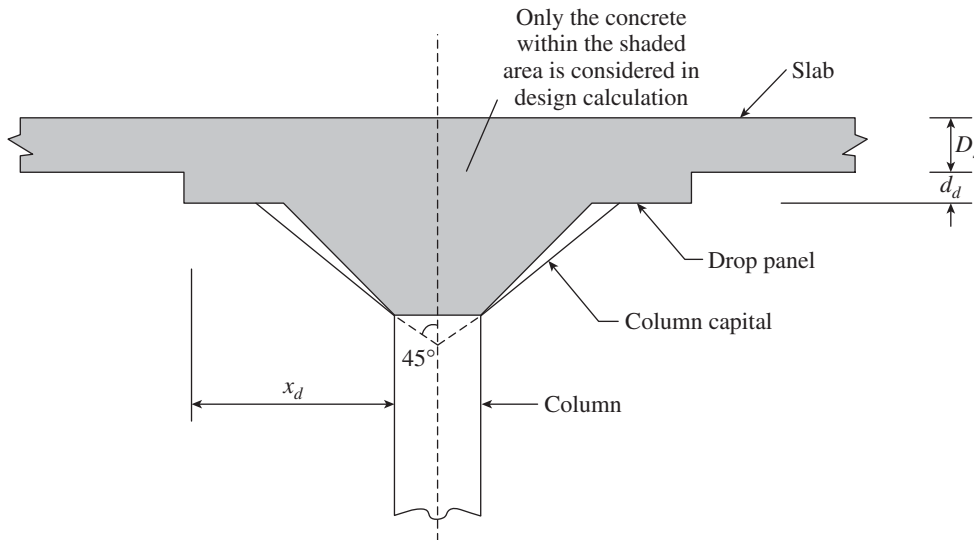


FIG. 10.9 Drop panel and column capital in flat slabs

This equation is valid only when the edge beams with a stiffness ratio of $\alpha_b \geq 0.8$ is provided along the discontinuous edges of the slab; otherwise, the value of thickness predicted by Eq. (10.2) has to be increased by 10 per cent.

For slabs with drop panels, the minimum thickness of a slab is given by (see Fig. 10.9)

$$D_s \geq \frac{L_n(0.6 + f_y/1000)}{30} - \frac{2x_d}{L_n}d_d \quad (10.3)$$

where d_d is the additional thickness of the drop panel below the soffit of the slab (see Fig. 10.9), which should be less than the depth of the slab, D_s , and x_d is the dimension from face of column to edge of drop panel. While using Eq. (10.3), the quantity $(2x_d/L_n)$ is calculated in two directions and only the smaller value is used; x_d should be less than $L_n/4$. Equations similar to Eqs (10.1)–(10.3) are also available in the US code. It has to be noted that these provisions do not address the sensitivity of slab deflections to early age construction loads, rate of construction, or concrete strength (Gardner 2011).

According to Clause B.3.1 of the Canadian code, the slab thickness determined from Eqs (10.1)–(10.3) should not be less than the following:

1. 100 mm
2. The perimeter of the slab divided by 140 in the case of slabs discontinuous on one or more edges
3. The perimeter of the slab divided by 160 in the case of fully continuous slabs

Equations (10.1)–(10.3) are based on the past experience of slabs with usual values of uniform gravity loading and good construction practice and may not be the economical or suitable thickness for all applications. For $f_y = 415 \text{ N/mm}^2$, these expressions will result in clear span to overall thickness ratios, L_n/D , in the range 30–46. Hence, caution should be

exercised in certain sequences of shoring during construction (see also Section 3.9.4 of Chapter 3) or when large imposed to dead load ratios or concentrated loads are encountered.

Scanlon and Lee (2006) and Gilbert (1985) also proposed generalized minimum thickness equations for one- and two-way slabs in terms of span to depth ratios considering the applied loads, long-term multipliers, effects of cracking, and so on. The span to depth provisions of various codes as well as the proposals of various authors are compared by Gardner (2011) and Lee and Scanlon (2010).

10.4 WALL- AND BEAM-SUPPORTED TWO-WAY SLABS

The analysis, design, and detailing of wall- and beam-supported two-way slabs are discussed in this section.

10.4.1 Analysis of Wall-supported Slabs

Clause 24.3 of IS 456 states that ‘bending moments in slabs (except flat slabs) constructed monolithically with supports shall be calculated by taking such slabs either continuous over supports and capable of free rotation, or as members of a *continuous framework* with the supports, taking into account the stiffness of supports. If such supports are formed due to beams, which justify fixity at the support of slabs, then the effect on the supporting beam, such as, the bending of the web in the transverse direction of the beam and the torsion in the longitudinal direction of the beam, whichever is applicable, shall also be considered in the design of the beam.’ In the Subclause 24.3.1, it also states that ‘for the purpose of calculating the moments in slabs in a monolithic structure, it will generally be sufficiently accurate to assume that members connected to the ends of such slabs are fixed in position and direction at the ends remote from their connections with the slabs.’ Thus, it implies that one must use the *equivalent frame method* for the analysis. However, the code also permits the use of moment coefficients (provided in Annexure D of IS 456) for two way-slabs. Hence, the designers often choose the simple procedure given in Annexure D, although it may be uneconomical (Purushothaman 1984).

In this context, it is interesting to quote the ACI code provision (Clause 13.5.1) that states a two-way slab system ‘may be designed by any procedure satisfying conditions of equilibrium and geometric compatibility, if shown that the design strength at every section is at least equal to the required

strength and that all serviceability conditions, including specified limits on deflections, are met.’ Clause 24.4 of IS 456 also reflects a similar view.

There are a number of possible approaches to the analysis of two-way systems, which include the following (NZS 3101-Part1: 2006):

1. Linear elastic analysis for thin plates (classical plate theory, finite difference method)
2. Non-linear analysis (finite element analysis)
3. Plastic or limit analysis (lower bound like the strip method and upper bound like the yield-line analysis method)
4. Idealized frame method of analysis (equivalent frame method)
5. Simplified methods of analysis (methods based on moment coefficients, direct design method)
6. Combination of elastic theory and limit analysis

The designer is permitted by the codes to adopt any of these approaches provided that all safety and serviceability criteria are satisfied. In general, finite element analysis (FEA) is used only when we encounter a complex two-way system or unusual loading; otherwise, it is not suitable for design office use, as it is time-consuming and expensive. In finite element method, plate or shell elements are typically employed to represent the behaviour of slabs. Designers using FEA often ignore twisting moments, an assumption that may be unconservative, especially in the corner regions of slabs. Wood and Armer (1968) proposed one of the most popular design methods that explicitly incorporate twisting moment in slab design. Other available methods to consider twisting moments are discussed by Shin, et al. (2009).

Though the ACI code allowed the use of moment coefficients until 1971, it now recommends either the *direct*

design method or *equivalent frame method* for the design of floor systems with or without beams. These procedures were derived from analytical studies based on the elastic theory in conjunction with the aspects of limit analysis and results of experimental tests. The primary difference between the direct design method and equivalent frame method is in the way the moments are computed for the two-way systems.

The *yield-line theory* is a limit analysis method devised for the slab design. Compared to elastic theory, the yield-line theory gives a more realistic representation of the behaviour of slabs at the ultimate limit state, and its application is particularly advantageous for irregular column spacing. Whereas the yield-line method is an upper bound limit design procedure, *strip method* is considered to give a lower bound design solution.

Design methods based on moment coefficients from elastic analysis are still favoured by many designers. These methods are easy to apply and give valuable insight into slab behaviour; their use is especially justified for many irregular slab cases where the preconditions of the direct design method are not met or when column interaction is not significant.

Before discussing the details of some of these methods of analysis, it may be useful to study the trajectories of principal moments in two-way slabs. We are aware of the fact that structures have a tendency to transmit loads to the supporting systems along the shortest possible path. As seen from the discussions of Section 10.2, this tendency is seen in slabs as well. This feature is illustrated in Fig. 10.10, which shows the principal moment directions in slabs with ratios of sides 1.0 and 2.0 for simply supported and fixed boundary conditions (Leonhardt and Mönning 1977). From this figure, it is seen that in the central region in the longer direction of the longer slabs, the direction of the principal moments, is nearly perpendicular

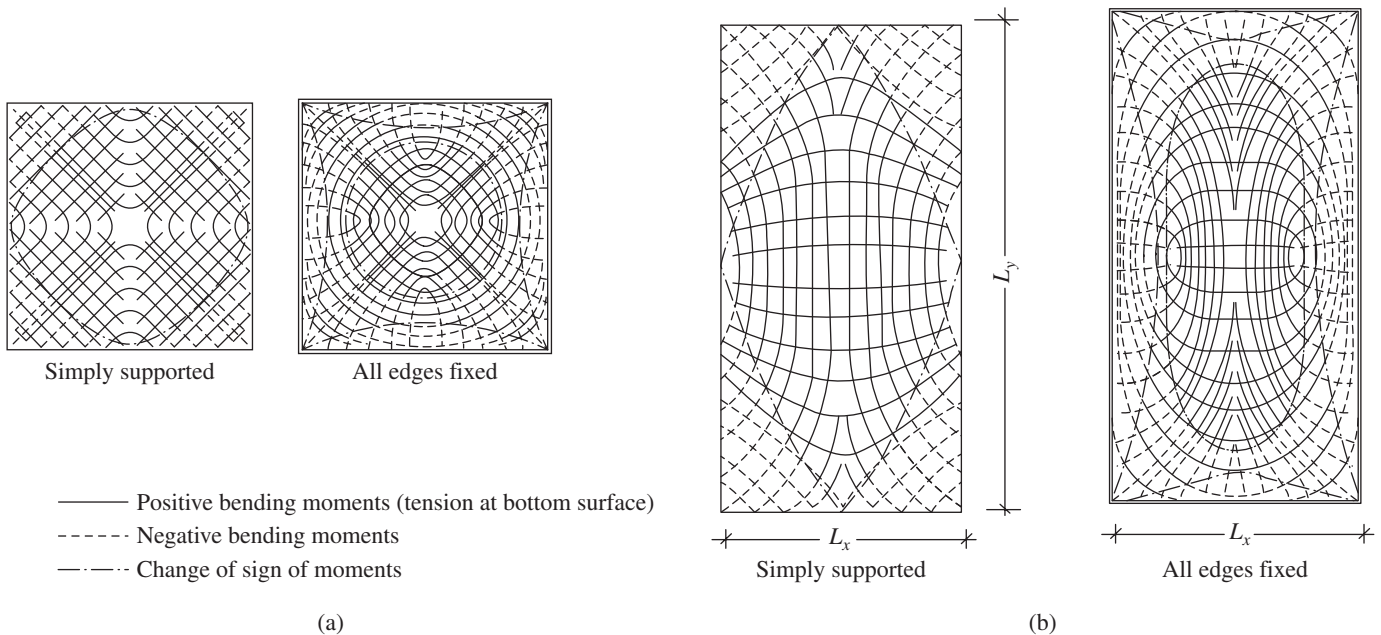
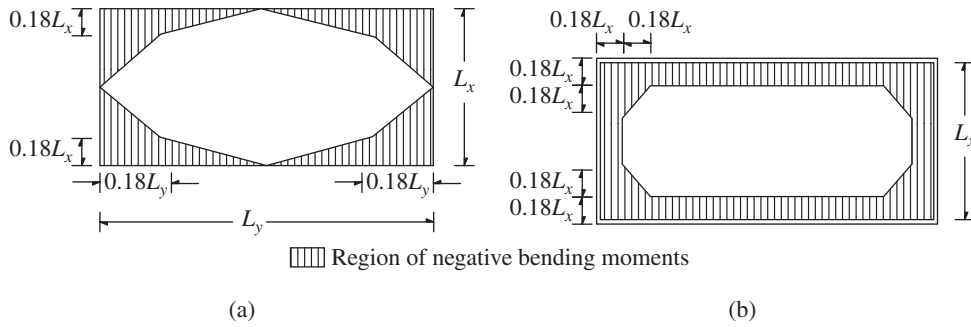


FIG. 10.10 Trajectories of principal moments in beam-supported rectangular slabs (a) $L_y/L_x = 1$ (b) $L_y/L_x = 2.0$



$$z = \frac{w}{k_p \pi^4 \left(\frac{1}{L_x^2} + \frac{1}{L_y^2} \right)^2} \quad (10.4b)$$

After obtaining the deflections, the bending moments and torsional moments may be obtained using the following relations:

$$M_x = -k_p \left(\frac{\partial^2 z}{\partial x^2} + \nu \frac{\partial^2 z}{\partial y^2} \right) \quad (10.5a)$$

$$M_y = -k_p \left(\frac{\partial^2 z}{\partial y^2} + \nu \frac{\partial^2 z}{\partial x^2} \right) \quad (10.5b)$$

$$M_{xy} = -M_{yx} = k_p (1 - \nu) \left(\frac{\partial^2 z}{\partial x \partial y} \right) \quad (10.5c)$$

FIG. 10.11 Regions of negative bending moments in rectangular slabs under uniformly distributed slabs (a) Simply supported slab (b) Slab with fixed ends

to the supports. Thus, the load is mainly transferred in the shorter direction, implying that the moments in the shorter direction, M_x , are greater than those in the longer direction, M_y . The principal moment directions in the corner regions are inclined to the support, indicating twisting moments.

Approximate regions of negative bending moments in simply supported rectangular slabs under uniformly distributed slabs are shown in Fig. 10.11(a) and these regions for slabs with fixed ends is shown in Fig. 10.11(b). These regions, extending to about 0.18 times the relevant span in the case of simply supported boundary conditions and to 0.18 times the short span in each direction in the case of fixed ends, should be provided with reinforcements on both the upper and lower faces of the slabs (Prakash Rao 1995).

Classical Theory of Plates

The exact determination of the bending and torsional moments is difficult, as the slabs are highly indeterminate. The fundamental assumption used in the analysis of plates under pure bending is that the deflection of the plate is small in comparison to its thickness. Similar to the case of beams, differential equations of equilibrium can also be established in the case of plates. The basic fourth-order differential equation for rectangular plates is given by

$$\frac{\partial^4 z}{\partial x^4} + 2 \frac{\partial^4 z}{\partial x^2 \partial y^2} + \frac{\partial^4 z}{\partial y^4} = \frac{w}{k_p} \quad (10.4a)$$

where z is the deflection of the plate, w is the uniform load, and k_p is the flexural rigidity or plate stiffness (similar to EI in beams) $= Et_p^3/[12(1-\nu^2)]$, E is the modulus of elasticity of plate, t_p is the thickness of plate, and ν is the Poisson's ratio. Solving this differential equation gives the deflection of the plate. The solution must satisfy the different boundary conditions. For example, for a simply supported plate the deflection along the edges must be zero, that is, $z = 0$ and $M_x = 0$ at $x = 0$ and $x = L_x$. Lévy, assuming the deflection in the form of a series of sin curves, presented a solution to this problem in 1899 (Timoshenko and Krieger 1959). The maximum deflection at mid-span for this case was obtained as

Exact solutions for two-way slabs of various shapes with various boundary conditions and subjected to different types of loadings have been presented by Timoshenko and Krieger (1959). As may be noted, the exact solutions are mathematically involved and not suitable for design office use.

Grashof-Rankine and Marcus Methods

Franz Grashof (1820–72) in Germany and William Rankine (1826–93) in the UK independently developed an approximate method for the analysis of simply supported rectangular slabs, as shown in Fig. 10.3. They considered the slab to be divided into a series of orthogonal unit beam strips (Grashof 1878). They ignored the torsion between the interconnecting strips and the influence of adjoining strips on either side. Hence, considering the two middle strips as shown in Fig. 10.3(a), the deflection at their common intersection point will be the same (as these two strips of beams belong to the same monolithic slab). Thus, equating the deflection in the longer and shorter directions results in the following equation:

$$\frac{5w_x L_x^4}{384EI_x} = \frac{5w_y L_y^4}{384EI_y} \quad (10.6a)$$

where w_x is the share of the load w in the shorter direction, w_y is the share of the load w in the longer direction, L_x is the short span, and L_y is the long span. Assuming that $I_x = I_y$ and simplifying Eq. (10.6a), we get

$$\frac{w_x}{w_y} = \frac{L_y^4}{L_x^4} \quad (10.6b)$$

From this equation, one may conclude that a larger share of the load is carried in the shorter direction and the ratio of these

two loads is proportional to the fourth power of the ratio of the spans.

From Eq. (10.6b), we get the relation between w_x and w_y as

$$w_x = w_y \left(\frac{L_y}{L_x} \right)^4 \tag{10.7}$$

We know that

$$w_y = w_x + w_y \tag{10.8}$$

Denoting the aspect ratio of spans, L_y/L_x , as r and substituting Eq. (10.8) in Eq. (10.7) and simplifying, we get

$$w_x = w \left(\frac{r^4}{1+r^4} \right) \tag{10.9a}$$

$$w_y = w \left(\frac{1}{1+r^4} \right) \tag{10.9b}$$

The maximum short- and long-span moments for these beams per unit width are

$$M_x = \frac{w_x L_x^2}{8} \tag{10.10a}$$

$$M_y = \frac{w_y L_y^2}{8} \tag{10.10b}$$

Substituting Eq. (10.9) in Eq. (10.10), we get the following equations, which are identical to the equations given in Clause D-2.1 of IS 456, for simply supported slabs that do not have adequate provision to resist torsion and to prevent the corners from lifting:

$$M_x = \alpha_x w_u L_x^2 \tag{10.11a}$$

$$M_y = \alpha_y w_u L_x^2 \tag{10.11b}$$

where M_x and M_y are the moments on strips of unit width spanning L_x and L_y , respectively, α_x and α_y are the bending moment coefficients, w_u is the uniformly distributed factored load on slab, and L_x and L_y are the lengths of short and long spans, respectively.

The bending moment coefficients α_x and α_y are given by

$$\alpha_x = \frac{1}{8} \left(\frac{r^4}{1+r^4} \right) \tag{10.12a}$$

$$\alpha_y = \frac{1}{8} \left(\frac{r^2}{1+r^4} \right) \tag{10.12b}$$

The values of α_x and α_y for different aspect ratios are given in Table 10.2, which is the same as that given in Table 27 of IS 456.

It is important to note that both M_x and M_y are given in terms of L_x^2 . Lévy's solution is also given in this table for comparison.

It is seen that the IS 456 coefficients, based on Grashof–Rankine formula, are conservative as compared to Lévy's solution, except for long span positive moments for $L_y/L_x > 1.5$ (Purushothaman 1984).

The approximate method of slab design developed by Marcus is similar in derivation to the Grashof–Rankine formula, but it introduced an important correction to allow for restraint at the corners and for the resistance given by torsion (Marcus 1932). Marcus suggested the following equations:

$$M'_x = C_x M_x \tag{10.13a}$$

$$M'_y = C_y M_y \tag{10.13b}$$

where M'_x and M'_y are the moments after correction for torsional effects, M_x and M_y are the moments without taking torsional effects and given by Eq. (10.11), and C_x and C_y are the Marcus correction factors given by

$$C_x = C_y = 1 - \frac{5}{6} \left(\frac{r^2}{1+r^4} \right) \tag{10.14}$$

The moment coefficients for the analysis of rectangular slabs subjected to a uniformly distributed load for various support conditions by the Grashof–Rankine formula with Marcus correction are given in Table 10.3.

The value of the Marcus correction works out to 0.583 for $r = 1.0$ and 0.909 for $r = 3.0$. Hence, there is 42 per cent reduction in moments for square slabs, which reduces to nine per cent for one-way slabs. For slabs with fixed ends, the corresponding reductions are 14 per cent and three per cent, respectively. It should be noted that corner reinforcement is necessary when torsion is taken into account (see Section 10.4.5). It has been shown that the bending moments obtained in this simple manner (using Grashof–Rankine formula with Marcus correction) vary by only three per cent from those that have been obtained from more rigorous analyses based on the elastic plate theory, with Poisson's ratio equal to zero (Purushothaman 1984; Reynolds and Steedman 1988). When the effect of Poisson's ratio has to be considered, the bending moments may be obtained by using the following relation:

$$M_x = M_{x0} + \nu M_{y0} \tag{10.15a}$$

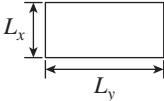





$$M_y = M_{y0} + \nu M_{x0} \tag{10.15b}$$

TABLE 10.2 Bending moment coefficients for slabs spanning in two directions at right angles, simply supported on four sides

$r = L_y/L_x$	1.0	1.1	1.2	1.3	1.4	1.5	1.75	2.0	2.5	3.0
α_x	0.0625 (0.048)	0.074 (0.053)	0.084 (0.063)	0.093 (0.069)	0.099 (0.075)	0.104 (0.081)	0.113 –	0.11 (0.102)	0.122 –	0.124 (0.119)
α_y	0.0625 (0.048)	0.061 (0.049)	0.059 (0.050)	0.055 (0.050)	0.051 (0.050)	0.046 (0.050)	0.037 –	0.029 (0.046)	0.020 –	0.014 (0.040)

Note: Values in parentheses are as per Lévy's method.

TABLE 10.3 Bending moments for rectangular panels with various support conditions based on Grashof–Rankine formula with Marcus correction

Support Conditions — Simply Supported — Continuous Edge	Proportion of Load in Each Direction		Span Moments Without Marcus Correction		Marcus Correction Factors		Support Moments	
	w_x/w	w_y/w	M_x^+	M_y^+	C_x	C_y	M_x^-	M_y^-
	$\frac{r^4}{1+r^4}$	$\frac{1}{1+r^4}$	$\frac{w_x L_x^2}{8}$	$\frac{w_y L_y^2}{8}$	$1 - \frac{5}{6} \left(\frac{r^2}{1+r^4} \right)$	$1 - \frac{5}{6} \left(\frac{r^2}{1+r^4} \right)$	0	0
	$\frac{5r^4}{2+5r^4}$	$\frac{2}{2+5r^4}$	$\frac{9}{128} w_x L_x^2$	$\frac{w_y L_y^2}{8}$	$1 - \frac{75}{32} \left(\frac{r^2}{2+5r^4} \right)$	$1 - \frac{5}{3} \left(\frac{r^2}{2+5r^4} \right)$	$\frac{w_x L_x^2}{8}$	0
	$\frac{5r^4}{2+5r^4}$	$\frac{1}{1+5r^4}$	$\frac{1}{24} w_x L_x^2$	$\frac{w_y L_y^2}{8}$	$1 - \frac{25}{18} \left(\frac{r^2}{1+5r^4} \right)$	$1 - \frac{5}{6} \left(\frac{r^2}{1+5r^4} \right)$	$\frac{w_x L_x^2}{12} \alpha$	0
	$\frac{r^4}{1+r^4}$	$\frac{1}{1+r^4}$	$\frac{9}{128} w_x L_x^2$	$\frac{9}{128} w_y L_y^2$	$1 - \frac{15}{32} \left(\frac{r^2}{1+r^4} \right)$	$1 - \frac{15}{32} \left(\frac{r^2}{1+r^4} \right)$	$\frac{w_x L_x^2}{8}$	$\frac{w_y L_y^2}{8}$
	$\frac{2r^4}{1+2r^4}$	$\frac{1}{1+2r^4}$	$\frac{1}{24} w_x L_x^2$	$\frac{9}{128} w_y L_y^2$	$1 - \frac{5}{9} \left(\frac{r^2}{1+2r^4} \right)$	$1 - \frac{15}{32} \left(\frac{r^2}{1+2r^4} \right)$	$\frac{w_x L_x^2}{12}$	$\frac{w_y L_y^2}{8}$
	$\frac{r^4}{1+r^4}$	$\frac{1}{1+r^4}$	$\frac{1}{24} w_x L_x^2$	$\frac{1}{24} w_y L_y^2$	$1 - \frac{5}{18} \left(\frac{r^2}{1+r^4} \right)$	$1 - \frac{5}{18} \left(\frac{r^2}{1+r^4} \right)$	$\frac{w_x L_x^2}{12}$	$\frac{w_y L_y^2}{12}$

Note: $r = L_y/L_x$

where M_{x0} and M_{y0} are the bending moments for Poisson's ratio $\nu = 0$ and M_x and M_y are the bending moments for any given Poisson's ratio. It is interesting to note that the Marcus method was specified in the 1964 version of IS 456 but deleted in the future versions of the code.

Pigeaud and Westergaard also analysed this problem and provided moment coefficients that were altered slightly to accommodate the experimental results obtained during 1921–26 (Westergaard and Slater 1921; Westergaard 1926). Stiglat and Wippel (1983) also developed extensive tables for slabs with various boundary conditions. It is to be noted that Westergaard's coefficients were adopted in several codes of practices including IS 456:1964, CP 114:1965, and ACI 318:1963. A comparison of the coefficients suggested by Westergaard, Grashof–Rankine, and Marcus has been provided by Purushothaman (1984).

Coefficients Based on Yield-line Theory

Restrained slabs are defined as those that are cast integrally with beams and in which the corners are prevented from lifting and provision for torsion is made at simply supported corners. They may be continuous or discontinuous at the edges.

As per Clause D-1 of IS 456, the maximum design moments per unit width of such restrained slabs may be calculated using the following equations:

$$M_x = \alpha_x w_u L_x^2 \quad (10.16a)$$

$$M_y = \alpha_y w_u L_x^2 \quad (10.16b)$$

where M_x and M_y are the moments on strips of unit width spanning L_x and L_y , respectively, α_x and α_y are the bending moment coefficients as given in Table 10.4 (Table 26 of IS 456), w_u is the uniformly distributed factored load on slab, and L_x and L_y are the lengths of short and long spans, respectively. It has to be noted that in Table 10.4, the ratio of support moment to span moment is about 1.30 irrespective of the support conditions or aspect ratio. This is a simplification of results by the yield-line theory. It is also interesting to note that for simply supported slabs with aspect ratio 2.0, Table 26 of the code gives a coefficient of 0.107, whereas for the same aspect ratio, Table 27 gives a coefficient of 0.118; this is because Table 26 assumes that the corners are prevented from lifting.

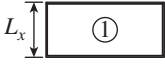
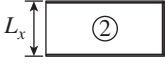

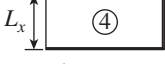
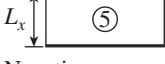
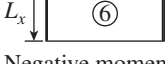

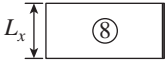
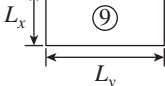
Eqs (10.16a and b) may be used only when the following conditions are satisfied:

1. The characteristic dead and imposed loads on adjacent panels are approximately equal to the loads on the panel being considered.
2. The spans of adjacent panels in each direction are approximately equal.
3. The slabs are essentially subjected to uniform loads.

The following are the rules to be observed when the equations are applied to restrained slabs (continuous or discontinuous):

1. Slabs are considered as divided in each direction into middle strips and edge strips as shown in Fig. 10.12.
2. The maximum design moments calculated as mentioned earlier apply only to the middle strips and no redistribution is allowed.

TABLE 10.4 Bending moment coefficients for rectangular panels supported on four sides with provision for torsion at corners

Type of Panel and Moment Considered — Simply Supported — Continuous Edge	Short Span Coefficients α_x (values of L_y/L_x)								Long Span Coefficients α_y for All Values of L_y/L_x
	1.0	1.1	1.2	1.3	1.4	1.5	1.75	2.0	
Interior panels:  Negative moment at continuous edge	0.032	0.037	0.043	0.047	0.051	0.053	0.060	0.065	0.032
Positive moment at mid-span	0.024	0.028	0.032	0.036	0.039	0.041	0.045	0.049	0.024
One short edge discontinuous:  Negative moment at continuous edge	0.037	0.043	0.048	0.051	0.055	0.057	0.064	0.068	0.037
Positive moment at mid-span	0.028	0.032	0.036	0.039	0.041	0.044	0.048	0.052	0.028
One long edge discontinuous:  Negative moment at continuous edge	0.037	0.044	0.052	0.057	0.063	0.067	0.077	0.085	0.037
Positive moment at mid-span	0.028	0.033	0.039	0.044	0.047	0.051	0.059	0.065	0.028
Two adjacent edges discontinuous:  Negative moment at continuous edge	0.047	0.053	0.060	0.065	0.071	0.075	0.084	0.091	0.047
Positive moment at mid-span	0.035	0.040	0.045	0.049	0.053	0.056	0.063	0.069	0.035
Two short edges discontinuous:  Negative moment at continuous edge	0.045	0.049	0.052	0.056	0.059	0.060	0.065	0.069	—
Positive moment at mid-span	0.035	0.037	0.040	0.043	0.044	0.045	0.049	0.052	0.035
Two long edges discontinuous:  Negative moment at continuous edge	—	—	—	—	—	—	—	—	0.045
Positive moment at mid-span	0.035	0.043	0.051	0.057	0.063	0.068	0.080	0.088	0.035
Three edges discontinuous (one long edge continuous):  Negative moment at continuous edge	0.057	0.064	0.071	0.076	0.080	0.084	0.091	0.097	—
Positive moment at mid-span	0.043	0.048	0.053	0.057	0.060	0.064	0.069	0.073	0.043
Three edges discontinuous (one short edge continuous):  Negative moment at continuous edge	—	—	—	—	—	—	—	—	0.057
Positive moment at mid-span	0.043	0.051	0.059	0.065	0.071	0.076	0.087	0.096	0.043
Four edges discontinuous:  Positive moment at mid-span	0.056	0.064	0.072	0.079	0.085	0.089	0.100	0.107	0.056

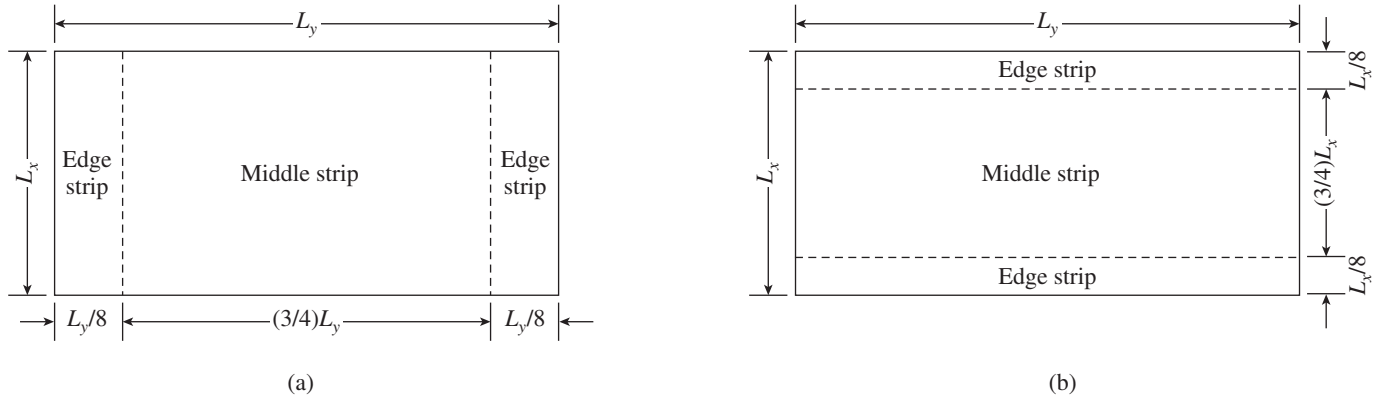


FIG. 10.12 Division of slab into middle and edge strips (a) For span L_x (b) For span L_y

3. Reinforcement in the middle strips should be detailed in accordance with Section 10.3.5.2.
4. Corner reinforcements are provided to resist the torsional moments.

The coefficients given in Table 10.4 were derived from yield-line analysis and corrected for the non-uniform distribution of reinforcement (Taylor, et al. 1969). It should be noted that similar coefficients are available in BS 8110-1:1997, AS 3600:2001, and NZS 3101-Part 1:2006.

The coefficients in Table 10.4 (Table 26 of IS 456) were derived based on the following equations (BS 8110-1:1997; Taylor, et al. 1969):

$$\alpha_y^+ = \frac{(24 + 2N_d + 1.5N_d^2)}{1000} \quad (10.17)$$

where N_d is the number of discontinuous edges ($0 \leq N_d \leq 4$). Thus, for $N_d = 0, 1, 2, 3$, and 4 , the values of α_y^+ are obtained as 0.0240, 0.0275, 0.0340, 0.0435, and 0.0560, respectively (it should be noted that they match with the values given in the last column of Table 10.4). Similarly, the expression for α_x^+ in terms of α_y^+ has been derived as (BS 8110-1:1997; Taylor, et al. 1969)

$$\alpha_x^+ = \frac{2}{9} \left[\frac{3 - (\sqrt{18\alpha_y^+}/r)(C_{s1} + C_{s2})}{(C_{l1} + C_{l2})^2} \right] \quad (10.18)$$

with $C_{s1} = C_{l1} = 1$ for discontinuous edges and $C_{s2} = C_{l2} = \sqrt{7/3}$ for continuous edges, where r is the aspect ratio of spans ($= L_y/L_x$), α_x^+ and α_y^+ are the coefficients for positive span moments per unit width in the short and long spans, respectively, subscripts s and l denote the short and long edges, respectively, and subscripts 1 and 2 denote the two edges in either direction. The negative moment coefficients for the continuous edge are taken $4/3$ times the coefficients for the span moment. Although the negative moment coefficient for a discontinuous support is zero, we may need to provide some reinforcement during detailing of the slabs to take care of any partial fixity. Thus,

$$\begin{aligned} \alpha^- &= 4/3\alpha^+ \text{ at continuous support} \\ \alpha^- &= 0 \text{ at discontinuous support} \end{aligned} \quad (10.19)$$

Example 10.4 shows the use of these equations.

Unbalanced moments in adjacent spans When there is a series of continuous slabs in one or both directions, the negative moments obtained at a common support (using the coefficients given in Table 10.4), on the left- and right-hand sides, may not be equal and may differ significantly, as shown in Fig. 10.13. This may be due to any one or more of the following reasons:

1. The two adjacent spans being unequal
2. The loading on one panel being different from that of the other
3. The boundary conditions in the two adjoining panels being different

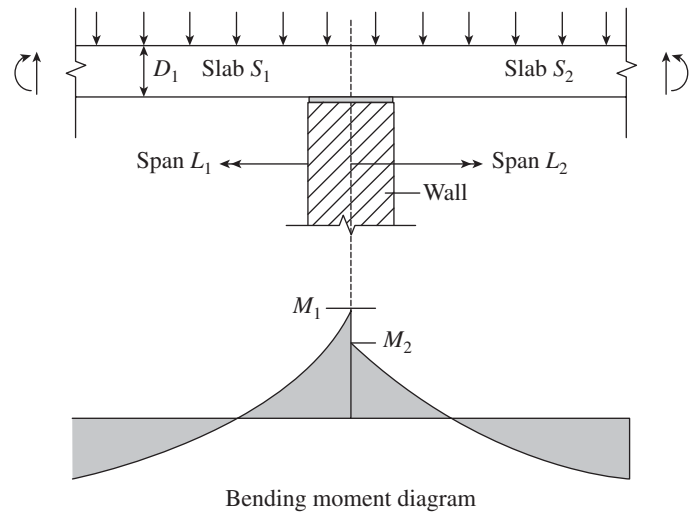


FIG. 10.13 Unbalanced moments in adjacent spans of a continuous slab

Clause 24.4.1 of IS 456 suggests the following procedure in such situations (the same procedure is found in BS 8110-1:1997):

1. Calculate the sum of the mid-span moment and average of the support moments (neglecting the signs) for each panel.
2. Treat the values found from Table 10.4 as fixed-end moments (FEMs).
3. Distribute the FEMs across the supports according to the relative stiffness of adjacent spans, giving new support moments.

4. Adjust the mid-span moment for each panel: this should be done in such a way that when it is added to the average of the support moments (neglecting signs) from step 3, the total should be equal to that from step 1.

If, for a given panel, the resulting support moments are significantly greater than the value obtained from Table 10.4, the code suggests that the tension steel over the supports should be extended beyond the provisions of Clause D-1.5. It also recommends the following procedure:

5. Take the span moment as parabolic between supports: the maximum value is found from step 4.
6. Determine the points of contraflexure of the new support moments (from step 3) with the span moment (from step 5).
7. Extend half the support tension steel at each end to at least an effective depth or 12 times the bar diameter beyond the nearest point of contraflexure.
8. Extend the full area of support tension steel at each end to half the distance 6.6 from step 7.

Even though this procedure has been specified in the code, several engineers consider it logical to take the larger value of moment (M_1 as shown in Fig. 10.13) as the design negative moment at the common continuous edge (this results in a conservative design). According to them, this is because the moment coefficients given in Table 10.4 are based on an inelastic analysis and not on an elastic analysis, and the code itself states in Clause D-1.4 that no redistribution should be made (Pillai and Menon 2009). In this context, it is interesting to note that the code also recommends the use of the same moment coefficients for design using the working stress method. Several others have proposed moment redistribution based on the relative stiffness of the adjacent slabs (Sinha 2002; Suryanarayana 1993). Purushothaman (1984) has provided a review of the various moment redistribution methods applicable to slabs and found that the method proposed by Hahn (1966) compares well with the method of averaging the negative bending moments at the common support.

The unbalanced moments ($M_1 - M_2$) in Fig. 10.13 may be distributed by using the following (assuming slab S_1 is free at the other end) formulae:

$$k_1 = \text{Distribution factor for slab } S_1$$

$$= \frac{\text{Stiffness of Slab } S_1}{\text{Stiffness of Slab } S_1 + \text{Stiffness of Slab } S_2}$$

$$= \frac{(3EI/L)_{S_1}}{(3EI/L)_{S_1} + (4EI/L)_{S_2}} \tag{10.20a}$$

$$k_2 = \text{Distribution factor for slab } S_2 = 1 - k_1 \tag{10.20b}$$

Distributed moment for slab $S_1 = \text{Unbalanced moment} \times k_1$

Distributed moment for slab $S_2 = \text{Unbalanced moment} \times k_2$

The span moments are modified by adding half of the distributed moments.

Influence of pattern loading Irrespective of the type of slab (one way or two way), the effect of variability in imposed loading, called *pattern loading*, should be considered in the design. The concept of pattern loading was introduced in Section 3.10 of Chapter 3, with reference to elastic analysis of frames. In the case of two-way slabs, it has been found that the *checker board pattern* of loading, as shown in Fig. 10.14(a), results in maximum positive bending moments and the *strip pattern* of loading, as shown in Fig. 10.14(b), results in maximum negative bending moments (Jirsa et al. 1969). Purushothaman (1984) compared the IS code coefficients for restrained slabs with the coefficients experimentally found by Siess and Newmark (1950), which include pattern loading, and found that the values of IS code coefficients are generally higher than those derived by Siess and Newmark. Hence, pattern loading will not be critical when we use the IS code coefficients for the design of two-way slabs.

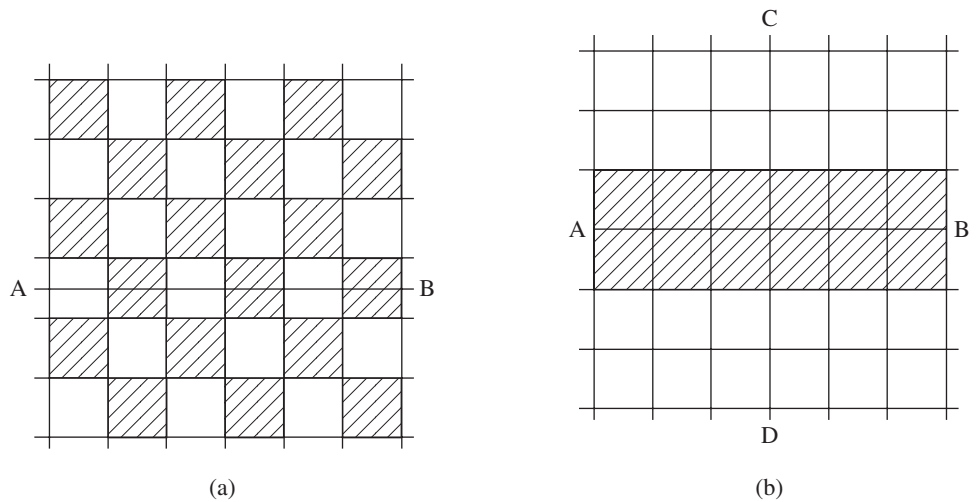


FIG. 10.14 Pattern loading (a) Checker board loading pattern for maximum positive moments (b) Strip loading pattern for maximum negative moments along panel edges (along AB)

Shear Forces in Two-way Slabs

Shear force does not usually govern the design of wall-supported concrete slabs subjected to uniform loads. This was discussed with reference to one-way slabs in Section 9.5 of Chapter 9. It may be noted that the magnitude of shear stresses are comparatively lesser in two-way slabs than in one-way slabs due to the two-way action. Hence, they will not govern the design.

The distribution of shear forces at the various edges of a two-way slab is not easy to determine. However, Clause 24.5 and Fig. 7 of the code (see also Fig. 10.1b) recommend a simple triangular distribution of load on the short edge and a trapezoidal distribution of load on the long edge. The critical section for shear is suggested to be at a distance d from the face of the support as per Clause 24.3.2.4 of IS 456. It has to be noted that this type of shear is often called a *one-way shear*, which is different from the *two-way shear* or *punching shear*, which also has to be checked in the case of flat slabs (see Section 11.5 of Chapter 11).

Thus, the factored maximum shear force per unit length V_u may be obtained as (see Fig. 10.15):

$$V_u = w_u(0.5L_{xn} - d) \quad (10.21a)$$

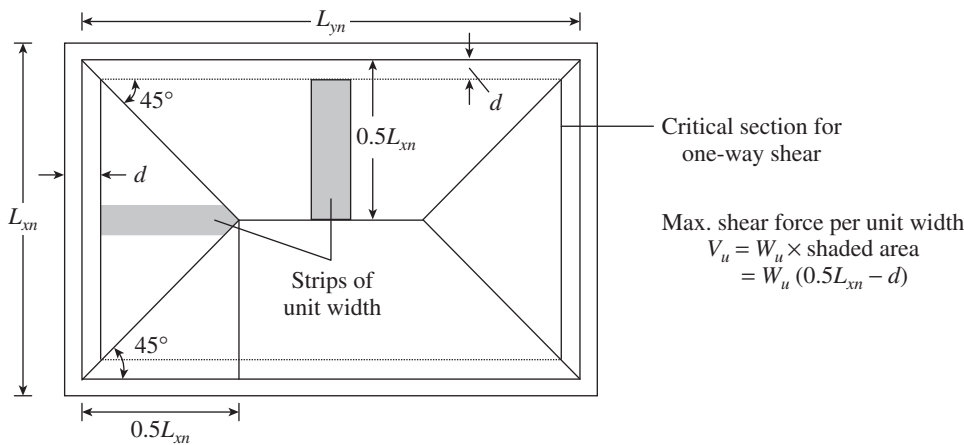


FIG. 10.15 Assumed distribution of loads for determination of shear force in two-way slabs

where L_{xn} is the clear span in the shorter direction, d is the effective depth, and w_u is the factored uniform load acting on the slab.

The corresponding nominal shear stress will be

$$\tau_v = \frac{V_u}{bd} \text{ with } b = 1000 \text{ mm} \quad (10.21b)$$

This stress should not exceed half the maximum shear stress $\tau_{c,max}$ given in Table 20 of IS 456 (see Clause 40.2.3.1). If τ_v is less than $k\tau_c$, no shear reinforcement is necessary; if it is greater than $k\tau_c$ but less than $0.5\tau_{c,max}$ shear reinforcement has to be provided, where k is the shear enhancement factor discussed in Section 9.5 of Chapter 9 (Clause 40.2.1.1 of IS 456).

Table 10.5 is provided in the UK code (BS 8110-1:1997)

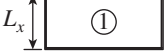



for calculating the shear forces in restrained slabs. The shear force is calculated as

$$V_{sy} = \alpha_{vy} w_u L_x \quad (10.22a)$$

$$V_{sx} = \alpha_{vx} w_u L_x \quad (10.22b)$$


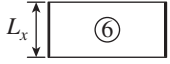
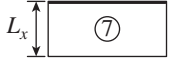

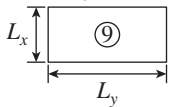
where α_{vx} and α_{vy} are the shear force coefficients as given in Table 10.5, w_u is the uniformly distributed factored load on the slab, and L_x is the short span. The coefficients in Table 10.5 have been derived with an assumed distribution of the load on a supporting

TABLE 10.5 Shear force coefficients for restrained rectangular panels with provision for torsion at corners

Type of Panel and Moment Considered — Simply Supported — Continuous Edge	Short Span Coefficients α_{vx} (Values of L_y/L_x)								Long Span Coefficients α_{vy} for All Values of L_y/L_x
	1.0	1.1	1.2	1.3	1.4	1.5	1.75	2.0	
Interior panels:  Continuous edge	0.33	0.36	0.39	0.41	0.43	0.45	0.48	0.50	0.33
One short edge discontinuous:  Continuous edge	0.36	0.39	0.42	0.44	0.45	0.47	0.50	0.52	0.36
Discontinuous edge	—	—	—	—	—	—	—	—	0.24
One long edge discontinuous:  Continuous edge	0.36	0.40	0.44	0.47	0.49	0.51	0.55	0.59	0.36
Discontinuous edge	0.24	0.27	0.29	0.31	0.32	0.34	0.36	0.38	—
Two adjacent edges discontinuous:  Continuous edge	0.40	0.44	0.47	0.50	0.52	0.54	0.57	0.60	0.40

(Continued)

TABLE 10.5 (Continued)

Type of Panel and Moment Considered — Simply Supported — Continuous Edge	Short Span Coefficients α_x (Values of L_y/L_x)								Long Span Coefficients α_y for All Values of L_y/L_x
	1.0	1.1	1.2	1.3	1.4	1.5	1.75	2.0	
Discontinuous edge	0.26	0.29	0.31	0.33	0.34	0.35	0.38	0.40	0.26
Two short edges discontinuous:  ⑤ Continuous edge	0.40	0.43	0.45	0.47	0.48	0.49	0.52	0.54	—
Discontinuous edge	—	—	—	—	—	—	—	—	0.26
Two long edges discontinuous:  ⑥ Continuous edge	—	—	—	—	—	—	—	—	0.40
Discontinuous edge	0.26	0.30	0.33	0.36	0.38	0.40	0.44	0.47	—
Three edges discontinuous (one long edge continuous):  ⑦ Continuous edge	0.45	0.48	0.51	0.53	0.55	0.57	0.60	0.63	—
Discontinuous edge	0.30	0.32	0.34	0.35	0.36	0.37	0.39	0.41	0.29
Three edges discontinuous (one short edge continuous):  ⑧ Continuous edge	—	—	—	—	—	—	—	—	0.45
Discontinuous edge	0.29	0.33	0.36	0.38	0.40	0.42	0.45	0.48	0.30
Four edges discontinuous:  ⑨ Discontinuous edge	0.33	0.36	0.39	0.41	0.43	0.45	0.48	0.50	0.33

beam as shown in Fig. 10.16; in this figure $V_s = V_{sx}$ when $L = L_y$ and $V_s = V_{sy}$ when $L = L_x$.

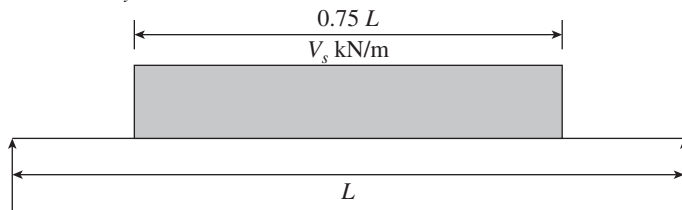


FIG. 10.16 Distribution of load on a beam supporting a two-way slab

Load on supporting beams The load to be carried by the supporting beams may be estimated based on the appropriate yield-line pattern, in which the slab may fail (see also Section 3.4.1 of Chapter 3 and Section 10.8). If the beam is simply supported on all four sides, we may assume 45° dispersion of loads as shown in Fig. 10.1(b), and the total load acting on one of the beams in the shorter direction is given by

$$\left(\frac{wL_x}{2}\right)\left(\frac{L_x}{2}\right) = \frac{w}{4}(L_x)^2$$

If this is assumed to be the uniformly distributed load w_x acting over the middle $0.75L_x$, then

$$w_x \text{ on short beam} = \frac{w}{4}(L_x)^2 \div 0.75L_x = \frac{wL_x}{3} \quad (10.23)$$

Similarly, the load acting on one of the beams in the longer direction is

$$\frac{wL_x L_y}{2} - \frac{wL_x^2}{4} = \frac{wL_x^2}{2}\left(r - \frac{1}{2}\right)$$

where $r = L_y/L_x$. Assuming that this load is uniformly distributed over the middle $0.75L_y$, the equivalent load on L_y is

$$w_y = \left[\frac{wL_x^2}{2}\left(r - \frac{1}{2}\right)\right] \div 0.75L_y = \frac{wL_x}{3}\left(2 - \frac{1}{r}\right) \quad (10.24)$$

For slabs with other boundary conditions, the load on beams may be calculated based on the coefficients provided in Fig. 10.17 (Reynolds and Steedman 1988).

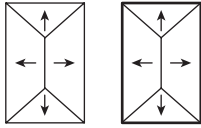
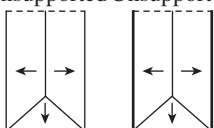
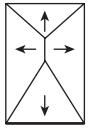
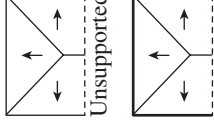
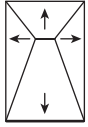
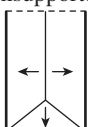
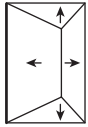
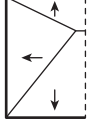
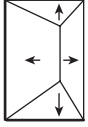
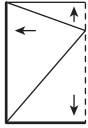
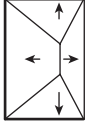
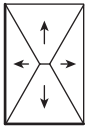
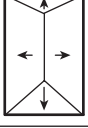
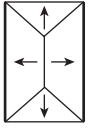
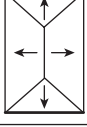
Panels Supported along Four Edges	Panels Unsupported along One Edge
 $r > 1: R_1 = R_3 = \frac{1}{4} wL_x^2$ $R_2 = R_4 = \frac{1}{2} \left(r - \frac{1}{2} \right) wL_x^2$ $\alpha = \beta = 1/2r$ $r = 1: R_1 = R_2 = R_3 = R_4 = \frac{1}{4} wL_x^2$	<p>Unsupported Unsupported</p>  $R_1 = 0$ $R_2 = R_4 = \frac{1}{2} \left(r - \frac{1}{4} \right) wL_x^2$ $R_3 = \frac{1}{4} wL_x^2$ $\beta = 1/2r$
 $r < 4/3: R_1 = \frac{1}{4} wL_x^2 (\text{min.}) \quad \alpha = 1/2r (\text{min.})$ $R_2 = R_4 = \frac{1}{2} \left(r - \frac{2}{3} \right) wL_x^2 \quad \beta = 5/6r (\text{max.})$ $R_3 = \frac{5}{12} wL_x^2 (\text{max.})$	<p>Unsupported Unsupported</p>  $r > 2: R_1 = R_3 = \frac{1}{2} r \left(1 - \frac{1}{4} r \right) wL_x^2$ $R_2 = 0$ $R_4 = \frac{1}{4} r^2 wL_x^2$ $\psi = r/2$
 $r \leq 4/3: R_1 = \frac{3}{5} R_3 \text{ approx. (min.)} \quad \alpha = 3/8 (\text{min.})$ $R_2 = R_4 = \frac{3}{16} r^2 wL_x^2 \quad \beta = 5/8 (\text{max.})$ $R_3 = \frac{5}{8} r \left(1 - \frac{3}{8} r \right) wL_x^2 \text{ approx. (max.)}$ $\psi = \xi = 3r/8$	<p>Unsupported</p>  $L_1 = 0 \quad \beta = 5/8r$ $R_2 = \frac{3}{5} R_4 (\text{min.}) \quad \psi = 5/8$ $R_3 = \frac{5}{16} wL_x^2$ $R_4 = \frac{5}{8} \left(r - \frac{5}{16} \right) wL_x^2 (\text{max.})$
 $R_1 = R_3 = \frac{3}{16} wL_x^2 \quad \alpha = \beta = 3/8r$ $R_2 = \frac{3}{5} R_4 (\text{min.}) \quad \psi = \frac{5}{8} (\text{max.})$ $R_4 = \frac{5}{8} \left(r - \frac{3}{8} \right) wL_x^2 (\text{max.})$	<p>Unsupported</p>  $r > 8/5: R_1 = \frac{3}{5} R_3 (\text{min.}) \quad R_2 = 0$ $R_3 = \frac{5}{8} r \left(1 - \frac{5}{16} r \right) wL_x^2 (\text{max.})$ $R_4 = \frac{5}{16} r^2 wL_x^2 \quad \alpha = 3/8r (\text{min.})$ $\psi = 5r/8 (\text{max.})$
 $R_1 = \frac{3}{16} wL_x^2 (\text{min.}) \quad \alpha = 3/8r (\text{min.})$ $R_2 = \frac{3}{5} R_4 (\text{min.}) \quad \beta = 5/8r (\text{max.})$ $R_3 = \frac{5}{16} wL_x^2 (\text{max.})$ $R_4 = \frac{5}{8} \left(r - \frac{1}{2} \right) wL_x^2 (\text{max.})$	<p>Unsupported</p>  $r \geq 8/5: R_1 = \frac{3}{10} wL_x^2 (\text{min.}) \quad R_2 = 0$ $R_3 = \frac{1}{2} wL_x^2$ $R_4 = \left(r - \frac{4}{5} \right) wL_x^2 (\text{max.})$ $\alpha = 3/5r \quad \beta = 1/r$
 $r < 5/4: R_1 = R_3 = \frac{5}{16} wL_x^2 \quad \alpha = \beta = 5/8r$ $R_2 = \frac{3}{5} R_4 (\text{min.}) \quad \psi = 5/8 (\text{max.})$ $R_4 = \frac{5}{8} \left(r - \frac{5}{8} \right) wL_x^2 (\text{max.})$	<p>Condition of supports</p> <p>----- Free edge</p> <p>———— Simply supported</p> <p>———— Continuous</p>
 $r \leq 5/4: R_1 = R_3 = \frac{1}{2} r \left(1 - \frac{2}{5} r \right) wL_x^2 \quad \alpha = \beta = 1/2$ $R_2 = \frac{3}{20} r^2 wL_x^2 (\text{min.}) \quad \xi = 3r/10$ $R_4 = \frac{1}{4} r^2 wL_x^2 (\text{max.})$	<p>Condition of supports</p> <p>----- Free edge</p> <p>———— Simply supported</p> <p>———— Continuous</p>
 $R_1 = \frac{3}{20} wL_x^2 (\text{min.}) \quad \alpha = 3/10r (\text{min.})$ $R_2 = R_4 = \frac{1}{2} \left(r - \frac{2}{5} \right) wL_x^2$ $R_3 = \frac{1}{4} wL_x^2 (\text{max.}) \quad \beta = 1/2r (\text{max.})$	<p>Condition of supports</p> <p>----- Free edge</p> <p>———— Simply supported</p> <p>———— Continuous</p>
 $R_1 = R_3 = \frac{3}{20} wL_x^2 (\text{min.})$ $R_2 = R_4 = \frac{1}{2} \left(r - \frac{3}{10} \right) wL_x^2 (\text{max.})$ $\alpha = \beta = 3/10r (\text{min.})$	<p>Condition of supports</p> <p>----- Free edge</p> <p>———— Simply supported</p> <p>———— Continuous</p>
 $r < 5/3: R_1 = R_3 = \frac{5}{12} wL_x^2 (\text{min.})$ $R_2 = R_4 = \frac{1}{2} \left(r - \frac{5}{6} \right) wL_x^2 (\text{max.})$ $\alpha = \beta = 5/6r (\text{min.})$	<p>Condition of supports</p> <p>----- Free edge</p> <p>———— Simply supported</p> <p>———— Continuous</p>

FIG. 10.17 Loads on beams supporting rectangular two-way slabs with various boundary conditions
 Source: Reynolds and Steedman 1988 (Adapted), *Reinforced Concrete Designer's Handbook*, 10th edition, E & FN Spon, Taylor & Francis Group, Table 63, p. 205, reprinted with permission from Taylor & Francis

10.4.2 Beam-supported Two-way Slabs

It should be noted that IS 456 does not provide any specific recommendations for the design of beam-supported two-way slabs. Designers often design continuous beam-supported slabs also using the coefficients provided in the code (Tables 12 and 13 of the code are for one-way slabs and Table 26 of the code is for two-way slabs), that is, treating them as continuous slabs on rigid supports.

Extending plate-based code methods to beam-supported continuous slabs introduces a degree of approximation with respect to the support rigidity. A major assumption in the plate-based methods is that a rectangular slab panel is rigidly supported on its four sides. If beams are provided along the column lines and if these beams are rigid, then the analysis and design of the slab may be considered in the same manner as wall-supported slabs.

Gamble, et al. (1969) tested a nine-panel two-way floor slab, and found that at the design load level, the response was essentially linear, the ratio of failure to total design load was 3.7, and that the design on the basis of rigid beams is unreasonable and misleading. According to the Swedish regulations, if the overall depth of beam, D_b , satisfies the following conditions, the beam may be considered adequately stiff (NS 3473:1998; Regan and Yu 1973):

$$\frac{D_b}{D_s} \geq 2.5 \quad \text{for } r \leq 1.5 \quad (10.25a)$$

$$\frac{D_b}{D_s} \geq 2.5r \quad \text{for } r > 1.5 \quad (10.25b)$$

where D_s is the thickness of slab and $r = L_y/L_x$. This empirical relation is shown graphically in Fig. 10.18. A similar guideline is given in Clause B.1.2 of the Canadian code (CSA A23.3:2004), which takes into account the width of the beam and also the clear span. According to the Canadian code, a stiff supporting beam satisfies the following condition:

$$\frac{D_b}{D_s} \geq \left(\frac{2.0L_n}{b_w} \right)^{1/3} \quad (10.26)$$

where b_w is the web width of the beam and L_n is the clear span of the supporting beam.

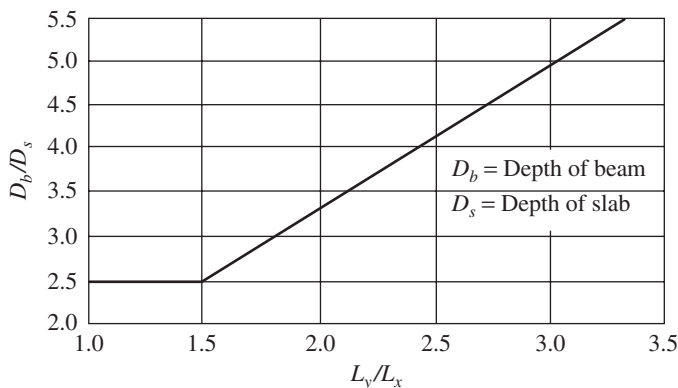


FIG. 10.18 Minimum depth of beam to ensure rigidity

Thus, for example, a 100mm thick slab requires a beam depth of 250mm for a square panel and 500mm depth for a rectangular panel, with $r = 2.0$, to be considered stiff as per the Swedish code. In contrast, as per the Canadian code, when the slab thickness is 100mm, the depth required for a beam with a width of 230mm for a square panel of size 3m is 297mm and for a rectangular panel of size 3m × 6m, it is 374mm in the longer direction and 297mm in the shorter direction. In practice, the size of beams chosen for these spans will be higher than those indicated by Eqs (10.25) and (10.26). Hence, one may use the coefficients given in Tables 10.4 and 10.5 and the design and detailing of two-way slabs supported on stiff beams may be carried out similar to the design and detailing of two-way slabs supported on the walls. With such an approach for design purposes, we are able to isolate the slab system from the integral slab-beam-column system; we may analyse and design the supporting beams separately for the loads as described in Section 3.4.1 of Chapter 3 and in Chapter 5.

If the beams are not stiff, the behaviour of the slab will be different from that supported on rigid beams or walls, as the behaviour is affected by the following factors:

1. Deflection of the supporting beams
2. Torsion in the supporting beams
3. Displacements and rotations in the supporting columns

When such flexible beams are encountered, we should not use the moment coefficients; it is better to analyse such slabs supported by flexible beams by using the equivalent frame method discussed in Chapter 11. The supporting beams may be designed for combined bending and torsion using the methods given in Chapter 8.

10.4.3 Design Procedure for Two-way Slabs

The different steps involved in the design of two-way slabs, considering them as ‘beams of one metre width’, are similar to the design of one-way slabs. It will have the 10 steps as discussed in Section 9.6 of Chapter 9, except that the bending moments are obtained using the coefficients provided in Tables 10.2–10.5 (Tables 26 and 27 of the code).

The required thickness of the slab may be estimated initially based on the serviceability limit state criteria of deflection, using the suggested value of effective span to depth ratio given in Clause 24.1 of the code or by using Eqs (10.1)–(10.3).

As discussed in Section 9.4.5 of Chapter 9, a check may be made for the effective depth, d , required for resisting the bending moments using Eq. (5.28) given in Chapter 5. As the depth chosen based on the deflection criteria will normally be greater than that required for bending, the tension steel required will be less than that for the balanced steel and the section will be under-reinforced. If the assumed depth is much greater than the required depth, all the design steps are to be redone

with the new value of slab thickness. This kind of iteration can be avoided by using the direct design method suggested by Pandian (1989) and is discussed in Section 10.11.

The area of reinforcement required in each direction at the mid-span and supports of the middle strip may be found by using Eq. (5.14) given in Chapter 5 and Eq. (9.10) given in Chapter 9 or by using the following approximate formula:

$$A_{st} = \frac{M_u}{0.8df_y} \quad (10.27)$$

This formula has been found to give a fairly good estimation of the area of bars. One may assume the average effective depth for both directions for calculating the steel area or use the actual effective depth in each direction.

It has to be noted that the reinforcements calculated for the bending moments occurring in the middle strip of the restrained discontinuous slabs have to be provided in the middle strip alone (see Fig. 10.12) and the edge strips require only minimum reinforcement. Furthermore, the restrained discontinuous two-way slabs are to be provided with torsional reinforcement at the corners to prevent cracking. As in one-way slabs, the spacing of reinforcements selected should be within the code-prescribed limits to control cracking (spacing less than $3d$ or 300 mm, whichever is less). These aspects are explained in Section 10.4.5.

The minimum area of steel in both directions is 0.12 per cent of the cross-sectional area for high-yield strength bars and 0.15 per cent for mild steel bars, as per Clause 26.5.2.1 of IS 456. The spacing of bars may be calculated using Eq. (9.11) given in Chapter 9. As discussed, smaller diameter and high-strength reinforcement (TOR-KARI) with $f_y = 550$ N/mm² can also be used in two-way slabs to gain considerable economy.

After calculating the reinforcements, the assumed thickness should be checked for L/d limits imposed by the code, using modification factors given in Figs 4 and 5 of the IS code. Finally, a check may be performed on shear strength, though normally two-way slabs will be safe in shear for the assumed depth based on the deflection criteria.

10.4.4 Use of Design Aids

As discussed in Section 9.6.1 of Chapter 9, design charts 1–18 and/or Tables 1–4 of SP 16-1980 may also be used for the design of two-way slabs, assuming $b = 1000$ mm. For a given value of M_u/bd^2 , the reinforcement percentage, p_t , can be read from these tables. Tables 5–44 give the moment of resistance of slabs, per metre width, of specific thicknesses in the range 100–250 mm for different values of f_{ck} and f_y . Table 96 may be used for finding the spacing of bars for the designed area of steel.

10.4.5 Detailing of Reinforcements

The detailing of reinforcement for simply supported two-way slabs and restrained two-way slabs is discussed in this section. The minimum and maximum reinforcement requirements as discussed in Section 9.4.5 of Chapter 9 for one-way slabs are also applicable to two-way slabs.

Simply Supported Two-way Slabs

The flexural reinforcements in the two directions are provided to resist the maximum bending moments M_x and M_y calculated as per Eq. (10.11). It has to be noted that the bending moments M_x and M_y are the maximum moments occurring at the mid-span and hence less steel is required at locations away from the mid-span and near the supports. However, in practice, bars are provided uniformly spaced throughout the span (in both directions), with a spacing not exceeding $3d$ or 300 mm (whichever is smaller).

For the special case of simply supported two-way slabs (torsionally unrestrained), Clause D–2.1.1 of IS 456 suggests to extend 50 per cent of the mid-span reinforcement to the supports. The remaining 50 per cent of the bars may be terminated within a distance of $0.1L_x$ or $0.1L_y$ from the support.

When the slab is truly *simply supported* at the edges, there will not be any *negative* moments near the supports. However, there may be some unforeseen partial fixity. Hence, in practice, to safeguard against partial fixity, either alternate bars are bent up or separate top steel is provided, with an area equal to 0.5 times of that provided at the bottom of the mid-span, with an extension of $0.1L_x$ or $0.1L_y$ from the face of the support (see Fig. 10.19). It should be noted that nowadays separate top and bottom layers of reinforcement are preferred instead of bent-up bars.

Detailing of torsional reinforcement at corners As discussed in Section 10.2, torsional stresses and torsional moments are developed near the corners of a simply supported slab, which will result in the lifting up of the corners as shown in Fig. 10.20(a) unless the slab is restrained at corners. This will result in cracking of the slab near the corners as shown in Fig. 10.20(b). Hence, torsional reinforcements are to be provided in the corners of the slab to take care of these torsional moments. Two types of reinforcement are indicated in Figs 10.20(c) and (d). The type shown in Fig. 10.20(d) is normally adopted as it is easy to fabricate and provide.

Detailing for Restrained Two-way Slabs

When restrained slabs are designed by using the moment coefficients given in Table 10.4, they should be detailed as per Clauses D-1.4–D-1.10 of the code. They are briefly discussed here:

1. The tension steel calculated for the positive design moments (per unit width) at the short and long spans should

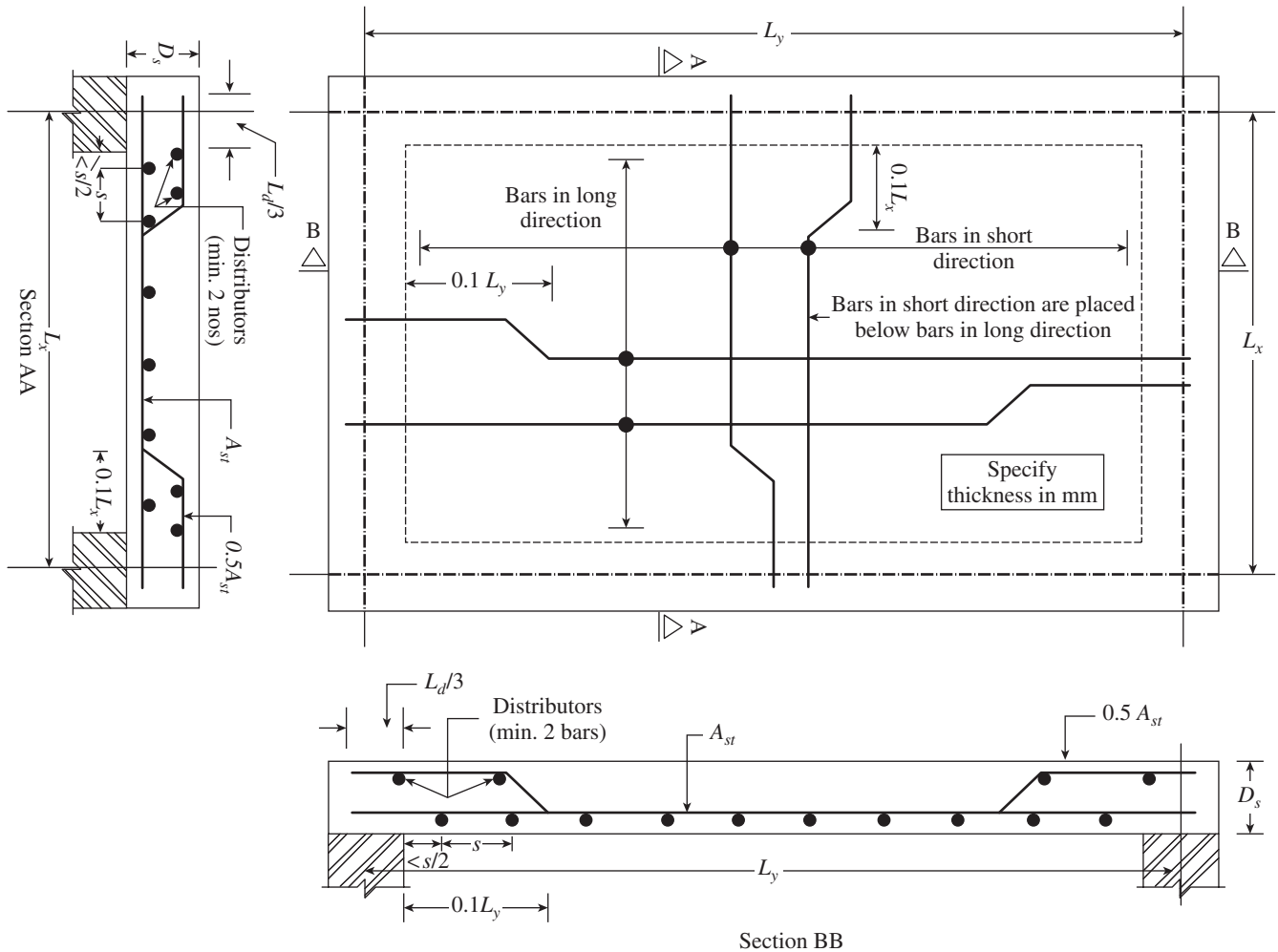


FIG. 10.19 Detailing of wall-supported two-way slabs with bent-up bars

- be provided, as shown in Fig. 10.21, at the bottom of the mid-span in the *middle strip* in the short- and long-span directions, respectively. These bars should extend to within $0.25L_x$ or $0.25L_y$ of a continuous edge or $0.15L_x$ or $0.15L_y$ of a discontinuous edge, as per Clause D-1.4. SP 34:1980 recommends that alternate bars (bottom steel) should extend fully into the support, as shown in Fig. 10.21.
- The tension steel calculated for the negative design moments in the short and long spans at continuous supports should be provided at the top and uniformly distributed across the edge strips of the short and long spans, respectively (see Fig. 10.21). According to Clause D-1.5 of the code, at least 50 per cent of these bars should extend to a distance of $0.3L_x$ or $0.3L_y$ from the face of the continuous support, on either side. The remaining bars may be curtailed at a distance of $0.15L_x$ or $0.15L_y$ from the face of the continuous support, as shown in Fig. 10.21.
 - At discontinuous edge, negative moments may arise due to partial fixity. Hence, to safeguard against such situations, Clause D-1.6 of the code recommends that 50 per cent of the bottom steel at the mid-span should be provided at

these edges and such steel should extend over a length of $0.1L_x$ or $0.1L_y$ from the face of the support, as shown in Fig. 10.21.

- Reinforcement in an edge strip parallel to the edge need not exceed the minimum area of tension reinforcement together with the recommendations for torsion given as per Clause D-1.7 of the code.

It has to be noted that straight reinforcements alone are shown in Fig. 10.21. Some designers prefer to provide cranked or bent-up reinforcement bars as shown in Fig. 10.22(a). For comparison, straight bars are also shown in Fig. 10.22(b).

Detailing of torsional reinforcement at corners Clause D-1.8 of the code stipulates that torsion reinforcement should be provided at any corner where the slab is simply supported on both edges meeting at that corner. The following points need to be noted:

- This torsion reinforcement should be provided at the top and bottom in a mesh or grid pattern, each with layers of bars placed parallel to the sides of the slab and extending from the edges to a minimum distance of one-fifth of the

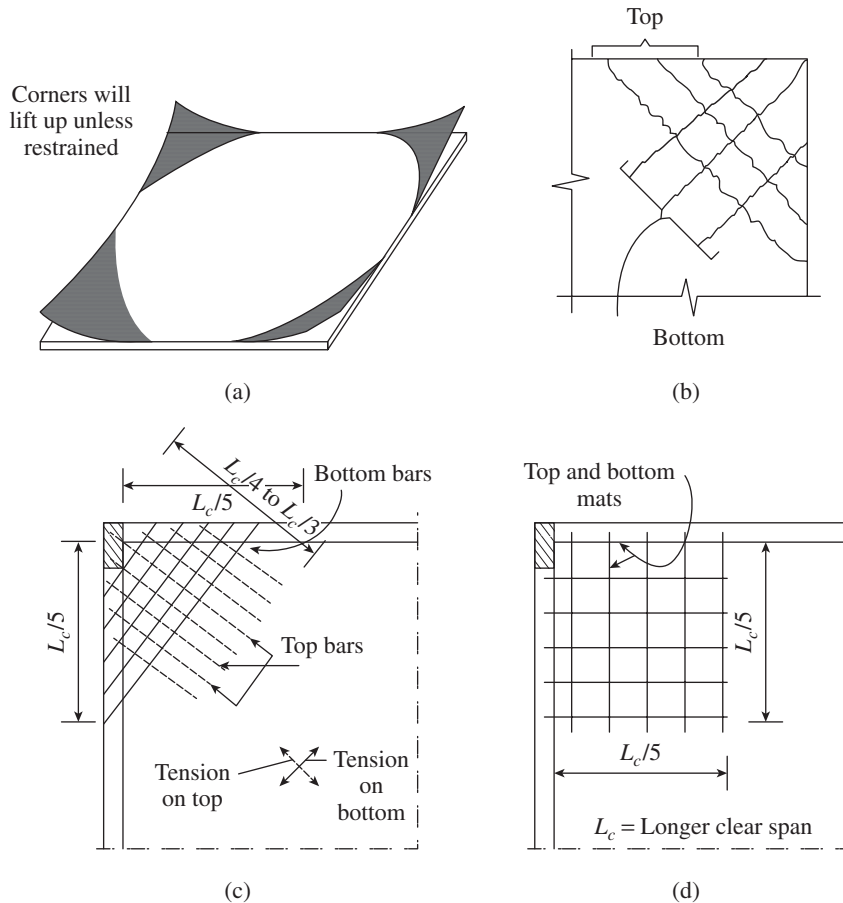


FIG. 10.20 Torsional effects and torsional reinforcements (a) Lifting of corners due to torsion (b) Potential crack pattern (c) Torsion reinforcement using skewed bars (d) Torsion reinforcement using top and bottom bars

shorter span (i.e., $0.2L_x$). The area of reinforcement in each of these four layers should be three-quarters of the area required for the maximum mid-span design moment in the slab, that is, $0.75A_{st,x}^+$. The bars can be made U-shaped (wherever convenient) and provided in the two orthogonal directions as shown in Fig. 10.23.

2. Torsion reinforcement equal to half that described in 1, that is, $0.375A_{st,x}^+$, should be provided at a corner where one edge of the slab is continuous and the other edge is discontinuous as per Clause D-1.9 of IS 456. They are shown in Fig. 10.23.
3. Torsion reinforcement need not be provided when both edges meeting at a corner are continuous, as per Clause D-1.10 of IS 456. However, such a location will have some reinforcements provided to resist the negative moment over supports in the middle strips and the distributor reinforcements in the edge strips.

Two-way slabs can be *pre-cambered* to counteract the effects of long-term deflection but care is needed in applying such cambers. It is desirable to limit the cambering to a maximum of half of the total deflection (C & CAA T36, 2003).

Roof slabs Roof slabs are subjected to weathering action in addition to supporting the self-weight, occasional imposed load, and the weathering course. The imposed load prescribed by IS 875 on roof slabs is $0.75\text{--}1.50\text{ N/mm}^2$. It is important to provide adequate drainage facilities; otherwise, there will be the problem of *ponding* and overloading and/or leakage of roof slab. A minimum slope of one per cent, that is, 10 mm per metre slope, is required, though 20 mm per metre is preferable for efficient drainage. Every 175 m^2 of roof area may require approximately one 100 mm diameter drain pipe for 100 mm per hour rainfall intensity.

Roofs in tropical areas are subjected to large variations of temperature (as much as 30°C). Strains due to thermal changes can be in the order of $12 \times 10^{-6} \times 30 = 3.6 \times 10^{-4}$ and due to moisture change (drying shrinkage) may be in the order of 4×10^{-4} to 10×10^{-4} (Purushothaman 1984). These strains are sufficient to cause micro-cracks in concrete. Moreover, variations in temperature will result in further thermal movements; for example, for a 6 m span roof, it will be around $3.6 \times 10^{-4} \times 6000 = 2.2\text{ mm}$. Hence, it is advisable to provide sliding joints between the roof and the wall in wide roofs, using elastomeric bearing pads. Expansion joints should also be provided not exceeding about 25 m (Purushothaman 1984).

Another aspect that deserves attention is the lifting of the corners. Purushothaman (1984) has shown that a 100 mm thick concrete roof of size $3\text{ m} \times 4.5\text{ m}$ requires about 4600 N as corner holding down force, which may be held down by a 200 mm thick *parapet wall* of 2 m length and 600 mm height. Thus, the function of a parapet wall in holding down the corners of slabs should not be underestimated.

Nowadays, to mitigate the heat-island effect of cities, *green roofs* are selected. When such green roofs are planned, the load due to it (typically $1\text{--}5\text{ kN/m}^2$) should be considered in the design. In addition, proper water proofing system, root repellent system, and drainage system should be selected.

10.5 DESIGN OF NON-RECTANGULAR SLABS

Non-rectangular slabs in shapes such as trapezoid, circle, and triangle, are sometimes encountered in practice. Circular slabs are often used in liquid-retaining structures. Sometimes, one may need to design a rectangular slab with one edge free and the other three edges continuous. The design of these slabs is briefly discussed in this section.

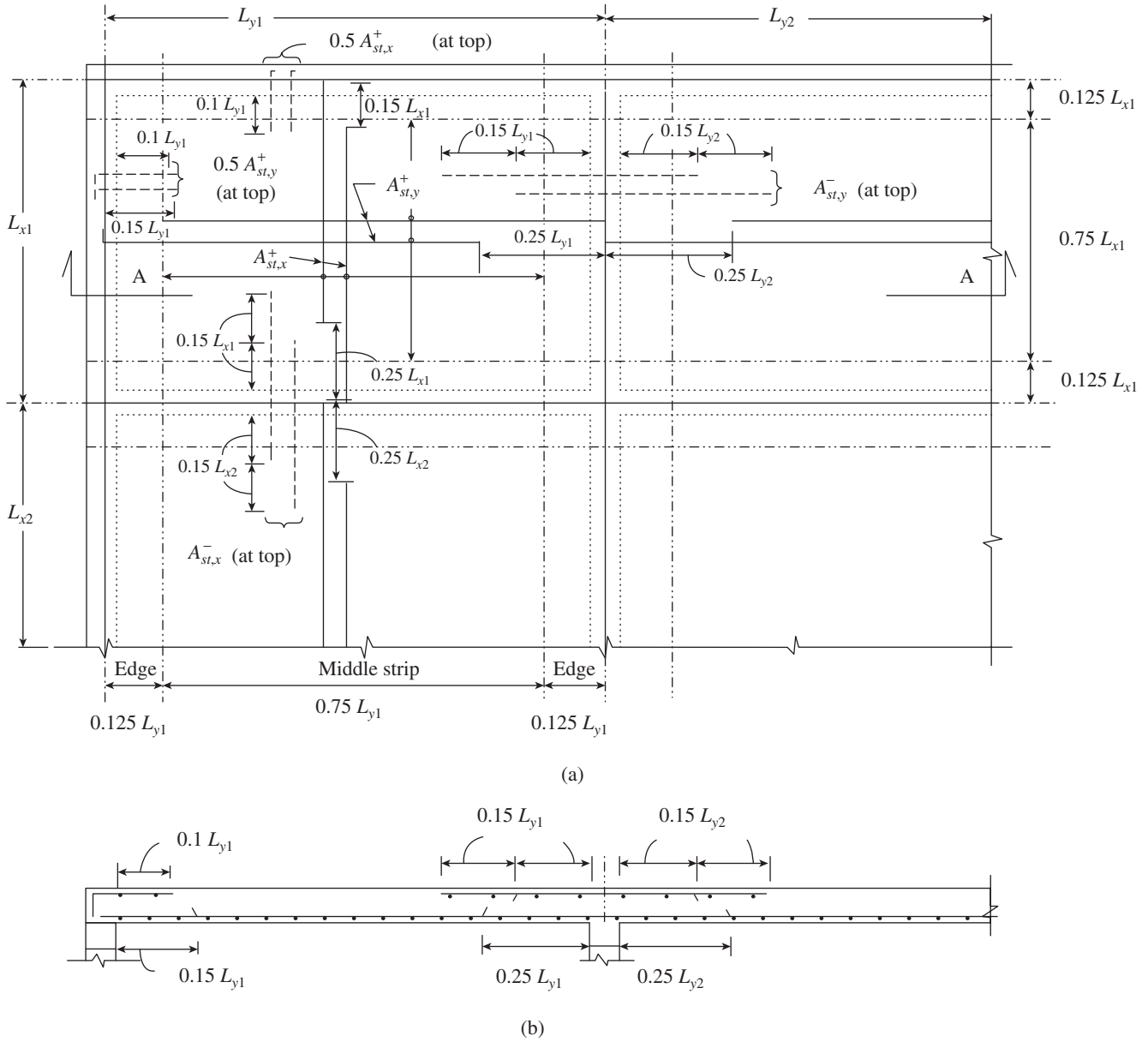


FIG. 10.21 Reinforcement detailing in restrained two-way slabs (a) Plan (b) Section 'AA'

10.5.1 Circular Slabs

Classical solutions based on the elastic plate theory are available for uniformly loaded circular slabs with various boundary conditions (Timoshenko and Krieger 1959). They are usually expressed in polar coordinates; hence, the bending moments are expressed as radial moments, M_r , and tangential moments, M_t . For example, for simply supported circular slabs subjected to uniformly distributed loads, the bending moments are given by

$$M_r = \frac{w}{16} (3 + \nu)(r^2 - a^2) \tag{10.28a}$$

$$M_t = \frac{w}{16} [r^2 (3 + \nu) - a^2 (1 + 3\nu)] \tag{10.28b}$$

where r is the radius of the circular slab, w is the uniformly distributed load, a is the radius where the bending moment is determined ($0 \leq a \leq r$), and ν is the Poisson's ratio, which may be taken as 0 or 0.15 for reinforced concrete. Assuming $\nu = 0$, we get the maximum moment at the centre of the slab as (see Fig. 10.24a)

$$M_{r,max} = M_{t,max} = 3wr^2/16 \tag{10.28c}$$

The maximum shear force, $V = 0.5wr$. (10.29)

The maximum deflection at the centre of the slab is given by

$$\Delta_{max} = \frac{(5 + \nu)wr^4}{64(1 + \nu)k_p} \text{ with } k_p = \frac{ED_s^3}{12(1 - \nu^2)} \tag{10.30}$$

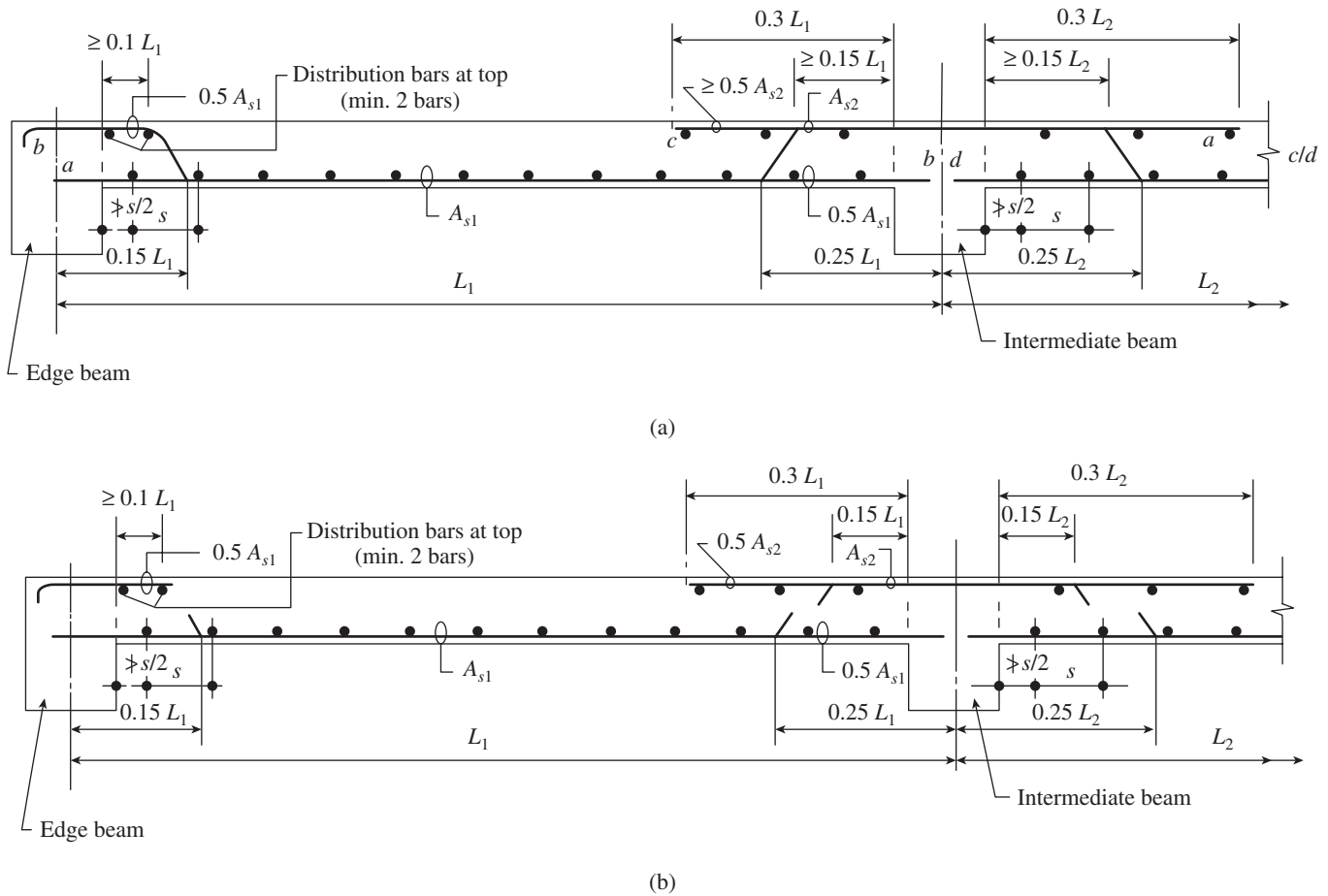


FIG. 10.22 Simplified rules for curtailment of bars in two-way slabs—section through middle strip (a) Using bent-up bars (b) Using straight bars

where k_p is the plate stiffness, D_s is the overall depth of slab, and E is the Young's modulus.

For circular slabs with fixed boundary subjected to uniformly distributed loads, the bending moments are given by

$$M_r = \frac{w}{16} [r^2(1+\nu) - a^2(3+\nu)] \quad (10.30a)$$

$$M_t = \frac{w}{16} [r^2(1+\nu) - a^2(1+3\nu)] \quad (10.30b)$$

$$\text{The maximum shear force, } V = 0.5wr \quad (10.31)$$

where r is the radius of circular slab, w is the uniformly distributed load, a is the radius where the bending moment is determined ($0 \leq a \leq r$), and ν is the Poisson's ratio, which may be taken as 0 or 0.15 for reinforced concrete.

The maximum deflection at the centre of the slab is given by

$$\Delta_{\max} = \frac{w(r^2 - a^2)^2}{64k_p} \quad \text{with } k_p = \frac{ED_s^3}{12(1-\nu^2)} \quad (10.32)$$

Similar expressions are available for simply supported annular plates and semicircular plates subjected to uniform loads (Timoshenko and Krieger 1959; Szilard 1974).

Reinforcement may be provided in the following two ways:

1. The ideal form of reinforcement for circular slabs is in the form of radial and circumferential reinforcement; however, it results in the stacking up of bars near the centre of the slab. Moreover, each circumferential bar has its own length and the length of all radial bars is not the same. Hence, the radial bars are usually provided in two or three sets from edge to edge and in the form of discontinuous bars in between the segments as shown in Fig. 10.24(b). The radial bars are also bent up near the edge and a few rings are provided in the top layer as well (see Section XX in Fig. 10.24b).
2. An alternative arrangement is in the form of grid pattern shown in Fig. 10.24(c). This type of reinforcement is simpler than the radial layout; however, the pattern of reinforcement deviates considerably from the directions of principal moments. This deviation is indicated along the radial lines inclined at 22.5° and 45° to the direction of reinforcement in Fig. 10.24(c). Grid type arrangement should also take into account this factor. In addition, ring reinforcement should be provided along the periphery for adequate stiffness. It should be noted that the reinforcement layout for fixed boundary is also similar, except that the top reinforcement should be provided in the radial and

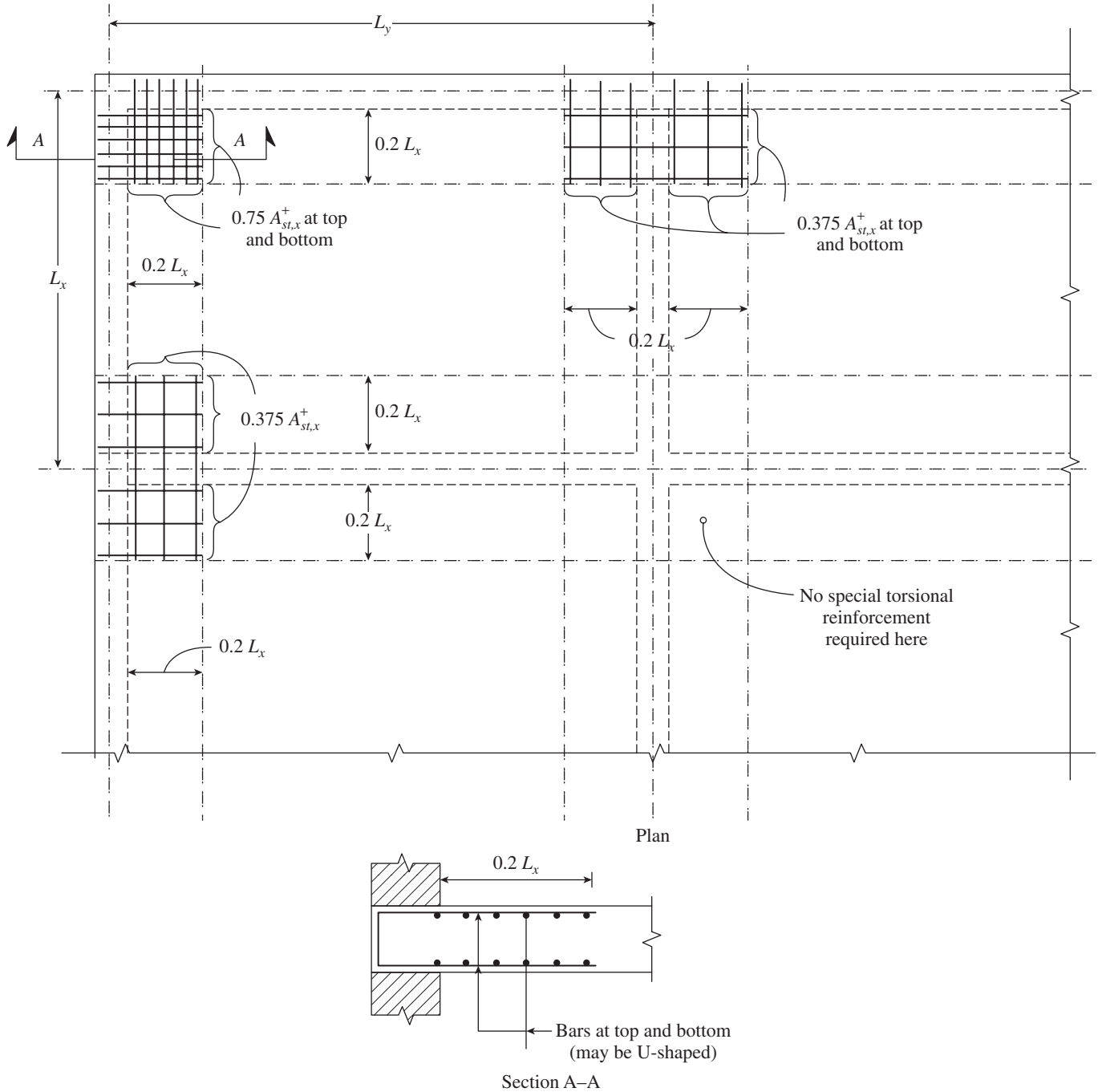


FIG. 10.23 Detailing of torsional reinforcement in restrained slabs

tangential directions up to a distance of $0.6r$ from the edge where r is the radius of the slab. These bars should be well-anchored beyond the edge.

Semicircular slabs may be designed idealizing them as rectangles, with the length of the short side as 0.866 times the radius of the circle.

10.5.2 Triangular Slabs

Triangular slabs are sometimes used from aesthetic considerations. The expressions for bending moments in an equilateral

triangular plate simply supported or fixed on all sides are available in classical texts on plates. They may be expressed in the following form (Timoshenko and Krieger 1959):

$$M_{x,max} = \alpha_{x1} wa^2 \tag{10.33a}$$

$$M_{y,max} = \alpha_{y1} wa^2 \tag{10.33b}$$

where a is the side of the triangle and α_{x1} and α_{y1} are the bending moment coefficients. Figure 10.25 shows the variation of these moments and support reactions in uniformly loaded equilateral triangular slabs of side a for both simply supported and fixed conditions (Stiglat and Wippel 1983).

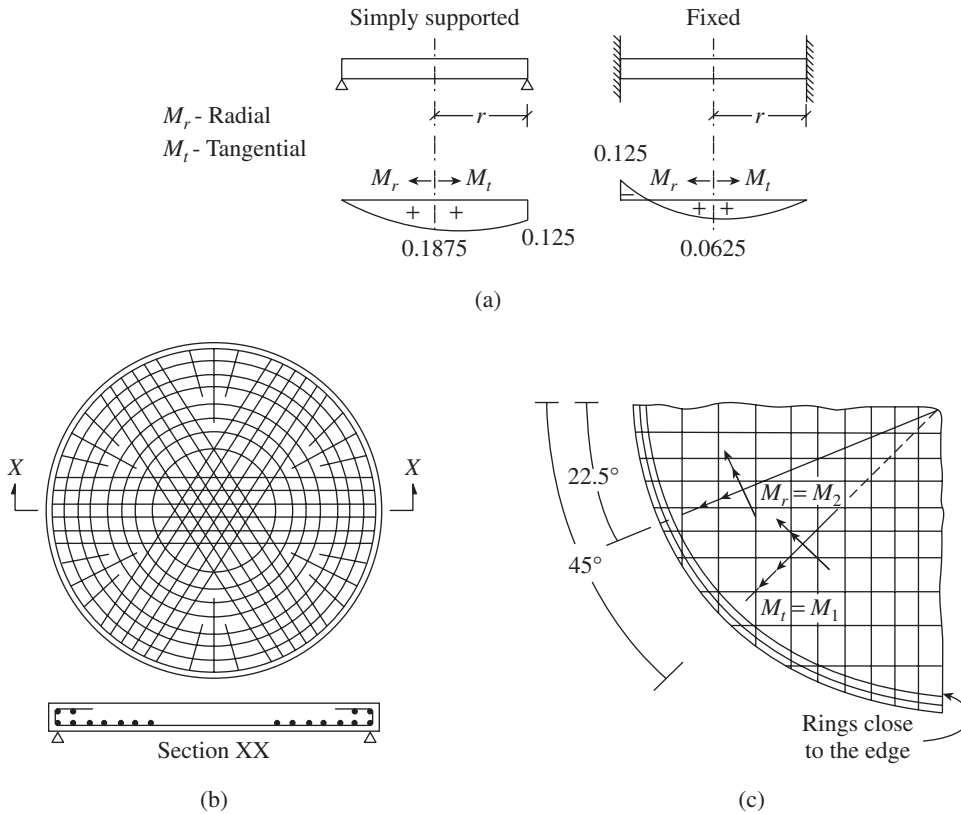


FIG. 10.24 Alternative methods of detailing circular slabs (a) Bending moments (factor = wr^2) (b) Rings and radial bars (c) Grid reinforcement

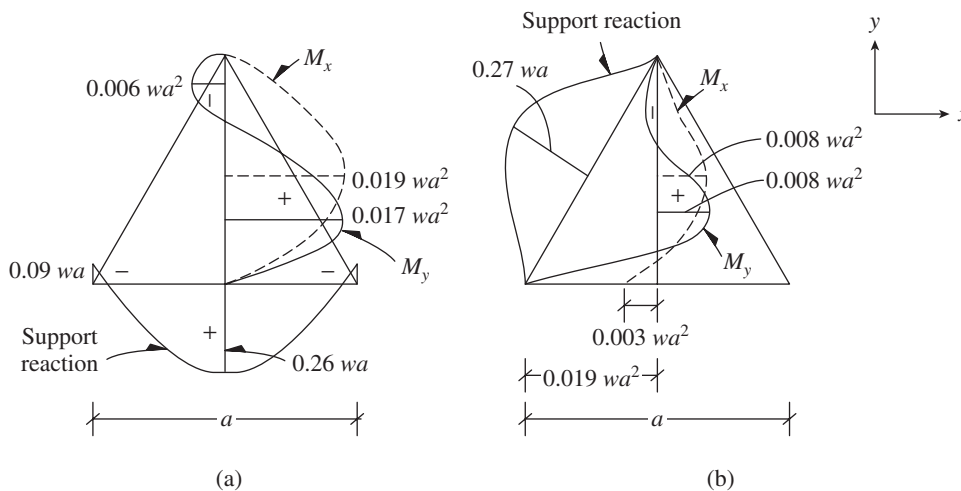


FIG. 10.25 Variation of bending moment and support reaction in triangular slabs (a) Simply supported slab (b) Fixed slab

The corners have a tendency to lift-off the supports as is evident from the negative reaction at the corners (see Fig. 10.25a). The moments M_x and M_y attain the maximum values near the centroid of the triangle. Hence, we should provide the reinforcement across the adjacent sides, parallel to the third side for M_x and parallel to the line bisecting the included angle for M_y (Leonhardt and Mönning 1977).

Two alternative arrangements of reinforcement are shown in Figs 10.26(a) and (b). The bottom reinforcement can be

provided parallel to the sides covering the entire slab to resist both M_x and M_y . The negative reinforcement should be provided across the adjacent sides of corners to a distance of about $0.3a$ and parallel to the line bisecting the corner angle and should be well-anchored into the support.

Alternatively, the reinforcement can be provided in the grid layout at the top and bottom as shown in Fig. 10.26(b), taking into account the deviation by 30° of the bottom reinforcement to the principal bending moments.

Slabs with fixed boundaries require negative reinforcement at the top, perpendicular to the sides close to the boundaries, and positive bottom reinforcement as shown in Fig. 10.26(c), designed for the respective moments as indicated in Fig. 10.25(b). The deviation by 30° of the bottom reinforcement to the principal bending moments should also be considered. The top reinforcement may be provided along each of the fixed edges for a distance of $0.3L$ as shown in Fig. 10.26(c) and anchored beyond the boundaries of the slab (Leonhardt and Mönning 1977). It has to be noted that the negative bars along only one edge have been shown in Fig. 10.26(c) for clarity and similar reinforcement should be provided along the other edges too.

10.5.3 Trapezoidal and Polygonal Slabs

Trapezoidal slabs having approximate symmetry about one of the axes can be designed as an equivalent rectangular slab with the L_y/L_x ratio computed as shown in Fig. 10.27(a).

Polygonal slabs including triangular slabs may be designed assuming them as equivalent circular or rectangular slabs. In the case of triangular slabs, with height h and side b , the diameter of the inscribed circle can be written as (see Fig. 10.27b)

$$d_{eq} = \frac{2bh}{b + \sqrt{b^2 + 4h^2}} \quad (10.34)$$

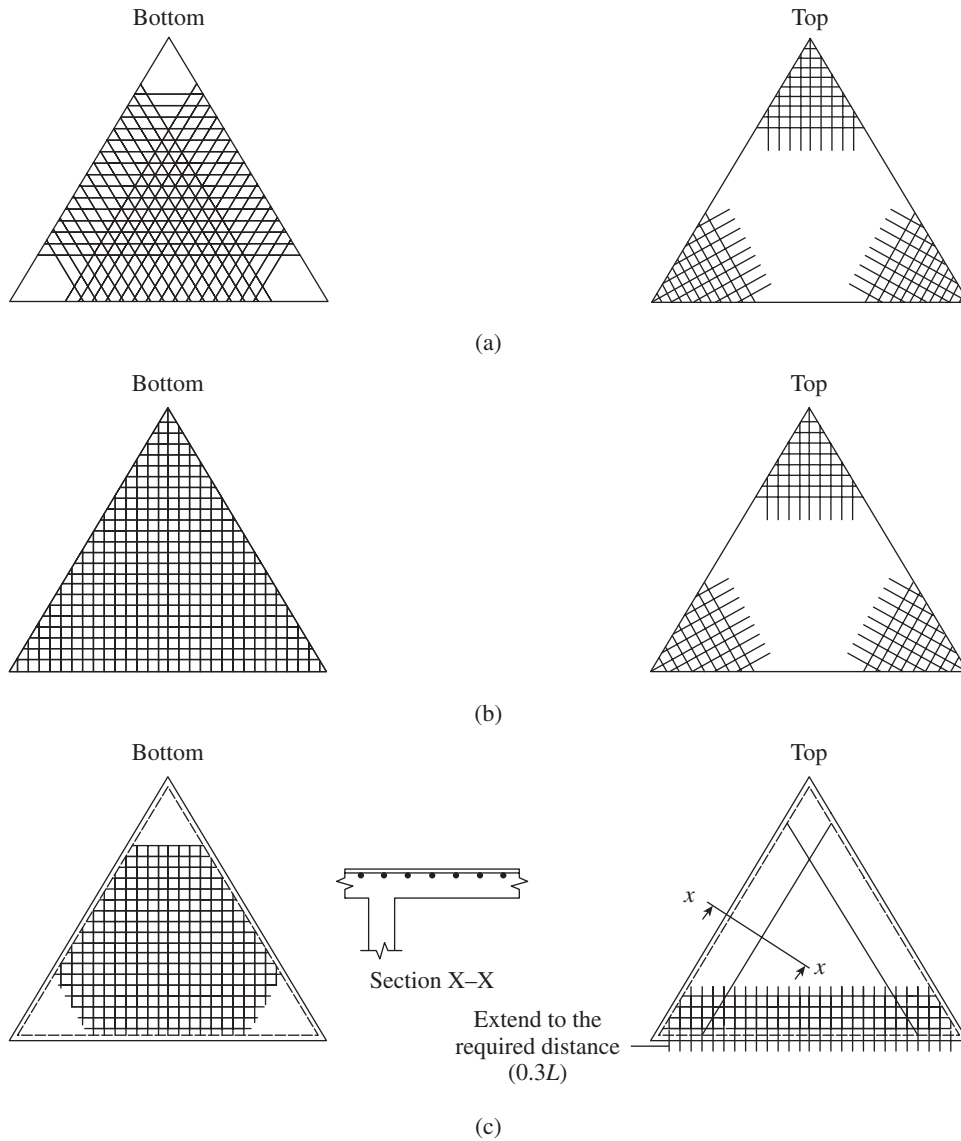


FIG. 10.26 Detailing of reinforcement in triangular slabs (a) Simply supported slab (b) Simply supported slab—alternate detailing (c) Fixed slab

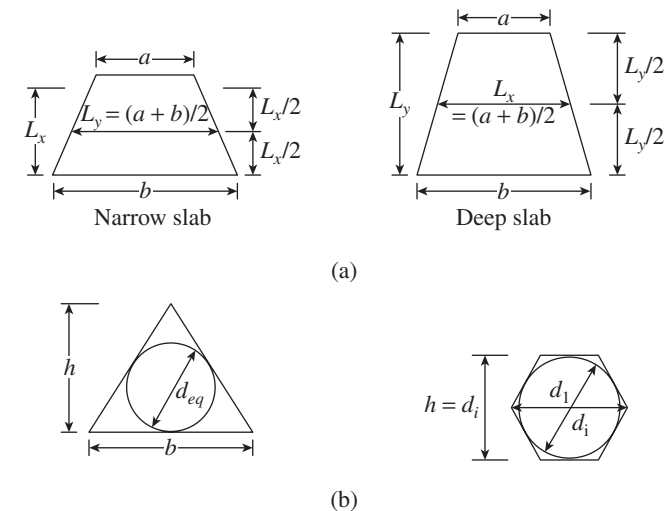


FIG. 10.27 Non-rectangular slabs (a) Trapezoidal slabs (b) Polygonal slabs

Reynolds and Steedman (1988) suggest that the bending moments in the two directions at the centre of the circle be calculated in the following way:

1. For slabs simply supported along all edges (corners restrained): $+wd_{eq}^2/16$
2. For continuous slabs along all edges: $+wd_{eq}^2/30$
3. The negative bending moment at sides for continuous slabs: $-wd_{eq}^2/30$

where w is the intensity of uniformly distributed load or intensity of pressure at the centre of the circle if the intensity varies uniformly.

For polygonal slabs with five or more sides (see Fig. 10.27b), the bending moments can be calculated as that of an equivalent circle with diameter d_{eq} given by

$$d_{eq} = \frac{(d_i + d_1)}{2} \quad (10.35)$$

The value of d_{eq} may be taken as $1.077d_i$ in the case of hexagons and $1.041d_i$ in the case of octagon, where d_i is the diameter of the inscribed circle (equals the distance across flats as shown in Fig. 10.27b) and d_1 is the diameter of the circumscribed circle (equals the distance across corners).

10.6 CONCENTRATED LOADS ON TWO-WAY SLABS

Clause 24.4 of IS 456 states that the bending moments in two-way slabs carrying concentrated loads like wheel loads, may be found by any accepted method approved by the engineer in charge. The note to this clause states that the most commonly used elastic methods are based on Pigeaud's or Westergaard's theory. The Pigeaud's method is normally adopted and is presented in the form of design curves (Pigeaud 1929; Reynolds and Steedman 1988). The curves for finding the maximum bending moments of a rectangular slab, simply supported along four edges, are given in Figs 10.28–10.30 for three different L_y/L_x ratios. Curves for other L_y/L_x ratios are available in Reynolds and Steedman (2008).

It has to be noted that these curves are applicable for loads placed at the centre of two-way simply supported slabs as shown in Fig. 10.31. In this figure, u and v are the loaded breadth and length, respectively and L_x and L_y are the short and

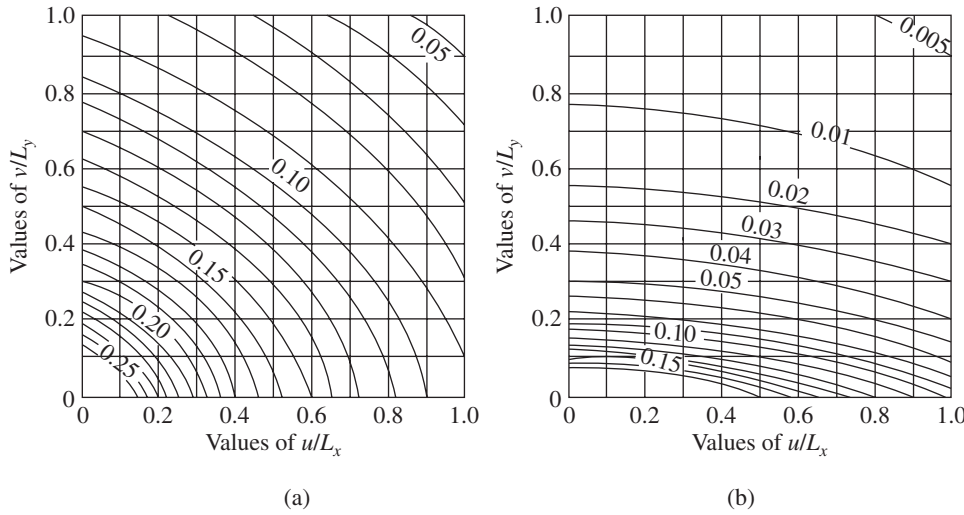


FIG. 10.28 Pigeaud's curves for $L_y/L_x = 2.5$ (a) Coefficient of m_x (b) Coefficient of m_y

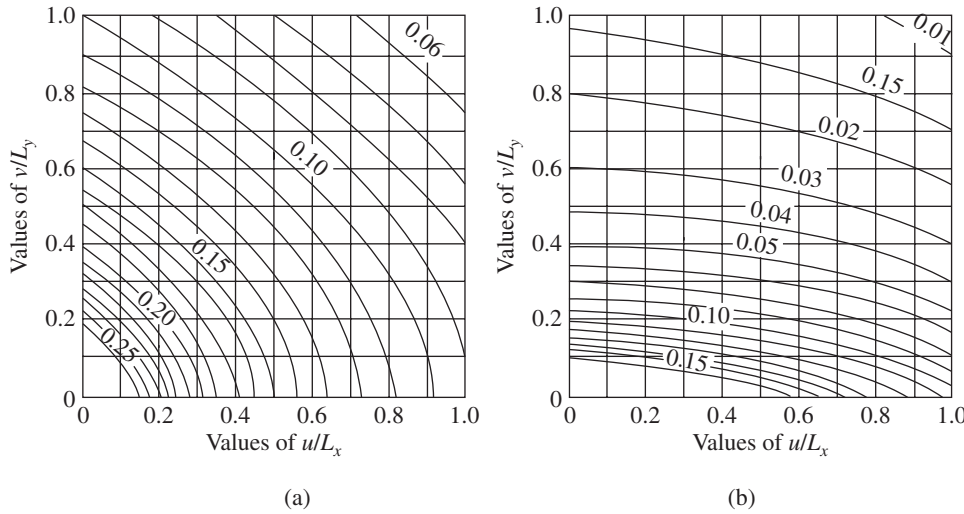


FIG. 10.29 Pigeaud's curves for $L_y/L_x = 2.0$ (a) Coefficient of m_x (b) Coefficient of m_y

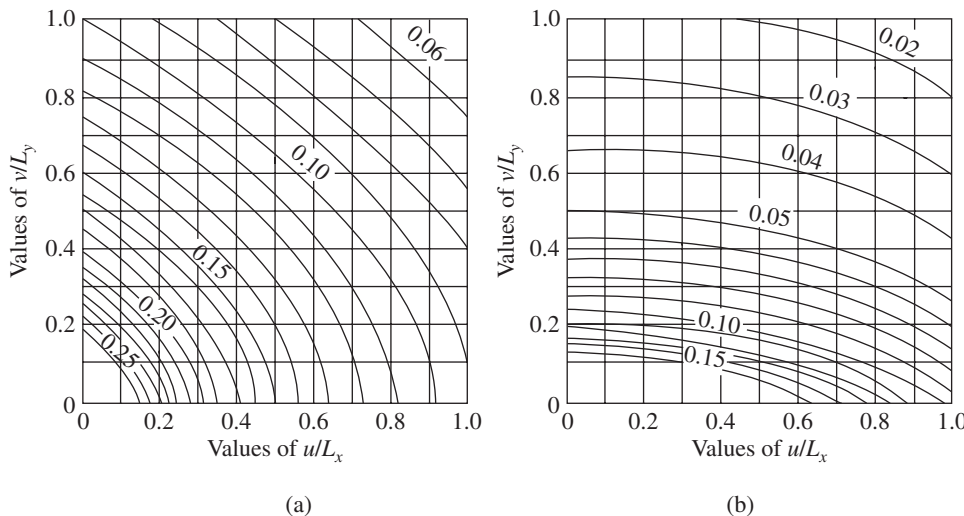


FIG. 10.30 Pigeaud's curves for $L_y/L_x = 1.67$ (a) Coefficient of m_x (b) Coefficient of m_y

long spans of the slab, respectively. For one-way slabs, the curve given in Reynolds and Steedman (2008) for $L_y/L_x = \infty$ may be used. It should be noted that these values may be added with the bending moments obtained for uniform loads using the methods discussed in the previous sections. Moreover, for other values of L_y/L_x , the values may be interpolated.

If P is the concentrated load acting on the loaded area $u \times v$, then the bending moments M_x and M_y may be obtained using the following equations:

$$M_x = P(m_x + \nu m_y) \quad (10.36a)$$

$$M_y = P(m_y + \nu m_x) \quad (10.36b)$$

where m_x and m_y are the coefficients from Figs 10.28–10.30 and ν is the Poisson's ratio; BS 8110 recommends the use of $\nu = 0.2$. The maximum shearing force, V per unit length, on a panel carrying a concentrated load is given by (Varghese 2006).

$$\text{Short span: } V = P(L_y - v/2)/(uL_y) \quad (10.37a)$$

$$\text{Long span: } V = P(L_x - u/2)/(vL_x) \quad (10.37b)$$

For slabs that are restrained along the four edges, Pigeaud recommends that the mid-span moments be reduced by 20 per cent.

Pigeaud's method can be extended to loads placed away from the centre of the panel (Reynolds and Steedman 2008; Varghese 2006). Suryanarayana (1990) has shown that this extension does not always work and in some cases the results will not be reliable.

10.7 OPENINGS IN TWO-WAY SLABS

Prakash Rao (1995) suggests that two-way slabs with openings may be split into different parts, as shown in Fig. 10.32, and analysed separately. The bending moments computed for the various segments are found to be on the safer side and thus adequate in most of the cases.

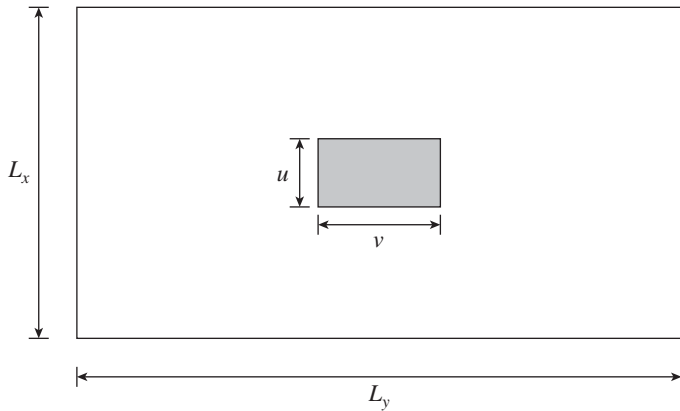


FIG. 10.31 Position of concentrated load for applying Pigeaud's curves

The computed bottom reinforcement should be provided throughout the slab without curtailment. The reinforcement transverse to the direction of the main (shorter) span should be of adequate length beyond the edges of opening, usually equal to half the width of the opening and anchorage length. U-bar type reinforcement should be provided along the edges of the opening (see Fig. 10.23). Alternatively, yield-line methods of analysis may be adopted to determine the quantity of reinforcement in slabs with openings.

10.8 YIELD-LINE ANALYSIS FOR SLABS

Most concrete slabs are designed for the moments found by the methods described in this chapter. These methods are based essentially upon the elastic theory. (It should be noted that a similar contradiction exists in the process by which frames are analysed, using elastic analysis, and different members are designed using limit state methods by multiplying the elastic moments by load factors). The reinforcement for slabs may also be calculated by strength methods that account for the actual inelastic behaviour of members at factored loads.

Limit analysis not only eliminates the inconsistency of combining elastic analysis with inelastic design but also accounts for the reserve strength available in most of the reinforced concrete structures. Limit analysis also permits, within certain limits, an arbitrary readjustment of moments found by elastic analysis to arrive at the design moments.

Although IS 456 and ACI 318 codes contain no specific provisions for limit or plastic analysis of slabs, Clause 24.4 of IS 456 permits the use of 'any acceptable method' for determining the bending moments including Johansen's *yield-line analysis*.

Yield-line analysis for slabs was first proposed by Ingerslev (1923) and was fully developed later by Johansen (1943; 1968). Johansen's method received wider attention after the English language summary by Hognestad (1953) and the book by Jones and Wood (1967). A review of these developments may be found in Park and Gamble (2000) and Kennedy and Goodchild (2003).

It is well known that when the loads acting on a frame are increased, *plastic hinges* will be formed at the maximum stressed locations in beams or columns. Upon overloading, there would be large inelastic rotations at these plastic hinges at essentially a constant resisting moment. In the case of slabs, such yielding will occur along the lines, called *yield lines*.

As already explained in Section 10.2, when the load is increased on a reinforced concrete slab, the regions of highest moments will yield first and hairline cracks occur in the soffit at the mid-span, where the flexural tensile capacity of the slab is exceeded. Increasing the loads further will increase the size of the cracks and yielding of the reinforcement will take place. On increasing the loads further, the cracks tend to migrate to the boundaries of the slab and the tensile reinforcement passing through the cracks also yield. The plastic hinges along the lines of the yielded reinforcement are called the *yield*

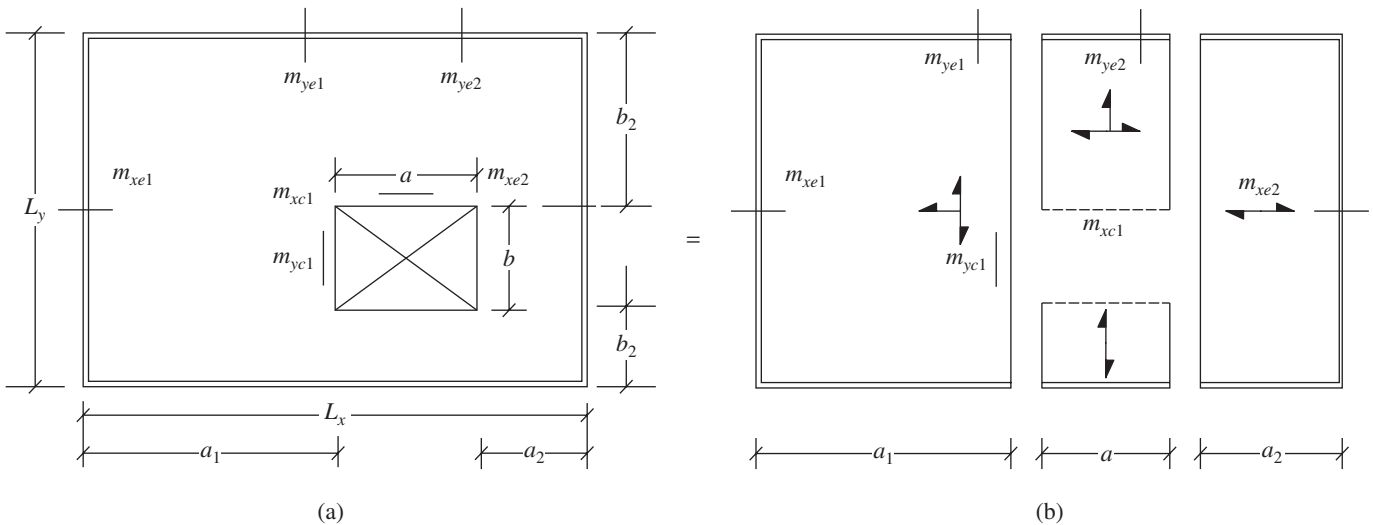


FIG. 10.32 Splitting of two-way slabs with opening for approximate analysis (a) Slab with opening (b) Slab split into different parts

lines. The final failure will take place by the rotation of the slab elements about the *axes of rotation*, which are usually the support edges of the slab. This kind of behaviour with the cracking pattern and yield lines for a simply supported square slab is shown in Fig. 10.33.

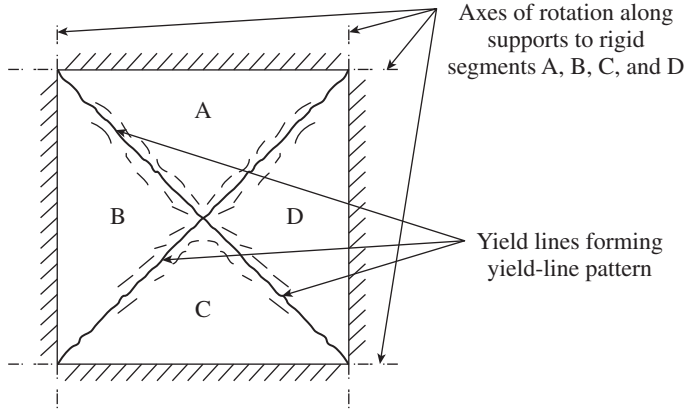


FIG. 10.33 Yield-line pattern in a simply supported square slab

It is important to note that for the complete yield-line pattern to develop, the slab must be under-reinforced (as we have seen in the previous sections, in most of the cases the slab will be under-reinforced), so that sufficient rotation capacity is available for the initiation and propagation of yield lines.

10.8.1 Upper and Lower Bound Theorems

Plastic analysis methods like the yield-line theory are derived from the general theory of structural plasticity, which states that the collapse load of a structure lies between two limits, an *upper bound* and a *lower bound*, of the true *collapse load*. These limits can be found by well-established methods. A full solution by the theory of plasticity would attempt to make the lower and upper bounds converge to a single correct solution.

The lower bound and upper bound theorems, when applied to slabs, can be stated as follows (Jones and Wood 1967; Kennedy and Goodchild 2003):

Lower bound theorem If, for a given external load, it is possible to find a distribution of moments that satisfies equilibrium requirements, with the moment not exceeding the yield moment at any location, and if the boundary conditions are satisfied, then the given load is lower bound of the true carrying capacity.

Upper bound theorem If, for a small increment of displacement, the internal work done by the slab, assuming that the moment at every plastic hinge is equal to the yield moment and that boundary conditions are satisfied, is equal to the external work done by the given load for that same small increment of displacement, then that load is an upper bound of the true carrying capacity.

The yield-line method of analysis for slabs is an upper bound method, and consequently, the failure load calculated

for a slab with known flexural resistances may be higher than the true value.

10.8.2 Characteristics of Yield Lines

The following characteristic features of yield lines help us in selecting the possible yield-line patterns and establishing the axes of rotations of a typical slab (Kennedy and Goodchild 2003):

1. Yield lines are straight lines.
2. Yield lines represent the axes of rotation.
3. Yield lines must end at a slab boundary.
4. Axes of rotation generally lie along the lines of support and pass over any column support.
5. A yield line between two slab segments must pass through the point of intersection of the axes of rotation of the adjacent slab segments.
6. Yield lines form under concentrated loads, radiating outward from the point of application.

The terms *positive yield line* and *negative yield line* are used to distinguish between those associated with tension at the bottom and at the top of the slab, respectively.

The notations used for yield lines and supports are given in Fig. 10.34.

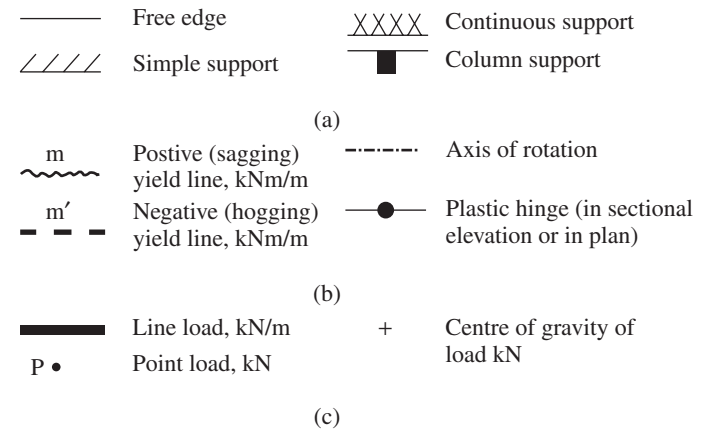


FIG. 10.34 Notations used (a) Supports (b) Yield lines (c) Loads

Yield-line patterns developed in slabs of different shapes and with different boundary conditions are shown in Fig. 10.35. Note the negative yield lines near the supports in the case of slabs with fixed or continuous supports. In square slabs, there are axes of rotation over all four simple supports. Positive yield lines form along the lines of intersection of the rotation segments of the slab. For a rectangular two-way slab on simple supports, the diagonal yield lines must pass through the corners, whereas the central yield line is parallel to the two longer sides (axes of rotation along opposite supports intersect at infinity in this case). Similar guidelines may be applied to the other slabs in Fig. 10.35 to obtain the pattern of yield lines as shown in the figure.

10.8.3 Orthotropic Reinforcement and Skewed Yield Lines

In general, slab reinforcement is placed orthogonally, that is, in two perpendicular directions. The same reinforcement is often provided in each direction, but the effective depths will be different. Such slabs are said to be *isotropically reinforced*. However, in many practical cases, economical designs are obtained by using reinforcement having different bar areas or different spacing in each direction. In such cases, the slab will have different moment capacities in the two orthogonal directions. Such slabs are said to be *orthotropically reinforced*.

When the yield line is perpendicular to the direction of the reinforcement, the yield line ultimate moment is given by the following equation as per under-reinforced flexural member (see Annexure G of IS 456):

$$m = M_u = 0.87 f_y A_{st} d \left(1 - \frac{A_{st} f_y}{b d f_{ck}} \right) \tag{10.38}$$

Often yield lines will form at an angle with the directions established by the reinforcement, as shown in Fig. 10.36(a). For yield-line analysis, it is necessary to calculate the resisting moment, per unit length, along such skewed yield lines. Hence, we need to calculate the contribution to resistance from each of the two sets of bars.

Let us consider the common case of an *orthotropically reinforced slab*, as shown in Fig. 10.36(a), with the yield line making an angle α with the bars in the x direction. Let us assume that the bars along the x direction have a spacing of v and moment resistance m_y per unit length about the y axis, whereas the bars along the y direction have a spacing of u and moment resistance m_x per unit length about the x axis. Let us determine the

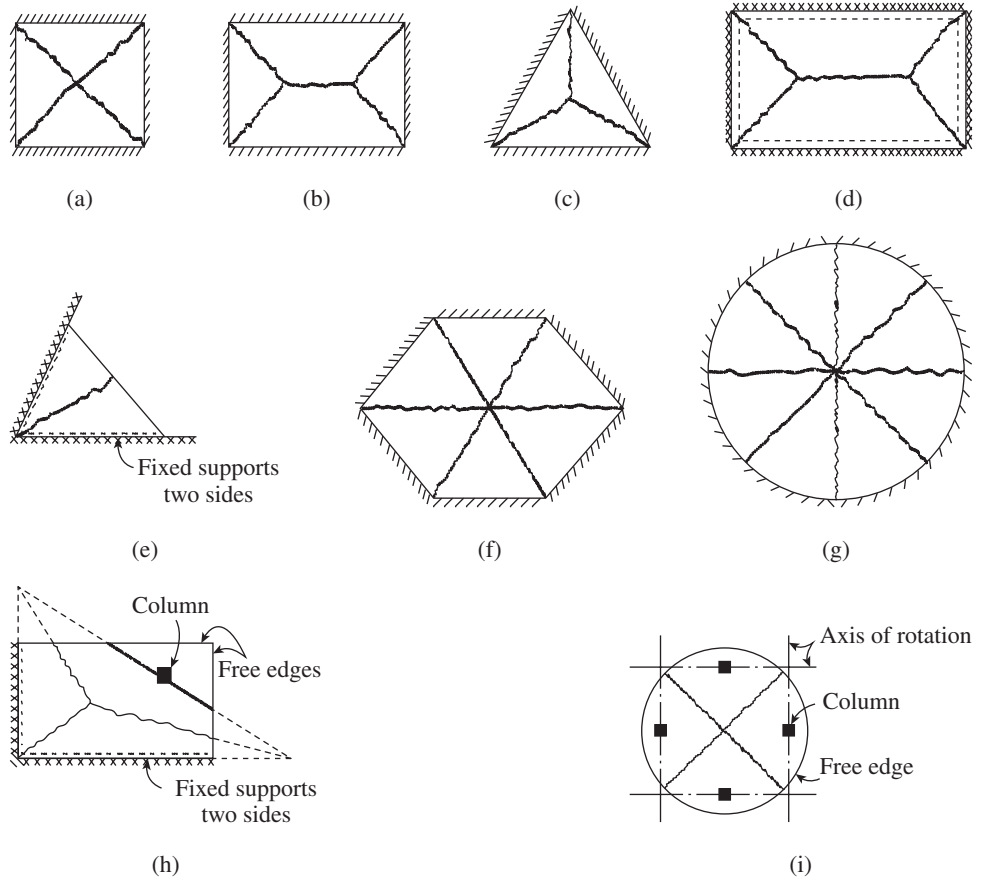


FIG. 10.35 Typical yield-line patterns in slabs of different shapes and support conditions (a) Square slab (b) Rectangular slab (c) Triangular slab (d) Rectangular slab (fixed supports) (e) Triangular slab (adjacent side supports) (f) Hexagonal slab (g) Circular slab (h) Rectangular slab (with a column support) (i) Circular slab (with four column supports)

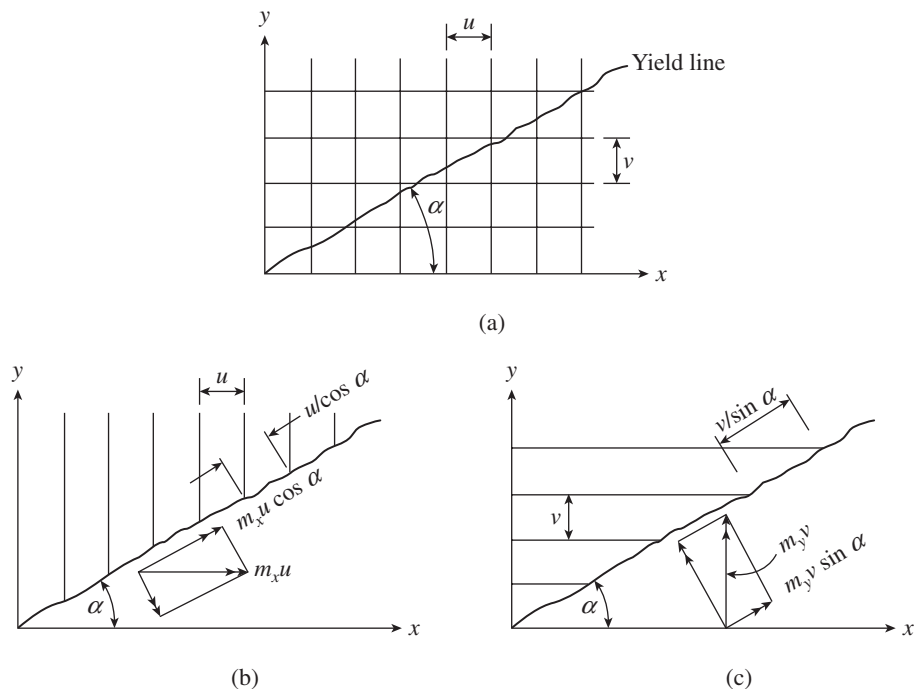


FIG 10.36 Yield line skewed with orthotropic reinforcement (a) Orthotropic reinforcement and yield line (b) y direction bars (c) x direction bars

resisting moments per unit length for the bars in the x and y directions separately.

With reference to Fig. 10.36(b), for the y direction bars, the resisting moment *per bar* about the x axis is $m_x u$ and the component of that resistance about the α axis is $m_x u \cos \alpha$. Thus, the resisting moment per unit length along the α axis for the bars in the y direction is

$$m_{\alpha y} = \frac{m_x u \cos \alpha}{u / \cos \alpha} = m_x \cos^2 \alpha \quad (10.39a)$$

If there is more than one mesh of reinforcement

$$m_{\alpha y} = \sum m_x \cos^2 \alpha \quad (10.39b)$$

Similarly, with reference to Fig. 10.36(c), for the bars in the x direction, the resisting moment *per bar* about the y axis is $m_y v$ and the component of that resistance about the α axis is $m_y v \sin \alpha$. Thus, the resisting moment per unit length along the α axis for the bars in the x direction is

$$m_{\alpha x} = \frac{m_y v \sin \alpha}{v / \sin \alpha} = m_y \sin^2 \alpha \quad (10.40a)$$

If there is more than one mesh of reinforcement

$$m_{\alpha x} = \sum m_y \sin^2 \alpha \quad (10.40b)$$

Thus, the resisting moment per unit length measured along the α axis for the combined sets of bars is given by the sum of the resistances given by Eqs (10.39) and (10.40) as

$$m_{\alpha} = m_x \cos^2 \alpha + m_y \sin^2 \alpha \quad (10.41)$$

When the same reinforcement is provided in each direction, we have $m_x = m_y = m$. Hence,

$$m_{\alpha} = m(\cos^2 \alpha + \sin^2 \alpha) = m \quad (10.42)$$

This equation indicates that in an *isotropically reinforced slab*, the yield moment is the same in all directions, regardless of the orientation of the yield line.

This analysis neglects any consideration of strain compatibility along the yield line and assumes that the displacements perpendicular to the yield line are sufficient to produce yielding in both sets of bars. This assumption has been validated by test data, except for values of α close to 0–90°. For such cases, however, neglecting the contribution of bars nearly parallel to the yield line was found to be conservative.

It has been shown that the analysis of an orthotropic slab can be simplified to that of a related isotropic slab, called the *affine slab*, when the ratio of the negative to positive reinforcement areas is the same in both the directions. The horizontal dimensions and slab loads must be modified to permit this transformation. More details about this may be found in Jones and Wood (1967).

10.8.4 Ultimate Load on Slabs

There are two methods for the determination of ultimate load capacity of slabs. They are based on the principles of (a) virtual work and (b) equilibrium.

Both the virtual work and equilibrium methods give an *upper bound* to the collapse load on the slab. Hence, it is important to investigate all possible yield-line patterns, such that the lowest value of the ultimate load is found. If a correct yield-line pattern is assumed, the lower-bound solution will coincide with the upper-bound solution; it should be noted that the lower-bound solutions are available only for a few simple cases of slabs (Rangan 1974). Experimental results have shown that the actual failure loads are greater than the loads predicted by the yield-line analysis, because of the membrane action of slabs, as discussed in Section 10.2. Hence, the upper-bound results obtained from the yield-line analysis can be used with a reasonable amount of safety.

10.8.5 Yield-line Analysis by Virtual Work Method

When the yield-line pattern has formed, since the moments and loads are in equilibrium, an infinitesimal increase in load will cause the structure to deflect further. The principle behind the virtual work method is that the external work done by the loads to cause a small arbitrary virtual deflection must equal the internal work done, as the slab rotates at the yield lines to accommodate this deflection.

The slab is given a virtual displacement and the corresponding rotations at the various yield lines are calculated. By equating the internal and external work, the relation between the applied loads and the resisting moments of the slab is obtained. Elastic rotations and deflections are not considered when writing the work equations, as they are very small compared with the plastic deformations (Kennedy and Goodchild 2003).

External work done The external work done by the loads is calculated as

$$\text{External work done} = \sum (W\delta) \quad (10.43)$$

where W is the load and δ is the virtual displacement.

More complicated trapezoidal shapes may always be subdivided into component triangles and rectangles. The total external work is then calculated by summing the work done by the loads on the individual parts of the failure mechanism. There is no difficulty in combining the work done by the concentrated loads, line loads, and distributed loads when they act together.

Internal work done The internal work done during the assigned virtual displacement is found by summing the products of yield moment m per unit length of hinge times the plastic rotation θ at the respective yield lines, consistent with the virtual displacement. If the resisting moment m is

constant along a yield line of length L and if the rotation is θ , the internal work is calculated as

$$\text{Internal work done} = \sum (M\theta) = \sum (mL\theta) \quad (10.44a)$$

where m is the ultimate moment per unit length of yield line, L is the length of yield line, and θ is the plastic rotation at the respective yield line.

If the resisting moment varies, as in cases where the bar size or spacing is not constant along the yield line, the yield line is divided into n segments, within each one of which the moment is constant. The internal work is then

$$W_i = (m_1l_1 + m_2l_2 + \dots + m_nl_n)\theta \quad (10.44b)$$

For the entire system, the total internal work done is the sum of the contributions from all the yield lines. In all cases, the internal work contributed is positive, regardless of the sign of m , because the rotation is in the same direction as the moment. The external work, on the other hand, may be either positive or negative, depending on the direction of the displacement of the point of application of the force resultant.

The following examples will help in better understanding of the yield-line analysis using the virtual work method.

1. Let us consider an example of an isotropically reinforced simply supported square slab supporting uniformly distributed load as shown in Fig. 10.37.

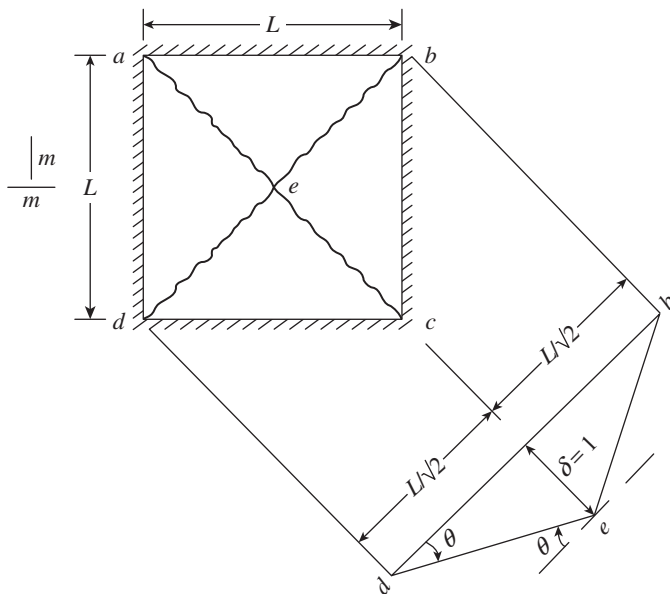


FIG. 10.37 Yield-line pattern in a simply supported square slab

For a virtual displacement of $\delta=1$ at point e , the external work done can be expressed as the area load w multiplied by the displaced volume. In this case, the displaced volume has the shape of an inverted pyramid; the volume is equal to the total area times one-third of δ .

$$\text{External work done} = \sum (W\delta) = wL^2/3 \quad (10.45a)$$

As the slab is isotropically reinforced, the ultimate moment along the yield line is also m . Since it is a square slab, the internal work done by the yield line bd is the same as that done by the yield line ac .

Internal work done =

$$\sum (M\theta) = \sum (mL\theta) = 2 \left[m(\sqrt{2}L)2 \left(\frac{\sqrt{2}}{L} \right) \right] = 8m \quad (10.45b)$$

Equating Eqs (10.45a and b) and simplifying, we get

$$m = \frac{wL^2}{24} \quad (10.45c)$$

2. Now let us consider another example of an isotropically reinforced square slab fixed at all edges supporting uniformly distributed load as shown in Fig. 10.38.

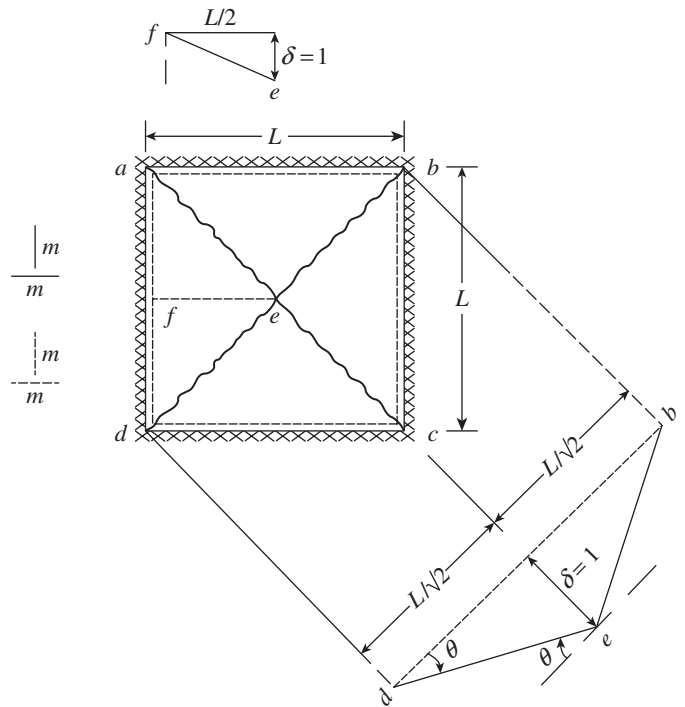


FIG. 10.38 Yield-line pattern in a fixed square slab

Since the edges are fixed, negative yield lines will also form along the edges as shown in Fig. 10.38.

$$\text{External work done} = \sum (W\delta) = wL^2/3 \quad (10.46a)$$

As the slab is isotropically reinforced, the ultimate moment along the yield line is also m . Since it is a square slab, the internal work done by the yield line bd is the same as that done by the yield line ac .

Internal work done along the positive yield lines ac and bd (from the previous example) = $\sum (mL\theta) = 8m$

Internal work done along the negative yield lines ab , bc , cd , and da

$$= \sum (mL\theta) = 4[mL(2/L)] = 8m$$

$$\text{Total internal work done} = 16m \quad (10.46b)$$

Equating Eqs (10.46a and b) and simplifying, we get

$$m = \frac{wL^2}{48} \quad (10.46c)$$

3. As a final example, let us consider an orthotropically reinforced simply supported rectangular slab, subjected to uniformly distributed load of w per square metre. The slab and yield-line pattern are shown in Fig. 10.39. Let us assume that the steel in the shorter Y direction provides a moment of resistance of m per unit length and the steel in the longer X direction provides a moment of resistance of μm per unit length. In the yield-line pattern shown, βL is the unknown dimension.

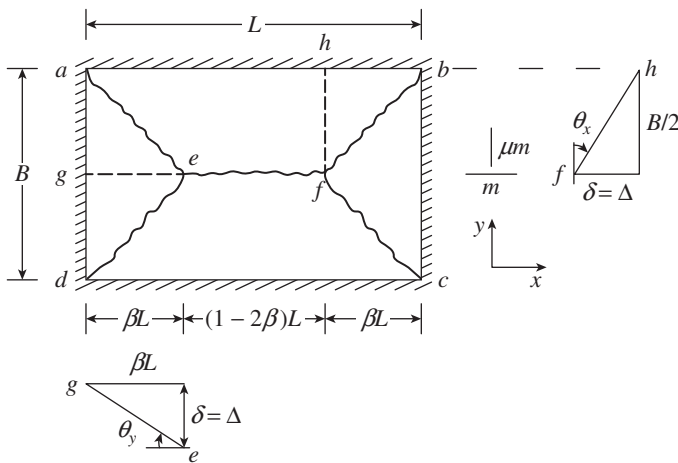


FIG. 10.39 Yield-line pattern in a rectangular simply supported slab

Let us first calculate the work done by the external loads. It is calculated by assuming that the points e and f deflect by Δ .

- (a) Triangles aed and bfc : Area = $0.5B\beta L$ and deflection of centroid = $\Delta/3$

Work done by external loads

$$W_1 = 2 \left[w \cdot 0.5B\beta L \frac{\Delta}{3} \right] = wBL\beta \frac{\Delta}{3}$$

- (b) Trapeziums $defc$ and $aefb$: Dividing the trapeziums into two triangles and a rectangle, we get the following:

Triangle: Area = $0.5B/2\beta L$, deflection at centroid = $\Delta/3$

Rectangle: Area = $B/2(L - 2\beta L)$, deflection at centroid = $\Delta/2$

Work done by external loads is

$$\begin{aligned} W_2 &= 2 \left[2 \left(w \cdot 0.5 \frac{B}{2} \beta L \frac{\Delta}{3} \right) + w \frac{B}{2} (L - 2\beta L) \frac{\Delta}{2} \right] \\ &= \frac{wLB}{6} (3 - 4\beta) \Delta \end{aligned}$$

$$\text{Total work done by the external loads, } W = W_1 + W_2 = w \frac{LB}{6} (3 - 2\beta) \Delta$$

Let us now calculate the internal work done by the yield lines.

- (a) Yield lines in triangles aed and bfc : The triangles rotate only about the y axis.

$$\theta_y = \frac{\Delta}{\beta L}; L_y = B; m_y = \mu m$$

Hence, internal work done on the yield lines in triangles aed and bfc is

$$\begin{aligned} WI_1 &= 2(L_x m_x \theta_x + L_y m_y \theta_y) \\ &= 2 \left(2\beta L m 0 + B \mu m \frac{\Delta}{\beta L} \right) = 2m \frac{B}{L} \frac{\mu}{\beta} \Delta \end{aligned}$$

- (b) Yield lines in trapeziums $aefb$ and $cfed$: The trapeziums rotate only about the x axis.

$$\theta_x = \frac{\Delta}{0.5B}; L_x = L; m_x = m$$

Hence, internal work done on the yield lines in trapeziums $aefb$ and $cfed$ is

$$WI_2 = 2 \left(2Lm \frac{\Delta}{0.5B} + B \mu m 0 \right) = 4m \frac{L}{B} \Delta$$

Total internal work done is

$$WI = WI_1 + WI_2 = \left(2m \frac{B}{L} \frac{\mu}{\beta} + 4m \frac{L}{B} \right) \Delta$$

Equating the work done by external loads to the internal work done at the yield lines, we get

$$\left(2m \frac{B}{L} \frac{\mu}{\beta} + 4m \frac{L}{B} \right) \Delta = w \frac{LB}{6} (3 - 2\beta) \Delta$$

Solving for m and denoting B/L as α , we get

$$m = \frac{wB^2}{12} \frac{(3\beta - 2\beta^2)}{(\mu\alpha^2 + 2\beta)} \quad (10.47a)$$

To get the maximum value of m , we should set $\frac{\partial m}{\partial \beta} = 0$. Thus, we get

$$(\mu\alpha^2 + 2\beta)(3 - 4\beta) - (3\beta - 2\beta^2)(2) = 0$$

Simplifying, we get

$$4\beta^2 + 4\beta\alpha^2\mu - 3\mu\alpha^2 = 0$$

By solving this quadratic equation in β , we get the value of β as

$$\beta = \frac{1}{2} \left[-\mu\alpha^2 + \sqrt{(\mu^2\alpha^4 + 3\mu\alpha^2)} \right] \quad (10.47b)$$

Substituting this value of β in Eq. (10.47a) and simplifying, we get

$$m = \frac{w\alpha^2 L^2}{24} \left[\sqrt{(3 + \mu\alpha^2)} - \alpha\sqrt{\mu} \right]^2 \tag{10.47c}$$

If $\mu = 1$ and $\alpha = 1$, we have an isotropically reinforced square slab. Thus, we get

$$m = \frac{wL^2}{24} (\sqrt{4} - 1)^2 = \frac{wL^2}{24} \tag{10.47d}$$

If $\mu = 1$, we get an isotropically reinforced rectangular slab. Thus, we get

$$m = \frac{w\alpha^2 L^2}{24} \left[\sqrt{(3 + \alpha^2)} - \alpha \right]^2 \tag{10.47e}$$

If $\mu = 1$, $\alpha = 0.5$ and $L = 2B$, where B is the length of the short span. Substituting these values, we get

$$\begin{aligned} m &= \frac{w(0.5)^2 L^2}{24} \left[\sqrt{(3 + 0.25)} - 0.5 \right]^2 = \frac{wL^2}{96} (1.6972) \\ &= 0.01768wL^2 \end{aligned} \tag{10.47f}$$

or $m = 0.01768w(2B)^2 = 0.0707wB^2$

This value can be compared with the code value of $0.107wB^2$ for such a rectangular slab.

10.8.6 Yield-line Analysis by Equilibrium Method

In the equilibrium method, the equilibrium of the individual segments of the slab formed by the yield lines under the action of the applied loads and moments acting on the edges of the segments is considered.

Let us consider two examples to show the calculations involved using the equilibrium method. First, consider an isotropically reinforced square slab subjected to uniformly distributed load. The yield-line pattern is as shown in Fig. 10.40(a).

Considering the equilibrium of the triangular element C , and taking moments about the edge ab , we get

$$mL = \left(\frac{L}{2}\right)\left(\frac{L}{2}\right)\left(\frac{L}{6}\right)w$$

Hence, $m = \frac{wL^2}{24}$.

For the isotropically reinforced hexagonal slab subjected to uniformly distributed loads and with simply supported boundary conditions, the yield-line pattern is shown in Fig. 10.40(b). Considering the equilibrium of the triangular element A , and taking moments about the edge, we get

$$mL = \left(\frac{L}{2}\right)\left(\frac{\sqrt{3}L}{2}\right)\frac{1}{3}\left(\frac{\sqrt{3}L}{2}\right)w$$

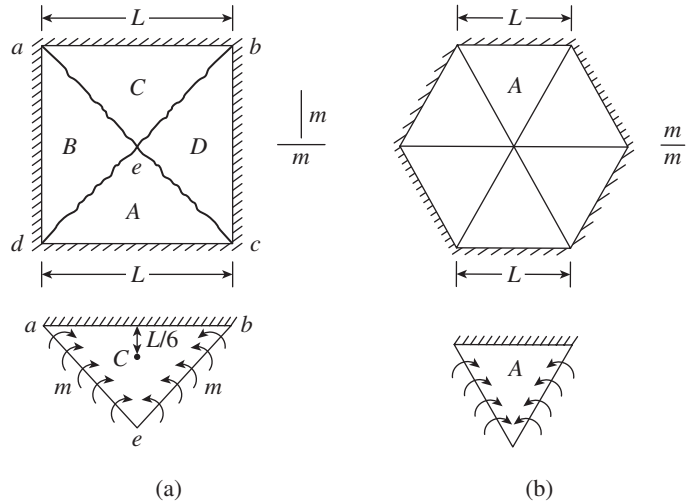


FIG. 10.40 Equilibrium of elements (a) Square slab (b) Hexagonal slab

Hence, $m = \frac{wL^2}{8}$.

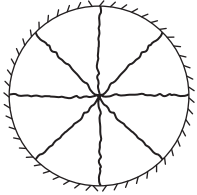
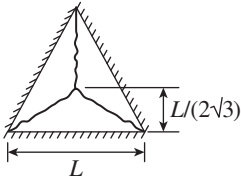
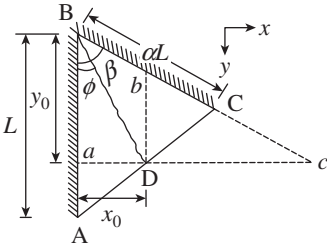
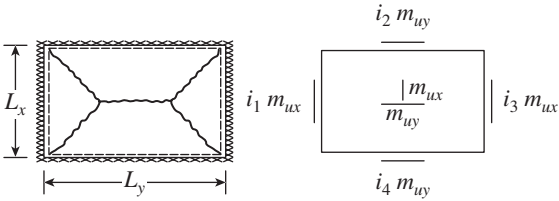
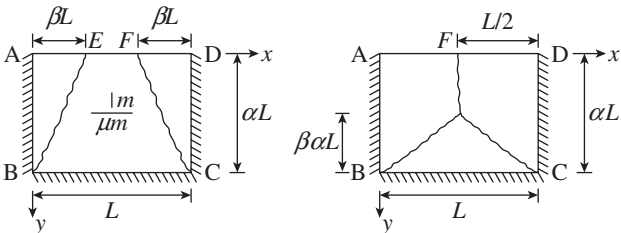
Table 10.6 shows some more results obtained by using the yield-line analysis for slabs with different shapes and boundary conditions. For more discussions on the use of the yield-line theory for the solution of slabs having other shapes and boundary conditions, slabs with openings, slabs with point loads, and formation of corner levers due to lifting of corners, the reader may refer to Purushothaman (1984), Jones and Wood (1967), Park and Gamble (2000), Kennedy and Goodchild (2003), Bhatt, et al. (2006), and Gambhir (2008).

10.8.7 Limitations of Yield-line Theory

The following are the limitations of the yield-line theory:

1. The analysis is based on the rotation capacity at the yield line, that is, lightly reinforced slabs.
2. The theory focuses on the moment capacity of the slab. It is assumed that an earlier failure would not occur due to shear, bond, or torsion and that cracking and deflections at service load will not be excessive.
3. As an upper-bound method, it will predict a collapse load that may be greater than the true collapse load; the *strip method of analysis*, which is not discussed in this book, may be considered superior in this respect. Details of the strip method of analysis may be found in Shukla (1973), Hillerborg (1996), and Park and Gamble (2000). Moreover, it should be noted that the strip method is a tool for design, whereas the yield-line theory provides the means for determining the capacity of a given slab with known reinforcement.
4. Neither the strip method nor the yield-line theory gives any information on stresses, deflections, or cracking at service load conditions.

TABLE 10.6 Yield-line analysis of slabs with different shapes and boundary conditions

S. No.	Slab Shape, Boundary Condition, and Yield-line Pattern	Formula
1.	 <p>Simply supported circular slab</p>	$m_u = \frac{w_u r^2}{6}$ <p>where r is the radius of the slab</p>
2.	 <p>Simply supported equilateral triangular slab</p>	$m_u = \frac{w_u L^2}{72}$
3.	 <p>General triangle with edges AB and BC simply supported and edge CA free</p>	$m_u = \frac{w_u \alpha L^2 \sin^2(\beta/2)}{6}$
4.	 <p>Yield-line pattern Moment capacities</p> <p>General orthotropic rectangular slab with fixed edges</p>	$m_{uy} = \frac{w_u L_{xr}^2}{24} \left[\sqrt{(3 + \alpha^2)} - \alpha \right]^2$ <p>where $\mu = m_{uy}/m_{ux}$, $X = \sqrt{1 + i_1} + \sqrt{1 + i_3}$, $Y = \sqrt{1 + i_2} + \sqrt{1 + i_4}$, $L_{xr} = \frac{2L_x}{Y}$, $L_{yr} = \frac{2L_y}{X\sqrt{\mu}}$, $\alpha = \frac{L_{xr}}{L_{yr}}$</p> <p>For simply supported edges, set the appropriate i value as zero.</p>
5.	 <p>Mode 1 Mode 2</p> <p>Rectangular slab with one of its longer sides free and the other three sides simply supported</p>	<p>Mode 1:</p> $m = \frac{w_u \alpha^2 L^2}{24 \mu} \left[\sqrt{\left(4 + \frac{9\mu}{\alpha^2}\right)} - 2 \right]$ <p>Mode 2:</p> $m = \frac{w_u L^2}{24} \left[\sqrt{\left(3 + \frac{\mu}{4\alpha^2}\right)} - \frac{\sqrt{\mu}}{2\alpha} \right]^2$ <p>For design, take the greater of the two values of m.</p>

10.9 SLOPED AND PYRAMIDAL ROOFS

Sloping roofs are generally provided for buildings in hilly areas of high altitude, so that snow will not get accumulated.

Such roofs are sometimes adopted for architectural reasons. The design of sloping-slab panels is to be done in the same way as level slab panels, by using a dead load equal to *dead load/cos θ*, where θ is the angle of the sloping slab with the

horizontal. The imposed load may be reduced if the angle is greater than 10° as per IS 875, Part 2. If the angle of slope is considerable, we need to design the supported edge beam for horizontal and vertical loads.

For covering large areas, pyramidal roofs on square or rectangular plans or even hexagonal or octagonal plans are adopted. A pyramidal roof on a square plan is shown in Fig. 10.41. It consists of four sloping triangular slab panels cast monolithic on beams supporting these sloping slab panels (the beams are not shown in the figure). The beams may be supported by walls or columns.

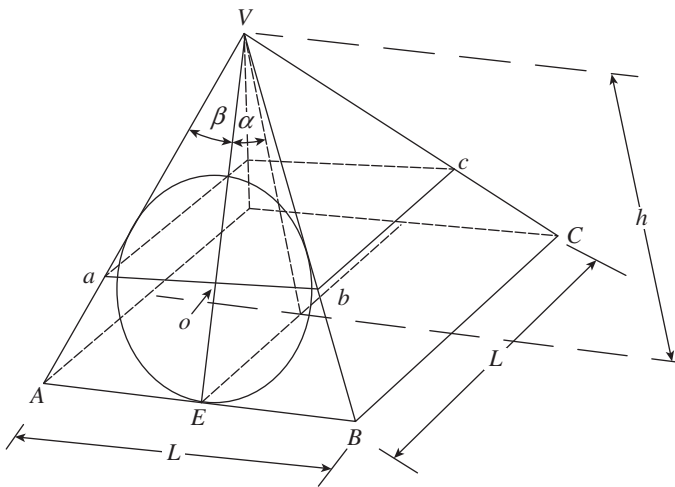


FIG. 10.41 Pyramidal roof on square plan

The triangular slab panels can be designed as a circular slab having a diameter of the inscribed circle as shown in Fig. 10.41. The diameter d may be found by using Eq. (10.34). The design of a circular slab may be done as described in Section 10.5.3. In sloping-slab panels, straight bars on the top and bottom are used both ways for ease of placing the bars. The beams supporting the triangular-slab panels are under bending and axial tension. When the span L is large, one may provide sloping beams along the sloping edges. More details of the analysis and design may be found in Terrington (1939) and Varyani (1999).

10.10 EARTHQUAKE CONSIDERATIONS

As discussed in Chapter 9, the floors or roofs of a structure tie the vertical structural elements (e.g., shear walls and frames) together to allow buildings to resist external loads such as gravity and lateral movements due to earthquakes or winds. When resisting the lateral loads, they act as a diaphragm, transferring the forces from the structure to the vertical

lateral load resisting elements (often referred to as VLLR elements), which in turn transfer the forces to the foundations.

No design provision is available in the Indian codes for the design of these diaphragms for horizontal loads. In the US code, a simplified analysis procedure is used in which the floor slab is assumed to act as the web of a continuous beam and the beams at the floor periphery are assumed to act as the compression and tension chords (flanges) of the (continuous) beam, as shown in Fig. 10.42(a).

Collector elements (also called drag struts or drag elements) are elements of floor or roof slabs that transmit lateral forces to the seismic force resisting system of the building (see Fig. 10.42b). Typically, collectors transfer earthquake forces in axial tension or compression. When a collector is a part of the gravity force resisting system, it is designed for seismic axial forces along with the bending moment and shear force from the applicable gravity loads acting simultaneously with the seismic forces. Based on a finite element parametric study, Thomas and Sengupta (2008) found that the chord forces increase with increasing spacing of frame or shear walls. They also developed a simplified method based on the analogy of beam-on-springs.

The chord reinforcements can be placed in the chord beam in addition to the reinforcement required for bending due to gravity loads. The bars will be in compression or tension. To prevent the buckling of bars in compression, they should be provided with closely spaced transverse ties. It is essential that splices of tensile reinforcement located in the chord and collector elements be fully developed and adequately confined (Clause 21.9.8.2 of ACI 318). When chord reinforcement is located within a wall, the joint between the diaphragm and the wall should be provided with adequate shear strength to transfer the shear forces.

The chord forces are calculated as (see Fig. 10.43)

$$P_u = M/z \tag{10.48}$$

where P is the compressive or tensile chord force, M is the in-plane bending moment in the slab, and z is the lever arm. The lever arm may be calculated based on two concepts (Thomas

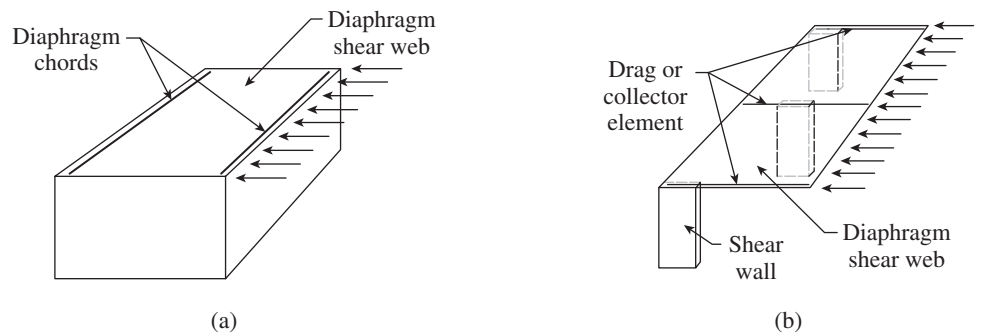


FIG. 10.42 Simple idealization of diaphragm chord and collector elements (a) Diaphragm chords resist tension or compression at edges of diaphragm (b) Drag or collector elements transfer forces from diaphragm to vertical elements

and Sengupta 2008). In the first method, the compressive stress in the slab is considered to locate the resultant of C . In this method, the lever arm is the distance between the resultant compression in the slab and the centroid of the chord beam under tension. In the second method, the compressive stress in the slab is neglected and the lever arm is the distance between the centroids of the two chord beams (see Fig. 10.43)

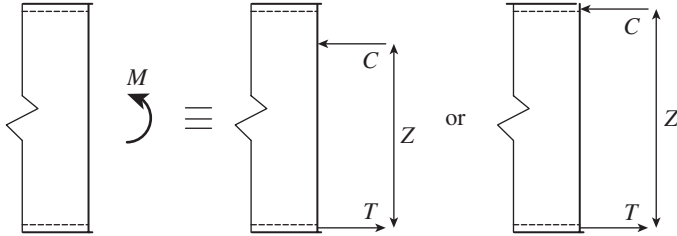


FIG. 10.43 Calculation of chord forces

The chord reinforcement, A_{st} , is calculated as

$$A_{st} = \frac{P_u}{0.87f_y} \quad (10.49)$$

Diaphragms are classified as rigid, flexible, and semi-rigid based on this relative rigidity. No diaphragm is perfectly rigid or perfectly flexible, and an exact analysis of structural systems containing *semi-rigid diaphragms* is complex. Another potential problem in diaphragms can be due to any abrupt and significant changes in wall stiffness below and above a diaphragm level. In buildings with significant plan irregularities, such as multi-wing plans and L-, H-, or V-shaped plans, particular attention should be paid to accurately assess the in-plane diaphragm stress at the joints of the wings and to design for them. Other classes of buildings deserving special attention to diaphragm design include those with relatively large and tall buildings resting on a significantly larger low-rise part, as shown in Fig. 9.16 of Chapter 9.

Various researchers have identified that the commonly employed *equivalent static analysis method* for the design of diaphragms underestimates the acceleration of floors, particularly in the lower levels of the buildings (Fleischman, et al. 2002; Rodriguez, et al. 2002; Gardiner, et al. 2008). More details about the analysis, design, and constructional aspects of diaphragms may be found in the ACI code (Section 21.11), Thomas and Sengupta (2008), and Moehle, et al. (2010). Sengupta and Shetty (2011) provide an analysis of the chord forces for slabs with large openings.

10.11 SIMPLIFIED DESIGN

The design of a slab is essentially an iterative process for the control of moment and deflection. Pandian (1989) derived simplified quadratic equations using which direct solutions can be obtained. The quadratic equation proposed by him is of the form

$$A(L/d)^2 + B(L/d) + C = 0 \quad (10.50)$$

where $A = a - w_1\alpha f^2$, $B = -(b + 31.25\alpha Lf)f$, $C = cf^2$, f is the factor for boundary conditions and equal to 1.3, 1, and 0.35 for continuous, simply supported, and cantilever slabs, respectively, and α is the bending moment coefficient from IS 456.

The solution to (L/d) is obtained as

$$(L/d) = \frac{-B - \sqrt{B^2 - 4AC}}{2A} \quad (10.51)$$

After getting this value, the value of p_t is obtained by solving another quadratic equation of the form

$$(L/d) = (A'p_t^2 + B'p_t + C')f \quad (10.52)$$

Pandian (1989) also tabulated the values of a , b , and c and A' , B' , and C' as given in Tables 10.7 and 10.8 respectively.

TABLE 10.7 Values of a , b , and c

f_{ck} N/mm ²	Values of a , b , and c	f_y N/mm ²		
		250	415	500
15	a	1.785	0.591	1.209
	b	174.020	86.227	124.847
	c	4712.786	2710.020	3116.768
20	a	2.153	0.764	1.545
	b	203.597	99.690	146.486
	c	5324.091	2973.250	146.486
25	a	2.408	0.867	1.746
	b	223.870	107.710	159.550
	c	5725.152	3129.060	3674.246

TABLE 10.8 Values of A' , B' , and C'

f_y N/mm ²	A'	B'	C'
250	16.400	-45.700	57.240
415	30.876	-59.770	45.670
500	38.886	-61.110	39.224

The design procedure consists of the following two steps: Determine L/d from Eq. (10.51), using the values of a , b , and c from Table 10.7 and calculating A , B , and C . After obtaining L/d , determine the value of p_t from Eq. (10.52) using the values of A' , B' , and C' from Table 10.8.

To illustrate the use of the procedure, take a continuous slab of span 6 m by 4 m, with total load w_1 of 5.25 kN/m², $f_{ck} = 20$, and Fe 415 steel; $\alpha = 0.053$ (Table 26 of IS 456) and $f = 1.3$. From Table 10.7, $a = 0.764$, $b = 99.69$, and $c = 2973.25$. Using these values, the values of A , B , and C are calculated as

$$A = a - w_1\alpha f^2 = 0.764 - 5.25 \times 0.053 \times 1.3^2 = 0.2938$$

$$B = -(b + 31.25\alpha Lf)f$$

$$= -(99.69 + 31.25 \times 0.053 \times 4 \times 1.3)1.3 = -140.79$$

$$C = cf^2 = 2973.25 \times 1.3^2 = 5024.8$$

From Eq. (10.51), we get $L/d = 38.84$.

It should be noted that this value of L/d satisfies both the moment and deflection criteria.

EXAMPLES

EXAMPLE 10.1 (Simply supported two-way slab):

The slab of a residential building of size 4.3 m × 6 m is simply supported on all the four sides on 230 mm walls. Assuming an imposed load of 2 kN/m² and load due to finishes of 1.0 kN/m², design the floor slab. Use M25 concrete and Fe 415 steel. Assume mild exposure.

SOLUTION:

Step 1 Calculate the thickness of the slab and effective spans.

$$L_x = 4.3 \text{ m}; L_y = 6 \text{ m}$$

Since the aspect ratio, that is, the ratio $L_y/L_x = 6/4.3 = 1.4 < 2$, we should design the slab as a two-way slab.

L/D ratio of simply supported slab (as per Clause 24.1 of IS 456) for Fe 415 steel

$$= 0.8 \times 30 = 24$$

(Note that this is valid only up to $L_x = 3.5$ m as per the code)

$$\text{Hence, } D = 4300/24 = 179 \text{ mm}$$

Provide $D = 175$ mm

Assuming 10 mm diameter bars are used, from Table 16 of IS 456, cover for mild exposure and M 25 concrete = 15 mm.

$$\text{Hence, } d_x = 175 - 15 - 5 = 155 \text{ mm and } d_y = 155 - 10 = 145 \text{ mm}$$

Effective span:

The effective span of the slab in each direction = Clear span + d (or width of support, whichever is smaller).

Thus, effective span

$$L_x = 4300 + 155 = 4455 \text{ mm}; L_y = 6000 + 145 = 6145 \text{ mm}$$

$$\text{Hence, } r = L_y/L_x = 6145/4455 = 1.38$$

Step 2 Calculate the loads on the slab.

$$\text{Self-weight of slab} = 0.175 \times 25 = 4.375 \text{ kN/m}^2$$

$$\text{Weight of finishes (given)} = 1.0 \text{ kN/m}^2$$

$$\text{Imposed load} = 2.0 \text{ kN/m}^2$$

$$\text{-----}$$

$$\text{Total load, } w = 7.375 \text{ kN/m}^2$$

$$\text{Factored load } w_u = 1.5 \times 7.375 = 11.06 \text{ kN/m}^2$$

Step 3 Design the moments (for strips at mid-span, with 1 m width in each direction).

For $L_y/L_x = 1.38$, from Table 10.2 (Table 27 of the code)

$$\alpha_x = 0.098$$

$$\alpha_y = 0.0515$$

$$\text{Hence, } M_x = \alpha_x w_u L_x^2 = 0.098 \times 11.06 \times 4.455^2 = 21.51 \text{ kNm/m}$$

$$M_y = \alpha_y w_u L_x^2 = 0.0515 \times 11.06 \times 4.455^2 = 11.30 \text{ kNm/m}$$

Check the depth for maximum bending moment.

$$M_{\text{max}} = 0.138 f_{ck} b d^2$$

$$d = \left(\frac{21.51 \times 10^6}{0.138 \times 25 \times 1000} \right)^{0.5} = 79 \text{ mm} < 155 \text{ mm}$$

Hence, the depth adopted is adequate and the slab is under-reinforced.

Step 4 Design the reinforcement.

$$\begin{aligned} \frac{x_u}{d} &= 1.2 - \sqrt{1.44 - \frac{6.68 M_u}{f_{ck} d b^2}} \\ &= 1.2 - \sqrt{1.44 - \frac{6.68 \times 21.51 \times 10^6}{25 \times 1000 \times 155^2}} = 0.105 \end{aligned}$$

$$z = d \left(1 - 0.416 \frac{x}{d} \right) = 155 (1 - 0.416 \times 0.105) = 148.23 \text{ mm}$$

$$A_{st} = \frac{M}{0.87 f_y z} = \frac{21.51 \times 10^6}{0.87 \times 415 \times 148.23} = 402 \text{ mm}^2$$

This result may also be got using Table 3 of SP 16.

$$\frac{M_u}{b d^2} = \frac{21.51 \times 10^6}{1000 \times 155^2} = 0.895$$

From Table 3 of SP 16, for M25 concrete, with $f_y = 415$ MPa,

$$p_t = 0.2595; A_{st} = \frac{0.2595 \times 1000 \times 153}{100} = 402 \text{ mm}^2$$

Note: We may also use the approximate formula.

$$A_{st} = \frac{M_u}{0.8 d f_y} = \frac{21.51 \times 10^6}{0.8 \times 155 \times 415} = 418 \text{ mm}^2 \approx 402 \text{ mm}^2$$

From Table 96 of SP 16, provide 10 mm diameter bars at 190 mm centre-to-centre distance (c/c) ($A_{st} = 413 \text{ mm}^2$); spacing $< 3d$. Hence, the crack width will be controlled.

Similarly, for the longer direction

$$\frac{M_u}{b d^2} = \frac{11.30 \times 10^6}{1000 \times 145^2} = 0.538$$

From Table 3 of SP 16, for M25 concrete, with $f_y = 415$ MPa,

$$p_t = 0.1526; A_{st} = \frac{0.1526 \times 1000 \times 145}{100} = 221 \text{ mm}^2$$

From Table 96 of SP 16, provide 8 mm diameter bars at 220 mm c/c ($A_{st} = 228 \text{ mm}^2$).

The reinforcement detailing for the slab is shown in Fig. 10.44 with alternate bars bent up at $0.1L_x$ and $0.1L_y$ in the shorter and longer directions, respectively. (It should be noted that at the support in the longer direction, the 8 mm bars are provided at 440 mm c/c; spacing $\approx 3 \times 145 = 435$ mm. Hence, it is adequate.)

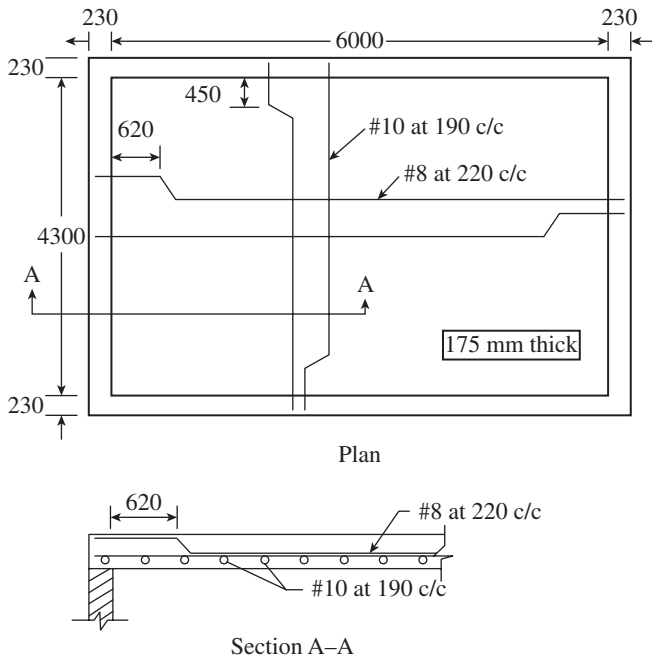


FIG. 10.44 Reinforcement detailing for slab of Example 10.1

Step 5 Check for deflection.

Let us check the deflection in the shorter direction, since it is critical.

$$p_t = \frac{100A_{st}}{bd} = \frac{100 \times 413}{1000 \times 155} = 0.266\%$$

$$f_s = 0.58 \times 415 \times \frac{402}{413} = 234 \text{ MPa}$$

Modification factor k_f from Fig. 4 of the code = 1.61

Basic span to depth ratio for simply supported slab = 20 (Clause 23.2.1)

$$\text{Allowable } L/d = 20 \times 1.61 = 32.2$$

$$\text{Provided span to depth ratio} = 4455/155 = 28.74 < 32.2$$

Hence, the assumed depth is enough to control deflection.

Note: As per this calculation, an effective depth of 140 mm is sufficient. We may redesign the slab with lesser depth slightly greater than 140 mm to achieve economy; this is left as an exercise to the reader. See also Example 10.3, where we have used a reduced depth.

Step 6 Check for shear.

Average effective depth $d = (155 + 145)/2 = 150 \text{ mm}$

The maximum shear force occurs at a distance of effective depth from the face of support.

$$V_u = w_u(0.5L_{xm} - d) = 11.06(0.5 \times 4.3 - 0.15) = 22.12 \text{ kN/m}$$

$$\tau_v = 22.12 \times 10^3 / (1000 \times 150) = 0.148 \text{ MPa}$$

For $p_t = 0.266$, τ_c for M25 concrete (Table 19 of IS 456) = 0.368 MPa

$$k\tau_c > 0.148 \text{ MPa}$$

Hence, the slab is safe in shear.

Note: It is clearly seen that the shear will not be critical in two-way slabs subjected to uniformly distributed loads.

Step 7 Check for cracking.

Steel more than 0.12 per cent in both directions,

Spacing of steel $< 3d = 3 \times 145 = 435 \text{ mm}$ or 300 mm in both directions.

Diameter of steel reinforcement $< 175/8 = 21 \text{ mm}$

Hence, no calculation is required for cracking.

Step 8 Check for development length.

As shown in Chapter 9, Example 9.1, as per Clause 26.2.3.3(d),

it should be checked whether $L_d \leq 1.3 \left(\frac{M_{nl}}{V_u} \right) + L_0$.

It is found that a 10 mm diameter bar is satisfactory.

Length of embedment available at the support

$$= 230 - \text{clear side cover} = 230 - 25$$

$$= 205 \text{ mm} > L_d/3$$

$$L_d = \frac{0.87 \times 415 \times 10}{4 \times (1.4 \times 1.6)} = 403 \text{ mm}; L_d/3 = 135 \text{ mm} < 205 \text{ mm}$$

Hence, the length provided is sufficient to develop the bond.

EXAMPLE 10.2 (Use of Marcus correction):

Compute the design moments for the slab analysed in Example 10.1 using the Marcus correction.

SOLUTION:

Step 1 Calculate the moments without Marcus correction.

From Example 10.1, for $L_y/L_x = 1.38$, from Table 10.2 (Table 27 of the code)

$$\alpha_x = 0.098$$

$$\alpha_y = 0.0515$$

Hence, $M_x = \alpha_x wL_x^2 = 0.098 \times 11.06 \times 4.455^2 = 21.51 \text{ kNm/m}$

$$M_y = \alpha_y wL_x^2 = 0.0515 \times 11.06 \times 4.455^2 = 11.30 \text{ kNm/m}$$

Step 2 Calculate the moments with Marcus correction.

$$\text{Marcus correction factor, } C_x = C_y = 1 - \frac{5}{6} \left(\frac{r^2}{1+r^4} \right) = 1 - \frac{5}{6} \left(\frac{1.38^2}{1+1.38^4} \right) = 1 - 0.343 = 0.657$$

Hence $M_x = 21.51 \times 0.657 = 14.13 \text{ kNm/m}$

$$M_y = 11.30 \times 0.657 = 7.42 \text{ kNm/m}$$

Thus, 34 per cent reduction in moments is possible by taking into account the torsional effects and corner restraint.

EXAMPLE 10.3:

Let us redesign the slab given in Example 10.1, assuming that the corners of the slab are prevented from lifting up by the wall loads due to the floor above.

SOLUTION:

Step 1 Calculate the thickness of the slab and effective spans.

Assume $D = 170 \text{ mm}$ (as a smaller depth was required in Step 5 of Example 10.1).

Assuming 10 mm diameter bars,

$$d_x = 170 - 20 - 5 = 145 \text{ mm and } d_y = 145 - 10 = 135 \text{ mm}$$

$$L_x = 4300 + 145 = 4445 \text{ mm and } L_y = 6000 + 135 = 6135 \text{ mm}$$

Step 2 Calculate the loads on the slab.

Self-weight of slab now is $0.17 \times 25 = 4.25 \text{ kN/m}^2$

Hence total load, $w = 7.25 \text{ kN/m}^2$

Factored load, $w_u = 1.5 \times 7.25 = 10.875 \text{ kN/m}^2$

Step 3 Design the moments (considering 1 m width in each direction at mid-span). As the ends of the slabs are restrained,

$M_{ux} = \alpha_x w_u L_x^2$ where α_x may be taken as per Table 26 of the code (Case 9)

$$L_y/L_x = \frac{6135}{4445} = 1.38$$

$$\text{Hence, } \alpha_x = 0.079 + (0.085 - 0.0079) \left(\frac{1.38 - 1.3}{1.4 - 1.3} \right) = 0.084$$

$$\text{Hence, } M_{ux} = 0.084 \times 10.875 \times 4.445^2 = 18.05 \text{ kNm/m}$$

It should be noted that due to the restraints the bending moment has reduced from 21.51 kNm/m to 18.05 kNm/m (as obtained in Example 10.1), that is, a reduction of 16 per cent.

From Table 26, Case 9, we get, $\alpha_y = 0.056$. Hence

$$M_{vy} = \alpha_y w_u L_x^2 = 0.056 \times 10.875 \times 4445^2 = 12.03 \text{ kNm/m}$$

(This value is slightly higher than the non-constraint value of 11.30 kNm/m obtained in Example 10.1.)

Step 4 Design the reinforcements.

For short span,

$$\frac{M_u}{bd^2} = \frac{18.05 \times 10^6}{1000 \times 145^2} = 0.859$$

From Table 3 of SP 16, for M25 concrete, with $f_y = 415 \text{ MPa}$,

$$p_t = 0.2487; A_{st} = \frac{0.2487 \times 1000 \times 145}{100} = 361 \text{ mm}^2$$

From Table 96 of SP 16, provide 10 mm diameter bars at 215 mm c/c ($A_{st} = 366 \text{ mm}^2, p_t = 0.252\%$).

Maximum permitted spacing = $3 \times 145 = 435 \text{ mm}$ or $300 \text{ mm} > 215 \text{ mm}$

For long span,

$$\frac{M_u}{bd^2} = \frac{12.03 \times 10^6}{1000 \times 135^2} = 0.66$$

Hence, from Table 3 of SP 16,

$$p_t = 0.189;$$

$$A_{st} = \frac{0.189 \times 1000 \times 135}{100} = 255 \text{ mm}^2$$

From Table 96 of SP 16, provide 8 mm diameter bars at 190 mm c/c ($A_{st} = 265 \text{ mm}^2$).

Maximum permitted spacing = $3 \times 135 = 405 \text{ mm}$ or $300 \text{ mm} > 190 \text{ mm}$

Step 5 Calculate the corner reinforcement. As the slab is torsionally restrained, corner reinforcement as per Clause D-1.8 should be provided for a distance of $L_x/5 = 4445/5 \approx 890 \text{ mm}$ in both directions in meshes at top and bottom (four layers).

Area of torsion reinforcement = 0.75 of area required for the maximum mid-span moment
 $= 0.75 \times 361 = 271 \text{ mm}^2$

Provide 8 mm diameter bars at 180 mm c/c ($A_{st} = 279 \text{ mm}^2$) both ways at top and bottom at each corner over an area of $890 \text{ mm} \times 890 \text{ mm}$, that is, five U-shaped bars (see Fig. 10.45 for reinforcement detailing).

Step 6 Check for deflection control.

$$p_t = 0.252\%$$

$$f_s \approx 0.58 \times 415 = 240.7 \text{ MPa}$$

Modification factor (from Fig. 4 of the code), $k_t = 1.6$

$$(L/d)_{\max} = 1.6 \times 20 = 32$$

$$(L/d)_{\text{provided}} = 4445/145 = 30.7 < 32$$

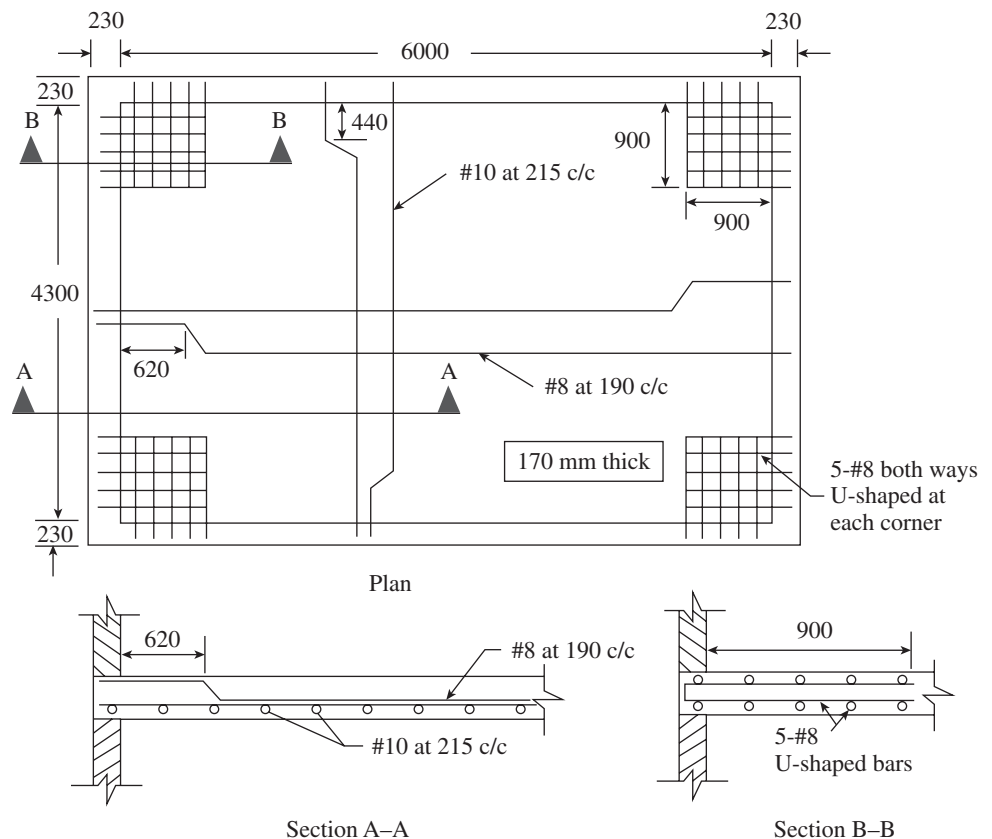


FIG. 10.45 Reinforcement detailing for slab of Example 10.3

Hence, the assumed depth is enough to control deflection. Check for shear will not be critical as shown in Example 10.1.

Step 7 Check for cracking.

Steel more than 0.12 per cent in both directions, spacing of steel $< 3d$ or 300 mm in both directions, and diameter of steel bar $< 170/8 = 21.25$ mm.

Hence, cracking will be within acceptable limits.

EXAMPLE 10.4:

Find the bending moment coefficients α_x and α_y for a slab having all edges continuous, that is, Case 1 in Table 10.4, with $r = 1.75$, using Eqs (10.17)–(10.19).

SOLUTION:

For this case, the number of discontinuous edges, $N_d = 0$. Hence, from Eq. (10.17), we get

$$\alpha_y^+ = \frac{(24 + 2N_d + 1.5N_d^2)}{1000} = \frac{24 + 0 + 0}{1000} = 0.024$$

$$C_{s1} + C_{s2} = C_{l1} + C_{l2} = \sqrt{7/3} + \sqrt{7/3} = 3.055$$

From Eq. (10.18), we get

$$\alpha_x^+ = \frac{2}{9} \left[\frac{3 - (\sqrt{18\alpha_y^+}/r)(C_{s1} + C_{s2})}{(C_{l1} + C_{l2})^2} \right]$$

$$= \frac{2}{9} \left[\frac{3 - (\sqrt{18 \times 0.024}/1.75)(3.055)}{(3.055)^2} \right] = 0.0441$$

Thus, we have the following values of moment coefficients for this slab:

In the shorter direction:

Positive at mid-span = 0.0441(0.045)

Negative at edges = $(4/3)0.0441 = 0.0588(0.060)$

In the longer direction:

Positive at mid-span = 0.024(0.024)

Negative at edges = $(4/3)0.024 = 0.032(0.032)$

Note: The values given in brackets are those obtained from Table 26 of the code.

EXAMPLE 10.5 (Design of two-way slabs with two adjustment edges continuous):

Design a rectangular slab panel of size 4 m by 5.5 m, which is continuous over two adjacent edges and simply supported on the other two edges. Assume that the slab supports an imposed load of 3 kN/m² and a floor finish of 1 kN/m². The slab is subjected to moderate exposure and is made of M20 concrete and Fe 415 steel.

SOLUTION:

Step 1 Calculate the thickness of the slab and effective span. As the slab is subjected to moderate exposure, from

Table 16 of the code, for M20, nominal cover = 30 mm. As the shorter span is 4 m, we shall use the Canadian code formula to estimate the minimum thickness of the slab. Assuming $\alpha_m = 2.0$ and $\beta = L_y/L_x = 5.5/4 = 1.375$,

$$D = \frac{L_n(0.6 + f_y/1000)}{30 + 4\beta\alpha_m} = \frac{5000(0.6 + 415/1000)}{30 + 4 \times 1.375 \times 2} = 124 \text{ mm}$$

$$\text{Moreover, } D \geq \frac{\text{Perimeter}}{140} = \frac{2 \times (4000 + 5500)}{140} = 135 \text{ mm}$$

Let us adopt $D = 130$ mm.

Using 10 mm bars, $d_x = 135 - 30 - 5 = 100$ mm and $d_y = 100 - 10 = 90$ mm

As the size of the supporting beams is not given, assume effective spans as 4 m and 5.5 m.

Step 2 Calculate the load on the slab.

Self-weight of slab = $0.135 \times 25 = 3.375$ kN/m²

Weight of finishes = 1 kN/m²

Imposed load = 3 kN/m²

Total load = 7.375 kN/m²

Factored load $w_u = 7.375 \times 1.5 = 11.06$ kN/m²

Step 3 Design the moments (for strips of 1 m width at each direction).

For $L_y/L_x = 1.375$, from Table 26 of the code, row 4, α_x values for negative moments at continuous edge at short and long spans are 0.0695 and 0.047, respectively. Similar positive moment coefficients at mid-span are 0.052 and 0.035, respectively, for short and long spans.

Factored negative bending moments in the short and long spans are

$$M_{nx} = 0.0695 \times w_u L_x^2 = 0.0695 \times 11.06 \times 4^2 = 12.3 \text{ kNm/m}$$

$$M_{ny} = 0.047 \times w_u L_x^2 = 0.047 \times 11.06 \times 4^2 = 8.32 \text{ kNm/m}$$

Required effective depth for resisting the bending moment

$$d = \left(\frac{M_u}{0.138 f_{ck} b} \right)^{0.5} = \left(\frac{12.3 \times 10^6}{0.138 \times 20 \times 1000} \right)^{0.5} = 67 \text{ mm} < 135 \text{ mm}$$

Hence, the adopted depth is sufficient and the slab is under-reinforced.

Step 4 Design the negative reinforcement.

$$\text{Approximate } A_{st} = \frac{M}{0.8df_y} = \frac{12.3 \times 10^6}{0.8 \times 100 \times 415} = 370 \text{ mm}^2/\text{m}$$

Alternatively, let us use Table 2 of SP 16.

$$\frac{M_u}{bd^2} = \frac{12.3 \times 10^6}{1000 \times 100^2} = 1.23$$

For $f_{ck} = 20$ N/mm² and $f_y = 415$ N/mm², we get

$$p_t = 0.3692\% \text{ and } A_{sx2} = \frac{0.3692 \times 1000 \times 100}{100} = 369.2 \text{ mm}^2/\text{m}$$

Note that the approximate value A_{st} matches the exact value in this case.

From Table 96 of SP 16, provide 10 mm diameter bars at 210 mm c/c ($A_{st} = 374 \text{ mm}^2$) in the short span direction at the top face at support; spacing $< 3d = 300 \text{ mm}$. Hence, it is adequate.

Reinforcement in the longer direction:

$$\text{Approximate } A_{st} = \frac{M}{0.8df_y} = \frac{8.32 \times 10^6}{0.8 \times 90 \times 415} = 278 \text{ mm}^2/\text{m}$$

Alternatively,

$$\frac{Mu}{bd^2} = \frac{8.32 \times 10^6}{1000 \times 90^2} = 1.027$$

From Table 2 of SP 16, for $f_y = 415 \text{ N/mm}^2$, we get $p_t = 0.3036\%$ and $A_{s_{y2}} = \frac{0.3036 \times 1000 \times 90}{100} = 273 \text{ mm}^2/\text{m} \approx 278 \text{ mm}^2/\text{m}$

From Table 96 of SP 16, provide 8 mm diameter bars at 180 mm c/c ($A_{st} = 279 \text{ mm}^2$).

Spacing $< 3d = 270 \text{ mm}$

Step 5 Design the positive reinforcement. The area of reinforcement required for the positive moment in the shorter direction can be computed proportionately, based on the bending moment coefficient, as the effective depth is the same.

$$A_{s_{x1}} = (0.052)369.2/0.0695 = 276 \text{ mm}^2/\text{m}$$

Provide 8 mm diameter bars at 180 mm c/c ($A_{st} = 279 \text{ mm}^2$).

Similarly, required area of steel for positive moment in the longer direction

$$A_{s_{y1}} = 0.035 \times 273/0.047 = 203 \text{ mm}^2/\text{m}$$

From Table 96 of SP16, provide 8 mm at 240 mm c/c ($A_{st} = 209 \text{ mm}^2/\text{m}$).

$$A_{s_{t,min}} = 0.12 \times 135 \times 1000/100 = 162 \text{ mm}^2/\text{m} \text{ (#8 at 270 mm c/c} \\ = 186 \text{ mm}^2/\text{m)}$$

Maximum spacing $= 3 \times 90 = 270 \text{ mm}$, which is greater than the adopted spacing.

Step 6 Detail the reinforcement. The detailing of reinforcement using straight bars is shown in Fig. 10.46. Alternate bars from positive bending moment may also be bent up to provide for negative steel; in such a case some additional bars have to be provided. For example, in the shorter direction, if alternate bars are bent up at support, we will have 8 mm bars at 360 mm centres, and hence area provided at support by these bars $= 140 \text{ mm}^2$. However, we need 370 mm^2 ; hence, additional bars of area $370 - 140 = 230 \text{ mm}^2$

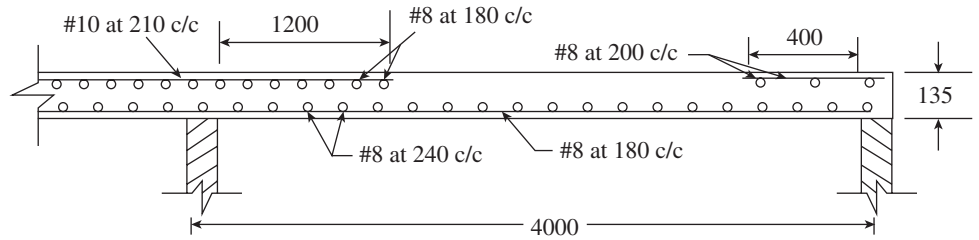


FIG. 10.46 Reinforcement detailing of Example 10.5

have to be provided. Hence, we need to provide additional #10 at 340 c/c (Area $= 231 \text{ mm}^2$). Since such an arrangement may be confusing at site, straight bars may be specified.

Step 7 Check for shear. From Table 10.5, shear force coefficient for $L_y/L_x = 1.375$ for two adjacent sides continuous case is $\beta_{vx} = 0.515$.

$$\text{Shear force} = 0.515w_uL_x = 0.515 \times 11.06 \times 4 = 22.78 \text{ kN}$$

The maximum shear force occurs at a distance d from the face of support.

$$V = 22.78 - dw_x = 22.78 - 0.1 \times 11.06 = 21.67 \text{ kN}$$

$$\text{Nominal shear stress, } \tau_c = \frac{V}{bd} = \frac{21.67 \times 1000}{1000 \times 100} = 0.217 \text{ N/mm}^2$$

This stress is less than the minimum value in Table 19 of IS 456 (0.28 MPa). Hence, the slab is safe in shear.

Step 8 Check for deflection control.

$$p_t = 0.37\%$$

$$f_s = 0.58 \times 415 = 240.7 \text{ MPa}$$

From Fig. 4 of the code, modification factor for $p_t = 1.38$ is $k_t = 1.38$.

$$\text{Basic } L/d = 28, \text{ maximum } L/d = 28 \times 1.38 = 38.6$$

$$(L/d) \text{ provided} = 4000/136 = 29.6 < 38.6$$

Hence, no additional calculation for deflection is necessary.

Step 9 Check for cracking. The spacing of reinforcement is less than $3d$ or 300 mm, steel more than 0.12 per cent in both directions has been provided and the diameter of the bar is less than $135/8 = 16.8 \text{ mm}$. Hence, additional calculation for cracking is not required.

EXAMPLE 10.6 (Continuous two-way slab):

Design a continuous two-way slab system for the layout shown in Fig. 10.47. It is subjected to an imposed load of 2 kN/m^2 and surface finish of 1 kN/m^2 . Consider M20 concrete, grade Fe 415 steel, and mild environment. Assume that the supporting beams are $230 \text{ mm} \times 500 \text{ mm}$.

SOLUTION:

Because of the symmetry, only one quadrant of the floor system has to be designed, that is, slabs S_1 to S_4 .

Step 1 Calculate the thickness of slabs. Let us assume uniform thickness for all slabs; it will be governed by the corner slab S_1 with two adjacent edges discontinuous.

The distribution factors, distributed moments, and final moments after distribution are shown in Fig. 10.49.

Step 4 Design the reinforcement. The bending moment and corresponding area of required reinforcements are given in Table 10.9:

Area of steel in edge strips = 0.12% of gross sectional area

$$= \frac{0.12}{100} \times 150 \times 1000 = 180 \text{ mm}^2/\text{m}$$

(say #8 at 250mm c/c, $A_{st} = 201 \text{ mm}^2/\text{m}$)

We will now calculate torsion reinforcement in the following scenarios:

1. Torsion reinforcement when both edges are discontinuous

$$= \frac{3}{4} \times \text{mid-span reinforcement}$$

$$= \frac{3}{4} \times 213 = 160 \text{ mm}^2$$

Provide #8 at 300 c/c ($A_{st} = 168 \text{ mm}^2$).

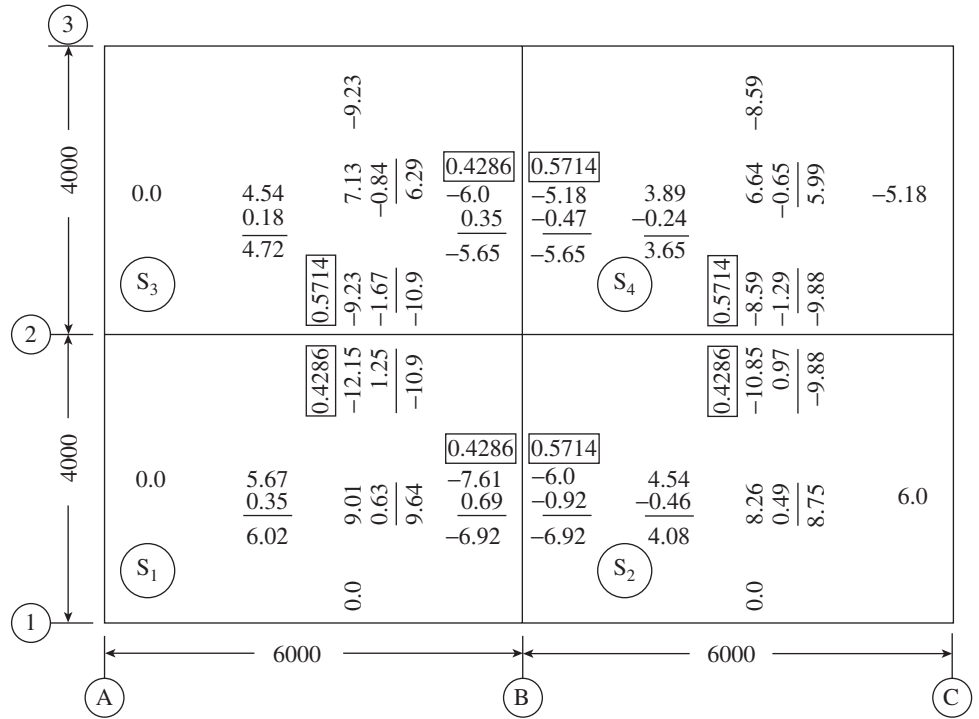


FIG. 10.49 Distribution of moments in slab panels

TABLE 10.9 Bending moment and area of reinforcement for the slabs in Fig 10.49

	Bending Moment kNm	M_u/bd^2	p_r Percentage Table 2 of SP 16 with Min. 0.12%	A_s mm ²	Reinforcement
Slab S ₁ $d_x = 130$ mm $d_y = 120$ mm	(a) Shorter direction				
	+9.64	0.570	0.1636	213	#8 at 230 (218 mm ²)
	-10.90	0.645	0.1855	241	#8 at 200 (251 mm ²)
	(b) Longer direction				
	+6.02	0.418	0.12	144	#8 at 300 (168 mm ²)
	-6.92	0.481	0.1373	165	#8 at 300 (168 mm ²)
Slab S ₂	(a) Shorter direction				
	+8.75	0.518	0.1484	193	#8 at 250 (201 mm ²)
	-9.88	0.585	0.1678	218	#8 at 230 (218 mm ²)
	(b) Longer direction				
	-6.92	0.481	0.1373	165	#8 at 300 (168 mm ²)
	+4.08	0.283	0.12	144	#8 at 300 (168 mm ²)
Slab S ₃	(a) Shorter direction				
	-10.90	0.645	0.1855	241	#8 at 200 (251 mm ²)
	+6.29	0.372	0.12	156	#8 at 300 (168 mm ²)
	(b) Longer direction				
	+4.72	0.328	0.12	144	#8 at 300 (168 mm ²)
	-5.64	0.395	0.12	144	#8 at 300 (168 mm ²)
Slab S ₄	(a) Shorter direction				
	-4.88	0.585	0.1678	218	#8 at 230 (218 mm ²)
	+5.99	0.354	0.12	156	#8 at 300 (168 mm ²)
	(b) Longer direction				
	-5.65	0.392	0.12	144	#8 at 300 (168 mm ²)
	+3.63	0.253	0.12	144	#8 at 300 (168 mm ²)

2. Torsion reinforcement when only one edge is discontinuous
 = $3/8 \times$ mid-span reinforcement
 = $3/8 \times 215 = 80 \text{ mm}^2$
 Provide #8 at 300 c/c.
 This reinforcement should be provided for a length of $L_x/5 = 4000/5 = 800 \text{ mm}$.

Step 5 Check for shear. From Table 10.4, shear force coefficient for $L_y/L_x = 6/4 = 1.5$ for two adjacent sides continuous is $\beta_{vx} = 0.54$.

$$V_{sx} = \beta_{vx} w_u L_x = 0.54 \times 10.125 \times 4 = 21.87 \text{ kN}$$

Maximum shear force at a distance 135 mm (d) from the face of support

$$V = 21.87 - 0.135 \times 10.125 = 20.5 \text{ kN}$$

$$\text{Nominal shear stress, } \tau_v = \frac{V}{bd} = \frac{20.5 \times 1000}{1000 \times 135} = 0.15 \text{ N/mm}^2$$

This stress is less than the minimum value in Table 19 of IS 456 for M20 concrete. Hence, the slab is safe in shear.

Step 6 Check for deflection.

$$p_t \text{ at mid-span} = \frac{218 \times 100}{1000 \times 130} = 0.167\%$$

$$f_s = 240.7 \text{ MPa}$$

Modification factor (from Fig. 4 of IS 456) = 2.0

$$\text{Maximum } L/d = 28 \times 2 = 56$$

$$L/d \text{ provided} = 4000/130 = 30.8 < 56$$

Hence, the deflection will be within limits.

Step 7 Check for cracking. The spacing of reinforcement is less than $3d$ ($3 \times 130 = 390 \text{ mm}$) or 300 mm and the steel provided is more than 0.12 per cent of gross cross section in both directions. Diameter of bars $< 150/8 = 18.75 \text{ mm}$. Hence, no separate check for cracking is required.

Step 8 Detail the reinforcement. The detailing of reinforcement in various middle stirrups and edge strips should be done as per Figs 10.21 and 10.23. It should be noted that for practical convenience only two bar spacing may be adopted.

EXAMPLE 10.7:

Design a circular slab of diameter 7 m subjected to an imposed load of 4 kN/m^2 . Assume that the slab is simply supported and is in mild environment. Use $f_{ck} = 20 \text{ MPa}$ and $f_y = 415 \text{ N/mm}^2$.

SOLUTION:

Step 1 Compute the loads. The usual span to depth ratio will be in the range 25–40.

Let us adopt $L/d = 32.5$.

$$\text{Thickness of slab, } t = 7000/32.5 = 215.38 \text{ mm}$$

Adopt 220 mm thickness.

Self-weight	= $0.22 \times 25 = 5.5 \text{ kN/m}^2$
Floor finish (assumed)	= 1.0 kN/m^2
Imposed load	= 4.0 kN/m^2
Total load	= 10.5 kN/m^2
Factored load	= $1.5 \times 10.5 = 15.75 \text{ kN/m}^2$

Step 2 Calculate the bending moment. Assuming $\nu = 0$, as per Eq. (10.27)

$$M_r = \frac{3w}{16}(r^2 - a^2)$$

$$M_t = \frac{w}{16}(3r^2 - a^2)$$

Bending moment at edge ($a = r$)

$$M_r = 0 \text{ and } M_t = 2/16wr^2$$

Bending moment at centre ($a = 0$)

$$M_r = \frac{3}{16}wr^2 \text{ and } M_t = \frac{3}{16}wr^2$$

Hence, maximum moment at centre = $\frac{3}{16} \times 15.75 \times 3.5^2 = 36.18 \text{ kNm/m}$

Note: According to the yield-line theory,

$$\text{Ultimate moment} = \frac{w_u r^2}{6} = \frac{15.75 \times 3.5^2}{6} = 32.15 \text{ kNm/m}$$

Hence, we will achieve economy by using yield-line theory.

Step 3 Check depth of slab. For $f_y = 415 \text{ N/mm}^2$

$$\text{Required depth } d = \sqrt{\frac{M_u}{kbf_{ck}}} = \left(\frac{36.18 \times 10^6}{0.138 \times 1000 \times 20} \right)^{0.5} = 115 \text{ mm}$$

Select an overall depth of 200 mm. The slab is under-reinforced. Assume a cover of 20 mm and the diameter of bar as 12 mm.

Provided effective depth in one direction = $200 - 20 - 6 = 174 \text{ mm}$

Effective depth in the other direction = $174 - 12 = 162 \text{ mm}$

Step 4 Calculate the area of reinforcement. The bending moment in the circumferential direction is the same as that of the radial direction.

The area of reinforcement is

$$A_{st} = \frac{M_u}{0.8df_y} = \frac{36.18 \times 10^6}{0.8 \times 162 \times 415} = 673 \text{ mm}^2/\text{m}$$

The same result may be obtained by calculating $M_u/(bd^2)$ and using Table 2 of SP16. From Table 96 of SP 16, provide 12 mm diameter bars at 160 mm c/c (area = 707 mm^2) in both the directions.

Maximum allowed spacing is the lesser of 486 mm ($3d$) or 300 mm. Hence, the spacing is within limits to control cracking. The overall diameter of the slab is chosen as 7.2 m and the reinforcement details are similar to that shown in Fig. 10.24(c).

Step 5 Check for shear. The critical section for shear is at a distance d from the support. The shear force at critical section is

$$V_u = w \left(\frac{R}{2} - d \right) = 15.75 \left(\frac{3.5}{2} - 0.162 \right) = 25.0 \text{ kN}$$

The actual width of the slab at a distance d from the support is slightly less than a unit width at the support because of the radial coordinates. However, let us check the shear stress using unit width as an approximation.

Thus, nominal shear stress of $\tau_v = \frac{V_u}{bd} = \frac{25.01 \times 10^3}{1000 \times 162} = 0.154 \text{ N/mm}^2$

This is less than τ_c (min.) as per Table 19 of IS 456. Hence, the slab is safe in shear.

EXAMPLE 10.8 (Design of circular well cap):

Design a well cap to support a circular pier of diameter 2 m. Assume that the internal diameter of the well is 9 m and that the load on the pier is 900 kN (see Fig. 10.50). Use Fe 415 steel and M35 concrete.

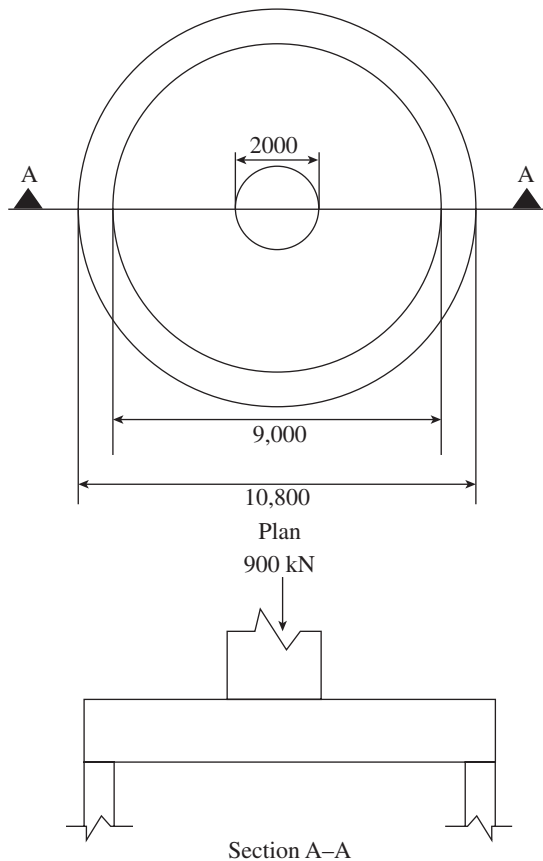


FIG. 10.50 Well cap

SOLUTION:

Step 1 Calculate the loads. As the well cap will be subjected to alternate wetting and drying, we assume that it is subjected to severe exposure; hence, minimum cover as per Tables 2 and 16 of IS 456 is 45 mm. As we are using M35 concrete, it

may be reduced by 5 mm. Hence, use cover = 40 mm. Assume $L/d = 20$; hence $d = 9000/20 = 450 \text{ mm}$. Assume $d = 440 \text{ mm}$, with 20 mm bars; total depth $D = 440 + 10 + 50 = 500 \text{ mm}$ and effective radius of slab, $R = 9/2 + 0.45 = 4.95 \text{ m}$.

Let the overall outside diameter = $2(4.95 + 0.45) = 10.8 \text{ m}$

Factored self-weight $w_c = 1.5 \times 0.5 \times 25 = 18.75 \text{ kN/m}^2$

Factored imposed load $w_l = 1.5 \times 900 = 1350 \text{ kN}$

Step 2 Calculate the bending moment. The maximum radial bending moment for this case at the face of the concentrated central load as per Timoshenko and Krieger (1959) (p. 67) is calculated here:

Diameter of pier = 2 m; hence, $a = 1 \text{ m}$

$$M_r = \frac{3w_c R^2}{16} + \frac{W_l}{4\pi} \left[\text{Log}_n \left(\frac{R}{a} \right) - \frac{1}{4} \left(1 - \frac{a^2}{R^2} \right) \right]$$

$$= \frac{3 \times 18.75 \times 4.95^2}{16} + \frac{1350}{4\pi} \left[\text{Log}_n \left(\frac{4.95}{1} \right) - \frac{1}{4} \left(1 - \frac{1}{4.95^2} \right) \right]$$

$$= 86.14 + 107.5(1.6 - 0.24) = 86.14 + 146.2 = 232.34 \text{ kNm/m}$$

The maximum circumferential bending moment at the edge of the pier support, that is, 1000 mm from the centre is given by

$$M_t = \frac{3w_c R^2}{16} + \frac{W_l}{4\pi} \left[\text{Log}_n \left(\frac{R}{a} \right) + \frac{1}{4} \left(3 - \frac{a^2}{R^2} \right) \right]$$

$$= 86.14 + \frac{1350}{4\pi} \left[\text{Log}_n \left(\frac{4.95}{1} \right) + 0.25 \left(3 - \frac{1}{4.95^2} \right) \right]$$

$$= 86.14 + 107.5(1.6 + 0.74) = 337.7 \text{ kNm/m} > M_r$$

Step 3 Check the depth for bending.

Required depth for a balanced section

$$d = \left(\frac{M}{0.138bf_{ck}} \right)^{0.5} = \left(\frac{337.37 \times 106}{0.138 \times 1000 \times 35} \right)^{0.5} = 264 \text{ mm}$$

However, provide an overall depth of 600 mm in order to resist the shear due to the pier. Using 20 mm bars, $d = 600 - 40 - 10 = 550 \text{ mm}$

Step 4 Calculate the reinforcement.

Area of reinforcement

$$A_{st} = \frac{337.37 \times 10^6}{0.8 \times 550 \times 415} = 1848 \text{ mm}^2/\text{m}$$

Provide 20 mm bars at 165 mm c/c spacing ($A_{st,provided} = 1905 \text{ mm}^2$) in the circumferential direction. The effective depth of reinforcement in the radial direction = $550 - 10 - 10 = 530 \text{ mm}$.

$$\text{Required } A_{st} = \frac{232.34 \times 10^6}{0.8 \times 530 \times 415} = 1320 \text{ mm}^2/\text{m}$$

Provide 20 mm diameter bars at 230 mm c/c ($A_{st,provided} = 1366 \text{ mm}^2$) at 1000 mm from the centre.

Minimum reinforcement =

$$\frac{0.12}{100} \times 600 \times 1000 = 720 \text{ mm}^2 < 1366 \text{ mm}^2$$

Maximum spacing = $3d > 230 \text{ mm}$

The reinforcement should be provided as shown in Fig. 10.24(b).

Note: As the depth of the slab is greater than 200 mm, provide minimum steel, that is, 16 mm at 270 mm also at the top of the slab as temperature and shrinkage steel.

Step 5 Check for shear.

$$\text{Shear force} = \frac{p}{2\pi a} = \frac{900}{2 \times \pi \times 1.0} = 143 \text{ kN/m}$$

$$\text{Nominal shear stress} = \frac{143 \times 10^3}{(1000 \times 550)} = 0.26 \text{ N/mm}^2$$

Design shear strength τ_c for M35 with minimum steel from Table 19 of IS 456

$$= 0.29 \text{ N/mm}^2 > 0.265 \text{ N/mm}^2$$

Hence, the slab is safe for shear.

EXAMPLE 10.9:

A simply supported semicircular slab of 2.8 m radius is subjected to a uniformly distributed imposed load of 4 kN/m^2 and floor finish of 1 kN/m^2 . Assuming moderate environment, design the slab with Fe 415 steel and M25 concrete.

SOLUTION:

Step 1 Convert to the equivalent rectangle. The semicircular slab can be idealized as a rectangle, as shown in Fig. 10.51. The shorter side of the rectangle may be selected as 0.866 times the radius of the circle = $0.866 \times 2800 = 2425 \text{ mm}$.

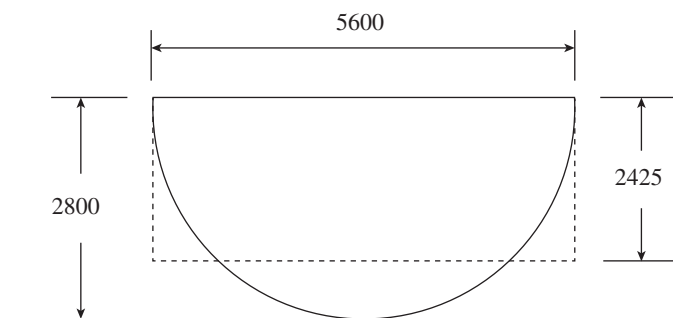


FIG. 10.51 Semi-circular slab

Hence, we need to design a rectangular slab of size $5600 \times 2425 \text{ mm}$. As $L_y > 2L_x$, we need to design it as a one-way slab.

Step 2 Calculate the loads and bending moments.

$$L/d = 20 \text{ (Simply supported slab as per Clause 23.2.1)}$$

$D = 2425/20 = 121.25 \text{ mm}$; we may reduce this by taking into account the reinforcement ratio.

Hence, assume $D = 115 \text{ mm}$.

$$\text{Self-weight} = 0.115 \times 25 = 2.875 \text{ kN/m}^2$$

$$\text{Floor finish} = 1.0 \text{ kN}^2$$

$$\text{Imposed load} = 3.0 \text{ kN}^2$$

$$\text{Total} = 6.875 \text{ kN/m}^2$$

$$\text{Factored load } w_u = 1.5 \times 6.875 = 10.31 \text{ kN/m}^2$$

$$\text{B.M.} = \frac{w_u L^2}{8} = \frac{10.31 \times 2.425^2}{8} = 7.58 \text{ kNm/m}$$

Step 3 Check the depth for bending.

Required depth for resisting bending moment

$$d = \left(\frac{M_u}{0.138 b f_{ck}} \right)^{0.5} = \left(\frac{7.58 \times 10^6}{0.138 \times 1000 \times 25} \right)^{0.5} = 47 \text{ mm}$$

Cover for moderate exposure = 50 mm (Table 16 of IS 456)

Assuming 10 mm bars,

$$\text{Effective depth provided} = 115 - 30 - 5 = 80 \text{ mm} > 50 \text{ mm.}$$

Hence, the slab is under-reinforced.

Step 4 Calculate the reinforcement.

Required area of steel

$$A_{st} = \frac{M_u}{0.8 d f_y} = \frac{7.58 \times 10^6}{0.8 \times 80 \times 415} = 285 \text{ mm}^2/\text{m. Provide 10 mm}$$

bars at 270 mm c/c in the shorter direction (Table 96 of SP 16); $A_{st, \text{provided}} = 291 \text{ mm}^2$.

Minimum reinforcement for shrinkage = $0.12 \times 80 \times 1000/100 = 96 \text{ mm}^2/\text{m}$

Provide 6 mm at 230 mm c/c in the longer direction ($A_{st, \text{provided}} = 123 \text{ mm}^2$).

Check for cracking; provided spacing $\leq 3 \times 80 = 240 \text{ mm}$ or 300 mm. Hence, cracking will be controlled.

Step 5 Check for shear.

Maximum shear force at a distance d from the face of support

$$V_u = w_u \left(\frac{L_x}{2} - d \right) = 10.31 \left(\frac{2.425}{2} - 0.08 \right) = 11.68 \text{ kN/m}$$

$$\text{Nominal shear stress} = \frac{V_u}{bd} = \frac{11.68 \times 10^3}{1000 \times 80} = 0.146 \text{ N/mm}^2$$

Minimum shear strength as per Table 19 for M25 concrete = $0.29 \text{ N/mm}^2 > 0.167 \text{ N/mm}^2$. Hence, the slab is safe in shear.

EXAMPLE 10.10 (Slab with opening):

A simply supported slab with effective short and long spans of 3.5 m and 4.55 m, respectively, is subjected to an imposed load of 2.0 kN/m^2 . An opening of $600 \text{ mm} \times 600 \text{ mm}$ is to be provided in the slab as shown in Fig. 10.52. Design the slab using M25 concrete and Fe 415 steel.

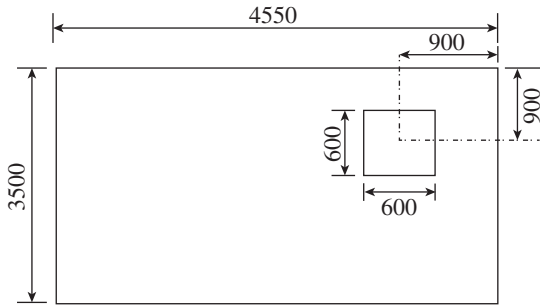


FIG. 10.52 Slab with opening

SOLUTION:

Step 1 Assume the depth of the slab.

Assuming mild environment, cover = 20 mm (Table 16 of the code)

L/d ratio for simply supported slab (Clause 24.1) = 28

$$D = L/28 = 3500/28 = 125 \text{ mm}$$

Assume overall depth of 150 mm. With 10 mm bars, effective depth = 150 – 20 – 5 = 125 mm

Step 2 Calculate the loads and bending moments.

Self-weight of slab	= 0.15 × 25	= 3.75 kN/m ²
Floor finish (assumed)		= 1 kN ²
Imposed load		= 2 kN ²
Total load		= 6.75 kN/m²

$$\text{Factored load} = 1.5 \times 6.75 = 10.125 \text{ kN/m}^2$$

$$L_x/L_y = 4.55/3.5 = 1.3$$

From Table 27 of the code, $\alpha_x = 0.093$ and $\alpha_y = 0.055$.

$$M_x = 0.093 \times 10.125 \times 3.5^2 = 11.53 \text{ kNm/m}$$

$$M_y = 0.055 \times 10.125 \times 3.5^2 = 6.82 \text{ kNm/m}$$

Step 3 Check the depth for bending.

Required depth

$$d = \left(\frac{M_u}{0.138bf_{ck}} \right)^{0.5} = \left(\frac{11.53 \times 10^6}{0.138 \times 1000 \times 25} \right)^{0.5} = 58 \text{ mm} < 125 \text{ mm}$$

Hence, the depth assumed is sufficient.

Step 4 Calculate the reinforcement.

$$\text{Area of reinforcement in short span} = \frac{M_u}{0.8df_y} = \frac{11.53 \times 10^6}{0.8 \times 125 \times 415} = 278 \text{ mm}^2/\text{m}$$

Provide 8 mm at 180 mm c/c ($A_{st, \text{provided}} = 279 \text{ mm}^2$).

$$\text{Area of reinforcement in longer direction} = \frac{6.82 \times 10^6}{0.8 \times (125 - 8) \times 415} = 176 \text{ mm}^2/\text{m}$$

Provide 8 mm at 280 mm c/c ($A_{st, \text{provided}} = 179 \text{ mm}^2$).

Spacing of bars $< 3d = 3 \times 125 = 375 \text{ mm}$ or 300 mm

Hence, the cracking will be within permissible limits.

$$\text{Minimum reinforcement} = (0.12/100) \times 125 \times 1000 = 150 \text{ mm}^2 < 176 \text{ mm}^2$$

Step 5 Check for shear.

$$\text{Load transferred to short span, } w_x = \frac{L_y^2}{L_x^2 + L_y^2} w_u = \frac{4.5^2 (10.125)}{4.5^2 + 3.5^2} = 6.3 \text{ kN/m}$$

Maximum shear force at a distance d from the face of

$$\text{support } V_u = w_x \left(\frac{L_x}{2} - d \right) = 6.3 \left(\frac{3.5}{2} - 0.125 \right) = 10.24 \text{ kN/m}$$

Nominal shear stress =

$$\frac{V_u}{bd} = \frac{10.24 \times 10^3}{1000 \times 125} = 0.08 \text{ N/mm}^2 < 0.29 \text{ N/mm}^2$$

(Table 19 of IS 456)

Hence, the slab is safe in shear. Alternate bars should be bent up at $0.2 \times \text{span}$ to resist any secondary bending moment occurring at support.

Step 6 Detailing at opening: The size of opening is 600 mm and the thickness of the slab is 150 mm. The opening is not at the critical zone of the slab. In the short span $600/180 = 3$ numbers 8 mm diameter bars and in the long span $600/280 = 2$ numbers 8 mm diameter bars will be intercepted by the opening. Hence, provide two 8 mm bars at each edge along the long- and short-span directions. Similarly, provide two 8 mm bars at the four diagonal corners of the opening as shown in Fig. 10.53.

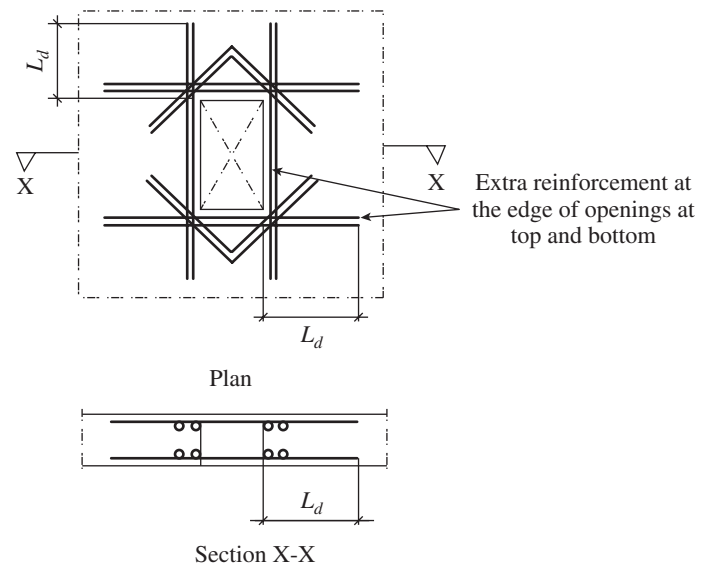


FIG. 10.53 Reinforcement around opening

Note: The edge reinforcement equals the amount of reinforcements interrupted due to opening.

EXAMPLE 10.11:

A two-way continuous slab of size 5 m × 8.35 m and 300 mm thickness has a central point load of 100 kN due to some electrical equipment of size 1 m × 2 m. Determine the bending moments and shear due to the concentrated load using Pigeaud's method. Assume a wearing coat of thickness 50 mm.

SOLUTION:

Step 1 Calculate u and v .

$$u = 1.0 + 2(0.3 + 0.05) = 1.7 \text{ m}$$

$$v = 2.0 + 2(0.3 + 0.05) = 2.7 \text{ m}$$

Step 2 Determine the coefficients using Pigeaud's curves.

$$\frac{u}{L_x} = \frac{1.7}{5} = 0.34; \quad \frac{v}{L_y} = \frac{2.7}{8.35} = 0.32; \quad \frac{L_y}{L_x} = \frac{8.35}{5} = 1.67$$

Using Fig. 10.30, $m_x = 0.145$ and $m_y = 0.075$.

Step 3 Calculate the bending moments.

$$M_x = P(m_x + \nu m_y) = 100(0.145 + 0.2 \times 0.075) = 16 \text{ kNm}$$

$$M_y = P(m_y + \nu m_x) = 100(0.075 + 0.2 \times 0.145) = 10.4 \text{ kNm}$$

Allowing a reduction of 20 per cent for continuity, we get $M_x = 12.8 \text{ kNm}$ and $M_y = 8.32 \text{ kNm}$ per metre width.

Step 4 Calculate the maximum shear force.

$$\text{Short span: } V = P(L_y - v/2)/(uL_x) = 100(8.35 - 1.35)/(1.7 \times 8.35) = 49.31 \text{ kN/m}$$

$$\text{Long span: } V = P(L_x - u/2)/(vL_x) = 100(5 - 0.85)/(2.7 \times 5) = 30.74 \text{ kN/m}$$

EXAMPLE 10.12:

Consider a rectangular slab of size 5 m by 4 m with one of its longer sides free and the other three sides simply supported. The reinforcement in two perpendicular directions are such that $m_x = 12 \text{ kNm/m}$ and $m_y = 18 \text{ kNm/m}$. Find its collapse load.

SOLUTION:

$m_x = 12 \text{ kNm/m}$ and $m_y = 18 \text{ kNm/m}$. Hence, $\mu = 18/12 = 1.5$.

Ratio of shorter to longer sides, $\alpha = 4/5 = 0.8$; $L = 5 \text{ m}$

For Mode 1 failure (see Table 10.6)

$$m = \frac{w_u \alpha^2 L^2}{24\mu} \left[\sqrt{\left(4 + \frac{9\mu}{\alpha^2}\right)} - 2 \right]$$

$$12 = \frac{w_u (0.8)^2 5^2}{24 \times 1.5} \left[\sqrt{\left(4 + \frac{9 \times 1.5}{0.8^2}\right)} - 2 \right] = 1.3375 w_u$$

Hence, $w_u = 8.97 \text{ kN/m}^2$

For Mode 2 failure,

$$m = \frac{w_u L^2}{24} \left[\sqrt{\left(3 + \frac{\mu}{4\alpha^2}\right)} - \frac{\sqrt{\mu}}{2\alpha} \right]^2$$

$$12 = \frac{w_u 5^2}{24} \left[\sqrt{\left(3 + \frac{1.5}{4 \times 0.8^2}\right)} - \frac{\sqrt{1.5}}{2 \times 0.8} \right]^2 = 1.3259 w_u$$

Hence, $w_u = 9.05 \text{ kN/m}^2$

We must take the lower value of the ultimate load, since we are using an upper bound approach. Hence, the first mode of failure with two positive yield lines govern the failure, with $w_u = 8.97 \text{ kN/m}^2$. It should be noted that it has already been shown by Jones that when $\mu/\alpha^2 \geq 2$, the first mode will govern; otherwise, the second mode of failure will govern. For our case, $\mu/\alpha^2 = 1.5/0.8^2 = 2.34 > 2$; hence, the first mode governs, which is also evident by the calculations.

EXAMPLE 10.13:

Design using the yield-line theory a simply supported square slab of size 5 m to support a service imposed load of 3 kN/m^2 . Adopt M20 concrete and Fe 415 grade reinforcement.

SOLUTION:

Step 1 Assume the depth of the slab.

As per Clause 24.1 of IS 456, L/d ratio for simply supported slab = $35 \times 0.8 = 28$

Hence, depth of slab = $L/28 = 5000/28 = 178.5 \text{ mm}$

Let us adopt $D = 180 \text{ mm}$; assuming cover = 25 mm and diameter of bars used as 10 mm,

$$d = 180 - 25 - 5 = 150 \text{ mm.}$$

Step 2 Calculate the loads.

$$\text{Self-weight of slab} = 0.18 \times 25 = 4.5 \text{ kN/m}^2$$

$$\text{Imposed load} = 3.0 \text{ kN/m}^2$$

$$\text{Floor finish (say)} = 1.00 \text{ kN/m}^2$$

$$\text{Total service load} = 8.5 \text{ kN/m}^2$$

$$\text{Design factored load, } w_u = 1.5 \times 8.5 = 12.75 \text{ kN/m}^2$$

Step 3 Calculate the bending moments and shear.

Ultimate bending moment as per yield-line theory

$$m = M_u = \frac{w_u L^2}{24} = \frac{12.75 \times 5^2}{24} = 13.28 \text{ kNm/m}$$

$$\text{Ultimate shear, } V_u = 0.5 w_u L = 0.5 \times 12.75 \times 5 = 31.875 \text{ kN}$$

Step 4 Check the limiting moment capacity of the slab.

$$M_{u,\text{lim}} = 0.138 f_{ck} b d^2 = 0.138 \times 20 \times 1000 \times 150^2 = 62.1 \text{ kNm}$$

$M_u < M_{u,\text{lim}}$. Hence, the section is under-reinforced.

Step 5 Calculate the reinforcement.

$$\frac{M_u}{bd^2} = \frac{12.75 \times 10^6}{1000 \times 150^2} = 0.567$$

From Table 2 of SP 16, we get for M20 concrete, $p_t = 0.1624\%$

$$A_{st} = \frac{0.1624}{100} \times 1000 \times 150 = 244 \text{ mm}^2$$

Provide 10 mm diameter bars at 300 mm c/c ($A_{st} = 262 \text{ mm}^2$).

Step 6 Check for shear stresses.

$$\text{Nominal shear stress} = \frac{V_u}{bd} = \frac{31875}{1000 \times 150} = 0.213 \text{ N/mm}^2$$

$$p_t = \frac{100A_{st}}{bd} = \frac{100 \times 262}{1000 \times 150} = 0.175\%$$

From Table 19 of IS 456,

$$k_s \tau_c = k_s \times 0.30 \text{ N/mm}^2 > 0.213 \text{ N/mm}^2$$

Hence, the slab is safe in shear.

SUMMARY

Slabs with longer to shorter span ratio less than 2.0 are called two-way slabs. In such slabs, unlike one-way slabs, load sharing is in both short and long spans and hence main reinforcements have to be provided in both directions, based on the bending moments. The reinforcement in the shorter direction should be placed below the reinforcement in the longer direction. Two-way slab systems include two-way solid slabs supported by the beams, flat plates, flat slabs, and waffle slabs. The choice between these different two-way slab systems is made based on the architectural, structural, and construction considerations.

The actual behaviour of a two-way slab is very complex; however, it is usually visualized as a slab made of a series of orthogonal (intersecting at right angles) beams in two directions. As the load on the slabs is increased, hairline cracks first appear at the maximum stressed regions, which propagate as yield or failure lines. Slabs usually carry loads even after the formation of the yield-line mechanism due to membrane action, which, however, is not considered in the design. The behaviour of flat slabs is also similar, though they fail mainly because of punching of the columns through the slab.

The main step in the design of the two-way slabs is the determination of the slab thickness, which governs serviceability, shear, and fire resistance requirements. The Indian code provisions on L/d ratios are inadequate and hence the provisions given in the ACI and Canadian codes are also discussed.

There are a number of possible approaches to the analysis of two-way slab systems, such as linear and non-linear analysis, and other simplified methods of analysis. The Indian code uses moment coefficients, whereas the ACI code uses direct design and equivalent frame method.

The moment coefficients as per IS 456 are provided, which are based on the work of Grashof and Rankine. Marcus introduced an important correction to the Grashof–Rankine formula that allows for restraint at the corners and the resistance given by torsion. When two spans are not equal, there will be unbalanced moments at the common edge; though we may safely take the maximum moment for design, methods for the redistribution of these unbalanced moments are also discussed.

Pattern loading will not be critical when we use coefficients given in Annexure D of IS 456. Shear forces will not be critical in two-way slabs except when there are concentrated loads. In such cases, they should be checked at a distance d away from the face of the support. The loads to be carried by the supporting beams of the slab

are estimated based on the appropriate yield-line pattern of the slab. It has to be noted that when the beams are not stiff, the behaviour of the slab will be different from the slabs supported on rigid beams or walls.

The design procedure is similar to that of one-way slabs, except that the tables given in Annexure D are used to determine the bending moments. To get the optimum slab thickness, satisfying both moment and deflection criteria, we need to adopt an iterative procedure. A method suggested by Pandian (1989) can be used to obtain optimal L/d ratios without iteration. Design charts and tables given in SP 16 are used in practice to rapidly design two-way slabs. Annexure D of IS 456 also provides the detailing of reinforcement in two-way slabs by considering them as divided into middle and edge strips in both directions. When the slab is unrestrained at the corners, it is necessary to provide torsional reinforcements to a length of one-fifth of the shorter span both at the top and bottom of the slab. For roof slabs, the temperature and shrinkage effects should be considered in the design in addition to additional loads due to rooftop gardens, if they are planned.

Circular and triangular slabs may be designed for the moments based on the plate theory or yield-line theory. Reinforcement in circular slabs may be provided in the radial and circumferential fashion or in the regular orthotropic grid fashion. Other non-rectangular slabs are often designed as equivalent circular or rectangular slabs.

Concentrated loads due to equipment or vehicles in bridges may be considered in the design using elastic methods such as Pigeaud's or Westergaard's theory or by using yield line methods. A few curves based on Pigeaud's theory are presented.

Smaller openings in slabs can be provided by providing extra reinforcements around the edges of openings. Larger openings require careful study and may be analysed using the yield-line theory. An introduction to the yield-line theory is provided and yield-line analyses based on virtual work method and the equilibrium method are explained with a few examples. The limitations of these upper bound approaches are also listed.

Guidance on the design of sloped and pyramidal roofs is provided. The action of roof and floor slabs in transferring the horizontal load to the vertical lateral resistant systems, like the shear walls, is explained. The diaphragm action of these slabs is complex and is presently considered similar to the behaviour of webs in continuous beams; the beams at the floor periphery are assumed to act as the compression and tension chords. The concepts presented are explained with ample examples and references are provided for further study.

REVIEW QUESTIONS

1. When are slabs considered as two-way slabs?
2. What are the main differences in behaviour of one-way and two-way slabs?
3. Name the different types of two-way slabs.
4. Describe the behaviour of two-way slabs.
5. Distinguish between isotropic and orthotropic slabs.
6. As per Clause 24.1 of IS 456, when the span is less than 3.5m and imposed load less than 3kN/m², the basic L/d ratio of continuous slabs with Fe 415 grade steel can be taken as _____.
(a) 40 (c) 35
(b) 32 (d) none of these
7. As per Clause 24.1 of IS 456, when the span is less than 3.5m and imposed load less than 3kN/m², the basic L/d ratio of simply supported slabs with Fe 415 grade steel can be taken as _____.
(a) 20 (c) 35
(b) 28 (d) none of these
8. Can we modify the basic L/d ratio given in Clause 24.1 of IS 456? How can it be done?
9. When are the deflection calculations required as per the code?
10. As per IS 456, the final deflection due to all loads should not exceed _____.
(a) span/350 (c) either span/350 or 20mm
(b) span/250 (d) none of these
11. IS 456 restricts the deflection to prevent cracking of brittle partitions to _____.
(a) span/350 (c) either span/350 or 20mm
(b) span/250 (d) none of these
12. State the two equations given in the Canadian code for calculating L/D ratio.
13. List the possible approaches used for the analysis of two-way systems.
14. Why is finite element analysis (FEA) not suitable for routine design office use?
15. Do an Internet search and write down the Wood and Armer equations that consider twisting moments.
16. Sketch the trajectories of principal moments in beam-supported rectangular slabs.
17. Why is the plate theory not used in routine office calculations?
18. What are the expressions for α_x and α_y in the Grashof–Rankine equations adopted in Table 27 of IS 456?
19. What are the Marcus correction factors C_x and C_y ?
20. What are the conditions to be satisfied while using Table 26 of the code (Table 10.4 of this chapter)?
21. State the equations for α_x^+ and α_y^+ , which were used to develop Table 26 of IS 456.
22. Under what situations will there be unbalanced moments in the slab boundaries?
23. Is it necessary to consider pattern loading while using IS 456 code coefficients? Why?
24. The critical section for one-way shear is taken at a distance of _____.
(a) $1.5d$ from the face of support
(b) $2.0d$ from the face of support
(c) d from the face of support
(d) none of these
25. If the beam is simply supported on all four sides, the dispersion of loads is assumed at _____.
(a) 30° (b) 45° (c) 60° (d) 42.5°
26. State the Swedish code formula for considering the supporting beam as adequately stiff.
27. What are the Canadian code formulae for considering the supporting beam as adequately stiff?
28. Why is the design of two-way slabs considered as iterative?
29. List the different steps involved in the design of a beam-supported two-way slab.
30. What is the approximate equation that can be used to estimate the slab reinforcement with reasonable accuracy?
31. What is the minimum amount of reinforcement to be provided in the longer and shorter directions as per IS 456?
32. How can the design tables provided in SP 16 be used in the design of two-way slabs?
33. List the detailing rules for simply supported two-way slabs as per Annexure D of IS 456.
34. What are the rules for providing torsional reinforcement in two-way slabs?
35. List the detailing rules for restrained two-way slabs as per Annexure D of IS 456.
36. What are the additional aspects to be considered for the design of roof slabs?
37. Assuming Poisson's ratio as zero, write down the equations for M_r and M_t for simply supported circular slabs.
38. Sketch the two alternate reinforcement detailing adopted for circular slabs.
39. Sketch the two alternate reinforcement detailing adopted for triangular slabs.
40. How can we approximately design (a) trapezoidal slabs, (b) triangular slabs, and (c) hexagonal slabs?
41. What is the method normally used for the design of two-way slabs subjected to concentrated loads?
42. How are the openings in two-way slabs considered in design?
43. What are the yield lines?
44. State the upper- and lower-bound theorems.
45. What are the characteristic features of yield lines?
46. State the two methods for the determination of ultimate load capacity of slabs based on the yield-line theory.
47. State the principle behind the virtual work method and the two equations for work done by external loads and internal work done by yield lines.
48. Derive the equation for the ultimate moment capacity of a simply supported square slab subjected to central concentrated load using the virtual work method.
49. What are the limitations of the yield-line theory?

50. How are pyramidal roofs designed?
 51. How are two-way slabs designed to resist lateral loads?

52. Describe the detailing of reinforcements to be provided in two-way slabs for resisting lateral loads.

EXERCISES

- The slab of a residential building of size $5\text{ m} \times 6.5\text{ m}$ is simply supported on all the four sides on 230 mm walls. Assuming an imposed load of 3 kN/m^2 and load due to finishes of 1.0 kN/m^2 , design the floor slab. Use M25 concrete and Fe 550 steel. Assume mild exposure.
- Compute the design moments for the slab analysed in Exercise 1 using the Marcus correction.
- Redesign the slab given in Exercise 1 assuming that the corners of the slab are prevented from lifting up by wall loads due to the floor above.
- Find the bending moment coefficients a_x and a_y for a slab having two long edges discontinuous, that is, Case 6 in Table 10.4, with $r = 1.5$, using Eqs (10.17)–(10.19).
- Design a rectangular slab panel of size 4.5 m by 6 m in which one long edge is discontinuous. Assume that the slab supports imposed load of 4 kN/m^2 and a floor finish of 1 kN/m^2 . The slab is subjected to mild exposure and is made of M25 concrete and Fe 415 steel.
- Design a continuous two-way slab system shown in Fig. 10.54. It is subjected to an imposed load of 3 kN/m^2 and surface finish of 1 kN/m^2 . Consider M25 concrete, grade Fe 415 steel, and moderate environment. Assume that the supporting beams are $230 \times 500\text{ mm}$.

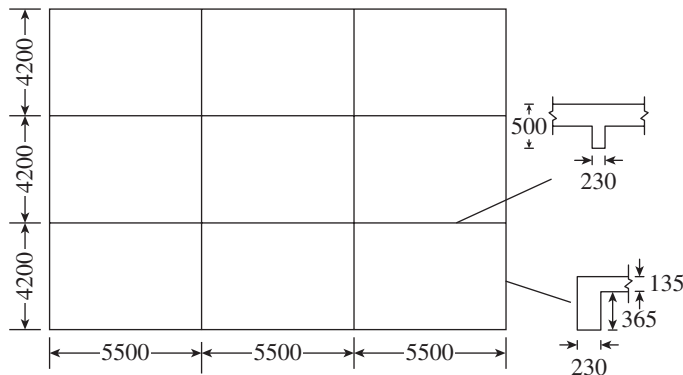


FIG. 10.54

7. Design a circular slab of diameter 5.5 m subjected to an imposed load of 5 kN/m^2 . Assume that the slab is simply supported

and is in a severe environment. Use $f_{ck} = 25\text{ MPa}$ and $f_y = 415\text{ N/mm}^2$.

- Design a well cap to support a circular pier of diameter 2 m . Assume that the internal diameter of the well is 7 m and that the load on the pier is 600 kN . Use Fe 415 steel and M35 concrete.
- A simply supported semicircular slab of 3.5 m radius is subjected to a uniformly distributed imposed load of 3 kN/m^2 and floor finish of 1 kN/m^2 . Assuming moderate environment, design the slab with Fe 500 steel and M20 concrete.
- A simply supported slab with effective short and long spans of 4 m and 6 m , respectively, is subjected to an imposed load of 3.0 kN/m^2 . An opening of $500\text{ mm} \times 500\text{ mm}$ is to be provided in the slab as shown in Fig. 10.55. Design the slab using M25 concrete and Fe 415 steel.

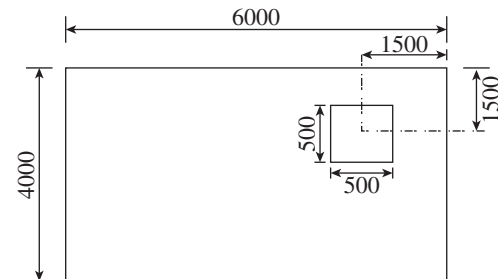


FIG. 10.55

- A two-way continuous slab of size 4 m by 8 m and 300 mm thickness has a central point load of 85 kN due to some electrical equipment of size 0.9 m by 1.8 m . Determine the bending moment and shear due to the concentrated load using Pigeaud's method. Assume a wearing coat of thickness 40 mm .
- Consider a rectangular slab of size 8 m by 6 m with one of its longer sides free and the other three sides simply supported. The reinforcement in two perpendicular directions are such that $m_x = 12\text{ kNm/m}$ and $m_y = 15\text{ kNm/m}$. Find its collapse load.
- Design the rectangular slab given in Exercise 1 using the yield-line theory and compare the results.

REFERENCES

- Aalami, B.O. 2008, ADAPT-TN290, *Vibration Design of Concrete Floors for Serviceability*, ADAPT Corporation, Redwood City, pp. 20. (also see http://www.adapsoft.com/resources/ADAPT_TN290_vibration_analysis.pdf, last accessed on 18 January 2012).
- Bhatt, P., T.J. MacGinley, and B.S. Choo 2006, *Reinforced Concrete: Design Theory and Examples*, 3rd edition, Taylor & Francis, London and New York, p. 686..
- BS 8110-1:1997, 1997, *Structural Use of Concrete-Part 1: Code of Practice for Design and Construction*, British Standards Institution, London, p. 151.
- C & CAA T36 2003, *Guide to Long-span Concrete Floors*, Cement and Concrete Association of Australia, 2nd edition, p. 45. (also see <http://www.concrete.net.au/publications/pdf/Long-span%20Floors.pdf>, last accessed on 18 January 2012).

- Fanella, D.A. 2001, 'Time Saving Design Aids for Reinforced Concrete, Part 2: Two-way Slabs', *Structural Engineer*, ZweigWhite, Vol. 2, No. 9, pp. 28–33.
- Fleischman, R.B., K.T. Farrow, and K. Eastman 2002, 'Seismic Response of Perimeter Lateral System Structures with Highly Flexible Diaphragms', *Earthquake Spectra*, Earthquake Engineering Research Institute, Vol. 18, No. 3, pp. 251–86.
- Gambhir, M.L. 2008, *Design of Reinforced Concrete Structures*, Prentice Hall of India, New Delhi, p. 723.
- Gamble, W.L., M.A. Sozen, and C.P. Siess 1969, 'Tests of a Two-way Reinforced Concrete Floor Slab', *Proceedings, ASCE*, Vol. 95, No. ST6, pp. 1073–96.
- Gardiner, D.R., D.K. Bull, and A.J. Carr 2008, 'Trends in Internal Forces in Concrete Floor Diaphragms of Multi-storey Structures During Seismic Shaking', *The 14th World Conference on Earthquake Engineering*, 12–17 October 2008, Beijing, China.
- Gardner, N.J. 2011, 'Span/Thickness Limits for Deflection Control', *ACI Structural Journal*, American Concrete Institute, Farmington Hills, Vol. 108, No. 4, pp. 453–60.
- Gilbert, R.I. 1985, 'Deflection Control of Slabs Using Allowable Span to Depth Ratios', *Proceedings, ACI Journal*, American Concrete Institute, Farmington Hills, Vol. 82, No. 1, pp. 67–72.
- Grashof, F. 1878, *Theorie der Elasticität und Festigkeit*, R. Gaertner, Berlin.
- Hahn, J. 1966, *Structural Analysis of Beams and Slabs*, Sir Isaac Pitman and Sons, London, p. 310.
- Hillerborg, A. 1996, *Strip Method Design Handbook*, E & FN Spon, London, p. 322.
- Hognestad, E. 1953, 'Yield Line Theory for Ultimate Flexural Strength of Reinforced Concrete Slabs', *Proceedings, ACI Journal*, American Concrete Institute, Farmington Hills, Vol. 24, No. 7, pp. 637–56.
- Ingerslev, A. 1923, 'The Strength of Rectangular Slabs', *The Structural Engineer*, The Institution of Structural Engineers, London, Vol. 1, No.1, pp. 3–14.
- Jirsa, J.O., M.A. Sozen, and C.P. Siess 1969, 'Pattern Loadings on Reinforced Concrete Floor Slabs', *Proceedings, ASCE*, Vol. 95, No. ST6, pp. 1117–37.
- Johansen, K.W. 1943, 'Bruklinieteorier', Jul. Gjellerups Forlag, Copenhagen, p. 191 (*Yield Line Theory*, Translated by Cement and Concrete Association, London, 1962, p. 181).
- Johansen, K.W. 1968, *Pladeformler*, Polyteknisk Forlag, Copenhagen, p. 240 (*Yield Line Formulae for Slabs*, Translated by Cement and Concrete Association, London, 1972, p. 106).
- Jones, L.L. and R.H. Wood 1967, *Yield Line Analysis of Slabs*, Thames and Hudson, London, p. 405.
- Kennedy, G. and C. Goodchild 2003, *Practical Yield Line Design*, Reinforced Concrete Council, British Cement Association, Berkshire, p. 175.
- Lee, Y.H. and A. Scanlon 2010, 'Comparison of One- and Two-way Slab Minimum Thickness Provisions in Building Codes and Standards', *ACI Structural Journal*, American Concrete Institute, Farmington Hills, Vol. 107, No. 2, pp. 157–63.
- Leonhardt, F. and E. Mönning 1977, *Vorlesungen über Massivbau, Dritter Teil, Grundlagen zum Bewehren im Stahlbetonbau*, 3rd edition, Springer Verlag, Berlin, p. 246.
- Marcus, H. 1932, *Die Theorie Elastischer Gewebe und ihre Anwendung auf die Berechnung biegsamer Platten*, Julius Springer, Berlin.
- Moehle, J.P., J.D. Hooper, D.J. Kelly, and T.R. Meyer 2010, 'Seismic Design of Cast-in-place Concrete Diaphragms, Chords, and Collectors: A Guide for Practicing Engineers', *NEHRP Seismic Design Technical Brief No. 3*, National Institute of Standards and Technology, Gaithersburg, p. 29, (also see <http://www.nehrp.gov/pdf/nistgcr10-917-4.pdf>, last accessed on 19 December 2011).
- NS 3473 (Norwegian Standards) 1998, *Concrete Structures, Design Rules*, 5th edition, Oslo, p. 78.
- Ockelton, A.J. 1955, 'Load Tests on Three Storey Reinforced Concrete Building in Johannesburg', *The Structural Engineer*, The Institution of Structural Engineers, London, Vol. 33, No. 10.
- Pandian, N. 1989, 'A Simplified Limit State Design of Slabs as per IS 456:1978', *The Indian Concrete Journal*, ACC Ltd, Vol. 63, No. 1, pp.45–6.
- Park, R. and Gamble W.L. 2000, *Reinforced Concrete Slabs*, 2nd edition, John Wiley and Sons, New York.
- Pigeaud, M. 1929, 'Calcul des Plaques Rectangulaires Minces Appuyées a Leur Pourtour', *Annales des Ponts et Chaussées, Memoirs*, Pt. II.
- Pillai, S.U. and D. Menon 2009, *Reinforced Concrete Design*, 3rd edition, Tata McGraw-Hill Publishing Company, New Delhi, p. 962.
- Purushothaman, P. 1984, *Reinforced Concrete Structural Elements: Behaviour, Analysis and Design*, Tata McGraw-Hill Publishing Company Ltd, New Delhi, p. 709.
- Rangan, B.V. 1974, 'Limit States Design of Slabs Using Lower Bound Approach', *Journal of the Structural Division*, ASCE, Vol. 100, No. 2, pp. 373–89.
- Rao, Prakash D.S. 1995, *Design Principles and Detailing of Concrete Structures*, Tata McGraw-Hill Publishing Company Ltd, p. 360.
- Regan, P.E. and C-W. Yu 1973, *Limit State Design of Structural Concrete*, Chatto and Windus, London, p. 325.
- Reynolds, C.E. and J.C. Steedman 1988, *Reinforced Concrete Designer's Handbook*, 10th edition, E & FN Spon, London, p. 436. (2008, 11th edition, CRC Press, Boca Raton).
- Rodriguez, M.E., J.I. Restrepo, and A.J. Carr 2002, 'Earthquake-induced Floor Horizontal Accelerations in Buildings', *Earthquake Engineering and Structural Dynamics*, Vol. 31, John Wiley & Sons, pp. 693–718.
- Scanlon, A. and Y.H. Lee 2006, 'Unified Span to Depth Ratio Equation for Nonprestressed Concrete Beams and Slabs', *ACI Structural Journal*, American Concrete Institute, Farmington Hills, Vol. 103, No. 1, pp. 42–8.
- Sengupta, A.K. and A.D. Shetty 2011, 'Analysis of Chord Forces in Floors with Large Openings or Re-entrant Corners in Reinforced Concrete Buildings', *ICI Journal*, Indian Concrete Institute, Chennai, Vol. 12, No. 2, pp. 7–15.
- Shin, M., A. Bommer, J.B. Deaton, and B.N. Alemdar 2009, 'Twisting Moments in Two-way Slabs', *Concrete International*, American Concrete Institute, Farmington Hills, Vol. 31, No. 7, pp. 35–40.
- Shukla, S.N. 1973, *Handbook for Design of Slabs by Yield-Line and Strip Methods*, Structural Engineering Research Centre, Roorkee, p. 180.
- Siess, C.P. and N.M. Newmark 1950, 'Moments in Two-way Concrete Floor Slabs: A Report of an Investigation', *University of Illinois Engineering Experiment Station, Bulletin No. 385*, Urbana, p. 124.

- Sinha, S.N. 2002, *Reinforced Concrete Design*, 2nd revised edition, Tata McGraw-Hill Publishing Company, New Delhi, p. 711.
- Stiglat, K. and H. Wippel 1983, *Platten*, 3rd edition, W. Ernst und Sohn, Berlin.
- Suryanarayana, P. 1990, 'When Pigeaud's Method fails', *Civil Engineering and Construction Review (CE & CR)*, Vol. 3, No. 11, pp. 25–30.
- Suryanarayana, P. 1993, 'Design of Slab Panels Continuous over Beam Supports', *ICI Bulletin*, Indian Concrete Institute, Chennai, Vol. No. 43, pp. 25–7.
- Szilard, R. 2004, *Theories and Applications of Plate Analysis: Classical, Numerical and Engineering Methods*, John Wiley and Sons, New York, p. 1056.
- Taylor, R., B. Hayes, and G.T. Mohamedbhai 1969, 'Coefficients for Designing Slabs of Beam-and-slab Panels by the Yield-line Theory', *Concrete*, Concrete Society, London, Vol. 3, No. 5, pp. 171–2.
- Terrington, J.S. 1939, *Design of Pyramid Roofs*, Concrete Publications Ltd, London, p. 24.
- Thomas, P. and A.K. Sengupta 2008, 'Analysis of Chord Forces in Reinforced Concrete Buildings Subjected to Seismic Loads', *ICI Journal*, Indian Concrete Institute, Chennai, Vol. 9, No. 3, pp. 21–27.
- Timoshenko, S.P. and S.W. Krieger 1959, *Theory of Plates and Shells*, 2nd edition, McGraw Hill, New York, p. 580.
- Varghese, P.C. 2006, *Limit State Design of Reinforced Concrete*, 2nd edition, Prentice-Hall of India Private Ltd, New Delhi, p. 545.
- Varyani, U.H. 1998, 'Slab Design of Minimum Concrete Thickness in Accordance with IS 456:1978 and SP 24:1983', *Civil Engineering and Construction Review (CE & CR)*, Trend-Set Engineers Pvt. Ltd, Vol. 11, No. 12, pp. 57–9.
- Varyani, U.H. 1999, *Structural Design of Multi-storied Buildings*, South Asian Publishers, New Delhi, p. 310.
- Vecchio, F.J. and K. Tang 1990, 'Membrane Action in Reinforced Concrete Slabs', *Canadian Journal of Civil Engineering*, Canadian Science Publishing, Vol. 17, pp. 686–97.
- Westergaard, H.M. 1926, 'Formulas for the Design of Rectangular Floor Slabs and the Supporting Girders', *Proceedings*, American Concrete Institute, Vol. 22, pp. 26–46.
- Westergaard, H.M. and W.A. Slater 1921, 'Moments and Stresses in Slabs', *Proceedings*, American Concrete Institute, Farmington Hills, Vol. 17, pp. 415–538.
- Wood, R.H. 1968, 'The Reinforcement of Slabs in Accordance to the Pre-determined Field of Moments', *Concrete*, Concrete Society, London, Vol. 2, No. 2, pp. 69–76. *Discussions*, Armer, G.S.T., *Concrete*, Aug. 1968, pp.319–320.

DESIGN OF FLAT PLATES AND FLAT SLABS

11.1 INTRODUCTION

Two-way slabs directly supported on columns, called *flat plates*, are preferred in many parts of the world due to their relatively simple formwork and reinforcement layout and the potential for shorter storey heights (thus increasing the number of floors that can be built within a specific height), fast construction, flat ceiling, and economy (especially where labour costs are high). Flat plates also provide more flexibility in the layout of columns, partitions, small openings, and so on. In addition, the slab thickness required for structural purposes in most cases provides the required fire resistance stipulated by the local bodies. The main limitation of flat plates is the problem posed by resisting two-way shear around the columns, which is called the *punching shear*. Hence, for heavy loads or long spans, *flat slabs*, which have drop panels around the column (which provide additional resistance to shear), are used (see Figs 11.1a–c). Moreover, for reasons of shear around the columns, the column tops are sometimes flared, creating *column heads* (also called column capitals). Flat slabs without drop panels or column heads are referred to as *flat plates*, especially in the USA (see Fig. 11.1d). It should be noted that for the purposes of design, a column capital is part of the column, whereas the drop panel is considered a part of the slab.

The flat plate system is often the system of choice in the USA in regions of low to moderate seismic risk, where it is allowed as a *lateral force resisting system* (LFRS), even though it provides questionable resistance to lateral loads. However, in regions of high seismic risk, it is designed to resist only gravity loads, and shear walls are often provided as the main LFRS. It has to be noted that these types of slabs are critical in punching shear, whereas beam-supported slabs are generally not critical in shear at all.

Historically, flat slabs predate both two-way slabs on beams and flat plates. Flat slabs were originally patented

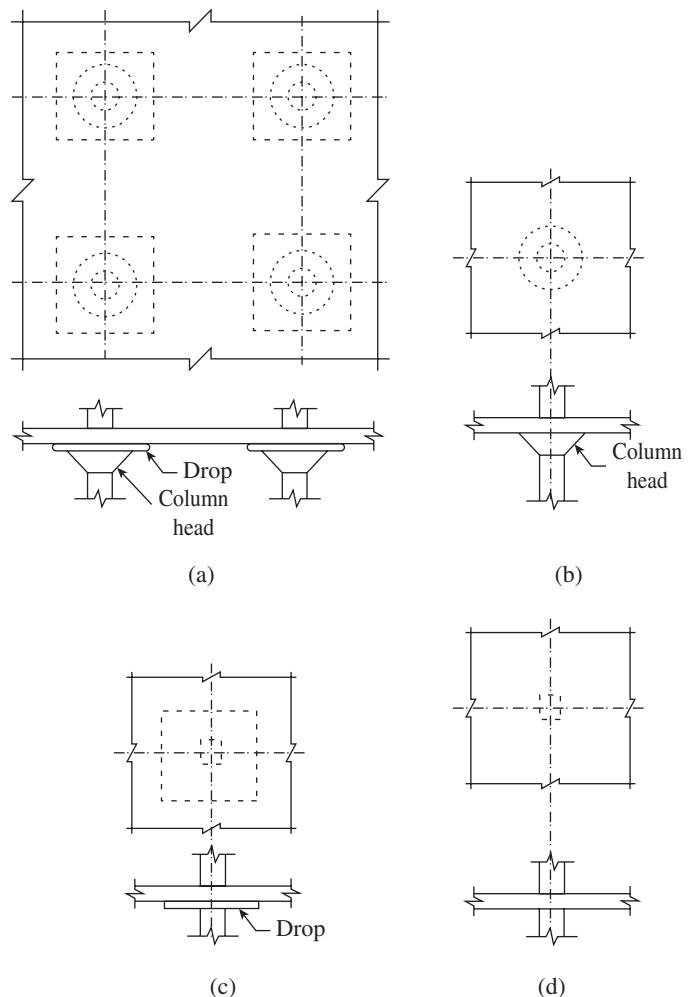


FIG. 11.1 Flat slabs and flat plates (a) Flat slab with drop and column head (b) Flat slab with column head (c) Flat slab with drop (d) Flat plate

by O.W. Norcross of the USA as early as 1902 and several systems of placing reinforcement have been developed and patented since then. Thus, as in other types of structures, construction of flat slabs preceded their theory and design.

C.A.P. Turner is credited with the construction of a flat slab system known as the *mushroom* system in 1906. In the same year, Maillart built a flat slab in Switzerland. By 1913, it was estimated that more than 1000 buildings had been constructed in the USA, without any appreciable design effort (Sozen and Siess 1963).

It was only in 1914 that Nichols proposed a method of analysis of these slabs based on simple statics (Nichols 1914). Though the equation for the *total static moment* derived by Nichols was correct, it was not accepted by Turner and others (his paper was only 10 pages long but had 54 pages of discussions). It was not until 1971 that the ACI code fully recognized Nichols' analysis and required flat slabs to be designed for 100 per cent of the moments predicted from statics (Sozen and Siess 1963; Wight and MacGregor 2009). These design provisions were based on monumental work of the analysis and design of slabs published by Westergaard and Slater in 1921 and Distasio and Van Buren in 1936 as well as the extensive testing program conducted at the University of Illinois and at the Portland Cement Association during 1956–68 (Hatcher, et al. 1965, 1969; Guralnick and La Fraugh 1963). Considerable rationalization of theory, tests, and computer simulations was also achieved through the studies undertaken by Guralnick and La Fraugh (1963), Hanson and Hanson (1968), Vanderbilt, et al. (1969), Gamble, et al. (1969), Corley and Jirsa (1970), Gamble (1972), Wiesinger (1973), and Rice (1973). A comprehensive review of these developments may be found in the works of Sozen and Siess (1963), Grossmann (1989), and Park and Gamble (2000). Punching resistance of flat plates under earthquake loading is still under active research.

11.2 PROPORTIONING OF FLAT SLABS

The thickness of the slab and the size of the drop and column head may be proportioned as per the suggestions given in Clause 31.2 of IS 456.

11.2.1 Thickness of Slab

The thickness of flat slabs, similar to other two-way slabs, is generally controlled by the span to effective depth ratio as discussed in Section 10.3.1 of Chapter 10. It has to be noted that the minimum thickness of the slab should be 125 mm and the longer span should be used in the calculation of the L/d ratio.

11.2.2 Drop Panel

When used to reduce the amount of negative moment reinforcement over a column or for reducing the shear stresses around the column supports, a *drop panel* should be rectangular in plan and should adhere to the following (see Fig. 11.2):

1. Project below the slab at least one-quarter of the adjacent slab thickness (for economy in formwork, the thickness

of the drop panel may be decided based on the available formwork dimensions).

2. Extend in each direction from the centre line of support a distance not less than one-sixth of the panel length in that direction.
3. For exterior panels, the width of the drop panel at a right angle to the non-continuous edge and measured from the centre line of columns should be equal to one-half the width of the drop panel in the interior panels.

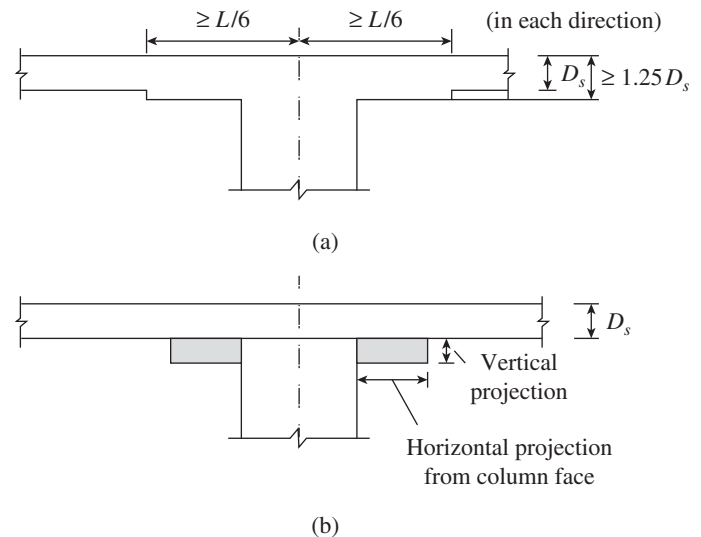


FIG. 11.2 Drop panels and shear caps provide increased shear strength (a) Drop panels (b) Shear cap

The drop panel stiffens the slab in the region of highest moments due to which the deflections will be reduced. Hence, the minimum thickness of slab required to limit the deflections (see Section 10.3.1 of Chapter 10) may be reduced by 10 per cent if drop panels are provided as shown in Fig. 11.2.

11.2.3 Column Heads

The columns supporting flat slabs should have a size of about one-sixteenth the length of the longer span of the slab and about one-eighth to one-ninth the storey height of the building (Varghese 2006). Occasionally, the tops of columns will be flared outward as shown in Fig. 11.1(a). The flared portion, called *column head* or *column capital*, provides increased punching resistance and reduces the clear span L_n . It is usually proportioned to be one-fifth but not more than one-fourth of the shorter span. Its height should not be less than 150 mm (Varghese 2006). A theoretical 45° failure plane is defined as shown in Fig. 10.9 of Chapter 10, outside which the flaring is considered ineffective in transferring shear into the column. While calculating the total moment M_o (see Section 11.4.2) the clear distance L_n is taken as the distance from face to face of the columns or column heads. Thus, it may be inferred that the maximum width of a column head is limited to $0.175L$ for design purposes. The stiffening effect of the column heads

is ignored in the analysis. Openings should not encroach on column heads.

Clause 6.4.7 of the ACI code stipulates that the concrete in the column head be placed at the same time as the slab concrete. As a result, the formwork will become complicated and expensive. Hence, column heads are not used in practice and instead other alternatives such as drop panels or shear reinforcements are used.

11.2.4 Shear Caps

The ACI code allows *shear caps*, also called *shear capitals*, which are projections below the slab, similar to drop panels, but may not satisfy the dimensional limits of drop panel specified in the code. They are used to locally increase the thickness of the slab. Their horizontal projection from the face of the column must be greater than their vertical projection below the slab (see Fig. 11.2b). In general, the vertical projection will be 0.5–1.0 times the slab thickness. Shear caps are provided to a distance such that the shear capacity on the critical perimeter outside the shear cap is greater than the applied shear (see Section 11.5.2). Megally and Ghali (2002) showed that the failure of shear capital is accompanied by the sudden separation of the shear capital from the slab along with brittle failure; hence, they do not recommend the use of shear capitals to increase the punching shear resistance, especially in earthquake zones (for the shear capital to be effective, their length should be greater than four times the slab thickness plus the largest column dimension and should also be reinforced like drop panels).

11.3 BEHAVIOUR OF FLAT SLABS

Though flat slabs and flat plates do not have beams, their behaviour is identical to that of two-way slabs with beams. The broad strips of the slab centred on the column lines in two *orthogonal* directions, designated as *column strips*, normally

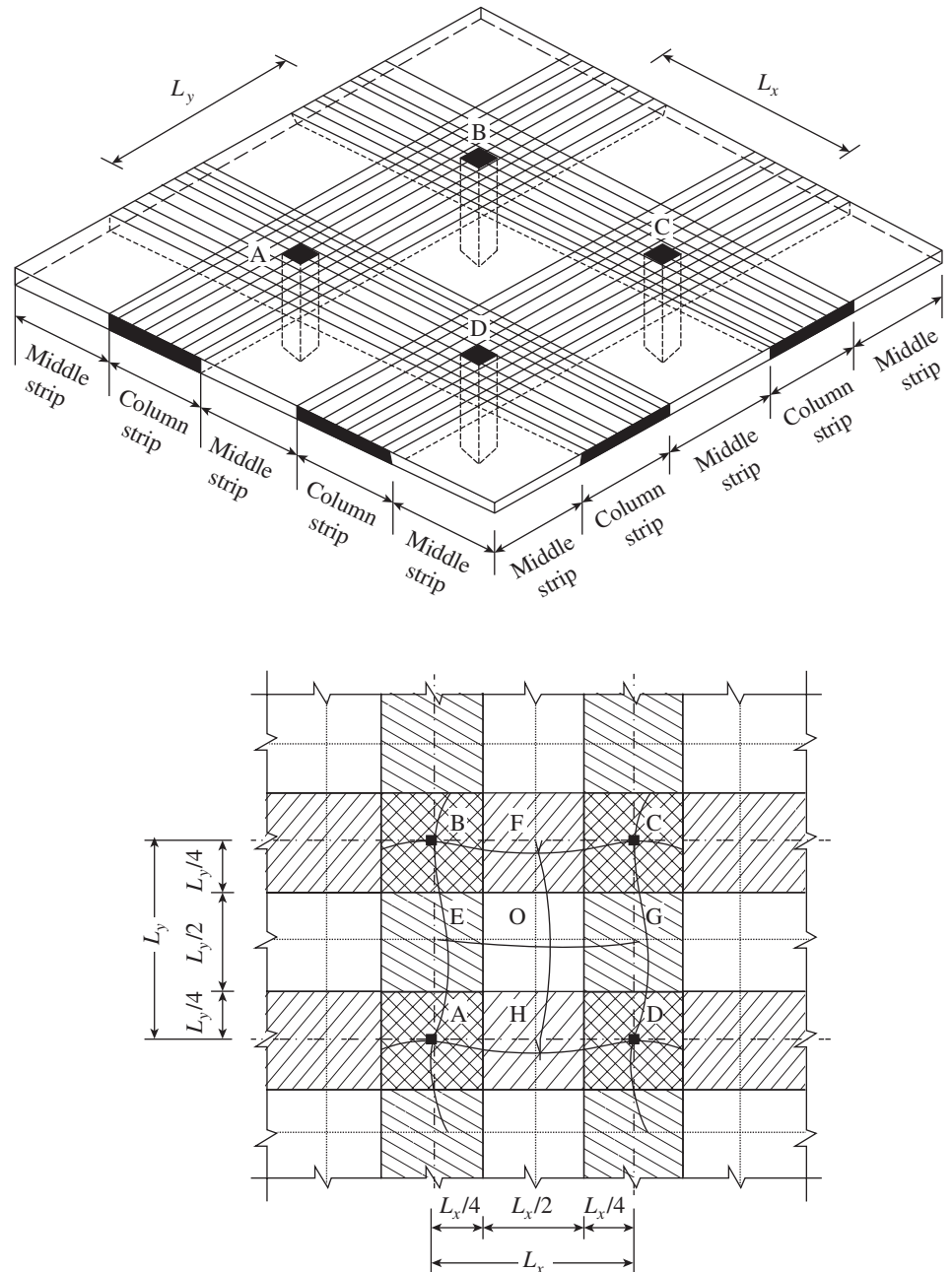


FIG. 11.3 Division of flat slabs into column and middle strips

act as broad beams. The strips at the middle of the slab, which do not pass through the columns, are referred to as the *middle strips*. A simplified scheme of column and middle strips of a typical flat slab as adopted in the various codes of practice is shown in Fig. 11.3.

The column strips behave as continuous beams supported on columns. The typical deflected shape of the interior panel of the flat slab is also shown in Fig. 11.3. It should be noted that unlike the beams of a slab-beam-column system, the column strips are flexible; hence, the deflections of a flat slab are generally larger than that of the more rigid beam-slab-column system. The column strip AHD will have negative moment at points A and D and positive moment at

point H. The middle strip EOG will have positive moments at points E, O, and G. The middle strips are supported by the column strips, which in turn transfer the load to the columns. As the column strips are heavily loaded when compared to the middle strips, they will carry higher bending moments than the middle strips.

If w is the uniformly distributed load acting on a flat plate shown in Fig. 11.4(a), the load w may be divided into two loads— w_1 acting in L_1 direction and w_2 acting in L_2 direction. The bending moment in span direction L_1 will be as shown in Fig. 11.4(b). The moment variation across the width and the trajectories of principal moments in flat slabs are shown in Figs 11.4(c) and (d), respectively. The load per metre of span is w_1L_2 . In continuous beams, the sum of the mid-span positive moment and the average of the negative moments at adjacent supports will be equal to the mid-span positive moment of a corresponding simply supported beam. This requirement of statics results in the following relation (see Fig. 11.4b):

$$M_{ef} + \frac{(M_{ab} + M_{cd})}{2} = \frac{w_1L_2L_1^2}{8} \tag{11.1a}$$

A similar requirement in the perpendicular direction results in the following relation:

$$M_{gh} + \frac{(M_{ac} + M_{bd})}{2} = \frac{w_2L_1L_2^2}{8} \tag{11.1b}$$

It has to be noted that these relations do not reveal the relative magnitudes at the support or span moments. For slabs on rigid beams, the maximum positive elastic moments are at the centre of the panels, and where there is fixity or continuity at the boundaries, the maximum negative moments are at the centres of the edges. In flat slabs, however, the maximum positive and negative moments are on the column lines. Intermediate situations arise when the edge beams have appreciable flexibility in the vertical plane. The variation of bending moment in flat slabs across the width is shown in Fig. 11.4(c) along with the assumed straight line variation normally assumed in design, based on experimental results (see Section 11.4 for the details of bending moment distribution suggested by the codes).

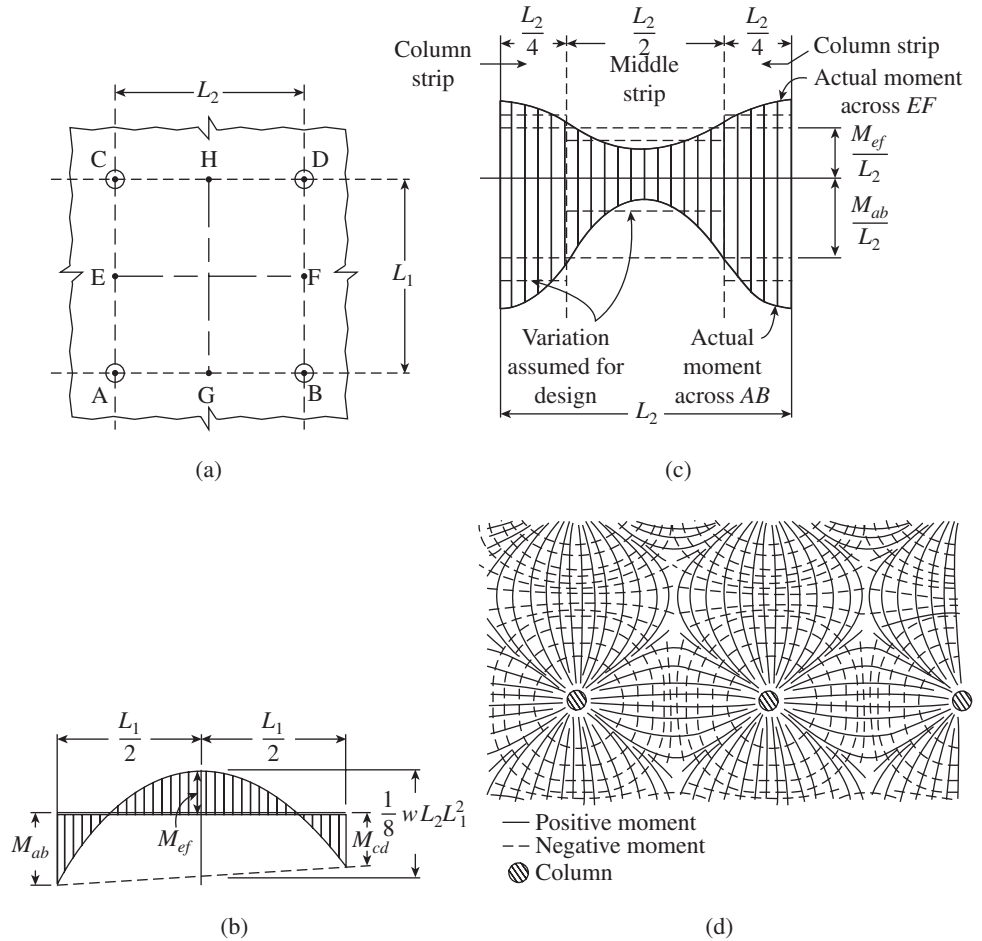


FIG. 11.4 Variation of bending moment in flat slabs (a) Critical moment sections (b) Moment variation along the span (c) Moment variation across the width of critical sections (d) Trajectories of principal moments in flat slabs

Tests were conducted on several nine-panel reinforced concrete (RC) slabs with and without drops and with welded wire mesh and high and medium strength reinforcements at the Structural Research Laboratory of the University of Illinois (Hatcher, et al. 1965, 1969; Xanthakis and Sozen 1963; Sozen and Siess 1963). Similar tests were conducted at the University of New South Wales (Rangan and Hall 1983; Rangan 1987). From these tests the following observations were made: At working loads the slabs had small deflections and stresses. It should be noted that in flat slabs, which tend to span in the longer direction, the deflection increases in proportion to the cube of the major span, whereas in beam-supported systems it depends on the cube of the shorter span (Regan 1981).

Upon loading, cracks appeared first on the top surface of the slab near the column, where maximum bending moment occurs. These were soon followed by cracking in the mid-span at the bottom. (In models with shallow beams, more pronounced cracking was observed on the bottom of the panels adjacent to the shallow beams. In models with drop

panels, cracking was observed at the top of the slab, confined to the surface within drop panels.) Further loading caused cracking and yield lines started forming at the end regions. The cracks at the top were concentrated around the column with the cracks radiating from the column in all directions.

Although the flexural capacity is significantly enhanced by the minimum reinforcement provided in the slab for the purpose of crack control at service loads, punching shear failure usually precedes a complete flexural failure (Hatcher, et al. 1965). Typical crack patterns at failure of flat plates and flat slabs as observed in tests are shown in Figs 11.5 and 11.6, respectively.

When the punching shear stress is exceeded, initiation of shear cracks seem to occur at a distance d from the face of the column, where d is the effective depth of the slab (see Fig. 10.6 of Chapter 10). Unless the slab is reinforced for shear, the slab will not have adequate reserve strength.

The resistance to punching shear will be provided by the concrete in the compression zone and the dowel action of the negative reinforcement, which occurs over a large perimeter of the slab around the column. As a result of the dowel action, there will be no immediate failure after the formation of the first crack. It has to be noted that unlike flexural failure, failure in punching shear is not ductile. The design for punching shear is provided in Section 11.5.2.

11.4 METHODS OF ANALYSIS

As already discussed, two-way flat slabs are highly statically indeterminate and generally lightly reinforced, and the sections are highly ductile. This ductility permits considerable amount of moment redistribution. Hence, the determination of the exact moments is not necessary. However, the distribution of the provided flexural reinforcement will affect the distribution of cracking of the concrete, which will directly affect the nature of the redistribution, the load–deflection response, and hence the overall serviceability of the slab.

Two analysis methods are usually prescribed by the codes for flat slabs and plates—the direct design method (DDM) and the equivalent frame method (EFM). These methods are primarily based on experience, supplemented by elastic analysis and laboratory tests of a limited number of slab geometries. Mulenga and Simmonds (1993) provide a detailed comparison of these two methods. It has to be noted that these procedures predate widespread availability of digital computers and the use of non-linear analysis. These methods

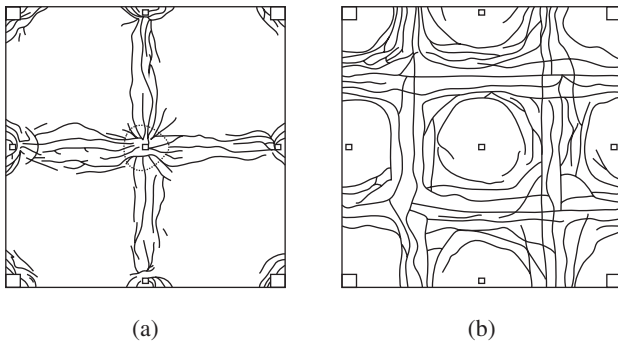


FIG. 11.5 Typical crack pattern in flat plates (a) At top (b) At bottom

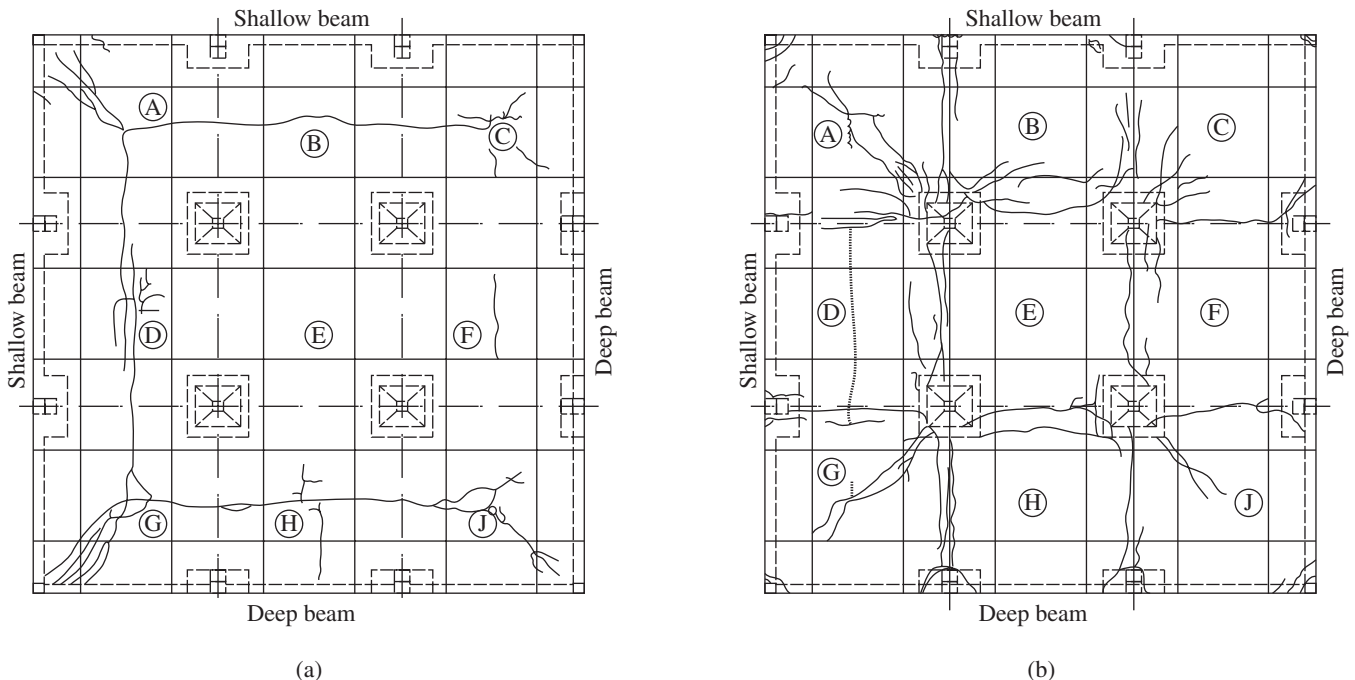


FIG. 11.6 Typical crack pattern in flat slabs with edge beams (a) At bottom (b) At top

Source: Xanthakis and Sozen 1963, reprinted with permission

are covered in Section 4 of IS 456 and are based on the 1977 version of the ACI 318 code. It is of interest to note that these provisions were modified in the 1989 version of the ACI code. Moreover, in the ACI code the design of two-way slabs is dealt in a unified way. Its provisions apply to slabs supported by beams as well as to flat slabs and flat plates.

In both the DDM and EFM, a typical panel is divided, for the purpose of design, into column strips and middle strips. As per Clause 31.1.1 of the code, a *column strip* is defined as a strip of slab having a width on each side of the column centre line equal to $0.25L_2$ but not greater than $0.25L_1$, where L_1 is the span in the direction the moments are being determined, measured centre to centre of supports, and L_2 is the span transverse to L_1 , measured centre to centre of supports (see Fig. 11.7). As per the ACI code, such a strip includes column line beams, if present. In the case of monolithic construction, as per ACI, beams are defined to include the part of the slab on each side of the beam extending a distance h_w

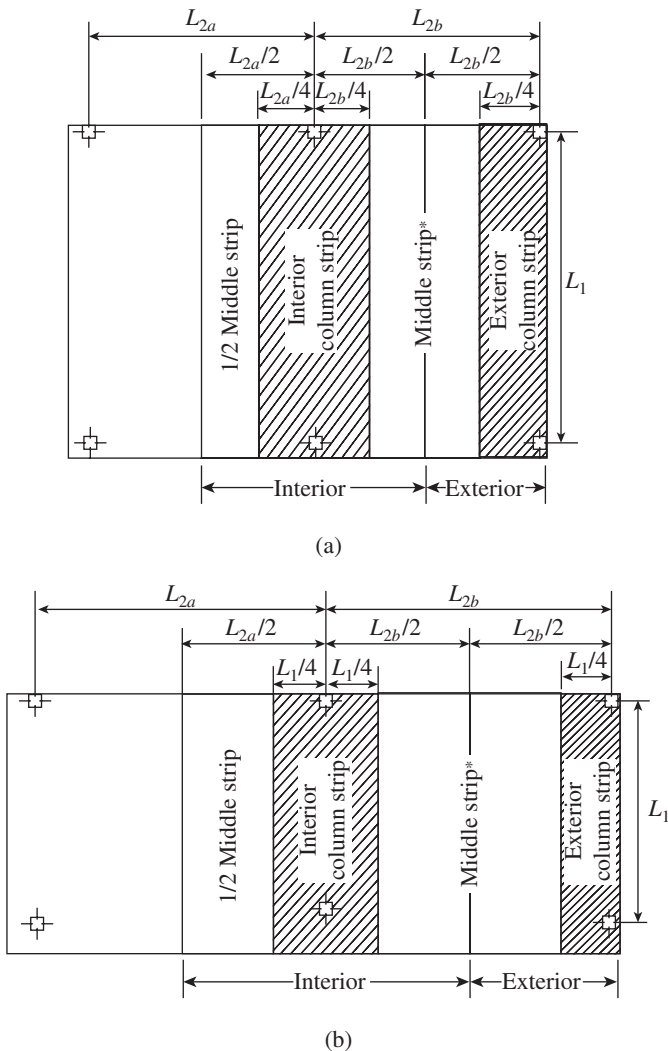


FIG. 11.7 Division of interior and exterior slab panels into column and middle strips (a) Column strip for $L_2 \leq L_1$ (b) Column strip for L_{2a} and $L_{2b} > L_1$

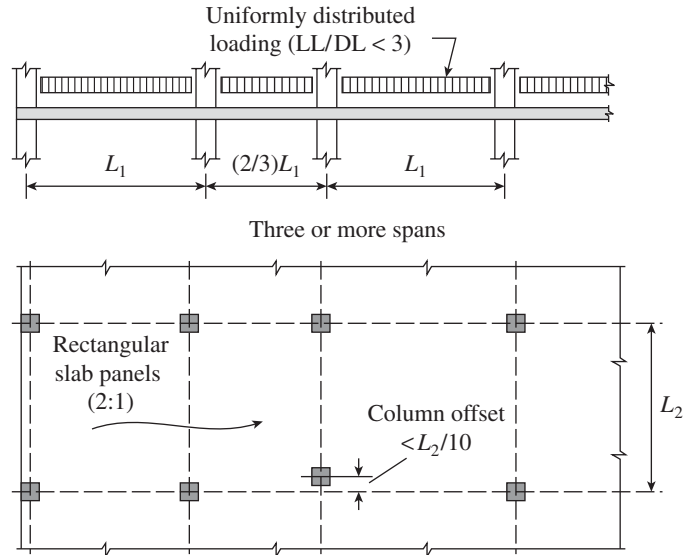


FIG. 11.8 Assumptions in direct design method

equal to the projection of the beam above or below the slab (whichever is greater) but not less than four times the slab thickness (see Fig. 10.8 of Chapter 10).

The *middle strip* is the design strip bounded on each of its opposite sides by the column strip. A *panel* refers to the part of a slab bounded on each of its four sides by the centre line of a column or the centre lines of adjacent spans.

11.4.1 Direct Design Method

The DDM is a semi-empirical method and as per Clause 31.4.1 of IS 456 it is applicable only when the following conditions are met (see Fig. 11.8):

1. There should be a minimum of three continuous spans in each direction. It is because the negative bending moment at an interior support in a two-way structure will exceed the values given in the code.
2. The panels should be rectangular, and the ratio of the longer to the shorter spans within a panel should not be greater than 2.0. This limitation excludes one-way slabs.
3. The successive span lengths (centre to centre of supports) in each direction must not differ by more than one-third of the longer span. (If this limit is exceeded, negative bending moments will be developed in the regions for which the DDM will consider only the positive moments). The end span may be shorter but not longer than the interior spans.
4. Columns may be offset to a maximum of 10 per cent of the span in the direction of offset. If the column offsets result in variation of spans in the transverse direction, as per Clause 31.4.2.4, the adjacent transverse spans should be averaged while carrying out the analysis.
5. Loads must be due to gravity loads alone, which are uniformly distributed over an entire panel, and the design

imposed loads must not exceed three times (two times in the ACI code) the dead load. This limit on the ratio of the imposed load to dead loads is to take care of the effects of pattern loading (see Section 3.9 of Chapter 3 for discussion on pattern loading).

6. If beams are used on the column lines, the relative stiffness of the beams in the two perpendicular directions given by the ratio $\alpha_1 L_2^2 / \alpha_2 L_1^2$ must be between 0.2 and 5.0, where $\alpha = E_{cb} I_b / E_{cs} I_s$. It has to be noted that this condition is specified in the ACI code.
7. Redistribution of bending moments is permitted up to 10 per cent, as per Clause 31.4.3.4 of IS 456, provided that the total design moment for the panel in the direction considered is not less than M_o computed as per Eq. (11.2).

Though the design by the DDM is to a large extent empirical, the given limitations conform to the available experimental results (Hatcher, et al. 1965, 1969; Jirsa, et al. 1966; Magura and Corley 1971). Van Buren (1971), by adopting the DDM for the analysis of flat slabs with staggered columns, has shown that this method can be used even if one of the conditions is violated. When lateral loads are considered, the DDM can be applied, provided separate systems to resist lateral loads, for example, shear walls, are used.

In the DDM, the bending moments are not computed but nominally defined in the code, as functions of column stiffness, span lengths, and design (dead and live) loads. The absolute sum of the positive and average negative bending moments along the span due to the total load on a panel, known as the *total static moment*, M_o , was derived by Nichols in 1914 as (Clause 31.4.2.2 of IS 456)

$$M_o = M_P + M_\lambda = \frac{wL_2L_1^2}{8} \left[1 - \frac{4d_c}{\pi L_1} + \frac{1}{3} \left(\frac{d_c}{L_1} \right)^3 \right] \quad (11.2a)$$

Nichols approximated this equation as

$$M_o = \frac{wL_2}{8} \left(L_1 - \frac{2D_c}{3} \right)^2 \approx \frac{wL_2L_n^2}{8} = \frac{WL_n}{8} \quad (11.2b)$$

where w is the uniformly distributed design load on the slab, d_c is the diameter of the column or the column capital, W is the design load on area L_2L_n (note that it is less than the load on L_2L_1), L_n is the clear span extending from the face of columns, capitals, brackets, or walls but greater than or equal to $0.65L_1$, L_1 is the length of span in the direction of M_o , L_2 is the length of span transverse to L_1 , and D_c is the diameter of the circular column. It should be noted that the term $(L_1 - 2D_c/3)$ derived in Nichols' expression for circular column was later approximated to the clear span L_n to consider rectangular or square columns as well. The moment M_o in the L_2 direction can be found in a similar fashion.

While considering the values of L_n , L_1 , and L_2 , the following points should be carefully considered (Clauses 31.4.2.3–31.4.2.5 and 31.5.3):

1. Circular supports should be treated as equivalent square supports having the same area, that is, square supports of size $0.886D_c$ (see Fig. 11.9).
2. When the transverse span of the panel on either side of the centre line of support varies, L_2 should be taken as the average of the transverse spans; hence, for the slab in Fig. 11.7, L_2 should be taken as $(L_{2a} + L_{2b})/2$.
3. When the span adjacent and parallel to an edge is being considered, the distance from the edge to the centre line of the panel should be substituted for L_2 .
4. The negative design moment should be located at the face of rectangular supports, treating circular supports as equivalent square supports. See Fig. 11.9.

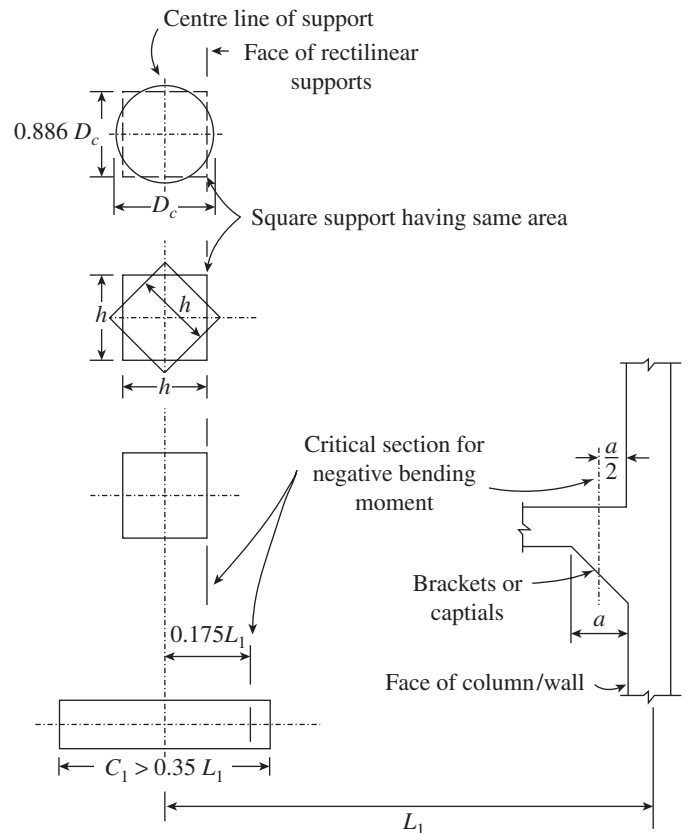


FIG. 11.9 Critical sections for negative design moment (Clause 31.5.3 of IS 456)

This total static moment is distributed longitudinally and transversely among various regions of the slab (column and middle zones) based on the panel (interior or exterior) and span (interior or exterior) conditions.

Interior spans As per Clause 31.4.3.2 of IS 456, this distribution in interior spans is simple and is approximately equal to the *fixed-end beam* moments. Thus, the support (negative) moment M_s is assumed to be 65 per cent of the total

static moment M_o and the span (positive) moment M_F to be the remaining 35 per cent. These moments are further divided between the column and middle strips as discussed later in this section.

Exterior spans As per Clause 31.4.3.3 of IS 456, the distribution of total static moment in exterior (end) spans depends upon the end support conditions and the relative stiffness of the columns and slab. The distribution coefficients for various moments in the end panel are given as follows (Clause 31.4.3.3):

Exterior negative design moment coefficient

$$= \frac{0.65}{(1.0 + \alpha)} \tag{11.3a}$$

Interior negative design moment coefficient

$$= 0.75 - \frac{0.10}{(1.0 + \alpha)} \tag{11.3b}$$

Mid-span positive design moment coefficient

$$= 0.63 - \frac{0.28}{(1.0 + \alpha)} \tag{11.3c}$$

where $\alpha = \frac{1}{\alpha_c} = \frac{K_s + K_b}{\sum K_c}$, $\tag{11.3d}$

K_s is the flexural stiffness of the slab, expressed as moment per unit rotation = EI_s/L_s , K_b is the flexural stiffness of the beam, if present = EI_b/L_b (and equal to zero for flat slabs), and $\sum K_c$ is the sum of the flexural stiffness of the columns meeting at the joint = $\sum EI_c/L_c = \sum Eh^4/(12L_c)$, where L is the length and h is the width of column (see also Fig. 10.9 of Chapter 10). These expressions for moments in the exterior spans in terms of α_{ec} were suggested by Gamble in 1970 (it should be noted that α_{ec} is different from α_c given in the IS code and is related to the stiffness of the equivalent column, which was considered in ACI 318-77). Since the computation of α_{ec} was tedious, these expressions were replaced in the future versions of the ACI code by a table of coefficients (see Table 11.1 and Fig. 11.10), which can be directly read for design. From this table, it is seen that the procedure given in the ACI code for the design of two-way slabs is unified and we have coefficients for all possible cases encountered in practice.

TABLE 11.1 Distribution of total static moment M_o for an end span as per ACI 318

Type of Moment	Slab Simply Supported on Concrete or Masonry Wall	Two-Way Beam-Supported Slabs	Flat Plates and Flat Slabs		Slab Monolithic with Concrete Wall
			Without Edge Beam	With Edge Beam	
Interior: Negative	0.75	0.70	0.70	0.70	0.65
Interior: Positive	0.63	0.57	0.52	0.50	0.35
Exterior: Negative	0	0.16	0.26	0.30	0.65

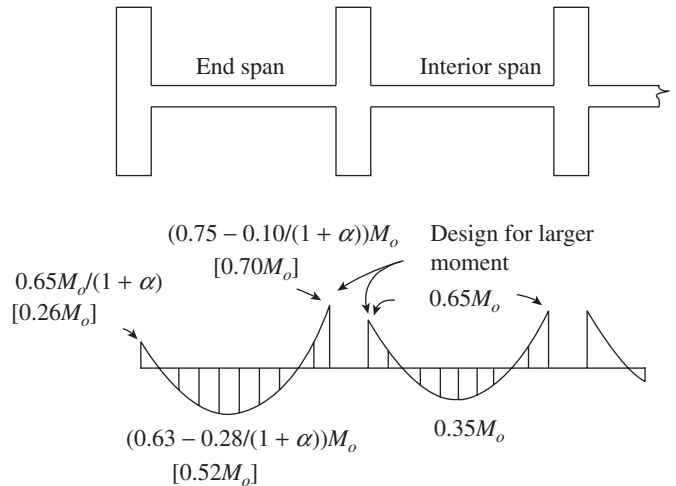


FIG. 11.10 Design moment coefficients used in DDM for flat slabs or flat plate

Note: Quantities in square brackets are as per ACI 318

As per Clause 31.4.3.1, negative factored moments should be located at the face of rectangular supports. Circular or regular polygon-shaped supports may be treated as square supports with the same area. Clause 31.4.3.5 stipulates that the negative moment sections should be designed to resist the larger of the two interior negative factored moments determined for spans framing into a common support unless an analysis is made to distribute the unbalanced moment in accordance with the stiffness of adjoining elements (see Fig. 11.10). Edge beams or edges of slab should be proportioned to resist the torsion due to their share of exterior negative factored moments.

Distribution of Bending Moments across Panel Width

After distributing the moment M_o longitudinally as a positive moment in span and negative moment at the two ends, the next step is to apportion them transversely to the column strip and middle strip of the respective sections, as per Clause 31.5.4 of IS 456.

1. Distribution to column strip The rules for distributing the moments in the column strip are shown in Table 11.2 and Fig. 11.11.

The transverse distribution of moments to column strips as per Clause 13.6.4 of ACI 318 is given in Table 11.3.

For slabs with beams between supports, the slab portion of the column strips should be proportioned to resist the portion of column strip moments not resisted by the beams. In the definition of β_t , the shear modulus has been taken as $E_{cb}/2$. The torsional constant, C , for T- or L-beams is calculated by subdividing the cross section into separate rectangular parts and summing the values of C for each part.

TABLE 11.2 Transverse distribution of moments to column strips as per IS 456 (percentages)

Moment to be Distributed	Column/Wall Width	Percentage of the Moment at that Support
Negative moment in interior spans	–	75
Negative moment in end spans	< 0.75L ₂	100
	> 0.75L ₂	Multiply the moment at support by (b _{cs} /L ₂)
Positive moment in all spans	–	60

Note: b_{cs} is the width of column support (see Fig. 11.11) and L₂ is the span that is transverse to the direction in which moments are determined.

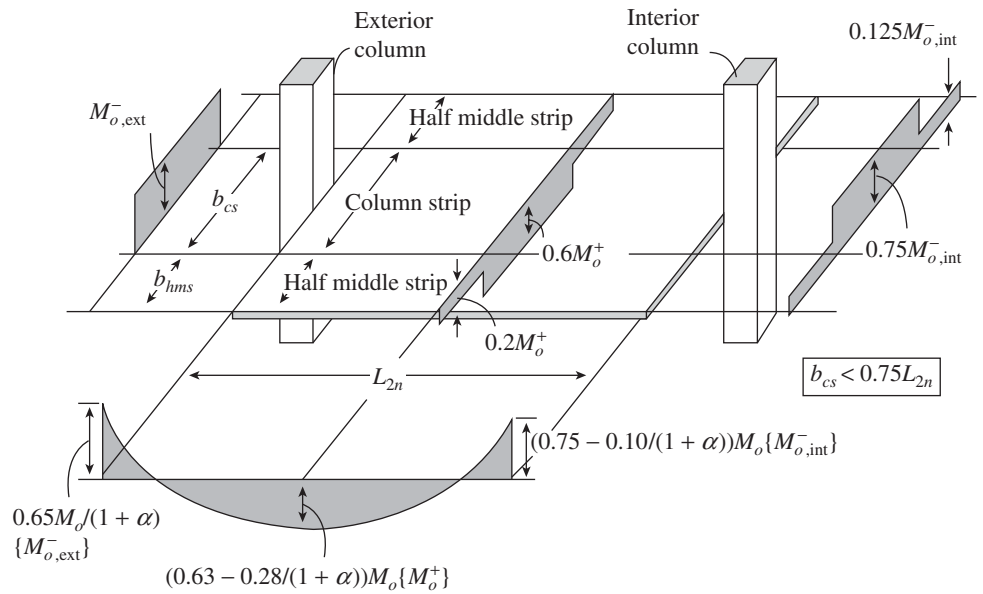


FIG. 11.11 Transverse distribution of bending moments in a typical end span

TABLE 11.3 Transverse distribution of moments to column strips as per ACI 318 (percentages)

Moment to be Distributed	Type of Beam Present	$\frac{\alpha_1 L_2}{L_1}$	β_t	L ₂ /L ₁		
				0.5	1.0	2.0
Negative moment in interior spans	No internal beam	0	–	75	75	75
	With internal beam	≥ 1	–	90	75	45
Negative moment in end spans	No internal beam and no edge beam	0	0	100	100	100
	No internal beam and with edge beam	0	≥ 2.5	75	75	75
	With internal beam and no edge beam	≥ 1	0	100	100	100
	With internal and edge beams	≥ 1	≥ 2.5	90	75	45
Positive moment in all spans	No internal beam	0	–	60	60	60
	With internal beam	≥ 1	–	90	75	45

Notes:

- Linear interpolation can be made between the values shown.
- The effect of the torsional stiffness parameter $\beta_t = \frac{E_{cb}C}{2E_{cs}I_b}$, where E_{cb} and E_{cs} are the Young’s moduli for beam and slab, respectively, and I_b is the moment of inertia of beam.
- $C = \sum \left(1 - 0.63 \frac{x}{y} \right) \left(\frac{x^3 y}{3} \right)$; x is the shorter side of the rectangle and y is the longer side.

2. Distribution to middle strip As per Clause 31.5.5.4 of IS 456, the moments in the middle strip are assigned as follows (see Fig. 11.11):

- The portion of negative and positive factored moments not resisted by the column strips is proportionately assigned to the corresponding half middle strips.
- Each middle strip is proportioned to resist the sum of the moments assigned to its two half middle strips.
- A middle strip adjacent to and parallel with a wall-supported edge is proportioned to resist twice the moment assigned to the half middle strip corresponding to the first row of interior supports.

Fanella (2001 and 2002) developed design aids in the form of tables for the design moments as per the ACI code, so that they

may be used directly in design. Tables 11.4 and 11.5 show these tables for flat slabs directly supported on columns and flat slabs with edge beams, respectively (see also Figs 11.12 and 11.13).

TABLE 11.4 Design moment coefficients for flat plates supported on columns; refer to Fig. 11.12 (Fanella 2002, SEAOC)

Location	Exterior		First Interior	Interior	
	Negative	Positive	Negative	Positive	Negative
Total moment	0.26M _o	0.52M _o	0.70M _o	0.35M _o	0.65M _o
Column strip	0.26M _o	0.31M _o	0.53M _o	0.21M _o	0.49M _o
Middle strip	0	0.21M _o	0.17M _o	0.14M _o	0.16M _o

Note: All negative moments are at the face of the support.

TABLE 11.5 Design moment coefficients for flat plates or flat slabs with edge beams; refer to Fig. 11.13 (Fanella 2002, SEAOC)

Location	Exterior		First Interior	Interior	
	Negative	Positive	Negative	Positive	Negative
Total moment	0.30M _o	0.50M _o	0.70M _o	0.35M _o	0.65M _o
Column strip	0.23M _o	0.30M _o	0.53M _o	0.21M _o	0.49M _o
Middle strip	0.07M _o	0.20M _o	0.17M _o	0.14M _o	0.16M _o

Notes:

1. All negative moments are at the face of the support.
2. Torsional stiffness of spandrel beam β_t ≥ 2.5; for values of β_t less than 2.5, exterior negative column strip moment increases to (0.30 – 0.03β_t)M_o.

For other cases, the reader may refer to the work of Fanella (2002).

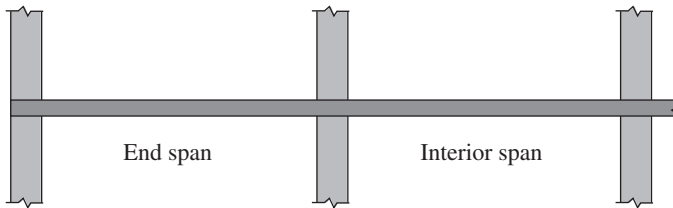


FIG. 11.12 Flat slabs supported directly on columns

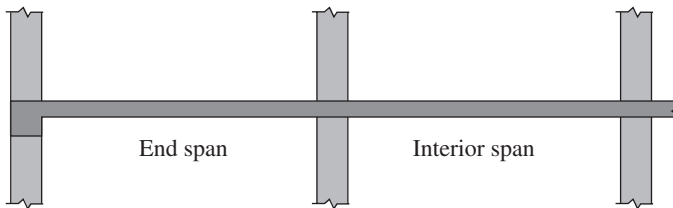


FIG. 11.13 Flat slabs with edge beams

Effects of Pattern Load

As indicated earlier, the positive moment in continuous slabs may change due to pattern loading. In the ACI code, the DDM is limited to cases where the live load to dead load ratio (*LL/DL*) is limited to 2.0. Hence, the necessity of checking the effects of pattern loading has been eliminated. However, in the IS code, the *LL/DL* ratio of up to 3.0 is permitted. Hence, Clause 31.4.6 of IS 456 suggests the following:

When the ratio of *LL/DL* exceeds 0.5, the following may be noted:

1. The sum of the flexural stiffness of columns above and below the slab, ΣK_c, should be such that α_c is not less than the approximate minimum value of α_{c,min} specified in Table 11.6 (this table is based on the work of Jirsa, et al. 1969).
2. If the sum of the flexural stiffness of columns, ΣK_c, does not satisfy the condition in point 1, the positive design moments for the panel should be multiplied by the coefficient β_L, which is given by the following equation:

$$\beta_L = 1 + \left(\frac{2 - \beta_t}{4 + \beta_t} \right) \left(1 - \frac{\alpha_c}{\alpha_{c,min}} \right) \text{ with } \beta_t = \frac{DL}{LL} \quad (11.4)$$

Here, α_c is the ratio of flexural stiffness of the column above and below the slab to the flexural stiffness of the slab at a joint taken in the direction the moments are being determined and is given as

$$\alpha_c = \frac{\sum K_c}{\sum K_s + \sum K_b} \quad (11.5)$$

where K_b, K_c, and K_s are the flexural stiffness of beam, column, and slab, respectively. It has to be noted that for flat slabs or plates ΣK_b = 0.

TABLE 11.6 Minimum permissible values of α_c

Imposed Load/Dead Load	Ratio L ₂ /L ₁	Value of α _{c,min} for Relative Beam Stiffness				
		α = $\frac{E_{cb}I_b}{E_{cs}I_s}$				
		0.0	0.50	1.00	2.0	4.0
0.5	0.5–2.0	0	0	0	0	0
	1.0	0.6	0	0	0	0
1.0	0.50	0.6	0	0	0	0
	0.80	0.7	0	0	0	0
	1.00	0.7	0.1	0	0	0
	1.25	0.8	0.4	0	0	0
2.0	2.00	1.2	0.5	0.2	0	0
	0.50	1.3	0.3	0	0	0
	0.80	1.5	0.5	0.2	0	0
	1.00	1.6	0.6	0.2	0	0
	1.25	1.9	1.0	0.5	0	0
3.0	2.00	4.9	1.6	0.8	0.3	0
	0.50	1.8	0.5	0.1	0	0
	0.80	2.0	0.9	0.3	0	0
	1.00	2.3	0.9	0.4	0	0
	1.25	2.8	1.5	0.8	0.2	0
	2.00	13.0	2.6	1.2	0.5	0.3

11.4.2 Equivalent Frame Method

The EFM is more general and is based on elastic analysis. In this method, the structure is divided into frames in longitudinal and transverse directions. Thus, the actual three-dimensional structure is considered as a series of equivalent plane frames, each consisting of a row of columns and a portion of the floor system tributary to it. In each direction, the equivalent frame consists of a row of columns (or supports) bounded laterally by the centre lines of panels on each side of the row of columns (or supports). Frames adjacent to and parallel to an edge are bounded laterally by the edge and centre line of the adjacent panel. The equivalent frames for a typical structure are shown in Fig. 11.14 (see Clause 31.5 of IS 456). Some more assumptions are made regarding the stiffness of the frame members. Gross concrete areas are assumed, and the stiffening effect of the flared columns is ignored. The equivalent frames can be analysed under both gravity and lateral loads using any standard computer program based on the *finite element method* (FEM). The concept of *substitute frames* can be made use of instead of analysing the

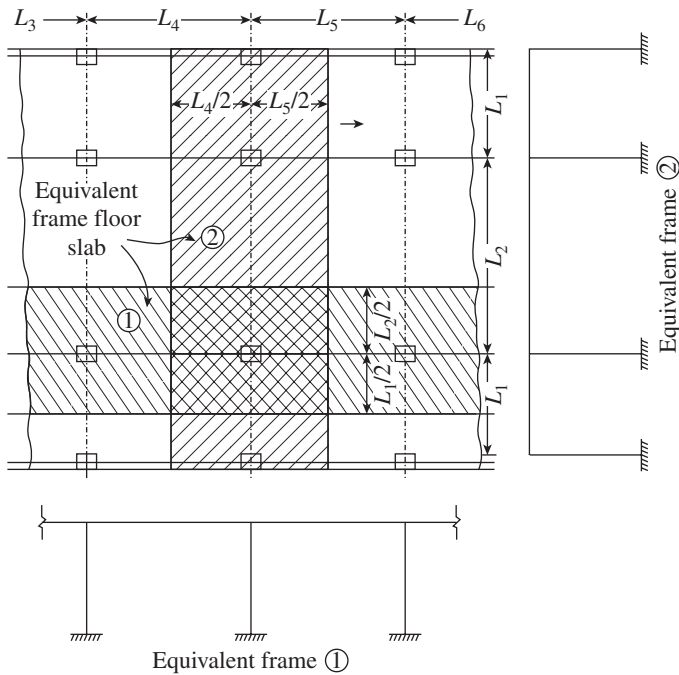


FIG. 11.14 Equivalent frames for various rows of columns

whole equivalent frame, when the geometry and loading are symmetrical.

The variation of the moment of inertia along the axis of slab on account of the provision of drops should be taken into account in the analysis. However, in the case of a recessed or coffered slab made solid in the region of columns, the influence of the solid part may be ignored if the length of such a solid part does not exceed 0.15 times the effective span measured from the centre line of the columns. Other conditions on loading are given in Clause 31.5.2 of the code.

The EFM requires greater effort but has wider applicability than the DDM. A further advantage of the EFM is that it can be used for lateral load analysis as well (see Section 11.9 for details). The EFM is better suited for computer analysis and the DDM for manual analysis. However, tables were developed to evaluate fixed-end moments, stiffness, and equivalent column stiffness for manual analysis of EFM using the moment distribution method; such tables may be found in SP 24:1983. If standard frame analysis software based on the stiffness method is to be used, the torsional member and the resulting equivalent column stiffness need to be incorporated into either the slab-beam or column elements (Wight and MacGregor 2009). The alternate

effective slab width method is discussed in Section 11.9.2. Since standard computer software is usually employed in the analysis, more details and examples using the EFM are not included here. They may be found in the works of Vanderbilt and Corley (1983), Pillai and Menon (2009), Varghese (2006), and Wight and MacGregor (2009) and in SP 24:1980.

11.4.3 Transfer of Moments to Columns

On many occasions, the maximum load that a flat slab can support is dependent upon the strength of the slab-column joint. In addition to the load that is transferred by shear from the slab to the column (along an area around the column), moments and torsion also have to be transferred to the exterior columns. Such a transfer may also be there in interior columns, when there are unbalanced gravity loads or other lateral loads such as wind and earthquake. The behaviour of slab-column joints subjected to shear, bending, and torsion is complex and has been reviewed by Hawkins (1974b) and Regan and Braestrup (1985) and in the report of ACI-ASCE Committee 426 (1974). Hawkins and Corley (1974) studied the moment transfer to column in slabs with shear-head reinforcement.

It has to be noted that such moment transfers will be very critical at the edge and exterior columns. These moment transfers will cause shear stresses of their own in the slabs. Moreover, shear forces resulting from the moment transfer must be considered in the design of transverse column reinforcement (ties and spirals) as well. The shear stresses due to moment and shear transfers in the interior columns and edge column-slab joints are shown in Figs 11.15 and 11.16, respectively. It is seen from these figures that the transfer is made by both flexure and eccentric shear; the latter is usually

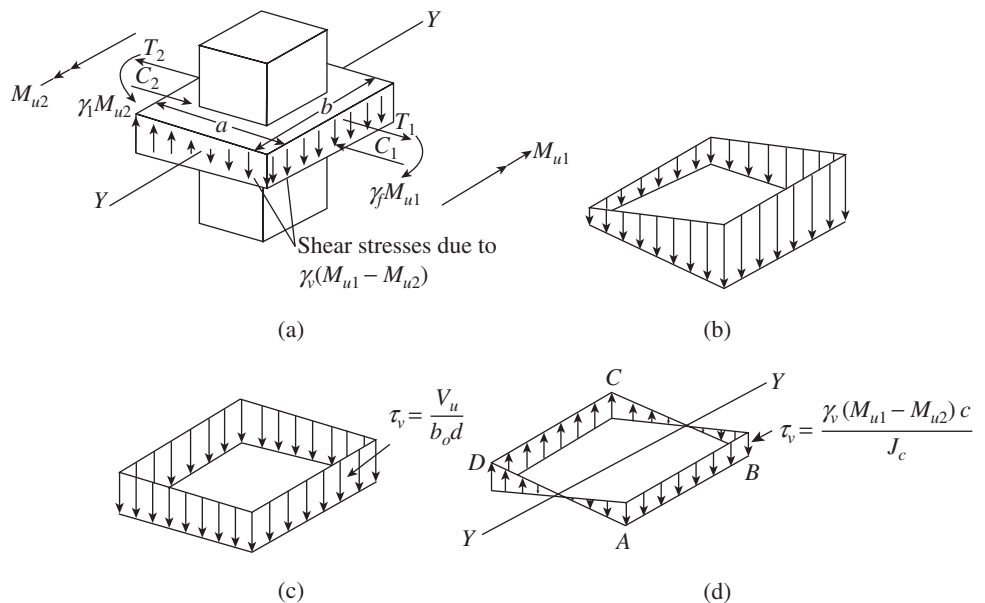


FIG. 11.15 Shear stresses due to transfer of shear and moment at interior columns (a) Transfer of unbalanced moments to column (b) Total shear stresses (c) Shear stress due to V_u (d) Shear due to unbalanced moment

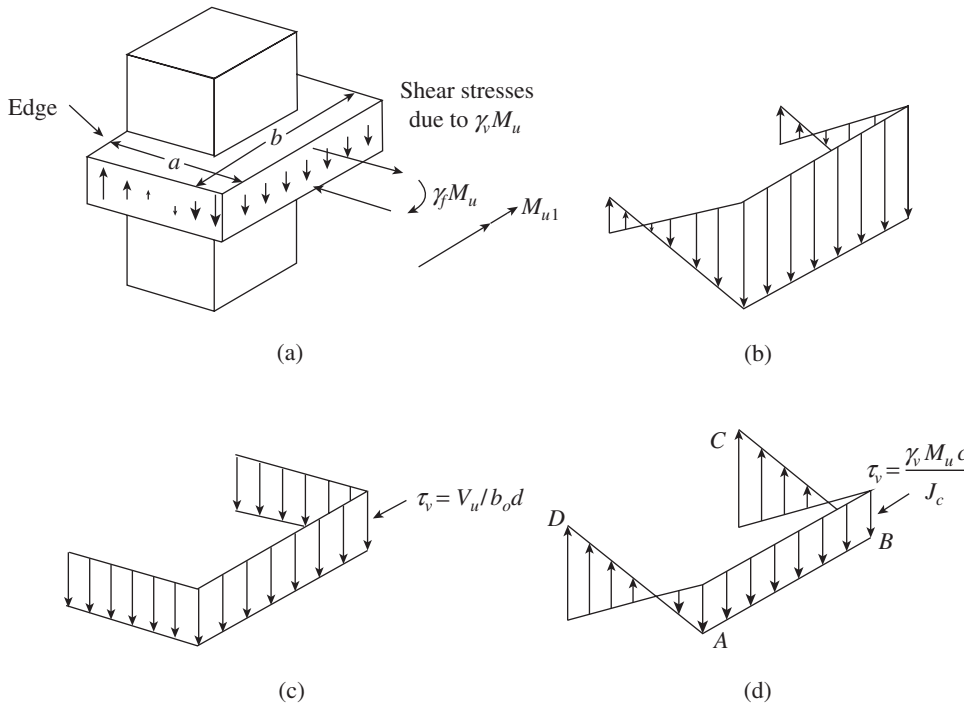


FIG. 11.16 Shear stresses due to transfer of shear and moment at edge columns (a) Transfer of moment at edge column (b) Total shear stresses (c) Shear stresses due to V_u (d) Shear stresses due to M_u

assumed to be located at a distance of $d/2$ from the column face, where d is the effective depth of the slab.

Clause 13.6.3.6 of the ACI code suggests that the moment transfer from the slab to the edge column due to gravity loads is to be taken as $0.3M_o$, where M_o is the factored statical moment. When there is an unbalanced moment, M_u , due to gravity load or wind, earthquake, or other lateral loads, a part of the moment equal to $\gamma_f M_u$ should be transferred by flexure. The remainder of the unbalanced moment $M_u(1 - \gamma_f) = \gamma_v M_u$ is assumed to be transferred by the eccentricity of the shear about the centroid of the critical section. As per Clause 31.3.3 of IS 456, the value of γ_f is given as (in IS 456 nomenclature it is α)

$$\gamma_f = \frac{1}{1 + \frac{2}{3} \left(\frac{a}{b}\right)^{0.5}} \quad (11.6)$$

fraction of the transfer moment $\gamma_f M_u$ (see Clause 31.3.3 of IS 456). It has been found from tests that the slab bars not anchored in the column will not be effective for transferring the moments to the column (Simmonds and Alexander 1987). Equation 11.6 was derived to give a value of $\gamma_f = 0.6$ for $a_1 = a_2$, as proposed by Hanson and Hanson (1968), to provide a transition to $\gamma_f = 1.0$ for slabs attached to the side of a wall and to $\gamma_f = 0$ for a slab attached to the end of a long wall (Wight and MacGregor 2009).

Equation 11.6 was found to overestimate the value of γ_f , especially when the rectangularity ratio of the column increases. For example, for interior columns with the values of a_2/a_1 as 1, 2, and 2.5, the values of γ_f equals 0.40, 0.32, and 0.30, respectively, whereas the values as found by Nazief, et al. (2010), using a boundary element method calculation,

where a and b are the sides of the control perimeter of a rectangular column (see Figs 11.15 and 11.16), a is the overall dimension of the critical section for shear in the direction in which the moment acts (perpendicular to the moment vector), and b is the overall dimension of the critical section for shear transverse to the direction in which the moment acts.

Based on experience and tests, this transfer is considered to be made within an effective slab width between lines that are located 1.5 times the slab or drop panel thickness outside the opposite faces of the column or capital (Clause 31.3.3 of IS 456). This width of size of column plus $1.5D_s$, where D_s is the slab or drop panel thickness, is called the *transfer width* (see Fig. 11.17). Sufficient reinforcements have to be provided within this transfer width to carry the

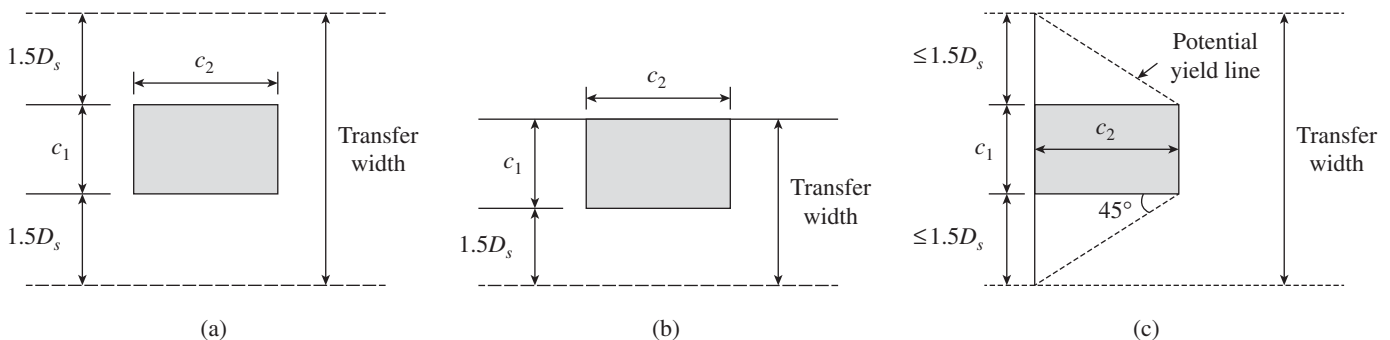


FIG. 11.17 Transfer width at slab-column connections (a) Interior column (b) Exterior column—moment transferred parallel to the edge (c) Exterior column—moment transferred perpendicular to the edge

are 0.36, 0.18, and 0.13, respectively. Hence, based on the FEM analysis results, Elgabri and Ghali (1996) proposed the following modified equation, which gives better values than the IS code equation (Nazief, et al. 2010):

$$\gamma_f = \frac{1}{1 + \frac{2}{3} \left(\frac{a_1}{a_2} - 0.2 \right)^{0.5}} \quad \text{for } a_1/a_2 \geq 0.2 \quad (11.7a)$$

$$\gamma_f = 0.4 \quad \text{for } a_1/a_2 < 0.2 \quad (11.7b)$$

Anggadajaja and Teng (2008) conducted tests on rectangular edge column–slab connections subjected to biaxial lateral loading and found that the ACI eccentric shear model accurately predicts the failure behaviour of edge connections in the cyclic moment transfer. Section 13.5.3.3 of the ACI code permits increasing the fraction γ_f used for moment transfer under certain conditions. Gayed and Ghali (2008) and Ritchie, et al. (2006), based on their extensive finite element studies and experimental results, suggested that such a reduction should not be permitted.

If there is an unbalanced loading of two adjoining spans, the result will be an additional moment at the connection of the walls and columns to slabs. To consider the effect of such situations, Eq. (11.8) is given in Clause 31.4.5.2 of IS 456. This equation was derived for two adjoining spans, one longer than the other. It was assumed that the longer span was loaded with the dead load plus one-half the live load and the shorter span with only the dead load. It has to be noted that in the ACI code (Clause 13.6.9.2) the coefficient 0.08 is replaced by 0.07 and the denominator is taken as 1.0.

$$M = \frac{0.08 \left[(w_d + 0.5w_l)L_2L_n^2 - w'_d L'_2L_n'^2 \right]}{\left(1 + \frac{1}{\alpha_c} \right)} \quad (11.8)$$

Here, w_d and w_l are the design factored dead and live loads, respectively, per unit area, L_2 is the length of span transverse to the direction of M , L_n is the length of clear span in the direction of M , and $\alpha_c = \Sigma K_c / \Sigma K_s$, where K_c and K_s have been defined earlier. It has to be noted that w'_d , L'_2 , and L'_n refer to the shorter span. The value of M given by Eq. (11.8) should be used for unbalanced moment transfer by gravity loading at the interior columns unless a more refined analysis is used.

11.5 SHEAR IN FLAT PLATES AND FLAT SLABS

For flat slabs and flat plates directly supported by columns, shear may be the critical factor in design. In almost

all tests of such structures, failures have been due to shear or perhaps shear and torsion. These conditions are particularly serious around the exterior columns.

The shear strength of flat slabs in the vicinity of columns is thus considered to be governed by the more severe of the following two conditions:

1. Wide beam action or one-way shear
2. Two-way action (also called *punching shear*)

In two-way action, it is also important to consider the shear caused by the moment transfer (combined with torsional moment) around the columns. Such a moment transfer will be critical to the corner and edge columns.

11.5.1 One-way or Beam Shear

The analysis for wide beam action considers the slab to act as a wide beam spanning between columns. The critical section extends in a plane across the entire width of the slab and is assumed to be located at a distance d (effective slab depth) from the face of the column or shear capital, as shown in Fig. 11.18(a). The area from which the load is transferred to the critical section is termed the *tributary area*. For this condition, the conventional beam theory can be applied, which has been covered in Section 10.4.2 of Chapter 10. Thus, the magnitude of shear stress is given by

$$\tau_v = \frac{V_u}{bd} \quad (11.9)$$

where $V_u = w_u(0.5L_n - d)$, w_u is the factored uniform load applied on the slab, L_n is the length of clear span in the longer direction, b is the length resisting shear (length of short span), and d is the effective depth of slab. It should be noted that for lateral loads the shear force V_u is obtained from the analysis of the equivalent frame.

In the case of flat slabs with drop panels, the one-way shear needs to be checked at two sections—at a distance d_1 from the face of the columns, where d_1 is the effective depth of the slab inside the panel, and at a section d_2 from the edge of the drop panel, where d_2 is the effective depth of the slab outside

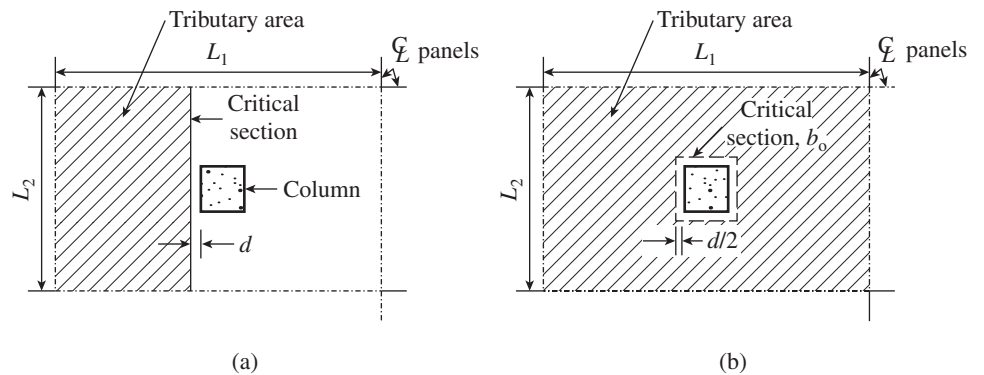


FIG. 11.18 Shear in flat plates (a) One-way or beam action (b) Two-way action (punching shear)

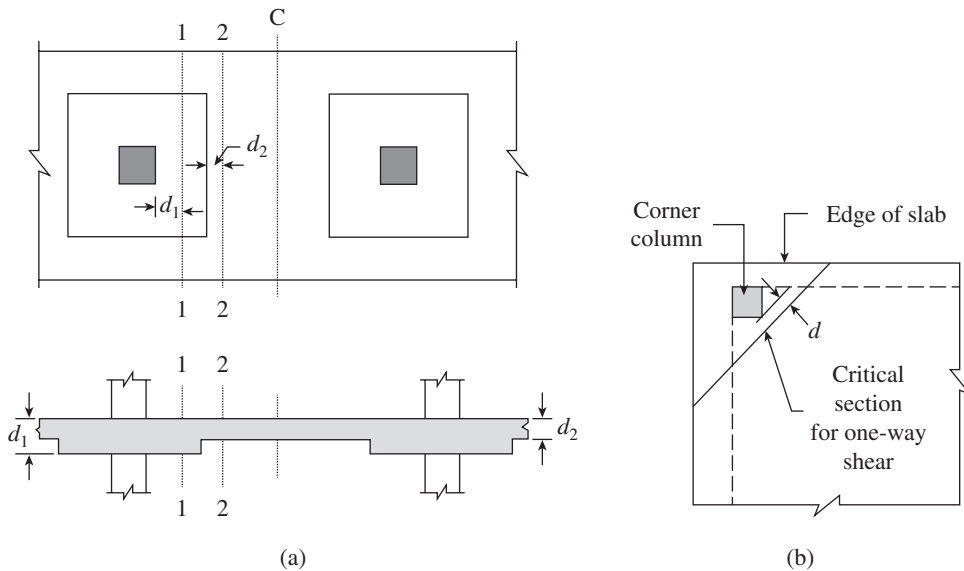


FIG. 11.19 Critical section for one-way shear (a) Flat slabs (b) Corner column

the panel (see Fig. 11.19a). In the case of corner columns, the critical section has to be taken along a straight line located at a distance d from the corner column, as shown in Fig. 11.19(b).

11.5.2 Two-way or Punching Shear

As discussed earlier, slab-column connections experience very complex behaviour when subjected to lateral displacements or unbalanced gravity loads. This involves the transfer of flexure, shear, and torsion in the portion of the slab around the column. Combined flexural and diagonal cracking is coupled with significant in-plane compressive forces in the slab induced by the restraint of the surrounding unyielding slab portions. When loaded incrementally, the slab around a column support fails in the shape of a truncated cone or pyramid with the failure surface inclined at about $25\text{--}35^\circ$ (see Fig. 10.6 of Chapter 10). This failure surface is accompanied by bending cracks in the same region in the circular and radial directions. In general, the punching shear capacity will be considerably less than the one-way shear capacity. Punching failure usually occurs suddenly without any warning. Once a punching failure occurs, the shear capacity of that joint is completely lost. The column load is transferred to the adjacent column-slab connection, thereby overloading them and causing them to fail. This kind of failure results in a progressive collapse (see also Section 2.6 of Chapter 2). Thus, a flat slab or flat plate may possess sufficient ductility if it fails in flexure but little ductility when punching shear is the failure mode.

Many slab-column connections in flat plate structures were damaged and failed after the 1985 Mexico City earthquake, the 1989 Loma Prieta earthquake, and the 1994 Northridge earthquake. In the event of punching failure at a connection, bottom slab reinforcement anchored through the columns has

been observed to be an effective means of preventing or delaying collapse; lack of such reinforcement has been observed to result in catastrophic failures (Moehle and Mahin 1991). This showed that slab-column connections are prone to punching shear failure when lateral forces cause substantial unbalanced moments to be transferred from the slab to column. Moreover, low percentages of longitudinal reinforcement in the column strip (about 0.5 per cent flexural reinforcement with no shear reinforcement) results in low shear strength and leads to failure.

In the codes, for the condition of two-way action, the critical section is assumed to be located at a distance

$d/2$ from the perimeter of the column or drop panel, with potential diagonal tension cracks occurring along a truncated cone or pyramid passing through the critical section (see Fig. 10.6 of Chapter 10 and Fig. 11.20). It should be noted that when there is a drop panel, there will be two critical sections as shown in Figs 11.20(b) and (d)—one at a distance of $d_1/2$ from the face of the column and within the drop panel and the other at a distance of $d_2/2$ from the edge of the drop panel, where d_1 and d_2 are the effective slab depths at the respective locations.

Several variables affect the punching shear strength of flat slabs, which include the concrete strength, ratio of the column size to slab effective depth, ratio of shear strength to flexural strength, shape of the column, amount of tension and compression reinforcement, and lateral constraints (Theodorakopoulos and Swamy 2002). Research by Moe (1961) showed that the critical section governing punching shear strength is located at the face of the column. However, ACI-ASCE Committee 326 in 1962 suggested it to be taken at the critical section $d/2$ from the face of the column, as shown in Fig. 11.20, for the sake of simplicity in calculation. This was referred to as *pseudo-critical section for shear*. This simplification was later adopted by the ACI code. Moreover, it considered the shear perimeter as consisting of straight lines, that is, without rounding off the corners. Similar provisions are also adapted in the IS 456 code. It has to be noted that the other codes consider the critical section at $1.5d$ or even $2d$ from the face of the column and rounded shear perimeters even for rectangular columns, as shown in Fig. 11.21. The ACI and IS codes assume that the ultimate shear strength at this section is a function of the square root of the concrete strength (other codes, such as EC2-2003 and DIN 1045-1:2001, consider the cube root of the concrete strength).

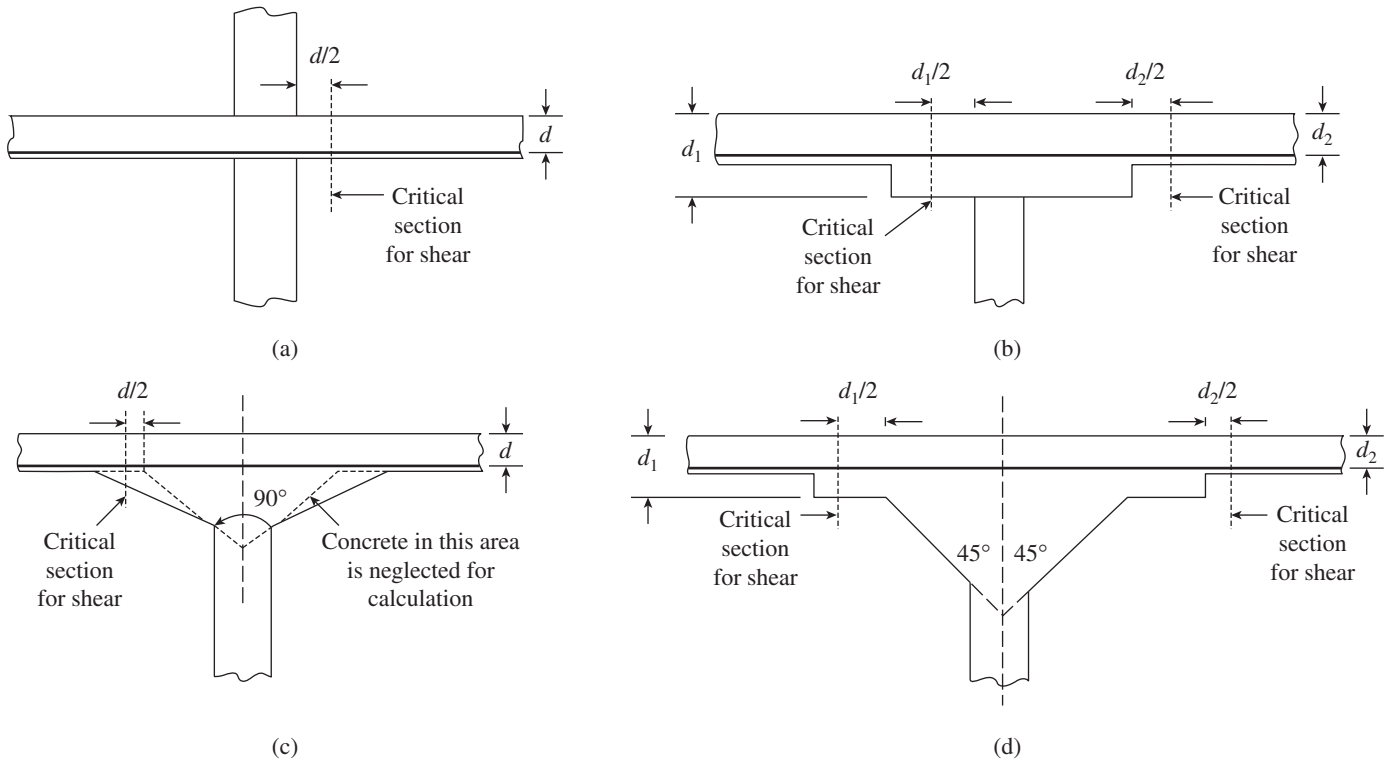


FIG. 11.20 Critical sections for two-way punching shear (a) Flat slab without drop and column head (b) Slab with drop but without column head (c) Slab without drop but with column head (d) Slab with drop and column head

For different shapes of columns, the perimeter in IS 456 is suggested to be similar to the shape of the column immediately below the slab, as shown in Fig. 11.22 (Clause 31.6.1, see also Table E8 of SP 24:1983). Critical sections for columns near the free edge of the slab are also shown in Figs 11.22(e) and (f).

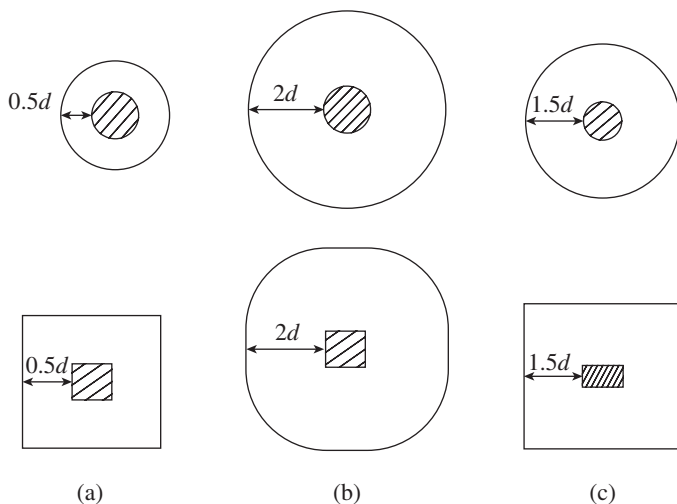


FIG. 11.21 Critical perimeters in different codes (a) ACI 318, AS 3600, and IS 456 (b) CEB-FIP MC-90 (c) BS 8110

Based on the results of a significant number of experimental tests involving slab-column specimens, Moe (1961) proposed an equation for predicting the punching shear strength of two-way slabs supported on columns. The ACI Committee

326 in 1962 simplified this equation and adopted an equation similar to that found in Clause 31.6.3 of IS 456 (see Clause 11.11.2.1 of ACI 318). The tributary area to be considered for calculating the value of V_u for the punching shear is the area bounded by the lines of zero shears, that is, the area within the centre lines of the spans minus the area within the critical section—the area shown shaded in Fig. 11.18(b). The exterior supports must resist a shear force due to the loads acting on half the span.

As per Clause 31.6.3 of the code, the nominal punching shear stress in flat slabs is calculated as

$$\tau_v = \frac{V_u}{b_o d} = \frac{V_u}{A_c} \quad (11.10)$$

where V_u is the shear force in flat slabs due to the design loads at the critical section, b_o is the perimeter of the critical section, d is the effective depth of the slab, and A_c is the concrete area of the assumed critical section. The maximum value of τ_v should not exceed $0.467\sqrt{f_{ck}}$ (NZS 3101:2006).

Design Punching Shear Strength

Early tests found that the punching shear strength of concrete, τ_c , is dependent on the following three parameters (ACI-ASCE Committee 326:1962 and 426:1974; SP 24:1983):

1. The ultimate compressive strength of concrete, f_{ck}
2. The ratio of shorter side to longer side of the column or column capital, β_c

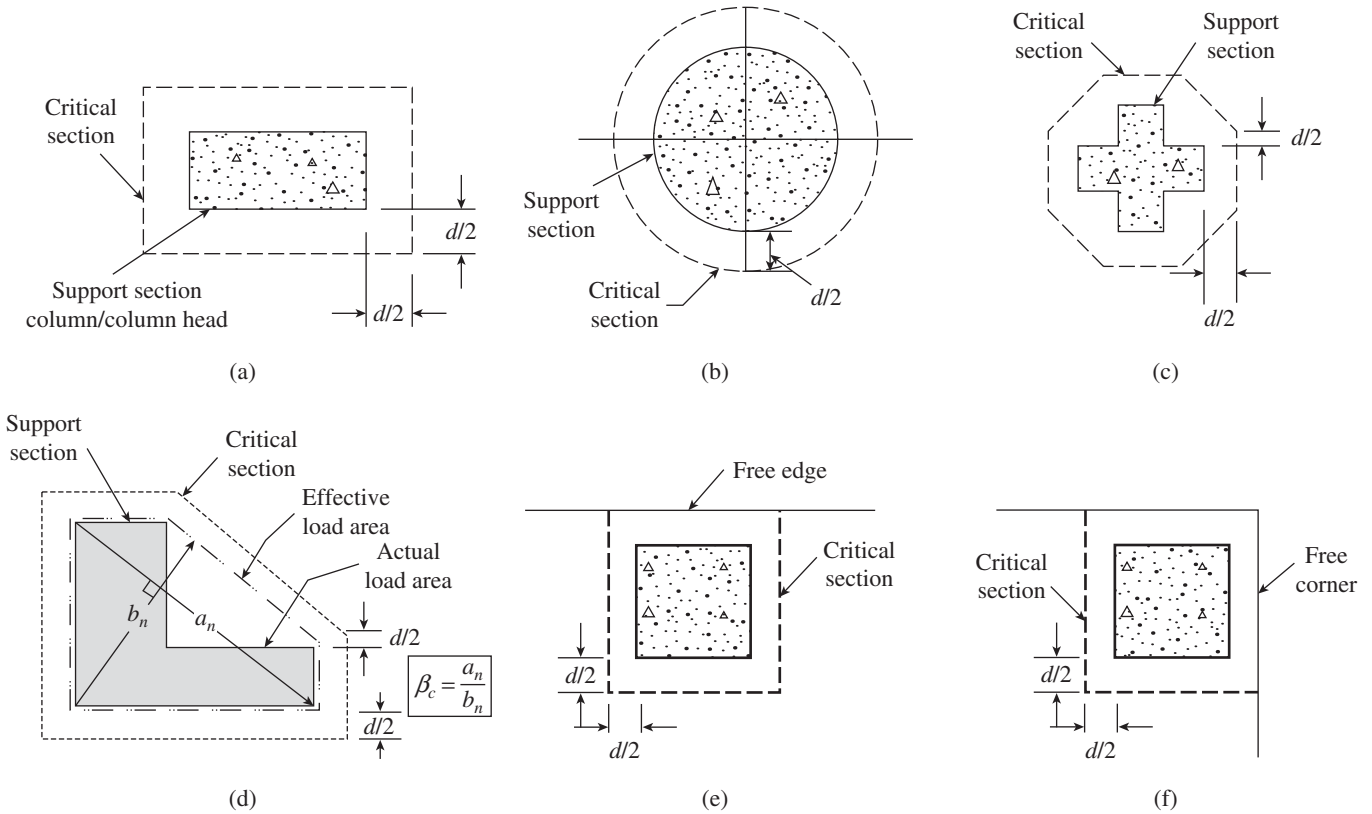


FIG. 11.22 Critical shear perimeters for different shapes of columns (a) Interior rectangular column (b) Circular column (c) +-shaped column (d) L-shaped column (e) Exterior square column at an edge (f) Exterior square column at a corner

3. The ratio of the dimension of column support to the effective depth d of the slab

Thus, Clause 31.6.3.1 of IS 456 stipulates that when shear reinforcement is not provided, the calculated shear stress at the critical section should not exceed the following design shear strength of concrete:

$$\tau_c = 0.25k_s\sqrt{f_{ck}} \quad (11.11a)$$

where $k_s = (0.5 + \beta_c) \leq 1$. (11.11b)

For columns with β_c less than 0.5, the shear stress at failure was found to vary between $0.25\sqrt{f_{ck}}$ (near the shorter sides) and $0.15\sqrt{f_{ck}}$ (along the longer sides). The factor k_s in Eq. (11.11) reflects this reduction in the shear strength. As per SP 24:1983, for non-rectangular columns like L-shaped columns, β_c may be taken as the ratio of the shortest overall dimension to the longest overall dimension of the effective loaded area, formed by enclosing all the re-entrant corners, as in Fig. 11.22(d).

The ACI 318 code formula evolved from the work of Moe (1961), ACI-ASCE Committee 326 (1962), ACI-ASCE Committee 426 (1974), and Vanderbilt (1972) and considers the reduction of shear stress with increasing rectangularity of the loaded area, that is, when the ratio of the longer to shorter sides of a rectangular column is greater than 2.0. The ultimate safe value of punching shear stress in the ACI code

(in IS 456 nomenclature) is the smallest of the following three equations:

$$\tau_c = 0.3\lambda\phi\sqrt{f_{ck}} \quad (11.12a)$$

$$\tau_c = 0.075\left(2 + \frac{4}{\beta_c}\right)\lambda\phi\sqrt{f_{ck}} \quad (11.12b)$$

$$\tau_c = 0.075\left(2 + \frac{\alpha_s d}{b_o}\right)\lambda\phi\sqrt{f_{ck}} \quad (11.12c)$$

The value of $0.3\lambda\phi\sqrt{f_{ck}}$ for the basic shear strength given by Eq. (11.12a) exceeds the normal shear strength used in beams of $0.15\lambda\phi\sqrt{f_{ck}}$ (see Eq. 6.9b of Chapter 6), because of the confinement afforded to the slab shear failure surface (ACI 352.1R 1989). As the supporting column cross section becomes elongated, the confinement due to lateral compression along the long face is diminished. This reduction in strength due to reduction in lateral confinement is reflected by the parameter β_c .

It has to be noted that β_c in ACI 318 is the inverse of that in IS 456. The value of α_c is taken as 40 for an interior column, 30 for an edge column, and 20 for a corner column, and the partial safety factor ϕ is taken as 0.75 for the punching shear. The ACI also considers the λ factor to account for concrete density (1.0 for normal density concrete). Normally, Eq. (11.12a) will govern; when β_c exceeds 2.0, Eq. (11.12b)

governs and for very large columns, Eq. (11.12c) will govern.

As the IS 456 provisions are based on the ACI code, the format of Eq. (11.11) and Eq. (10.12) given in Chapter 10 are similar. However, other code formulae (for example, Eurocode 2, CEB-FIP model code, and BS 8110) also consider the size effect and the effect of reinforcement ratio. As mentioned previously, other codes also consider the cube root of f_{ck} instead of its square root and take the critical section at $1.5d$ or $2.0d$ from the face of the column. A comparison of the different codal provisions is provided by Subramanian (2005), Widiyanto, et al. (2009), and Gardner (2011). Most of the codal equations are generally applicable only for concretes up to M40 (Subramanian 2005). Since Eurocode 2 and CEB-FIP model code are found to predict the punching shear strength of flat slabs consistently for high-strength normal weight and high-strength lightweight concretes, a similar format has been proposed to be included in the Indian code (Subramanian 2005). A state-of-the-art report on punching shear in RC Slabs is provided by Polak (2005).

Combined Shear and Moment Transfer at Columns

When gravity load or wind, earthquake, or other lateral loads cause transfer of moment M_u from a slab to the column, as discussed in Section 11.4.3, a fraction $M_u(1 - \gamma_f) = \gamma_c M_u$ is assumed to be transferred by the eccentricity of shear, which is assumed to vary linearly about the centroid of the critical section as shown in Figs 11.15 and 11.16. The value of γ_f is found from Eq. (11.6). As per the eccentric shear stress model originally suggested in the ACI code, the nominal shear stress of slab-column connections transferring the shear and moment is calculated using the following formulae:

$$\tau_{v1,max} = \frac{V_u}{A_c} + \frac{\gamma_{vx} M_{ux}}{J_{cx}} c \tag{11.13a}$$

$$\tau_{v1,min} = \frac{V_u}{A_c} - \frac{\gamma_{vx} M_{ux}}{J_{cx}} c' \tag{11.13b}$$

where V_u and M_{ux} are the factored shear force and factored unbalanced bending moment, respectively, determined at the centroidal axis of the critical section, A_c is the concrete area of the assumed critical section $= b_o d$, and c and c' are the distances from the centroidal axis to the sections where the maximum and minimum shear stresses occur. The quantity J_{cx} is a calculated property of the assumed critical section analogous to the polar moment of inertia (ACI 318:2011). This eccentric shear stress model is based on the work by DiStasio and Van Buren (1960) and adopted by the ACI-ASCE Committee 326 (1962). It is an extrapolation of the working stress method of calculation to an ultimate strength situation.

To compute the polar moment of inertia of a critical shear perimeter, the critical section is broken down into two or four individual plates. The polar moment of inertia of a rectangle with depth d and width a about an axis $z-z$ perpendicular to the plane of the rectangle and displaced a distance \bar{x} from the centroid of the rectangle is given by (Wight and MacGregor 2009)

$$J_c = (I_x + I_y) + A\bar{x}^2 = \left(\frac{ad^3}{12} + \frac{da^3}{12} \right) + (ad)\bar{x}^2 \tag{11.14}$$

Table 11.7 gives the values of J/c and J/c' for the four typical slab-column connections as shown in Fig. 11.23. ACI 421.1 R:2008 gives the following approximate expression for J_c , which will differ from Eq. (11.14) by only 2.5 per cent but is quick to compute:

$$J_c = \frac{d}{3} \sum [l_{ij}(x_i^2 + x_i x_j + x_j^2)] \tag{11.15}$$

where the summation is for all the sides of the polygon and l_{ij} and (x_i, x_j) are the length and coordinates, respectively, of the edges of a typical side ij . The value of J_c for circular columns may be calculated by considering them as equivalent square columns having sides equal to $0.886D_c$, where D_c is the diameter of the circular column.

TABLE 11.7 Section properties for shear stress computations—rectangular columns

Case (See Fig. 11.23)	Area of Critical Section, A_c , mm ²	Modulus of Critical Section		c (mm)	c' (mm)
		J/c (mm ³)	J/c' (mm ³)		
A (interior column)	$2(a + b)d$	$\frac{ad(a + 3b) + d^3}{3}$	$\frac{ad(a + 3b) + d^3}{3}$	$\frac{a}{2}$	$\frac{a}{2}$
B (edge column—bending parallel to edge)	$(a + 2b)d$	$\frac{ad(a + 6b) + d^3}{6}$	$\frac{ad(a + 6b) + d^3}{6}$	$\frac{a}{2}$	$\frac{a}{2}$
C (edge column—bending perpendicular to edge)	$(2a + b)d$	$\frac{2a^2d(a + 2b) + d^3(2a + b)}{6a}$	$\frac{2a^2d(a + 2b) + d^3(2a + b)}{6(a + b)}$	$\frac{a^2}{2a + b}$	$\frac{a(a + b)}{2a + b}$
D (corner column)	$(a + b)d$	$\frac{a^2d(a + 4b) + d^3(a + b)}{6a}$	$\frac{a^2d(a + 4b) + d^3(a + b)}{6(a + 2b)}$	$\frac{a^2}{2(a + b)}$	$\frac{a(a + 2b)}{2(a + b)}$

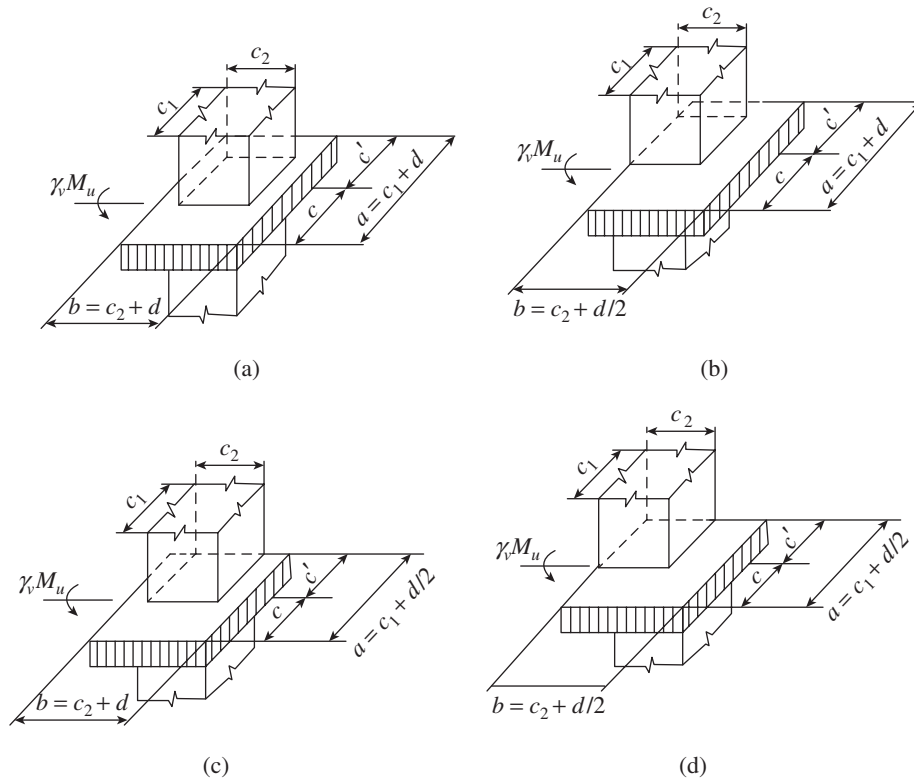


FIG. 11.23 Critical shear section of slab-column connections (a) Case A: Interior column (b) Case B: Edge column (bending parallel to edge) (c) Case C: Edge column (bending perpendicular to edge) (d) Case D: Corner column

Design aids in the form of tables were developed by Fanella (2002) to calculate J_c . Two such tables for interior rectangular column (see Fig. 11.23a) and edge columns (see Fig. 11.23c) are given in Tables 11.8 and 11.9, respectively.

When moments act simultaneously about both the principal axes, the maximum shear stress due to them may be calculated by using the following relation:

$$\tau_{v,\max} = \frac{V_u}{A_c} \pm \frac{\gamma_{v1} M_{u1}}{J_{c1}} c_1 \pm \frac{\gamma_{v2} M_{u2}}{J_{c2}} c_2 \tag{11.16}$$

where V_u , M_{u1} , and M_{u2} are the shear and moments about the two principal axes, respectively, and J_{c1} and J_{c2} (and the corresponding values of c) are the corresponding properties of the critical shear perimeter. The calculated stress as per Eq. (11.16) should be less than the ultimate allowable shear stress given by Eq. (11.12).

It has to be noted that the punching shear failure surface is accompanied

TABLE 11.8 Properties of critical section—interior rectangular column (Fanella 2002, SEAOC)

c_1/d	f_1							f_2						
	c_2/c_1							c_2/c_1						
	0.50	0.75	1.00	1.25	1.50	1.75	2.00	0.50	0.75	1.00	1.25	1.50	1.75	2.00
1.00	7.00	7.50	8.00	8.50	9.00	9.50	10.00	2.33	2.58	2.83	3.08	3.33	3.58	3.83
1.50	8.50	9.25	10.00	10.75	11.50	12.25	13.00	3.40	3.86	4.33	4.80	5.27	5.74	6.21
2.00	10.00	11.00	12.00	13.00	14.00	15.00	16.00	4.67	5.42	6.17	6.92	7.67	8.42	9.17
2.50	11.50	12.75	14.00	15.25	16.50	17.75	19.00	6.15	7.24	8.33	9.43	10.52	11.61	12.71
3.00	13.00	14.50	16.00	17.50	19.00	20.50	22.00	7.83	9.33	10.83	12.33	13.83	15.33	16.83
3.50	14.50	16.25	18.00	19.75	21.50	23.25	25.00	9.73	11.70	13.67	15.64	17.60	19.57	21.54
4.00	16.00	18.00	20.00	22.00	24.00	26.00	28.00	11.83	14.33	16.83	19.33	21.83	24.33	26.83
4.50	17.50	19.75	22.00	24.25	26.50	28.75	31.00	14.15	17.24	20.33	23.43	26.52	29.61	32.71
5.00	19.00	21.50	24.00	26.50	29.00	31.50	34.00	16.67	20.42	24.17	27.92	31.67	35.42	39.17
5.50	20.50	23.25	26.00	28.75	31.50	34.25	37.00	19.40	23.86	28.33	32.80	37.27	41.74	46.21
6.00	22.00	25.00	28.00	31.00	34.00	37.00	40.00	22.33	27.58	32.83	38.08	43.33	48.58	53.83
6.50	23.50	26.75	30.00	33.25	36.50	39.75	43.00	25.48	31.57	37.67	43.76	49.85	55.95	62.04
7.00	25.00	28.50	32.00	35.50	39.00	42.50	46.00	28.83	35.83	42.83	49.83	56.83	62.83	70.83
7.50	26.50	30.25	34.00	37.75	41.50	45.25	49.00	32.40	40.36	48.33	56.30	64.27	72.24	80.21
8.00	28.00	32.00	36.00	40.00	44.00	48.00	52.00	36.17	45.17	54.17	63.17	72.17	81.17	90.17
8.50	29.50	33.75	38.00	42.25	46.50	50.75	55.00	40.15	50.24	60.33	70.43	80.52	90.61	100.71
9.00	31.00	35.50	40.00	44.50	49.00	53.50	58.00	44.33	55.58	66.83	78.08	89.33	100.58	111.83
9.50	32.50	37.25	42.00	46.75	51.50	56.25	61.00	48.73	61.20	73.67	86.14	98.60	111.07	123.54
10.00	34.00	39.00	44.00	49.00	54.00	59.00	64.00	53.33	67.08	80.83	94.58	108.33	122.08	135.83

Note: $c = c' = (c_1 + d)/2$; $A_c = f_1 d^2$; $J/c = J/c' = 2f_2 d^3$; for c_1 , c_2 , c , and c' , refer to Fig. 11.23.

TABLE 11.9 Properties of critical section—edge column, bending perpendicular to edge (Fanella 2002, SEAOC)

c_1/d	f_1							f_2							f_3						
	c_2/c_1							c_2/c_1							c_2/c_1						
	0.50	0.75	1.00	1.25	1.50	1.75	2.00	0.50	0.75	1.00	1.25	1.50	1.75	2.00	0.50	0.75	1.00	1.25	1.50	1.75	2.00
1.0	4.50	4.75	5.00	5.25	5.50	5.75	6.00	1.38	1.51	1.65	1.79	1.93	2.07	2.21	0.69	0.70	0.71	0.72	0.72	0.73	0.74
1.5	5.75	6.13	6.50	6.88	7.25	7.63	8.00	2.07	2.34	2.60	2.87	3.14	3.40	3.67	1.11	1.13	1.16	1.18	1.19	1.21	1.22
2.0	7.00	7.50	8.00	8.50	9.00	9.50	10.00	2.94	3.38	3.81	4.24	4.68	5.1	5.54	1.63	1.69	1.73	1.77	1.80	1.82	1.85
2.5	8.25	8.87	9.50	10.13	10.75	11.38	12.00	3.98	4.62	5.26	5.91	6.55	7.19	7.83	2.27	2.36	2.43	2.49	2.53	2.58	2.61
3.0	9.60	10.25	11.00	11.75	12.50	13.25	14.00	5.18	6.08	6.97	7.86	8.76	9.65	10.54	3.02	3.15	3.25	3.34	3.41	3.46	3.51
3.5	10.75	11.62	12.50	13.37	14.25	15.12	16.00	6.56	7.74	8.93	10.11	11.30	12.48	13.67	3.89	4.06	4.20	4.31	4.41	4.49	4.56
4.0	12.00	13.00	14.00	15.00	16.00	17.00	18.00	8.10	9.62	11.13	12.65	14.17	15.69	17.21	4.86	5.09	5.27	5.42	5.55	5.65	5.74
4.5	13.25	14.37	15.50	16.62	17.75	18.87	20.00	9.80	11.70	13.59	15.49	17.38	19.27	21.17	5.94	6.24	6.47	6.66	6.82	6.95	7.06
5.0	14.50	15.75	17.00	18.25	19.50	20.75	22.00	11.68	13.99	16.30	18.61	20.92	23.23	25.54	7.14	7.51	7.80	8.03	8.22	8.38	8.51
5.5	15.75	17.12	18.50	19.87	21.25	22.62	24.00	13.72	16.49	19.26	22.03	24.80	27.56	30.33	8.44	8.89	9.24	9.52	9.76	9.95	10.11
6.0	17.00	18.50	20.00	21.50	23.00	24.50	26.00	15.93	19.20	22.46	25.73	29.00	32.27	35.54	9.86	10.40	10.82	11.15	11.43	11.65	11.85
6.5	18.25	19.87	21.50	23.12	24.75	26.37	28.00	18.30	22.11	25.92	29.73	33.54	37.36	41.17	11.39	12.02	12.51	12.91	13.23	13.50	13.72
7.0	19.50	21.25	23.00	24.75	26.50	28.25	30.00	20.84	25.24	29.63	34.02	38.42	42.81	47.21	13.03	13.77	14.34	14.79	15.17	15.47	15.74
7.5	20.75	22.62	24.50	26.37	28.25	30.12	32.00	23.55	28.57	33.59	38.61	43.63	48.65	53.67	14.78	15.63	16.29	16.81	17.24	17.59	17.89
8.0	22.00	24.00	26.00	28.00	30.00	32.00	34.00	26.42	32.11	37.80	43.48	49.17	54.86	60.54	16.64	17.61	18.36	18.95	19.44	19.84	20.18
8.5	23.25	25.37	27.50	29.62	31.75	33.87	36.00	29.47	35.86	42.25	48.65	55.04	61.44	67.83	18.61	19.71	20.56	21.23	21.78	22.23	22.61
9.0	24.50	26.75	29.00	31.25	33.50	35.75	38.00	32.67	39.82	46.96	54.11	61.25	68.40	75.54	20.69	21.93	22.88	23.63	24.25	24.75	25.18
9.5	25.75	28.12	30.50	32.87	35.25	37.62	40.00	36.05	43.98	51.92	59.86	67.79	75.73	83.67	22.89	24.27	25.33	26.17	26.85	27.41	27.89
10.0	27.00	29.5	32.00	34.50	37.00	39.50	42.00	39.59	48.36	57.13	65.90	74.67	83.44	92.21	25.19	26.72	27.90	28.83	29.59	30.21	30.74

Note: $c = [f_3/(f_2 + f_3)] [c_1 + d/2]$, $c' = [f_2/(f_2 + f_3)] [c_1 + d/2]$, $A_c = f_1 d^2$, $Jc = 2f_2 d^3$, $Jc' = 2f_3 d^3$; for c_1 , c_2 , c and c' , refer to Fig. 11.23.

by bending cracks in the same region in circular and radial directions (Leonhardt and Mönning 1977; Dilger, et al. 1978). Thus, it is recommended that there should be adequate flexural reinforcement in addition to shear reinforcement in this region. In general, a minimum flexural reinforcement ratio of 0.5 per cent is provided in both the directions within a region 1.5–2 times the depth of the slab outside the opposite faces of the column or capital, the upper limit of flexural reinforcement ratio being 1.5 per cent (Leonhardt and Mönning 1977). In addition, it is desirable to anchor the flexural reinforcement in the column.

Load Patterns for Maximum Shear Stress due to Combined Shear and Moment Transfer

The maximum shear stress on the critical section around the columns should be computed using a consistent load case that produces a sum of shear stresses due to gravity load and moment that is likely to be the maximum. For an interior column, the maximum value of V_u occurs when all adjacent panels are loaded with full factored dead and live loads, whereas the maximum value of M_u occurs when two differing adjacent spans are loaded with full factored live load. For edge columns, maximum V_u occurs when full factored dead and live loads act simultaneously on both the edge panels adjoining the column, whereas for maximum M_u two cases are to be considered—one in which full factored dead and live loads act in both adjacent panels and the other in which full factored live load is applied only to the longer of the two adjacent panels. For corner columns, full factored dead and live loads are applied to all panels in the floor system.

Calculation of Moment about Centroid of Shear Perimeter

The distribution of stresses calculated using Eq. (11.13) and illustrated in Figs 11.15 and 11.16 assumes that V_u acts through the centroid of the shear perimeter and M_u acts about the centroidal axis of this perimeter. When the DDM is used, V_u and M_u are normally calculated at the face of the columns. The equilibrium of the simple free body diagram can be used to determine the values of V_u and M_u acting at the centroids.

Simplified Analysis for Shear and Moment Transfer at Edge Columns

Alexander and Simmonds (2005) proposed the following equation for determining the maximum shear stress at the front face of an exterior column transferring the combined shear and moment.

$$\tau_{v(AB)} = \frac{0.65[V_u + M_{u,\text{face}}/(4d)]}{(c_1 + c_2)d} \quad (11.17)$$

where V_u is the factored shear to be transferred, $M_{u,\text{face}}$ is the factored moment at the face of the column, d is the effective

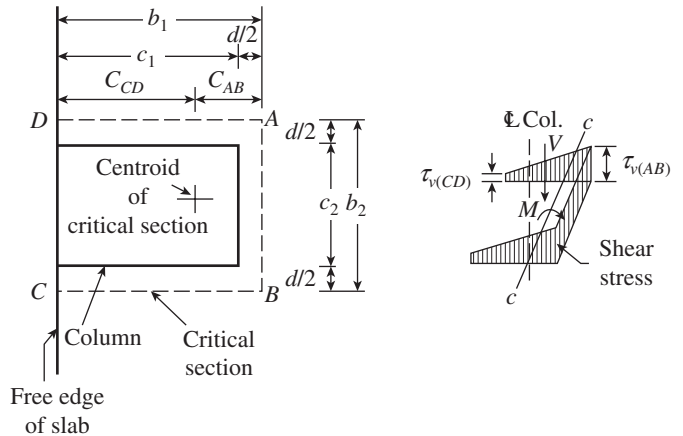


FIG. 11.24 Geometry and shear stress distribution of edge slab-column connection

depth of slab, and c_1 and c_2 are the column dimensions perpendicular and parallel to the edge of the slab, respectively (see Fig. 11.24). In addition to being simple to apply, Eq. (11.17) was shown to give similar results as obtained by Eq. (11.13) (Alexander and Simmonds 2005).

As already mentioned, the eccentric shear stress model explained here was originally developed by DiStasio and Van Buren in 1960 and adopted in the USA as well as several other codes of practices. Based on a large number of large-scale tests conducted at the University of New South Wales, another different method was developed to guard against punching shear failure by Rangan and Hall (1983) and Rangan (1987; 1990). This method covers flat slab floors with or without spandrel beams as well as slabs with or without closed ties. This method has been adopted in the Australian code AS 3600. More details and design examples using this method may be found in the work of Rangan (1990).

Effect of Thick Slabs and Some Analytical Models

Until now, the design rules for the punching shear provided in the design codes have been generally based on experimental results performed on isolated slab elements representing a part of the slab close to a column. Most of these tests have been performed on relatively thin slabs, typically 100–200 mm in depth. However, these test results are commonly extrapolated to design flat slabs with a thickness two to three times larger, and even for foundation mats with thicknesses 10–20 times larger. Increasing the flexural reinforcement ratio may increase the punching capacity, but it significantly decreases the deformation capacity and ductility of the slab. Similarly, there is a significant reduction in the punching shear resistance with increasing slab thickness. These facts were established by the experimental work done by Birkle and Dilger (2008) and Rizk, et al. (2011). Yang, et al. (2010) found that direct replacement of conventional Fe 415 steel bars with high-strength ASTM A 1035 steel bars ($f_y = 840 \text{ N/mm}^2$) having the same area results in a 27 per cent increase of the

punching shear strength, as the high-strength bars do not yield prior to punching failure.

Kinnunen and Nylander (1960) was the first to develop a rational theory for the estimation of the punching shear strength, which is based on the assumption that the punching strength is reached for a given critical rotation ψ . Although its application was too complex, it served as the basis for the Swedish and Swiss design codes of the 1960s. Recently, a new failure criterion for punching shear based on the *critical shear crack theory* was presented by Muttoni and his associates; this model also takes into account the size effect (Muttoni 2008; Guandalini, et al. 2009; Ruiz and Muttoni 2009). Another analytical model was presented by Theodorakopoulos and Swamy (2002), who also extended it to fibre-reinforced polymer (FRP) RC flat slabs (Theodorakopoulos and Swamy 2007).

Strategies to Avoid Punching Shear Failure

If the calculated punching shear strength exceeds the actual punching shear strength, we may adopt any one of the following strategies to avoiding punching shear failure:

1. Increase the overall thickness of the slab (this will be uneconomical and also increase V_u due to increase in self-weight of the slab).
2. Increase the thickness of the slab locally with a drop panel.
3. Increase b_o by increasing the size of the column or by adding column capital or shear cap (see Section 11.2.4 for details).
4. Provide some kind of shear reinforcement.

The first three solutions either increase the overall floor height or are impractical, architecturally unacceptable, or expensive. Consequently, very often, to achieve an elegant thin flat slab or flat plate, shear reinforcement is required. Properly designed shear reinforcement can prevent brittle punching failure and increase the strength and ductility of the slab-column connection.

Provision of *spandrel beams* along the edges of the slab will also improve the punching shear capacity of the slab (Falamaki and Loo 1992). However, the existence of spandrel beams will complicate the already complex punching shear performance of the column–slab connection. In view of these considerations, many researchers have found that the introduction of shear reinforcement is more economical and reduces the chances of brittle failure at the slab-column connection.

11.5.3 Reinforcement for Punching Shear

The performance of several types of shear reinforcements such as inclined stirrups, structural shear heads (in the form of steel I- or channel sections), bent-up bars, hooked bars, and welded wire fabric has been tested extensively in the last three decades (Hawkins, et al. 1975; Mokhtar, et al. 1985; Broms 1990; Ghali and Hammill 1992; Lim and Rangan 1995; Ghali and Dilger 1998). It has been found that the introduction of

such shear reinforcement results in ductile failure caused by the yielding of flexural reinforcement and improves the punching shear resistance. The following reinforcement schemes have been used in the past:

1. Shear stirrups
2. Headed shear studs
3. Structural steel shear heads
4. Shear bands

A summary of the different types of shear reinforcement is provided by Hawkins (1974a).

Shear Stirrups

One of the common practices is to provide *shear stirrups* connecting the top and bottom reinforcement. This layout may be circular or rectangular in plan. Figure 11.25 shows a shear reinforcement in the form of rings and vertical stirrups as per US practice (ACI 318:2011). Two types of shear stirrups as suggested by SP 24:1983 are shown in Fig. 11.26. The stirrups may be closed (Fig. 11.26a) or castellated (Fig. 11.26b) and should pass around one row of tension steel running perpendicular to them at each face as per Fig. 11.26. The first ring of stirrups is provided within a distance of $d/2$ and the successive stirrups are placed at a spacing less than $d/2$ as per ACI 318. (Moreover, the distance between the column face and the first line of stirrup legs should not exceed $d/2$; see Fig. 11.25d). SP 24 suggests that the spacing should not exceed $0.75d$ and the stirrups should be continued to a distance d beyond the section at which the shear stress is within the prescribed limits.

Shear stirrups are designed in the same manner as the stirrups in beams so far as the design principles, code requirements, and anchorages are concerned. As mentioned earlier, when the actual shear stress at the critical section τ_v exceeds $k_s \tau_c$ but is less than $1.5 \tau_c$, shear reinforcement is provided. When it is provided, the critical section for punching shear gets shifted farther away from the column. Hence, Clause 31.6.3.2 of IS 456 requires that the shear stresses be investigated at successive sections (at intervals of $0.75d$ as per SP 24:1983) up to a section where the shear stress does not exceed $0.5 \tau_c$. While designing shear reinforcement, the shear carried by concrete is assumed to be 0.5 times τ_c and the shear reinforcement is designed to carry the remaining shear. Thus, the area of stirrups is found as

$$A_{sv} = \frac{(V_u - 0.5k_s \tau_c b_o d) s_v}{0.87 f_y d} \quad (11.18)$$

where A_{sv} is the total cross-sectional area of all stirrup legs in the perimeter, b_o is the perimeter of the critical section, V_u is the factored shear force, τ_c is the design shear strength of concrete (see Eq. 11.11), f_y is the specified yield strength of shear reinforcement (should be less than or equal to 415 N/mm^2 as per IS 456), s_v is the spacing of stirrups, and d is the effective

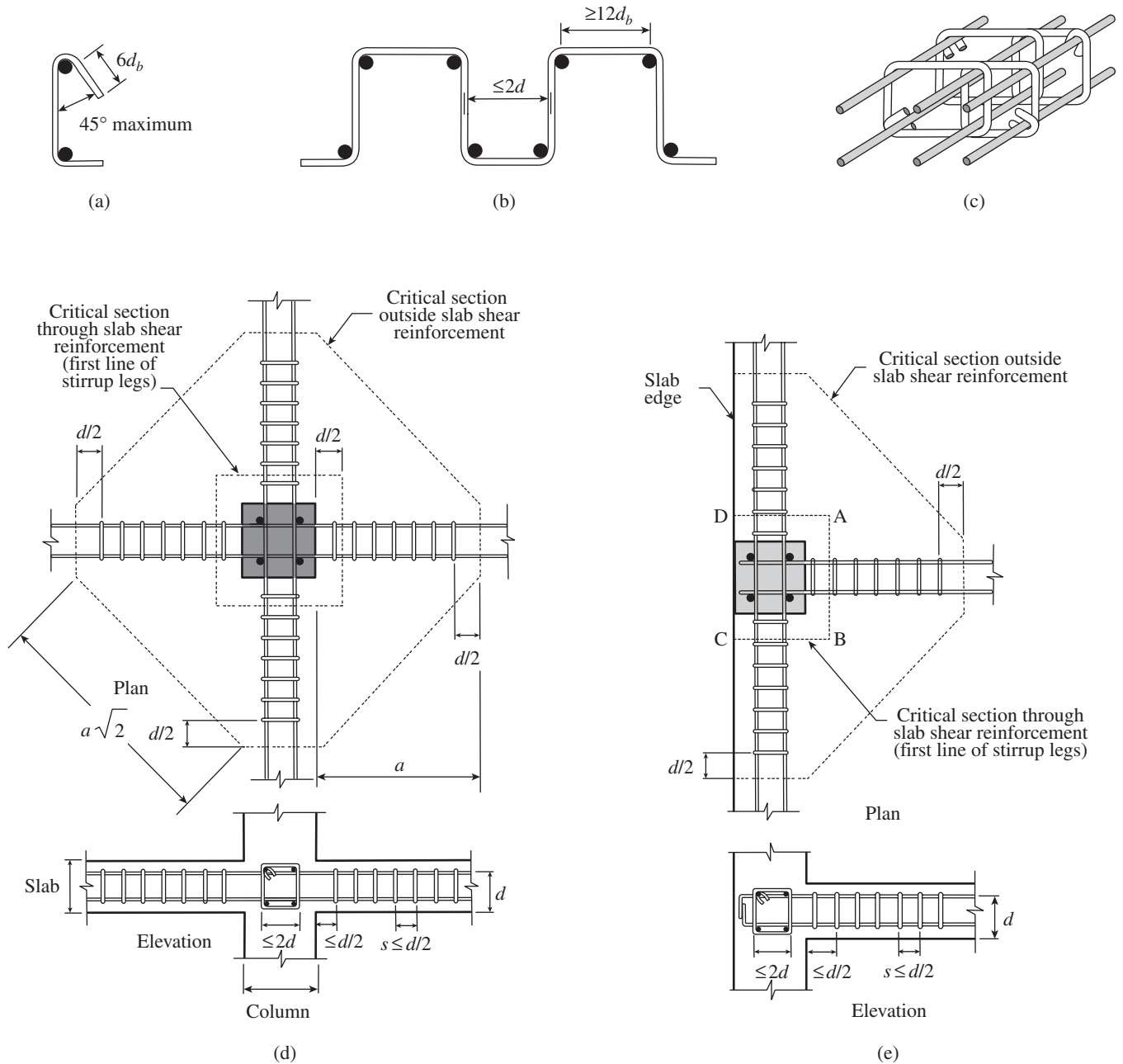


FIG. 11.25 Stirrup-type shear reinforcement in flat slabs as per ACI 318 (a) Single-leg stirrup (b) Multiple-leg stirrup (c) Closed stirrups (d) Arrangement of shear stirrup reinforcement—interior column (e) Arrangement of shear stirrup reinforcement—edge column (Reprinted with permission from ACI)

depth. If the shear stress exceeds $1.5\tau_c$, the thickness of the flat slab has to be revised. As per ACI, the spacing between adjacent stirrup legs in the shear reinforcement should not exceed $2d$ measured in a direction parallel to the column face.

It has to be noted that Clause 11.11.3.1 of the ACI code permits a shear stress of $\tau_c = 0.15\lambda\phi\sqrt{f_{ck}}$ at the inner critical shear section at $d/2$ from the column in a slab with stirrup-type reinforcement, even though Clause 11.11.2 of the code allows $\tau_c = 0.3\lambda\phi\sqrt{f_{ck}}$ at the same critical section in a slab without shear reinforcement. This is because of the measured shear strengths in slabs with stirrups reported in tests by Hawkins

(1974a) and ACI-ASCE Committee 326 (now 426) (1962). Hence, in the ACI code the nominal shear strength of two-way flat slabs with stirrup-type reinforcement is

$$V_n = V_c + V_s \leq 0.45\sqrt{f_{ck}}b_o d \quad (11.19)$$

where $V_c = 0.15\lambda\phi\sqrt{f_{ck}}b_o d$, $V_s = A_{sv}f_y d/s$, s is the spacing of stirrups, and ϕ is the strength reduction factor = 0.75 as per the ACI code.

In most of the slabs, the thickness being too small, it is difficult to obtain proper anchorage to shear reinforcement without specifying small diameter bars and close tolerances.

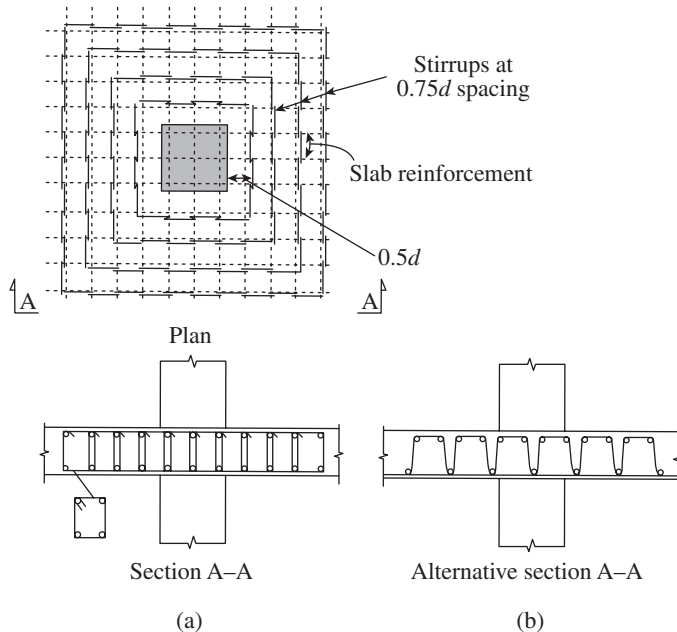


FIG. 11.26 Shear stirrups as suggested in SP 24:1983 (a) Closed stirrups (b) Castellated stirrups

ACI stipulates that stirrups should generally be considered in slabs only when the effective thickness d is greater than or equal to 150 mm and not less than 16 times the shear reinforcement bar diameter. (The commentary also cautions that anchorage of shear reinforcement according to the requirements of the ACI code is difficult in slabs thinner than 250 mm.) Even then, the stirrups should be executed only under strict inspection and control. They should engage the longitudinal flexural reinforcement in the direction being considered.

Some designers discourage the use of shear stirrups in slabs for the following reasons:

1. Congestion of reinforcement, unless they are planned carefully considering the sequence of layout
2. Difficulty in obtaining proper anchorages to short lengths of bars and required close dimensional tolerances
3. Likely damage to small-sized bars during handling and concreting
4. Risk of omitting small-sized bars, as they may be considered inconsequential at site
5. Considerable expense in fabricating, handling, and placing small-sized stirrups

Stirrup shear reinforcement was investigated by Kinnunen and Nylander (1960), Broms (1990), and others. Much of the experimental work reported until now led to the conclusion that shear reinforcement consisting of bars is not fully effective, because it does not reach its yield strength before slab failure. Inclined reinforcement, though effective, is difficult to design, manufacture, and place. It is also not suited for earthquake-resistant design, where a reversal of moment may occur; hence, it is not used extensively at present.

Headed Shear Studs

Headed shear studs act in the same mechanical manner as hooked stirrup legs, but the head of shear studs provide better anchorage than a bar hook. Extensive tests in Germany by Andrä, et al. (1979) and in Canada by Dilger and Ghali (1981), Dilger, et al. (1978), Mokhtar, et al. (1985), and Elgabry and Ghali (1987) on full-size slab-column connections confirmed that the use of shear studs increases the load-carrying capacity, punching shear strength, and ductility of flat slabs. The tests also revealed that such studs are easy to install, reduce congestion, and do not interfere with flexural reinforcement. Headed stud type reinforcement consists of rows of vertical studs, each with a circular head welded or forged on the top and a steel strip welded to the bottom (see Figs 11.27 and 11.28; it can be seen that the stud rail is fixed at the bottom of the slab and double-headed rails dropped from top of reinforcement cage). It should be noted that in Europe the studs are arranged in a radial fashion from the centre of the column, usually at angles not exceeding 45° . Recent research by Matzke (2012) has indicated that the radial arrangement of shear studs may be better than the orthogonal arrangement as shown in Fig. 11.27(a).

The anchorage is mechanically achieved by the forged heads or the steel strip. The full yield strength of the stud was found to be developed without appreciable slip when the anchor head has an area greater than 10 times the cross-sectional area of the stud (Ghali and Dilger 1998). The steel strip, also called the *rail*, acts as an anchor and spacer, holding the studs in a vertical position at the appropriate spacing in the formwork until the concrete is cast. Two makes of stud rail are available: (a) The first type has the spacing bar at the bottom and is fixed in position before placing the main reinforcement (as shown on Fig. 11.28a), although they can also be fixed from above (e.g., DEHA stud rails). (b) The second type is fixed from the top after all the main reinforcement has been positioned as shown in Fig. 11.28b (e.g., Max Frank Ltd, UK shear studs). Provisions for the design of flat slabs with stud-shear reinforcements were introduced in the ACI code in Section 11.11.5 in 2005. According to the ACI code, the overall height of the shear stud assembly should not be less than the thickness of the member less the sum of (a) the concrete cover on the top flexural reinforcement, (b) the concrete cover on the base rail, and (c) one-half the bar diameter of the tension flexural reinforcement.

The design of headed shear reinforcement is not provided in IS 456. As per ACI-318, the design is similar to that of stirrup-type shear reinforcement with a few significant changes. As the bearing stresses under the heads of studs confine the slab around the columns effectively when compared to the stirrup-type reinforcement, the following equations are used (ACI Committee 421.1R 1992; Clause 11.11.5 of ACI 318):

$$\phi V_n \geq V_u \quad (11.20a)$$

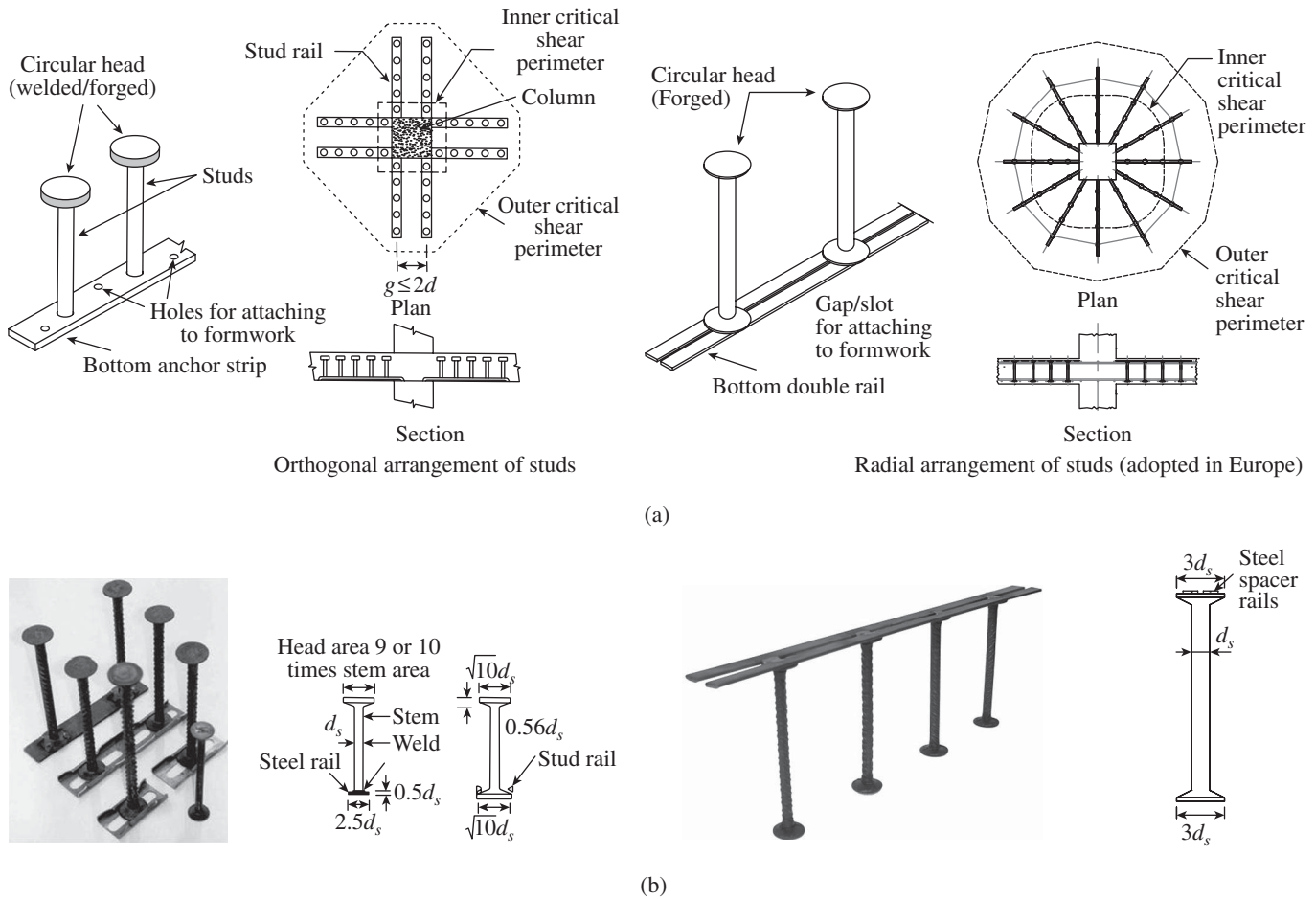


FIG. 11.27 Headed shear studs (a) Headed shear stud reinforcement (b) Details of double-headed studs (Reprinted with permission from ACI)

Source: Elgabry and Ghali (1990), reprinted with permission from ACI

Photo courtesy: Max Frank Ltd UK

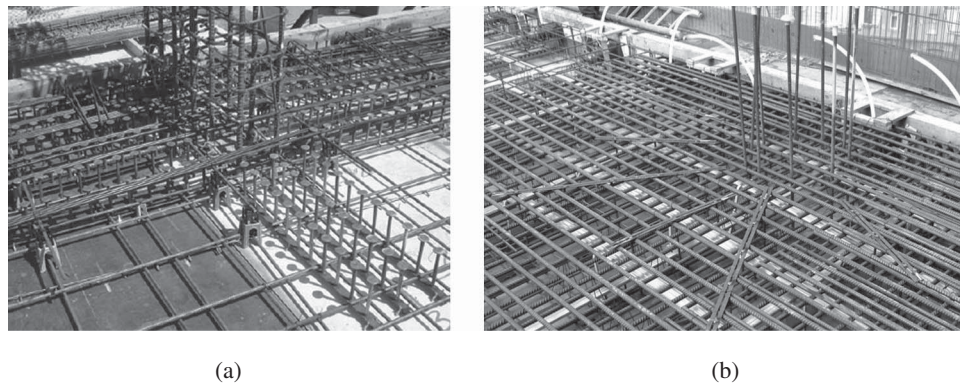


FIG. 11.28 Examples of the use of headed shear stud reinforcement (a) Single-headed stud rail fixed at the bottom of the slab (b) Double-headed stud rail dropped in place after the slab reinforcement is fixed

Courtesy: HALFEN GmbH, Germany and Max Frank Ltd, UK

$$V_n = V_c + V_s \leq 0.6\sqrt{f_{ck}} b_o d \quad (11.20b)$$

where $V_c = 0.225\lambda\sqrt{f_{ck}} b_o d$, $V_s = A_{sv} f_y d/s_v$, A_{sv} is the cross-sectional area of all the headed shear studs on one peripheral line that is approximately parallel to the perimeter of the column section, s_v is the spacing of headed shear studs, b_o is

the perimeter of the critical section, λ equals one for normal weight concrete, and ϕ is the strength reduction factor = 0.75. The quantity $A_{sv} f_y / (b_o s_v)$ should be greater than $0.15\sqrt{f_{ck}}$. The ACI code also permits a greater spacing of $0.75d$ for headed studs when the maximum shear stresses due to factored loads are less than or equal to $0.45\phi\sqrt{f_{ck}}$; otherwise, a spacing of $0.5d$ is to be adopted. The spacing between the adjacent shear head reinforcements measured on the perimeter of the first peripheral line of shear reinforcement, denoted by g in Fig. 11.25a, should not exceed $2d$.

The ACI code stipulates that the shear stress due to factored shear force and moment should not exceed $0.15\phi\lambda\sqrt{f_{ck}}$ at *outer critical section* (i.e., at the critical section located $d/2$ outside the outermost peripheral line of shear reinforcement) and it should not exceed $0.225\phi\lambda\sqrt{f_{ck}}$ at the *inner critical*

section, at a distance $d/2$ from the face of the column (see Fig. 11.25a). ACI 421.1R-99 also allows a higher value of $f_y = 500\text{MPa}$ for headed shear stud reinforcement, as tests have shown almost slip-free anchorage of the studs. It was also found that the mechanical anchorage at the top and bottom of the stud (heads) is capable of developing forces in excess of the specified yield strength at all sections of the stud stem.

The use of headed shear studs has increased substantially in recent years due to the following reasons: (a) relatively easy installation and cost effectiveness, (b) adequate anchorage of these studs even in thin slabs, (c) use of entire effective slab thickness, and (d) introduction of provisions in the ACI code in the 2008 version. More information on the methods of design and worked out design examples are available in the works of Dilger and Ghali (1981), Elgabry and Ghali (1990), and Hammill and Ghali (1994), and in the report of ACI-ASCE Committee 421-1999.

Steel Section Shear Head Reinforcement

Shear head reinforcement, as shown in Fig. 11.29, includes the use of I-sections, channel sections, or steel plates (Moe 1961; Corley and Hawkins 1968). Structural steel sections when used as shear head reinforcement reduce congestion and result in ease of fabrication and installation. However, steel sections tend to be heavy and are expensive compared to conventional shear stirrup reinforcement and normally require full penetration welding at the intersections right above the column. They are difficult to integrate with conventional reinforcement and may obstruct passage of the column bars through the connection. Due to their high stiffness, they attract extra moment to the connection, which can lead to problems at the ends of the steel sections.

The I-sections are welded fully to form identical arms of equal length in orthogonal directions; the arms may be just one in each direction as indicated in Fig. 11.29(a) or more than one as required, but not more than four in any direction. The arms should have adequate length beyond which (outer critical section) the shear stresses in concrete are within the permissible limits.

The design of shear heads is provided in Section 11.11.4 of ACI 318. The depth of the structural sections h_v should be chosen keeping in view the requirements of the slab for minimum concrete cover and reinforcement. Adequate clearance should be available at the top for accommodating two layers of

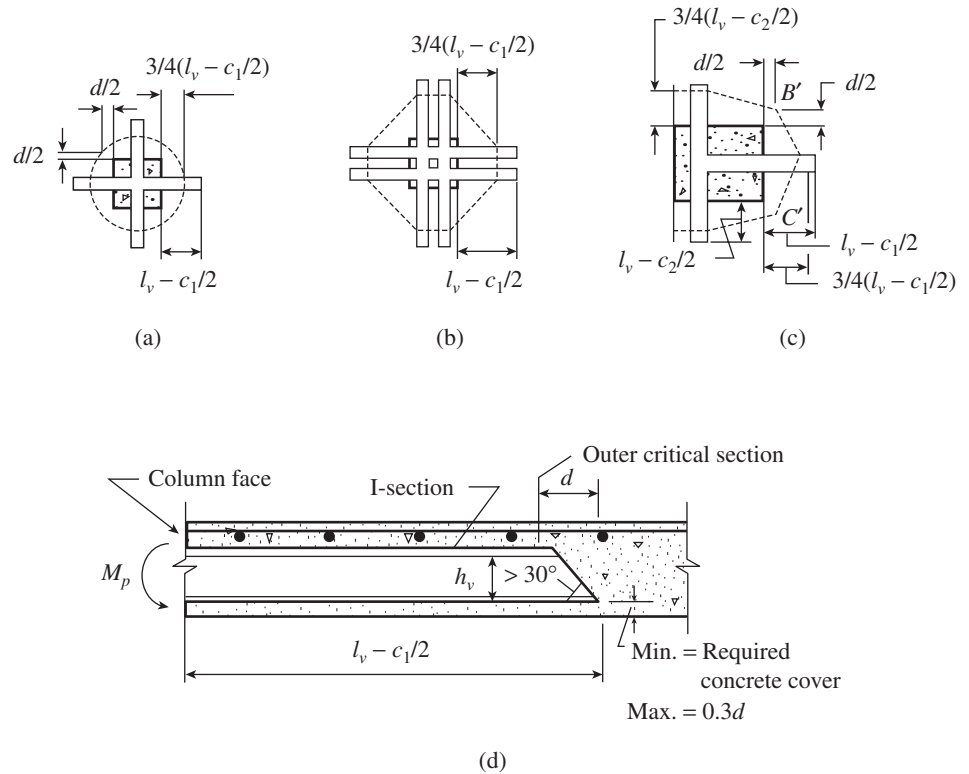


FIG. 11.29 Shear head reinforcement (a) Small interior shear head ($n = 4$) (b) Large interior shear head ($n = 4$) (c) Small edge shear head ($n = 3$) (d) Section through shear head

Source: ACI 318:2011, reprinted with permission from ACI

reinforcement and the specified minimum concrete cover. The minimum concrete cover should be provided for the bottom flange as well; it should be ensured that the bottom flange is within a distance of $0.3d$ for effective shear transfer. A shear head shall not be deeper than 70 times the web thickness of the steel shape. These restrictions on structural sections are indicated in Fig. 11.29. The length of the arms of the shear head should be such that the shear stress at the exterior critical perimeter should be less than $0.3\sqrt{f_{ck}}$. The required plastic moment strength, M_p , for each arm of the shear head is given in the ACI code as

$$M_p = \frac{V_u}{2(0.85)n} \left[h_v + \alpha_v \left(l_v - \frac{c_1}{2} \right) \right] \quad (11.21)$$

where V_u is the factored shear force around the column, h_v is the depth of steel section, n is the number of shear head arms, l_v is the minimum required length of each shear head arm, c_1 is the size of column along the shear head (see Fig. 11.29), and α_v is the ratio of the stiffness of each shear head arm to the stiffness of the surrounding composite cracked slab having a width equal to $c_2 + d$, where c_2 is the size of the column perpendicular to the shear head arm. Taking the modular ratio m as E_s/E_c and I_{xx} as the moment of inertia of the shear head arm,

$$\alpha_v = \frac{mI_{xx}}{I_{\text{comp}}} \geq 0.15 \quad (11.22)$$

More details about the design of shear heads may be had from ACI 318:2011 or the work of Varghese (2006). Shear heads

are not extensively used because of the expense involved and also due to the difficulty of placing the top and bottom reinforcements in the slab in the region where they are provided.

Shear Band Reinforcement

Research undertaken at the Centre for Cement and Concrete, University of Sheffield, UK, has led to a new concept in shear reinforcement called the *shear band system* (Pilakoutas and Li 2003). This patented new shear reinforcement system is made of high-strength steel strips ($f_y = 1100\text{MPa}$) of high ductility. The strip is punched with holes, because this has been demonstrated experimentally to increase its anchoring characteristics over short lengths. The strip can be bent to a

variety of shapes (see Fig. 11.30). Due to its small thickness, the reinforcement can be placed from the top, after all flexural reinforcement is in place, with minimal loss of cover. This system has the following benefits:

1. It anchors above the outermost layer of reinforcement.
2. It acts over the entire concrete core, maximizing its effectiveness in resisting shear.
3. It does not decrease the effective depth of flexural reinforcement.
4. It is very simple to place and efficient.
5. It does not increase the flexural capacity of the slab.

This system is adaptable and can accommodate greater tolerances in placement and enables quick addition of extra reinforcement where required at a later stage. In addition, this system has the following features:

1. It can enable the construction of thinner slabs.
2. It can be designed by using the existing design procedures for shear stirrups.
3. It can be used in addition to other systems.

Experimental validation of shear band reinforcement was done by Pilakoutas and Li (2003). Kang and Wallace (2008) tested and found that this system is effective in both non-participating and lateral force resistant systems.

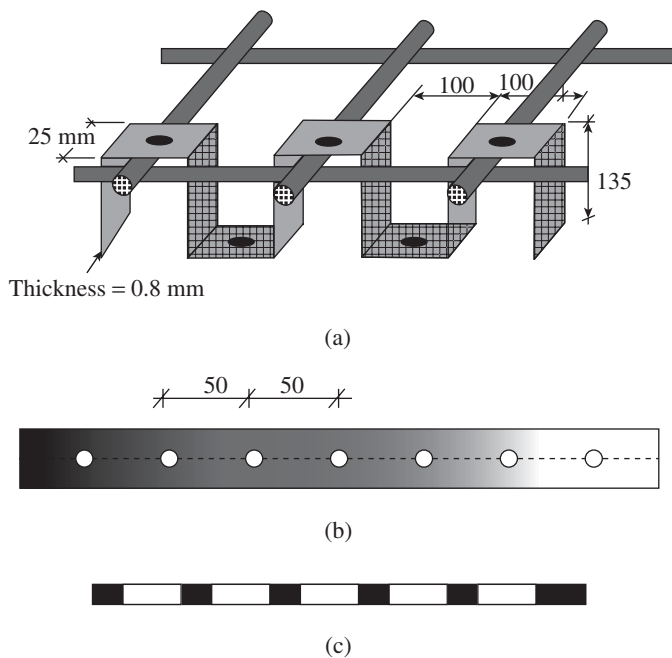


FIG. 11.30 Shear band reinforcement (a) Placement in slab (b) Flat steel strip punched with holes (c) Schematic way of representing shear band reinforcement

Lattice Shear Reinforcement

A new type of shear reinforcement called *lattice shear reinforcement* was used by Park, et al. (2007) (see Fig. 11.31). It was found that this type of shear reinforcement improved the punching shear strength of the slab-column connections. They also developed a method for estimating the shear strength of the slab-column connections with lattice shear reinforcement.

In addition to these systems, a UFO *punching preventer*, made of steel plate material, has been developed in Europe

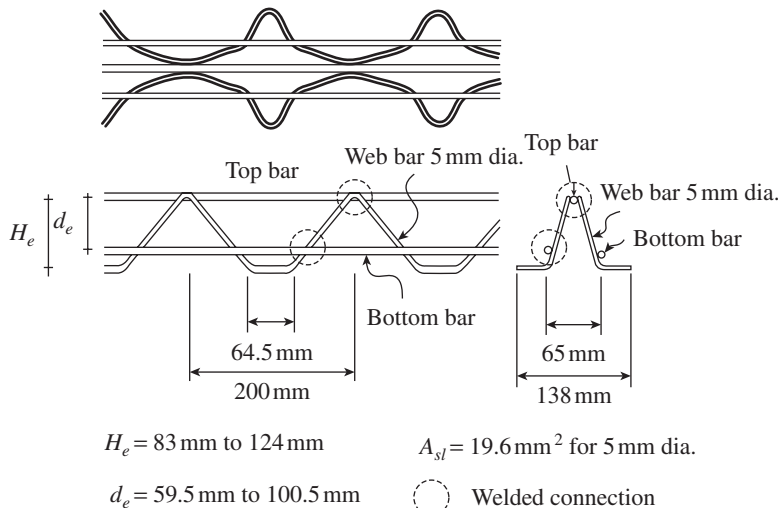


FIG. 11.31 Lattice shear reinforcement suggested by Park, et al. (2007) (Reprinted with permission from ACI)

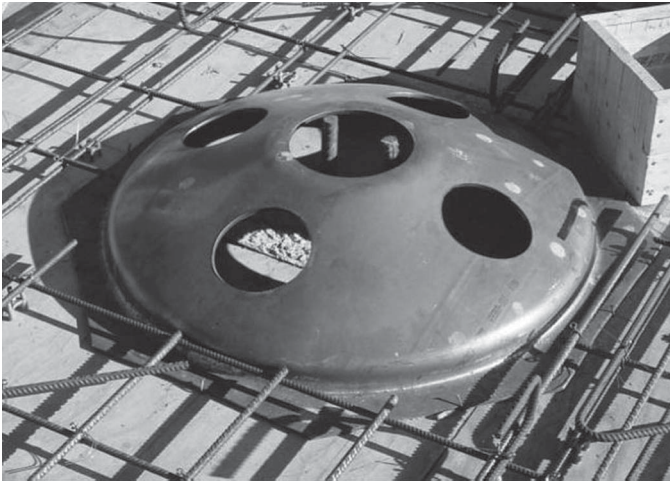


FIG. 11.32 Flat slab with UFO punching preventer and Bamtec carpet reinforcement

Courtesy: Casper Ålander, Celsa-Steelservice

and is shown in Fig. 11.32. (The name UFO might have been given because of its resemblance to a flying saucer.) Its location of use is inside the slab centrally on top of the column. The UFO increases the punching capacity beyond the level that can be reached by the punching shear reinforcement. The bottom flange and the lower part of the product function like a support for the slab in the outer area. In the inner area, the UFO collects the reactions from the slab and transfers them by membrane action to the area on top of the column. Thus, it functions like a mushroom-shaped column head. The punching capacity of the slab can be calculated in accordance with the relevant concrete code, using the size of the UFO as the size of the support. More details about this product are provided by Ålander (2005).

11.6 DESIGN PROCEDURE FOR FLAT SLABS AND PLATES

The steps required for the design of flat slabs are similar to that of other two-way slabs, except that the bending moment determination in different locations requires a three-step procedure. Moreover, we need to check for punching shear in addition to one-way shear. The various steps are as follows:

1. Determine whether the slab geometry and loading allow the use of the DDM. Assuming a depth of slab, calculate the factored dead and live loads.
2. Select a slab thickness to satisfy the deflection and shear requirements using Eqs (10.2) and (10.3) of Chapter 10, remembering that the minimum thickness should be 125 mm. Such calculations also require the supporting beam or column dimensions. A reasonable approximation for such a dimension of columns or beams would be 8–15 per cent of the average of the long and short span dimensions, that is, 8–15 per cent of $(L_1 + L_2)/2$. For shear

check, the critical section is at a distance of $d/2$ from the face of support. If the thickness shown for deflection is not adequate to carry the shear, use one or more of the following:

- (a) Increase column dimension.
- (b) Increase concrete strength.
- (c) Use drop panels or column capitals to improve shear strength.
- (d) Increase slab thickness.
- (e) Use shear reinforcement.

As discussed, option (e) is preferable in most of the situations and option (d) is least preferred.

3. Divide the flat slab into column and middle strips (Clause 31.1.1).
4. The DDM is essentially a three-step procedure:
 - (a) Compute the total statical factored moment M_o using Eq. (11.2) (Clause 31.4.2.2).
 - (b) Divide M_o as negative and positive moments within each span, ($0.65M_o$ and $0.35M_o$ as per Clause 31.4.3.2 in interior spans and as per Clause 31.4.3.3 in exterior spans).
 - (c) Distribute the negative and positive moment from step 4(b) to the column and middle strips within each span, as per Clause 31.5.5.
5. Determine whether the trial slab thickness chosen is adequate for the moment–shear transfer in the case of flat plates at the interior or exterior column junctions by computing the portion of the moment transferred by shear (using the equation given in Clause 31.3.3) and considering the properties of the critical shear section at a distance $d/2$ from the column face. If not, design the punching shear reinforcement.
6. Design the flexural reinforcement to resist the factored moments computed in step 4.
7. Select the size and spacing of the reinforcement to fulfil the requirements for crack control, bar development lengths, and shrinkage and temperature stresses using Fig. 11.33 (Fig. 16 of IS 456).

A comparison of the design made as per IS 456, ACI 318, BS 8110, and CP 110 of an interior panel of flat and waffle slabs of size 6 m × 6 m was made by Suryanarayana (2001).

11.7 DETAILING OF REINFORCEMENTS

The area of reinforcement in each direction of flat slab systems should be determined from the moments at critical sections, using the usual equations for flexure (Eq. 9.10 of Chapter 9 or Eq. 10.27 of Chapter 10) but they should not be less than the minimum steel requirements. In flat plate or flat slab, the moments are larger in the column or middle strips spanning the longer direction of the panels. As a result, the reinforcement in the longer span is usually

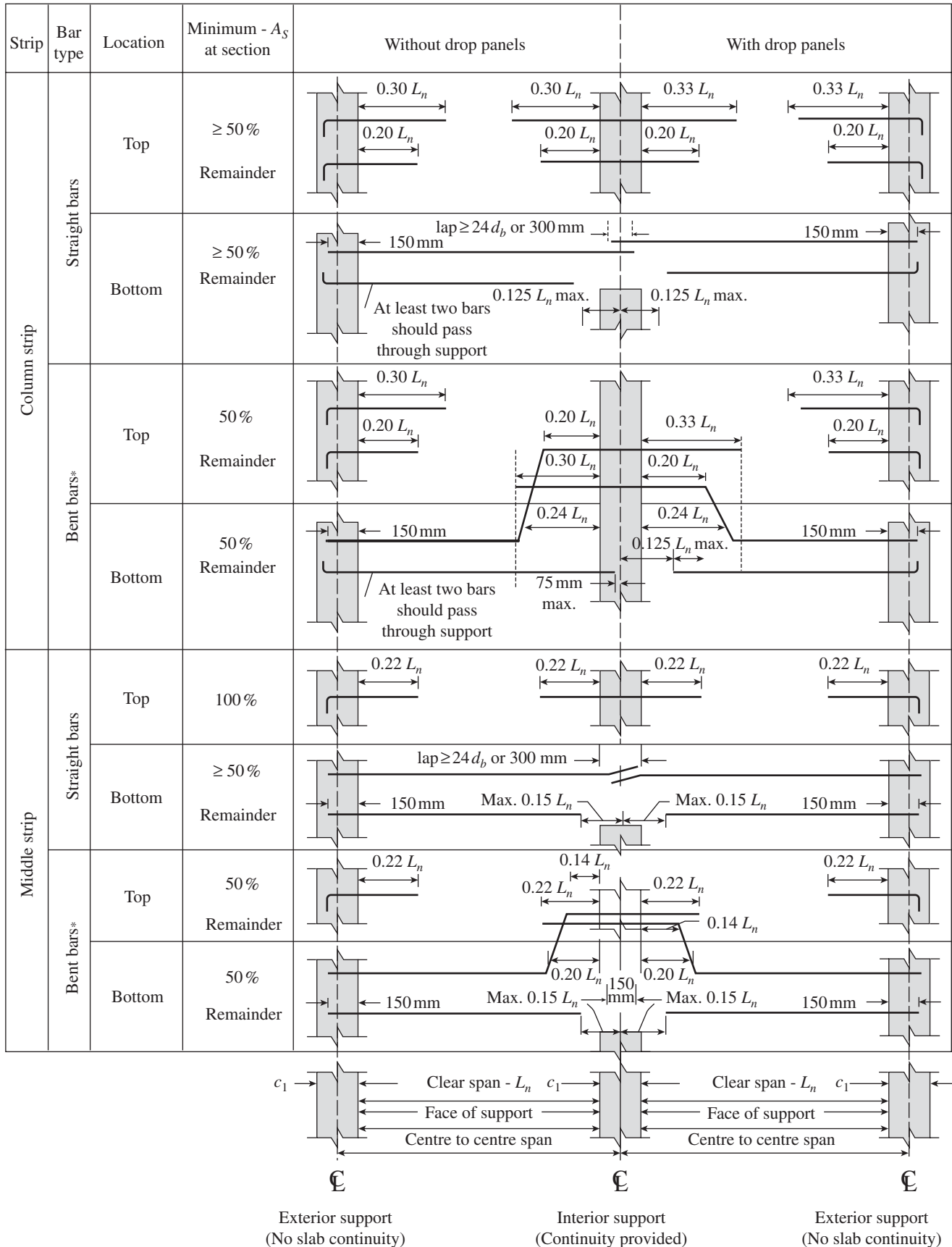


FIG. 11.33 Minimum extensions and bend joint locations for reinforcement in flat slabs

*Bent bars may be used at exterior supports if a general analysis is made.

placed closer to the top and bottom of the slab than in the shorter span. Such an arrangement will give a larger effective depth for the larger moment. For slabs supported on beams having α_b greater than about 1.0, the opposite is true; hence, the reinforcement pattern should be reversed (Wight and MacGregor 2009).

The detailing of reinforcement in flat slabs must be done as specified in Clause 31.7 of IS 456. These rules are listed as follows:

1. The spacing of reinforcement in the flat slab should not exceed *twice the slab thickness*, except where a slab is of cellular or ribbed construction. ACI has an additional limit of 450 mm.
2. When drop panels are used, the thickness of the drop panel for the determination of the area of reinforcement should be the lesser of the thickness of the drop and that of the slab, plus one-fourth the distance from the edge of the drop panel to the face of the column or column capital (see Clause 31.7.2). If the drop panel has greater depth, the full depth will not be effective and hence the aforementioned limit is specified.
3. Reinforcement in flat slabs should have minimum lengths as specified in Fig. 16 of IS 456. (A modified figure taking into account the latest provisions in ACI 318 is shown in Fig. 11.33.) Larger lengths as per Clauses D-1.4 to D-1.10 of IS 456 should be provided when the analysis is done by the EFM. It has to be noted that ACI permits bent bars only when the depth to span ratio permits the use of bends of 45° or less; it is because bent bars are seldom used and are difficult to place properly.
4. Where adjacent panels are unequal in span, the extension of the negative reinforcement beyond each face of the common column should be based on the *longer span*.
5. All slab reinforcements perpendicular to a discontinuous edge should have an anchorage (straight, bent, or otherwise anchored) past the internal face of the spandrel beam, wall, or column equal to the following:
 - (a) For *positive reinforcement*, it should not be less than 150 mm; however, with fabric reinforcement having a fully welded transverse wire directly over the support, it should be possible to reduce this length to one-half the width of the support or 50 mm, whichever is greater.
 - (b) For *negative reinforcement*, it should be such that the design stress is developed at the internal face in accordance with the development requirements of the code.

6. Where the slab is not supported by a spandrel beam or wall or where the slab cantilevers beyond the support, the anchorage is permitted within the slab.
7. In frames where flat slabs act as primary members resisting lateral loads, the lengths of reinforcement should be determined by analysis but should not be less than those prescribed in Fig. 11.33.

The US practice is to use 16 mm or smaller diameter bars in spans up to 7.5 m and to use 16–20 mm diameter bars if the spans exceed 7.5 m. In addition, the Concrete Reinforcing Steel Institute recommends that the top steel should not be less than 12 mm diameter placed at 300 mm centres in order to provide adequate rigidity such that they will not be displaced during the concrete operations or when people walk on them.

11.7.1 Detailing at Edge Columns

The shear and moment transfers from the slab to an exterior or a corner column will result in the slab acting as a torsional member. Moehle (1988) and Wight and Macgregor (2009) suggest the following reinforcement detail at these locations:

1. The top steel required to transfer the moment $\gamma_f M_u$ should be placed in a width equal to the smaller of $2(1.5D_s) + c_2$ and $2c_t + c_2$ centred on the column (see Fig. 11.34), where c_1 and c_2 are the dimensions of the column, c_t is the distance from the inner face of the column to the edge of the slab, and D_s is the depth of the flat slab. This width is referred to as the *effective transfer width*.

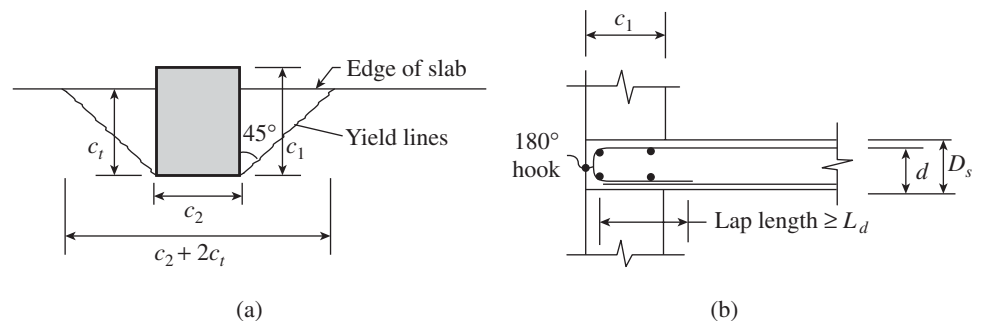


FIG. 11.34 Effective transfer width at exterior slab-column connections (a) Effective width (b) Detailing of reinforcement

2. As suggested by ACI-ASCE Committee 352.1R:1989, torsional reinforcement should be provided along the edge of the slab, within the dimensions defined in point 1 and extending away from the side face of the column to at least two times the slab thickness. The reinforcement placed outside this width is considered ineffective for moment transfer.

However, it is advisable to provide a stiff edge beam to prevent the excessive deflections taking place at the free end of the slab. Clause 31.3.2 of the code suggests the following when a

beam of depth greater than 1.5 times the thickness of the slab or wall is provided:

1. The loads directly coming on the beam or wall plus one-fourth of the total uniformly distributed load on slab should be considered for the design of the beam or wall.
2. The bending moments on the half-column strip adjacent to the beam or wall should be taken as one-fourth of the bending moments for the first interior column strip.

11.7.2 Structural Integrity Reinforcement

Research shows that several flat plate structures have collapsed in a progressive manner (see the case study). The basic mechanism of this failure consists of one overloaded slab-column connection failing in punching shear, subsequently overloading the slab below, resulting in the progressive collapse of several floors in a building. As shown in Fig. 11.35, the top reinforcement is inadequate to provide the post-punching resistance because it can be torn from the top surface of the slab at relatively low loads (Moehle, et al. 1988). To avoid this failure, researchers have suggested the provision of a secondary mechanism to suspend a slab after initial shear failure. Hence, bottom slab reinforcement passing through the column cage, which will act as a membrane to suspend the slab after the initial punching shear failure, has been suggested by them (Hawkins and Mitchell 1979; Mitchell and Cook 1984). Hawkins and Mitchell (1979) derived the following equation for the required area, A_{sb} , of such bottom reinforcement:

$$A_{sb} = \frac{0.5w_u L_1 L_2}{0.87f_y} \quad (11.23)$$

where w_u is the factored load to be carried by the slab and L_1 and L_2 are the centre-to-centre dimensions of the slab panels. Edge connections may require two-thirds of the reinforcement calculated by Eq. (11.23) and corner connections only half the reinforcement.

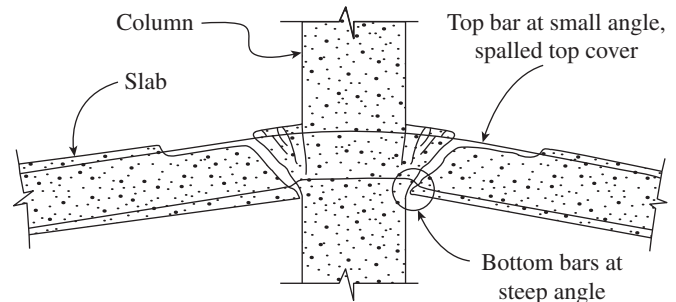


FIG. 11.35 Mechanism by which bottom reinforcement prevents progressive collapse

Source: Moehle, et al. 1988, reprinted with permission from ACI

Based on these recommendations, ACI 318 specified an integrity reinforcement in which at least two of the column strip bottom bars in each direction should pass within the region bounded by the longitudinal reinforcement of the column and shall be anchored at the exterior supports (see Figs 2.34 and 2.35). In slabs with shear heads and in lift slab construction (see Section 2.3.3 of Chapter 2) where it is not practical to pass these bottom bars through the column, the ACI code suggests that at least two bottom bars in each direction should pass through the shear head or lifting collar as close to the column as practicable. As already noted, in order to limit deformation demands under earthquake excitation, other stiffer structural systems like shear walls should be provided.

CASE STUDY

Collapse of Skyline Plaza, Virginia, USA

Skyline Plaza apartment building in Bailey's Crossroads, Virginia, USA, is an example of a catastrophic collapse of a 30-storey cast-in-place RC structure. This flat plate structure collapsed while under construction due to punching shear on the 23rd floor, which resulted in a progressive collapse.

In the midst of construction on 2 March 1973, one apartment building A-4 and the parking garage adjoining it collapsed. The following figure shows the damage following the collapse. The incident occurred at around 2:30 in the afternoon and resulted in the death of 14 construction workers and the injury of 34 others. It was designed as a 26-storey apartment complex with a 4-storey basement and a penthouse level. All floor slabs were 200 mm thick and the floor-to-floor height was 2.75 m.

The Center for Building Technology of the National Bureau of Standards (now the National Institute of Standards and Technology,

or NIST) investigated this collapse. A three-dimensional finite element analysis was conducted on the 22nd and 23rd floors to determine the magnitude of forces exerted on the floor slabs and whether the slabs could properly handle those forces. Upon completion of the analysis, it was determined that the moments in the column strips of the slab were not great enough to cause failure. On the other hand, the analysis did show that the slab around a few columns experienced shear stress greater than the shear capacity of the concrete slab. The improper and early removal of forms supporting the 23rd floor resulted in increased shear force around the columns. The recently poured concrete had strength less than the design strength of 20 MPa at the time of the collapse and was unable to withstand these increased forces. Hence, it triggered a punching shear collapse mechanism around a number of columns on the 23rd storey. Without the support of these columns, other

(Continued)

(Continued)

columns on that storey were overstressed, which ultimately led to the collapse of the entire 23rd floor slab onto the floor below. The increased loading on the 22nd floor from the weight of the collapsed floors above was too great and led to a progressive collapse all the way to the ground level (Leyendecker and Fattal 1977).

The important lessons learnt from the partial collapse of the Skyline Plaza are as follows (Leyendecker and Fattal 1977; Schellhammer, et al. 2012):

1. Redundancy within structural design is essential to prevent progressive collapse.
2. Construction loads, which will govern the design, must always be estimated and considered in the design.
3. Preconstruction plans of concrete casting, formwork plans, removal of formwork schedules, or reshoring program should be decided in consultation with the contractor.
4. Before the removal of shoring, the concrete strength should be ascertained.
5. Proper shoring of floors above and that of the currently executed floor should be verified, especially in flat plate systems.

Following this failure, the Portland Cement Association (PCA) and the Prestressed Concrete Institute both issued new design guides with provisions included to prevent progressive collapse. The importance of designing for construction loads as well as normal design loads was emphasized in the ACI journals (Agarwal and Gardner 1974). The ACI code included a provision to place rebar continuously through the slab-column intersection at the top and bottom of the slab. If the slab fails in punching shear, the bottom bars act as a catenary and prevent the collapse of the slab onto the structure below.

Several other failures of flat slab structures have been reported in the literature, which include New York Coliseum on 9 May 1955 (waffle slab); 2000 Commonwealth Avenue on 5 January 1971; the five-storey Harbour Cay Condominium collapse at Cocoa Beach, Florida, on 27 March 1981 (11 workers killed and 23 injured); the Tropicana Casino parking garage in Atlantic City,



Progressive collapse of Skyline Plaza building in Virginia, USA

(Source: Ellingwood, et al. 2007)

New Jersey, on 30 October 2003; the four-storey warehouse at Ontario, Canada, on 4 January 1978; the five-storey Sampoong Department Store, Seoul, Korea, on 29 June 1995 (this collapse is the largest peacetime disaster in South Korean history; 502 people died, 6 went missing, and 937 sustained injuries); Piper's Row Car Park, Wolverhampton, UK, in 1997; underground parking structure, Geneva, Switzerland, in 1976; underground car parking, Bluche, Switzerland, in 1981; office building, Cagliari, Italy, in 2004; and the parking garage flat slab at Gretzenbach, Switzerland, in 2004. In addition, several flat plate systems have failed during earthquakes.

11.8 OPENINGS IN FLAT SLABS

Clause 31.8 of IS 456 permits openings of any size in a flat slab system, provided it can be shown by suitable analysis that the requirements of strength and serviceability, including the limits on deflections, are met. However, in the following situations no special analysis is required:

1. In the area within the middle half of the span in each direction, opening of any size is permitted, provided the total amount of reinforcement required for the panel without openings, in both directions, is maintained.
2. In the area common to the intersecting column strips, an opening size of one-eighth the width of column strip in either span is permitted. The equivalent of reinforcement interrupted should be added on all sides of the openings (see Fig. 10.53)

3. In the area common to one column strip and one middle strip, the maximum permitted opening size is limited in such a way that a maximum of one-quarter of the slab reinforcement in either strip may be interrupted. The equivalent of reinforcement interrupted should be added on all sides of the openings.

These provisions are explained in Fig. 11.36 for slabs with $L_2 > L_1$.

Effect of Openings on Shear Strength of Slabs

As per Clause 31.6.1.2 of the code, the effect of an opening on the concrete shear strength has to be considered in flat slabs when any opening is located anywhere within the column strip or within 10 times the slab thickness from the concentrated load or reaction area. The effect of the opening on the shear strength may

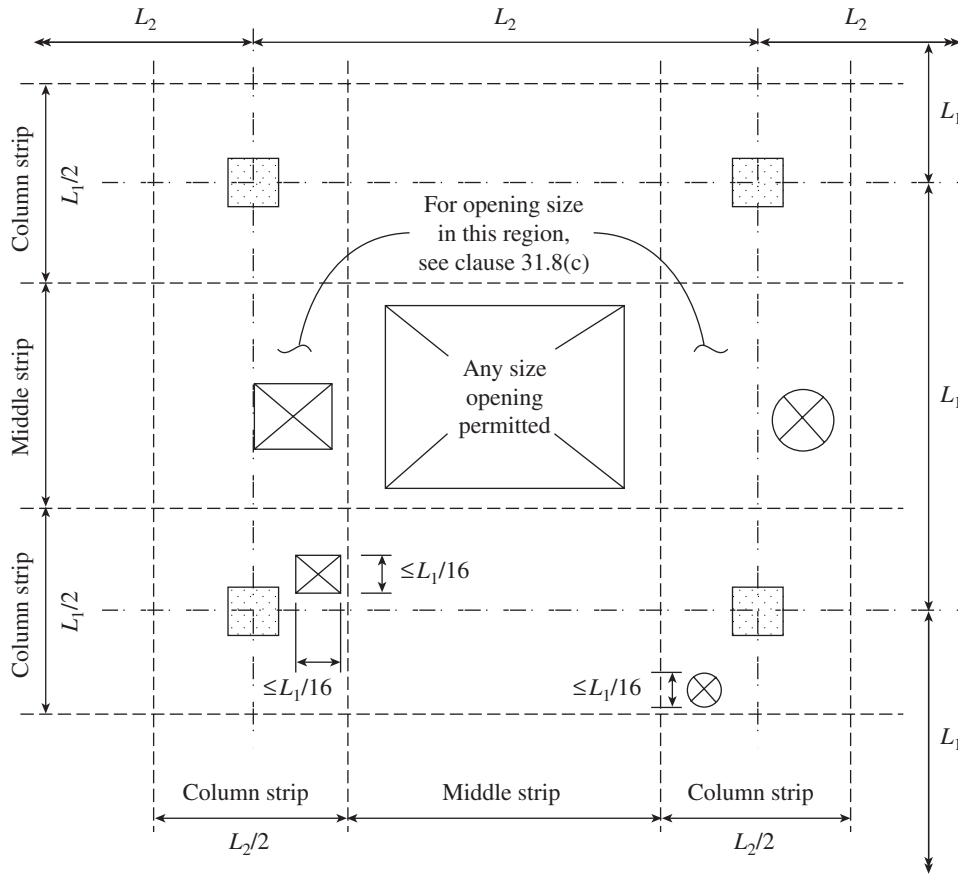


FIG. 11.36 Permitted openings in flat slabs

be considered by reducing the perimeter of the critical section by a length equal to the projection of the opening on the critical length. This reduction is determined by the enclosed radial projections of the openings to the centroid of the reaction area as shown in Figs 11.37 and 11.38. Clause 31.6.1.2 of the code also stipulates that openings should not encroach upon the column head. As per the ACI code, for slabs with shear reinforcement the ineffective portion of the perimeter b_o is taken as one-half of that without shear reinforcement (see Fig. 11.38b). The one-half factor may also be adopted for shear head reinforcement and stirrup reinforcement. Teng, et al. (2004) studied the punching shear strength of slabs with openings and supported

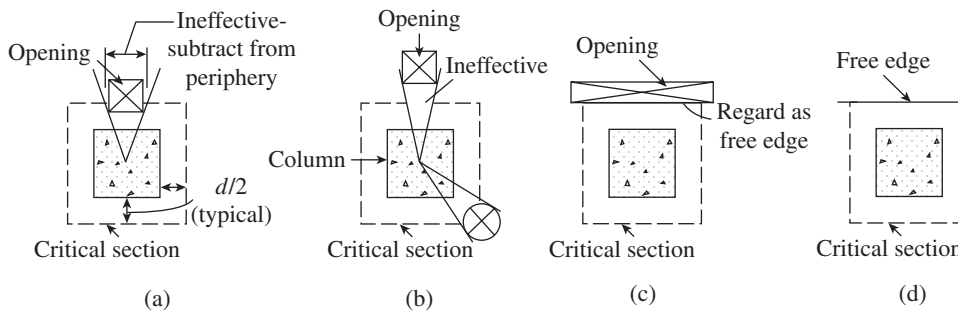


FIG. 11.37 Effect of opening on shear strength of slabs (a) Opening on the critical perimeter (b) Opening away from the critical perimeter (c) Large opening near critical perimeter (d) Column near the edge of building

on rectangular columns; they proposed a shear stress formula that was found to correlate well with test results.

11.9 EARTHQUAKE EFFECTS

As already mentioned, earthquakes have demonstrated that slab-column connections of flat slabs are vulnerable to brittle punching shear failures, which are expensive to repair. Though the ACI code stipulates that moment frames or shear walls are to be provided to resist lateral loads in regions of high seismic risk, it allows flat slabs without such LFRSs in regions of low or moderate seismic risk.

The ACI code gives several rules for detailing of flat slabs in earthquake zones (see Clause 21.3.6 of ACI 318:2011). Some of these rules are illustrated in Fig. 11.39.

Other rules are as follows:

1. Not less than one-half of the reinforcement in the column strip at support should be placed within the effective transfer width (see Figs 11.17 and 11.34).
2. Not less than one-half of all bottom middle strip reinforcements and all bottom column strip reinforcements at mid-span shall be continuous and shall develop f_y at the face of the support.
3. At discontinuous edges of the slab, all top and bottom reinforcements at support shall be developed at the face of support.
4. At the critical sections for punching shear, the two-way shear caused by factored gravity loads shall not exceed $0.4\phi V_c$.

Where precast flooring elements are used, an adequately reinforced in situ topping of at least 65 mm in thickness (50 mm for concrete slabs and composite topping slabs) should be placed in order to provide suitable diaphragm action. It is essential to ensure that this topping is adequately bonded to the precast elements, if composite action is required, by the use of mechanical connectors or chemical (e.g., epoxy) bonding in conjunction with adequate interface

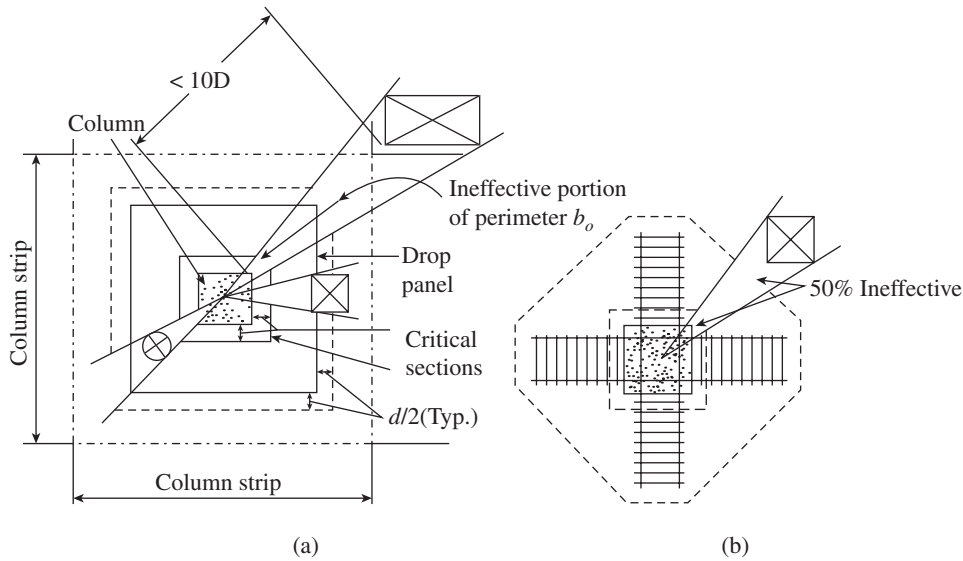


FIG. 11.38 Effect of opening in slab (a) With drop panel (b) With shear reinforcement

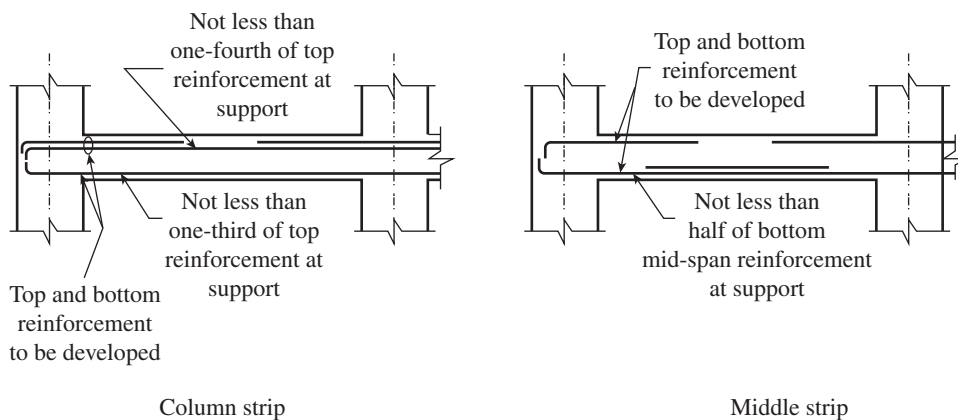


FIG. 11.39 Detailing of reinforcement in flat slabs in earthquake zones as per ACI 318 (Reprinted with permission from ACI)

roughening. Without this, separation can occur and the topping may buckle when subjected to diagonal compression resulting from diaphragm shear and be unable to transmit the floor inertial forces to the shear walls or columns (RCD D4-1995).

11.9.1 Diaphragm Action

Designers should ensure that there is an adequate load path for the forces to be transferred between a diaphragm and any lateral force resisting elements, such as walls or frames. In addition, the connections between them should be detailed in such a way that they adequately transfer the anticipated loads. The *strut-and-tie* method may be used for the design of these details. The design for a diaphragm action is similar to those explained in Section 10.10 of Chapter 10, but now the slab will act as a horizontal diaphragm between shear walls. The chord forces developed in buildings with flat plates and shear walls are found to be substantially higher than those in framed buildings without shear walls; hence, more chord reinforcement may be required in buildings with flat plates or flat slabs and shear walls (Dhar

and Sengupta 2010). The locations and spacing of shear walls also have a significant effect on the variation of the chord forces at any level (Dhar and Sengupta 2010). Barron and Hueste (2004) studied the impact of diaphragm flexibility on the structural response of rectangular RC building structures using a performance-based approach.

11.9.2 Effective Slab Width for Earthquake Loads

Two approaches are used in the modelling of the slab-column behaviour for two-dimensional frame analysis—torsional member and effective slab width methods. The most common *torsional member method* is the *equivalent column method*, developed originally for gravity loads and adopted for lateral loads (Corley and Jirsa 1970; Vanderbilt 1979). It defines a transverse torsional spring to model the torsional stiffness of the slab adjacent to the slab-column connection. This stiffness is combined with the column stiffness to provide the properties of an equivalent column. Although this method has been adopted in the ACI code, it is inconvenient to implement in typical two-dimensional elastic frame software.

The *effective slab width method* models the slab as a beam and hence can be used easily with standard frame analysis software. The equivalent width of the slab-beam element is adjusted to simulate the actual behaviour of the three-dimensional system, whereas the depth is taken as the actual depth of the slab. The effective width accounts for the behaviour of the slab that is not fully effective across its transverse width. More recent proposals for effective slab widths are calibrated to match the experimental behaviour of laterally loaded slab-column systems.

The following parameters have been identified to affect the effective slab width in the model for determining the strength and stiffness—the aspect ratio of the columns and panels, the type of connection (interior, exterior, corner, and edge), the level of gravity load, differing negative and positive moment response, the amount of initial cracking, and the presence of drop panel (Dovich and Wight 2005). Different authors have proposed different effective widths (for example, see Vanderbilt and Corley 1983; Leo and Durrani 1995; Grossman 1997;

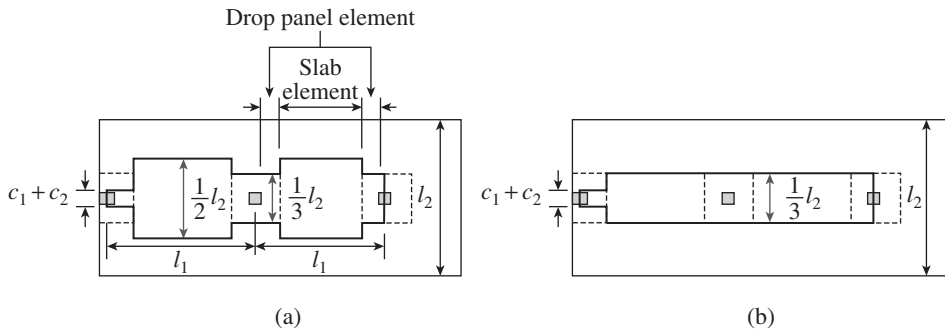


FIG. 11.40 Effective slab width model (a) Effective width for strength (b) Effective width for initial stiffness

Source: Dovich and Wight 2005, reprinted with permission from ACI

Hwang and Moehle 2000; Dovich and Wight 2005; and Han, et al. 2009). The effective width model developed by Dovich and Wight is shown in Fig. 11.40. These models are intended to give an estimate of the strength and stiffness contributions of flat slab frames at relatively low drift levels. More discussions and suggestions on deciding the effective slab width may be found in Section 13.9 of the work of Wight and MacGregor (2009).

Eurocode 2 suggests that the structure be divided into frames consisting of strips of slabs contained between the centre lines of adjacent panels. The stiffness of these equivalent beams, computed based on the gross cross section of the slab, is reduced to one-half in the case of horizontal loading to reflect the increased flexibility of the flat slab structures.

11.9.3 Deformation Capacity of Slab-column Connections

Even when other structural components, such as shear walls or perimeter moment frames, are used to resist lateral loads, slab-column connections should have sufficient rotational capacity to avoid punching failure so that the gravity load-carrying capacity is maintained under seismic excitations. Hence, deformation capacity is of particular concern for slab-column connections subjected to lateral loads.

Test data has convincingly shown the trend of connection deformation capacity being reduced by the increased gravity load. The connection deformation capacity is often expressed as the *inter-storey drift ratio*. This ratio was empirically formulated by Pan and Moehle (1989), Megally and Ghali (2000), Durani, et al. (1995), Hueste and Wight (1999), and Robertson and Johnson (2006). Until now, the ratio V_{ug}/V_c is identified as the only variable that affects the connection deformation capacity.

In Clause 21.13.6 of the ACI code, the effect of the gravity load on the drift capacity of flat plates was recognized and the following percentage drift ratio limitation, in the absence of shear reinforcement, was recommended (see Fig. 11.41):

$$DR = \begin{cases} 3.5 - 5.0VR & (\text{for } VR < 0.6) \\ 0.5 & (\text{for } VR \geq 0.6) \end{cases} \quad (11.24a)$$

where DR is the *design storey drift ratio* (storey drift divided by storey height, which should be taken as the largest value for the adjacent storeys above and below the connection), and

$$VR = \frac{V_{ug}}{\phi V_n} \quad (11.24b)$$

where V_n is calculated using Eq. (11.20), V_{ug} is the factored shear force on the slab critical section due to gravity loads, and $\phi = 0.75$. If DR exceeds the limit given by Eq. (11.24), shear reinforcement should be provided or the connection

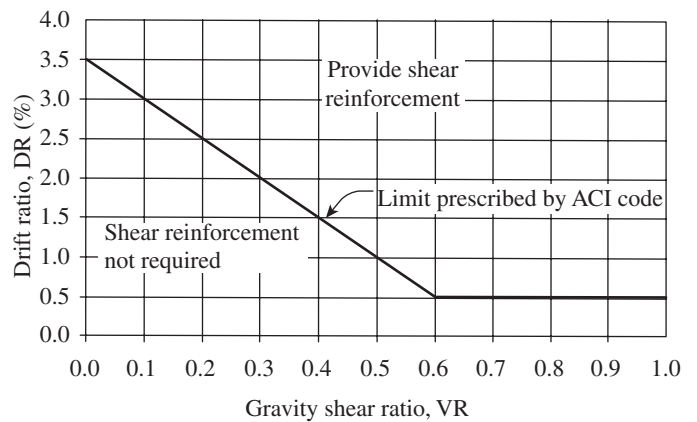


FIG. 11.41 ACI code criterion for adequacy of slab-column connection in seismic zones

Source: Hueste, et al. 2007, reprinted with permission from ACI

should be redesigned. In addition, Clause 21.13.6 of ACI 318:11 prescribes that V_s in Eq. (11.20) should not be less than $0.26\sqrt{f_{ck}} b_o d$ and the shear reinforcement should extend at least four times the slab thickness from the face of the support. The required design steps are shown in Fig. 11.42.

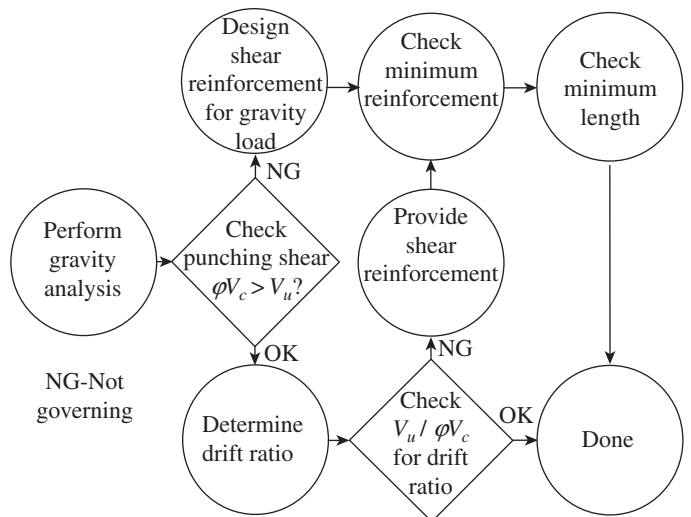


FIG. 11.42 Design steps for resisting punching shear in earthquake zones
Source: Hueste, et al. 2007 reprinted with permission from ACI

Hueste, et al. (2007) suggested the following performance-based seismic design limit for slab-column connection, based on a linear regression analysis of the test data.

$$DR = 5 - 7 \frac{V_{ug}}{\tau_c b_o d} \quad (11.24c)$$

where τ_c is calculated using Eq. (11.12).

11.10 WAFFLE SLABS

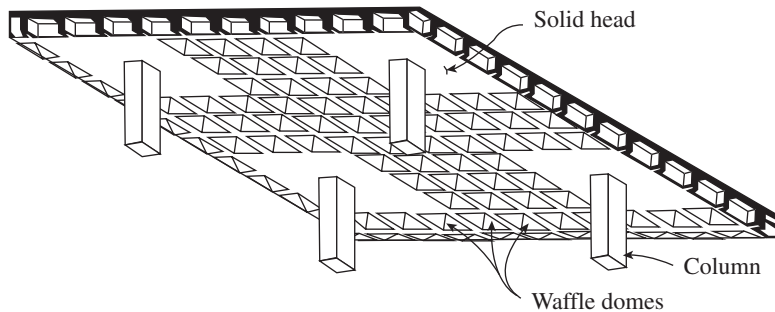
A *waffle slab*, also called a *two-way joist*, *ribbed slab system*, or a *coffered slab*, essentially consists of a thin top slab acting compositely with a closely spaced orthogonal grid of beam ribs, as shown in Fig. 11.43 (the name waffle slab is due to its appearance, which is similar to pancakes made in countries such as Belgium and the USA). The joists are commonly formed by using standard glass fibre reinforced plastic (GFRP) square *dome* forms. Standard GFRP pan dimensions are given in Table 11.10. Thin precast concrete domes with a thickness of 25–40 mm may also be used as *left-in-place shuttering*, in which case they act monolithically with the waffle slab system. In *flat* waffle slabs, these domes are omitted around the columns to form solid heads to resist the high bending and shear stresses in these critical areas. In contrast to a joist,

which carries loads in a one-way action, a waffle system carries the loads simultaneously in two directions. The system is more suitable for square bays than rectangular bays.

Instead of using dome forms, it is also possible to incorporate hollow blocks, which are left in place, to give a flat ceiling. Waffle slabs result in considerable reduction in dead loads compared to conventional flat slabs, and their soffit provides architecturally desirable appearance. Waffle slabs are more efficient for spans in the range 9–12 m because they have greater overall depth and may have less dead weight than comparable flat slabs. However, the overall depth of a waffle slab will be 50–100 per cent more than that of an equivalent solid flat slab. Normally, the width of web of the ribs is greater than 65 mm, the spacing of ribs is less than 1.5 m (usually less than 12 times the thickness of topping slab), and the depth of rib, excluding any topping, is kept less than 4 times the width of web of ribs (see Clause 30.5 of the code).

The self-weight of a two-way ribbed slab with filler block is given by the following relation (Varyani and Radhaji 2005):

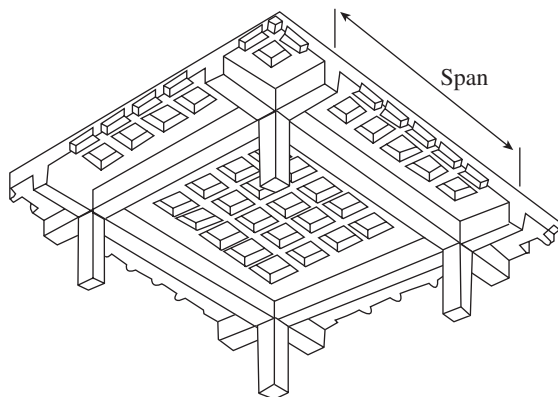
$$w_s = \rho_c \left[D_f + \left(2 - \frac{b_w}{b_f} \right) (D - D_f) \frac{b_w}{b_f} \right] + \rho_h \left(1 - \frac{b_w}{b_f} \right)^2 (D - D_f) \quad (11.25)$$



(a)



(b)



(c)



(d)

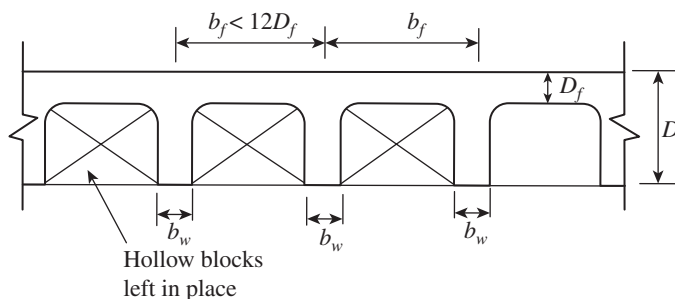
FIG. 11.43 Waffle slabs (a) Waffle slab (flat plate) (b) Building with waffle slab (c) Waffle slab supported on beams (d) Waffle slab ceiling in Washington, DC, Metro station

TABLE 11.10 Standard GFRP dome pans (Hurd 1997)

Void Plan, mm	Depths Available, mm	Joist Centres, mm	Joist Width, mm
475 × 475	100, 150, 200, 250, 300, 350, and 400	600 × 600	125
600 × 600	150, 200, 250, 300, 350, and 400	750 × 750	150
750 × 750	200, 250, 300, 350, 400, 450, and 500	900 × 900	150
1000 × 1000	400 and 600	1200 × 1200	200
1025 × 1025	300, 350, 400, 450, 500, and 600	1200 × 1200	200
1300 × 1300	250, 300, 350, 400, 450, 500, 550, and 600	1500 × 1500	200

Note: All sizes may not be available from a single manufacturer.
Courtesy: W. Palmer Jr. of Concrete Construction

where ρ_c is the unit weight of concrete (kN/m^3), ρ_h is the volumetric unit weight of filler block (kN/m^3), and D , D_f , b_w , and b_f are as shown in Fig. 11.44 and are in metres.

**FIG. 11.44** Two-way ribbed slab with filler blocks

The overall behaviour of the system shown in Fig. 11.43(a) is similar to a flat slab (Schwetz, et al. 2009). Hence, waffle slabs are designed as flat slabs by treating the solid heads as drop panels. The bending moments per metre width obtained for solid slabs (in case of waffle slab supported by beams—see Fig. 11.43c) should be multiplied by the spacing of the ribs to obtain the bending moments per rib. In the case of waffle slabs without beams, as shown in Fig. 11.43(a), bending moments in column and middle strips can be determined using the DDM. These bending moments may be apportioned to the number of ribs present in the column and middle strips. The ribs may be designed as T- or rectangular beams.

At least 50 per cent of the total tension reinforcement at the bottom should be extended to the support and anchored properly, as per Clause 26.2.3.3 of IS 456. At least one bar at each corner of the rib is extended throughout the length for holding transverse reinforcement in the form of stirrups. Minimum reinforcement is provided in the topping slab, usually in the form of welded wire mesh.

The one-way shear force per metre width obtained should be multiplied by the spacing of the ribs to obtain the shear force per rib. When the shear stress calculated using Eq. (11.9) exceeds the permissible shear stress given in Table 19 of IS 456, any one of the following measures should be adopted:

1. Increase the width of rib.
2. Reduce the spacing of ribs.
3. Provide solid concrete at the supports.
4. Provide shear reinforcement only if none of the other measures mentioned are possible.

For ribbed and coffered flat slabs, solid areas should be provided at the columns, and the punching shear stress should be checked in a similar manner to the shear around the columns in solid flat slabs.

11.11 GRID SLABS

When the spacing of ribs is greater than 1.5 m, the slab is referred to as a grid slab (see also Section 2.3.4 of Chapter 2). The behaviour of the grid slabs is different from that of a solid or waffle slab, as torsional rigidity is negligible in grids (Varyani and Radhaji 2005). Grids are suitable for spans greater than 10.0 m. They are generally analysed by using grid analysis programs, with the slab load acting on them as triangular or trapezoidal loads. The beams are then designed as T- or rectangular beams for the bending and torsional moments as well as shear forces obtained from the computer results. The slabs over the grid beams are designed as two-way slabs.

11.12 HOLLOW-CORE SLABS

Hollow-core slabs are produced using the following two methods: (a) In the dry-cast (or extrusion) system, a very low slump concrete is forced through the casting machine and the concrete is compacted around the cores. (b) The second system uses a higher slump concrete and the sides are created by stationary forms (or by slip forming) with forms attached to the machine (Hawkins and Ghosh 2006). Cores are typically created by pneumatic tubes attached to the form or by slip forming with long tubes attached to the casting machine. Information on the dimensions, section properties, and load-carrying capacities of hollow-core slabs is provided in PCI Design Handbook (2010). The design handbook shows cross sections and section properties of proprietary hollow-core slabs along with load tables for uniform loading that apply for non-proprietary sections varying from 150 mm to 300 mm in depth. The load tables in the design handbook are based on the ACI 318 requirements for flexural strength, service load flexural stresses, and shear strength. It should be noted that for loading conditions other than uniform loading, the designers should perform separate calculations. The use of

shear reinforcement is generally not feasible for hollow-core slabs, and therefore, the shear strength, particularly of deep slabs, may be limited to the shear strength of the concrete. Tests on hollow-core units with depths greater than 320 mm have shown that web-shear strengths can be less than strengths computed using the equations provided in the ACI 318 code coupled with a critical section, located at $d/2$ from the face of the support (Hawkins and Ghosh 2006).

EXAMPLES

EXAMPLE 11.1 (Design of flat plate):

Design a flat plate supported on columns spaced at 5.5 m in both directions. The size of the column is 500 mm by 500 mm and the imposed load on the panel is 4 kN/m². The height of each floor is 3.5 m. The floor slab is exposed to moderate environment. Assume floor finishing load to be 1 kN/m² and use M25 concrete and Fe 415 grade steel.

SOLUTION:

Step 1 Select the thickness of the slab. As the slab experiences moderate environment, choose cover as 30 mm (Table 16 of IS 456). As per Clauses 31.2.1 and 24.1 of the code,

$$L/d \text{ ratio with Fe 415 steel} = 0.9(0.8 \times 40) = 28.8.$$

$$\text{Minimum effective depth} = \frac{\text{Span}}{28.8} = \frac{5500}{28.8} = 190 \text{ mm} > 125 \text{ mm (as per the code)}$$

Assuming 12 mm diameter bars,

$$\text{Total depth} = 190 + 6 + 30 = 226 \text{ mm}$$

Assume $D = 225$ mm and $d = 189$ mm.

Step 2 Calculate the loads.

$$\text{Self-weight of slab} = 0.225 \times 25 = 5.625 \text{ kN/m}^2$$

$$\text{Weight of finishing} = 1 \text{ kN/m}^2$$

$$\text{Imposed load} = 4 \text{ kN/m}^2$$

$$\text{Total working load, } w = 10.625 \text{ kN/m}^2$$

$$\text{Design factored load, } w_u = 1.5 \times 10.625 = 15.94 \text{ kN/m}^2$$

$$\text{Clear spacing between the columns, } L_n = L_1 - c_1 = 5.5 - 0.5 = 5 \text{ m}$$

$$\text{Total design load on the panel, } W = w_u L_n L_2 = 15.94 \times 5 \times 5.5 < 5.5 = 438.35 \text{ kN}$$

Step 3 Calculate the bending moments. The sum of the positive and average negative bending moments (Clause 31.4.2.2)

$$M_o = \frac{WL_n}{8} = \frac{438.35 \times 5}{8} = 273.97 \text{ kNm/panel}$$

Interior panel:

Panel negative design moment (Clause 31.4.3.2)

$$= 0.65M_o = 0.65 \times 273.97 = 178.08 \text{ kNm/5.5 m}$$

Panel positive design moment

$$= 0.35M_o = 0.35 \times 273.97 = 95.89 \text{ kNm/5.5 m}$$

As per Clause 31.4.3.3, the relative stiffness of the columns and the slab determines the distribution of the negative and positive moments in the exterior panel.

The building is not restrained against lateral sway; hence, the effective height of the column can be taken as 1.2 times the clear height (Clause E-1 of IS 456). Hence, the effective length of the column is calculated as follows:

$$L = H - D = 3.5 - 0.225 = 3.275 \text{ m}$$

$$L_e = 1.2 \times 3.275 = 3.93 \text{ m}$$

Relative stiffness of column

$$K_c = \frac{I_c}{L_e} = \frac{h^4}{12L_e} = \frac{0.5^4}{12 \times 3.93} = 1.325 \times 10^{-3}$$

Relative stiffness of slab panel

$$K_s = \frac{I_s}{L_{se}} = \frac{bt^3}{12L_{se}} = \frac{5.5 \times 0.225^3}{12 \times 5.5} = 9.492 \times 10^{-4}$$

$$\alpha_c = \frac{\sum K_c}{K_s} = \frac{2 \times 1.325 \times 10^{-3}}{9.492 \times 10^{-4}} = 2.79$$

$$\text{Imposed load/Dead load} = 4/(5.625 + 1) = 0.6$$

$L_2/L_1 = 1$; hence, from Table 17 of IS 456, $\alpha_{c,\min} = 0.14$.

$\alpha_c > \alpha_{c,\min}$; hence, the stiffness is sufficient.

The factor that decides the relative distribution of bending moment between the negative and positive bending moments as per Clause 31.4.3.3 of IS 456 is

$$\alpha = 1 + \frac{1}{\alpha_c} = 1 + \frac{1}{2.79} = 1.358$$

End span:

In an end span,

$$\text{Exterior negative bending moment coefficient} = 0.65/\alpha = 0.479$$

$$\text{Interior negative bending moment coefficient} = 0.75 - 0.1/\alpha = 0.676$$

$$\text{Positive bending moment coefficient} = 0.63 - 0.28/\alpha = 0.424$$

The corresponding end panel bending moments are as follows:

$$\text{Negative bending moment at outer support} = 0.479 \times 273.97 = 131.23 \text{ kNm/panel}$$

$$\text{Negative bending moment at inner support} = 0.676 \times 273.97 = 185.20 \text{ kNm/panel}$$

$$\text{Positive bending moment in the panel} = 0.424 \times 273.97 = 116.16 \text{ kNm/panel}$$

It should be noted that these three values as per ACI 318 (Table 11.4) are $0.26 \times 273.97 = 71.23$ kNm, $0.7 \times 273.97 = 191.78$ kNm, and $0.52 \times 273.97 = 143.46$ kNm. Thus, there is a significant difference in the negative bending moment at the outer support using the IS code.

The bending moments are to be distributed between the column and middle strips as shown in Table 11.11 (Clause 31.5.5).

$$\text{Width of column strip} = 0.5 \times 5.5 = 2.75 \text{ m}$$

TABLE 11.11 Bending moment and area of steel

	Column Strip in kNm/2.75 m	A_{st} , mm ²	Middle Strip in kNm/2.75 m	A_{st} , mm ²
Interior panel: Negative moment	$0.75 \times 178.08 = 133.56$	2128	44.52	710
Positive moment	$0.60 \times 95.89 = 57.53$	914	38.36	611
Outer panel: Negative at exterior support	$1.0 \times 131.23 = 131.23$	2091	0	–
Negative at inner support	$0.75 \times 185.20 = 138.90$	2190	46.30	740
Positive at panel	$0.60 \times 116.16 = 69.70$	1111	46.46	740

Step 4 Check the slab depth for bending. The thickness of the slab is controlled by the absolute maximum bending moment. From the table, it can be seen that the critical bending moment occurs at the interior support of the outer panel column strip and is

$$M_{cip} = 138.9 \text{ kNm/2.75 m}$$

The depth required to resist this bending moment

$$d = \left(\frac{M_c}{Kb f_{ck}} \right)^{0.5} = \left(\frac{138.9 \times 10^6}{0.138 \times 2750 \times 25} \right)^{0.5} = 121 \text{ mm} < \text{chosen} \\ = 189 \text{ mm}$$

Hence, the adopted depth is satisfactory and the slab is under-reinforced.

Step 5 Design the reinforcement.

Effective depth for upper layer of reinforcement = $189 - 12 = 177 \text{ mm}$

Let us use this effective depth to calculate the reinforcement.

$$M_u = 0.87 f_y A_{st} d \left[1 - \frac{A_{st} f_y}{bd f_{ck}} \right]$$

Hence, for maximum negative moment at the interior support of the outer panel column strip

$$138.9 \times 10^6 = 0.87 \times 415 \times A_{st} \times 189 \left[1 - \frac{A_{st}}{2750 \times 189} \frac{415}{25} \right]$$

Simplifying, we get

$$A_{st}^2 - 31308 A_{st} + 63.73 \times 10^6 = 0$$

Solving, we get $A_{st} = 2189 \text{ mm}^2$.

The same result may be got by using design aids in SP 16:

$$\frac{M_u}{bd^2} = \frac{138.9 \times 10^6}{2750 \times 189^2} = 1.414$$

From Table 3 of SP 16, for $f_y = 415 \text{ N/mm}^2$

$$p_t = 0.4215; A_{st} = (0.4215/100) \times 189 \times 2750 = 2190 \text{ mm}^2$$

We may also use the approximate formula

$$A_{st} = \frac{M_u}{0.8 f_y d} = \frac{138.9 \times 10^6}{0.8 \times 415 \times 189} = 2213 \text{ mm} \text{ (1\% increase over exact results)}$$

From Table 96 of SP 16, provide 12 mm bars at 140 mm centre-to-centre distance (c/c) at top face of slab over the columns in the column strip (area provided = 2222 mm^2).

The reinforcement at different locations may be calculated by using proportionate spacing compared with the other bending moments as shown. For example,

Spacing of 12 mm bars at outer support at top = $140 \times 138.9/131.23 = 148 \text{ mm}$

Spacing at middle span at bottom = $140 \times 138.9/69.70 = 279 \text{ mm}$

Spacing at inner support at top = $140 \times 138.9/133.56 = 146 \text{ mm}$

Minimum reinforcement:

$A_{st, \min} = 0.12 \times 2750 \times 225/100 = 742 \text{ mm}^2 > A_{st}$ required at middle strip

Allowable maximum spacing (Clause 31.7.1 of IS 456) = $2D = 2 \times 225 = 450 \text{ mm}$

Spacing of 10 mm bars for minimum steel = $79 \times 2750/742 = 292 \text{ mm}$

Hence, provide 10 mm diameter bars at 275 mm c/c at middle strip to take up positive and negative moments. Since the span is the same in both the directions, provide similar reinforcement in the other direction as well.

Integrity reinforcement:

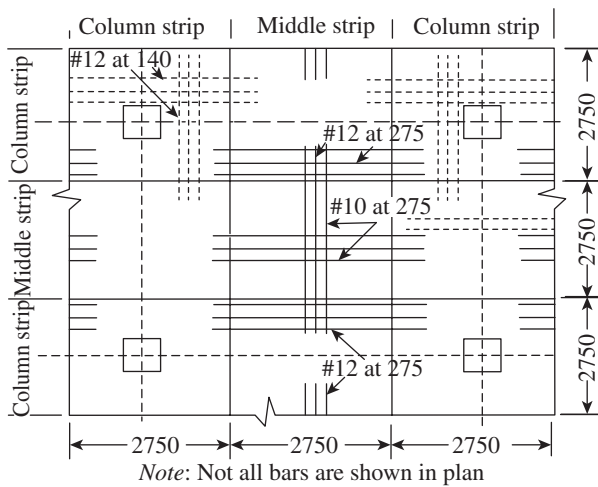
To control progressive collapse, we need to provide steel as per Eq. (11.23).

$$A_s = \frac{0.5 w_u L_1 L_2}{0.87 f_y} = \frac{0.5 \times 15.94 \times 5.5^2 \times 10^3}{0.87 \times 415} = 667 \text{ mm}^2$$

Provide two extra #20 bars each way, with a length of $2L_d$ ($2 \times 806 = 1612 \text{ mm}$) passing through the column cage. The steel provided (628 mm^2) is only slightly less than that suggested by Hawkins and Mitchell (1979) (94% of 667 mm^2); hence, it is sufficient.

To simplify detailing, only two spacings are selected, as shown in Fig. 11.45 (see Fig. 16 of the code).

Step 6 Check for punching shear. The critical shear plane is at a distance of $0.5d$ from the face of the column. The perimeter of critical section


Legend

- - - - - Top reinforcement ——— Bottom reinforcement

FIG. 11.45 Reinforcement details of flat plate of Example 11.1

$$b_o = 4(a + d) = 4(0.5 + 0.189) = 4(0.689) = 2.756 \text{ m}$$

The shear force on this plane is

$$\begin{aligned} V_u &= w_c [L \times L - (a + d)(a + d)] \\ &= 15.94(5.5 \times 5.5 - 0.689 \times 0.689) = 474.6 \text{ kN} \end{aligned}$$

$$\text{Nominal shear stress} = \frac{V_u}{b_o d} = \frac{474.6 \times 1000}{2756 \times 189} = 0.91 \text{ N/mm}^2$$

Shear strength of concrete (Clause 31.6.3) = $k_s \tau_c$

$$k_s = 0.5 + \beta_c < 1$$

$$\beta_c = 0.5/0.5 = 1; \text{ hence } k_s = 1.$$

$$\tau_c = 0.25 \sqrt{f_{ck}} = 0.25 \sqrt{25} = 1.25 \text{ N/mm}^2 > 0.91 \text{ N/mm}^2$$

Hence, there is no need to provide shear reinforcement or thickening of slab.

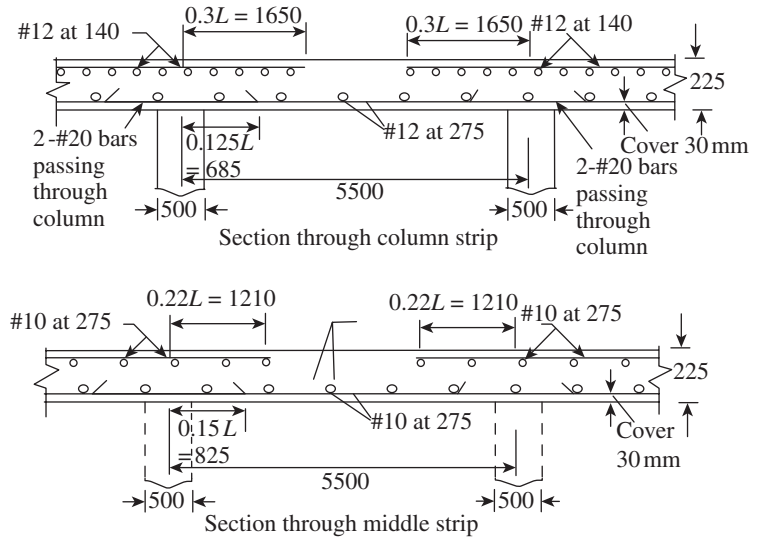
Note: In addition, we need to check for one-way shear (which will not be critical as seen in the examples of Chapter 10) and development length (as shown in Example 10.1 of Chapter 10).

EXAMPLE 11.2 (Flat slab with drop panels):

Design the interior panel of a large single-storey warehouse flat slab roof with a panel size of 6 m × 6 m supported by columns of size 500 mm × 500 mm. The height of the columns is 5 m. Take live load as 3.0 kN/m² and the weight of finishes including waterproof treatment as 2.5 kN/m². Use M25 concrete and Fe 415 steel. Assume mild environment.

SOLUTION:

Step 1 Select the thickness of the slab. For mild environment, minimum cover is 20 mm, which can be reduced by 5 mm if we use bars less than 12 mm (as per Table 16 of IS 456).



As per Clauses 31.2.1 and 24.1 of the code, for flat slab with Fe 415 steel

$$L/d = 0.8 \times 40 = 32$$

Minimum effective depth

$$= \text{Span}/32 = 6000/32 = 187.5 \text{ mm} > 125 \text{ mm (minimum as per code)}$$

Adopt a cover of 20 mm and assume 12 mm diameter bars. Hence,

$$\text{Required depth} = 187.5 + 20 + 6 = 213.5 \text{ mm}$$

$$\text{Adopt a depth of 215 mm and } d = 215 - 26 = 189 \text{ mm.}$$

Step 2 Calculate the size of the drop panel. As per Clause 31.2.2 of the code, a drop should not be less than 6000/3 = 2000 mm.

$$\text{Minimum depth of drop panel} = \frac{1}{4} D_s = \frac{1}{4} \times 215 = 53.75 \text{ mm}$$

Provide a drop panel of depth 60 mm and size 3000 mm × 3000 mm.

$$\text{Take total depth at drop panel} = 215 + 60 = 275 \text{ mm} > 1.25 \times 215 = 269 \text{ mm}$$

$$\text{Width of column strip} = \text{Width of middle strip} = 6000/2 = 3000 \text{ mm}$$

Step 3 Calculate the loads.

$$\text{Self-weight of slab} = 0.215 \times 25 = 5.375 \text{ kN/m}^2 \text{ in middle strip}$$

$$\text{Dead load due to extra thickness of slab at drops} = 0.06 \times 25 = 1.5 \text{ kN/m}^2$$

$$\text{Live load} = 3 \text{ kN/m}^2$$

$$\text{Finishes} = 2.5 \text{ kN/m}^2$$

$$\text{Total working load, } w = 12.375 \text{ kN/m}^2$$

$$\text{Design factored load, } w_u = 1.5 \times 12.375 = 18.56 \text{ kN/m}^2$$

$$\text{Clear span, } L_n = 6 - 0.5 = 5.5 \text{ m}$$

$$\text{Design load} = W = w_u L_n = 18.56 \times 6 \times 5.5 = 612.48 \text{ kN}$$

Step 4 Calculate the bending moment.

$$\text{Design static moment, } M_o \text{ (Clause 31.4.2.2)} = \frac{WL_n}{8} = \frac{612.48 \times 5.5}{8} = 421.08 \text{ kNm}$$

As per Clause 31.4.3.2

$$\text{Total negative design moment} = 0.65M_o = 0.65 \times 421.08 = 273.7 \text{ kNm}$$

$$\text{Total positive design moment} = 0.35M_o = 0.35 \times 421.08 = 147.4 \text{ kNm}$$

These moments are distributed into the column and middle strips as shown in Table 11.12, as per Clauses 31.5.5.1 and 31.5.5.3.

TABLE 11.12 Moment in column and middle strip of Example 11.2

Type	Column Strip, kNm	Middle Strip, kNm
Negative moment	$0.75 \times 273.7 = 205.3$	68.4
Positive moment	$0.60 \times 147.4 = 88.4$	59.0

Step 5 Check the slab depth for bending.

Thickness of slab required at drops

$$d = \left(\frac{M_u}{0.138 f_{ck} b} \right)^{0.5} = \left(\frac{205.3 \times 10^6}{0.138 \times 25 \times 3000} \right)^{0.5} = 141 \text{ mm}$$

Total depth provided at drop is $215 + 60 = 275$ mm with effective depth 247 mm and effective depth provided at middle strip 189 mm. Hence, the depth provided is sufficient and the slab is under-reinforced.

Step 6 Check for punching shear. The critical section is at a distance $d/2 = 247/2 = 123.5$ mm from the face of the column.

Perimeter of critical section, $b_o = 4(a + d) = 4(500 + 247) = 2988$ mm

Shear force on this plane

$$V_u = w_c [L \times L - (a + d)(a + d)] = 18.56(6^2 - 0.747^2) = 657.8 \text{ kN}$$

$$\text{Nominal shear stress} = \frac{V_u}{b_o d} = \frac{657.8 \times 1000}{2988 \times 247} = 0.89 \text{ N/mm}^2$$

Shear strength of concrete (Clause 31.6.3) = $k_s \tau_c$

$$k_s = 0.5 + \beta_c < 1; \beta_c = 0.5/0.5 = 1; \text{ hence, } k_s = 1.$$

$$\tau_c = 1 \times 0.25 \sqrt{f_{ck}} = 0.25 \sqrt{25} = 1.25 \text{ N/mm}^2 > 0.89 \text{ N/mm}^2$$

Hence, the slab is safe in punching shear and there is no need to provide shear reinforcement.

The shear strength at a distance $d/2$ from the drop also has to be checked. It will be safe as the drop size is large and hence the shear force at that section will be considerably reduced.

Step 7 Design the reinforcement.

1. The maximum negative reinforcement in the column strip, M_u , is 205.3 kNm and the effective depth at the drop is 247 mm. Hence,

$$\frac{M_u}{bd^2} = \frac{205.3 \times 10^6}{3000 \times 247^2} = 1.12$$

From Table 3 of SP 16 we get $p_t = 0.3284$.

$A_{st} = \frac{0.3284}{100} \times 3000 \times 247 = 2434 \text{ mm}^2$ to be provided in 3000 mm width

Required spacing = $(113/2434) \times 3000 = 139$ mm

Hence, provide 12 mm diameter bars at 135 mm c/c at the top face of the slab over the columns in the column strip ($A_{st, \text{provided}} = 2517 \text{ mm}^2$).

2. For the positive moment in column strip, M_u is 88.4 kNm and the effective depth of the slab is 189 mm.

$$A_{st} = \frac{88.4 \times 10^6}{0.8 \times 415 \times 189} = 1409 \text{ mm}^2$$

$$\text{Minimum } A_{st} = \frac{0.12}{100} \times 3000 \times 215$$

$$= 774 \text{ mm}^2 < 1409 \text{ mm}^2$$

$$\text{Required spacing} = \frac{113}{1409} \times 3000 = 240 \text{ mm} < 2D\delta = 430 \text{ mm}$$

Provide 12 mm diameter bars at 240 mm c/c at the bottom in the column strip.

3. For the negative moment in the middle strip, M_u is 68.4 kNm and the effective depth of the slab is 189 mm.

$$A_{st} = \frac{68.4 \times 10^6}{0.8 \times 415 \times 189} = 1090 \text{ mm}^2$$

Required spacing for 10 mm bar = $(79/1090) \times 3000 = 217 \text{ mm} < 430 \text{ mm}$

Provide 10 mm diameter bars at 215 mm c/c at top in the middle strip.

4. For the positive moment in the middle strip, M_u is 59.0 kNm, and the effective depth of slab is 189 mm.

$$A_{st} = 1090 \times 59/68.4 = 940 \text{ mm}^2$$

Spacing of 10 mm bar = 252 mm

Provide 10 mm diameter bars at 215 mm c/c at the bottom of the middle strip.

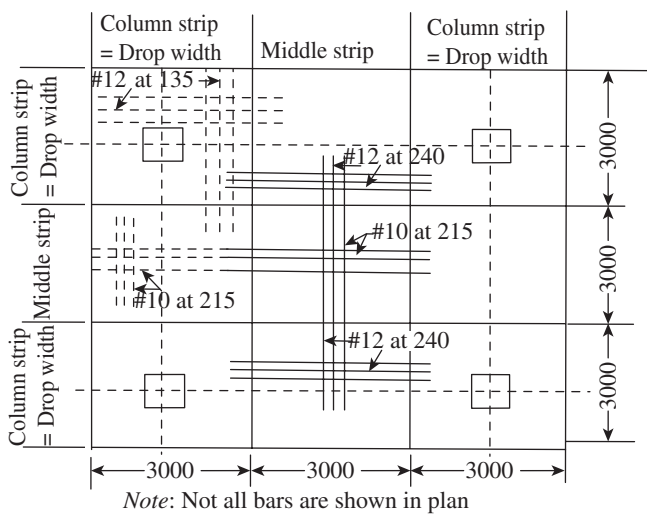
Since the span is the same in both directions, the same reinforcement may be provided in both the directions. The reinforcement detailing as per Fig. 16 of IS 456 code is shown in Fig. 11.46.

Integrity reinforcement:

Integrity reinforcement (Eq. 11.23)

$$A_s = \frac{0.5 w_u L_1 L_2}{0.87 f_y} = \frac{0.5 \times 18.56 \times 6 \times 6 \times 10^3}{0.87 f_y} = 925 \text{ mm}^2$$

Provide two 25 diameter bars, with a length of $2L_d (2 \times 1007 = 2014 \text{ mm})$ passing through the column cage each way.


Legend

--- Top bars — Bottom bars

FIG. 11.46 Reinforcement details of flat slab of Example 11.2

EXAMPLE 11.3 (Flat slab with drop and column head):
Redesign Example 11.2 assuming the flat slab is supported by a circular column of 500 mm diameter and is with suitable column head.

SOLUTION:

Step 1 Calculate the equivalent column head and design load. Let the diameter of the column head be $0.25L = 0.25 \times 6 = 1.5$ m. The circular section may be considered as an equivalent square of size a . Hence,

$$\frac{\pi}{4} \times 1.5^2 = a^2$$

Solving, we get $a = 1.329$ m ≈ 1.33 m

Hence $L_n = 16 - 1.33 = 4.67$ m

$$W = w_u L_2 L_n = 18.56 \times 6 \times 4.67 = 520 \text{ kN}$$

Step 2 Calculate the bending moment.

$$M_o = \frac{WL_n}{8} = \frac{520 \times 4.67}{8} = 303.55 \text{ kNm}$$

Total negative moment = $0.65 \times 303.55 = 197.31$ kNm

Total positive moment = $0.35 \times 303.55 = 106.24$ kNm

The distribution of these positive and negative moments in the column and middle strips is done as shown in Table 11.13.

TABLE 11.13 Distribution of positive and negative moments

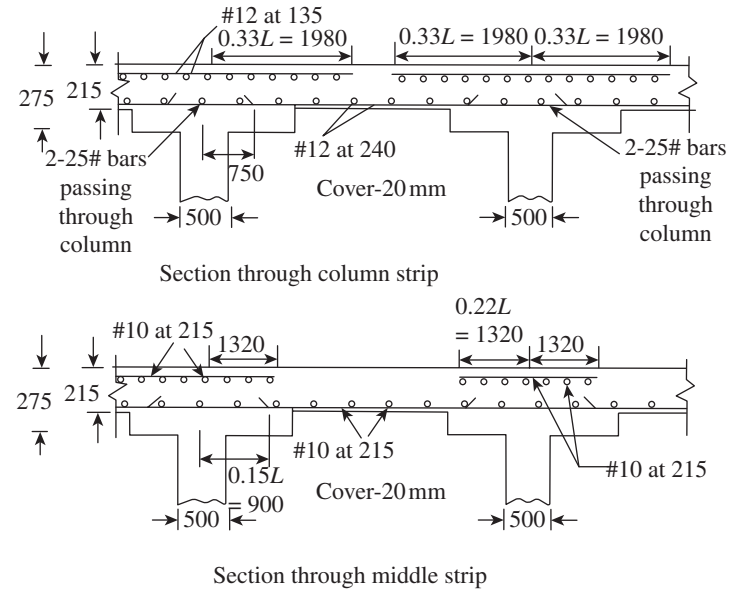
Type	Column Strip, kNm	Middle Strip, kNm
Negative moment	$0.75 \times 197.31 = 148$	49.31
Positive moment	$0.60 \times 106.24 = 63.74$	42.80

Width of middle strip = Width of column strip = 3000 mm

Step 3 Check the depth for bending.

Required depth for resisting bending moment

$$d = \left(\frac{M_u}{0.138 f_{ck} b} \right)^{0.5} = \left(\frac{148 \times 10^6}{0.138 \times 25 \times 3000} \right)^{0.5} = 119.6 \text{ mm}$$



The effective depth provided at the drop is 247 mm and at the middle strip is 189 mm. Hence, the depth is sufficient for bending and the slab is under-reinforced.

Step 4 Check for punching shear. The critical section is at a distance of $d/2 = 247/2$ mm from the face of the column.

Diameter of the critical section = $1500 + 247 = 1747$ mm

Perimeter of the critical section = $\pi d = \pi \times 1747 = 5488.4$ mm

Shear on this section $V_u = 18.56 \left(6^2 - \pi \times \frac{1.747^2}{4} \right) = 623.67$ kN

Nominal shear stress, $\tau_v = \frac{623.67 \times 10^3}{5488.4 \times 247} = 0.46$ N/mm²

As per Clause 31.6.3 of IS 456

$$\tau_c = k_s 0.25 \sqrt{f_{ck}}$$

$$k_s = 0.5 + \beta_c < 1; \beta_c = 1.5/1.5 = 1; \text{ hence } k_s = 1.$$

$$\tau_c = 0.25 \times \sqrt{25} = 1.25 \text{ N/mm}^2 > 0.46 \text{ N/mm}^2$$

Hence, the slab is safe in punching shear and no shear reinforcement is necessary.

Step 5 Design the reinforcement. The reinforcement at different locations has been calculated and is shown in Table 11.14.

TABLE 11.14 Reinforcement at various locations for Example 11.3

Bending Moment	M_u , kNm	d , mm	A_s , mm ²	Diameter and Spacing of Bars
Negative moment in column strip	148	247	1805	12 mm diameter at 185 mm c/c
Positive moment in column strip	63.74	189	1016	10 mm diameter at 230 mm c/c
Negative moment in middle strip	49.41	189	787	10 mm diameter at 290 mm c/c
Positive moment in middle strip	42.50	189	677	10 mm diameter at 290 mm c/c

Note: Minimum steel = $(0.12/100) \times 3000 \times 215 = 774$ mm²

As the span is the same in both directions, provide the same reinforcement in both the directions. The reinforcement detail will be similar to that shown in Fig. 11.45, including the integrity reinforcement.

EXAMPLE 11.4:

Design the slab reinforcement at the exterior column of Example 11.1 for moment transfer between slab and column and check for combined stresses. In addition, calculate the moments to be carried by the columns.

SOLUTION:

Step 1 Determine the portion of M_u to be transferred by the flexure.

Moment at exterior column = 131.23 kNm

It should be noted that as per ACI 318, this value is only 71.23 kNm. Hence, we will also consider the moment as 71.23 kNm in this example; otherwise, we may get uneconomical results.

From Example 11.1, we have the effective depth as 189 mm and the total depth as 225 mm.

Portion of unbalanced moment transferred by flexure = $\gamma_f M_u$
From Fig. 11.21 (Case c)

$$a = c_1 + \frac{d}{2} = 500 + \frac{189}{2} = 594.5 \text{ mm}$$

$$b = c_2 + d = 500 + 189 = 689 \text{ mm}$$

From Eq. (11.6), we get

$$\gamma_f = \frac{1}{1 + \frac{2}{3} \left(\frac{a}{b} \right)^{0.5}} = \frac{1}{1 + \frac{2}{3} \left(\frac{594.5}{689} \right)^{0.5}} = 0.62$$

$$\gamma_f M_u = 0.62 \times 71.23 = 44.16 \text{ kNm}$$

Effectivetransferwidth = $c_2 + 3D_s = 500 + 3 \times 225 = 1175 \text{ mm}$

Step 2 Determine the area of reinforcement.

$$\frac{M_u}{bd^2} = \frac{44.16 \times 10^6}{1175 \times 189^2} = 1.05$$

From Table 3 of SP16, for Fe 415 steel,

$$p_t = 0.307; A_t = (0.307/100) \times 1175 \times 189 = 682 \text{ mm}^2$$

We need six 12# bars at 190 mm c/c. We have already provided 12# bars at 140 mm c/c in the column strip. Hence, no additional reinforcement is necessary.

Step 3 Calculate the fraction of unbalanced moment carried by the eccentric shear.

$$\gamma_v = 1 - \gamma_f = 1 - 0.62 = 0.38$$

$$\gamma_v M_u = 0.38 \times 71.23 = 27.06 \text{ kNm}$$

Step 4 Calculate the properties of the critical section for shear.

$$A_c = (2a + b)d = 2 \times (594.5 + 689) \times 189 = 4,85,163 \text{ mm}^2$$

From Table 11.7,

$$\begin{aligned} \frac{J}{c} &= \frac{2a^2d(a+2b) + d^3(2a+b)}{6a} \\ &= \frac{2 \times 594.5^2 \times 189(594.5 + 2 \times 689) + 189^2(485,163)}{6 \times 594.5} \\ &= 78.735 \times 10^6 \text{ mm}^4 \end{aligned}$$

A similar result can be obtained by using Table 11.8.

With $c_1/d = 500/189 = 2.65$ and $c_2/c_1 = 1$, we get $f_2 = 5.773$.

$$J/c = 2f_2d^3 = 2 \times 5.773 \times 189^3 = 77.95 \times 10^6 \text{ mm}^4$$

Step 5 Check for the combined stresses.

Gravity load shear to be carried by exterior column

$$V_u = \frac{w_u L_1 L_2}{2} = \frac{15.94 \times 5.5 \times 5.5}{2} = 241.09 \text{ kN}$$

Combined stresses (Eq. 11.13)

$$\begin{aligned} \tau_{v,\max} &= \frac{V_u}{A_c} + \gamma_v M_u \frac{c}{J} = \frac{241.09 \times 1000}{485,163} + \frac{27.06 \times 10^6}{78.735 \times 10^6} \\ &= 0.497 + 0.344 = 0.841 \text{ N/mm}^2 \end{aligned}$$

$$\tau_{v,\min} = 0.497 - 0.344 = 0.153 \text{ N/mm}^2$$

Design the punching shear stress (Eq. 11.12).

$$\tau_c = 0.25 \sqrt{f_{ck}} = 1.25 \text{ N/mm}^2 > 0.841 \text{ N/mm}^2$$

Hence, the slab is safe to transfer the combined stresses.

Step 6 Calculate the factored moments in the columns.

1. For interior columns, using Eq. (11.8)

$$M_u = \frac{0.08 \left[(w_d + 0.5w_l)L_2L_n^2 - w'_dL'_2L_n'^2 \right]}{(1 + 1/\alpha_c)}$$

Since the spans are equal, $L_n = L'_n$. Thus, we get

$$M_u = \frac{0.08(0.5w_lL_2L_n^2)}{(1 + 1/\alpha_c)}$$

We already have $1 + 1/\alpha_c = 1.358$ and $w_l = 4 \text{ kN/m}^2$, $L_2 = 5.5 \text{ m}$, and $L_n = 5 \text{ m}$ from Example 11.1. Hence,

$$M_u = \frac{0.08(0.5 \times 4 \times 5.5 \times 5^2)}{1.358} = 16.2 \text{ kNm}$$

With the same column size and length above and below the slab

$$M_c = 16.2/2 = 8.1 \text{ kNm}$$

This moment should be combined with the factored axial load (for each storey) for the design of interior columns.

For the exterior columns, the total exterior negative moment from the slab must be transferred directly to the column.

$$M_u = 71.23 \text{ kNm}$$

$$M_c = 71.23/2 = 35.62 \text{ kNm}$$

This moment is to be combined with the factored axial load (for each storey) for the design of the exterior columns.

EXAMPLE 11.5:

Assume a corner column of size 400 mm × 1000 mm supporting a 200 mm thick flat slab with effective depth 160 mm. The factored moment due to gravity loads at the face of the column is 98.4 kNm, the factored shear force at the face of the column

is 232.3 kN, and the shear force at the edge is 30 kN. Check the stresses due to the combined forces assuming that the slab is made using M25 concrete and Fe 415 steel.

SOLUTION:

We have $c_1 = 400$ mm, $c_2 = 1000$ mm, and $d = 160$ mm. The use of Eq. (11.13) requires the calculation of shear and moment relative to the centroid of the critical section (see Fig. 11.47).

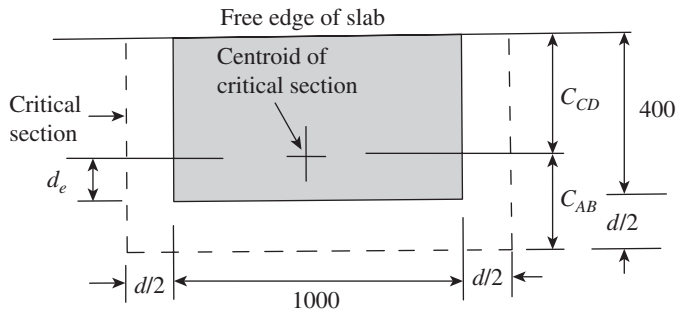


FIG. 11.47 Edge column and critical section

$$b_1 = c_1 + d/2 = 400 + 160/2 = 480 \text{ mm}$$

$$b_2 = c_2 + d = 1000 + 160 = 1160 \text{ mm}$$

Perimeter of critical section $b_0 = 2b_1 + b_2 = 2 \times 480 + 1160 = 2120$ mm

Distance from the centroid to the extreme fibre of critical section (Alexander and Simmonds 2005)

$$C_{AB} = \frac{b_1^2}{b_0} = \frac{480^2}{2120} = 108.7 \text{ mm}$$

$$C_{CD} = b_1 - C_{AB} = 480 - 108.7 = 371.3 \text{ mm}$$

$$d_e = C_{AB} - \frac{d}{2} = 108.7 - 80 = 28.7 \text{ mm}$$

Polar moment of the shear perimeter

$$\begin{aligned} J &= \frac{2b_1^3 d}{3} + \frac{b_1 d^3}{6} - b_0 d C_{AB}^2 \\ &= \frac{2 \times 480^3 \times 160}{3} + \frac{480 \times 160^3}{6} - 2120 \times 160 \times 108.7^2 \\ &= 8.116 \times 10^9 \text{ mm}^4 \end{aligned}$$

Calculate the moment at the centroid of the critical section, which is given by

$$\begin{aligned} M_u &= M_{u,\text{face}} + V_{u,\text{span}} d_e - V_{u,\text{edge}} \left(\frac{c_1}{2} - d_e \right) \\ &= 98.4 + 232.3 \times 0.0287 - 30 (0.4/2 - 0.0287) \\ &= 98.4 + 6.67 - 5.14 = 99.93 \text{ kNm} \end{aligned}$$

Shear at the centroid, $V_u = 232.3 + 30 = 262.3$ kN

Shear stress

$$\tau_v = \frac{V_u}{b_o d} + \frac{\gamma_v M_u C_{AB}}{J}$$

$$\gamma_f = \frac{1}{1 + \frac{2}{3} \left(\frac{b_1}{b_2} \right)^{0.5}} = \frac{1}{1 + \frac{2}{3} \left(\frac{480}{1160} \right)^{0.5}} = 0; \quad \gamma_v = 1 - 0.7 = 0.36$$

$$\text{Hence } \tau_v = \frac{262.3 \times 10^3}{2120 \times 160} + \frac{0.3 \times 99.93 \times 10^6 \times 108.7}{8.116 \times 10^9} = 0.773 +$$

$$0.402 = 1.175 \text{ N/mm}^2$$

Design punching shear stress $\tau_c = 0.25\sqrt{25} = 1.25 \text{ N/mm}^2 > 1.175 \text{ N/mm}^2$

Hence, the slab is safe to carry the shear and bending moment. Let us check the stress using the approximate formula (Eq. 11.17).

$$\begin{aligned} \tau_v &= \frac{0.65 [V_u + M_{u,\text{face}} / (4d)]}{(c_1 + c_2) d} \\ &= \frac{0.65 [262.3 \times 10^3 + 98.4 \times 10^6 / (4 \times 160)]}{(400 + 1000) 160} = 1.207 \text{ N/mm}^2 \end{aligned}$$

Note: The approximate method is simple to apply and predicts the stresses with reasonable accuracy (in this case, the percentage of error is only 2.7%).

EXAMPLE 11.6:

A flat plate panel of dimensions 6 m \times 7 m supported by columns of size 450 mm \times 450 mm has a slab thickness of 180 mm and is designed for a working (total) load of 10 kN/m². Check the safety of the slab in punching shear and provide shear reinforcement, if required. Assume M25 concrete and Fe 415 steel.

SOLUTION:

Assuming that 10 mm diameter bars are used and the cover is 25 mm,

$$\text{Effective depth, } d = 180 - 25 - 5 = 150 \text{ mm}$$

$$\text{Factored design load} = 1.5 \times 10 = 15 \text{ kN/m}^2$$

Step 1 Check for punching shear.

$$\text{Critical perimeter } b_o = 4(c + d) = 4(450 + 150) = 2400 \text{ mm}$$

$$V_u = 15 [7 \times 6 - (0.45 + 0.15)^2] = 624.6 \text{ kN}$$

$$\text{Stress due to punching shear} = \frac{V_u}{b_o d} = \frac{624.6 \times 10^3}{2400 \times 150} = 1.74 \text{ N/mm}^2$$

Allowable punching shear stress

$$\tau_c = k_s 0.25 \sqrt{f_{ck}}$$

$$k_s = (0.5 + \beta_c) < 1; \quad \beta_c = \frac{450}{450} = 1; \quad \text{hence } k_s = 1.$$

$$\tau_c = 1 \times 0.25 \sqrt{25} = 1.25 \text{ N/mm}^2 < 1.74 \text{ N/mm}^2$$

Hence, shear reinforcement has to be provided.

Note: Increasing the strength of concrete may also solve this problem. Thus, $0.25 \sqrt{f_{ck}} = 1.6$ or $f_{ck} = \left(\frac{1.74}{0.25} \right)^2 = 48.44 \text{ N/mm}^2$

Hence, we may have to use M50 concrete to keep the punching shear stress within limits.

Step 2 Check the suitability of shear reinforcement. As per Clause 31.6.3.2 of the code, check whether the stress is below $1.5\tau_c$.

$$1.5\tau_c = 1.5 \times 1.25 = 1.875 \text{ N/mm}^2 > 1.74 \text{ N/mm}^2$$

Hence, shear reinforcement can be used.

Note: If the stress exceeds $1.5\tau_c$, we need to increase the depth of the slab.

Step 3 Calculate the shear to be carried by the reinforcement (Clause 31.6.3.2).

Shear stress assumed to be carried by concrete = $0.5\tau_c = 0.5 \times 1.25 = 0.625 \text{ N/mm}^2$

Shear force carried by concrete = $0.625 \times b_o d = 0.625 \times 2400 \times 150/10^3 = 225 \text{ kN}$

Shear to be carried by reinforcement = $624.6 - 225 = 399.6 \text{ kN}$

Note: As per ACI, shear force carried by concrete =

$$0.15\phi\sqrt{f_{ck}}b_o d = 0.15 \times 0.75 \times \sqrt{25} \times 2400 \times 150/10^3 = 202.5 \text{ kN}$$

Step 4 Calculate the total area of shear stirrups (Eq. 11.18).

Maximum spacing of stirrups = $0.75d$ (SP 24:1983) = $0.75 \times 150 = 112.5 \text{ mm}$

Adopt $s_v = 80 \text{ mm} \approx d/2$ as suggested by ACI 318.

Assuming $f_y = 415 \text{ N/mm}^2$

$$A_{sv} = \frac{399.6 \times 10^3}{0.87f_y} \times \frac{s_v}{d} = \frac{399.6 \times 10^3}{0.87 \times 415} \times \frac{80}{150} = 590 \text{ mm}^2$$

Required stirrup area on each side of column = $590/4 = 148 \text{ mm}^2$

With two-legged U stirrups as shown in Figs 11.23(c) and (d), Area of each leg = $148/2 = 74 \text{ mm}^2$

Provide two-legged 10mm diameter stirrups with area 78.5 mm^2 .

Alternatively, using Table 62 of SP 16, we get (per each side of column)

$$\frac{V_u/4}{d} = \frac{399.6/4}{15} = 6.66 \text{ kN/cm}$$

Fe 415 grade 10mm diameter stirrups at 80mm c/c provide 7.089 kN/cm .

It has to be noted that the spacing between adjacent legs should not exceed $2d = 2 \times 150 = 300 \text{ mm}$.

Step 5 Calculate the length up to which stirrups are to be provided. As per SP 24:1983, shear reinforcement should be provided up to a section where the shear stress does not exceed $0.5\tau_c = 0.5 \times 1.25 = 0.625 \text{ N/mm}^2$ or where $V_u \leq b_o d(0.5\tau_c)$.

Let this distance be a from the face of the column (see Fig. 11.23d). For a square column

$$b_o = 4(450 + a\sqrt{2})$$

Thus, $624.6 \times 10^3 \leq [4(450 + a\sqrt{2})] \times 150 \times 0.625$

Solving, $a\sqrt{2} = 1215.6 \text{ mm}$ or $a = 860 \text{ mm}$.

Provide the first set of stirrups at 60mm from each face of the column and provide 11 sets of 10mm diameter stirrups of width 300mm and depth 125mm, spaced at 80mm c/c at each face of the column (similar to the arrangement given in Fig. 11.23d).

EXAMPLE 11.7:

For the slab in Example 11.6, design headed shear studs as shear reinforcement, instead of shear stirrups.

SOLUTION:

Step 1 Calculate the initial area of shear studs. The ACI code provisions are used as the IS code does not have provisions for headed shear studs. From Example 11.6, size of column = $450 \text{ mm} \times 450 \text{ mm}$, $d = 150 \text{ mm}$, $b_o = 2400 \text{ mm}$, $f_{ck} = 25 \text{ N/mm}^2$, and $V_u = 624.6 \text{ kN}$.

Shear force carried by concrete =

$$0.225\lambda\phi\sqrt{f_{ck}}b_o d = 0.225 \times 1 \times 0.75 \times \sqrt{25} \times 2400 \times 150/10^3 = 304 \text{ kN}$$

Shear force to be carried by headed shear studs = $624.60 - 304 = 320.6 \text{ kN}$

The maximum value of shear allowed with headed shear studs is

$$0.6\sqrt{f_{ck}}b_o d = 0.6 \times \sqrt{25} \times 2400 \times 150/10^3 = 1080 \text{ kN} < 624.60 \text{ kN}$$

Hence, the chosen column size and slab depth can be used.

From Example 11.6, $\frac{V_u}{b_o d} = 1.74 \text{ N/mm}^2 > 0.45\phi\sqrt{f_{ck}} = 0.45 \times 0.75 \times \sqrt{25} = 1.69 \text{ N/mm}^2$

Adopt spacing of studs = $0.50d = 0.50 \times 150 = 75 \text{ mm}$.

Assuming $f_{yt} = 415 \text{ N/mm}^2$

$$A_{sv} = \frac{320.60 \times 10^3}{0.87f_y} \times \frac{s_v}{d} = \frac{320.60 \times 10^3}{0.87 \times 415} \times \frac{75}{150} = 419 \text{ mm}^2$$

Headed stud area for each side of column = $419/4 = 105 \text{ mm}^2$.

With two studs at a section as shown in the plan of Fig. 11.25(a),

Area of each stud = $105/2 = 52.5 \text{ mm}^2$

Provide 10mm diameter studs of length 125mm (area = 78.5 mm^2).

Step 2 Calculate the length up to which studs are required. At the outer critical section, the shear stress should be less than $0.15\phi\sqrt{25}$.

$$b_o = 4(450 + a\sqrt{2})$$

Thus, $624.6 \times 10^3 \leq [4(450 + a\sqrt{2})] \times 150 \times 0.15 \times 0.75 \times \sqrt{25}$
 $624.6 \times 10^3 \leq (450 + a\sqrt{2})337.5$

Solving, $a = 990 \text{ mm}$.

Provide 14 sets of headed shear studs on each face, each of length 125mm, with a spacing of 75mm and the value of g 300mm ($\leq 2d$); place the first set of headed studs at a distance of $d/2 = 75 \text{ mm}$ from the face of the column.

Step 3 Check shear strength at the inner critical section. The area provided by the inner row of shear studs is

$$A_v = 8 \times 78.5 = 628 \text{ mm}^2$$

Assuming only one line of shear studs is crossed by the potential critical shear crack near the column

$$V_s = A_v f_{yt} = 628 \times 415/1000 = 260 \text{ kN} > 219.6 \text{ kN}$$

Hence, the slab is safe.

Provide 14 sets of 10 mm diameter headed studs with a lengths of 125 mm and head diameter of 32 mm at a spacing of 75 mm; the arrangement should be as shown in Fig. 11.25.

EXAMPLE 11.8:

Design a waffle slab for an internal panel of a floor system that is constructed in an 8.4 m square module. Assume the imposed load to be 2.5 kN/m² and the use of M25 concrete and Fe 415 steel. The slab is to be supported on square columns of size 450 mm × 450 mm. The slab is subjected to mild exposure.

SOLUTION:

Step 1 Determine the proportioning of the slab elements. As per Clauses 24.1 and 31.2.1 of IS 456,

$$L/d = 0.9(0.8 \times 40) = 28.8$$

Required minimum effective depth = 8400/28.8 = 292 mm

Assume that the waffle slab is as shown in Fig. 11.48.

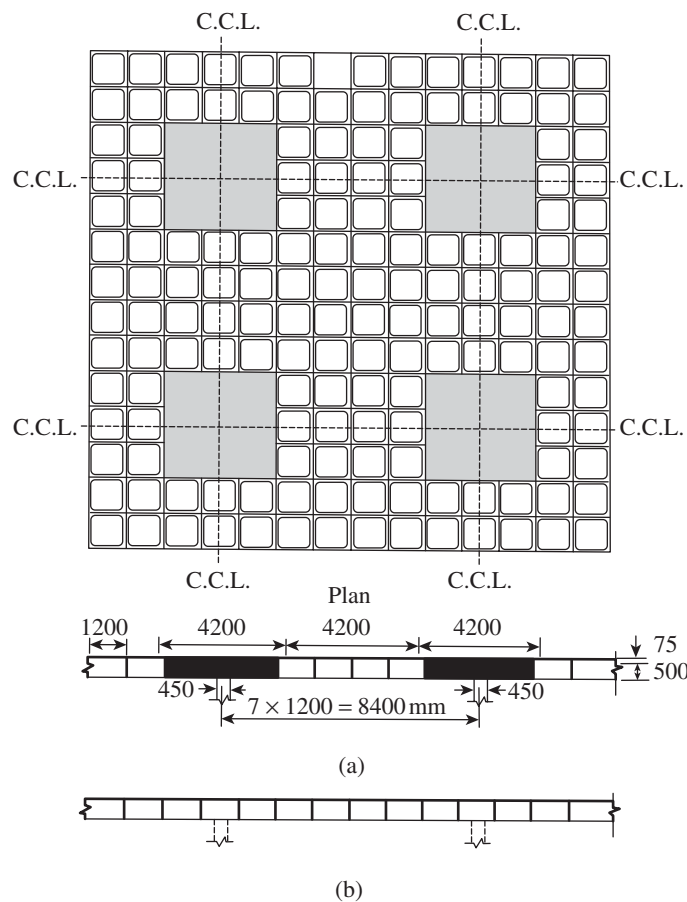


FIG. 11.48 Waffle slab of Example 11.8 (a) Section at column strip (b) Section at middle strip

Let us choose a GFRP dome pan of size 1200 mm × 1200 mm, with void plan of 1025 mm × 1025 mm, joist (rib) width 200 mm, and depth 500 mm. Let us provide a 75 mm thick top slab.

Clause 30.5 of IS 456 stipulates the following:

1. The rib width should be greater than 65 mm; provided 200 mm.
2. The c/c of ribs should be less than 1.5 m; provided 1.2 m.
3. The depth of rib should be less than four times the width, that is, $4 \times 200 = 800$ mm; provided 500 mm.
4. The depth of the topping slab should be greater than 50 mm or less than $(1/10) \times 1200 = 120$ mm (Table 3.17 of BS 8110); provided 75 mm.

$$\text{Total depth} = 575 \text{ mm} > 292 \text{ mm}$$

Hence, the proportions chosen are as per the code requirements. From Table 16 of IS 456, cover for mild exposure is 20 mm. Let the solid portion of the slab over the column be three modules wide, that is, $3 \times 1200 + 200 = 3800$ mm wide in both directions.

Step 2 Calculate the loads.

$$\begin{aligned} \text{Self-weight } w_s &= \rho_c \left[D_f + \left(2 - \frac{b_w}{b_f} \right) (D - D_f) \left(\frac{b_w}{b_f} \right) \right] \\ &= 25 \left[\frac{75}{1000} + \left(2 - \frac{200}{1200} \right) \left(\frac{575 - 75}{1000} \right) \left(\frac{200}{1200} \right) \right] \\ &= 5.70 \text{ kN/m}^2 \end{aligned}$$

Weight of solid head = $0.5 \times 25 = 12.5 \text{ kN/m}^2$

$$\begin{aligned} \text{Hence, self-weight of slab} &= \frac{12.5 \times 3.8 + 5.7 \times (8.4 - 3.8)}{8.4} \\ &= 8.78 \text{ kN/m}^2 \end{aligned}$$

Finishes = 1.25 kN/m²

Imposed load = 2.50 kN/m²

Total load $w = 12.53 \text{ kN/m}^2$

Factored load, $w_u = 12.53 \times 1.5 = 18.8 \text{ kN/m}^2$

Step 3 Calculate the bending moments. The DDM is applicable for this system.

Imposed load/Dead load = $2.5/6.95 = 0.36$

$$L_2/L_1 = 8.4/8.4 = 1.0$$

Hence, from Table 17 of IS 456, $\alpha_{c,\min} = 0$. Hence, the effect of the pattern load need not be considered.

$$M_0 = \frac{wL_2L_n^2}{8}; L_n = 8.40 - 0.45 = 7.95 \text{ m}$$

$$\text{Thus, } M_0 = \frac{18.8 \times 8.4 \times 7.95^2}{8} = 1248 \text{ kNm}$$

Column strip:

Negative bending moment = $-0.65 \times 0.75 \times 1248 = 608.4 \text{ kNm}/4.2 \text{ m}$

Positive bending moment = $0.35 \times 0.60 \times 1248 = 262.1 \text{ kNm}$, to be resisted by four ribs

Middle strip:

Negative bending moment = $-0.65 \times 0.25 \times 1248 = 202.8 \text{ kNm}/4.2 \text{ m}$

Positive bending moment = $0.35 \times 0.40 \times 1248 = 174.7 \text{ kNm}/4.2 \text{ m}$

Step 4 Check for punching stress.

In the solid head portion:

Assuming 12 m bars, the effective depth = $575 - 20 - 6 = 549$ mm.

$$b_o = 4(c_1 + d) = 4(450 + 549) = 3996 \text{ mm}$$

$$V_u = 18.8 \times \left[8.4^2 - \frac{(450 + 549)^2}{1000} \right] = 1308 \text{ kN}$$

$$\tau_v = \frac{V_u}{b_o d} = \frac{1308 \times 1000}{3996 \times 549} = 0.60 \text{ N/mm}^2$$

$$\tau_c = k_s \times 0.25 \sqrt{f_{ck}} \text{ with } k_s = 1 \text{ for square column}$$

$$= 1 \times 0.25 \sqrt{25} = 1.25 \text{ N/mm}^2 > 0.45 \text{ N/mm}^2$$

Hence, it is safe in punching shear.

Shear stress at the ribs:

Nominal shear stress is checked at a distance d from the edge of the solid head.

Width of solid head = $3 \times 1.2 + 0.2 = 3.8$ m in both directions

$$b_o = 4(3.8 + 0.549) = 17.396 \text{ m}$$

Total shear at this section = $[8.42 - (3.8 + 0.549)^2] \times 18.8 = 971$ kN

This shear is resisted by 12 ribs of 200 mm width and 549 mm effective depth. Hence,

$$\tau_v = \frac{971 \times 1000}{12 \times 200 \times 549} = 0.74 \text{ N/mm}^2 < 1.25 \text{ N/mm}^2$$

Hence, the adopted waffle slab is safe in punching shear.

Note: Punching shear reinforcement in waffle slabs should be avoided.

Step 5 Check the depth to resist the bending moment.

$$d = \left(\frac{M}{k_b f_{ck}} \right)^{0.5} = \left(\frac{608.4 \times 10^6}{0.138 \times 3800 \times 25} \right)^{0.5} = 215.4 \text{ mm} < 549 \text{ mm}$$

Hence, the depth adopted is adequate and the slab is under-reinforced.

Step 6 Design the reinforcement. The bending moment of 608.4 kNm is to be shared by four ribs. Hence,

Bending moment per rib = $608.4/4 = 152.1$ kNm

For M25 concrete, $\frac{M_{u,lim}}{bd^2} = 3.45$ (Table D of SP 16)

Hence $M_{u,lim} = 3.45 \times 200 \times 549^2/10^6 = 208$ kNm > 152.1 kNm

Hence, the ribs can be designed as singly reinforced (under-reinforced rectangular section).

$$\frac{M_u}{bd^2} = \frac{152.1 \times 10^6}{200 \times 549^2} = 2.523$$

From Table 3 of SP 16, we get for Fe 415 and M25 concrete,

$$p_t = 0.808; A_{st} = \frac{0.808}{100} \times 200 \times 549 = 887 \text{ mm}^2$$

Provide three 20 diameter bars with area = 942 mm².

For positive bending moment,

Moment in each rib = $262.1/4 = 65.53$ kNm

$$\frac{M_u}{bd^2} = \frac{65.53 \times 10^6}{200 \times 549^2} = 1.09$$

From Table 3 of SP 16, we get

$$p_t = 0.319; A_{st} = \frac{0.319}{100} \times 200 \times 549 = 350.2 \text{ mm}^2$$

Provide two 16 diameter bars with area = 402 mm².

Note: For positive moment, the ribs may be considered as T-beams to reduce the reinforcement.

Design of ribs in the middle strip:

For negative moment, only three ribs carry this moment. Hence,

Moment in each rib = $202.8/3 = 67.6$ kNm

Hence, provide two 16 diameter bars.

For positive moment, each rib carries $174.7/3 = 58.2$ kNm

Hence, provide two 16 diameter bars.

Check for shear in ribs:

Maximum shear force at distance d for support,

$$V_u = w_u (0.5L_n - d) = 18.8 \times (0.5 \times 7.95 - 0.549) = 64.4 \text{ kN/m}$$

Shear force carried by rib = $64.4 \times 1.2 = 77.3$ kN

$$\text{Nominal shear stress, } \tau_v = \frac{V_u}{bd} = \frac{77.3 \times 1000}{200 \times 549} = 0.70 \text{ N/mm}^2$$

$$\frac{100A_s}{bd} = \frac{100 \times 942}{200 \times 549} = 0.86\%$$

From Table 19 of IS 456, for M25 concrete, $\tau_c = 0.6$ N/mm².

$$\tau_{c, \max} = 3.1 \text{ N/mm}^2 > 0.70 \text{ N/mm}^2$$

Hence, spacing of 8 mm stirrups

$$s_v = \frac{0.87 f_y A_{sv} d}{V_u - \tau_c b d} = \frac{0.87 \times 415 \times 50.2 \times 549}{77.3 \times 1000 - 0.6 \times 200 \times 549} = 871 \text{ mm}$$

Maximum spacing of stirrups (Clause 26.5.1.5) = $0.75 \times 549 = 411$ mm or 300 mm

Hence, provide 8 mm diameter stirrups at 300 mm c/c. The reinforcement details for the rib in the column strip are shown in Fig. 11.49 (for the sake of clarity, slab reinforcements are not shown in the figure).

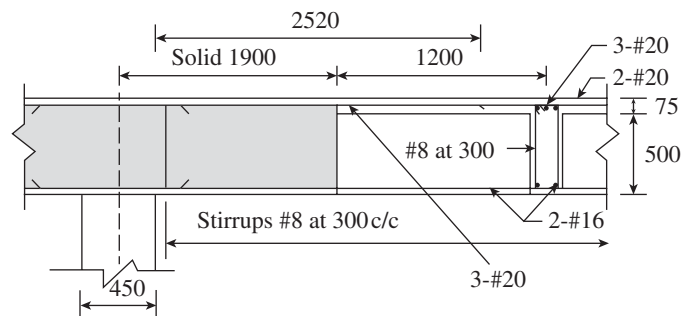


FIG. 11.49 Reinforcement detail in the rib including shear reinforcement

Reinforcement in topping slab:

Minimum reinforcement has to be provided in the 75 mm thick topping slab.

$$A_{st,min} = 0.12 \times \frac{75}{100} \times 1000 = 90 \text{ mm}^2/\text{m}$$

The spacing of rods should not be greater than one-half of the c/c distance of rib or 300 mm. Provide 5 mm TOR-KARI bars

at 200 mm c/c in the centre of the topping slab both ways (area provided = 98 mm²/m).

Reinforcement in the solid portion of width 3800 mm is calculated as follows:

$$A_{st,min} = 0.12 \times (500/100) \times 1000 = 600 \text{ mm}^2/\text{m}$$

Provide 10 mm diameter bars at 130 mm c/c both ways ($A_{st} = 604 \text{ mm}^2$) at the top and bottom of the solid portion.

SUMMARY

Two-way slabs directly supported on columns, called flat plates, are preferred due to the several advantages offered by them and also due to their architectural appearance. The main limitation of flat plates is the problem posed by resisting the two-way shear around the columns, which is called the punching shear. Hence, for heavy loads or long spans, flat slabs with drop panels around the columns are used. It is preferable to use flat plate systems with LFRSs, especially in moderate to severe earthquake zones.

Similar to other two-way slabs, the thickness of flat slabs is generally controlled by the span to effective depth ratio. Rules are prescribed in the codes for fixing the dimensions of drop panels, column heads, and shear capitals. The behaviour of flat slabs is similar to that of two-way slabs with beams, and different amounts of reinforcement are provided in the column and middle strips. The deflections of a flat slab are generally larger than that of the more rigid beam-slab-column system.

The behaviour of a flat slab system is complex. Tests revealed that the failure is mostly by punching shear, unless shear reinforcements are provided. The empirical design rules specified in various codes are based on the extensive experimental results conducted in the USA. The two analysis methods adopted in the codes are the DDM and the EFM. These methods are covered in Section 4 of IS 456 and are based on the 1977 version of the ACI 318 code. Later versions of the ACI code proposed several modifications to these analysis methods.

The DDM is a semi-empirical method and is applicable only when certain conditions are met; otherwise, we need to use the EFM or FEM.

In both DDM and EFM, regular slabs subjected to uniformly distributed loads are divided in each direction into strips or frames centred on the column lines and bounded laterally by the centre lines of panels on each side. In the EFM, these strips or frames are then analysed as two-dimensional structures for the purpose of determining the bending moments at critical sections located at either the mid-spans or the faces of supports.

In the DDM, the total static moment is calculated first, which is then divided into negative and positive moments in the proportion of 65 per cent to 35 per cent. These positive and negative moments are then distributed laterally across the strip according to some preset rules, including the effect of pattern loading. These moments are also used to determine the magnitude of the unbalanced moment that must be transferred between the slab and the supporting column. In this manner, the complex three-dimensional analysis is simplified considerably into a two-dimensional frame. Tables are provided, which can be directly used by the designers, thereby avoiding the complex calculation of some parameters like J . It is important to provide reinforcement in the slab near the column region, called the transfer width, for the moment that is transferred by flexure.

Although one-way shear may not be critical in flat slabs as in two-way slabs, several failures due to accidental loads including earthquake loads is due to punching shear—column punching through the slab. The critical section is assumed to be located around the column at a distance $d/2$ from either face of the column in the Indian and US codes. The Indian code provisions for calculating the punching shear strength, which are based on the ACI code, do not consider reinforcement ratio and size effects. The European code provisions include these parameters as well and are based on the cube root of compressive strength of concrete unlike the square root of compressive strength as in the IS code. They are also found to predict the punching shear strength of flat slabs consistently for high-strength normal weight and high-strength lightweight concretes (lightweight aggregates are being increasingly used to reduce the self-weight of concrete or due to the unavailability of natural coarse aggregates).

The punching shear resistance of RC flat slabs can be enhanced by various means. (Enhancement is necessary especially in flat slabs located in seismic areas. During an earthquake, the unbalanced moment transferred between the slabs and column may produce significant shear stresses that will increase the likelihood of brittle fracture.) The enlargement of column cross section and thickening of the portion of the slab around the column (by the use of drop panels or column shear capitals) will enhance the shear resistance. Tests indicate that we should not use shear capitals to increase the punching shear resistance especially in earthquake zones. Provision of spandrel beams along the edges of the slab will improve the punching shear capacity of the slab. However, the existence of spandrel beams will complicate the already-complex punching shear performance of the column-slab connection. Hence, many researchers have found that the introduction of shear reinforcement is more economical and reduces the chances of brittle failure at the slab-column connection. The performance of several types of shear reinforcements such as stirrups, structural shear heads (in the form of steel I- or channel sections), bent-up bars, headed shear studs, lattice shear reinforcement, and shear bands have been tested extensively in the last three decades. It has been found that the introduction of such shear reinforcement results in ductile failure caused by the yielding of flexural reinforcement and improves the punching shear resistance. Headed stud shear reinforcement has several advantages over other types of shear reinforcement and hence provisions for its design were introduced in the 2005 version of the ACI code.

The design procedure with and without shear reinforcement is described and the detailing of these slabs explained, as per Fig. 16 of IS 456. In order to prevent progressive collapse, it is necessary

to provide at least two bars passing through the column cage in the slab-column connection. The expression for area required for this reinforcement is provided.

The effect and detailing around the opening and the detailing for flat slabs located in seismic zones are discussed. Flat slabs in such seismic zones should be analysed with reduced slab width. Research has shown that storey drift limits, although primarily

related to serviceability, also improve the frame stability and seismic performance of such systems. These provisions limiting the storey drift are also provided.

The design of waffle, grid, and hollow-core slabs is also briefly discussed. Examples are given to explain the concepts and the application of the equations provided. Chapter 12 deals with the serviceability aspects of the limit states design.

REVIEW QUESTIONS

- Distinguish between flat slabs and flat plates with sketches of both.
- What are the advantages offered by flat plates over conventional two-way slabs with supporting beams?
- The minimum thickness of flat slabs or flat plates _____.
 - is decided based on the span to effective depth ratio similar to two-way slabs
 - should be greater than 125 mm
 - both of these
 - none of these
- What is the purpose of a drop panel?
- The size of a drop panel in the interior panels should project _____.
 - one-fourth of slab thickness and have length greater than one-third the panel length
 - one-fifth of slab thickness and have length greater than one-third the panel length
 - one-fifth of slab thickness and have length greater than one-fourth the panel length
 - one-fourth of slab thickness and have length greater than one-fourth the panel length
- Write short notes on the following:
 - Column head
 - Shear cap
 - Behaviour of flat slabs under increasing loads
- What are the two methods of analysis prescribed in the codes for flat slabs?
- State the conditions that should be satisfied while using the DDM.
- What is the expression for total static moment M_o ?
- How are circular supports considered in the DDM?
- In interior spans, the total static moment is distributed as negative and positive bending moments in the ratio _____ per cent.
 - 50:50
 - 60:40
 - 65:35
 - 70:30
- How are the positive and negative bending moments distributed in the column and middle strips in the interior span?
- How is the effect of pattern load considered in the DDM as per the IS 456 code?
- In what way is the EFM better than the DDM?
- How is the moment transfer between the slab and column due to unbalanced gravity loads or lateral loads considered in IS 456?
- As per IS 456, the transfer width around the interior column is taken as _____.
 - 1.2 times the depth of slab or drop panel on each side of column
 - 1.5 times the depth of slab or drop panel on each side of column
 - 2.0 times the depth of slab or drop panel on each side of column
 - None of these
- How is the moment acting on a column determined using the DDM?
- How is one-way shear considered in flat slabs?
- Why is two-way shear more critical than one-way shear in flat slabs?
- Sketch the failure surface of a flat slab around a column in punching shear.
- What are the two critical sections in flat slabs with drop panels to be considered for punching shear?
- As per the IS 456 code, punching shear is checked at a distance _____ from the face of the column.
 - 0.5d
 - 1.0d
 - 1.5d
 - 2.0d
- List a few factors that affect the punching shear strength of flat slabs.
- How is a flat slab designed for punching shear? State the equations for nominal shear stress and design shear stress.
- How is the combined shear and moment transfer in a flat slab considered?
- State the simplified expression for moment and shear transfer in edge columns developed by Alexander and Simmonds.
- List the strategies to avoid punching shear failure.
- List a few types of punching shear reinforcements adopted in practice.
- How are shear stirrups designed to resist punching shear? Provide a sketch to show how they can be provided in slabs.
- What are the reasons for not adopting shear stirrups in slabs?
- What is headed stud shear reinforcement? Provide a sketch to explain it.
- What are the equations available in the ACI code for the design of headed shear studs?
- List a few advantages of headed shear studs.
- What is shear head reinforcement? Why is it not popular?
- What is shear band reinforcement? What are its advantages?
- Describe the various steps involved in the design of flat slabs.
- The spacing of reinforcements in flat slabs is restricted to _____.
 - 2 times the slab depth
 - 300 mm
 - 3 times the slab depth
 - 450 mm
- The negative moment reinforcement in a flat slab without drop panel is provided over the support for a length of _____.
 - 0.25 L_n
 - 0.33 L_n
 - 0.30 L_n
 - 0.35 L_n

39. The negative moment reinforcement in a flat slab with drop panel is provided over the support for a length of _____.
 (a) $0.25L_n$ (c) $0.30L_n$
 (b) $0.33L_n$ (d) $0.35L_n$
40. All positive slab reinforcements perpendicular to a discontinuous edge should be anchored to a minimum distance of _____.
 (a) L_d (b) 150 mm (c) 200 mm (d) 300 mm
41. How can we prevent the progressive collapse of flat plates? State the expression for the required area of steel for this requirement.
42. Under what conditions can openings be provided without rigorous analysis?
43. Discuss the effect of openings on punching shear strength.
44. List a few rules to be followed in the detailing of flat slabs in seismic zones.
45. Write short notes on the following:
 (a) Effective slab width for seismic analysis
 (b) Drift control in seismic zones
 (c) Waffle slabs
 (d) Grid slabs
 (e) Hollow-core slabs

EXERCISES

- Design the interior panel of a flat plate supported on columns spaced at 6 m in both directions. The size of the column is 450 mm by 450 mm and the imposed load on the panel is 3 kN/m^2 . The floor slab is exposed to moderate environment. Assume the floor finishing load as 1 kN/m^2 and use M30 concrete and Fe 415 grade steel.
- Design the interior panel of a building with flat slab roof having a panel size of $7 \text{ m} \times 7 \text{ m}$ supported by columns of size $600 \text{ mm} \times 600 \text{ mm}$. Take live load as 4.0 kN/m^2 and the weight of finishes as 1.0 kN/m^2 . Use M25 concrete and Fe 415 steel. Assume mild environment.
- Redesign Exercise 2 assuming the flat slab is supported by a circular column of 500 mm diameter and is with suitable column head.
- Design the slab reinforcement at the exterior column of Exercise 1 for moment transfer between the slab and column and check for combined stresses. In addition, calculate the moments to be carried by the columns.
- Assume a corner column of size $400 \text{ mm} \times 800 \text{ mm}$ supporting a 175 mm thick flat slab with effective depth 150 mm. The factored moment due to gravity loads at the face of the column is 80 kNm, the factored shear force at the face of the column is 200 kN, and the shear force at the edge is 25 kN. Check the stresses due to the combined forces assuming that the slab is made using M25 concrete and Fe 415 steel.
- A flat plate panel of dimensions $5 \text{ m} \times 6 \text{ m}$ supported by columns of size $450 \text{ mm} \times 450 \text{ mm}$ has a slab thickness of 150 mm and is designed for a working (total) load of 9 kN/m^2 . Check the safety of the slab in punching shear and provide shear reinforcement, if required. Assume M20 concrete and Fe 415 steel.
- For the slab in Exercise 6, design headed shear studs as shear reinforcement, instead of shear stirrups.
- Design a waffle slab for an internal panel of a floor system that is constructed in a 6.3 m square module and subjected to a total design service load of 9.0 kN/m^2 , out of which the live load is 3 kN/m^2 . Use M25 concrete and Fe 415 steel. The slab is to be supported on square columns of size $750 \text{ mm} \times 750 \text{ mm}$ and constructed using removable forms of size $750 \text{ mm} \times 750 \text{ mm} \times 500 \text{ mm}$. The slab is subjected to mild exposure.

REFERENCES

- ACI-ASCE Committee 326 1962, 'Shear and Diagonal Tension, Part 3: Slabs and Footings', *Proceedings, ACI Journal*, Vol. 59, No. 3, pp. 353–96.
- ACI-ASCE Committee 352 2002 (ACI 352.1R-1989, reapproved 2004), *Recommendations for Design of Slab-column Connections in Monolithic Reinforced Concrete Structures*, American Concrete Institute, Farmington Hills, p. 37.
- ACI-ASCE Committee 421 1999 (ACI 421.1R-99, reapproved 2006), *Shear Reinforcement for Slabs*, American Concrete Institute, Farmington Hills, p. 15.
- ACI-ASCE Committee 426 1974, 'The Shear Strength of Reinforced Concrete Members—Slabs', *Proceedings, ASCE*, Vol. 100, No. ST8, pp. 1543–91.
- Agarwal, R.K. and N.J. Gardner 1974, 'Form and Shore Requirements for Multi-story Flat Slab Type Buildings', *Proceedings, ACI Journal*, Vol. 71, No. 11, pp. 559–69.
- Ålander, C. 2005, *Advanced Systems for Rational Slab Reinforcement*, p. 14, [http://213.182.3.55/bamtec/database/library.nsf/626e6035eadbb4cd85256499006b15a6/3c136610c0b3636fc1256eca004881ca/\\$FILE/E2_Final_ALANDER.pdf](http://213.182.3.55/bamtec/database/library.nsf/626e6035eadbb4cd85256499006b15a6/3c136610c0b3636fc1256eca004881ca/$FILE/E2_Final_ALANDER.pdf), last accessed on 3 March 2012.
- Alexander, S.D.B. and S.H. Simmonds 2005, 'Shear and Moment Transfer at an Edge Column: A Simplified Analysis Method', *Concrete International*, ACI, Vol. 27, No. 8, pp. 69–74.
- Andrä, H.P., W.H. Dilger, and A. Ghali 1979, 'Durchstanzbewehrung für Flachdecken', *Beton und Stalbetonbau* (Berlin), Vol. 74, No. 5, pp. 129–32.
- Anggadajaja, E. and S. Teng 2008, 'Edge-Column slab connection under gravity and lateral loading', *ACI Structural Journal*, Vol. 105, No. 5, pp. 541–51.
- Barron, J.M. and M.B.D. Huete 2004, 'Diaphragm Effects in Rectangular Reinforced Concrete Buildings', *ACI Structural Journal*, Vol. 101, No. 5, pp. 615–24.
- Birkle, G. and W.H. Dilger 2008, 'Influence of Slab Thickness on Punching Shear Strength', *ACI Structural Journal*, Vol. 105, No. 2, pp. 180–8.
- Broms, C.E. 1990, 'Shear Reinforcement for Deflection Ductility of Flat Plates', *ACI Structural Journal*, Vol. 87, No. 6, pp. 696–705.
- Corley, W.G. and J.O. Jirsa 1970, 'Equivalent Frame Analysis for Slab Design', *Proceedings, ACI Journal*, Vol. 67, No. 11, pp. 875–84.

- Corley, W.G. and N.M. Hawkins 1968, 'Shearhead Reinforcement for Slabs', *Proceedings, ACI Journal*, Vol. 65, No. 10, pp. 811–24.
- Dhar, S. and A.K. Sengupta 2010, 'Analysis of Chord Forces in Reinforced Concrete Buildings with Flat Plates or Flat Slabs', *ICI Journal*, Indian Concrete Institute, Vol. 10, No. 4, pp. 21–7.
- Dilger, W.H. and A. Ghali 1981, 'Shear Reinforcement for Concrete Slabs', *Journal of the Structural Division*, ASCE, Vol. 107, No. ST12, pp. 2403–20.
- Dilger, W.H., Z.E. Mahmoud, and A. Ghali 1978, 'Flat Plates with Special Shear Reinforcement Subjected to Static and Dynamic Moment Transfer', *Proceedings, ACI Journal*, Vol. 76, No. 10, pp. 543–9.
- DiStasio, J. and M.P. Van Buren 1936, 'Slabs Supported on Four Sides', *Proceedings, ACI Journal*, Vol. 32, No. 3, pp. 350–64.
- DiStasio, J. and M.P. Van Buren 1960, 'Transfer of Bending Moment between Flat Plate Floor and Column', *Proceedings, ACI Journal*, Vol. 57, No. 3, pp. 299–314.
- Dovich, L.M. and J.K. Wight 2005, 'Effective Slab Width Model for Seismic Analysis of Flat Slab Frames', *ACI Structural Journal*, Vol. 102, No. 6, pp. 868–75.
- Durrani, A.J., Y. Du, and Y.H. Luo 1995, 'Seismic Resistance of Nonductile Slab-column Connections in Existing Flat-slab Buildings', *ACI Structural Journal*, Vol. 92, No. 4, pp. 479–87.
- Elgabri, A.A. and A. Ghali 1987, 'Tests on Concrete Slab-column Connections with Stud Shear Reinforcement Subjected to Shear-Moment Transfer', *ACI Structural Journal*, Vol. 84, No. 5, pp. 433–42.
- Elgabri, A.A. and A. Ghali 1990, Design of stud-shear reinforcement for slabs, *ACI Structural Journal*, Vol. 87, No. 3, pp. 350–361.
- Elgabri, A.A. and A. Ghali 1996, 'Transfer of Moments between Columns and Slabs: Proposed Code Revisions', *ACI Structural Journal*, Vol. 93, No. 1, pp. 56–61.
- Ellingwood, B.R., R. Smilowitz, D.O. Dusenberry, D. Dithinh, and N.J. Carino, 'Best Practices for Reducing the potential for progressive Collapse in Buildings', NIST Report No: NISTIR 7396, National Institute of Standards and Technology, US Dept. of Commerce, Gaithersburg, MD, 2007, p. 216, <http://www.bfrl.nist.gov/861/861pubs/collapse/NISTIR7396.pdf>, last accessed on 10 July 2013.
- Falamaki, M. and Y.C. Loo 1992, 'Punching Shear Tests of Half Scale Reinforced Concrete Flat Plate Models with Spandrel Beams', *ACI Structural Journal*, Vol. 89, No. 3, pp. 263–71.
- Fanella, D.A. 2002, 'Time Saving Design Aids for Reinforced Concrete', proceedings of the 71st Annual Convention of Structural Engineers Association of California (SEAOC), Sept. 25–29, Santa Barbara, California, pp. 453–72.
- Gamble, W.L. 1972, 'Moments in Beam Supported Slabs', *Proceedings, ACI Journal*, Vol. 69, No. 3, pp. 149–57.
- Gamble, W.L., M.A. Sozen, and C.P. Siess 1969, 'Tests of a Two-way Reinforced Concrete Floor Slab', *Proceedings, ASCE*, Vol. 95, No. ST6, pp. 1073–96.
- Gardner, N.J. 2011, 'Verification of Punching Shear Provisions for Reinforced Concrete Flat Slabs', *ACI Structural Journal*, Vol. 108, No. 5, pp. 572–80.
- Gayed, R.B. and A. Ghali 2008, 'Unbalanced Moment Resistance in Slab-column Joints: Analytical Assessment', *Journal of Structural Engineering*, ASCE, Vol. 134, No. 5, pp. 859–64.
- Ghali, A. and W.H. Dilger 1998, 'Anchoring with double-head Studs', *Concrete International*, ACI, Vol. 20, No. 11, pp. 21–4.
- Ghali, A. and N. Hammill 1992, 'Effectiveness of Shear Reinforcement in Slabs', *Concrete International*, ACI, Vol. 14, No. 2, pp. 60–5.
- Grossman, J.S. 1989, 'Code Procedures, History, and Shortcomings: Column-slab Connections', *Concrete International*, Vol. 11, No. 9, pp. 73–7.
- Grossman J.S. 1997, 'Verification of Proposed Design Methodologies for Effective Width of Slabs in Slab-column Frames', *ACI Structural Journal*, Vol. 94, No. 2, pp. 181–96.
- Guandalini, S., O.L. Burdet, and A. Muttoni 2009, 'Punching Tests of Slabs with Low Reinforcement Ratios', *ACI Structural Journal*, Vol. 106, No. 1, pp. 87–95.
- Guralnick S.A. and R.W. La Fraugh 1963, 'Laboratory Study of a 45-Foot Square Flat Plate Structure', *Proceedings, ACI Structural Journal*, Vol. 60, No. 9, pp. 1107–86.
- Hammill, N. and A. Ghali 1994, 'Punching shear resistance of corner slab-column connections', *ACI Structural Journal*, Vol. 91, No.6, pp. 697–707.
- Han, S.-W., Y.-M. Park, S.-H. Kee 2009, 'Stiffness Reduction Factor for Flat Slabs Structures under Lateral Loads', *Journal of Structural Engineering*, Vol. 135, No. 6, pp. 743–50.
- Hanson, N.W. and J.M. Hanson 1968, 'Shear and Moment Transfer between Concrete Slabs and Columns', *Journal of the PCA Research and Development Laboratories*, Portland Cement Association, Vol. 10, No. 1, pp. 2–16.
- Hatcher, D.S., M.A. Sozen, and C. P. Siess 1965, 'Test of a Reinforced Concrete Flat Plate', *Proceedings, ASCE*, Vol. 91, No. ST5, pp. 205–31.
- Hatcher, D.S., M.A. Sozen, and C.P. Siess 1969, 'Test of a Reinforced Concrete Flat Slab', *Journal of the Structural Division*, ASCE, Vol. 95, No. ST6, pp. 1051–72.
- Hawkins, N.M. 1974a, 'Shear Strength of Slabs with Shear Reinforcement', *Shear in Reinforced Concrete*, SP-42, Vol. 2, American Concrete Institute, Detroit, pp. 785–815.
- Hawkins, N.M. 1974b, 'Shear Strength of Slabs with Moments Transferred to Columns,' *Shear in Reinforced Concrete*, SP-42, American Concrete Institute, Detroit, pp. 817–46.
- Hawkins, N.M. and W.G. Corley 1974, 'Moment Transfer to Columns in Slabs with Shear-head Reinforcement', *Shear in Reinforced Concrete*, SP-42, American Concrete Institute, Detroit, pp. 847–79.
- Hawkins, N.M. and S.K. Ghosh 2006, 'Shear Strength of Hollow Core Slabs', *PCI Journal*, Vol. 51, No. 1, pp. 110–4.
- Hawkins, N.M., and D. Mitchell 1979, 'Progressive Collapse of Flat Plate Structures', *Proceedings, ACI Journal*, Vol. 76, No. 7, pp. 775–808.
- Hawkins, N.M., D. Mitchell, S.N., and Hannah 1975, 'The Effects of Shear Reinforcement on Reversed Cyclic Loading Behavior of Flat Plate Structures', *Canadian Journal of Civil Engineering* (Ottawa), Vol. 2, pp. 572–82.
- Hueste, M.B.D., J. Browning, A. Lepage, and J.W. Wallace 2007, 'Seismic Design Criteria for Slab-column Connections', *ACI Structural Journal*, Vol. 104, No. 4, pp. 448–57.
- Hueste, M.B.D. and J.K. Wight 1999, 'Nonlinear Punching Shear Failure Model for Interior Slab-column Connections', *Journal of Structural Engineering*, ASCE, Vol. 125, No. 9, pp. 997–1008.

- Hurd, M.K 1997. 'Using Glass-fiber-reinforced-plastic Forms', *Concrete Construction*, Vol. 42, No. 9, pp. 725–8, (also see http://www.concreteconstruction.net/Images/Using%20Glass-Fiber-Reinforced-Plastic%20Forms_tcm45-343261.pdf, last accessed on 14 November 2012).
- Hwang, S.-J. and J.P. Moehle 2000, 'Models for Laterally Loaded Slab-column Frames', *ACI Structural Journal*, Vol. 97, No. 2, pp. 345–53.
- Jirsa, J.O., M.A. Sozen, and C.P. Siess 1966, 'Test of a Flat Slab Reinforced with Welded Wire Fabric', *Proceedings, ASCE*, Vol. 92, No. ST3, pp. 199–224.
- Kang, T.H.-K and J.W. Wallace 2008, 'Seismic Performance of Reinforced Concrete Slab-column Connections with Thin Plate Stirrups', *ACI Structural Journal*, Vol. 105, No. 5, pp. 619–27.
- Kinnunen, S. and H. Nylander 1960, *Punching Shear of Concrete Slabs without Shear Reinforcement*, Meddelande No. 38, Institutionen för Byggnadsstatik, Kungliga Tekniska Högskolan, Stockholm.
- Leo, Y.H. and A.J. Durrani 1995, 'Equivalent Beam Model for Flat Slab Buildings, Part I: Interior Connections and Part II: Exterior Connections', *ACI Structural Journal*, Vol. 92, No. 1, pp. 115–24 and Vol. 92, No. 2, pp. 250–7.
- Leonhardt, F. and E. Mönig 1977, *Vorlesungen über Massivbau, Grundlagen zum Bewehren im Stahlbetonbau*, 3rd edition, Springer-Verlag, Berlin, p. 246.
- Leyendecker, E.V. and S.G. Fattal, 1977, *Investigation of the Skyline Plaza Collapse in Fairfax County, Virginia*, Center for Building Technology, Institute for Applied Technology, National Bureau of Standards, Washington, DC, Report No. 94, p. 91.
- Lim, F.K. and B.V. Rangan 1995, 'Studies on Concrete Slabs with Stud Shear Reinforcement in Vicinity of Edge and Corner Columns', *ACI Structural Journal*, Vol. 92, No. 5, pp. 515–25.
- Matzke, E.M. 2012, 'Punching Shear Strength and Drift Capacity of Slab-Column Connections with Headed Shear Stud Reinforcement Subjected to Combined Gravity Load and Biaxial-Lateral Displacements', M.S. Thesis, University of Minnesota, p. 230 (https://nees.org/data/get/NEES-2010-0983.groups/Documentation/Thesis_Matzke_090912%20submitted.pdf).
- Magura, D.D. and W.G. Corley 1971, 'Tests to Destruction of a Multipanel Waffle Slab Structure: 1964–1965 New York World's Fair', *Proceedings, ACI Journal*, Vol. 68, No. 9, pp. 699–703.
- Megally, S. and A. Ghali 2000, 'Punching Shear Design of Earthquake Resistant Slab-column Connections', *ACI Structural Journal*, Vol. 97, No. 5, pp. 720–30.
- Megally, S. and A. Ghali 2002, 'Cautionary Note On Shear Capitals', *Concrete International*, ACI, Vol. 24, No. 3, pp. 75–82.
- Mitchell, D. and W.D. Cook 1984, 'Preventing Progressive Collapse of Slab Structures', *Journal of Structural Engineering*, ASCE, Vol. 110, No. 7, pp. 1513–32.
- Moe, J. 1961, *Shearing Strength of Reinforced Slabs and Footings under Concentrated Load*, Bulletin D47, Portland Cement Association, Skokie, p. 130.
- Moehle, J.P. 1988, 'Strength of Slab-column Edge Connections', *ACI Structural Journal*, Vol. 85, No. 1, pp. 89–98, 'Discussions and Closure', Vol. 85, No. 6, pp. 703–9.
- Moehle, J.P., M.E. Kreger, and R. Leon 1988, 'Background to Recommendations for Design of Reinforced Concrete Slab-column Connections', *ACI Structural Journal*, Vol. 85, No. 6, pp. 636–44.
- Moehle, J.P. and S.A. Mahin 1991, 'Observations on the Behavior of Reinforced Concrete Buildings during Earthquakes', in S. K. Ghosh (ed.), *SP 127 Earthquake-resistant Concrete Structures: Inelastic Response and Design*, (also see <http://nisee.berkeley.edu/lessons/concretemm.html>, last accessed on 19 February 2012).
- Mokhtar, A., A. Ghali, and W.H. Dilger 1985, 'Stud Shear Reinforcement for Flat Concrete Plates', *ACI Structural Journal*, Vol. 82, No. 5, pp. 676–83.
- Mulenga, M.N. and S.H. Simmonds 1993, 'Frame Methods for Analysis of Two-way Slabs', *Structural Engineering Report No. 183*, Department of Civil and Environmental Engineering, University of Alberta, Canada, p. 247.
- Muttoni, A. 2008, 'Punching Shear Strength of Reinforced Concrete Slabs without Transverse Reinforcement', *ACI Structural Journal*, Vol. 105, No. 4, pp. 440–50.
- Nazief, M.A., Y.F. Rashed, and W.M. El-Degwy 2010, 'Boundary Element Method Calculation for Moment Transfer Parameters in Slab-column Connections', *ACI Structural Journal*, Vol. 107, No. 2, pp. 164–9.
- Nichols, J.R. 1914, 'Statical Limitations upon the Steel Requirement in reinforced Concrete Flat Slab Floors', and 'Discussions', *Transactions of The American Society of Civil Engineers*, Vol. 77, pp. 1670–736.
- Pan, A. and J.P. Moehle 1989, 'Lateral Displacement Ductility of Reinforced Concrete Flat Plates', *ACI Structural Journal*, Vol. 86, No. 3, pp. 250–8.
- Park, H-G, K-S Ahn, K-K Choi, and L. Chung 2007, 'Lattice Shear Reinforcement for Slab-column Connections', *ACI Structural Journal*, Vol. 104, No. 3, pp. 294–303, and Gayed R.B. 2008, 'Discussion', Vol. 105, No. 2, pp. 237–8.
- Park R. and W.L. Gamble 2000, *Reinforced Concrete Slabs*, 2nd edition, John Wiley and Sons, New York, p. 736.
- PCI Design Handbook 2010, *Precast and Prestressed Concrete*, 7th edition, Precast/Prestressed Concrete Institute, Chicago, p. 804.
- Pilakoutas, K. and X. Li 2003, 'Alternative Shear Reinforcement for Reinforced Concrete Flat Slabs', *Journal of Structural Engineering*, ASCE, Vol. 129, No. 9, pp. 1164–72.
- Pillai, S.U. and D. Menon 2009, *Reinforced Concrete Design*, 3rd edition, Tata McGraw Hill Publishing Company Ltd, New Delhi, p. 962.
- Polak, M.A. (ed.) 2005, *Punching Shear in Reinforced Concrete Slabs*, SP-232, American Concrete Institute, Farmington Hills, p. 302.
- Rangan, B.V. 1987, 'Punching Shear Strength of Reinforced Concrete Slabs', *Civil Engineering Transactions (Barton)*, Vol. CE29, No. 2, pp. 71–8.
- Rangan, B.V. 1990, 'Punching Shear Design in the New Australian Standard for Concrete Structures', *ACI Structural Journal*, Vol. 87, No. 2, pp. 140–4.
- Rangan B.V. and A.S. Hall 1983, 'Moment and Shear Transfer between Slab and Edge Column', *Proceedings, ACI Journal*, Vol. 80, No. 3, pp. 183–91.
- RCD D4-1995, *Seismic Detailing for Reinforced Concrete Buildings in Australia*, Reinforced Concrete Digest D4, Steel Reinforcement Institute of Australia, p. 23.
- Regan, P.E. 1981, *Behaviour of Reinforced Concrete Flat Slabs*, Construction Industry Research and Information Association (CIRIA) Report 89, London, p. 91.

- Regan, P.E. and M.W. Braestrup 1985, *Punching Shear in Reinforced Concrete*, Bulletin d'Information 168, Comité Euro-International du Beton, Lausanne, p. 232.
- Rice, P.F. 1973, 'Practical Approach to Two-way Slab Design', *Proceedings, Journal of the Structural Division*, ASCE, Vol. 99, No. 1, pp. 131–43.
- Ritchie, M., A. Ghali, W. Dilger, and R.B. Gayed 2006, 'Unbalanced Moment Resistance by Shear in Slab-column Connections: Experimental Assessment', *ACI Structural Journal*, Vol. 103, No. 1, pp. 74–82.
- Rizk, E., H. Marzouk, and A. Hussein 2011, 'Punching Shear of Thick Plates with and without Shear Reinforcement', *ACI Structural Journal*, Vol. 108, No. 5, pp. 581–91.
- Robertson, I. and G. Johnson 2006, 'Cyclic Lateral Loading of Nonductile Slab-column Connections', *ACI Structural Journal*, Vol. 103, No. 3, pp. 356–64.
- Ruiz, M.F. and A. Muttoni 2009, 'Applications of Critical Shear Crack Theory to Punching of Reinforced Concrete Slabs with Transverse Reinforcement', *ACI Structural Journal*, Vol. 106, No. 4, pp. 485–94.
- Schellhammer, J., N.J. Delatte, and P.A. Bosela, 2012, 'Another Look at the Collapse of Skyline Plaza at Bailey's Crossroads, Virginia', *Journal of Performance of Constructed Facilities*, ASCE.
- Schwetz, P.F., F.P. S.L. Gastal, and L. C. P. Silva 2009, 'Numerical and Experimental Study of a Real Scale Waffle Slab', *IBRACON Structures and Materials Journal*, Vol. 2, No. 4, pp. 380–403.
- Simmonds, S.H. and S.D.B. Alexander 1987, 'Shear and Moment Transfer at an Edge Connection', *ACI Structural Journal*, Vol. 84, No. 4, pp. 296–303.
- Sozen, M.A. and C.P. Siess 1963, 'Investigation of Multiple-panel Reinforced Concrete Floor Slabs: Design Methods—Their Evolution and Comparison', *Proceedings, Journal of the American Concrete Institute*, Vol. 60, No. 8, pp. 999–1027.
- Subramanian, N. 2005, 'Evaluation and Enhancing the Punching Shear Resistance of HSC Flat Slabs', *The Indian Concrete Journal*, Vol. 79, No. 4, pp. 31–7.
- Suryanarayana, P. 2001, 'Design Alternatives for Flat Plate Structures', *New Building Materials and Construction World (NBM & CW)*, Vol. 7, No. 4, pp. 20–4.
- Teng, S., H.K. Cheong, K.L. Kuang, and J.Z. Geng 2004, 'Punching Shear Strength of Slabs with Openings and Supported on Rectangular Columns', *ACI Structural Journal*, Vol. 101, No. 5, pp. 678–87.
- Theodorakopoulos D.D. and R.N. Swamy 2002, 'Ultimate Punching Shear Strength Analysis of Slab-column Connections', *Cement and Concrete Composites*, Vol. 24, pp. 509–21.
- Theodorakopoulos, D.D. and R.N. Swamy 2007, 'Analytical Model to Predict Punching Shear Strength of FRP Reinforced Concrete Flat Slabs', *ACI Structural Journal*, Vol. 104, No. 3, pp. 257–66.
- Van Buren M.P. 1971, 'Staggered Columns in Flat Plates', *Journal of the Structural Division*, ASCE, Vol. 97, No. ST6, pp. 1791–7.
- Vanderbilt, M.D. 1972, 'Shear Strength of Continuous Plates', *Journal of the Structural Division*, ASCE, Vol. 98, No. ST5, pp. 961–973.
- Vanderbilt, M.D. 1979, 'Equivalent Frame Analysis for Lateral Loads', *Journal of the Structural Division*, ASCE, Vol. 105, No. ST10, pp. 1981–98.
- Vanderbilt, M.D. and W.G. Corley 1983, 'Frame Analysis of Concrete Buildings', *Concrete International: Design and Construction*, Vol. 5, No. 12, pp. 33–43.
- Vanderbilt, M.D., M.A. Sozen, and C.P. Siess 1969, 'Test of a Modified Reinforced Concrete Two-way Slab', *Proceedings, ASCE*, Vol. 95, No. ST6, pp. 1097–116.
- Varghese, P.C. 2006, *Limit States Design of Reinforced Concrete*, 2nd edition, Prentice Hall of India Ltd, New Delhi, p. 545.
- Varyani, U.H. and A. Radhaji 2005, *Design Aids for Limit State Design of Reinforced Concrete Members*, 2nd edition, Khanna Publishers, Delhi, p. 419.
- Westergaard, H.M. and W.A. Slater 1921, 'Moments and Stresses in Slabs', *Proceedings, American Concrete Institute*, Vol. 17, pp. 415–538.
- Widianto, O. Bayrak, and J.O. Jirsa 2009, 'Two-way Shear Strength of Slab-column Connections: Reexamination of ACI 318 Provisions', *ACI Structural Journal*, Vol. 106, No. 2, pp. 160–70.
- Wiesinger, F.P. 1973, 'Design of Flat Plates with Irregular Column Layout', *Proceedings, American Concrete Institute*, Vol. 70, No. 2, pp. 117–23.
- Wight, J.K. and J.G. MacGregor 2009, *Reinforced Concrete: Mechanics and Design*, 5th edition, Pearson Prentice Hall, Upper Saddle River, p. 1112.
- Xanthakis, M. and M. A., Sozen 1963, 'An Experimental Study of Limit Design in Reinforced Concrete Flat Slabs', *Structural Research Series No. 277*, Civil Engineering Studies, University of Illinois, p. 159.
- Yang, J.-M., Y.-S. Yoon, W.D. Cook, and D. Mitchell 2010, 'Punching Shear Behavior of Two-way Slabs Reinforced with High-strength Steel', *ACI Structural Journal*, Vol. 107, No. 4, pp. 468–475.

SERVICEABILITY LIMIT STATES: DEFLECTION AND CRACK CONTROL

12.1 INTRODUCTION

When working stress method was used in the 1970s (although IS 456 introduced the ultimate load method in an appendix in the 1964 edition of the code, limit states method was introduced only in 1978), concretes with compressive strength ranging from 15 MPa to 20 MPa and reinforcements with a yield strength of 250 MPa were primarily used. The use of these materials along with conservative allowable stresses of the working stress method resulted in large sections with small deflections. The working stress method limited the stress in concrete to about 45 per cent of its specified compressive strength, and the stress in the steel reinforcement to less than 50 per cent of its specified yield strength. The use of limit states method changed this scenario and we now use steels with f_y ranging from 415 MPa to even 690 MPa (MMFX 2 bars) and concretes with strength f_{ck} ranging from 20 MPa to 60 MPa or greater. Moreover, we now use the specified compressive strength of concrete and yield strength of steel in the calculations. Hence, the use of limit states method with higher strength materials resulted in smaller, slender sections. These slender sections resulted in excessive deflections coupled with the cracks. The higher stresses allowed in these thin sections have also resulted in deterioration of structures all over the world (Subramanian 1989). As discussed in Section 4.8 of Chapter 4, limit states philosophy is concerned not only with the *strength limit states*, which are based on the safety or load-carrying capacity of members, but also with the *serviceability limit states*, which are concerned with the performance of structures and their elements under service loads. Until now, we have been discussing the strength aspects of limit states design. In this chapter, we shall discuss the serviceability limit states of design.

Serviceability is measured by considering the magnitudes of deflection, cracking, and vibration of structures as well as consideration of durability (amounts of surface deterioration

of the concrete and corrosion of reinforcing steel). Since we do not have adequate information on durability, it is often satisfied, in most existing standards and guidelines, by prescriptive requirements (see Section 4.4.5 of Chapter 4). For example, carbonation-initiated corrosion requirements, such as water/cementitious material (w/cm) ratio, cement type and content, compressive strength, and concrete cover based on exposure condition, are specified in the codes. In future, these requirements will be based on performance and service life of structures defined according to a probabilistic approach (FIB Bulletin No. 34:2006). It has to be noted that serviceability limit state is not concerned with the collapse of structures, though in some rare cases it may result in collapse, as may be seen from the case study discussed later in this chapter.

Computation of deflections can help in the proper design of adjustable props (*shores* in American terminology) in the formwork, in setting out proper cambers, in planning the sequence of removal of formwork, and also in verifying whether undue distress arises in the structure due to inadequate design or construction even at the stage of decentering. Deflection measurements can give an idea of shrinkage effects and the adequacy of curing (Purushothaman 1984). Excessive deflections may also indicate a tendency towards undesirable vibrations. The age of concrete at the time of loading has an important effect on deflections. Ambient weather and initial curing have significant effects on subsequent deflections (Purushothaman 1984). The composite action of walls on beams and in-filled frames may reduce the actual deflections considerably, but until now, no recommendations are available in codes to consider these effects.

This chapter presents the treatment of initial and time-dependent deflection of reinforced concrete (RC) elements such as simple and continuous beams and one-way and two-way slab systems. Since serviceability is checked at

working loads, we should perform another analysis to get deflections at various parts of a structure, using load factors equal to 1.0.

Tension cracks in beams may reduce durability; in many cases, they are visually disturbing and objectionable to clients. Hence, a discussion of cracking and methods to calculate crack widths are also included in this chapter. Crack and deflection control strategies are also discussed.

Due to the use of high-strength materials, we are now able to design slender sections, which may result in problems such as vibration and fatigue. These problems are also briefly discussed.

12.2 DESIGN FOR LIMIT STATE OF DEFLECTION

Excessive deflections may result in cracking of supporting walls or partitions, and excessive deflection of a spandrel beam above a window opening may even crack the glass panels or result in ill-fitting of doors and windows. In the case of roofs, such excessive deflection may lead to ponding of water, which will result in additional loads not considered in design. It may also cause poor drainage of rain water and misalignment of sensitive machinery or equipment (see Table 12.1). Sometimes, the excessive sag may be visually unacceptable. Construction loads and procedures can also have a significant effect on deflection, particularly in floor slabs. Hence, in addition to preventing the failure of any concrete element due to the ultimate limit states of bending and shear, the designer must ensure that the deflections under working loads do not adversely affect the efficiency and the appearance of the structure.

Current codes adopt two approaches for deflection control. The first is an indirect method in which the span to effective

depth (L/d) ratio of the beam or slab is not allowed to exceed the appropriate limiting values. The limiting L/d ratios as per Clause 23.2.1 may be modified depending on the area and stress of tension steel (Fig. 4 of IS 456), area of compression steel (Fig. 5 of IS 456), and the ratio of web width to flange width in the case of flanged beams (Fig. 6 of IS 456). Such an indirect method was used in the designs presented in Chapter 5 (Sections 5.5.7 and 5.7.6), Chapter 9 (Sections 9.4.2 and 9.8), Chapter 10 (Sections 10.3), and Chapter 11 (Section 11.2). This method is simple and found to be satisfactory in several situations where spans, loads and their distributions, member sizes, and proportions are in the usual ranges. When these parameters are not within the usual ranges, the second method is used, which requires deflections to be calculated and checked with the limiting values imposed by the codes. The provisions for the calculation of deflection may be found in Annexure C of IS 456.

For understanding the principles involved in arriving at the basic values of span to effective depth ratios given in IS 456, let us consider a fully elastic, simply supported rectangular beam of span length L , supporting a uniformly distributed load of w per unit length. If the permissible bending stress is f , the section can withstand a bending moment M given by

$$M = fZ_e = f \frac{D^2}{6} = \frac{wL^2}{8} \quad (12.1)$$

where D is the overall depth of the rectangular section and Z_e is the elastic section modulus.

The deflection of the beam is given by

$$\Delta = \frac{5}{384} \frac{wL^4}{EI} \quad (12.2)$$

where E is the Young's modulus and I is the moment of inertia of the section.

From Eq. (12.1), we get

$$w = \frac{4}{3} f \left(\frac{D}{L} \right)^2 \quad (12.3)$$

Substituting the value of w in Eq. (12.2) and using $I = bD^3/12$, we get for unit breadth

$$\frac{\Delta}{L} = \frac{5}{24} \frac{f}{E} \left(\frac{L}{D} \right) \quad (12.4)$$

This equation can be generalized for other types of loads and end conditions as (SP 24:1980)

$$\frac{\Delta}{L} = K \left(\frac{L}{D} \right) \quad (12.5)$$

This equation shows that for a given elastic material, if the L/D ratio is kept constant, the ratio of the deflection to span will remain constant. By setting a limit to the ratio

TABLE 12.1 Effect of deflection or drift (AS 4100 Supplement 1:1999 Clause 3.5.3 and Appendix B)

Deflection or Drift Index	Nature of Cracks	Typical Behaviour
$L/1000$	Not visible	Cracking of brickwork
$H/500$	Not visible	Cracking of partition walls and general architectural damage
$L/300$ and $H/300$	Visible	Cracking in reinforced walls, damage to ceiling and flooring, cladding leakage, and visually annoying
$L/200$ to $L/300$ $H/200$ to $H/300$	Visible	Damage to lightweight partitions, display windows, and finishes
$L/100$ to $L/200$ or $H/100$ to $H/200$	Visible	Impaired operations of movable components—doors, windows, and sliding partitions

Note: L is the span of the horizontal flexural member and H is the storey height.

of span to depth, the deflection will be limited to a given fraction of the span. Though the overall depth D is to be used in L/D calculations in some codes, IS 456 considers effective depth, to offset the effects due to cracking and the consequent reduction in stiffness of the member (SP 24:1983). The span/thickness limits for deflection control provided in various codes and other proposals by various authors have been compared by Gardner (2011). These span/depth limits provided in codes do not address the sensitivity of slab deflections to early-age construction loads, rate of construction, and strength of concrete at the time of loading (Gardner 2011). Span/Depth expressions, considering several practical parameters, have been developed for one-way slabs and beams by Grossman (1981), Rangan (1982), Gilbert (1985), Scanlon and Lee (2006), and Bischoff and Scanlon (2009). A comparison of the minimum thickness provisions of slabs in different codes was provided by Lee and Scanlon (2010).

The best method to control deflection, without increasing the depth, is to increase the amount of compression steel. If a shallow member is desired, the designer may also choose to provide more tension reinforcement than that required from strength consideration, thus reducing the service stress in the member (SP 24:1980); however, in this case, the total tension steel should not violate the limit state condition that the maximum strain in tension steel should be greater than $\frac{0.87f_y}{E_s} + 0.002$. It is worthwhile to note that the code recommends performing actual deflection calculations for beams or slabs when the span exceeds 10 m in length.

It is difficult to precisely calculate the deflections, due to several uncertainties regarding the material properties, effects of cracking, degree of restraint at the supports, and load history for the member under consideration. In general, the codal provisions ensure that under loads up to full-service loads, stresses in both steel and concrete remain within the elastic limits. In service, members usually sustain full dead load and a fraction of the specified live load, which is difficult to assess. The deflections that occur in the members as soon as the loads are applied are called *immediate deflections* or *short-term deflections*.

Asymmetric reinforcement in beams ($A_{st} > A_{sc}$) leads to shrinkage deflections of concrete, which increase the gravity load deflections. Creep of concrete leads to gradual increase in deflection under sustained service loads. The shrinkage and creep of concrete are influenced by several parameters that include temperature and humidity, curing conditions, age of concrete at the time of load, water–cement ratio, and aggregate content in concrete. Due to the creep and shrinkage of concrete, the deflections gradually increase over an extended period. These *time-dependent deflections* over several years may be three or more times the initial elastic

deflections (Ghali, et al. 2011). Some approximate methods for calculating such time-dependent deflections are also provided in the codes.

12.2.1 Limiting Deflection

As discussed in Section 4.8.2 and Table 4.18 of Chapter 4, the following limiting criteria are adopted in IS 456 for ensuring proper performance of beams and slabs (see Clause 23.2 of IS 456):

1. The final deflection due to all loads (including the effects of temperature, creep, and shrinkage) should not exceed span/250—this limitation is to control the cracks.
2. The deflection occurring after the construction of finishes and partitions (including the effects of temperature, creep, and shrinkage) should not exceed span/350 or 20 mm, whichever is less—this limit is intended to avoid damage of partitions and finishes.

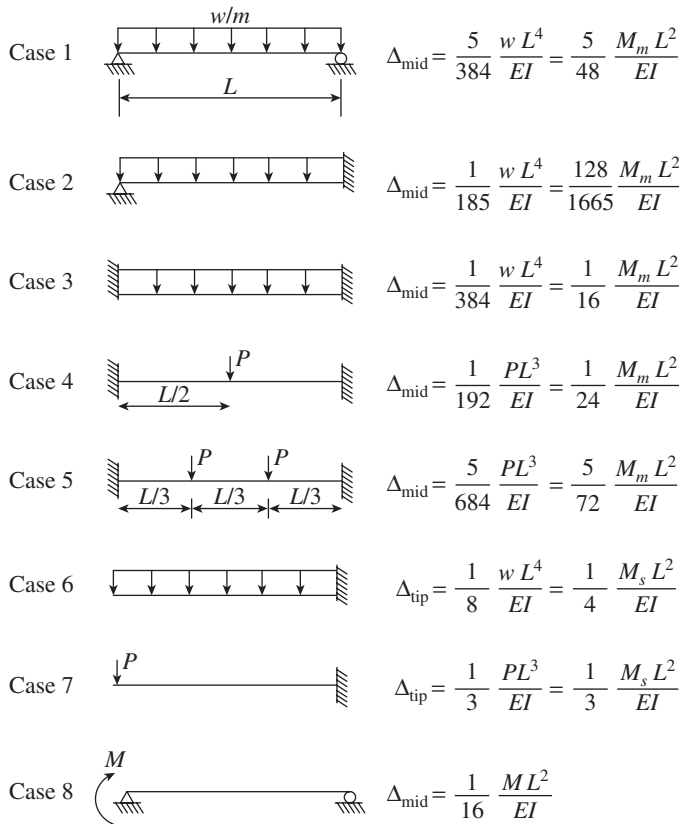
The limiting deflection as per the ACI code is given here:

1. For roofs or floors supporting or attached to non-structural elements likely to be damaged by large deflections— $L/360$
2. For roofs or floors not supporting or attached to non-structural elements likely to be damaged by large deflections— $L/180$

These limits are decreased to $L/480$ and $L/240$, respectively, when long-term deflection is considered along with immediate deflection. ACI also permits to exceed these limits when a camber is provided; in such a case, the total deflection minus camber should not exceed the prescribed limits.

12.3 SHORT-TERM DEFLECTIONS

The short-term or *instantaneous deflection* caused by the service loads may be calculated using the usual elastic theory equations of deflections. For example, the central deflection of a simply supported beam with span L and flexural rigidity EI , carrying a uniform load w per unit length, is $5wL^4/(384EI)$. The equations for calculating the instantaneous mid-span deflections of beams with different end conditions and tip deflection of cantilevered beams are shown in Fig. 12.1 and Table 12.2. Except cases 2 and 8, the calculations give the maximum deflection; even in cases 2 and 8, they provide a good estimate of the maximum deflection. Since the deflections are calculated at working loads, the method of superposition can be used to obtain maximum deflection due to different loads acting on the beam, if the member is not cracked. It has to be noted that the deflection for a simply supported beam is five times that of the same beam with the same load, but has fully restrained condition against rotation at both ends (see Fig. 12.1). Hence, it is important to consider the influence of support conditions in deflection calculations.



M_m : Mid-span moment; M_s : Support moment

FIG. 12.1 Deflections for beams with various end conditions

TABLE 12.2 Deflection coefficient K for uniformly distributed loads and moment M_a at critical section for different support conditions

S. No.	Type of Beam	K^*	$C = M_a/M_o$
1.	Cantilever (fixed-end deflection due to rotation at supports not included, see Section 12.11)	2.4	4.0
2.	Simply supported beam	1.0	1.0
3.	One end continuous with discontinuous end unrestrained ($K = 1.20 - 0.20M_o/M_m$) ⁺	0.925	0.73
4.	One end continuous with discontinuous end integral with the end support ($K = 1.20 - 0.20M_o/M_m$) ⁺	0.8 to 0.85	0.50 to 0.57
5.	Fixed-hinged beam (mid-span deflection)	0.738	0.5
6.	Both ends continuous ($K = 1.20 - 0.20M_o/M_m$) ⁺	0.7 to 0.8	0.4 to 0.5
7.	Fixed-Fixed	0.60	0.33

Note: * $\Delta = K \frac{5 M_a L^2}{48 E_c I_{eff}}$ with $M_a = \frac{(wL^2)}{8}$

⁺ M_m is the mid-span moment for continuous member and M_a is the mid-span moment except for cantilevers where it is moment at support face.

While calculating deflection, it is better to use the effective span (Clause 22.2 of IS code) than the clear span. In continuous beams, the length of adjacent spans and the loads on those spans will affect the value of deflection in the span under consideration. To account for end restraint of such continuous beams, it is often accurate enough to calculate the central deflection of the member as if simply supported and subtract from it the opposite deflection caused by the average negative moments at the two ends (Park and Paulay 1975). Thus, if the end moments are M_1 and M_2 , the average negative moment is $M_{av} = (M_1 + M_2)/2$, and hence, the amount to be subtracted from the simple beam deflection is $M_{av}L^2/8EI$.

Continuous Beams

The length and loading in adjacent spans in a continuous beam will affect the deflection in the span under consideration. For example, the mid-span deflection of a continuous beam with uniform loads but with unequal end moments may be computed using superposition in the following way:

$$\Delta = \Delta_m + \Delta_1 + \Delta_2$$

From Fig. 12.1, and assuming that the moments at the ends of the beam M_1 and M_2 are all negative and M_o is the positive moment at mid-span due to uniform loads for a comparable simply supported beam, we get

$$\Delta = \frac{5 M_o L^2}{48 EI} - \frac{1 M_1 L^2}{16 EI} - \frac{1 M_2 L^2}{16 EI}$$

and the mid-span moment M_m is

$$M_m = M_o - \frac{M_1 + M_2}{2}$$

Expressing the deflection in terms of the moments M_m , M_1 , and M_2 and simplifying, we get

$$\Delta = \frac{5L^2}{48EI} [M_m - 0.1(M_1 + M_2)] \tag{12.6}$$

Similar expressions can be worked out for concentrated loadings (Branson 1977). More discussions on continuous beam deflections may be found in the work of Wight and MacGregor (2009).

12.3.1 Moment of Inertia of Member

The moment of inertia, I , depends on the amount of cracking that has taken place in the member. Depending on the load level, the beam will be cracked at a few sections and will remain uncracked in the portions between these cracks. If the maximum tensile stress in the concrete, calculated on the basis of uncracked section, is smaller than the modulus

of the rupture of concrete, it can be assumed that the concrete is not cracked in the tension zone. In this case, the value of I can be taken as I_{gr} where I_{gr} is the moment of inertia of the uncracked gross section about the centroidal axis, ignoring the transformed area of reinforcement. However, for accurate calculation, we should use the moment of inertia taking into account the transformed area of steel reinforcement, as it may increase the moment of inertia of the uncracked section up to 30 per cent. The method of calculating the moment of inertia of the transformed section is explained here.

Transformed Section

The elastic bending equation can be written as

$$\sigma = \frac{M_s y}{I} \tag{12.7}$$

where σ is the stress, M_s is the applied service moment, I is the moment of inertia, and y is the distance of extreme fibre from the neutral axis. When a beam made of two different materials are loaded, the different E values of these materials lead to different stress distributions. In the elastic theory, this problem is overcome by transforming the beam as an all-concrete beam by replacing the area of steel with an area of concrete having the axial stiffness AE . Since m is E_s/E_c , the resulting area of concrete is mA_{st} or mA_{sc} . (It should be noted that in the working stress method as explained in Section 4.7.1 of Chapter 4, the modular ratio is defined as $280/3\sigma_{cbc}$ to take care of creep effects). This transformed area of steel is assumed to be concentrated at the same point where the steel reinforcement is placed as shown in Fig. 12.2(b). It is important to realize that this steel in the compression zone or in the uncracked tension zone displaces an area of concrete equal to A_{sc} or A_{st} , respectively. Hence, the compression and tension steel in uncracked concrete is transformed to an

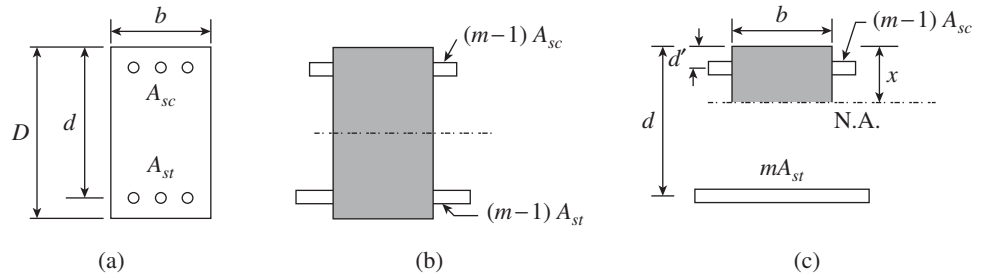


FIG. 12.2 Transformed sections (a) Cross section (b) Uncracked transformed section (c) Cracked transformed section

equivalent area of concrete equal to $(m - 1)A_{sc}$ and $(m - 1)A_{st}$, respectively (see Fig. 12.2b). It has to be noted that in the usual working stress method, the compression steel is transformed to $(1.5m - 1)A_{sc}$ to take care of the effect of creep on the stresses.

The cracked transformed section is shown in Fig. 12.2(c). Here, the steel in the compression zone displaces an area of concrete equal to A_{sc} and hence has a transformed area of $(m - 1)A_{sc}$. However, the tension steel does not displace any concrete and hence is considered to have an area equal to $m A_{st}$ (see Fig. 12.2c).

The moment of inertia about the neutral axis of the cracked rectangular section considering tension and compression reinforcement is given by

$$I_{cr} = \frac{bx^3}{3} + mA_{st}(d - x)^2 + (m - 1)A_{sc}(x - d')^2 \tag{12.8}$$

where m is the modular ratio = E_s/E_c , A_{sc} is the area of compression reinforcement, A_{st} is the area of tension reinforcement, d' is the effective cover for compression reinforcement, x is the depth of neutral axis, E_s is the modulus of elasticity of steel = 2×10^5 N/mm², and E_c is the short-term static modulus of elasticity of concrete = $5000\sqrt{f_{ck}}$ N/mm² as per Clause 6.2.3.1 of IS 456.

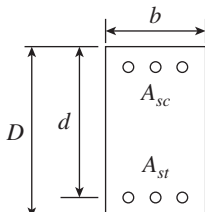
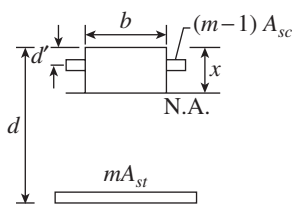
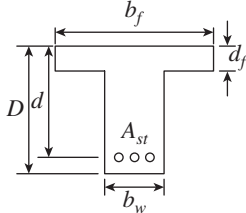
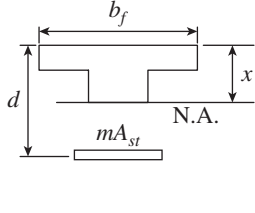
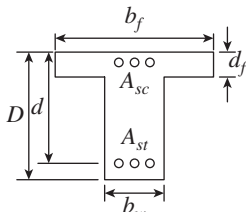
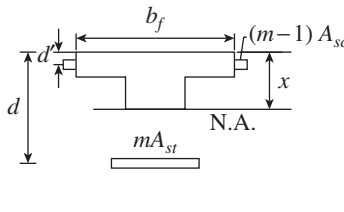
Expressions for gross and cracked moment of inertia of rectangular and flanged sections, with and without compression steel, are given in Table 12.3. Example 12.1 illustrates the considerable reduction in stiffness of beams due to cracking.

TABLE 12.3 Gross and cracked moment of inertia of rectangular and flanged sections

Gross Section	Cracked Transformed Section	Gross and Cracked Moment of Inertia
		$m = \frac{E_s}{E_c}; B = \frac{b}{mA_{st}}; I_g = \frac{bD^3}{12}$ $x = \left[\left(\sqrt{1 + 2Bd} \right) - 1 \right] / B$ $I_{cr} = \frac{bx^3}{3} + mA_{st}(d - x)^2$

(Continued)

TABLE 12.3 (Continued)

Gross Section	Cracked Transformed Section	Gross and Cracked Moment of Inertia
		$\frac{x}{d} = \sqrt{\left[(m\rho + \{m-1\}\rho')^2 + 2\left(m\rho + \{m-1\}\rho' \frac{d'}{d} \right) \right]} - [m\rho + \{m-1\}\rho']$ $I_{cr} = \frac{bx^3}{3} + mA_{st}(d-x)^2 + (m-1)A_{sc}(x-d')^2$ <p>These equations are valid for flanged sections also when $x \leq b_f$.</p>
		<p>When $x > b_f$</p> $A = \left[mp + (m-1)\rho' + \left(1 - \frac{b_w}{b_f} \right) \frac{d_f}{b_f} \right]^2$ $B = \left[mp + (m-1)\rho' \frac{d'}{d} + 0.5 \left(1 - \frac{b_w}{b_f} \right) \left(\frac{d_f}{b_f} \right)^2 \frac{b_w}{b_f} \right]$ $C = \left[mp + (m-1)\rho' + \left(1 - \frac{b_w}{b_f} \right) \left(\frac{d_f}{b_f} \right)^2 \right] \frac{b_f}{b_w}$ $\frac{x}{d} = \sqrt{A + 2B} - C$ $E = \left(\frac{x}{d} \right)^3 - \left(1 - \frac{b_w}{b_f} \right) \left(\frac{x}{d} - \frac{d_f}{d} \right)^3$ $F = m\rho \left(1 - \frac{x}{d} \right)^2 + (m-1)\rho' \left(\frac{x}{d} - \frac{d'}{d} \right)^2$ $\frac{I_{cr}}{bd^3} = \frac{E}{3} + F$
		<p>(This row contains the same equations as the T-section row above.)</p>

Note: $\rho = \frac{A_{st}}{bd}$, $\rho' = \frac{A_{sc}}{bd}$

Service Load Stresses in a Cracked Beam

The service load stresses in steel and concrete can be computed using the equations derived in Chapter 4. Hence, using Eq. (4.9a), we may obtain compressive stress in concrete as

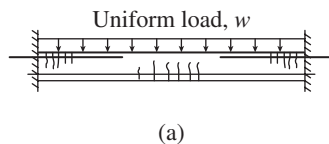
$$\sigma_{cbc} = \frac{2M_s}{jkb d^2} \tag{12.9a}$$

Using Eq. (4.10a), we may obtain stress in steel as

$$\sigma_{st} = \frac{M_s}{A_{st} j d} \tag{12.9b}$$

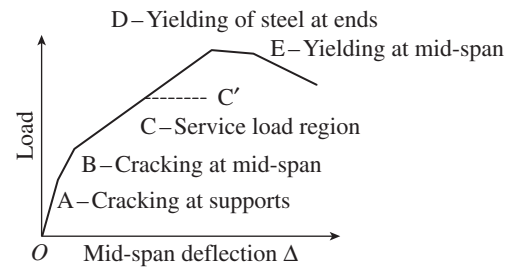
12.3.2 Load-Deflection Behaviour of RC Beam

The load-deflection response of a fixed-ended RC beam is shown in Fig. 12.3(b). As shown in this figure, initially the beam is uncracked and stiff and the load deflection curve is shown as O-A. When the load is increased further, the bending moments at the ends of the beam



(a)

exceed the cracking moment, thus the beam cracks at the ends, leading to a reduction of the moment of inertia at the ends. Due to this, the stiffness of beam decreases, and further deflection is shown as A-B. Further increase in load results in the cracking of the beam at the mid-span as well, which results in the reduction of the moment of inertia at the mid-span and consequent reduction of stiffness (shown as B-D). Eventually, the steel reinforcement will yield at the ends (point D) and subsequently at the mid-span (point E), resulting in large increases in deflection with little change in the load. The service



(b)

FIG. 12.3 Load-Deflection behaviour of fixed-fixed beam (a) Beam and loading (b) Load vs deflection curve

load deflection is shown as point C. The beam is considered elastic at point C, even though increasing the load results in progressive reduction in stiffness and non-linear load deflection behaviour. It has to be noted that due to the creep in concrete, the service load deflection at point C will eventually be increased to point C'.

Tension Stiffening and Effective Moment of Inertia

The tensile capacity of the concrete is usually neglected in strength design calculations, assuming that tensile forces are resisted entirely by the reinforcement at a crack. However, concrete continues to carry tension between the cracks through the transfer of bond forces from the reinforcing bars into the concrete. The concrete contribution between cracks is called *tension stiffening*, and this phenomenon has an effect on member stiffness, deflection, and crack widths under service load conditions (Gilbert and Warner 1978). Although tension stiffening may only have a relatively minor effect on the deflection of heavily reinforced beams, it is found to have very significant effect in lightly reinforced members, like most RC floor slabs, where the ratio I_{gr}/I_{cr} is high (Gilbert 1999, 2007). Tension stiffening may be best understood by considering the axial response of an RC tension member as illustrated in Figs 12.4(a) and 12.5.

The member is initially uncracked and hence the response is governed more by the concrete than the reinforcement. Once cracked, the member response is affected by the stiffness of the reinforcing bar, and there is a gradual transition towards the bare bar response, as more and more cracks develop in the member. Cracking is accompanied by a gradual reduction in the average load carried by the concrete between cracks (\bar{P}_c) as more cracks develop. Once cracking has stabilized, the load carried by the concrete continues to decrease as secondary internal cracks develop between the primary cracks (Goto 1971; Bischoff 2005).

The effects of cracking and reinforcement on member stiffness can be taken into account in a number of different ways, for example, by using the effective member rigidity EA_{eff} in the calculations. The CEB-FIP Model Code (1993)

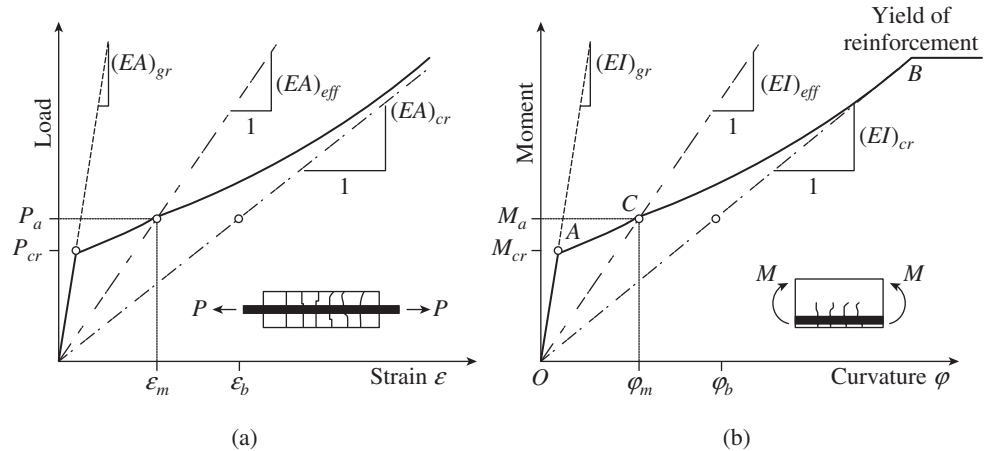


FIG. 12.4 Member deformation (a) Axial member (b) Flexural member

Source: Bischoff 2005, reprinted with permission from ASCE

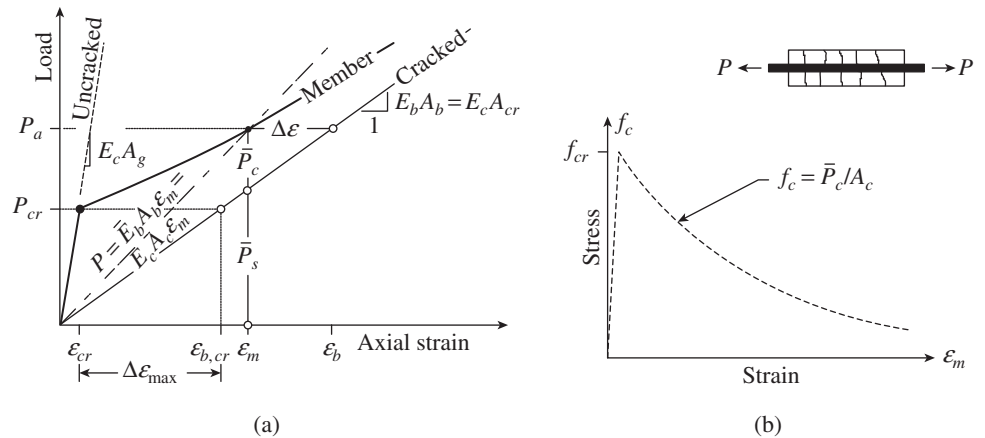


FIG. 12.5 Tensile member response (a) Load vs axial strain curve (b) Stress–Strain curve

Source: Bischoff 2005, reprinted with permission from ASCE

has adopted the tension stiffening strain approach based on the work of Rao (1966). This method ignores the concrete tensile stresses but increases the apparent stiffness of the reinforcement to account for the concrete contribution between cracks.

An alternative approach for modelling the post-cracking member response is to account for the tensile contribution of the concrete between cracks with an average stress–strain response for the cracked concrete (see Fig. 12.5b). This gives a concrete tensile response with a descending branch after cracking and is equivalent to assuming that the concrete has a reduced effective modulus of elasticity, which depends on the level of strain in the member. Expressing the effective member stiffness with a concrete modulus E_c and effective concrete area A_{eff} gives

$$A_{eff} = \frac{A_{cr}}{1 - \eta(P_{cr}/P_a)^2} \quad (12.10)$$

where $\eta = 1 - A_{cr}/A_{gr}$, A_{cr} is the transformed concrete area of the cracked section given by $A_c + (m - 1)A_{st}$, A_{st} is the area of reinforcement, A_{gr} is the gross area of section, A_c is the area

of concrete in the section, P_a is the applied axial load, and P_{cr} is the axial cracking load. Results of such an approach were found to agree well with experimental results (Bischoff 2005).

Similarly, for a concrete beam, the deflection of a beam can be calculated by integrating the curvatures along the length of the beam (Ghali 1993; Ghali, et al. 2011). For an elastic beam, the curvature, $1/r$, equals M/EI , where EI is the flexural stiffness of the beam. Due to the cracking of RC beams, there will be three different values of EI as shown in Fig. 12.4(b). As can be observed in this figure, before cracking, the entire cross section is effective and the corresponding EI can be represented by the radial line OA with a slope $(EI)_{unc}$. Usually, the gross moment of inertia, I_{gr} , is used for representing this zone of behaviour; the uncracked transformed moment of inertia, as described in Section 12.3.1 is seldom used. As the load approaches the point where the steel reinforcements yield, the EI value approaches $(EI)_{cr}$, and is represented by the radial line OB. At service loads, the concrete participates in resisting tensile stresses because of the bond between the reinforcement and concrete (tension stiffening effect). This effect may be taken into account by considering an effective moment of inertia, I_{eff} , which will be somewhere between the moment of inertia of the gross section, I_{gr} , and the moment of inertia of the fully-cracked section, I_{cr} . The value of I_{eff} will depend on the relative magnitudes of the service moment M , cracking moment M_{cr} , and the yield moment M_y .

Branson (1963) derived the following equation to express the transition from I_{gr} to I_{cr} , based on the experimental data of beams and slabs:

$$I_{eff} = \left(\frac{M_{cr}}{M}\right)^a I_{gr} + \left[1 - \left(\frac{M_{cr}}{M}\right)^a\right] I_{cr} \leq I_{gr} \quad (12.11)$$

where I_{cr} is the moment of inertia of the cracked section considering equivalent area of tension and compression reinforcement, I_{gr} is the moment of inertia of the uncracked section neglecting reinforcement, M_{cr} is the cracking moment of the section, and M is the maximum moment under service load. Branson's effective moment of inertia expression (Eq. 12.11) has been adopted by several codes including ACI 318-11. All these codes set the value of exponent a to three to obtain an average moment of inertia for the entire span of a beam. Al-Shaikh and Al-Zaid (1993) proposed that in order to obtain better correlation with experimental results, the value of a should be decreased as the reinforcement ratio (ρ) of a concrete beam increases. Accordingly, they proposed the following equation for a :

$$a = 3 - 0.8\rho \quad (12.12)$$

It has to be noted that the equation for I_{eff} proposed by Branson was developed empirically based on the test results of simply supported rectangular RC beams with reinforcement ratios

between one per cent and two per cent. Branson's expression accurately estimates the moments of inertia of concrete beams with medium to high reinforcement ratios ($\rho > 1\%$).

Bischoff (2005) developed the following effective moment of inertia expression, which is a weighted average of the flexibilities of the uncracked and cracked portions of an RC beam:

$$\frac{1}{I_{eff}} = \left(\frac{M_{cr}}{M}\right)^a \frac{1}{I_{gr}} + \left[1 - \left(\frac{M_{cr}}{M}\right)^a\right] \frac{1}{I_{cr}} \geq \frac{1}{I_{gr}} \quad (12.13a)$$

By rearranging the terms, this equation may be rewritten as

$$I_{eff} = \frac{I_{cr}}{1 - \left(1 - \frac{I_{cr}}{I_{gr}}\right) \left(\frac{M_{cr}}{M}\right)^a} \leq I_{gr} \quad (12.13b)$$

It must be noted that the Branson's approach models the uncracked and cracked portions of a concrete beam as springs in parallel, whereas Bischoff's approach models them as springs in series (see Fig. 12.6). In the springs-in-parallel model, the stiffnesses of the uncracked and cracked portions are averaged, whereas in the springs-in-series model, the flexibilities are averaged. Bischoff (2005) proposed a value of two for the power a in Eq. (12.13), based on the deflection equation given in Eurocode 2.

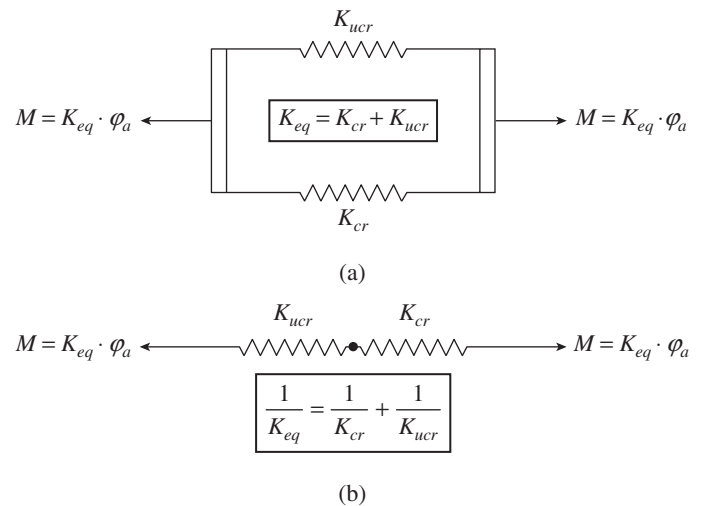


FIG. 12.6 Simple spring models (a) Branson's effective moment of inertia (b) Bischoff's effective moment of inertia

Source: Bischoff and Scanlon 2007, reprinted with permission from ACI

To account for both shrinkage-induced cracking and the reduction in tension stiffening with time, Gilbert (2007) and Gilbert and Kilpatrick (2011) introduced a parameter β in Eq. (12.13b) as described here:

$$I_{eff} = \frac{I_{cr}}{1 - \beta \left(1 - \frac{I_{cr}}{I_{gr}}\right) \left(\frac{M_{cr}}{M}\right)^2} \leq 0.6I_{gr} \quad (12.13c)$$

If no significant shrinkage occurs before first loading, a value of $\beta = 1.0$ can be used. However, in practice, significant shrinkage usually occurs before first loading, and hence the following values have been suggested by Gilbert and Ranzi (2010):

1. $\beta = 0.7$ at early ages (less than 28 days)
2. $\beta = 0.5$ at ages greater than six months and when predicting long-term deflections

The upper limit of $0.6I_{gr}$ is specified by Gilbert (2010, 2011), because the value of I_{eff} is very sensitive to the calculated value of M_{cr} . For lightly loaded members, failure to account for cracking due to unanticipated shrinkage restraint, temperature gradient, or constructed loads can result in significant underestimates of deflection.

Gilbert (2007) and Bischoff and Scanlon (2007) compared the experimental results of beams and slabs with different reinforcement ratios to the analytical deflection estimates obtained from the two approaches (Branson 1963; Bischoff 2005) and showed that the expression proposed by Bischoff (2005) is in closer agreement with the experimental results, particularly for lightly reinforced concrete elements.

The Indian code, IS 456, in Clause C-2.1 gives an expression for I_{eff} , which is an empirical fit to the results of several deflection tests on RC beams, as

$$I_{eff} = \frac{I_{cr}}{1.2 - \frac{M_{cr}}{M} \frac{z}{d} \left(1 - \frac{x}{d}\right) \frac{b_w}{b_f}} \quad \text{with } I_{cr} \leq I_{eff} \leq I_{gr} \quad (12.14a)$$

where d is the effective depth of the section, b_w is the breadth of web, b_f is the breadth of compression flange, z is the lever arm $= d - x/3$, and x is the depth of neutral axis. Other terms have been defined earlier. The similarity in format of Eqs (12.13c) and (12.14a) should be noted. However, Eq. (12.14a) is more difficult to evaluate. Al-Shaikh (1994) proposed the following modification to the formula given in the Indian code to improve its accuracy:

$$I_{eff} = \frac{I_{cr}}{1.02 - 1.37 \frac{M_{cr}}{M} \frac{z}{d} \left(1 - \frac{x}{d}\right) \frac{b_w}{b_f}} \quad \text{with } I_{cr} \leq I_{eff} \leq I_{gr} \quad (12.14b)$$

Another approach to using an effective moment of inertia is to carry out a transformed section analysis using the effective modulus \bar{E}_s of the reinforcement to give an effective modular ratio $\bar{m} = \bar{E}_s/E_c$. This is then used to calculate an effective value for the cracked transformed moment of inertia \bar{I}_{cr} that is equivalent to I_{eff} . This approach was developed by Murashev as early as 1940 (see Murashev, et al. 1971) and a comparison of this approach with that of Bischoff (2005) has shown that both the approaches are similar.

The moment of inertia of an uncracked rectangular section neglecting the reinforcements is given by

$$I_{gr} = bD^3/12 \quad (12.15)$$

where b is the width of the rectangular section and D is its overall depth.

The cracking moment of inertia, neglecting reinforcements, is given by

$$M_{cr} = \frac{I_{gr} f_{cr}}{y_t} \quad (12.16a)$$

where f_{cr} is the modulus of rupture of concrete $= 0.7\sqrt{f_{ck}}$ in N/mm^2 , as per Clause 6.2.2 of IS 456 ($0.55\lambda\sqrt{f_{ck}}$ as per ACI 318), and y_t is the distance of extreme fibre from the centroid of the section; for rectangular section, $y_t = D/2$.

Restraint stresses decrease the cracking moment M_{cr} of the member under applied loads by reducing the effective tensile strength or modulus of rupture of concrete. Hence, Gilbert (1999) proposed the following equation for M_{cr} :

$$M_{cr} = Z(f_{cr} - f_{cs}) \geq 0.0 \quad (12.16b)$$

where Z is the section modulus of the uncracked section and f_{cs} is the maximum shrinkage-induced tensile stress on the uncracked section. At the extreme fibre at which cracking occurs, f_{cs} may be taken as (Gilbert 1999; Scanlon and Bischoff 2008)

$$f_{cs} = \left(\frac{2.5\rho}{1 + 50\rho} \right) E_s \varepsilon_{sh} \quad (12.16c)$$

where ρ is the reinforcement ratio $= A_{st}/(bd)$ and ε_{sh} is the design shrinkage strain. Murashev, et al. (1971) also proposed a similar expression. The design shrinkage strain ε_{sh} should be calculated from the basic shrinkage strain $\varepsilon_{sh,b}$. The Australian code suggests that $\varepsilon_{sh,b}$ should be taken as 850×10^{-6} and provides graphs to find the design shrinkage strain ε_{sh} for various environments. Typical shrinkage strains are given in Table 12.4.

TABLE 12.4 Typical shrinkage strains after 30 years in various environments for normal concrete as per AS 3100-2009

Condition of Environment	Final Design Shrinkage Strain ε_{sh} , 10^{-6} for Hypothetical Thickness, t_h , mm			
	50	100	200	400
Arid	1100	940	730	500
Interior	1000	860	670	450
Temperate-inland	900	760	590	410
Tropical and near coastal	650	570	440	300

Shrinkage restraint effects on cracking are being recognized by building codes. The Australian code AS 3600-2001 initially adopted Eq. (12.16c) with a 1.5 factor in the numerator instead of 2.5, but switched over to the 2.5 factor in the 2009 version. The Canadian code A 23.3 in 1994 adopted a 50 per cent

reduction in cracking moment for two-way slabs, whereas ACI 318 in 2008 stipulated a lower cracking moment (two-thirds of the code-specified value) for evaluating deflections of slender tilt-up walls. Scanlon and Bischoff (2008) provide the derivation of Eq. (12.16c) and a comparison of different proposals.

Nayak and Menon (2004) compared the codal provisions on deflections and found considerable disparities in the prediction of the cracking moment, moment–curvature and load–deflection behaviour. Based on the experimental studies on six one-way slab specimens, they found that the Eurocode 2 method of calculating the cracking moment is in good agreement with the test results, whereas ACI 318 method of calculating deflections correlates well with the load–deflection behaviour of the experimental results, albeit with a higher slope. Based on the experimental results, they proposed an improved procedure, based on the Eurocode 2 cracking moment formula combined with a modified ACI 318 code formula.

12.3.3 Other Factors that Influence Deflection

The other factors that are used in the deflection equation are the length L , Young's modulus of concrete, E_c , and the value of sustained load.

It is advisable to use the effective span length, L , when calculating deflections (see Clause 22.2 of IS 456), instead of the clear span L_n (Wight and MacGregor 2009). To obtain the flexural rigidity EI of the section, the secant modulus of concrete E_c may be taken as $5000\sqrt{f_{ck}}$ for normal weight concrete as per Clause 6.2.3.1 of IS 456. ACI 318 provides an equation using which we may consider the lightweight concrete as well. A different formula is proposed for high-strength concrete (HSC) by the ACI Committee 363-1984. Recently Noguchi, et al. (2009) performed a statistical analysis on more than 3000 test results and proposed a universal formula for E_c (see Section 1.8.6 of Chapter 1 for more details). When very high-strength concrete with strength 140 MPa or higher is used or when deformation is critical, it may be advisable to determine the stress–strain relationship from actual cube compression test results and deduce the value of secant modulus E_c .

Sustained Loads

While determining creep deformations, the term 'sustained or permanent loads' is often used. It is necessary to assess how much of the load is permanent and how much is transitory. Two quantities pertaining to *sustained load* are important—the first is the *magnitude* and the second is the *duration*. The determination of these two quantities is often left to the designer.

Some designers consider only the dead load as the sustained load. However, usually a portion of the live load will also be sustained. The proportion of the live load that should be

considered as permanent will, however, depend on the type of structure. For example, in an office building, the desks, bookshelves, file cabinets, equipment, and so on are all part of the live load and are sustained over a long period. However, a part of the live load, such as people coming in and out of the space and temporary office equipment, is not sustained for a long time.

Other occupancies may have different estimates of sustained loading. There are no guidelines for determining the magnitudes or durations for any given design situation. These are left to the judgment of the designer. BS 8110—Part 2 (1985) suggests that for normal domestic or office occupancy, 25 per cent of the live load should be considered as permanent, and for structures used for storage, at least 75 per cent should be considered permanent when the upper limit to the deflection is being assessed. As an approximation, we may assume 50–60 per cent of the live loads as permanent loads. The Australian code (AS 3600-2009) suggests that for deflection calculations, the characteristic live load can be multiplied by 0.6 for offices (1.0 for storage) for immediate deflections and 0.25 for long-term deflections (0.5–0.8 for storage). See Table 12.5.

TABLE 12.5 Live load factors to calculate permanent loads (AS 3600-2009)

Item	Long-term Factor	Short-term Factor
Residential floor	0.3	0.7
Office floor	0.2	0.5
Floor—retail	0.25	0.6
Roof with access	0.2	0.7
Floor—storage	0.5–0.8	1.0

12.3.4 Deflection of Continuous Beams

The deflection calculated using the expression for I_{eff} given in Eq. (12.13) or (12.14) is valid for simply supported beams. When restraints are present at the ends of a beam element, such as interior supports in continuous beams and *encastre* ends in fixed beams, deflection will be considerably less. Moreover, for continuous beams, the I_{eff} value may be different in the negative and positive moment regions. The use of mid-span section properties for continuous prismatic members is considered satisfactory in approximate calculations primarily because the mid-span rigidity including the effect of cracking has the dominant effect on deflections (ACI 435R-95).

Clause 9.5.2.4 of ACI 318 suggests the use of average I_{eff} values, obtained from Eq. (12.11) for the critical positive and negative moment sections. ACI Committee 435R-95 suggests using the following weighted average formulas:

For beams continuous on both ends,

$$\text{Average } I_{eff} = 0.70I_{em} + 0.15(I_{e1} + I_{e2}) \quad (12.17a)$$

For beams continuous on one end alone,

$$\text{Average } I_{eff} = 0.85I_{em} + 0.15(I_{e1}) \quad (12.17b)$$

where I_{em} , I_{e1} , and I_{e2} are the values of I_{eff} at mid-span and the two ends of the beam, respectively.

The weighted average expression given in Clause C-2.1 of IS 456 for continuous beams is a bit complicated and is based on the methods of Beeby (1968) and Beeby and Miles (1969). It has a format similar to Eq. (12.14a) and is given by

$$I_{eff,ave} = \frac{I_{cr,ave}}{1.2 - \frac{M_{cr,ave}}{M} z \left(1 - \frac{x}{d}\right) \frac{b_w}{b_f}} \quad \text{with } I_{cr,ave} \leq I_{eff,ave} \leq I_{gr,ave} \quad (12.18)$$

where $I_{cr,ave}$, $I_{gr,ave}$, and $M_{cr,ave}$ are computed as weighted average using the following equation suggested by Beeby and Miles (1969):

$$X_{ave} = k_1 \left(\frac{X_1 + X_2}{2} \right) + (1 - k_1)X_m \quad (12.19)$$

Here, subscripts 1 and 2 denote the two continuous support locations, X_{ave} is the modified value of X , X is the value of I_{gr} , I_{cr} , and M_{cr} as appropriate, X_1 and X_2 are the values of X at support, X_m is the value of X at mid-span, and k_1 is the coefficient given in Table 12.6.

TABLE 12.6 Values of coefficient k_1

$k_2 = \frac{M_1 + M_2}{M_{f1} + M_{f2}}$	≤ 0.5	0.6	0.7	0.8	0.9	1.0	1.1	1.2	1.3	1.4
k_1	0	0.03	0.08	0.16	0.30	0.50	0.73	0.91	0.97	1.0

Note: M_1 and M_2 are support moments and M_{f1} and M_{f2} are fixed-end moments.

Let us check the applicability of the formula given in Table 12.6 for standard cases. For simply supported beam, $M_1 = M_2 = 0$ and hence $k_2 = 0$. Thus, from Table 12.6, we get $k_1 = 0$, $M_{ave} = M_m$, and $I_{ave} = I_m$. For fixed-ended beam, $M_1 = M_2 = WL/12$, $M_{f1} = M_{f2} = WL/12$, and hence $k_2 = 1.0$. Thus, from Table 12.6, we get $k_1 = 0.5$. Using Eq. (12.19), we get

$$M_{ave} = \left(\frac{M_1 + M_2}{4} \right) + \frac{M_m}{2}$$

$$I_{ave} = \left(\frac{I_1 + I_2}{4} \right) + \frac{I_m}{2}$$

It may be seen that the weighted average obtained from IS code includes the ACI 318 code recommendation as a special case.

12.3.5 Design Aids

Charts and tables are provided by SP 16:1980 for calculating I_{gr} and also I_{eff} based on Eq. (12.14a). Chart 88 can be used

to calculate the I_{gr} value of T-beams, based on the b_f/b_w ratio. Chart 89 of SP 16 can be used for finding the value of I_{eff}/I_{cr} . Using the values of M_{cr}/M , x/d and b_f/b_w , we can directly read the value of I_{eff}/I_{cr} from Chart 89. This chart takes into account the condition $I_{eff}/I_{cr} \geq 1$. After finding the value of I_{eff} , it has to be compared with I_{gr} , and the lesser of the two values should be used for calculating the deflection. Table 86 can be used to calculate the values of moment of inertia, I_{gr} , based on the breadth and effective depth of section. The moment of inertia of cracked section, I_{cr} , can be calculated for different d'/d ratios (0.05, 0.10, 0.15, and 0.20) using Tables 87–90 of SP 16. Similarly, the depth of the neutral axis values of x/d by elastic theory can be calculated for different d'/d ratios (0.05, 0.10, 0.15, and 0.20) using Tables 91–94 of SP 16. While using Tables 87–90, the required values are read from the tables based on the values of p, m and $p_c(m-1)/(p, m)$, where $p_t = 100A_{st}/(bd)$, $p_c = 100A_{sc}/(bd)$, and m is the modular ratio $= E_s/E_c$.

Das (2004) presented a direct design method for singly reinforced rectangular concrete slabs, which simultaneously satisfies the condition of bending and serviceability. Design charts were also provided allowing practical application of this method to enable the design engineer to adjust the steel reinforcement and depth. Design charts were also provided to find the effective depth when the area of steel to resist the bending is just adequate for deflection criteria.

12.4 LONG-TERM DEFLECTIONS

Shrinkage, temperature, and creep due to sustained loads cause additional long-term deflections over and above those of instantaneous deflection. For convenience of computation, the code suggests to consider the total deflection occurring over a period of time as consisting of the following three parts:

1. The instantaneous or short-term deflection under permanent loads
2. The creep deflection due to permanent loads
3. The short-term deflection under the total load

12.4.1 Deflection due to Creep

The deflection caused by permanent loads goes on increasing with time due to creep, as shown in Fig. 12.7. As discussed in Section 1.8.9 of Chapter 1, *creep* is the tendency to deform inelastically with time under sustained loads. It is considered at stresses within the accepted elastic range (say, below $0.5\sqrt{f_{ck}}$). It occurs in addition to the stress-induced elastic deformation and also stress-independent shrinkage strains and thermal movement. Creep occurs under both compressive and tensile stresses (Neville, et al. 1983). Creep is more severe in materials that are subjected to heat for long periods and near melting point. It always increases with temperature. It has to be noted that steel will creep only above 700°F.

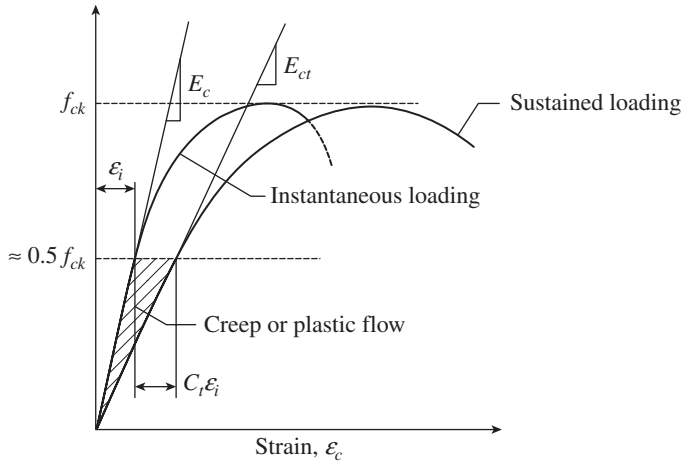


FIG. 12.7 Typical stress–strain curves for instantaneous and long-time loading

The deformation in concrete elements due to creep and shrinkage are considered as ‘time-dependent’ deformation (Ghali, et al. 2002). The rate of this creep deformation is a complex function of concrete constituents, concrete mixture proportions, curing temperature and humidity, size of the concrete member, age and duration of loading, quantity of compression reinforcement, and magnitude of the sustained load (ACI Committee 209R-92; Branson 1977; Neville, et al. 1983). Rangan (1982) and Desayi, et al. (1989) also studied the influence of the ratio of sustained load to total load on the creep deflections. The inelastic deformation increases at a decreasing rate during the time of loading. Moderate creep in concrete is sometimes welcomed, because it relieves tensile stresses induced by shrinkage, temperature changes, or movement of supports that might otherwise lead to cracking. However, the relief offered by creep decreases with age.

As seen in Fig. 12.7, the result of creep is to increase strain with constant stress; we may account for it by using the modified modulus of elasticity E_{ct} (see Fig. 12.7). An alternative procedure of applying a multiplier C_t to the elastic deflection Δ_i is adopted in many codes.

To study the effect of creep deformation, let us consider a singly reinforced beam as shown in Fig. 12.8. Due to permanent loads and creep, the compressive strain in concrete increases with time, resulting in an increase in curvature, as shown in Fig. 12.8(b). The distribution of creep strain across the depth at any cross section of a flexural member is non-uniform, with a linear variation similar to that produced by the applied loads

(see Fig. 12.8b). It is to be noted that the strain at tension steel is unchanged, because concrete contributes little in taking tension and steel reinforcement exhibits little creep. This linear variation of creep strains results in a *creep curvature*, ϕ_{cp} , over and above the *initial elastic curvature*, ϕ_i , due to the applied loads.

There is a slight increase in the depth of neutral axis, with a corresponding reduction in the internal lever arm. To maintain static equilibrium with the applied moment at the section, there has to be a slight increase in the steel stress and a corresponding increase in the strain (which is not shown in Fig. 12.8).

At service loads, the creep curvature, ϕ_{cp} , may be assumed to be proportional to the *initial elastic curvature*, ϕ_i . Hence, from Fig. 12.8(b), we may derive

$$\frac{\phi_{cp}}{\phi_i} = \frac{\epsilon_{cp}/x_{cp}}{\epsilon_i/x_i} = k_r C_t \tag{12.20}$$

where C_t is called the creep coefficient = ϵ_{cp}/ϵ_i and k_r is the ratio of the initial neutral axis depth (x_i) to the neutral axis depth due to creep (x_{cp}). Since $x_i < x_{cp}$, the value of k_r is always less than unity. The ACI Committee 209 has recommended the following hyperbolic-type equation suggested by Branson (1977) for the creep coefficient:

$$C_t = \left(\frac{t^{0.60}}{10 + t^{0.60}} \right) C_u \tag{12.21}$$

where C_t is the creep coefficient at any time t after a basic curing period, t is the time in days after loading, and C_u is the ultimate creep coefficient, with a recommended value of 2.35 for 40 per cent humidity. The ultimate creep coefficient is dependent on six factors: (a) relative humidity, (b) age of concrete at load application, (c) minimum member dimension, (d) concrete consistency, (e) fine aggregate content, and (f) air content

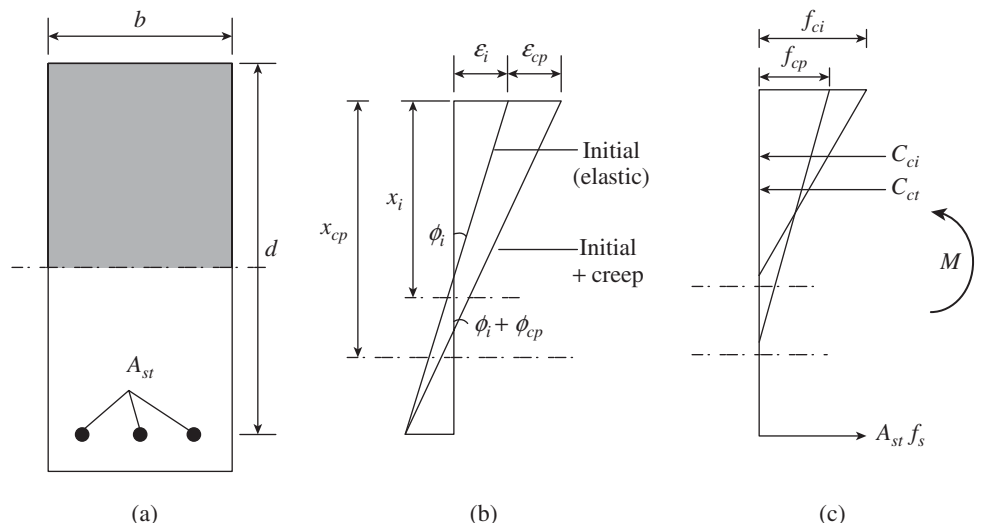


FIG. 12.8 Strain and stress distribution in an RC beam subjected to creep (a) Cross section (b) Strains (c) Stresses

(Fanella and Rabbat 2002). Equation 12.21 is applicable to the standard condition of 40 per cent ambient relative humidity, loading age of seven days, average thickness of member of 150 mm, slump of 100 mm or less, 50 per cent fine aggregate, six per cent air content, and moist-cured concrete or three days of steam-cured concrete. For other conditions, some correction factor has to be applied as per ACI 209 R-92. The Australian code provides more detailed provisions and suggests the basic creep coefficient (creep factor in AS 3600 terminology) as per Table 12.7.

TABLE 12.7 Basic creep factor as per AS 3600-2009

Characteristic strength f_{ck} , MPa	18	20	25.6	32	≥ 40
Basic creep factor	5.2	4.2	3.4	2.5	2.0

The basic creep factor given in Table 12.7 should be modified based on the charts given in AS 3600; typical design creep factors are as per Table 12.8.

TABLE 12.8 Typical design creep factor after 30 years in various environments as per AS 3600-2009 for a basic factor of 2.5

Condition of Environment	Age of Concrete at Loading Days	Design Creep Factor for Hypothetical Thickness t_h , mm			
		50	100	200	400
Arid	0 to 7	3.9	3.3	2.7	2.3
	8 to 28	3.0	2.5	2.1	1.8
	>28	2.7	2.3	1.9	1.6
Interior	0 to 7	3.5	3.1	2.5	2.1
	8 to 28	2.7	2.3	1.9	1.6
	>28	2.5	2.1	1.7	1.5
Temperate-inland	0 to 7	3.2	2.8	2.3	1.9
	8 to 28	2.5	2.1	1.8	1.5
	>28	2.2	1.9	1.6	1.3
Tropical and near-coastal	0 to 7	2.7	2.3	1.9	1.6
	8 to 28	2.1	1.8	1.5	1.3
	>28	1.9	1.6	1.4	1.1

Compression Steel Effect on Creep

The presence of compression steel decreases the deformation due to creep as well as shrinkage. The effect of compression steel on deformations was studied by Yu and Winter (1960), Branson (1977), Desayi, et al. (1989) on the basis of which the following value of k_r was recommended:

$$k_r = \frac{0.85}{1 + 0.5p_c} \quad (12.22)$$

where p_c is the percentage of compression steel reinforcement = $100A_{sc}/(bd)$.

Codal Equations for Creep Deflection

Clause 9.5.2.5 of ACI 318 suggests that the additional long-term deflection resulting from creep and shrinkage of flexural members (normal weight or lightweight concrete) should be determined by multiplying the immediate deflection by the factor, λ_Δ . Thus, the total instantaneous and sustained load deflection is $(1 + \lambda_\Delta)\Delta_i$, where λ_Δ is given by the following expression (Branson 1971):

$$\lambda_\Delta = \frac{\xi}{1 + 0.5p_c} \quad (12.23a)$$

Here, the value of p_c should be considered at the mid-span for simple and continuous spans and at the support for cantilevers. The value of time-dependent factor for sustained loads, ξ , is taken as given in Table 12.9 and Fig. 12.9. While using the ACI code formula, it has to be noted that the long-term deflection is strongly affected by the predicted instantaneous deflection; long-term deflection is expressed as a multiple of instantaneous deflection. Paulson, et al. (1991) found that the creep coefficient for HSC may be about 50 per cent of the value for normal strength concrete and that the influence of compression steel in reducing creep deflections is less pronounced. Hence, based on their experimental long-term studies, they suggested the following equation, which is a modified version of Eq. (12.23a):

$$\lambda_\Delta = \frac{\mu\xi}{1 + 0.5\mu p_c} \quad (12.23b)$$

where $\mu = 1.4 - f_{ck}/87.5$ with $0.4 \leq \mu \leq 1.0$.

TABLE 12.9 Value of ξ as per ACI 318

Duration of Loading	Value of ξ
5 years or more	2.0
12 months	1.4
6 months	1.2
3 months	1.0

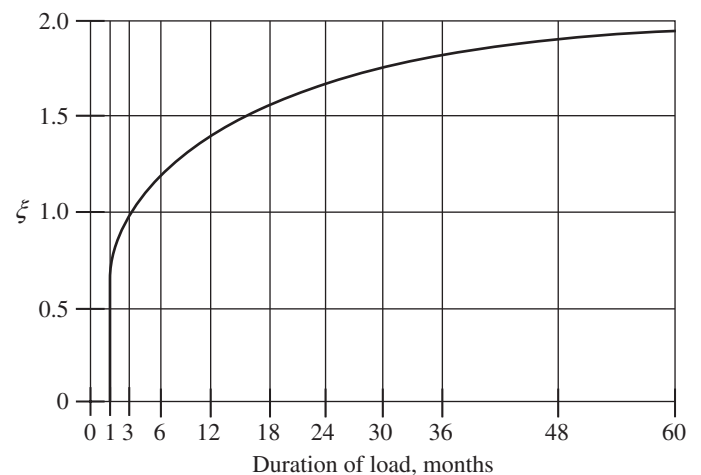


FIG. 12.9 Multiplier for long-term deflection as per ACI-318 (Reprinted with permission from ACI)

Maghsoudi and Akbarzadeh (2007), based on their tests, also concluded that the serviceability and post-serviceability performance of RC structures can be improved using HSC.

The Indian code, IS 456, uses the *sustained modulus method* for calculating the creep deflection (Bazant 1972). In this case, a reduced or *effective modulus of elasticity*, E_{ct} , is used for computing initial plus creep deflections:

$$E_{ct} = \frac{f}{\varepsilon_i + \varepsilon_{cp}} = \frac{f}{\varepsilon_i + C_t \varepsilon_i} = \frac{E_c}{1 + C_t} \quad (12.24)$$

where f is the stress in concrete, ε_i is the elastic strain, and ε_{cp} is the creep strain. The value of creep coefficient, C_t (θ in IS code nomenclature), is given in Clause 6.2.5.1 and is provided in Table 12.10.

Clause C-4 of IS 456 suggests that the creep deflection due to permanent loads may be obtained from the following equation:

$$\Delta_{cp} = \Delta_{i, cp} - \Delta_{ip} \quad (12.25)$$

where Δ_{cp} is the additional deflection due to creep, Δ_{ip} is the maximum initial (short-term) elastic deflection due to permanent loads using E_c and I_{eff} , and $\Delta_{i, cp}$ is the total deflection including creep due to permanent loads calculated using an elastic analysis with E_{ct} and the corresponding I_{eff} . It has to be noted that the increased modular ratio $m' = E_s/E_{ce}$ is generally quite high, and hence, the moment of inertia of the corresponding cracked transformed section will also be high, but it has to be limited to I_{gr} . In case the calculated I_{cr} is less than I_{gr} , then I_{eff} has to be calculated using Eq. (12.14) and considering the moment due to dead load plus permanent live load.

TABLE 12.10 Value of creep coefficient as per IS 456

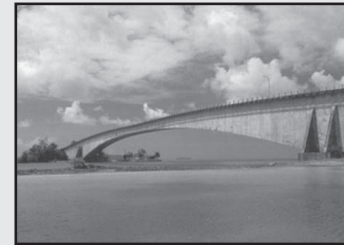
Age of Loading	Creep Coefficient
7 days	2.2
28 days	1.6
1 year	1.1

CASE STUDY

Collapse of Koror–Babeldaob Bridge, Republic of Palau, Micronesia

The Koror–Babeldaob Bridge was completed in 1977, to connect the two main islands of Koror and Babeldaob in the Republic of Palau. It is an RC, balanced cantilever prestressed concrete box girder bridge with a total length of 385.6m. The main span had a length of 241 m and once set the world record for the longest span in post-tensioned concrete box girder bridges. Its two-lane single-cell box girder superstructure was built using cast-in-place segments and a permanent mid-span hinge. After 18 years, the deflection in the main span was found to be excessive (the total deflection was 1.61 m compared to the calculated final sag of 0.46 m to 0.58 m, measured from the design camber of -0.3 m), and the prestress loss was measured as 50 per cent. Two independent studies were carried out by Louis Berger International and the Japan International Cooperation Agency. They concluded that the bridge was safe, and the large deflections were due to a creep and the lower value of modulus of elasticity of the concrete than those adopted in design.

It was decided to install additional prestressing and eliminate the hinge at the mid-span. The retrofit began on 17 October 1995, with the removal of the concrete overlay. However, the bridge collapsed suddenly on 26 September 1996, three months after the reopening, with two fatalities. At the time of collapse, there was negligible traffic load and no apparent external trigger. The construction of a new cable-stayed bridge began in 1997 by a Japanese construction company (Kajima Corporation) and completed in December 2001. The main span of the new bridge is still a prestressed concrete box girder, but is only 7 m deep at the main pier and 3.5 m deep at the centre; it is now supported by stay cables. The new bridge was opened on 11 January 2002 and named Japan–Palau Friendship Bridge (Burgoyne and Scantlebury 2006).



Koror–Babeldaob bridge—Before and after collapse

(Source: Bazant, et al. 2010, reprinted with permission from *Concrete International*, ACI)

It was not until 2008 that the technical data necessary for the complete analysis, to find the reasons for the collapse of the Koror–Babeldaob bridge, was released. Bazant, et al. (2010 and 2011) described the following as the main lessons from this failure: (a) The use of a realistic creep and shrinkage model is important (existing models for creep and shrinkage prediction grossly underestimate the deflections and prestress loss). (b) Three-dimensional finite element analysis is required. (c) The differences in drying rates among slabs of different thicknesses and exposures must be taken into account. They also showed that the Model B3, as per 1995 RILEM recommendation, when modified, could be used to estimate the long-time deflections reliably.

12.4.2 Deflection due to Differential Shrinkage

Shrinkage of concrete is the volume decrease in concrete caused by drying and chemical changes. It is the time-dependent strain measured in an unloaded and unrestrained specimen at constant temperature (Gilbert 2001). There are three types of shrinkage: *plastic*, *chemical*, and *drying*. Concrete shrinkage strain is considered as the sum of drying and chemical shrinkage (Gilbert 2001). Drying shrinkage in HSC is smaller than in normal concrete due to the smaller water–cement ratio used. However, the *endogenous shrinkage* is significantly higher (Gilbert 2001).

Shrinkage of concrete in beams may have a similar effect on the deflection as creep. Shrinkage of an isolated plain concrete member will shorten it without causing any curvature. However, when steel reinforcements are provided, the bond between the concrete and steel will restrain the shrinkage. Restraint to shrinkage is probably the most common cause of cracking in concrete structures. When reinforcement is placed symmetrically in the cross section, shrinkage does not produce any curvature in the member—except in statically indeterminate frames, where it may produce overall change in geometry of the whole frame, which may be similar to the effect of temperature in these frames (see Fig. 12.10).

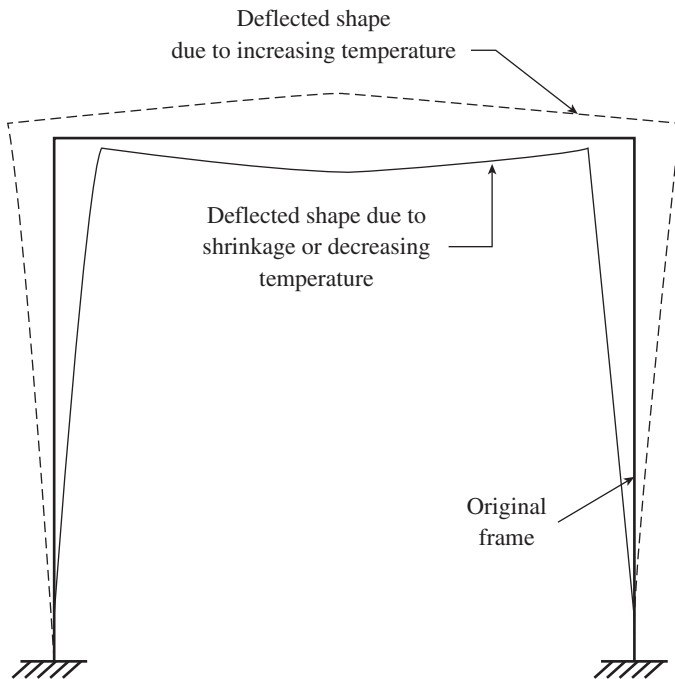


FIG. 12.10 Deflections in statically indeterminate frames due to temperature or shrinkage

In a singly reinforced beam or beams with asymmetric reinforcement, there will be considerable curvature due to restrained shrinkage at the heavily reinforced face and unrestrained effect at the lightly reinforced face. Such a differential shrinkage in a simply supported beam (with tension reinforcement at the bottom) and a cantilever beam (with main

tension bars at the top and compression bars at the bottom) is shown in Fig. 12.11. It has to be noted that the curvature ϕ_{sh} due to differential shrinkage is in the same direction as that due to flexure under loading. Thus, the deflection due to shrinkage increases the deflection of the beam.

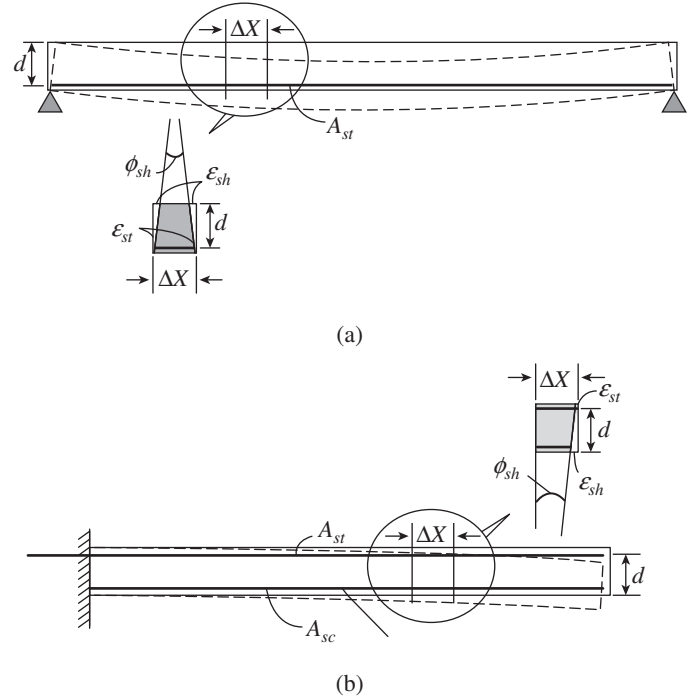


FIG. 12.11 Curvature due to differential shrinkage (a) Simply supported beam (b) Cantilever beam

The shrinkage curvature ϕ_{sh} , as shown in Fig. 12.11, may be expressed in terms of the shrinkage strains ϵ_{sh} (at the extreme concrete compression face) and ϵ_{st} (at the level of tension steel) as

$$\phi_{sh} = \frac{\epsilon_{sh} - \epsilon_{st}}{d} \quad (12.26)$$

where d is the effective depth of beam. This equation may be expressed in the form

$$\phi_{sh} = \frac{\epsilon_{sh}}{d} \left(1 - \frac{\epsilon_{st}}{\epsilon_{sh}} \right) \quad \text{or} \quad \phi_{sh} = \frac{\epsilon_{sh}}{D} k_4 \quad (12.26a)$$

$$\text{where } k_4 = \frac{1 - \epsilon_{st}/\epsilon_{sh}}{d/D}$$

The relationship between the shrinkage deflection, Δ_{cs} , and the curvature, ϕ_{sh} , can be established by using a structural analysis method such as the *conjugate beam method* or *moment area method*. Thus, Clause C-3 of IS 456 gives the following expression for computing the shrinkage deflection:

$$\Delta_{cs} = k_3 \phi_{sh} L^2 \quad (12.27)$$

where k_3 is a constant depending on the support condition (see Table 12.11), ϕ_{sh} is the shrinkage curvature = $k_4 \epsilon_{sh}/D$, L is the

length of span, D is the total depth of the section, and ϵ_{sh} is the ultimate shrinkage strain in concrete. (Clause 6.2.4.1 of IS 456 suggests that in the absence of any test data, the approximate value of the total shrinkage strain for design may be taken as 0.0003 mm/mm. ACI Committee 435 has suggested the use of $\epsilon_{sh} = 0.0004$ mm/mm, though values as high as 0.0010 mm/mm have been reported for concretes with high water content and hot and low-humidity conditions. See also Table 12.4 for provisions in AS 3600.). The constant k_4 is given by the following equation:

$$k_4 = 0.72 \times \frac{p_t - p_c}{\sqrt{p_t}} \leq 1.0 \quad \text{for } 0.25 \leq (p_t - p_c) < 1.0 \quad (12.28a)$$

$$k_4 = 0.65 \times \frac{p_t - p_c}{\sqrt{p_t}} \leq 1.0 \quad \text{for } (p_t - p_c) \geq 1.0 \quad (12.28b)$$

where $p_t = 100A_{st}/(bd)$ and $p_c = 100A_{sc}/(bd)$.

TABLE 12.11 Coefficient k_3 for shrinkage

Support Condition	Coefficient k_3
Cantilever	1/2 = 0.50
Simply supported beam	1/8 = 0.125
Continuous at one end alone (propped cantilever)	11/128 = 0.086
Continuous at both ends (fixed beams)	1/16 = 0.063

Equations (12.28a and b) suggested by IS 456 are based on experimental fit with test data (SP 24-1983). It has to be noted that when $p_t = p_c$, the beam is symmetrically reinforced, and Eq. (12.28) yields $k_4 = 0$ and hence $\phi_{sh} = 0$. It should be pointed out the empirical method given in the code avoids the complications of computing E and I for shrinkage curvature but is found to be fairly accurate for practical purposes. It is also interesting that the ACI code does not give any separate equation for computing shrinkage deflection. A single multiplier as given in Eq. (12.23) is used for predicting the additional long-term deflection resulting from creep and shrinkage.

The procedure for calculating Δ_{cp} may be summarized in the following points (SP 24-1983):

1. Compute the short-term deflection, $\Delta_{i(D+L)}$, due to characteristic dead plus live loads using the short-term modulus E_c .
2. Compute the short-term deflection, Δ_i , due to the permanent load alone, considering E_c .
3. Compute the initial plus creep deflection, $\Delta_{i,cp}$, for the permanent load using the effective modulus E_{cr} .
4. Compute the creep deflection under permanent load as $\Delta_{cp} = \Delta_{i,cp} - \Delta_i$.
5. Compute the deflection due to shrinkage Δ_{cs} .
6. The total deflection, which includes the effect of creep and shrinkage, is computed as the sum of steps 1, 4, and 5.

Gilbert and Kilpatrick (2011), Gilbert and Ranzi (2010), and Gilbert (2011) have presented a detailed creep and shrinkage modification factors, using which the time-dependent deflections could be estimated more precisely. More details about the time-dependent deflection due to creep and shrinkage may also be found in the report of the ACI Committee 435-1995 and the works of Branson (1977); Gilbert (1988), Samra (1997); Gilbert (2001); and Ghali, et al. (2011). Mazzotti and Savoia (2009), based on their experimental work, found that creep and shrinkage deflection of self-compacting concrete beams are higher than in normal concrete beams.

12.4.3 Deflection due to Temperature

As mentioned in Section 12.4.2, significant deformations and curvatures may result in statically indeterminate frames due to seasonal changes in temperature (see Fig. 12.10). The bending moments due to temperature loading may be determined using standard software packages such as ANSYS and abacus. An appropriate value of the coefficient of thermal expansion for concrete should be used in the analysis. See Section 3.9.2 of Chapter 3 for guidance. Once the bending moments are determined using software, the deflections in the various beam members may be determined using Eq. (12.6) and the procedure used for the determination of short-term deflection in continuous beams (refer to Section 12.3.4). The same procedure is applicable to the calculation of deflections induced by overall shrinkage in statically indeterminate frames.

In addition to overall curvatures in the whole structure, local deflections may also be introduced in beams and slabs because of asymmetric reinforcement. Such deflections can be calculated using the procedure described in Section 12.4.2 for differential shrinkage. More information on thermal and shrinkage effects is provided in Section 3.9.2 of Chapter 3.

Deflections due to temperature effects are rarely computed in normal design situations (unless the structure is subjected to large fluctuations of temperatures or to heat such as those experienced in chimneys and cooling towers)—it is because such deflections are not usually significant and are reversible. However, the tensile stresses (and consequent cracks) induced by restraints against temperature changes can be significant—they are usually taken care of by proper detailing of reinforcement, as explained in Section 3.9.2 of Chapter 3. It has to be noted that the shrinkage and temperature reinforcement required for fully restrained slabs could be double the amount specified by the codes. ACI 224R-01 states that the minimum reinforcement percentage specified in ACI 318 (between 0.18% and 0.20%) does not normally control cracks to within generally accepted design limits; to control cracks to a more acceptable level, the percentage requirement is of the order of 0.60 per cent.

12.5 DEFLECTION OF TWO-WAY SLABS

Excessive deflections of two-way slabs present a serious serviceability problem not easily remedied, particularly after the installation of non-structural elements and mechanical services. Hence, it is better to provide thicker slabs than thinner slabs. The deflection of two-way slabs has been a subject of extensive research in several countries (Rangan 1976; Kripanarayanan and Branson 1976; Branson 1977; Sbarounis 1984; Scanlon and Murray 1982). Some of the important variables that affect the two-way slab deflection are (a) the ratio of the spans (L_x/L_y), (b) the deformation of the supporting beams, (c) the extent and distribution of cracking, (d) creep and shrinkage of concrete, (e) the ratio of live load to sustained load, and (f) the stiffening effects of drop panels and column capitals in the case of flat slabs. The large number of variables defies a simple solution to the deflection of two-way slabs.

Although it is possible to compute deflections using theory of plates, for slabs with simple boundary conditions, or by using the finite element method, the extent of cracking affects the stiffness and hence accurate predictions of deflections are not possible (Adan, et al. 2010).

Approximate methods of computing deflections in slabs have been introduced wherein the real structure is divided into column and beam strips, and using an equivalent EI_{eff} , the deflections of these strips are computed to yield the final deflections. Figure 12.12 shows a rectangular panel in a column-supported two-way slab system. In this figure, it is assumed that the edges parallel to L_y do not deflect. The dotted areas represent a set of crossing beams for which the column strip deflection, Δ_{cx} , and the middle strip deflection, Δ_{mx} , can be obtained for x -direction bending. Similarly, by assuming that the edges parallel to L_x do not deflect, we will have another set of deflections Δ_{my} and Δ_{cy} for y -direction bending.

The deflection Δ_{mp} at mid-panel of a two-way slab can be considered as the sum of the column-strip deflection Δ_{cx} and the perpendicular middle-strip deflection Δ_{my} (Nilson and Walters 1975).

$$\Delta_{mp} = \Delta_{cx} + \Delta_{my} = \Delta_{cy} + \Delta_{mx} \quad (12.29)$$

Both column and middle strips can be treated as continuous beams for which the end moments and mid-span moments are M_1 , M_2 , and M_m , respectively. These moments would have been calculated at factored load levels (using direct design method or equivalent frame method, explained in Chapter 11) for proportioning flexural reinforcement. To calculate the deflections, these moments have to be scaled down at the working load level. The column- and middle-strip deflections can then be calculated using the following equation:

$$\Delta = K \frac{5}{48} \frac{ML_n^2}{E_c I_{eff}} \quad (12.30)$$

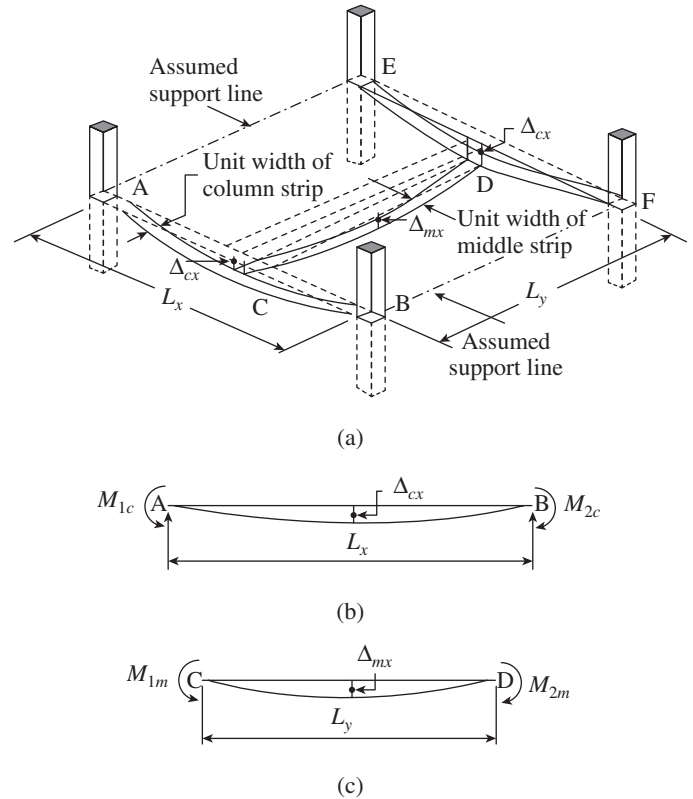


FIG. 12.12 Slab deflection using crossing beam approach (a) Rectangular panel in a column supported two-way slab (b) Deflection of column strip (c) Deflection of middle strip

where K is a coefficient as defined in Table 12.2. However, in determining the coefficient K , the total static moment M_o should be calculated on the basis of the end moment and mid-span moment, rather than the uniformly distributed load w . Hence, M_o and K should be determined by using

$$M_o = M_m + 0.5(M_1 + M_2) \quad (12.31)$$

$$K = 1.20 - 0.2M_o/M_m \quad (12.32)$$

For irregular panels or non-uniform loading, finite element method should be used to determine the deflections. However, any such analysis that does not include the effect of cracked stiffness will considerably underestimate the deflections.

Worked out examples using the given procedure may be found in the works of Scanlon and Gardner (2006), ACI 435R-1995, and Nawy (2005).

Gilbert and Guo (2005) conducted long-term testing (750 days) of large scale RC flat slabs and found that the actual long-term deflection is not accounted adequately in the current codes. There are relatively few reports in the literature that provide comparison between measured and predicted deflections in flat plates in multi-storey buildings (Sbarounis 1984 and Hossain, et al. 2011). Hossain, et al. (2011) measured the long-term deflections in the seven-storeyed concrete building in Cardington, UK, and also studied the influence of construction

loading on deflections in flat-plate slabs. It was shown that slabs constructed using adjustable vertical supports called *props* in multi-storey structures are subjected to loads that exceed the total design service load. Application of these loads often occurs before the slab has reached the specified design strength. The combination of early-age loading and reduced concrete material properties leads to increased cracking and loss of slab stiffness. As a result, immediate as well as long-term deflections will increase and precise calculation of deflection is impossible. Hence, Hossain, et al. suggest setting upper and lower bounds to likely deflections. They found the deflection multiplier approach of ACI 318 code more attractive in such a situation and found it to have good correlation with the measured long-term deflections. The combined effect of shrinkage restraint and construction loading on deflection calculations was also considered by Scanlon and Bischoff (2008), who showed that the stiffness (I_{eff}/I_g ratio) is highly sensitive to these effects in slabs typically used in practice, with reinforcement ratio between 0.2 per cent and 0.4 per cent. The effects of shore stiffness and concrete cracking on the distribution and magnitude of construction loads were studied by Park, et al. (2011). El-Salakawy and Benmokrane (2004) conducted experiments on 10 full-size one-way slabs reinforced with fibre-reinforced polymer (FRP) bars and found that the slabs with a carbon FRP or glass FRP reinforcement ratio equivalent to the balanced reinforcement ratio satisfy serviceability and strength requirements of ACI 440.1R-01 and CAN/CSA-S806-02 codes.

Chapter 5 of ACI 435R-95 provides some design techniques (increasing section depth, increasing section width, adding compression reinforcement, adding tension reinforcement, prestressing, and revising structure geometry), construction techniques (providing extra curing to allow gain in strength, using high early strength concrete, controlling shoring and re-shoring procedures, delaying the first loading, delaying the installation of deflection sensitive elements, building camber into floor slabs, and ensuring that top bars are not displaced downward, especially in cantilevers), and material selection techniques (using aggregates, cement, silica fume, and admixtures that reduce shrinkage and creep or increase modulus of elasticity and adding short fibres in concrete) using which elements can be designed to meet both strength and serviceability requirements.

12.6 CRACKING IN REINFORCED CONCRETE MEMBERS

It is of interest to note that structures built in the past using working stress design method and reinforcements with a yield strength of 250 MPa had low tensile stresses in the reinforcements at service loads. It has been found in laboratory investigations that cracking is generally proportional to the tensile stress in steel (Gergely and Lutz 1968; Beeby 1979). Thus, with low tensile stresses in the reinforcements at service

loads, these structures served their intended functions with very limited flexural cracking.

However, the use of high-strength steel having yield stress of 415 MPa and higher and the use of limit states design methods (which allow higher stresses in the reinforcements) result in visible cracks, and hence, the detailing of reinforcement to control cracking assumes more importance.

Concrete has a high compressive strength but its tensile strength is comparatively very low. Hence, small tensile stresses can easily cause cracks, but these cracks are harmless for serviceability, durability, and safety of structures as long as they remain as hairline cracks, that is, as long as the crack widths remain under 0.2–0.4 mm depending on the environmental conditions. It is necessary to avoid such cracks only in liquid storage tanks and other containers of gases.

Cracking in RC members may be due to the following causes (ACI Committee 224R-01):

1. Flexural tensile stress due to bending under applied loads
2. Volume changes due to creep, shrinkage, thermal, and chemical effects
3. Additional curvatures due to continuity effects, settlement of supports, and so on

We will confine our attention to the cracking due to the first cause. It is difficult to predict the crack width due to the other two causes. However, it has been found that they are greatly controlled by good quality concrete, proper detailing of shrinkage and temperature reinforcement, proper location of expansion or control joints, and so on. It has to be noted that even if we keep the tensile stresses well below the tensile strength of concrete, we cannot avoid cracks. Due to the heat of the hydration, large temperature differentials will be generated within the concrete mass, resulting in temperature stresses. Since concrete might not have developed any tensile strength during this young age (a few hours after setting), the stresses will create micro-cracks between coarse aggregates and mortar. These micro-cracks also reduce the final tensile strength (Leonhardt 1977, 1987). It is also important to realize that cracks cannot be prevented by reinforcements; reinforcing bars can only prevent the opening of cracks and enforce small spacing of cracks and thereby small crack width (Leonhardt 1977). Cracks can also occur due to differential shrinkage or temperature differentials when thin members are connected to thick members, as found in several box girder bridges, where transverse cracks are developed in thin bottom slabs in spite of high prestressing (Leonhardt 1987). Leonhardt (1987) and ACI 224R-2001 also suggest measures, such as using cement with low-initial heat of hydration and proper curing including by thermal insulation, to prevent early-age cracking. Leonhardt (1987) also presented design charts for sizing reinforcement for crack control.

12.6.1 Types of Cracks

Tensile stresses may be induced by loads, moments, shears, and torsion, which produce different crack patterns as shown in Fig. 12.13 (Leonhardt 1977). Members loaded in direct tension crack through the entire cross section, as shown in Fig. 12.13(a), with a crack spacing of 0.75 to 2 times the minimum thickness of the member. In the case of large tension members, with reinforcement at each face, as shown in Fig. 12.13(c), smaller surface cracks develop near the surface of reinforcement, in addition to larger cracks right through the entire cross section at larger intervals. Members subjected to bending develop flexural cracks as shown in Fig. 12.13(b), which can extend up to the neutral axis of beams. In T-beams having a depth of more than about 800 mm, the cracking is closely spaced at the level of reinforcement, which tends to join the web cracks with a larger spacing, and may be termed as *forking cracks* (Leonhardt 1977). Crack widths can be very large, if sufficient reinforcement is not provided in the web.

Bond stresses lead to splitting along the reinforcement as shown in Fig. 12.13(d). Concentrated loads may also cause similar splitting or bursting cracks, especially in bearing areas. It has to be noted that under service loads, the final cracking pattern will not be seen, and there will be only a few cracks at the maximum stressed locations.

In beams with heavy shear forces, we may have cracks with an inclination between 25° and 50° as shown in Fig. 12.13(e).

Such cracks may start vertically at the bottom but will become inclined as they approach the neutral axis due to shear stress. They may extend as high as the neutral axis and sometimes into the compression zone as well. In thin webbed beams, as in I-section beams, *web shear cracks* can form (see Fig. 12.13e). Appropriate shear reinforcement has to be provided to prevent the propagation of these cracks. Torsion causes similar inclined cracks, crossing the whole depth on all faces of the beam, as shown in Fig. 8.4(d) of Chapter 8.

As mentioned earlier, cracks will be formed due to differential settlement, shrinkage, and temperature stresses. Moreover, shrinkage may increase the width of already formed load-induced cracks. Though drying shrinkage may take over a year, thermal shrinkage affects the concrete in a short period of time (a few days); thus, concrete cannot creep and mitigate cracking. As long as the contraction is less than the threshold of approximately 225 microstrain, cracking is not expected (TRC Circular E-C107, 2006). Surface cracks as shown in Fig. 12.13(f) are harmless, as they do not have any special direction and are not deep. They may be found in massive structures and may be avoided by proper curing. Settlement cracks as shown in Fig. 12.13(g) are formed along the reinforcing bars, due to the settlement of fresh concrete, above thick bars, if the concrete used has too much slump. As the volume of rust is typically two to three times the thickness of the corresponding section loss in the base metal, bursting forces are generated, resulting in eventual loss of cover. Such

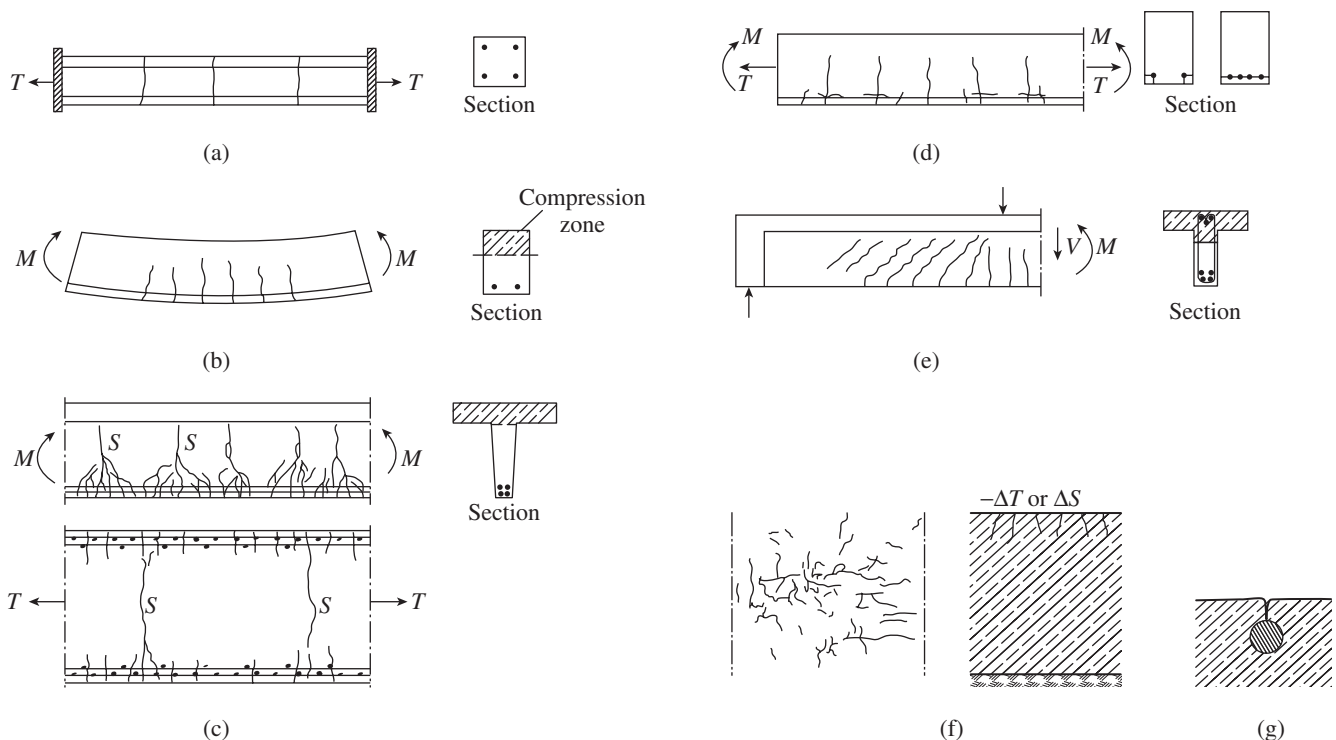


FIG. 12.13 Types of cracks (a) Tension cracks (b) Bending with or without axial load (c) Thick sections (d) Secondary and bond cracks (e) Shear cracks (f) Surface cracks (g) Longitudinal cracks along reinforcing bars

cracking due to rusting will be along the reinforcement and may look similar to bond cracking. Cracks may also form due to freezing and thawing in cold climates, excess load due to ponding, poor detailing at corners, differential settlement, and so on (Subramanian 1979). Concrete should be resistant to damage from freeze–thaw cycles if the concrete has gained sufficient compressive strength (above 27 MPa) and has more than nine per cent entrained air by volume of mortar (ACI 201, TRC Circular E-C107).

12.6.2 Mechanism of Cracking

When a member is subjected to direct tension, cracks start when the tensile stress in the concrete reaches its tensile strength. Slip occurs between concrete and steel at the cracks. At the crack, the concrete is free from stress and the entire tensile force is carried by the reinforcement. Further increase in load results in the stress reaching the tensile strength at some other location and subsequent cracking. Tensile stress is present in the concrete between the cracks, however, because tension is transferred from the steel to concrete by the bond. The magnitude and distribution of the bond stress determines the distribution of tensile stress in the concrete and steel between the cracks. At higher loads, further cracks will form between the initial ones, when the tensile strength of concrete is exceeded. The crack spacing can be reduced only to a certain minimum value, S_{min} . This limit is reached when a tensile force of sufficient magnitude to form an additional crack between two existing cracks can no longer be transmitted by the bond from the steel to the concrete. The crack spacing may be expected to vary from S_{min} to $2S_{min}$, with an average spacing of $1.5S_{min}$, so that $S_{max} = 4/3S_{ave}$ and $S_{min} = 2/3S_{ave}$.

At this stage, the crack pattern is stabilized and further loading merely increases the width of already formed cracks. The foregoing hypothesis was formulated by Watstein and Parsons (1943) and considered the classical theory. Based on this, the following equation for maximum crack width can be derived (Park and Paulay 1975):

$$W_{max} = \frac{d_b f_s}{\rho_e K_1} \tag{12.33}$$

where $K_1 = \frac{2\tau_b E_s}{f_{ct}}$, τ_b is the average bond stress, ρ_e is effective reinforcement ratio = A_{st}/A_e , A_{st} is the steel area, A_e is the effective area of concrete in tension, f_{ct} is the tensile strength of concrete, d_b is the diameter of bar, E_s is the modulus of elasticity of steel, and f_s is the stress in steel.

Modified forms of Eq. (12.33) have been suggested based on comparison with test results; examples of such equations are those given by CEB-FIP and suggested by Kaar and Hognestad (1965) and Gergely and Lutz (1968).

Base, et al. (1966) proposed a fundamentally different approach by assuming that there is no slip of steel relative to concrete. Thus, they assumed that the crack will have zero width at the surface of reinforcing steel and will increase in width as the surface of the member is approached. They proposed the following formula:

$$W_{max} = 3.3a_{cr} \frac{f_s}{E_s} \frac{h_2}{h_1} \tag{12.34}$$

where a_{cr} is the distance from the point at which crack width is to be determined to the surface of the nearest reinforcing bar, f_s is the stress in steel, E_s is the modulus of elasticity of steel, h_1 is the distance from centroid of tension steel to the neutral axis, and h_2 is the distance from the point at which the crack width is to be determined to the neutral axis (see also Fig. 12.14 for h_1 , h_2 , and a_{cr}).

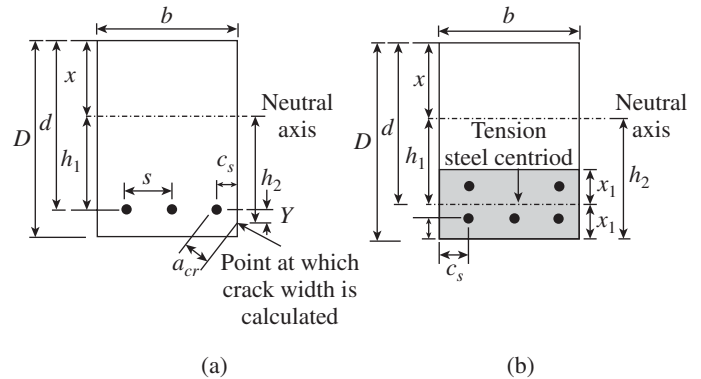


FIG. 12.14 Notation for crack width equation (a) Base, et al. approach (b) Gergely–Lutz approach

12.6.3 Limiting Crack Width

There are three reasons for limiting the crack width in concrete. These are appearance, corrosion, and water tightness. It has to be noted that all the three are not applicable simultaneously in a particular structure. Appearance is important for exposed concrete for aesthetic reasons. Similarly, corrosion is important for concrete exposed to aggressive environments. Water tightness is required for liquid storage structure and for marine and sanitary structures. Appearance requires limiting crack widths on the surface. This can be ensured by locating the reinforcement as close as possible to the surface (by using small covers), which will prevent the cracks from widening. Corrosion control, on the contrary, requires increased thickness of concrete cover and better quality of concrete. Water tightness requires control on crack widths but is applicable only to special structures. Hence, a single provision in the code is not sufficient to address the control of cracking due to all these three reasons.

Traditionally, the codes specified permissible crack widths in order to solve this problem. The permissible crack widths as specified by some codes are given in Table 12.12.

It is interesting to note that the earlier version of IS 456 recommended a limiting crack width of 0.004 times the nominal cover for severe environment. (Crack widths can easily be measured using optical comparators, hand-held crack injection scope, as made by Chemco Systems, and crack width gauges or rulers; see ACI 224.1R-07.)

TABLE 12.12 Tolerable crack widths according to ACI 224R-01, CEB-FIP Model Code-1990, and IS 456 (Subramanian 2005)

S. No.	Exposure Condition	Tolerable Crack Widths, mm		
		ACI 224 R-01	CEB-FIP-90*	IS 456-2000
1.	Low humidity, dry air, or protective environment	0.40	0.4–0.6	0.30
2.	High humidity, moist air, or soil	0.30	0.2–0.3	0.20
3.	De-icing chemicals	0.175	0.10–0.15	0.10
4.	Sea water and sea water spray	0.15	0.10–0.15	0.10
5.	Water retaining structures	0.10	–	–

Note: *Lower crack width limit is for cases with minimum cover; upper limit = $1.5 \times$ minimum cover.

Early investigations of crack width in beams and members subject to axial tension indicated that crack width was proportional to steel stress and bar diameter but was inversely proportional to reinforcement percentage (Fanella and Rabbat 2002). Other variables, such as the quality of the concrete, the thickness of the concrete cover and the area of concrete in the zone of maximum tension surrounding each individual reinforcing bar, depth of member and location of neutral axis, and bond strength and tensile strength of the concrete, were also found to be important (ACI 318-2011; Fanella and Rabbat 2002). Some of these factors are interrelated. There is a high correlation between surface crack width and cover c_c as shown in Fig. 12.15. For a particular magnitude of strain

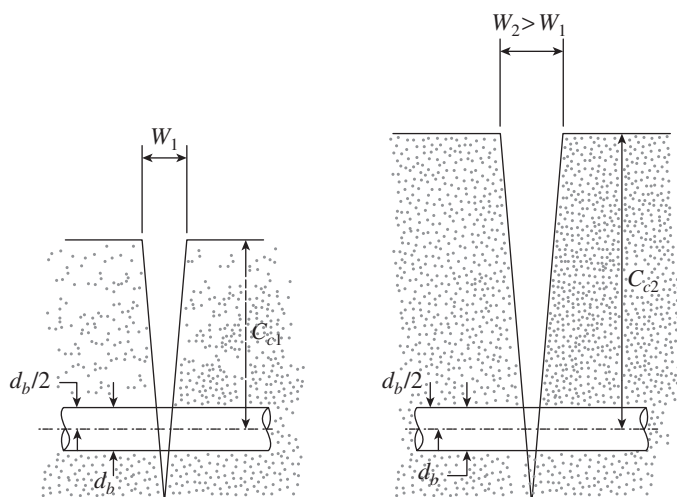


FIG. 12.15 Crack width for different cover thicknesses

in the steel, the larger the cover, the larger will be the surface crack width affecting the appearance.

12.6.4 Crack Control Provisions in Codes

According to the explanatory handbook SP 24-1983, the width of flexural crack at a particular point on the surface of a flexural member is found to increase with the increase in the following three major influencing factors:

1. Average tensile strain at surface, which in turn increases with increase in the mean tensile strain (ϵ_{sm}) in the neighbouring reinforcement
2. Distance between the point on the surface and the nearest longitudinal bar that runs perpendicular to the crack
3. Distance between the point on the surface and the neutral axis

Due to the several interrelated variables, the estimate of the probable maximum width of surface cracks in a flexural member is a fairly complex problem. As discussed in Section 12.6.2, a number of widely different equations have been proposed (with semi-empirical formulations) in the past. The formulation given in Annexure F of the recent revision of the IS 456 is exactly similar to that given in the British code BS 8110: Part 2: 1985.

Provided the strain in tension reinforcement is limited to $0.8f_y/E_s$, the design surface crack width is given by Annexure F of IS 456 as (see also Fig. 12.16)

$$W_{cr} = \frac{(3a_{cr}\epsilon_m)}{1 + 2\frac{(a_{cr} - c_{min})}{(D - kd)}} \quad (12.35)$$

where a_{cr} is the distance from the point considered to the surface of the nearest longitudinal bar. In Fig. 12.16(a), $a_{cr} = [(0.5s)^2 + c_{min}^2]^{0.5}$ where s is the spacing between bars, c_{min} is the minimum cover to the longitudinal bar, ϵ_m is the average steel strain at the level considered, D is the overall depth of the member, kd is the depth of neutral axis, E_s is the modulus of elasticity of the reinforcement, and f_y is the yield stress of reinforcement.

In general, the point for considering the maximum crack width is located on the surface of the beam or slabs (on the tension side), mid-way between two reinforcing bars as shown in Fig. 12.16. As an approximation, the steel stress is calculated on the basis of the cracked section and reduced by an amount equal to the tensile force generated by the triangular distribution, having a value equal to zero at the neutral axis and a value of 1 N/mm^2 at the centroid of tension steel in the short term (reducing to 0.55 N/mm^2 in long term), acting over the tension zone divided by the steel area. For rectangular tension zone, the formula for mean strain ϵ_m is given by the code as

$$\epsilon_m = \epsilon_1 - \frac{b(D - kd)(a' - kd)}{3E_s A_{st}(d - kd)} \quad (12.36)$$

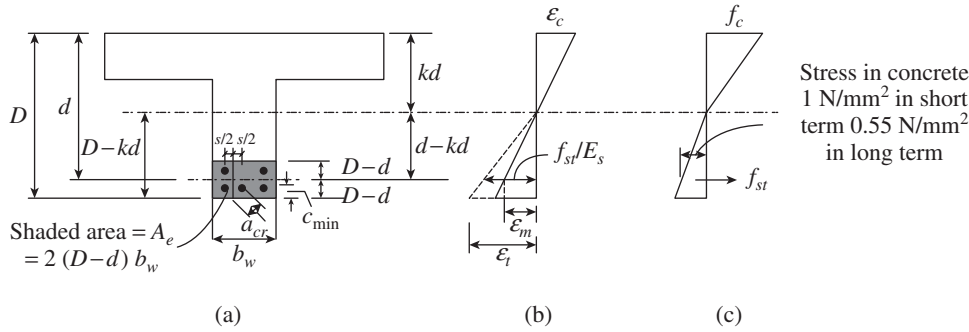


FIG. 12.16 Parameters for crack width calculation (a) Beam section (b) Strains (c) Stress

where ϵ_1 is the strain at the level considered (calculated ignoring the stiffening of the concrete in tension zone), b is the width of the section at the centroid of the tension steel ($b = b_w$ for a rectangular web as in Fig. 12.16), a' is the distance from the compression face to the point at which the crack width is being calculated, d is the effective depth, and A_{st} is the area of tension steel. It has to be noted that a negative value for ϵ_m indicates that the section is uncracked.

American Code Formula

From 1971 through 1995, the American code formulation was based on the formula suggested by Gergely and Lutz (1968), which gives the maximum probable crack width as

$$w_{cr} = 11 \times 10^{-6} \sqrt[3]{c_{\min} \left(\frac{A_e}{n} \right) \left(\frac{h_2}{h_1} \right) f_{st}} \quad (12.37)$$

where c_{\min} is the thickness of concrete cover measured from the extreme tension fibre to the centre of the nearest bar, A_e is the effective area of concrete in tension surrounding the main tension reinforcement, having the same centroid as the tension steel $= 2(D - d)b_w$, as shown in Fig. 12.16, n is the number of bars in tension (in case different diameters are used, n should be taken as the total steel area divided by the area of the largest bar diameter), f_{st} is the stress at the centroid of the tension steel and may be taken as $0.6f_y$, and h_1 and h_2 are as defined in Fig. 12.14(b).

It has to be noted that Eq. (12.36) is empirical, and for dimensional homogeneity, the constant three in the denominator evidently has the inverse unit of stress. Similarly, the same applies to the constant 11×10^{-6} in Eq. (12.37), which was obtained from statistical analysis of the experimental data.

The 1995 edition of the ACI code as well as Clause 10.6.1 of CSA A 23.3-04 code require that when the yield strength of reinforcement exceeds 275 MPa, the detailing of the flexural tension reinforcement must satisfy the following equation:

$$z = f_{st} \sqrt[3]{c_{\min} (A_e/n)} \begin{cases} \leq 30 \text{ kN/mm for interior exposures} \\ \leq 25 \text{ kN/mm for exterior exposures} \end{cases} \quad (12.38)$$

This equation was derived from Eq. (12.37) with an approximate value of 1.2 for h_2/h_1 and by dividing the crack width by the constant value, yielding the parameter z . The numerical limitations of z for interior and exterior exposure correspond to limiting crack widths of 0.4 mm and 0.33 mm, respectively.

Ganesan and Sivananda (1996) compared the various formulae with the available experimental results and concluded that the best results are predicted by the formula proposed by Gergely and Lutz.

As already pointed out, increased cover results in increased crack widths at the surface. However, increased cover is highly desirable from the point of view of durability and protection against corrosion of reinforcement (Subramanian and Geetha 1997). These two aspects appear to be contradictory. The ACI code-specified z factors (Eq. 12.38) essentially encourage reduction of the reinforcement cover, which could be detrimental to corrosion protection (Fanella and Rabbat 2002). Moreover, the method severely penalized structures with covers more than 50 mm by either reducing the spacing or the service load stress of the reinforcement.

The role of cracks in the corrosion of reinforcement has also been found to be controversial. Research shows that corrosion is not clearly correlated with surface crack widths in the range normally found with reinforcement stresses at service load levels (Darwin 1985; Oesterle 1997). Further, it has been found that actual crack widths in structures are highly variable. A scatter of the order of ± 50 per cent in crack widths was observed even in careful laboratory work (Fanella and Rabbat 2002). Moreover, shrinkage and other time-dependent effects influence crack widths.

The behaviour of the two-way reinforced slabs with respect to cracking may be different from that of beams. Nawy (1972) developed an expression for crack width based on his tests on 20 clamped and simply supported square slabs reinforced with welded wire fabric. A state-of-the-art report on the design for crack control in reinforced and prestressed concrete beams, two-way slabs, and circular tanks is presented by Nawy (2001).

Exposure tests on concrete specimens indicated that concrete quality, adequate compaction, and ample concrete cover may be of greater importance for corrosion protection than crack width at the concrete surface. Moreover, a better crack control was obtained when the steel reinforcement is well distributed over the zone of maximum concrete tension. Hence, it was decided to replace the ACI clause to predict crack widths by a clause restricting the spacing of bars.

From the 1999 edition of the ACI code, the maximum bar spacing is specified directly. The spacing s of reinforcement closest to a surface in tension should not exceed that given by (Frosch 1999)

$$s = 380 \left(\frac{280}{f_{st}} \right) - 2.5c_c \leq 300 \left(\frac{280}{f_{st}} \right) \quad (12.39)$$

where s is the centre-to-centre spacing of flexural tension reinforcement nearest to the extreme tension face (where there is only one bar nearest to the extreme tension face, s is the width of the extreme tension face), f_{st} is the calculated stress in reinforcement at service load, computed as the unfactored moment divided by the product of the steel area and internal moment arm (ACI code permits the designer to take f_{st} as 60 % of the specified yield strength), and c_c is the clear cover from the nearest surface in tension to the surface of flexural tension reinforcement.

It has to be noted that the spacing limitation is independent of the exposure condition and bar size used. Thus, for a required amount of flexural reinforcement, this approach would encourage use of smaller bar sizes to satisfy the spacing criteria of Eq. (12.39).

The maximum reinforcement spacings as per Eqs (12.38) and (12.39) for slabs with a single layer of reinforcement were compared by Fanella and Rabbat (2002), and it was shown that Eq. (12.39) significantly relaxes the spacing requirements for larger cover between 50 mm and 100 mm. It has to be noted that Eq. (12.39) is not applicable to structures subject to very aggressive exposure or designed to be watertight. Special precautions are required and must be investigated for such cases.

The tests conducted by Treece and Jirsa (1989) found that epoxy coating significantly increased the width and spacing of cracks with the average width of cracks increasing up to twice the width of cracks in specimens with uncoated bars. Hence, the following equation was proposed for the maximum spacing of reinforcement, which includes the effect of epoxy-coated bars:

$$s = 300\alpha_s \left(1.25 - \frac{c_c}{120\alpha_s} \right) \leq 300\alpha_s \quad (12.40)$$

where $\alpha_s (= 250\gamma_c/f_{st})$ is the reinforcement factor, c_c is the thickness of concrete cover, γ_c is the reinforcement coating factor (1.0 for uncoated and 0.5 for epoxy-coated bars), and f_{st} is the calculated stress in reinforcement at service level, which may be taken as $0.60f_y$.

CEB-FIP Model Code 1990 and the Australian code AS 3600-2009 suggest that crack width calculations are not required if the calculated maximum steel stress and spacing do not exceed those given in Table 12.13 for a given bar diameter.

TABLE 12.13 Maximum steel stress and spacing for tension or flexure in beams

Nominal Bar Diameter (d_b), mm	Maximum Steel Stress, MPa	Centre-to-Centre Spacing (s), mm
10	360	50
12	330	87.5
16	280	150
20	240	200
24	210	237.5
28	185	268
32	160	300
36	140	–
40	120	–

Note: Maximum steel stress = $760 - 173 \log_e(d_b)$ or $400 - 0.8s$

Maghsoudi and Akbarzadeh (2007) found that for doubly reinforced HSC beams, the measured value of crack width and experimental cracking stresses are less than the values predicted by CSA and ACI codes. Rizk and Marzouk (2010) developed a new formula to calculate crack spacing for two-way concrete slabs. Marzouk, et al. (2010) investigated the cracking criteria for thick concrete two-way slabs used for offshore and nuclear containment structures. Their test results showed that the concrete cover has a major effect on the crack width when compared to bar spacing. They also compared the different code predictions and developed a method to predict the crack width of such thick slabs. Gilbert (2001, 2008) developed an analytical design method (as opposed to the empirical methods employed in current codes) for flexural crack control, taking into account the time-dependent development of cracking and increase in crack widths with time due to shrinkage. The results of this method correlated well with the test results. A review of the methods to predict cracking is provided by Carino and Clifton (1995). TRB Circular E-C107 discusses the precautions to be taken to minimize cracking during design, selection of materials, proportioning, and construction.

12.6.5 Distribution of Tension Reinforcement in Flanges of I-beams

The ACI 318 code also suggests that for control of flexural cracking in the flanges of T-beams, the flexural reinforcement must be distributed over a flange width not exceeding the effective flange width or a width equal to 1/10 the span, whichever is less. If the effective flange width is greater than 1/10 the span, additional longitudinal reinforcement as shown in Fig. 12.17 should be provided in the outer portion of the flange.

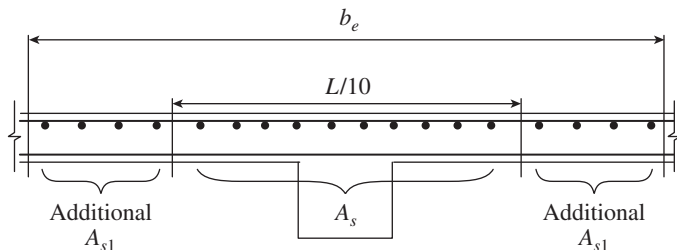


FIG. 12.17 Negative moment reinforcement for flanged floor beam

12.7 SIDE FACE REINFORCEMENT IN BEAMS

Clause 26.5.1.3 of IS 456 suggests that side face reinforcements should be provided along the two faces when the depth of the web in a beam exceeds 750 mm. The total area of such reinforcement should not be less than 0.1 per cent of the web area and should be distributed equally on the two faces at a spacing not exceeding 300 mm or web thickness, whichever is less (see Fig. 5.14 of Chapter 5).

The ACI 318 building code requires special side face reinforcement in all beams that are deeper than 914 mm. Frantz and Breen (1980) proposed that the amount of side face reinforcement in large beams is independent of the amount of flexural reinforcement and depends mainly on the member depth also on the clear concrete cover to the side face reinforcement c_s and the diameter of the side face reinforcing bars d_b . The current version of the American code suggests that the required skin reinforcement (see Fig. 12.18) must be uniformly distributed along both side faces of the member for a distance $d/2$ nearest the flexural tension reinforcement. The spacing is not to exceed the minimum of $d/6$, 300 mm, and $1000A_b/(d - 750)$, where A_b is the area of an individual bar.

The total area of skin reinforcement provided on both faces need not be greater than one-half the total area of the main tensile reinforcement. Table 12.14 gives the maximum spacing and the minimum bar area of that spacing.

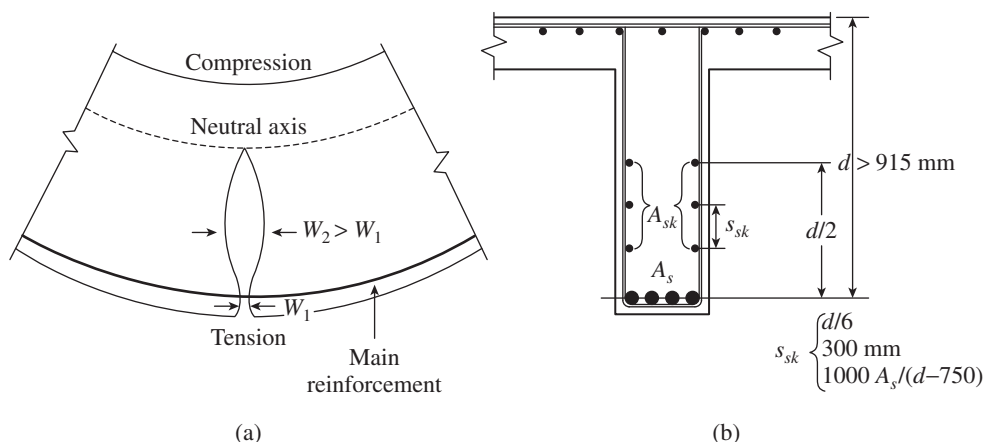


FIG. 12.18 Side face reinforcement (a) Side face cracking (b) Crack control skin reinforcement for deep beams

TABLE 12.14 Spacing and bar size for skin reinforcement

Depth D , mm	Maximum Spacing, s_{sk} (mm)	Minimum Bar Area A_b at Maximum Spacing (mm ²)
900	150	22.5
1050	175	52.5
1200	200	90.0
1500	250	187.50
1800	300	315.0
2100	300	405.0

It is of interest to note that the ACI code does not give any area for the skin reinforcement but only specifies the maximum spacing.

Adebar and Leeuwen (1999) compared different North American requirements for side face reinforcement and have shown that there are considerable differences regarding how much side face reinforcement is appropriate. They also concluded that the ACI code provision may be unconservative under certain exposure conditions when there are diagonal cracks. They also proposed an equation to predict the spacing of side face reinforcement.

Crack Control in Compression Members

Clause 43.2 of IS 456 suggests that cracking need not be checked in compression members subjected to compression and bending when it is subjected to design axial load greater than $0.2f_{ck}A_g$, where f_{ck} is the characteristic compressive strength of concrete and A_g is the area of gross section of the member. If the member is subjected to a load lesser than $0.2f_{ck}A_g$, it may be considered like a flexural member for the purpose of crack control.

12.8 FRAME DEFLECTIONS

In addition to beam and slab deflections dealt with in Sections 12.2 to 12.5, we must also consider several other types of deflections in the design of RC frames. One important deflection that has to be controlled is the lateral deflection of the frame. This is because such lateral deflections lead to second-order $P-\Delta$ effects, which are inversely proportional to the lateral stiffness. Lateral deflections are to be considered at service loads and at factored loads. The evaluation of deflection at factored load level should consider the effective stiffness for beams and columns in the analysis. A discussion on effective stiffness is provided in Section 4.5.1 of Chapter 4. As cracking will be

less predominant at service loads, one may consider the gross section properties in the service load analysis. Commentary to the ACI code Clause 10.10.4.1 suggests using $1/0.7 = 1.43$ times the stiffness values given in Table 4.10 for service load analysis.

As per Clause 7.11.1 of IS 1893: Part 1 (2002), the storey drift in any storey due to design service lateral loads should not exceed 0.004 times the storey height or $H/250$, where H is the storey height. Also as per Clause 7.11.3 of the same code, two adjacent buildings should be separated by a distance equal to the amount R times the calculated storey displacement, where R is the response reduction factor defined in Table 7 of IS 1893. When the floor levels of two similar adjacent buildings are at the same level, the factor R may be reduced to $R/2$. More elaborate drift considerations are specified in Clause 12.8.6 and Table 12.12-1 of ASCE 7-10. Some guidance to calculate the axial shortening of columns in multi-storey buildings is provided in Section 3.9.6 of Chapter 3.

12.9 VIBRATION CONTROL

It should be noted IS 456 does not prescribe any design criteria for the control of vibration. Clause 19.6 merely requires that vibration be considered and appropriate action taken to ensure that vibration does not adversely affect the safety and serviceability of the structure (see also Section 4.8.2). Aerobics, dancing, and other rhythmic human activities have caused annoying vibrations in a number of buildings in recent years (particularly in cantilevers) in both in situ and precast construction. These activities may induce vibrations of about 2–4 cycles per second (Hz). The two main factors behind these problems are resonance (when the natural frequency of the floor structure is equal to or close to the forcing frequency of the rhythmic activity or less than 5 Hz) and the perception of occupants to vibration (vibrations that are imperceptible or barely perceptible to some people can be very objectionable to others). While vibrations can cause an uncomfortable sensation to the occupant, it can also interfere with the operation of laboratory or medical equipment sensitive to vibration. Hence, hospitals and certain laboratories are likely to be subject to more strict levels of vibration. Cracking reduces floor stiffness and, consequently, lowers its natural frequency.

The first natural frequency, f_n , of a rectangular slab panel can be calculated as (ArcelorMittal 2008)

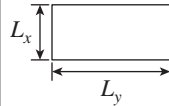





$$f_n = \frac{c}{L_y^2} k_1 \quad (12.41a)$$

where

$$c = \sqrt{\frac{E_{cd} D^3}{12(1 - \nu^2)} \frac{g}{w}} \quad (12.41b)$$

f_n is first natural frequency in Hertz, L_y is the long span length, E_{cd} is the dynamic modulus of elasticity of concrete (may be taken as 1.25 times the static modulus, E_c), D is the slab thickness in mm, ν = Poisson's ratio (may be taken as 0.2 for concrete), g is the acceleration due to gravity (9810 mm/s^2), and w is the weight per unit surface area of the slab. The value of constant k_1 is given in Table 12.15 for different boundary conditions.

TABLE 12.15 First natural frequency constant k_1 for rectangular slab panels of uniform thickness

Case	Boundary Condition — Simply Supported — Continuous Edge	Value of k_1
1.		$1.57(1 + r^2)$
2.		$1.57\sqrt{1 + 2.5r^2 + 5.14r^4}$
3.		$1.57\sqrt{5.14 + 2.92r^2 + 2.44r^4}$
4.		$1.57\sqrt{1 + 2.33r^2 + 2.44r^4} \delta$
5.		$1.57\sqrt{2.44 + 2.72r^2 + 2.44r^4}$
6.		$1.57\sqrt{5.14 + 3.13r^2 + 5.14r^4}$

Note: $r = L_y/L_x$

Alternatively, the natural floor frequency (f_n in Hz) can also be found from the general frequency equation

$$f_n = \frac{1}{2\pi} \sqrt{\frac{K}{M}} \quad (12.42a)$$

where M is the total mass of the vibrating system in Kg and K is the stiffness in N/mm . The stiffness K can be approximated by the expression

$$K = \frac{Mg}{(3/4)\Delta} \quad (12.42b)$$

where Δ is the total deflection of the floor structure due to the weight supported by all its members, in mm, g is the acceleration due to gravity = 9810 mm/s^2 , and $3/4\Delta$ is the average deflection. Substituting Eq. (12.42b) in Eq. (12.42a) and simplifying, we get the following simple formula:

$$f_n = \frac{18}{\sqrt{\Delta}} \quad (12.42c)$$

It has to be noted that while calculating Δ , full dead load and 10 per cent of live load may be considered (ArcelorMittal 2008).

Clause C-3 of IS 800:2007 suggests the following formula for simply supported one-way systems:

$$f_n = 156 \sqrt{\frac{EI}{WL^4}} \quad (12.43)$$

IS 800:2007 suggests that floor systems with a natural frequency less than 8 Hz in the case of floors supporting rhythmic activity and less than 5 Hz in the case of floors supporting normal human activity should be avoided.

Worked out examples on vibration control and more details may be found in the works of Murray, et al. (1997), ArcelorMittal (2008), Aalami (2008), ATC Design Guide 1 (1999), and Naeim (1991).

The methods to minimize floor vibrations include the following (Naeim 1991):

1. *Changing the frequency of the floor:* This can be accomplished by changing bay sizes, increasing the depth of the floor system, or in some cases just by switching the orientation of the framing.
2. *Adding weight to the floor:* This can be accomplished by thickening a slab, using normal weight instead of lightweight concrete.
3. *Damping the floor:* Damping a floor decreases the magnitude of vibrations that have been introduced. This can be accomplished by architectural components such as ceilings, partition walls, and furniture. Different construction types offer different levels of damping.
4. *Isolating the affected area from the rest of the structure:* When extreme vibration-producing situations, such as running tracks, aerobic studios, and dance halls, are not on a slab on grade, sometimes the only way to effectively control the vibration is to provide separate framing for the area so that it is completely isolated from the rest of the structure.

If floor vibrations are encountered after a floor is constructed, the options for addressing floor vibrations are limited and may be expensive or impractical. If the floor has additional load capacity, ballast can be added to the floor. Columns can be added to decrease span lengths. Active damping systems can be used to reduce vibrations but these are very expensive.

12.10 FATIGUE CONTROL

Fatigue is a strength limit state but fatigue strength is checked at service loads; hence, it is discussed in this chapter. When concrete is subjected to fluctuating loads rather than sustained loads, its *fatigue strength*, like all other materials, is considerably smaller than its static strength. An overview of the fatigue strength of RC structures is given in ACI 215R-74. The lack of explicit provisions in ACI 318 and IS 456 is indicative of a lack of observed fatigue-related problems in existing buildings. However, fatigue strength may govern the

design, due to the use of HSC and resulting thin sections, especially in cantilever bridges.

Fatigue failure of concrete occurs due to the progressive growth of micro-cracks. The fatigue strength of plain concrete in compression or tension is 50–60 per cent of static strength for two million cycles. Concrete loaded in flexural compression has 15–20 per cent higher fatigue strength than axially-loaded concrete (ACI 215R-74). The parameters that govern fatigue behaviour include the range of load, rate and frequency of loading, loading eccentricity, material properties, and environmental conditions.

In general, three phases can be found in a fatigue process: crack initiation, crack propagation, and failure. Crack initiation is the phase where micro-cracks are initiated at discontinuities and stress concentration points are formed during the hardening process of concrete. Crack propagation is the phase where a crack grows a small amount with each load change and eventually leads to failure. The ACI Committee 215R-74 recommends that the compression stress range in concrete, f_{cr} , should not exceed

$$f_{cr} = 0.33f_{ck} + 0.47f_{\min} \quad (12.44)$$

where f_{\min} is the minimum compressive stress in the cycle (positive in compression). In bridge design, the compressive stress at service load is also limited to $0.4f_{ck}$.

The formula to determine the allowable steel stress range f_r for reinforcing bars is given in Clause 5.5.3.2 of the AASHTO-2007 specifications as

$$f_r = 166 - 0.33f_{\min} \quad (12.45a)$$

where f_r is the allowable steel stress range (MPa), and f_{\min} is the minimum live load stress combined with the more severe stress from either the permanent loads or the shrinkage- and creep-induced external loads and is positive if in tension and negative if in compression (MPa).

Amorn, et al. (2007) studied the fatigue of deformed welded-wire reinforcement (WWR) and proposed the following fatigue equation for WWR with a cross weld in the high-stress region:

$$f_r = 110 - 0.33f_{\min} \quad (12.45b)$$

They suggested the use of Eq. (12.45a) for WWR with no cross weld in the high-stress region and provided numerical examples to determine the fatigue strength. Ayyub, et al. (1994) observed that the WWR, available in the USA, met the fatigue requirements of structural reinforcement for bridge decks.

A safe fatigue life for cases not reaching the endurance limit was suggested by Hanson, et al. (1976) as follows:

$$\begin{aligned} \log N = & 6.1 - 2.8 \times 10^{-4} f_r - 9.7 \times 10^{-5} f_{\min} + 4.8 \times 10^{-5} f_u \\ & - 0.39A_s + 0.32 \left(\frac{r}{h} \right) \end{aligned} \quad (12.46)$$

where N is the number of cycles to failure, f_u is the ultimate steel strength (MPa), A_s is the bar area (mm^2), and r/h is the ratio of base radius to height of rolled-on transverse deformations; if the actual value of r/h is not known, a value of 0.3 may be used. It was found that with a decrease in the bend-to-bar diameter ratio, the resistance to fatigue is reduced.

12.11 SLENDERNESS LIMITS FOR BEAMS FOR STABILITY

When slender beams are used, they may fail by lateral buckling accompanied by twist. Information on slenderness limits and calculation of critical moment M_{cr} , which will govern the strength of the beam, are provided in Section 5.5.6 of Chapter 5.

12.12 DEFLECTION OF CANTILEVERS

For cantilevers, the effective span is taken as the clear span plus one-half the effective depth of cantilever. While calculating the deflection of cantilever, the rotation at its base should also be considered, as shown in Fig. 12.19.

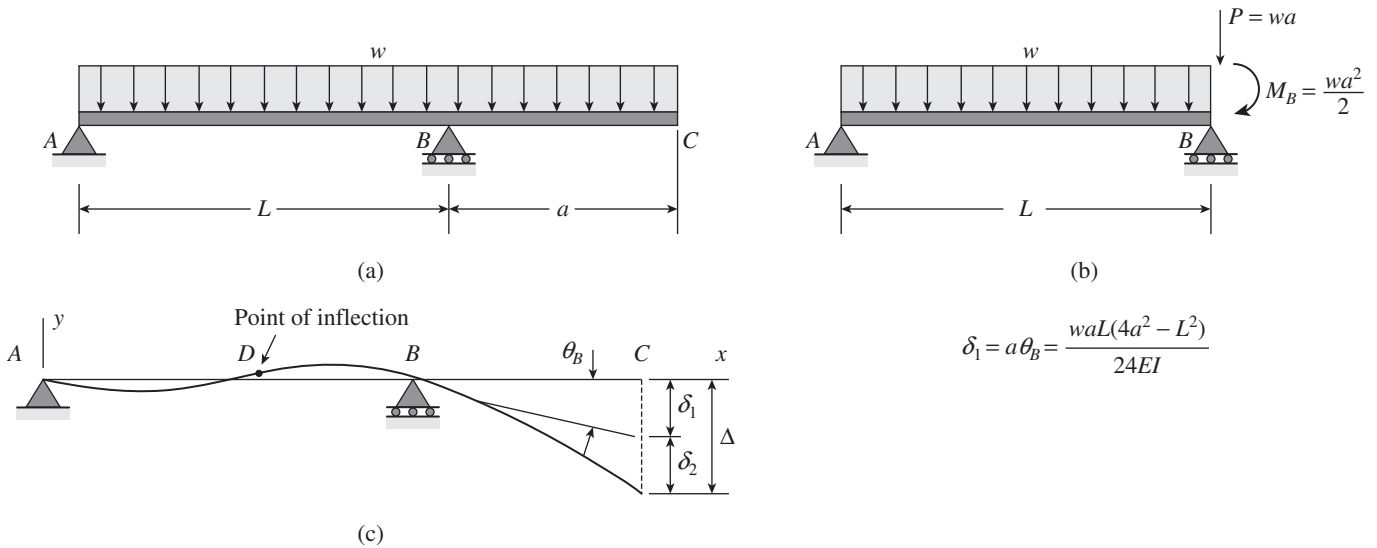


FIG. 12.19 Deflection of cantilever (a) Beam with cantilever (b) Equivalent beam (c) Deflection of beam

EXAMPLES

EXAMPLE 12.1 (Calculation of transformed section properties):

An RC beam of rectangular section has the cross-sectional dimensions shown in Fig. 12.20(a). Assuming M25 concrete and Fe 415 steel, compute the moment of inertia for both the uncracked and the cracked sections.

SOLUTION:

Step 1 Calculate the material properties for M25 concrete.

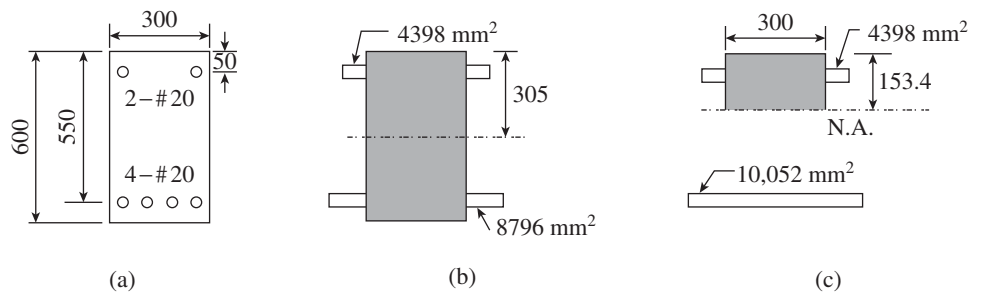


FIG. 12.20 (a) Cross section (b) Uncracked transformed section (c) Cracked transformed section

Modulus of elasticity (Clause 6.2.3.1)

$$E_c = 5000\sqrt{f_{ck}} = 5000\sqrt{25} = 25,000 \text{ N/mm}^2$$

Modular ratio, $m = E_s/E_c = 2 \times 10^5/25,000 = 8$

Note: Modular ratio as per Clause B-2.1.2 and Table 21 of code is $m = 280/3\sigma_{cbc} = 280/(3 \times 8.5) = 10.98$ (greater than eight as this takes into account the effects of the creep)

Modulus of rupture

$$f_{cr} \text{ (Clause 6.2.2)} = 0.7\sqrt{f_{ck}} = 0.7\sqrt{25} = 3.5 \text{ MPa}$$

Step 2 Calculate the approximate cracking moment (assuming gross section).

$$\text{Section modulus } Z = \frac{bD^2}{6} = \frac{300 \times 600^2}{6} = 18 \times 10^6 \text{ mm}^3$$

Cracking moment, $M_{cr} = f_{cr}Z = 3.5 \times 18 \times 10^6 = 63 \times 10^6 \text{ kNm}$

Step 3 Calculate the uncracked transformed section.

$$\text{Area of tension steel } A_{st} = 4 \times \pi \times 20^2/4 = 1256.6 \text{ mm}^2$$

Area of compression steel $A_{sc} = 2 \times \pi \times 20^2/4 = 628.3 \text{ mm}^2$

Transformed area of tensile steel $= (m - 1)A_{st} = (8 - 1)1256.6 = 8796 \text{ mm}^2$

Transformed area of compression steel = $(m - 1)A_{sc} = (8 - 1)628.3 = 4398 \text{ mm}^2$

Note: The compression area of steel is taken as $(m - 1)A_{sc}$ and not as $(1.5m - 1)A_{sc}$ as considered in stress calculation, because the factor $1.5m$, which takes into account creep effects, is not applicable in short-term deflection calculations.

The centroid of transformed section can be located as shown in Table 12.16.

TABLE 12.16 Determination of centroid

Part	Area (mm ²)	y_{top} (mm)	Ay_{top} (mm ³)
Concrete	$300 \times 600 = 180 \times 10^3$	300	54×10^6
Compression steel	4398	50	21.99×10^4
Tension steel	8796	550	4.84×10^6
	$\Sigma A = 1,93,594$		$\Sigma Ay_{top} = 59.06 \times 10^6$
$\bar{y}_{top} = \frac{59.06 \times 10^6}{1,93,594} = 305 \text{ mm}$			

The moment of inertia of the section can be calculated as shown in Table 12.17 (it should be noted that the moment of inertia of the steel layers about their centroids are negligible).

TABLE 12.17 Moment of inertia of uncracked transformed section

Part	Area (mm ²)	\bar{y} (mm)	$I_{own \text{ axis}}$ (mm ⁴)	$A\bar{y}^2$ (mm ⁴)
Concrete	180×10^3	$300 - 305 = -5$	$\frac{bd^3}{12} = 5.4 \times 10^9$	4.5×10^6
Compression steel	4398	$305 - 50 = 255$	–	285.98×10^6
Tension steel	8796	$305 - 550 = -245$	–	527.98×10^6
$I_{gv} = \Sigma(I_{own} + A\bar{y}^2) = 6.218 \times 10^9$				

It should be noted that the moment of inertia of uncracked transformed section is 15 per cent larger than the gross moment of inertia of concrete alone.

Step 4 Calculate the cracked transformed section. Let us assume that the neutral axis in this case is below compression steel. The following are the transformed areas of steel:

Compression steel $(m - 1)A_{sc} = (8 - 1)628.3 = 4398 \text{ mm}^2$

Tension steel $mA_{st} = 8 \times 1256.6 = 10,052 \text{ mm}^2$

The centroid is calculated as given in Table 12.18 assuming the depth of neutral axis as x .

TABLE 12.18 Determination of centroid

Part	Area (mm ²)	\bar{y} (mm)	$A\bar{y}$ (mm ³)
Compression zone of concrete	$300x$	$x/2$	$300x^2/2 = 150x^2$
Compression steel	4398	$x - 50$	$4398x - 219.9 \times 10^3$
Tension steel	10,052	$x - 550$	$10,052x - 5.5286 \times 10^6$

By definition, at x , $\Sigma A\bar{y} = 0$. Hence, we have

$$150x^2 + 14,450x - 5.7485 \times 10^6 = 0$$

or

$$x^2 + 96.33x - 38,323 = 0$$

$$\text{Thus, } x = \frac{-96.33 \pm \sqrt{96.33^2 + 4 \times 38,323}}{2} = \frac{-96.33 \pm 403.2}{2}$$

$$= 153.4 \text{ mm (from top fibre)}$$

The moment of inertia of the cracked section may be computed as shown in Table 12.19.

TABLE 12.19 Moment of inertia of cracked section

Part	Area (mm ²)	y (mm)	$I_{own \text{ axis}}$ (mm ⁴)	Ay^2 (mm ⁴)
Compression zone of concrete	$300 \times 153.4 = 46,020$	$153.4 / 2 = 76.7$	$\frac{bx^3}{12} = 90.244 \times 10^6$	270.731×10^6
Compression steel	4398	$153.4 - 50 = 103.4$	–	47.021×10^6
Tension steel	10,052	$153.4 - 550 = -396.6$	–	1581.095×10^6
$I = \Sigma(I_{own \text{ axis}} + Ay^2) = 1989.091 \times 10^6 \text{ mm}^4$				

In this beam, I_{cr} is approximately 32 per cent of the moment of inertia of uncracked transformed section and 36.8 per cent of the concrete section alone. This indicates that the stiffness reduces considerably due to cracking.

Note: This procedure can be used to locate the neutral axis of any shape of cross section under uniaxial bending.

EXAMPLE 12.2:

A simply supported beam of span 5 m, as shown in Fig. 12.21, is made of M20 grade concrete and is reinforced with three 20 mm bars of Fe 415 grade steel. If it is subjected to an imposed load of 15 kN/m and a concentrated dead load of 10 kN at mid-span, calculate the short-term deflection due to live loads alone.

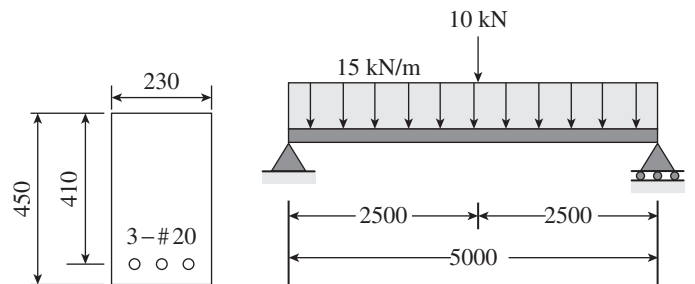


FIG. 12.21 Beam of Example 12.2

SOLUTION:

Step 1 Calculate the bending moments.

Self-weight of beam = $25 \times 0.45 \times 0.23 = 2.59 \text{ kN/m}$

Bending moment due to dead load alone

$$= 2.59 \times 5^2 / 8 + 10 \times 5 / 4 = 8.10 + 12.5 = 20.6 \text{ kNm}$$

Bending moment due to dead and live loads

$$= 15 \times 5^2 / 8 + 20.6 = 46.9 + 20.6 = 67.5 \text{ kNm}$$

Step 2 Calculate m , E_c , and f_{cr} .

Modulus of elasticity of concrete, E_c (Clause 6.2.3.1)

$$= 5000 \sqrt{f_{ck}} = 5000 \sqrt{20} = 22,360 \text{ MPa}$$

$E_s = 2 \times 10^5$ MPa. Hence, modular ratio,

$$m = \frac{E_s}{E_c} = \frac{2 \times 10^5}{22,360} = 8.9$$

Modulus of rupture f_{cr} (Clause 6.2.2)

$$= 0.7 \sqrt{f_{ck}} = 0.7 \sqrt{20} = 3.13 \text{ N/mm}^2$$

Step 3 Calculate the gross and cracked section properties

Moment of inertia,

$$I_{gr} = bD^3 / 12 = 230 \times 450^3 / 12 = 1746.56 \times 10^6 \text{ mm}^4$$

$$A_{st} = 3 \times 314 = 942 \text{ mm}^2, \rho = \frac{A_{st}}{bd} = \frac{942}{230 \times 410} = 0.00999$$

$$\text{From Table 12.3, } B = \frac{b}{mA_{st}} = \frac{230}{8.9 \times 942} = 0.0274$$

$$x = \left[\left(\sqrt{1 + 2Bd} \right) - 1 \right] / B = \left[\left(\sqrt{1 + 2 \times 0.0274 \times 410} \right) - 1 \right] / 0.0274 = 140.3 \text{ mm}$$

$$\begin{aligned} \frac{I_{cr}}{bd^3} &= \frac{1}{3} \left(\frac{x}{d} \right)^3 + m\rho \left(1 - \frac{x}{d} \right)^2 \\ &= \frac{1}{3} \left(\frac{140.3}{410} \right)^3 + 8.9 \times 0.00999 \left(1 - \frac{140.3}{410} \right)^2 = 0.0518 \end{aligned}$$

$$I_{cr} = 0.0518 \times 230 \times 410^3 = 821.58 \times 10^6 \text{ mm}^4$$

Using design aids:

Alternatively, the x/d value may be calculated using Tables 91–94 of SP 16: 1980:

$$p_t m = \frac{100 \times 942}{230 \times 410} \times 8.9 = 8.89$$

From Table 91, $x/d = 0.342$, $x = 0.342 \times 410 = 140.2 \text{ mm}$

Similarly, the value of $I_{cr}/(bd^3/12)$ may be obtained from Tables 87–90.

From Table 87, for $p_t m$ of 8.89, $I_{cr}/(bd^3/12) = 0.622$

$$I_{cr} = \frac{0.622}{12} \times 230 \times 410^3 = 821.6 \times 10^6 \text{ mm}^4$$

$$\begin{aligned} M_{cr} &= \frac{f_{cr} I_{gr}}{y_t} = \frac{3.13 \times 1746.56 \times 10^6}{(0.5 \times 410)} = 26.67 \times 10^6 \text{ Nmm} \\ &= 26.67 \text{ kNm} < M_{DL+LL} = 67.5 \text{ kNm} \end{aligned}$$

Step 4 Calculate the effective moment of inertia.

(a) As per IS 456, $z = d - x/3 = 410 - 140.3/3 = 363.2 \text{ mm}$.
From Clause C.2.1 of IS 456:

$$I_{eff} = \frac{I_{cr}}{1.2 - \frac{M_{cr}}{M} \left(\frac{z}{d} \right) \left(1 - \frac{x}{d} \right) \frac{b_w}{b}} \text{ but } I_{cr} \leq I_{eff} \leq I_{gr}$$

Hence

$$\begin{aligned} I_{eff} &= \frac{821.58 \times 10^6}{1.2 - \left(\frac{26.67}{67.5} \right) \left(\frac{363.2}{410} \right) \left(1 - \frac{140.3}{410} \right) \times 1} \\ &= \frac{821.58 \times 10^6}{0.9698} \\ &= 1.031 \times 821.58 \times 10^6 = 847 \times 10^6 \text{ mm}^4 \end{aligned}$$

(b) As per Bischoff (2005):

$$I_{eff} = \frac{I_{cr}}{1 - \left(\frac{M_{cr}}{M} \right)^2 \left[1 - \frac{I_{cr}}{I_{gr}} \right]} \leq I_{gr}$$

$$\begin{aligned} I_{eff} &= \frac{821.58 \times 10^6}{1 - \left(\frac{26.67}{67.5} \right)^2 \left[1 - \frac{821.58}{1746.56} \right]} \\ &= 1.09 \times 821.58 \times 10^6 \\ &= 895.63 \times 10^6 \text{ mm}^4 \end{aligned}$$

(c) As per Branson's formula (ACI 318):

$$\begin{aligned} I_{eff} &= \left(\frac{M_{cr}}{M_a} \right)^3 I_{gr} + \left[1 - \left(\frac{M_{cr}}{M_a} \right)^3 \right] I_{cr} \leq I_{gr} \\ &= \left(\frac{26.67}{67.5} \right)^3 \times 1746.56 \times 10^6 + \left[1 - \left(\frac{26.67}{67.5} \right)^3 \right] \\ &\quad \times 821.58 \times 10^6 \\ &= (107.73 + 770.9) \times 10^6 = 847 \times 10^6 \text{ mm}^4 \end{aligned}$$

It is seen that the IS code formula yields the minimum value for I_{eff} (in this case, it is equal to the ACI code formula) and all the values are greater than I_{cr} ; Hence, take $I_{eff} = 847 \times 10^6 \text{ mm}^4$.

Step 5 Calculate the deflection.

$$\Delta_{D+L} = \frac{5}{384} \frac{wL^4}{EI_{eff}} + \frac{1}{48} \frac{WL^3}{EI_{eff}} = \frac{5}{48} \frac{L^2}{EI_{eff}} [M_1 + 0.8M_2]$$

where M_1 and M_2 are mid-span moments due to uniformly distributed load and concentrated load, respectively.

(a) Due to dead load + imposed load:

$$\begin{aligned} \Delta_{D+L} &= \frac{5 \times 5000^2}{48 \times 22,360 \times 847 \times 10^6} [46.9 + 0.8 \times 20.6] \times 10^6 \\ &= 8.71 \text{ mm} \end{aligned}$$

(b) Due to dead load alone (for this $M_{cr} < M$; hence, we use I_{gr}):

$$\Delta_D = \frac{5 \times 5000^2}{48 \times 22,360 \times 1746.56 \times 10^6} [8.10 + 0.8 \times 12.5] \times 10^6 = 1.21 \text{ mm}$$

The admissible deflection due to live load alone is (Clause 23.2b)

$$\Delta_{all} = \frac{L}{350} = \frac{5000}{350} = 14.3 \text{ mm} > 8.71 - 1.21 = 7.5 \text{ mm}$$

Hence, deflection is within limits.

EXAMPLE 12.3:

Determine the short-term deflection due to dead and live loads and long-term shrinkage and creep deflection due to permanent load of a cantilever beam of span 4.0m and subjected to a dead load of 3.75 kN/m and live load of 15 kN/m at service level. The width and overall depth of beam are 300 mm and 500 mm, respectively, and reinforced with five 25 mm diameter bars in tension zone and two 20 mm diameter bars in compression zone and a clear cover of 25 mm (see Fig. 12.22). Consider a support width of 300 mm, M25 concrete, and Fe 415 grade steel.

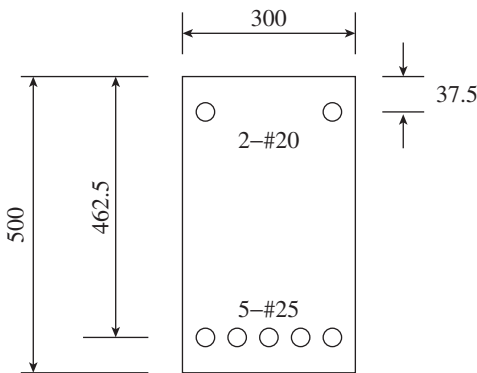


FIG. 12.22 Cross section of beam of Example 12.3

SOLUTION:

Step 1 Calculate I_{cr} .

$$E_c = 5000 \sqrt{f_{ck}} = 5000 \sqrt{25} = 25,000 \text{ N/mm}^2$$

$$m = E_s / E_c = 2 \times 10^5 / 25,000 = 8; A_{st} = 5 \times 490 = 2450 \text{ mm}^2$$

$$A_{sc} = 2 \times 314 = 628 \text{ mm}^2$$

$$\rho = \frac{A_{st}}{bd} = \frac{2450}{300 \times 462.5} = 0.0177,$$

$$\rho' = \frac{A_{sc}}{bd} = \frac{628}{300 \times 462.5} = 4.52 \times 10^{-3}$$

Cover, $d'' = d' = 25 + 25/2 = 37.5 \text{ mm}$, $d = 500 - 37.5 = 462.5 \text{ mm}$

Effective length, $L = 4000 + 462.5/2 = 4231.3 \text{ mm}$ (Clause 22.2d of IS 456)

Analyse whether a deflection check is required.

$$p_t = (100A_{st})/(bd) = 1.77$$

$$p_c = (100A_{sc})/(bd) = 0.452$$

Modification factor for tension steel (for $p_t = 1.77$) = 0.866 (Fig. 4 of IS 456)

Modification factor for compression steel (for $p_t = 0.452$) = 1.13 (Fig. 5 of IS 456)

Effective depth ratio for cantilever (Clause 23.2.1) = $7 \times 0.866 \times 1.13 = 6.85$

Hence, effective required depth = $4231.3/6.85 = 617.7 \text{ mm} > 462.5 \text{ mm}$

Hence, check for deflection is required.

From Table 12.3

$$\begin{aligned} \frac{x}{d} &= \sqrt{\frac{[m\rho + (m-1)\rho']^2 + 2[m\rho + (m-1)\rho' \frac{d'}{d}]}{[m\rho + (m-1)\rho']}} \\ &= \sqrt{\frac{[8 \times 0.0177 + 7 \times 4.52 \times 10^{-3}]^2 + 2\left(8 \times 0.0177 + 7 \times 4.52 \times 10^{-3} \times \frac{37.5}{462.5}\right)}{-(8 \times 0.0177 + 7 \times 4.52 \times 10^{-3})}} \\ &= 0.5642 - 0.1732 = 0.391 \end{aligned}$$

Neutral axis depth, $x = 0.391 \times 462.5 = 180.8 \text{ mm}$

$$\begin{aligned} I_{cr} &= \frac{bx^3}{3} + mA_{st}(d-x)^2 + (m-1)A_{sc}(x-d')^2 \\ &= \frac{300}{3}(180.8)^3 + 8 \times 2450(462.5 - 180.8)^2 \\ &\quad + 7 \times 628(180.8 - 37.5)^2 \\ &= 2236.64 \times 10^6 \text{ mm}^4 \end{aligned}$$

Alternatively, the same result may be obtained using Table 88 of SP 16:1980.

$$d'/d = 37.5/462.5 = 0.08 \approx 0.10$$

$$p_t m = 1.77 \times 8 = 14.16$$

$$p_c(m-1)/p_t m = 7 \times 0.452/14.16 = 0.22$$

From Table 88 of SP 16, for $d'/d = 0.10$; $I_{cr} = \frac{bd^3}{12} \times 0.90$

$$I_{cr} = \frac{300 \times 462.5^3}{12} \times 0.9 = 2226 \times 10^6 \text{ mm}^4$$

Similarly, from Table 92 of SP 16, $x/d = 0.392$

Step 2 Calculate I_{eff} .

$$f_{cr} = 0.7\sqrt{f_{ck}} = 0.7\sqrt{25} = 3.5 \text{ N/mm}^2$$

$$I_{gr} = bD^3/12 = 300 \times 500^3/12 = 3125 \times 10^6 \text{ mm}^4$$

$$y_t = D/2 = 500/2 = 250 \text{ mm}$$

$$M_{cr} = f_{cr}I_{gr}/y_t = 3.5 \times 3125 \times 10^6/250 = 43.75 \times 10^6 \text{ Nmm} \\ = 43.75 \text{ kNm}$$

$$M = (15 + 3.75) \times 4.231^2/2 = 167.83 \text{ kNm} > M_{cr}$$

Lever arm distance, $z = d - x/3 = 462.5 - 180.8/3 = 402.2 \text{ mm}$

As per Clause C-2.1 of IS 456

$$I_{eff} = \frac{I_{cr}}{1.2 - \frac{M_{cr}}{M} \left(\frac{z}{d} \right) \left(1 - \frac{x}{d} \right) \frac{b_w}{b}} \quad \text{but } I_{cr} \leq I_{eff} < I_{gr}$$

$$= \frac{2236.64 \times 10^6}{1.2 - \left(\frac{43.75}{167.83} \right) \left(\frac{402.2}{462.5} \right) \left(1 - \frac{180.8}{462.5} \right) \times 1} = 2106.2 \times 10^6 < I_{cr}$$

Hence, $I_{eff} = I_{cr} = 2236.64 \times 10^6 \text{ mm}^4$

As per Bischoff (2005):

$$I_{eff} = \frac{I_{cr}}{1 - \left(\frac{M_{cr}}{M} \right)^2 \left[1 - \frac{I_{cr}}{I_{gr}} \right]} = \frac{2236.64 \times 10^6}{1 - \left(\frac{43.75}{167.83} \right)^2 \left[1 - \frac{2236.64}{3125} \right]} \\ = 2280.7 \times 10^6 \text{ mm}^4 > I_{cr}$$

Step 3 Calculate the short-term deflection.

$$\text{Hence, } \Delta_s = \frac{1}{8} \frac{WL^3}{E_c I_c} = \frac{1}{8} \times \frac{18.75 \times 4.231 \times 10^3 \times (4.231 \times 1000)^3}{25,000 \times 2236.64 \times 10^6} \\ = 13.43 \text{ mm}$$

It has to be noted that the deflection due to rotation as shown in Fig. 12.19 should be added to this value.

Step 4 Calculate the long-term deflection due to shrinkage.

Deflection due to shrinkage (Clause C-3.1) for cantilevers:

$$\Delta_{sh} = 0.5\varphi_{sh}L^2$$

$$\text{where } \varphi_{sh} = k_4 \frac{\varepsilon_{cs}}{D} \quad \text{where } \varepsilon_{cs} = 0.0003$$

$$p_t - p_c = 1.77 - 0.452 = 1.318$$

$$\text{Hence, } k_4 = 0.65 \frac{p_t - p_c}{\sqrt{p_t}} \leq 1.0 \text{ for } p_t - p_c \geq 1.0$$

$$k_4 = 0.65 \times \frac{1.318}{\sqrt{1.77}} = 0.644$$

$$\varphi_{sh} = \frac{0.644 \times 0.0003}{500} = 3.864 \times 10^{-7}$$

$$\Delta_{sh} = 0.5 \times 3.864 \times 10^{-7} \times 4231^2 = 3.46 \text{ mm}$$

Step 5 Calculate the long-term deflection due to creep.

As per Clause C-4.1 of IS 456:

$$\Delta_{cp} = \Delta_{i,cp} - \Delta_i$$

$$\Delta_{i,cp} = \frac{1}{8} \frac{W_d L^3}{E_{cc} I_e} \quad \text{and} \quad E_{cc} = \frac{E_c}{1 + C_t}$$

Let us assume the age at loading as 28 days. Hence, from Clause 6.2.5.1, $C_t = 1.6$.

$$E_{cc} = \frac{25,000}{1 + 1.6} = 9615.4 \text{ N/mm}^2$$

$$m = \frac{E_s}{E_{cc}} = \frac{2 \times 10^5}{9615.4} = 20.8; \quad p_t m = 1.77 \times 20.8 = 36.8$$

$$p_c(m-1)/(p_t m) = 0.452(20.8-1)/(1.77 \times 20.8) = 0.243$$

From Table 88 of SP 16, for $d'/d = 0.10$

$$I_{cr} = \frac{bd^3}{12} \times 1.540 = \frac{300 \times 462.5^3}{12} \times 1.540 = 3809 \times 10^6 \text{ mm}^4 \\ > I_{gr} = 3125 \times 10^6 \text{ mm}^4$$

Hence, use the I_{gr} value.

Assuming 60 per cent of the imposed load as permanent load,

$$W = (3.75 + 0.6 \times 15) \times 4.231 \times 10^3 = 53,945.25 \text{ kN}$$

$$\Delta_{i,cp} = \frac{1}{8} \frac{53,945.25 \times (4.231 \times 1000)^3}{9615.4 \times 3125 \times 10^6} = 17 \text{ mm}$$

$$\Delta_{ip} = \frac{1}{8} \frac{53,945.25 \times (4.231 \times 1000)^3}{25,000 \times 2236.64 \times 10^6} = 9.13 \text{ mm}$$

Hence, $\Delta_{cp} = 17.0 - 9.13 = 7.87 \text{ mm}$

Total long-term deflection = $13.43 + 3.46 + 7.87 = 24.76 \text{ mm}$

Permissible deflection (Clause 23.2a) = $L/250 = 4231/250 = 16.92 \text{ mm} < 24.76 \text{ mm}$

Hence, the depth has to be revised based on the deflection criteria. It has to be noted that increasing the compression reinforcement will also reduce the creep deflection.

EXAMPLE 12.4:

A three-span continuous beam of rectangular section 250 mm by 500 mm, each 5 m span, is provided with three 16 mm bars at support and two 16 mm bars and one 12 mm bar at mid-span. The beam is subjected to a live load of 15 kN/m and is made of M25 concrete and Fe 415 steel. Compute the deflection at service loads.

SOLUTION:

Step 1 Calculate I_{gr} and M_{cr} .

$$\text{Young's modulus of concrete, } E_c = 5000\sqrt{f_{ck}} = 5000\sqrt{25} \\ = 25,000 \text{ Mpa}$$

$$\text{Modular ratio, } m = E_s/E_c = 2 \times 10^5/25,000 = 8$$

The gross moment of inertia of the section at mid-span and end span is the same and is given as

$$I_{gr} = \frac{bD^3}{12} = \frac{250 \times 500^3}{12} = 2604.17 \times 10^6 \text{ mm}^4$$

Assuming a clear cover of 25 mm, effective depth, $d = 500 - 25 - 8 = 468 \text{ mm}$

$$d' = 25 + 8 = 33 \text{ mm}$$

Step 2 Calculate M_{cr} and I_{cr} at mid-span.

$$f_{cr} = 0.7\sqrt{f_{ck}} = 0.7\sqrt{25} = 3.5 \text{ N/mm}^2$$

$$M_{cr} = \frac{I_{gr}f_{cr}}{y_b} = \frac{2604.17 \times 10^6 \times 3.5}{(500/2)} = 36.46 \times 10^6 \text{ Nmm}$$

Moment of inertia of cracked section at mid-span

$$A_{st} = 2 \times 201 + 113 = 515 \text{ mm}^2$$

$$\text{From Table 12.3, } B = \frac{b}{mA_{st}} = \frac{250}{8 \times 515} = 0.0607$$

Neutral axis depth,

$$x = \frac{\sqrt{(1+2Bd)} - 1}{B} = \frac{\sqrt{(1+2 \times 0.0607 \times 468)} - 1}{0.0607} = 108.8 \text{ mm}$$

$$I_{cr,m} = \frac{bx^3}{3} + mA_{st}(d-x)^2$$

$$= \frac{250 \times 108.8^3}{3} + 8 \times 515 \times (468 - 108.8)^2 = 638.9 \times 10^6 \text{ mm}^4$$

Step 3 Calculate I_{cr} at the support.

$$A_{st} = 3 \times 201 = 603 \text{ mm}^2$$

$$\text{From Table 12.3, } B = \frac{b}{mA_{st}} = \frac{250}{8 \times 603} = 0.0518$$

Neutral axis depth,

$$x = \frac{\sqrt{(1+2Bd)} - 1}{B} = \frac{\sqrt{(1+2 \times 0.0518 \times 468)} - 1}{0.0518} = 116.52 \text{ mm}$$

$$I_{cr,m} = \frac{bx^3}{3} + mA_{st}(d-x)^2$$

$$= \frac{250 \times 116.52^3}{3} + 8 \times 603 \times (468 - 116.52)^2$$

$$= 727.8 \times 10^6 \text{ mm}^4$$

Step 4 Calculate service-level bending moment.

$$\text{Dead load} = 0.25 \times 0.5 \times 25 = 3.125 \text{ kN/m}$$

$$\text{Total load on beam} = 15 + 3.125 = 18.125 \text{ kN/m}$$

Let us use the moment coefficients used in Table 12 of IS 456 to determine the bending moments.

At mid-span of end span:

$$\text{Bending moment} = \frac{w_{DL}L^2}{12} + \frac{w_{LL}L^2}{10} = \frac{3.125 \times 5^2}{12} + \frac{15 \times 5^2}{10}$$

$$= 44 \text{ kNm}$$

At middle of interior span:

$$\text{Bending moment} = \frac{w_{DL}L^2}{16} + \frac{w_{LL}L^2}{12} = \frac{3.125 \times 5^2}{16} + \frac{15 \times 5^2}{12}$$

$$= 36.13 \text{ kNm}$$

At support next to end support:

$$\text{Bending moment} = -\frac{w_{DL}L^2}{10} - \frac{w_{LL}L^2}{9} = -\frac{3.125 \times 5^2}{10}$$

$$- \frac{15 \times 5^2}{9} = -49.48 \text{ kNm}$$

At other interior supports:

$$\text{Bending moment} = -\frac{w_{DL}L^2}{12} - \frac{w_{LL}L^2}{9} = -\frac{3.125 \times 5^2}{12}$$

$$- \frac{15 \times 5^2}{9} = -48.18 \text{ kNm}$$

Step 5 Calculate the effective moment of inertia.

At mid-span:

$$\text{Lever arm distance, } z = d - x/3 = 468 - 108.8/3 = 431.73 \text{ mm}$$

As per Clause C-2.1 of IS 456

$$I_{eff,m} = \frac{I_{cr}}{1.2 - \frac{M_{cr}}{M} \left(\frac{z}{d} \right) \left(1 - \frac{x}{d} \right) \frac{b_w}{b}} \text{ but } I_{cr} \leq I_{eff} < I_{gr}$$

$$= \frac{638.9 \times 10^6}{1.2 - \left(\frac{36.46}{44} \right) \left(\frac{431.73}{468} \right) \left(1 - \frac{108.8}{468} \right) \times 1} = 1041.8 \times 10^6 > I_{cr}$$

At support in end span:

$$\text{Lever arm distance, } z = d - x/3 = 468 - 116.52/3 = 429.16 \text{ mm}$$

$$I_{eff,s} = \frac{727.8 \times 10^6}{1.2 - \left(\frac{36.46}{49.48} \right) \left(\frac{429.16}{468} \right) \left(1 - \frac{116.52}{468} \right) \times 1}$$

$$= 1050.9 \times 10^6 > I_{cr}$$

Step 6 Calculate the average effective moment of inertia for end span.

$$M_{f1} = M_{f2} = wL^2/12 = 18.125 \times 5^2/12 = 37.76 \text{ kNm}$$

$$M_1 = 0 \text{ kNm and } M_2 = 49.48 \text{ kNm}$$

The factor k_2 in Table 25 of IS 456 is given here:

$$k_2 = \frac{M_1 + M_2}{M_{f1} + M_{f2}} = \frac{0 + 49.48}{2 \times 37.76} = 0.655$$

Value of k_1 from Table 25 of IS 456 is 0.0575.

$$I_{eff,av} = k_1 \left[\frac{X_1 + X_2}{2} \right] + (1 - k_1) X_0$$

$$= 0.0575 \left(\frac{2 \times 1050.9 \times 10^6}{2} \right) + (1 - 0.0575) \times 1041.8 \times 10^6$$

$$= 1038.8 \times 10^6 \text{ mm}^4$$

Note: As per the weighted average method of ACI 318,

$$I_{eff,av} = 0.7I_{eff,m} + 0.15(I_{eff,1} + I_{eff,2})$$

$$= [0.7 \times 1041.8 + 0.15(2 \times 1050.9)] \times 10^6$$

$$= 1044.53 \times 10^6 \text{ mm}^4$$

Although both IS code and ACI code methods yield similar results, ACI method is simpler to use.

Step 7 Calculate short-term deflection.

$$\Delta = \frac{5}{384} \frac{wL^4}{EI_{eff}} = \frac{5}{384} \frac{18.125 \times 5000^4}{25,000 \times 1050.9 \times 10^6} = 5.61 \text{ mm} (= L/883)$$

Hence, the deflection is within allowable limits

EXAMPLE 12.5 (Crack width in beams):

Determine the possible crack width at a point midway between the bars on the tension face at a section of maximum bending moment of the beam in Example 12.3.

SOLUTION:

From Example 12.3, we have the following data:

$$A_{st} = 5 \times 490 = 2450 \text{ mm}^2, D = 500 \text{ mm}, d = 462.5 \text{ mm}, c_{min} = 25 + 12.5 = 37.5 \text{ mm},$$

$$s = 50 \text{ mm}, M = 167.83 \text{ kNm}, m = 7, E_c = 25,000 \text{ N/mm}^2, x = 180.8 \text{ mm}, \text{ and } I_{cr} = 2236.64 \times 10^6 \text{ mm}^4$$

$$\text{Hence, } a_{cr} = [(0.5s)^2 + c_{min}^2]^{0.5} = [0.5(50)^2 + 37.5^2]^{0.5} = 51.54 \text{ mm}$$

Step 1 Calculate the strain in concrete at the extreme fibre.

$$y = 500 - 180.8 = 319.2 \text{ mm}$$

$$\varepsilon_1 = \frac{f_c}{E_c} = \frac{My}{I_{cr} E_c} = \frac{167.83 \times 10^6 \times 319.2}{2236.64 \times 10^6 \times 25000} = 9.58 \times 10^{-4}$$

As per Annexure F of IS 456,

$$\varepsilon' = \frac{b(D-x)(a-x)}{3E_s A_s (d-x)} = \frac{300 \times (500 - 180.8)(500 - 180.8)}{3 \times 2 \times 10^5 \times 2450 \times (462.5 - 180.8)}$$

$$= 7.38 \times 10^{-5}$$

$$\varepsilon_m = \varepsilon_1 - \varepsilon' = 9.58 \times 10^{-4} - 7.38 \times 10^{-5} = 8.84 \times 10^{-4}$$

Step 2 Calculate the crack width as per IS code.

Design surface crack width as per Annexure F of IS 456 is

$$W_{cr} = \frac{(3a_{cr} \varepsilon_m)}{1 + 2 \frac{(a_{cr} - c_{min})}{(D - kd)}} = \frac{3 \times 51.54 \times 8.84 \times 10^{-4}}{1 + 2 \frac{(51.54 - 37.5)}{(500 - 180.8)}}$$

$$= 0.06 \text{ mm} < 0.3 \text{ mm (normal exposure)}$$

Hence, the crack width is within allowable limits.

Step 3 Calculate the crack width as per Gergely and Lutz formula.

A_e/n = Effective concrete area in tension per bar

$$= 2(D - d)b_w/5 = 2(500 - 462.5) \times 300/5 = 4500 \text{ mm}^2$$

$$\text{Using Table 21 of IS 456, } m = \frac{280}{3\sigma_{cbc}} = \frac{280}{3 \times 8.5} = 11$$

Lever arm distance, $jd = d - x/3 = 462.5 - 180.8/3 = 402.2 \text{ mm}$

$$\text{Stress in steel, } f_{st} = \frac{M_s}{A_{st} jd} = \frac{167.83 \times 10^6}{2450 \times 402.2} = 170.3 \text{ MPa}$$

It has to be noted that ACI 318 allows one to take f_{st} as $0.6f_y = 0.6 \times 415 = 249 \text{ MPa} > 170.3 \text{ MPa}$. It should also be noted that f_{st} is less than the allowable stress 230 MPa as per Table 22 of IS 456 for Fe 415 steel.

$$h_1 = d - x = 462.5 - 180.8 = 281.7 \text{ mm};$$

$$h_2 = D - x = 500 - 180.8 = 319.2 \text{ mm}$$

Crack width

$$w_{cr} = 11 \times 10^{-6} \sqrt[3]{c_{min} \left(\frac{A_e}{n} \right) \left(\frac{h_2}{h_1} \right) f_{st}}$$

$$= 11 \times 10^{-6} \sqrt[3]{37.5 \times 4500 \left(\frac{319.2}{281.7} \right) \times 170.3} = 0.09 \text{ mm}$$

Thus in this case, crack width as per Gergely and Lutz formula (0.09 mm) is higher than the value obtained from the IS code formula (0.06 mm).

EXAMPLE 12.6:

The interior span of a typical level of a multi-storey office building has L_x and L_y as 7.0 m and 6.1 m, respectively. Evaluate the in-service vibration response of the floor and its acceptability for the following data.

Thickness of slab, $D = 200 \text{ mm}$

Concrete strength, $f_{ck} = 25 \text{ MPa}$

Poisson's ratio, $\nu = 0.2$

Live load = 3 kN/m²

SOLUTION:

Let us assume a simply supported boundary condition as it is more conservative.

As per Clause 6.2.3.1,

$$E_c = 5000 \sqrt{f_{ck}} = 5000 \sqrt{25} = 25,000 \text{ N/mm}^2$$

$$E_{cd} = 1.25 \times 25,000 = 31,250 \text{ N/mm}^2$$

$$g = 9810 \text{ mm/sec}^2$$

$$r = L_y/L_x = 7/6.1 = 1.15$$

Hence, from Table 12.15, $k_1 = 1.57(1 + r^2) = 1.57(1 + 1.15^2) = 3.65$

Approximately 10 per cent of the full live load may be considered for vibration calculation.

$$w_{LL} = 0.1 \times 3.0 = 0.3 \text{ kN/m}^2$$

Dead load, $w_{DL} = 0.2 \times 25 + 1.0$ (partition load) $= 6 \text{ kN/m}^2$

$$I_x = \frac{bd^3}{12} = \frac{1 \times 200^3}{12} = 0.667 \times 10^6 \text{ mm}^4/\text{mm}$$

Using approximate formula:

$$\Delta_{slab} = \frac{5}{384} \frac{(6 + 0.3) \times 10^{-3} \times 7000^4}{0.667 \times 10^6 \times 25,000} = 11.81 \text{ mm} < L/350$$

$$= 20 \text{ mm (Clause 23.2b)}$$

$$f_n = \frac{18}{\sqrt{11.81}} = 5.24 \text{ Hz} > 5 \text{ Hz (Clause C-3 IS 800:2007)}$$

Using Eq. (12.41):

$$c = \sqrt{\frac{E_{cd} D^3 g}{12(1 - \nu^2) w}} = \sqrt{\frac{31,250 \times 200^3 \times 9810}{12 \times (1 - 0.2^2) \times 6.3 \times 10^{-3}}}$$

$$= 183.8 \times 10^6 \text{ mm}^2/\text{sec}$$

$$f_n = \frac{c}{L_y^2} k_1 = \frac{183.8 \times 10^6 \times 3.65}{7000^2} = 13.69 \text{ Hz} > 5 \text{ Hz}$$

Hence, the vibration characteristics of the slab are within limits.

SUMMARY

According to the design philosophy of the limit states method, two distinct classes of limit states should be satisfied, namely ultimate limit states and serviceability limit states. Whereas the former deals with safety in terms of strength, overturning, sliding, fatigue fracture, buckling, and so on, the latter is concerned with serviceability in terms of deflection, cracking, durability, vibration, and so on. IS 456 (Clauses 42 and 43) does not require the designer to perform any explicit check on deflection or crack width for all normal cases, provided the codal recommendations for limiting L/d ratios (for deflection control) and spacing of flexural reinforcement (for crack control) are complied with.

It has been recognized that many of the modern concrete structures are safe with respect to ultimate limit states. However, many times structural 'failures' are often reported in terms

of serviceability. In particular, it is the serviceability limit state of durability that is often ignored all over the world. In this chapter, durability is covered in terms of prescriptive specifications in the code. The other serviceability criteria, such as control of deflection, cracking, vibration, and fatigue, are covered and code provisions of other countries are compared, wherever necessary. The use of design aids presented in SP 16 are also explained. The methods to calculate instantaneous as well as long-term deflections due to creep and shrinkage are provided. Crack width calculations as well as other methods to control cracks are explained. All the calculation methods are explained with ample examples. The serviceability design will result in elements that will not sag or vibrate as well as result in fewer cracks, which are responsible for corrosion and deterioration of concrete structures all over the world.

REVIEW QUESTIONS

- Why is control of deflections and cracking more important in limit states design than in working stress design?
- Why are the serviceability limit states considered important in design?
- What are the quantities considered in serviceability limit states?
- What are the problems with excessive deflection?
- What are the two approaches for deflection control adopted in recent codes?
- Name the two methods using which deflections can be reduced.
- IS 456 recommends checking for actual deflection, when the span exceeds _____.
(a) 6 m (b) 8 m (c) 10 m (d) 12 m
- Why is it difficult to make accurate predictions of deflections and crack widths in flexural members?
- Name any three parameters that affect shrinkage and creep deflection.
- As per IS 456, the final deflection due to all loads should not exceed _____.
(a) span/200 (c) span/350 and 20 mm
(b) span/350 (d) span/250
- As per IS 456, the deflection occurring after the construction of partitions should not exceed _____.
(a) span/200 (c) span/350 and 20 mm
(b) span/350 (d) span/250
- The central deflection of a simply supported beam with span L and flexural rigidity EI , carrying a uniform load w per unit length is _____.
(a) $5wL^4/(384EI)$ (c) $wL^4/(384EI)$
(b) $5wL^4/(48EI)$ (d) $wL^4/(48EI)$
- Distinguish between instantaneous and long-term deflections?
- Write a short note on the transformed area of steel.
- Write the expressions to compute the service load stresses in concrete and steel of a member subjected to flexure.
- Describe the load-deflection behaviour of a flexural member.
- Explain with suitable sketches what is meant by tension stiffening effect in a flexural member.
- Write down the expression given in Annexure C of IS 456 for calculating I_{eff} . How was this expression derived?
- In addition to I_{eff} , what are the other factors that affect the deflection response of flexural members?

20. As an approximation, which of the following percentage of live loads may be assumed as permanent loads?
 - (a) 50–60%
 - (b) 30–40%
 - (c) 20–30%
 - (d) 55–65%
21. How is I_{eff} considered to compute the deflection of continuous beams in the IS and ACI codes?
22. Explain the use of Tables 87–90 of SP 16 while computing deflections.
23. Name a few parameters that may affect creep deformation.
24. Explain the IS code method of calculating creep deflection. How does it differ from the ACI code method?
25. How does shrinkage of concrete lead to deflections in flexural members?
26. How does compression reinforcement affect deflection due to shrinkage and creep?
27. Summarize the procedure for calculating total deflection including that due to creep and shrinkage as per IS 456.
28. Explain how temperature effects lead to deflections in flexural members.
29. List a few variables that affect two-way slab deflection.
30. How does construction sequence affect slab deflections?
31. What are the design, construction, and material selection techniques that can be used to reduce deflection in flexural members?
32. Why has cracking become more important while using limit states design?
33. What are the three causes of cracking?
34. How will you distinguish between flexural, shear, and torsional cracks?
35. Why is it necessary to limit the width of cracks?
36. The crack width that is allowed in low humidity and protective environment as per IS 456 is _____.
 - (a) 0.1 mm
 - (b) 0.2 mm
 - (c) 0.3 mm
 - (d) 0.4 mm
37. Name a few parameters that control crack width.
38. State the equation given in IS 456 to compute crack width.
39. How can we control flexural cracking in the flanges of T-beams?
40. What is the suggestion given in IS 456 for side face reinforcement?
41. Why is it necessary to control lateral deflection of frames?
42. What are the main problems associated with the vibration of slabs?
43. How can we calculate the natural frequency of slabs using the deflections?
44. What are the methods adopted to minimize floor vibrations?
45. List a few parameters that govern fatigue behaviour of RC members.

EXERCISES

1. An RC beam of span 6 m has a rectangular cross section as shown in Fig. 12. 23. Assuming M25 concrete and Fe 415 steel, compute the moment of inertia of both uncracked and cracked transformed sections.

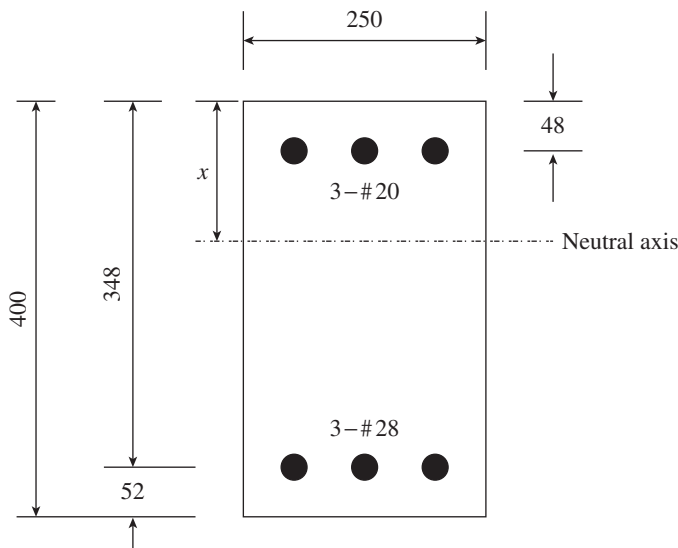


FIG. 12.23

2. A one-way slab of effective span 4.2 m is subjected to a total load, inclusive of self-weight, of 10 kN/m² and is reinforced with 10 mm bars at 125 mm centre to centre in the short span and with distributors of 8 mm bars at 200 mm centre to centre. If the total depth of the slab is 200 mm

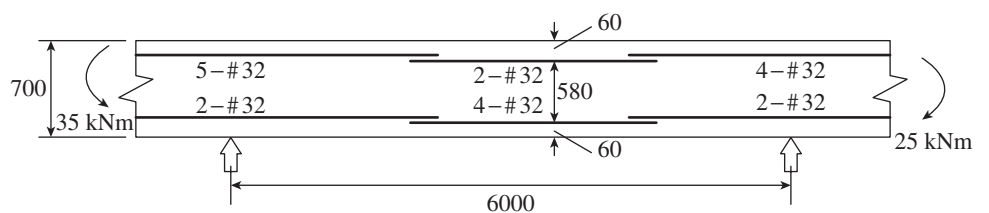


FIG. 12.24

- with effective width 165 mm, calculate the maximum short-term deflection as per IS 456.
3. If the beam shown in Exercise 1 is subjected to a superimposed service load (including dead load) of 17.5 kN/m and a central concentrated load of 30 kN, calculate the instantaneous deflection as per the IS 456 and ACI 318 methods.

[Hint:
$$\Delta = \frac{5}{384} \frac{wL^4}{EI_{eff}} + \frac{5}{48} \frac{WL^3}{EI_{eff}},$$

- where w is the uniformly distributed load and W is the concentrated load]
4. For the beam of Exercise 3, determine the maximum long-term deflection due to creep and shrinkage and check whether the total deflection is within code limits. Assume ultimate shrinkage strain of 0.004 and ultimate creep coefficient of 1.6.
 5. For the one-way slab of Exercise 2, determine the long-term deflection due to creep and shrinkage and check whether the total deflection is within code limits.
 6. The interior span of a continuous beam is shown in Fig. 12.24. The beam has the following basic dimensions: $b = 380$ mm, $D = 700$ mm, $d = 640$ mm, and $d' = 60$ mm. The negative reinforcement

at left support is five 32 diameter bars (area = 4021 mm²) and compression steel is two 32 diameter bars (1608 mm²). The negative reinforcement at right support is four 32 diameter bars (area = 3217 mm²) and compression steel is two 32 diameter bars (1608 mm²). The span is 6 m and the superimposed load, inclusive of self-weight, is 15 kN/m². The end moment at left support is 35 kNm and at right support is 25 kNm. Calculate the deflection at service load using M25 concrete and Fe 415 grade steel.

7. The interior span of a typical level of a multi-storey office building has L_x and L_y as 6.2 m and 5.5 m, respectively. Evaluate the in-service vibration response of the floor and its acceptability for the following data: thickness of slab, $D = 180$ mm; concrete strength, $f_{ck} = 25$ MPa; Poisson's ratio, $\nu = 0.2$; and live load = 4 kN/m².
8. Determine the maximum probable crack width for the one-way slab of Exercise 2.
9. For the T-beam designed in Example 5.27 of Chapter 5, calculate the following:
 - (a) Short-term deflection due to service loads
 - (b) Long-term deflection due to creep
 - (c) Long-term deflection due to shrinkage
 - (d) Maximum possible crack width
 Verify whether the calculated deflection and crack widths are within the code stipulated limits.

10. A beam shown in Fig. 12.25 is subjected to a service bending moment of 106 kNm. Using M20 concrete and Fe 415 steel, calculate the crack width at the following locations:

- (a) At a point 100 mm below the neutral axis at the side of the beam
- (b) At a point midway between bars at the tension face
- (c) At the bottom corner

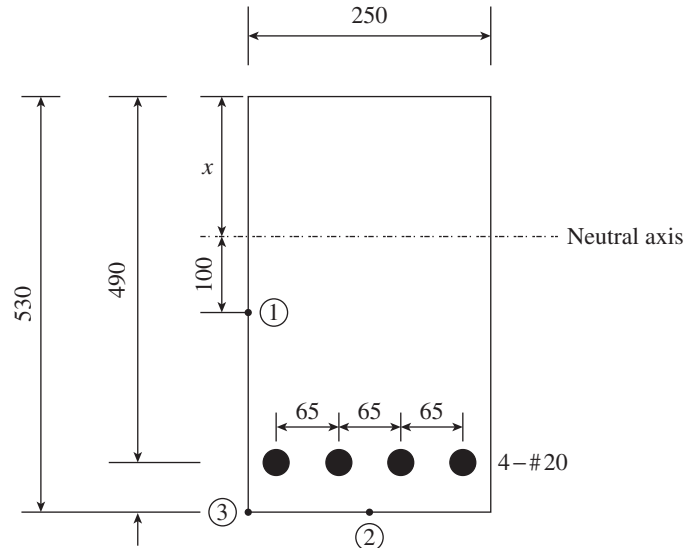


FIG. 12.25

REFERENCES

- Aalami, B.O. 2008, ADAPT-TN290, *Vibration Design of Concrete Floors for Serviceability*, ADAPT Corporation, Redwood City, pp. 20, (also see http://www.adaptsoft.com/resources/ADAPT_TN290_vibration_analysis.pdf, last accessed on 13 September 2013).
- ACI Committee 209 (ACI 209R-92, reapproved 1997), *Prediction of Creep, Shrinkage, and Temperature Effects in Concrete Structures*, American Concrete Institute, Farmington Hills, p. 47.
- ACI Committee 215 1974 (ACI 215R-74), *Considerations for Design of Concrete Structures Subjected to Fatigue Loading*, American Concrete Institute, Farmington Hills, p. 24.
- ACI Committee 224 2001 (ACI 224R-01), *Control of Cracking in Concrete Structures*, American Concrete Institute, Farmington Hills, p. 12.
- ACI Committee 224.1 2007 (ACI 224.1R-07), *Causes, Evaluation and Repair of Cracks in Concrete Structures*, American Concrete Institute, Farmington Hills, p. 22.
- ACI Committee 435 1974 (ACI 435R-95, reapproved 2000), *Control of Deflection in Concrete Structures*, American Concrete Institute, Farmington Hills, p. 89.
- Adan, S.M., R. Luft, and W.I. Naguib 2010, 'Deflection Considerations in Two-way Reinforced Concrete Slab Design', *Proceedings of the ASCE 2010 Structures Congress*, ASCE, pp. 1991–2002, (also see <ftp://ftp.eng.auburn.edu/pub/hza0002/ASCE%202010/data/papers/227.pdf>, last accessed on 2 June 2012).
- Adebar, P. and J. van Leeuwen 1999, 'Side Face Reinforcement for Flexural and Diagonal Cracking in Large Concrete Beams', *ACI Structural Journal*, American Concrete Institute, Farmington Hills, Vol. 96, No. 5, pp. 693–705.
- Al-Shaikh, A.H. 1994, 'A Modified Model for the Effective Moment of Inertia Computations', *The Indian Concrete Journal*, ACC Ltd, Vol. 68, No. 5, pp. 275–8.
- Al-Shaikh, A.H. and R.Z. Al-Zaid 1993, 'Effect of Reinforcement Ratio on the Effective Moment of Inertia of Reinforced Concrete Beams', *ACI Structural Journal*, American Concrete Institute, Farmington Hills, Vol. 90, No. 2, pp. 144–9.
- Amorn, A., J. Bowers, A. Girgis, and M.K. Tadros 2007, 'Fatigue of Deformed Welded-wire Reinforcement', *PCI Journal*, PCI, Chicago, Vol. 52, No. 1, pp. 106–20.
- ArcelorMittal 2008, *Design Guide for Floor Vibrations*, Luxembourg, p. 56, (also see http://www.arcelormittal.com/sections/fileadmin/redaction/pdf/Brochures/25_Novembre_2008_Vibration_EN.pdf, last accessed on 30 April 2012).
- ATC Design Guide 1 1999, *Minimizing Floor Vibration*, Applied Technology Council, Redwood City, p. 49.
- Ayyub, B.M., P.C. Chang, and N.A. Al-Mutairi 1994, 'Welded Wire Fabric for Bridges. II: Fatigue Strength', *Journal of Structural Engineering*, ASCE, Vol. 120, No. 6, pp. 1882–92.
- Bares, R. 1971, *Tables for the Analysis of Plates, Slabs and Diaphragms Based on the Elastic Theory*, Bauverlag GmbH, Wiesbaden and Berlin, p. 626.
- Base, G.D., J.B. Reed, A.W. Beeby, and H.P.J. Taylor 1966, *An Investigation of the Crack Control Characteristics of Various Types of Bar in Reinforced Concrete Beams*, Research Report No. 18, Cement and Concrete Association, London, p. 44.

- Bazant, Z.P. 1972, 'Prediction of Concrete Creep Effects using Age-adjusted Effective Modulus Method', *Proceedings, ACI Journal*, Farmington Hills, Vol. 69, No. 4, pp. 212–7.
- Bazant, Z.P., M.H. Hubler, and Q. Yu 2011, 'Pervasiveness of Excessive Segmental Bridge Deflections: Wake-Up Call for Creep', *ACI Structural Journal*, Farmington Hills, Vol. 108, No. 6, pp. 766–74.
- Bazant, Z.P., Q. Yu, G-H Li, G.J. Klein, and V. Kristek 2010, 'Excessive Deflections of Record-span Prestressed Box Girder', *Concrete International*, American Concrete Institute, Farmington Hills, Vol. 32, No. 6, pp. 44–52.
- Beeby, A.W. 1968, *Short-term Deformations of Reinforced Concrete Members*, Technical Report, TRA 408, Cement and Concrete Association, London.
- Beeby, A.W. and J.R. Miles 1969, 'Proposals for the Control of Deflection in the New Unified Code', *Concrete*, Concrete Society, London, Vol. 3, No. 3, pp. 101–10.
- Beeby, A.W. 1977, 'The Prediction of Crack Widths in Hardened Concrete', *The Structural Engineer*, Vol. 57A, No.1. pp. 9–17.
- Bischoff, P.H. 2005, 'Re-evaluation of Deflection Prediction for Concrete Beams Reinforced with Steel and Fiber Reinforced Polymer Bars', *Journal of Structural Engineering*, ASCE, Vol. 131, No. 5, pp. 752–67, and Gilbert, R.I. 2006, 'Discussion', Vol. 132, No. 8, pp. 1328–30.
- Bischoff, P.H. and A. Scanlon 2007, 'Effective Moment of Inertia for Calculating Deflections of Concrete Members Containing Steel Reinforcement and Fiber-Reinforced Polymer Reinforcement', *ACI Structural Journal*, American Concrete Institute, Farmington Hills, Vol. 104, No. 1, pp. 68–75.
- Bischoff, P.H. and A. Scanlon 2009, 'Span-depth Ratios for One-way Members based on ACI 318 Deflection Limits', *ACI Structural Journal*, American Concrete Institute, Farmington Hills, Vol. 106, No. 5, pp. 617–26.
- Branson, D.E. 1963, *Instantaneous and Time-dependent Deflections of Simple and Continuous Reinforced Concrete Beams*, Research Report No. 7, Alabama Highway Department, Montgomery, p. 94.
- Branson, D.E. 1971, 'Compression Steel Effect on Long-time Deflections', *Proceedings, ACI Journal*, American Concrete Institute, Farmington Hills, Vol. 68, No. 8, pp. 555–9.
- Branson, D.E. 1977, *Deformation of Concrete Structures*, McGraw-Hill, New York, p. 546.
- BS 8110: Part 2, 1985, *Structural Use of Concrete, Part 2: Code of Practice for Special Circumstances*, British Standards Institution, p. 57.
- Burgoyne, C. and R. Scantlebury 2006, 'Why did Palau Bridge collapse?', *The Structural Engineer*, The Institution of Structural Engineers, London, Vol. 84, No. 11, pp. 30–7.
- Carino, N.J. and J.R. Clifton 1995, *Prediction of Cracking in Reinforced Concrete Structures*, Report No: NISTIR 5634, Building and Fire Research Laboratory, National Institute of Standards and Technology, Gaithersburg, MD 20899, p. 51, (also see <http://www.fire.nist.gov/bfrlpubs/build95/PDF/b95081.pdf>, last accessed on 1 May 2012).
- CEB-FIP 1970, *International Recommendations for the Design and Construction of Concrete Structures*, Paris, p. 80 and CEB-FIP Model Code 1990, 1993, Design Code, Thomas Telford, London and Comité Euro-International du Béton, Switzerland, p. 462.
- Darwin, D. 1985, 'Debate: Crack Width, Cover, and Corrosion', *Concrete International*, American Concrete Institute, Farmington Hills, Vol. 7, No. 5, pp. 20–32.
- Das, S.K. 2004, 'Design of RC Slabs to Satisfy Both Bending and Deflection Criteria', *The Indian Concrete Journal*, ACC Ltd, Vol. 78, No. 3, pp.144–7.
- Desayi, P., K.U. Muthu, and K. Amarnath 1989, 'Deflection Control of Doubly Reinforced Beams', *International Journal of Structures*, Vol. 9, pp. 43–57.
- El-Salakawy, E. and B. Benmokrane 2004, 'Serviceability of Concrete Bridge Deck Slabs Reinforced with Fiber-reinforced Polymer Composite Bars', *ACI Structural Journal*, American Concrete Institute, Farmington Hills, Vol. 101, No. 5, pp. 727–36.
- Fanella, D.A. and B.G. Rabbat (ed.) 2002, *PCA Notes on ACI 318-02 Building Code Requirements for Structural Concrete with Design Applications*, 8th edition, Portland Cement Association, Illinois.
- FIB Bulletin No. 34: 2006, 'Model Code for Service Life Design', FIB Secretariat, Case Postale 88, CH-1015, Lausanne, Switzerland.
- Frantz, G.C. and J.E. Breen 1980, 'Design Proposal for Side Face Crack Control Reinforcement for Large Reinforced Concrete Beams', *Concrete International: Design and Construction*, American Concrete Institute, Farmington Hills, Vol. 2, No. 10, pp. 29–34.
- Frosch, R.J. 1999, 'Another Look at Cracking and Crack Control in Reinforced Concrete', *ACI Structural Journal*, Vol. 96, No. 3, pp. 437–42.
- Ganesan, N. and K.P. Shivananda 1996, 'Comparison of International Codes for the Prediction of Maximum Width of Cracks in Reinforced Concrete Flexural Members', *The Indian Concrete Journal*, ACC Ltd, Vol. 70, No. 11, pp. 635–41.
- Gardner N.J. 2011, 'Span/Thickness Limits for Deflection Control', *ACI Structural Journal*, American Concrete Institute, Farmington Hills, Vol. 108, No. 4, pp. 453–60.
- Gergely, P. and L.A. Lutz 1968, 'Maximum Crack Width in Reinforced Concrete Flexural Members', in R.E. Philleo (ed.), *Causes, Mechanism, and Control of Cracking in Concrete*, SP-20, American Concrete Institute, Detroit, pp. 87–117.
- Ghali, A. 1993, 'Deflection of Reinforced Concrete Members: A Critical Review', *ACI Structural Journal*, American Concrete Institute, Farmington Hills, Vol. 90, No. 4, pp. 364–73.
- Ghali, A., R. Favre, and M. El-Badry 2002, *Concrete Structures: Stresses and Deformations*, 3rd edition, E & FN Spon, London and New York, 2002, p. 605.
- Ghali, A., R. Favre, and M. Elbadry 2011, *Concrete Structures: Stresses and Deformations: Analysis and Design for Sustainability*, 4th edition, CRC Press, Boca Raton, p. 646.
- Gilbert, R.I. 1985, 'Deflection Control of Slabs Using Allowable Span to Depth Ratios', *Proceedings, ACI Journal*, American Concrete Institute, Farmington Hills, Vol. 82, No. 1, pp. 67–82.
- Gilbert, R.I. 1988, *Time Effects in Concrete Structures*, Elsevier Science Publishers, Amsterdam, p. 321.
- Gilbert, R.I. 1999, 'Deflection Calculation for Reinforced Concrete Structures—Why We Sometimes Get it Wrong', *ACI Structural Journal*, American Concrete Institute, Farmington Hills, Vol. 96, No. 6, pp. 1027–32.
- Gilbert, R.I. 2001, 'Shrinkage, Cracking and Deflection—The Serviceability of Concrete Structures', *Electronic Journal of Structural Engineering*, EJSE International, Melbourne, Vol. 1, No. 1, pp. 2–14, (also see <http://www.ejse.org/Archives/Full-text/200101/02/20010102.htm>, last accessed on 2 May 2012).

- Gilbert, R.I. 2007, 'Tension Stiffening in Lightly Reinforced Concrete Slabs', *Journal of Structural Engineering*, ASCE, Vol. 133, No. 6, pp. 899–903.
- Gilbert, R.I. 2008, 'Control of Flexural Cracking in Reinforced Concrete', *ACI Structural Journal*, American Concrete Institute, Farmington Hills, Vol. 105, No. 3, pp. 301–7.
- Gilbert, R.I. 2010. *The Serviceability of Concrete Structures—Design for Deflection and Crack Control*, Concrete Institute of Australia, Sydney, p. 234.
- Gilbert, R.I. 2011, 'The Serviceability Limit States in Reinforced Concrete Design', *Procedia Engineering*, Vol. 14, pp. 385–95.
- Gilbert, R.I. and X.H. Guo 2005, 'Time-dependent Deflection and Deformation of Reinforced Concrete Flat Slabs—an Experimental Study', *ACI Structural Journal*, American Concrete Institute, Farmington Hills, Vol. 102, No. 3, pp. 363–73.
- Gilbert, R.I. and A. Kilpatrick 2011, 'Improved Predictions of the Long-term Deflections of RC Flexural Members', *Proceedings of the FIB Symposium*, Prague, pp. 187–90, (also see http://ww2.integer.it/Web_1/database_locale/Fib%20Praga_2011/pdf/030%20596%20065%201%20Gilbert%20SE.pdf, last accessed on 14 April 2012).
- Gilbert, R.I. and G. Ranzi 2010, *Time Dependent Behaviour of Concrete Structures*, Taylor & Francis, London, p. 426.
- Gilbert, R.I. and R.F. Warner 1978, 'Tension Stiffening in Reinforced Concrete Slabs', *Proceedings, Structural Engineering Division*, ASCE, Vol. 104, No. ST12, pp. 1885–900.
- Goto, Y. 1971, 'Cracks Formed in Concrete around Deformed Tension Bars', *ACI Journal*, Vol. 68, No. 4, pp. 244–51.
- Grossman, J.S. 1981, 'Simplified Computations for Effective Moment of Inertia (I_e) and Minimum Thickness to Avoid Deflection Computations', *Proceedings, ACI Journal*, American Concrete Institute, Farmington Hills, Vol. 78, No. 6, pp. 423–39. In addition, 1982, 'Author Closure', *Proceedings, ACI Journal*, American Concrete Institute, Farmington Hills, Vol. 79, No. 5, pp. 414–9.
- Hanson, J.M., N.F. Somes, T. Helgason, W.G. Corley, and E. Hognestad 1976, *Fatigue Strength of High Yield Reinforcing Bars*, National Cooperative Highway Research Program Report 164, Transportation Research Board, Washington, DC.
- Hossain, T.R., R. Vollum, and S.U. Ahmed 2011, 'Deflection Estimation of Reinforced Concrete Flat Plates using ACI Method', *ACI Structural Journal*, American Concrete Institute, Farmington Hills, Vol. 108, No. 4, pp. 405–13.
- Kaar, P.H. and E. Hognestad 1965, 'High Strength Bars as Concrete Reinforcement, Part 7: Control of Cracking in T-beam Flanges', *Journal, Portland Cement Association Research and Development Laboratories*, Vol. 7, No. 1, pp. 42–53.
- Kripanarayanan, K.M. and D.E. Branson 1976, 'Short-time Deflections of Flat Plates, Flat Slabs, and Two-way Slabs', *Proceedings, ACI Journal*, American Concrete Institute, Farmington Hills, Vol. 73, No. 12, pp. 686–90.
- Lee, Y.H. and A. Scanlon 2010, 'Comparison of One- and Two-way Slab Minimum Thickness Provisions in Building Codes and Standards', *ACI Structural Journal*, American Concrete Institute, Farmington Hills, Vol. 107, No. 2, pp. 157–63.
- Leonhardt, F. 1977, 'Crack Control in Concrete Structures', *IABSE Surveys*, No. S-4/77, International Association for Bridge and Structural Engineering, Zurich, p. 26.
- Leonhardt, F. 1987, 'Cracks and Crack Control in Concrete Structures', *IABSE Proceedings*, P109/87, International Association for Bridge and Structural Engineers, Zurich, pp. 25–44.
- Maghsoudi, A.A. and B.H. Akbarzadeh 2007, 'Effect of Tension and Compression Reinforcements on the Serviceability of HSC Beams with Relatively Small Shear Span to Depth Ratio', *The Arabian Journal for Science and Engineering*, Vol. 32, No. 2B, pp. 219–38, (also see http://ajse.kfupm.edu.sa/articles/322B_P.03.pdf, last accessed on 12 May 2012).
- Marzouk, H., M. Houssin, and A. Hussein 2010, 'Crack Width Estimation for Concrete Plates', *ACI Structural Journal*, Vol. 107, No. 3, American Concrete Institute, Farmington Hills, pp. 282–90.
- Mazzotti C. and M. Savoia 2009, 'Long-term Deflection of Reinforced Self-consolidating Concrete Beams', *ACI Structural Journal*, American Concrete Institute, Farmington Hills, Vol. 106, No. 6, pp. 772–81.
- Murashev, V.I., E.E. Sigalov, and V.N. Baikov 1971, *Design of Reinforced Concrete Structures*, 2nd edition, Mir Publishers, Moscow, p. 579.
- Murray, T.M., D.E. Allen, and E.E. Unger 1997, *Design Guide 11: Floor Vibrations due to Human Activity*, American Institute of Steel Construction, Chicago, p. 71.
- Naeim, F. 1991, 'Design Practice to Prevent Floor Vibrations', *Steel Tips*, Structural Steel Educational Council, California, p. 28, (also see <http://www.johnmartin.com/publications/Vibration/Design.pdf>, last accessed on 18 January 2012).
- Nayak, S.K. and D. Menon 2004, 'Improved Procedure for Estimating Short Term Deflections in RC Slabs', *The Indian Concrete Journal*, ACC Ltd, Vol. 78, No. 7, pp. 19–25.
- Nawy, E.G. 1972, 'Crack Control through Reinforcement Distribution in Two-way Slabs and Plates', *Proceedings, Journal of ACI*, American Concrete Institute, Farmington Hills, Vol. 69, No. 4, pp. 217–9.
- Nawy, E.G. 2001, 'Design for Crack Control in Reinforced and Prestressed Concrete Beams, Two-way Slabs and Circular Tanks—A State-of-the art', in SP-204, *Design and Construction Practices to Mitigate Cracking*, American Concrete Institute, Farmington Hills, pp. 1–42.
- Nawy, E.G. 2005, *Reinforced Concrete—A Fundamental Approach*, 5th edition, Pearson-Prentice Hall, New Jersey, pp. 500–7.
- Neville, A.M., W.H. Dilger, and J.J. Brooks 1983, *Creep of Plain and Structural Concrete*, Construction Press, London, p. 380.
- Nilson, A.H. and D.B. Walters 1975, 'Deflection of Two-way Floor Systems by the Equivalent Frame Method', *Proceedings, ACI Journal*, American Concrete Institute, Farmington Hills, Vol. 72, No. 5, pp. 210–8.
- Noguchi, T., F. Tomosawa, K.M. Nemati, B.M. Cjiaia, and A.P. Fantilli 2009, 'A Practical Equation for Elastic Modulus of Concrete', *ACI Structural Journal*, American Concrete Institute, Farmington Hills, Vol. 106, No. 5, pp. 690–6.
- Oesterle, R.G. 1997, *The Role of Concrete Cover in Crack Control Criteria and Corrosion Protection*, RD Serial No. 2054, Portland Cement Association, Skokie.
- Park, H.-G., H.-J. Hwang, G.-H. Hong, Y.-N. Kim, and J.-Y. Kim 2011, 'Slab Construction Load Affected by Shore Stiffness and Concrete Cracking', *ACI Structural Journal*, American Concrete Institute, Farmington Hills, Vol. 108, No. 6, pp. 679–88.
- Park, R. and T. Paulay 1975, *Reinforced Concrete Structures*, John Wiley and Sons, New York, p. 769.

- Paulson, K., A.H. Nilson, and K.C. Hover 1991, 'Long-term Deflection of High-strength Concrete Beams', *ACI Materials Journal*, American Concrete Institute, Farmington Hills, Vol. 88, No. 2, pp. 197–206.
- Purushothaman, P. 1984, *Reinforced Concrete Structural Elements—Behaviour, Analysis and Design*, Tata McGraw Hill Publishing Company Ltd, New Delhi and Torsteel Research Foundation in India, Bangalore, p. 709.
- Rangan, B.V. 1976, 'Prediction of Long-term Deflections of Flat Plates and Slabs', *Proceedings, ACI Journal*, American Concrete Institute, Farmington Hills, Vol. 73, No. 4, pp. 223–6.
- Rangan, B.V. 1982, 'Control of Beam Deflections by Allowable Span to Depth Ratios', *Proceedings, ACI Journal*, American Concrete Institute, Farmington Hills, Vol. 79, No. 5, pp. 372–7.
- Rao, P.S. 1966, *Die Grundlagen zur Berechnung der bei statisch unbestimmten Stahlbeton konstruktionen im plastischen Bereich auftretenden Umlagerungen der Schnittkräfte (Basic laws governing moment redistribution in statically indeterminate reinforced concrete structures)*, DAfStb, Ernst and Sohn, Berlin, Heft 177.
- Rizk, E. and H. Marzouk 2010, 'A New Formula to Calculate Crack Spacing for Concrete Plates', *ACI Structural Journal*, American Concrete Institute, Farmington Hills, Vol. 107, No. 1, pp. 43–52.
- Samra, R.M. 1997, 'Time-dependent Deflection of Reinforced Concrete Beams Revisited', *Journal of Structural Engineering*, ASCE, Vol. 123, No. 6, pp. 823–30.
- Sbarounis, J.A. 1984, 'Multi-story Flat Plate Buildings: Measured and computed One-year Deflections', *Concrete International*, American Concrete Institute, Farmington Hills, Vol. 6, No. 8, pp. 31–5.
- Scanlon, A. and Bischoff, P.H. 2008, 'Shrinkage Restraint and Loading History Effects on Deflections of Flexural Members', *ACI Structural Journal*, American Concrete Institute, Farmington Hills, Vol. 105, No. 4, pp. 498–506.
- Scanlon, A. and N.J. Gardner 2006, 'Deflection', in *Concrete Design Handbook*, 3rd edition, Cement Association of Canada, Ottawa, Chapter 6, pp. 6-1 to 6-38.
- Scanlon, A. and Y.H. Lee 2006, 'Unified Span-to-depth Ratio Equation for Non-prestressed Concrete Beams and Slabs', *ACI Structural Journal*, American Concrete Institute, Farmington Hills, Vol. 103, No. 1, pp. 142–8.
- Scanlon, A. and D.W. Murray 1982, 'Practical Calculation of Two-way Slab Deflections', *Concrete International: Design and Construction*, American Concrete Institute, Farmington Hills, Vol. 4, No. 11, pp. 43–50.
- SP 24(S&T):1983, *Explanatory Handbook on Indian Standard Code of Practice for Plain and Reinforced Concrete*, Bureau of Indian Standards, New Delhi, p. 164.
- Subramanian, N. 1979, 'Deterioration of Concrete Structures: Causes and Remedial Measures', *The Indian Highways*, Indian Roads Congress, New Delhi, Vol. 7, No. 3, pp. 5–10.
- Subramanian, N. 1989, 'Diagnosis of the Causes of Failures', *The Bridge and Structural Engineer, Journal of the Indian National Group of the IABSE*, Vol. 19, No. 1, pp. 24–42.
- Subramanian, N. 2005, 'Controlling the Crack Width of Flexural RC Members', *The Indian Concrete Journal*, ACC Ltd, Vol. 79, No. 11, pp. 31–6.
- Subramanian, N. and K. Geetha 1997, 'Concrete Cover for Durable RC Structures', *The Indian Concrete Journal*, ACC Ltd, Vol. 71, No. 4, pp. 197–201.
- TRC Circular E-C107 2006, *Control of Cracking in Concrete: State-of-the-Art*, Transportation Research Board, Washington, DC, p. 56, (also see <http://onlinepubs.trb.org/onlinepubs/circulars/ec107.pdf>, last accessed on 31 March 2012).
- Treece, R.A. and J.O. Jirsa 1989, 'Bond Strength of Epoxy Coated Reinforcing Bars', *ACI Materials Journal*, American Concrete Institute, Farmington Hills, Vol. 86, No. 2, pp. 167–74.
- Watstein, D. and D.E. Parsons 1943, 'Width and Spacing of Tensile Cracks in Axially Reinforced Concrete Cylinders', *Journal of Research of the National Bureau of Standards*, Vol. 31, No. RP545, pp. 1–24.
- Wight, J. K. and J. G. MacGregor 2009, *Reinforced Concrete: Mechanics and Design*, 5th edition, Pearson Prentice Hall, New Jersey, p. 1112.
- Yu, W.W. and G. Winter 1960, 'Instantaneous and Long-term Deflections of Reinforced Concrete Beams under Working Loads', *Proceedings, ACI Journal*, American Concrete Institute, Farmington Hills, Vol. 57, No. 1, pp. 29–50.

DESIGN OF AXIALLY LOADED SHORT COLUMNS

13.1 INTRODUCTION

As mentioned in Section 2.2.2 of Chapter 2, a structural element that is predominantly subjected to axial compressive forces is termed a *compression member*. When a compression member is vertical, it is called a *column*, and when it is horizontal or inclined, it is called a *strut*. Struts are usually found in concrete trusses. The cross-sectional dimensions of a column are generally considerably lesser than its height. Many times, columns may carry a secondary bending moment about the major or minor axis or about both the axes. These may produce tensile stresses over some part of the cross section. However, still columns are referred to as the compression members because they predominantly carry compressive forces. A column that springs from a beam is referred to as a *floating column*, which is to be avoided; if unavoidable, it should be interconnected to other structural systems to ensure the safe transfer of lateral loads to the foundation. Proper care should also be taken in detailing the column-beam joint, from where the floating column springs. Columns transmit all the forces applied on them through floors and beams of upper floors to the lower levels and then to the soil through the foundations. Thus, they are very important for the proper functioning of the building, as the failure of a column in a critical location may result in the collapse of the entire building.

In this chapter, the term column will be used interchangeably with the term compression member, for the sake of brevity. Upright compression members that support decks in bridges are often called *piers*. A short compression member, with a height less than three times its least lateral dimension, placed at the base of columns to transfer the load of columns to a footing, pile cap, or mat is called a *pedestal* or a *stub column* (see note under Clause 26.5.3.1h of IS 456). Upright slender

members mostly circular in shape and subjected to dominant bending moment and nominal compression are called *poles*, *pillars*, or *posts*. As per Clause 25.1.1 of IS 456, a column or strut is defined as a compressive member whose effective length exceeds three times the least lateral dimension. In this chapter, we will be concerned with the design and detailing of short columns subjected predominantly to axial compression. Detailing of columns in earthquake zones is also discussed. Design of long columns, as well as columns with axial compression and bending, is discussed in Chapter 14.

13.2 CLASSIFICATION OF COLUMNS

Columns can be classified based on their shape, type of reinforcement used, type of loading to which they are subjected, and their slenderness.

13.2.1 Based on Cross Section

Based on architectural requirements, columns may have cross sections such as rectangular, square, circular, hexagonal, T, L, or + shapes, as shown in Fig. 2.4 of Chapter 2 and Fig. 13.1.



(a)



(b)

FIG. 13.1 Classification of columns (a) Tall circular columns supporting a highway in Pittsburgh, USA (b) Rectangular building columns in India

Courtesy: Akshaya Pvt. Ltd

13.2.2 Based on Type of Reinforcement

Based on the type of reinforcement provided, reinforced concrete (RC) columns are classified into the following three types:

Tied columns Columns reinforced with longitudinal reinforcement and lateral (transverse) ties (see Fig. 2.5a of Chapter 2 and Fig. 13.1b)

Spiral columns Columns with longitudinal reinforcement tied by continuous spiral reinforcement (see Fig. 2.5b of Chapter 2).

Composite columns Columns reinforced longitudinally with structural steel sections, such as hollow tubes and I-sections, with or without additional longitudinal reinforcement or transverse reinforcement (see Fig. 2.5c of Chapter 2).

The first two types of columns are most commonly used in RC structures. Tied columns are applicable to all cross-sectional shapes, whereas spiral reinforcement is used mainly in columns of circular cross section, though they can have hexagonal, octagonal, or even square shapes. This chapter primarily deals with only the first two types of columns. Information on composite columns may be found in the works of Suryanarayana (1993), Roik and Bergmann (1992), and Leon, et al. (2007).

13.2.3 Based on Types of Loading

Columns may also be classified into the following three types, based on the loads acting on them:

Columns with concentrically applied loads Such columns (see Fig. 13.2a) with zero bending moment are rare. In multi-storey frames, as shown in Fig. 13.3, interior columns like A will be subjected to axial compression and shear, under gravity

loads (in columns, shear resistance will be high due to the presence of axial compression and the lateral ties).

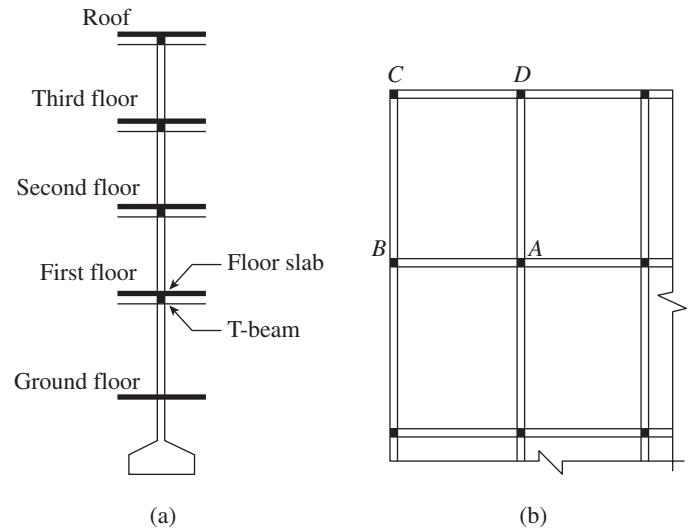


FIG. 13.3 Columns in typical multi-storey buildings (a) Section through column (b) Part floor plan

Columns with uniaxial eccentricity— $e_x = 0$, $e_y \neq 0$ or $e_x \neq 0$, $e_y = 0$ Edge columns such as B and D in Fig. 13.3 are subjected to uniaxial bending moments. Practically, a small bending moment in the other direction is also present but may be neglected in most of the cases. A column with axial compression, P , and bending moment, M , may be analysed as an equivalent column subjected to an axial compressive force P acting at an eccentricity $e = M/P$, as shown in Fig. 13.2(b).

Columns with biaxial eccentricity— $e_x \neq 0$ and $e_y \neq 0$ Corner columns like C in multi-storey buildings (see Fig. 13.3) are subjected to biaxial bending moments in addition to the compressive force. In this case $e_x = M_x/P$ and $e_y = M_y/P$. When subjected to lateral loads, most of the columns in a building will be subjected to uniaxial or biaxial bending moments (see Fig. 13.2c).

13.2.4 Based on Slenderness Ratio

Columns, struts, beams, and ties are often *slender members*. *Slenderness ratio* of a member is defined as the ratio of the effective length to the radius of gyration of the section. Thus,

$$\text{Slenderness ratio} = \frac{L_e}{r} \quad (13.1a)$$

$$\text{and} \quad r = \sqrt{\frac{I}{A}} \quad (13.1b)$$

where L_e is the *effective length* of the member (see Section 13.3.2), r is the *radius of gyration* of the section about the effective length axis (for rectangular section, $r_x = D/\sqrt{12} = 0.3D$

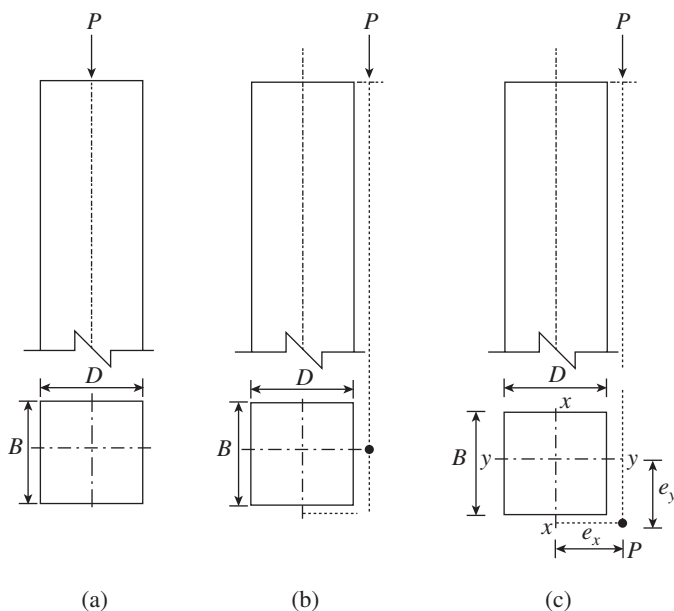


FIG. 13.2 Cross section of column with different types of loading (a) Concentric axial loading (b) Loading with one axis eccentricity (c) Loading with biaxial eccentricities

about major axis and $r_y = 0.3B$ about minor axis, and for circular section, $r = 0.25D_c$, I is the moment of inertia (also called the *second moment of area*), A is the area of the section, D and B are the width and depth, respectively, of the rectangular column, and D_c is the diameter of the circular column.

The cross section of slender members has two axes and hence there are two moments of inertia. Similarly, the support to the column may be different for the two axes. Hence, the radius of gyration must be calculated for the two axes separately and the higher L_e/r ratio should be considered in the design. Since solid sections are often used in RC, a factor called *slenderness factor* is used instead of the slenderness ratio. It is given by the following expression:

$$\text{Slenderness factor, } g = \frac{L_e}{d} \quad (13.2)$$

where d is the depth of the cross section of column about which the column is likely to buckle (least lateral dimension) and L_e is the effective length of the column in the plane of buckling.

Based on the slenderness factor, columns can be classified as follows:

Short columns These types of columns generally fail after reaching the ultimate load carrying capacity of columns.

Slender columns These types of columns generally fail suddenly at relatively low compressive loads due to buckling.

Thus, slenderness factor represents the vulnerability of column failure by buckling. As per Clause 25.1.2 of IS 456:2000, columns are considered as short columns when the slenderness factor about both the axes (i.e., L_{ex}/D and L_{ey}/B , where B and D are breadth and depth, respectively, of column, L_{ex} is the effective length in major axis, and L_{ey} is the effective length in minor axis) is less than 12. According to Clause 10.10.1 of ACI 318, columns may be considered as slender if L_e/r is greater than $[34 - 12(M_1/M_2) \leq 40]$ in the case of braced columns and is greater than 22 in the case of unbraced columns, where M_1 and M_2 are the bending moments acting at the two ends of the column; M_1/M_2 is positive if the column is bent in single curvature and negative if the member is bent in double curvature.

13.3 UNSUPPORTED AND EFFECTIVE LENGTHS OF COLUMNS

In the design of columns, we should distinguish between the unsupported length and effective length. The difference between the two is explained in this section.

13.3.1 Unsupported Length

The unsupported length, L , of a compression member is taken as the clear height of the column. Clause 25.1.3 of IS 456 defines unsupported length for various types of constructions as follows:

1. In flat slab or flat plate construction, it is the clear distance between the floor and the extremity of the slab, the drop

panel, or column capital, whichever is the minimum (see Figs 13.4a–c).

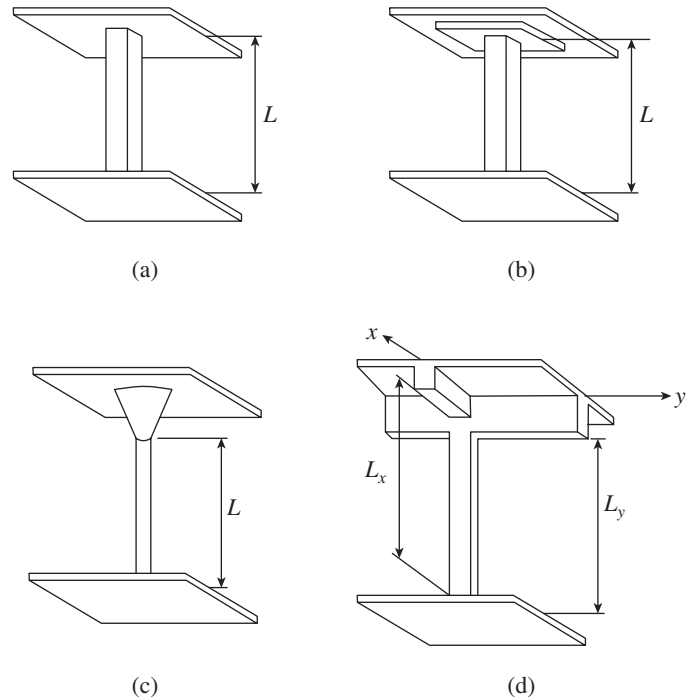


FIG. 13.4 Unsupported length of columns (a) Flat plate (b) Flat slab (c) Column capital (d) Slab with beams

- In beam slab construction, it is taken as the clear distance between the floor and the underside of the beam. It has to be noted that the unsupported length of a column may be different in two orthogonal directions depending on the supporting elements in the respective directions. Figure 13.4(d) shows this case where unsupported lengths L_x and L_y are different. Each coordinate and subscript x and y in the figure indicates the plane of the frame in which the stability of the column is investigated.
- In columns restrained laterally by intermediate struts, it should be taken as the clear distance between consecutive struts in each vertical plane. To provide adequate support, two such struts should meet the column at the same level and the angle between vertical planes through the struts should not be more than 30° from the right angle. Such struts are expected to have sufficient size and sufficient anchorage to restrain the column against lateral deflection.
- In columns with haunches, it is taken as the clear distance between the floor and lower edge of the haunch in the plane considered.
- In columns with brackets, it is the clear distance between the floor and lower edge of the bracket, provided the width of the bracket is equal to at least half the width of the column.

13.3.2 Buckling of Columns and Effective Length

Columns, when concentrically loaded, may fail in one of the following modes of failure, depending on the slenderness ratio:

Pure compression failure Short columns, with L_e/b ratio less than 12, will fail by the crushing of concrete without undergoing any lateral deformation.

Buckling failure Slender columns, with L_e/b ratio greater than 30, will become unstable even under small loads, well before the materials reach their yield stresses. When such columns are loaded, at a particular load, called the *buckling load*, the column undergoes buckling with lateral deflection transverse to the applied load of undefined magnitude as shown in Fig. 13.5. The horizontal line in this figure indicates the lateral deflection and instability of the column. If the column is also subjected to bending moment or transverse load, the column deflects as shown by the curved line in Fig. 13.5(b). The buckling of the column is initiated in the plane about which the slenderness ratio is the largest. Such buckling failures are rare in RC columns, as the slenderness factor of practical columns is less than 30.

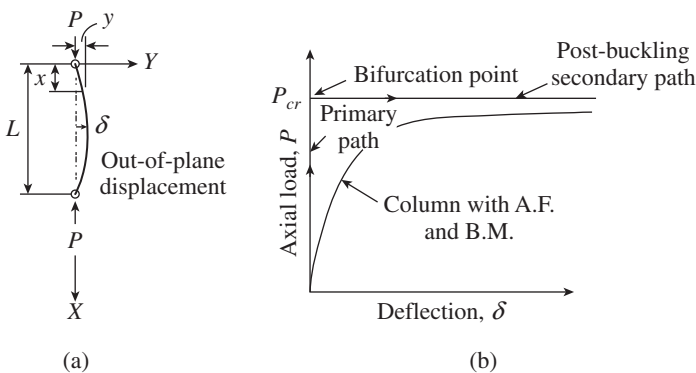


FIG. 13.5 Buckling behaviour of columns (a) Column (b) Load vs deflection curve

Combined compression and bending failure Most of the RC columns may be subjected to axial load and bending moment due to eccentricity of load or from connecting beams or slabs. Such slender columns will undergo deflection along their length as beam columns, and these deflections produce additional secondary bending moments in the columns. When material failure is reached under the combined action of these direct loads and bending moments, the failure is termed as combined compression and bending failure.

The differential equation for axially loaded column with hinged ends as shown in Fig. 13.5(a) is

$$\frac{d^2 y}{dx^2} + \left(\frac{P}{EI} \right) y = 0 \quad (13.3)$$

Euler (1759) derived the solution to this differential equation as

$$P_{cr} = \frac{n^2 \pi^2 EI}{L^2} \quad (13.4a)$$

where EI is the flexural rigidity of the column cross section, L is the length of the column, and n is the number of half sine waves in the deformed shape of the column. The lowest value of P_{cr} will occur with $n = 1.0$. This value is referred to as *Euler's buckling load* and is given by

$$P_{cr} = \frac{\pi^2 EI}{L^2} \quad (13.4b)$$

The critical load for fixed-end column has been derived as

$$P_{cr} = \frac{4\pi^2 EI}{L^2} \quad (13.4c)$$

The buckling loads of columns with different boundary conditions may also be considered by the concept of effective lengths. The *effective length* of a column in the considered plane may be defined as the distance between the *points of inflection* (zero moment) in the buckled configuration of the column in that plane.

Thus, the effective length of a column is different from the unsupported length L of the column. The effective length L_e depends on the unsupported length and the type of end restraints. The relation between the effective and unsupported lengths of any column is given by

$$L_e = kL \quad (13.5)$$

where k is the ratio of the effective length to the unsupported length.

Effective length factors for columns with idealized support conditions are shown in Fig. 13.6. In a frame, when relative transverse displacement between the upper and lower ends of a column is prevented, the frame is considered to be *braced against side sway*. Similarly, when relative transverse displacement between the upper and lower ends of a column is not prevented, the frame is considered to be *unbraced against side sway*. It has to be noted that the value of k varies between 0.5 and 1.0 for laterally braced columns and 1.0 and ∞ for unbraced columns.

When there is relative transverse displacement between the upper and lower ends of a column, the points of inflection may not lie within the member. In such a case, they may be located by extending the deflection curve beyond the column ends and by applying conditions of symmetry as shown in Figs 13.6(d)–(e).

Table 28 of IS 456 suggests effective length L_e of columns, in a given plane, for idealized support conditions, as shown in Table 13.1.

Columns with hinged ends are rare in cast in situ concrete construction, though they may occur in precast structures. Most concrete buildings may be assumed as fully braced

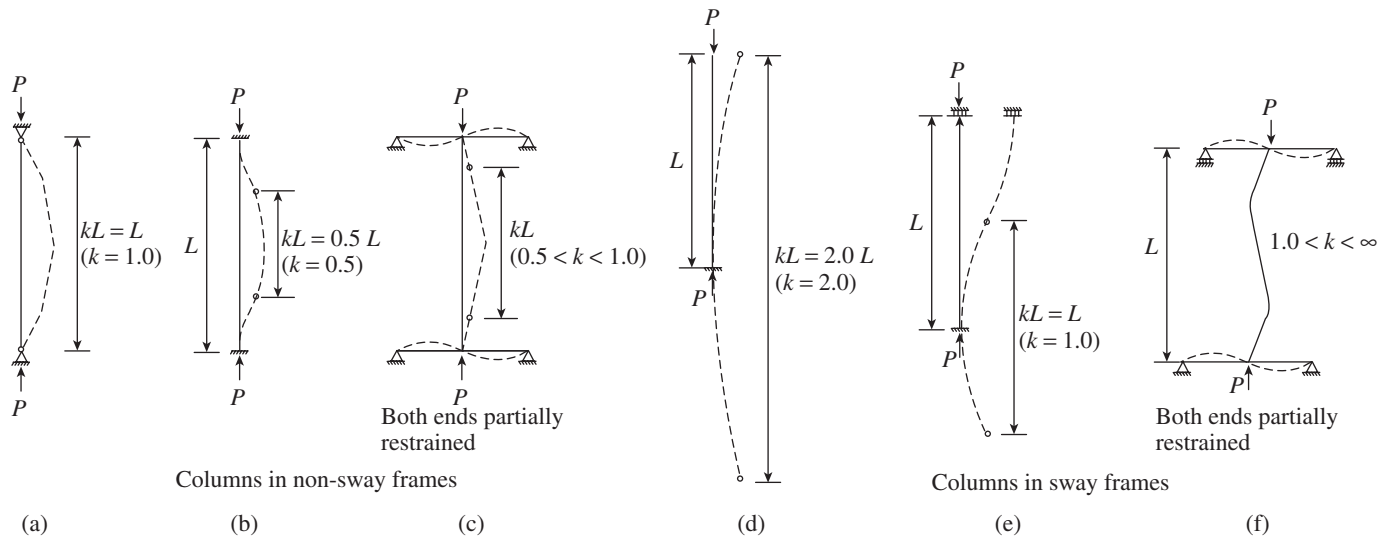
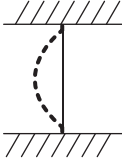
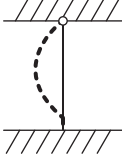
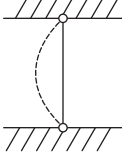
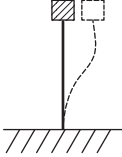


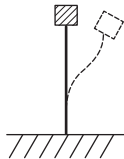
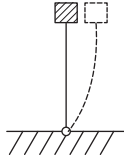
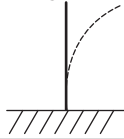
FIG. 13.6 Effective length factor k for columns (a) Hinged ends (b) Fixed ends (c) Partially restrained ends (d) Cantilevered (e) One end fixed and the other end restrained against rotation but not held in position (f) Partially restrained ends

TABLE 13.1 Effective length of columns for different support conditions

S. no.	Description	Theoretical Effective Length	Recommended Effective Length, L_e
1.	Effectively held in position and restrained against rotation at both ends 	$0.50L$	$0.65L$
2.	Effectively held in position at both ends, restrained against rotation at one end 	$0.70L$	$0.80L$
3.	Effectively held in position at both ends, but not restrained against rotation 	$1.00L$	$1.00L$
4.	Effectively held in position and restrained against rotation at one end, and restrained against rotation but not held in position at the other end 	$1.00L$	$1.20L$

(Continued)

TABLE 13.1 (Continued)

S. no.	Description	Theoretical Effective Length	Recommended Effective Length, L_e
5.	Effectively held in position and restrained against rotation in one end, and partially restrained against rotation but not held in position at the other end 	–	$1.50L$
6.	Effectively held in position at one end but not restrained against rotation, and restrained against rotation but not held in position at the other end 	$2.00L$	$2.00L$
7.	Effectively held in position and restrained against rotation at one end but not held in position nor restrained against rotation at the other end 	$2.00L$	$2.00L$

Note: L is the unsupported length of the column.

(non-sway), as they will have bracing elements such as shear walls, stairwells, or elevator shafts, which are considerably stiffer than columns. Occasionally, unbraced frames may be found in industrial buildings where an open bay may be required to accommodate a travelling crane. When there are in-filled walls, the building frame may be assumed as partially braced. Most columns in practice are short columns and will also have partial rotational fixity at both ends. For such a case, we may assume $k = 0.85$ for preliminary designs, if the frame is braced. However, if the frame is partially braced, a more conservative value of $k = 1.0$ may be assumed (SP 24:1983). In the case of unbraced frames, the code clause E-1 recommends a minimum value of $k = 1.2$. Some bridge piers may be classified as slender columns (see Fig. 13.7).



FIG. 13.7 Piers of Millau Viaduct, France

Source: http://www.leviaducdemillau.com/version_html/phototheque.php, reprinted with permission.
Copyright: Eiffage CEVM/Foster + Partners/D.Jamme.

The highest piers-cum-pylons in the world were constructed for the Millau Viaduct, France, shown in Fig. 13.7. The piers have heights varying between 77.56 m and 244.96 m. These were designed by the structural engineer Michel Virlogeux and British architect Norman Foster.

13.4 DETERMINATION OF EFFECTIVE LENGTH OF COLUMNS IN FRAMES

End restraints of columns in building frames cannot be easily categorized into the simple end restraints as shown in Table 13.1. Real columns have partially restrained ends and their effective length depends on the ratio of the flexural stiffness of the column to the summation of column stiffness and flexural stiffness of beams connected to the ends. Different methods have been suggested to predict the effective length of such columns. Two sets of curves (one set for columns in non-sway frames and another set for columns in sway frames) are provided in Annexure E of IS 456:2000 and are based on the curves originally proposed by Wood (1974) (see Figs 13.8 and 13.9).

It is interesting to note that Wood's curves are also used in IS 800:2007 for determining the effective length of steel columns. The code also gives the following equations for the effective length factor k , based on Wood's curves:

1. For non-sway frames:

$$k = \frac{1 + 0.145(\beta_1 + \beta_2) - 0.265\beta_1\beta_2}{2 - 0.364(\beta_1 + \beta_2) - 0.247\beta_1\beta_2} \quad (13.6a)$$

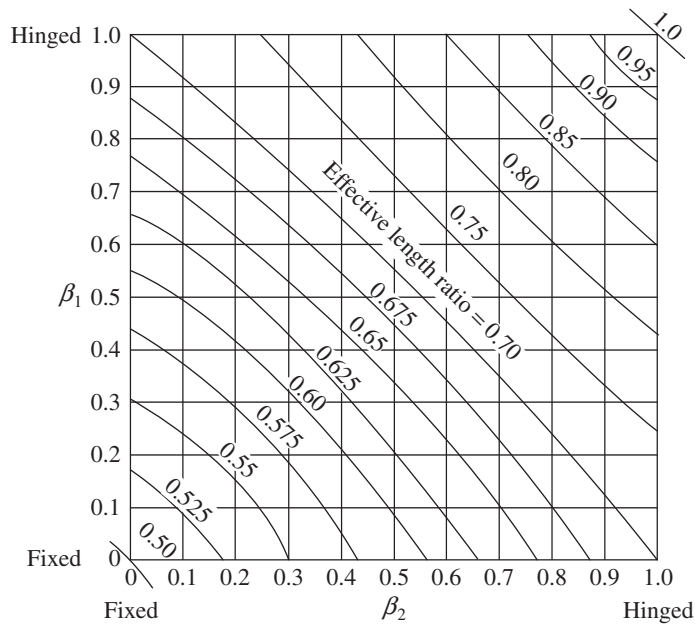


FIG. 13.8 Effective length ratios for a column in a non-sway frame

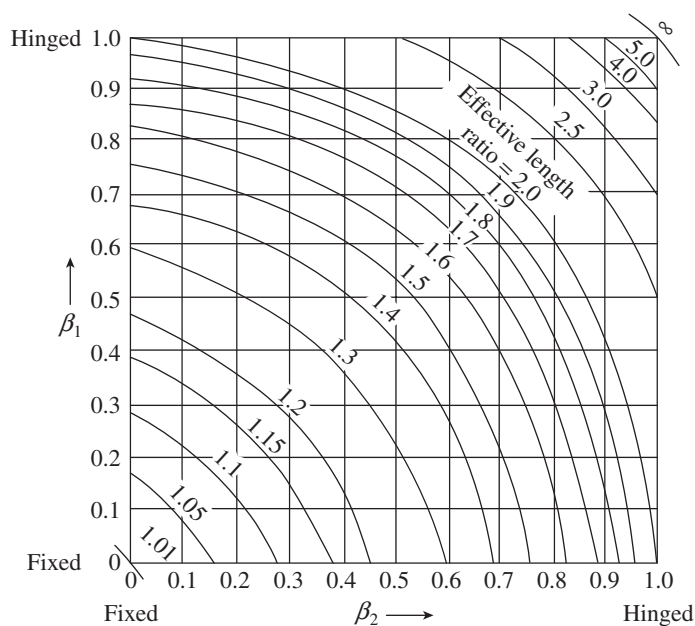


FIG. 13.9 Effective length ratios for a column in a sway frame

2. For sway frames:

$$k = \left(\frac{1 - 0.2(\beta_1 + \beta_2) - 0.12\beta_1\beta_2}{1 - 0.8(\beta_1 + \beta_2) + 0.6\beta_1\beta_2} \right)^{0.5} \quad (13.6b)$$

where $\beta_i = \frac{\Sigma K_c}{\Sigma K_c + \Sigma K_b}$, with $i = 1, 2$ (13.6c)

and ΣK_c and ΣK_b = summation of effective flexural stiffness of columns and beams (EI/L) framing into top joint and bottom joint, respectively, for calculating β_1 and β_2 .

While using Wood's curves, the following stiffness factors are used for computation (SP 24:1983):

$$K_c = \frac{I_c}{L_c} \quad (13.7a)$$

$$K_b = \frac{1}{2} \frac{I_b}{L_b} \quad \text{for braced columns} \quad (13.7b)$$

$$K_b = 1.5 \frac{I_b}{L_b} \quad \text{for unbraced columns} \quad (13.7c)$$

where I_b and I_c are the second moments of area of the beam and column, respectively, and L_b and L_c are the lengths of the beam and column, respectively, taken as centre-to-centre distance of the intersecting member. The increased beam stiffness for the unbraced columns (Eq. 13.7c) compared to braced columns (Eq. 13.7b) is because the braced columns will be bent in *single curvature* and the unbraced columns will be bent in *double curvature*. It has to be noted that in the case of a column fixed at its base, $\Sigma K_b = \infty$ and hence $\beta_2 = 0.0$. Conversely, for a hinged column $\Sigma K_b = 0$ and hence $\beta_2 = 1.0$. As already mentioned, in the case of unbraced (sway) frames, it is good practice to adopt a minimum value of $k = 1.2$. A review of the IS code provisions for effective length of columns in frames is provided by Dafedar, et al. (2001).

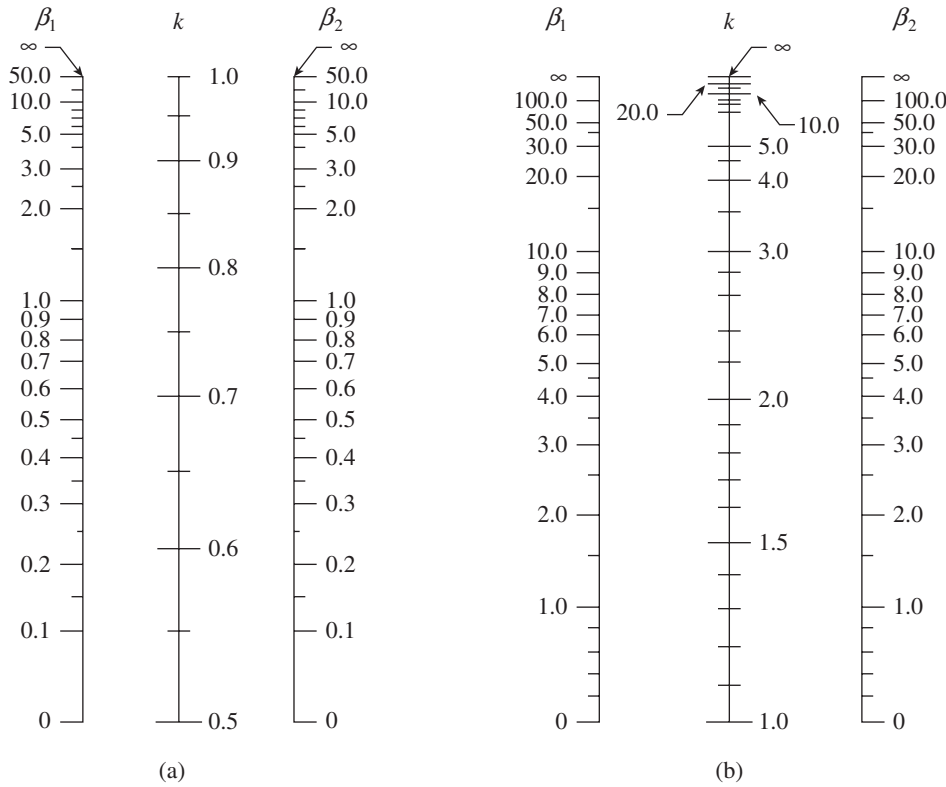
The American code suggests the use of *Jackson and Moreland alignment charts* (also called *Julian and Lawrence nomograph*) developed in 1959 (see Fig. 13.10), which allow graphical determination of the effective length factor, k , for a column of constant cross section in a multi-bay frame (Johnston 1966; Kavanagh 1962). These charts were derived by considering a typical interior column in an infinitely high and infinitely wide frame, in which all the columns and beams have the same cross section and length. Equal loads were applied at the tops of each of these columns, while the beams remained unloaded. Due to these assumptions, these charts may tend to underestimate the value of k for elastic frames of practical dimensions by up to 15 per cent, which in turn underestimate the magnified moments (Lai, et al. 1983). To use these charts, β_1 and β_2 values are calculated at both ends of the column using Eq. (13.6c) and then a line is drawn connecting the values of β at the top and bottom of the column; the intersection of this line with the line labelled k in Fig. 13.10 gives the value of the effective length factor k .

The British code BS 8110, Part 2:1985, provides the following simple equations for calculating the effective length factor, k :

1. For braced columns (in non-sway frames), the lesser of the following:

$$k = 0.7 + 0.05(\alpha_1 + \alpha_2) \leq 1 \quad (13.8a)$$

$$k = 0.85 + 0.05\alpha_{\min} \leq 1 \quad (13.8b)$$



$\beta =$ Ratio of $\sum(EI/L_c)$ of column to $\sum(EI/L_b)$ of flexural members in a plane at one end of column
 L_b and $L_c =$ Length of column and beam, respectively, measured centre to centre of joints

FIG. 13.10 Jackson and Moreland alignment charts as per ACI 318 (a) Non-sway frames (b) Sway frames, reprinted with permission from ACI

2. For unbraced columns (in sway frames), the lesser of the following:

$$k = 1.0 + 0.15(\alpha_1 + \alpha_2) \quad (13.9a)$$

$$k = 2.0 + 0.30\alpha_{\min} \quad (13.9b)$$

where α_{\min} is the lesser of the α values at the two ends of the column and $\alpha_i = \frac{\sum I_c / L_c}{\sum I_b / L_b}$; with $i = 1, 2$. For fully fixed condition and hinged condition, α is taken as 0 and 10, respectively.

ACI Committee 340:1978 suggested the following formulae for unbraced columns (in sway frames):

$$\text{For } \alpha_{\text{ave}} < 2, \quad k = \frac{20 - \alpha_{\text{ave}}}{20} \sqrt{1 + \alpha_{\text{ave}}} \quad (13.9c)$$

$$\text{For } \alpha_{\text{ave}} \geq 2, \quad k = 0.9 \sqrt{1 + \alpha_{\text{ave}}} \quad (13.9d)$$

where α_{ave} is the average of the α values at the two ends of the column.

13.4.1 Sway and Non-sway Frames

It is seen from the foregoing discussions that the effective lengths of sway and non-sway frames differ considerably. A column may be assumed non-sway when the ratio of the total

lateral stiffness of the bracing elements to that of the columns in a storey is considerable. Clause 10.10.1 of ACI 318 allows compression members to be considered as braced against side sway when bracing elements like shear walls have a total stiffness of at least 12 times the gross stiffness of all the columns in the storey. If not readily apparent by inspection, the following two different criteria may be used:

1. A storey in a frame can be considered as non-sway if the increase in the lateral load moments resulting from the $P-\Delta$ effects (also called *second-order effects*, which are explained in Chapter 14) does not exceed five per cent of the first-order end moments.
2. The storey within a structure may be considered non-sway if the computed *stability index*, Q , is less than 0.04 (MacGregor and Hage 1977). The *elastic stability index*, Q , is given by Clause E-2 of IS 456 as

$$Q = \frac{\sum P_u \Delta_u}{H_u h_s} \quad (13.10)$$

where $\sum P_u$ is the sum of axial loads on all columns in the storey, Δ_u is the elastically computed first-order relative lateral deflection between the top and bottom of that storey due to H_u (the total lateral force acting within the storey), and h_s is the height of the storey. While computing Q , P_u should correspond to the lateral loading case for which P_u is the greatest. A frame may contain both non-sway and sway storeys. The criterion given in Eq. (13.10) is not suitable if H_u is zero.

It has to be noted that ACI 318 has a similar criterion, but the limit considered in the stability index is set as 0.05 instead of 0.04. (The Indian code provision is based on an earlier version of the ACI code.) Commentary to Clause 10.10.5.2 of the ACI code states that if the lateral load deflections of the frame have been computed using service loads and the service load moments of inertia, we may compute Q in Eq. (13.10) using 1.2 times the sum of the service gravity loads, the service load storey shear, and 1.43 times the first-order service load storey deflections. MacGregor and Hage (1977) recommend that for Q values between 0.0475 and 0.2, a second-order analysis is required and frames having $Q > 0.2$ should be avoided. The value of Q should be computed at the ultimate load

level using the stiffness representative of this load level (see Section 4.5.1 and Table 4.10 of Chapter 4). A modified stability index, Q_r , which relates P - Δ effects to maximum expected displacements rather than elastic displacements, was derived by Paulay and Priestley (1992), who suggest that when $Q_r \geq 0.15$, P - Δ effects should be considered.

In the absence of bracing elements, the lateral flexibility measure of the storey Δ_u/H_u (storey drift per unit storey shear) may be taken for a typical intermediate storey as (Taranath 1988).

$$\frac{\Delta_u}{H_u} = \frac{h_s^2}{12E_c \Sigma(I_c/h_s)} + \frac{h_s^2}{12E_c \Sigma(I_b/L_b)} \quad (13.11)$$

where $\Sigma(I_c/h_s)$ is the sum of ratios of second moment of area to height of all columns in the storey in the plane under consideration, $\Sigma(I_b/L_b)$ is the sum of ratios of second moment of area to span of all floor beams in the storey in the plane under consideration, and E_c is the Young's modulus of elasticity of concrete. Other terms have been defined earlier.

The application of this concept is demonstrated in Example 13.2. It should be noted that Eq. (13.11) does not consider the effect of in-fills, bracings, or shear walls. However, it gives an idea of the lateral flexibility of the storey under consideration.

13.4.2 Fixity at Footing

The usual assumption of full fixity at the column base may be valid only for columns supported by a raft foundation, a thick pile cap, or an individual footing on the rock. Individual footing supported on deformable soil may have considerable rotational flexibility and offer only partial fixity. In such cases, there will be rotation in addition to settlement at the base as shown in Fig. 13.11, and the calculation of β_1 may be done in the following manner.

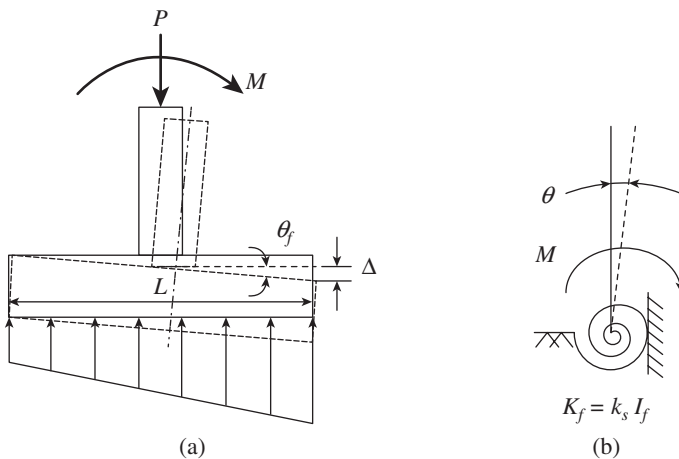


FIG. 13.11 Modelling of column base rotational stiffness (a) Rotation and settlement of footing (b) Rotational spring

At the column-to-foundation joint, K_c for a braced column restrained at its top end may be taken as $4E_c I_c/L_c$. The rotational

stiffness of the beam is replaced by the rotational spring stiffness of the footing and soil, which can be taken as (Paulay and Priestley 1992)

$$K_f = \frac{M}{\theta_f} \quad (13.12)$$

where M is the moment applied to the footing and θ_f is the rotation of the footing. It has to be noted that the stress under the footing is the sum of uniform stress due to axial force (P/A), which causes a uniform downward settlement, and varying stress due to bending moment (My/I), which causes a rotation. The rotation θ_f is

$$\theta_f = \frac{\Delta}{y} \quad (13.13)$$

where y is the distance from the centroid of the footing area and Δ is the displacement of that point, y -distance from the centroid, relative to the displacement of the footing centroid. If k_s is the modulus of sub-grade reaction (defined as the stress required for compressing the soil by unit amount = f/Δ), then θ_f can be defined as

$$\theta_f = \frac{f}{k_s y} = \frac{My}{I_f} \times \frac{1}{k_s y} \quad (13.14)$$

Substituting in Eq. (13.12), we get

$$K_f = I_f k_s \quad (13.15)$$

where I_f is the moment of inertia of the contact area between the bottom of the footing and the soil and k_s is the modulus of sub-grade reaction. The approximate relationship between allowable soil bearing pressure and coefficient of sub-grade reaction, k_s , is provided in Fig. 13.12, based on the PCI

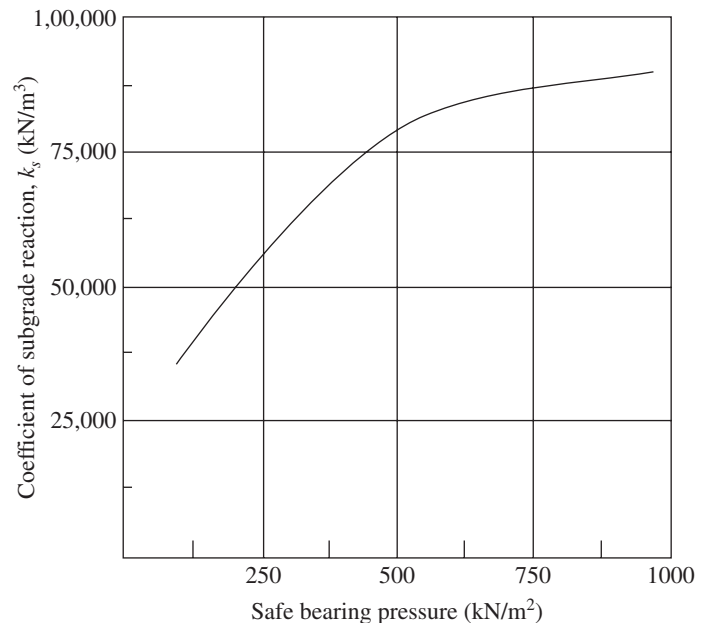


FIG. 13.12 Approximate relationship between allowable soil bearing pressure and coefficient of subgrade reaction, k_s

Handbook 1999. Typical values of modulus of sub-grade reaction are given in Appendix A.

Thus, the value of β_1 at the bottom of a column restrained by a footing is given by

$$\beta_1 = \frac{4E_c I_c / L_c}{I_f k_s} \tag{13.16}$$

The axis about which the footing rotates is the plane of the footing–soil interface. Hence, in Eq. (13.16), L_c should be taken as the length of the column plus the depth of the footing.

13.5 BEHAVIOUR OF SHORT COLUMNS

Research into the behaviour of RC short columns subjected to axially or eccentrically applied loads of short duration was started in the early 1900s (Considère 1902, 1903; Talbot 1906; and Withey 1911). As early as 1911, Withey observed that as the load is increased beyond the service load range, the concrete creeps and tries to transfer the load to the relatively stiff steel reinforcement. The classical elastic theory predicts that the stress in column reinforcement is modular ratio ($m = E_s/E_c$) times the stress in the surrounding concrete. However, the 564 laboratory column tests conducted in the early 1930s, primarily in the University of Illinois and Lehigh University, indicated that due to shrinkage and creep effects prevailing in concrete, the predictions of the elastic theory (working stress method) were erroneous (ACI Committee 105:1930). The steel reinforcements were found to have more compression than the value predicted by the elastic theory. It was also found that actual stresses under service loads cannot be meaningfully computed. When the load was increased, the steel reached the yield strength before the concrete could reach its full strength. The column carried further load, because the steel sustained the yield stress, while the deformations increased, until the concrete reached its full strength. The criterion for failure is the limiting strain, and the columns are deemed to have failed when the axial strain reaches a limit of 0.002. Hence, during the 1940s, design procedures for axially loaded columns were developed based on the ultimate strength results of these extensive experimental investigations.

These tests also revealed that only 0.85 times the compressive strength of concrete was realized in the full-scale column tests (Richart and Brown 1934; Hognestad 1951). The strength in the column is lower than that of the test cylinder because of the differences in specimen shape and size and also due to the vertical casting of the column leading to sedimentation and water gain in the top region of the column

(Park and Paulay 1975). Thus, the ultimate nominal strength of concentrically loaded rectangular or square column, consisting of the strength of steel and strength of concrete, $P_o = P_n$, is obtained as

$$P_o = 0.85f'_c(A_g - A_{sc}) + f_y A_{sc} \tag{13.17}$$

where A_{sc} is the total area of longitudinal steel, A_g is the gross area of the cross section, f_y is the yield strength of longitudinal reinforcement, and f'_c is the cylinder strength of concrete.

The tests conducted in the USA also revealed the enormous ductility of columns with spiral reinforcement. Transverse reinforcements such as lateral ties or spirals are often provided to prevent the buckling of longitudinal bars. As can be seen from Fig. 13.13(a), up to the load P_u , transverse steel adds very little to the strength of the column and the behaviours of tied and spiral columns are almost identical. Once the ultimate load is reached, a tied column with not very closely spaced ties fails immediately, with an ‘hourglass’ type of concrete failure and buckling of longitudinal bars between the ties (see Fig. 13.13b).

On the other hand, when a corresponding spirally reinforced concrete column with an equal area is tested, the shell of concrete outside the spiral cracks or spalls off completely at the predicted ultimate load. At this stage, the load capacity is reduced, due to the loss of concrete area, but the small spacing of the spiral steel prevents the buckling of longitudinal bars between the spirals. Hence, the longitudinal bars continue to carry the load with large increases in deflection (see Fig. 13.13a). Now, as the column shortens due to vertical compression, it extends laterally due to *Poisson effect*; the core concrete bears against the spiral, causing it to exert a confining reaction to the core. The resulting radial compressive stress increases the load carrying capacity of the core concrete. Thus, even after the loss of the outer concrete shell, the ultimate

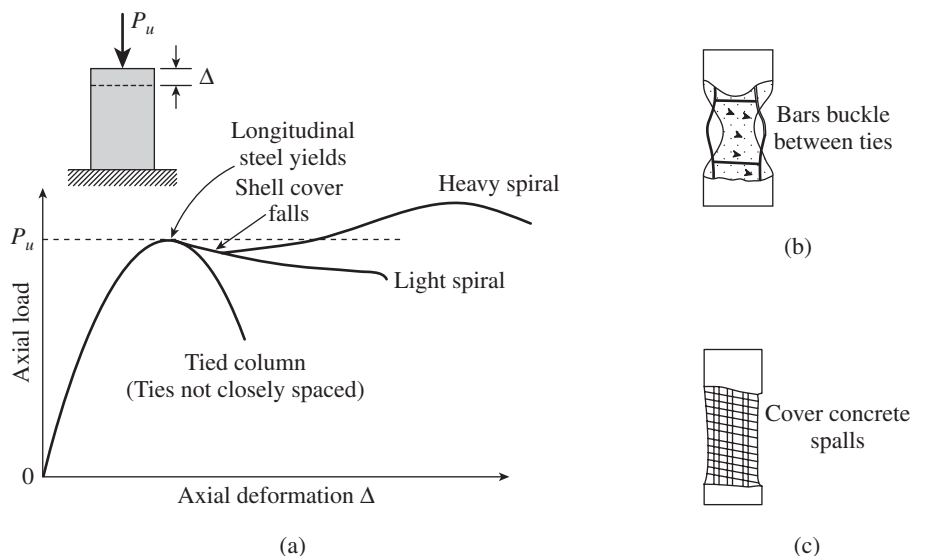


FIG. 13.13 Behaviour of short columns (a) Load-deformation curve (b) Tied column (c) Spiral column

load of the column with heavy spiral increases beyond P_u (see Fig. 13.13a). The column fails when the spiral steel yields and the confining effect is totally lost (see Fig. 13.13c). The criterion for failure in this case is also the limiting strain of 0.002.

13.5.1 Confining Reinforcement for Circular Columns

Assuming that the spirals are sufficiently close to apply a near-uniform pressure, the confining pressure can be calculated from the hoop tension developed by the spiral steel. Let us consider the free body of a half spiral turn, with D_k as the diameter of the core measured to the outside of the spiral or hoop, A_{sp} as the area of hoops or spiral bar, and s as the pitch of the spiral (see Fig. 13.14). The lateral pressure on the concrete f_l reaches the maximum when the spiral reinforcement reaches its yield strength f_{yt} . Considering the equilibrium of the forces acting on the half turn of the spiral, we get (Park and Paulay 1975)

$$f_l s D_k = 2 f_{yt} A_{sp}; \text{ thus, } f_l = \frac{2 f_{yt} A_{sp}}{s D_k} \quad (13.18)$$

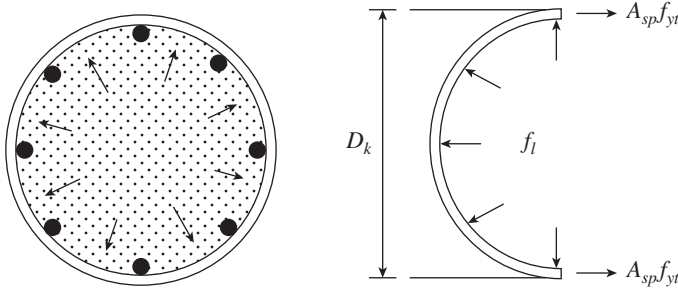


FIG. 13.14 Confinement of core concrete by spiral reinforcement

Based on the results of extensive experimental program, Richart, et al. (1929, 1934) assumed that the strength gain in core concrete loaded axially to failure while subjected to confining fluid pressure as

$$f_{cc} = f_{cp} + 4.1 f_l \quad (13.19)$$

where f_{cc} is the strength of confined core concrete, f_{cp} is the compressive strength of plain concrete in column (as discussed earlier, $f_{cp} \approx 0.85 f'_c$), and f_l is the passive compressive pressure provided by transverse reinforcement.

Substituting Eq. (13.19) into Eq. (13.18), we get the axial compressive strength of concrete confined by a spiral as

$$f_{cc} = 0.85 f'_c + \frac{8.2 f_{yt} A_{sp}}{s D_k} \quad (13.20)$$

Now, using this value of f_{cc} instead of $0.85 f'_c$ in Eq. (13.17), we get the nominal ultimate strength of a spiral column as

$$P_n = \left(0.85 f'_c + \frac{8.2 f_{yt} A_{sp}}{s D_k} \right) A_k + f_y A_{sc} \quad (13.21a)$$

where A_k is the area of concrete in the column core; other terms are already defined. The area of concrete in the column core is

$$A_k = \frac{\pi D_k^2}{4} - A_{sc}$$

Thus,

$$\begin{aligned} \frac{8.2 f_{yt} A_{sp}}{s D_k} A_k &= \frac{8.2 f_{yt} A_{sp}}{s D_k} \left(\frac{\pi D_k^2}{4} - A_{sc} \right) \\ &= 2.05 f_{yt} V_s - \frac{8.2 f_{yt} A_{sp} A_{sc}}{s D_k} \end{aligned} \quad (13.21b)$$

where $V_s = A_{sp} \pi D_k / s$ is the volume of spiral steel per unit length of column core and A_{sc} is the total area of longitudinal steel in the circular column. Substituting this value in Eq. (13.21a) and assuming $f_{yt} = f_y$, we get

$$P_n = 0.85 f'_c A_k + 2.05 f_y V_s + f_y A_{sc} \left(1 - \frac{8.2 A_{sp}}{s D_k} \right) \quad (13.21c)$$

If the spiral steel is replaced by an equivalent volume of longitudinal steel, V_s will be equal to the area of the longitudinal steel. Hence, Eq. (13.21c) indicates that the spiral steel is approximately twice as effective as the same volume of longitudinal steel in contributing to the strength of the column (Park and Paulay 1975).

It is interesting to note that the earlier versions of Indian and British codes included this additional strength due to spirals in the strength of circular columns. However, in the later editions of these codes, this practice has been discontinued, as the extra load carrying capacity of columns having heavy spirals can be realized only after the shell concrete has spalled and at the expense of very large deformations (see Fig. 13.13a). Thus, spirals add little to strength prior to reaching yield, but they provide ductility. Although both tied and spirally reinforced columns have the same strength, a higher factor of safety should be provided for tied columns because of the lack of ductility.

The design criterion adopted in codes for column confinement is based on the premise that confined columns should maintain their concentric capacities even after the spalling of concrete cover (Park and Paulay 1975). Thus, equating the concentric capacity of cover concrete to strength gain in the core, we get

$$0.85 f'_c (A_g - A_k) = 4.1 f_l (A_k - A_{sc}) \quad (13.22)$$

where f'_c is the compressive cylinder strength of concrete, A_g is the gross area of column cross section, A_k is the area of concrete core within perimeter transverse reinforcement (commonly taken as centre to centre), and A_{sc} is the area of longitudinal steel reinforcement.

Substituting f_l from Eq. (13.18) into Eq. (13.22) and dividing both sides by $2.05f_{yt}A_k$, we get

$$0.415 \frac{f'_c}{f_{yt}} \left(\frac{A_g}{A_k} - 1 \right) = \frac{4A_{sp}}{sD_k} - \frac{4A_{sp}A_{sc}}{sD_k A_k} \quad (13.23a)$$

Denoting $[4A_{sp}/(sD_k)]$ as ρ_{st} and rearranging, we get

$$\rho_{st} = 0.415 \frac{f'_c}{f_{yt}} \left(\frac{A_g}{A_k} - 1 \right) + \frac{4A_{sp}A_{sc}}{sD_k A_k} \quad (13.23b)$$

This equation was adopted in the ACI 318 code, after dropping the last term and changing the coefficient 0.415 to 0.45, as

$$\rho_{st} = 0.45 \frac{f'_c}{f_{yt}} \left(\frac{A_g}{A_k} - 1 \right) \quad (13.24a)$$

Using the relations $f'_c = 0.8f_{ck}$ and $\rho_{st} = 4A_{sp}/(sD_k)$ and rearranging, we get the formula suggested in Clause 39.4.1 of IS 456 and Clause 7.4.7 of IS 13920:1993, that is,

$$A_{sp} = 0.09sD_k \frac{f_{ck}}{f_{yt}} \left(\frac{A_g}{A_k} - 1 \right) \quad (13.24b)$$

For large columns, the ratio of cross-sectional area to confined core area (A_g/A_k) may approach unity, and Eq. (13.24b) results in small values of ρ_{st} . Hence, a lower-bound expression is provided by setting a limit to the (A_g/A_k) ratio as follows:

$$\rho_{st} = 0.12 \frac{f'_c}{f_{yt}} \quad (13.25a)$$

Using the relation $f'_c = 0.8f_{ck}$ and rearranging this equation, we may obtain the equation provided in draft IS 13920 as (<http://www.iitk.ac.in/nicee/IITK-GSDMA/EQ11.pdf>)

$$A_{sp} = 0.024sD_k \frac{f_{ck}}{f_{yt}} \quad (13.25b)$$

It has to be noted that the amount of confinement steel provisions in the ACI 318 and IS 13920 codes are independent of the axial force level. Recent theoretical and experimental research has shown that the amount of confinement steel required for a given curvature ductility factor is strongly dependent on the axial force level (Paulay and Priestley 1992; Saatcioglu and Razvi 2002, Sharma, et al. 2005). More discussions on confining reinforcement are provided in Section 13.10.3.

13.5.2 Confining Reinforcement for Rectangular and Square Columns

The confinement steel requirements for square and rectangular columns were derived as an arbitrary extension of the formulae mentioned in Section 13.5.1, recognizing that rectangular or square hoops are not as effective as spirals. It was assumed in ACI 318 that the rectangular or square hoops will be only 75 per cent as effective as circular spirals. Thus, the constants in Eqs (13.24a) and (13.25) were changed to give hoops

with about one-third *more* cross-sectional area than those of spirals, to give the following formula (note that the following is for one leg of hoop, with $0.415 \times 0.75 \approx 0.3$):

$$\rho_{st} = 0.3 \frac{f'_c}{f_{yt}} \left(\frac{A_g}{A_k} - 1 \right) \quad (13.26a)$$

For large columns, the ratio of cross-sectional area to confined core area (A_g/A_k) may approach unity. Hence, a lower-bound expression is provided in ACI 318 as

$$\rho_{st} = 0.09 \frac{f'_c}{f_{yt}} \quad (13.26b)$$

where $\rho_{st} = \frac{A_{sh}}{sh}$ and A_{sh} is the area of one leg of rectangular or square hoop; other terms have been defined already.

Thus, the strength enhancement in the core ($f_{cc} - f_{cp}$) implied by these formulae are $3.8f_l$ and $2.8f_l$ for circular columns with spirals and rectangular or square columns, respectively (as against the value of $4.1f_l$ suggested by Richart, et al. 1929). Equations (13.25a and b) and (13.26b) govern for large-diameter columns and are intended to ensure adequate flexural curvature capacity in the yielding regions (Watson, et al. 1994; Paultre and Légeron 2008).

Clause 7.4.8 of IS 13920:1993 assumes that rectangular hoops are only 50 per cent as efficient as spirals in improving confinement to concrete. Hence, from Eq. (13.24b), giving hoops twice the cross-sectional area as those of spirals, we get

$$A_{sh} = 0.18sh \frac{f_{ck}}{f_{yt}} \left(\frac{A_g}{A_k} - 1 \right) \quad (13.27)$$

where h is the longer dimension of the rectangular confining hoop measured to its outer face (should not exceed 300 mm) and gives the area of only one leg.

For large columns, draft IS 13920 provides the following lower-bound limit (<http://www.iitk.ac.in/nicee/IITK-GSDMA/EQ11.pdf>):

$$A_{sh} = 0.05sh \frac{f_{ck}}{f_{yt}} \quad (13.27b)$$

Comparing Eq. (13.27) with Eq. (13.26), we note that the A_{sh} value prescribed by IS 13920 is only 0.75 times the value given by the ACI code.

13.6 PRACTICAL PROVISIONS ON REINFORCEMENT DETAILING

The proportioning of columns and their reinforcement, especially in earthquake zones, should be given careful consideration. This is because the failure of one column may result in the progressive collapse of the whole structure. In this section, the detailing rules as given in IS 456 and IS 13920 are explained.

13.6.1 Dimensions

As indicated in Table 4.1 of Chapter 4 and shown in Fig. 13.15, the minimum dimension of column in earthquake zones should not be less than 300 mm or 15 times the largest longitudinal bar diameter (Clause 7.1.2 of draft IS 13920). This limit is necessary because of two reasons. Firstly, in smaller-size columns, the moment capacity of the column may be low due to the smaller lever arm between the compression and tension steel. Hence, the strong column–weak beam theory cannot be fulfilled (see also Section 13.10.1). Secondly, with smaller columns, the beam bars will not get enough anchorage length in the column (see Fig. 13.15). Other seismic codes recommend that the dimension of an interior column should not be less than 20–30 times the diameter of the largest beam bar running parallel to that column dimension. That is, if the beam uses 20 mm diameter bars, the minimum column width should be 400–600 mm.

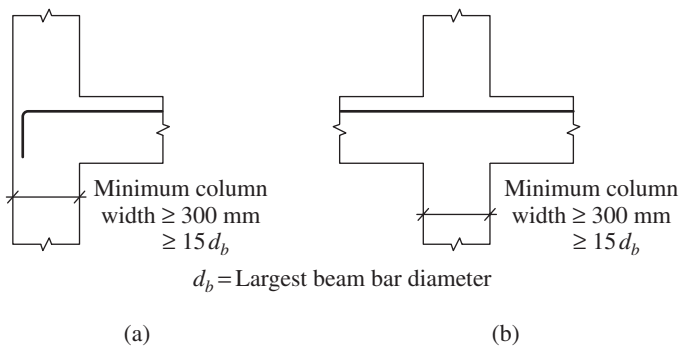


FIG. 13.15 Minimum width of columns in earthquake zones (a) Exterior column (b) Interior column

In addition, the confinement of concrete will be better in a relatively square column than a column with large width-to-depth ratio. Hence, Clause 7.1.3 of IS 13920 stipulates that the ratio of the shortest cross-sectional dimension to the perpendicular dimension should be greater than 0.4.

13.6.2 Concrete Cover

As indicated in Tables 4.6 and 4.7 of Chapter 4, depending on the exposure conditions, we should adopt different concrete grades and cover for columns (Clause 26.4.2, Table 16 of IS 456); the nominal concrete cover for fire resistance is 40 mm (Clause 26.4.3, Table 16A of IS 456). In addition, as per Clause 26.4.2.1 of IS 456, the nominal cover to the longitudinal reinforcement should not be less than either 40 mm or the diameter of the bar. Although this criterion has been reduced to 25 mm for columns with minimum dimension of 200 mm or below, whose reinforcing bars do not exceed 12 mm, 200 mm size columns are not advisable. It is better to apply the minimum cover provision to the transverse reinforcement of column and not to the main bars.

13.6.3 Longitudinal Reinforcement

Clause 26.5.3.1 of IS 456 suggests the following with regard to longitudinal reinforcement in column:

1. The minimum and maximum percentages of longitudinal reinforcement in columns should be 0.8 per cent and 6 per cent, respectively. (The minimum and maximum limits as per ACI 318 are one per cent and eight per cent, respectively; the maximum limit as per NZS 3101:2006 is $18A_g/f_y$ and in the region of lap splices up to $24A_g/f_y$ is permitted.) The minimum limit is to provide resistance to bending (moments may arise due to inaccuracies in construction and loading or due to lateral deflection of column) and to prevent failure due to the effect of creep and shrinkage under sustained loading; the maximum limit is to provide proper clearance between the bars. The maximum limit of six per cent will result in practical difficulties of placing and compacting concrete. Hence, in practice only three to four per cent is used as the maximum limit. Moreover, when bars from the columns below are to be lapped with those in the column under consideration, more than three per cent will result in congestion of reinforcement.
2. In certain situations, larger column sizes than required by design may have to be adopted due to architectural considerations, for meeting local building regulations (e.g., for fire resistance), or to use standard formworks or moulds. In such cases, the code permits the use of minimum percentage of longitudinal reinforcement based on the required area of concrete instead of the actual area of concrete. SP 24:1983 clarifies that in such cases the minimum limit will be that corresponding to pedestals, that is, 0.15 per cent of gross area. In a framework, accidental removal of a column in the lower storey may convert the column under consideration into a tension member. To consider this situation, SP 24 suggests a minimum steel of $0.15 P/f_y$, where P is the ultimate load on column in Newtons and f_y is the yield strength of reinforcement in N/mm^2 .
3. A minimum of four longitudinal bars of 12 mm diameter for rectangular columns and a minimum of six longitudinal bars of 12 mm diameter for circular columns should be provided. Only in columns of less than 400 mm, four corner longitudinal bars may be used, as the spacing of longitudinal bars should be less than 300 mm. More bars are desirable in columns of size greater than 400 mm. Columns with helical reinforcement should also have at least six longitudinal bars within and in contact with the helical reinforcement; these longitudinal bars should be provided equidistant around the inner circumference of the helical reinforcement. For sections with several corners such as L, T, or + shapes, at least one bar should be provided at each

corner with proper transverse reinforcement. Furthermore, the spacing of longitudinal bars, measured along the periphery of any column, should not be more than 300 mm. It is important to realize that the specified minimum diameter of bar (12 mm) is based on the requirement of stiffness and hence independent of the strength or type of steel.

4. Different types of reinforcing bars, such as plain bars and deformed bars, of various grades should not be used side by side, as it may lead to confusion and error. However, secondary reinforcement like ties may be of mild steel throughout, even though the main steel may be of high-strength deformed bars (SP 24:1983). It has to be noted that Clause 5.3 of IS 13920 allows thermo-mechanically treated (TMT) bars of grades Fe 500 and Fe 550, in addition to Fe 415, provided they have an elongation of more than 14.5 per cent and conform to other requirements of IS 1786.

The additional requirements in earthquake zones are provided in Section 13.10.1.

13.6.4 Transverse Reinforcement

Transverse reinforcement serves several purposes such as (a) to provide shear and torsional resistance to the member and to avoid shear failure, (b) to confine the concrete core and thereby increase the ultimate strain of concrete and, in turn, to improve ductility, (c) to provide lateral resistance against buckling to the longitudinal (main) reinforcement, (d) to prevent loss of bond strength within column bar splices, and (e) to help keep the longitudinal reinforcement in place during construction. As stated in Section 13.6.3, although Clause 5.3 of IS 13920 allows the use of high-strength TMT bars when they have elongation of more than 14.5 per cent, it does not specifically state that these grades can be used for transverse reinforcement. Clause 39.4.1 of IS 456 restricts the strength of helical reinforcement to less than or equal to 415 MPa. It may be of interest to note that commentary to Clause 10.9.3 of ACI 318 allows the use of up to 700 MPa yield strength reinforcement for confinement, based on the research of Richart, et al. (1929), Pessiki, et al. (2001), and Saatcioglu and Razvi (2002).

As discussed in Section 6.13 of Chapter 6, Clause 40.2.2 of IS 456 allows an increase in the design shear strength of concrete due to compressive forces using the following factor, which should be multiplied with the design shear strength of concrete, τ_c , given in Table 19 of the code (Table 6.2 of Chapter 6 in this book):

$$\delta = 1 + \frac{3P_u}{A_g f_{ck}} \leq 1.5 \quad (13.28)$$

where P_u is the axial compressive force acting on the member in N, A_g is the gross area of concrete section in mm^2 , and f_{ck}

is the characteristic compressive strength of concrete in MPa. As discussed in Chapter 6, the nominal shear capacity, V_n , of the column with transverse reinforcement is considered as the sum of the contributions of concrete, V_c , and that of the transverse reinforcement, V_s , as follows:

$$V_n = V_c + V_s = \tau_c b d + 0.87 f_{yt} A_{sv} (d/s_v) \geq V_u \quad (13.29)$$

where V_c is the nominal shear resistance provided by the concrete, V_s is the nominal shear strength provided by the shear reinforcement, A_{sv} is the total cross-sectional area of 'single' leg of transverse reinforcement effective in shear, f_{yt} is the yield strength of ties, s_v is the hoop spacing along the length of the column, and b and d are the width and effective depth of column, respectively. From Eq. (6.25c) of Chapter 6, we get

$$\frac{A_{sv}}{s} = \frac{(\tau_v - \tau_c) b}{0.87 f_{yt}} \quad (13.30)$$

where τ_v is the calculated nominal shear stress (V_u/bd) in MPa, τ_c is the design shear strength of concrete in MPa, and f_{yt} is the yield stress of the ties. The shear in the two directions has to be checked and sufficient transverse reinforcement in both the directions are to be provided. Even when τ_v is less than τ_c (calculated using Table 19 of the code), minimum shear reinforcement has to be provided, as described in the following paragraphs.

In general, transverse reinforcement is provided in the form of rectangular or polygonal links (lateral ties) with internal angles less than 135° or by circular rings, which are capable of resisting circumferential tension. The following are the general provisions of IS 456 about transverse reinforcement (Clause 26.5.3.2). The ends of transverse reinforcement should be properly anchored. (As per Clause 26.2.2.4b of IS 456, anchorage of ties is considered to have been provided when the bar is bent through an angle of at least 90° round a bar of at least its own diameter and is continued beyond the end of the curve for a length of at least eight times the diameter; if the bent angle is 135° , it should be continued for a length of at least eight times the diameter, and if the bent angle is 180° , it should be continued for at least four times the bar diameter.) Other requirements are listed as follows:

1. *Pitch and diameter of lateral ties:* The pitch or spacing of transverse reinforcement should not be more than the least of (a) the least lateral dimension of column, (b) 16 times the smallest diameter of the longitudinal (main) reinforcement, and (c) 300 mm. Ties must be stiff enough to prevent lateral displacement of the main bars during ultimate failure conditions. In such situations, the stiffness governs rather than the strength. Hence, the size of ties is independent of

the type or grade of steel used (SP 24:1983). Thus, the code stipulates that the diameter of the polygonal links or lateral ties should not be less than one-fourth the diameter of the largest longitudinal bar, or 6mm, whichever is greater (see Fig. 13.16a). IS 456 does not specify any maximum size; from practical considerations, it is better to restrict the size of lateral ties to 16mm. It is recommended to commence and end the ties or spirals from the column ends at a distance of one-fourth the spacing or pitch. The first two ties or the first turn of spiral should be at half the spacing or pitch (see Fig. 13.16).

2. *Pitch and diameter of helical reinforcement:* Helical reinforcement should be of regular formation with the turns of the helix spaced evenly, and its ends should be anchored properly by providing one and a half extra turns of the spiral bar. Where an increased load on the column on the strength of the helical reinforcement is allowed for, the pitch of helical turns should not be more than 75 mm or more than one-sixth the core diameter of the column. At the same time, it should not be less than 25 mm or three times the diameter of the bar forming the helix (see Fig. 13.16b). The diameter of the helical reinforcement should also follow the rules of lateral ties, as given in point 1.

In most rectangular sections, a single peripheral tie will not be sufficient to confine the concrete properly or to provide lateral restraint against buckling to longitudinal bars. Hence, an arrangement of overlapping rectangular hoops or supplementary cross-ties will be necessary. A longitudinal bar is deemed to be restrained by ties only if the bar is not spaced more than 75mm away from another fully restrained bar (see Fig. 13.17a). In a set of overlapping hoops, it is preferable to have one peripheral hoop enclosing all the longitudinal bars, together with one or more hoops covering smaller areas of the section. The detail in Fig. 13.17(b), which has two hoops each enclosing six bars, though effective, is not preferable as compared to the arrangement in Fig. 13.17(a), as it is more difficult to construct.

3. The unsupported length of transverse ties should not exceed 48 times the diameter of the tie in two directions

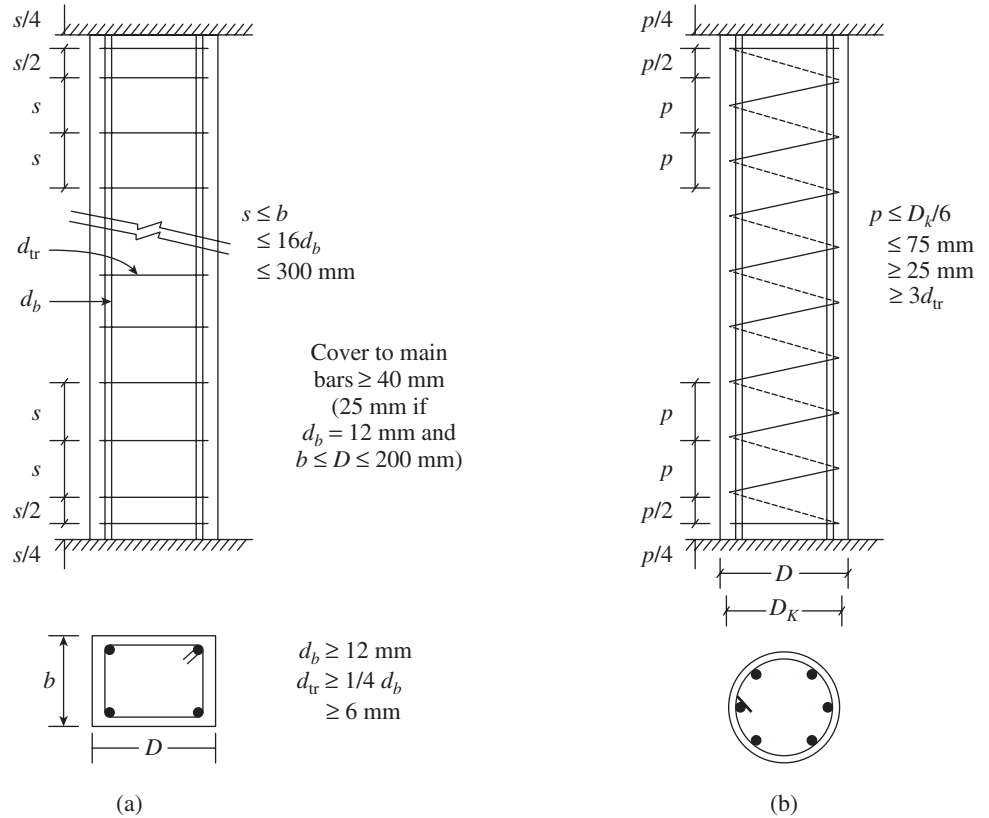


FIG. 13.16 Pitch and arrangement of transverse steel in column (a) Rectangular (b) Circular

nor 300 mm (see Figs 13.17b and c). In the case of large columns, more than one tie may be used to provide adequate restraint to the longitudinal bar, as shown in Figs 13.17(a) and (b). More ties in a single plane are also necessary for L-, T-, and +-shaped columns (see Fig. 13.17d).

- When the longitudinal reinforcement is placed in more than one row, effective lateral support to the longitudinal reinforcement in inner row is assumed only if transverse reinforcement is provided for the outermost row and no bar of the inner row is closer to the nearest compression face than three times the diameter of largest bar on inner row (see Fig. 13.17e).
- Longitudinal bars may also be grouped at each corner and each group tied together with transverse reinforcement in accordance with point 1, as shown in Fig. 13.17(f). In such a case, transverse reinforcement for the column as a whole may be provided on the assumption that each group is a single longitudinal bar for the purpose of determining the pitch and diameter of transverse reinforcement (it should not, however, exceed 20 mm).

Some more arrangements of column ties are shown in Fig. 13.18 (also see Fig. 7.5 of SP 34-1987). Additional transverse reinforcement should be provided at splices of longitudinal bars as shown in Fig. 7.34 of Chapter 7 (also see Section 7.7.1). Additional requirements in earthquake zones are provided in Section 13.10.2.

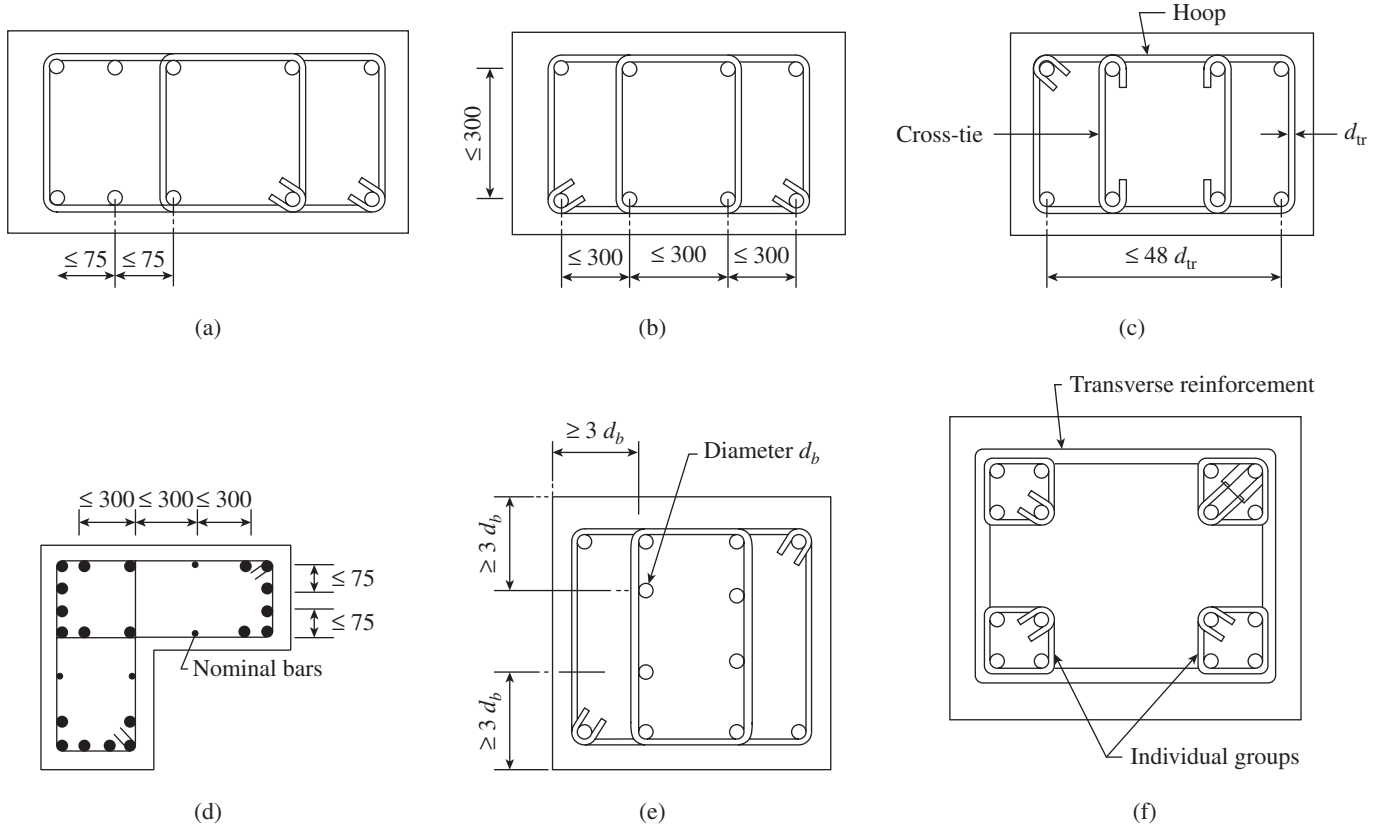


FIG. 13.17 Different types of arrangement of transverse reinforcement (a) Two overlapping hoops (b) Two overlapping hoops (not preferable) (c) Single hoops plus two cross-ties bent around longitudinal bars (d) T-shaped column (e) Longitudinal bars in more than one row (f) Grouping of longitudinal bars

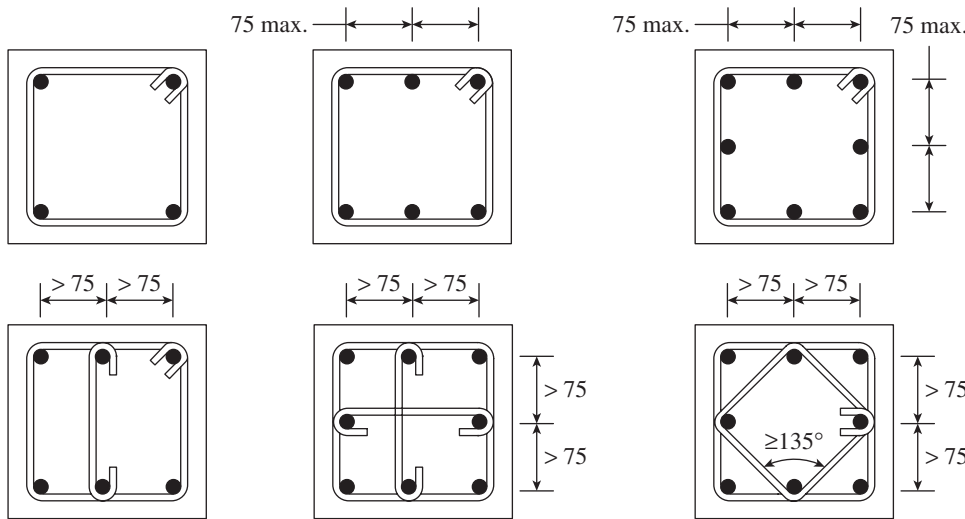


FIG. 13.18 Some more arrangements of column ties

13.6.5 Columns in Multi-storey Frames

In multi-storeyed buildings, since the column reinforcement cannot be continuous over the entire height of the building, they are spliced at each floor for ease of construction. In such cases, the bars from the footing or the lower floor, as the case may be, form the *starter bars* for the column bars above that level. The length of these starter bars (also known as *dowel bars*) should

be equal to at least the development length L_d of the bars. When there is a small offset, the bars from the lower floor are cranked into the column at the floor level (with a maximum slope of 1:6, as suggested by Clause 26.5.3.3 of IS 456), so that the main bars are in proper location (see Fig. 13.19a). This type of detail is often practised when the size of the column is not altered or when the change in column size is small (when the offset is less than half the floor slab depth or 75 mm). Alternatively, the dowel bars may be left to continue without cranking and the main bars can be cranked (as shown in Fig. 7.34b of Chapter 7).

When the offset is greater than $D/2$ or 75 mm, it is not advisable to crank the bars. In this case, a different set of dowel bars are to be provided for continuity and should be well anchored in both segments of column, and the column bars from lower floor are terminated within the slab as shown in Fig. 7.34(c) of Chapter 7. The column bars should be terminated at the top floor as shown in Fig. 7.33(c) of Chapter 7.

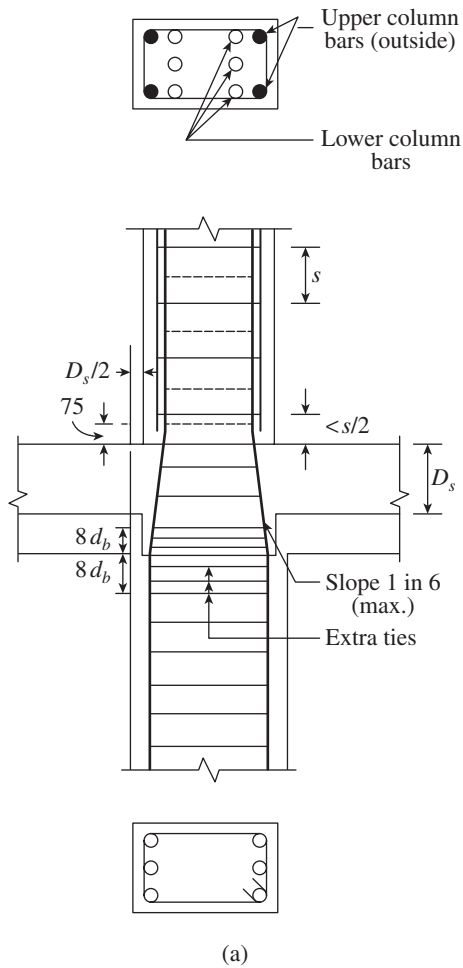


FIG. 13.19 Continuous columns (a) Small offset in continuous columns (b) Kinking of bars

When column vertical bars are bent, additional ties are to be provided as shown in Fig. 13.19(a); these additional ties should be designed to carry 1.5 times the horizontal component of the force in the inclined portion of the bars and should be placed not more than $8d_b$ from the point of bend (Clause 26.5.3.3). It is important to note the extra ties at the beam-column junction as well in Fig. 13.19(a). They are required for the proper functioning of the frame system while resisting the lateral loads (see Chapter 19 for discussions on beam-column joints). Construction workers often kink the longitudinal bars of columns for better alignment at site, as shown in Fig. 13.19(b). This type of kinking will lead to heavy local shear and bending moments and is dangerous for the safety of columns; hence, such a practice should be discouraged. It should also be noted that the splicing near the beam-column joint, as shown in Fig. 13.19(a) or Fig. 7.35(c) of Chapter 7, is not suitable for earthquake zones, where the splicing should be located at mid-height between floors (see also Section 13.10). In addition, it is preferable to splice only less than 50 per cent of the vertical bars at a particular location (also see Section 13.10).

13.7 OTHER CODAL PROVISIONS

IS 456 also has the following provisions for slenderness limit and minimum eccentricity, which should be considered by the designer.

13.7.1 Slenderness Limit

As stated earlier, columns should never be sized in such a way that they fail by buckling under concentric loading or lateral torsional buckling when subjected to axial force and bending. All columns should be proportioned in such a way that they fail only by material failure. For this purpose, and to prevent the development of significant torsional deformation, Clause 25.3.1 of IS 456 stipulates that the clear distance between restraints should never exceed 60 times the least lateral dimension of the column. For unbraced columns, it is better to keep this value as 30. In addition, Clause 25.3.2 of IS 456 suggests that the clear height of cantilever columns should not exceed $100 \times B^2/D$, where

B is the width of the cross section and D is the depth of cross section measured in the plane under consideration.

13.7.2 Minimum Eccentricity

Real columns will have accidental eccentricities caused by imperfections in construction, inaccuracy in loading, and lateral deflection of column. Hence, the codes of practices always prescribe some minimum eccentricities to be considered in the design of columns. Where the calculated eccentricity is larger, the minimum eccentricity should be ignored (Clause 39.2 of IS 456).

Clause 25.4 of IS 456:2000 specifies this minimum eccentricity for rectangular or square columns as

$$e_{x,\min} = \text{Unsupported length}/500 + (\text{Lateral dimension}/30) \geq 20 \text{ mm} \quad (13.31a)$$

$$e_{y,\min} = \text{Unsupported length}/500 + (\text{Lateral dimension}/30) \geq 20 \text{ mm} \quad (13.31b)$$

Furthermore, when biaxial bending is considered, it is sufficient to ensure that eccentricity exceeds the minimum about one axis at a time. For other shapes of cross section, SP 24:1983 suggests a value of $L_{ef}/300$, based on the German code DIN 1045, where L_{ef} is the effective length.

13.8 DESIGN OF SHORT COLUMNS UNDER AXIAL COMPRESSION

We shall consider the design of rectangular and circular columns with spiral reinforcement separately in this section, as their behaviours are different, as explained in Section 13.5.

13.8.1 Design of Rectangular Columns with Axial Loading

As discussed in Section 13.5, the ultimate failure of any column is reached when the uniform compressive strain reaches a value of 0.002. Clause 39.7.1 of IS 456 gives the additional moments to be considered for slender compression members; rearranging it in the form of eccentricity, we get

$$e = \frac{M}{P} = \frac{D}{2000} \left(\frac{L_e}{D} \right)^2$$

Substituting the limit of 12 specified for L_e/d for short columns (Clause 25.1.2), we get

$$e = \frac{M}{P} = \frac{D}{2000} (12)^2 = 0.072 D$$

where D is the least lateral dimension; Clause 39.3 of IS 456 considers this limiting eccentricity to be approximately $0.05D$. It also suggests the following equation to predict the nominal axial load capacity of short column, P_n , when the minimum eccentricity does not exceed $0.05D$ times the lateral dimension:

$$P_n = 0.4 f_{ck} A_c + 0.67 f_y A_{sc} \quad (13.32)$$

where f_{ck} is the characteristic compressive strength of concrete, A_c is the area of concrete ($= A_g - A_{sc}$), f_y is the characteristic strength of the compressive reinforcement, A_{sc} is the area of longitudinal steel in column, and A_g is the gross area of cross section of column. Equation 13.32 is derived based on the following considerations:

1. For equilibrium, the applied axial force should be equal to the load carried by concrete plus the load carried by steel. Assuming f_c and f_s to be the stresses in concrete and steel at the uniform strain of 0.002, we have

$$P_n = A_c f_c + A_{sc} f_s \quad (13.33a)$$

2. Assuming that the strength of concrete in column is 0.85 times, the cylinder strength (see Section 13.5), the design compressive stress in concrete f_c (i.e., at strain = 0.002) is given by (see Fig. 13.20a)

$$f_c = 0.85 f'_c / \gamma_m = 0.85 (0.8 f_{ck}) / 1.5 = 0.45 f_{ck}$$

3. The design compressive stress in steel f_s (i.e., at strain = 0.002) is $0.87 f_y$ for Fe 215 steel (see Fig. 13.20a) and $0.790 f_y$ and $0.746 f_y$ for Fe 415 and Fe 500 steel, respectively (see Fig. 13.20c and Table 5.2 of Chapter 5). Hence, for Fe 500 steel, substituting these values, we get

$$P_n = 0.45 f_{ck} A_c + 0.75 f_y A_{sc} \quad (13.33b)$$

The formula given in Clause 39.3 of IS 456 (Eq. 13.32) is obtained by reducing the given capacity by approximately 10 per cent to take into account the eccentricity of $0.05D$ (the reduction in f_s is 15 per cent in case of Fe 415 steel and 23 per cent in case of Fe 250 steel). If the minimum eccentricity is greater than $0.05D$, the design should be made as per Clause 39.5 of IS 456. It should be noted that Eq. (13.33b) has been designated as P_{uz} in Clause 39.6 of IS 456.

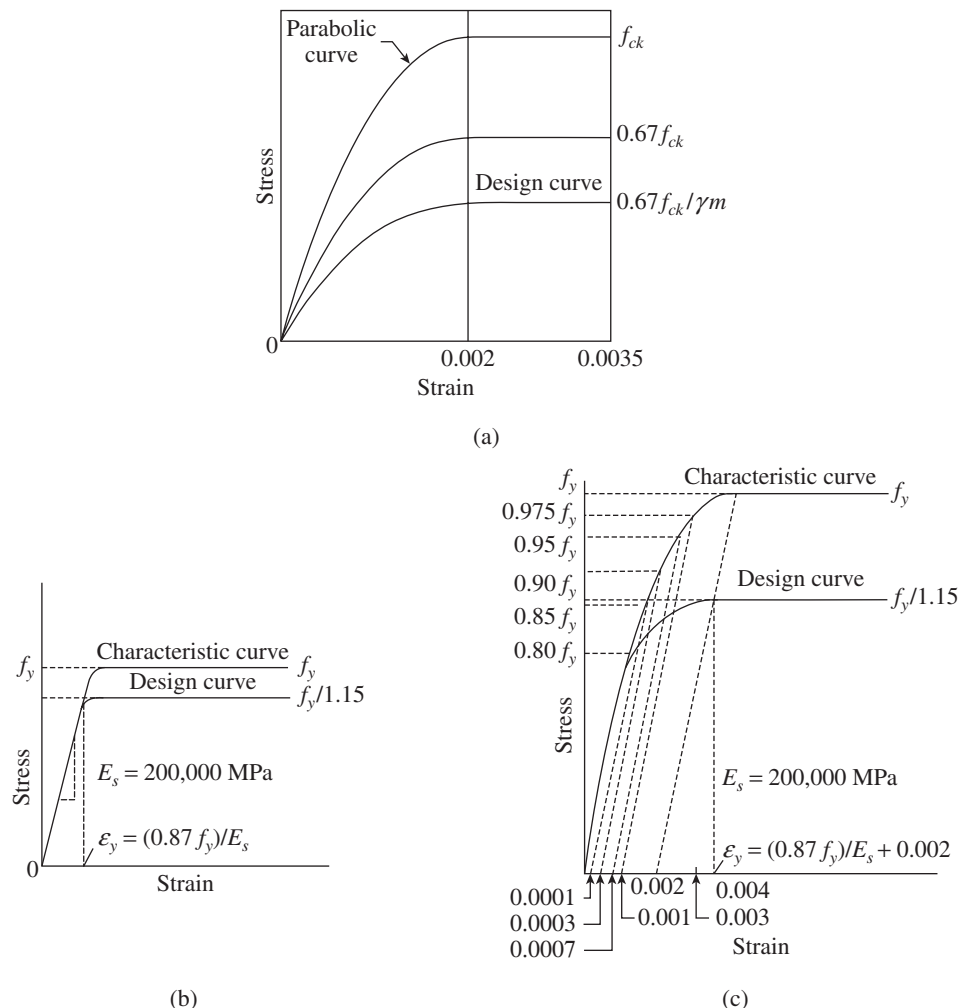


FIG. 13.20 Stress–Strain curves as per IS 456 (a) Concrete (b) Mild steel bars (c) High-yield strength-deformed bars

The use of Eq. (13.32) has been found to yield conservative results compared to the design involving axial compression and bending with minimum eccentricities; this equation can be used for columns up to a size of 400 mm, above which we need to design only for axial force and minimum eccentricity.

Clause 10.3.6.2 of the ACI 318 code uses a similar equation, but limits the design axial strength of a section in pure compression to 80 per cent of the nominal strength. It also applies a capacity reduction factor, ϕ , of 0.65 for tied columns. Thus, it has the following format:

$$\begin{aligned} P_{n,\max} &= 0.80\phi[0.85f'_cA_c + f_yA_{sc}] \\ &= 0.80 \times 0.65[0.85 \times (0.8f_{ck})A_c + f_yA_{sc}] \\ &= 0.3536f_{ck}A_c + 0.52f_yA_{sc} \end{aligned} \quad (13.33c)$$

It is important to note that prior to ACI 318-77, columns were required to be designed for a minimum eccentricity of $0.1D$ for tied columns or $0.05D$ for spiral columns. This requirement resulted in tedious computations to find the axial load capacity of a column at these minimum eccentricities. Hence, from the 1977 version of the ACI code, the minimum design eccentricity provisions were replaced by reduced axial load strengths of 0.8 times the nominal strength for tied column (represents e/D of 0.1) and 0.85 times the nominal strength for spiral columns (represents e/D of 0.05).

As stated earlier, any attempt to predict the concrete and steel stresses, f_c and f_s , respectively, under service load will not yield correct results due to the effect of creep and shrinkage. As per the conventional working stress method of design, substituting the permissible stresses σ_{cc} and σ_{sc} in lieu of f_c and f_s , respectively, in Eq. (13.33a), we get the design equation as given in Clause B-3-1 of IS 456 as

$$P = \sigma_{cc}A_c + \sigma_{sc}A_{sc} \quad (13.33d)$$

where σ_{cc} is the permissible stress in concrete in direct compression, σ_{sc} is the permissible compressive stress for column bars, A_c is the cross-sectional area of concrete excluding reinforcing steel, and A_{sc} is the cross-sectional area of longitudinal steel.

The code attempts to provide a solution to the problem of creep and shrinkage by suggesting values of σ_{sc} as 130 MPa for Fe 250 steel and 190 MPa for high-yield strength-deformed bars (see Table 4.13 of Chapter 4). The permissible stress in concrete in direct compression, σ_{cc} , for various grades of concrete is given in Table 4.12 of Chapter 4. The use of Eq. (13.33d) is shown in Example 4.2, just for illustration purposes. As explained in Section 13.5, it is not advisable to design columns using the elastic theory.

In addition to the longitudinal reinforcement estimated by the formula given in Eq. (13.33), we need to follow the general provisions of reinforcement suggested in Section 13.6.

It should also be noted that it is not advisable to use Fe 250 grade bars as longitudinal (main) steel in columns.

13.8.2 Design of Circular or Square Columns with Spiral Reinforcement

Realizing the superior performance of spiral columns compared to similar columns with lateral ties (see Section 13.5), Clauses 39.4 and B-3.2 of IS 456 allow the strength of these columns to be taken as 1.05 times the strength of similar columns with lateral ties. This increase is allowed provided the volume of helical reinforcement satisfies the following relation (Clause 39.4.1 of IS 456), which can be derived directly from Eq. (13.24b) as

$$\frac{V_{sp}}{A_k} > 0.36 \frac{f_{ck}}{f_{yt}} \left(\frac{A_g}{A_k} - 1 \right) \quad (13.34)$$

where A_g is the gross area of the column cross section, A_k is the core area of helically reinforced column measured to the outside diameter of the helix, f_{ck} is the characteristic compressive strength of the concrete, f_{yt} is the characteristic strength of the helical reinforcement, which is limited to 415 N/mm² in IS 456, and V_{sp} is the volume of spiral steel per unit length = $A_{sp}\pi D_k/s$.

It has to be noted that in spiral columns, the load capacity of the column depends on the area of concrete available within the core. If the full capacity of the core is to be mobilized, it should be confined effectively, thereby ensuring a *triaxial state of stress* inside the core. Hence, the code specifies a small pitch for the helical reinforcement (see Fig. 13.16b). If the condition specified in Eq. (13.34) is satisfied, then the strength of the column can be considered as (Clause 39.4 of IS 456)

$$\begin{aligned} P_n &= 1.05(0.4f_{ck}A_c + 0.67f_yA_{sc}) \\ &= 0.42f_{ck}A_c + 0.704f_yA_{sc} \end{aligned} \quad (13.35a)$$

Clause 10.3.6.1 of the ACI 318 code uses a similar equation, but limits the design axial strength of a section in pure compression to 85 per cent of the nominal strength. It also applies a capacity reduction factor, ϕ , of 0.75 for spiral columns. Thus, it has the following format:

$$\begin{aligned} P_{n,\max} &= 0.80\phi(0.85f'_cA_c + f_yA_{sc}) \\ &= 0.80 \times 0.75[0.85 \times (0.8f_{ck})A_c + f_yA_{sc}] \\ &= 0.408f_{ck}A_c + 0.6f_yA_{sc} \end{aligned} \quad (13.35b)$$

The design strength of composite columns as shown in Fig. 2.5(c) of Chapter 2, with steel I section and longitudinal bars, may be estimated as follows:

$$P_n = 0.4f_{ck}A_c + 0.67f_yA_{sc} + 0.67f_{ys}A_{ss} \quad (13.35c)$$

where f_{ys} is the yield strength of rolled steel section (sections rolled in India generally have yield strength of 250 MPa) and A_{ss} is the area of rolled steel section. It has to be noted that such composite columns are not popular due to the problems of interconnections and constructional details.

13.8.3 Steps in Design of Short Columns

The design of a column is usually an iterative process. The following are the various steps involved in the design of a concentrically loaded short column:

1. Compute the load on the column.
2. Choose a suitable size for the column, based on either architectural requirements or the size of the beam that will be placed on it. It is good practice to accommodate the beam bars within column bars (see Section 4.4.8 and Fig. 4.12 of Chapter 4). When wide shallow beams are encountered, details as discussed in Section 5.10 of Chapter 5 should be considered (see Fig. 5.37 of Chapter 5).

The initial size may be chosen based on the following equation, which can be derived by rearranging the terms in Eq. (13.32):

$$A_c = \frac{P_u}{0.4(f_{ck} + 1.67f_y\rho_g)} \text{ mm}^2 \quad (13.36)$$

where $\rho_g = A_{sc}/A_g$, which may be initially chosen as two per cent.

3. Decide whether the column in the frame is a sway or non-sway column by computing the stability index Q (see Section 13.4.1). If $Q \leq 0.04$, then the column can be considered as a non-sway column. It should be noted that only internal columns with equal spans on either side and not subjected to lateral loads can be designed as concentrically loaded columns.
4. Using Wood's curves given in Annexure E of IS 456 (Figs. 13.8 and 13.9), determine the effective length of column; for idealized conditions, Table 28 of IS 456 (Table 13.1) may be used.
5. Compute the slenderness of the column about the principal axes. The column can be considered as a short column only when the value is less than 12; otherwise, the column has to be designed as a long column using the methods presented in Chapter 14.
6. Compute the area of steel using Eq. (13.33b) or (13.35a). Check for minimum ($\geq 0.8\%$) and maximum ($\leq 3\text{--}4\%$ to allow for lapping and to reduce congestion) percentage of steel. If the calculated area of steel is not within limits, repeat steps 4–6 by changing the size of the column.
7. Detail longitudinal steel by choosing suitable size and numbers (size ≥ 12 mm; the minimum number of bars should be four or six depending on whether the column is rectangular or circular, respectively. See Sections 13.6.3 and

13.10.1). Adopt suitable cover to steel (minimum 40 mm; see Section 13.6.2) and also check the perimeter spacing of bars (≤ 300 mm as per Clause 26.5.3.1 of IS 456).

8. Design and detail transverse steel by choosing suitable size, spacing, and so on (see Sections 13.6.4 and 13.10.2).

13.8.4 Design Aids

The capacity of a rectangular or square column is given by Eq. (13.32) as

$$P_n = 0.4f_{ck}A_c + 0.67f_yA_{sc}$$

where $A_c = A_g - A_{sc}$. If p is the percentage of steel, $p = 100A_{sc}/A_g$.

Hence, $A_{sc} = pA_g/100$. Substituting it in the expression for A_c , we get

$$A_c = A_g - A_{sc} = A_g \left(1 - \frac{p}{100}\right)$$

Rewriting the equation for P_n using these quantities, we get

$$P_n = 0.4f_{ck}A_g \left(1 - \frac{p}{100}\right) + 0.67f_yA_g \frac{p}{100}$$

Rearranging the terms, we get

$$\frac{P_n}{A_g} = 0.40f_{ck} + \frac{p}{100}(0.67f_y - 0.40f_{ck})$$

Using this equation, design charts for axially loaded short columns have been prepared and presented in Charts 24–26 of SP 16 for Fe 250, Fe 415, and Fe 500 steel respectively. There are two parts to these charts. In the lower part, P_u/A_g (In SP 16, P_u is used instead of P_n) is plotted against reinforcement percentage p for different grades of concrete. If the cross section of the column is known, from the value of P_u/A_g , the reinforcement percentage can be directly read from the chart. In the upper section of these charts, P_u/A_g is plotted against P_u for various values of A_g . To use this chart for the given value of P_u , proceed horizontally until the A_g corresponding to the size of the column is reached, then proceed vertically and read the value of p for the adopted value of f_{ck} .

13.9 DESIGN OF PEDESTALS

A pedestal is a compression member, the effective length of which does not exceed three times the least lateral dimension. Clause B-3.1 of IS 456 allows the design of RC pedestals as short columns. When the longitudinal reinforcement of a pedestal is not taken into account in strength calculations, nominal longitudinal reinforcement of not less than 0.15 per cent of the cross-sectional area should be provided as per Clause 26.5.3.1(h) of IS 456. Pedestals can also be of plain concrete (see Clause 34.1.3 of IS 456).

13.10 EARTHQUAKE AND OTHER CONSIDERATIONS

The proportioning of columns and their reinforcement in earthquake resistant frames should be given careful consideration. The following requirements are based on IS 13920:1993 code and draft IS 13920 (<http://www.iitk.ac.in/nicee/IITK-GSDMA/EQ11.pdf>) and are applicable to members that have factored axial stress greater than $0.08f_{ck}$ under the effect of earthquake loads. If the factored axial stress is less than the specified limit, the member has to be designed as a flexural member.

13.10.1 Strong Column–Weak Beam Concept

When buildings are subjected to earthquake loads, plastic hinges will be formed at the ends of the members where there are heavy bending moments, and subsequently the structure will fail when there are enough plastic hinges to form a mechanism. (It is because structures are often designed only for a fraction of the actual earthquake loads; see Section 3.8 of Chapter 3.) A few possible mechanisms in which a structure may fail are shown in Fig. 13.21 (Paulay 1996). The distribution of damage over the height of the building depends on the distribution of lateral drift. If the building has weak columns or long columns in a particular storey, the drift will concentrate in this storey and may exceed the drift capacity of the column (see Figs 13.21a and 13.22). It should be noted that in the current design practice, contribution of masonry in-fill is considered in the mass of the building but neglected in the estimation of stiffness; thus, the actual behaviour of the building is not captured in design. Such soft storey columns have to be

designed and detailed carefully (Subramanian 2004). Due to the failure of several buildings having soft storey columns, Clause 7.10.3(a) was included in IS 1893, which states that the columns and beams of a soft storey should be designed for 2.5 times the storey shears and moments calculated under seismic loads. On the other hand, if strong columns are provided throughout the building height, drift will be more uniformly distributed (Fig. 13.21c) and localized damage will be reduced. Buildings with columns having the same strength as beams may result in an intermediate mechanism as shown in Fig.13.21(b).

It is also important to recognize that the columns in a given storey support the weight of the entire building above those columns, whereas the beams support only the gravity loads of the particular floor; hence, the failure of a column is of greater importance than that of a beam, as column failure will result in the collapse of the entire building. Recognizing this fact, building codes often specify that columns should be stronger than the beams that frame into them. This *strong-column weak-beam* principle is fundamental to achieving safe behaviour of frames during strong earthquake ground shaking (Moehle, et al. 2008). Buildings following this principle will fail in *beam-hinge mechanism* (beams yielding before the columns) and not in the *storey mechanism* (columns yielding before the beams). Storey mechanism must be avoided as it causes greater damage to the building. It has to be noted that the beam-hinge mechanism also has a plastic hinge at the base of ground floor column (see Fig. 13.21c); hence it is important not to have any splicing at this location and to have ductile detailing, so that the required rotation capacity is achieved.

Kuntz and Browning (2003) and Murty, et al. (2012) have shown that the beam mechanism as shown in Fig. 13.21(c)

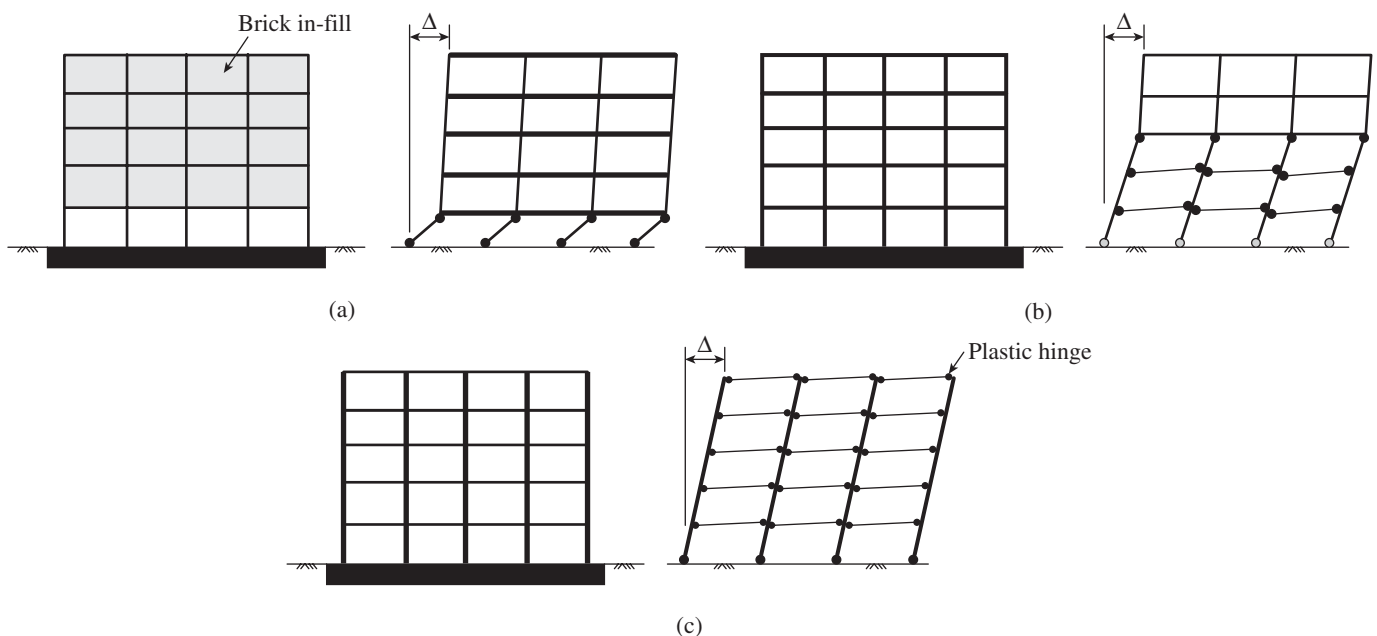


FIG. 13.21 Different failure mechanisms of multi-storey frames (a) Storey mechanism (soft storey or strong beam–weak column design) (b) Intermediate mechanism (c) Beam mechanism (strong column–weak beam design)

can be achieved only when the strength ratio of the column to beam is about 4.0. Murty, et al. (2012), based on parametric studies, found that an increase in the column to beam strength ratio increases (a) the lateral load (base shear) capacity of the building and (b) the lateral deformation and ductility capacity of the building (see Fig. 13.23). The sequence of hinge formation is critical in a building in addition to its capacity curve and the location of plastic hinges in the building. It is preferable that the hinges form in beams before they are formed in columns. Such a possibility is found to occur when the column to beam strength ratio is more than 3.6 (Murty, et al. 2012). As the column to beam strength ratio of about 3–4 is impractical in most cases, a lower strength ratio of 1.2 and 1.1 is adopted by ACI 318 and draft IS 13920, respectively. (However, Park and Paulay, (1975) have shown that the formation of plastic

column yielding associated with an intermediate mechanism, as shown in Fig. 13.21(b), is to be expected, and the columns must be detailed accordingly.

At the plastic hinge locations, it is necessary to provide sufficient confining reinforcement such that the required ductility is achieved (see Section 13.10.3).

13.10.2 Detailing of Longitudinal Reinforcement

The requirements for longitudinal reinforcement as per IS 13920 are as follows:

1. As mentioned earlier, Clause 7.2.1 of draft IS 13920 stipulates that at a joint in a frame resisting earthquake forces, the sum of moment of resistance of the column should be at least 1.1 times the sum of moment of resistance of the beam along



(a)



(b)

FIG. 13.22 Typical building in urban areas of India with open ground-storey parking (a) Soft storey (b) Typical failure of a soft storey column in Bhuj earthquake of 26 January 2001

Courtesy: Earthquake Engineering Research Institute, USA, and National Information Centre of Earthquake Engineering, Indian Institute of Technology, Kanpur

hinges in columns of a framed structure, at locations other than the column bases at the foundation level, is still possible as a result of a severe earthquake despite the application of the ‘strong column–weak beam’ concept in the design according to various design code recommendation.) Due to this, some

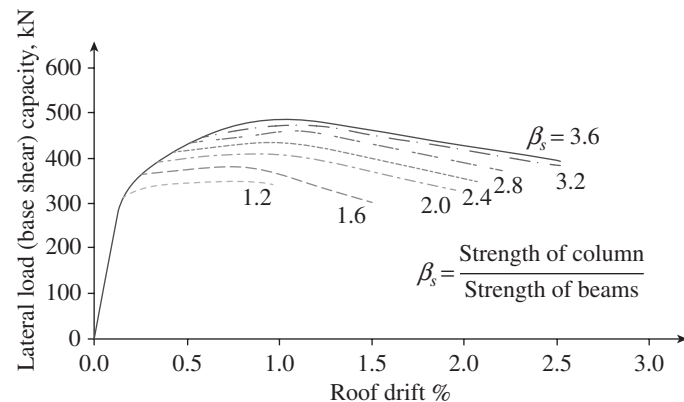


FIG. 13.23 Increase in ductility with increase in column to beam strength
Source: Murty, et al. 2012, reprinted with permission

each principal plane of the joint (see Fig. 13.24). The moment of resistance of the column should be calculated considering the factored axial forces on the column. Determination of moment of resistance (also called nominal moment capacity) is discussed in Section 14.2.2 of Chapter 14. The moment of resistance should be summed in such a way that the column moments oppose the beam moments. This requirement should be satisfied for beam moments acting in both directions in the principal plane of the joint considered. Columns not satisfying this requirement should have special confining reinforcement over their full height instead of the critical end regions alone.

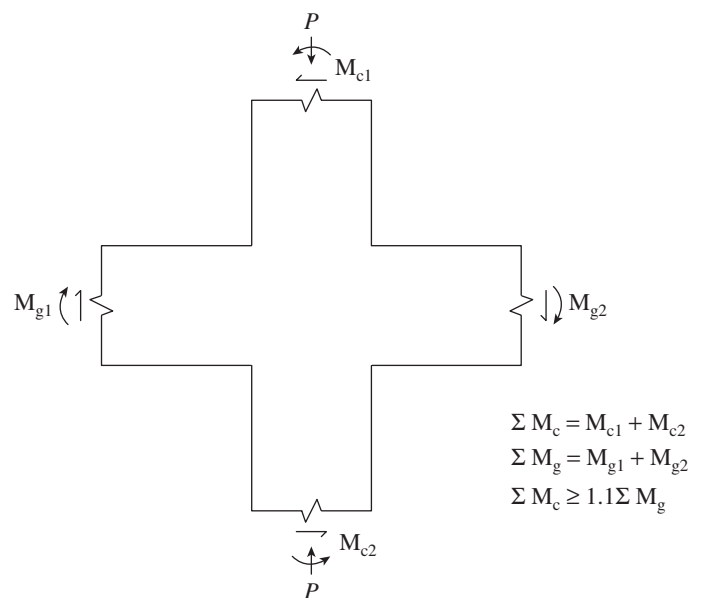


FIG. 13.24 Strong column–Weak beam concept

When determining the nominal flexural strength of a beam section in negative bending (top in tension), longitudinal reinforcement contained within the effective flange width of a top slab that acts monolithically with the beam increases the strength of beams. Research by French and Moehle (1991) on beam-column sub-assemblies subjected to lateral loading indicates that using the effective flange widths defined in Clause 8.12 of ACI 318 (similar to Clause 23.1.2 of IS 456) reasonably estimates girder negative bending strengths of interior connections at inter-storey displacement levels approaching two per cent of storey height. This effective width is conservative where the slab terminates in a weak spandrel beam.

2. Clause 7.2.2 of draft IS 13920 requires that at least one intermediate bar be provided between the corner bars along each column face; thus, as per this clause, rectangular columns in lateral load resisting frames should have a minimum of eight bars, instead of the four bars suggested in IS 456. Intermediate bars are required to ensure the integrity of the beam-column joint and increase confinement to the column core (see Section 19.2.6 of Chapter 19).
3. Seismic moments are the maximum in columns just above and just below the beam (see Fig. 7.47 of Chapter 7). Hence, reinforcement must not be changed in these locations. Since the seismic moments are minimum away from the ends of columns, it is preferable to provide lap splices *only* in the central half of the columns, and the splicing should not extend into the plastic hinge regions (the usual procedure of providing splices just above floor levels, as shown in Fig. 13.19, should not be adopted in earthquake zones, unless it is ensured that plastic hinges do not form in these locations). This clause of draft IS 13920 (Clause 7.2.3) requires the designers to specify column reinforcement from a mid-storey height to the next mid-storey height. This clause has an impact on the dowels to be left for future extension. If inadequate projected length of reinforcement is left for future vertical extensions of columns, it will result in a very serious seismic threat to the future upper storeys. It is because such a connection creates a very weak section in all the columns at a single location, and all upper storeys are prone to collapse at that level.

Moreover, when subjected to seismic forces, columns can develop substantial reversible moments. Hence, all the bars are liable to be subjected to tension, requiring the designers to proportion the lap splices as only tension splices. Hoops should be provided over the entire splice length at spacing not exceeding 150 mm centre to centre. It is also preferable to splice less than 50 per cent of the bars at one section. Thus, in buildings of normal proportions, only half the bars can be spliced in one storey and the other half has to be spliced in the next storey. In case of construction difficulty in lapping only 50 per cent of the column reinforcement in a storey, draft IS 13920 allows all bars to be lapped at the same location but with

an increased lap length of $1.3L_d$, where L_d is the development length in tension as per IS 456. Closely spaced stirrups or spirals around the length of the splice may be desirable (see Fig. 7.31 of Chapter 7). Welded splices and mechanical couplers (see Section 7.7.2 of Chapter 7 and Clause 26.2.5.2 of IS 456) can be used in locations where yielding of bars are likely, and the couplers or welded connection should be capable of developing 1.0 time or 1.25 times the specified tensile strength of the bar, respectively. More information on splices may be found in Sections 7.7.1 and 7.7.2 of Chapter 7.

4. Even non-structural column extensions contribute to the stiffness of the column. If the extensions are not properly tied with the column core, earthquake forces may cause spalling of this portion, leading to a sudden change in the stiffness of the column. Hence, such extensions must be detailed at least as per IS 456 requirements for columns. When this extra area has been considered in the strength calculations, it should be provided with the minimum longitudinal and transverse reinforcement as per Clause 7.2.2 of IS 13920. However, when this area is considered as non-structural, minimum longitudinal and transverse reinforcement must be provided as per IS 456 provisions (see Fig. 13.25).

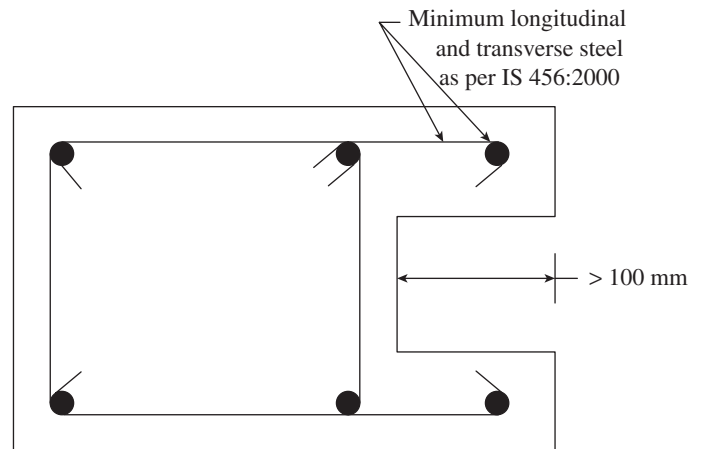


FIG. 13.25 Column with more than 100 mm projection beyond the core

Bars passing through a beam-column joint may create severe bond stress demands on the joint; hence, Clause 21.7.2.3 of the ACI code restricts beam bar sizes.

13.10.3 Detailing of Transverse Reinforcement

Full confinement of concrete at beam-column junctions at possible plastic hinge locations, and sometimes over the full length of columns, is required to achieve the required ductility.

The requirements for transverse reinforcement as per IS 13920 are as follows:

1. Usually, a minimum bar diameter is specified for transverse reinforcement in columns to ensure minimum ductility and to prevent local buckling of longitudinal bars. Clause 7.3.5 of draft IS 13920 specifies the minimum diameter as

8 mm (as per IS 456 it is 6 mm or one-fourth the largest longitudinal bar). However, for columns with longitudinal bar diameter larger than 25 mm, the minimum diameter of transverse reinforcement is specified as 10 mm.

2. Transverse reinforcement for circular columns should consist of spiral or circular hoops. In rectangular columns, rectangular hoops may be used. A rectangular hoop is a closed stirrup, having a 135° hook with a six diameter extension (but not less than 65 mm) at each end, which is embedded in the confined core (see Fig. 13.26a). It has to be noted that 135° hooks ensure that the stirrup does not open out during strong earthquake shaking. The 1993 edition of IS 13920 required 10 diameter extension, but not less than 75 mm at each end (see Clause 7.3.1). A large value of extension leads to considerable construction difficulties. Laboratory testing in the USA confirmed that six diameter extension may be adequate. Hence, ACI 318 and draft 13920 codes have changed the requirement of ten diameter extension to six diameter extension (but not less than 65 mm). Cross-ties with a 90° hook are not as effective as either cross-ties with 135° hook or hoops in providing confinement. Construction problem arises in placing cross-ties with 135° hooks at both ends. Tests show that if the cross-tie ends with 90° hooks are alternated, confinement will be sufficient. Not all bars need to be laterally supported by a bend of a transverse hoop or cross-tie, provided the

bar is not spaced more than 75 mm away from another fully restrained bar (see Fig. 13.17a).

3. The parallel legs of a rectangular hoop should be spaced less than 300 mm centre to centre. If the length of any side of the hoop exceeds 300 mm, it is necessary to provide a cross-tie, as shown in Fig. 13.26(b). Alternatively, a pair of overlapping hoops may be provided within the column as shown in Fig. 13.26(c). It is important to ensure that the hooks engage the peripheral longitudinal bars. Consecutive cross-ties engaging the same longitudinal bars should have their 90° hooks on the opposite sides of the column, as shown in Fig. 13.26 (c).
4. Closer spacing of hoops is desirable to ensure better seismic performance. Although IS 456 allows the hoop spacing to be equal to the least lateral dimension of the column, Clause 7.3.3 of IS 13920 restricts it to half the least lateral dimension.
5. Ties, lap spliced in the cover concrete, as shown in Fig. 13.27(a), should not be assumed to make any contribution to strength or stability (as the cover concrete will spall during ultimate loads) and hence should not be used. Similarly, lapped splices of circular hoops or spirals in the cover concrete must be avoided, as they have resulted in the collapse of bridge piers during earthquakes when the cover concrete spalled. Sometimes, J-type intermediate ties, with 135° hook at one end and 90° hook at the other end, are preferred

due to ease of construction. Such ties when arranged in such a way that the positions of different hooks alternate, as shown in Fig. 13.27(b), can effectively stabilize compression bars but can make only limited contribution to the confinement of the concrete core (Paulay and Priestley 1992). In the presence of high compressive forces and ductility demands, the strength of such a tie is fully mobilized and the 90° hook may open out; hence, they should be used only in members exposed to restricted ductility demands (Paulay and Priestley 1992).

The use of intermediate ties with a 135° or 180° hook on each end may not be possible due to construction difficulties. A spliced tie, as shown in Fig. 13.27(c), may be used in the compression core only when ductility demand is restricted. However, the use of such ties should be avoided as shear reinforcement in beams. They are also not recommended in potential plastic hinge locations of

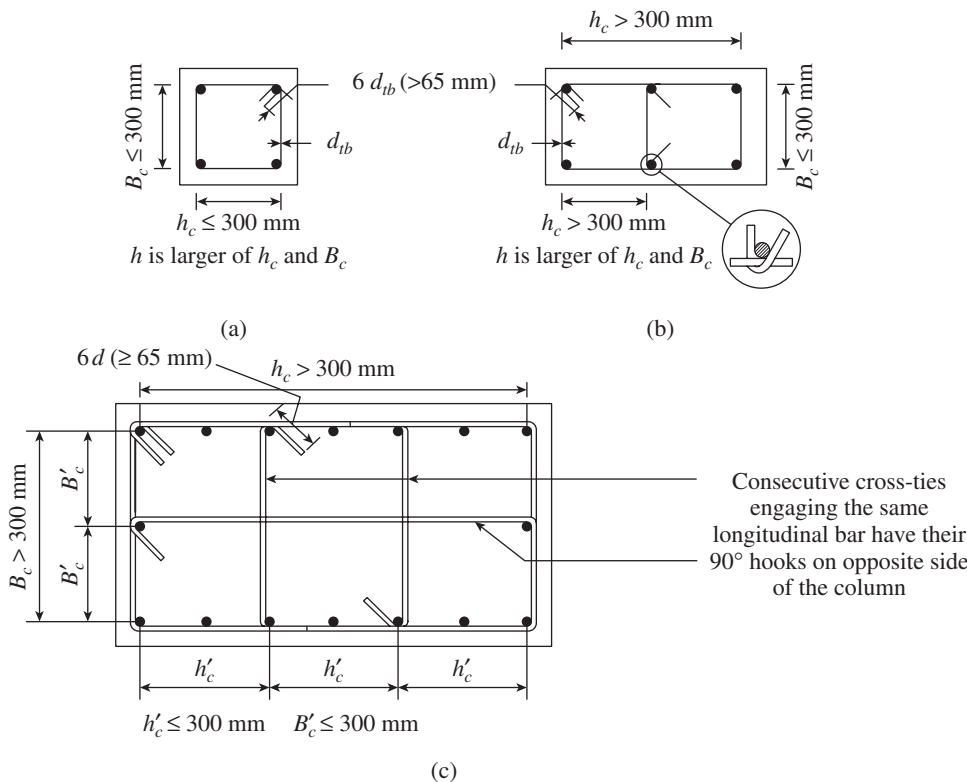


FIG. 13.26 Transverse reinforcement in columns (a) Single hoop (b) Single hoop with a cross-tie (c) Overlapping hoops with cross-ties

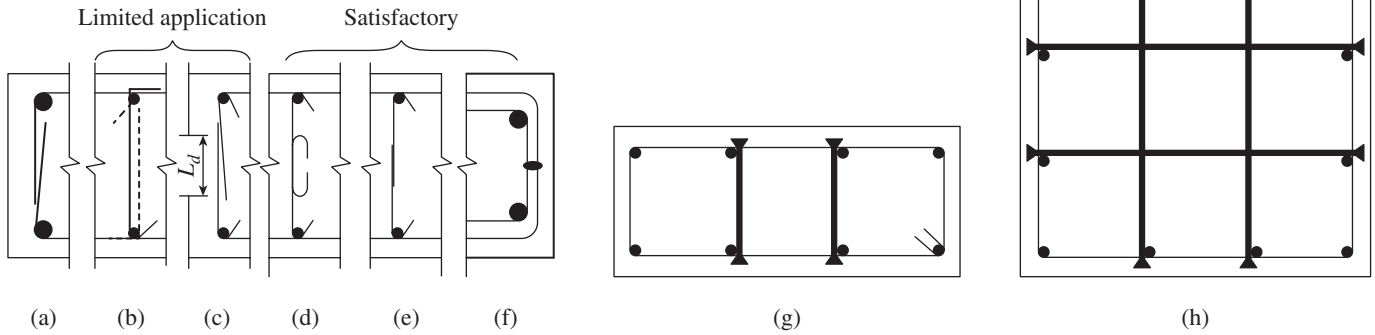


FIG. 13.27 Alternative tie arrangements (a) Lap-splicing of ties near cover concrete (b) Alternating J-type intermediate ties (c) Spliced tie inside the compression core (d) Splicing of plain ties (e) Lap welding of spliced ties (f) Prefabricated hoops with butt-welds (g)–(h) Double-headed studs as cross-ties

columns, where reversal of moments can occur. For plain bars, the splicing as shown in Fig. 13.27(d) may be more effective. As ties are not subjected to alternating inelastic strains, lap welding as shown in Fig. 13.27(e) is acceptable, provided good quality weld is assured. Prefabricated hoops with proper butt welds, as shown in Fig. 13.27(f), may result in less congestion due to the elimination of hooks and their extensions (see also Section 4.4.8 and Fig. 4.14b of Chapter 4). Double-headed studs are also found suitable for use as cross-ties, with the conventional closed stirrups following the perimeter of the cross section as shown in Figs. 3.27(g) and (h). Columns with headed studs as cross-ties have exhibited improved ductility and equal or greater strength than companion columns with conventional tie reinforcement (Youakim and Ghali 2002). More details on headed studs are provided in Section 6.2.3 of Chapter 6.

6. Based on the strong column–weak beam theory, Clause 7.3.4 of IS 13920 stipulates that the design shear force for columns should be the maximum of the following:

- (a) Calculated factored shear force as per analysis
- (b) A factored shear force given by

$$V_u = 1.4 \left[\frac{M_u^{bL} + M_u^{bR}}{h_{st}} \right] \quad (13.37)$$

where M_u^{bL} and M_u^{bR} are moment of resistance, of opposite sign, of beams framing into the column from opposite faces (see Fig. 13.28) and h_{st} is the storey height. The moment capacity of the beam is to be calculated as per IS 456:2000. Hence, in IS 13920, the column shear is evaluated based on beam flexural yielding, with the assumption that yielding will occur in beams rather than in columns. The factor of 1.4 is based on the consideration that the plastic moment capacity of a section is usually calculated by assuming the stress in flexural reinforcement as $1.25f_y$ as against $0.87f_y$ in the moment capacity calculation.

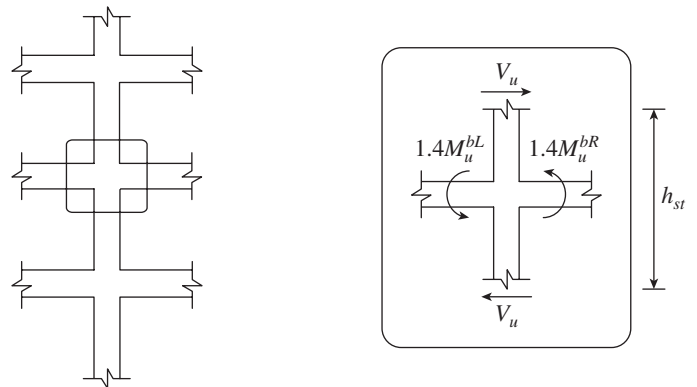


FIG. 13.28 Calculation of design shear force for column

7. Welding of stirrups, ties, or inserts to longitudinal reinforcement is not permitted as per Clause 21.1.7.2 of ACI 318.

13.10.4 Special Confining Reinforcement

Ductile response requires that members yield in flexure and shear failure is avoided. Shear failure, especially in columns, is relatively brittle and can lead to rapid loss of lateral strength and axial load carrying capacity (Moehle, et al. 2008). Column shear failure is the most frequently cited cause of concrete building failure and collapse during the past earthquakes (see Fig. 13.29). The shear strength of concrete reduces considerably in plastic hinge locations, which are often subjected to multiple stress reversals, especially if the axial compressive loads are low. In these locations, in order to have the desired ductility and rotation capacity, special confining reinforcement has to be provided and splicing of longitudinal bars should not be considered. These are discussed in the following subsections.

Shear Strength Degradation due to Cyclic Loading

When an RC member is subjected to load, flexural and shear cracks develop as shown in Fig. 13.30(a). When the load is reversed, these cracks close and a new set of cracks form

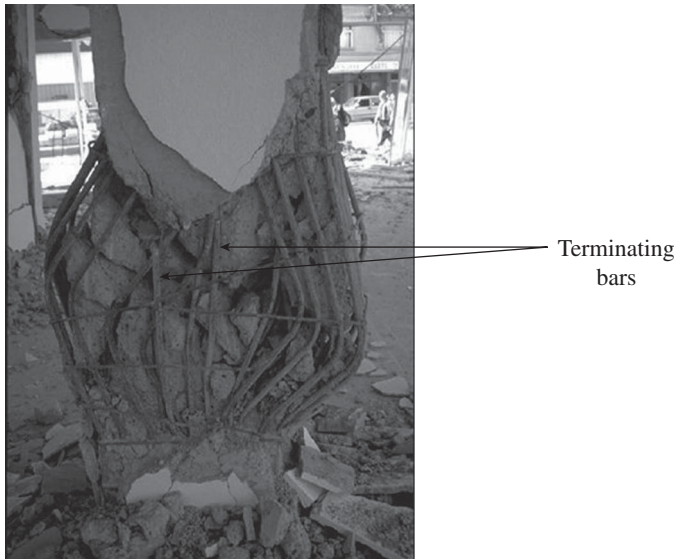


FIG. 13.29 Shear failure leading to a storey mechanism and subsequent collapse of building
Source: FEMA 451

(Scribner and Wight 1980). The crack pattern after several cycles of loading will be similar to that shown in Fig. 13.30(b). The left end of the beam will resemble a series of blocks of concrete held together by the reinforcement cage. The shear is now transferred across the crack only by the dowel action of the longitudinal reinforcement and grinding friction along the crack.

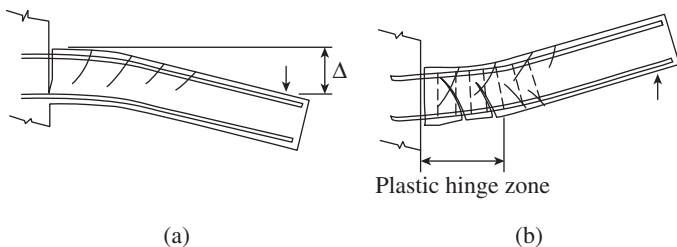


FIG. 13.30 Shear strength degradation due to cyclic loads (a) Cracks due to load acting in one direction (b) Cracks due to load acting in opposite direction

According to the experimental studies performed by Aschheim and Moehle (1992) and Wong, et al. (1993), the inelastic deformation capacity of RC members subjected to cyclic loading is less than that expected under monotonic loading. Wight and Sozen (1975) found that more shear reinforcement is required to ensure a flexural failure. As seen in Fig. 13.30, the low deformation capacity of RC members is attributed to the fact that under cyclic loading, the shear capacity of concrete deteriorates as the flexure–shear cracks in the plastic hinge zones widen; therefore, the aggregate interlock at the crack surface weakens (Priestley, et al. 1994). To address the degradation of the shear strength of RC members subjected to cyclic loading, ACI 318 (Clause 21.5.4.2), IS 13920 (Clause 6.3.3) and NZS 3101 codes neglect the concrete contribution, V_c , to the shear resistance of the members in the

earthquake design of the special moment frames in the plastic hinge locations. Several theoretical models for predicting the shear capacity of columns degraded by inelastic deformation have also been developed in the past and verified by experimental results (Priestley, et al. 1994; Sezen and Moehle 2004; Elwood and Moehle 2005; Mostafaei, et al. 2009; Choi and Park 2010).

As mentioned earlier, potential plastic hinge zones are provided with special confining reinforcement to enhance ductile behaviour—to ensure adequate rotational ductility of columns and to provide restraint against buckling to the compression reinforcement. Such confining reinforcement needs to be provided unless a larger amount of transverse reinforcement is required from shear strength considerations. However, shear-dominated columns subjected to cyclic reversals at low temperatures (-36°C) exhibited an increase in flexural strength, shear, and displacement capacity (Montejo, et al. 2009).

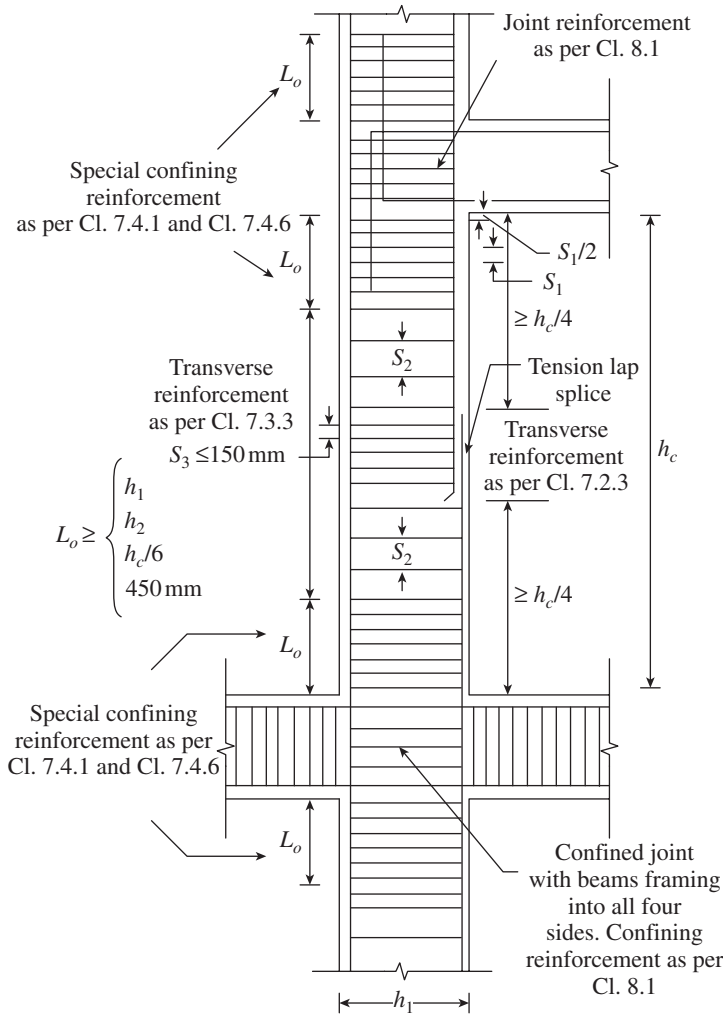
Confining Reinforcement as per Codes

The following are the rules given in codes regarding confining reinforcement:

1. Special confining reinforcement shall be provided over a length L_o (*length of plastic hinge*) from each joint face, towards mid-span, and on either side of any section, where flexural yielding may occur under the effect of earthquake forces (see Fig. 13.31). As per Clause 7.4.1 of IS 13920, the length L_o should not be less than the following:
 - (a) Larger lateral dimension of the member (h) at the section where yielding occurs
 - (b) One-sixth of clear span of the member
 - (c) 450 mm

Several factors influence the length of plastic hinge, such as the (a) level of axial load, (b) moment gradient, (c) value of shear stress in the plastic hinge region, (d) amount and mechanical properties of longitudinal and transverse reinforcement, (e) strength of concrete, and (f) level of confinement provided in the potential plastic hinge zone. The simplified equations available in literature do not contain all or most of these factors (Paulay and Priestley 1992). Bae and Bayrak (2008) identified that the plastic hinge length L_o has to be increased from the present $1.0h$ (as per ACI 318 and IS 13920) to a minimum of $1.5h$ and proposed a formula for calculating it. Subramanian (2009) also provides a comparison of the available formulae to predict the plastic hinge length.

2. Clause 7.4.6 of IS 13920 suggests that the spacing of hoops used as special confining reinforcement should not exceed one-fourth of the minimum member dimension or six times the diameter of the longitudinal bar; the spacing need not be less than 75 mm nor more than 100 mm to ensure proper compaction of concrete (see Fig. 13.31).



ACI 318	IS 13920
$S_1 \leq \begin{cases} h_1/4 \\ h_2/4 \\ 6d_b \\ S_o \end{cases}$	$\begin{cases} h_1/4 \\ h_2/4 \\ 6d_b \\ 100 \text{ mm but} \\ > 75 \text{ mm} \end{cases}$
$S_2 \leq \begin{cases} 6d_b \\ 150 \text{ mm} \end{cases}$	$0.5h_1 \text{ or } h_2$

d_b = Diameter of smallest longitudinal bar
 $150 \text{ mm} \geq S_o = 100 + \left(\frac{350 - h_x}{3}\right) \geq 100 \text{ mm}$

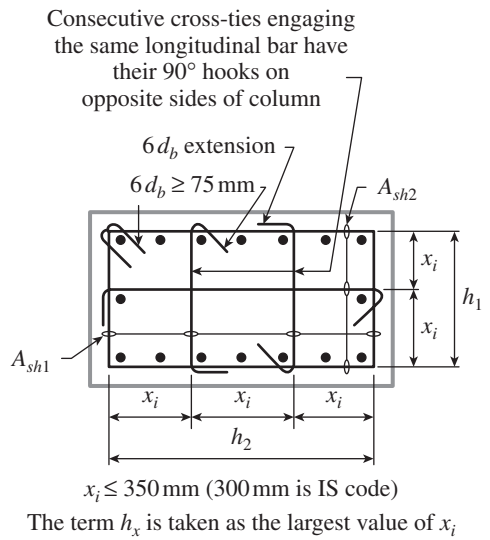


FIG. 13.31 Columns and joint detailing as per IS 13920

- As mentioned earlier, during severe shaking, a plastic hinge may form at the bottom of a column that terminates into a footing or raft foundation. Hence, special confining reinforcement of the column must be extended to at least 300 mm into the foundation, as per Clause 7.4.2 of IS 13920 (see Fig. 13.32).
- The point of contraflexure is usually in the middle half of the column, except for columns in the top and bottom storeys of a multi-storey frame (see Fig. 7.47 of Chapter 7). When the calculated point of contraflexure, under the effect of gravity and earthquake loads, is not within the middle half of the column, the zone of inelastic deformation may extend beyond the region that is provided with closely spaced hoop reinforcement. In such cases, Clause 7.4.3 of IS 13920 stipulates that special confining reinforcement should be provided over the full height of the column.

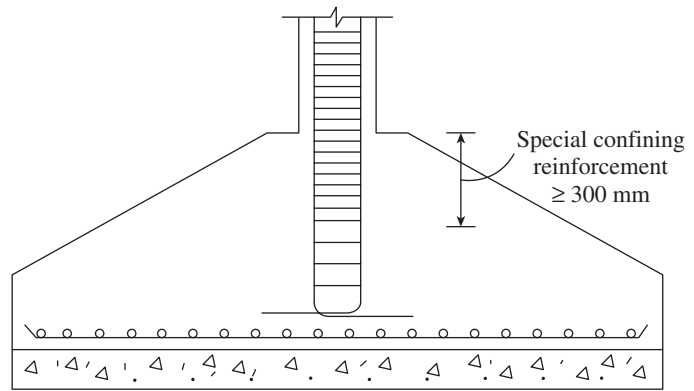


FIG. 13.32 Special confining reinforcement in footing

- Observations in past earthquakes indicate very poor performance of buildings where a wall in the upper storey terminates on the columns in the lower storeys. Hence, when such a situation cannot be avoided, special confining

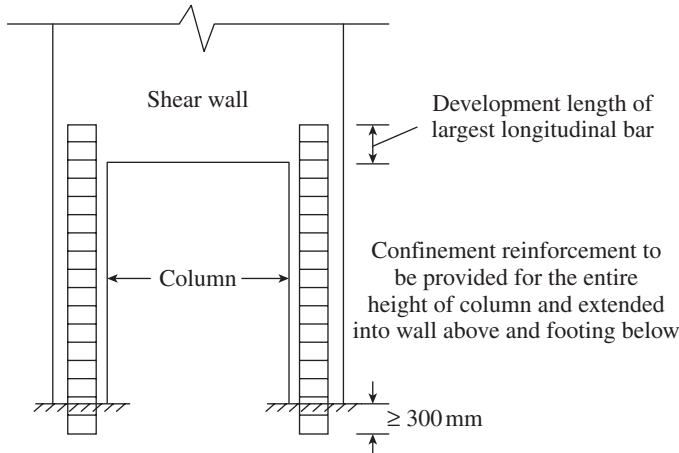
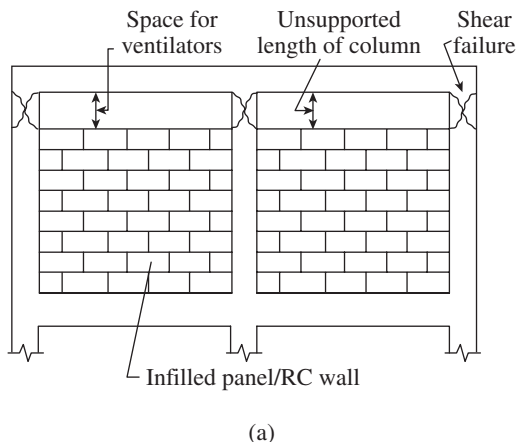


FIG. 13.33 Special confining reinforcement for columns supporting discontinued wall

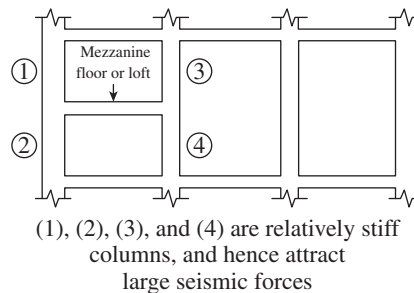
reinforcement must be provided over the full height in such columns (see Fig. 13.33). The transverse reinforcement in columns supporting discontinued walls should be extended above the discontinuity by at least the development length of the largest vertical bar and below the base by the same amount where the column rests on a wall. Where the column terminates in a footing or mat, the transverse reinforcement is to be extended below the top of the footing or mat to a distance of at least 300 mm, as shown in Fig. 13.32.

- Column stiffness is inversely proportional to the cube of the column height. Hence, columns with significantly lesser height than other columns in the same storey have much higher lateral stiffness and consequently attract much greater seismic shear force. There is a possibility of brittle shear failure occurring in the unsupported zones of such short columns. This has been observed in several earthquakes in the past.

Semi-basements require ventilators to be provided between the soffit of beams and the top of the wall (see Fig. 13.34a); in such cases, the columns become ‘short-columns’ as compared to the other interior columns. Another



(a)



(1), (2), (3), and (4) are relatively stiff columns, and hence attract large seismic forces

example is a mezzanine floor or a loft, which also results in the stiffening of some of the columns while leaving other columns of the same storey unbraced over their full height (see Fig. 13.34b). Hence, special confining reinforcement shall be provided over the full height in such columns to give them adequate confinement and shear strength. More information on the behaviour and ductility of short columns are provided by Moretti and Tassios (2006). An explosive cleavage type shear failure is also possible as occurred in the RC short bridge piers during the 1995 Hanshin-Awaji earthquake in Japan (Yamada 1996).

It has to be noted that as per draft IS 13920, ductile requirements are mandatory for all structures located in seismic zones III, IV, and V. Only in the case of zone II structures, the designer may choose to design structures for non-seismic force with ductile detailing or for seismic force with non-seismic detailing. Hence, moment-resisting frame structures located in seismic zones III–V shall comply with Sections 5–8 of IS 13920, that is, as special moment-resisting frames (SMRF) with response reduction factor $R = 5.0$. Moment-resisting frame structures located in seismic zone III are permitted to comply with only Section 10 of IS 13920, that is, as intermediate moment-resisting frame (IMRF). Sheth (2003) may be consulted for more details of IMRF.

Parameters Affecting Confinement Reinforcement

The state of knowledge on concrete confinement has improved substantially since the pioneering work of Richart, et al. in 1929, which is described in Sections 13.5.1 and 13.5.2. A large volume of experimental data has been generated and a number of improved analytical models have been developed. Various design parameters that are overlooked by the Indian and ACI codes have been identified and studied (Saatcioglu and Razvi 2002; Elwood, et al. 2009). The confinement requirements of IS 13920 may not be appropriate even for normal strength concrete (NSC) at high axial load levels and

are quite unsafe in the case of high-strength concrete (HSC) under high load levels to impart enough ductility to critical hinge regions of columns (Sharma, et al. 2005). A good review of the research in this area is provided by Sakai and Sheikh (1989), Sharma, et al. (2005), Sharma, et al. (2006), and Subramanian (2011). Recent research has shown that the following important parameters influence the confinement of concrete:

Axial load level It has been well established that columns with low compressive axial loads may require

FIG. 13.34 Columns with variable stiffness (a) Columns with partial in-filled panel (b) Columns supporting mezzanine floor or loft

less confinement than those with high axial loads. The Canadian and New Zealand codes include the effect of axial load. Elwood, et al. (2009) suggest that it is enough to include the term $P_u/A_g f'_c$ (which has a range of 0.1–0.7) in the equation, since the inclusion of the term $A_s f_{yt}$, as done in the Canadian code, does not appreciably change the value of confining reinforcement. The moment–curvature response of members subjected to axial tensions would be dominated by the behaviour of longitudinal reinforcement; hence, columns with axial tension are not critical as they will sustain large ultimate curvatures.

Effective confining pressure or ratio of concrete strength to tie strength The required A_{sh} will be proportional to $sD_k f'_c/f_{yt}$. It has to be noted that as the yield strength is increased, the quantity of the required confining reinforcement will be reduced. Based on the assumption of the amount of strain that will occur in transverse reinforcement, limits are often placed on the value of f_{yt} that can be used in the calculations. As HSC is more brittle than NSC, it may require more confining steel.

Unconfined cover concrete thickness As the load is increased, the unconfined concrete in the cover portion of the column will begin to spall, when the compressive strain in concrete reaches about 0.003–0.005, resulting in loss of strength. This loss will be considerable when the area of unconfined concrete cover is a larger proportion of the total concrete. Hence, this effect has to be included in the confinement provisions, by specifying the ratio A_g/A_k , where A_g is the gross area and A_k is the area of confined core (the normal range for this ratio is 0.7–0.81). The fact that A_{sh} will be directly proportional to A_g/A_k has been confirmed using the moment–curvature studies (Watson, et al. 1994; Elwood and Eberhard 2009). However, ACI (as well as IS 13920) equations, as shown earlier, were set up to equate the concentric capacity of cover concrete to strength gain in the core, rather than considering the effect of A_g/A_k on lateral deformation capacity. Hence, the ACI and IS codes have a factor of $(A_g/A_k - 1)$ instead of A_g/A_k . For larger columns to have sufficient confinement, the ratio A_g/A_k should not exceed 1.3.

Longitudinal reinforcement and spacing It has been found from experiments that the amount and transverse support of longitudinal reinforcement will also influence the confinement of concrete core (see Figs 13.35 and 13.36). Canadian and New Zealand codes allow for this, though the approach taken and the resultant impact on the requirements are different in these

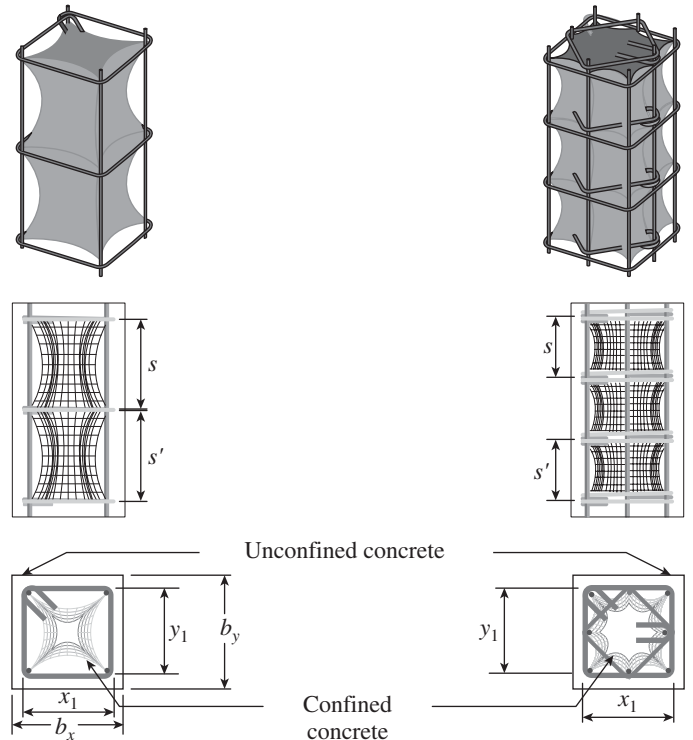


FIG. 13.35 Confinement of concrete in rectangular or square columns
Source: Paultre and Légeron 2008, reprinted with permission from ASCE

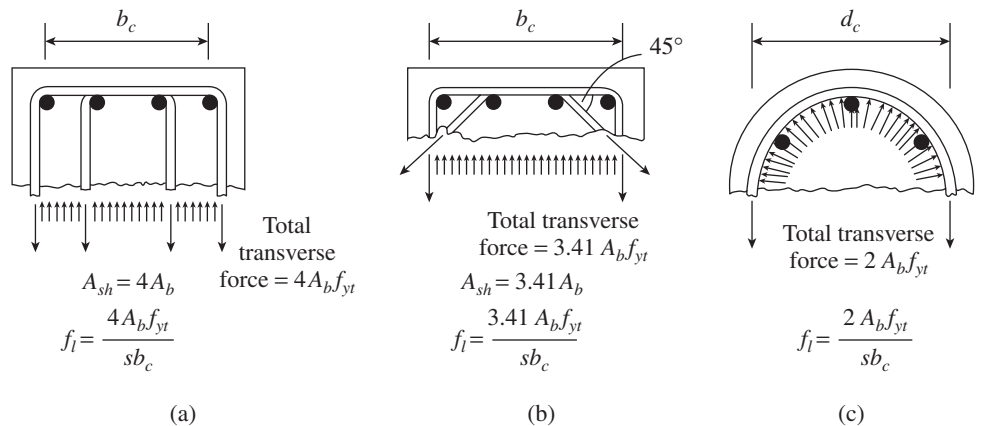


FIG. 13.36 Confining stresses provided by different arrangements of transverse reinforcement (a) Two overlapping hoops (b) Two overlapping hoops with one diamond shaped (c) Circular column with spiral ties

codes (Elwood, et al. 2009). The Canadian code recognizes the fact that when more longitudinal bars are restrained by hoops or cross-ties, the effectiveness of confinement is improved, since the confined concrete arches horizontally between the restrained longitudinal bars (see Fig. 13.35). This effect is reflected in the factor k_n , which relates to the number of longitudinal bars restrained by the corners of hoops or hooks of seismic cross-ties, n_l , as shown in Fig. 13.37. The k_n factor also encourages good column detailing for confinement and provides effective restraint to prevent bar buckling (Elwood, et al. 2009). It should be noted that when the longitudinal reinforcement ratio is high, steel congestion problems will

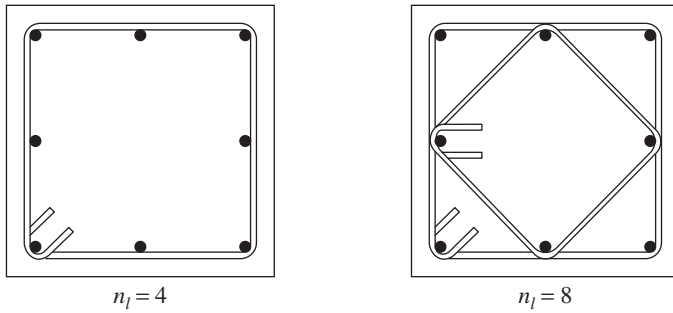


FIG. 13.37 Consideration of the effect of longitudinal rods in confinement

arise, and hence a larger size of column is preferable in such cases. The required confining reinforcement increases when flexural steel content ρ_l decreases.

Based on the foregoing discussions, the following equation is proposed for confining reinforcement (Elwood, et al. 2009; Subramanian 2011):

$$\frac{A_{sh}}{sh} = 0.3k_n k_p \frac{A_g f'_c}{A_c f_{yt}} \quad (13.38a)$$

where

$$k_n = \left(0.6 + 0.4 \frac{n}{n_l} \right) \left(\frac{h_x + 12}{20} \right) \quad \text{and} \quad k_p = \frac{0.8 P_u}{A_g f_{ck}} \geq 0.2 \quad (13.38b)$$

with $f_{yt} \leq 689 \text{ MPa}$; $\frac{A_g}{A_c} \leq 1.3$; and $\left(\frac{h_x + 12}{20} \right) \geq 1.0$

where A_k is the area of concrete core within perimeter transverse reinforcement, A_g is the gross area of column, A_{sh} is the total cross-sectional area of transverse reinforcement (including cross hoops) with spacing s and perpendicular to dimension b_c , b_c is the cross-sectional dimension of column core measured to the outside edges of transverse reinforcement composing area A_k , d_b is the diameter of longitudinal bar, f_{ck} is the specified cube compressive strength of concrete, f_{yt} is the specified yield strength of transverse reinforcement, h is the longer dimension of the rectangular confining hoop measured to its outer edge, h_x is the centre-to-centre horizontal spacing of cross-ties or hoop legs, P_u is the factored load on column, n is the total number of longitudinal bars, and n_l is the number of longitudinal bars of column laterally supported by corner of hoops or by seismic hooks of cross-ties that are greater than or equal to 135° .

A comparison of Eqn. 13.38 with the equations available in various codes is provided by Subramanian 2011 and Elwood, et al. 2009.

Curvature ductility factor It is well known that the quantity of confining reinforcement provided in the potential plastic hinge zones of columns has a significant effect on the curvature ductility factor $\mu_\phi = \phi_u / \phi_y$. Columns are considered to have adequate ductility if they are able to sustain a curvature

ductility factor μ_ϕ of approximately 20 (Watson, et al. 1994; Elwood and Eberhard 2009). This order of curvature ductility should enable the plastic hinges at the bases of columns to undergo sufficient plastic rotation to reach a displacement ductility factor of 4 to 6. Frames where limited ductility is sufficient should be designed to sustain a curvature ductility factor μ_ϕ of approximately 10 (Li and Park 2005).

The relationship between the *curvature ductility* and *displacement ductility* was derived by Park and Paulay (1975), neglecting the P - Δ effect, rebar slip, and shear deformations, as follows:

$$\mu_\Delta = 1 + 3(\mu_\phi - 1) \frac{L_p}{L} \left(1 - 0.5 \frac{L_p}{L} \right) \quad (13.39)$$

where μ_Δ is the displacement ductility ($=\Delta_u / \Delta_y$), μ_ϕ is the curvature ductility ($=\phi_u / \phi_y$), L is the length of column, L_p is the plastic hinge length, Δ_u and ϕ_u are the deflection and curvature, respectively, at the end of post-elastic range, and Δ_y and ϕ_y are the deflection and curvature, respectively, when the first yield is reached. There is no real consensus on the level of ductility required by concrete structures in seismic loading; typical values of displacement ductility factor may range from 4 to 6. Curvature ductility factors may be four times the displacement ductility factors (Sharma, et al. 2005). The plastic hinge length, L_p , will be typically in the range of 0.5 to 1.5 times the member depth, h (Bae and Bayrak 2008). A simple equation [$\delta = 20(e/L) \leq 4\%$, where $e = M/P \leq 0.2L$ (M and P are the moment and the axial load acting on the column)] was presented by Bae and Bayrak (2009) to calculate the drift capacity of concrete columns, when $L/h > 2$.

Based on the reasoning given earlier, the following confinement equation is proposed for circular columns (Elwood, et al. 2009):

$$\rho_s = 0.44 k_p \left(\frac{f_{ck}}{f_{yt}} \right) \left(\frac{A_g}{A_k} \right) \quad (13.40)$$

where ρ_s is the volumetric ratio of transverse reinforcement, $k_p = 0.8 P_u / A_g f_{ck} \geq 0.2$. It has to be noted that the term k_n is not required for circular columns, as spirals provide better effective confinement than rectangular hoops. The circular HSC columns designed as per CSA A23.3-04 (similar to Eq.13.40) were found to behave in a ductile manner regardless of the yield strength of transverse steel or axial load level (Paultre, et al. 2009)

The superiority of helical reinforcement in circular column over rectangular links in square or rectangular columns in providing greater ductility has been proved in several earthquakes. For example, Fig. 13.38 shows the damage to Olive View Hospital building during the earthquake on 9 February 1971 in San Fernando, California (Jennings 1971). It should be noted that the circular column has withstood

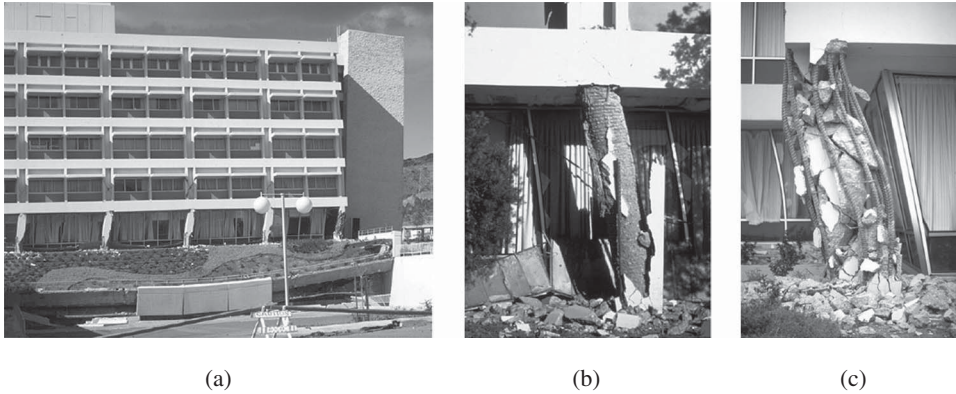


FIG. 13.38 Damage to Olive View Hospital (a) A wing of the building showing approximately 600 mm drift in its first storey (b) Damaged spirally reinforced column in first storey still carrying load (c) Completely collapsed tied rectangular corner column in the same storey

Source: Jennings 1971, reprinted with permission from NISEE, University of California, Berkeley

approximately 600 mm drift in the ground floor and carries load even after the spalling of the cover concrete.

It should also be noted that very high-strength concrete is extremely brittle when not confined adequately and the required confinement may be considerably greater than for NSC columns (Li and Park 2004). HSC can be made to behave in a ductile manner under high levels of axial force, provided that a lateral confining reinforcement of high-yield strength is used in an efficient configuration (Bayrak and Sheikh 1998; Sharma, et al. 2005; Canbay, et al. 2006). High-strength lightweight concrete columns were also found to have high ductility under seismic loads (Hendrix and Kowalsky 2010). Self-consolidating concrete (SCC) columns were found to have better structural performance and are more ductile than comparable NSC or HSC columns, provided SCC is properly proportioned (Lin, et al. 2008; Galano and Vignoli 2008).

Use of steel fibres was found to delay the spalling of concrete cover and increase the strain capacity and ductility of columns (Campione, et al. 2010; Ganesan and Ramana Murthy 1990; Foster and Attard 2001). Elliptical columns with *interlocking spiral reinforcement* to confine an oblong column core were found to perform satisfactorily with displacement ductility capacity ranging from 7.4 to 10 (Correal, et al. 2007). When *superelastic shape memory alloy* longitudinal reinforcements or *engineered cementitious composites* (ECC), or both, are used in the plastic hinge zone of bridge columns, they exhibit large drift capacity and experience less damage compared to the conventional concrete columns (Saiidi, et al. 2009).

EXAMPLES

EXAMPLE 13.1 (Effective Length of Column):

An unbraced portal frame ABCD is having a span of 5 m and height 6 m with pinned supports at bottom. Columns AB and CD are having a size of 400 mm × 600 mm and beam BC is having a size 300 mm × 600 mm. The beam is connected to

the face of column, which is 400 mm wide. Estimate the effective length of columns in the plane of portal frame using Wood's charts.

SOLUTION:

Unsupported length of column = 6000 – 600 = 5400 mm

$$\Sigma I_c / h_s = 2 \times (400 \times 600^3 / 12) / 6000 = 24,00,000 \text{ mm}^3$$

$$\Sigma I_b / L_b = (300 \times 600^3 / 12) / 5000 = 10,80,000 \text{ mm}^3$$

As the frame or column is unbraced, we have

$$K_c = \Sigma I_c / h_s = 24,00,000 \text{ mm}^3$$

$$K_b = 1.5 \Sigma I_b / L_b = 1.5 \times (10,80,000) = 16,20,000 \text{ mm}^3$$

$$\beta_1 = K_c / (K_c + K_b) = \frac{24,00,000}{24,00,000 + 16,20,000} = 0.597 \text{ at top}$$

$$\beta_2 = 1 \text{ (as bottom is hinged)}$$

From Wood's curves for column with sway (see Fig. 27 of IS 456), $k = 2.75 > 1.20$

$$\text{Effective length} = 2.75 \times 5400 = 14,850 \text{ mm}$$

Note: The same value of k can be obtained by using Eq. (13.6b)

$$k = \left(\frac{1 - 0.2(\beta_1 + \beta_2) - 0.12\beta_1\beta_2}{1 - 0.8(\beta_1 + \beta_2) + 0.6\beta_1\beta_2} \right)^{0.5} = \left(\frac{1 - 0.2 \times 1.597 - 0.12 \times 0.597 \times 1}{1 - 0.8 \times 1.597 + 0.6 \times 0.597 \times 1} \right)^{0.5} = \left(\frac{0.609}{0.0806} \right)^{0.5} = 2.75$$

EXAMPLE 13.2 (Effective length of column in a portal frame):

A plane frame, as shown in Fig. 13.39, has all its columns of size 400 mm × 400 mm and all its beams of size 400 mm × 600 mm. All the beams are subjected to a uniformly distributed load of 100 kN/m, including self-weight. Calculate the effective length of column marked C1 using Wood's charts. Assume M 25 concrete.

SOLUTION:

Unsupported length of column C1 = 3000 – 600 = 2400 mm

Relative stiffness estimation:

$$\Sigma I_c / h_s = 3 \times (400 \times 400^3 / 12) / 3000 = 2.13 \times 10^6 \text{ mm}^3$$

$$\Sigma I_b / L_b = 2 \times (400 \times 600^3 / 12) / 3000 = 4.80 \times 10^6 \text{ mm}^3$$

Check to find if the column is braced or unbraced:

$$E_c = 5000 \times \sqrt{25} = 25,000 \text{ N/mm}^2$$

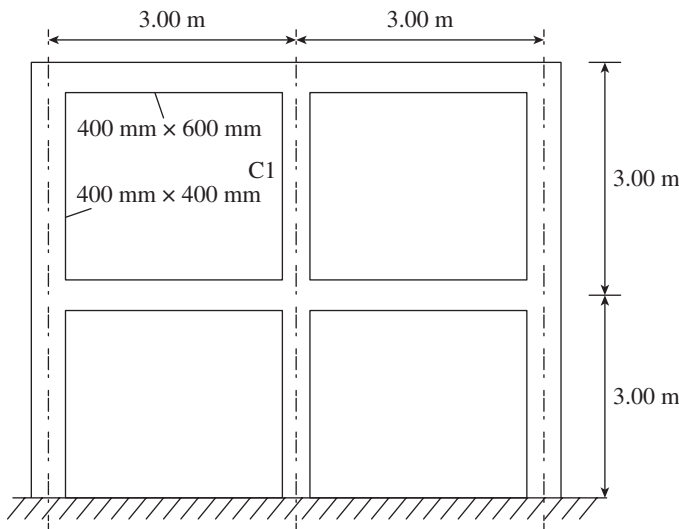


FIG. 13.39 Frame of Example 13.2

$$\begin{aligned} \frac{\Delta_u}{H_u} &= \frac{h_s^2}{12 E_c \Sigma(I_c/h_s)} + \frac{h_s^2}{12 E_c \Sigma(I_b/L_b)} \\ &= \frac{3000^2}{12 \times 25,000(2.13 + 4.8) \times 10^6} = 4.33 \times 10^{-6} \text{ mm/N} \end{aligned}$$

$$P_u = 1.5 \times (100 \times 3) = 450 \text{ kN}$$

Stability index

$$Q = \frac{\Sigma P_u \Delta_u}{H_u h_s} = \frac{450 \times 1000 \times 4.33 \times 10^{-6}}{2400} = 0.0008 < 0.04$$

Hence, the frame can be considered as 'braced'.

$$\beta_1 = \beta_2 = \frac{\Sigma I_c / h_s}{\Sigma I_c / h_s + \Sigma 0.5 I_b / L_b} = \frac{2.13}{2.13 + 0.5 \times 4.8} = 0.47$$

From Wood's curves for column without sway (see Fig. 26 of IS 456)

$$\text{Effective length} = 0.675 \times 2400 = 1620 \text{ mm}$$

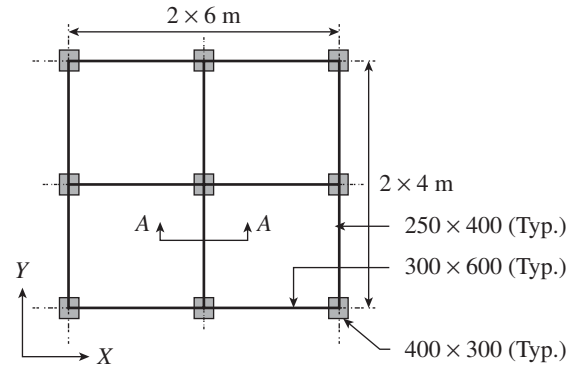
Note: The same value of k can be obtained by using Eq. (13.6a)

$$\begin{aligned} k &= \frac{1 + 0.145(\beta_1 + \beta_2) - 0.265\beta_1\beta_2}{2 - 0.364(\beta_1 + \beta_2) - 0.247\beta_1\beta_2} \\ &= \frac{1 + 0.145(0.47 + 0.47) - 0.265 \times 0.47 \times 0.47}{2 - 0.364(0.47 + 0.47) - 0.247 \times 0.47 \times 0.47} \\ &= \frac{1.078}{1.603} = 0.672 \end{aligned}$$

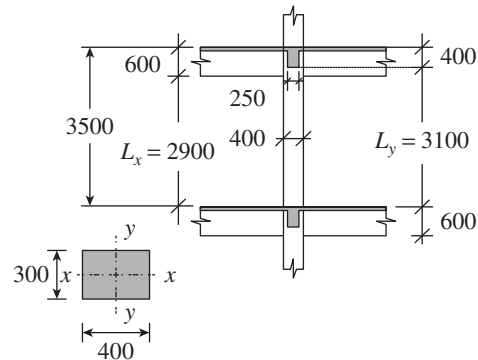
EXAMPLE 13.3 (Effective length of multi-storey column):

The plan of a G + 4 building is shown in Fig. 13.40. The sizes of all columns are 400 mm × 300 mm, sizes of all beams along

the x -direction are 300 mm × 600 mm, and sizes of all beams along the y -direction are 250 mm × 400 mm. Typical storey height is 3500 mm. Assume total uniform floor load of 50 kN/m² from all the floors (combined) and consider M25 concrete for columns and M20 for beams. Estimate effective lengths about the local x -axis and z -axis of the internal column at the first floor level.



Plan



Column and its local axes

Section A-A

FIG. 13.40 Building of Example 13.3

SOLUTION:

Unsupported length of the column

$$L_x = 3500 - 600 = 2900 \text{ mm (for buckling about } x\text{-axis)}$$

$$L_y = 3500 - 400 = 3100 \text{ mm (for buckling about } y\text{-axis)}$$

Step 1 Estimate the relative stiffness.

(a) Columns—nine numbers, $h_s = 3.5$ m

$$\Sigma I_c / h_s = 9 \times (300 \times 400^3 / 12) / 3500 = 4114.3 \times 10^3 \text{ mm}^3$$

(for sway in x -direction)

$$\Sigma I_c / h_s = 9 \times (400 \times 300^3 / 12) / 3500 = 2314.3 \times 10^3 \text{ mm}^3$$

(for sway in y -direction)

(b) Longitudinal beams—six numbers, size: 300 × 600 mm,

$$L_b = 6.0 \text{ m}$$

$$\Sigma I_b / L_b = 6 \times (300 \times 600^3 / 12) / 6000 = 5400 \times 10^3 \text{ mm}^3$$

(c) Transverse beams—six numbers, size: 250 × 400 mm,
 $L_b = 4.0$ m
 $\Sigma I_b / L_b = 6 \times (250 \times 400^3 / 12) / 4000 = 2000 \times 10^3 \text{ mm}^3$

Step 2 Check to decide whether column is braced or unbraced.
 Modulus of elasticity for columns, $E_{c,col} = 5000 \times \sqrt{25} = 25,000 \text{ N/mm}^2$
 Modulus of elasticity for beams, $E_{c,beam} = 5000 \times \sqrt{20} = 22,361 \text{ N/mm}^2$
 Contributory axial load to internal lower storey column

$$\Sigma P_u = (12 \times 8) \times 50 = 4800 \text{ kN}$$

$$\left(\frac{\Delta_u}{H_u} \right)_x = \frac{h_s^2}{12 E_c \Sigma(I_c / h_s)} + \frac{h_s^2}{12 E_c \Sigma(I_b / L_b)}$$

$$= \frac{3500^2}{12 \times 25,000 \times 4114.3 \times 10^3} + \frac{3500^2}{12 \times 22,361 \times 5400 \times 10^3}$$

$$= 18.38 \times 10^{-6} \text{ mm/N}$$

$$\left(\frac{\Delta_u}{H_u} \right)_y = \frac{3500^2}{12 \times 25,000 \times 2314.3 \times 10^3} + \frac{3500^2}{12 \times 22,361 \times 2000 \times 10^3}$$

$$= 40.47 \times 10^{-6} \text{ mm/N}$$

Stability Index: $Q = \frac{\Sigma P_u \Delta_u}{H_u h_s}$

Longitudinal direction: $Q_x = \frac{4800 \times 1000 \times 18.38 \times 10^{-6}}{3500} = 0.025 < 0.04$

Hence, it may be considered as braced in the x -direction.

Transverse direction: $Q_y = \frac{4800 \times 1000 \times 40.47 \times 10^{-6}}{3500} = 0.056 > 0.04$

Hence, it may be considered as *not* braced in the y -direction.

Buckling about minor axis—sway in x -direction

$$K_c = \Sigma I_c / h_s = 2 \times (300 \times 400^3 / 12) / 3500 = 9,14,286 \text{ mm}^3$$

$$K_b = \Sigma I_b / L_b = 2 \times (300 \times 600^3 / 12) / 6000 = 18,00,000 \text{ mm}^3$$

$$\beta_1 = \beta_2 = \frac{\Sigma I_c / h_s}{\Sigma I_c / h_s + \Sigma 0.5 I_b / L_b}$$

$$= 914,286 / (914,286 + 0.5 \times 18,00,000) = 0.504$$

From Fig. 26 of the code or Eq. (13.6a), $k_x = 0.69$.

Effective length, $L_x = 0.69 \times 2900 = 2001 \text{ mm}$

Buckling about major axis—sway in y -direction

$$K_c = \Sigma I_c / h_s = 2 \times (400 \times 300^3 / 12) / 3500 = 5,14,286 \text{ mm}^3$$

$$K_b = \Sigma I_b / L_b = 2 \times (250 \times 400^3 / 12) / 4000 = 6,66,667 \text{ mm}^3$$

$$\beta_1 = \beta_2 = \frac{\Sigma I_c / h_s}{\Sigma I_c / h_s + \Sigma 1.5 I_b / L_b}$$

$$= 5,14,286 / (5,14,286 + 1.5 \times 6,66,667) = 0.34$$

From Fig. 27 of IS 456 or Eq. (13.6a), $k_y = 1.27 > 1.20$
 Effective length = $1.27 \times 3100 = 3937 \text{ mm}$

EXAMPLE 13.4 (Design of square column):

Design a column of height 3 m, which is effectively held in position and restrained against rotation at bottom and effectively restrained against rotation but not held in position at top. It is subjected to an axial load of 1650 kN under dead and live load condition. Use M25 concrete, Fe 415 steel, and assume moderate environment.

SOLUTION:

Step 1 Determine the size of the column.

Factored load = $1.5 \times 1650 = 2475 \text{ kN}$

Assuming $\rho_g = A_{sc} / A_g = 2\%$,

Using Eq. (13.36),

$$A_c = \frac{P_u}{0.4(f_{ck} + 1.67 f_y \rho_g)} = \frac{2475 \times 1000}{0.4(25 + 1.67 \times 415 \times 2/100)}$$

$$= 159,221 \text{ mm}^2$$

Assuming a square column, size of column = $\sqrt{159,221} = 399 \text{ mm}$; adopt 400 mm.

Step 2 Determine whether the column is a short or long column.

Boundary condition for columns:

Bottom: Effectively held in position and restrained against rotation

Top: Effectively restrained against rotation but not held in position

Refer to Table 13.1 (Table 28 of IS 456).

Effective length factor, $k = 1.20$

Effective length of column, $L_e = k \times L = 1.20 \times 3.00 = 3.60 \text{ m}$

Ratio: $L_e / \text{least lateral dimension} = 3.60 / 0.4 = 9 < 12$

Hence, the column can be classified as a short column.

Step 3 Calculate the minimum eccentricity (Clause 25.4 of IS 456).

Minimum eccentricity = $(L/500) + (b/30) = (3000/500) + (400/30) = 19.33 \text{ mm} < 20 \text{ mm}$

$$0.05 \times b = 0.05 \times 400 = 20$$

Hence, the formula for the short column capacity suggested by IS 456:2000 can be used.

Step 4 Estimate longitudinal reinforcement.

Minimum reinforcement (Clause 26.5.3.1) = $(0.8/100) \times 400 \times 400 = 1280 \text{ mm}^2$

As per Clause 39.3 of IS 456, $P_u = 0.4 f_{ck} A_c + 0.67 f_y A_{sc}$

Substituting the values, we get

$$2475 \times 1000 = 0.4 \times 25 \times 400 \times 400 + 0.67 \times 415 \times A_{sc}$$

Solving, we get, $A_{sc} = 3147 \text{ mm}^2$ ($p = 1.96\%$) $> 1280 \text{ mm}^2$

Hence, provide eight 25 mm bars; area provided = 3927 mm^2

Provided percentage of reinforcement = $3927 / (400 \times 400) \times 100 = 2.45\% < 4\%$

Hence, the selected area is within limits.

Use of design aids The same value of A_{sc} may be obtained by using Chart 25 of SP 16. In the top of the chart, go along the line for $P_u = 2475 \text{ kN}$, hit the line for $A_g = 1500 \text{ cm}^2$; now come down on the same line and hit the line for M25 concrete and read the reinforcement percentage as 2.1%.

Step 5 Estimate transverse reinforcement.

Diameter of transverse reinforcement [Clause 26.5.3.2(c)-(2)]

Criteria 1: Diameter of longitudinal bar/4 = $25/4 = 6.25 \text{ mm}$

Criteria 2: 6 mm

Adopt a diameter of 8 mm for the transverse reinforcement.

Spacing of transverse reinforcement [Clause 26.5.3.2(c)-(1)]

Criteria 1: Least lateral dimension of column = 400 mm

Criteria 2: $16 \times$ Diameter of smallest longitudinal bar = $16 \times 25 = 400 \text{ mm}$

Criteria 3: 300 mm

Hence, provide transverse reinforcement of 8 mm bars at 300 mm centre to centre.

Step 6 Detail the reinforcement. Adopt the column as shown in Fig. 13.41, with 40 mm cover to reinforcement.

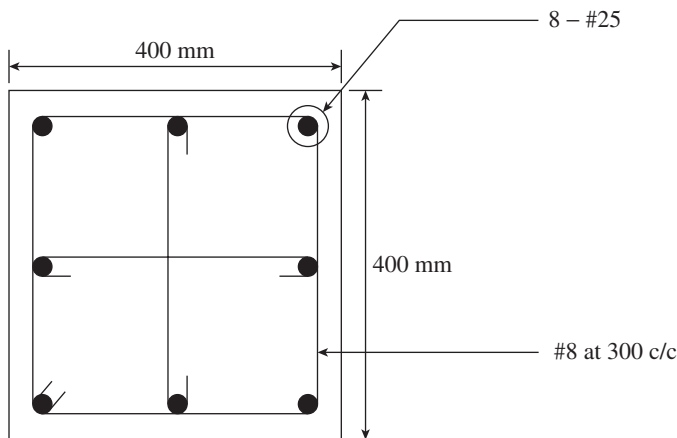


FIG. 13.41 Reinforcement details of column in Example 13.4

EXAMPLE 13.5 (Design of rectangular column):

Design a rectangular column subjected to an axial load of 3000 kN under dead and live loads case. The column is braced against side sway in both the directions and is having

an unsupported length of 3.20 m. Use M25 concrete, Fe 415 steel, and assume moderate environment.

SOLUTION:

Step 1 Determine the size of the column.

$$\text{Factored load} = 1.5 \times 3000 = 4500 \text{ kN}$$

Adding one per cent as self-weight of column,

$$\text{Total load} = 1.01 \times 4500 = 4545 \text{ kN}$$

Since the load is high, assume $\rho_g = A_{sc}/A_g = 3\%$. Using Eq. (13.36),

$$A_c = \frac{P_u}{0.4(f_{ck} + 1.67f_y\rho_g)} = \frac{4545 \times 1000}{0.4(25 + 1.67 \times 415 \times 3/100)} = 248,136 \text{ mm}^2$$

Assume a size of 450 mm \times 600 mm (area provided = 270,000 mm²).

Note: We need to add the self-weight of column in the load to determine the size. Self-weight of column in this case is $(0.45 \times 0.6) \times 3.2 \times 25 = 21.6 \text{ kN}$. It is seen that the self-weight of column is negligible compared to the load acting on it. Hence, it may be neglected in most of the cases.

Step 2 Determine whether the column is a short or long column.

Since the column is braced, effective length factor, k , may be taken equal to 1.00.

$$\text{Ratio: } L_x/b = 3.20/0.45 = 7.11 < 12$$

$$L_y/D = 3.20/0.60 = 5.33 < 12$$

Hence, the column can be classified as short column.

Step 3 Check for minimum eccentricity.

$$0.05b = 0.05 \times 450 = 22.5 \text{ mm}$$

$$0.05D = 0.05 \times 600 = 30.0 \text{ mm}$$

$$e_{x,\min} = (L_x/500) + (b/30) = (3200/500) + (450/30) = 21.4 \text{ mm} < 22.5 \text{ mm}$$

$$e_{y,\min} = (L_y/500) + (D/30) = (3200/500) + (600/30) = 26.4 \text{ mm} < 30.0 \text{ mm}$$

Hence, formula for short column capacity suggested by IS 456:2000 can be used.

Step 4 Estimate longitudinal reinforcement.

$$4545 \times 1000 = (0.4 \times 25 \times 450 \times 600) + (0.67 \times 415 \times A_{sc})$$

Area of reinforcement, $A_{sc} = 6635 \text{ mm}^2$

Minimum reinforcement = $(0.8/100) \times 450 \times 600 = 2160 \text{ mm}^2 < 6635 \text{ mm}^2$

Provide six 28 mm bars and four 32 mm bars; area provided = 6911 mm^2 ; use 32 mm bars at the four corners as shown in Fig. 13.42.

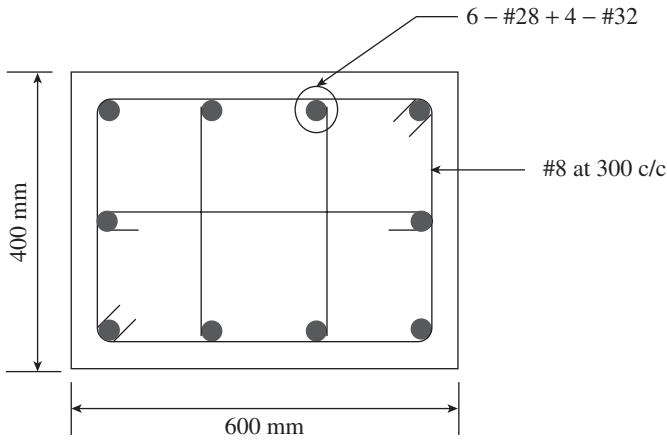


FIG. 13.42 Reinforcement details of column in Example 13.5

Provided percentage of reinforcement = $6911 / (450 \times 600) \times 100 = 2.56\% < 4\%$ (maximum)

Hence, the selected area is within limits.

Note: In such heavily loaded columns, it may be advantageous to go in for high-strength concrete and steel, using which we may reduce the size of columns, thus maximizing the usable floor space. For example, using M50, we may reduce the size of column to 300 mm × 500 mm and need to use ten 25 mm Fe 500 bars, with area = 4908 mm².

Step 5 Estimate transverse reinforcement.

Diameter of transverse reinforcement [Clause 26.5.3.2(c)-(2)]

Criteria 1: Diameter of largest longitudinal bar/4 = 32/4 = 8 mm

Criteria 2: 6 mm

Provide transverse reinforcement of diameter 8 mm.

Spacing of transverse reinforcement [Clause 26.5.3.2(c)-(1)]

Criteria 1: Least lateral dimension of column = 450 mm

Criteria 2: 16 × Diameter of smallest longitudinal bar = 16 × 28 = 448 mm

Criteria 3: 300 mm

Hence, provide transverse reinforcement of 8 mm bars at 300 mm centre to centre.

Step 6 Detail the reinforcement.

Provide the steel bars as shown in Fig. 13.42 with 40 mm cover to reinforcement.

EXAMPLE 13.6 (Design of circular column):

Design a spiral column subjected to an unfactored load of 1600 kN. Effective length of column is 3.5 m. Use M25 concrete, Fe 415 steel, and assume moderate environment.

SOLUTION:

Step 1 Determine the size of column.

$$\text{Factored load} = 1.5 \times 1600 = 2400 \text{ kN}$$

Adding one per cent as the weight of column,

$$\text{Total load} = 1.01 \times 2400 = 2424 \text{ kN}$$

Assuming $\rho_g = A_{sc}/A_g = 2\%$, from Eq. (13.36),

$$A_c = \frac{P_u}{0.4(f_{ck} + 1.67f_y\rho_g)} = \frac{2424 \times 1000}{0.4(25 + 1.67 \times 415 \times 2/100)} = 1,55,940 \text{ mm}^2$$

Diameter of column = $\sqrt{\frac{1,55,940 \times 4}{\pi}} = 446 \text{ mm}$; adopt $D = 500 \text{ mm}$.

Step 2 Check whether the column is short or long.

Ratio: $L/D = 3.50/0.5 = 7.00 < 12$

Hence, the column can be classified as a short column.

Step 3 Calculate the minimum eccentricity.

$$0.05D = 0.05 \times 500 = 25.0 \text{ mm}$$

$e_{\min} = (L/500) + (D/30) = (3500/500) + (500/30) = 23.67 \text{ mm} < 25.00 \text{ mm}$

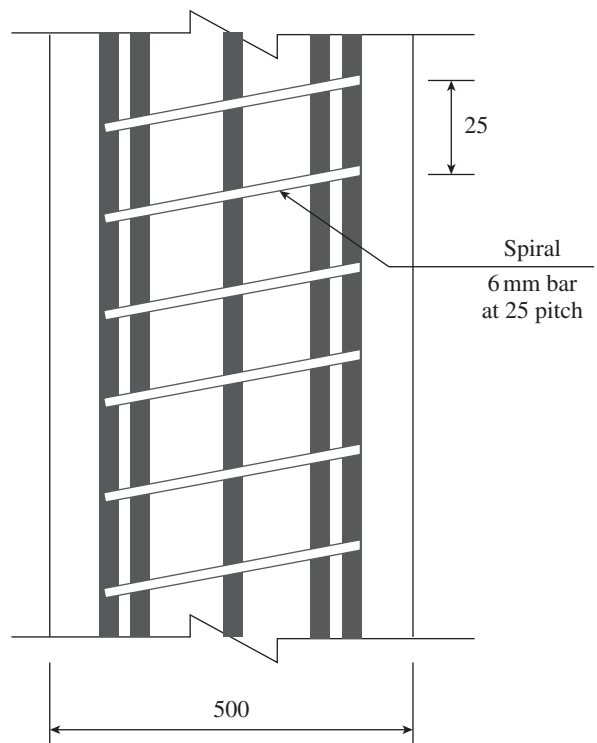
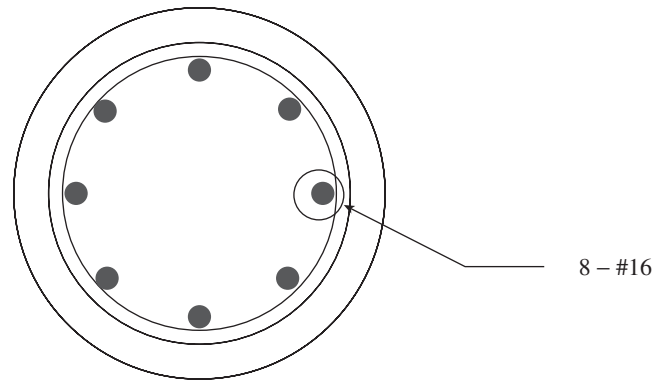


FIG. 13.43 Reinforcement details of column in Example 13.6

Hence, formula for the short column capacity suggested by IS 456:2000 can be used.

Step 4 Estimate longitudinal reinforcement.

$$2424 \times 1000 = 1.05 \{ [0.40 \times 25 \times (\pi/4) \times 500 \times 500] + [0.67 \times 415 \times A_{sc}] \}$$

$$\text{Area of reinforcement, } A_{sc} = 1241 \text{ mm}^2$$

$$\text{Minimum reinforcement} = (0.8/100) \times (\pi/4) \times 500 \times 500 = 1571 \text{ mm}^2$$

$$\text{Required reinforcement} = \max(1241, 1571) = 1571 \text{ mm}^2$$

$$\text{Hence, provide eight 16 mm bars; area provided} = 1608 \text{ mm}^2$$

Step 5 Estimate spiral reinforcement. Assume 6 mm diameter of spiral reinforcement, 40 mm clear cover and pitch equal to s .

$$\text{Core diameter} = 500 - 40 \times 2 = 420 \text{ mm}$$

Ratio of volume of spiral reinforcement to volume of core per unit length of column is given by

$$\rho_s = \frac{\left(\pi \times \frac{6^2}{4} \right) \times \frac{\pi(420-6)}{s}}{\pi \times 420^2 / 4} = \frac{0.2654}{s}$$

As per Clause 39.4.1 of IS 456: 2000

$$\rho_s \geq 0.36 \left(\frac{A_g}{A_c} - 1 \right) \left(\frac{f_{ck}}{f_y} \right)$$

Thus,

$$\frac{0.2654}{s} \geq 0.36 \left(\frac{\pi \times 500^2 / 4}{\pi \times 420^2 / 4} - 1 \right) \left(\frac{25}{415} \right) \text{ or } s \leq 29.33 \text{ mm}$$

Limits on pitch as per Clause 26.5.3.2(d) of IS 456:2000

Maximum spacing:

Criteria 1: 75 mm

Criteria 2: Core diameter/6 = 420/6 = 70 mm

Minimum spacing:

Criteria 1: 25 mm

Criteria 2: 3 × diameter of bar = 3 × 6 = 18 mm

As per Clause 26.5.3.2 (c)-(2): Diameter should be greater than the largest longitudinal bar diameter/4 (16/4 = 4 mm) or 6 mm.

Provide 6 mm diameter spiral at 25 mm with centre to centre pitch.

Step 6 Detail the reinforcement. Provide the main bars and spirals as shown in Fig. 13.43 with 40 mm cover to reinforcement.

SUMMARY

Vertical compression members are called columns. Compression members may be present in bridges and trusses and are called piers and struts, respectively. As the columns carry the loads from different floors and finally transmit them to the soil below through footings, they are to be designed carefully. Moreover, failure of a single column may jeopardize the functioning of the whole building, as it may lead to progressive collapse. The classification of columns may be based on the shape of cross section (rectangular, square, circular, etc.), type of transverse steel (tied, spiral, or composite), type of loading (concentric and eccentric), and length (long and short). In this chapter, only short columns with concentric loads are considered. As per IS 456 when L_{ex}/D and L_{ey}/b are less than 12, the columns are considered as short columns. The effective length L_e differs from the unsupported length L and is determined based on the support conditions at the top and bottom of columns.

Short columns are considered to fail by the crushing of concrete without undergoing any lateral deformation, whereas long columns may fail by buckling. The effective length of columns with definable boundary conditions can be found by using Euler's theory. The effective length of multi-storey columns can be found by Wood's curves presented in the IS 456 code or by Jackson and Moreland alignment charts, adopted by the ACI 318 code. Two separate curves or charts are presented for sway and non-sway frames.

A column may be assumed non-sway when the ratio of the total lateral stiffness of the bracing elements to that of the columns in a storey is considerable. Thus, frames with stiff lateral force resisting elements, like shear walls, are usually considered as non-sway. The stability index Q may be calculated and used to judge whether a frame is sway or non-sway.

Tests conducted in the 1940s revealed that the working stress method does not predict the stresses in concrete and steel, due to the effects of creep and shrinkage. The limit states method, using a limiting strain of 0.002 in compression, is found to predict the collapse load reasonably. It was also found that the columns with spiral reinforcement have more ductility than columns with ties as transverse reinforcement. It was observed that only 0.85 times the compressive strength of concrete was realized in the full-scale column tests. The necessary amount of reinforcement, as per codes, for transverse reinforcement of spiral and tied columns is derived.

Practical provisions on size and reinforcement detailing (both longitudinal and transverse), as per IS 456, are discussed. The slenderness and minimum eccentricity (which arises due to imperfections in construction, inaccuracy in loading, etc.) provisions are also presented. Expressions provided in IS 456 and ACI 318 for predicting the ultimate load on columns are derived for rectangular columns with ties and circular columns with spiral reinforcement. The steps necessary for the design are listed. The use of design aids presented in SP 16 is also explained. Pedestals may be designed similar to short columns.

During earthquakes, the failure of columns is cited as the main reason for the collapse of buildings. Hence, the detailing requirements (for longitudinal and transverse reinforcement) as per IS 13920, which are more stringent than the provisions of IS 456, are also explained. The strong column-weak beam concept, which prevents storey mechanism and facilitates plastic hinges to form in beams, is discussed. The need for providing close spacing of ties (confinement reinforcement) in plastic hinge locations and in soft storey columns is stressed.

The cyclic shear force acting along with axial compression during earthquakes causes degradation of shear strength of concrete.

Although a few analytical models have been proposed to predict the shear strength, the ACI 318 code suggests ignoring the shear strength of concrete in the design of confinement reinforcement. The confining reinforcement to be adopted in plastic hinge regions, as per IS 13920, is discussed and a proposal based on the Canadian code

(which considers the effects of several parameters) is also provided. Ample examples are given to explain the use of equations presented in the chapter and for the design and detailing of short columns. Chapter 14 deals with the design of columns with axial force and bending moments and the design of long columns.

REVIEW QUESTIONS

- What are the different types of classifications of columns?
- How are columns classified based on the type of reinforcement?
- How are columns classified based on the type of loading?
- Define slenderness ratio and slenderness factor.
- How are concrete columns classified as short and long columns?
- Distinguish between unsupported length and effective length of columns.
- How does buckling affect column strength? What is the Euler's buckling load for a column with fixed ends?
- The effective length of a column with fixed-fixed end is _____.
(a) $1.0L$ (c) $0.5L$
(b) $1.2L$ (d) $0.75L$
- The effective length of a column effectively held in position and restrained against rotation in one end and partially restrained against rotation but not held in position at the other end is _____.
(a) $1.0L$ (c) $1.2L$
(b) $2.0L$ (d) $1.5L$
- The effective length of cantilever columns is _____.
(a) $1.0L$ (c) $1.5L$
(b) $1.2L$ (d) $2.0L$
- The minimum value of effective length factor for columns in sway frames recommended by IS 456 is _____.
(a) 1.0 (c) 1.5
(b) 1.2 (d) 3.0
- How are effective lengths of columns in multi-storey frames determined?
- How do we determine whether the given frame is sway or non-sway?
- Define stability index. How is it useful in the design of columns?
- How can the fixity at the base of a column be determined?
- Explain the difference in behaviour between tied columns and columns with spiral reinforcement.
- Why should we not consider working stress method in the design of columns?
- How can spirals increase the axial load capacity of a column? How is the effect of spirals considered in design using IS 456?
- Derive the formula for A_{sp} used in IS 13920 for spiral columns. How is the formula for A_{sh} for rectangular columns derived from the A_{sp} of spiral column?
- The minimum size of columns in earthquake zones is _____.
(a) 200 mm
(b) 230 mm or 15 times the diameter of the largest longitudinal bar
(c) 300 mm
(d) 300 mm or 15 times the diameter of the largest longitudinal bar
- The minimum diameter of longitudinal bar to be used in a column is _____.
(a) 10 mm (b) 12 mm (c) 16 mm (d) 8 mm
- The minimum and maximum recommended practical reinforcement percentages in column are _____, respectively.
(a) 0.8% and 6% (c) 1.0% and 8%
(b) 0.8% and 4% (d) 0.8% and 0.3%
- The minimum numbers of bars required in rectangular and circular columns are _____, respectively.
(a) 4 and 6 (c) 6 and 6
(b) 8 and 6 (d) none of these
- What is the criterion for using high-yield strength-deformed bars in columns in earthquake zones?
- What are the functions of transverse reinforcement in an RC column?
- How is the effect of shear force considered in the design of columns?
- When a larger size is adopted, due to architectural reasons, what is the minimum area of steel required to be provided?
- When is anchorage considered to have been provided in transverse reinforcement?
- The spacing of transverse reinforcement as per IS 456 should be the least of (B and D —size of column; d_b —diameter of the smallest longitudinal bar) _____.
(a) B , $8d_b$, and 300 mm
(b) B , $16d_b$, and 300 mm
(c) D , $16d_b$, and 450 mm
(d) None of these
- The spacing of transverse reinforcement as per IS 456 should be the greater of _____.
(a) $d_b/2$ and 6 mm
(b) $d_b/3$ and 8 mm
(c) $d_b/4$ and 8 mm
(d) $d_b/4$ and 6 mm
- The spacing of spirals as per IS 456 should be (D_k —diameter of core, d_{tr} —diameter of spiral) _____.
(a) <150 mm, $<D_k/6$, >25 mm, $>3d_{tr}$
(b) <75 mm, $<D_k/8$, >25 mm, $>3d_{tr}$
(c) <75 mm, $<D_k/6$, >25 mm, $>3d_{tr}$
(d) <75 mm, $<D_k/6$, >25 mm, $>4d_{tr}$
- A longitudinal bar is deemed to be restrained by ties when the bar is spaced from another fully restrained bar at _____.
(a) <75 mm (b) <100 mm (c) <150 mm (d) <200 mm
- The unsupported length of transverse ties should not exceed _____.
(a) $40d_{tr}$ or 150 mm (c) $45d_{tr}$ or 300 mm
(b) $45d_{tr}$ or 200 mm (d) $48d_{tr}$ or 300 mm
- Sketch the possible ways in which column bars are doweled for the next floor columns as per IS 456.
- Clause 25.3.1 of IS 456 stipulates that the clear distance between restraints, should never exceed (D and b are large and small sides of column cross section, respectively) _____.

- (a) $50b$ (c) $60b$
 (b) $50D$ (d) $60D$
36. The minimum eccentricity for rectangular column should be taken as _____.
 (a) unsupported length/400 + (Lateral dimension/20)
 (b) unsupported length/450 + (Lateral dimension/25)
 (c) unsupported length/500 + (Lateral dimension/30)
 (d) none of these
 37. What is the reason behind the consideration of minimum eccentricity?
 38. What is the assumed value of uniform strain in column at failure as per IS 456?
 39. Derive the column strength equation as given in Clause 38.3 of IS 456.
 40. What is the permissible slenderness ratio for rectangular columns?
 41. Under what condition can spiral columns be considered to have 1.05 times the strength of a similar rectangular column?
 42. List the different steps to be taken while designing rectangular or spiral short columns.
 43. Why is it necessary to restrict the maximum percentage of reinforcement in columns?
 44. Explain the strong column–weak beam concept. Why is it necessary to adopt this concept for the design of columns situated in earthquake zones?
 45. What is the minimum number of bars to be provided in rectangular or square columns in earthquake zones? Is it different from the IS 456 provision?
 46. Why is it preferable to provide lap splices only at the mid-height of columns situated in earthquake zones? Can we splice all column bars in the same location?
 47. How does the transverse reinforcement requirements of IS 13920 differ from that of IS 456?
 48. Why is it necessary to provide 135° hooks at the end of transverse reinforcement in columns situated in earthquake zones?
 49. Why should we not use J-type ties (one end with 135° hook and the other with 90° hook) in earthquake zones?
 50. Write a short note on double-headed studs as ties in columns.
 51. How is the shear force calculated for columns situated in earthquake zones?
 52. Write a short note on special confining reinforcement in columns.
 53. Sketch column transverse reinforcement in earthquake zones.
 54. Special confining reinforcement of the column must be extended into the foundation by at least _____.
 (a) 250 mm (c) 400 mm
 (b) 300 mm (d) 450 mm
 55. What precautions should be adopted in case of short columns in earthquake zones?
 56. List the parameters that affect the confining reinforcement.

EXERCISES

1. A four-storeyed building has a plan dimension of $20\text{ m} \times 30\text{ m}$ with floor to floor height of 3.5 m. Columns are spaced at an interval of 4 m along the transverse direction and at an interval of 6 m along the longitudinal direction. The size of all columns is $500\text{ mm} \times 500\text{ mm}$ and size of all beams is $300\text{ mm} \times 600\text{ mm}$. Calculate the effective length of interior first floor column by considering M25 grade concrete. Assume uniformly distributed floor load of 40 kN/m^2 from all the floors above (combined).
2. A single-storey single-bay portal frame, which is pinned at bottom, is subjected to a uniformly distributed load of 250 kN/m . Consider size of frame as $5\text{ m} \times 5\text{ m}$ along with size of columns as $400\text{ mm} \times 400\text{ mm}$ and size of beams as $200\text{ mm} \times 400\text{ mm}$. Estimate the effective length of column by considering M20 concrete.
3. A column of height 1.5 m is pinned at the bottom and effectively restrained against rotation but not held in position at the top. It is subjected to a factored axial load of 2500 kN under the combination of dead load and live load. Design the column, using M30 concrete and Fe 415 steel.
4. Design a column subjected to an axial load of 3000 kN under dead load and live load case. The column is braced against side sway in one direction and is fixed at the bottom and free at the top in the other direction. Unsupported length of column is 2.0 m. Use M25 concrete and Fe 415 steel.
5. A short rectangular column having an effective length of 3 m carries a factored axial compressive load of 2000 kN . Architectural requirements dictate the column size as $600\text{ mm} \times 450\text{ mm}$. Design the column using M25 concrete and Fe 415 steel.
6. Design a spiral column subjected to an unfactored load of 2000 kN . The effective length of the column is 3 m. Use M25 concrete and Fe 415 steel.
7. A circular column is subjected to a factored load of 2500 kN . The effective length of the column is 2.5 m. Use M50 concrete and Fe 415 steel.
8. A short circular column of diameter 500 mm and height 4 m is hinged at the top and the bottom. It is reinforced with six 20 mm high-yield strength-deformed bars and has 6 mm MS spiral at 25 mm pitch. Assuming M25 concrete and Fe 415 steel, estimate the capacity of the column. Check whether it can support a factored axial load of 2450 kN .

REFERENCES

- ACI Committee 105, 'Reinforced Concrete Column Investigation', *ACI Journal, Proceedings*, Vol. 26, April 1930, pp. 601–12, Vol. 27, February 1931, pp. 675–6, Vol. 28, November 1931, pp. 157–8, Vol. 29, September 1932, pp. 53–6, February 1933, pp. 275–84, Vol. 30, September–October 1933, pp. 78–90, and November–December 1933, pp. 153–6.

- ACI Committee 340 1978, *Design Handbook in Accordance with the Strength Design Method of ACI 318-77, Vol. 2: Columns*, SP 17A(78), American Concrete Institute, Farmington Hills, p. 228.
- Aschheim, M. and J.P. Moehle 1992, *Shear Strength and Deformability of RC Bridge Columns Subjected to Inelastic Cyclic Displacements*, Report No. UCB/EERC-92/04, Earthquake Engineering Research Center, University of California at Berkeley, Berkeley, p. 99.
- Bae, S. and O. Bayrak 2008, 'Plastic Hinge Length of Reinforced Concrete Columns', *ACI Structural Journal*, Vol. 105, No. 3, pp. 290–300.
- Bae, S. and O. Bayrak 2009, 'Drift Capacity of Reinforced Concrete Columns', *ACI Structural Journal*, Vol. 106, No. 4, pp. 405–15.
- Bayrak, O. and S.A. Sheikh 1998, 'Confinement Reinforcement Design Considerations for Ductile HSC Columns', *Journal of Structural Engineering, ASCE*, Vol. 124, No. 9, pp. 999–1010.
- Campione, G., M. Fossetti, and M. Papia 2010, 'Behavior of Fiber-reinforced Concrete Columns under Axially and Eccentrically Compressive Loads', *ACI Structural Journal*, Vol. 107, No. 3, pp. 272–81.
- Canbay, E., G. Ozcebe, and U. Ersoy 2006, 'High-strength Concrete Columns under Eccentric Load', *Journal of Structural Engineering, ASCE*, Vol. 132, No. 7, pp. 1052–60.
- Choi, K-K, and H-G. Park 2010, 'Evaluation of Inelastic Deformation Capacity of Beams Subjected to Cyclic Loading', *ACI Structural Journal*, Vol. 107, No. 5, pp. 507–15.
- Considère, A., 'Compressive Resistance of Concrete Steel and Hooped Concrete, Part I', *Engineering Record*, 20 December 1902, pp. 581–3, 'Part II', 27 December 1902, pp. 605–6.
- Considère, A. 1903, 'Concrete Steel and Hooped Concrete', *Reinforced Concrete*, pp. 119.
- Correal, J.F., M.S. Saiidi, D. Sanders, and S. El-Azazy 2007, 'Shake Table Studies of Bridge Columns with Double Interlocking Spirals', *ACI Structural Journal*, Vol. 104, No. 4, pp. 393–401.
- Dafedar, J.B., Y.M. Desai, and M.R. Shiyekar 2001, 'Review of Code Provisions for Effective Length of Framed Columns', *The Indian Concrete Journal*, Vol. 75, No. 6, pp. 402–7.
- Elwood, K.J. and M.O. Eberhard 2009, 'Effective Stiffness of Reinforced Concrete Columns', *ACI Structural Journal*, Vol. 106, No. 4, pp. 476–84.
- Elwood, K.J., J. Maffei, K.A. Riederer, and K. Telleen 2009, 'Improving Column Confinement, Part 1: Assessment of Design provisions, and Part 2: Proposed New Provisions for the ACI 318 Building Code', *Concrete International, ACI*, Vol. 31, No. 11, pp. 32–9 and Vol. 31, No. 12, pp. 41–48.
- Elwood K.J. and J.P. Moehle 2005, 'Drift Capacity of Reinforced Concrete Columns with Light Transverse Reinforcement', *Earthquake Spectra*, Vol. 21, No. 1, pp.71–89.
- Euler, L. 1759, 'Sur le Force de Colonnes' (Concerning the Strength of Columns), *Memoires de l'academie des sciences de Berlin*, Vol. 13, pp. 252–82 (English translation by J. A. Van den Broek 1947, *American Journal of Physics*, Vol. 15, pp. 309).
- Foster, S.J. and M.M. Attard 2001, 'Strength and Ductility of Fiber-reinforced High-strength Concrete Columns', *Journal of Structural Engineering, ASCE*, Vol. 127, No. 1, pp. 28–34.
- French, C.W. and J.P. Moehle 1991, 'Effect of Floor Slab on Behavior of Slab-beam-column Connections', *ACI SP-123, Design of Beam-column Joints for Seismic Resistance*, American Concrete Institute, Farmington Hills, pp. 225–58.
- Galano, L. and A. Vignoli 2008, 'Strength and Ductility of HSC and SCC Slender Columns Subjected to Short Term Eccentric Load', *ACI Structural Journal*, Vol. 105, No. 3, pp. 259–69.
- Ganesan, N. and J.V. Ramana Murthy 1990, 'Strength and Behavior of Confined Steel Fiber-reinforced Concrete Columns', *ACI Materials Journal*, Vol. 87, No. 3, pp. 221–7.
- Hendrix, S.E. and M.J. Kowalsky 2010, 'Seismic Shear Behavior of Lightweight Aggregate Concrete Square Columns', *ACI Structural Journal*, Vol. 107, No. 6, pp. 680–8.
- Hognestad 1951, *A Study of Combined Bending and Axial Load in Reinforced Concrete Members*, University of Illinois Engineering Experimental Station, Bulletin No. 399, p. 128.
- Jennings, P.C. (ed.) 1971, *Engineering Features of the San Fernando Earthquake of February 9, 1971*, Report EERL 71-02, National Science Foundation and Earthquake Research Affiliates of the California Institute of Technology, Pasadena, p. 515, (also see <http://authors.library.caltech.edu/26440/1/7102.pdf>, last accessed on 17 July 2012).
- Johnston, B.G. 1966, *Guide to Design Criteria for Metal Compression Members*, 2nd edition, Column Research Council, Fritz Engineering Laboratory, Lehigh University, Bethlehem.
- Kavanagh, T.C. 1962, 'Effective Length of Framed Columns, Part 2', *Transactions ASCE*, Vol. 127, pp. 81–101.
- Kuntz, G.L. and J. Browning 2003, 'Reduction of Column Yielding during Earthquakes for Reinforced Concrete Frames', *ACI Structural Journal*, Vol. 100, No. 5, pp. 573–580.
- Lai, S-M.A., J.G. MacGregor, and J. Helleland 1983, 'Geometric Non-linearities in Non-sway Frames', *Journal of Structural Division, ASCE*, Vol. 109, No. ST12, pp. 2770–85.
- Leon, R.T., D.K. Kim, and J. Hajjar, 'Limit State Response of Composite Columns and Beam-columns, Part 1: Formulation of Design Provisions for 2005 AISC Specification', *Engineering Journal, AISC*, Vol. 44, No. 4, 4th quarter, 2007, pp. 341–57 and 'Part 2: Application of Design Provisions for the 2005 AISC Specification', *Engineering Journal, AISC*, Vol. 45, No. 1, 1st quarter, 2008, pp. 21–46.
- Li, B. and R. Park 2004, 'Confining Reinforcement for High Strength Concrete Columns', *ACI Structural Journal*, Vol. 101, No. 3, pp. 314–24.
- Lin, C.-H., C.-L. Hwang, S.-P. Lin, and C.-H. Liu 2008, 'Self-consolidating Concrete Columns under Concentric Compression', *ACI Structural Journal*, Vol. 105, No. 4, pp. 425–32.
- MacGregor, J.G. and S.E. Hage 1977, 'Stability Analysis and Design of Concrete Frames', *Journal of Structural Division, ASCE*, Vol. 103, No. ST10, pp. 1953–70.
- Moehle, J.P., J.D. Hooper, and C.D. Lubke 2008, 'Seismic Design of Reinforced Concrete Special Moment Frames: A Guide to Practicing Engineers', *NEHRP Seismic Design Technical Brief No.1*, produced by the NEHRP Consultants Joint Venture, a partnership of the Applied Technology Council and the Consortium of Universities for Research in Earthquake Engineering, for the National Institute of Standards and Technology, Gaithersburg, MD., NIST GCR 8-917-1, p. 27, (also see <http://www.nehrp.gov/pdf/nistgcr8-917-1.pdf>, last accessed on 29 May 2012).
- Montejo, L.A., M.J. Kowalsky, and T. Hassan 2009, 'Seismic Behavior of Shear-dominated Reinforced Concrete Columns at Low Temperatures', *ACI Structural Journal*, Vol. 106, No. 4, pp. 445–54.

- Moretti, M.L. and T.P. Tassios 2006, 'Behavior and Ductility of Reinforced Concrete Short Columns using Global Truss Model', *ACI Structural Journal*, Vol. 103, No. 3, pp. 319–27.
- Mostafaei, H., F.J. Vecchio, and T. Kabeyasawa 2009, 'Deformation Capacity of Reinforced Concrete Columns', *ACI Structural Journal*, Vol. 106, No. 2, pp. 187–95.
- Murty, C.V.R., R. Goswami, A.R. Vijayanarayanan, and V.V. Mehta 2012, *Some Concepts in Earthquake Behaviour of Buildings*, under print.
- Park, R. and T. Paulay 1975, *Reinforced Concrete Structures*, John Wiley and Sons, New York, p. 769.
- Paulay, T. 1996, 'Seismic Design of Concrete Structures: The Present Needs of Societies', *Proceedings of the Eleventh World Congress on Earthquake Engineering*, Acapulco, Mexico, 23–28 June 1996, Paper No. 2001, Elsevier, p. 65, (also see http://www.iitk.ac.in/nicee/wcee/article/11_2001.PDF, last accessed on 2 June 2012).
- Paulay, T. and M.J.N. Priestley 1992, *Seismic Design of Reinforced Concrete and Masonry Buildings*, John Wiley and Sons Inc., New York, p. 768.
- Paultre, P., R. Eid, H.I. Robles, and N. Bouaanani 2009, 'Seismic Performance of Circular High-strength Concrete Columns', *ACI Structural Journal*, Vol. 106, No. 4, pp. 395–404.
- Paultre, P. and F. Légeron 2008, 'Confinement Reinforcement Design for Reinforced Concrete Columns', *Journal of Structural Engineering*, ASCE, Vol. 134, No. 5, pp. 738–49.
- Pessiki, S., B. Graybeal, and M. Mudlock 2001, 'Proposed Design of High-strength Spiral Reinforcement in Compression Members', *ACI Structural Journal*, Vol. 98, No. 6, pp. 799–810.
- Priestley, M.J.N., R. Verma, and Y. Xiao 1994, 'Seismic Shear Strength of Reinforced Concrete Columns', *Journal of Structural Engineering*, ASCE, Vol. 120, No. 8, pp. 2310–29.
- PCI Design Handbook* 1999, 5th edition, Precast/Prestressed Concrete Institute, Chicago.
- Richart, F.E., A. Brandtzaeg, and R.L. Brown 1929, *The Failure of Plain and Spirally Reinforced Concrete in Compression*, University of Illinois Engineering Experimental Station, Bulletin No. 190, p. 74.
- Richart, F.E. and R.L. Brown 1934, *An Investigation of Reinforced Concrete Columns*, University of Illinois Engineering Experimental Station, Bulletin No. 267, p. 91.
- Roik, K. and R. Bergmann 1992, 'Composite Columns', in P. Dowling, J.E. Harding, and R. Bjorhovde (eds), *Constructional Steel Design*, Elsevier Science Publishers, New York, pp. 443–70.
- Saatcioglu, M. and S.R. Razvi 2002, 'Displacement-based Design of Reinforced Concrete Columns for Confinement', *ACI Structural Journal*, Vol. 99, No. 1, pp. 3–11.
- Saiidi, M.S., M. O'Brien, and M. Sadrossadat-Zadeh 2009, 'Cyclic Response of Bridge Columns using Superelastic Nitinol and Bendable Concrete', *ACI Structural Journal*, Vol. 106, No. 1, pp. 69–77.
- Sakai, K. and S.A. Sheikh 1989, 'What Do We Know about Confinement in Reinforced Concrete Columns? (A Critical Review of Previous Work and Code Provisions)', *ACI Structural Journal*, Vol. 86, No. 2, pp. 192–207.
- Scribner, C.F. and J.K. Wight 1980, 'Strength Decay in R.C. Members under Load Reversals', *Journal of Structural Division*, ASCE, Vol. 106, No. 4, pp. 861–76.
- Sezen, J. and J.P. Moehle 2004, 'Shear Strength Model for Lightly Reinforced Concrete Columns', *Journal of Structural Engineering*, ASCE, Vol. 130, No. 11, pp. 1692–1703.
- Sharma, U., P. Bhargava, and S.K. Kaushik 2006, 'Confinement of High Strength Concrete Columns: State of Knowledge', *ICI Journal*, Vol. 7, No. 1, pp. 7–17.
- Sharma, U., P. Bhargava, S.K. Kaushik, and R. Bhowmick 2005, 'Evaluation of Confinement Reinforcement Requirements of IS 13920:1993 for RC Columns', *The Indian Concrete Journal*, Vol. 79, No. 3, pp. 51–59.
- Sheth, A. 2003, 'Use of Intermediate RC Moment Frames in Moderate Seismic Zones', *The Indian Concrete Journal*, Vol. 77, No. 11, pp. 1431–5.
- Subramanian, N. 2004, *Discussion* on the paper 'Seismic Performance of Conventional Multi-storey Building with Open Ground Floors for Vehicular Barking', *The Indian Concrete Journal*, Vol. 78, No. 4, pp. 11–2.
- Subramanian, N. 2009, *Discussion* on the paper 'Plastic Hinge Length of Reinforced Concrete Columns', *ACI Structural Journal*, Vol. 106, No. 2, pp. 233–4.
- Subramanian, N. 2011, 'Design of Confinement Reinforcement for RC Columns', *The Indian Concrete Journal*, Vol. 85, No. 8, pp. 25–36.
- Suryanarayana, P. 1993, 'Design Alternatives for Composite Columns', *Civil Engineering and Construction Review (CE & CR)*, Vol. 15, No. 8, pp. 30–3.
- Talbot, A.N., *Tests of Concrete and Reinforced Concrete Columns*, Bulletin No. 10, 1906, and Bulletin No. 20, 1907, University of Illinois, Urbana.
- Taranath B.S. 1988, *Structural Analysis and Design of Tall Buildings*, McGraw-Hill International Edition, p. 739.
- Watson, S., F.A. Zahn, and R. Park 1994, 'Confining Reinforcement for Concrete Columns', *Journal of Structural Engineering*, ASCE, Vol. 120, No. 6, pp. 1798–1824.
- Wight, J.K. and M.A. Sozen 1975, 'Shear Strength Decay of RC Columns under Shear Reversals', *Proceedings, ASCE*, Vol. 101, No. ST5, pp. 1053–65.
- Withey, M.O., *Tests on Reinforced Concrete Columns*, Bulletin No. 300, 1910, and Bulletin No. 466, 1911, University of Wisconsin, Madison.
- Wong, Y.L., T. Paulay, and M.J.N. Priestley 1993, 'Response of Circular Reinforced Concrete Beams to Multi-directional Seismic Attack', *ACI Structural Journal*, Vol. 90, No. 2, pp. 180–91.
- Wood, R.H. 1974, 'Effective Lengths of Columns in Multistory Buildings', *The Structural Engineer*, Vol. 52, No. 7, pp. 235–43, No. 8, pp. 295–302, and No. 9, pp. 341–6.
- Yamada, M. 1996, 'Cleavage Shear Explosion of Reinforced Concrete Short Columns Broken Down Buildings and Hanshin-Express Highways at the Recent Hanshin-Awaji Earthquake in Japan on 17 January 1995', *Proceedings, Eleventh World Conference on Earthquake Engineering*, Mexico.
- Youakim, S.A. and A. Ghali 2002, 'Ductility of Concrete Columns with Double-head Studs', *ACI Structural Journal*, Vol. 99, No. 4, pp. 480–7.

DESIGN OF COLUMNS WITH MOMENTS

14.1 INTRODUCTION

Axially loaded columns were discussed in Chapter 13. Such columns are rare in actual practice. Even Clause 39.2 of IS 456 stipulates that all compression members should be designed for a minimum eccentricity, which has already been discussed in Section 13.6.2 of Chapter 13. (Though such minimum eccentricities were included in the ACI code until 1977, they are now incorporated directly in the design equations to limit the maximum design axial strength of columns to 80–85% of the nominal strength.) Most of the columns we encounter in practice are subjected to bending moments, about one or both the axes of cross section, in addition to direct compressive loads. The bending action may produce tensile forces over a part of the cross section depending on the magnitude of the axial compressive force as well as the bending moment. Despite the presence of tensile stresses, columns are generally referred to as *compression members* or *beam-columns*, as the compressive forces or stresses dominate their behaviour. Such compression members include columns rigidly connected to beams, columns of multi-storeyed buildings, portal frames, columns supporting crane loads in industrial buildings, and arches. In multi-storeyed buildings, the edge columns are usually subjected to uniaxial bending and the corner columns are subjected to biaxial bending. Even the internal columns may be subjected to bending if there are lateral loads or when the adjoining spacing of columns are different on either side of the column.

When combined axial compression and bending moment act on a member having low slenderness ratio (ratio of unbraced length to radius of gyration), where column buckling is not a criterion, the strength of the member is governed by the material strength of the cross section. In such short columns, load stages below the ultimate load are not so important. Cracking of concrete at service loads, even for large eccentricity, does not pose a problem. Similarly, the

deflections at service loads are seldom a factor. For short columns, as usual, the design is based on factored load, which must not exceed the design strength. Thus,

$$M_n \geq M_u \quad (14.1a)$$

$$P_n \geq P_u \quad (14.1b)$$

The values of M_n and P_n may be found using the strain compatibility analysis. As this analysis results in repetitive and tedious calculations, interaction curves are often drawn and used; such interaction curves are provided in SP 16 and help the designer to arrive at the design quickly. Such interaction diagrams have been developed for square, rectangular, circular, T, L, and + sections.

Corner columns in multi-storey buildings are subjected to biaxial bending in addition to axial compression. Even though it is possible to solve such cases using strain compatibility analysis of the cross section, further analysis is involved as the neutral axis is skewed. Hence, some approximate solutions are adopted, which consider the biaxial bending problem as that of uniaxial bending with an equivalent bending moment.

Slender columns are also rarely encountered in practice. The behaviour of slender columns is non-linear and the design bending moments should also consider the $P-\Delta$ and $P-\delta$ effects ($P-\delta$ effects are due to the deformations along the column and $P-\Delta$ effects are those due to the storey drifts in buildings). In addition, they are susceptible to buckling. It is preferable to compute the bending moments of such slender columns using a second-order analysis. However, codes also suggest approximate methods to compute these bending moments by using a linear analysis and considering some additional bending moments to take care of the $P-\Delta$ effects. It is interesting to note that Clause B4.3 of IS 456 makes it mandatory that columns subjected to combined direct load and flexure be designed only by limit state design.

14.2 DESIGN OF COLUMN WITH AXIAL LOAD AND UNIAXIAL BENDING

Before considering the design of columns subjected to axial load and moments, let us first discuss the assumptions made in IS 456 for such columns.

14.2.1 Assumptions Made in Limit States Design for Columns

In addition to the assumptions made for flexure (see Section 5.4.1 of Chapter 5 and Clause 38.1 of IS 456), the following assumptions are made in the analysis of columns subjected to axial compression and bending, as per Clause 39.1 of IS 456:

1. The failure of concrete is governed by the maximum strain criteria. For members under concentric load, the ultimate compressive strain in concrete, ϵ_c , is taken uniformly as 0.002 across the section. The ultimate strain in concrete at the outermost compression fibre for bending is taken as 0.0035. This value of maximum compressive strain of 0.0035 is also applicable when the neutral axis lies within the section and in the limiting case when the neutral axis lies along one edge of the section (see Fig. 14.1). In the latter case, the strain varies from 0.0035 at the highly stressed compressed edge to zero at the opposite edge. As shown in Fig. 14.1, the strain distribution lines for these two cases intersect each other at a depth of $3D/7$ (Point F in Fig. 14.1) from the highly compressed edge.
2. This point F is assumed to act as a fulcrum for the strain distribution line when the neutral axis falls outside the section, as shown in Fig. 14.1. Let the maximum compressive strain at the highly compressed extreme fibre in concrete subjected to axial compression and bending be ϵ_c and the minimum strain at the least compressed extreme fibre be ϵ'_c . Thus, the magnitude of the maximum failure strain ϵ_c is taken as

$$\epsilon_c = 0.0035 - 0.75\epsilon'_c \quad (14.2)$$

For pure bending ϵ'_c is taken as zero, and for axial compression load $\epsilon_c = \epsilon'_c$ so that at failure $\epsilon_c = 0.002$.

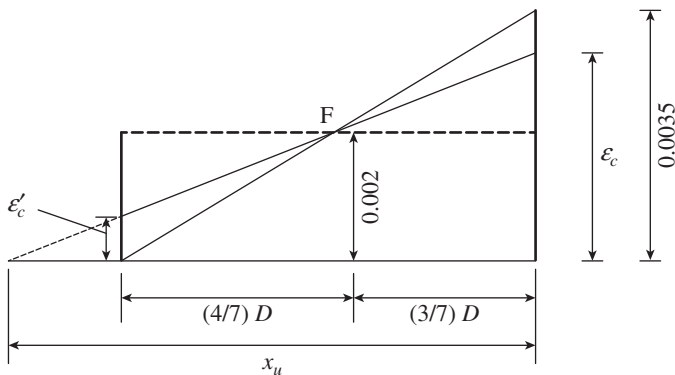


FIG. 14.1 Failure strain in concrete under compressive load and moment

The design stress–strain curve of concrete is already shown in Fig. 13.20(a) of Chapter 13. As already mentioned in Chapter 5, the compressive strength of concrete in a structure is assumed to be 0.67 times its characteristic strength. In addition, a partial factor of safety equal to 1.5 is applied to the strength of concrete. Thus, the design strength of concrete is taken as $0.67f_{ck}/1.5 = 0.447f_{ck}$. The equation of the parabolic part of the curve is taken as

$$f_{cc} = 447f_{ck}(\epsilon_c - 250\epsilon_c^2) \quad (14.3)$$

The design stress–strain curves for mild steel bars and high-yield strength-deformed (HYSD) bars have already been presented in Figs 13.20(b) and (c), respectively, of Chapter 13. The partial factor of safety for the strength of steel reinforcement is taken in IS 456 as 1.15, and hence the design strength is $f_y/1.15$ or $0.87f_y$. The design stress at salient strain for HYSD bars as per Fig. 13.20(c) of Chapter 13 is given in Table 5.2 of Chapter 5. Thus, for these HYSD bars, the design stress–strain curve is linear up to a stress of $0.8 \times 0.87f_y = 0.696f_y$ and thereafter non-linear up to the design stress of $0.87f_y$, corresponding to a strain equal to or greater than $(0.87f_y/E_s) + 0.002$. The f_{yd} values given in Table 5.2 of Chapter 5 may also be obtained using the following equations, with ϵ taken as strain $\times 1000$:

For Fe 415 steel:

$$f_{yd} = -109.1569 + 537.27\epsilon - 250.9\epsilon^2 + 55.28\epsilon^3 - 4.7\epsilon^4 \quad (14.4a)$$

For Fe 500 steel:

$$f_{yd} = 1707.624 - 2356.6\epsilon - 1444\epsilon^2 + 366.7\epsilon^3 - 33.2\epsilon^4 \quad (14.4a)$$

For mild steel bars, however, the stress–strain curve is linear up to a stress of $0.87f_y$ (see Fig. 5.5a of Chapter 5) and thereafter the strain increases at a constant stress. As mild steel bars are rarely used as main reinforcement in columns, we will consider only HYSD bars in the following discussion.

14.2.2 Derivation of Basic Equations

Let us consider a symmetrically reinforced rectangular column section. The relation between the axial force, P , and moment, M , will be derived by considering different positions of neutral axis. Throughout the computations, it is necessary to rigorously observe the sign convention for stresses, strains, forces, and directions. Compression is taken as positive in all cases.

Case 1—Eccentricity $e \leq e_{min}$ The stress and strain diagrams for this case are shown in Fig. 14.2. Considering the equilibrium of axial forces, we get

$$P_u = 0.447f_{ck}BD + (f_{sc} - f_{cc})A_{sc} \quad (14.5a)$$

or

$$P_u = 0.447f_{ck}BD + (f_{sc} - 0.447f_{ck})pBD/100$$

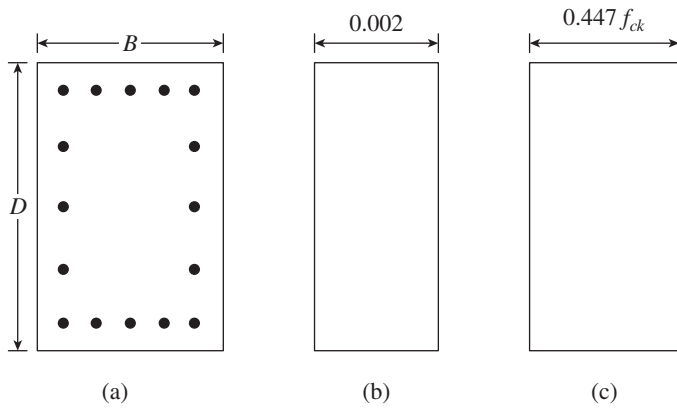


FIG. 14.2 Stress and strain diagrams for $e \leq e_{min}$ (a) Section (b) Strain (c) Stress

This equation can be written in the form

$$\frac{P_u}{f_{ck}BD} = 0.447 + \frac{p}{100f_{ck}}(f_{sc} - 0.447f_{ck}) \quad (14.5b)$$

where B is the breadth of column, D is the depth of column, p is the percentage of steel reinforcement in the section, f_{ck} is the characteristic compressive strength of concrete, and f_{sc} is the compressive stress in steel corresponding to a strain of 0.002 (equals $0.79f_y$ for Fe 415 grade steel and $0.746f_y$ for Fe 500 steel).

The second term within parenthesis represents the deduction for the concrete replaced by the reinforcement bars, which is usually neglected for convenience. (In the interaction diagrams presented in SP 16, as a better approximation, a constant value corresponding to M20 concrete has been used, so that the error is considerably small over the range of concrete grades normally used. It has to be noted that an accurate consideration of the second term in the parentheses of Eq. 14.5b would have necessitated the preparation of separate charts for each grade of concrete, which will increase

the number of charts; as the accuracy so obtained is not very significant, such attempts were not made.)

It has to be noted that Clause 39.3 of IS 456 stipulates that Eq. (13.32) of Chapter 13 be used in the design of columns, where the minimum eccentricity does not exceed 0.05 times the lateral dimension. However, SP 16 uses both these equations. Charts 24–26 of SP 16 for axially loaded short columns are based on Eq. (13.32) of Chapter 13, whereas Charts 27–62 for columns subjected to axial compression and moments, including those cases in which the eccentricity is less than the minimum specified eccentricity of the code, are based on Eq. (14.5). The basic difference between these two equations is the value of stress in the compression steel. Equation (13.32) of Chapter 13 uses a constant value of $0.67f_y$, whereas Eq. (14.5) uses the actual value of stress based on a strain of 0.002 for different types of steel, which is slightly higher, as explained in Section 13.8.1.

Case 2—Neutral axis lies outside section The stress–strain diagram in this case is shown in Fig. 14.3. The stress is uniformly $0.447f_{ck}$ for a distance of $3D/7$ from the highly compressed edge because the strain is more than 0.002 and hence the stress diagram is as shown in Fig. 14.3.

Using similar triangles it can be shown that the maximum strain in concrete is

$$\epsilon_{cc} = 0.002 \left[1 + \frac{3D/7}{x_u - 3D/7} \right] \quad \text{for } x_u \geq D \quad (14.6)$$

Let $x_u = kD$ and let g be the difference between the stress at the highly compressed edge and that at the least compressed edge (see Fig. 14.3). Considering the geometric properties of the parabola, we get

$$g = 0.447f_{ck} \left[\frac{\frac{4}{7}D}{kD - \frac{3}{7}D} \right]^2 = 0.447f_{ck} \left(\frac{4}{7k - 3} \right)^2 \quad (14.7)$$

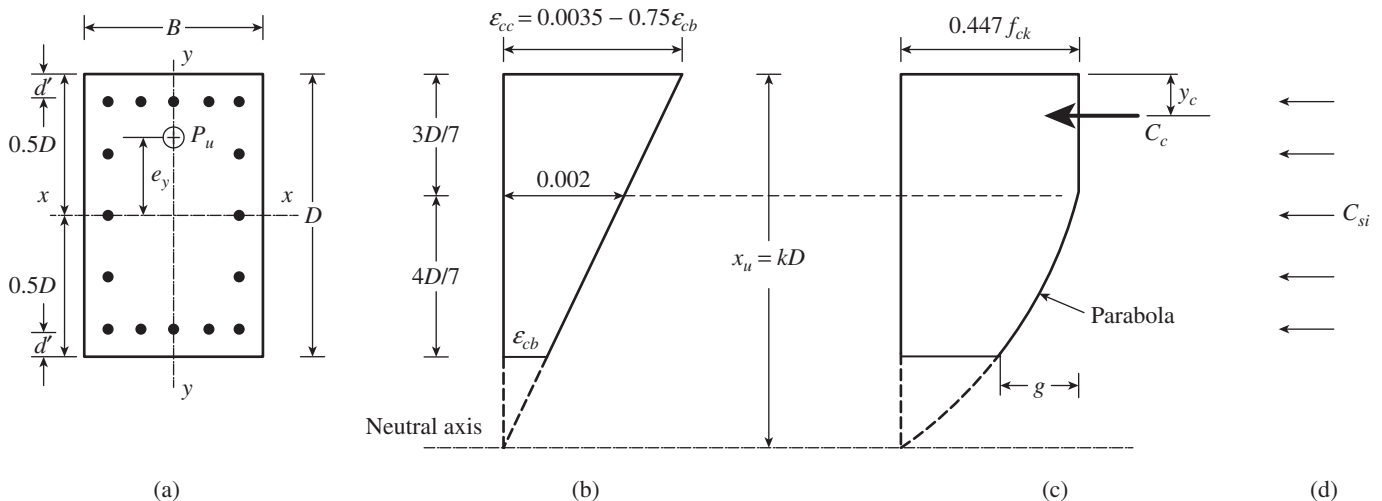


FIG. 14.3 Stress–Strain diagram when neutral axis is outside the section (a) Column section (b) Strain diagram (c) Concrete stress diagram (d) Steel forces

$$\begin{aligned} \text{Area of the stress block} &= 0.447f_{ck}D - \frac{g}{3}\left(\frac{4}{7}D\right) = \\ &0.447f_{ck}\left[1 - \frac{4}{21}\left(\frac{4}{7k-3}\right)^2\right] \end{aligned} \quad (14.8)$$

The compressive force due to concrete stress block can be written as

$$C_c = k_1f_{ck}BD, \text{ where } k_1 = 0.447\left[1 - \frac{4}{21}\left(\frac{4}{7k-3}\right)^2\right] \quad (14.9)$$

Similarly, the stresses in the reinforcements at various levels can be calculated from the known strains using Fig. 5.5 and Table 5.2 of Chapter 5. The compressive force in steel reinforcement is

$$C_{si} = \sum_{i=1}^n A_{si}(f_{si} - f_{ci}) \quad (14.10)$$

where A_{si} is the area of i th row of reinforcement, f_{si} is the stress in the i th row of reinforcement, compression being positive and tension being negative, f_{ci} is the stress in concrete at the level of the i th row of reinforcement, and n is the number of rows of reinforcement. From Eq. (5.45) of Chapter 5, we get

$$\begin{aligned} f_{ci} &= 0.447f_{ck} \text{ for } \varepsilon \geq 0.002 \\ &= 447f_{ck}\varepsilon(1 - 250\varepsilon) \text{ for } \varepsilon < 0.002 \end{aligned} \quad (14.11)$$

The axial capacity can be determined as

$$P_n = C_c + \sum_{i=1}^n C_{si} = k_1f_{ck}BD + \sum_{i=1}^n A_{si}(f_{si} - f_{ci}) \quad (14.12)$$

The distance of the centroid of the concrete stress block from the most compressed edge of column, y_c , can be found by taking moments about the highly stressed compressive edge divided by the area of stress block.

This moment is given by

$$\begin{aligned} &0.447f_{ck}BD\left(\frac{D}{2}\right) - \frac{4}{21}gBD\left[\frac{3}{7}D + \frac{3}{4}\left(\frac{4}{7}D\right)\right] \\ &= 0.224f_{ck}BD^2 - \frac{8}{49}gBD^2 \end{aligned}$$

$$\text{Hence, } y_c = \frac{0.224f_{ck}BD^2 - \frac{8}{49}gBD^2}{0.447f_{ck}BD - \frac{4}{21}gBD} = k_2D \quad (14.13)$$

$$\text{where } k_2 = \frac{0.224f_{ck} - \frac{8}{49}g}{0.447f_{ck} - \frac{4}{21}g} \quad (14.14)$$

Taking moment of the forces about the centroid of the section, we get

$$M_n = C_c(0.5D - y_c) + \sum_{i=1}^n C_{si}y_{si} \quad (14.15a)$$

where y_c is the distance of the centroid of the concrete stress block, measured from the highly stressed compressive edge and y_{si} is the distance from the centroid of the section to the i th row of reinforcement, positive towards the highly compressed edge and negative towards the least compressed edge.

Using Eqs (14.9) and (14.10), we may rewrite Eq. (14.15a) as

$$M_n = k_1f_{ck}BD^2(0.5 - k_2) + \sum_{i=1}^n A_{si}(f_{si} - f_{ci})y_{si} \quad (14.15b)$$

The values of coefficients k_1 and k_2 for different values of k have been calculated and provided in Table 14.1 (SP 16:1980).

TABLE 14.1 Values of coefficients k_1 and k_2 when neutral axis lies outside the section

$k = x_u/D$	Coefficient k_1	Coefficient k_2
1.00	0.361	0.416
1.05	0.374	0.432
1.10	0.384	0.443
1.20	0.399	0.458
1.30	0.409	0.468
1.40	0.417	0.475
1.50	0.422	0.480
2.00	0.435	0.491
2.50	0.440	0.495
3.00	0.442	0.497
4.00	0.444	0.499

Note: k values up to 1.2 are adequate for constructing interaction diagrams.

Introducing $p_{si} = 100A_{si}/BD$, Eqs (14.12) and (14.15b) may be rearranged and rewritten as

$$\frac{P_n}{f_{ck}BD} = k_1 + \sum_{i=1}^n \frac{p_{si}}{100f_{ck}}(f_{si} - f_{ci}) \quad (14.12a)$$

$$\frac{M_n}{f_{ck}BD^2} = k_1(0.5 - k_2) + \sum_{i=1}^n \frac{p_{si}}{100f_{ck}}(f_{si} - f_{ci})\left(\frac{y_{si}}{D}\right) \quad (14.15c)$$

Case 3—Neutral axis lies inside section The stress–strain diagram in this case is shown in Fig. 14.4.

In this case, the stress block parameters are simpler and they can be directly incorporated into the expressions derived for the case of neutral axis outside the section. Now, the distance of the centroid of the concrete stress block from the most compressed edge of column is

$$k_2D = 0.416kD$$

It has to be noted that unlike flexural members, we cannot limit the depth of neutral axis kD in the case of compression members.

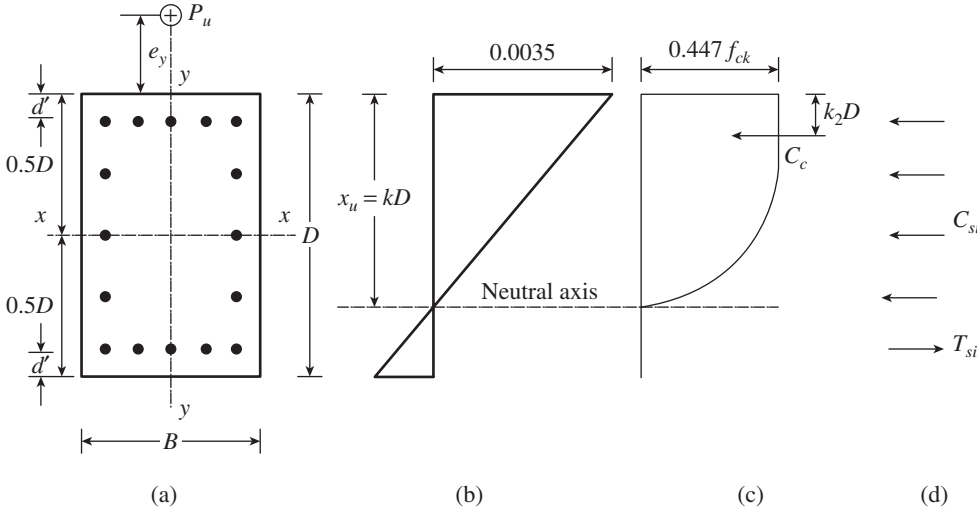


FIG. 14.4 Stress–Strain diagram when neutral axis is inside the section (a) Column section (b) Strain diagram (c) Concrete stress diagram (d) Steel forces

Balancing the axial forces on the section, we get

$$P_n = C_c + \sum_{i=1}^m C_{si} = 0.36 f_{ck} B k D + \sum_{i=1}^n A_{si} (f_{si} - f_{ci}) \quad (14.16)$$

It has to be noted that tension is taken into account in f_{si} , which is the stress in the i th row of reinforcement, compression being positive and tension being negative.

Balancing moments on the section, that is, taking moment of the forces about the centroid of the section, we get

$$M_n = 0.36 f_{ck} B k D^2 (0.5 - 0.416k) + \sum_{i=1}^n A_{si} (f_{si} - f_{ci}) y_{si} \quad (14.17)$$

Again, tension is taken into account through y_{si} , which is the distance from the centroid of the section to the i th row of reinforcement, positive towards the highly compressed edge and negative towards the least compressed edge.

Introducing $p_{si} = 100 A_{si}/BD$, Eqs (14.16) and (14.17) may be rearranged and rewritten as

$$\frac{P_n}{f_{ck} BD} = 0.36k + \sum_{i=1}^n \frac{p_{si}}{100 f_{ck}} (f_{si} - f_{ci}) \quad (14.16a)$$

$$\frac{M_n}{f_{ck} BD^2} = 0.36k(0.5 - 0.416k) + \sum_{i=1}^n \frac{p_{si}}{100 f_{ck}} (f_{si} - f_{ci}) \left(\frac{y_{si}}{D} \right) \quad (14.17a)$$

where $k = x_u/D$ and x_u is the depth of neutral axis (see Fig. 14.4).

From the foregoing computations, it is evident that the ultimate load carrying capacity of a uniaxially eccentrically loaded column depends on the following parameters: the size of the column, the disposition of reinforcements, the stress–strain curves of the materials used, the yield limits of the materials, and, above all, the eccentricity of the load. At this

juncture, it is important to note that the top-storey columns of multi-storey buildings will have small loads and large bending moments, whereas the bottom-storey columns will have heavy loads and more or less the same bending moments. Hence, in such situations it is advisable to keep the same column size throughout a few storeys, say every five storeys. (Only when columns are considerably stiffer than beams framing into them, the cantilever action may dominate their behaviour in the lower storeys.)

Rectangular stress block If an equivalent rectangular stress block, as adopted in the ACI and other

national codes and as shown in Fig. 5.1(h) of Chapter 5, is used, then the corresponding equations are much simpler than the rectangular-parabolic stress block assumption of the Indian code. Assume that the depth of stress block $a = 0.8x_u$.

Case 1— $0.8x < D$: In this case, the whole cross section is under compression

$$C_c = 0.45 f_{ck} BD$$

Taking moment about the centroid of the section, we get

$$C_c y_c = C_c \left(0.5D - \frac{D}{2} \right) = 0.225 f_{ck} BD^2$$

Hence, we get

$$P_n = C_c + \sum_{i=1}^m C_{si} = 0.45 f_{ck} BD + \sum_{i=1}^n A_{si} (f_{si} - f_{ci}) \quad (14.18)$$

$$M_n = 0.225 f_{ck} BD^2 + \sum_{i=1}^n A_{si} (f_{si} - f_{ci}) y_{si} \quad (14.19)$$

Case 2— $0.8x \leq D$: In this case, part of the column cross section is in compression and part is in tension.

$$C_c = 0.45 f_{ck} B(0.8x_u) = 0.36 f_{ck} Bx_u$$

$$P_n = C_c + \sum_{i=1}^m C_{si} = 0.36 f_{ck} Bx_u + \sum_{i=1}^n A_{si} (f_{si} - f_{ci}) \quad (14.20)$$

Taking moment about the centroid of the section, we get

$$C_c y_c = C_c \left(0.5D - \frac{a}{2} \right) = C_c \left(0.5D - \frac{0.8x_u}{2} \right)$$

$$M_n = 0.36 f_{ck} Bx_u (0.5D - 0.4x_u) + \sum_{i=1}^n A_{si} (f_{si} - f_{ci}) y_{si} \quad (14.21)$$

The difference between the values of P_u and M_u calculated based on the rectangular stress block will not differ much from those calculated based on rectangular–parabolic stress block.

As such, the analysis of eccentrically loaded columns is tedious and time consuming and may require several hours of computational effort. As shown in Example 14.2, this difficulty is overcome by generating and using a series of P – M interaction curves (Clause 39.5 of IS 456) (these interaction curves are discussed in Section 14.2.5). As an approximation, the deduction for the concrete replaced by the reinforcement bars (i.e., the value of f_{ci}) in Eqs (14.12a), (14.15c), (14.16a), and (14.17a) may be neglected. In the interaction charts of SP 16, a constant value corresponding to M20 concrete is used instead in order to minimize the error.

14.2.3 Sections with Asymmetric Reinforcement and Plastic Centroid

Usually, reinforced concrete (RC) columns are symmetrically reinforced about the axis of bending. However, in certain situations, such as columns of portal frames or arches where the eccentricity is large, it may be economical to provide asymmetric reinforcement, with more rods on the tension side, as shown in Fig. 14.5 (it has to be noted that when such frames are situated in earthquake zones, equal reinforcement has to be provided in both faces). Such columns can also be analysed using the strain compatibility method discussed in Section 14.2.2.

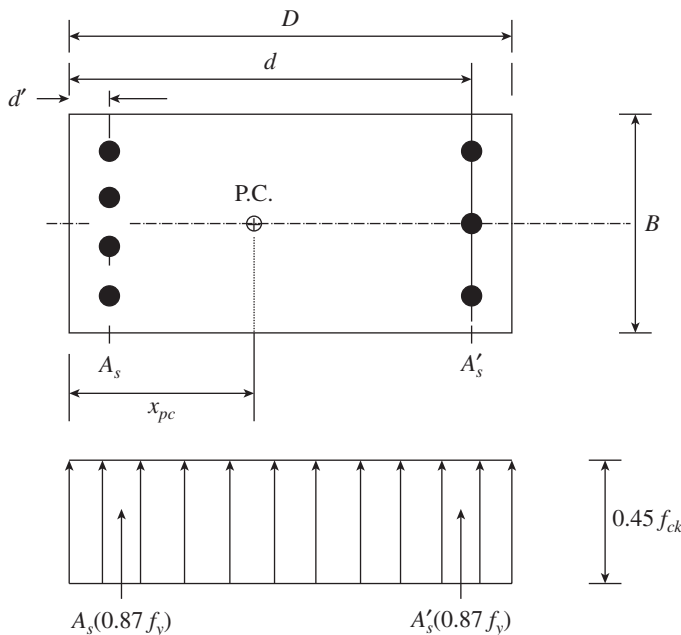


FIG. 14.5 Plastic centroid of an asymmetrically reinforced column

However, for an asymmetrically reinforced column, the resultant load must pass through the *plastic centroid* to produce uniform strain at failure. The plastic centroid represents the location of the resultant force produced by the steel and

concrete. For locating the plastic centroid, the entire concrete section is assumed to be stressed uniformly in compression (to the ultimate strain $\epsilon_{cu} = 0.0035$) and all the steel to f_y in compression. The eccentricity of the applied load should be measured with respect to the plastic centroid, because only then will $e = 0$ correspond to an axial load with zero moment. The location of plastic centroid for the column from the left face shown in Fig. 14.5 is given by

$$x_{pc} = \frac{0.45 f_{ck} B D^2}{2} + A'_s (0.87 f_y) d + A_s (0.87 f_y) d' \quad (14.22)$$

$$0.45 f_{ck} B D + A'_s (0.87 f_y) + A_s (0.87 f_y)$$

For symmetrical sections, the plastic centroid coincides with the centroid of the column cross section. The moments are taken about the plastic centroid. An example to calculate the ultimate load carrying capacity of such asymmetrically reinforced column sections is provided by Purushothaman (1984).

14.2.4 Analysis of Circular Columns

The determination of the ultimate strength of circular columns is based on the same principles as in the case of rectangular or square columns. However, in this case, the geometry of the compression zone and the circular arrangement of steel bars pose complications. Several approximate methods have been suggested to simplify the calculations. In SP 16, the interaction diagrams for circular sections were obtained by dividing the circle into slices. In the method proposed by Whitney (1942), the circular column is replaced by an equivalent rectangular column. The area of the equivalent column is made equal to the area of the actual circular column, and its depth in the direction of bending is taken as 0.8 times the outside diameter of the real column. Fifty per cent of the steel is assumed to be placed on each side of the equivalent column, at a distance $2/3 D_s$ apart, where D_s is the diameter of a circle passing through the centre of the bars in the real column, as shown in Fig. 14.6. Once the equivalent column is established, the values of P_n and M_n are calculated as for rectangular columns.

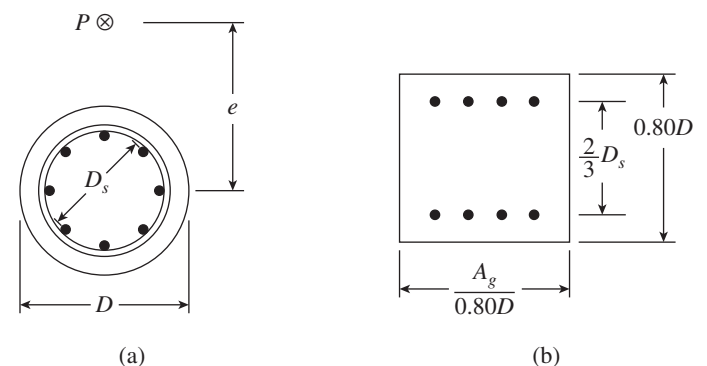


FIG. 14.6 Replacing circular column with an equivalent rectangular column (a) Actual circular column (b) Equivalent rectangular column

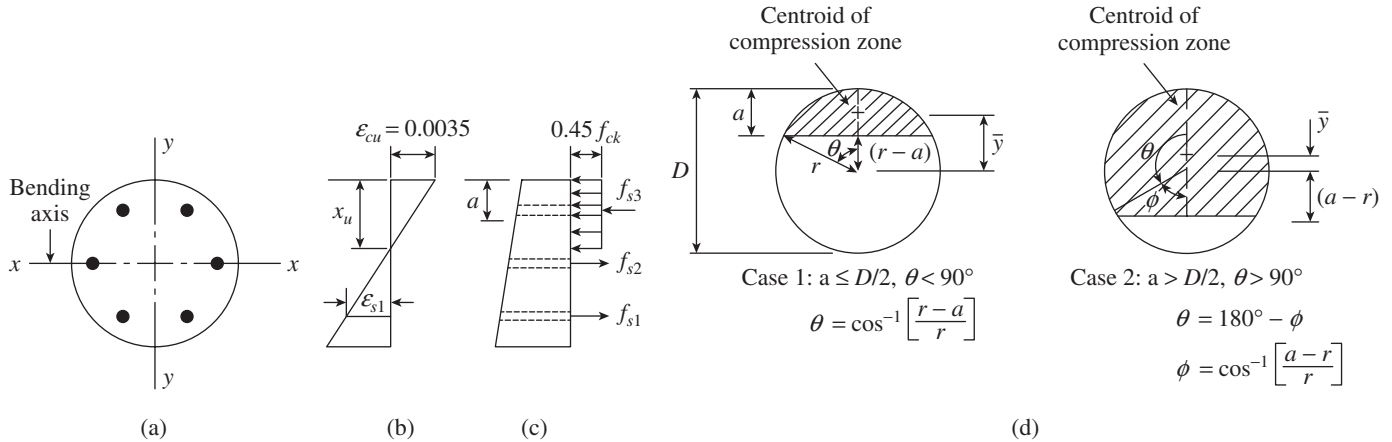


FIG. 14.7 Circular column under direct load and moments (a) Section (b) Strains (c) Stresses (d) Compression zones

This equivalent column method was found to give satisfactory results and corresponds closely with experimental results.

The stress block parameters for rectangular sections are not applicable to circular sections. The extreme fibre strain for circular section may be taken as 0.0035, even though the failure strain in compression for circular sections may be less than that of rectangular sections. The use of rectangular stress block of $0.45f_{ck}$ will result in simplified calculations (see Fig. 14.7). While developing the interaction curves of SP 16, the circular section was divided into strips and the forces on each of these strips were summed up for determining the total forces and moments due to stresses in concrete.

The compression zone of a circular column is a segment of a circle having depth a , as shown in Fig. 14.7(d). To compute the compressive force and its moment about the centroid of the column, we need to compute the area and centroid of the segment. These can be expressed as a function of angle θ (see Fig. 14.7d). The area of the segment is given by

$$A = r^2(\theta - \sin \theta \cos \theta) \tag{14.23}$$

where r is the radius of circle and θ is the angle expressed in radians (1 radian = $180^\circ/\pi$). The distance of the centre of gravity from the centre of the column is

$$\bar{y} = \frac{2r}{3} \left[\frac{\sin^3 \theta}{\theta - \sin \theta \cos \theta} \right] \tag{14.24}$$

An example of circular column based on the strain compatibility method may be found in the work of Purushothaman (1984). As the calculations based on this method are tedious and lengthy, designers often use the interactions curves, such as those presented in SP 16:1980, for their analysis and design.

14.2.5 Interaction Curves

In Section 14.2.2, we have seen that the values of P_n and M_n for a given column can be determined using the strain compatibility method. Preparing an interaction curve by hand, even for just one column, for various strain distributions is time consuming.

In a design office, various sizes of columns with various concrete strengths and steel percentages are to be dealt with and the results obtained quickly. Hence, designers often resort to spreadsheets, computer programs, or computer-generated interaction curves or tables for column design. The remainder of this chapter is concerned primarily with computer-generated interaction curves such as the one shown in Fig. 14.8. As can be seen in Example 14.2, such a curve is drawn for a column as the load changes from one of pure axial load through varying combinations of axial loads and moments to a pure bending case. (Hereafter, the tension part of the interaction curve will not be discussed.) Figure 14.8 also shows the shape of the interaction curve when the column concrete is confined and not confined (confined columns have spiral or transverse ties at close spacing and usually have 135° hooks; under earthquake loads, they carry loads even after spalling of concrete cover; see Section 13.10.4 of Chapter 13 for more details). The interaction curve for confined concrete based on Indian codes is presented by Rohit, et al. (2013).

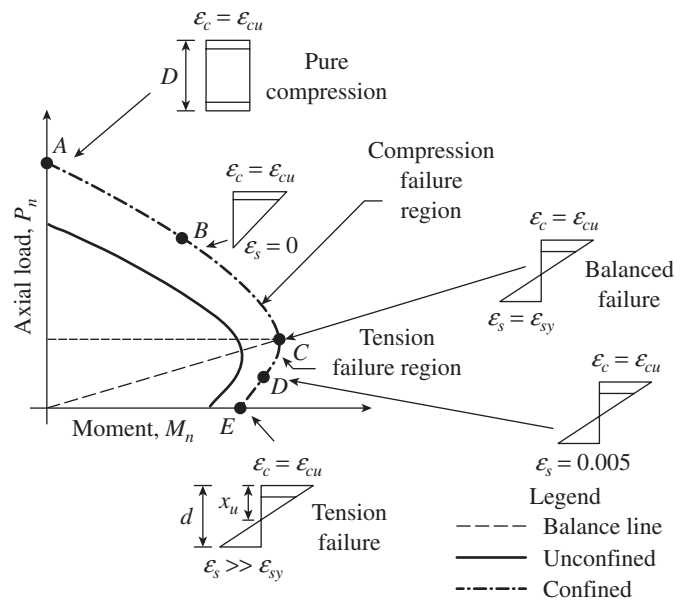


FIG. 14.8 Column interaction curve

Interaction curves are useful for studying the strength of columns with various proportions of loads and moments. Any combination of loading that falls inside the curve is generally satisfactory, whereas any combination falling outside the curve is not satisfactory and may represent failure.

The points and regions on the interaction curve that are important are as follows:

Point A—pure axial load This point corresponds to a strain distribution that represents uniform axial compression without moment, sometimes referred to as *pure axial load*.

Point B—zero tension, onset of cracking The strain distribution at this point corresponds to the axial force and moment on the onset of the crushing of the concrete, when the strain in the concrete at the least compressed edge is zero and the concrete begins to crack. Since the tensile strength of concrete is ignored in strength calculations, failure loads below point B in the interaction curve represent cases where the section is partially cracked.

Region A–C—compression-controlled failure The columns with axial load capacity P_n and moment capacity M_n that fall in this region of interaction curve initially fail due to the crushing of concrete in the compression face, before the yielding of tensile steel. Hence, they are called *compression-controlled columns*.

Point C—balanced failure This point is called the *balanced failure* point and represents the balanced loading case, where theoretically both the crushing of the concrete in the compression face and the yielding of reinforcement in the tension face develop simultaneously. It has to be noted that in the ACI code, the definition of balanced failure when there are several layers of tension steel was changed from the 2002 version; now it corresponds to the yielding of the extreme layer of the tension reinforcement rather than the yielding of the centroid of the tension reinforcement.

Point D—tension-controlled limit This point denotes the *ductile failure of column*, where the tensile strain in the extreme layer of the tension steel is sufficiently large, that is, equal to or great than about 2.5 times the yield strain in steel [yield strain in Fe 415 steel, $\epsilon_s = f_y/E = 415/(2 \times 10^5) = 0.0021$]. Clause 10.3.4 of the ACI code denotes this as *tension-controlled column*, which has a strain in the extreme layer of the tensile steel equal to or greater than 0.0005. In such columns, there will be ample warning of failure with excessive deflection and cracking.

Region C–D—transition region The columns that fall in the region CD are termed *transition region columns*. It may be of interest to note that Clause 9.3.2.2 of the ACI code specifies the appropriate strength reduction factor, ϕ , for tension- and compression-controlled sections and for cases in the transition region, as shown in Table 14.2 (see also Section 5.5.5 and Fig. 5.9

of Chapter 5). A lower ϕ factor is used for compression-controlled sections because these sections have less ductility and are more sensitive to variations in concrete strength. Members with spiral reinforcement are assigned a higher ϕ than those with tied columns because they have greater ductility or toughness. The Indian code does not consider strength reduction factors and uses partial safety factors on materials; in addition, the spirally reinforced columns are considered to have an augmented capacity of 1.05 times the corresponding tied columns.

Point E—pure bending This point represents the bending strength of the member, that is, when it is subjected to moment alone with zero axial loads.

TABLE 14.2 Values of strength reduction factor, ϕ , for columns as per the ACI code

Type of Column	Compression Controlled	Transition Region	Tension Controlled
Tied column	0.65	$0.65 + (\epsilon_t - 0.002)250/3$	0.90
Spiral column	0.75	$0.75 + (\epsilon_t - 0.002)50$	0.90

14.2.6 Design Aids

The interaction curves discussed until now are applicable only for the sections that were considered. The application of the interaction curves can be made more general by making the coordinates P_u and M_u independent of the cross-sectional dimensions, that is, by using the non-dimensional parameters, $p_u = P_u/(f_{ck}BD)$ and $m_u = M_u/(f_{ck}BD^2)$, and by plotting curves for various values of p/f_{ck} , where $p = 100A_s/(BD)$. Such interaction curves can be used for any size of column sections, area of reinforcement, and values of f_{ck} . Several such curves were generated and provided in the design handbook SP 16:1980. These interaction curves are available for rectangular and circular columns with symmetrical arrangement of steel. Typical curves for rectangular and circular columns are shown in Figs 14.9 and 14.10, respectively. It has to be noted that the general form of the interaction curves in the ACI handbook SP 17 and the curves in SP 16 are the same; however, in SP 16, the curves are generated for the parameter p/f_{ck} rather than $p f_y/f_{ck}$, and hence, different sets of curves are required for different types of steel. Moreover, in SP 16, the e/h concept has been de-emphasized and the state of stress in steel has been given more importance.

The non-dimensional interaction curves given in SP 16:1980 consider the following three types of symmetrically reinforced columns:

Rectangular columns with reinforcement on two sides—Charts 27 to 38 The two sides refer to the sides parallel to the axis of bending. There are no interior rows of bars, and each outer row has an area of $0.5A_s$ and includes four-bar reinforcement.

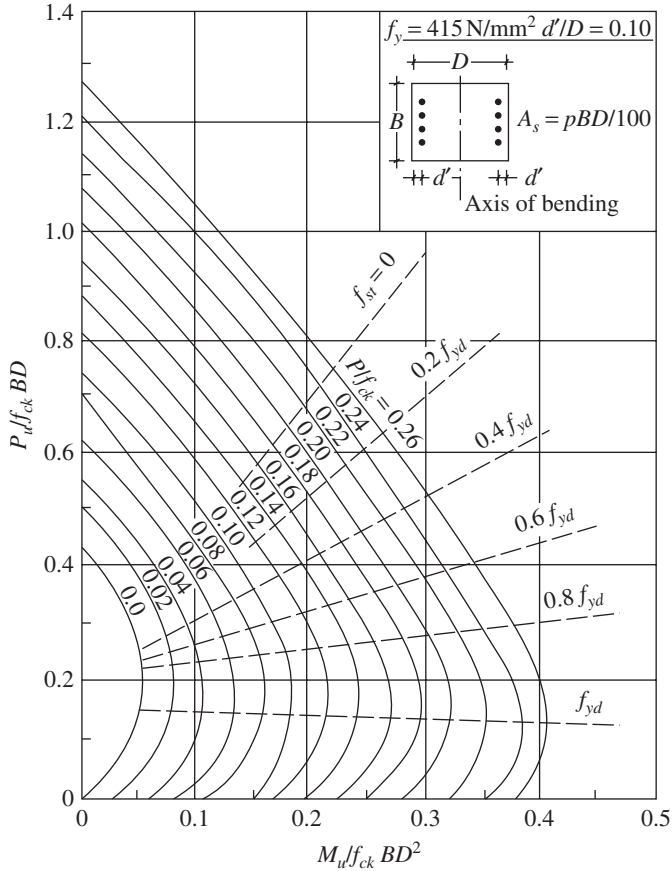


FIG. 14.9 Typical interaction diagram for rectangular columns (Chart 32 of SP 16)

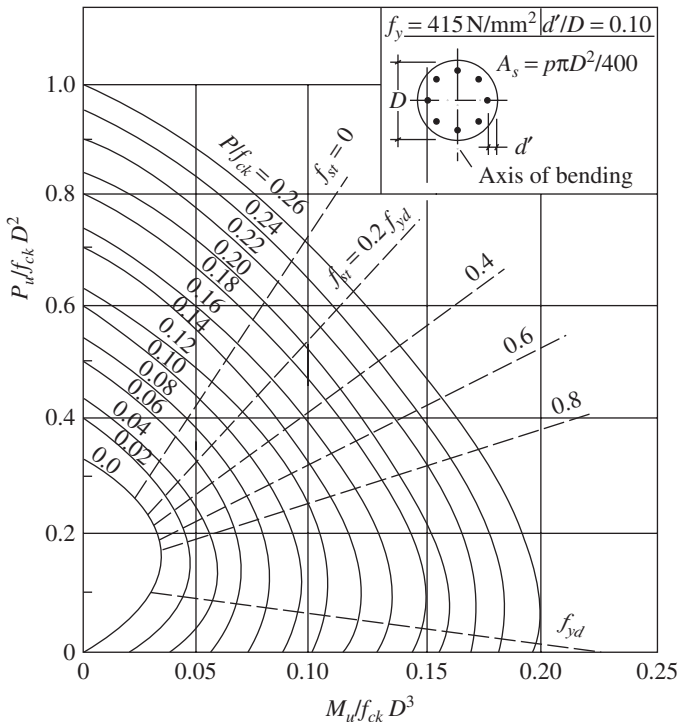


FIG. 14.10 Interaction diagram for circular columns (Chart 56 of SP 16)

Rectangular columns with reinforcement on four sides—Charts 39 to 50 These charts have been prepared for a section with 20 bars equally distributed on all four sides, but they can be used for any number of bars greater than eight.

Circular columns—Charts 51 to 62 These charts have been prepared for a section with eight bars, but can be used for any section having more than six bars.

These charts have been prepared for three grades of steel (Fe 250, Fe 415, and Fe 500) and for four values of cover ratio d'/D (0.05, 0.10, 0.15, and 0.20) for each of the three types of columns. For intermediate values of d'/D , linear interpolation is recommended. Each of these twelve charts of SP 16 contains a set of curves with p/f_{ck} ranging from 0.0 to 0.26. Similar charts are available in the work of Iyengar and Viswanatha (1990).

The dotted lines in these charts (see Figs 14.9 and 14.10) indicate the stress in the bars nearest to the tension face of the column. Thus, the line $f_{st} = 0$ indicates that the neutral axis lies along the outermost row of reinforcement. For points lying above this line on the chart, all the bars in the section will be in compression. The line for $f_{st} = f_{yd}$ indicates that the outermost tension reinforcement will reach the design yield strength. For points lying below this line on the chart, all outermost tension reinforcement will undergo inelastic deformation, whereas successive inner rows may reach the stress of f_{yd} . It has to be noted that some interaction charts also include radial lines representing different eccentricity ratios e/D or lines representing values of strains $\epsilon_t = 0.002$ and 0.005 in the extreme tension steel. A radial line through the origin has a slope equal to $(P_u/A_g)/(M_u/A_gD)$. Realizing that $M_u = P_u e$, we may deduce that the slope is D/e or $1/(e/D)$, where e/D represents the ratio of eccentricity to the column thickness.

Sinha (1995 and 1996b) has developed interaction curves and tables for different types of reinforcement detailing for rectangular columns with different D/B ratios. A different set of interaction curves for columns have been developed by Varyani and Radhaji (2005).

14.2.7 Design Procedure

The design procedure for columns subjected to axial force and uniaxial bending moment is iterative and consists of the following steps:

1. Determine the axial load and bending moments acting on the column, based on a suitable analysis program, for different load cases. From this, determine the maximum axial force and bending moment that has to be supported by the column. Calculate the factored load and factored bending moment.
2. Select trial cross-sectional dimensions B and D based on experience, grade of concrete, minimum permissible column size (200 mm but preferably not less than 300 mm in earthquake zones), and minimum size and cover based

on fire resistance and environment exposure requirements (see Fig. 1 of IS 456).

3. Check for minimum eccentricity:

$$e \left(= \frac{M_u}{P_u} \right) > e_{\min} \left[= \left\{ \left(\frac{L}{500} \right) + \left(\frac{D}{30} \right) \right\} \text{ or } 20\text{mm} \right]$$

4. Choose rebar size and size of cover based on exposure condition. Calculate d'/D .
5. Calculate $p_u = P_u/f_{ck}BD$ and $m_u = M_u/f_{ck}BD^2$.
6. Depending on the values of p_u , m_u , d'/D , and grade of steel, select the corresponding chart from SP 16. If there is no exact match for the calculated d'/D value, the values from two charts should be taken and interpolated. It is better to select the chart based on the nearest higher value of d'/D . Read the value of p/f_{ck} from the chart. Be sure that the column diagram shown at the upper right side of the interaction curve matches with the column being considered. In other words, check whether the bars are on two faces of the column or on all the four faces. Selecting a wrong chart may result in the wrong design.
7. Calculate the steel area $A_s = pBD/100$. Check whether the calculated area of reinforcement is within the bounds of the specified code (Clause 26.5.3.1a), that is, above 0.8 per cent and below 3–4 per cent; revise the section if necessary and repeat the calculations.
8. Design ties as per Clause 26.5.3.2 and detail the reinforcements taking into consideration Clause 26.5.3.1 of IS 456.

It has to be noted that for eccentricity ratios, e/D , less than about 0.1, a spiral circular column is more efficient in terms of load capacity. However, this economy may be offset by the more expensive formwork and the cost of spiral reinforcement. For e/D ratios greater than 0.2, a rectangular column with bars in the faces farthest from the axis of bending is economical. Increasing the depth of the column perpendicular to the axis of bending will result in economy, although in practice the sizes may be restricted due to architectural and formwork considerations.

Rectangular column with bars in all the four faces is economical when there is biaxial bending and when the e/D ratio is less than about 0.2. In seismic areas where ductility is important, spiral columns are used.

In tall buildings, high-strength concrete (HSC) columns are often used to achieve economy and to reduce column size. When such HSC columns transfer load through normal-strength concrete (NSC) floor slabs, the designer must consider this effect in the design, as discussed in Section 9.4.7 of Chapter 9. For lower columns in tall buildings, when limited by architectural reasons, bundled bars may be used with high reinforcement ratio, as per Clause 7.4 of SP 34:1987. When the longitudinal reinforcements are grouped, but not in contact, Clause 7.2.5 of SP 34:1987

should be followed. Various arrangements of column ties and detailing of bars may be found in Section 7 of SP 34:1987.

14.2.8 Splicing of Reinforcement

As discussed in Sections 7.7.1 and 7.7.2 of Chapter 7, in non-seismic zones, the longitudinal bars of columns are spliced just above each floor using indirect splices (lap splicing), as shown in Fig. 7.34 of Chapter 7, or by direct splicing (welded splices or mechanical splices), as shown in Figs 7.35–7.38 of Chapter 7. As discussed in Section 13.10.2 of Chapter 13, in seismic zones, the lap splices should be located only in the mid-height of the column. As mentioned in Section 14.2.6, the design interaction curves contain dotted lines (see Figs 14.9 and 14.10), which indicate various tensile stresses occurring in the reinforcement closest to the tension face of the column. Until $f_{st} = 0$, compression lap splice is sufficient. Between $f_{st} = 0$ and $f_{st} = 0.5f_{yd}$, a lap length of L_d should be provided, if half and fewer bars are spliced at a section; if more bars are spliced, a splice length of $1.3L_d$ needs to be adopted. Beyond $f_{st} = 0.5f_{yd}$, a lap length of $1.3L_d$ needs to be provided. These requirements, as per Clause 7.2.3 of Draft IS 13920, are shown in Fig. 14.11, on a typical interaction curve.

It has to be noted that when we need to provide $1.3L_d$, the lap length will be long, up to half or more than half the height of the storey. In such situations, it may be economical

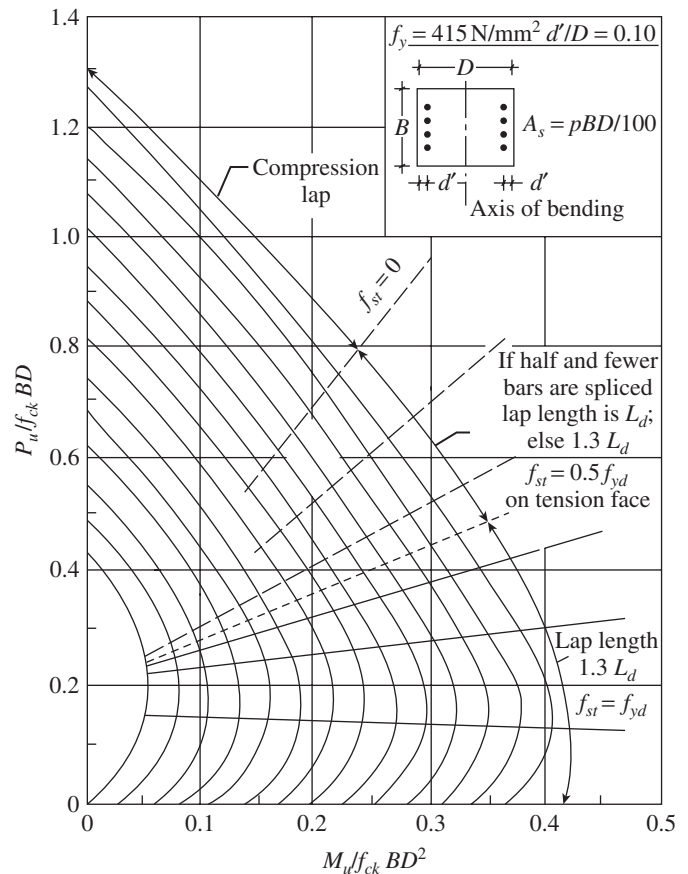


FIG. 14.11 Required lap splice length

to provide welded or mechanical splices. As per Clause 7.2.3 of IS 13920:1993, additional transverse reinforcement, at a spacing not exceeding 150mm, should be provided at these splices (see also Fig.13.31 of Chapter 13).

14.2.9 Transverse Reinforcement

Other transverse reinforcement requirements have already been discussed in Sections 13.10.3 and 13.10.4 of Chapter 13. A few examples of column ties are illustrated in Fig. 14.12

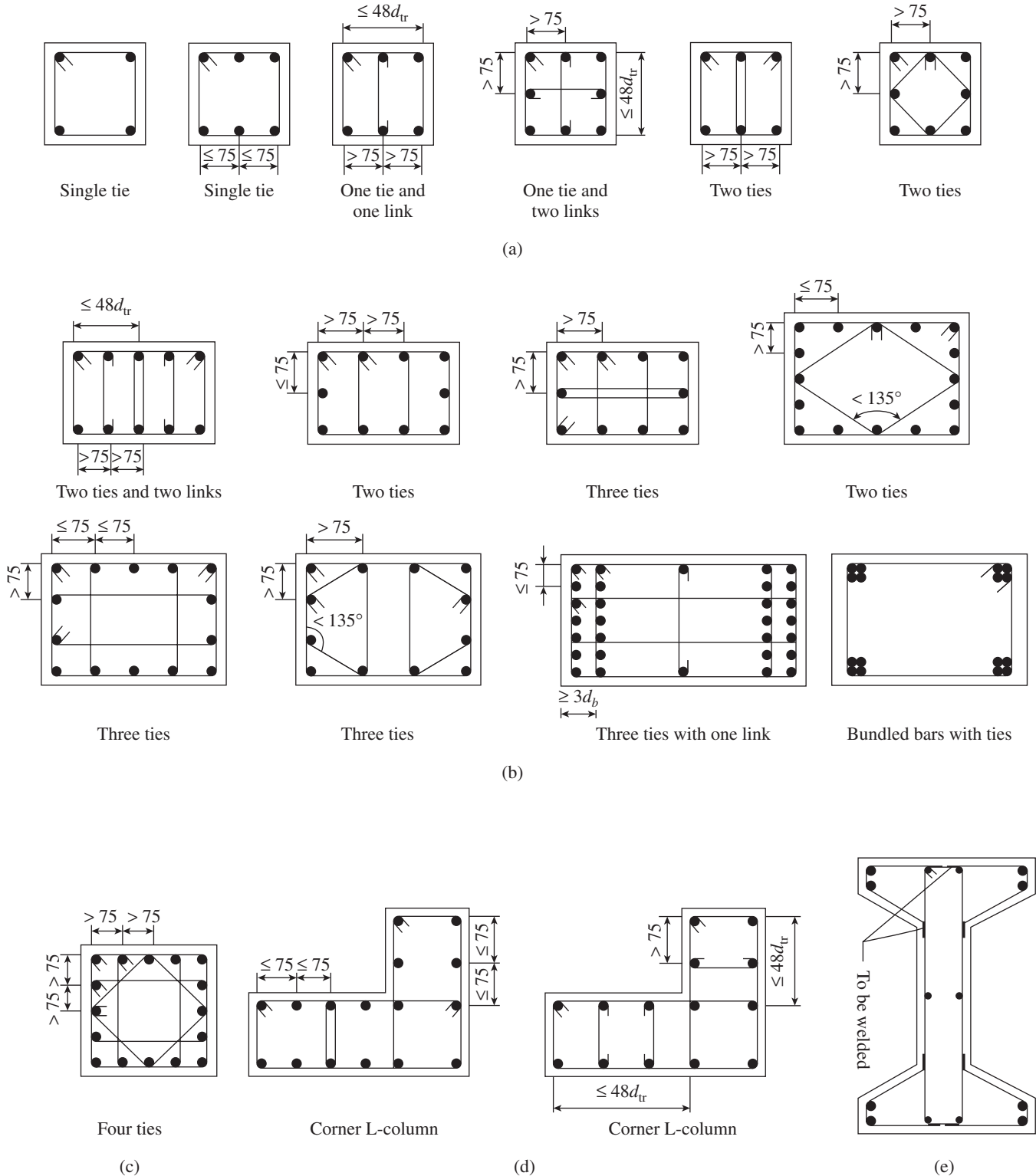


FIG. 14.12 Typical arrangements of column ties (a) Square columns (b) Rectangular columns (c) Large square column (d) L-shaped columns (e) I-shaped column

(see also Figs 13.17 and 13.18 of Chapter 13). Diamond- and octagonal-shaped ties facilitate to keep the centre of the column open and free of cross-ties, resulting in easy placing and vibration of concrete. Welded reinforcement grids as shown in Fig. 4.14 of Chapter 4 will improve the constructability and speed of construction. Specially fabricated welded wire reinforcement cages incorporating the longitudinal bars and ties can also be used (Lambert-Aikhionbare and Tabsh 2001; Razvi and Saatcioglu 1989; Saatcioglu and Grira 1999). Bigger column sizes will also result in better reinforcement detailing (see Fig. 4.12 of Chapter 4). Even though the use of welded wire fabric (WWF) as confinement reinforcement considerably improves the concrete strength and ductility, it should be used with ties with 135° hooks with a spacing of $d/2$, in order to prevent the buckling of longitudinal reinforcement (Razvi and Saatcioglu 1989). The amount of spiral reinforcement to be provided has already been discussed in Section 13.5.1 of Chapter 13, and as per the ACI code, the yield strength for spiral reinforcement can be up to 700 MPa. More information on detailing of column ties, lap splices, longitudinal bars, and so forth may be found in CRSI Staff (2011, 2013).

14.3 DESIGN OF COLUMNS WITH AXIAL LOAD AND BIAxIAL BENDING

Many columns are subjected to biaxial bending, that is, bending about both axes. The most common ones are the corner columns in buildings, where beams frame into the corner column in two perpendicular directions and transfer their end moments into the column. Similar loading may also

occur in the interior columns if the column layout is irregular, at the columns supporting heavy spandrel beams, and at the bridge piers. In addition, beams supporting helical or free-standing stairs, or oscillating and rotating machinery, have to resist biaxial bending with or without axial load (Varyani and Radhaji 2005).

Clause 39.6 of IS 456 mentions two methods for the design of members subjected to combined axial load and biaxial bending. The first method is based on the conditions of equilibrium, on the basis of assumptions given in the code in Clauses 39.1 and 39.2, with a suitably chosen inclined neutral axis. This method is described briefly in this section. The second method is described in Section 14.3.3.

A symmetrically reinforced concrete column section subjected to biaxial bending is shown in Fig. 14.13. The stress–strain diagrams are based on the assumptions listed in Section 14.2.1. The equations of strain compatibility and equilibrium as given in Section 14.2.2 can be used to analyse this section as well.

Thus, we get

$$P_n = C_c + \sum_{i=1}^n C_{si} \quad (14.25)$$

$$M_{nx} = P_n e_x (0.5D - \bar{y}) + \sum_{i=1}^n A_{si} (f_{si} - f_{ci}) y_{si} \quad (14.26)$$

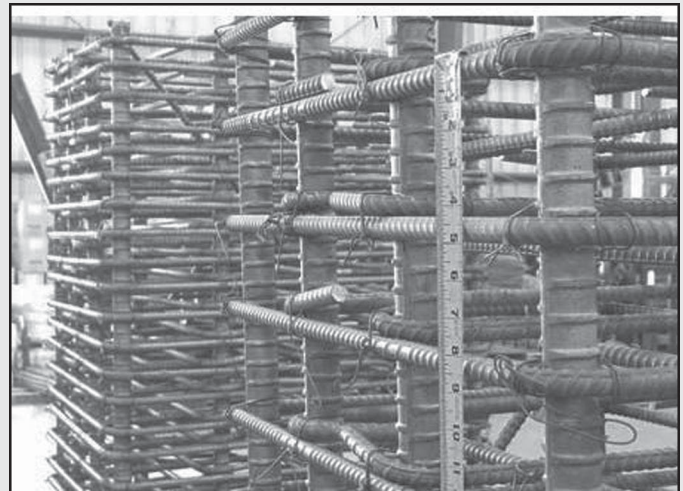
$$M_{ny} = P_n e_y (0.5D - \bar{x}) + \sum_{i=1}^n A_{si} (f_{si} - f_{ci}) x_{si} \quad (14.26a)$$

CASE STUDY

Use of Fe 690 Grade Steel as Seismic Ties for the First Time

With 31 storeys above grade and eight floors of parking area below, the 76,180 m² Escala is the largest residential tower in Seattle, Washington, USA. Escala features a dual seismic system of concrete shear walls and ductile frames, instead of a more conventional central core. It is the first structure in North America to use M96 concrete in columns and Fe 690 steel as seismic column ties. The structural engineering firm Cary Kopczynski & Co. (CKC) obtained special permission from the City of Seattle to use HSS in the new condominium tower, though Fe 690 steel was approved by ACI 318 in 2006.

The use of Fe 690 seismic confinement reduced tie quantities in columns and shear walls as much as 40 per cent when compared to Fe 415 steel. The use of Fe 690 steel also saved additional bars, since the number of required supplementary seismic ties is reduced. This allowed reduction in the vertical bars, further reducing tonnage and simplifying placement. The use of M96 concrete also resulted in significant reduction in column sizes, offering more usable floor space. More details of the design and construction of this building may be had from the work of Kopczynski (2008).



Reinforcing mockups for M96 concrete columns shows constructability improvements with Fe 690 ties over the Fe 415 ties shown in the background (Source: Cary Kopczynski & Company)

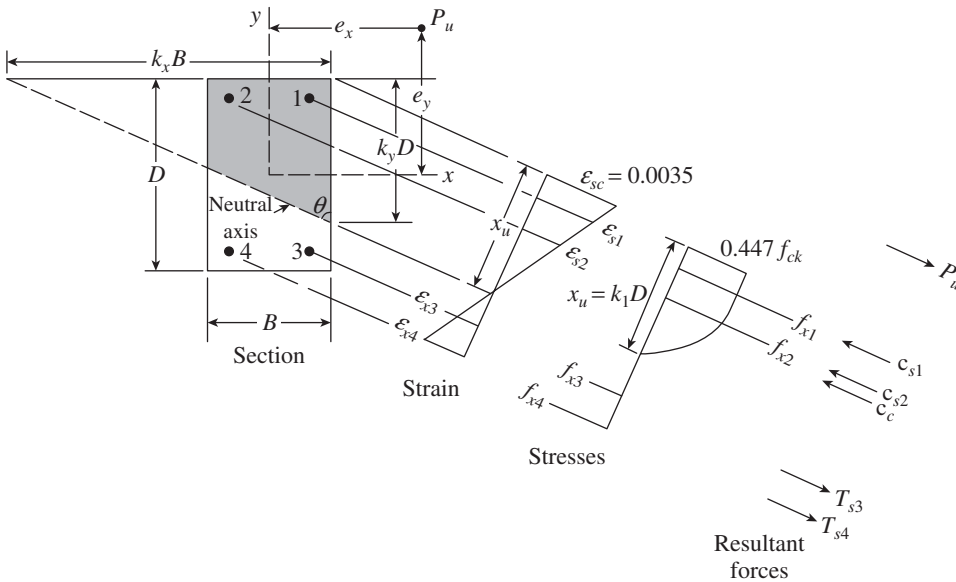


FIG. 14.13 Biaxial bending of symmetrically reinforced concrete columns

The appropriate signs (positive for compression and negative for tension) should be used in these equations. If the column has more than four bars, the extra steel forces should also be considered. The use of rectangular stress block will simplify the calculations. The analysis involves a triangular or trapezoidal area of compressed concrete, as well as a neutral axis that is not usually perpendicular to the direction of eccentricity; it is inclined with an angle depending on the moment values as well as the section properties (Park and Paulay 1975; Warner, et al. 1976). In general, the lateral deflection along the longitudinal axis of the column under biaxially eccentric compression load is in a direction different from the direction of eccentricity (Furlong, et al. 2004).

Such an analysis is tedious, as a trial and adjustment procedure is required to find the inclination and depth of neutral axis, satisfying the equilibrium equations [see the study of Purushothaman (1984) for the complete treatment and worked out examples]. To use these equations in design, it is necessary to assume an initial section and reinforcement and the area of reinforcement successively corrected until the section capacity approaches the required value. Thus, it is clear that the use of these equations is not recommended for design offices unless they are solved with the use of computer software.

For a given cross section and reinforcement, by varying the inclination of

the neutral axis, a series of interaction diagrams can be drawn. The development of interaction diagrams for biaxially loaded columns is described by Furlong, et al. 2004. A typical set of one quadrant of interaction diagram for a typical section is shown in Fig. 14.14. It is seen that the complete set of diagrams for all angles will result in an *interaction surface*, which is the failure surface for the given section. Each point on this surface will represent a particular set of axial load P_n , and moments M_{nx} and M_{ny} , which together produce the failure of the section.

If a horizontal section is taken through the interaction surface of Fig. 14.14, we get an interaction curve, which gives the possible combinations of M_{nx} and M_{ny} that will cause failure at a given axial load P_n . This line is a constant *load contour* of the interaction surface. An expression for the shape of the interaction curve in a general case is difficult to derive, because the shape varies with the section geometry, the strength of materials, the arrangement and area of steel reinforcement, and the level of axial load (Park and Paulay 1975). Hence, a number of approximate methods have been developed for the analysis and design of an RC column with biaxial bending, which are discussed in the following sections.

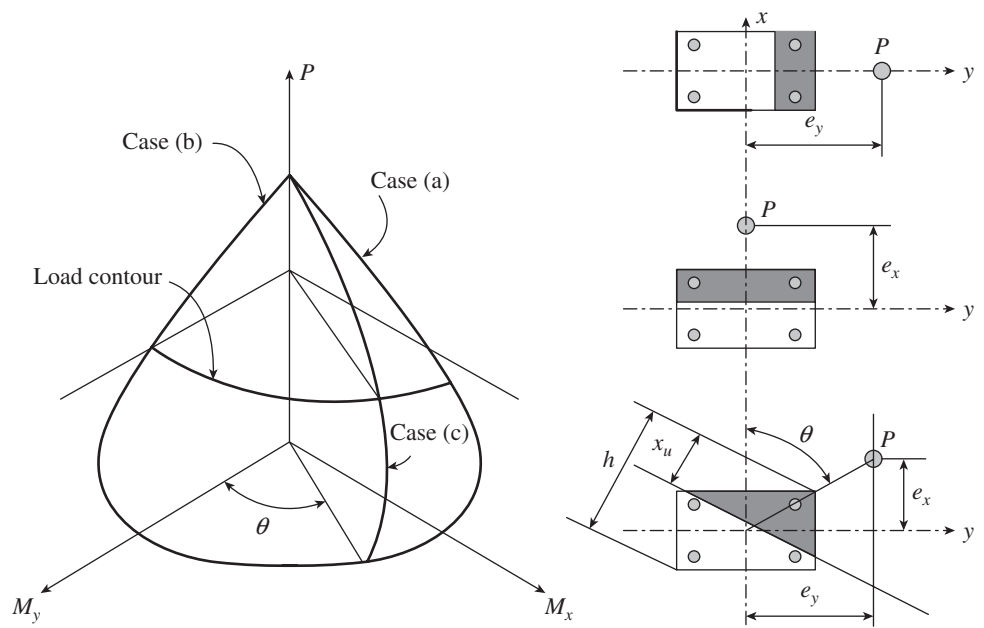


FIG. 14.14 Three-dimensional interaction surface for an RC column with biaxial bending
Source: Furlong 1961 (adapted), reprinted with permission from ACI

14.3.1 Methods of Superposition

Some simple methods of superposition have been developed, which reduce the inclined bending to bending about major axis of the section, thus allowing the use of interaction diagrams developed for uniaxial bending (Moran 1972).

One such method involves the following steps: (a) Determine the required A_s in the x -direction considering P_u and M_{ux} . (b) Determine the required A_s in the y -direction considering P_u and M_{uy} . (c) Determine the total required area of steel by adding the two areas obtained in steps (a) and (b). This method has no theoretical basis and may lead to unsafe designs because the full strength of concrete is considered twice in the design (Park and Paulay 1975). However, this method can be conveniently used in the design of long L-, T-, and +-shaped columns as the overlapping area in the x - and y -directions will be small. Example 14.10 explains the use of this method. Two alternative methods similar to this superposition method have been suggested and found to produce conservative designs. The details of these methods may be found in the works of Moran (1972) and Park and Paulay (1975).

14.3.2 Methods of Equivalent Uniaxial Eccentricity

In these methods, the biaxial eccentricities e_x and e_y are replaced by an equivalent uniaxial eccentricity, e_{ox} , and the column is designed for uniaxial bending and axial load. An approximate method suggested by MacGregor (1973) is described here. If we consider e_x as the eccentricity parallel to side D and the x -axis, as shown in Fig. 14.15, so that $M_{uy} = P_u e_x$ and $M_{ux} = P_u e_y$, and if $\frac{e_x}{D} \geq \frac{e_y}{B}$, then it can be shown that the column can be designed for P_u and a factored moment $M_{oy} = P_u e_{ox}$ (MacGregor 1973), where

$$e_{ox} = e_x + \frac{\alpha e_y D}{B} \quad (14.27a)$$

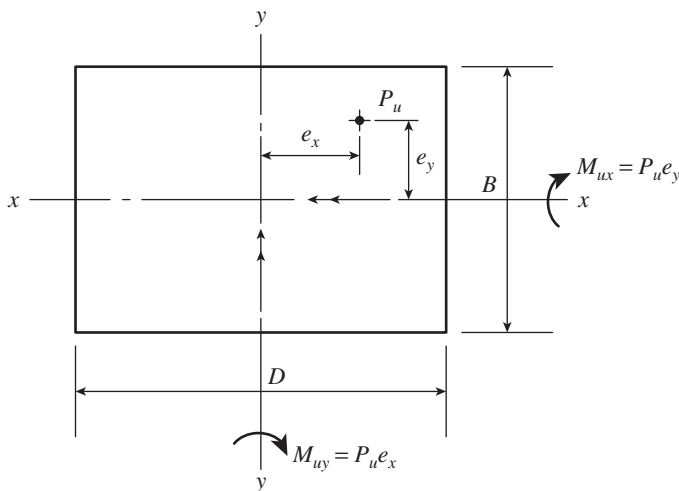


FIG. 14.15 Definition of terms for biaxially loaded columns

The value of α may be taken as follows:

$$\text{For } P_u/f_{ck}A_g \leq 0.4, \alpha = \left(0.5 + \frac{P_u}{f_{ck}A_g}\right) \left(\frac{f_y + 275}{700}\right) \geq 0.6 \quad (14.27b)$$

$$\text{For } P_u/f_{ck}A_g > 0.4, \alpha = \left(1.3 - \frac{P_u}{f_{ck}A_g}\right) \left(\frac{f_y + 275}{700}\right) \geq 0.5 \quad (14.27c)$$

If the inequality in Eq. (14.27a) is not satisfied, the definition of the x - and y -axes should be interchanged. This procedure is limited in application to columns with doubly symmetric cross sections having the ratio of longer to shorter dimension between 0.5 and 2 and reinforced with equal reinforcement on all the four faces (Furlong, et al. 2004).

Few researchers advocate the use of an equivalent bending moment of the following form:

$$M'_{ux} = \sqrt{M_{ux}^2 + M_{uy}^2} \quad (14.28)$$

where M'_{ux} is the equivalent bending moment about the x -axis. This approximation is found to be more appropriate for circular columns.

Everard (1974) suggests using the following modified bending moment about the x -axis:

$$M'_{ux} = M_{ux} + M_{uy} \frac{D}{B} \quad (14.29a)$$

If M_{uy} is more prominent than M_{ux} , then the modified bending moment about the y -axis should be taken as

$$M'_{uy} = M_{uy} + M_{ux} \frac{B}{D} \quad (14.29b)$$

This approach was found to result in safe and conservative designs.

Clause 3.8.4.5 of the UK code BS 8110-Part 1: 1997 suggests an approximate method for symmetrically reinforced rectangular sections, which is an improvement over Everard's method. It suggests that the two moments M_x and M_y acting on the column can be reduced to a single moment about a given axis by using the following:

$$\text{When } M_x/d \geq M_y/b, M'_x = M_x + \beta \frac{d}{b} M_y \quad (14.30a)$$

$$\text{When } M_x/d < M_y/b, M'_y = M_y + \beta \frac{b}{d} M_x \quad (14.30b)$$

where b and d are shown in Fig. 14.16 and the coefficient $\beta = 1 - \frac{7}{6} \frac{P}{f_{ck}BD}$ may be obtained from Table 14.3.

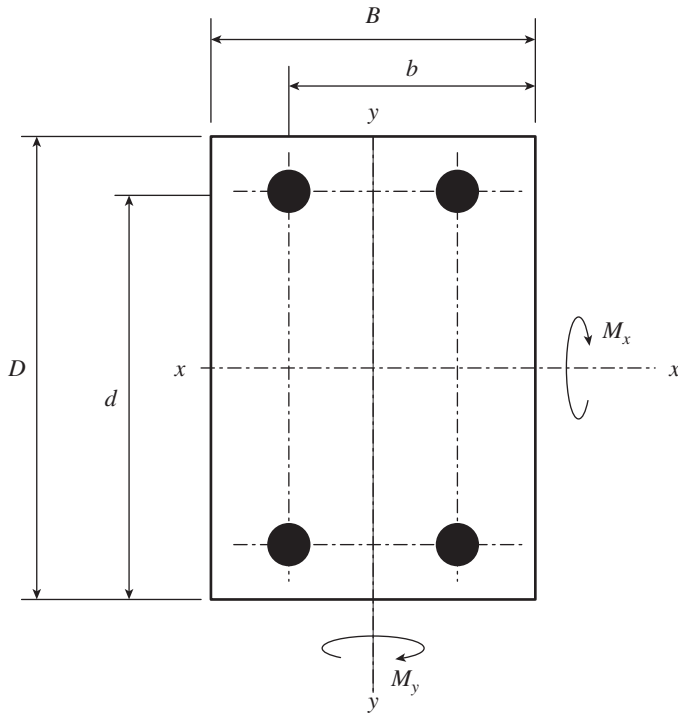


FIG. 14.16 Column under biaxial bending as per BS 8110

TABLE 14.3 Values of coefficient β

$\frac{P}{f_{ck}BD}$	0	0.1	0.2	0.3	0.4	0.5	≥ 0.6
β	1.00	0.88	0.77	0.65	0.53	0.42	0.30

This method is found to produce accurate results and avoids iterations.

14.3.3 Methods Based on Approximations for Shape of Interaction Surface

A few suggestions have been made for the shape of the interaction surface with which the biaxial bending strength may be calculated using the uniaxial bending strength.

Bresler’s Reciprocal Load Method

Bresler (1960) derived the following expression for calculating the capacity of columns under biaxial bending, which has been included in the commentary of Clauses 10.3.6 and 10.3.7 of the ACI 318 code:

$$\frac{1}{P_n} = \frac{1}{P_{nx}} + \frac{1}{P_{ny}} - \frac{1}{P_{no}} \tag{14.31}$$

where P_n is the nominal axial load strength at given eccentricity along both axes, P_{nx} is the nominal axial load strength at given eccentricity along the x-axis, P_{ny} is the nominal axial load strength at given eccentricity along the y-axis, and P_{no} is the nominal axial load strength at zero eccentricity. If the value of P_n from Eq. (14.31) reduced by a strength

reduction factor, ϕ , exceeds the applied factored axial load P_u at the biaxial eccentricity, the section will be adequate. This relationship is found to be most suitable when the values P_{nx} and P_{ny} are greater than the balanced axial force P_b for the particular axis. Equation (14.31) is more suitable for analysis than for design and, hence, is often used to check designs. Bresler (1960) and Ramamurthy (1966) found the capacity predicted by Eq. (14.31) to be in reasonable agreement with theoretical as well as experimental results. The results obtained by Bresler’s reciprocal formula are not realistic for columns with high-end restraints or columns that are very slender (Suryanarayana 2013).

Bresler’s Load Contour Method

Bresler (1960) also suggested that the family of interaction lines corresponding to various levels of constant loads P_u can be approximated by the following expression:

$$\left(\frac{M_{ux}}{M_{nx}}\right)^m + \left(\frac{M_{uy}}{M_{ny}}\right)^n \leq 1 \tag{14.32}$$

where M_{nx} and M_{ny} are the maximum uniaxial moment capacities for an axial load of P_u , bending about x- and y-axes, respectively, M_{ux} and M_{uy} are the moments about x- and y-axes, respectively, due to design loads, and the constants m and n depend on the column properties and are determined experimentally.

Parme, et al. (1966) restated Eq. (14.32) as

$$\left(\frac{M_{ux}}{M_{nx}}\right)^{\log 0.5/\log \beta} + \left(\frac{M_{uy}}{M_{ny}}\right)^{\log 0.5/\log \beta} \leq 1 \tag{14.33}$$

where β is the parameter dictating the shape of the interaction line. Other suggestions for the shape of interaction surfaces have been made by Pannell (1963) and Furlong (1961). Hsu (1988) proposed the equation of failure surface method and showed that this method provides a more logical approach over the reciprocal load and load contour methods. A unified formula for calculating the ultimate state of RC members under combined loading conditions, including axial compression, shear, bending, and torsion, has been proposed recently by Huang, et al. (2013).

Clause 39.6 of IS 456 has adopted Eq. (14.32) as an alternative method, in the following form

$$\left(\frac{M_{ux}}{M_{nx}}\right)^\alpha + \left(\frac{M_{uy}}{M_{ny}}\right)^\alpha \leq 1 \tag{14.34}$$

where α is a coefficient related to P_u/P_{nz} . For values of $P_u/P_{nz} = 0.2$ to 0.8 , the values of α vary linearly from 1.0 to 2.0. For values less than 0.2, α is 1.0 (indicating a straight line); for values greater than 0.8, α is 2.0 (indicating an ellipse).

For intermediate values, that is, 0.2 to 0.8, it is calculated as followed:

$$\alpha = \frac{2}{3} + \frac{5}{3} \left(\frac{P_u}{P_{nz}} \right) \quad \text{for} \quad 0.2 < \frac{P_u}{P_{nz}} < 0.8 \quad (14.35)$$

P_{nz} is the axial load capacity of the column and is given in the code as

$$P_{nz} = 0.45f_{ck}A_c + 0.75f_yA_{sc} \quad (14.36)$$

where A_c is the area of concrete in the column, A_{sc} is the area of steel reinforcement, f_{ck} is the characteristic compressive strength of concrete in the column, f_y is the characteristic yield strength of reinforcement, P_u is the axial load, and P_{nz} is the axial load capacity of the column. It has to be noted that P_{nz} is the design load capacity for the column when the load is applied concentrically and not the load capacity, which takes into account an eccentricity of $0.05D$.

A plot of interaction curves given by Eq. (14.34) for different values of P_u/P_{nz} are shown in Fig. 14.17 (SP 16:1980). Any combination of biaxial moments falling inside these curves for the given value of P_u/P_{nz} is considered safe.

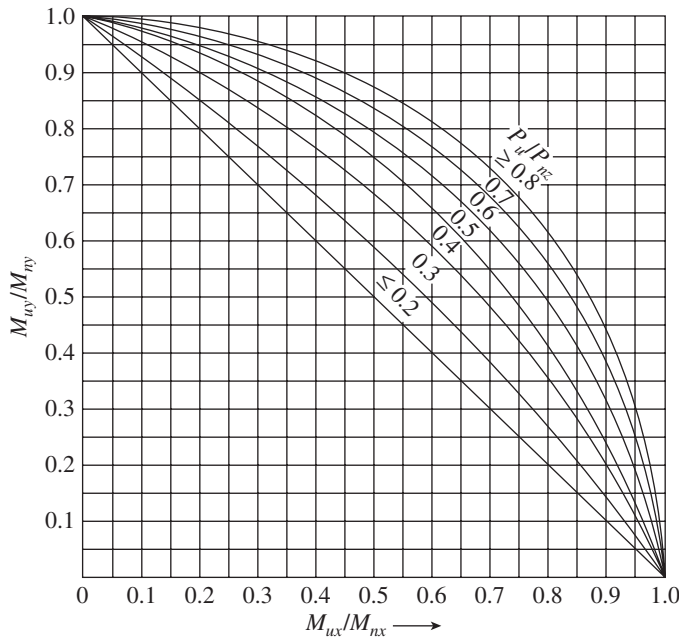


FIG. 14.17 Interaction curves for biaxial moments for different values of P_u/P_{nz}

It has to be remembered that this alternative method, given in the code, involves a trial and error process and does not provide any clue to the location of the neutral axis.

14.3.4 Design Procedure for Columns with Biaxial Moments

The procedure for the design of columns subjected to factored axial load P_u and biaxial moments M_{ux} and M_{uy} consists of the following steps:

1. Assume cross-sectional dimensions and the area of steel and its distribution.

2. Compute concentric load capacity P_{nz} as per Eq. (14.36) and P_u/P_{nz} . Chart 63 of SP 16 can also be used to evaluate the value of P_{nz} .
3. Determine the uniaxial capacities M_{nx} and M_{ny} of the section combined with the given axial load P_u with the use of interaction curves for axial load and uniaxial moment.
4. Determine the adequacy of the column section using Eq. (14.34) or Fig. 14.17. When using Eq. (14.34), use Eq. (14.35) to calculate α , which should be greater than 1.0 and less than 2.0. When Eq. (14.34) results in a value greater than 1.0, the selected section is unsafe, and when it is much lower than 1.0, the section is not economical; in such cases, the section should be modified and steps 1–4 are to be repeated again, until the resulting value of Eq. (14.34) is nearly equal to 1.0.

For practical designs, $\alpha = 1.15$ – 1.55 for rectangular columns and $\alpha = 1.5$ – 2.0 for square columns is generally satisfactory (Bresler 1960).

14.3.5 Design Aids

It has been shown in Section 14.2.4 that the design of columns subjected to factored axial load P_u and biaxial moments M_{ux} and M_{uy} is iterative. Sinha and his associates have developed interaction curves for typical reinforcement distribution in rectangular and square columns for axial load, biaxial moments, effective cover to reinforcement, and area of steel (Banerjee and Sinha 1994; Sinha 1995; Sinha 1996b; Sinha and Kumar 1992). These curves can be used directly to determine the area of steel, without any trial and error process. Similar design charts are provided by Varyani and Radhaji (2005) and Ghanekar and Jain (1982), but they require interpolation with respect to $P_u/f_{ck}BD$. Gupta developed the following equations for columns with $f_y = 415 \text{ N/mm}^2$ and $f_{ck} = 20 \text{ N/mm}^2$, which could be used directly to get the area of steel (Gupta 2010):

For rectangular columns:

$$A_s = 3.307P_u - 0.0295BD + 57.317D (M_{ux}/P_u) + 57.317B (M_{uy}/P_u) + 114634.538 (M_{ux}M_{uy}/P_u^2) \quad (14.37)$$

For circular columns:

$$A_s = 3.307P_u - 0.0231D^2 + 90.033D (M_{ux}/P_u) + 90033.755 (M_{ux}M_{uy}/P_u^2) \quad (14.38)$$

where B is the size of column along the x -direction and D is the size of column along the y -direction or the diameter of column in the case of circular columns. The other terms have been defined already. It has to be noted that these equations are valid only if the summation of the first two terms is not less than zero. Design aids have also been developed by Row and Paulay (1973), Sun and Lu (1992), Weber (1966), Fanella (2001), ACI design handbook SP 17:2009, and CRSI handbook (2008).

14.3.6 Design of L, T, and + Columns

L-, T-, and cross (+)-shaped columns are often used at outside and re-entrant building corners for architectural purposes. The codes, such as IS 456 and ACI 318, do not provide any guidance on the design of these columns, though the basic strain compatibility and equilibrium equations given in Section 14.2.2 can be used for the analysis of such columns. These columns have been considered by several researchers (Park and Paulay 1975; Ramamurthy and Kahn 1983; Wsu 1985; Hsu 1985, 1987, 1989; Sinha 1996a, 1996b; Sinha 1994). Interaction curves of L, T, and + columns subjected to axial load and biaxial bending are available in the works of Martin (1979), Sinha (1996b), and Sinha and Sinha (1989).

Gupta (2010) developed the following equation for L-columns with $f_y = 415 \text{ N/mm}^2$ and $f_{ck} = 20 \text{ N/mm}^2$, which could be used directly to get the area of steel:

$$A_s = 3.332P_u - 0.0371(A_g) + 71.646D(M_{ux}/P_u) + 71.646B(M_{uy}/P_u) + 143293.172(M_{ux}M_{uy}/P_u^2) \quad (14.39)$$

It has to be noted that this equation is valid only if the summation of the first two terms is not less than zero.

Charts for the design of hollow rectangular sections are provided by Kumar and Sinha (1994) and of circular ring-shaped columns by Varyani and Radhaji (2005). A number of computer programs for biaxial bending, like PCAColumn (current version 4.10), developed by Portland Cement Association, Illinois, are also commercially available.

14.4 SLENDER COLUMNS

The discussion until now dealt with concentrically or eccentrically loaded short columns, whose strength is governed entirely by the strength of the materials used and the cross-sectional shape. Most of the columns met with in practice belong to this category. However, with the increasing use of HSC, columns may become slender. Slender columns are prone to *buckling*. Many designers assume that concrete members are sufficiently thick, and hence, buckling can be ignored. Though this may be true for braced frames (where side sway is prevented), the possibility of buckling should be considered in the case of unbraced frames. A *slender column* may be defined as a column that has significant reduction in its axial load capacity due to moments resulting from lateral deflections of the column. Figure 14.18 shows



(a)



(b)

FIG. 14.18 Examples of slender columns (a) 50 m tall column for runway in Portugal (b) Slender columns in a building in Chicago

Source: (a) Muntalip, Mohd Huzaifah, <http://www.akademifantasia.org/europe/incredible-funchals-airport-runway-in-portugal>

examples of slender columns. Slender concrete columns may fail by buckling in the elastic or inelastic stress state or they may fail when the compressive strain in the concrete reaches its limit of 0.0035. The former is classified as *instability failure* and the latter as *material failure* (Purushothaman 1984). Slender columns are best avoided by novice designers, and if they are to be used, expert advice should be sought.

14.4.1 Definition

As per Clause 25.1.2 of IS 456, a compression member is considered slender when either of the slenderness factors L_{ex}/D and L_{ey}/B is greater than 12, where L_{ex} and L_{ey} are the effective lengths with respect to the major and minor axis, respectively, and B and D are the width and depth of the column [this may be considered as applicable to non-sway (braced) columns bent in double curvature with equal end moments ($M_1 = M_2$), as shown in Fig. 14.19c]. In addition, Clauses 25.3.1 and 25.3.2 recommend the following limits as discussed in Section 13.7.1 of Chapter 13:

Columns with both ends restrained Unsupported length should not exceed 60 times the least lateral dimension of a column.

Columns with one end unrestrained Unsupported length should not exceed $100 \times B^2D$, where B is the width and D is the depth of column measured in the plane under consideration.

It is important to remember that the effective length of column, $L_e = kL_u$, in braced (non-sway) frames will always be less than its unsupported length (L_u), whereas it is always greater than its unsupported length in unbraced (sway) frame (see also Section 13.4).

Clause 10.10.1 of ACI 318 considers a column as slender in a sway frame if $\lambda = \frac{L_e}{r} > 22$ and in a non-sway frame if

$$\lambda = \frac{L_e}{r} > 34 - 12 \frac{M_1}{M_2} \quad (14.40)$$

where $L_e (= kL_u)$ is the effective length, r is the radius of gyration, and M_1/M_2 is the ratio of end moments. M_1 is the smaller factored end moment and has a positive sign if the column is bent in *single curvature* (C shaped), and negative sign if it is bent in *double curvature* (S shaped). Single and double curvature bending is illustrated in Fig. 14.19. M_2 is the larger factored end moment and always has a positive sign. In Eq. (14.40), the term $(34 - 12M_1/M_2)$ should not be taken larger than 40, according to Clause 10.10.1 of ACI 318. It is interesting to note that the Australian and Canadian codes consider the effect of axial load also in the braced limit (see Table 14.4).

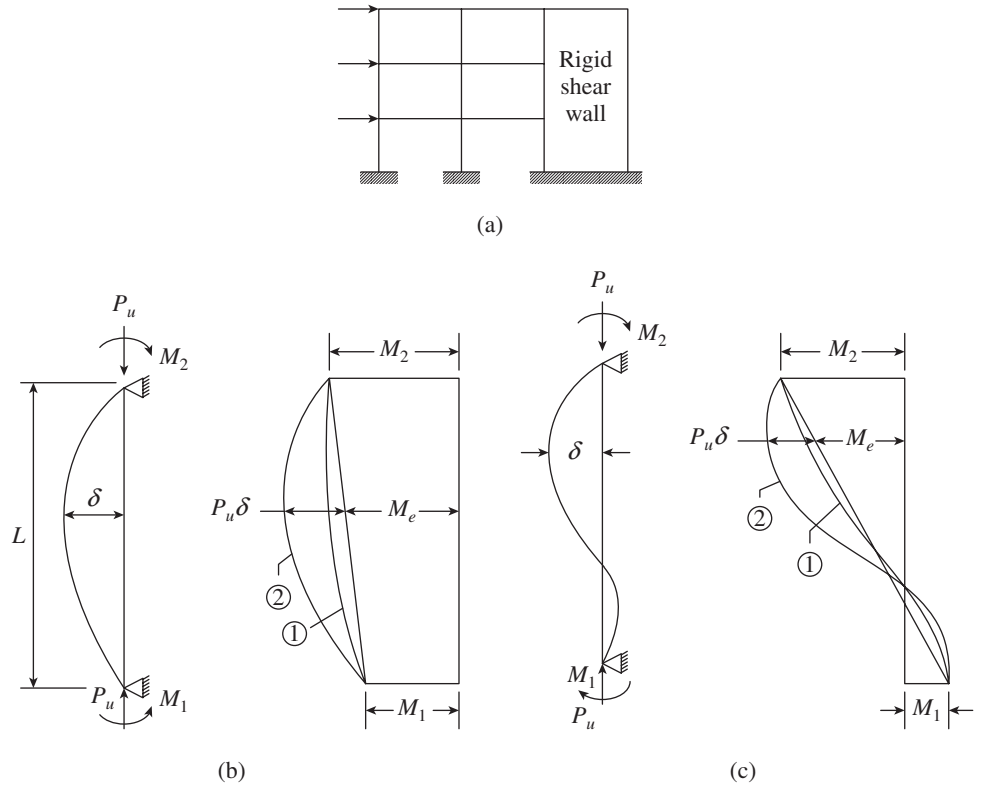


FIG. 14.19 Single and double curvature bending in braced frames (a) Braced (non-sway) frame (b) Single curvature bending (c) Double curvature bending

TABLE 14.4 Lower slenderness limits in codes (adapted from Hellesland 2005, reprinted with permission from ACI)

Code	Parameter	Unbraced Limit	Braced Limit, No Transverse Loading
ACI 318:2011 and NZS 3101:Part1:2006	λ	22	$34 - 12\mu_o \geq 40$
BS 8110-1:1997	$kL/D(\lambda)$	10 (35) (also $L_u \leq 100B^2/D \leq 60B$)	15 (52)
IS 456:2000, BS 8110-1:1997	$kL/B(\lambda)$	$L_u \leq 100B^2/D \leq 60B$	12 (42)
AS 3600:2009	λ	25	$60(1 - \mu_o) \left(1 - \frac{P_u}{0.6P_o} \right) \geq 25$
CSA A23.3:2004	λ	-	$\frac{25 - 10\mu_o}{\sqrt{P_u/f'_c A_g}}$ with $\mu_o \geq -0.5$

Note: $\lambda = L_e/r$, $\mu_o = M_1/M_2$, and $P_o = 0.85f'_c A_c + f_y A_s$

See Sections 13.3 and 13.4 of Chapter 13 for the discussions and determination of effective length of columns in braced

and unbraced frames. Earlier versions of ACI 318 contained a clause that stated that if $L_e/r > 100$, a second-order analysis must be made. Hellesland (2005) studied the non-slender column limits for braced and unbraced columns prescribed in various codes and suggested an alternative limit.

14.4.2 Behaviour

The behaviour of a slender column shown in Fig. 14.20(a) under increasing load is illustrated by the $P-M$ interaction diagram of Fig. 14.20(c). The maximum moment in the column occurs at section A-A due to the combination of the initial eccentricity e in the column and the deflection δ at this point. Two types of failure are possible. If the additional eccentricity δ is negligible, as in the column that is braced against sway, the maximum moment will equal Pe in all stages and a linear $P-M$ path will be followed with increasing load. This is short column behaviour, and the material failure of the section will be reached eventually, when the interaction line is reached at point A. If the column is slender, the maximum moment M will be $P(e + \delta)$, and since δ increases more rapidly at higher load levels, the $P-M$ path will be non-linear. When the column is stable at lateral deflection δ_1 , it will reach the interaction curve at point B and the material failure of the section occurs. Again, this kind of failure usually occurs in practical columns that are braced against sway. However, when the column is very slender, it may become unstable at lateral deflection δ_2 ,

before reaching the interaction curve; this kind of instability or buckling failure may occur in unbraced (sway) frames, as indicated at point C in Fig. 14.20(c) (MacGregor, et al. 1970).

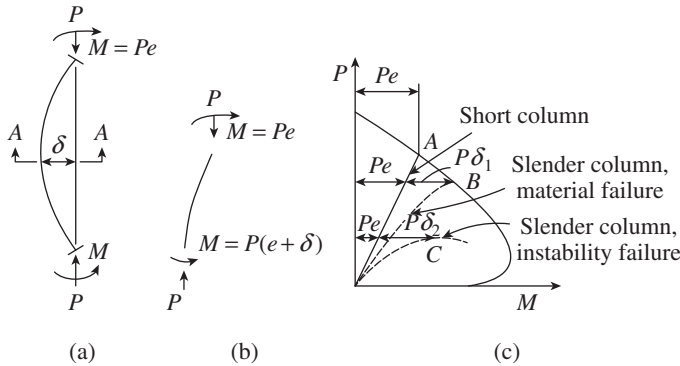


FIG. 14.20 Behaviour of slender columns (a) Column with eccentric loads (b) Free body diagram (c) P - M interaction diagram

Source: MacGregor, et al. 1970, reprinted with permission from ACI

Slender column behaviour for particular loading and end condition can be illustrated by the use of slender column interaction diagrams. Figure 14.21 is such a diagram as illustrated by MacGregor, et al. (1970). The interaction diagram for the critical section A-A of the column shown in Fig. 14.20(a) is drawn in Fig. 14.21(a), in which short and slender column behaviours are illustrated. This particular column has an unsupported length-to-thickness of column ratio of $L_u/h = 30$. Failure of this column occurs at point B under the load and the amplified moment. The load and primary moment Pe at failure of this column is given by point A in Fig. 14.21(a). This point A for a range of e/h and L_u/h ratios can be determined, and based on this, a set of curves as shown in Fig. 14.21(b) can be generated (MacGregor, et al. 1970), which will give the load P and the failure moment M of the column. Such P - M interaction diagrams are useful in finding the reduced strength due to slenderness for various L_u/h ratios. It is also evident from Fig. 14.19 that there is more likelihood of the maximum bending moment being increased by the additional moment

in the single curvature case than in the double curvature case, because in the former the lateral deflections will be greater and the primary moments are near maximum over a large part of the column. Moreover, although in both cases of loading the bending deformations cause additional moments, these moments do not amplify the maximum primary moments that occur at the ends of the column (Park and Paulay 1975).

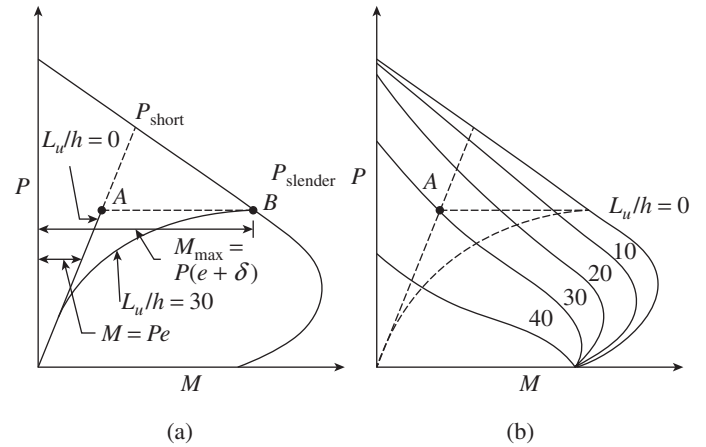


FIG. 14.21 Construction of slender column interaction diagrams (a) Slender column behaviour (b) Slender column P - M interaction diagrams

Source: MacGregor, et al. 1970, reprinted with permission from ACI

The three most significant variables affecting the strength and behaviour of slender columns have been identified as the slenderness ratio L_u/h , the end eccentricity ratio e/h , and the ratio of end eccentricities e_1/e_2 (MacGregor, et al. 1970). As shown in Fig. 14.22, the effects of these variables are strongly interrelated (MacGregor, et al. 1970). In slender hinged columns subjected to single curvature bending (Figs 14.22a and b), the interaction diagrams for all L_u/B ratios greater than zero fall inside the interaction diagram for the cross section ($L_u/B = 0$). This is not true in the case of double curvature bending, since the maximum applied moment occurs at one or both ends of the column, while the maximum deflection moments occur between the ends of the column.

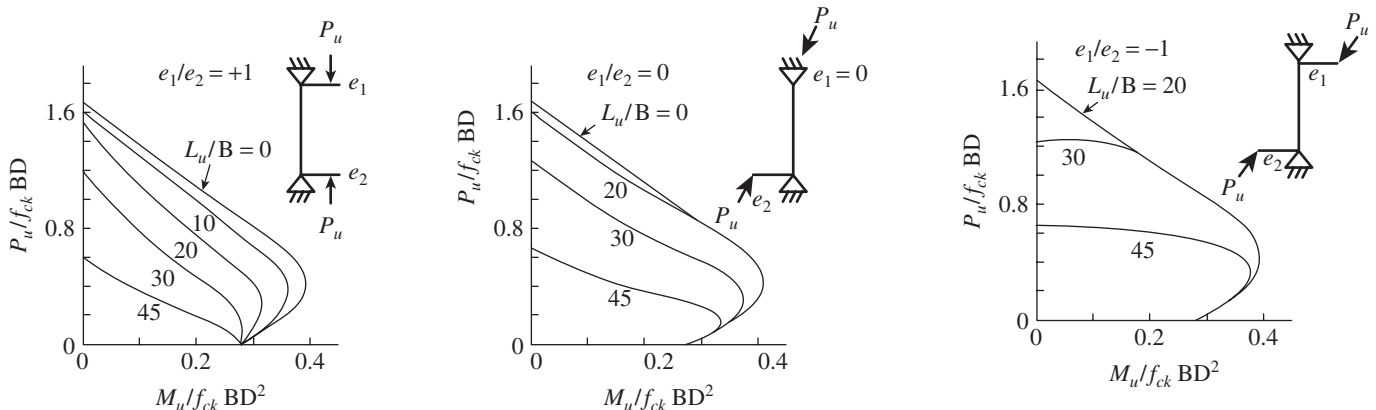


FIG. 14.22 Effect of curvature on interaction diagrams for slender hinged columns

Source: MacGregor, et al. 1970, reprinted with permission from ACI

This is illustrated by the interaction diagram for $L_u/B = 30$ in Fig. 14.22(c). For large eccentricities, however, the maximum moments will always occur at the ends of the column, and as a result, there is no weakening due to length (MacGregor, et al. 1970).

It has also been shown by researchers that an increase in the proportion of the load carried by the reinforcement led to a more stable column. Thus, columns with high concrete strength and/or low reinforcement percentages tended to be most strongly affected by length (Broms and Viest 1961). In other words, for the column to be stable, it is important to increase the p/f_{ck} ratio.

Creep due to sustained loads tends to weaken a hinged slender column by increasing the column deflections. Columns bent in symmetrical single curvature will be much weakened by sustained load, whereas those bent in double curvature are not affected much, especially when the end eccentricities are large (MacGregor, et al. 1970).

The end moments in columns of frames also depend on the relative stiffness of the columns and beams. During loading, the stiffness of beams and columns is reduced by the cracking of concrete and later by inelastic deformations. The stiffness of columns will also be reduced by the additional moments caused by the lateral $P-\Delta$ deflection of the columns. Thus, changes in column moments will occur during the loading due to the changes in relative stiffness and due to the additional moments caused by deflection.

From the foregoing discussion on slender column behaviour, the major variables affecting the slender column are summarized as follows (MacGregor, et al. 1970):

1. The ratio of unsupported length to section depth L_u/h , the end eccentricity ratio e/h , and the ratio and signs of end eccentricities e_1/e_2 —the effects of these variables are strongly interrelated.
2. The degree of rotational restraint—stiffer beams at the ends of columns provide greater column strength.
3. The degree of lateral restraint—a braced column is significantly stronger than a column unbraced against end displacements.
4. The amount of steel reinforcement and the strength of concrete—an increase in the p/f_{ck} ratio provides increased stability.
5. The duration of loading—creep of concrete during sustained loading increases the concrete deflections and decreases the strength of slender columns.

14.4.3 Design Approaches

In the absence of interaction diagrams for slender columns, the following four methods of design are often used:

1. Exact method based on non-linear second-order analysis
2. Moment magnifier method

3. Additional moment method
4. Reduction factor method

The first method is an ‘exact design method’ and the other three are approximate design methods. They are discussed briefly in this section.

Exact Method Based on Non-linear Second-order Analysis

The design of slender columns may be based on the moments and forces found from the second-order analysis of the structure taking into account material non-linearity, member curvature and lateral drift, duration of loading, shrinkage and creep, and interaction with the supporting foundation. Such a non-linear second-order analysis has shown to predict ultimate loads within 15 per cent of tests conducted on columns in statically indeterminate RC structures (ACI 318:2011). The sections may be proportioned to resist these actions without any modification, as the effect of column slenderness has been considered in the determination of member forces and moments. The main factors to be included in the second-order analysis are the $P-\Delta$ and $P-\delta$ moments due to the lateral deflections of the columns in the structure. These geometric non-linear effects are typically distinguished between $P-\delta$ effects, associated with deformations along the members, measured relative to the member chord, and $P-\Delta$ effects, measured between member ends and commonly associated with storey drifts in buildings. In buildings subjected to earthquakes, $P-\Delta$ effects are much more of a concern than $P-\delta$ effects, and provided that members conform to the slenderness limits for special systems in high seismic regions, $P-\delta$ effects do not generally need to be modelled in non-linear seismic analysis (Deierlein, et al. 2010).

Clause 39.1 of IS 456 and Clause 10.10.3 of ACI 318 recommend this type of second-order analysis. To allow for the variability in the actual cracked member properties, the ACI code suggests a stiffness reduction factor of 0.8 to be multiplied with the section properties used in the analysis (MacGregor and Hage 1977). Two-dimensional models of three-dimensional frames ignore the interactions among biaxial bending, biaxial shear, torsion, and axial effects in their structural components and connections. Most importantly, they are not capable of capturing the stability and second-order behaviour of the framed structures within the elastic range. Hence, it is better to conduct a three-dimensional second-order analysis of the frames to capture the actual behaviour. Due to the inherent variability in the response of structures to earthquake ground motions and the many simplifying assumptions made in analysis, the results of any linear or non-linear analysis, especially for earthquake performance, should be interpreted with care (Deierlein, et al. 2010). Clause 10.10.4 of ACI 318 also allows the use of elastic second-order analysis. In this analysis, consideration must be

made for the influence of axial loads, the presence of cracked regions along the length of the member, and the effects of load duration. The moment of inertia of columns and beams can be assumed as discussed in Section 4.5.1 and Table 4.10 of Chapter 4. Though these methods are very rational, they are not usually used in design offices because of their time-consuming complex analysis and lack of availability of non-expensive suitably written computer software.

Moment Magnifier Method

In this approximate *moment magnifier method*, suggested by ACI 318 in Clause 10.10.5, moments computed from the first-order analysis are multiplied by a moment magnifier to account for the second-order effects (a first-order frame analysis is an elastic analysis that does not include the internal force effects resulting from deflections). The moment magnifier is a function of the factored axial load, P_u , and the critical buckling load, P_{cr} , for the column. Using this method, non-sway and sway frames are treated separately. As already discussed in Section 13.4.1 of Chapter 13, sway and non-sway frames can be identified based on two criteria: increase in column end moments from second-order effects not exceeding five per cent of the first-order end moments or the stability index, Q , is less than 0.04.

Columns in non-sway or braced frames *Braced column* is not subjected to side sway, and hence, there is no significant relative lateral displacement between the top and bottom ends of the column. The pinned ended column of Fig. 14.19 may be taken as an example of braced column. Normally, the ends of a braced column will be partially restrained against rotation by the connecting beams. For each load combination, the factored moments at the top and bottom of the column are calculated using first-order frame analysis. For each column, the smaller and larger factored end moments are designated as M_1 and M_2 , respectively. The column may be bent in single or double curvature, as shown in Fig. 14.19. As shown in this figure, if M_1/M_2 is +1, the column is bent in single curvature and will result in increased moment near the centre of column (curve 2 of Fig. 14.19a). However, when M_1/M_2 is not equal to +1, the moment near the centre need not be greater than M_2 (as shown by curve 1 of Fig. 14.19a). Such an increase is less likely in columns bent in double curvature (Fig. 14.19b), especially when M_1/M_2 is less than about +0.5 and approaches the lower limit of -1.0.

The magnified moment, M_c (for each load combination), is calculated by multiplying the larger factored end moment, M_2 , by a magnification factor δ_{ns} for non-sway frame (Mirza, et al. 1987). The following is a summary of the code moment magnification equations for non-sway frame (MacGregor 1993).

$$M_c = \delta_{ns} M_2 \quad (14.41a)$$

where the *moment magnification factor*, δ_{ns} , is given by

$$\delta_{ns} = \frac{C_m}{1 - \frac{P_u}{0.75P_{cr}}} \geq 1.0 \quad (14.41b)$$

$$P_{cr} = \frac{\pi^2 EI}{(kL_u)^2} \quad (14.41c)$$

P_{cr} is the critical buckling load for the column and the subscript ns denotes non-sway frame. The term 0.75 in Eq. (14.41a) is a *stiffness reduction factor*, which is included to provide a conservative estimate of P_{cr} . When calculating P_{cr} , the effect of cracking, creep, and the non-linear behaviour of concrete on the stiffness, EI , can be accounted for using the following equations:

$$EI = \frac{(0.2E_c I_g + E_s I_{se})}{1 + \beta_{dns}} \quad (14.42a)$$

or

$$EI = \frac{0.4E_c I_g}{1 + \beta_{dns}} \quad (14.42b)$$

Alternatively, EI may be calculated using the value of EI from the more accurate Eq. (10.8) of the ACI code as follows (Khuntia and Ghosh 2004) and dividing the value by $(1 + \beta_{dns})$.

$$EI = \left(0.80 + 25 \frac{A_s}{A_g} \right) \left(1 - \frac{M_u}{P_u h} - 0.5 \frac{P_u}{P_o} \right) E_c I_g \leq 0.875 E_c I_g \quad (14.42c)$$

β_{dns} is a factor to account for the reduction in the column stiffness due to the effect of sustained axial load. The term β_{dns} is the ratio of the maximum factored axial sustained load to the maximum factored axial load associated with the same load combination, but shall not be taken greater than 1.0. ACI 318 allows β_{dns} to be taken as 0.6, in which case $EI = 0.25E_c I_g$. For heavily reinforced columns, Eq. (14.42a) underestimates the effect of the reinforcement; hence Eq. (14.42b) is more accurate for those columns.

The factor C_m used in Eq. (14.41b) is a correction factor relating the actual moment diagram to an equivalent uniform moment diagram and is adopted from AISC specification. Its value is given by

$$C_m = 0.6 + 0.4 \frac{M_1}{M_2} \geq 0.4 \quad (14.43)$$

The term M_1/M_2 in this equation is taken as positive if the column is bent in single curvature and negative if it is bent in double curvature. For columns with transverse loads between support, C_m must be taken as 1.0. Figure 14.23 shows some values of C_m for different end moment cases. The factored end moment, M_2 , must not be taken less than $M_{2,\min} = P_u(15 + 0.03h)$, about each axis separately, where h is the column

cross-sectional dimension in mm at the direction of analysis. The effective length $L_e = kL_u$ may be calculated using the procedures discussed in Section 13.4 of Chapter 13. Sarkar and Rangan (2003) and Tikka and Mirza (2004) found that the use of Eq. (14.43) may result in an unsafe estimation of equivalent eccentricity for the columns with low and medium slenderness and hence developed modified equations.

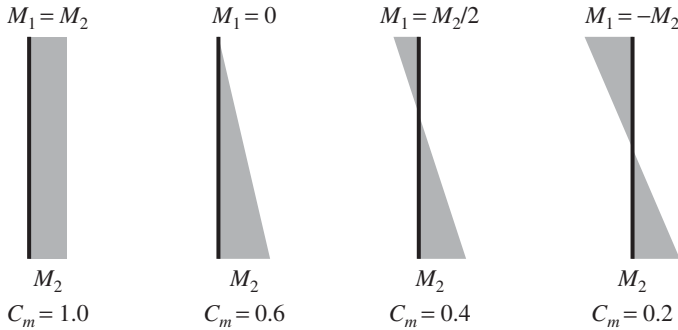


FIG. 14.23 Values of C_m for different end moment cases

Columns in sway or unbraced frames Unbraced frame is subjected to side sway, and hence, there will be significant displacement between the top and bottom ends of the column. Such a sway is possible in asymmetric frames or in frames subjected to lateral loads. A simple frame subjected to side sway is shown in Fig. 14.24(a). The additional moments at the ends of the column caused by the action of the vertical load acting on the deflected configuration of the unbraced column is called *lateral drift effect* (see Fig. 14.24b).

In unbraced frames, the action of primary moments M_1 and M_2 generally result in double curvature, as shown in Fig. 14.24(b). Moreover, the moments at the unbraced column ends will be the maximum; it is due to the primary moments being enhanced by the lateral drift effect (see Fig. 14.24c).

For each load combination, the factored non-sway moments, M_{ns} , and the factored sway moments, M_s , are calculated at the top and bottom of the column using first-order elastic frame analysis. The magnified sway moments are added to the unmagnified non-sway moments, M_{ns} , at each end of the column. The magnified moments at each end of the column (M_1 and M_2) are calculated as follows:

$$M_1 = M_{1ns} + \delta_s M_{1s} \quad (14.44a)$$

$$M_2 = M_{2ns} + \delta_s M_{2s} \quad (14.44b)$$

where δ_s is the moment magnification factor for frames not braced against side sway and accounts for the effects of lateral drift resulting from lateral and gravity loads. The ACI code gives two alternative methods to calculate δ_s . In the first method, it is taken as (MacGregor and Hage 1977; Lai and MacGregor 1983)

$$\delta_s = \frac{1}{1-Q} \geq 1.0 \quad (14.45a)$$

If δ_s calculated by this equation exceeds 1.5, the magnified moments must be calculated using the second-order elastic analysis or by using

$$\delta_s = \frac{1}{1 - \frac{\sum P_u}{0.75 \sum P_{cr}}} \quad (14.45b)$$

where $\sum P_u$ is the summation of all factored vertical loads in a storey and $\sum P_{cr}$ is the summation of the critical buckling loads for all sway-resisting columns in the storey and is calculated using Eq. (14.41c).

Design aids for the moment magnifier method are available in the ACI handbooks (SP 17:2009) and are also provided by Furlong (1971). More information on this method can be had from the work of Wight and MacGregor (2009). Recently, Wytroval and Tuchscherer (2013) observed that the moments estimated by the moment magnification procedure may be

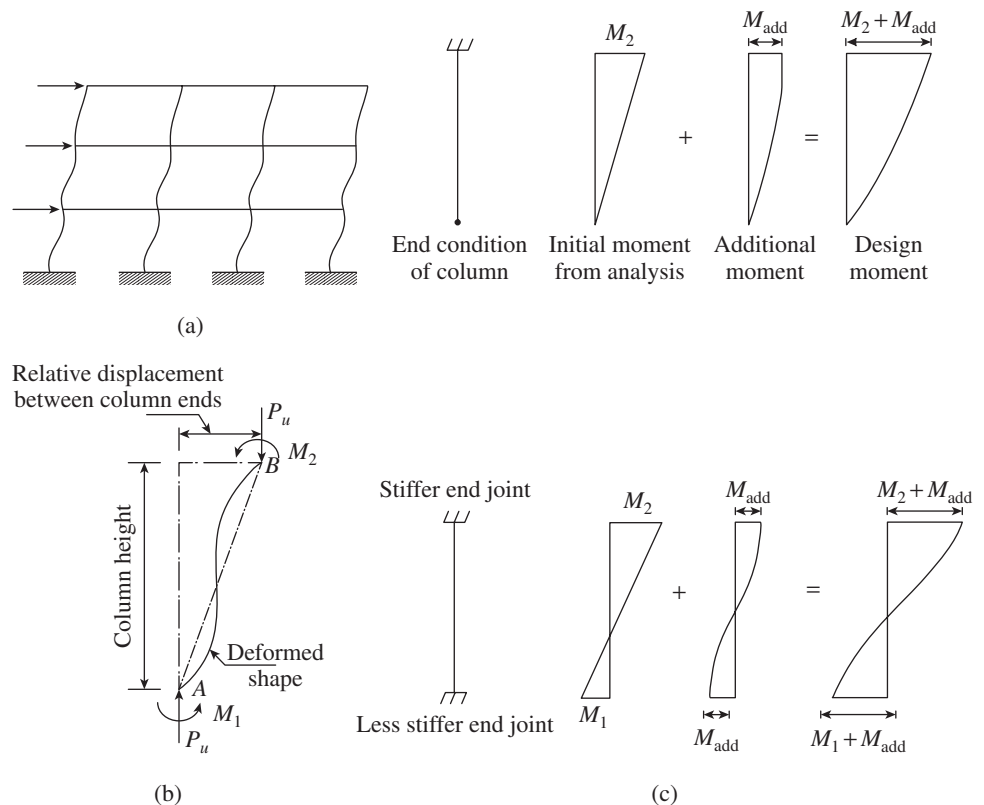


FIG. 14.24 Unbraced column-lateral drift effect (a) Sway frame (b) Deflected shape of column (c) Moments

five times larger than those estimated by using the second-order analysis. They suggest that the main source of these inconsistencies is the approximation of the column's flexural stiffness, EI , and suggest the removal of Eqs (14.42a) and (14.42b) from the ACI code.

Additional Moment Method

This *additional moment method* has been adopted in the code IS 456. The moment at the failure section of the column can also be taken as equal to the sum of the applied moment M and a complementary or additional moment M_a equal to load times the complementary eccentricity. This complementary moment represents the moment induced by the column deflections. The column is designed for the axial load P_u and the moment $(M_e + M_a)$. The value of M_a is based on the CEB-FIP recommendations of 1964. The additional moment is assumed to be a function of the slenderness ratio and the eccentricity ratio, eh . The accuracy of the additional moment method has been established through a series of comparisons of analytical and experimental results over the total range of slender columns (Cranston 1972). In this method, the deflection δ of the column is computed from the curvature diagram as shown in Fig. 14.25. The ultimate curvature at a cross section of the column is given by

$$\phi_{max} = \frac{1}{r_u} \cong \frac{\epsilon_c + \epsilon_s}{d} \tag{14.46}$$

where ϵ_c and ϵ_s are the strains in the extreme fibre of compression concrete and in the extreme tension steel, respectively, and d is the depth of the section between the extreme compression fibre of concrete and the extreme tension steel.

For an idealized case of linear moment–curvature relationship, the curvature diagram may have the shape shown in full line in Fig. 11.25(d). For design purposes, the curvature diagram

may be assumed to be somewhere between the triangular (unconservative) and rectangular (conservative) distribution, with maximum curvature denoted by $1/r_u$. By integrating the curvature diagram, we get the deflection for triangular distribution as $L^2/(12r_u)$ and for the rectangular distribution as $L^2/(8r_u)$. Let us consider it as $L^2/(10r_u)$ for design purposes (Cranston 1972). Hence, the additional moment M_a is given by

$$M_a = P_u \delta = \frac{P_u L^2}{10r_u} \tag{14.47}$$

For the balanced condition defined in Clause 39.7.1.1, the values of ϵ_c and ϵ_s are 0.0035 and 0.002, respectively. Hence, the ultimate curvature for the *balanced condition* from Eq. (14.46) is

$$\frac{1}{r_u} = \frac{0.0035 + 0.002}{d} = \frac{1}{182d} \tag{14.48}$$

Hence,
$$M_a = \frac{P_u d}{1820} \left(\frac{L}{d} \right)^2 \tag{14.49}$$

The expression given in Clause 39.7.1 of IS 456 is a modified version of this equation. In the code, the column length L is replaced by the effective length L_e to allow for the effects of various end conditions occurring in practical columns. The code expressions for M_a will yield conservative results in most cases even if the failure is not a balanced one (SP 24:1983).

As per Clause 39.7.1 of IS 456, the additional moments M_{ax} and M_{ay} should be calculated by the following formulae:

$$M_{ax} = \frac{P_u D}{2000} \left(\frac{L_e}{D} \right)^2 \tag{14.50a}$$

$$M_{ay} = \frac{P_u B}{2000} \left(\frac{L_e}{B} \right)^2 \tag{14.50b}$$

where P_u is the axial load in the member, L_{ex} is the effective length in respect of major axis, L_{ey} is the effective length in respect of minor axis, D is the depth of column at right angles to the major axis, and B is the width of column [Cranston (1972) derived an expression for additional moments as an average of four curvature distributions over the column height: rectangular, triangular, parabolic, and sinusoidal. The number 2000 in the denominator of Eq. (14.50) is the rounded off value of 1960 considered by Cranston, which itself is the average of the results from the four curvature distributions].

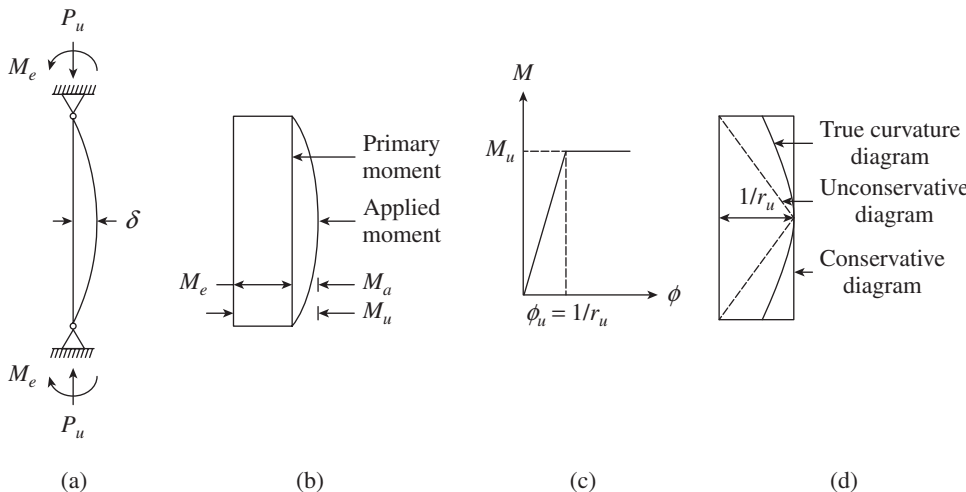


FIG. 14.25 Deflection of beam-column based on curvature (a) Deflected shape of slender column at ultimate load (b) Moment diagram (c) Idealized M – ϕ relationship (d) Curvature diagram

If the failure is not a *balanced* one (since column is a compression member, it generally fails in compression mode), the sum ($\varepsilon_c + \varepsilon_s$) will obviously be less than the assumed balanced values. Hence, a moment reduction factor, k , may be used, and this is specified in Clause 39.7.1.1 as (k is obtained from the P – M interaction curve, by approximating it to a straight line)

$$k = \frac{P_{nz} - P_u}{P_{nz} - P_b} \leq 1.0 \quad (14.51)$$

where P_u is the axial load on the compression member, P_{nz} is the axial load capacity of the section $= 0.45f_{ck}A_c + 0.75f_yA_s$, and P_b is the axial load corresponding to the condition of maximum compressive strain of 0.0035 in extreme compressive fibre of concrete and tension strain of 0.002 in the outermost layer of tension steel (it has to be noted that the use of the moment reduction factor, k , is optional but is strongly recommended in SP 16 for the sake of economy). The value of P_b will depend on the arrangement of reinforcement and cover ratio, d'/D , in addition to the grade of steel and concrete. The value of P_b may be evaluated for rectangular and circular sections as follows (Table 60 of SP 16):

For rectangular sections:

$$P_b = \left(k_1 + k_2 \frac{p}{f_{ck}} \right) f_{ck} BD \quad (14.52a)$$

For circular sections:

$$P_b = \left(k_1 + k_2 \frac{p}{f_{ck}} \right) f_{ck} D^2 \quad (14.52a)$$

where the values of k_1 and k_2 are as given in Tables 14.5 and 14.6, respectively.

TABLE 14.5 Values of k_1

Section	d'/D			
	0.05	0.10	0.15	0.20
Rectangular	0.219	0.207	0.196	0.184
Circular	0.172	0.160	0.149	0.138

TABLE 14.6 Values of k_2

Section	f_y (N/mm ²)	d'/D			
		0.05	0.10	0.15	0.20
Rectangular, equal reinforcement on two opposite sides	250	−0.045	−0.045	−0.045	−0.045
	415	0.096	0.082	0.046	−0.022
	500	0.213	0.173	0.104	−0.001
Rectangular, equal reinforcement on four sides	250	0.215	0.146	0.061	−0.011
	415	0.424	0.328	0.203	0.028
	500	0.545	0.425	0.256	0.040
Circular	250	0.193	0.148	0.077	−0.020
	415	0.410	0.323	0.201	0.036
	500	0.543	0.443	0.291	0.056

Notes under Clause 39.7.1 of IS 456 suggest the following:

1. A column may be considered braced in a given plane if the lateral stability of the structure as a whole is provided by walls or bracings designed to resist all lateral loads in that plane. It should otherwise be considered as unbraced.
2. In the case of braced columns without any transverse loads, the additional moment can be added to an initial moment equal to

$$M_u = 0.4M_{u1} + 0.6M_{u2} \geq 0.4M_{u2}$$

where M_{u2} is the larger column end moment and M_{u1} is the smaller end moment (assumed negative if the column is bent in double curvature).

3. Unbraced columns at any given storey of a frame are constrained to deflect equally. In such cases, the slenderness ratio of each column may be taken as the average of all columns acting in the same direction.

Reduction Factor Method

The *reduction factor method* is the earliest and a highly simplified procedure, which was used in an earlier version of ACI 318 (1963) and is still used in IS 456 for the working stress method of design. According to Clause B-3.3 of IS 456, the permissible stresses in concrete and steel are reduced using a strength reduction factor C_r given by

$$C_r = 1.25 - \frac{L_e}{48B} \quad (14.52a)$$

where B is the least lateral dimension of the column (or diameter of the core in a spiral column) and L_e is the effective length of column. Alternatively, the code also gives another equation for 'more exact' calculations as

$$C_r = 1.25 - \frac{L_e}{160r_{\min}} \quad (14.52b)$$

where r_{\min} is the least radius of gyration.

The reduction factor method implies that the same eccentricity is maintained in both the slender and analogous short columns. This is contrary to the actual behaviour of slender columns, where the reduction in load carrying capacity is caused by the increased eccentricity due to secondary deflection moments. This is a severe shortcoming in the case of unbraced frames, since the magnitude of the secondary moments is extremely important. Moreover, owing to practical considerations, many important variables are neglected to keep the formula simple. Hence, reduction factors are considered as extreme lower bounds and are unduly conservative for many practical cases (Purushothaman 1984).

14.4.4 Slender Columns Bent about Both Axes

When slender columns are subjected to significant bending about both the axes, additional moments have to be calculated

for both directions of bending. These additional moments are combined with the initial moments found from the first-order analysis to obtain the design moments in the principal directions. However, the minimum eccentricity is to be assumed to act only about one axis at a time, as per Clause 25.4 of IS 456. With these moments, the columns may be designed for biaxial bending using the design charts given in SP 16.

A review of the currently available methods of design of short and slender columns under biaxial bending was provided by Suryanarayana (1991) who, by using 10 design examples, concluded that the Indian code method is simple and reliable. Design aids for slender column are also available in Goris (2012).

14.4.5 Design Procedure

The following are the various steps involved in the design of slender columns:

1. Normally, initial sizes are assumed based on experience; such initial sizes are also required for frame analysis software. Determine the effective length and slenderness ratio in the principal $X-X$ and $Y-Y$ axes of the column. If the slenderness factor is greater than 12 or more, about any of the axes, the column has to be designed as a slender column about that axis. If it is slender about both axes, the additional moments about both the axes should be considered. The following steps are done in the $X-X$ axis.
2. Determine the end moments M_{u1} and M_{u2} by first-order analysis.
3. Determine the moments caused by accidental eccentricity, M_{\min} .
4. Choose M_{ux1} as the larger of M_{u1} and M_{\min} and M_{ux2} as the larger of M_{u2} and M_{\min} .
5. Now calculate the additional moment, $M_{\text{add}} = k_x M_{ax}$, using Eqs (14.50) and (14.51). P_{nz} and P_b can be determined using an assumed area of longitudinal reinforcement of about 2.5–3 per cent. Chart 63 of SP 16 may be used to find P_{nz} , Table 60 of SP 16 may be used to calculate P_{bx} , and using the value of P_{bx}/P_{nz} , the value of k_x can be determined using Chart 65 of SP 16.
6. Calculate

$$\begin{aligned} M'_{ux} &= 0.6 \times \text{larger of } M_{ux1} \text{ and } M_{ux2} \\ &\quad + 0.4 \times \text{smaller of } M_{ux1} \text{ and } M_{ux2} \\ &> 0.4 \times \text{larger of } M_{ux1} \text{ and } M_{ux2} \end{aligned}$$

7. Determine the value of design moments M_{dx} by adding the additional moment M_{add} with M'_{ux} . Alternatively, the design moments may be found by second-order analysis programs.
8. Calculate $P_u/f_{ck}BD$, and using the appropriate interaction diagram of SP 16, determine M_{nx} for the assumed area of steel.
9. If the column is slender in the $Y-Y$ axis, repeat steps 2 to 8 for the $Y-Y$ axis as well.

10. Check the following:

$$\left(\frac{M_{ux}}{M_{nx}} \right)^\alpha + \left(\frac{M_{uy}}{M_{ny}} \right)^\alpha \leq 1$$

11. Change reinforcement or size and repeat the calculation given in step 10, if the left-hand side of the equation results in values higher than 1.0 or much lower than 1.0.

14.5 EARTHQUAKE CONSIDERATIONS

For columns situated in earthquake zones, the axial loads and bending moment(s) acting on them can be found by a suitable first-order or second-order analysis; the design is similar to that in non-seismic zones. Though a minimum size of 300 mm by 300 mm is suggested in Clause 7.1.2 of IS 13920 for columns supporting beams having a span of 5 m or more, it is often not followed. For bond limitations of beam bars passing through interior beam-column joints to be satisfied, the depth of the column needs to be up to 30 times the diameter of beam bars (Paulay and Priestley 1992). In general, designers use column section having a width of 230 mm and a depth ranging from 230 mm to 450 mm, so that the columns merge with the brick walls, which have a thickness of 230 mm. Such a practice results in the designed section occupying a place towards the apex of the $P-M$ diagram. IS 456 does not have provisions that stress the importance of designing such columns as *under-reinforced* (*tension controlled* and ductile), even though the consequences of designing over-reinforced column sections (*compression controlled* and brittle) are more serious than in beams. Moreover, smaller column sizes relative to that of beams will result in a *strong beam-weak column* system, leading to catastrophic storey (or side sway) collapse mechanisms (Murty 2001). To meet the strong column-weak beam requirement, the sum of the nominal flexural strengths, M_n , of the columns framing into a joint must be at least 1.1 to 1.2 times the sum of the nominal flexural strengths of the beams framing into the joint (see Section 13.10). It is required to include the developed slab reinforcement within the effective flange width as beam flexural tension reinforcement when computing beam strength. This check must be verified independently for sway in both directions and in each of the two principal framing directions (Moehle, et al. 2008). Small column sizes will also result in constructability problems (see Fig. 4.12 of Chapter 4). With reference to the familiar $P-M$ diagrams (see Figs 14.9 and 14.10 of Chapter 14), the designed column should be made to lie at or below the balanced point (below the diagonal $0.87f_y$ line), so that the failure of the column is by yielding of steel and not by crushing of concrete (Murty 2001; Moehle, et al. 2008).

The minimum number of bars in seismic columns should be eight in square and rectangular columns and six in the case of circular columns. Longitudinal bars should not be farther

apart than 200 mm centre to centre (c/c) or one-third of the cross-sectional dimension in the direction considered in the case of rectangular columns, or one-third the diameter in the case of circular columns (Paulay and Priestley 1992). Bundled bars grouped in the four corners of a column are undesirable in seismic zones (Paulay and Priestley 1992).

The shear strength of members with axial loads is discussed in Section 6.13 of Chapter 6. It is important to provide ties at closer spacing near probable plastic hinge locations (see Fig. 13.31 of Chapter 13), with 135° hooks (see Section 13.10.4 of Chapter 13 for more details), and the amount of confining reinforcement must be as per Eq. (13.38) of Chapter 13. Youakim and Ghali (2003) studied the behaviour of concrete columns with double-headed studs under earthquake loading and have highlighted their advantages over conventional cross-ties. As per IS 13920:1993, splicing of column bars should be provided only in the middle half of a column and not near its top or bottom ends, where plastic hinges are likely to form (see Fig. 13.31 of Chapter 13). Moreover, only up to 50 per cent of the vertical bars in the column are to be lapped at a section in any storey. Furthermore, when laps are provided, ties must be provided along the length of the lap at a spacing not more than 150 mm (see Section 13.10 of Chapter 13). *Mechanical couplers* should be used where the reinforcement ratio is greater than three per cent. *Welded splices* should never be located in potential plastic hinge regions. It is also necessary to anchor the column rods in the foundations and provide special confining reinforcements in footings as shown in Fig. 13.32 of Chapter 13. Special confining reinforcement throughout the column is also necessary in several occasions as discussed in Section 13.9.4 (see Figs 13.33 and 13.34) of Chapter 13.

During earthquakes, corner and edge columns may be subjected to combined biaxial bending and tension. Hsu (1986) proposed two design formulae for RC members under combined biaxial bending and axial tension for square and rectangular sections. These two non-dimensional design formulae were considered as an improvement over the load contour methods. SP 16 also contains charts (Charts 66 to 85) for the design of rectangular columns (with reinforcement on two sides and on four sides) subjected to bending and tension. It has to be noted that these charts are meant only for strength calculations; they do not take into account crack control, which may be important for tension members (see Chapter 18 on tension members). L-, T-, or +-shaped columns should not be used in earthquake zones as they may crack at the re-entrant corners and fail subsequently without reaching their ultimate capacities. Similarly, slender columns should not be used in seismic-dominated ductile frames. More information on column design in seismic zones may be found in Paulay and Priestley (1992).

Seismic behaviour of RC circular and square columns under combined loadings including torsion was studied by

Li and Belarbi (2009) and Prakash, et al. (2012). Seismic performance assessment of inadequately detailed RC columns was studied by Boys, et al. (2008). Seismic tests on full-scale concrete columns were reported by Sezen and Moehle (2006) and Bae and Bayrak (2008). Han and Jee (2005) investigated the seismic behaviours of columns in ordinary moment-resisting concrete frames (OMRCF) and intermediate moment-resisting concrete frames (IMRCF). Based on the test results, they concluded that the OMRCF and IMRCF column specimens had drift capacities greater than 3.0 per cent and 4.5 per cent, respectively; ductility capacity of these specimens exceeded 3.01 and 4.53, respectively. Dasgupta and Murty (2005a, 2005b) suggested modifications to the flexural limit state design as per IS 456 and proposed a limiting strain value for steel of $0.002 + (f_y/1.15E_s)$ in the extreme layer of steel on the tension side; based on this modification, they have drawn P - M interaction curves for columns and shear walls without boundary elements. Based on their tests on a one-third scale, three-bay, and three-storey RC planar frame, Ghannoum and Moehle (2012) developed an analytical model for the dynamic collapse analysis of such frames and implemented on open-source OpenSees software (McKenna, et al. 2000). Tan and Tang (2004) have provided an interaction formula for reinforced columns in fire conditions.

EXAMPLES

EXAMPLE 14.1 (Calculation of P and M for tension failure of steel):

A short column of size 250 mm \times 300 mm is reinforced with four 20 mm bars and two 16 mm bars as shown in Fig. 14.26. Calculate P and M for tension failure of steel by bending on the major axis. Assume M25 concrete and Fe 415 steel and clear cover of 40 mm.

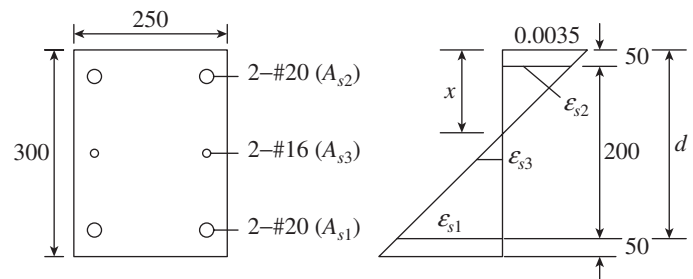


FIG. 14.26 Column and strain diagram of Example 14.1

SOLUTION:

Step 1 Calculate the strains.

Cover to centre of steel reinforcement = $40 + 20/2 = 50$ mm

Let us denote tension and compression steel as A_{s1} and A_{s2} , respectively, and the steel at mid-depth as A_{s3} .

Maximum strain in concrete at outermost compression fibre = 0.0035 (Clause 38.1 of IS 456)

$$\text{Strain in tension steel } \epsilon_{s1} = \frac{f_y}{1.15E_s} + 0.002 = \frac{415}{1.15 \times 2 \times 10^5} + 0.002 = 0.0038$$

From similar triangles of strain diagram

$$\frac{x}{d} = \frac{0.0035}{(0.0035 + 0.0038)}$$

Hence $x = 250 \times 0.0035/0.0073 = 119.86 \text{ mm}$

Stress in steel $= 0.87 \times f_y = 0.87 \times 415 = 361 \text{ N/mm}^2$

$$\text{Strain, } \epsilon_{s3} = \frac{0.0035}{119.86} \times 30 = 8.76 \times 10^{-4} \text{ (less than yield)}$$

Stress for $\epsilon_{s3} = f_{s3} = 8.76 \times 10^{-4} \times E_s = 175.2 \text{ N/mm}^2$

$$\epsilon_{s2} = \frac{0.0035}{119.86} \times (119.86 - 50) = 2.04 \times 10^{-3} \text{ (less than yield)}$$

From Fig. 3 or Table A of SP 16

Stress in compression steel for $\epsilon_{s2} = 2.04 \times 10^{-3}$, $f_{s2} = 330 \text{ N/mm}^2$

Note: This value of stress may also be obtained using Eq. (14.4).

Step 2 Calculate P under this condition. As strain in steel is greater than 0.002, stress in concrete at the level of compression steel is $f_{ck} = 0.446 \times 25 = 11.15 \text{ N/mm}^2$.

$$\begin{aligned} \text{Hence, } P &= 0.36f_{ck}bx + \sum(f_{si} - f_{cci})A_{sci} - \sum A_{sti}f_{sti} \\ &= [0.36 \times 25 \times 250 \times 119.86 + (330 - 11.25) \\ &\quad \times 628 - 361 \times 628 - 175.2 \times 402] \times 10^{-3} \\ &= 269.69 + 200.18 - 226.71 - 70.43 = 172.73 \text{ kN} \end{aligned}$$

Step 3 Calculate moment under this condition. Taking moment of all forces about the centre of gravity of column section, we get

$$\begin{aligned} M &= [269.69(150 - 0.416x) + 200.18 \times 100 \\ &\quad + 226.71 \times 100] \times 10^{-3} \\ &= [269.69(150 - 0.416 \times 119.86)] \times 10^{-3} + 20.02 + 22.67 \\ &= 69.70 \text{ kNm} \end{aligned}$$

EXAMPLE 14.2:

Draw the $P_u - M_{ux}$ interaction curve for a column section shown in Fig. 14.27. Use M25 concrete, Fe 415 steel, and clear cover of 40 mm.

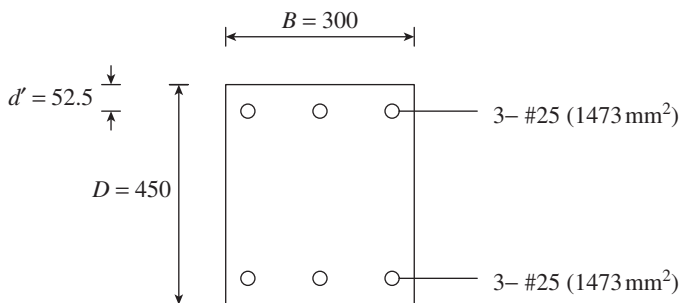


FIG. 14.27 Column of Example 14.2

SOLUTION:

The $P_u - M_{ux}$ interaction curve is obtained by considering several positions of neutral axis parallel to the x -axis.

Neutral axis at very large distance, so that $e_y = 0$ When $e_y = 0$, the capacity of the column

$$P_u = 0.447f_{ck}BD + (0.75f_y - 0.447f_{ck})A_s$$

$$A_s = 6 \times 491 = 2946 \text{ mm}^2$$

$$\begin{aligned} P_u &= [0.447 \times 25 \times 300 \times 450 + (0.75 \times 415 - 0.447 \times 25) \\ &\quad \times 2946] \times 10^{-3} \\ &= 1508.63 + 884.02 = 2392.65 \text{ kN} \end{aligned}$$

$$M_u = P_u e_y = 0 \text{ (as } e_y = 0)$$

Neutral axis at minimum eccentricity $e_y = 0.05D$ Now P_u and M_u are determined as (Clause 39.3 of IS 456)

$$\begin{aligned} P_u &= 0.4f_{ck}BD + (0.67f_y - 0.4f_{ck})A_s \\ &= [0.4 \times 25 \times 300 \times 450 + (0.67 \times 415 - 0.4 \times 25) \\ &\quad \times 2946] \times 10^{-3} \\ &= 1350 + 789.67 = 2139.67 \text{ kN} \end{aligned}$$

$$M_u = P_u e_y = 2139.6 \times 0.05 \times 450 \times 10^{-3} = 48.14 \text{ kNm}$$

Neutral axis lies outside section Let the depth of neutral axis $kD = 1.1D$ (with $k = 1.1$) $= 1.1 \times 450 = 495 \text{ mm}$

$$P_u = k_1 f_{ck}BD + \sum A_{si}(f_{sci} - f_{cci})$$

where

$$\begin{aligned} k_1 &= 0.447 \left[1 - \frac{4}{21} \left(\frac{4}{7k - 3} \right)^2 \right] \\ &= 0.447 \left[1 - \frac{4}{21} \left(\frac{4}{7 \times 1.1 - 3} \right)^2 \right] = 0.384 \end{aligned}$$

Strain at the highly compressed extreme fibre (Clause 39.1b of IS 456)

$$\begin{aligned} \epsilon_{cu} &= 0.002 \left[1 + \frac{3D/7}{x_u - 3D/7} \right] = 0.002 \left[1 + \frac{3 \times 450/7}{1.1 \times 450 - 3 \times 450/7} \right] \\ &= 3.276 \times 10^{-3} \end{aligned}$$

Strain at the top steel level

$$\epsilon_{s1} = \frac{3.276 \times 10^{-3}}{495} \times (495 - 52.5) = 2.928 \times 10^{-3}$$

Hence, stress in top steel (Fig. 3 of SP 16)

$$f_{s1} = 355.14 \text{ MPa}$$

Stress in concrete $f_{cc1} = 0.447f_{ck} = 0.447 \times 25 = 11.18 \text{ MPa}$

Strain at the bottom steel level

$$\varepsilon_{s2} = \frac{3.276 \times 10^{-3}}{495} (45 + 52.5)$$

$$= 0.645 \times 10^{-3} \text{ Stress in bottom steel}$$

$$f_{s2} = 0.645 \times 10^{-3} \times 2 \times 10^5 = 129 \text{ MPa}$$

Stress in concrete at this level

$$f_{cc2} = 447 \varepsilon_{s2} (1 - 250 \varepsilon_{s2}) f_{ck}$$

$$= 447 \times 0.645 \times 10^{-3} (1 - 250 \times 0.645 \times 10^{-3}) \times 25 = 6.04 \text{ MPa}$$

From Table 14.2, $k_1 = 0.384$ and $k_2 = 0.443$

Hence,

$$P_u = [0.384 \times 25 \times 300 \times 450 + (355.14 - 11.18) \times 1473$$

$$+ (129 - 6.04) \times 1473] \times 10^{-3}$$

$$= 1296 + 477.19 + 181.12 = 1954.31 \text{ kN}$$

$$M_u = [1296 \times (0.5 - 0.443) \times 450 + 477.19(0.5 \times 450 - 52.5)$$

$$+ 181.12(0.5 \times 450 - 52.5)] \times 10^{-3}$$

$$= 33.24 + 82.32 + 31.24 = 146.8 \text{ kNm}$$

Neutral axis within section resulting in balanced section

For this case (see Fig. 14.28), the axial load and moment capacity are given by

$$P_u = 0.36 f_{ck} B x_u + (f_{sci} - f_{cci}) A_{si}$$

$$- 0.87 f_y A_{s2}$$

$$M_{ux} = 0.36 f_{ck} B x_u (0.5D - 0.416 x_u)$$

$$+ (f_{sci} - f_{cci}) A_{s1} (0.5D - d')$$

$$+ 0.87 f_y A_{s2} (0.5D - d')$$

From Fig. 14.28, we get

$$x_u = \frac{0.0035}{0.0055 + 0.87 f_y / E_s} (D - d')$$

$$= \frac{0.0035}{0.0055 + 0.87 \times 415 / (2 \times 10^5)}$$

$$(450 - 52.5) = 190.45 \text{ mm}$$

Strain in compression steel =

$$\varepsilon_{sc} = \frac{0.0035}{190.45} \times (190.45 - 52.5) =$$

$$2.535 \times 10^{-3}$$

Stress in compression steel, f_{sci} (from Fig. 3 of SP 16) = 346.9 N/mm²

$$P_u = (0.36 \times 25 \times 300 \times 190.45 + (346.9 - 11.18$$

$$\times 1473 - 0.87 \times 415 \times 1473) \times 10^{-3}$$

$$= 514.22 + 494.52 - 531.82 = 476.92 \text{ kN}$$

$$M_{ux} = [514.22 \times (0.5 \times 450 - 0.416 \times 190.45)$$

$$+ 494.52(0.5 \times 450 - 52.5)$$

$$+ 531.82(0.5 \times 450 - 52.5)] \times 10^{-3}$$

$$= 74.96 + 85.30 + 91.74 = 252 \text{ kNm}$$

Neutral axis within section with strain in steel = 0.005

From Fig. 14.29, we get

$$\frac{x_u}{0.0035} = \frac{397.5 - x_u}{0.005} \text{ or } 1.391 - 0.0035 x_u = 0.005 x_u$$

Thus $x_u = 163.68 \text{ mm}$

$$\text{Strain in compression steel} = \varepsilon_{sc} = \frac{0.0035}{163.68} \times (163.68 -$$

$$52.5) = 2.377 \times 10^{-3}$$

Stress in compression steel (from Fig. 3 of SP 16) = 342.7 N/mm²

Stress in concrete at this level = $0.447 \times 25 = 11.18 \text{ N/mm}^2$

$$P_u = [0.36 \times 25 \times 300 \times 163.68 + (342.7 - 11.18)$$

$$\times 1473 - 0.87 \times 415 \times 1473] \times 10^{-3}$$

$$= 441.94 + 488.33 - 531.82 = 398.45 \text{ kN}$$

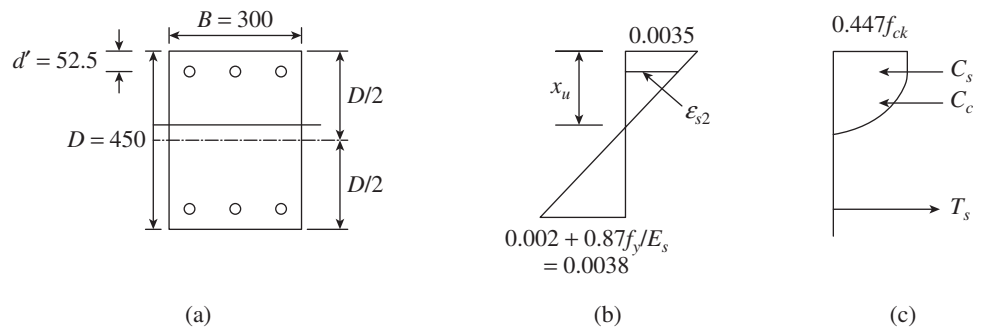


FIG. 14.28 Neutral axis within the section (a) Section (b) Strain diagram (c) Stress diagram

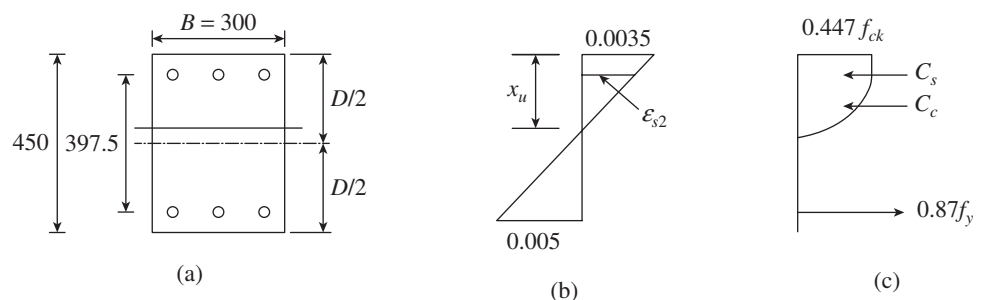


FIG. 14.29 Neutral axis within section with strain in steel = 0.005 (a) Section (b) Strain diagram (c) Stress diagram

$$\begin{aligned}
 M_{ux} &= [441.94 \times (0.5 \times 450 - 0.416 \times 163.68) \\
 &\quad + 488.33(0.5 \times 450 - 52.5) \\
 &\quad + 531.82(0.5 \times 450 - 52.5)] \times 10^{-3} \\
 &= 69.34 + 84.24 + 91.74 = 245.32 \text{ kNm}
 \end{aligned}$$

Neutral axis within section resulting in pure flexure In this case, the tension steel would have definitely yielded.

$$\begin{aligned}
 \text{Tension capacity} &= 0.87 \times 415 \times 1473 \times 10^{-3} = 531.82 \text{ kN} \\
 \text{Compression capacity up to compression steel} \\
 &= 0.36 \times 25 \times 300 \times 52.5 = 141.75 \text{ kN}
 \end{aligned}$$

Hence, the neutral axis lies below the compression steel. Denoting the distance of neutral axis from extreme compression fibre as x_u

$$\begin{aligned}
 C_c &= 0.36 \times 25 \times 300 \times x_u \times 10^{-3} = 2.7x_u \\
 T &= 531.82 \text{ kN} \\
 C_s &= \left[\frac{(x_u - 52.5)}{x_u} \times 1473 \times (0.0035 \times 2 \times 10^5) \right] \times 10^{-3} \\
 &= 1031.1 \left(\frac{x_u - 52.5}{x_u} \right)
 \end{aligned}$$

Using force equilibrium,

$$1031.1 \left(\frac{x_u - 52.5}{x_u} \right) + 2.7x_u = 531.82$$

$$\begin{aligned}
 1031.1x_u - 54132.75 + 2.7x_u^2 - 531.82x_u &= 0 \\
 \text{or } x_u^2 + 184.92x_u - 20049.2 &= 0
 \end{aligned}$$

$$x_u = \frac{-184.92 \pm \sqrt{34195.4 + 4 \times 20049.2}}{2} = 76.65 \text{ mm}$$

$$\text{Hence, } C_c = 0.36 \times 25 \times 300 \times 76.65 \times 10^{-3} = 206.96 \text{ kN}$$

acting at $(397.5 - 0.416 \times 76.65) = 365.6 \text{ mm}$ from tension steel.

$$\begin{aligned}
 C_s &= \left[\frac{(76.65 - 52.5)}{76.65} \times (0.0035 \times 2 \times 10^5) \times 1473 \right] \times 10^{-3} \\
 &= 324.87 \text{ kN}
 \end{aligned}$$

acting at 345 mm from tension steel.

$$M_u = [206.96 \times 365.6 + 324.87 \times 345] \times 10^{-3} = 187.74 \text{ kNm}$$

Capacity in axial tension

$$P_u = 6 \times 491 \times 0.87 \times 415 \times 10^{-3} = 1063.65 \text{ kN}$$

The P_u - M_{ux} interaction curve obtained by plotting P_u and M_{ux} values for different neutral axis position considered in this example is shown in Fig. 14.30.

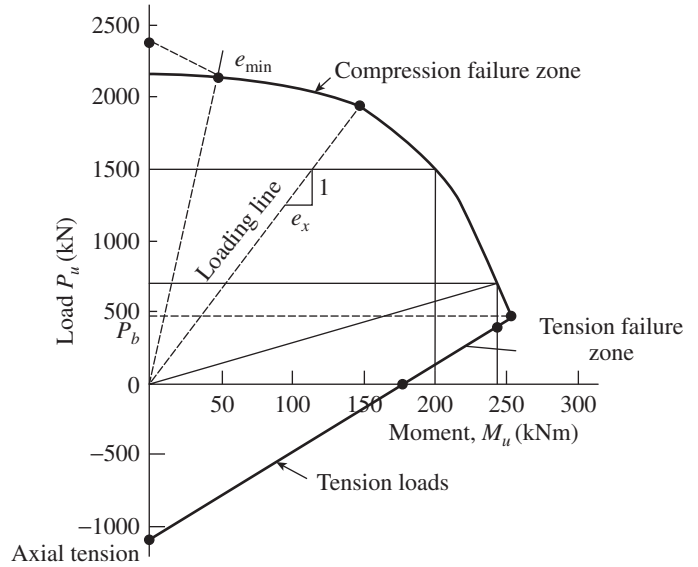


FIG. 14.30 Interaction curve for column of Example 14.2

EXAMPLE 14.3 (Determination of maximum eccentricity): Using the interaction curve obtained in Example 14.2, determine (a) the maximum eccentricity e_x with which a factored load $P_u = 1500 \text{ kN}$ can be safely applied and (b) the design strength corresponding to an eccentricity of $e_x = 0.8D$.

SOLUTION:

(a) From Fig. 14.30, the flexural strength corresponding to $P_u = 1500 \text{ kN}$ is obtained as $M_u = 200 \text{ kNm}$.

$$\begin{aligned}
 \text{The corresponding eccentricity } e &= \frac{M_u}{P_u} = \frac{200 \times 10^3}{1500} \\
 &= 133.33 \text{ mm}
 \end{aligned}$$

(b) $e_x = 0.8D = 0.8 \times 450 = 360 \text{ mm}$

Draw a radial line with $e_x = 0.36$ and locate its intersection with the interaction curve. Consider a point with coordinates $P_u = 500 \text{ kN}$ and $M_u = 500 \times 0.36 = 180 \text{ kNm}$. Now, draw a line from the origin to this point and extend it so that it intersects the interaction curve. From this line, we get $P_u = 700 \text{ kN}$ and $M_u = 245 \text{ kNm}$ (see Fig. 14.30).

EXAMPLE 14.4 (Design of a short column using interaction curves):

Design a short rectangular column subjected to a factored load of 1400 kN and a factored moment of 90 kNm . Adopt M25 concrete and Fe 415 grade steel and assume mild environment.

SOLUTION:

Step 1 Determine the size of column.

$$\text{From Eq. (13.36) of Chapter 13 } A_c = \frac{P_u}{0.4(f_{ck} + 1.67f_y\rho_g)}$$

$$\text{Assuming } \rho_g = \frac{A_{sc}}{A_g} = 2\%$$

$$A_c = \frac{1400 \times 10^3}{0.4(25 + 1.67 \times 415 \times 2/100)} = 90,065 \text{ mm}^2$$

Since a moment is also acting on the column along with the axial force, adopt a slightly bigger size. Assuming 300 mm as the breadth, depth $> 90,065/300 = 300$.

Adopt 300 mm \times 400 mm size.

As per Clause 26.4.2.1 of IS 456, adopt clear cover = 40 mm.

Assuming ties of 8 mm and main bar of 25 mm, $d' = 40 + 8 + 25/2 = 60.5$ mm

$$d'/D = 60.5/400 = 0.15$$

Step 2 Calculate p_u and m_u .

$$p_u = \frac{P_u}{f_{ck}BD} = \frac{1400 \times 10^3}{25 \times 300 \times 400} = 0.467$$

$$m_u = \frac{M_u}{f_{ck}BD^2} = \frac{90 \times 10^6}{25 \times 300 \times 400^2} = 0.075$$

Step 3 Use design aids to calculate the area of steel.

Let us use charts for $d'/D = 0.15$.

From Chart 33 of SP 16, we get $p/f_{ck} = 0.07$ (for this $f_{st} = 0$, that is, compression controlled)

Percentage of reinforcement $p = 0.07 \times 25 = 1.75\%$

$$A_s = \frac{pBD}{100} = 1.75 \times 300 \times \frac{400}{100} = 2100 \text{ mm}^2$$

Provide six 22 mm bars (area = 2280 mm²). As per Clause 26.5.3.1(g) of IS 456,

spacing of steel = $400 - 2 \times 60.5 = 279 \text{ mm} < 300 \text{ mm}$, Hence, spacing is sufficient.

Step 4 Design lateral ties.

Diameter of ties $> 1/4d_b$, and $6 \text{ mm} = 22/4 = 5.5 \text{ mm}$ and 6 mm

Tie spacing $< 16d_b$, 300 mm, and $B = 16 \times 22 = 352 \text{ mm}$, 300 mm, and 300 mm

Provide 6 mm diameter ties at 300 mm c/c as shown in Fig. 14.31.

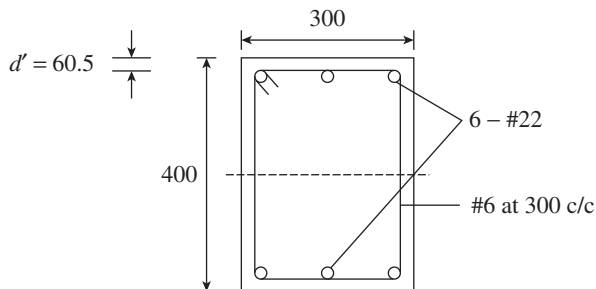


FIG. 14.31 Designed column of Example 14.4

EXAMPLE 14.5 (Design of a rectangular column with reinforcement on four sides):

Design the column given in Example 14.4 for the same data but when reinforcement is provided on four sides of the column.

SOLUTION:

From Example 14.4, $p_u = 0.467$, $m_u = 0.075$, and $d'/D = 0.15$

Taking d'/D as 0.15 and using Chart 45 of SP 16, we get $p/f_{ck} = 0.075$

Percentage of reinforcement $p = 0.075 \times 25 = 1.875\%$

$$A_s = \frac{pBD}{100} = 1.875 \times 300 \times \frac{400}{100} = 2250 \text{ mm}^2$$

Provide six 22 mm bars (area = 2280 mm²).

Note: In this case, because of the discrete diameter of available bars, we get the same reinforcement. However, if we look at the required reinforcement, we find that the required reinforcement is about 7.15 per cent higher if we adopt this arrangement of reinforcement on all four sides of the column.

EXAMPLE 14.6 (Design of a short column with minor axis bending moment):

Design the column given in Example 14.4 for the same data, except that a moment of 90 kNm is applied about the minor axis.

SOLUTION:

From Example 14.4, $p_u = 0.467$ and $d'/B = 60.5/300 = 0.20$.

$$m_u = \frac{M_u}{f_{ck}DB^2} = \frac{90 \times 10^6}{25 \times 400 \times 300^2} = 0.10$$

From Chart 34 of SP16, we get $p/f_{ck} = 0.105$

Percentage of reinforcement $p = 0.105 \times 25 = 2.625\%$

$$A_s = pBD = 2.625 \times 300 \times \frac{400}{100} = 3150 \text{ mm}^2$$

Provide four 25 mm bars and four 20 mm bars (area = 3219 mm²), as shown in Fig. 14.32.

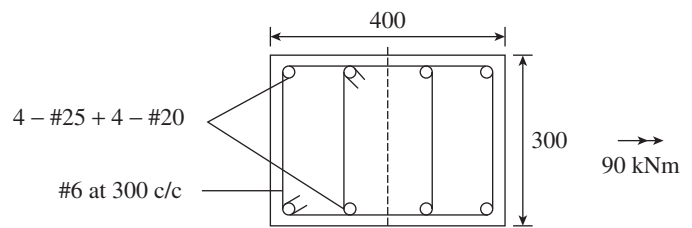


FIG. 14.32 Designed column of Example 14.6

Note: When the same moment is applied about the minor axis, we need to provide more reinforcement.

EXAMPLE 14.7 (Design of a short circular column):

Design a short circular column subjected to a factored load of 1400 kN and a factored moment of 90 kNm. Adopt M25 concrete and Fe 415 grade steel and assume mild environment. Design (a) with helical reinforcement and (b) with hoop reinforcement.

SOLUTION:

(a) With helical reinforcement

Step 1 Determine the size of the column. This example is similar to Example 14.4, except that this is a circular column. From Example 14.4,

Required area of column, assuming helical reinforcement = $90,065/1.05 = 85,776 \text{ mm}^2$

Note: As per Clause 39.4. of IS 456, the strength of a column with helical reinforcement is 1.05 times greater than a member with lateral ties.

Hence, required diameter of column = $\sqrt{85776 \times \frac{4}{\pi}} = 330.5 \text{ mm}$

Let us provide a 390 mm column.

Step 2 Calculate p_u and m_u .

$$p_u = \frac{P_u}{f_{ck} D^2} = \frac{1400 \times 10^3}{(25 \times 390^2) \times 1.05} = \frac{0.368}{1.05} = 0.35$$

$$m_u = \frac{M_u}{f_{ck} D^3} = \frac{90 \times 10^6}{(25 \times 390^3) \times 1.05} = \frac{0.061}{1.05} = 0.058$$

Assuming a cover of 40 mm, 25 mm main rods, and 8 mm spiral

$$d' = 40 + 8 + 12.5 = 60.5 \text{ mm}; d'/D = 60.5/350 = 0.173$$

Step 3 Determine the area of steel.

Assume $d'/D = 0.20$ and $f_y = 415 \text{ N/mm}^2$.

From Chart 58 of SP 16, $p/f_{ck} = 0.10$; hence $p = 0.10 \times 25 = 2.5\%$

$$A_{st} = p\pi D^2/400 = 2.5 \times \pi \times 390^2/400 = 2986 \text{ mm}^2$$

Provide six 25 mm bars (area = $2945 \text{ mm}^2 \approx 2986 \text{ mm}^2$).

Note: Even though both the rectangular and circular columns have the same concrete area, the reinforcement required for the circular column is 42 per cent more than that for the rectangular column. This is due to the fact that the lever arm available for all the steel bars in a rectangular column is larger than that available in the circular column.

Step 4 Calculate the helical reinforcement. As per Clause 39.4.1 of IS 456

$$\frac{\text{Volume of helical reinforcement}}{\text{Volume of core}} > 0.36 \left(\frac{A_g}{A_c} - 1 \right) \left(\frac{f_{ck}}{f_y} \right)$$

Assuming 6 mm bars for the helix,

$$\text{Core diameter } d = 390 - 2(40) = 310 \text{ mm}$$

$$0.36 \left(\frac{A_g}{A_c} - 1 \right) \left(\frac{f_{ck}}{f_y} \right) = 0.36 \left(\frac{390^2}{310^2} - 1 \right) \frac{25}{415} = 0.0126$$

For 6 mm spiral, $A_{sh} = \pi \times \frac{6^2}{4} = 28.27 \text{ mm}^2$

$$V_{us} = A_{sh} \pi \left(\frac{d'_c}{s_h} \right) = 28.27 \times \pi \times (310 - 6) = 27,003/s_h$$

$$V_c = \frac{\pi}{4} d_c^2 = \frac{\pi}{4} \times 310^2 = 75,476.8$$

Thus, $\frac{27,003}{75,476.8 s_h} > 0.0126$ or $s_h \leq 28 \text{ mm}$

Provide 6 mm diameter spiral at 25 mm pitch as shown in Fig. 14.33.

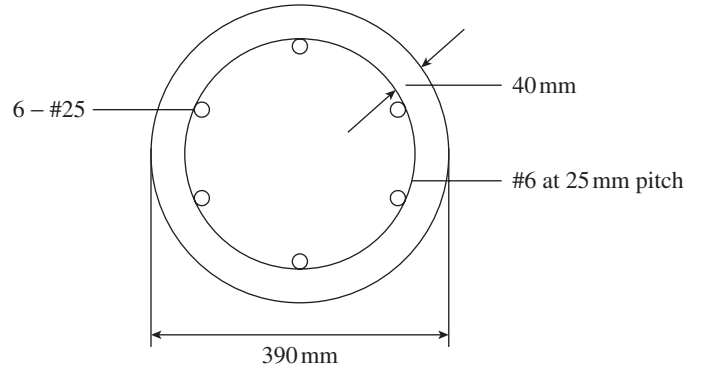


FIG. 14.33 Designed circular column of Example 14.7

(b) With hoop reinforcement

From Step 2, $p_u = 0.368$ and $m_u = 0.061$.

From Chart 58 of SP16, $p/f_{ck} = 0.115$.

Hence $p = 0.115 \times 25 = 2.875\%$

$$A_{st} = 2.875 \times \pi \times 390^2/400 = 3434 \text{ mm}^2$$

Provide six 28 mm bars with area = 3694.

Provide 8 mm hoops at 300 mm c/c (as per Clause 26.5.3.2 of IS 456).

EXAMPLE 14.8 (Design of a column with large bending moment):

Design a short rectangular column in moderate environment subjected to an axial load of 1400 kN and bending moment of 380 kNm. Adopt M25 concrete and Fe 415 grade steel.

SOLUTION:

Step 1 Determine the size of column. Such columns with dominant bending moment may be found in the upper storeys of multi-storey buildings. Assuming three per cent reinforcement, from Eq. (13.36) of Chapter 13,

$$A_c = \frac{1400 \times 10^3}{0.4(25 + 1.67 \times 415 \times 3/100)} = 76,433 \text{ mm}^2$$

Since the bending moment is larger, this area will not be sufficient. Let us assume a size of 300 mm × 550 mm.

Step 2 Calculate p_u and m_u

$$p_u = \frac{P_u}{f_{ck} BD} = \frac{1400 \times 10^3}{25 \times 300 \times 550} = 0.34$$

$$m_u = \frac{M_u}{f_{ck} BD^2} = \frac{380 \times 10^6}{25 \times 300 \times 550^2} = 0.167$$

With $d' = 40 + 8 + 12.5 = 60.5 \text{ mm}$, $d'/D = 60.5/550 = 0.11$.

Step 3 Calculate the reinforcement. From Chart 32 of SP16, with $f_y = 415 \text{ N/mm}^2$ and $d'/D = 0.10$,

$$p/f_{ck} = 0.11, p = 0.11 \times 25 = 2.75\%$$

$$A_{st} = 2.75 \times 300 \times 550/100 = 4537 \text{ mm}^2$$

Provide six 32 mm bars and two 20 mm bars with area = 4825 + 628 = 5453 mm².

Step 4 Design the ties. Diameter of ties > 6 mm and $d_b/4 = 32/4 = 8$ mm. With 8 mm ties, the spacing should not be less than 300 mm or $16 \times 25 = 400$ mm. Hence, provide 8 mm ties at 300 mm c/c as shown in Fig. 14.34.

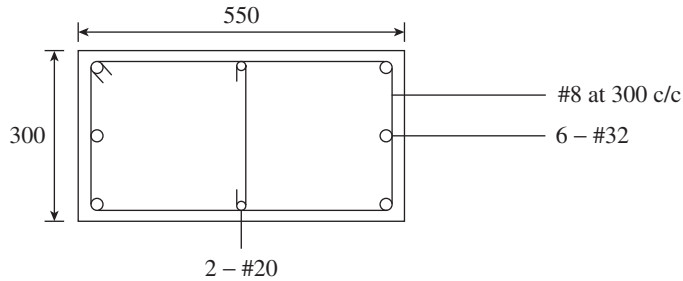


FIG. 14.34 Designed column of Example 14.8

Note: Some designers prefer to provide the main bars in two faces in two rows. However, for better constructability, it is better to provide the rebars in a single row at each face of the column.

EXAMPLE 14.9 (Design a rectangular column with biaxial bending):

Design the reinforcement of a short column of size 300 mm × 500 mm and unsupported length of 3 m subjected to a factored axial load P_u of 1400 kN and factored moment M_{ux} about major axis of 130 kNm and M_{uy} about minor axis of 60 kNm. Adopt M30 concrete and Fe 500 grade steel and assume moderate environment.

SOLUTION:

Step 1 Check for bending moment due to minimum eccentricity.

As per Clause 25.4 of IS code

$$e_{y,\min} = \frac{L_u}{500} + \frac{D}{30} = \frac{3000}{500} + \frac{500}{30} = 22.67 \text{ mm} > 20 \text{ mm}$$

$$e_{x,\min} = \frac{3000}{500} + \frac{300}{30} = 16 \text{ mm} < 20 \text{ mm}$$

Moment due to eccentricity

$$M_{uxe} = 1400 \times 22.67/1000 = 31.74 \text{ kNm} < M_{ux}$$

Hence, moments due to minimum eccentricity do not govern.

Step 2 Determine the uniaxial capacity about the X–X axis. At first trial, let us assume reinforcement percentage at 1.5 per cent.

$$p/f_{ck} = 1.5/30 = 0.05$$

Assuming 45 mm cover (severe environment as per Table 16 of IS 456), 8 mm ties, and 25 mm main bars, $d' = 45 + 8 + 12.5 = 65.5$; $d'/D = 65.5/500 = 0.13$. Let us use Chart 45 of SP 16 with $d'/D = 0.15$.

$$\frac{P_u}{f_{ck}BD} = \frac{1400 \times 10^3}{30 \times 300 \times 500} = 0.31$$

From Chart 45, $\frac{M_n}{f_{ck}BD^2} = 0.085$

$$M_{nx} = 0.085 \times 30 \times 300 \times 500^2/10^6 = 191.25 \text{ kNm}$$

Step 3 Determine the uniaxial capacity about the Y–Y axis.

$$d'/D = 65.5/300 = 0.218$$

Let us use Chart 46 of SP16 with $d'/D = 0.2$.

From Chart 46, $\frac{M_n}{f_{ck}BD^2} = 0.08$.

$$M_{ny} = 0.08 \times 30 \times 500 \times 300^2/10^6 = 108 \text{ kNm}$$

Step 4 Calculate P_{nz} . From Chart 63 of SP 16 corresponding to $p = 1.5$, $f_y = 415$ MPa, and $f_{ck} = 30$ MPa,

$$P_{nz}/A_g = 18 \text{ N/mm}^2; P_{nz} = 18 \times A_g = 18 \times 300 \times 500/10^3 = 2700 \text{ kN}$$

Step 5 Check the capacity of the assumed section.

$$\frac{P_u}{P_{nz}} = \frac{1400}{2700} = 0.519; \frac{M_{ux}}{M_{nx}} = \frac{130}{191.25} = 0.68; \frac{M_{uy}}{M_{ny}} = \frac{60}{108} = 0.556$$

$$\alpha = \frac{2}{3} + \frac{5}{3} \left(\frac{P_u}{P_{nz}} \right) = \frac{2}{3} + \frac{5}{3} \times 0.519 = 1.532$$

$$\text{Hence } \left(\frac{M_{ux}}{M_{nx}} \right)^\alpha + \left(\frac{M_{uy}}{M_{ny}} \right)^\alpha = 0.68^{1.532} + 0.556^{1.532} = 0.554 + 0.407 = 0.961 < 1.0$$

Therefore, the assumed section and reinforcement are safe.

$$\text{Provide } A_s = 1.5 \times 500 \times 300/100 = 2250 \text{ mm}^2$$

Provide eight 20 mm bars (area = 2513 mm²) as shown in Fig. 14.35.

Step 6 Design the transverse reinforcement. As per Clause 26.5.3.2(c) of IS 456

$$\text{Diameter} > (1/4)d_b \text{ or } 6 \text{ mm} = 1/4 \times 20 = 5 \text{ mm or } 6 \text{ mm}$$

$$\text{Pitch} < B, 16 \times d_b, \text{ or } 300 \text{ mm} = 300, 16 \times 20, \text{ or } 300 \text{ mm}$$

Provide 6 mm diameter ties at 300 mm c/c as shown in Fig. 14.35.

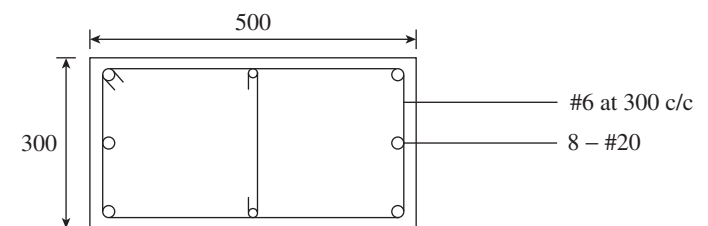


FIG. 14.35 Designed column of Example 14.9

EXAMPLE 14.10 (Design of a circular column with biaxial loading):

Design a biaxially loaded braced circular column for the following data: Factored axial load, $P_u = 1875$ kN, ultimate biaxial moments, $M_{ux} = 190$ kNm and $M_{uy} = 100$ kNm,

unsupported length, $L_u = 3.25$ m, and diameter of column = 500 mm. Use M25 concrete and Fe 415 grade steel and assume moderate environment.

SOLUTION:

Step 1 Determine the equivalent uniaxial moment. Biaxially loaded circular columns can be designed for a uniaxial bending with

$$M_u = (M_{ux}^2 + M_{uy}^2)^{0.5}$$

Thus $M_u = (190^2 + 100^2)^{0.5} = 214.71$ kNm

Step 2 Check for moment due to minimum eccentricity.

$$e_{mix} = \frac{L_u}{500} + \frac{D}{30} = \frac{3250}{500} + \frac{500}{30} = 23.17$$
 mm

$$M_{ue} = 1800 \times \frac{23.17}{1000} = 41.7$$
 kNm $< M_u$

Hence, moment due to minimum eccentricity does not govern. As we may adopt lateral ties or spirals, we can choose either of them.

(a) Column with lateral ties

Step 3 Determine the steel reinforcement using the chart from SP 16. With 40 mm cover (as per Clause 26.4.2.1 of IS 456), 25 mm main bars, and 8 mm ties,

$$d' = 40 + 8 + 25/2 = 60.5$$
 mm; $d'/D = 60.5/500 = 0.121$

$$\frac{P_u}{f_{ck} D^2} = \frac{1875 \times 1000}{25 \times 500^2} = 0.30$$

$$\frac{M_u}{f_{ck} D^3} = \frac{214.71 \times 10^6}{25 \times 500^3} = 0.0687$$

Using Chart 57 of SP 16 with $d'/D = 0.15$, we get $p/f_{ck} = 0.10$. $p = 0.10 \times 25 = 2.5\% < 4\%$. Hence, it is within limits. $A_s = 2.5 \times \pi \times 500^2 / (4 \times 100) = 4908.7$ mm². Provide ten 25 mm bars ($A_{st} = 4908$ mm²).

Step 4 Design the transverse reinforcement.

Diameter $> (1/4 d_b)$ and 6 mm $= 1/4 \times 25 = 6.25$ mm and 6 mm Pitch $< D$, $16 \times d_b$, and 300 mm $= 500$, 16×25 , and 300 Provide 8 mm lateral ties at a spacing of 300 mm c/c as shown in Fig. 14.36.

(b) Column with spirals

As per Clause 39.4 of IS 456, the strength of a column with spirals can be taken to be 1.05 times the strength of a column with lateral ties. Hence

$$\frac{P_u}{f_{ck} D^2} = \frac{1875 \times 1000}{1.05 \times 25 \times 500^2} = 0.286$$

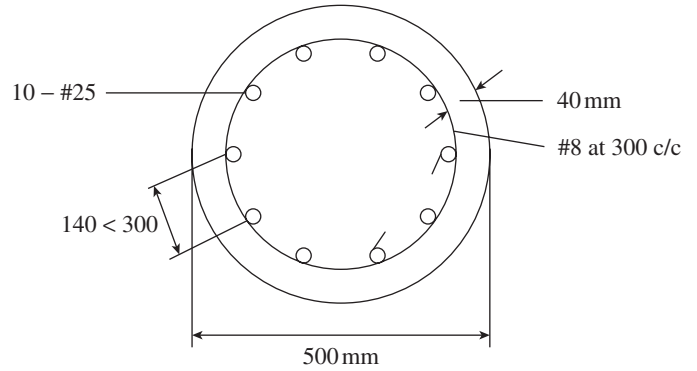


FIG. 14.36 Designed column of Example 14.10

$$\frac{M_u}{f_{ck} D^3} = \frac{214.71 \times 10^6}{1.05 \times 25 \times 500^3} = 0.065$$

$d'/D = 0.121$ as in (a)

Using Chart 57 of SP 16, $p/f_{ck} = 0.085$.

$$p = 0.085 \times 25 = 2.125\%$$

$$A_s = 2.125 \times \pi \times 500^2 / (4 \times 100) = 4172.4$$
 mm²

Provide seven 28 mm bars ($A_s = 4310$ mm²).

Transverse reinforcement The calculations are similar to that provided in Example 14.7, as per Clause 26.5.3.2(d) of IS 456; provide 8 mm diameter spirals at 50 mm pitch.

EXAMPLE 14.11 (Design of an L column subjected to biaxial bending):

Design a biaxially loaded L column for the following data: $B = 250$ mm, $D = 1000$ mm, factored axial load, $P_u = 4000$ kN, and factored moments $M_{ux} = 750$ kNm and $M_{uy} = 750$ kNm. Assume M25 concrete, Fe 415 steel, and moderate environment.

SOLUTION:

This design is made as suggested by Varyani (1999). Let us consider the column as two rectangles of 250 mm \times 1000 mm and apply $P_u = 4000$ kN and $M_u = 750$ kNm.

Step 1 Calculate the area of steel for one axis. Assuming a cover of 40 mm, 28 mm bars, and 8 mm ties,

Effective cover, $d' = 40 + 8 + 28/2 = 62$ mm; $d'/D = 62/1000 = 0.062$

$$\frac{P_u}{f_{ck} BD} = \frac{4000 \times 1000}{25 \times 250 \times 1000} = 0.64$$

$$\frac{M_u}{f_{ck} BD^2} = \frac{750 \times 10^6}{25 \times 250 \times 1000^2} = 0.12$$

From Chart 32 of SP 16, with $d'/D = 0.10$

$$p/f_{ck} = 0.15; p = 0.14 \times 25 = 3.5\%$$

$$A_{s1} = \frac{3.5}{100} \times 250 \times 1000 = 8750$$
 mm²

Step 2 Calculate the area of steel for the other axis. Now applying $P_u = 0$ and $M_y = 750$ kNm

$$\frac{M_u}{f_{ck}BD^2} = 0.12$$

From Chart 32 of SP 16, $p/f_{ck} = 0.08$, $p = 0.08 \times 25 = 2\%$

$$A_{s2} = \frac{2}{100} \times 250 \times 1000 = 5000 \text{ mm}^2$$

Total area of steel = $8750 + 5000 = 13,750 \text{ mm}^2$

Provide twenty four 28 mm bars with area = $14,784 \text{ mm}^2$ as shown in Fig. 14.37.

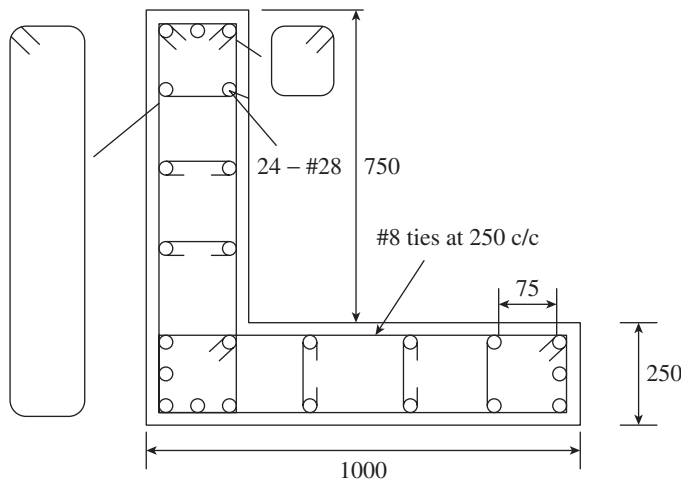


FIG. 14.37 Designed L-column of Example 14.11

Note: Sinha (1996b) designed the same column using the interaction diagrams developed by him and obtained $A_{st} = 14,875 \text{ mm}^2$ as against $13,750 \text{ mm}^2$ (8.18% more steel). This is due to the fact that $250 \text{ mm} \times 250 \text{ mm}$ (14.2%) concrete area is taken in our calculation in both directions. The error may be significant if the overlapping area is large.

EXAMPLE 14.12 (Design of a slender column):

Design a biaxially loaded braced rectangular column deforming in single curvature for the following data: Factored axial load $P_u = 1750$ kN, factored bending moments M_{ux1} and M_{uy1} at bottom are 200 kNm and 100 kNm, respectively, factored bending moments M_{ux2} and M_{uy2} at top are 100 kNm and 60 kNm, respectively, unsupported length L_u is 8.5 m, and effective lengths L_{ex} and L_{ey} are 7.5 m and 6 m, respectively. Consider the size of column as 400 mm by 500 mm. Assume M25 concrete, Fe 415 steel, and moderate environment.

SOLUTION:

Step 1 Check for moment due to minimum eccentricity.

$$e_{y,\min} = L_u/500 + D/30 = 8500/500 + 550/30 = 35.35 \text{ mm} > 20 \text{ mm}$$

$$e_{x,\min} = L_u/500 + B/30 = 8500/500 + 400/30 = 30.33 \text{ mm} > 20 \text{ mm}$$

Hence $M_{uxe} = P_u \times e_{y,\min} = 1750 \times 35.33/1000 = 61.83 \text{ kNm} < M_{ux1}$ and M_{ux2}

$M_{uye} = P_u \times e_{x,\min} = 1750 \times 30.33/1000 = 53.08 \text{ kNm} < M_{uy1}$ and M_{uy2}

Hence, moments due to minimum eccentricity do not govern the design.

Step 2 Check for slenderness (Clauses 25.1.2 and 25.3 of IS 456).

$$\frac{L_{ex}}{D} = \frac{7500}{550} = 13.64 > 12; \quad \frac{L_{ey}}{B} = \frac{6000}{400} = 15 > 12$$

In addition, $60B = 60 \times 400/1000 = 24 \text{ m} > L_u = 8.5 \text{ m}$ and $100B^2/D = (100 \times 400^2)/(1000 \times 550) = 29.1 \text{ m} > L_u = 8.5 \text{ m}$

Hence, the column is slender in both directions and the assumed column dimensions satisfy the slenderness limits.

Step 3 Determine the additional moments due to slenderness.

$$M'_{ax} = kM_{ax} \text{ and } M'_{ay} = k_yM_{ay}$$

As per Clause 39.7.1 of IS 456

$$M_{ax} = \frac{P_u D}{2000} \left(\frac{L_{ex}}{D} \right)^2 = \frac{1750 \times 550}{2000 \times 10^3} \left(\frac{7500}{550} \right)^2 = 89.49 \text{ kNm}$$

$$M_{ay} = \frac{P_u B}{2000} \left(\frac{L_{ey}}{B} \right)^2 = \frac{1750 \times 400}{2000 \times 10^3} \left(\frac{6000}{400} \right)^2 = 78.75 \text{ kNm}$$

From Clause 39.7.1.1 of IS 456

$$k_x = \frac{P_{nz} - P_u}{P_{nz} - P_{bx}} \text{ and } k_y = \frac{P_{nz} - P_u}{P_{nz} - P_{by}}$$

Let us assume 2.5 per cent of steel reinforcement and 40 mm clear cover.

$$A_{sc} = \frac{2.5}{100} \times 400 \times 550 = 5500 \text{ mm}^2;$$

$$A_c = 400 \times 550 - 5500 = 214,500 \text{ mm}^2$$

From Clause 39.6 of IS 456

$$\begin{aligned} P_{nz} &= 0.45f_{ck}A_c + 0.75f_yA_{sc} \\ &= (0.45 \times 25 \times 214500 + 0.75 \times 415 \times 5500) \times 10^{-3} \\ &= 4125 \text{ kN} \end{aligned}$$

From Table 60 of SP 16 (Tables 14.5 and 14.6)

$$P_b = (k_1 + k_2 p/f_{ck}) f_{ck} BD$$

Assume 8 mm ties, 28 mm main bars, and equal reinforcement on four sides.

For $d'/D = (40 + 8 + 14)/550 = 0.113$; hence $k_1 = 0.204$ and $k_2 = 0.296$;

$$\begin{aligned} P_{bx} &= \left(0.204 + 0.296 \times \frac{2.5}{25} \right) \times 25 \times 550 \times 400 \times 10^{-3} \\ &= 1284.80 \text{ kN} \end{aligned}$$

For $d'/B = 62/400 = 0.155$; hence $k_1 = 0.1948$ and $k_2 = 0.1855$

$$P_{by} = \left(0.1948 + 0.1855 \times \frac{2.5}{25}\right) \times 25 \times 550 \times 400 \times 10^{-3}$$

$$= 1173.43 \text{ kN}$$

Hence, $k_x = \frac{4125 - 1750}{4125 - 1284.8} = 0.836$ and $k_y = \frac{4125 - 1750}{4125 - 1173.43} = 0.805$

Thus $M'_{ax} = 0.836 \times 89.49 = 74.81 \text{ kNm}$ and $M'_{ay} = 0.805 \times 78.75 = 63.37 \text{ kNm}$

Step 4 Calculate the design moments.

$$M_{dx} = M_{ux} + M'_{ax} \text{ and } M_{dy} = M_{uy} + M'_{ay}$$

From Note 2 of Clause 39.7.1 of IS 456, for braced frame,

$$M_{ux} = 0.6 \times \text{larger of } M_{ux1} \text{ and } M_{ux2}$$

$$+ 0.4 \times \text{smaller of } M_{ux1} \text{ and } M_{ux2}$$

$$= 0.6 \times 200 + 0.4 \times 100 = 160 \text{ kNm} > 0.4 \times 200$$

$$M_{uy} = 0.6 \times \text{larger of } M_{uy1} \text{ and } M_{uy2} + 0.4$$

$$\times \text{smaller of } M_{uy1} \text{ and } M_{uy2}$$

$$= 0.6 \times 100 + 0.4 \times 60 = 84 \text{ kNm} > 0.4 \times 100$$

$M_{dx} = 160 + 74.81 = 234.81 \text{ kNm}$ and $M_{dy} = 84 + 63.37 = 147.37 \text{ kNm}$

Step 5 Determine M_{nx} and M_{ny} .

$$\frac{P_u}{f_{ck}BD} = \frac{1750 \times 1000}{25 \times 400 \times 550} = 0.318$$

$d'/D = 62/550 = 0.062$, $d'/B = 62/400 = 0.155$, and $pf_{ck} = 2.5/25 = 0.1$

From Chart 45 of SP 16, with $d'/D = 0.15$,

$$\frac{M_{nx}}{f_{ck}BD^2} = 0.125 \text{ and } \frac{M_{ny}}{f_{ck}DB^2} = 0.125$$

$$M_{nx} = 0.125 f_{ck}BD^2 = (0.125 \times 25 \times 400 \times 550^2) \times 10^{-6}$$

$$= 378.13 \text{ kNm}$$

$$M_{ny} = 0.125 f_{ck}DB^2 = (0.125 \times 25 \times 550 \times 400^2) \times 10^{-6}$$

$$= 275 \text{ kNm}$$

Step 6 Check with interaction equation.

$$\alpha = \frac{2}{3} + \frac{5}{3} \left(\frac{P_u}{P_{nz}} \right) = \frac{2}{3} + \frac{5}{3} \times \frac{1750}{4125} = 1.374$$

$$\text{Hence } \left(\frac{M_{ux}}{M_{nx}} \right)^\alpha + \left(\frac{M_{uy}}{M_{ny}} \right)^\alpha = \left(\frac{234.81}{378.13} \right)^{1.374} + \left(\frac{147.37}{275} \right)^{1.374} =$$

$$0.520 + 0.424 = 0.944 < 1.0$$

Hence, the assumed percentage of steel is safe. $A_s = 5500 \text{ mm}^2$; provide twelve 25 mm bars.

Step 7 Design the transverse reinforcement.

Diameter $> (1/4)d_b$ and $6 \text{ mm} = 1/4 \times 25 = 6.25 \text{ mm}$ and 6 mm

Pitch $< B$, $16d_b$, and $300 \text{ mm} = 400$, 16×25 , and 300 mm

Provide 8 mm diameter ties at 300 mm c/c as shown in Fig. 14.38.

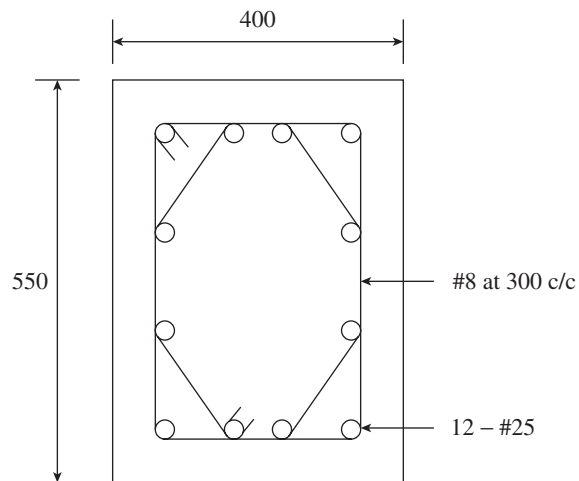


FIG. 14.38 Designed column of Example 14.12

SUMMARY

In practice, all columns are subjected to axial force and bending moments. Even the codes specify that the columns are to be designed for axial load applied at minimum eccentricity. Such columns with uniaxial or biaxial moments can be analysed and designed using strain compatibility and equilibrium equations. As shown in Section 14.2.2, such a method involves lengthy calculations and trial and error. Hence, the use of interaction diagrams has been suggested in the code. The plastic centroid may be used in the case of sections with asymmetric reinforcement. Circular columns can also be analysed or designed using strain compatibility and equilibrium equations, but the complications can be reduced by the use of a rectangular stress block.

The development of interaction curves is explained. Such curves are presented in SP 16, for (a) rectangular columns with reinforcement on two sides, (b) rectangular columns with reinforcement on four sides, and (c) circular columns. Such interaction curves for other shapes of columns are also available. The design procedure for columns subjected to uniaxial and biaxial bending based on interaction diagrams has been explained. Splicing of reinforcement and transverse reinforcement requirements of such columns are also discussed.

Columns with biaxial bending moments may be designed by approximate methods, developed in the past. These methods are categorized into (a) methods of superposition, (b) methods

of equivalent uniaxial eccentricity, and (c) methods based on approximations for the shape of interaction surface, which include Bresler's reciprocal load method and Bresler's load contour method. The load contour method is adopted in IS 456; the various steps involved in the design procedure are explained. Various design aids have also been developed to simplify the calculations. The design of T-, L-, and +-shaped columns is briefly outlined.

The use of HSC has resulted in slender columns in which the material strength may not be attained due to the possibility of buckling. The limits prescribed in the Indian and US codes for the column to be considered as slender are discussed. The behaviour of slender columns has been described by considering the interaction diagram. Slender columns should be designed for additional moments, which result due to $P-\Delta$ effects. It is shown that there is more likelihood of the maximum bending moment being increased by the additional

moment in the single curvature bending of slender column than in the double curvature bending. The major variables affecting the slender column are summarized. The four methods that are employed for the design of slender columns include (a) exact method based on second-order analysis (which is the best rational method and recommended by the codes, but is time-consuming and complex), (b) moment magnifier method (adopted in the ACI 318 code), (c) additional moment method (adopted in the IS 456 code), and (d) reduction factor method (adopted in IS 456 for working stress design, which does not consider the actual behaviour of slender columns and is rather extremely simplified). The details of these methods are discussed and the design procedure for slender columns based on additional moment method is described. Earthquake considerations of columns with axial force and moments are also discussed. Ample examples are included to explain the concepts presented.

REVIEW QUESTIONS

1. What are the assumptions made in the limit state design of columns?
2. What is the magnitude of the maximum failure strain ϵ_c considered in the design of columns? How does it differ from beam design?
3. What are the parameters that affect the ultimate load carrying capacity of a uniaxially eccentrically loaded column?
4. What is plastic centroid? When is it necessary to locate plastic centroid instead of centroid?
5. How is the design of circular columns considered in the method suggested by Whitney?
6. Sketch a typical axial load–moment interaction curve for a column and explain its salient points.
7. A column is subjected to axial force and uniaxial moment and the calculated design point (p_u, m_u) lies (a) marginally outside and (b) inside the envelope of the design interaction curve. Comment on the safety of the column in these two situations. What is the action to be taken in situation (a)?
8. Which column can be considered as a tension-controlled column?
9. What are the sections for which interaction diagrams are available in SP 16?
10. When should we consider the interaction diagram for (a) rectangular columns with reinforcement on two sides and (b) rectangular columns with reinforcement on four sides?
11. What is the significance of the diagonal dotted lines of the interaction diagrams?
12. List the various steps involved in the design of columns subjected to axial force and uniaxial bending moment.
13. What is the location and length of splicing of bars in columns in seismic zones?
14. What are the approximate methods used for columns subjected to biaxial bending?
15. What is the advantage of using the UK code method for the design of biaxially loaded columns?
16. Explain Bresler's load contour method, adopted in IS 456, for the design of biaxially loaded columns.
17. Describe the procedure for designing columns with biaxial moments, as per IS 456.
18. What is a slender column?
19. As per IS 456, under which of the following conditions is a compression member considered slender?
 - (a) $L_{ex}/D > 12$
 - (b) $L_{ey}/B > 12$
 - (c) Both L_{ex}/D and $L_{ey}/B > 12$
 - (d) Either L_{ex}/D or $L_{ey}/B > 12$
20. When both ends of a column are restrained by beams, the unsupported length should not exceed _____.
 - (a) $60B$
 - (b) $100B^2D$
 - (c) $60D$
 - (d) $100BD^2$
21. When one end of a column is restrained by beams, the unsupported length should not exceed _____.
 - (a) $60B$
 - (b) $100B^2D$
 - (c) $60D$
 - (d) $100BD^2$
22. What are the major variables that affect the strength and behaviour of slender columns?
23. What are the four methods that are used to design slender columns?
24. Write short notes on the following:
 - (a) Non-linear second-order analysis
 - (b) Moment magnifier method
 - (c) Additional moment method
 - (d) Reduction factor method
25. How do braced and unbraced columns differ in their behaviour?
26. Differentiate the behaviour of a slender column from that of a short column.
27. List the various steps involved in the design of slender columns.
28. List the various precautions to be undertaken in the case of columns subjected to earthquake loads.

EXERCISES

1. A short column of size $300\text{ mm} \times 400\text{ mm}$ is reinforced with six 20 mm bars as shown in Fig. 14.39. Calculate P and M for tension failure of steel by bending on major axis. Assume M25 concrete, Fe 415 steel, and clear cover of 40 mm.

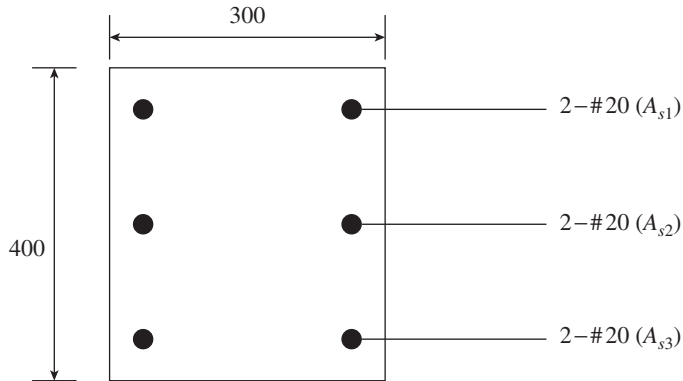


FIG. 14.39

2. A column of size 400 mm \times 400 mm is reinforced with three 25 mm HYSD bars of grade Fe 415 in the compression and tension sides, with an effective cover of 52.5 mm, as shown in Fig. 14.40. Develop the P - M interaction curve for M25 concrete.

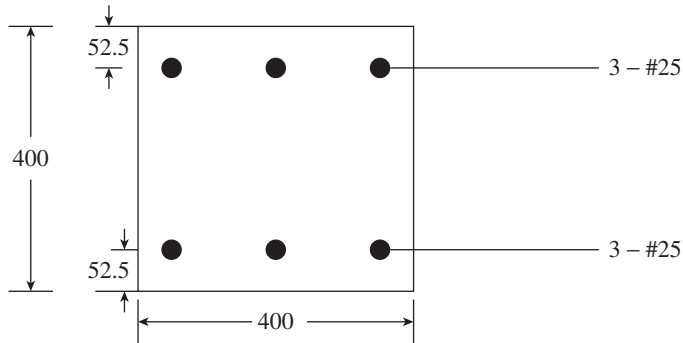


FIG. 14.40

3. Using the interaction curve obtained in Exercise 2, determine (a) the maximum eccentricity e_x with which a factored load $P_u = 1750$ kN can be safely applied and (b) the design strength corresponding to an eccentricity of $e_x = 0.7D$.

4. Design a short rectangular column subjected to a factored load of 2000 kN and a factored moment of 120 kNm. Adopt M30 concrete and Fe 500 grade steel and assume mild environment.
5. Design the column given in Exercise 4 for the same data but when reinforcement is provided on four sides of the column.
6. Design the column given in Exercise 4 for the same data except that the moment of 120 kNm is applied about the minor axis.
7. Design a short circular column subjected to a factored load of 2000 kN and a factored moment of 120 kNm. Adopt M30 concrete and Fe 415 grade steel and assume mild environment. Design (a) with helical reinforcement and (b) with hoop reinforcement.
8. Design a short rectangular column in moderate environment subjected to an axial load of 2000 kN and bending moment of 350 kNm. Adopt M30 concrete and Fe 500 grade steel.
9. Design a short column with unsupported length of 3.25 m and subjected to biaxial bending for the following data: Effective lengths, $L_{ex} = 3$ m and $L_{ey} = 2.75$ m, size of column = 400 mm \times 600 mm, factored axial load, $P_u = 2200$ kN, and factored moments, $M_{ux} = 250$ kNm and $M_{uy} = 150$ kNm. Assume M30 concrete, Fe 415 steel, and moderate exposure.
10. Design a biaxially loaded braced circular column for the following data: Factored axial load, $P_u = 2000$ kN, ultimate biaxial moments, $M_{ux} = 250$ kNm and $M_{uy} = 150$ kNm, unsupported length, $L_u = 3.25$ m, and diameter of column = 550 mm. Use M25 concrete and Fe 415 grade steel and assume moderate environment.
11. Design a biaxially loaded T column for the following data: $B = 250$ mm, $D = 1000$ mm, factored axial load, $P_u = 4000$ kN, and factored moments, $M_{ux} = 750$ kNm and $M_{uy} = 750$ kNm. Assume M20 concrete, Fe 415 steel, and moderate environment. Check your results with those found in Sinha 1996b (Example 5.9).
12. Design a slender unbraced rectangular column subjected to biaxial bending for the following data: Size of column = 250 mm \times 300 mm, unsupported length, $L_u = 5$ m, effective length, $L_{ex} = 4$ m, $L_{ey} = 3.0$ m, factored axial load, $P_u = 800$ kN, and factored moments, $M_{ux} = 25$ kNm and $M_{uy} = 20$ kNm. Assume M25 concrete, Fe 500 steel, and moderate exposure.

REFERENCES

- ACI 2009, *ACI Design Handbook SP 17*, American Concrete Institute, Farmington Hills, p. 252.
- Bae, S. and O. Bayrak 2008, 'Seismic Performance of Full-scale Reinforced Concrete Columns', *ACI Structural Journal*, Vol. 105, No. 2, pp. 123–33.
- Banerjee and S. N. Sinha 1994, 'Design Aids for RC Rectangular Beams Subjected to Biaxial Moments', *The Indian Concrete Journal*, Vol. 68, No. 5, pp. 245–50.
- Boys, A., D.K. Bull, and S. Pampanin 2008, 'Seismic Performance Assessment of Inadequately Detailed Reinforced Concrete Columns', *NZSEE Conference*, Paper no. 29, p. 10, (also see <http://www.nzsee.org.nz/db/2008/Paper29.pdf>, last accessed on 13 February 2013).
- Bresler, B. 1960, 'Design Criteria for Reinforced Concrete Columns under Axial Load and Biaxial Bending', *ACI Structural Journal*, Vol. 57, No. 5, pp. 481–90; 'Discussion', pp. 1621–38.
- Broms, B. and I.M. Viest 1961, 'Long Reinforced Concrete Columns: A Symposium', *Transactions, ASCE*, Vol. 126, Part 2, pp. 308–400.
- CEB-FIP 1964, *Recommendations for an International Code of Practice for Reinforced Concrete*, Comité Européen du Béton, Paris, p. 155.
- Cranston, W.B. 1972, *Analysis and Design of Reinforced Concrete Columns*, Research Report 20, Cement and Concrete Association, London, p. 54.
- CRSI 2008, *CRSI Design Handbook*, 10th edition, Concrete Reinforcing Steel Institute, Schaumburg, p. 1605.
- CRSI Staff 2011, 'RFIs on Circular Ties, Rotating Hooks, Staggered Lap Splices, and Closure Strips', *Concrete International*, ACI, Vol. 33, No. 10, pp. 59–64, and 2013, 'Column Tie Configurations', *Concrete International*, Vol. 35, No. 3, pp. 45–51.
- Dasgupta, K. and C.V.R. Murty 2005a, 'Seismic Design of RC Columns and Wall Sections, Part 1: Consistent Limit State Design Philosophy', *The Indian Concrete Journal*, Vol. 79, No. 3, pp. 33–41.
- Dasgupta, K. and C.V.R. Murty 2005b, 'Seismic Design of RC Columns and Wall Sections, Part 2: Proposal for Limiting Strain in Steel', *The Indian Concrete Journal*, Vol. 79, No. 4, pp. 22–6.

- Deierlein, D.G., A.M. Reinhorn, and M.R. Willford 2010, *Nonlinear Structural Analysis For Seismic Design: A Guide for Practicing Engineers*, NEHRP Seismic Design Technical Brief No. 4., NIST GCR 10-917-5, National Institute of Standards and Technology (NIST), Gaithersburg, p. 32, (also see <http://www.nehrp.gov/pdf/nistgcr10-917-5.pdf>, last accessed on 1 February 2013).
- Everard, N. J. 1974, 'Proportioning of Sections: Ultimate Strength Design', in Mark Fintel (ed.), *Handbook of Concrete Engineering*, Von Nostrand Reinhold Company, New York.
- Fanella, D.A. 2001, 'Time Saving Design Aids for Reinforced Concrete, Part 3: Columns and Walls', *Structural Engineer*, Vol. 2, No. 11, pp. 42–7.
- Furlong, R.W. 1961, 'Ultimate Strength of Square Columns under Biaxially Eccentric Loads', *ACI Journal*, Vol. 57, No. 9, pp. 1129–40.
- Furlong, R.W. 1971, 'Columns Slenderness and Charts for Design', *ACI Journal*, Vol. 68, No. 1, pp. 9–17.
- Furlong, R.W., C.-T. T. Hsu, and S.A. Mirza 2004, 'Analysis and Design of Concrete Columns for Biaxial Bending: Overview', *ACI Structural Journal*, Vol. 101, No. 3, pp. 413–23.
- Ghanekar, V.K. and J.P. Jain 1982, *Handbook for Limit State Design of Reinforced Concrete Members*, Tata McGraw-Hill Publishing Company Ltd, New Delhi, p. 776.
- Ghannoum, W.M. and J.P. Moehle 2012, 'Dynamic Collapse Analysis of a Concrete Frame Sustaining Column Axial Failures', *ACI Structural Journal*, Vol. 109, No. 3, pp. 403–12.
- Goris, A. (ed.) 2012, *Schneider-Bautabellen für Ingenieure*, 20. Auflage, Düsseldorf, p. 1616.
- Gupta, R.G. 2010, 'Magic Equations for Designing Short RCC Columns of Different Shapes with Axial, Uniaxial, Biaxial Loads', *The Indian Concrete Journal*, Vol. 84, No. 10, pp. 57–60.
- Han, S.W. and N.Y. Jee 2005, 'Seismic Behaviors of Columns in Ordinary and Intermediate Moment Resisting Concrete Frames', *Engineering Structures*, Vol. 27, pp. 951–62.
- Hellesland, J. 2005, 'Nonslender Column Limits for Braced and Unbraced Reinforced Concrete Members', *ACI Structural Journal*, Vol. 102, No. 1, pp. 12–21.
- Hsu, C-T. T. 1985, 'Biaxially Loaded L-shaped Reinforced Columns', *Journal of Structural Engineering*, ASCE, Vol. 111, No. 12, pp. 2576–95, 'Errata', Vol. 114, No. 11, November 1988, p. 240.
- Hsu, C-T. T. 1986, 'Reinforced Concrete Members Subjected to Combined Biaxial Bending and Tension', *ACI Journal, Proceedings*, Vol. 83, No.1, pp.137–44.
- Hsu, C-T. T. 1987, 'Channel-shaped Reinforced Concrete Compression Members under Biaxial Bending', *ACI Structural Journal*, Vol. 84, No. 3, pp. 201–11.
- Hsu, C-T. T. 1988, 'Analysis and Design of Square and Rectangular Columns by Equation of Failure Surface', *ACI Structural Journal*, Vol. 85, No. 2, pp. 167–78.
- Hsu, C-T. T. 1989, 'T-shaped Reinforced Concrete Members under Biaxial Bending and Axial Compression', *ACI Structural Journal*, Vol. 86, No. 4, pp. 460–8.
- Huang, L., Y. Lu, and C. Shi 2013, 'Unified Calculation Method for Symmetrically Reinforced Concrete Section Subjected to Combined Loading', *ACI Structural Journal*, Vol. 110, No. 1, pp. 127–36.
- Iyengar, K.T.S. and C.S. Viswanatha 1990, *Torsteel Design Handbook for Reinforced Concrete Members with Limit State Design*, Torsteel Research Foundation in India, Mumbai, and Tata McGraw-Hill Publishing Company Ltd, New Delhi, p. 190.
- Kopczynski, C. 2008, 'High-strength Rebar Expanding Options in Concrete Towers', *Structure Magazine*, ASCE, pp. 30–1.
- Khuntia, M., and Ghosh, S.K. 2004, 'Flexural Stiffness of Reinforced Concrete Columns and Beams: Analytical Approach' *ACI Structural Journal*, Vol. 101, No. 3, pp. 351–63.
- Kumar, R. and S.N. Sinha 1994, 'Design Aids for Hollow Rectangular Reinforced Concrete Columns', *Journal of Structural Engineering*, Vol. 20, No. 4, pp. 195–206.
- Lambert-Aikhionbare N. and S.W. Tabsh 2001, 'Confinement of High-strength Concrete with Welded Wire Reinforcement', *ACI Structural Journal*, Vol. 98, No. 5, pp. 677–85.
- Lai, S-M.A. and J.G. MacGregor 1983, 'Geometric Nonlinearities in Unbraced Multistory Frames', *Journal of the Structural Division*, ASCE, Vol. 109, No.11, pp. 2528–45.
- Li, Q. and A. Belarbi 2009, *Seismic Performance of Square RC Bridge Columns under Combined Loading including Torsion with Low Shear*, Report No. NUTC R231, Center for Transportation Infrastructure and Safety/NUTC program, Missouri, University of Science and Technology, Rolla, p. 11, (also see http://ntl.bts.gov/lib/32000/32300/32342/R231_Li_CR.pdf, last accessed 10 February 2013).
- MacGregor, J.G. 1973, 'Simple Design Procedures for Concrete Columns, Introductory Report', *Symposium on Design and Safety of Reinforced Concrete Compression Members, Report of the Working Commissions*, Vol. 15, International Association of Bridge and Structural Engineering (IABSE), Zurich, pp. 23–49.
- MacGregor, J.G. 1993, 'Design of Slender Concrete Columns—Revisited', *ACI Structural Journal*, Vol. 90, No. 3, pp. 302–9.
- MacGregor, J.G., J.E. Breen, and E.O. Pfrang 1970, 'Design of slender Concrete Columns', *ACI Structural Journal*, Vol. 67, No. 1, pp. 6–28.
- MacGregor, J.G. and S.E. Hage 1977, 'Stability Analysis and Design of Concrete Frames', *Journal of Structural Division, Proceedings ASCE*, Vol. 103, No. ST10, pp. 1953–70.
- Martin, J. 1979, 'Design Aids for L-shaped Reinforced Concrete Columns', *ACI Structural Journal*, Vol. 76, No. 11, pp. 1197–216.
- McKenna, F., G.L. Fenves, M.H. Scott, and B. Jeremie 2000, 'Open System for Earthquake Engineering Simulation', *OpenSees*, Berkeley, (also see <http://opensees.berkeley.edu/>, last accessed on 11 March 2013).
- Mirza, S.A., P.M. Lee, and D.L. Morgan 1987, 'ACI Stability Resistance Factor for RC Columns', *Journal of Structural Engineering, ASCE*, Vol. 113, No. 9, pp. 1963–76.
- Moehle, J.P., J.D. Hooper, and C.D. Lubke 2008, *Seismic Design of Reinforced Concrete Special Moment Frames; A Guide for Practicing Engineers*, NEHRP Seismic Design Technical Brief No. 1, Report no. NIST GCR 8-917-1, National Institute of Standards and Technology, Gaithersburg, p. 27. (also see <http://www.nehrp.gov/pdf/nistgcr8-917-1.pdf>, last accessed on 29 January 2013).
- Moran, F. 1972, *Design of Reinforced Concrete Sections under Normal Loads and Stresses in the Ultimate Limit State*, Bulletin d'Information No. 83, Comité Européen du Béton, Paris, p. 134.
- Murty, C.V.R. 2001, 'Shortcomings in Structural Design Provisions of IS 456:2000', *The Indian Concrete Journal*, Vol. 75, No. 2, pp. 150–7, and 'Discussion' by N. Prabhakar, May 2001, pp. 312–4.

- Pannell, F.N. 1963, 'Failure Surfaces for Members in Compression and Biaxial Bending', *Journal of ACI*, Vol. 60, No. 1, pp. 129–40.
- Park, R. and T. Paulay 1975, *Reinforced Concrete Structures*, John Wiley and Sons, New York, p. 769.
- Parne, A.L., J.M. Nieves, and A. Gouwens 1966, 'Capacity of Reinforced Rectangular Columns Subject to Biaxial Bending', *ACI Structural Journal*, Vol. 63, No. 9, pp. 911–23.
- Paulay, T. and M.J.N. Priestley 1992, *Seismic Design of Reinforced Concrete and Masonry Buildings*, John Wiley and Sons, Inc., New York, p. 744.
- Prakash, S.S., Q. Li, and A. Belarbi 2012, 'Behavior of Circular and Square Reinforced Concrete Bridge Columns under Combined Loadings Including Torsion', *ACI Structural Journal*, Vol. 109, No. 3, pp. 317–28.
- Purushothaman, P. 1984, *Reinforced Concrete Structural Elements: Behaviour, Analysis and Design*, Tata McGraw-Hill Publishing Company Ltd, New Delhi, and Torsteel Research Foundation in India, Bengaluru, p. 709.
- Ramamurthy, L.N. 1966, 'Investigation of the Ultimate Strength of Square and Rectangular Columns under Biaxially Eccentric Loads', *Reinforced Concrete Columns, SP-13*, American Concrete Institute, Farmington Hills, pp.263–98.
- Ramamurthy, L.N. and T.A.H. Khan 1983, 'L-shaped Reinforced Concrete Columns', *Journal of Structural Engineering*, ASCE, Vol. 109, No. 8, pp. 1903–17.
- Razvi, S.R. and M. Saatcioglu 1989, 'Confinement of Reinforced Concrete Columns with Welded Wire Fabric', *ACI Structural Journal*, Vol. 86, No. 5, pp. 615–23.
- Rohit, D.H.H., A.K. Jaiswal, and C.V.R. Murty 2013, 'Expressions for Moment of Resistance of RC Structural Walls', *The Indian Concrete Journal*, Vol. 87, No. 10, pp. 48–62.
- Row, D.G. and T. Paulay 1973, 'Biaxial Flexure and Axial Load Interaction in Short Rectangular Reinforced Concrete Columns', *Bulletin of the New Zealand Society for Earthquake Engineering*, Vol. 6, No. 3, pp.110–21.
- Saatcioglu, M. and M. Grira 1999, 'Confinement of Reinforced Concrete Columns with Welded Reinforcement Grids', *ACI Structural Journal*, Vol. 96, No. 1, pp. 29–39.
- Sarkar, P.K. and B.V. Rangan 2003, 'Reinforced Concrete Columns under Unequal Load Eccentricities', *ACI Structural Journal*, Vol. 100, No. 4, pp. 519–28.
- Sezen, H. and J.P. Moehle 2006, 'Seismic Tests of Concrete Columns with Light Transverse Reinforcement', *ACI Structural Journal*, Vol. 103, No. 6, pp. 842–9.
- Sinha, S.N. 1994, 'Effect of Different Shapes of Column Sections on their Moment Capacities', *The Bridge and Structural Engineer, Journal of ING-IABSE*, Vol. 24, No. 4, pp. 1–15.
- Sinha, S.N. 1995, 'Design of Rectangular Column Section', *The Indian Concrete Journal*, Vol. 69, No. 12, pp. 707–10.
- Sinha S.N. 1996a, 'Design of Cross (+) Section of Column', *The Indian Concrete Journal*, Vol. 68, No. 5, pp. 153–8.
- Sinha, S.N. 1996b, *Handbook of Reinforced Concrete Design*, Tata McGraw-Hill Publishing Company Ltd, New Delhi, p. 530.
- Sinha, S.N. and N.A. Kumar 1992, 'Direct Method of Design of Rectangular Column Section', *Journal of Structural Engineering*, Vol. 19, No. 2, pp. 61–4.
- Sinha, S.N. and A.K. Sinha 1989, 'Design Aid for Cross Shaped Column Section', *The Bridge and Structural Engineer, Journal of ING-IABSE*, Vol. 19, No.1, pp. 1–10.
- SP 16:1980, *Design Aids for Reinforced Concrete to IS 456:1978*, Bureau of Indian Standards, New Delhi, p. 232.
- Sun, B-J. and Z-T. Lu 1992, 'Design Aids for Reinforced Concrete Columns', *Journal of Structural Engineering*, ASCE, Vol. 118, No. 11, pp. 2986–95.
- Suryanarayana, P. 1991, 'Design of Short and Slender Columns under Biaxial Bending: The State-of-art', *ICI Bulletin*, No. 37, pp. 22–30.
- Suryanarayana, P., an email dated 28 February 2013.
- Tan, K.H. and C.Y. Tang 2004, 'Interaction Formula for Reinforced Columns in Fire Conditions', *ACI Structural Journal*, Vol. 101, No. 1, pp. 19–28.
- Tikka, T.K. and S.A. Mirza 2004, 'Equivalent Uniform Moment Diagram Factor for Reinforced Concrete Columns', *ACI Structural Journal*, Vol. 101, No. 4, pp. 521–31.
- Varyani, U.H. 1999, *Structural Design of Multi-storeyed Buildings*, South Asian Publishers, New Delhi, pp. 310.
- Varyani, U.H. and A. Radhaji 2005, *Design Aids for Limit States Design of Reinforced Concrete Members*, Khanna Publishers, Delhi, p. 420.
- Warner, R.F., B.V. Rangan, and A.S. Hall 1976, *Reinforced Concrete*, Pitman Australia, p. 475.
- Weber, D.C. 1966, 'Ultimate Strength Design Charts for Columns with Biaxial Bending', *ACI Structural Journal*, Vol. 63, No. 11, pp. 1205–30.
- Whitney, C. 1942, 'Plastic Theory of Reinforced Concrete Design', *Transactions of ASCE*, Vol. 107, pp. 251–326.
- Wight, J.K. and J.G. MacGregor 2009, *Reinforced Concrete: Mechanics and Design*, 5th edition Pearson-Prentice Hall, Upper Saddle River, p.1112.
- Wsu, C-T.T. 1985, 'Biaxially Loaded L-shaped Reinforced Concrete Columns', *Journal of Structural Engineering*, ASCE, Vol. 111, No. 12, pp. 2576–95.
- Wyetroval, T. and R. Tuchscherer 2013, 'Design of Slender Concrete Columns', *Structure Magazine*, ASCE, pp. 10–13.
- Youakim, S.A. and A. Ghali 2003, 'Behavior of Concrete Columns with Double-head Studs under Earthquake Loading: Parametric Study', *ACI Structural Journal*, Vol. 100, No. 6, pp. 795–803.

DESIGN OF FOOTINGS AND PILE CAPS

15.1 INTRODUCTION

Structures built below the ground are called *substructures* or *foundation structures* as opposed to the term *superstructure*, which denotes structures built above the ground. Even though foundation structures include the floors built below the ground, they can be designed using the principles discussed in the earlier chapters. Hence, we will consider only the footings and pile caps in this chapter. The function of a *footing* or a *foundation* is to safely and effectively transmit the load from the columns and walls to the underlying soil. Reinforced concrete (RC) is admirably suitable for footings and RC footings in turn are used in RC, structural steel, or wooden buildings, bridges, towers, and other structures.

The permissible pressure on the soil beneath a footing, called the *safe bearing capacity* (SBC), will be considerably less than the compressive stresses in walls and columns. Hence, it is necessary, in general, to spread these loads over sufficient soil area to ensure that the loads are safely carried by the soil. In addition to providing foundations that will carry the loads without excessive or uneven settlements and rotations, it is also necessary to check whether they provide sufficient resistance to sliding and overturning or pull-out in case of tensile loads.

Foundation structures may be categorized as (a) shallow foundations, (b) deep foundations, and (c) special foundations (built for transmission line or microwave towers, cooling towers, and chimneys). The choice of a suitable type of foundation depends on the depth at which the bearing strata lies, the soil condition, the type of superstructure, and the magnitude and type of reaction at the base of the superstructure. The type of soil available at the site, the depth at which the foundation can be laid, and the safe load the soil can carry have to be determined by a geotechnical consultant. Normally, this information is available in a soil report. The geotechnical design of foundations (e.g., calculation of SBC

of soil and piles) is usually found in books on soil mechanics and foundation engineering. In this book, we are mainly concerned with the *structural design* of commonly used foundations. However, some guidance on soil design is also provided (see Appendix A for some data on soils).

SP 24:1983 states that ‘the recommendations in Clause 34 of IS 456 are confined to the design of footings that support isolated columns or walls and rest directly on soil or on a group of pile’. Accordingly, the design of these simple types of footings (including combined footings supporting two columns) alone is covered in this chapter. These simple types of footings are the most common and are widely used; they are also more economical than the other types of foundations.

15.2 TYPES OF FOOTINGS

Various types of RC foundations are available. They are mainly classified as *shallow foundations* and *deep foundations*. In general, this classification is based on the value of D_f/B , where D_f is the depth of foundation and B is the width of base of foundation. The value of D_f/B commonly ranges between 0.25 and 1 for shallow foundations and between 5 and 20 for deep foundations.

There are five types of shallow foundations, namely (a) strip or continuous wall footings, (b) isolated or spread footings, (pad and sloped), (c) combined footings, (d) raft or mat foundations, and (e) floating rafts. The first three types are more common (see Fig. 2.3 of Chapter 2). *Strip or continuous wall footings* behave as cantilevers on each side of the wall and spread the wall load over a large soil area. *Isolated or spread footings* may be of uniform thickness; *stepped or sloped*; or have *pedestals* to save materials (see Fig. 15.1). Depending on the shape of the column, isolated footings may be square, rectangular, or circular in shape. When the length to breadth ratio of rectangular footing is more than 2.5, a central longitudinal beam may be provided to make the footing more

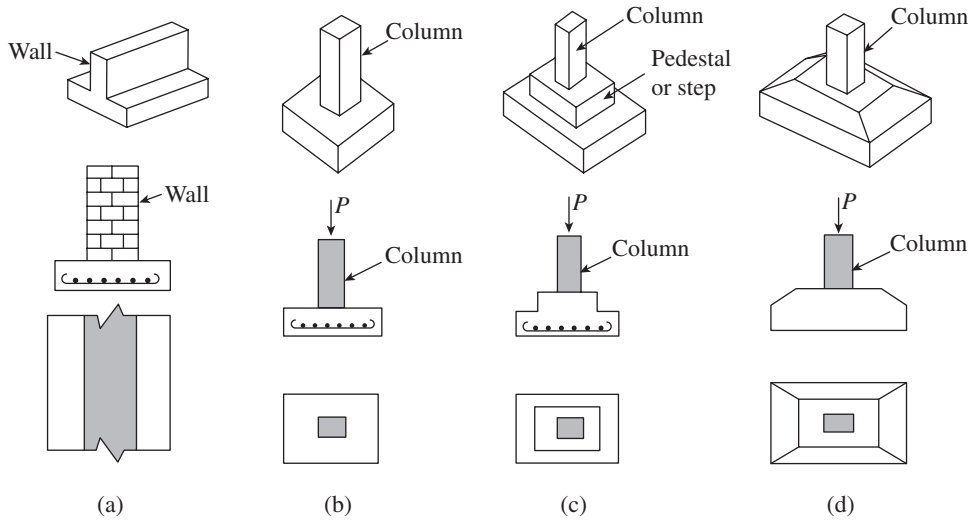


FIG. 15.1 Types of isolated footings (a) Strip or wall footing (b) Spread footing (c) Stepped footing (d) Sloped footing

rigid and have more uniform soil pressure (this will also help reduce the depth of slab in the footing and achieve economy). *Combined footings* transmit load from two or more columns to the soil and may have rectangular, trapezoidal, or other shapes (see Fig. 15.2). Such combined footings are used when one column is near the property line. When the distance between the columns is large, it may be economical to connect two isolated footings by a *strap beam* (see Fig. 15.2d). The strap beam will not transfer any load to the soil. A *mat or raft foundation* transfers loads from all the columns in the building to the soil beneath; it is used in soils of low bearing capacity or where the areas of individual footings overlap (Fig. 15.3a). Mat foundations may also be used to reduce differential settlements when the loads in adjacent columns vary considerably or when there are variable soils within the same building.

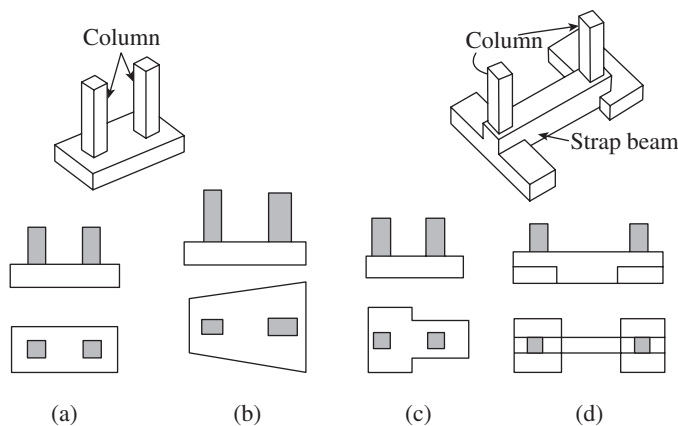


FIG. 15.2 Combined footings for two columns (a) Combined rectangular (b) Combined trapezoidal (c) Combined T-shaped (d) Combined strap

Piles and caissons are the common types of *deep foundations* and transmit loads from columns through the upper layers of poor soil to a strong soil layer at some depth below the

surface. Deep foundations are also employed when it is necessary to provide resistance to uplift or when there is a possibility of erosion due to flowing water as in bridge piers. *Piles* are small diameter shafts driven or cast in bored holes in the ground and are usually provided in groups connected by a pile cap (see Fig. 15.3b). A *pile cap* transmits the column load to a series of piles, which, in turn, transmits the load to the soil. Concrete piles are classified into (a) driven cast in situ piles, (b) bored cast in situ piles, (c) driven precast piles, (d) precast piles in pre-bored holes (IS 2911, Part 1, Sections 1 to 4), and (e) under-reamed piles

(IS 2911, Part 3). They may have enlarged (belled) bottom to transmit the load to a large area.

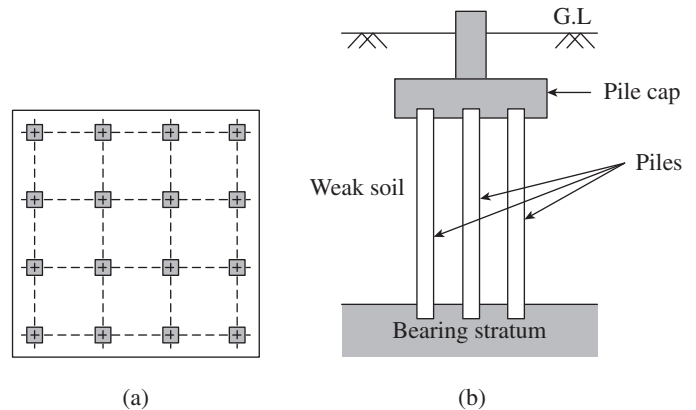


FIG. 15.3 Mat and pile foundation (a) Mat foundation (b) Pile foundation

Caissons, also called *well foundations*, are about 0.6–1.5 m in diameter and are sometimes used instead of piles, especially in bridges (Saran 2006). Three types of caissons are used—open, box, or pneumatic (see Figs 15.4a–c).

A *floating raft foundation* is a special type of foundation that is used where deep deposits of compressible cohesive soils exist. The foundation is so designed that the net foundation pressure is zero. This condition is achieved by excavating the soil to such a depth that the weight of soil removed is equal to the weight of the building including that of the substructure (see Fig. 15.4d). In addition, a combination of piles and raft called the *piled raft foundation* has also been employed.

The choice of foundation for a particular site is usually selected based on the geotechnical report. The factors to be considered are the type and properties of soil, variability of the soil over the area and with increasing depth, position of water table, type of structure along with loadings, and susceptibility of the structure to settlement and tilt. McCarthy (2006) has

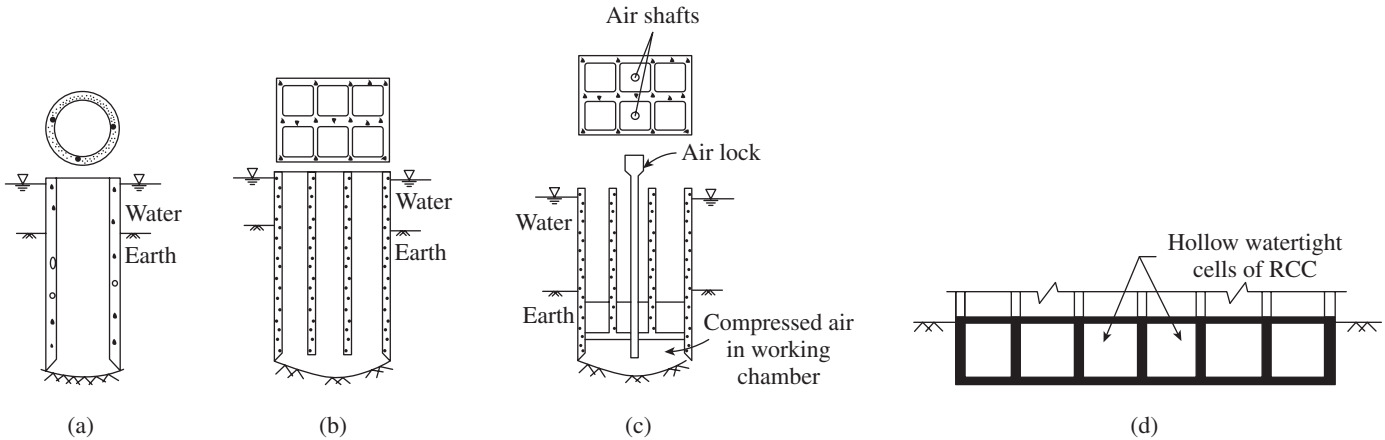


FIG. 15.4 Caissons and floating raft (a) Open caisson (b) Box caisson (c) Pneumatic caisson (d) Floating raft

suggested guidelines for selecting an appropriate foundation type based on soil conditions.

The design of strip, spread, and combined footings and simple pile and pile caps alone is covered in this chapter as these are the most basic and common types. The design of more complex types of foundations (raft, piled-raft, various types of pile, wells and caissons, towers, chimneys, shell, etc.) is outside the scope of this book. For details and design of foundations not covered in this book, interested readers may refer to the books by Bowles (1996), Reese, et al. (2005), Kameswara Rao (2011), Kurian (2006), Saran (2006), Teng (1962), Tomlinson (2001, 2008), Manohar (1985), and Varghese (2009), and the related IS codes (IS 2950:1981, IS 4091:1979, IS 9456:1980, IS 11089:1984, and IS 11233:1985).

15.3 SOIL PRESSURE UNDER FOOTINGS

The distribution of soil pressure under a footing is a function of the type of soil and the relative rigidity of the soil and the footing. When the load is applied at the centre of gravity (C.G.) of the footing, the actual soil pressure distribution under the base resting on cohesionless soil (e.g., sand) and cohesive soil (e.g., clay) will be as shown in Figs 15.5(a) and (b). When the footing is loaded, the sand near the edges of the footing will try to displace laterally, causing a decrease in soil pressure near the edges, as shown in Fig. 15.5(a). On the other hand, when the footing is loaded, the clayey soil under the footing deflects in the shape of a bowl, relieving the pressure near the middle of footing, as shown in Fig. 15.5(b). The design of footings considering such a non-uniform soil pressure is complex. Hence, an idealized uniform pressure distribution as shown in Fig. 15.5(c) is commonly adopted in the structural design.

Tabsh and Al-Shawa (2005) developed the following equation for the relative stiffness factor, K'_r , to determine whether a shallow footing can be considered rigid for the purposes of structural design:

$$K'_r = \frac{E_s D^3}{k_s (1 - \nu_s^2) (B - c_1)^2 (L - c_2)^2} \quad (15.1)$$

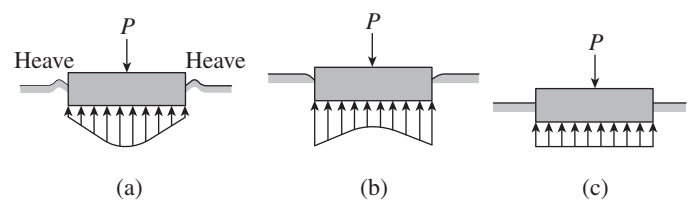


FIG. 15.5 Pressure distribution under footings (a) Cohesionless soil (b) Cohesive soil (c) Assumed uniform pressure

where E_s is the Young's modulus of concrete, D is the average thickness of foundation, k_s is the modulus of subgrade reaction of soil (N/mm^3) as given in Table A.3 of Appendix A, B and L are the breadth and length of footing, respectively, c_1 and c_2 are the column dimensions along the breadth and length of footing, respectively, and ν_s is the Poisson's ratio of soil (see Table A.4 of Appendix A). They have shown that $K'_r = 1$ is the limit between a flexible and rigid footing. When the value of K'_r is greater than or equal to 1, the footing can be safely assumed as rigid.

15.3.1 Soil Pressure under Footings Subjected to Lateral Moments

Walls and columns often transfer moments along with axial force to their footings. These moments may be due to wind, earthquake, or lateral earth pressure. The effect of these moments will produce uniformly varying soil pressure as shown in Fig. 15.6(a). The soil pressure q at any point can be determined as

$$q = \frac{P}{A} \pm \frac{(Pe_x)x}{I_y} = \frac{P}{A} \pm \frac{Mx}{I_y} \quad (15.2)$$

where P is the vertical load (positive in compression), A is the area of contact surface between the soil and footing, I_y is the moment of inertia of this area = $BL^3/12$, M is the moment about the y -axis ($= Pe_x$), e_x is the eccentricity of the axial load from the centroid of the footing along the x -axis, and x is the distance from the centroidal axis to the point where the

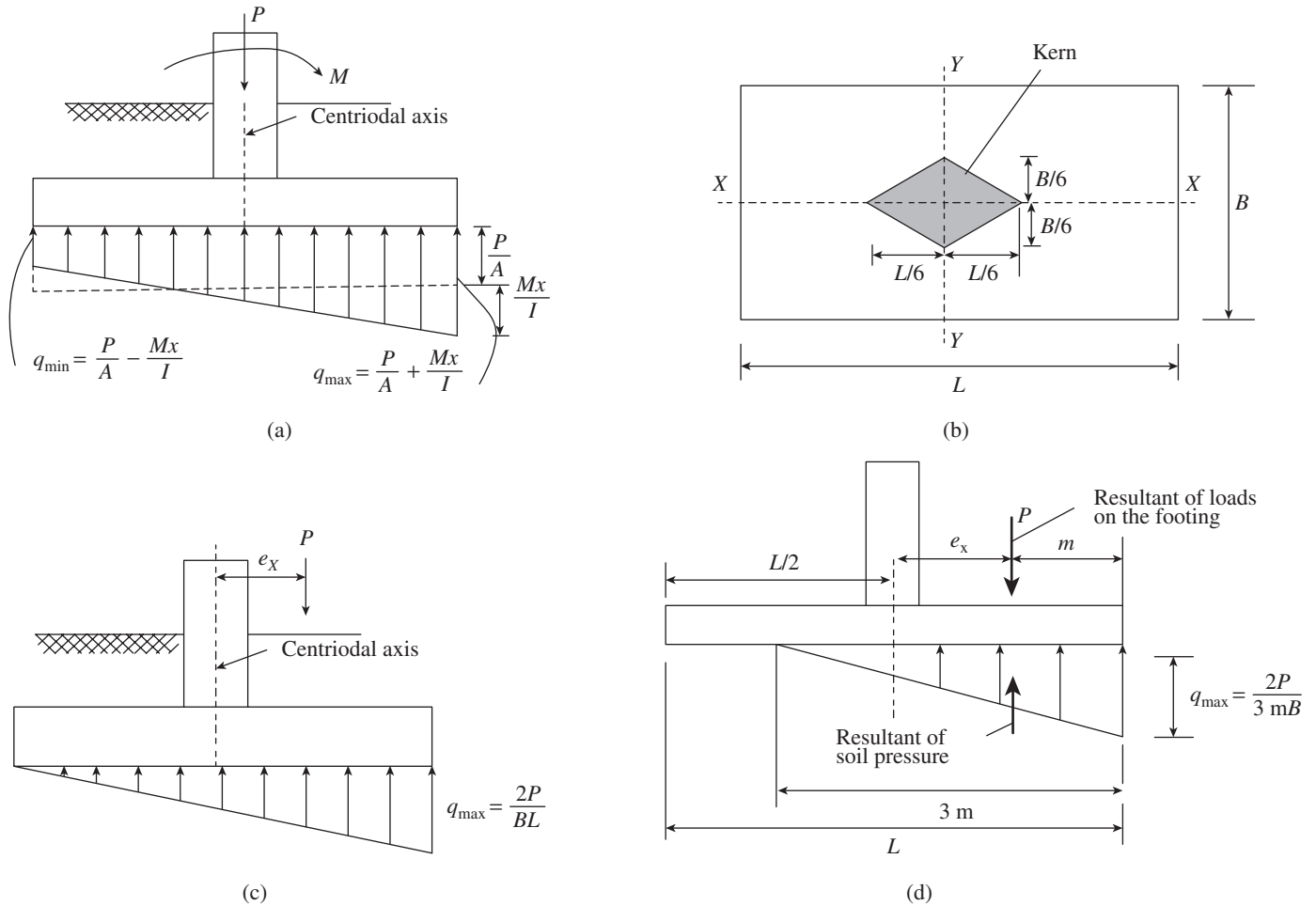


FIG. 15.6 Non-uniform soil pressure under the base of footing (a) Resultant load within the kern (b) Plan view showing kern dimensions (c) Eccentricity $e_x = L/6$ (d) Resultant load outside the kern ($e_x > L/6$)

pressure is calculated. The maximum and minimum values of soil pressure at the extreme edges of the footing will be

$$q_{\max} = \frac{P}{LB} + \frac{6Pe_x}{BL^2}; \quad q_{\min} = \frac{P}{LB} - \frac{6Pe_x}{BL^2} \quad (15.3)$$

In the case of wall footings, unit length of the wall is considered and hence the value of B becomes unity and the load P corresponds to the load acting on unit length of the wall.

The moment M can be expressed as Pe_x , where e_x is the eccentricity of the load P relative to the centroidal axis of the area A . The maximum eccentricity is one that causes $q = 0$ at one end of footing (see Fig. 15.6c). Eccentricities larger than this will result in the footing lifting off the soil, as the soil-footing interface cannot resist tension. For rectangular footing as shown in Fig. 15.6, $e_{\max} = L/6$ or $B/6$. This distance is called the *kern distance*. Loads applied within the *kern* (the area shown as shaded in Fig. 15.6b) will cause compression over the entire area of footing, and hence Eq. (15.4) can be used to compute q , which should

be less than the SBC. It should be noted that when $e_x = L/6$, $q_{\min} = 0$ and q_{\max} will be twice the average pressure, as shown in Fig. 15.6(c). When the eccentricity of load is greater than e_{\max} , the resultant upward load may be located by using the fact that this upward load must be equal and opposite of the resultant downward load, as shown in Fig. 15.6(d). In general, such a situation is not advisable; it makes inefficient use of the footing concrete since part of the base is not in contact with the soil, and may also cause differential settlement in soils like clays and may cause the structure to tilt. In Fig. 15.6(d), it is assumed that the distance of the resultant upward load from the right edge of the footing is m . Then, the soil pressure will spread over a distance of $3m$. Now, equating the total upward soil pressure to the downward load, we get

$$(1/2)(3mB)(q_{\max}) = P$$

Hence,

$$q_{\max} = \frac{2P}{3mB} = \frac{2P}{3B(0.5L - e_x)} \quad (15.4)$$

where B is the width of footing. The determination of the required area of footing subjected to load and lateral moment is a trial and error process. We assume a size, calculate the maximum soil pressure, and compare it with the allowable pressure; if it is greater than the allowable pressure, we need to assume another size, and so on. Once the area is fixed, the remaining design will be similar to that of other footings.

When a footing is subjected to eccentricities about both the axes, the resulting soil pressures at any point (x, y) is given by

$$q = \frac{P}{A} \pm \frac{(Pe_x)x}{I_y} \pm \frac{(Pe_y)y}{I_x} \quad (15.5)$$

where e_x and e_y are the eccentricities of the load from the centroid of the footing along the x - and y -axes, respectively, I_x and I_y are the moments of inertia of the section about the x - and y -axes, respectively, and x and y are the distances of the point from the x - and y -axes, respectively. Teng (1962) has developed a chart, which can be used to calculate the maximum soil pressure when there is double eccentricity in a rectangular footing. Teng's chart is divided into four zones and the factor and formulae to calculate maximum soil pressure for each zone is given. For non-rectangular footing areas of various configurations, kern distances and other aides for calculation of soil pressures can be found in the works of Teng (1962), Kramrisch (1985), and Peck, et al. (1974). It has to be noted that on compressible soils, footings should be loaded concentrically to avoid tilting; eccentrically loaded footings can be used only on highly compacted soils and on rock.

15.3.2 Safe Bearing Capacity

Terzaghi (1943) identified three modes of failure of footings as shown in Fig. 15.7. The *ultimate bearing capacity* of soils corresponding to general shear failure may be obtained by using the following formula developed by Terzaghi (1943):

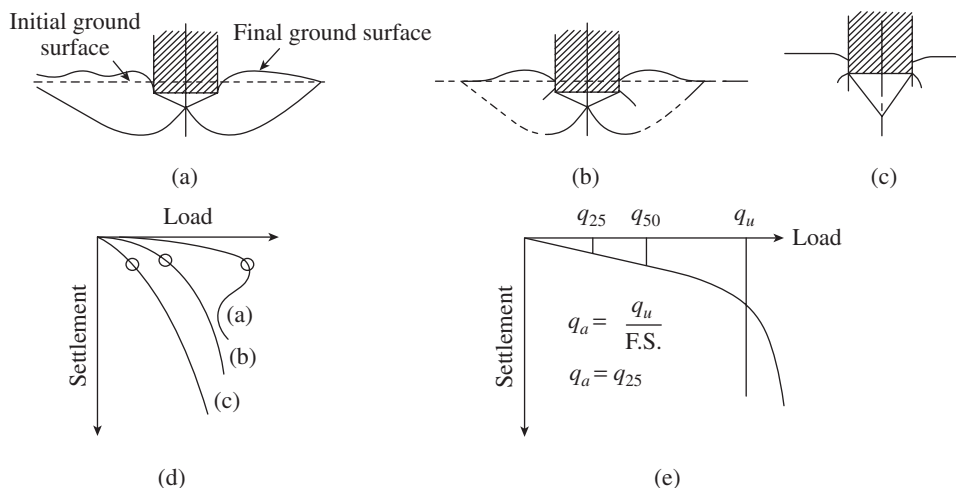


FIG. 15.7 Shear failure of soil due to bearing (a) General shear (large heave—dense sand) (b) Local shear (small heave) (c) Punching shear (no heave) (d) Load settlement curves for (a), (b), and (c) (e) Allowable pressure q_a taken as the lesser of q_u/FS or q_{25}

$$q_u = cN_c + \gamma_0 DN_q + 0.5B\gamma_1 N_\gamma \quad (15.6)$$

where N_c , N_q , and N_γ are known as *bearing capacity factors*, γ_0 is the unit weight of the surcharge with depth D , γ_1 is the unit weight of soil below the foundation, and B is the width of footing. From this equation, the net ultimate bearing capacity can be obtained by deducting $\gamma_0 D$ from q_u as

$$q_n = cN_c + \gamma_0 D(N_q - 1) + 0.5B\gamma_1 N_\gamma \quad (15.7)$$

The values of bearing capacity factors N_c , N_q , and N_γ are functions of the effective friction angle of the soil, ϕ , and were derived by Terzaghi (1943) and later modified by Meyerhof (1951, 1953), Hansen (1961), and Vesic (1973, 1975) as

$$N_q = e^{\pi \tan \phi} \left(\frac{1 + \sin \phi}{1 - \sin \phi} \right) \text{ with } \phi \rightarrow 0, N_q \rightarrow 1 \quad (15.8a)$$

$$N_c = (N_q - 1) \cot \phi \text{ with } \phi \rightarrow 0, N_c \rightarrow \pi + 2 \quad (15.8b)$$

$$N_\gamma = 2(N_q + 1) \tan \phi \text{ with } \phi \rightarrow 0, N_\gamma \rightarrow 0 \quad (15.8c)$$

The SBC, q_a , is obtained by applying a factor of safety, FS , as follows

$$q_a = \frac{q_n}{FS} + \gamma_0 D \quad (15.9)$$

It has to be noted that no factor of safety is applied to the surcharge; the usual factor of safety adopted for soil is 3.0. Equation (15.8) has been adopted in IS 6403:1981. The ultimate net bearing capacity for strip footing as given in Eq. (15.8) has to be modified to take into account the shape of the footing, inclination of loading, depth of embedment, and effect of water table. Equations that take into account these factors are given in IS 6403:1981. Varghese (2009) suggests a thumb rule of $SBC = N$ t/m², where N is the standard penetration test (SPT) value. Typical SBCs for soft clays range from 50 kN/m² to 100 kN/m², for medium stiff clays from 200 kN/m² to 250 kN/m², for very stiff clays from 200 kN/m² to 450 kN/m², and for soft rocks from 450 kN/m² to 900 kN/m² (see Table A.5 of Appendix A).

15.3.3 Settlement of Foundation

In the design of footings, the settlement analysis should be given more importance than the calculation of bearing capacity. When foundation failure does occur, it is usually the result of differential settlement or heaving of the soil that supports the foundation (Venugopal and Subramanian 1977). However, there is a rough correlation between the

bearing capacity and settlement. Soils of high bearing capacity tend to settle less than soils of low bearing capacity. Hence, it is advisable to carefully check the settlement of structures founded on weak soils. As a guide, settlement analysis should be considered with care when the SBC falls below 125 kN/m². Where settlement criteria dominate, the bearing pressure is restricted to a suitable value below that of the SBC, known as the *allowable bearing pressure*. The allowable maximum and differential settlements of RC buildings as per IS 1904:1986 are given in Table 15.1.

TABLE 15.1 Allowable maximum and differential settlements of RC buildings

Type of Soil	Type of Settlement	Isolated Footing	Raft Foundation
Sand and hard clay	Maximum (mm)	50	75
	Differential (mm)	0.0015L	0.0021L
	Angular distortion	1/666	1/500
Plastic clay	Maximum (mm)	75	100
	Differential (mm)	0.0015L	0.002L
	Angular distortion	1/666	1/500

Note: *L* is the length of the deflected part of raft or the centre-to-centre distance between columns.

According to Clause 6.1 of IS 6403:1981, the allowable bearing capacity used in design has to be taken as the *lesser of* that given by Eq. (15.8) and the net soil pressure that can be imposed on the footing without exceeding the permissible settlement as given in Table 15.1 (also see Fig. 15.7e). For calculation of settlement of foundations, IS 8009 (Part 1:1976 and Part 2:1980) may be referred. Clause 34.1 of IS 456 stipulates that the footings should be designed to sustain the applied loads and moments without any differential settlement and without exceeding the SBC of the soil.

15.3.4 Depth of Foundation

The depth of foundation is fixed based on the following (IS 1904:1986):

1. The depth is usually based on the availability of soil of adequate bearing capacity. Strata of varying thickness, even at appreciable depth, may increase differential settlement. Hence, Clause 12.1 IS 1904:1986 stipulates that necessary calculations should be made to estimate settlement from different thicknesses of strata and the structure should be designed accordingly. Usually, it is necessary to check the value of the bearing capacity up to a depth of $2B$ from the base of footing, where B is the width of footing. The least value of SBC within this distance has to be considered for design.
2. Due to seasonal changes of alternate wetting and drying, clayey soils will undergo shrinkage and swelling, resulting in appreciable movements. Hence, in the case of swelling soils like black cotton soils, it is better to keep the base of footing below a depth of 2.5–4 m.
3. In regions where the temperature goes down below freezing point, the base of the footing should be kept at a depth that is not affected by frost action, especially in fine sand and silt.
4. When the ground surface slopes downwards adjacent to a footing, the sloping surface shall not intersect a frustum of bearing material under the footing, having sides that make an angle of 30° with the horizontal for soil. Footing on the sloping ground should have adequate edge distance from the sloping ground for protection against erosion, as shown in Fig. 15.8(a); the horizontal distance from the lower edge of the footing to the sloping surface should be at least 600 mm for rock and 900 mm for soil.
5. In the case of footings in granular soil, a line drawn between the lower adjacent edges of adjacent footings should not have a steeper slope than one vertical to two horizontal (see Fig. 15.8b). In the case of footing on clayey soils, a

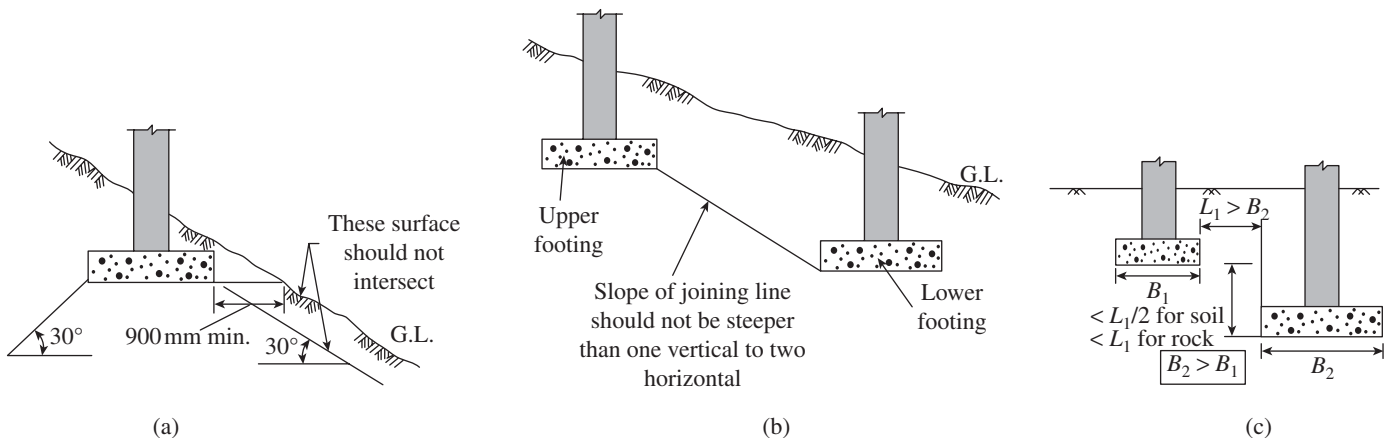


FIG. 15.8 Footing depth in sloping ground or when they are at different levels (a) Footing on sloping ground (b) Footing in granular or clayey soil (c) Footing at two levels

- line drawn between the lower adjacent edge of the upper footing and the upper adjacent edge of lower footing shall not have a steeper slope than one vertical to two horizontal.
- The adjacent excavation or foundation that is very close to the current foundation should be carefully evaluated. If the new foundation is deeper and closer to the existing one, the damage will be greater. As per Clause 14.1 of IS 1904:1986, the minimum horizontal spacing between the existing and new footings should be equal to the width of the wider one (see also Fig. 15.8c).
 - Depth of ground water table plays an important role in the depth of foundation.

The approximate depth of foundation D_f may be determined using the following Rankine's formula:

$$D_f = \frac{q_a}{\gamma_s} \left(\frac{1 - \sin \phi}{1 + \sin \phi} \right)^2 > 500 \text{ mm} \quad (15.10)$$

where q_a is the SBC of soil, γ_s is the unit weight of soil, and ϕ is the angle of repose of soil. For typical values of $q_a = 150 \text{ kN/m}^2$, $\gamma_s = 20 \text{ kN/m}^3$, and $\phi = 30^\circ$, the depth D_f based on this equation works out to 0.833 m. All foundations shall extend to a depth of at least 500 mm below natural ground level (N.G.L.) to allow removal of top soil and variations in ground level (Clause 7.2 of IS 1904:1986). Clause 15.7 of ACI 318 stipulates that the minimum depth of footing above bottom reinforcement is 150 mm for footings on soil and 300 mm for footings on piles.

Hence, the best-recommended depth of foundation is from 1 m to 1.5 m from original ground level.

15.3.5 Gross and Net Soil Pressures

The soil pressure may be expressed in terms of gross or net pressure at the foundation level. The *gross soil pressure* is the total soil pressure produced by all loads above the foundation level. Thus, it consists of (a) the column load, (b) the weight of the footing, and (c) the weight of the soil from the foundation level to the ground level. On the other hand, the *net soil pressure* does not include either the weight of the soil above the base of the footing or the weight of the footing. For example, let us consider a 600 mm thick isolated pad-type footing of size $3 \text{ m} \times 3 \text{ m}$, supporting a concentrically loaded column with its top surface located 2 m below the ground level, as shown in Fig. 15.9(a). Let us assume that there is no column load. Hence, the total downward load from the weights of soil and foundation is 51 kN/m^2 (assuming the weight of soil as 18 kN/m^3 and that of concrete as 25 kN/m^3). This will be balanced by an equal and opposite soil pressure. As a result, the net effect on the concrete footing is zero.

When the column load of 1125 kN is added, the pressure under the footing increases by $q_{\text{net}} = P/A = 1125/9 = 125 \text{ kN/m}^2$, as shown in Fig. 15.9(b). The total soil pressure is 176 kN/m^2 . This is referred to as the gross soil pressure and should not exceed the allowable bearing capacity of the soil q_a . However,

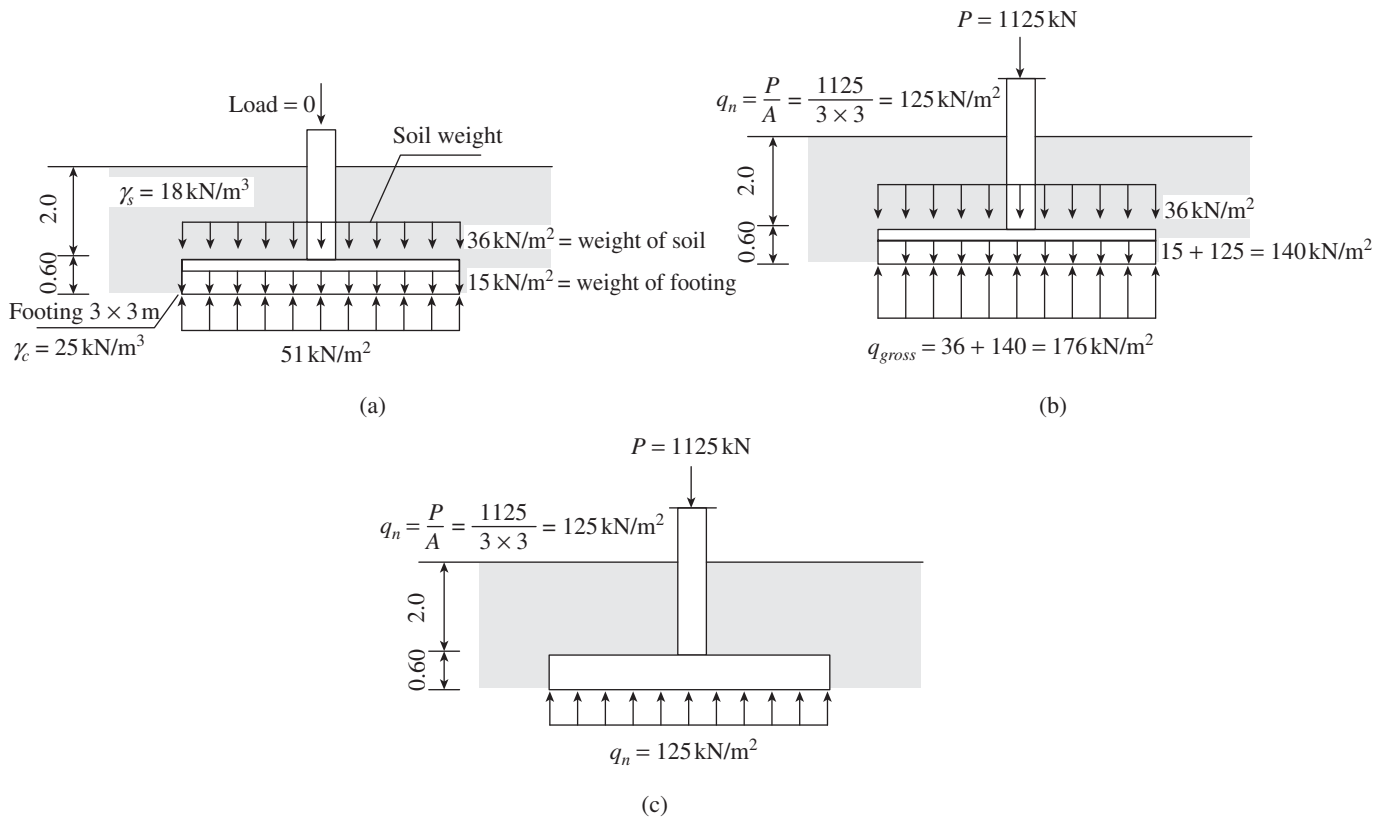


FIG. 15.9 Gross and net bearing pressure (a) Self-weight and soil weight (b) Gross soil pressure (c) Net soil pressure

when the bending moments and shear in the concrete footing are calculated, the upward and downward pressures of 51 kN/m^2 cancel out, leaving only the net soil pressure, q_n , to cause internal forces in the footing, as shown in Fig. 15.9(c).

In design, the area of footing is selected based on the criteria of *gross soil pressure* not exceeding the SBC of soil. However, the flexural reinforcement is calculated and the shear strength of footing is checked based on the *net soil pressure*. This area of footing is selected as

$$\text{Area} = \frac{\text{DL (structure, footing, and surcharge)} + \text{LL on column or wall}}{q_a} \quad (15.11a)$$

It should be noted that for service load combinations including wind or earthquake, most codes allow a 33 per cent increase in q_a ; for such load combinations, the required area is

$$\text{Area} = \frac{\text{DL (structure, footing, and surcharge)} + \text{LL} + \text{WL on column or wall}}{1.33q_a} \quad (15.11b)$$

However, it should not be less than the value given by Eq. (15.11a). The loads used in Eq. (15.11) are the unfactored service loads. Algin (2007) developed a comprehensive formula for dimensioning rectangular footings. Once the area of footing is determined, all other calculations are done based on the soil pressure due to factored loads. The load combinations prescribed in Table 18 of IS 456 should be used in the foundation design.

The factored net soil pressure used to design the footing is

$$q_{nu} = \frac{\text{Factored loads}}{\text{Area of footing}} \quad (15.12)$$

It has to be noted that the factored net soil pressure q_{nu} will exceed the value of SBC. It is acceptable, because the factored loads are 1.5 times the service loads, whereas the factor of safety considered in determining SBC will be about 2.5 to 3. Hence, even the factored net soil pressure will be less than the pressure that will cause failure of the soil.

CASE STUDY

Foundation Failure

The *Tower of Pisa* is a free-standing bell tower of the cathedral of the Italian city of Pisa. The tower is a 56.4 m tall, circular, eight-storey structure made of white marble. Although intended to stand vertically, the tower began leaning to the southeast soon after the onset of construction in 1173 due to a poorly laid 3 m deep foundation and weak, unstable subsoil. Prior to restoration work performed between 1990 and 2001, the tower leaned at an angle of 5.5° , but the tower now leans at about 3.99° . This means that the top of the tower is 3.9 m from where it would stand if the tower were perfectly vertical. Several attempts have been made to stabilize the foundation movement. Details of these may be found in the works of Subramanian and Muthukumar (1998) and Burland, et al. (2009). After a decade of corrective reconstruction and stabilization efforts, it was declared stable in 2008 for at least another 200 years. It may be of interest to note that in June 2010, the *Capital Gate* building in Abu Dhabi, UAE, was certified as the 'world's furthest leaning man-made tower'; it has a 18° slope, almost five times as that of the Leaning Tower of Pisa; however, this tower is deliberately engineered to slant.



Tower of Pisa
(Source: Sundaragopal, Er Srinivas)

15.4 DESIGN CONSIDERATIONS

Design of foundations consists of two phases—soil design and structural design. Due to the complex nature of soils and their behaviour, a hybrid approach to foundation design is adopted in most of the codes in which bearing pressures are checked based on the working stress method and members of foundation are designed using the limit state method.

It should be noted that some codes such as Eurocode 7 and AASHTO follow the limit state method for both soil and structural designs (for details of such an approach, refer to Paikowsky, et al. 2010). Using the unfactored or service loads for soil design, in concentrically loaded isolated footing, the following condition should be satisfied:

$$\sum P_s \leq q_a A \quad (15.13)$$

where P_s is the specified service load (unfactored) acting on the footing, A is the area of footing in contact with the soil, and q_a is the SBC of soil.

Both ultimate limit state and serviceability limit state checks are to be satisfied (Wight and MacGregor 2009).

The following are the ultimate limit states to be checked for soil design:

1. Bearing resistance failure caused by shear failure of the supporting soil (see Fig. 15.7)
2. Serviceability failure in which excessive *differential settlement* between adjacent footings cause structural damage
3. Excessive settlement and resulting excessive angular distortion (settlement may be of two types: *immediate settlement* as in sands and long-term settlement called *consolidation* as in clays)
4. Stability under lateral loads due to sliding
5. Stability against overturning, in case of slender tall structures
6. Failure due to soil liquefaction (*soil liquefaction* describes a phenomenon whereby a saturated soil substantially loses strength and stiffness during earthquakes, causing it to behave like a liquid)

Bearing failures of the soil supporting the footing can be prevented by limiting the service load stresses under the footing to that of the SBC. Stability of the footing under lateral loads will be dependent upon the amount of passive pressure P_{pi} , mobilized in the adjoining soil and the friction between the soil and footing.

Clause 20 of IS 456 recommends a factor of safety of 1.4 against both sliding and overturning under the most adverse

combination of the applied characteristic loads. As per Clause 20.2, for sliding, only 0.9 times the characteristic dead loads should be considered. The resistance against sliding is provided by the friction between the base of the footing and the soil below and by the passive resistance of the soil in contact with the vertical faces of the footing. Thus, the factor of safety against sliding is calculated as

$$FS = \frac{\mu P + \sum P_{pi}}{P_h} > 1.4 \quad (15.14)$$

where P is the compressive load on footing, μ is the coefficient of friction, which may vary between 0.35 (for silt) and 0.55 (coarse-grained soil without silt), P_h is the lateral force, and P_{pi} is the sum of passive pressure components of the soil, as shown in Fig. 15.10(a) (passive pressure is discussed in Chapter 16). It has to be noted that in clayey soil, μP should be replaced by $c_a B$, where c_a is the base cohesion = $0.5c$ to $0.75c$, c is the unit cohesion of base soil, and B is the base width of foundation.

If the required factor of safety against sliding cannot be achieved by the provided footing, it is usual to provide a *shear key* below the base of footing, especially in the case of retaining walls, as shown in Fig. 15.10(b). If a construction joint has to be provided at the interface of wall or column and the footing, then a kind of 'shear key' is provided at this interface, as shown in Fig. 15.10(c), to transfer the horizontal shear forces due to lateral forces to the footing. Suprenant (1987) discusses the construction problems and possible solutions of providing such a shear key.

When lateral loads act on the structure, the stability of the structure as a whole should be ensured at the foundation

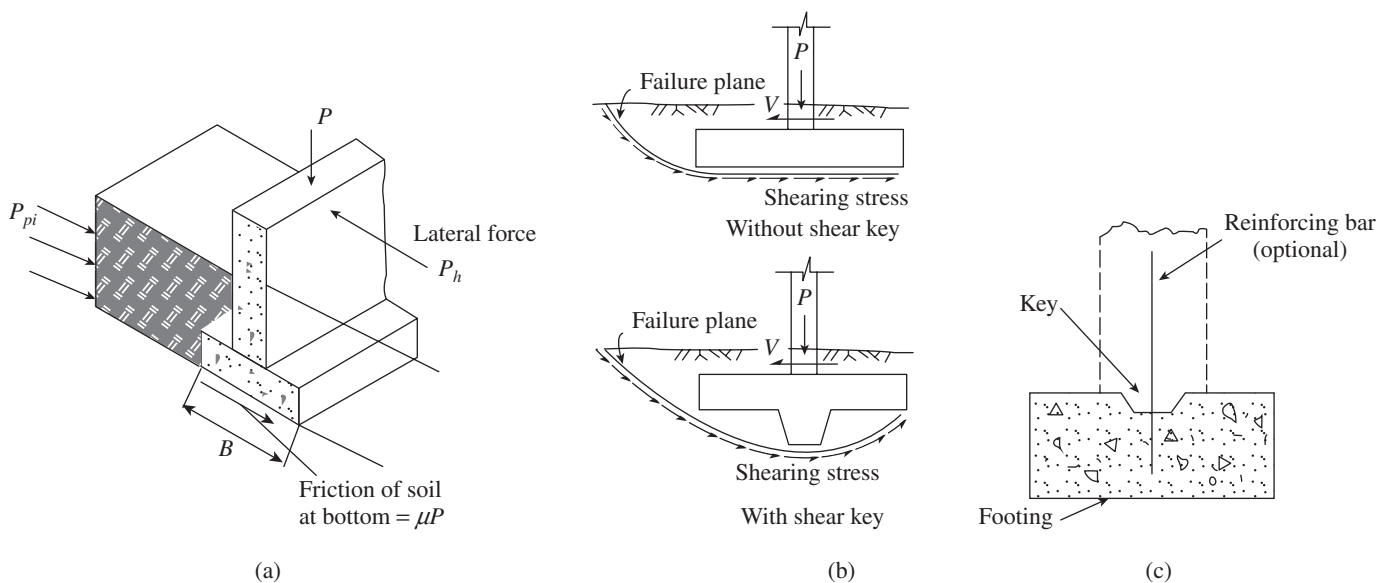


FIG. 15.10 Stability against sliding (a) Forces resisting sliding (b) Concept of shear key (c) Shear key at the footing–column or footing–wall interface

level. Such overturning checks are also necessary for footings supporting large cantilevered beams or slabs. The factor of safety against overturning is given by (see Fig. 15.11)

$$FS = \frac{M_{\text{restoring}}}{M_{\text{overturning}}} > 1.4 \quad (15.15)$$

where $M_{\text{restoring}}$ is the summation of moments about O that resist rotation, typically including the moment due to the weight of the foundation and structure (W_f), weight of backfill (W_s), and the moment due to the passive pressure (P_p), and $M_{\text{overturning}}$ is the moment due to the active pressure, P_a , about O .

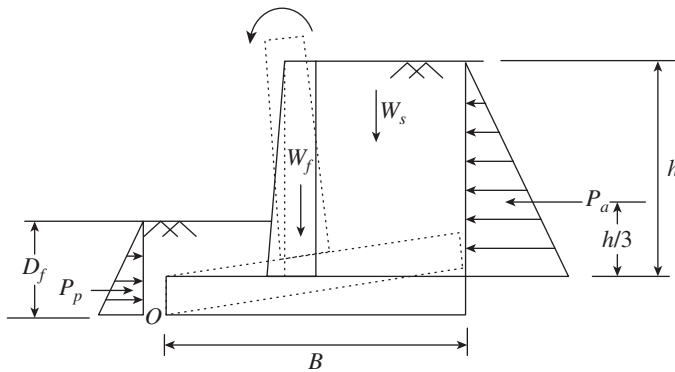


FIG. 15.11 Stability against overturning

In cases where the dead load alone provides the restoring moment, only 0.9 times the characteristic dead loads should be considered as per Clause 20.1 of the code; in this case, the restoring moments due to imposed loads should be ignored. It has to be noted that Clause 20.1 of IS 456 permits a reduced factor of safety of 1.2 when the overturning moment is entirely due to dead loads; however, it is a better practice to use a factor of safety of 1.4 or more in all cases of loading.

In general, the problems of overturning and sliding are rare in RC buildings but common in retaining walls. Hence, calculations for stability against overturning and sliding are provided in Chapter 16. In addition, when the column it is supporting is subjected to tension (due to wind or earthquake load, especially in the case of tall towers), footing has to be designed for *uprooting* or *pull-out*. Details of design to resist uprooting may be found in the works of Bowles (1996) and Subramanian and Vasanthi (1990).

The following are the ultimate limit states that apply to the structural design:

1. Flexural failure of the footing
2. One-way or two-way (punching) shear failure of the footing
3. Inadequate anchorage of the flexural reinforcement in the footing
4. Bearing failure at column–footing interface

15.5 STRUCTURAL DESIGN OF INDIVIDUAL FOOTINGS

Design of foundations with variable types of foundation structures will be different, but the following steps are typical to any design:

1. Calculate loads from structure due to various loading cases and surcharge.
2. Obtain soil properties from soil report provided by a geotechnical expert.
3. Based on the soil report, determine the footing location and depth; shallow footings are less expensive, but usually the geotechnical report will determine the type of footing to be adopted.
4. Determine footing size based on Eq. (15.11).
5. Calculate contact pressure and check stability if required.
6. Estimate settlements.
7. Design the footing based on limit state design.

Until now, we have discussed steps 1–6. The structural design of footing will be discussed in the remaining parts of this chapter.

Foundations are not easily accessible for periodic inspection and maintenance and hence durability considerations should be considered with care. While deflection control may be neglected (as footings are buried under the soil and are not visible), control of crack width is an important serviceability consideration, especially for footing subjected to aggressive environments. The following are the requirements as per IS 456:

1. As per Clause 26.4.2.2, the minimum cover to reinforcement is 50 mm under normal exposure and the corresponding minimum grade of concrete is M20; under extreme exposure conditions, it is 75 mm (Table 16) and M25 concrete. However, it is a better practice to adopt 75 mm cover under all exposure conditions.
2. Clause 8.2.2.4 and Table 4 give guidance regarding the type of cement, minimum free water to cement ratio, and minimum cement content for situations in which chlorides are encountered along with sulphates in soil or ground water.
3. Footings are considered to be in moderate category of exposure as they are buried in soil, and hence it is sufficient to restrict the crack width to 0.3 mm (SP 24:1980). However, for severe and above categories, the assessed surface crack width should not exceed 0.004 times the nominal cover to main steel, as per SP 24:1980 (for a cover of 75 mm, it once again works out to 0.3 mm). Hence, for a majority of footings, the general detailing rules given in Clause 26.3 will be sufficient for crack control, except for footings exposed to aggressive chemicals in soils.
4. Minimum reinforcement and spacing should be as per the requirement of solid slabs, as per Clause 34.5.1. Hence,

minimum percentage in each direction is 0.12 per cent of the total cross-sectional area for high-strength deformed bars or welded wire fabric and 0.15 per cent for Fe 250 grade steel. Moreover, spacing of main bars should not exceed three times the effective depth or 300 mm, whichever is smaller (Clause 26.3.3b). Further, Clause 34.5.2 stipulates a nominal reinforcement of 360 mm^2 per metre length in each direction on each face for thick foundations with thickness greater than 1 m.

5. As per Clause 34.1.2, in reinforced or plain concrete footings, the thickness at the edge should be greater than 150 mm (and 300 mm in the case of pile caps). This ensures that the footing will have enough rigidity to support the bearing pressures acting on them.
6. Usually, a *levelling course* of lean cement concrete (1:5:10 or 1:4:8 proportion) of thickness 80–100 mm is provided below the footing base, which serves as a separating layer between the natural soil and the footing so that any harmful chemical present in the soil will not react with the footing concrete.

The structural design procedures for isolated spread footings were derived largely on the experimental investigations by Talbot (1913), Richart (1948), Hognestad (1953), and ACI-ASCE Committee 326 (1962). These tests and recommendations have been re-evaluated subsequently by researchers, focusing on one-way and two-way shears (Dieterle and Steinle 1981; Kordina and Nölting 1981; Hallgren, et al. 1998; Gesund 1983; Hegger, et al. 2006, 2009). Collins and Kuchma (1999) and Hegger, et al. (2009) point out that the ACI code (as well as IS 456) provisions do not account for the size effect on shear and punching shear strength. Hence, these codes tend to be less conservative for footings with large effective depths. Size effect may be significant in high-strength concrete (Collins and Kuchma 1999). Moreover, when the shear slenderness, L_0/d (where L_0 is the distance from the face of the column or wall to the point of zero shear and d is the effective depth), is greater than 2.5, Uzel, et al. (2011) suggest providing shear reinforcement in the footing.

The design of a footing must consider bending, development length of reinforcement, one-way shear and punching shear, and the transfer of load from the column or wall to the footing. In general, shear considerations predominate and hence thickness is governed by one-way or punching shear rather than bending. As a result, foundations are always under-reinforced.

15.5.1 Shear Design Considerations

In many cases, the thickness of footing will be governed by the requirements of shear rather than by flexure. Hence, in footings, the design for shear is considered before the design for flexure. The shear capacity of footings has to be checked in one-way bending action as well as in two-way (punching) shear as per Clause 34.2.4.1 of IS 456. The requirements as per one-way and two-way shears are discussed here.

One-way shear One-way shear in footing is considered similar to that of slabs. Considering the footing as a wide beam, the critical section is taken along a vertical plane extending the full width of the footing, located at a distance equal to the effective depth of footing (i.e., considering a dispersion angle of 45°) from the face of the column, pedestal, or wall, as shown in Fig. 15.12(a).

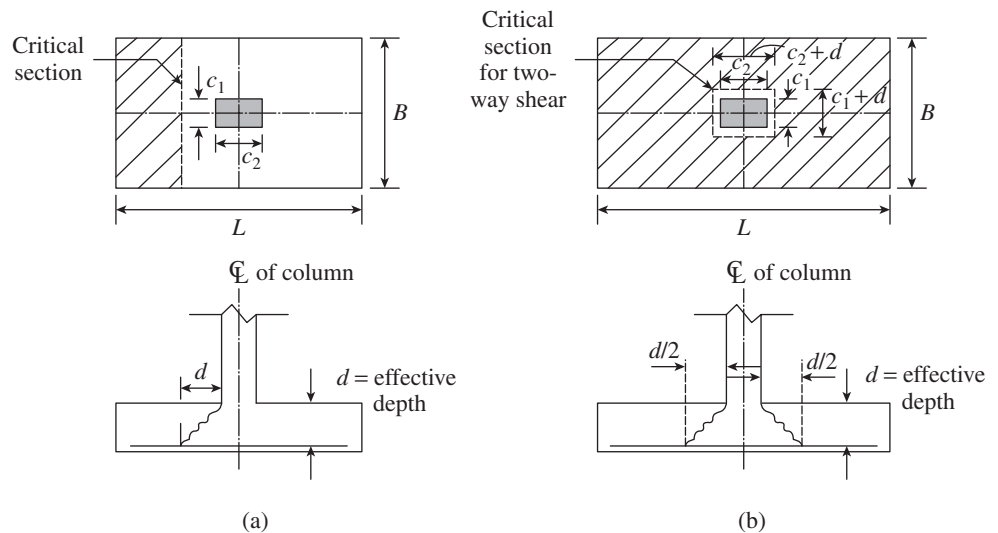


FIG. 15.12 Critical sections for shear (a) One-way shear (b) Two-way punching shear

In one-way shear, the shear force to be resisted, V_{u1} , is the sum of the upward forces in the footing from the critical section to the edge of footing. The consequent shear stress is given by

$$\tau_{v1} = \frac{V_{u1}}{Bd} \quad (15.16)$$

where B is the breadth and d is the effective depth of footing. This value of τ_{v1} should not exceed the design shear strength of concrete τ_c as per Table 19 of IS 456.

As Table 19 of IS 456 for the determination of shear strength of concrete requires the percentage of reinforcement (in footing design, the area of steel as per flexure is determined only after the determination of depth based on shear considerations), it may be assumed that the footing is provided with 0.25–0.50 per cent of tension steel and the corresponding value of design shear stress, τ_c , is taken as per Table 19 of IS 456. It has to be noted that while calculating the steel as per bending

moment (B.M.) requirements, it is necessary to check whether the assumed steel as per shear requirements is provided.

Two-way shear The behaviour of footing in two-way (punching) shear is identical to that of two-way flat slabs supported on columns, as discussed in Section 11.5.2 of Chapter 11. However, punching shear in footing is not as critical as in flat slabs, since the footing is supported by the soil below. Hence, it is desirable to check the tendency of the column punching through the footing, along the surface of a truncated pyramid around the column, called the *critical perimeter*. Thus, the critical section for the two-way shear is taken at a distance $d/2$ from the periphery of the column, as shown in Fig. 15.12(b).

It has to be noted that in wall footings (Fig. 15.1a) and combined footings provided with a central beam (Fig. 15.2d), the footing slab is subjected only to one-way bending; hence, they need to be checked for one-way shear alone.

As discussed in Section 11.5.2 of Chapter 11, when shear reinforcement is not provided, the calculated punching shear stress at the critical section, τ_{v2} , should not exceed $k_s \tau_{cp}$, where

$$\tau_{v2} = \frac{V_{u2}}{b_o d} \tag{15.17a}$$

$$k_s = (0.5 + \beta_c) \leq 1 \tag{15.17b}$$

$$\tau_{cp} = 0.25 \sqrt{f_{ck}} \tag{15.17c}$$

Here, β_c is the ratio of the short side to the long side of the column, f_{ck} is the characteristic compressive strength of concrete, V_{u2} is the punching shear force, which is the total upward reaction from the area bounded by the critical perimeter and edge of the footing (see Fig. 15.12b), b_o is the length of critical perimeter = $2(c_1 + c_2 + 2d)$, c_1 and c_2 are the short and long sides of the column, respectively, and d is the effective depth of footing.

For the purposes of computing stresses in footings that support a round or octagonal column or pedestal, Clause 34.2.2 of IS 456 recommends the use of an equivalent inscribed square column, as shown in Fig. 15.13, which will result in conservative design.

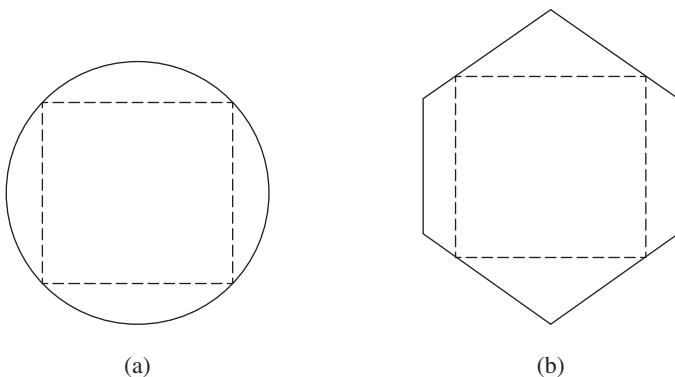


FIG. 15.13 Equivalent square column (a) For round column (b) For octagonal column

It has to be noted that the depth of footing will be chosen in such a way that shear reinforcement is avoided in footing slabs.

15.5.2 Bending Moment Considerations

The bending moment at any section of a footing is determined by considering a vertical plane at this section, which extends completely across the footing, and then computing the moment due to soil pressure acting over the entire area of the footing on one side of this plane (Clause 34.2.3.1 of IS 456). The maximum bending moment to be used in the design of an isolated footing that supports a column, pedestal, or wall occurs at the following locations, as per Clause 34.2.3.2 of IS 456:

1. For footings supporting a wall, column, or pedestal, the maximum bending moment occurs at the face of the wall, column, or pedestal, as shown in Figs 15.14(a) and (b).
2. Since brick walls are generally less rigid than concrete walls, the maximum bending moment location is assumed at halfway between the centre line and the edge of the wall for footings supporting masonry walls, as shown in Fig. 15.14(c).
3. For footings supporting steel columns, the critical section is taken at halfway between the face of the column or pedestal and the edge of the base plate, as shown in Fig. 15.14(d).

The total tensile reinforcement, calculated to resist the maximum bending moment, has to be distributed as follows, as per Clause 34.3 of IS 456:

In one-way reinforced footing The total reinforcement is distributed evenly across the full width of the footing.

In two-way square footing The calculated reinforcement is distributed evenly across the width in both directions.

In two-way rectangular footing The calculated reinforcement in the long direction is distributed evenly across the full width of the footing, whereas in the short span direction, it is distributed in different proportions in the central zone and the edge zones (see Fig. 15.15). The amount of reinforcement in the central zone is given by

$$A_{s1} = \frac{2A_{sL}}{1 + L/B} \tag{15.18}$$

where A_{s1} is the area of reinforcement in central zone, A_{sL} is the total area of reinforcement in the shorter direction, B is the length of the shorter side, and L is the length of the longer side. The remainder of the reinforcement is evenly distributed in the two outer zones of the footing.

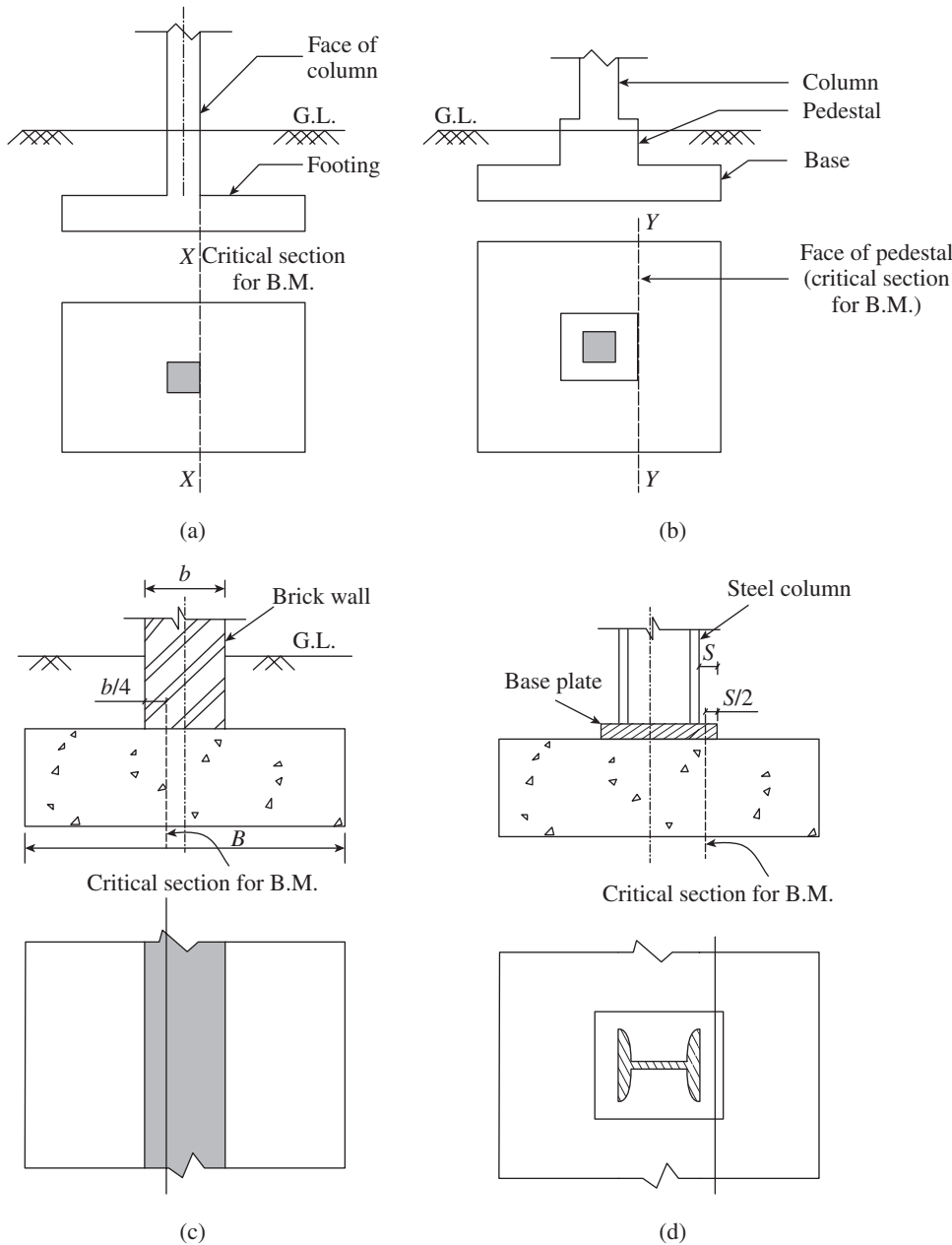
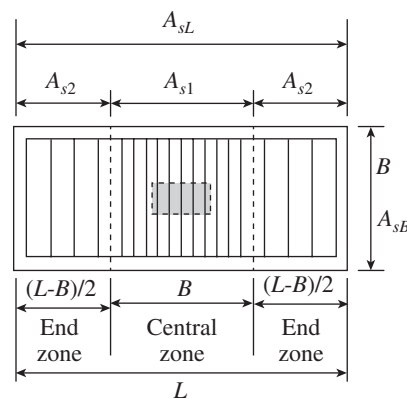


FIG. 15.14 Critical section for moment (a) Concrete column or wall (b) Pedestal footing (b) Masonry wall (c) Column with steel base plate



$$A_{s1} = \left(\frac{2 A_{sL}}{1 + L/B} \right)$$

$$A_{s2} = \left(\frac{A_{sL} - A_{s1}}{2} \right)$$

FIG. 15.15 Zones for reinforcement in a rectangular footing

15.5.3 Providing Development Length

The design bond strength and development length in footing is the same as that in beams and slabs (as per Clause 26.2.1 of IS 456). Clause 34.2.4.3 of the code stipulates that the critical section for checking the development length in footing should be the same planes where the maximum bending moment occurs. In addition, it should be checked at all other vertical planes where abrupt changes of sections occur. In locations where the reinforcement is curtailed, anchorage requirements must be satisfied as in the case of beams.

15.5.4 Transfer of Load at Base of Column

The axial load, moments, and shear acting at the base of a column or pedestal are transferred to the footing by any one of the following means:

1. Compressive forces by bearing on concrete surface as well as by reinforcement
2. Tensile forces due to moment by reinforcement bars, which are properly anchored into column as well as footing, with adequate development length
3. Lateral forces by shear friction or shear keys

Though all these types of forces are to be transferred from column to footing, the code recommendations (Clause 34.4 of IS 456) are confined only to compressive forces.

Compressive forces are transferred through direct bearing, and bearing stresses are checked both at the column-footing interface and at the bottom of footing. Under factored load, the permissible bearing stress, f_{br} , is limited by Clause 34.4 of IS 456 as

$$f_{br} = 0.45 f_{ck} \left(\sqrt{\frac{A_1}{A_2}} \right) \leq 0.9 f_{ck} \quad (15.19)$$

where A_1 is the area of the supporting surface that is geometrically similar to and concentric with the loaded area, A_2 is the actual bearing area at the column base, and f_{ck} is the compressive strength of concrete. Equation 15.19 is based on

experiments conducted by Hawkins (1968) on unreinforced concrete blocks supported on a stiff support and loaded through a stiff plate.

In sloped or stepped footings, area A_1 may be taken as the area of the lower base of a frustum of a pyramid or cone contained wholly within the footing, with its upper area equal to the actual bearing area (A_2) and having sides extending at two horizontal to one vertical, until they first reach the edge of the footing, as shown in Fig. 15.16. The 2:1 rule used to define A_1 does not imply that the load spreads at this rate; it is only an empirical relationship derived by Hawkins (1968).

As shown in Eq. (15.19), the basic bearing stress of $(0.45f_{ck})$ may be increased by the factor $\sqrt{A_1/A_2}$, taking advantage of confinement of bearing area (which is subjected to triaxial state of compressive stress), in the immediate vicinity of the loaded area of footing. However, as this factor $\sqrt{A_1/A_2}$ cannot be increased infinitely, an upper limit of $\sqrt{A_1/A_2} = 2$ is imposed in the code (SP 24:1983).

If the permissible bearing stress is exceeded either in the base of the column or in the footing, reinforcement must be

provided for developing the excess force. The reinforcement may be provided either by extending the longitudinal bars of column into the footing or by providing dowels as follows (Clauses 34.4.2–34.4.4 of IS 456):

1. Minimum area of extended longitudinal bars or dowels must be 0.5 per cent of the cross-sectional area of the supported column or pedestal.
2. A minimum of four bars must be provided.
3. If dowels are used, their diameter should not exceed the diameter of the column bars by more than 3 mm.
4. Enough development length should be provided to transfer the compression or tension to the supporting member.
5. Only column bars of diameter larger than 36 mm in compression can be doweled into the footings with bars of smaller diameter of necessary area. The dowel must extend into the column a distance equal to the development length, L_{dc} , of the column bar. At the same time, the dowel must extend vertically into the footing up to a distance equal to the development length (L_{dc} or L_{dt} , depending on whether the column is subjected to compression or tension) as shown in Fig. 15.17. (for the sake of clarity, footing bars are not shown in the figure)

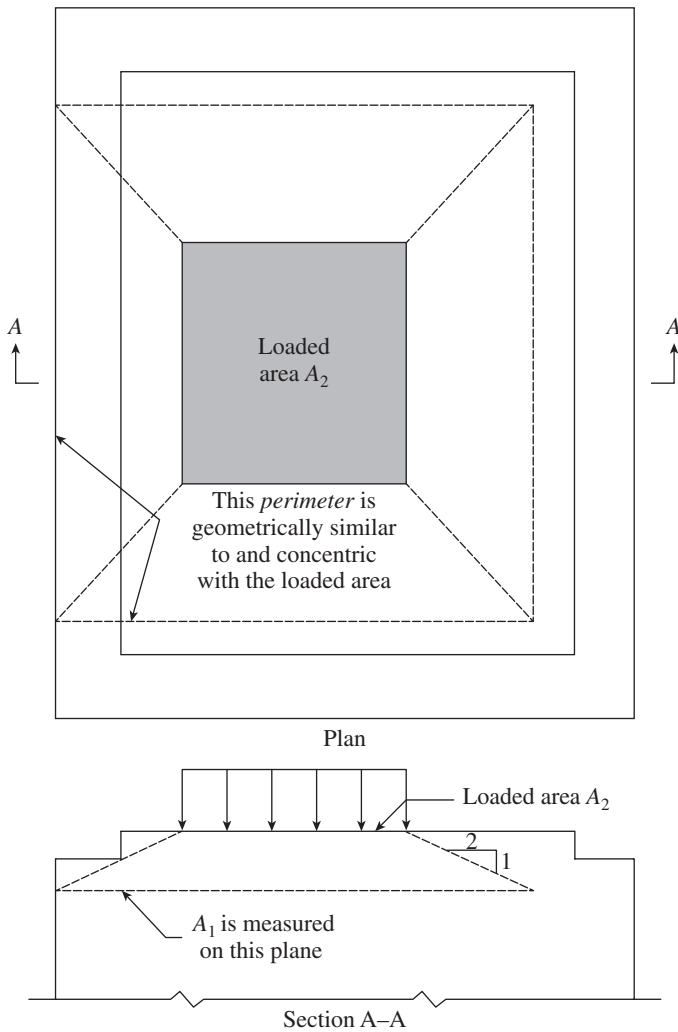


FIG. 15.16 Bearing area in a stepped or sloped footing

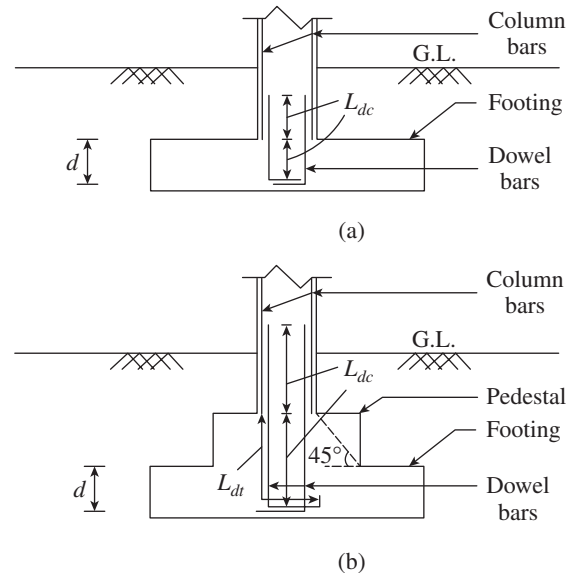


FIG. 15.17 Development length requirement (a) Column in compression (b) Column in tension

It has to be noted that the column or dowel bars of Fig. 15.17 are bent into the footing according to Clause 21.12.2.2 of the ACI 318 code, which states that ‘longitudinal reinforcement resisting flexure shall have 90° hooks near the bottom of the foundation with the free end of the bars oriented toward the center of the column’. In Indian practice, the bars are bent in the opposite direction, which is not correct. It is because this anchorage detail cannot provide an effective node point for the development of the diagonal compression strut mechanism. The bent length usually rests on the bottom mat

of reinforcement of footing, and a minimum length of 300 mm should be provided (see Fig. 6.1 of SP 34:1987). Similar detailing should be adopted when terminating the column reinforcement at the top of a building.

15.5.5 Design of Wall Footings

The design principles used for beam actions also apply to the wall footings with minor modifications. As a result of the very large rigidity of the wall, the footing below the wall behaves like a cantilever on both sides of the wall, as shown in Fig. 15.18. The soil pressure causes the cantilevers to bend upwards, and as a result, reinforcement is required at the bottom of the footing, as shown in Fig. 15.18. Experiments on footings showed the type of cracks as shown in Fig. 15.18.

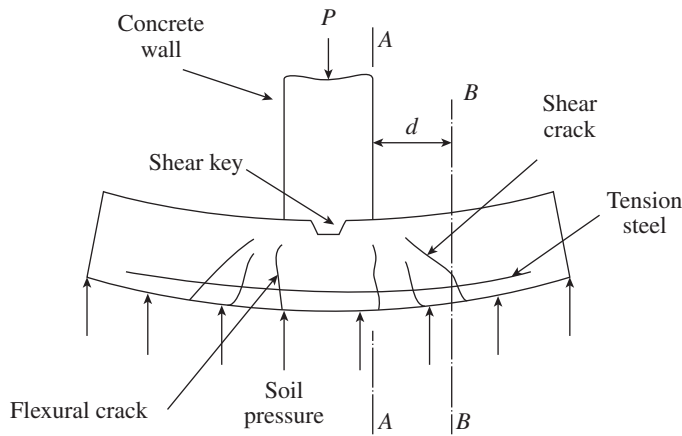


FIG. 15.18 Behaviour of wall footing

The calculation of development length is based on the section where maximum moment occurs. The maximum bending moment in footing supporting a concrete wall is given by

$$M_u = \frac{q_u(B-b)^2}{8} \quad (15.20)$$

where q_u is the soil pressure acting below the footing, B is the width of footing, and b is the width of the wall. For one-way shear, the critical section is at a distance d from the face of the wall, as in beams (section B-B in Fig. 15.18a). Thus the maximum shear force is calculated as

$$V_u = q_u \left(\frac{B-b}{2} - d \right) \quad (15.21)$$

The presence of the wall prevents two-way shear. Thicknesses of wall footings are usually chosen in 25 mm increments and the widths in 50 mm increments.

15.5.6 Design of Square Column Footings

The various steps involved in the design of footings and the expressions involved are given in this section. Let P be the service load on the column footing from the column and q_a be the SBC of soil. Let P_1 be the self-weight of footing (it can generally be taken as 10–20% of P).

Step 1 Determine the plan size of footing.

$$A = \frac{P + P_1}{q_a} \quad (15.22)$$

Provide this area in a form depending upon the type of footing as follows:

- (a) Square footing: $B = \sqrt{A}$
- (b) Rectangular footing: $B \times L = A$
- (c) Circular footing: $\frac{\pi D^2}{4} = A$

Step 2 Calculate upward soil pressure. After deciding the dimensions of the footing, the upward soil pressure acting on the base of footing is determined as

$$q_u = \frac{\text{Factored load}}{\text{Area of footing provided}} = \frac{\gamma_f P}{\text{Area}} \quad (15.23)$$

where γ_f is the load factor. Let us now consider the required equations for a square footing of uniform depth as shown in Fig. 15.19.

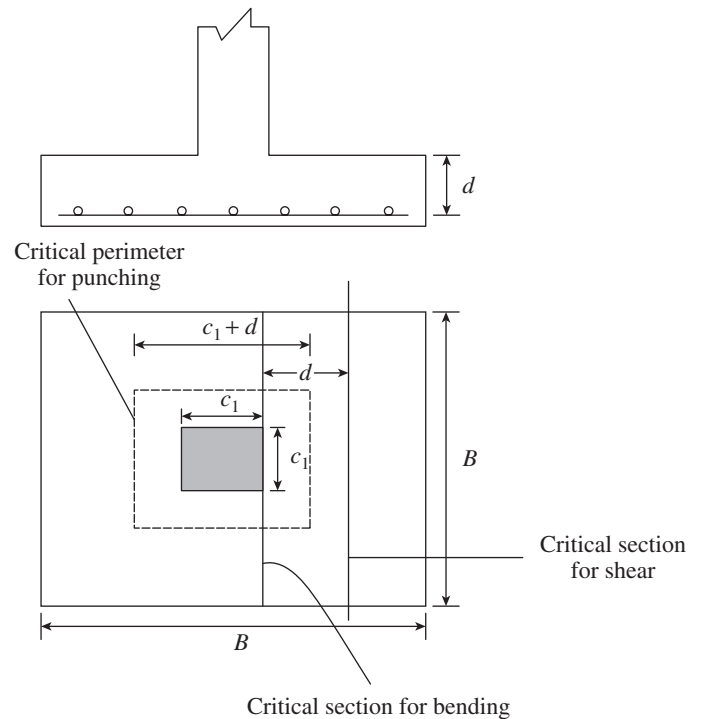


FIG. 15.19 Design of square footing

Step 3 Determine the depth of footing based on one-way shear considerations. By considering one-way shear, the depth is obtained from a section at d from the face of the column (see Fig. 15.19).

Shear force,

$$V_{u1} = q_u B \left(\frac{B - c_1}{2} - d \right) = \frac{q_u B}{2} (B - c_1 - 2d) \quad (15.24a)$$

If τ_c is the design shear strength,

$$\tau_c B d = V_{u1} \quad (15.24b)$$

Equating these two equations and assuming a value of τ_c from Table 19 of IS 456 for $100A_s/Bd = 0.15\text{--}0.50$ per cent (for example $\tau_c = 0.36 \text{ N/mm}^2$ for M20 concrete for $p_t = 0.25\%$), we may obtain the required depth of footing.

Step 4 Check for punching shear.

$$\text{Critical perimeter, } b_0 = 4(c_1 + d) \tag{15.25a}$$

Punching shear force,

$$V_{u2} = q_u[B^2 - (c_1 + d)^2] \tag{15.25b}$$

Punching shear resistance (Clause 31.6.3.1 of IS 456)

$$V_{n2} = k_s \tau_c [b_o d] \tag{15.25c}$$

where $k_s = (0.5 + \beta_c) \leq 1$ and $\tau_c = 0.25\sqrt{f_{ck}}$; for square column, $\beta_c = 1$ and hence $k_s = 1$, b_0 is the critical shear perimeter $= 4(c_1 + d)$. V_{n2} should be greater than V_{u2} .

Step 5 Calculate the area of steel. Taking moments at the face of the column, we get

$$M_u = \frac{q_u B}{2} \left[\frac{B - c_1}{2} \right]^2 = \frac{q_u B}{8} [B - c_1]^2 \tag{15.26}$$

The value of d required from bending moment consideration may be found by using

$$d = \sqrt{\frac{M_u}{k_2 f_{ck} B}} \tag{15.27}$$

where the value of k_2 may be obtained from Table 5.3 of Chapter 5 ($k_2 = 0.138$ for Fe 415 steel). We need to adopt the largest of the three depths calculated from bending, one-way shear, and punching shear considerations. Usually, the depth based on bending considerations will not govern. The area of steel may be determined by using

$$A_{st} = \frac{M_u}{j d f_y} \tag{15.28}$$

where the value of j may be obtained from Table 5.3 of Chapter 5 ($j = 0.8$ for Fe 415 steel). We may also determine the area of steel using Tables 2–4 of SP 16, after calculating $R = M_u/Bd^2$.

Check for minimum percentage of steel and bar spacing for crack control as given in Section 15.5 (as per Clauses 34.5.1, 34.5.2, and 26.3.3b of IS 456).

Step 6 Check for development length. Select the bar size whose development length is less than $[0.5(B - c_1) - \text{cover}]$. If it is not possible to get the required development length, provide 90° bends at the end.

Step 7 Check for transfer of force at the base of column. This may be checked as per Section 15.5.4.

Step 8 Check for development length of column bars. This may be checked as per Section 15.5.4 and Fig. 15.17. It has to be noted that the column bars should project into the footing for a length equal to the development length in compression, L_{dc} (see Fig. 15.20). Bars subjected to tension should be provided with a length of L_{dt} but the extra length ($L_{dt} - L_{dc}$) may be provided by bending the bars as shown in Fig. 15.20. If pedestals are not provided, this requirement (L_{dc}) alone will govern the footing depth (Subramanian 1993). Pedestals may be provided to reduce the depth, based on development length requirement. Typical reinforcement detailing for isolated square footing is shown in Fig. 15.20.

15.5.7 Design of Rectangular Footing

The expressions are derived in this section for a rectangular pad-type footing as shown in Fig. 15.21. Let M_{XX} be the moment at the face of the column at section X–X normal to the shorter span, B , and M_{YY} be the moment at the face of the column at section Y–Y normal to the larger span, L , due to the soil pressure q_u .

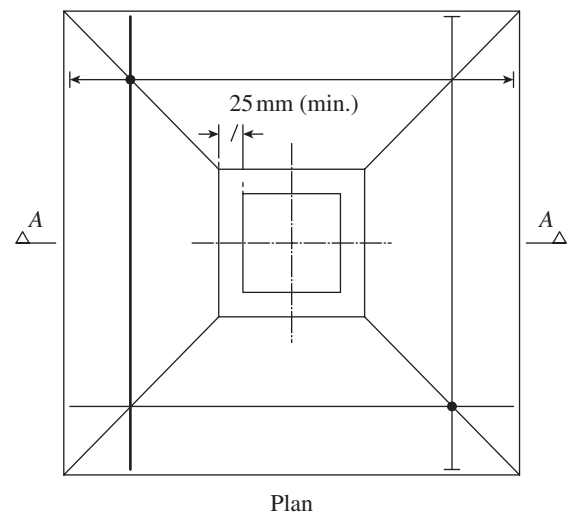
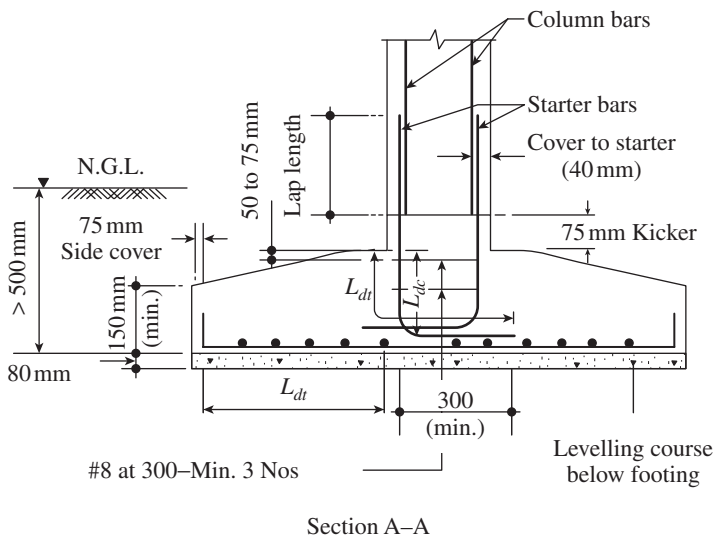


FIG. 15.20 Detailing of reinforcement in footing

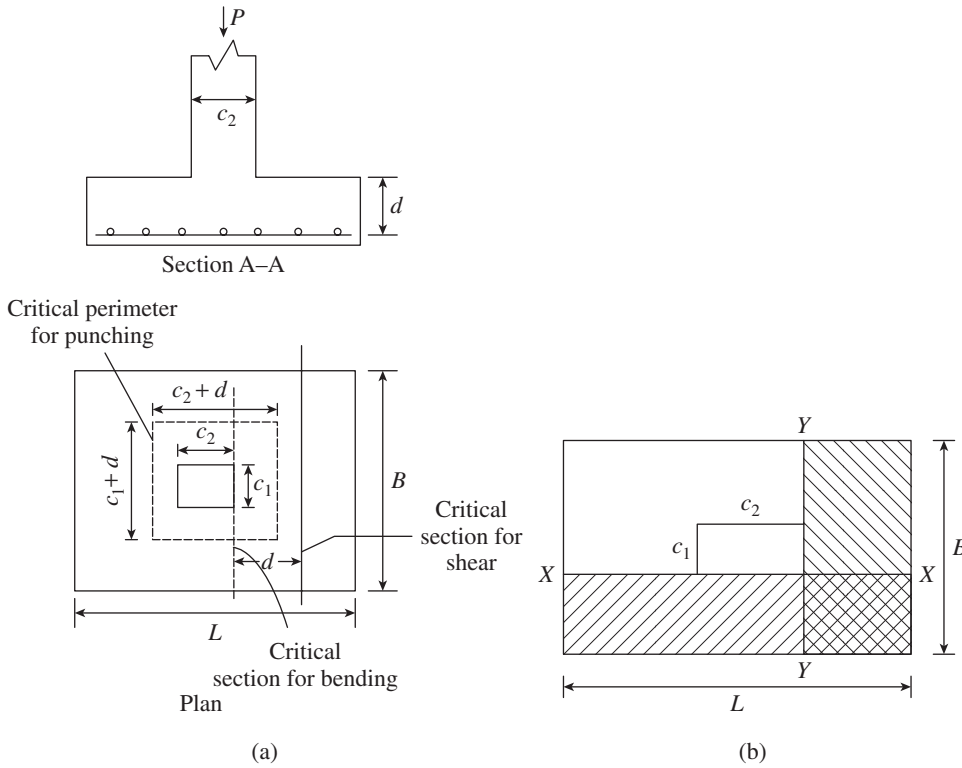


FIG. 15.21 Design of rectangular footing (a) Plan and elevation (b) Critical sections for bending moment

Thus we get,

$$M_{XX} = q_u L \left(\frac{B - c_1}{2} \right) \left(\frac{B - c_1}{4} \right) = \frac{q_u L}{8} (B - c_1)^2 \text{ with } q_u = \frac{P_u}{LB} \quad (15.29a)$$

Similarly,

$$M_{YY} = \frac{q_u B}{8} (L - c_2)^2 \quad (15.29b)$$

The design procedure is similar to that of square footings, except that the reinforcements are calculated in two directions and the check for one-way shear is to be made in both directions at a distance d from the face of the footing. All other checks are similar. In addition, the distribution of reinforcement should be made as discussed in Section 15.5.2 and Fig. 15.15. The step-by-step procedure for the design of concentrically loaded rectangular footings is illustrated in Example 15.4 and for eccentrically loaded rectangular footings in Example 15.5.

15.5.8 Design of Sloped Footings

In India, sloped footings are used when the thickness of footing exceeds about 300–350 mm and they have a sloped

top surface as shown in Fig. 15.22. This type of footing may require more depth but lesser reinforcement than uniform pad-type footing and hence may be economical. Moreover, the projection of the footing beyond the column face bends as a cantilever, and hence, the required flexibility is obtained by reducing the depth towards the free end, as is usually done in cantilever beams or slabs. As mentioned earlier, the edge thickness should be greater than 150 mm as per IS 456. Clause 34.1.1 of IS 456 states that in sloped or stepped footings, the effective cross section in compression should be limited by the area above the neutral plane, and the angle of slope or depth and location of steps should be such that the design requirements are satisfied at every section. Hence, there is no specific recommendation regarding the maximum slope. Dunham (1962) has recommended that the slope

should not exceed one in three for construction considerations ($\alpha = 18.4^\circ$). Practically, when the slope exceeds 20° , it will be difficult to vibrate the concrete and top forms need to be provided, which will increase the cost of construction. As the strength of the footing depends on the compressive strength

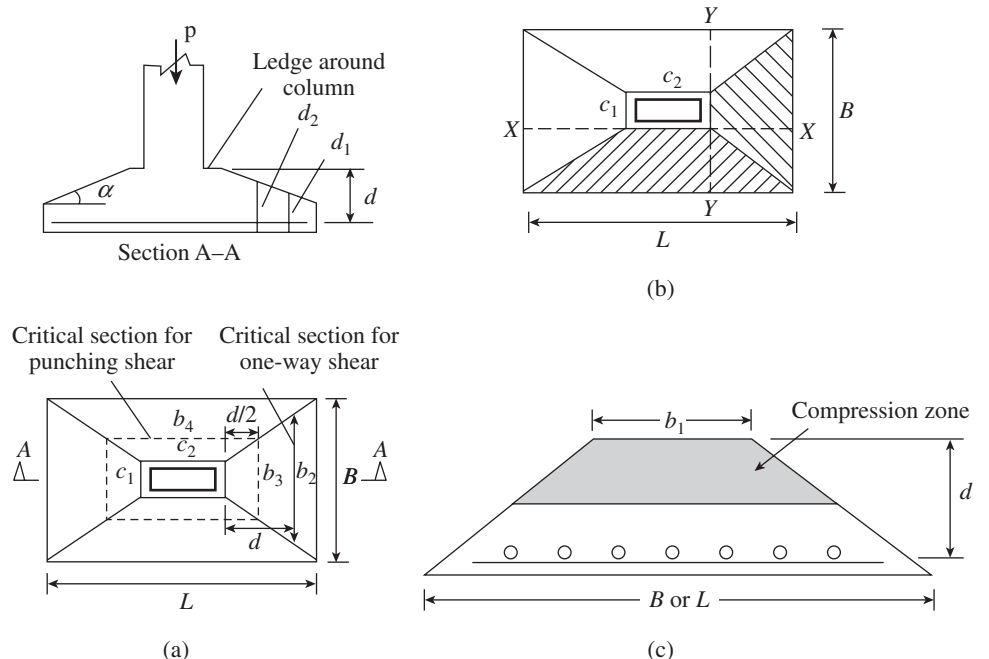


FIG. 15.22 Sloped rectangular footing (a) Sloped footing (b) Critical sections for bending (c) Trapezoidal section

of the concrete in the sloped portion, special care should be taken during placement, compaction, and curing such that concrete quality is maintained in this portion as well. There are three approaches to the calculation of bending moment and determination of depth of sloped footing (Subramanian 1995b).

Step 1 Determine the bending moment and corresponding depth.

- (a) In the first method, it is assumed that the bending moment is the same as in uniform pad-type footing. Thus, Eq. (15.29) can be used to calculate M_{XX} and M_{YY} .
- (b) A less conservative method assumes that the failure plane will be along the diagonals and the moment to be resisted is due to the loads in the trapezoidal area alone (Subramanian and Vasanthi 1989; Subramanian 1995b). Accordingly, the bending moments based on the trapezoidal area are derived as (see Fig. 15.22a)

$$M_{XX} = q_u \left[\left(\frac{L+c_2}{2} \right) \left(\frac{B-c_1}{2} \right) \right] \left[\left(\frac{2L+c_2}{L+c_2} \right) \frac{1}{3} \left(\frac{B-c_1}{2} \right) \right]$$

$$= \frac{q_u}{24} (2L+c_2)(B-c_1)^2 \quad (15.30a)$$

$$M_{YY} = \frac{q_u}{24} (2B+c_1)(L-c_2)^2 \quad (15.30b)$$

The bending moment capacity, M_n , of the trapezoidal footing, as shown in Fig. 15.22(c), and the lever arm, j , can be derived, and is given here (Dayaratnam, 2004):

$$M_n = Kb_1d^2f_{ck} + K_2(B-b_1)d^2f_{ck} \quad (15.31)$$

$$j = \frac{(K-K_2)b_1 + K_2B}{0.36k_u b_1 + 0.204(B-b_1)k_u^2} \quad (15.32)$$

where the values for the coefficients K , K_2 , and k_u for two grades of steel are given in Table 15.2.

TABLE 15.2 Design moment and neutral axis coefficients

Steel Grade	K	K_2	k_u
Fe 415	0.138	0.025	0.479
Fe 500	0.133	0.023	0.456

Equating Eq. (15.31) with M_{XX} and M_{YY} , the required effective depth in the two directions can be determined and the maximum value adopted. Similarly, equating Eq. (15.28) with Eq. (15.31), we may determine the required steel (using appropriate effective depth) in both directions.

- (c) When adopting method (a), the width of the column (or the dimension at the column base) is usually considered as the effective width to obtain the depth of footing, which is very conservative. However, some designers assume that the moment is resisted by an

effective width larger than the dimension at column base (Bhavnagri 1974; Jain and Jaikrishna 1977). One such approximation assumed is to use the formula

$$b_{eff} = c_1 + \frac{(B-c_1)}{8} \text{ and } b_{eff1} = c_2 + \frac{(L-c_2)}{8} \quad (15.33)$$

It has been found that method (b) yields a saving of 8.5 per cent in concrete and about 20 per cent in steel (Subramanian 1995b).

Step 2 Check for one-way shear. As discussed for uniform thickness (pad-type) footing, one-way shear has to be checked at a distance equal to the effective depth, d , from the face of the column (not from the edge of top of the footing). The shear force V_{u1} to be resisted is taken as that acting in the corresponding quadrant of footing. The area of concrete resisting the shear is taken as the breadth of the quadrant b_2 at the section, multiplied by the depth of the section d_1 (see Fig. 15.22a). The values of b_2 and d_1 can be determined from the geometry of the quadrant.

At critical section in the YY axis,

$$\text{Shear force, } V_{u1} = q_u \left(\frac{L-c_2}{2} - d \right) \left(\frac{B+b_2}{2} \right) \quad (15.34a)$$

If τ_c is the design shear strength, the capacity of the section for one-way shear

$$V_{n1} = \tau_c b_2 d_1 \quad (15.34b)$$

where τ_c is the design shear strength of concrete obtained from Table 19 of IS 456.

V_{n1} should be greater than V_{u1} ; else the depth has to be increased. Similar checks have to be done at critical sections along the XX axis at a distance d from the face of the column.

Step 3 Check for two-way shear. As in the case of pad-type footing, the depth of the footing has to be checked at a distance of $d/2$ from the face of the column for two-way shear. The lengths b_3 and b_4 as well as the depth d_2 at this section have to be calculated (see Fig. 15.22a). The punching shear force is given by

$$V_{u2} = q_u (LB - b_3 b_4) \quad (15.35a)$$

Punching shear resistance (Clause 31.6.3.1 of IS 456) is calculated as

$$V_{n2} = k_s \tau_c [b_o d_2] = k_s \tau_c [2(b_3 + b_4)d_2] \quad (15.35b)$$

V_{n2} should be greater than V_{u2} ; else the depth has to be increased.

The other checks for development length (in both directions), transfer of force at the base of column, and development length of column bars have to be done as already discussed in Section 15.5.6 for square pad-type footing. The design of sloped square footings is illustrated in Example 15.3.

15.6 DESIGN OF COMBINED FOOTINGS

When the distance between two columns is small, the individual footings of these columns will overlap and hence it may be necessary to provide a *combined footing* (see Fig. 15.2).

Such combined footings are also adopted when one of the columns is very close to the property line. In such a case, designing an eccentric footing will not be possible unless the load acting on the edge column is small. A better alternative will be to combine the footing of this edge column with that of another column in the same line. When one column is near the property line and the next column in that row is far away, connecting these columns by a combined footing may be expensive. In such cases, counterweights called 'dead man' may be provided for the edge column to take care of the eccentric loading (Kramrisch 1985). Combined footing can be divided into two categories: (a) Those supporting only two columns and (b) those supporting multiple columns (more than two columns). Combined footing supporting two columns is discussed in Section 15.6.1.

When the SBC of the soil is low, the footings of individual columns merge, and hence, individual footings are combined to form a *strip column footing* that supports more than two columns that are placed in rows (see Fig. 15.23). The longitudinal bending moment on the base at any section is the sum of the anticlockwise moments of each load to the left of the section minus the clockwise moment of the upward pressure between the section and the left-hand end of the base. The shearing force at any section is the algebraic sum of the vertical forces on one side of the section. In the transverse direction, the moment due to the cantilevering slab from the face of the column has to be considered.

It has to be noted that strip footings can support the loads more economically than single footings because the individual strips behave like continuous beams whose moments are much smaller than the cantilever moments in large single footings. An end overhang on either side of footing will reduce the end moment equal to that of span moment (Subramanian 1995a); for a two-column footing, the overhang should be about $L/\sqrt{8} = 0.354L$, where L is the inner span (Varghese 2009). Once the bending moments and shear forces are determined, the design and other checks are done similar to individual footings.

When there is irregular column spacing or there are varying column loads, a slab with upstanding T-beam may be used. These beams make the foundation more rigid and the loads will be more effectively distributed to the foundation. The degree of rigidity that must be given to the foundation beam is governed by the limiting differential movements that can be tolerated by the superstructure and by economies in the size and amount of reinforcement in the beams. Too great a rigidity should be avoided since it will result in high bending moments and shearing forces and the possibility of forming a wide crack if moments and shears are underestimated (this is always a possibility since it is difficult to accurately calculate settlements). When the beam is provided, it is designed as a continuous beam and the base slab as cantilevering from either side of the beam. More discussions on design, detailing, and exact methods of analysis of such foundations may be found in the work of Varghese (2009).

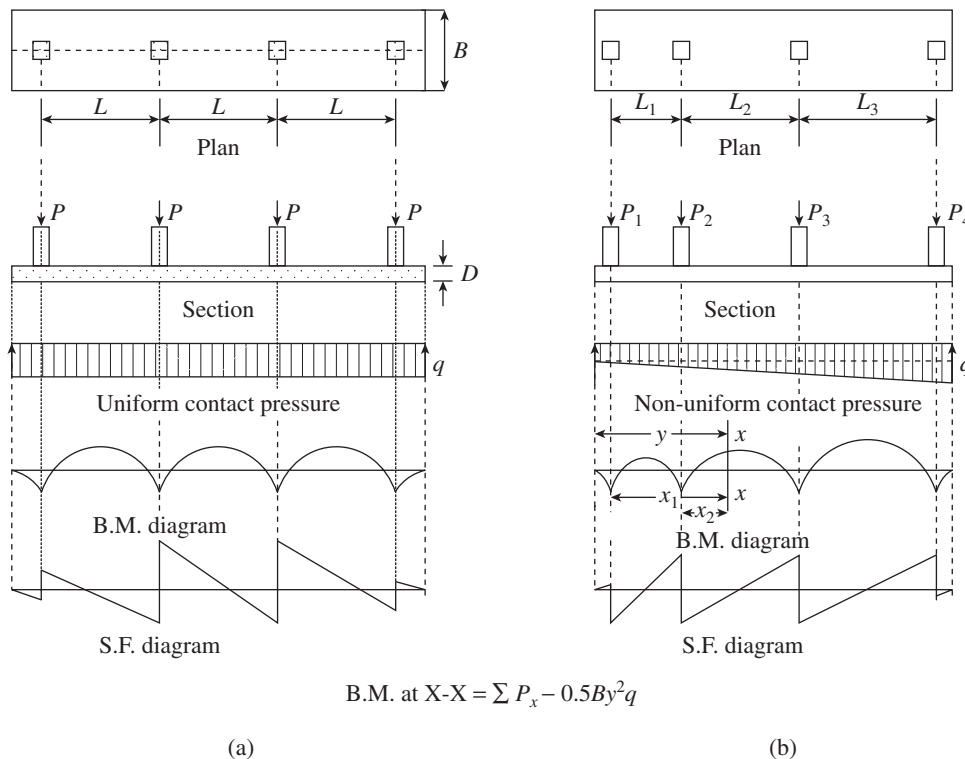


FIG. 15.23 Strip column footing (a) With equal column spacings and loads (b) With unequal column spacings and loads

When the strips are arranged in both directions, a *grid foundation* is formed as shown in Fig. 15.24(a). In many cases, especially when the SBC is very low, the strips may merge resulting in a *mat foundation* or *raft foundation*, as shown in Fig. 15.24(b). The structural action of such a mat is similar to a flat slab or flat plate but acting upside down, that is, loaded upwards by the soil pressure and downwards by the concentrated column reactions. However, it has to be noted that the soil pressures on the raft are not uniform; soil pressures near the column locations will be larger than those away from columns, due to the flexibility of the raft slab. Hence, rafts are often analysed by using finite element methods or finite grid methods (Bowles 1996). The raft may also be provided with beams connecting the columns, making it more rigid. Strip or mat foundations may also be provided with column

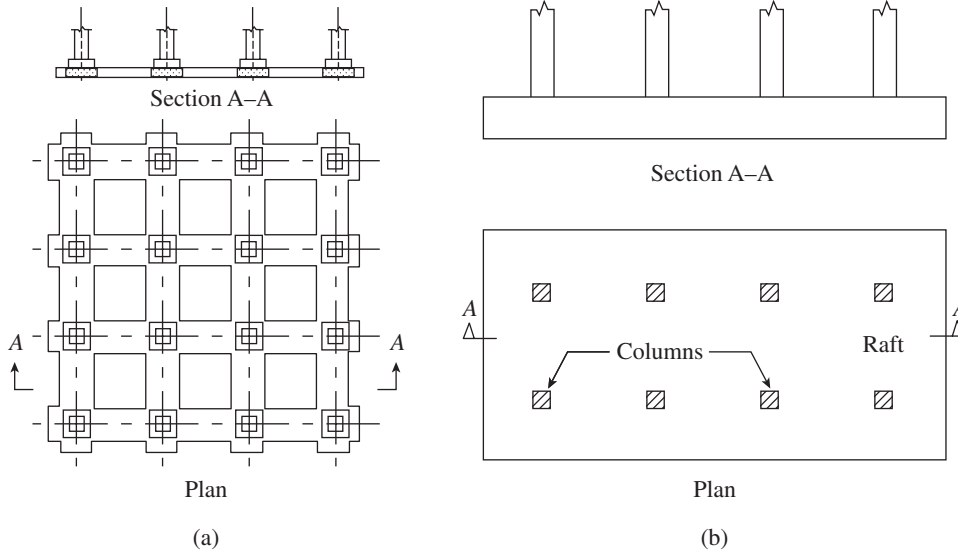


FIG. 15.24 Arrangement of strips (a) Grid foundation (b) Mat foundation

pedestals, as shown in Fig. 15.24(a), in order to provide the required shear strength or development length for dowels. In addition to providing large bearing areas, the strip and mat foundations, due to their continuity and rigidity, reduce the differential settlement of individual columns relative to each other. Hence, they are used when differential settlements, due to local variations in the quality of soil, are expected. The design of mat foundations is outside the scope of this book and interested readers may find them in ACI 336 (1988) and the works of Baker (1948), Varghese (2009), Gupta (1997), Curtin, et al. (2006), and Dayaratnam (2004). When the SBC of the soil is so low that even rafts cannot be supported, deep foundations like piles have to be used. It is also possible to combine piles with raft to have a piled-raft foundation (Clancy and Randolph 1996).

15.6.1 Two-column Footings

The first step in the design of combined footings is to make the centroid of the footing area coincide with the resultant of the two-column loads. This produces uniform bearing pressure over the entire area and avoids tilting of the footing. In plan, the footing may be rectangular, trapezoidal, or T-shaped (see Fig. 15.25). The simple relationships as shown in Fig. 15.25 may be used to determine the shape of the bearing area, so that the centroid of the footing and the resultant of loads coincide. In general, the distance from the centre of the exterior column to the property line, m , will be known. Using this value, the SBC of soil, the loads P_1 and P_2 acting on the footing,

the distance from the centre of the exterior column to the resultant of both column loads, n , and the breadth and length of footing can be fixed using the relationships given in Fig. 15.25 (Kramrisch and Roberts 1961; Kramrisch 1985).

Behaviour of Combined Two-column Footing

As in isolated footings, the factored net soil pressure q_u is computed as the resultant factored load divided by the selected base area. This pressure is assumed to act as uniformly distributed load. It has to be noted that when there are moments in addition to loads, the pressure distribution will be non-uniform. However, it may be conservative to assume uniform distribution.

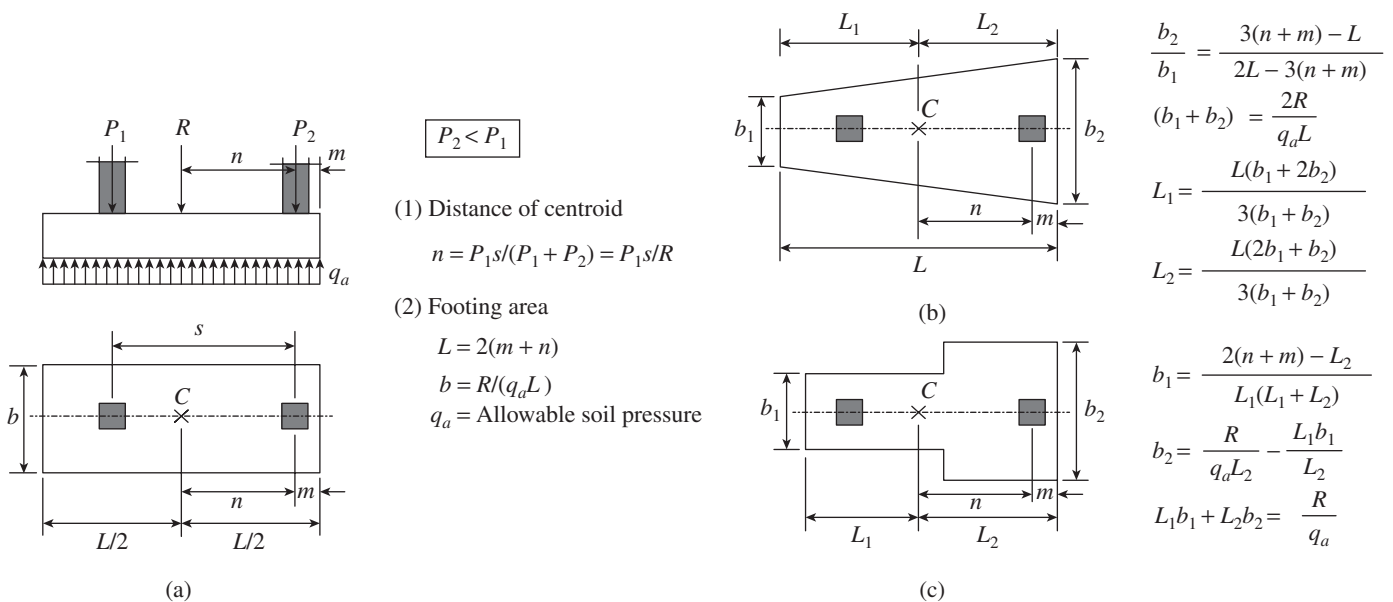


FIG. 15.25 Two-column footings (a) Rectangular (b) Trapezoidal (c) T-shaped

The footing slab is subjected to two-way bending and one-way as well as punching shear. In most cases, the width of footing, B , will be considerably less than the length, L . Hence, there will be a predominant flexural behaviour in the longitudinal direction (as shown in longitudinal beam strips $A-B-C$ of Figs 15.26a and b), and the two-way action will be limited and present only in the transverse strips in the neighbourhood of columns (as shown by strips $A-D$ and $B-E$ in Fig. 15.26a). It may be conservative to assume that the wide longitudinal beam of width B and length L (subjected to

a factored load $w = q_u B$) is supported on two-column strips, which in turn act as transverse beams cantilevering from the columns. The width of the column strip is usually assumed as the width of column plus $0.5-1.0d$ on either side of the column, as shown in Fig. 15.26(a), where d is the effective depth of footing. It has to be noted that IS 456 and ACI 318 codes do not specify the exact width for the transverse column strip. The width selected will have little influence on the transverse bending capacity of the footing, but it can affect the punching shear resistance and perhaps the shear resistance.

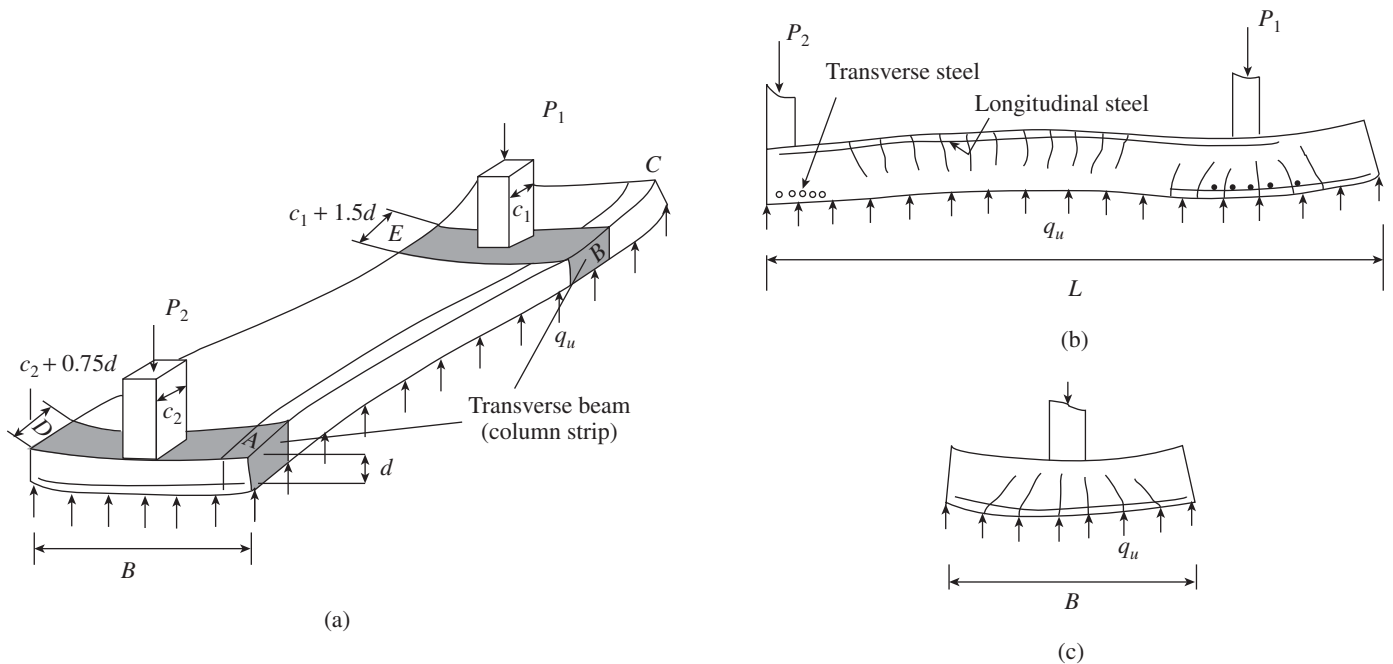


FIG. 15.26 Behaviour of two-column footing (a) Load distribution (b) Behaviour of longitudinal beam strips (c) Behaviour of transverse beam strips

Design Considerations

The design of combined footings has not been standardized by the codes. Hence, practising designers use slightly varying approaches. The following are the various steps of one such approach:

Step 1 Determine the size of footing. As in the case of isolated footings, the area of footing is determined for the service loads, and the footing dimensions are selected so that the centroid of the column loads coincide with the centroid of footing.

Step 2 Calculate the bending moment and shear at various locations. The loads are then multiplied by the appropriate load factors, and the shear and bending moments are calculated from statics for these loads, considering the footing slab as simply supported on the two-column strips, with overhangs (if any) beyond each column strip, and assuming the supports at the column centre lines, as shown in Fig. 15.27.

Step 3 Determine the thickness of the footing. The thickness of the footing will usually be governed by shear considerations. The critical section for one-way shear is taken at a distance d from the face of each column. As shear reinforcement is generally not provided for slab footings, determine the depth required for shear by assuming the value of τ_c from Table 19 of IS 456 corresponding to $p_t = 0.25-0.50$.

Step 4 Check for punching shear. Check the calculated depth for safety of punching shear, taking the critical section for punching shear at a distance $d/2$ from the face of each column. As per Clause 31.6.3.1 of IS 456, the punching shear stress should not exceed $\tau_p = k_s(0.25\sqrt{f_{ck}})$, where $k_s = 0.5 + \beta_c \leq 1$, where β_c is the ratio of the short side to the long side of the column. It has to be noted that if the column is near the boundary line, punching will be resisted by only three sides of the critical perimeter. In such a situation, Wight and MacGregor (2009) suggest checking of shear stresses due to direct shear and the shear due to moment transfer as in flat plates, using Eq. (11.13) of Chapter 11.

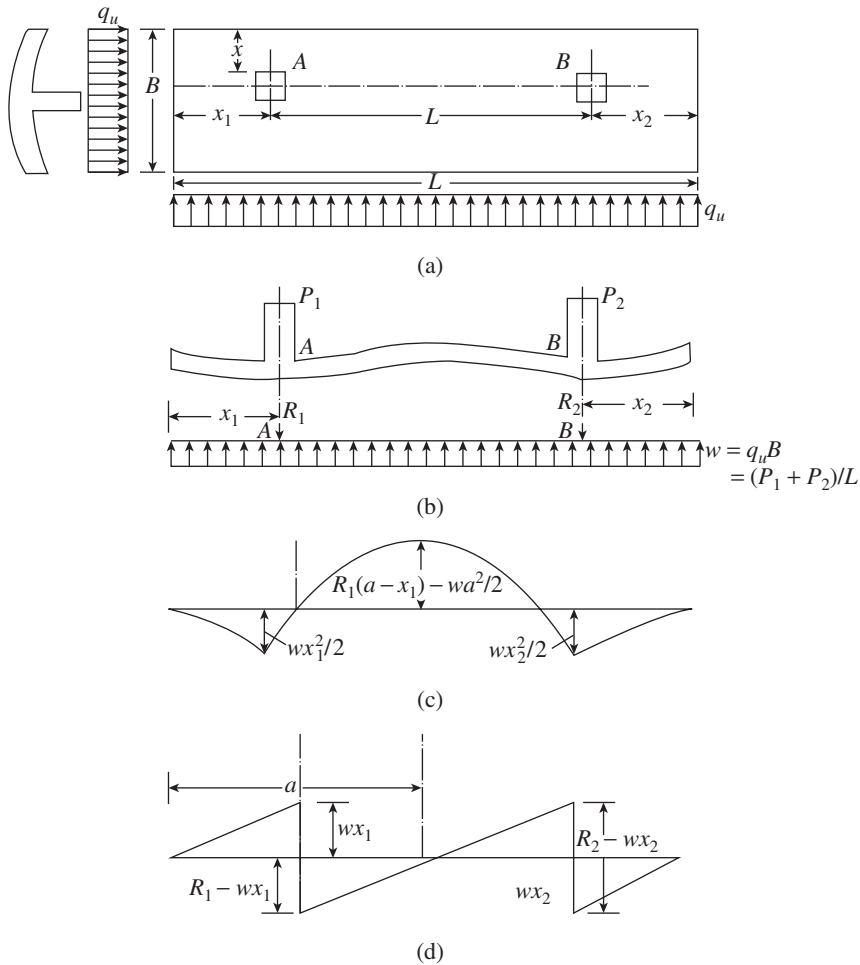


FIG. 15.27 Bending moment and shear force in two-column footing (a) Rectangular combined footing (b) Bending of footing and loading (c) Bending moment diagram (d) Shear force diagram

Step 5 Determine the reinforcement in the long direction. Find the bending moment where shear $V = 0$ and determine reinforcement in the long direction for the chosen depth. Check whether minimum steel requirements and the reinforcement required for resisting shear are satisfied. Provide minimum steel in the remaining parts of the footing.

Step 6 Check for development length for the chosen diameter of steel.

Step 7 Determine the reinforcement in the short direction. Design for transfer of column loads in the transverse direction by assuming that the column load is spread over a width in the long direction equal to column width plus $0.5-1.0d$ on either side of the column, if that much footing is available. This transverse steel is designed for the cantilever action of the slab projecting from the face of the column and placed on top of the longitudinal steel. Provide minimum steel in the remaining parts of the footing in the transverse direction.

Step 8 Check for development length in the transverse direction as well for the chosen diameter of steel. In many

cases, it may be necessary to bend the bars at the ends to get the necessary development length.

Step 9 Check for shear in the transverse direction as well at a distance d from the face of the column; in many cases this check may not be necessary, as the width of the footing resisting shear will be large and the critical section will be near the edge of the footing.

Step 10 Check for transfer of force at the column face. This check is similar to that done for individual footings. If the limiting bearing resistance is less than the column load, dowels must be provided.

Step 11 Detail the reinforcement as per design and provide nominal reinforcement wherever necessary. Typical detailing for combined rectangular footing is shown in Fig. 15.28. It has to be noted that shear stirrups have been provided to reduce the depth of footing. In order to prevent shear failure along the inclined plane (corbel type of failure) in footing, where a column is placed on the edge, SP 34:1987 suggests providing horizontal U-bars around the vertical starter bars, as shown in Fig. 15.29.

The design of trapezoidal combined footing is similar to that of rectangular combined footing; however, in such footings the longitudinal bars are usually arranged in a fan shape with alternate bars cut off at some distance away from the narrow end (typical detailing is shown in Fig. 15.30).

15.6.2 Design of Combined Slab and Beam Footing

When the depth required for slab footing is large based on shear considerations, it will become uneconomical. In such cases, a combined slab and beam footing may be provided as shown in Fig. 15.31, in which a central longitudinal beam connects the two columns.

The base slab bends transversely under the action of uniform soil pressure from below and behaves like a one-way cantilevered slab. The loads transferred from the slab are resisted by the longitudinal beam. The depth of the beam is usually governed by shear considerations, at a distance d away from the face of the column or pedestal. The width of the beam is chosen to be equal to or greater than the sides of columns at a right angle to the beam. The pedestal may be used to provide the required development length. The top and bottom reinforcements in the beam are decided based on the longitudinal bending moment diagram and designed as a rectangular or T-beam. The beam will be subjected to high

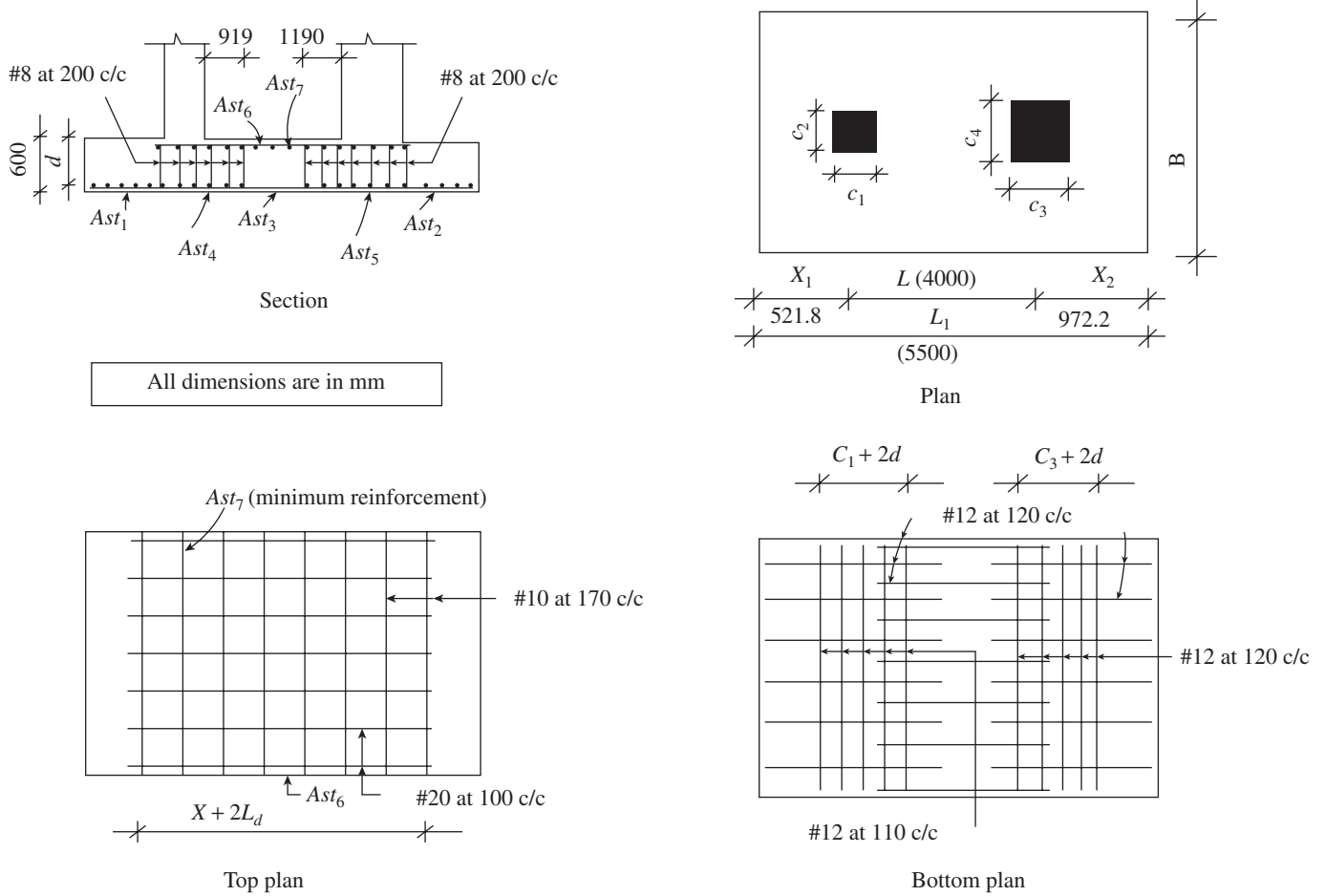


FIG. 15.28 Typical detailing of combined rectangular footing
 Note: $(X + 2L_d)$ may be greater than EL_1 , in which case, the bars must be well anchored in the slab.

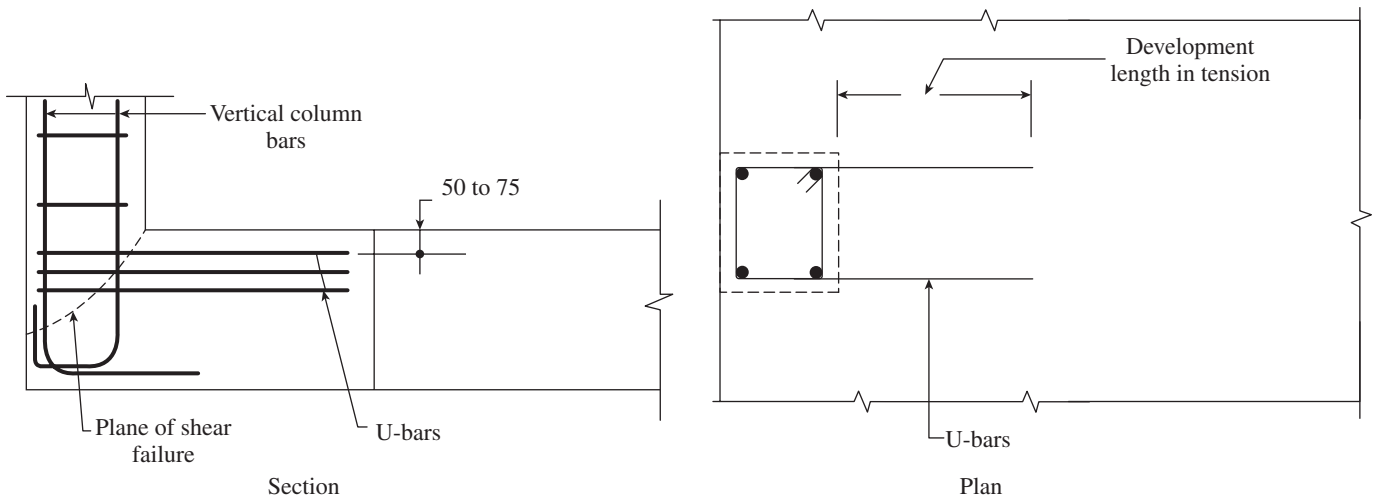


FIG. 15.29 Column at the edge of footing

shear forces, which may be resisted by providing multi-legged stirrups, as shown in Fig. 15.31.

The base slab may be flat or tapered for economy. The thickness of slab should be checked for one-way shear at a distance d away from the face of the beam. The flexural

reinforcement in the slab, designed for the cantilever moment at the face of the beam, should be provided at the bottom of the slab, as shown in Fig. 15.31. Punching shear will not govern such beam and slab footings. The reinforcements should be checked for development length requirements.

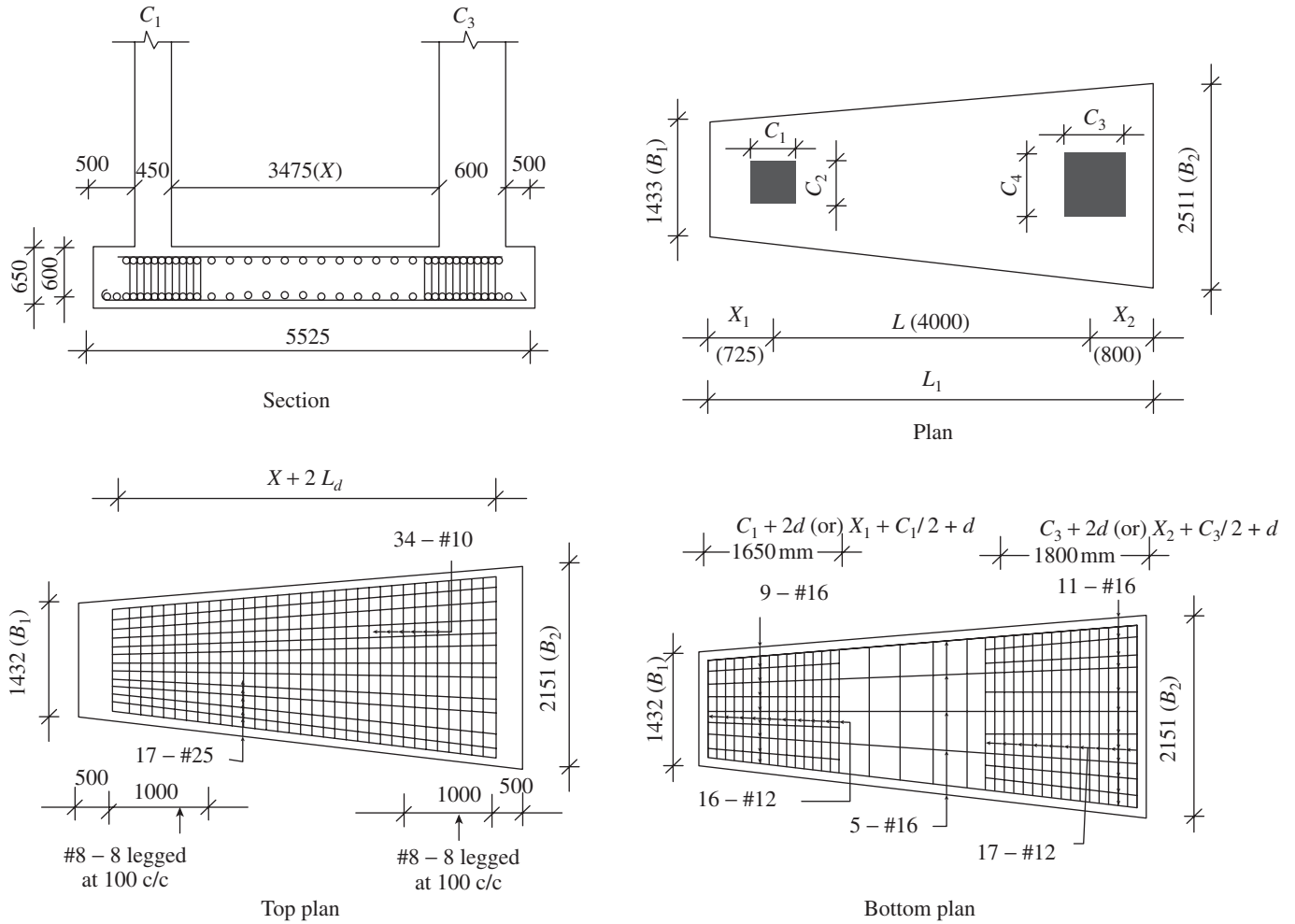


FIG. 15.30 Detailing of trapezoidal footing

Note: $(X + 2L_d)$ may be greater than L_1 , in which case, the bars must be well anchored in the slab. L_d is the development length.

15.6.3 Design of Combined Footing with Strap Beam

When the distance between the two columns is large, it is economical to provide *strap footings*, in which a beam connecting the two-column footings is provided, as shown in Fig. 15.2(d). It is assumed that the *strap beam* is rigid and that it transfers the load from the columns to the footings and not directly to the soil. The column loads are transferred to the soil only through the independent footings. The areas of independent footings are so chosen that the soil pressure acting on the footings is uniform and the resultant soil pressure on the footing areas coincide with the C.G. of the column loads (usually a breadth is chosen for

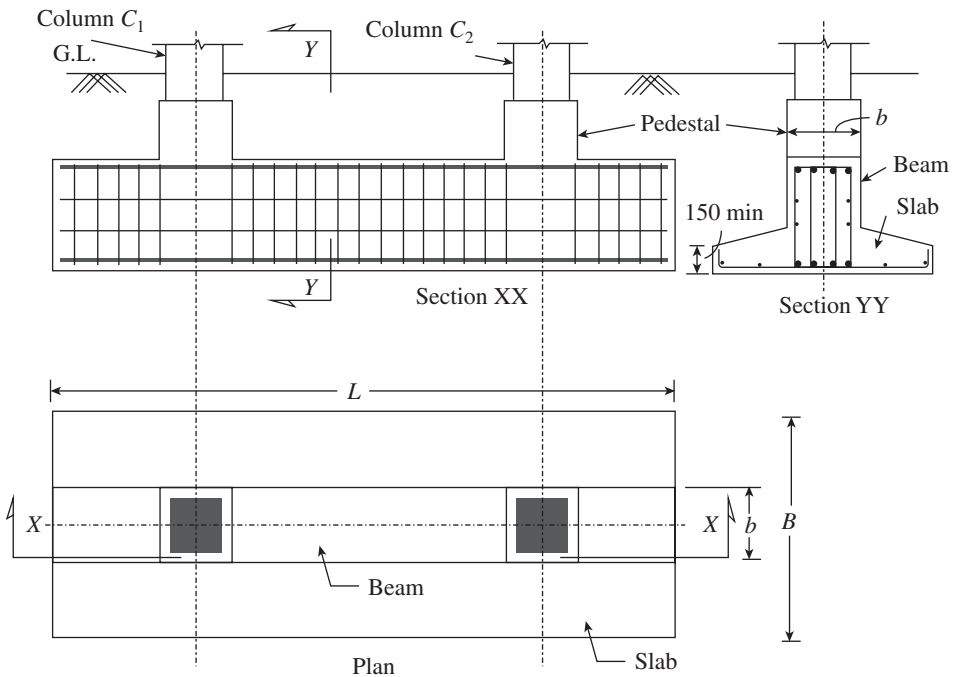


FIG. 15.31 Combined slab and beam footing

the footings and the length of each determined based on C.G. consideration). The footings for columns C_1 and C_2 are designed as isolated footings for cantilever bending moment of the slab (on both sides of the rigid strap beam) and shear force considerations.

The width of strap beam is generally equal to or greater than the sides of columns at a right angle to the strap beam. The strap beam is designed as a rectangular beam by assuming that the loads are acting uniformly on it from (a) columns in

the downward direction and (b) footings of columns C_1 and C_2 in the upward direction, as shown in Fig. 15.32.

The depth of the strap beam is decided based on bending moment and shear force considerations. Longitudinal reinforcements are provided based on bending moment considerations and transverse stirrups based on shear considerations. More details on design of combined footings may be found at <http://osp.mans.edu.eg> and the work of Varghese (2009).

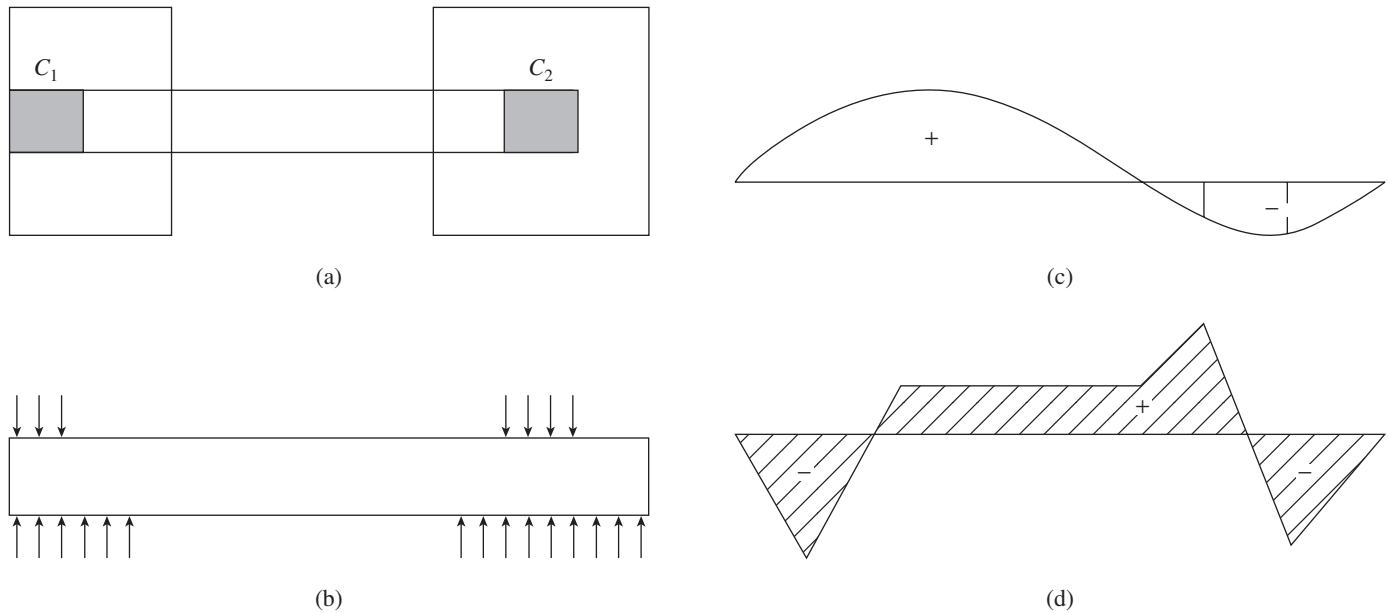


FIG. 15.32 Bending moment and shear force in strap beam (a) Plan (b) Loading on strap beam (c) Bending moment diagram (d) Shear force diagram

15.7 DESIGN OF PLAIN CONCRETE FOOTINGS

Occasionally, plain concrete footings are used to support light loads, especially when the supporting soil has good SBC. Such footings are also called *pedestal footings*. The footing will be in the form of a solid rectangular unreinforced concrete block. The depth of the plain concrete pedestal can be determined based on the *angle of dispersion* of the load as follows (Clause 34.1.3 of IS 456):

$$D = 0.5(L - b) \tan \alpha \quad (15.36a)$$

where

$$\tan \alpha < 0.9 \sqrt{1 + \frac{100q_u}{f_{ck}}} \quad (15.36b)$$

q_u is the calculated maximum bearing pressure at the base of the pedestal, N/mm^2 , and α is the angle with the horizontal as shown in Fig. 15.33.

In practice, the dispersion is taken as 45° , that is, one horizontal to one vertical, in cement concrete footings (this value will be obtained when $q_u = f_{ck}/400$) and one vertical to two-thirds horizontal for lime concrete (IS 1080:1985). Though no tension steel is required in such a footing, it is always

advisable to provide minimum shrinkage steel. Moreover, when the depth to transfer the load to the ground bearing is less than the permissible angle of spread, the foundations should be reinforced (IS 1080:1985).

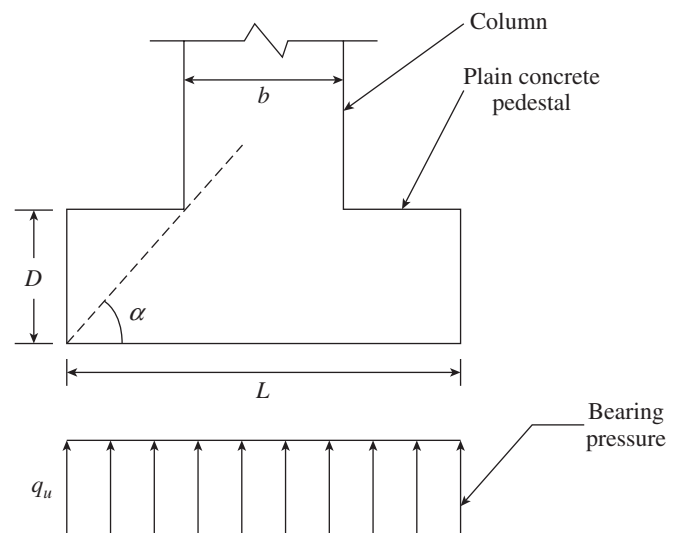


FIG. 15.33 Thickness of plain concrete footing

15.8 DESIGN OF PILES

Pile foundation is provided under the following conditions:

1. Top layers of soil are highly compressible and have very low SBC for it to support structural loads through shallow foundations.
2. Rock level at site is shallow enough to make end-bearing pile foundation economical.
3. Lateral forces are relatively predominant.
4. Expansive soils like black cotton soil are present at the site.
5. The structure is at an offshore location.
6. The foundation is subjected to strong uplift forces.
7. The structure is near flowing water (e.g., bridge abutments), where it is required to safeguard foundation against erosion.

A *pile* is a slender column provided with a cap to receive the column load and transfer it to the underlying soil layer or layers. As mentioned earlier, concrete piles are categorized as (a) driven cast in situ piles, (b) bored cast in situ piles,

(c) driven precast piles, and (d) precast piles in pre-bored holes. Based on their function, they are classified as end-bearing piles, friction piles, compaction piles, anchor piles, and uplift piles. Based on their effect of installation, they are classified as displacement piles (examples are driven concrete piles) and non-displacement piles (examples are bored cast in situ or pre-cast piles). Some of these piles are shown in Fig. 15.34. For a complete description of different types of piles, refer to the work of Tomlinson and Woodward (2008).

Soil Design

Similar to footings, piles should also be designed for soil and structural considerations. Piles transmit the loads to the ground either by skin friction with soils made of sandy materials, by cohesion with soils that contain clay, or by compression at the tip when the pile reaches bedrock or other resistant layer of soil. Usually, a combination of upward skin friction along the pile and vertical compressive force at the tip of the pile is used to calculate the bearing capacity of a pile.

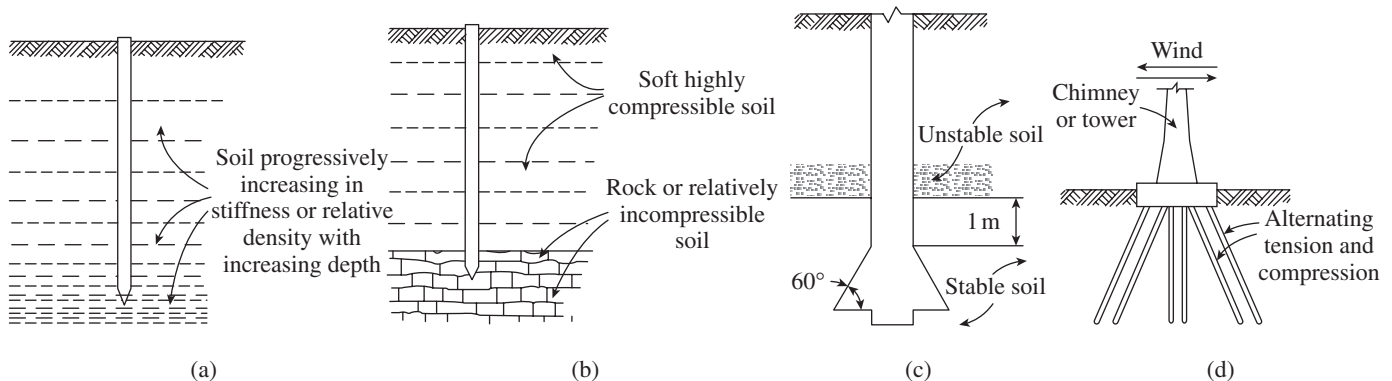


FIG. 15.34 Different types of piles (a) Friction pile (b) End-bearing pile (c) Bored cast in situ under-reamed pile (d) Racking or batter pile
Source: Tomlinson and Woodward 2008 (adapted)

15.8.1 Behaviour of Piles

The bearing capacity of a pile depends on (a) type, size, and length of pile, (b) type of soil, and (c) method of installation. Let us consider a pile loaded gradually by increasing the load at top, as shown in Fig. 15.35(a). The load–settlement curve for this pile can be obtained, as shown in Fig. 15.35(b), by plotting the settlement of the pile tip at every stage of loading. The behaviour of the pile in increasing load is described as follows (Saran 2006):

1. When an initial load Q_1 is applied on the top of the pile, the axial load at the top of the pile will be Q_1 , and

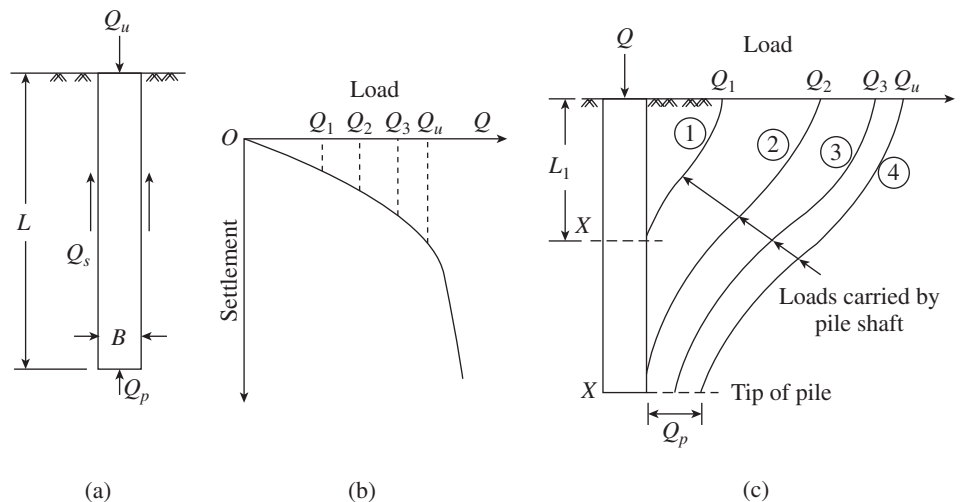


FIG. 15.35 Behaviour of piles (a) Single pile (b) Load–Settlement curve (c) Load transfer mechanism

at a distance L_1 from the top this load diminishes to zero. That is, the load Q_1 applied on the pile is resisted by skin friction alone, as shown by curve 1 of Fig. 15.35(c).

2. When the load is increased to Q_2 , the total load Q_2 is resisted by the skin friction along the entire pile, as shown by curve 2 of Fig. 15.35(c).
3. When the load exceeds Q_2 , part of this load is transferred to the soil at the base of the pile as compressive force and the remaining load is transferred by skin friction, as shown by curve 3 of Fig. 15.35(c). The friction load attains the ultimate value Q_s at this load level, and any further increase in load will only increase the compressive load at the pile tip.
4. When the load is increased further, the compressive load at the pile tip also reaches its ultimate value Q_p , as shown by curve 4 of Fig. 15.35(c), and the pile will fail by punching shear.

Thus, the ultimate bearing capacity of the pile, Q_u , can be calculated as

$$Q_u = Q_p + Q_s \quad (15.37)$$

where Q_p is the compressive force at the tip of the pile and Q_s is the upward skin friction along the pile.

15.8.2 Static Formula for Pile Capacity

The methods used to estimate the ultimate load carrying capacity of piles are categorized as (a) static analysis, (b) dynamic analysis, and (c) static in situ test. The static formula, which is in more common use than the dynamic formula, as given in IS 2911 is discussed here. The dynamic formula is more useful to predict the bearing capacity of driven piles in cohesionless soils. Static In situ test, often referred to as *pile load test*, is more reliable than the other two methods but is expensive and time-consuming. IS 2911(Part 4):1985 recommends that one-half to two per cent of the total number of piles are to be tested. Pile load tests are very useful to confirm the ultimate load in cohesionless soils. In cohesive soils, the results of pile load tests should be viewed cautiously as the test results may be affected by pile driving, development of pore pressure, and inadequate time allowed for consolidation settlement.

Pile Capacity in Granular Soils

The static formula for determining the ultimate load capacity, Q_u , of piles in granular soils is given, as per IS 2911(Part1-Sec1):2010, by

$$Q_u = A_p(0.5D\gamma N_\gamma + P_D N_q) + \sum_{i=1}^n K_i P_{Di} \tan \delta_i A_{si} \quad (15.38a)$$

where A_p is the cross-sectional area of pile tip in m^2 ; D is the diameter of shaft in m, γ is the effective unit weight of the soil at pile tip in kN/m^3 , N_γ and N_q are the bearing capacity factors (given by Eq. 15.8), depending on the angle of internal friction of the soil, ϕ , at pile tip, P_D is the effective

overburden pressure at pile tip in kN/m^2 , K_i is the coefficient of earth pressure applicable to the i th layer, P_{Di} is the effective overburden pressure for the i th layer in kN/m^2 , δ_i is the angle of wall friction between the pile and soil for the i th layer, A_{si} is the surface area of pile shaft in the i th layer in m^2 , and the summation is done for layers 1 to n in which the pile is installed and which contribute to positive skin friction. The first term of Eq. (15.38a) gives the end-bearing capacity and the second term gives the skin friction resistance.

The earth pressure coefficient, K_i , depends on the nature of soil strata, type of pile, spacing of pile, and its method of construction. For driven piles in dense sand and with ϕ varying between 30° and 40° , IS 2911 suggests using K_i in the range of 1–2. Similarly, the value of δ may be taken equal to the friction angle of the soil around the pile shaft. The maximum effective overburden at the pile tip, P_D , should correspond to the critical depth, and for $\phi = 30^\circ$, it may be taken as 15 times the diameter of the pile and is increased to 20 times for $\phi = 40^\circ$.

Pile Capacity in Cohesive Soils

The ultimate load capacity of pile, in kN , in cohesive soils is given by IS 2911 as

$$Q_u = A_p N_c c_p + \sum_{i=1}^n \alpha_i c_i A_{si} \quad (15.38b)$$

where A_p is the cross-sectional area of pile in m^2 , N_c is the bearing capacity factor, which may be taken as 9, c_p is the average cohesion at pile tip in kN/m^2 , α_i is the adhesion factor for the i th layer (see Fig. 15.36), c_i is the average cohesion for the i th layer in kN/m^2 , and A_{si} is the surface area of pile shaft in the i th layer in m^2 . The first term of Eq. (15.38b) gives the end-bearing resistance and the second term gives the skin friction resistance.

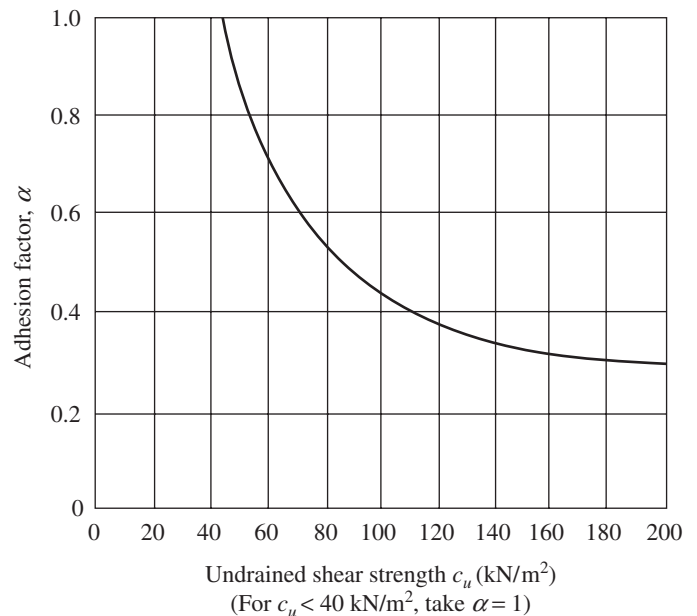


FIG. 15.36 Variation of adhesion factor with undrained shear strength

IS 2911 (Part 1, Section 1):2010 also provides equations to estimate the ultimate load-bearing capacity of piles based on static cone penetration data. A minimum factor of safety equal to 2.5 is used while arriving at the safe pile capacity from the ultimate load capacities obtained using the static formula. Codes usually allow 25 per cent excess pile capacity when acted upon by wind or earthquake loads.

It has to be noted that when a pile is installed in a fill, loose sand deposits, or any soil that will undergo considerable consolidation, or where piles are driven through a strata of soft clay into firmer soils, there will be *negative skin friction*. Reconsolidation of the remoulded clay layer around any driven pile and lowering of water table in clays initiating significant settlement may also result in negative skin friction. IS 2911 stresses that pile capacity should be reduced to compensate for the downward drag due to negative skin friction. Downward drag forces can be mitigated by providing friction-reducing material such as bitumen coating or sleeves around the piles.

15.8.3 Dynamic Pile Formula

The Engineering News formula is the simplest and most used dynamic pile formula. Using a factor of safety of six, the allowable pile capacity is given by

$$Q_a = \frac{166.7WH}{S+C} \tag{15.39}$$

where Q_a is the allowable pile load in kN, W is the weight of pile hammer in kN, H is the drop of hammer in m, S is the average penetration of pile per blow for the first 150 mm of driving in mm, and C is the additional penetration of pile tip that would have happened if there were no energy losses (taken as 25.4 mm for piles driven with drop hammer and 2.54 mm for piles driven with stream hammer). It has to be noted that the modified Hiley’s formula is superior to the Engineering News formula and was included in the 1979 version of IS 2911. The modern wave equation, developed by E.A.L. Smith of Raymond Pile Co., gives a better prediction of dynamic pile capacity in all types of piles (Smith 1960). The use of *pile driving analyser* (PDA) equipment can accurately predict the capacities of piles during installation of piles and can be used for *integrity testing of piles* that have already been installed.

15.8.4 Pile Groups

Usually piles are installed in groups. It is economical to use a few high-capacity deep piles under the column than a large number of low-capacity short piles. A single pile foundation is incapable of taking moment, whereas a two-pile group foundation is capable of taking moment in only one direction. A minimum of three piles is required under a column to resist the column load as well as the moment in two directions.

The top of piles is usually connected by a pile cap, which helps the piles to act as a single integral unit. A pile cap when in contact with the soil or buried below ground level may, under certain conditions, transmit a part of the load to the soil on which it rests.

The supporting capacity of a group of vertically loaded piles in many situations is considerably less than the sum of the capacities of the individual piles. This is because the zone of soil that is stressed by the entire group extends to a much greater width and depth than the zone beneath the single pile (as shown in Fig. 15.37). Group action in piled foundations has resulted in many recorded cases of failure or excessive settlement, even though loading tests made on a single pile have indicated satisfactory performance (Tomlinson and Woodward 2008). *Group efficiency of piles* mainly depends on the spacing between piles, type of soils, and method of pile installation (Saran 2006).

The ultimate bearing capacity of a pile group may be obtained as (Terzaghi, et al. 1996)

$$Q_g = c_u Lp + q_u A - \gamma LA < nQ_u \tag{15.40}$$

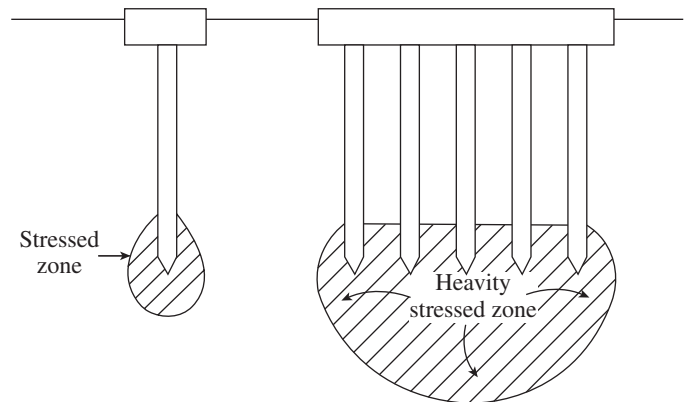


FIG. 15.37 Stressed zones beneath a single pile and a group of piles (a) Single pile (b) Group of piles

where c_u is the unit undrained cohesion of the soil along the vertical surface of the block (see Fig. 15.38) ($= 0.5 \times$ unconfined compressive strength for cohesive soils, $=$ earth pressure at rest $\times \tan \phi$ for granular soil with angle

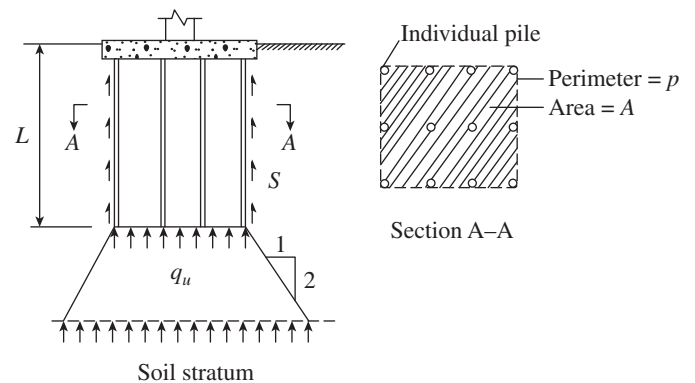


FIG. 15.38 Maximum capacity of pile group

of internal friction ϕ , L is the length of pile embedment in soil, p is the perimeter of area enclosing all piles in the group (see Fig. 15.38), q_u is the ultimate bearing capacity of soil at the level of pile tip, Q_u is the ultimate load capacity of single pile, A is the area enclosing all piles in the group (see Fig. 15.38), γ is the unit weight of soil within the block, average for length L (use buoyant weight for the portion below ground water level), and n is the number of piles in the group.

The negative skin friction of a pile group, Q_{ns} , in a cohesive soil is given by the smaller of the following (see Fig. 15.39):

$$Q_{ns} = c_u L p + \gamma L A \quad (15.41a)$$

$$Q_{ns} = n c_u L \pi d \quad (15.41b)$$

where d is the diameter of the pile; other terms have been defined earlier. Thus, the pile has to resist a load equal to $P + Q_{ns}$, where P is the load acting on the pile group.

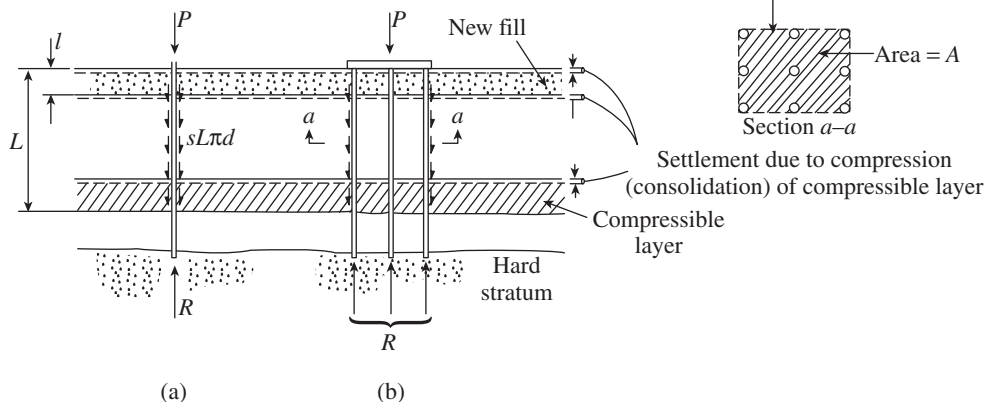


FIG. 15.39 Negative skin friction of piles (a) Single pile (b) Group of piles
Source: Teng 1962

Spacing of Piles

IS 2911 recommends a minimum spacing of 2.5 times the shaft diameter (2.5 times the diameter of the circumscribing circle for non-circular sections) for end-bearing piles, three times the shaft diameter for friction piles, and two times the shaft diameter for piles resting on rock. In loose sand, smaller spacing is desired because of the benefit of compaction. Smaller spacing is also advantageous where negative skin friction is significant.

15.8.5 Structural Design of Piles

When a pile is wholly embedded in soil having an undrained shear strength greater than 0.01 N/mm^2 , its axial capacity is not limited by its strength as a long column. Hence, it may be designed as a short column using Eq. (13.32) of Chapter 13. IS 2911 (Part 1, Section 1):2010 stipulates that the minimum grade of concrete to be used in pile foundation is M25.

In general, the soil design governs the design and it is necessary to provide only minimum steel in the pile; hence, even mild steel bars can be used. The minimum area of reinforcement of any type or grade within the pile should be 0.4 per cent of the cross-sectional area of the pile shaft. Clear cover to all main reinforcement in pile shaft should not be less than 50 mm or 60 mm in corrosive environment. Minimum six vertical bars should be used for a circular pile and the minimum diameter of the vertical bar should be 12 mm. Precast piles are square or hexagonal in shape, whereas bored piles are circular in shape. IS 2911 (Part 1, Section 3):2010 recommends the following extra reinforcements (both longitudinal and transverse) for driven precast concrete piles to resist vibration loads due to driving:

Longitudinal reinforcement The area of main longitudinal reinforcement should not be less than the following percentages of the cross-sectional area of piles:

- For piles with length less than 30 times the least width, 1.25 per cent
- For piles with a length 30–40 times the least width, 1.50 per cent
- For piles with length greater than 40 times the least width, 2 per cent

The clear horizontal distance between adjacent vertical bars should be four times the maximum aggregate size of concrete.

Transverse reinforcement It should be in the form of links or spirals and

should not be less than 8 mm in diameter and their spacing need not be less than 150 mm. The provisions are the same for driven cast in situ piles, bored cast in situ piles, and bored precast piles. SP 34:1987 stipulates the minimum steel reinforcement for driven precast piles as shown in Fig. 15.40. Piles should be provided with steel or cast iron shoes as shown in Fig. 15.40 if they are driven through rock, coarse gravel, or clay with cobbles.

Stiffener rings These rings of size 16 mm in diameter should be provided along the length of the cage at every 1.5 m centre-to-centre (c/c) to provide rigidity to reinforcement cage.

Stresses induced by bending in the cross section of precast pile during lifting and handling may be estimated and the design should consider these bending moments. The bending moments for different support conditions during handling are given in Table 15.3, as per IS 2911 (Part 1, Section 3):2010.

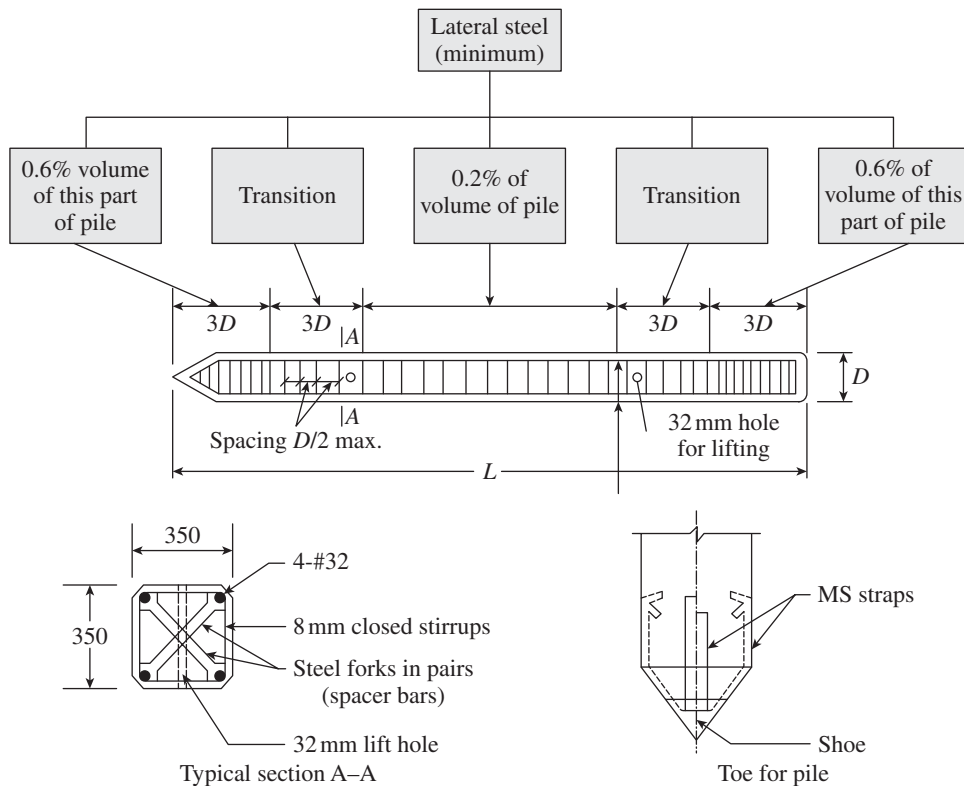


FIG. 15.40 Minimum steel requirement for precast piles

TABLE 15.3 Bending moment for different support conditions

S. No.	Number of Points of Pickup	Location of Support From End in Terms of Length of Pile for Minimum Moments	Bending Moment to be Considered in Design (KNm)
1.	One	$0.293L$	$4.3WL$
2.	Two	$0.207L$	$2.2WL$
3.	Three	$0.145L$, the middle point will be at the centre	$1.05WL$

Note: W is the weight of pile in kN and L is the length of pile in m.

As per IS 2911, the pile has to be checked for buckling and considered as long column only when the undrained shear strength of the soil is less than 0.01 N/mm^2 . However, for the size of concrete piles used in practice, buckling will not take place unless the soil is extremely soft (Bowles 1996).

Piles that are used to support tall towers and chimneys will be subjected to tension under uplift loads and overturning moments. Similarly, expansion of top layers of expansive soils like black cotton soils will also induce uplift in piles. Further, a factor of safety of three should be used with tension piles. Tension piles are discussed in detail by Tomlinson and Woodward (2008).

Lateral Load Capacity

A pile may be subjected to lateral force due to wind, earthquake, water current, earth pressure, plant and equipment,

and so on. The lateral load carrying capacity of a single pile depends not only on the horizontal sub-grade modulus of the surrounding soil but also on the structural strength of the pile shaft against bending. An approximate method is suggested for the pile analysis under lateral load in Appendix C of IS 2911. Other methods developed by Matlock and Reese (1962) and Broms (1964a, 1964b) can also be used. Raker piles can also be used to resist horizontal loads. The design of piles for lateral

CASE STUDY

Rare Foundation Failure in China

On 27 June 2009, an unoccupied 13-storey block of an apartment complex, still under construction, at Lianhuanan Road in the Minhang district of Shanghai city, China, toppled over and ended up lying on its side in a muddy construction field. One worker was killed.

According to an investigation report, the cause of this building collapse was the pressure difference on two sides of the structure. Earth was excavated along the building on one side with a depth of 4.6 m, for an underground car park, and piled up on the other side of the structure to depths of up to 10 m. The weight of the overburdened earth led to an increase in lateral soil pressure, eventually weakening the pile foundation and causing it to fail. This situation might have been aggravated by several days of heavy rain leading up to the collapse, but investigators did not cite this as a crucial factor. The sequence of failure of this building is shown in the figure. More details about this failure may be found in the work of Subramanian (2009).

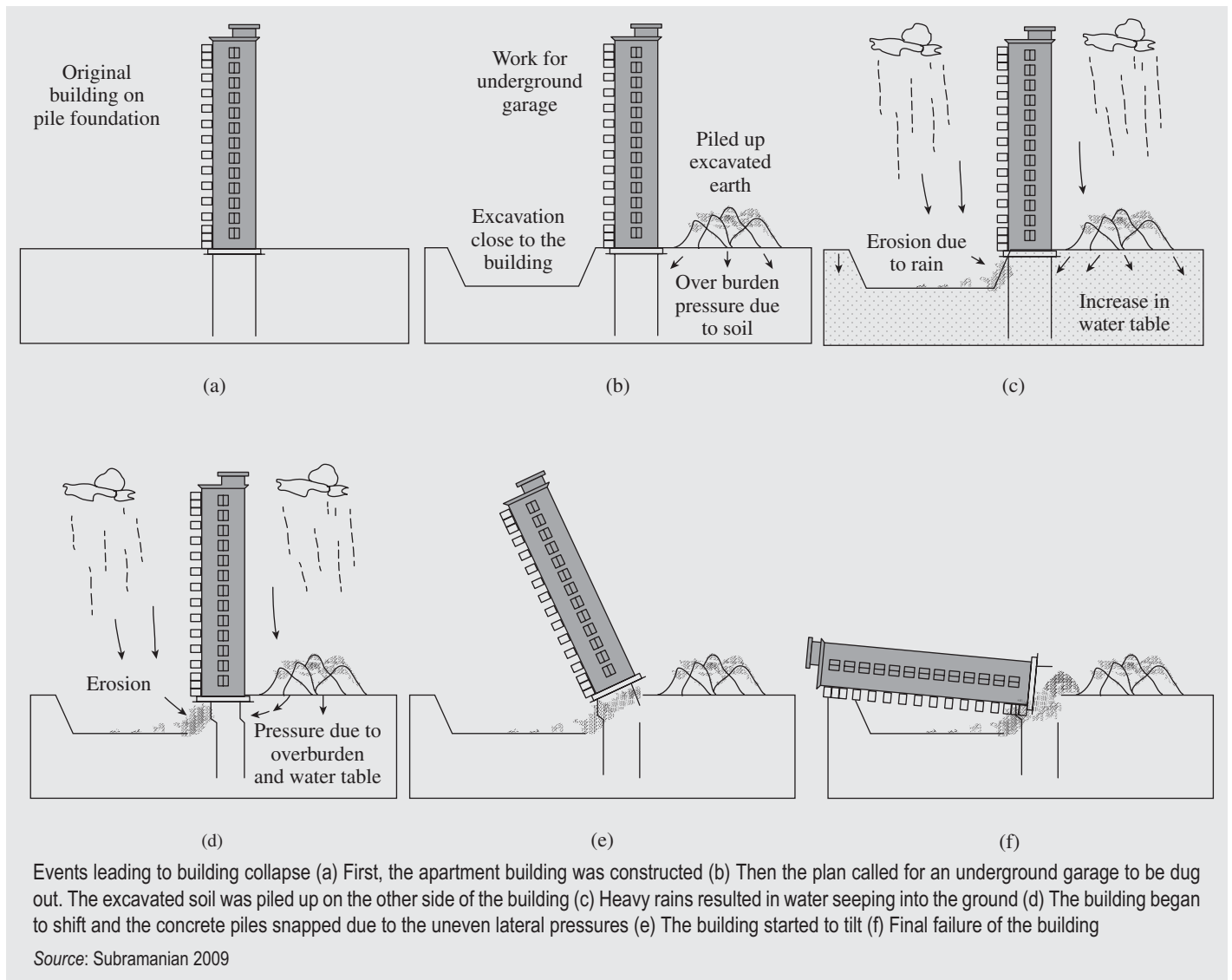


Toppling of building in China

(Source: Basulto, David, 30 June 2009, 'Building collapse in Shanghai', <http://www.archdaily.com/27245>, last accessed on 2 June 2013.)

(Continued)

(Continued)



loads is outside the scope of this book; interested readers may go through the mentioned references or the works of Varghese (2009) and Saran (2006).

15.8.6 Design of Under-reamed Piles

The six major natural hazards in terms of property damage are earthquakes, hurricanes, tornadoes, floods, landslides, and expansive soils. A study reveals that *expansive soils* tie with hurricane winds or storm surges for second place among America's most destructive natural hazards in terms of dollar losses to buildings. This study had projected that by the year 2000 losses due to expansive soil would exceed \$4.5 billion annually (Chen 1988). Recent estimates by the Federal Emergency Management Agency (FEMA) put the annual damage from expansive soils to be as high as \$7 billion. However, as this hazard develops gradually and is seldom life threatening, it has received limited attention, despite

its expensive effects. In India, expansive and *swelling soils* like black cotton soil are found in the entire Deccan plateau. These soils cover an area of about 518,000 km² and thus form about 20 per cent of the total area of India (Chen 1988). The plasticity index (PI), which is defined as the liquid limit (LL) minus the plastic limit (PL), is generally a good indicator of swelling potential. Expansive soils have a liquid limit of 40–100, plasticity index of 20–60, and shrinkage limit of 9–14.

Clays beneath the water table have no swelling potential as they are completely saturated, with no capacity for moisture absorption. Variation in moisture content and volume changes are the greatest in clays found in regions of moderate to high precipitation, where prolonged periods of drought are followed by long periods of rainfall. The depth of seasonal moisture change is referred to as the *depth of the active zone*. It has been found that most changes that cause engineering problems occur at depths less than 3 m, though volume changes

can occur up to 10m from the ground surface. The best means of preventing or reducing the damage from expansive soils is to avoid building on them. When that is not possible, the following methods can be applied: (a) removal of the upper zone of expansive soil and replacement with non-expansive soil, termed *over-excavation* (the practical economic depth for over-excavation is about 1.2m, though it has been used up to a depth of 3.5 m in the USA), (b) remoulding and compaction (beneficial for soils having low potential for expansion, high dry density, and low natural water content and soils in a fractured condition), (c) application of heavy loads to offset the swelling pressure, (d) prevention of access to water, (e) provision of chemical stabilization, (f) use of helical piers, (g) use of under-reamed piles, and (h) provision of pier and grade beam foundation (in the USA, such foundation has been used, using piers of length ranging from 6 m to 15 m).

The discussion here is confined to under-reamed piles, which were invented and thoroughly investigated by Prof. Dinesh Mohan and Jain of CBRI, Roorkee. The design of under-reamed piles is covered in IS 2911(Part 3):1980. The bulbs of the under-reamed piles provide necessary anchorage to withstand the upward pull and downward push, created by the expansive soil during the swelling and shrinkage due to change in moisture content. The bulbs are generally anchored below the region of pronounced seasonal variation of the groundwater table. When the groundwater table is not struck, they are taken

to a depth of moisture stabilized zone. Under-reamed piles can be (a) bored cast in situ concrete piles having one or more bulbs (see Figs 15.41a and b) or (b) bored compaction piles.

In general, the diameter of the bulb is kept 2.5 times the diameter of the stem. A minimum bucket length of 300 mm is provided at the bottom of the lowest under-ream. In case of multiple under-reams, the spacing between the under-reams is generally limited to 1.25–1.5 times the under-ream diameter. The minimum spacing of under-reamed piles is kept twice the size of the under-ream, D_u . It shall not be less than $1.5D_u$.

For piles placed under grade beams, the maximum spacing of piles should generally not exceed 3m. The minimum diameter of stem for borehole needing stabilization by drilling mud should be 250 mm, and for strata consisting of harmful constituents, like sulphates, it should be 300 mm.

According to IS 2911 (Part 3):1980, the minimum area of longitudinal reinforcement in stem should be 0.4 per cent of mild steel (or equivalent deformed steel). Reinforcement is to be provided in the full length and a minimum number of three 10 mm diameter mild steel or three 8 mm diameter high-strength steel bars should be provided. The transverse reinforcement as circular stirrups shall not be less than 6 mm diameter mild steel bars at a spacing of not more than the stem diameter or 300 mm, whichever is lesser. Similar stipulations are specified for under-reamed compaction piles, where the minimum number of bars is four 12 mm or 10 mm bars depending on whether mild or

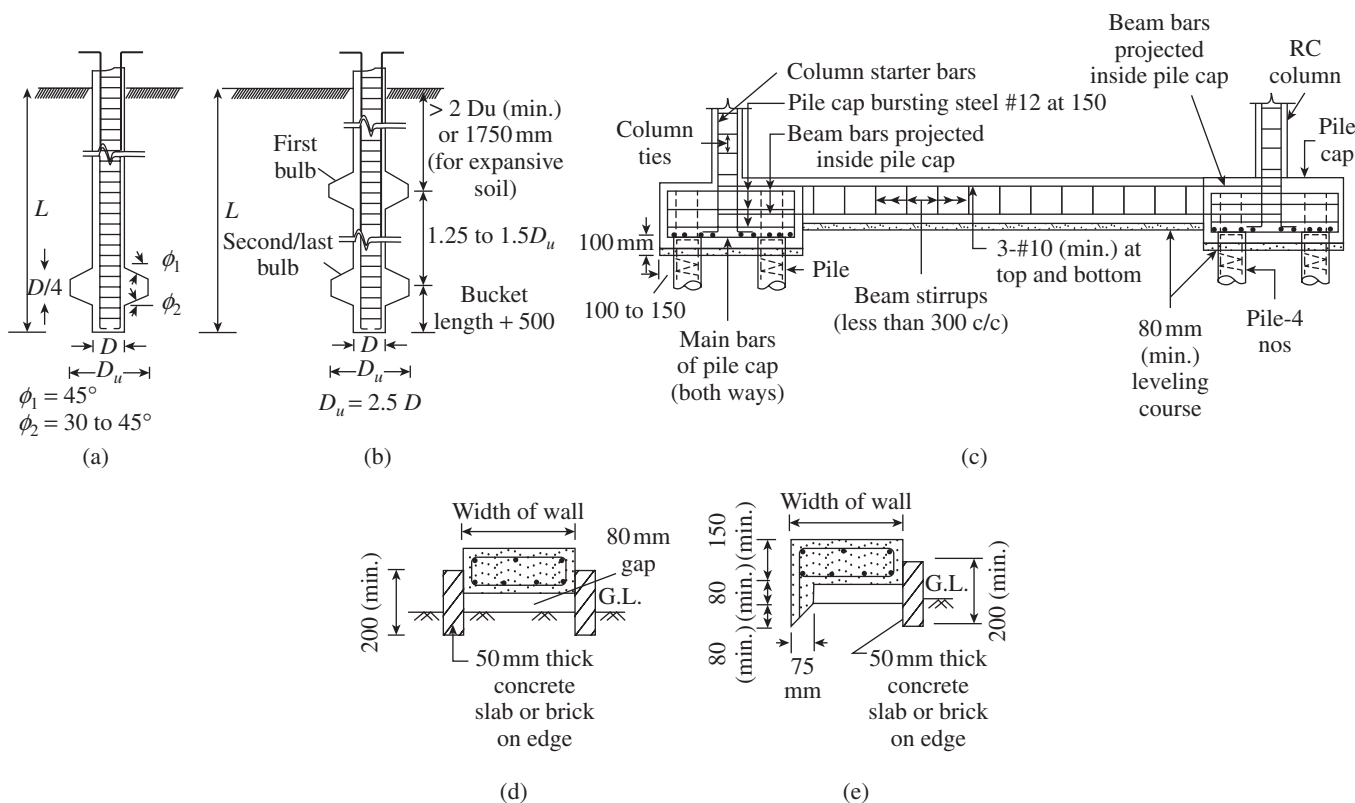


FIG. 15.41 Typical details of bored cast in situ under-reamed pile foundation (a) Section of single under-reamed pile (b) Section of multiple under-reamed pile (c) Typical longitudinal section of grade beam (d) and (e) Typical section of grade beam

high-strength steel bars are used. For piles of length exceeding 5 m and diameter exceeding 375 mm, a minimum of six 12 mm diameter bars of mild or high-strength steel shall be provided. For piles exceeding 400 mm diameter, a minimum of six 12 mm diameter mild or high-strength steel bars should be provided. The circular stirrups for piles of length exceeding 5 m and diameter exceeding 375 mm should be of 8 mm diameter bars.

As per IS 2911 (Part 3):1980, the ultimate load carrying capacity, Q_u , of under-reamed pile in clayey soils is given by

$$Q_u = 9A_p C_p + 9A_a C'_a + C_a (A'_s + \alpha A_s) \quad (15.42)$$

where A_p is the cross-sectional area of pile stem at toe level, C_p is the cohesion of the soil around toe, $A_a = \frac{\pi}{4}(D_u^2 - D^2)$, where D_u and D are the under-ream and stem diameters, respectively, C'_a is the average cohesion of soil around the under-reamed bulbs, α is the reduction factor (usually taken as 0.5 for clays), C_a is the average cohesion of the soil along the pile stem; A_s is the surface area of the stem, and A'_s is the surface area of the cylinder circumscribing the under-reamed bulbs. Equation (15.42) holds for the usual spacing of under-reamed bulbs, spaced at not more than 1.5 times their diameter. It has to be noted that the first two terms of Eq. (15.42) are for bearing and the last two are for friction components. If the pile has only one bulb the third term will not occur, and the first term should not be considered for the calculation of the uplift capacity. While calculating the capacity, the negative skin friction, if any, should also be considered. Tomlinson and Woodward (2008) recommend that in the calculation of skin friction, a length of 3 m should be deducted from the overall pile length to allow for possible loss of adhesion due to shrinkage of soil. They also suggest that the shaft skin friction should be ignored for a distance of two shaft diameters above the top of each under-ream.

Furthermore, IS 2911 (Part 3):1980 includes another equation for calculating the ultimate load capacity of under-reamed pile located in sandy soils. If the soil has both cohesion and friction or in layered strata having different types of soil, the bearing capacity may be estimated using these two formulae for clayey as well as sandy soils; However, in such cases, pile load tests should be conducted to estimate the actual capacity. A factor of safety of 2.5 and 3 is used to obtain safe load in compression and uplift from the ultimate load predicted by Eq. (15.42). However, in case of bored compaction piles with bulb diameter twice the shaft diameter, the factor of safety in compression may be taken as 2.25. Under-reamed piles are normally used only for low loads, say, 250–400 kN. Under-reamed piles can be used up to about 8–10 m depth. For higher depths, under-reamed piles should not be adopted, as forming of bulb is difficult. In such cases, bored cast in situ piles may be adopted. Tests performed at the Anna University, Chennai have shown that the bulbs collapse in sandy soils, especially under the water table.

According to IS 2911(Part 3):1980, in the absence of actual tests and detailed investigations, the safe load on under-reamed piles of bulb diameter 2–5 times the stem diameter may be taken as given in the table of Appendix B of the code. The safe loads given in the table are only for medium sandy or medium clayey soil. For other soil conditions, appropriate increase or decrease has to be made by the factors given in the code. Moreover, a load reduction factor has to be applied for water table. This table has been removed in the new draft code, as it was not considered to give reliable results. More information on the design of under-reamed piles may be obtained from the works of Sharma, et al. (1978) and Subramanian (1994a).

Grade Beams

The grade beams supporting the walls may be designed taking into account the arching effect due to masonry above the beam. The beam with masonry due to composite action behaves as a deep beam. For the design of beams, a maximum bending moment of $wL^2/50$, where w is the uniformly distributed load per metre run (worked out by considering a maximum height of two storeys in structures with load-bearing walls and one storey in framed structures) and L is the effective span in metres, will be taken if the beams are supported during construction until the masonry above it gains strength. The value of bending moment shall be increased to $wL^2/30$ if the beams are not supported. For considering composite action, the minimum height of wall shall be 0.6 times the beam span. The brick strength should not be less than 3 N/mm². For concentrated loads and other loads that come directly over the beam, full bending moment should be considered.

The minimum overall depth of grade beams should be 150 mm. The reinforcement at the bottom should be kept continuous in all the beams, and an equal amount may be provided at the top to a distance of quarter span both ways from the pile centres. The longitudinal reinforcements both at the bottom and at the top should not be less than three 10 mm bars. Stirrups of 6 mm diameter bars should be provided at a spacing of 300 mm, and the spacing should be reduced to 100 mm at the door openings near the wall edge, up to a distance of three times the depth of the beam. The typical longitudinal section of a grade beam is shown in Fig. 15.41(c). In expansive soils, the grade beams shall be kept a minimum of 80 mm clear off the ground, as shown in Fig. 15.41(d).

15.9 DESIGN OF PILE CAPS

A pile cap is a structural member whose function is to transfer load from a column to a group of piles. The column is positioned at the C.G. of the pile group, so that the pile cap incorporates column dowel bars exactly in the same way as

they are provided in individual footings. The plan dimension of the pile cap should be arrived at in such a way that there can be a deviation of up to 100 mm in the theoretical central line of piles. In practice, the pile caps are extended as much as 150 mm beyond the outer face of the piles to provide for this deviation. The shape of the pile cap should be such that the C.G. of the piles and the pile cap should coincide, so that all the piles are equally loaded with gravity loads. Wherever possible, the piles should be arranged in the most compact geometric form to keep the stresses in the pile cap to a minimum. Some pile arrangements are shown in Fig. 15.42.

Assuming the pile cap to be rigid, the load in each pile, P_p , can be determined using the equation (see Fig. 15.43) (Bowles 1996)

$$P_p = \frac{P}{n} \pm \frac{M_x y}{\sum y^2} \pm \frac{M_y x}{\sum x^2} \tag{15.43}$$

where P is the total vertical load acting at the centroid of the pile group, n is the number of piles in the group, M_x and M_y are the moments with respect to X and Y axes, respectively, and x and y are the distance of pile from Y and X axes, respectively.

The pile caps are designed in such a way that they are capable of safely carrying the bending moments and shear forces and are deep enough to provide adequate anchorage length to the pile reinforcements and column starter bars. The depth of a pile cap is usually not less than 600 mm. Based on experience, the following relationship between pile diameter, D_p , and thickness of pile cap, D , is suggested by Reynolds and Steedman (1988).

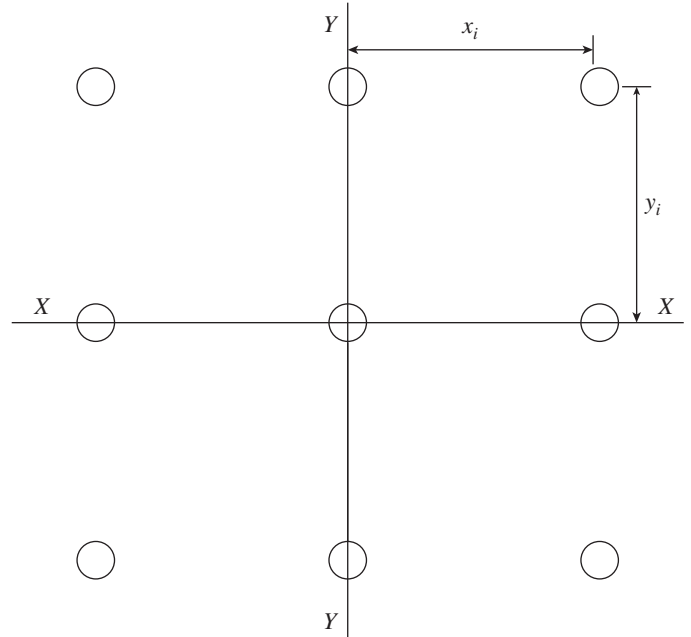


FIG. 15.43 Distribution of load to the individual pile of a pile group

If $D_p < 550$ mm, $D = 2D_p + 100$ (15.44a)

If $D_p > 550$ mm, $D = \frac{(8D_p - 600)}{3}$ (15.44b)

15.9.1 Sectional Method of Design of Pile Cap

There are two common approaches to the design of pile caps. In the first approach, as adopted in Clause 34 of IS 456, the cap is considered to be a deep beam and is designed for flexure and shear at assumed critical sections. This method is

referred to as the sectional method of design. Varghese (2009) and Souza, et al. (2009) suggest that this method can be adopted in shallow pile caps, where the shear span (distance between face of column and pile centres) to effective depth ratio is more than 1.5, as the bending action will be more predominant than the truss action. Pile caps designed by sectional method are likely to exhibit brittle failures when overloaded (Souza, et al. 2009). This is because, unlike deep beams, pile caps contain a small percentage of longitudinal reinforcement and usually may not have any transverse shear reinforcement.

The pile cap is designed as a footing on pile, and computations of moments and shears are based on the

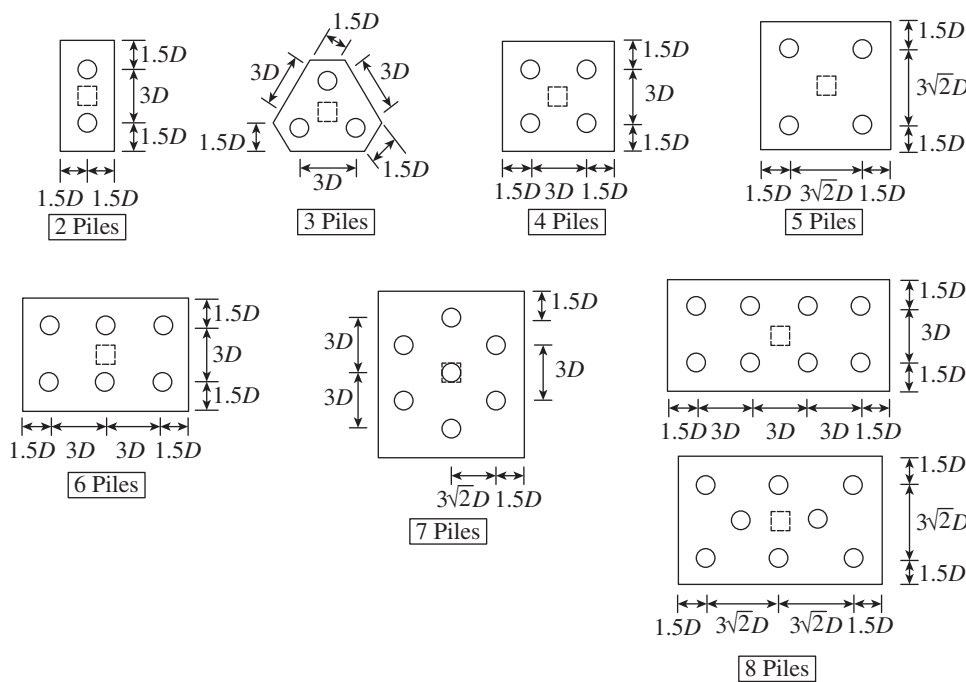


FIG. 15.42 Typical pile cap layouts

assumption that the reaction from any pile is concentrated at the centre of the pile (as per Clause 34.2.1 of IS 456). Thus, the action of a pile cap is considered similar to that of isolated footing. The main difference is that instead of a uniform soil pressure in the case of isolated footing, the pile cap has concentrated reactions acting at the centre of piles from below. The critical section for moment is taken at the face of the column or pedestal, whereas for both beam shear and punching shear, the critical section is taken at $d/2$ away from the face of the column or pedestal, where d is the effective depth of pile cap. Similar to footing, the calculated shear stress in punching should not exceed $k_s (0.25\sqrt{f_{ck}})$ (Clause 31.6.3.1 of IS 456). Minimum steel considering the pile cap as beam and as per Clause 26.5.1.1 of IS 456 is to be provided both ways. Provision of a pedestal of size 300 mm all around the column shifts beam shear 300 mm outwards and gives reasonable depth to pile cap. The pedestal should be designed for bearing stresses, which should not exceed $0.45f_{ck}$ and should be provided with a minimum of 0.15 per cent steel.

The following cases are to be considered while checking one-way shear at a distance $d/2$ away from column face, as per Clause 34.2.4.2 of IS 456 (see Fig. 15.44):

Centre of pile $D_p/2$ away from section The entire reaction from pile is considered.

Centre of pile $D_p/2$ inwards to section The entire reaction from pile is ignored.

For intermediate positions of pile centres Straight line interpolation of pile reaction between the full value at $D_p/2$ outside the section and zero value at $D_p/2$ inside the section has to be considered.

The allowable punching shear is usually high. Moreover, the depth of pile caps will be larger than in ordinary slabs. Hence, punching shear will usually not govern. Pile caps can

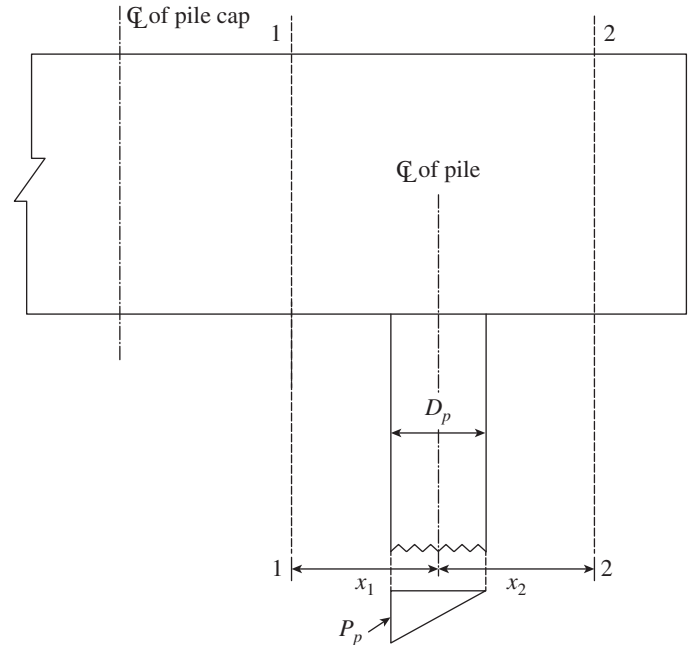


FIG. 15.44 Consideration of shear in pile caps

be designed quickly using readily available computer software (Subramanian 1994b).

15.9.2 Strut-and-tie Model for Pile Caps

The second approach, recommended by CSA A23.3-94, ACI 318, is the *strut-and-tie model*, where the forces in the pile cap are derived from an idealized equilibrium model. In this model, the compression forces are assumed to be distributed through unreinforced compressive struts to nodal regions at each pile, and the resulting tension forces between piles are carried by tension ties formed by the reinforcement. The structural action of a four-pile group is shown schematically in Fig. 15.45(a). The pile cap is a special case of a 'deep beam' and can be idealized as a three-dimensional truss or

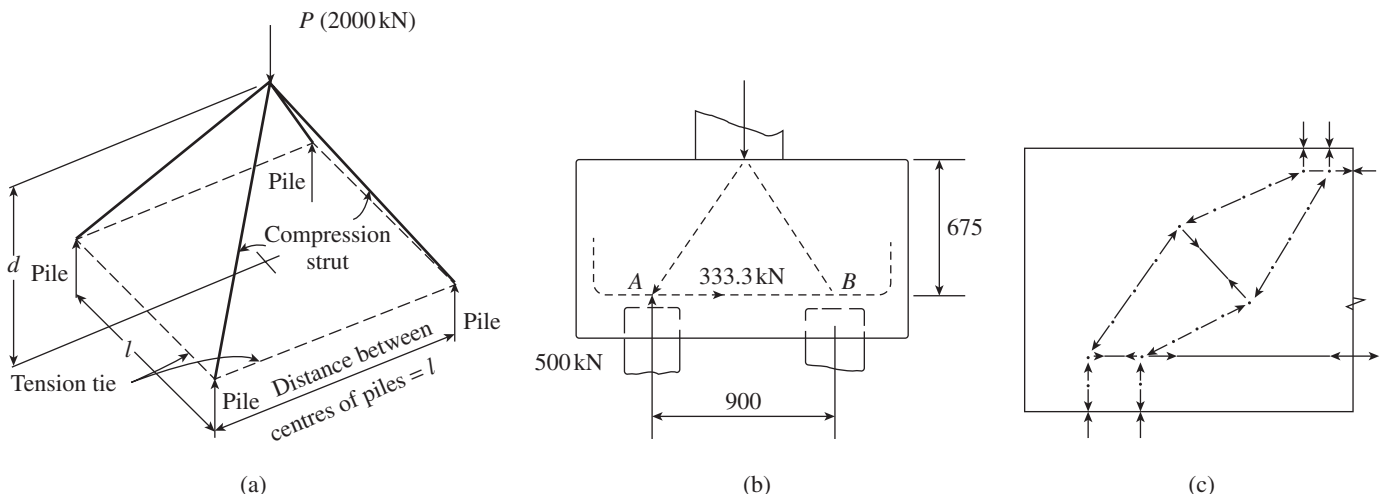


FIG. 15.45 Strut-and-tie model of pile cap (a) Three-dimensional truss model (b) Force in tie (c) Refined truss model that includes a concrete tension tie to resist transverse tension

strut-and-tie model, with four compression struts transferring load from the column to the tops of the piles and four tension ties equilibrating the outward components of the compression thrusts. Since the tension ties have constant force in them, they must be anchored for the full horizontal tie force outside the intersection of the pile and the compression strut (outside points *A* and *B* in Fig. 15.45b). Hence, the bars either must extend a distance equal to L_d past the centre lines of the piles or must be bent with 90° hook as shown in Fig. 15.45(b).

For the four-pile cap shown in Fig. 15.45(a) and with the dimensions given in Fig. 15.45(b), reaction in each pile = $2000/4 = 500$ kN. Considering the equilibrium at joint *A*, the horizontal shear force in tie $A - B = PL/8d = 2000 \times 900/(8 \times 675) = 333.3$ kN. Hence, required A_{st} to resist this tension = $333.3 \times 1000/(0.87 \times 415) = 923$ mm². Five 16mm bars may be provided within a width of $3D_p$ centred on each pile (when the pile spacing is less than or equal to three times the pile diameter, the tension steel can be spread over the entire width). It is also necessary to provide minimum steel in other portions where the tie action is not there to control crack widths, as shown in Fig. 15.46. Leonhardt and Mönning (1977) also suggest providing shear stirrups as shown in Fig. 15.46, though it is not followed in practice. The tie forces in pile caps supported by two, three, four, and five piles can be found using Table 15.4 (Reynolds and Steedman 1988).

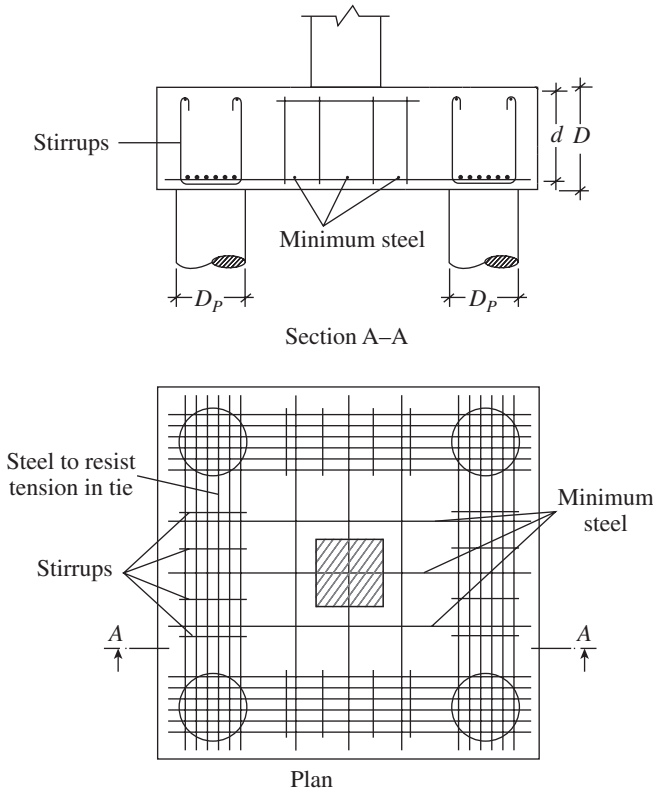


FIG. 15.46 Detailing of pile cap as per strut-and-tie model

It has been found from experiments that spreading out the reinforcement uniformly (as suggested by IS 456) in a pile

cap supported by four piles reduced the failure load by 14–20 per cent compared to pile cap with the same quantity of reinforcement, but with all reinforcement concentrated over the pile (as suggested by strut-and-tie models). In pile caps supported by three piles, the reduction in load due to uniformly distributed reinforcement was 50 per cent (Adebar, et al. 1990). Adebar, et al. (1990) also found that the usual assumption of plane sections remaining plane after bending is not valid in pile caps. They also found that deep pile caps deform very little prior to failure, do not have necessary flexibility to ensure uniformity of pile loads at failure, and do not behave like wide beams.

The modes of failure to be considered in limit state design for such a pile cap are (a) crushing under the column or over the pile (bearing stresses should be checked), (b) bursting of the side cover where the pile transfers its load to the pile cap (usually bursting steel around pile rods are provided), (c) yielding of the tension tie, (d) anchorage failure of the tension tie (development length should be checked), (e) two-way shear failure where the cone of material inside the piles punches downward, and (f) failure of the compression struts. Of these, the two-way shear failure mode is least understood (Wight and MacGregor 2009).

On the basis of the experimental results of six four-pile caps of varying geometry, Adebar, et al. (1990) concluded that their results clearly indicated that the strut-and-tie model predicts the behaviour of deep pile caps more accurately. They observed that the compression struts in deep pile caps do not fail by crushing of concrete. Rather, failure occurs after the compression strut splits longitudinally due to transverse tension caused by spreading of the compressive stresses. To consider this splitting, they also proposed a refined strut-and-tie model as shown in Fig. 15.45(c). Based on these observations, they suggested that the ‘shear strength’ of deep pile caps with steep compression struts is better enhanced by increasing the bearing area of the concentrated loads rather than further increasing the depth of the pile cap. Adebar and Zhou (1993, 1996) again confirmed that the maximum bearing stress was a better indicator of shear strength than shear resistance based on any pseudo-critical section. They suggested the following equation to limit the bearing stress of struts, which has been adopted in the Canadian code CSA A23.3-2004.

$$f_b = 0.6\phi_c f'_c + 6\alpha\beta\phi_c \sqrt{f'_c} \tag{15.45a}$$

With $\phi_c = 0.65$ and $f'_c = 0.8f_{ck}$, Eq. (15.45a) may be rewritten as

$$f_b = 0.3f_{ck} + 3.5\alpha\beta\sqrt{f_{ck}} \tag{15.45b}$$

The coefficient α in this equation accounts for confinement and is given by

$$\alpha = \frac{1}{3} \left(\sqrt{\frac{A_2}{A_1}} - 1 \right) \leq 1. \text{ Thus } \sqrt{\frac{A_2}{A_1}} \leq 4 \tag{15.45c}$$

TABLE 15.4 Tensile force in ties for pile caps

Number of Piles	Dimensions of Pile Cap	Tensile Force to be Resisted by Reinforcement	
		Neglecting Size of Column	Considering the Size of Column
2		$\frac{Pl}{4d}$	$\frac{P}{12ld}(3l^2 - a^2)$
3		$\frac{Pl}{9d}$	Parallel to X-X: $\frac{P}{36ld}(4l^2 + b^2 - 3a^2)$ Parallel to Y-Y: $\frac{P}{18ld}(2l^2 - b^2)$
4		$\frac{Pl}{8d}$	Parallel to X-X: $\frac{P}{24ld}(3l^2 - a^2)$ Parallel to Y-Y: $\frac{P}{24ld}(3l^2 - b^2)$
5		$\frac{Pl}{10d}$	Parallel to X-X: $\frac{P}{30ld}(3l^2 - a^2)$ Parallel to Y-Y: $\frac{P}{30ld}(3l^2 - b^2)$

Note: D_p is the diameter of pile, a and b are the dimensions of column, and α is the spacing factor of piles and ranges between two and three depending on soil conditions.

The coefficient β accounts for the aspect ratio of the strut and is given by

$$0.0 \leq \beta = 0.33 \left(\frac{h_s}{b_s} - 1 \right) \leq 1.0 \quad (15.45d)$$

The term h_s/b_s is the aspect ratio of the strut, where h_s is the length and b_s is the breadth of strut (see Fig. 15.47). The aspect ratio at the column end may be taken as $h_s/b_s = 2d/b_{col}$ and at piles, where only one compressive strut acts, $h_s/b_s = d/D_p$,

where d is the effective depth of pile cap, D_p is the diameter of pile, and b_{col} is the width of column. For the purposes of bearing stress check, circular, polygonal, and rectangular sections can be transformed into a square pile of equal area.

The use of strut-and-tie method will lead to more longitudinal reinforcement to support the same loading than the sectional method (Nori and Tharval (2007)). However, the strut-and-tie method is a more rational and safe method, and its use results in ductile behaviour of the pile cap.

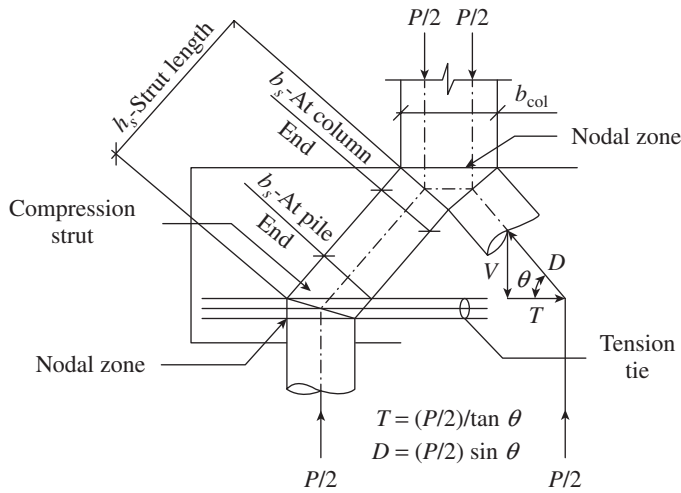


FIG. 15.47 Idealized strut-and-tie model of pile cap

15.9.3 Detailing of Pile Caps

As discussed in Section 15.9.2, there is a tendency for the pile cap to fail in bursting due to high principal tension. This is resisted by providing reinforcement that goes around the outer pile reinforcement in the group (usually 12 mm bars at 150 mm centres are provided). The dowel bars for column should be well anchored in the pile cap. The size of the pile cap is made to overhang beyond the outermost pile in the group by 100–150 mm, depending on the pile size. A levelling course of plain concrete of about 80 mm thickness is provided under the pile cap. The clear cover for the main reinforcement, at the bottom of pile cap, should be greater than 60 mm. These details, as per SP 34:1987, are shown in Fig. 15.48.

15.10 EARTHQUAKE CONSIDERATIONS

An important criterion for the design of foundations of earthquake-resistant structures is that the foundation system should be capable of supporting the design gravity loads while maintaining the chosen seismic energy-dissipating mechanisms (Paulay and Priestley 1992). In conventional seismic design of structures, designers use the non-linear deformation of elements of the

structures for dissipation of the input energy, although a number of active and passive energy dissipation systems can also be employed (Soong Spencer 2002; Symans, et al. 2008). It is also desirable to have the inelastic response to occur only above the foundations, as repairs to foundations are extremely difficult and quite expensive. In other words, the footing and the components of the foundation structure should elastically respond to earthquakes (Paulay and Priestley 1992). If the footing is not large enough, *rocking* or tipping can occur.

The widely used detailing of an individual footing, supporting a seismic column, is shown in Fig. 15.49(a). The following are the unacceptable features of such a detailing (Paulay 1996):

1. The column starter bars are spliced with the main bars where a plastic hinge is expected to form.
2. The outward bending of column bars at the bottom of the footing does not ensure continuity of earthquake-induced moment transfer from the column to footing.

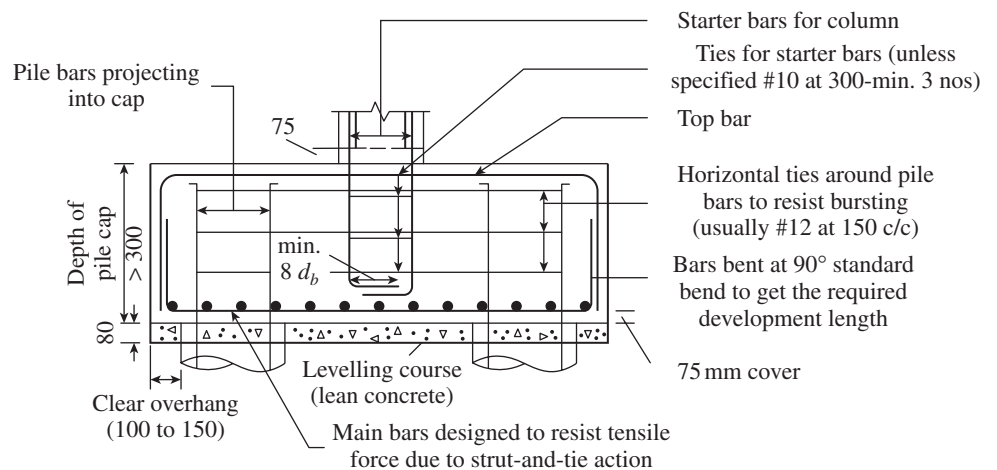


FIG. 15.48 Typical detailing of pile cap

Source: SP 34:1987 (adapted)

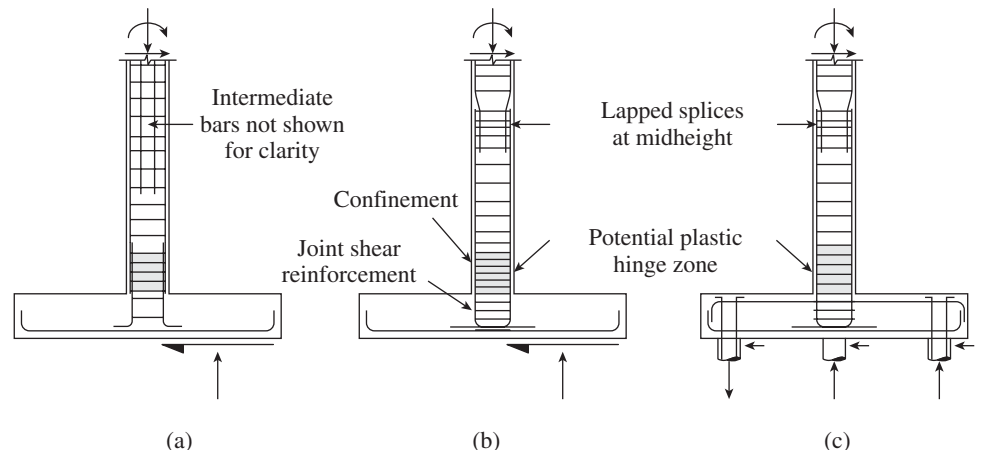


FIG. 15.49 Seismic design considerations for footings (a) Conventional wrong detail for footing (b) Correct detail for footing (c) Detail for pile cap

Source: Paulay 1996

3. The column–footing junction, behaving like a knee joint of a portal frame, has insufficient joint shear reinforcement.

The correct detailing for footing in seismic regions is shown in Fig. 15.49(b), where the splice is located approximately at the mid-height of column (as discussed in Section 13.10.2 of Chapter 13). The column bars that are bent inwards will enable effective moment transfer. Properly designed joint shear reinforcement is assumed to be provided. Similar details for a pile cap are shown in Fig. 15.49(c). Under large ductility demands, the flexural over-strength of the plastic hinge at the base of the column may be much larger than the initial design moment, resulting in tension in some piles (Paulay 1996). This will require reinforcement at the top of the pile cap.

As discussed in Section 15.5.4, the longitudinal reinforcement of columns or structural walls resisting seismic forces should be extended into the footing, mat, or pile cap and fully developed for tension at the interface. Experiments conducted by Nilsson and Losberg (1976) demonstrated that columns subjected to moments should have their hooks turned inwards towards the axis of the column in the footing, as shown in Figs 15.17 and 15.49(b) and (c), for the joint to effectively resist the flexure in column. Clause 7.4.2 of IS 13920 stipulates that special confining reinforcement of the column must be extended to at least 300 mm into the foundation, as shown in Fig. 13.32 of Chapter 13.

Foundations typically do not contain top reinforcement and may be susceptible to brittle flexural failures during an earthquake. Hence, Clause 21.12.2.4 of ACI 318 suggests providing flexural reinforcement in the top of the footing, mat, or pile cap to resist uplift forces in boundary elements of special structural walls or columns and such reinforcement should not be less than that calculated using Eq. (5.36c) of Chapter 5. In addition, columns or boundary members of walls that are placed close to the edge of the foundation should be detailed to prevent an edge failure of the footing, pile cap, or mat (such situations occur when the columns are placed near the boundary line, as shown in Fig. 15.29).

When structural walls are provided, seismic resistance is concentrated at a few selected locations rather than being distributed over the entire plan area of the building. As a result, the local demand on the foundation may be very large and indeed critical (Binney and Paulay 1980). Due to the scarcity of experimental evidence relating to ductile response of such foundation systems, conservative detailing procedures should be adopted. Several examples of foundations supporting wall are provided in the works of Binney and Paulay (1980) and Paulay and Priestley (1992). A discussion on the effects

of lateral forces on piles may also be found in the study by Paulay and Priestley (1992).

15.10.1 Use of Grade Beams

Stiff grade beams provided between the footings can absorb large moments transmitted by plastic hinges. As shown in Fig. 15.50(a), they provide high degree of elastic restraint against column rotations. When such grade beams are provided, the footings may be designed to transmit only axial loads from the columns due to gravity and earthquake forces (Paulay and Priestley 1992). Clause 21.12.3.1 of ACI 318 suggests that these grade beams, which are designed to act as horizontal ties between pile caps or footings, should have continuous longitudinal reinforcement that should be developed within or beyond the supported column or anchored within the pile cap or footing at all discontinuities.

Clause 21.12.3.2 stipulates that the smallest cross-sectional dimension of the grade beam should be equal to or greater than the clear spacing between the connected columns divided by 20 but need not be greater than 450 mm. Closed ties should be provided in these beams, with the spacing not exceeding the lesser of one-half the smallest cross-sectional dimension and 300 mm. Grade beams resisting seismic flexural stresses from column moments should have reinforcement details similar to the beams of the frame above the foundation. Due consideration must be given to the joints between columns and grade beams. Design of grade beams is discussed in Section 5.12 of Chapter 5. The footings may be joined to provide a continuous footing (as shown by dotted lines in Fig. 15.50a), thus reducing the bearing pressure under footings. When the foundation is provided at a greater depth, stub columns or pedestals are often used between the footing and grade beams, as shown in Fig. 15.50(b). In such cases, it is better to restrict energy dissipation to plastic hinges in columns above the beams. The stub columns should be designed in such a way that inelastic deformation and shear failure are avoided (Paulay and Priestley 1992).

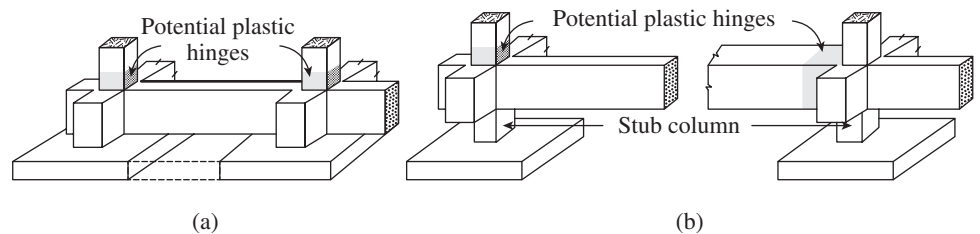


FIG. 15.50 Footing with grade beams (a) Footing at shallow depth (b) Footing at deeper depth

15.10.2 Failures due to Liquefaction

Strong ground shaking can cause a loss of strength in saturated cohesionless soils. This loss of strength is referred to as *liquefaction*. Liquefaction of saturated sands during earthquakes

was first identified as a major source of secondary damage after the 1964 Niigata and Alaska earthquakes and was further observed during the 1989 Loma-Prieta, 1995 Hyogoken-Nambu (Kobe), 2001 Bhuj, and 2004 Sumatra earthquakes. Significant damage can occur to structures supported on soils that liquefy. *Bearing capacity failure* may result in the structure settling and rotating (tilting) as in Niigata in 1964 (see case study). It has to be noted that seismically induced bearing capacity failure can also occur without liquefaction of the underlying soil. In addition to bearing capacity failures, the following may occur due to soil liquefaction:

1. Catastrophic flow failures
2. Lateral spreading and ground failures
3. Excessive settlement
4. Increase in active lateral earth pressures behind retaining walls
5. Loss of passive resistance in anchor systems

It is better to avoid locations where liquefaction may occur. It can occur most commonly in sandy and silty soils. Moreover,

the soils that are loose have a greater propensity to compress due to shaking and are thus more susceptible to liquefaction. Soils containing clays are not generally prone to liquefaction.

Soil mitigation options include densification, drainage, reinforcement, mixing, or replacement. The implementation of these techniques may be designed to fully or partially eliminate the liquefaction potential, depending on the amount of deformation that the structure can tolerate. The most widely used techniques for in situ densification of liquefiable soils are vibro-compaction, vibro-replacement (also known as vibro-stone columns), deep dynamic compaction, and compaction (pressure) grouting (Cooke and Mitchell 1999).

The seismic performance of pile foundations in liquefiable soils remains a topic of intensive research (Liyanapathirana and Poulos 2005; Bhattacharya 2006; Puri and Prakash 2008). Piles have to be designed by neglecting the friction capacity in the liquefied soils and by considering down-drag forces due to settlement of the liquefied soils. Deep piles should be designed to resist lateral forces if lateral spreading is also a concern.

CASE STUDY

Soil Liquefaction Failure

The Niigata earthquake (off the north-west coast of Honshu, Japan) together with the Alaska earthquake, which occurred in 1964, brought liquefaction phenomenon and its devastating effects to the attention of engineers and seismologists. Ground failure occurred near the bank of Shinano River where the Kawagishi-cho apartment buildings suffered bearing capacity failures and tilted severely. Despite the extreme tilting, the buildings, remarkably, suffered little structural damage.



Tilting of apartments

(Source: http://earthquake.usgs.gov/earthquakes/world/events/1964_06_16.php)

EXAMPLES

EXAMPLE 15.1 (Design of wall footing):

Design an RC footing for a 300 mm thick concrete wall that carries a service load (inclusive of dead load) of 330 kN/m. The allowable soil pressure, q_a , is 240 kN/m² at a depth of 1.5 m below ground. Assume M20 concrete and Fe 415 steel.

SOLUTION:

Given $P = 330$ kN/m and $q_a = 240$ kN/m² at 1.5 m.

Step 1 Determine the size of footing. Assuming the weight of footing as 10 per cent of the applied load,

$$\text{Required width of footing} = \frac{P \times 1.1}{q_a} = \frac{330 \times 1.1}{240} = 1.513 \text{ m}$$

Provide 1.55 m wide footing.

$$\text{Factored net pressure, } q_u = \frac{330 \times 1.5}{1.55 \times 1} = 319.4 \text{ kN/m}^2 = 0.319 \text{ N/mm}^2$$

Step 2 Check for shear (determine the depth). Shear usually governs the thickness of footing. The critical section for one-way shear is at a distance d mm away from the face of the wall (see Fig. 15.51).

$$\begin{aligned} V_u &= q_u \times 1000 \left[\frac{(B - t_w)}{2} - d \right] \\ &= 0.319 \times 1000 \left[\frac{(1550 - 300)}{2} - d \right] \\ &= 199,375 - 319d \text{ N} \end{aligned}$$

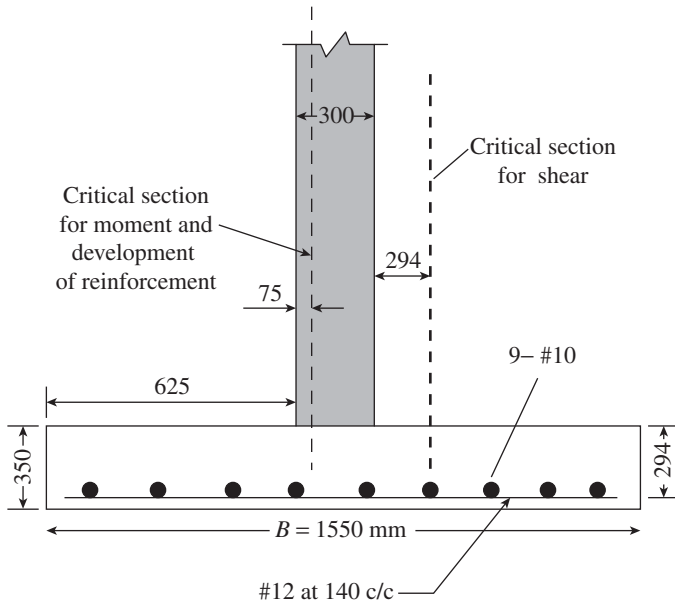


FIG. 15.51 Wall footing of Example 15.1

Assuming nominal flexural reinforcement of $p_t = 0.25\%$, from Table 19 of IS 456, for M20 concrete, we get $\tau_c = 0.36$ MPa.

Shear resistance of concrete, $V_n = \tau_c \times 1000 \times d = 360d$

However, $V_n \geq V_u$. Hence,

$$360d \geq 199,375 - 319d \quad \text{or} \quad d \geq 293.6 \text{ mm}$$

Assuming a clear cover of 50 mm (Clause 26.4.2.2 of IS 456) and 12 mm bars,

Thickness of footing, $D \geq 294 + 50 + 12/2 = 350$ mm

Provide $D = 350$ mm and $d = 350 - 56 = 294$ mm.

Step 3 Design the flexural reinforcement. The critical section for moment is halfway between the centre line and the edge of the masonry wall as per Clause 34.2.3.2(b) of IS 456, that is, $1550/2 - 300/4 = 700$ mm.

Considering 1 m strip of footing,

$$M_u = \left(0.319 \times 1000 \times \frac{700^2}{2} \right) \times 10^{-6} = 78.16 \text{ kNm}$$

$$\frac{M_u}{bd^2} = \frac{78.16 \times 10^6}{1000 \times 294^2} = 0.9043 \text{ MPa}$$

From Table 2 of SP 16, for Fe 415 steel and M20 concrete, $p_t = 0.2654\% > 0.25\%$ assumed for one-way shear.

Required $A_{st} = \frac{0.2654}{100} \times 1000 \times 294 = 780.3 \text{ mm}^2$ per metre length

Spacing of 12 mm bars = $(1000 \times 113)/780.3 = 144 \text{ mm} < 3d$ or 300 mm

Provide 12 mm bars at 140 mm c/c.

Step 4 Check for development length. For M20 concrete and Fe 415 steel, required development length for 12 mm bar from Table 65 of SP 16 = 564 mm.

Length available = $625 - 50 = 575 \text{ mm} > 564 \text{ mm}$

Step 5 Determine the distributors. Minimum reinforcement along the length of the footing

$$A_s = \frac{0.12}{100} BD = \frac{0.12}{100} \times 1550 \times 350 = 651 \text{ mm}^2$$

$$\text{Spacing of 10 mm bars} = \frac{1550 \times 78.5}{651} = 187 \text{ mm}$$

Provide 10 mm bars at 185 mm c/c (nine bars).

Step 6 Check for the transfer of force at the base of the wall. Maximum ultimate bearing stress at wall-footing interface (300 mm loaded area)

$$f_{br} = \frac{330 \times 10^3 \times 1.5}{1000 \times 300} = 1.65 \text{ MPa}$$

As per Clause 34.4 of IS 456, $f_{br, \max} = 0.45 f_{ck} \sqrt{\frac{A_1}{A_2}}$
 $9 \sqrt{\frac{A_1}{A_2}} = 9 \text{ MPa}$ in the footing face. Hence, it is safe.

EXAMPLE 15.2 (Centrally loaded square footing):

Design an isolated footing for a square column of size 400 mm \times 400 mm, supporting a service load of 2200 kN. Assume SBC of soil as 250 kN/m² at a depth of 1.5 m below the ground. Use M20 concrete and Fe 415 steel for the footing and M30 concrete and Fe 415 steel for the column. Assume that the column is reinforced with eight 25 mm bars.

SOLUTION:

Given $P = 2200$ kN and $q_a = 250$ kN/m² at 1.5 m below ground level.

Step 1 Determine the size of footing. Assuming the weight of footing and backfill as 10 per cent of column load,

$$\text{Required area of footing} = \frac{1.1P}{q_a} = \frac{1.1 \times 2200}{250} = 9.68 \text{ m}^2$$

$$\text{Size of square footing} = \sqrt{9.68} = 3.11 \text{ m}$$

Provide a square footing of side 3.2 m.

$$\text{Factored net soil pressure } q_u = \frac{P\gamma_f}{B^2} = \frac{2200 \times 1.5}{3.2 \times 3.2} = 322.3 \text{ kN/m}^2 = 0.322 \text{ N/mm}^2$$

Step 2 Check for shear (determine the depth). The critical section for one-way shear is at a distance d from the face of column (see Fig. 15.52). Factored shear force

$$V_{u1} = \frac{q_u B}{2} (B - c_1 - 2d) = \frac{0.322 \times 3200}{2} (3200 - 400 - 2d) \text{ N} = 1,442,560 - 1030.4d$$

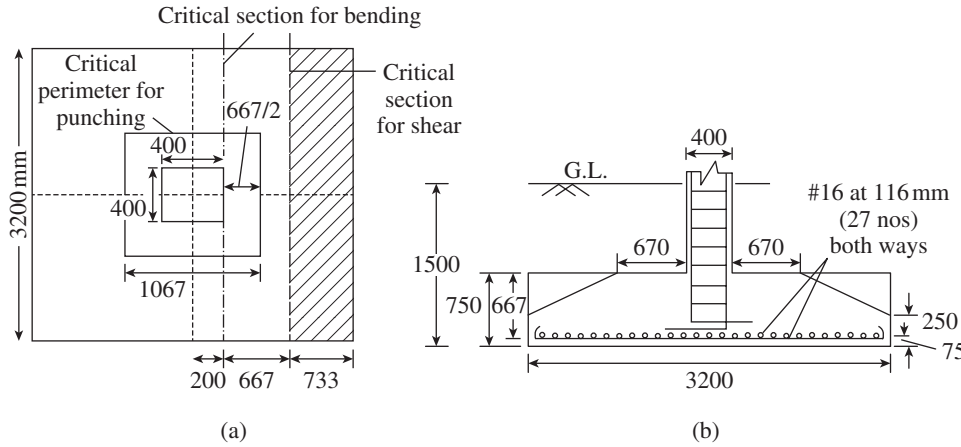


FIG. 15.52 Details of square footing of Example 15.2 (a) Plan (b) Section

Assuming $p_t = 0.25\%$, from Table 19 of IS 456 for M20 concrete, $\tau_c = 0.36$ MPa.

One-way shear resistance $V_n = \tau_c B d = 0.36 \times 3200 \times d = 1152d$
 Since $V_n > V_{u1}$, we get

$$1152d \geq 1,442,560 - 1030.4d \text{ or } d \geq 661 \text{ mm}$$

Adopt $d = 667$ mm. Assuming 16 mm bars and 75 mm clear cover,

$$D = 667 + 75 + 16/2 = 750 \text{ mm}$$

Step 3 Check thickness for two-way shear. The critical section for two-way shear is at $d/2$ mm from the periphery of the column (see Fig. 15.52)

$$\begin{aligned} \text{Factored shear force} &= V_{u2} = q_u [B^2 - (c_1 + d)^2] \\ &= 0.322 \times [3200^2 - (400 + 667)^2] \times 10^{-3} = 2930.7 \text{ kN} \end{aligned}$$

As per Clause 31.6.3.1 of IS 456, two-way shear resistance

$$V_{n2} = k_s \tau_c [4 \times (c_1 + d)d], k_s = [0.5 + \beta_c] \leq 1$$

As $\beta_c = 1$ for square column, $k_s = 1.0$.

$$\tau_c = 0.25 \sqrt{f_{ck}} = 0.25 \sqrt{20} = 1.118 \text{ MPa}$$

$$\begin{aligned} \text{Hence } V_{n2} &= 1.0 \times 1.118 \times 4 \times 667(400 + 667) \times 10^{-3} \\ &= 3182.8 \text{ kN} > 2930.7 \text{ kN} \end{aligned}$$

Step 4 Check for q_a with the actual size of footing. With the weight of concrete and soil as 24 kN/m³ and 18 kN/m³, respectively, the actual pressure below the footing is

$$\begin{aligned} q &= 2200/(3.2 \times 3.2) + (24 \times 0.75) + (18 \times 0.75) \\ &= 214.84 + 18 + 13.5 = 246.34 \text{ kN/m}^2 < 250 \text{ kN/m}^2 \text{ (SBC of soil)} \end{aligned}$$

Step 5 Design the flexural reinforcement. Factored moment at the face of column (in either direction) (see Fig. 15.52)

$$\begin{aligned} M_u &= \frac{q_u}{8} B(B - c_1)^2 = \frac{0.322}{8} \times 3200 \times (3200 - 400)^2 \times 10^{-6} \\ &= 1009.8 \text{ kNm} \end{aligned}$$

$$\frac{M_u}{Bd^2} = \frac{1009.8 \times 10^6}{3200 \times 667^2} = 0.7093$$

From Table 2 of SP16 with $f_{ck} = 20$ N/mm² and $f_y = 415$ N/mm², $p_t = 0.2050\%$.

As this steel percentage is less than the percentage assumed for calculating shear strength, that is, 0.25 per cent in Step 2, shear strength requirement governs the design. Hence, Required $A_{st} = 0.25 \times 3200 \times 667/100 = 5336 \text{ mm}^2$

Using 16 mm bars, required number of bars = $5336/201 = 27$ bars.

$$\begin{aligned} \text{Spacing} &= [3200 - (75 \times 2) - 16]/(27 - 1) = 116 \text{ mm} \\ \text{Provide 16 mm bars at 116 mm c/c both ways.} \end{aligned}$$

Step 6 Check for development length. For M20 concrete and Fe 415 steel, required development length for 16 mm bar from Table 6.5 of SP16 is 752 mm.

$$\text{Length available} = 1400 - 75 = 1325 \text{ mm} > 752 \text{ mm.}$$

Step 7 Calculate transfer of force at the base of column.

$$\begin{aligned} \text{Factored compressive force at base of column} &= 1.5 \times 2200 = 3300 \text{ kN} \end{aligned}$$

As per Clause 30.6 of IS 456, limiting bearing stress

$$f_{br,max} = 0.45 f_{ck} \sqrt{\frac{A_1}{A_2}}$$

(a) At column face, $A_1 = A_2 = 400 \times 400 \text{ mm}^2$ and $f_{ck} = 30$ MPa; hence,

$$f_{br} = 0.45 \times 30 \times 1 = 13.5 \text{ MPa}$$

(b) At footing face, $f_{ck} = 20$ MPa, $A_1 = 3200^2 \text{ mm}^2$, and $A_2 = 400^2 \text{ mm}^2$

$$\sqrt{\frac{A_1}{A_2}} = \frac{3200}{400} = 8 > 2. \text{ Hence, adopt a value of 2.0.}$$

$$f_{br} = 0.45 \times 20 \times 2 = 18 \text{ MPa}$$

The critical face is the column face.

$$\begin{aligned} \text{Limiting bearing resistance} &= 13.5 \times 400^2 \times 10^{-3} = 2160 \text{ kN} < P_u = 3300 \text{ kN} \end{aligned}$$

The excess force of $3300 - 2160 = 1140$ kN may be resisted by providing dowels or by continuing the column bars into the footing.

Step 8 Check for development length of column bars. For fully stressed 25 mm bars in compression (M20 and Fe 415), development length from Table 65 of SP 16 is 1175 mm.

$$\text{Required } L_d = 1175 \times 1140/3300 = 406 \text{ mm}$$

Available vertical embedment length in footing, $d = 667 \text{ mm} > 406 \text{ mm}$.

The column bars are bent (with 90° standard bend) into the footing and rest on top of bottom mesh of footing reinforcement, as shown in Fig. 15.52(b).

Note: The effective depth of 667 mm is required only near the face of the column (due to shear considerations). As per IS 456, only a minimum depth of 150 mm needs to be provided at the edge. Hence, keep the edge depth as 250 mm and provide the shape as shown in Fig. 15.52(b).

EXAMPLE 15.3 (Design of concentrically loaded sloped square footing):

Design a sloped square footing for a circular column of size 500 mm diameter and subjected to an unfactored load of 1200 kN. Assume SBC of 200 kN/m² and use M20 concrete and Fe 415 steel.

SOLUTION:

Step 1 Determine the size of footing.

Required area of footing = $1.1 \times 1200/200 = 6.6 \text{ m}^2$

Hence size of footing = $\sqrt{6.6} = 2.57 \text{ m}$

Adopt 2.6 m × 2.6 m footing.

Step 2 Determine the size of equivalent square column.

As per Clause 34.2.2 of IS 456

$$c_1 = c_2 = \frac{500}{\sqrt{2}} = 354 \text{ mm}$$

Let us provide a square ledge of size 700 mm × 700 mm around the column and proceed with the calculations with a column size of 354 mm × 354 mm.

Step 3 Calculate the soil pressure on footing.

Factored load = $1.5 \times 1200 = 1800 \text{ kN}$

$$\text{Upward soil pressure} = \frac{1800 \times 10^3}{2600 \times 2600} = 0.266 \text{ N/mm}^2$$

Step 4 Calculate the depth of footing.

Depth of footing based on moment considerations

$$\begin{aligned} M_x &= \frac{P}{8L} (B - c_1)^2 = \frac{1800 \times 10^3}{8 \times 2600} (2600 - 354)^2 \times 10^{-6} \\ &= 436.54 \text{ kNm} \end{aligned}$$

Note that the breadth resisting the moment can be taken as 700 mm.

$$\begin{aligned} M_n &= 0.138 b_1 d^2 f_{ck} + 0.025 (B - b_1) d^2 f_{ck} \\ &= [0.138 \times 700 + 0.025 (2600 - 700)] 20 d^2 = 2882 d^2 \end{aligned}$$

$$\text{Equating the external moment, we get } d = \sqrt{\frac{436.54 \times 10^6}{2882}} =$$

389 mm

As the depth will be governed by shear consideration, let us adopt an effective depth of 600 mm at the face of column and edge depth of 250 mm. Let us adopt a clear cover of 75 mm. With 20 mm rods, effective cover = 85 mm.

Step 5 Check depth for one-way shear. The critical section is at a distance $d = 600 \text{ mm}$ from the face of column.

$$\text{Distance of this section from the edge of footings} = \left(\frac{2600 - 354}{2} \right) - 600 = 523 \text{ mm}$$

Breadth of footing at this section with 45° diagonal (refer to Fig. 15.53)

$$b_2 = 2600 - 2 \times 523 = 1554 \text{ mm}$$

$$\text{Shear at this section} = \left(\frac{2600 + 1554}{2} \right) \times 523 \times 0.266 \times 10^{-3} = 289 \text{ kN}$$

Effective depth at this section,

$$d_1 = (250 - 85) + \frac{(700 - 250) \times 523}{(2600 - 700)/2} = 412 \text{ mm}$$

$$\text{Shear stress, } \tau_v = \frac{289 \times 1000}{412 \times 1554} = 0.451 \text{ N/mm}^2$$

From Table 19 of IS 456, τ_c for M20 concrete with $p_t = 0.50\% = 0.48 \text{ N/mm}^2$.

Hence, the footing is safe in one-way shear with $p_t = 0.50\%$.

Step 6 Check depth for two-way shear. Two-way shear has to be checked at a distance of $d/2 = 600/2 = 300 \text{ mm}$ from the face of column.

$$\text{Distance of this section from the edge of footing} = \left(\frac{2600 - 354}{2} \right) - 300 = 823 \text{ mm}$$

Width of footing at this section (refer to Fig. 15.53) $b_3 = 2600 - 2 \times 823 = 954 \text{ mm}$

$$\text{Depth of footing at this section } d_2 = (250 - 85) + \frac{(700 - 250) \times 823}{950} = 555 \text{ mm}$$

Punching shear at this section

$$V_s = (2600^2 - 954^2) \times 0.266 \times 10^{-3} = 1556 \text{ kN}$$

Punching shear stress (Clause 31.6.2.1 of IS 456)

$$\tau_{vp} = \frac{1556 \times 10^3}{(4 \times 954) \times 555} = 0.735 \text{ N/mm}^2$$

Permissible shear stress (Clause 31.6.3 of IS 456)

$$= k_s \tau_c \text{ where } k_s = 0.5 + \beta_c < 1.0 \text{ and } \tau_c = 0.25 \sqrt{f_{ck}}$$

$$\beta_c = \frac{354}{354} = 1.0; k_s = 1.0$$

Hence, permissible shear stress = $1 \times 0.25 \sqrt{20} = 1.118 \text{ N/mm}^2 > 0.735 \text{ N/mm}^2$

Footing is safe in two-way shear.

Step 7 Calculate the area of steel. The lever arm of the trapezium section is given by

$$j = \frac{(K - K_2)b_1 + K_2b_2}{0.36k_u b_1 + 0.204(B - b_1)k_u^2}$$

$$= \frac{(0.138 - 0.025)0.7 + 0.025 \times 2.6}{0.36 \times 0.479 \times 0.7 + 0.204(2.6 - 0.7) \times 0.479^2}$$

$$= \frac{0.1855}{0.2096} = 0.885$$

$$A_{st} = \frac{M_u}{0.87f_y j d} = \frac{436.54 \times 10^6}{0.87 \times 415 \times 0.885 \times 600} = 2277 \text{ mm}^2$$

If we consider only the rectangular portion

$$\frac{M_u}{bd^2} = \frac{436.54 \times 10^6}{700 \times 600^2} = 1.732$$

From Table 2 of SP16, for Fe 415 steel and M20 concrete $p_t = 0.541\% > p_t$ required for shear in Step 5 = 0.50%.

$$A_{st} = \frac{0.541}{100} \times 700 \times 600 = 2272 \text{ mm}^2$$

Thus, there is not much difference in A_{st} if we ignore the triangular portion of the trapezium in this case.

From Table 95 of SP16, provide twelve 16 mm bars ($A_{st} = 2412 \text{ mm}^2$)

$$\text{Spacing} = (2600 - 2 \times 75)/11 = 220 \text{ mm}$$

It has to be noted that a more economical solution will be obtained if the soil pressure is assumed to act on the trapezoids of the footing.

$$M_x = \frac{q_u}{24} (2L + c_2)(B - c_1)^2$$

$$= \frac{0.266}{24} (2 \times 2600 + 354)$$

$$(2600 - 354)^2 \times 10^{-6}$$

$$= 310.52 \text{ kNm (as compared to } 436.54 \text{ kNm)}$$

$$\text{Now } \frac{M_u}{bd^2} = \frac{310.52 \times 10^6}{700 \times 600^2} = 1.232$$

From Table 2 of SP16, for Fe 415 steel and M20 concrete $p_t = 0.37\%$

However, we need to provide 0.5 per cent steel as per shear consideration.

$$\text{Hence } A_{st} = 0.5/100 \times 700 \times 600 = 2100 \text{ mm}^2$$

From Table 95 of SP 16, provide eleven 16 mm bars both ways ($A_{st} = 2211 \text{ mm}^2$).

$$\text{Spacing} = (2600 - (2 \times 75) - 16)/10 = 243 \text{ mm}$$

Spacing is less than 300 mm or 3d (Clause 34.5 of IS 456). Hence it is adequate.

Step 8 Check for development length.

$$\text{Length available} = (2600 - 700)/2 = 950 \text{ mm}$$

L_d of 16 mm bar for M20 concrete (Table 65 of SP 16) = 752 mm < 950 mm.

Hence, it is adequate.

Step 9 Check for transfer of force at the base of column.

Factored compressive force at the base of column = 1.5 × 1200 = 1800 kN

Assuming the column to be M25 at column face

$$f_{br} = 0.45 \times 25 \times 1 \left(\text{as } \sqrt{\frac{A_1}{A_2}} = 1 \right) = 11.25 \text{ MPa}$$

At the footing face, $\sqrt{A_1/A_2} = \sqrt{\frac{2600^2}{\pi \times 500^2/4}} = 5.86 > 2$; $f_{br} = 0.45 \times 20 \times 2 = 18 \text{ MPa}$

Limiting bearing resistance = 11.25 × π × 500²/4 × 10⁻³ = 2209 kN > 1800 kN

Hence, it is safe. However, extend the column bars into the footing.

Step 10 Calculate the overall dimensions of the footing.

$$\text{Required overall depth} = 600 + 12 + 12/2 + 75 = 693 \text{ mm}$$

Provide 700 mm depth at centre and 250 mm depth at edges and adopt 2600 mm² footing with eleven 16 mm bars, as shown in Fig. 15.53.

EXAMPLE 15.4 (Design of concentrically loaded rectangular footing):

Design a rectangular footing for the column in Example 15.2, assuming that there is a spatial restriction of 2.8 m on one of the plan dimensions of the footing.

SOLUTION:

Step 1 Determine the size of footing. As given in Example 15.2,

$$\text{Required area of footing} = 9.68 \text{ m}^2$$

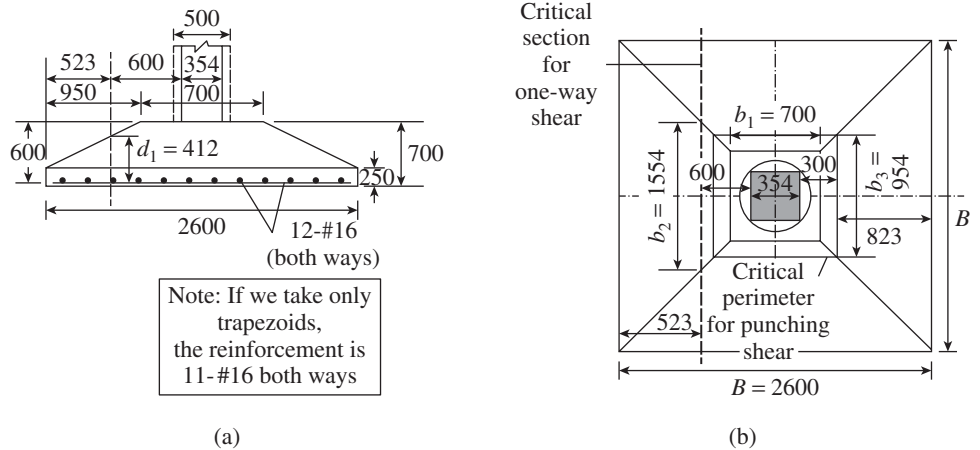


FIG. 15.53 Sloped footing of Example 15.3 (a) Section (b) Plan

Since width B is restricted to 2.8 m,

Length $L = 9.68/2.8 = 3.46$ m

Provide a rectangular footing of size 2.8 m \times 3.5 m.

Net factored soil pressure, $q_u = \frac{2200 \times 1.5}{2.8 \times 3.5} = 336.7 \text{ kN/m}^2 = 0.337 \text{ N/mm}^2$

Step 2 Determine the thickness of footing based on one-way shear. For maximum V_{u1} , take section along the breadth of footing at a distance d from the column.

$$V_{u1} = q_u B \left(\frac{L - c_2 - 2d}{2} \right) = 0.337 \times 2.8 \left(\frac{3.5 - 0.4 - 2d}{2} \right) = 0.4718(3.1 - 2d)$$

As shown in Example 15.2, this value should be equal to $\tau_c B d$.

Assuming $p_t = 0.25\%$ from Table 19 of IS 456, for M20 concrete $\tau_c = 0.36 \text{ N/mm}^2$.

Hence, $0.4718(3.1 - 2d) = 0.36 \times 2.8 \times d$

Solving, $d = 0.75 \text{ m} = 750 \text{ mm}$

Step 3 Check depth for two-way shear. As in Example 15.2,

Punching shear strength $= 0.25 \sqrt{f_{ck}} = 1.118 \text{ N/mm}^2$

Taking a section at $d/2$ around the column, we get

$$\begin{aligned} V_{u2} &= q_u [LB - (c_1 + d)(c_2 + d)] \\ &= 0.337 [2800 \times 3500 - (400 + 750)^2] = 2857 \times 10^3 \text{ N} \\ \tau_{v2} &= \frac{V_{u2}}{2[(c_1 + d) + (c_2 + d)]d} \\ &= \frac{2857 \times 10^3}{4(400 + 750) \times 750} = 0.828 \text{ N/mm}^2 < 1.118 \text{ N/mm}^2 \end{aligned}$$

Hence, it is safe in two-way shear.

Step 4 Design the flexural reinforcement in the long direction. Bending moment in long direction (section x-x in Fig. 15.54)

$$\begin{aligned} M_{ux} &= q_u B \frac{(L - c_2)^2}{8} = \frac{0.337 \times 2800(3500 - 400)^2}{8} \\ &= 1133.5 \times 10^6 \text{ Nmm} \\ R &= \frac{M_u}{Bd_x^2} = \frac{1133.5 \times 10^6}{2800 \times 750^2} = 0.72 \text{ MPa} \end{aligned}$$

Hence, from Table 2 of SP 16, for M20 concrete and Fe 415 steel, $p_t = 0.209\%$. This is less than $p_t = 0.25\%$ assumed for one-way shear.

Hence, required $A_{st} = 0.25 \times 2800 \times 750/100 = 5250 \text{ mm}^2$

From Table 95 of SP16, provide seventeen 20 mm bars ($A_{st} = 5340 \text{ mm}^2$) at uniform spacing in the long direction.

Check for development length Required development length for M20 concrete and Fe 415 steel (Table 65 of SP 16) = 940 mm.

Available length $= \frac{(L - c_2)}{2} - \text{cover} = \frac{(3500 - 400)}{2} - 75 = 1475 \text{ mm} > 940 \text{ mm}$

Step 5 Design the reinforcement in the short direction.

Bending moment in the short direction

$$\begin{aligned} M_{uy} &= q_u L \left(\frac{B - c_1}{8} \right)^2 = \frac{0.337 \times 3500(2800 - 400)^2}{8} \\ &= 849.3 \times 10^6 \text{ Nmm} \end{aligned}$$

Assuming 16 mm bars $d_y = 750 - 20/2 - 16/2 = 732 \text{ mm}$

$$R = \frac{M_u}{Ld_y^2} = \frac{849.3 \times 10^6}{3500 \times 732^2} = 0.453 \text{ MPa}$$

From Table 2 of SP 16, for M20 concrete and Fe 415 steel, $p_t = 0.129\%$.

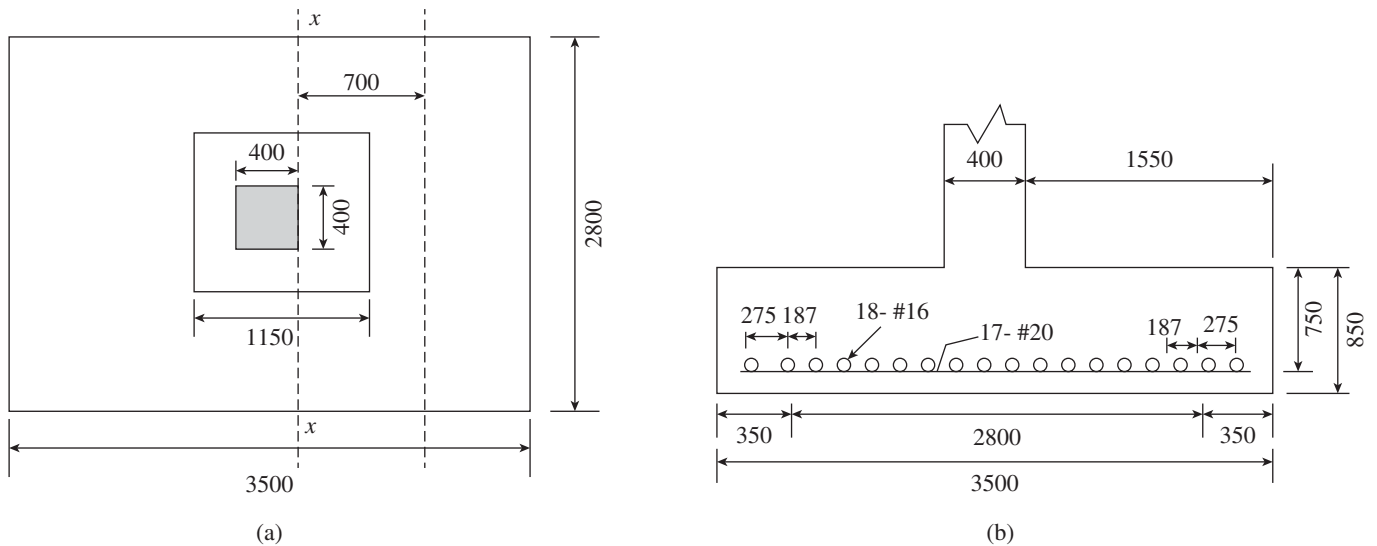


FIG. 15.54 Rectangular footing of Example 15.4 (a) Plan (b) Section

Check for p_t for one-way shear One-way shear in the short direction

$$\begin{aligned} V_{u1} &= q_u L \left(\frac{B - c_1 - 2d_y}{2} \right) \\ &= 0.337 \times 3500 \left(\frac{2800 - 400 - 2 \times 732}{2} \right) \\ &= 552 \times 10^3 \text{ N} \\ \tau_{v1} &= \frac{V_{u1}}{L \times d_y} = \frac{552 \times 10^3}{3500 \times 732} = 0.215 \text{ N/mm}^2 \end{aligned}$$

From Table 19 of IS 456, for M20 concrete and for minimum $p_t \leq 0.15\%$, $\tau_c = 0.28$. Hence,

$$\text{Required } A_{st} = 0.129 \times 3500 \times 750/100 = 3386 \text{ mm}^2$$

$$\text{Required overall depth} = 750 + 10 + 75 = 835 \text{ mm}$$

Provide an overall depth of 850 mm.

$$\text{Minimum } A_{st} = 0.12 \times 3500 \times 850/100 = 3570 \text{ mm}^2 > 3386 \text{ mm}^2$$

From Table 95 of SP16, provide eighteen 16 mm bars ($A_{st} = 3619 \text{ mm}^2$). According to Clause 34.3.1(c) of IS 456, area of steel to be provided within the central band width $B = 2800 \text{ mm}$

$$= 3570 \times \frac{2}{\beta + 1} = 3570 \times \frac{2}{\left(\frac{3.5}{2.8} + 1\right)} = 3173 \text{ mm}^2$$

Number of required 16 mm bars = $3173/201 = 16$ bars

Hence, provide sixteen 16 mm bars at uniform spacing within the central band of 2.8 m at a spacing of $2800/(16 - 1) = 187 \text{ mm c/c}$.

In addition, provide one bar each at the end of the two other segments making a total of 18 bars; width of end segment = $(3500 - 2800)/2 = 350 \text{ mm}$.

Spacing of bar = $350 - \text{end cover} = 350 - 75 = 275 \text{ mm}$ (see Fig. 15.54).

Check for spacing

$$\text{Maximum spacing} = 275 \text{ mm} < 300 \text{ or } 3d$$

Hence, it is adequate.

Check for development length From Table 65 of SP 16, development length for 16 mm bar (for M20 concrete and Fe 415 steel) = 752 mm.

$$\text{Available length} = (B - c_1)/2 - \text{cover} = (2800 - 400)/2 - 75 = 1125 \text{ mm} > 752 \text{ mm}$$

Hence, it is safe.

Step 6 Check for the transfer of force at column base. The calculations are identical to those given in Example 15.2, except for the footing face, where $A_2 = 2.8 \times 3.5 = 9.8 \text{ m}^2$.

$$\text{However, } \sqrt{\frac{A_1}{A_2}} > 2. \text{ Hence } f_{br} = 0.45 \times 20 \times 2 = 18 \text{ MPa}$$

At column face, $f_{br} = 13.5 \text{ MPa}$ as per Example 15.2.

$$\text{Limiting bearing resistance} = 13.5 \times 400^2 \times 10^{-3} = 2160 \text{ kN} < P_u = 3300 \text{ kN}$$

The excess force of 1140 kN may be transferred by simply extending the column bars.

Note: A sloped footing will be more economical than the pad-type footing of this example. The reader may design this example as a sloped footing and compare the results.

EXAMPLE 15.5 (Eccentrically loaded isolated rectangular footing):

Design the footing for the column of Example 14.4 of Chapter 14. Assume SBC of soil as 200 kN/m^2 at 1.5 m depth and use M20 concrete and Fe 415 steel for the footing. Note that the moment is reversible.

SOLUTION:

From Example 14.4, we get $P_u = 1400 \text{ kN}$ and $M_u = 90 \text{ kNm}$.

Step 1 Determine the size of footing. Since the given moment is reversible, we need to have a footing that is symmetric with respect to the column. Assume the weight of footing as 10 per cent of the column load.

$$\text{Let us assume } e < L/6, \text{ with } e = \frac{90 \times 10^6}{(1400 \times 10^3) \times 1.1} = 58.44 \text{ mm.}$$

$$\text{Hence } L > 6 \times 58.44 = 350.6 \text{ mm.}$$

For determination of footing size we need working loads and moments. Assuming that the load factor is 1.5, $P = 1400/1.5 = 933.3 \text{ kN}$ and $M = 90/1.5 = 60 \text{ kNm}$. Hence

$$\frac{P}{BL} + \frac{M}{BL^2/6} \leq \text{SBC} \quad \text{or} \quad \frac{933.3 \times 1.1}{BL} + \frac{60 \times 6}{BL^2} < 200$$

From this, we get

$$200BL^2 - 1026.6L - 360 = 0$$

Assuming $L = 1.2$ times B and simplifying, we get

$$L^3 - 6.16L - 2.16 = 0$$

Solving this using online solver at <http://easycalculation.com/algebra/cubic-equation.php>,

$$\text{we get } L = 2.6415 \text{ m.}$$

The economical footing is one that has equal projections beyond the face of column in both directions, that is, when $(L - c_2)/2 = (B - c_1)/2$. Hence, adopt $2.65 \text{ m} \times 2.55 \text{ m}$.

Step 2 Calculate the net pressure below foundation.

$$\text{Factored net soil pressure, } q_{u,\max} = \frac{P_u}{BL} + \frac{6M_u}{BL^2}$$

$$q_1 = q_{u,\max} = \frac{1400}{2.55 \times 2.65} + \frac{90 \times 6}{2.55 \times 2.65^2}$$

$$= 207.17 + 30.16 = 237.3 \text{ kN/m}^2$$

$$q_2 = q_{u,\min} = 207.17 - 30.16 = 177 \text{ kN/m}^2$$

Step 3 Determine the depth of footing. Even though the depth has to be fixed based on one-way shear, to simplify the calculation let us first determine the depth due to bending considerations.

$$\text{Cantilever span } L_c = \frac{(L - c_2)}{2} = \frac{(2650 - 400)}{2} = 1125 \text{ mm}$$

Then soil pressure at the face of column (see Fig. 15.55)

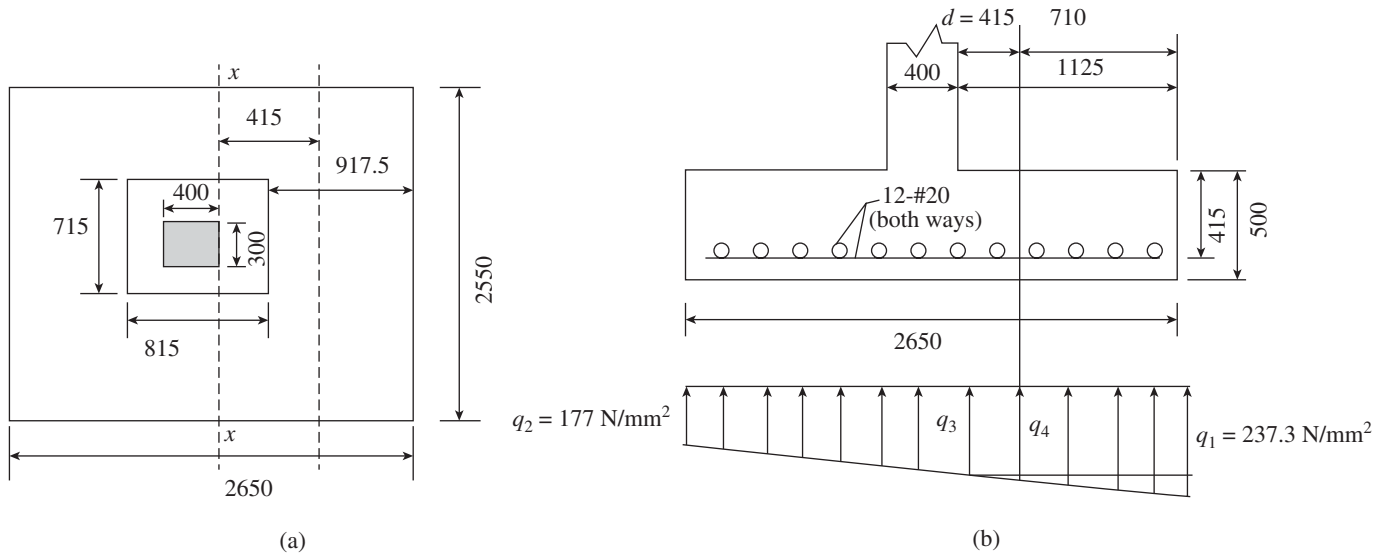


FIG. 15.55 Rectangular footing with axial force and moment for Example 15.5 (a) Plan (b) Section

$$q_3 = q_1 - \frac{(q_1 - q_2)L_c}{L}$$

$$= 237.3 - \frac{(237.3 - 177) \times 1.125}{2.65} = 211.7 \text{ kN/m}^2$$

$$= 0.2117 \text{ N/mm}^2$$

The maximum bending moment at the face of column (taking rectangular and triangular distribution of pressure diagram separately)

$$M_c = \frac{q_3 BL_c^2}{2} - \frac{(q_3 - q_1)}{2} BL_c^2 (2/3)$$

$$M_c = (0.2117 \times 2550 \times 1125^2 / 2) + \frac{(0.2373 - 0.2117)}{2}$$

$$\times 2550 \times 1125^2 \times \frac{2}{3}$$

$$= (341.61 + 27.54) \times 10^6 = 369.15 \times 10^6 \text{ Nmm}$$

$$d = \sqrt{\frac{M_c}{0.138 \times f_{ck} B}} = \sqrt{\frac{369.15 \times 10^6}{0.138 \times 20 \times 2550}} = 229 \text{ mm}$$

As the thickness will be governed by shear stress considerations, assume $d = 415 \text{ mm}$, with 20 mm bars and clear cover of 75 mm. Hence, overall depth = 500 mm.

Step 4 Check for one-way shear. The critical section is at a distance $d = 415 \text{ mm}$ from the face of the column.

Shear span $L_s = (L - c_2)/2 - d = 1125 - 415 = 710 \text{ mm}$

The soil pressure at this location

$$q_4 = q_1 - \frac{(q_1 - q_2)L_s}{L} = 237.3 - \frac{(237.3 - 177) \times 0.71}{2.65}$$

$$= 221.1 \text{ kN/mm}^2 = 0.2211 \text{ MPa}$$

The factored shear force at this plane is

$$V_u = \frac{(q_1 + q_4)}{2} BL_s = \frac{(0.2373 + 0.2211)}{2} \times 2550 \times 710 \times 10^{-3}$$

$$= 415 \text{ kN}$$

$$\text{Nominal shear stress } \tau_v = \frac{V_u}{Bd} = \frac{415 \times 10^3}{2550 \times 415} = 0.392 \text{ N/mm}^2$$

From Table 19 of IS 456, for M20 concrete, $\tau_c = 0.408 \text{ N/mm}^2$ for $p_t = 0.35\%$. Hence, we need to provide 0.35 per cent reinforcement.

Step 5 Check for punching shear. The critical section is at a distance $d/2 = 415/2 = 207.5 \text{ mm}$ from the face of the footing.

$$L_{ps} = 1125 - 207.5 = 917.5 \text{ mm}$$

The soil pressure at this location

$$q_5 = q_1 - \frac{(q_1 - q_2)}{L} \times L_{ps} = 237.3 - \frac{(237.3 - 177)}{2.65} \times 0.9175$$

$$= 216.4 \text{ kN/m}^2$$

$$\text{Average pressure} = (237.3 + 216.4)/2 = 226.9 \text{ kN/m}^2$$

$$\text{Punching shear force } V_{u2} = q[LB - (c_1 + d)(c_2 + d)]$$

$$= 0.2269 [2550 \times 2650 - (400 + 415)(300 + 415)] = 1401 \times 10^3 \text{ N}$$

$$\text{Nominal shear stress } \tau_{v2} = \frac{V_{u2}}{b_o d}$$

$$b_o = 2 \times [(400 + 415) + (300 + 415)] = 3060 \text{ mm}$$

$$\tau_{v2} = \frac{1401 \times 10^3}{3060 \times 415} = 1.103 \text{ N/mm}^2$$

$$\text{Limiting shear stress } \tau_c = k_s (0.25 \sqrt{f_{ck}})$$

$$k_s = 0.5 + c_1/c_2 < 1$$

$$= 0.5 + 300/400 = 1.25; \text{ hence, } k_s = 1.0.$$

$$\tau_c = 1.0 \times 0.25 \sqrt{20} = 1.118 \text{ N/mm}^2 > 1.103 \text{ N/mm}^2$$

Hence, it is safe in punching shear.

Step 6 Design the flexural reinforcement.

$M_c = 369.15 \times 10^6$ Nmm from Step 3

$$R = \frac{M_u}{Bd_x^2} = \frac{360.15 \times 10^6}{2550 \times 415^2} = 0.84$$

From Table 2 of SP 16, $p_t = 0.245\% < p_t = 0.35\%$ required for one-way shear.

Hence, provide $0.35 \times 2550 \times 415/100 = 3704$ mm²

Using 20 mm bars, required number = $3704/314 = 12$

Corresponding spacing = $(2550 - 2 \times 75 - 20)/11 = 216$ mm

Provide twelve 20 mm bars in the long direction at a spacing of 216 mm c/c.

Check for development length Required development length for 20 mm bars (for M20 with Fe 415) = 940 mm

Available length = $L_c - \text{cover} = 1125 - 75 = 1050$ mm > 940 mm

Hence, it is safe.

Step 7 Design the reinforcement in the short direction.

The projection on both sides of the column in the short direction is the same as that in the long direction. However, $d_y = 415 - 20 = 395$ mm. Since the percentage reinforcement is governed by one-way shear considerations, provide the same reinforcement in this direction as well. In addition, the difference in dimensions between the two sides ($B = 2550$ mm and $L = 2650$ mm) is not significant. Hence, provide the bars at uniform spacing as in the long direction.

Step 8 Check for the transfer of forces at column base. In this case, some bars are in tension due to the bending moment. Hence, no transfer of the tensile force is possible through bearing at the column-footing interface. Hence, the column bars should be extended into the footing.

Required development length of 22 mm column bars in tension $47 \times 22 = 1034$ mm

Length available (including 90° bend on top of the upper layer of footing reinforcement, with equivalent anchorage length for bend = $8 \times d_b$) = $(500 - 75 - 20 - 20 - 22/2) + 8 \times 22 = 550$ mm

The balance of $1034 - 550 = 484$ mm should be made up by extending these bars into the footing beyond the bend. As the moment in the column is reversible, all bars should be provided with this extension.

Note: Alternatively, a pedestal of size 450 mm × 550 mm may be provided with small diameter bars to reduce the development length requirement.

EXAMPLE 15.6 (Design of combined footing):

Design a rectangular combined footing to support two columns of size 300 mm × 300 mm (with six 16 bars) and 400 mm × 400 mm (with six 20 bars), carrying 800 kN and 1200 kN (service live + dead loads), respectively. These columns are located 3.6 m apart and the column carrying 800 kN is flush with the property line. Assume SBC of 200 kN/m². Assume

M25 concrete in the columns and M20 concrete in the footing and Fe 415 steel in the columns as well as footing.

SOLUTION:

Step 1 Calculate the size of footing. Assuming the self-weight of footing plus backfill as 15 per cent of column loads

$$\text{Required area of footing} = \frac{(800+1200) \times 1.15}{200} = 11.5 \text{ m}^2$$

Spacing between columns = 3600 mm

The C.G. distance from centre of edge column

$$n = \frac{P_2 s}{P_1 + P_2} = \frac{1200 \times 3600}{(1200 + 800)} = 2160 \text{ mm}$$

Since $n > s/2$, rectangular footing can be adopted.

Length of footing = $2(2160 + 150) = 4620$ mm

Provide $L = 4.62$ m

Required breadth = $11.50/4.62 = 2.49$ m

Provide $B = 2.5$ m

See Fig. 15.56(a) for the configuration of this combined footing.

Step 2 Calculate the bending moment and shear force in the longitudinal direction.

Ultimate loads are

$$P_{u1} = 800 \times 1.5 = 1200 \text{ kN}$$

$$P_{u2} = 1200 \times 1.5 = 1800 \text{ kN}$$

Treating the footing as a wide beam with width = 2.5 m, soil pressure acting upward is

$$w = q_u B = \frac{(P_{u1} + P_{u2})}{L} = \frac{(1200 + 1800)}{4.62} = 650 \text{ kN/m}$$

The bending moment and shear force are calculated as follows:

Shear force at A = 0

Shear force left of point B = $1200 - wx_1 = 1200 - 650 \times 0.15 = 1102.5$ kN

Distance at which shear is zero from left end

$0 = 1200 - 650a$; hence $a = 1.85$ m

Shear force left of point C

$1800 - 650 \times 0.87 = 1234.5$ kN

Maximum bending moment where the shear force is zero is = $P_1(a - x_1) - wa^2/2$; with $a = 1.85$ m

= $1200(1.85 - 0.15) - 650 \times 1.85^2/2 = 928$ kNm

Bending moment at the face of column C₂ = $650 \times (0.87 - 0.2)^2/2 = 146$ kNm

Shear force at a distance d from the inside face of column C₂
 $V_{u1} = 1800 - 650(870 + 200 + d) \times 10^{-3} = (1104.5 - 0.65d)$ kN

The shear force and bending moment diagrams are shown in Fig. 15.56(c).

Step 3 Determine the thickness based on shear.

Assuming $p_t = 0.5\%$ from Table 19 of IS 456 and

$$\tau_c = 0.48 \text{ N/mm}^2 \text{ for M20 concrete}$$

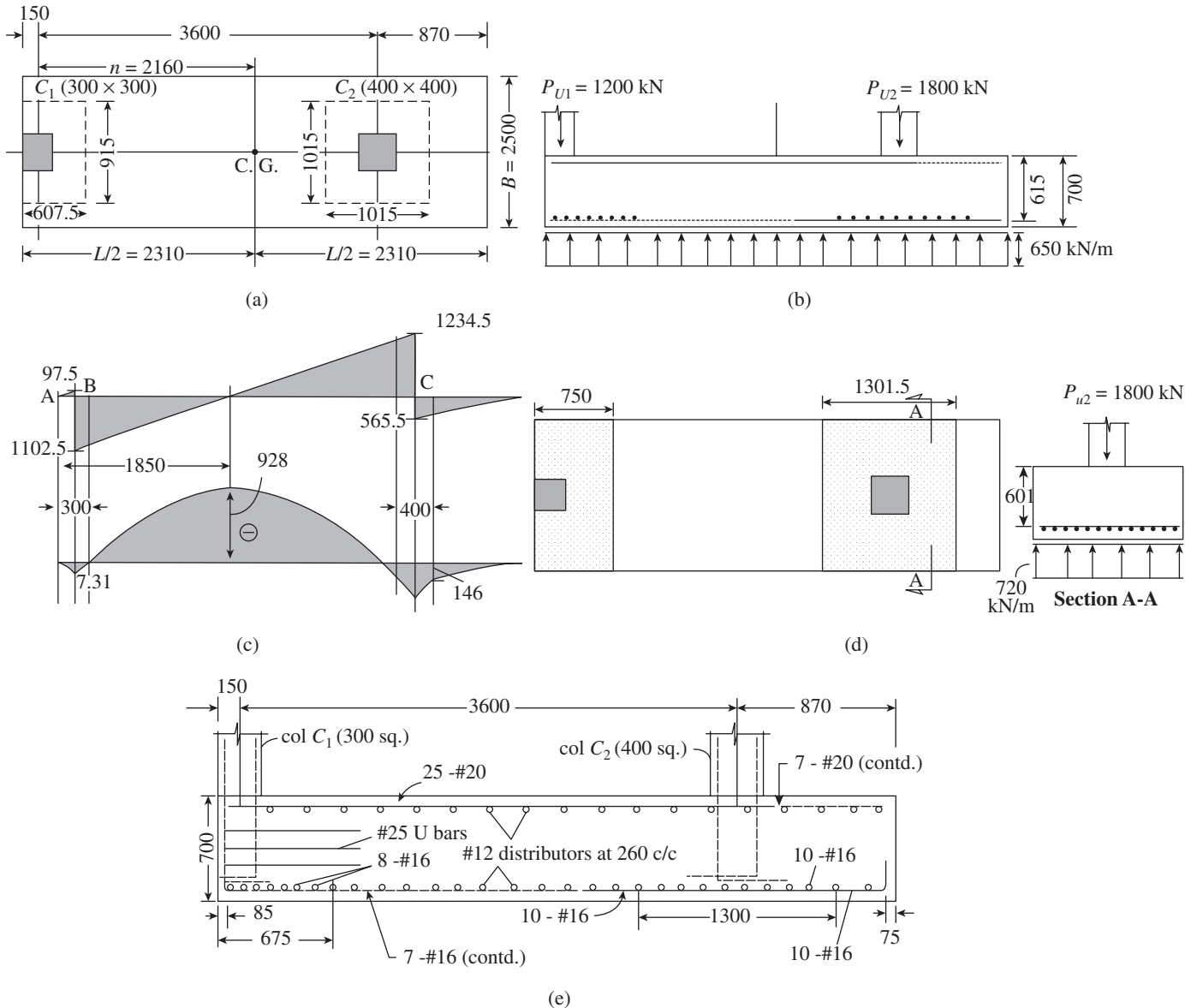


FIG. 15.56 Combined footing of Example 15.6 (a) Plan (b) Footing (c) Shear force and bending moment diagram (d) Column strips acting as transverse beams (e) Reinforcement detailing

$$V_{nc} = 0.48 \times 2500 \times d \times 10^{-3} = 1.2d$$

Equating V_{u1} and V_{nc} , we get

$$1104.5 - 0.65d \leq 1.2d \text{ or } d \geq 597 \text{ mm}$$

Assume an overall depth of 700 mm. With clear cover of 75 mm and 20 mm bars, effective depth, $d = 700 - 75 - 20/2 = 615$ mm.

Step 4 Check for two-way punching shear.

$$\text{Soil pressure} = \frac{1200 + 1800}{4.62 \times 2.5} = 260 \text{ kN/m}^2$$

Column C₂

Load 1800 kN; critical section at $(615/2)$ mm on either face of column

$$\text{Shear perimeter} = 4(400 + 615) = 4060 \text{ mm}$$

$$V_{u2} = 1800 - 260(1.015)^2 = 1532 \text{ kN}$$

$$\text{Punching shear stress } \tau_p = k(0.25\sqrt{f_{ck}}) = 0.25 \times \sqrt{20} = 1.12 \text{ N/mm}^2$$

$$\text{Hence capacity} = 4060 \times 615 \times 1.12 \times 10^{-3} = 2796 \text{ kN} > 1532 \text{ kN}$$

Column C₁

Load = 1200 kN

Shear perimeter only on three sides, as the column is at the edge

$$\text{Shear perimeter} = (300 + 615) + 2(300 + 615/2) = 2130 \text{ mm}$$

$$\text{Capacity} = 2130 \times 615 \times 1.12 \times 10^{-3} = 1467 \text{ kN} > 1200 \text{ kN}$$

(Note: V_{u1} will be less than 1200 kN and equals $1200 - 260 \times 0.915 \times 0.6075 = 1055$ kN)

Step 5 Check for base pressure. Assuming $\gamma_s = 18 \text{ kN/m}^3$ for the backfill, $\gamma_c = 24 \text{ kN/m}^3$ for concrete, and depth of footing as 1.5 m,

$$q = (800 + 1200)/(4.62 \times 2.5) + 24 \times 0.7 + 18(1.5 - 0.7)$$

$$= 173.2 + 16.8 + 14.4 = 204.4 \text{ kN/m}^2 \approx 200 \text{ kN/m}^2 \text{ (SBC)}$$

Hence, it is adequate.

Step 6 Calculate the longitudinal steel.

Maximum bending moment = 928 kNm

$$R = \frac{M_u}{Bd^2} = \frac{928 \times 10^6}{2500 \times 615^2} = 0.982 \text{ MPa}$$

Hence, from Table 2 of SP 16 for M20 concrete and Fe 415 steel, $p_t = 0.2896\% > 0.12\%$ (minimum steel).

Note: It is less than that assumed for shear consideration in Step 3, that is, 0.5 per cent.

Hence, required steel = $0.5 \times 2500 \times 615/100 = 7687.5 \text{ mm}^2$

Required number of 20 mm bars = $7687.5/314 = 25$

Spacing of bars = $(2500 - 75 \times 2 - 20)/24 = 97 \text{ mm}$

Provide twenty-five 20 mm bars at the top as shown in Fig. 15.56(e) between the two columns.

Step 7 Check for development length. For M20 concrete and Fe 415 steel, required L_d for 20 mm bar is 940 mm (Table 65 of SP16). Adequate length is available on both sides of the section where maximum bending moment occurs.

Step 8 Calculate the reinforcement for bending moment at the face of column C_2 .

Bending moment = 146 kNm

$$\frac{M_u}{Bd^2} = \frac{146 \times 10^6}{2500 \times 615^2} = 0.155;$$

From Table 2 of SP16, $p_t = 0.085\% < 0.12\%$ (minimum).

Hence, area required = $0.12 \times 2500 \times 615/100 = 1845 \text{ mm}^2$

Provide ten 16 mm bars ($A_{st} = 2010 \text{ mm}^2$).

Spacing = $(2500 - 75 \times 2 - 16)/9 = 259 \text{ mm} < 300 \text{ mm}$ (maximum spacing)

Required development length for 16 mm bar = $47 \times 16 = 752 \text{ mm}$

Available length on right side = $870 - 200 - 75 = 595 \text{ mm}$.

Hence, provide 90° bend and $4d_b$ mm extension; anchorage value (Table 67 of SP 16) = 128 mm.

Thus, $595 + 128 = 723 \text{ mm} < 752 \text{ mm}$. Hence, provide extension of $6d_b$ (i.e., 32 mm extra).

Step 9 Calculate the reinforcement in transverse direction.

(a) *Under column C_1*

Factored load per unit length of beam = $1200/2.5 = 480 \text{ kN/m}$

Projection from the column face = $(2500 - 300)/2 = 1100 \text{ mm}$

Maximum bending moment at column face = $480 \times 1.1^2/2 = 290.4 \text{ kNm}$

Effective depth (16 mm bars will be placed above the 16 mm longitudinal bars)

$$d = 700 - 75 - 16 - 16/2 = 601 \text{ mm}$$

Let us assume that the load is spread over a width of $0.75d$ on either side of the column. Hence, width of beam = $300 + 0.75d = 300 + 0.75 \times 601 = 750 \text{ mm}$

$$R = \frac{M_u}{Bd^2} = \frac{290.4 \times 10^6}{750 \times 601^2} = 1.072$$

From Table 2 of SP 16, $p_t = 0.318\%$ for Fe 415 and M20 concrete.

$A_{st} = 0.318 \times 750 \times 601/100 = 1434 \text{ mm}^2$

Required number of 16 mm bars = $1434/201 = 8$

Spacing = $(750 - 75 - 16)/7 = 94 \text{ mm}$

Provide eight 16 mm bars below column C_1 .

Required development length = $47 \times 16 = 752 \text{ mm} < (1100 - 75) \text{ mm}$ available.

(b) *Under column C_2*

Factored load per unit length of beam = $1800/2.5 = 720 \text{ kN/m}$

Projection from column face = $(2500 - 400)/2 = 1050 \text{ mm}$

Moment at column face = $720 \times 1.05^2/2 = 396.9 \text{ kNm}$

Width of beam = $400 + 2 \times (0.75 \times 601) = 1301.5 \text{ mm}$

$$R = \frac{M_u}{Bd^2} = \frac{396.9 \times 10^6}{1301.5 \times 601^2} = 0.844 \text{ MPa}$$

From Table 2 of SP 16 for M20 concrete and Fe 415 steel, $p_t = 0.2462\% > 0.12\%$ (minimum steel).

Required $A_{st} = 0.2462 \times 1301.5 \times 601/100 = 1926 \text{ mm}^2$

Required number of 16 mm bars = $1926/201 = 10$

Spacing = $1301.5/9 = 145 \text{ mm}$

Provide ten 16 mm bars. The required development length of $47 \times 16 = 752 \text{ mm}$ is available beyond the column face.

Note: As the entire width of 4.62 m is available to resist one-way shear, it will not be critical in this direction.

Step 10 Check for the transfer of force at column face.

(a) *Column C_1*

Limiting bearing stress

(i) At column face = $0.45f_{ck} = 0.45 \times 25 = 11.25 \text{ MPa}$

(ii) At footing face = $0.45f_{ck} \sqrt{A_1/A_2} = 0.45 \times 25 \times 1 = 9.0 \text{ MPa}$

Since the column is located at the edge of the footing, Bearing resistance = $9 \times 300^2/10^3 = 810 \text{ kN} < P_{u1} = 1200 \text{ kN}$

Hence, the column reinforcement should be extended into the footing or sufficient dowels should be provided.

(b) *Column C_2*

For column C_2 , $A_2 = 400^2$ and $A_1 = 2500^2$

Hence $\sqrt{A_1/A_2} = 6.25 > 2.0$; hence, take as 2.0.

Limiting bearing stress

- (i) At column face = 11.25 MPa (as in column C_1)
 (ii) At footing face = $0.45 \times 20 \times 2 = 18 \text{ MPa} > 11.25 \text{ MPa}$

Hence limiting bearing resistance = $11.25 \times 400^2/10^3 = 1800 \text{ kN} = P_{u2}$

Hence, no reinforcement is necessary across the interface. However, extend the column bars into the footing.

Step 11 Design U bars at the edge around vertical starter bars of columns.

Angle of dispersion of the edge column load = $\tan^{-1}(350/150) = 66.8^\circ$

Horizontal component at mid-depth of footing, due to dispersion = $1200 \times \cos 66.8 = 473 \text{ kN}$

Required area = $473 \times 1000/(0.87 \times 415) = 1310 \text{ mm}^2$

Provide three 25 mm U bars around the vertical starter bars of columns, with length on each face as 1175 mm (L_d of 25 mm bar).

Step 12 Detail the reinforcement. The reinforcement details are shown in Fig. 15.56(e). It has to be noted that a few bottom bars (7-#16) are extended throughout the length to provide nominal reinforcement. In addition, some nominal transverse reinforcement is also provided at the top and bottom (0.06% on each face- #12 at 260 c/c) to tie up with the main bars.

EXAMPLE 15.7 (Design of plain concrete footing):

Design a plain concrete footing for a column of size 250 mm × 250 mm carrying a service load of 250 kN. Assume allowable soil pressure of 250 kN/m² at 1.2 m below ground level. Assume M20 concrete and Fe 415 steel.

SOLUTION:

Step 1 Determine the size of footing. Assuming weight of footing + back fill as 10 per cent of axial load

$$\text{Required area} = 250 \times 1.1/250 = 1.1 \text{ m}^2$$

Provide 1.05 m × 1.05 m footing as shown in Fig. 15.57.

Step 2 Determine the thickness of footing.

$$\text{Soil pressure, } q_u = \frac{1.5 \times 250}{1.05^2} = 340 \text{ kN/m}^2 = 0.34 \text{ N/mm}^2$$

$$\text{Thickness of footing } D = \left(\frac{1050 - 250}{2} \right) \tan \alpha$$

$$\text{where } \tan \alpha > 0.9 \sqrt{\frac{100q_u}{f_{ck}} + 1} = 0.9 \sqrt{\frac{100 \times 0.34}{20} + 1} = 1.48$$

$$D = \left(\frac{1050 - 250}{2} \right) \times 1.48 = 592 \text{ mm}$$

Provide 600 mm depth. Check gross base pressure assuming weight of soil as 18 kN/m³ and weight of concrete as 24 kN/m³.

Actual soil pressure = $250/1.05^2 + 24 \times 0.6 + 18 \times 0.6 = 252 \text{ kN/m}^2 \approx 250 \text{ kN/m}^2$ (SBC)

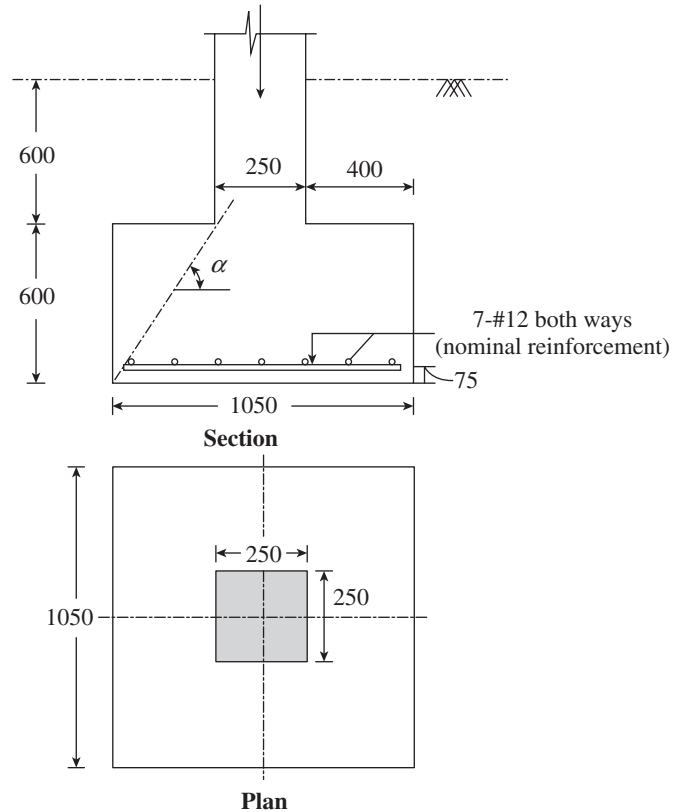


FIG. 15.57 Plain concrete footing of example 15.7

Step 3 Provide minimum steel.

$$\text{Minimum steel} = 0.12/100 \times 600 \times 1050 = 756 \text{ mm}^2$$

Provide seven 12 mm bars both ways ($A_{st} = 791 \text{ mm}^2$).

Step 4 Check for transfer of axial force at base.

$$\text{Limiting bearing stress, } f_{br} = 0.45 f_{ck} \sqrt{A_1/A_2}$$

The bearing stress at column face will govern.

$$\text{Hence } A_1 = A_2 = 250 \times 250 \text{ mm}^2$$

Capacity in bearing = $0.45 \times 20 \times 250^2 \times 10^{-3} = 562.5 \text{ kN} > 250 \times 1.5 = 375 \text{ kN}$

Hence, the load can be transferred without any reinforcement.

EXAMPLE 15.8 (Design of RC pile):

Design a precast pile of diameter 400 mm carrying an axial load of 275 kN, placed in submerged medium dense sandy soil having an angle of internal friction of 32°. The density of soil is 18 kN/m³ and the submerged density of soil is 10 kN/m³. Angle of wall friction between concrete pile and soil, δ is $0.75\phi = 24^\circ$. Assume the following data: Depth of top of pile cap below ground level is 500 mm, thickness of pile cap is 1.5 m, grade of concrete in pile is M25, Fe 415 steel is used, and clear cover to reinforcement is 75 mm. Determine the vertical carrying capacity of the pile in accordance with IS 2911 (Part 1, Section 1) and design the pile.

SOLUTION:

Step 1 Perform soil design.

Cross-sectional area of pile at the toe, $A_p = \pi \times 0.4^2/4 = 0.126 \text{ m}^2$

Let us conservatively assume that the water table is up to the ground level.

Effective unit weight of soil at pile toe, $\gamma = \gamma_{sub} = 10 \text{ kN/m}^3$

$$N_q = e^{\pi \tan \phi} \left(\frac{1 + \sin \phi}{1 - \sin \phi} \right) = e^{\pi \tan 32} \left(\frac{1 + \sin 32}{1 - \sin 32} \right) = 7.121 \times 3.255 = 23.18$$

$$N_\gamma = 2(N_q + 1) \tan \phi = 2(23.18 + 1) \tan 32 = 30.22$$

Assuming the critical depth as 17.5 times the diameter of the pile,

Effective overburden pressure at pile tip, $P_D = 10(0.5 + 1.5 + 17.5 \times 0.4) = 90 \text{ kN/m}^2$

Coefficient of earth pressure, K_i , is taken as 1.5, as $\phi = 32^\circ$.

P_{D1} = Effective overburden pressure at bottom of pile cap = $10(0.5 + 1.5) = 20 \text{ kN/m}^2$

P_{D2} = Effective overburden pressure at pile toe = $P_D = 90 \text{ kN/m}^2$

A_{s1} = Surface area of pile stem in the first layer = $\pi \times \text{diameter} \times L = 1.257L$

$$Q_u = 2.5 \times 275 = 687.5 \text{ kN}$$

Substituting the various quantities in the following static capacity equation,

$$Q_u = A_p(0.5D\gamma N_\gamma + P_D N_q) + \sum_{i=1}^n K_i P_{Di} \tan \delta_i A_{si}$$

$$687.5 = 0.126(0.5 \times 0.4 \times 10 \times 30.22 + 90 \times 23.18) + \left[1.5 \times \frac{90 + 20}{2} \times \tan 24 \times 1.257L \right]$$

Solving, $L = 8.69 \text{ m}$

Provide 9.0 m pile.

Step 2 Perform structural design.

Factored load = $1.5 \times 275 = 412.5 \text{ kN}$

$L/D = 9.0/0.4 = 22.5 < 30$. Hence, minimum percentage of steel = 1.25%

$$A_{st, \min} = 1.25 \times \pi \times 400^2/400 = 1570 \text{ mm}^2$$

Provide eight 16 mm bars with area = 1608 mm^2 .

Axial load capacity of short column

$$= 0.4A_c f_{ck} + 0.67A_{sc} f_y = [0.4 \times (\pi \times 400^2/4 - 1608) \times 25 + 0.67 \times 1608 \times 415]/1000$$

$$= 1240 + 447 = 1687 \text{ kN} > 412.5 \text{ kN}$$

Assume 8 mm ties with a 45 mm cover to the centre of tie bar.

$$\text{Total length of one tie bar, } s = 4(400 - 2 \times 45) = 1240 \text{ mm}$$

$$\text{Volume of one tie bar, } v = 1240 \times \pi \times 8^2/4 = 62,329 \text{ mm}^3$$

$$\text{The minimum volume of ties in the end zone of } 3d \text{ length} = (0.6/100) \times \pi \times 400^2/4 \times (3 \times 400) = 904,778 \text{ mm}^3$$

$$\text{Number of ties in the end } 1200 \text{ mm length} = 9,04,778/62,329 = 15$$

$$\text{Spacing of these ties} = 1200/14 = 85 \text{ mm}$$

Spacing of ties in the middle zone is three times this spacing or $3 \times 85 = 255 \text{ mm}$

In addition, stiffener rings of size 16 mm diameter should be provided along the length of the cage at every 1.5 m c/c (see Fig. 15.58).

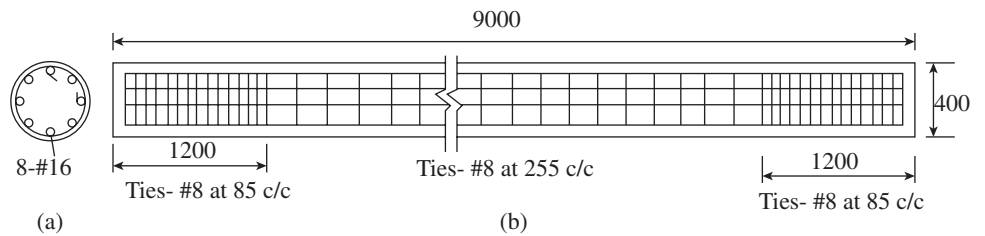


FIG. 15.58 Precast concrete pile of Example 15.8 (a) Cross section (b) Longitudinal section

EXAMPLE 15.9 (Design of pile cap):

An RC column of size $500 \text{ mm} \times 500 \text{ mm}$ is supported on four piles of 300 mm diameter (bored cast in situ piles). The column carries a load of 1000 kN , a moment of 300 kNm in the $x-x$ direction, and a shear force of 50 kN on top of the pile. Design the pile cap assuming M25 concrete and Fe 415 steel. Further, assume that the piles are capable of resisting the reaction from the pile cap.

SOLUTION:

Step 1 Fix the size of pile cap.

Assume a spacing of pile = $3 \times \text{diameter of pile} = 3 \times 300 = 900 \text{ mm}$ with 150 mm projection on either side.

$$\text{Length of pile cap} = 900 + 300 + 2 \times 150 = 1500 \text{ mm}$$

$$D_p = 300 \text{ mm} < 550 \text{ mm}$$

$$\text{Thickness of pile cap} = 2D_p + 100 = 2 \times 300 + 100 = 700 \text{ mm}$$

Step 2 Calculate the forces on piles.

$$\text{Weight of pile cap} = 1.5 \times 1.5 \times 0.7 \times 25 = 39.38 \text{ kN} \approx 40 \text{ kN}$$

$$\text{Total vertical load on four piles} = 1000 + 40 = 1040 \text{ kN}$$

The shear force at the top of the pile cap will cause a moment

$$M_s = VD = 50 \times 0.7 = 35 \text{ kNm}$$

$$\text{Total bending moment } M_t = M + M_s = 300 + 35 = 335 \text{ kNm}$$

This bending moment will cause equal and opposite forces on the pair of piles.

$$\text{The axial load on a pair of piles due to bending moment}$$

$$\Delta P = M_t/\text{Spacing} = 335/0.9 = 372.2 \text{ kN}$$

Maximum working load on each pile at forward end (piles 1 and 4)

$$P_p = P/n + \Delta P/2 = 1040/4 + 372.2/2 = 446.1 \text{ kN}$$

$$\begin{aligned} \text{Maximum working load on piles 2 and 3} \\ = 1040/4 - 372.2/2 = 73.9 \text{ kN} \end{aligned}$$

$$\text{Maximum factored load on pile } P_{pu} = 1.5 \times 446.1 = 669.15 \text{ kN} \approx 670 \text{ kN}$$

Step 3 Calculate the tension in the tie.

Assuming clear cover of 75 mm and 20 mm bars,

$$\text{Effective depth, } d = 700 - 75 - 20/2 = 615 \text{ mm}$$

Angle the diagonal compression strut makes with the diagonal of the bottom square

$$= \tan^{-1} \left(\frac{615}{450\sqrt{2}} \right) = 44^\circ$$

$$\text{Force in diagonal} = P_{pu}/\tan \theta = 670/\tan 44 = 693 \text{ kN}$$

$$\text{Tension in tie} = \frac{693}{\sqrt{2}} = 490 \text{ kN}$$

$$\text{Required } A_{st} = \frac{490 \times 10^3}{0.87 \times 415} = 1357 \text{ mm}^2 \text{ per tie}$$

Provide five 20 mm bars (area = 1570 mm²), connecting the piles at bottom (under each tie) within a width of 1.5 × 300 = 450 mm.

Step 4 Check for minimum steel.

Required minimum steel as wide beam (Clause 26.5.1.1)

$$A_s = \frac{0.85}{f_y} bd = \frac{0.85}{415} \times 1500 \times 615 = 1890 \text{ mm}^2$$

$$A_{st} \text{ provided} = 1570 \times 2 = 3140 \text{ mm}^2 > 1890 \text{ mm}^2$$

However, provide 16 mm bars at 160 mm spacing, both ways, in the remaining portions of the pile cap to control cracking.

Note: As per strut-and-tie method, one-way shear check is not required as the column load is transferred as tension in tie steel.

Step 5 Check for bearing resistance. At column, A_2 —pile cap area, A_1 —column area

$$\sqrt{\frac{A_2}{A_1}} = \sqrt{\frac{1.5^2}{0.5^2}} = 3; \text{ hence } \alpha = \frac{1}{3} \left(\sqrt{\frac{A_2}{A_1}} - 1 \right) = \frac{1}{3} (3 - 1) = 0.67$$

$$\beta = 0.33 \left(\frac{2d}{b_c} - 1 \right) = 0.33 \left[\frac{2 \times 0.615}{0.5} - 1 \right] = 0.48$$

$$\text{Hence } f_b = 0.3f_{ck} + 3.5\alpha\beta\sqrt{f_{ck}}$$

$$= 0.3 \times 25 + 3.5 \times 0.67 \times 0.48 \times \sqrt{25} = 13.13 \text{ N/mm}^2$$

Note: As per IS 456, $f_b = 0.45 \times 25 = 11.25 \text{ N/mm}^2$

Actual bearing stress under column

$$= 1000 \times 10^3/500^2 + 300 \times 10^6/(500 \times 500^2/6) = 4 + 14.4 = 18.4 \text{ N/mm}^2$$

Provide a pedestal of depth 200 mm and width 600 mm.

$$\text{Actual bearing stress} = 1000 \times 10^3/600^2 + 300 \times 10^6/(600 \times 600^2/6)$$

$$= 2.78 + 8.33 = 11.1 \text{ N/mm}^2 < f_b$$

Hence, it is adequate.

At pile

$$\sqrt{\frac{A_2}{A_1}} = \sqrt{\frac{300^2 \pi}{150^2 \pi}} = 2 < 4$$

$$\text{Hence } \alpha = \frac{1}{3} (2 - 1) = 0.33$$

$$\beta = 0.33 \left(\frac{615}{300} - 1 \right) = 0.347$$

$$f_b = 0.3f_{ck} + 3.5\alpha\beta$$

$$= 0.3 \times 25 + 3.5 \times 0.33 \times 0.347 \sqrt{25}$$

$$= 9.5 \text{ N/mm}^2$$

$$\text{Actual bearing stress} = \frac{P_{pu}}{A_p} = \frac{670 \times 10^3}{\pi \times 150^2} = 9.48 \text{ N/mm}^2 < 9.5 \text{ N/mm}^2$$

Hence, it is safe.

Step 6 Check for development length. Development length required for 20 mm rod (for M25 concrete and Fe 415 steel) is 806 mm (Table 65 of SP16).

$$\text{Available length beyond centre line of pile} = 150 + 150 - 75 = 225 \text{ mm}$$

$$\text{Required length beyond the edge of pile cap with } 90^\circ \text{ bend} \\ (806 - 225 - 160) = 421 \text{ mm}$$

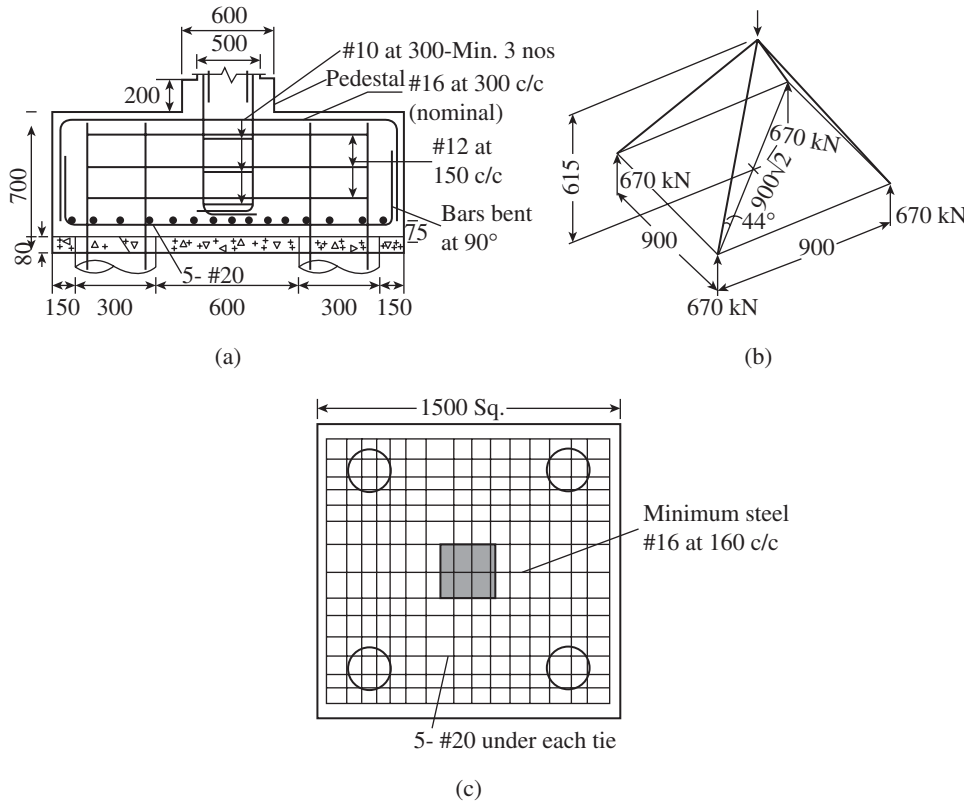
Note: Anchorage value of 90° bend with 20 mm rod = 160 mm (Table 67 of SP16). Provide 421 + 4 d_b = 421 + 4 × 20 = 501 mm length after 90° bend (see Fig. 15.59).

Step 7 Provide horizontal bursting steel around the outer pile rods of 12 mm at 150 c/c.

Step 8 Provide dowels from piles into the pile cap (Clause 34.4.3).

$$A_{\text{dowel}} = 0.005 \times \pi \times 300^2/4 = 353 \text{ mm}^2$$

It is good practice to provide a minimum of four vertical dowels. Provide four 16 mm dowels with 12 mm tie at 250 mm c/c extending into cap and pile for a length of 516 mm (development length). Alternatively, the pile rods can be extended into the pile cap.



Step 3 Check for one-way shear. One-way shear will be checked at a distance $0.5d$ from the face of column, that is, at 307.5 mm from face, which falls 107.5 mm away from the centre line of pile (see Fig. 15.60).

Shear force by linear interpolation
 $(2 \times 670) \times 42.5/300 = 190 \text{ kN}$

From Table 19 of IS 456 shear strength of M25 concrete for 0.218% = 0.34 N/mm^2

Nominal shear stress = $(190 \times 1000)/(1500 \times 615) = 0.21 \text{ N/mm}^2 < 0.34 \text{ N/mm}^2$

Hence, it is safe against one-way shear.

Step 4 Check for punching shear. Critical section is at $d/2$ (307.5 mm) around the face of column.

From Example 15.9, working load on column = 1000 kN

Factored load = $1.5 \times 1000 = 1500 \text{ kN}$

$$\text{Nominal shear stress} = \frac{V_u}{b_0 d} = \frac{1500 \times 1000}{[4 \times (500 + 615)]615} = 0.547 \text{ N/mm}^2$$

Punching shear strength of concrete (Clause 31.6.3.1 of Is 456)

$$= k_s \tau_c \text{ with } k_s = (0.5 + \beta_c) \leq 1 \text{ and } \tau_c = 0.25 \sqrt{f_{ck}}$$

$$\beta_c = 0.5/0.5 = 1; \text{ hence } k_s = 1$$

FIG. 15.59 Pile cap of Example 15.9 (a) Section (b) Stru-and-tie forces (c) Plan

EXAMPLE 15.10:

Design the pile cap of Example 15.9 as per sectional method.

SOLUTION:

From Example 15.9, maximum factored reaction on pile = 670 kN

Step 1 Calculate the bending moment and depth.

Maximum bending moment at the face of column = $2 \times 670(0.45 - 0.25) = 268 \text{ kNm}$

Effective depth based on the bending moment

$$d = \sqrt{\frac{268 \times 10^6}{0.138 \times 25 \times 1500}} = 228 \text{ mm}$$

As in Example 15.9 adopt $d = 615 \text{ mm}$.

Step 2 Calculate the reinforcement based on the moment.

$$\frac{M_u}{bd^2} = \frac{268 \times 10^6}{1500 \times 615^2} = 0.472 \text{ MPa}$$

From Table 3 of SP 16 for Fe 415 and M25 concrete, $p_t = 0.1336\% < 0.2\%$ (minimum as per wide beam)

$$\text{Min. } A_{st} = \frac{0.85}{f_y} bd = \frac{0.85}{415} \times 1500 \times 615 = 1890 \text{ mm}^2$$

Required number of 16 mm bars = $1890/201 = 10$ bars

Spacing = $(1500 - 75 - 75 - 16)/9 = 148 \text{ mm} < 300 \text{ mm}$

Hence provide ten 16 mm bars ($A_{st} = 2010 \text{ mm}^2$, $p_t = 0.218\%$).

Note: In Example 15.9, A_{st} provided was 3140 mm^2 (56% more steel).

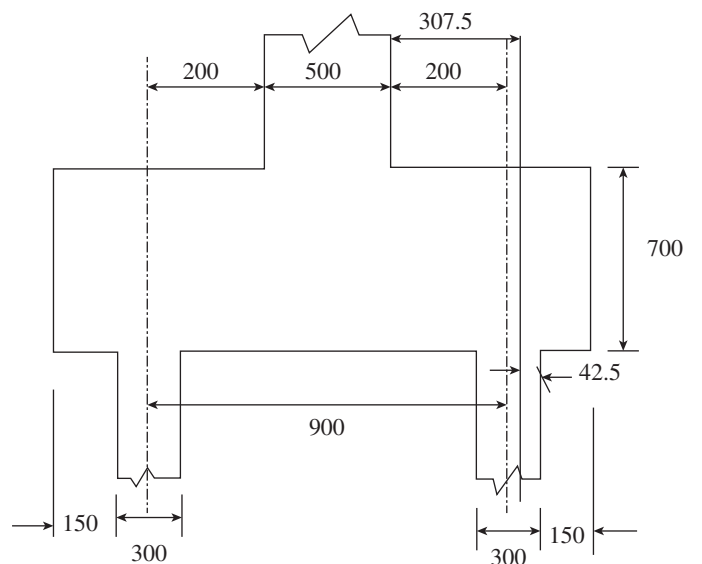


FIG. 15.60 Pile cap of Example 15.10

Punching shear strength $= 0.25\sqrt{25} = 1.25 \text{ N/mm}^2 > 0.547 \text{ N/mm}^2$
Hence, it is safe against punching.

Step 5 Check for development length. L_d of 16 mm bars (M25 concrete and Fe 415 steel), as per Table 65 of SP 16 is 645 mm.

Available length (from Example 15.9) = 225 mm

Hence, bend rods with 90° bend and provide $(645 - 225 - 128 + 4 \times 16) = 356 \text{ mm}$ length after the bend.

Note: 128 mm is the anchorage value of 16 mm bar.

Step 6 Provide bursting steel and dowels for piles. The provision of bursting steel and dowels for piles are the same as in Example 16.9.

SUMMARY

Foundations are very important elements of any structure and they distribute the load from the column to the soil below. The safety of foundations will affect the safety of the structure and hence they have to be designed and detailed carefully. The permissible pressure on the soil beneath the footing, called the safe bearing capacity (SBC), will be considerably lesser than the compressive stresses in walls and columns. Foundations are broadly classified into shallow foundations and deep foundations. Five types of shallow foundations exist, namely (a) strip or continuous wall footings, (b) isolated or spread footings (pad and sloped), (c) combined footings, (d) raft or mat foundations, and (e) floating rafts. Piles and caissons are the common types of deep foundations and they transmit column loads through the upper layers of poor soil to a strong soil layer at some depth below the surface.

The factors to be considered in selecting a suitable footing are the type and properties of soil, variability of the soil over the area and with increasing depth, position of water table, type of structure along with loadings, and susceptibility of the structure to settlement and tilt. In general, an idealized uniform pressure distribution is assumed under the footing, which under service loads should not exceed the SBC of soil. Moments produce uniformly varying soil pressure under the footing. Loads applied within the kern will cause compression over the entire area of footing and such a situation is often preferred. The SBC of the soil is often provided by the geotechnical consultant, based on shear failure of soil and settlement considerations. The depth of foundation is usually based on the type of soil at the site and its characteristics.

Design of foundations consists of two phases—soil design and structural design. Soil design is concerned with avoiding shear failure of the soil, excessive and differential settlement, sliding and overturning, and liquefaction. In contrast, in structural design the following limit states are checked: flexural failure of the footing, one-way or two-way (punching) shear failure of the footing, inadequate anchorage of the flexural reinforcement in the footing, and bearing failure at the column–footing interface. All these structural design considerations with respect to wall footings, square, rectangular, and sloped individual footings, and combined footings are discussed and the required equations are derived. Detailing aspects of these types of footings are explained. Further, design and detailing of plain concrete footings are provided.

The behaviour of piles is explained and the soil design of piles is illustrated. A brief discussion on the design of under-reamed piles, which are used in expansive soils, is provided. Piles usually are grouped and tied by means of a pile cap. The strut-and-tie method of design of pile caps is explained along with the sectional method adopted in the present IS 456 code. Detailing of pile cap based on these two methods is also considered. The earthquake considerations of footings are also explained. The concepts presented are amply illustrated by adequate examples.

The design of foundations in rocks is not considered; information on shallow foundations on rock may be found from IS 12070:1987, IS 13063:1991, and IS 14593:1998 and the works of Wyllie (1999) and Paikowsky, et al. (2010). Brick-infilled vierendeel girders have been suggested as an alternative foundation for soils having low SBC by Sundaramurthy and Santhakumar (2005).

REVIEW QUESTIONS

- How are RC foundations classified?
- List the five types of shallow foundations with sketches.
- What are the common types of deep foundations? When are deep foundations selected over shallow foundations?
- How are piles classified?
- What are the factors to be considered while choosing a foundation system?
- The maximum eccentricity that can be allowed in a square footing without footing lift off is _____.
(a) $B/3$ (c) $B/5$
(b) $B/4$ (d) $B/6$
- Write down the equation to calculate soil pressure under footing when it is subjected to axial load that has eccentricities about both axes.
- Typical SBC of soft clay is of range _____.
(a) 20–30 kN/m² (c) 50–100 kN/m²
(b) 30–60 kN/m² (d) 200–300 kN/m²
- Settlement analysis should be considered when SBC is below _____.
(a) 300 kN/m² (c) 200 kN/m²
(b) 400 kN/m² (d) 125 kN/m²
- How is the depth of foundation fixed based on IS 1904?
- Write down Rankine's formula for calculating the depth of the foundation.
- Compare the following terms:
(a) SBC (c) net soil pressure
(b) gross soil pressure (d) factored soil pressure
- Why is it desirable to eliminate eccentricity in loading on a footing, wherever possible, by means of proper proportioning?
- List the ultimate limit states that are to be checked for soil design of footings.
- List the ultimate limit states that are to be checked for structural design of footings.

16. Minimum cover to reinforcement under normal exposure and the corresponding minimum grade of concrete as per IS 456 are _____.
(a) 40 mm and M20 (c) 75 mm and M30
(b) 50 mm and M25 (d) 50 mm and M20
17. As per IS 456, what is the minimum steel that has to be provided in footings?
18. What is the minimum edge distance that has to be provided in footings as per IS 456?
19. Explain how one-way shear and two-way shear are considered in isolated footings.
20. Critical section for one-way shear is taken from the face of the column at a distance of _____.
(a) $d/2$ (c) $d/4$
(b) $d/3$ (d) d
21. How can we design a footing supporting a round or octagonal column?
22. Where is the bending moment considered critical in the following cases?
(a) Footing supporting a brick wall
(b) Footing supporting a steel column
(c) Footing supporting a pedestal
23. How is the steel reinforcement distributed in the case of (a) one-way reinforced footing, (b) two-way square footing, and (c) two-way rectangular footing?
24. How are axial load, moments, and shear acting at the base of column transferred to the footing?
25. How do we check the transfer of compressive forces through direct bearing?
26. What are the rules for providing dowels connecting footing and column?
27. Describe the various steps adopted in the design of wall footings.
28. Describe the various steps adopted in the design of isolated square footings.
29. What are the advantages of providing pedestals to columns?
30. What is the main difference in the design of rectangular footings over square footings?
31. What are the precautions to be taken while designing and constructing sloped footings?
32. What are the situations in which combined footings are preferred over isolated footings?
33. Explain the behaviour of combined two-column footing.
34. Give the various steps involved in the design of two-column footing.
35. Draw typical reinforcement details of (a) combined rectangular footing and (b) combined trapezoidal footing.
36. How is the design of combined slab and beam footing different from combined slab footing?
37. Explain the design of plain concrete footing.
38. Under what circumstances are pile foundations preferred?
39. Explain the behaviour of piles under increasing load.
40. What is the static formula used for the design of piles as per IS 2911?
41. What is the Engineering News formula? What is its purpose?
42. State reasons for the group capacity to be lower than the number of piles multiplied by individual capacity of piles.
43. What is meant by negative skin friction? When should it be considered?
44. Minimum spacing of end-bearing piles as per IS 2911 is _____.
(a) 2.0 times the shaft diameter
(b) 2.5 times the shaft diameter
(c) 3.0 times the shaft diameter
(d) none of these
45. When are piles designed as long columns?
46. The minimum area of reinforcement to be provided in any type of pile is _____.
(a) 0.2% (c) 0.4%
(b) 1.2% (d) 0.8%
47. In what way does the reinforcement detailing of driven precast concrete piles differ from other types of piles?
48. Write short notes on under-reamed piles and grade beams.
49. Sketch the economical pile layout for (a) five piles, (b) six piles, and (c) eight piles.
50. What is the usual relationship between pile diameter, D_p , and thickness of pile cap, D , adopted in practice?
51. Differentiate between the sectional method and strut-and-tie method of design of pile caps.
52. Sketch the detailing of reinforcement as per the sectional method and the strut-and-tie method of design.
53. What are the modes of failure to be considered in limit state design of pile caps?
54. Sketch the usual detailing of individual footing and list the drawbacks of this type of detailing in earthquake zones.
55. How do grade beams help footing in earthquake zones?
56. What are the effects of liquefaction and how are they mitigated?

EXERCISES

1. Design an RC wall footing to carry a dead load of 120 kN/m and a live load of 80 kN/m. The allowable soil pressure, q_a , is 200 kN/m² at a depth of 1.5 m below ground. Assume M20 concrete, Fe 415 steel, and $\gamma_s = 20$ kN/m³.
2. Design a square footing to support a 350 mm square column. The column carries a dead load of 450 kN and a live load of 380 kN. The allowable soil pressure is 150 kN/m². Use M20 concrete and Fe 415 steel for the footing and M30 concrete and Fe 415 steel for the column. Assume that the column is reinforced with eight 25 mm bars. Unit weight of the soil above footing base = 20 kN/m³.
3. Design a sloped square footing for a rectangular column of size 300 mm × 400 mm and subjected to an unfactored load of 1000 kN. Assume SBC of 200 kN/m²; use M20 concrete and Fe 415 steel.
4. Design a rectangular footing for the column in Exercise 2, assuming that there is a spatial restriction of 2.0 m on one of the plan dimensions of the footing.
5. Design the footing for the column subjected to an axial force of 900 kN and moment of 60 kNm. Assume SBC of soil as 200 kN/m² at 1.5 m depth; use M20 concrete and Fe 415 steel for the footing. Note that the moment is reversible.

6. Design a rectangular combined footing to support two columns of size 450 mm × 450 mm (with six 20 bars) and 600 mm × 600 mm (with six 25 bars), carrying 1000 kN and 1400 kN (service live + dead loads), respectively. These columns are located 4.0 m apart and the column carrying 1000 kN is flush with the property line. Assume SBC of 200 kN/m². Assume M25 concrete in the columns and M20 concrete in the footing and Fe 415 steel in the columns as well as footing.
7. Design a plain concrete footing for a column of size 300 mm × 300 mm carrying a service load of 300 kN. Assume allowable soil pressure of 250 kN/m² at 1.2 m below ground level. Assume M20 concrete and Fe 415 steel.
8. Design a square precast pile of size 350 mm carrying an axial load of 200 kN, placed in submerged medium dense sandy soil having an angle of internal friction of 36°. The density of soil is 20 kN/m³ and submerged density of soil is 12 kN/m³. Angle of wall friction between concrete pile and soil, δ , is $0.75\phi = 27^\circ$. Assume the following data: depth of top of pile cap below ground level is 500 mm, thickness of pile cap is 1.2 m, grade of concrete in pile is M25, Fe 415 steel is used, and clear cover to reinforcement is 75 mm. Determine the vertical carrying capacity of the pile in accordance with IS 2911 (Part 1, Section 1) and design the pile.
9. An RC column of size 400 mm × 400 mm is supported on four piles of 300 mm diameter (bored cast in situ piles). The column carries a load of 750 kN and a moment of 250 kNm in the $x-x$ direction. Design the pile cap assuming M25 concrete and Fe 415 steel. Further, assume that the piles are capable of resisting the reaction from the pile cap.
10. Design the pile cap of Exercise 9 as per the sectional method.

REFERENCES

- ACI 336.2R-88 1966, *Suggested Analysis and Design Procedures for Combined Footings and Mats*, American Concrete Institute, Farmington Hills, p. 21 (also see *Journal of ACI*, Vol. 63, No. 10, pp. 1041–57).
- ACI-ASCE Committee 326 1962, 'Shear and Diagonal Tension, Part 3: Slabs and Footings', *ACI Journal, Proceedings*, Vol. 59, No. 3, pp. 353–96.
- Adebar, P., D. Kuchma, and M.P. Collins 1990, 'Strut and Tie Models for the Design of Pile Caps: An Experimental Study', *ACI Structural Journal*, Vol. 87, No. 1, pp. 81–92.
- Adebar, P. and Z. Zhou 1993, 'Bearing Strength of Concrete Compression Struts', *ACI Structural Journal*, Vol. 90, No. 5, pp. 534–41.
- Adebar, P. and Z. Zhou 1996, 'Design of Deep Pile Caps by Strut-and-tie Models', *ACI Structural Journal*, Vol. 93, No. 4, pp. 437–48.
- Algin, H.M. 2007, 'Practical Formula for Dimensioning a Rectangular Footing', *Engineering Structures*, Vol. 29, No. 6, pp. 1128–34.
- Baker, A.L.L. 1948, *Raft Foundations: The Soil-line Method of Design*, 2nd edition, Concrete Publications, London, p. 141.
- Bhattacharya, S. 2006, 'A Review of Methods for Pile Designs in Seismically Liquefiable Soil', *Design of Foundations in Seismic Areas: Principles and Applications*, NICEE, IIT, Kanpur.
- Bhavnagri, V.S. 1974, 'Flexural Resistance of Sloped Footings', *The Indian Concrete Journal*, Vol. 48, No. 9, pp. 292–9.
- Binney, J.R. and T. Paulay 1980, 'Foundations for Shear Wall Structures', *Bulletin of the New Zealand National Society for Earthquake Engineering*, Vol. 13, No. 2, pp. 171–81, (also see <http://www.nzsee.org.nz/db/Bulletin/Archive/13%282%290171.pdf>, last accessed on 26 March 2013).
- Bowles, J.E. 1996, *Foundation Analysis and Design*, 5th edition, The McGraw-Hill Companies, Inc., New York, p. 1175.
- Broms, B.B. 1964a, 'Lateral Resistance of Piles in Cohesionless Soils', *Journal of Soil Mechanics and Foundation Engineering*, Proceedings ASCE, Vol. 90, No. SM3, pp. 123–56.
- Broms, B.B. 1964b, 'Lateral Resistance of Piles in Cohesive Soils', *Journal of Soil Mechanics and Foundation Engineering*, Proceedings ASCE, Vol. 90, No. SM2, pp. 27–63.
- Burland, J.B., M.B. Jamiolkowski, and C. Viggiani 2009, 'Leaning Tower of Pisa: Behaviour after Stabilization Operations', *International Journal of Geotechnique*, Vol. 3, Issue 1, pp. 156–69, (http://casehistories.geoengineer.org/volume/volume1/issue3/IJGCH_1_3_2.pdf, last accessed on 26 June 2013).
- Chen, F.H. 1988, *Foundation on Expansive Soils*, 2nd edition, Elsevier, Amsterdam, p. 464.
- Clancy, P. and M.F. Randolph 1996, 'Simple Design Tools for Piled Raft Foundation', *Géotechnique*, Vol. 46, No. 2, pp. 313–28.
- Collins, M.P. and D. Kuchma 1999, 'How Safe are our Large, Lightly Reinforced Concrete Beams, Slabs, and Footings?', *ACI Structural Journal*, Vol. 96, No. 4, pp. 482–90.
- Cooke, H.G. and J.K. Mitchell 1999, *Guide to Remedial Measures for Liquefaction Mitigation at Existing Highway Bridge Sites*, Multidisciplinary Center for Earthquake Engineering Research, Report No. MCEER-99-0015, p. 162.
- Curtin, W.G., G. Shaw, G.I. Parkinson, J.M. Golding, and N.J. Seward 2006, *Structural Foundation Designers' Manual*, 2nd edition, Wiley-Blackwell Publishing, Oxford, p. 370.
- Dayaratnam, P. 2004, *Limit State Design of Reinforced Concrete Structures*, Oxford and IBH Publishing Co. Pvt. Ltd, New Delhi, p. 532.
- Dieterle, H. and A. Steinle 1981, *Blockfundamente für Stahlbetonfertigungsstützen*, Deutscher Ausschuss für Stahlbeton, Heft 326, Berlin, p. 49.
- Dunham, C.W. 1962, *Foundations for Structures*, 2nd edition, McGraw-Hill Publishing Co., New York, p. 722.
- Gesund, H. 1983, 'Flexural Limit Analysis of Concentrically Loaded Column Footings', *ACI Journal Proceedings*, Vol. 80, No. 3, pp. 223–8.
- Gupta, S.C. 1997, *Raft Foundation Design and Analysis with A Practical Approach*, New Age International, New Delhi, p. 148.
- Hallgren, M., S. Kinnunen, and B. Nylander 1998, 'Punching Shear Tests on Column Footings', *Nordic Concrete Research*, Vol. 21, No. 3, pp. 1–22.
- Hansen, J.B. 1970, 'A Revised and Extended Formula for Bearing Capacity', *Bulletin No. 28*, Danish Geotechnical Institute, Copenhagen.
- Hawkins, N.M. 1968, 'The Bearing Strength of Concrete Loaded through Rigid Plates', *Magazine of Concrete Research*, Vol. 20, No. 62, pp. 31–40.
- Hegger, J., M. Ricker, and A.G. Sherif 2009, 'Punching Strength of Reinforced Concrete Footings', *ACI Structural Journal*, Vol. 106, No. 5, pp. 706–16.

- Hegger, J., A.G. Sherif, and M. Ricker 2006, 'Experimental Investigations on Punching Behavior of Reinforced Concrete Footings', *ACI Structural Journal*, Vol. 103, No. 4, pp. 604–13.
- Hognestad, E. 1953, 'Shearing Strength of Reinforced Column Footings', *ACI Journal, Proceedings*, Vol. 50, No. 11, pp. 189–208, (also see <http://osp.mans.edu.eg/sfoundation/foundation.htm>, last accessed on 26 March 2013).
- IS 1080:1985, *Code of Practice for Design and Construction of Shallow Foundations in Soils (Other than Raft, Ring and Shell)*, Bureau of Indian Standards, New Delhi, p. 7.
- IS 1904:1986, *Code of Practice for Design and Construction of Foundations in Soils: General Requirements*, Bureau of Indian Standards, New Delhi, p. 22.
- IS 2911 (Part 1, Section 1):2010, *Part 1: Concrete Piles, Section 1 Driven Cast-in-situ Concrete Piles*, p. 44, (Part 1, Section 2) 2010, *Section 2 Bored Cast-in-situ Concrete Piles*, p. 22., (Part 1, Section 3): 2010, *Section 3 Driven Precast Concrete Piles*, p. 24, and (Part 1, Section 4):2010, *Section 4 Precast Concrete Piles in Prebored Holes*, p. 23, Bureau of Indian Standards, New Delhi.
- IS 2911 (Part 3):1980, *Under Reamed Piles*, Bureau of Indian Standards, New Delhi, p. 33.
- IS 2950 (Part 1):1981, *Code of Practice for Design and Construction of Raft Foundations, Part 1: Design*, 2nd revision, Bureau of Indian Standards, New Delhi, p. 24.
- IS 4091:1979, *Code of Practice for Design and Construction of Foundations for Transmission Line Towers and Poles*, Bureau of Indian Standards, New Delhi, p. 17.
- IS 6403:1981, *Code of Practice for Determination of Bearing Capacity of Shallow foundations*, 1st revision, Bureau of Indian Standards, New Delhi, p. 16.
- IS 8009 (Part 1):1976, *Code of Practice for Calculation of Settlements of Foundations, Part 1: Shallow Foundations Subjected to Symmetrical Static Vertical Loads*, p. 40, (Part 2):1980, *Part 2: Deep Foundations Subjected to Symmetrical Static Vertical Loading*, p. 20, Bureau of Indian Standards, New Delhi.
- IS 9456:1980, *Code of Practice for Design and Construction of Conical and Hyperbolic Paraboloidal types of Shell Foundations*, Bureau of Indian Standards, New Delhi, p. 29.
- IS 11089:1984, *Code of Practice for Design and Construction of Ring Foundations*, Bureau of Indian Standards, New Delhi, p. 14.
- IS 11233:1985, *Code of Practice for Design and Construction of Radar Antenna, Microwave and TV Tower Foundations*, Bureau of Indian Standards, New Delhi, p. 15.
- IS 12070:1987, *Code of Practice for Design and Construction of Shallow Foundations on Rocks*, Bureau of Indian Standards, New Delhi, p. 13.
- IS 13063:1991, *Code of Practice for Structural Safety of Buildings on Shallow Foundations on Rocks*, Bureau of Indian Standards, New Delhi, p. 15.
- IS 14593:1998, *Bored Cast-in-situ Piles Founded on Rock: Guidelines*, Bureau of Indian Standards, New Delhi, p. 9.
- Jain, O.P. and Jaikrishna 1977, *Plain and Reinforced Concrete*, Nem Chand and Bros, Roorkee.
- Kameswara Rao, N.S. V. 2011, *Foundation Design: Theory and Practice*, John Wiley, New York, p. 544.
- Kordina, K. and D. Nölting 1981, *Tragverhalten von ausmittig beanspruchten Einzelfundamenten aus Stahlbeton*, Technical report, DFG-research Ko 204/27+30, Brunschweig, Germany, p. 155.
- Kramrisch, F. 1985, 'Footings', Chapter 5 in M. Fintel (ed.), *Handbook of Concrete Engineering*, 2nd edition, Van Nostrand Reinhold, New York, p. 813.
- Kramrisch, F. and P. Roberts 1961, 'Simplified Design of Combined Footings', *Journal of the Soil Mechanics and Foundations Division, ASCE*, Vol. 87, No. SM5, pp. 19–44.
- Kurian, N.P. 2006, *Shell Foundations: Geometry, Analysis, Design and Construction*, Narosa Publishing House, New Delhi, p. 379.
- Leonhardt, F. and E. Mönnig 1977, *Vorlesungen über Massivbau*, Dritter Teil-Grundlagen zum Bewehren im Stahlbetonbau, 3rd edition, Springer Verlag, Berlin, p. 246.
- Liyanapathirana, D.S. and H.G. Poulos 2005, 'Seismic Lateral Response of Piles in Liquefying Soils', *Journal of the Geotechnical and Geoenvironmental Engineering, ASCE*, Vol. 131, No. 12, pp. 1466–79.
- Matlock, H. and L.C. Reese 1962, 'Generalized Solution to Laterally Loaded Piles', *Transactions of the American Society of Civil Engineers*, Vol. 127, Part I, pp. 1220–47.
- McCarthy, D.F. 2006, *Essentials of Soil Mechanics and Foundations: Basic Geotechnics*, 7th edition, Prentice Hall, Englewood Cliffs, p. 864.
- Manohar, S.N. 1985, *Tall Chimneys*, Tata McGraw Hill and Torsteel Research Foundation of India, New Delhi.
- Meyerhof, G.G. 1951, 'The Ultimate Bearing Capacity of Foundations', *Geotechnique*, Vol. 2, No. 4, pp. 301–31.
- Meyerhof, G.G. 1953, 'The Bearing Capacity of Foundations under Eccentric and Inclined Loads', *3rd International Conference on Soil Mechanics and Foundation Engineering*, Zurich, Vol. 1, p. 669.
- Nilsson, I.H.E. and A. Losberg 1976, 'Reinforced Concrete Corners and Joints Subjected to Bending Moment', *Journal of the Structural Division, ASCE*, Vol. 102, No. ST6, pp. 1229–54.
- Nori, V.V. and M.S. Tharval 2007, 'Design of Pile Caps: Strut and Tie Model Method', *The Indian Concrete Journal*, Vol. 81, No. 4, pp. 13–19.
- Paikowsky, S.G., M.C. Canniff, K. Lesny, A. Kisse, S. Amatya, and R. Muganga 2010, *LRFD Design and Construction of Shallow Foundations for Highway Bridge Structures, NCHRP Report 651*, National Cooperative Highway Research Program, Transportation Research Board, Washington D.C., p. 149, (also see http://onlinepubs.trb.org/onlinepubs/nchrp/nchrp_rpt_651.pdf, last accessed on 1 March 2013).
- Paulay, T. 1996, 'Seismic Design of Concrete Structures: The Present Needs of Societies', Paper No. 2001, *Eleventh World Conference on Earthquake Engineering*, Acapulco, p. 23–8, (also see http://www.iitk.ac.in/nicee/wcee/article/11_2001.PDF, last accessed on 26 March 2013).
- Paulay, T. and M.J.N. Priestley 1992, *Seismic Design of Reinforced Concrete and Masonry Buildings*, John Wiley and Sons, Inc., New York, p. 744.
- Peck, R.B., W.E. Hanson, and T.H. Thornburn 1974, *Foundation Engineering*, 2nd edition, John Wiley and Sons, New York, p. 514.
- Puri, V.K. and S. Prakash 2008, 'Pile Design in Liquefying Soil', *14th World Conference on Earthquake Engineering*, 12–17 October 2008, Beijing, p. 8.
- Reese, L.C., W.M. Isenhower, and S-T. Wang 2005, *Analysis and Design of Shallow and Deep Foundations*, John Wiley, New York, p. 608.

- Reynolds, C.E. and J.C. Steedman 1988, *Reinforced Concrete Designer's Handbook*, E & FN Spon, London, p. 436.
- Richart, F.E. 1948, 'Reinforced Concrete Wall and Column Footings', *ACI Journal*, Vol. 45, Part 1, No. 2, pp. 97–127, and Part 2, No. 3, pp. 237–60.
- Saran, S. 2006, *Analysis and Design of Substructures-Limit state Design*, 2nd edition, Oxford and IBH Publishing Co. Pvt. Ltd, New Delhi, p. 870.
- Sharma, D., M.P. Jain, and C. Prakash 1978, *Handbook on Under-reamed and Bored Compaction Pile Foundations*, Central Building Research Institute, Roorkee.
- Smith, E.A.L. 1960, 'Pile-driving Analysis by the Wave Equation', *Journal of the Engineering Mechanics Division, Proceedings ASCE*, Vol. 86, No. EM 4, pp. 35–61.
- Soong, T.T. and B.F. Spencer Jr. 2002, 'Supplemental Energy Dissipation: State-of-the-art and State-of-the-practice', *Engineering Structures*, Vol. 24, No. 3, pp. 243–59.
- Souza, R., D. Kuchma, J.W. Park, and T. Bittencourt 2009, 'Adaptable Strut-and-tie Model for Design and Verification of Four-pile Caps', *ACI Structural Journal*, Vol. 106, No. 2, pp. 142–50.
- Symans, M.D., F.A. Charney, A.S. Whittaker, M.C. Constantinou, C.A. Kircher, M.W. Johnson, and R.J. McNamara 2008, 'Energy Dissipation Systems for Seismic Applications: Current Practice and Recent Developments', *Journal of Structural Engineering, ASCE*, Vol. 134, No. 1, pp. 3–21.
- Subramanian, N. 1993, 'Development Length Paradox in Foundation Design', *Bulletin of the Indian Concrete Institute*, No. 44, pp. 10–11.
- Subramanian, N. 1994a, 'Design of Under Reamed Piles', *Bulletin of the Indian Concrete Institute*, No. 46, pp. 17–19, and *Discussions*, pp. 6–7.
- Subramanian, N. 1994b, 'A Program for the Design of Piles and Pile Caps', *Civil Engineering and Construction Review*, Vol. 7, No. 8, pp. 33–9.
- Subramanian, N. 1995a, 'Economy in Building Construction', *Bulletin of the Indian Concrete Institute*, No. 50, pp. 15–21.
- Subramanian, N. 1995b, 'Computer Aided Design of Footings', *International Journal of Foundation Engineer*, Vol. 1, No. 1, pp. 25–33.
- Subramanian, N. 2009, 'Rare Foundation Failure of a Building in Shanghai, China', *New Building Materials and Construction World*, Vol. 16, No. 2, pp. 100–4.
- Subramanian, N. and D. Muthukumar 1998, 'Leaning Tower of Pisa: Will It Be Reopened for Tourists?' *Bulletin of the Indian Concrete Institute*, No. 63, pp. 13–6.
- Subramanian, N. and V. Vasanthi 1989, 'Modified Method Saves Foundation Cost', *Bulletin of the Indian Concrete Institute*, No. 28, pp. 35–8, *Discussions*, March 1990, pp. 18–21.
- Subramanian, N. and V. Vasanthi 1990, 'Design of Tower Foundations', *The Indian Concrete Journal*, Vol.64, No. 3, pp. 135–41.
- Sundaramurthy, S. and A.R. Santhakumar 2005, 'Brick-infilled Vierendeel Girders as Foundation for Low-lying, Low Bearing-capacity Soil Terrain', *The Indian Concrete Journal*, Vol. 79, No. 1, pp. 57–60.
- Suprenant, B.A. 1987, 'Shear Keys for Basement Walls: Pros and Cons', *Publication No. #C870620*, The Aberdeen Group, p. 3, (also see <http://www.concreteconstruction.net/concrete-articles/shear-keys-for-basement-walls-pros-and-cons.aspx>, last accessed on 7 March 2013).
- Tabsh, S.W. and A.R. Al-Shawa 2005, 'Effect of Spread Footing Flexibility on Structural Response', *Practice Periodical on Structural Design and Construction*, ASCE, Vol. 10, No. 2, pp. 109–14.
- Talbot, A.N. 1913, *Reinforced Concrete Wall Footings and Column Footings, Bulletin 67*, Engineering Experiment Station, University of Illinois, Urbana, p. 96.
- Teng, W.C. 1962, *Foundation Design*, Prentice Hall of India Pvt. Ltd, New Delhi, p. 466.
- Terzaghi, K. 1943, *Theoretical Soil Mechanics*, John Wiley and Sons, New York, p. 511.
- Terzaghi, K., R.B. Peck, and G. Mesri 1996, *Soil Mechanics in Engineering Practice*, 3rd edition, John Wiley and Sons, New York, p. 592.
- Tomlinson, M.J. 2001, *Foundation Design and Construction*, 7th edition, Pearson-Prentice Hall, p. 584.
- Tomlinson, M.J. and J. Woodward 2008, *Pile Design and Construction Practice*, 5th edition, Taylor and Francis, London and New York, p. 568.
- Uzel, A., B. Podgorniak, E.C. Bentz, and M.P. Collins 2011, 'Design of Large Footings for One-way Shear', *ACI Structural Journal*, Vol. 108, No. 2, pp.131–8.
- Varghese, P.C. 2009, *Design of Reinforced Concrete Foundations*, PHI Learning Pvt. Ltd, New Delhi, p. 433.
- Venugopal, M.S. and N. Subramanian 1977, 'Differential Movements in Soils', *Seminar on Problems of Building Foundations*, Chennai.
- Vesic, A.S. 1973, 'Analysis of Ultimate Loads of Shallow Foundation', *Journal of the Soil Mechanics and Foundation Engineering, ASCE*, Vol. 99, No. SM1, pp. 45–73.
- Vesic, A.S. 1975, 'Bearing Capacity of Shallow Foundations', In H.F. Winterkorn and H-Y Fang (eds), *Foundation Engineering Handbook*, Von Nostrand Reinhold Co., New York, pp.121–47.
- Wyllie, D.C. 1999, *Foundations on Rock: Engineering Practice*, 2nd edition, E & FN Spon, London, p. 435.
- Wight, J.K. and J.G. MacGregor 2009, *Reinforced Concrete: Mechanics and Design*, 5th edition, Pearson-Prentice Hall, Upper Saddle River, p. 1112.

DESIGN OF RC WALLS AND STRUCTURAL WALLS

16.1 INTRODUCTION

A vertical load-bearing element in a building whose length exceeds four times its thickness is usually considered a wall (see Fig. 16.1). This definition distinguishes a wall from a column. The main functions of the walls are to carry loads, enclose and divide space, exclude weather, and retain heat. Loads are applied to a wall in the following ways:

1. Gravity loads on the wall due to load from slab and beam (Fig. 16.1b)
2. Lateral loads perpendicular to the plane of the wall due to wind, earthquake, water, or soil (Fig. 16.1d)
3. Horizontal in-plane loads due to wind or earthquake when the wall is used to provide lateral stability, as in the case of structural walls (Fig. 16.1c)

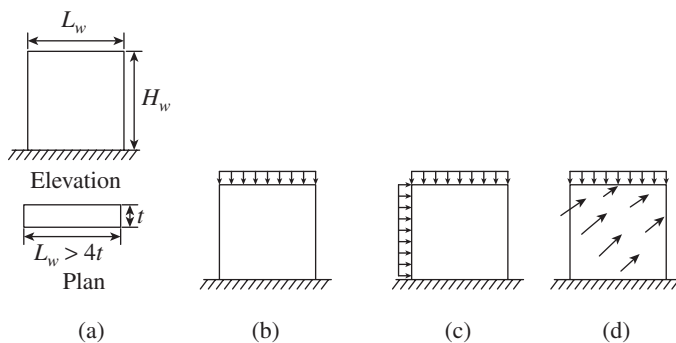


FIG. 16.1 Concrete wall and loads acting on it (a) Definition (b) Gravity loads (c) Lateral loads (d) Horizontal in-plane loads

The design methods used to design walls for various types of loading are listed in Table 16.1.

Walls are of several types and may be classified as non-load-bearing walls, load-bearing walls, and structural walls (see Section 16.2). The strength and behaviour of the walls will normally depend upon their geometry [aspect ratio (H_w/L_w), slenderness ratio (H_w/t), and thickness ratio (L_w/t)], material properties [strength of concrete and steel, mode

TABLE 16.1 Design methods of concrete walls

Type of Load on the Wall	Design Method
In-plane vertical loads (Fig. 16.1b)	(a) When there is only compressive load, may be designed as plain wall; however, minimum reinforcements are provided to control cracking
	(b) When there is eccentric loading, must be designed as reinforced concrete wall as per empirical method (Clause 32.2 of IS 456)
In-plane vertical and lateral loads (Fig. 16.1c)	(a) When the whole section is under compression, designed separately for compression and shear; in-plane bending may be neglected as per Clause 32.3.1 of IS 456
	(b) When part of the section is tension, designed as per Annex A of IS 13920 for combined bending and axial loads and separately for shear
In-plane vertical loads but horizontal loads acting perpendicular to the plane of wall (Fig. 16.1d)	If axial load does not exceed $0.04f_{ck}A_g$, designed as slab (height to thickness ratio should be less than 50), otherwise designed as wall (Clause 32.3.2 of IS 456)

of disposition of steel (single layer or double layer), and steel ratio in vertical and horizontal directions], end conditions (fixed, free, or its combinations at the ends), loading pattern (concentrated or uniformly distributed, axial or eccentric), and the nature of opening [size, location, and disposition of opening (symmetric or asymmetric, single or multiple)]. The design of reinforced concrete (RC) walls is covered by Clause 32 of IS 456, which is based on the provisions of the Australian code, AS 3600:2001. Design of structural (shear) walls should be done as per Clause 9 of IS 13920. The behaviour of different types of walls, the design methods, and their detailing are discussed in this chapter. Some of these provisions are also compared with the ACI 318 or BS 8110 code provisions.

16.2 TYPES OF REINFORCED CONCRETE WALLS

Reinforced concrete walls may be classified as follows:

Non-load-bearing walls They support their own weight and some lateral pressures or loads acting on one or both sides of the wall. Examples of such walls include basement walls and retaining walls (see Fig. 16.2a and Fig. 2.9 of Chapter 2). The types and design of retaining walls are discussed in Section 16.4.

Load-bearing walls Most of the concrete walls in buildings are load-bearing walls, which may carry concentric or eccentric vertical loads (see Fig. 16.2b). These walls are laterally supported and braced by the rest of the structure. Load-bearing walls with solid rectangular cross section may be designed as columns subjected to axial load and bending. Braced walls mainly subjected to vertical compressive loads with some eccentricity (with respect to the wall thickness) may be designed by the empirical method given in Clause 32.2 of IS 456, as described in Section 16.3. The eccentric load causes weak-axis bending in these walls.

Structural or shear walls In tall buildings, RC walls are placed at strategic locations so that the structure has adequate stiffness to resist the lateral loads caused by wind or earthquakes. These walls, which primarily resist lateral loads due to wind or earthquakes, are called *shear walls* or *structural walls*. They basically act as deep vertical cantilever beams that provide lateral stability to the building and resist the in-plane shear and bending moment caused by the lateral loads (see Fig. 16.2c and Fig. 2.8 of Chapter 2). They also resist tributary gravity loads transferred by the structure, in addition to the shear and strong axis bending caused by lateral loads. These types of walls are discussed in Section 16.5.

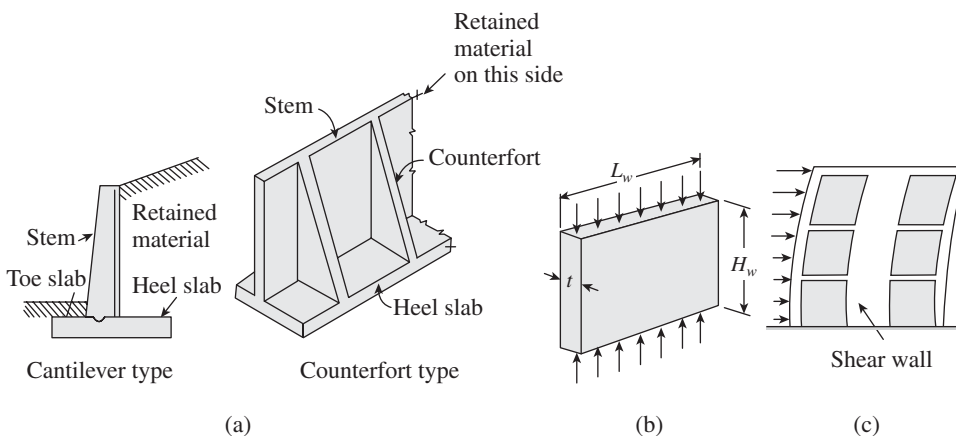


FIG. 16.2 Types of RC walls (a) Retaining walls (b) Load-bearing wall (c) Shear wall

In addition to this classification, walls may be further classified as follows:

Braced walls These are walls that are supported and restrained against lateral deflections along one to four sides.

The supports may be in the form of a buttress, floor, cross wall, or other horizontal or vertical element. In order to consider the wall as braced, the lateral supports should be able to transmit lateral forces from the braced wall to the principal structural bracing or to the foundation.

Unbraced walls These are walls that provide their own lateral stability. These walls are generally supported solely along the lower edge of the wall. For example, cantilever-retaining walls act as vertical flexural cantilevers while resisting the lateral load due to the retained soil.

Stocky walls These walls are thick walls and the ratio of the effective height to thickness, called the *slenderness ratio*, does not exceed 15 for a braced wall or 10 for an unbraced wall (BS 8110-1:1997).

Slender walls These are walls that have a slenderness ratio exceeding those of stocky walls. However, as per Clause 32.2.3 of IS 456, this ratio should not exceed 30, irrespective of whether the wall is braced or unbraced. (BS 8110 relaxes this limit to 40 for braced RC walls with less than one per cent reinforcement and to 45 for braced RC walls with greater than one per cent reinforcement.)

It has to be noted that the slenderness ratio is generally higher for walls than for columns, and the reinforcement ratios are usually about a fifth to a tenth of those in columns.

16.3 LOAD-BEARING WALLS

Load-bearing walls in which the resultant of the loads falls within the middle third of its thickness may be considered as concentrically loaded (i.e., when the eccentricity is less than or equal to one-sixth the thickness of the wall). As indicated in

Table 16.1, the design method of these walls differ depending on whether they are braced or unbraced and on whether they are subjected to only vertical compression or to vertical compression and horizontal loads.

16.3.1 Braced and Unbraced Walls

The definition of braced walls has been provided in Section 16.2. As per Clause 32.1 of IS 456, braced walls subjected to only vertical compression may be designed as per the empirical method given in Clause 32.2 of IS 456. The minimum

thickness of these walls should be greater than or equal to 100 mm. As per Clause 14.5.3 of ACI, the thickness of bearing walls should not be less than the minimum of 100 mm and $1/25$ times the supported height (H_w) or length (L_w).

It also suggests that the thickness of the exterior basement walls and foundation walls should not be less than 190 mm. These provisions are meant to provide a wall thickness that is sufficient for the easy placement of concrete at site, thus avoiding honeycombing.

Walls can be assumed to be braced if they are laterally supported by a structure that satisfies the following conditions, as per Clause 32.2.1 of IS 456:

1. Walls or vertical bracing elements are provided in two directions, such that lateral stability of the whole structure is ensured.
2. Lateral forces are resisted by shear in the planes of these walls or by other braced elements.
3. The roof and floor systems are designed to transfer lateral loads effectively as diaphragms.
4. The connection between the wall and the lateral supports is designed in such a way to resist horizontal forces not less than (a) simple static reaction to the total horizontal forces at the level of lateral support and (b) 2.5 per cent of the total vertical load that the wall is designed to carry at the level of lateral support but not less than 2 kN per metre length of wall (AS 3600:2001).

Walls that do not comply with these requirements are considered as unbraced. It has to be noted that in multi-storey buildings, unbraced walls should not be relied upon to provide stability to the building. The overall stability and structural integrity should be ensured by providing various types of ties (see Section 2.6 and Fig. 2.33 of Chapter 2), which may provide alternate load paths in the case of framed buildings, or by providing structural walls.

16.3.2 Eccentricities of Vertical Load

Reinforced concrete walls are designed for vertical loads as well as transverse eccentricity. The following guidelines are used to assess the transverse eccentricity of loads (Clause 32.2.2 of IS 456 and Clause 3.9.4 of BS 8110-1:1997):

1. The design vertical loads on a wall due to discontinuous concrete floor or roof acting on only one side of the wall produce eccentricity of loading. The load may be assumed to act at one-third the thickness of the wall from the loaded face (see Fig. 16.3). When there is in situ concrete floor on either side of the wall, the load may be assumed to act at the centre of the wall and the common bearing area may be assumed to be shared equally on each floor.
2. For braced walls, only the eccentricity of the individual wall needs to be considered in the design. The resultant eccentricity of all the vertical loads immediately above a lateral support can be assumed to be zero.
3. For unbraced walls, however, at any level, full allowance should be made for the eccentricity of all vertical loads and

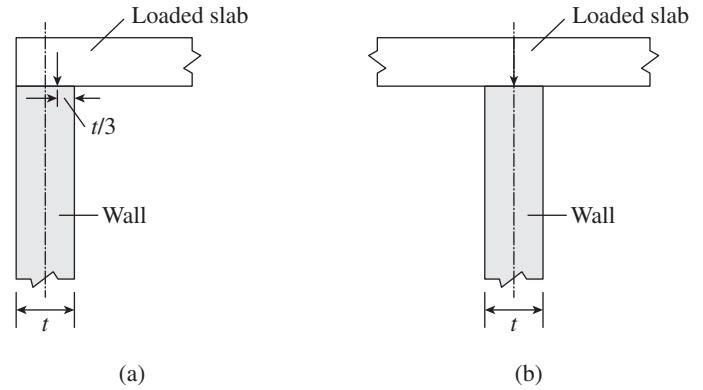


FIG. 16.3 Eccentricity of loads on walls (a) Slab on one side of the wall (b) Slab on both sides of the wall

- the overturning moments produced by any lateral forces above that level.
4. Loads may be applied to walls at eccentricities greater than half the thickness of the wall through special fittings, like joist hangers.
 5. The design of the wall should take into account the actual eccentricity of the vertical load, but in any case consider a minimum eccentricity of not less than $t/20$ (or 20 mm as per BS 8110).
 6. When there are local concentrated loads, such as at beam bearings or column bases, they must be assumed to be immediately dispersed through the wall, provided the bearing stress does not exceed $0.45f_{ck}$ (Clause 34.4 of IS 456). The horizontal length of the wall considered effective in carrying the concentrated load may be taken as the smaller of the contact area plus four times the wall thickness or the centre-to-centre (c/c) distance between the loads.

16.3.3 Slenderness Ratio and Effective Height of Walls

Similar to columns, the load-carrying capacity of RC walls depends on their slenderness ratio. Clause 32.2.4 of IS 456 specifies that the *effective height* of the braced wall should be taken as per Table 16.2. As mentioned earlier, according to Clause 32.2.3 of IS 456, the value of H_{we}/t should not exceed 30 and when it exceeds 12, the wall is considered slender.

TABLE 16.2 Effective height, H_{we} , of braced concrete walls

Restrained by	Restrained Against Rotation at Both Ends	Not Restrained Against Rotation at Both Ends
Floors	$0.75H_w$	$1.0H_w$
Intersecting walls or similar members	$0.75L_1$	$1.0L_1$

Note: H_w is the unsupported height of the wall and L_1 is the horizontal distance between the centres of lateral restraints.

When cross walls are provided as stiffeners, the slenderness ratio of plain concrete walls may be taken as the effective length divided by thickness, as per IS 1905:1980. In other words, if the

cross walls are placed sufficiently close, the horizontal distance between the cross walls may lead to an effective length smaller than the usual effective height of the wall (SP 24:1983).

16.3.4 Empirical Design Method

The design axial strength, P_{nw} , per unit length of a braced slender wall in compression is given by Clause 32.2.5 of IS 456 as

$$P_{nw} = 0.3f_{ck}(t - 1.2e_x - 2e_a) \quad (16.1a)$$

where t is the thickness of wall, f_{ck} is the characteristic compressive strength of concrete, e_x is the eccentricity of load at right angles to the plane of the wall with a minimum value of $t/20$, e_a is the additional eccentricity due to slenderness effect (similar to that in columns as per Clause 39.7.1), which is taken as $(H_e/t)^2(t/2500)$, and H_e is the effective height of the wall. It has to be noted that the formula does not include contribution due to steel reinforcement, as tests have shown that steel reinforcement does not contribute to the overall compressive strength of the wall (Oberlender and Everard 1977; Pillai and Parthasarathy 1977). It is important to realize that this equation is to be used only for rectangular cross sections and only when the resultant load acts within the middle third of the thickness of the wall (kern distance).

The ACI 318 code provides a similar empirical design method in its Clause 14.5 and provides the following equation:

$$P_{uw} = 0.55\phi f'_c A_g \left[1 - \left(\frac{kH_w}{32t} \right)^2 \right] \quad (16.1b)$$

In Eq. (16.1b), ϕ is the strength reduction factor for compression-controlled sections, taken equal to 0.65, A_g is the area of gross cross section ($= L_w t$), H_w and t are the height and thickness of the wall, respectively, and k is the effective length factor. Equation (16.1b) is based on the 54 wall tests reported by Oberlender and Everard (1977) and the subsequent modification done by Kripanarayanan (1977). Pillai and Parthasarathy (1977), based on their experiments on eighteen wall models, with five H_w/t ratios ranging from 5 to 30, suggested that the term $32t$ may be modified as $50t$ and the coefficient 0.55 is to be taken as 0.57. It can be shown that the Indian code formula given in Eq. (16.1a) is very conservative and contains a coefficient of 2.0 for e_a , whereas the suggestion made by Pillai and Parthasarathy (1977), which has the same format of Eq. (16.1a), considers a coefficient of 1.0 for e_a and is found to correlate well with experimental results.

Stocky Braced Plain and RC Walls

Although IS 456 and ACI 318 do not give a separate formula for stocky braced plain walls, Clause 3.9.4.15 of BS 8110 (Part 1):1997 gives the following formula:

$$P_{uw} = 0.3f_{ck}(t - 2e_x) \quad (16.2a)$$

From this formula, it may be observed that when $e_x = t/2$, the wall will not carry any load.

Similarly, BS 8110 provides the following formula for stocky braced RC walls:

$$P_{uw} = 0.35f_{ck}A_c + 0.7f_yA_{sc} \quad (16.2b)$$

where A_c is the area of concrete, A_{sc} is the area of longitudinal reinforcement in wall, f_{ck} is the characteristic compressive strength of concrete, and f_y is the characteristic strength of compressive reinforcement. It has to be noted that it is similar to the equation given in Clause 39.3 of IS 456 for short axially loaded column.

Unbraced Plain Walls

The effective height of unbraced walls will be larger than the actual height of the wall. BS 8110 gives the following guidelines for determining the effective height of unbraced plain concrete walls:

1. Wall with a roof or floor spanning at right angles on top of the wall— $1.5L_1$
2. Wall with no roof or floor on top of the wall— $2L_1$

where L_1 is the clear distance of wall between lateral supports (unsupported height of the wall).

The ultimate strength of short and unbraced plain concrete walls can be taken as the lesser of the following formulae, as per BS 8110:

$$P_{nw} = 0.3f_{ck}(t - 2e_{x1}) \quad (16.3a)$$

$$P_{nw} = 0.3f_{ck}(t - 2e_{x2} - 2e_a) \quad (16.3b)$$

where e_{x1} and e_{x2} are the resultant eccentricities calculated at the top and bottom of the wall, respectively, and e_a is the additional eccentricity due to deflections.

16.3.5 Design of Walls Subjected to Combined Horizontal and Vertical Loads

In plain concrete walls, the transverse reinforcements are not susceptible to buckling, as they are not designed to carry any load and are provided only to control cracking. However, in RC walls where the vertical steel is designed to carry the load, the transverse horizontal steel has to be designed properly as in columns to restrain the vertical steel against buckling. When walls are subjected to in-plane horizontal forces in addition to vertical load, Clause 32.3 of IS 456 suggests that the wall may be designed as per Clause 32.2 (as explained in Section 16.3.4) for vertical loads and as per Clause 32.4 for horizontal shear as explained here. This clause also suggests neglecting in-plane bending when the horizontal cross section of the wall is always under compression, due to the effect of horizontal and vertical loads.

It has to be noted that the behaviour of walls subjected to shear depends on their height-to-length ratio (H_w/L_w). Shear in the plane of the wall is of primary importance for walls with a small height-to-length ratio (see also Section 16.5.1). The design of slender walls, particularly walls with uniformly distributed reinforcement, will probably be controlled by flexural considerations. Hence, Clause 32.4 of IS 456 has given a different formula for predicting the shear strength of concrete in short walls, also called *squat walls* ($H_w/L_w \leq 1$), and slender walls, also called *flexural walls* ($H_w/L_w > 1$). It has to be noted that as per ACI 318, walls are considered as squat walls when their height-to-length ratio (H_w/L_w) is less than or equal to 2.0.

Critical Section for Shear

As per Clause 32.4.1, the critical section for maximum shear can be taken at a distance that is lesser of $0.5L_w$ or $0.5H_w$ (see Fig. 16.4).

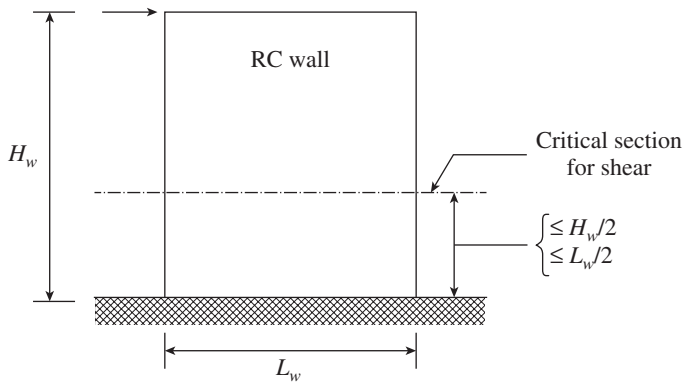


FIG. 16.4 Critical section for shear

Nominal Shear Stress

The nominal shear stress, τ_{vw} , in walls can be calculated as

$$\tau_{vw} = V_u / td \quad (16.4a)$$

where V_u is the shear force due to design loads, t is the thickness of wall, and d is the effective depth of wall, taken as $0.8L_w$, and L_w is the length of the wall. Clause 32.4.2.1 of IS 456 states that the calculated nominal shear stress should never exceed the maximum allowable shear stress,

$$\tau_{c,max} = 0.17f_{ck} \quad (16.4b)$$

It has to be noted that the value of $\tau_{c,max} \approx 0.6315\sqrt{f_{ck}}$ provided in Table 20 of IS 456 for beams is lower than that given by Eq. (16.4b). Clause 11.9.3 of ACI 318 gives this value as $0.745\sqrt{f_{ck}}$, based on tests conducted by Cardenas, et al. (1973) on structural walls with a thickness equal to $L_w/25$.

Design Shear Strength of Concrete

The design shear strength of concrete in walls without shear reinforcement is given by Clause 32.4.3 of IS 456 as follows:

1. For $H_w/L_w \leq 1$

$$\tau_{cw} = \sqrt{f_{ck}} \left(0.6 - \frac{0.2H_w}{L_w} \right) \quad (16.5a)$$

2. For $H_w/L_w > 1$

Lesser of the value calculated from Eq. (16.5a) and the value given by

$$\tau_{cw} = 0.045\sqrt{f_{ck}} \left[\frac{\left(\frac{H_w}{L_w} \right) + 1}{\left(\frac{H_w}{L_w} \right) - 1} \right] \quad (16.5b)$$

It has to be noted that Eq. (16.5b) differs from the equation given in AS 3600:2001, which is as follows, for the same condition of $H_w/L_w > 1$:

$$\tau_{cw} = 0.045\sqrt{f_{ck}} + \left[\frac{0.09\sqrt{f_{ck}}}{\left(\frac{H_w}{L_w} \right) - 1} \right] \quad (16.5c)$$

However, in any case,

$$\tau_{cw} \geq 0.15\sqrt{f_{ck}} \quad (16.5c)$$

The shear strength is taken as $V_{nc} = \tau_{cw}(0.8L_w)t$, where the terms f_{ck} , H_w , and L_w have already been defined.

The shear strength of concrete in walls, V_c , as per Clause 11.9.6 of ACI 318 may be computed as the lesser of Eqs (16.6a and b):

$$V_{uc} = 0.24\lambda\sqrt{f_{ck}}td + \frac{P_u d}{4L_w} \quad (16.6a)$$

$$V_c = \left[0.045\lambda\sqrt{f_{ck}} + \frac{L_w \left(0.09\lambda\sqrt{f_{ck}} + \frac{0.2P_u}{L_w d} \right)}{\left(\frac{M_u}{V_u} - \frac{L_w}{2} \right)} \right] td \quad (16.6b)$$

where λ is the modification factor for lightweight concrete, d is the effective depth, taken as $0.8L_w$. The ultimate axial load on wall, P_u , is positive for compression and negative for tension. The other terms have already been defined. If $(M_u/V_u - L_w/2)$ is negative, Eq. (16.6a) should be used. Equation (16.6a) corresponds to the occurrence of a principal tensile stress of $0.30\lambda\sqrt{f_{ck}}$ at the centroid of the wall cross section, whereas Eq. (16.6b) corresponds to the occurrence of a flexural tensile stress of $0.45\lambda\sqrt{f_{ck}}$ at a section $L_w/2$ above the section being investigated (ACI 318:2011).

As in the case of beams, when τ_{vw} is greater than τ_{cw} , shear reinforcements have to be provided in the wall. As the effective depth is taken as $0.8L_w$, we need to provide shear reinforcement to carry a shear force given by

$$V_s = V_u - \tau_{cw}t(0.8L_w) \tag{16.7}$$

The required amount of shear ties can be computed by using the conventional formula

$$A_{sv} = \frac{V_s s_v}{0.87 f_y d} \tag{16.8}$$

where A_{sv} is the area of horizontal shear reinforcement within spacing s_v .

Clause 32.4.4 of IS 456 suggests the following while providing shear reinforcement:

For $H_w/L_w \leq 1$, that is, for squat walls, where shear will govern the design, the vertical steel should be computed first. Then, the maximum of this steel and the minimum specified for walls (0.12% for high-yield strength-deformed, HYSD, bars) has to be determined and provided in the vertical direction. If this amount is more than the specified minimum horizontal steel (0.20% for HYSD bars), then the same steel is to be provided in the horizontal direction as well. This means, more reinforcement has to be provided horizontally than vertically.

For $H_w/L_w > 1$, that is, for slender walls, where flexure will govern, the design is made for horizontal steel and should be provided in the horizontal direction. This steel should not be less than the specified minimum (0.20% for HYSD bars). It has to be noted that the minimum steel (0.12% for HYSD bars) should also be checked for vertical reinforcement.

both vertical and horizontal directions should not be greater than three times the wall thickness or 450 mm, whichever is less. For walls of thickness more than 200 mm, the vertical and horizontal reinforcement should be provided in two grids, one near each face of the wall (Clause 32.5.1). Clause 32.5.2 also states that the vertical reinforcement need not be enclosed by transverse reinforcement as in columns, provided the vertical steel is not greater than 0.01 times the gross sectional area or where the vertical reinforcement is not required for compression. These provisions are the same in ACI 318 as well (see Clause 14.3). In addition to these requirements, ACI 318 suggests to provide a minimum of two 16 mm bars in walls having two layers of reinforcement in both directions and one 16mm bar in walls having a single layer of reinforcement in both directions around window or door openings. Such bars should be anchored to develop f_y in tension at the corners of the openings.

Standard detailing for walls, as given in the IS handbook on detailing, are shown in Fig. 16.5 (SP 34:1987). Figure 16.5(b) shows the section of a wall with thickness less than 170 mm with single layer of vertical and horizontal nominal reinforcement, provided at the centre of the wall, whereas Fig. 16.5(c) shows a thick wall having thickness greater than 170 mm, with more than nominal reinforcement placed in two layers. In this case, the vertical reinforcement is placed inside the horizontal reinforcement. When only nominal reinforcements are provided, then horizontal reinforcement may be placed inside the vertical

16.3.6 Detailing of Concrete Walls

The requirement of minimum ratio of vertical and horizontal reinforcement to gross area, as per Clause 32.5 of IS 456, is given in Table 5.10 of Chapter 5. Thus, for Fe 415 grade steel and with diameter not larger than 16 mm, this ratio in vertical and horizontal directions is 0.0012 and 0.0020, respectively. The spacing in

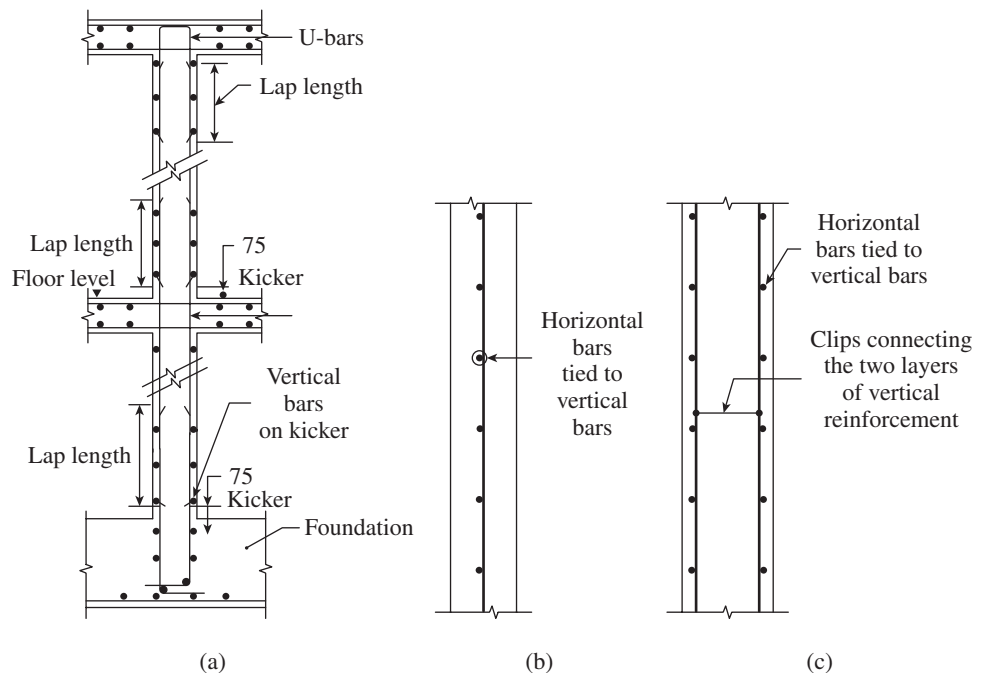


FIG. 16.5 Detailing of wall reinforcement as per SP 34:1987 (a) General section through the wall (b) Vertical section of wall with single layer of reinforcement (thickness less than 170 mm) (c) Vertical section of wall with double layer of reinforcement

Note: Horizontal bars are placed outside vertical bars

steel to reduce the possibility of coarse aggregates being 'hung up' on the horizontal bars (SP 34:1987). It is mandatory to provide clips for vertical bars at a horizontal spacing less than twice the wall thickness. Similarly, vertical spacing of clips should be the lesser of 300 mm and $15d_b$, where d_b is the diameter of vertical reinforcement. In addition, at all splices, the top of each lower bar and the bottom of each upper bar should be restrained by clips. The clips should be alternately reversed; or else, truss-type clips as shown in Fig. 16.6 may be used (SP 34:1987).

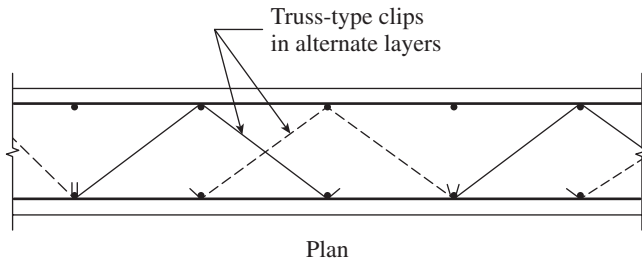


FIG. 16.6 Truss-type clips for walls

Splices at top of walls When a roof slab is cast over an RC wall, the connection between the two is established as follows (SP 34:1987):

1. When the diameter of wall reinforcement is less than or equal to 10 mm, the wall reinforcement can be bent into the roof slab as shown in Fig. 16.7(a).
2. When the diameter of the wall reinforcement is greater than 10 mm, the slab as well as wall reinforcements are bent into one another as shown in Fig. 16.7(b) or U-type bars can be used to connect the two elements as shown in Fig. 16.7(c).

When walls are constructed using sliding and climbing shuttering, proper detailing is to be adopted in consultation with the contractor.

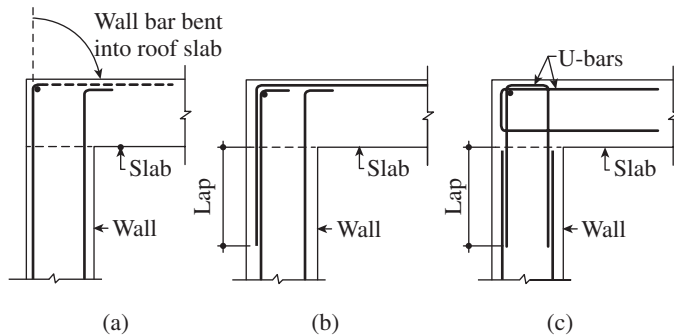


FIG. 16.7 Splices at top of walls (a) Wall bars bent into roof slab (b) Wall and slab bars bent into one another (c) Use of U-bars to connect wall and slab

Vertical cracks in walls are more likely to form due to restrained horizontal shrinkage or temperature stresses than horizontal cracks as a result of restrained vertical stresses.

Hence, IS 456 and ACI 318 stipulate more reinforcement horizontally (0.20%), than vertically (0.12%).

16.4 DESIGN OF RETAINING WALLS

A *retaining wall* is defined as a structure whose primary purpose is to retain some material on one or both sides of it. In some cases, the retaining wall may also support vertical loads. Usually, it is used to retain soil, at two different levels on either side. The materials to be retained on either side may be different, for example, the walls of a swimming pool, which retain soil on one side and water on the other side. Retaining walls are mostly used at the ends of bridges in the form of abutments; for roads in hilly areas, swimming pools, basement walls, and underground water tanks; and while constructing a building on a site where filling is required.

The retained material exerts a lateral pressure causing the retaining wall to bend, overturn, or slide. Hence, the retaining wall and its foundation should be designed in such a way that it is stable under the effects of lateral earth pressure, in addition to the usual requirements of strength and serviceability.

16.4.1 Types of Retaining Walls

Some of the more common types of retaining walls are gravity and semi-gravity walls, gabions, crib walls, cantilevered walls, basement walls, counterfort walls, buttressed retaining walls, anchored walls, and segmental retaining walls (see Fig. 16.8).

Gravity-retaining walls These walls are built of plain concrete or stone, and their stability against overturning and sliding depends primarily on their massive weight (see Fig. 16.8a). They are so proportioned that there are no tensile stresses developed in any portion of the wall. Little reinforcement is required in this type of wall; however, gravity-retaining walls are not economical, especially for high walls (greater than about 3 m), as they consume large quantities of materials. *Semi-gravity-retaining walls* are lighter than gravity-retaining walls and contain small amount of reinforcement in the stem as well as toe, to reduce the mass of concrete.

Gabions These are large cages or baskets usually made of steel wire or square welded mesh, rectangular in shape, filled with stone, and used to build retaining walls (see Fig. 16.8b). They are suitable for walls of small to moderate height (about 3–6 m).

Crib walls These walls consist of interlocking precast concrete or timber members that form cells, which are then filled with granular materials (see Fig. 16.8c). Except for the exposed front face, crib walls are completely covered with soil and hence the cribbing will not be visible. They are suitable

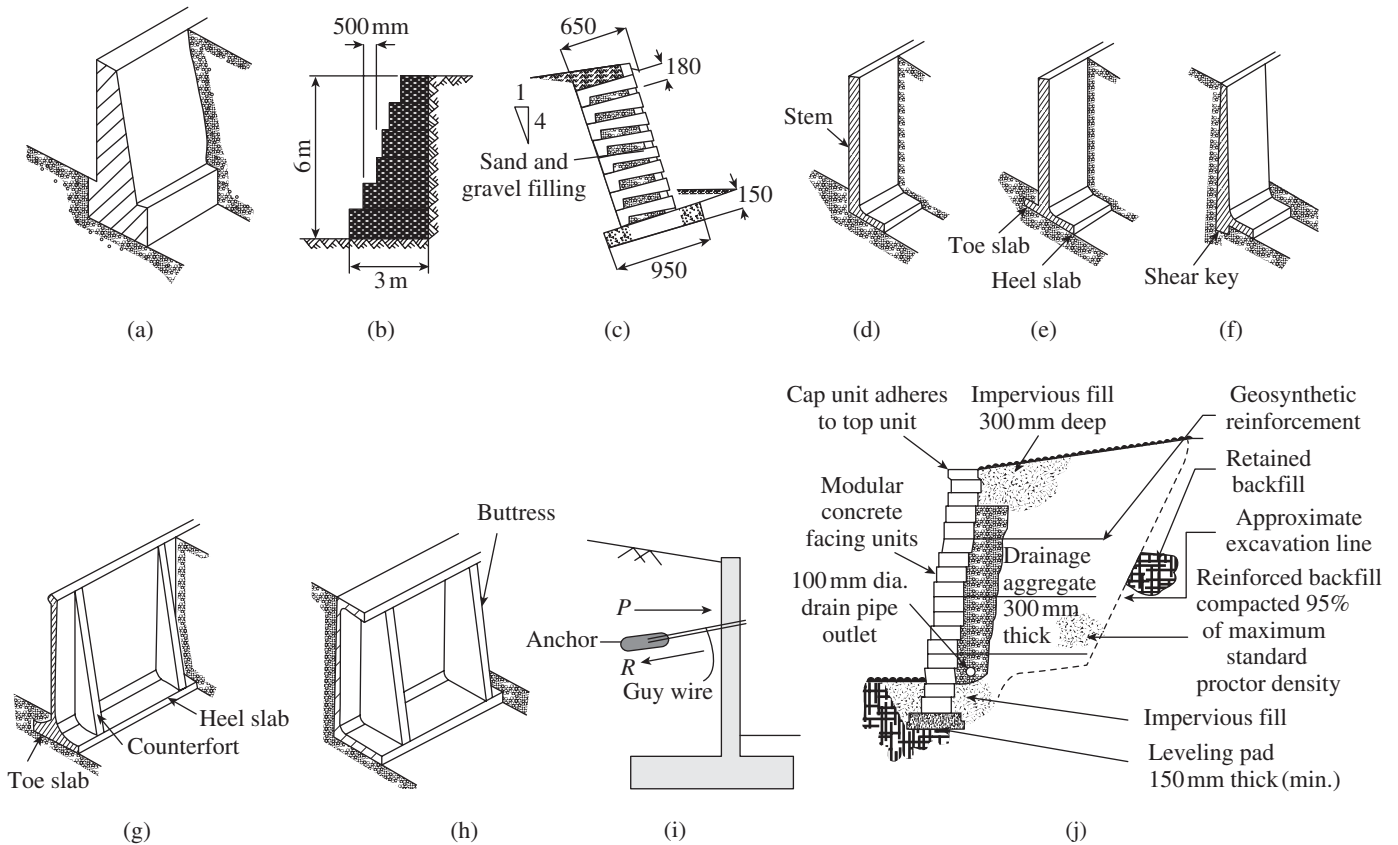


FIG. 16.8 Types of retaining walls (a) Gravity (b) Gabion (c) Crib (d) T-type cantilever (e) L-type cantilever (f) L-type with shear key (g) Counterfort (h) Buttress (i) Anchored (j) Segmental

for walls of small to moderate height (about 4–6 m) subjected to moderate earth pressure.

Cantilever-retaining walls These are the most commonly used retaining walls. They may be T- or L-type walls (see Figs 16.8d–f). The base slab of a T-type wall consists of a *toe slab* (on the front side of the wall) and a *heel slab* (see Fig. 16.8e), whereas that of an L-type wall has only the heel slab (see Fig. 16.8d). The stability of the wall is provided essentially by the weight of earth on the heel slab and the self-weight of the structure. These retaining walls can be provided with shear keys to resist shear forces (see Fig. 16.8f). Walls of this type are economical for small to moderate heights (6–7.5 m).

Counterfort-retaining walls When the height of a retaining wall exceeds about 6 m, and when the thickness of stem, toe, and heel of a cantilever-retaining wall becomes uneconomical, counterforts may be provided to economize the design of various components of the retaining wall (see Fig. 16.8g). Counterfort walls consist of a footing slab (toe and heel slab), a vertical stem, and intermittent vertical ribs (called *counterforts*) that tie the footing and vertical stem together. The heel slab and the vertical stem span horizontally between these counterforts. Thus, the stem and heel slabs are designed as continuous slabs supported over counterforts. The sizes

of concrete components and the steel reinforcement will be reduced considerably, as the bending moments are less than those occurring in cantilever-retaining wall. However, extra cost is incurred for the formwork to make counterforts. The counterforts are generally provided on the side of retained earth. Sometimes counterforts may also be provided on the side of the toe slab in addition to that on the side of the heel slab. This type is suitable for high walls, greater than about 6.5–7 m.

Buttressed-retaining walls When the counterforts are provided in the front of the wall and not on the soil side, they are known as *buttressed-retaining walls* (see Fig. 16.8h). Buttresses reduce the clearance in front of the wall. The contribution of backfill is less towards the stability of the wall because heel projection is small.

Anchored-retaining walls The cantilever stem of retaining walls can also be propped by high-strength prestressed guy wires instead of counterforts (see Fig. 16.8i). These guy wires are anchored in the rock or soil behind it. As it is technically complex, this type of wall is used only when high loads are expected or where the wall is very slender.

Segmental-retaining walls This system consists of concrete masonry units that are placed without the use of mortar (dry

stacked) and rely on a combination of mechanical interlock and mass to prevent overturning and sliding (see Fig. 16.8j). The units may also be used in combination with horizontal layers of soil reinforcement, which extend into the backfill to increase the effective width and weight of the gravity mass. When soil reinforcement is provided, they are also called *mechanically stabilized earth retaining walls* (MSE RW) or *reinforced earth walls*.

Segmental retaining walls have the ability to function equally well in large-scale applications (highway walls, bridge abutments, erosion control, parking area supports, etc.) as well as smaller residential landscape projects. They can easily accommodate curves and other unique layouts. As they are available in a variety of sizes, shapes, textures, and colours, they are more aesthetic than conventional retaining walls. The flexible nature of segmental retaining walls allows the units to move and adjust relative to one another, and hence, there will not be any visible signs of distress (cracks). Moreover, they are more economical than conventional retaining walls. A typical (curved) segmental retaining wall is shown in Fig. 16.9(a). Such walls provide an attractive, cost-effective alternative to conventional cast-in-place concrete retaining walls. Many proprietary systems are available including Allan Block, Anchor Retaining Wall Systems, Contech Engineered Solutions, Redi-Rock International, The Reinforced Earth Company, and Tensar International Corporation. Reinforced earth walls have been used successfully in numerous bridge projects all over the world. One such wall is shown in Fig. 16.9(b). More details of these walls and their design and construction may be found in NCMA Manual (2010) and the works of Elias, et al. (2001) and Subramanian and Sundararaj (1980).

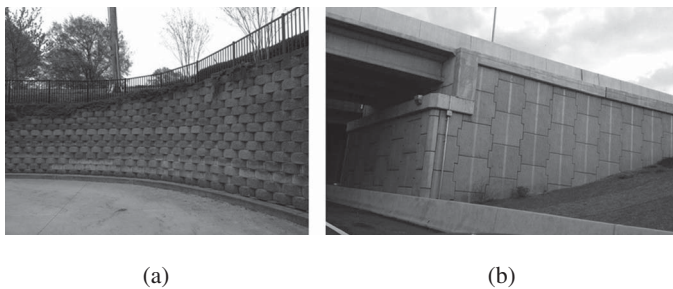


FIG. 16.9 Typical segmental walls in the USA (a) Segmental-retaining wall (b) Reinforced earth wall

Basement walls Walls in the basement of a building also act as retaining walls.

The rest of this chapter considers only the cantilever- and counterfort-retaining walls. Interested readers should consult the works of Clayton, et al. (1993), Brooks and Nielsen (2012), Budhu (2008), and NCMA (2010) for the design of other types of retaining walls.

16.4.2 Theories of Earth Pressure

As mentioned earlier, earth pressure is the main force acting on the retaining wall and makes it bend, overturn, and slide. There are two theories for calculating the earth pressure on the retaining walls: (a) Coulomb’s theory, developed in 1773, and (b) Rankine’s theory, developed in 1857. However, only in 1934, Terzaghi pointed out the validity and limitations of these two theories and explained the fundamental principles of the action of earth pressures (Terzaghi, et al. 1996). Based on a series of tests conducted at MIT, he identified the following three types of earth pressures (see also Fig. 16.10):

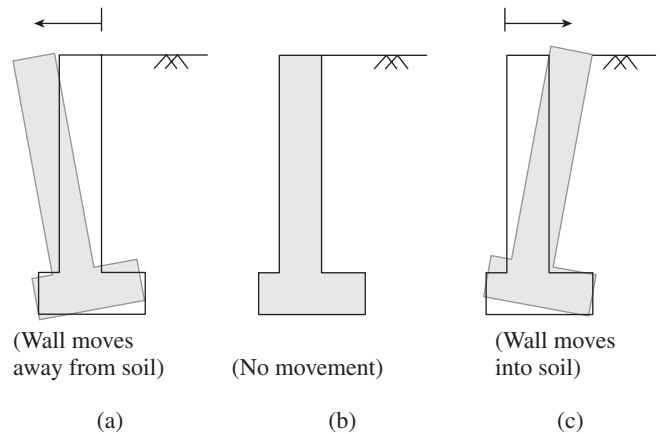


FIG. 16.10 Three types of earth pressures (a) Active (b) At rest (c) Passive

1. *Active earth pressure*: In general, the behaviour of lateral earth pressure is analogous to that of a fluid, with the magnitude of pressure p increasing linearly with increasing depth z for moderate depths below the surface and is given by

$$p = K\gamma z \tag{16.9a}$$

where γ is the unit weight of earth (may be taken as 17–19 kN/m³ for sands, 19–20 kN/m³ for sand and gravel mixes, and 14–18 kN/m³ for clays) and K is the coefficient of earth pressure that depends on the physical properties of soil and on whether the pressure is active or passive.

Active earth pressure develops when the wall moves away from the backfill as shown in Fig. 16.10(a). Here, the soil mass is active in exerting pressure on the wall and hence termed as *active earth pressure*. The coefficient of active earth pressure is denoted by K_a . The force P_a caused by the active pressure on a wall of height H may be expressed as

$$P_a = K_a \gamma \frac{H^2}{2} \tag{16.9b}$$

A deflection at the top of the wall in the range $0.001H-0.05H$ (where H is the height of the wall) is necessary to develop full active pressure.

2. *Earth pressure at rest*: Earth pressure at rest develops when the wall does not deform laterally (see Fig. 16.10b). This typically occurs when the wall is restrained from movement, for example, in the case of a basement wall that is restrained at the bottom by the foundation slab and at the top by the floor slab (thus they are termed *non-yielding walls*). The pressure at any depth, h , is given by

$$p_r = K_0 \gamma h \tag{16.10a}$$

where K_0 is the coefficient of earth pressure at rest and γ_e is the unit weight of earth. The value of K_0 is given by (Jaky 1944; Michalowski 2005)

$$K_0 = 1 - \sin \phi \tag{16.10b}$$

where ϕ is the *effective internal friction angle* of the soil (also called *angle of shearing resistance*). Equation (16.10) is found to give good results when the backfill is loose sand. For dense sand backfill, it may grossly underestimate the lateral earth pressure at rest (Das 2010). Equations for K_0 for such soils as well as fine grained normally consolidated soils, over-consolidated clays, and partly submerged soils is provided by Das (2010). Test results indicated that K_0 is in the range of 0.35–0.60 for sand and gravel, 0.45–0.75 for clay and silt, and 1.0 for over-consolidated clays. The magnitude of earth pressure at rest will lie somewhere between the active and passive earth pressures. The values of soil friction angle, ϕ , for different types of soils are provided in Table 16.3.

TABLE 16.3 Internal friction angle, ϕ , for different types of soils

Soil Type	Soil Friction Angle, ϕ (Degrees)
Well-graded gravel, sandy gravel, with little or no fines	40 ± 5
Poorly graded gravel, sandy gravel, with little or no fines	38 ± 6
Well-graded sands, gravelly sands, with little or no fines	38 ± 5
Poorly graded sands, gravelly sands, with little or no fines	34 ± 4
Silty sands	34 ± 3
Clayey sands	32 ± 4
Inorganic silts, silty or clayey fine sands, with slight plasticity	33 ± 4
Inorganic clays, silty clays, sandy clays of low plasticity	27 ± 4

Source: www.geotechdata.info/parameter/angle-of-friction

3. *Passive earth pressure*: When the wall moves into the soil, the soil mass is compressed and passive pressure is developed (see Fig. 16.10c). This situation might occur along the section of a wall that is below grade and on the opposite side of the retained section of fill. The coefficient of passive earth pressure is denoted by K_p . It has to be noted that the passive pressure is several times larger than the active pressure for the same type of soil. Roughly $K_p = 1/K_a$. The force P_p caused by the active pressure on a wall of height H may be expressed as

$$P_p = K_p \gamma \frac{H^2}{2} \tag{16.11}$$

The factors that affect the active or passive pressure applied to a particular wall include the type of backfill material used, drainage of backfill material, level of water table, seasonal conditions such as dry, wet, or frozen, consolidation of backfill, the presence of trucks or other equipment (surcharge) on the backfill, type of soil below the footing, and possibility of vibration in the vicinity of the wall (especially for granular backfill). The most important factor is the accumulation of water behind the wall; hence, proper drainage is very important (see Section 16.4.5 for the methods adopted). Clays should not be used as backfill material as their shear characteristics change easily and they tend to creep against the wall, increasing the active earth pressure, at later ages (McCormac and Brown 2013). Frost action, which may occur at about 1–2 m below ground level, may be considered by adding a surcharge load of 8.75–10 kN/m at the top of the stem (McCormac and Brown 2013).

Rankine's Earth Pressure Theory

Rankine was the first to investigate the state of stress in a semi-infinite mass of homogenous, elastic, and isotropic soil mass under the influence of its own weight at failure (Rankine 1857). Rankine's theory (also called *plasticity theory*) assumes the following:

1. There is no adhesion or friction between the wall and soil.
2. Lateral pressure is limited to vertical walls.
3. Failure (in the backfill) occurs as a sliding wedge along an assumed failure plane defined by ϕ .
4. Lateral pressure varies linearly with depth and the resultant pressure is located one-third of the height (H) above the base of the wall.
5. The resultant force is parallel to the backfill surface.

According to Rankine's theory, the active earth pressure coefficient K_a for a retaining wall with earthfill sloping at an angle δ to horizontal is given by (see Fig. 16.11)

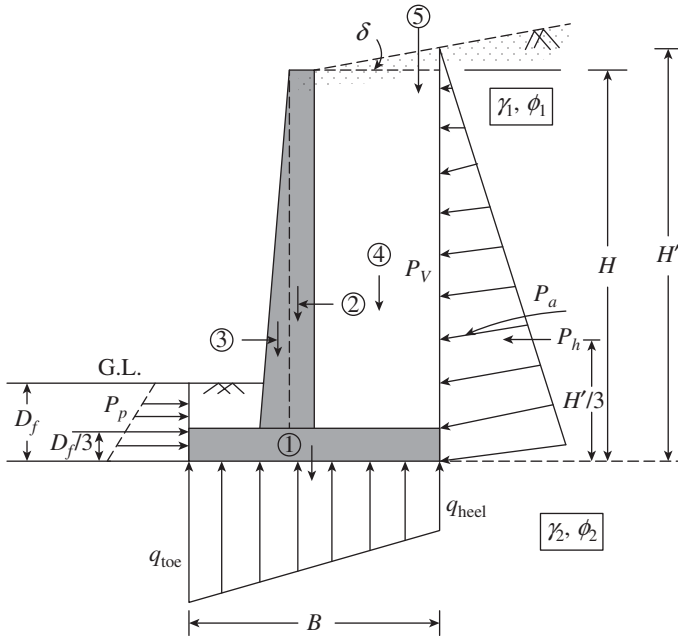


FIG. 16.11 Rankine's active and passive earth pressure

$$K_a = \cos \delta \frac{\cos \delta - \sqrt{(\cos^2 \delta - \cos^2 \phi)}}{\cos \delta + \sqrt{(\cos^2 \delta - \cos^2 \phi)}} \quad (16.11a)$$

The force exerted by the active pressure due to the backfill, per unit length of the wall, based on triangular pressure distribution, is given by

$$P_a = K_a \gamma \frac{H'^2}{2} \quad (16.11b)$$

The resultant force acts at a distance $H/3$ measured from the bottom of the wall and is inclined at an angle δ to the horizontal (parallel to the surface of the backfill). Table 16.4 gives the values of K_a for various combinations of δ and ϕ ; the usual range of K_a is 0.27–0.4.

TABLE 16.4 Values of K_a for various values of δ and ϕ

δ (Degrees)	ϕ (Degrees)						
	28	30	32	34	36	38	40
0	0.361	0.333	0.307	0.283	0.260	0.238	0.217
5	0.366	0.337	0.311	0.286	0.262	0.240	0.219
10	0.380	0.350	0.321	0.294	0.270	0.246	0.225
15	0.409	0.373	0.341	0.311	0.283	0.258	0.235
20	0.461	0.414	0.374	0.338	0.306	0.277	0.250
25	0.573	0.494	0.434	0.385	0.343	0.307	0.275

Passive earth pressure In a similar manner, the Rankine's passive earth pressure coefficient, K_p , for a wall of height H with a granular sloping backfill is given by (Das 2010)

$$K_p = \cos \delta \frac{\cos \delta + \sqrt{(\cos^2 \delta - \cos^2 \phi)}}{\cos \delta - \sqrt{(\cos^2 \delta - \cos^2 \phi)}} \quad (16.12a)$$

The active force per unit length of the wall is given by

$$P_p = K_p \gamma \frac{H'^2}{2} \quad (16.12b)$$

As in the case of active earth pressure, the resultant force P_p acts at a distance $H/3$ measured from the bottom of the wall and is inclined at angle δ to the horizontal.

Table 16.5 gives the values of K_p for various combinations of δ and ϕ ; the usual range of K_p is 2.5–4.0. It has to be noted that the passive pressure developed on the toe side of the retaining wall (see Fig. 16.11) will not be considerable (due to the smaller height) and hence is generally not considered in the design; omission of the contribution of passive pressure produces a conservative design. In addition, the top 300 mm depth of soil above the toe slab is usually not considered in the calculation of passive pressure.

TABLE 16.5 Values of K_p for various values of δ and ϕ

δ (Degrees)	ϕ (Degrees)						
	28	30	32	34	36	38	40
0	2.770	3.000	3.255	3.537	3.852	4.204	4.599
5	2.715	2.943	3.196	3.476	3.788	4.136	4.527
10	2.551	2.775	3.022	3.295	3.598	3.937	4.316
15	2.284	2.502	2.740	3.003	3.293	3.615	3.977
20	1.918	2.132	2.362	2.612	2.886	3.189	3.526
25	1.434	1.664	1.894	2.135	2.394	2.676	2.987

For horizontal earthfill, $\delta = 0$, the active earth pressure is given by

$$P_A = \frac{\gamma H^2}{2} \left(\frac{1 - \sin \phi}{1 + \sin \phi} \right) = \frac{\gamma H^2}{2} \tan^2 \left(45 - \frac{\phi}{2} \right) \quad (16.13)$$

acting at $H/3$ from the bottom of the wall in the horizontal direction and normal to the vertical stem.

Similarly for horizontal earthfill, the passive earth pressure is given by

$$P_p = \frac{\gamma H^2}{2} \left(\frac{1 + \sin \phi}{1 - \sin \phi} \right) = \frac{\gamma H^2}{2} \tan^2 \left(45 + \frac{\phi}{2} \right) \quad (16.14)$$

acting at $H/3$ in the horizontal direction from the bottom of wall.

Effect of surcharge on a level backfill Loads are often imposed on the backfill surface behind a retaining wall in the form of buildings or highways, with moving traffic. These loads are often considered as equivalent static loads for the purposes of design and are assumed to be uniformly distributed. The earth pressure computation is often made by substituting the uniformly distributed load by an equivalent surcharge layer.

The thickness of this surcharge layer is equal to the distributed load divided by the unit weight of the underlying soil. Thus, this equivalent height of earth, H_a , is obtained as

$$H_a = w_s / \gamma \tag{16.15}$$

The computation of lateral pressure due to the uniform surcharge is relatively simple. In the case of Rankine’s theory, the pressure caused by the uniform surcharge, w_s , is taken as a rectangle of pressure of magnitude, $K_a \gamma H_a$, behind the wall with a total lateral surcharge force assumed to act at its mid-height, as shown in Fig. 16.12. This pressure should be added with the triangular pressure distribution due to actual backfill, with the resultant force acting at $H/3$ from the base. Thus, the total force acting on the wall is

$$P = P_a + P_{a1} \tag{16.16}$$

where

$$P_a = K_a \gamma H^2 / 2 \tag{16.17a}$$

$$P_{a1} = K_a \gamma H_a H \tag{16.17b}$$

These forces P_a and P_{a1} act at a distance of $H/3$ and $H/2$ from the top of the heel slab, respectively.

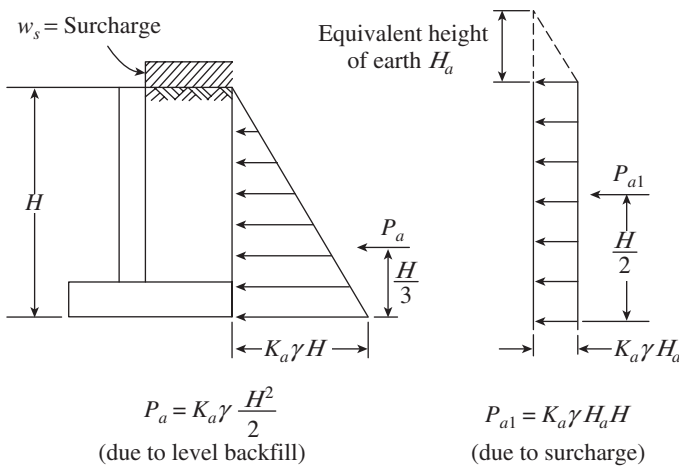


FIG. 16.12 Effect of surcharge

Partly submerged backfill For partly submerged backfill as shown in Fig. 16.13(a), the active pressure distribution is computed on the basis of the bulk unit weight of the soil, γ_e ,

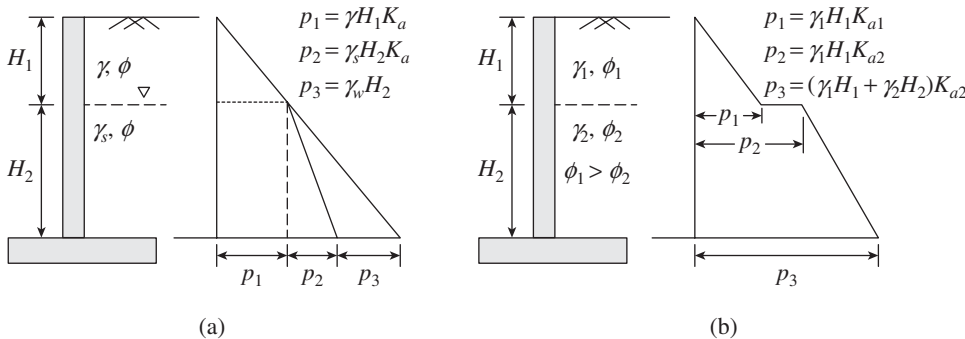


FIG. 16.13 Active earth pressure distribution (a) Partly submerged backfill (b) Stratified backfill

above the water table and the submerged unit weight of the soil, γ_s , below the water table. The hydrostatic water pressure below the water table must be added to the active earth pressure to obtain the total lateral pressure.

Stratified backfill When there are two or more layers of backfilled soil, the pressure will change abruptly at the strata interfaces. The pressure distribution has to be computed by using the appropriate values of K_a for each stratum. For a particular layer, the weight of the overlying layers is considered as surcharge. A typical pressure diagram for two different layers of soil backfill is shown in Fig. 16.13(b).

Coulomb’s Earth Pressure Theory

Coulomb’s theory (also called *wedge theory*) is similar to Rankine’s theory except that it considers the following (Coulomb 1773):

1. The friction between the wall and the backfill soil is taken into account by using a soil–wall friction angle of β . Note that β ranges from $\phi/2$ to $2\phi/3$ and $\beta = 2\phi/3$ is commonly used.
2. Lateral pressure is not limited to vertical walls.
3. The resultant force is not necessarily parallel to the backfill surface because of the soil–wall friction value β .

Coulomb considered a rigid mass of soil sliding upon a plane (straight line) shear surface and derived the equation for active earth pressure by resolving the forces acting in the parallel and perpendicular directions to the shear surface. It has to be noted that a number of experiments have revealed that the actual failure surface is not a plane surface, as assumed in the wedge theory, but a logarithmic spiral or a combination of spiral and straight lines. The total active earth pressure acting on the retaining wall based on Coulomb’s theory is given by (Teng 1983)

$$P_a = K_a \frac{\gamma_e H^2}{2} \cos \theta \tag{16.18a}$$

where the active earth pressure coefficient is given by

$$K_a = \frac{\cos^2(\phi - \theta)}{\cos^2 \theta \cos(\theta + \beta) \left[1 + \frac{\sin(\beta + \phi) \sin(\phi - \delta)}{\cos(\theta + \beta) \cos(\theta - \delta)} \right]^2} \tag{16.18b}$$

where θ is the angle made by the back of wall with vertical, ϕ is the angle of internal friction of soil, and β is the angle of friction between the retaining wall and earth, which may be taken as $\phi/3$ or $2\phi/3$, but not greater than δ . For design purposes, the value of β may be taken as 20° for concrete walls. It has to be noted that when $\delta = 0^\circ$, $\theta = 0^\circ$ and $\beta = 0^\circ$,

Coulomb's active earth pressure coefficient becomes equal to Rankine's active earth pressure coefficient.

The resultant earth pressure acts at $H/3$ from the base and is inclined at an angle β to the normal to the face of the wall as shown in Fig. 16.14(a).

For horizontal earthfill, $\delta = 0$. Hence the equation for the active pressure coefficient becomes

$$K_a = \frac{\cos^2(\phi - \theta)}{\cos^2 \theta \cos(\theta + \beta) \left[1 + \frac{\sin(\beta + \phi) \sin \phi}{\cos(\theta + \beta) \cos \theta} \right]^2} \quad (16.19)$$

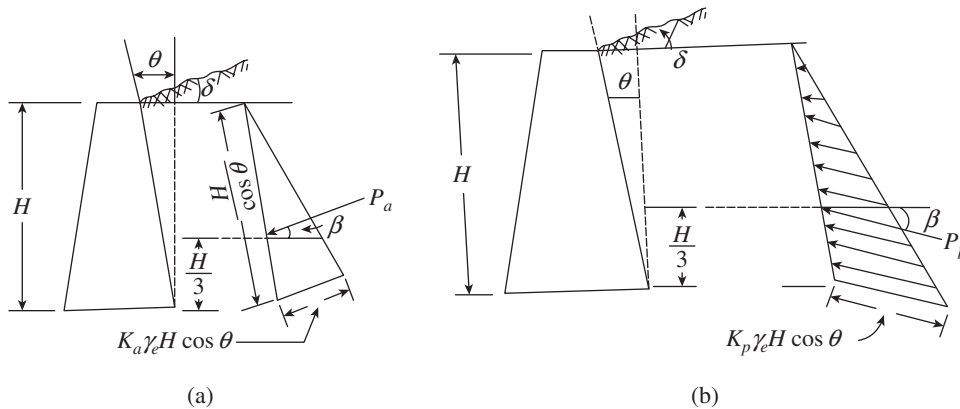


FIG. 16.14 Coulomb's theory (a) Active earth pressure (b) Passive earth pressure

Culmann (1875) also developed a graphical solution for Coulomb's active earth pressure, which can be used for any wall friction, regardless of the irregularity of backfill and surcharges. See the work of Das (2010) and Draft IS 1893 (Part 3) for the details of this method. Donkada and Menon (2012) based on their studies found that Coulomb's theory, which accounts for wall friction, gives a better cost-effective design than Rankine's theory, which is used in practice for convenience.

Passive earth pressure When the wall is forced against the soil, passive earth pressure (P_p) develops. The total passive earth pressure acting on the retaining wall based on Coulomb's theory is given by (Teng 1983)

$$P_p = K_p \frac{\gamma_e H^2}{2} \cos \theta \quad (16.20a)$$

where the passive earth pressure coefficient K_p is given by

$$K_p = \frac{\cos^2(\phi + \theta)}{\cos^2 \theta \cos(\theta - \beta) \left[1 - \frac{\sin(\beta + \phi) \sin(\phi + \delta)}{\cos(\theta - \beta) \cos(\theta - \delta)} \right]^2} \quad (16.20b)$$

This pressure acts at $H/3$ from the base and is inclined at an angle β to the face of the wall as shown in Fig. 16.14(b).

For horizontal earth-fill, $\delta = 0$. Hence, Eq. (16.20b) transforms to

$$K_p = \frac{\cos^2(\phi + \theta)}{\cos^2 \theta \cos(\theta - \beta) \left[1 - \frac{\sin(\beta + \phi) \sin \phi}{\cos(\theta - \beta) \cos \theta} \right]^2} \quad (16.20c)$$

It may be noted that for a given value of ϕ , the value of K_p increases with wall friction (Das 2010).

Since Coulomb's theory takes into account the friction of the wall, it is considered to be more accurate and often used for walls over 6.5 m height. The two methods give identical results if the friction of the soil on the wall is neglected. It has to be noted that both Rankine's and Coulomb's formulae were developed for cohesionless soils. Usually, designers assume that cohesionless granular backfill will be placed behind the walls. Thus, typical values of K_a and K_p will be in the range of 0.3–0.4 and 3.0–3.3, respectively, for granular materials.

The lateral pressure exerted by clays and silts or sloped backfill can be very high. It is because the angle of internal friction is in the range of 0–10° for soft clays and 30–40° for granular soils. Hence, K_a values can be as high as 0.9 or even 1.0 or more for clayey soils (Peck, et al. 1974).

16.4.3 Earth Pressure during Earthquakes

In the seismic zones, the retaining walls are subjected to dynamic earth pressure, the magnitude of which is more than the static earth pressure due to ground motion. The dynamic earth pressure is influenced by a range of factors, which include (a) nature of seismic wave, (b) thickness of different soil layers and the wall dimensions, (c) properties of the soil and wall material, and (d) groundwater conditions and their dynamic response. A rigorous analysis considering these factors into account is often difficult to develop. Hence, simplifying assumptions are made in the analysis methods.

The available analysis methods may be grouped into two broad categories, namely pseudo-static approach and dynamic response analysis using finite element methods (FEM). Due to its simplicity, the pseudo-static approach is often adopted and one such method called the *Mononobe–Okabe method* is recommended by draft IS 1893 Part 3.

The earliest method for determining the combined static and dynamic earth pressures on a retaining wall was developed by

Okabe (1924) and Mononobe and Matsuo (1929) after the great Kanto earthquake of 1923. This method, generally referred to as the Mononobe–Okabe method, is based on plasticity theory and is essentially an extension of the Coulomb sliding wedge theory, in which the transient earthquake forces are represented by an equivalent static force. The latter is expressed in terms of the weight of the wedge multiplied by the seismic coefficient. This method gives the following equations for computing the total dynamic active earth pressure exerted against the wall (see Fig. 16.15):

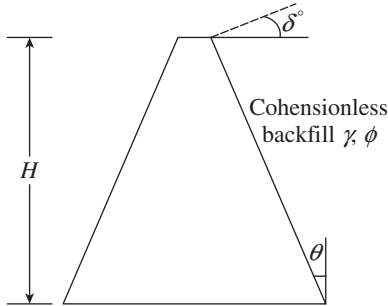


FIG. 16.15 Cross section of retaining wall

$$(P_a)_{dyn} = \frac{1}{2} \gamma H^2 (1 \mp A_v) (K_a)_{dyn} \quad (16.21a)$$

where

$$(K_a)_{dyn} = \frac{\cos^2(\phi - \psi - \theta)}{\cos \psi \cos^2 \theta \cos(\psi + \theta + \beta) \left(1 + \sqrt{\frac{\sin(\phi + \beta) \sin(\phi - \psi - \delta)}{\cos(\beta + \psi + \theta) \cos(\theta - \delta)}} \right)^2} \quad (16.21b)$$

The expression $(K_a)_{dyn}$ gives two values depending on the sign of A_v . For design purposes, the higher of the two values should be taken.

The total dynamic passive pressure exerted against the wall is given by

$$(P_p)_{dyn} = \frac{1}{2} \gamma H^2 (1 \mp A_v) (K_p)_{dyn} \quad (16.22a)$$

where

$$(K_p)_{dyn} = \frac{\cos^2(\phi - \psi + \theta)}{\cos \psi \cos^2 \theta \cos(\psi - \theta + \beta) \left(1 - \sqrt{\frac{\sin(\phi + \beta) \sin(\phi - \psi + \delta)}{\cos(\beta + \psi - \theta) \cos(\delta - \theta)}} \right)^2} \quad (16.22b)$$

For design purposes, the lesser value of $(K_p)_{dyn}$ shall be considered out of the two values corresponding to $\pm A_v$.

The seismic inertia angle ψ is given by

$$\psi = \tan^{-1} \left(\frac{A_h}{1 \mp A_v} \right) \quad (16.23)$$

where γ is the unit weight of soil in kN/m^3 , H is the height of the structure in m, ϕ is the angle of internal friction of soil, β is the angle of friction between the retaining wall and earth, θ is the inclination of wall with respect to vertical (this definition of θ is different from θ in Coulomb's equations), δ is the slope inclination, ψ is the seismic inertia angle, and A_v and A_h are the vertical and horizontal seismic coefficients, respectively. A_v may be taken as $2/3 A_h$. $(P_a)_{dyn}$ and $(P_p)_{dyn}$ are the combined static and dynamic forces due to the driving and resisting wedges, respectively. These equations are subject to the same limitations that are applicable to Coulomb's equations.

It has to be noted that the seismic inertia angle ψ must always be less than or equal to the difference of the angle of internal friction and the ground surface inclination (i.e., $\phi - \delta$). If it is greater, then the value of ψ may be assumed as $\phi - \delta$. In the case of passive earth pressure, the value of seismic inertia angle ψ must always be less than or equal to the sum of the angle of internal friction and the ground surface inclination (i.e., $\phi + \delta$). More information on seismic analysis and design of retaining walls is provided in the works of Anderson, et al. (2008).

16.4.4 Preliminary Proportioning of Retaining Walls

Proper proportioning of a retaining wall is as important to its construction as its structural design. Choosing correct proportions facilitate proper concrete placement and provide sufficient room for structural reinforcement. The foundation depth should be kept at a minimum of 600 mm from ground level (see Fig. 16.16a). However, it should always be below the seasonal frost line. In order to achieve stability, retaining walls are usually proportioned so that the width of the base (B) is equal to approximately 0.5–0.7 times the height of the wall (H). The toe projection is generally smaller than that of the heel slab. In general, the top of the vertical stem of any cast in situ concrete retaining wall should not be less than 200–300 mm for the proper placement of concrete. For cantilever and counterfort walls, the stem thickness at the base is often about 10 per cent of the total wall height (Teng 1983). For economy, the vertical stem may be tapered linearly. For heights up to about 3.6 m, the stems of cantilever-retaining walls are made of constant thickness, because the extra cost of setting tapered formwork may offset the saving made in concrete volume. The sloping face of the wall can be either in the back or in the front face of the wall; the taper on the front (outside) face is preferred as it will tend to counteract the deflection and tilting due to lateral pressure.

The base slab thickness can also be chosen similar to that of the stem thickness but in any case should not be less than about 300 mm. Due to lateral pressure, the retaining wall will deflect a small amount at the top. Moreover, unless it rests on rock foundation, it will tilt or lean a small distance away from the soil, due to the compressible nature of the supporting soil. Therefore, the front face of the vertical stem wall should have

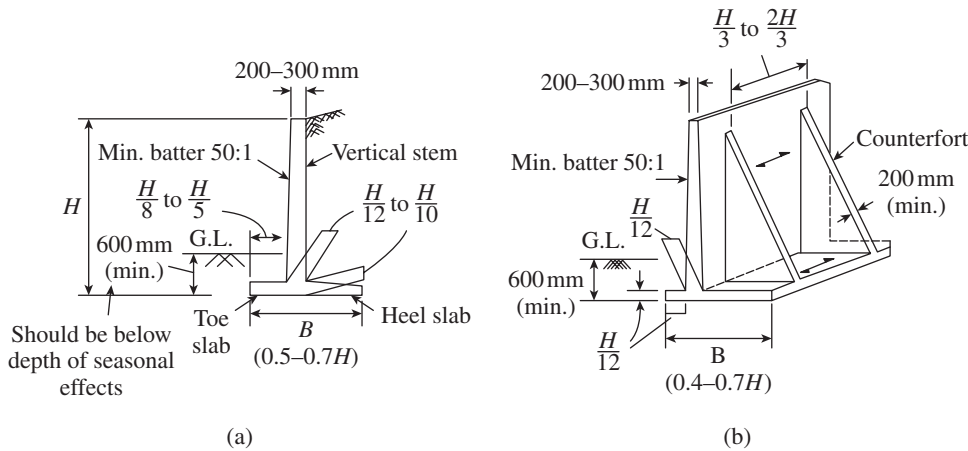


FIG. 16.16 Common proportions of retaining walls (a) Cantilever-retaining wall (b) Counterfort-retaining wall

Source: Teng 1983

a batter, or inclination of 1:50, so that the deformations are not obvious to the passer-by (see Fig. 16.16). Different depths may be chosen for the toe slab and the heel slab; if the depth of the heel or toe slab is excessive, the slab may be tapered.

For walls of moderate height, the counterforts may be spaced at a c/c distance of about one-third to two-thirds of the total wall height (see Fig. 16.16b). For walls higher than about 9 m, the spacing may be reduced to less than one-half the height. From a construction point of view, counterforts should not be placed at spacing less than about 2.5 m. The thickness of counterforts may be chosen as 200–300 mm (about 1/16th of the height of the wall). Sometimes, buttresses are provided below the ground level, interconnecting the toe slab with the lower portion of the vertical stem slab. They may have the same thickness and spacing as those of counterforts. The counterforts enable the designer to reduce the vertical stem and heel slab thickness, which can be chosen as $0.05H-0.08H$. When buttresses are provided over the toe slab, the toe slab thickness can also be chosen as $0.05H$. In some cases, a *shear key* is included to increase resistance to sliding, as shown in Fig. 16.8(f). The shear key is generally an extension of the vertical stem and extends below the bottom of the base. The proportioning shown in Fig. 16.16 is based on the walls constructed successfully. They are usually conservative.

Donkada and Menon (2012) performed parametric studies to establish ‘heuristic’ rules for proportioning retaining wall dimensions and proposed the following for the optimal length of heel slab:

$$\text{Heel slab length} = H \sqrt{\frac{K_a}{3}} \quad (16.24)$$

They also found that cantilevered walls are cost effective than counterfort walls even when the height of the walls exceeds 8 m. For tall walls, the most cost-effective solution was provided by retaining walls with relieving platforms as shown

in Fig. 16.17. The optimal length of the relieving platform, L_{rp} , was found to be

$$L_{rp} = 0.33H \tan \left(\frac{\pi}{4} - \frac{\phi}{2} \right) \quad (16.25)$$

where H is the height of the retaining wall and ϕ the angle of friction of backfill.

Donkada and Menon (2012) also provided a table for selecting the optimal wall or slab thicknesses of cantilever, counterfort, and cantilever walls with two relieving platforms, for three different values of safe bearing capacity (SBC).

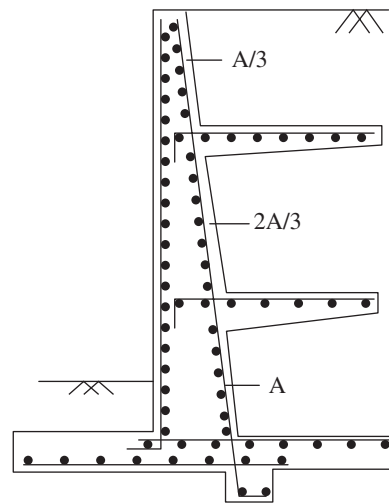


FIG. 16.17 Cantilever-retaining walls with relieving platforms

16.4.5 Drainage and Compaction of Backfill

One of the most important aspects of designing and constructing retaining walls is the prevention of water accumulation behind the walls. When water accumulates in the backfill, it considerably increases the lateral pressure acting on the wall; in cold climates, the situation may become worse due to frost action. If no drainage is provided in the backfill, water percolates through the backfill in the downward direction, continues under the base of the retaining wall, and rises through the soil in front of the wall. The seepage of water will increase the weight of the soil due to saturation or partial saturation, reduce the passive resistance in the front face of the wall, and lessen the resistance to sliding, and may tend to uplift the base of the wall. Many failures have occurred in the past due to the improper provision of drainage behind the retaining walls. Such failures can easily be prevented by using a well-drained and cohesionless soil for the backfill.

In general, it is more economical to make provisions for reducing the seepage pressure than designing the retaining wall for the water pressure. This can be done by using granular backfill and providing weep holes at the bottom of the retaining wall (see Figs 16.8j and 16.18). Granular backfill material offers the benefits of good drainage, easy compaction, and increased sliding resistance. For large walls, weep holes of diameter 100 mm or more are common (larger sizes are easy to clean). For uniform drainage, adequate spacing between weep holes should be provided (normal spacing is about 1.5–3 m horizontally and vertically). Filter fabric material should be used between the wall and the backfill to prevent fines migration, clogging of weep holes, loss of backfill, and caving. Water draining through weep holes may cause softening of the soil under the toe slab where the soil pressure is the highest, which may become unsightly. A better method includes the use of 150–200 mm diameter perforated pipes often wrapped in geo-textile or buried in a granular filter bed running along the heel slab, as shown in Fig. 16.8(j), and serve to carry water to the weep holes. Sometimes, the surface of the backfill (up to a distance greater than the width of the heel slab) may also be paved with non-porous material such as asphalt to divert the water away from the backfill.

It is common practice to compact the backfill in layers. This kind of compaction may increase the lateral pressure due to the heavy weight of compaction equipment. To avoid this, the compaction work adjacent to the retaining wall (within an area approximately equal to the sliding wedge) should be done with lightweight tampers.

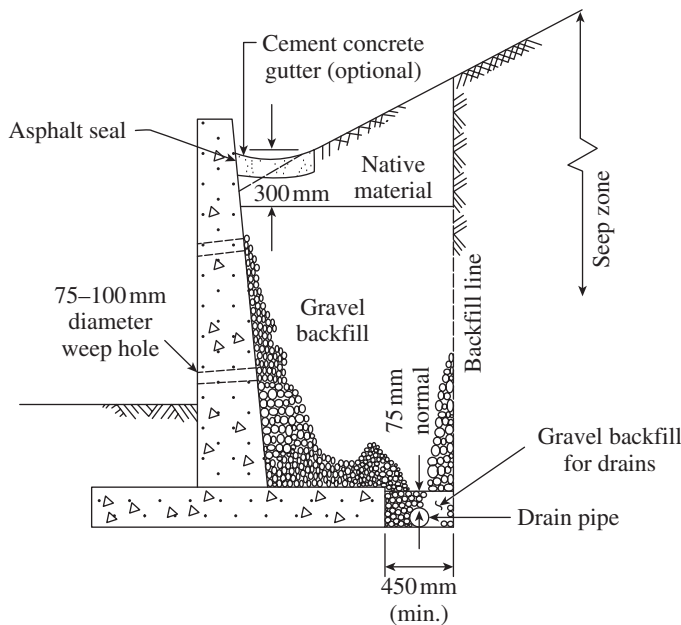


FIG. 16.18 Drainage of backfill

16.4.6 Stability Requirements

The retaining wall should satisfy stability requirements of overturning and sliding, in addition to strength and serviceability.

Overturning and sliding are checked at service load conditions, whereas design of stem, toe, and heel slabs are done using limit state design.

Stability Against Overturning

As already discussed in Section 15.4 of Chapter 15, the factor of safety against sliding and overturning as per Clause 20 of IS 456 should be greater than 1.4 (many other codes and authors suggest that the factor of safety should be greater than 2.0). When the stabilizing forces are mainly due to dead loads, the code suggests using only 0.9 times the characteristic dead loads, while calculating the factor of safety. While making the computations, the backfill on the toe slab is usually neglected, as it may get eroded in due course.

The retaining wall will overturn due to the earth pressure, with a point at the edge of the toe slab acting as the centre of rotation. Considering a sloping backfill as shown in Fig. 16.11, the overturning moment about the bottom edge of the toe slab, M_o , may be calculated as

$$M_o = \frac{(P_a \cos \delta)H'}{3} = \frac{K_a \gamma (H')^3}{6} \cos \delta \quad (16.26a)$$

The restoring (stabilizing) moment about the bottom edge of the toe slab, M_r , provided by the self-weight of the retaining wall and the earth resting on the heel slab is calculated as

$$M_r = \sum W(B-x) + (P_a \sin \delta)B \quad (16.26b)$$

where B is the width of base slab, W is the weight of each component, and x is its distance from the tip of toe.

For the case of level backfill with surcharge, the overturning moment is given by (see Fig. 16.12)

$$M_o = P_a \left(\frac{H}{2} \right) + P_{a1} \left(\frac{H}{3} \right) \quad (16.27)$$

where P_a and P_{a1} are given by Eqs (16.17a) and (16.17b), respectively.

The factor of safety for overturning is given by

$$FS_{(\text{overturning})} = \frac{0.9M_r}{M_o} \geq 1.4 \quad (16.28)$$

Stability Against Sliding

Consideration of sliding is very important for retaining walls, as a large percentage of retaining wall failures have occurred due to sliding (McCormac and Brown 2013). The retaining wall has the tendency to slide under the action of the horizontal component of active earth pressure, which is resisted essentially by the frictional force acting at the base of the retaining wall and the passive earth pressure. The passive earth pressure is generally small, especially when the height of earth at the front of the retaining wall is small and hence is often neglected and the unfactored loads are used.

Considering a sloping backfill as shown in Fig. 16.11, the factor of safety against sliding is given by

$$FS_{(\text{sliding})} = \frac{\mu(0.9 \sum W + P_a \sin \delta)}{P_a \cos \delta} \geq 1.4 \quad (16.29a)$$

where μ is the coefficient of friction between soil and the concrete base slab—its value may be assumed as 0.55 for coarse-grained soil without silt, 0.45 for coarse-grained soil with silt, 0.35 for silt, and 0.60 for rough rock surface (Teng 1983), W is the weight of each component of wall and soil above the heel slab, $P_a \sin \delta$ is the vertical component of active earth pressure, and $P_a \cos \delta$ is the horizontal component of active earth pressure.

For retaining walls with horizontal backfill and surcharge (Fig. 16.12), the active earth pressure acts in the horizontal direction and hence the factor of safety against sliding is given by

$$FS_{(\text{sliding})} = \frac{\mu(0.9 \sum W)}{P_a + P_{a1}} \geq 1.4 \quad (16.29b)$$

When the value of the active earth pressure is high, especially when there is surcharge, the frictional resistance alone will not provide the required factor of safety against sliding. In such cases, it is advantageous to provide a shear key, as shown in Fig. 16.19, projecting below the base of footing in line with the vertical stem slab (at least 125–150 mm in front of the back face of the stem), and extending throughout the length of the wall. From a soil mechanics point of view, keys are more effective when placed at the end of the heel slab. Another common practice is to widen the footing on the heel side (McCormac and Brown 2013). The shear key will develop considerable passive resistance if the concrete in the shear key and toe slab is placed against the undisturbed soil, without the use of vertical forms. Hence, the shear key should not be placed in front of the toe slab, where the soil is likely to be disturbed. If the soil is soft or purely granular, the sides of the key should have a slope of 1 vertical to at least 1.5 horizontal (Teng 1983). Many designers select the size of keys by rules of thumb. One such rule is to provide a depth of key between two-thirds to full depth of the footing slab (McCormac and Brown 2013).

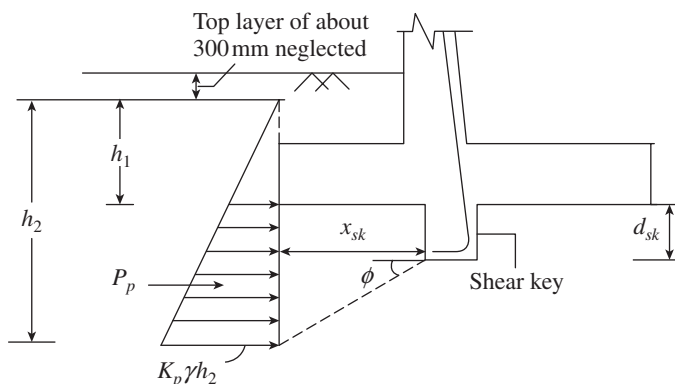


FIG. 16.19 Passive pressure due to shear key

The provision of shear key results in additional resistance to sliding due to the development of passive pressure in front of the retaining wall. A conservative estimate of passive pressure can be made by considering the passive pressure developed over a height $h_2 - h_1$, below the toe slab as shown in Fig. 16.19, and is given by

$$P_p = \frac{K_p \gamma}{2} (h_1 + d_{sk} + x_{sk} \tan \phi)^2 - \frac{K_p \gamma}{2} (h_1)^2 \quad (16.30)$$

Now the factor of safety against sliding is given by

$$FS_{(\text{sliding})} = \frac{\mu(0.9 \sum W + P_a \sin \delta) + P_p}{P_a \cos \delta} \geq 1.4 \quad (16.31)$$

The top 300 mm of soil below the ground level is usually ignored in the calculation of passive pressure.

16.4.7 Soil Bearing Pressure Requirements

The width of the base slab, B , should be chosen in such a way that it distributes the vertical reaction from the retaining wall to the foundation soil without excessive settlement or rotation. As explained in Section 15.3 of Chapter 15, the resultant reaction should be checked to lie within the middle third of the base. The calculated maximum pressure below the base slab should not exceed the SBC of the soil and the minimum pressure should not be negative. The minimum and maximum pressures are calculated as

$$q_{\max} = \frac{\sum W}{B} \left(1 + \frac{6e}{B} \right) \leq \text{SBC} \quad (16.32a)$$

$$q_{\min} = \frac{\sum W}{B} \left(1 - \frac{6e}{B} \right) \geq 0.0 \quad (16.32b)$$

where the eccentricity e is calculated by taking moments of all the weights from the end of heel as

$$e = \frac{\sum M + M_o}{\sum W} - \frac{B}{2} \leq B/6 \quad (16.32c)$$

The designer should also ensure that the tilting of the footing is avoided in weak soils by proportioning the base slab in such a way that more or less uniform pressure is present below the base slab.

16.4.8 Procedure for Design

The design of cantilever or counterfort-retaining walls consists of the following steps:

1. Calculate the depth of foundation, D_f , based on Rankine's formula given by

$$D_f = \frac{q_a}{\gamma_e} \left(\frac{1 - \sin \phi'}{1 + \sin \phi'} \right)^2 \quad (16.33)$$

where q_a is the SBC of soil in kN/m^2 , γ_e is the unit weight of soil in kN/m^3 , and ϕ' is the angle of repose of soil [for well-drained sand or gravel backfills, the angle of repose, ϕ' , is approximately equal to the angle of internal friction, ϕ ; recently, a relation was derived for sands by Ghazavi, et al. (2008) as $\phi' = 0.36\phi + 21.2$]. The minimum depth of foundation should be 600 mm (see Section 16.4.4). In the case of expansive soils, the chosen depth of foundation should be below the seasonal volume changes, say at about 3.5–4 m.

2. Select initial sizes for the stem, heel, and toe slabs as well as counterforts, if any, as discussed in Section 16.4.4.
3. Calculate the weight of various elements and soil on heel slab, active pressure of soil, and moments due to these forces acting on the retaining wall. It is advantageous to calculate them in a tabular format to minimize possible errors.
4. Calculate soil pressure below base slab as per Section 16.4.7. It should not exceed the SBC of the soil and no tension should be developed in the soil. If these conditions are not satisfied, the base slab dimensions should be modified and the calculations in steps 3 and 4 should be repeated until they are satisfied.
5. Check for safety against overturning as per Section 16.4.6. The factor of safety against overturning should be at least 1.4; otherwise, the dimensions of the retaining wall should be modified and the calculations in steps 3 and 5 should be repeated until they are satisfied.
6. Check for safety against sliding as per Section 16.4.6. The factor of safety against sliding should be at least 1.4; otherwise, a shear key may be provided.
7. Design the toe, heel, and stem slabs. Calculate the bending moment and shear force acting on these elements. Provide sufficient depth and reinforcements to resist these moments and shear forces (see also Section 16.4.9).
8. Design the counterfort and the interface between the counterfort and the stem and heel slab. If the retaining wall has counterforts, design the counterfort wall as a T-beam and provide the required depth and reinforcement. In addition, design vertical ties at the connection between the counterfort and the vertical slab as well as between the counterfort and the heel slab for tension (see also Section 16.4.10).
9. Detail the construction joints. Vertical or horizontal *construction joints* are to be provided between two successive pours of concrete. Keys are used to increase the shear resistance at the joint (see Fig. 16.20a). The keyway is normally formed by pushing a bevelled timber into the

top of the footing slab when it is cast; after the concrete hardens, the wooden member is removed and when the stem is cast over it, the keyway is formed. If keys are not used, the surface of the footing slab is roughened and cleaned, and the concrete for the stem wall is placed over it. This practice is found to be as satisfactory as the use of keyway (McCormac and Brown 2013).

10. Provide expansion and contraction joints in the retaining wall. If the length of the retaining wall exceeds 30–45 m, *vertical expansion joints* are to be incorporated into the wall to account for expansion due to temperature changes. They completely separate the different parts of a retaining wall. The spacing of such joints would depend upon the temperature variation, exposure to weather, and the conditions while laying the concrete. These joints may be filled with 12–20 mm thick flexible joint fillers (see Fig. 16.20b). Reinforcing bars are generally run through the joints so that vertical and horizontal alignments are maintained. When the bars pass through a joint, one end of the bars on one side of the joint is greased or sheathed so that the desired expansion takes place smoothly (McCormac and Brown 2013). A rough value for the width of an expansion joint can be determined using Eq. (3.27) of Chapter 3.

Contraction joints are weakened places provided in the retaining wall so that shrinkage cracks will occur at prepared locations. These are vertical joints or grooves formed or cut into the wall (see Fig. 16.20c); they are constructed using rubber strips that are left in place or with wooden strips that are later removed and may be replaced by caulking. In addition to handling shrinkage problems, contraction joints are useful in mitigating differential settlements. Contraction joints are usually about 6 mm wide and about 12–20 mm deep and are provided at intervals of 7.5–10 m.

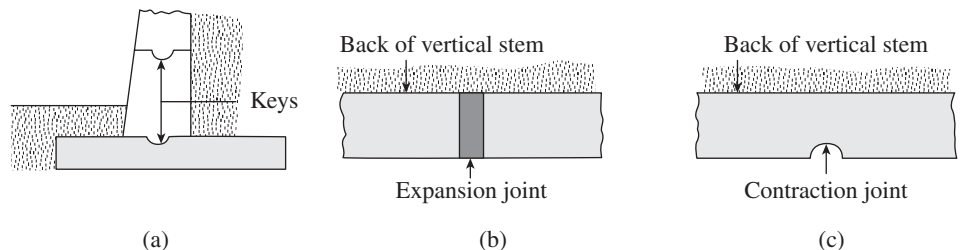


FIG. 16.20 Joints in retaining walls (a) Construction (b) Expansion (c) Contraction

16.4.9 Behaviour and Design of Cantilever-retaining Walls

The design of a cantilever-retaining wall involves the design of the stem, toe, and heel slabs, which essentially act as cantilever slabs. Limit state design is used for the design, and a load factor of 1.5 is assumed as per the IS code.

Design of Vertical Stem Slab

The stem slab acts as a cantilever when subjected to lateral earth pressure. The critical section for maximum bending moment is at the junction of the stem and the base slab. The critical section for shear force may be taken at a distance d from the top of the base slab, where d is the effective depth of the stem slab. However, shear may not be critical in the stem as in the base slab. The assumed thickness should be checked and reinforcement calculated. For high and heavily loaded walls, greater thickness of concrete may be economical. The moment in the stem causes tension on the inside face, where the earth is retained, and hence, flexural reinforcement should be provided in this face (see Fig. 16.21c). The thickness and reinforcement can be reduced proportionately over the height. A cover of 50 mm may be provided for these reinforcements, and the reinforcement may be curtailed in stages (usually at one-third and two-thirds height) to achieve economy. It is better not to curtail all the bars at the same location (see Section 7.7.1 of Chapter 7). Clause 26.2.3 of IS 456 requires that the bars cut off must be continued for a distance of at least $12d_b$ (where d_b is the diameter of bar) or the effective depth, d , beyond their theoretical cut-off points and must also meet the necessary development length requirements (see Section 7.8.1 of Chapter 7). Temperature reinforcement ($A_{st,min} = 0.12\%$ of gross cross-sectional area) is provided transverse to the main reinforcement. Nominal reinforcement should be provided in the vertical and horizontal directions near the front face, which is exposed to the atmosphere.

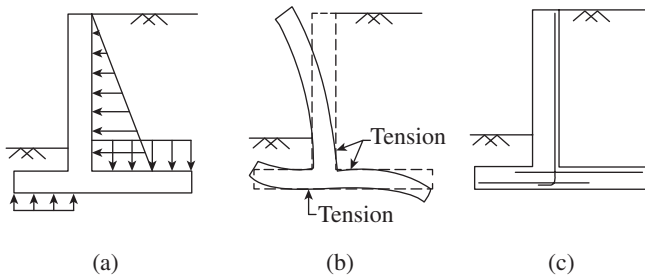


FIG. 16.21 Behaviour of cantilever-retaining wall (a) Loads on stem, toe, and heel slabs (b) Deflected shape (c) Location of main reinforcement

Design of Base Slab

The various forces acting on the wall are the earth pressure, weight of earth supported on heel, weight of stem, and weight of base slab; weight of earth on toe, if any, is neglected.

The toe slab acts as a cantilever from the front face of the vertical stem slab. It is subjected to upward pressure from the soil and the self-weight acting downwards (see Fig. 16.21a). The downward load of earth on the toe slab is usually neglected. The net loading acts upwards, similar to normal footings. The critical section for bending moment occurs at the face of the

stem whereas the critical section for shear force occurs at a distance d from the face of stem, where d is the effective depth of toe slab. The assumed thickness has to be checked for adequacy and the required steel should be calculated. A cover of 75 mm may be provided and the reinforcements are placed near the bottom of the toe slab (see Fig. 16.21c). Different thicknesses may be adopted for the toe slab and the heel slab.

The heel slab also acts like a cantilever. The lateral earth pressure tends to cause the retaining wall to rotate about its toe. This action tends to push the heel slab into the backfill, making the weight of the backfill on the heel slab to push it down. Thus, the heel slab is subjected to upward pressure from the soil and the downward loads due to self-weight and earth above the heel. The bending moment due to the downward loads is more than that due to the upward loads and causes tension at the top of the slab (see Fig. 16.21a). Since the upward soil pressure is relatively small compared to the downward loads, many designers choose to neglect it (McCormac and Brown 2013). The maximum bending moment and shear force occurs at the junction of the heel and the stem, for which adequate thickness and steel have to be provided. Steel is placed near the upper face of the heel slab. Minimum reinforcement, as applicable to beam (Clause 26.5.1.1 of IS 456), should also be checked. The required development length of these main bars is 1.3 times the normal development length to take care of the 'top-bar' effect (see Section 7.4.2 of Chapter 7).

It has to be noted that the critical section for shear in the heel slab is taken at the face of the support and *not* at a distance d away from it. It is because the reaction in the direction of shear does not introduce compression into the heel part of the footing in the region of the stem, and the possible crack may extend ahead of the rear face of the stem slab (see Fig. 6.27d of Chapter 6). This shear may control the thickness and reinforcement of the heel slab. It has to be noted that as the load is due to soil and concrete, a load factor as applicable to dead loads can be applied. As IS 456 uses a load factor of 1.5 for both dead load and imposed load, the load factor of 1.5 is used in the computations.

16.4.10 Behaviour and Design of Counterfort-retaining Walls

The design of counterfort-retaining walls involves the design of the vertical stem, toe, and heel slabs and the design of counterforts. As mentioned earlier, counterforts tie the footing and vertical stem together. The heel slab and the vertical stem span horizontally between these counterforts. Thus, the stem and heel slabs are designed as continuous slabs supported over counterforts. The sizes of the concrete components and the steel reinforcement will be reduced considerably, as the bending moments are less than those occurring in cantilever-retaining walls.

Design of Heel, Toe, and Stem Slabs

Each panel of the stem and heel slab between two adjacent counterforts may be designed as two-way slabs fixed on three edges and free on the fourth side. These boundary conditions are also applicable to the toe slab if buttresses are provided; otherwise, the toe slab is designed as a cantilever slab as in a cantilever-retaining wall. The loads acting on these elements are identical to those acting on cantilever-retaining walls.

Bending moment coefficients for slabs fixed on three edges and free on one edge subjected to uniformly distributed load and triangular load are available from the theory of plates. Critical bending moment locations are indicated in Figs 16.22(a) and (b) for the uniformly distributed loading case and the triangularly distributed loading case, respectively. The critical moment coefficients for these two loading cases are shown in Tables 16.6 and 16.7, respectively. The magnitudes of these bending moments are maximum at the middle of the fixed edges.

The loads acting on the heel or toe slab can be divided into uniformly and triangularly distributed loads. The bending moments at the critical locations on the slab caused by uniformly distributed loads are given as

$$M = \alpha_i w L^2 \tag{16.34}$$

where α_i is the bending moment coefficient at the i th location, w is the uniformly distributed load, L is the clear span between the fixed edges, and $i = 1, 2, 3,$ and 4 are locations, and the directions are as marked in Fig. 16.22(a).

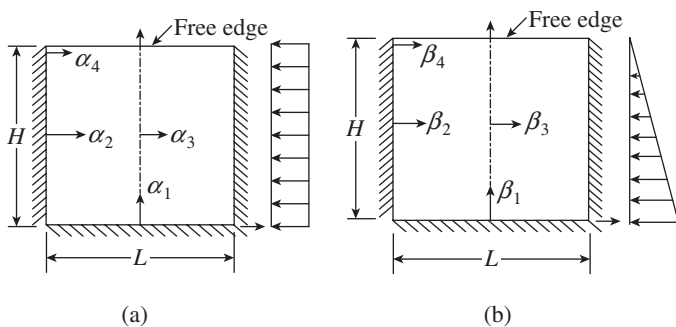


FIG. 16.22 Moment coefficients for three-sided fixed slab (a) Uniformly distributed load (b) Triangularly distributed load

The bending moments at the critical locations on the slab caused by triangularly distributed loads are given as

$$M = \beta_i w L^2 \tag{16.34}$$

where β_i is the bending moment coefficient at the i th location, w is the uniformly distributed load, L is the clear span between the fixed edges, and $i = 1, 2, 3,$ and 4 are locations, and the directions are as marked in Fig. 16.22(b). Using these

coefficients, the bending moments may be calculated and the required thickness and reinforcements are computed. It has to be noted that an approximate and conservative estimate of the bending moments can also be obtained by treating the slabs as one-way continuous slabs spanning between the counterforts.

TABLE 16.6 Bending moment coefficients in plates with three fixed edges and uniformly distributed loads (see Fig. 16.22a)

H/L	$y = 0$ and $x = 0$	$y = H/2$ and $x = \pm L/2$	$y = H/2$ and $x = 0$	$y = H$ and $x = \pm L/2$
0.6	-0.055	-0.037	0.017	-0.075
0.7	-0.054	-0.044	0.021	-0.078
0.8	-0.053	-0.051	0.025	-0.081
0.9	-0.052	-0.056	0.029	-0.084
1.0	-0.051	-0.061	0.032	-0.085
1.25	-0.047	-0.071	0.037	-0.087
1.50	-0.042	-0.076	0.040	-0.084
2.0	-0.040	-0.083	0.041	-0.083

Source: Timoshenko and Woinowsky-Krieger, 1959

TABLE 16.7 Bending moment coefficients in plates with three fixed edges and triangularly distributed loads (see Fig. 16.22b)

H/L	$y = 0$ and $x = 0$	$y = H/2$ and $x = \pm L/2$	$y = H/2$ and $x = 0$	$y = H$ and $x = \pm L/2$
0.6	-0.024	-0.013	0.006	0.0
0.7	-0.026	-0.017	0.008	0.0
0.8	-0.028	-0.021	0.010	0.0
0.9	-0.029	-0.024	0.012	0.0
1.0	-0.030	-0.027	0.014	0.0
1.25	-0.031	-0.033	0.017	0.0
1.50	-0.029	-0.037	0.019	0.0
2.0	-0.029	-0.040	0.021	0.0

Source: Timoshenko and Woinowsky-Krieger, 1959

In the vertical stem slab, the bending moment in the horizontal direction between counterforts will generally be more than the bending moment in the vertical direction. The behaviour of various elements of counterfort-retaining wall is shown in Fig. 16.23. The deflected shape of the stem slab in the horizontal direction is shown in Fig. 16.23(b). Hence, the main reinforcement has to be placed close to the rear face of the stem near the counterforts (for the negative moment); in between the counterforts, the reinforcement has to be placed close to the front face as shown in Fig. 16.23(b). The vertical section through the heel slab shows the deflected shape in Fig. 16.23(c). Due to this behaviour, the main reinforcement has to be placed at the top of the heel slab near the counterforts; in between the counterforts, it has to be placed at the bottom of the heel slab as shown in Fig. 16.23(c).

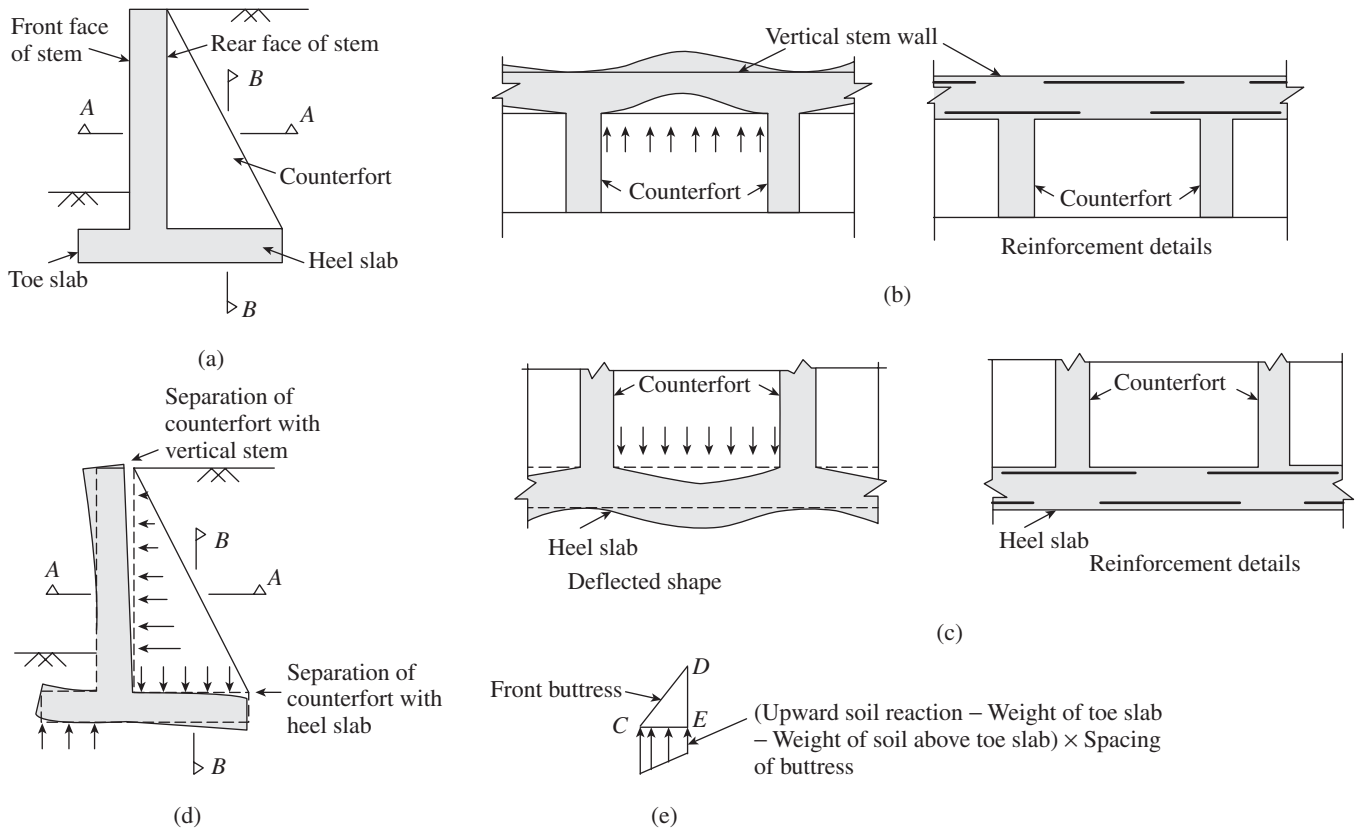


FIG. 16.23 Behaviour of counterfort-retaining walls (a) Counterfort-retaining wall (b) Horizontal section of vertical stem wall (Section A–A) (c) Vertical section through heel slab (Section B–B) (d) Counterfort interface with stem and heel slabs (e) Forces on toe buttress (if provided)

Design of Counterforts

The counterforts act as a cantilever beam. They are designed for active earth pressure for the load from the stem portion between the adjacent counterforts. As the stem acts integrally with the counterfort, the counterfort can be designed as T-beams, with the depth of the section varying linearly from the top (free edge) to the bottom (fixed edge). This produces tension on the inclined side of the counterfort and compression in the flange of the counterfort (stem). Therefore, main steel has to be provided on the inclined face of the counterfort. Since the reinforcement bars are inclined and not parallel to the compression face, this has to be considered while computing the required area of steel.

The stem will have a tendency to separate itself from the counterforts due to the action of the earth pressure. Similarly, the downward load acting on the heel slab will tend to separate it from the counterfort. These actions are shown in Fig. 16.23(d). Hence, the counterfort should be secured firmly to the vertical stem and heel slab. This is achieved by providing vertical and horizontal ties in the counterfort, which are anchored in the heel slab and stem, respectively. These ties will be in tension.

Sometimes, buttresses are also provided in the toe portions to reduce the thickness of the toe slab. The front buttress is subjected to the forces as shown in Fig. 16.23(e), which

consist of the self-weight of the toe slab and the weight of soil above the toe slab acting downwards and the soil reaction on the toe slab between two buttresses acting upwards. It is designed as a cantilever beam. The bending moment and shear force for carrying out the design is obtained at section D–E. The main reinforcement has to be provided at the bottom. The section is checked for shear and end anchorage.

Buttress-retaining Wall

It has to be noted that the behaviour of the buttress-retaining wall, as shown in Fig. 16.8(h), is similar to that of counterfort-retaining wall. The vertical stem and the toe slab can be designed as continuous slab supported by buttresses. The heel slab behaves like a cantilever slab with fixity at the junction between the heel slab and vertical stem. The buttresses are more efficient than counterforts because they act as compression members due to the active earth pressure acting on the vertical stem, whereas as we discussed earlier, counterforts are subjected to tension and need to be tied carefully with the stem wall and heel slab with stirrups. Occasionally, high walls are designed with both buttresses and counterforts.

16.4.11 Bridge Abutments or Basement Walls

For abutments such as rigid frame abutments or propped abutments, which do not deflect sufficiently to create an active wedge in the backfill soil, the lateral earth pressure

distributions as shown in Fig. 16.24 may be considered and the governing distribution should be used. In addition, live load surcharge effects should also be considered.

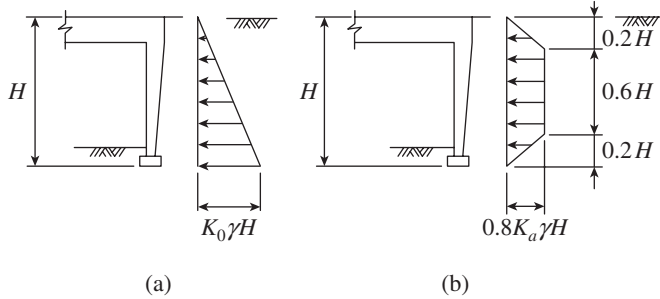


FIG. 16.24 Lateral earth pressure distribution for bridge abutment (a) Case 1 (b) Case 2

In the case of basement wall as well, the top and bottom of the wall is restrained by the ground floor slab and the slab below basement, respectively (see Fig. 2.9e of Chapter 2). The wall will be subjected to lateral earth pressure at rest and vertical load from the superstructure. The lateral restraint provided by the two slabs at the top and bottom may be considered as simply supported. The two pressure distributions as shown in Fig. 16.24 should be considered and the controlling distribution should be used in the design. Thus, the maximum bending moment will be at the mid-span.

The initial dimensions of the wall may be determined similar to that of a cantilever-retaining wall. The base slab behaves similar to the base slab of a cantilever-retaining wall.

16.5 STRUCTURAL WALLS

For tall buildings, it is necessary to provide adequate stiffness to resist the lateral loads caused by wind or earthquake, so that the deflections are within limits. When these buildings are not properly designed for the lateral loads, they may be subjected to very high stresses, vibrations, and side sway, which could damage the buildings severely and may also cause considerable discomfort to their occupants.

When RC walls with very large in-plane stiffness are placed as shown in Fig. 16.25, they provide the needed resistance to the lateral loads, have the ability to dampen vibration, and keep the lateral drift within limits. Such walls, often called *shear walls*, generally act as deep vertical cantilever beams and resist the in-plane shears and bending moments caused by lateral loads in the plane of the walls and also carry vertical gravity loads, thus providing lateral stability to the structure. As these walls predominantly exhibit flexural deformations and their strength is normally controlled by their flexural resistance, their name is a misnomer, although they are provided with shear reinforcement to prevent diagonal tension failures. Hence, they are referred to as *structural walls* in ACI 318 and also in this book, and sometimes as *flexural walls*. They have large strength and high stiffness and provide greater

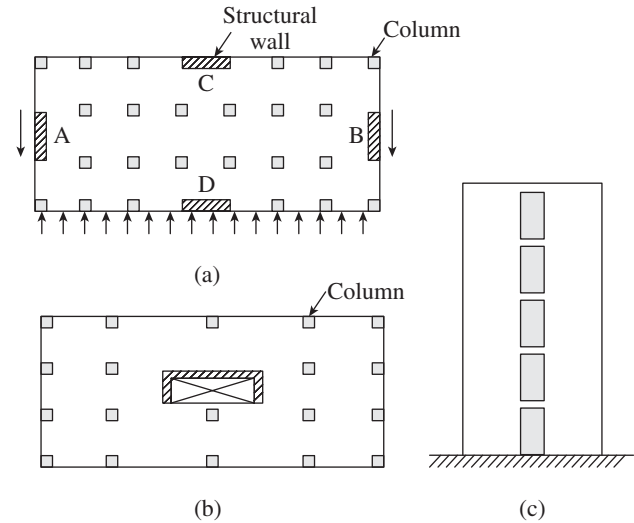


FIG. 16.25 Types of structural walls (a) Rectangular shear walls (b) Structural wall around elevators and stairwells (c) Coupled structural walls

ductility than RC framed buildings. Fintel (1991), based on his observation of collapsed buildings during several earthquakes throughout the world since 1963, concluded that structural walls exhibit extremely good earthquake performance [it is interesting to note that the R value, which signifies the ductility provided by the system, for ductile structural walls (designed as per IS 13920) is given as 4.0 in Table 7 of IS 1893(Part1):2002, whereas for special RC moment-resisting frame (SMRF) it is 5.0; only ductile shear wall with SMRF has $R = 5.0$].

When a building has structural walls, it can be modelled in STAAD using *surface elements*. The modelling can be done using a single surface element or a combination of surface elements. The use of the surface element enables the designer to treat the entire wall as one entity. It greatly simplifies the modelling of the wall and adds clarity to the analysis and design output. The results are presented by STAAD in the context of the entire wall rather than individual finite elements, thereby allowing users to quickly locate required information. The relative stiffness to be considered in the analysis is discussed in Section 4.5.1 of Chapter 4. More information on the modelling of structural walls are presented by Agarwal and Shrikhande (2006), Dharanidaran and Sengupta (2012), Paulay and Priestley (1992), and Smith and Coull (1991).

16.5.1 Types of Structural Walls

As discussed in Section 2.5.2 of Chapter 2, structural walls can be constructed in a variety of shapes such as rectangular, T-, C-, or L-shaped, circular, curvilinear, or box type. When the flanges of T-, C-, or L-shaped walls are in compression, they exhibit large ductility; however, T- and L-section walls have only limited ductility when the flange is in tension. The structural

walls must be provided symmetrically along the length and width of the building, as shown in Figs 16.25(a) and (b), to avoid torsional stresses and better performance during earthquakes. If the wall is provided in only one direction, a proper moment-resisting frame must be provided in the other direction. Structural walls should also be continuous throughout the height (also see Section 3.8.3 and Fig. 3.11 of Chapter 3 and Fig. 13.33 of Chapter 13). They are more effective when located along the exterior perimeter of a building but need not extend over the full width of the building (see Fig. 16.25a). They may be used to enclose stairwells, elevators, or toilets, as shown in Fig. 16.25(b); even in this case, it is better to locate them symmetrically. It is to be noted that such an arrangement of walls in the interior of a building may not be as effective as the walls located on the periphery of the building; however, because of the box shape they provide torsional resistance during earthquakes.

In many situations, it is not possible to use structural walls without some openings in them for doors, windows, and service ducts. Such openings should be placed in one or more vertical and symmetrical rows in the walls throughout the height of the structure, as shown in Fig. 16.25(c). The walls on either side of the opening are interconnected by short deep beams called *coupling beams* or *link beams*. Such walls are called *coupled structural walls*. Walls with openings arranged in a regular and rational pattern have very good energy dissipation characteristics. Because of their low span-to-depth ratio, typically between one and four, the short beams require special detailing requirements to ensure adequate deformation capacity during earthquakes (more discussions on coupled structural walls are provided in Section 16.5.5). Undesirable forms for earthquake-resistant structural walls and the failure of third floor columns due to large openings in the shear wall of Macuto-Sheraton hotel in Venezuela during the 1967 Caracas earthquake are discussed by Park and Paulay (1975). A rational approach to the design of walls with significant irregular openings is provided by Paulay and Priestley (1992).

Boundary elements are portions along the wall edges that are strengthened by longitudinal and transverse reinforcements. They may have the same thickness as that of the walls, as shown in Fig. 16.26(a), though it is advantageous to provide them with greater thickness as shown in Fig. 16.26(b). The increased thickness boundary elements are also known as *barbells*. The increased thickness gives sufficient space for the concentrated vertical reinforcement, which is tied like a column and also helps to prevent buckling of flanges. When structural walls have webs and flanges that act together to form H-, C-, T-, and L-shaped wall cross sections, they are known as wall assemblies; Fig. 16.26(c) shows a H-type structural wall.

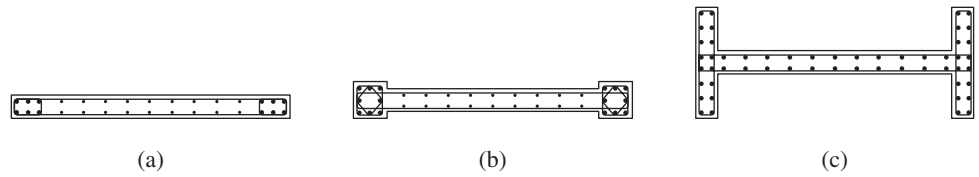


FIG. 16.26 Structural walls with boundary elements (a) Rectangular wall—boundary element has the same thickness as the wall (b) Rectangular wall with enlarged boundary element (c) Flanged wall

The shape of the cross section, coupled with the distribution of steel in the section, influences the flexural capacity of the structural wall.

Clause 9.4.1 of IS 13920 stipulates that boundary elements should be provided when the extreme fibre compressive stress in the wall due to factored gravity loads plus factored earthquake force exceeds $0.2f_{ck}$. Clause 21.9.6.2 of ACI 318 suggests a condition based on displacement-based approach to determine whether boundary elements are required [see also Moehle (1992) and Wallace and Orakcal (2002)]. In regions subjected to earthquakes, Clause 9.1.3 of IS 13920 limits the effective flange widths to be used in the design of flanged walls to the smaller of the following:

1. Half the distance to an adjacent structural wall web
2. One-tenth of the total wall height (ACI Clause 21.9.5.2 allows 25% of total wall height)

Clause 9.1.3 also suggests that boundary elements may be discontinued when the calculated compressive stresses are less than $0.15f_{ck}$.

16.5.2 Behaviour of Structural Walls

The behaviour of walls will depend on their geometry. Based on the geometry, walls may be classified as *squat walls* (with $H_w/L_w < 2$), *intermediate walls* (with $2 < H_w/L_w < 3$), and *slender* or *cantilever walls* (with $H_w/L_w > 3$). Slender and squat/intermediate walls are shown in Fig. 16.27. Squat walls are generally dominated by shear, whereas in slender walls lateral loads are resisted mainly by flexural action; when the

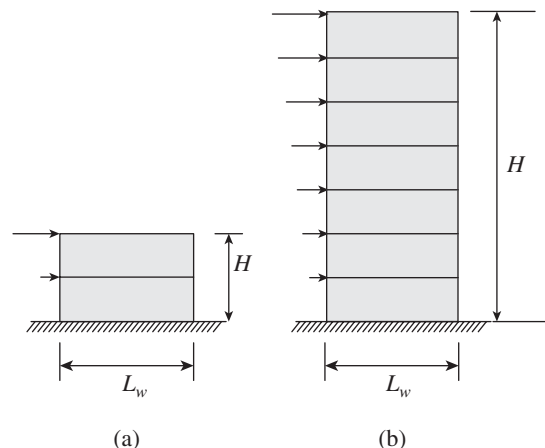


FIG. 16.27 Classification based on H_w/L_w (a) Squat/Intermediate wall (b) Cantilever wall

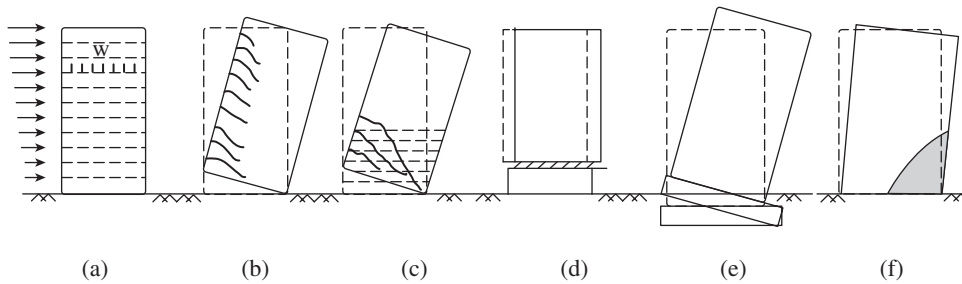


FIG. 16.28 Failure modes in cantilever walls (a) Wall (b) Flexural tension (c) Flexural shear (d) Sliding (e) Overturning (f) Flexural compression

value of H_w/L_w is between two and three, the walls exhibit a combination of shear and flexural behaviour.

Five basic modes of failure are possible in slender walls. They are shown in Fig. 16.28 and are listed as follows (Paulay and Priestley 1992; Rohit, et al. 2011):

1. Ductile flexural tension failure with yielding of vertical steel as shown in Fig. 16.28(b)
2. Flexural shear failure with diagonal shear cracks in the web of wall as shown in Fig. 16.28(c)
3. Horizontal sliding failure near wall foundation interface or at a construction joint as shown in Fig. 16.28(d)
4. Overturning (stability) failure as shown in Fig. 16.28(e)
5. Flexural compression failure with the crushing of concrete at the bottom regions of the wall as shown in Fig. 16.28(f)

Brittle failure mechanisms or even those with limited ductility should not be permitted to occur. The observed hysteretic behaviour of well-detailed structural walls is similar to that of beams. However, shear deformations in the plastic hinge regions of a cantilever wall may be significantly larger than in other predominantly elastic regions (Paulay and Priestley 1992).

Squat walls are generally governed by their shear strength. They are usually subjected to high nominal shear stress. The possible failure modes of a squat shear wall are shown in Fig. 16.29 (Paulay, et al. 1982; Paulay and Priestley 1992). They are listed as follows:

1. When adequate horizontal reinforcement is not provided, diagonal tension failure occurs, along a diagonal crack, as

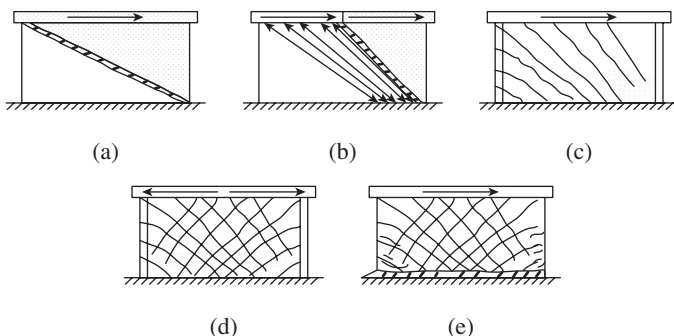


FIG. 16.29 Shear failure modes of squat structural walls (a) and (b) Diagonal tension (c) and (d) Diagonal compression (e) Sliding shear

shown in Fig. 16.29(a). It has to be noted that for slender walls ($H_w/L_w \geq 2.0$) only horizontal reinforcement needs to be provided (as for beams and columns), and only nominal vertical bars are required. However, in squat walls, vertical shear reinforcement is also necessary for the development of truss mechanism.

2. As seen in Fig. 16.29(b), diagonal tension failure may also develop

along a steeper failure plane. If a path is available to transfer the shear force to the rest of the wall, such a diagonal crack may not result in failure (Paulay and Priestley 1992). A tie beam, provided at the top of the wall, will distribute the shear force along the top edge and minimize diagonal tension. In addition, it will enhance force transfer more efficiently to the foundation by diagonal compression.

3. When shear reinforcement is adequate, a diagonal compression failure may occur as shown in Fig. 16.29(c). It results in the crushing of concrete compression struts in the web of the wall. As mentioned earlier while discussing slender walls, the web crushing failure may occur in walls with boundary elements (columns or flanges) subjected to high level of shear stress.
4. The compressive strength of these struts is drastically reduced under cyclic loading, since inclined cracks in two directions develop as shown in Fig. 16.29(d). This mode of failure can be avoided if the average shear stress in the wall's critical section is limited to a range $0.45\sqrt{f_{ck}}$ to $0.8\sqrt{f_{ck}}$, depending on the ductility requirements imposed on the wall (Park and Paulay 1975).
5. Another failure mode of squat walls is due to horizontal sliding shear, associated with low levels of axial load and high levels of shear stress, and is shown in Fig. 16.29(e). This shear failure mode occurs at the wall–foundation interface and is similar to that observed in beams subjected to high levels of cyclic shear.

Squat structural walls under reverse cycling loads generally have relatively poor energy dissipation characteristics, showing pinched hysteresis loops, and experience significant stiffness degradation and possible sudden loss in lateral capacity (Paulay, et al. 1982; Gulec, et al. 2009). Gulec, et al. (2009) compared the shear strengths of 217 squat shear walls with boundary elements available in the literature with the equations given in ACI 318 and ASCE/SEI 43-05 as well as those proposed by Barda, et al. (1977) and Wood (1990). They concluded that the effect of barbells and flanges on the ultimate shear strength of squat walls is significant and none of the equations evaluated by them takes into account

the presence of these elements. The equation by Wood (1990) provided a conservative estimate of shear strength. Gulec and Whittaker (2011) proposed an empirical equation for predicting the peak shear strength of symmetrical shear-critical squat structural walls with boundary elements.

Interaction of Structural Walls and Rigid Jointed Frames

In buildings of moderate height, frame–wall interactions may be neglected, since walls are stiff enough to attract the majority of the effects from lateral loads. Thus, the frame can be considered as non-sway frames. However, frame–wall interactions must be considered for high-rise structures, where the walls have significant effect on the frame. Fig. 16.30 shows a cantilever structural wall and a frame, both carrying the same load at a certain height. The structural wall suffers bending distortions and assumes a constant slope above the loaded level. The originally horizontal sections at each floor tilt. The moment-resisting frame mainly experiences translator displacements and tends to become vertical above the load level.

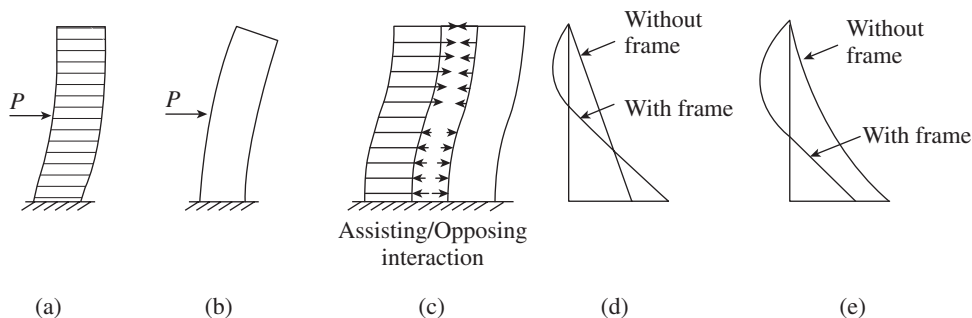


FIG. 16.30 Wall–Frame interaction (a) Frame shear mode (b) Wall flexural mode (c) Interaction of wall and frame (d) Shear force (e) Bending moments

When wall shortening is neglected, the floor remains horizontal. Due to the incompatibility of displacements, a shear wall can oppose a moment-resisting frame at the upper floors. Only at the lower floors do these two structures assist each other in carrying the external load. Thus, in upper storeys, the frame must resist more than 100 per cent of the storey shear caused by the lateral loads. Neglecting frame–wall interactions will not be conservative at these levels. In addition, a more economical solution will be obtained when frame–wall interactions are considered. As mentioned previously, the FEM-based computer programs may be used to access the interaction of structural walls and moment-resisting frames. More details about the modelling, behaviour, and design of dual systems may be found in the work of Paulay and Priestley (1992).

Normally, the floor slabs of multi-storey buildings act as horizontal diaphragms and provide lateral support; hence, the critical height with respect to buckling will be equal to the floor height. Paulay and Priestley (1993), based on observed responses in tests of rectangular structural walls, have given recommendations for the prediction of the onset of

out-of-plane buckling. Information on critical loads for axially loaded walls is also provided by Wight and MacGregor (2009).

It is also necessary to have adequate foundation for giving full fixity and sufficient connection of structural wall at each floor, so that the horizontal loads are transmitted properly to the walls. Sometimes, the foundation of structural walls may not be anchored adequately. This will limit the lateral load capacity of the wall to its overturning capacity. Such walls may ‘rock’ on their foundation during severe ground shaking. The importance of modelling rocking of structural wall foundations as a means of energy dissipation has also been discussed by Pauley and Priestley (1992), who acknowledge that the satisfactory response of some structures in earthquakes can be attributed only to foundation rocking. Rocking may be avoided by providing tension piles below footings. Wyllie (1987) and Pauley and Priestley (1992) provide more information on wall foundations.

16.5.3 Design of Structural Walls

As discussed in Section 16.5.2, different reinforcement requirements are necessary for squat and cantilever walls

to ensure diagonal tension failure in squat walls and flexural tensile failures in cantilever walls. (It has to be noted that contrary to slender walls, inelastic response in shear rather than flexural yielding provides ductility in squat walls.) A ductile failure mode is achieved by providing a shear capacity that is greater than the flexural capacity of the wall. Clause 9.1.2 of IS 13920:1993 suggests that the thickness of any part of the wall should not be less than 150 mm.

In case of coupled structural walls, it is preferable to have a minimum thickness of 200 mm. The wall thickness and cover may be governed by the fire code requirements.

Flexural Strength

Traditionally, walls are provided with 0.25 per cent of reinforcement in both directions. Naturally, such an arrangement does not efficiently utilize steel because many bars operate on relatively small internal lever arm. Moreover, the ultimate curvature, hence the curvature ductility, is considerably reduced when a large amount of flexural reinforcement is provided in this fashion, as shown in Fig. 16.31 (Cardenas and Magura 1973). It is clearly seen from this figure that uniform steel distribution across the section is not only uneconomical but highly undesirable for larger steel contents wherever energy absorption in post-elastic range is required (in earthquake zones).

When the structural walls are subjected to considerable moments, greater efficiency is achieved when the bulk of the

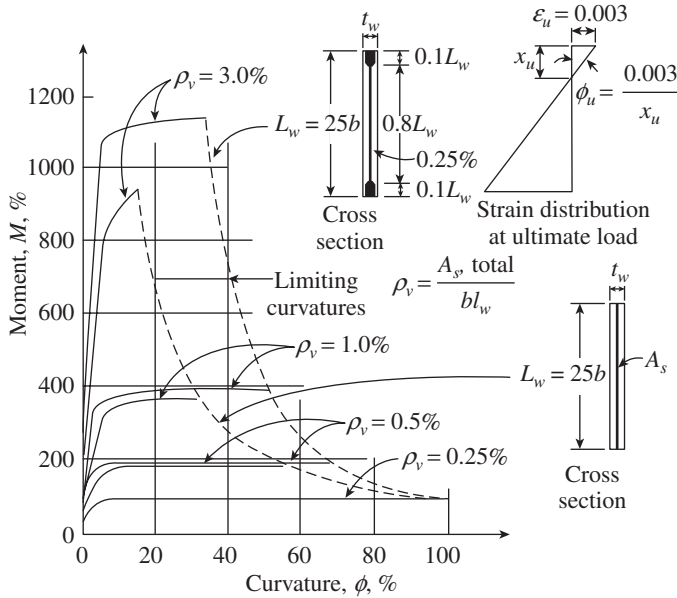


FIG. 16.31 Effect of amount and distribution of vertical reinforcement on ultimate curvature

Source: Cardenas and Magura 1973, reprinted with permission from ACI

flexural reinforcement is placed close to the tensile edge, as in columns. During earthquakes or wind loads, moment reversals occur and hence equal reinforcements are to be provided at both extremities. In the sections with non-uniform steel distribution as shown in Fig. 16.31, minimum vertical reinforcement of 0.25 per cent steel has been placed over the inner 80 per cent of the depth and the remainder of steel is provided in the outer (10%) zones of the cross section. The increased strength and ductility due to this arrangement is self-evident from this figure.

Because of the larger cross-sectional area, the axial compressive load on structural wall is often considerably smaller than what would cause a balanced failure condition. As a result, moment capacity is usually increased by gravity forces inducing axial compression. However, it should be remembered that axial compression reduces ductility (Park and Paulay 1975).

The flexural strength of slender rectangular structural wall sections containing uniformly distributed vertical reinforcement and subjected to axial and lateral load can be derived by using the same assumptions as for RC beams. The stress-strain curve is assumed for concrete as per IS 456, whereas that of steel is assumed to be bilinear (as shown in Figs 5.4 and 5.5(a) of Chapter 5).

In addition, the following assumptions are made while deriving the expressions for flexural strength:

1. Instead of using discrete reinforcement bars, an equivalent thin steel plate is considered, distributed uniformly throughout the section.
2. When the neutral axis is within the section, the maximum strain in the extreme fibre of concrete in compression is 0.0035.

Two types of flexural failures may take place in this section: (a) *Flexural tension failure* takes place when the tension steel yields prior to crushing of concrete in the extreme compression fibre. (b) *Flexural compression failure* takes place when tension steel does not yield while the concrete crushes in the extreme compression fibre (Medhekar and Jain 1993).

Flexural tension failure The assumed strain distribution for a rectangular wall subjected to combined uniaxial bending and axial load is as shown in Fig. 16.32.

The various forces and their lever arm with respect to the bottom fibre are given in Table 16.8 (Medhekar and Jain 1993).

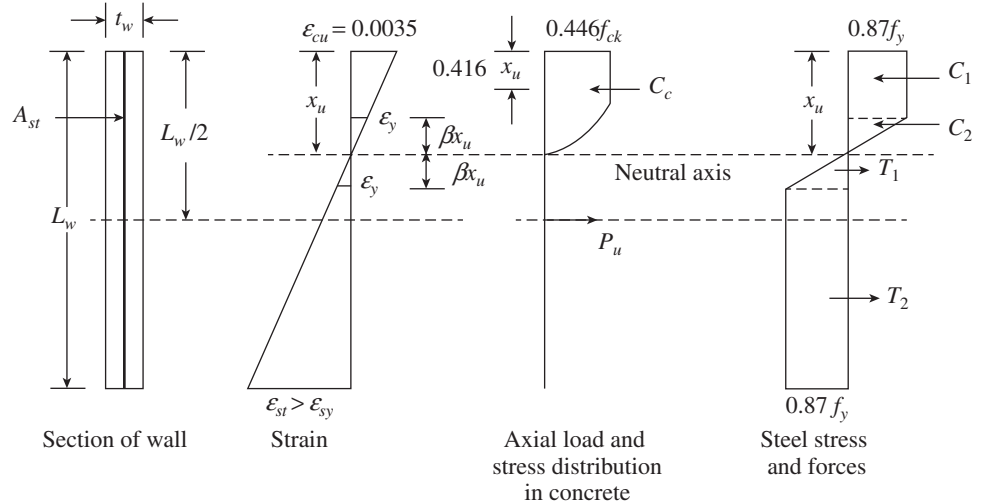


FIG. 16.32 Stress-Strain distribution in structural wall (flexural tension failure)

TABLE 16.8 Forces and their lever arms for the wall section shown in Fig. 16.32

Force	Lever Arm from the Bottom Fibre
$C_c = 0.36f_{ck}x_u t_w j680$	$L_w - 0.416x_u$
$C_1 = 0.87f_y t_w \rho x_u (1 - \beta)$	$L_w - 0.5x_u (1 - \beta)$
$C_2 = 0.435f_y t_w \rho x_u \beta$	$L_w - x_u \left(1 - \frac{2}{3}\beta\right)$
$T_1 = 0.435f_y t_w \rho x_u \beta$	$L_w - x_u \left(1 + \frac{2}{3}\beta\right)$

(Continued)

TABLE 16.8 (Continued)

Force	Lever Arm from the Bottom Fibre
$T_2 = 0.87f_y t_w \rho [L_w - x_u(1 + \beta)]$	$0.5[L_w - x_u(1 + \beta)]$
P_u	$0.5L_w$

Note: f_{ck} is the characteristic strength of concrete, f_y is the yield stress of reinforcement, L_w is the horizontal length of wall in plan, t_w is the thickness of wall, x_u is the depth of neutral axis from extreme compression fibre, ρ is the vertical reinforcement ratio = $A_{st}/(t_w L_w)$, A_{st} is the area of uniformly distributed vertical reinforcement, $\beta = \frac{0.87f_y}{0.0035E_s}$, E_s is the elastic modulus of steel, and P_u is the axial compressive load on wall.

The depth of the neutral axis may be found by equating the tensile and compressive forces. Thus, we have

$$C_c + C_1 + C_2 = T_1 + T_2 + P_u \quad (16.35)$$

Substituting the necessary expressions from Table 16.8 into this equation yields

$$\frac{x_u}{L_w} = \left(\frac{\phi + \lambda}{2\phi + 0.36} \right) \quad (16.36a)$$

where
$$\phi = \left(\frac{0.87f_y \rho}{f_{ck}} \right) \quad (16.36b)$$

and
$$\lambda = \left(\frac{P_u}{f_{ck} t_w L_w} \right) \quad (16.36c)$$

By taking moment of all the forces about the bottom fibre of the section, the moment capacity of the section is obtained as

$$\frac{M_n}{f_{ck} t_w L_w^2} = \phi \left[\left(1 + \frac{\lambda}{\phi} \right) \left(0.5 - 0.416 \frac{x_u}{L_w} \right) - \left(\frac{x_u}{L_w} \right)^2 \left(0.168 \frac{\beta^3}{3} \right) \right] \quad (16.37)$$

This equation is valid when the non-dimensional depth of neutral axis $\frac{x_u}{L_w}$ is less than the

critical non-dimensional depth of neutral axis, $\frac{x_u^*}{L_w}$, where

$$\frac{x_u^*}{L_w} = \frac{0.0035}{0.0035 + \frac{0.87f_y}{E_s}} \quad (16.38)$$

When $\frac{x_u}{L_w} < 0.5$, the term containing $\left(\frac{x_u}{L_w} \right)^2$ in Eq. (16.37) may be neglected for simplicity without introducing any significant error (Medhekar and Jain 1993)

Flexural compression failure For this condition, the strain in the tension steel at the extreme fibre will be less than the yield strain. Hence, the tension steel does not yield. As a result, the contribution of force T_2 should not be considered in the analysis. The strain distribution in concrete and the stress distribution in steel and concrete for this case are shown in Fig. 16.33. The non-dimensional neutral axis $\frac{x_u}{L_w}$ lies between the critical non-dimensional depth of neutral axis $\frac{x_u^*}{L_w}$ and unity.

The depth of neutral axis may be found by equating the tensile and compressive forces. Thus, we have

$$C_c + C_1 + C_2 = T_1 + P_u \quad (16.39)$$

Substituting the necessary expressions from Table 16.8 into this equation yields

$$\alpha_1 \left(\frac{x_u}{L_w} \right)^2 + \alpha_2 \left(\frac{x_u}{L_w} \right) - \alpha_3 = 0 \quad (16.40a)$$

where
$$\alpha_1 = \left[0.36 + \phi \left(1 - \frac{\beta}{2} - \frac{1}{2\beta} \right) \right] \quad (16.40b)$$

$$\alpha_2 = \left(\frac{\phi}{\beta} - \lambda \right) \quad (16.40c)$$

and
$$\alpha_3 = \left(\frac{\phi}{2\beta} \right) \quad (16.40d)$$

The quadratic equation given in Eq. (16.40a) should be solved to get the value of $\frac{x_u}{L_w}$.

By taking moment of all the forces about the bottom fibre of the section, the moment capacity of the section is obtained as

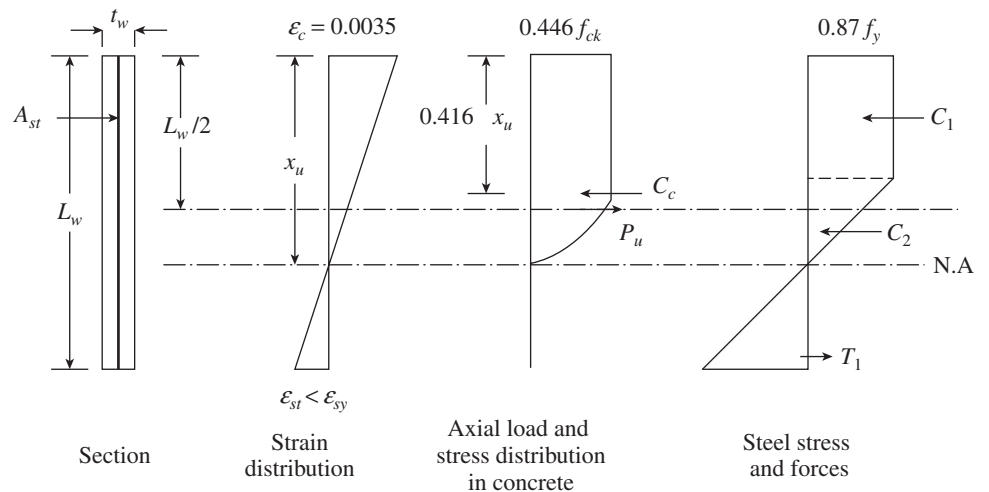


FIG. 16.33 Stress–Strain distribution in structural wall (flexural compression failure)

$$\frac{M_n}{f_{ck}t_wL_w^2} = \alpha_1 \left(\frac{x_u}{L_w} \right) - \alpha_4 \left(\frac{x_u}{L_w} \right)^2 - \alpha_5 - \frac{\lambda}{2} \quad (16.41a)$$

$$\text{where} \quad \alpha_4 = 0.15 + \frac{\varphi}{2} \left(1 - \beta + \frac{\beta^3}{3} - \frac{1}{3\beta} \right) \quad (16.41b)$$

$$\text{and} \quad \alpha_5 = \frac{\varphi}{6\beta} \left[\frac{1}{(x_u/L_w)} - 3 \right] \quad (16.41c)$$

These equations are provided in Annex A of IS 13920:1993. It has to be noted that there is a small error in the expression for α_4 in IS 13920, which has been corrected in Eq. (16.41b). The term $+\beta^3/3$ is given as $-\beta^2/2$ in IS 13920. In addition, Rohit, et al. (2012, 2013) point out that the limiting strain in steel should be taken as $0.002 + 0.87f_y/E_s$ and not just as $0.87f_y/E_s$ to achieve the desired ductility. Hence, the values of β and x_u^*/L_w in the earlier equations should be taken as

$$\beta = \frac{0.0020 + 0.87f_y/E_s}{0.0035}$$

$$\frac{x_u^*}{L_w} = \frac{0.0035}{0.0035 + \left(0.0020 + \frac{0.87f_y}{E_s} \right)} \quad (16.38a)$$

Using slightly different assumptions, and using a rectangular stress block, Cardenas and his colleagues developed simpler expressions for calculating the neutral axis and nominal moment strength of structural walls (Cardenas and Magura 1973; Cardenas, et al. 1973). Wight and MacGregor (2009) point out that for all structural walls, the neutral axis depth, calculated by using these expressions, will be less than $0.375d_w$ and hence the wall will always be tension controlled. Moment–Axial force interaction diagrams, similar to that discussed in Chapter 13 for columns, can be generated (Park and Paulay 1975; Paulay and Priestley 1992).

Wight and MacGregor (2009) suggest that when the rectangular walls contain boundary elements or enlarged barbells, vertical reinforcement in the web can be ignored because their contribution to M_n will be quite small compared to the contribution from the vertical reinforcement concentrated at the edge of the walls. They also show that the compression stress block in this case will normally be contained within the boundary element and derive simple expressions for M_n .

The instability of the wall section may be improved by increasing the flexural rigidity of the wall by providing wall returns as shown in Fig. 16.34. Such returns may be necessary between the ground and first floors of a building, where there will be maximum moments and axial loads. Paulay and Priestley (1992) presented a method for computing

the required reinforcement in flanged wall sections (see Fig. 16.26c). An equivalent eccentricity method is presented by Wight and MacGregor (2009) to compute the moment strength of biaxially loaded walls.

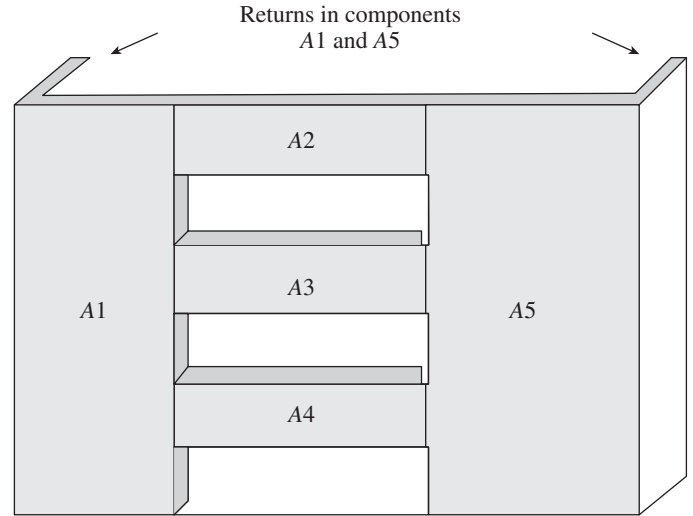


FIG. 16.34 Wall returns to increase stability

Shear Strength Requirements

The design basis for structural walls has the same general form as that used for ordinary beams:

$$V_u \leq V_n \quad (16.42a)$$

where

$$V_n = V_c + V_s = \tau_c t_w d_w + \frac{0.87f_y A_h d_w}{s_v} \quad (16.42b)$$

where V_u is the factored shear force and V_n is the nominal shear capacity of the section, V_c is the shear strength of concrete, V_s is the shear strength of steel reinforcement, A_h is the area of horizontal shear reinforcement, s_v is the spacing of horizontal reinforcement, τ_c is the design shear strength of concrete, and t_w and d_w are the thickness and effective depth of structural wall, respectively.

As per Clause 9.2 of IS 13920, the nominal shear stress, τ_v , should be calculated by

$$\tau_v = \frac{V_u}{t_w d_w} \quad (16.43)$$

where t_w is the thickness of the web of the structural wall and d_w is the effective depth of wall section. This may be taken as $0.8L_w$ for rectangular sections.

The design shear strength of concrete, τ_c , can be calculated based on Table 19 of IS 456:200. It has to be noted that as per Clause 40.2.2 of IS 456, for members subjected to axial compressive load, P_u , the design shear strength can be increased by the following factor:

$$\delta = 1 + \frac{3P_u}{A_g f_{ck}} \quad (16.44)$$

where A_g is the gross area of the concrete section. However, for structural walls, Medhekar and Jain (1993) suggest that only 80 per cent of the factored axial compressive load should be considered effective, due to the possible effect of vertical acceleration.

The nominal shear stress, τ_v , should not exceed the maximum shear stress, $\tau_{c,max}$ ($\approx 0.63\sqrt{f_{ck}}$), given in Table 20 of IS 456:2000 [based on tests by Cardenas et al. (1973), Clause 21.9.4.5 ACI 318 restricts the maximum shear stress to $0.75\sqrt{f_{ck}}$]. When τ_v is greater than τ_c but less than $\tau_{c,max}$, horizontal shear reinforcement has to be provided. The area of such reinforcement, A_h , with a vertical spacing of s_v is given by

$$V_s = \frac{0.87f_y A_h d_w}{s_v} \quad (16.45)$$

where $V_s = (V_u - \tau_c t_w d_w)$ is the shear force to be resisted by the horizontal reinforcement. It has to be noted that the horizontal reinforcement should not be less than the minimum specified in Clause 9.1.4 of IS 13920 (0.25% of gross area).

Shear reinforcement for structural walls always consists of evenly distributed vertical and horizontal reinforcement. In many cases, the inclination of shear cracks in walls with respect to a horizontal line will be less than 45° , and hence, the vertical reinforcement will be as effective as the horizontal reinforcement. Experimental results showed that for long and low structural walls, vertical web reinforcement will be more effective in enabling diagonal compression struts to form (Barda, et al. 1977). Hence, in walls with H_w/L_w less than 0.5, the ACI code requires that the vertical (longitudinal) web steel, ρ_t , should be equal to the amount of horizontal shear reinforcement (this is similar to Clause 9.2.6 of IS 13920). For structural walls having H_w/L_w ratios between 0.5 and 2.5, a linear interpolation is suggested between this steel and the minimum of 0.25 per cent, giving (see Clause 11.9.9.4 of ACI 318)

$$\rho_t = 0.0025 + 0.5 \left(2.5 - \frac{H_w}{L_w} \right) (\rho_t - 0.0025) \quad (16.46)$$

For walls with $H_w/L_w \geq 2.5$, this equation will not govern. In shorter walls where the horizontal wall percentage, ρ_t , exceeds 0.0025, the value of ρ_t , calculated using Eq. (16.46), need not exceed the amount of horizontal reinforcement required for shear strength. Rohit, et al. (2011) have compared the Indian, American, and New Zealand code provisions and based on that proposed minimum reinforcement ratios in vertical and horizontal directions of walls for three H_w/L_w ratios, namely $H_w/L_w < 1$, $1 \leq H_w/L_w \leq 2$, and $H_w/L_w > 2.0$.

It has to be noted that the equations given in ACI 318 can be used for calculating the nominal shear strength, V_n . The two equations given in Clause 11.9.6 are to be used for designing walls resisting lateral wind loads and the equation given in Clause 21.9.4 should be used when the wall is subjected to

lateral earthquake forces. The equation given in the latter clause alone is considered here and is of the form

$$V_n = A_{cv} (\alpha_c \lambda \sqrt{f'_c} + \eta \rho_t f_y) \leq 0.6 A_{cv} \sqrt{f_{ck}} \quad (16.47)$$

where A_{cv} is the width of the web of wall t_w , multiplied by the total length of the wall L_w . The first term represents the concrete contribution to shear strength, V_c . The coefficient α_c represents the difference between the expected occurrence of flexure-shear cracking in slender walls and web-shear cracking in short walls. The value of α_c is taken as 2.0 for walls with $H_w/L_w \geq 2.0$ and 3.0 for walls with $H_w/L_w \leq 1.5$. A linear variation for the value of α_c is to be used for walls with H_w/L_w ratios in between 1.5 and 2.0. The second term inside the parenthesis of Eq. (16.47) represents the contribution to shear strength by horizontal reinforcement. The parameter η is introduced by Carrillo and Alcocer (2013) to take care of the type of reinforcement; they suggest $\eta = 0.8$ for deformed bars and 0.7 for welded-wire mesh. Carrillo and Alcocer (2013) also suggest an expression for α_c , based on shake-table tests, which is dependent on M/VL_w . The maximum allowable value for the nominal shear strength, V_n from Eq. (16.47) is limited to $0.6 A_{cv} \sqrt{f_{ck}}$ in Clause 21.9.4.4 of ACI 318.

A review of the code provisions of seismic shear design of RC structural walls was made by Dasgupta, et al. (2003), and they suggested that separate seismic design provisions for slender and squat walls need to be provided in IS 13920. They also proposed improvements to the clauses of IS 13920:1993.

Design of Boundary Elements

The boundary element should have adequate axial load-carrying capacity, similar to short columns, so that it can carry an axial compression equal to the sum of the factored gravity load plus an additional compressive load induced by the seismic forces. Clause 9.4.2 of IS 13920 suggests that this additional compressive load due to seismic forces be calculated as

$$P_{u,add} = \frac{M_u - M_n}{C_w} \quad (16.47)$$

where M_u is the factored design moment on the entire wall section, M_n is the moment of resistance provided by distributed vertical reinforcement across the wall section, and C_w is the c/c distance between the boundary elements. Thus, IS 13920 assumes that the moment capacity of RC structural walls with boundary elements is the sum of the moment capacity of web portion of the wall and that due to the couple produced by the axial capacity of the boundary elements and the lever arm between them. Rohit, et al. (2012) points out that this superposition principle made in IS 13920 leads to gross over-estimation of design moment capacity; they provide alternate expressions for walls with boundary elements.

If the gravity load adds to the strength of the wall, Clause 9.4.3 of IS 13920 suggests taking the load factor as 0.8. A comparison of various codes on seismic design of RC structural walls was made by Dasgupta and Murty (2005) and Dasgupta, et al. (2010); based on these comparisons, they suggested modifications to the clauses of IS 13920:1993. Similarly, Wallace and Moehle (2012) reviewed the performance of structural walls in recent earthquakes as well as in laboratory tests, identified possible shortcomings, and suggested improvements to the ACI 318 provisions.

High-strength Concrete Walls

Current models developed for the shear design of walls cast with normal-strength concrete (NSC) are empirical and cannot be directly used for the design of high-strength concrete (HSC) walls, which are more brittle than NSC. Rangan (1997), Gupta and Rangan (1998), and Farvashany, et al. (2008) provide some understanding of the shear behaviour of HSC walls. Rangan (1997) also developed a simple method for calculating the shear strength of structural HSC walls subjected to in-plane vertical and horizontal loads and provides a numerical example.

The behaviour of NSC and HSC walls subjected to both standard and hydrocarbon fires were studied by Ngo, et al. (2013). They conclude that the thermal behaviour of HSC walls differs significantly from that of NSC walls, with HSC walls having less fire resistance periods—31 minutes—compared to 120 minutes for NSC walls in hydrocarbon fires. They suggest the use of polypropylene fibres in HSC walls, which may increase the fire resistance by 100 per cent.

16.5.4 Detailing of Structural Walls

The reinforcement in a structural wall must be designed in accordance with Clause 9 of IS 13920 and should be provided as follows (see Fig. 16.35):

1. The minimum amount of vertical and horizontal reinforcement should be 0.25 per cent of the gross

concrete area (Clause 9.1.4). This reinforcement should be distributed uniformly across the cross section of the wall. The New Zealand code NZS 3101:2006 stipulates a minimum limit of $0.22\sqrt{f_{ck}}/f_y$ and a maximum limit of $16/f_y$ for the ratio $\rho_l (= A_s/t_w s_v)$ of vertical bars; the upper limit is to reduce congestion of reinforcement.

2. The vertical reinforcement should not be less than the horizontal reinforcement (Clause 9.2.6). Curtailment of flexural reinforcement in cantilever walls is discussed in the work of Paulay and Priestley (1992).
3. When the factored shear stress in the wall exceeds $0.25\sqrt{f_{ck}}$ ($0.15\lambda\sqrt{f_{ck}}$ as per ACI 318:2011) or when the thickness of the wall exceeds 200 mm, reinforcements should be provided in two curtains, each having bars running in the longitudinal and transverse directions (Clause 9.1.5).
4. The diameter of bars used in any part of the wall should not exceed one-tenth of the thickness of the wall (Clause 9.1.6).
5. The maximum spacing of reinforcement in either direction should not exceed the smallest of $L_w/5$, $3t_w$, and 450 mm, where L_w is the horizontal length of wall and t_w is the thickness of wall (Clause 9.1.7).
6. The percentage of vertical reinforcement in the boundary element (with same or greater thickness than the wall) should not be less than 0.8 per cent nor greater than 4 per cent (Clause 9.4.5).
7. When the entire wall section is provided with special confining reinforcement, as per column and given in Clause 7.4.8 of IS 13920, boundary elements need not be provided (Clause 9.4.6).
8. In walls that do not have boundary elements, vertical reinforcement should be concentrated at the ends of the wall; each concentration should consist of a minimum of four 12 mm bars arranged in at least two layers (Clause 9.3.3).
9. When boundary elements are required, they should be provided throughout the height of the wall, with confining

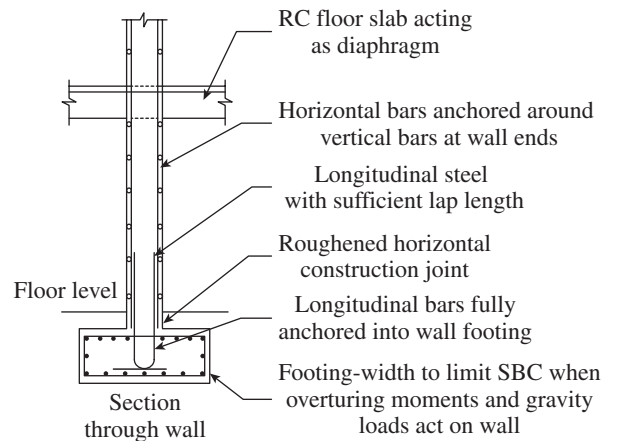
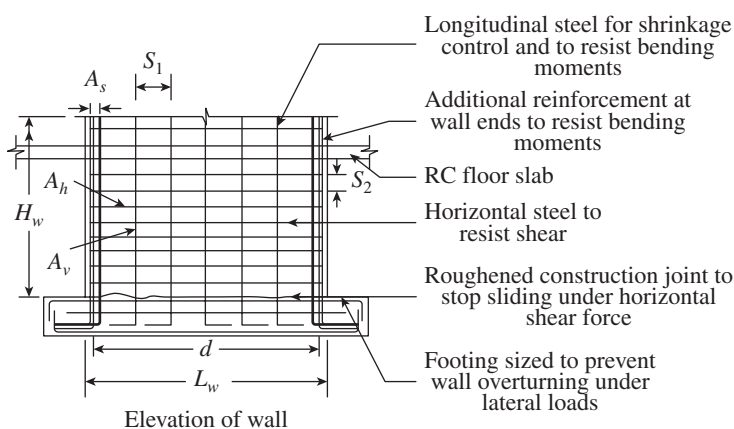


FIG. 16.35 Geometry and reinforcement detailing of typical structural wall

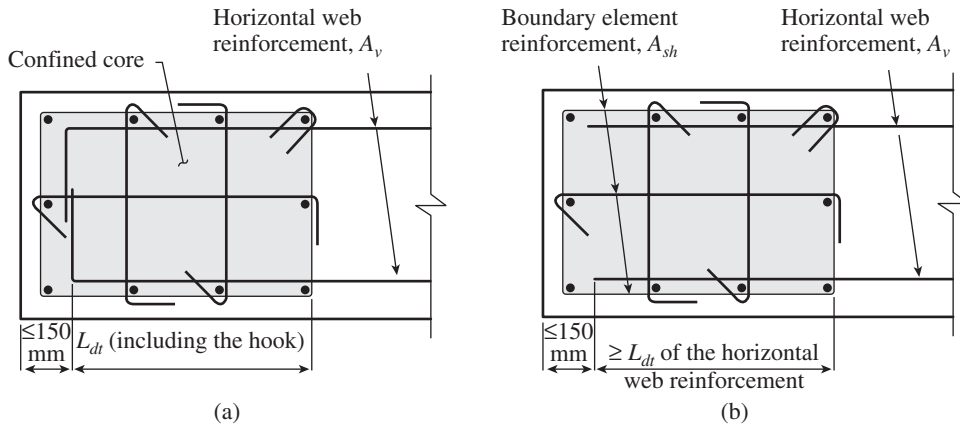


FIG. 16.36 Development of wall horizontal reinforcement in confined boundary element (a) With standard hooks or headed reinforcement (b) With straight bars

Source: ACI 318, reprinted with permission from ACI

reinforcement as per column and given in Clause 7.4.8 of IS 13920 (Clause 9.4.5). The area of cross section, A_{sh} , of the bar forming the rectangular hoop of the special confining reinforcement should not be less than

$$A_{sh} = 0.05sh \frac{f_{ck}}{f_y} \quad (16.48)$$

where h is the longer dimension of the rectangular confining hoop measured to its outer face, and should not exceed 300 mm (see Fig. 7 of IS 13920:1993), and s is the spacing of hoops.

10. Horizontal reinforcement should be anchored near the edges of the wall or in the confined core of the boundary elements, as shown in Fig. 16.36 (Clause 9.9.1 of IS 13920).
11. Splicing of vertical flexural reinforcement should be avoided in plastic hinge regions where yielding may take place. This zone is considered in Clause 9.9.2 to extend to a distance of L_w from the base of the wall or one-sixth the wall height, whichever is larger. However, this height need not be taken greater than $2L_w$. [Bohl and Adebar (2011) proposed an equation for estimating the lower-bound plastic hinge length of isolated walls.] Not more than one-third of the vertical reinforcement should be spliced at such a location. Splices in adjacent bars should be staggered by a minimum of 600 mm.

12. Lateral ties should be provided around lapped spliced bars that are larger than 16 mm in diameter. The diameter of the tie should not be less than one-fourth the diameter of the spliced

bar or 6 mm. The spacing of such ties should be less than 150 mm c/c (Clause 9.9.3 of IS 13920)

13. Welded splices or mechanical connections are allowed by Clause 9.9.4 of IS 13920 and should confirm to Clause 25.2.5.2 of IS 456. When they are used, not more than 50 per cent of the bars should be spliced at a section where flexural yielding of the bars may occur, that is, at plastic hinge locations.

14. Diagonal reinforcements, as shown in Fig. 16.37, may be used in the web of the wall to reduce

shear distortion and to resist sliding shear. Such reinforcement is more effective in squat structural walls. They will also contribute to flexural strength and increase the energy dissipation capacity of walls (Paulay, et al. 1982). More details about the design of diagonal reinforcement may be found in the study of Paulay and Priestley (1992).

Figure 16.38 shows the details of reinforcement in a typical structural wall with and without the boundary element. It also shows reinforcement detailing when single and double curtains are adopted. It should be noted that equal amount of vertical flexural reinforcement should be provided near the left and right edges of the wall to account for reversal of lateral loads, as shown in Figs 16.35 and 16.38. The vertical reinforcement must be firmly anchored in the foundations, as shown in Fig. 16.35, to account for tensile forces due to the overturning moments. Keys or roughened construction joints should be provided at the foundation and wall junction to

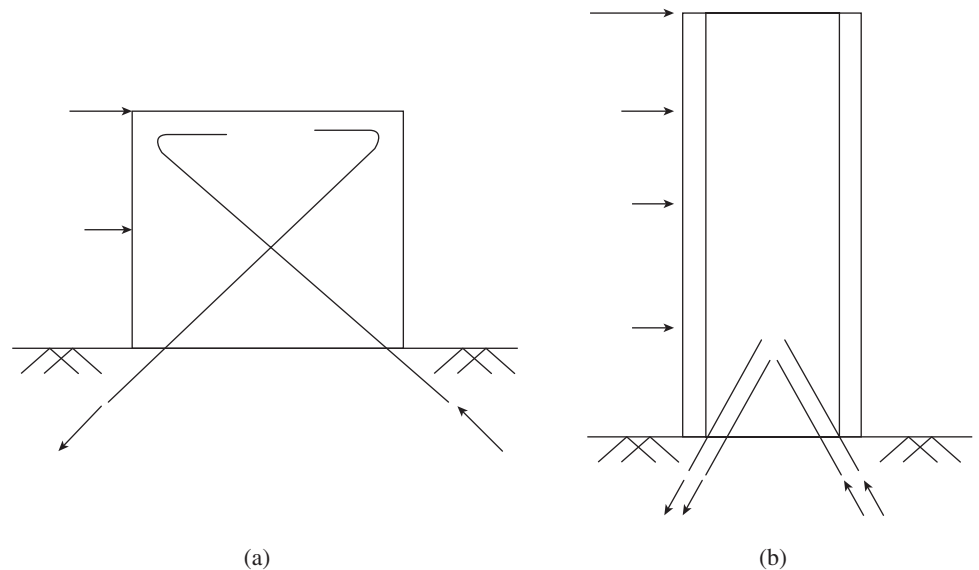


FIG. 16.37 Diagonal reinforcement in walls (a) Squat walls (b) Cantilever walls

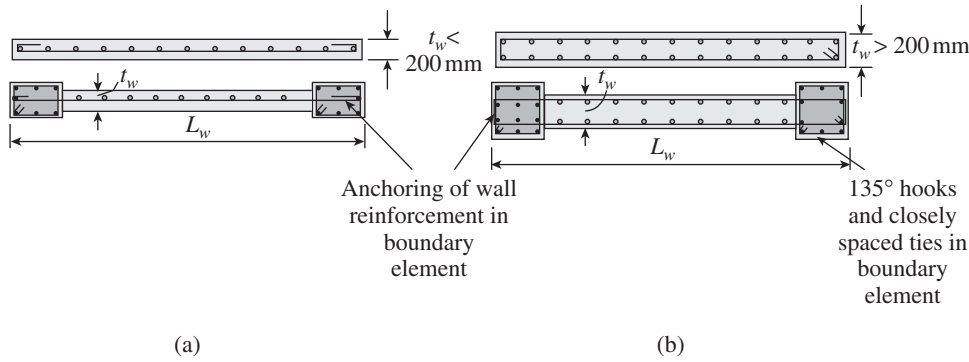


FIG. 16.38 Detailing of walls with and without boundary elements (a) Single curtain of reinforcement (b) Double curtains of reinforcement

resist sliding under horizontal shear force. The foundation of the structural wall should be suitably proportioned such that the SBC of soil is not exceeded and that there is no tension in the underlying soil.

Since the structural walls carry large horizontal earthquake forces, the overturning effects on them are large. Hence, the foundations should be carefully designed and detailed. Double-headed studs can be used to replace hooked cross-ties in structural walls to reduce the congestion of steel (Dilger and Ghali 1997; Mobeen, et al. 2005).

16.5.5 Procedure for Design of Reinforced Concrete Structural Walls

The following are the steps required in the design of rectangular RC structural walls, after the moments, shear force, and axial forces are determined using an FEM-based computer program (the clauses given here pertain to IS 13920:1993):

Step 1 Check whether a boundary element is required. This can be determined by calculating the stress in the wall using the following equation:

$$\text{Stress} = \frac{P_u}{A_g} + \frac{M_u \left(\frac{L_w}{2} \right)}{I} \quad (16.49)$$

where P_u is the factored axial load, M_u is the factored moment acting on the wall, A_g is the gross area of the wall, L_w is the length of wall, and I is the moment of inertia of the wall = $t_w L_w^3 / 12$. When this stress is greater than $0.2f_{ck}$, boundary elements are to be provided (Clause 9.4.1). They may be discontinued when the compressive stress is less than $0.15f_{ck}$. It should be noted that boundary elements need not be provided when the entire wall is provided with special confining reinforcement as per Clause 9.4.6. However, the provision of boundary walls will result in better performance during earthquakes. Clause 21.9.6.4 of ACI 318 suggests that the boundary element should extend horizontally from the extreme compression fibre to a distance not less than the larger of $x_u - 0.1L_w$ and $x_u/2$, where x_u is the neutral axis depth.

Step 2 Check for section requirements of Clause 9.1.2. The thickness of the wall should be greater than 150 mm.

Step 3 Check for minimum reinforcement and maximum spacing as per Clauses 9.1.4–9.1.7. $A_{st,min} = 0.0025t_w L_w$. If the thickness is greater than or equal to 200 mm, reinforcement should be provided in two layers. The maximum allowable spacing is the smallest of $L_w/5$, $3t_w$, and 450 mm. The chosen diameter

of the bar should be less than $t_w/10$. The area of vertical reinforcement in the boundary element should be greater than 0.6 per cent and less than 4 per cent (Clause 9.4.4).

Step 4 Design for shear. Calculate the nominal shear stress, $\tau_v = \frac{V_u}{t_w d_w}$, where $d_w = 0.8L_w$. Using Table 19 of IS 456, find the design shear strength of concrete, τ_c . In addition, find the value of $\tau_{c,max}$ from Table 20 of IS 456 for the chosen grade of concrete. If $\tau_v \geq \tau_{c,max}$, then the thickness of the section should be increased and the calculation repeated. If $\tau_v \leq \tau_c$, the minimum percentage of horizontal steel (0.25% of gross area) specified in Clause 9.1.4 is adequate. If $\tau_v \geq \tau_c$, calculate the shear to be carried by the stirrups as

$$V_{us} = (\tau_v - \tau_c)t_w d_w \quad (16.50)$$

From this, the spacing of two-legged stirrups of chosen diameter can be calculated as

$$s_v = \frac{0.87f_y A_h d_w}{V_{us}} \quad (16.51)$$

where A_h is the area of the two legs of the chosen diameter of stirrup.

Step 5 Design for flexural strength. Calculate the moment of resistance of the rectangular structural wall as per Annex A

of IS 13920. Calculate $\frac{x_u^*}{L_w}$ and $\frac{x_u}{L_w}$ using Eqs (16.36) and (16.38). If $\frac{x_u}{L_w} < \frac{x_u^*}{L_w}$ calculate $\frac{M_n}{f_{ck} t_w L_w^2}$ using Eq. (16.37). For $\frac{x_u^*}{L_w} < \frac{x_u}{L_w} < 1.0$, calculate $\frac{M_n}{f_{ck} t_w L_w^2}$ using Eq. (16.41). From this, calculate M_n . If $M_n > M_u$, then the moment ($M_u - M_n$) should be resisted by the boundary elements.

As discussed in Section 5.5.5 of Chapter 5, and as per ACI 318, a section can be designated as a *tension-controlled section* when the steel strain in the extreme layer of tension

reinforcement ϵ_t reaches 0.0050 in tension and the concrete compressive strain in the most compressed face of the wall reaches ϵ_{cu} (= 0.0035 in IS 456). Wight and MacGregor (2009) have shown that when the depth of the neutral axis x_u is less than or equal to $0.375d_t$, the wall is tension controlled (where d_t is the distance from the extreme compression fibre to the centroid of the bars farthest from the compression face of the wall). Similarly, the wall will be *compression controlled* when x_u is greater than or equal to $0.6d_t$.

Step 6 Design the boundary element. Calculate the c/c distance of boundary element, C_w . The additional compressive force to be resisted by the boundary element, in addition to its own axial force, $P_{add} = (M_u - M_n)/C_w$. Total load on column, $P_{u1} = P_u + P_{add}$. Assuming minimum steel (0.8% of gross area of boundary element), calculate the nominal axial load capacity, P_n , of the boundary element as a short column:

$$P_n = 0.4f_{ck}A_g + (0.67f_y - 0.4f_{ck})A_s \quad (16.52)$$

Check whether $P_n < P_{u1}$; if not, increase the area of steel or the size of boundary element and repeat the calculation.

Special confining reinforcement should be provided throughout the boundary element as per Clauses 9.4.6 and 7.4.8. The area of confining steel, A_{sh} , is given by the greater of

$$A_{sh} = 0.18sh \left(\frac{f_{ck}}{f_y} \right) \left(\frac{A_g}{A_k} - 1.0 \right) \quad (16.53a)$$

and
$$A_{sh} = 0.05sh \left(\frac{f_{ck}}{f_y} \right) \quad (16.53b)$$

where s is the spacing of confining reinforcement, h is the longer dimension of the rectangular confining hoop, and A_k and A_g are the area of confined core and gross area of boundary element, respectively. The spacing s should be greater than 75 mm and less than 100 mm (Clause 7.4.6). It should also be less than one-fourth the size of boundary element or $6d_b$, where d_b is the diameter of the main bar.

Step 7 Detail the reinforcement as given in Section 16.5.4.

A design of ductile flexural wall is provided in Example 15.6. More design examples may be found in the works of Singh (2011), Agarwal and Shrikhande (2006), and Paulay and Priestley (1992). Fanella (2001) provides design aids for structural

walls. Designers of cast-in-place concrete structural walls and coupling beams will find the NEHRP guide by Moehle, et al. (2011) to be quite useful, as it offers code requirements (ACI 318) and accepted approaches to their implementation. It also identifies good practices, background information, detailing, and constructability challenges. Wallace and Moehle (2012) identified some of the shortcomings of ACI 318 provisions and offer possible improvements.

Results of the tests done by Wallace and associates indicate that the walls detailed using displacement-based design have lateral drift capacities in excess of 2 per cent of the specimen height, which was greater than that required by design of 1.5 per cent (Thomsen IV and Wallace 2004; Massone and Wallace 2004; Wallace and Thomsen IV 1995; Wallace 1995).

16.5.6 Coupling Beams

For the desired behaviour of coupled walls to be attained, the coupling (link) beams must be sufficiently strong and stiff. However, the coupling beams must also yield before the wall piers, behave in a ductile manner, and exhibit sufficient energy dissipation. In many cases, geometric limits result in coupling beams that are deep in relation to their clear span. Deep coupling beams may be controlled by shear and may be susceptible to strength and stiffness deterioration under earthquake loading. The efficiency and performance of coupled structural walls greatly depend on the behaviour of the coupling beams under high shear reversals. The vulnerability of coupling beams having conventional detailing, consisting of distributed horizontal and vertical reinforcement as shown in Fig. 16.39(a), to large load reversals was demonstrated during the 1964 Alaska earthquake (see Fig. 16.40).

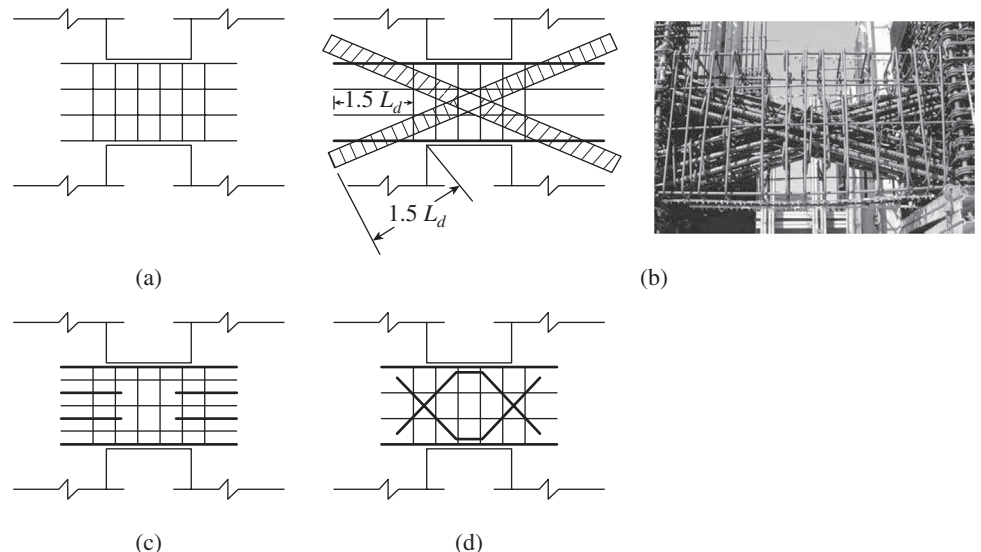


FIG. 16.39 Reinforcement details in RC coupling beams (a) Conventional reinforcement (b) Diagonal reinforcement (c) Conventional reinforcement with dowels (d) Diagonal reinforcement at beam-wall interface

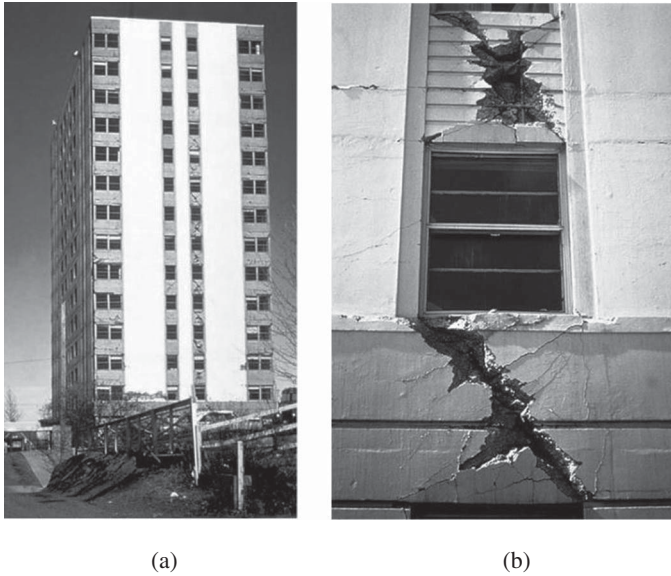


FIG. 16.40 14-storey 1200 L Street apartment building, Anchorage, Alaska, after damage from the 1964 earthquake (a) Overall view of damage (b) Close-up of characteristic X-shaped cracks and failure of coupling beams

Source: NISEE, University of California, Berkeley

Extensive experimental studies on the seismic behaviour of coupling beams were conducted to develop a better reinforcement layout (Paulay and Binney 1974; Paulay and Santhakumar 1976). This resulted in an improved reinforcement detailing, in which two groups of diagonal reinforcing bars were introduced (with one group serving as the tension member and the other as the compression member) to resist the entire shear demand, within the span of the coupling beam as shown in Fig. 16.39(b). This kind of detailing has been adopted in the ACI code. In this reinforcement detail, the diagonal bars need to be carefully anchored in the walls and confined by closely spaced transverse reinforcement, similar to that used in RC columns. In the design of this type of coupling beam, the whole shear transfer mechanism is assigned to the heavily reinforced diagonal cages. Experimental results have shown that diagonally reinforced coupling beams are capable of maintaining their shear strength with good stiffness retention and energy dissipation capacity under large displacement reversals (Paulay and Binney 1974; Barney, et al. 1980; Tassios, et al. 1996).

The diagonal reinforcement detailing, however, results in reinforcement congestion and constructability problems associated with the placement of the diagonal bars and closely spaced transverse reinforcement. These drawbacks have led the researchers to develop other alternate reinforcement details, such as the addition of dowels or diagonal reinforcement only at the beam–wall interface, as shown in Figs 16.39(c) and (d). However, experimental investigations on model coupling beams have shown that for coupling beams with a span-to-depth

less than or equal to 2.0, diagonal reinforcement as shown in Fig. 16.39(b) will be the most efficient solution (Tassios, et al. 1996; Galano and Vignoli 2000). Architecturally practical span-to-depth ratios will fall between three and four (and greater).

Diagonal reinforcement is designed based on the assumption that the shear force can be resolved into diagonal compression and tension forces, intersecting each other at mid-span where no moment is resisted, as shown in Fig. 16.41. Initially, the diagonal compression is transmitted by the concrete and the contribution of the compression steel is considered insignificant. Once the tension steel yields, large cracks form and will remain open. When the loads are reversed, as during earthquakes, these bars are subjected to large compression stresses, perhaps yields, and the previously formed cracks were found to close (Park and Paulay 1975). Based on this, the ultimate tensile force in the steel can be calculated as

$$T_u = C_u = A_s(0.87f_y)$$

and

$$V_u = 2T_u \sin \alpha$$

Hence,

$$A_s = \frac{V_u}{1.74f_y \sin \alpha} \quad (16.54a)$$

and

$$\tan \alpha = \frac{h - 2d'}{L_s} \quad (16.54b)$$

where V_u is the factored shear force, α is the angle made by the diagonal reinforcement with the horizontal, h is the height of coupling beam, d' is the cover for top and bottom longitudinal steel in coupling beam, and L_s is the clear span of the coupling beam. Equation (16.54a) is specified in Clause 9.5.2 of IS 13920:1993, which also specifies that at least four bars of 8 mm diameter should be provided along each diagonal.

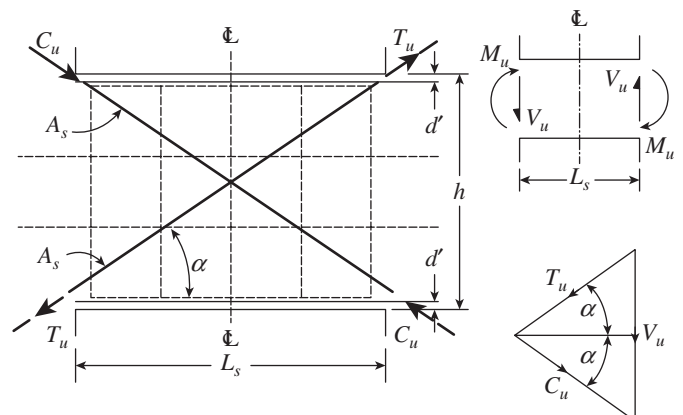


FIG. 16.41 Model of diagonally reinforced coupling beam—geometry of beam with reinforcement

The resisting moment at the supports of the beam (see Fig. 16.37b) may be found from the shear force as (Park and Paulay 1975)

$$M_u = \frac{V_u L_s}{2} = L_s T_u \sin \alpha \quad (16.55)$$

Since equal amount of steel has to be provided in both diagonal bands, the loss of contribution from concrete may not be critical, provided the diagonal compression bars are stable. Hence, in seismic situations, it is important to have closely spaced ties around the diagonal bars to retain the concrete around the bars (see Clause 7.4 of IS 13920:1993 for the requirements of confining reinforcement, which are the same as discussed for columns in Section 13.9.4 and shown in Fig. 13.31 of Chapter 13). Clause 9.5.2 of IS 13920 stipulates that the pitch of spirals or spacing of ties should not exceed 100 mm. Nominal transverse reinforcement should also be provided around the entire beam cross section. The main purpose of the confined concrete in the diagonal band area is to provide some lateral flexural rigidity to the diagonal struts, so that they will enable the compression yielding of the main diagonal bars (Park and Paulay 1975). The ductile behaviour of this type of detailing, as shown in Fig. 16.39(b), has been demonstrated in the tests conducted at the University of Canterbury (Park and Paulay 1975; and Paulay and Binney 1974). It has to be noted that providing transverse reinforcement around the diagonal bar bundles as discussed here (also see Fig. 16.42a) is difficult where the diagonal groups intersect at the beam mid-span, particularly for shallow beams, as well as at the beam-wall interface due to interference with the wall boundary vertical reinforcement.

Clause 9.5.1 stipulates that when $L_s/D \leq 3$, where D is the overall depth of coupling beam, or when the earthquake-induced shear stress, τ_v , in the coupling beam exceeds $0.1\sqrt{f_{ck}}$ (L_s/D), the entire earthquake-induced shear and flexure should preferably be resisted by the diagonal reinforcement (in Clause 21.9.7.2 of ACI 318, these limits are set as $L_s/D \leq 2$ and $\tau_v \geq 0.3\lambda\sqrt{f_{ck}}$).

As per Clause 9.5.3 of IS 13920, we should anchor the diagonal and horizontal bars of the coupling beam in the adjacent walls with an anchorage length of $1.5L_d$, where L_d is the development length in tension. In this connection, it is

interesting to note that as per Clause 21.9.7.4(b) of ACI 318 only diagonal bars need to be embedded into the walls for an anchorage length of $1.25L_d$. The ACI code also gives two confinement options for the coupling beams: (a) *Diagonal confinement*, as discussed earlier and (b) *full-section confinement*. Both these options are shown in Fig. 16.42. Full-section confinement was introduced in the 2008 version of ACI 318 as an alternative detailing option, where transverse reinforcement is placed around the beam cross section to provide confinement and suppress buckling, and no transverse reinforcement is provided directly around the diagonal bar bundles (see Fig. 16.42b). Use of this detailing option avoids the constructability problems of diagonal confinement where the diagonal bars intersect and at the beam-wall interfaces. It may reduce the construction time for a typical floor by a day or two.

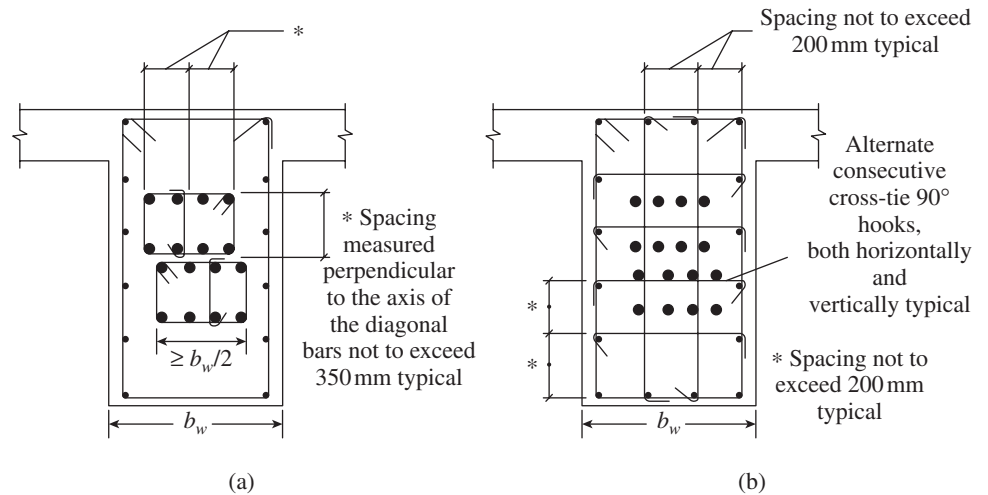


FIG. 16.42 Confinement options for coupling beams as per ACI 318 (a) Diagonal confinement (b) Full-section confinement

Harries, et al. (2005), with the help of a number of design examples, showed that it is not possible to design practically constructible diagonally reinforced concrete coupling beams having shear stress approaching the ACI 318 prescribed limit of $0.75\sqrt{f_{ck}}$. Hence, they suggest using $0.75\sqrt{f_{ck}}$ or the equation suggested by them as the practical upper limit of gross section shear stress for which diagonally reinforced concrete coupling beams may be designed.

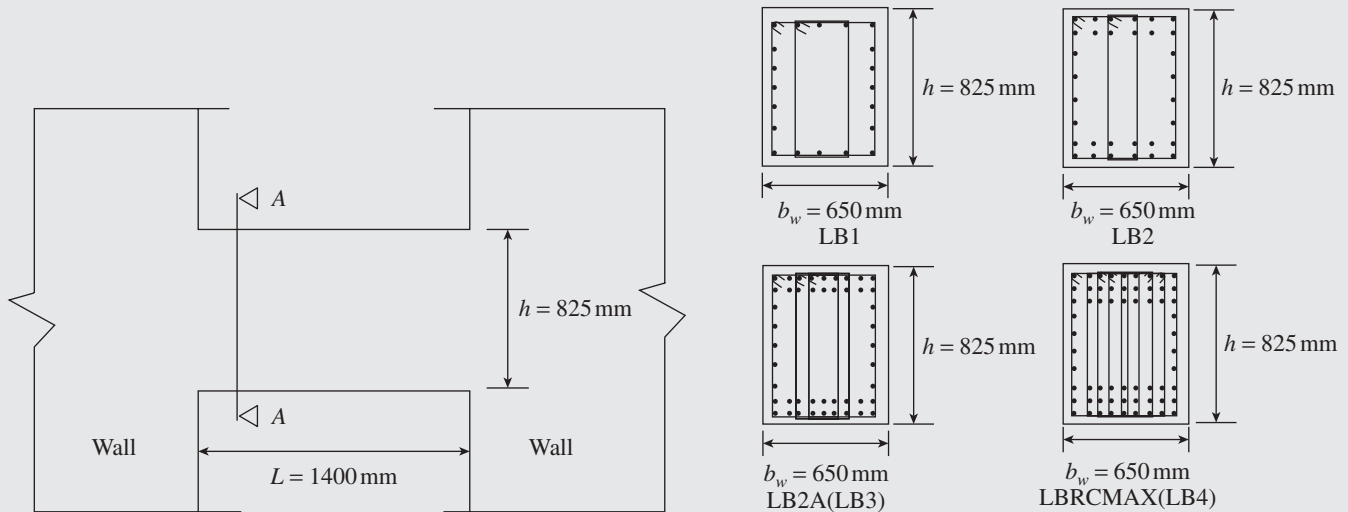
It has to be noted that in beams with aspect ratio (L_s/D) approaching four, the angle of inclination (α) of the diagonal reinforcement will be very small (approximately about 10°). This makes the placement of the diagonal reinforcement more difficult, as it will be obstructed by transverse reinforcement. Hence, in these situations, straight (longitudinal) flexural reinforcement may be used if the shear demand and required ductility are low.

CASE STUDY

Reinforced Concrete Link Beams of Burj Khalifa

In Burj Khalifa, the world’s tallest building, several thousand RC link beams were used to interconnect structural walls. Lee, et al. (2008) describe the design and analysis of the coupling beams for the Burj Khalifa (formerly Burj Dubai) skyscraper in accordance with Appendix A of ACI 318. Typical link beams used in this structure are quite stocky, as shown in the sketch, with shear–span ratio ($L/2D$) of 0.85, width of 650mm, and height of

825 mm. Details of reinforcements in these link beams are given in the following table. Link beams LB1 and LB2 were designed as per ACI 318, the former as deep beam and the latter by using the strut-and-tie method. M80 concrete was used in the link beams and the yield strength of reinforcements was 460MPa (effective strength of stirrup steel was limited in the design to 420MPa as per ACI).



Details of link beams of Burj Khalifa

Details of reinforcements of link beams

Beam ID	Geometry			Factored Loads		Main Reinforcement			Stirrups		
	Width (mm)	Depth (mm)	Span (mm)	Shear (kN)	Moment (kNm)	Top Bar	Bottom Bar	Side Bars, Each Face	Size	Spacing	Type
LB1	650	825	1400	1705	1194	5, #32	5, #32	5, #12	#16	150	Two hoops
LB2	650	825	1400	2805	1164	12, #32	12, #32	4, #12	#16	125	Two hoops
LB3	650	825	1400	3750	2625	18, #32	18, #32	4, #12	#16	80	Three hoops
LB4	650	825	1400	5250	3675	27, #32	27, #32	4, #12	#16	75	Five hoops

Source: Lee, et al. 2008, reprinted with permission from ACI

Notes: LB3 and LB4 are hypothetical beams designed by Lee, et al. (2008) to show that pure RC solutions are possible to support the very large shear forces in these link beams. In reality, LB3 was provided with steel plate and LB4 with built-up steel I beams within the core of the link beam to carry the entire shear and flexural demand.

Walls adjacent to the link beams are 650mm thick and typically reinforced with a minimum of 20mm bars at a spacing of 350mm on each vertical and horizontal face. It has to be noted that the link beams in the Burj Khalifa are not diagonally-reinforced. Lee, et al. (2008) concluded that the strut-and-tie method permits RC

coupling beams to be designed for substantially higher loads than would be possible by ACI sectional design methods, with the capacity of the compression strut determining the resistance of the beam to loading. More details may be found in the work of Lee, et al. (2008).

16.5.7 Openings in Structural Walls

An opening in the structural wall causes high shear stresses in the region of the wall adjacent to it. Hence, it is necessary to check such regions for adequacy of horizontal shear reinforcement in order to prevent diagonal tension failure due to shear. Clause 9.6.1 of IS 13920 stipulates checking of the shear strength along critical planes that pass through the opening. It is also necessary to provide reinforcements along the edges of opening in the walls. Clause 9.6.2 of IS 13920 suggests that the area of the vertical and horizontal bars should be such that they are equal to the respective interrupted bars. The vertical bars should extend for the full storey height. The horizontal bars should be extended beyond the sides of the openings by a distance equal to the

development length in tension. A typical detailing of structural wall with opening is shown in Fig. 16.43. An example of design of structural wall with opening is provided by Medhekar and Jain (1993) and Ingle and Jain (2008).

16.5.8 Construction Joints

The shear strength of the construction joint, τ_{vj} , must be equal to but preferably greater than the shear strength, τ_v , required at that particular level. This shear strength, representing the diagonal tension strength of the wall, may be calculated as $\tau_v = V_v / 0.8t_wL_w$. The design shear force at any construction joint, V_j , can be calculated by using the shear friction concept as

$$V_j = \mu(0.8P_u + 0.87f_yA_{vj}) \quad (16.56)$$

where μ is the coefficient of friction at the joint (may be assumed as 1.0) and A_v is the area of vertical reinforcement in the wall. To account for vertical acceleration, the axial compressive load, P_u , is taken as $0.8P_u$.

The shear stress, τ_{vj} , that can be safely transferred across a well-prepared rough horizontal joint (see Section 16.5.4), with $\mu = 1$, is

$$\tau_{vj} = \frac{0.8P_u + 0.87f_yA_{vj}}{A_g} \quad (16.57)$$

where A_g is the gross sectional area of the wall, which may be taken as $0.8t_wL_w$ (Park and Paulay 1975). Thus, when $\tau_{vj} \geq \tau_v$, the required vertical reinforcement ratio across a horizontal construction joint, $\rho_{vj} = A_{vj}/A_g$ can be written using Eq. (16.57) as

$$\rho_{vj} = \left(1.25\tau_v - \frac{P_u}{A_g} \right) \frac{0.92}{f_y} \geq 0.0025 \quad (16.58a)$$

where τ_v is the factored nominal shear stress at the joint, P_u is the factored axial load (positive for compression), and A_g is the gross cross-sectional area of the joint. It has to be noted that Clause 9.8 of IS 13920 gives the value of ρ_{vj} as

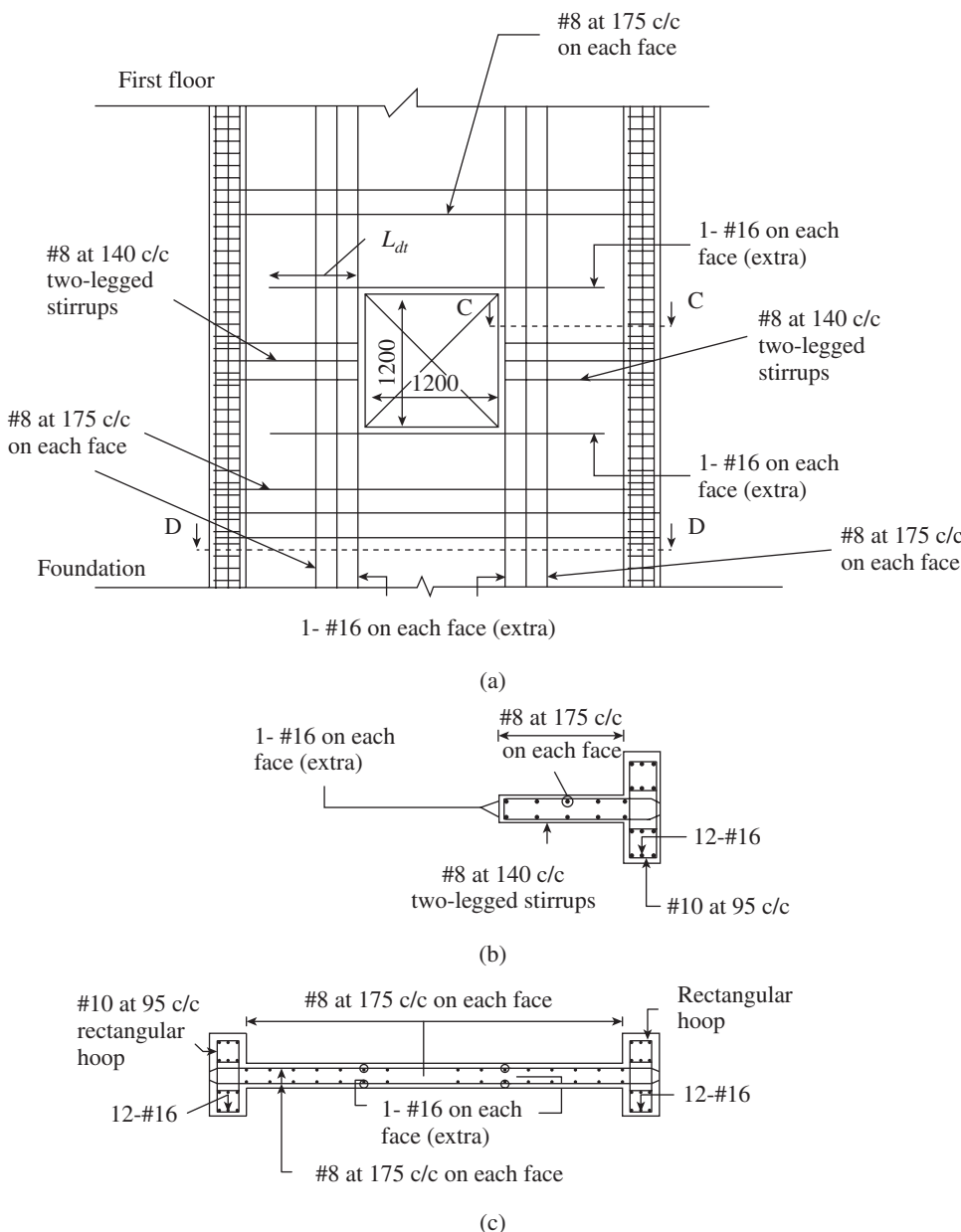


FIG. 16.43 Detailing at openings in structural walls (a) Elevation (b) Section C-C (c) Section D-D

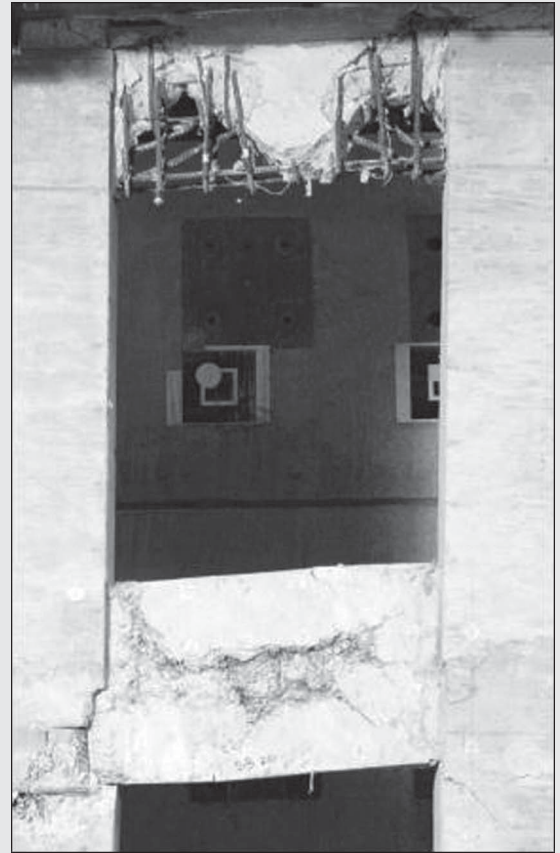
Source: Ingle and Jain 2008

CASE STUDY

Alternative Coupling Beams

Several alternative coupling beam approaches have been proposed for use. These systems include steel sections (Harries and Shahrooz 2005), hybrid coupling beams: steel sections encased in concrete (Harries and Shahrooz 2005), steel beams having a fused link (Shahrooz, et al. 2003), unbonded post-tensioned coupling beams (Kurama and Shen 2004), hybrid beams having steel shear plates and conventional flexural reinforcement (Fortney, et al. 2004), and innovative self-centring concrete core shear wall with composite link beams adopted in the San Francisco Public Utilities Commission's (SFPUC) new headquarters in San Francisco, California (Panian, et al. 2012). In addition, the use of headed bars to provide confinement has been proposed (Mobeen, et al. 2005). These alternatives have been successfully implemented in a number of constructions (Harries and Shahrooz 2005).

Parra-Montesinos, et al. (2010, 2011) investigated the use of high-performance fibre-reinforced concrete (HPFRC) in critical regions of earthquake-resistant wall systems (i.e., link beams and plastic hinge regions of the wall) in order to simplify their construction and improve their behaviour during strong earthquakes (see the given photograph). The tensile and compression behaviour of HPFRCs allows a substantial reduction in the reinforcement used for shear resistance and confinement, which facilitates easy construction and reduces costs. In the case of link or coupling beams connecting structural walls, the use of HPFRC leads to reductions in diagonal reinforcement used for shear resistance between 60 per cent and 100 per cent depending on the beam span-to-depth ratio. In wall plastic hinge regions, transverse reinforcement spacing could be increased to double the normal spacing (Naish 2009).



Damage in link beams after being subjected to earthquake-type loading; Top: regular concrete link beam; Bottom: HPFRC link beam

(Courtesy: Profs Gustavo J. Parra-Montesinos and James K. Wight from the University of Michigan)

$$\rho_{vj} = \frac{0.92}{f_y} \left(\tau_v - \frac{P_u}{A_g} \right) \quad (16.58b)$$

Park and Paulay (1975) showed that, in the absence of axial compression, the minimum vertical reinforcing content of 0.25 per cent in the core of the wall will not be adequate unless the shear stress developed at the ultimate load is very small.

EXAMPLES

EXAMPLE 16.1 (Design of braced plain concrete wall):

A concrete-bearing wall, 3 m high and 4 m in length between cross walls, carries a factored load of 400 kN/m width through a floor at the top. Assuming that there are no openings in the wall, design the wall, considering M20 concrete and Fe 415 steel.

SOLUTION:

Step 1 Determine the thickness of the wall.

- (a) Minimum thickness = 100 mm (Clause 32.1 of IS 456)
- (b) Lesser of $H/25$ or $L/25 = 3000/25 = 120$ mm (as per ACI 318)

Adopt a thickness of 120 mm.

Step 2 Determine the slenderness. As per Clause 32.2.4,

Effective height $H_{we} = 0.75H_w$ or $0.75L$, whichever is less
 $= 0.75 \times 3000$ or $0.75 \times 4000 = 2250$ mm

As per Clause 32.2.3, $H_{we}/t < 30$.

$$H_{we}/t = 2250/120 = 18.75 < 30$$

Hence, it is adequate. As $H_{we}/t > 12$, the wall is slender.

Step 3 Determine the design strength of the wall. As per Clause 32.2.5,

Design strength $p_{nw} = 0.3(t - 1.2e - 2e_a)f_{ck}$

Minimum $e_x = t/20$ (Clause 32.2.2) = $120/20 = 6$ mm

$$e_a = \frac{H^2 w_e}{2500t} = \frac{2250^2}{2500 \times 120} = 16.88 \text{ mm}$$

Hence $P_{nw} = 0.3(120 - 1.2 \times 6 - 2 \times 16.88)20 = 474.24 \text{ N/mm}$

For 1 m length $P_{nw} = 474.24 \text{ kN} > 400 \text{ kN/m}$

Hence, the wall can safely carry the applied load.

Step 4 Design of reinforcement.

Maximum spacing = $3t$ or $450 \text{ mm} = 3 \times 120 = 360 \text{ mm}$

Vertical $A_{st} = 0.0012 \times 1000 \times 120 = 144 \text{ mm}^2/\text{m}$

Horizontal $A_{st} = 0.0020 \times 1000 \times 120 = 240 \text{ mm}^2/\text{m}$

Provide 8 mm at 300 mm c/c on both faces vertically and horizontally (A_{st} provided = $168 \times 2 = 336 \text{ mm}^2/\text{m}$).

Step 5 Check the capacity as per ACI 318.

$$P_{nw} = 0.286 f_{ck} A_g \left[1 - \left(\frac{kH_w}{32t} \right)^2 \right]$$

$$= 0.286 \times 20 \times (4000 \times 120) \left[1 - \left(\frac{0.8 \times 3000}{32 \times 120} \right)^2 \right] \times 10^{-3}$$

$$= 1672 \text{ kN}$$

For 1 m length = $1672/4 = 418 \text{ kN}$ (less than 474.24 kN as per IS 456)

The detailing of wall as per the design is shown in Fig. 16.44.

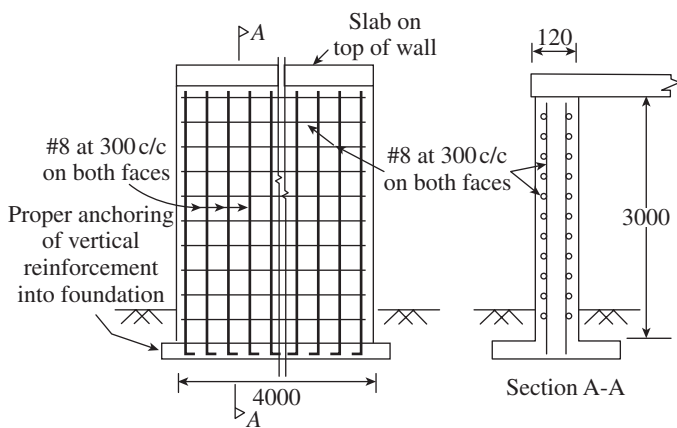


FIG. 16.44 Detailing of bearing wall

EXAMPLE 16.2 (Design of braced RC wall subject to shear and axial loads):

Design a braced 6 m tall concrete wall, 4 m long and 200 mm thick. Assume that it is restrained against rotation at its base and unrestrained at the other ends. If it has to carry a factored vertical load of 400 kN and a factored horizontal load of 10 kN

at the top, design the wall. Assume M20 concrete and Fe 415 steel.

SOLUTION:

Step 1 Check whether the wall is wholly in compression.

Maximum bending moment in wall $M_u = 10 \times 6 = 60 \text{ kNm}$

Maximum load $P_u = 400 \text{ kN}$

$e = M_u/P_u = 60/400 = 0.15 \text{ m}$

$L/6 = 4/6 = 0.67 \text{ m} > 0.15 \text{ m}$

As $e < L/6$, the entire wall will be under compression.

Step 2 Determine the slenderness of the wall.

$H_{we} = 0.75 \times 6 = 4.5 \text{ m}$; Slenderness ratio = $4500/200 = 22.5 < 30$

Since $H_{we}/t > 12$, the wall is slender.

Step 3 Determine the minimum and the additional eccentricity.

$$e_x = e_{\min} = t/20 = 200/20 = 10 \text{ mm}$$

Additional eccentricity (Clause 32.2.5)

$$e_a = \left(\frac{H_{we}}{t} \right)^2 \frac{t}{2500} = \left(\frac{4500}{200} \right)^2 \frac{200}{2500} = 40.5 \text{ mm}$$

Step 4 Determine the design axial strength of the wall.

$$P_{uw} = 0.3(t - 1.2e - 2e_a) f_{ck} = 0.3(200 - 1.2 \times 10 - 2 \times 40.5)20$$

$$= 642 \text{ N/mm}$$

Total capacity of wall = $642 \times 4000/1000 = 2568 \text{ kN} > 400 \text{ kN}$

Step 5 Determine minimum steel required.

p_t = Horizontal steel = 0.20% (Clause 32.5)

p_v = Vertical steel = 0.12%

Hence $A_{sh} = 0.002 \times 200 \times 1000 = 400 \text{ mm}^2/\text{m}$

As per Clause 32.5.1, since thickness is 200 mm, reinforcement has to be provided in two layers—each layer $200 \text{ mm}^2/\text{m}$. Provide 8 mm bars at 250 mm c/c ($A_h = 201 \text{ mm}^2/\text{m}$). Provide the same steel in the vertical direction as well.

Step 6 Check for shear (Clause 32.4).

$$\frac{H_w}{L_w} = \frac{6}{4} = 1.5 > 1. \text{ Hence, consider it as slender wall.}$$

Effective depth of wall, $d = 0.8L_w = 0.8 \times 4 = 3.2 \text{ m}$

Critical section is at $0.5 \times 4 = 2 \text{ m}$ or $0.5 \times 6 = 3 \text{ m}$ from base.

$$\tau_v = \text{Shear stress} = \frac{V_u}{bd} = \frac{10 \times 1000}{200 \times 3200} = 0.016 \text{ N/mm}^2$$

Maximum allowable shear stress (Clause 32.4.2.1)

$$\tau_{\max} = 0.17 f_{ck} = 0.17 \times 20 = 3.4 \text{ N/mm}^2 > \tau_v$$

Design shear strength of concrete wall without steel (Clause 32.4.3b)

Lesser of

$$\tau_{cw1} = [0.6 - 0.2(H_w/L_w)]\sqrt{f_{ck}} = (0.6 - 0.2 \times 1.5)\sqrt{20} = 1.34 \text{ N/mm}^2$$

$$\tau_{cw2} = 0.045\sqrt{f_{ck}} \left(\frac{H_w + 1}{L_w} \right) = 0.045\sqrt{20} \left(\frac{1.5 + 1}{1.5 - 1} \right) = 1.0 \text{ N/mm}^2$$

and $\tau_{cw3} = 0.15\sqrt{f_{ck}} = 0.15\sqrt{20} = 0.67 \text{ N/mm}^2$

All these above values are greater than the actual shear stress, τ_v ; hence, the wall is safe in shear.

Step 7 Design the steel for shear. For the sake of calculation, let us assume that the shear force is high and design the steel to resist shear.

Assume $V = 750 \text{ kN}$

$$\text{Now, } \tau_v = \frac{750 \times 1000}{200 \times 3200} = 1.17 \frac{\text{N}}{\text{mm}^2} < 3.4 \text{ N/mm}^2 \text{ but } \tau_v > \tau_{cw}$$

$$V_c = (0.8L_w)t\tau_c = 3200 \times 200 \times 0.67 \times 10^{-3} = 428.8 \text{ kN}$$

Shear to be taken by steel = $750 - 428.8 = 321.2 \text{ kN}$

With minimum steel as calculated in Step 5,

$$\frac{A_{sh}}{S_h} = p_w t = 0.002 \times 200 = 0.4 \text{ mm}^2$$

$$V_s = 0.87 f_y d \frac{A_{sh}}{s_h} = 0.87 \times 415 \times 3200 \times 0.4 \times 10^{-3} = 462 \text{ kN} > 321.2 \text{ kN}$$

Hence, it is safe with minimum steel. The detailing of wall in this example is similar to that of Example 16.1 (see Fig. 16.44).

EXAMPLE 16.3 (Design of cantilever-retaining wall):

A cantilever-retaining wall is required to retain earth 3.8 m high above the ground level. The backfill surface is inclined at an angle of 15° with the horizontal and the backfilled soil has a unit weight of 18 kN/m^3 and an angle of internal friction of 30° . The exposure condition is moderate. Assume that the SBC of soil is 150 kN/m^2 and that the coefficient of friction between the soil and concrete is 0.5. Design the RC retaining wall.

SOLUTION:

Step 1 Determine the depth of the foundation. Select M20

concrete and Fe 415 steel.
 Depth of foundation = $\frac{q_a}{\gamma_s} \left[\frac{1 - \sin \phi}{1 + \sin \phi} \right]^2 = \frac{150}{18} \left[\frac{1 - \sin 30}{1 + \sin 30} \right]^2 = 0.93 \text{ m}$

Assume depth = 1.2 m

Overall depth of retaining wall = $1.2 + 3.8 = 5 \text{ m}$

Step 2 Select the initial sizes.

Width of footing $B = 0.5H$ to $0.7H = 0.5 \times 5$ to $0.7 \times 5 = 2.5 \text{ m}$ to 3.5 m

Adopt $B = 3 \text{ m}$

Width of heel = $0.5B = 0.5 \times 3.0 = 1.5 \text{ m}$; adopt 1.5 m

Thickness of base slab = $H/12 = 5000/12 = 417 \text{ mm}$; adopt 420 mm

Adopt stem thickness at base = 420 mm

Adopt top thickness of stem = 200 mm

Height of stem = $5000 - 420 = 4580 \text{ mm}$

The preliminary proportioning is shown in Fig. 16.45.

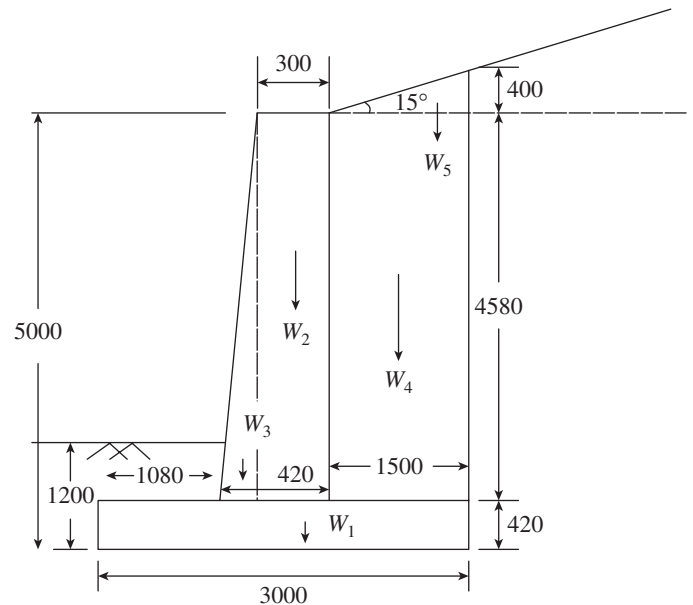


FIG. 16.45 Dimensions of the cantilever-retaining wall

Step 3 Calculate the forces and moments acting on the wall.

The pressure on the soil is obtained from equilibrium of the forces acting on the wall. The line of action of the resultant vertical forces (see Fig. 16.45) with respect to the heel can be located by applying statics, considering 1 m length of the wall, as shown in Table 16.9.

TABLE 16.9 Forces and moments on one metre length of retaining wall

No.	Notation	Item	Force (kN)	Distance from Heel (m)	Moment about Top of Toe (kNm)
1.	W_1	Footing	$0.42 \times 3.0 \times 25 = 31.5$	$3/2 = 1.5$	47.25
2.	W_2	Rectangular portion of wall	$0.2 \times 4.58 \times 25 = 22.9$	$1.5 + 0.2/2 = 1.6$	36.64
3.	W_3	Triangular portion of wall	$(0.42 - 0.2)/2 \times 4.58 \times 25 = 12.6$	$1.5 + 0.2 + 0.22/3 = 1.77$	22.30
4.	W_4	Soil on heel	$1.5 \times 4.58 \times 18 = 123.7$	$1.5/2 = 0.75$	92.78

5.	W_5	Soil in inclined slope	$(0.40 \times 1.5)/2 \times 18 = 5.4$	$1.5/3 = 0.5$	2.70
		Sum	196.1	-	201.67

Step 4 Calculate the earth pressure.

Height of inclined portion of soil = $1.5 \times \tan 15^\circ = 0.40$ m

Earth pressure coefficients

$$K_a = \frac{\cos \delta - \sqrt{\cos^2 \delta - \cos^2 \phi}}{\cos \delta + \sqrt{\cos^2 \delta - \cos^2 \phi}} \cos \delta$$

$$= \frac{\cos 15 - \sqrt{\cos^2 15 - \cos^2 30}}{\cos 15 + \sqrt{\cos^2 15 - \cos^2 30}} \cos 15$$

$$= \frac{0.966 - 0.427}{0.966 + 0.427} \times 0.966 = 0.374$$

$$K_p = \frac{1 + \sin \phi}{1 - \sin \phi} = \frac{1 + \sin 30}{1 - \sin 30} = 3.0$$

Force due to active earth pressure

$P_a = K_a \gamma_e H^2 / 2$, with $H = 5 + 0.4 = 5.4$ m

$P_a = 0.374 \times 18 \times 5.4^2 / 2 = 98.15$ kN (per metre length of wall)

Horizontal component = $P_a \cos \delta = 98.15 \times \cos 15 = 94.8$ kN

Vertical component = $P_a \sin \delta = 98.15 \times \sin 15 = 25.4$ kN

Step 5 Check for stability.

Overturning moment $M_o = (P_a \cos \delta) H' / 3 = 94.8 \times 5.4 / 3 = 170.64$ kNm

Distance of resultant vertical force from heel (from Table 16.9)

$$x = \frac{\sum M}{\sum W} = \frac{201.67}{196.1} = 1.03 \text{ m}$$

Stabilizing moment (about toe)

$M_r = \sum W(B - x) = 196.1(3.0 - 1.03) = 386.32$ kNm (permetre length of wall)

Factor of safety against overturning

$FS_{\text{overturning}} = 0.9M_r / M_o = 0.9 \times 386.32 / 170.64 = 2.04 > 1.4$

Hence, it is safe against overturning.

Step 6 Calculate soil pressure below the footing.

Distance of resultant reaction from heel

$$x_1 = \frac{(\sum M + M_o)}{\sum W} = \frac{201.67 + 170.64}{196.1} = 1.9 \text{ m}$$

Eccentricity = $x_1 - B/2 = 1.9 - 3.0/2 = 0.40$ m $< B/6 = 0.5$ m

Hence, the resultant reaction is within middle third of the base.

$$6e/B = 6 \times 0.4/3.0 = 0.8$$

$$q_{\max} = \frac{\sum W}{B} \left(1 + \frac{6e}{B} \right) = \frac{196.1}{3.0} (1 + 0.80) = 118 \text{ kN/mm}^2 <$$

150 kN/mm² (q_a)

Hence, it is safe.

$$q_{\min} = \frac{196.1}{3.0} (1 - 0.80) = 13 \text{ N/mm}^2 > 0 \text{ kN/mm}^2$$

Hence, there is no tension in the soil below the footing.

Step 7 Check for stability against sliding.

Sliding force = $P_a \cos \delta = 94.8$ kN

Let us neglect the passive pressure on the toe side.

Resisting force = $F = \mu \sum W = 0.5 \times 196.1 = 98.05$ kN

Factor of safety against sliding = $0.9F / P_a \cos \delta = 0.9 \times 98.05 / 94.8 = 0.93 < 1.4$

Hence, a shear key has to be provided.

Step 8 Design the shear key. Assume a shear key of 300 mm \times 400 mm at a distance of 1.1 m from toe. The effect of the shear key is to develop passive resistance over a depth h_2 as shown in Fig. 16.46.

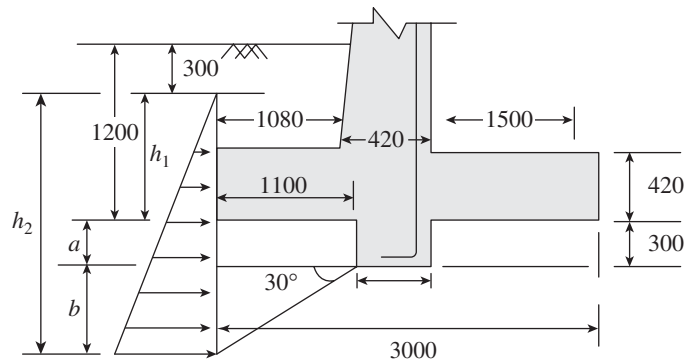


FIG. 16.46 Shear key and passive earth pressure

For computing the passive pressure below the toe, the top overburden of 300 mm is usually neglected.

Hence, $h_1 = 1.2 - 0.3 = 0.9$ m

$$\phi = 30^\circ$$

$$b = 1.1 \times \tan 30^\circ = 0.635 \text{ m}$$

$$P_p = \frac{1}{2} \gamma K_p (h_1 + a + b)^2 - \frac{1}{2} \gamma K_p h_1^2$$

$$= \frac{1}{2} \times 18 \times 3(0.9 + 0.3 + 0.635)^2 - \frac{1}{2} \times 18 \times 3 \times 0.9^2$$

$$= 90.92 - 21.87 = 69.05 \text{ kN}$$

$$\text{Factor of safety against sliding} = \frac{0.9(P_p + F)}{P_a \cos \delta} = \frac{0.9(69.05 + 98.05)}{94.8} = 1.59 > 1.4$$

Hence, it is safe against sliding.

Step 9 Design the toe slab. The loads considered for the design of toe slab are shown in Fig. 16.47. The net pressure is obtained by reducing the pressure due to self-weight of toe slab from gross pressure at base.

Pressure due to self-weight of toe slab = $25 \times 0.42 = 10.5 \text{ kN/m}^2$

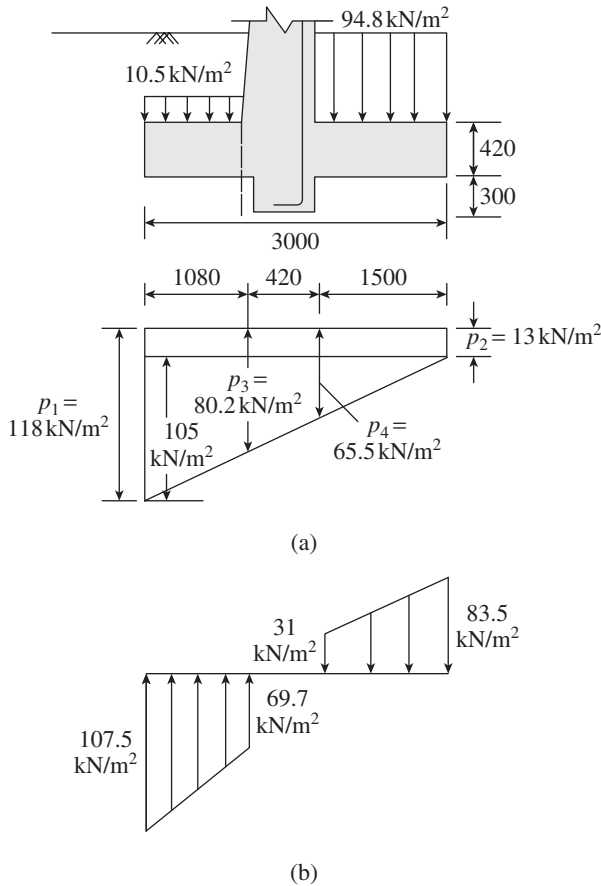


FIG. 16.47 Gross and net pressure below the base slab
(a) Pres-sure below footing (b) Net pressure diagram

As shown in Fig. 16.47, the net upward pressure varies from 107.5 kN/m^2 to 69.7 kN/m^2 . Assuming a clear cover of 75 mm and 16 mm bars,

effective depth of footing, $d = 420 - 75 - 8 = 337 \text{ mm}$

Using a load factor of 1.5, the design shear force at d (337 mm) from the face of the stem is

$$V_u = 1.5 \times [(107.5 + 69.7)/2] \times (1.08 - 0.337) = 98.7 \text{ kN/m}$$

The bending moment at the face of the stem is

$$\begin{aligned} M_u &= 1.5 \times [(69.7 \times 1.08^2 / 2) + (107.5 - 69.7) \\ &\quad \times 0.5 \times 1.08^2 \times 2/3] \\ &= 83 \text{ kNm/m} \end{aligned}$$

$$\text{Nominal shear stress} = \tau_v = \frac{V_u}{bd} = \frac{98.7 \times 10^3}{1000 \times 337} = 0.293 \text{ MPa}$$

From Table 19 of IS 456, for M20 concrete with $p_t = 0.20$, $\tau_c = 0.32 \text{ MPa}$

$$R = \frac{M_u}{bd^2} = \frac{83 \times 10^6}{1000 \times 337^2} = 0.731 \text{ MPa}$$

From Table 2 of SP 16, $p_t = 0.2123\% > p_t = 0.20\%$ required for shear

$$A_{st} = \frac{p_t bd}{100} = \frac{0.2123 \times 1000 \times 337}{100} = 716 \text{ mm}^2/\text{m}$$

Using 16 mm bars, spacing = $201 \times 1000/716 = 281 \text{ mm}$

Provide 16 mm bars at 275 mm c/c at the bottom of the toe slab. The bars should extend a distance of $L_d = 47 \times 16 = 752 \text{ mm}$ beyond the front face of the vertical stem. As the toe slab has a length of only 1.08 m, no curtailment is necessary.

Distribution steel = $0.0012 \times 1000 \times 420 = 504 \text{ mm}^2/\text{m}$

Spacing of 10 mm bars = $(78.5 \times 1000)/504 = 150 \text{ mm}$

Provide distributors of 10 mm at 150 mm c/c.

Step 10 Design the heel slab. The distributed loads acting downwards on the heel slab are as follows:

(a) Due to soil = $18 \times (4.58 + 0.4/2) = 86.0 \text{ kN/m}^2$

(b) Due to self-weight = $25 \times 0.42 = 10.5 \text{ kN/m}^2$

Total = 96.5 kN/m^2

The net pressure acting downwards varies between 31 kN/m^2 and 83.5 kN/m^2 as shown in Fig. 16.47.

Considering a load factor of 1.5, the design shear force at the rear face of the stem is

$$V_u = \frac{1.5(31 + 83.5)}{2} \times 1.5 = 128.8 \text{ kN/m}$$

$$\begin{aligned} M_u &= 1.5[(31 \times 1.5^2 / 2) + (83.5 - 31) \times 0.5 \times 1.5^2 \times 2/3] \\ &= 111.4 \text{ kNm/m} \end{aligned}$$

$$\text{Nominal shear stress, } \tau_v = \frac{V_u}{bd} = \frac{128.8 \times 10^3}{1000 \times 337} = 0.382 \text{ N/mm}^2$$

From Table 19 of IS 456, for M20 concrete, p_t required to get design shear strength of 0.382 N/mm^2 is 0.296 per cent.

$$R = \frac{M_u}{bd^2} = \frac{111.4 \times 10^6}{1000 \times 337^2} = 0.981 \text{ MPa}$$

From Table 2 of SP 16, p_t required = $0.2893\% < 0.296\%$ required for shear

$$\text{Hence required } A_{st} = \frac{0.296}{100} \times 1000 \times 337 = 998 \text{ mm}^2$$

With 16 mm bars, spacing = $201 \times 1000/998 = 202 \text{ mm}$

Provide 16 mm bars at 200 mm c/c at the top of the heel slab. The bars should extend by a distance of at least $1.3L_d = 1.3 \times 47 \times 16 = 978 \text{ mm}$ beyond the rear face of stem. Since the length of the heel slab is only 1.5 m, curtailment of rods is not attempted.

Step 11 Design the vertical stem.

Height of cantilever = 4.58 m
 Assuming clear cover of 50 mm and 20 mm bars,
 Effective depth d at the base of stem = $420 - 50 - 10 = 360$ mm
 Force due to active earth pressure
 $P_a = K_a \gamma_e H^2 / 2$
 $H = 4.58 + 0.4 = 4.98$ m
 $P_a = 1.5(0.374 \times 18 \times 4.98^2 / 2) = 125.22$ kN/m
 Horizontal component = $P_a \cos \delta = 125.22 \times \cos 15 = 120.95$ kN/m
 Bending moment, $M_u = 1.5(P_a \cos \delta) \frac{H}{3} = 120.95 \times \frac{4.98}{3} = 200.78$ kN/m

$$R = \frac{M_u}{bd^2} = \frac{200.78 \times 10^6}{1000 \times 360^2} = 1.55 \text{ MPa}$$

From Table 2 of SP 16, for M20 concrete
 Required $p_t = 0.477\%$
 Required $A_{st} = (0.477/100) \times 1000 \times 360 = 1717$ mm²/m
 With 16 mm bars, required spacing = $201 \times 1000/1717 = 117$ mm
 Provide 16 mm bars at 115 mm c/c. Extend the bars into the shear key as shown in Fig. 16.19.

Required anchorage length = $47 \times 16 = 752$ mm
 Available anchorage length = $420 + 300 - 75 = 645$ mm.
 Hence, bend the rods into the shear key with 90° bend. For 16 mm bar, anchorage value for 90° bend = 128 mm. Hence, the anchorage length is sufficient.

Check for shear at base of stem

Critical section is at $d = 360$ mm above the base, that is, at $z = 4.58 - 0.36 = 4.22$ m below top edge.
 Shear force at 4.22 m = $1.5[0.374 \times 18 \times (4.22 + 0.4)^2 / 2] = 107.77$ kN/m
 Horizontal component = $107.77 \times \cos 15 = 104.1$ kN/m

$$\tau_v = \frac{104.1 \times 10^3}{1000 \times 360} = 0.29 \text{ MPa}$$

From Table 19 of IS 456, τ_c (for $p_t = 0.477\%$) = 0.468 MPa
 Hence, it is safe for shear.

Curtailement of reinforcement

A_{sty} required at any section is proportional to M /thickness at the section.

Hence A_{sty} is proportional to $\frac{y^3}{dy}$ or $\frac{A_{sty}}{A_{st}} = \frac{y^3}{h^3} \frac{d}{dy}$

At 2.30 m above the bottom of the stem slab

$$\frac{A_{sty}}{1717} = \left(\frac{2.28}{4.58}\right)^3 \times \left(\frac{420}{310}\right) \text{ or } A_{sty} = 287 \text{ mm}^2$$

Hence, curtail alternate bars at this section and extend the curtailed bar up to $12 \times 16 = 192$ mm or d (d at this section = $200 + (420 - 200) \times 2500/4580 - 50 - 10 = 260$ mm) above the theoretical section.

Temperature and shrinkage reinforcement

Minimum steel = $0.0012 \times 4.58 \times 1000 \times (420 + 200) / 2 = 1704$ mm²
 Required number of 10 mm bars = $1704 / 78.5 = 22$
 Provide 15 bars on the exposed face at 320 mm spacing and 11 bars on the inner face at 450 mm spacing.

Step 12 Detail the reinforcement. Detailing of the cantilever-retaining wall of this example is shown in Fig. 16.48

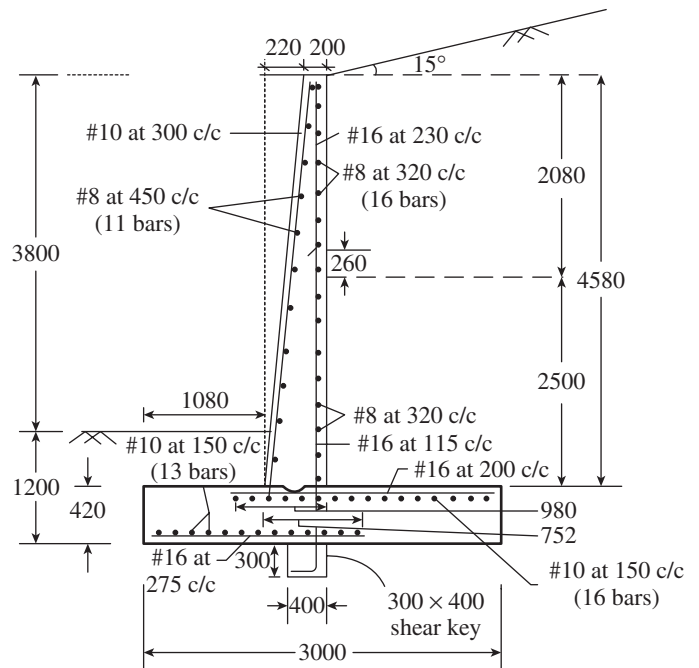


FIG. 16.48 Detailing of cantilever-retaining wall

EXAMPLE 16.4 (Design of counterfort-retaining wall):
 Design a counterfort-type retaining wall to retain a 6.8 m high backfill above the ground level. The unit weight and SBC of the soil at site are 18 kN/m³ and 170 kN/m², respectively. The angle of internal friction of soil and coefficient of friction are 30° and 0.6, respectively. The exposure condition is moderate.

SOLUTION:

The exposure condition is moderate; hence select M25 concrete with Fe 415 grade steel.

Step 1 Fix the dimensions of the retaining wall.

$$\text{Minimum depth of foundation} = \frac{q_a}{\gamma_s} \left(\frac{1 - \sin \phi}{1 + \sin \phi} \right)^2 = \frac{170}{18} \left(\frac{1 - \sin 30}{1 + \sin 30} \right)^2 = 1.05 \text{ m}$$

Assume depth of foundation as 1.2 m.
 Overall height of the wall $H = 6.8 + 1.2 = 8\text{ m}$
 Spacing of counterforts may be determined using the following empirical equations:

$L = 0.8\sqrt{H}$ to $1.2\sqrt{H} = 0.8\sqrt{8}$ to $1.2\sqrt{8} = 2.26\text{ m}$ to 3.39 m
 and $L = 3.5(H/\gamma_e)^{0.25} = 3.5(8/18)^{0.25} = 2.86\text{ m}$
 Adopt a spacing of counterfort $L = 3\text{ m c/c}$.
 Thickness of base slab = $2LH\text{ cm} = 2 \times 3 \times 8 = 48\text{ cm} = 480\text{ mm}$
 Base width $B = 0.6H$ to $0.7H = 0.6 \times 8$ to $0.7 \times 8 = 4.8\text{ m}$ to 5.6 m
 Adopt a base width of 5.0 m .
 Toe projection = $1/4 \times B = 5/4 = 1.25\text{ m}$
 Vertical stem thickness = $H/40 = 8000/40 = 200\text{ mm}$
 Hence heel length = 3.55 m
 Thickness of counterfort = $L/10 = 3000/10 = 300\text{ mm}$
 Height of vertical section $h = 8 - 0.48 = 7.52\text{ m}$
 The assumed cross section is shown in Fig. 16.49.

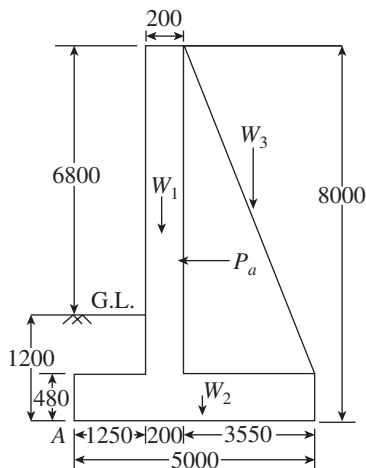


FIG. 16.49 Preliminary dimensions of the counterfort-retaining wall

Step 2 Check for stability against overturning. The forces and moments about the tip of the toe slab (point A in Fig. 16.49) are shown in Table 16.10. The stability check is done by neglecting the earth on the toe slab as it is small and may not exist during construction.

TABLE 16.10 Forces and moments acting on counterfort-retaining wall

No.	Element	Load (kN)	Distance from A (m)	Moment about A (kNm)
1	Stem (W_1)	$0.2 \times 7.52 \times 25 = 37.60$	$1.25 + 0.1 = 1.35$	50.76
2	Footing (W_2)	$0.48 \times 5 \times 25 = 60$	$5/2 = 2.5$	150.0
3	Soil on heel (W_3)	$3.55 \times 7.52 \times 18 = 480.53$	$1.25 + 0.2 + 3.55/2 = 3.225$	1549.71
	Sum	578.13	–	1750.47

Force due to active earth pressure $P_a = K_a \gamma_e H^2/2$

where $K_a = \frac{1 - \sin \phi}{1 + \sin \phi} = \frac{1 - \sin 30}{1 + \sin 30} = \frac{1}{3}$

$P_a = 18 \times 8^2 / (2 \times 3) = 192\text{ kN}$

Overturning moment due to earth pressure,

$M_o = P_a H/3 = 192 \times 8/3 = 512\text{ kNm}$ (per metre length of wall)

Factor of safety against overturning = $0.9 \times 1750.47/512 = 3.97 > 1.55$

Hence, it is safe against overturning.

Step 3 Check for stability against sliding.

Sliding force $P_a = 192\text{ kN}$

Ignoring passive pressure, factor of safety against sliding

$$= \frac{0.9(\mu \sum W)}{P_a} = 0.9 \times 0.6 \times \frac{578.13}{192} = 1.626 > 1.4$$

Hence, it is safe against sliding.

Step 4 Calculate soil pressure under the footing slab.

Resultant vertical reaction, $R = \sum W = 578.13$

Distance of R from the toe = $(M_w - M_o)/R = (1750.47 - 512)/578.13 = 2.142\text{ m}$

Eccentricity, $e = B/2 - 2.142 = 5/2 - 2.142 = 0.358 < B/3 = 5/6 = 0.83$

Thus, the resultant lies within the middle third of the base slab.

$$p_{\max}, p_{\min} = \frac{R}{B} \left(1 \pm \frac{6e}{B} \right) = \frac{578.13}{5} \left(1 \pm \frac{6 \times 0.358}{5} \right)$$

$p_{\max} = 165.3\text{ kN/m}^2 < q_a = 170\text{ kN/m}^2$

$p_{\min} = 66\text{ kN/m}^2 > 0$

Hence, the maximum pressure is below the SBC and there is no tension in the soil below the footing slab.

Step 5 Design the toe slab. The net pressures acting upwards under the toe slab are obtained by reducing the uniformly distributed self-weight of the toe slab from the gross pressures at the base.

Pressure due to self-weight = $25 \times 0.48 = 12\text{ kN/m}^2$

Downward pressure on heel slab

= Pressure (due to earth on heel slab + due to self-weight)

= $18 \times 7.52 + 25 \times 0.48 = 147.36\text{ kN/m}^2$

The net soil pressure acting on the base slab is shown in Fig. 16.50.

Let us assume 16 mm bars with a clear cover of 75 mm.

The effective depth, $d = 480 - 75 - 8 = 397\text{ mm}$

Assuming a load factor of 1.5, the design shear force at a distance d ($= 397\text{ mm}$) from the front face of stem is $V_u = 1.5(153.3 + 128.5)/2 \times (1.25 - 0.397) = 180.28\text{ kN/m}$

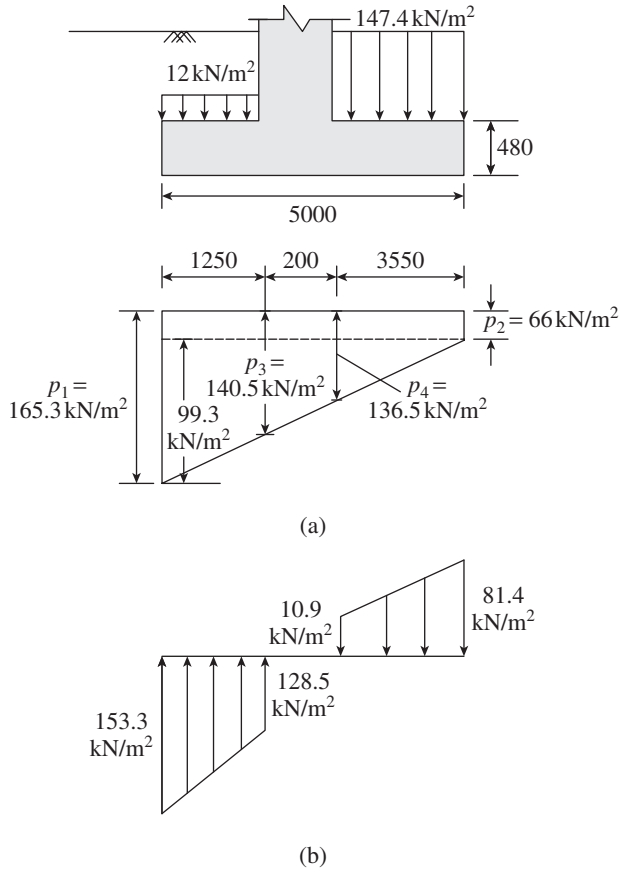


FIG. 16.50 Gross and net pressure below the base slab
(a) Pressure below footing (b) Net pressure diagram

Design moment at the face of the stem slab is

$$M_u = 1.5 \left[(128.5 \times 1.25^2 / 2) + (153.3 - 128.5) \times \frac{1.25^2}{2} \times 2/3 \right]$$

$$= 169.96 \text{ kNm/m}$$

Effective depth required for bending moment =

$$\sqrt{\frac{M_u}{0.138 f_{ck} b}} = \sqrt{\frac{169.96 \times 10^6}{0.138 \times 25 \times 1000}} = 222 \text{ m} < 397 \text{ mm}$$

Hence, the assumed depth is sufficient.

$$\text{Nominal shear stress } \tau_v = \frac{V_u}{bd} = \frac{180.28 \times 10^3}{100 \times 397} = 0.454 \text{ N/mm}^2$$

From Table 19 of IS 456, for M25 concrete, required $p_t = 0.44\%$

$$R = \frac{M_u}{bd^2} = \frac{169.96 \times 10^6}{1000 \times 397^2} = 1.08 \text{ MPa}$$

From Table 3 of SP 16, required $p_t = 0.316\% < 0.44\%$ required for shear

$$\text{Hence required } A_{st} = \frac{0.44}{100} \times 1000 \times 397 = 1747 \text{ mm}^2$$

With 16 mm bars, spacing = $201 \times 1000 / 1747 = 115 \text{ mm}$

With 20 mm bars, spacing = $314 \times 1000 / 1747 = 179.7 \text{ mm}$

Provide 20 mm bars at 170 mm c/c at the bottom of the toe slab. The bars should extend a distance of $40.3 \times 20 = 806 \text{ mm}$ beyond the front face of the stem slab.

Distributors

Distribution steel = $0.12/100 \times 1000 \times 397 = 477 \text{ mm}^2$

With 10 mm bars, spacing = $78.5 \times 1000 / 477 = 164.6 \text{ mm}$

Provide 10 mm bars at a spacing of 160 mm c/c.

Step 6 Design the heel slab. The soil pressure under the heel slab is shown in Fig. 16.51. It is divided into equivalent contributions of uniformly and triangularly distributed loads. The equivalent distribution is also shown in Fig. 16.51.

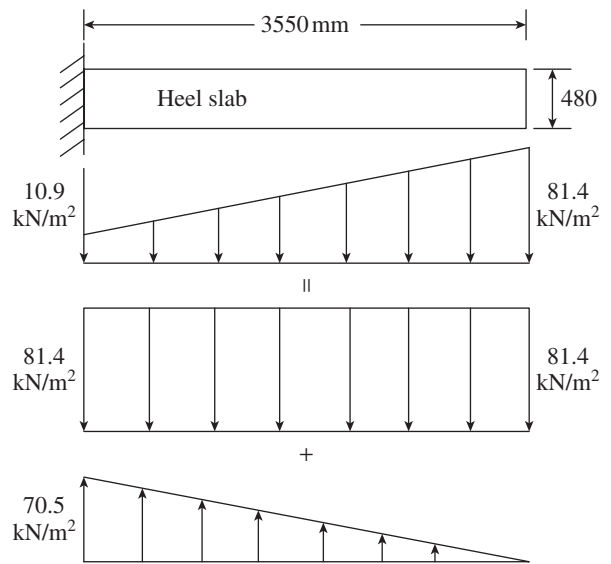


FIG. 16.51 Soil pressure acting on heel slab

Aspect ratio of the heel slab = $3.55/3 = 1.183$ (see Fig. 16.52)

It is usually assumed that the end 1 m of the heel slab is subjected to continuous beam action (see Fig. 16.52); hence, more reinforcement is provided in this 1 m width.

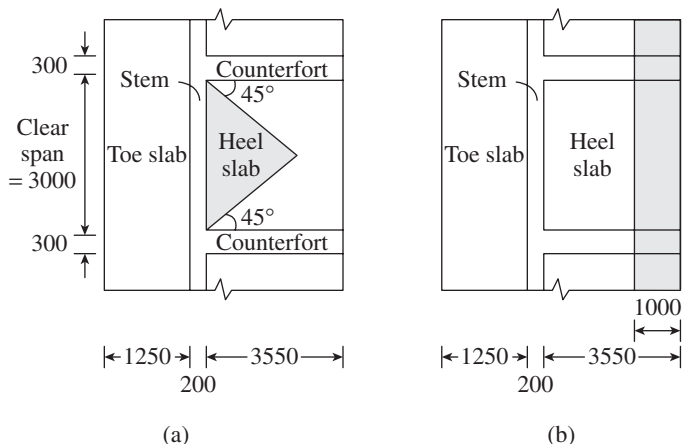


FIG. 16.52 Assumed behaviour of heel slab (a) Cantilever action (b) Continuous beam action

The bending moment coefficients for the aspect ratio interpolated from Tables 16.6 and 16.7 are given as follows:

$$\alpha_1 = -0.048; \alpha_2 = -0.068; \alpha_3 = 0.036; \alpha_4 = 0.086$$

$$\beta_1 = -0.031; \beta_2 = -0.031; \beta_3 = 0.016; \beta_4 = 0$$

Effective span = c/c spacing of counterforts + $d = 3 + 0.397 = 3.397$ m (see Fig. 16.52a)

The maximum (positive) bending moment occurs at the middle of the heel slab.

The gross and net pressure below the base slab is shown in Fig. 16.50.

The factored bending moment is

$$M_u = 1.5[0.068 \times 81.4 - (0.031) \times 70.5]3.397^2 = 57.98 \text{ kNm/m}$$

Alternatively, the approximate maximum mid-span moment can be calculated as

$$M_u = \frac{w_u L^2}{16} = 1.5[(10.9 + 81.4)/2] \times \frac{3.397^2}{16} = 49.93 \text{ kNm/m}$$

This value is approximately 14 per cent less than the accurate value.

Maximum factored negative bending moment at the counterfort location, near the free edge, is

$$M_u = 1.5[0.086 \times 81.4 - 0.0 \times 70.5] \times 3.397^2 = 121.5 \text{ kNm/m}$$

Design shear force

$$V_u = w_u(\text{clear span}/2 - d) = [1.5(10.9 + 81.4)/2] \left(\frac{3}{2} - 0.397 \right) = 76.36 \text{ kN/m}$$

$$\text{Nominal shear stress } \tau_v = \frac{V_u}{bd} = \frac{76.36 \times 1000}{1000 \times 397} = 0.193 \text{ N/mm}^2$$

From Table 19 of IS 456, for M25 concrete, p_t required = 0.15%

Design of reinforcement (for negative moment) at the counterfort

$$R = \frac{M_u}{bd^2} = \frac{121.5 \times 10^6}{1000 \times 397^2} = 0.771 \text{ MPa}$$

From Table 3 of SP 16, required $p_t = 0.2223\% > 0.15\%$ required for shear

$$\text{Hence required } A_{st} = \frac{0.2223}{100} \times 1000 \times 397 = 883 \text{ mm}^2$$

Spacing of 16 mm bars = $201 \times 1000/883 = 228$ mm

Provide five 16 mm bars at the top near the free edge between counterforts for 1 m length and in the remaining portion provide 16 mm at 220 mm c/c.

Provide 16 mm at 220 mm c/c in the perpendicular direction as well at the top. Extend it 645 mm beyond the stem.

Design of reinforcement for positive moment at mid-span

$$R = \frac{M_u}{bd^2} = \frac{57.98 \times 10^6}{1000 \times 397^2} = 0.368 \text{ MPa}$$

From Table 3 of SP 16, required $p_t = 0.104\% < 0.12\%$ (min.)

Hence required $A_{st} = 0.12/100 \times 1000 \times 397 = 476 \text{ mm}^2$

Spacing of 12 mm bars = $113 \times 1000/476 = 237$ mm

Provide 12 mm bars at 230 mm c/c.

Distribution steel

Provide 12 mm at 230 mm c/c.

Step 7 Design the vertical stem slab. The counterforts support the vertical stem wall with a clear span of 3 m and of cantilever height = 7.52 m.

Aspect ratio of the slab = $7.52/3 = 2.5$

For triangular soil load, the bending moment coefficients for the aspect ratio from Table 16.6 are

$$\beta_1 = -0.029; \beta_2 = -0.04; \beta_3 = 0.021; \beta_4 = 0$$

The active earth pressure at the base of the wall is

$$p_a = K_a \gamma_e h = 18 \times \frac{7.52}{3} = 45.12 \text{ kN/mm}^2 \text{ (linearly varying to zero at top)}$$

Applying a load factor of 1.5, $w_u = 1.5 \times 45.12 = 67.68 \text{ kN/m}^2$

Clear spacing between counterforts = 3 m

Assuming 50 mm cover and 12 mm bars, effective depth, $d = 200 - 50 - 6 = 140$ mm

Hence effective span = $3000 + 140 = 3140$ mm

The factored negative bending moment occurs at the counterfort support. This may be taken as

$$M = \frac{w_u L^2}{12} = 67.68 \times \frac{3.14^2}{12} = 55.6 \text{ kNm/m}$$

Required effective depth,

$$d = \sqrt{\frac{M_u}{0.138 f_{ck} b}} = \sqrt{\frac{55.6 \times 10^6}{0.138 \times 25 \times 1000}} = 126 \text{ mm} < 140 \text{ mm (assumed)}$$

Maximum mid-span moment may be taken as

$$M = w_u L^2/16 = 0.75 \times 55.6 = 41.7 \text{ kNm/m}$$

Design shear force

$$V_u = w_u(\text{clear span}/2 - d) = 67.68 (3/2 - 0.14) = 92 \text{ kN/m}$$

Check for shear at base

Nominal shear stress

$$\tau_v = \frac{V_u}{bd} = \frac{92 \times 1000}{1000 \times 140} = 0.657 \text{ N/mm}^2$$

As the shear stress is high, increase the thickness of stem as 300 mm, $d = 300 - 56 = 244$ mm

$$\tau_v = \frac{92 \times 1000}{1000 \times 244} = 0.377 \text{ N/mm}^2$$

From Table 19 of IS 456, required p_t for M25 concrete = 0.283%

Design of reinforcement for negative moment at the counterfort

$$R = \frac{M_u}{bd^2} = \frac{55.6 \times 10^6}{1000 \times 244^2} = 1.11 \text{ MPa}$$

From Table 3 of SP 16, for M25 concrete and Fe 415 steel,

$$p_t = 0.3252\% > 0.283\% \text{ required for shear}$$

Required $A_t = (0.3252/100) \times 1000 \times 244 = 793 \text{ mm}^2/\text{m}$

Required spacing of 12 mm bars = $113 \times 1000/793 = 142$ mm

Provide 12 mm bars at 140 mm c/c at rear face of the stem up to one-third height (2.5 m). In the next one-third, provide 12 mm at 240 c/c, and in the last one-third, provide minimum steel of 12 mm at 350 c/c.

Design of front face reinforcement for positive moment

$$R = \frac{M_u}{bd^2} = \frac{41.7 \times 10^6}{1000 \times 244^2} = 0.70 \text{ MPa}$$

From Table 3 of SP 16, for M25 concrete and Fe 415 steel

$$p_t = 0.201\% > 0.12\% \text{ (min.)}$$

Required $A_t = (0.201/100) \times 1000 \times 244 = 490 \text{ mm}^2/\text{m}$

Required spacing of 12 mm bars = $113 \times 1000/490 = 230$ mm

Provide 12 mm horizontal bars at 230 mm c/c on front faces of the stem up to two-thirds height (5.0 m) above the base; above that provide minimum steel (12 mm at 350 c/c).

Step 8 Design the stem for cantilever action. Consider the triangular loading on the stem (Fig. 16.53) to be carried by cantilever action. The intensity of horizontal pressure at the base of the stem is 45.12 kN/m^2 and at a distance 1.5 m above the base it is $18 \times (7.52 - 1.5)/3 = 36.12 \text{ kN/m}^2$

Total bending moment due to the loading on the triangular portion

$$\begin{aligned} &= \left(\frac{1}{2} \times 3 \times 1.5\right) \left(36.12 \times \frac{1.5}{2} + (45.12 - 36.12) \times \frac{1.5}{2 \times 3}\right) \\ &= 66.02 \text{ kNm} \end{aligned}$$

This moment is distributed non-uniformly across the width of 3 m. Let us assume that the maximum moment is two-thirds of this value.

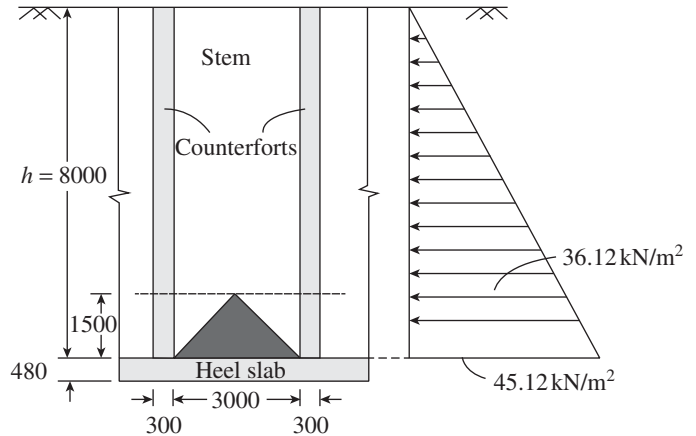


FIG. 16.53 Design of stem for cantilever action

$$M_{\max} = 66.02 \times 2/3 = 44.01 \text{ kNm}$$

Effective depth = $244 - 12 = 232$ mm

$$R = \frac{M_u}{bd^2} = \frac{1.5 \times 44.01 \times 10^6}{1000 \times 232^2} = 1.226 \text{ MPa}$$

From Table 3 of SP 16, required $p_t = 0.361\% > 0.12\%$ (minimum)

Required $A_{st} = 0.361/100 \times 1000 \times 232 = 838 \text{ mm}^2$ (required up to 1.5 m height from base)

Spacing of 12 mm bars = $113 \times 1000/838 = 135$ mm

Provide 12 mm bars at 130 mm c/c up to 1.5 m height, and above that provide minimum steel of 12 mm bars at 360 mm c/c on both the faces.

The reinforcement details of toe, heel, and vertical stem slabs are shown in Fig. 16.54.

Step 9 Design the counterfort. The interior counterfort acts as a T-beam of varying section cantilevering from the base slab.

Height of counterfort = 7.52 m

Assumed thickness = 300 mm

Clear spacing = 3 m

Thus, each counterfort receives earth pressure from a width of $L_1 = 3 + 0.3 = 3.3$ m

The earth pressure at the base $P_a = 45.12 \text{ kN/m}^2$

The factored bending moment in one counterfort is

$$M_u = 1.5 \left(\frac{1}{2} \times 45.12 \times 7.52\right) \times 3.3 \times \frac{7.52}{3} = 2105 \text{ kNm}$$

$$V_u = 1.5 \left(\frac{1}{2} \times 45.12 \times 7.52\right) \times 3.3 = 839.8 \text{ kN}$$

The compressive face of the beam is not upright but at an inclination of $\tan \theta = 3450/7520$ or $\theta = 24.64^\circ$ (see Fig. 16.55).

$$D \text{ at base} = L \cos \theta = 3450 \cos 24.64 = 3135 \text{ mm}$$

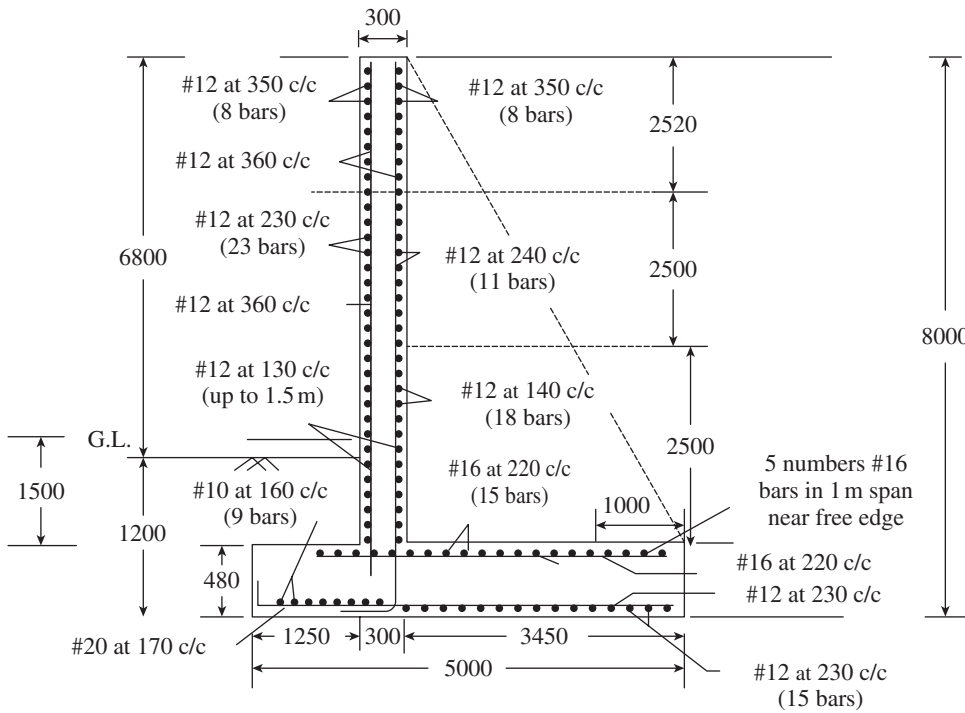


FIG. 16.54 Detailing of stem, toe, and heel slabs

With a clear cover of 50 mm and with 25 mm bars,

$$\text{Effective depth, } d = 3135 - 50 - 12.5 = 3072.5 \text{ mm}$$

$$\text{Required depth} = \sqrt{\frac{2105 \times 10^6}{0.138 \times 300 \times 25}} = 1426 \text{ mm} < 3072.5 \text{ mm}$$

Hence, the considered depth is sufficient.

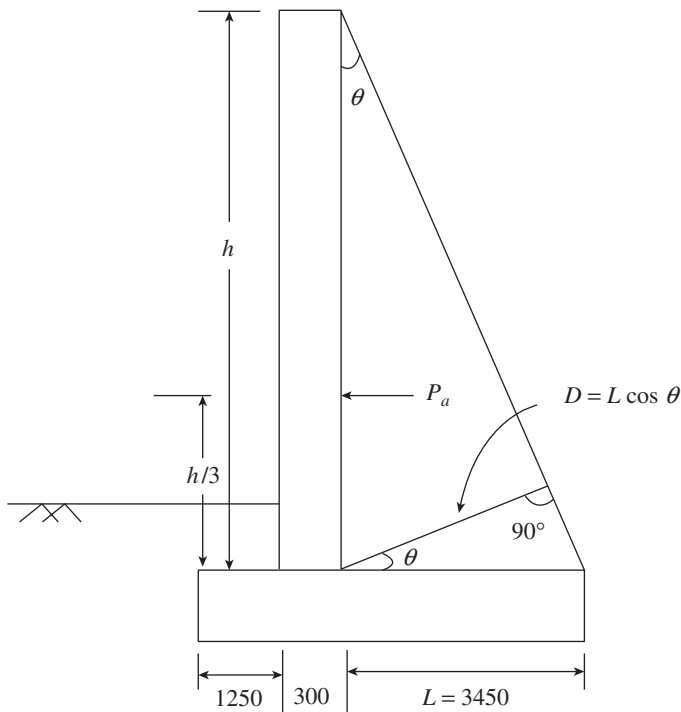


FIG. 16.55 Assumed depth for counterfort

The area of tension steel is calculated as

$$\begin{aligned} A_{st} &= \frac{M_u}{jd(0.87f_y)} \\ &= \frac{2105 \times 10^6}{0.8 \times 3072.5 \times 0.87 \times 415} \\ &= 2105 \text{ mm}^2 \end{aligned}$$

Percentage of reinforcement = $2105 / (300 \times 3072.5) \times 100 = 0.23\%$

Minimum reinforcement in beam

$$\frac{A_s}{bd} = \frac{0.85}{f_y}$$

Hence, $A_s = 0.85 \times 300 \times 3072.5 / 415 = 1887 \text{ mm}^2 < 2105 \text{ mm}^2$

Required number of 20 mm bars = $2105 / 314 = 7$

Provide seven 20 mm bars (Area = 2198 mm^2) in two rows.

Curtailement of bars

Let h_1 be the depth at which one bar can be curtailed. Then

$$\left(\frac{7-1}{7}\right) = \left(\frac{h_1}{7.52}\right)^2$$

$h_1 = 6.96 \text{ m}$ from top; curtail one bar at 7 m from top.

The remaining bars are required ($6 \times 314 = 1884 \text{ mm}^2$) to satisfy minimum reinforcement requirement.

Shear reinforcement (connection between counterfort and stem slab)

$$V_{u,net} = V_u - \frac{M_u}{d} \tan \theta = 839.8 - \frac{2105}{3.072} \tan 24.64 = 525.5 \text{ kN}$$

$$\text{Nominal shear stress} = \frac{V_{u,net}}{bd} = \frac{525.5 \times 1000}{300 \times 3072.5} = 0.57 \text{ N/mm}^2$$

$$p_t = \frac{100A_{st}}{bd} = \frac{100 \times 2198}{300 \times 3072.5} = 0.238\%$$

From Table 19 of IS 456, for M25 concrete

$$\tau_c = 0.352 \text{ N/mm}^2 < 0.57 \text{ N/mm}^2$$

Hence, shear reinforcement has to be provided for a shear force of

$$\begin{aligned} V_{ns} &= (\tau_v - \tau_c)bd = (0.570 - 0.352) \times 300 \times 3072.5 \times 10^{-3} \\ &= 200.94 \text{ kN} \end{aligned}$$

Assume two-legged 8 mm stirrup, $A_{sv} = 2 \times 50 = 100 \text{ mm}^2$

Required spacing

$$s_v = \frac{0.87 f_y A_{sv} d}{V_{us}} = \frac{0.87 \times 415 \times 100 \times 3072.5}{200.94 \times 10^3}$$

$$= 552 > 300 \text{ mm (maximum as per code)}$$

Hence, provide two-legged 8 mm stirrups at 300 mm c/c.

Check for tension

The tension to be resisted by the ties is given by the lateral pressure multiplied by the tributary area.

Thus $T = 45.12 \text{ kN/m}^2 \times 3.3 = 149 \text{ kN/m}$

With a load factor of 1.5, required area of steel

$$= \frac{1.5 \times 149 \times 10^3}{0.87 \times 415} = 619 \text{ mm}^2/\text{m}$$

Spacing of two-legged 8 mm stirrups = $2 \times 50 \times 10^3 / 619 = 161.5 \text{ mm}$

Spacing of two-legged 10 mm stirrups = $2 \times 78.5 \times 10^3 / 619 = 253 \text{ mm}$

Hence, provide two-legged 10 mm stirrups at 250 mm c/c at the base.

At one-third height from the base,

Required $A_{st} = 2/3 \times 619 = 413 \text{ mm}^2/\text{m}$

Spacing of two-legged 8 mm stirrups = $2 \times 50 \times 103 / 413 = 242 \text{ mm}$

Provide two-legged 8 mm stirrups at 240 mm c/c from a distance of 2500 mm from the base.

Design of vertical ties

As in the case of connection between the counterfort and vertical stem, the connection between the counterfort and heel slab has to be designed for the tension due to the net downward pressure acting on the heel slab (see Fig. 16.50). Considering 1 m width near the end of heel slab, the average downward pressure

$$= \frac{\left[81.4 + \left(10.9 + \frac{81.4 - 10.9}{3.55} \times 1 \right) \right]}{2}$$

$s = 56.08 \text{ kN/m}^2$

Average tension force = $56.08 \times 3.3 = 185.06 \text{ kN/m}$

With a load factor of 1.5, required area of reinforcement =

$$\frac{1.5 \times 185.06 \times 10^3}{0.87 \times 415} = 769 \text{ mm}^2$$

Spacing of two-legged 10 mm ties = $2 \times 78.5 \times 10^3 / 769 = 204 \text{ mm}$

Provide two-legged 10 mm ties at 200 mm c/c. The spacing may be increased to 300 mm beyond 1 m, due to the reduction in net pressure. The reinforcement details

of stem and counterfort are shown in Fig. 16.56, and the reinforcement in counterfort is shown in the section through counterfort in Fig. 16.57.

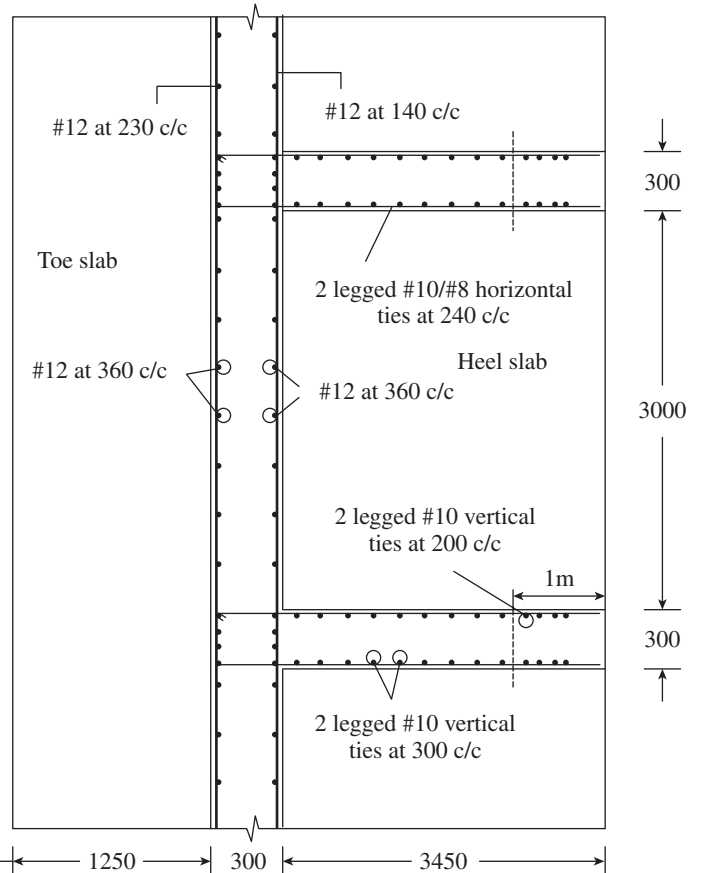


FIG. 16.56 Reinforcement details of stem and counterfort

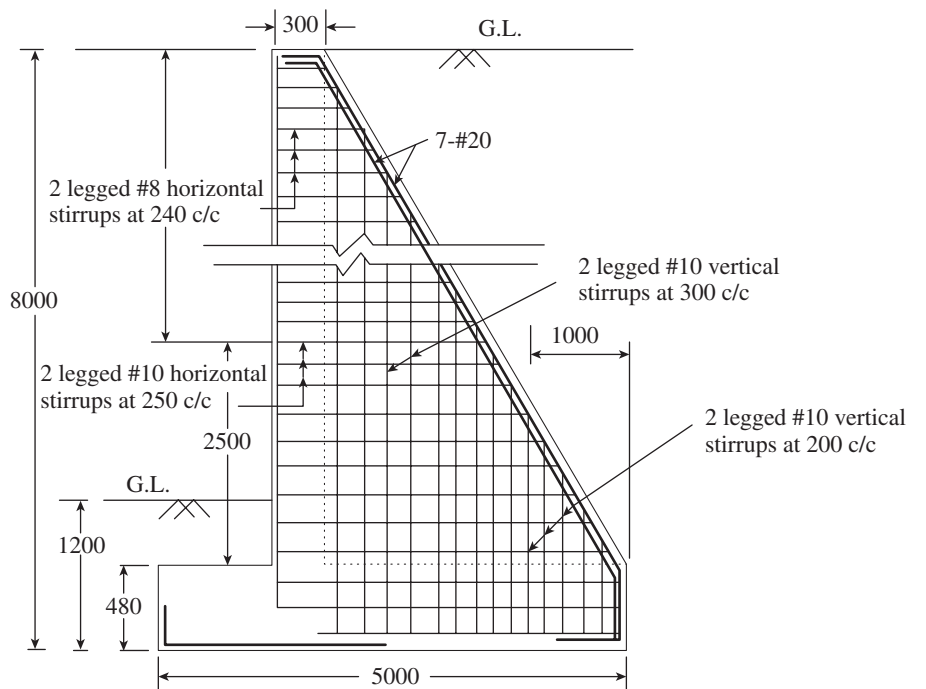


FIG. 16.57 Section through counterfort showing the reinforcement detail

EXAMPLE 16.5:

A 5 m high retaining wall with back face inclined at 20° to the vertical retains cohesionless backfill with $\gamma_c = 18 \text{ kN/m}^3$, $\phi = 32^\circ$ and $\beta = 20^\circ$. The backfill surface is sloping at an angle of 18° to the horizontal. Determine the active dynamic earth pressure acting on the retaining wall using Mononobe–Okabe method, assuming that the wall is located in a seismic region with $A_h = 0.21$.

SOLUTION:

Given $\gamma_c = 18 \text{ kN/m}^3$, $\phi = 32^\circ$, $\beta = 20^\circ$, $\delta = 18^\circ$, $\theta = 20^\circ$ and $A_h = 0.21$.

The dynamic active earth pressure as per Mononobe–Okabe method is given by

$$(P_a)_{dyn} = \frac{1}{2} \gamma H^2 (1 \pm A_v) (K_a)_{dyn} \quad (16.21a)$$

where

$$(K_a)_{dyn} = \left[\frac{\cos^2(\phi - \psi - \theta)}{\cos \psi \cos^2 \theta \cos(\psi + \theta + \beta)} \times \left(1 + \sqrt{\frac{\sin(\phi + \beta) \sin(\phi - \psi - \delta)}{\cos(\beta + \psi + \theta) \cos(\theta - \delta)}} \right)^2 \right] \quad (16.21b)$$

Assuming $A_v = (2/3)A_h = (2/3) \times 0.21 = 0.14$

The seismic inertia angle ψ is given by

$$\psi = \tan^{-1} \left(\frac{A_h}{1 \mp A_v} \right) = \tan^{-1} \left(\frac{0.21}{1 \mp 0.14} \right) = 10.4^\circ \text{ for } +A_v \text{ and } 13.7^\circ \text{ for } -A_v.$$

The value of ψ must always be less than or equal to the difference of the angle of internal friction and the ground surface inclination (i.e., $\phi - \delta$). If it is greater, then the value of ψ may be assumed as $\phi - \delta$. It should be noted that in our case $\psi < \phi - \delta = 32 - 18 = 14$.

Value of $(P_a)_{dyn}$ with $+A_v$

$$\begin{aligned} &= \frac{1}{2} \times 18 \times 5^2 \frac{\cos^2(32 - 10.4 - 20)}{\cos 10.4 \cos^2 20 \cos(10.4 + 20 + 20)} \\ &\quad \times \left(1 + \sqrt{\frac{\sin(32 + 20) \sin(32 - 10.4 - 18)}{\cos(20 + 10.4 + 20) \cos(20 - 18)}} \right)^2 \\ &= 225 \times \frac{0.9992}{0.9836 \times 0.8830 \times 0.6374} \\ &\quad \times \left(1 + \sqrt{\frac{0.7880 \times 0.0628}{0.6374 \times 0.9994}} \right)^2 \\ &= 248 \text{ kN/m} \end{aligned}$$

Value of $(P_a)_{dyn}$ with $-A_v$

$$\begin{aligned} &= \frac{1}{2} \times 18 \times 5^2 \\ &\quad \frac{\cos^2(32 - 13.7 - 20)}{\cos 13.7 \cos^2 20 \cos(13.7 + 20 + 20)} \\ &\quad \times \left(1 + \sqrt{\frac{\sin(32 + 20) \sin(32 - 13.7 - 18)}{\cos(20 + 13.7 + 20) \cos(20 - 18)}} \right)^2 \\ &= 225 \times \frac{0.9996}{0.9715 \times 0.8830 \times 0.5920} \\ &\quad \times \left(1 + \sqrt{\frac{0.7880 \times 0.0052}{0.5920 \times 0.9994}} \right)^2 \\ &= 94.11 \text{ kN/m} \end{aligned}$$

The $+A_v$ case governs and hence $(P_a)_{dyn} = 248 \text{ kN/m}$.

EXAMPLE 16.6:

Design the shear wall of a 10-storey building having a dual system consisting of SMRF and structural walls. The floor to floor height is 3.1 m. The design forces in the wall have been obtained from a computer analysis and are shown in Table 16.11. Design the structural wall assuming M25 concrete and Fe 415 steel. The following sizes were assumed in the computer analysis: Length and height of wall are 4 m and 31 m, respectively, wall thickness is 200 mm, boundary element (column) size is 450 mm \times 450 mm, and beam size is 300 mm \times 450 mm.

TABLE 16.11 Design forces under different loading cases

Load Case	Moment (kNm)	Shear (kN)	Axial Force (kN)	Axial Load on Boundary Element (kN)
1.5(DL + LL)	446	25.4	3710	377
1.2(DL + LL + EL)	4571	949	3001	1619
1.2(DL + LL - EL)	5296	990	2935	1800
1.5(DL + EL)	5773	1190	3075	1938
1.5(DL - EL)	6559	1234	3172	2132
0.9DL + 1.5EL	5928	1198	1970	1717
0.9DL - 1.5EL	6406	1232	1886	1829

SOLUTION:

Step 1 Check for boundary columns requirement. Although a boundary element was considered in the analysis, let us

check whether it is required, assuming a rectangular wall of size 4000 mm × 200 mm.

From Table 16.8, maximum design forces at the base of the wall

$$P_u = 3710 \text{ kN} \quad \text{and} \quad M_u = 6559 \text{ kNm}$$

$$\text{Stress} = \frac{P_u}{A_g} + \frac{M_u \left(\frac{L_w}{2} \right)}{I} = \frac{3710 \times 10^3}{4000 \times 200} + \frac{6559 \times 10^6 \times \left(\frac{4000}{2} \right)}{4000^3 \times \frac{200}{12}}$$

$$= 4.64 + 12.29 = 16.69 \text{ N/mm}^2 > 0.2f_{ck} = 5 \text{ N/mm}^2$$

Since the stress in the extreme fibre exceeds the limit, boundary element should be provided (Clause 9.4.1 of IS 13920). The boundary element provided in the form of column of size 450 mm × 450 mm is shown in Fig. 16.58.

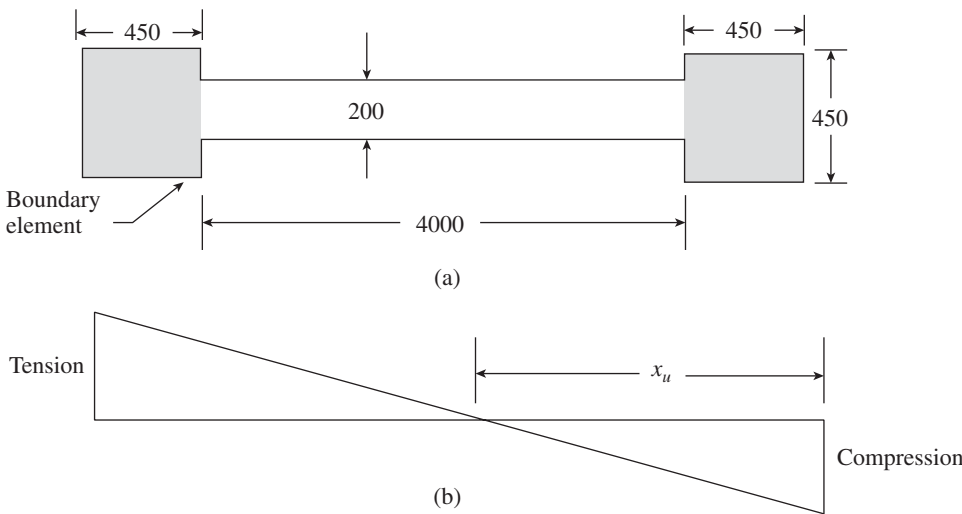


FIG. 16.58 Dimensions and stress distribution of structural wall

Step 2 Check for section requirements (Clause 9.1.2 of IS 13920).

Thickness of wall = 200 mm > 150 mm

Hence, minimum thickness is satisfied.

Step 3 Check for minimum reinforcement (Clause 9.1.4).

$$A_{st} = 0.0025t_w l_w = 0.0025 \times 200 \times 4000 = 2000 \text{ mm}^2$$

Thickness is 200 mm; hence, reinforcement should be provided in two layers (Clause 9.1.5). Provide 8 mm bars at 200 mm c/c in the two layers in both horizontal and vertical directions; area provided = 251 × 4 × 2 = 2008 mm².

Maximum allowed spacing (Clause 9.1.7):

Smaller of $L_w/5$, $3t_w$, and 450 or $4000/5 = 800$, $3 \times 200 = 600$, and 450

$$450 \text{ mm} > 200 \text{ mm}$$

Hence, the adopted spacing is adequate. As per Clause 9.1.6, diameter of bar should be less than $t_w/10 = 200/10 = 20 \text{ mm} > 8 \text{ mm}$. Hence, the adopted diameter is sufficient.

Maximum area of vertical reinforcement in boundary element (Clause 9.4.4)

$$A_{st} < 0.04 \times \text{Area of boundary element}$$

$$= 0.04 \times 450 \times 450 = 8100 \text{ mm}^2$$

$$\text{Minimum area} = 0.008 \times 450 \times 450 = 1620 \text{ mm}^2$$

$$\text{Provide twelve 16 mm bars. Area} = 2412 \text{ mm}^2 > 1620 \text{ mm}^2$$

Step 4 Design for shear (Clause 9.2 of IS 13920).

$$\text{Effective depth of wall } d_w = 0.8L_w = 0.8 \times 4000 = 3200$$

$$\text{Nominal shear stress} = \frac{V_w}{t_w d_w} = \frac{1234 \times 1000}{200 \times 3200} = 1.925 \text{ N/mm}^2$$

As per Table 19 of IS 456, design shear strength for M25 concrete with 0.25 per cent steel is 0.36 N/mm².

$$\tau_{c,max} \text{ (Table 20 of IS 456)} = 3.1 \text{ N/mm}^2 > 1.925 \text{ N/mm}^2$$

Hence, shear has to be carried by shear reinforcement.

$$V_{u,s} = (\tau_v - \tau_c)t_w d_w = (1.925 - 0.36) \times 200 \times 3200 \times 10^{-3} = 1001.6 \text{ kN}$$

Spacing required for two-legged 8 mm bar

$$s_v = \frac{0.87f_y A_h d_w}{V_{us}} = \frac{0.87 \times 415 \times (2 \times 50) \times 3200}{1001.6 \times 10^3} = 115.4 \text{ mm} < 200 \text{ mm} \text{ (minimum assumed)}$$

$$\text{Spacing of 10 mm bars} = \frac{115.4}{100} \times (2 \times 78.5) = 181.2 \text{ mm}$$

Provide 10 mm bars at 180 mm c/c in two curtains in the horizontal and vertical directions

$$\text{(area of vertical steel} = 4 \times 2 \times 436 = 3488 \text{ mm}^2\text{)}.$$

Step 5 Design for flexural strength (Annex A of 13920).

Axial load on wall, $P_u = 3710 \text{ kN}$

$$\frac{x_u^*}{L_w} = \frac{0.0035}{0.0035 + 0.87f_y/E_s} = \frac{0.0035}{0.0035 + 0.87 \times 415 / (2 \times 10^5)} = 0.66$$

$$\frac{x_u}{L_w} = \frac{\phi + \lambda}{2\phi + 0.36}$$

$$\text{where } \phi = \frac{0.87 f_y \rho}{f_{ck}} \text{ and } \lambda = \frac{P_u}{f_{ck} t_w L_w}$$

$$\rho = \text{vertical steel ratio} = A_{sv} / (t_w L_w)$$

$$\rho = \frac{A_{sv}}{t_w S_v} = \frac{3488}{200 \times 4000} = 4.36 \times 10^{-3}$$

$$\phi = \frac{0.87 \times 415 \times 4.36 \times 10^{-3}}{25} = 0.063$$

$$\lambda = \frac{3710 \times 10^{-3}}{25 \times 200 \times 4000} = 0.1855$$

$$\text{Hence } \frac{x_u}{L_w} = \frac{0.063 + 0.1855}{2 \times 0.063 + 0.36} = 0.511 < \frac{x_u^*}{L_w} = 0.66$$

Hence

$$\frac{M_n}{f_{ck} t_w L_w^2} = \phi \left[\left(1 + \frac{\lambda}{\phi} \right) \left(\frac{1}{2} - 0.416 x_u / L_w \right) - \left(\frac{x_u}{L_w} \right)^2 \left(0.168 + \frac{\beta^2}{3} \right) \right]$$

$$\text{where } \beta = \frac{0.87 f_y}{0.0035 E_s} = \frac{0.87 \times 415}{0.0035 \times 2 \times 10^5} = 0.5158$$

$$\frac{M_n}{f_{ck} t_w L_w^2} = 0.063 \left[\left(1 + \frac{0.1855}{0.063} \right) \left(\frac{1}{2} - 0.416 \times 0.511 \right) - (0.511)^2 \left(0.168 + \frac{0.5158^2}{3} \right) \right]$$

$$= 0.063 [3.944 \times 0.2874 - 0.067] = 0.0672$$

Thus, $M_n = 0.0672 \times 25 \times 200 \times 4000^2 \times 10^{-6} = 5375.2 \text{ kNm}$

The remaining moment, that is, $M_u - M_n = 6559 - 5375.2 = 1183.8 \text{ kNm}$, should be resisted by reinforcement in the boundary elements.

Step 6 Design the boundary elements. The maximum compressive axial load on boundary element (column) as per Table 16.8,

$$P_u = 2132 \text{ kN}$$

c/c of boundary element, $C_w = 4 + 0.45 = 4.45 \text{ m}$

Additional compressive force induced by seismic force (Clause 9.4.2 of IS 13920)

$$= \frac{M_u - M_{uv}}{C_w} = \frac{1183.8}{4.45} = 266 \text{ kN}$$

Total axial load = $2132 + 266 = 2398 \text{ kN}$

Size of the boundary element = $450 \text{ mm} \times 450 \text{ mm}$

$$A_g = 450 \times 450 = 202.5 \times 10^3 \text{ mm}^2$$

Assuming minimum longitudinal reinforcement of 0.8 per cent of gross area, as per Clause 9.4.4 of IS 13920

$$A_s = 0.008 \times 202.5 \times 10^3 = 1.62 \times 10^3 \text{ mm}^2$$

Axial load capacity of boundary element acting as short column

$$P_n = 0.4 f_{ck} A_g + (0.67 f_y - 0.4 f_{ck}) A_s$$

$$= 0.4 \times 25 \times 202.5 \times 10^3 + (0.67 \times 415 - 0.4 \times 25) 1.62 \times 10^3$$

$$= 2459 \times 10^3 \text{ N} = 2459 \text{ kN} > 2398 \text{ kN}$$

Hence provide eight 16 mm bars (area = 1608 mm^2).

Confining reinforcement in boundary element

Special confining reinforcement should be provided throughout the height of the boundary element (Clauses 9.4.6 and 7.4.8 of IS 13920)

$$A_{sh} = 0.18 s h \left[\frac{f_{ck}}{f_y} \right] \left[\frac{A_g}{A_k} - 1.0 \right]$$

Let us assume an effective cover of 50 mm.

$$h = \text{Longer dimension of the rectangular confining hoop}$$

$$= (450 - 50 \times 2) = 350 \text{ mm} > 300 \text{ mm}$$

Hence, provide a cross-tie in both directions. Now, $h = 175 \text{ mm}$.

A_k = Area of confined core in the rectangular hoop measured to its outside dimensions

$$= (450 - 100) \times (450 - 100) = 122,500 \text{ mm}^2$$

$$A_g = \text{Cross area} = 450 \times 450 = 202,500 \text{ mm}^2$$

$$A_{sh} = 0.18 s \times 175 (25/415) [(202,500/122,500) - 1.0] = 1.24 s$$

$s \leq$ one-fourth size of boundary element or $6d_b = (1/4 \times 450)$ or $(6 \times 16) = 112.5 \text{ mm}$ or 96 mm

$75 \text{ mm} \leq s \leq 100 \text{ mm}$ (Clause 7.4.6 of IS 13920) using $s = 90 \text{ mm}$

$$A_{sh} = 1.24 \times 90 = 111.5 \text{ mm}^2$$

$$\text{Moreover, } A_{sh} > 0.05 s h (f_{ck}/f_y) = 0.05 \times 90 \times 175 \times (25/415) = 47.5 \text{ mm}^2$$

Hence, provide 12 mm ties at 90 mm c/c. The details of the structural wall are shown in Fig. 16.59.

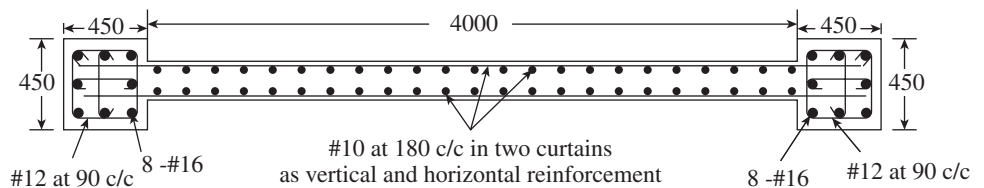


FIG. 16.59 Reinforcement details of structural wall

SUMMARY

Similar to a column, a reinforced concrete (RC) wall is a vertical member in a building. When the length is less than four times the thickness, it is called a column; otherwise, it is considered a wall. Walls may be classified as non-load-bearing walls (basement and retaining walls, which are subjected to lateral earth or water pressure but usually not subjected to in-plane axial loads), load-bearing walls (carrying in-plane vertical loads), and structural (shear) walls (designed to carry lateral loads). IS 456 does not contain provisions for designing structural walls, which may be designed using the provisions of IS 13920. In addition to these types, walls may be classified as braced or unbraced as well as stocky or slender. The empirical design method given in Clause 32.2 of IS 456 may be used to find the design strength of walls subjected to in-plane vertical loads. Clause 32.3 of IS 456 gives a procedure to design walls subjected to combined horizontal and vertical forces. These procedures are compared with ACI 318 and BS 8110 procedures for both braced and unbraced walls. The shear strength provisions of IS 456 and ACI 318 codes are also compared. The detailing of walls with in-plane loads is also provided.

Retaining walls, which are used to retain material on one or both sides, may be of the following types: Gravity and semi-gravity walls; gabions; crib walls; basement walls; cantilever, counterfort, or buttressed walls; anchored walls; and segmental retaining walls. The design of the cantilever, counterfort, or buttressed walls requires the knowledge of earth pressure theories. There are three types of earth pressures: Active, passive, and at rest. Active or passive earth pressure is affected by several factors, which include the type of backfill material used, drainage of backfill material, level of water table, consolidation of backfill, amount of surcharge on the backfill, type of soil below the footing, and possibility of vibration in the vicinity of the wall. Drainage of backfill is an important practical criterion and several failures of retaining walls have been reported due to improper drainage.

The two earth pressure theories, namely Rankine's theory, developed in 1857, and Coulomb's theory, developed in 1773, are discussed and the expressions for calculating active and passive earth pressures are provided. While calculating earth pressures, the effect of surcharge, submerged or stratified backfill, and horizontal or sloped nature of backfill should be considered. The simplified Mononobe–Okabe method is usually specified in codes to calculate

the earth pressure due to earthquakes, although some sophisticated methods have also been developed in the recent past.

Design of retaining walls is an iterative process. This involves assumptions of some preliminary dimensions, the guidelines for which are provided. Practical aspects such as drainage and compaction of backfill are also discussed. Expressions for checking the stability against overturning and sliding (with and without considering passive earth pressure) are derived. The use of shear key, which will increase the factor of safety against sliding, is explained.

The various steps involved in the design and detailing of retaining walls are enumerated and practical aspects such as provision of construction, expansion, and contraction joints are also considered. The behaviour and design of cantilever- and counterfort-retaining walls are explained. The difference in the design of basement walls is explained.

There may be different types of structural walls, which are also known as shear walls. They include rectangular or flanged walls, box type walls, and coupled walls. Depending on the height-to-length ratio, walls may be classified as flexural (slender) walls and squat walls. Shear strength in squat walls has to be checked carefully. Past earthquakes have demonstrated the importance of boundary elements. The behaviour of structural walls and failure modes of slender and squat structural walls are illustrated. A short discussion on the interaction of dual system (consisting of structural walls and rigid jointed frames) has been included. Proper software should be used to consider the interaction, and proper foundation systems should be used to resist the applied lateral as well as in-plane loads.

The expressions provided in IS 13920 for calculating the flexural strength of these walls are derived, and shear strength requirements are also discussed. The design of boundary elements as per IS 13920 is explained, and the drawback of this procedure is also indicated. A brief discussion on high-strength concrete structural walls is included. The detailing aspects of structural walls are enumerated. The steps required for the design of structural walls are provided. The design of coupling beams and the various reinforcement options are discussed. Methods to take care of opening in structural walls are also provided. Recent research on coupled walls is also included and the readers may consult the list of references for further study. Complete design examples are provided to explain the concepts and use the expressions developed for the design of various types of RC walls.

REVIEW QUESTIONS

- Both wall and column are vertical elements of a building. How is a wall distinguished from a column?
- How is the wall designed under the following conditions?
 - In-plane vertical loading with eccentricity
 - In-plane vertical and lateral loads with part of the section in tension
 - In-plane vertical loads and horizontal loads acting perpendicular to the plane of the wall
- What are the three types of walls? Give examples of each type with appropriate sketches.
- Define slenderness ratio for a wall. Give the slenderness limit of a wall as per IS 456.
- An unbraced wall can be considered stocky when the slenderness ratio of the unbraced wall does not exceed _____.
 - 10
 - 12
 - 15
 - 30
- Load-bearing walls can be considered as concentrically loaded when the eccentricity is less than _____.
 - one-fourth the wall thickness
 - one-third the wall thickness
 - one-sixth the wall thickness
 - one-fifth the wall thickness
- The thickness of braced walls should be equal to or greater than _____.

- (a) 100 mm (c) 175 mm
(b) 150 mm (d) 200 mm
8. List the conditions given in Clause 32.2.1 of IS 456 for the wall to be considered as braced.
 9. When the wall supports a slab on only one side, the load from the slab is assumed to act at _____.
(a) one-fourth of the thickness from the loaded face
(b) one-third of the thickness from the loaded face
(c) one-fifth of the thickness from the loaded face
(d) none of these
 10. The wall design should anyhow consider a minimum eccentricity of _____.
(a) $t/10$ (c) $t/20$
(b) $t/15$ (d) none of these
 11. How is the effective height of a braced wall determined as per IS 456? Will cross walls, provided as stiffeners, affect the strength of walls?
 12. State the empirical design method given in Clause 32.2.5 of IS 456. Why does it not take the reinforcement into account?
 13. When is a wall considered a squat wall as per IS 456?
 14. How are walls designed to resist shear force as per Clause 32.4 of IS 456?
 15. The effective depth of a wall is taken as _____.
(a) $0.75L_w$ (c) $0.85L_w$
(b) $0.8L_w$ (d) $0.9L_w$
 16. What are the minimum vertical and horizontal steel requirements in walls as per IS 456?
 17. How are cracks controlled in walls by spacing of rebars?
 18. When are vertical and horizontal reinforcements provided in walls in two grids?
(a) $t > 150$ mm (c) $t > 250$ mm
(b) $t > 200$ mm (d) $t > 300$ mm
 19. Sketch the standard detailing in RC walls as per SP 34.
 20. How is the connection between roof slab and RC wall established as per SP 34?
 21. What is the reason for specifying more minimum horizontal reinforcement than vertical reinforcement in walls?
 22. What is the purpose of a retaining wall? List and sketch the different types of retaining walls encountered in practice.
 23. Write short notes on segmental retaining walls.
 24. What are the two theories for calculating earth pressure on retaining walls?
 25. Compare active, passive, and at rest earth pressures.
 26. What are the factors that affect the active or passive pressure applied on a wall?
 27. Why is clay not used as backfill material?
 28. What are the expressions for active and passive earth pressure coefficients for a retaining wall with sloping backfill as per Rankine's theory?
 29. What is meant by surcharge? How is it considered in earth pressure calculations?
 30. How is the effect of water in the backfill considered in the calculation of active earth pressure?
 31. What is the main difference between Rankine's and Coulomb's earth pressure theories?
 32. What are the expressions for active and passive earth pressure coefficients for a retaining wall with straight backfill as per Coulomb's theory?
 33. How can the earth pressure due to earthquake be considered in the analysis?
 34. The width of base is often chosen as _____.
(a) 0.3–0.5 times the height of wall
(b) 0.4–0.6 times the height of wall
(c) 0.5–0.7 times the height of wall
(d) none of these
 35. Why is it preferable to taper the outside face of the stem of retaining walls?
 36. The counterforts are usually spaced at a c/c distance of _____.
(a) 3 m
(b) one-third to one-half the total height
(c) one-third to two-thirds the total wall height
(d) one-third the projecting height from the ground level
 37. Why is it important to consider drainage of backfill? What methods are adopted for the effective drainage of backfill?
 38. How is the check for overturning performed on retaining walls? State the equation for the factor of safety against overturning for level backfill.
 39. How is the check for sliding performed on retaining walls? State the equation for the factor of safety against sliding for level backfill.
 40. What is the purpose of shear key? How does it increase the shearing resistance?
 41. What are the soil bearing pressure requirements of retaining walls?
 42. List the various steps involved in the design of retaining walls.
 43. Write short notes on joints in retaining walls.
 44. Briefly describe the behaviour and design of the various elements of a cantilever-retaining wall.
 45. Where are the critical sections for shear located in the case of (a) the toe slab and (b) the heel slab of a cantilever-retaining wall? Why is the critical section for shear in a heel slab taken differently?
 46. The development length of bars in a heel slab is taken as _____.
(a) L_d (c) $1.3L_d$
(b) $2L_d$ (d) none of these
 47. Briefly describe the behaviour and design of the various elements of a counterfort-retaining wall.
 48. How does the design of stem slab and heel slab differ between counterfort-retaining walls and cantilever-retaining walls?
 49. Are buttresses more efficient than counterforts? Justify your answer.
 50. What are structural walls? Why should they not be called shear walls? What are their advantages while resisting earthquake loads?
 51. Write a short note on the types of structural walls.
 52. What are boundary elements in structural walls and when should they be provided as per IS 13920? How do they improve the performance of structural walls?

53. How do squat structural walls behave differently from slender structural walls?
54. What are the five possible failure modes of slender structural walls?
55. What are the possible failures modes of squat structural walls?
56. Write short notes on the interaction of structural walls with moment-resisting frames?
57. The minimum thickness of structural walls as per IS 13920 should be _____.
(a) 100 mm (c) 200 mm
(b) 150 mm (d) 250 mm
58. The minimum thickness of coupled structural walls as per IS 13920 should be
(a) 100 mm (c) 200 mm
(b) 150 mm (d) 250 mm
59. What are the assumptions made while deriving the expressions for flexural strength as per IS 13920?
60. What are the two equations provided in Annex A of IS 13920 for calculating the flexural strength of rectangular structural walls? Derive these equations.
61. How can we obtain expressions for calculating the flexural strength of structural walls with barbells?
62. How is the shear strength of a structural wall computed and shear reinforcement designed?
63. How is the design of boundary element considered in IS 13920?
64. List the detailing requirements of structural walls as per IS 13920.
65. The diameter of bars used in any part of the structural wall should not exceed _____.
(a) one-twelfth of the thickness of wall
(b) one-tenth of the thickness of wall
(c) one-eighth of the thickness of wall
(d) none of these
66. The maximum spacing of reinforcement in either direction should not exceed the smaller of _____.
(a) $L_w/5$, $2t_w$, and 300 mm
(b) $L_w/5$, $3t_w$, and 450 mm
(c) $L_w/5$, $3t_w$, and 300 mm
(d) none of these
67. Describe the steps involved in the design of structural walls.
68. Write short notes on coupling beams and their design.
69. Discuss the two confinement options for the coupling beams as given in ACI 318.
70. How are the openings in structural walls considered in IS 13920?
71. What are the alternative coupling beam arrangements envisaged by researchers?
72. Write short notes on construction joints in structural walls.

EXERCISES

1. A concrete-bearing wall, 3.5 m high and 5 m in length between cross walls, carries a factored load of 360 kN/m width through a floor at the top. Assuming that there are no openings in the wall, design the wall, considering M20 concrete and Fe 415 steel.
 2. Design a braced 5 m tall concrete wall, 4 m long and 200 mm thick. Assume that it is restrained against rotation at its base and unrestrained at the other ends. If it has to carry a factored vertical load of 350 kN and a factored horizontal load of 12 kN at the top, design the wall. Assume M20 concrete and Fe 415 steel.
 3. A cantilever-retaining wall is required to retain earth 4.0 m high above the ground level. The backfill surface is level but subjected to a surcharge pressure of 40 kN/m², and the backfilled granular soil is having a unit weight of 16 kN/m³ and angle of internal friction of 30°. The exposure condition is moderate. The SBC of soil at 1.25 m below ground level is 160 kN/m² and the coefficient of friction between the soil and concrete is 0.5. Design the RC retaining wall, assuming M20 concrete and Fe 415 steel.
 4. Design a counterfort-type retaining wall to retain a filling of 7.5 m height above the ground level. The unit weight and SBC of the soil at site are 15 kN/m³ and 150 kN/m², respectively.
- The angle of internal friction of soil and coefficient of friction are 30° and 0.5, respectively. The exposure condition is moderate.
5. An eight metre-high retaining wall with back face inclined at 20° to the vertical retains cohesionless backfill with $\gamma_c = 18 \text{ kN/m}^3$, $\phi = 30^\circ$, and $\beta = 20^\circ$. The backfill surface is sloping at an angle of 10° to the horizontal. Determine the active dynamic earth pressure acting on the retaining wall using Mononobe–Okabe method, assuming that the wall is located in a seismic region with horizontal seismic coefficient of 0.10.
 6. Design the structural wall of a 20-storey building having a dual system consisting of SMRF and structural walls. The floor-to-floor height is 3.1 m. The design forces in the wall obtained from a computer analysis are $P_u = 16,000 \text{ kN}$, $M_u = 14,550 \text{ kNm}$, and $V_u = 800 \text{ kN}$. Design the structural wall assuming M25 concrete and Fe 415 steel. The following sizes were assumed in the computer analysis: Total length (including the boundary element) and height of wall are 6 m and 62 m, respectively, wall thickness is 200 mm, and boundary element (column) size is 600 mm × 600 mm.

REFERENCES

- Agarwal, P. and M. Shrikhande 2006, *Earthquake Resistant Design of Structures*, Prentice Hall of India Pvt. Ltd, New Delhi, p. 634.
- Anderson, D.G., G.R. Martin, I. Lam, and J.N. Wang 2008, *Seismic Analysis and Design of Retaining Walls, Buried Structures, Slopes, and Embankments*, NCHRP Report 611, Transportation Research Board, Washington D.C., p. 148.
- AS 3600:2001, *Concrete Structures*, 3rd edition, Standards Australia International Ltd, Sydney, p. 176.
- ASCE/SEI 43-05 2005, *Seismic Design Criteria for Structures, Systems, and Components in Nuclear Facilities*, American Society of Civil Engineers, Reston, p. 96.
- BS 8110-1:1997, *Structural Use of Concrete, Part 1: Code of Practice for Design and Construction*, British Standards Institution, London, p. 148.
- Barda, F., J.M. Hanson, and W.G. Corley 1977, 'Shear Strength of Low-rise Walls with Boundary Elements', *Reinforced Concrete Structures*

- in *Seismic Zones, SP-53*, American Concrete Institute, Farmington Hills, pp. 149–202.
- Barney, G.B., K.N. Shiu, B.G. Rabbat, A.E. Fiorato, H.G. Russell, and W.G. Corley 1980, *Behavior of Coupling Beams under Load Reversals (RD068.01B)*, Portland Cement Association, Skokie, p. 25.
- Bohl, A. and P. Adebbar 2011, 'Plastic Hinge Lengths in High-rise Concrete Shear Walls', *ACI Structural Journal*, Vol. 108, No. 2, pp. 148–57.
- Brooks, H. and J.P. Nielsen 2012, *Basics of Retaining Wall Design—A Design Guide for Earth Retaining Structures*, 9th edition, HBA Publications, Inc., Corona del Mar, p. 240.
- Budhu, M. 2008, *Foundations and Earth Retaining Structures*, John Wiley and Sons Inc., New York, p. 500.
- Cardenas, A.E., J.M. Hanson, W.G. Corley, and E. Hognestad 1973, 'Design Provisions for Shear Walls', *ACI Journal, Proceedings*, Vol. 99, No. 3, pp. 221–30.
- Cardenas, A.E. and D.D. Magura 1973, Strength of High-rise Shear Walls—Rectangular Cross Sections, *ACI Special Publication 36, Response of Multistory Concrete Structures to Lateral Forces*, pp. 119–50.
- Carrillo, J. and S.M. Alcocer 2013, 'Shear Strength of Reinforced Concrete Walls for Seismic Design of Low-rise Housing', *ACI Structural Journal*, Vol. 110, No. 3, pp. 415–26.
- Clayton, C.R.I., J. Milititsky, and R.I. Woods 1993, *Earth Pressure and Earth-retaining Structures*, 2nd edition, CRC Press, Boca Raton, p. 408.
- Coulomb C.A. 1773, 'Essai Sur une application des règles de maximis et de minimis à quelques problèmes de statique, relatifs à l'architecture', *Mémoires de Mathématique et de Physique*, Présentés à l'Académie des Sciences, par divers Savans, Paris, Vol. 7, pp. 343–82.
- Culmann, C. 1875, *Die Graphische Statik*, Mayer and Zeller, Zurich.
- Das, B.M. 2010, *Principles of Geotechnical Engineering*, 7th edition, Cengage Learning, Stamford, p. 666.
- Dasgupta, K., R. Goswami, and C.V.R. Murty 2010, 'Seismic Shear Design of Deep RC Vertical Members: A Review of Codal Provisions', *The Indian Concrete Journal*, Vol. 84, No. 9, pp. 39–50, and 'Recommended Provisions for Indian Codes', pp. 59–63.
- Dasgupta, K. and C.V.R. Murty 2005, 'Seismic Design of RC Columns and Wall Sections, Part 1: Consistent Limit State Design Philosophy', *The Indian Concrete Journal*, Vol. 79, No. 3, pp. 33–41, and 'Part 2: Proposal for Limiting Strain in Steel', No. 4, pp. 22–6.
- Dasgupta, K., C.V.R. Murty, and S.K. Agrawal 2003, 'Seismic Shear Design of RC Structural Walls, Part I: Review of Code Provisions', *The Indian Concrete Journal*, Vol. 77, No. 11, pp. 1423–30, and 'Part II: Proposed Improvements in IS 13920:1993 Provisions', pp. 1459–68.
- Dharanidaran, S. and A.K. Sengupta 2012, 'Modeling of Tall Shear Walls for Non-linear Analysis of RC Buildings under Cyclic Lateral Loading', *The Indian Concrete Journal*, Vol. 86, No. 6, pp. 32–40.
- Dilger, W.H. and A. Ghali 1997, 'Double-head Studs as Ties in Concrete Walls and Columns', *Concrete International, ACI*, Vol. 19, No. 6, pp. 59–66.
- Donkada, D. and D. Menon 2012, 'Optimal Design of Reinforced Concrete Retaining Walls', *The Indian Concrete Journal*, Vol. 86, No. 4, pp. 9–18.
- Elias, V., B.R. Christopher, and R. R. Berg 2001, *Mechanically Stabilized Earth Walls and Reinforced Soil Slopes Design and Construction Guideline*, Report No. FHWA-NHI-00-043, National Highway Institute, Federal Highway Administration, Washington, D.C., p. 418, (also see <http://isddc.dot.gov/OLPFiles/FHWA/010567.pdf>, last accessed on 9 May 2013).
- Fanella, D.A. 2001, 'Time Saving Design Aids for Reinforced Concrete, Part 3: Columns and Walls', *Structural Engineer*, Vol. 2, No. 11, pp. 42–7.
- Farvashany, F.E., S.J. Foster, and B.V. Rangan 2008, 'Strength and Deformation of High-strength Concrete Shear Walls', *ACI Structural Journal*, Vol. 105, No. 1, pp. 21–9.
- Fintel, M. 1991, 'Shear Walls: An Answer for Seismic Resistance?', *Concrete International, ACI*, Vol. 13, No. 7, pp. 48–53.
- Fortney, P.J., G.A. Rassati, B.M. Shahrooz, I. Clemente, and S. Noé 2004, 'Cyclic Test on Steel Plate Reinforced Coupling Beam', *Proceedings of Atti del VI Workshop Italiano sulle Strutture Composte*, Trieste, Italy.
- Galano, L. and A. Vignoli 2000, 'Seismic Behavior of Short Coupling Beams with Different Reinforcement Layouts', *ACI Structural Journal*, Vol. 97, No. 6, pp. 876–85.
- Ghazavi, M., M. Hosseini, and M. Mollanouri 2008, 'A Comparison between Angle of Repose and Friction Angle of Sand', *The 12th International Conference of the International Association for Computer Methods and Advances in Geomechanics (IACMAG)*, 1–6 October 2008, Goa, India, p. 4, (also see <http://www.civil.iitb.ac.in/~dns/IACMAG08/pdfs/E01.pdf>, last accessed on 9 May 2013).
- Gulec, C.K., and A.S. Whittaker 2011, 'Empirical Equations for Peak Shear Strength of Low Aspect Ratio Reinforced Concrete Walls', *ACI Structural Journal*, Vol. 108, No. 1, pp. 80–9.
- Gulec, C.K., A.S. Whittaker, and B. Stojadinovic 2009, 'Shear Strength of Squat Reinforced Concrete Walls with Boundary Flanges or Barbells', *ACI Structural Journal*, Vol. 106, No. 3, pp. 368–77.
- Gupta, A. and B.V. Rangan 1998, 'High-strength Concrete (HSC) Structural Walls', *ACI Structural Journal*, Vol. 95, No. 2, pp. 194–205.
- Harries, K.A., P.J. Fortney, B.M. Shahrooz, and P.J. Brien 2005, 'Practical Design of Diagonally Reinforced Concrete Coupling Beams: Critical Review of ACI 318 Requirements', *ACI Structural Journal*, Vol. 102, No. 6, pp. 876–82.
- Harries, K.A. and B.M. Shahrooz 2005, 'Hybrid Coupled Wall Systems: State-of-the-art', *Concrete International, ACI*, Vol. 27, No. 5, pp. 45–51.
- Ingle, R.K. and S.K. Jain 2008, *Explanatory Examples for Ductile Detailing of RC Buildings*, National Information Centre of Earthquake Engineering (NICEE), IIT, Kanpur, p. 72, (also see <http://www.iitk.ac.in/nicee/IITK-GSDMA/EQ22.pdf>, last accessed on 20 May 2013).
- IS 1893 (Part 3) Draft Doc: CED 39(7739):2009 *Criteria for Earthquake Resistant Design of Structures (Part 3) Bridges and Retaining Walls*, Bureau of Indian Standards, New Delhi, p. 54.
- IS 1905:1987 1989, *Code of Practice for Structural Use of Unreinforced Masonry*, 3rd revision, Bureau of Indian Standards, New Delhi, p. 26.
- IS 13920:1993, *Indian Standard Code of Practice for Ductile Detailing of Reinforced Concrete Structures Subjected to Seismic Forces*, Bureau of Indian Standards, New Delhi, p. 14, (also see <http://www.iitk.ac.in/nicee/IITK-GSDMA/EQ11.pdf> for the draft revised edition of code, last accessed on 23 July 2013).

- Jaky, J. 1944, 'The Coefficient of Earth Pressure at Rest', In Hungarian 'A nyugalmi nyomas tenyezoje', *Journal of the Society of Hungarian Architects and Engineers* (Magyor Mernok es Epitesz-Egyelet Kozlonye), pp. 355–8.
- Kripanarayanan, K.M. 1977, 'Interesting Aspects of the Empirical Wall Design Equation', *ACI Journal, Proceedings*, Vol. 74, No. 5, pp. 204–7.
- Kurama, Y. and Q. Shen 2004, 'Post-tensioned Hybrid Coupled Walls under Lateral Load', *Journal of Structural Engineering*, ASCE, Vol. 130, No. 2, pp. 297–309.
- Lee, H.J., D.A. Kuchma, W. Baker, and L.C. Novak 2008, 'Design and Analysis of Heavily Loaded Reinforced Concrete Link Beams for Burj Khalifa', *ACI Structural Journal*, Vol. 105, No. 4, pp. 451–9.
- Massone, L.M., and J.W. Wallace 2004, 'Load–Deformation Response of Slender Reinforced Concrete Walls', *ACI Structural Journal*, Vol. 101, No. 1, pp. 103–13.
- McCormac, J.C. and R.H. Brown 2013, *Design of Reinforced Concrete*, 9th edition, John Wiley and Sons, New York, p. 714.
- Medhekar, M.S. and S.K. Jain 1993, 'Seismic Behavior, Design and Detailing of RC Shear Walls, Part I: Behaviour and Strength', *The Indian Concrete Journal*, Vol. 67, No. 7, pp. 311–8, and 'Part II: Design and Detailing', No. 9, pp. 451–57.
- Michalowski, R.L. 2005, 'Coefficient of Earth Pressure at Rest', *Journal of Geotechnical and Geoenvironmental Engineering*, ASCE, Vol. 131, No. 11, pp. 1429–33.
- Mobeen, S.S., A.E. Elwi, and A. Ghali 2005, 'Double-headed Studs in Shear Walls', *Concrete International, ACI*, Vol. 27, No. 3, pp. 59–63.
- Moehle, J.P. 1992, 'Displacement-based Design of RC Structures Subjected to Earthquakes', *Earthquake Spectra*, Vol. 8, No. 3, pp. 403–28.
- Moehle, J.P., T. Ghodsi, J.D. Hooper, D.C. Fields, and R. Gedhada 2011, *Seismic Design of Cast-in-place Concrete Special Structural Walls and Coupling Beams: A Guide for Practicing Engineers*, NEHRP Seismic Design Technical Brief No. 6, NIST GCR 11-917-11, National Institute of Standards and Technology, Gaithersburg, p. 37 (also see <http://www.nehrp.gov/pdf/nistger11-917-11.pdf>, last accessed on 3 October 2012).
- Mononobe, N. and H. Matsuo 1929, 'On the Determination of Earth Pressures during Earthquakes', *Proceedings of World Engineering Congress*, Vol. 9, pp. 177–85.
- Naish, D., J.W. Wallace, J.A. Fry, and R. Klemencic 2009, *Reinforced Concrete Link Beams: Alternative Details for Improved Construction*, UCLA-SGEL Report 2009/06, Report to Charles Pankow Foundation and School of Engineering and Applied Science, University of California, Los Angeles, 11 August 2009, p. 116.
- NCMA 2010, *Design Manual for Segmental Retaining Walls* (also design software SRWall 4.0), 3rd edition, National Concrete Masonry Association, Herndon, p. 206.
- Ngo, T., S. Fragomeni, P. Mendis, and B. Ta 2013, 'Testing of Normal- and High-strength Concrete Walls Subjected to Both Standard and Hydrocarbon Fires', *ACI Structural Journal*, Vol. 110, No. 3, pp. 503–10.
- Oberlender, G.D. and N.J. Everard 1977, 'Investigation of Reinforced Concrete Walls', *ACI Journal, Proceedings*, Vol. 74, No. 6, pp. 256–63.
- Okabe S. 1924, 'General Theory on Earth Pressure and Seismic Stability of Retaining Wall and Dam', *Koboku Gakkaishi, Journal of the Japanese Society of Civil Engineers*, Vol. 10, No. 6, pp. 1277–323.
- Panian, L., P. Williams, and M. Donovan 2012, 'Redefining High-performance Concrete Structures', *Concrete International, ACI*, Vol. 34, No. 11, pp. 23–30.
- Park, R. and T. Paulay 1975, *Reinforced Concrete Structures*, John Wiley & Sons, New York, p. 769.
- Parra-Montesinos, G.J., J.K. Wight, R. Lequesne, and M. Setkit 2011, 'A Summary of Ten Years of Research on HPFRC Coupling Beams', *Proceedings of the 6th International Workshop on High-performance Fibre Reinforced Cement Composites (HPFRCC 6)*, Ann Arbor, 20–22 June 2011, Springer, pp. 355–62.
- Parra-Montesinos, G.J., J.K. Wight, and M. Setkit 2010, M., 'Earthquake-resistant Coupling Beams without Diagonal Reinforcement', *Concrete International, ACI*, Vol. 32, No. 12, pp. 36–40.
- Paulay, T. and J.R. Binney 1974, 'Diagonally Reinforced Coupling Beams of Shear Walls', *Shear in Reinforced Concrete, SP-42*, American Concrete Institute, Farmington Hills, pp. 579–98.
- Paulay, T. and M.J.N. Priestley 1992, *Seismic Design of Reinforced Concrete and Masonry Buildings*, John Wiley and Sons, Inc., New York, p. 744.
- Paulay, T. and M.J.N. Priestley 1993, 'Stability of Ductile Structural Walls', *ACI Structural Journal*, Vol. 90, No. 4, pp. 385–92.
- Paulay, T., M.J.N. Priestley, and A. J. Syngé 1982, 'Ductility in Earthquake Resisting Squat Shear Walls', *Journal of the American Concrete Institute*, Vol. 79, No. 4, pp. 257–69.
- Paulay, T. and A.R. Santhakumar 1976, 'Ductile Behavior of Coupled Shear Walls', *Journal of the Structural Division, ASCE*, Vol. 102, No. 1, pp. 93–108.
- Peck, R.B., W.E. Hanson, and T.H. Thornburn 1974, *Foundation Engineering*, 2nd edition, John Wiley and Sons, New York, p. 513.
- Pillai S.U. and C.V. Parthasarathy 1977, 'Ultimate Strength and Design of Concrete Walls', *Building and Environment*, Vol. 12, pp. 25–9.
- Rangan, B.V. 1997, 'Rational Design of Structural Walls', *Concrete International, ACI*, Vol. 19, No. 11, pp. 29–33.
- Rankine, W. 1857, 'On the Stability of Loose Earth', *Philosophical Transactions of the Royal Society of London*, Vol. 147, pp. 9–27.
- Rohit, D.H.H., A.K. Jaiswal, and C.V.R. Murty 2013, 'Expressions for Moment of Resistance of RC Structural Walls', *The Indian Concrete Journal*, Vol. 87, No. 10.
- Rohit, D.H.H., P. Narahari, R. Sharma, A.K. Jaiswal, and C.V.R. Murty 2011, 'When RC Columns Become RC Structural Walls', *The Indian Concrete Journal*, Vol. 85, No. 5, pp. 35–45.
- Rohit, D.H.H., P. Narahari, A.K. Jaiswal, and C.V.R. Murty 2012, 'Superposition Principle Invalid in IS 13920 Design of Slender RC Walls with Boundary Elements', *The Indian Concrete Journal*, Vol. 86, No. 3, pp. 43–52.
- Shahrooz, B.M., P.J. Fortney, and G.A. Rassati 2003, 'Seismic Performance of Hybrid Core Wall Buildings', *Proceedings of the International Workshop on Steel and Concrete Composite Construction*, Taipei, pp. 79–88.
- Singh, B. 2011, 'Structural Design of a Ductile Shear Wall', *The Indian Concrete Journal*, Vol. 85, No. 5, pp. 51–56.
- Smith, B.S. and A. Coull 1991, *Tall Building Structures: Analysis and Design*, John Wiley and Sons, Inc., p. 537.
- SP 34:1987, *Handbook on Concrete Reinforcement and Detailing*, Bureau of Indian Standards, New Delhi, p. 232.
- Subramanian, N. and M. Sundararaj 1980, 'Strengthening of Soils using Earth Reinforcement', *The Indian Highways*, Vol. 8, No. 6, pp. 25–34.

- Tassios, T.P., M. Moretti, and A. Bezas 1996, 'On the Behavior and Ductility of Reinforced Concrete Coupling Beams of Shear Walls', *ACI Structural Journal*, Vol. 93, No. 6, pp. 711–20.
- Teng, W.C. 1983, *Foundation Design*, Prentice Hall of India Pvt. Ltd, New Delhi, p. 466.
- Terzaghi, K., R.B. Peck, and G. Mesri 1996, *Soil Mechanics in Engineering Practice*, 3rd edition, John Wiley and Sons, New York, p. 592.
- Thomsen IV, J.H. and J.W. Wallace 2004, 'Displacement-based Design of Slender Reinforced Concrete Structural Walls—Experimental Verification', *Journal of Structural Engineering, ASCE*, Vol. 130, No. 4, pp. 618–30.
- Timoshenko, S. and S. Woinowsky-Krieger 1959, *Theory of Plates and Shells*, 2nd edition, McGraw-Hill, New York, p. 580.
- Wallace, J.W. 1995, 'Seismic Design of RC Structural Walls. Part I: New Code Format', *Journal of Structural Engineering, ASCE*, Vol. 121, No. 1, pp. 75–87.
- Wallace, J. and J. Moehle 2012, 'Behavior and Design of Structural Walls: Lessons from Recent Laboratory Tests and Earthquakes', *Proceedings of the International Symposium on Engineering Lessons Learned from the 2011 Great East Japan Earthquake*, 1–4 March 2012, Tokyo, Japan, pp. 1132–44.
- Wallace, J.W. and K. Orakcal 2002, 'ACI 318-99 Provisions for Seismic Design of Structural Walls', *ACI Structural Journal*, Vol. 99, No. 4, pp. 499–508.
- Wallace, J.W. and J.H. Thomsen IV 1995, 'Seismic Design of RC Shear Walls; Part II: Applications', *Journal of Structural Engineering, ASCE*, Vol. 121, No. 1, pp. 88–101.
- Wight, J.K. and J.G. MacGregor 2009, *Reinforced Concrete: Mechanics and Design*, Pearson Prentice Hall, Upper Saddle River, p. 1112.
- Wood, S.L. 1990, 'Shear Strength of low-rise Reinforced Concrete Walls', *ACI Structural Journal*, Vol. 87, No. 1, pp. 99–107.
- Wyllie, Jr., L.A. 1987, 'Chapter 7 Structural Walls and Diaphragms—How They Function?', In R. White and C.G. Salmon (eds), *Building Structural Design Handbook*, Wiley-Interscience, New York, pp. 188–215.

DESIGN OF STAIRCASES

17.1 INTRODUCTION

Reinforced concrete (RC) stairs are an important component of a building and often the only means of providing access between the various floors of a building. The staircase essentially consists of landings and flights. Often, the flight is an inclined slab consisting of risers and treads (collectively called the *going of staircase*), whereas the landing is a horizontal slab (see Fig. 17.1). From a structural point of view,

a staircase consists of slab or beam elements, whose design principles have already been covered in the previous chapters.

The following are the definitions of a few technical terms that are often used in connection with the design of staircases (see also Fig. 17.1b):

Tread or going of step Tread is the horizontal upper portion of a step where the foot rests. Going of step (g) is the horizontal distance of the tread minus the nosing.

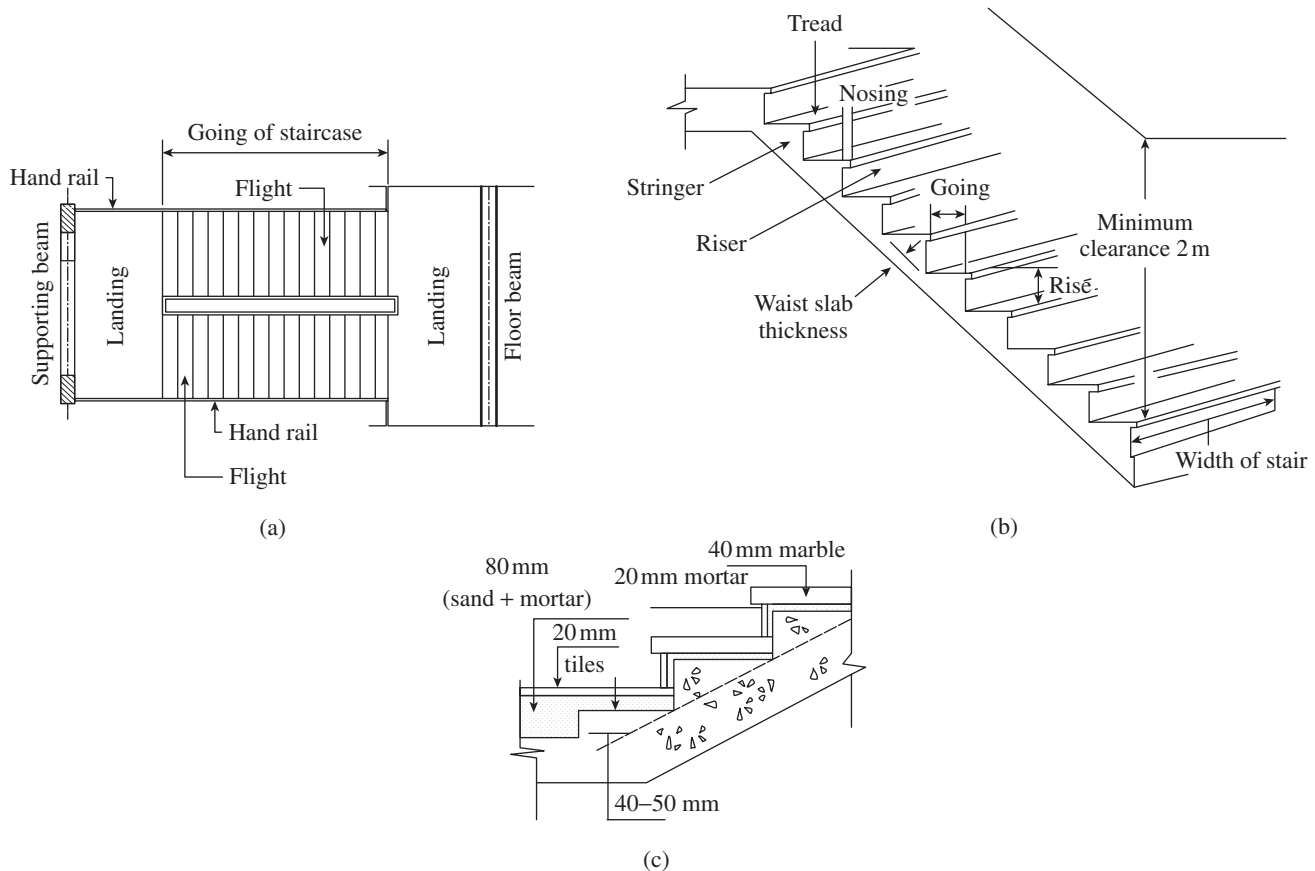


FIG. 17.1 Components of a staircase (a) Plan of staircase (b) Terminology used (c) Part section

Nosing Sometimes, the tread is projected outwards for aesthetics or to provide more space; this projection is called the nosing. Many times, the nosing is provided by the finishing over the concrete tread (see Fig. 17.1c).

Riser and rise Rise (r) is the vertical distance between two consecutive treads and riser is the vertical portion of the step.

TABLE 17.1 Rise and going of steps as per BS 5395-1:2010

Category of stair	Rise, r^1		Going, g		Pitch	Clear Width of Stair ²	Hand-rail Height
	Min. (mm)	Max. (mm)	Min. (mm)	Max. (mm)	Max. (degrees)	Min. (mm)	Min. (mm)
Private stair	100	220	225	350	41.5	800	900
Public stair	100	190	250	350	38	1000	900
Assembly stair	100	180	280	350	33	1000	900

Notes:

¹ $g + 2r$ should be between 550 mm and 700 mm.

² For hospitals, the minimum clear width of stair is 1200 mm.

The minimum and maximum values of rise and going of steps as well as the minimum clear width of stairs for different types of buildings, as per British code BS 5395-1:2010, are given in Table 17.1. A good design of the stair should comply with the following rule of thumb:

$$(2r + g) > 550 \text{ mm to } 700 \text{ mm} \quad (17.1)$$

The pitch expressed in degrees is obtained from

$$\theta = \tan^{-1} \left(\frac{r}{g} \right) \quad (17.2)$$

The maximum pitch for different types of buildings is also given in Table 17.1. The rise and tread must be equal in all the steps in a stair and preferably the same in all the floors of the building.

Flight or going of stair Flight is a series of steps provided between two landings. Going of stair (G) is the horizontal projection of the flight.

Landing Landing is the horizontal slab provided between two flights. It is provided every 10–14 steps for

comfort in climbing. Landing is also provided when there is a change in the direction of the stairs.

Overlap The amount by which the nosing of a tread (or landing) oversails the next lower tread (or landing) is called the overlap.

Waist It is the least thickness of a stair slab.

Winder The radiating or angular tapering step is called winder.

Soffit It is the bottom surface of a stair slab.

Headroom The vertical distance of a line connecting the nosings of all treads and the soffit is referred to as the headroom. A minimum of 2 m headroom is often recommended.

Steps may be of three types: (a) brick or concrete steps on inclined slab, (b) tread-riser steps, and (c) isolated steps. These are shown in Fig. 17.2. The behaviour and design of various types of staircases are presented in this chapter.

17.2 TYPES OF STAIRCASES

Concrete stairs may be of a variety of shapes and support conditions, and hence, design considerations also vary accordingly for each type. Some of the most common

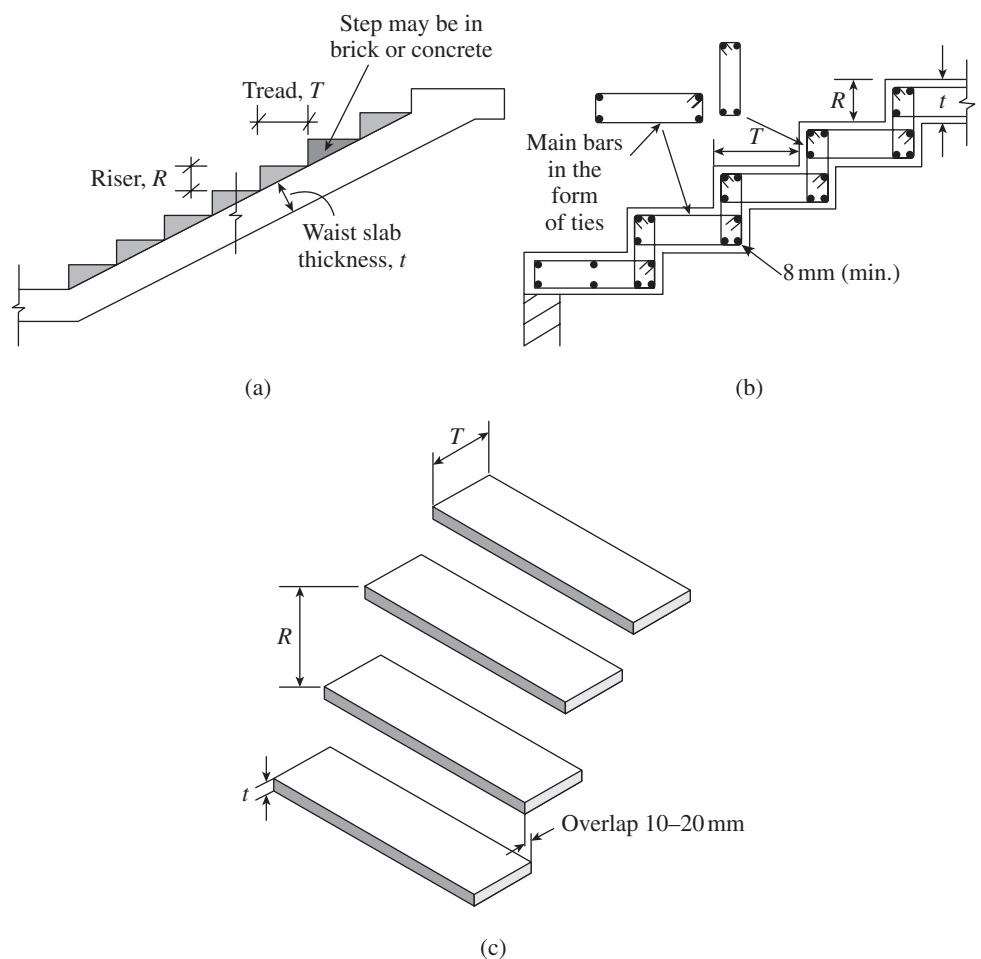


FIG. 17.2 Type of steps (a) Steps on waist slab (b) Slabless tread-riser (c) Isolated steps

geometrical configurations are shown in Fig. 17.3, which include the following:

1. Straight flight stairs with or without intermediate landing (Figs 17.3a and b)
2. Quarter-turn stairs (Fig. 17.3c)
3. Half-turn stairs, also referred to as *dog-legged* or *scissor-type* stairs (Fig. 17.3d)
4. Branching stairs (Fig. 17.3e)
5. Open-well stairs (half-turn) (Fig. 17.3f) and quarter-turn landing (Fig. 17.3g)
6. Spiral stairs (Figs 17.3h and i)
7. Helicoidal stairs (Fig. 17.3j)

Spiral, helical, circular, and elliptical stairs are also referred to as *geometrical stairs*. The type of stair and its location are selected based on architectural considerations, such as accessibility, function, comfort, lighting, ventilation, and aesthetics, as well as structural and economic considerations. By reducing the depth of stair slabs, a marked improvement in appearance may be obtained. *Free-standing stairs*,

which are similar to dog-legged stairs in plan, but with their landing unsupported, provide an elegant appearance. They are three-dimensional structures and have to be fixed at both the top and bottom ends for stability, as shown in Fig. 17.4.

17.2.1 Structural Classifications

For design purposes, stairs are classified into the following two types, depending on the predominant direction in which the slab of the stair deflects in flexure:

1. Transversely supported (transverse to the direction of movement in the stair)
2. Longitudinally supported (in the direction of movement)

Transversely Supported Stairs

Transversely supported stairs include the following types:

1. Simply supported steps supported by two walls or beams or a combination of both (see Fig. 17.5a)

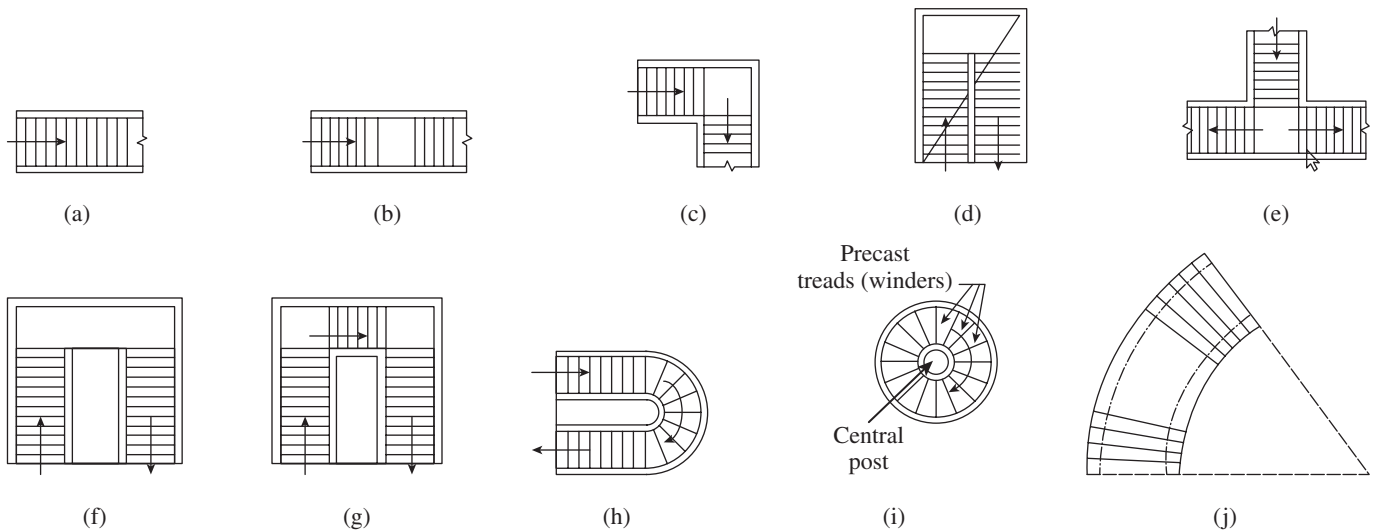


FIG. 17.3 Plan views of various types of stairs (a) and (b) Straight flight stairs (c) Quarter-turn stairs (d) Half-turn stairs (e) Branching stairs (f) Open-well (half-turn) stairs (g) Open-well stairs with quarter-turn landing (h) Part-circular stairs (i) Spiral stairs (j) Helicoidal stairs

2. Stairs cantilevering from a central spine beam (see Fig. 17.5b)
3. Steps cantilevering from a wall or a beam (see Fig. 17.5c). The detailing of stair slab when concrete or brick step is adopted is also shown in Fig. 17.5(d). It has to be noted that the tread-riser type of arrangement is also employed as cantilevers.

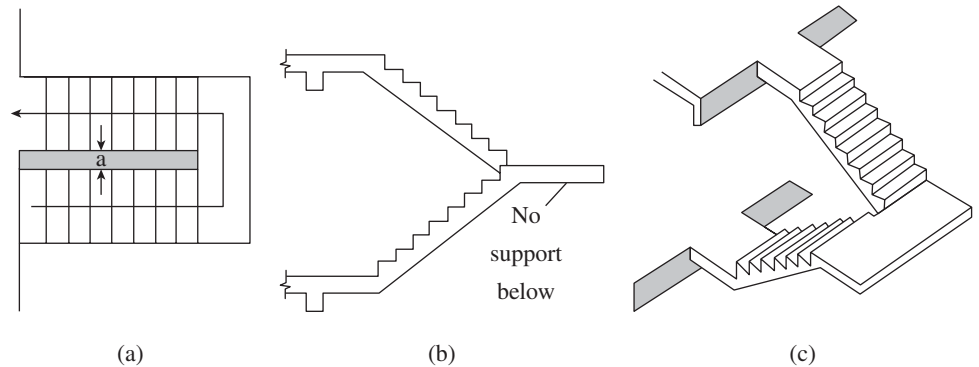


FIG. 17.4 Typical free-standing stair (a) Plan (b) Section (c) Isometric view

In all these cases, the slab supports gravity loads by bending in the

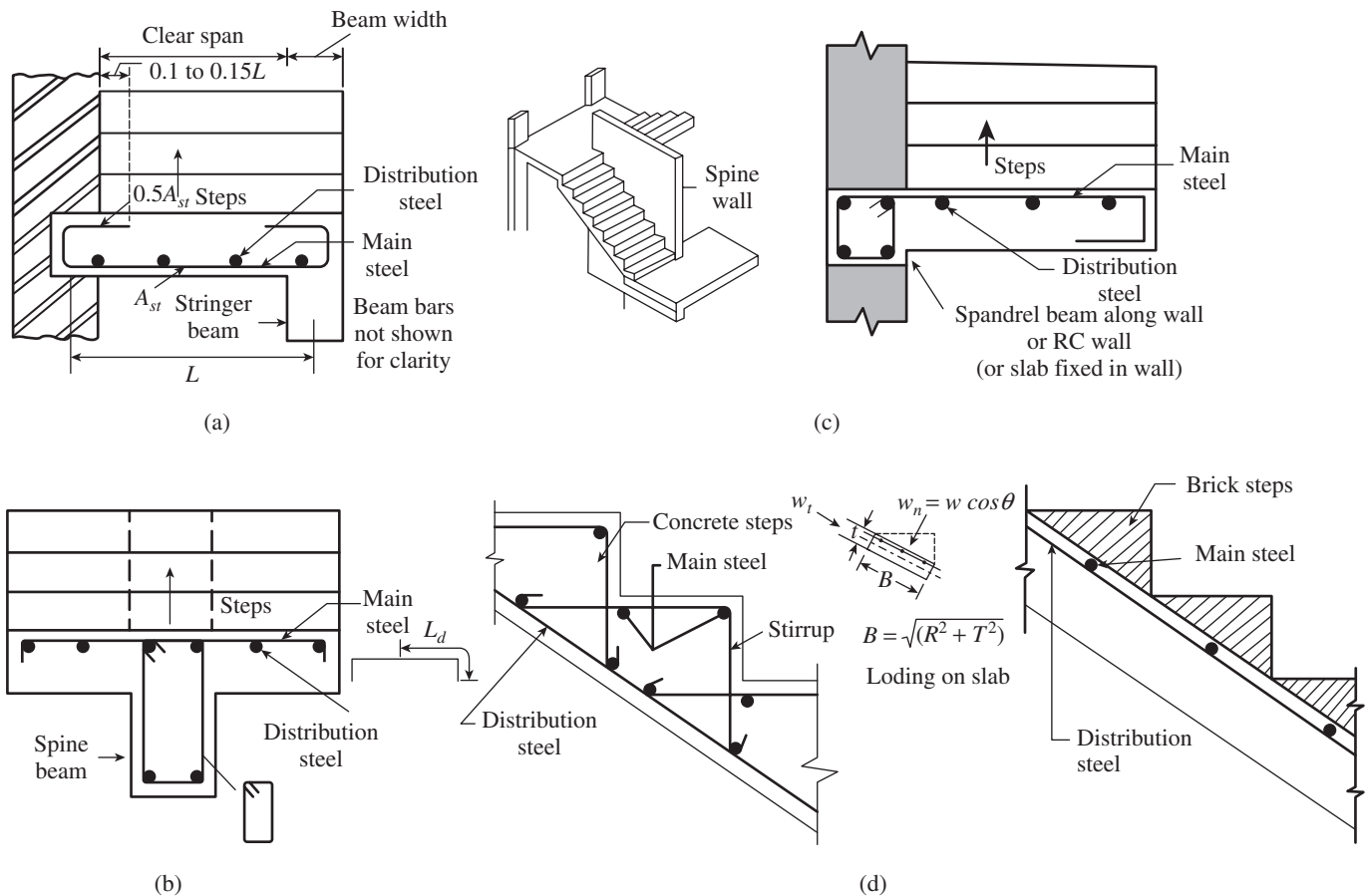


FIG. 17.5 Transversely supported stairs (a) Supported between two stringer beams or walls (b) Doubly cantilevered from a central spine beam (c) Cantilevered from spandrel beam or wall (d) Detailing of cantilever stair for concrete and brick steps

transverse vertical plane, with the span along the width of the stair. When the slab is supported at the two sides by stringer beams or walls as shown in Fig. 17.5(a), it should be designed as simply supported; however, at supports, reinforcements are to be provided at the top to resist the negative bending moments that may arise due to partial fixity. The stringer beam in Fig. 17.5(a) may also be provided as an upstand stringer. It has to be noted that the spandrel beam (see Fig. 17.5c) is subjected to *equilibrium* torsion in addition to bending moment and shear. Although the slab may be spanning transversely, the spandrel and spine beams of Figs 17.5(a) and (c), respectively, span longitudinally (along the slope of the stair) between the supporting columns and hence have to be designed and detailed accordingly. The methods of design of these beams for flexure, shear, and torsion have already been covered in Chapters 5–7 and hence are not discussed in this chapter.

When the slab is doubly cantilevered from the central spine beam as in Fig. 17.5(b), it is better to check for the case of loading on one side of the stair slab, which may induce torsion in the spine beam. This condition may also dislodge the slab from the beam if proper detailing is not provided. The detail

as shown in Fig. 17.5(b) may prevent such a separation, as the stirrups of the beam will anchor the slab into the beam, provided the stirrups are designed to take into account torsion as well. It is important to provide closed stirrups, preferably with 135° hooks, so that they effectively resist the torsional moment.

Longitudinally Supported Stairs

These stairs span between the supports at the top and bottom of a flight and are unsupported at the sides. Longitudinally supported stairs may be supported in any of the following ways:

1. Internal beams at the ends of the flight in addition to beams or walls at the outside edges of the landings (see Fig. 17.6a)
2. Beams or walls at the outside edges of the landings (see Fig. 17.6b)
3. Landings that are supported by beams or walls running in the longitudinal direction (see Fig. 17.6c)
4. A combination of these three methods
5. Stairs with quarter landings associated with the open-well stairs

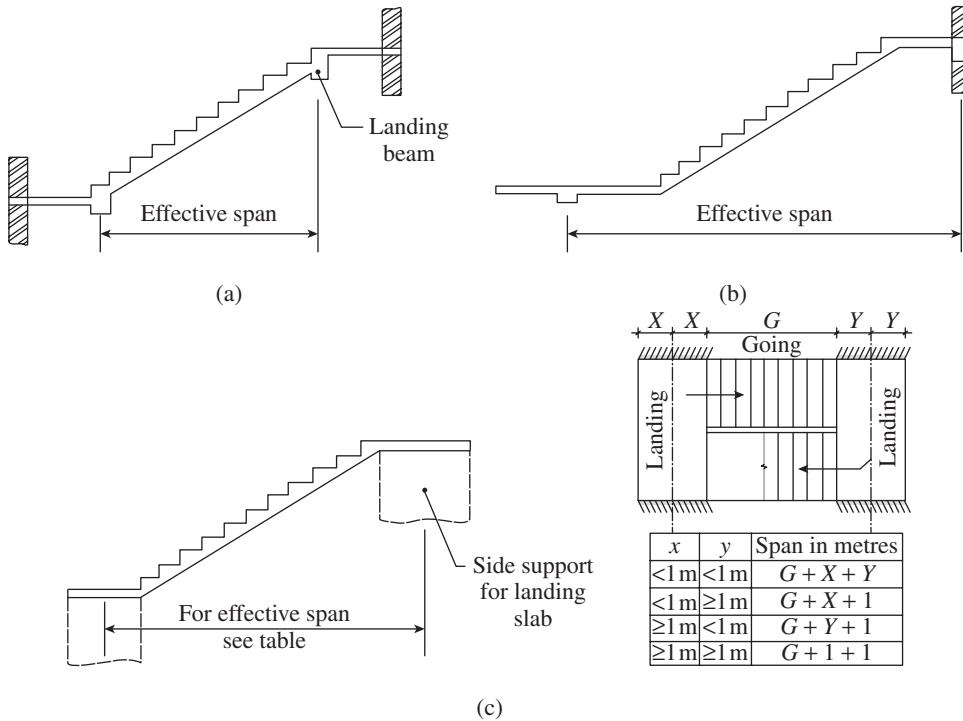


FIG. 17.6 Types of stairs spanning longitudinally (a) Support at top and bottom risers (b) Landing slab spanning in the same direction as stairs (c) Supported on the edge of landing slab

In all these cases, we may adopt either the waist slab (Fig. 17.2a) or the tread-riser type (Fig. 17.2b). The slab thickness depends on the effective span, which should be calculated according to the boundary condition as discussed in Section 17.2.2. In most cases, the waist slab may be between 110 mm and 250 mm thick. If the thickness works out to 300 mm, which may not be elegant, a small amount of compression reinforcement may be used in the mid-span to reduce the waist slab thickness to about 200 mm. However, when the span is greater than 6 m, central beams may be used to support flight slabs, which in turn may be cantilevered on either side, as in Fig. 17.5(b). In general, all these staircases require four columns in plan. Of these, two columns should be used to support the landing beam. Stringers, treads, or complete flights and landings can be precast, depending upon the nature of the project, site, and size of the crane, as shown in Fig. 17.7. Care should be exercised when detailing the junctions of in situ

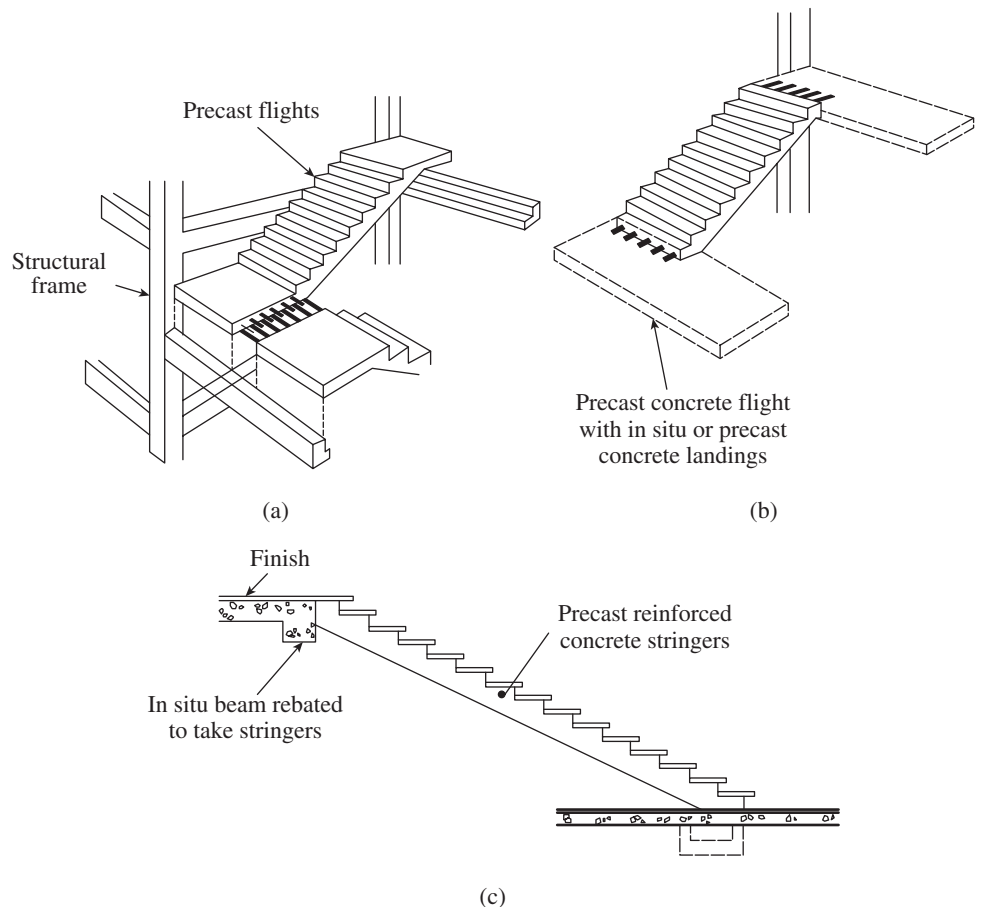


FIG. 17.7 Precast concrete flight, landing, or stringers (a) Precast flight (b) Precast concrete flight with landing (c) Precast stringers

concrete with precast units to avoid unsightly finishes (BS 5395-1:2010).

When additional intermediate supports are provided as in Fig 17.6(a), negative bending moments develop at the junction of the landing slab and waist slab; hence, necessary reinforcement needs to be provided to resist them.

17.2.2 Effective Span

Clause 33 of IS 456 gives the following rules for calculating the effective spans, depending on the way the stair slab is supported:

1. When the stairs span longitudinally and are supported at the top and bottom by beams, as shown in Fig. 17.6(a), the effective span is the distance between the respective centres of beams.

- When the stairs span longitudinally with the landing slab also spanning in the same direction as the stairs, as shown in Fig. 17.6(b), the effective span is the centre-to-centre distance (c/c) between the supporting beams or walls.
- When the stairs span longitudinally and are supported by landings on top and bottom, which span in the transverse direction (perpendicular to the stairs), as shown in Fig. 17.6(c), the effective span is to be taken as the total going of the stair plus half the width of the landing on each end or one metre, whichever is smaller.
- In the case of stairs spanning transversely (horizontally in the transverse direction), as shown in Fig. 17.5, the effective width of the stair is taken as the effective span.

Ahmed, et al. (1995, 1996) considered the case of the landing slab running at right angles to the direction of the flight and supported by walls or beams on three sides, as shown in Fig. 17.8, as they are common in residential buildings. The Indian code does not have provisions for this case. Based on their finite element study on the behaviour of stairs with such a supporting condition, they found that for this case the effective length, L , may be taken as the going of the stair measured horizontally. They identified two critical locations for the flexural design of such stairs: (a) The mid-span location for positive moment and (b) the kink location, where the landing slab meets the inclined waist slab, for negative moment. The design negative moments near the kink were found to be of the same order as those of the positive moment and have a magnitude of $wL^2/8$. Their study showed that even when the landing slab is supported on the two edges parallel to the direction of the span, as in Fig. 17.6(c), the behaviour is similar and that the effective length, L , may be taken

as the going of the stair, indicating that the IS 456 provisions are quite conservative. The Bangladesh National Building Code, in its 1993 version, has included these recommendations by Ahmed, et al. (1996). It has to be noted that ACI 318 does not contain any provision for the design of staircases.

17.3 LOADS ON STAIR SLABS

The dead load to be considered on the stairs includes the (a) self-weight of stair slab (waist slab, tread-riser slab, or individual steps), (b) self-weight of step (in the case of waist slab-type stairs, it is taken as $25 \text{ kN/m}^3 \times \text{average thickness of step}$; the average thickness of step can be taken as $\text{riser}/2$), and (c) self-weight of finish (may be taken as $0.6\text{--}1.0 \text{ kN/m}^2$).

The imposed loads are assumed to act as uniformly distributed loads on the horizontal projection of the flight, that is, on the going of staircase, as well as on the landing. The imposed loads as recommended by IS 875 (Part 2):1987 are given in Table 17.2. A horizontal load of 0.75 kN/m is to be considered as acting on the balustrade or parapet.

As the dead and imposed loads are the characteristic values, for limit states design they should be multiplied by the appropriate partial load factors.

TABLE 17.2 Imposed load on staircases as per IS 875(Part 2):1987

Type of Staircase	Imposed Load (kN/m^2)
Service stairs for maintenance in water tanks, catwalks, etc.	1.5
Staircase in residential buildings	3.0
Staircase in offices and public buildings	5.0
Staircase with isolated steps	1.3 kN/step^*

* This concentrated load should be applied at the free end of each cantilever step.

Distribution of Loads on Stairs

According to Clause 33.2 of IS 456, the following distribution of loads may be taken:

- In the case of stairs with open wells, when a staircase takes a right-angled turn, the load on areas common to any such span (usually in landings) may be taken as 50 per cent in each direction, as shown in Fig. 17.9(a).
- When a longitudinally spanning flight or landing is embedded by at least 110 mm into walls, the loading may be assumed to act on a reduced width of flight, due to partial two-way action. The code permits this reduction in width as 150 mm, as shown in Fig. 17.9(b). It also suggests increasing the effective breadth of the section by 75 mm.

17.4 DESIGN OF STAIR SLABS SPANNING TRANSVERSELY

In this section, we look at the design of isolated tread slabs, slabless chairs, and stairs with waist slab.

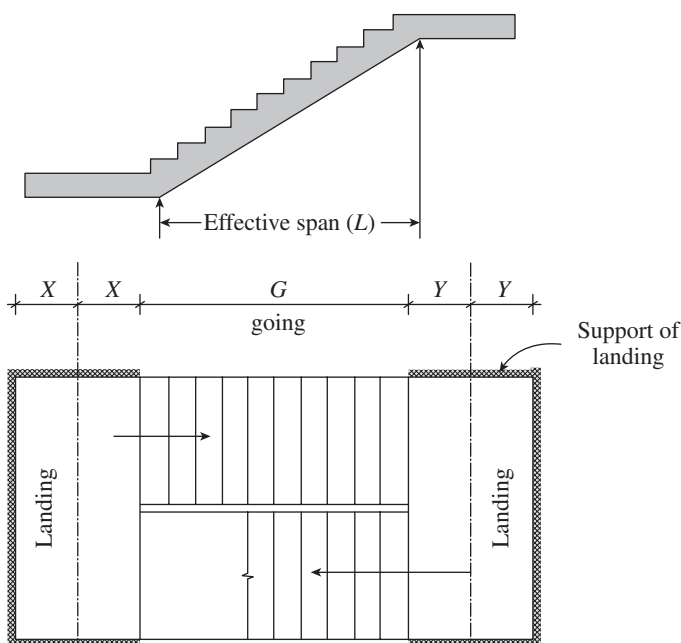


FIG. 17.8 Stair with landing slab supported on three sides

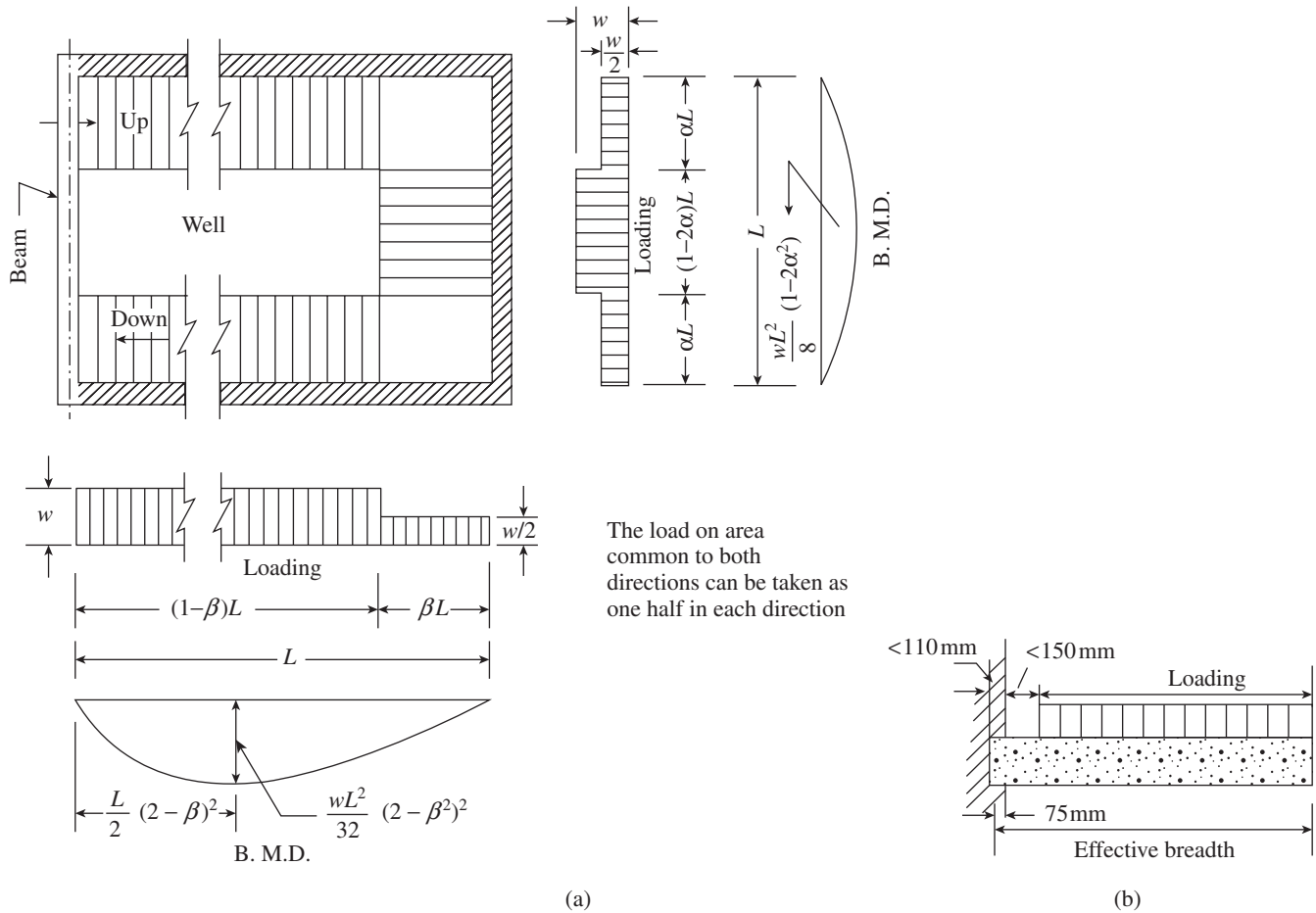


FIG. 17.9 Distribution of loading on stairs (a) Open well stairs (b) Stairs built into the walls

Isolated tread slabs These slabs, as shown in Fig. 17.2(c), are designed as cantilever slabs. A concentrated load of 1.3 kN acting at the free edge of the step should also be considered for the design of cantilevered steps. Although Clause 23.2.1(a) of IS 456 recommends that the depth of cantilevers based on deflection criteria be $L/7$, where L is the effective span (which may be modified using the factors given in Fig. 4 of IS 456), we may adopt a depth of $L/8$ or $L/10$ for such cantilever steps, as the length will only be about 1.2 m. For larger spans, it may be economical to taper the slab thickness to a minimum value of 80 mm at the free end. The design of cantilever tread slab is explained in Example 17.1. It is important to anchor the top bars into the support. The shear stresses will usually be very small and hence a check for the same is not required. In earthquake zones, equal amount of bottom bars with adequate anchoring has to be provided to resist stress reversals. It is necessary to provide proper chairs for the main bars so that they remain at the top face during concreting operations.

Slabless stairs In these stairs, each tread-riser unit, consisting of the riser slab and one half of tread slab on either side, is assumed to act independently as a beam having a Z-section, as shown in Fig. 17.10. The overall depth of the beam is $R + t$, where R is the riser and t is the thickness of slab.

Usually a thickness of about 100 mm is sufficient. To simplify calculations, the flange portions are omitted for calculations and the rectangular portion alone is taken to resist the external loads (see Fig. 17.10b). The detailing is to be done as per Fig. 17.10(c). The main bars are placed at the top or bottom of the riser portion, depending upon whether the system is cantilevered or simply supported. Nominal distributors in the form of stirrups are provided (say, 6 mm bars at 200 mm c/c).

At every bend of these stirrups where there is no main bar, an 8 mm diameter bar (minimum) should be provided. The cover requirements are as per Table 16 of IS 456. The design of transversely supported tread-riser stair is explained in Example 17.2.

Stairs with waist slab In this type of stair, the longitudinal axis of the flight is inclined to the horizontal, and the steps form a series of triangles on top of the waist slab. If the steps are also made of concrete, nominal reinforcement, in the form of stirrups, as shown in Fig. 17.5(d) are provided in the steps to prevent the cracking of nosing. The vertically acting gravity loads w are resolved into two orthogonal components, $w_n = w \cos \theta$ acting normal to the waist slab, causing flexure, and $w_t = w \sin \theta$ acting tangential to the waist slab; the tangential component may be neglected in design as the waist slab will

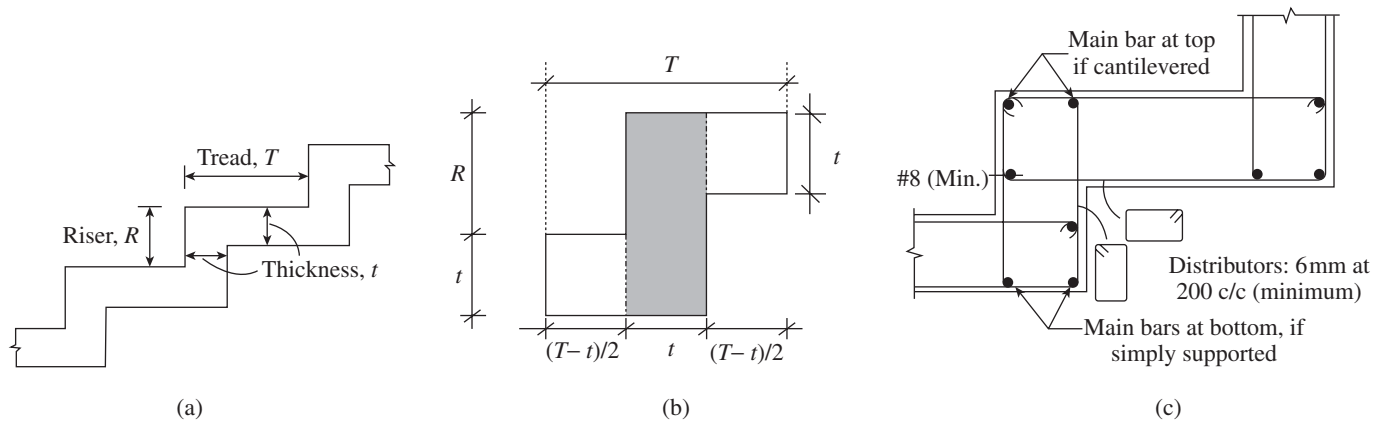


FIG. 17.10 Transversely spanning tread-riser stair (a) Typical tread-riser arrangement (b) Tread-riser unit taken for design as Z-section (c) Detailing of tread-riser stair

be extremely deep in that plane. As shown in Fig. 17.5(d), the main bars are provided transversely, either at the top or bottom, depending upon whether the slab is cantilevered or simply supported (in Fig. 17.5d cantilevered waist slab is shown). The design of stringer beam supported waist slab-type stair is explained in Example 17.3 and that of transversely spanning stair with waist slab is given in Example 17.4.

17.5 DESIGN OF STAIR SLABS SPANNING LONGITUDINALLY

In this section, we look at the design of slabless stairs, stairs with waist slab, and free standing stairs.

Slabless stairs The aesthetic appeal of tread-riser stair is lost if the slab thickness exceeds the riser, R . Hence, the effective span for these stairs is usually kept below 3.5m. The tread-riser slab has many folds in the span and hence its analysis is complicated (Bangash and Bangash 1999; Cusans 1966; Bangash 2010; Solanki 1975). Sharma, et al. (1995), based on their experimental studies on saw tooth (tread-riser) stairs, concluded the following: (a) The load-carrying capacity of these stairs is much more than those predicted by the simplified

method (by assuming their behaviour to be similar to that of longitudinally spanning waist slabs), Cusan's method, and the stiffness method. (b) There is no significant difference in the strength and behaviour of the odd and even number stepped stairs. (c) The results of the simplified method are in good agreement with the results of the stiffness method and provides conservative estimates of bending moment compared with the experimental results. Hence, the overall behaviour of this type of stair, including the calculation of bending moment, may be considered similar to that of stairs with waist slab.

The bending moments are considered to occur in the longitudinal direction in the riser as well as treads. Each tread slab is subjected to a bending moment combined with shear force, whereas the riser slab is subjected to a constant bending moment and an axial force (which may be compressive or tensile), as shown in Fig. 7.11(a). We may assume that the connection between the riser slab and the adjoining tread slab is rigid. As the shear stresses in the tread slab and axial stresses in the riser slab are relatively small, it is enough to design both tread and riser slabs for flexure alone. The slab thicknesses of both tread and riser slabs are kept the same and are assumed as span/25 for simply supported slabs and span/30 for continuous stairs.

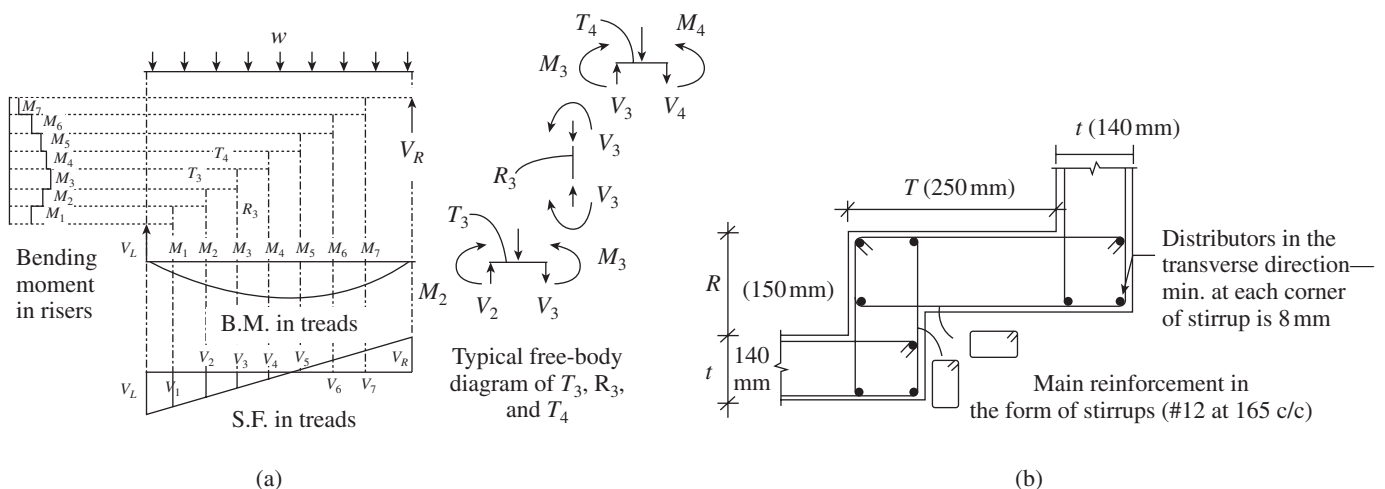


FIG. 17.11 Longitudinally supported tread-riser stairs (a) Bending moment and shear force diagram (b) Detailing of reinforcement

The reinforcement detailing is shown in Fig. 17.11(b); this is similar to the detailing shown in Fig. 17.10(c) for transversely supported tread-riser slabs, except that in this case the main bars are in the form of closed stirrups and the distributors (usually 8mm bars) are placed transversely. This type of detailing provides reinforcement at the top as well and hence can resist the negative bending moment near the supports, arising out of any partial fixity. The closed stirrups may also enhance the resisting capacity of shear as well as axial force, as we are not considering the axial force in the design. The design of such a slab is illustrated in Example 17.8 and the reinforcement detailing of this example is shown in Fig. 17.11(b).

Stairs with waist slab The slab is designed as a simply supported slab. The slab thickness t may be taken as approximately $L/20$ for simply supported conditions and $L/25$ for continuous end conditions. The vertically acting gravity loads w are resolved into two orthogonal components, $w_n = w \cos \theta$ acting normal to the waist slab, causing flexure, and $w_t = w \sin \theta$ acting tangential to the waist slab. The tangential component may be neglected in design. The main bars are designed for the bending moments induced in the vertical plane $= w_n L^2/8$, where L is the effective span as discussed in Section 17.2.2. The reinforcements are placed longitudinally as shown in Figs 17.12 and 17.13 (Figure 17.12 shows the detailing for stairs supported at the ends of landing and

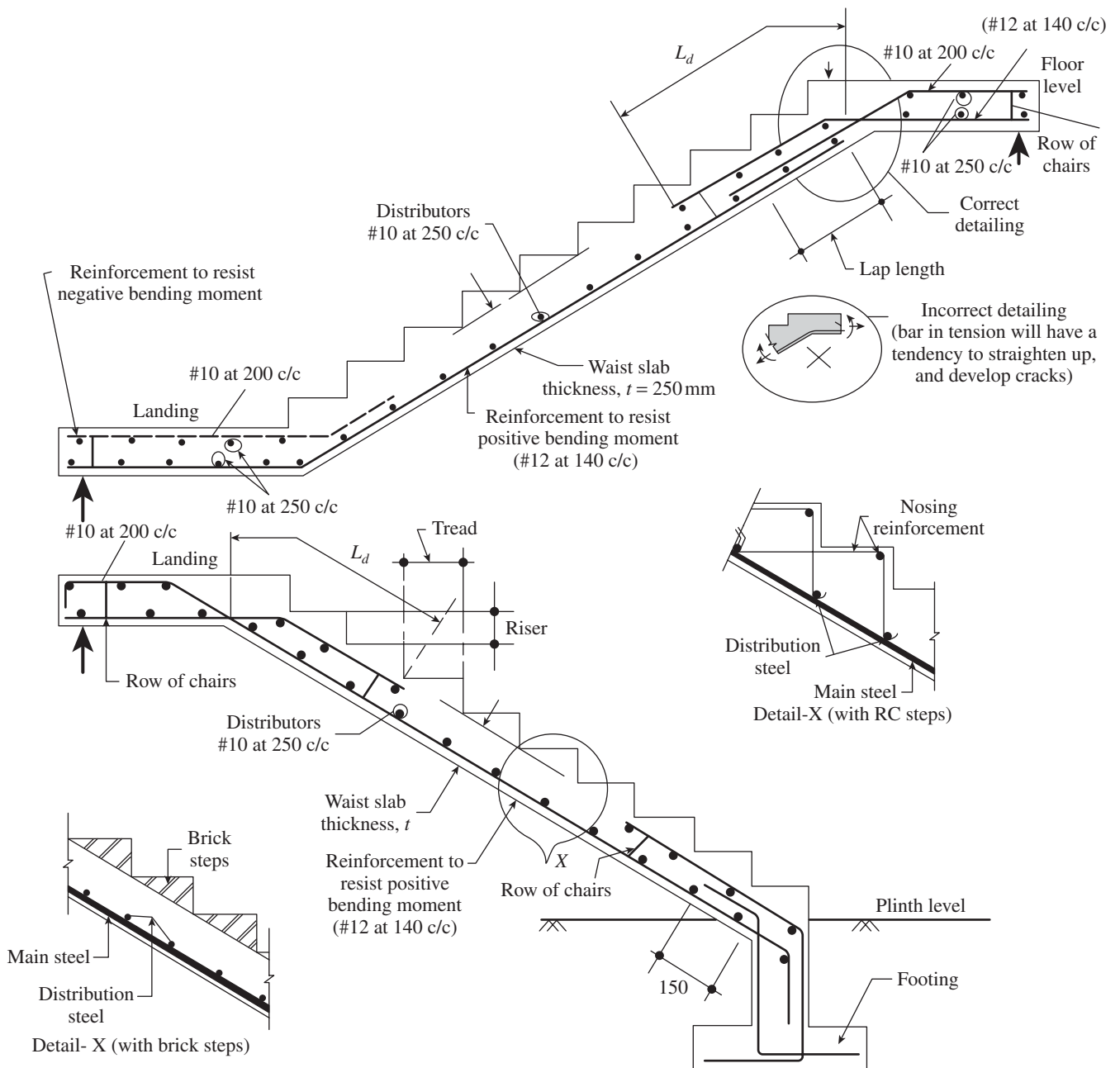


FIG. 17.12 Detailing of dog-legged stair supported at the ends of landing

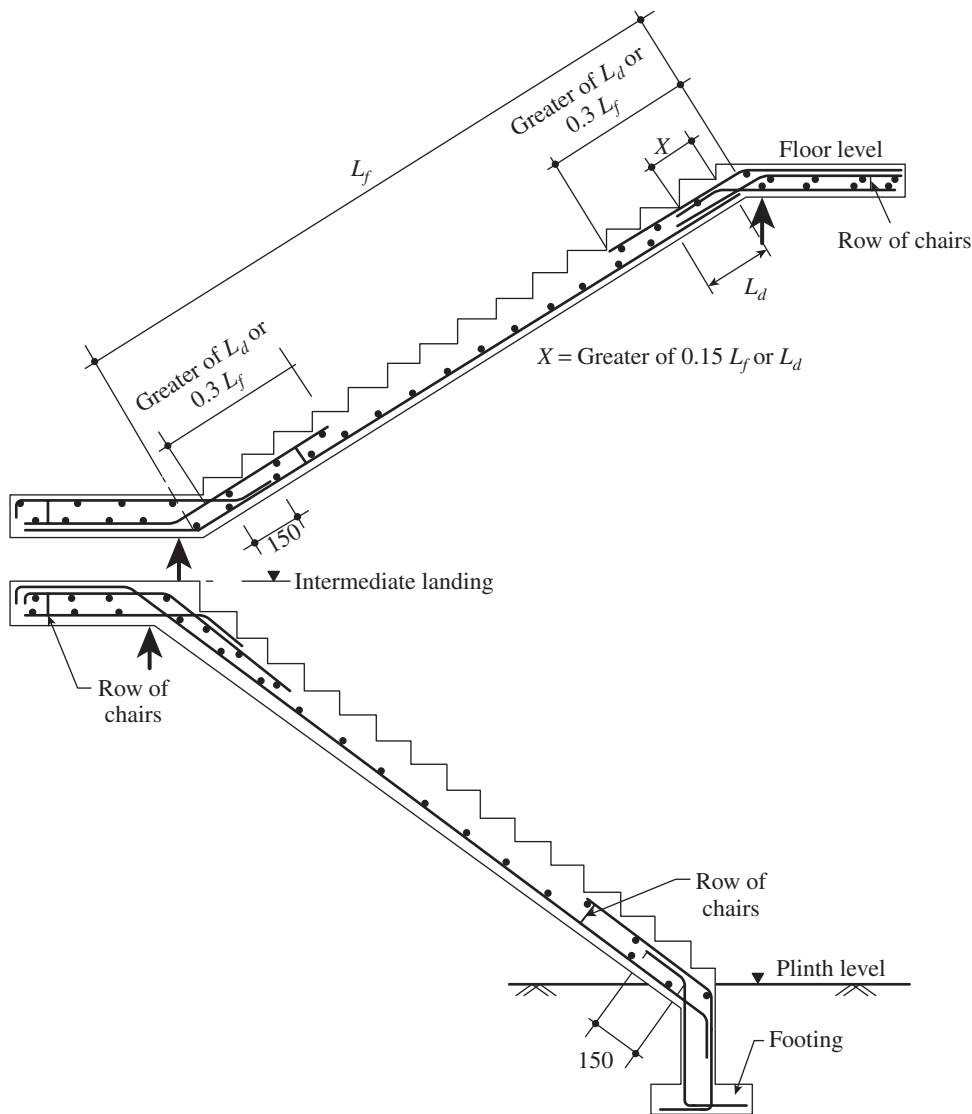


FIG. 17.13 Detailing of dog-legged stair supported at the ends of flights

Fig. 17.13 shows the detailing for stairs supported at the ends of flights, as per SP 34:1987. Detailing of bars should be properly done at the junction of the flight and landing slab. The bottom bars in the waist slab should not be bent in the bottom of the top landing slab at the re-entrant corner; it should be taken straight to the top face and then bent (see Fig. 17.12). This is because these bars, in tension, will try to straighten up and result in the cracking of the concrete cover. The distributor bars are provided in the transverse direction, along the width of the waist slab. Shear stresses may be checked at a distance of effective depth away from the support; in general, they are not critical. Examples 17.5–17.7 illustrate the design of longitudinally supported waist slab-type staircases.

Free-standing stairs Although free-standing stairs have the same structural shape as that of longitudinally supported stairs with waist slab, their behaviour is different since the landing slab is not supported (see Fig. 17.4). Several approximate methods

have been proposed (Cusans and Kuang 1965; Reynolds and Steedman 1988; Varyani 1999; Bangash and Bangash 1999; Bangash 2010) for the analysis of free-standing stairs. However, free-standing stairs can be analysed more accurately by using any available three-dimensional analysis software. The lower flight is subjected to axial compression, bending, and torsion, whereas the upper flight has to resist axial tension, bending, and torsion. The landing slab has to be stiff in its own plane in order to connect the two out-of-plane flights effectively. Hence, the clear distance between the flights in plan (distance a in Fig. 17.4) must be made as less as possible, say 150 mm to 300 mm (Varyani 1999). The flight reinforcement should be well anchored into the supporting beams at the top and bottom floor levels, and these beams should be designed and detailed carefully to resist the forces and moments introduced by the flights. Both the flights and the landing slab will require rebars at both top and bottom and torsional reinforcement in the form of closed stirrups. A complete design of such a stair is provided by Karunakar Rao (1983) and Varyani (1999). Stripping of the formwork should start from the free edge of mid-landing and proceed towards both the supports. At all stages

of construction, the staircase as a whole should be considered as a cantilever.

17.6 HELICOIDAL STAIRCASES

A *helicoidal stair* is a stair describing a helix around a central void and the shape is generated by moving a straight line touching a helix such that the moving line is always perpendicular to the axis of the helix; see Fig. 17.14 (Chatterjee 1978). A helicoidal staircase provides an impressive appearance and hence is increasingly adopted by architects. It is a three-dimensional structure and requires a three-dimensional structural analysis (Scordelis 1960). The analysis of this type of staircase may be simplified by considering its horizontal projection, thus idealizing it as a fixed-ended curved beam (Bergman 1956). This approach has been found to result in a conservative estimate of forces

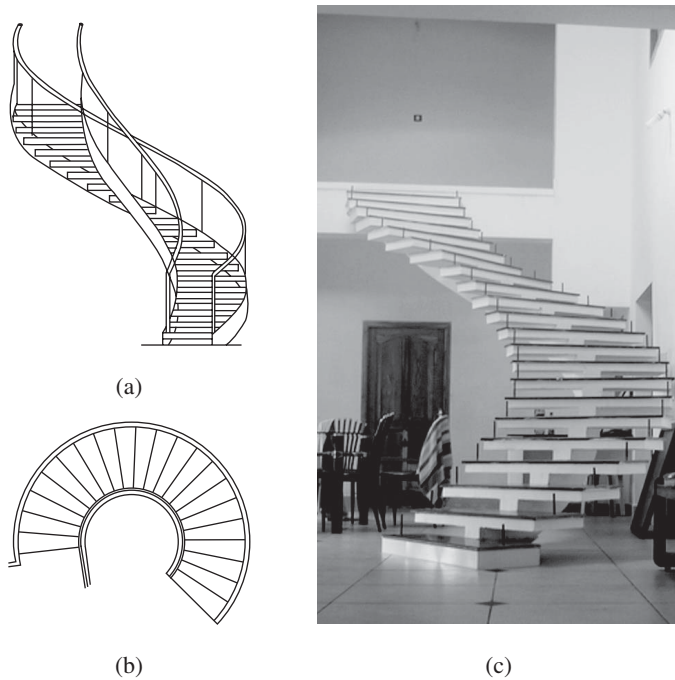


FIG. 17.14 Helicoidal staircase (a) Elevation (b) Plan (c) In a hospital-cum-residence in Panruti, Tamil Nadu

Courtesy: Er T. Vetrikarasi

(Chatterjee 1978). The critical stress resultants acting on the girder are the bending moment about the two principal planes and torsional moment, transverse shear, and axial thrust. It

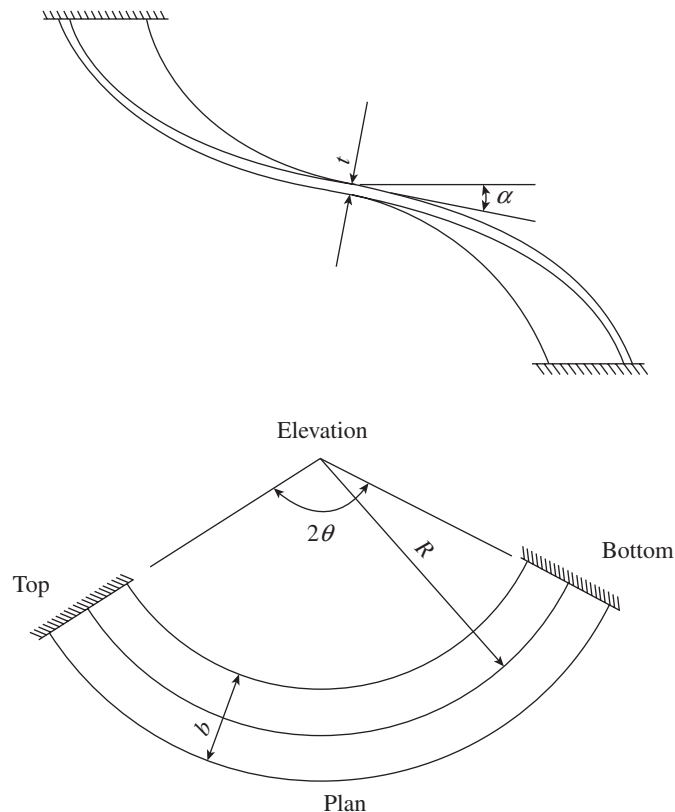


FIG. 17.15 Helicoidal stair notations

has to be noted that when the helicoidal girder is treated as a curved girder, the axial thrust is considered; however, the effect of axial thrust is not significant.

The notations for the approximate curved beam analysis are shown in Fig. 17.15. These are as follows:

1. R = Radius to the centre line of curve
2. 2θ = Subtended angle in plan
3. α = Slope of the helicoidal slab; $\tan(\alpha) = \text{rise/tread}$ for equal size steps
4. t = Thickness of slab, which should be less than the width of slab

The vertical load acting on the curved beam is multiplied by the cosine of the slope of the slab. This load is considered acting normal to the surface of the slab. The radial and torsional moments on the slab for fixed support boundary conditions are given by (Bergman 1956; Chatterjee 1978)

$$M_r = w_u R_c^2 (c \cos \phi - 1)$$

$$M_t = w_u R_c^2 (c \sin \phi - \phi)$$

where R_c is the radius of the centroidal axis of the slab, including the effect of eccentricity of loading, $e = b^2/12R$ (Chatterjee 1978); hence, $R_c = R + e = R + b^2/12R$, where b is the width of the slab, ϕ is the angle measured from the middle point of the curve of the slab,

$$c = \frac{2(g+1)\sin\theta - 2g\theta\cos\theta}{(g+1)\theta - (g-1)\sin\theta\cos\theta} \quad \text{and} \quad g = \frac{EI}{GC}$$

where EI is the flexural rigidity and GC is the torsional rigidity. The value of g for concrete slabs may be calculated by using the following approximate values: $E/G = 2.4$, $I = \text{moment of inertia} = bh^3/12$, and $C = \text{torsional constant} = bh^3/3.5$. Using these values, the value of g is calculated as $2.4 \times 3.5/12 = 0.7$. Chatterjee (1978) suggests that the effect of the eccentricity of loading may be neglected when $(b/R) \leq (1/3)$.

It is important to note that the connecting slabs or beams at the floor levels must be designed to provide the required fixity at the ends of the helicoidal girder. The method of design is illustrated in Example 17.9. Various methods of analysis of helicoidal stairs may be found in Bangash and Bangash (1999). Santathadaporn and Cusens (1966) and Reynolds and Steedman (1988) provide design aids for fixed-ended helicoidal girders. Solanki (1976) analysed fixed-ended helicoidal girders with intermediate landings, whereas Wadud and Ahmed (2005) provided the design aids for such girders.

17.7 EARTHQUAKE CONSIDERATIONS

In general, RC staircases are built integrally with the structural system of the building, even though they are analysed as isolated systems. The elements of these staircases, such as the flight slabs and landing slab, act as diagonal braces and attract large

lateral forces during an earthquake, thereby incurring damage (Fig. 17.16a). The provision of a sliding support will prevent the stair slab from acting as diagonal bracing (Fig. 17.16b and c). Stairs with landings are not normally reinforced to act as compression braces and can be expected to fail in a very brittle manner. Such behaviour was observed in the earthquakes of San Fernando (1971), Nicaragua (1972), Lima (1974), El Asnam (1980), Guam (1993), and Northridge (1994). The beams supporting the landing slab of dog-legged stairs will also cause the secondary effect of *short columns*, in addition to causing the twist of the building due to stiffness irregularity in plan, if they are not located centrally. Short-column effect results in enhanced shear demand with additional stiffness introduced at intermediate levels. Axial load also increases in these columns due to increased rigidity of the particular bay. This increase in both axial and shear forces may result in

brittle failure of these short columns. Hence, it is important to include the stairs in the modelling of the structure.

Other strategies that may be adopted include the following (IS 4326:1993):

Separated staircases The staircases are completely separated and built on a separate RC structure by providing adequate gap between the staircase tower and the building to ensure that they do not pound each other during shaking caused by a strong earthquake (see Fig. 17.17). The opening at the vertical joints between the floor and the staircase may be either covered with a tread plate attached to one side of the joint and sliding on the other side or covered with some appropriate material that could crumble or fracture during an earthquake without causing structural damage.

Built-in staircase This is done by providing rigid walls at the stair opening, as shown in Fig. 17.18. Under such circumstances, the joints as provided in separated staircases will not be necessary. The two walls enclosing the staircase should extend through the entire height of the stairs and to the building foundations.

Staircases with sliding joints This strategy is used where it is not possible to provide rigid walls around stair openings; to adopt the separated staircase, sliding joints should be provided as shown in Fig. 17.16(b) so that they will not act as diagonal bracing.

As the stairs provide vital link of communication and services, they should be designed for higher safety factor when compared with the other

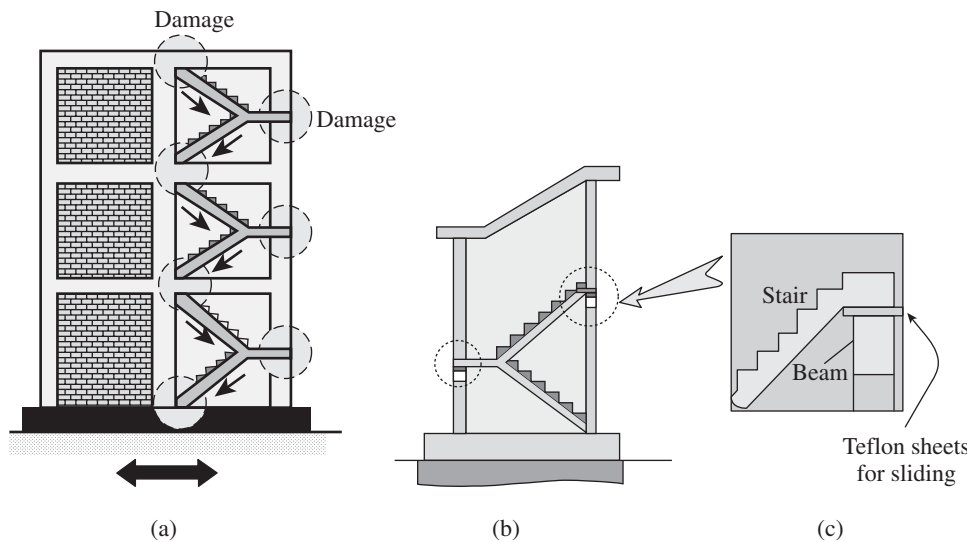


FIG. 17.16 Earthquake effects (a) Damage locations due to diagonal bracing effect (b) Location for sliding support (c) Detail at the sliding support

Source: Murty, et al. 2006, NICEE, IIT Kanpur

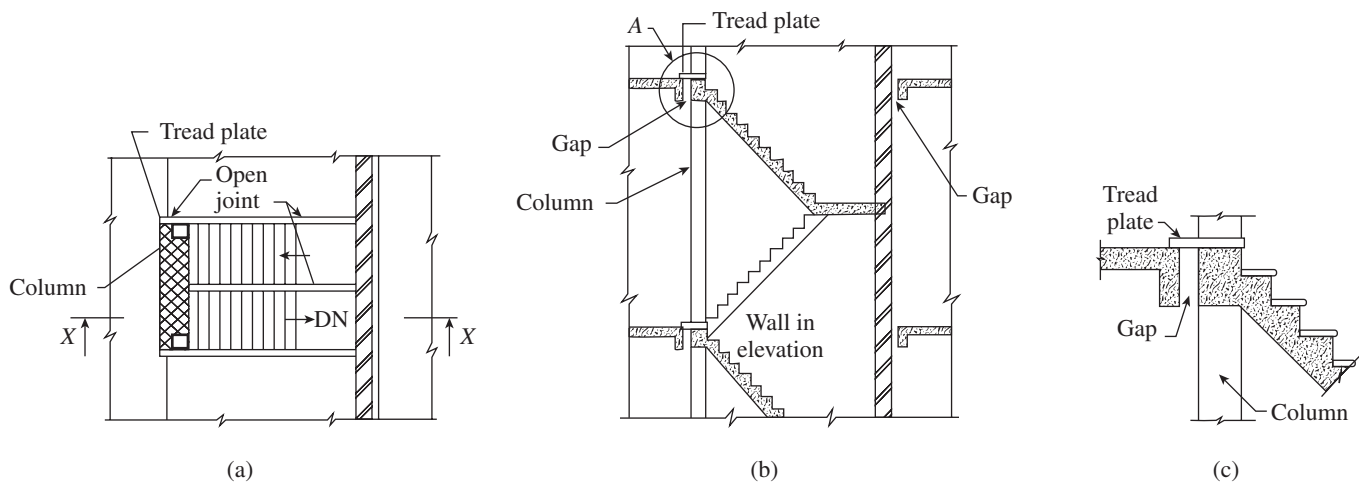


FIG. 17.17 Separated staircases (a) Plan (b) Section at X-X (c) Detail at A

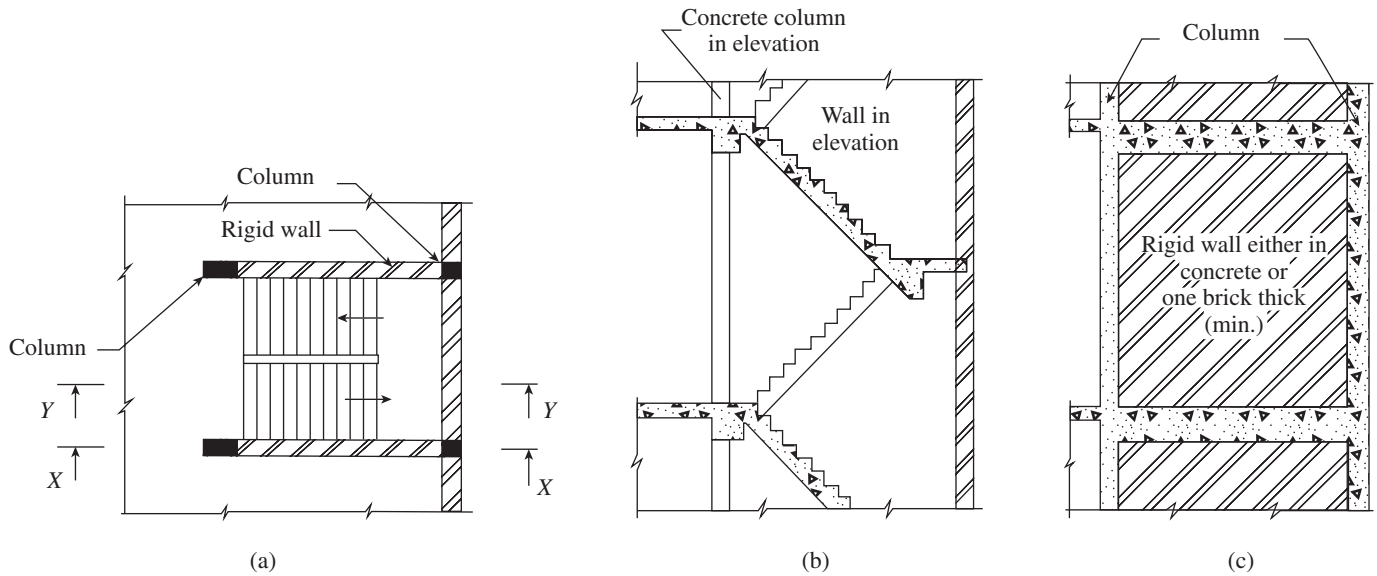


FIG. 17.18 Rigidly built-in staircase (a) Plan (b) Section Y–Y (c) Section at X–X

structural elements. An important factor of 1.5 must be applied to the staircases located in earthquake zones.

Fire Protection

The fire protection rating for the staircase should be at least 30 minutes more than that assigned to the building. It is better to provide a cover not less than 25 mm. The minimum thickness of slabs in the staircase should be 110 mm. More

importantly, the fixtures and railings must be fireproof. Fire-resistant fibreglass covers should be used for the railings and steps instead of plastic covers.

EXAMPLES

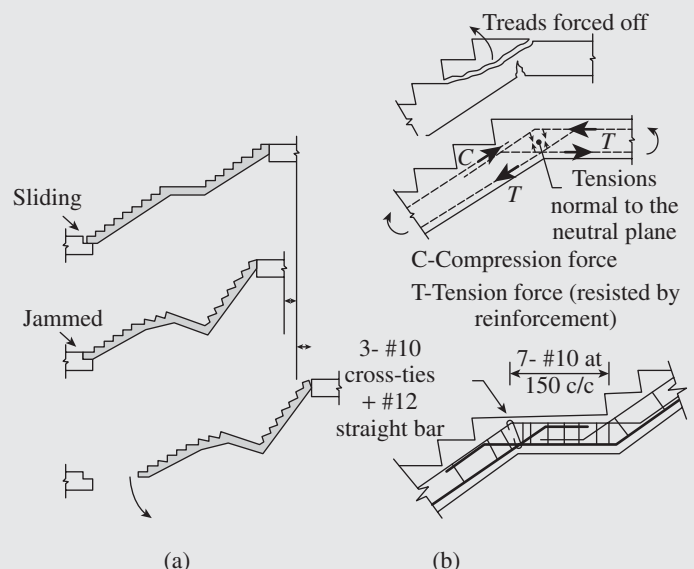
EXAMPLE 17.1 (Design of cantilever tread slab staircase): A straight staircase with independent steps cantilevering from the face of the wall has to be designed for a residence.

CASE STUDY

Collapse of and Damage to Stairs and Ramps during Earthquakes in New Zealand

During the earthquakes in New Zealand (on 4 September 2010 at Darfield and on 22 February 2011 at Lyttelton), the stairs in at least four multi-storey buildings collapsed; in many other cases, the stairs sustained serious damages. In the Forsyth Barr Building, Christchurch, the provided seismic gaps were reduced by construction tolerances and debris, among others. This resulted in insufficient space to accommodate even small amounts of inter-storey drifts, leading to compression of the stair slab and subsequent collapse and trapping office workers in the 18-storey building (see the given figure).

Where a straight stair or ramp had a mid-landing, the front part of the mid-height landing failed. It is called an ‘opening knee’ failure, wherein the top of the landing at the first step will be squeezed off when the top of the stair is compressed (Williams 2012). Simmons and Bull (2000), based on their research, recommended transverse ties to be placed at the knee (as shown in the figure) to resist the bursting forces and to reduce the buckling of any longitudinal reinforcement, should cracking through the knee occur.



Inter-storey drift along the stair (a) Compression forces shortening the stair (b) The knee of the stair or landing ‘opens’ and the landing fails

(Source: Williams 2012, adapted)

Given data: width of flight = 1.2 m, tread = 300 mm, and riser = 150 mm. Use M20 concrete and Fe 415 steel and assume mild exposure.

SOLUTION:

Step 1 Calculate the loads.

Given: Effective length = 1.2 m, $T = 300$ mm, $R = 150$ mm.

To have marginal overlap between adjacent tread slabs, let us assume the actual width of the tread slab to be

$$B = 300 + 10 = 310 \text{ mm}$$

The thickness at support (t) is assumed to be

$$t = L/10 = 1200/10 = 120 \text{ mm}$$

Let us adopt a depth of 80 mm at the free end and 120 mm at the support. Hence, average thickness is $(80 + 120)/2 = 100$ mm.

Dead load

Self-weight of tread slab

$$= \gamma_c bt = 25 \times (0.10 \times 0.31) = 0.775 \text{ kN/m}$$

Finishes (assumed as 0.6 kN/m^2)

$$= 0.6 \times 0.31 = 0.186 \text{ kN/m}$$

Total dead load = 0.961 kN/m

Factored dead load = $1.5 \times 0.961 = 1.44 \text{ kN/m}$

Imposed load

As per IS 875 (Part 2), imposed load on stairs liable to overloading is 5 kN/m^2 and 1.3 kN at the free edge of cantilever. Hence, for

Case 1 factored imposed load = $1.5(5 \times 0.3) = 2.25 \text{ kN/m}$ and

Case 2 factored imposed load = $1.5 \times 1.3 = 1.95 \text{ kN}$

Step 2 Calculate the bending moment.

Bending moment due to dead load = $1.44 \times 1.2^2/2 = 1.04 \text{ kNm}$

Bending moment due to imposed load = $2.25 \times 1.2^2/2 = 1.62 \text{ kNm}$

or $1.95 \times 1.2 = 2.34 \text{ kNm}$ (governs)

Hence, $M_u = 1.04 + 2.34 = 3.38 \text{ kNm}$

Step 3 Check for depth.

$$d = \sqrt{\frac{M_u}{kbf_{ck}}} = \sqrt{\frac{3.38 \times 10^6}{0.138 \times 310 \times 20}} = 63 \text{ mm} < 120 \text{ mm (cover)}$$

Hence, the adopted depth is sufficient.

Step 4 Design the reinforcement.

Assuming a clear cover of 20 mm (Table 16 of IS 456) and bar diameter of 10 mm, effective depth

$$d = 120 - 20 - 10/2 = 95 \text{ mm}$$

$$\frac{M_u}{bd^2} = \frac{3.38 \times 10^6}{310 \times 95^2} = 1.208 \text{ MPa}$$

From Table 2 of SP 16 for M20 concrete and $f_y = 415 \text{ MPa}$, $p_t = 0.362\%$. Hence,

$$A_{st} = 0.362 \times 310 \times 95 / 100 = 107 \text{ mm}^2$$

We may also get the same result by using the expressions developed in Chapter 5 or by using the approximate formula

$$A_{st} = \frac{M_u}{0.8df_y} = \frac{3.38 \times 10^6}{0.8 \times 95 \times 415} = 107 \text{ mm}^2$$

Provide three 10 mm diameter bars.

Area provided = $3 \times 78.5 = 235.5 \text{ mm}^2 > 107 \text{ mm}^2$; provided

$$p_t = \frac{235.5 \times 100}{310 \times 95} = 0.8$$

Distributors

$(A_{st})_{\min} = 0.0012bt$ (for Fe 415 bars, Clause 26.5.2.1)

$= 0.0012 \times 1000 \times 120 = 144 \text{ mm}^2/\text{mm}$ (assuming uniform slab thickness)

Spacing of 8 mm bars = $(50.2 \times 1000)/144 = 348 \text{ mm}$

Provide 8 mm diameter distributors at 300 mm c/c.

Step 5 Check for anchorage.

Required anchorage length (Clause 26.2.1), $L_a = \frac{0.87f_y d_b}{4\tau_b} = \frac{0.87 \times 415 \times 8}{4(1.2 \times 1.6)} = 376 \text{ mm}$

Each of the main bars must be anchored into the supporting wall for a length of 380 mm with an L bend.

Step 6 Check for shear (which usually will not be critical).

Factored shear force at support = $(1.44 + 2.25) 1.2 = 4.428 \text{ kN}$

$$\tau_v = \frac{V_u}{bd} = \frac{4.428 \times 1000}{310 \times 95} = 0.15 \text{ N/mm}^2$$

$$\tau_c = 0.57 \times 1.30 > \tau_v \text{ (Clause 40.2.1.1. of IS 456)}$$

Hence, it is safe in shear.

Detailing of tread slab is shown in Fig. 17.19.

Notes:

1. It is important to provide proper chairs to the top bars to ensure that they remain in top face during concreting.
2. As the cantilever steps transfer considerable moment to the supporting wall, the wall has to be designed to resist the additional moment due to the cantilever steps.
3. During seismic loading there may be reversal of stresses, and to resist it bottom reinforcement as shown in Fig. 17.19 is necessary.

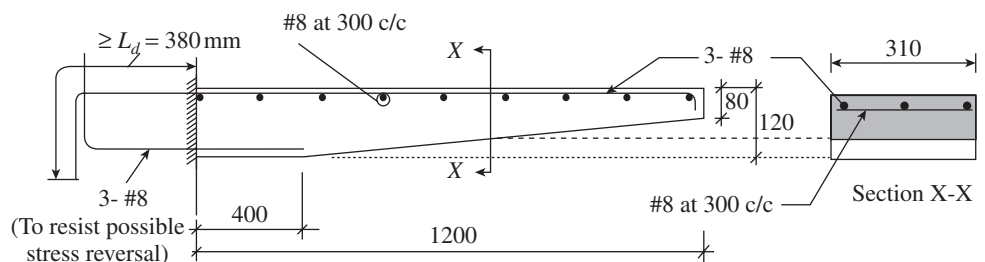


FIG. 17.19 Detailing of tread slab of Example 17.1

EXAMPLE 17.2 (Design of cantilever slabless stair):

Design the cantilevered staircase given in Example 17.1 as a slabless stair.

SOLUTION:

Step 1 Calculate the loads. From Example 17.1, we have $R = 150\text{ mm}$, $T = 300\text{ mm}$, and $L = 1.2\text{ m}$.

Let us assume a slab thickness of 100 mm (see Fig. 17.20a). With 20 mm cover, 10 mm diameter bars, and 8 mm diameter stirrups

$$d = (150 + 100) - 20 - 8 - 10/2 = 217\text{ mm}$$

Calculate the load on typical tread and riser unit.

Dead load

- Self-weight = $25 \times (0.3 \times 0.1 + 0.15 \times 0.1) = 1.125\text{ kN/m}$
- Finishes (assumed as 0.6 kN/m^2) = $0.6 \times 0.3 = 0.180\text{ kN/m}$
- Total dead load = 1.305 kN/m
- Factored dead load = $1.5 \times 1.305 = 1.958\text{ kN/m}$

Imposed load

- As given in Example 17.1, imposed load for
- Case 1 = $1.5(5 \times 0.3) = 2.25\text{ kN/m}$ and
- Case 2 = $1.5 \times 1.3 = 1.95\text{ kN}$

Step 2 Calculate the bending moments. As given in Example 17.1, the bending moment will be critical for the concentrated imposed load. Hence,

$$\text{bending moment} = 1.958 \times 1.2^2/2 + 1.95 \times 1.2 = 3.75\text{ kNm}$$

Step 3 Design the reinforcement. Ignoring the contribution of flanges and considering only the rectangular section, we have $b = 100\text{ mm}$ and $d = 217\text{ mm}$.

$$\frac{M_u}{bd^2} = \frac{3.75 \times 10^6}{100 \times 217^2} = 0.8\text{ MPa}$$

From Table 2 of SP 16, for M20 concrete and $f_y = 415\text{ MPa}$, $p_t = 0.233\%$. Hence,

$$A_{st} = 0.233 \times 100 \times 217/100 = 50.56\text{ mm}^2$$

Provide two 8 mm bars on top (A_{st} provided = $2 \times 50.2 = 100.4\text{ mm}^2$)

Anchorage length = 376 mm as in Example 17.1.

Distributors

Assuming mild steel bars

$$(A_{st})_{\min} = 0.0015bt = 0.0015 \times 1000 \times 100 = 150\text{ mm}^2/\text{m}$$

$$\text{Spacing of } 6\text{ mm bars} = 28.27 \times 1000/150 = 188\text{ mm}$$

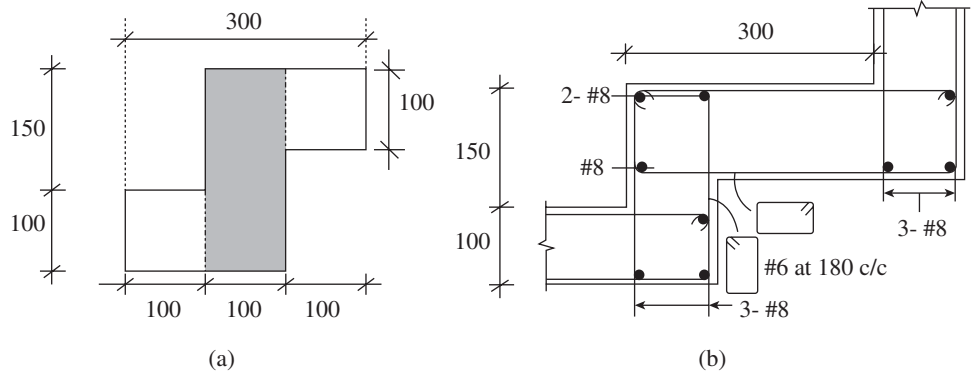


FIG. 17.20 Tread-riser stair of Example 17.2 (a) Typical unit (b) Detailing

Provide 6 mm bars at 180 mm c/c in the form of closed stirrups with an 8 mm bar placed transversely at each bend as shown in Fig. 17.20(b).

EXAMPLE 17.3 (Design of stair with slab cantilevering from spine beam):

Design a staircase consisting of 10 steps having 300 mm tread and 160 mm rise and two landings. The width of the staircase is 1500 mm and the length of each landing is 1200 mm . The arrangement of staircase is shown in Fig. 17.21. Assume the imposed load as 5 kN/m^2 and mild exposure, and use M20 concrete and Fe 415 steel.

SOLUTION:

Step 1 Design the step.

$$\text{Effective cantilever length of the step} = 1500/2 = 750\text{ mm}$$

$$\text{Assume depth} = L/10 = 750/10 = 75\text{ mm}$$

$$\text{Self-weight} = 25 \times (0.3 \times 0.075) = 0.563\text{ kN/m}$$

$$\text{Finishes (assumed as } 0.6\text{ kN/m}^2) = 0.6 \times 0.3 = 0.18\text{ kN/m}^2$$

$$\text{Total dead load} = 0.743\text{ kN/m}$$

$$\text{Factored dead load} = 1.5 \times 0.743 = 1.115\text{ kN/m}$$

Imposed load

$$\text{Case 1} = 1.5 \times 5 \times 0.3 = 2.25\text{ kN/m}$$

$$\text{Case 2} = 1.5 \times 1.3 = 1.95\text{ kN}$$

$$\text{Bending moment due to dead load} = 1.115 \times 0.75^2/2 = 0.314\text{ kNm}$$

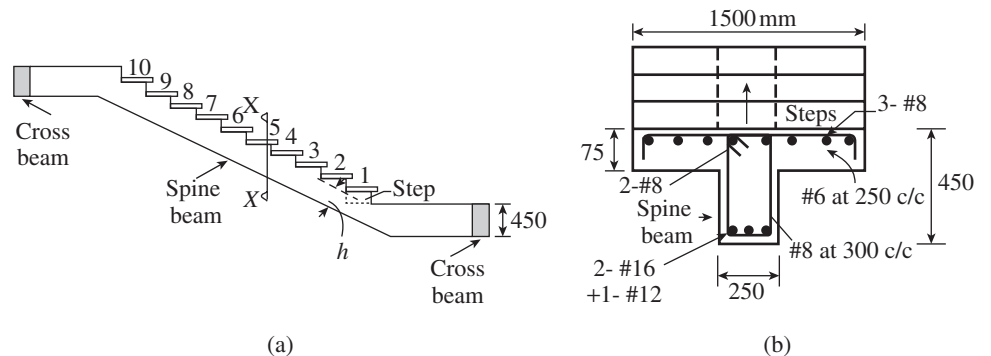


FIG. 17.21 Cantilevered step from spine beam of Example 17.3 (a) Spine beam with steps (b) Section X-X

$$\begin{aligned} \text{Bending moment due to imposed load} &= 2.25 \times 0.75^2/2 \\ &= 0.633 \text{ kNm} \end{aligned}$$

$$\text{or } 1.95 \times 0.75 = 1.463 \text{ kNm (governs)}$$

$$\text{Hence, } M_u = 0.314 + 1.463 = 1.777 \text{ kNm}$$

$$\begin{aligned} \text{Required depth} &= \sqrt{\frac{1.777 \times 10^6}{0.138 \times 300 \times 20}} = 46 \text{ mm} \\ &< 75 \text{ mm (cover)} \end{aligned}$$

Adopt a total depth of 75 mm, with clear cover = 20 mm (Table 16 of IS 456 for mild exposure) and 10 mm diameter bar.

$$\begin{aligned} d &= 75 - 20 - 10/2 = 50 \text{ mm} \\ \frac{M_u}{bd^2} &= \frac{1.777 \times 10^6}{300 \times 50^2} = 2.37 \text{ MPa} \end{aligned}$$

From Table 2 of SP 16, for M20 concrete and $f_y = 415 \text{ MPa}$, $p_t = 0.7855\%$. Hence,

$$A_{st} = 0.7855 \times 300 \times 50/100 = 118 \text{ mm}^2$$

Provide three 8 mm bars at top. Provide 6 mm bars at 250 mm as distribution steel as shown in Fig. 17.21. From Table 65 of SP 16, L_d for M20 concrete and 8 mm bar = 376 mm < 1500/2. Hence, the anchorage is sufficient.

Step 2 Design the beam.

Length of stair = 10 × 300	= 3000 mm
Length of two landings = 1200 × 2	= 2400 mm
Total length	= 5400 mm
Less width of cross beam	= 300 mm
Effective length of beam	= 5100 mm
Weight of steps = 25 × 1.5 × 0.075	= 2.81 kN/m
Assume self-weight = 25 × 0.5 × 0.25	= 3.13 kN/m
Add extra for finishes	= 1.0 kN/m
Total dead weight	= 6.94 kN/m
Live load	= 5.0 kN/m
Total factored load = 1.5(5 + 6.94)	= 17.91 kN/m

$$M_u = \frac{wL^2}{8} = \frac{17.91 \times 5.1^2}{8} = 58.23 \text{ kNm}$$

$$\text{Required depth } d = \sqrt{\frac{M_u}{kbf_{ck}}} = \sqrt{\frac{58.23 \times 10^6}{0.138 \times 250 \times 20}} = 290 \text{ mm}$$

Provide overall depth as 450 mm with effective depth as 410 mm.

$$\frac{M_u}{bd^2} = \frac{58.23 \times 10^6}{250 \times 410^2} = 1.39 \text{ MPa}$$

From Table 2 of SP 16, for M20 concrete and $f_y = 415 \text{ MPa}$, $p_t = 0.422\%$. Hence,

$$A_{st} = 0.422 \times 410 \times 250/100 = 433 \text{ mm}^2$$

Provide two 16 mm bars and one 12 mm bar (A_{st} provided = 515 mm²) at bottom and two 8 mm bars at top as hanger reinforcement.

Design for shear

Critical shear force occurs at a distance of effective depth from the support. Hence,

$$V_u = w \left(\frac{L}{2} - d \right) = 17.91 \left(\frac{5.1}{2} - 0.41 \right) = 38.33 \text{ kN}$$

Nominal shear stress

$$\tau_v = \frac{V_u}{bd} = \frac{38.33 \times 1000}{250 \times 410} = 0.374 \text{ N/mm}^2$$

Percentage of reinforcement at critical shear zone = 515 × 100/(250 × 410) = 0.50%

Allowable shear strength, from Table 19 of IS 456, $\tau_c = 0.48 \text{ N/mm}^2$

$\tau_v < \tau_c$ and $\tau_v < \tau_{c,\max}$ (2.8 N/mm² as per Table 20 of IS 456 for M20)

Hence, only nominal shear stirrups need to be provided. Select two-legged 8 mm bars.

$$\begin{aligned} \text{Spacing } s_v &= \frac{A_{sv} f_y}{0.4b} = \frac{100 \times 415}{0.4 \times 250} \\ &= 415 \text{ mm} > 300 \text{ mm (maximum)} \end{aligned}$$

Hence, provide two-legged 8 mm bars at 300 mm spacing.

Note: The landing slab has the same cantilever span as that of the steps. Hence, provide 75 mm depth and 8 mm bars at 250 mm spacing at the top face of the landing; in addition, provide 8 mm bars at 300 mm spacing as distribution steel.

EXAMPLE 17.4 (Design of transversely spanning waist slab-type stair):

Design a waist slab-type staircase with a straight flight supported by two stringer beams along the two sides. Assume an effective span of 1.35 m, a riser of 150 mm, and a tread of 300 mm. Assume imposed load of 4 kN/m². Use M25 concrete and Fe 415 steel. Assume mild exposure.

SOLUTION:

Step 1 Calculate the loads. Given:

Effective length, $L = 1.35 \text{ m}$, $R = 150 \text{ mm}$, $T = 300 \text{ mm}$

$$\text{Hence, } \sqrt{R^2 + T^2} = \sqrt{150^2 + 300^2} = 335 \text{ mm}$$

Let us assume a waist slab thickness of 80 mm. Clear cover as per Table 16 of IS 456 is 20 mm (mild exposure). Let us assume 10 mm bars. Hence,

$$\text{Effective depth} = 80 - 20 - 10/2 = 55 \text{ mm}$$

Loads acting vertically over each tread width are calculated as follows:

$$\text{Self-weight of slab} = 25 (0.08 \times 0.335) = 0.67 \text{ kN/m}$$

$$\text{Self-weight of step} = 25 \times (0.15/2 \times 0.30) = 0.56 \text{ kN/m}$$

$$\text{Finishes (assumed)} = 0.6 \times 0.30 = 0.18 \text{ kN/m}$$

$$\text{Imposed load} = 4.0 \times 0.3 = 1.20 \text{ kN/m}$$

$$\text{Total load, } w = 2.61 \text{ kN/m}$$

$$\text{Factored load} = 1.5 \times 2.61 = 3.92 \text{ kN/m}$$

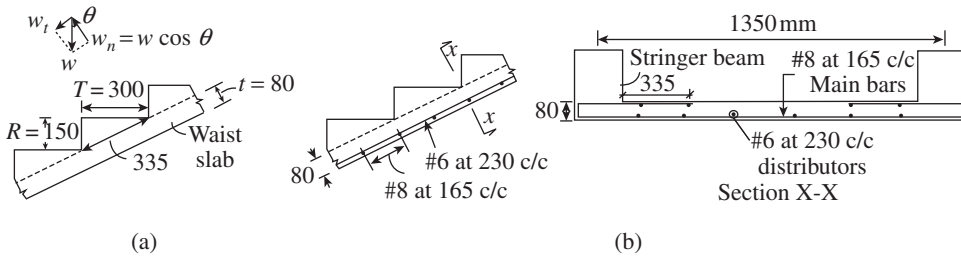


FIG. 17.22 Transversely supported waist slab stair of Example 17.4 (a) Configuration (b) Detailing

Step 2 Calculate the bending moment.

Factored load causing flexure in the transverse direction

$$= w \cos \theta = 3.92 \times \left(\frac{300}{335}\right) = 3.51 \text{ kN/m}$$

Distributed factored load per metre width along inclined slab

$$w_u = \frac{3.51}{0.335} = 10.48 \text{ kN/m}$$

Maximum bending moment at mid-span

$$M_u = \frac{w_u L^2}{8} = \frac{10.48 \times 1.35^2}{8} = 2.39 \text{ kNm/m}$$

Step 3 Design the reinforcement.

$$\frac{M_u}{bd^2} = \frac{2.39 \times 10^6}{1000 \times 55^2} = 0.79 \text{ MPa}$$

From Table 3 of SP 16 for M25 concrete and Fe 415 steel, $p_t = 0.228\%$. Hence,

$$A_{st} = (0.228/100) \times 10^3 \times 55 = 125 \text{ mm}^2/\text{m}$$

Required spacing of 8 mm bars = $50 \times 10^3 / 125 = 400 \text{ mm}$
 Maximum permissible spacing = $3d = 3 \times 55 = 165 \text{ mm}$
 Provide 8 mm diameter bars at 165 mm spacing as shown in Fig. 17.22.

Distributors

Assuming 6 mm mild steel bars,
 Minimum $A_{st} = 0.0015bt = 0.0015 \times 1000 \times 80 = 120 \text{ mm}^2/\text{m}$
 Spacing of 6 mm bars = $28.3 \times 10^3 / 120 = 235 \text{ mm}$
 Provide 6 mm mild steel bars at 230 mm c/c (see Fig. 17.22).

EXAMPLE 17.5 (Longitudinally supported dog-legged stair):
 Design the waist slab for the staircase shown in Fig. 17.23.

Assume rise of step = 150 mm, tread = 250 mm, width of stair = 1 m, and weight of finishes = 0.75 kN/m². Use M20 concrete and Fe 415 steel. Assume mild exposure and stairs not liable for overcrowding.

SOLUTION:

Step 1 Calculate the loads. Given

$$R = 150, T = 250 \text{ mm}$$

$$\text{Hence, } \sqrt{R^2 + T^2} = \sqrt{150^2 + 250^2} = 292 \text{ mm}$$

Gradient of staircase, $\tan \theta = 150/250 = 0.6$; hence, $\theta = 31^\circ$.

As the landing slab is supported on three sides, as per Ahmed, et al. (1995, 1996)

Effective span = $9 \times 0.25 = 2.25 \text{ m}$
 Assume a waist slab thickness = $L/20 = 2.25 \times 1000/20 = 112.5 \text{ mm}$, say 115 mm.

Assuming 20 mm clear cover (Table 16 of IS 456) and 12 mm main bars,
 Effective depth, $d = 115 - 20 - 12/2 = 89 \text{ mm}$

Loads on going of stair (on projected plan area)

Self-weight of waist slab = $25 \times (0.115 \times 292/250) = 3.36 \text{ kN/m}^2$
 Self-weight of steps = $25 \times (0.15/2) = 1.88 \text{ kN/m}^2$
 Finishes (given) = 0.75 kN/m^2
 Imposed load (as per IS 875 Part 2) = 3.00 kN/m^2

Total load = 8.99 kN/m^2
 Factored load = $8.99 \times 1.5 = 13.49 \text{ kN/m}^2$

Loads on landing

Self-weight of slab = $25 \times 0.115 = 2.88 \text{ kN/m}^2$
 Finishes (given) = 0.75 kN/m^2
 Imposed load = 3.00 kN/m^2

Total load = 6.63 kN/m^2
 Factored load = $1.5 \times 6.63 = 9.95 \text{ kN/m}^2$

Step 2 Calculate the bending moment.

$$M_u = \frac{wL^2}{8} = \frac{13.49 \times 2.25^2}{8} = 8.54 \text{ kNm}$$

Required depth $d = \sqrt{\frac{M_u}{kbf_{ck}}} = \sqrt{\frac{8.54 \times 10^6}{0.138 \times 1000 \times 20}} = 56 \text{ mm}$
 $< 89 \text{ mm}$

The assumed overall depth is sufficient.

Step 3 Design the reinforcement.

$$\frac{M_u}{bd^2} = \frac{8.54 \times 10^6}{1000 \times 89^2} = 1.08 \text{ MPa}$$

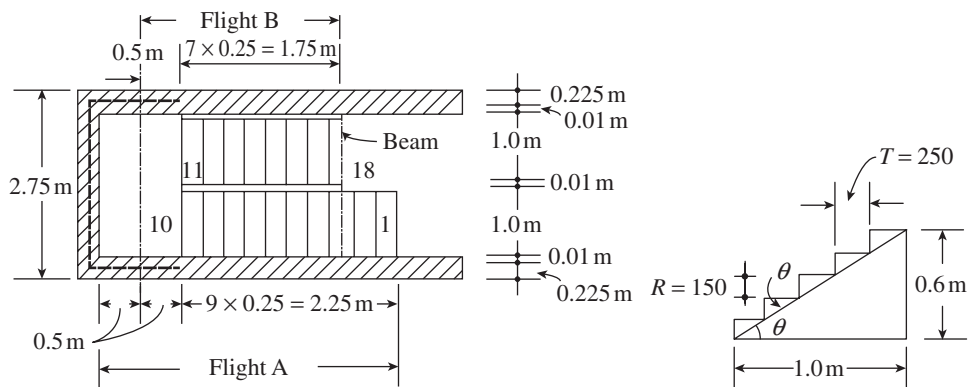


FIG. 17.23 Longitudinally supported waist-type stair of Example 17.5

From Table 2 of SP 16, for Fe 415 steel and M20 concrete, $p_t = 0.3206\%$. Hence,

$$A_t = 0.3206/100 \times 1000 \times 89 = 285 \text{ mm}^2/\text{m}$$

Required spacing of 8 mm diameter bars = $(50 \times 10^3)/285 = 175 \text{ mm}$

Maximum spacing = $3d = 3 \times 89 = 267 \text{ mm}$

Hence, provide 8 mm diameter bars at 170 mm c/c.

Distribution steel

$$A_s = (0.12/100) \times 1000 \times 115 = 138 \text{ mm}^2$$

Assuming 8 mm diameter bars,

$$\text{Spacing} = (50.2 \times 10^3)/138 = 363 \text{ mm}$$

Provide 8 mm mild steel bars at 300 mm c/c.

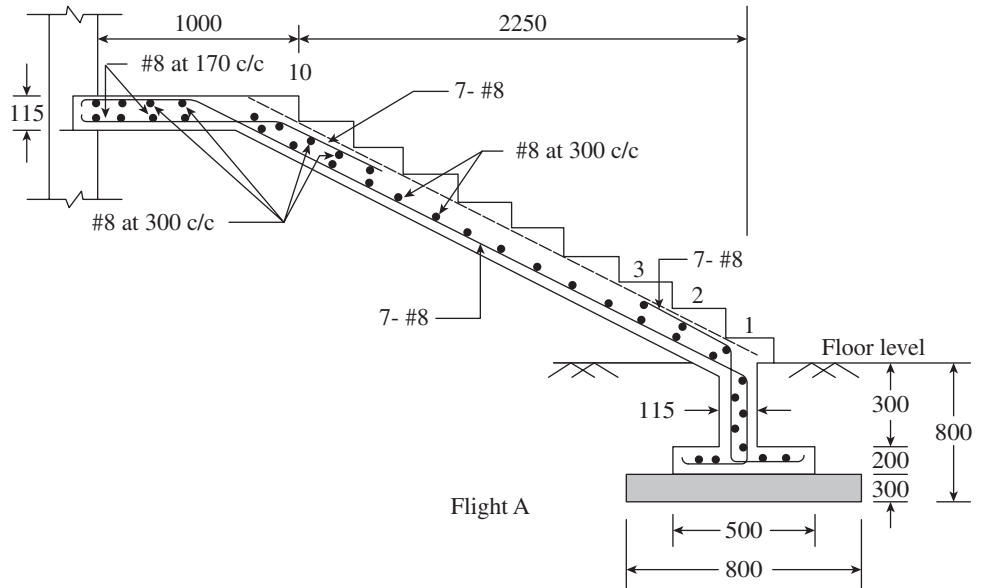


FIG. 17.24 Detailing of stair of Example 17.5

Step 4 Check for shear.

$$V_u = \frac{wL}{2} = \frac{13.49 \times 2.25}{2} = 15.18 \text{ kN}$$

Nominal shear stress

$$\tau_v = \frac{V_u}{bd} = \frac{15.18 \times 1000}{1000 \times 89} = 0.17 \text{ N/mm}^2$$

From Table 19 of IS 456, τ_c (for $f_{ck} = 20$ and $p_t = 0.33\%$) = $0.40 \text{ N/mm}^2 > 0.17 \text{ N/mm}^2$

Hence, it is safe in shear.

Note: Usually well-proportioned slabs will be safe in shear.

Step 5 Design the landing slab.

Effective span = c/c of well or clear span of landing + effective depth of slab, whichever is less

$$= (2.75 - 0.225) \text{ or } 2.3 + 0.089 = 2.525 \text{ or } 2.389 \text{ m; hence, } L = 2.389 \text{ m}$$

$$M_u = \frac{wL^2}{8} = \frac{9.95 \times 2.389^2}{8} = 7.10 \text{ kNm} < 8.54 \text{ kNm}$$

Hence, provide the same reinforcement on the waist slab, that is, 8 mm diameter bar at 170 mm c/c at bottom and 8 mm diameter at 300 mm c/c as distributor (see Fig. 17.24). As flight B has a smaller span, provide the same reinforcement as in flight A.

EXAMPLE 17.6 (Design of dog-legged staircase supported longitudinally):

Design a waist slab-type dog-legged staircase for a building, given the following data:

- (a) Height between floors = 3 m
- (b) Riser, $R = 150 \text{ mm}$; tread, $T = 250 \text{ mm}$
- (c) Width of flight and landing width = 1.25 m
- (d) Imposed load = 4.0 kN/m^2
- (e) Floor finishes = 0.6 kN/m^2

Assume that the stair is to be supported on 230 mm width beams at the outer edges of the landing, parallel to the risers (Fig. 17.25). Use M20 concrete and Fe 415 steel. Assume mild exposure.

SOLUTION:

Step 1 Calculate the loads. Given:

$$R = 150 \text{ mm, } T = 250 \text{ mm}$$

$$\text{Hence, } \sqrt{R^2 + T^2} = \sqrt{150^2 + 250^2} = 292 \text{ mm}$$

Effective span = c/c distance between supports = $9 \times 250 + 1250 \times 2 + 230 = 4980 \text{ mm}$

Assume waist slab thickness = $L/20 = 4980/20 = 249 \text{ mm}$, say 250 mm

Assuming 20 mm clear cover (IS 456, Table 16) and 12 mm diameter bars,

$$\text{Effective depth} = 250 - 20 - 12/2 = 224 \text{ mm}$$

Assume 200 mm thick slab for the landing, as the span is small.

Load on going on projected plan area

Self-weight of waist slab	$= 25 \times 0.25 \times 292/250 = 7.30 \text{ kN/m}^2$
Self-weight of steps	$= 25 \times (0.15/2) = 1.88 \text{ kN/m}^2$
Finishes (given)	$= 0.60 \text{ kN/m}^2$
Imposed load (given)	$= 4.0 \text{ kN/m}^2$

$$\text{Total load} = 13.78 \text{ kN/m}^2$$

$$\text{Factored load} = 1.5 \times 13.78 = 20.67 \text{ kN/m}^2$$

Load on landing

Self-weight of slab	$= 25 \times 0.20 = 5.00 \text{ kN/m}^2$
Finishes (given)	$= 0.60 \text{ kN/m}^2$
Imposed load (given)	$= 4.0 \text{ kN/m}^2$

$$\text{Total load} = 9.60 \text{ kN/m}^2$$

$$\text{Factored load} = 9.6 \times 1.5 = 14.4 \text{ kN/m}^2$$

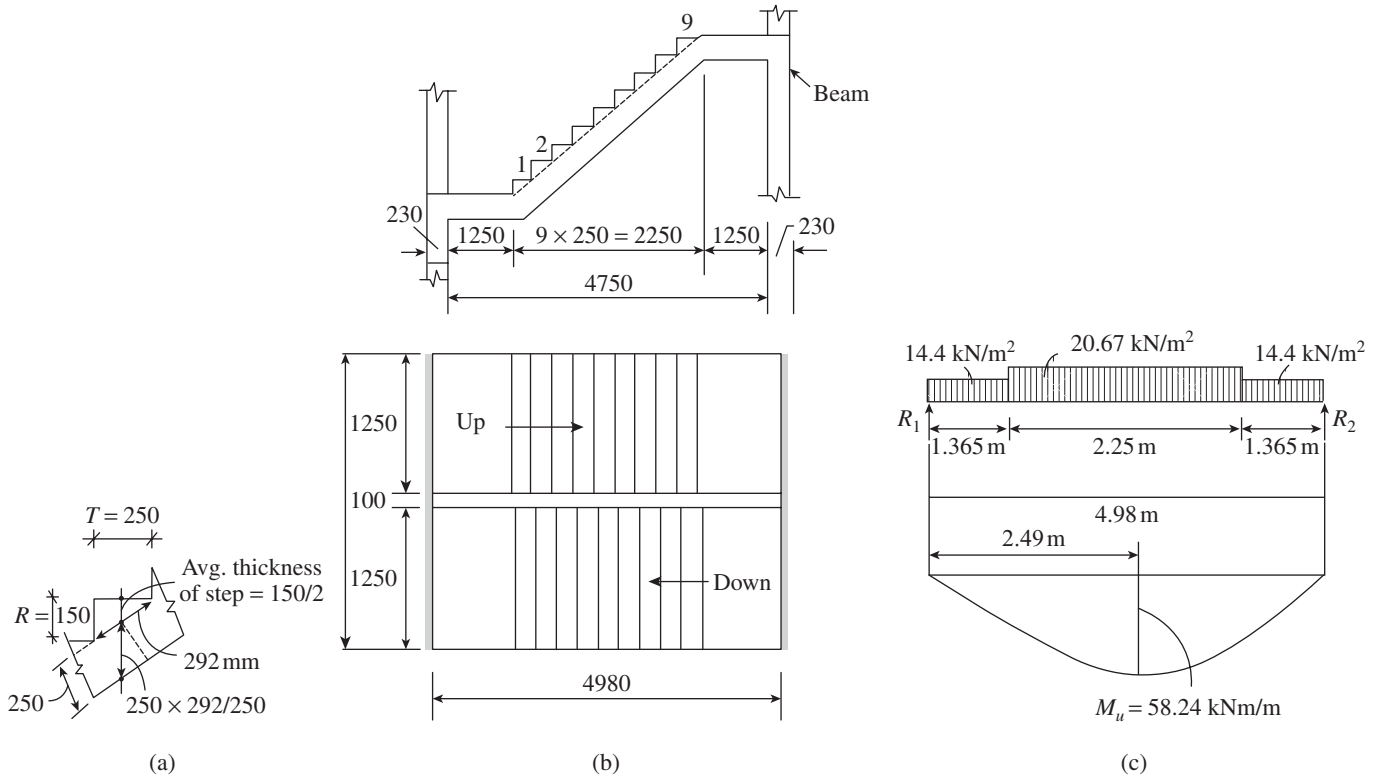


FIG. 17.25 Dog-legged staircase of Example 17.6 (a) Steps (b) Stair (c) Loading

Step 2 Calculate the bending moment. The loading diagram is shown in Fig. 17.25(c).

$$\text{Reaction } R = (14.4 \times 1.365) + (20.67 \times 2.25)/2 = 42.91 \text{ kN/m}$$

Maximum bending moment at mid-span

$$\begin{aligned} M_u &= 42.91 \times 2.49 - (14.4 \times 1.365)(2.49 - 1.365/2) - 20.67 \\ &\quad \times (2.49 - 1.365)^2/2 \\ &= 58.24 \text{ kNm/m} \end{aligned}$$

Step 3 Design the reinforcement.

$$\frac{M_u}{bd^2} = \frac{58.24 \times 10^6}{1000 \times 224^2} = 1.16 \text{ MPa}$$

From Table 2 of SP 16, for Fe 415 steel and M20 concrete, $p_t = 0.3462\%$. Hence,

$$A_t = 0.3462/100 \times 1000 \times 224 = 776 \text{ mm}^2/\text{m}$$

Required spacing of 12 mm diameter bars = $(113 \times 10^3)/776 = 145 \text{ mm}$

Hence, provide 12 mm diameter bars at 140 mm c/c.

Distribution steel

$$A_s = (0.12/100) \times 1000 \times 250 = 300 \text{ mm}^2$$

Assuming 10 mm diameter bars

$$\text{Spacing} = (78.5 \times 10^3)/300 = 261 \text{ mm}$$

Provide 10 mm mild steel bars at 250 mm c/c. The detailing of bars is shown in Fig. 17.12. It has to be noted that nominal reinforcement (50% of A_{st}) of ten bars at 200 mm c/c is provided in the landing slab near the support at the top to

resist any negative moment that may arise due to partial fixity; distributors of eight numbers at 250 c/c are also provided.

EXAMPLE 17.7 (Design of dog-legged staircase with supports perpendicular to the risers):

Repeat the design of Example 17.6 assuming that the landing is supported only on the two edges perpendicular to the risers as in Fig. 17.26.

SOLUTION:

Step 1 Calculate the loads. As the flight is supported as given in Fig. 17.26, and as the width of landing is less than 2 m, the effective span as per Clause 33.2 of IS 456 can be taken as the c/c between the landings. Hence, $L = 2.25 + 2 \times 0.625 = 3.5 \text{ m}$

Assume waist slab thickness = $L/20 = 3500/20 = 175 \text{ mm}$.

Assuming 20 mm clear cover (IS 456, Table 16) and 12 mm diameter bars,

$$\text{effective depth} = 175 - 20 - 12/2 = 149 \text{ mm}$$

Load on going on projected plan area

Self-weight of waist slab	$= 25 \times 0.175 \times 292/250 = 5.11 \text{ kN/m}^2$
Self-weight of steps	$= 25 \times (0.15/2) = 1.88 \text{ kN/m}^2$
Finishes (given)	$= 0.60 \text{ kN/m}^2$
Imposed load (given)	$= 4.0 \text{ kN/m}^2$

$$\text{Total load} = 11.59 \text{ kN/m}^2$$

$$\text{Factored load} = 1.5 \times 11.59 = 17.39 \text{ kN/m}^2$$

$$\text{Load on landing} = 25 \times 0.175 + 0.6 + 4.0 = 8.98 \text{ kN/m}^2$$

$$\text{Factored load} = 1.5 \times 8.98 = 13.47 \text{ kN/m}^2$$

Fifty per cent of this load may be assumed to act longitudinally.

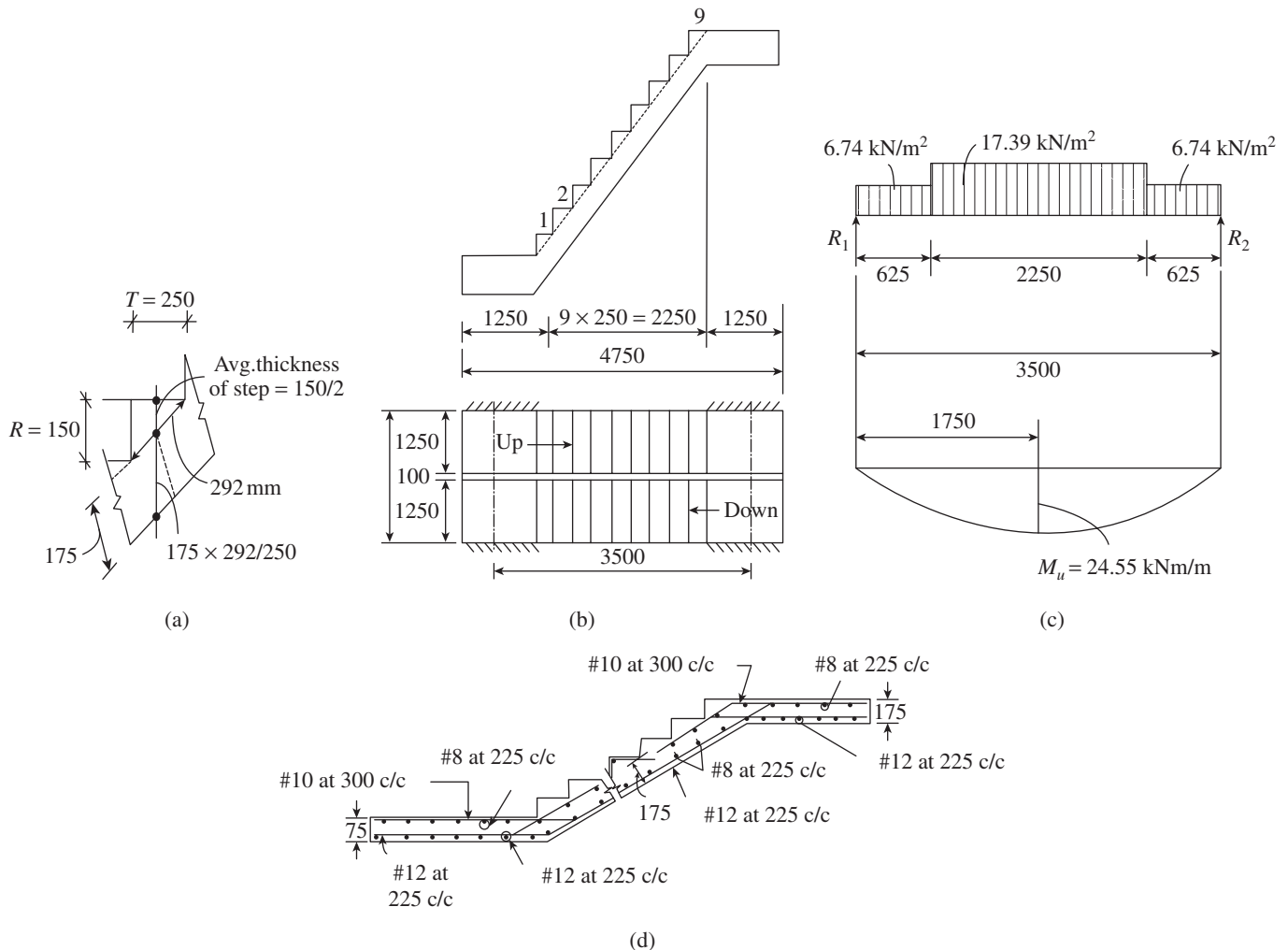


FIG. 17.26 Dog-legged staircase of Example 17.7 (a) Steps (b) Stair (c) Loading (d) Detailing

Step 2 Calculate the bending moment. The loading diagram is shown in Fig. 17.26(c).

$$\text{Reaction } R = (6.74 \times 0.625) + (17.39 \times 2.25)/2 = 23.78 \text{ kN/m}$$

Maximum bending moment at mid-span

$$\begin{aligned} M_u &= 23.78 \times 1.75 - (6.74 \times 0.625)(1.75 - 0.625/2) \\ &\quad - 17.39 \times (1.75 - 0.625)^2/2 \\ &= 24.55 \text{ kNm/m} \end{aligned}$$

Step 3 Design the reinforcement.

$$\frac{M_u}{bd^2} = \frac{24.55 \times 10^6}{1000 \times 149^2} = 1.11 \text{ MPa}$$

From Table 2 of SP 16, for Fe 415 steel and M20 concrete, $p_t = 0.3302\%$. Hence,

$$A_t = 0.3302/100 \times 1000 \times 149 = 492 \text{ mm}^2/\text{m}$$

Required spacing of 12 mm diameter bars = $(113 \times 10^3)/492 = 229 \text{ mm}$

Hence, provide 12 mm diameter bars at 225 mm c/c.

Distribution steel

$$A_s = (0.12/100) \times 1000 \times 175 = 210 \text{ mm}^2$$

Assuming 8 mm diameter bars

$$\text{Spacing} = (50.3 \times 10^3)/210 = 239 \text{ mm}$$

Provide 8 mm bars at 225 mm c/c.

Step 4 Design the landing slab. The entire loading on the waist slab is transferred to the supporting edges by the bending of the landing slab in the direction parallel to the risers. Considering the full width of landing of 1.25 m, loads on landing slab (assuming as uniformly distributed) are calculated as follows:

$$\text{Load acting directly} = 13.47 \times 1.25 = 16.84 \text{ kN/m}$$

$$\text{Load from waist slab} = 17.39 \times 2.25/2 = 19.56 \text{ kN/m}$$

$$\text{Total load} = 36.40 \text{ kN/m}$$

$$\text{Loading on 1 m strip of slab} = 36.40/1.25 = 29.12 \text{ kN/m}$$

$$\text{Effective span} = 2.6 \text{ m}$$

Maximum bending moment at mid-span

$$M_u = wL^2/8 = 29.12 \times 2.6^2/8 = 24.6 \text{ kNm/m}$$

As this value is similar to the value obtained for waist slab, we may provide the same reinforcement of 12 mm bars at 225 mm c/c as main bars (in a direction parallel to risers at bottom) and 8 mm bars at 225 mm c/c as distributors. The detailing is shown in Fig. 17.26(d). It has to be noted that in the landing, the bars of the waist slab are kept above the main bars of landing in order to provide the effective depth. Moreover, such a detailing is also required due to the fact that the waist slab is supported by the landing. Fifty per cent of the main reinforcement (10 mm at 300 mm c/c) is provided at the top, as research by Ahmed, et al. (1995, 1996) showed that there will be negative bending moment at the support regions of the waist slab.

EXAMPLE 17.8 (Design of longitudinally supported tread-riser-type staircase):

Repeat the design of Example 17.7 considering it as tread-riser-type stair and the imposed load as 5 kN/m².

SOLUTION:

As in Example 17.7, the effective span, $L = 2.25 + 2 \times 0.625 = 3.5$ m

Step 1 Calculate the loads.

Let us assume waist slab thickness = $L/25 = 3500/25 = 140$ mm

Assuming 20 mm clear cover (IS 456, Table 16) and 12 mm bars,

$$\text{effective depth} = 140 - 20 - 12/2 = 114 \text{ mm}$$

Load on going on projected plan area See Fig. 17.11.

$$\begin{aligned} \text{Self-weight of tread-riser slab} &= 25 \times (0.15 + 0.25) \times 0.14/0.25 \\ &= 5.60 \text{ kN/m}^2 \end{aligned}$$

$$\text{Finishes (given)} = 0.60 \text{ kN/m}^2$$

$$\text{Imposed load (given)} = 5.0 \text{ kN/m}^2$$

$$\text{Total load} = 11.20 \text{ kN/m}^2$$

$$\text{Factored load} = 1.5 \times 11.20 = 16.8 \text{ kN/m}^2$$

$$\text{Load on landing} = 25 \times 0.175 + 0.6 + 5.0 = 9.98 \text{ kN/m}^2$$

$$\text{Factored load} = 1.5 \times 9.98 = 14.97 \text{ kN/m}^2$$

As in Example 17.7, 50 per cent of this load may be assumed to act longitudinally.

Step 2 Calculate the bending moment. The loading diagram is similar to that shown in Fig. 17.26(c).

$$\text{Reaction } R = (7.49 \times 0.625) + (16.8 \times 2.25)/2 = 23.58 \text{ kN/m}$$

Maximum bending moment at mid-span

$$\begin{aligned} M_u &= 23.58 \times 1.75 - (7.49 \times 0.625)(1.75 - 0.625/2) \\ &\quad - 16.8 \times (1.75 - 0.625)^2/2 \\ &= 23.90 \text{ kNm/m} \end{aligned}$$

Step 3 Design the reinforcement.

$$\frac{M_u}{bd^2} = \frac{23.90 \times 10^6}{1000 \times 114^2} = 1.84 \text{ MPa}$$

From Table 2 of SP 16, for Fe 415 steel and M20 concrete, $p_t = 0.5802\%$. Hence,

$$A_t = 0.5802/100 \times 1000 \times 114 = 661 \text{ mm}^2/\text{m}$$

Required spacing of 12 mm diameter bars = $(113 \times 10^3)/661 = 170$ mm

Hence, provide 12 mm diameter bars at 165 mm c/c in the form of closed ties. Provide 8 mm bars transversely at each bend as distributor. The detailing is shown in Fig. 17.11b.

Step 4 Design the landing slab. The design of landing slab is similar to Example 17.7. Hence, provide 12 mm bars at 225 mm c/c as main bars (in a direction parallel to risers at bottom and below the bars of waist slab, so that the required effective depth is achieved) and 8 mm bars at 225 mm c/c as distributors. In addition, provide 50 per cent of the main reinforcement (10 mm at 300 mm c/c) at the top of the landing slab, as in Example 17.7.

EXAMPLE 17.9 (Design of helicoidal stair):

Design a helicoidal stair for a building with floor height 4 m. The width of stair is 1.2 m and the tread and riser are 280 mm and 200 mm, respectively. The included angle of the stair is 180°. There is a mid-landing of 1.2 m length. The building is used for commercial purposes and subjected to mild exposure. Use M25 concrete and Fe 415 steel.

SOLUTION:

Given: $R = 150$ mm, $T = 250$ mm, $b = 1.2$ m

Height of the building = 3000 mm

Hence, the number of risers = $4000/200 = 20$

Length of tread at the centre line = $20 \times 280 = 5600$ mm

Going of the staircase including the mid-landing = $5600 + 1200 = 6800$ mm

Since the included angle is 180°, the radius of helicoid = $\pi R = 6800$ mm. Hence,

$$R = 6800/\pi = 2164.5 \text{ mm}$$

The gradient of staircase, $\alpha = \tan^{-1}(R/T) = \tan^{-1}(200/280) = 35.54^\circ$

Effective span = c/c distance between supports = $9 \times 250 + 1250 \times 2 + 230 = 4980$ mm

Step 1 Calculate the loads.

Assume thickness of slab = $L/25 = 6800/25 = 272$ mm, say 275 mm

Assuming 20 mm clear cover (IS 456, Table 16) and 12 mm bars

Effective depth = $275 - 20 - 12/2 = 249$ mm

Self-weight of slab = $25 \times (0.275 \times 1.2) = 8.25$ kN/m

Self-weight of steps = $25 \times (0.2/2 \times 1.2) = 3.00$ kN/m

Imposed load (given) = $5.0 \times 1.2 = 6.00$ kN/m

$$\text{Total load} = 17.25 \text{ kN/m}$$

Factored load normal to the surface of the slab

$$= 1.5 \times 17.25 \times \cos 35.54 = 21.05 \text{ kN/m}$$

Step 2 Calculate the bending moment.

Radius of the centroidal axis of the slab, $R_c = R + b^2/12R$

$$= 2164.5 + 1200^2/(12 \times 2164.5) = 2220 \text{ mm}$$

The value of $c = \frac{2(g+1)\sin\theta - 2g\theta\cos\theta}{(g+1)\theta - (g-1)\sin\theta\cos\theta}$

$$= \frac{2(0.7+1)\sin 90 - 2 \times 0.7 [90 \times (\pi/180)] \cos 90}{(0.7+1)[90 \times (\pi/180)] - (0.7-1)\sin 90 \cos 90}$$

$$= \frac{3.4}{2.67}$$

$$= 1.273$$

At mid-span, $\phi = 0^\circ$

Bending moment, $M_r = w_u R_c^2 (c \cos \phi - 1) = 21.05 \times 2.22^2 (1.273 - 1) = 28.32 \text{ kNm}$

Torsional moment, $M_t = w_u R_c^2 (c \sin \phi - \phi) = 0 \text{ kNm}$

At supports, $\phi = 90^\circ$

Bending moment, $M_t = w_u R_c^2 (c \cos \phi - 1) = 21.05 \times 2.22^2 (1.273 \cos 90 - 1) = -103.74 \text{ kNm}$

Torsional moment, M_t

$$w_u R_c^2 (c \sin \phi - \phi) = 21.05 \times 2.22^2 (1.273 \sin 90 - 90 \times \pi/180) = -30.89 \text{ kNm}$$

Step 3 Check for depth of slab. Equivalent bending moment (Clause 41.4.2 of IS 456)

$$M_e = M_r + M_t \left[\frac{1+h/b}{1.7} \right] = 103.74 + 30.89 \left[\frac{1+275/1200}{1.7} \right] = 126.07 \text{ kNm}$$

Required depth $d = \sqrt{\frac{M_e}{kbf_{ck}}} = \sqrt{\frac{126.07 \times 10^6}{0.138 \times 1200 \times 25}} = 175 \text{ mm} < 249 \text{ mm}$

Hence, the selected depth is safe.

Step 4 Design the reinforcement.

$$\frac{M_u}{bd^2} = \frac{126.09 \times 10^6}{1200 \times 249^2} = 1.70 \text{ MPa}$$

From Table 3 of SP 16, for Fe 415 steel and M25 concrete, $p_t = 0.515\%$. Hence,

$$A_t = 0.515/100 \times 1200 \times 249 = 1538 \text{ mm}^2$$

Hence, provide eight 16 mm bars at the top face of the slab (area provided = 1608 mm^2) at support for a distance of span/3 ($6800/3 \approx 2270 \text{ mm}$) and provide only four bars at mid-span. The positive bending moment at mid-span is only 28.32 kNm , and hence, the required reinforcement is about 345 mm^2 .

$$\begin{aligned} \text{Minimum reinforcement} &= 0.12/100 \times 1200 \times 275 \\ &= 396 \text{ mm}^2 \end{aligned}$$

Provide five 12 mm bars throughout, as shown in Fig. 17.27.

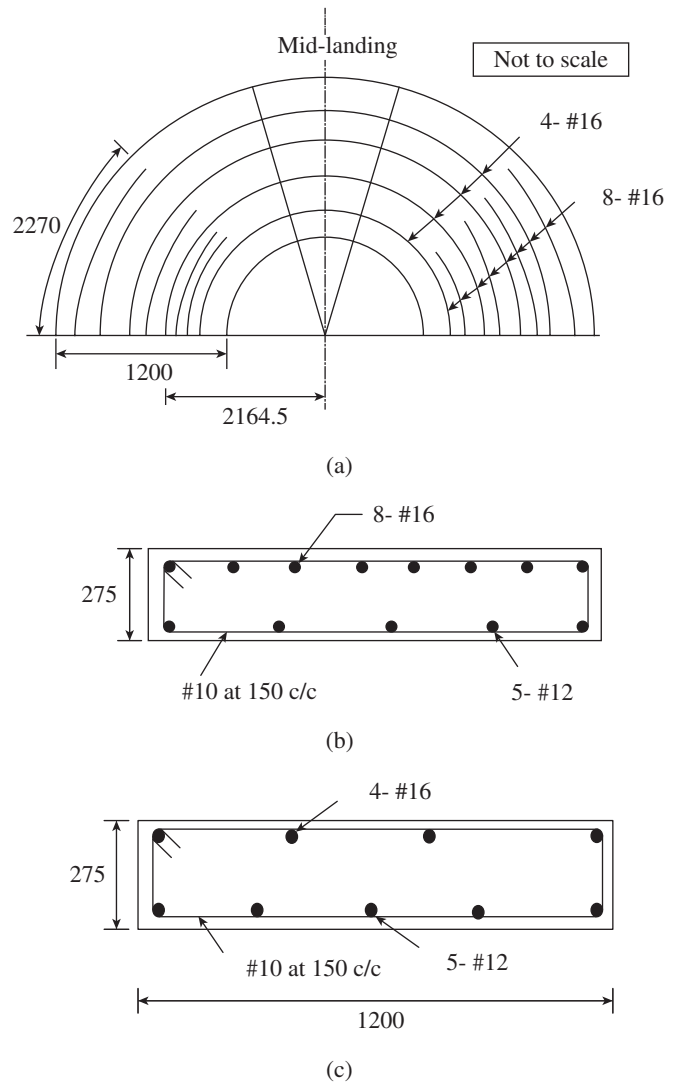


FIG. 17.27 Helicoidal stair of Example 17.9 (a) Plan (reinforcement at top) (b) Cross section at support (c) Cross section at mid-span

Step 5 Check for shear. Shear force acting at a distance of 249 mm from the support

$$V_u = 21.05(6.8/2 - 0.249) = 66.33 \text{ kN}$$

Equivalent shear force (Clause 41.3.1 of IS 456)

$$V_e = V_u + 1.6 \left(\frac{M_t}{b} \right) = 66.33 + 1.6 \left(\frac{30.89}{1.2} \right) = 107.52 \text{ kN}$$

Nominal shear stress

$$\tau_v = \frac{V_u}{bd} = \frac{107.52 \times 1000}{1200 \times 249} = 0.36 \text{ N/mm}^2$$

From Table 19 of IS 456, τ_c (for $f_{ck} = 25 \text{ N/mm}^2$ and $p_t = 0.19\%$)

$$= 0.318 \text{ N/mm}^2 < 0.36 \text{ N/mm}^2$$

(It has to be noted that since the slab is subjected to torsion, smaller reinforcement is used for p_t).

Hence, shear reinforcement has to be provided. As torsion is present, closed stirrups with 135° hooks are provided. From Clause 41.4.3 of IS 456,

$$A_{sv} = \left[\frac{T_u}{b_1 d_1} + \frac{V_u}{2.5 d_1} \right] \left(\frac{s_v}{0.87 f_y} \right) > \frac{(\tau_v - \tau_c) b s_v}{0.87 f_y}$$

Assuming two-legged 10mm diameter stirrups, we have

$$b_1 = b - 2c_s = 1200 - 2(20 + 10 - 16/2) = 1124 \text{ mm}$$

$$d_1 = D - 2c_s = 275 - 2(20 + 10 - 16/2) = 199$$

$$A_{sv} = \left[\frac{30.89 \times 10^6}{1124 \times 199} + \frac{107.52 \times 10^3}{2.5 \times 199} \right] \left(\frac{s_v}{0.87 \times 415} \right) = 0.981 s_v$$

$$\text{For 10 mm stirrup, } s_v = 2 \times 78.5 / 0.981 = 160 \text{ mm}$$

$$\text{Moreover, } s_v \leq \frac{A_{sv} (0.87 f_y)}{(\tau_v - \tau_c) b} = \frac{2 \times 78.5 \times 0.87 \times 415}{(0.36 - 0.318) \times 1200} = 1125 \text{ mm}$$

As per Clause 26.5.1.7 of IS 456, spacing should be less than x_1 , $(x_1 + y_1)/4$, and 300 mm, that is, $(275 - 2 \times 20 - 10)$, $(225 + 1150)/4$, and 300 mm.

Hence, provide two-legged 10mm stirrup at 150 mm c/c throughout the length.

Note: The landing slabs or beams must be designed to resist the fixed end moments of the staircase; it is desirable to provide reinforcement in these supporting elements at both the top and bottom.

SUMMARY

Reinforced concrete stairs are often the only means of providing access to various floors of a building (during fires, lifts are not used for obvious reasons; moreover, lifts are provided only in buildings having three or more floors). The terminology of terms used in connection with the stairs is explained first and then the different types of stairs are listed. With regard to structural design, stairs may be classified as transversely supported and longitudinally supported. Both these types and their design aspects are explained. Stairs are

usually designed as one-way slabs. The determination of effective length for various support conditions is also provided. Detailing of different types of stairs is also illustrated. Building the stairs integrally with the structural system will result in failure of stairs and columns, as they will act as diagonal braces during earthquakes, for which they are not designed. The methods by which such failures could be avoided are discussed. The principles presented are illustrated with ample examples.

REVIEW QUESTIONS

1. Explain the following terms:
 - (a) Going of step and going of stair
 - (b) Riser and tread
 - (c) Landing slab and waist slab
2. List any three common geometrical configurations of staircases with suitable sketches.
3. Explain the basic difference in structural behaviour between transversely supported stairs and longitudinally supported stairs.
4. Describe any two transversely supported stairs with sketches.
5. Describe any two longitudinally supported stairs with sketches.
6. State the rules for determining the effective span of longitudinally supported stairs as per IS 456.
7. How do we determine the effective span if the landing slab, running at right angles to the direction of the flight, is supported by walls or beams on three sides?
8. How are the loads to be distributed as per Clause 33.2 of IS 456?
9. Explain the design of the following transversely supported stairs:
 - (a) Isolated tread slabs
 - (b) Tread-riser stair
 - (c) Stairs with waist slab
10. Explain the design of the following longitudinally supported stairs:
 - (a) Tread-riser stair
 - (b) Stairs with waist slab
11. Sketch the reinforcement detailing of dog-legged stair supported at (a) the edge of landing and (b) the end of flights.
12. Write short notes on (a) free standing stairs and (b) helicoidal stairs.
13. What are the three ways by which we may prevent stairs from collapse during earthquake loading?

EXERCISES

1. A straight staircase with independent steps cantilevering from the face of the wall has to be designed for a residence. Given data: width of flight = 1.5 m, tread = 275 mm, and riser = 160 mm. Use M25 concrete and Fe 415 steel and assume mild exposure.
2. Design the cantilevered staircase given in Exercise 1 as a slabless stair.
3. Design a staircase consisting of 10 steps having 280mm tread and 150mm rise and two landings. The width of the staircase is 1300mm and the length of each landing is 1300mm. The arrangement of staircase is shown in Fig. 17.21. Assume the imposed load as 4kN/m² and mild exposure, and use M25 concrete and Fe 415 steel.
4. Design a waist slab-type staircase with a straight flight supported by two stringer beams along the two sides. Assume an effective span of 1.50m, a riser of 150 mm, and a tread of 275 mm. Assume imposed load of 4kN/m². Use M20 concrete and Fe 415 steel. Assume mild exposure.
5. Design the waist slab for the staircase similar to that shown in Fig. 17.23. Assume rise of step = 175 mm, tread = 300 mm, width of stair = 1.2 m, and weight of finishes = 0.75 kN/m². Use M25 concrete and Fe 415 steel. Assume mild exposure and stairs not liable for overcrowding.
6. Design a waist slab-type dog-legged staircase for a building, given the following data: Height between floors = 3.3 m, riser = 150 mm,

- tread = 250 mm, width of flight and landing = 1.50 m, imposed load = 3.0 kN/m², and floor finishes = 0.6 kN/m². Assume that the stair is to be supported on 230 mm width beams at the outer edges of the landing, parallel to the risers (similar to that shown in Fig. 17.25). Use M25 concrete and Fe 415 steel. Assume mild exposure.
7. Repeat the design of Exercise 6 considering that the landing is supported only on the two edges perpendicular to the risers as in Fig. 17.26.
 8. Repeat the design of Exercise 7 considering it as tread-riser type of stair.
 9. Design a helicoidal stair for a building with floor height 2.975 m. The width of stair is 1.2 m and the tread and riser are 300 mm and 175 mm respectively. The included angle of the stair is 120°. There is a mid-landing of 1.2 m length. The building is used for commercial purposes and subjected to mild exposure. Use M25 concrete and Fe 415 steel.

REFERENCES

- Ahmed, I., A. Muqtadir, and S. Ahmad 1995, 'Design Provisions for Stair Slabs in the Bangladesh Building Code', *Journal of Structural Engineering, ASCE*, Vol. 121, No. 7, pp. 1051–7.
- Ahmed, I., A. Muqtadir, and S. Ahmad 1996, 'Design Provisions for Stair Slabs in the Bangladesh Building Code', *Journal of Structural Engineering, ASCE*, Vol. 122, No. 3, pp. 262–6 and 1997, 'Discussions', pp. 1115–6.
- Bangash, M.Y.H. 2010, *Handbook of Staircases, Escalators and Moving Walkways*, Whittles Publishing, London, p. 384.
- Bangash, M.Y.H. and T. Bangash 1999, *Staircases: Structural Analysis and Design*, A.A. Balkema, Rotterdam, p. 337.
- Bergman, V.R. 1956, 'Helicoidal Staircases of Reinforced Concrete', *ACI Journal, Proceedings*, Vol. 53, No. 10, pp. 403–12.
- BS 5395-1:2010, *Stairs, Ladders and Walkways, Part 1: Code of Practice for the Design, Construction and Maintenance of Straight Stairs and Winders*, 3rd edition, British Standards Institution, London, p. 42.
- Chatterjee, B.K. 1978, *Theory and Design of Concrete Shells*, 2nd edition, Oxford and IBH Publishing Company, New Delhi, pp. 179–98.
- Cusans, A.R. 1966, 'Analysis of Slabless Stairs', *Concrete and Constructional Engineering*, Vol. 61, No. 10, pp. 359–64.
- Cusans, A.R. and J-G. Kuang 1965, 'A Simplified Method for Analysing Free Standing Stairs', *Concrete and Constructional Engineering*, Vol. 60, No. 5, pp. 167–72, 194.
- IS 4326:1993 2002, *Code of Practice for Earthquake Resistant Design and Construction of Buildings*, Bureau of Indian standards, New Delhi, p. 33.
- Karunakar Rao, P. 1983, 'Analysis, Detailing and Construction of a Free-standing Staircase', *The Indian Concrete Journal*, Vol. 57, No. 5, pp. 111–5, 123.
- Murty C.V.R., S. Brzev, H. Faison, C.D. Comartin, and A. Irfanoglu 2006, *At Risk: The Seismic Performance of Reinforced Concrete Frame Buildings with Masonry Infill Walls*, Earthquake Engineering Research Institute, Oakland, (also see http://www.world-housing.net/uploads/WHETutorial_RCFrame_English.pdf, last accessed on 12 June 2012).
- Reynolds, C.E. and J.C. Steedman 1988, *Reinforced Concrete Designer's Handbook*, 10th edition, E and FN Spon, London.
- Santathadaporn, S. and A.R. Cusans 1966, 'Charts for Design of Helical Stairs', *Concrete and Constructional Engineering*, Vol. 61, No. 2, pp. 46–54.
- Scordelis A.C. 1960, 'Internal Forces in Uniformly Loaded Helicoidal Girders', *ACI Journal, Proceedings*, Vol. 56, No. 4, pp. 1013–26, and 'Discussions', pp. 1491–502.
- Sharma, C.M., Harpal Singh, and C.B. Kukreja 1995, 'Saw Tooth Stairs: An Experimental Study', *ICI Bulletin*, No. 50, pp. 11–4.
- Simmons, P.W. and D.K. Bull 2000, *The Safety of Single Storey Straight Stair flights with Mid-Height Landings Under Simulated Seismic Displacements*, Research Report 2000-09, Department of Civil Engineering, University of Canterbury, p. 293.
- Solanki, H.T. 1975, 'Free Standing Stairs with Slabless Tread-risers', *Journal of the Structural Division, ASCE*, Vol. 101, No. 8, pp. 1733–8.
- Solanki, H.T. 1976, 'Helicoidal Girders', *Journal of the Structural Division, ASCE*, Vol. 102, No. 4, pp. 869–73.
- Varyani, U.H. 1999, *Structural Design of Multi-storeyed Buildings*, South Asia Publishers, New Delhi, p. 310.
- Wadud, Z. and S. Ahmad 2005, 'Simple Design Charts for Helicoidal Stair Slabs with Intermediate Landings', *Institution of Engineers (India) Journal, Civil Engineering Division*, Vol. 85, pp. 269–75.
- Williams, S., M.J.N. Priestly, H. Anderson, M. Cook, P. Fehl, C. Hyland, R. Jury, P. Millar, S. Pampanin, G. Skimming, and A. Thornton 2012, *Expert Panel Report. Structural Performance of Christchurch CBD Buildings in the 22 February 2011 Aftershock*, p. 136, (also see <http://www.dbh.govt.nz/UserFiles/File/Reports/quake-final-expert-panel-report.pdf>, last accessed on 10 January 2013).

DESIGN OF TENSION MEMBERS

18.1 INTRODUCTION

Concrete is strong in compression and weak in tension; this is why reinforcements are provided where tensile stresses occur in concrete members. The tensile strength of concrete is about 1/10th to 1/15th of its compressive strength. As mentioned in the previous chapters, the cracked concrete in the tension zone of beams and eccentrically loaded columns is normally neglected; however, in shear and bond, the contribution due to cracked concrete, which is capable of resisting a small amount of tension between the cracks, is also included. Similarly, in deflection calculation as well, the tension stiffening effect of concrete between the cracks is taken into consideration while estimating the effective flexural rigidity (see Chapter 12). This method of sometimes including and often neglecting concrete in the tension zone has been followed by designers for a number of years. It shows that researchers and designers always want to consider the limited tensile strength of concrete in a rational manner.

There are a few situations in which concrete will be entirely subjected to tension or to combined tension and bending. These include walls of cylindrical tanks (with a sliding joint at the base), walls of rectangular tanks, hangers and ties of bow-girder bridges, reinforced concrete (RC) truss members, hopper walls of bunkers and silos, columns subjected to earthquake loads, cylindrical pipes, and suspended roofs.

There are several ways in which the basic weakness of concrete in tension may be overcome. One of the best solutions to this problem is to prestress the member in such a way that the resulting stresses after application of the load is compressive in nature. There have also been attempts to increase the tensile strength of concrete by using a variety of fibres or epoxy admixtures (Walraven 2009; Popovics 1985). A parallel development in this direction is *ferrocement*, which is being used for building boats and water tanks (Naaman 2000).

In this chapter, we will discuss the design of members in which tension predominates. In such members, it is assumed that the tension is primarily carried by the reinforcement and concrete is considered only to provide a protective cover to the steel reinforcement. These members are classified into two groups based on the crack width limitation—members in which the crack width is less than 0.1 mm (often considered as uncracked section) and those where it is greater than 0.1 mm (considered as a cracked section). Crack width is closely linked with the tensile stress of the transformed concrete cross section and the stress in the reinforcement. The tensile stresses in the reinforcement and concrete are limited to indirectly control the crack width. The members under tension are often designed using elastic theory and those subjected to both bending and tension are designed using limit states or elastic theory. When designing members using limit states theory, we need to check whether the crack widths are within the prescribed limits. Since water tank walls are also subjected to tension and bending moment, a few provisions of IS 3370-Part 2:2009 are also discussed and some examples are provided.

18.2 BEHAVIOUR OF TENSION MEMBERS

The behaviour of tension members and the tension stiffening effect have already been discussed in Chapter 12 (see Fig. 12.4(a) of Chapter 12 and Fig. 18.1). Tests of reinforced tension members were carried out as early as 1899 by Considere. In 1908, Mörsch observed that uncracked concrete between two adjacent cracks was able to decrease the extent to which steel reinforcement is stretched as compared to bare steel samples. This effect was referred to as *tension stiffening* and was attributed to the bond between the concrete and steel.

When a member is subjected to tension, it is initially uncracked; hence, the response is governed more by the concrete section than the reinforcement. Even after cracking, the member maintains a stiffness that is greater than a bare

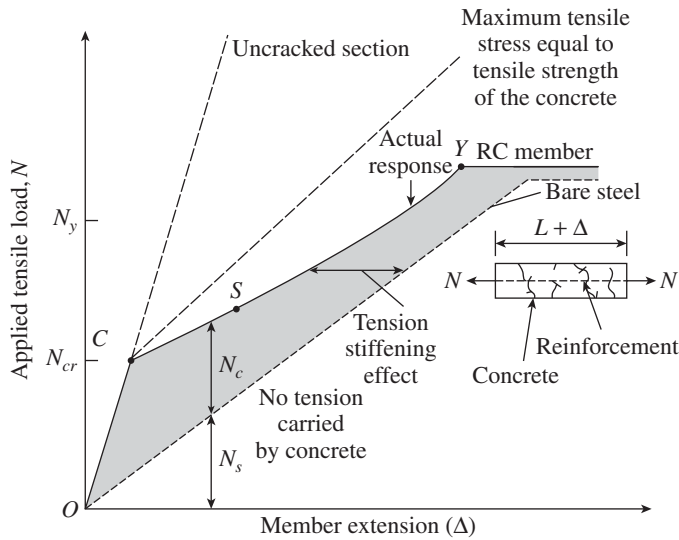


FIG. 18.1 Typical load–deformation response for a concrete member

steel sample, that is, the tension stiffening effect shown by the shaded area in Fig. 18.1, and passes through four distinct phases under increasing axial tension. These four phases are the uncracked linear elastic behaviour, represented by line OC; initial and continued cracking, line CS; stabilized crack development, line SY; and finally, post-yielding. The values N_c and N_s in Fig. 18.1 represent the average load carried by the concrete and the steel over the length of the member. Thus, once the member is cracked, its response is affected by the stiffness of the reinforcing bar, and there is a gradual transition towards the bare bar response as more and more cracks develop in the member. Once the cracking has stabilized, the load carried by the concrete continues to decrease as secondary internal cracks develop between the primary cracks (Goto 1971; Beeby 1979; Bischoff 2005; Beeby and Scott 2005).

It can be seen from this behaviour that when an RC member is subjected to tensile forces, the concrete between the cracks carries the tensile stresses that are transferred by the bond and thus contributes to the stiffness of the member. The post-cracking member response can be taken into account by considering the tension stiffening effect (see Fig. 12.5b of Chapter 12). This gives a concrete tensile response with a descending branch after cracking and is equivalent to assuming that the concrete has a reduced effective modulus of elasticity that depends on the level of strain in the member. The effective member stiffness with the modulus of elasticity of concrete E_c and effective concrete area A_{eff} can be expressed as

$$A_{eff} = \frac{A_{cr}}{1 - \eta(N_{cr}/N)^2} \quad (18.1)$$

where $\eta = 1 - A_{cr}/A_{gr}$, A_{cr} is the transformed concrete area of the cracked section given by $A_c + (m-1)A_{st}$, A_c is the area of concrete, A_{gr} is the gross area of section, A_c is the area of concrete, A_{st} is the area of reinforcement, N is the applied axial tensile load, and N_{cr} is the axial cracking load. Results of

such an approach were found to agree well with experimental results (Bischoff 2005). The ability of concrete to carry tension between cracks in an RC member helps control member stiffness, deformation, and crack widths that are mostly related to satisfying serviceability requirements.

The post-cracking response of RC tensile members was found to be not affected by the compressive strength of concrete; thus, the same response may be assumed for normal-strength concrete (NSC) and high-strength concrete (HSC) (Fields 1998). It was also found that well-distributed reinforcement with a minimum of $15d_b$ concrete around it will result in better distribution of cracks (Fields 1998). Tension stiffening was found to be time-dependent, and this effect decays over time with increase in the degree of cracking; it is estimated to reach a final value equal to approximately half its initial value in a period of less than 20 to 30 days (Beeby and Scott 2006). Wenkenbach (2011) found that as bar diameter increases, the decay time decreases. Wu and Gilbert (2008) also studied the tension stiffening effect in RC members under short- and long-term loads.

18.3 DESIGN METHODS FOR MEMBERS IN DIRECT TENSION

The serviceability limit state governs the design of tension members that are exposed to severe exposure conditions. In general, while designing members subjected to direct tension, the following criteria are considered:

1. The total tension force is considered to be resisted only by the reinforcement.
2. The stress in the reinforcement must be less than the allowable stress in the serviceability limit state.
3. The allowable stress in concrete of the transformed section must be less than the allowable tension in concrete in serviceability limit state to prevent excessive cracking.

These criteria may be expressed as follows (Dayaratnam 2004):

$$A_{st} \geq \frac{N_u}{(0.87f_y)} \quad (18.2)$$

$$\frac{N}{A_{st}} \leq f_{ast} \quad (18.3)$$

$$\frac{N}{A_c + A_{st}(m-1)} \leq f_{act} \quad (18.4a)$$

If the effects of shrinkage are also included, the equation can be written as

$$\frac{\epsilon_{sh}E_sA_{st} + N}{A_c + A_{st}(m-1)} \leq f_{act} \quad (18.4b)$$

where N is the axial tensile force in the member, N_u is the factored axial tensile force in the member, A_{st} is the area of tensile reinforcement, A_c is the area of the concrete in the member, f_y is the yield strength of reinforcement, f_{ast} is the

allowable tensile stress in steel, f_{act} is the allowable direct tensile stress in concrete, m is the modular ratio (taken as $280/3\sigma_{bc}$ or E_s/E_c), ϵ_{sh} is the average shrinkage coefficient or strain (may be taken as 300×10^{-6}), and E_s is the Young's modulus of steel reinforcement.

The following provisions relate to tension members like walls in *liquid storage tanks*.

The allowable tensile stresses in steel and minimum lap length as per BS 8007, IS 3370, and IS 456 are shown in Table 18.1. It has to be noted that bars in tension members should be lapped only when it is unavoidable (see Section 18.8). In circular tanks, the locations of horizontal splices should be staggered by not less than one lap length or 900 mm. The allowable tensile stresses in concrete as per IS 3370-Part 2 and IS 456 are shown in Table 18.2. As per Clause 4.4.2 of IS 3370, the characteristic strength f_y of reinforcement should not exceed 500N/mm^2 . A minimum thickness of 125 mm is preferable in liquid retaining structures.

TABLE 18.1 Permissible stresses in steel under direct tension and lap length (BS 8007, IS 3370, and IS 456)

Code	Exposure Category (Minimum Grade of Concrete and Design Crack Width)	Permissible Stress, MPa (Lap Length)	
		Plain Bars Fe 250	High-yield Strength-deformed Fe 415
BS 8007:1987	Very severe (M40 and 0.1 mm)	85 ($19d_b$)	100 ($14d_b$)
BS 8007 and S 3370-Part 2:2009	Moderate to severe (M30 and 0.2 mm)	115 ($26d_b$)	130 ($18.5d_b$)
IS 456:2000 (Clause 35.3.2, Tables 5 and 22)	Mild (M25 and 0.3 mm)	140 for $d_b \leq 20\text{ mm}$ ($35d_b$) 130 for $d_b > 20\text{ mm}$ ($32.5d_b$)	230 ($36d_b$)

Note: d_b is the diameter of bar.

TABLE 18.2 Permissible stresses in concrete under direct tension (IS 3370 and IS 456)

Cracking Condition	M25	M30	M35	M40	M45	M50
Direct tension: Cracking not permitted (IS 3370-Part 2:2009)	1.3	1.5	1.6	1.8	2.0	2.1
Cracking permitted (IS 456- Clause B-2.1.1)	3.2	3.6	4.0	4.4	4.8	5.2
Tension due to bending (IS 3370-Part 2:2009)	1.8	2.0	2.2	2.4	2.6	2.8

18.3.1 Minimum Concrete Grade and Cover of Reinforcement for Liquid Retaining Structures

The cover for surfaces in contact with any liquid should be provided by considering severe environmental exposure conditions as per Clause 3 of IS 3370-Part 1. As per Table 16 of IS 456, the minimum nominal cover for severe condition is

45 mm, which may be reduced by 5 mm for concrete grades M35 and above. As per the British code BS 8007, both faces of a liquid containing structure, together with any internal walls and columns of a containment structure, should be considered as subject to severe exposure and should be designed for a maximum design crack width of 0.2 mm; the nominal cover should not be less than 40 mm; For critical aesthetic appearance or in very severe environments, a crack width of 0.1 mm should be considered. The minimum grade of concrete to be used for severe condition as per Table 3.3 of the British code BS 8110-1:1997 is M40, with a maximum water/cement ratio of 0.55 and a minimum cement content of 325kg/m^3 .

The maximum cement content, not including fly ash and ground granulated blast furnace slag (GGBS), should be less than 400kg/m^3 (it is 450kg/m^3 as per Clause 8.2.4.2 of IS 456) and the minimum cement content is 320kg/m^3 without fly ash or GGBS, as per Clause 5 and Table 1 of IS 3370-Part 1. The minimum concrete grade is M30 and the maximum water/cement ratio is 0.45.

18.3.2 Minimum Reinforcement

A minimum amount of reinforcement should be provided in two principal directions perpendicular to each other to take care of shrinkage and temperature effects. As per Clause 8.1 of IS 3370-Part 2, this minimum reinforcement within each surface zone (see Fig. 18.2) should not be less than 0.35 per cent for high-yield strength-deformed (HYSD) bars and 0.64 per cent for mild steel bars. For tanks having any dimension less than 15 m, this minimum reinforcement can be reduced to 0.24 per cent for HYSD bars and 0.40 per cent for mild steel bars.

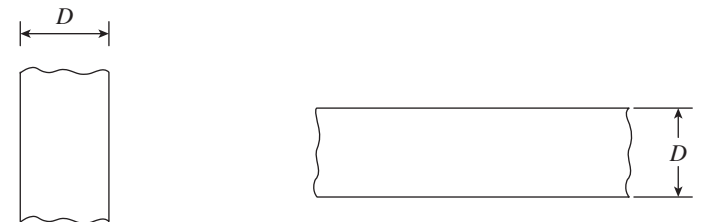


FIG. 18.2 Surface zones—walls and suspended slabs

Note: For $D < 500\text{ mm}$, assume each reinforcement face controls $D/2$ depth of concrete. For $D > 500\text{ mm}$ assume each reinforcement face controls 250 mm depth of concrete, ignoring any central core beyond this surface depth.

In order to be effective in distributing cracking, at least the following amount of reinforcement has to be provided (Clause A-1.2 of IS 3370-Part 2):

$$\rho_{crit} = \frac{f_{ct}}{f_y} \tag{18.5}$$

where ρ_{crit} is the critical steel ratio of steel area to the gross area of the whole concrete section, f_{ct} is the direct tensile strength of the immature concrete, taken as per Table 18.3, and f_y is the characteristic strength of reinforcement. It is also recommended to use small size bars at close spacing to avoid high steel ratios well in excess of ρ_{crit} (also see Table 2 of

IS 3370-Part 1 for the methods to control thermal contraction and restrained shrinkage).

TABLE 18.3 Direct tensile strength of immature concrete as per IS 3370-Part 2

Grade of concrete	M25	M30	M35	M40	M45	M50
f_{ct} N/mm ²	1.15	1.3	1.45	1.6	1.7	1.8

Note: $f_{ct} = 0.12(f_{ck})^{0.7}$

18.3.3 Spacing of Reinforcement

In walls, roofs, and floors having a thickness of less than 200 mm, the calculated amount of reinforcement may be placed in one face. In walls that are over 200 mm thick and in ground slabs that are over 300 mm thick, steel should be equally divided on both faces. As per Clause 8.1 of IS 3370-Part 2, bar spacing shall not generally exceed 300 mm or the thickness of the section, whichever is less.

18.4 DESIGN PROCEDURE FOR DIRECT TENSION

The following are the steps required for designing a member subjected to direct tension:

1. Calculate the area of steel required by using Eqs (18.2) and (18.3). Usually, Eq. (18.3) governs. It has to be noted that this area of steel should be greater than the minimum area of steel, which is determined as given in step 3. Provide this area of steel in the direction of force. In slabs or walls, determine the size and spacing of bars. The spacing should be less than 300 mm or the depth of the member.
2. Calculate the required area of concrete based on Eq. (18.4). The value of f_{act} to be used in this equation is chosen from Table 18.2 depending on the extent of cracking that is permitted (in liquid retaining structures, only limited cracking is permitted).
3. Minimum secondary steel should be provided based on Eq. (18.5).
4. Check cover and detailing of reinforcement. Minimum cover should be provided based on exposure conditions. As already mentioned, the spacing should be less than the maximum permitted spacing to limit the crack width. Special attention should also be paid to the lap length of bars in tension (see Section 18.8).
5. If limit states design is used for sizing the member, crack widths should be calculated and checked against permissible values (see Section 18.5.3).

18.5 DESIGN OF MEMBERS SUBJECTED TO TENSION AND BENDING

Many tie members, like the horizontal girder in a bow-string girder bridge (see Fig. 18.3), are subjected to primary tension and secondary bending. These members can be designed as a cracked or uncracked section depending on the environmental

exposure condition. Such sections can be analysed in a manner similar to that of combined compression and bending. However, it is not easy to replace the compressive force by the tensile force, since concrete in tension should be neglected. This problem can be better tackled by the working stress method since the cracking limit state can control the design. It may be noted that in most practical cases, we have either large bending with small axial force (as in rectangular water tanks) or large tension with very small bending moments (as in circular tanks). Thus, there is very little possibility of large bending and large tension occurring simultaneously.

Figure 18.3 shows the Godavari Arch Bridge, a bow-string girder arch or tied arch in Rajahmundry, Andhra Pradesh, India. This bridge was built between 1991 and 1997. It is one of the longest span prestressed concrete arch bridges in Asia (longest span 97.6 m and total length 2745 m). It was built by Hindustan Construction Company for the Indian Railways and was designed by M/S Bureau BBR, Switzerland.



FIG. 18.3 Godavari arch bridge

Source: <http://en.wikipedia.org/wiki/File:Archbridgegodavari.JPG>

Two possible cases of failure exist in such members subjected to axial tension and bending. If the tension force is very large compared to the bending moment, the whole member will be in tension and it will fail by the fracture of tension reinforcement. If the bending moment is very large and the tension is nominal, then the failure will be by the crushing of concrete or by the yielding of steel.

18.5.1 Tension with Small Eccentricity

Consider a rectangular section as shown in Fig. 18.4 that is subjected to tension and bending moment. Let N be the axial tensile force and M be the bending moment acting on the section. The two forces can be combined into an equivalent eccentric tension force N acting at an eccentricity of e given by

$$e = \frac{M}{N} \quad (18.6)$$

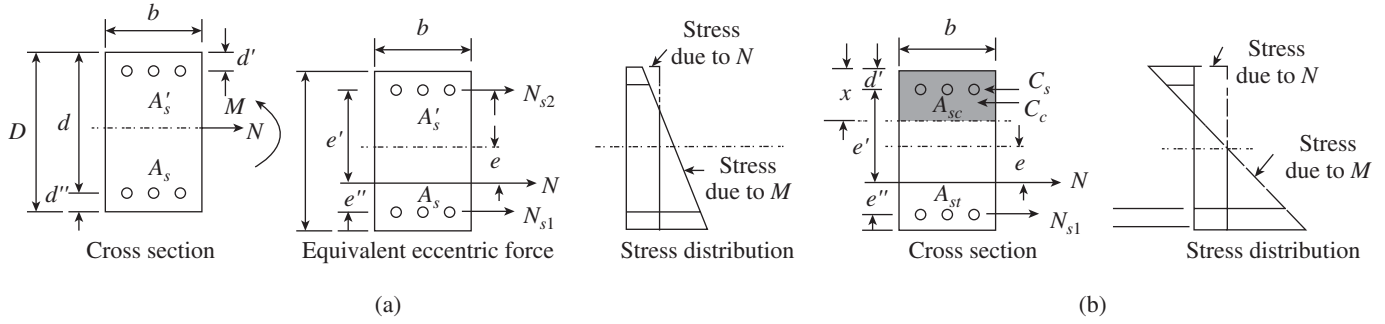


FIG. 18.4 Elastic behaviour of members under tension and bending (a) Small eccentricity (b) Large eccentricity

If this eccentricity is less than $(D/2) - d''$, where D is the total depth and d'' is the effective cover for tension steel, then the total section will be in tension and the section is considered as tension dominated.

Let A_s be the area of steel reinforcement subjected to larger tension and A'_s be the area of steel reinforcement subjected to smaller tension. Moreover, let N_{s1} and N_{s2} be the tensions developed in these reinforcements, respectively.

For force equilibrium,

$$N_{s1} + N_{s2} = N \tag{18.7}$$

Taking moment about the centroid of top steel (see Fig. 18.4a), we get

$$Ne' = A_s f_s (d - d'') \quad \text{or} \quad A_s = \frac{Ne'}{f_s (d - d'')} \tag{18.8}$$

Similarly, by taking moments about the centroid of bottom steel, we get

$$Ne'' = A'_s f'_s (d - d') \quad \text{or} \quad A'_s = \frac{Ne''}{f'_s (d - d')} \tag{18.9}$$

By considering the fact that the tension in the top and bottom steel should be restricted to the values given in Table 18.1, depending on the exposure condition, we can determine A_s and A'_s . This method is explained in Example 18.4.

18.5.2 Tension with Large Eccentricity

In certain situations, the members may be subjected to heavy bending moment with small tension. An example of members in such a situation is the walls of *rectangular water tanks* as shown in Fig. 18.5. In these tanks, the normal load acting on the side walls is resisted by the shear forces at the base and at the sides. The shear forces on the side walls act as tensile forces on the front and back walls, as shown in Fig. 18.5. Similarly, as discussed earlier, in the case of circular water tanks, the radial pressure causes circumferential hoop tension, and if the wall is fixed at base, it will be subjected to bending moment as well. According to Clause 6.1.1 of IS 13920, we need not consider any axial force effect as long as the factored axial stress on the member under earthquake loading does not exceed $0.1f_{ck}$.

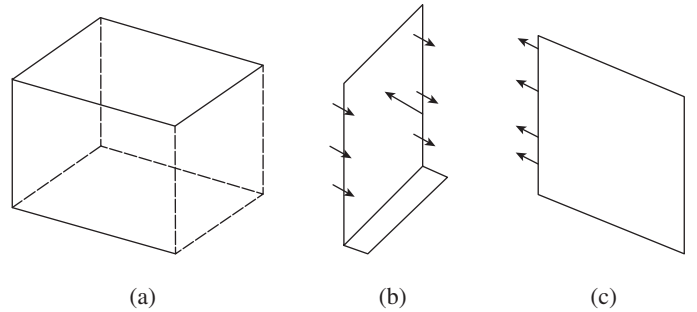


FIG. 18.5 Tank walls subjected to bending moment and axial tension (a) Rectangular tank (b) Side wall (c) Front and back wall

If the tensile force is not so large as to crack the whole section, the equations for calculating the neutral axis depth x as well as the stresses in concrete and steel can be developed, as was done in Chapter 5 in the case of pure flexure.

The stress distribution in this case and the internal forces are shown in Fig. 18.4(b). We may use the same assumptions as in flexural analysis and ignore the contribution of concrete in the tension zone. The stress distribution is as shown in Fig. 18.4(b). The maximum strain and stress in the top fibre of concrete are ϵ_c and f_c , respectively. Now, we have

$$f_c = E_c \epsilon_c \tag{18.10}$$

where E_c is the Young's modulus for concrete. Since the average stress in the compressive zone is $0.5f_c$, the total compressive force C_c is

$$C_c = 0.5bxf_c \tag{18.11}$$

Since the stress distribution is triangular, this force acts at a distance of $x/3$ from the top fibre.

The strain in tension steel is ϵ_s . From Fig. 18.4(b), we may deduce that

$$\epsilon_s = \epsilon_c \frac{d - x}{x} \tag{18.12}$$

The stress in steel is

$$f_s = E_s \epsilon_s \tag{18.13}$$

where E_s is the Young's modulus for steel. Using Eqs (18.10) and (18.12), we may write

$$f_s = E_s \varepsilon_s = \frac{E_s}{E_c} E_c \varepsilon_c \left(\frac{d-x}{x} \right) = m f_c \left(\frac{d-x}{x} \right) \quad (18.13)$$

where $m = E_s/E_c$ is the modular ratio.

Total tensile force N_{s1} is

$$N_{s1} = A_{st} f_s = A_{st} m f_c \left(\frac{d-x}{x} \right) \quad (18.14)$$

Force in compression steel is

$$C_s = A_{sc} f_s = A_{sc} m f_c \left(\frac{x-d'}{x} \right) \quad (18.15)$$

where A_{sc} is the area of compression steel.

Hence, total compressive force, C , is

$$C = C_c + C_s = 0.5 b x f_c + A_{sc} m f_c \left(\frac{x-d'}{x} \right) \quad (18.16)$$

For equilibrium in the axial direction,

$$N_{s1} - C = \text{Applied axial tensile force } N$$

Thus, we may write

$$A_{st} m f_c \left(\frac{d-x}{x} \right) - 0.5 b x f_c - A_{sc} m f_c \left(\frac{x-d'}{x} \right) = N \quad (18.17)$$

Taking moments about the tension steel, we get

$$0.5 b x f_c \left(d - \frac{x}{3} \right) + A_{sc} m f_c \left(\frac{x-d'}{x} \right) (d-d') = M - N \frac{D}{2} \quad (18.18)$$

where M is the applied moment and D is the overall depth of the section.

We now have two unknowns (f_c and x) in these equations. Eliminating f_c from Eqs (18.17) and (18.18), we get

$$\begin{aligned} & \left(M - \frac{ND}{2} \right) A_{st} m (d-x) - A_{sc} m (x-d') \left[M + N \left(d-d' - \frac{D}{2} \right) \right] \\ & = 0.5 b x^2 \left[N \left(d - \frac{x}{3} - \frac{D}{2} \right) + M \right] \end{aligned} \quad (18.19)$$

The solution of this cubic equation (obtained using a trial and error procedure) will give the value of the neutral axis depth, x . The compressive stress in concrete may then be obtained by using Eq. (18.10) or (18.11) and should be within the allowable limits. It has to be noted that the equations are valid only if $x \leq d$, as we have initially assumed that the top steel is in compression.

A method of design for strength at the ultimate state followed by verification of stresses using working stress method for symmetrically reinforced rectangular section subjected to tension and bending was provided by Mallick (1983).

18.5.3 Checking for Crack Width

A review of the causes of direct tension cracking and the methods for controlling cracking caused by direct tension are

provided by ACI Committee 224.2R-92. IS 3370-Part 2:2009 provides two different equations for crack width calculation: one for members in direct tension and the other for members in flexure. These are based on BS 8007:1987.

Crack Widths in Flexure

When the strain in the tension reinforcement is limited to $0.8 f_y/E_s$ and the stress in concrete is limited to $0.45 f_{ck}$, the design surface crack width is calculated by using the following expression (see also Fig. 12.16 of Chapter 12):

$$W_{cr} = \frac{(3 a_{cr} \varepsilon_m)}{1 + 2 \frac{(a_{cr} - c_{\min})}{(D-x)}} \quad (18.20)$$

where a_{cr} is the distance from the point considered to the surface of the nearest longitudinal bar, $a_{cr} = [(0.5s)^2 + c_{\min}^2]^{0.5}$, s is the spacing between bars, c_{\min} is the minimum cover to the longitudinal bar, ε_m is the average steel strain at the level considered, D is the overall depth of the member, x is the depth of neutral axis, E_s is the modulus of elasticity of the reinforcement, and f_y is the yield strength of reinforcement.

Average strain in flexure The average strain at the level where cracking is being investigated may be found by calculating the apparent strain using characteristic loads and normal elastic theory. Where there is prominent flexure, but with some tension, we need to adjust the depth of the neutral axis for the effect of this tension. The calculated apparent strain ε_1 is then adjusted to take into account the stiffening effect of the concrete between cracks. The average strain at the surface, ε_m , is given by Clause B-1 of IS 3370 (Part 2) as

$$\varepsilon_m = \varepsilon_1 - \varepsilon_2 \quad (18.21)$$

where ε_1 is the strain at the considered level and ε_2 is the strain due to stiffening effect of concrete between the cracks. Thus,

$$\varepsilon_1 = \varepsilon_s \frac{D-x}{d-x} \quad (18.22)$$

where strain $\varepsilon_s = f_s/E_s$, D is the overall depth of the member, d is the effective depth, and x is the depth of neutral axis.

Stiffening effect of concrete between the cracks The stiffening effect of the concrete may be included by deducting from the apparent strain a value obtained from Eq. (18.23) or (18.24).

For a limiting surface crack width of 0.2 mm:

$$\varepsilon_2 = \frac{b_t (D-x)(a' - x)}{3 E_s A_{st} (d-x)} \quad (18.23)$$

For a limiting surface crack width of 0.1 mm:

$$\varepsilon_2 = \frac{1.5 b_t (D-x)(a' - x)}{3 E_s A_{st} (d-x)} \quad (18.24)$$

where b_t is the width of section at the centroid of the tension steel, a' is the distance from the compression face to the point at which the crack width is being calculated, A_{st} is the area of tension steel, D is the overall depth of the member, d is the effective depth, E_s is the modulus of elasticity of reinforcement, and x is the depth of neutral axis. It has to be noted that a negative value for ϵ_m indicates that the section is uncracked. It should also be noted that the stiffening effect factors should not be interpolated or extrapolated and should be applied only for the crack widths stated.

It is interesting to note that Eqs (18.20)–(18.23) presented here and the equations given in IS 3370 (Part 2) are the same as those found in Annexure F of IS 456 and explained in Section 12.6.4 of Chapter 12; these equations were originally derived by Beeby (1979).

Crack Widths in Direct Tension

As per Clause B-4 of IS 3370-Part 2, when the strain in the reinforcement is limited to $0.8f_y/E_s$, the design crack width, W_{cr} , may be calculated from

$$W_{cr} = 3a_{cr}\epsilon_m \quad (18.25)$$

where a_{cr} is the distance from the point mid-way between two bars at the surface of the member to the surface of the nearest longitudinal bar (see Fig. 18.6) and ϵ_m is the average strain at the level where the cracking is being considered.

As mentioned earlier, $\epsilon_m = \epsilon_1 - \epsilon_2$

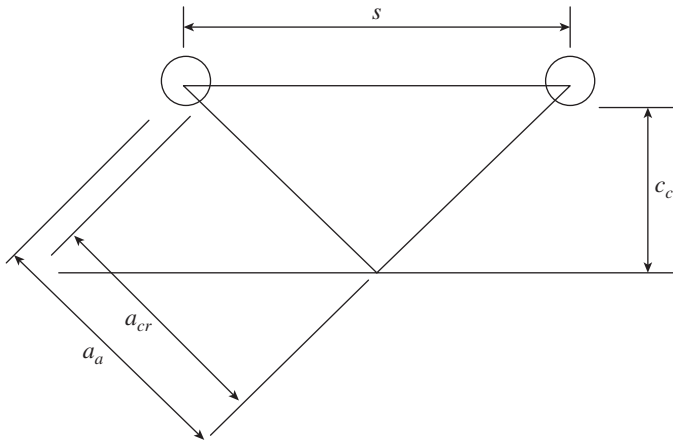


FIG. 18.6 Definition of a_{cr}

The stiffening effect of the concrete may be included by deducting from the apparent strain a value obtained from Eq. (18.26) or (18.27).

For a limiting design surface crack width of 0.2 mm:

$$\epsilon_2 = \frac{2b_t D}{3E_s A_s} \quad (18.26)$$

For a limiting design surface crack width of 0.1 mm:

$$\epsilon_2 = \frac{b_t D}{E_s A_s} \quad (18.27)$$

All the terms used in these equations have already been defined. The stiffening effect factors should not be interpolated or extrapolated and should be applied only for the crack widths stated. It has to be noted that the crack width formula given in IS 3370 does not include the diameter of bars, which may be an important parameter in determining crack widths.

Muttoni and Ruiz (2007) developed an analytical model for studying the cracking behaviour of bridge decks that are subjected to continuous unloading and reloading processes, which tend to increase the crack width in a tension member. They also developed a simple design formula for such bridge decks. Gouthaman and Menon (2001) showed that crack width control is most effectively achieved by reducing the tensile stress in the steel and by minimizing bar spacing. The parametric study conducted by them showed that it is difficult to obtain crack widths below 0.3 mm when large cover is provided; such cases may necessitate an increase in the slab thickness. Recently, a unified approach was developed for the design of reinforcement to control cracking in concrete resulting from restrained contraction (Bamforth 2007; Bamforth, et al. 2010).

18.6 INTERACTION CURVES FOR BENDING AND TENSION

The following linear interaction formula is considered to be conservative from the design point of view (Dayaratnam 2004):

$$\frac{N_u}{N_n} + \frac{M_u}{M_n} = 1 \quad (18.28a)$$

where N_u is the factored axial load, M_u is the factored bending moment, N_n is the nominal axial force capacity, and M_n is the nominal moment capacity of the section. The values of N_n and M_n may be obtained as (see also Eq. 5.22 and Table 5.3 of Chapter 5)

$$N_n = (f_y/1.15)(A_{st} + A_{sc}) = 0.87f_y(A_{st} + A_{sc}) \quad (18.28b)$$

$$M_n = \text{Min} \left[(k_2 f_{ck} b d^2); (0.87 f_y A_{st} j d) \right] \quad (18.28c)$$

with $k_2 = 0.149, 0.138, \text{ and } 0.133$ and $j = 0.78, 0.80, \text{ and } 0.81$ for Fe 250, Fe 415, and Fe 500 grade steels, respectively.

Interaction diagrams for rectangular sections under combined bending and tension are provided in Charts 66–85 of SP 16 (Charts 66–75 are for sections with reinforcement on two sides and Charts 76–85 are for sections with reinforcement on all four sides). These interaction diagrams are based on the limit state of strength and suitable for limited application only, as they have been developed without taking cracking into account. In the charts of SP 16, $N_u/(f_{ck} b D)$ is plotted in the y-axis and $M_u/(f_{ck} b D^2)$ on the x-axis, as in column interaction diagrams. The necessary steel ratio p/f_{ck} can be read from these charts.

18.7 DESIGN FOR BENDING, SHEAR, AND TENSION

It has been found that axial tensile forces tend to decrease the shear strength of concrete; tensile forces directly increase the stress and, hence, the strain in the longitudinal reinforcement. Axial tension increases the inclined crack width and reduces aggregate interlock, and hence, the shear strength provided by concrete is reduced. For members subject to significant axial tension, the following equation is suggested by ACI 318-08 (Clause 11.2.2.3):

$$V_c = 0.15 \left(1 + \frac{0.29P_u}{A_g} \right) \lambda \sqrt{f_{ck}} b_w d \geq 0 \quad (6.34)$$

where P_u is taken as negative for tension and P_u/A_g is expressed in MPa. More details and references may be found in Section 6.13 of Chapter 6.

18.8 DETAILING FOR TENSION MEMBERS

Much importance should be given to the detailing of splices in tension members, as the whole load is assumed to be transferred by the reinforcements. Clause 26.2.2.1 of IS 456 stipulates that hooks should be provided for plain bars in tension. Clause 26.2.5.1(c) states that the lap length including the anchorage value of hooks for bars in direct tension should be $2L_d$ or $30d_b$, whichever is greater (where L_d is the development length and d_b is the diameter of bar). In addition, the straight length of the lap should not be less than $15d_b$ or 200mm. The note under this clause stipulates that splices in tension members should be enclosed in spirals made of bars not less than 6 mm diameter and with pitch less than 100 mm. The *top-cast bar effect* should also be considered (see Section 7.4.2—point 12—of chapter 7 and Clause 26.2.5.1c of IS 456).

Clause 12.15.6 of the ACI code requires that the splices in tension members be made with full mechanical or full-welded splice and splices in adjacent bars shall be staggered at least 750 mm. As per Clause R 15.12.4 of the ACI code, a mechanical or welded splice should develop at least 125 per cent of the specified yield strength when located in regions of high tensile stress in the reinforcement (see also Clause 26.2.5.2). Such mechanical or welded splices need not be staggered, although such staggering is encouraged by the code when the area of reinforcement provided is less than twice that required by the analysis.

The second important consideration is the provision of transverse reinforcements in these members. Unlike compression members, transverse reinforcements (links) are required in tension members to account for the straightening of bars encased in concrete, when the tensile force is applied. These links may have to resist some shear force as well in the case of bottom tie members of trusses. The minimum transverse reinforcement, as per Clause 26.5.1.6 of IS 456,

may be calculated and provided. Such links may be of 6 mm bars (minimum) spaced at intervals of 0.75 times the least dimension of section or 300 mm, whichever is lesser, as per Clause 26.5.1.5 of IS 456.

The third important detailing aspect is the connection at the end of the tension members to other members of the structure. For light loads, the bars may be bent round in a large hook and brought back again into the member as shown in Fig. 18.7(a). The hook on bar a alone is shown in the figure, but all other bars are also bent similarly, and extra links are provided to prevent the hooks from opening out when loaded. Sufficient depth h should be provided in the connected member. The strength of such joints may be considerably increased by anchoring these rebars into the main members by providing special anchor bars in the main members as shown in Fig. 18.7(b).

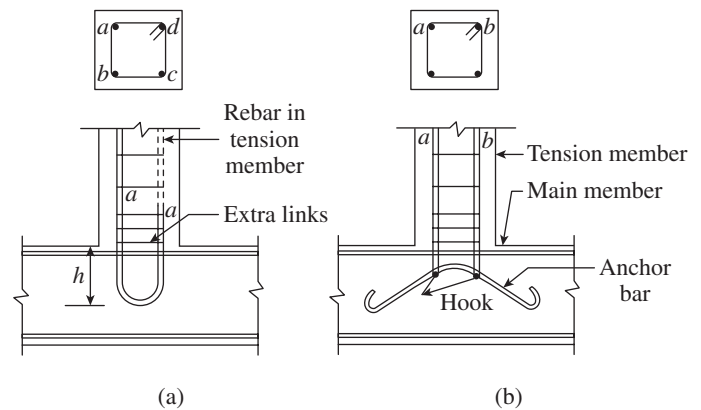


FIG. 18.7 Anchorage for tension member reinforcement (a) Anchorage of rebars (b) Hooked anchorage

Source: Purushothaman 1984

18.9 EARTHQUAKE AND OTHER CONSIDERATIONS

During earthquakes, because of load reversal, a tension member may become a compression member; hence, it is important to check the member for compressive forces as well. Moreover, when there is flexure in addition to tension, the sign of bending moment may change; hence, it is important to provide equal reinforcement at the top and bottom to take care of such reversal of moment. Plastic hinges may form at the ends of members. Hence, close links need to be provided at each end for a distance equal to twice the effective depth of the member, at spacing not less than $d/4$ or $8d_b$, where d is the effective depth and d_b is the diameter of the longitudinal bar.

If the tension member is subjected to fire conditions, due to the increase in temperature, the tension in the member may increase and the design should cater to this extra tension. In addition, the cover should be chosen based on the anticipated fire exposure.

The changes in temperature and moisture content of the concrete may cause movements. If these movements are restrained, they lead to tensile stresses in concrete and possible

cracks. The restraint of movement can be reduced by proper sequence of construction. Figure 18.8(a) shows the preferred sequence; in this sequence, after each bay is cast the slab is unrestrained at one edge and can contract during cooling. On the other hand, the sequence shown in Fig. 18.8(b) is not recommended because the middle slab is restrained on both sides.

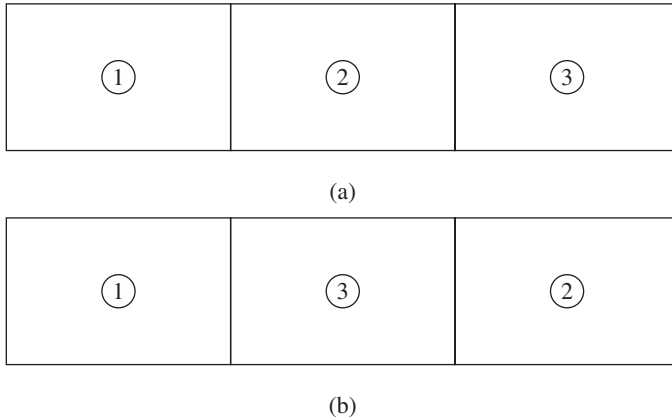


FIG. 18.8 Sequence of construction (a) Preferred sequence (b) Not recommended

When designing large members, the *size effect* may play a role. Very little is known about size effects in tension members. More information on size effects can be had from the work of Bažant and Planas (1998).

18.10 DESIGN OF WATER TANKS

Most of the discussions presented in this chapter are also applicable to *water tanks* or liquid storage structures (Fig. 18.9). Hence, a brief note about their design is given here.

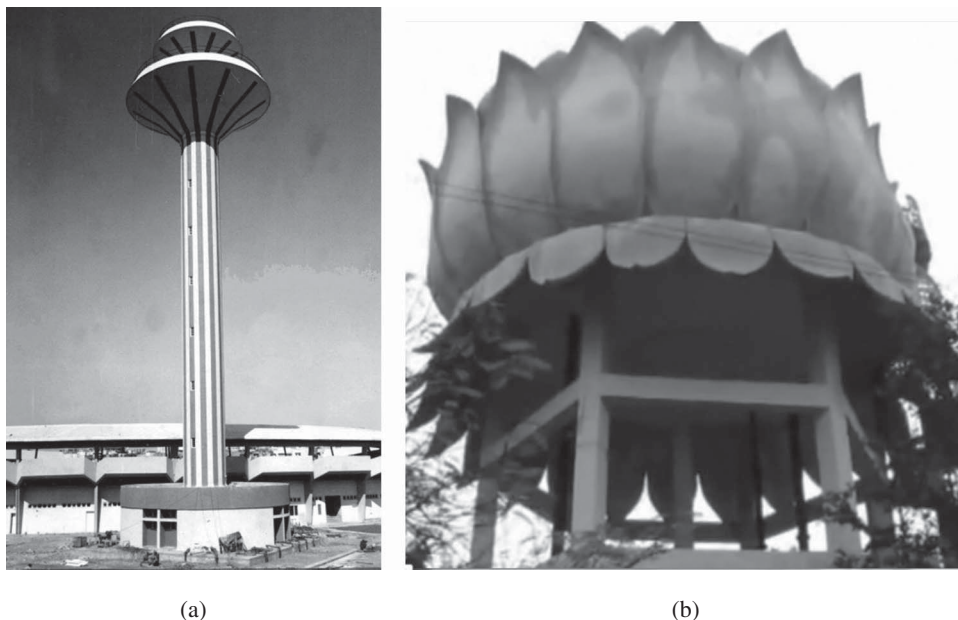


FIG. 18.9 RC water tanks (a) Andheri water tower in Mumbai (b) Lotus-shaped tank in Tamil Nadu
Courtesy: Er N. Prabhakar, Mumbai

In these tanks, the cracks are restricted for the sake of durability as well as to prevent leakage. RC circular tanks are mainly subjected to direct tension due to hoop force. On the other hand, in tanks with fixed bases, the walls are subjected to bending moments as well as hoop tension. The water load is considered as a dead load. IS 3370-Part 4 gives tables, using which the hoop tension and bending moments at different heights and shear at base may be found for circular tanks.

Rectangular tanks are used for smaller capacity, as they are uneconomical for larger capacities. The vertical walls are subjected to bending moment and tension. IS 3370-Part 4 provides tables for rectangular walls as well. Once the bending moments, tension, and shear are known, these walls can be designed as per the methods discussed in this chapter, using IS 3370-Parts 1 and 2. The base slabs can be designed for the water load and self-weight as circular and two-way slabs with partially restrained ends, in the case of circular and rectangular slabs, respectively (see Chapter 10 for the design of such slabs). It is important to consider tank full and tank empty conditions for the design. Joints such as contraction joint, expansion joint, sliding joint, and construction joint should be provided, especially in large tanks, to reduce cracking and leakage (see IS 3370 for details). When the tanks are designed as per limit states method, calculations for crack widths have to be made to check whether they are within allowable limits. Overhead water tanks require additional calculations for the design of staging to resist wind or earthquake loading. In addition, the water tank itself may be subjected to wind and earthquake loads. More information, guidance for the design, and examples are provided in the works of Anchor (1992), Gambhir (2008), Srinivas and Menon (2000), Pratapa and Menon (2011), and IITK-GSDMA Guidelines, (2007).

EXAMPLES

EXAMPLE 18.1 (Design of a tie member in a truss):

Design the tie member of an RC truss subjected to a tensile force of 450 kN, including dead and imposed loads. Assume M35 grade concrete, Fe 415 steel, and mild environment. Check for the crack width.

SOLUTION:

From Tables 18.1 and 18.2, the admissible stresses in the mild environment for Fe 415 steel and M35 concrete are as follows:

$f_{ast} = 230 \text{ MPa}$, $f_{act} = 4 \text{ MPa}$ (as per IS 456)

$$\text{Modular ratio, } m = \frac{280}{3\sigma_{cbc}} = \frac{280}{3 \times 11.5} = 8.1$$

Factored tension force, $N_u = 1.5 \times 450 = 675 \text{ kN}$

Step 1 Calculate the required area of steel reinforcement. As per IS 456, it is given by the following expression:

$$A_{st} \geq \frac{N_u}{(0.87f_y)} = \frac{675 \times 1000}{0.87 \times 415} = 1869 \text{ mm}^2$$

The required area of tension reinforcement as per serviceability criteria is

$$A_{st} = \frac{N}{f_{ast}} = \frac{450 \times 1000}{230} = 1957 \text{ mm}^2$$

It has to be noted that the area of reinforcement required by the serviceability criteria is more than that of strength consideration. Provide four 20 mm bars and four 16 mm bars ($A_{st} = 2060 \text{ mm}^2$).

Step 2 Calculate the total area of concrete section. From Eq. (18.4), the required area of concrete section is given by

$$\begin{aligned} A_c = bt &= \frac{N}{f_{act}} - A_{st}(m-1) \\ &= \frac{450 \times 1000}{4.0} - (8.1 - 1) \times 2060 \\ &= 97,874 \text{ mm}^2 \end{aligned}$$

Provide a section of size 260 mm by 400 mm with area = 104,000 mm². Distribute the main reinforcement uniformly across the cross section, with two 20 mm plus one 16 mm bars at top and bottom and one 16 mm bar on the two sides, as shown in Fig. 18.10, with a clear cover of 45 mm.

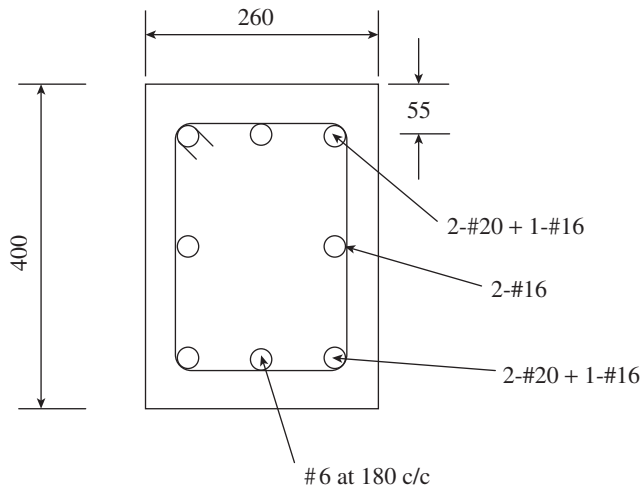


FIG. 18.10 Cross section of member of Example 18.1

Step 3 Check for minimum area of steel. From Table 18.3, for M35,

$$f_{ct} = 1.45 \text{ N/mm}^2$$

Minimum area of steel as per Eq. (18.5) is

$$p_{crit} = \frac{f_{ct}}{f_y} \times 100 = \frac{1.45}{415} \times 100 = 0.35\%$$

$$p_t \text{ provided} = \frac{2060}{400 \times 260} \times 100 = 1.98\% > 0.35\%$$

Step 4 Calculate the transverse reinforcement. Even in tension members, it is necessary to provide transverse reinforcement. As per Clause 26.5.1.6, the area of transverse reinforcement is

$$A_{sv} = \frac{0.4b s_v}{0.87f_y}$$

where s_v should not exceed 0.75 times the least dimension of section, as per Clause 26.5.1.5.

Adopting s_v as 180 mm $< 0.75 \times 260 = 195 \text{ mm}$,

$$A_{sv} = \frac{0.4b s_v}{0.87f_y} = \frac{0.4 \times 260 \times 180}{0.87 \times 415} = 52 \text{ mm}^2$$

Provide 6 mm ties at 180 mm centre-to-centre distance (c/c).

Step 5 Check for crack width. Assuming that the limiting design crack width is 0.2 mm,

$$\epsilon_2 = \frac{2b_t D}{3E_s A_s} = \frac{2 \times 260 \times 400}{3 \times 2 \times 10^5 \times 2060} = 1.68 \times 10^{-4}$$

Tensile stress at steel, $f_s = \frac{450 \times 1000}{2060} = 218.45 \text{ N/mm}^2$

Hence, strain, $\epsilon_1 = f_s / E_s = 218.45 / 2 \times 10^5 = 1.09 \times 10^{-3}$

Average strain = $\epsilon_m = \epsilon_1 - \epsilon_2 = 1.09 \times 10^{-3} - 1.68 \times 10^{-4} = 0.922 \times 10^{-3}$

$$\begin{aligned} a_{cr} &= \sqrt{[(s/2)^2 + c^2] - d_b/2} = \sqrt{(75/2)^2 + 61^2} - 20/2 \\ &= 61.60 \text{ mm} \end{aligned}$$

Crack width, $W = 3a_{cr}\epsilon_m = 3 \times 61.60 \times 0.922 \times 10^{-3} = 0.17 \text{ mm} < 0.2 \text{ mm}$

Hence, the crack width is within limits.

EXAMPLE 18.2 (Design of wall of cylindrical water tank):

Design the wall of an RC cylindrical tank (with a sliding joint at the base) subjected to a hoop tension of 230 kN per metre. Assume M30 grade concrete, Fe 415 steel, and mild environment.

SOLUTION:

From Tables 18.1 and 18.2, the admissible stresses in the mild environment for Fe 415 steel and M30 concrete are as follows:

$f_{ast} = 130 \text{ MPa}$, $f_{act} = 1.5 \text{ MPa}$ (cracking not permitted as per IS 3370)

$$\text{Modular ratio, } m = \frac{280}{3\sigma_{cbc}} = \frac{280}{3 \times 10} = 9.3$$

Factored tension force, $N_u = 1.5 \times 230 = 345 \text{ kN}$

Step 1 Calculate the required area of steel reinforcement. As per IS 456, it is given by the expression

$$A_{st} \geq \frac{N_u}{(0.87f_y)} = \frac{345 \times 1000}{0.87 \times 415} = 956 \text{ mm}^2$$

The required area of tension reinforcement as per serviceability criteria (IS 3370) is

$$A_{st} = \frac{N}{f_{ast}} = \frac{230 \times 1000}{130} = 1769 \text{ mm}^2$$

It has to be noted that the area of reinforcement required by the serviceability criteria is more than that of strength consideration. Provide 16 mm diameter bars at 110 mm c/c at the centre of the wall ($A_{st} = 1828 \text{ mm}^2$).

Step 2 Calculate the thickness of concrete section. From Eq. (18.4), the required area of concrete section is given by

$$A_c = bt = \frac{N}{f_{act}} - A_{st}(m-1) = \frac{230 \times 1000}{1.5} - (9.3-1) \times 1828 = 1,38,161 \text{ mm}^2$$

Hence, required thickness, $t = 1,38,161/1000 = 138 \text{ mm}$

Provide a 150 mm thick wall with 16 mm diameter bars at 110 mm c/c at the centre of the wall. The spacing is less than 150 mm (thickness of wall) or 300 mm. Hence, it is adequate.

Step 3 Check for minimum area of steel for crack control. From Table 18.3, for M30,

$$f_{ct} = 1.3 \text{ N/mm}^2$$

Minimum area of steel as per Eq. (18.5) is

$$p_{\text{crit}} = \frac{f_{ct}}{f_y} \times 100 = \frac{1.3}{415} \times 100 = 0.31\%$$

$$p_t \text{ provided} = \frac{1828}{150 \times 1000} \times 100 = 1.22\%$$

Hence, the provided reinforcement is sufficient.

Assuming that the tank is less than 15 m in diameter, the required amount of secondary steel is 0.24 per cent for HYSD bars (Clause 8.1 of IS 3370-Part 2). Hence,

$$A_{sd} = \frac{0.24}{100} \times (150 \times 1000) = 360 \text{ mm}^2$$

Provide 8 mm bars at 140 mm c/c with $A_{sd} = 359 \text{ mm}^2$ vertically with a nominal cover of 45 mm.

EXAMPLE 18.3 (Design of water pipe):

An RC water pipe line of 400 mm radius is carrying water at a pressure of 7 m head of water. Design the pipe with grade 415 steel and M30 concrete.

SOLUTION:

From Tables 18.1 and 18.2, the admissible stresses in the mild environment for Fe 415 steel and M30 concrete are as follows:

$f_{ast} = 130 \text{ MPa}$, $f_{act} = 1.5 \text{ MPa}$ (cracking not permitted as per IS 3370)

$$\text{Modular ratio, } m = \frac{280}{3\sigma_{cbc}} = \frac{280}{3 \times 10} = 9.3$$

Specific weight of water = 9.807 kN/m^3

Water pressure in the pipe, $p = 7 \text{ m}$ of head = $7 \times 9.807 = 68.7 \text{ kN/m}^2$

Hoop tension in the pipe, $N = pR = 68.7 \times 0.4 = 27.5 \text{ kN/m}$

Neglecting the self-weight of pipe and considering 1 m length of pipe,

Factored hoop tension = $1.5 \times 27.5 = 41.25 \text{ kN/m}$

Step 1 Calculate the required area of steel reinforcement. As per IS 456, it is

$$A_{st} \geq \frac{N_u}{(0.87f_y)} = \frac{41.25 \times 1000}{0.87 \times 415} = 114 \text{ mm}^2/\text{m}$$

The required area of tension reinforcement as per serviceability criteria (IS 3370) is

$$A_{st} = \frac{N}{f_{ast}} = \frac{27.5 \times 1000}{130} = 212 \text{ mm}^2/\text{m}$$

The serviceability criterion controls the design. Provide 8 mm diameter bars at 200 mm c/c at the centre of the cross section ($A_{st} = 250 \text{ mm}^2$).

Step 2 Calculate the thickness of concrete section. From Eq. (18.4), the required area of concrete section is given by

$$A_c = bt = \frac{N}{f_{act}} - A_{st}(m-1) = \frac{27.5 \times 1000}{1.5} - (9.3-1) \times 250 = 16,258 \text{ mm}^2/\text{m}$$

Hence, required thickness of pipe, $t = 16,258/1000 = 16.26 \text{ mm}$

As this thickness is too small, provide a 75 mm thick wall, so that about 30 mm cover is available for the reinforcement.

Step 3 Check for minimum area of steel for crack control. From Table 18.3, for M30,

$$f_{ct} = 1.3 \text{ N/mm}^2$$

Minimum area of steel as per Eq. (18.4) is

$$p_{\text{crit}} = \frac{f_{ct}}{f_y} \times 100 = \frac{1.3}{415} \times 100 = 0.31\%$$

Required area = $0.31 \times 75 \times 1000/100 = 232.5 \text{ mm}^2/\text{m} < 250 \text{ mm}^2/\text{m}$

Hence, the provided reinforcement is sufficient.

Required longitudinal reinforcement = $0.31 \times$ area of cross section/100

$$= 0.31/100 \times 2\pi \times (400 + 37.5) \times 75 = 639 \text{ mm}^2/\text{m}$$

Provide nine 10mm bars uniformly distributed along the circumference of the pipe, as shown in Fig. 18.11.

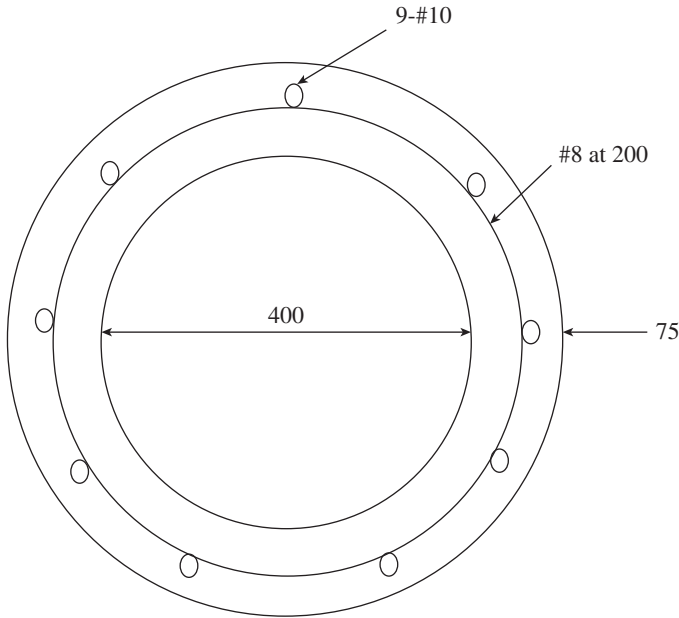


FIG. 18.11 Cross section of RC pipe of Example 18.3

EXAMPLE 18.4 (Member subjected to tension with small eccentricity):

An RC truss member of length 6 m in a moderate environment is subjected to a direct tensile force of 140 kN and a bending moment of 8.4 kNm. Design the member.

SOLUTION:

Step 1 Choose the grade of steel and concrete. The beam is subjected to moderate environment; hence, as per Table 5 of IS 456, the minimum grade of concrete to be adopted is M25. Let us select M25 concrete and Fe 415 grade steel. As per Table 18.1, the permissible tensile stress in reinforcement is 130 N/mm^2 and the allowable direct tensile stresses in concrete in direct tension and bending are 1.3 N/mm^2 and 1.8 N/mm^2 , respectively (Table 1 of IS 3370-Part 2).

Step 2 Calculate the eccentricity and assume section.

$$\text{Eccentricity } e = \frac{M}{N} = \frac{8.4}{140} \times 1000 = 60 \text{ mm}$$

The length of the member is 6 m. Hence, the depth may be taken greater than $L/20 = 300 \text{ mm}$ (Clause 23.2.1). Let us assume a size of 400 mm by 250 mm and a cover of 30 mm for both faces (Table 16 of IS 456) and 20 mm bars. Hence, $d' = d'' = 30 + 10 = 40 \text{ mm}$, $d = 400 - 40 = 360 \text{ mm}$.

Step 3 Check whether the eccentricity is small.

$$\text{Eccentricity} = 60 \text{ mm} < D/2 - d' = 200 - 40 = 160 \text{ mm}$$

The eccentricity is small, and hence, the entire section will be in tension.

Step 4 Calculate the area of steel.

$$e' = D/2 + e - d' = 400/2 + 60 - 40 = 220 \text{ mm}$$

$$e'' = D/2 - e - d' = 400/2 - 60 - 40 = 100 \text{ mm}$$

From Eq. (18.7)

$$A_s = \frac{Ne'}{f_s(d-d')} = \frac{140 \times 1000 \times 220}{130 \times (360 - 40)} = 740 \text{ mm}^2$$

From Eq. (18.8)

$$A_s' = \frac{Ne''}{f_s'(d-d')} = \frac{140 \times 1000 \times 100}{130 \times (360 - 40)} = 336 \text{ mm}^2$$

Select three 20 bars at bottom ($3 \times 314 = 942 \text{ mm}^2$) and two 16 bars at top (402 mm^2).

Step 5 Check whether the provided cross section is adequate.

$$\text{Modular ratio, } m = \frac{280}{3\sigma_{cbc}} = \frac{280}{3 \times 8.5} = 11$$

Transformed area of cross section, $A_{tr} = A_c + (m-1)(A_s + A_s')$

$$= 250 \times 400 + (11-1)(942 + 402) = 100,000 + 13,440 = 1,13,440 \text{ mm}^2$$

Axial tensile stress in concrete = $140 \times 1000 / 1,13,440 = 1.23 \text{ N/mm}^2 < 1.3 \text{ N/mm}^2$

Since the combined bending and tension stress may govern, let us provide a 300 mm by 400 mm section.

Step 6 Check for allowable bending and tensile stresses.

Transformed area of cross section, $A_{tr} = 300 \times 400 + 13,440 = 1,33,440 \text{ mm}^2$

Axial tensile stress in concrete = $140 \times 1000 / 1,33,440 = 1.05 \text{ N/mm}^2 < 1.3 \text{ N/mm}^2$

Hence, it is within allowable limits.

The centroid of the transformed section is obtained by taking moments of areas about the centre of the concrete cross section.

$$\text{Depth of neutral axis, } x = \frac{bD^2/2 + (m-1)(A_s d + A_s' d')}{A_{tr}}$$

$$= \frac{300 \times 400^2/2 + (11-1)(942 \times 360 + 402 \times 40)}{133440} = 206.5 \text{ mm}$$

$$\text{Moment of inertia } I_{tr} = b/3[x^3 + (D-x)^3] + (m-1)[A_s(d-x)^2 + A_s'(x-d')^2]$$

$$= 300/3[206.5^3 + (400-206.5)^3] + (11-1)[942(360-206.5)^2 + 402(206.5-40)^2]$$

$$= 1605 \times 10^6 + 333.4 \times 10^6 = 1988.4 \times 10^6 \text{ mm}^4$$

The maximum tensile stress due to combined tension and bending occurs at the bottom fibre of the section and is given by

$$f_{\max} = \frac{N}{A_r} + \frac{My}{I_r}$$

$$= \frac{140 \times 1000}{1,33,440} + \frac{8.4 \times 10^6 \times 200}{1988.4 \times 10^6} = 1.05 + 0.84 = 1.89 \text{ N/mm}^2$$

As it is only slightly greater than the allowable value of 1.80 N/mm², the section is safe.

EXAMPLE 18.5 (Member subjected to moment with small tension):

An RC wall of a rectangular tank is subjected to a direct tension of 50 kN/m and a moment of 90 kNm/m. Design the section using M25 concrete and Fe 415 grade steel reinforcement. Assume moderate environment.

SOLUTION:

Step 1 Determine a trial section. Let us initially make a guess on the thickness of wall based on tension considerations and later suitably increase the size based on the bending moment.

The allowable direct and bending stresses for M25 concrete are 1.3 N/mm² and 1.8 N/mm², respectively, as per Table 1 of IS 3370-Part 2. Neglecting the area of steel, the required area of concrete section is

$$\text{Approximate } A_c = \frac{N}{f_{act}} = \frac{50 \times 1000}{1.3} = 38,462 \text{ mm}^2$$

Considering 1 m width, approximate required thickness = 39 mm. It should be noted that the section has to resist bending moment as well.

$$m = \frac{280}{3\sigma_{cbc}} = \frac{280}{3 \times 8.5} = 11 \text{ (Clause B-2.1.2 and Table 21$$

of IS 456)

$$k = \frac{1}{1 + \frac{\sigma_{st}}{m\sigma_{cbc}}} = \frac{1}{1 + \frac{130}{11 \times 8.5}}$$

$$= 0.418 \text{ (Table 4 of IS 3370-Part 2)}$$

$$j = 1 - k/3 = 1 - 0.418/3 = 0.86,$$

$$Q = 0.5kj\sigma_{cbc} = 0.5 \times 0.418 \times 0.86 \times 8.5 = 1.528$$

Depth required for resisting bending moment,

$$d = \sqrt{\frac{M}{Qb}} = \sqrt{\frac{90 \times 10^6}{1.528 \times 1000}} = 243 \text{ mm}$$

Assuming 20 mm bars and a cover of 40 mm, adopt $D = 350$ mm with $d = 350 - 40 - 10 = 300$ mm.

Equivalent moment = $M - T(d - d')/2 = 90 - 50(0.30 - 0.04)/2 = 83.5$ kNm

Approximate reinforcement to resist bending

$$A_{st} = \frac{M}{\sigma_{st}jd} = \frac{83.5 \times 10^6}{130 \times 0.86 \times 300} = 2489 \text{ mm}^2$$

Area of tension reinforcement required to resist the axial force

$$A_{st1} = \frac{N}{f_s} = \frac{50 \times 1000}{130} = 385 \text{ mm}^2$$

Total area required = 2489 + 385 = 2874 mm²

Provide 20 mm bars at 110 mm c/c ($A_{st} = 2856 \text{ mm}^2$).

Step 2 Calculate the neutral axis depth.

From Eq. (18.19), with $A_{sc} = 0$, we get

$$\left(M - \frac{ND}{2}\right)A_{st}m(d - x) = 0.5bx^2 \left[N\left(d - \frac{x}{3} - \frac{D}{2}\right) + M\right]$$

$$\left(90 \times 10^6 - 50 \times 10^3 \times \frac{350}{2}\right)2856 \times 11 \times (300 - x)$$

$$= 0.5 \times 1000x^2 \left[50 \times 10^3 \left(300 - \frac{x}{3} - \frac{350}{2}\right) + 90 \times 10^6\right]$$

Simplifying, we get

$$x^3 - 5775x^2 - 3,06,306x + 91.89 \times 10^6 = 0$$

This cubic equation may be solved by trial and error method or by using online calculators (e.g., <http://www.easycalculation.com/algebra/cubic-equation.php>).

Thus, $x = 103.1$ mm

Step 3 Check for compressive stress in concrete.

The compressive stress in concrete is found using Eq. (18.18).

$$bx \frac{f_c}{2} \left(d - \frac{x}{3}\right) = M - N \frac{D}{2}$$

$$1000 \times 103.1 \times \frac{f_c}{2} \left(300 - \frac{103.1}{3}\right) = 90 \times 10^6 - 50 \times 10^3 \times \frac{350}{2}$$

Thus $f_c = 5.93 \text{ N/mm}^2 < 8.5 \text{ N/mm}^2$ (as per Table 2 of IS 3370-Part 2).

Step 4 Check for tensile stress in steel. The tensile stress in steel is found from the stress diagram as

$$f_s = mf_c \left(\frac{d - x}{x}\right) = 11 \times 5.93 \times \left(\frac{300 - 103.1}{103.1}\right)$$

$$= 124.5 \text{ N/mm}^2 < 130 \text{ N/mm}^2 \text{ (Table 4 of IS 3370-Part 2)}$$

Hence, the stresses are within the permissible limits.

Note: You can also design using limit states method, in which case the stresses should be within $0.87f_y$ and $0.45f_{ck}$, respectively, for steel and concrete. Moreover, while using the limit states method, it is necessary to calculate the crack widths and check whether they are within the allowable limits.

EXAMPLE 18.6 (Crack width for members with large moment and small tension):

Calculate the crack width for the wall in Example 18.5.

SOLUTION:

Step 1 Calculate the strain at steel level.

From Example 18.5, the tensile stress in steel is,

$$f_s = 124.5 \text{ N/mm}^2$$

Hence, strain, $\varepsilon_s = f_s/E_s = 124.5/2 \times 10^5 = 6.225 \times 10^{-4}$

Step 2 Calculate the apparent strain at the surface of the wall.

$$\varepsilon_1 = \varepsilon_s \frac{D-x}{d-x} = 6.225 \times 10^{-4} \frac{350-103.1}{300-103.1} = 7.806 \times 10^{-4}$$

Step 3 Calculate the tension stiffening effect. Let us assume that the crack width is less than 0.2 mm.

$$\begin{aligned} \varepsilon_2 &= \frac{b_t(D-x)(a'-x)}{3E_sA_s(d-x)} = \frac{1000 \times (350-103.1)(350-103.1)}{3 \times 2 \times 10^5 \times 2856 \times (300-103.1)} \\ &= 1.806 \times 10^{-4} \end{aligned}$$

Step 4 Calculate the average strain at the surface.

$$\varepsilon_m = \varepsilon_1 - \varepsilon_2 = (7.806 - 1.806) \times 10^{-4} = 5.0 \times 10^{-4}$$

Step 5 Calculate a_{cr} .

$$\begin{aligned} a_{cr} &= \sqrt{[(s/2)^2 + (c + d_b/2)^2]} - d_b/2 \\ &= \sqrt{[(110/2)^2 + (40 + 20/2)^2]} - 20/2 \\ &= 64.33 \text{ mm} \end{aligned}$$

Step 6 Calculate the crack width.

$$\begin{aligned} W_{cr} &= \frac{3a_{cr}\varepsilon_m}{1 + 2 \frac{(a_{cr} - c_{\min})}{(D-x)}} = \frac{3 \times 64.33 \times 5.0 \times 10^{-4}}{1 + 2 \frac{(64.33 - 40)}{(350 - 103.1)}} \\ &= 0.08 \text{ mm} < 0.2 \text{ mm} \end{aligned}$$

Hence, the crack width is within the allowable limits.

EXAMPLE 18.7 (Crack width for members subjected to direct tension):

Calculate the crack width for a section of depth 280 mm and breadth 1000 mm subjected to a direct tension of 400 kN/m. Assume a clear cover of 40 mm and that the section is provided with 16 mm bars of Fe 415 grade on each face at 200 mm c/c.

SOLUTION:

$$A_s = (201 \times 5) \times 2 = 2010 \text{ mm}^2/\text{m}$$

$$\text{Strain in steel, } \varepsilon_1 = \frac{N}{A_s E_s} = \frac{400 \times 1000}{2010 \times 2 \times 10^5} = 9.95 \times 10^{-4}$$

Assuming that the crack width is to be restricted within 0.2 mm, the strain due to stiffening effect of concrete

$$\varepsilon_2 = \frac{2bD}{3E_sA_s} = \frac{2 \times 1000 \times 280}{3 \times 2 \times 10^5 \times 2010} = 4.64 \times 10^{-4}$$

$$\begin{aligned} \text{Average strain, } \varepsilon_m &= \varepsilon_1 - \varepsilon_2 = 9.95 \times 10^{-4} - 4.64 \times 10^{-4} \\ &= 5.31 \times 10^{-4} \end{aligned}$$

$$\begin{aligned} \text{Distance to the point considered, } a_{cr} &= \sqrt{(100^2 + 48^2)} - 8 \\ &= 102.92 \text{ mm} \end{aligned}$$

$$\begin{aligned} \text{Crack width, } W_{cr} &= 3a_{cr}\varepsilon_m = 3 \times 102.92 \times 5.31 \times 10^{-4} \\ &= 0.164 \text{ mm} < 0.20 \text{ mm} \end{aligned}$$

Note: If the calculation results in a crack width that is higher than 0.20 mm, the reinforcement has to be increased.

EXAMPLE 18.8 (Use of design aids and interaction equation): Design a tension member of size 300 mm by 300 mm subjected to a working tensile force of 200 kN and a bending moment of 60 kNm, using the P-M design charts given in SP 16. Use M25 concrete and Fe 415 steel. Check the section using interaction equation.

SOLUTION:

We will use the charts presented in the design aids provided in SP 16 for designing this member.

$$N_u = 1.5 \times 200 = 300 \text{ kN}; M_u = 1.5 \times 60 = 90 \text{ kNm}$$

Thus,

$$\frac{N_u}{f_{ck}bD} = \frac{300 \times 1000}{25 \times 300 \times 300} = 0.133$$

$$\frac{M_u}{f_{ck}bD^2} = \frac{90 \times 10^6}{25 \times 300 \times 300^2} = 0.133$$

Assuming 20 mm bars and a clear cover of 35 mm, $d' = 35 + 10 = 45 \text{ mm}$,

$$d'/D = 45/300 = 0.15$$

Let us assume that the reinforcement is equally distributed on two sides.

From Chart 70, we get $p/f_{ck} = 0.14$. Hence,

$$p = \frac{A_{st}}{bD} \times 100 = 0.14 \times 25 = 3.5$$

Thus

$$A_{st} = \frac{3.5 \times 300 \times 300}{100} = 3150 \text{ mm}^2$$

Provide five 20 mm bars at the top and bottom (area = $2 \times 1570.5 = 3141 \text{ mm}^2$).

It has to be noted that when a member is subjected to bending and tension, unsymmetrical reinforcement is required to be provided—more reinforcement at the tension face and less at the compression face. The application of elastic method will result in $A_{st} = 1589 \text{ mm}^2$ and $A_{sc} = 1114 \text{ mm}^2$. Thus, in this case, the use of charts as given in SP 16 forces the designer to use uneconomical symmetrical reinforcement.

Check for interaction

$$N_n = 0.87f_y(A_{st} + A_{sc}) = 0.87 \times 415 \times 3141/1000 = 1134 \text{ kN}$$

$$M_n = \text{Min} \left[(k_2 f_{ck} b d^2); (0.87 f_y A_{st} j d) \right]$$

$$M_{n1} = 0.138 \times 25 \times 300 \times (300 - 45)^2 / 10^6 = 67.3 \text{ kNm}$$

$$M_{n2} = 0.87 \times 415 \times 1570.5 \times 0.8 \times 255 / 10^6 = 115.67 \text{ kNm}$$

Hence, $M_n = 67.3 \text{ kNm}$. Now, using the interaction equation, we get

$$\frac{N_u}{N_n} + \frac{M_u}{M_n} = \frac{300}{1134} + \frac{90}{67.3} = 0.265 + 1.337 = 1.602 > 1.0$$

It shows that the depth has to be increased to 390 mm to satisfy the interaction equation.

SUMMARY

In this chapter, the design of members predominantly subjected to tension or members with bending and direct tension is considered. Such members may be found in the walls of water tanks and in trusses. The design is carried out by considering that the tension is primarily resisted by steel reinforcements; moreover, the concrete is considered to provide only protective cover to the steel. The members under tension are often designed using elastic theory and those subjected to bending and tension are designed using limit states or elastic theory. When designing members using limit states theory, we need to check whether the crack widths are within the prescribed limits.

The behaviour of tension members and the tension stiffening effect are explained. The design methods for members in direct tension are discussed. The provisions in the latest version of the IS code on liquid storage tanks (IS 3370-Parts 1 and 2) for minimum concrete grade, cover, minimum reinforcement, and spacing of reinforcement are explained. The design procedure for members in direct tension is included.

The design of members subjected to bending as well as tension, which can be considered in two separate categories as tension with small eccentricity and as tension with large eccentricity, is then discussed. The provisions in IS 3370 for checking crack widths in members subjected to flexure as well as tension are explained. The interaction curve for members in bending and tension and the design aids provided in SP 16 are also discussed. The design of members subjected to bending, shear, and tension is briefly indicated.

Engineers must be careful while detailing splices, member end connections, and transverse reinforcements in tension members. Due to reversal of stresses, there is a possibility for a member to become a compression member during earthquakes. Such considerations along with construction methods to reduce restraining effects are to be given importance in such tension members. As the discussions in this chapter are applicable to water tanks, a brief discussion on water tanks is also included. The examples provided explain the main concepts presented in this chapter, and the references provided may aid the reader to get more information and guidelines.

REVIEW QUESTIONS

- List two examples where an RC member will be subjected to the following:
 - Direct tension
 - Direct tension combined with bending
- Sketch and describe the behaviour of members subjected to direct tension.
- What is meant by tension stiffening effect?
- What are the criteria considered while designing members subjected to direct tension?
- The average shrinkage strain is usually assumed as _____.
 - 300×10^{-6}
 - 400×10^{-6}
 - 600×10^{-6}
 - 800×10^{-6}
- The minimum cover for severe conditions as per Table 16 of IS 456 is _____.
 - 40 mm and may be reduced by 5 mm for M35 and above
 - 45 mm and may be reduced by 5 mm for M35 and above
 - 45 mm
 - none of these
- Discuss the classification of exposure conditions used in IS 456 and BS 8007. What are the crack widths allowed in each of the exposure conditions for durability?
- The permissible stress in direct tension in Fe 415 grade steel as per IS 456 is _____.
 - 110 MPa
 - 130 MPa
 - 230 MPa
 - 360 MPa
- The minimum amount of grade Fe 415 reinforcement within each surface zone as per IS 3370-Part 2:2009 is _____.
 - 0.30%
 - 0.35%
 - 0.40%
 - 0.12%
- Why is some minimum critical steel ratio prescribed in IS 3370?
- As per IS 3370, the spacing of reinforcement should not exceed _____.
 - 250 mm or the thickness of section
 - 300 mm or the thickness of section
 - 300 mm or twice the thickness of section
 - 400 mm or twice the thickness of section
- List the steps necessary for designing a member subjected to direct tension.
- How is a member subjected to tension with small eccentricity designed?
- How is a member designed when there is large moment and small tension?
- State the equations provided in IS 3370-Part 2 for calculating the crack widths for the following:
 - Members subjected to direct tension
 - Members subjected to flexure
- Explain how the P-M design charts given in SP 16 can be used for members subjected to direct tension combined with bending. What are the drawbacks of using these charts?
- Write the interaction equation that may be used to check the members subjected to direct tension combined with bending. What are the different terms and how can they be calculated?
- Explain the detailing of reinforcement in members subjected to direct tension.
- List a few requirements that are necessary when a tension member is subjected to earthquake loads.

20. Why is the sequence of construction important? With a sketch give the preferred sequence of construction of walls in tanks.
21. Briefly describe how the walls in circular water tanks are designed.

EXERCISES

- Design the tie member of an RC truss subjected to a tensile force of 400 kN, including dead and imposed loads. Assume M30 grade concrete, Fe 415 steel, and mild environment. Check for crack width.
- Design the wall of an RC cylindrical tank (with a sliding joint at the base) subjected to a hoop tension of 150 kN per metre. Assume M 35 grade concrete, Fe 415 steel, and moderate environment.
- An RC water pipe line of 350 mm radius is carrying water at a pressure of 6 m head of water. Design the pipe with grade 415 steel and M30 concrete.
- An RC truss member of length 5 m in a mild environment is subjected to a direct tensile force of 100 kN and a bending moment of 5.5 kNm. Design the member.
- An RC wall of a rectangular tank is subjected to a direct tension of 60 kN/m and a moment of 100 kNm/m. Design the section using M30 concrete and Fe 415 grade steel reinforcement. Assume moderate environment.
- Calculate the crack width for the wall in Exercise 5.
- Calculate the crack width for a section of depth 400 mm and breadth 1000 mm subjected to a direct tension of 500 kN/m. Assume a clear cover of 40 mm and that the section is provided with 20 mm bars of Fe 415 grade on each face at 200 mm c/c.
- Design a tension member of size 250 mm by 400 mm subjected to a working tensile force of 150 kN and a bending moment of 45 kNm, using the charts given in SP 16. Use M25 concrete and Fe 415 steel. Check the section using the interaction equation.

REFERENCES

- ACI Committee 224.2R-92 (reapproved 1997), *Cracking of Concrete Members in Direct Tension*, American Concrete Institute, Farmington Hills, p. 12.
- Anchor, R.D. 1992, *Design of Liquid Retaining Concrete Structures*, 2nd edition, Edward Arnold, London, p. 185.
- Bamforth, P.B. 2007, *Early-age Thermal Crack Control in Concrete*, CIRIA Report C660, Construction Industry Research and Information Association, London.
- Bamforth, P B., S. Denton, and J. Shave 2010, *The Development of a Revised Unified Approach for the Design of Reinforcement to Control Cracking in Concrete Resulting from Restrained Contraction*, Final Report, Institution of Civil Engineers, UK, ICE/0706/012, p. 67, (also see <http://www.ice.org.uk/getattachment/444f47bb-685c-4d13-b95d-973d42050e99/The-development-of-a-revised-unified-approach-for-.aspx>, last accessed on 25 May 2012).
- Bazant, Z.P. and J. Planas 1998, *Fracture and Size Effect in Concrete and Other Quasibrittle Materials*, CRC Press, Boca Raton, p. 640.
- Beeby, A.W. 1979, 'The Prediction of Crack Widths in Hardened Concrete', *The Structural Engineer (UK)*, Vol. 57A, No. 1, pp. 9–17 and 1980, 'Discussions', Vol. 58A, October, pp. 326–32.
- Beeby, A.W. and R.H. Scott 2005, 'Cracking and Deformation of Axially Reinforced Members Subjected to Pure Tension', *Magazine of Concrete Research*, Vol. 57, No. 10, pp. 611–21, (also see <http://dx.doi.org/10.1680/macr.2005.57.10.611>, last accessed on 20 May 2012).
- Beeby, A.W. and R.H. Scott 2006, 'Mechanisms of Long-term Decay of Tension Stiffening', *Magazine of Concrete Research*, Vol. 58, No. 5, pp. 255–66, (also see <http://dro.dur.ac.uk/1824/1/1824.pdf>, last accessed on 10 June 2012).
- Bischoff, P.H. 2005, 'Re-evaluation of Deflection Prediction for Concrete Beams Reinforced with Steel and Fiber Reinforced Polymer Bars', *Journal of Structural Engineering*, ASCE, Vol. 131, No. 5, pp. 752–767 and Gilbert, R.I. 2006, 'Discussion', Vol. 132, No. 8, pp. 1328–30.
- BS 8007:1987, *Code of Practice for Design of Concrete Structures for Retaining Aqueous Liquids*, British Standards Institution, London, p. 31.
- Considere, M. 1899, 'Influence des armatures métalliques sur les propriétés des mortiers et bétons', *Compte Rendu de L'Academic des Sciences*, Vol. 127, pp. 992–5.
- Dayaratnam, P. 2004, *Limit States Design of Reinforced Concrete Structures*, Oxford and IBH Publishing Co. Pvt. Ltd, New Delhi, p. 532.
- Fields, K.L. 1998, *Tension Stiffening Response of High-strength Reinforced Concrete Tensile Members*, M.S. thesis, The University of New Brunswick, Canada, p. 195.
- Gambhir, M.L. 2008, *Design of Reinforced Concrete Structures*, Prentice-Hall of India Pvt. Ltd, New Delhi, p. 723.
- Goto, Y. 1971, 'Cracks Formed in Concrete around Deformed Tension Bars', *Journal of the American Concrete Institute*, Vol. 68, No. 4, pp. 244–51.
- Gouthaman, A. and D. Menon 2001, 'Increased Cover Specifications in IS 456: 2000: Crack-width Implications in RC Slabs', *The Indian Concrete Journal*, Vol. 75, No. 9, pp. 581–6.
- IITK-GSDMA 2007, *Guidelines for Seismic Design of Liquid Storage Tanks, Part 1: Provisions with Commentary, Part 2: Explanatory Examples*, National Information Centre of Earthquake Engineering, IIT, Kanpur, p. 112, (also see <http://www.iitk.ac.in/nicee/IITK-GSDMA/EQ08.pdf>, last accessed on 15 May 2012).
- IS 3370 (Part 1):2009, *Concrete Structures for Storage of Liquids—Code of Practice, Part 1: General Requirements*, Bureau of Indian Standards, New Delhi, p. 16.
- IS 3370 (Part 2):2009, *Concrete Structures for Storage of Liquids—Code of Practice, Part 2: Reinforced Concrete Structures*, Bureau of Indian Standards, New Delhi, p. 12.
- Mallick, S.K. 1983, 'Limit States Design of Tension Members under Tension and Bending in One Plane', *The Indian Concrete Journal*, Vol. 57, No. 8, pp. 202–4, 219.
- Mörsch, E. 1909, *Concrete–Steel Construction* (English translation by E.P. Goodrich from 3rd edition of *Der Eisenbetonbau*), The Engineering News Publishing Company, New York, p. 368.
- Muttoni, A. and M.F. Ruiz 2007, 'Concrete Cracking in Tension Members and Application to Deck Slabs of Bridges', *Journal of Bridge Engineering*, ASCE, Vol. 12, No. 5, pp. 646–53.

- Naaman A.E. 2000, *Ferrocement and Laminated Cementitious Composites*, Techno Press 3000, Michigan.
- Pratapa, P.P. and D. Menon 2011, 'Optimal Design of Cylindrical Reinforced Concrete Water Tanks', *The Indian Concrete Journal*, Vol. 85, No. 2, pp. 19–25.
- Popovics, S. 1985, 'Modification of Portland Cement Concrete with Epoxy as Admixture', *SP 89-11*, American Concrete Institute, Farmington Hills, pp. 207–30.
- Purushothaman, P. 1984, *Reinforced Concrete Structural Elements—Behaviour, Analysis and Design*, Tata McGraw Hill Publishing Company Ltd, New Delhi and Torsteel Research Foundation in India, Bangalore, p. 709.
- Srinivas, N. and D. Menon 2000, 'Design Criteria for Crack Control in RC Liquid Retaining Structures: Need for a Revision of IS 3370 (Part II) 1965', *The Indian Concrete Journal*, Vol. 74, No. 8, pp. 451–8.
- Walraven, J.C. 2009, 'High Performance Fiber Reinforced Concrete: Progress in Knowledge and Design Codes', *Materials and Structures*, Vol. 142, pp. 1247–60.
- Wenkenbach, I. 2011, *Tension Stiffening in Reinforced Concrete Members with Large Diameter Reinforcement*, Masters thesis, Durham University, (also see <http://etheses.dur.ac.uk/3250/>, last accessed on 31 May 2012).
- Wu, H.Q. and R.I. Gilbert 2008, *An Experimental Study of Tension Stiffening in Reinforced Concrete Members under Short-term and Long-term Loads*, Report No. R-449, the University of New South Wales, Sydney, <http://www.civeng.unsw.edu.au>, last accessed on 1 June 2012.

DESIGN OF JOINTS

19.1 INTRODUCTION

Capacity design is a powerful design tool, which was initially developed in New Zealand about 40 years ago (Park and Paulay 1975). As we have seen in the earlier chapters, this philosophy has been adopted with some modifications for the seismic design of reinforced concrete (RC) structures and elements in several countries. In the capacity design of structures, a building is usually envisaged as a chain and the different components, such as columns, beams, joints, and walls, as its links. On the basis of the underlying principle of ‘a chain is as strong as its weakest link’, the overall strength of a building is correlated to the strength of its weakest component. This analogy can be used not only for a building but for all structural systems; if an RC bridge is idealized as a chain, then the piers, deck, and the knee joints are the links. In fact, the same analogy can also be applied to each structural element. In the context of design, if a structure is idealized as a chain and its components as the links, then the design force can be idealized as two persons pulling the chain at its two ends (see Fig. 19.1).

The objective of any design will then be to ensure that the chain (or its weakest link) does not break when it is pulled with the design force. In order to ensure this, the designers need to (a) identify the weakest link; (b) accurately (and conservatively) evaluate the strength of the weakest link; and, most importantly, (c) know with reasonable certainty the higher-bound value of the design force with which the chain will be pulled. If the ductile link is the weak one (i.e., its capacity to take the load is less), then the chain will show large final elongation (see Fig. 19.1). Instead, if the brittle link is the weak one, then the chain will fail suddenly and show small final elongation. Therefore, if such a ductile chain is required, the ductile link should be made to be the weakest link (Murty 2005). It is important to evaluate the strength of all the links in the chain unless it is obvious that a particular link is stronger than other links. Otherwise, there is a possibility of unknowingly missing the weakest link, thereby overestimating the overall strength of the chain, resulting in disastrous consequences. As we have seen in the earlier chapters, it is better to make beams as the ductile weak links than columns (strong column–weak beam design method), as failure of columns may result in the complete collapse of the structure.

Even though designers often take care to design and detail elements such as beams, columns, footings, and walls for ductile behaviour, they often ignore beam-column joints. As a result, joints often become the weakest links in the structural system. Joints are crucial zones for the effective transfer of forces and moments between the connecting elements such as beams and columns. When a building is located in a non-seismic zone and designed only for gravity loads, the design check for joints may not be critical and hence is not attempted. However, the catastrophic failures reported in the past earthquakes, especially during the past several earthquakes in India as well as those in Turkey and Taiwan in 1999, were attributed to beam-column joints (Saatcioglu, et al. 2001; Rai and Seth 2002; Arslan and Korkmaz 2007). Some of these failures are shown in Fig. 19.2.

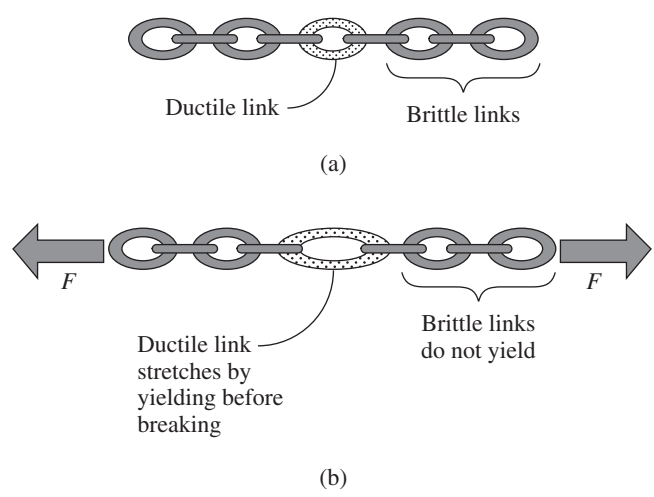


FIG. 19.1 Capacity design concept (a) Original chain (b) Loaded chain

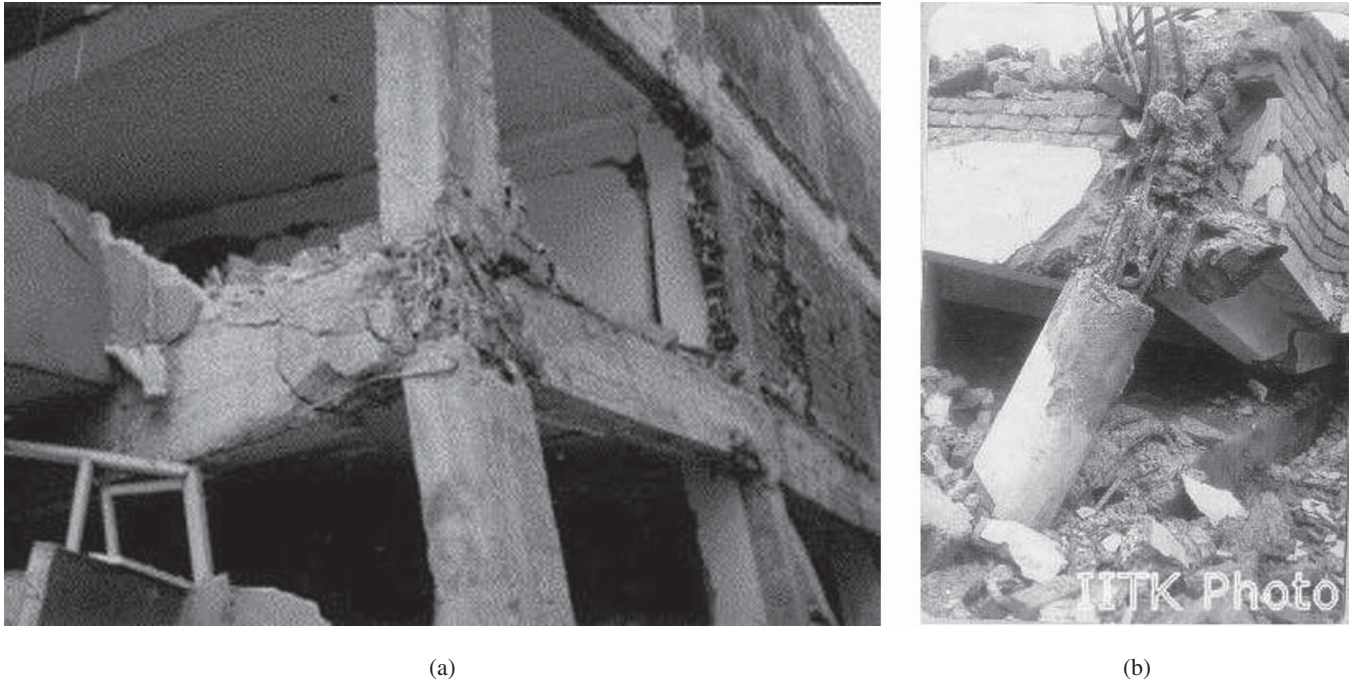


FIG. 19.2 Failure of beam-column joints (a) During the Turkey earthquake (b) During the 1988 Bihar earthquake
 Source: (a) Reprinted from Arslan and Korkmaz 2007 with permission from Elsevier (b) NICEE, Kanpur

Hence, in this chapter the design and detailing of beam-column joints for seismic loads is discussed. The beam-to-beam joints, which are generally not given importance during design, are also covered. The design and detailing of corbels, which are often found in industrial or precast concrete buildings, is discussed. Anchors or fasteners are employed to connect precast concrete components or to connect steel columns to concrete foundations. Indian codes do not have provisions for their design. The ACI code provisions for the design of anchors are provided for the benefit of designers.

19.2 BEAM-COLUMN JOINTS

The performance of framed structures not only depends upon the individual structural elements but also upon the integrity of the joints. In most of the cases, joints of framed structures are subjected to the most critical loading under seismic conditions. Despite the significance of the joints in sustaining large deformations and forces during earthquakes, until recently, specific guidelines have not been explicitly included in the Indian codes of practice for their design and detailing (IS 456:2000 and IS 13920:1993). However, some provisions have been included recently in Draft IS 13920 based on the ACI 318 and ACI 352 (ACI-ASCE Committee 352) provisions (Jain, et al. 2006).

Whereas considerable attention is devoted to the design of individual elements (slabs, beams, and columns), in the absence of suitable guidelines no conscious efforts are made to design joints. It appears that the integrity and strength of

such joints are assumed to be satisfied by anchoring the beam reinforcement.

One of the basic assumptions of the frame analysis is that the joints are strong enough to sustain the forces (moments, axial, and shear forces) generated by the loading and to transfer the forces from one structural member to another (beams to columns, in most of the cases). It is also assumed that all the joints are rigid and the members meeting at a joint deform (rotate) by the same angle. Hence, it is clear that unless the joints are designed to sustain these forces and deformations, the performance of structures will not be satisfactory under all the loading conditions, especially under seismic conditions. Since the mid-1960s, numerous experimental tests and analytical studies have been conducted to investigate the performance of RC beam-column connections subjected to lateral earthquake loading (Hanson and Connor 1967). Post-earthquake analyses of structures, accidental loading, or laboratory tests show that the distress in the joint region is the most frequent cause of failure rather than the failure of the connected elements (Saatcioglu 2001; Rai and Seth 2002; Park and Paulay 1975). Analytical models that simulate the response of RC interior beam-column joints have been developed (e.g., Mitra and Lowes 2007). Even though such models are currently available and documented on the *OpenSees* website (www.opensees.berkeley.edu), they are complicated and not suitable for design office use.

Beam-column joint is defined as the portion of the column within the depth of the deepest beam that frames into the column (ACI 352-02). The beam-column joints in a moment resistant frame can be classified as (a) interior joints, (b) exterior joints,

(c) corner joints, and (d) knee joints (see Fig. 19.3). When four beams frame into the vertical faces of a column, the joint is called an *interior joint*. When one beam frames into the vertical face of a column and two more beams frame into the column in the perpendicular direction, it is called an *exterior joint*. A *corner joint* is one in which the beams frame into two adjacent vertical faces of a column. In a *roof joint* (also called *knee joint*), the columns will not extend above the joint, whereas in a floor joint the columns will extend above the joint as shown in Fig. 19.3.

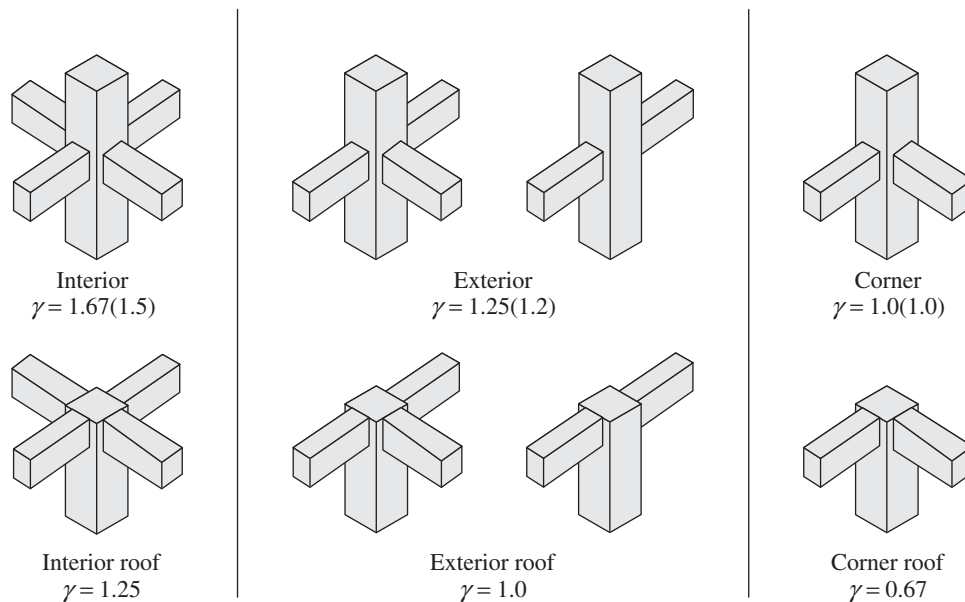


FIG. 19.3 Types of beam-column joints and strength coefficients as per ACI 352-02 (Reprinted with permission from ACI)

Note: Values in brackets are those suggested by Draft IS 13920

Considerable research and test results are reported on the strength and behaviour of beam-column joints (Subramanian and Prakash Rao 2003; Paulay and Priestley 1992; ACI SP 123:1991). The revised IS 1893:2002 has considerably enhanced the lateral forces on structures compared to the previous version, which makes the design of joints imperative. Recommendations on the design and detailing are available, which were developed based on the test results (ACI 318-2011; ACI 352-02; NZS 3101-2006; Draft IS 13920; EN 1998-1:2003). The design and detailing procedures as per draft IS 13920 (Jain and Murty 2005) and ACI 352-02 (which was first published in 1976) are summarized in this chapter. Beam-column joints in buildings located in earthquake zones and built before the development of current design guidelines need to be repaired and strengthened. A state of the art on repair and rehabilitation of RC beam-column joints is provided by Engindeniz, et al. (2005).

19.2.1 Requirements of Beam-column Joints

A beam-column joint undergoes serious stiffness and strength degradation when subjected to earthquake loads. The essential

requirements for the satisfactory performance of a joint in an RC structure, during earthquakes, can be summarized as follows (Park and Paulay 1975; Paulay and Priestley 1992):

1. A joint should exhibit a service load performance equal to or greater than that of the members it joins; that is, the failure should not occur within the joints. Should there be a failure due to overloading, it should occur in beams through large flexural cracking and plastic hinge formation and not in columns (normally the joint is considered as a part of the column).
2. A joint should possess strength not less than the maximum demand corresponding to the development of the structural plastic hinge mechanism of the structure. This requirement will eliminate the need for repair in an inaccessible region in the structure.
3. The joint should respond elastically during moderate earthquakes.
4. The deformation of joints should not significantly increase the storey drift.
5. The joint configuration should ensure ease of fabrication and good access for placing and compacting concrete in the joint region.

19.2.2 Design and Detailing of Joints

The problems involved in the detailing and construction of beam-column joints are often not appreciated by designers. Because of the restricted space available in the joint block, the detailing of reinforcement assumes more significance in the joints than anywhere else. Indeed, the conflicting requirement of small-sized bars for good performance and large-sized bars for ease of placement and concreting is more obvious at the joints than anywhere else (Subramanian and Prakash Rao 2003). This is particularly true at internal joints, where the beams intersect in both the horizontal directions and where large moments are to be sustained by the connections. In the absence of specifications from the designers, site engineers often adopt expedient procedures for detailing, which are not always conducive for satisfactory structural performance.

Some of the incorrect detailing practices adopted by the site engineers in India are (Subramanian and Prakash Rao 2003) (a) incorrect bending of beam reinforcement into the beam-column joint for anchorage (the beam bars at the top are bent upwards instead of downwards; such a detailing prevents diagonal strut formation in the joint and may cause

diagonal cracking, leading to shear failure of the joint); (b) inadequate anchorage of beam bars into the beam-column joint; (c) poor quality concrete at the critical region of the joint, obviously due to poor quality formwork coupled with inadequate compaction, and (d) kinking of column bars near beam-column joints (this can damage concrete at the joint, may cause excessive stresses in the column, and may lead to early distress, especially under lateral forces induced by earthquakes) (Subramanian and Prakash Rao 2003). It may also be noted that shear reinforcements are usually not provided in these joints; even when provided, they are not as per IS 13920. Further, some site engineers provide the extreme bars of the beam reinforcement outside the column bars, which is not a correct practice. Unless there is a wide beam, the beam reinforcement should be placed within the column cage, without much kinking (see Fig. 4.12 of Chapter 4).

19.2.3 Corner Joints

The external joints (corner joints) of a frame can be broadly classified into opening and closing corners. The corners that tend to open (increase the included angle when loaded), as circled in Fig. 19.4, are termed *opening corners*, whereas those that tend to decrease the included angle are termed *closing corners*. Opening corners occur at the corners of frames, bottom of water tanks, and in L-shaped retaining walls. In bridge abutments, the joint between the wing walls and abutment will act as an opening joint.

The joints in multi-storeyed buildings will be subjected to alternate opening and closing forces under seismic loading. For closing corners, tests have shown that the usual detailing will be satisfactory.

The elastic distribution of stresses before cracking of an opening corner knee joint is shown in Fig. 19.5(b). As shown in this figure, large tensile stresses occur at the re-entrant corner and the middle of the joint. Due to these stresses, cracking will develop as shown in Fig. 19.5(c). If reinforcements are not provided crossing these cracks,

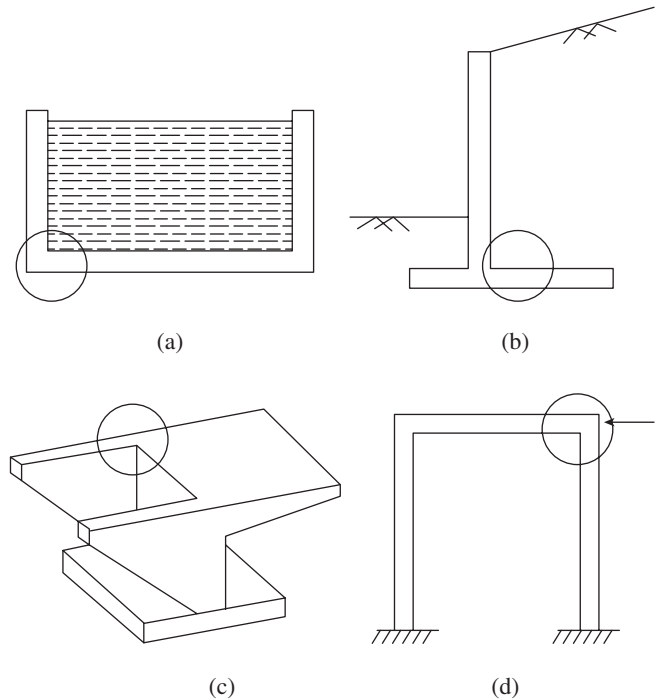


FIG. 19.4 Examples of opening joints (a) Water tank (b) Retaining wall (c) Bridge abutment (d) Portal frame

the joint will fail immediately after the development of the diagonal crack. When the internal load path in the form of a truss system is envisaged and steel provided to carry the tension, with concrete carrying the compression, the resulting details will have a good chance of working safely. Such a truss system could be determined using the strut-and-tie model—a possible model for the joint is shown in Fig. 19.5(d). In all the strut-and-tie models of this chapter, the compression struts are shown by dashed lines and tension ties are shown by solid lines.

The efficiency of joints, η , is usually defined as the ratio of failure moment of the joint to the capacity of the adjoining members (Skettrup, et al. 1984). Nilsson and Losberg (1976) and Desayi and Kumar (1989) measured the efficiencies of open and closing joints for a number of reinforcement configurations. They found that for the normal detailing

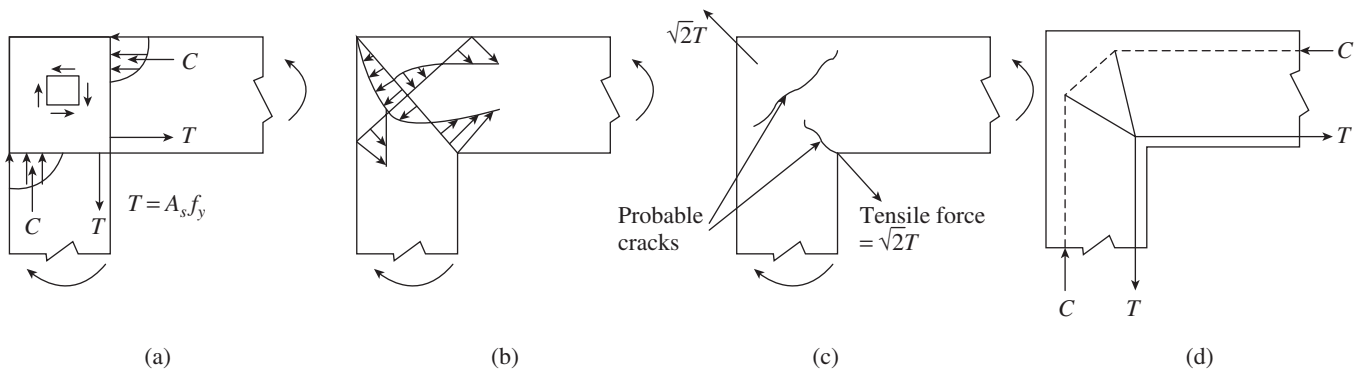


FIG. 19.5 Stresses in an opening joint (a) Stresses at ultimate load (b) Elastic distribution of stresses (c) Possible cracks (d) Strut-and-tie model

adopted in practice for an opening joint (Fig. 19.6a), the flexural efficiency may be only about 25 per cent of the strength of the members meeting at the joint. Nilsson and Losberg (1976) experimentally showed that the detail shown in Fig. 19.6(g) will develop the required moment capacity without excessive deformation. This is because the diagonal bar limits the growth of crack at the re-entrant corner (this crack is shown in Fig. 19.5c) and the two hooked bars resist the tension at the centre of the joint. Desayi and Kumar (1989) showed that similar behaviour may be attained by providing horizontal and vertical stirrups in the beam-column joint (the intermediate column bars may serve as vertical stirrups). The inclined diagonal fan-type stirrups shown in Fig. 19.6(a) should be designed for a tensile force of $\sqrt{2}T$.

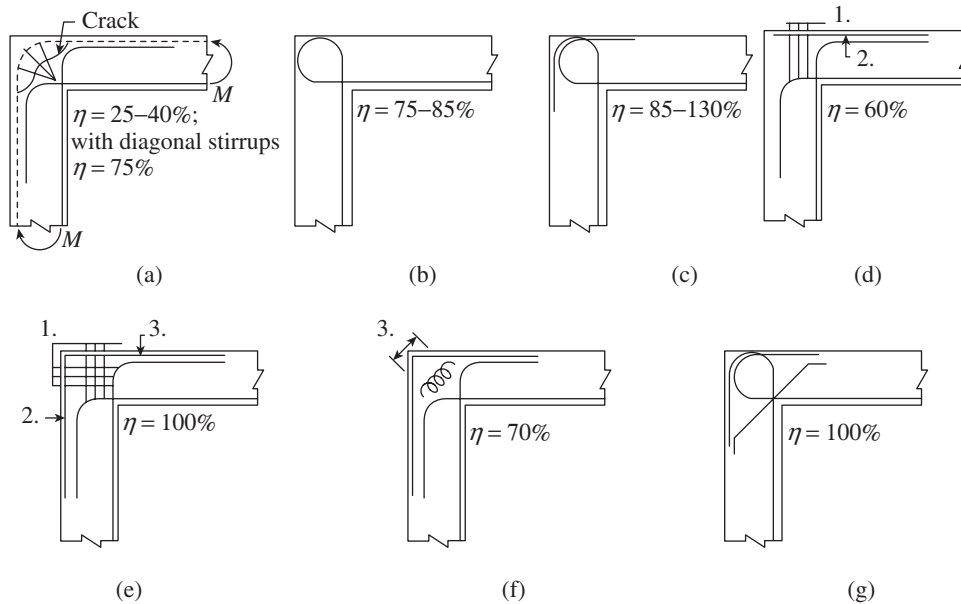


FIG. 19.6 Measured efficiency of opening joints (a) Detail A—Simple detail (b) Detail B—Loop detail (c) Detail C—Two U hooks (d) Detail D—Vertical stirrups (e) Detail E—Simple detail (f) Detail F—Cross-diagonal spiral (g) Detail G—With diagonal bar

Source: Subramanian and Prakash Rao 2003

Notes:

1. 2-legged stirrups; 2 nos in (d1), 3 nos in (d2), 4 nos in (d3) and (e)
2. 2 nos 6 mm hanger bars
3. Circular spiral diameter = 75 mm and pitch = 100.0 mm

Closing Corner Joints

The stresses and behaviour of a closing corner joint are opposite to those in an opening corner joint (see Fig. 19.7). Hence, a major diagonal crack is formed on the diagonal of the joint, as shown in Fig. 19.7(b). Unlike the opening corner joints, closing corner joints develop efficiencies in the range of 85–100 per cent. In these joints, the top tension bars in the beams have to be bent to a sufficient radius to anchor them in the column to prevent bearing or splitting failure inside the bent bars at the corner, as they transmit a force of $\sqrt{2}A_s$ ($0.87f_y$) to the concrete in the diagonal direction. The tension

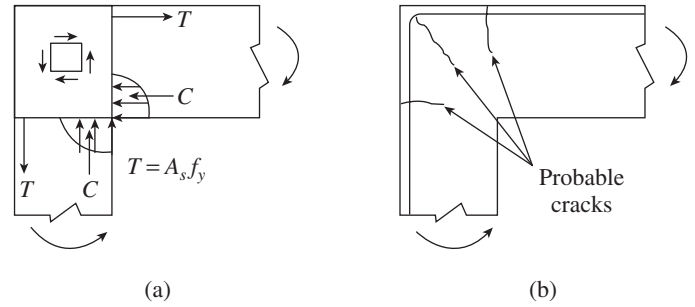


FIG. 19.7 Closing corner joint (a) Stresses at ultimate load (b) Cracking pattern

steel should be continuous around the corner (i.e., it should not be lapped within the joint).

It has to be noted that the relative size of the beam and column in a joint will affect its strength and detailing (Wight and Macgregor 2009; Prakash Rao 1985, 1995).

Knee joints may be subjected to load reversals during wind or seismic loads and hence require greater care in detailing. Since the joints subjected to alternating loads close as well as open, both systems of diagonal reinforcement will be required. In such a situation, an orthogonal mesh will be ideal (Prakash Rao 1995).

19.2.4 T-joints

T-joints are encountered in exterior column-beam connections, continuous roof beams over columns, and at the base of retaining walls. The forces acting at a T-joint are shown in Fig. 19.8(a). The shear force in the joint gives rise to diagonal cracks, thus requiring stirrups in the joint. The detailing of longitudinal reinforcement also significantly affects the efficiency of the joint. A commonly found detail is shown in Fig. 19.8(b) and an improved detail is shown in Fig. 19.8(c). As the bars are bent away from the joint core in the detail of Fig. 19.8(b), the efficiency was found to be in the range of only 25–40 per cent. However, the detail of Fig. 19.8(c), where the bars are anchored in the joint core, showed better performance in tests and had efficiency in the range of 80–100 per cent (Nilsson and Losberg 1976). However, it has to be noted that stirrups have to be provided to confine the concrete core within the joint.

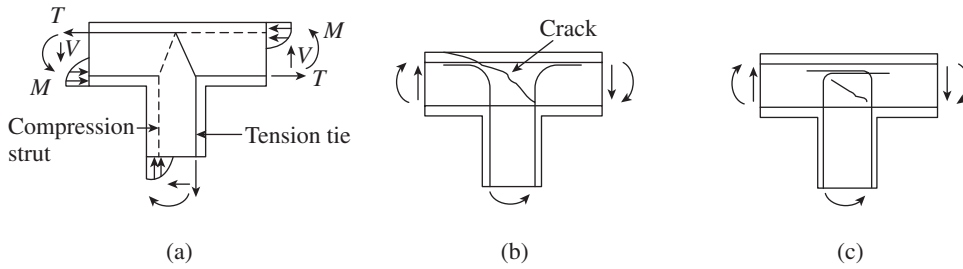


FIG. 19.8 T-joints (a) Forces and strut-and-tie model (b) Poor detail (c) Satisfactory detail

In the case of T-joints at the base of retaining walls, Nilsson and Losberg (1976) found that the normal detailing as shown in Fig. 19.9(a) results in wide corner cracks. To reduce the crack width, they suggest a detail with an inclined reinforcement as shown in Fig. 19.9(b).

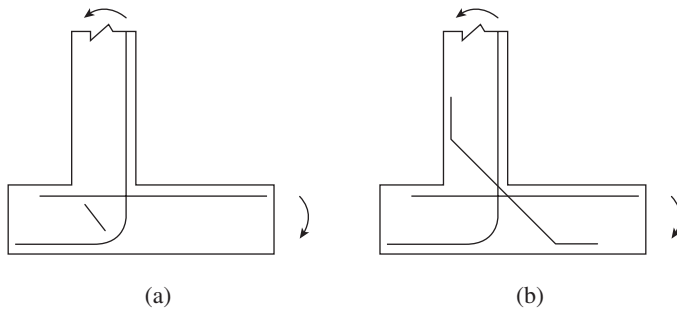


FIG. 19.9 Layout of reinforcement in retaining wall corners (a) Normal detail (b) Addition of diagonal bar

19.2.5 Beam-column Joints in Frames

The beam-column joint in a multi-storey frame transfers the loads and moments at the ends of the beams into the columns. The interior roof beam-column joint in a frame has the same flow of forces as the T-joint of Fig. 19.8(a) and its crack pattern is also similar to Fig. 19.8(b). The forces acting on an interior joint subjected to gravity loading is shown in Fig. 19.10(a). As shown in this figure, the tension and compression from the beam ends and the axial loads from the columns are transmitted directly through the joint. For a four-member connection as shown in Fig. 19.10(a), if the two beam moments are in equilibrium with one another then no additional reinforcement is required.

In the case of lateral loading like seismic loading, the equilibrating forces from beams and columns, as shown in Fig. 19.10(b), develop diagonal tensile and compressive stresses within the joint. Cracks develop perpendicular to the tension

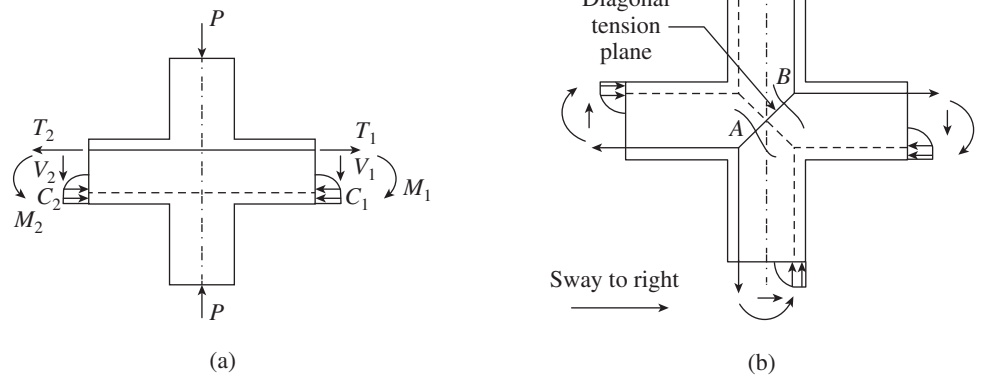


FIG. 19.10 Forces in interior beam-column joints (a) Gravity loading (b) Seismic loading

diagonal A-B in the joint and at the faces of the joint where the beams frame into the joint. As concrete is weak in tension, transverse reinforcements have to be provided in such a way that they cross the plane of failure to resist the diagonal tensile forces (Uma and Meher Prasad 2005).

19.2.6 Design of Beam-column Joints

Because the joint block area is smaller relative to the member sizes, it is essential to consider localized stress distribution within the joints. A simplified force system may be adopted in designing beam-to-column connections. The quantity of steel required is calculated on the assumption that steel reaches the design yield stress and the concrete its design compressive stress. Where local bearing or bond failure is expected, the lower of the two capacities should be adopted based on experimental results. It is essential to prevent bond and anchorage failure within the joints, especially at the external joints, through proper design and detailing practices.

The principal mechanisms of failure of a beam-column joint are as follows:

1. Shear failure within the joint
2. Anchorage failure of bars, if anchored within the joint
3. Bond failure of beam or column bars passing through the joint

As mentioned earlier, the joint has to be designed based on the fundamental concept that failure should not occur within the joint; that is, the joint is strong enough to withstand the yielding of connecting beams (usually) or columns.

Types of Joints

Typical beam-column joints are grouped as Type 1 and Type 2 joints, as per ACI 352.

Type 1 joints These joints have members that are designed to satisfy strength requirements without significant inelastic deformation. These are non-seismic joints.

Type 2 joints These joints have members that are required to dissipate energy through reversals of deformation into the inelastic range. These are seismic joints.

Joint Shear and Anchorage

Joint shear is a critical check and will govern the size of the columns of moment-resisting frames. To illustrate the procedure, consider the column bound by two beams as shown in Fig. 19.11. As discussed in the earlier chapters, for ductile behaviour, it is assumed that the beams framing into the column will develop plastic hinges at the ends and develop their probable moment of resistance (M_{pr}) at the column faces. This action determines the demands on the column and the beam-column joint.

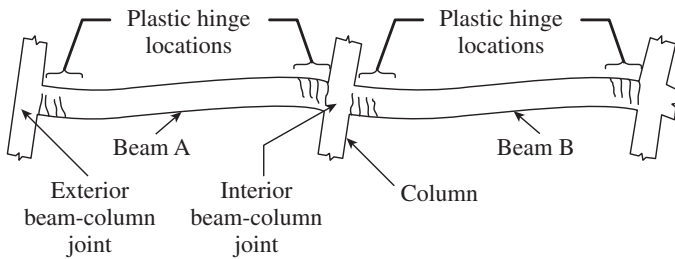


FIG. 19.11 Beam-column joint and frame yielding mechanism

Hanson and Connor (1967) first suggested a quantitative definition of RC joint shear, namely that it could be determined from a free body diagram at mid-height of a joint panel. Figure 19.12 is a free body diagram of the joint for calculation of column shear, V_{col} . It is made by cutting through the beam plastic hinges on both sides of the column and cutting through the column one-half storey height above and below the joint. In this figure, subscripts A and B refer to beams A and B on the opposite sides of the joint, and $V_{e2,A}$ and $V_{e1,B}$ are the shears in the beams at the joint face corresponding to development of M_{pr} at both ends of the beam. For a typical storey, it is sufficiently accurate to assume that the point of contraflexure is at the mid-height of the column. Thus, the column shears for sway to the right and left (see also Clause 7.3.4 of IS 13920-1993) may be found as

$$V_{col} = \left(\frac{M_{pr,A}^- + M_{pr,B}^+}{h_{st}} \right) \quad (19.1a)$$

$$V_{col} = \left(\frac{M_{pr,A}^+ + M_{pr,B}^-}{h_{st}} \right) \quad (19.1b)$$

where h_{st} is the storey height. It has to be noted the probable (plastic) moment capacity of beams ($M_{pr,A}$ and $M_{pr,B}$) are usually calculated by assuming the stress in flexural reinforcement as $1.25f_y$ as against $0.87f_y$ in the moment capacity calculation. Hence, a factor of 1.4 is used in the equations given in Clause 7.3.4 of IS 13920, which is similar to Eq. (19.1).

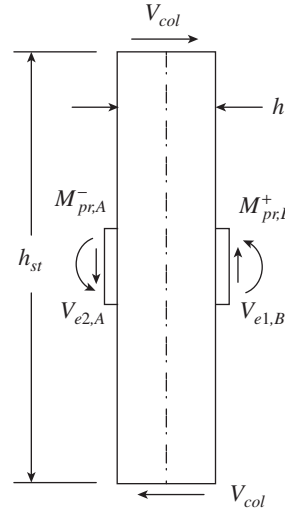


FIG. 19.12 Free body diagram of interior beam-column joint

Once the column shear, V_{col} , is found, the design horizontal joint shear V_j can be obtained by considering the equilibrium of horizontal forces acting on the free body diagram of the joint shear, as shown in Fig. 19.13. Assuming the beam to have zero axial load, the flexural compression force in the beam on one side of the joint may be taken equal to the flexural tension force on the same side of the joint (Moehle, et al. 2008).

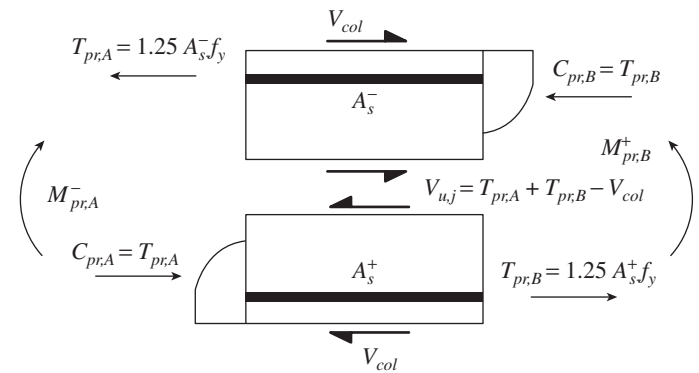


FIG. 19.13 Free body diagram of joint shear

Thus, the joint shear, $V_{u,j}$ is given by

$$\begin{aligned} V_{u,j} &= T_{pr,A} + C_{pr,B} - V_{col} \\ &= T_{pr,A} + T_{pr,B} - V_{col} \end{aligned}$$

$$= \alpha A_s^- f_y + \alpha A_s^- f_y - V_{col} \quad (19.2a)$$

For an external joint, where the joint has beam on only one side of the joint, Eq. (19.2a) is written as

$$V_{u,j} = T_{pr,A} - V_{col} \quad (19.2b)$$

The force T_{pr} is the tension in the reinforcement in the beam at its probable capacity and is given by

$$T_{pr} = \alpha A_s f_y \quad (19.3)$$

The factor α is a stress multiplier; $\alpha \geq 1$ for Type 1 joints, where only limited ductility is required, and $\alpha \geq 1.25$ for Type 2 joints, which require considerable ductility. The value of $\alpha \geq 1.25$ is intended to account for (a) the actual yield stress of a typical reinforcing bar being commonly 10–25 per cent higher than the nominal value and (b) the effect of strain hardening at high strain (ACI 352-02).

Numerous studies have shown the presence of a slab to have a significant effect on the performance of Type 2 connections (e.g., Durrani and Wight 1987; Durrani and Zerbe 1987; Ehsani and Wight 1985a; Wolfram-French and Boroojerdi 1989). Hence, ACI 352-02 recommends including the longitudinal reinforcement in the slab within the effective width in the quantity A_s used to calculate the joint shear force. For now, the effective width may be assumed as given in ACI 318:11 or IS 456:2000 (see also Section 5.7.1 and Table 5.9 of Chapter 5). For corner and exterior connections without transverse beams, the effective width is taken as the beam width plus a distance on each side of the beam equal to the length of the column cross section measured parallel to the beam generating the shear (see also Fig. 3.2 of ACI 352-02).

The nominal shear strength of the joint $\phi V_{n,j}$ should be at least equal to the required strength $V_{u,j}$. Thus we get,

$$\phi V_{n,j} \geq V_{u,j} \quad (19.4a)$$

$$\phi V_{n,j} = \phi \gamma \sqrt{f'_c} A_{ej} \quad (19.4b)$$

Here, A_{ej} is the effective shear area of the joint = $b_j h_j$, b_j is the effective width of the joint, and h_j is the effective depth of the joint, ϕ is the strength reduction factor = 0.85, and γ is the strength coefficient, which is dependent on the configuration and confinement of the joint provided by the beams. The values of this coefficient for Type 2 connections are provided in Fig. 19.3. (The coefficients for Type 1 connections are about 1.2–1.5 times higher; see Table 1 of ACI 352-02.) It has to be noted that Draft IS 13920 does not define different strengths for roof and typical floor levels

but instead specifies using typical values (upper row of Fig. 19.3) for all levels. It has to be noted that the NZS 3101 code suggests a limiting value of $V_{n,j} = 0.2 f'_c A_{ej}$ irrespective of the confinement offered by the framing members. Thus, the NZS criterion is based on the diagonal compression failure of concrete in the joint core and hence is assumed to be proportional to the compressive strength f'_c of concrete, whereas the ACI code criterion is based on the tensile strength of concrete, which is usually expressed as proportional to $\sqrt{f'_c}$.

It is important to consider the effect of high axial load in the column on the nominal shear strength of the joint (Hakuto, et al. 2000). Though it is not considered in the ACI and NZS codes, Eurocode 8 (EN 1998-1:2003) includes this important factor (Uma and Jain 2006). Recently, Kim and LaFave (2008) developed joint shear strength models, using the Bayesian parameter estimation method and experimental observations, which are found to predict joint shear strength more reliably than the models suggested in the ACI and NZS codes.

For connections with beams framing in from two perpendicular directions, the horizontal shear in the joint should be checked independently in each direction. For the joint to be considered as a fully confined interior joint, the beams on the four faces of the joint must cover at least three-quarters of the width and depth of the joint face, where the depth of the joint is taken as the depth of the deepest beam framing into the joint. If a beam covers less than three-quarters of the column face at the joint, it must be ignored in the determination of the coefficient γ that applies as per Fig. 19.3. For lightweight concrete frames, the ACI 318 code suggests that the shear capacity from Eq. (19.4b) be multiplied by 0.75. If Eq. (19.4a) is not satisfied, the size of the column has to be increased.

The area effective in resisting joint shear may not be as large as the entire cross-sectional area of the column since the (web) width of beam, b , and of the column, b_c , may differ from each other. The codes recommend effective joint shear area based on engineering judgment. Concentric and eccentric joints are shown in Fig. 19.14, and a comparison of effective joint width, b_j , as per different codes is given in Table 19.1. ACI 318:2011 suggests that the effective joint width may be taken as the smallest of b_c , $b + 2x$, and $b + h_c$ (see Fig. 19.14 for the definitions of these terms). The effective depth of the joint, h_j , may be taken as the depth of column, h_c , in the considered direction of shear (see Fig. 19.14). In ACI 352:2002, the shear strength of the eccentric beam-column connection is reduced by using a smaller effective width if the eccentricity of the spandrel beam with respect to the column centroid exceeds one-eighth of the column width.

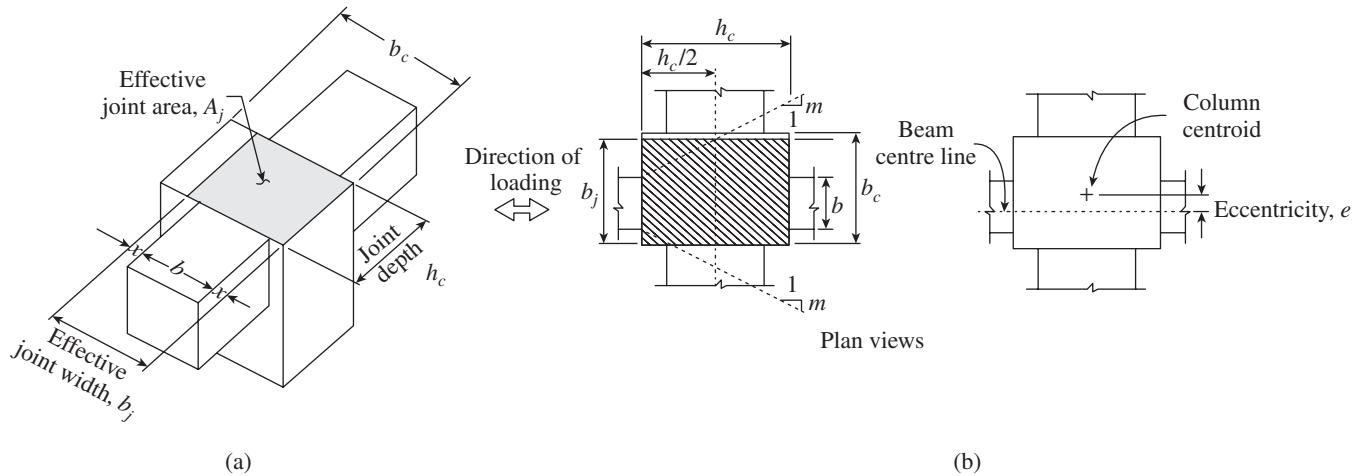


FIG. 19.14 Determination of effective joint width as per ACI 352-02 (a) Concentric joint (b) Eccentric joint (Reprinted with permission from ACI)

TABLE 19.1 Effective width of joint, b_j (see Fig. 19.14)

S. No.	Category	ACI 352 R-02	NZS 3101-06, Draft IS 13920
1.	$b_c > b$	Minimum of [b_c , $(b + \Sigma mh_c/2)^*$, $(b + b_c)/2$]	Minimum of (b_c , $b + 0.5h_c$)
2.	$b > b_c$	b_c	Minimum of (b , $b_c + 0.5h_c$)

Note:

* When the eccentricity between the beam centre line and the column centroid exceeds $b/8$, $m = 0.3$; otherwise, $m = 0.5$. The summation term should be applied on each side of the joint where the edge of the column extends beyond the edge of the beam. The value of $mh_c/2$ should not be taken larger than the extension of the column beyond the edge of the beam.

When beams of different widths frame into opposite sides of the column in the direction of loading, b should be taken as the average of two widths. The average of the beam and column widths usually governs the effective joint shear width, b_j , as per ACI 352-02, for RC beam-column connections without joint eccentricity.

Eccentrically connected beams were found to be the cause of the collapse of a four-storey school building at Hakodate University, Japan, during the 1968 Tokachi-oki earthquake and several damages to beam-column joints were reported during the 1995 Hyogo-ken Nanbu earthquake in Japan. However, based on experimental research, LaFave, et al. (2005) and Canbolat and Wight (2008) determined that the floor slabs significantly reduced the influence of spandrel beam eccentricity on the behaviour of the connection region under lateral loading. Hence, they argue that the effective joint width suggested in codes is conservative and proposed the following effective width:

$$b_{j, \text{proposed}} = \frac{b + b_c}{2} \quad (19.5)$$

After determining the design horizontal shear, V_{jh} , the vertical shear, V_{jv} , can be approximated as follows when the columns do not form plastic hinges (Uma and Meher Prasad 2005):

$$V_{jv} = V_{jh} \left(\frac{h_b}{h_c} \right) \quad (19.6)$$

where h_b and h_c are the heights of beam and column, respectively.

Design of Shear Reinforcement

The role of transverse reinforcement and the mechanism of shear transfer in a beam-column joint for seismic resistance are much debated and two schools of thoughts prevail. Currently, there is little consensus within the design and research communities as to whether joint hoops serve to confine the core concrete or to carry joint shear directly. Paulay, et al. (1978) proposed shear transfer mechanisms of a joint as shown in Fig. 19.15, referred to as *diagonal strut mechanism* and *truss mechanism*. They assumed that the strength of the diagonal strut controls the joint strength before cracking. When the joint shear becomes large, diagonal cracking occurs in the joint core and the joint reinforcements come into play; finally, the joint fails by the crushing of the concrete in the joint core. Both mechanisms are incorporated in the NZS 3101 code. Thus, NZS 3101 requires a large amount of transverse reinforcement in a joint to resist a dominant part of the joint shear by the truss mechanism, relying on the good bond stress transfer along the longitudinal reinforcement. The use of larger-diameter and higher-strength bars for beam flexural reinforcement is limited in NZS 3101 to reduce the bar slippage within the joint (Kitayama, et al. 1991).

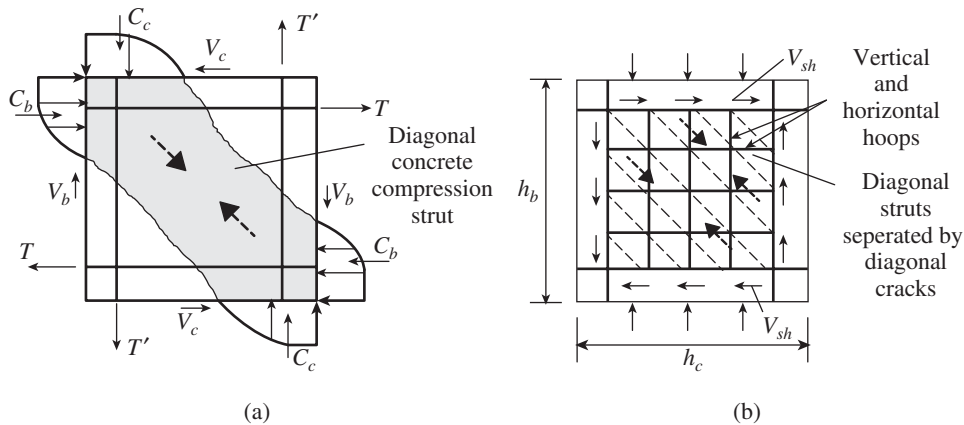


FIG. 19.15 Joint shear resistance mechanisms (a) Concrete strut mechanism (b) Concrete truss mechanism

The US codes (ACI 318 as well as ACI 352) assume severe bond deterioration of the reinforcing bars in the joint and hence the internal shear forces are resisted only by the diagonal compressive strut of concrete. Thus, the role of transverse reinforcement is only to confine the core concrete. These conflicting concepts about the function of transverse reinforcement lead to different demands for hoop bars as well as disparity in detailing criteria (Hwang, et al. 2005). The real behaviour of the structure may be due to the combination of the diagonal strut and the truss mechanisms with the bond deterioration of longitudinal reinforcement to a certain degree during cyclic loading.

Joints Confined by Beams

The behaviour of a beam-column joint is influenced by several variables, which include concrete strength, arrangement of joint reinforcement, size and quantity of beam or column reinforcement, bond between concrete and longitudinal bars in the beam or column, and axial load in the column. As per ACI 352-02, for Type 1 joints the hoop reinforcement can be omitted when the joints are confined by beams framing into the sides of the column. Such confinement may be assumed under the following circumstances:

1. When beams frame into all four sides of the joint and each beam width is at least three-quarters of the column width, leaving no more than 100mm of the column width uncovered on either side of the beam
2. When beams frame into two opposite sides of a joint, and each beam width is at least three-quarters of the column width, leaving no more than 100mm of the column width uncovered on either side of the beam. In this case, however, horizontal transverse reinforcement should be provided in the perpendicular direction.

When such confining beams are not present, ACI 352-02 recommends that at least two layers of transverse reinforcement

be provided for Type 1 joints, between the top and bottom levels of longitudinal reinforcement, in the deepest beam framing into the joint. The primary functions of ties in a tied column are to restrain the outward buckling of the column longitudinal bars, to improve bond capacity of column bars, and to provide some confinement to the joint core.

Confinement Reinforcement

Confinement of the joint core is intended to maintain the integrity of joint concrete, to improve joint

concrete toughness, and to reduce the rate of stiffness and strength deterioration (ACI 352-02). Currently, the US as well as the Indian (Draft IS 13920) code provisions emphasize the importance of the confinement of joint core. The required area of confinement reinforcement in the joint, when spiral reinforcement is used, as per ACI 352 is given by Eqs (13.24a) and (13.25a) of Chapter 13. The Draft IS 13920 provisions are similar and are given by Eqs (13.24b) and (13.25b) of Chapter 13. When rectangular hoops are used, the ACI provisions are as per Eq. (13.26) of Chapter 13 and the Draft IS 13920 provisions are as per Eq. (13.27) of Chapter 13. It has to be noted that both the codes suggest the column confinement steel to be continued into the joint as well. For Type 2 joints, when the joint is confined by beams, transverse reinforcement equal to at least half the confining reinforcement required at the end of the column should be provided within the depth of the shallowest framing member. The spacing of the hoops should not exceed 150 mm (see Clause 8.1 of IS 13920) in seismic joints. Hwang, et al. (2005) experimentally found that the ACI requirement of providing hoops to confine the joint is unnecessary and difficult to construct. Their tests indicated that hoop reinforcement with wider vertical spacing of up to 300 mm could be used without significantly affecting the joint performance. They also developed a softened strut-and-tie (SST) model to design the hoops.

Spacing requirement for horizontal and vertical transverse reinforcement as per ACI and NZS codes are compared in Table 19.2 (see Fig. 13.31 of Chapter 13 for the definition of the terms used). The ties within the joint should be provided as closed hoops with the ends bent as 135° hooks. For single-leg cross-tie most of the codes suggest a 135° bend at both ends, though ACI recommends alternate placement of 90° hooks on opposite faces of the column for easy constructability. A comprehensive comparison of the provisions of ACI, NZS, and Eurocode 8 codes on

TABLE 19.2 Spacing requirement for horizontal and vertical transverse reinforcement

Code	Vertical Spacing for Horizontal Stirrups	Horizontal Spacing for Vertical Stirrups
ACI 318 and ACI 352	Minimum of ($h_1/4$, $6d_b$, s_o)	Not more than 350 mm
NZS 3101	Minimum of ($10d_b$, 200 mm)	Minimum of ($h_1/4$, 200 mm)

Notes:

- All dimensions are in mm; $S_o = 100 + \left(\frac{350 - h_x}{3}\right)$ where $100 < s_o < 150$.
- Provisions in IS 13920 are the same as in ACI except s_o ; it is 75–100 mm.

beam-column joints is provided by Uma and Jain (2006) and Joshi (2001).

When wide beams are used, confining reinforcement should be provided through the joint to provide confinement for longitudinal beam reinforcement outside the column core if such confinement is not provided by a beam framing into the joint. In the exterior and corner joints, all the 135° hooks of the cross-ties should be along the outer face of the column (see Clauses 8.1.4 and 8.1.5 of IS 13920).

For best behaviour of the joint, the longitudinal column bars should be uniformly distributed around the perimeter of the column core. Au, et al. (2005), Lu, et al. (2012), and Bindhu, et al. (2009), based on their experimental results, found that additional diagonal bars along the column or beam within the joint region result in additional strength and ductility of the beam-column joint.

19.2.7 Anchorage of Bars at Joints

In interior joints, the flexural reinforcement in the beam entering one face of the joint is usually continued through the joint to become the flexural steel for the beam entering the opposite side. However, in exterior or corner joints, one or more beams do not continue beyond the joint, and hence it is difficult to anchor the beam bars within the column width. For Type 1 joints, the critical section for development of yield strength of the beam bars may be taken at the face of the column. However, during seismic loading, moment reversals take place at the beam-column connections; these reversals cause stress reversals in the beams, column, and slab longitudinal reinforcement at the connection. Due to such stress reversals,

splitting cracks develop along the outer column cover, subsequently separating the cover concrete from the column core (Paulay and Priestley 1992). Hence, ACI 352-02 suggests that the critical section for development be taken at the face of the confined column core. However, Paulay and Priestly (1992) state that this assumption is satisfactory only in elastic joints, where yielding of beam bars at the face of the column is not expected.

When plastic hinge develops in the beams adjacent to the joint, the top bars of beams may go into the strain hardening range and yielding may penetrate into the joint core with simultaneous bond deterioration (Paulay and Priestley 1992). A splitting crack may appear along the bar as shown in Fig. 19.16(a) and the bond stress distribution around the bar will not be uniform.

Column dimensions seldom permit providing the development length by straight embedment alone; hence, hooks are often required to anchor negative (top) beam

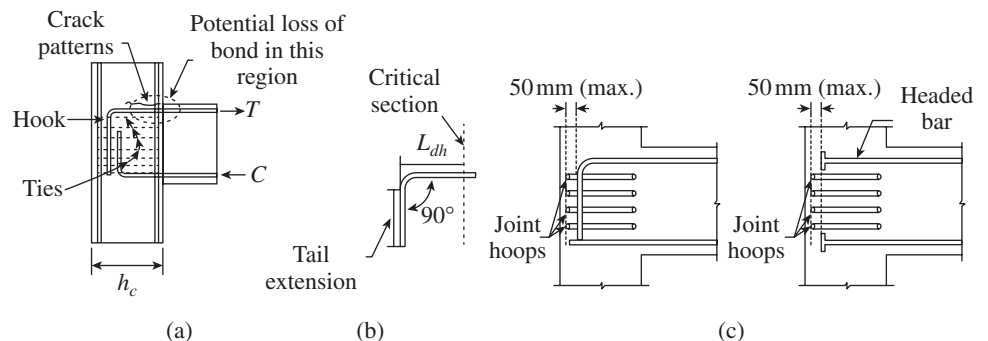


FIG. 19.16 Anchoring of beam bars in exterior joints (a) Anchorage details (b) Hook details (c) Location of hoops and headed bars (Reprinted with permission from ACI)

reinforcement at the far side of exterior beam-column joints. In general, 90° hooks are used, with the hook projecting downwards and extending beyond the mid-depth of the joint, so that joint diagonal compression strut, as shown in Fig. 19.15, can be developed. If the bottom bars are also required to develop their strength at the face of the joint, they should also be provided with 90° hooks, which should be turned upwards and extended towards the mid-depth of the joint (Hakuto, et al. 2000). Hooks should be located within 50 mm of the confined core, as shown in Fig. 19.16(c) (column bars not shown for clarity). If the beam has more than one layer of flexural reinforcement, the tails of subsequent layers of bars should be located within $3d_b$ of the adjacent tail.

A comparison of the different code provisions for hooks is provided in Table 19.3 (some more discussions are provided in Section 7.6 of Chapter 7). The development length equation in ACI and NZS codes consider the beneficial effect of anchoring the bar in the well-confined joint core and also the adverse effect of the bar being subjected to load reversals during earthquake.

TABLE 19.3 Comparison of code provisions for hooks (see also Fig. 19.16)

Code	Critical Section from the Face of the Column	Tail Extension	Development Length, L_{dh}
ACI 318:2011	At the face of the column	$12d_b$	$\frac{f_y d_b}{4.83\sqrt{f_{ck}}} \geq 8d_b$ or 150 mm
ACI 352:2002	Type 1: at the face of the column Type 2: outside edge of the column core (50 mm from the face of the column)	$12d_b$	Type 1: $\frac{f_y d_b}{3.75\sqrt{f_{ck}}}$ Type 2: $\frac{\alpha f_y d_b}{5.55\sqrt{f_{ck}}}$ $\geq 8d_b$ or 150 mm; $\alpha = 1.25$
NZS 3101:2006 ¹	Minimum of ($h_c/2$, $8d_b$)	$12d_b$	$\frac{f_y d_b}{3.73\sqrt{f_{ck}}} \geq 8d_b$
Draft IS 13920 ²	At the face of the column (but a total length of $L_d + 10d_b$ has to be provided, as shown in Fig. 7.45 of Chapter 7)	$>4d_b$	$L_d = \frac{0.136 f_y d_b}{\tau_{bd}}$ $= \frac{f_y d_b}{1.177(f_{ck})^{2/3}}$

Notes:

¹ L_{dh} is the horizontal development length; as per the NZS code, L_{dh} can be reduced based on the diameter of bar, cover, and confinement. For example, ACI 352 suggests that the L_{dh} as given by the aforementioned equations could be multiplied by 0.8 if transverse joint reinforcement is provided at a spacing less than or equal to $3d_b$.

² In IS 13920 and IS 456, τ_{bd} is taken as per Table 7.1 of Chapter 7. The development length L_d as per the Indian code includes the anchorage value of hooks and tail extension in tension (see also Section 7.6.1 of Chapter 7).

Use of Headed Reinforcement

The use of hooks in external beam-column joints often results in steel congestion, difficult fabrication and construction, and greater potential for poor concrete placement. Moreover, cyclic loading tends to degrade the anchorage capacity due to slip. Anchor plates or heads, either welded or threaded to the longitudinal bar, can be used as an alternative to the use of hooked bars in exterior beam-column joints (Wallace, et al. 1998; Chun, et al. 2007). The use of headed bars offers a potential solution to the problems posed by hooked bars and may ease fabrication, construction, and concrete placement. On the basis of the works of Bashandy (1996), Wallace, et al. (1998), and Wright and McCabe (1997), ACI 352:2002 was revised to allow the use of headed bars with a development length L_{dh} equal to 75 per cent of the development length of a standard 90° hooked bar (see also Section 7.6.2 of Chapter 7). The head of the bar should be located within 50 mm from the back of the confined core, as per ACI 352:2002, and as shown in Fig. 19.16(c).

When the side cover at the free face of the joint is less than $3d_b$, ACI 352:2002 suggests that each head should be transversely restrained by a stirrup that is anchored in the joint. As Type 2 connections may experience significant inelastic deformations, the hoop leg should be designed for 50 per cent of the yield strength of the bar being developed. In Type 1 joints, it can be designed for 25 per cent of the yield strength of the bar being developed. If the side cover is greater than $3d_b$, the restraining force should be determined using the *concrete capacity design (CCD) approach* (see Section 19.5.2). However, minimum transverse reinforcement should always be provided.

Head size with a net area of three to four times the bar area was found to be sufficient to effectively anchor the beam reinforcement (Chun, et al. 2007). A new model that accounts for head bearing and bond capacity of the anchored bars was proposed by Chun, et al. (2009). Various strut-and-tie models have also been proposed to consider material strength and also the structural configuration of the system (Hong, et al. 2007; Thompson, et al. 2002).

Beam and Column Bars Passing through Interior Joint

The uneven distribution of bond stress around a bar may affect the top beam bars, the underside of which may be embedded in inferior quality concrete, due to sedimentation. The following factors influence the bond response of bars at the beam-column joint (Paulay and Priestley 1992):

1. Confinement, transverse to the direction of the embedded bar, significantly improves bond performance under seismic conditions.
2. The bar diameter, d_b , has a significant effect on the bond strength in terms of bond stress.
3. The bar deformations (i.e., the area of ribs of deformed bars) improve resistance against slip and increase the bond strength.
4. The clear distance between the bars moderately affects the bond strength.
5. The compression strength of concrete is not a significant parameter.

Experimental research has revealed that a displacement ductility factor of at least $\mu_\Delta = 6$ or inter-storey drift of at least 2.5 per cent can be achieved if the ratio of the largest bar diameter in the beam, d_b , to the column depth, h_c , at an interior joint was limited to the following (Paulay, et al. 1978):

$$\frac{d_b}{h_c} f_y \leq 11 \text{ to } 17 \quad (19.7a)$$

Paulay and Priestley (1992) also recommend that the average design bond stress should be around $1.2\sqrt{f_{ck}}$. Considering several factors that affect the top bar behaviour and assuming that the bar stress in compression does not exceed f_y , Paulay and Priestley (1992) modified the basic limitation of d_b/h_c as

$$\frac{d_b}{h_c} \leq k_j k_{ji} \frac{\sqrt{f_{ck}}}{f_y} \quad (19.8)$$

where k_{ji} is a product of several factors discussed earlier. Clause 10.4.6.6 of NZS 3101:2006 code approximates the product $k_j k_{ji}$ in the range 2.86–3.6.

The purpose of the recommended value of h/d_b is to limit the slippage of beam and column bars through the joint. ACI 352:2002 has the following limitation for Type 2 joints:

$$\frac{h_c}{d_b \text{ (beam bars)}} \geq 20 \frac{f_y}{415} \geq 20 \quad (19.9a)$$

No limitation is provided in ACI 352:2002 for Type 1 joints. Interestingly, ACI 352:2002 has a limitation for the height of beams as

$$\frac{h_b}{d_b \text{ (column bars)}} \geq 20 \frac{f_y}{415} \geq 20 \quad (19.9b)$$

Clause 7.1.2 of Draft IS 13920 stipulates the following:

$$\frac{h_c}{d_b \text{ (beam bars)}} \geq 15; h_c \geq 300 \text{ mm} \quad (19.9c)$$

It is important to note that this length (h_c) is not sufficient to fully anchor the bars in tension, but it delays the deterioration of bond between the bars and concrete in the joint. ACI 352:2002 states that bar slippage is likely to occur with the $20d_b$ dimension of interior column, which will considerably reduce the stiffness and energy dissipation capacity of the connection zone (as per ACI 352, a column size of $32d_b$ would be necessary to substantially reduce the slip). Larger development lengths are highly desirable, especially when the joint is subjected to high shear stresses and when the column-to-beam flexural strength ratio is low (ACI 352:2002; Leon 1991; Jirsa 1991; Zhu and Jirsa 1983). Tests on half-scale specimens have shown that anchorage lengths of 24–28 times the bar diameter performed better than those of 16–20 times the bar diameter. As a result of the smaller size of columns currently being used in India, compared to those used in the USA and New Zealand, an h/d_b limitation of 15 was chosen in IS 13920 (Jain, et al. 2006).

Larger beam-to-column flexural strength ratios considerably improve the behaviour of connections; in order to avoid the formation of plastic hinges in joints, the flexural strength

ratio should not be less than 1.4 (Ehsani and Wight 1985b). It has to be noted that the NZS 3101 code stipulates a beam-to-column flexural strength ratio of 1.4, whereas ACI 318 and IS 13920 stipulate ratios of 1.2 and 1.1, respectively.

19.2.8 Constructability Issues

Detailing beam-column joints is an art requiring careful attention to several code requirements as well as construction requirements. Many builders omit ties in beam-column joints as they may require some extra effort. Murty (2005) suggests a three-stage procedure for installing the horizontal ties in a beam-column joint as shown in Fig. 19.17.

In stage 1, as shown in Fig. 19.17(a), top bars of the beam are not placed and horizontal ties in the joint region are stacked up. In stage 2, top bars of the beam are inserted in the beam stirrups, and beam reinforcement cage is lowered into the formwork. In stage 3, ties in the joint region are raised in their final locations and tied with binding wires, and column ties are continued. Er Rangarajan of Coimbatore suggests a two-step scheme. In the first step, beams are placed in the usual way, except that the top bars near the column are stopped at a minimum distance of $3d$ from the face of the column (so that lapping is avoided in the plastic hinge zones) for the column ties to be placed and tied easily. In the next step, the required top bars of the beam are added and tied to the existing top bars.

As already discussed in Section 4.4.8 and Fig. 4.12 of Chapter 4, beams should be made at least 100 mm narrower than columns to facilitate easy passing of beam bars within the core of the column, without bending of the beam bars. Multiple layers of longitudinal reinforcement should be avoided wherever possible, as they make the placement difficult, especially in exterior beam-column joints. In this case, as well as in cases where shallow columns are joined with relatively deep beams, the beam bars may be terminated

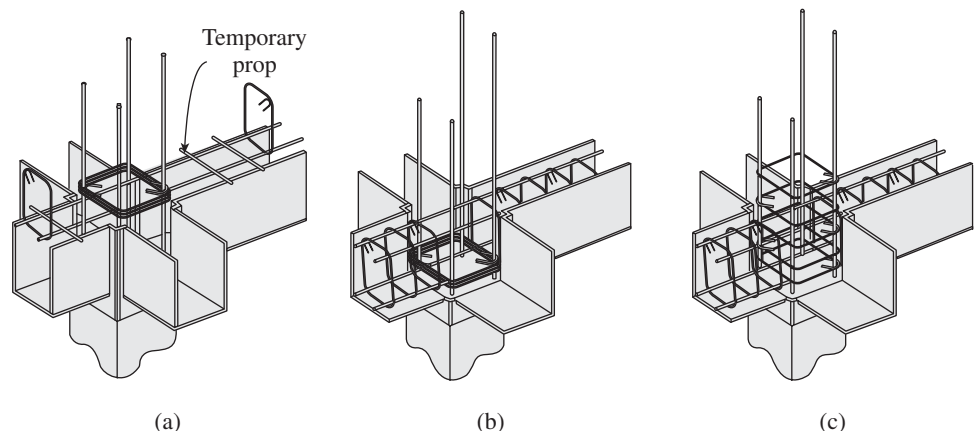


FIG. 19.17 Three stages of providing horizontal ties in beam-column joints (a) Stage 1 (b) Stage 2 (c) Stage 3

Source: Murty 2005, NICEE, IIT Kanpur

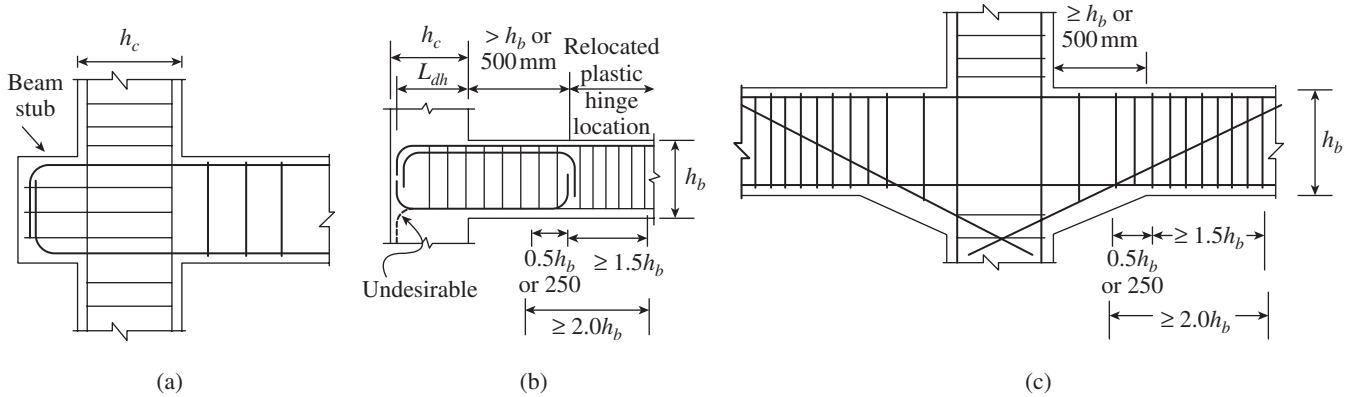


FIG. 19.18 Measures to improve constructability

in an extended beam stub as shown in Fig. 19.18(a). In this case, ties should be extended into the beam stub to control cracks (Park and Paulay 1975). Such a detailing has been adopted in Christchurch, New Zealand (Park and Paulay 1975). Architects may, however, object to this solution on aesthetic grounds.

To avoid unfavourable plastic hinge mechanism and to reduce congestion at beam-column joints, the beam plastic hinge region can be moved slightly away from the face of the beam-column joint. This will eliminate the bond deterioration between the beam bars and the surrounding concrete in the beam-column joint. Moving the beam plastic hinge region can be achieved by detailing the beam as shown in Figs 19.18(b) and (c). NZS 3101:2006 suggests that the critical section should be located at a distance equal to at least the beam depth, h_b , or 500 mm away from the column face. This section may be located by abruptly terminating the flexural reinforcement by bending it into the beam, by bending a significant part of the flexural reinforcement diagonally across the web, or by providing a haunch (see Figs 19.18b and c). It is possible that under reversed loading yielding can encroach into the zone between the critical section and the column face. Hence, transverse reinforcement must be provided at closer spacing of at least $0.5h_b$ or 250 mm before that section and extended over a distance of $2h_b$ to a point $1.5h_b$ past the critical section into the span (NZS 3101:2006). Detailing of such regions should be done carefully.

19.3 BEAM-TO-BEAM JOINTS

In RC construction, secondary beams are often supported by primary beams/girders. Many designers often assume that the reaction from the supported beam is uniformly distributed through

the depth of the interface between the beam and girder. This assumption may be due to the Indian (as well as ACI) code approach in shear design where the shear strength is considered as the summation of concrete and steel strengths ($V_c + V_s$) and the concrete strength is determined assuming a uniform distribution of shear stress through the web of the beam of $\tau_c = V_c/b_w d$. However, tests conducted on actual beam-to-beam joints show a different behaviour, which can be represented in a simplified form by a truss model, as discussed here.

On the basis of extensive experimental studies conducted at the University of Stuttgart on the behaviour of such joints, Leonhardt and Mönning (1977) suggested strut-and-tie models for the flow of forces of such interconnected systems as shown in Fig. 19.19 (Rausch 1972).

The strut-and-tie models of Fig. 19.19 indicate tensile stresses at the beam-to-beam junction, and hence additional vertical stirrups are to be provided to support them. Such stirrups are also referred to as *hanger reinforcement* or *hanger stirrups*. The main reaction from the secondary beam to the girder was found to be delivered by a diagonal compression strut, as shown in Fig. 19.20, which tends to

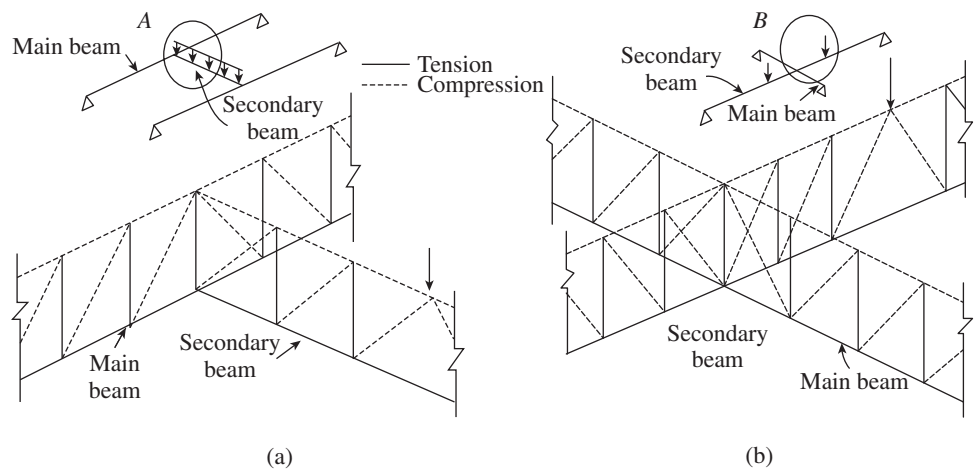


FIG. 19.19 Strut-and-tie model for beam-to-beam joints (a) System A (b) System B

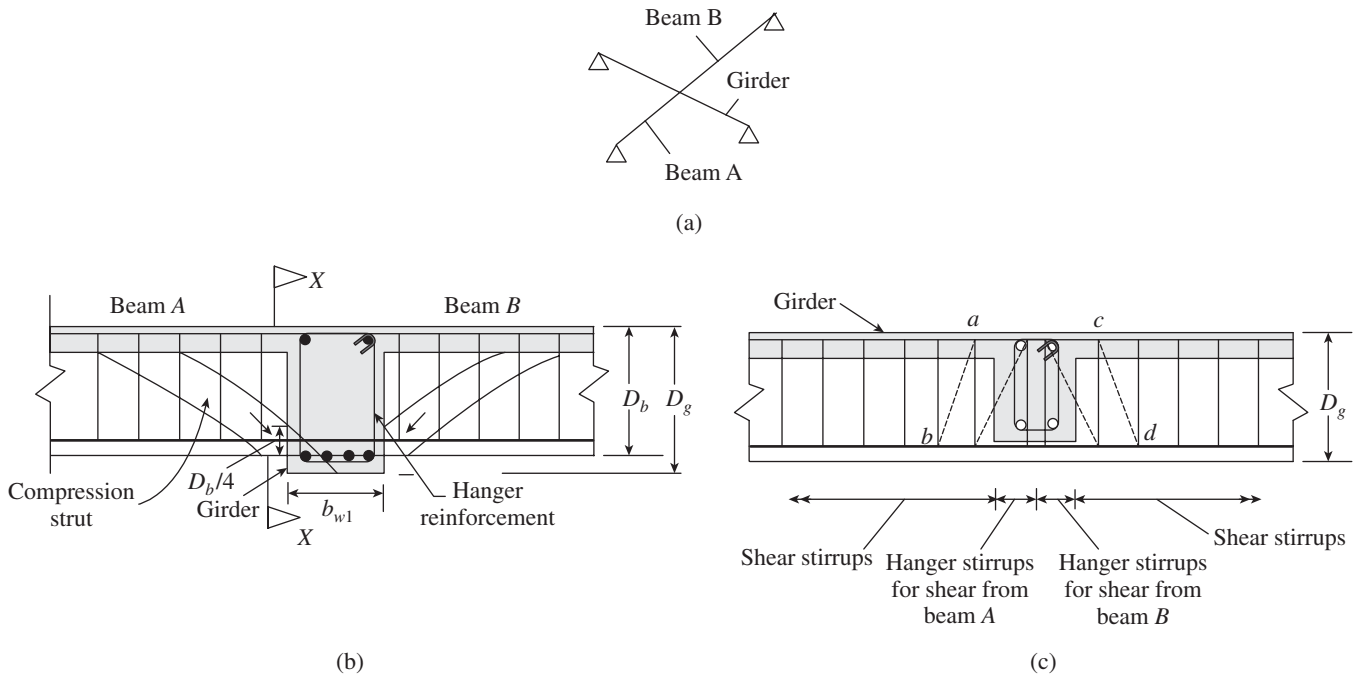


FIG. 19.20 Girder supporting secondary beams (a) System of beams (b) Section through secondary beam (c) Section X-X through the girder

apply its thrust near the bottom of the supporting girder. This inclined compressive force will tend to push the bottom of the supporting girder/main beam, eventually splitting the concrete at the bottom of the girder and resulting in the subsequent failure of the girder. These compressive forces should be resisted by providing hanger stirrups, which are designed to equilibrate the downward component of the diagonal compression struts (see Fig. 19.20a). It has to be noted that the hanger stirrups are to be provided in addition to the normal girder stirrups required for shear, as shown in Fig. 19.20.

The transfer of beam reaction into the girder may be visualized using the strut-and-tie model, as shown in Fig. 19.20(c). Thus, the compression struts ab and cd (shown as dotted lines in the figure) complete the shear transfer into the girder. If the depths of the girder and secondary beams are similar, the hangers should be designed to resist the full reaction. However, if the depth of the secondary beam is much smaller than that of the girder, it may not be necessary to provide hanger stirrups. Leonhardt and Mönnig (1977) and Mattock and Shen (1992) suggest that the hanger stirrups must be designed to resist a downward force of V_s^* , where

$$V_s^* = \frac{D_b}{D_g} V_{ur} \quad (19.10)$$

Here, D_b is the overall depth of secondary beam, D_g is the overall depth of the supporting girder, and V_{ur} is the factored applied reaction from the secondary beam. Bauman and Rüschi (1970) recommend that the hanger stirrups be designed for

the entire shear force V_{ur} without any reduction as suggested by Leonhardt and Mönnig (1977). It has to be noted that the difference in the cost of the hangers designed by the two approaches is not significant. Equating the tensile capacity of hanger stirrups, we have

$$A_h(0.87f_{yh}) = \frac{D_b}{D_g} V_{ur} \quad (19.11)$$

where A_h is the area of hanger stirrups adjacent to one face of the supporting beam and f_{yh} is the yield strength of hanger stirrups. If shears are transferred to both side faces of the supporting girder, Eq. (19.11) should be evaluated separately for each face.

According to the Canadian code CSA A23.3-04, the hanger stirrups are to be placed in the supporting girder to intercept 45° planes starting on the shear interface at one-quarter of the depth of the supported beam, D_b , above its bottom face and spreading down into the supporting girder, as shown in Fig. 19.21(a). The distribution of hanger stirrups according to Leonhardt and Mönnig (1977) and as suggested in Eurocode is shown in Fig. 19.21(b); it should be distributed within a zone extending to a distance of half the depth of the relevant beam on each side of the point of intersection of the beam axes. This zone is referred to as the *transition* or *transfer zone* (see Fig. 19.21).

The hanger stirrups should be well anchored at the top and the bottom. When the beam and girder are of the same depth, the lower layer of reinforcement in the supported beam can be cranked up at the junction, so that it is above the lower layer of reinforcement of the supporting girder.

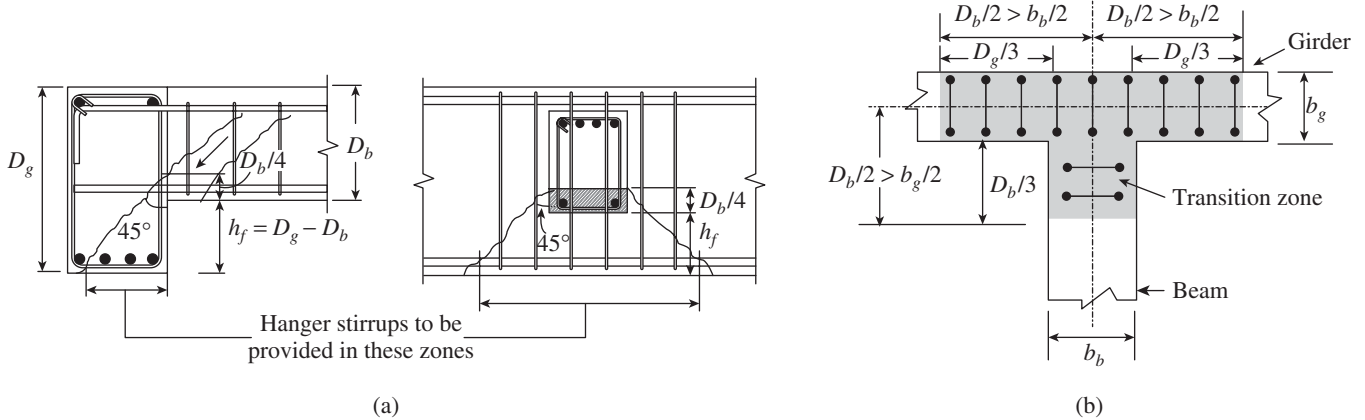


FIG. 19.21 Location of hanger stirrups (a) As per Canadian code (b) As per Leonhardt and Mönning (1977) and Euro code

Hanger stirrups may not be necessary when the factored reaction, V_{ur} , is less than about $0.22\sqrt{f_{ck}}b_bD_b$, since diagonal cracks will not form at this shear in the supporting girder. In this case, the prediction of truss model will not be valid.

When the reaction due to the secondary beam is large, SP 34-1987 suggests using bent-up bars in addition to hanger stirrups as shown in Fig. 19.22. Such reinforcement helps reduce cracking and should be placed within the transition zone.

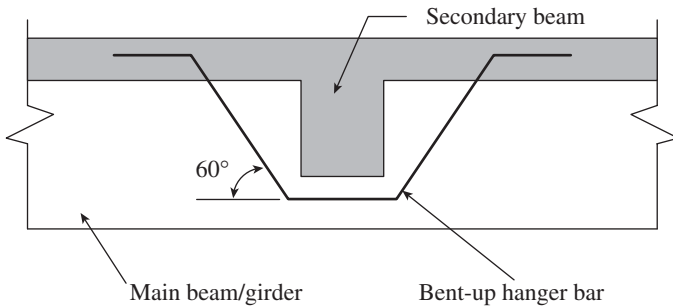


FIG. 19.22 Bent-up hanger bars

19.4 DESIGN OF CORBELS

Corbels or brackets are short stub-like projections from the column or wall faces (see Fig. 19.23). The term corbel is generally used to denote cantilevers having shear span to effective depth ratios, a_v/d , less than or equal to 1.0 (Clause 28.1a of IS 456). They are generally found in the columns of industrial buildings to support gantry girders, which, in turn, support rails over which overhead cranes are mounted. They are extensively used in precast concrete construction to provide seating for beams; in such cases, corbels are cast integrally with precast columns. Usually, the width of the corbel is restricted to the width of

the columns. The principal function of corbels is to support the prefabricated beam and at the same time transmit the reactions to vertical structural members such as walls or columns. Corbels are designed to resist the ultimate shear force V_u applied to them by the beam and the ultimate horizontal reaction N_u due to shrinkage, creep, or temperature changes.

Corbels are usually provided with a steel-bearing plate or an angle on its top surface, as shown in Fig. 19.23a, to distribute the reaction evenly and to have uniform contact surface. A similar bearing plate or angle will be provided in the lower part of the supported beam. Sometimes, these two plates are welded together; in such situations, it is important to consider horizontal forces in the design of corbel. Elastomeric or Teflon-bearing pads are sometimes provided between the corbel and the supported beam; however, even in this case, frictional forces may develop due to volumetric changes in the concrete. Clause 28 of IS 456 covers the design of corbels.

The principal failure modes for corbels are as follows (Kriz and Rath 1965; Mattock, et al. 1976):

1. Flexural tension failure is the most common mode and results in the crushing of the concrete at the bottom of the sloping face of the corbel after extensive yielding of the tension reinforcement.

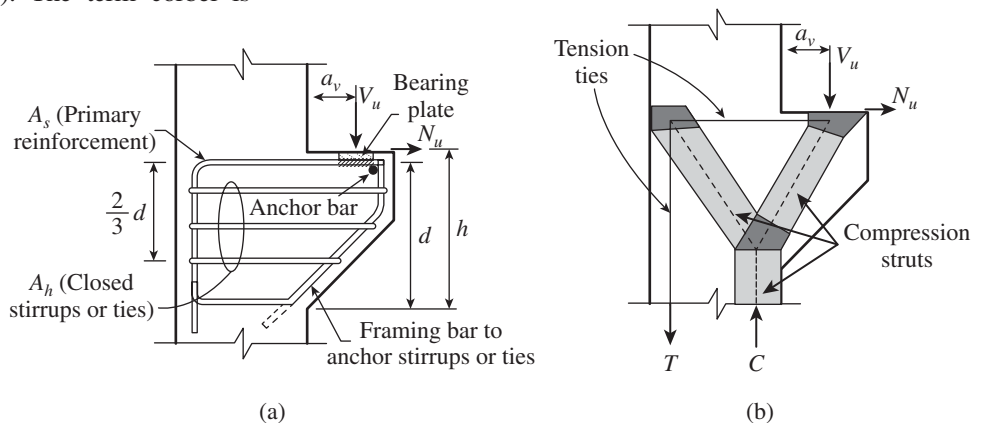


FIG. 19.23 Typical corbel (a) Reinforcement details (b) Strut-and-tie model (Reprinted with permission from ACI)

2. Flexural compression failure results in the crushing of the concrete strut at the base of the corbel before the yielding of the reinforcement.
3. Diagonal splitting failure leads to sudden splitting along the line from the bearing plate to the base of the corbel.
4. Shearing failure results in a series of short inclined cracks along the weakened plane. Another possibility is the failure in direct shear along a plane more or less flush with the vertical face of the column.
5. If the reinforcement is not detailed properly, shearing of a portion outside the reinforcing bars takes place.
6. If the corbel depth is too shallow, the diagonal cracks may intersect the sloping surface of the corbel.

Direct tension failure is also possible when the horizontal force N_u is abnormally large. Some of these failure modes are shown in Fig. 19.24. In corbels with proper detailing, all these failure modes tend to converge into a single failure mode called the *beam-shear failure* (Russo, et al. 2006). This failure mode is characterized by the opening of one or more diagonal cracks followed by shear failure in the compression strut. To avoid the failure mode shown in Fig. 19.24(d), both IS 456 (Clause 28.1b) and ACI 318 (Clause 11.8.2) require

that the depth measured at the outside edge of the contact area of the supported load must be at least one-half of the depth at the face of the column.

The behaviour of a corbel may be visualized using the strut-and-tie model shown in Fig. 19.23(b). The downward reaction V_u is resisted by the vertical component of the diagonal compression strut, which carries the load down into the column. The horizontal load N_u is directly resisted by the tension in the bars kept at the top of the corbel; these bars also resist the outward thrust at the top of the concrete strut. At the other end of the corbel, the tension in the ties is kept in equilibrium by the horizontal component of the second compression strut. The vertical component of the thrust in the strut acts as a tensile force acting downwards into the supporting column. The required reinforcement to resist the forces as per the strut-and-tie model is shown in Fig. 19.23(a).

For the corbel shown in Fig. 19.25(a), the stress in the reinforcement at ultimate loads will be approximately f_y from the face of support to the load point. Hence, it is important to anchor the main bars A_s as they have to develop their full yield strength f_y at the loaded end. Hence, it is suggested in Clause 28.2.2 of IS 456 to anchor the reinforcement by the following:

1. Welding the primary tension reinforcement to the underside of the bearing plate or angle, especially when corbels are designed to resist horizontal forces, or welding to a transverse bar of equal diameter, in which case the bearing area should stop short of the face of the support by a distance equal to the cover of the reinforcement (the welding details as per ACI 318 are shown in Fig. 19.25b)

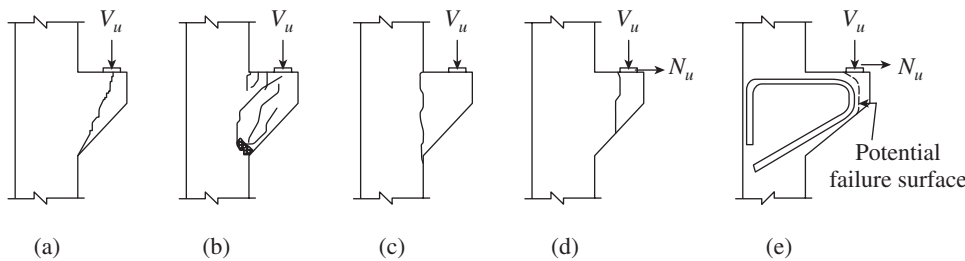


FIG. 19.24 Failure modes of corbel (a) Diagonal splitting failure (b) Shear failure (c) Direct shear failure (d) Vertical splitting (too shallow outer face) (e) Shearing of a portion outside the reinforcement

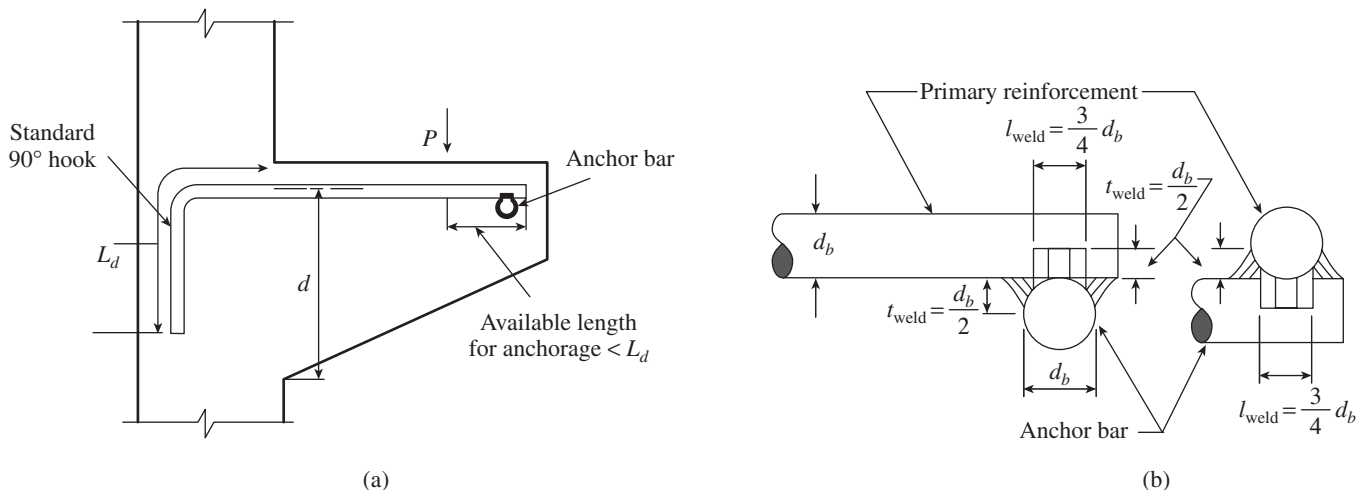


FIG. 19.25 Anchorage of main reinforcement in corbels (a) Required anchorage (b) Details of welding main bar to anchor bar (Reprinted with permission from ACI)

2. Bending back the bars to form a loop, in which case, the bearing area of the load should not project beyond the straight portion of the bars forming the main tension reinforcement

It has to be noted that an end hook in the vertical plane, with the minimum diameter bend, is not totally effective, because an essentially plain concrete corner will exist near the loads applied close to the corner and will result in failure due to shearing of the edge portion (see Fig. 19.24e). U-shaped bars in a horizontal plane provide effective end hooks for wide brackets (perpendicular to the plane of the figure) and when loads are not applied close to the edge. However, bending in two directions may be a little difficult. It is also important to provide a 90° hook for anchorage at the other side of corbel as shown in Fig. 19.25(a).

The closed stirrups with area A_h (see Fig. 19.23a) must be provided to confine the concrete in the two compression struts and to prevent the splitting in the direction parallel to the thrust. The framing bars may be of the same diameter as the stirrups and mainly serve to improve the stirrup anchorage.

The corbel may also be considered as a very short cantilevered beam, with flexural tension at the column face resisted by the top bars A_s . The strut-and-tie model and the aforementioned method are found to give the same area of reinforcement.

Design of Corbels

As IS 456 does not give any design method for corbels, the methods given in ACI 318 are described here. Clause 11.8.1 of ACI 318 requires that brackets and corbels with a shear span-to-depth ratio a_v/d between one and two are to be designed using the strut-and-tie model. Corbels having a_v/d ratio between zero and one may be designed using the strut-and-tie model or by the method described in Section 11.8 of Chapter 11, which is partly based on the strut-and-tie method and partly on the shear friction. This latter method was developed mainly based on the results of tests done on corbels (Kriz and Rath 1965; Mattock, et al. 1976). This procedure is limited to a_v/d ratios less than 1.0 due to the non-availability of test data on larger corbels. The usual design basis is employed; that is, $M_n \geq M_u$ and $V_n \geq V_u$ (the ACI code considers a strength reduction factor of 0.75 while calculating the nominal strengths, including flexure, direct tension, and shear).

The section of corbel at the face of the supporting column must simultaneously resist the following: the shear V_u , the bending moment M_u [$= V_u a_v + N_u(h - d)$], and the horizontal tension N_u , where V_u and N_u are the vertical and horizontal loads acting on the corbel, a_v is the distance from the load to the face of the column, d is the depth of the corbel below the tie, and h is the total depth of corbel (see Fig. 19.23a). Clause 11.8.3.4 of ACI 318 stipulates that the factored tensile

force, N_u , should not be taken less than $0.2V_u$ and this tensile load should be regarded as a live load, even if tension results from the restraint of creep, shrinkage, or temperature change. The factored horizontal tensile force, N_u , should not be greater than V_u , because this method of design has been validated experimentally only for such a condition.

The reinforcement to resist the moment, M_u , can be determined by the usual methods of flexure design. Thus, from Eqs (5.16) and (5.18b) of Chapter 5, we have

$$A_f = \frac{M_u}{\phi f_y (d - 0.5a)}, \text{ where } a = \frac{A_f f_y}{0.85 f'_c b} = \frac{A_f f_y}{0.68 f_{ck} b} \quad (19.12)$$

An additional area of reinforcement, A_n , is required to resist the factored tensile force N_u .

$$A_n = \frac{N_u}{\phi f_y} \quad (19.13)$$

Thus, the total required area of steel, A_s , at the top of the corbel to resist flexure and tension is

$$A_s \geq A_f + A_n \quad (19.14)$$

The design for shear reinforcement is based on shear–friction method, and the shear–friction reinforcement is given by

$$A_{vf} = \frac{V_u}{\phi \mu f_y} \quad (19.15)$$

where the friction factor μ can be taken as per Clause 11.6.4.3 of IS 456 as follows:

1. For normal weight concrete placed monolithically—1.4
2. For lightweight concrete placed monolithically—1.05

Clause 11.8.3.2 of ACI 318 suggests that the value of $V_n = V_u/\phi$ must not exceed the smallest of $0.16f_{ck}b_wd$, $11b_wd$, and $(3.3 + 0.064f_{ck})b_wd$ for normal weight concrete or the smaller of $(0.16 - 0.056a_v/d)f_{ck}b_wd$ and $(5.5 - 1.9a_v/d)b_wd$ for lightweight concrete.

As per Clause 11.8.3.5 of ACI 318, the total area of reinforcement required for tension A_s should not be less than the larger of $(A_f + A_n)$ and $(2A_{vf}/3 + A_n)$. Clause 11.8.4 of ACI 318 stipulates that the total area, A_h , of closed stirrups or ties parallel to primary tension reinforcement should not be less than $0.5(A_s - A_n)$ and this area of reinforcement, A_h , should be uniformly distributed within $(2/3)d$ adjacent to the primary tension reinforcement, as shown in Fig. 19.23(a). This requirement means that A_h should be greater than $0.5A_f$ and also $A_{vf}/3$. To avoid the possibility of sudden failure when there is a crack under the action of flexural moment and outward tensile force, the ACI code specifies a minimum amount of reinforcement, $A_{s,\min} = 0.032(f_{ck}/f_y)b_wd$.

Russo, et al. (2006) have proposed a new model for determining the shear strength of RC corbels. By comparing

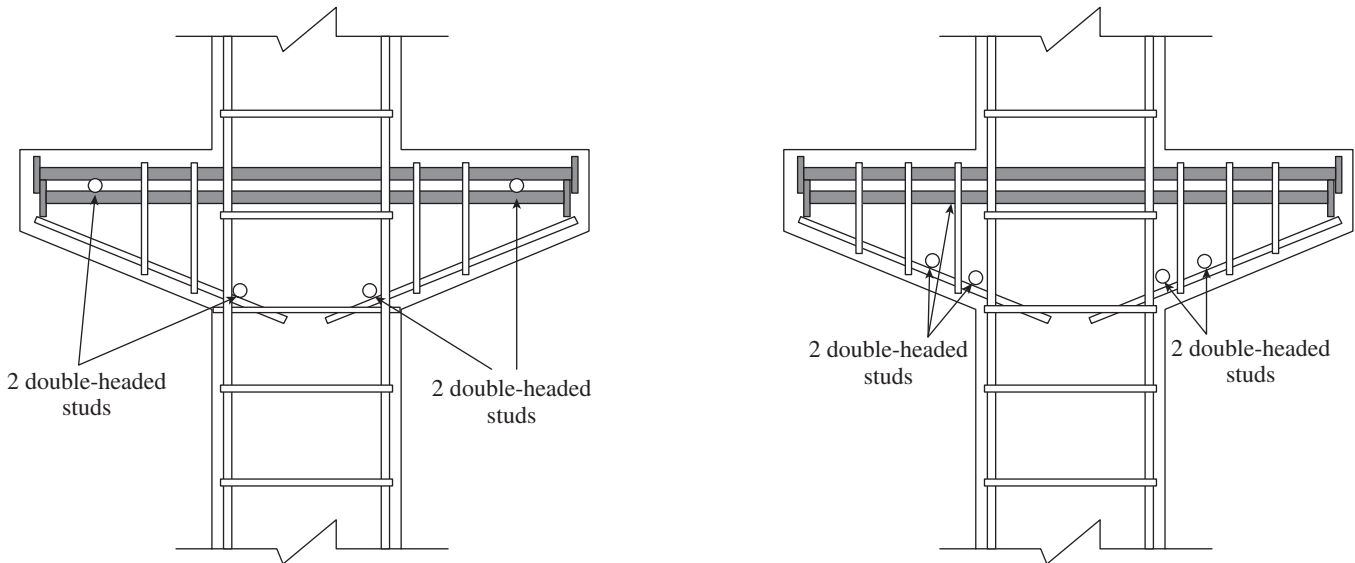


FIG. 19.26 Double-headed studs in corbels

the results of the model with test data of 243 specimens and ACI and other formulae, they showed that the proposed model correlated well with the test data. Hwang, et al. (2000) proposed a softened strut-and-tie model for determining the shear strength of corbels; they compared the model with the empirical formulae of ACI 318 and experimental data of 178 corbels and found that their model performed better on all the parameters that affect the shear strength. Birkle, et al. (2002) showed that double-headed studs provide sufficient anchorage when used as top reinforcement in corbels. They also showed from their experimental studies that the double-headed studs when placed in the compression zone, in the direction normal to the corbel face, significantly improve the ductility of the corbel. They suggested that for best efficiency the confining studs should be placed at the bottom face just outside the column corbel interface (see Fig. 19.26).

19.5 DESIGN OF ANCHORS

Before describing the design of anchors, a brief discussion on the different types of anchors is provided.

19.5.1 Types of Anchors

Anchors (sometimes known as fasteners) are embedded in concrete and used to connect and support structural steel columns, light poles, highway sign structures, bridge rail, equipment, and many other applications. They are basically used to connect two elements of a structure and are increasingly used in both retrofit and new constructions.

The type of anchors used in practice may be broadly classified as cast-in-place anchors and post-installed anchors (CEB Report 1994).

Cast-in-place anchors These include the following types: (a) headed hexagonal bolt; (b) L-bolt; (c) J-bolt; and (d) welded headed stud. In the precast concrete industry, precast components are typically connected by the use of an embedded plate, which is usually anchored with *welded headed studs*. As per PCI Design Handbook, the minimum plate thickness to which studs are attached should be one-half the diameter of the stud (thicker plates may be required for bending resistance or to ensure a more uniform load distribution to the attached studs). The size of anchors ranges from 16 mm to 60 mm in diameter. These types of anchors are shown in Fig. 19.27. The most recommended anchor rod for commercial construction, according to the American Institute of Steel Construction, is a straight rod with hexagonal head

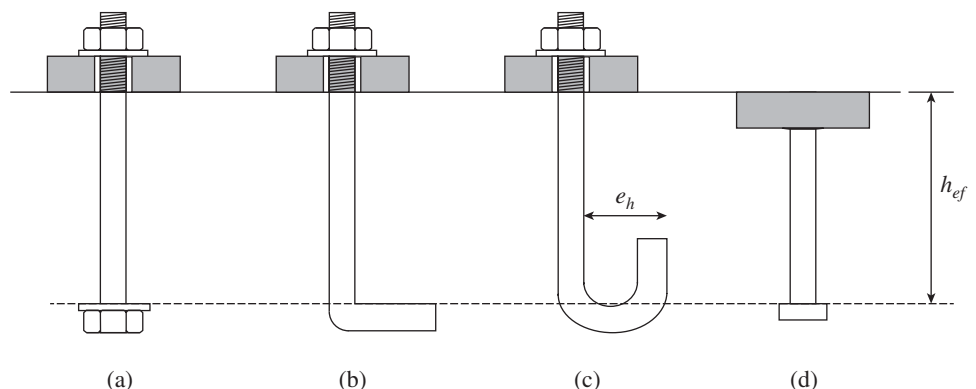


FIG. 19.27 Cast-in-place anchors (a) Headed hexagonal bolt with washer (b) L-bolt (c) J-bolt (d) Welded headed stud

Source: ACI 318:2011, reprinted with permission from ACI

or threaded nut and minimum rod diameter of 18 mm. The physical material properties for normal headed studs as per the American Welding Society's AWS D1.1-02 code are as follows:

1. Minimum tensile strength—415 MPa
2. Minimum yield strength (0.2% offset)—345 MPa
3. Minimum elongation in 50 mm—20 per cent
4. Minimum reduction of area—50 per cent

Cast-in-place anchors are set in place inside the formwork along with the steel reinforcement prior to concrete placement. Anchor groups may be set using a steel or plywood template to ensure proper geometry and placement. As these pre-installed anchors do not allow any clearance, they need very accurate positioning. Cast-in-place anchors are recommended when the applied loads require large embedment lengths and high tensile strength. The headed anchors transfer tensile load by mechanical bearing of the head, nut, or bent portion and possibly by the bond between the anchor shank and the surrounding concrete (Klingner 2001).

Post-installed anchors Installed in hardened concrete, these are classified as adhesive and mechanical anchors, based on their load transfer mechanisms (see Fig. 19.28).

Adhesive anchors Adhesive or bonded anchors (Fig. 19.28a) are inserted into hardened concrete with an anchor hole diameter not greater than 1.5 times the anchor diameter. These anchors transfer tensile loads to the concrete by the bond between the anchor and the adhesive as well as the bond between the adhesive and the concrete. Steel elements for adhesive anchors include threaded rods, deformed reinforcing bars, or internally threaded steel sleeves with external deformations (ACI 318:11). Details of installation and behaviour of these types of anchors are provided by Subramanian and Cook (2002, 2004). Epoxy is

the most widely used adhesive (which may take up to 24 hours to cure) though resins such as vinyl esters, polyesters, methacrylates, and acrylics have also been used. As per ACI, adhesive anchors should be installed in concrete having a minimum age of 21 days.

Mechanical anchors These transfer load by friction or bearing and include expansion anchors and undercut anchors. *Expansion anchors* work by the expansion of a wedge or sleeve mechanism against the surrounding concrete (Klingner 2001). *Undercut anchors* (Fig. 19.28b) are placed in a drilled hole, which is locally widened at the bottom (called the undercut) using a special drilling tool. These are then set by projecting elements from the anchor against the sides of the undercut portion of the hole, usually by applying a torque to the anchor. In *torque-controlled expansion anchors* (Fig. 19.28c), the expansion is generated by applying a predetermined torque. In *displacement-controlled expansion anchors* (Fig. 19.28d), the expansion is generated when the anchors are driven inside the hole. Mechanical anchors loaded in tension apply reaction forces to the concrete at the expansion mechanism, usually near the end of the embedded part of the anchor. It has been found that post-installed anchors do not have predictable pull-out strengths; hence, qualification tests and evaluation should be done as per ACI 355.2 (for mechanical anchors) or ACI 355.4 (for adhesive anchors) before adopting them.

A *grouted anchor* is a headed bolt or a threaded rod with a nut at the embedded end, placed in a drilled hole filled with a pre-mixed grout or a Portland cement–sand grout. These anchors are often not as strong as other post-installed anchor systems because aggregates are generally not used in the holes in which these are placed and grouted. Grouted anchor failures most often occur between the grout and original concrete. Proprietary cement-based grouts can achieve a compressive strength of 27.5 MPa within 3 hours and 48 MPa

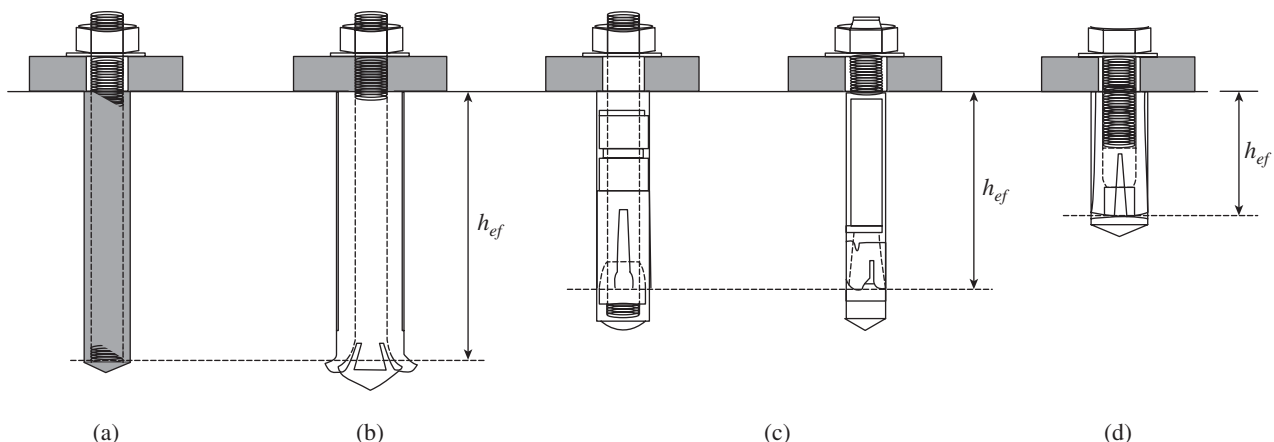


FIG. 19.28 Post-installed anchors (a) Adhesive or bonded anchor (b) Undercut anchor (c) Torque-controlled expansion anchors—sleeve and stud types (d) Drop-in type displacement-controlled expansion anchor

Source: ACI 318:2011, reprinted with permission from ACI

within 24 hours. Average bond stress varies in the range 7.3–21.5 MPa for cementitious grouts and 17.8–19.4 MPa for polymer grouts (Subramanian and Cook 2004). Allowable design loads of post-installed anchors are generally based on tested capacity divided by a factor of safety of about four.

As shown in Fig. 19.29, anchors under tension loading can exhibit five different types of failures (ACI 318:2011; Subramanian and Vasanthi 1991):

1. Steel anchor failure (Fig. 19.29a—due to yield and fracture of the anchor shank)
2. Pull-out or pull-through failure (Fig. 19.29b—due to the progressive crushing of concrete over the anchor head)
3. Concrete breakout (Fig. 19.29c, where a cone-shaped concrete failure surface propagates from the head of the anchor; this is usually the most critical failure mode)
4. Concrete splitting (Fig. 19.29d, which is characterized by the formation of cracks vertically along the length of the anchor)
5. Side-face blowout (Fig. 19.29e, which involves the side-face blowing out of concrete surface adjacent to the anchor head; studs cannot be closer to an edge than 40% of the effective height of the studs)

Failures in bonded anchors may occur due to pull-out of a cone of concrete, slip out of the hole, or steel failure (see Fig. 19.29f).

Failure of anchors under shear loading is discussed in Section 19.5.7.

19.5.2 Code Provisions for Design

There are no provisions for the design of anchors in IS 456. In the early 1970s, formal design concepts for headed-stud anchors were introduced in the Precast/Prestressed Concrete Institute’s (PCI) PCI Design Handbook (1971). The PCI design model was adopted by ACI Committee 349-76, a standard for concrete nuclear structures. ACI 349-90 used a 45° cone breakout model for determining the concrete breakout strength.

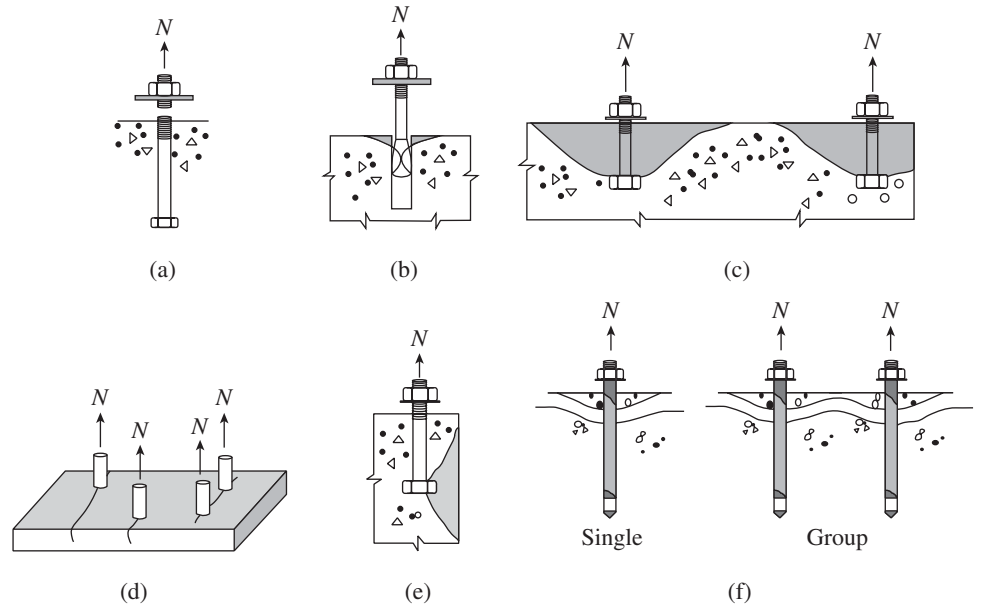


FIG. 19.29 Failure modes for anchors under tensile loading (a) Steel failure (b) Pull-out (c) Concrete breakout (d) Concrete splitting (e) Side-face blowout (f) Bonded anchors

Source: ACI 318:2011, reprinted with permission from ACI

This method assumed a constant tensile stress of $\sqrt{f'_c}/3$ acting on the projected area of a 45° cone radiating towards the free surface from the bearing edge of the anchor (see Fig. 19.30).

Extensive testing and analytical studies by Eligehausen and his associates at the Technical University of Stuttgart in the 1980s resulted in a design procedure known as the κ (Kappa) method (Eligehausen 1988). This method suggested a truncated pyramid failure model (with a 35° slope of failure cone), which was incorporated in the Eurocode (CEB Report 1994; CEB Guide 1997; Eligehausen, et al. 2006; Subramanian 2000). This corresponds to the widespread observation that the horizontal extent of the failure surface is about three times the effective embedment depth (see Fig. 19.31).

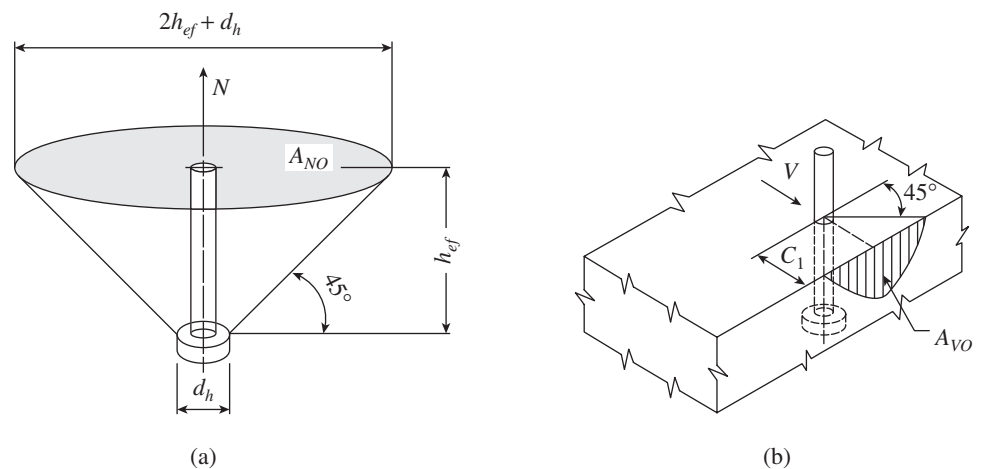


FIG. 19.30 Concrete breakout bodies according to ACI 349 (a) Tensile loading (b) Shear loading

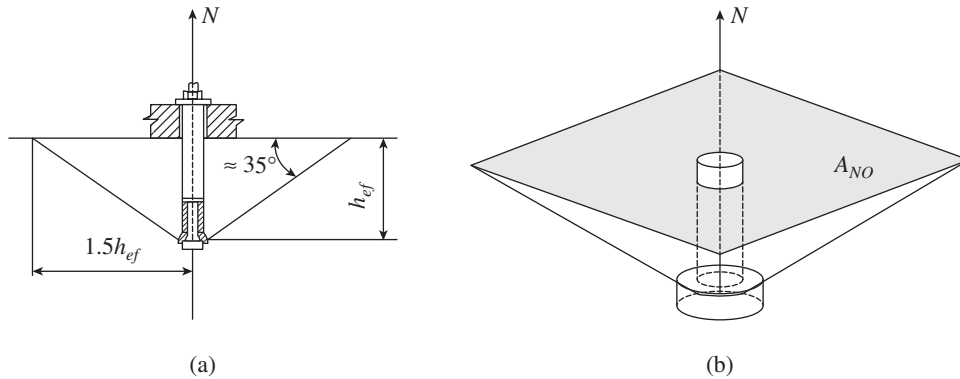


FIG. 19.31 Concrete breakout failure under tensile loading according to ACI 318 (a) Tensile loading on anchor (b) Assumed truncated pyramidal concrete breakout

Additional refinement of the Kappa method at the University of Texas, Austin, to make it user friendly, resulted in the CCD approach to fastenings in concrete, based on the 35° truncated pyramid failure model (Fuchs, et al. 1995). In the earlier ACI 349/PCI method, the calculation of breakout capacity is based on a 45° concrete cone failure model, which resulted in an equation based on the embedment length squared (h_{ef}^2). The CCD method accounts for fracture mechanics and results in an equation for concrete breakout based on 1.5th power of h_{ef} (i.e., $h_{ef}^{1.5}$). The basic advantage of the CCD method is that it is user-friendly and the calculations of capacity considering factors such as edge distance and spacing between anchors are determined using relatively simple relationships based on rectangular prisms (Fuchs, et al. 1995; Subramanian 2000). The CCD method was adopted in the 2002 edition of the ACI code (Appendix D of ACI 318) and with improvements in subsequent 2005, 2008, and 2011 versions of the code. However, the precast concrete industry, which uses embedded plates that are anchored with welded headed studs, was sceptical about the ACI method, as the CCD method was calibrated using an extensive database of post-installed anchors (Anderson and Meinheit 2007).

It has to be noted that anchor group effects should be considered whenever two or more anchors have spacing less than the critical spacing as follows:

Concrete breakout failure in tension	: $3h_{ef}$
Bond strength in tension	: $2c_{Na}$
Concrete breakout failure in shear	: $3c_1$

where c_{Na} is the projected distance from the centre of an anchor shaft on one side of the anchor required to develop the full bond strength of a single adhesive anchor (mm) and c_1 is the distance from the centre of an anchor shaft to the edge of the concrete in one direction (mm); if shear is applied to the anchor, c_1 is taken in the direction of the applied

shear and if tension is applied to the anchor, c_1 is the minimum edge distance.

Appendix D of ACI 318:11 provides design requirements for anchors in concrete used to transmit structural loads by means of tension, shear, or a combination of tension and shear between the connected structural elements (Subramanian 2000). Hence, the ACI method of design is described in Sections 19.5.3–19.5.16.

19.5.3 Steel Strength of Anchor in Tension

In the ACI 318 code, design equations are presented to check the following different failure modes:

1. Steel capacity (tension and shear)
2. Concrete breakout capacity (tension and shear)
3. Pull-out strength and side-face blowout strength (only in tension and cast-in-place anchor)
4. Concrete pryout strength (only in shear)
5. Bond strength (only for adhesive anchor)

The designer should aim to achieve steel failure as it will be ductile and will provide sufficient warning before failure.

The nominal steel strength of an anchor in tension, N_{sa} , is determined as per ACI 318-11 as

$$N_{sa} = A_{se,N} f_{uta} \quad (19.16)$$

where $A_{se,N}$ is the effective cross-sectional area of an anchor in tension (mm²) and f_{uta} is the specified tensile strength of the anchor steel (MPa) and should not be taken greater than $1.9f_{ya}$ and 860 MPa, where f_{ya} is the specified yield strength of the anchor steel (MPa). This limitation on f_{uta} is to ensure that the stress in anchor will not exceed f_{ya} under service load conditions. For threaded rods and headed bolts, the value of $A_{se,N}$ may be obtained by using the following equation:

$$A_{se,N} = \frac{\pi}{4} \left(d_a - \frac{0.9743}{n_t} \right)^2 \quad (19.17)$$

where d_a is the diameter of the anchor bolt and n_t is the number of threads per millimetre.

19.5.4 Concrete Breakout Strength of Anchor in Tension

As per ACI 318-11, the nominal concrete breakout strength of a single anchor in tension in cracked concrete, N_{no} , may be determined using the following formula:

$$N_{no} = k_c \lambda_a \sqrt{f'_c} (h_{ef})^{1.5} \quad (19.18a)$$

where k_c is the coefficient for basic concrete breakout strength in tension, f'_c is the concrete cylinder compressive

strength (MPa), h_{ef} is the effective embedment depth of anchor (mm) (see Figs 19.27 and 19.28 for the definition of h_{ef}), and λ_a is the modification factor reflecting the reduced mechanical properties of lightweight concrete in certain concrete anchorage applications. (ACI 318-11 suggests that the value of λ_a be taken as follows: cast in situ and undercut anchor concrete failure = 1.0λ , expansion and adhesive anchor concrete failure = 0.8λ , adhesive anchor bond failure = 0.6λ , where λ is the modification factor for lightweight concrete and equals 0.85 for sand-lightweight concrete and 0.75 for all-lightweight concrete.)

The values of k_c in Eq. (19.18a) were determined from a large database of test results in uncracked concrete based on the five per cent fractile strength (meaning that 95 per cent of anchors will have higher strength than predicted by this equation). The values were obtained by adjusting them to the corresponding k_c values for cracked concrete (Fuchs, et al. 1995). The current 2011 version of ACI code suggests the value of k_c as 7 for post-installed anchors and as 10 for cast in situ headed studs and headed anchor bolts in cracked concrete. ACI 318 also stipulates that the values of f'_c should not exceed 70 MPa for cast in anchors and 55 MPa for post-installed anchors; testing is required for post-installed anchors when f'_c is greater than 55 MPa.

In ACI 318-08, there was a limitation on anchor embedment depth of 625 mm for the calculation of concrete breakout strength, which has been removed in ACI 318-11. For anchors with deeper embedment ($h_{ef} > 280$ mm), test results by Lee, et al. (2007) indicated that the use of $h_{ef}^{1.5}$ could be overly conservative. Hence, the following alternative equation has been provided in the 2011 edition of the ACI 318 code for cast in headed studs and headed bolts with $280 \text{ mm} \leq h_{ef} \leq 635$ mm.

$$N_{no} = 3.9\lambda_a\sqrt{f'_c}(h_{ef})^{5/3} \quad (19.18b)$$

Experimental and numerical investigations by Ožbolt, et al. (2007) indicated that this equation may not be conservative for $h_{ef} > 635$ mm.

When fasteners are located so close to an edge or to an adjacent anchor, there will not be enough space for the complete concrete cone to develop and hence the load-bearing capacity of

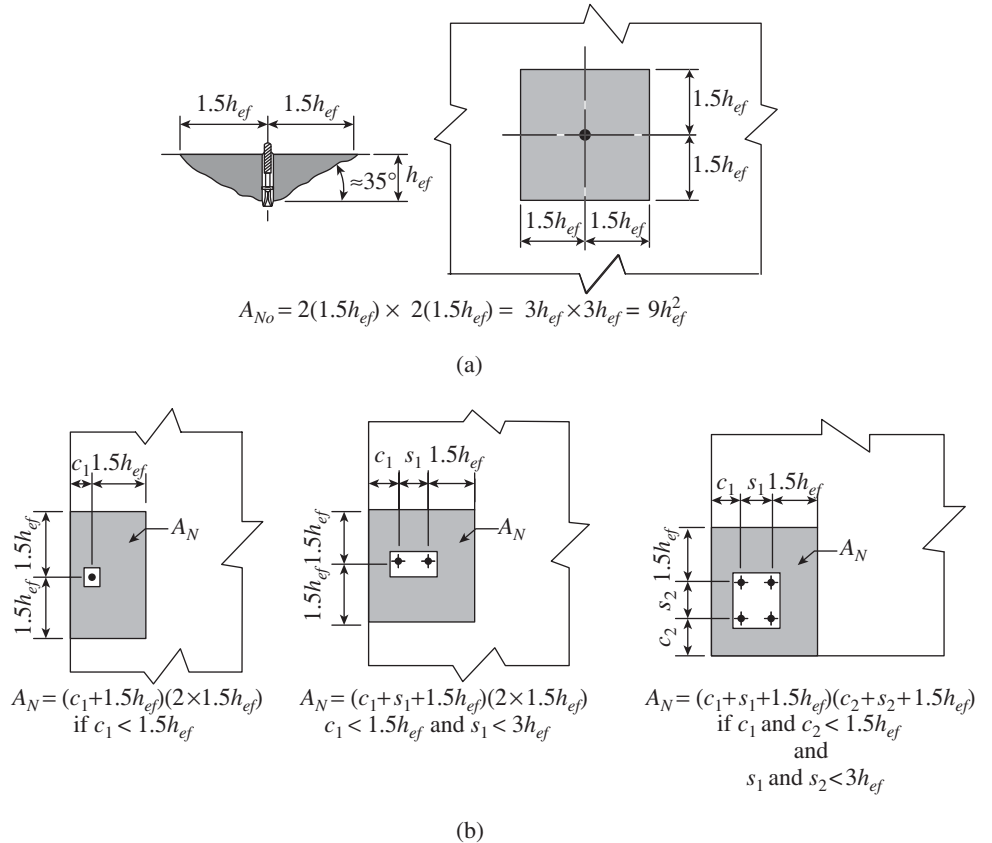


FIG. 19.32 Projected areas for single and group of anchors (a) Single anchor (b) Group of anchors (Reprinted with permission from ACI)

the anchor has to be reduced (see Fig. 19.32). This is also valid for fasteners at close spacing, since the breakout cones may overlap. The nominal concrete capacity for a single anchor in such cases is calculated based on the following equation:

$$N_n = \frac{A_N}{A_{No}}\psi_2\psi_3\psi_4N_{no} \quad (19.19)$$

For a group of anchors, it is given by

$$N_{ng} = \frac{A_N}{A_{no}}\psi_1\psi_2\psi_3\psi_4N_{no} \quad (19.20)$$

where A_N is the projected concrete failure area of a single anchor or group of anchors, for calculation of strength in tension (mm^2), A_{no} is the projected area of one anchor at the concrete surface unlimited by edge influences or neighbouring anchors (idealizing the failure cone as a pyramid with a base length $s_{cr} = 3h_{ef}$, as shown in Fig. 19.32a, we get $A_{no} = 9h_{ef}^2$), and ψ_1 is the modification factor for anchor groups loaded eccentrically in tension; in cases where eccentric loading exists about two axes, ψ_1 should be calculated for each axis individually and the product of the factors used as ψ_1 . The value of ψ_1 is given by

$$\psi_1 = \frac{1}{1 + \frac{2e'_N}{3h_{ef}}} \quad (19.21)$$

where e'_N is the distance between the resultant tensile force of tensioned anchor bolts of a group and the centroid of tensioned anchor bolts (see Fig. 19.33); if the loading on an anchor group is such that only some anchors are in tension, only those anchors that are in tension should be considered when determining the eccentricity e'_N .

If anchors are located close to an edge such that it is not possible for a complete breakout prism to develop, the strength of the anchor is further reduced beyond that reflected in A_N/A_{No} . Such a modification factor for edge effects for single anchor or anchor groups loaded in tension, ψ_2 , is given by

$$\psi_2 = 1 \text{ if } c_1 \geq 1.5h_{ef} \tag{19.22a}$$

$$\psi_2 = 0.7 + 0.3 \frac{c_{a,\min}}{1.5h_{ef}} \text{ if } c_1 \leq 1.5h_{ef} \tag{19.22b}$$

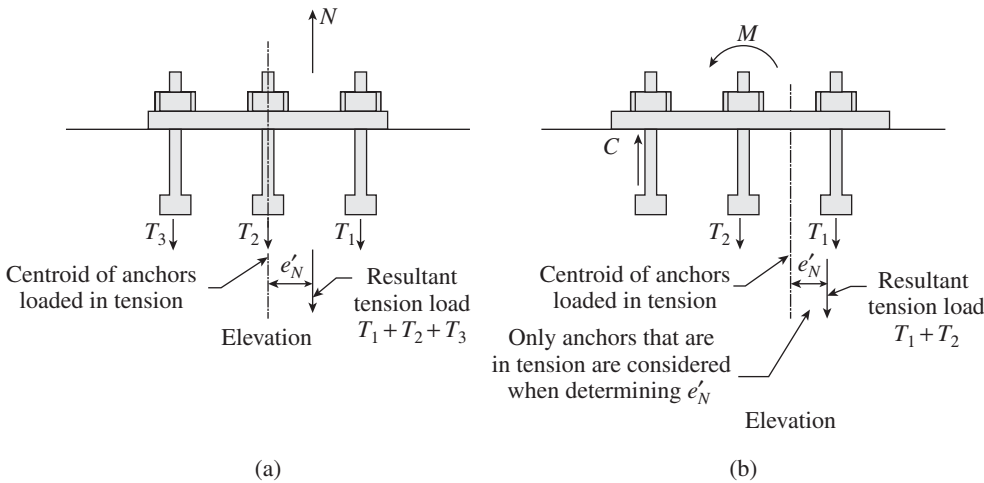


FIG. 19.33 Definition of e'_N for a group of anchors (a) All anchors are in tension (b) Only a few anchors are in tension

Source: ACI 318:2011, reprinted with permission from ACI

where $c_{a,\min}$ is the minimum distance from the centre of an anchor shaft to the edge of concrete (mm).

If an analysis indicates that there is no cracking at service load levels, then the modification factor, ψ_3 , may be applied:

$$\psi_3 = 1.25 \text{ for cast-in-place anchors} \tag{19.23a}$$

$$\psi_3 = 1.4 \text{ for post-installed anchors} \tag{19.23b}$$

Experimental studies indicated that many torque-controlled and displacement-controlled expansion anchors and some undercut anchors require minimum edge distances exceeding $1.5h_{ef}$ to achieve the basic concrete breakout strength when tested in uncracked concrete without supplementary reinforcement to control splitting. To account for this potential splitting mode of failure, the basic concrete breakout strength has to be reduced by a factor ψ_4 , when the edge distance c_1 is less than the critical edge distance c_{ac} . As per ACI 318, the critical edge distance, c_{ac} , should not be less than the values given in Table 19.4.

TABLE 19.4 Critical and minimum edge distance for post-installed anchors

Type of Post-installed Anchor	Critical Edge Distance, c_{ac}	Minimum Edge Distance
Adhesive anchors	$2h_{ef}$	$6d_a$
Undercut anchors	$2.5h_{ef}$	$6d_a$
Torque-controlled expansion anchors	$4h_{ef}$	$8d_a$
Displacement-controlled expansion anchors	$4h_{ef}$	$10d_a$

This modification factor ψ_4 is applicable only to post-installed anchors and is determined as follows:

$$\text{If } c_1 \geq c_{ac}, \text{ then } \psi_4 = 1.0 \tag{19.24a}$$

$$\text{If } c_1 < c_{ac}, \text{ then } \psi_4 = \frac{c_{a,\min}}{c_{ac}} > \frac{1.5h_{ef}}{c_{ac}} \tag{19.24b}$$

It has to be noted that for anchors located less than $1.5h_{ef}$ from three or more edges, the tensile breakout strength computed by the CCD method may give overly conservative results.

Research was initiated by PCI to check the validity of ACI Appendix D design equations and 412 tests were conducted by Wiss, Janney, Elstner Associates Inc. (WJE) on headed studs in the structural laboratory in Northbrook, Illinois. This research showed that the provisions for tension strength modified for the effects of edges and spacings in the

ACI code are generally conservative, except where there is influence of spacing in two directions. In this case, the CCD design model is slightly unconservative (about less than 10%) for anchor spacings that are less than $2h_{ef}$ (Anderson and Meinheit 2007, 2008). Hence, PCI also adopted the ACI code approach in the sixth edition of its design handbook.

19.5.5 Pull-out Strength in Tension

Pull-out capacity is dictated by a failure of the concrete around the head of the anchor. When the bearing area of the head is small, crushing of concrete occurs at the head and the anchor can pull-out and crush the concrete without forming a concrete breakout cone (see Fig. 19.29b). Local crushing under the head of the anchor significantly reduces the stiffness of the anchor connection and increases displacement (Anderson and Meinheit 2007). The nominal pull-out strength of a single

cast in, post-installed expansion and post-installed undercut anchor in tension, N_{pn} , may be calculated as

$$N_{pn} = \psi_p N_p \tag{19.25}$$

where N_p is determined based on the five per cent fractile of test results conducted as per ACI 355.2. The value of ψ_p is taken as 1.4 if the analysis results show no cracking at service loads in the zone where the anchor is located and as 1.0 if there is cracking.

For single-headed stud or headed bolt, the value of N_p to be used in Eq. (19.25) is found to be

$$N_p = 8A_{brg} f'_c \tag{19.26}$$

where A_{brg} is the net bearing area of the head of stud, anchor bolt, or headed deformed bar (mm^2) and f'_c is the cylinder compressive strength of concrete (MPa). The value computed from Eq. (19.26) corresponds to the load at which crushing of concrete occurs due to bearing of the anchor head (CEB Guide, 1997).

The pull-out strength in tension of a single-hooked bolt, N_p , to be used in Eq. (19.25) was derived by Lutz (Fuchs, et al. 1995), with limits based on the test results of Kuhn and Shaikh (1996), as

$$N_p = 0.9 f'_c e_h d_a \text{ with } 3d_a \leq e_h \leq 4.5d_a \tag{19.27}$$

where e_h is the distance from the inner surface of the shaft of a J- or L-bolt to the outer tip of the J- or L-bolt (mm) and d_a is the diameter of anchor bolt (mm).

19.5.6 Concrete Side-face Blowout Strength in Tension

Side-face blowout failures are unique to embedded, headed anchors. This failure is affected by edge condition but not the same edge condition associated with concrete breakout failure. If the head of an anchor is close to the free edge, the compression stress bulb at the bearing region of the head can cause concrete to spall. It has to be noted that this condition applies to very small edge distances and relatively deep embedment depth. For a single-headed anchor with deep embedment close to an edge ($h_{ef} > 2.5c_1$), the nominal side-face blow out strength, N_{sb} , can be calculated as

$$N_{sb} = \lambda_a \left(13c_1 \sqrt{A_{brg}} \right) \sqrt{f'_c} \tag{19.28}$$

If c_2 is less than $3c_1$, this value of N_{sb} should be multiplied by the factor $(1 + c_2/c_1)/4$ where $1.0 \leq c_2/c_1 \leq 3.0$. It has to be noted that side-face blowout is not critical in post-installed anchors.

For multiple-headed anchor with deep embedment close to an edge ($c_1 < 0.4h_{ef}$) and anchor spacing less than $6c_1$,

the nominal side-face blowout strength, N_{sb} , can be calculated as

$$N_{sb} = \left(1 + \frac{s}{6c_1} \right) N_{sb} \tag{19.29}$$

where s is the distance between outer anchors along the edge (it has to be noted that it is not the spacing between the adjacent anchors) and N_{sb} is obtained from Eq. (19.28) without modification for a perpendicular edge distance.

19.5.7 Failure Modes in Shear Loading

In the case of shear loading with large edge distance, the mode of failure of anchors will normally be by steel fracture as shown in Fig. 19.34(a) preceded by spalling of concrete. Fastening with short anchors may fail by prying out a concrete cone on the side opposite to the load application as shown in Fig. 19.34(b). Concrete breakout failures may be due to concrete spalling and lateral cone or edge failures as shown in Fig. 19.34(c). As with tension loading, the failure load will be influenced by the concrete tensile capacity, side cover, flexural stiffness of the anchor shaft, and embedment depth (CEB Report, 1994).

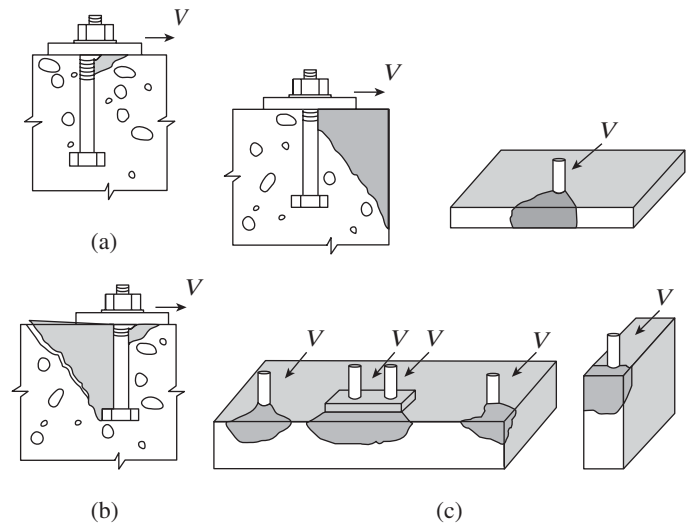


FIG. 19.34 Failure modes for anchors under shear loading (a) Steel failure (b) Concrete pryout failure (c) Concrete breakout failure

Source: ACI 318:2011, reprinted with permission from ACI

19.5.8 Steel Strength of Anchor in Shear

The nominal steel strength of an anchor in shear, V_{sa} , according to Clause D.6.1 of ACI 318-11 is

$$V_{sa} = A_{se,v} f_{uta} \tag{19.30a}$$

$$V_{sa} = 0.6 A_{se,v} f_{uta} \tag{19.30b}$$

where $A_{se,v}$ is the effective cross-sectional area of an anchor in shear (mm^2) and f_{uta} is the specified tensile strength of anchor steel (MPa). For threaded rods and bolts, the value of $A_{se,v}$ may be obtained by using an equation similar to that of Eq. (19.17).

Equation (19.30a) is used for cast in headed stud anchor and Eq. (19.30b) is used for cast in headed bolt and hooked bolt anchors and for post-installed anchors where sleeves do not extend through the shear plane. In Eq. (19.30), the value of f_{uta} should not be taken greater than $1.9f_{ya}$ or 860 MPa, according to ACI 318, where f_{ya} is the specified yield strength of anchor steel (MPa). For post-installed anchors where sleeves extend through the shear plane, the strength should be determined according to ACI 355.2. It has to be noted that CEB Design Guide suggests the following equation (CEB Guide, 1997):

$$V_{sa} = 0.6A_{se,v}f_{ya} \quad (19.30c)$$

19.5.9 Concrete Breakout Strength of Anchor in Shear

The basic concrete breakout capacity in shear of an individual anchor in cracked concrete, V_{no} , according to ACI 318-11 is the smaller of the following two equations:

$$V_{no1} = \lambda_a \left[0.6 \left(\frac{l_e}{d_a} \right)^{0.2} \sqrt{d_a} \right] \sqrt{f'_c} (c_1)^{1.5} \quad (19.31a)$$

$$V_{no2} = 3.7 \lambda_a \sqrt{f'_c} (c_1)^{1.5} \quad (19.31b)$$

where l_e is the activated load-bearing length of the fastener, which is considered as follows: $l_e = h_{ef}$ for anchors with constant overall stiffness over the full length, such as headed studs, undercut anchors, and torque-controlled expansion anchors, where there is no distance sleeve or the expansion sleeve also has the function of the distance sleeve (Fuchs, et al. 1995), $l_e = 2d_a$ for torque-controlled expansion anchors, with the distance sleeve separated from the expansion sleeve, and, $l_e \leq 8d_a$ in all other cases. c_1 is the edge distance in the loading direction (mm) and d_a is the diameter of the anchor (mm). All other terms have already been defined. Equation (19.31b) was included based on the research by Lee, et al. (2010) who performed shear tests on large anchors with diameters of 63.5–88.9 mm, embedment depths greater than 635 mm (635–889 mm), and relatively short edge distance ($c_{a1}/d_a < 6-8$).

It has to be noted that Eq. (19.31) does not increase with the failure surface area, which is in turn proportional to c_1^2 . However, it is proportional to $c_1^{1.5}$ and is influenced by anchor stiffness and diameter. This is due to size effect and has been

verified by theoretical and experimental studies (Eligehausen and Fuchs 1988; Eligehausen, et al. 2006). The maximum diameter for which the provisions of concrete breakout strength in tension and shear (Clauses D.5.2 and D.6.2 of ACI 318) are applicable has been increased from 50 mm to 100 mm based on recent tests on large diameter anchors with deep embedment (Lee, et al. 2007, 2010).

As in the case of direct tension, the effects of multiple anchors, spacing of anchors, edge distance, and thickness of concrete member on nominal concrete breakout strength in shear may be included by applying reduction factors. In tension loading, the size of failure cone is dependent on the anchorage depth, whereas in shear loading it is dependent on the edge distance. Thus, when there is shear force perpendicular to the edge on a single anchor, the nominal concrete breakout strength in shear, V_n , is calculated based on the following equation:

$$V_n = \frac{A_v}{A_{vo}} \psi_6 \psi_7 \psi_8 V_{no} \quad (19.32)$$

For a group of anchors, it is given by

$$V_{ng} = \frac{A_v}{A_{vo}} \psi_5 \psi_6 \psi_7 \psi_8 V_{no} \quad (19.33)$$

where A_v is the actual projected area of the failure surface on the side of concrete member at its edge for a single anchor or group of anchors (mm^2). It is calculated as the base of a truncated half pyramid projected on the side face of the member where the top of the half pyramid is given by the axis of the anchor row selected as critical. A_{vo} is the projected area for a single anchor in a deep member with a distance from edges equal or greater than $1.5c_1$ in the direction perpendicular to the shear force. (It is the full breakout prism for an anchor unaffected by edge distance, spacing, or depth of member.) We may evaluate A_{vo} as the base of a half pyramid with a side length parallel to the edge of $3c_1$ and a depth of $1.5c_1$, as shown in Fig. 19.35(a). Hence, we get $A_{vo} = 4.5c_1^2$.

ψ_5 is the modification factor for anchor groups loaded eccentrically in shear and is given by

$$\psi_5 = \frac{1}{1 + \frac{2e'_N}{3C_1}} \quad (19.34)$$

e'_N is the distance between the resultant shear force of the group of fasteners resisting shear and centroid of sheared anchor bolts (see Fig. 19.36). If the loading on an anchor group is such that only some anchors are in shear in the same direction, only those anchors that are loaded in shear should be considered when determining the eccentricity e'_N .

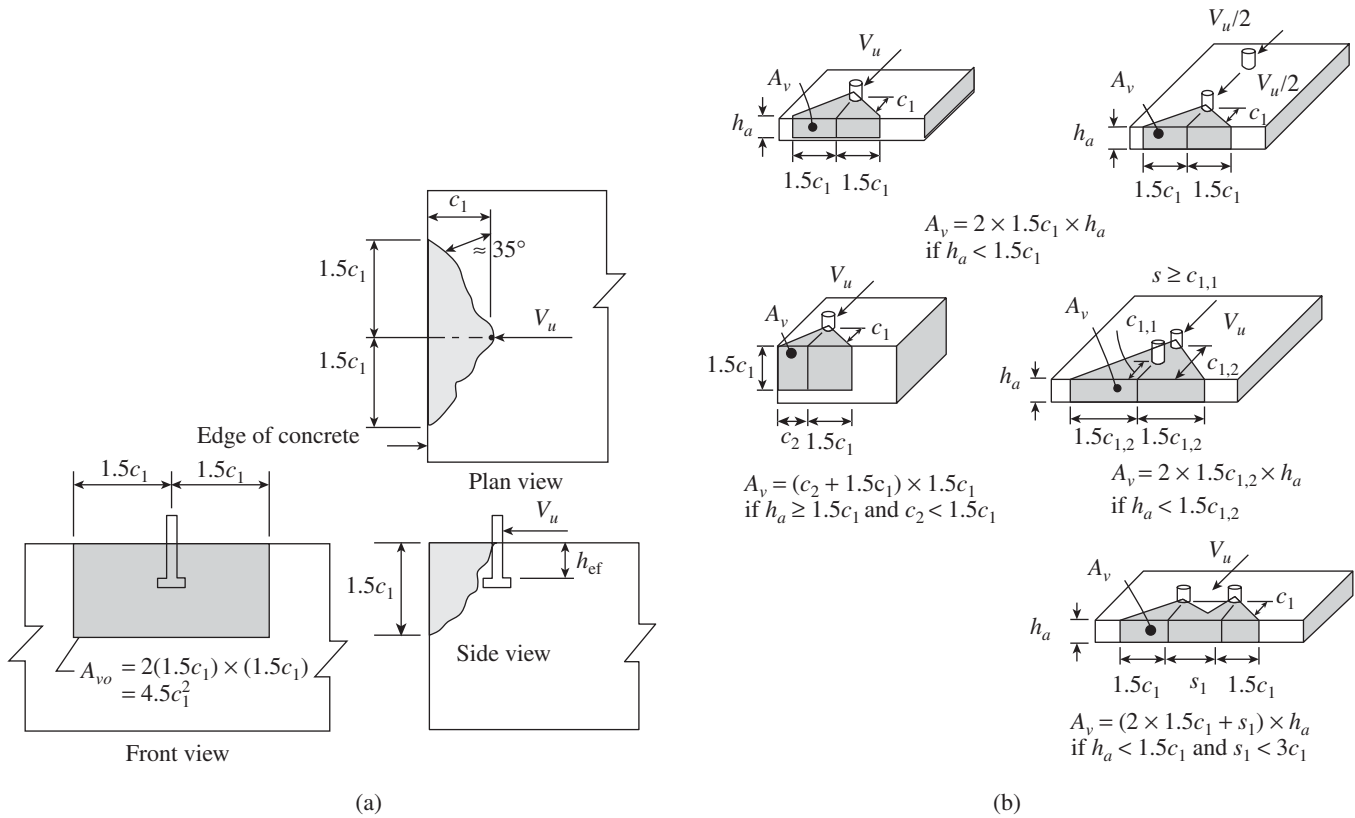


FIG. 19.35 Projected area for single and group of anchors under shear loading (a) Single anchor (b) Group of anchors

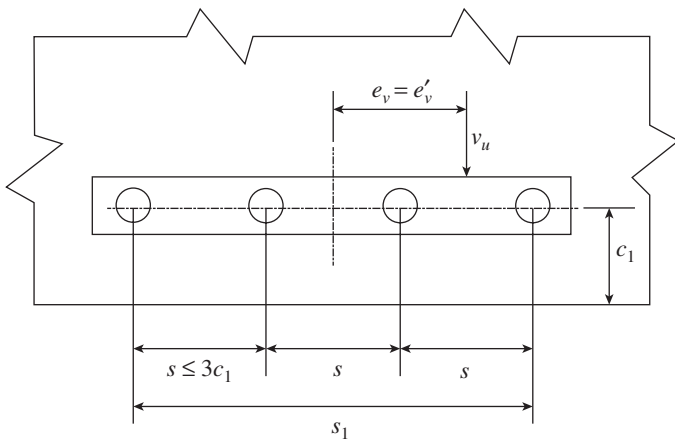


FIG. 19.36 Example of multiple fastening with cast in situ headed studs close to edge under eccentric shear loading

The modification factor for edge effects for single anchor or anchor groups loaded in shear, ψ_6 , is given by (see Fig. 19.37)

$$\psi_6 = 1 \text{ if } c_2 \geq 1.5c_1 \quad (19.35a)$$

$$\psi_6 = 0.7 + 0.3 \frac{c_2}{1.5c_1} \text{ if } c_2 \leq 1.5c_1 \quad (19.35b)$$

where c_1 is the edge distance in the loading direction (see Fig. 19.37) for fastenings in a narrow thin member

with $c_{2,max} < 1.5c_1$ ($c_{2,max}$ is the maximum value of edge distance perpendicular to the loading direction) and $h < 1.5c_1$, the value of edge distance, c_1 , to be used in Eqs (19.33) to (19.35) is limited to $c_1 = \max(c_{2,max}/1.5; h/1.5; s/3)$, where h is the thickness of concrete member and s is the maximum spacing perpendicular to the direction of shear (Fig. 19.35b). This gives a constant failure load independent of edge distance c_1 (Fuchs, et al. 1995; Eligehausen, et al. 1992).

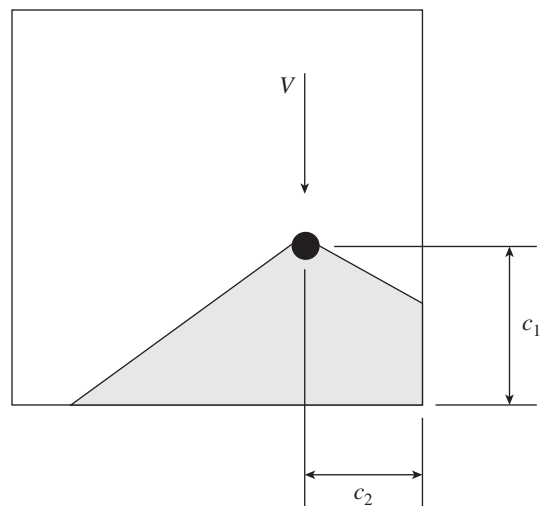


FIG. 19.37 Edge effect in shear

If an analysis indicates that there is no cracking at service load levels, then the modification factor, ψ_7 , may be applied:

$$\psi_7 = 1.25 \tag{19.36a}$$

For anchors located in a region of a concrete member where analysis indicates cracking at service load levels, the following modification factors may be used: For anchors in cracked concrete without supplementary reinforcement or with edge reinforcement smaller than 12 mm bars

$$\psi_7 = 1.0 \tag{19.36b}$$

For anchors in cracked concrete with supplementary reinforcement or with edge reinforcement greater than 12 mm bars

$$\psi_7 = 1.2 \tag{19.36c}$$

For anchors in cracked concrete with supplementary reinforcement of 12 mm bars or greater between the anchor and the edge, and with reinforcement enclosed within stirrups at a spacing of less than 100 mm

$$\psi_7 = 1.4 \tag{19.36d}$$

The modification factor, ψ_8 , for anchors located in concrete members where $h_a < 1.5c_1$, is calculated as

$$\psi_8 = \sqrt{\frac{1.5c_1}{h_a}} \geq 1.0 \tag{19.37}$$

Anderson and Meinheit (2000, 2008) showed that for a multiple-stud connection the breakout capacity in shear is defined by the *catty-corner stud*, that is, the stud diagonally opposite to the geometric corner (see Fig. 19.38). On the basis of their work, the PCI code introduced the concept of side edge distance to the catty-corner stud. It has been shown that corner influences are much better modelled by the WJE/PCI equations than the ACI code provisions and ACI provisions are very conservative for small side edge distances.

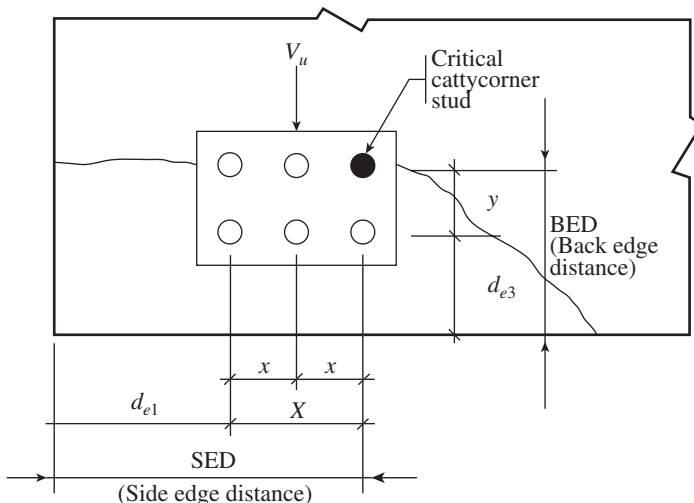


FIG. 19.38 Corner concrete breakout when headed stud anchor is located near a member corner

19.5.10 Concrete Pryout Strength of Anchor in Shear

Pryout failure normally occurs when short, stocky studs or post-installed anchors are loaded in shear away from an edge (see Fig. 19.34b). The nominal pryout strength V_{cp} , for a single anchor can be found using the following expression (Clause 6.3.1 of ACI 318):

$$V_{cp} = k_{cp} N_{cp} \tag{19.38}$$

For cast in, expansion, and undercut anchors, N_{cp} may be taken as N_n determined using Eq. (19.19); for adhesive anchors, N_{cp} is the lesser of N_n determined from Eq. (19.19) and bond strength N_a as per Eq. (19.40) (see Section 19.5.11).

The nominal pryout strength V_{cpg} for a group of anchors can be found using the expression

$$V_{cpg} = k_{cp} N_{cpg} \tag{19.39a}$$

For cast in, expansion, and undercut anchors, N_{cpg} may be taken as N_{ng} determined using Eq. (19.20); for adhesive anchors, N_{cpg} is the lesser of N_{ng} determined from Eq. (19.19) and bond strength N_{ag} as per Eq. (19.40) (see Section 19.5.11). In Eqs (19.38) and (19.39), $k_{cp} = 1.0$ for $h_{ef} < 65$ mm and $k_{cp} = 2.0$ for $h_{ef} \geq 65$ mm.

The research by Anderson and Meinheit (2005) showed that pryout failure will result in anchors with a h_{ef}/d_a ratio less than 4.5 in normal strength concrete and about 5.4–7.4 in lightweight concrete. They experimentally determined that the characteristic of the headed stud that dominates the pryout capacity is its stiffness and that the diameter of anchor may be used to represent the stiffness of the anchor. They suggested the following equation for calculating the concrete breakout strength:

$$V_{cp} = \phi V_{cpo} \psi_y \leq n A_{se} f_{uta} \tag{19.39b}$$

where the nominal pryout shear strength of one y-row of anchors, V_{cpo} , is

$$V_{cpo} = 18.43 \lambda_a n \sqrt{f'_c} (d_a)^{1.5} (h_{ef})^{0.5} \tag{19.39c}$$

The y-spacing factor, ψ_y , is given by

$$\psi_y = \frac{5\sqrt{y}}{4d_a} \text{ for } \frac{y}{d_a} \leq 20 \tag{19.39d}$$

The value of ψ_y is taken equal to 1 if $y = 0$. In this equation, n is the number of anchors, y is the spacing of anchors in the direction of shear force, and $\phi = 0.85$. Other terms have been defined already.

19.5.11 Bond Strength of Adhesive Anchor in Tension

The basic bond strength of a single adhesive anchor in tension in cracked concrete, N_{ba} , can be calculated as (Subramanian and Cook 2002)

$$N_{ba} = \lambda_a \tau_{cr} \pi d_a h_{ef} \quad (19.40)$$

The characteristic bond strength τ_{cr} in cracked concrete should be taken as five per cent fractile of test results conducted as per ACI 355.4M. When analysis indicates no cracking at service load levels, τ_{ucr} may be used instead of τ_{cr} in Eq. (19.40), where τ_{ucr} is the characteristic bond stress of adhesive anchor in uncracked concrete (MPa). Minimum characteristic bond strength as given in Table 19.5 may be used, provided anchors meet the requirements of ACI 355.4M, anchor holes are drilled with a rotary impact drill or rock drill (these drills produce non-uniform hole configuration, which provided better bond), concrete has a compressive strength of 17MPa and has attained a minimum age of 21 days at the time of installation, and concrete temperature at that time is at least 10°C.

TABLE 19.5 Minimum characteristic bond strength (ACI 318-11)

Service Environment During Installation	Moisture Content of Concrete at Installation	Peak Temperature of Concrete at Installation	τ_{cr} (MPa)*+	τ_{ucr} (MPa)*+
Outdoor	Dry to fully saturated	79	1.4	4.5
Indoor	Dry	43	2.1	7.0

Notes:

* When anchor is subjected to sustained tension loading, multiply values of τ_{cr} and τ_{ucr} by 0.4.

+ When anchor is subjected to major earthquake loads, multiply values of τ_{cr} by 0.8 and τ_{ucr} by 0.4.

The nominal bond strength for single adhesive anchor in tension may be calculated as

$$N_a = \frac{A_{Na}}{A_{Nao}} \psi_{10} \psi_{11} N_{ao} \quad (19.41)$$

For a group of anchors, it is given by

$$N_{ag} = \frac{A_{Na}}{A_{Nao}} \psi_9 \psi_{10} \psi_{11} N_{ao} \quad (19.42)$$

where A_{Na} is the projected influence area of a single adhesive anchor or group of adhesive anchors (mm²); this may be approximated as a rectilinear area projected outwards at a distance of c_{Na} from the centre line of a single adhesive anchor or, in the case of group of adhesive anchors, from a line through a row of adjacent adhesive anchors. A_{na} should not exceed nA_{Nao} , where n is the number of anchors in that group. A_{Nao} is the projected influence area of one adhesive anchor with an edge distance equal to or greater than c_{Na} (the critical edge distance, c_{Na} , is the projected distance from the centre of an anchor shaft on one side of the anchor, which is

required to develop the full bond strength of a single adhesive anchor, mm). Thus

$$A_{Nao} = (2c_{Na})^2 \quad (19.43)$$

The critical edge distance c_{Na} has been derived by Eligehausen, et al. (2006a) as

$$c_{Na} = 10d_a \sqrt{\frac{\tau_{ucr}}{7.6}} \quad (19.44)$$

In this equation, the constant 7.6 has the unit of MPa.

The modification factor for adhesive anchor groups loaded eccentrically in tension is given by

$$\psi_9 = \frac{1}{\left(1 + \frac{e'_N}{c_{Na}}\right)} \leq 1.0 \quad (19.45)$$

If the loading on an adhesive anchor group is such that only some adhesive anchors are in tension, only those adhesive anchors that are in tension should be considered when determining the eccentricity, e'_N for use in Eq. (19.45) and for calculating N_{ag} in Eq. (19.42).

When there is eccentric loading about two axes, the modification factor ψ_9 should be computed separately for each axis and the product of these factors should be used in Eq. (19.42).

The modification factor for edge effects for single adhesive anchor or adhesive anchor groups loaded in tension, ψ_{10} , is given by (Eligehausen, et al. 2006)

$$\psi_{10} = 1 \text{ if } c_{a,\min} \geq c_{Na}$$

$$\psi_{10} = 0.7 + 0.3 \frac{c_{a,\min}}{c_{Na}} \text{ if } c_{a,\min} < c_{Na} \quad (19.46b)$$

The modification factor for adhesive anchors designed for uncracked concrete without supplementary reinforcement to control concrete splitting, ψ_{11} , is given by

$$\psi_{11} = 1 \text{ if } c_{a,\min} \geq c_{ac} \quad (19.47a)$$

$$\psi_{11} = \left(\frac{c_{a,\min}}{c_{ac}}\right) > \left(\frac{c_{Na}}{c_{ac}}\right) \text{ if } c_{a,\min} < c_{Na} \quad (19.47b)$$

where c_{ac} is the critical edge distance required to develop the basic strength as controlled by bond, mm. For all other cases, ψ_{11} can be taken as 1.0.

More information on adhesive bonded anchors may be found in the works of Eligehausen, et al. (2006). The recommended procedures for development and splicing of post-installed bonded reinforcing bars are provided by Charney, et al. (2013).

CASE STUDY

Boston’s Big Dig Ceiling Collapse

On 10 July 2006, about 26 tons of concrete and associated suspension hardware fell on a passenger car when it was passing the Interstate 90 connector tunnel in Boston (often referred to as the ‘Big Dig’), killing a passenger and injuring the driver. A later investigation found that hundreds of dangerous adhesive anchors were holding together the tiles on the tunnel ceilings.

The National Transportation Safety Board’s (NTSB) investigation of that accident determined that the ceiling collapse was due to the use of an epoxy anchor adhesive with poor creep resistance, that is, an epoxy formulation that was not capable of sustaining long-term loads. Over time, the epoxy deformed and fractured until several ceiling support anchors pulled out and allowed a portion of the ceiling to collapse. The use of an inappropriate epoxy formulation resulted from the failure of engineers at Gannett Fleming, Inc. and Bechtel/Parsons Brinckerhoff to detect potential creep in the anchor adhesive as a critical long-term failure mode and to account for possible anchor creep in the design, specifications, and approval process for the epoxy anchors used in the tunnel. The use of such epoxy formulation also resulted from a general lack of understanding and knowledge in the construction

community about creep in adhesive anchoring systems. Selection of a better adhesive could have prevented the accident.

NTSB found the adhesive suppliers at fault and ordered Powers Fasteners, a distributor, and its supplier Sika Corp. to revise product literature and packaging to clearly state that the fast-setting materials are approved only for short-term loads. Powers Fasteners has increased the safety factor on its fast-setting materials by a factor of four since the Big Dig collapse. NTSB recommended that federal and state highway authorities develop standards and protocols for the testing of adhesive anchors used in sustained tensile load overhead highway applications and consider the creep characteristics of polymers. A mandatory tunnel inspection was also suggested. More information about this failure and recommendations by NTSB may be found at NTSB/HAR-07/02 (2007).

In this connection, it is important to note that ACI 503.5R-92, ‘Guide for the Selection of Polymer Adhesives with Concrete’, which was first published in 1992 and reapproved in 1997 and 2003, cautions about creep failure of adhesive anchors and suggests pre-testing of such anchors. ACI Committee 355 also developed ACI 355.2-07, *Qualification of Post-installed Mechanical Anchors in Concrete*.

19.5.12 Required Strength of Anchors

After calculating the nominal strength, the following condition has to be satisfied as per ACI 318-11:

$$\phi(N_{Sn}, N_n, N_p, N_{sb}) \geq N_{ua} \quad (19.48)$$

$$\phi(V_{sn}, V_n, V_{cp}) \geq V_{ua} \quad (19.49)$$

where ϕ is the strength reduction factor and N_{ua} and V_{ua} are the applied factored tension and shear loads on anchor, respectively. Clause 4.3 of ACI 318 gives various ϕ factors for different conditions. They are summarized in Table 19.6. In this table, condition A pertains to the presence of supplementary reinforcement except for pull-out and pryout strengths and condition B for the absence of such reinforcement and for pull-out and pryout strengths. Similarly, categories 1 to 3 are applicable to post-installed anchors: Category 1 pertains to low sensitivity to installation and high reliability, category 2 to medium sensitivity to installation and medium reliability,

Concrete breakout	Cast-in-place	0.75	0.75	0.70	0.70
	Category 1	0.75	0.75	0.65	0.70
	Category 2	0.65	0.75	0.55	0.70
	Category 3	0.55	0.75	0.45	0.70
Pull-out of anchor	Cast-in-place	Use condition B		0.70	0.70
	Category 1			0.65	0.70
	Category 2			0.55	0.70
	Category 3			0.45	0.70
Pryout	Cast-in-place	Use condition B		0.70	0.70
	Category 1			0.65	0.70
	Category 2			0.55	0.70
	Category 3			0.45	0.70

TABLE 19.6 Strength reduction factor, ϕ , for various conditions

Failure Mode	Anchor Property	Strength Reduction Factor ϕ			
		Condition A		Condition B	
		Tension	Shear	Tension	Shear
Steel	Ductile	Use condition B		0.75	0.65
	Brittle			0.65	0.60
Side-face blowout	Cast-in-place	0.75	0.75	0.70	0.70

and category 3 to high sensitivity to installation and lower reliability.

From Table 19.6, it is clear that the ACI code uses a lower capacity reduction factor ($\phi = 0.65$) on steel shear strength than when loaded in tension ($\phi = 0.75$). Anderson and Meinheit (2007) observe that a factor of $\phi = 0.75$ is more appropriate for headed studs welded to plate, as the steel plate can plastically redistribute the shear to headed studs better than post-installed anchors.

19.5.13 Interaction of Tensile and Shear Forces

Anchors and group of anchors that are subjected to shear and tensile loads should be designed to satisfy the following:

1. When $V_{ua}/(\phi V_n) \leq 0.2$ for the governing strength in shear, full strength in tension may be permitted: $\phi N_n \geq N_{ua}$.
2. When $N_{ua}/(\phi N_n) \leq 0.2$ for the governing strength in tension, full strength in shear may be permitted: $\phi V_n \geq V_{ua}$.
3. When $V_{ua}/(\phi V_n) > 0.2$ for the governing strength in shear and $N_{ua}/(\phi N_n) > 0.2$ for the governing strength in tension, ACI 318-11 suggests the following interaction equation

$$\frac{N_{ua}}{\phi N_n} + \frac{V_{ua}}{\phi V_n} \leq 1.2 \quad (19.50)$$

It has been found that Eq. (19.50) yields conservative results for steel failure (CEB Guide 1997). Traditionally, the shear-tension interaction equation has been expressed as

$$\left(\frac{N_{ua}}{\phi N_n}\right)^\alpha + \left(\frac{V_{ua}}{\phi V_n}\right)^\alpha \quad (19.51)$$

where the exponent α varies from 1 to 2. More accurate results may be obtained if the value of α is taken as 2 if N_u and V_u are governed by steel failure and as 1.5 for all other failure modes (CEB Guide, 1997). The tri-linear recommendation of the ACI code is the simplification of Eq. (19.51) where $\alpha = 5/3$ (see Fig. 19.39). Any other interaction expression determined by test data can also be used.

Clause D.8 of the ACI code contains the required edge distances, spacings, and thicknesses to preclude spitting failure (see Table 19.4) and Clause D.9 gives the requirements for the installation and inspection of anchors. Swiatek and Whitbeck (2004) discuss many practical problems connected with anchor rods and provide some easy solutions.

19.5.14 Seismic Design Requirements

When the seismic component of the total factored tension demand on an anchor or group of anchors exceeds 20 per cent, the following four options are suggested by ACI 318 (see Section D.3.3.4.3):

1. Ensure failure of ductile steel anchor ahead of brittle failure of concrete. This involves the new concept of 'stretch length'. Observations from earthquakes indicated that a stretch length of about eight times the diameter of anchor results in good structural performance (see Fig. 19.40).

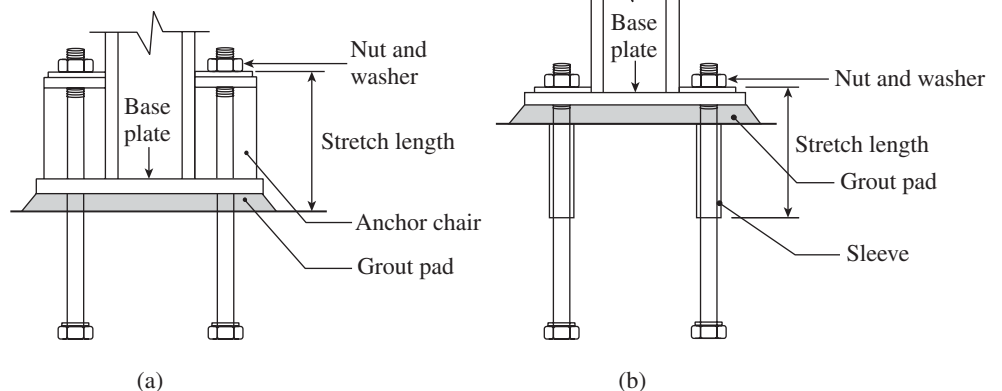


FIG. 19.40 Provision of stretch length in anchors (a) Anchor chair (b) Sleeve (Reprinted with permission from ACI)

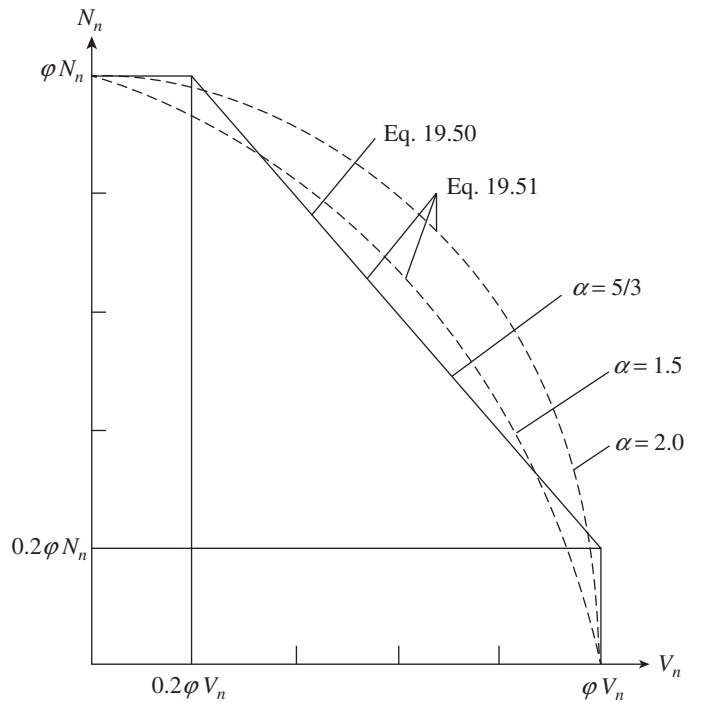


FIG. 19.39 Interaction diagram for combined tension and shear

2. Design anchor for the maximum tension force that can be transmitted to the anchor based on the development of a ductile yield mechanism in the attachment in flexure, shear, or bearing, or its combinations, and considering both material over-strength and strain hardening effects of the attachment.
3. Design anchor for the maximum tension force that can be transmitted to the anchor by a non-yielding attachment.
4. Design anchor for the maximum tension force obtained from design load combinations involving earthquake load E , with E multiplied by an amplification factor (Ω_0) to account for over-strength of the seismic force-resisting system.

For an anchor or a group of anchors subjected to shear, three options similar to (2) to (4) have been made available in the ACI code. However, unlike the earlier version of the code, ductile anchor failure in shear is not allowed as an option. Additional guidance on the use of options (1) to (4) is provided in NEHRP Provisions (2010).

19.5.15 Influence of Reinforcements to Resist Shear

In general, the procedure to predict the strength of anchors exhibiting concrete cone failures assumes absence of

reinforcement in the anchorage area. Parallel reinforcement near the anchor heads (e.g., hairpin reinforcement) has been shown to increase the ultimate load when the reinforcement is well anchored, as shown in Fig. 19.41 (Bode and Hanenkamp 1985). To ensure yielding of the anchor reinforcement, the reinforcement should be in contact with the anchor and must be placed as close to the concrete surface as possible, as shown in Fig. 19.41 (Rehm, et al. 1985). As the larger bent radii associated with the larger diameter bars may significantly influence the effectiveness of the anchor reinforcement, the ACI code restricts the anchor reinforcement to 18 mm bars.

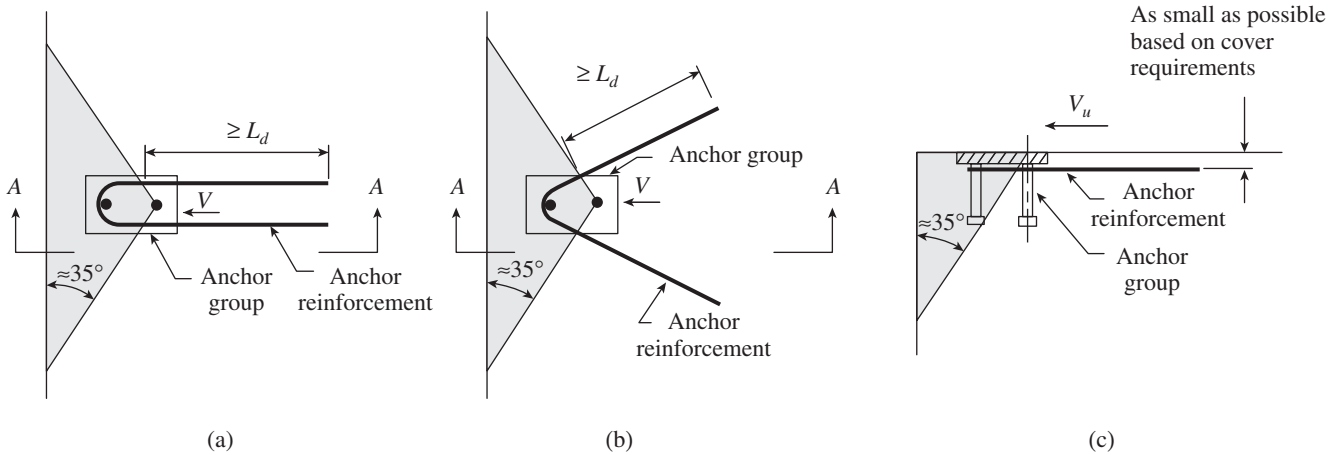


FIG. 19.41 Hairpin anchor reinforcement for shear (a) U-loops (b) V-loops (c) Section A-A (Reprinted with permission from ACI)

When anchor reinforcement is used, the ACI code allows the use of design strength of the anchor reinforcement instead of concrete breakout strength in the determination of ϕV_n . A strength reduction factor of 0.75 is suggested to be used for the design of anchor reinforcement.

Hence

$$A_{sa} = \frac{V_u}{0.75 f_{ya}}$$

where V_u is the applied shear force, A_{sa} is the area of anchor reinforcement, and f_{ya} is the yield strength of anchor reinforcement. The reinforcement could also consist of stirrups and ties enclosing the edge reinforcement embedded in the breakout cone and as close to the anchors as possible (see Fig. 19.42). Only reinforcement spaced less than the lesser of $0.5c_1$ and $0.3c_2$ from the anchor centre line should be considered as anchor reinforcement. In this case, the anchor reinforcement should be developed

on both sides of the breakout surface; edge reinforcement is also necessary for equilibrium considerations (see Fig. 19.42). The use of anchor reinforcement is attempted only in the case of cast-in-place anchors.

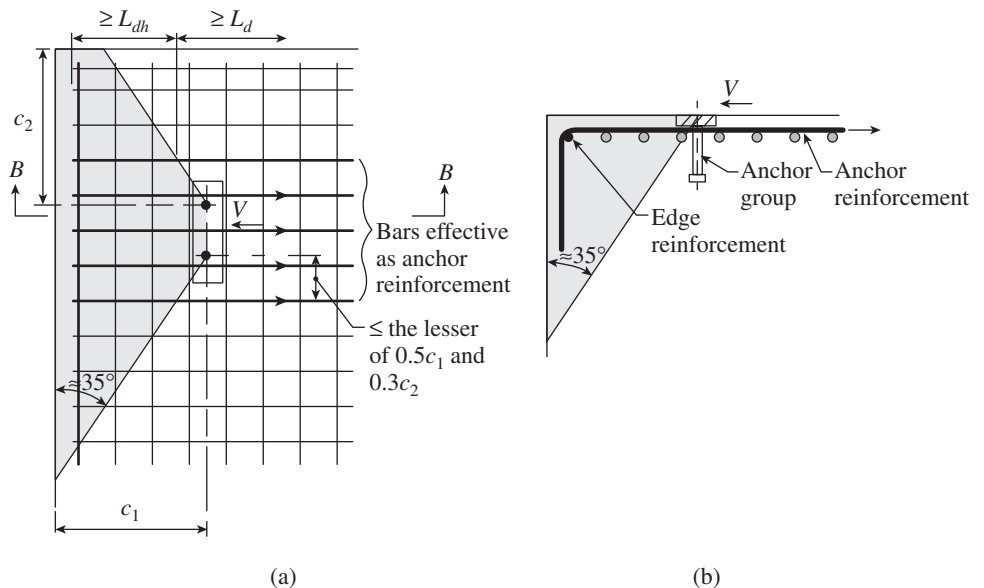


FIG. 19.42 Edge and anchor reinforcement for shear (a) Plan (b) Section B-B (Reprinted with permission from ACI)

Recently, Petersen and Zhao (2013) proposed anchor shear reinforcement consisting of closed stirrups, which prevented concrete breakout failures and resulted in anchor steel fracture in 25 mm diameter anchors with a front edge distance of 150 mm. They observed that cover concrete in front of the anchor bolts spalled, causing the top portion of the anchor bolt close to the concrete surface to become exposed. As a result, the full anchor capacity in shear is not achieved, as the exposed anchors are subjected to combined shear, tension, and bending at failure, thus reducing the capacity. Hence, reinforcing bars are to be provided along all concrete surfaces to minimize concrete damage in front of anchors for consistent seismic shear behaviour.

19.5.16 Required Edge Distances and Spacing to Prevent Splitting of Concrete

Splitting failure mode, which is highly dependent on a number of factors that are difficult to quantify, is not directly accounted for in ACI 318. Rather than explicitly calculating the splitting resistance, Clause D.8 of ACI 318 specifies the following minimum edge distances and spacings to preclude splitting failure, unless supplementary reinforcements are provided to control splitting:

1. The minimum centre-to-centre (*c/c*) spacing of anchors should be $4d_a$ for cast in anchors that will not be torqued and $6d_a$ for torqued cast in anchors and post-installed anchors.
2. The minimum edge distances of anchors that will not be torqued should be based on specific cover requirements for reinforcements (Table 16 of IS 456), and for torqued cast-in anchors the minimum edge distance should be $6d_a$.
3. The minimum edge distances for anchors should not be less than those given in Table 19.4.
4. The value of h_{ef} for an expansion or undercut post-installed anchor should not exceed two-thirds of member thickness and member thickness minus 100 mm.

19.6 OBTUSE-ANGLED AND ACUTE-ANGLED CORNERS

Corners with obtuse and acute angles occur in bridge abutments between the wing walls and the front wall and in folded plate roof. Tests on V-shaped beams with 135° to 145° corners have been conducted by Nilsson and Losberg (1976) and Abdul-Wahab and Ali (1989) for various reinforcement details. On the basis of these investigations, they concluded the following:

1. The efficiency of the joint detail is improved when inclined bars are added to take up the tensile force at the inner corner. Loops with inclined bars, as shown in Fig. 19.43(a), are preferable for continuous corners between lightly reinforced slabs (since their efficiency is of the order of 80–130%).

2. The efficiency of the corners improved significantly when the thicknesses of the adjoining members were different. (The efficiency increased to 197% when the thickness of one leg was increased from 100 mm to 300 mm.) Further, the mode of failure changed from diagonal tensile failure to flexural failure.
3. The efficiency of the corner increased by about 32 per cent when the length ratio of the two legs was changed from one to two.

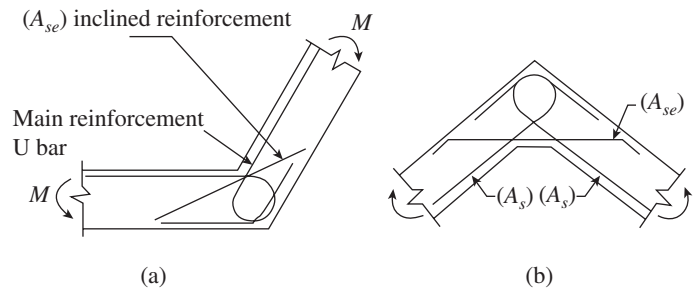


FIG. 19.43 Reinforcement details for obtuse and acute corners (a) Obtuse angle (b) Acute angle

The main reinforcement should be restricted to about 0.65–1.0 per cent of the section in order to avoid brittle failure of the corner. If the area of inclined reinforcement, A_{se} , is the same as that of main reinforcement, A_s , the main reinforcement percentage may be increased to about 0.8–1.2 per cent. If the reinforcement percentage is higher than this, the corner must be provided with a reinforced haunch and stirrups (Nilsson and Losberg 1976).

Nilsson and Losberg (1976) also tested 60° acute angle specimens and observed that the failure had the same characteristics as in the tests with 90° and 135° corners. Based on their tests, they suggested a reinforcement layout shown in Fig 19.43(b). The inclined reinforcement in acute-angled corner is laid in a haunch. The length of this haunch is at least one-half the thickness of the wing wall and the reinforcement is less than 0.5–0.75 per cent and at least equal to the thickness of wing wall when it is about 0.8–1.2 per cent. The bars must not be spliced in the corner region. Further, recesses or openings should not be made at or in the immediate vicinity of corners or joints, since they considerably reduce the strength and stiffness of the connection. More information and examples on the design and detailing of joints may be found in the works of Ingle and Jain (2002), Park and Paulay (1975), Paulay and Priestley (1992), Prakash Rao (1995), and Taylor and Clarke (1976).

EXAMPLES

EXAMPLE 19.1:

Design an interior (Type 2) joint of a building. The details of the column and beam meeting at the joint are given in Table 19.7 (Uma and Jain 2006).

TABLE 19.7 Section details of interior joint

Parameter	Column	Beam	Slab
	625 mm × 625 mm	500 mm × 625 mm	150 mm thick
Longitudinal reinforcement	12–25 mm diameter (5890 mm ²) $f_y = 415$ MPa	Top: 6–22 mm diameter (2280 mm ²) Bottom: 3–22 mm diameter (1140 mm ²) $f_y = 415$ MPa	Top: 10 mm at 150 c/c Bottom: 10 mm at 200 c/c
Height/Span	3500 mm	5000 mm	

Assume M25 concrete and Fe 415 steel reinforcement and moderate environment. Further, assume that beams of similar size are provided in the perpendicular direction as well.

SOLUTION:

It is important to point out that for Type 2 connections, the column sizes that are adequate for member strength requirements may not be adequate to satisfy anchorage and shear requirements within the joint. Wider beam sections may be necessary to cover column faces (at least 75% of the column width) and to allow the use of higher joint shear values (ACI 352:2002). Since L_d given in IS 456 results in large values (as it does not consider the confined core), L_d as per ACI 352 is considered. Table 19.8 is based on anchorage requirements for hooked bars terminating in exterior joint ($f_y = 415$ MPa and $f_{ck} = 25$ MPa are assumed with $\alpha = 1.25$).

TABLE 19.8 Minimum column depth for Type 2 beam-column joints

d_b (mm)	$L_{dh} = \frac{\alpha f_y d_b}{5.55 \sqrt{f_{ck}}} \text{ (mm)}$	h (mm) for column = $20d_b(f_y/415)$	
		With hoop spacing $> 3d_b$ (mm)	With hoop spacing $\leq 3d_b$ (mm)
12	225	315	270
16	300	390	330
20	375	465	390
22	412	502	420
25	468	558	465
28	524	614	510
32	600	690	570

In Table 19.8, an extra 90 mm has been added to L_{dh} to determine the minimum column dimension to anchor a given bar. The quantity 90 mm has been assumed based on twice the clear cover (typical 40 mm) plus one tie-bar diameter (assumed 10 mm). The 0.8 multiplier given in ACI 352:2002 for close spacing of transverse reinforcement is included in column 4 of Table 19.8. Table 19.9 is based on requirements for the ratio of joint dimension to the diameter of beam and column bars of interior joints for $f_y = 415$ MPa (it should be

noted that it is not dependent on f_{ck}). These tables will be useful for selecting bar diameters and joint dimensions.

TABLE 19.9 Minimum column or beam depth of Type 2 interior beam-column joints

d_b (mm)	Column or Beam Size (mm)
12	240
16	320
20	400
22	440
25	500
28	560
32	640

Step 1 Check the depth of the beam and column. For 22 mm bar, the depth required for beam (Table 19.9) is 440 mm. Beam depth provided = 625 mm. Hence, depth is sufficient. Similarly, for 25 mm bar, column width required = 500 mm, column width provided = 625 mm. Hence, width is sufficient.

Step 2 Compute the tension force in beam bars.

Force developed in top bars

$$T_1 = \alpha f_y A_{st} = 1.25 \times 415 \times \frac{2280}{1000} = 1182.75 \text{ kN} = C_1$$

Force developed in bottom bars

$$T_2 = \alpha f_y A_{st} = 1.25 \times 415 \times \frac{1140}{1000} = 591.4 \text{ kN} = C_2$$

Step 3 Compute column shear.

$$V_{cd} = \frac{M_{pr,A}^- + M_{pr,B}^+}{h_{st}}$$

$$M_{pr,A}^- = A_s \alpha f_y (d - 0.416x_u)$$

$$\text{with } x_u = \frac{1.25 f_y A_{st}}{0.36 f_{ck} b} = \frac{1.25 \times 415 \times 2280}{0.36 \times 25 \times 500} = 262.83 \text{ mm}$$

From Table 16 of IS 456, cover for moderate environment = 30 mm

Assuming 8 mm stirrups in beam

$$d = 625 - 30 - 8 - 22/2 = 576 \text{ mm}$$

$$\begin{aligned} M_{pr,A}^- &= 2280 \times 1.25 \times 415 (576 - 0.416 \times 262.83) / 10^6 \\ &= 551.94 \text{ kNm} \end{aligned}$$

$$M_{pr,B}^+ = A_s \alpha f_y (d - 0.416x_u)$$

$$x_u = \frac{1.25 f_y A_{st}}{0.36 f_{ck} b} = \frac{1.25 \times 415 \times 1140}{0.36 \times 25 \times 500} = 131.42 \text{ mm}$$

$$M_{pr,B}^+ = 1140 \times 1.25 \times 415(576 - 0.416 \times 131.42)/10^6$$

$$= 308.3 \text{ kNm}$$

$$V_{cd} = \frac{551.94 + 308.3}{3.5} = 245.78 \text{ kN}$$

Step 4 Compute joint shear.

$$\text{Joint shear } V_j = T_1 + C_2 + T_{s1} + T_{s2} - V_{co1}$$

where T_{s1} and T_{s2} are the tension force due to slab reinforcement within effective width of T-beam.

As per Clause 23.1.2 of IS 456, the effective width of flange in T-beam should not exceed the following:

- (a) $L_o/6 + b_w + 6D_f = (0.7 \times 5000)/6 + 500 + 6 \times 150 = 1983 \text{ mm}$
- (b) $b_w + b_o$ (see Table 5.9 of Chapter 5) = $500 + 3000 = 3500 \text{ mm}$

(assuming clear span b_o on either side as 3000 mm and slab thickness as 150 mm)

Hence, effective width of slab = 1983 mm

Within this width we have $(1983 - 500)/150 = 9$ top bars and $(1983 - 500)/200 = 7$ bottom bars in the slab. Both bottom and top bars are assumed to be continuous through the connection.

$$\text{Hence } T_{s1} + T_{s2} = (19 + 7) \times 78.5 \times 1.25 \times 415/1000 = 651.55 \text{ kN}$$

$$\text{Joint shear} = 1182.75 + 591.4 + 651.55 - 245.78 = 2179.92 \text{ kN}$$

Step 5 Compute joint shear strength.

$$V_n = \gamma \sqrt{f_{ck}} b_j h_c$$

Width of beam = 500 mm $> 3/4 \times 625 = 469 \text{ mm}$

$\gamma = 1.5$ as per Clause 8.2.1 Draft IS 13920 (assuming joint confined on all four faces) with similar beams.

As per Clause 8.2.2 of Draft IS 1920, since $b_c > b_b$

$$\text{Joint width } b_j = \text{Min}(b_c; b_b + 0.5h_c) = \text{Min}(625; 500 + 0.5 \times 625) = 625 \text{ mm}$$

Shear strength of joint

$$= 1.5 \sqrt{25} \times 625 \times \frac{625}{1000}$$

$$= 2929.7 \text{ kN} > 2179.92 \text{ kN}$$

Step 6 Compute transverse reinforcement in joint. As per Clauses 8.1.2 and 8.1.3, since the joint is confined by beams, at least half the special confining reinforcement required at the end of columns should be provided in the joint.

As per Clause 7.4.8 of IS 13920, the area of rectangular hoop

$$A_{sh} = 0.18sh \frac{f_{ck}}{f_y} \left[\frac{A_g}{A_k} - 1.0 \right]$$

or

$$A_{sh} = 0.05sh \frac{f_{ck}}{f_y}$$

Assuming nominal cover of 40 mm and tie of 10 mm, the size of core is $(625 - 90 = 535 \text{ mm})$ by $(625 - 90 = 535 \text{ mm})$. As it is greater than 300 mm, overlapping hoops or single hoop with cross-ties have to be provided. Thus, h will be $535/2 = 267.5 \text{ mm}$.

$$A_g = 625 \times 625 = 3,90,625 \text{ mm}^2$$

$$A_k = 535 \times 535 = 2,86,225 \text{ mm}^2$$

$$A_g/A_k - 1 = 0.3647$$

The spacing of hoops should not exceed the following (Clause 7.4.6 of Draft IS 13920):

- (a) One-fourth of the minimum column size = $625/4 = 156.25 \text{ mm}$
- (b) Not less than 75 mm and not more than 100 mm
- (c) Six times the diameter of longitudinal bar = $6 \times 25 = 150 \text{ mm}$

Hence choose $s = 100 \text{ mm}$

$$\text{Hence } A_{sh} = 0.18 \times 100 \times 267.5 \times 25/415 \times 0.3647 = 105.8 \text{ mm}^2$$

$$A_{sh} \text{ as per second equation} = 0.05 \times 267.5 \times 100 \times 25/415 = 80.6 \text{ mm}^2 < 105.8 \text{ mm}^2$$

As beams confine the joint in four faces, only 50 per cent of the confining reinforcement has to be provided; adopt 8 mm hoops (area of one leg = $50.26 \text{ mm}^2 \approx 52.4 \text{ mm}^2$)

The hoop details are given in Fig. 19.44.

Step 7 Check for flexural strength ratio.

$$\text{Area of steel in column} = 12 \times 25 \text{ mm bars} = 5890 \text{ mm}^2$$

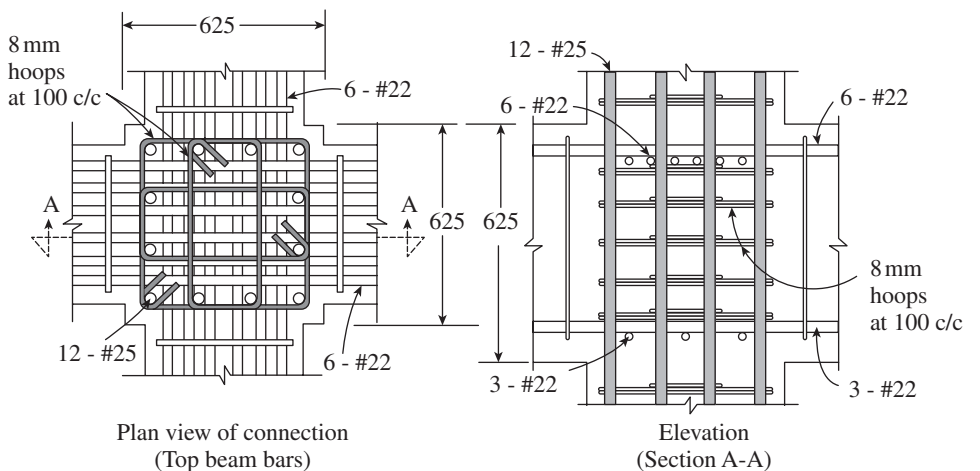


FIG. 19.44 Detailing of joint of Example 19.1

$$p = (5890/625^2) \times 100 = 1.508\%; p/f_{ck} = 1.508/20 = 0.075$$

$$d' = 40 + 8 + 25/2 = 60.5 \text{ mm}$$

$$d'/D = 60.5/625 = 0.097 \approx 0.10$$

From Chart 44 of SP 16:1980, for $P_u/(f_{ck}bD) = 0$, $p/f_{ck} = 0.025$
 $M_u/f_{ck}bD^2 = 0.105$; $M_u = 0.105 \times 25 \times 625^3/106 = 640.87 \text{ kNm}$

Note: This will be conservative. In practice, P_u will be known and hence the exact value of $P_u/(f_{ck}bD)$ should be used.

$$\Sigma M_c = 2 \times 640.87 = 1281.74 \text{ kNm}$$

$$\Sigma M_B = 551.94 + 308.3 = 860.24 \text{ kNm}$$

The ratio $\frac{\Sigma M_c}{\Sigma M_B} = \frac{1281.74}{860.24} = 1.49 > 1.2$ (As per IS 13920 it should only be 1.1)

Hence, it is safe.

Note: The design of a non-seismic exterior beam-column joint is given in Example 7.4 of Chapter 7. More examples on beam-column design may be found in ACI 352:2002 and on the website <http://www.iitk.ac.in/nicee/IITK-GSDMD/EQ22.pdf>.

EXAMPLE 19.2 (Design of hanger stirrups):

Design the hanger stirrups for a beam-to-girder joint as shown in Fig. 19.45(a). The factored reaction from the secondary beam of size 300 mm × 500 mm on each side of the joint is 200 kN. Assume Fe 415 steel and M25 concrete. Assume that the shear reinforcement in the beam and girder is two-legged 10 mm of Fe 415 grade.

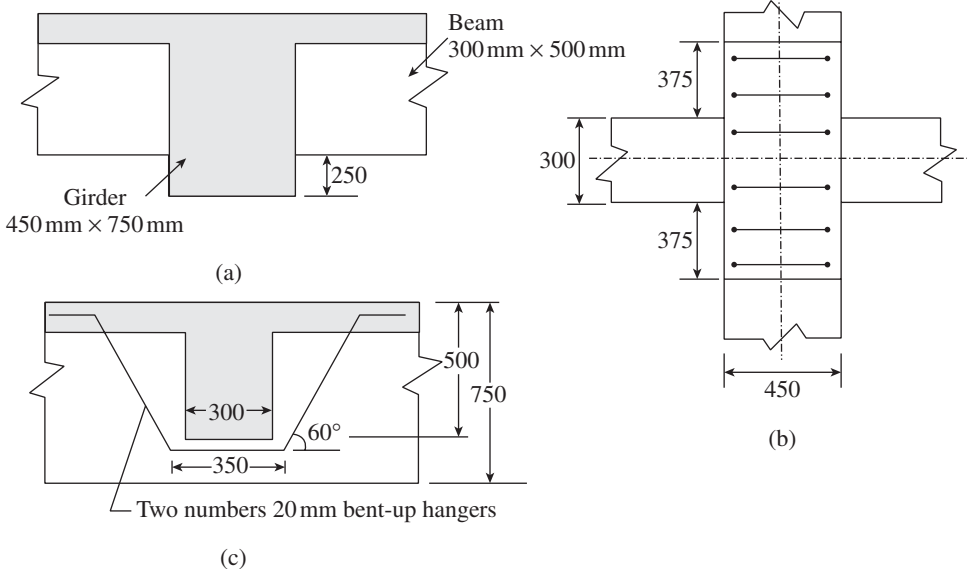


FIG. 19.45 Hanger stirrups of Example 19.2 (a) Beam-girder joint (b) Plan view of joint zone (c) Alternate bent-up hangers

SOLUTION:

Reaction, $V_{ur} = 200 \text{ kN}$

Step 1 Check whether hanger stirrups are required.

Check $V_{ur} > 0.22\sqrt{f_{ck}}b_bD_b = 0.22 \times \sqrt{25} \times 300 \times \frac{500}{10^3}$
 $= 165 \text{ kN} < 200 \text{ kN}$

Hence, hanger stirrups are required.

Step 2 Compute tensile force to be carried by hangers. Tensile force to be carried by hanger stirrups on each side

$$T_h = V_{ur} \frac{D_b}{D_g} = 200 \left(\frac{500}{750} \right) = 133.33 \text{ kN}$$

Step 3 Design hanger reinforcement. Equating the tensile force to the strength of hanger reinforcement,

$$A_h(0.87f_y) = 133.33 \times 10^3$$

Thus, $A_h = \frac{133.33 \times 1000}{0.87 \times 415} = 370 \text{ mm}^2$

Providing two-legged 10 mm bars as hanger stirrups, we need $370/(2 \times 78.5) = 3$ sets on either side of the joint. This should be provided within a distance of $D_g/2 > b_b/2$ on either side, that is, $750/2 = 375 \text{ mm}$, as shown in Fig. 19.45(b). As $D_b/2 = 500/2 = 250 \text{ mm}$ is only 25 mm greater than $450/2 = 225 \text{ mm}$, no hanger bars are necessary in the secondary beam. It is important to note that these hanger stirrups are to be provided in addition to the shear reinforcement already provided in the girder.

Step 4 Provide alternate bent-up hanger bars. We can also provide alternate bent-up bars as shown in Fig. 19.44(c).

Equating the strength of bent-up bars with the reaction, we get

$$0.87f_y \sin 60 \times 2 \times A_{bh} = 2 \times 133.33 \times 1000$$

Hence, $A_{bh} = 426 \text{ mm}^2$

Provide two sets of bent-up hangers of size 20 mm, with area = 628 mm^2 .

EXAMPLE 19.3 (Design of corbel):

Design a corbel to support a factored vertical load of 300 kN, applied at a distance of 350 mm from the column face. The column is 300 mm × 500 mm in plan. Assume M30 concrete, Fe 415 steel, and moderate environment.

SOLUTION:

Step 1 Determine ultimate loads on the corbel.

Factored vertical load = $V_u = 300$ kN, acting at a distance $a_v = 350$ mm

In the absence of a roller or low-friction support pad,

Horizontal tensile force, $N_u = 0.2 \times V_u = 0.2 \times 300 = 60$ kN

Size of column = 300 mm \times 500 mm

Corbel will be placed along the major axis of column.

Hence,

Width of corbel, $b_w = 300$ mm

Step 2 Determine corbel geometry.

Permissible bearing stress, f_{br} (Clause 34.4 of IS 456) = $0.45f_{ck} = 0.45 \times 30 = 13.5$ MPa

Assume length of bearing plate, $l_{bp} = 300$ mm

Width of bearing plate $l_w = \frac{V_u}{f_{br} \times l_{bp}} = \frac{300 \times 1000}{13.5 \times 300} = 74$ mm.
Provide 80 mm.

Clear cover for moderate environment (Table 16 of IS 456) = 30 mm

Assuming main bar and anchor bar of 20 mm and stirrups of 10 mm, length of corbel

$L = a_v + l_w/2 + \text{Diameter of (anchor bar + framing bar + stirrup) + clear cover}$

$$= 350 + 80/2 + (20 + 10 + 10) + 30 = 460 \text{ mm}$$

According to the shear friction provisions of the ACI code, the nominal shear strength, V_n , should not exceed $0.16f_{ck}b_wd$, $11b_wd$, and $(3.3 + 0.064f_{ck})b_wd$. With $f_{ck} = 30$ MPa, this limitation becomes the smallest of $4.8b_wd$, $11b_wd$, and $5.22b_wd$. The first limit controls. With $V_u = \phi V_n$, $\phi = 0.75$, $b_w = 300$ mm, we get

$$300 \times 1000 = 0.75 \times 4.8 \times 300 \times d \text{ or } d = 278 \text{ mm}$$

Let us assume $d = 400$ mm.

[Check: As per Table 20 of IS 456, $\tau_{c,max} = 3.5$ N/mm², $V_u/bd = 300 \times 1000/(300 \times 400) = 2.5$ N/mm² $<$ $\tau_{c,max}$. Hence, the chosen value of d is sufficient.]

Choose $h = 450$ mm. Adopt the depth at the other end (near the load) = 250 mm $>$ $d/2$.

Check for $a_v/d = 350/d = 350/400 = 0.875$. Hence, the ACI method is applicable.

The adopted size is shown in Fig. 19.46.

Step 3 Compute reinforcement required for shear friction.

The shear friction reinforcement is given by

$$A_{vf} = \frac{V_u}{\phi \mu f_y} = \frac{300 \times 1000}{0.75 \times 1.4 \times 415} = 689 \text{ mm}^2$$

Step 4 Compute reinforcement required for flexure. The bending moment to be resisted

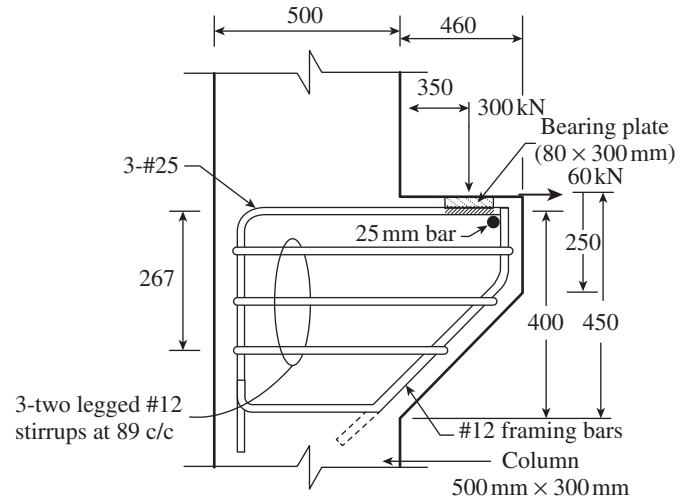


FIG. 19.46 Corbel of Example 19.4

$$M_u = [V_u a_v + N_u (h - d)] = \frac{[300 \times 350 + 60(450 - 400)]}{1000} = 108 \text{ kNm}$$

Required area of flexural steel

$$A_f = \frac{M_u}{\phi f_y (d - 0.5a)}, \text{ where } a = \frac{A_f f_y}{0.68 f_{ck} b}$$

As a first trial, let us assume $(d - 0.5a) = 0.9d$

$$A_f = \frac{M_u}{\phi f_y (d - 0.5a)} = \frac{108 \times 10^6}{0.75 \times 415 \times (0.9 \times 400)} = 964 \text{ mm}^2$$

Checking the stress block depth gives

$$a = \frac{A_f f_y}{0.68 f_{ck} b} = \frac{964 \times 415}{0.68 \times 30 \times 300} = 65.4 \text{ mm}$$

Hence, the revised steel area

$$A_f = \frac{M_u}{\phi f_y (d - 0.5a)} = \frac{108 \times 10^6}{0.75 \times 415 \times (400 - 0.5 \times 65.4)} = 944.7 \text{ mm}^2$$

Step 5 Compute reinforcement for direct tension. The required reinforcement to resist direct tension

$$A_n = \frac{N_u}{\phi f_y} = \frac{60 \times 1000}{0.75 \times 415} = 193 \text{ mm}^2$$

Step 6 Compute total area of reinforcement at top of corbel. Total steel area at the top of the bracket should not be less than the following:

$$(a) A_s \geq A_f + A_n = 945 + 193 = 1138 \text{ mm}^2$$

$$(b) A_s \geq \frac{2}{3} A_{vf} + A_n = \frac{2}{3} \times 689 + 193 = 653 \text{ mm}^2$$

Minimum steel, $A_{s,min} = 0.032(f_{ck}/f_y)b_wd = 0.032(30/415) \times 300 \times 400 = 278 \text{ mm}^2$

Hence provide three 25 mm bars (area provided = 1472 mm^2).

Step 7 Compute the area of horizontal stirrups. Area of horizontal stirrups,

$$A_h \geq 0.5(A_s - A_n) \geq 0.5(1298 - 193) = 553 \text{ mm}^2$$

Provide three 12 mm diameter double-legged stirrups, with area = 678 mm². As per the ACI code, these should be placed within $2/3d = 2/3 \times 400 = 267$ mm, measured from the tension steel. A spacing of 89 mm may be adopted. Provide a pair of 12 mm framing bars at the inside corner of the hoops to improve anchorage, as shown in Fig. 19.46.

Step 8 Check for anchorage of bars. Anchorage for the 25 mm main bars has to be provided at the loaded end by welding these bars to the underside of the bearing plate and at the other end by a standard 90° bend. The required development length for 25 mm bar in M30 concrete (Table 65 of SP 16) = 940 mm (measured from the face of the column). Assuming a cover of 50 mm and 25 mm bars for the column, available length with 90° bend = $(500 - 50 - 25) + 200$ (anchorage value of 90° bend from Table 67 of SP 16) = 625 mm. Extra length required $940 - 625 = 315$ mm. Extend the bars into the column for a minimum length of 320 mm. The hooks should be placed inside the column cage. For the stirrups, a standard 135° hook should be provided.

EXAMPLE 19.4 (Tension capacity of anchor without edge effects):

Design a single-headed bolt installed at the bottom of a 150 mm thick slab to support a service dead load of 20 kN. Assume M20 concrete and no cracking under service loads.

SOLUTION:

Step 1 Determine factored design load.

$$N_u = 1.5 \times 20 = 30 \text{ kN}$$

Step 2 Compute steel strength of anchor in tension.

Nominal strength of anchor in tension $N_{sn} = A_{se,N} f_{uta}$

Let us assume 16 mm diameter grade 4.6 bolt, in the yield stress, $f_{ya} = 240$ MPa and $f_{uta} = 400$ MPa. Threaded area of bolt = 157 mm²; size of head = $1.65D = 1.65 \times 16 = 26.4$ mm (see Subramanian 2008).

$$N_{sn} = 157 \times \frac{400}{1000} = 62.8 \text{ kN}$$

$$\phi N_{sn} = 0.75 \times 62.8 = 47.1 \text{ kN} > 30 \text{ kN}$$

Step 3 Calculate concrete breakout capacity. The concrete breakout strength of a single anchor in tension in cracked concrete

$$\phi N_n = \phi k_c \lambda_a \sqrt{f'_c} h_{ef}^{1.5}$$

$k_c = 10$, $\lambda_a = 1$ (normal concrete), $\phi = 0.70$
 $\psi_3 = 1.25$ (no cracking under service load)
 $f_{ck} = 30$ MPa; hence $f'_c = 30 \times 0.8 = 24$ MPa

$$30 \times 1000 = 0.7 \times 10 \times 1 \times \sqrt{24} \times h_{ef}^{1.5}$$

$$h_{ef}^{1.5} = 874.8; h_{ef} = (874.8)^{2/3} = 91.5 \text{ mm}$$

Provide $h_{ef} = 100$ mm;

$$\phi N_n = 0.7 \times 10 \times 1 \times \sqrt{24} \times \frac{100^{1.5}}{10^3} = 34.3 \text{ kN} > 30 \text{ kN}$$

Note: The value of h_{ef} can be determined directly only in the case of a single fastener away from the edge. Whenever the edges are near or there are other adjacent fasteners, the determination of h_{ef} is iterative.

Step 4 Calculate pull-out strength in tension.

$$N_{pn} = \psi_p N_p$$

$\psi_p = 10$ if there is cracking

$N_p = \phi(8A_{brg}f'_c)$ for a headed bolt

The bearing area of heads and nuts A_{brg} is not found in Appendix D of ACI 318. It can approximately be calculated as

$$A_{brg} = \frac{\pi(d_{head}^2 - d_a^2)}{4} = \frac{\pi}{4}(26.4^2 - 16^2) = 346.3 \text{ mm}^2$$

$$N_p = 0.70 \times 8 \times 346.3 \times 24 = 46,543 \text{ N}$$

$$= 46.54 \text{ kN} > 30 \text{ kN}$$

$$N_{pn} = 1 \times 46.54 = 46.54 \text{ kN}$$

Hence, provide grade 4.6 headed bolt of 16 mm diameter with an embedment length of 100 mm (see Fig. 19.47).

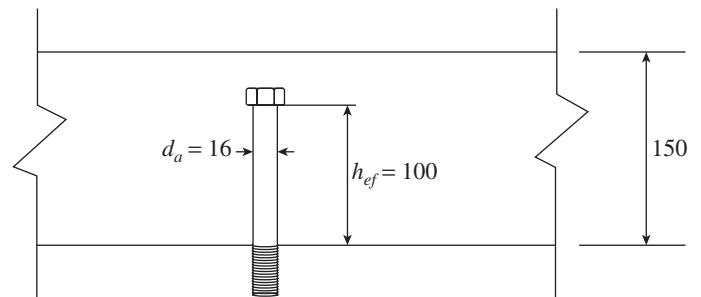


FIG. 19.47 Designed anchor of Example 19.4

Note: Concrete side-face blowout in tension is not applicable as there is no free edge near the anchor. It has to be noted that concrete break-out capacity governs.

EXAMPLE 19.5:

Determine the ultimate shear capacity of a hexagonal head cast-in-place anchor of diameter 16 mm and 100 mm embedment depth. Assume M30 concrete and the concrete is cracked.

SOLUTION:

Step 1 Compute steel strength in shear.

$$V_{sa} = 0.6A_{se,V}f_{uta}$$

Assuming $f_{ya} = 240$ MPa and $f_{uta} = 400$ MPa

$$A_{se,V} = 157 \text{ mm}^2 \text{ (as in Example 19.4)}$$

$$V_{sa} = 0.6 \times 157 \times 400/10^3 = 37.68 \text{ kN}$$

$$\phi V_{sa} = 0.65 \times 37.68 = 24.49 \text{ kN}$$

Step 2 Compute concrete breakout strength in shear. The anchor is not located near a free edge; hence, concrete breakout does not apply to this anchor.

Step 3 Compute concrete pryout strength in shear.

Concrete pryout strength, $V_{cp} = k_{cp}N_{cp}$

Since $h_{ef} > 65$ mm, $k_{cp} = 2.0$.

$N_{cp} = N_a$ from tension calculations (see Example 19.4)

$$= k_c \lambda_a \sqrt{f'_c} h_{ef}^{1.5} = 10 \times 1 \times \frac{\sqrt{24}(100)^{1.5}}{10^3} = 48.99 \text{ kN}$$

$$V_{cp} = 2 \times 48.99 = 97.98 \text{ kN}$$

$\phi = 0.70$ for concrete pryout under condition B (in the absence of supplementary reinforcement)

$$\phi V_{cp} = 0.70 \times 97.98 = 68.59 \text{ kN}$$

Hence design shear strength = 24.49 kN

Note: Steel strength governs the design because the anchor is not near a free edge.

EXAMPLE 19.6 (Shear capacity of anchor with edge effects):

Determine the concrete breakout capacity in shear for a 12 mm diameter threaded anchor embedded in a 200 mm deep uncracked concrete section. Assume M30 concrete with $h_{ef} = 120$ mm, $c_1 = 140$ mm, and $c_2 = 110$ mm (see Fig. 19.48).

SOLUTION:

Calculate concrete breakout capacity in shear.

$$V_n = \frac{A_v}{A_{vo}} \psi_6 \psi_7 \psi_8 V_{no}$$

$$A_{vo} = 4.5c_1^2 = 4.5 \times 140^2 = 88,200 \text{ mm}^2$$

Step 1 Determine A_v . This edge distance will not allow the full concrete breakout cone to develop. Hence, A_v should be calculated accordingly (see Fig. 19.35).

$1.5c_{a1} = 1.5 \times 140 = 210$ mm $>$ 200 mm. Hence, use 200 mm in calculating A_v .

$$c_2 = 110 \text{ mm} < 1.5c_1$$

$$\text{Hence } A_v = 200(1.5 \times 140 + 110) = 64,000 \text{ mm}^2$$

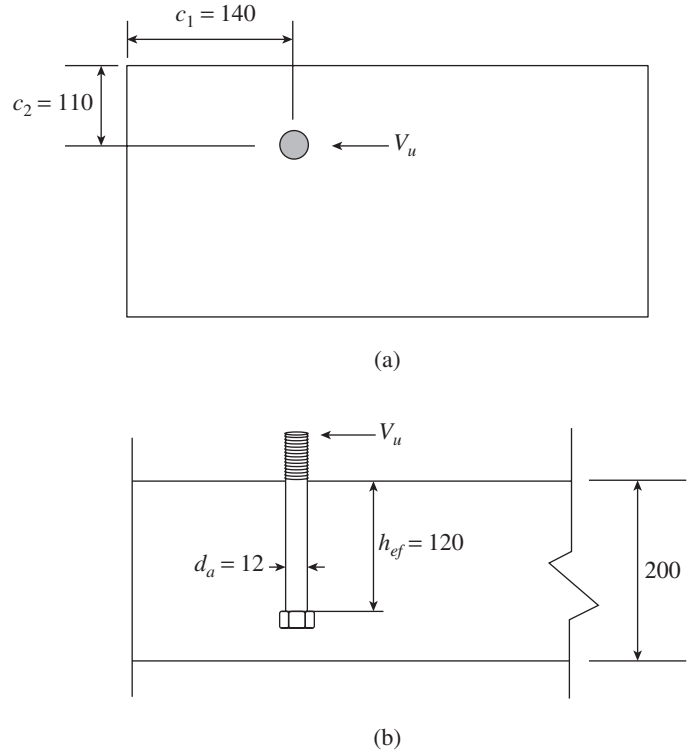


FIG. 19.48 Anchor of Example 19.6

Step 2 Calculate basic breakout capacity in shear.

$$V_{no} = \lambda_a \left[0.6 \left(\frac{l_e}{d_a} \right)^{0.2} \sqrt{d_a} \right] \sqrt{f'_c} (c_1)^{1.5}$$

$l_e = h_{ef}$ for headed studs = 120 mm

$d_a = 12$ mm, $\lambda_a = 1$ (normal concrete)

$$V_{n01} = 1 \times \left[0.6 \left(\frac{120}{12} \right)^{0.2} \sqrt{12} \right] \sqrt{24}(140)^{1.5} = 26,732.5 \text{ N}$$

$$= 26.73 \text{ kN}$$

$$V_{n02} = 3.7 \lambda_a \sqrt{f'_c} (c_1)^{1.5} = 3.7 \times 1 \times \sqrt{24}(140)^{1.5}/10^3 = 30.03 \text{ kN}$$

Hence, 26.73 kN is chosen.

Step 3 Calculate modification factors.

$$\psi_6 = 0.7 + 0.3 \frac{c_2}{1.5c_1} \text{ (since } c_2 < 1.5c_1)$$

$$= 0.7 + 0.3(110/210) = 0.857$$

$$\psi_7 = 1.25 \text{ (uncracked concrete)}$$

$$\psi_8 = \sqrt{\frac{1.5c_1}{h_a}} \geq 1.0 \text{ (since } h_a < 1.5c_1)$$

$$\psi_8 = \sqrt{210/120} = 1.323$$

Step 4 Compute nominal breakout capacity in shear.

Hence, $V_{n1} = (64,000/88,200) \times 0.857 \times 1.25 \times 1.323 \times 26.73 = 27.49 \text{ kN}$

$$\phi V_{n1} = 0.7 \times 27.49 = 19.24 \text{ kN}$$

It has to be noted that the breakout capacity of the concrete near a corner should be calculated in both orthogonal directions towards the free edge. Hence, the given calculations should be performed with $c_1 = 110 \text{ mm}$ and $c_2 = 140 \text{ mm}$ and V_{n2} is to be determined. The lesser of V_{n1} and V_{n2} is taken as the critical breakout capacity of the embedment in shear.

EXAMPLE 19.7:

Determine the ultimate capacity of the cast-in-place anchor group with the configuration shown in Fig. 19.49.

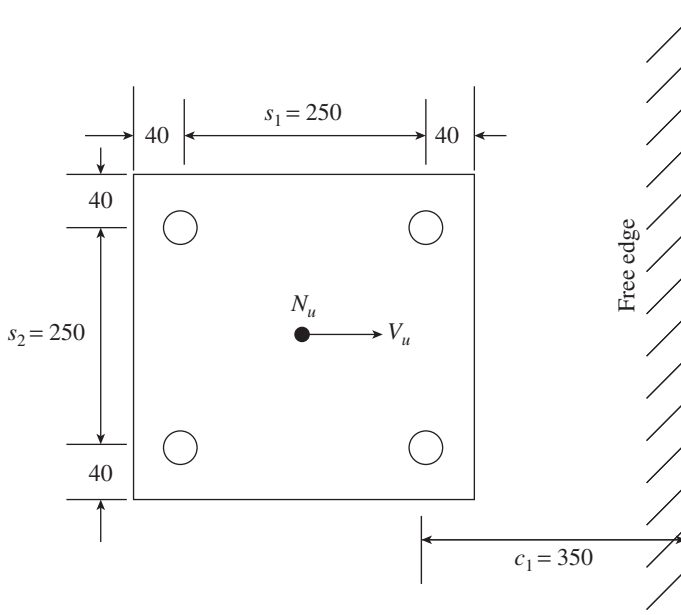


FIG. 19.49 Configuration of the cast-in-place anchor group of Example 19.7

Assume 20 mm diameter hexagonal head anchors, $h_{ef} = 300 \text{ mm}$, thickness of concrete = 1000 mm, M30 concrete, $f_{uta} = 40 \text{ MPa}$, applied tension $N_u = 200 \text{ kN}$, and shear $V_u = 40 \text{ kN}$.

SOLUTION:

Since the anchor group is concentrically loaded, each anchor is subjected to the same tension and shear forces.

Step 1 Compute steel strength in tension.

$$N_{sn} = A_{se} f_{uta}$$

Threaded area for 20 mm diameter anchor bolt = 245 mm^2

$$N_{sn} = 245 \times 40/10^3 = 98 \text{ kN}$$

$$\phi N_{sn} = 0.75 \times 98 = 73.5 \text{ for single anchor}$$

$$= 4 \times 73.5 = 294 \text{ kN for the anchor group } > 200 \text{ kN } (N_u)$$

Step 2 Calculate concrete breakout strength in tension.

$$N_{ng} = \frac{A_N}{A_{N0}} \psi_1 \psi_2 \psi_3 \psi_4 N_{no}$$

For this example, A_N and A_{N0} will not be equal, as the multi-anchor group will have larger breakout area than a single anchor. The edge distance of 350 mm is less than $1.5h_{ef} (= 1.5 \times 300)$; hence, the full failure cone cannot be developed.

$$\begin{aligned} A_N &= (c_1 + s_1 + 1.5h_{ef})(1.5h_{ef} + s_2 + 1.5h_{ef}) \\ &= (350 + 250 + 1.5 \times 300)(1.5 \times 300 + 250 + 1.5 \times 300) \\ &= 1050 \times 1150 = 120.75 \times 10^6 \text{ mm}^2 \end{aligned}$$

$$A_{N0} = 9h_{ef}^2 = 9 \times 300^2 = 81 \times 10^4 \text{ mm}^2.$$

$\psi_1 = 1$, as the tensile force is applied at the centroid of the anchor group.

Since $c_1 \leq 1.5h_{ef}$, edge effects have to be considered.

$$\psi_2 = 0.7 + 0.3 \frac{c_1}{1.5h_{ef}} = 0.7 + 0.3 \frac{350}{1.5 \times 300} = 0.933$$

$\psi_3 = 1.0$ as concrete cracking is expected.

$\psi_4 = 1.0$ for cast-in-place anchors.

$$N_{no} = k_c \lambda_a \sqrt{f'_c} (h_{ef})^{1.5} = 10 \times 1 \times \frac{\sqrt{24}(300)^{1.5}}{10^3} = 254.56 \text{ kN}$$

$$\begin{aligned} N_{ng} &= \frac{120.75 \times 10^4}{81 \times 10^4} \times (1.0)(0.933)(1.0)(1.0) \times 254.56 \\ &= 354.18 \text{ kN} \end{aligned}$$

$\phi = 0.70$ for concrete breakout under condition B.

$$\phi N_{ng} = 0.70 \times 354.18 = 247.93 \text{ kN for the group } > 200 \text{ kN } (N_u).$$

Step 3 Compute pull-out strength in tension.

$$N_{pn} = \psi_p N_p$$

$\psi_p = 1.0$ as cracking is expected

$$N_p = 8A_{brg} f'_c$$

Assuming head size = $1.65 \times 20 = 33 \text{ mm}$

$$\text{Approximate } A_{brg} = \frac{\pi(33^2 - 20^2)}{4} = 541 \text{ mm}^2$$

$$f'_c = 0.8 \times 30 = 24 \text{ MPa}$$

$$N_{pn} = 8 \times 541 \times 24/1000 = 103.87 \text{ kN}$$

$\phi = 0.70$ for pull-out under condition B.

$$\phi N_{pn} = 0.7 \times 103.87 = 72.71 \text{ kN for a single anchor}$$

$$= 4 \times 72.71 = 290.84 \text{ kN for the anchor group } > 200 \text{ kN } (N_u)$$

Step 4 Calculate concrete side-face blowout in tension.

Concrete side-face blowout applies only when

$$h_{ef} > 2.5c_1 = 2.5 \times 350 = 875 \text{ mm}$$

As $h_{ef} = 300 \text{ mm}$, this failure mode is not applicable.

The governing case in tension is concrete breakout = 247.93 kN.

Step 5 Compute steel strength in shear.

$$V_{sa} = 0.6A_{se} f_{uta} = 0.6 \times 245 \times 40/10^3 = 58.8 \text{ kN}$$

Since Fe 240 steel is ductile, the strength reduction factor for steel failure $\phi = 0.65$.

$$\begin{aligned}\phi V_{sa} &= 0.65 \times 58.8 = 38.22 \text{ kN for single anchor} \\ &= 4 \times 38.22 = 152.88 \text{ kN for anchor group}\end{aligned}$$

Step 6 Compute concrete breakout strength in shear.

$$V_{ng} = \frac{A_v}{A_{v0}} \psi_5 \psi_6 \psi_7 \psi_8 V_{n0}$$

For this example, there are two anchors located along the free edge.

$$\begin{aligned}A_v &= [2(1.5c_1) + s_1](1.5c_1) = [2(1.5 \times 350) + 250](1.5 \times 350) \\ &= 1300 \times 525 = 68.2 \times 10^4 \text{ mm}^2\end{aligned}$$

$$A_{v0} = 4.5c_1^2 = 4.5 \times 350^2 = 55.125 \times 10^4 \text{ mm}^2$$

$\psi_5 = 1.0$ as shear force is applied at the centroid.

$\psi_6 = 1.0$ as there is only a single free edge.

$\psi_7 = 1.0$ as concrete cracking is expected.

$\psi_8 = 1.0$ as $h_a > 1.5c_1$; bottom surface is below the failure cone.

$$l_e = h_{ef} = 300 \text{ mm}, d_a = 20 \text{ mm}$$

$$\begin{aligned}V_{n01} &= \lambda_a \left[0.6 \left(\frac{l_e}{d_a} \right)^{0.2} \sqrt{d_a} \right] \sqrt{f'_c} (c_1)^{1.5} \\ &= 1 \times \frac{\left[0.6 \left(\frac{300}{20} \right)^{0.2} \sqrt{20} \right] \sqrt{24} (350)^{1.5}}{10^3} \\ &= 147.94 \text{ kN}\end{aligned}$$

$$\begin{aligned}V_{n02} &= 3.7 \lambda_a \sqrt{f'_c} (c_1)^{1.5} = 3.7 \times 1.0 \times \frac{\sqrt{24} (350)^{1.5}}{10^3} \\ &= 118.69 \text{ kN}\end{aligned}$$

Hence $V_{n0} = 118.69 \text{ kN}$

$$\begin{aligned}V_{ng} &= \frac{68.2 \times 10^4}{55.125 \times 10^4} \times 1.0 \times 1.0 \times 1.0 \times 1.0 \times 118.69 \\ &= 146.84 \text{ kN}\end{aligned}$$

$\phi = 0.70$ for concrete breakout under condition B.

$$\phi V_{ng} = 0.7 \times 146.84 = 102.79 \text{ kN for the group.}$$

Step 7 Compute concrete pryout strength in shear.

$$V_{cpg} = k_{cp} N_{cpg}$$

$$k_{cp} = 2.0 \text{ for } h_{ef} \geq 65 \text{ mm}$$

$$N_{cpg} = N_{ng} \text{ from tension calculation} = 354.18 \text{ kN}$$

$$V_{cpg} = 2 \times 354.18 = 708.36 \text{ kN}$$

$\phi = 0.70$ for concrete pryout under condition B.

$$\phi V_{cpg} = 0.70 \times 708.36 = 495.85 \text{ kN}$$

Governing case in shear is concrete breakout strength in shear = $102.79 \text{ kN} > 40 \text{ kN} (V_u)$

Step 8 Calculate tension and shear interaction. Tension and shear interaction is considered when both the tension and shear stresses are greater than 20 per cent.

$$\text{Tension } \frac{N_u}{\phi N_n} = \frac{200}{247.93} = 0.807 > 0.2$$

$$\text{Shear } \frac{V_u}{\phi V_n} = \frac{40}{102.79} = 0.389 > 0.2$$

Both are greater than 20 per cent. Hence, interaction must be considered.

$$\frac{N_u}{\phi N_n} + \frac{V_u}{\phi V_n} \leq 1.2; 0.807 + 0.389 = 1.196 < 1.2$$

Hence, the anchor group is adequate to carry both tension and shear.

Step 9 Calculate splitting failure. The minimum c/c spacing

$$s_{\min} = 4d_a = 4 \times 20 = 100 \leq s_1 \text{ and } s_2 = 250 \text{ mm.}$$

Minimum edge requirement = Minimum cover = $40 \text{ mm} < c_1 = 350 \text{ mm}$

Hence, there is no danger of splitting failure.

SUMMARY

The performance of framed structures not only depends upon the individual structural elements but also upon the integrity of the joints. However, despite the significance of the joints in sustaining large deformations and forces during earthquakes, specific guidelines were not explicitly included in the Indian codes of practice until recently for their design and detailing.

Beam-column joints in a moment resistant frame can be classified as (a) interior joints, (b) exterior joints, (c) corner joints, and (d) knee joints. The requirements for the satisfactory performance of joints are listed. Some of the incorrect detailing practices adopted in India

are highlighted. The various types of joints and their behaviour under lateral forces are discussed.

The principal mechanisms of failure of a beam-column joint are (a) shear failure within the joint, (b) anchorage failure of bars, if anchored within the joint, and (c) bond failure of beam or column bars passing through the joint.

For design, beam-column joints can be categorized as non-seismic joints (Type 1) and seismic joints (Type 2). The joint shear can be determined from a free body diagram at the mid-height of a joint panel. By assuming the point of contraflexure at the mid-height

of a column, the column shears can be determined. The tensile force in reinforcement is taken as $\alpha A_s f_y$, where α is taken as 1.25 for seismic joints. Test data show that the longitudinal reinforcement in the slab within the effective width of beam has to be considered while calculating the joint shear force. The nominal shear strength is prescribed in ACI 352:2002 or Draft IS 13920 for different joint configurations, based on experimental results. This nominal shear (with a strength reduction factor) should be greater than the calculated joint shear force. Eccentricity of joints is considered by defining effective shear area of joint.

The role of transverse reinforcement and the mechanism of shear transfer in a beam-column joint are considered differently in the US and New Zealand codes. When joints are confined by beams (with width greater than or equal to three-fourths the column width) on all the four sides of the column, no joint reinforcement is required for Type 1 joints and only 50 per cent of confining reinforcement needs to be provided for Type 2 joints with a maximum spacing of 150 mm. The ties within the joint should be provided as closed hoops with the ends bent as 135° hooks. For best joint behaviour, the longitudinal column bars should be uniformly distributed around the perimeter of the column core.

In exterior beam-column joints, column dimensions seldom permit providing the development length by straight embedment alone; hence, hooks are often required to anchor negative (top) beam reinforcement, at the far side of joint. These 90° hooks should project inwards to facilitate the formation of diagonal compressive strut in the joint. Similarly, the bottom bars of beams should be projected upwards into the external beam-column joint. Such hooks should be located within 50 mm of the confined core. To reduce the congestion of reinforcement in beam columns, headed bars could be used instead of 90° hooks. To limit slippage of beam and column bars through the joint, ACI 352:2002 suggest that h_c/d_b and h_b/d_b should be greater than or equal to 20 (15 as per Draft IS 13920). While detailing beam-column joint reinforcement, constructability issues should be considered.

In beam-to-beam joints, additional vertical stirrups, called hanger stirrups, are to be provided to take care of tensile stresses occurring in such joints. The design and detailing of beam-to-beam joints are discussed.

Corbels are used extensively in precast concrete construction to provide seating for beams; they are short stub-like projections from the column or wall faces. The principal failure modes for corbels are discussed. Design of corbels can be done by using the strut-and-tie method (when a_v/d is between one and two) or by a combination of strut-and-tie and shear friction methods (when a_v/d is between one and two). On the basis of the ACI code, a method of design is explained and detailing of reinforcement is provided.

Anchors or fasteners are embedded in concrete and used to connect two elements of a structure, for example, structural steel columns to foundations. Anchors are broadly classified into cast-in-place anchors and post-installed anchors. Different types of cast-in-place and post-installed anchors are described. Anchors under tension loading can exhibit five different types of failure: (a) steel failure, (b) pull-out or pull-through failure, (c) concrete breakout, (d) concrete splitting, (b) side-face blowout. Failures in bonded anchors may occur due to pull-out of a cone of concrete, slip out of the hole, or steel failure. Under shear loading, the anchors may experience (a) steel failure, (b) concrete pryout failure, and (c) concrete breakout failure. As IS 456 does not contain provisions for the design of anchors, the design as per ACI 318 (Appendix D) is discussed. Designers should aim to achieve steel failure, as it will be ductile and provide sufficient warning before failure.

The various equations for finding the nominal steel strength of anchor in tension and shear, concrete breakout for single and group of anchors in tension and shear, pull-out in tension, concrete side-face blowout in tension, concrete pryout in shear for single and group of anchors, and bond strength of adhesive anchors in tension for single and group of anchors are provided. The interaction equation for anchors subjected to combined tension and shear is also provided. Brief discussions are included for considering earthquake effects, influence of reinforcements to resist shear, and required edge distances and spacing to prevent splitting of concrete. Some guidelines are also provided for obtuse- or acute-angled corners. Guidelines for joints between steel beams and RC columns are available in the ASCE Task Committee Report (1994).

REVIEW QUESTIONS

1. Explain capacity design concept.
2. How are beam-column joints classified?
3. What are the essential requirements for the satisfactory performance of a joint in an RC structure?
4. List a few of the incorrect detailing practices adopted in India for beam-column joints.
5. Sketch the elastic stresses that may occur in a knee opening-type joint and identify the cracking pattern.
6. Sketch a reinforcement detailing of an opening-type knee joint, which will have an efficiency of (a) above 85 per cent and (b) nearly 100 per cent.
7. How does the behaviour of a closing joint differ from that of an opening joint? Sketch the cracking pattern for this type of joint.
8. Where do we get T-joints? Sketch the correct detailing of a T-joint.
9. Explain the behaviour of beam-column joints during seismic loading.
10. List the principal mechanisms of failure of a beam-column joint.
11. How are beam-column joints classified as per ACI 352?
12. How is column shear at a beam-column joint calculated?
13. Sketch the free body diagram of a beam-column joint to determine joint shear.
14. How is the probable capacity in tension of reinforcement in beam calculated? Why is the value of $\alpha > 1.25$ considered in seismic joints?
15. Why is it necessary to include the slab reinforcement in the calculation of T_{pr} ? What is the width of slab normally considered contributing to joint strength?
16. What is the equation used to calculate nominal shear strength of the joint? How does the NZS code formula differ from that

- specified in IS 13920 and ACI 352? When can we consider a joint as fully confined? How is a joint with lightweight concrete considered?
17. How is an eccentric beam in a beam-column joint considered in ACI 318 and IS 13920?
 18. What is the difference in the philosophy of design of transverse stirrups in beam-column joints in ACI 318 and NZS 3101?
 19. When can we reduce the confining transverse tie requirement of a beam-column joint to half of that required at the end of columns?
 20. How many minimum layers of transverse reinforcement are required within the beam-column joint?
 21. What are the vertical spacing requirements of horizontal stirrups within a beam-column joint as per ACI 318?
 22. Why is anchorage requirement more important in beam-column joints? In what way do the external joints differ from the internal joints in this aspect?
 23. Why is it necessary to provide the top 90° hook pointing downwards in the joint?
 24. Hooks should be located within _____ mm of the confined core at the farther end of external joint.
 - (a) 30mm
 - (b) 50mm
 - (c) 80mm
 - (d) 100mm
 25. As per the ACI code, a tail extension of more than _____ is not effective.
 - (a) $4d_b$
 - (b) $8d_b$
 - (c) $12d_b$
 - (d) $16d_b$
 26. How does IS 13920 development length requirement for anchorage differ from ACI 318 requirement?
 27. What are the advantages of using headed bars in external beam-column joints? By how much can the required development length be reduced if we choose to use headed bars?
 28. What are the factors that influence the bond response of bars at the beam-column joint?
 29. To limit slippage of beam bars through the beam-column joint, ACI 352 recommends that the ratio of width of column to maximum diameter of beam bar should exceed _____.
 - (a) 12
 - (b) 15
 - (c) 20
 - (d) 25
 30. To limit slippage of beam bars through the beam-column joint, IS 13920 recommends that the ratio of width of column to maximum diameter of beam bar should exceed _____.
 - (a) 12
 - (b) 15
 - (c) 20
 - (d) 25
 31. Why are constructability issues more important in beam-column joints than in structural members?
 32. Can we shift the probable plastic hinge location away from a beam-column joint? Sketch a few possibilities.
 33. Why is it necessary to provide hanger reinforcement in beam-to-beam joints? Sketch the transfer zones where such reinforcement is to be placed.
 34. When is it necessary to provide bent up bars at the beam-to-beam joint?
 35. What are corbels? What is their function? What forces are they designed for?
 36. What are the principal failure modes for corbels?
 37. Why is anchoring of main bar important in corbels? What are the methods suggested in IS 456 for anchoring the main bars of corbels?
 38. Sketch the typical reinforcement detailing of a corbel.
 39. List the different types of cast-in-place anchors and post-installed anchors.
 40. How do mechanical anchors differ from adhesive or bonded anchors?
 41. What are the five different types of failures of anchors?
 42. What are the main differences between the concrete capacity design and the earlier design method for calculating concrete breakout strength?
 43. How is the nominal steel strength of an anchor in tension computed?
 44. How is the nominal concrete breakout strength of a single anchor in tension in cracked concrete computed? What is the factor used to get the strength in uncracked concrete?
 45. What is the alternative equation provided in ACI 318 for calculating the concrete breakout strength of anchors with embedment length greater than 280 mm.
 46. How is the concrete breakout strength of a group of anchors determined?
 47. How is the concrete breakout capacity of an eccentrically loaded anchor group in tension determined?
 48. When edge distance c_1 is less than critical edge distance c_{ac} breakout strength has to be reduced by a factor ψ_4 . In adhesive anchors, c_{ac} is _____.
 - (a) $2h_{ef}$
 - (b) $4h_{ef}$
 - (c) $6d_a$
 - (d) $8d_a$
 49. To avoid splitting of concrete, a minimum edge distance is prescribed. For adhesive anchors, this is prescribed in the ACI code as _____.
 - (a) $2h_{ef}$
 - (b) $4h_{ef}$
 - (c) $6d_a$
 - (d) $8d_a$
 50. How is the nominal pull-out strength of a single cast in anchor determined?
 51. How is the nominal side-face blowout strength, N_{sb} , of a headed anchor determined?
 52. What are the failure modes for anchors under shear loading?
 53. How is the nominal steel strength of an anchor in shear, V_{sa} , computed?
 54. How is the basic concrete breakout capacity in shear of an individual anchor in cracked concrete, V_{no} , computed?
 55. What is the reduction factor applied to the basic breakout capacity in shear to consider the effects of (a) eccentrically loaded multiple anchors in shear, (b) edge effects, and (c) cracked concrete?
 56. What is the equation used to compute nominal pryout strength, V_{cp} , for a single anchor?
 57. How is the basic bond strength of a single adhesive anchor computed?
 58. What is the interaction equation used in ACI 318 to consider combined tension and shear acting on anchors?

- 59. What are the options provided in the ACI code for considering seismic loads in anchors?
- 60. Can reinforcement be provided to increase the strength of anchors? What are the types and positions of reinforcements

suggested in ACI 318? How are these reinforcements designed?

- 61. Sketch the reinforcements to be adopted in acute- and obtuse-angled corners.

EXERCISES

- 1. Design an interior (Type 2) joint of a building. The details of the column and beam meeting at the joint are given in Table 19.10.

TABLE 19.10

Parameter	Column	Beam	Slab
	600 mm × 600 mm	450 mm × 550 mm	125 mm Thick
Longitudinal reinforcement	12–22 mm diameter (4561 mm ²) $f_y = 415$ MPa	Top: 5–20 mm diameter (1570 mm ²) Bottom: 3–20 mm diameter (942 mm ²) $f_y = 415$ MPa	Top: 8 mm at 200 c/c Bottom: 8 mm at 300 c/c
Height/Span	3200	4200	

Assume M25 concrete and Fe 415 steel reinforcement and moderate environment. Further, assume that similar size beams are provided in the perpendicular direction as well.

- 2. Design the hanger stirrups for a beam-to-girder joint as shown in Fig. 19.50. The factored reaction from the secondary beam of size 250 mm × 375 mm on each side of the joint is 120 kN. Assume Fe 415 steel and M25 concrete. Further, assume that the shear reinforcement in the beam and girder is two-legged 8 mm of Fe 415 grade.

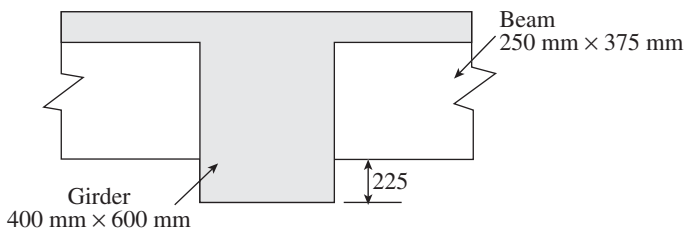


FIG. 19.50

- 3. Design a corbel to support a factored vertical load of 500 kN, applied at a distance of 140 mm from the column face. The column is 300 mm × 350 mm in plan. Assume M30 concrete, Fe 415 steel, and moderate environment.
- 4. Design a single-headed bolt installed at the bottom of a 150 mm thick slab to support a service dead load of 30 kN. Assume M25 concrete and no cracking under service loads.
- 5. Determine the ultimate shear capacity of a hexagonal head cast-in-place anchor of diameter 20 mm and 120 mm embedment depth. Assume M25 concrete and the concrete is cracked.
- 6. Determine the concrete breakout capacity in shear for a 16 mm diameter threaded anchor embedded in a 150 mm deep uncracked concrete section. Assume M25 concrete with $h_{ef} = 100$ mm, $c_1 = 150$ mm, and $c_2 = 120$ mm (see Fig. 19.51).

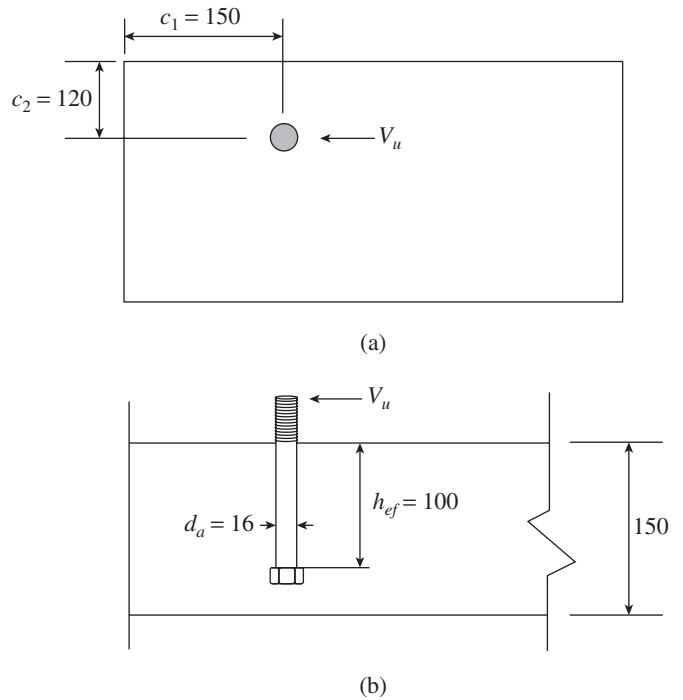


FIG. 19.51

- 7. Determine the ultimate capacity of the cast-in-place anchor group with the configuration shown in Fig. 19.52.

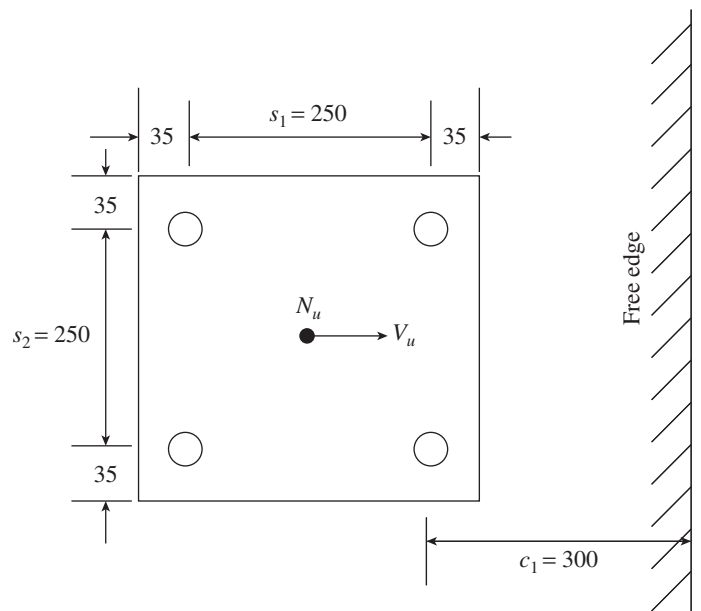


FIG. 19.52

Assume 16 mm diameter hexagonal head anchors, $h_{ef} = 200$ mm, thickness of concrete = 750 mm, M25 concrete, $f_{uta} = 40$ MPa, applied tension $N_u = 175$ kN, and shear $V_u = 30$ kN.

REFERENCES

- Abdul-Wahab, H.M.S and W.M. Ali 1989, 'Strength and Behavior of Reinforced Concrete Obtuse Corners under Opening Bending Moments', *ACI Structural Journal*, Vol. 86, No. 6, pp. 679–85.
- ACI SP 123 1991, Jirsa, J.O. (ed.), *Design of Beam-column Joints for Seismic Resistance*, American Concrete Institute, Detroit, p. 518.
- ACI Committee 349 1978, '349-76: Code Requirements for Nuclear Safety Related Concrete Structures', *Proceedings, ACI Journal*, Vol. 75, No. 8, pp. 329–35.
- ACI-ASCE Committee 352 2002, *352R-02: Recommendation for Design of Beam-column Joints in Monolithic Reinforced Concrete Structures*, American Concrete Institute, Farmington Hills, p. 37.
- ACI 355.2-07 2007, *Qualification of Post-installed Mechanical Anchors in Concrete and Commentary*, American Concrete Institute, Farmington Hills, p. 35.
- ACI 355.4-11 2011, *Qualification of Post-installed Adhesive Anchors in Concrete and Commentary*, American Concrete Institute, Farmington Hills, p. 55.
- Anderson, N.S. and D.F. Meinheit 2000, 'Design Criteria for Headed Stud Groups in Shear: Part 1- steel capacity and Back Edge Effects', *PCI Journal*, Vol. 45, No.5, pp. 46–75.
- Anderson, N.S. and D.F. Meinheit 2005, 'Pryout Capacity of Cast-in Headed Stud Anchors', *PCI Journal*, Vol. 50, No. 2, pp. 90–112.
- Anderson, N.S. and D.F. Meinheit 2007, 'A Review of Headed-stud Design Criteria in the Sixth Edition of the PCI Design Handbook', *PCI Journal*, Vol. 52, No. 1, pp. 2–20.
- Anderson, N.S. and D.F. Meinheit 2008, 'The PCI Headed Stud Anchorage Research Program: Scope and Highlights of findings', In J.C. Walraven and D. Stoelhorst (eds), *Tailor Made Concrete Structures—New Solutions for our Society, Proceedings of the International fib Symposium 2008*, Amsterdam, 19–22 May, pp. 127–31.
- Arslan, M.H. and H.H. Korkmaz 2007, 'What is to be Learned from Damage and Failure of Reinforced Concrete Structures during Recent Earthquakes in Turkey?', *Engineering Failure Analysis*, Vol. 14, No. 1, pp. 1–22.
- ASCE Task Committee Report 1994. 'Guidelines for Joints between Steel Beams and Reinforced Concrete Columns', *Journal of Structural Engineering*, ASCE, Vol. 120, No. 8, pp. 2330–57.
- Au, F.T.K., K. Huang, and H.J. Pam 2005, 'Diagonally Reinforced Beam-column Joints Reinforced under Cyclic Loading', *Proceedings, Institution of Civil Engineers: Structures and Buildings*, Vol. 158, No. 1, pp. 21–40.
- Bashandy, T.R. 1996, *Application of Headed Bars in Concrete Members*, PhD dissertation, The University of Texas at Austin, p. 303.
- Baumann, T. and H. Rüschi 1970, Schubversuche mit indirekter Krafteinleitung, Versuche zum Studium der Verdübellungswirkung der Biegezugbewehrung eines Stahlbetonbalkens, Deutscher Ausschuss für Stahlbeton, Heft 210, Wilhelm Ernst and Sohn, Berlin, pp. 1–41.
- Bindhu, K.R., K.P. Jaya, and V.K. Manicka Selvam 2009, 'Behaviour and Strength of Exterior Joint Sub-assembly Subjected to Reversal Loadings', *The Indian Concrete Journal*, Vol. 83, No. 11, pp. 9–20.
- Birkle, G., A. Ghali, and K. Schafer 2002, 'Double-headed Studs Improve Corbel Reinforcement', *Concrete International, ACI*, Vol. 24, No. 9, pp. 77–84.
- Bode and Hanenkamp 1985, 'Zur Tragfähigkeit von Kopfbolzen bei Zugbeanspruchung', *Bauingenieur*, Vol. 60, pp. 361–7.
- Canbolat, B.B. and J.K. Wight 2008, 'Experimental Investigation on Seismic Behavior of Eccentric Reinforced Concrete Beam-column-slab Connections', *ACI Structural Journal*, Vol. 105, No. 2, pp. 154–62.
- CEB Guide 1997, *Design of Fastenings in Concrete: Design Guide*, Comité Euro-International du Béton and Thomas Telford Services Ltd, London, p. 83.
- CEB Report 1994, *Fastenings to Concrete and Masonry Structures: State of the Art Report*, Comité Euro-International du Béton and Thomas Telford Services Ltd, London, p. 249.
- Charney, F., K. Pal, and J. Silva 2013, 'Recommended Procedures for Development and Splicing of Post-installed Bonded Reinforcing Bars in Concrete Structures', *ACI Structural Journal*, Vol. 110, No. 3, pp. 437–46.
- Chun, S.-C., S.-H. Lee, T.H.-K. Kang, B. Oh, and J.W. Wallace 2007, 'Mechanical Anchorage in Exterior Beam-column Joints Subjected to Cyclic Loading', *ACI Structural Journal*, Vol. 104, No. 1, pp. 102–12.
- Chun, S.-C., B. Oh, S.-H. Lee, and C.J. Naito 2009, 'Anchorage Strength and Behavior of Headed Bars in Exterior Beam-column Joints', *ACI Structural Journal*, Vol. 106, No. 5, pp. 579–90.
- Desayi, P. and A. Kumar 1989, 'Detailing of Opening L-joints in RC Frames', in N. Subramanian (ed.), *Proceedings of the National Seminar on Detailing of RC and Steel Structures*, Association of Consulting Engineers and Indian Concrete Institute, 22–23 December 1989, Chennai.
- Durrani, A.J. and J.K. Wight 1987, 'Earthquake Resistance of Reinforced Concrete Interior Connections Including a Floor Slab', *ACI Structural Journal*, Vol. 84, No. 5, pp. 400–6.
- Durrani, A.J. and H.E. Zerbe 1987, 'Seismic Resistance of R/C Exterior Connections with Floor Slab', *Journal of Structural Engineering*, ASCE, Vol. 113, No. 8, pp. 1850–64.
- Ehsani, M.R. and J.K. Wight 1985a, 'Effect of Transverse Beam and Slab on the Behavior of Reinforced Concrete Beam-to-column Connections', *ACI Journal*, Vol. 82, No. 2, pp. 188–95.
- Ehsani, M.R. and J.K. Wight 1985b, 'Exterior Reinforced Concrete Beam-to-column Connections Subject to Earthquake-type Loading', *ACI Journal*, Vol. 82, No. 4, pp. 492–9.
- Eligehausen, R. 1988, 'Design of Fastenings with Steel anchor-Future Concept', *Betonwerk + Fertigteil-technik*, No. 5, pp. 88–100.
- Eligehausen, R., P. Bouska, V. Cervenka, and R. Pukl 1992, 'Size Effect on the Concrete Cone Failure load of Anchor Bolts', *Fracture Mechanics of Concrete Structures*, Elsevier Applied Science, pp. 517–25.
- Eligehausen, R., R.A. Cook, and J. Appl 2006a, 'Behaviour and Design of Adhesive Bonded Anchors', *ACI Structural Journal*, Vol. 103, No. 6, pp. 822–31.
- Eligehausen, R. and W. Fuchs 1988, 'Load Bearing Behavior of Anchor Fastenings under Shear, Combined Tension and Shear or Flexural Loadings', *Betonwerk + Fertigteil-technik*, No. 2, pp. 48–56.
- Eligehausen, R., R. Mallée, and J.F. Silva 2006b, *Anchorage in Concrete Construction*, Ernst and Sohn, Berlin, p. 378.

- EN 1998-1:2003, *Eurocode 8: Design of Structures for Earthquake Resistance, Part 1: General Rules, Seismic Actions and Rules for Buildings*, European Committee for Standardization, Brussels, p. 215.
- Engindeniz, M., L.F. Kahn, and A.-H. Zureick 2005, 'Repair and Strengthening of Reinforced Concrete Beam-column Joints: State of the Art', *ACI Structural Journal*, Vol. 102, No. 2, pp. 187–97.
- Fuchs, W., R. Eligehausen, and J.E. Breen 1995, 'Concrete Capacity Design (CCD) Approach for Fastening to Concrete', *ACI Structural Journal*, Vol. 92, No. 1, pp. 73–94, *Discussion* by Lutz, L. and *Authors' Closure*, Vol. 92, No. 6, pp. 787–802.
- Hakuto, S., R. Park, and H. Tanaka 2000, 'Seismic Load Tests on Interior and Exterior Beam-column Joints with Substandard Reinforcing Details', *ACI Structural Journal*, Vol. 97, No. 1, pp. 11–25.
- Hanson, N.W. and H.W. Connor 1967, 'Seismic Resistance of Reinforced Concrete Beam-column Joints', *Journal of Structural Div., ASCE*, Vol. 93, No. ST5, pp. 533–59.
- Hong, S.-G., S.-C. Chun, S.-H. Lee, and B. Oh 2007, 'Strut-and-tie Model for Development of Headed Bars in Exterior Beam-column Joints', *ACI Structural Journal*, Vol. 104, No. 5, pp. 590–600.
- Hwang, S.-J., H.-J. Lee, T.-F. Liao, K.-C. Wang, and H.-H. Tsai 2005, 'Role of Hoops on Shear Strength of Reinforced Concrete Beam-column Joints', *ACI Structural Journal*, Vol. 102, No. 3, pp. 445–53.
- Hwang, S.-J., W.-Y. Lu, and H.-J. Lee 2000, 'Shear Strength Prediction for Reinforced Concrete Corbels', *ACI Structural Journal*, Vol. 97, No. 4, pp. 543–52.
- Ingle, R.K. and S.K. Jain 2002, *Explanatory Examples for Ductile Detailing of RC Buildings*, Document No. IITK-GSDMA-EQ22-V3.0, IITK-GSDMA Project on Building Codes, p. 72, (also see <http://www.iitk.ac.in/nicee/IITK-GSDMA/EQ22.pdf>, last accessed on 13 June 2013).
- Jain, S.K., R.K. Ingle, and G. Mondal 2006, 'Proposed Codal Provisions for Design and Detailing of Beam-column Joints in Seismic Regions', *The Indian Concrete Journal*, Vol. 80, No. 8, pp. 27–35.
- Jain, S.K. and C.V.R. Murty 2002, *Proposed Draft Provisions and Commentary on Ductile Detailing of RC Structures Subjected to Seismic Forces (IS 13920)*, Document No. IITK-GSDMA-EQ11-V4.0, IITK-GSDMA Project on Building Codes, p. 67, (also see <http://www.iitk.ac.in/nicee/IITK-GSDMA/EQ11.pdf>, last accessed on 17 July 2013).
- Jirsa, J.O. (ed) 1991, *ACI SP-123: Design of Beam-column Joints for Seismic Resistance*, American Concrete Institute, Michigan, pp. 518.
- Joshi, D.S. (ed.) 2001, *Design of Reinforced Concrete Structures for Earthquake Resistance*, Indian Society of Structural Engineers, Mumbai.
- Kim, J. and J.M. LaFave 2008, 'Probabilistic Joint Shear Strength Models for Design of RC Beam-column Connections', *ACI Structural Journal*, Vol. 105, No. 6, pp. 770–80.
- Kitayama, K., S. Otani, and H. Aoyama, 'Development of Design Criteria for RC Interior Beam-column Joints', in Jirsa, James O. 1991, *ACI SP-123: Design of Beam-column Joints for Seismic Resistance*, American Concrete Institute, Michigan, pp. 97–123.
- Klingner, R.E. 2001, 'ACI-355.2: What's it all about?' *STRUCTURE Magazine*, ASCE, Vol. 8, No. 10, pp. 28–32.
- Kriz, L.B. and C.H. Raths 1965, 'Connections in Precast Concrete Structures - Strength of Corbels', *Journal of the Prestressed Concrete Institute*, Vol. 10, No.1, pp. 16–47.
- Kuhn, D. and F. Shaikh 1996, 'Slip-Pullout Strength of Hooked Anchors', *Research Report*, University of Wisconsin-Milwaukee.
- LaFave, J.M., J.F. Bonacci, B. Burak, and M. Shin 2005, 'Eccentric Beam-column Connections', *Concrete International, ACI*, Vol. 27, No. 9, pp. 58–62.
- Lee, N.H., K.S. Kim, C.J. Bang, and K.R. Park 2007, 'Tensile Headed Anchors with Large Diameters and Deep Embedment in Concrete', *ACI Structural Journal*, Vol. 104, No. 4, pp. 479–86.
- Lee, N.H., K.R. Park, and Y.P. Suh 2010, 'Shear Behavior of Headed Anchors with Large Diameters and Deep Embedments', *ACI Structural Journal*, Vol. 107, No. 2, pp. 146–56.
- Leon, R.T. 1989, 'Interior Joints with Variable Anchorage Lengths', *Journal of Structural Engineering*, ASCE, Vol. 115, No. 9, pp. 2261–75.
- Leonhardt, F. and E. Mönning 1977, *Vorlesungen über Massivebau: Dritter Teil, Grundlagen zum Bewehren im Stahlbetonbau*, Dritte Auflage, Springer-Verlag, Berlin, p. 246.
- Lu, X., T.H. Urukup, S. Li, and F. Lin 2012, 'Seismic Behavior of Interior RC Beam-column Joints with Additional Bars under Cyclic Loading', *Earthquakes and Structures*, Vol. 3, No. 1, pp. 37–57, (also see <http://technop.kaist.ac.kr/samplejournal/pdf/eas0301003.pdf>, last accessed on 13 June 2013).
- Mattock, A.H., and J.F. Shen 1992, 'Joints Between Reinforced Concrete Members of Similar Depth', *ACI Structural Journal*, Vol. 89, No. 3, pp. 290–295.
- Mitra, N. and L.N. Lowes 2007, 'Evaluation, Calibration, and Verification of a Reinforced Concrete Beam-column Joint Model', *Journal of Structural Engineering*, ASCE, Vol. 133, No. 1, pp. 105–20.
- Moehle, J.P., J.D. Hooper, and C.D. Lubke 2008, *Seismic Design of Reinforced Concrete Special Moment Frames: A Guide for Practicing Engineers*, NEHRP Seismic Design Technical Brief No. 1, NIST GCR 8-917-1, National Institute of Standards and Technology, Gaithersburg, p. 27.
- Murty, C.V.R. 2005, *Earthquake Tips: Learning Earthquake Design and Construction*, Department of Civil Engineering, IIT Kanpur, and Building Material and Technology Promotion Council, Ministry of Urban Development and Poverty Alleviation, Govt. of India, p. 48.
- NEHRP Provisions 2010, *NEHRP Recommended Seismic Provisions for New Buildings and Other Structures, Part 3: Resource Paper 8, Appropriate Seismic Load Combinations for Base Plates, Anchorages, and Foundations (FEMA P-750)*, Building Seismic Safety Council, Washington, D.C., (also see <http://www.fema.gov/library/viewRecord.do?id=4103>, last accessed on 10 July 2013).
- Nilsson, I.H.E. and R. Losberg 1976, 'Reinforced Concrete Corners and Joints Subjected to Bending Moment', *Journal of the Structural Div., ASCE*, Vol. 102, No. ST6, pp. 1229–53.
- NTSB/HAR-07/02 2007, 'Ceiling Collapse in the Interstate 90 Connector Tunnel, Boston, Massachusetts, July 10, 2006', *Highway Accident Report NTSB/HAR-07/02*, National Transportation Safety Board, Washington, D.C., p. 120, (also see http://www.nts.gov/news/events/2007/boston_ma/har0702.pdf, last accessed on 30 July 2013).
- Ožbolt, J., R. Eligehausen, G. Periškić, and U. Mayer 2007, '3D FE Analysis of Anchor Bolts with Large Embedments', *Engineering Fracture Mechanics*, Vol. 74, No. 1–2, pp. 168–78.

- Park, R. and T. Paulay 1975, *Reinforced Concrete Structures*, John Wiley and Sons, New York, p. 769.
- Paulay, T. 2001, 'Seismic Design of Concrete Structures: The Present Needs of Societies', *Proceedings of the Eleventh World Congress on Earthquake Engineering*, 23–28 June, Acapulco, Paper no. 2001, Elsevier, p. 65, (also see http://www.iitk.ac.in/nicee/wcee/article/11_2001.PDF, last accessed on 2 June 2012).
- Paulay, T., R. Park, and M.J.N. Priestley 1978, 'Reinforced Concrete Beam-column Joints under Seismic Actions', *ACI Journal*, Vol. 75, No. 11, pp. 585–93.
- Paulay, T. and M.J.N. Priestley 1992, *Seismic Design of Reinforced Concrete and Masonry Buildings*, John Wiley and Sons, New York, p. 744.
- PCI Design Handbook 1971, *PCI Design Handbook: Precast and Prestressed Concrete*, 1st edition, Prestressed Concrete Institute, Chicago (Current edition: 7th edition, 2010, p. 828).
- Petersen, D. and J. Zhao 2013, 'Design of Shear Reinforcement for Seismic Shear Loads', *ACI Structural Journal*, Vol. 110, No. 1, pp. 53–62.
- Prakash Rao, D.S. 1985, 'Detailing of Reinforcement in Concrete Structures, Part 2', *The Indian Concrete Journal*, Vol. 59, No. 1, pp. 22–5.
- Prakash Rao, D.S. 1995, *Design Principles and Detailing of Concrete Structures*, Tata McGraw-Hill Publishing Company Ltd, New Delhi, p. 360.
- Rai, D.C. and Alpa Sheth, 'E-conference on Indian Seismic Codes', *The Indian Concrete Journal*, Vol. 76, No. 6, pp. 376–8.
- Rausch, E. 1972, 'Schubsicherung bei der Einmündung von Nebenträgern in Hauptträger (indirekte Auflagerung)', *Beton und Stahlbetonbau*, Vol. 67, No. 12, pp. 285–93.
- Rehm, G., J. Schlaich, K. Schäfer, and R. Eligehausen 1985, 'Fritz-Leonhardt-Kolloquium-Forschungskolloquium des Deutschen Ausschusses für Stahlbeton', *Beton und Stahlbetonbau*, Vol. 80, No. 6 and 7, pp. 156–61 and 190–4.
- Russo, G., R. Venir, M. Pauletta, and G. Somma 2006, 'Reinforced Concrete Corbels: Shear Strength Model and Design Formula', *ACI Structural Journal*, Vol. 103, No. 1, pp. 3–10.
- Saatcioglu, M., N.J. Gardner, and A. Ghobarah, '1999 Turkey Earthquake/Performance of RC Structures', *Concrete International*, *ACI*, Vol. 23, No. 3, pp. 47–56.
- Skettrup, E., J. Strabo, N.H. Andersen, and T. Brøndum-Nielsen 1984, 'Concrete Frame Corners', *ACI Journal*, Vol. 81, No. 6, pp. 587–93.
- Subramanian, N. 2008, *Design of Steel Structures*, Oxford University Press, New Delhi, p. 1211.
- Subramanian, N. and D.S. Prakash Rao 2003, 'Design of Joints in RC Structures with Particular Reference to Seismic Conditions', *The Indian Concrete Journal*, Vol. 77, No. 2, pp. 883–92.
- Subramanian, N. and V. Vasanthi 1991, 'Design of Anchor Bolts in Concrete', *The Bridge and Structural Engineer, Journal of ING/IABSE*, Vol. XXI, No. 3, pp. 48–73.
- Subramanian, N. 2000, 'Recent Developments in the Design of Anchor Bolts', *The Indian Concrete Journal*, Vol. 74, No. 7, pp. 407–14.
- Subramanian, N. and R.A. Cook 2002, 'Installation, Behaviour and Design of Bonded Anchors', *The Indian Concrete Journal*, Vol. 76, No. 1, pp. 47–56.
- Subramanian N. and R.A. Cook 2004, 'Behaviour of Grouted Anchors', *The Indian Concrete Journal*, Vol. 78, No. 4, pp. 14–21, *Reply to the Discussion*, Vol. 78, No. 12, p. 12.
- Swiatek, D. and E. Whitbeck 2004, 'Anchor Rods', *Modern Steel Construction*, Vol. 44, No. 12, pp. 31–3.
- Taylor, H.P.J. and J.L. Clarke 1976, 'Some Detailing Problems in Concrete Framed Structures', *The Structural Engineer, U.K.*, Vol. 54, No. 1, pp. 19–32.
- Thompson, M. K., M.J. Young, J.O. Jirsa, J.E. Breen, and R.E. Klingner 2002, *Anchorage of Headed Reinforcement in CCT Nodes*, Center for Transportation Research Report 1855-2, Austin, p. 160.
- Uma, S.R. and A. Meher Prasad 2005, *Seismic Behaviour of Beam-column Joints in Reinforced Concrete Moment Resisting Frames*, Document No. IITK-GSDMA-EQ31-V1.0, IITK-GSDMA Project on Building Codes, p. 29, (also see <http://www.iitk.ac.in/nicee/IITK-GSDMA/EQ31.pdf>, last accessed on 17 July 2013).
- Uma, S.R. and S.K. Jain 2006, 'Seismic Design of Beam-column Joints in RC Moment Resisting Frames: Review of Codes', *Structural Engineering and Mechanics*, Vol. 23, No. 5, pp. 579–97, (also see <http://www.iitk.ac.in/nicee/IITK-GSDMA/EQ32.pdf>, last accessed on 17 July 2013).
- Wallace, J.W., S.W. McConnell, P. Gupta, and P.A. Cote 1998, 'Use of Headed Reinforcement in Beam-column Joints Subjected to Earthquake Loads', *ACI Structural Journal*, Vol. 95, No. 5, pp. 590–606.
- Wight, J.K. and J.G. MacGregor 2009, *Reinforced Concrete: Mechanics and Design*, 5th edition, Pearson Prentice Hall, New Jersey, p. 1112.
- Wolfgang-French, C. and A. Boroojerdi 1989, 'Contribution of R/C Floor Slab in Resisting Lateral Loads', *Journal of Structural Engineering*, ASCE, Vol. 115, No. 1, pp. 1–18.
- Wright, J.L. and S.L. McCabe 1997, *The Development Length and Anchorage Behavior of Headed Reinforcing Bars*, SM Report No. 44, Structural Engineering and Engineering Materials, University of Kansas Center for Research, Lawrence, p. 147.
- Zhu, S. and J.O. Jirsa 1983, *Study of Bond Deterioration in Reinforced Concrete Beam-column Joints*, PMFSEL Report No. 83-1, Department of Civil Engineering, University of Texas at Austin, Texas.

DESIGN OF MULTI-STOREY BUILDINGS

20.1 INTRODUCTION

The world's urban population reached 7.1 billion in 2013 (of which the Indian population is 1.27 billion) and is growing at an annual rate of 1.2 per cent or 77 million people per year. Currently, about half the world's population is living in urban areas. By 2030, urban dwellers will make up roughly 60 per cent of the world's population. The urban population in India increased from 18 per cent in 1961 to 27.8 per cent in 2001. McKinsey Global Institute's projections show India's urban population soaring from 340 million in 2008 to 590 million in 2030. It is projected that Asia and Africa will have more urban dwellers than any other continent of the world and Asia will contain 54 per cent of the world's urban population by 2030. Such urbanization calls for massive efforts to provide housing and other infrastructure facilities. Though the urban population is growing at an alarming rate, the land available for construction is limited—though many agricultural lands are rapidly being converted illegally to construction sites. Housing the millions is possible only by constructing multi-storey buildings. Already, most of the buildings in Indian cities have ground plus three floors. The recent trend is to construct buildings with at least 10–15 storeys, so that the massive housing and commercial needs are satisfied (see Fig. 20.1). Most of these buildings are made of reinforced concrete (RC). Mass of concrete floor slabs, beams, and columns of RC construction is higher than that of comparable steel construction. This results in larger earthquake-induced bending moments and axial forces. As the height of a building increases, the behaviour of the structure becomes more complex. Such buildings are more sensitive to wind and earthquake loads and hence, need to be very carefully designed and detailed (Taranath 2010).

Clustering of buildings in the form of tall buildings in densely built-up areas is efficient in terms of transportation and reducing carbon footprint. Such tall buildings offer the



FIG. 20.1 Construction of a multi-storey building in Chennai

opportunity for creating open spaces such as plazas, parks, and other community spaces at the ground level. Agglomeration also reduces the per capita carbon footprint, which in turn improves the ecological environment and contributes to environmental economy (Ali and Aksamija 2008). It has to be remembered that the design of tall buildings is also influenced by several other factors, which include city by-laws, vertical transportation, fire protection, security, plumbing for water supply and sanitation, maintenance and repair arrangements, indoor air quality, daylight and ventilation, congestion of the surrounding movement systems (public transportation, private and commercial vehicles, pedestrian on the sidewalk, and the additional load on the utilities and infrastructure), aesthetics, and energy use (Dayaratnam 2004; Ali and Aksamija 2008). Wind influences the design of structural system of tall buildings as well as their shape and form. The different structural systems to efficiently resist wind loads may be found in Chapter 2. The effect of wind and

earthquake loads may be reduced by the use of supplementary damping systems and base isolators (see Section 3.8.4 of Chapter 3).

Since daylighting design has a large impact on the sustainability of the design, the *façade* may be one of the most important factors in controlling the daylight and shadow that enters a high-rise structure. The latest trend is the use of double skin, and occasionally triple skin, façade with ventilation systems. Double glazing with argon-filled cavities, triple-glazing, and glass coating can increase U-values. (A U-value is a measure of heat loss in a building element such as a wall, floor, or roof. It is defined as the heat flux density through a given structure divided by the difference in environmental temperatures on either side of the structure in steady-state conditions. It is expressed as watts per square meter per degree of temperature difference, $W/m^2/^\circ C$. A low U-value usually indicates high levels of insulation). With careful design, high-rise structures can be aerodynamically designed to resist high wind speeds and to simultaneously utilize them, by using strategically placed wind turbines, thus producing more energy with no risk to the safety of the building's users (Irwin, et al. 2008). More discussions on environmental and socio-economic factors are presented by Ali and Aksamija (2008) and Ali and Armstrong (1995).

In practice, multi-storey buildings are often analysed, designed, and detailed using commercially available software. The commercial software packages available in the market include STAAD.Pro, SAP 2000, ETABS, SAFE, Nastran, Midas NFX, ANSYS, and STRUDS. In addition, a number of free or open-source programs are also available, which include OpenSees, Frame3DD, and IDARC 2D. Many of these programs have analysis and design capabilities. Special structural design packages are also available and some engineers have developed their own spreadsheets for the design of structural elements (e.g., FRAME, RC Slab, RC Beam, and RC Foundation developed by Computer Design Consultants). AutoCAD is the most preferred detailing tool.

However, before using these programs, the engineer should know about the working of these programs, their assumptions, and the input–output details. It is better to solve some benchmark problems before analysing any project. The main inputs required for these software are the geometry, stiffness, loading, and boundary conditions. Modelling is the most important aspect. Usually, centre line dimensions are considered and the thickness of the member is assumed to have no influence. Three-dimensional models provide more accurate results, especially when there are lateral loads. Modelling of a standard skeletal building is not difficult, but complex structures need experience and engineering judgement. The beams and columns may be modelled as line elements and the walls and slabs as plate elements.

The loads and load combinations as discussed in Chapter 3, and as specified in IS 1893 (Part 1):2002, are to be used. In some software, the loads can be generated automatically, whereas in a few others the loads are calculated manually and placed at the appropriate nodes. Thus, modelling of these buildings with suitable assumptions becomes the biggest challenge to the designer while using these kinds of software. More discussions on modelling can be had from the work of Jones (2013).

Linear analysis is considered sufficient for buildings having 15 storeys, whereas dynamic analysis is preferred for regular buildings in high seismic zones and having height greater than 40m, irregular buildings, and slender buildings subjected to heavy wind loads. Soil–Structure interaction may be considered for important structures. Response spectrum method of analysis using a site-specific design spectrum is to be used in important projects. Geometric and material non-linearity are to be considered in the non-linear analysis.

In this chapter, the use of STAAD.Pro, which is popular in India, is illustrated by considering the linear analysis and design of a multi-storey building. Modelling requirements of the building, loading, and other assumptions involved in the design are explained in detail. A design summary of the various structural elements is also presented. However, elements like staircase are not considered.

20.2 EXAMPLE FRAME

A seven-storey RC building, as shown in Fig. 20.2, having three bays in one direction with spans of 8 m, 5 m, and 8 m and three

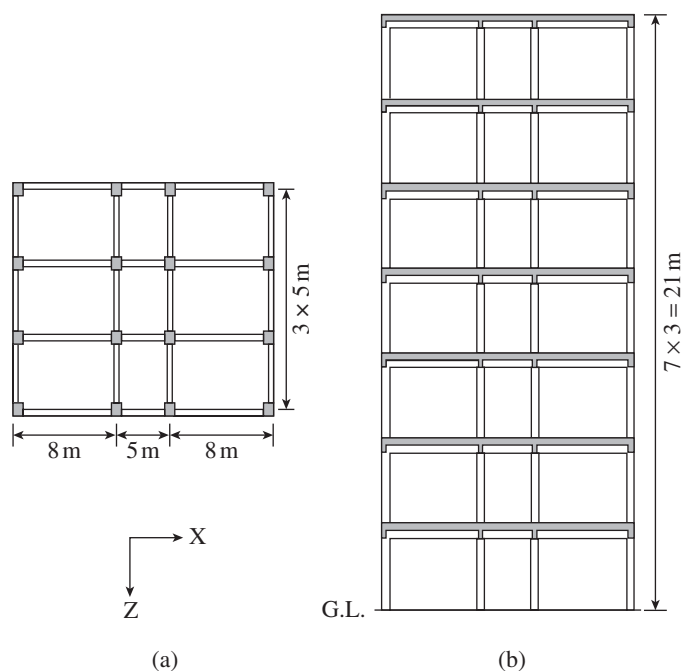


FIG. 20.2 Example frame (a) Plan (b) Elevation

equal bays of 5 m each in the other direction, is considered in this case study. The following are some of the other pertinent details required for the analysis and design:

Details of Structure

Details of building	= Ground plus six-storey building, as shown in Fig. 20.2
Location	= Mumbai
Walls	= 230 mm thick brick masonry
Typical floor-to-floor height	= 3000 mm
Height of plinth	= 450 mm
Depth of foundation	= 2000 mm below ground level
Bearing capacity of soil	= 400 kN/m ²

Loading on Structure

Dead load	Roof finish	= 1.5 kN/m ²
	Floor finish	= 1.0 kN/m ²
Live load	Roof	= 1.5 kN/m ²
	Floor	= 5.0 kN/m ²

Wind load	= Not considered for design
Seismic load	= Seismic zone III
Type of soil	= Medium soil

Other Information

Concrete grade	= M30
Reinforcement grade	= Fe 415
Exposure condition	= Very severe (clear cover = 50)
Water table	= At ground level

20.3 DETAILED STRUCTURAL LAYOUTS

The foundation and column layouts of the example frame are shown in Fig. 20.3.

The beam layout for floors is shown in Fig. 20.4(a) and the roof beam layout is shown in Fig. 20.4(b).

The slab layout for floors is shown in Fig. 20.5(a) and the roof slab layout is shown in Fig. 20.5(b).

The column numbers in grids 1 and 4 are shown in Fig. 20.6(a) and those in grids 2 and 3 are shown in Fig. 20.6(b).

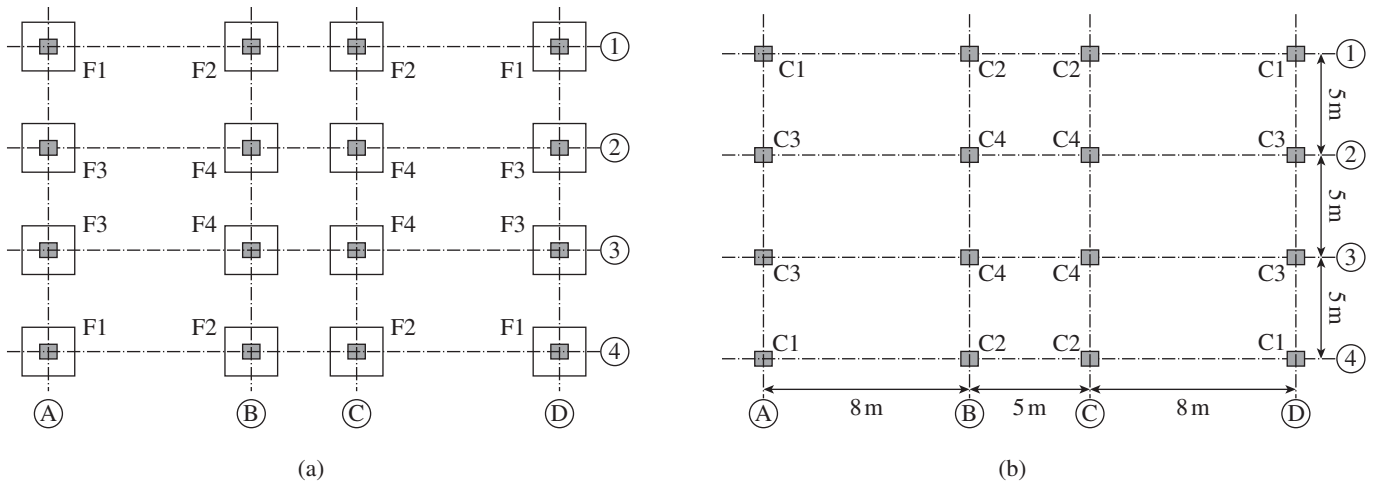


FIG. 20.3 Foundation and column layouts (a) Foundation layout (b) Column layout

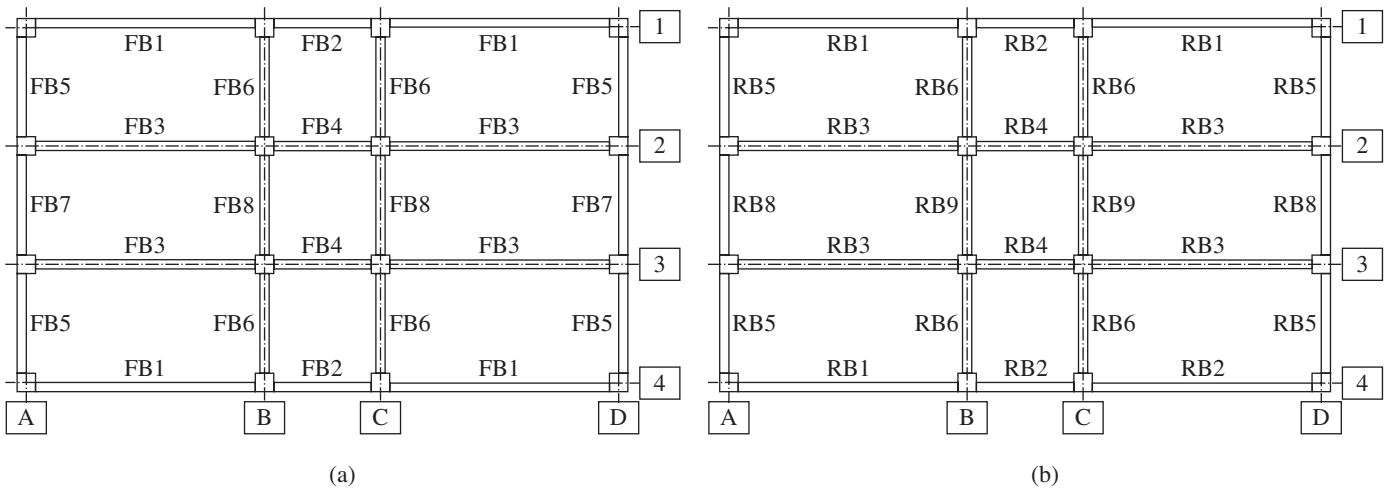


FIG. 20.4 Beam layout (a) First to sixth floors (b) Roof

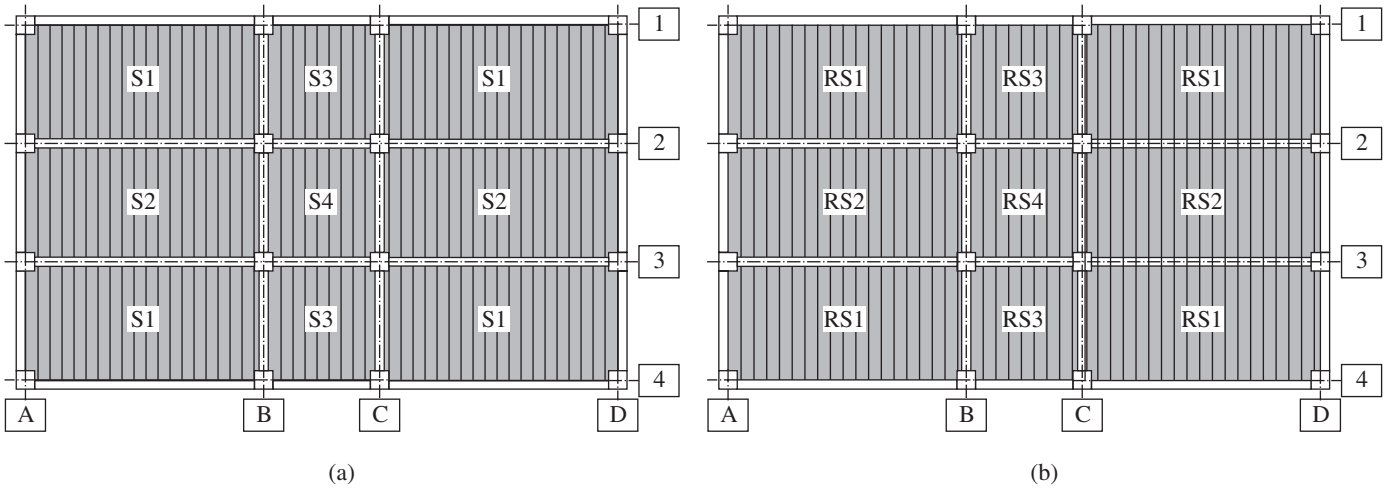


FIG. 20.5 Slab layout (a) First to sixth floors (b) Roof

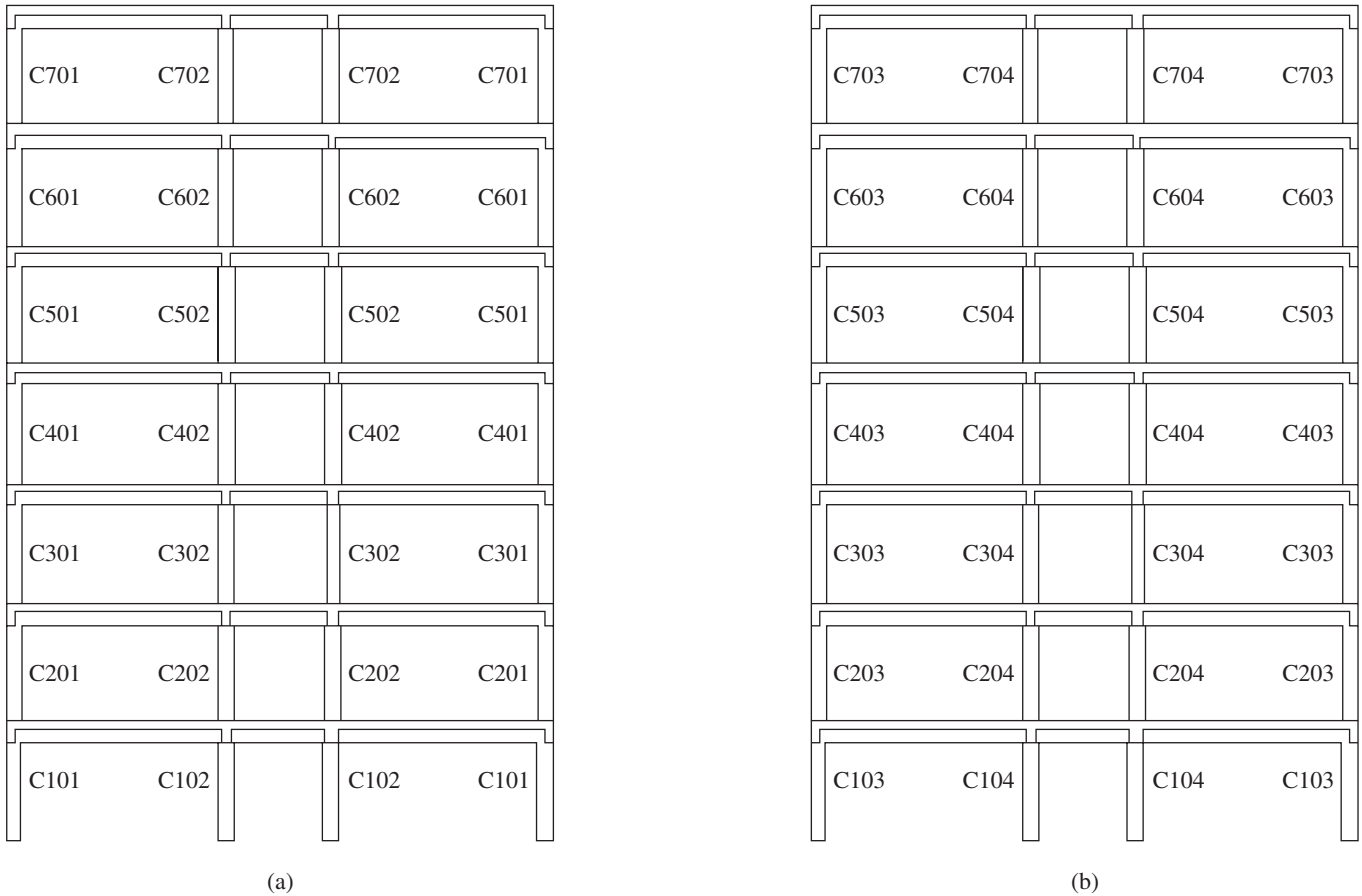


FIG. 20.6 Elevation showing the columns (a) Grids 1 and 4 (b) Grids 2 and 3

Preliminary Sizes of Structural Members

As any structural finite element analysis will require preliminary member sizes, the following member sizes have been chosen based on experience.

Column	C1	=	400 × 700 (Z × X)	Floor beams	FB1 to FB2	=	300 × 600
	C2 and C3	=	400 × 700		FB3 to FB4	=	400 × 700
	C4	=	450 × 800		FB5 and FB7	=	300 × 450
				Roof beams	RB1 to RB2	=	300 × 600
					RB3 to RB4	=	400 × 700
					RB5 and RB7	=	300 × 450
					RB6 and RB8	=	300 × 600
				Slab (all floors)	ts	=	180 mm thick (all slabs)

20.4 ESTIMATION OF LOADS

STAAD.Pro is capable of estimating self-weight of the frame elements modelled. However, there are many elements, namely slab, brick wall, glazing, and floor finish, which are generally not required to be defined. Hence, the user needs to provide the input for the loadings, which needs to be considered for the analysis. In the following sections, the different loadings, which need to be defined for the analysis of buildings are briefly described.

20.4.1 Calculation of Dead Load—STAAD.Pro Load Case 11

The following loads are considered under this load case:

Self-weight of structures An RC frame loading is to be considered in this category. Self-weight command is used in STAAD.Pro to assign the self-weight of the structural members that are physically modelled.

Self-weight of slabs Slab weight needs to be calculated manually and applied as uniformly distributed load (UDL) on beams. STAAD.Pro has a floor load command, which may be used to calculate and assign the distributed load to beams.

$$\text{Intensity of slab weight} = 0.18 \times 25 = 4.50 \text{ kN/m}^2$$

The following additional loads are also considered in the dead load:

$$\text{Roof finish} = 2.0 \text{ kN/m}^2$$

$$\text{Floor finish} = 1.0 \text{ kN/m}^2$$

Self-weight of brick walls Assume unit weight of brick wall as 18 kN/cum.

$$\text{Weight of brick wall} = 0.23 \times 3 \times 18 = 12.42 \text{ kN/m}$$

It has to be noted that stiffness of the brickwork is not included in the analysis and only the dead load of brickwork is considered. In this case, all the brick walls are assumed to be 230 mm thick, though in practice the interior walls may have a thickness of only 115 mm.

Typical distribution of slab loads on beams in STAAD.Pro is shown Fig. 20.7.

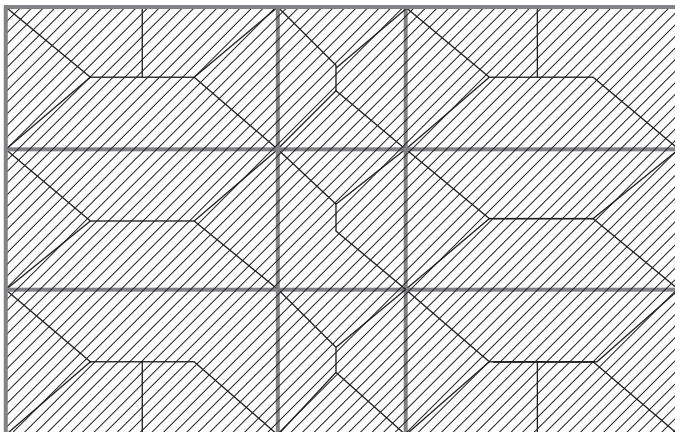


FIG. 20.7 Floor load distribution by STAAD.Pro

20.4.2 Calculation of Live Load—STAAD.Pro Load Case 12

The following loads are considered in the live load:

$$\text{Roof} = 1.5 \text{ kN/m}^2$$

$$\text{Floor} = 5.0 \text{ kN/m}^2$$

The distribution of live load is similar to that of self-weight of slab, and the floor load command is used in STAAD.Pro for this calculation.

20.4.3 Calculation of Earthquake Load

As per Clause 7.8.1a, IS 1893 (Part 1):2002, dynamic analysis needs to be carried out only for buildings greater than 40 m in height in zones IV and V and those greater than 90 m in height in zones II and III. Hence, the configuration of the building does not demand dynamic analysis. However, it has been considered for demonstration purposes. Furthermore, static analysis has also been carried out for the base shear enhancement as per Clause 7.8.2 of IS 1893 (Part 1):2002. The following are the general parameters for an earthquake load:

Location	= Mumbai
Seismic zone	= III
Zone factor (Z)	= 0.16
Importance factor (I)	= 1.5 [as per Table 6, IS 1893 (Part 1):2002]
Response reduction factor (R)	= 5.0 [as per Table 7, IS 1893 (Part 1):2002]
Type of soil	= Medium
Type of building	= All other [Clause 7.6.2 of IS 1893 (Part 1):2002]
Type of earthquake	= DBE
Seismic mass	= DL + 50% LL of floor + 25% LL of roof
Height of the building	= 21.0 m
Length of the building	
Along X-direction	= 21.0 m
Along Z-direction	= 15.0 m

Primary Load Cases for Seismic Analysis

The following primary load cases are considered for the application of seismic loads:

1. Static seismic—X : STAAD.Pro Load Case 1
2. Static seismic—Z : STAAD.Pro Load Case 2
3. Response spectrum—X : STAAD.Pro Load Case 21
4. Response spectrum—Z : STAAD.Pro Load Case 22

In STAAD.Pro, static seismic load cases shall be defined only in the first two load cases.

Equivalent Static Analysis Using STAAD.Pro

The following are the steps for the equivalent static analysis in STAAD.Pro:

Lump the applicable seismic weight as per IS 1893 Part 1

Applicable seismic weight on floors = $(4.5 + 2.0) + 0.50 \times 5.00 = 9.00 \text{ kN/m}^2$

Applicable seismic weight on roof = $(4.5 + 1.0) = 5.50 \text{ kN/m}^2$

Applicable seismic weight of brick walls = 12.42 kN/m

Define rigid diaphragm In-plane rigidity of the slab is simulated through rigid diaphragm specifications. This provision is applicable for structures having RC floors. In STAAD.Pro, master-slave specifications are used to simulate rigid diaphragm action when the slab is not modelled.

Define equivalent static parameters Z, I, R , type of structure (namely 1, 2, 3) to find the fundamental time period based on structure types defined in IS 1893 (Part 1) or fundamental time periods, soil type, and damping ratio need to be defined.

Define or apply equivalent static loads In STAAD.Pro, equivalent static loads need to be applied along with an appropriate factor. These load cases can be defined only for the horizontal direction.

Analyse structure and interpret results After completing the modelling and inputting the loading, the user needs to analyse the structure. This will generate the output, namely SFD, BMD, and RC/Steel design as requested by the user. These results need to be interpreted properly and used for the final design and detailing.

Response Spectrum Analysis

The following are the steps for the response spectrum analysis in STAAD.Pro:

Lump the applicable seismic mass as per IS 1893 Part 1

Seismic mass can be defined as the appropriate loads from applicable load cases or can be defined as the nodal loads based on the contributory mass at the node. Applicable seismic weight is similar to the one defined in the equivalent static method.

Define rigid diaphragm This procedure is similar to the one specified in the equivalent static method.

Define response spectrum parameters Z, I, R , codal response spectrum or site-specific response spectrum (if available), ratio of base shear by response spectrum analysis and by equivalent static method (ratio ≥ 1), and damping ratio need to be defined.

Note: In STAAD.Pro, site-specific response spectrum needs to be defined in the units of m/s^2 . If it is available after normalization, then an appropriate scale factor can be given in scale. For example, if the response spectrum is normalized by g , then we can give scale equal to 9.81.

Analyse structure and interpret results After completing the modelling and inputting the loading, the user needs to analyse the structure. This will generate the output, namely SFD, BMD, and RC/Steel design as requested by the user. These results need to be properly interpreted and used for the final design and detailing.

Results of Seismic Analysis

Results of equivalent static analysis

Fundamental time period

Applicable formula = $0.09h/\sqrt{d}$ [Clause 7.6.2 of IS 1893 (Part 1);2002]

X-direction = $0.09 \times 21.0/\sqrt{21} = 0.412 \text{ s}$

Z-direction = $0.09 \times 21.0/\sqrt{15} = 0.488 \text{ s}$

Seismic mass lumped in STAAD.Pro = $37,024.15 \text{ kN}$

Spectral acceleration (S_a/g) [Refer to IS 1893(Part 1)]:

Response spectrum for medium soil

X-direction (S_{ax}/g) = 2.5

Z-direction (S_{az}/g) = 2.5

Horizontal seismic coefficient

$A_{hx} = (Z/2) \times (I/R) \times (S_{ax}/g) = (0.16/2) \times (1.5/5) \times 2.5 = 0.06$

$A_{hz} = (Z/2) \times (I/R) \times (S_{az}/g) = (0.16/2) \times (1.5/5) \times 2.5 = 0.06$

Base shear

$V_{bx} = 0.06 \times 37,024.15 = 2221.45 \text{ kN}$;

$V_{bz} = 0.06 \times 37,024.15 = 2221.45 \text{ kN}$

Base shear from STAAD.Pro

$V_{bx} = 2062.64 \text{ kN}$; $V_{bz} = 1947.05 \text{ kN}$

Results of response spectrum analysis in STAAD.Pro (first cycle)

Base shear from STAAD.Pro

$V_{bx} = 1069.25 \text{ kN}$; $V_{bz} = 904.76 \text{ kN}$

Scale factor for scaling base shear obtained by response spectrum method

Refer to Clause 7.8.2, IS 1893 (Part 1).

Ratio of base shear from seismic static analysis to base shear by response spectrum analysis

X-direction = $2221.45/1069.25 = 2.078$

Z-direction = $2221.45/904.76 = 2.455$

STAAD.Pro has also suggested same scale factors based on the response spectrum analysis and equivalent static analysis. All results of response spectrum need to be scaled by the aforementioned figures.

20.5 ANALYSIS OF STRUCTURE

A structure needs to be analysed for gravity and earthquake/wind loads. Gravity loads are those that are more or less constant over the lifetime of a structure. The static analysis for gravity loads is much simpler compared to the dynamic analysis for the earthquake/wind loads.

20.5.1 Gravity Load Analysis

The space frame is modelled using software STAAD.Pro. The gravity loads are considered as specified in Section 20.4.

20.5.2 Lateral Load Analysis

Two different seismic analyses, namely equivalent static and response spectrum, are considered for this purpose. Both the analyses are carried out using the STAAD.Pro software.

20.6 LOAD COMBINATIONS

The building being considered for this analysis is symmetrical about both the axes; hence as per Clause 6.3.2.1 of IS 1893 (Part 1):2002, we can consider full seismic force in one horizontal direction at a time. Furthermore, it is not necessary to consider the effect of vertical seismic force for the type of building under consideration. The load combinations that are considered for the analysis and design are provided in Table 20.1.

TABLE 20.1 Load combinations considered in the analysis

Limit State of Serviceability		Limit State of Strength	
Number	Details	Number	Details
101	DL + LL	1001	1.50DL + 1.50LL
201	DL + EL _x	2001	0.90DL + 1.50EL _x
202	DL - EL _x	2002	0.90DL - 1.50EL _x
203	DL + EL _z	2003	0.90DL + 1.50EL _z
204	DL - EL _z	2004	0.90DL - 1.50EL _z
205	DL + LL + EL _x	2005	1.50DL + 1.50EL _x
206	DL + LL - EL _x	2006	1.50DL - 1.50EL _x
207	DL + LL + EL _z	2007	1.50DL + 1.50EL _z
208	DL + LL - EL _z	2008	1.50DL - 1.50EL _z
		2009	1.20DL + 1.20LL + 1.20EL _x
		2010	1.20DL + 1.20LL - 1.20EL _x
		2011	1.20DL + 1.20LL + 1.20EL _z
		2012	1.20DL + 1.20LL - 1.20EL _z

20.7 REINFORCED CONCRETE DESIGN USING STAAD.PRO FOR INDIAN CODES

STAAD. Pro has the capacity to design the frame elements through its in-built subroutines. It has different country codes in its library; hence, the given frame can be designed for the Indian, American, British codes, etc. The user needs to provide different parameters as mentioned in the following section to obtain correct results using STAAD.Pro.

20.7.1 Design Parameters as per IS 456

We need to specify the load list (for which design is to be performed) followed by design parameters in STAAD.Pro.

Important Design Parameters

- F_ymain* : Yield stress for main reinforcing steel
- F_ysec* : Yield stress for secondary reinforcing steel
- F_c* : Concrete yield stress
- Clear* : Clear cover
- Minmain* : Minimum main reinforcement bar size
- Maxmain* : Maximum main reinforcement bar size
- Minsec* : Minimum secondary reinforcement bar size
- Maxsec* : Maximum secondary reinforcement bar size
- Bracing* : Beam design
= 1.0: Axial force will be taken into account for beam design
- Column design
= 1.0: Column is unbraced about major axis
= 2.0: Column is unbraced about minor axis
= 3.0: Column is unbraced about both axes
- Ratio* : Maximum percentage of longitudinal reinforcement in columns
- R_{face}* : = 4.0: Reinforcement distributed equally on four faces in column
= 2.0: Reinforcement distributed equally on two faces about major axis
= 3.0: Reinforcement distributed equally on two faces about minor axis
- Reinf* : = 1.0 for spiral reinforcement
- Torsion* : = 0.0: Torsion considered in beam design
= 1.0: Torsion neglected in beam design
- Ensh/Rensh* : Used when beam is divided into two or more parts; refer to the STAAD.Pro help manual for details
- Ensh* : A default value equal to zero means enhanced shear strength check as per IS 456:2000 (Clause 40.5). A value equal to one is proposed for the ordinary shear check.

If a positive distance is entered, then enhanced shear strength check will be performed up to that distance from start of member, valid if the beam is split up into two or more parts.

- Rensh* : A default value equal to zero means distance of start or end points of the member from its nearest support; valid if the beam is split up into two or more parts
- ELZ/ELY* : Ratio of effective length to actual length of column about major or minor axis
- ULZ/ULY* : Ratio of unsupported length to actual length of column about major or minor axis

An example of *ELZ/ELY/ULZ/ULY* is provided in Fig. 20.8.

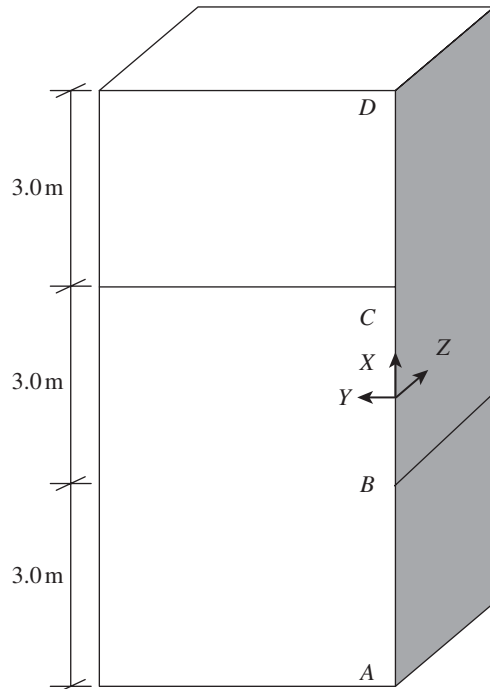


FIG. 20.8 Interpretation of effective length in STAAD.Pro

$$\begin{aligned}
 ULY_{AB} &= 3.0/3.0 && = 1.0 \\
 ELY_{AB} &= 1.2 \times 3.0/3.0 && = 1.2 \\
 ULZ_{AB} &= (3.0 + 3.0)/3.0 && = 2.0 \\
 ELZ_{AB} &= 1.2 \times (3.0 + 3.0)/3.0 && = 2.4 \\
 ULY_{BC} &= (3.0 + 3.0)/3.0 && = 2.0 \\
 ELY_{BC} &= 1.2 \times (3.0 + 3.0)/3.0 && = 2.4 \\
 ULZ_{BC} &= (3.0 + 3.0)/3.0 && = 2.0 \\
 ELZ_{BC} &= 1.2 \times (3.0 + 3.0)/3.0 && = 2.4 \\
 ULZ_{CD} &= (3.0 + 3.0)/3.0 && = 2.0 \\
 ELZ_{CD} &= 1.2 \times (3.0 + 3.0)/3.0 && = 2.4 \\
 ULY_{CD} &= 3.0/3.0 && = 1.0 \\
 ELY_{CD} &= 1.2 \times 3.0/3.0 && = 1.2
 \end{aligned}$$

20.7.2 Design Parameters as per IS 13920

All the general parameters for design are the same as that of IS 456. The following additional points or parameters need to be considered for design.

Design Parameter Gravity Load Design

Gravity load design (GLD) is used to satisfy Clause 6.3.3 of IS 13920. As per the clause, shear force to be resisted by the vertical hoops shall be the maximum of the following:

1. Calculated factored shear force as per analysis
2. Shear force due to formation of plastic hinges at both ends of the beam plus the factored gravity load on the span

In STAAD.Pro, we need to specify gravity load case number to generate UDL on beam. Gravity load case can be generated by using repeat load or unfactored load combination. However, the user can use EUDL (equivalent UDL) parameter as a substitute to GLD. The parameter should not be factored as the program will automatically multiply it with 1.2.

If both GLD and EUDL are used, the program ignores the GLD parameter and proceeds with EUDL.

Design Parameter PLASTIC

To calculate the plastic hogging and sagging moments of resistance at beam ends, the parameter is entered as one. If this parameter is not given (default value = 0), then STAAD.Pro calculates the plastic hogging and sagging moments of resistance.

Design Parameter IPLM

This parameter is specified if it is not necessary to calculate the plastic or elastic hogging and sagging moments of resistance at either the start or end of the beam. This means support may or may not be there at the beam start or end.

- IPLM=1 : No plastic or elastic moments of resistance to be calculated at beam start
- IPLM=-1: Plastic or elastic moments of resistance to be calculated at beam start
- IPLM=2 : No plastic or elastic moments of resistance to be calculated at beam end
- IPLM=-2: Plastic or elastic moments of resistance to be calculated at beam end
- IPLM=0 : Default value, which will calculate plastic or elastic moments of resistance at both ends of the beam

Design Parameter IMB

- IMB = 1.0 : No plastic or elastic moments of resistance to be calculated at beam start and end
- IMB = -1.0 : Plastic or elastic moments of resistance to be calculated at beam start and end
- IMB = 0 : Default value, which also implies the same

If physical member command is used, then IPLM and IMB are ignored.

Design Parameter COMBINE

- Combine = 1: No printout available for sectional force and critical load for combined member in output

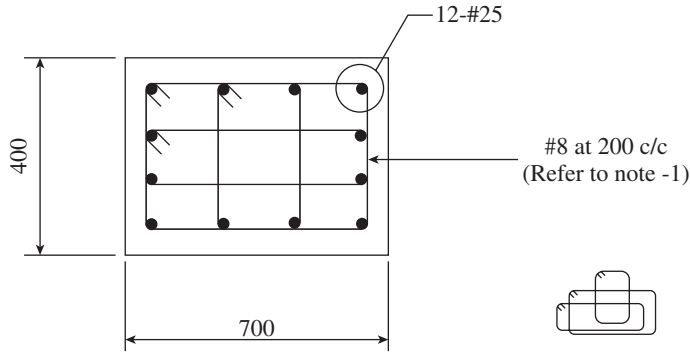


FIG. 20.9 Typical reinforcement detail for column marked C101

TABLE 20.4 Reinforcement in columns as per STAAD.Pro

Column Number	Column Size		Main Reinforcement	Confining Reinforcement	Stirrups
	B (Parallel to X)	D (Parallel to Z)			
C101	400	700	12 #25	#16 @ 100mm c/c	#8 @ 200mm c/c
C201	400	700	12 #20	#16 @ 100mm c/c	#8 @ 200mm c/c
C301	400	700	12 #20	#16 @ 100mm c/c	#8 @ 200mm c/c
C401	400	700	12 #20	#16 @ 100mm c/c	#8 @ 200mm c/c
C501	400	700	12 #20	#16 @ 100mm c/c	#8 @ 200mm c/c
C601	400	700	12 #20	#16 @ 100mm c/c	#8 @ 200mm c/c
C701	400	700	12 #20	#16 @ 100mm c/c	#8 @ 200mm c/c
C102	400	700	20 #25	#12 @ 100mm c/c	#8 @ 200mm c/c
C202	400	700	20 #20	#16 @ 100mm c/c	#8 @ 200mm c/c
C302	400	700	20 #20	#12 @ 100mm c/c	#8 @ 200mm c/c
C402	400	700	20 #16	#16 @ 100mm c/c	#8 @ 200mm c/c
C502	400	700	20 #16	#16 @ 100mm c/c	#8 @ 200mm c/c
C602	400	700	20 #16	#16 @ 100mm c/c	#8 @ 200mm c/c
C702	400	700	20 #16	#16 @ 100mm c/c	#8 @ 200mm c/c
C103	400	700	24 #20	#10 @ 100mm c/c	#8 @ 200mm c/c
C203	400	700	24 #20	#12 @ 100mm c/c	#8 @ 200mm c/c
C303	400	700	20 #20	#12 @ 100mm c/c	#8 @ 200mm c/c

C403	400	700	20 #16	#16 @ 100mm c/c	#8 @ 200mm c/c
C503	400	700	20 #16	#16 @ 100mm c/c	#8 @ 200mm c/c
C603	400	700	20 #16	#16 @ 100mm c/c	#8 @ 200mm c/c
C703	400	700	20 #16	#16 @ 100mm c/c	#8 @ 200mm c/c
C104	450	800	24 #25	#10 @ 100mm c/c	#8 @ 225mm c/c
C204	450	800	24 #25	#10 @ 100mm c/c	#8 @ 225mm c/c
C304	450	800	24 #20	#10 @ 100mm c/c	#8 @ 225mm c/c
C404	450	800	16 #20	#12 @ 100mm c/c	#8 @ 225mm c/c
C504	450	800	12 #20	#16 @ 100mm c/c	#8 @ 225mm c/c
C604	450	800	12 #20	#16 @ 100mm c/c	#8 @ 225mm c/c
C704	450	800	12 #20	#16 @ 100mm c/c	#8 @ 225mm c/c

Note: In practice, stirrup of 16 mm diameter is not recommended. Hence, column size can be increased to reduce the diameter of stirrups.

20.10 STRENGTH DESIGN OF BEAMS

Beams are designed in STAAD.Pro through its inbuilt program. IS 13920 is used for the design. Typical design details are shown here.

Beam No. 205 Design Results

M30 Fe 415 (Main) Fe 415 (Sec.)

Length: 5000.0 mm Size: 400.0 mm × 600.0 mm Cover: 50.0 mm

STAAD space Page no. 1070

Summary of REINF. area (mm²)

Section	0.0 mm	1250.0 mm	2500.0 mm	3750.0 mm	5000.0 mm
Top REINF.	2144.78 (mm ²)	1618.91 (mm ²)	1557.06 (mm ²)	1784.86 (mm ²)	2604.17 (mm ²)
Bottom REINF.	1343.37 (mm ²)	1841.28 (mm ²)	2153.14 (mm ²)	1951.65 (mm ²)	1579.55 (mm ²)

Summary of provided REINF. area

Section	0.0 mm	1250.0 mm	2500.0 mm	3750.0 mm	5000.0 mm

Top REINF.	7-20í	6-20í	5-20í	6-20í	9-20í
	1 layer(s)	1 layer(s)	1 layer(s)	1 layer(s)	2 layer(s)
Bottom REINF.	5-20í	6-20í	7-20í	7-20í	6-20í
	1 layer(s)	1 layer(s)	1 layer(s)	1 layer(s)	1 layer(s)
Shear REINF.	2-legged 8í @ 130 mm c/c	2-legged 8í @ 190 mm c/c	2-legged 8í @ 190 mm c/c	2-legged 8í @ 190 mm c/c	2-legged 8í @ 130 mm c/c

Shear design results at distance *d* (effective depth) from face of the support

Shear design results at 740.0 mm away from start support

$$VY = 194.48 \quad MX = -1.33 \quad LD = 2007$$

Provide two-legged 8í at 190 mm c/c.

Shear design results at 740.0 mm away from end support

$$VY = -198.47 \quad MX = -1.38 \quad LD = 2008$$

Provide two-legged 10í at 190 mm c/c.

EUDL Considered on member # 209 IS 20.01 N/mm

Reinforcement recommended by STAAD.Pro needs to be customized to meet the practical conditions. Typical reinforcement details for beam FB5 are shown in Fig. 20.10 (SP 34:1987).

Results of the beam design are summarized in Tables 20.5 and 20.6. The number of bars and diameter of bars are adjusted to account for the detailing requirement.

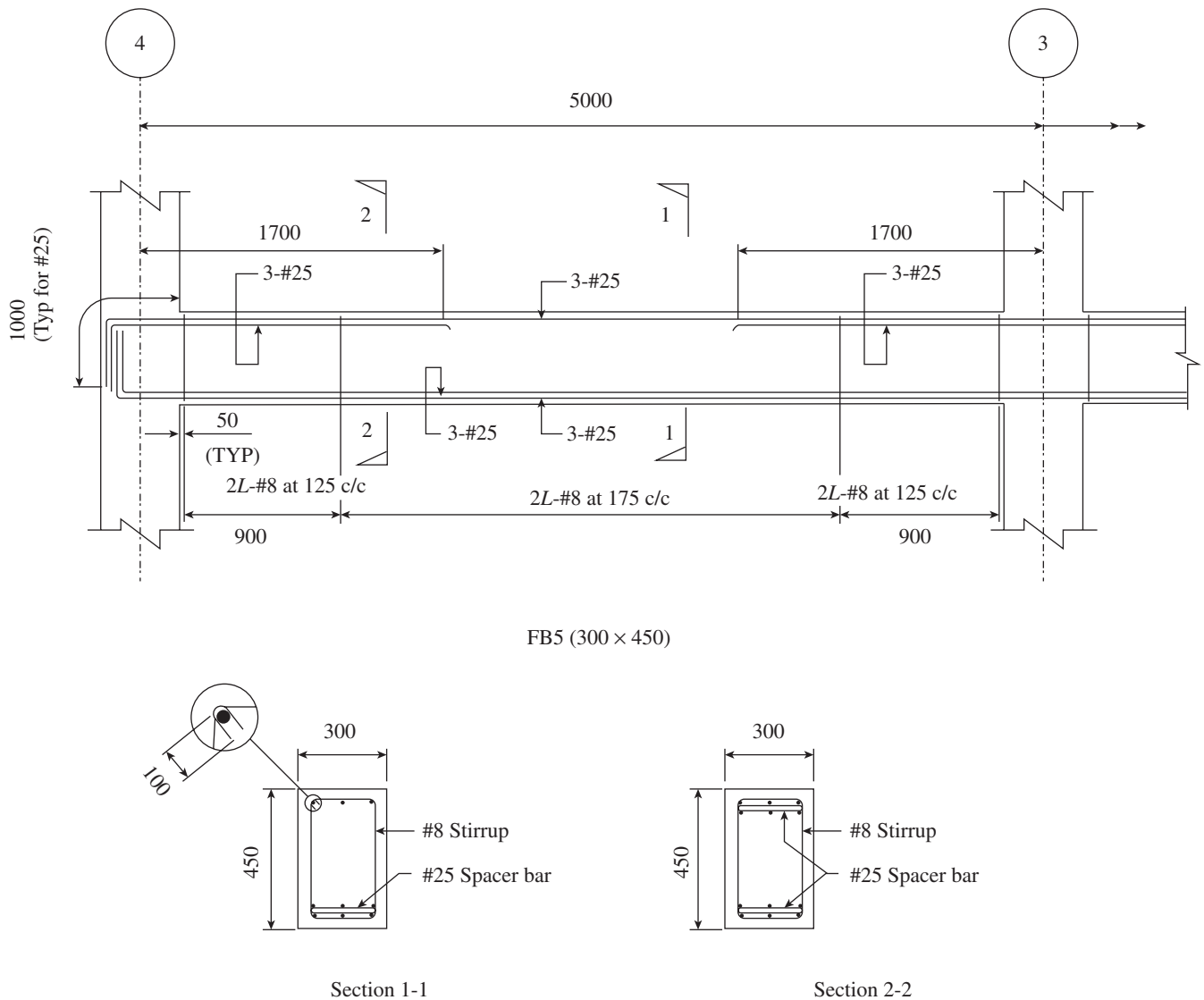


FIG. 20.10 Typical reinforcement details for beam marked FB5

TABLE 20.5 Reinforcement in beams as per STAAD.Pro

Beam Number	Column Size		Top Reinforcement			Bottom Reinforcement		
	Width B	Depth D	Left	Centre	Right	Left	Centre	Right
FB1	400	650	6#25	3#25	6#25	5#25	5#25	5#25
FB2	400	650	5#25	5#25	5#25	5#25	5#25	5#25
FB3	400	750	8#25	4#25	8#25	6#25	6#25	6#25
FB4	400	750	8#25	8#25	8#25	8#25	8#25	8#25
FB5	400	600	6#25	4#25	6#25	6#25	6#25	6#25
FB6	400	750	6#25	4#25	6#25	6#25	6#25	6#25
FB7	400	600	5#25	5#25	5#25	6#20	6#20	6#20
FB8	400	750	6#25	4#25	6#25	6#25	6#25	6#25
RB1	400	650	3#20	3#20	3#20	3#20	3#20	3#20
RB2	400	650	3#20	3#20	3#20	3#20	3#20	3#20
RB3	400	750	4#20	4#20	4#20	4#20	4#20	4#20
RB4	400	750	3#20	3#20	3#20	3#20	3#20	3#20
RB5	400	600	3#20	3#20	3#20	3#20	3#20	3#20
RB6	400	750	3#20	3#20	3#20	3#20	3#20	3#20
RB7	400	600	3#20	3#20	3#20	3#20	3#20	3#20
RB8	400	750	3#20	3#20	3#20	3#20	3#20	3#20

Table 20.6 shows the summary of shear reinforcement in beams.

TABLE 20.6 Shear reinforcement in beams

Beam No.	Stirrups		
	Left	Centre	Right
FB1	#8 @ 140 mm c/c (2L)	#8 @ 200 mm c/c (2L)	#8 @ 140 mm c/c (2L)
FB2	#8 @ 140 mm c/c (2L)	#8 @ 200 mm c/c (2L)	#8 @ 140 mm c/c (2L)
FB3	#10 @ 160 mm c/c (2L)	#10 @ 225 mm c/c (2L)	#10 @ 160 mm c/c (2L)
FB4	#10 @ 160 mm c/c (2L)	#10 @ 300 mm c/c (2L)	#10 @ 160 mm c/c (2L)
FB5	#8 @ 130 mm c/c (2L)	#8 @ 190 mm c/c (2L)	#8 @ 130 mm c/c (2L)
FB6	#8 @ 160 mm c/c (2L)	#8 @ 200 mm c/c (2L)	#8 @ 160 mm c/c (2L)
FB7	#8 @ 130 mm c/c (2L)	#8 @ 200 mm c/c (2L)	#8 @ 130 mm c/c (2L)
FB8	#8 @ 160 mm c/c (2L)	#8 @ 200 mm c/c (2L)	#8 @ 160 mm c/c (2L)
RB1	#8 @ 140 mm c/c (2L)	#8 @ 200 mm c/c (2L)	#8 @ 140 mm c/c (2L)
RB2	#8 @ 140 mm c/c (2L)	#8 @ 200 mm c/c (2L)	#8 @ 140 mm c/c (2L)
RB3	#8 @ 160 mm c/c (2L)	#8 @ 160 mm c/c (2L)	#8 @ 160 mm c/c (2L)
RB4	#8 @ 160 mm c/c (2L)	#8 @ 200 mm c/c (2L)	#8 @ 160 mm c/c (2L)
RB5	#8 @ 130 mm c/c (2L)	#8 @ 190 mm c/c (2L)	#8 @ 130 mm c/c (2L)

RB6	#8 @ 160 mm c/c (2L)	#8 @ 200 mm c/c (2L)	#8 @ 160 mm c/c (2L)
RB7	#8 @ 130 mm c/c (2L)	#8 @ 200 mm c/c (2L)	#8 @ 130 mm c/c (2L)
RB8	#8 @ 160 mm c/c (2L)	#8 @ 200 mm c/c (2L)	#8 @ 160 mm c/c (2L)

20.11 DESIGN OF FOUNDATIONS

STAAD.Pro does not have an inbuilt facility for the design of foundations. There are separate specialized software for the design of foundations (e.g., STAAD Foundation Advanced, Foundation 3D, Mat 3D, etc.)

In the present case study, all the foundations are designed manually. Refer to the details given in the following section.

20.11.1 Design Parameters

Factor of safety against overturning

Stability due to dead load : 1.20

Stability due to live load : 1.40

Factor of safety against sliding : 1.40

Factor of safety against uplift (based on engineering judgement) : 1.20

Allowable loss of contact (based on engineering judgement) : 15%

20.11.2 Design Forces

It is better to design the foundation for each and every load combination. However, this substantially increases efforts in design. Based on good engineering judgement, it is recommended to use the following load cases for the design of foundation:

Case 1—Representing maximum compression case

Case 2—Representing maximum tension case

Case 3—Representing maximum shear in X-direction case

Case 4—Representing maximum shear in Z-direction case

Case 5—Representing maximum moment about X (i.e., M_x) case

Case 6—Representing maximum moment about Z (i.e., M_z) case

Case 7—Representing maximum resultant shear or moment on foundation

STAAD.Pro produces the summary of reactions for Cases 1–6 for a particular set of load combinations. Case 7 needs to be decided by the engineer based on likely maximum resultant shear or moment.

20.11.3 Summary of Foundation Design

Typical reinforcement details for foundation are shown in Fig. 20.11. Table 20.7 shows the summary of foundation reinforcement.

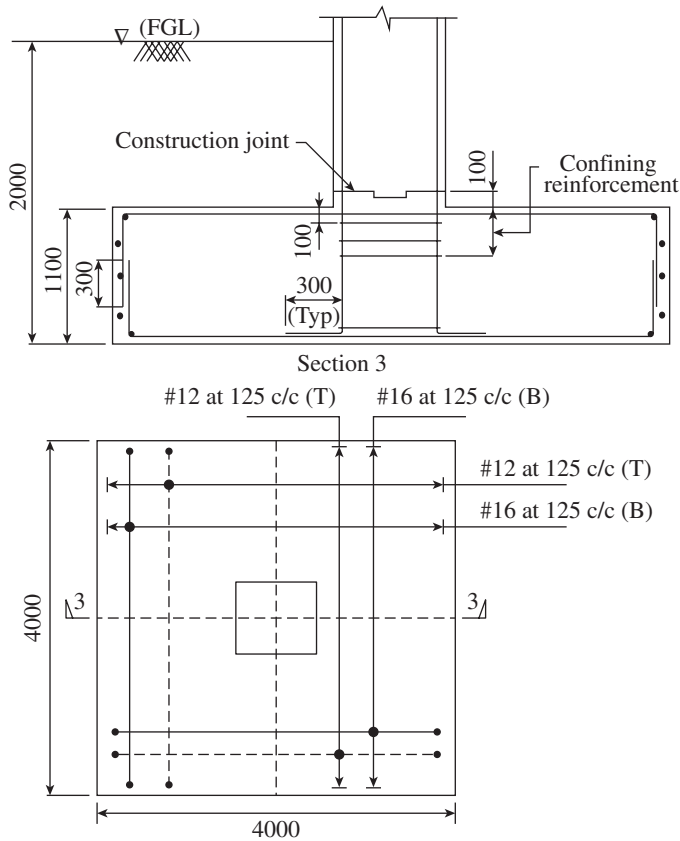


FIG. 20.11 Reinforcement details of foundation marked F1

TABLE 20.7 Reinforcement in foundations as per STAAD.Pro

Type	Foundation Size			Reinforcement along Length		Reinforcement along Width	
	L	B	t	Top	Bottom	Top	Bottom
F1	4.0	4.0	1.1	#12 @ 125 c/c	#16 @ 125 c/c	#12 @ 125 c/c	#16 @ 125 c/c
F2	3.0	3.0	0.9	#12 @ 175 c/c	#16 @ 175 c/c	#12 @ 175 c/c	#16 @ 175 c/c
F3	3.2	3.2	0.9	#12 @ 175 c/c	#16 @ 175 c/c	#12 @ 175 c/c	#16 @ 175 c/c
F4	3.7	3.7	1.1	#12 @ 150 c/c	#16 @ 150 c/c	#12 @ 150 c/c	#16 @ 150 c/c

20.12 DESIGN OF SLABS

Slabs have been analysed and designed as two-way slabs as per IS 456:2000.

20.12.1 Summary of Loading on Slab

- Weight of slab = $0.18 \times 25 = 4.5 \text{ kN/m}^2$
- Weight of floor finish (1st to 6th floors) = 2 kN/m^2
- Weight of floor finish (terrace) = 1 kN/m^2
- Live load on floor (1st to 6th floors) = 5 kN/m^2
- Live load on floor (terrace) = 1.5 kN/m^2

Hence,

Total UDL on 1st to 6th floor slab = $4.5 + 2.0 + 5 = 11.5 \text{ kN/m}^2$
 Total UDL on terrace slab = $4.5 + 1 + 1.5 = 7 \text{ kN/m}^2$

All the slabs have been designed for this loading.

20.12.2 Design Data

- Thickness of slab = 180 mm
- Clear cover = 15 mm
- Effective cover = 25 mm
- Effective thickness = 155 mm
- Load factor = 1.5

20.12.3 Summary of Slab reinforcement

Table 20.8 shows the summary of slab reinforcement.

TABLE 20.8 Reinforcement in slabs as per STAAD.Pro

Slab mark	Reinforcement along X-direction		Reinforcement along Z-direction	
	Span	Continuous Support	Span	Continuous Support
S1	#10 @ 150 c/c	#10 @ 150 c/c	#10 @ 100 c/c	#10 @ 100 c/c
S2	#10 @ 200 c/c	#10 @ 200 c/c	#10 @ 100 c/c	#10 @ 100 c/c
S3	#12 @ 300 c/c	#12 @ 300 c/c	#10 @ 250 c/c	#10 @ 250 c/c
S4	#8 @ 200 c/c	#10 @ 200 c/c	#10 @ 250 c/c	#10 @ 250 c/c
RS1	#8 @ 175 c/c	#8 @ 175 c/c	#10 @ 150 c/c	#10 @ 150 c/c
RS2	#8 @ 225 c/c	#8 @ 225 c/c	#8 @ 150 c/c	#10 @ 150 c/c
RS3	#8 @ 175 c/c	#8 @ 175 c/c	#8 @ 250 c/c	#8 @ 250 c/c
RS4	#8 @ 225 c/c	#8 @ 225 c/c	#8 @ 250 c/c	#8 @ 250 c/c

20.13 STAAD.PRO INPUT FILE

For the convenience of the readers, the complete STAAD.Pro input file for the example building is provided here:

```

STAAD SPACE
START JOB INFORMATION
ENGINEER DATE 18-Sep-11
END JOB INFORMATION
INPUT WIDTH 79
UNIT METER KN
*****
    
```


JOINT COORDINATES

1 0 0 0; 3 8 0 0; 4 12 0 0; 6 20 0 0; 7 0 0 5; 8 8 0 5;
 9 12 0 5; 10 20 0 5;
 11 0 0 10; 12 8 0 10; 13 12 0 10; 14 20 0 10; 15 0 0 15;
 17 8 0 15; 18 12 0 15;
 20 20 0 15; 21 0 3 0; 23 8 3 0; 24 12 3 0; 26 20 3 0; 27
 0 3 5; 28 8 3 5;
 29 12 3 5; 30 20 3 5; 31 0 3 10; 32 8 3 10; 33 12 3 10;
 34 20 3 10; 35 0 3 15;
 37 8 3 15; 38 12 3 15; 40 20 3 15; 45 0 6 0; 47 8 6 0;
 48 12 6 0; 50 20 6 0;
 51 0 6 5; 52 8 6 5; 53 12 6 5; 54 20 6 5; 55 0 6 10; 56
 8 6 10; 57 12 6 10;
 58 20 6 10; 59 0 6 15; 61 8 6 15; 62 12 6 15; 64 20 6 15;
 65 0 9 0; 67 8 9 0;
 68 12 9 0; 70 20 9 0; 71 0 9 5; 72 8 9 5; 73 12 9 5; 74
 20 9 5; 75 0 9 10;
 76 8 9 10; 77 12 9 10; 78 20 9 10; 79 0 9 15; 81 8 9 15;
 82 12 9 15;
 84 20 9 15; 85 0 12 0; 87 8 12 0; 88 12 12 0; 90 20 12
 0; 91 0 12 5; 92 8 12 5;
 93 12 12 5; 94 20 12 5; 95 0 12 10; 96 8 12 10; 97 12 12
 10; 98 20 12 10;
 99 0 12 15; 101 8 12 15; 102 12 12 15; 104 20 12 15; 105
 0 15 0; 107 8 15 0;
 108 12 15 0; 110 20 15 0; 111 0 15 5; 112 8 15 5; 113 12
 15 5; 114 20 15 5;
 115 0 15 10; 116 8 15 10; 117 12 15 10; 118 20 15 10; 119
 0 15 15; 121 8 15 15;
 122 12 15 15; 124 20 15 15; 125 0 18 0; 127 8 18 0; 128
 12 18 0; 130 20 18 0;
 131 0 18 5; 132 8 18 5; 133 12 18 5; 134 20 18 5; 135 0
 18 10; 136 8 18 10;
 137 12 18 10; 138 20 18 10; 139 0 18 15; 141 8 18 15;
 142 12 18 15;
 144 20 18 15; 145 0 21 0; 147 8 21 0; 148 12 21 0; 150
 20 21 0; 151 0 21 5;
 152 8 21 5; 153 12 21 5; 154 20 21 5; 155 0 21 10; 156 8
 21 10; 157 12 21 10;
 158 20 21 10; 159 0 21 15; 161 8 21 15; 162 12 21 15;
 164 20 21 15;
 201 10 3 7.5; 202 10 6 7.5; 203 10 9 7.5; 204 10 12 7.5;
 205 10 15 7.5;
 206 10 18 7.5; 207 10 21 7.5;

MEMBER INCIDENCES

1 1 21; 3 3 23; 4 4 24; 6 6 26; 7 7 27; 8 8 28; 9 9 29;
 10 10 30; 11 11 31;
 12 12 32; 13 13 33; 14 14 34; 15 15 35; 17 17 37; 18 18
 38; 20 20 40; 21 21 23;

23 23 24; 24 24 26; 26 27 28; 28 28 29; 30 29 30; 31 31
 32; 33 32 33; 35 33 34;
 36 35 37; 38 37 38; 39 38 40; 41 21 27; 42 27 31; 43 31
 35; 47 23 28; 48 28 32;
 49 32 37; 50 24 29; 51 29 33; 52 33 38; 56 26 30; 57 30
 34; 58 34 40; 59 21 45;
 61 23 47; 62 24 48; 64 26 50; 65 27 51; 66 28 52; 67 29
 53; 68 30 54; 69 31 55;
 70 32 56; 71 33 57; 72 34 58; 73 35 59; 75 37 61; 76 38
 62; 78 40 64; 79 45 65;
 81 47 67; 82 48 68; 84 50 70; 85 51 71; 86 52 72; 87 53
 73; 88 54 74; 89 55 75;
 90 56 76; 91 57 77; 92 58 78; 93 59 79; 95 61 81; 96 62
 82; 98 64 84; 99 65 85;
 101 67 87; 102 68 88; 104 70 90; 105 71 91; 106 72 92;
 107 73 93; 108 74 94;
 109 75 95; 110 76 96; 111 77 97; 112 78 98; 113 79 99;
 115 81 101; 116 82 102;
 118 84 104; 119 85 105; 121 87 107; 122 88 108; 124 90
 110; 125 91 111;
 126 92 112; 127 93 113; 128 94 114; 129 95 115; 130 96
 116; 131 97 117;
 132 98 118; 133 99 119; 135 101 121; 136 102 122; 138
 104 124; 139 105 125;
 141 107 127; 142 108 128; 144 110 130; 145 111 131; 146
 112 132; 147 113 133;
 148 114 134; 149 115 135; 150 116 136; 151 117 137; 152
 118 138; 153 119 139;
 155 121 141; 156 122 142; 158 124 144; 159 125 145; 161
 127 147; 162 128 148;
 164 130 150; 165 131 151; 166 132 152; 167 133 153; 168
 134 154; 169 135 155;
 170 136 156; 171 137 157; 172 138 158; 173 139 159; 175
 141 161; 176 142 162;
 178 144 164; 183 45 47; 185 47 48; 186 48 50; 188 51 52;
 190 52 53; 192 53 54;
 193 55 56; 195 56 57; 197 57 58; 198 59 61; 200 61 62;
 201 62 64; 203 45 51;
 204 51 55; 205 55 59; 209 47 52; 210 52 56; 211 56 61;
 212 48 53; 213 53 57;
 214 57 62; 218 50 54; 219 54 58; 220 58 64; 225 65 67;
 227 67 68; 228 68 70;
 230 71 72; 232 72 73; 234 73 74; 235 75 76; 237 76 77;
 239 77 78; 240 79 81;
 242 81 82; 243 82 84; 245 65 71; 246 71 75; 247 75 79;
 251 67 72; 252 72 76;
 253 76 81; 254 68 73; 255 73 77; 256 77 82; 260 70 74;
 261 74 78; 262 78 84;
 267 85 87; 269 87 88; 270 88 90; 272 91 92; 274 92 93;
 276 93 94; 277 95 96;
 279 96 97; 281 97 98; 282 99 101; 284 101 102; 285 102
 104; 287 85 91;

```

288 91 95; 289 95 99; 293 87 92; 294 92 96; 295 96 101; 3 4 7 10 11 14 17 18 61 62 65 68 69 72 75 76 81 82 85 88
296 88 93; 297 93 97; 89 92 95 96 101 102 105 108 109 112 115 116 121 122 125
298 97 102; 302 90 94; 303 94 98; 304 98 104; 309 105 128 129 132 135 136 141 142 145 148 149 152 155 156 161
107; 311 107 108; 162 165 168 169 172 175 176 PRIS YD 0.7 ZD 0.4
312 108 110; 314 111 112; 316 112 113; 318 113 114; 319 *
115 116; 321 116 117; 8 9 12 13 66 67 70 71 86 87 90 91 106 107 110 111 126
323 117 118; 324 119 121; 326 121 122; 327 122 124; 329 127 130 131 146 147 150 151 166 167 170 171 PRIS YD 0.8
105 111; 330 111 115; ZD 0.45
331 115 119; 335 107 112; 336 112 116; 337 116 121; 338 MEMBER PROPERTY INDIAN
108 113; 339 113 117; 41 TO 43 56 TO 58 203 TO 205 218 TO 220 245 TO 247 260
340 117 122; 344 110 114; 345 114 118; 346 118 124; 351 TO 262 287 TO 289 302 303 TO 304 329 TO 331 344 TO 346
125 127; 353 127 128; 371 TO 373 386 TO 388 413 TO 415 428 TO 429 430 PRIS YD
354 128 130; 356 131 132; 358 132 133; 360 133 134; 361 0.6 ZD 0.4
135 136; 363 136 137; *
365 137 138; 366 139 141; 368 141 142; 369 142 144; 371 21 23 24 36 38 39 183 185 186 198 200 201 225 227 228
125 131; 372 131 135; 240 242 243 267 269 270 282 284 285 309 311 312 324 326
373 135 139; 377 127 132; 378 132 136; 379 136 141; 380 327 351 353 354 366 368 369 393 395 396 408 410 411 PRIS
128 133; 381 133 137; YD 0.65 ZD 0.4
382 137 142; 386 130 134; 387 134 138; 388 138 144; 393 *
145 147; 395 147 148; 26 28 30 31 33 35 47 TO 52 188 190 192 193 195 197 209 TO
396 148 150; 398 151 152; 400 152 153; 402 153 154; 403 214 230 232 234 235 237 239 251 TO 256 272 274 276 277
155 156; 405 156 157; 279 281 293 TO 298 314 316 318 319 321 323 335 TO 340 356
407 157 158; 408 159 161; 410 161 162; 411 162 164; 413 358 360 361 363 365 377 TO 382 398 400 402 403 405 407
145 151; 414 151 155; 419 TO 424 PRIS YD 0.75 ZD 0.4
415 155 159; 419 147 152; 420 152 156; 421 156 161; 422 *****
148 153; 423 153 157;
424 157 162; 428 150 154; 429 154 158; 430 158 164;
*****
START GROUP DEFINITION
JOINT
_FIRSTFLOOR 21 23 24 26 TO 35 37 38 40 201
_SECONDSFLOOR 45 47 48 50 TO 59 61 62 64 202
_THIRDFLOOR 65 67 68 70 TO 79 81 82 84 203
_FOURTHFLOOR 85 87 88 90 TO 99 101 102 104 204
_FIFTHFLOOR 105 107 108 110 TO 119 121 122 124 205
_SIXTHFLOOR 125 127 128 130 TO 139 141 142 144 206
_SEVENTHFLOOR 145 147 148 150 TO 159 161 162 164 207
END GROUP DEFINITION
*****
DEFINE MATERIAL START
ISOTROPIC CONCRETE
E 2.17185e+007
POISSON 0.17
DENSITY 23.5616
ALPHA 1e-005
DAMP 0.05
END DEFINE MATERIAL
*****
MEMBER PROPERTY INDIAN
1 6 15 20 59 64 73 78 79 84 93 98 99 104 113 118 119 124
133 138 139 144 153 158 159 164 173 178 PRIS YD 0.7 ZD 0.4
*
3 4 7 10 11 14 17 18 61 62 65 68 69 72 75 76 81 82 85 88
89 92 95 96 101 102 105 108 109 112 115 116 121 122 125
128 129 132 135 136 141 142 145 148 149 152 155 156 161
162 165 168 169 172 175 176 PRIS YD 0.7 ZD 0.4
*
8 9 12 13 66 67 70 71 86 87 90 91 106 107 110 111 126
127 130 131 146 147 150 151 166 167 170 171 PRIS YD 0.8
ZD 0.45
MEMBER PROPERTY INDIAN
41 TO 43 56 TO 58 203 TO 205 218 TO 220 245 TO 247 260
TO 262 287 TO 289 302 303 TO 304 329 TO 331 344 TO 346
371 TO 373 386 TO 388 413 TO 415 428 TO 429 430 PRIS YD
0.6 ZD 0.4
*
21 23 24 36 38 39 183 185 186 198 200 201 225 227 228
240 242 243 267 269 270 282 284 285 309 311 312 324 326
327 351 353 354 366 368 369 393 395 396 408 410 411 PRIS
YD 0.65 ZD 0.4
*
26 28 30 31 33 35 47 TO 52 188 190 192 193 195 197 209 TO
214 230 232 234 235 237 239 251 TO 256 272 274 276 277
279 281 293 TO 298 314 316 318 319 321 323 335 TO 340 356
358 360 361 363 365 377 TO 382 398 400 402 403 405 407
419 TO 424 PRIS YD 0.75 ZD 0.4
*****
CONSTANTS
MATERIAL CONCRETE ALL
*****
SUPPORTS
1 3 4 6 TO 15 17 18 20 FIXED
*****
DEFINE 1893 LOAD
ZONE 0.16 RF 5 I 1.5 SS 2 ST 3 DM 0.05 PX 0.423 PZ 0.488
DT 0
*
SELFWEIGHT 1
*
MEMBER WEIGHT
21 23 24 26 28 30 31 33 35 36 38 39 41 TO 43 47 TO 52 56
TO 58 183 185 186 188 190 192 193 195 197 198 200 201 203
TO 205 209 TO 214 218 TO 220 225 227 228 230 232 234 235
237 239 240 242 243 245 TO 247 251 TO 256 260 TO 262 267
269 270 272 274 276 277 279 281 282 284 285 287 TO 289
293 294 TO 298 302 TO 304 309 311 312 314 316 318 319 321
323 324 326 327 329 330 TO 331 335 TO 340 344 TO 346 351
353 354 356 358 360 361 363 365 366 368 369 371 TO 373
377 TO 382 386 TO 388 UNI 12.42
*
FLOOR WEIGHT
YRANGE 2.9 21.1 FLOAD 4.5
YRANGE 2.9 18.1 FLOAD 2
YRANGE 20.9 21.1 FLOAD 1

```

```

*
YRANGE 2.9 18.1 FLOAD 2.5
*****
CUT OFF MODE SHAPE 100
CUT OFF FREQUENCY 33
*****
LOAD 1 STATIC SEISMIC X
1893 LOAD X 1
PERFORM ANALYSIS
CHANGE
*****
LOAD 2 STATIC SEISMIC Z
1893 LOAD Z 1
PERFORM ANALYSIS
CHANGE
*****
LOAD 11 DEAD LOAD
*****
SELFWEIGHT Y -1
*****
FLOOR LOAD
** LOAD = 0.18 x 25 = 4.5kN/mm2 (180 mm thickness of
slab)
YRANGE 2.9 21.1 FLOAD 4.5 GY
** FLOOR FINISH = 2kN/sqm
YRANGE 2.9 18.1 FLOAD -2 GY
** TERRACE FINISH = 1kN/sqm
YRANGE 20.9 21.1 FLOAD -1 GY
** WEIGHT OF BRICK WALL = 0.23 x 3 x 18 = 12.42kN/sqm
MEMBER LOAD
21 23 24 26 28 30 31 33 35 36 38 39 41 TO 43 47 TO 52 56
TO 58 183 185 186 188 190 192 193 195 197 198 200 201 203
TO 205 209 TO 214 218 TO 220 225 227 228 230 232 234 235
237 239 240 242 243 245 TO 247 251 TO 256 260 TO 262 267
269 270 272 274 276 277 279 281 282 284 285 287 TO 289
293 294 TO 298 302 TO 304 309 311 312 314 316 318 319 321
323 324 326 327 329 330 TO 331 335 TO 340 344 TO 346 351
353 354 356 358 360 361 363 365 366 368 369 371 TO 373
377 TO 382 386 TO 388 UNI GY -12.42
*****
LOAD 12 LIVE LOAD
FLOOR LOAD
** LIVE LOAD ON FLOOR = 5kN/sqm
YRANGE 2.9 18.1 FLOAD-5 GY
** LIVE LOAD ON TERRACE = 1.5kN/sqm
YRANGE 20.9 21.1 FLOAD-1.5 GY

```

```

*****
LOAD 21 SEISMIC X
***** LUMPING DL *****
SELFWEIGHT X 1
*
SELFWEIGHT Y 1
*
SELFWEIGHT Z 1
*
FLOOR LOAD
YRANGE 2.9 21.1 FLOAD 4.5 GX
YRANGE 2.9 18.1 FLOAD 2 GX
YRANGE 20.9 21.1 FLOAD 1 GX
*
YRANGE 2.9 21.1 FLOAD 4.5 GY
YRANGE 2.9 18.1 FLOAD 2 GY
YRANGE 20.9 21.1 FLOAD 1 GY
*
YRANGE 2.9 21.1 FLOAD 4.5 GZ
YRANGE 2.9 18.1 FLOAD 2 GZ
YRANGE 20.9 21.1 FLOAD 1 GZ
*
MEMBER LOAD
21 23 24 26 28 30 31 33 35 36 38 39 41 TO 43 47 TO 52
56 TO 58 183 185 186 188 190 192 193 195 197 198 200
201 203 TO 205 209 TO 214 218 TO 220 225 227 228 230
232 234 235 237 239 240 242 243 245 TO 247 251 TO 256
260 TO 262 267 269 270 272 274 276 277 279 281 282
284 285 287 TO 289 293 294 TO 298 302 TO 304 309 311
312 314 316 318 319 321 323 324 326 327 329 330 TO
331 335 TO 340 344 TO 346 351 353 354 356 358 360 361
363 365 366 368 369 371 TO 373 377 TO 382 386 TO 388
UNI GX 12.42
*
21 23 24 26 28 30 31 33 35 36 38 39 41 TO 43 47 TO 52
56 TO 58 183 185 186 188 190 192 193 195 197 198 200
201 203 TO 205 209 TO 214 218 TO 220 225 227 228 230
232 234 235 237 239 240 242 243 245 TO 247 251 TO 256
260 TO 262 267 269 270 272 274 276 277 279 281 282
284 285 287 TO 289 293 294 TO 298 302 TO 304 309 311
312 314 316 318 319 321 323 324 326 327 329 330 TO
331 335 TO 340 344 TO 346 351 353 354 356 358 360 361
363 365 366 368 369 371 TO 373 377 TO 382 386 TO 388
UNI GY 12.42
*
21 23 24 26 28 30 31 33 35 36 38 39 41 TO 43 47 TO 52 56
TO 58 183 185 186 188 190 192 193 195 197 198 200 201 203
TO 205 209 TO 214 218 TO 220 225 227 228 230 232 234 235
237 239 240 242 243 245 TO 247 251 TO 256 260 TO 262 267
269 270 272 274 276 277 279 281 282 284 285 287 TO 289

```

293 294 TO 298 302 TO 304 309 311 312 314 316 318 319 321
 323 324 326 327 329 330 TO 331 335 TO 340 344 TO 346 351
 353 354 356 358 360 361 363 365 366 368 369 371 TO 373
 377 TO 382 386 TO 388 UNI GZ 12.42

***** LUMPING LL *****

* 50% LL ON FLOOR * NO NEED TO CONSIDER LL ON ROOF *
 FLOOR LOAD
 YRANGE 2.9 18.1 FLOAD 2.5 GX
 YRANGE 2.9 18.1 FLOAD 2.5 GY
 YRANGE 2.9 18.1 FLOAD 2.5 GZ

* SCALE FACTOR = $(0.16/2) \times (1.5 / 5) = 0.024$
 SPECTRUM CQC 1893 X 2.078 ACC SCALE 0.024 DAMP 0.05 MIS
 SOIL TYPE 2

LOAD 22 SEISMIC Z
 SPECTRUM CQC 1893 Z 2.455 ACC SCALE 0.024 DAMP 0.05 MIS
 SOIL TYPE 2

***** SERVICEABILITY LOAD COMBINATIONS ***

***** 1.00DL + 1.00LL *****

LOAD COMB 101 COMBINATION 101
 11 1.0 12 1.0

***** 1.00DL +/- 1.00EL_x

LOAD COMB 201 COMBINATION 201
 11 1.0 21 1.0

LOAD COMB 202 COMBINATION 202
 11 1.0 21 -1.0

LOAD COMB 203 COMBINATION 203
 11 1.0 22 1.0

LOAD COMB 204 COMBINATION 204
 11 1.0 22 -1.0

***** 1.00 DL 1.00LL +/- 1.00EL_x

LOAD COMB 205 COMBINATION 205
 11 1.0 12 1.0 21 1.0

LOAD COMB 206 COMBINATION 206
 11 1.0 12 1.0 21 -1.0

LOAD COMB 207 COMBINATION 207
 11 1.0 12 1.0 22 1.0

LOAD COMB 208 COMBINATION 208
 11 1.0 12 1.0 22 -1.0

***** STRENGTH LOAD COMBINATIONS *****

***** 1.50DL + 1.50LL *****

LOAD COMB 1001 COMBINATION 1001
 11 1.5 12 1.5

***** 0.90DL +/- 1.50EL_x

LOAD COMB 2001 COMBINATION 2001
 11 0.9 21 1.5

LOAD COMB 2002 COMBINATION 2002
 11 0.9 21 -1.5

LOAD COMB 2003 COMBINATION 2003
 11 0.9 22 1.5

LOAD COMB 2004 COMBINATION 2004
 11 0.9 22 -1.5

***** 1.50DL +/- 1.50EL_x

LOAD COMB 2005 COMBINATION 2005
 11 1.5 21 1.5

LOAD COMB 2006 COMBINATION 2006
 11 1.5 21 -1.5

LOAD COMB 2007 COMBINATION 2007
 11 1.5 22 1.5

LOAD COMB 2008 COMBINATION 2008
 11 1.5 22 -1.5

***** 1.50DL + 1.50LL +/- 1.50EL_x

LOAD COMB 2009 COMBINATION 2009
 11 1.2 12 1.2 21 1.2

LOAD COMB 2010 COMBINATION 2010
 11 1.2 12 1.2 21 -1.2

LOAD COMB 2011 COMBINATION 2011
 11 1.2 12 1.2 22 1.2

LOAD COMB 2012 COMBINATION 2012
 11 1.2 12 1.2 22 -1.2

PERFORM ANALYSIS PRINT ALL
 DEFINE ENVELOP
 101 201 TO 208 ENVELOP 1 TYPE SERVICEABILITY
 1001 2001 TO 2012 ENVELOP 2 TYPE STRESS
 END DEFINE ENVELOP

LOAD LIST 1001 2001 TO 2012
 START CONCRETE DESIGN
 CODE IS13920
 CLEAR 0.05 ALL
 FC 30000 ALL
 FYMAIN 415000 ALL
 FYSEC 415000 ALL
 MAXMAIN 25 ALL
 MAXSEC 16 ALL
 MINMAIN 20 ALL
 MINSEC 8 ALL
 TORSION 0 ALL
 GLD 101 ALL

```

PLASTIC 1 MEMB 21 23 24 26 28 30 31 33 35 36 38 39 41 TO
43 47 TO 52 56 TO 58 183 185 186 188 190 192 193 195 197
198 200 201 203 TO 205 209 TO 214 218 TO 220 225 227 228
230 232 234 235 237 239 240 242 243 245 246 TO 247 251 TO
256 260 TO 262 267 269 270 272 274 276 277 279 281 282
284 285 287 TO 289 293 TO 298 302 TO 304 309 311 312 314
316 318 319 321 323 324 326 327 329 TO 331 335 TO 340 344
TO 346 351 353 354 356 358 360 361 363 365 366 368 369
371 TO 373 377 TO 382 386 TO 388 393 395 396 398 400 402
403 405 407 408 410 411 413 TO 415 419 TO 424 428 TO 430
BRACE 3 MEMB 1 3 4 6 TO 15 17 18 20 59 61 62 64 TO 73 75
76 78 79 81 82 84 85 TO 93 95 96 98 99 101 102 104 TO 113
115 116 118 119 121 122 124 TO 133 135 136 138 139 141 142
144 TO 153 155 156 158 159 161 162 164 TO 173 175 176 178
BRACE 1 MEMB 21 23 24 26 28 30 31 33 35 36 38 39 41 TO 43
47 TO 52 56 TO 58 183 185 186 188 190 192 193 195 197 198
200 201 203 TO 205 209 TO 214 218 219 TO 220 225 227 228
230 232 234 235 237 239 240 242 243 245 TO 247 251 252 TO
256 260 TO 262 267 269 270 272 274 276 277 279 281 282 284
285 287 288 TO 289 293 TO 298 302 TO 304 309 311 312 314
316 318 319 321 323 324 326 327 329 TO 331 335 TO 340 344
TO 346 351 353 354 356 358 360 361 363 365 366 368 369
371 TO 373 377 TO 382 386 TO 388 393 395 396 398 400 402
403 405 407 408 410 411 413 TO 415 419 TO 424 428 TO 430
RFACE 4 MEMB 1 3 4 6 TO 15 17 18 20 59 61 62 64 TO 73 75
76 78 79 81 82 84 85 TO 93 95 96 98 99 101 102 104 TO 113
115 116 118 119 121 122 124 TO 133 135 136 138 139 141 142
144 TO 153 155 156 158 159 161 162 164 TO 173 175 176 178
DESIGN COLUMN 1 3 4 6 TO 15 17 18 20 59 61 62 64 TO 73 75
76 78 79 81 82 84 85 TO 93 95 96 98 99 101 102 104 TO 113
115 116 118 119 121 122 124 TO 133 135 136 138 139 141 142
144 TO 153 155 156 158 159 161 162 164 TO 173 175 176 178
DESIGN BEAM 21 23 24 26 28 30 31 33 35 36 38 39 41 TO 43
47 TO 52 56 TO 58 183 185 186 188 190 192 193 195 197 198
200 201 203 TO 205 209 TO 214 218 219 TO 220 225 227 228
230 232 234 235 237 239 240 242 243 245 TO 247 251 252 TO
256 260 TO 262 267 269 270 272 274 276 277 279 281 282
284 285 287 288 TO 289 293 TO 298 302 TO 304 309 311 312
314 316 318 319 321 323 324 326 327 329 TO 331 335 TO 340
344 TO 346 351 353 354 356 358 360 361 363 365 366 368 369
371 TO 373 377 TO 382 386 TO 388 393 395 396 398 400 402
403 405 407 408 410 411 413 TO 415 419 TO 424 428 TO 430
TRACK 2 ALL

END CONCRETE DESIGN
*****
FINISH
*****

```

SUMMARY

Increasing population coupled with urbanization has made the construction of multi-storey buildings a necessity to house the millions without jeopardizing agricultural lands. A number of innovations in this field have resulted in the construction of tall buildings, which will not only efficiently resist the wind and earthquake loads but also provide enclosures that give comfort and energy efficiency. RC is ideally suited for such multi-storey buildings. High-strength concrete and high-yield strength-deformed bars are increasingly used in today's skyscrapers. The current trend in tall buildings is to incorporate wind energy systems, which make them self-sufficient and sustainable.

It is impossible to manually perform the analysis and design of such tall buildings because of the nature of computations involved and the complexity of the analysis procedures. Hence, designers often invoke the use of commercial software. Many commercial software applications are available now. However, designers should understand their shortcomings and limitations before selecting a particular software application. The modelling of tall buildings of complex nature and geometry always poses a challenge to the designer. In this chapter, the use of a popular software application called STAAD.Pro is discussed considering a specific example of

a seven-storey building. Static and dynamic seismic analyses of the building have been considered and the results are presented.

It has to be noted that designers should not directly accept the results produced by the computer. A few checks, such as matching the reactions with the applied downward loads, performing simple equilibrium and compatibility checks using hand calculations, and checking for abnormal deflections or forces in particular locations, are necessary for validating the results. The input data also needs to be checked thoroughly. It is important to realize that the design of any structure based on the results obtained from erroneous computer analysis will lead to structural failures, costly disputes, and poorly performing structures. In this context, we should remember the words of Emkin (1998) who cautioned that the structural engineers are unfortunately becoming so dependent on computers that they are rapidly losing the skills to be able to do any computational work without computers. Structural engineers should be aware that real engineering knowledge includes considerable experience, insight, intuition, creativity, spontaneous thought, gut feeling, ability to imagine the behaviour of structures, and a lot more 'awareness' of structural engineering than any computer program or programmer can have (Emkin 1998; Subramanian 2011).

EXERCISES

- Design the building given in this chapter (see Fig. 20.2) using STAAD.Pro or any other software available with you by considering seismic zone IV and soft soil for the following cases:
 - Considering provisions of IS 13920
 - Without considering provisions of IS 13920
 Compare the quantities.
- The plan of a G + 7 building located in Delhi is shown in Fig. 20.12.

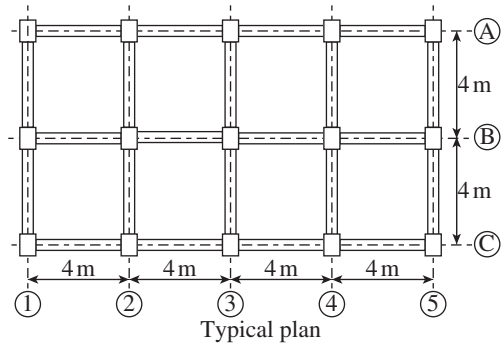


FIG. 20.12

Design the building using STAAD.Pro or any other software available with you for the following cases:

- (a) Considering provisions of IS 13920
- (b) Without considering provisions of IS 13920

Compare the quantities. Assume each floor has a height of 3 m.

- 3. The plan of a G + 5 building located in Mumbai is shown in Fig. 20.13.

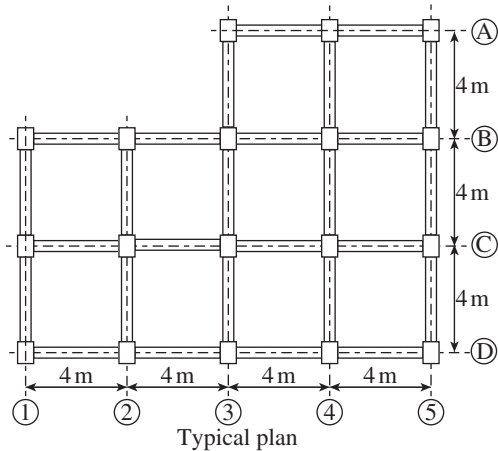


FIG. 20.13

Ali, M.M. and A. Aksamija 2008, 'Toward a Better Urban Life: Integration of Cities and Tall Buildings', *The 4th Architectural Conference on High Rise Buildings*, 9–11 June 2008, Amman, Jordan, p. 21, (also see <http://www.ctbuh.org/LinkClick.aspx?fileticket=v6e2fV1J2sg%3D&tabid=53&language=en-US>, last accessed on 10 April 2013).

Ali, M.M. and P. Armstrong 1995, *Architecture of Tall Buildings*, Council on Tall Buildings and Urban Habitat, McGraw-Hill, Inc., New York.

Dayaratnam, P. 2004, *Limit State Design of Reinforced Concrete Structures*, Oxford and IBH Publishing Co. Pvt. Ltd, New Delhi, p. 532.

Emkin, L.Z. 1998, 'Misuse of Computers by Structural Engineers: A Clear and Present Danger', *Proceedings of the First Structural Engineers World Congress*, SEWC'98, 19–23 July, San Francisco.

Irwin, P., J. Kilpatrick, J. Robinson, and A. Frisque 2008, 'Wind and Tall Buildings: Negatives and Positives', *Structural Design of Tall and Special Buildings*, Vol. 17, pp. 915–28.

Design the building using STAAD.Pro or any other software available with you, for the following cases:

- (a) Considering provisions of IS 13920
- (b) Without considering provisions of IS 13920

Compare the quantities. Assume each floor has a height of 3.2 m.

- 4. The plan of a G + 8 building located in Chennai is shown in Fig. 20.14.

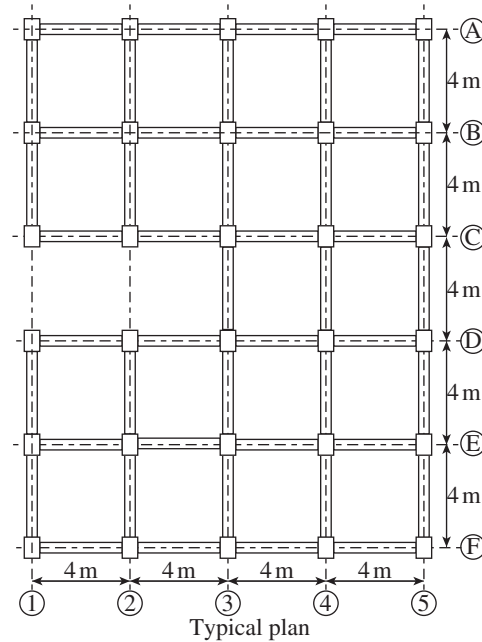


FIG. 20.14

Design the building using STAAD.Pro or any other software available with you for the following cases:

- (a) Considering provisions of IS 13920
- (b) Without considering provisions of IS 13920

Compare the quantities. Assume each floor has a height of 3.2 m.

REFERENCES

IS 1893 (Part 1):2002, *Criteria for Earthquake Resistant Design of Structure, Part 1: General Provisions and Buildings*, 5th revision, Bureau of Indian Standards, New Delhi, p. 39.

IS 13920:1993, *Ductile Detailing of Reinforced Concrete Structures Subjected to Seismic Forces: Code of Practice*, Bureau of Indian Standards, New Delhi, p. 14, (also see *Draft Code* available at <http://www.iitk.ac.in/nicee/IITK-GSDMA/EQ11.pdf>, last accessed on 16 April 2013, p. 67).

Jones, T. 2013, *Analysis and Design of Structures: A Practical Guide to Modeling*, Bentley Institute Press, Exton, p. 263.

SP 34 (S&T):1987, *Handbook on Concrete Reinforcement and Detailing*, Bureau of Indian Standards, New Delhi.

STAAD.Pro v8i (SELECT Series 1) 2009, *Technical Reference Manual*, Bentley Systems Inc., p. 668.

Subramanian, N. 2011, 'Are Our Structural Engineers Geared Up for the Challenges of the Profession?', *The Indian Concrete Journal*, Vol. 85, No. 1, pp. 20–26.

Taranath, B.S. 2010, *Reinforced Concrete Design of Tall Buildings*, CRC Press, Boca Raton, p. 923.

FEATURES OF THE BOOK

6.6.1 Maximum Spacing

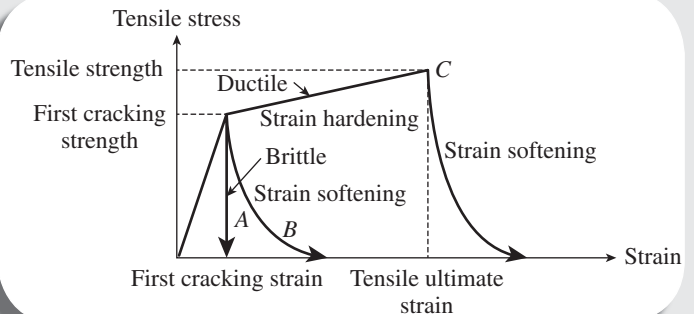
As per Clause 26.5.1.5 of IS 456, for vertical stirrups, the maximum spacing of shear reinforcement shall not exceed $0.75d$ or 300 mm, whichever is less. It should be noted that the code limits the maximum yield strength of web reinforcement to 415 N/mm^2 to avoid the difficulties encountered in bending high-strength stirrups (they may be brittle near sharp bends) and also to prevent excessively wide inclined cracks. For inclined stirrups at 45° , the same clause of the code stipulates

Based on the Latest Code for Reinforced Concrete

The latest versions of IS 456:2000 and IS 13920:1993 have been used throughout the book. However, even though IS 456 was revised in 2000, most of the design provisions remain unchanged from the previous 1978 edition of the code. Hence, IS 456 code provisions are compared with the provisions of other recent codes, especially with those of ACI 318:2011.

Illustrations

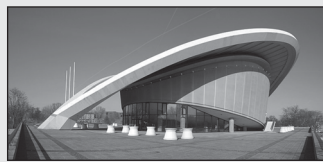
Plenty of photographs of structures as well as clear and well-labelled illustrations are interspersed in the text for better understanding of the theories discussed.



CASE STUDY

Failure of Congress Hall, Berlin, Germany

The Benjamin Franklin Hall, as the building was officially known, also called the conference hall (Der Kongresshalle) and nicknamed 'pregnant oyster' (Schwangere Auster), is a gift from the USA to the Berlin International Building Exhibition in 1957. The American architect Hugh A. Stubbins Jr designed the building in collaboration with two Berlin architects, Werner Duetman and Franz Mocken. This one-third curved and cantilevered roof (see figure) collapsed on 21 May 1980, killing one and injuring numerous people. It started rumbling and vibrating in the morning and hence most people inside had time to leave the building before it collapsed. The 76 mm thick RC shell roof resembles an open human eye with a tension ring as the pupil and the two arches at the edges representing the upper and lower lids. The two arch support points represent the corners of the 'eye'. The report of the failure cited that the collapse was mainly due to the planning and execution of the roof, which lead to cracks and corrosion



Congress Hall, Germany

and finally to the failure of the tensioning elements. The hall was rebuilt in its original style and reopened again in 1987 at the 750th anniversary of Berlin. More details of the failure may be found in Subramanian (1982).

Case Studies

Case studies have been provided in all the chapters to help students relate to the concepts discussed.

Solved Examples

Numerous solved examples and lucid step-wise solutions are provided throughout the book. These will help students understand the formulae used and the procedure followed.

EXAMPLE 8.6 (Design of T-beam):

The T-beam given in Example 8.4 is subjected to the following factored loads: bending moment of 150 kNm , shear of 120 kN and torsion of 60 kNm . Assuming M30 concrete and Fe 415 steel, design the reinforcements as per IS 456. Assume severe environment.

SOLUTION:

As per Clause 40.1.1 of IS 456, we will design the flange of the T-beam by ignoring the contribution of flanges.

REVIEW QUESTIONS

- Distinguish between flat slabs and flat plates with sketches of both.
- What are the advantages offered by flat plates over conventional two-way slabs with supporting beams?
- The minimum thickness of flat slabs or flat plates _____
 - is decided based on the span to effective depth ratio similar to two-way slabs
 - should be greater than 125 mm
 - both of these
 - none of these
- What is the purpose of a drop panel?
- The size of a drop panel in the interior panels should project _____
 - one-fourth of slab thickness and have length greater than one-third the panel length
 - one-fifth of slab thickness and have length greater than one-third the panel length
 - one-fifth of slab thickness and have length greater than one-fourth the panel length
 - one-fourth of slab thickness and have length greater than one-third the panel length
- State the conditions that should be satisfied while using DDM.
- What is the expression for total static moment M_s ?
- How are circular supports considered in the DDM?
- In interior spans, the total static moment is distributed between negative and positive bending moments in the ratio _____ per cent.
 - 50:50
 - 60:40
 - 65:35
 - 70:30
- How are the positive and negative bending moments distributed in the column and middle strips in the interior span?
- How is the effect of pattern load considered in the DDM as per IS 456 code?
- In what way is the EFM better than the DDM?
- How is the moment transfer between the slab and column due to unbalanced gravity loads or lateral loads considered in IS 456 code?
- As per IS 456, the transfer width around the interior column is taken as _____.
 - 1.2 times the depth of slab or drop panel on each side of column

Review Questions

The review questions given at the end of each chapter cover all the theoretical concepts dealt within the chapter. Students would do well to go through all the review questions, try to answer them, and revisit the chapter for answers to questions they could not answer.

Exercises

Numerous multiple-choice and numerical exercises are given at the end of the chapters for students to practise.

EXERCISES

- Design the interior panel of a flat plate supported on columns of size 450 mm \times 450 mm and the imposed load on the panel is 3 kN/m². The slab is exposed to moderate environment. Assume the floor shing load as 1 kN/m² and use M30 concrete and Fe 415 steel.
- Design the interior panel of a building with flat slab roof of a panel size of 7 m \times 7 m supported by columns of size 450 mm \times 600 mm. Take live load as 4.0 kN/m² and the weight finishes as 1.0 kN/m². Use M25 concrete and Fe 415 steel. Assume mild environment.
- Design Exercise 2 assuming the flat slab is supported by a circular column of 500 mm diameter and is with suitable column diameter.
- Design the slab reinforcement at the exterior column of Exercise 2 for moment transfer between the slab and column and check combined stresses. Also calculate the moments to be carried by the columns.
- Design a corner column of size 400 mm \times 800 mm supporting a factored moment due to gravity loads at the face of the column is 80 kNm, the factored shear force at the face of the column is 200 kN, and the shear force at the edge is 25 kN. Check the stresses due to the combined forces assuming that the slab is made using M25 concrete and Fe 415 steel.
- A flat plate panel of dimensions 5 m \times 6 m supported by columns of size 450 mm \times 450 mm has a slab thickness of 150 mm and is designed for a working (total) load of 9 kN/m². Check the safety of the slab in punching shear and provide shear reinforcement, if required. Assume M20 concrete and Fe 415 steel.
- For the slab in Exercise 6, design headed shear studs as shear reinforcement, instead of shear stirrups.
- Design a waffle slab for an internal panel of a floor system that is constructed in a 6.3 m square module and subjected to a total design service load of 9.0 kN/m², out of which the live load is 3 kN/m². Use M25 concrete and Fe 415 steel. The slab is to be supported on square columns of size 750 mm \times 750 mm and constructed using removable forms of size 750 mm \times 750 mm \times 500 mm. The slab is subjected to p

REFERENCES

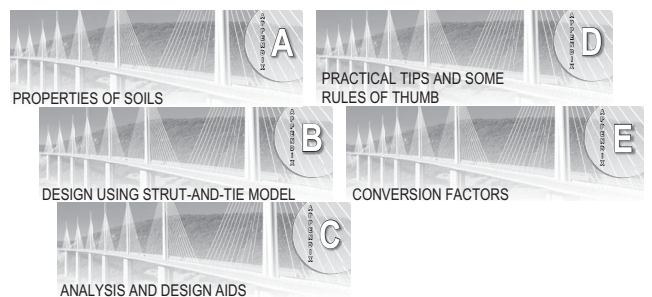
- | | |
|-----------------------------------------------------------------------------------------------------------------------------------------------------------------------------------------------------------------------------------|---------------------------------------------------------------------------------------------------------------------------------------------------------------|
| ACI-ASCE Committee 326 1962, 'Shear and Diagonal Tension, Part 3: Slabs and Footings', <i>Proceedings, ACI Journal</i> , Vol. 59, No. 3, pp. 353–96. | DiStasio, J. and M.P. Van Buren, 'Behavior of Slabs between Flat Plate Floor and Column', <i>ACI Structural Journal</i> , Vol. 57, No. 3, pp. 299–314. |
| ACI-ASCE Committee 352 2002 (ACI 352.1R-1989, reapproved 2004), <i>Recommendations for Design of Slab-Column Connections in Monolithic Reinforced Concrete Structures</i> , American Concrete Institute, Farmington Hills, p. 37. | Dovich, L.M. and J.K. Wight 2004, 'Seismic Analysis of Flat Slab-Column Connections', <i>ACI Structural Journal</i> , Vol. 102, No. 6, pp. 868–75. |
| ACI-ASCE Committee 421 1999 (ACI 421.1R-99, reapproved 2006), <i>Shear Reinforcement for Slabs</i> , American Concrete Institute, Farmington Hills, p. 15. | Durrani, A.J., Y. Du, and Y.H. Kim, 'Nonductile Slab-Column Connections in Buildings', <i>ACI Structural Journal</i> , Vol. 102, No. 6, pp. 868–75. |
| ACI-ASCE Committee 426 1974, 'The Shear Strength of Reinforced Concrete Members—Slabs', <i>Proceedings, ASCE</i> , Vol. 100, No. ST8, pp. 1543–91. | Elgabry, A.A. and A. Ghali 1999, 'Connections with Stud Shear Reinforcement for Moment Transfer', <i>ACI Structural Journal</i> , Vol. 97, No. 6, pp. 868–75. |

References and Weblinks

For interested readers and researchers in this area, the book provides plenty of reference material at the end of each chapter as well as a separate bibliography at the end of the book.

Appendices

Appendices on strut-and-tie-method, properties of soils, design aids, conversion factors, and practical tips and thumb rules for practising structural engineers have been provided for easy reference.



LIST OF SYMBOLS

- A Area, mm²
- A_b Area of bar = $\pi d_b^2/4$, mm²
- A_{brg} Net bearing area of the head of the bolt, mm²
- A_c Area of concrete, concrete area of the assumed critical section of flat slab = $b_o d$
- A_{cp} Area of the full concrete cross section, mm²
- A_{cr} Transformed concrete area of the cracked section = $A_c + (m - 1)A_{st}$
- A_e Effective frontal area, also the effective area of concrete in tension surrounding the main tension reinforcement, mm²
- A_{ej} Effective shear area of the joint
- A_{gr} Gross cross-sectional area of concrete, mm²
- A_h Design horizontal acceleration spectrum value (IS 1893)
- A_k Area of the confined concrete core measured to the outside of spiral or hoop, mm²
- A_N Projected concrete failure area of a single anchor or a group of anchors
- A_{Na} Projected influence area of a single adhesive anchor or a group of adhesive anchors for the calculation of bond strength in tension, mm²
- A_{Na0} Projected influence area of a single adhesive anchor for the calculation of bond strength in tension if not limited by edge distance or spacing, mm²
- $A_{N,o}$ Projected area of one anchor on the concrete surface not limited by edge influences
- A_o Area enclosed by the centre line of the thickness of a hollow member, mm²
- A_{oh} Area enclosed by the centre line of the outermost closed transverse torsional reinforcement, mm²
- A_p Cross-sectional area of the pile tip, in m²
- A_s Area of steel, mm²
- A_{sa} Area of anchor reinforcement, mm²
- A_{sb} Structural integrity reinforcement, mm²
- A_{sc} Area of compression steel, mm²
- $A_{se,N}$ Effective cross-sectional area of an anchor in tension, mm²
- $A_{se,V}$ Effective cross-sectional area of an anchor in shear, mm²
- A_{si} Surface area of the pile shaft in the i th layer, m²
- A_{st} Area of tension steel, mm²
- A_{st}^+ and A_{st}^- Reinforcement for positive and negative moments, respectively, mm²
- $A_{st,min}$ Minimum tensile steel, mm²
- A_{sh} Area of transverse reinforcement, mm²
- A_{sp} Area of spiral reinforcement, mm²
- A_v Area of stirrup, also the projected concrete failure area of a single anchor or a group of anchors, for the calculation of strength in shear, mm²
- A_{vo} Projected concrete failure area of a single anchor, for the calculation of strength in shear, if not limited by corner influence, spacing, or member thickness, mm²
- A_{sv} Area of cross section of the transverse reinforcement or headed shear stud ('single' stirrup leg), mm²
- A_r Projected rib area normal to reinforcing bar axis, mm²
- A_{tr} Total cross-sectional area of transverse reinforcement within the spacing s , mm² (ACI 318)
- A_{vf} Area of shear-friction reinforcement placed normal to the possible crack, mm²
- a Side of triangle, mm
- a and b Sides of the control perimeter of a rectangular column, mm
- a_{cr} Distance from the point at which crack width is determined to the surface of the nearest reinforcing bar, mm
- a_g Maximum course aggregate size, mm
- a_v Shear span = M_u/V_u , mm
- b Breadth of beam, or shorter dimension of a rectangular column, mm
- b_0 Beam spacing, mm
- b_c Cross-sectional dimension of the column core measured to the outside edges of transverse reinforcement composing area A_k , mm
- b_e Effective width of slab, mm
- b_f Breadth of flange, mm
- b_o Perimeter of the critical section, mm
- b_w Breadth of web, mm
- C Torsional stiffness, also the total compressive force, kN and minimum clearance, m
- C_c Compressive force due to concrete stress block, N
- C_f Force coefficient of the structure
- C_L Limiting value of concrete compression
- C_m Correction factor to convert actual moment diagram to an equivalent uniform moment diagram
- C_r Strength reduction factor for a slender column
- C_{pe} External pressure coefficient
- C_{pi} Internal pressure coefficient
- C_{si} Compressive force in steel reinforcement, N
- C_t Creep coefficient = ϵ_{cp}/ϵ_i
- C_u Ultimate creep coefficient
- CE Carbon equivalent
- C_x and C_y Marcus correction factors (slabs)
- c and c' Distances from the centroidal axis to the sections where the maximum and minimum shear stress occur, mm
- c_a Cohesion of soil, kN/m²
- c_{ac} Critical edge distance for anchors, mm
- $c_{a,min}$ Minimum distance from the centre of an anchor shaft to the edge of the concrete, mm
- c_b Cover for the bar or wire, mm
- c_c Clear cover, mm
- c_{min} Thickness of the concrete cover measured from the extreme tension fibre to the centre of the nearest bar, mm
- c_n Nominal cover, mm
- c_{Na} Projected distance from the centre of an anchor shaft on one side of the anchor required to develop the full bond strength of a single adhesive anchor, mm
- c_r Average centre-to-centre rib spacing, mm
- c_s Side cover, mm
- c_t Distance from the inner face of the column to the edge of the slab, mm
- c_u Cohesion of clayey soil, kN/m²
- c_1 and c_2 Column dimensions, mm
- D Overall depth of beam/slab or diameter of a column; dimension of a rectangular column in the direction under consideration, mm
- DBE Design basis earthquake
- DL Dead load
- DR Design storey drift ratio
- D_b Overall depth of the beam, mm
- D_c Diameter of the circular column, mm
- d_{eq} Diameter of an equivalent circle, mm

D_f	Thickness of flange, also the depth of foundation, mm	f_{sr}	Compressive stress range, N/mm ²
D_k	Diameter of core measured to the outside of spiral/hoop, mm	f_t	Tensile strength of concrete, N/mm ²
D_p	Diameter of the pile, mm	f_{uta}	Specified tensile strength of anchor steel, N/mm ²
D_s	Overall depth or thickness of slab, mm	f_y	Characteristic yield strength of steel rebar or wire, N/mm ²
D_u	Diameter of the under-ream of an under-reamed pile	f_{ya}	Specified yield strength of anchor steel, N/mm ²
d	Effective depth of a beam or slab, mm, also the base dimension of the building at the plinth level (IS 875), m	f_{ys}, f_{yv}	Yield strength of stirrup, N/mm ²
d_1	Diameter of the circumscribed circle, mm	f_{yt}	Specified yield strength of transverse reinforcement, N/mm ²
d'	Cover for compression steel, mm	f_x	Flexural stress, N/mm ²
d''	Cover for tension steel, mm	G	Modulus of rigidity = $E/[2(1 + \nu)]$
d_b	Nominal diameter of a bar or wire in mm	G_f	Gust factor, also the fracture energy, N/m
d_d	Thickness of drop panel below the soffit of the slab, mm	g	Acceleration due to gravity- 9.807 m/sec ² , also the slenderness factor = L_e/d
d_o	Depth or diameter of opening, mm	g_1	Centroidal distance of bars from the bottom fibre, mm
d_i	Diameter of the inscribed circle, mm	H	Height of the building, mm
d_v	Effective shear depth, mm $\approx 0.9d$	H_e	Effective height of the wall, mm
E	Young's modulus, N/mm ²	h	Longer dimension of the rectangular confining hoop, measured to its outer face, mm
E_c	Modulus of elasticity of concrete, $(5000 \sqrt{f_{ck}})$ N/mm ²	h_c	Overall depth of column in mm
E_{cd}	Dynamic modulus of elasticity of concrete, N/mm ²	h_{ef}	Effective embedment length of anchor, mm
E_s	Modulus of elasticity of steel reinforcement = 2×10^5 N/mm ²	h_s	Storey height, mm
EL	Earthquake load	h_x	Centre-to-centre horizontal spacing of cross-ties or hoop legs, mm
e	Eccentricity, mm, also the ratio of the width of support to the effective span of beam	h_v	Depth of the shear-head steel section, mm
e_a	Additional eccentricity due to slenderness effect or deflection, mm	h_1	Distance from centroid of tension steel to the neutral axis, mm
e_h	Distance from the inner surface of the shaft of to the outer tip of the J- or L-bolt, mm	h_2	Distance from the point where the crack width is determined to the neutral axis, mm
e_{min}, e_{max}	Minimum and maximum eccentricity, mm	H_u	Total lateral force acting within the storey, kN
e'_N	Distance between the resultant tensile force of tensioned anchor bolts of a group and the centroid of tensioned anchor bolts, mm	H_w	Unsupported height of wall, mm
F	Net wind force on the element, kN	H_{we}	Effective height of wall, mm
F'	Frictional drag force, kN	I	Importance factor (IS 1893), second moment of area (moment of inertia), mm ⁴
FS	Factor of safety	IL	Imposed load
f	Permissible bending stress, N/mm ²	I_b	Moment of inertia (M.I.) of beam, mm ⁴
f_1, f_2	Principal stresses, N/mm ²	I_{eff}	Effective moment of inertia, moment of inertia of the cracked section considering equivalent area of tension and compression reinforcement, mm ⁴
f_{act}	Allowable direct tensile stress in concrete, N/mm ²	I_f	Moment of inertia of the contact area of footing and soil, mm ⁴
f_{ast}	Allowable tensile stress in steel, N/mm ²	I_g	Gross moment of inertia of cross section, mm ²
f_{br}	Bearing stress at bends, N/mm ²	I_{gr}	Moment of inertia of gross section excluding reinforcement, mm ⁴
f_c	Design compressive stress corresponding to any strain ϵ_c	I_{cr}	Moment of inertia of the cracked section, mm ⁴
f'_c	Cylinder compressive strength of concrete (ACI 318) $\approx 0.8 f_{ck}$, N/mm ²	I_s	Moment of inertia of the slab, mm ⁴
f_{cc}	Stress in concrete at the level of centroid of compression steel, also the strength of confined core of concrete in column, N/mm ²	J_c	Calculated property of the assumed critical section analogous to the polar moment of inertia, mm ⁴ = $(I_x + I_y) + A\bar{x}^2$
f_{ce}	Cube or cylinder strength of some hypothetical concrete, N/mm ²	jd	Leaver arm distance, mm
f_{cp}	Compressive strength of plain concrete in columns $\approx 0.85f'_c$, N/mm ²	K	Stiffness of member, N/mm
f_{ck}	Characteristic cube compressive strength of concrete, N/mm ²	K_a	Coefficient of the active earth pressure
f_{cr}	Modulus of rupture of concrete (flexural tensile strength) = $0.7 \sqrt{f_{ck}}$, N/mm ² , also the compression stress range in concrete, N/mm ²	K_b	Flexural stiffness of the beam = EI_b/L_b
f_{cs}	Cube or cylinder strength of slab concrete, maximum shrinkage induced tensile stress on the uncracked section, N/mm ²	K_c	Flexural stiffness of the column = EI_c/L_{cs}
f_{ct}	Splitting tensile strength of concrete, N/mm ²	K_f	Rotational spring stiffness of the footing and soil
f_d	Design strength, N/mm ²	K_p	Coefficient of the passive earth pressure
f_i	Passive compressive pressure provided by transverse reinforcement, N/mm ²	K_s	Flexural stiffness of the slab = EI_s/L_s
f_m	Mean value of the normal distribution	K_t	Torsional stiffness = T/ϕ
f_{min}	Minimum compressive stress in the cycle, N/mm ²	K'_{tr}	Transverse reinforcement index (ACI 318)
f_n	First natural frequency, Hertz	K_0	Coefficient of earth pressure at rest
f_r	Allowable steel stress range, N/mm ²	k	Constant or coefficient or factor, also the effective length factor for column and moment reduction factor for slender column
f_s	Stress in steel, N/mm ²	k_1	Probability factor or risk coefficient for wind (IS 875)
f_{sc}	Stress in compression steel, N/mm ²	k_2	Terrain, height and structure size factor for wind (IS 875)
		k_3	Topography (ground contours) factor for wind (IS 875)

- k_c Modification factor for compression reinforcement to be applied on basic L/d ratio
 k_p Flexural rigidity or plate stiffness of slab = $Et^3 / [12(1 - \nu^2)]$, Nmm
 k_s Modulus of sub-grade reaction, N/mm³
 k_t Ratio of average tensile stress to the maximum tensile stress in concrete, modification factor for tension reinforcement to be applied on basic L/d ratio
 k_{tr} Transverse reinforcement index (ACI 318) = $40A_{tr}/s_n$
 L Length of a column or beam between adequate lateral restraints or the unsupported length of a column, effective span of beam, span length of slab, mm
 LL Live load or imposed load
 L_0 Distance between the points of contraflexure (zero moments)
 L_c Longer clear span
 L_d Development length of bar in tension, mm
 L_{dc} Development length of bars in compression, mm
 L_{dh} Development length including standard hook, mm
 L_{dt} Development length of headed deformed bars in tension, mm
 L_{dw} Development length of welded deformed wire reinforcement in tension, mm
 L_{sp} Length of lap splice, mm
 L_w Length of wall
 L_{ex}, L_{ey} Effective length about major and minor axis respectively, mm
 L_n Clear span, face-to-face of supports, mm
 L_p Plastic hinge length, mm
 L'_n Shorter of the two spans at right angles, mm
 L_x Length of the shorter side of a slab, mm
 L_u Unsupported length of column, mm
 L_y Length of the longer side of a slab, mm
 L_o Embedment length beyond the centre of support
 L_1 Span in the direction in which moment is determined, centre-to-centre (c/c) of supports, also the horizontal distance between centres of lateral restraint of wall, mm
 L_2 Span transverse to L_1 , centre-to-centre of supports, mm
 L'_2 Shorter of the continuous spans, mm
 l Clear distance between lateral restraints
 l_{ch} Characteristic length in fracture mechanics calculations, mm
 l_v Minimum required length of each shear-head arm, mm
 M Bending moment, kNm or mass, kg
 MCE Maximum Considered Earthquake
 M_{ax}, M_{ay} Additional moment in slender columns about x - and y -axis respectively, Nmm
 M_{cr} Cracking moment, kNm
 M_d Design moment, kNm
 M_m Mid-span moment, kNm
 M_{nx}, M_{ny} Nominal moment of resistance about x - and y -axis respectively, Nmm
 M_o Total static moment in flat slabs/flat plates, Nmm
 M_{pr} Probable (plastic) moment capacity of beams, Nmm
 M_r Radial bending moment, Nmm
 M_s Moment at service load, Nmm
 M_t Additional bending moment due to torsion, also the tangential bending moment, Nmm
 $M_{u,lim}$ Limiting moment of resistance of a singly reinforced section, Nmm
 M_{ux}, M_{uy} Factored moment about x - and y -axis respectively, Nmm
 $M_{w,lim}$ Limiting moment of resistance of the web, Nmm
 M_x, M_y Moment about x - and y -axis respectively, Nmm
 M_{xy} Torsional moment, Nmm
 M'_x and M'_y Bending moments considering torsional effects in slabs, Nmm
 M_{x0} and M_{y0} Bending moments for Poisson's ratio $\nu = 0$, Nmm
 M_1 and M_2 Moments at the ends of the beam, Nmm
 m Modular ratio [= $280/(3\sigma_{cbc})$] as per working stress method] = E_s/E_c
 m_x and m_y Pigeaud's moment coefficients for concentrated loads
 m_u $M_u/f_{ck}BD^2$
 N Applied axial tensile load, kN
 N_a Nominal bond strength in tension of a single adhesive anchor, N
 N_{ag} Nominal bond strength in tension of group of adhesive anchors, N
 N_{ba} Basic bond strength in tension of a single adhesive anchor, N
 N_c, N_q , and N_γ Bearing capacity factors
 N_d Number of discontinuous edges in slabs
 N_n Nominal axial force capacity, also the nominal concrete breakout capacity for single anchor, N
 $N_{n,g}$ Nominal concrete breakout capacity for a group of anchors, N
 N_{ua} Factored tensile force applied to an anchor or individual anchors in a group of anchors, N
 N_{no} Nominal concrete breakout strength of a single anchor in tension in cracked concrete, N
 N_p Pullout strength in tension of a single anchor in cracked concrete, N
 N_{pn} Nominal pullout strength of a single cast-in and post-installed anchor, N
 N_{sb} Side-face blowout strength of a single anchor, N
 N_{sbg} Side-face blowout strength of a group of anchors, N
 N_u Factored axial load, kN
 n Number of samples
 n_l Number of longitudinal bars of column laterally supported by a corner of hoops
 P Axial load on a compression member, kN
 P_a Applied axial load, kN, force due to active earth pressure of soil, kN
 P_{cr} Critical load or Euler's buckling load, kN
 P_D Effective overburden pressure at pile tip, kN/m²
 P_h Lateral force, kN
 P_{noz}, P_{nz} Nominal axial load strength at zero eccentricity, kN
 P_{nx}, P_{ny} Nominal axial load strength at given eccentricity along x - and y -axis, respectively, N
 P_p Force due to passive earth pressure of soil, kN
 P_u Factored axial compressive load on column, kN
 P_{uw} Design axial compressive strength per unit length of a braced slender wall, kN
 p Pressure, N/mm²
 p_b Balanced steel ratio
 p_c Percentage of compression steel = $A_{sc}/bd \times 100$
 $p_{c,lim}$ Limiting compression reinforcement for the balanced section
 p_{cp} Perimeter of the full concrete cross section, mm
 p_d Design wind pressure, N/mm²
 p_e Active earth pressure
 p_f Probability that the load exceeds the characteristic load Q_c
 p_h Perimeter of the closed stirrup, mm
 p_t Percentage of tension steel = $A_{st}/bd \times 100$
 $p_{t,lim}$ Limiting percentage tensile steel
 p_u $P_u/f_{ck}BD$
 $p_{v,max}$ Maximum amount of shear reinforcement for ductile failure = $A_{sv}/(s_v b_w)$
 Q A constant = $0.5\sigma_{cbd}jk$ (working stress method), also the stability index
 Q_c Characteristic load
 Q_d Design loads
 Q_m Statistical mean of the observed maximum loads
 Q_p Compressive force at the tip of the pile, kN
 Q_s Upward skin friction along the pile, kN
 Q_u Ultimate bearing capacity of the pile, kN

- Q_v First moment of the area about the neutral axis of the portion of the section above the layer at distance y from the neutral axis = $\int_A y dA = \bar{\Sigma} \bar{y}_j A_j$
- q_a Safe or allowable bearing capacity of soil, kN/m^2
- q_{nu} Factored net soil pressure, kN/m^2
- q_u Calculated maximum bearing pressure of soil, kN/m^2
- R Response reduction factor (IS 1893), also the radius of curvature, mm
- R_d Design strength (or resistance)
- R_m Mean value of resistance
- R_n Nominal strength of the member
- R_u Characteristic material strength
- r Radius, mm, aspect ratio = L_y/L_x , and radius of gyration of the section
- S_d/g Response acceleration coefficients (IS 1893)
- s Centre-to-centre spacing of reinforcement, pitch of spiral, mm, and standard deviation
- s_v Spacing of stirrups, mm, also the minimum vertical spacing between bars, mm
- $s_{v,max}$ Maximum stirrup spacing, mm
- s_{ze} Equivalent crack spacing factor (MCFT), mm
- SBC Safe bearing capacity of soil, kN/m^2
- T Torsional/twisting moment, kNm
- T_a Approximate fundamental natural period of vibration, seconds
- T_{cr} Cracking torsion or torque, kNm or axial cracking load
- T_n Nominal strengths in torsion, kNm
- T_{no} Nominal strength under torsion alone, kNm
- T_{th} Threshold torsion, kNm
- T_u Factored torque, kNm
- t_p Thickness of plate, mm
- t_w Thickness of wall, mm
- t_o Equivalent thickness, mm
- t_d Bar diameter factor (ACI 318)
- t_x, t_y Width of the contact area of load on slab
- u, v Length and width of the area on which the concentrated load acts, mm
- V Shear force, kN
- V_{az} Shear transferred across the crack by interlock of aggregate particles, kN
- V_b Basic wind speed, m/s
- V_B Total design seismic base shear, kN
- V_c Nominal shear resistance provided by concrete, N
- V_{cp} Nominal concrete pryout strength of a single anchor, N
- V_{cpg} Nominal concrete pryout strength of a group of anchors, N
- V_{cr} Shear force at which the diagonal tension crack occurs, kN
- V_{cz} Shear in the compression zone of concrete, kN
- V_d Shear resisted by dowel action of the longitudinal reinforcement, also the design shear force, kN
- V_e Equivalent shear force including torsion, kN
- V_n Nominal shear capacity or strength, nominal concrete breakout strength of an anchor in shear, N
- V_{no} Nominal strength under shear alone, also the basic concrete breakout capacity in shear of an individual anchor in a cracked concrete, N
- V_s Nominal shear carried by vertical shear reinforcement, N
- V_{sa} Nominal steel strength of an anchor in shear, N
- V_{sp} Volume of spiral steel per unit length of column core = $A_{sp} \pi D_k / s$, mm^3/mm
- V_{si} Nominal shear carried by inclined shear reinforcement or bent-up bars, kN
- V_{sn} Nominal shear resistance due to friction between the crack surfaces, kN
- V_u Factored shear force, kN
- V_{ua} Factored shear force applied to one anchor or group of anchors, N
- V_{ug} Factored shear force on a critical section of a flat slab due to gravity loads, kN
- V_{us} Shear to be resisted by shear reinforcements, kN
- V_z Design wind speed at any height z in m/s ,
- W Load or total load, kN
- W_{cr} Crack width, mm
- W_f Weight of the foundation and structure, kN
- W_{max} Maximum crack width, mm
- W_s Weight of soil or backfill, kN
- WL Wind load, kN/m^2
- w Uniformly distributed load per unit area, kN/m^2
- w_d Distributed dead load per unit area, kN/m^2
- w_l Distributed imposed load per unit area, kN/m^2
- w/cm Water/cementitious material ratio
- w_x Share of the load w in the short direction, kN/m^2
- w_y Share of the load w in the long direction, kN/m^2
- x Depth of neutral axis, mm
- x_{cp} Neutral axis depth due to creep
- x_d Dimension from face of column to edge of drop panel, mm
- x_u Depth of neutral axis at ultimate failure of under-reinforced beam, mm
- $x_{u,lim}$ Limiting depth of neutral axis, mm
- y Distance of extreme fibre from the neutral axis, mm
- y_c Distance of the centroid of the concrete stress block, measured from the highly stressed compressive edge, mm
- y_f Depth of the equivalent rectangular stress block, mm
- y_{si} Distance from the centroid of the section to the i th row of reinforcement
- Z Modulus of section, mm^3 , also the zone factor as per IS 1893
- Z_e Elastic section modulus, mm^3
- z Lever arm distance, mm
- α Reinforcement location factor (ACI 318), flexural rigidity coefficient.
- α_b Ratio of flexural stiffness of the beam ($4E_b I/L$) to the flexural stiffness of slab
- α_{bm} Average value of α_b
- α_c Coefficient of thermal expansion for concrete (6×10^{-6} per degree Celsius to 12×10^{-6} per degree Celsius), also the ratio of flexural stiffness of the column above and below the slab to the flexural stiffness of the slabs
- α_s Coefficient of thermal expansion for steel = 11×10^{-6} per degree Celsius to 13×10^{-6} per degree Celsius, also the reinforcement factor = $250 \gamma_c / f_{st}$
- α_v Ratio of the stiffness of each shear head arm to the stiffness of the surrounding composite cracked slab
- α_{vx} and α_{vy} Shear force coefficients for slabs
- α_x and α_y Bending moment coefficients for slabs
- β Coating factor for epoxy-coated bars (ACI 318), reliability index, and torsional rigidity coefficient, ratio of $\Sigma(EI/L)$ of column to $\Sigma(EI/L)$ of flexural members
- β_1 Factor for stress block depth (ACI 318)
- β_b Ratio of area of bars cut-off to the total area of bars at section
- β_c Ratio of the short side to the long side of the column or capital
- β_{dms} Factor to account for the reduction in the column stiffness due to the effect of sustained axial load
- β_L Coefficient to consider the effect of pattern loading
- β_m Factor which models the ability of cracked concrete to transfer shear (MCFT)
- β_s Ratio of clear spans = L_y/L_x
- β_{ss} Empirical factor for shear strength

β_t	Torsional stiffness parameter = $E_{cb}C/2E_{cs}I_b$	μ	Coefficient of friction
γ	Reinforcement size factor (ACI 318) = 0.8 for rebars of size 20 mm or less, = 1.0 for 22 mm	μ_Δ	Displacement ductility factor = Δ_u/Δ_y
γ_c	Reinforcement coating factor (1.0 for uncoated and 0.5 for epoxy-coated bars)	μ_ϕ	Curvature ductility factor = ϕ_u/ϕ_y
γ_e	Unit weight of earth or soil, kg/m ³	ν	Poisson's ratio
γ_f	Partial safety factors for load, also the factor used to determine the unbalanced moment transferred by flexure at slab-column connections,	ν_s	Poisson's ratio of soil
γ_m	Partial safety factor for material	ρ	A_{st}/b_wd
γ_s	Factor used to determine the unbalanced moment transferred by eccentricity of shear at slab-column connections = $(1 - \gamma_f)$	ρ'	A_{sc}/b_wd
γ_{mw}	Partial material safety factor for weld	ρ_c	Unit weight of concrete (kg/m ³),
γ_w	Weight of wall material, kg/m ³ also the unit weight of water = 10 kN/m ³	ρ_{crit}	Ratio of steel area to the gross area of the whole concrete section,
Δ	Deflection of beam or column, mm	ρ_e	Effective reinforcement ratio = A_{st}/A_e
Δ_{cp}	Additional deflection due to creep	ρ_h	Volumetric unit weight of filler block (kN/m ³)
Δ_{cx}	Deflection at column strip of a two-way slab, mm	ρ_{st}	Volumetric ratio of transverse reinforcement
Δ_i	Lateral displacement at level i , mm	ϕ	Strength reduction factor (ACI 318), = 0.9 for flexure, = 0.75 for shear and torsion, = 0.65 for compression controlled sections
Δ_{ip}	Maximum initial (short-term) elastic deflection due to permanent loads, mm	ϕ	Angle of twist or rotation, curvature of the beam or column, effective friction angle of the soil, and angle of repose of soil.
$\Delta_{i,cp}$	Total deflection including creep due to permanent loads, mm	ϕ_{cp}	Creep curvature
Δ_{max}	Ultimate or maximum deformation, mm	ϕ_{cr}	Curvature of section at cracking
Δ_{mp}	Deflection at mid-panel of a two-way slab, mm	f_c	Cumulative normal distribution function
Δ_{my}	Deflection at middle strip of a two-way slab, mm	ϕ_i	Initial elastic curvature
Δ_y	Yield deformation, mm	ϕ_{sh}	Shrinkage curvature
δ	Factor to increase/decrease design shear strength of concrete for considering the effect of axial compressive/tensile force, deflection/displacement, mm, and angle of wall friction between pile and soil	ϕ_y	Yield curvature
δ_{ns}	Moment magnification factor for non-sway frames	σ or s	Standard deviation
δ_s	Moment magnification factor for sway frames	σ^2	Variance
δM	Percentage reduction in moment	σ_R	Standard deviation of resistance
ϵ_{cc}	Creep strain of concrete	σ_Q	Standard deviation of the loads
ϵ_c	Compressive strain in concrete	σ_{cbc}	Permissible stress in concrete in bending compression, N/mm ²
ϵ_{cp}	Creep strain	σ_{cc}	Permissible stress in concrete in direct compression, N/mm ²
ϵ_{cu}	Ultimate compressive strain in concrete (0.003 to 0.008 in IS 456 taken as 0.0035)	σ_{sc}	Permissible stress in steel in compression, N/mm ²
ϵ_i	Elastic strain	σ_{st}	Permissible stress in steel in tension, N/mm ²
ϵ_m	Average steel strain	σ_{sv}	Permissible tensile stress in shear reinforcement, N/mm ²
ϵ_s	Strain in steel	τ	Shear stress, N/mm ²
ϵ_{sc}	Strain in compression steel	τ_b	Average bond stress, N/mm ²
ϵ_{sh}	Design shrinkage strain in concrete	τ_{ba}	Anchorage bond stress, N/mm ²
$\epsilon_{sh,b}$	Basic shrinkage strain	τ_{bd}	Design bond stress, N/mm ²
ϵ_{st}	Strain at the centroid of tension steel	τ_c	Design shear strength (stress) of concrete, N/mm ²
ϵ_{su}	Strain in steel at ultimate failure	τ_{ce}	Enhanced design shear strength of concrete, N/mm ²
ϵ_t	Net tensile strain in the extreme tension steel (ACI 318)	τ_{cp}	Punching shear strength of concrete, N/mm ²
ϵ_x	Longitudinal strain at the mid-depth of the member (MCFT)	τ_{cr}	Average critical shear stress at which the diagonal tension crack appears, characteristic bond stress of adhesive anchor in cracked concrete, N/mm ²
ϵ_y	Yield strain in steel (0.12 – 0.20)	$\tau_{c,max}$	Maximum shear stress in concrete with shear reinforcement, N/mm ²
θ	Crack angle, slope angle of strut, angle of repose of soil, and rotation of yield lines	$\tau_{c,w}$	Design shear strength of concrete in walls, N/mm ²
θ_f	Rotation of footing	τ_n	Nominal shear strength resisted by concrete and steel, N/mm ²
λ	Modification factor for lightweight concrete (ACI 318) = $f_{cr}/(0.5 \sqrt{f_{ck}})$ taken as 1.0 for normal concrete, 0.85 for sand-lightweight concrete and 0.75 for other lightweight aggregate concrete, also the slenderness ratio = L_e/r	τ_s	Shear for which stirrups at cut-off point should be designed, kN
λ_Δ	Deflection factor for creep and shrinkage	$\tau_{s,max}$	Maximum stress in shear reinforcement, N/mm ²
		τ_t	Torsional shear stress, N/mm ²
		τ_{ucr}	Characteristic bond stress of adhesive anchor in uncracked concrete, N/mm ²
		τ_v	Nominal shear stress = V_u/bd , N/mm ²
		τ_{vw}	Nominal shear stress in walls, N/mm ²
		τ_{ve}	Equivalent nominal stress, = V_e/bd , N/mm ²
		ξ	Time-dependent factor for sustained load deflection
		Ψ_i	Correction factors used to calculate capacity of anchors

Note: All other symbols are explained appropriately in the text.

PROPERTIES OF SOILS

This appendix presents some information about the properties of soils, which are tabulated along with other related values for easy reference. This will be of interest to a structural designer.

A.1 SOIL TESTS

For low-rise buildings, the depth of borings may be specified to be about 6 m below the anticipated foundation level, with at least one boring continuing deeper, to 30 m, the least building dimension, or refusal, whichever is the least. At least one soil boring should be specified for every 230 m² of the building area for buildings over 12 m height or having more than three storeys. For large buildings founded on poor soils, borings should be spaced at less than 15 m intervals. It is recommended to have a minimum of five borings, one at the centre and the rest at the corners of the building.

A.2 RANK ORDER OF SOIL SUITABILITY FOR FOUNDATION SUPPORT

- Best: Bedrock
- Very good: Sand and gravel
- Good: Medium to hard clay (which is kept dry)
- Poor: Silts and soft clay
- Undesirable: Organic silts and organic clay
- Unsuitable: Peat

A.3 PLASTICITY INDEX

The plasticity index (PI) of the soil provides an indication of how much clay will shrink or swell. The higher the PI, the greater is the shrink–swell potential.

- PI of 0–15%: Low expansion potential
- PI of 15–25%: Medium expansion potential
- PI of 25% and above: High expansion potential

A.3.1 Precautions for Foundations in Expansive Soils

Clays with liquid limits exceeding 50 per cent and PI over 25 per cent may be considered as expansive. Expansive soil does

not preclude building construction, but special precautions must be taken to prevent structural problems. Arid regions are much more susceptible to damage from expansive soils than others that have moist soil conditions throughout the year. Expansive soils swell and shrink, and lift up and crack lightly loaded individual or continuous strip footings, causing differential settlements and frequent distress in floor slabs (Venugopal and Subramanian 1977). Hence, buildings in such soils must be supported on footings located well below the zone of seasonal moisture fluctuation (normally assumed as 2.5–3.0 m), preferably on non-expansive soil. If non-expansive soil is not available at a reasonable depth or when the depth of seasonal moisture fluctuation is high (up to 10 m depth has been identified in some parts of the world), under-reamed piles or drilled pier foundation should be adopted and the piles should go well below the zone of seasonal moisture fluctuation (Subramanian 1994). The design must be made with the assumption that the upper portions of the pile or pier will lose contact with the adjacent soil (Reese, et al. 2006). To maintain the water content of soil below the foundation, it may be advisable to cut vegetation around the building as the roots of trees and plants will absorb the water below the foundation, causing the soil to shrink. Impermeable aprons of about 1 m width may also be provided along the periphery of the building to prevent water evaporation from the soil below the ground level. The various soil properties and related values are provided in Tables A.1–A.8.

TABLE A.1 Soil properties* (www.dot.ca.gov)

Soil Type	Unit Weight Moist (kN/m ³)	Unit Weight Saturated (kN/m ³)	Undrained Shear Strength	
			Cohesion (kN/m ²)	Angle of Internal Friction, ϕ
Loose sand	15–19.6	18.8–20.4	0	28
Medium dense sand	17–20.4	19.6–21.2	0	32

(Continued)

TABLE A.1 (Continued)

Soil Type	Unit Weight Moist (kN/m ³)	Unit Weight Saturated (kN/m ³)	Undrained Shear Strength	
			Cohesion (kN/m ²)	Angle of Internal Friction, ϕ
Dense sand	17–22	20.4–22	0	38
Very soft clay	13.3–15.7	13.3–15.7	0–12	0
Soft clay	15.7–18.8	15.7–18.8	12–24	0
Medium clay	17–19.6	17–19.6	24–48	0
Stiff clay	18–20.4	18–20.4	48–96	0
Very stiff clay	18.8–22	18.8–22	96–192	0

*Values approximated

TABLE A.2 Typical values for modulus of elasticity (E_s) for different types of soils (Bowles 1996 and Dowrick 2003)

Soil	E_s (N/mm ²)	
Clay		
Very soft	2–15	
Soft	5–25	
Medium	15–50	
Hard	50–100	
Sandy	25–250	
Glacial till	Loose	10–153
	Dense	144–720
	Very dense	478–1440
	Loess	14–57
Sand	Silty	7–21
	Loose	10–24
	Dense	48–81
Sand and gravel	Loose	48–148
	Dense	96–192
Shale	144–14,400	
Silt	2–20	

TABLE A.3 Typical values for modulus of subgrade modulus (k_s) for different types of soils (Bowles 1996)

Soil	k_s (kN/m ³)
Loose sand	4800–16,000
Medium dense sand	9600–80,000
Dense sand	64,000–1,28,000
Clayey medium dense sand	32,000–80,000
Silty medium dense sand	24,000–48,000
Clayey soil	
$q_u \leq 200$ kN/m ²	12,000–24,000

Soil	k_s (kN/m ³)
$200 < q_u \leq 400$ kN/m ²	24,000–48,000
$q_u > 800$ kN/m ²	>48,000

Note: q_u is the safe bearing capacity (SBC); approximate value of subgrade modulus is SBC/Settlement corresponding to this pressure.

TABLE A.4 Typical values for Poisson's ratio (ν_s) for soils

Type of Soil	ν_s
Clay (saturated)	0.4–0.5
Clay (unsaturated)	0.1–0.3
Sandy clay	0.2–0.3
Silt	0.3–0.35
Sand (dense)	0.2–0.4
• Course (void ratio = 0.4–0.7)	0.15
• Fine grained (void ratio = 0.4–0.7)	0.25
Rock	0.1–0.4 (depends on the type of rock)
Loess	0.1–0.3
Ice	0.36
Concrete	0.15

TABLE A.5 Allowable bearing pressures on soils for preliminary design

Type of Rock/Soil	Allowable Bearing Pressures (kN/m ²)	Standard Penetration Blow Count (N)	Apparent Cohesion c_u (kN/m ²)		
Hard rock without lamination and defects (e.g., granite, trap, and diorite)	3200	>30	–		
Laminated rocks (e.g., sandstone and limestone in sound condition)	1600	>30	–		
Soft or broken rock, hard shale, and cemented material	900	>30	–		
Soft rock	450	>30	–		
Gravel	Dense	450	>30	–	
	Medium	96–285	>30	–	
Sand*	Compact and dry	Loose and dry			
		Coarse	450	250	30–50
	Medium	250	48–120	15–30	–
	Fine or silt	150	100	<15	–
Clay ⁺	Very stiff	190–450	15–30	100–200	
	Medium stiff	200–250	4–15	25–100	
	Soft	50–100	0–4	0–25	

(Continued)

TABLE A.5 (Continued)

Type of Rock/Soil	Allowable Bearing Pressures (kN/m ²)	Standard Penetration Blow Count (N)	Apparent Cohesion c_u (kN/m ²)
Peat, silts, and made-up ground	To be determined after investigation		

Notes:

* Reduce bearing pressures by half below the water table.

+ Alternatively, allow 1.2 times c_u for round and square footings and 1.0 times c_u for length/width ratios of more than 4.0. Interpolate for intermediate values.

TABLE A.6 Typical interface friction angles (NAVFAC 1982)

	Interface Materials	Interface Friction Angle δ
Mass concrete against	Clean sound rock	25
	Clean gravel, gravel-sand mixtures, and coarse sand	29-31
	Clean fine to medium sand, silty medium to coarse sand, and silty or clayey gravel	24-29
	Clean fine sand and silty or clayey fine to medium sand	19-24
	Fine sandy silt and non-plastic silt	17-19
	Medium stiff, stiff, and silty clay	17-19
Formed concrete against	Clean gravel, gravel-sand mixture, and well-graded rockfill with spalls	22-26
	Clean gravel, silty sand-gravel mixture, and single-size hard rockfill	17-22
	Silty sand, gravel, or sand mixed with silt or clay	17
	Fine sandy silt and non-plastic silt	14
Steel sheet piles against	Clean gravel, gravel-sand mixture, and well-graded rockfill with spalls	22
	Clean sand, silty sand-gravel mixture, and single-size hard rockfill	17
	Silty sand, gravel, or sand mixed with silt or clay	14
	Fine sandy silt and non-plastic silt	11

TABLE A.7 Typical values of fundamental period for soil deposits—for rock motions with $a_{max} = 0.4g$ (SEAOC 1980)

Soil Depth (m)	Dense Sand (s)	5 m of Fill Over Normally Consolidated Clay* (s)
10	0.3-0.5	0.5-1.0
30	0.6-1.2	1.5-2.3
60	1.0-1.8	1.8-2.8
90	1.5-2.3	2.0-3.0
150	2.0-3.5	-

Note:

* Representative of San Francisco Bay area

TABLE A.8 Mean shear wave velocities (m/s) for the top 30 m of ground (Borchardt 1994 and Day 2003)

General Description	Mean Shear Wave Velocity		
	Minimum	Average	Maximum
<ul style="list-style-type: none"> Firm and hard rocks <ul style="list-style-type: none"> – <i>Hard rocks</i> (e.g., metamorphic rocks with very widely spaced fractures) – <i>Firm to hard rocks</i> (e.g., granites, igneous rocks, conglomerates, sandstones, and shales with closely to widely spaced fractures) Gravelly soils and soft to firm rocks (e.g., soft igneous sedimentary rocks, sandstones, shales, gravels, and soils with >20% gravel) Stiff clays and sandy soils (e.g., loose to very dense sands, silt loams, sandy clays, and medium stiff to hard clays and silty clays, $N > 5$ blows/300 mm) Soft soils (e.g., loose submerged fills and very soft clays, $N < 5$ blows/ft, and silty clays, < 37 m thick) Very soft soils (e.g., loose saturated sand, marshland, and recent reclamation) 	1400	1620	-
	700	1050	1400
	375	540	700
	200	290	375
	100	150	200
	50	75	100

Note: The fundamental time period T of soil layer of thickness H having an average shear wave velocity V_s is approximately $T = 4H/V_s$.

If we assume the weighted average shear wave velocity for 30–50 m soil layer as 290 m/s, then the fundamental period of soil layer will range from 0.41 s to 0.69 s. The fundamental time period of four- to six-storey buildings including the soil-structure interaction should be within this range, that is, 0.41 s–0.69 s. Therefore, there will be quasi-resonance of the buildings and the soil layer. If the seismic damaging energy entering the building is more than the capacity of the structure, the building will show distress and may lead to collapse.

Similarly, if we assume the weighted average shear wave velocity for 150–300 m soil layer to be around 500 m/s, then the fundamental time period will range from 1.2 s to 2.4 s. The fundamental time period of 10- to 15-storey buildings including soil-structure interaction will fall in this range of time period of vibrations. Therefore, there will be quasi-resonance of the buildings and the soil layer; the seismic waves will affect this group of buildings, which will result

in damage or collapse of the buildings. Hence, it is important to know the depth of soil layers above the bedrock and their

properties, like shear wave velocities, which are related in the microzonation of a region.

REFERENCES

- Borcherdt, R. 1994, 'Estimates of Site Dependent Response Spectra for Design (Methodology and Justification)', *Earthquake Spectra*, Vol. 10, No. 4, pp. 617–53.
- Bowles, J.E. 1996, *Foundation Analysis and Design*, 5th edition, McGraw-Hill, New York.
- Day, R.W. 2003, *Foundation Engineering Handbook*, McGraw-Hill/ASCE Press, p. 930.
- Dowrick, D. 2003, *Earthquake Risk Reduction*, Wiley, Chichester.
- NAVFAC 1982, *Foundations and Earth Structures*, Design Manual 7.2, Naval Facilities Engineering Command, Dept of Navy, Alexandria.
- Reese, L.C., W.M. Isenhower, and S-T. Wang 2005, *Analysis and Design of Shallow and Deep Foundations*, John Wiley, New York, p. 608.
- SEAOC 1980, *Recommended Lateral Force Requirements and Commentary*, Structural Engineers Association of California.
- Subramanian, N. 1994, 'Design of Under Reamed Piles', *ICI Bulletin*, No. 46, pp. 17–9.
- Venugopal, M.S. and N. Subramanian 1977, 'Differential Movements in Soils', *Seminar on Problems of Building Foundations*, 20 February, Chennai.
- www.dot.ca.gov/hq/esc/construction/OSCCCompleteManuals/TrenchingandShoringManual2011.pdf, last accessed on 3 March 2013.

DESIGN USING STRUT-AND-TIE MODEL

B.1 INTRODUCTION

While designing reinforced concrete members, we usually assume that the strain varies linearly with the depth of the member and as a result plane sections remain plane. This assumption is validated by Saint-Venant's principle, which states that a system of forces in equilibrium applied to some segment of a solid body produces stresses in that body, which rapidly diminish with increasing distance from the segment. Thus, the principle indicates that the stresses due to axial load and bending approach a linear distribution at a distance approximately equal to the overall height of the member, h , away from the discontinuity. Saint-Venant's principle, however, does not apply at points that are closer than the distance h to discontinuities in applied load or geometry. Hence, reinforced concrete structures may be divided into two regions—one where the beam theory is valid,

called the *bending region (B-region)*, and the other near the concentrated loads, openings, or changes in cross section, where discontinuities affect the member behaviour, which is referred to as the *Discontinuity region (D-region)*. Figure B.1 shows the occurrences of D-regions (shaded areas) due to geometric discontinuities and combined geometrical and loading discontinuities.

When the stresses are within the elastic range and the concrete is uncracked, the stresses within the D-regions may be computed using finite element analysis and elastic theory. However, when the concrete cracks, redistribution of internal stresses takes place; hence, the results of the finite element analysis will not represent the actual state of stresses. At this stage, the internal forces may be determined safely by the use of statically determinate trusses, the members of which represent the internal forces. This truss model is referred to as the *strut-and-tie model (STM)*, and it transforms a complex situation to

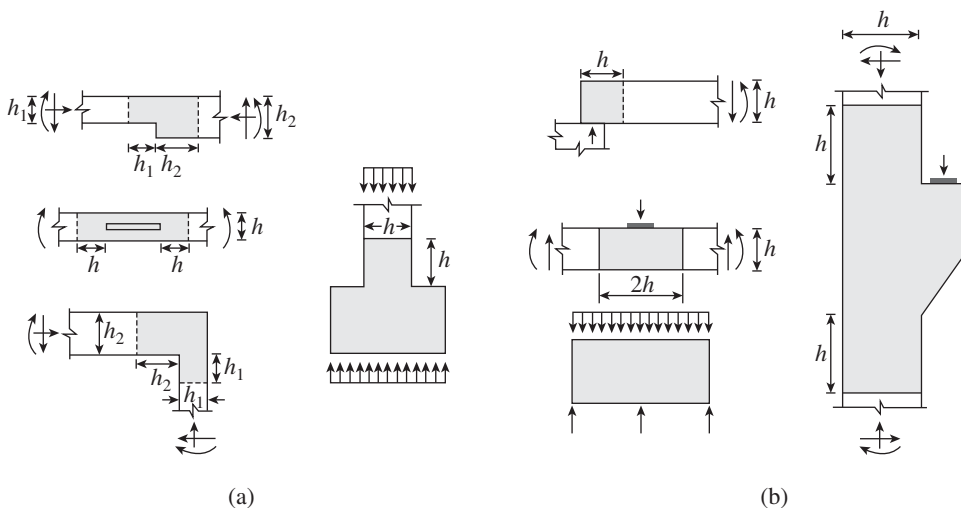


FIG. B.1 D-regions and discontinuities (a) Geometric discontinuities (b) Loading and geometric discontinuities

Source: ACI 318:11, reprinted with permission from ACI

a greatly simplified design process. STM is not a cookbook approach and requires some judgement on the part of the designer. Moreover, it also requires a few iterations to arrive at the correct configuration of truss members, size of nodes, and a reinforcement layout that would satisfy the code requirements. Such STMs consist of concrete *compression struts*, steel *tension ties*, and joints that are called *nodal zones*. Usually, in the design, struts are represented by dashed (discontinuous) lines and ties by solid lines.

B.2 STRUT-AND-TIE MODELS

ASCE-ACI Committee 445 on Shear and Torsion (1998) provides a

history of the development of truss models in concrete beams. The truss analogy, which is a specialized form of the STM, was introduced by Ritter (1899) and was refined by Mörch (1909), as discussed in Section 6.7.1 of Chapter 6, and is used exclusively in the design of B-regions. As already indicated in Section 6.7.1 of Chapter 6, the truss model has been modified by several others. The foundations for the present-day STMs were mainly provided by Schlaich and co-researchers (Schlaich and Weischede 1982; Schlaich and Schäfer 1989; Schlaich, et al. 1987) and Marti (1985). They oriented the geometry of struts and ties using elastic stress fields and designed following the theory of plasticity (Schlaich, et al. 1987). The STM approach was introduced in ACI 318-02 as Appendix A. However, IS 456 has not yet adopted this design method.

As mentioned earlier, STMs divide members into B- and D-regions. Any general region in which the strain distribution in the cross section is substantially non-linear due to load and/or geometrical discontinuities is defined as a D-region. As shown in Figs B.1 and B.2, a D-region is the portion of the member that is within a distance equal to the member height h from a load or geometric discontinuity. Naturally, any region outside the D-region is considered a B-region. STM is applied within the D-region.

The struts and ties of the D-regions can be determined from the loads applied to them by equilibrium analysis. If a structure or member consists of only a D-region, the analysis of sectional effects by a conventional structural analysis may be omitted and the internal forces or stresses may be directly determined from the applied loads using the STM. In corbels and deep beams with span less than two times the depth (see

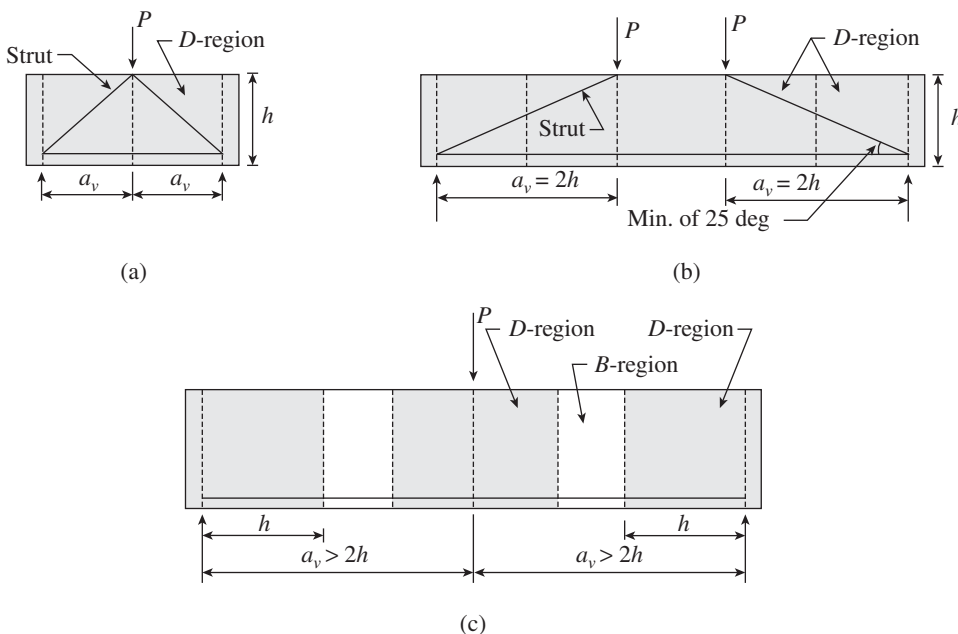


FIG. B.2 Beams with different spans and the definition of D-region and B-region (a) Deep beam with shear span $a_v < 2h$ (b) Deep beam with shear span $a_v = 2h$ (c) Slender beam with shear span $a_v > 2h$

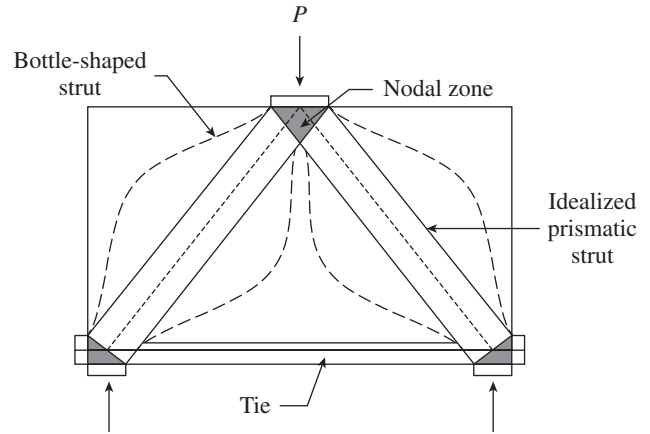


FIG. B.3 Strut-and-tie model of a deep beam
Source: ACI 318-11, reprinted with permission from ACI

Fig. B.1), there will be no B-region. A typical STM for a deep beam is shown in Fig. B.3.

B.2.1 Components of Strut-and-tie Model

The three different components of an STM, namely (a) struts, (b) ties, and (c) nodes, are explained here.

Struts

Struts are the compression members of an STM and represent concrete stress fields whose principal compressive stresses are predominantly along the centre line of the strut. Along its length, a strut may be rectangular (prismatic), fan shaped, or bottle shaped, as shown in Fig. B.4. ACI 318-11 classifies struts as (a) struts with uniform cross section over their length, (b) bottle-shaped struts with reinforcement satisfying Clause A.3.3, (c) bottle-shaped struts without reinforcement satisfying Clause A.3.3, (4) struts in tension members (these struts can occur in the tension flange of a T beam), and (e) all other types of struts. The dimensions of the cross section of the strut are fixed by the contact area between the strut and the nodal zone. As shown in Fig. B.4(c), bottle-shaped struts are wider at the centre than at the ends and from where the width of the compressed concrete at mid-length of the strut can spread laterally (ACI 318-11). Even though bottle-shaped struts have a larger cross section at mid-length, they are weaker than rectangular struts because of their tendency to longitudinal splitting. Struts can be strengthened by steel reinforcement; such struts are termed reinforced struts.

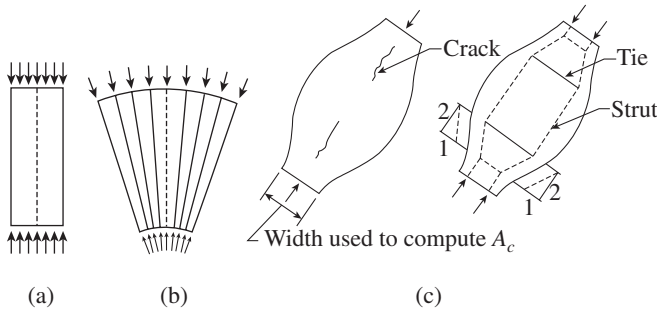


FIG. B.4 Types of struts in STM (a) Prism (b) Fan (c) Bottle

Source: ACI 318-11, reprinted with permission from ACI

To simplify design, bottle-shaped struts are idealized either as prismatic or as uniformly tapered, and crack control reinforcement is provided to resist the transverse tension. The cross-sectional area A_c of a bottle-shaped strut is taken as the smaller of the cross-sectional area at the two ends of the strut. Near the end of the bottle-shaped struts, a linear taper, as shown in Fig. B.4(c), with a slope of 1:2 to the axis of the compressive force, is suggested in ACI 318. As the compression spreads out from the support, tension is developed. When the induced tensile stress exceeds the tensile strength of the concrete, a crack will form parallel to the axis of the strut, as shown in Fig. B.4(c). Without any transverse reinforcement, the strut will split, causing brittle failure. (This phenomenon is the basis of the split cylinder test used to determine the tensile strength of concrete.) However, when sufficient transverse reinforcement is available, the strut can continue to carry load beyond the cracking load. The amount of confining transverse reinforcement can be computed using the STM shown in Fig. B.4(c). Alternatively, when f_{ck} is less than 50 MPa, ACI 318-11 suggests the use of the following equation (see Fig. B.5):

$$\sum \frac{A_{si}}{bs_i} \sin \alpha_i \geq 0.003 \quad (B.1)$$

where A_{si} is the area of surface reinforcement in the i th layer crossing a strut, s_i is the spacing of rebars in the i th layer adjacent to the surface of the member, b is the width of the strut, and α_i is the angle between the axis of the strut and the bars in the i th layer of reinforcement crossing the strut.

Brown and Bayrak (2006) showed that these two methods (reinforcement ratio greater than 0.003 and slope of dispersion equal to 2:1) result in significantly different amounts of reinforcement. Hence, they suggested a variable angle of dispersion to model bottle-shaped struts. More information on bottle-shaped struts may be found in the works of Brown and Bayrak (2006); Brown, et al. (2006); and Sahoo, et al. (2009).

No guidance is available to indicate when the strut should be considered as rectangle or bottle shaped. Some researchers

suggest the use of rectangular struts when the struts are horizontal, and bottle-shaped when the struts are inclined (ACI SP 208:2002; Nilson, et al. 2005).

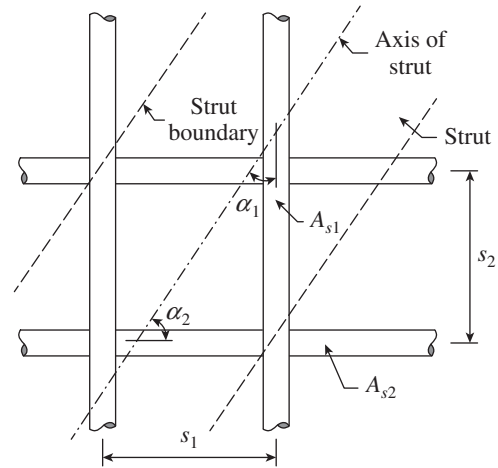


FIG. B.5 Reinforcement crossing a strut

Ties

A tie is a tension member within an STM. It consists of conventional reinforcing steel or prestressing steel, or both, plus a portion of the surrounding concrete that is concentric with the axis of the tie. It should be noted that the surrounding concrete is not considered to resist axial tension in the model. However, it defines the tie area and the region that is available to anchor the struts and ties. Even though the tensile capacity of the concrete is not used in the design, it reduces tie deformation under service loads.

Nodal Zones

Nodes are the intersection points of the axes of the struts, ties, and concentrated forces, representing the joints of an STM. A *nodal zone* is the volume of concrete around the node where the force transfer occurs. A nodal zone may be treated as a single zone as shown in Fig. B.6(a) or may be subdivided into two smaller zones, as shown in Fig. B.6(b), to equilibrate forces. Thus, in Fig. B.6(b), the two reactions R_1 and R_2 equilibrate the vertical components of strut forces C_1 and C_2 .

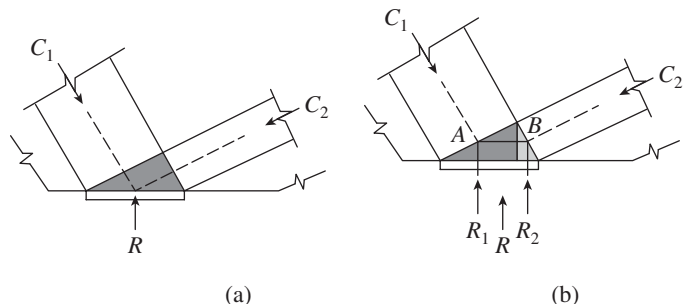


FIG. B.6 Subdivision of nodal zones (a) Nodal zone (b) Subdivided nodal zone

Source: ACI 318-11, reprinted with permission from ACI

To maintain equilibrium, at least three forces should act on a given node of an STM. Nodes are classified according to the signs of these forces. Thus, a node can be classified as a *C-C-C node* if all the members intersecting at the node are in compression, as a *C-C-T node* if one of the members acting on the node is in tension, and so on, as shown in Fig. B.7.

One way of laying out nodal zones is to orient the sides of the nodes at right angles to the axes of the struts or ties meeting at that node, as shown in Fig. B.8, such that the bearing pressure on each side of the node is the same. When this is done for a C-C-C node, the ratio of the lengths of the sides of the node, $w_{n1}:w_{n2}:w_{n3}$, is the same as the ratio of the forces in the three members meeting at the node, $C_1:C_2:C_3$, as shown in Fig. B.8(a). It is important to note that both tensile and compressive forces place nodes in compression, because tensile forces are treated as if they pass through the node and apply a compressive force on the far side or anchorage face (Nilson, et al. 2005). Nodal zones laid out in this fashion are referred to as *hydrostatic nodal zones* because the in-plane stresses in the node are the same in all directions. In such a case, the Mohr's circle for the in-plane

stresses reduces to a point. If one of the forces is tensile, the width of that side of the node is calculated from a hypothetical bearing plate on the end of the tie, which is assumed to exert a bearing pressure on the node equal to the compressive stress in the strut at that node, as shown in Fig. B.8(b). The dimensions of the remaining sides are established to maintain a constant level of stress p within the node.

The length of such a hydrostatic zone may not be sufficient to allow for adequate anchorage of tie reinforcement. In such situations, an extended nodal zone, as shown in Fig. B.8(b), is used. The reinforcement may be extended through the nodal zone to be anchored by bond, hooks, or mechanical anchorage before the reinforcement reaches point A on the right-hand side of the extended nodal zone, as shown by Fig. B.8(c).

B.3 DESIGN OF D-REGION USING STRUT-AND-TIE MODELS

A design with an STM typically involves the following steps:

1. *Define and isolate D-regions from B-regions:* As mentioned earlier, the D-regions extend on both sides of discontinuity or concentrated loads for a distance h , where h is the depth of the beam. (Hence, the length of a D-region near a concentrated load is $2h$ since it extends in both directions of the load.) At geometric discontinuities, a D-region may have different dimensions on either side of discontinuity, as shown in Fig. B.1.
2. *Determine the boundary conditions on the D-region:* If the entire beam consists of D-regions (as shown in Figs B.2a and b), the boundary conditions on the D-region are simply the boundary conditions on the beam (support reactions). If only a portion of the beam is designed using an STM, the D-region can be designed by assigning appropriate boundary conditions and loading to the sections, considering it to be congruent with the rest of the beam.
3. *Develop a truss model to represent the flow of forces:* The selection of struts and ties can be done by considering the flow

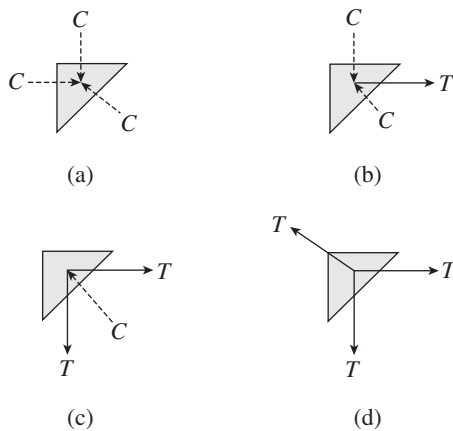


FIG. B.7 Classification of nodes (a) C-C-C node (b) C-C-T node (c) C-T-T node (d) T-T-T node

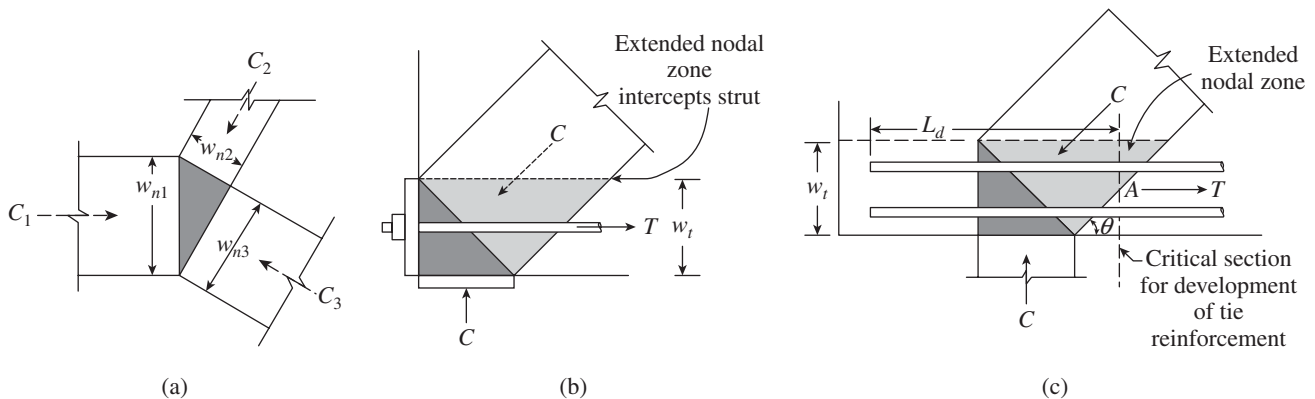


FIG. B.8 Nodal zones and extended nodal zones (a) Geometry (b) Tension force anchored by a plate (c) Tension force anchored by bond

of stresses through the D-region, which can be determined using a finite element analysis software. It should be noted that multiple solutions are possible. Systematic approach is required to select the geometry and members of the STM as hastily drawn models may not satisfy either equilibrium or compatibility conditions (Nori and Tharval 2007). The layout of a truss model is constrained by the geometric requirement that struts must intersect only at nodal zones. Ties may cross struts. Since the contribution of the tensile forces to displacement is much more than that of concrete struts, a model with the shortest and minimum number of ties and the least tie forces is the most effective (Nori and Tharval 2007). The STM should be in equilibrium with the applied loads and the reactions. The axes of the struts and ties, respectively, are chosen to approximately coincide with the axes of the compression and tension fields. It may be beneficial to iterate to find the most efficient and economical model dimensions. It is also important to consider the location of loads and supports during the development of an STM. Angles between struts and ties should be at least 45° whenever possible. An exception to this rule is when a diagonal compression strut meets two ties in the orthogonal direction. Angles smaller than 30° are unrealistic and involve high compatibility strains (Nori and Tharval 2007). The ACI code recommends that the angle, θ , between the axes of any strut and any tie entering a single node should be greater than 25° . This is specified to mitigate cracking and to avoid incompatibilities due to shortening of the struts and lengthening of the ties occurring in almost the same directions.

4. *Calculate forces in struts and ties:* If the STM produces a statically determinate truss, member forces can be calculated using statics. When a statically indeterminate truss is chosen, the determination of forces in the members is complex, as the stiffness of each member is unknown. Stiffness values have to be assumed initially. Forces can be calculated using an iterative method or computer software based on the stiffness method. It is better to choose determinate truss for STMs, so that the member forces are calculated easily.
5. *Estimate member dimensions and size the ties:* To control cracking in the D-region, ties are designed so that the stresses in the reinforcement are below yield at service loads. The geometry of the tie must be selected in such a way that the reinforcement could be provided within the tie dimensions. It may be necessary to spread the reinforcement into layers to avoid overstressing the concrete in the nodal zones. If sufficient length is not available to anchor reinforcement within the nodal or extended nodal zones, the reinforcement should be extended beyond the node; otherwise, a hook or mechanical anchor must be used to fully develop the reinforcement.

6. *Check stresses in the nodal zones and struts:* The struts should be proportioned based on their required compressive resisting force. If a strut does not have sufficient capacity, the design may be revised by increasing the size of the nodal zone or by providing compression reinforcement. It has to be noted that such a revision may affect the size of the bearing plate or column. The nodal zones allow the transfer of stress between truss members. It is important to ensure that the concrete will not be overstressed in these nodal zones. Stress limitations depend on the members that intersect at the node (ties and struts).

A complete design will include verification of the following: (a) Tie reinforcements are placed within the tie member dimensions, (b) nodal zones are confined by compressive forces or tension ties, and (c) requirement of minimum reinforcement is satisfied. As STMs represent strength limit states, code requirements for serviceability should also be satisfied. Traditional elastic analysis can be used for deflection calculations and the deflection should be within limits (Clause 23.2 of IS 456). Similarly, crack control provisions given in Clause 26.3 of IS 456 should also be satisfied.

B.4 ACI PROVISIONS FOR STRUT-AND-TIE MODELS

According to Clause A.2.6 of the ACI code, the design of struts, ties, and nodal zones should satisfy the following:

$$\phi F_n \geq F_u \quad (\text{B.2})$$

where F_u is the factored force acting in a strut or tie or on one face of a nodal zone; F_n is the nominal capacity of the strut, tie, or nodal zone; and ϕ is the strength reduction factor. (It is taken as 0.75 for struts, ties, and nodal zones in the ACI 318-11 code.)

B.4.1 Strength of Struts

The strength of a strut is limited by the strength of the concrete in the strut and the strength of the nodal zones at the ends of the strut. The nominal compressive strength of a strut without longitudinal reinforcement, F_{ns} , is taken, according to Clause A.3.1 of ACI 318, as the smaller of the value of

$$F_{ns} = f_{ce} A_{cs} \quad (\text{B.3})$$

at the two ends of the strut, where A_{cs} is the cross-sectional area at one end of the strut, which is equal to the product of the strut thickness and strut width, and f_{ce} is the effective compressive strength of the concrete in the strut or nodal zone. The width of strut w_s used to compute A_{cs} is the smaller dimension perpendicular to the axis of the strut at the ends of the strut. This strut width is illustrated in Fig. B.8(a). In two-dimensional structures like deep beams, the thickness of the struts may be taken as the width of the member.

The effective compressive strength of the concrete, f_{ce} , in a strut should be taken as

$$f_{ce} = 0.68\beta_s f_{ck} \quad (\text{B.4})$$

where the factor β_s accounts for the effects of cracking and confining reinforcement within the strut and f_{ck} is the characteristic (cube) compressive strength of concrete. The suggested values of β_s as per Clause B3.2 of ACI 318-11 are given in Table B.1.

TABLE B.1 Node and strut efficiency factors as per ACI 318-11

	Strut and Node Efficiencies	Efficiency Factor*
Struts	Strut with uniform cross section over its length	$\beta_s = 1.00$
	Bottle-shaped struts with reinforcement satisfying Clause A.3.3	$\beta_s = 0.75$
	Bottle-shaped struts without reinforcement satisfying Clause A.3.3	$\beta_s = 0.60\lambda^+$
	Struts in tension members or tension flanges of members	$\beta_s = 0.40$
	All other types of struts	$\beta_s = 0.60\lambda^+$
Nodes	Nodes bounded by struts or bearing areas (C-C-C nodes)	$\beta_n = 1.00$
	Nodes anchoring one tie (C-C-T nodes)	$\beta_n = 0.80$
	Nodes anchoring more than one tie (C-T-T and T-T-T nodes)	$\beta_n = 0.60$

Notes:

*Brown, et al. (2006), based on their experimental results, suggest a constant value of strut efficiency factor, $\beta_s = 0.60$, which will provide adequate safety and simplify the code rules.

+ λ equals 1.0 for normal weight concrete, 0.85 for sand lightweight concrete, and 0.75 for all lightweight concrete.

Compression reinforcement can be used to increase the strength of a strut; such compression reinforcement should be properly anchored, parallel to the axis of the strut, located within the strut, and enclosed in ties or spirals. The nominal strength of a longitudinally reinforced strut may be determined as

$$F_{ns} = f_{ce}A_{cs} + A_s f_s \quad (\text{B.5})$$

where f_s is the stress in steel and is based on the strain in the concrete at peak stress and A_s is the area of steel in strut. For Fe 250 and Fe 415 grade steel, $f_s = f_y$.

B.4.2 Strength of Nodal Zones

The nominal compression strength of a nodal zone, F_{mz} , should be

$$F_{mz} = f_{ce}A_{nz} \quad (\text{B.6})$$

where f_{ce} is the effective compressive strength of the concrete in the nodal zone and A_{nz} is the smaller of the following:

1. The area of the face of the nodal zone taken perpendicular to the line of action of the force from the strut or tie.

2. The area of a section through the nodal zone taken perpendicular to the line of action of the resultant force on the section; this condition occurs when multiple struts intersect a node.

The effective concrete strength in a nodal zone, f_{ce} , may be taken as per Clause A.5 of ACI 318-11 as

$$f_{ce} = 0.68\beta_n f_{ck} \quad (\text{B.7})$$

where the factor β_n reflects the increasing degree of disruption of the nodal zones due to the incompatibility of tension strains in the ties and compression strains in the struts and f_{ck} is the characteristic (cube) compressive strength of concrete. The suggested values of β_n as per Clause A5.2 of ACI 318-11 are given in Table B.1.

B.4.3 Strength of Ties

The nominal strength of a tie, F_{nt} , is the sum of the reinforcing steel and prestressing steel within the tie and may be calculated as per Clause A.4.1 of ACI 318-11 as

$$F_{nt} = A_{st}f_y + A_{ps}(f_{pe} + \Delta f_p) \quad (\text{B.8})$$

where A_{st} and f_y are the area and yield strength of reinforcing steel, A_{ps} and f_{pe} are the area and effective stress in prestressing steel, and Δf_p is the increase in stress in prestressing steel due to factored load. The value of $(f_{pe} + \Delta f_p)$ should not exceed the yield stress of the prestressing reinforcement, f_{py} . The value of A_{ps} is zero for non-prestressed members. Clause A.4.1 of ACI 318-11 permits the value of Δf_p to be taken as 420 MPa for bonded tendons and 70 MPa for unbonded tendons. It has to be noted that the axis of the reinforcement in a tie should coincide with the axis of the tie in the STM.

The effective width of a tie, w_t , depends on the distribution of reinforcement. If the reinforcement is placed in single layer, the effective tie width can be taken as the diameter of the largest bars in the tie plus twice the cover to the surface of the bars, as shown in Fig. B.8(b). Alternatively, the width of a tie may be taken as the width of the anchor plate. A practical upper limit of the tie width can be taken as the width corresponding to the width in a hydrostatic nodal zone calculated as

$$w_{t,\max} = \frac{F_{nt}}{bf_{ce}} \quad (\text{B.9})$$

where f_{ce} is the effective nodal zone compressive stress as per Eq. (B.7). The tie reinforcement should be distributed approximately uniformly over the width and thickness of the tie, as shown in Fig. B.8(c).

B.4.4 Shear Requirements for Deep Beams

The ACI code allows deep beams to be designed using STMs regardless of how they are loaded and supported. Clause 11.7.3 of ACI 318-11 stipulates that the shear in a deep beam may

not exceed $0.74\phi\sqrt{f_{ck}} b_w d$, where b_w is the width of the web, d is the effective width, and ϕ is the strength reduction factor = 0.75. Clause 11.7.4 provides minimum steel requirements for horizontal and vertical reinforcements within a deep beam (see also Section 5.9 and Table 5.10 of Chapter 5).

B.5 COMPUTER SOFTWARE FOR STRUT-AND-TIE MODELS

Computer-aided strut-and-tie (CAST) is a Windows-based design tool for STM with rich graphical user interfaces. CAST was developed in 1999 by Kuchma and associates at the University of Illinois (Kuchma and Tjhin 2001). CAST allows designers to quickly optimize their design, handle multiple load cases, and generate final drawings. This program also serves as an instructional device, familiarizing students and practitioners with both the program and the strut-and-tie design philosophy. CAST can be downloaded from <http://dankuchma.com/stm/CAST>.

EXAMPLE OF DEEP BEAM

The design of a deep beam is considered here to explain the concepts presented. A transfer girder to carry two 450 mm square columns, each with a factored load of 1575 kN located

at one-third points of its 6 m span, is shown in Fig. B.9(a). This girder has a thickness of 500 mm and a height of 2 m. Assume $f_{ck}=30\text{ MPa}$, $f_y=415\text{ MPa}$, and moderate environment. Design the girder for the given loads, ignoring self-weight.

SOLUTION

The span-to-depth ratio for this girder is three; hence, it can be considered as a deep beam (Clause 11.7.1 of ACI 318) and STM can be used.

Step 1 Define and isolate D-regions from B-regions. All the supports and loads are within a distance h from each other; hence, the entire beam is designated as a D-region.

The following preliminary checks need to be carried out:

(a) *Check for shear capacity:* The thickness of struts and ties is equal to the thickness of the beam, $b = 500\text{ mm}$. Assume an effective depth for shear design, $d = 0.9h = 0.9 \times 2 = 1.8\text{ m}$. The maximum design shear capacity of the beam as per the ACI code is

$$V_n = \phi 0.74 \sqrt{f_{ck}} b_w d = 0.75 \times 0.74 \times \sqrt{30} \times 500 \times \frac{1800}{1000} = 2735\text{ kN} > V_u = 1575\text{ kN}$$

Hence, the beam is safe in shear.

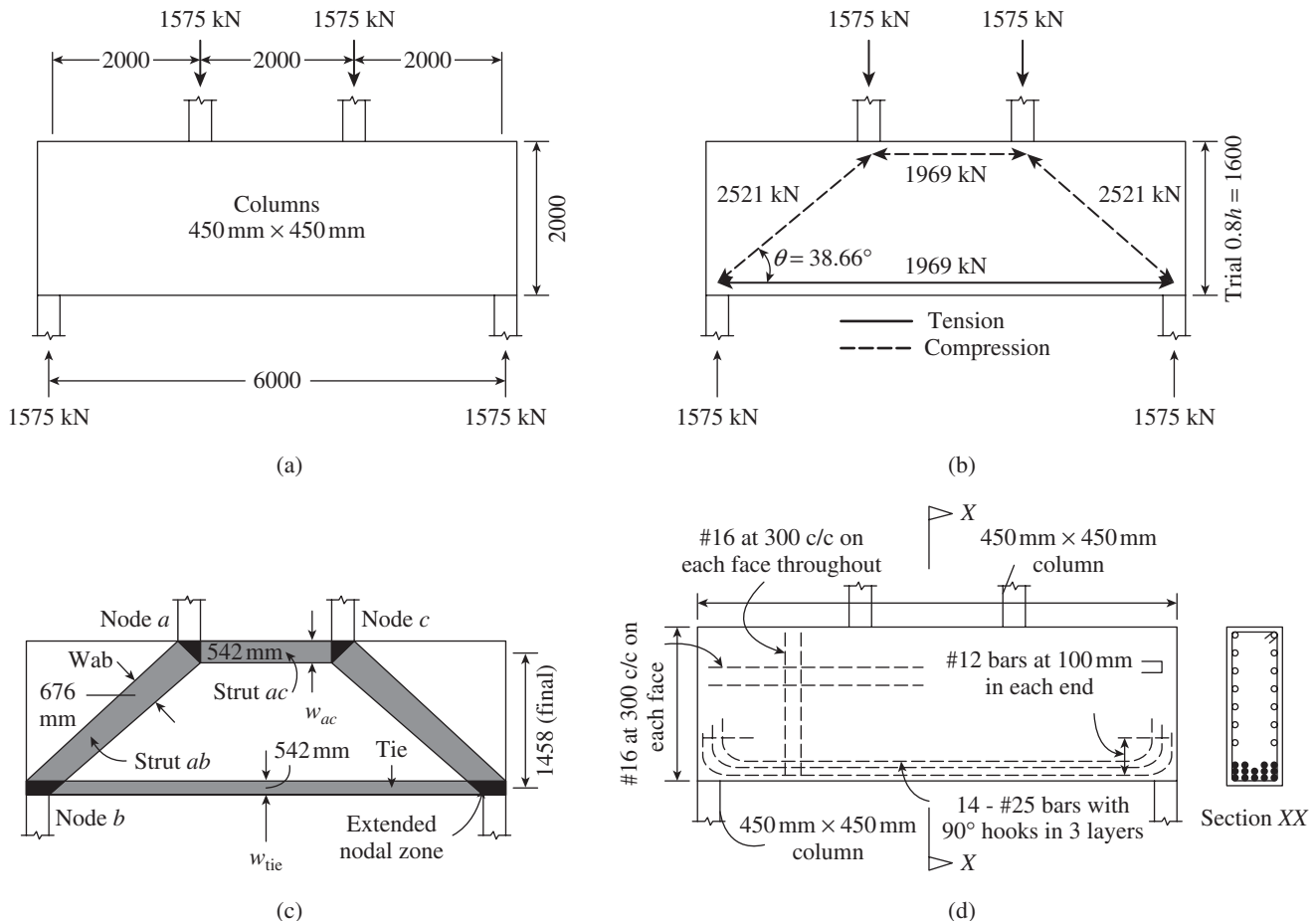


FIG. B.9 Example design of deep beam (a) Beam dimension and loading (b) Beam internal forces and trial STM (c) Final STM with struts, ties, and nodes (d) Details of reinforcement

(b) Check the bearing capacity at loading and support locations: Bearing strength at points of loading (as per Clause A.5 of ACI 318-11) is

$$F_{m1} = \phi 0.85 \beta_n (0.8 f_{ck}) A_{nz} = 0.75(0.85)(1.0)(0.8 \times 30)(450)(450)/1000 = 3098 \text{ kN} > 1575 \text{ kN. Hence, it is acceptable.}$$

(As per Clause 34.4 of IS 456, bearing strength = $0.45 f_{ck} A_c = 0.45 \times 30 \times 450 \times \frac{450}{1000} = 2733 \text{ kN} > 1575 \text{ kN.}$)

Bearing strength at supports (Clause A.5 of ACI 318-11)

$$F_{m2} = \phi 0.85 \beta_n (0.8 f_{ck}) A_{nz} = 0.75(0.85)(0.8)(0.8 \times 30)(450)(450)/1000 = 2478 \text{ kN} > 1575 \text{ kN. Hence, it is acceptable.}$$

Step 2 Determine the boundary conditions of the D-region. The two 1575 kN loads acting at the top of the girder are equilibrated by the two reactions at support, each having a value of 1575 kN. Let us assume the centre-to-centre distance between the top horizontal strut and the bottom tie is $0.8h = 1.6 \text{ m}$. Now, the diagonal strut forms at an angle = $\tan^{-1} \left(\frac{1.6}{2.0} \right) = 38.66^\circ$. The force in the diagonal strut is $F_{ba} = 1575/\sin 38.66 = 2521 \text{ kN}$.

Step 3 Develop a truss model to represent the flow of forces. Based on the girder geometry and loading, an STM as shown in Fig. B.9(b) is chosen. The selected STM is in equilibrium with the applied loads and the reactions. The axes of the struts and ties, respectively, coincide with the axes of the compression and tension fields. The angle, θ , between the axes of any strut and any tie entering a single node is $38.66^\circ > 25^\circ$ (Clause A.2.5 of ACI 318); hence, the chosen model may be sufficient to carry the applied loads.

Step 4 Calculate the forces in struts and ties. As the selected truss is determinate, the forces in struts and ties can be calculated from statics. The calculated forces in struts and ties are shown in Fig. B.9(b).

Step 5 Estimate member dimensions and size the ties. The nodal stress p is determined by the average stress under the columns. Thus, average stress $p = 1575 \times 1000/(450 \times 450) = 7.78 \text{ N/mm}^2$. The width of strut ac may be found using p as

$$w_{ac} = \frac{F_{ac}}{b \times p} = 1969 \times \frac{1000}{500 \times 7.78} = 506 \text{ mm}$$

Similarly, the widths of w_{ab} and w_{tie} are found to be 648 mm and 506 mm, respectively. The centre-to-centre distance between the horizontal strut at the top and the bottom tie is $2000 - 506 = 1494 \text{ mm}$, or $0.747h$. The angle θ between the diagonal strut ab and the tie is now 36.76° . The revised force in the diagonal strut is $F_{ba} = 1575/\sin 36.76 = 2632 \text{ kN}$. Similarly, the revised force in the strut ac and the tie is 2108 kN. Revised widths w_{ab} , w_{ac} , and w_{tie} are found to be 676 mm, 542 mm, and 542 mm, respectively. Since the difference between the first

and the second iterations is less than five per cent, no further iteration is attempted.

Step 6 Design the ties and anchorages. The tie design consists of three steps—selection of area of steel, design of anchorage, and check to find whether the rebars fit within the available width.

$$\text{Area of steel, } A_{st} = \frac{F_{tu}}{\phi_y^f} = \frac{2108 \times 1000}{0.75 \times 415} = 6773 \text{ mm}^2$$

Provide fourteen 25 mm bars, with area = 6872 mm^2 . Place 10 bars in two layers and the remaining four bars in the third layer as shown in Fig. B.9(d). With a clear cover of 35 mm for moderate environment (Table 16 of IS 456) and 200 mm clear spacing between the layers, the required tie width = $2 \times 35 + 3 \times 25 + 2 \times 200 = 545 \text{ mm} \approx 542 \text{ mm}$.

The anchorage length L_d for 25 mm bars in M30 concrete (Table 65 of SP 16:1980) is 806 mm. The length of nodal zone plus extended nodal zone is $(450 + 0.5 \times 542 \cot 36.76) = 812.7 \text{ mm}$. Available anchor length = $812.7 - \text{side cover} = 812.7 - 30 = 782.7 \text{ mm} < 806 \text{ mm}$. Hence, provide a 90° hook at the end to achieve the required anchorage.

Using 30 mm covers on the sides, 16 mm bars for transverse and horizontal reinforcement, and 75 mm spacing between bars, the required width, $b_{req} = 2 \times 30 + 5 \times 25 + 4 \times 75 = 485 \text{ mm} < 500 \text{ mm}$ (thickness of girder).

Step 7 Check stresses in the nodal zones and struts. Let us assume uniform cross section for the horizontal strut ac and bottle shape for the diagonal strut ab .

$$\text{Capacity of strut } ac = \phi 0.68 \beta_s f_{ck} A_{cs} = 0.75 \times 0.68 \times (1.0) \times 30 \times \frac{500 \times 542}{1000} = 4146 \text{ kN} > 2108 \text{ kN. Hence, it is adequate.}$$

$$\text{Capacity of bottle-shaped strut } ab = \phi 0.68 \beta_s f_{ck} A_{cs} = 0.75 \times 0.68 \times (0.75) \times 30 \times \frac{500 \times 676}{1000} = 3878 \text{ kN} > 2632 \text{ kN. Hence, it is adequate.}$$

$$\text{Capacity of nodal zone at } a \text{ (C-C-C node, hence from Table B.1, } \beta_n = 1.0) = \phi 0.68 \beta_n f_{ck} A_{nz} = 0.75 \times 0.68 \times (1.0) \times 30 \times \frac{500 \times 676}{1000} = 5171 \text{ kN} > 2632 \text{ kN}$$

$$\text{Capacity of nodal zone at } b \text{ (C-C-T node, hence from Table B.1, } \beta_n = 0.80) = \phi 0.68 \beta_n f_{ck} A_{nz} = 0.75 \times 0.68 \times (0.80) \times 30 \times \frac{500 \times 676}{1000} = 4137 \text{ kN} > 2632 \text{ kN}$$

Step 8 Calculate the minimum vertical and horizontal web reinforcements. As per Clause 11.7.4.1 of ACI 318-11, the area of shear reinforcement perpendicular to the longitudinal axis of the beam, A_v , should be greater than $0.0025 b_w s$, and the spacing of bars should not exceed the smaller of $d/5$ and 300 mm, that is, smaller of 300 mm and $1600/5 = 320 \text{ mm}$; hence, adopt 300 mm.

Provide one 16 mm bar on each face at a spacing of 300 mm over the entire length. $A_v/(bs_v) = 2(201)/(500 \times 300) = 0.00268 > 0.0025$

Hence, it is sufficient.

Clause 11.7.4.2 of ACI 318-11 suggests that the area of shear reinforcement parallel to the longitudinal axis of the beam, A_{vh} , should not be less than $0.0025bws_2$ and s_2 should not exceed the smaller of $d/5$ and 300 mm. Hence, provide 16 mm bars on each face at a spacing of 300 mm in the horizontal direction as well.

Step 9 Check the reinforcement to resist bursting forces in bottle-shaped struts (Eq. B.1). With two 16 mm bars in the vertical and horizontal directions, we have $A_v = A_{sh} = 402 \text{ mm}^2$. As per Eq. (B.1), we have

$$\sum \frac{A_{si}}{bs_i} \sin \alpha_i \geq 0.003$$

Thus,

$$\begin{aligned} \sum \frac{A_{si}}{bs_i} \sin \alpha_i &= \frac{402 \times \sin 36.76 + 402 \times \sin 53.24}{500 \times 300} \\ &= 0.00375 \geq 0.003 \end{aligned}$$

This shows that the provided horizontal and vertical shear reinforcements satisfy both minimum steel requirements as well as prevent longitudinal splitting of bottle-shaped struts. The detailing of steel is provided in Fig. B.9(d). It has to be noted that horizontal U-shaped 12 mm bars are also used at a spacing of 100 mm centre-to-centre distance across the end of the girder to confine the hooks of bottom tie-bars.

More details about the STM method and examples of design using STM may be found in ACI SP-208 (2002) and ACI SP-273 (2010) and in the works of Marti (1985), Nilson, et al. (2005), Nori and Tharval (2007), and Wight and MacGregor (2009).

REFERENCES

- ACI 318-11 2011, *Building Code Requirements for Structural Concrete and Commentary*, American Concrete Institute, Farmington Hills, Appendix A, pp. 387–402.
- ASCE-ACI Committee 445 on Shear and Torsion 1998, 'Recent Approaches to Shear Design of Structural Concrete', *Journal of Structural Engineering*, ASCE, Vol. 124, No. 12, pp. 1375–417.
- ACI SP 208 2002, *Examples for the Design of Structural Concrete with Strut-and-tie Models*, Karl-Heinz Reineck (ed.), American Concrete Institute, Farmington Hills, p. 250.
- ACI SP 273 2010 *Further Examples for the Design of Structural Concrete with Strut-and-tie Models*, Karl-Heinz Reineck and Lawrence C. Novak (eds), American Concrete Institute, Farmington Hills, p. 288.
- Brown, M.D. and O. Bayrak 2006, 'Minimum Transverse Reinforcement for Bottle-shaped Struts', *ACI Structural Journal*, Vol. 103, No. 6, pp. 813–21.
- Brown, M.D., C.L. Sankovich, O. Bayrak, and J.O. Jirsa 2006, 'Behavior and Efficiency of Bottle-shaped Struts', *ACI Structural Journal*, Vol. 103, No. 3, pp. 348–55.
- Kuchma, D.A. and T.N. Tjhin 2001, 'CAST (Computer Aided Strut-and-tie) Design Tool', In P.C. Change (ed.), *Proceedings of the 2001 Structures Congress and Exposition, Structures 2001: A Structural Engineering Odyssey*, Washington, D.C., 21–23 May 2001, American Society of Civil Engineers, Reston, pp. 1–7.
- Marti, P. 1985, 'Basic Tools of Reinforced Concrete Beam Design', *ACI Journal, Proceedings*, Vol. 82, No. 1, pp. 46–56.
- Mörsch, E. 1909, *Der Eisenbetonbau, seine Theorie und Anwendung (Reinforced Concrete Theory and Application)*, Third edition, Verlag Konrad Wittner, Stuttgart, Germany, p. 118.
- Nilson, A.H., D. Darwin, and C.W. Dolan 2005, *Design of Concrete Structures*, 13th edition, Tata McGraw-Hill Edition, New Delhi, pp. 321–46.
- Nori, V.V. and M.S. Tharval 2007, 'Design of Pile Caps: Strut and Tie Model Method', *The Indian Concrete Journal*, Vol. 81, No. 4, pp. 13–9.
- Ritter, W. 1899, *Die Bauweise Hennebique*, *Schweizerische Bauzeitung*, Vol. 33, No. 7, pp. 59–61.
- Sahoo, D.K., B. Singh, and P. Bhargava 2009, 'Investigation of Dispersion of Compression in Bottle-shaped Struts', *ACI Structural Journal*, Vol. 106, No. 2, pp. 178–86.
- Schlaich, J. and K. Schäfer 1989, 'Konstruieren im Stahlbetonbau (Design for Concrete Structures)', In *Beton-kalender*, Ernst and Sohn, Berlin, pp. 563–715.
- Schlaich, J., K. Schäfer, and M. Jennewein 1987, 'Toward a Consistent Design of Structural Concrete', *PCI-Journal*, Special Report, Vol. 32, No.3, pp. 74–150.
- Schlaich, J. and D. Weischede 1982, 'A Practical Method for the Design and Detailing of Structural Concrete (in German)', *Bulletin d'Information no.150*, Comité Euro- International du Béton, Paris, p. 163.
- Wight, J.K. and J.G. MacGregor 2009, *Reinforced Concrete: Mechanics and Design*, 5th edition, Pearson Prentice Hall, New Jersey, p. 1112.

ANALYSIS AND DESIGN AIDS

The design tables presented in this appendix will be quite useful for the quick analysis and design of beams.

TABLE C.1 Reinforcement percentage, ρ_t , for singly reinforced rectangular beam sections ($f_{ck} = 20 \text{ N/mm}^2$)

M_u/bd^2 (N/mm ²)	f_y (N/mm ²)			M_u/bd^2 (N/mm ²)	f_y (N/mm ²)		
	250	415	500		250	415	500
0.3	0.140	0.085	0.070	2.25	1.222	0.736	0.611
0.35	0.164	0.099	0.082	2.3	1.255	0.756	0.627
0.4	0.188	0.114	0.094	2.35	1.289	0.776	0.644
0.45	0.213	0.128	0.106	2.4	1.323	0.797	0.661
0.5	0.237	0.143	0.119	2.45	1.357	0.818	0.679
0.55	0.262	0.158	0.131	2.5	1.392	0.839	0.696
0.6	0.286	0.172	0.143	2.55	1.428	0.860	0.714
0.65	0.311	0.187	0.156	2.6	1.464	0.882	0.732
0.7	0.336	0.202	0.168	2.65	1.500	0.904	0.750
0.75	0.361	0.218	0.181	2.7	1.537	0.926	
0.8	0.387	0.233	0.193	2.75	1.575	0.949	
0.85	0.412	0.248	0.206	2.8	1.613		
0.9	0.438	0.264	0.219	2.85	1.652		
0.95	0.464	0.279	0.232	2.9	1.692		
1	0.490	0.295	0.245	2.95	1.732		
1.05	0.516	0.311	0.258				
1.1	0.543	0.327	0.271		Steel grade	Limiting ρ_t	
1.15	0.570	0.343	0.285		Fe 250	1.757	
1.2	0.596	0.359	0.298		Fe 415	0.955	
1.25	0.624	0.376	0.312		Fe 500	0.754	
1.3	0.651	0.392	0.325				
1.35	0.679	0.409	0.339				
1.4	0.706	0.426	0.353				
1.45	0.734	0.442	0.367				
1.5	0.763	0.459	0.381				
1.55	0.791	0.477	0.396				

M_u/bd^2 (N/mm ²)	f_y (N/mm ²)			M_u/bd^2 (N/mm ²)	f_y (N/mm ²)		
	250	415	500		250	415	500
1.6	0.820	0.494	0.410				
1.65	0.849	0.512	0.425				
1.7	0.878	0.529	0.439				
1.75	0.908	0.547	0.454				
1.8	0.938	0.565	0.469				
1.85	0.968	0.583	0.484				
1.9	0.999	0.602	0.499				
1.95	1.029	0.620	0.515				
2	1.061	0.639	0.530				
2.05	1.092	0.658	0.546				
2.1	1.124	0.677	0.562				
2.15	1.156	0.696	0.578				
2.2	1.189	0.716	0.594				

Note: Blanks indicate inadmissible reinforcement percentage.

TABLE C.2 Reinforcement percentage, ρ_t , for singly reinforced rectangular beam sections ($f_{ck} = 25 \text{ N/mm}^2$)

M_u/bd^2 (N/mm ²)	f_y (N/mm ²)			M_u/bd^2 (N/mm ²)	f_y (N/mm ²)		
	250	415	500		250	415	500
0.3	0.140	0.085	0.070	2.25	1.172	0.706	0.586
0.35	0.164	0.099	0.082	2.3	1.203	0.724	0.601
0.4	0.188	0.113	0.094	2.35	1.233	0.743	0.617
0.45	0.211	0.127	0.106	2.4	1.264	0.761	0.632
0.5	0.236	0.142	0.118	2.45	1.295	0.780	0.647
0.55	0.260	0.156	0.130	2.5	1.326	0.799	0.663
0.6	0.284	0.171	0.142	2.55	1.357	0.818	0.679
0.65	0.309	0.186	0.154	2.6	1.389	0.837	0.694

(Continued)

TABLE C.2 (Continued)

M_u/bd^2 (N/mm ²)	f_y (N/mm ²)			M_u/bd^2 (N/mm ²)	f_y (N/mm ²)		
	250	415	500		250	415	500
0.7	0.333	0.201	0.167	2.65	1.421	0.856	0.710
0.75	0.358	0.216	0.179	2.7	1.453	0.875	0.727
0.8	0.383	0.231	0.191	2.75	1.486	0.895	0.743
0.85	0.408	0.246	0.204	2.8	1.519	0.915	0.759
0.9	0.433	0.261	0.216	2.85	1.552	0.935	0.776
0.95	0.458	0.276	0.229	2.9	1.585	0.955	0.793
1	0.483	0.291	0.242	2.95	1.619	0.975	0.810
1.05	0.509	0.307	0.254	3	1.653	0.996	0.827
1.1	0.535	0.322	0.267	3.05	1.688	1.017	0.844
1.15	0.560	0.338	0.280	3.1	1.723	1.038	0.861
1.2	0.586	0.353	0.293	3.15	1.758	1.059	0.879
1.25	0.613	0.369	0.306	3.2	1.794	1.081	0.897
1.3	0.639	0.385	0.319	3.25	1.830	1.102	0.915
1.35	0.665	0.401	0.333	3.3	1.866	1.124	0.933
1.4	0.692	0.417	0.346	3.35	1.903	1.147	
1.45	0.719	0.433	0.359	3.4	1.941	1.169	
1.5	0.746	0.449	0.373	3.45	1.978	1.192	
1.55	0.773	0.465	0.386	3.5	2.017		
1.6	0.800	0.482	0.400	3.55	2.056	Steel grade	Limiting p_t
1.65	0.827	0.498	0.414	3.6	2.095	Fe 250	2.197
1.7	0.855	0.515	0.428	3.65	2.135	Fe 415	1.193
1.75	0.883	0.532	0.441	3.7	2.175	Fe 500	0.943
1.8	0.911	0.549	0.455	3.72	2.196		
1.85	0.939	0.566	0.470				
1.9	0.968	0.583	0.484				
1.95	0.996	0.600	0.498				
2	1.025	0.618	0.513				
2.05	1.054	0.635	0.527				
2.1	1.083	0.653	0.542				
2.15	1.113	0.670	0.556				
2.2	1.143	0.688	0.571				

Note: Blanks indicate inadmissible reinforcement percentage.

TABLE C.3 Reinforcement percentage, p_t , for singly reinforced rectangular beam sections ($f_{ck} = 30$ N/mm²)

M_u/bd^2 (N/mm ²)	f_y (N/mm ²)			M_u/bd^2 (N/mm ²)	f_y (N/mm ²)		
	250	415	500		250	415	500
0.3	0.140	0.084	0.070	2.4	1.230	0.741	0.615
0.35	0.163	0.098	0.082	2.45	1.259	0.759	0.630
0.4	0.187	0.113	0.093	2.5	1.288	0.776	0.644
0.45	0.211	0.127	0.105	2.55	1.318	0.794	0.659

M_u/bd^2 (N/mm ²)	f_y (N/mm ²)			M_u/bd^2 (N/mm ²)	f_y (N/mm ²)		
	250	415	500		250	415	500
0.5	0.235	0.141	0.117	2.6	1.347	0.812	0.674
0.55	0.259	0.156	0.129	2.65	1.377	0.830	0.689
0.6	0.283	0.170	0.141	2.7	1.407	0.848	0.703
0.65	0.307	0.185	0.153	2.75	1.437	0.866	0.719
0.7	0.331	0.199	0.166	2.8	1.467	0.884	0.734
0.75	0.356	0.214	0.178	2.85	1.498	0.902	0.749
0.8	0.380	0.229	0.190	2.9	1.529	0.921	0.764
0.85	0.405	0.244	0.202	2.95	1.560	0.940	0.780
0.9	0.429	0.259	0.215	3	1.591	0.958	0.795
0.95	0.454	0.274	0.227	3.05	1.622	0.977	0.811
1	0.479	0.289	0.240	3.1	1.654	0.996	0.827
1.05	0.504	0.304	0.252	3.15	1.686	1.016	0.843
1.1	0.529	0.319	0.265	3.2	1.718	1.035	0.859
1.15	0.555	0.334	0.277	3.25	1.750	1.054	0.875
1.2	0.580	0.349	0.290	3.3	1.783	1.074	0.891
1.25	0.606	0.365	0.303	3.35	1.816	1.094	0.908
1.3	0.631	0.380	0.316	3.4	1.849	1.114	0.924
1.35	0.657	0.396	0.328	3.45	1.882	1.134	0.941
1.4	0.683	0.411	0.341	3.5	1.916	1.154	0.958
1.45	0.709	0.427	0.354	3.55	1.950	1.175	0.975
1.5	0.735	0.443	0.368	3.6	1.984	1.195	0.992
1.55	0.761	0.459	0.381	3.65	2.019	1.216	1.009
1.6	0.788	0.475	0.394	3.7	2.053	1.237	1.027
1.65	0.814	0.491	0.407	3.75	2.088	1.258	1.044
1.7	0.841	0.507	0.420	3.8	2.124	1.279	1.062
1.75	0.868	0.523	0.434	3.85	2.160	1.301	1.080
1.8	0.895	0.539	0.447	3.9	2.196	1.323	1.098
1.85	0.922	0.555	0.461	3.95	2.232	1.345	1.116
1.9	0.949	0.572	0.475	4	2.269	1.367	
1.95	0.976	0.588	0.488	4.05	2.306	1.389	
2	1.004	0.605	0.502	4.1	2.344	1.412	
2.05	1.032	0.622	0.516	4.15	2.382	Steel grade	Limiting p_t
2.1	1.060	0.638	0.530	4.2	2.420	Fe 250	2.636
2.15	1.088	0.655	0.544	4.25	2.459	Fe 415	1.432
2.2	1.116	0.672	0.558	4.3	2.498	Fe 500	1.132
2.25	1.144	0.689	0.572	4.35	2.538		
2.3	1.173	0.706	0.586	4.4	2.578		
2.35	1.201	0.724	0.601	4.45	2.618		

Note: Blanks indicate inadmissible reinforcement percentage.

TABLE C.4 Reinforcement percentage, p_t , for singly reinforced rectangular beam sections ($f_{ck} = 35 \text{ N/mm}^2$)

M_u/bd^2 (N/mm ²)	f_y (N/mm ²)			M_u/bd^2 (N/mm ²)	f_y (N/mm ²)		
	250	415	500		250	415	500
0.3	0.139	0.084	0.070	3.05	1.582	0.953	0.791
0.35	0.163	0.098	0.081	3.1	1.611	0.971	0.806
0.4	0.186	0.112	0.093	3.15	1.641	0.989	0.821
0.45	0.210	0.127	0.105	3.2	1.672	1.007	0.836
0.5	0.234	0.141	0.117	3.25	1.702	1.025	0.851
0.55	0.258	0.155	0.129	3.3	1.732	1.044	0.866
0.6	0.282	0.170	0.141	3.35	1.763	1.062	0.882
0.65	0.306	0.184	0.153	3.4	1.794	1.081	0.897
0.7	0.330	0.199	0.165	3.45	1.825	1.099	0.912
0.75	0.354	0.213	0.177	3.5	1.856	1.118	0.928
0.8	0.378	0.228	0.189	3.55	1.887	1.137	0.944
0.85	0.403	0.243	0.201	3.6	1.919	1.156	0.960
0.9	0.427	0.257	0.214	3.65	1.951	1.175	0.975
0.95	0.452	0.272	0.226	3.7	1.983	1.194	0.991
1	0.476	0.287	0.238	3.75	2.015	1.214	1.008
1.05	0.501	0.302	0.250	3.8	2.047	1.233	1.024
1.1	0.526	0.317	0.263	3.85	2.080	1.253	1.040
1.15	0.551	0.332	0.275	3.9	2.113	1.273	1.056
1.2	0.576	0.347	0.288	3.95	2.146	1.293	1.073
1.25	0.601	0.362	0.300	4	2.179	1.313	1.090
1.3	0.626	0.377	0.313	4.05	2.213	1.333	1.106
1.35	0.651	0.392	0.326	4.1	2.246	1.353	1.123
1.4	0.677	0.408	0.338	4.15	2.280	1.374	1.140
1.45	0.702	0.423	0.351	4.2	2.315	1.394	1.157
1.5	0.728	0.438	0.364	4.25	2.349	1.415	1.175
1.55	0.754	0.454	0.377	4.3	2.384	1.436	1.192
1.6	0.779	0.470	0.390	4.35	2.419	1.457	1.209
1.65	0.805	0.485	0.403	4.4	2.454	1.478	1.227
1.7	0.831	0.501	0.416	4.45	2.490	1.500	1.245
1.75	0.858	0.517	0.429	4.5	2.526	1.521	1.263
1.8	0.884	0.532	0.442	4.55	2.562	1.543	1.281
1.85	0.910	0.548	0.455	4.6	2.598	1.565	1.299
1.9	0.937	0.564	0.468	4.65	2.635	1.587	1.317
1.95	0.963	0.580	0.482	4.7	2.672	1.610	
2	0.990	0.596	0.495	4.75	2.709	1.632	
2.05	1.017	0.613	0.508	4.8	2.747	1.655	
2.1	1.044	0.629	0.522	4.85	2.785		
2.15	1.071	0.645	0.535	4.9	2.823		
2.2	1.098	0.662	0.549	4.95	2.862		
2.25	1.125	0.678	0.563	5	2.901		

M_u/bd^2 (N/mm ²)	f_y (N/mm ²)			M_u/bd^2 (N/mm ²)	f_y (N/mm ²)		
	250	415	500		250	415	500
2.3	1.153	0.695	0.576	5.05	2.941		
2.35	1.181	0.711	0.590	5.1	2.981		
2.4	1.208	0.728	0.604	5.15	3.021		
2.45	1.236	0.745	0.618	5.2	3.061		
2.5	1.264	0.762	0.632				
2.55	1.292	0.778	0.646				
2.6	1.321	0.796	0.660				
2.65	1.349	0.813	0.674				
2.7	1.378	0.830	0.689		Steel grade	Limiting p_t	
2.75	1.406	0.847	0.703		Fe 250	3.075	
2.8	1.435	0.865	0.718		Fe 415	1.671	
2.85	1.464	0.882	0.732		Fe 500	1.32	
2.9	1.493	0.900	0.747				
2.95	1.523	0.917	0.761				
3	1.552	0.935	0.776				

Note: Blanks indicate inadmissible reinforcement percentage.

TABLE C.5 Reinforcement percentage, p_t , for singly reinforced rectangular beam sections ($f_{ck} = 40 \text{ N/mm}^2$)

M_u/bd^2 (N/mm ²)	f_y (N/mm ²)			M_u/bd^2 (N/mm ²)	f_y (N/mm ²)		
	250	415	500		250	415	500
0.3	0.139	0.084	0.070	3.05	1.554	0.936	0.777
0.35	0.163	0.098	0.081	3.1	1.583	0.953	0.791
0.4	0.186	0.112	0.093	3.15	1.611	0.971	0.806
0.45	0.210	0.126	0.105	3.2	1.640	0.988	0.820
0.5	0.233	0.141	0.117	3.25	1.669	1.005	0.835
0.55	0.257	0.155	0.129	3.3	1.698	1.023	0.849
0.6	0.281	0.169	0.140	3.35	1.728	1.041	0.864
0.65	0.305	0.184	0.152	3.4	1.757	1.058	0.878
0.7	0.329	0.198	0.164	3.45	1.786	1.076	0.893
0.75	0.353	0.213	0.176	3.5	1.816	1.094	0.908
0.8	0.377	0.227	0.188	3.55	1.846	1.112	0.923
0.85	0.401	0.242	0.201	3.6	1.876	1.130	0.938
0.9	0.425	0.256	0.213	3.65	1.906	1.148	0.953
0.95	0.450	0.271	0.225	3.7	1.936	1.166	0.968
1	0.474	0.286	0.237	3.75	1.967	1.185	0.983
1.05	0.499	0.300	0.249	3.8	1.997	1.203	0.999
1.1	0.523	0.315	0.262	3.85	2.028	1.222	1.014
1.15	0.548	0.330	0.274	3.9	2.059	1.240	1.029

(Continued)

TABLE C.5 (Continued)

M_u/bd^2 (N/mm ²)	f_y (N/mm ²)			M_u/bd^2 (N/mm ²)	f_y (N/mm ²)		
	250	415	500		250	415	500
1.2	0.572	0.345	0.286	3.95	2.090	1.259	1.045
1.25	0.597	0.360	0.299	4	2.121	1.278	1.061
1.3	0.622	0.375	0.311	4.05	2.153	1.297	1.076
1.35	0.647	0.390	0.324	4.1	2.184	1.316	1.092
1.4	0.672	0.405	0.336	4.15	2.216	1.335	1.108
1.45	0.697	0.420	0.349	4.2	2.248	1.354	1.124
1.5	0.723	0.435	0.361	4.25	2.280	1.373	1.140
1.55	0.748	0.451	0.374	4.3	2.312	1.393	1.156
1.6	0.773	0.466	0.387	4.35	2.345	1.412	1.172
1.65	0.799	0.481	0.399	4.4	2.377	1.432	1.189
1.7	0.824	0.497	0.412	4.45	2.410	1.452	1.205
1.75	0.850	0.512	0.425	4.5	2.443	1.472	1.222
1.8	0.876	0.528	0.438	4.55	2.476	1.492	1.238
1.85	0.902	0.543	0.451	4.6	2.510	1.512	1.255
1.9	0.928	0.559	0.464	4.65	2.543	1.532	1.272
1.95	0.954	0.575	0.477	4.7	2.577	1.552	1.289
2	0.980	0.590	0.490	4.75	2.611	1.573	1.306
2.05	1.006	0.606	0.503	4.8	2.645	1.594	1.323
2.1	1.033	0.622	0.516	4.85	2.680	1.614	1.340
2.15	1.059	0.638	0.530	4.9	2.715	1.635	1.357
2.2	1.086	0.654	0.543	4.95	2.749	1.656	1.375
2.25	1.112	0.670	0.556	5	2.785	1.677	1.392
2.3	1.139	0.686	0.570	5.05	2.820	1.699	1.410
2.35	1.166	0.702	0.583	5.1	2.856	1.720	1.428
2.4	1.193	0.719	0.596	5.15	2.892	1.742	1.446
2.45	1.220	0.735	0.610	5.2	2.928	1.764	1.464
2.5	1.247	0.751	0.624	5.25	2.964	1.786	1.482
2.55	1.275	0.768	0.637	5.3	3.001	1.808	1.500
2.6	1.302	0.784	0.651	5.35	3.038	1.830	
2.65	1.329	0.801	0.665	5.4	3.075	1.852	
2.7	1.357	0.818	0.679				
2.75	1.385	0.834	0.692		Steel grade	Limiting p_t	
2.8	1.413	0.851	0.706		Fe 250	3.515	
2.85	1.441	0.868	0.720		Fe 415	1.91	
2.9	1.469	0.885	0.734		Fe 500	1.509	
2.95	1.497	0.902	0.749				
3	1.525	0.919	0.763				

Note: Blanks indicate inadmissible reinforcement percentage.

TABLE C.6 Analysis aids for singly reinforced rectangular beam sections—values of M_u/bd^2 (N/mm²) for given value of p_t

p_t	M 20			M 25		
	Fe 250	Fe 415	Fe 500	Fe 250	Fe 415	Fe 500
0.2	0.424	0.692	0.827	0.426	0.698	0.835
0.25	0.527	0.856	1.020	0.530	0.865	1.033
0.3	0.628	1.016	1.207	0.633	1.029	1.227
0.35	0.728	1.172	1.389	0.735	1.190	1.416
0.4	0.827	1.324	1.566	0.835	1.348	1.601
0.45	0.924	1.473	1.737	0.935	1.503	1.781
0.5	1.020	1.618	1.903	1.033	1.655	1.958
0.55	1.114	1.759	2.064	1.130	1.804	2.129
0.6	1.207	1.897	2.219	1.227	1.951	2.297
0.65	1.299	2.030	2.368	1.322	2.094	2.460
0.7	1.389	2.160	2.512	1.416	2.234	2.619
0.75	1.478	2.286	2.651	1.509	2.371	2.773
0.8	1.566	2.409		1.601	2.505	2.923
0.85	1.652	2.528		1.692	2.636	3.069
0.9	1.737	2.643		1.781	2.764	3.210
0.95	1.821	2.754		1.870	2.889	
1	1.903			1.958	3.011	
1.05	1.984			2.044	3.130	
1.1	2.064			2.129	3.246	
1.15	2.142			2.214	3.359	
1.2	2.219			2.297		
1.25	2.294			2.379		
1.3	2.368			2.460		
1.35	2.441			2.540		
1.4	2.512			2.619		
1.45	2.582			2.696		
1.5	2.651			2.773		
1.55	2.718			2.849		
1.6	2.784			2.923		
1.65	2.849			2.997		
1.7	2.912			3.069		
1.75	2.974			3.140		
1.8				3.210		
1.85				3.279		
1.9				3.347		
1.95				3.414		
2				3.480	Steel grade	$[M_u/(f_{ck} bd^2)]_{lim}$
2.05				3.545	Fe 250	0.149
2.1				3.608	Fe 415	0.138
2.15				3.671	Fe 500	0.133

(Continued)

TABLE C.6 (Continued)

p_t	M 20			M 25		
	Fe 250	Fe 415	Fe 500	Fe 250	Fe 415	Fe 500
2.2						
2.25						
2.3						
2.35						
2.4						
2.45						
2.5						
2.55						
2.6						

Note: Blanks indicate conditions corresponding to $x_u > x_{u,max}$, which is not permitted in design.

TABLE C.6 (Continued)

p_t	M 30			M 35			M 40		
	Fe 250	Fe 415	Fe 500	Fe 250	Fe 415	Fe 500	Fe 250	Fe 415	Fe 500
0.2	0.428	0.702	0.841	0.429	0.705	0.845	0.430	0.707	0.848
0.25	0.532	0.871	1.042	0.534	0.876	1.049	0.535	0.879	1.054
0.3	0.636	1.038	1.240	0.639	1.045	1.249	0.640	1.049	1.256
0.35	0.739	1.202	1.434	0.742	1.211	1.446	0.745	1.218	1.456
0.4	0.841	1.364	1.624	0.845	1.376	1.641	0.848	1.384	1.653
0.45	0.942	1.524	1.811	0.947	1.538	1.832	0.951	1.549	1.847
0.5	1.042	1.680	1.994	1.049	1.698	2.020	1.054	1.712	2.039
0.55	1.141	1.835	2.173	1.149	1.856	2.205	1.155	1.872	2.228
0.6	1.240	1.986	2.349	1.249	2.012	2.386	1.256	2.031	2.414
0.65	1.337	2.136	2.521	1.348	2.166	2.565	1.356	2.189	2.598
0.7	1.434	2.283	2.690	1.446	2.318	2.741	1.456	2.344	2.779
0.75	1.529	2.427	2.855	1.544	2.467	2.913	1.555	2.497	2.957
0.8	1.624	2.569	3.016	1.641	2.614	3.082	1.653	2.649	3.132
0.85	1.718	2.708	3.174	1.737	2.760	3.249	1.751	2.798	3.305
0.9	1.811	2.845	3.328	1.832	2.903	3.412	1.847	2.946	3.475
0.95	1.903	2.979	3.478	1.926	3.044	3.572	1.944	3.092	3.642
1	1.994	3.111	3.625	2.020	3.182	3.729	2.039	3.236	3.806
1.05	2.084	3.240	3.768	2.112	3.319	3.882	2.134	3.378	3.968
1.1	2.173	3.367	3.908	2.205	3.454	4.033	2.228	3.518	4.127
1.15	2.262	3.492		2.296	3.586	4.181	2.321	3.657	4.283
1.2	2.349	3.613		2.386	3.716	4.325	2.414	3.793	4.437
1.25	2.436	3.733		2.476	3.844	4.467	2.506	3.928	4.588
1.3	2.521	3.850		2.565	3.970	4.605	2.598	4.061	4.736
1.35	2.606	3.964		2.653	4.094		2.689	4.191	4.882
1.4	2.690	4.076		2.741	4.216		2.779	4.321	5.024
1.45	2.773			2.827	4.335		2.868	4.448	5.164
1.5	2.855			2.913	4.453		2.957	4.573	5.302

p_t	M 30			M 35			M 40		
	Fe 250	Fe 415	Fe 500	Fe 250	Fe 415	Fe 500	Fe 250	Fe 415	Fe 500
1.55	2.936			2.998	4.568		3.045	4.696	
1.6	3.016			3.082	4.681		3.132	4.818	
1.65	3.095			3.166	4.792		3.219	4.938	
1.7	3.174			3.249			3.305	5.055	
1.75	3.251			3.330			3.390	5.171	
1.8	3.328			3.412			3.475	5.285	
1.85	3.403			3.492			3.559	5.397	
1.9	3.478			3.572			3.642	5.508	
1.95	3.552			3.651			3.724		
2	3.625			3.729			3.806		
2.05	3.697			3.806			3.887		
2.1	3.768			3.882			3.968		
2.15	3.838			3.958			4.048		
2.2	3.908			4.033			4.127		
2.25	3.976			4.107			4.206		
2.3	4.044			4.181			4.283		
2.35	4.110			4.253			4.361		
2.4	4.176			4.325			4.437		
2.45	4.241			4.396			4.513		
2.5	4.305			4.467			4.588		
2.55	4.368			4.536			4.662		
2.6	4.430			4.605			4.736		
2.65				4.673			4.809		
2.7		Steel grade	$[M_u/(f_{ck} bd^2)]_{lim}$	4.740			4.882		
2.75		Fe 250	0.149	4.806			4.953		
2.8		Fe 415	0.138	4.872			5.024		
2.85		Fe 500	0.133	4.937			5.095		
2.9				5.001			5.164		
2.95				5.064			5.233		
3				5.127			5.302		
3.05				5.189			5.369		
3.1							5.436		
3.15							5.502		
3.2							5.568		
3.25							5.633		
3.3							5.697		
3.35							5.761		
3.4							5.824		
3.45							5.886		
3.5							5.947		

Note: Blanks indicate conditions corresponding to $x_u > x_{u,max}$, which is not permitted in design.

TABLE C.7 Design aid for doubly reinforced beams, $f_{ck} = 20 \text{ N/mm}^2$, $f_y = 415 \text{ N/mm}^2$

$M_{u,l} / bd^2 \text{ N/mm}^2$	$d'/d = 0.05$		$d'/d = 0.10$		$d'/d = 0.15$		$d'/d = 0.20$	
	p_t	p_c	p_t	p_c	p_t	p_c	p_t	p_c
2.775	0.961	0.006	0.961	0.006	0.962	0.007	0.962	0.008
2.800	0.968	0.014	0.969	0.014	0.970	0.016	0.971	0.017
2.825	0.976	0.021	0.977	0.022	0.978	0.025	0.980	0.027
2.850	0.983	0.029	0.985	0.031	0.986	0.033	0.988	0.037
2.875	0.990	0.036	0.992	0.039	0.994	0.042	0.997	0.047
2.900	0.998	0.044	1.000	0.047	1.003	0.051	1.005	0.056
2.925	1.005	0.052	1.008	0.055	1.011	0.060	1.014	0.066
2.950	1.012	0.059	1.015	0.063	1.019	0.069	1.023	0.076
2.975	1.019	0.067	1.023	0.071	1.027	0.078	1.031	0.086
3.000	1.027	0.074	1.031	0.079	1.035	0.086	1.040	0.096
3.025	1.034	0.082	1.038	0.087	1.043	0.095	1.049	0.105
3.050	1.041	0.090	1.046	0.095	1.051	0.104	1.057	0.115
3.075	1.049	0.097	1.054	0.103	1.060	0.113	1.066	0.125
3.100	1.056	0.105	1.061	0.111	1.068	0.122	1.075	0.135
3.125	1.063	0.112	1.069	0.119	1.076	0.131	1.083	0.144
3.150	1.070	0.120	1.077	0.127	1.084	0.139	1.092	0.154
3.175	1.078	0.128	1.085	0.135	1.092	0.148	1.101	0.164
3.200	1.085	0.135	1.092	0.144	1.100	0.157	1.109	0.174
3.225	1.092	0.143	1.100	0.152	1.108	0.166	1.118	0.183
3.250	1.100	0.150	1.108	0.160	1.117	0.175	1.127	0.193
3.275	1.107	0.158	1.115	0.168	1.125	0.184	1.135	0.203
3.300	1.114	0.166	1.123	0.176	1.133	0.192	1.144	0.213
3.325	1.121	0.173	1.131	0.184	1.141	0.201	1.153	0.222
3.350	1.129	0.181	1.138	0.192	1.149	0.210	1.161	0.232
3.375	1.136	0.188	1.146	0.200	1.157	0.219	1.170	0.242
3.400	1.143	0.196	1.154	0.208	1.165	0.228	1.179	0.252
3.425	1.151	0.204	1.161	0.216	1.174	0.236	1.187	0.261
3.450	1.158	0.211	1.169	0.224	1.182	0.245	1.196	0.271
3.475	1.165	0.219	1.177	0.232	1.190	0.254	1.205	0.281
3.500	1.173	0.226	1.185	0.240	1.198	0.263	1.213	0.291
3.525	1.180	0.234	1.192	0.249	1.206	0.272	1.222	0.301

$M_{u,l} / bd^2 \text{ N/mm}^2$	$d'/d = 0.05$		$d'/d = 0.10$		$d'/d = 0.15$		$d'/d = 0.20$	
	p_t	p_c	p_t	p_c	p_t	p_c	p_t	p_c
3.550	1.187	0.242	1.200	0.257	1.214	0.281	1.231	0.310
3.575	1.194	0.249	1.208	0.265	1.222	0.289	1.239	0.320
3.600	1.202	0.257	1.215	0.273	1.231	0.298	1.248	0.330
3.625	1.209	0.264	1.223	0.281	1.239	0.307	1.256	0.340
3.650	1.216	0.272	1.231	0.289	1.247	0.316	1.265	0.349
3.675	1.224	0.280	1.238	0.297	1.255	0.325	1.274	0.359
3.700	1.231	0.287	1.246	0.305	1.263	0.334	1.282	0.369
3.725	1.238	0.295	1.254	0.313	1.271	0.342	1.291	0.379
3.750	1.245	0.303	1.262	0.321	1.280	0.351	1.300	0.388
3.775	1.253	0.310	1.269	0.329	1.288	0.360	1.308	0.398
3.800	1.260	0.318	1.277	0.337	1.296	0.369	1.317	0.408
3.825	1.267	0.325	1.285	0.345	1.304	0.378	1.326	0.418
3.850	1.275	0.333	1.292	0.353	1.312	0.387	1.334	0.427
3.875	1.282	0.341	1.300	0.362	1.320	0.395	1.343	0.437
3.900	1.289	0.348	1.308	0.370	1.328	0.404	1.352	0.447
3.925	1.296	0.356	1.315	0.378	1.337	0.413	1.360	0.457
3.950	1.304	0.363	1.323	0.386	1.345	0.422	1.369	0.467
3.975	1.311	0.371	1.331	0.394	1.353	0.431	1.378	0.476
4.000	1.318	0.379	1.338	0.402	1.361	0.440	1.386	0.486
4.025	1.326	0.386	1.346	0.410	1.369	0.448	1.395	0.496
4.050	1.333	0.394	1.354	0.418	1.377	0.457	1.404	0.506
4.075	1.340	0.401	1.362	0.426	1.385	0.466	1.412	0.515
4.100	1.347	0.409	1.369	0.434	1.394	0.475	1.421	0.525
4.125	1.355	0.417	1.377	0.442	1.402	0.484	1.430	0.535
4.150	1.362	0.424	1.385	0.450	1.410	0.493	1.438	0.545
4.175	1.369	0.432	1.392	0.458	1.418	0.501	1.447	0.554
4.200	1.377	0.439	1.400	0.466	1.426	0.510	1.456	0.564
4.225	1.384	0.447	1.408	0.475	1.434	0.519	1.464	0.574
4.250	1.391	0.455	1.415	0.483	1.442	0.528	1.473	0.584
4.275	1.398	0.462	1.423	0.491	1.451	0.537	1.482	0.593
4.300	1.406	0.470	1.431	0.499	1.459	0.546	1.490	0.603

(Continued)

TABLE C.7 (Continued)

M_u/l $bd^2 N/mm^2$	$d'/d = 0.05$		$d'/d = 0.10$		$d'/d = 0.15$		$d'/d = 0.20$	
	p_t	p_c	p_t	p_c	p_t	p_c	p_t	p_c
4.325	1.413	0.477	1.438	0.507	1.467	0.554	1.499	0.613
4.350	1.420	0.485	1.446	0.515	1.475	0.563	1.507	0.623
4.375	1.428	0.493	1.454	0.523	1.483	0.572	1.516	0.632
4.400	1.435	0.500	1.462	0.531	1.491	0.581	1.525	0.642
4.425	1.442	0.508	1.469	0.539	1.499	0.590	1.533	0.652
4.450	1.449	0.515	1.477	0.547	1.508	0.599	1.542	0.662
4.475	1.457	0.523	1.485	0.555	1.516	0.607	1.551	0.672
4.500	1.464	0.531	1.492	0.563	1.524	0.616	1.559	0.681
4.525	1.471	0.538	1.500	0.571	1.532	0.625	1.568	0.691
4.550	1.479	0.546	1.508	0.580	1.540	0.634	1.577	0.701
4.575	1.486	0.553	1.515	0.588	1.548	0.643	1.585	0.711
4.600	1.493	0.561	1.523	0.596	1.556	0.652	1.594	0.720
4.625	1.500	0.569	1.531	0.604	1.565	0.660	1.603	0.730
4.650	1.508	0.576	1.538	0.612	1.573	0.669	1.611	0.740
4.675	1.515	0.584	1.546	0.620	1.581	0.678	1.620	0.750
4.700	1.522	0.591	1.554	0.628	1.589	0.687	1.629	0.759
4.725	1.530	0.599	1.562	0.636	1.597	0.696	1.637	0.769
4.750	1.537	0.607	1.569	0.644	1.605	0.705	1.646	0.779
4.775	1.544	0.614	1.577	0.652	1.614	0.713	1.655	0.789
4.800	1.552	0.622	1.585	0.660	1.622	0.722	1.663	0.798
4.825	1.559	0.629	1.592	0.668	1.630	0.731	1.672	0.808
4.850	1.566	0.637	1.600	0.676	1.638	0.740	1.681	0.818
4.875	1.573	0.645	1.608	0.684	1.646	0.749	1.689	0.828
4.900	1.581	0.652	1.615	0.693	1.654	0.757	1.698	0.838
4.925	1.588	0.660	1.623	0.701	1.662	0.766	1.707	0.847
4.950	1.595	0.667	1.631	0.709	1.671	0.775	1.715	0.857
4.975	1.603	0.675	1.638	0.717	1.679	0.784	1.724	0.867
5.000	1.610	0.683	1.646	0.725	1.687	0.793	1.733	0.877
5.025	1.617	0.690	1.654	0.733	1.695	0.802	1.741	0.886
5.050	1.624	0.698	1.662	0.741	1.703	0.810	1.750	0.896
5.075	1.632	0.706	1.669	0.749	1.711	0.819	1.758	0.906
5.100	1.639	0.713	1.677	0.757	1.719	0.828	1.767	0.916

M_u/l $bd^2 N/mm^2$	$d'/d = 0.05$		$d'/d = 0.10$		$d'/d = 0.15$		$d'/d = 0.20$	
	p_t	p_c	p_t	p_c	p_t	p_c	p_t	p_c
5.125	1.646	0.721	1.685	0.765	1.728	0.837	1.776	0.925
5.150	1.654	0.728	1.692	0.773	1.736	0.846	1.784	0.935
5.175	1.661	0.736	1.700	0.781	1.744	0.855	1.793	0.945
5.200	1.668	0.744	1.708	0.789	1.752	0.863	1.802	0.955
5.225	1.675	0.751	1.715	0.797	1.760	0.872	1.810	0.964
5.250	1.683	0.759	1.723	0.806	1.768	0.881	1.819	0.974
5.275	1.690	0.766	1.731	0.814	1.776	0.890	1.828	0.984
5.300	1.697	0.774	1.739	0.822	1.785	0.899	1.836	0.994
5.325	1.705	0.782	1.746	0.830	1.793	0.908	1.845	1.003
5.350	1.712	0.789	1.754	0.838	1.801	0.916	1.854	1.013
5.375	1.719	0.797	1.762	0.846	1.809	0.925	1.862	1.023
5.400	1.726	0.804	1.769	0.854	1.817	0.934	1.871	1.033
5.425	1.734	0.812	1.777	0.862	1.825	0.943	1.880	1.043
5.450	1.741	0.820	1.785	0.870	1.833	0.952	1.888	1.052
5.475	1.748	0.827	1.792	0.878	1.842	0.961	1.897	1.062
5.500	1.756	0.835	1.800	0.886	1.850	0.969	1.906	1.072
5.525	1.763	0.842	1.808	0.894	1.858	0.978	1.914	1.082
5.550	1.770	0.850	1.815	0.902	1.866	0.987	1.923	1.091
5.575	1.777	0.858	1.823	0.911	1.874	0.996	1.932	1.101
5.600	1.785	0.865	1.831	0.919	1.882	1.005	1.940	1.111
5.625	1.792	0.873	1.839	0.927	1.890	1.014	1.949	1.121
5.650	1.799	0.880	1.846	0.935	1.899	1.022	1.958	1.130
5.675	1.807	0.888	1.854	0.943	1.907	1.031	1.966	1.140
5.700	1.814	0.896	1.862	0.951	1.915	1.040	1.975	1.150
5.725	1.821	0.903	1.869	0.959	1.923	1.049	1.984	1.160
5.750	1.828	0.911	1.877	0.967	1.931	1.058	1.992	1.169
5.775	1.836	0.918	1.885	0.975	1.939	1.067	2.001	1.179
5.800	1.843	0.926	1.892	0.983	1.947	1.075	2.009	1.189
5.825	1.850	0.934	1.900	0.991	1.956	1.084	2.018	1.199
5.850	1.858	0.941	1.908	0.999	1.964	1.093	2.027	1.209
5.875	1.865	0.949	1.915	1.007	1.972	1.102	2.035	1.218
5.900	1.872	0.956	1.923	1.015	1.980	1.111	2.044	1.228

(Continued)

TABLE C.7 (Continued)

$M_u / bd^2 N/mm^2$	$d'/d = 0.05$		$d'/d = 0.10$		$d'/d = 0.15$		$d'/d = 0.20$	
	p_t	p_c	p_t	p_c	p_t	p_c	p_t	p_c
5.925	1.880	0.964	1.931	1.024	1.988	1.120	2.053	1.238
5.950	1.887	0.972	1.939	1.032	1.996	1.128	2.061	1.248
5.975	1.894	0.979	1.946	1.040	2.005	1.137	2.070	1.257
6.000	1.901	0.987	1.954	1.048	2.013	1.146	2.079	1.267
6.025	1.909	0.994	1.962	1.056	2.021	1.155	2.087	1.277
6.050	1.916	1.002	1.969	1.064	2.029	1.164	2.096	1.287
6.075	1.923	1.010	1.977	1.072	2.037	1.173	2.105	1.296
6.100	1.931	1.017	1.985	1.080	2.045	1.181	2.113	1.306
6.125	1.938	1.025	1.992	1.088	2.053	1.190	2.122	1.316
6.150	1.945	1.032	2.000	1.096	2.062	1.199	2.131	1.326
6.175	1.952	1.040	2.008	1.104	2.070	1.208	2.139	1.335
6.200	1.960	1.048	2.015	1.112	2.078	1.217	2.148	1.345
6.225	1.967	1.055	2.023	1.120	2.086	1.225	2.157	1.355
6.250	1.974	1.063	2.031	1.128	2.094	1.234	2.165	1.365
6.275	1.982	1.071	2.039	1.137	2.102	1.243	2.174	1.374
6.300	1.989	1.078	2.046	1.145	2.110	1.252	2.183	1.384
6.325	1.996	1.086	2.054	1.153	2.119	1.261	2.191	1.394
6.350	2.003	1.093	2.062	1.161	2.127	1.270	2.200	1.404
6.375	2.011	1.101	2.069	1.169	2.135	1.278	2.209	1.414
6.400	2.018	1.109	2.077	1.177	2.143	1.287	2.217	1.423
6.425	2.025	1.116	2.085	1.185	2.151	1.296	2.226	1.433
6.450	2.033	1.124	2.092	1.193	2.159	1.305	2.235	1.443
6.475	2.040	1.131	2.100	1.201	2.167	1.314	2.243	1.453
6.500	2.047	1.139	2.108	1.209	2.176	1.323	2.252	1.462
6.525	2.054	1.147	2.115	1.217	2.184	1.331	2.261	1.472
6.550	2.062	1.154	2.123	1.225	2.192	1.340	2.269	1.482
6.575	2.069	1.162	2.131	1.233	2.200	1.349	2.278	1.492
6.600	2.076	1.169	2.139	1.242	2.208	1.358	2.286	1.501
6.625	2.084	1.177	2.146	1.250	2.216	1.367	2.295	1.511
6.650	2.091	1.185	2.154	1.258	2.224	1.376	2.304	1.521
6.675	2.098	1.192	2.162	1.266	2.233	1.384	2.312	1.531
6.700	2.105	1.200	2.169	1.274	2.241	1.393	2.321	1.540

$M_u / bd^2 N/mm^2$	$d'/d = 0.05$		$d'/d = 0.10$		$d'/d = 0.15$		$d'/d = 0.20$	
	p_t	p_c	p_t	p_c	p_t	p_c	p_t	p_c
6.725	2.113	1.207	2.177	1.282	2.249	1.402	2.330	1.550
6.750	2.120	1.215	2.185	1.290	2.257	1.411	2.338	1.560
6.775	2.127	1.223	2.192	1.298	2.265	1.420	2.347	1.570
6.800	2.135	1.230	2.200	1.306	2.273	1.429	2.356	1.580
6.825	2.142	1.238	2.208	1.314	2.281	1.437	2.364	1.589
6.850	2.149	1.245	2.216	1.322	2.290	1.446	2.373	1.599
6.875	2.156	1.253	2.223	1.330	2.298	1.455	2.382	1.609
6.900	2.164	1.261	2.231	1.338	2.306	1.464	2.390	1.619
6.925	2.171	1.268	2.239	1.346	2.314	1.473	2.399	1.628
6.950	2.178	1.276	2.246	1.355	2.322	1.482	2.408	1.638
6.975	2.186	1.283	2.254	1.363	2.330	1.490	2.416	1.648
7.000	2.193	1.291	2.262	1.371	2.339	1.499	2.425	1.658
7.025	2.200	1.299	2.269	1.379	2.347	1.508	2.434	1.667
7.050	2.208	1.306	2.277	1.387	2.355	1.517	2.442	1.677
7.075	2.215	1.314	2.285	1.395	2.363	1.526	2.451	1.687
7.100	2.222	1.321	2.292	1.403	2.371	1.535	2.460	1.697

TABLE C.8 Design aid for doubly reinforced beams, $f_{ck} = 25 N/mm^2$, $f_y = 415 N/mm^2$

$M_u / bd^2 N/mm^2$	$d'/d = 0.05$		$d'/d = 0.10$		$d'/d = 0.15$		$d'/d = 0.20$	
	p_t	p_c	p_t	p_c	p_t	p_c	p_t	p_c
3.450	1.196	0.002	1.196	0.002	1.196	0.002	1.196	0.002
3.475	1.203	0.009	1.204	0.010	1.204	0.011	1.205	0.012
3.500	1.211	0.017	1.211	0.018	1.212	0.020	1.214	0.022
3.525	1.218	0.025	1.219	0.026	1.221	0.029	1.222	0.032
3.550	1.225	0.032	1.227	0.034	1.229	0.038	1.231	0.042
3.575	1.232	0.040	1.235	0.042	1.237	0.046	1.240	0.051
3.600	1.240	0.048	1.242	0.051	1.245	0.055	1.248	0.061
3.625	1.247	0.055	1.250	0.059	1.253	0.064	1.257	0.071
3.650	1.254	0.063	1.258	0.067	1.261	0.073	1.266	0.081
3.675	1.262	0.071	1.265	0.075	1.269	0.082	1.274	0.091
3.700	1.269	0.078	1.273	0.083	1.278	0.091	1.283	0.101
3.725	1.276	0.086	1.281	0.091	1.286	0.100	1.291	0.110
3.750	1.283	0.094	1.288	0.099	1.294	0.109	1.300	0.120

(Continued)

TABLE C.8 (Continued)

$M_u / b d^2$ N/mm ²	$d'/d = 0.05$		$d'/d = 0.10$		$d'/d = 0.15$		$d'/d = 0.20$	
3.775	1.291	0.101	1.296	0.107	1.302	0.118	1.309	0.130
3.800	1.298	0.109	1.304	0.116	1.310	0.126	1.317	0.140
3.825	1.305	0.117	1.311	0.124	1.318	0.135	1.326	0.150
3.850	1.313	0.124	1.319	0.132	1.326	0.144	1.335	0.160
3.875	1.320	0.132	1.327	0.140	1.335	0.153	1.343	0.169
3.900	1.327	0.140	1.335	0.148	1.343	0.162	1.352	0.179
3.925	1.334	0.147	1.342	0.156	1.351	0.171	1.361	0.189
3.950	1.342	0.155	1.350	0.164	1.359	0.180	1.369	0.199
3.975	1.349	0.162	1.358	0.172	1.367	0.189	1.378	0.209
4.000	1.356	0.170	1.365	0.181	1.375	0.198	1.387	0.219
4.025	1.364	0.178	1.373	0.189	1.384	0.206	1.395	0.228
4.050	1.371	0.185	1.381	0.197	1.392	0.215	1.404	0.238
4.075	1.378	0.193	1.388	0.205	1.400	0.224	1.413	0.248
4.100	1.385	0.201	1.396	0.213	1.408	0.233	1.421	0.258
4.125	1.393	0.208	1.404	0.221	1.416	0.242	1.430	0.268
4.150	1.400	0.216	1.411	0.229	1.424	0.251	1.439	0.278
4.175	1.407	0.224	1.419	0.238	1.432	0.260	1.447	0.287
4.200	1.415	0.231	1.427	0.246	1.441	0.269	1.456	0.297
4.225	1.422	0.239	1.435	0.254	1.449	0.278	1.465	0.307
4.250	1.429	0.247	1.442	0.262	1.457	0.287	1.473	0.317
4.275	1.436	0.254	1.450	0.270	1.465	0.295	1.482	0.327
4.300	1.444	0.262	1.458	0.278	1.473	0.304	1.491	0.337
4.325	1.451	0.270	1.465	0.286	1.481	0.313	1.499	0.346
4.350	1.458	0.277	1.473	0.294	1.489	0.322	1.508	0.356
4.375	1.466	0.285	1.481	0.303	1.498	0.331	1.517	0.366
4.400	1.473	0.293	1.488	0.311	1.506	0.340	1.525	0.376
4.425	1.480	0.300	1.496	0.319	1.514	0.349	1.534	0.386
4.450	1.487	0.308	1.504	0.327	1.522	0.358	1.542	0.396
4.475	1.495	0.316	1.511	0.335	1.530	0.367	1.551	0.405
4.500	1.502	0.323	1.519	0.343	1.538	0.375	1.560	0.415
4.525	1.509	0.331	1.527	0.351	1.546	0.384	1.568	0.425
4.550	1.517	0.338	1.535	0.359	1.555	0.393	1.577	0.435
4.575	1.524	0.346	1.542	0.368	1.563	0.402	1.586	0.445

$M_u / b d^2$ N/mm ²	$d'/d = 0.05$		$d'/d = 0.10$		$d'/d = 0.15$		$d'/d = 0.20$	
4.600	1.531	0.354	1.550	0.376	1.571	0.411	1.594	0.455
4.625	1.539	0.361	1.558	0.384	1.579	0.420	1.603	0.464
4.650	1.546	0.369	1.565	0.392	1.587	0.429	1.612	0.474
4.675	1.553	0.377	1.573	0.400	1.595	0.438	1.620	0.484
4.700	1.560	0.384	1.581	0.408	1.603	0.447	1.629	0.494
4.725	1.568	0.392	1.588	0.416	1.612	0.455	1.638	0.504
4.750	1.575	0.400	1.596	0.424	1.620	0.464	1.646	0.513
4.775	1.582	0.407	1.604	0.433	1.628	0.473	1.655	0.523
4.800	1.590	0.415	1.611	0.441	1.636	0.482	1.664	0.533
4.825	1.597	0.423	1.619	0.449	1.644	0.491	1.672	0.543
4.850	1.604	0.430	1.627	0.457	1.652	0.500	1.681	0.553
4.875	1.611	0.438	1.635	0.465	1.660	0.509	1.690	0.563
4.900	1.619	0.446	1.642	0.473	1.669	0.518	1.698	0.572
4.925	1.626	0.453	1.650	0.481	1.677	0.527	1.707	0.582
4.950	1.633	0.461	1.658	0.489	1.685	0.535	1.716	0.592
4.975	1.641	0.469	1.665	0.498	1.693	0.544	1.724	0.602
5.000	1.648	0.476	1.673	0.506	1.701	0.553	1.733	0.612
5.025	1.655	0.484	1.681	0.514	1.709	0.562	1.742	0.622
5.050	1.662	0.492	1.688	0.522	1.718	0.571	1.750	0.631
5.075	1.670	0.499	1.696	0.530	1.726	0.580	1.759	0.641
5.100	1.677	0.507	1.704	0.538	1.734	0.589	1.768	0.651
5.125	1.684	0.515	1.712	0.546	1.742	0.598	1.776	0.661
5.150	1.692	0.522	1.719	0.554	1.750	0.607	1.785	0.671
5.175	1.699	0.530	1.727	0.563	1.758	0.615	1.793	0.681
5.200	1.706	0.537	1.735	0.571	1.766	0.624	1.802	0.690
5.225	1.713	0.545	1.742	0.579	1.775	0.633	1.811	0.700
5.250	1.721	0.553	1.750	0.587	1.783	0.642	1.819	0.710
5.275	1.728	0.560	1.758	0.595	1.791	0.651	1.828	0.720
5.300	1.735	0.568	1.765	0.603	1.799	0.660	1.837	0.730
5.325	1.743	0.576	1.773	0.611	1.807	0.669	1.845	0.740
5.350	1.750	0.583	1.781	0.619	1.815	0.678	1.854	0.749
5.375	1.757	0.591	1.788	0.628	1.823	0.687	1.863	0.759
5.400	1.764	0.599	1.796	0.636	1.832	0.695	1.871	0.769
5.425	1.772	0.606	1.804	0.644	1.840	0.704	1.880	0.779
5.450	1.779	0.614	1.812	0.652	1.848	0.713	1.889	0.789

(Continued)

TABLE C.8 (Continued)

M_u / $lb\,d^2$ N/mm ²	$d'/d = 0.05$		$d'/d = 0.10$		$d'/d = 0.15$		$d'/d = 0.20$	
	5.475	1.786	0.622	1.819	0.660	1.856	0.722	1.897
5.500	1.794	0.629	1.827	0.668	1.864	0.731	1.906	0.808
5.525	1.801	0.637	1.835	0.676	1.872	0.740	1.915	0.818
5.550	1.808	0.645	1.842	0.684	1.880	0.749	1.923	0.828
5.575	1.815	0.652	1.850	0.693	1.889	0.758	1.932	0.838
5.600	1.823	0.660	1.858	0.701	1.897	0.767	1.941	0.848
5.625	1.830	0.668	1.865	0.709	1.905	0.775	1.949	0.858
5.650	1.837	0.675	1.873	0.717	1.913	0.784	1.958	0.867
5.675	1.845	0.683	1.881	0.725	1.921	0.793	1.967	0.877
5.700	1.852	0.691	1.888	0.733	1.929	0.802	1.975	0.887
5.725	1.859	0.698	1.896	0.741	1.937	0.811	1.984	0.897
5.750	1.867	0.706	1.904	0.749	1.946	0.820	1.993	0.907
5.775	1.874	0.714	1.912	0.758	1.954	0.829	2.001	0.917
5.800	1.881	0.721	1.919	0.766	1.962	0.838	2.010	0.926
5.825	1.888	0.729	1.927	0.774	1.970	0.847	2.019	0.936
5.850	1.896	0.736	1.935	0.782	1.978	0.855	2.027	0.946
5.875	1.903	0.744	1.942	0.790	1.986	0.864	2.036	0.956
5.900	1.910	0.752	1.950	0.798	1.994	0.873	2.044	0.966
5.925	1.918	0.759	1.958	0.806	2.003	0.882	2.053	0.976
5.950	1.925	0.767	1.965	0.814	2.011	0.891	2.062	0.985
5.975	1.932	0.775	1.973	0.823	2.019	0.900	2.070	0.995
6.000	1.939	0.782	1.981	0.831	2.027	0.909	2.079	1.005
6.025	1.947	0.790	1.988	0.839	2.035	0.918	2.088	1.015
6.050	1.954	0.798	1.996	0.847	2.043	0.927	2.096	1.025
6.075	1.961	0.805	2.004	0.855	2.051	0.935	2.105	1.035
6.100	1.969	0.813	2.012	0.863	2.060	0.944	2.114	1.044
6.125	1.976	0.821	2.019	0.871	2.068	0.953	2.122	1.054
6.150	1.983	0.828	2.027	0.879	2.076	0.962	2.131	1.064
6.175	1.990	0.836	2.035	0.888	2.084	0.971	2.140	1.074
6.200	1.998	0.844	2.042	0.896	2.092	0.980	2.148	1.084
6.225	2.005	0.851	2.050	0.904	2.100	0.989	2.157	1.094
6.250	2.012	0.859	2.058	0.912	2.109	0.998	2.166	1.103
6.275	2.020	0.867	2.065	0.920	2.117	1.007	2.174	1.113
6.300	2.027	0.874	2.073	0.928	2.125	1.015	2.183	1.123
6.325	2.034	0.882	2.081	0.936	2.133	1.024	2.192	1.133
6.350	2.041	0.890	2.089	0.944	2.141	1.033	2.200	1.143

M_u / $lb\,d^2$ N/mm ²	$d'/d = 0.05$		$d'/d = 0.10$		$d'/d = 0.15$		$d'/d = 0.20$	
	6.375	2.049	0.897	2.096	0.953	2.149	1.042	2.209
6.400	2.056	0.905	2.104	0.961	2.157	1.051	2.218	1.162
6.425	2.063	0.912	2.112	0.969	2.166	1.060	2.226	1.172
6.450	2.071	0.920	2.119	0.977	2.174	1.069	2.235	1.182
6.475	2.078	0.928	2.127	0.985	2.182	1.078	2.244	1.192
6.500	2.085	0.935	2.135	0.993	2.190	1.087	2.252	1.202
6.525	2.092	0.943	2.142	1.001	2.198	1.095	2.261	1.212
6.550	2.100	0.951	2.150	1.009	2.206	1.104	2.270	1.221
6.575	2.107	0.958	2.158	1.018	2.214	1.113	2.278	1.231
6.600	2.114	0.966	2.165	1.026	2.223	1.122	2.287	1.241
6.625	2.122	0.974	2.173	1.034	2.231	1.131	2.295	1.251
6.650	2.129	0.981	2.181	1.042	2.239	1.140	2.304	1.261
6.675	2.136	0.989	2.189	1.050	2.247	1.149	2.313	1.271
6.700	2.143	0.997	2.196	1.058	2.255	1.158	2.321	1.280
6.725	2.151	1.004	2.204	1.066	2.263	1.167	2.330	1.290
6.750	2.158	1.012	2.212	1.074	2.271	1.175	2.339	1.300
6.775	2.165	1.020	2.219	1.083	2.280	1.184	2.347	1.310
6.800	2.173	1.027	2.227	1.091	2.288	1.193	2.356	1.320
6.825	2.180	1.035	2.235	1.099	2.296	1.202	2.365	1.330
6.850	2.187	1.043	2.242	1.107	2.304	1.211	2.373	1.339
6.875	2.195	1.050	2.250	1.115	2.312	1.220	2.382	1.349
6.900	2.202	1.058	2.258	1.123	2.320	1.229	2.391	1.359
6.925	2.209	1.066	2.265	1.131	2.328	1.238	2.399	1.369
6.950	2.216	1.073	2.273	1.139	2.337	1.247	2.408	1.379
6.975	2.224	1.081	2.281	1.148	2.345	1.255	2.417	1.389
7.000	2.231	1.089	2.289	1.156	2.353	1.264	2.425	1.398
7.025	2.238	1.096	2.296	1.164	2.361	1.273	2.434	1.408
7.050	2.246	1.104	2.304	1.172	2.369	1.282	2.443	1.418
7.075	2.253	1.111	2.312	1.180	2.377	1.291	2.451	1.428
7.100	2.260	1.119	2.319	1.188	2.385	1.300	2.460	1.438
7.125	2.267	1.127	2.327	1.196	2.394	1.309	2.469	1.448
7.150	2.275	1.134	2.335	1.204	2.402	1.318	2.477	1.457
7.175	2.282	1.142	2.342	1.213	2.410	1.327	2.486	1.467
7.200	2.289	1.150	2.350	1.221	2.418	1.335	2.495	1.477
7.225	2.297	1.157	2.358	1.229	2.426	1.344	2.503	1.487

(Continued)

TABLE C.8 (Continued)

$M_u / b d^2$ N/mm ²	$d'/d = 0.05$		$d'/d = 0.10$		$d'/d = 0.15$		$d'/d = 0.20$	
	7.250	2.304	1.165	2.365	1.237	2.434	1.353	2.512
7.275	2.311	1.173	2.373	1.245	2.443	1.362	2.521	1.506
7.300	2.318	1.180	2.381	1.253	2.451	1.371	2.529	1.516
7.325	2.326	1.188	2.389	1.261	2.459	1.380	2.538	1.526
7.350	2.333	1.196	2.396	1.269	2.467	1.389	2.546	1.536
7.375	2.340	1.203	2.404	1.278	2.475	1.398	2.555	1.546
7.400	2.348	1.211	2.412	1.286	2.483	1.407	2.564	1.556
7.425	2.355	1.219	2.419	1.294	2.491	1.416	2.572	1.565
7.450	2.362	1.226	2.427	1.302	2.500	1.424	2.581	1.575
7.475	2.369	1.234	2.435	1.310	2.508	1.433	2.590	1.585
7.500	2.377	1.242	2.442	1.318	2.516	1.442	2.598	1.595
7.525	2.384	1.249	2.450	1.326	2.524	1.451	2.607	1.605

$M_u / b d^2$ N/mm ²	$d'/d = 0.05$		$d'/d = 0.10$		$d'/d = 0.15$		$d'/d = 0.20$	
	7.550	2.391	1.257	2.458	1.334	2.532	1.460	2.616
7.575	2.399	1.265	2.465	1.343	2.540	1.469	2.624	1.624
7.600	2.406	1.272	2.473	1.351	2.548	1.478	2.633	1.634
7.625	2.413	1.280	2.481	1.359	2.557	1.487	2.642	1.644
7.650	2.420	1.288	2.489	1.367	2.565	1.496	2.650	1.654
7.675	2.428	1.295	2.496	1.375	2.573	1.504	2.659	1.664
7.700	2.435	1.303	2.504	1.383	2.581	1.513	2.668	1.674
7.725	2.442	1.310	2.512	1.391	2.589	1.522	2.676	1.683
7.750	2.450	1.318	2.519	1.399	2.597	1.531	2.685	1.693
7.775	2.457	1.326	2.527	1.408	2.605	1.540	2.694	1.703
7.800	2.464	1.333	2.535	1.416	2.614	1.549	2.702	1.713

TABLE C.9 Analysis aids for doubly reinforced rectangular beam sections—values of $M_u / f_{ck} b d^2$ for Fe 415 steel and $d'/d = 0.05$ (N/mm²)

p_c / f_{ck}	p_t / f_{ck}														
	0.01	0.02	0.03	0.04	0.05	0.06	0.07	0.08	0.09	0.10	0.11	0.12	0.13	0.14	0.15
0.01	0.0348	0.0687	0.1001	0.1285	0.1539	–	–	–	–	–	–	–	–	–	–
0.02	0.0348	0.0691	0.1028	0.1342	0.1625	0.1877	–	–	–	–	–	–	–	–	–
0.03	0.0348	0.0691	0.1033	0.1369	0.1682	0.1964	0.2216	–	–	–	–	–	–	–	–
0.04	0.0348	0.0691	0.1034	0.1376	0.1710	0.2023	0.2304	0.2554	–	–	–	–	–	–	–
0.05	0.0348	0.0691	0.1034	0.1376	0.1718	0.2052	0.2363	0.2643	0.2892	–	–	–	–	–	–
0.06	0.0348	0.0691	0.1034	0.1377	0.1719	0.2060	0.2393	0.2704	0.2982	0.3231	–	–	–	–	–
0.07	0.0348	0.0691	0.1034	0.1377	0.1719	0.2062	0.2403	0.2734	0.3044	0.3322	0.3569	–	–	–	–
0.08	0.0348	0.0691	0.1034	0.1377	0.1719	0.2062	0.2404	0.2745	0.3076	0.3384	0.3661	0.3907	–	–	–
0.09	0.0348	0.0691	0.1034	0.1377	0.1720	0.2062	0.2405	0.2747	0.3087	0.3417	0.3725	0.4000	0.4245	–	–
0.10	0.0348	0.0691	0.1034	0.1377	0.1720	0.2062	0.2405	0.2748	0.3090	0.3429	0.3758	0.4065	0.4339	0.4583	–
0.11	0.0348	0.0691	0.1034	0.1377	0.1720	0.2062	0.2405	0.2748	0.3090	0.3432	0.3771	0.4099	0.4405	0.4678	0.4921
0.12	0.0348	0.0691	0.1034	0.1377	0.1720	0.2062	0.2405	0.2748	0.3090	0.3433	0.3775	0.4113	0.4440	0.4745	0.5017
0.13	0.0348	0.0691	0.1034	0.1377	0.1720	0.2062	0.2405	0.2748	0.3091	0.3433	0.3776	0.4117	0.4455	0.4782	0.5085
0.14	0.0348	0.0691	0.1034	0.1377	0.1720	0.2062	0.2405	0.2748	0.3091	0.3433	0.3776	0.4118	0.4460	0.4797	0.5123
0.15	0.0348	0.0691	0.1034	0.1377	0.1720	0.2062	0.2405	0.2748	0.3091	0.3433	0.3776	0.4119	0.4461	0.4802	0.5139

Note: – indicates over-reinforced section, ($k > x_{u,max}/d$).

TABLE C.10 Analysis aids for doubly reinforced rectangular beam sections—values of $M_u / f_{ck} b d^2$ for Fe 415 steel and $d'/d = 0.10$ (N/mm²)

p_c / f_{ck}	p_t / f_{ck}														
	0.01	0.02	0.03	0.04	0.05	0.06	0.07	0.08	0.09	0.10	0.11	0.12	0.13	0.14	0.15
0.01	0.0346	0.0670	0.0982	0.1266	0.1520	–	–	–	–	–	–	–	–	–	–
0.02	0.0346	0.0671	0.0993	0.1304	0.1587	0.1840	–	–	–	–	–	–	–	–	–
0.03	0.0346	0.0671	0.0995	0.1317	0.1625	0.1907	0.2160	–	–	–	–	–	–	–	–
0.04	0.0346	0.0671	0.0996	0.1319	0.1640	0.1947	0.2228	0.2480	–	–	–	–	–	–	–
0.05	0.0346	0.0671	0.0996	0.1320	0.1643	0.1963	0.2268	0.2548	0.2800	–	–	–	–	–	–

(Continued)

TABLE C.10 (Continued)

p_c/f_{ck}	p_t/f_{ck}														
	0.01	0.02	0.03	0.04	0.05	0.06	0.07	0.08	0.09	0.10	0.11	0.12	0.13	0.14	0.15
0.06	0.0346	0.0671	0.0996	0.1320	0.1644	0.1967	0.2286	0.2589	0.2869	0.3120	–	–	–	–	–
0.07	0.0346	0.0671	0.0996	0.1321	0.1645	0.1969	0.2292	0.2609	0.2911	0.3190	0.3440	–	–	–	–
0.08	0.0346	0.0671	0.0996	0.1321	0.1645	0.1969	0.2293	0.2616	0.2932	0.3233	0.3510	0.3760	–	–	–
0.09	0.0346	0.0671	0.0996	0.1321	0.1645	0.1970	0.2294	0.2617	0.2939	0.3255	0.3554	0.3831	0.4080	–	–
0.10	0.0346	0.0671	0.0996	0.1321	0.1645	0.1970	0.2294	0.2618	0.2942	0.3263	0.3578	0.3876	0.4152	0.4400	–
0.11	0.0346	0.0671	0.0996	0.1321	0.1645	0.1970	0.2295	0.2619	0.2943	0.3266	0.3587	0.3900	0.4198	0.4472	0.4720
0.12	0.0346	0.0671	0.0996	0.1321	0.1645	0.1970	0.2295	0.2619	0.2943	0.3267	0.3590	0.3910	0.4223	0.4519	0.4793
0.13	0.0346	0.0671	0.0996	0.1321	0.1645	0.1970	0.2295	0.2619	0.2944	0.3268	0.3592	0.3915	0.4234	0.4545	0.4841
0.14	0.0346	0.0671	0.0996	0.1321	0.1645	0.1970	0.2295	0.2620	0.2944	0.3268	0.3592	0.3916	0.4239	0.4558	0.4868
0.15	0.0346	0.0671	0.0996	0.1321	0.1645	0.1970	0.2295	0.2620	0.2944	0.3269	0.3593	0.3917	0.4240	0.4563	0.4881

Note: – indicates over-reinforced section, ($k > x_{u,max}/d$).

TABLE C.11 Analysis aids for doubly reinforced rectangular beam sections—values of $M_u/f_{ck}bd^2$ for Fe 415 steel and $d'/d = 0.15$ (N/mm²)

p_c/f_{ck}	p_t/f_{ck}														
	0.01	0.02	0.03	0.04	0.05	0.06	0.07	0.08	0.09	0.10	0.11	0.12	0.13	0.14	0.15
0.01	0.0351	0.0662	0.0964	0.1247	0.1501	–	–	–	–	–	–	–	–	–	–
0.02	0.0352	0.0661	0.0968	0.1268	0.1549	0.1801	–	–	–	–	–	–	–	–	–
0.03	0.0353	0.0661	0.0968	0.1273	0.1571	0.1851	0.2102	–	–	–	–	–	–	–	–
0.04	0.0353	0.0661	0.0969	0.1274	0.1578	0.1875	0.2152	0.2402	–	–	–	–	–	–	–
0.05	0.0353	0.0661	0.0968	0.1275	0.1580	0.1883	0.2178	0.2454	0.2703	–	–	–	–	–	–
0.06	0.0353	0.0661	0.0968	0.1275	0.1581	0.1886	0.2188	0.2482	0.2756	0.3004	–	–	–	–	–
0.07	0.0353	0.0661	0.0968	0.1275	0.1582	0.1887	0.2191	0.2493	0.2785	0.3057	0.3305	–	–	–	–
0.08	0.0353	0.0661	0.0968	0.1275	0.1582	0.1888	0.2193	0.2497	0.2798	0.3088	0.3359	0.3606	–	–	–
0.09	0.0353	0.0661	0.0968	0.1275	0.1582	0.1888	0.2194	0.2499	0.2802	0.3103	0.3392	0.3661	0.3907	–	–
0.10	0.0353	0.0661	0.0968	0.1275	0.1582	0.1889	0.2195	0.2500	0.2805	0.3108	0.3408	0.3695	0.3963	0.4208	–
0.11	0.0353	0.0661	0.0968	0.1275	0.1582	0.1889	0.2195	0.2501	0.2806	0.3111	0.3414	0.3712	0.3999	0.4265	–
0.12	0.0353	0.0661	0.0968	0.1275	0.1582	0.1889	0.2195	0.2501	0.2807	0.3112	0.3417	0.3720	0.4016	0.4302	0.4567
0.13	0.0353	0.0661	0.0968	0.1275	0.1582	0.1889	0.2195	0.2502	0.2808	0.3113	0.3418	0.3723	0.4025	0.4321	0.4604
0.14	0.0353	0.0661	0.0968	0.1275	0.1582	0.1889	0.2195	0.2502	0.2808	0.3114	0.3419	0.3724	0.4029	0.4330	0.4625
0.15	0.0354	0.0661	0.0968	0.1275	0.1582	0.1889	0.2195	0.2502	0.2808	0.3114	0.3420	0.3726	0.4030	0.4335	0.4635

Note: Shaded values indicate neutral axis lies within the cover ($k < d'/d$) and – indicates over-reinforced section, ($k > x_{u,max}/d$).

TABLE C.12 Analysis aids for doubly reinforced rectangular beam sections—values of $M_u/f_{ck}bd^2$ for Fe 415 steel and $d'/d = 0.20$ (N/mm²)

p_c/f_{ck}	p_t/f_{ck}														
	0.01	0.02	0.03	0.04	0.05	0.06	0.07	0.08	0.09	0.10	0.11	0.12	0.13	0.14	0.15
0.01	0.0364	0.0661	0.0951	0.1229	0.1482	–	–	–	–	–	–	–	–	–	–
0.02	0.0367	0.0661	0.0952	0.1237	0.1512	0.1764	–	–	–	–	–	–	–	–	–
0.03	0.0369	0.0661	0.0952	0.1240	0.1522	0.1796	0.2046	–	–	–	–	–	–	–	–
0.04	0.0370	0.0661	0.0952	0.1240	0.1526	0.1808	0.2080	0.2328	–	–	–	–	–	–	–
0.05	0.0370	0.0661	0.0951	0.1241	0.1528	0.1813	0.2094	0.2363	0.2609	–	–	–	–	–	–
0.06	0.0370	0.0661	0.0951	0.1241	0.1529	0.1815	0.2100	0.2380	0.2647	0.2891	–	–	–	–	–
0.07	0.0371	0.0661	0.0951	0.1240	0.1529	0.1817	0.2103	0.2386	0.2666	0.2930	–	–	–	–	–
0.08	0.0371	0.0661	0.0951	0.1240	0.1529	0.1817	0.2104	0.2390	0.2673	0.2951	0.3214	–	–	–	–
0.09	0.0371	0.0661	0.0951	0.1240	0.1529	0.1818	0.2105	0.2392	0.2677	0.2960	0.3237	0.3498	–	–	–
0.10	0.0371	0.0661	0.0951	0.1240	0.1529	0.1818	0.2106	0.2393	0.2679	0.2964	0.3247	0.3522	0.3782	–	–
0.11	0.0371	0.0661	0.0951	0.1240	0.1529	0.1818	0.2106	0.2394	0.2681	0.2967	0.3251	0.3534	0.3807	0.4066	–

(Continued)

TABLE C.12 (Continued)

p_c/f_{ck}	p_r/f_{ck}														
	0.01	0.02	0.03	0.04	0.05	0.06	0.07	0.08	0.09	0.10	0.11	0.12	0.13	0.14	0.15
0.12	0.0371	0.0661	0.0951	0.1240	0.1529	0.1818	0.2107	0.2395	0.2682	0.2969	0.3254	0.3539	0.3820	0.4092	0.4350
0.13	0.0371	0.0661	0.0950	0.1240	0.1529	0.1818	0.2107	0.2395	0.2683	0.2970	0.3256	0.3542	0.3826	0.4106	0.4377
0.14	0.0371	0.0661	0.0950	0.1240	0.1529	0.1818	0.2107	0.2395	0.2683	0.2971	0.3258	0.3544	0.3829	0.4113	0.4393
0.15	0.0371	0.0661	0.0950	0.1240	0.1529	0.1818	0.2107	0.2395	0.2684	0.2971	0.3259	0.3545	0.3832	0.4117	0.4401

Note: Shaded values indicate neutral axis lies within the cover ($k < d'/d$) and – indicates over-reinforced section, ($k > x_{u,max}/d$).

TABLE C.13 Analysis aids for doubly reinforced rectangular beam sections—values of $M_u/f_{ck}bd^2$ for Fe 500 steel and $d'/d = 0.05$ (N/mm²)

p_c/f_{ck}	p_r/f_{ck}														
	0.01	0.02	0.03	0.04	0.05	0.06	0.07	0.08	0.09	0.10	0.11	0.12	0.13	0.14	0.15
0.01	0.0418	0.0823	0.1190	0.1513	–	–	–	–	–	–	–	–	–	–	–
0.02	0.0418	0.0830	0.1233	0.1598	0.1920	–	–	–	–	–	–	–	–	–	–
0.03	0.0418	0.0831	0.1243	0.1643	0.2007	0.2328	–	–	–	–	–	–	–	–	–
0.04	0.0418	0.0831	0.1244	0.1655	0.2052	0.2415	0.2735	–	–	–	–	–	–	–	–
0.05	0.0418	0.0831	0.1244	0.1657	0.2067	0.2462	0.2823	0.3142	–	–	–	–	–	–	–
0.06	0.0418	0.0831	0.1244	0.1657	0.2069	0.2479	0.2872	0.3232	0.3549	–	–	–	–	–	–
0.07	0.0418	0.0831	0.1244	0.1657	0.2070	0.2482	0.2890	0.3282	0.3640	0.3956	–	–	–	–	–
0.08	0.0418	0.0831	0.1244	0.1657	0.2070	0.2483	0.2894	0.3302	0.3692	0.4049	0.4364	–	–	–	–
0.09	0.0418	0.0831	0.1244	0.1658	0.2070	0.2483	0.2895	0.3307	0.3714	0.4102	0.4457	0.4771	–	–	–
0.10	0.0418	0.0831	0.1244	0.1658	0.2070	0.2483	0.2896	0.3308	0.3719	0.4125	0.4512	0.4866	0.5178	–	–
0.11	0.0418	0.0831	0.1244	0.1658	0.2071	0.2483	0.2896	0.3309	0.3721	0.4132	0.4537	0.4922	0.5274	0.5585	–
0.12	0.0418	0.0831	0.1244	0.1657	0.2071	0.2483	0.2896	0.3309	0.3722	0.4134	0.4544	0.4948	0.5332	0.5682	0.5993
0.13	0.0418	0.0831	0.1245	0.1658	0.2071	0.2484	0.2896	0.3309	0.3722	0.4134	0.4547	0.4956	0.5359	0.5742	0.6091
0.14	0.0418	0.0831	0.1244	0.1658	0.2071	0.2484	0.2897	0.3309	0.3722	0.4135	0.4547	0.4959	0.5369	0.5770	0.6152
0.15	0.0418	0.0831	0.1244	0.1658	0.2071	0.2484	0.2897	0.3309	0.3722	0.4135	0.4548	0.4960	0.5372	0.5781	0.6181

Note: – indicates over-reinforced section, ($k > x_{u,max}/d$).

TABLE C.14 Analysis aids for doubly reinforced rectangular beam sections—values of $M_u/f_{ck}bd^2$ for Fe 500 steel and $d'/d = 0.10$ (N/mm²)

p_c/f_{ck}	p_r/f_{ck}														
	0.01	0.02	0.03	0.04	0.05	0.06	0.07	0.08	0.09	0.10	0.11	0.12	0.13	0.14	0.15
0.01	0.0413	0.0801	0.1166	0.1489	–	–	–	–	–	–	–	–	–	–	–
0.02	0.0412	0.0804	0.1188	0.1551	0.1872	–	–	–	–	–	–	–	–	–	–
0.03	0.0412	0.0804	0.1193	0.1577	0.1936	0.2255	–	–	–	–	–	–	–	–	–
0.04	0.0412	0.0804	0.1195	0.1583	0.1965	0.2322	0.2639	–	–	–	–	–	–	–	–
0.05	0.0412	0.0804	0.1195	0.1585	0.1972	0.2352	0.2707	0.3022	–	–	–	–	–	–	–
0.06	0.0412	0.0804	0.1195	0.1586	0.1975	0.2362	0.2740	0.3092	0.3406	–	–	–	–	–	–
0.07	0.0412	0.0804	0.1195	0.1586	0.1976	0.2365	0.2752	0.3127	0.3477	0.3789	–	–	–	–	–
0.08	0.0412	0.0804	0.1195	0.1587	0.1977	0.2367	0.2755	0.3141	0.3515	0.3862	0.4173	–	–	–	–
0.09	0.0412	0.0804	0.1195	0.1587	0.1977	0.2368	0.2757	0.3145	0.3530	0.3902	0.4247	0.4557	–	–	–
0.10	0.0412	0.0804	0.1195	0.1587	0.1978	0.2368	0.2758	0.3148	0.3536	0.3919	0.4290	0.4632	0.4940	–	–
0.11	0.0412	0.0804	0.1195	0.1587	0.1978	0.2369	0.2759	0.3149	0.3538	0.3926	0.4309	0.4677	0.5017	–	–
0.12	0.0412	0.0804	0.1195	0.1587	0.1978	0.2369	0.2760	0.3150	0.3540	0.3929	0.4316	0.4697	0.5064	0.5402	–
0.13	0.0412	0.0804	0.1195	0.1587	0.1978	0.2369	0.2760	0.3151	0.3541	0.3930	0.4319	0.4706	0.5086	0.5451	0.5787
0.14	0.0412	0.0804	0.1195	0.1587	0.1978	0.2369	0.2760	0.3151	0.3541	0.3931	0.4321	0.4710	0.5096	0.5474	0.5837
0.15	0.0412	0.0804	0.1195	0.1587	0.1978	0.2369	0.2760	0.3151	0.3542	0.3932	0.4322	0.4711	0.5100	0.5486	0.5863

Note: – indicates over-reinforced section, ($k > x_{u,max}/d$).

TABLE C.15 Analysis aids for doubly reinforced rectangular beam sections—values of $M_u/f_{ck}bd^2$ for Fe 500 steel and $d'/d = 0.15$ (N/mm²)

p_c/f_{ck}	p/f_{ck}														
	0.01	0.02	0.03	0.04	0.05	0.06	0.07	0.08	0.09	0.10	0.11	0.12	0.13	0.14	0.15
0.01	0.0415	0.0787	0.1143	0.1465	–	–	–	–	–	–	–	–	–	–	–
0.02	0.0416	0.0787	0.1153	0.1506	0.1825	–	–	–	–	–	–	–	–	–	–
0.03	0.0416	0.0787	0.1156	0.1518	0.1868	0.2186	–	–	–	–	–	–	–	–	–
0.04	0.0416	0.0787	0.1157	0.1523	0.1884	0.2231	0.2546	–	–	–	–	–	–	–	–
0.05	0.0416	0.0787	0.1157	0.1525	0.1890	0.2250	0.2595	0.2907	–	–	–	–	–	–	–
0.06	0.0416	0.0787	0.1157	0.1526	0.1893	0.2257	0.2616	0.2957	0.3267	–	–	–	–	–	–
0.07	0.0416	0.0787	0.1157	0.1526	0.1894	0.2260	0.2624	0.2982	0.3320	–	–	–	–	–	–
0.08	0.0416	0.0787	0.1157	0.1526	0.1895	0.2262	0.2628	0.2991	0.3347	0.3683	–	–	–	–	–
0.09	0.0416	0.0787	0.1157	0.1527	0.1896	0.2264	0.2631	0.2995	0.3358	0.3712	0.4046	–	–	–	–
0.10	0.0416	0.0787	0.1157	0.1527	0.1896	0.2264	0.2632	0.2999	0.3363	0.3725	0.4077	0.4409	–	–	–
0.11	0.0416	0.0787	0.1157	0.1527	0.1896	0.2265	0.2633	0.3000	0.3366	0.3731	0.4092	0.4442	0.4772	–	–
0.12	0.0416	0.0787	0.1157	0.1526	0.1896	0.2265	0.2634	0.3002	0.3369	0.3734	0.4098	0.4459	0.4807	0.5135	–
0.13	0.0416	0.0787	0.1157	0.1526	0.1896	0.2265	0.2634	0.3003	0.3370	0.3737	0.4102	0.4466	0.4825	0.5171	0.5497
0.14	0.0416	0.0787	0.1157	0.1526	0.1896	0.2266	0.2635	0.3003	0.3371	0.3739	0.4105	0.4470	0.4834	0.5191	0.5536
0.15	0.0416	0.0786	0.1157	0.1526	0.1896	0.2266	0.2635	0.3004	0.3372	0.3740	0.4107	0.4473	0.4838	0.5202	0.5558

Note: Shaded values indicate neutral axis lies within the cover ($k < d'/d$) and – indicates over-reinforced section, ($k > x_{u,max}/d$).

TABLE C.16 Analysis aids for doubly reinforced rectangular beam sections—values of $M_u/f_{ck}bd^2$ for Fe 500 steel and $d'/d = 0.20$ (N/mm²)

p_c/f_{ck}	p/f_{ck}														
	0.01	0.02	0.03	0.04	0.05	0.06	0.07	0.08	0.09	0.10	0.11	0.12	0.13	0.14	0.15
0.01	0.0425	0.0781	0.1123	0.1442	–	–	–	–	–	–	–	–	–	–	–
0.02	0.0428	0.0781	0.1128	0.1464	0.1779	–	–	–	–	–	–	–	–	–	–
0.03	0.0429	0.0780	0.1129	0.1472	0.1804	0.2117	–	–	–	–	–	–	–	–	–
0.04	0.0429	0.0780	0.1129	0.1475	0.1815	0.2145	0.2455	–	–	–	–	–	–	–	–
0.05	0.0430	0.0780	0.1129	0.1476	0.1820	0.2158	0.2487	–	–	–	–	–	–	–	–
0.06	0.0430	0.0780	0.1129	0.1477	0.1822	0.2164	0.2501	0.2829	–	–	–	–	–	–	–
0.07	0.0430	0.0780	0.1129	0.1477	0.1824	0.2168	0.2508	0.2844	0.3170	–	–	–	–	–	–
0.08	0.0430	0.0780	0.1129	0.1477	0.1824	0.2170	0.2513	0.2852	0.3187	0.3510	–	–	–	–	–
0.09	0.0430	0.0780	0.1129	0.1477	0.1825	0.2171	0.2516	0.2858	0.3197	0.3531	0.3851	–	–	–	–
0.10	0.0430	0.0780	0.1129	0.1477	0.1825	0.2172	0.2517	0.2861	0.3203	0.3541	0.3875	0.4192	–	–	–
0.11	0.0431	0.0780	0.1128	0.1477	0.1825	0.2172	0.2518	0.2863	0.3207	0.3548	0.3885	0.4218	–	–	–
0.12	0.0431	0.0780	0.1128	0.1477	0.1825	0.2172	0.2519	0.2865	0.3209	0.3552	0.3893	0.4230	0.4560	–	–
0.13	0.0431	0.0780	0.1128	0.1477	0.1825	0.2173	0.2520	0.2866	0.3211	0.3555	0.3898	0.4238	0.4575	0.4903	–
0.14	0.0431	0.0780	0.1128	0.1477	0.1825	0.2173	0.2520	0.2867	0.3213	0.3557	0.3901	0.4243	0.4583	0.4920	0.5245
0.15	0.0431	0.0779	0.1128	0.1477	0.1825	0.2173	0.2520	0.2867	0.3214	0.3559	0.3904	0.4247	0.4588	0.4928	0.5265

Note: Shaded values indicate neutral axis lies within the cover ($k < d'/d$) and – indicates over-reinforced section, ($k > x_{u,max}/d$).

TABLE C.17 Moment of resistance factors for doubly reinforced T-beam section, $M_u/f_{ck}b_wd^2 - f_y = 415 \text{ N/mm}^2$, $\rho_f/f_{ck} = 0.0075$, $D_f/d = 0.20$, $d'/d = 0.05 \text{ (N/mm}^2\text{)}$

p_f/f_{ck}	b_f/b_w									
	1.0	2.0	3.0	4.0	5.0	6.0	7.0	8.0	9.0	10.0
0.02	0.0683	0.0696	0.0702	0.0707	**	**	**	**	**	**
0.03	0.099	0.1029	0.1042	0.105	0.1055	0.106	**	**	**	**
0.04	0.1267	0.1348	0.1375	0.1389	0.1397	0.1403	0.1409	0.1413	**	**
0.05	0.1513	0.1653	0.1698	0.1721	0.1735	0.1744	0.1751	0.1757	0.1762	0.1766
0.06	–	0.1942	0.201	0.2046	0.2067	0.2081	0.2091	0.2099	0.2105	0.2111
0.07	–	0.2203	0.2315	0.2363	0.2392	0.2412	0.2427	0.2437	0.2446	0.2453
0.08	–	–	0.261	0.2672	0.2712	0.2739	0.2758	0.2772	0.2784	0.2793
0.09	–	–	0.2886	0.2977	0.3026	0.3061	0.3085	0.3104	0.3118	0.313
0.1	–	–	0.3132	0.3274	0.3334	0.3377	0.3408	0.3431	0.345	0.3464
0.11	–	–	–	0.3561	0.3639	0.3688	0.3727	0.3755	0.3777	0.3795
0.12	–	–	–	0.3823	0.3937	0.3995	0.4041	0.4075	0.4102	0.4123
0.13	–	–	–	–	0.423	0.43	0.4351	0.4391	0.4423	0.4449
0.14	–	–	–	–	0.4505	0.46	0.4656	0.4704	0.4741	0.4771
0.15	–	–	–	–	0.475	0.4895	0.4962	0.5012	0.5055	0.509
0.16	–	–	–	–	–	0.5181	0.5262	0.5317	0.5366	0.5406
0.17	–	–	–	–	–	0.5442	0.5559	0.5624	0.5674	0.5719
0.18	–	–	–	–	–	–	0.585	0.5924	0.5978	0.6029

Note: ** indicates neutral axis lies within the covering concrete (i.e., $k < d'/d$) and – indicates over-reinforced section (i.e., $k > x_{u,max}/d$)

TABLE C.18 Moment of resistance factors for doubly reinforced T-beam section, $M_u/f_{ck}b_wd^2 - f_y = 415 \text{ N/Sq mm}$, $\rho_f/f_{ck} = 0.0075$, $D_f/d = 0.30$, $d'/d = 0.05 \text{ (N/mm}^2\text{)}$

p_f/f_{ck}	b_f/b_w									
	1.0	2.0	3.0	4.0	5.0	6.0	7.0	8.0	9.0	10.0
0.02	0.0683	0.0696	0.0702	0.0707	**	**	**	**	**	**
0.03	0.099	0.1029	0.1042	0.105	0.1055	0.106	**	**	**	**
0.04	0.1267	0.1348	0.1375	0.1389	0.1397	0.1403	0.1409	0.1413	**	**
0.05	0.1513	0.1652	0.1698	0.1721	0.1735	0.1744	0.1751	0.1757	0.1762	0.1766
0.06	–	0.194	0.201	0.2046	0.2067	0.2081	0.2091	0.2099	0.2105	0.2111
0.07	–	0.2215	0.2313	0.2363	0.2392	0.2412	0.2427	0.2437	0.2446	0.2453
0.08	–	0.2476	0.2605	0.2672	0.2712	0.2739	0.2758	0.2772	0.2784	0.2793
0.09	–	0.2714	0.2887	0.2974	0.3026	0.3061	0.3085	0.3104	0.3118	0.313
0.1	–	–	0.3163	0.3268	0.3334	0.3377	0.3408	0.3431	0.345	0.3464
0.11	–	–	0.3429	0.3555	0.3635	0.3688	0.3727	0.3755	0.3777	0.3795
0.12	–	–	0.3683	0.3834	0.3931	0.3995	0.4041	0.4075	0.4102	0.4123
0.13	–	–	–	0.4111	0.422	0.4296	0.4351	0.4391	0.4423	0.4449
0.14	–	–	–	0.4379	0.4503	0.4592	0.4656	0.4704	0.4741	0.4771
0.15	–	–	–	0.464	0.478	0.4884	0.4957	0.5012	0.5055	0.509
0.16	–	–	–	0.4888	0.5059	0.517	0.5254	0.5317	0.5366	0.5406
0.17	–	–	–	–	0.5328	0.5451	0.5547	0.5618	0.5674	0.5719
0.18	–	–	–	–	0.5592	0.5727	0.5835	0.5915	0.5978	0.6029

Note: ** indicates neutral axis lies within the covering concrete (i.e., $k < d'/d$) and – indicates over-reinforced section (i.e., $k > x_{u,max}/d$)

TABLE C.19 Moment of resistance factors for doubly reinforced T-beam section, $M_u/f_{ck}b_wd^2 - f_y = 415$ N/Sq mm, $\rho_d/f_{ck} = 0.0075$, $D_f/d = 0.20$, $d'/d = 0.10$ (N/mm²)

ρ_d/f_{ck}	b_f/b_w									
	1.0	2.0	3.0	4.0	5.0	6.0	7.0	8.0	9.0	10.0
0.02	0.0669	0.0691	**	**	**	**	**	**	**	**
0.03	0.0976	0.1017	0.1037	**	**	**	**	**	**	**
0.04	0.1253	0.1334	0.1363	0.1383	**	**	**	**	**	**
0.05	0.1499	0.1639	0.1684	0.171	0.1728	**	**	**	**	**
0.06	–	0.1927	0.1996	0.2032	0.2056	0.2074	**	**	**	**
0.07	–	0.2189	0.2301	0.2348	0.2379	0.2402	0.242	**	**	**
0.08	–	–	0.2595	0.2658	0.2698	0.2726	0.2748	0.2766	**	**
0.09	–	–	0.2872	0.2962	0.3012	0.3047	0.3073	0.3094	0.3111	**
0.1	–	–	0.3118	0.326	0.3319	0.3363	0.3394	0.3419	0.344	0.3457
0.11	–	–	–	0.3547	0.3624	0.3674	0.3712	0.3742	0.3766	0.3786
0.12	–	–	–	0.3808	0.3923	0.398	0.4026	0.4061	0.4089	0.4112
0.13	–	–	–	–	0.4216	0.4286	0.4336	0.4377	0.4409	0.4436
0.14	–	–	–	–	0.4491	0.4586	0.4642	0.4689	0.4727	0.4757
0.15	–	–	–	–	0.4736	0.4881	0.4948	0.4998	0.5041	0.5076
0.16	–	–	–	–	–	0.5166	0.5248	0.5303	0.5352	0.5391
0.17	–	–	–	–	–	0.5428	0.5545	0.561	0.566	0.5704
0.18	–	–	–	–	–	–	0.5836	0.591	0.5964	0.6014

Note: ** indicates neutral axis lies within the covering concrete (i.e., $k < d'/d$) and – indicates over-reinforced section (i.e., $k > x_{u,max}/d$)

TABLE C.20 Moment of resistance factors for doubly reinforced T-beam section, $M_u/f_{ck}b_wd^2 - f_y = 415$ N/Sq mm, $\rho_d/f_{ck} = 0.0075$, $D_f/d = 0.30$, $d'/d = 0.10$ (N/mm²)

ρ_d/f_{ck}	b_f/b_w									
	1.0	2.0	3.0	4.0	5.0	6.0	7.0	8.0	9.0	10.0
0.02	0.0669	0.0691	**	**	**	**	**	**	**	**
0.03	0.0976	0.1017	0.1037	**	**	**	**	**	**	**
0.04	0.1253	0.1334	0.1363	0.1383	**	**	**	**	**	**
0.05	0.1499	0.1637	0.1684	0.171	0.1728	**	**	**	**	**
0.06	–	0.1926	0.1996	0.2032	0.2056	0.2074	**	**	**	**
0.07	–	0.2201	0.2299	0.2348	0.2379	0.2402	0.242	**	**	**
0.08	–	0.2462	0.2591	0.2658	0.2698	0.2726	0.2748	0.2766	**	**
0.09	–	0.27	0.2873	0.296	0.3012	0.3047	0.3073	0.3094	0.3111	**
0.1	–	–	0.3149	0.3254	0.3319	0.3363	0.3394	0.3419	0.344	0.3457
0.11	–	–	0.3415	0.354	0.3621	0.3674	0.3712	0.3742	0.3766	0.3786
0.12	–	–	0.3669	0.382	0.3916	0.398	0.4026	0.4061	0.4089	0.4112
0.13	–	–	–	0.4097	0.4205	0.4282	0.4336	0.4377	0.4409	0.4436
0.14	–	–	–	0.4365	0.4489	0.4578	0.4642	0.4689	0.4727	0.4757
0.15	–	–	–	0.4626	0.4766	0.4869	0.4943	0.4998	0.5041	0.5076
0.16	–	–	–	0.4874	0.5044	0.5155	0.524	0.5303	0.5352	0.5391
0.17	–	–	–	–	0.5313	0.5436	0.5532	0.5604	0.566	0.5704
0.18	–	–	–	–	0.5578	0.5712	0.582	0.5901	0.5964	0.6014

Note: ** indicates neutral axis lies within the covering concrete (i.e., $k < d'/d$) and – indicates over-reinforced section (i.e., $k > x_{u,max}/d$)

TABLE C.21 Design aids for vertical stirrups—values of V_{US}/d for two-legged stirrups, kN/cm

Stirrup Spacing, cm	$f_y = 250 \text{ N/mm}^2$ Diameter, mm					$f_y = 415 \text{ N/mm}^2$ Diameter, mm				
	6	8	10	12	16	6	8	10	12	16
50	2.460	4.373	6.833	9.839	17.492	4.083	7.259	11.343	16.334	29.037
60	2.050	3.644	5.694	8.200	14.577	3.403	6.049	9.452	13.611	24.198
70	1.757	3.124	4.881	7.028	12.495	2.917	5.185	8.102	11.667	20.741
80	1.537	2.733	4.271	6.150	10.933	2.552	4.537	7.089	10.208	18.148
90	1.367	2.429	3.796	5.466	9.718	2.269	4.033	6.302	9.074	16.132
100	1.230	2.187	3.416	4.920	8.746	2.042	3.630	5.671	8.167	14.519
110	1.118	1.988	3.106	4.472	7.951	1.856	3.300	5.156	7.424	13.199
120	1.025	1.822	2.847	4.100	7.288	1.701	3.025	4.726	6.806	12.099
130	0.946	1.682	2.628	3.784	6.728	1.571	2.792	4.363	6.282	11.168
140	0.879	1.562	2.440	3.514	6.247	1.458	2.593	4.051	5.833	10.370
150	0.820	1.458	2.278	3.280	5.831	1.361	2.420	3.781	5.445	9.679
160	0.769	1.367	2.135	3.075	5.466	1.276	2.269	3.545	5.104	9.074
170	0.723	1.286	2.010	2.894	5.145	1.201	2.135	3.336	4.804	8.540
180	0.683	1.215	1.898	2.733	4.859	1.134	2.016	3.151	4.537	8.066
190	0.647	1.151	1.798	2.589	4.603	1.075	1.910	2.985	4.298	7.641
200	0.615	1.093	1.708	2.460	4.373	1.021	1.815	2.836	4.083	7.259
250	0.492	0.875	1.367	1.968	3.498	0.817	1.452	2.269	3.267	5.807
300	0.410	0.729	1.139	1.640	2.915	0.681	1.210	1.890	2.722	4.840
350	0.351	0.625	0.976	1.406	2.499	0.583	1.037	1.620	2.333	4.148
400	0.307	0.547	0.854	1.230	2.187	0.510	0.907	1.418	2.042	3.630
450	0.273	0.486	0.759	1.093	1.944	0.454	0.807	1.260	1.815	3.226

TABLE C.22 Design aids for bent-up bars to resist shear—values of V_{US} for single bar, kN

Bar Diameter, mm	$f_y = 250 \text{ N/mm}^2$		$f_y = 415 \text{ N/mm}^2$	
	$\alpha = 45^\circ$	$\alpha = 60^\circ$	$\alpha = 45^\circ$	$\alpha = 60^\circ$
10	12.08	14.79	20.05	24.56
12	17.39	21.30	28.87	35.36
16	30.92	37.87	51.33	62.87
18	39.14	47.93	64.97	79.57
20	48.32	59.18	80.21	98.23
22	58.46	71.60	97.05	118.86
25	75.49	92.46	125.32	153.49
28	94.70	115.98	157.20	192.53
32	123.69	151.49	205.32	251.47
36	156.54	191.73	259.86	318.27

Note: α is the angle between the bent-up bar and the axis of the member

Tables C.7 to C.20 were developed by Er R.K. Desai, former Chief Engineer (Civil), ITI Ltd, Bangalore. The author thanks him for giving permission to include these tables.

PRACTICAL TIPS AND SOME RULES OF THUMB

D.1 THUMB RULES FOR REINFORCED CONCRETE DESIGNERS

The following are some of the rules of thumb and tables, which will be useful to the practising structural engineer (www.eng-tips.com).

Minimize floor-to-floor height By minimizing the floor-to-floor height and using the same floor-to-floor height, the costs associated with mechanical services, stairs, and exterior building cladding can be significantly reduced. The limiting factor will be deflection considerations.

Use repetitive formwork The cost of formwork may be very high and is not given due consideration by the designers. The cost can be minimized when the framing system is used repetitively (ten or more times) on a structure.

Adopt uniform column layout Uniform column layout results in simpler formwork, which can be used repetitively from floor to floor. Similarly, regular-shaped buildings will be economical than irregular-shaped buildings with L- or T-shaped columns.

Use expansion joints Use of expansion joints in a building is a controversial issue, as some experts consider it unnecessary. Joints are required when a building spans different ground conditions or when the shape or height changes considerably. Joint spacing of roughly 30–60 m for concrete structures seems to be the typical range recommended by various authorities (IS 456 suggests 45 m). Without detailed calculation, joints should be detailed to permit 15–25 mm movement; when seismic pounding is an issue, this should be increased to a minimum of 200 mm (see Section 3.9.2 of Chapter 3).

Use high-strength concrete in columns The high strength may reduce the column size or the amount of reinforcing steel required for the column. High-strength concrete (HSC) may also allow for the use of one standard column size throughout the structure.

Specify self-consolidating concrete Heavily reinforced concrete columns and beams can be very congested with rebar, which prevents the proper placement of the concrete. Self-consolidating concrete (SCC) maximizes concrete flowability without harmful segregation and dramatically reduces honeycombing and air pockets.

Specify locally available materials The use of local aggregates and recycled materials (slag and fly ash) in concrete makes it a ‘green’ product, which is requested by environmentally responsible owners.

Use high early strength concrete This will allow for earlier form stripping and will reduce total construction time.

Consider accidental loads for important buildings For high-risk facilities such as public and commercial tall buildings, accidental loads such as bomb blast or high velocity impact should be considered.

Use standard column size This can be achieved by varying the amount of reinforcing steel and the concrete strength within the column. This will allow for a single column form and will minimize the number of variations to meet slab or beam forms.

Place construction joints at points of minimum shear Place construction joints at the point of minimum shear, at approximately mid-points or near the mid-points. They should be formed vertically and not in a sloped manner.

Use good quality cover blocks Cover blocks should be of the same mix as the concrete used in the members in order to achieve durability.

As far as possible, use the same depth for beams The savings in formwork and shoring costs will exceed any additional costs for concrete and reinforcing steel. This will

also provide a uniform ceiling elevation and minimize mechanical service installation difficulties.

Use the largest bar size that satisfies the design requirements Use larger size bars in columns and smaller size bars in slabs. Larger size bars reduce the total number of bars that must be placed and minimize installation costs.

Use commonly available size of bars and spirals For a single structural member, the number of different sizes of bars should be kept to a minimum.

Eliminate bent bars wherever possible Bent bars increase fabrication costs and require greater storage area and sorting time on the job site.

Increase beam sizes to avoid minimum bar spacing Minimum bar spacing results in tight rebar installations and requires more time to properly place the material. Rebar lapping can also result in bar congestion, which makes proper concrete placement difficult.

Use lap splices whenever possible The cost of additional bar length is usually less than the cost of material and labour for mechanical splices. However, lap splices should not be used for bars larger than 36 mm diameter except where welded.

Avoid congestion of steel Congestion of bars should be avoided, especially at beam-column or other joints, so that all reinforcements can be properly placed.

Estimation of initial member sizes The design of even a simply supported beam requires the designer to guess the beam size before including its self-weight in the analysis. Suggestions for the initial depth of beams and slabs are given in Table D.1 (see also C & CAA T36 2003). It is better to provide higher depth for beams; this will lead to less consumption of steel. Increased width of beams will have no effect on steel consumption and may help in increasing the shear resistance. On the other hand, thicker slabs will lead to expensive design. It is better to use minimum grade of concrete (M20–M25) for slabs and beams.

TABLE D.1 Initial depth of beams and slabs

Member		Span/ Overall Depth Ratio	Maximum Recommended Span
Rectangu- lar beam	Simply supported	10–14	8 m
	Continuous	20–26	
Flanged beam	Simply supported	12–18	12 m
	Continuous	18–21	
One-way slab	Single span	24	3–3.5 m
	Continuous	30	

Member		Span/ Overall Depth Ratio	Maximum Recommended Span
Two-way slab	Simply supported	28	9 m
	Continuous	36	
Flat plate or slab	Simply supported	28–32 (see Fig. 10.7 of Chapter 10)	7 m
	Continuous	Span is longer span	9 m
Cantilever		6–7	5 m

Note: The width (b) of a rectangular beam should be between one-third and two-thirds of the effective length (d).

Design of beams

(a) Beams should be designed taking the following into consideration:

(i) Beams should be designed for moment value at the column face and not the value at centre line as per computer analysis. By this, the value of bending moment will be reduced by 15–25 per cent, leading to a saving in steel.

(ii) Beams should be designed for shear values at a distance d from the column face and not the value at centre line as per computer analysis.

(iii) Moment redistribution should be allowed only for static loads.

(iv) Even though the entire beam length is considered as uniform T-section in the analysis, for design of reinforcement, mid-span should be considered as a T-beam and support sections as rectangular beams.

(b) Higher grade of concrete should be used in most of the beams that are doubly reinforced.

(c) Approximate value of moment of resistance of beam may be found using

$$M_r = k_1 f_{ck} b_w d^2 \text{ in kNm,}$$

where $k_1 = 0.138$ and 0.133 for Fe 415 and Fe 500 steel, respectively.

If the area of steel is known (under-reinforced beam), then

$$M_r = 0.71 A_s f_y d$$

(d) Approximate area of steel reinforcement may be obtained using

$$A_{st} = \frac{M_u}{0.8 d f_y}$$

This value should be less than $19.82 f_{ck} / f_y$ and $18.87 f_{ck} / f_y$ for Fe 415 and Fe 500 steel, respectively.

(e) A minimum of 0.2 per cent should be used for compression reinforcement to aid in controlling the deflection, creep, and other long-term deflections.

- (f) Length of curtailment should be checked with the required development length (L_d for M20, M25, M30, M35, and M40 concrete is $47db$, $40db$, $38db$, $33db$, and $29.7db$, respectively.)
- (g) Keep the higher diameter bars away from the neutral axis (N.A.) (i.e., the layer nearest to the tension face) so that maximum lever arm will be available.
- (h) The maximum area of either the tension or the compression reinforcement in a horizontal element is four per cent of the gross cross-sectional area of the concrete.
- (i) The shear stress $\tau_v = V_u/bd$ for beams should be less than $0.63\sqrt{f_{ck}}$ N/mm². When the calculated shear stress $\tau_v > \tau_c$ [= $0.64(100A_s/bd)^{0.33}(f_{ck}/25)^{0.25}$], shear reinforcements have to be designed; when $\tau_v < \tau_c$, minimum shear reinforcement has to be provided.
- (j) Where splices are provided in bars, they should be, as far as possible, away from the sections of maximum stresses and should be staggered.
- (k) Where the depth of the beams exceeds 750 mm in case of beams without torsion and 450 mm with torsion, provide side face reinforcement.
- (l) Deflection in slabs and beams may be reduced by providing compression reinforcement.
- (m) Only closed stirrups should be used for transverse reinforcement for members subjected to torsion (compatibility torsion) and for members likely to be subjected to reversal of stresses due to seismic loads.
- (n) To accommodate bottom bars, it is good practice to make secondary beams smaller than the main beams by at least 50 mm.

Design of slabs

- (a) Provide a maximum spacing of 250–300 mm for main reinforcement in order to control the crack width.
- (b) A minimum of 0.24 per cent should be used for the roof slabs since they are subjected to higher temperatures.
- (c) There is evidence that early striking and early loading through rapid floor construction has some impact on long-term deflections.
- (d) Thin flat slab construction will almost certainly require punching shear reinforcement at columns.
- (e) Minimum recommended thickness for slabs for fire is 120 mm.
- (f) When openings in floors or roofs are required, the area of reinforcement interrupted by such openings should be replaced by an equivalent amount, half of which should be placed along each edge of the opening. Openings in the column strips should be avoided for flat slabs.
- (g) Designing slabs with mesh reinforcement can result in substantial cost savings; however, certain kinds of detailing should be given importance.

Design of columns

- (a) Use higher grade of concrete when the axial load is predominant.
- (b) Opt for higher section properties when the moment is predominant.
- (c) Restrict the maximum percentage of reinforcement to about three per cent.
- (d) Provide a minimum size of 300 mm × 300 mm for columns in earthquake zones. Higher size columns and richer concrete mixes at the lower floors result in economy. Moreover, avoid slender columns.
- (e) For preliminary sizing, it is best to aim for columns with one to two per cent reinforcement.
 - (i) Column $H/10$ – 20
 - (ii) Edge columns $H/7$ – 9
 - (iii) Corner column $H/6$ – 8
 (H is the height)
- (f) Using about 2.5 per cent of steel, the design load of an axially loaded short column is calculated (when the minimum eccentricity does not exceed 0.05 times the lateral dimension of column) as

$$P_u = 0.4f_{ck}A_c + 0.67f_yA_{sc}$$

where P_u is the factored axial load on the member, A_c is the area of concrete, and A_{sc} is the area of longitudinal reinforcement.

- (g) The approximate method for allowing for moments is to multiply the axial load from the floor immediately above the column being considered by the following:
 - (i) 1.25 for interior columns (allows for pattern loading)
 - (ii) 1.50 for edge columns
 - (iii) 2.00 for corner columns
 Keep the same column size for the entire building (and reduce only the reinforcement) or at least for four to five storeys.
- (h) The approximate method of designing columns subjected to biaxial moments is given in Section 14.3.2 of Chapter 14, which is found to give better results.
- (i) A reinforced column should have at least six bars of longitudinal reinforcement for circular sections and at least four bars, one at each corner of the column, in the case of rectangular sections (eight bars in the case of earthquake zones).
- (j) In general, a column section is considered as a wall when the length is more than four times the thickness; however, for fire purposes, if the fire can get to all the four sides, it should be considered as a column.

Design of reinforced concrete walls

- (a) Approximate thickness of reinforced concrete walls is given as $H/30$ – 45 , where H is the height.

(b) Shear walls are essentially vertical cantilevers and may be sized as such; therefore, a height-to-width ratio equal to seven is reasonable for a shear wall. However, at this aspect ratio, tension will be developed at the base and this requires justification in the design. Pad foundations should be designed to resist overturning and piles may be required to resist tension. The minimum practical thickness is 200 mm. The wall should be preferably ‘braced’, that is, there should be another shear wall in the orthogonal direction.

Design of retaining walls

- (a) Approximate thickness is given as $H/(10-12)$, where H is the height.
- (b) For cantilever-retaining walls, the preliminary dimensions may be fixed as given in Fig. 16.16 of Chapter 16.
- (c) Retaining walls should be attempted with ‘traditional’ dimensions first. Make every effort to correctly size and balance the heel and toe. There are good reasons why these shapes (toe to heel from 0.45–0.55 of the height) are so commonly found. Stability and sliding are easy to satisfy with an oversized heel or toe, but the strength of these members will be very difficult to achieve.

Tables D.2–D.4 provide the standard design for columns with Fe 415 steel and M20 and M25 concrete (multiply by 1.5 to get P_u values).

TABLE D.2 Standard design for axial loaded short square columns

Column Size $B \times D$ (mm)	Main Steel			Lateral Ties		Safe Load Carrying Capacity of Column (kN)		
	No.	Dia-meter (mm)	%	Dia-meter (mm)	Pitch (mm)	M20	M25	
230 × 230	4	12	0.85	6	190	363	433	
	4	16	1.52	6	230	427	496	
	8	12	1.71	6	190	445	514	
	4	20	2.37	6	230	508	577	
	4	16	2.37	6	190	508	577	
	4	12						
	8	16	3.03	6	230	571	639	
	4	25	3.71	8	230	635	703	
300 × 300	4	20	3.89	6	230	653	720	
	4	16						
	4	16	0.89	6	250	624	743	
	8	12	1.00	6	190	642	761	
	4	20	1.40	6	300	707	825	
	4	16	1.40	6	190	707	825	
	4	12						
	8	16	1.79	6	250	770	888	
400 × 400	4	25	2.18	8	300	833	951	
	4	20	2.29	6	250	851	968	
	4	16						
	4	16						

Column Size $B \times D$ (mm)	Main Steel			Lateral Ties		Safe Load Carrying Capacity of Column (kN)		
	No.	Dia-meter (mm)	%	Dia-meter (mm)	Pitch (mm)	M20	M25	
400 × 400	8	20	2.79	6	300	932	1049	
	8	16	1.00	6	300	1141	1353	
	4	25	1.23	8	300	1208	1418	
	4	20	1.29	6	250	1225	1436	
	4	16						
	12	16	1.51	6	250	1288	1498	
	8	20	1.57	6	300	1306	1516	
	16	16	2.01	6	300	1432	1641	
	4	25	2.01	8	300	1432	1641	
	4	20						
	12	20	2.36	6	300	1533	1741	
	8	25	2.45	8	300	1559	1767	
	16	20	3.14	6	300	1758	1964	
	12	25	3.68	8	300	1913	2119	
	450 × 450	4	25	0.97	8	300	1434	1701
		12	16	1.19	6	300	1514	1781
4		28	1.21	8	300	1521	1788	
8		20	1.24	6	300	1532	1799	
4		25	1.59	8	300	1660	1925	
4		20						
12		20	1.86	6	300	1758	2023	
8		25	1.94	8	300	1787	2052	
8		28	2.43	8	300	1966	2229	
8		32	3.18	8	300	2239	2500	
500 × 500		12	16	0.96	6	300	1765	2096
		8	20	1.00	6	300	1783	2113
	8	22	1.22	6	300	1882	2212	
	4	25	1.29	8	300	1914	2243	
	4	20						
	16	16	1.29	6	300	1914	2243	
	12	20	1.51	6	300	2013	2341	
	8	25	1.57	8	300	2040	2368	
	20	16	1.61	6	300	2058	2386	
	16	20	2.01	6	300	2238	2565	
	12	25	2.36	8	300	2396	2721	
	20	20	2.51	6	300	2463	2788	
16	25	3.14	8	300	2747	3069		

- Notes:
1. Clear cover assumed is 40 mm for M20 and 45 mm for M25.
 2. Minimum eccentricity $\leq D/20$ mm

(Continued)

TABLE D.2 (Continued)

Column Size $B \times D$ (mm)	Main Steel			Lateral Ties		Safe Load Carrying Capacity of Column (kN)	
	No.	Dia-meter (mm)	%	Dia-meter (mm)	Pitch (mm)	M20	M25
230 × 300	6	12	0.98	6	190	499	581
	4	16	1.17	6	230	513	604
	8	12	1.31	6	190	531	622
	6	16	1.75	6	230	585	676
	4	20	1.82	6	230	594	684
	4	16	1.82	6	190	594	684
	4	12					
	8	16	2.33	6	230	657	747
	6	20	2.73	6	230	707	797
	4	25	2.84	8	230	721	810
	4	20	2.99	6	230	739	829
	4	16					
230 × 350	8	20	3.64	6	230	820	909
	4	16	1.00	6	230	574	681
	8	12	1.12	6	190	592	698
	6	16	1.50	6	230	647	752
	4	20	1.56	6	230	655	761
	4	16	1.56	6	190	655	761
	4	12					
	4	20	1.82	6	230	693	798
	4	16					
	8	16	2.00	6	230	718	824
	6	20	2.34	6	230	768	873
	4	25	2.44	8	230	783	888
230 × 400	8	20	3.12	6	230	882	985
	6	25	3.67	8	230	961	1065
	4	16	0.87	6	230	635	756
	8	12	0.98	6	190	653	774
	6	16	1.31	6	230	708	829
	4	20	1.37	6	230	718	839
	4	16	1.37	6	190	718	839
	4	12					
	8	16	1.75	6	230	781	901
	6	20	2.05	6	230	830	950
	4	25	2.13	8	230	843	964
	4	16	2.24	6	230	862	982
230 × 450	8	20	2.73	6	230	943	1062
	6	25	3.2	8	230	1021	1139
	8	12	0.87	6	190	714	851
	10	12	1.09	6	190	755	892
	6	16	1.17	6	230	770	906

Column Size $B \times D$ (mm)	Main Steel			Lateral Ties		Safe Load Carrying Capacity of Column (kN)	
	No.	Dia-meter (mm)	%	Dia-meter (mm)	Pitch (mm)	M20	M25
	4	16	1.21	6	230	777	914
	4	12					
	12	12	1.31	6	190	796	932
	8	16	1.55	6	230	841	977
	6	20	1.82	6	230	891	1027
	10	16	1.94	6	230	842	1049
	4	20	1.99	6	230	923	1058
	4	16					
	8	20	2.42	6	230	1005	1139
	8	25	3.79	8	230	1258	1391

TABLE D.3 Standard design for axial loaded short rectangular columns

Column Size $B \times D$ (mm)	Main Steel			Lateral Ties		Safe Load Carrying Capacity of Column (kN)	
	No.	Diameter (mm)	%	Diameter (mm)	Pitch (mm)	M20	M25
230 × 500	10	12	0.98	6	190	816	968
	6	16	1.05	6	230	831	982
	4	16	1.09	6	190	839	991
	4	12					
	12	12	1.18	6	190	858	1009
	8	16	1.40	6	230	903	1054
	6	20	1.64	6	230	953	1104
	10	16	1.75	6	230	976	1126
	4	20	1.79	6	230	984	1135
	4	16					
	12	16	2.10	6	230	1048	1198
	8	20	2.18	6	230	1065	1215
230 × 600	4	25	2.80	8	230	1194	1342
	4	20					
	12	20	3.28	6	230	1292	1441
	8	25	3.42	8	230	1321	1469
	10	12	0.82	6	190	940	1122
	6	16	0.87	6	230	952	1135
	4	16	0.91	6	230	962	1144
	4	12					
	12	12	0.98	6	190	979	1162
	8	16	1.17	6	230	1027	1209
	6	20	1.37	6	230	1076	1258
	10	16	1.46	6	230	1099	1280
300 × 350	4	20	1.49	6	230	1106	1287
	4	16					
	12	20	2.73	6	230	1414	1593
	8	25	2.85	8	230	1444	1623

(Continued)

TABLE D.3 (Continued)

Column Size $B \times D$ (mm)	Main Steel			Lateral Ties		Safe Load Carrying Capacity of Column (kN)	
	No.	Diameter (mm)	%	Diameter (mm)	Pitch (mm)	M20	M25
	6	16	1.15	6	230	777	916
	4	20	1.20	6	230	787	925
	4	16	1.20	6	190	787	925
	4	12					
	8	16	1.53	6	230	849	987
	6	20	1.79	6	230	898	1036
	4	25	1.87	8	230	913	1051
	4	20	1.96	6	230	931	1068
	4	16					
	8	20	2.39	6	230	1012	1148
	6	25	2.81	8	230	1091	1227
300 × 400	6	16	1.005	6	230	857	1016
	4	16	1.047	6	190	866	1025
	4	12					
	8	16	1.34	6	230	929	1087
	4	25	1.63	8	230	992	1150
	4	20	1.72	6	230	1011	1169
	4	16					
	8	20	2.09	6	230	1092	1248
	6	25	2.45	8	230	1169	1325
	4	25	2.68	8	230	1219	1375
	4	20					
	8	25	3.27	8	230	1347	1501
300 × 450	4	16	0.93	6	190	946	1124
	4	12					
	8	16	1.19	6	230	1009	1187
	4	20	1.53	6	230	1092	1269
	4	16					
	12	16	1.79	6	230	1155	1332
	8	20	1.86	6	230	1172	1349
	12	20	2.79	6	230	1398	1573
	8	25	2.91	8	230	1427	1602
300 × 500	6	16	0.80	6	250	1016	1214
	4	16	0.84	6	250	1027	1225
	4	12					
	12	12	0.90	6	190	1042	1241
	8	16	1.07	6	250	1089	1287
	6	20	1.26	6	250	1140	1338
	10	16	1.34	6	250	1162	1359
	4	20	1.37	6	250	1170	1367
	4	16					
	12	16	1.61	6	250	1235	1432
	8	20	1.67	6	250	1251	1448
	4	25	2.15	8	300	1381	1576
	4	20					
	12	20	2.51	6	300	1478	1673
	8	25	2.62	8	300	1508	1702

Column Size $B \times D$ (mm)	Main Steel			Lateral Ties		Safe Load Carrying Capacity of Column (kN)	
	No.	Diameter (mm)	%	Diameter (mm)	Pitch (mm)	M20	M25
300 × 600	8	16	0.89	6	300	1248	1486
	12	16	1.34	6	300	1394	1631
	8	20	1.40	6	300	1414	1650
	12	20	2.09	6	300	1637	1872
	12	25	3.27	8	300	2020	2252
300 × 700	12	16	1.15	6	250	1555	1832
	8	20	1.20	6	300	1574	1850
	12	20	1.79	6	300	1797	2072
	8	25	1.87	8	300	1827	2102
	12	25	2.80	8	300	2179	2451
	8	28	2.35	8	300	2008	2382
	8	32	3.06	8	300	2277	2548
300 × 750	12	16	1.07	6	250	1633	1930
	8	20	1.12	6	300	1654	1950
	16	16	1.43	6	250	1779	2075
	12	20	1.68	6	300	1881	2175
	16	20	2.23	6	300	2103	2397
	12	25	2.62	8	300	2261	2553
	16	25	3.49	8	300	2614	2903

TABLE D.4 Standard design for axial loaded short circular columns

Column Diameter (mm)	Main Steel			Lateral Ties		Safe Load Carrying Capacity of Column (kN)	
	No.	Diameter (mm)	%	Diameter (mm)	Pitch (mm)	M20	M25
230	6	12	1.63	6	150	344	398
	8	12	2.18	6	150	385	439
	6	16	2.9	6	200	439	492
	8	16	3.87	6	200	511	564
300	6	12	0.96	6	200	499	593
	8	12	1.28	6	200	540	633
	6	16	1.71	6	200	595	687
	8	16	2.28	6	200	667	759
	6	20	2.67	6	200	717	809
380	8	12	0.80	6	200	768	918
	6	16	1.06	6	200	821	971
	8	16	1.42	6	200	895	1044
	6	20	1.66	6	200	944	1098
	8	20	2.22	6	200	1058	1206
	6	25	2.60	8	250	1136	1283
	12	20	3.32	6	200	1283	1429
400	8	16	1.28	6	200	960	1125
	8	20	2.00	6	200	1123	1287

(Continued)

TABLE D.4 (Continued)

Column Diameter (mm)	Main Steel			Lateral Ties		Safe Load Carrying Capacity of Column (kN)	
	No.	Diameter (mm)	%	Diameter (mm)	Pitch (mm)	M20	M25
	8	25	3.13	8	250	1378	1541
	8	28	3.92	8	250	1557	1718
450	8	16	1.01	6	200	1137	1347
	8	20	1.58	6	200	1301	1509
	8	25	2.47	8	250	1555	1762
	8	28	3.1	8	250	1736	1941
500	8	20	1.28	6	200	1500	1758
	12	20	1.92	6	200	1726	1983
	8	25	2.00	8	250	1754	2011
	8	28	2.51	8	250	1934	2190
	12	25	3.00	8	250	2109	2362
600	8	20	0.89	6	200	1961	2335
	12	20	1.33	6	200	2185	2557
	8	25	1.39	8	250	2215	2587
	8	28	1.74	8	250	2394	2764
	12	25	2.08	8	250	2567	2936

Notes:

1. Clear cover assumed is 40 mm for M15 and M20 and 45 mm for M25.
2. The load arrived at in the table are for circular ties.
3. For helical ties, the load shall be multiplied by 1.05.

Tables D.5 and D.6 provide the footing design for square columns for two different safe bearing capacities (SBCs) of soil.

TABLE D.5 Square footing for square columns (SBC: 150 kN/m²; concrete: M20; steel: Fe 415)

Load in kN	Size of Footing in m L × B	Least Lateral Dimension of Column in mm	Depth of Footing in mm		Reinforcement in Each Direction
			D	D _{edge}	
100	0.90 × 0.90	300	200	200	5 #10
150	1.10 × 1.10	300	250	200	5 #10
200	1.20 × 1.20	300	300	200	5 #10
250	1.40 × 1.40	400	300	200	7 #10
300	1.50 × 1.50	400	300	200	9 #10
350	1.60 × 1.60	400	350	200	9 #10
400	1.70 × 1.70	400	350	200	12 #10
450	1.90 × 1.90	400	350	200	14 #10
500	1.90 × 1.90	400	400	200	11 #12
550	2.00 × 2.00	400	400	200	11 #12
600	2.10 × 2.10	400	450	200	11 #12
650	2.20 × 2.20	400	500	200	13 #12
700	2.30 × 2.30	400	550	200	13 #12

Load in KN	Size of Footing in m L × B	Least Lateral Dimension of Column in mm	Depth of Footing in mm		Reinforcement in Each Direction
			D	D _{edge}	
800	2.50 × 2.50	400	600	200	16 #12
850	2.50 × 2.50	400	600	200	17 #12
900	2.60 × 2.60	400	650	200	17 #12
950	2.70 × 2.70	400	650	200	19 #12
1000	2.70 × 2.70	500	650	200	20 #12
1100	2.90 × 2.90	500	650	200	13 #16
1200	3.00 × 3.00	500	700	200	13 #16
1300	3.10 × 3.10	500	750	200	14 #16
1400	3.20 × 3.20	500	750	200	16 #16
1500	3.40 × 3.40	600	750	200	17 #16
1600	3.50 × 3.50	600	750	200	19 #16

TABLE D.6 Square footing for square columns (SBC: 200 kN/m²; concrete: M20; steel: Fe 415)

Load in KN	Size of Footing in m L × B	Least Lateral Dimension of Column in mm	Depth of Footing in mm		Reinforcement in Each Direction
			D	D _{edge}	
100	0.80 × 0.80	300	200	200	4 #10
150	0.90 × 0.90	300	250	200	4 #10
200	1.10 × 1.10	300	300	200	5 #10
250	1.20 × 1.20	400	300	200	5 #10
300	1.30 × 1.30	400	300	200	7 #10
350	1.40 × 1.40	400	350	200	7 #10
400	1.50 × 1.50	400	350	200	10 #10
450	1.60 × 1.60	400	400	200	10 #10
500	1.70 × 1.70	400	400	200	13 #10
550	1.80 × 1.80	400	400	200	16 #10
600	1.90 × 1.90	400	450	200	16 #10
650	2.00 × 2.00	400	450	200	17 #10
700	2.00 × 2.00	400	500	200	17 #10
750	2.10 × 2.10	400	500	200	15 #12
800	2.10 × 2.10	400	550	200	13 #12
850	2.20 × 2.20	400	550	200	16 #12
900	2.30 × 2.30	400	600	200	16 #12
950	2.30 × 2.30	500	650	200	16 #12
1000	2.40 × 2.40	500	650	200	18 #12
1100	2.50 × 2.50	500	650	200	11 #16
1200	2.60 × 2.60	500	650	200	11 #16
1300	2.70 × 2.70	500	650	200	14 #16
1400	2.80 × 2.80	500	700	200	14 #16
1500	2.90 × 2.90	600	700	200	16 #16
1600	3.00 × 3.00	600	700	200	16 #16

(Continued)

TABLE D.6 (Continued)

Load in kN	Size of Footing in m $L \times B$	Least Lateral Dimension of Column in mm	Depth of Footing in mm		Reinforcement in Each Direction
			D	D_{edge}	
1800	3.20 × 3.20	700	800	200	19 #16
1900	3.30 × 3.30	700	750	200	19 #16
2000	3.40 × 3.40	700	750	200	21 #16

Table D.7–D.14 provide information on steel reinforced bars.

TABLE D.7 Data for steel reinforcement bars

Diameter of Bar (mm)	Area (mm ²)	Weight (kg/m)	Perimeter of One Bar (mm)	Length/Tonne (m)
6	28.3	0.222	18.8	4505
8	50.3	0.395	25.1	2534

Diameter of Bar (mm)	Area (mm ²)	Weight (kg/m)	Perimeter of One Bar (mm)	Length/Tonne (m)
10	78.5	0.616	31.4	1623
12	113	0.888	37.7	1126
16	201	1.578	50.3	634
18	254	1.998	56.5	501
20	314	2.466	62.8	405
22	380	2.984	69.1	335
25	491	3.853	78.5	260
28	616	4.834	88.0	207
32	804	6.313	100.5	158
36	1018	7.990	113.1	125

TABLE D.8 Area of given number of bars (mm²)

Diameter of Bar (mm)	Number of Bars									
	1	2	3	4	5	6	7	8	9	10
6	28.3	56.5	84.8	113	141	170	198	226	254	283
8	50.3	101	151	201	251	302	352	402	452	503
10	78.5	157	235	314	392	471	549	628	706	785
12	113	226	339	452	565	679	792	905	1018	1131
16	201	402	603	804	1005	1206	1407	1608	1810	2011
18	254	509	763	1018	1272	1527	1781	2036	2290	2545
20	314	628	942	1257	1571	1885	2199	2513	2827	3142
22	380	760	1140	1521	1901	2281	2661	3041	3421	3801
25	491	982	1473	1963	2454	2945	3436	3927	4418	4909
28	616	1232	1847	2463	3079	3695	4310	4926	5542	6158
32	804	1608	2413	3217	4021	4825	5630	6434	7238	8042
36	1018	2036	3054	4072	5089	6107	7125	8143	9161	10179

TABLE D.9 Area of bars at given spacing (per meter width mm²)

Spacing mm	Diameter of Bar in mm											
	5	6	8	10	12	16	18	20	22	25	28	32
50	392	565	1005	1570	2262	4021	–	–	–	–	–	–
60	327	471	837	1309	1885	3351	4241	5236	–	–	–	–
70	280	404	718	1122	1615	2872	3635	4488	5430	–	–	–
75	261	377	670	1047	1508	2681	3392	4189	5068	6545	–	–
80	245	353	628	982	1414	2513	3181	3927	4751	6136	–	–
90	218	314	558	873	1257	2234	2827	3491	4223	5454	6841	–
100	196	283	503	785	1131	2011	2545	3142	3801	4909	6157	8042
110	178	257	457	714	1028	1828	2313	2856	3456	4462	5598	7311
120	163	236	419	654	942	1675	2121	2618	3167	4090	5131	6702
125	157	226	402	628	905	1608	2035	2513	3041	3927	4926	6433
130	151	217	387	604	870	1547	1957	2417	2924	3776	4737	6186

(Continued)

TABLE D.9 (Continued)

Spacing mm	Diameter of Bar in mm											
	5	6	8	10	12	16	18	20	22	25	28	32
140	140	202	359	561	808	1436	1818	2244	2715	3506	4398	5745
150	130	188	335	524	754	1340	1696	2094	2534	3272	4105	5362
160	122	177	314	491	707	1257	1590	1963	2376	3068	3848	5027
170	115	166	296	462	665	1183	1497	1848	2236	2887	3622	4731
175	112	162	287	449	646	1149	1454	1795	2172	2805	3518	4595
180	109	157	279	436	628	1117	1414	1745	2112	2727	3421	4468
190	103	149	265	413	595	1058	1339	1653	2001	2584	3241	4233
200	98	141	251	393	565	1005	1272	1571	1901	2454	3079	4021
210	93	135	239	374	539	957	1212	1496	1810	2337	2932	3830
220	89	128	228	357	514	914	1157	1428	1728	2231	2799	3656
225	87	126	223	349	503	894	1130	1396	1689	2182	2737	3574
230	85	123	218	341	492	874	1106	1366	1653	2134	2677	3497
240	81	118	209	327	471	838	1060	1309	1584	2045	2566	3351
250	78	113	201	314	452	804	1018	1257	1520	1963	2463	3217
260	75	109	193	302	435	773	979	1208	1462	1888	2368	3093
270	72	105	186	291	419	745	942	1164	1408	1818	2281	2979
275	71	103	183	286	411	731	925	1142	1382	1785	2239	2924
280	70	101	179	280	404	718	909	1122	1358	1753	2199	2872
290	67	97	173	271	390	693	877	1083	1311	1693	2123	2773
300	65	94	168	262	377	670	848	1047	1267	1636	2052	2681
350	56	81	144	224	323	574	727	898	1086	1402	1759	2298
400	49	71	126	196	283	503	636	785	950	1227	1539	2011
450	43	62	111	174	251	446	565	698	844	1090	1368	1787

TABLE D.10 Weight of bars at specified spacing

Diameter of Bar (mm)	Weight (kg/m)	Weight of Bar in kg per m ² for Spacing of Bar (mm)								
		75	100.0	125	150	175	200	225	250	275
6	0.222	2.959	2.220	1.776	1.480	1.268	1.110	0.986	0.888	0.807
8	0.395	5.261	3.946	3.157	2.631	2.255	1.973	1.754	1.578	1.435
10	0.617	8.220	6.165	4.932	4.110	3.523	3.083	2.740	2.466	2.242
12	0.888	11.838	8.878	7.103	5.919	5.073	4.439	3.946	3.551	3.228
14	1.208	16.112	12.084	9.667	8.056	6.905	6.042	5.371	4.834	4.394
16	1.578	21.044	15.783	12.627	10.522	9.019	7.892	7.015	6.313	5.739
18	1.998	26.634	19.976	15.981	13.317	11.415	9.988	8.878	7.990	7.264
20	2.466	32.882	24.661	19.729	16.441	14.092	12.331	10.961	9.865	8.968
22	2.984	39.787	29.840	23.872	19.894	17.052	14.920	13.262	11.936	10.851
25	3.853	51.378	38.534	30.827	25.689	22.019	19.267	17.126	15.413	14.012
28	4.834	–	48.337	38.669	32.224	27.621	24.168	21.483	19.335	17.577
32	6.313	–	63.133	50.507	42.089	36.076	31.567	28.059	25.253	22.958
36	7.990	–	–	63.923	53.269	45.659	39.952	35.513	31.961	29.056

TABLE D.13 Effective cover in mm for bars of different diameters in different numbers of horizontal rows

Number of Rows	Diameter of Bars in mm							
	12	16	18	20	22	25	28	32
1	31	33	34	35	36	38	42	48
2	45	49	52	55	58	63	70	90
3	58	65	70	75	80	88	98	112

TABLE D.14 Approximate steel (HYSD bars) consumption in reinforced concrete members

S. No.	Member (Percentage of Steel)	Quantity in kg/m ³	Required Diameter of Bars
1	Column footings or combined footings (0.4–0.6%)	50/100	12–16 mm
2	Rafts (1.75%)	150	16–20 mm 80–85% Stirrups: 8–12 mm 15–20%
3	Grade beams (1.25%)	100	12 mm, 16 mm 85% Stirrups: 8 mm 15%
4	Plinth beams (1.5%)	125	8 mm 85%, Stirrups: 6 mm 15%
5	Columns (2.5–3%)	200–250	16 mm, 20 mm, 25 mm 90% Ties: 8 mm 10%
6	Lintel beams (1%)	125	12 mm, 16 mm 85% Stirrups: 8 mm 15%
7	Sunshades (0.75%)	60	8 mm 75% Distributor: 6 mm 25%

S. No.	Member (Percentage of Steel)	Quantity in kg/m ³	Required Diameter of Bars
8	Canopy slabs up to 2.0 m span (1.5%)	125	10 mm 80% Distributor: 8 mm 20%
9	Staircase waist slabs (0.4%)	150	12 mm or 16 mm 85% Distributor: 8 mm 15%
10	Slabs		
	(a) One way (0.3%)	80	8–10 mm 70% Distributor: 6 mm 30%
	(b) Two way (0.25%)	100	8–10 mm 100%
	(c) Square slab 4–6 m size (0.4%)	150	10–12 mm 100%
11	Beams (1.8–3%)	150–250	12 mm, 16 mm, 20 mm 80–85% Stirrups: 8 mm 15–20%

Note: The sum total of all reinforcing steel, on an average, is about 85–100 kg/m³. The steel consumption in reinforced concrete buildings varies between 25 kg/m² and 70 kg/m², depending on the number of floors (3-storey to 10-storey buildings) and the type of construction (residential, commercial, etc.). Of the total steel quantity in a building, about 35 per cent is used in slabs, 20 per cent in beams, 25 per cent in columns, and the rest 20 per cent in foundations (Varyani 1996).

Concrete quantity in buildings Out of the total concrete quantity in buildings, about 50 per cent is consumed in slabs, 15 per cent in beams, 10 per cent in columns, 20 per cent in foundations, and the remaining five per cent in items such as staircase, lintels, and sunshade (Varyani 1996). Cement consumption is of the order of four bags per square metre of the covered area (i.e., 0.2 tonne per m² of the covered area). More tips and suggestions may be found at www.sefindia.org and in Subramanian 1995.

REFERENCES

C&CAA T36 2003, *Guide to Long-span Concrete Floors*, Cement and Concrete Association of Australia, 2nd edition, p. 45, (also see <http://www.concrete.net.au/publications/pdf/Long-span%20Floors.pdf>, last accessed on 20 September 2013).
<http://www.eng-tips.com/faqs.cfm?fid=1574>, last accessed on 23 September 2013.

Subramanian, N. 1995, 'Economy in Building Construction', *Bulletin of the Indian Concrete Institute*, No. 50, pp. 15–21.
Varyani, U.H. 1996, 'A Note on How to Reduce Steel Consumption in Reinforced Concrete Buildings', *Civil Engineering and Construction Review*, Vol. 9, No. 11, pp. 59–61.
www.sefindia.org, last accessed on 23 September 2013.

CONVERSION FACTORS

Some conversion factors useful in structural concrete design, especially when the designer is using the ACI codes (metric version of ACI 318M-2011 is available), are provided in this appendix.

Quantity	To Convert	To	Multiply By
Length	inch (in)	mm	25.4
	foot (ft)	m	0.3048
	m	ft	3.2808
	mile (mi)	km	1.609
Area	in ²	mm ²	645.16
	ft ²	m ²	0.0929
	m ²	ft ²	10.764
Volume	in ³	mm ³	16,387
	ft ³	m ³	0.02832
	m ³	ft ³	35.315
	gallon	litre	3.7853
	litre	gallon	0.2642
Mass per unit volume	lb/ft ³	kg/m ³	16.0185
	kg/m ³	lb/ft ³	0.062428
Force	Kilo pound (kip)	kN	4.448
	lb	N	4.448
	ton (2000 lb)	kN	8.896
	N	lb	0.2248
	kN	kip	0.2248
Pressure, stress	psi	MPa	0.006895
	ksi	MPa	6.895
	kN/m ²	kip/ft ²	0.02089
	psf	N/m ²	47.88
	N/m ²	psf	0.02088

Quantity	To Convert	To	Multiply By
	MPa	ksi	0.145
	MPa	psi	145.0
Moments	in-lb	Nm	0.1130
	kip-in	kNm	0.1130
	kip-ft	kNm	1.3558
	kNm	ft-kip	0.7376
Uniform loading	kip/ft	kN/m	14.59
	kip/in	kN/m	175.2
	kN/m	kip/ft	0.06852
Speed	mi/h	m/s	4.470
Acceleration	ft/s ²	m/s ²	0.3048
Density	lb/in ³	kg/m ³	27,680
	lb/ft ³	kg/m ³	16.02
Temperature	degree Fahrenheit (°F)	degree Celsius (°C)	(F° - 32)/1.8 ≈ (F° - 30)/2
Inertia	in ⁴	mm ⁴	416,231
Energy	ft-lb	Joule (Nm/9.81)	1.356

Note: 1 Pa = 1 N/m², 1 MPa = 10⁶ Pa = 1 N/mm², g = 32.17 ft/s² = 9.807 m/s², 1 erg = 10⁻⁷ J, 1 Hz (Hertz) = 1 cycles, °K (Kelvin) = °C + 273

Basic SI units relating to structural design

Quantity	Unit	Symbol
Length	metre	m
Mass	kilogram	kg
Time	second	s

The SI unit of force is Newton (N), which is the force that causes a mass of 1 kg to have an acceleration of 1 m/s². The acceleration due to gravity is 9.807 m/s² approximately, and hence the weight of a mass of 1 kg is 9.807 N.

Derived SI units relating to structural design

Quantity	Unit	Symbol	Formula
Force	Newton	N	kg.m/s ²
Pressure, stress	Pascal	Pa	N/m ²
Energy or work	Joule	J	Nm

The common multiple units of the pascal are the hectopascal (1 hPa≡100 Pa), kilopascal (1 kPa≡1000 Pa), megapascal (1 MPa ≡ 1,000,000 Pa), and gigapascal (1 GPa ≡ 1,000,000,000 Pa).

Grade of steel

Fps (ksi)	SI (N/mm ²)
Grade 40	Fe 275
Grade 50	Fe 345
Grade 60	Fe 415
Grade 75	Fe 520
Grade 80	Fe 550
Grade 100 (MMFX)	Fe 690

Concrete designation

f'_c (psi)	f'_c (MPa)	f_{ck} (MPa)*	
		Using Formula	Approximate
3000	20	26.3	25.00
4000	27.5	34.9	34.38
5000	35	43.3	43.75

f'_c (psi)	f'_c (MPa)	f_{ck} (MPa)*	
		Using Formula	Approximate
6000	40	48.8	50.00
7000	48	57.4	60.00
8000	55	64.9	68.75
9000	62	72.2	77.5

*Cube strength, $f_{ck} = f'_c / [0.76 + 0.2 \log(f'_c/20)]$; Approximate value of cube strength = $f'_c/0.8$

Steel bar designation

Fps (Bar No.)*	Diameter, in	Diameter, mm
3	0.375	10
4	0.500	13
5	0.625	16
6	0.750	19
7	0.875	22
8	1.000	25
9	1.128	29
10	1.270	32
11	1.410	36
14	1.693	43
18	2.257	57

*Bar number denotes approximately one-eighth of an inch. Thus, bar no. 3 denotes a bar having an approximate diameter of 3/8 inch.

BIBLIOGRAPHY

While each chapter contains an extensive list of references, the following is the list of books, codes, and handbooks that were referenced multiple times.

- ACI 318M-2011, *Building Code Requirements for Structural Concrete and Commentary*, American Concrete Institute, Farmington Hills, p. 503.
- BS 8110-1:1997, *Structural Use of Concrete-Part 1: Code of Practice for Design and Construction*, 2nd edition, British Standards Institution, London, p. 151.
- Dayaratnam, P. 2004, *Limit State Design of Reinforced Concrete Structures*, Oxford & IBH Publishing Co. Pvt. Ltd, New Delhi, p. 532.
- Duggal, S.K. 2007, *Earthquake Resistant Design of Structures*, Oxford University Press, New Delhi, p. 448.
- Fanella, D.A. and B.G. Rabbat (ed.) 2002, *PCA Notes on ACI 318-02 Building Code Requirements for Structural Concrete with Design Applications*, 8th edition, Portland Cement Association, Illinois.
- Gambhir, M.L. 2008, *Design of Reinforced Concrete Structures*, Prentice Hall of India Pvt. Ltd, New Delhi, p. 723.
- Ghoneim, M.A. and M.T. El-Mihilmy 2008, *Design of Reinforced Concrete Structures*, Vol.1 to 3, 2nd edition, Al-Balagh Lel Tebaah Wal-Nashr Wattawoza, Cairo.
- IS 456: 2000, *Indian Standard Code of Practice for Plain and Reinforced Cement Concrete*, 4th revision, Bureau of Indian Standards, New Delhi.
- IS 13920:1993, *Indian Standard Code of Practice for Ductile Detailing of Reinforced Concrete Structures Subjected to Seismic Forces*, Bureau of Indian Standards, New Delhi, p. 14.
- Iyengar, K.T.S. and C.S. Viswanatha 1990, *Torsteel Design Handbook for Reinforced Concrete Members with Limit State Design*, Torsteel Research Foundation in India, Mumbai, p. 190.
- Leonhardt, F. and E. Mönig 1977, *Vorlesungen über Massivebau, Dritter Teil, Grundlagen zum Bewehren im Stahlbetonbau*, Dritte Auflage, Springer-Verlag, Berlin, p. 246.
- Nilson, A.H., D. Darwin, and C.W. Dolan 2004, *Design of Concrete Structures*, 13th edition, Tata McGraw Hill Publishing Company Ltd, New Delhi, p. 779.
- McCormac, J.C., and R.H. Brown 2009, *Design of Reinforced Concrete-ACI 318-08 Code edition*, 8th edition, John Wiley & Sons Inc., New York, p. 720.
- NZS 3101:2006, *Part 1: The Design of Concrete Structures, Part 2: Commentary*, Standards, Wellington.
- Park, R. and T. Paulay 1975, *Reinforced Concrete Structures*, John Wiley & Sons, New York, p. 769.
- Paulay, T. and M.J.N. Priestley 1992, *Seismic Design of Reinforced Concrete and Masonry Buildings*, John Wiley & Sons, New York, p. 744.
- Pillai, S.U. and Menon, D. 2009, *Reinforced Concrete Design*, 3rd edition, Tata McGraw Hill Publishing Company Ltd, New Delhi, p. 962.
- Prakash Rao, D.S. 1995, *Design Principles and Detailing of Concrete Structures*, Tata McGraw-Hill Publishing Company Ltd, p. 360.
- Purushothaman, P. 1984, *Reinforced Concrete Structural Elements-Behaviour, Analysis and Design*, Tata McGraw Hill Publishing Company Ltd, New Delhi and Torsteel Research Foundation in India, Bangalore, p. 709.
- Reynolds, C.E., J.C. Steedman, and A.J. Threlfall 2008, *Reinforced Concrete Designer's Handbook*, 11th edition, CRC Press, Boca Raton, Florida, p. 416.
- Sinha, S.N. 2002, *Reinforced Concrete Design*, 2nd revised edition, Tata McGraw-Hill Publishing Company Ltd, New Delhi, p. 708.
- Sinha, S.N. 1996, *Handbook of Reinforced Concrete Design*, Tata McGraw-Hill Publishing Company Ltd, New Delhi, p. 530.
- SP 16:1980, *Design Aids for Reinforced Concrete to IS 456:1978*, Bureau of Indian Standards, New Delhi, p. 232.
- SP 24(S&T):1983, *Explanatory Handbook on Indian Standard Code of Practice for Plain and Reinforced Concrete*, Bureau of Indian Standards, New Delhi, p. 164.
- SP 34:1987, *Handbook on Concrete Reinforcement and Detailing*, Bureau of Indian Standards, New Delhi, p.192.
- Varghese, P.C. 2006, *Limit States Design of Reinforced Concrete*, 2nd edition, Prentice Hall of India Ltd, New Delhi, p. 545.
- Varghese, P.C. 2005, *Advanced Reinforced Concrete Design*, 2nd edition, PHI Learning Pvt. Ltd, New Delhi, p. 534.
- Varyani, U.H. and Radhaji 2005, *Design Aids for Limit State Design of Reinforced Concrete Members*, Khanna Publishers, Delhi, p. 420.
- Wang, C.-K., C.G. Salmon, and J.A. Pincheira 2006, *Reinforced Concrete Design*, 7th edition, John Wiley & Sons Inc., New York, p. 960.
- Wight, J. K. and J. G. MacGregor 2009, *Reinforced Concrete: Mechanics and Design*, 5th edition, Pearson Prentice Hall, New Jersey, p. 1112.

INDEX

<u>Index Terms</u>	<u>Links</u>
A	
Admixtures	11
Chemical	11
Mineral	12
Aggregates	122
Analysis	122
Computer programs	122
Redistribution of moments	124
Relative stiffness	122
Analysis methods	419
Direct design method	420
Equivalent frame method	424
Anchorage bond	264
Axial shortening of column	89
B	
Basic structural elements	46
Columns	47
Retaining walls	49
Trusses	49
Walls	48
Beams	48
Grade	186
Lintel	186
Plinth	186
Behaviour of RC beams under shear	215
Beams without shear reinforcement	218
Beams with shear reinforcements	227
Behaviour of uncracked beams	215
Modes of failure of deep beams	219
Principal stress distribution	217
Types of cracks	217

Index Terms

Links

Behaviour of RC beams under shear (<i>Cont.</i>)		
Typical crack pattern	218	
Variation in shear capacity	218	
Bending	143	
Cracked section	145	
Cracking moment	145	
Euler–Bernoulli equations	143	
Neural axis	143	
Uncracked section	143	
Bond behaviour	266	
Cracking mechanisms	266	
Factors affecting bond strength	267	
Bond force transfer mechanism	262	
C		
Cement	4	
Hydration	16	
Portland cement	7	
Portland pozzolana cement	7	
Portland slag cement	5	
Tests	8	
Characteristic load	70	131
Dead	72	
Design actions	71	
Earthquake	80	
Impact	75	
Imposed	72	
Loads on beam	73	
Snow and ice	75	
Wall loads on beam	74	
Wind	75	
Characteristic strength	131	
Classification of columns	506	
Cross section	506	
Slenderness ratio	507	
Type of reinforcement	507	
Types of loading	507	
Codes	126	

Index Terms

Links

Columns	506	508	
Buckling	508		
Effective length	508		
Unsupported length	508		
Column with axial load	547		
Biaxial bending	557		
Biaxial eccentricity	560		
Uniaxial	546		
Uniaxial eccentricity	559		
Compressive strength of concrete	30		
Factors affecting	30		
Influence of size of specimen	31		
Concrete	1	16	17
Advantages	3		
Autoclaved aerated	20		
Carbonation	26		
Creep	36		
Curing	30		
Disadvantages	3		
Durability	36	109	
Fibre-reinforced	21		
High-performance	18		
History	39	40	
Mixing	28		
Modulus of elasticity	33		
Poisson's ratio	33		
Ready-mixed	17		
Removal of forms	28		
Self-compacting	19		
Strength under combined stresses	35		
Stress–Strain curves	32	49	
Structural lightweight	20		
Temperature effects	35		
Types	17		
Confining reinforcement	532		
Circular columns	523		
Rectangular columns	523		
Square columns	524		

Index Terms

Links

Controlled permeability formwork	116	
Corrosion	111–116	
Cover	111	
Clear	112	
Nominal	111	113
Required	112	
Spacers and chairs	113	
Super cover system	113	
Cracking in RC members	484	
Control provisions	487	
Crack width limit	487	
Mechanism	486	
Types of cracks	485	
Critical section for shear	234	
Enhanced shear strength	235	
Curing of concrete	111	
Curtailement of reinforcement	293	
Bundled bars	274	294
Flexural members	293	
Negative moment reinforcement	294	
Positive moment reinforcement	293	
Special member	295	

D

Deep beams	181	
Bearing strength	184	
Distribution of reinforcement	183	
Lateral buckling	184	
Strut-and-tie model	136	181
Termination of reinforcement	183	
Vertical reinforcement	183	
Deflection of cantilevers	497	
Deflection of two-way slab	483	
Design considerations	105	
Aesthetics	116	
Economy	109	
Environment friendliness	116	
Functional requirements	118	

Index Terms

Links

Design considerations (<i>Cont.</i>)		
Safety	105	
Serviceability	109	
Stability	108	
Design method of concrete walls	647	
Design of anchors	761	
Design of corbels	758	
Design of pedestals	525	
Design of slabs	335	
Concrete cover	338	
Confinement factor	343	
Effective span	336	
General considerations	335	
High-strength concrete	341	
High-strength steel	342	
Minimum thickness	336	
Shear and size effect	343	
Design of water tanks	734	
Design philosophies	126	
Limit states design	133	
Ultimate load design	128	
Working stress method	127	
Design shear strength	231	
Loading condition	234	
Maximum shear stress	233	
Design using load tests	136	
Detailing of reinforcements	379	443
Edge columns	457	
Structural integrity reinforcement	444	
Development length	269	
Analytical development length	270	
Bars in compression	274	
Codal provisions	271	
Critical sections for development	270	
Excess reinforcement	274	
Welded wire fabric	26	275

Index Terms

Links

Devices to reduce earthquake effects	85			
Base isolation	85			
Dampers	86			
Energy-absorbing devices	86			
Doubly reinforced rectangular beams	162			
Analysis	165			
Behaviour	164			
Design	166			
Design using charts	168			
Limiting moment of resistance	166			
Ductile fibre-reinforced cementitious composites	21			
Engineered cementitious composites (ECC)	22			
SIFCON	23			
SIMCON	23			
Ultra-high-performance concrete	23			
Ductility	120			
Hysteretic curve	120			
Durability	109			
Carbonation	110			
Cover	111			
Exposure requirements	110			
Prescriptive requirements	110			
Durability of concrete	36			
Dynamic effects	78			
E				
Earth pressure	655			
Coulomb's theory	655			
During earthquakes	656			
Rankine's theory	656			
Earthquake considerations	20	34	349	396
	526	570	622	712
Built-in staircases	713			
Confining reinforcement	532			
Diaphragm	349	396		
Longitudinal reinforcement	534			
Semi-rigid diaphragm	349	397		
Separated staircases	713			

Index Terms

Links

Earthquake considerations (<i>Cont.</i>)		
Staircases with sliding joints	713	
Strong column–Weak beam concept	527	
Transverse reinforcement	528	556
Earthquake effects	446	
Deformation capacity	448	
Diaphragm action	447	
Effective slab width	447	
Earthquake loads	80	
Damping	82	
Design horizontal seismic coefficient	82	
Equivalent static method	83	
Importance factor	82	
MMI scale	80	
Mode shape	82	
MSK scale	80	
Natural frequencies	82	
Probabilistic Seismic Hazard Map	82	
Response reduction factor	82	
Response spectrum	82	
Richter scale	80	
Rules to be followed	84	
Soil liquefaction	80	
Tsunami	81	
Zone factor	82	
Environment friendliness	116	
Geopolymer concrete	118	
Erection and construction loads	89	
F		
Factors affecting shear strength	229	
Axial forces	229	
Lightweight aggregate concrete	229	
Longitudinal reinforcement ratio	229	
Shear span to effective depth ratio	229	
Size effect	229	
Size of beam	229	
Size of coarse aggregate	229	

Index Terms

Links

Factors affecting shear strength (<i>Cont.</i>)		
Tensile strength	33	229
Failures	66	
Congress Hall, Berlin	113	
Ferrybridge Cooling Towers	66	
Roman Point Collapse	65	
Fatigue behaviour of beams	188	
Ferrocement	23	
Fire resistance	115	
Flanged beams	168	256
Analysis	171	
Behaviour	170	
Design	178	
Doubly reinforced	176	
Effective width	169	
L-beams	180	
Negative moment	178	
Positive moment	178	
Transverse reinforcement	174	
Flat slabs	415	
Behaviour	417	
Column heads	416	
Design procedure	441	
Drop panel	416	
Openings	445	
Proportioning	416	
Shear cap	417	
Thickness	416	
Flexural bond stress	263	
Flexure	146	
Analysis	146	
Effective span	146	
Flood loads	89	
Floor and roof systems	51	
Bearing wall	51	
Composite floors	56	
Grid	56	
Insulated RC walls	52	

Index Terms

Links

Floor and roof systems (*Cont.*)

Masonry wall	51	
One-way and two-way slab	52	
Tilt-up concrete walls	52	
Footings	47	587
Combined footings	602	
Plain concrete footings	609	
Soil pressure	587	
Two-column footings	604	
Types	585	
Foundation movements	87	
Frames	511	
Non-sway	513	
Sway	513	
Functional requirements	118	
Constructability	119	
Welded reinforcement grids	119	

G

Grid slab	450	
-----------	-----	--

H

Hidden beams	185	
Hollow-core slab	450	

I

Internal curing	20	
-----------------	----	--

J

Joints	746	
Beam-to-beam joints	756	
Beam-column joints	744	
Closing corner joints	747	
Corner joints	747	
Design	445	
Detailing	445	
T-joints	747	

Index Terms

Links

Jump-form construction	66
L	
Lateral load resisting systems	57
Braced-tube	60
Bundled-tube	61
Buttressed core	62
Diagrid	62
Framed tube	60
Outrigger and belt truss	59
Rigid or moment-resisting	58
Shear-walled frame	58
Transfer girders	62
Tube-in-tube	61
Limit state of deflection	468
Design	468
Effect of deflection	468
Immediate deflection	336
Limiting deflection	135
Time-dependent deflection	503
Limit states format	133
Load and resistance factor	133
Multiple safety factor	133
Partial safety factor	133
Limit states method	132
Levels of reliability methods	130
Limit states	130
Serviceability limit states	130
Special limit states	130
Ultimate limit states	130
Uncertainties in design	129
Load combinations	592
For non-orthogonal buildings	91
Long-term deflection	447
Codal equations	479
Compression steel effect	479
Due to creep	479
Due to differential shrinkage	481

Index Terms

Links

Long-term deflection (*Cont.*)

Due to temperature	481
Long-time loading	478
Typical stress–strain curves	478

M

Methods of curing	111		
Minimum flexural ductility	180		
Minimum requirements	184		
Shear reinforcement in beam	231		
Size	232		
Spacing of stirrups in beams	106		
Steel in columns	524		
Steel requirements in beam	106		
Tensile steel in beam	107		
Mix design	10	13	17
Multi-storey building	790		

N

Natural frequency	34		
Moment-resisting frame	749		
Other building	83		
Shear walled buildings	83		
Non-destructive testing	105		
Non-rectangular slabs	381		
Circular	381		
Polygonal	385		
Trapezoidal	391		
Triangular	394		

O

One-way slabs	407		
Analysis	410		
Behaviour	410		
Concentrated load on	410		
Design of culvert	345		
Design procedure	368		

Index Terms

Links

P

Partial load factors	134
For loads	134
For material	135
Pattern loading	339
Performance-based design	102
Pile caps	619
Piles	613
Precast and prestressed buildings	56
Project specifications	126
Properties of concrete	62
Bond strength	263
Compressive strength	267
Cube and cylinder tests	30
Shear strength	33
Workability	37
Proportioning of concrete mixes	39

R

Reinforcing bars	303	
Anchoring	330	
Bends in tension	276	
Bent-up bars	223	281
Headed bars	302	
Reinforced concrete stairs	724	
Components	743	
Helicoidal staircases	711	
Longitudinally supported	711	
Structural classification	707	
Transversely supported	708	
Reinforcement detailing	710	
Columns in multi-storey frames	521	
Concrete cover	534	
Longitudinal reinforcement	555	
Reinforcing steel	582	
Basalt bars	27	
Corrosion	27	

Index Terms

Links

Reinforcing steel (<i>Cont.</i>)	
FRP bars	27
Fusion bonded epoxy-coated reinforcing bars	27
Galvanized reinforcing bars	27
HYSB bars	40
Stainless steel bars	27
TMT bars	39
Retaining walls	45
Anchored-retaining	651
Basement	652
Buttressed-retaining	651
Cantilever-retaining	651
Counterfort-retaining	651
Crib walls	696
Design	696
Gabions	696
Gravity-retaining	650
Segmental-retaining	651
Types	651
Ribbed slabs	354
Arrangement of reinforcement	125
Hollow block	347
Voided slabs	347
Roles and responsibilities of designer	103
Roofs	135
Pyramidal	395
Sloped	395
 S 	
Sampling and acceptance criteria	30
Self-desiccation of concrete	20
Serviceability limit state	72
Crack widths	88
Deflections	469
Vibration	491
Shear design	595
Beams located in earthquake zones	244
Beams with varying depth	243

Index Terms

Links

Shear design (<i>Cont.</i>)		
Beams with web opening	246	
Members with axial force	247	
Shear friction	248	
Shear in flat plates	427	
Beam shear	427	
Punching shear	427	
Punching shear strength	428	
Shear reinforcement	184	428
Design aids	432	
Design procedure	440	
Modified compression field theory	240	
Ritter–Mörsch truss model	257	
Short-term deflection	469	
Continuous beams	473	470
Deflection coefficient	473	
Instantaneous deflection	469	
Load-deflection behaviour	475	
Moment of inertia	473	
Service load stresses	500	
Simple spring models	474	
Tension stiffening	500	
Transformed section	475	
Typical shrinkage strains	475	
Short columns	527	
Behaviour	526	
Design	233	
Rectangular columns with axial loading	523	
Spiral columns	507	
Shrinkage	88	
Compensating concrete	88	
Strip	88	
Shrinkage and temperature reinforcement	87	
Shrinkage of concrete	42	
Autogenous	20	
Side face reinforcement	501	
Crack control	497	
Fatigue control	495	

Index Terms

Links

Side face reinforcement (<i>Cont.</i>)			
Vibration control	491		
Singly reinforced rectangular sections	189		
Analysis	165		
Balanced section	165		
Clear cover	159		
Clear side cover	159		
Compression-controlled section	647		
Design	553		
Ductile failure	553		
Effective depth	481		
Minimum depth	153		
Over-reinforced section	162		
Parabolic-rectangle stress block	142		
Slenderness limit	157		
Tension-controlled section	156		
Ultimate moment of resistance	146		
Under-reinforced section	150		
Skew bending theory	318		
Lateral bending failure	319		
Modified bending failure	319		
Negative bending failure	319		
Torsion-flexure interaction curves	320		
Torsion-shear interaction curves	320		
Slab-on-grade	350		
Compacted subgrade	350		
Shrinkage-compensating concrete	350		
Slab-on-ground	350		
Vapour barrier	350		
Slabs	2	48	802
Flat plates	54		
Flat slab	54		
One-way slabs	52	335	
Voided two-way flat	54		
Voided two-way slab	54		
Waffle flat	54		

Index Terms

Links

Slender columns	562
Behaviour	563
Definition	562
Design approaches	565
Design procedure	570
Slip-form construction	66
Soil and hydrostatic pressure	88
Splicing of reinforcement	282
Compression splices	286
Direct splices	288
Indirect splices	282
Inline couplers	291
Lap splices	284
Mechanical lap splice	291
Mechanical splices	290
Offset couplers	291
Offset mechanical splice	291
Welded splices	288
STAAD.Pro	795
Beams	799
Columns	778
Equivalent static analysis	795
Estimation of loads	794
Example frame	791
Foundations	798
Gravity load analysis	796
Input file	802
Lateral load analysis	796
Load combinations	796
Response spectrum analysis	795
Seismic analysis	794
Structural layouts	792
Stair slabs	707
Distribution of loads	707
Spanning longitudinally	709
Spanning transversely	707
Steps involved in construction	102
Strength reduction factor	133

Index Terms

Links

Structural integrity	64		
Demand-to-capacity ratio (DCR)	64		
Structural walls	665		
Behaviour	666		
Design	668		
Openings	680		
Types	665		
T			
Tall buildings	808		
Tension members	726		
Behaviour	726		
Design methods	727		
Detailing	733		
Large eccentricity	730		
Small eccentricity	729		
Thermal effects	87		
Coefficient of thermal expansion	87		
Torsion	306		
Behaviour of beams	309		
Compatibility torsion	306		
Equilibrium torsion	306		
In curved beams	308		
Plastic space truss model	313		
Primary torsion	306		
Secondary torsion	306		
Statically indeterminate torsion	307		
Theoretical models	312		
Torsional analysis	309		
Elastic analysis	309		
Plastic analysis	310		
Two-way slabs	52	335	362
Beam-supported	367	378	
Behaviour	332		
Concentrated loads	386		
Design procedure	378		
Openings	377		
Restrained two-way slabs	379		

Index Terms

Links

Two-way slabs (<i>Cont.</i>)		
Shear forces	374	
Simply supported	335	379
Wall-supported	367	
Types of reinforced concrete walls	645	
Braced	645	
Load-bearing	645	
Non-load-bearing	645	
Shear	645	
Slender	645	
Stocky	645	
Structural	645	
Unbraced	645	
Types of shear reinforcements	220	
Headed studs	224	
Inclined stirrups	224	
Spirals	224	
Steel fibres	226	
Vertical stirrups	221	
Types of slabs	334	
Cantilevered	334	
Continuous	334	
Types of staircases	703	
Branching	704	
Half-turn	704	
Helicoidal	704	
Open-well	704	
Quarter-turn	704	
Spiral	704	
Straight flight	704	
V		
Vortex shedding	77	
W		
Waffle slabs	54	449
Left-in-place shuttering	449	
Two-way ribbed slab	449	

Index Terms

Links

Wide shallow beams	185
Wind load	2
As source of energy	29
Working stress method	127
Limitations	128
Permissible stresses in concrete	127
Permissible stresses in steel	127
Response reduction factor	121

Y

Yield-line analysis	388
Equilibrium method	394
Limitations	394
Lower bound theorem	389
Orthotropic reinforcement	390
Skewed yield lines	390
Upper bound theorem	389
Virtual work method	391